ACTA CHEMICA SCANDINAVICA 27 (1973) 2001–2012

Thermal Fragmentations

VI. The Preparation of Aryl *N*-Monoalkyldithiocarbamates and Their Behaviour upon Heating

CHARLES LARSEN[a] and PALLE JAKOBSEN[b]

[a]*Department of General and Organic Chemistry, University of Copenhagen, The H. C. Ørsted Institute, DK-2100 Copenhagen, Denmark and* [b]*Institute for Chemistry, University of Copenhagen, Rådmandsgade 71, DK-2200, Copenhagen, Denmark*

The reaction between aliphatic isothiocyanates and aromatic thiols forming *N*-monosubstituted dithiocarbamates, and the thermal stability of these compounds have been investigated. Most dithiocarbamates were easily accessible by mixing equimolar amounts of isothiocyanate and thiol without addition of solvent. The ^{1}H NMR spectra of the compounds were interpreted, and a case of hindered rotation about the CN bond is demonstrated and discussed. The thermal stability of some of the compounds were estimated from ^{1}H NMR spectra recorded at various temperatures. In one case $\Delta H°$ for the dissociation of the dithiocarbamate into isothiocyanate and thiol was calculated. Mass spectra have demonstrated that the first step in the main degradation route due to electron impact is identical to the thermal induced one.

The fragmentation of alkyl *N*,*N*-dialkyldithiocarbazates upon heating to give *N*-isothiocyanatoamines and thiols [1] led us to investigate the similar reaction with aryl *N*-monoalkyldithiocarbamates. As early as 1869 Hofmann [2] observed that on distillation of ethyl *N*-ethyldithiocarbamate at atmospheric pressure it fragmented into ethyl isothiocyanate and ethanethiol. Later, Delépine [3] and Braun [4] found that Hofmann's observation was characteristic of both alkyl *N*-alkyldithiocarbamates and the corresponding alkyl *N*-aryl compounds. In support Ottenbrite [5] reported the preparation of aryl isothiocyanates by thermal decomposition of methyl *N*-aryldithiocarbamates.

Since information about aryl *N*-monosubstituted dithiocarbamates is sparse in the literature, it was necessary to investigate not only the formation and fragmentation, but also the physical and chemical properties of these compounds.

The reaction between aliphatic isothiocyanates and aromatic thiols proceeds remarkably simply. Mixing equimolar amounts of the starting materials

without addition of solvent resulted usually in formation of analytically pure *N*-alkyl dithiocarbamates. The yields range from 30 to 100 % (see Table 1). The necessity of adding basic catalysts

$$R^1NCS + R^2SH \rightarrow R^1NHCSSR^2$$

to the reaction mixture, claimed by Roshdestwenski [6] and later by Cherbuliez *et al.*,[7] was not confirmed as illustrated by the reaction between methyl isothiocyanate and benzenethiol. One h after mixing the two components crystals began to separate. After 2 h the whole mixture had solidified and a quantitative yield of phenyl *N*-methyldithiocarbamate (Ia) was obtained. Nor was it found necessary to irradiate the mixture of the two compounds with an unfrosted incandescent lamp, as claimed in a Belgian patent [8] for the preparation of 4-chlorophenyl *N*-methyldithiocarbamate (Ii). Some of the compounds listed in Table 1 are mentioned in this patent, with melting points which in some cases are lower than the ones found by us. Also, the yields are improved by our method.

To obtain information about whether differences in reactivity, yields, and stability could be correlated with steric and electronic properties of the starting materials or the products, the reaction was performed with differently substituted aromatic thiols and various isothiocyanates. The identity of the products was confirmed by elemental analyses, IR [9] and ^{1}H NMR spectroscopy. In individual cases the mass spectrum also was recorded. Methods of preparation, yields, melting points, and elemental analyses are presented in Table 1.

The reactivity of alkyl isothiocyanates towards thiols is fairly high, but is exceeded by that of *N*-isothiocyanatodialkylamines, as pointed out by Anthoni, Larsen and Nielsen.[10] In most reactions the time necessary for complete solidification of the mixture was *ca.* 24 h, though great variations were found. For those mixtures which had solidified before the end of the investigation, the time varied from 2 h to 2 months. Thus formation of Ia was accomplished in 2 h, while the formation of 2,4,6-trimethylphenyl *N*-methyldithiocarbamate (If) lasted 2 months.

It was expected that the acidity of the thiol would have considerable effect on the time of reaction, assuming a mechanism consisting of a nucleophilic attack of the thiolate ion on the carbon atom of the NCS group. The results, however, seem to indicate that other factors are more important. Thus the time for solidification is approximately the same for the reactions between methyl isothiocyanate and benzenethiol, 4-methoxybenzenethiol, 4-methylbenzenethiol, and 4-fluorobenzenethiol though these thiols present pronounced differences in stability of the anions.

To explore if steric crowding affects the reaction, 2,4,6-trimethylbenzenethiol was treated with methyl, ethyl, and isopropyl isothiocyanates. The times of reaction were 2 months, 1 day, and 1 week, respectively. When methyl isothiocyanate was treated with benzenethiol, 2-methylbenzenethiol, and 2,4,6-trimethylbenzenethiol, the times were 2 h, 2 days, and 2 months, respectively. Mixing the same three thiols with isopropyl isothiocyanate gave respective times of 1 day, 2 days and 1 week.

Even if the preceding information reveals no simple relationship between steric effects and reactivity, the fact that *t*-butyl isothiocyanate did not react

Table 1. *N*-Monoalkyldithiocarbamates $R^1NHCSSR^2$

Compound	R^1	R^2	Method	Yield	M.p. °C	Formula	Analyses (C, H, N, S)
Ia	Me	C_6H_5	A[8]	100	131 – 132	$C_8H_9NS_2$	Found: 52.48; 5.02; 7.66; 34.72 Calc.: 52.42; 4.95; 7.64; 34.99
Ib	Me	2-MeC_6H_4	A[8]	100	92 – 93	$C_9H_{11}NS_2$	Found: 54.60; 5.57; 7.01; – Calc.: 54.78; 5.62; 7.10; –
Ic	Me	3-MeC_6H_4	A	100	83 – 84	$C_9H_{11}NS_2$	Found: 54.80; 5.70; 7.07; 32.31 Calc.: 54.78; 5.62; 7.10; 32.50
Id	Me	4-MeC_6H_4	A[8]	100	90 – 91	$C_9H_{11}NS_2$	Found: 54.60; 5.53; 7.05; 32.36 Calc.: 54.78; 5.62; 7.10; 32.50
Ie	Me	4-$Bu^tC_6H_4$	A[8]	50	161 – 162	$C_{12}H_{17}NS_2$	Found: 60.01; 7.20; 5.86; 26.61 Calc.: 60.21; 7.14; 5.85; 26.79
If	Me	2,4,6-$Me_3C_6H_2$	A	70	106 – 107	$C_{11}H_{15}NS_2$	Found: 58.45; 6.83; 6.20; – Calc.: 58.65; 6.71; 6.22; –
Ig	Me	4-$MeOC_6H_4$	A	100	129 – 130	$C_9H_{11}NOS_2$	Found: 50.45; 5.23; 6.53; 29.87 Calc.: 50.67; 5.20; 6.57; 30.06
Ih	Me	4-FC_6H_4	A	100	132 – 133	$C_8H_8NS_2F$	Found: 47.50; 4.04; 6.91; – Calc.: 47.74; 4.01; 6.96; –
Ii	Me	4-ClC_6H_4	B[8]	100	111 – 112	$C_8H_8NS_2Cl$	Found: 44.10; 3.75; 6.49; 29.93 Calc.: 44.13; 3.70; 6.43; 29.45
Ij	Me	4-BrC_6H_4	B	80	136 – 137	$C_8H_8NS_2Br$	Found: 36.61; 3.09; 5.36; 24.28 Calc.: 36.65; 3.08; 5.34; 24.46
Ik	Me	2-$NH_2C_6H_4$	C[12]	80	91 – 92	$C_8H_{10}N_2S_2$	Found: 48.25; 5.16; 14.14; – Calc.: 48.45; 5.08; 14.12; –
Il	Me	4-$NH_2C_6H_4$	C[12]	77	103 – 104	$C_8H_{10}N_2S_2$	Found: 48.05; 5.05; 13.94; 32.18 Calc.: 48.45; 5.08; 14.12; 32.34
Im	Me	4-$NHCOCH_2C_6H_4$	D	84	167 – 169	$C_{10}H_{12}N_2OS_2$	Found: 49.80; 5.00; 11.63; 26.80 Calc.: 49.97; 5.03; 11.66; 26.68

Table 1. Continued.

In	Me	$C_6H_5CH_2$	A[3,11]	37	47 – 48	$C_9H_{11}NS_2$	Found:	54.99;	5.70;	7.24;	–
							Calc.:	54.78;	5.62;	7.10;	–
Io	Me	$4\text{-}ClC_6H_4CH_2$	A	45	75 – 76	$C_9H_{10}NS_2Cl$	Found:	46.80;	4.45;	5.89;	27.52
							Calc.:	46.64;	4.35;	6.04;	27.67
Ip	Me	$2,3,4,5,6\text{-}F_5C_6$	A	100	131 – 132	$C_9H_4NS_2F_5$	Found:	35.04;	1.49;	5.09;	23.40
							Calc.:	35.16;	1.48;	5.13;	23.47
Iq	Me	$2\text{-}COOHC_6H_4$	–	50	149 – 150	$C_9H_9NO_2S_2$	Found:	47.39;	4.04;	6.05;	–
							Calc.:	47.55;	3.99;	6.16;	–
IIa	Et	C_6H_5	E	30	33 – 34	$C_9H_{11}NS_2$	Found:	54.96;	5.65;	7.16;	–
							Calc.:	54.78;	5.62;	7.10;	–
IIb	Et	$2\text{-}MeC_6H_4$	A	37	35 – 36	$C_{10}H_{13}NS_2$	Found:	57.04;	6.34;	6.66;	–
							Calc.:	56.83;	6.20;	6.63;	–
IIc	Et	$3\text{-}MeC_6H_4$	A	70	56 – 57	$C_{10}H_{13}NS_2$	Found:	56.80;	6.28;	6.60;	–
							Calc.:	56.83;	6.20;	6.63;	–
IId	Et	$4\text{-}MeC_6H_4$	A	62	61 – 62	$C_{10}H_{13}NS_2$	Found:	56.60;	6.26;	6.55;	30.07
							Calc.:	56.83;	6.20;	6.63;	30.34
IIe	Et	$2,4,6\text{-}Me_3C_6H_2$	A	100	51 – 52	$C_{12}H_{17}NS_2$	Found:	60.35;	7.16;	5.76;	26.64
							Calc.:	60.20;	7.16;	5.85;	26.79
IIf	Et	$4\text{-}MeOC_6H_4$	A	100	99 – 100	$C_{10}H_{13}NOS_2$	Found:	52.88;	5.88;	6.18;	28.09
							Calc.:	52.83;	5.76;	6.16;	28.21
IIIa	Pr^i	C_6H_5	A	47	77 – 78	$C_{10}H_{13}NS_2$	Found:	57.20;	6.37;	6.68;	–
							Calc.:	56.83;	6.20;	6.63;	–
IIIb	Pr^i	$2\text{-}MeC_6H_4$	A	76	53 – 54	$C_{11}H_{15}NS_2$	Found:	58.85;	6.75;	6.21;	28.59
							Calc.:	58.64;	6.71;	6.22;	28.46
IIIc	Pr^i	$3\text{-}MeC_6H_4$	A	75	50 – 51	$C_{11}H_{15}NS_2$	Found:	58.52;	6.70;	6.10;	–
							Calc.:	58.64;	6.71;	6.22;	–

Table 1. Continued.

IIId	Pr^i	4-MeC_6H_4	A	55	54 – 55	$C_{11}H_{15}NS_2$	Found:	58.84;	6.71;	6.15;	–
							Calc.:	58.64;	6.71;	6.22;	–
IIIe	Pr^i	2,4,6-$Me_3C_6H_2$	A	36	65 – 66	$C_{13}H_{19}NS_2$	Found:	61.60;	7.62;	5.54;	–
							Calc.:	61.61;	7.56;	5.53;	–
IIIf	Pr^i	$C_6H_5CH_2$	A[11]	71	35 – 36	$C_{11}H_{15}NS_2$	Found:	58.55;	6.78;	6.21;	–
							Calc.:	58.64;	6.71;	6.22;	–
IVa	Bu^s	4-MeC_6H_4	A	63	34 – 35	$C_{12}H_{17}NS_2$	Found:	59.96;	7.21;	5.83;	–
							Calc.:	60.20;	7.16;	5.85;	–
Va	cyclohexyl	C_6H_5	A	100	87 – 88	$C_{13}H_{17}NS_2$	Found:	62.02;	6.88;	5.60;	25.59
							Calc.:	62.10;	6.82;	5.57;	25.51
Vb	cyclohexyl	3-MeC_6H_4	A	100	68 – 69	$C_{14}H_{19}NS_2$	Found:	63.50;	7.22;	5.25;	23.94
							Calc.:	63.35;	7.22;	5.28;	24.16
Vc	cyclohexyl	4-MeC_6H_4	A	50	50 – 60	$C_{14}H_{19}NS_2$	Found:	63.32;	7.30;	5.28;	–
							Calc.:	63.35;	7.22;	5.28;	–
VIa	Ph	C_6H_5	A	100	133 – 134	$C_{13}H_{11}NS_2$	Found:	63.30;	4.51;	5.61;	–
							Calc.:	63.64;	4.52;	5.71;	–
VIb	Ph	4-MeC_6H_4	A	60	151 – 152	$C_{14}H_{13}NS_2$	Found:	64.88;	5.17;	5.33;	–
							Calc.:	64.82;	5.05;	5.40;	–
VIc	Ph	4-ClC_6H_4	A	40	145 – 146	$C_{13}H_{10}NS_2Cl$	Found:	55.85;	3.67;	4.93;	–
							Calc.:	55.80;	3.60;	5.01;	–
VId	Ph	4-BrC_6H_4	A	100	137 – 138	$C_{13}H_{10}NS_2Br$	Found:	48.02;	3.20;	4.22;	–
							Calc.:	48.15;	3.11;	4.32;	–

within 6 months with benzenethiol, 4-methoxybenzenethiol, or phenylmethanethiol indicates that steric effects do have importance. One might object that the reason for these results was that the corresponding dithiocarbamates might be unstable at room temperature and fragment into thiol and isothiocyanate (see later), but as Wakamori *et al.*[11] have prepared benzyl *N-tert*-butyldithiocarbamate from the corresponding sodium salt and benzyl chloride and purified it by distillation (b.p. 130 – 133°C/0.04 mmHg), this possibility seems very unlikely.

A part of the explanation may be the absence of solvent. This means that the surroundings of the reactants were different in the various experiments. As different reactants will differ in ability to solvate one another, the degree of freedom with which the molecules can "move around" differs far more in these experiments than in comparable series where both reactants are solvated with the same solvent. The rate at which crystallization occurs might in some cases be of importance to the time of reaction found, but infrared spectroscopy showed that in the reaction between methyl isothiocyanate and 2,4,6-trimethylbenzenethiol it was impossible to detect any trace of If after the mixture had been left for 1 month at room temperature. This suggests that the reaction does not just proceed slowly, but that other factors play a dominant role.

Some experiments were carried out with added solvent (ethanol), but in all cases the time of reaction was prolonged; *e.g.* the formation of Ia from methyl isothiocyanate and benzenethiol was not accomplished in 5 h when the reaction was performed in ethanol, compared to a reaction time of 2 h without the use of solvent.

The reaction between methyl isothiocyanate and 2- and 4-aminobenzenethiols was shown by Anthoni *et al.*[12] to give dithiocarbamates. It was concluded that the reactivity of the aromatic groups concerned towards the isothiocyanate function appears to decrease in the order $SH > NH_2 > OH$. As an extension of this investigation we examined the reaction of methyl isothiocyanate and 2-mercaptobenzoic acid. After prolonged standing of an ethanolic solution of the two compounds at room temperature, 3-methyl-2-thioxo-3,4-dihydro-2H-benzo[e]-1,3-thiazin-4-one was obtained.

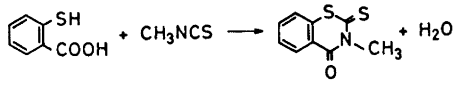

This product was earlier prepared from the same compounds + "cation exchange resin KU-2" [13] by reflux in toluene for 2 h. However, reducing the time of reaction to 1 week resulted in the formation of the expected 2-carboxyphenyl *N*-methyldithiocarbamate (Iq). The reactivity of the aromatic SH group towards isothiocyanates thus seems to exceed that of the COOH group.

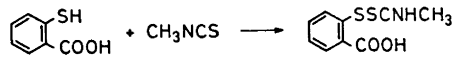

Iq

In the ^{1}H-NMR spectrum of phenyl *N*-methyldithiocarbamate (Ia) (Table 2) the phenyl protons occurred as a singlet (5H) at $\tau = 2.43$ ppm, the NH proton gave a broad signal (1H) at $\tau = 2.5 - 3.3$ ppm and the methyl signal (3H) consisted of a doublet centered at $\tau = 6.87$ ppm ($J = 4.9$ Hz). After shaking the solution of Ia with deuterium oxide it produced a spectrum consisting of a singlet at $\tau = 2.43$ ppm and a singlet at $\tau = 6.87$ ppm (intensities 5:3). This shows that the doublet at $\tau = 6.87$ ppm arises from coupling with a labile hydrogen atom, so a structure like (a) seems most likely.

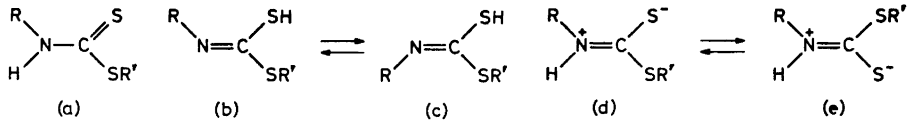

Accordingly nonequivalence of the methyl protons due to hindered rotation about a double bond as in the structures (b) and (c) is of no importance. This was also seen from the IR spectrum of the compound, which showed no absorption in the SH-stretching region but did show a NH-stretching absorption. Cooling the $CDCl_3$ solution of Ia to -40°C caused no change in the ^{1}H-NMR spectrum. Consequently hindered rotation about the CN bond caused by structures like (d) and (e) does not contribute in the temperature interval investigated. A similar investigation on IIIa, in which a greater tendency to hindered rotation could be expected, gave the same result.

In contrast to this behaviour, cooling of benzyl *N*-methyldithiocarbamate (In) produced a splitting of the doublet from the methyl signal into two doublets. Following the temperature dependence of the change in the methyl doublet showed that at 40°C there was one broad doublet, which on cooling showed a minor change in chemical shift ($\tau = 6.81$ to $\tau = 6.77$ ppm, $J = 4.8$ Hz) and at the same time became sharper and of lower intensity, while a new doublet appeared at $\tau = 6.95$ ppm, ($J = 5.3$ Hz). Simultaneously the singlet from the CH_2-group split up into two singlets. In the interval -15 to -40°C the integrals of the two doublets had a ratio of 2:1. A similar investigation of 4-chlorobenzyl *N*-methyldithiocarbamate (Io) yielded one doublet at 45°C and a ratio of 18:7 between the two doublets formed by cooling to -40°C. In IIIf it was not possible to detect any splitting of the methine signal on cooling, but at temperatures below 30°C there was a clear splitting of the methylene singlet, showing that a new singlet arises at *ca.* 4 Hz lower field. Simultaneously a faint change in the methyl signal could be detected (a new doublet appeared at a slightly higher field).

We therefore conclude that there definitely is hindered rotation about the CN bond in the benzyl compounds investigated, when the solutions are cooled. This hindrance may arise from structures like (d) and (e) which Holloway and Gitlitz found of importance for methyl *N*,*N*-dimethyldithiocarbamate.[14]

The absence of splitting in the low temperature spectra of the *S*-phenyl dithiocarbamates might result from (1) coincidence of chemical shift in the two forms (2) predominance of one form, *e.g.* (a) or (a′), to a high degree, or (3) a low barrier to rotation.

For some *N*,*N*-disubstituted carbamates [15] and for some thioamide derivatives [16] differences in barrier to internal rotation has been explained as arising from cross conjugation. In the present case the difference between the low

Table 2. Chemical shift[a] (τ, ppm) and coupling constants (J, Hz) of some aliphatic protons of *N*-monoalkyldithiocarbamates in $CDCl_3$ (5 % solution, 40°C). Multiplicity given in parentheses.

Compound	H^1	H^2	H^3	NH	J_{CH-NH}
$C_6H_5SCSNHCH_3^1$	6.87 (2)			2.5 – 3.3	4.9
o-$CH_3^2C_6H_4SCSNHCH_3^1$	6.87 (2)	7.53 (1)		3.1 – 3.8	5.0
m-$CH_3^2C_6H_4SCSNHCH_3^1$	6.86 (2)	7.58 (1)		2.8 – 3.5	5.0
p-$CH_3^2C_6H_4SCSNHCH_3^1$	6.87 (2)	7.57 (1)		3.0 – 4.0	5.0
p-$(CH_3^2)_3CC_6H_4SCSNHCH_3^1$	6.85 (2)	8.63 (1)		2.7 – 3.5	4.8
$2,^24,^36^2$-$(CH_3)_3C_6H_2SCSNHCH_3^{1c}$	6.89 (2)	7.60 (1)	7.67 (1)	3.1 – 3.6	4.8
p-$CH_3^2OC_6H_4SCSNHCH_3^1$	6.88 (2)	6.12 (1)		3.1 – 3.8	4.8
p-$FC_6H_4SCSNHCH_3^1$	6.82 (2)			3.0 – 4.0	4.9
p-$ClC_6H_4SCSNHCH_3^1$	6.83 (2)			2.7 – 3.9	5.0
p-$BrC_6H_4SCSNHCH_3^1$	6.84 (2)			2.8 – 3.8	5.0
o-$NH_2^2C_6H_4SCSNHCH_3^1$	6.88 (2)	5.5		3.0 – 3.5	4.9
p-$NH_2^2C_6H_4SCSNHCH_3^1$	6.90 (2)	5.9		3.0 – 3.5	4.8
p-$CH_3^2CONH^3C_6H_4SCSNHCH_3^{1b}$	7.01 (2)	7.92 (1)	– 0.13	0.8 – 1.2	4.8
$C_6H_5CH_2^2SCSNHCH_3^1$	6.78 (2)	5.44 (1)		2.7 – 4.3	4.5
p-$ClC_6H_4CH_2^2SCSNHCH_3^1$	6.77 (2)	5.47 (1)		2.7 – 2.8	4.5
$F_5C_6SCSNHCH_3^1$	6.75 (2)			2.5 – 3.0	4.8
o-$COOH^2C_6H_4SCSNHCH_3^{1b}$	6.99 (2)	0.3 – 0.8		2.0 – 2.6	4.5
$C_6H_5SCSNHCH_2^1CH_3^2$	6.33 (2 4)	9.80 (3)		3.0 – 4.0	5.2
o-$CH_3^3C_6H_4SCSNHCH_2^1CH_3^2$	6.32 (2 4)	8.90 (3)	7.55 (1)	3.1 – 4.1	5.2
m-$CH_3^3C_6H_4SCSNHCH_2^1CH_3^2$	6.32 (2 4)	8.87 (3)	7.57 (1)	3.0 – 4.0	5.3
p-$CH_3^3C_6H_4SCSNHCH_2^1CH_3^2$	6.32 (2 4)	8.90 (3)	7.58 (1)	2.9 – 3.9	5.2
$2^3,4,6^3$-$(CH_3)_3C_6H_2SCSNHCH_2^1CH_3^2$	6.37 (2 4)	8.92 (3)	7.60 (1)	3.0 – 3.6	5.2
p-$CH_3^3OC_6H_4SCSNHCH_2^1CH_3^2$	6.33 (2 4)	8.89 (3)	6.12 (1)	3.1 – 3.8	5.0
$C_6H_5SCSNHCH^1(CH_3^2)_2$	5.35 (2 7)	8.88 (2)		3.1 – 4.1	–
o-$CH_3^3C_6H_4SCSNHCH^1(CH_3^2)_2$	5.37 (2 7)	8.90 (2)	7.55 (1)	3.3 – 4.3	–
m-$CH_3^3C_6H_4SCSNHCH^1(CH_3^2)_2$	5.35 (2 7)	8.90 (2)	7.58 (1)	3.2 – 4.0	–
p-$CH_3^3C_6H_4SCSNHCH^1(CH_3^2)_2$	5.35 (2 7)	8.88 (2)	7.58 (1)	3.1 – 4.1	–
$2,4^3,6$-$(CH_3)_3C_6H_2SCSNHCH^1(CH_3^2)_2$	5.35 (2 7)	8.91 (2)	7.68 (1)	3.5 – 4.1	–
$C_6H_5CH_2^3SCSNHCH^1(CH_3^2)_2$	5.4 –	8.75 (2)	5.45 (1)	2.9 – 3.9	–
p-$CH_3^2C_6H_4SCSNHCH^1(CH_3)CH_2CH_3$	5.46 (2 6)	7.56 (1)		3.1 – 4.2	–
$C_6H_5SCSNHCH^1(CH_2)_5$	5.3 – 6.0			3.2 – 4.2	–
m-$CH_3^2C_6H_4SCSNHCH^1(CH_2)_5$	5.4 – 6.1	7.48 (1)		3.0 – 4.0	–
p-$CH_3^2C_6H_4SCSNHCH^1(CH_2)_5$	5.3 – 6.0	7.58 (1)		3.0 – 3.9	–
$C_6H_5SCSNHC_6H_5$				1.5 – 2.0	–
p-$CH_3^1C_6H_4SCSNHC_6H_5$	7.57 (1)			1.5 – 2.0	–
p-$ClC_6H_4SCSNHC_6H_5$				1.5 – 2.0	–

[a] The values given in the table are the centers of the multiplets.
[b] In $(CD_3)_2SO$ solution.
[c] Indices refer to the signals of the corresponding methyl groups.

temperature spectra of the *S*-benzyl and the *S*-phenyl compounds can be explained partly from cross conjugation. Thus it seems clear that a form like (f) will contribute more in the *S*-phenyl than in the *S*-benzyl compounds thus lowering the barrier to rotation about the CN bond in the former case.

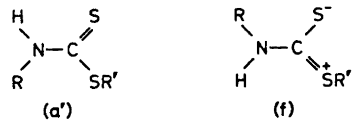

In Table 2 the chemical shifts of the aromatic protons are omitted. They were all found in the region $\tau = 2.4$ to 2.7 ppm and showed the expected pattern. The chemical shift of the NH proton was significantly different in the *N*-alkyl and the *N*-aryl compounds ($\tau = 2.5$ to 2.0 and 2.0 to 1.5 ppm, respectively), a behaviour which can be explained from the difference in acidity of the NH proton in the two cases.

As mentioned above, dithiocarbamates dissociate on heating forming isothiocyanates and thiols. The dissociation could conveniently be followed by heating the solutions used for the NMR measurements in the probe and observing not only the change in intensity and chemical shift of the alkyl signal, but also the growth of the SH signal. For Ia the dissociation temperature was estimated for solutions in bromobenzene, deuteriobromoform, and pentadeuterionitrobenzene, and it was found that the temperature of beginning dissociation was independant of the solvent used. Pentadeuterionitrobenzene

Table 3. The temperature dependence of the equilibrium $RNHCSSR' \rightleftharpoons RNCS + R'SH$. The dithiocarbamates were dissolved in pentadeuterionitrobenzene.

Compound	Temp. °C for beginning dissociation [a]	Temp. °C for 50 % dissociation [a]
Ia	60	120
Ib	> 160	–
Ic	110	> 160
Id	135	> 160
Ie	> 160	–
Ig	> 160	–
Ih	140	160
Ii	120	155
Ij	60	120
Ik	100	140
Im	145	> 160
In	140	> 160
Ip	120	140
IIa	120	160
IIIa	145	> 160
IIIb	> 160	–
VIb	90	140

[a] ±10°C.

was used as the solvent in the following experiments. The temperatures for beginning and 50 % dissociation are given in Table 3 for some dithiocarbamates. The highest temperature at which experiments could be performed was 160°C. An attempt to correlate the dissociation temperatures for the ringsubstituted *S*-phenyldithiocarbamates with Hammet σ-values showed no regularity.

A more detailed investigation of the temperature dependence of the dissociation equilibrium was carried out for Ia. The equilibrium concentrations were estimated from the integrals of the rising SH signal at $\tau = 6.47$ ppm, the total dithiocarbamate methyl signal centered at $\tau = 6.82$ ppm, and a growing singlet from methyl isothiocyanate at $\tau = 6.87$ ppm. A 0.577 M solution in pentadeuterionitrobenzene was used. The compositions estimated and the K_c's calculated are given in Table 4. From the graph of log K_c against T^{-1} (Fig. 1) $\Delta H°$ was calculated as 77.6 kJ/mol for the dissociation of Ia.

Table 4. Equilibrium constants at different temperatures for the process Ia $\rightleftharpoons$ $CH_3NCS + C_6H_5SH$ in pentadeuterionitrobenzene solution.

Temp. K	% (Ia)	K_c mol/l	$T^{-1} \times 10^3$ K^{-1}	log K_c
373	71.6	6.48	2.68	0.8116
383	63.7	11.92	2.62	1.0762
393	53.8	22.85	2.54	1.3589
403	46.4	35.80	2.48	1.5539
413	37.2	66.00	2.42	1.8195
423	27.0	113.8	2.36	2.0561

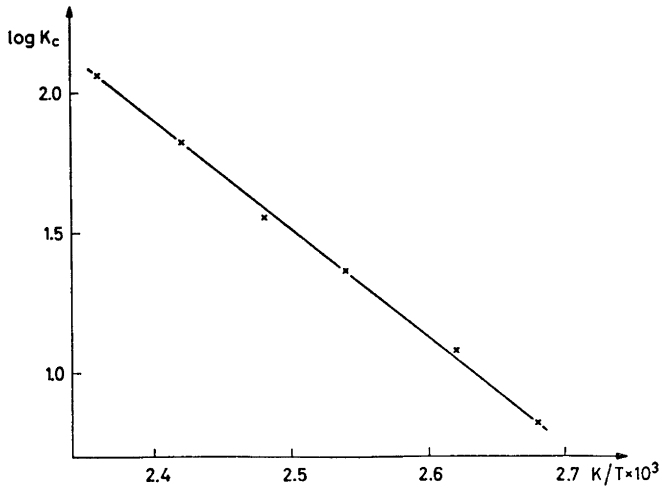

Fig. 1.

The mass spectra of Ia and methyl *N*-phenyldithiocarbamate have been studied in a paper by Thomson, Brown and Djerassi.[17] It was found that the spectra, apart from the molecular ions, could be interpreted as the spectra of the isothiocyanates superimposed on the spectra of the thiols. In the case of Ia a weak (0.2 % intensity relative to $\sum^{M}_{40}$) rearrangement peak corresponding to M – HNCS was observed. We have recorded the spectra of Ia, Ic, Id, Ie, Ii, In, and Va. With the exception of Ie and In the base peaks in the spectra corresponded to those of the thiols, and the spectra could be interpreted as mentioned above. The fragmentation pattern of Ie was analogous to previous findings, but the base peak was here found at *m/e* 151 ($C_9H_{11}S$), which corresponds to the loss of a methyl group from 4-*t*-butylbenzenethiol. In the spectrum of In $C_7H_7^+$ formed the base peak. An interesting deviation from the usual pattern is a peak corresponding to the loss of SH from the molecular ion (supported by a metastable ion at *m/e* 136.5).

In the paper by Thomson *et al.*[17] it was concluded that the absence of metastable ions for the fragmentation of the molecules into isothiocyanates and thiols indicated the possibility of a considerable amount of thermal dissociation taking place. We agree with this viewpoint when the temperature of the ion source is 200°C; however, since the results found by us are approximately identical using an ion source temp. of 70°C, this shows that the fragmentation routes due to electron impact are identical with the thermally induced ones, and that metastable ions for this fragmentation are not detected.

EXPERIMENTAL

Microanalyses were carried out in the microanalysis department of Chemical Laboratory II. Nuclear magnetic resonance spectra were obtained on a Varian A-60 instrument with tetramethylsilane as internal reference. IR spectra were obtained on a Perkin Elmer model 137 grating spectrograph. The mass spectra were obtained using an AEI MS-902 mass spectrometer operating at 70 eV. The ion source temperature was kept at 70°C.

Methods of synthesis of the compounds listed in Table 1. The directions given below correspond to entries ("Method") in Table 1. *Method A.* Equimolar amounts of thiol and isothiocyanate were mixed without addition of solvent. After standing at room temperature (from 1 h to 2 months) colourless crystals were obtained. In most cases the compounds were analytically pure. Sometimes it was necessary to cool and scratch with a spatula to induce crystallization. When necessary the products were recrystallized by dissolving the compounds in benzene and precipitating them with pentane. *Method B.* Equimolar amounts (0.01 mol) of thiol and isothiocyanate were heated to form a homogenous melt. After standing for 1 – 2 weeks at room temperature, the crystallized material was recrystallized from benzene-pentane to give colourless crystals. *Method C.* Isothiocyanate (0.01 mol) and thiol (0.01 mol) were dissolved in ethanol (25 ml). The reaction mixture was allowed to stand for 24 h at room temperature and water was added dropwise to induce precipitation. By cooling and scratching crystallization was effected, and the product was finally recrystallized from a mixture of benzene and pentane. *Method D.* Methyl isothiocyanate (0.01 mol, 0.73 g) was added to a solution of 4-acetamidobenzenethiol (0.01 mol, 1.67 g) in ethanol (25 ml). After standing for 24 h crystals had separated from the solution. These were filtered off and washed with pentane. *Method E.* Ethyl isothiocyanate (0.01 mol, 0.87 g) was mixed with benzenethiol (0.01 mol, 1.10 g) without addition of solvent. After 24 h at room temperature the mixture was chilled, and scratching with a spatula afforded crystals which melted below room temperature. The oily product was dissolved in boiling ethanol and water and treated with active carbon. The hot solution was filtered and left overnight in a refrigerator. The yield was 30 % of colourless crystals with a m.p. of 33 – 34°C.

2,4,6-Trimethylbenzenethiol. This compound was prepared by the same method as described for the preparation of benzeneselenol.[18] The product obtained was a colourless liquid b.p. 58 – 62°C at 0.6 mmHg.[19] Yield 25 %.

3-Methyl-2-thioxo-3,4-dihydro-2H-benzo[e]-1,3-thiazin-4-one. Methyl isothiocyanate (0.01 mol, 0.73 g) and 2-mercaptobenzoic acid (0.01 mol, 1.54 g) were dissolved in ethanol (25 ml). After 1 month yellow crystals had separated. The crystals were filtered off and washed on the filter with acetone. On this treatment the crystals became colourless, and after washing with ether the material was analytically pure. M.p. 146 – 147°C.[13] The yield was 15 %. (Found: C 51.80; H 3.35; N 6.68. Calc. for $C_9H_7ONS_2$: C 51.65; H 3.37; N 6.69.) *IR-spectrum* (KBr, in cm^{-1}): 3062vw, 1790vs, 1595s, 1450s, 1418s, 1290vs, 1128m, 1098s, 1076s, 1005m, 948s, 790w, 745s, 685m, 572w, and 486w. *^1H NMR-spectrum* ($CDCl_3$): methyl signal at $\tau = 6.09$ ppm, a complex signal at $\tau = 1.7$ ppm (1 H) and a complex signal at $\tau = 2.34 - 2.90$ ppm (3 H).

2-Carboxyphenyl N-methyldithiocarbamate. Methyl isothiocyanate (0.01 mol, 0.73 g) and 2-mercaptobenzoic acid (0.01 mol, 1.54 g) were dissolved in ethanol. After 1 week at room temperature the solvent was evaporated *in vacuo* and the residue was recrystallized from ethanol. Yield 50 % of colourless crystals, mp. 149 – 150°C.

REFERENCES

1. Larsen, Ch. *Proceedings of the 2nd International Symposium on Isothiocyanates*, Smolenice 1969, 175.
2. Hofmann, A. W. *Ber.* **2** (1869) 116.
3. Delépine, M. *Ann. Chim. Phys.* [VII] **29** (1903) 102.
4. v. Braun, J. *Ber.* **35** (1902) 3368.
5. Ottenbrite, R. M. *J. Chem. Soc. Perkin 1* **1972** 88.
6. Roshdestwenski, M. *J. Russ. Phys. Chem. Soc.* **41** (1909) 107.
7. Cherbuliez, E., Marszalek, J. and Rabinowitz, J. *Helv. Chim. Acta* **47** (1964) 1666.
8. Shell Internationale Research Maatschappij N. V., Belgian Patent 633.277, *Chem. Abstr.* **61** (1963) 3022c.
9. Jakobsen, P. and Larsen, Ch. *To be published*
10. Anthoni, U., Larsen, Ch. and Nielsen, P. H. *Acta Chem. Scand.* **23** (1969) 3385.
11. Wakamori, S., Yoshida, Y. and Ishii, Y. *Agr. Biol. Chem.* **33** (1969) 1367.
12. Anthoni, U., Larsen, Ch. and Nielsen, P. H. *Acta Chem. Scand.* **22** (1968) 1898.
13. Kretov, A. E., Bespalyi, A. S. and Levin, Y. A. *Khim. Geterotsikl. Soedin.* **1967** (6) 1053.
14. Holloway, C. E. and Gitlitz, M. H. *Can. J. Chem.* **45** (1967) 2659.
15. Rogers, M. T. and Woodbrey, J. C. *J. Phys. Chem.* **66** (1962) 540.
16. Sandström, J. *J. Phys. Chem.* **71** (1967) 2318.
17. Thomson, J. B., Brown, P. and Djerassi, C. *J. Am. Chem. Soc.* **88** (1966) 4049.
18. *Org. Syn. Coll. Vol.* III 553, 771
19. Truce, W. E. and Norman, O. L. *J. Am. Chem. Soc.* **75** (1953) 6023.

Received January 29, 1973.

ACTA CHEMICA SCANDINAVICA 27 (1973) 2013–2019

Structure and Aging of $Ni(OH)_2$ Precipitated from Sulfate and Chloride Solutions

E. SUONINEN,* T. JUNTUNEN,** H. JUSLÉN and M. PESSA

Institute of Materials Research, University of Turku, Turku, Finland

Kinetics of aging of $Ni(OH)_2$ particles precipitated from $(NiSO_4)_n + (NiCl_2)_{1-n}$ parent solutions by NaOH solutions are studied by means of X-ray diffraction. Three stoichiometric ratios, R, are used. The growth of primary $Ni(OH)_2$ particles is found to be strongly dependent on R. From sulphate solutions a smaller size and a relatively long incubation time for the growth of fresh nuclei are generally found in the understoichiometric case, $R = 0.8$. For $R \geq 1.0$, the crystal growth is prevented because of free OH^- ions in solution. These observations are explained on the basis of the nature and behavior of the double layer formed at the [001] surfaces of the primary particles.

The precipitation of nickel(II) hydroxide from an aqueous solution has been the subject of numerous studies.[1] In particular, the size and shape of the primary particles of the precipitate have been studied by X-ray diffraction.[2–8] The sorption processes on the [001] faces of the platelike, thin crystals of hexagonal $Ni(OH)_2$ have been shown to control the aging processes in the precipitate. The [001] faces of the crystals are first covered with Ni^{2+} ions, which accounts for the fact that the amount of hydroxide ions needed for a superficially complete precipitation of nickel is less than stoichiometric.[9] The adsorbed nickel ions attract anions from the solution, thus forming an electric double layer on the surface of the crystals. The aging of the precipitates is caused by the desorption of the anions from the double layer, followed either by their substitution with hydroxide ions, or by a subsequent desorption of the Ni^{2+} ions as well.

Since the type of anion is obviously important in the desorption process, a comparison of the aging of precipitates aged in solutions containing different anions is interesting. The drastic slowing-down of the aging caused by the presence of carbonate ions is already well established.[4,6] Furthermore, dependence of the strength of the double-layer formation on the nature of the

* Address during the academic year 1972–1973: Institute of Materials Science, University of Connecticut, Storrs, Conn. 06268, USA.

** Present address: Typpi Oy, Oulu, Finland.

ions is revealed by the differing behavior of the pH of the solution during the precipitation: the sulfate ions seem to produce a considerably stronger deviation from stoichiometry in the precipitate than do the chloride or nitrate ions.[9] However, most studies of the aging process seem to be limited to precipitates obtained from pure chloride or nitrate solutions. In the present work, the aging process of nickel hydroxide, precipitated from $(NiSO_4)_n + (NiCl_2)_{1-n}$ solutions, was studied by using X-ray diffraction.

EXPERIMENTAL

The samples were prepared by slowly adding NaOH solutions with various OH^- concentrations (see below) to a $(NiSO_4)_n + (NiCl_2)_{1-n}$ solution at 24°C with constant stirring. The values of n used were 0, 0.1, 0.9, and 1.0. The values 0.8, 1.0, and 1.2 were used for the stoichiometric ratio, R; the value 1.0 corresponding to the amount needed for stoichiometric precipitation of Ni^{2+}. The Ni^{2+} concentration of all solutions was 10 g/l. In this way twelve different solutions were obtained, the volume of each was 1 l after 0.55 N, 0.69 N, and 0.83 N NaOH had been added to set $R = 0.8$, 1.0, and 1.2, respectively.

The precipitates were aged at 24°C in the mother liquor until investigated. They were then filtered and placed into a Philips wide angle X-ray goniometer (PW 1380).

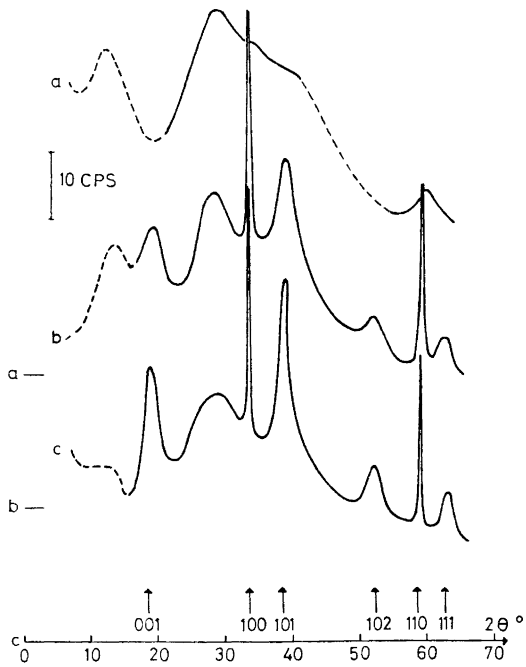

Fig. 1. Diffraction spectra of $Ni(OH)_2$ samples precipitated stoichiometrically from a $NiSO_4$ solution at 24°C. Aged in the parent solution (a) 6 h, (b) 8 days, (c) 90 days. The zero level of the curves is indicated in the left margin. Curve for the case (a) was not run between $42° \leq 2\theta \leq 54°$. The dashed parts in the low 2θ region indicate interference caused by the specimen holder.

A Cu$K\alpha$ diffraction tube (Ni filter) with the power of 45 kV × 30 mA was used. The divergence of the beam was 1°.

Samples of the precipitates were examined at times up to three months from precipitation. A diffraction spectrum was run at $2\theta = 30°...36°$ and 56°...62°. The form of the diffraction peaks was carefully recorded by running the spectrometer at a sufficiently slow speed (0.5° 2θ/min) in these regions. In order to permit an analysis of the intensity along [001], as made in Ref. 7, an attempt was made to prepare oriented samples with the [001] direction parallel to the diffraction vector. To this end, a diffraction spectrum on a sample precipitated from $NiSO_4$ was run up to $2\theta = 65°$. This spectrum is shown in Fig. 1. It proved very difficult to obtain a sufficiently strong [001] orientation of the sample, particularly at the start of aging. Samples prepared from chloride solutions were clearly different in this respect. Nevertheless, the [001] reflection of all samples was found to be too weak for quantitative measurements. Furthermore, the masking effect of the adjacent diffuse peak at $2\theta \simeq 13°$, caused by the plastic sample holder, proved disturbing (Fig. 1). Hence, only the crystallization in the [hk0] directions (hexagonal plane) of $Ni(OH)_2$ has been studied here.

Fig. 1. also shows another diffuse peak at $2\theta \simeq 28°$. It is caused by water remaining in the sample. This peak is, within the resolution of our measurement, identical to the diffuse peak obtained from a pure water sample. This does not, of course, prove that all water in the precipitates is similarly bonded; *cf.* Refs. 10, 11. The remaining peaks in Fig. 1 can be attributed to different [hkl] reflections of $Ni(OH)_2$, as indicated by vertical arrows.

The full widths at half maximum of the [100] and [110] peaks were measured for each run from recordings similar to the ones shown in Fig. 2. These widths were then corrected for instrumental broadening by a graphical method.[12] The average diameter of the primary disc-shaped particles in the precipitate was determined as an arithmetic mean of the sizes in the [100] and [110] directions from the corrected half widths, β, by using the Scherrer formula [10]

$$D = \frac{K\lambda}{\beta \cos \theta}$$

Here, D is the average diameter of the particles in the direction of the hexagonal base plane, $K = 0.9$ and $\lambda = 1.541$ Å.

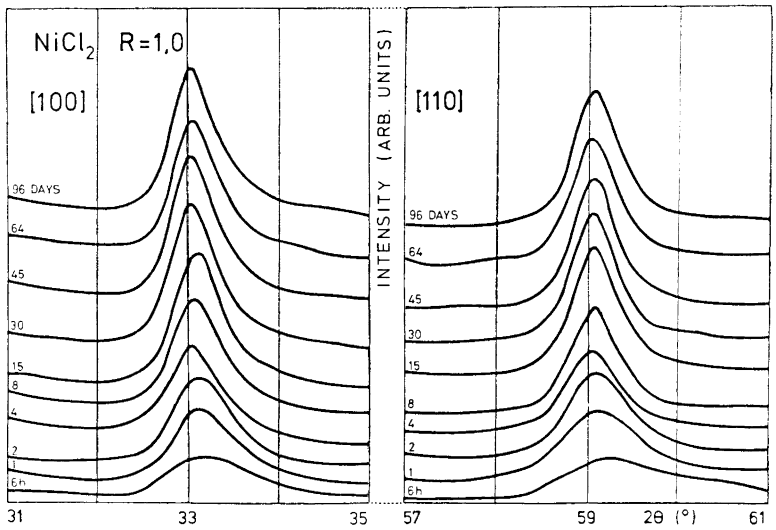

Fig. 2. Effect of aging on the primary particle size of $Ni(OH)_2$ precipitated from $NiCl_2$ solution. $R = 1.0$. Directions are [100] and [110].

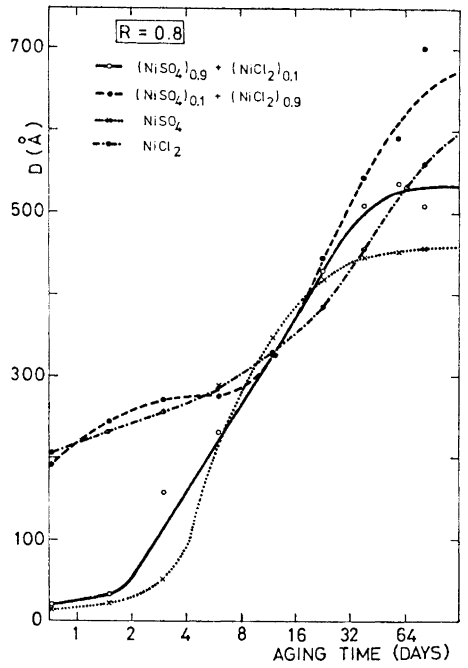

Fig. 3. The average particle size, D, in the hexagonal plane [100] and [110] as a function of the aging time for an understoichiometric amount of NaOH ($R = 0.8$).

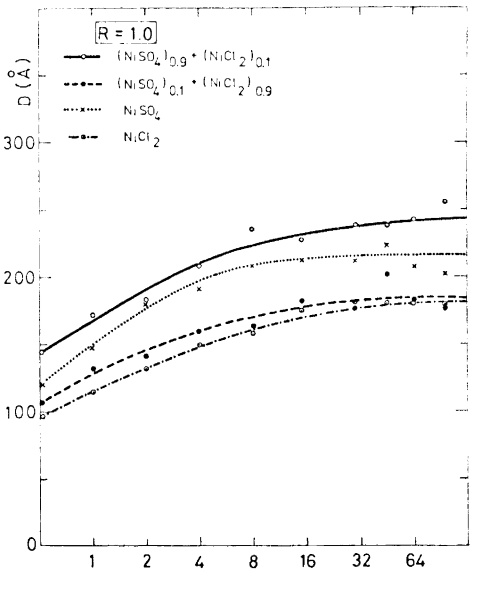

Fig. 4. The data corresponding to Fig. 3 for $R = 1.0$.

Figs. 3 to 5 shows the effect of the aging time on the particle size of $Ni(OH)_2$ precipitated from the above mentioned solutions for the three values of the stoichiometric ratio, R.

DISCUSSION

A comparison of a part of the present work with the results previously obtained for precipitates prepared from a pure chloride solution under similar conditions [11] shows that the structure and the aging mechanism of the precipitates are basically the same in both cases. It has been found, however, that the quantitative values of D may show quite a considerable amount of variance because of certain difficulties in the sample preparation. The anomalous behavior of the growth rate of the primary particles precipitated from the $(NiSO_4)_{0.9} + (NiCl_2)_{0.1}$ solution at $R = 1.2$ (Fig. 5) remains unexplained, but is probably associated with the preparation conditions which could have changed drastically during precipitation (impurities likely to be present). This curve has been disregarded in the following considerations.

A qualitative comparison of Figs. 3 to 5 is interesting. For the understoichiometric case, $R = 0.8$ (Fig. 3), a clearly distinguishable initiation of the growth after an incubation time (about 3 days) is found for the growth of the

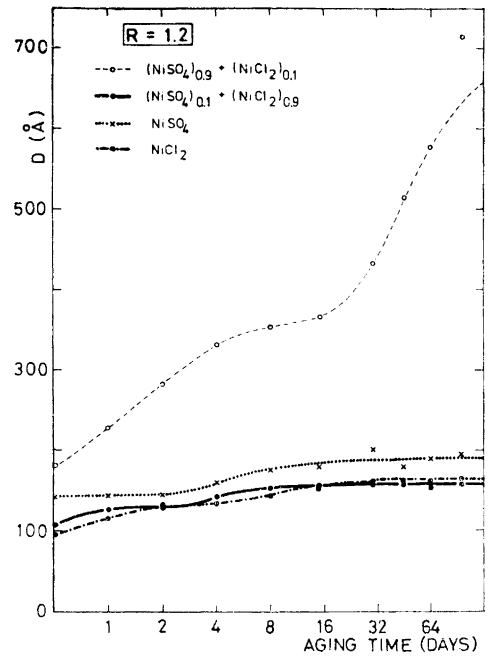

Fig. 5. The data corresponding to Fig. 3 for $R = 1.2$.

particles prepared from solutions with sulfate predominating ($n = 0.9$, 1), whereas the particles prepared from solutions with large amounts of chloride ions ($n = 0.1$, 0) begin to grow without a clearly distinguishable incubation time. Furthermore, the size of fresh nuclei is considerably smaller in sulfate dominated solutions (about 20 Å) than in predominantly chloride solutions

Table 1. Parent solutions from which the $Ni(OH)_2$ particles were precipitated, the average sizes of fresh nuclei (1 day) and aged particles (90 days) with estimated error limits (possible systematic errors neglected) for different stoichiometric ratios R.

Parent solution	D (1 day), Å	D (90 days), Å	R
$NiSO_4$	15 ± 5	460 ± 120	0.8
$(NiSO_4)_{0.9} + (NiCl_2)_{0.1}$	25 ± 5	530 ± 170	0.8
$(NiSO_4)_{0.1} + (NiCl_2)_{0.9}$	220 ± 45	650 ± 200	0.8
$NiCl_2$	220 ± 45	570 ± 190	0.8
$NiSO_4$	150 ± 25	215 ± 45	1.0
$(NiSO_4)_{0.9} + (NiSl_2)_{0.1}$	165 ± 30	240 ± 55	1.0
$(NiSO_4)_{0.1} + (NiCl_2)_{0.9}$	125 ± 20	185 ± 35	1.0
$NiCl_2$	115 ± 20	180 ± 35	1.0
$NiSO_4$	145 ± 25	190 ± 35	1.2
$(NiSO_4)_{0.9} + (NiCl_2)_{0.1}$	—	—	—
$(NiSO_4)_{0.1} + (NiCl_2)_{0.9}$	130 ± 20	165 ± 30	1.2
$NiCl_2$	115 ± 20	160 ± 30	1.2

(about 200 Å). On the other hand, the size of fresh nuclei are rather similar (about 100 Å) for all solutions when $R = 1.0$, see also Table 1.

Widely varying, but systematic, behavior of the crystal growth is found when R and the anion composition are changed. Where a clearly distinguishable incubation time is found, the growth, once started, progresses rapidly and is almost complete in two months. In the other cases, the growth is more gradual and seems to continue later. An overstoichiometric amount of NaOH always yields very low growth rates, indicating an efficient inhibition process in the presence of free hydroxyde ions in all solutions (Fig. 5).

The above observations show that the attachment of the sulfate ions to the double layer is obviously stronger than that of the chloride ions. A likely bonding mechanism for sulfate ions is the formation of a complex involving the top layer atoms of the hydroxide precipitate. Such a mechanism is not likely in the case of chloride ions. This explains the incubation time needed for the growth in understoichiometric, sulfate-dominated solutions. It seems likely, however, that sulfate ions are not adsorbed into the double layer in preference to chloride ions, despite the stronger bonding of the former. This is shown by the behavior of the solution with $n = 0.1$, which closely resembles the behavior of a pure chloride solution. Hence, the kind of anions initially attached to the double layer is determined by statistics rather than by the strength of the bonding (the number of Cl^- is twice the amount of SO_4^{2-}).

The growth behavior in the overstoichiometric region suggests a virtually permanent double layer inhibiting growth, irrespective of the kind of anions in the solution. The natural explanation is that the anion attached to the double layer is in this case the OH^- ion, which is now abundant in the solution.

Finally, it should be noted that the above description in terms of simple free ions in the solution is, of course, an over-simplification of the real situation, in which solvated complexes, including the above ions, in fact exist. This does not, however, alter the conclusion concerning the effect of the relative abundances of the simple ions on the growth mechanism.

The aging structures produced here resemble the "turbostratic" structure obtained by pressure washing precipitates from nitrate solutions.[8,13] Unfortunately, no data for the aging kinetics of these precipitates have so far been published.

Acknowledgements. We are deeply indebted to Outokumpu Oy for allowing us the use of the X-ray diffraction equipment. Thanks are also due to several persons in our laboratory for assistance in the measurements.

This work was financially supported by the *National Research Council for Technical Sciences* (Finland).

REFERENCES

1. *Gmelins Handbuch der anorganischen Chemie:* Nickel, Pt. B-2nd printing, Verlag Chemie GmbH, Weinheim 1966, pp. 434–494.
2. Berger, A. *Kolloid-Z.* **103** (1943) 185.
3. Longuet, J. *Compt. Rend.* **223** (1946) 150.
4. Longuet-Escard, J. and Bagno, O. *Compt. Rend.* **232** (1951) 1205.
5. Longuet-Escard, J. and Mering, J. *Compt. Rend.* **236** (1953) 1683.

6. Bagno, O. and Longuet-Escard, J. *J. Chim. Phys.* **51** (1954) 434.
7. Longuet-Escard, J. and Mering, J. *Compt. Rend.* **246** (1958) 440.
8. Le Bihan, S., Guenot, J. and Figlarz, M. *Compt. Rend.* **270** (1970) 2131.
9. Singley, W. J. and Carriell, J. T. *J. Am. Chem. Soc.* **75** (1953) 778.
10. Figlarz, M. and Le Bihan, S. *Compt. Rend.* **272** (1971) 580.
11. Juntunen, T. *Diploma engineer's thesis*, University of Oulu 1969.
12. Bartram, S. F. In Kaelbe, E. F., Ed., *Handbook of X-Rays*, McGeaw, New York 1967, Chapter 17.
13. Déportes, J., Mollard, P. Pénelon, J., Le Bihan, S. and Figlarz, M. *Compt. Rend.* **272** (1971) 449.

Received January 15, 1973.

ACTA CHEMICA SCANDINAVICA 27 (1973) 2020–2022

A Case of Reduction in the Reactions between Phenylmagnesium Bromide and Ethyl Chromone-2-carboxylate

GUST.-AD. HOLMBERG and RAINER SJÖHOLM

Institutionen för organisk kemi, Åbo Akademi, SF-20500 Åbo, Finland

When phenylmagnesium bromide reacts with ethyl chromone-2-carboxylate, 2-benzoylchromone and 2-(diphenylhydroxymethyl)-chromone were formed as primary and secondary products. A large excess of the Grignard reagent causes the formation of 1-(*o*-hydroxyphenyl)-3,4,4-triphenyl-3-buten-1-one. A reductive fission of the ether bond between the atoms in the positions 1 and 2 or a direct or indirect reduction of the double bond of the chromone nucleus is apparently involved in the reactions.

The reaction between arylmagnesium bromides and ethyl 3-phenylchromone-2-carboxylate has previously been examined in this laboratory.[1] It was then established that the primary reaction was a 1,2-addition to the carbonyl group of the carbethoxy portion of the molecule. The order, and in part even the nature of the subsequent reactions were not easy to elucidate in detail. Nevertheless, it seemed apparent that either a reductive fission of the ether bond between the atoms in the positions 1 and 2 or a reduction of the double bond between the atoms in the positions 2 and 3 occurred.

Because no reduction had been observed in the reactions between phenylmagnesium bromide and ethyl chromone-2-carboxylate (I),[2] investigations of these reactions were resumed. It was again established that the first reactions were 1,2-additions of the Grignard reagent to the carbonyl group of the carbethoxy portion, and the primary and secondary products, 2-benzoylchromone (II) and 2-(diphenylhydroxymethyl)chromone (III), were isolated when the molar ratio of the ester and the Grignard reagent was 1:2.5. If the excess of phenylmagnesium bromide was increased until the ratio was 1:5, 1-(*o*-hydroxyphenyl)-3,4,4-triphenyl-3-buten-1-one (IV) was formed and isolated. The quantities of the reaction products, evaluated from gas chromatograms of the reaction mixtures, clearly showed that the latter substance had formed from 2-(diphenylhydroxymethyl)chromone. One reaction sequence for this transformation would be a reductive fission of the ether bond between the atoms in the positions 1 and 2, followed by a 1,4-addition of phenylmagnesium bromide to the conjugated double bond system C=C–C=O. The double bond

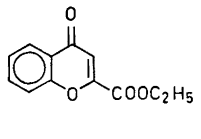

I

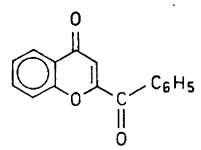

II

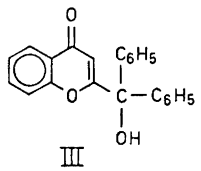

III

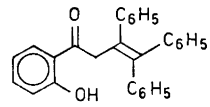

IV

in the butene chain is formed by elimination of water upon treatment with hydrochloric acid. Several equally possible reaction sequences can be constructed for the transformation. Either a reductive fission of the ether bond or a direct or indirect reduction of the ethylenic double bond of the chromone nucleus is included in all these sequences. The mechanisms and the reducing agents have to some extent been discussed previously.[1]

EXPERIMENTAL

Experiment 1 (molar ratio of ethyl chromone-2-carboxylate and phenylmagnesium bromide 1:2.5, inverse addition). A Grignard reagent, prepared from magnesium (0.60 g), bromobenzene (3.92 g), and dry ether (30 ml), was gradually added to a solution of ethyl chromone-2-carboxylate (2.18 g) in dry ether (30 ml). The temperature of the reaction mixture was kept at 0° during the addition (1 h). The reaction mixture was poured into a mixture of hydrochloric acid, water, and ice. The ether phase was separated and washed with water and 5 % potassium hydrogen carbonate solution. After drying with sodium sulphate, the solvent was evaporated. When cold ether was added to the remaining oil, a small quantity of 2-(diphenylhydroxymethyl)chromone (III) crystallized. The solvent was evaporated from the mother-liquor, the remaining oil dissolved in a small quantity of ethanol, and the solution placed in a refrigerator. After some days, a substance had crystallised. It was repeatedly recrystallised from ethanol. The pure compound, 2-benzoylchromone (II), melted at 92 – 93°. (Found: C 76.72; H 3.93. Calc. for $C_{16}H_{10}O_3$: C 76.79; H 4.03.) MS: $M^{+\cdot}$ at *m/e* 250, calc. 250, r.a. 16.5 %; $(M+1)^+$ at *m/e* 251, r.a. 2.8 %, calc. 2.9 %; $(M-CO)^{+\cdot}$ at *m/e* 222, r.a. 15.1 %; benzoyl ion at *m/e* 105, r.a. 100 %; phenyl ion at *m/e* 77, r.a. 54.3 %. NMR spectrum: aromatic protons at τ 1.6 – 2.7; methine proton at τ 3.14; ratio of the intensities 9:1. Gas chromatographic analysis of the original reaction product oil revealed that 2-benzoylchromone was the main product but that considerable amounts of 2-(diphenylhydroxymethyl)chromone were also present.

Experiment 2 (molar ratio of ethyl chromone-2-carboxylate and phenylmagnesium bromide 1:5). A solution of ethyl chromone-2-carboxylate (2.18 g) in dry ether (30 ml) was gradually added to a Grignard reagent, prepared from magnesium (1.21 g), bromobenzene (7.90 g), and dry ether (30 ml). After the reaction mixture had been held at 40° for 1 h, it was worked up as described above. The oil obtained was dissolved in ethanol and, after some days in a refrigerator, a substance crystallised. The pure product, obtained by recrystallisation from chloroform, melted at 183 – 184°. Analytical and spectroscopical data showed it to be 1-(*o*-hydroxyphenyl)-3,4,4-triphenyl-3-buten-1-one. (Found: C 86.05; H 5.59. Calc. for $C_{28}H_{22}O_2$: C 86.13; H 5.68.) IR spectrum: CO absorption at 1645 cm^{-1}. MS: $M^{+\cdot}$ at *m/e* 390, calc. 390, r.a. 28.3 %; $(M+1)^+$ at *m/e* 391, r.a. 8.9 %, calc. 8.7 %; $(M-HOC_6H_4CO)^+$ at *m/e* 269, r.a. 24.8 %; unknown ions at *m/e* 223, r.a.

9.6 %, and 191, r.a. 21.7 %; $(HOC_6H_4CO)^+$ at *m/e* 121, r.a. 100 %; self-explanatory ions at *m/e* 105, 91, 77, and 65 with r.a. less than 20 %. NMR spectrum: hydroxyl proton at τ −2.12; aromatic protons at τ 2.3 − 3.1; uncoupled methylene protons at τ 5.74; ratio of intensities 1:19:2. Gas chromatographic analysis showed that the isolated compound was the main product.

Experiment 3 (molar ratio of ethyl chromone-2-carboxylate and phenylmagnesium bromide 1:3.5). The above experiment was repeated with a Grignard reagent prepared from magnesium (0.84 g) and bromobenzene (5.50 g). Gas chromatographic analysis revealed that the amounts of 2-benzoylchromone, 2-(diphenylhydroxymethyl)chromone, and 1-(*o*-hydroxyphenyl)-3,4,4-triphenyl-3-buten-1-one were almost equal.

The elemental analyses were performed by Janssen Pharmaceutica, Analytical Department, Beerse, Belgium.

Statens naturvetenskapliga kommission (*Finland*) has supported the work.

REFERENCES

1. Holmberg, G.-A. and Jalander, L. *Acta Acad. Aboensis, Ser. B* **30** (1970) No. 14.
2. Holmberg, G.-A., Malmström, F. and Blom, U. Å. *Acta Chem. Scand.* **22** (1968) 1375.

Received January 19, 1973.

ACTA CHEMICA SCANDINAVICA 27 (1973) 2023–2026

Reactions between Grignard Reagents and Ethyl 4-Methyl-3-coumarincarboxylate

GUST.-AD. HOLMBERG, FOLKE MALMSTRÖM and ULF WENNSTRÖM

Institutionen för organisk kemi, Åbo Akademi, SF-20500 Åbo, Finland

Ethyl 4-methyl-3-coumarincarboxylate reacts with methylmagnesium iodide and isopropylmagnesium bromide forming 1,4-addition products. In contrast to these Grignard reagents, phenylmagnesium bromide gives 1,2-addition reactions. The carbonyl group in the carbethoxy portion is first attacked, and this reaction is then followed by a double 1,2-addition to the carbonyl group of the lactone ring.

The reactions of ethyl 3-coumarincarboxylate with phenylmagnesium bromide and *o*-methoxyphenylmagnesium iodide have been examined earlier in this laboratory.[1,2] A 1,4-addition of the Grignard reagent to the conjugated double bond system C=C–C=O occurred in both cases. This reaction was, however, followed by different 1,2-additions to the carbonyl groups.

When Munch-Petersen [3] recapitulated the results of earlier investigations into the reactions of Grignard reagents with α,β-unsaturated carboxylic esters, he noted among other things that the presence of two substituents at the β carbon atom of the ester prevents, or strongly represses, the 1,4-addition reactions and so often favours 1,2-addition reactions.

Against this background, it seemed justifiable to examine the reactions between Grignard reagents and ethyl 4-methyl-3-coumarincarboxylate (I), in which the methyl group may be taken as the second substituent at the β carbon atom. Methylmagnesium iodide, isopropylmagnesium bromide, and phenylmagnesium bromide were chosen as suitable Grignard reagents.

Methylmagnesium iodide gave exclusively a 1,4-addition reaction with the coumarin derivative. The product, ethyl 4,4-dimethyl-3,4-dihydro-3-coumarincarboxylate (II a), was transformed into 4,4-dimethyl-3,4-dihydrocoumarin (III a) by alkaline hydrolysis. Isopropylmagnesium bromide reacted in the same way, but gave a mixture of 4-isopropyl-4-methyl-3,4-dihydrocoumarin (III b) and its 3-carbethoxy derivative (II b). Apparently, the ester was the primary product. It was obviously partly hydrolysed when the products were isolated.

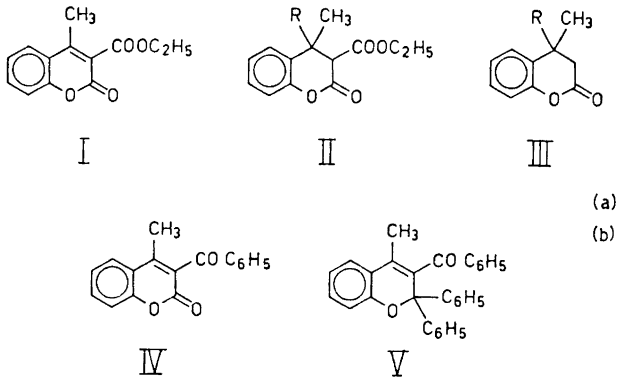

Phenylmagnesium bromide reacted in quite a different way. A large excess of the Grignard reagent gave, besides biphenyl, 3-benzoyl-2,2-diphenyl-4-methyl-2*H*-1-benzopyran (V). If a smaller excess was used, 3-benzoyl-4-methylcoumarin (IV) was also formed. It follows that the first reaction to occur was a 1,2-addition of the Grignard reagent to the carbonyl group of the ester portion. This reaction was then followed by a double 1,2-addition to the carbonyl group of the lactone ring. The dihydroxy derivative formed as primary product in the latter reaction apparently splits off water to form the benzopyran derivative during the work up. Similar reactions have been reported by Heilbron and Hill.[4]

It is interesting to note that the course of the reactions was dependent on the aliphatic or aromatic nature of the Grignard reagent.

The NMR spectra of 4,4-dimethyl- and 4-isopropyl-4-methyl-3,4-dihydrocoumarin are of note. The spectrum of the former compound is composed of a singlet from the methylene protons in position 3, a singlet from the methyl protons, and a complex signal from the phenylene protons. The spectrum of the latter shows a distinct AB quartet signal from the methylene protons in position 3 and signals with the appropriate multiplicity from the protons of the methyl, isopropyl, and phenylene groups. Thus, the 4,4-dimethyl-3,4-dihydrocoumarin molecule is not rigid, but the conformations can easily pass over one into the other. On the other hand, the isopropyl group in the molecule of 4-isopropyl-4-methyl-3,4-dihydrocoumarin prevents, or at least represses, conformation changes.

EXPERIMENTAL

Ethyl 4-methyl-3-coumarincarboxylate (I) was prepared from ethyl cyanoacetate and *o*-hydroxyacetophenone according to Wiener *et al.*[5] An attempt to hydrolyse the first intermediate, 3-cyano-4-methylcoumarin in alkaline solution in the presence of pyridine at ordinary temperature according to Schroeder and Link [6] was not successful.

Action of methylmagnesium iodide. A solution of ethyl 4-methyl-3-coumarincarboxylate (2.00 g) in dry ether (150 ml) was gradually added to a Grignard reagent prepared from methyl iodide (3.77 g), magnesium (0.63 g), and dry ether (20 ml). The reaction mixture was warmed for 15 min and then poured into a mixture of ice, water, and hydrochloric acid. The ether phase was separated and dried with sodium sulphate. The oil that remained

when the solvent had been evaporated was analysed by gas chromatography (column 1/8″ × 1.5 m, stationary phase 5 % SE-30 on Chromosorb W, flow rate of nitrogen 22 ml/min, initial temperature 150°, temperature programming 10°/min). Only one component was detected. The mass spectrum taken on a combined gas chromatograph/mass spectrometer showed the following important ions: $M^{+\cdot}$ at *m/e* 248, calc. 248; $(M-CH_3)^+$ at *m/e* 233; $(M-OC_2H_5)^+$ at *m/e* 203; $(M-CH_4-OC_2H_5)^+$ at *m/e* 187. These data indicated that the compound was ethyl 4,4-dimethyl-3,4-dihydro-3-coumarincarboxylate.

A sample (1.58 g) of the oil obtained above was dissolved in ethanol (40 ml), and a solution of potassium hydroxide (0.4 g) in water (0.5 ml) and ethanol (16 ml) was added. The mixture was boiled for 4 h under reflux. Because no crystals separated despite the chilled mixture being stored overnight in the refrigerator, the solvent was evaporated and the residue dissolved in a mixture of ether and water. The ether phase was dried with sodium sulphate and the solvent was evaporated. Gas chromatographic analysis of the remaining oil (0.49 g) showed only one compound, the mass spectrum of which was identical with that of 4,4-dimethyl-3,4-dihydrocoumarin. The sample of this compound prepared according to Colonge and Chambard [7] gave the following NMR spectrum: 4 aromatic protons at τ 2.4 – 3.2, 2 methylene protons (singlet) at τ 7.49, and 6 methyl protons (singlet) at τ 8.68.

The alkaline water solution was acidified and extracted several times with ether. The ether solutions were combined and dried with sodium sulphate. After the solvent had been evaporated, an oil (0.56 g) remained. The main part consisted of 4,4-dimethyl-3,4-dihydrocoumarin.

Action of isopropylmagnesium bromide. A solution of ethyl 4-methyl-3-coumarincarboxylate (5.00 g) in dry ether (400 ml) was gradually added to a Grignard reagent prepared from isopropyl bromide (5,31 g), magnesium (1.04 g), and dry ether (40 ml). After 12 h, the mixture was poured into a mixture of ice, water, and hydrochloric acid. The ether phase was separated and dried with sodium sulphate. When the ether had been evaporated, an oil (4.62 g) remained. The gas chromatographic analysis revealed that it consisted of 4-isopropyl-4-methyl-3,4-dihydrocoumarin (56.4 mol %), ethyl 4-isopropyl-4-methyl-3,4-dihydro-3-coumarincarboxylate (30.5 mol %), and unreacted ethyl 4-methyl-3-coumarincarboxylate (13.1 mol %). The compounds were identified by the aid of mass spectra.

4-Isopropyl-4-methyl-3,4-dihydrocoumarin: $M^{+\cdot}$ at *m/e* 204, calc. 204; $(M-C_3H_7)^+$ at *m/e* 161.

Ethyl 4-isopropyl-4-methyl-3,4-dihydro-3-coumarincarboxylate: $M^{+\cdot}$ at *m/e* 276, calc. 276, $(M-C_3H_7)^+$ at *m/e* 233; $(M-OC_2H_5)^+$ at *m/e* 231; $(M-C_3H_7-H)^+$ at *m/e* 232, $(M-COOC_2H_5)^+$ at *m/e* 203; $(M-C_3H_8-OC_2H_5)^+$ at *m/e* 187.

Because the products could not be separated, they were hydrolysed in the way described above for the alkaline hydrolysis of ethyl 4,4-dimethyl-3,4-dihydro-3-coumarincarboxylate. Only one substance, 4-isopropyl-4-methyl-3,4-dihydrocoumarin, could be detected in the resulting ether solution. The substance was very pure. After a careful evaporation of the solvent, the remaining oil gave an excellent NMR spectrum (Table 1). The IR spectrum of the substance shows a strong carbonyl absorption at 1785 cm^{-1}.

Table 1. Chemical shifts (τ), coupling constants (*J*), intensties, and multiplicities of the signals in the NMR spectrum of 4-isopropyl-4-methyl-3,4-dihydrocoumarin.

	Proton(s)	τ	Intensity	Multiplicity	*J*
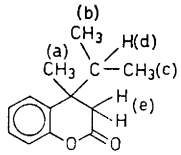	Aromatic	2.6 – 3.3	4		
	a	8.83	3	Singlet	
	b, c	9.20	3	Doublet	
		9.26	3	Doublet	6.7
	d	8.26	1	Septet	
	e	7.22	2	AB system	15.7
		7.92			

The alkaline water solution contained mainly 4-methyl-3-coumarincarboxylic acid.

Action of phenylmagnesium bromide. Experiment 1. Ethyl 4-methyl-3-coumarincarboxylate (5.80 g) dissolved in dry benzene (60 ml) was gradually added to a Grignard reagent prepared from bromobenzene (13.74 g, 3.5 equiv.), magnesium (2.10 g), and dry ether (40 ml). The addition was completed in 20 min and the mixture was warmed in a water-bath for 15 min. The reaction mixture was poured into a mixture of ice, water, and hydrochloric acid. The ether phase was separated, washed with water and potassium hydrogen carbonate, and finally dried with sodium sulphate. The gas chromatographic analysis of the oil obtained after evaporation of the solvent showed that biphenyl, unreacted ethyl 4-methyl-3-coumarincarboxylate, and a new compound (main product) were present. A smeary sample of the last-mentioned compound was obtained when the oil was dissolved in ethanol and ligroin was added to the cold solution. After the mixture had been kept for some days in the refrigerator, the precipitate was filtered and repeatedly recrystallised from either ethanol, tetrachloromethane, or a mixture of chloroform and ligroin. The pure product, pale yellow needles, melted at 204.5°. The mass spectrum shows the molecular ion at *m/e* 402 and abundant ions at *m/e* 387 ($[M-CH_3]^+$), 325 ($[M-C_6H_5]^+$), 297 ($[M-C_6H_5CO]^+$), 105 (benzoyl ion), and 77 (phenyl ion). These facts indicate that the substance is 3-benzoyl-2,2-diphenyl-4-methyl-2*H*-1-benzopyran. (Found: C 86.30; H 5.59. Calc. for $C_{29}H_{22}O_2$: C 86.54; H 5.51.)

Experiment 2. When the experiment was repeated with the reactants in the ratio 1:2.5 (3.32 g of ethyl 4-methyl-3-coumarincarboxylate, 3.93 g of bromobenzene, and 0.60 g of magnesium), the gas chromatogram showed the presence of biphenyl, unreacted ethyl 4-methyl-3-coumarin-3-carboxylate, a new compound, and 3-benzoyl-2,2-diphenyl-4-methyl-2*H*-1-benzopyran. A sample of the reaction mixture was dissolved in tetrachloromethane, applied on a bentonite column and eluted with tetrachloromethane. Fractions containing pure or almost pure samples of the new compound were combined and the solvent was evaporated. When the residue was treated with ligroin, a substance separated. After repeated recrystallisation from ligroin combined with charcoal treatment, the product melted at 137.5 – 138.5°. The IR spectrum shows two carbonyl peaks (1710 and 1670 cm^{-1}). The most abundant ions in the mass spectrum are the molecular ion at *m/e* 264, and the ions at *m/e* 263 ($[M-H]^+$), 245 ($[M-29]^+$), 187 ($[M-C_6H_5]^+$), 159 ($[M-C_6H_5CO^+]$), 105 (benzoyl ion), and 77 (phenyl ion). These facts indicate that the substance was 3-benzoyl-4-methylcoumarin. (Found: C 77.10; H 4.65. Calc. for $C_{17}H_{12}O$: C 77.26; H 4.58.)

Statens naturvetenskapliga kommission (Finland) has supported the work.

REFERENCES

1. Holmberg, G.-A. *Acta Chem. Scand.* **15** (1961) 1255.
2. Holmberg, G.-A. and Johansson, J. E. *Acta Acad. Aboensis, Ser. B* **30** (1970) No. 13.
3. Munch-Petersen, J. *Konjugeret addition af Grignard-reagenser till alfa, beta-umættede estere, Diss.*, University, Copenhagen 1962, p. 18.
4. Heilbron, I. M. and Hill, D. W. *J. Chem. Soc.* **1927** 2205.
5. Wiener, C., Schroeder, C. H. and Link, K. P. *J. Am. Chem. Soc.* **79** (1957) 5301.
6. Schroeder, C. H. and Link, K. P. *J. Am. Chem. Soc.* **75** (1953) 1886.
7. Colonge, J. and Chambard, R. *Bull. Soc. Chim. France* **1953** 573.

Received January 19, 1973.

ACTA CHEMICA SCANDINAVICA 27 (1973) 2027–2034

Remarks on the Assignment of Vibronic Satellites Exhibited by CaF_2, SrF_2, and BaF_2 Containing Substitutional Divalent Rare-earth Ions

ØYSTEIN RA

Tinius Olsens Tekniske Skole, N-3600 Kongsberg, Norway

When reexamined on the basis of lattice dynamics calculations some earlier vibronic assignments turn out to be questionable. A well known type of analysis involving local XY_8 complexes is shown to be of dubious validity even when restricted to satellites known to originate from semilocalized modes. Theoretical perfect lattice frequency distributions are reported for the three alkaline-earth fluorides.

Valuable information on the vibrations of even perfect crystals may often be uncovered by applying imperfections as probes. This paper, which is a sequel to previous lattice dynamics studies,[1–6] contains defect calculations concerning the frequency distributions of CaF_2, SrF_2, and BaF_2. The following remarks relate to substitutional rare-earth ions in the mass defect limit. Force field models and the attendant diagonal Green's functions put to use below are those reported on earlier occasions.[1–6] Information about phonon spectra may be obtained from vibronic satellites (satellite bands associated with electronic transitions of impurity atoms due to the combination of the electronic transition with the creation or annihilation of one or more phonons). In this respect CaF_2, SrF_2, and BaF_2 have been receiving some considerable attention. These fluorides frequently serve as host lattices for paramagnetic ions, and the simultaneous excitations of lanthanide ions and lattice waves have been studied by a number of authors. However, as I hope to demonstrate below, it is desirable to reconsider some of the earlier assignments. Preferably, a few conjectures should be put on a safer basis by relating them to detailed lattice dynamics calculations.

THE LOW LYING CaF_2:Tm^{2+} VIBRONIC

To begin with, we turn to the vibronic spectrum of Tm^{2+} in CaF_2 where the predominant contribution to the electronic transition appears to be of the $4f^n \rightarrow 4f^n$ type.[7] This system shows a strong vibronic satellite at an energy

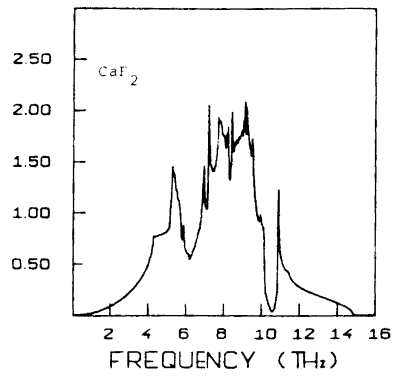

Fig. 1a. Unsmoothed computer plot of the frequency spectrum for CaF_2 as calculated by the method of Gilat and Raubenheimer [17] on the basis of the central force shell-model described in Ref. 6. The spectrum is normalized to one chemical unit.

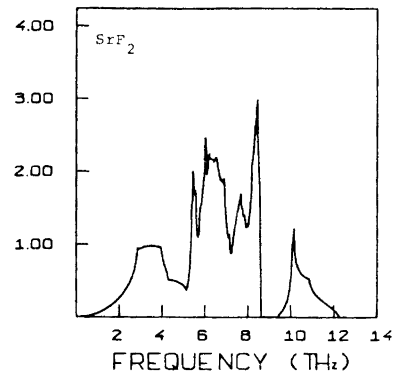

Fig. 1b. Unsmoothed computer plot of the frequency spectrum for SrF_2 as calculated by the method of Gilat and Raubenheimer [17] on the basis of the central force shell-model described in Ref. 6. The spectrum is normalized to one chemical unit. The gap is possibly an artifice of the model (see the discussion of parameter fitting in Ref. 6).

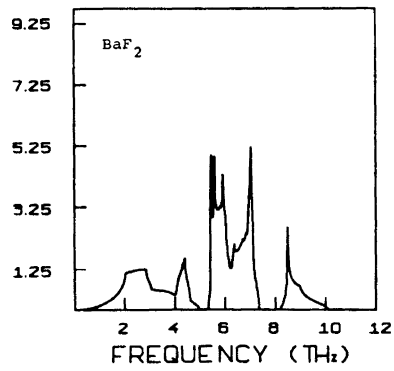

Fig. 1c. Unsmoothed computer plot of the frequency spectrum for BaF_2 as calculated by the method of Gilat and Raubenheimer [17] on the basis of the central force shell-model described in Ref. 6. The spectrum is normalized to one chemical unit. Note that the model predicts a complete separation of acoustic and optical frequency branches throughout the Brillouin zone. The acoustic part of the spectrum has the typical shape of the frequency distribution function for an f.c.c. monoatomic solid (see for instance the Ni spectrum calculated by Gilat and Raubenheimer [17] and shown in their Fig. 2)

shift of 93 cm^{-1} from the purely electronic line. However, there is probably no critical point in the perfect lattice, one-phonon density of states at this low energy value as indicated by the theoretical spectrum shown in Fig. 1a. It has been suggested by Loudon [8] that the satellite in question may originate in a quasilocalized mode brought about by the comparatively large mass difference between Ca and Tm. As far as symmetry arguments are concerned only odd-parity phonons can contribute a vibronic satellite for a $4f^n \rightarrow 4f^n$ transition. Thus, a Γ_{15} type resonance mode would be effective (a Γ_{15} semilocalized vibration is the only kind of resonance mode which can appear in the mass defect limit). Can such a mode exist? Invoking Figs. 2a, b we tentatively

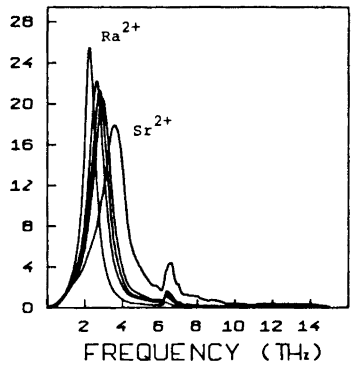

Fig. 2a. $\omega_L^2 M_{01}$ Im $G(l1\alpha,l1\alpha; \omega_L^2 x+i0)$, $0< x <1$, for Ra^{2+}, Tm^{2+}, Sm^{2+}, Ba^{2+}, and Sr^{2+} in CaF_2. The curve for Dy^{2+} is intermediate between those for Tm^{2+} and Sm^{2+}. Here ω_L is the largest (circular) frequency of the host lattice, M_{01} is the alkaline-earth ion mass, and $G(l1\alpha, l1\alpha; \omega_L^2 x+i0)$ is the limiting Green's function obtained for the impurity in the mass defect approximation on approaching the real axis from above. For a comparison with the perfect lattice cation Green's function, which differs from impurity Green's functions by the absence of a resonance denominator, the reader should consult Fig. 1a in Ref. 4. On so doing one will note the reappearence of perfect lattice features in the Sr^{2+} case for which the mass difference between the host cation and the impurity cation is the least.

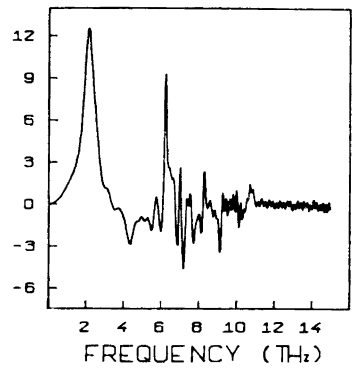

Fig. 2b. Large N (= the number of unit cells in a cyclic macrocell) limit of the CaF_2 $3nN\Delta F(\omega^2) \times 10^{-1}\ \omega_L^2$; where $n(=3)$ is the number of ions in a unit cell, and where $\Delta F(\omega^2)$ is the perturbance in the distribution of squared frequencies caused by a substitutional Ra^{2+} ion. The structure appearing for frequency values above ~11 THz consists of spurious fluctuations resulting from a representation of the imaginary part of the perfect lattice Green's function in terms of truncated sine series expansions (Ref. 4). The shapes assumed by the corresponding function for divalent rare-earth substitutions are similar, although the heights of the two main peaks decrease when the impurity mass approaches that of Ca^{2+}. Also, on decreasing the impurity mass through the sequence Ra^{2+}, Tm^{2+}, Dy^{2+}, Sm^{2+} the position of the low-frequency peak maximum shifts from 2.41 THz (~80.5 cm^{-1}) through 2.88 THz (~96.2 cm^{-1}) and 2.96 THz (~98.6 cm^{-1}) to 3.11 THz (~103.8 cm^{-1}). In units of ω_L^2, the corresponding widths are 0.02, 0.04, 0.04, and 0.04, respectively. On lowering the impurity mass from Ra^{2+} to Sm^{2+} the peak maximum of the other main maximum changes from 6.32 THz (~210.9 cm^{-1}) to 6.45 THz (~215.0 cm^{-1}). Nominal widths can be calculated, but would not be very instructive, the peak shapes differing considerably from a Lorentzian for this resonance.

answer this question in the affirmative and attribute the vibronic satellite to a pseudolocalized mode; the wavenumber value predicted for this mode by the mass defect approximation being 96 cm^{-1}.

THE CaF_2:Dy^{2+}, SrF_2:Dy^{2+}, AND BaF_2:Dy^{2+} SYSTEMS

The above assignment receives support from the existence of a similar phenomenon in the fluorescence spectrum obtained by Kiss [9] for a $4f \rightarrow 4f$ transition in CaF_2:Dy^{2+}. Again, there is a low-lying satellite, the peak maximum of which is separated from the no-phonon line by an amount of energy being significantly smaller than the predicted energy of any host crystal critical point phonon. This time the shift amounts to ~ 100 cm^{-1}. In the mass defect approximation the replacement of a Ca^{2+} ion by a Dy^{2+} ion brings about a pseudolocalized mode at ~ 99 cm^{-1}. However, an interpretation involving a Γ_{15} type vibration is at variance with Kiss' own explanation of his CaF_2:Dy^{2+} results. Kiss adheres to the type of analysis devised by Axe and Sorokin [10] and classifies several of the vibronics in terms of a vibrating XY_8 cluster constituted by the substitional rare-earth and a cage of nearest neighbour F^- ions. Although

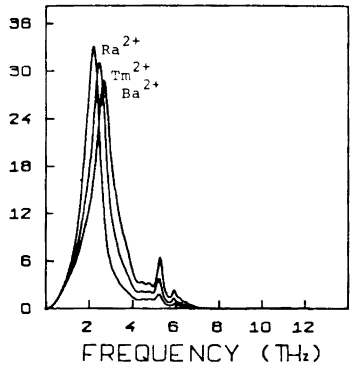

Fig. 3a. $\omega_L^2 M_{01}$ Im $G(l1\alpha, l1\alpha; \omega_L^2 x + i0)$ (the significance of the symbols involved is obtainable from the legend to Fig. 2a) for Ra^{2+}, Tm^{2+}, and Ba^{2+} in SrF_2. The curves for Dy^{2+} and Sm^{2+} impurities are intermediate between those for Tm^{2+} and Ba^{2+}. The two minor peaks show impurity resonances superposed on the perfect lattice structure shown in Fig. 2a of Ref. 4, the resonance frequencies being nearly coincident with two perfect lattice critical point frequencies as discussed in the text.

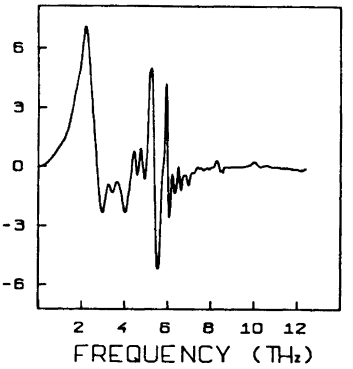

Fig. 3b. $3nN\Delta F(\omega^2) \times 10^{-1}$ ω_L^2 for a substitutional Ra^{2+} in SrF_2 (the significance of the symbols is explained in the legend to Fig. 2b). Due to the reduced difference between impurity and host ion mass the (dimensionless) width ($=0.07$) of the low-frequency maximum is more than three times that of its CaF_2:Ra^{2+} counterpart shown in Fig. 2b. For substitutional lanthanides in SrF_2 the perturbancies in frequency spectra are similar to the above curve, apart from the fact that the low-frequency peaks are more diffuse and the asymmetry in the peak shapes becomes more pronounced. In fact, the usual resonance condition is not fulfilled for any of the lanthanides since the appropriate multiple of the real part of the perfect lattice cation Green's function does not quite equal unity at peak maximum. However, in view of the crudeness of the mass defect approximation there is, in the present context, little difference in physical significance between resonance and near resonance.

this kind of interpretation has been rejected by Richman [11] on the grounds that the majority of vibronics discussed by Axe and Sorokin can be accounted for by host lattice phonons alone, Kiss maintains that an XY_8 analysis still applies to those experimentally detected effects which he ascribes to semilocalized vibrations. This reasoning makes him attach an E_u label to the 100 cm^{-1} vibronic of CaF_2:Dy^{2+}. However, for reasons to become clear shortly an XY_8 interpretation is of dubious validity even when the interest is confined to quasilocalized effects. Of the vibronics observed by Kiss in the fluorescence spectra of SrF_2:Dy^{2+} and BaF_2:Dy^{2+} there is for each compound one regarded by Kiss as originating in semilocalized vibrations and being of symmetry E_u. The frequency values are $\sim$ 85 cm^{-1} and $\sim$ 79 cm^{-1}, respectively. If, as a consequence of the doubt expressed above concerning the XY_8 analysis, we change the E_u assignment and take these modes to be of the Γ_{15} type (T_{1u} in the notation used by Kiss) then their wavenumbers are in fair agreement with those obtained for the lowermost semilocalized modes in the mass defect limit; namely 80 cm^{-1} (SrF_2:Dy^{2+}) and 72 cm^{-1} (BaF_2:Dy^{2+}). As indicated by Figs. 3 and 4a,b these resonance modes decay more rapidly into the neighbouring part of the phonon continuum than the corresponding ones occurring in the CaF_2:Tm^{2+} (Dy^{2+}) cases. As for BaF_2:Dy^{2+}, part of the lowermost observed vibronic peak may possibly be contributed also by lattice phonons since according to the lattice dynamics calculations described previously [6] (see also Fig. 1c) there is an L_3' phonon with odd-parity components at $\sim$ 69 cm^{-1}.

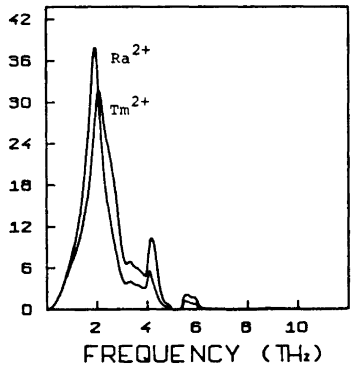

Fig. 4a. $\omega_L^2 M_{01}$ Im $G(l1\alpha, l1\alpha; \omega_L^2 x + i0)$ (the significance of the symbols involved is obtainable from the legend to Fig.2a) for Ra^{2+} and Tm^{2+} in BaF_2. The Dy^{2+} and Sm^{2+} curves are rather similar to the shown Tm^{2+} graph. The perfect lattice case is displayed in Fig. 3a of Ref. 4.

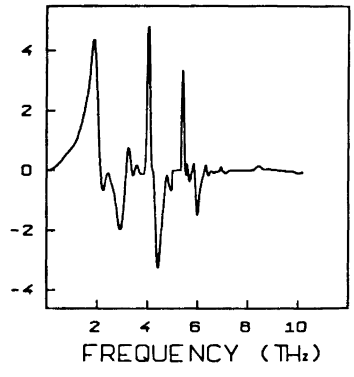

Fig. 4b. $3nN\Delta F(\omega^2) \times 10^{-1}$ ω_L^2 for a substitutional Ra^{2+} in BaF_2 (the significance of the symbols is explained in the legend to Fig. 2b). Since the critical impurity mass for (true) low-frequency resonance to take place is 337 (a.u.), the resonance condition is not satisfied even in the Ra^{2+} case. The rare-earth plots are similar to the one shown here. On decreasing the impurity mass from that of Ra^{2+}, the low-frequency maximum does, however, become even broader, and less symmetrical.

THE $SrF_2:Sm^{2+}$ AND $BaF_2:Sm^{2+}$ SYSTEMS

Having introduced L_3' phonons into the discussion, we turn to the systems $SrF_2:Sm^{2+}$ and $BaF_2:Sm^{2+}$ both of which have fluoroscence spectra associated with parent transitions within the $4f$ configuration.[12] This may be contrasted with $CaF_2:Sm^{2+}$ where all the low-temperature emission originates at a $4f^5$ $5d$ level.[12] The fluoroscence spectra of Sm^{2+} in SrF_2 and in BaF_2 have been studied experimentally by Wood and Kaiser.[12] Their $SrF_2:Sm^{2+}$ work has later been confirmed and extended by Cohen and Guggenheim[13] who reported data also on the Zeeman effect on the transitions. In the spectrum of $SrF_2:Sm^{2+}$ the two lowest lying vibronics are situated on the wavenumber axis at 86 cm^{-1} and 97 cm^{-1}, respectively. From symmetry and the Zeeman effect the 97 cm^{-1} vibronic may be ascribed to lattice vibrations which prior to the breakdown of translational symmetry carried labels L_3' or $X_3'(M_3')$. According to the calculations of dispersion relations reported earlier [6] there is a critical point phonon with symmetry label L_3' at $\sim$ 96 cm^{-1}, see also Fig. 1b. I tentatively identify this phonon with the 97 cm^{-1} observed vibronic line. However, there is in the dispersion relations for high symmetry **k**'s and in the predicted frequency distribution, Fig. 1 b, no sign of another perfect lattice critical point in the vicinity of and below this energy value. In fact, ignoring the possibility of an unresolved critical point due to branch crossing at a general **k**-value, the second lowest theoretical critical point, which is of the $X_5'(M_5')$ type, appears at $\sim$ 133 cm^{-1}. This critical point can be identified as the second slope discontinuity from the left in Fig. 1 b. Now, 133 cm^{-1} is rather close to the wavenumber of the third lowest vibronic line of $SrF_2:Sm^{2+}$, 131 cm^{-1}. Upon the reduction $O_h^5 \rightarrow O_h$ an irreducible $O_h^5 - X_5'$ amplitude subspace splits into $O_h - \Gamma_{15}$ and $O_h - \Gamma_{25}'$ spaces. The symmetry assigned to the odd-parity 131 cm^{-1} level by Cohen and Guggenheim [13] is Γ_{15}. I consider this to be sufficient reason for asking whether the lowest vibronic observed at 86 cm^{-1} might not possibly be due to an impurity effect on the lattice vibrations, *i.e.* a semilocalized mode. As pointed out by Cohen and Guggenheim the similar "sizes" of host and impurity cations makes it reasonable to assume that the SrF_2 lattice becomes only mildly distorted on replacing a few and well separated Sr^{2+} ions with Sm^{2+} ions. By invoking the results of Bron and Wagner [14] and of Timusk and Buchanan [15] on pseudolocalized modes generated by lattice distortions, Cohen and Guggenheim conclude that for the system $SrF_2:Sm^{2+}$ the phonons contributing to the vibronic spectra are those of the host crystal. On the other hand, in keeping with the "moderate distortion" hypothesis we may take the mass defect approximation to be quite good in this case. The mass defect model leads to a comparatively broad and not quite symmetric, yet discernible, peak in the perturbed frequency spectrum, Figs. 3a, b, with a maximum increase in the density of one-phonon states at $\sim$87 cm^{-1}. Consequently, I believe a semilocalized mode to provide a plausible explanation for the observed 86 cm^{-1} level. In the $BaF_2:Sm^{2+}$ case the difference between impurity and host mass is smaller than for $SrF_2:Sm^{2+}$, and the calculated low-frequency maximum in the perturbed frequency spectrum is more diffuse and of lower height than the corresponding $SrF_2:Sm^{2+}$ peak, Fig. 4a, b. If there should be a feeble resonance effect in the real system, it would probably

occur at an energy value close to that of the previously mentioned BaF_2 L_3' phonon at 69 cm^{-1}, and might be difficult to resolve.

SHORTCOMINGS OF THE XY_8 TYPE ANALYSIS

At this point a few comments are in order regarding the validity of the XY_8 type analysis. In so far as the mass defect approximation can be trusted, Figs. 2, 3, and 4a, b show that for a substitutional lanthanide ion in an alkaline-earth fluoride the possibility of the occurence of a Γ_{15} resonance is not exhausted by the low-lying and main maximum in the diagonal lanthanide ion Green's function. Among the additional maxima in the perturbed frequency spectra, some are fairly narrow and of appreciable height. The fact that these do not show up very clearly in the Green's function plots is a direct consequence of the closure conditions on the eigenvectors of the dynamical matrix in conjunction with the appreciable rare-earth amplitude in modes located on the frequency axis in the proximity of the lowermost peak in the Green's function. It is still possible for the other semilocalized modes to take part in vibronic formation, though, since for an electronic transition to couple to lattice waves it is not necessary for the rare-earth itself to move provided the remaining part of the lattice can furnish a suitable and oscillating crystal field. In view of the crudeness of the mass defect model, the predicted width, height, and peak position of even the major maxima occurring in Figs. 2b, 3b, and 4b are probably inaccurate. In fact, seemingly important peaks may represent mass defect artifices rather than physical occurrences. Nevertheless, our results serve to show that more than two distinct Γ_{15} resonances *could* very well turn up in alkaline-earth fluorides doped with rare-earth ions. This points to a serious shortcoming of the kind of analysis based on a local XY_8 complex, at least in the form proposed by Axe and Sorokin.[10] Their oscillatory space contains only two irreducible Γ_{15} (in their notation T_{1u}) subspaces.

It may be noted that rare-earth induced peaks in the density of one-phonon states may easily appear quite close to frequency values for perfect lattice critical point phonons, as evidenced by SrF_2:Sm^{2+}. In addition to the previously mentioned semilocalized mode at ~ 87 cm^{-1} there are two predicted Γ_{15} type semilocalized vibrations both of which occur in the vicinity of peaks in the host crystal frequency spectrum, Figs. 1b, 3b. The two semilocalized modes have frequency values ~ 178 cm^{-1} and ~ 199 cm^{-1}, respectively, while the two critical points, having symmetry labels Σ_1 and Σ_4, are at 183 cm^{-1} and 202 cm^{-1}. This proximity of frequencies is in the present case of some consequence since Cohen and Guggenheim have observed vibronic levels corresponding to frequencies which coincide with those of the two Σ_1 and Σ_4 critical points.[13] Upon the reduction $O_h^5 \rightarrow O_h$, carrier spaces for irreducible O_h^5 representations of the Σ_1 and the Σ_4 type both precipitate point group carrier spaces with labels compatible with what is kown about the two above-mentioned vibronics. However, since the latter may both be of the Γ_{15} type,[13] the two quasilocalized modes may also contribute.

In ending these remarks on vibronic satellites it seems safe to assert that additional and refined theoretical calculations may be useful in extracting

further information on vibrational properties from the quite ample experimental data already in existence.

AVAILABLE MATERIAL PREREQUISITE TO FURTHER CALCULATIONS

The author hopes to find the opportunity to indulge in further and more detailed studies of defective alkaline-earth fluorides in the future. It may be mentioned that extensive numerical material (*e. g.* numerical eigensystems for Fourier transformed dynamical matrices corresponding to a grid of 64 000 **k**-values + additional wave vector triplets going into the procedure used in Ref. 4 for generating Green's functions) needed in performing Kanzaki-type lattice statics[16] and Green's function lattice dynamics calculations has been stored on magnetic tape for use as required. This material is available from the author on request.

REFERENCES

1. Ra, Ø. *J. Chem. Phys.* **52** (1970) 3765.
2. Ra, Ø. *Phys. Status Solidi* **39** (1970) 265.
3. Ra, Ø. and Borgen, O. S. *Kgl. Norske Vidensk. Selsk. Skrifter* No. 8 1972.
4. Ra, Ø. *Z. Naturforsch.* **26a** (1971) 111.
5. Ra, Ø. *Z. Naturforsch.* **27a** (1972) 1196.
6. Ra, Ø. *J. Chem. Phys. In press.*
7. Kiss, Z. J. *Phys. Rev.* **127** (1962) 718.
8. Loudon, R. *Proc. Phys. Soc.* **84** (1964) 379.
9. Kiss, Z. J. *Phys. Rev.* **137** (1965) A1749.
10. Axe, J. D. and Sorokin, P. P. *Phys. Rev.* **130** (1963) 945.
11. Richman, I. *Phys. Rev.* **133** (1964) A1364.
12. Wood, D. L. and Kaiser, W. *Phys. Rev.* **126** (1962) 2079.
13. Cohen, E. and Guggenheim, H. J. *Phys. Rev.* **175** (1968) 354.
14. Wagner, M. and Bron, W. E. *Phys. Rev.* **139** (1965) A273.
15. Timusk, T. and Buchanan, M. *Phys. Rev.* **164** (1967) 345.
16. Hardy, J. R. and Lidiard, A. B. *Phil. Mag.* **15** (1967) 825.
17. Gilat, G. and Raubenheimer, L. J. *Phys. Rev.* **144** (1966) 390.

Received August 31, 1972.

ACTA CHEMICA SCANDINAVICA 27 (1973) 2035–2042

The Enthalpies of Fusion of Li_2BeF_4, $LiBeF_3$, and Na_2BeF_4, and the Heat Capacities of the Liquid Mixtures

JAN LÜTZOW HOLM,[a] BIRGIT JENSSEN HOLM[b] and FREDRIK GRØNVOLD[c]

[a] *Institute of Physical Chemistry*, [b] *Institute of Inorganic Chemistry, The University of Trondheim, NTH, N-7034 Trondheim-NTH, Norway and,* [c] *Institute of Chemistry, The University of Oslo, Blindern, Oslo 3, Norway*

As a part of an extended investigation of the thermochemistry of liquid and solid compounds in $AX–BX_2$ and $AX–CX_3$ systems, the heat capacities of solid and liquid Li_2BeF_4 and Na_2BeF_4, and of a liquid mixture of the $LiBeF_3$-composition have been measured. Furthermore, the enthalpies of fusion of the congruently melting compounds Li_2BeF_4 and Na_2BeF_4 have been determined. The following molar enthalpies of fusion were obtained in the temperature range investigated:

$$Li_2BeF_4: \Delta H_f = -336 + 14.06\ T \text{ cal mol}^{-1}$$
$$Na_2BeF_4: \Delta H_f = -9735 + 18.32\ T \text{ cal mol}^{-1}$$

The stability of the two solid compounds Li_2BeF_4 and $LiBeF_3$ has been discussed on the basis of data originally given by Holm and Kleppa and the heat capacities and enthalpies of fusion obtained in this work.

In the course of an extended investigation of the thermochemistry of liquid and solid metal halide mixtures, the enthalpies of fusion of some 2:1 and 1:1 compounds of alkali fluorides (LiF and NaF) and beryllium fluoride have been determined by means of a high precision drop calorimeter with adiabatic shields. With this calorimeter rather precise values for the heat capacities for the molten salt mixtures can also be obtained, as has been shown in a recent paper on alkali chloride-magnesium chloride mixtures by Holm *et al.*[1]

The thermodynamic properties as well as the structures of molten alkali fluoride-beryllium fluoride mixtures have for some time attracted the attention of several investigators. The enthalpy of mixing of liquid LiF-BeF_2, KF-BeF_2, and RbF-BeF_2 mixtures has been measured by Holm and Kleppa.[2] They suggested from the obtained ΔH^M-data that BeF_4^{2-} is an important anionic species in these mixed systems, particularly in the systems KF-BeF_2 and RbF-BeF_2, and to a lesser extent also in the system LiF-BeF_2.

Another contribution in the same field has been made by Braunstein *et al.*,[3] who calculated partial excess Gibbs free energies of AlkF in AlkF-BeF_2 mixtures from phase diagram data, and correlated their data with the chemical potential interaction parameter in charge-unsymmetrical mixtures. Raman spectra of BeF_4^{2-} in a molten LiF-NaF mixture has been reported by Quist *et al.*[4] They kept the BeF_2 content constant at 33 mol %, and were therefore unable to report upon any change in the spectra with composition. They concluded, however, that strong $Be^{2+} - F^-$ interactions are present in these mixtures, and also that Be^{2+} is tetrahedrally surrounded by F^- ions.

The phase diagram of the system LiF-BeF_2, and the phase equilibria in this system, have recently been reinvestigated by Romberger *et al.*,[5] who for the first time established Li_2BeF_4 as a congruently melting compound with a phenacite (Be_2SiO_4)-type structure. This system also contains the compound $LiBeF_3$, which disproportionates in the solid state at 290°C to Li_2BeF_4 and BeF_2.

The system NaF-BeF_2 contains a congruently melting compound corresponding to Na_2BeF_4, as shown in the phase diagram by Roy *et al.*[6]

In the paper by Holm *et al.*[1] the possible formation and stability of complex ions in the binary systems KCl-$MgCl_2$, RbCl-$MgCl_2$, and CsCl-$MgCl_2$ were discussed on the basis of the heat capacities of the liquid mixtures, and the enthalpies of mixing between the compounds. It was stressed that complex formation should not be considered as a *static* phenomenon in these systems. The results were rather indicative of changes in the stability of the complex ions as the temperature is varied. In this work the same methods will be used to elucidate the stability of the BeF_4^{2-} ion in molten lithium fluoride and sodium fluoride.

EXPERIMENTAL

A. Chemicals. Lithium fluoride (LiF, Fisher Certified Reagent) and sodium fluoride (NaF, *p.a.* from E. Merck, Germany) were melted in platinum crucibles in an atmosphere of purified nitrogen. Only clear crystals were selected from the samples. Beryllium fluoride (BeF_2, from the Brush Beryllium Co., USA) was a high purity product, which, according to the manufacturer, contains 99.5 % BeF_2.

For the preparation of Li_2BeF_4, $LiBeF_3$, and Na_2BeF_4 stoichiometric amounts of the alkali fluoride and beryllium fluoride were melted together in a platinum crucible in a purified nitrogen atmosphere.

B. Calorimetry. Duplicate samples of each of the compounds were loaded into platinum containers of known mass. The containers were evacuated carefully inside a glove box to get rid of the air. The glove-box was filled with purified nitrogen. After evacuation, the containers were filled with purified argon. They were then sealed by arc-welding a cup-shaped platinum lid to the rim of the container.

The sample was equilibrated in a vertical laboratory furnace and lifted into the silver calorimeter, which was placed above the furnace. The calorimeter was surrounded by silver shields, electrically heated to maintain quasi-adiabatic conditions. The furnace temperature was measured by a quartz thermometer. Temperatures are in terms of the International Practical Temperature Scale of 1968. The calorimeter proper, the calibration of the calorimeter, and the method of calculating the enthalpy increments $H_T - H_{298.15}$ have been described in detail by Grønvold.[7]

Steady state conditions were usually obtained after 10 – 20 min, depending on the furnace temperature. The calorimeter temperature during the period of experiments ranged from 298 to 330 K with a mean of 315 K. The heat capacity values for the compounds were estimated from those for the binary compounds by the relationship

$$c_p = nC_p(\mathrm{AlkF}) + C_p(\mathrm{BeF_2}),\ (n = 1 \text{ or } 2) \quad (1)$$

The heat capacity values at 315 K, used for adjusting the enthalpies to 298 K, are listed in Table 1.

Table 1. Heat capacity values at 315 K (from JANAF [8]).

Compound	C_p/cal K^{-1} mol^{-1}
LiF	10.19
NaF	11.31
BeF_2	12.70
Li_2BeF_4	33.08
$LiBeF_3$	22.89
Na_2BeF_4	35.26

RESULTS

(a) *Na_2BeF_4*. The enthalpy increments are listed in Tables 2 and 3 and plotted in Fig. 1. From our data we obtain the following relations (σ is the standard deviation)

Na_2BeF_4(s):

$$H_T - H_{298.15} = -10986 + 44.68\ T \text{ cal} \quad (\sigma = 185) \quad (2)$$

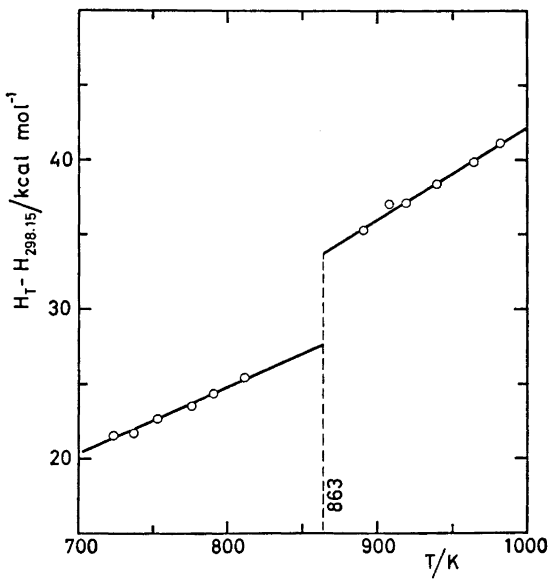

Fig. 1. Enthalpy curve, $H_T - H_{298.15}$ for Na_2BeF_4, this work.

Table 2. Experimental and calculated enthalpy increments for solid Li_2BeF_4 and Na_2BeF_4.

T/K	$\frac{H_T - H_{298.15}}{\text{cal mol}^{-1}}$ exp.	calc.
	Li_2BeF_4	
572.8	10539	10555
601.5	12009	11921
625.1	13024	13043
650.1	14075	14233
677.1	15549	15518
693.0	16451	16274
707.0	16837	16940
	Na_2BeF_4	
724.2	21615	21373
737.3	21777	21958
753.3	22632	22673
776.7	23554	23718
790.2	24339	24322
811.5	25400	25273

Table 3. Experimental and calculated enthalpy increments for liquid Li_2BeF_4, $LiBeF_3$, and Na_2BeF_4.

T/K	$\frac{H_T - H_{298.15}}{\text{cal mol}^{-1}}$ exp.	calc.
	Li_2BeF_4	
758.2	29200	29703
771.8	30427	30541
781.1	31413	31115
788.7	31924	31583
797.0	32326	32095
803.2	32216	32477
811.4	33051	32982
822.5	33767	33667
831.9	34519	34246
840.9	34593	34801
873.0	36554	36780
	$LiBeF_3$	
704.1	17044	17169
724.8	18177	18025
747.9	18962	18991
757.4	19458	19374
777.5	20113	20206
	Na_2BeF_4	
891.2	35269	35424
908.5	36999	36514
919.5	37020	37207
940.4	38346	38524
963.5	39833	39979
980.5	41232	41950

Na_2BeF_4(l):

$$H_T - H_{298.15} = -20721 + 63.00\ T \text{ cal} \quad (\sigma = 200) \tag{3}$$

This gives an equation for the enthalpy of fusion of Na_2BeF_4:

$$\Delta H_f(Na_2BeF_4) = -9735 + 18.32\ T \text{ cal mol}^{-1} \tag{4}$$

The enthalpy of fusion of Na_2BeF_4 at the melting point, 863 K, is 6.1 ± 0.2 kcal mol^{-1}. Values for this compound have not been reported in the literature.

(b) *Li_2BeF_4 and $LiBeF_3$.* The obtained enthalpy increments for these two compounds are listed in Tables 2 and 3 and plotted in Fig. 2. For lithium tetrafluoroberyllate we obtain the following results:

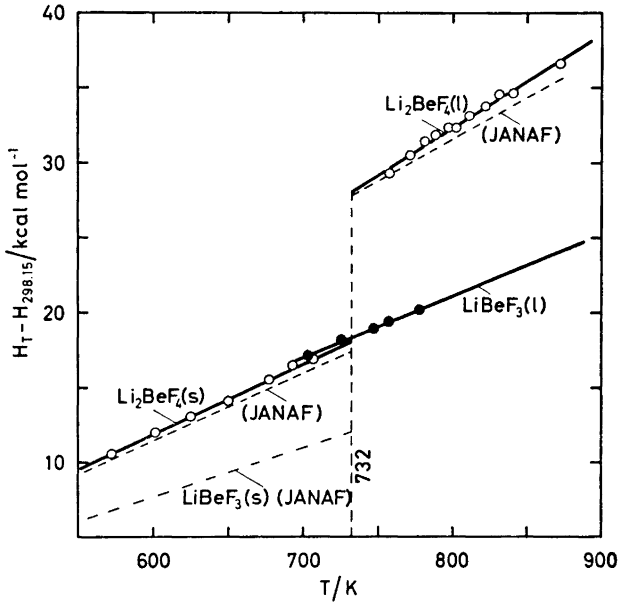

Fig. 2. Enthalpy curve, $H_T - H_{298.15}$ for Li_2BeF_4 and $LiBeF_3$. ○, Li_2BeF_4, this work; ●, $LiBeF_3$(l), this work; dotted line, Li_2BeF_4, data from JANAF;[8] dash-dotted line, $LiBeF_3$(s), data from JANAF.[8]

Li_2BeF_4(s):

$$H_T - H_{298.15} = -16698 + 47.58\ T \text{ cal} \quad (\sigma = 124) \tag{5}$$

Li_2BeF_4(l):

$$H_T - H_{298.15} = -17034 + 61.64\ T \text{ cal} \quad (\sigma = 194) \tag{6}$$

For liquid $LiBeF_3$ we find:

$LiBeF_3$(l):

$$H_T - H_{298.15} = -11965 + 41.38\ T \text{ cal} \quad (\sigma = 135) \tag{7}$$

On the basis of eqns. (5) and (6) we derive for the enthalpy of fusion of Li_2BeF_4:

$$\Delta H_f(Li_2BeF_4) = -336 + 14.06\ T \text{ cal mol}^{-1} \quad (8)$$

At the melting point 723.1 K this corresponds to $\Delta H_f = 10.0 \pm 0.15$ kcal mol^{-1}. This value should be compared with that given in JANAF,[8] $\Delta H_f = 10.6$ kcal mol^{-1}, which is based on the enthalpy determinations by Douglas and Payne.[9]

DISCUSSION

(a) *Enthalpy cycle calculations.* In the first part of the discussion we wish to demonstrate the use of two enthalpy cycles in calculations of enthalpy of reactions, since enthalpy of fusion and enthalpy of mixing data are available.

Cycle I at 732 K:

$$\begin{array}{ccccc} 2LiF(s) & + & BeF_2(s) & \xrightarrow{\Delta H_1} & Li_2BeF_4(s) \\ \downarrow 2\Delta H_f(LiF) & & \downarrow \Delta H_f(BeF_2) & & \downarrow \Delta H_f(Li_2BeF_4) \\ 2LiF(l) & + & BeF_2(l) & \xrightarrow{\Delta H_1^M} & Li_2BeF_4(l) \end{array}$$

According to the cycle

$$\Delta H_1^M = \Delta H_1 + \Delta H_f(Li_2BeF_4) - 2\Delta H_f(LiF) - \Delta H_f(BeF_2) \quad (9)$$

By inserting

$\Delta H_1 = -4.0$ kcal (Gross,[10] JANAF [8])
$\Delta H_f(Li_2BeF_4) = 10.0$ kcal mol^{-1} (this work)
$\Delta H_f(LiF) = 5.9$ kcal mol^{-1} (JANAF [8] and Douglas and Dever [11])
$\Delta H_f(BeF_2) = 1.2$ kcal mol^{-1} (JANAF [8] and Holm and Kleppa [2])

one finds

$$\Delta H_1^M(732\text{ K}) = -4.0 + 10.0 - 11.8 - 1.2$$
$$= -7.0 \text{ kcal (mol } Li_2BeF_4)^{-1}$$

This calculated value might be compared with the experimental enthalpy of mixing found by Holm and Kleppa [2] at 1135 K for the composition $X_{BeF_2} = 0.33$, $\Delta H^M = -1070$ cal (mol mixture)$^{-1}$. For the reaction

$$2LiF(l) + BeF_2(l) = Li_2BeF_4(l)$$

one therefore has

$$\Delta H_1^M(1135\text{ K}) = -3.2 \text{ kcal mol}^{-1}$$

This clearly shows the large temperature dependence of the enthalpy of mixing. The change in ΔH^M from 730 to 1135 K corresponds to an average change in the heat capacity of mixing of

$$\Delta C_p^M = \frac{-3200 + 7000}{400} = 9.5 \text{ cal K}^{-1} \text{ mol}^{-1}$$

This shows a very good agreement with the experimental value found in this work at 732 K:

$$\Delta C_p^M = 3.1 \text{ cal K}^{-1} \text{ (mol mixture)}^{-1} \text{ (Table 4)}$$

or

$$\Delta C_p^M = 9.3 \text{ cal K}^{-1} \text{ (mol } Li_2BeF_4)^{-1}$$

Cycle II at 732 K:

$$\begin{array}{ccccc} LiF(s) & + & BeF_2(s) & \xrightarrow{\Delta H_2} & LiBeF_3(s) \\ \downarrow \Delta H_f(LiF) & & \downarrow \Delta H_f(BeF_2) & & \downarrow \Delta H_f(LiBeF_3) \\ LiF(l) & + & BeF_2(l) & \xrightarrow{\Delta H_2^M} & LiBeF_3(l) \end{array}$$

According to cycle II

$$\Delta H_2 = \Delta H_f(LiF) + \Delta H_f(BeF_2) - \Delta H_f(LiBeF_3) + \Delta H_2^M \quad (10)$$

By inserting the values

$\Delta H_f(LiF) = 5.9$ kcal mol^{-1} (JANAF [8] and Douglas and Dever [11])
$\Delta H_f(BeF_2) = 1.2$ kcal mol^{-1} (JANAF [8] and Holm and Kleppa [2])
$\Delta H_f(LiBeF_3) = 6.3$ kcal mol^{-1} (this work)

one finds

$$\Delta H_2 = 0.8 + \Delta H_2^M \quad (11)$$

The enthalpy of mixing, ΔH_2^M, can be calculated from the enthalpies of mixing given by Holm and Kleppa.[2] For the 50:50 composition they found $\Delta H^M = -280$ cal (mol mixture)$^{-1}$ at 1135 K. By use of the calculated ΔC_p^M for this composition, $\Delta C_p^M = 4.8$ cal K^{-1} (mol $LiBeF_3)^{-1}$, it is possible to calculate the enthalpy of the reaction between liquid LiF and BeF_2 at 732 K:

$$LiF(l) + BeF_2(l) = LiBeF_3(l)$$

$$\Delta H_2^M(732 \text{ K}) = (-560 - 403 \times 4.8) = -2.5 \text{ kcal mol}^{-1}$$

Using this value in eqn. (11) we obtain

$$\Delta H_2 = -1.7 \text{ kcal mol}^{-1}$$

This value is in good agreement with the value reported by Gross [10] (see JANAF [8]) for reaction (II) at 298.15 K

$$LiF(s) + BeF_2(s) = LiBeF_3(s)$$

which is $= -1.8$ kcal mol^{-1}.

(b) *The heat capacities of the mixture.* From the slope of the enthalpy increment curves we find the heat capacities of the solids as well as of the liquids. From the heat capacities of the pure liquids we have calculated the changes in the heat capacity on mixing for some compositions. The results are summarized in Table 4. In the calculations we have used the following heat capacities:

LiF: 15.5 cal K^{-1} mol^{-1}, NaF: 16.4 cal K^{-1} mol^{-1} and
BeF_2: 17.9 at 700 K and 21.0 cal K^{-1} mol^{-1} at 1100 K (JANAF [8]).

The obtained heat capacities of mixing indicate that the BeF_4^{2-} ion is subject to dissociation in the LiF-BeF_2 melt as well as in the NaF-BeF_2 melt as the temperature increases. The BeF_3^- ion does not seem to be a pre-

Table 4. Changes in heat capacity on mixing x AlkF(l) + $(1-x)$$BeF_2$(l).

x	Alk	C_p/cal K^{-1} mol^{-1} comp.[a]	mix.	ΔC_p^M/cal K^{-1} mol^{-1} mix. − comp.	Temp. range K
0.67	Li	16.3 − 17.4	20.5	+4.2 − +3.1	700 − 1100
0.67	Na	16.6 − 17.7	21.0	+4.4 − +3.3	700 − 1100
0.50	Li	16.6 − 18.3	20.7	+4.1 − +2.4	700 − 1100

[a] As the heat capacity of liquid BeF_2 changes considerably with temperature, the C_p (comp.) and the C_p^M values will not be constant.

ferred complex ion in the melt in the actual temperature range, T above 1000 K. This can be seen from the fact that ΔC_p^M is about the same for the two mixtures 2/3 LiF + 1/3 BeF_2 and 1/2 LiF + 1/2 BeF_2. We therefore suggest that the most probable dissociation reaction for the tetrafluoro beryllate ion will be given as

$$BeF_4^{2-}{}_{(l)} = \text{“}BeF_2\text{”}_{(l)} + 2F^-{}_{(l)}$$

where “BeF_2“ denotes the inner and stable part (the non-polarizable part) of the complex.

Acknowledgements. Financial support has been received from the following sources and is gratefully acknowledged: *Norges Almenvitenskapelige Forskningsrad* (to F.G.), *Norges tekniske høgskoles fond* (to J.L.H.) and *Kaltenborn Griegs Stipendiefond* (to J.L.H. and B.J.H.).

REFERENCES

1. Holm, J. L., Jenssen Holm, B., Rinnan, B. and Grønvold, F. *J. Chem. Thermodynamics.* **5** (1973) 97.
2. Holm, J. L. and Kleppa, O. J. *Inorg. Chem.* **8** (1969) 207.
3. Braunstein, J., Romberger, K. A. and Ezell, R. *J. Phys. Chem.* **74** (1970) 4383.
4. Quist, A. S., Bates, J. B. and Boyd, G. E. *J. Phys. Chem.* **76** (1972) 78.
5. Romberger, K. A., Braunstein, J. and Thoma, R. E. *J. Phys. Chem.* **76** (1972) 1154.
6. Roy, D. M., Roy, R. and Osborn, E. F. *J. Am. Ceram. Soc.* **36** (1953) 185.
7. Grønvold, F. *Acta Chem. Scand.* **26** (1972) 2216.
8. *JANAF Thermochemical Tables*, Clearinghouse, Springfield, Virginia 1971.
9. Douglas, T. B. and Payne, W. H. *Natl. Bur. Std. Report* **8186**, 1964.
10. Gross, P. *Fulmer Research Institute, Report* **163/23**, May 1966.
11. Douglas, T. B. and Dever, J. L. *J. Am. Chem. Soc.* **76** (1954) 4826.

Received January 22, 1973.

ACTA CHEMICA SCANDINAVICA 27 (1973) 2043–2050

Enthalpies of Fusion of the Alkali Cryolites Determined by Drop Calorimetry

BIRGIT JENSSEN HOLM[a] and FREDRIK GRØNVOLD[b]

[a] *Institute of Inorganic Chemistry, The Technical University of Norway, N-7034 Trondheim-NTH, Norway and* [b] *Institute of Chemistry, University of Oslo, Blindern, Oslo 3, Norway*

Enthalpies of the alkali cryolites have been determined in the fusion region with an aneroid, inverse drop calorimeter with adiabatic shields. The values for the enthalpy of fusion are Li_3AlF_6: 21.0 ± 0.3; Na_3AlF_6: 27.1 ± 0.5; K_3AlF_6: 29.3 ± 0.4; Rb_3AlF_6: 31.5 ± 0.8; Cs_3AlF_6: 29.3 ± 0.9 kcal mol^{-1}. Measurements carried out on sodium chloride and sodium fluoride for comparison purposes are also reported.

Investigations of systems connected with the electrolytic production of aluminium have been carried out at the Institute of Inorganic Chemistry, The Technical University of Norway, during a number of years. In the course of these investigations, knowledge of the enthalpies of fusion of the alkali cryolites became of importance. Of these enthalpies of fusion, only the ones for lithium cryolite [1–3] and sodium cryolite [4,5] had then been measured calorimetrically. Values for potassium cryolite had been calculated from phase diagrams.[6,7] Some of the systems chosen for the calculations show extensive solid solubility, and the derived values are therefore rather unreliable. It was therefore decided to determine the enthalpy of fusion of all the alkali cryolites by drop calorimetry. Results of these determinations are presented in this work, together with data obtained for sodium chloride and sodium fluoride for comparison purposes.

EXPERIMENTAL

A. Materials. The sodium cryolite, Na_3AlF_6, was natural, hand-picked crystals from Ivigtut, Greenland. Aluminium trifluoride (AlF_3, technical grade, Riedel de Haën AG, Germany) was purified by repeated sublimations. Clear hexagonal crystals were picked from the samples. Sodium chloride (NaCl, *p.a. fusum* E. Merck AG, Germany), lithium fluoride (LiF, Fisher Certified Reagent, Fisher Scientific Co., USA), sodium fluoride (NaF, sample 1, min. 99 %, Baker & Adamson, USA, sample 2, (used for synthetic Na_3AlF_6) *p.a.*, E. Merck AG, Germany), rubidium fluoride (RbF, min. 99.8 %, Koch-Light Laboratories Ltd., England), cesium fluoride (CsF, sample 1, min. 98 %, The

British Drug House Ltd., England, sample 2, 99.9 %, Koch-Light Laboratories Ltd., England), were all melted in platinum crucibles and clear crystals were selected for use.

The alkali cryolites were made by fusing alkali fluoride and aluminium trifluoride in stoichiometric proportions. The compositions were checked by differential thermal analysis (DTA). If the sample was deficient in AlF_3 due to evaporation, more AlF_3 was added, and the process was repeated until no eutectic reaction could be observed by DTA.

All high-temperature work was carried out in an inert atmosphere of 99.99 % nitrogen.

B. Apparatus and method of operation. The determinations were carried out in a previously described [8] apparatus of the inverse drop type, operated with adiabatic shields. The finely crushed samples were loaded into platinum capsules, which were then evacuated inside a glove-box filled with purified nitrogen. After evacuation the capsules were filled with purified argon and the top lid was welded shut. The amount of sample used ranged from 2.9 to 5.3 g, and the mass of the empty platinum capsule was about 12 g.

The calorimetric measurements and calculations were carried out as described in the earlier paper.[8] The reported temperatures are in terms of the International Practical Temperature Scale of 1968. Steady state conditions were usually present after 10 – 25 min, depending on the sample studied and on the furnace temperature. The calorimeter temperature during the experiments ranged from 300 to 340 K with an estimated mean of 315 K. The heat capacities at 315 K, used in the adjustment of the enthalpies to 298 K, are given in Table 1.

Table 1. C_p values at 315 K.

	C_p/cal mol^{-1}K^{-1}	Reference
NaCl	12.01	JANAF [9]
NaF	11.31	»
Li_3AlF_6	49.05	»
Na_3AlF_6	52.50	»
K_3AlF_6	53.94	»
Rb_3AlF_6	54.9	[a]
Cs_3AlF_6	55.9	[a]

[a] Estimated.

Table 2. Enthalpy increments, experimental and calculated from $H_T - H_{298.15} = a + bT$.

T/K	$H_T - H_{298.15}$/cal mol^{-1}		T/K	$H_T - H_{298.15}$/cal mol^{-1}	
	exp.	calc.		exp.	calc.
	NaF, 3.3413 g; 1 mol ≙ 41.9882 g				
1195.1	11984	11989	1277.2	19090	–
1212.7	12256	12258	1288.5	21468	21450
1231.7	12556	12555	1296.5	21637	21588
1247.7	12805	12805	1307.6	21674	21772
			1315.6	21844	21905
	NaCl, 3.1698 g; 1 mol ≙ 58.4428 g				
1002.0	9568	9590	1082.1	16522	–
1028.7	9800	–	1085.4	17426	–
1039.1	10221	10171	1106.3	18005	17953
1049.3	10357	10331	1107.4	17860	17972
1058.4	10419	10474	1135.3	18513	18447
			1136.4	18462	18466

Table 2. Continued.

Li_3AlF_6; 1 mol ≙ 161.7889 g

Sample 1, 3.1566 g			Sample 2, 3.8094 g		
974.7	44290	44364	985.6	44122	–
994.3	45664	45668	1017.0	47065	47178
1011.9	47046	46838	1041.2	48480	48787
1035.1	48672	48381	1073.2	72056	72301
1069.5	72071	71960	1092.2	73995	74053
1086.1	73632	73491	1119.6	76466	76579
1098.8	74771	74661			
1113.1	76033	75980			

Na_3AlF_6; 1 mol ≙ 209.9413 g

Sample 1, natural cryolite, 3.4344 g			Sample 3, synthetic cryolite, 3.4140 g		
1173.1	59616	59528	1081.8	53379	53232
1184.0	60650	–	1102.7	54911	54673
1196.8	61837	–	1122.2	55913	56018
1203.0	61039	–	1122.8	55725	56059
1216.2	63164	–	1130.3	56560	56577
1223.1	63825	–	1139.6	57080	57218
1223.2	63750	–	1148.0	57817	57797
1234.7	64865	–	1156.2	58028	58362
1241.5	66012	–	1167.2	59558	59121
1290.3	95626	94857	1189.7	61355	–
1298.0	95296	95588	1214.3	63319	–
1303.3	95850	96091	1293.3	94788	95142
1309.3	97533	–	1295.4	95605	95341
1310.4	96542	96765	1303.0	95992	96062
1317.6	97368	97448	1307.7	96295	96509
1325.2	98516	98169	1308.9	96346	96622
1329.5	99562	–	1311.6	96775	96879
			1319.2	97795	97600

Sample 2, natural cryolite, 4.0912 g		
1198.6	61821	–
1212.3	63001	–
1226.8	64424	–
1249.4	67010	–
1293.6	95076	95170
1307.4	95684	–
1319.5	97493	97628
1333.1	99137	98919

K_3AlF_6, 3.1380 g; 1 mol ≙ 258.2779 g

1126.2	56608	56763	1290.5	98122	98264
1145.4	58111	58141	1298.7	99042	99034
1162.9	59414	59396	1305.9	99694	99709
1177.1	60481	60415	1313.7	100684	100441
1190.1	61294	61348	1316.6	100719	100713

Rb_3AlF_6; 1 mol ≙ 397.3819 g

Sample 1, 5.2556 g			Sample 2, 2.8822 g		
1053.6	49272	50016	1066.7	51178	50932
1064.4	50101	50771	1084.0	52846	52142
1083.2	51327	52086	1099.6	54161	53233
1095.9	52836	52974	1115.8	55812	–
1107.1	54192	53758	1144.5	60453	–
1135.0	60784	–	1203.7	92566	–

Table 2. Continued.

1166.9	65078	–	1223.4	94169	93907
1216.1	93231	93226	1238.7	95421	95336
1224.5	93811	94010	1253.6	96878	96728
1234.4	94778	94935			
1249.4	96186	96335			
		Cs_3AlF_6; 1 mol ≙ 539.6869 g			
Sample 1, 5.3079 g			Sample 2, 5.1218 g		
946.2	43203	43398	952.9	43777	43851
962.9	44229	44528	963.8	44895	44588
974.9	45757	–	974.3	45506	45299
994.2	47660	–	983.1	45874	45894
1013.5	49986	–	993.5	46671	46597
1047.5	56682	–	1103.8	83491	83915
1094.1	83838	83014	1111.9	83868	84668
1108.1	85052	84315	1127.1	85259	86080
1122.8	86228	85680	1143.5	86803	87603
1133.3	87222	86656			
1143.7	86151	–			
1156.6	89088	88820			

RESULTS AND DISCUSSION

The results of the enthalpy measurements are given in Table 2, and plotted in Figs. 1 – 3 together with some literature values. The measured values were fitted to equations of the type

$$H_T - H_{298.15} = a + bT$$

by a least squares treatment. Here b corresponds to the heat capacity, C_p, and is assumed constant over the limited temperature range in question.

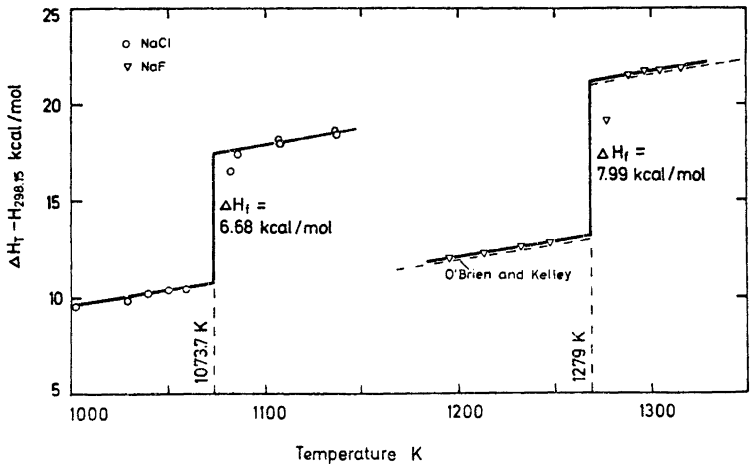

Fig. 1. The enthalpy and enthalpy of fusion of NaCl and NaF, ○ NaCl; ▽ NaF.

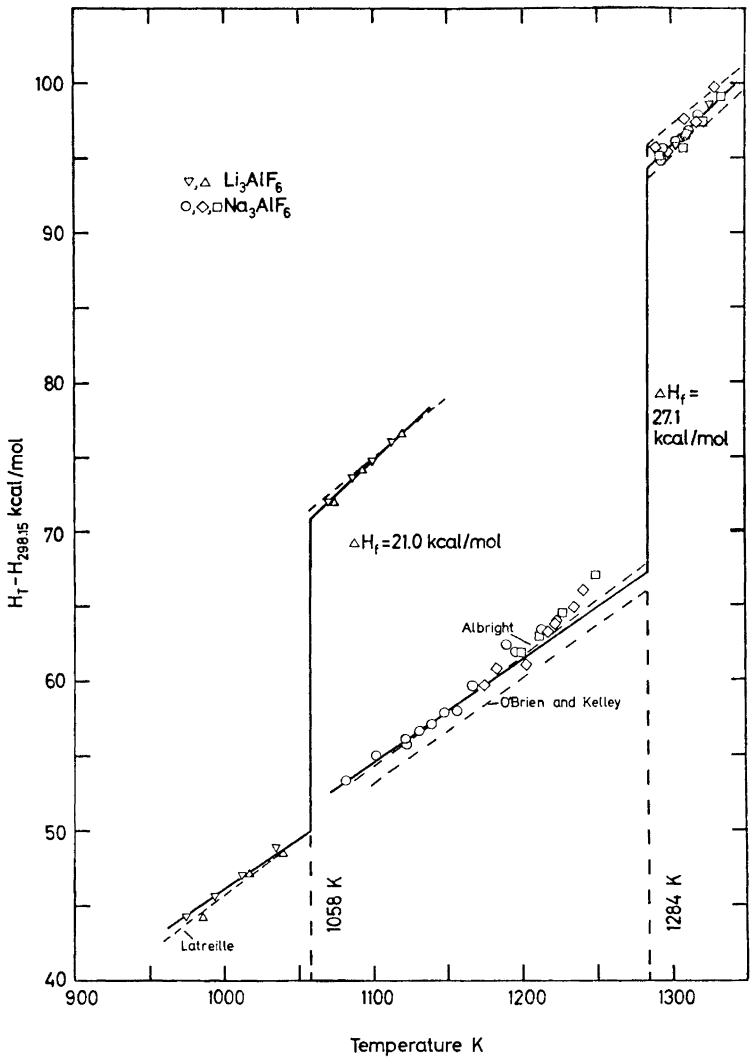

Fig. 2. The enthalpy and enthalpy of fusion of Li_3AlF_6 and Na_3AlF_6. ▽ Li_3AlF_6, sample 1; △ Li_3AlF_6, sample 2; ◇ Na_3AlF_6, sample 1, natural cryolite; □ Na_3AlF_6, sample 2, natural cryolite; ○ Na_3AlF_6, sample 3, synthetic cryolite.

Values which gave unreasonable C_p values were not included in the calculations of the straight lines. As is clearly seen from Figs. 2 – 3, the alkali cryolites exhibit a strong tendency to pre-melting. The exception seems to be Li_3AlF_6, which did not show deviations from the straight line up to 1040 K (melting point 1058 K). Na_3AlF_6 followed the straight line only up to 1170 K (melting point 1284 K), in very good agreement with the observations of

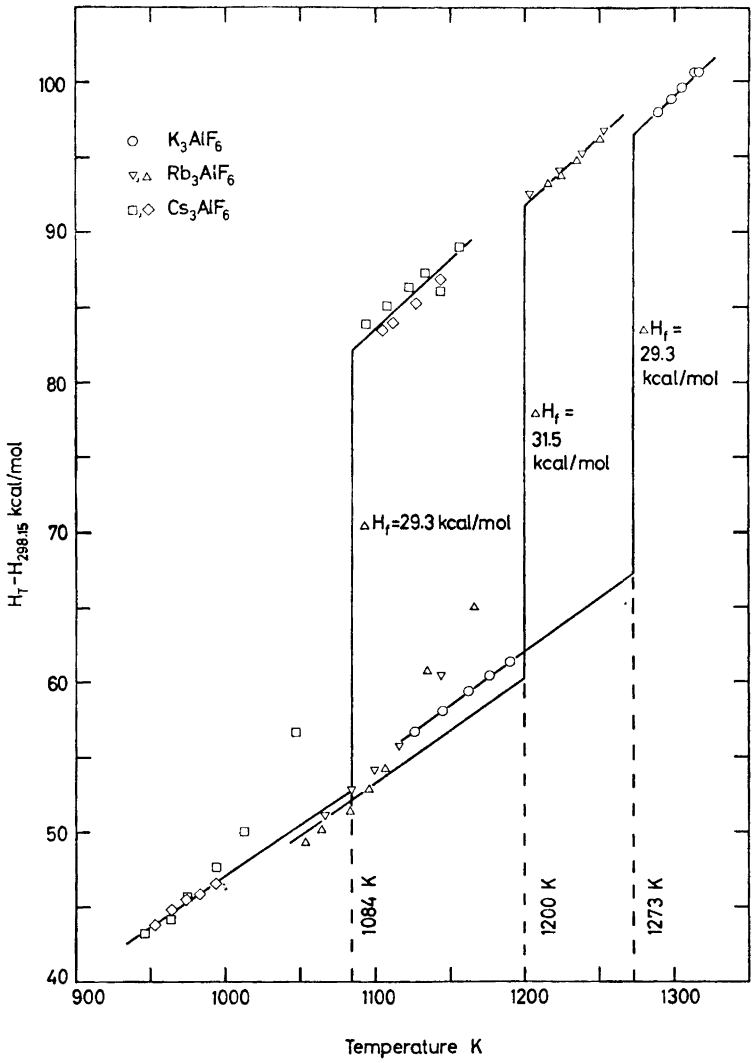

Fig. 3. The enthalpy and enthalpy of fusion of K_3AlF_6, Rb_3AlF_6, and Cs_3AlF_6. ○ K_3AlF_6; △ Rb_3AlF_6; sample 1; ▽ Rb_3AlF_6, sample 2; □ Cs_3AlF_6, sample 1; ◇ Cs_3AlF_6, sample 2.

Albright.[4] For this compound measurements were made on samples of both the natural mineral and of synthetic Na_3AlF_6, made from NaF and AlF_3. Within the experimental errors, no systematic differences could be detected between the results for the various samples. The enthalpy of K_3AlF_6 was not measured between 1190 K and 1290 K (melting point 1273 K). No pre-melting effects were observed below 1190 K, but DTA investigations[10] indicate that pre-melting does indeed take place in K_3AlF_6. The results for Rb_3AlF_6 and

Cs_3AlF_6 indicate pre-melting from approximately 1110 K and 990 K, respectively (melting points 1200 K and 1084 K). The constants in the enthalpy equations for the various compounds, and the temperature range in which the measurements were made, are given in Table 3.

Table 3. The constants in the equation $H_T - H_{298.15} = a + bT$.

Compound	Solid phase			Liquid phase		
	Temperature range T/K	a cal mol^{-1}	$b = C_p$ cal mol^{-1}K^{-1}	Temperature range T/K	a cal mol^{-1}	$b = C_p$ cal mol^{-1}K^{-1}
NaF	1180 – 1260	– 6694	15.63	1280 – 1330	57	16.61
NaCl	990 – 1070	– 6123	15.68	1080 – 1150	– 870	17.02
Li_3AlF_6	960 – 1050	– 20462	66.51	1065 – 1130	– 26645	92.20
Na_3AlF_6	1070 – 1175	– 21661	68.95	1290 – 1340	– 27605	94.91
K_3AlF_6	1120 – 1200	– 24030	71.74	1280 – 1330	– 22842	93.84
Rb_3AlF_6	1045 – 1100	– 23671	69.94	1205 – 1260	– 20334	93.38
Cs_3AlF_6	935 – 995	– 20598	67.64	1090 – 1170	– 18622	92.90

The enthalpy equations were extrapolated to the melting point, and the enthalpy of fusion was calculated. In cases were pre-melting occurs, this extrapolation was done from below the pre-melting region. The enthalpies of fusion are given in Table 4, together with literature values. The melting points were determined by thermal analysis or by DTA.[10]

Table 4. Enthalpies and entropies of fusion.

	Melting point T/K	ΔH_f/kcal mol^{-1}			ΔS_f cal mol^{-1}K^{-1} this work
		This work	Other calorimetric work	Calculated from phase diagrams	
NaF	1269	7.99 ± 0.05	8.03 [5]		6.22
NaCl	1073.7	6.68 ± 0.14	6.69,[11] 6.76 [12]		6.30
Li_3AlF_6	1058	21.0 ± 0.3	20.2,[1] 21.5 [2-3]	20.7,[6,13] 21.1,[14] 22.0,[2-3] (24.5 [7])[a]	19.8
Na_3AlF_6	1284	27.1 ± 0.5	27.91,[4] 27.64 [5]	27.4 [6]	21.1
K_3AlF_6	1273	29.3 ± 0.4		27.6 [6] (44.4 – 44.7 [7])[a]	23.0
Rb_3AlF_6	1290	31.5 ± 0.8			26.2
Cs_3AlF_6	1084	29.3 ± 0.9			27.0

[a] From phase diagrams with solid solubility.

As can be seen from Fig. 1 and Table 4 the agreement between our results for NaCl and those reported in earlier work [11,12] is very good. Dworkin and Bredig [11] do not give the actual enthalpies or the heat capacities, only the enthalpy of fusion, while the results of Dawson *et al.* are practically coinciding with ours. The agreement between the results from this work and those of O'Brien and Kelley [5] for NaF and Na_3AlF_6 is also satisfactory. The heat

capacity values reported for Li_3AlF_6 by Latreille [2] and for Na_3AlF_6 by Albright [4] are, however, somewhat different from those found in this work, while their enthalpy of fusion values are in fairly good agreement with ours. On the basis of comparing the heat capacities for all the alkali cryolites, and also taking into consideration the heat capacities of the alkali fluorides (JANAF [9]) and of AlF_3 (Douglas and Ditmars [15]), we judge our heat capacity values to be more accurate than those obtained earlier.

In Table 4 are also included the entropies of fusion of the alkali cryolites, $\Delta S_f = \Delta H_f/T_f$. These entropies can be seen to increase with increasing size of the alkali ion. Except for Rb_3AlF_6, a plot of $\Delta S_f(Me_3AlF_6)$ *versus* r_{Me^+} or $r_{Me^+}^2$ (Me = Li, Na, K, Rb, Cs) gives a smooth curve (Fig. 4).

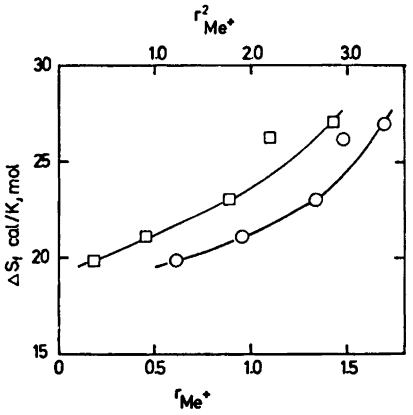

Fig. 4. The entropy of fusion of the alkal cryolites, *versus* the size of the alkali ion ○ ΔS_f *vs.* r_{Me^+}; □ ΔS_f *vs.* $r_{Me^+}^2$.

Acknowledgements. Financial support from *Guldberg og Waages Fond*, *Norges Tekniske Høgskoles Fond* and *Norges Almenvitenskapelige Forskningsråd*, is gratefully acknowledged. Dr.techn. J. L. Holm is thanked for valuable discussions, and Ing. Th. Tharaldsen for assistance with the preparation of samples.

REFERENCES

1. Bjørge, B. and Jenssen, B. *Acta Chem. Scand.* **22** (1968) 1347.
2. Latreille, H. *Contribution à l'étude thermodynamique de la cryolithe de lithium*, Thesis, Université de Lyon, 1968.
3. Rolin, M., Latreille, H. and Pham, H. *Bull. Soc. Chim. France* **1969** 2271.
4. Albright, D. M. *The High Temperature Thermodynamic Properties of Cryolite*, Thesis, Carnegie Institute of Technology, 1956.
5. O'Brien, J. C. and Kelley, K. K. *J. Am. Chem. Soc.* **79** (1957) 5616.
6. Yoshida, Y. and Matsushima, T. *Keikinzoku* **19** (1969) 488.
7. Yoshioka, T. and Kuroda, T. *Denki Kagaku* **36** (1968) 797.
8. Grønvold, F. *Acta Chem. Scand.* **26** (1972) 2216.
9. *JANAF Thermochemical Tables*, Clearinghouse, Springfield, Virginia 1965.
10. Jenssen, B. *Fase- og strukturforhold for noen komplekse alkali-aluminiumfluorider*, Lic. Thesis, Institute of Inorganic Chemistry, The Technical University of Norway, 1969.
11. Dworkin, A. S. and Bredig, M. A. *J. Phys. Chem.* **64** (1960) 269.
12. Dawson, R., Brackett, E. B. and Brackett, T. E. *J. Phys. Chem.* **67** (1963) 1669.
13. Matsushima, T. *Denki Kagaku* **37** (1969) 778.
14. Malinovsky, M. *Chem. Zvesti* **21** (1967) 783.
15. Douglas, T. B. and Ditmars, D. A. *J. Res. Natl. Bur. Std.* **71 A** (1967) 185.

Received January 25, 1973.

ACTA CHEMICA SCANDINAVICA 27 (1973) 2051–2074

Reactions between Azolium Salts and Nucleophilic Reagents

IX. Further Investigations of the *cine*-Substitution of Pyrazolium Salts

MIKAEL BEGTRUP

Department of Organic Chemistry, Technical University of Denmark, DK-2800 Lyngby, Denmark

A number of halogeno-pyrazoles and pyrazolium salts *1* have been prepared and base-catalyzed deuterium exchange and substitution of *1* have been studied. 1-Methyl-2-phenyl-4-halogeno pyrazolium tosylates *1f* when treated with sodium hydroxide afford only one of the possible *cine* substitution products, namely 1-phenyl-2-methyl-pyrazol-4-in-3-one *5f*. Analysis of the relative deuterium exchange rates of the 3- and 5-protons of 1-methyl-2-phenyl-pyrazolium tosylates leads to an exclusion of the intramolecular halogenation-substitution mechanism. Other experimental evidence indicates that *1f* reacts *via* an anomalous addition-elimination mechanism; the addition step being rate limiting. The product distribution being controlled by competition between pyrazolone formation from and ring cleavage of the initial addition compound. 1-Methyl-2-benzyl-4-halogeno pyrazolium tosylates *1d* when treated with base afford both of the possible *cine*-substitution products *5d* and *9d* indicating that the product distribution is influenced to a minor extent by competing ring-cleavage processes when the *N*-substituents are non-vinylic.

Recently it was found that 1,2-dimethyl-4-bromo-pyrazolium tosylate *1b*, when treated with sodium hydroxide or methoxide reacted with *cine*-substitution to give 1,2-dimethyl-pyrazol-4-in-3-one *5b*.[1] Although several mechanisms could be imagined for this reaction experiments showed that only two of these mechanisms were likely. One of these was an anomalous addition-elimination reaction (Fig. 2) (to be explained below). The other involved an intramolecular 1,2-migration of a bromonium ion from the 4-position to the 3-position followed by nucleophilic displacement with hydroxide or methoxide ions (Fig. 1) (to be explained below). Both possibilities are of considerable theoretical interest. Anomalous addition-elimination reactions are rare, especially in 5-membered rings;[2,3] intramolecular halogen migration-substitution mechanisms have been considered in aromatic systems,[4,5] but so far they have never been proved. In order to find evidence for a single mechanism the reaction between 4-halogeno substituted pyrazolium salts with two different *N*-substituents and sodium hydroxide or sodium methoxide has now been investigated.

Table 1. Preparation, melting points, and analytical data of 1,2-disubstituted pyrazolium tosylates.

Compound [a]	Starting material	Method of preparation	Yield of crude product [c] %	Melting point of crude product °C	Melting point after the second crystallisation °C	Analytical data Found: Calculated: C %	H %	N %	S %		%
1,2-Dimethyl-3-chloro-pyrazolium tosylate *1b* (X = Cl)	1-Methyl-5-chloro-pyrazole [b]	B	79	106–126	121–126	47.42 47.59	5.03 4.99	9.17 9.25	10.46; 10.59	Cl	11.61 11.71
1-Methyl-2-benzyl-pyrazolium tosylate *1c*	1-Benzyl-pyrazole [20]	B	100	oil	oil	62.64 62.77	5.83 5.85	8.27 8.13	9.45 9.31		
1-Methyl-2-benzyl-3-chloro-pyrazolium tosylate *8d* (X = Cl)	1-Benzyl-5-chloro-pyrazole [b]	B	71	oil	oil	56.87 57.06	5.16 5.05	7.30 7.39	8.43; 8.46	Cl	9.20 9.36
1-Methyl-2-benzyl-4-chloro-pyrazolium tosylate *1d* (X = Cl)	1-Benzyl-4-chloro-pyrazole [b]	B	100	oil	oil	53.45 57.06	4.99 5.05	7.42 7.39	8.38; 8.46	Cl	9.42 9.36
1-Methyl-2-benzyl-4-bromo-pyrazolium tosylate *1d*	1-Benzyl-4-bromo-pyrazole [20]	B	100	oil	oil	50.94 51.07	4.54 4.53	6.76 6.62	7.76; 7.58	Br	18.78 18.88
1-Methyl-2-benzyl-4-iodo-pyrazolium tosylate *1d* (X = I)	1-Benzyl-4-iodo-pyrazole [b]	B	88	63–66	119–126	46.16 45.97	4.07 4.07	5.89 5.96	6.99; 6.82	I	27.16 26.98
1-Methyl-2-benzyl-5-chloro-pyrazolium tosylate *4d* (X = Cl)	1-Methyl-5-chloro-pyrazole [b]	F	33	oil	oil	55.01 57.06	4.95 5.05	8.12 7.39	6.27; 8.46	Cl	13.80 9.36
	1-Benzyl-3-chloro-pyrazole [b]	B	40								

1-Methyl-2-phenyl-pyrazolium tosylate *1e*	1-Phenyl-pyrazole [25]	A	100	106–108	107–109	61.70 61.80	5.61 5.49	8.57 8.48	9.54 9.71		
1,3-Dimethyl-2-phenyl-pyrazolium tosylate *10f*	1-Phenyl-5-methyl-pyrazole [22]	A	100	oil	oil	61.27 62.77	6.14 5.85	8.29 8.13	9.57 9.31		
1,5-Dimethyl-2-phenyl-pyrazolium tosylate *12f*	1-Phenyl-3-methyl-pyrazole [23]	A	100	oil	oil	62.92 62.77	5.98 5.85	8.00 8.13	9.12 9.31		
1-Methyl-2-phenyl-3-chloro-pyrazolium tosylate *8f* (X=Cl)	1-Phenyl-5-chloro-pyrazole [18]	A	100	oil	oil	55.86 55.96	4.84 4.69	7.82 7.68	8.58; 8.79	Cl	9.61 9.71
1-Methyl-2-phenyl-3-bromo-pyrazolium tosylate *8f*	1-Phenyl-5-bromo-pyrazole [b]	E	100	oil	oil	48.78 49.88	4.12 4.19	6.58 6.85	7.55; 7.84	Br	19.25 19.52
1-Methyl-2-phenyl-4-chloro-pyrazolium tosylate *1f* (X=Cl)	1-Phenyl-4-chloro-pyrazole [26]	A	97	152	152	55.88 55.96	4.64 4.69	7.53 7.68	8.55; 8.79	Cl	9.54 9.71
1-Methyl-2-phenyl-4-bromo-pyrazolium tosylate *1f*	1-Phenyl-4-bromo-pyrazole [27]	A	97	171	179–180	49.74 49.88	4.31 4.19	6.75 6.85	7.67; 7.84	Br	19.42 19.52
1-Methyl-2-phenyl-4-iodo-pyrazolium tosylate *1f* (X=I)	1-Phenyl-4-iodo-pyrazole [b]	C	91	156	156	44.60 44.74	3.91 3.76	5.95 6.14	7.19; 7.03	I	27.70 27.83
1,3-Dimethyl-2-phenyl-4-bromo pyrazolium tosylate *11f*	1-Phenyl-4-bromo-5-methyl pyrazole [b]	D	100			50.87 51.07	4.68 4.53	6.42 6.62	7.61; 7.58	Br	18.75 18.88
1,5-Dimethyl-2-phenyl-4-bromo pyrazolium tosylate *13f*	1-Phenyl-3-methyl-4-bromo-pyrazole [b]	D	98	164–168	164–168	50.87 51.07	4.62 4.53	6.49 6.62	7.67; 7.58	Br	18.89 18.88
1-Methyl-2-phenyl-5-chloro-pyrazolium tosylate *4f* (X=Cl)	1-Phenyl-3-chloro-pyrazole [b]	D	75	87–104	108–110	55.87 55.96	4.74 4.69	7.78 7.68	8.91; 8.79	Cl	9.53 9.71
1-Methyl-2-phenyl-5-bromo-pyrazolium tosylate *4f*	1-Phenyl-3-bromo-pyrazole [b]	E	74	oil	oil	49.63 49.88	4.14 4.19	6.92 6.85	7.68; 7.84	Br	19.70 19.52

[a] All pure pyrazolium tosylates were colourless. [b] Preparation of the starting material is described above. [c] In all cases the crude product contained only traces of impurities and could be used directly for synthetic purposes. The loss by the different purification procedures is only a few per cent except in the case of method E which results in an appreciable loss.

Table 2. NMR-spectra of 1,2-disubstituted pyrazolium salts in deuterium oxide with DSS as an internal standard.

Pyrazolium tosylate	H-3 ppm	H-4 ppm	H-5 ppm	N_1-CH_3 N_2-CH_2 ppm	C-CH_3 ppm	J_{H3H4}[b] Hz	J_{H4H5} Hz	J_{H3H5} Hz	J_{CH_3H5} Hz	J_{CH_3H4} Hz
1,2-Dimethyl-3-chloro- *1b* (X=Cl)		6.80	8.14	4.07 3.98[c]			3.2		0.6	
1-Methyl-2-benzyl- *1c*	8.18	6.81		3.98 5.65		3.1	3.1			
1-Methyl-2-benzyl-3-chloro- *8d* (X=Cl)		7.00	8.29	4.02 5.78			3.1		0.6	
1-Methyl-2-benzyl-4-chloro- *1d* (X=Cl)	8.24[d]		8.32[d]	4.03 5.62				1.2	0.6	
1-Methyl-2-benzyl-4-bromo- *1d*	8.27[d]		8.34[d]	4.05 5.64				1.2	0.6	
1-Methyl-2-benzyl-4-iodo- *1d*	8.25[d]		8.32[d]	4.05 5.65				0.9	0.6	
1-Methyl-2-benzyl-5-chloro- *4d* (X=Cl)	8.25	6.93		3.96 5.69		3.1				
1-Methyl-2-phenyl- *1e*	8.36[a]	6.96	8.41[a]	3.92		3.0	3.0	1.1	0.6	
1,3-Dimethyl-2-phenyl- *10e*		6.78	8.27	3.78	2.27		3.0		0.5	0.8

1,5-Dimethyl-2-phenyl- *12e*	8.24	6.82	8.24	3.75	2.57		3.1		0.2	0.4
1-Methyl-2-phenyl-3-chloro- *8f* (X=Cl)		7.12	8.49	3.89			3.2		0.6	
1-Methyl-2-phenyl-3-bromo- *8f*		7.15	8.42	3.88			3.1		0.5	
1-Methyl-2-phenyl-4-chloro- *1f* (X=Cl)	8.51[a]		8.55	3.91				1.1	0.6	
1-Methyl-2-phenyl-4-bromo- *1f*	8.50[a]		8.56[a]	3.91				1.1	0.6	
1-Methyl-2-phenyl-4-iodo- *1f* (X=I)	8.39[a]		8.47[a]	3.92				1.1	0.6	
1,3-Dimethyl-2-phenyl-4-bromo- *11f*			8.47	3.80	2.37				0.6	
1,5-Dimethyl-2-phenyl-4-bromo- *13f*	8.42			3.80	2.55					
1-Methyl-2-phenyl-5-chloro- *4f* (X=Cl)		7.14	8.45	3.87			3.2			
1-Methyl-2-phenyl-5-bromo- *4f*	8.37	7.17		3.88		3.2				

[a] The assignment of the H-3 and H-5 signals was based on the fact that H-3 of *12f* and *13f* resonates at a higher field than H-5 of *10f* and *11f*, respectively (see also Ref. 14). Furthermore H-5 couples with the N-CH_3 group whereas H-3 does not. [b] All coupling constants were obtained by first order analysis. [c] N_2-CH_3. [d] The assignment of the H-3 and H-5 signals was based on the fact that H-3 of *4d* (X=Cl) absorbs at a higher field than H-5 of *8d* (X=Cl). Furthermore, the coupling between H-5 and the N-CH_3 group is larger than the coupling between H-5 and the N-CH_2 group.

RESULTS

The pyrazolium salts were prepared from 1-substituted pyrazoles and methyl tosylate (see Experimental) and they were identified through their NMR-spectra (Table 2).

The heteroaromatic protons of pyrazolium salts are acidic and the rate of the base-catalyzed exchange of these protons with deuterium was measured (see Table 3).

When 1-methyl-2-benzyl-4-bromo-pyrazolium tosylate *1d* was treated with sodium hydroxide both possible isomers, namely 1-benzyl-2-methyl-

Table 3. Deuterium exchange rates of 1-methyl-2-phenyl-pyrazolium tosylates.*

Pyrazolium tosylate	Proton	pD	$T_{1/2}$[a] min	Relative rate[b]
1-Methyl-2-benzyl-	H-3[h]	12.63[e]	6.5	0.81
1c	H-5[h]	12.63[e]	7.3	0.72
1-Methyl-2-benzyl-4-bromo-	H-3	9.86[g]	5.8	501
1e	H-5	9.86[g]	6.7	426
1-Methyl-2-phenyl-	H-3	11.67[e]	13.7[c]	3.47
1e	H-4			
	H-5	11.67[e]	13.7[d]	3.47
1,3-Dimethyl-2-phenyl-	H-4			
10f	H-5	12.63[e]	7.0[d]	0.76
1,5-Dimethyl-2-phenyl-	H-3	12.63[e]	5.4[d]	0.98
12f	H-4			
1-Methyl-2-phenyl-3-chloro-	H-5	9.86[g]	92	34
8f, X = Cl	H-4	12.63[e]	80	0.066
1-Methyl-2-phenyl-3-bromo-	H-5	9.86[g]	109	28
8f	H-4	12.44[e]	148	0.055
1-Methyl-2-phenyl-4-chloro-	H-3	7.96[f]	26.2	9430
1f, X = Cl	H-5	7.96[f]	32.1	7710
1-Methyl-2-phenyl-4-bromo-	H-3	9.86[g]	6.0[c]	513
1f	H-5	9.86[g]	6.0[c]	513
1,3-Dimethyl-2-phenyl-4-bromo-	H-5	9.86[g]	8.6	3.64
11f				
1,5-Dimethyl-2-phenyl-4-bromo-	H-3	9.86[g]	6.3	490
13f				
1-Methyl-2-phenyl-5-chloro-	H-3	9.86[g]	78	40
4f	H-4	12.63[e]	99	0.046
1-Methyl-2-phenyl-5-bromo	H-3	9.86[g]	87.5	36
4f	H-4	12.44[e]	133	0.062

[a] The rates were measured by NMR at 33°C except in the cases of *8f* and *4f* which were studied at 40°C. [b] In comparison to 1,2-dimethyl-pyrazolium tosylate.[1] [c] Mean value for the 3- and 5-proton, since these signals almost coincide. [d] No exchange after 60 days at room temperature at pD 12. [e] Glycine buffer. [f] Phosphate buffer. [g] Borate buffer. [h] H-3 and H-5 were separated in the basic solution.

* It is noteworthy that the exchange rates of pyrazolium tosylates are less influenced by *N*-substituents or 4-substituents than 1,3-disubstituted 1,2,3-triazolium tosylates.[28] This indicates that the transmission of inductive effects is less efficient through the C=N and C=C bonds of pyrazolium ions than of triazolium ions. Probably, the bond order of these bonds are higher in the triazolium salt series. The exchange rate ratio between H-3 and H-5 of unsymmetric pyrazolium ions is less than that between H-4 and H-5 of the corresponding triazolium ions.[28]

Table 4. Reaction of 3-halogeno-substituted pyrazolium salts with sodium hydroxide.

Starting material	Product	Yield %	Melting point °C	Melting point after recrystallization [a] °C	Reported melting point °C	Analytical data C %	H %	Found: Calculated: N %
1,2-Dimethyl-3-chloro-pyrazolium tosylate *16* (X=Cl)	1,2-Dimethyl-pyrazol-4-in-3-one *5b*	100	72–73	72–73	47–63 [1]			
1-Methyl-2-benzyl-3-chloro-pyrazolium tosylate *8d* (X=Cl)	1-Methyl-2-benzyl-pyrazol-4-in-3-one *9d*	93	91–93	93–94		69.93 70.20	6.33 6.42	14.58 14.88
1-Methyl-2-benzyl-5-chloro-pyrazolium tosylate *4d* (X=Cl)	1-Benzyl-2-methyl-pyrazol-4-in-3-one *5d*	82	61–62	61–62		66.31 70.20	6.54 6.42	14.56 14.88
1-Methyl-2-phenyl-3-chloro-pyrazolium tosylate *8f* (X=Cl)	1-Methyl-2-phenyl-pyrazol-4-in-3-one *9f*	85	117–119	117–119	117 [29,30]	68.92 68.95	5.65 5.79	16.09 16.08
1-Methyl-2-phenyl-3-bromo-pyrazolium tosylate *8f*	1-Methyl-2-phenyl-pyrazol-4-in-3-one *9f*	76	96–98	117–119				
1-Methyl-2-phenyl-5-chloro-pyrazolium tosylate *4f* (X=Cl)	1-Phenyl-2-methyl-pyrazol-4-in-3-one *5f*	45	118	123–124		69.09 68.95	5.95 5.79	16.24 16.08
1-Methyl-2-phenyl-5-bromo-pyrazolium tosylate *4f*	1-Phenyl-2-methyl-pyrazol-4-in-3-one *5f*	31	118	123–124				

[a] All compounds were colourless and hygroscopic.

Table 5. NMR-spectra in deuteriochloroform with TMS as an internal standard and infrared absorptions of the carbonyl groups of 1,2-disubstituted pyrazol-4-in-3-ones.

Compound	IR[a] cm^{-1}	Phenyl group	NMR H-4 ppm	NMR H-5 ppm	NMR N-CH_3 ppm	NMR N-CH_2 ppm	NMR $J_{^{13}C\text{-}H_3}$ Hz	NMR J_{H4H5} Hz
1-Methyl-2-benzyl-pyrazol-4-in-3-one *9d*	1620	broad singlet	5.50	7.17	3.23	5.07	141	3.4
1-Benzyl-2-methyl-pyrazol-4-in-3-one *5d*	1625	multiplet	5.46	7.39[b]	3.30	4.83	141	3.4
1-Methyl-2-phenyl-pyrazol-4-in-3-one *9f*	1645	broad singlet	5.56	7.45	3.14		142	3.6
1-Phenyl-2-methyl-pyrazol-4-in-3-one *5f*	1630	broad multiplet	5.64	7.57[b]	3.28		142	3.7

[a] IR-spectra obtained in potassium discs. [b] The H-5 doublet was detected by homonuclear INDOR.

pyrazol-4-in-3-one *5d* and 1-methyl-2-benzyl-pyrazol-4-in-3-one *9d*, were formed in the ratio 1.62 (total yield 51 %). The pyrazolones *5d* and *9d* were identified through their spectra (Table 5). The IR-spectra showed a carbonyl absorption in the region where other 1,2-disubstituted pyrazol-4-in-3-ones absorb.[1] The NMR-spectra confirmed the structures exhibiting a CH_3-signal, a CH_2-signal, two doublets due to the 4- and 5-protons, and a phenyl group. In *5d* the doublet arising from H-5 was hidden by the multiplet of the phenyl group but was detected by homonuclear INDOR. All δ-values agreed well with the corresponding signals of other 1,2-disubstituted pyrazol-4-in-3-ones.[1] One of the pyrazolones isolated was identical with that formed by treatment of 1-methyl-2-benzyl-3-chloro-pyrazolium tosylate *8d* (X = Cl) with sodium hydroxide and therefore has the structure *9d*. The other pyrazolone was identical with that formed by similar treatment of 1-methyl-2-benzyl-5-chloro-pyrazolium tosylate *4d* (X = Cl) and therefore has the structure *5d*.

As a further proof of the structures, 1-methyl-2-benzyl-pyrazol-4-in-3-one *9d* was treated with benzoyl chloride; this produced 1-methyl-3-benzoyloxy-pyrazole, identified through its hydrolysis to 1-methyl-3-hydroxy-pyrazole. Similarly, 1-benzyl-2-methyl-pyrazol-4-in-3-one *5d* and benzoyl chloride afforded 1-methyl-5-benzoyloxy-pyrazole which, in turn by hydrolysis, gave 1-methyl-5-hydroxy-pyrazole.[6]

When 1-methyl-2-benzyl-4-iodo-pyrazolium tosylate *1d* (X = I) was treated with sodium hydroxide, the pyrazolones *5d* and *9d* were formed in the same ratio (1.66) and in a total yield of 20 %. When the chloro compound *1d* (X = Cl) was used as the starting material, the total yield of *5d* and *9d* dropped to 4 % (product ratio 1.99).

When 1-methyl-2-phenyl-4-bromo-pyrazolium tosylate *1f* was treated with 1 N sodium hydroxide or methoxide only one pyrazol-4-in-3-one was isolated. The compound was identified through its spectra (Table 5).

The pyrazolone isolated was identical with that formed by treatment of 1-phenyl-2-methyl-3-chloro-pyrazolium tosylate *4f* with sodium hydroxide and therefore has the structure *5f*. This was confirmed through its reaction with benzoyl chloride [6] which afforded 1-phenyl-3-benzoyloxy-pyrazole, identified through its hydrolysis to the previously described 1-phenyl-3-hydroxy-pyrazole.[7,8] The isomeric pyrazol-4-in-3-one *9f*, prepared independently by treatment of 1-methyl-2-phenyl-3-chloro-pyrazolium tosylate *8f* (X = Cl) with sodium hydroxide, was stable under the conditions of the reaction between the 4-bromo-pyrazolium salt *1f* and sodium hydroxide. The crude product from the latter process did not contain the pyrazol-4-in-3-one *9f*, as shown by NMR and TLC. It may therefore be concluded that the 5-position of 1-methyl-2-phenyl-4-bromo-pyrazolium salts differs markedly in reactivity from the 3-position. This agreed with the fact that 1,3-dimethyl-2-phenyl-4-bromo-pyrazolium tosylate *11f* reacted with sodium hydroxide to give 1-phenyl-2,5-dimethyl-pyrazol-4-in-3-one *14f* ("isoantipyrin"), whereas the isomeric pyrazolium salt *13f* decomposed under similar conditions and failed to give a pyrazol-4-in-3-one *15f*.

It was found that 1-methyl-2-phenyl-4-chloro-pyrazolium tosylate *1f* (X = Cl) gave a much lower yield of the pyrazol-4-in-3-one *5f* than the bromo and iodo compounds *1f* (X = Br) and *1f* (X = I).

DISCUSSION

The intramolecular halogen migration-substitution mechanism. The first step in an intramolecular halogen migration-substitution mechanism is a base-catalyzed abstraction of a proton adjacent to the halogen with formation of the 3-anion *2* (Fig. 1). If the halogen subsequently migrates as a halogen cation

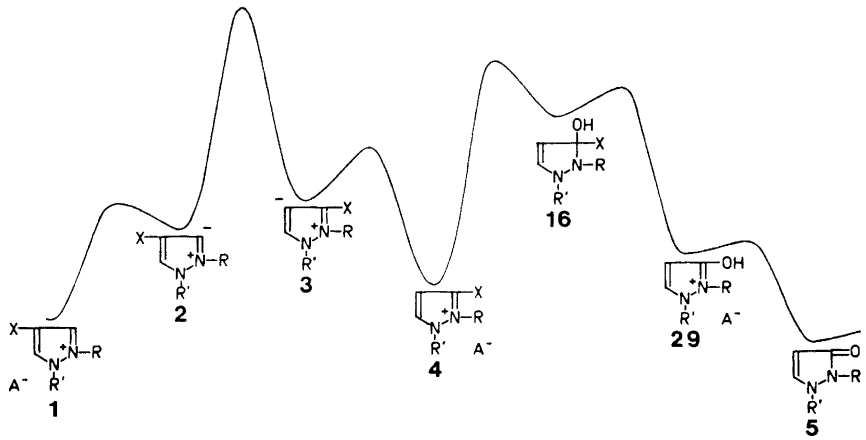

Fig. 1. The intrahalogenation-substitution mechanism of the reaction of 1,2-dimethyl-4-bromo-pyrazolium tosylate *1* (R = R′ = CH_3, X = Br) with sodium hydroxide. The energy diagram for the intrahalogenation (*1*→*2*→*3*→*4*) is discussed in the text. In the addition-elimination reaction with hydroxide ions the addition step is rate limiting,[32] the energy barrier between *4* and *16* being higher than that between *16* and *29*. The heteroaromatic protons of 3- and 4-bromo-pyrazolium tosylates are readily replaced by deuterium at pD's where no substitution of halogen takes place (Tables 3 and 6). Therefore, the barrier between *4* and *16* is considered to be higher than those between *1* and *2* and between *3* and *4*. Since transformation of 3- to 4-bromo-pyrazolium tosylates has never been observed, even under conditions where 3-bromo-pyrazolium tosylates undergo substitution, the barrier between *2* and *3* is considered to be higher than that between *4* and *16*. The barrier between *16* and *29* has arbitrarily been set higher than the *1*→*2* and *3*→*4* barriers. The barrier between *29* and *5* has been set low since 1,2-disubstituted pyrazol-4-in-3-ones *5* are very weak bases.

the 4-ion *3* is formed. Reprotonization gives the 3-halo compound *4*, which is expected to react readily with substitution, since halogen in the 3-position of pyrazolium salts react readily with nucleophilic reagents.[1] With hydroxide ions *4* gives rise to the hydroxy compound *16* which, in turn, by deprotonization produces the pyrazol-4-in-3-one *5*. The latter substitution is formulated as a normal addition-elimination mechanism.[2,3] When methoxide ions are used as the nucleophile *4* similarly gives a methoxypyrazolium salt which then, by loss of the *O*-methyl group yields *5*.[1]

Following this reaction course, a pyrazolium salt with two different *N*-substituents, *e.g. 1f*, could give rise to the two isomeric 3-anions *2f* and *6f* (Scheme 1, path A1 and A2). These anions would then rearrange to the 4-anions *3f* and *7f*, respectively, and the latter would by protonization, substitu-

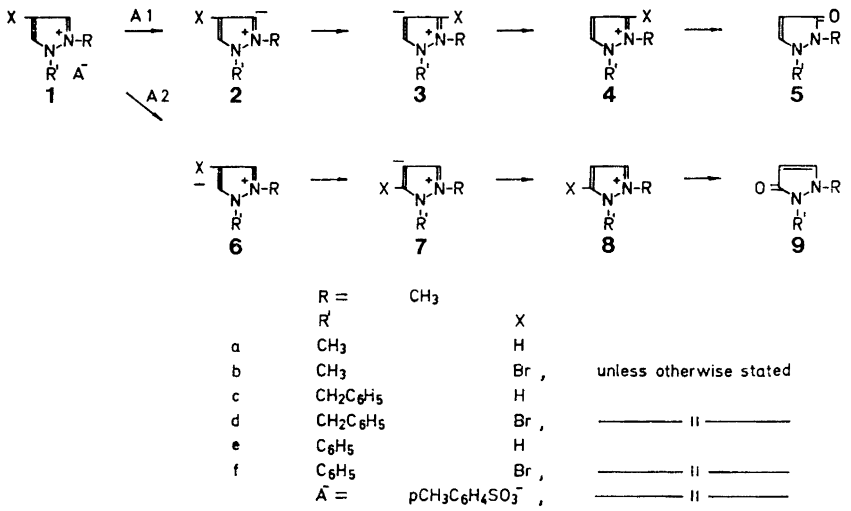

Scheme 1.

tion, and deprotonization (or dealkylation when sodium methoxide is used as the nucleophile) yield the two isomeric pyrazol-4-in-3-ones *5f* and *9f* .

The pure 3-bromo-pyrazolium tosylate *4f* afforded *5f* as the sole pyrazolone when treated with sodium hydroxide. The isomeric pyrazolone *9f* was not found. Similarly, the 3-bromo-pyrazolium tosylate *8f* and sodium hydroxide produced the pyrazolone *9f*, exclusively. Since *1f* only gave *5f* with sodium hydroxide (see above) a halogen migration-substitution mechanism would imply that of the two possible anions *3f* and *7f* only *3f* was formed as an intermediate.

The base catalyzed deuterium exchange experiments indicated that the 3- and 5-protons of the 4-bromo-pyrazolium tosylate *1f* were exchanged *ca.* 8900 times faster than the 4-protons of the 3-bromo-pyrazolium tosylates *4f* or *8f* (see Table 3). Consequently, the transition states leading from the 3-bromo compounds *4f* or *8f* to the 4-anions *3f* or *7f* must have higher energy than the transition states involved in the conversion of the 4-bromo compound *1f* to the 3- and 5-anions *2f* and *6f*.

When the pure 3-bromo compounds *4f* or *8f* were treated with base no isomerization to the 4-bromo isomer *1f* was observed. However, exchange of the 4-protons of *4f* and *8f* took place readily. Hence, the transition states leading from the 4-anions *3f* or *7f* to the 5- and 3-anions *2f* or *6f*, respectively, have a higher energy than the transition states leading from the 4-anions to the 3-bromo-pyrazolium tosylates *4f* or *8f*. Thus, the energy profile sketched in Fig. 1 may be proposed.

If the 4-anion is considered to be a valid representation of the transition state with the highest energy the distribution between the pyrazol-4-in-3-ones *5f* and *9f*, formed from *1f*, should depend on the difference in stability between the 4-anions *3f* and *7f*. This difference in turn is reflected by the relative

deuterium exchange rate of the 4-protons of the two 3-bromo-pyrazolium tosylates *4f* and *8f*. This ratio was found to be 1.1 (Table 3). A large difference in the stability between the 5- and 3-anions *2f* and *6f* could, however, influence the relative activation energy of the two transformations, *2f* to *3f*, and *6f* to *7f*, and hence, the distribution between the pyrazol-4-in-3-ones *5f* and *9f*.

The relative stability between the 5- and 3-anions *2f* and *6f* could not be determined accurately by deuterium exchange studies on the 4-bromo-pyrazolium tosylate *1e* (Table 3) since the 3- and 5-protons of this compound almost coalesced in NMR (Table 2). The relative stability could, however, be evaluated from deuterium exchange measurements in the 5- and 3-methyl-derivatives of *1f*. Thus, the 3-proton of 1,5-dimethyl-2-phenyl-4-bromo-pyrazolium tosylate *13f* was exchanged 1.36 times faster than the 5-proton of 1,3-dimethyl-2-phenyl-pyrazolium tosylate *11f* under identical conditions (Table 3). This ratio corresponds to the relative stability of the 3- and 5-anions *6f* and *2f*.

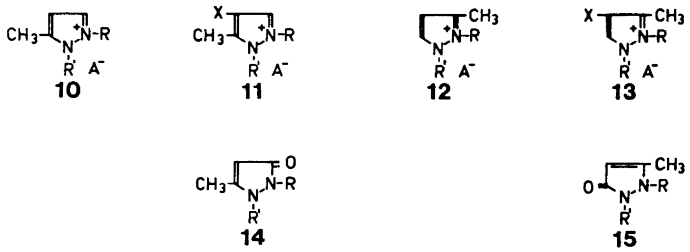

Scheme 2.

As a consequence, the distribution between the pyrazol-4-in-3-ones *5f* and *9f*, which could be formed from *1f via* an intrahalogenation-substitution mechanism, is expected to be *ca.* 1:1 and should never exceed 1:1.36.

Analogously, the distribution between the pyrazol-4-in-3-ones *5d* and *9d*, formed from *1d via* this mechanism, is expected to be *ca.* 1:1 and should never exceed 1:1.16. The formation of the pyrazol-4-in-3-one *5f* as the sole pyrazolone in the reaction between the pyrazolium salt *1f* and base excludes the intrahalogenation-substitution mechanism in this case.

The formation of the pyrazol-4-in-3-ones *5d* and *9d* in the ratio found *via* an intramolecular halogenation-substitution mechanism seems highly unlikely.

The elimination-addition mechanism. Of the previously discarded mechanisms[1] the elimination-addition mechanism is the only one which has to be analyzed again in the light of the present experimental results. The elimination-addition mechanism still remains unlikely for the previously mentioned reasons.[1] Furthermore, a rapid formation of a highly strained five-membered hetaryne in 1 N sodium hydroxide at only 100° seems unbelievable.* Superficially, the elimination-addition mechanism can, however, explain the formation of *5f* as the sole product arising from *1f*. Following an elimination-addition

* In fact, complete conversion of 1-methyl-2-phenyl-4-bromo-pyrazolium tosylate *1f* with 1 N sodium hydroxide may be performed even at room temperature, in the course of *ca.* 7 days.

mechanism, *1f* may give rise to the hetarynes *28f* and *30f* (Scheme 4) which then, by addition of water and subsequent deprotonization, could produce the pyrazol-4-in-3-ones *5f* and *9f*, respectively. The rate limiting step in an elimination-addition process is the elimination.[2,3,9] Therefore, the distribution of *5f* and *9f* should be reflected by the relative stability of the hetarynes *28f* and *30f*. In contrast to *30f*, the phenyl group and the triple bond are apparently conjugated in *28f*. However, the pyrazole ring and the benzene ring are presumably not coplanar in *28f*.[6] Therefore an overwhelming dominance of the pyrazol-4-in-3-one *5f* over the isomer *9f* is indeed not expected.

The anomalous addition-elimination mechanism. Thus, the only likely mechanism for the reaction of 1,2-disubstituted 4-halo-pyrazolium salts with base, is an anomalous addition-elimination reaction. In this case, the nucleophilic reagent initially attacks *1* (Fig. 2) at the electron deficient carbon atoms

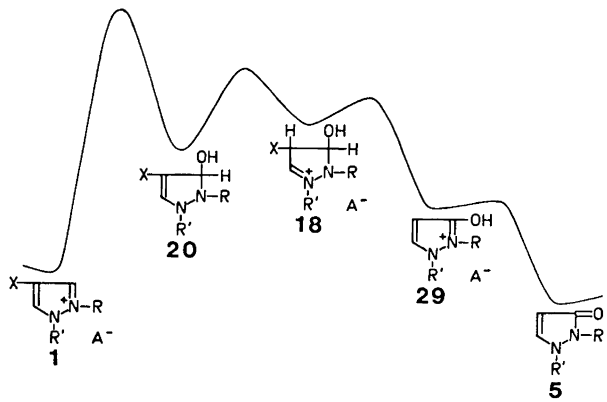

Fig. 2. The anomalous addition-elimination mechanism for the reaction of 1,2-dimethyl-4-bromo-pyrazolium tosylate *1* (R = R' = CH_3; X = Br) with sodium hydroxide. The addition step (*1* → *20*) is rate limiting, see the discussion in the text. The neutral intermediate *20* is considered more stable than the protonated derivative *18*. The elimination step (*18* → *29*) is assumed to be more favourable than the protonization (*20* → *18*) because it leads to a regain of aromaticity. The deprotonization (*29* → *5*) is discussed in the text to Fig. 1.

adjacent to the quaternary N-atoms giving rise to the neutral intermediate *20*. This is easily protonated at the 4-position, since the nitrogen atom may adopt the positive charge. This yields the species *18* which eliminates hydrogen halide producing the hydroxy-compound *29* which subsequently, by deprotonation, yields the pyrazol-4-in-3-one *5*. When methoxide ions are used as the nucleophile a similar reaction course takes place with formation of a methoxy-pyrazolium salt, which then, by cleaving off the *O*-methyl group, produces the pyrazolone *5*. Following the pathway depicted in Fig. 2, a pyrazolium salt with two different *N*-substituents, *e.g. 1f*, may be attacked in either the 5- or 3-position giving rise to the isomeric intermediates *20f* and *22f* and subsequently to the pyrazol-4-in-3-ones *5f* and *9f* (Scheme 3). It seems reasonable

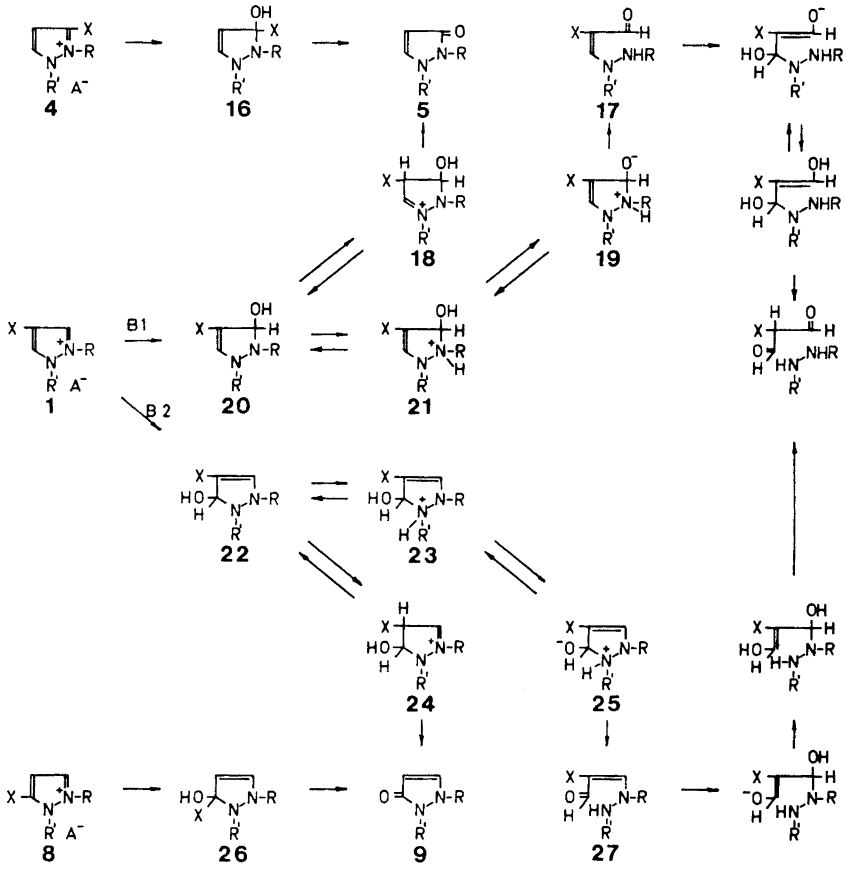

Scheme 3.

that the rate limiting step in this sequence is either the addition of the nucleophile to *1* or the protonization of the intermediate *20*. The elimination step (*18*→*29*) is obviously more favorable than the protonization since it leads to a regain of aromaticity.

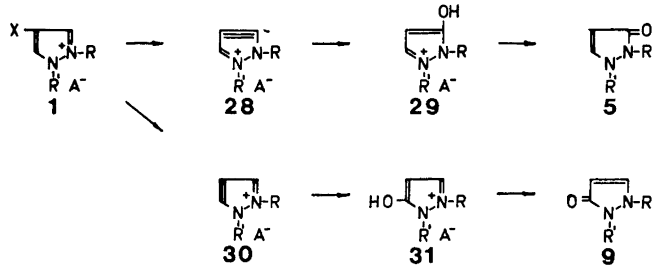

Scheme 4.

If the protonization step is rate limiting a kinetical H/D-isotope effect should be present. This is, however, not the case. Thus, 1-methyl-2-phenyl-4-bromo-pyrazolium tosylate *1f*, when heated with 1 N sodium hydroxide in a 1:1 mixture of water and deuterium oxide, gave the four H, D combinations of the pyrazolone *5f* and these were present in equal amounts as seen from the NMR-spectra. A separate experiment showed that the pyrazolone *5f* itself, when heated with 1 N sodium hydroxide in deuterium oxide under the usual reaction conditions, was deuterated quantitatively in the 5-position but only to an extent of a few per cent in the 4-position. Therefore, a kinetical H/D isotope effect is absent in the protonization of the 4-position. This protonization (and the elimination of hydrogen bromide from *18f*, as well) can therefore not be rate limiting. Consequently, the rate limiting step, if an anomalous addition-elimination mechanism is working, is the addition. In this case the intermediates *20f* and *20b* are similar to the intermediates *16f* (X = Cl) and *16b* (X = Cl), formed in the normal substitution reaction of 1-methyl-2-phenyl-5-chloro-pyrazolium tosylate *4f* (X = Cl) and 1,2-dimethyl-3-chloro-pyrazolium tosylate *4b* (X = Cl), respectively. Compound *4f* (X = Cl) reacts much faster with base than *4b* (X = Cl), (see Table 6). Therefore, *20f* is expected to react

Table 6. Rate of conversion of pyrazolium tosylate to pyrazol-4-in-3-ones in 1 N potassium hydroxide at 59.6°C.

Starting material	Product	$T_{1/2}$ min	Total amount of byproduct at the time of 50% conversion to pyrazol-4-in-3-one in %
1,2-Dimethyl-3-chloro-pyrazolium tosylate *16* (X = Cl)	1,2-Dimethyl-pyrazol-4-in-3-one *5b*	118.6	< 1
1-Methyl-2-benzyl-3-chloro-pyrazolium tosylate *8d* (X = Cl)	1-Methyl-2-benzyl-pyrazol-4-in-3-one *9d*	59.6	< 1
1-Methyl-2-benzyl-5-chloro-pyrazolium tosylate *4d* (X = Cl)	1-Benzyl-2-methyl-pyrazol-4-in-3-one *5d*	16.9	< 1
1-Methyl-2-phenyl-3-chloro-pyrazolium tosylate *8f* (X = Cl)	1-Methyl-2-phenyl-pyrazol-4-in-3-one *9f*	18.2	7.5
1-Methyl-2-phenyl-5-chloro-pyrazolium tosylate *4f* (X = Cl)	1-Phenyl-2-methyl-pyrazol-4-in-3-one *5f*	5.1	16
1-Methyl-2-phenyl-3-bromo-pyrazolium tosylate *8f*	1-Methyl-2-phenyl-pyrazol-4-in-3-one *9f*	31.0	< 1
1-Methyl-2-phenyl-5-bromo-pyrazolium tosylate *4f*	1-Phenyl-2-methyl-pyrazol-4-in-3-one *5f*	5.5	55

much faster than *20b* if the addition step is rate limiting. In fact, complete conversion of 1,2-dimethyl-4-bromo-pyrazolium tosylate *1b* required several hours heating to reflux with 1 N sodium hydroxide,[1] whereas 1-methyl-2-phenyl-4-bromo-pyrazolium tosylate *1f*, under identical conditions, was completely converted in 10 min.

The reason for the difference in reactivity between the dimethyl and the methylphenyl compounds is not clear. Mesomeric stabilization of the inter-

mediate by the phenyl group seems unlikely since the pyrazole and the benzene rings presumably are noncoplanar [6] and since an *N*-benzyl group exhibits a similar activation as a phenyl group (see Table 6). The activation decreases when the *N*-benzyl- or *N*-phenyl group is adjacent to the halogen (see Table 6), probably due to steric hindrance. Analogous results were found in the normal substitution of the 1-methyl-2-phenyl-5-bromo-1,2,3-triazolium ion, isosteric with *1f*, which is converted much faster than the 1,2-dimethyl-5-bromo-triazolium ion, isosteric with *1b*.[10]

If the addition step is rate limiting *and product determining*, the distribution between the pyrazol-4-in-3-ones *5f* and *9f* in the reaction of 1-methyl-2-phenyl-4-bromo-pyrazolium tosylate and base should be reflected by the relative stability of the intermediates *20f* and *22f*. No structural features justify that *20f* differs so markedly from *22f* in energy that only the former arises during the reaction. Indirectly, the *relative* energy of *20f* and *22f* can be roughly estimated by comparison with the *relative* stability of the structurally analogous compounds *16f* and *26f*, formed as intermediates in the normal substitution of the 3-bromo-pyrazolium tosylates *4f* and *8f*, respectively. The relative stability of *16f* and *26f* corresponds to the ratio between the substitution rates of *4f* and *8f* which was found to be 5.6. Therefore, 1-methyl-2-phenyl-4-bromo-pyrazolium tosylate *1f* should give the pyrazol-4-in-3-ones *5f* and *9f* in a ratio of *ca.* 5.6, in contrast to the fact that only *5f* arises. If an anomalous addition-elimination mechanism is working, the rate limiting addition step can therefore not be product determining.

In order to test this, the substitution of 1-methyl-2-phenyl-4-bromo-pyrazolium tosylate *1f* with sodium hydroxide was examined more carefully by following the reaction in NMR. The spectra indicated that 1-methyl-2-phenylhydrazine and the anion of bromomalonaldehyde were formed simultaneously with the pyrazolone. The crude product contained 33, 37, and 26 % of the three components, respectively. No other compounds or intermediates could be detected. The formation of the two byproducts is similar to the previously reported base induced ring cleavage of 1,2-dimethyl-pyrazolium iodide to give 1,2-dimethyl-hydrazine [11] and also to the cleavage of 1-methyl-2-phenyl-pyrazolium iodide [12] to 1-methyl-2-phenyl-hydrazine. These ring cleavages ,in analogy to the hydrolysis of immonium ions [13] and of 1,2-disubstituted pyrazolin-2-ium salts,[14] may be formulated as sketched in Scheme 3. Initially, a hydroxide ion attacks the carbon atom next to the positive N-atom, *1e* giving rise to *20f* and *22f*. Protonization at the ring-*N* and *O*-deprotonization followed by ring cleavage then produces *17f* and *27f*, respectively. By repetition of this sequence, *17f* and *27f* then afford bromomalonaldehyde and 1-methyl-2-phenyl-hydrazine. 1,2-Disubstituted hydrazines, when treated with 1,3-dicarbonyl compounds under acidic conditions, react with ring closure to give 1,2-disubstituted pyrazolium salts.[15] Therefore, bromomalonaldehyde and 1,2-dimethyl-hydrazine or 1-methyl-2-phenyl-hydrazine were treated with 1 N sodium hydroxide, both at room temperature and with prolonged heating to reflux. However, no pyrazol-4-in-3-ones, *5b* or *5f*, were produced. Consequently, ring-closure does not take place in basic solution, and hence, pyrazolone formation *via* a ring opening is unlikely. The intermediates *20f* and *22f* are common both for the pyrazolone generating

processes and for the ring cleavage. The formation of bromomalonaldehyde and of 1-methyl-2-phenyl-hydrazine demonstrates that the intermediate *20f* and/or *22f* are in fact formed. The product distribution may therefore depend on the relative ring cleavage rate of *20f* and *22f*. A faster ring cleavage of *22f* than of *20f* would cause a decrease in the relative yield of the pyrazol-4-in-3-one *9f*. If, on the other hand, *22f* is cleaved much faster than *20f*, virtually no pyrazol-4-in-3-one *9f* would arise in accordance with the experimental data. In contrast, the intrahalogenation-substitution process has no intermediate in common with the ring cleavage reaction. In this case, the latter is therefore not able to influence the distribution between the pyrazol-4-in-3-ones *5f* and *9f*.

This hypothesis is in excellent agreement with the results found by Maas *et al.* on the acid hydrolysis of tertiary enamines.[13]

Initially, the enamine is protonated producing an iminium ion which in turn is hydrated to an *N*-protonated α-amino alcohol analogous to *21* and *23*. The next steps are analogous to the sequence *23*→*25*→*27* (Scheme 3). It was found that the slowest step in the hydrolysis of the α-amino alcohol is the C–N cleavage reaction (corresponding to *25*→*27*). The rate of this step was found to be strongly dependent on the *N*-substituent. The more electron-attracting the *N*-substituent, the faster C–N-cleavage reaction. Thus the intermediate *23* is expected to undergo ring cleavage much faster than *21* due to the fact that a phenyl group is more electron attracting than a methyl group. Similarly, a more electron withdrawing halogen at C-4 may lead to a faster ring cleavage. At the same time, a more electron withdrawing 4-halogen will result in less protonization at the 4-position of *20f* and will therefore reduce the rate of formation of the pyrazol-4-in-3-one *5f*. The iodo compound *1f* (X = I) produces *5f* in a somewhat lower yield than the bromo compound *1f*. This is probably due to the fact that *1f* (X = I) gives off iodonium ions to a considerable extent during the reaction with formation of *1e*.

The differences between the 1-methyl-2-benzyl-4-chloro-, bromo-, and iodo-pyrazolium tosylates *1d* (X = Cl, Br, or I), respectively, are similar to those found between the phenyl analogs *1f* (X = Cl, Br, or I). This confirms that the reaction between 1-methyl-2-benzyl-4-halo-pyrazolium salts and sodium hydroxide follows an anomalous addition-elimination mechanism. If the addition step is product determining the ratio between *5d* and *9d* should be reflected by the relative substitution rates of 1-methyl-2-benzyl-5-chloro-pyrazolium tosylate *4d* and 1-methyl-2-benzyl-3-chloro-pyrazolium tosylate *8d*. This ratio was determined to be 3.35; therefore, the addition step is again not product determining. In the 1-methyl-2-benzyl substituted compounds the *N*-substituents are rather similar and the ring cleavage rates of the intermediates *20d* are therefore comparable. Consequently, the product ratio is only influenced to a minor extent by the ring cleavage reactions and both isomeric pyrazolones *5d* and *9d* arise. This may indicate that mesomeric delocalization of the nitrogen lone pair over the phenyl group plays a role during the rapid ring cleavage of the intermediate *22f*.

CONCLUSION

All experimental observations strongly support that 1-methyl-2-phenyl-4-halogeno-pyrazolium salts react with sodium hydroxide or sodium methoxide to form pyrazol-4-in-3-ones by an anomalous addition-elimination mechanism. The addition step is rate limiting (a proposed energy diagram is sketched in Fig. 2). The competition between pyrazol-4-in-3-one formation and ring cleavage is the product determining factor. The results obtained with 1-methyl-2-benzyl-4-halogeno-pyrazolium tosylates indicate that when the *N*-substituents are nonvinylic the ring cleavage processes influence the product distribution to a minor extent. The mechanism and the results are probably general for the reaction between 1,2-disubstituted 4-halogeno-pyrazolium tosylates *1* and sodium hydroxide or sodium methoxide.

EXPERIMENTAL

Column chromatography was carried out on silica gel (Merck, 0.05 – 0.2 mm). When non-aromatic eluents were used, 2 % of a fluorescent indicator (Riedl de Haën, Leuchtpigment ZS Super) was added to the silica gel and columns of clear quartz were used. The zones could then be visualized by illumination with a 254 mμ UV lamp. Preparative thin layer chromatography (TLC) was carried out on 20 × 40 cm plates with a 1 mm layer of silica gel (Merck, PF_{254}). Melting points are uncorrected. NMR-spectra were obtained on a Varian A-60 or a HA-100 instrument. Position of signals are given in ppm (δ-values) relative to tetramethylsilane (TMS) when deuteriochloroform was used as the solvent. When deuterium oxide was used as the solvent 2,2-dimethyl-2-silapentane-5-sulfonate (DSS) was used as an internal standard. IR-spectra were measured in potassium bromide pellets. The purity of all non-ionic compounds were checked by TLC. All compounds were identified through their melting point, IR- and NMR-spectra.

1-Phenyl-3-hydroxy-pyrazole.[7] 1-Phenyl-pyrazolidon-3 (10.74 g) (commercially available) was dissolved in ethanol (50 ml) and 0.4 M aqueous iron(III) chloride solution, 0.25 N in HCl, (210 ml) was added with stirring and heating in a 100°C bath during 30 min. Stirring and heating was continued for 1 h. The solution was then diluted with water (1 l) and extracted with methylene chloride (3 × 200 ml). The organic layer was dried (magnesium sulfate) and the solvent was removed. The residue was dissolved in ethanol (40 ml) and boiling water (50 ml) was added. Cooling, filtration, and washing with water (5 × 20 ml) yielded 6.53 g (61 %) of 1-phenyl-3-hydroxy-pyrazole as light yellow crystals, m.p. 153 – 156°C (reported [7] m.p. 153°).

1-Methyl-5-chloro-pyrazole. 1-Methyl-5-hydroxy-pyrazole [16] (1.50 g) and phosphoryl chloride (3.06 ml) were heated in a sealed tube to 155°C for 8 h. The mixture was dissolved in methylene chloride (30 ml), water (30 ml) was added and the mixture was stirred at room temperature for 1 h. During this period hydrolysis takes place, and the heat evolution causes gentle reflux of the methylene chloride. The organic phase was isolated and the aqueous phase was extracted with two additional portions of methylene chloride (30 ml). The methylene chloride was distilled off through a steam distillation apparatus at a bath temperature of 100°C. The methylene chloride was kept in the receiver and the residue was steam distilled collecting 200 ml of distillate. The distillate was extracted with two additional portions of methylene chloride. The organic extract was dried (magnesium sulfate) and the methylene chloride was distilled off through a Vigreux column at bath temperature 85°C. The residue consisted of 817 mg (46 %) of 1-methyl-5-chloro-pyrazole as a highly volatile colourless oil. (Found: C 41.01; H 4.39; N 23.88; Cl 30.25. Calc. for $C_4H_4N_2Cl$: C 41.20; H 4.32; N 24.03; Cl 30.41.) NMR-data are given in Table 7.

1-Benzyl-5-chloro-pyrazole. Similarly, "1-benzyl-5-hydroxy-pyrazole"[17] (2.19 g) and phosphoryl chloride (2.3 ml) after the steam distillation afforded 1.49 g of a mixture of

Table 7. NMR-spectra of pyrazoles described in the experimental section.

Compound	NMR Phenyl group	H-3 ppm	H-4 ppm	H-5 ppm	N-CH_3 ppm	N-CH_2 ppm	$J_{H_3H_4}$ Hz	$J_{H_4H_5}$ Hz	$J_{H_3H_5}$ Hz
1-Benzyl-3-chloro-pyrazole	narrow multiplet		6.18	7.3		5.23		2.3	
1-Phenyl-3-chloro-pyrazole	broad multiplet		6.26	7.71				2.4	
1-Phenyl-3-bromo-pyrazole	broad multiplet		6.37	7.69				2.6	
1-Benzyl-4-chloro-pyrazole	narrow multiplet		7.3	7.43		5.14			0.7
1-Benzyl-4-iodo-pyrazole	narrow multiplet		7.54	7.37		5.27			
1-Phenyl-4-iodo-pyrazole	multiplet		7.92						0.7
1-Methyl-5-chloro-pyrazole		7.48	6.20		3.84		2.1		
1-Benzyl-5-chloro-pyrazole	singlet	7.49	6.19			5.30	1.9		
1-Phenyl-5-chloro-pyrazole [18]	narrow multiplet	7.65	6.35				1.9		
1-Phenyl-5-bromo-pyrazole	broad doublet	7.70	6.50				1.9		
1-Phenyl-5-methyl-pyrazole [22,31]	singlet	7.64	6.24				1.8		

1-benzyl-5-chloro-pyrazole and 1-benzyl-3-chloro-pyrazole.* The mixture was chromatographed on a column of silica gel (50 g) using benzene as the eluent. This gave 281 mg (12 %) of 1-benzyl-3-chloro-pyrazole, m.p. 63 – 65°C. Recrystallization from hexane did not raise the melting point. (Found: C 62.45; H 4.72; N 14.43; Cl 18.33. Calc. for $C_{10}H_9N_2Cl$: C 62.33; H 4.71; N 14.55; Cl 18.41.) The compound was identified through its NMR-spectrum (Table 7). Furthermore, the compound, when treated with methyl tosylate (see Table 1), produced 1-methyl-2-benzyl-5-chloro-pyrazolium tosylate *4d* (X = Cl) identical with the pyrazolium salt obtained by treatment of 1-methyl-5-chloro-pyrazole with benzyl bromide and subsequent exchange of the bromide ion with tosylate ion (see Table 1).

The next fraction contained 41 mg (2 %) of a mixture of 1-benzyl-3-chloro- and 5-chloro-pyrazole. The third fraction contained 661 mg (27 %) of 1-benzyl-5-chloro-pyrazole as a colourless oil. (Found: C 62.27; H 4.79; N 14.50; Cl 18.43.) NMR-data are given in Table 7.

1-Phenyl-3-chloro-pyrazole.[18] 1-Phenyl-3-hydroxy-pyrazole (3.52 g) and phosphoryl chloride (4.0 ml) were heated in a sealed tube to 200°C for 24 h. After hydrolysis, the organic phase was isolated and the aqueous phase was extracted with two additional portions of methylene chloride (30 ml). The extract was dried (magnesium sulfate) and the methylene chloride was removed. The residue was chromatographed on a column of silica gel (100 g) using benzene as the eluent. This gave 2.12 g (54 %) of 1-phenyl-3-chloro-pyrazole as a colourless oil which crystallized on cooling, m.p. 30 – 32°C (reported[18] m.p. 31.5°). NMR-data are given in Table 7.

* The presence of 1-benzyl-3-chloro-pyrazole in the product indicates that the starting material is contaminated with 1-benzyl-3-hydroxy-pyrazole. This explains the very large range of the melting point reported[17] for 1-benzyl-5-hydroxy-pyrazole. 1-Benzyl-3-hydroxy-pyrazole may arise if the initial benzoylation of pyrazolidone-3, in contrast to that supposed,[17] produces a mixture of N-benzoylated derivatives.

1-Phenyl-3-bromo-pyrazole.[27] 1-Phenyl-3-hydroxy-pyrazole (3.53 g) and phosphoryl bromide (3.5 ml) were mixed and heated in a sealed tube to 200°C for 24 h. The mixture was then worked up as described in the preceding experiment. The first fraction to leave the column contained 837 mg (13 %) of 1-phenyl-3,4-dibromo-pyrazole as colourless crystals, m.p. 46 – 48°C. Recrystallization from hexane raised the melting point to 50 – 51°C. (Found: C 35.84; H 2.10; N 9.32; Br 52.86. Calc. for $C_9H_6N_2Br_2$: C 35.79; H 2.00; N 9.28; Br 52.92.) The product was identical with that obtained by bromination of 1-phenyl-3-bromo-pyrazole.[6] The next fraction contained 584 mg of a mixture of 1-phenyl-3,4-dibromo-pyrazole and 1-phenyl-3-bromo-pyrazole. Finally, 1.39 g (29 %) of 1-phenyl-3-bromo-pyrazole came off the column. NMR-data are given in Table 7.

1-Phenyl-5-bromo-pyrazole.[18] 1-Phenyl-5-hydroxy-pyrazole [19] (3.03 g) and phosphoryl bromide (3.5 ml) were heated with stirring to 155°C for 8 h. The mixture was then worked up as in the preceding experiment. (After the hydrolysis, filtration of the mixture was necessary. The residue was washed with methylene chloride (3 × 10 ml). The aqueous phase was then extracted further with methylene chloride as before.) The first fraction contained 1.29 g (23 %) of 1-phenyl-4,5-dibromo-pyrazole as colourless crystals, m.p. 106 – 108°C. Recrystallization from ethanol-water (1:1) did not raise the melting point. (Found: C 35.58; H 2.02; N 9.11; Br 52.74.) The next fraction contained 1.96 g (47 %) of 1-phenyl-5-bromo-pyrazole as colourless crystals, m.p. 54 – 56°C. Recrystallization from ethanol-water did not raise the melting point (reported [18] m.p. 56°). NMR-data are given in Table 7.

1-Benzyl-4-chloro-pyrazole. 1-Benzyl-pyrazole [20] (4.00 g) was dissolved in ether (115 ml) and sulfuryl chloride (7.25 ml) was added with stirring and cooling in an ice-salt bath during 20 min. Stirring was continued for 30 min at 0°C and then for 1 h at room temperature. Water (30 ml) was then added with cooling in ice. The ether phase was isolated and the aqueous phase was extracted with ether (3 × 25 ml). The combined organic extracts were extracted with 4 N hydrochloric acid (30 ml), 20 % aqueous sodium carbonate (3 × 30 ml), dried (magnesium sulfate), and filtered through activated carbon. Removal of the ether gave 4.90 g (100 %) of 1-benzyl-4-chloro-pyrazole as colourless crystals, m.p. 32 – 33°C. Recrystallization from ethanol-water raised the melting point to 33 – 34°C. (Found: C 62.32; H 4.82; N 14.45; Cl 18.27. Calc. for $C_{10}H_9N_2Cl$: C 62.33; H 4.71; N 14.55; Cl 18.41.)

1-Benzyl-4-iodo-pyrazole. 1-Benzyl-pyrazole [20] (4.00 g) and sodium acetate (15.3 g) were dissolved in water (28 ml) and a solution of iodine (28.3 g) and potassium iodide (27.8 g) in water (56 ml) was added. The mixture was heated to reflux for 7 h. After cooling to room temperature a concentrated aqueous solution of potassium hydroxide was added until the solution turned clear light in colour. Sodium thiosulfate (10 g) was then added and the mixture was extracted with methylene chloride (4 × 50 ml). The organic phase was dried (magnesium sulfate) and the methylene chloride was removed. This afforded 6.40 g (89 %) of 1-benzyl-4-iodo-pyrazole, colourless crystals, m.p. 58 – 59°C. Recrystallization from ethanol-water did not raise the melting point. (Found: C 42.26; H 3.21; N 9.80; I 44.57. Calc. for $C_{10}H_9N_2I$: C 42.27; H 3.19; N 9.86; I 44.67.) NMR-data are given in Table 7.

1-Phenyl-4-iodo-pyrazole.[20] Similarly, 1-phenyl-pyrazole (3.99 g) afforded 6.90 g (92 %) of 1-phenyl-4-iodo-pyrazole, m.p. 82 – 84°C (reported [21] m.p. 77°).

1-Phenyl-4-bromo-5-methyl-pyrazole. 1-Phenyl-5-methyl-pyrazole [22] (1.03 g) was dissolved in acetic acid (1.0 ml) and a solution of bromine (0.39 ml) in acetic acid (2.0 ml) was added with stirring during 15 min. Stirring was continued for 1 h. Water (60 ml) was then added and the mixture was cooled to 0°C. The precipitate was isolated and the aqueous phase was extracted with methylene chloride (10 ml). The extract was combined with the separated material and the methylene chloride was removed. The residue was reprecipitated from ethanol-water. The product was then dissolved in ether and filtered through activated carbon. Removal of the ether gave 1.40 g (90 %) of 1-phenyl-4-bromo-5-methyl-pyrazole as a yellow oil which crystallized on cooling to – 30°C, m.p. 34 – 36°C. Recrystallization from 90 % ethanol raised the melting point to 38°C. (Found: C 50.48; H 3.91; N 11.68; Br 33.59. Calc. for $C_{10}H_9N_2Br$: C 50.67; H 3.83; N 11.80; Br 33.71.)

1-Phenyl-3-methyl-4-bromo-pyrazole. 1-Phenyl-3-methyl-pyrazole [23] (1.11 g) was brominated as described above. Water (60 ml) was then added and the mixture was extracted with methylene chloride (3 × 10 ml). The methylene chloride was removed and the crude product was chromatographed on a column of silica gel (100 g) using benzene

as the eluent. The first fraction contained 177 mg (8 %) of a compound which, on the basis of an NMR-spectrum, is assumed to be 1-(*p*-bromo-phenyl)-3-methyl-4-bromo-pyrazole. (NMR-data: δ 7.84, singlet, (1H); δ 7.53, singlet, (4H); δ 2.31, singlet (3H)). The compound melted at 102 – 105°C. The next fraction contained 1.34 g (81 %) of 1-phenyl-3-methyl-4-bromo-pyrazole as an oil which crystallized on cooling, m.p. 28°C. The compound was dissolved in ether and filtered through activated carbon. Removal of the ether and recrystallization from 90 % ethanol gave colourless crystals, m.p. 31°C. (Found: C 50.62; H 3.96; N 11.60; Br 33.45.)

Preparation of pyrazolium tosylates

The pyrazolium tosylates were prepared by one of the following six methods (see Table 4).

A. The pyrazole (*ca.* 5 g) and methyl tosylate (1.2 equiv.) were heated to 145°C for 3 h. The mixture was then washed with ether (5 × 20 ml) and recrystallized from methanol-ether to give the crude product which was crystallized once more from methanol-ether. The product was dried *in vacuo* at room temperature.

B. As *A*, but the mixture of pyrazole and methyl tosylate was heated to 100°C for 3 h.

C. As *A*, but the mixture of pyrazole and methyl tosylate was heated to 100°C for 3 h and then to 145°C for 3 h.

D. As *A*, but after the first recrystallization the product was dissolved in methanol and filtered through activated carbon. Evaporation of the methanol *in vacuo* afforded the crude product which was recrystallized once more from methanol-ether.

E. As *A*, but after the first recrystallization the product was dissolved in water (5 ml per g of product). The aqueous phase was extracted with ether (2 × 10 ml per g of product) and then with methylene chloride (5 × 15 ml per g of product). The methylene chloride solution was dried (magnesium sulfate) and the solvent was removed. The residue was dissolved in methanol and filtered through activated carbon. Evaporation of the methanol and recrystallization from methanol-ether afforded the pure compound.

F. The pyrazole (5 g), benzyl bromide (1.2 equiv.), and dry acetonitrile (3.0 ml) were heated to reflux for 3 h. The mixture was washed with ether (5 × 20 ml), dissolved in water and passed through a column of Amberlite IRA-400 (190 ml) as its salt with *p*-toluene-sulfonic acid. The water was removed *in vacuo* and the residue was recrystallized from methanol-ether.

Reaction of 4-halogeno-substituted pyrazolium tosylates with sodium hydroxide

1-Methyl-2-phenyl-4-bromo-pyrazolium tosylate 1f (994 mg) was added with stirring to boiling 1 N aqueous sodium hydroxide (8.00 ml). The solution was heated to reflux for 10 min and the water was then removed *in vacuo* at room temperature. The residue was extracted with boiling chloroform (50 ml + 4 × 10 ml). The chloroform was removed and the residue was dried *in vacuo* in a desiccator. The residue was then extracted with boiling ethyl acetate (30 ml + 4 × 10 ml), the extracts were filtered through activated carbon and the solvent was removed. The crude product could be purified by recrystallization but chromatography on a column of silica gel (10 g) using ethyl acetate as the eluent was considered to be more convenient. The first fraction contained a small amount of a brown oil which was not identified further. The column was then eluted with ethyl acetate-methanol (1:1). This gave 141 mg (33 %) of 1-phenyl-2-methyl-pyrazol-4-in-3-one *5f*, m.p. 108 – 109°C. The compound was dissolved in ethyl acetate and the solution was filtered through activated carbon. Removal of the ethyl acetate yielded 109 mg of *5f* as colourless crystals, m.p. 119 – 122°C. Recrystallization from ethyl acetate-hexane raised the melting point to 123 – 124°C. The compound is hygroscopic. Melting point, IR- and NMR-spectra proved the identity with the material described below.

In a separate experiment, 1-methyl-2-phenyl-4-bromo-pyrazolium tosylate *1f* (41 mg) was dissolved in 1 N sodium hydroxide (0.40 ml) in an NMR-tube. The tube was heated in the NMR probe to 90°C. After *ca.* 1 min three peaks at δ 2.62, 3.30, and 8.77, relative to DSS, appeared. In the following minutes these peaks grew at the expense of the peak at δ 3.84, corresponding to the starting material *1f*. After *ca.* 10 min no more starting material was present. The signals were identified by adding, one by one, the pure substances to the solution. The three signals corresponded to 1-methyl-2-phenylhydrazine, 1-phenyl-2-methyl-pyrazol-4-in-3-one *5f*, and bromomalonaldehyde, respectively. The yields, calculated on basis of the integral of the methyl group signal of the tosylate anion, were 33 %, 26 %, and 37 %, respectively. In a similar experiment, the solution was acidified with hydrochloric acid after the reaction. The NMR-spectrum of the acidic solution showed three singlets at δ 3.10, 3.55, and 8.73. Again, addition of the pure substances demonstrated the presence of the above mentioned products. In a third experiment, the alkaline reaction mixture was extracted with deuteriochloroform. The organic solution, in addition to phenyl group absorptions and signals due to impurities, exhibited a doublet at δ 5.64 and a singlet at δ 3.29 in the NMR-spectrum. The signals corresponded to 1-phenyl-2-methyl-pyrazol-4-in-3-one *5f* as shown by addition of the authentic substance to the solution.

Deuterium exchange experiments. 1-Methyl-2-phenyl-4-bromo-pyrazolium tosylate *1f* (868 mg) was heated in a mixture of 1 N aqueous sodium hydroxide (4.30 ml) and deuterium oxide (4.30 ml) and the mixture was worked up as described above. The NMR-spectrum of the product, obtained after column chromatography, showed three signals (intensity 1:2:1) symmetrically centered at δ 5.64. The distance between the peaks was 1.8 Hz. This proves the presence of 1-phenyl-2-methyl-pyrazol-4-in-3-one *5f*, (4H5H) and *5f*, (4H5D) in the ratio 1:1. The ratio between the intensity of the triplet and the *N*-methyl group was 1:6.0 indicating that 50 % of the total amount of pyrazol-4-in-3-one present had deuterium incorporated at the 4-position. The 5-proton doublet of *5f* was reduced in intensity and a new peak appeared in the center of the doublet. The relative intensities could not be determined accurately due to overlap with minor phenyl group signals. However, integration indicated that H-5 had been replaced with deuterium to an extent of *ca.* 50 %. Therefore *5f*, (4D5H) and *5f*, (4D5D) are present in the ratio 1:1 and in the same amount as *5f*, (4H5H) and *5f*, (4H5D). In a separate experiment 1-phenyl-2-methyl-pyrazol-4-in-3-one *5f* was heated with 1 N sodium deuteriooxide in deuterium oxide (5.1 ml) and the mixture worked up as described above. The NMR-spectrum of the product, obtained after column chromatography, showed a singlet at δ 5.64. The ratio between the intensity of this signal and the methyl group signal was 1:3.50 indicating that 14 % of H-4 in *5f* had been replaced by deuterium. The doublet corresponding to H-5 in *5f* had disappeared and integration confirmed that *ca.* 100 % of H-4 in *5f* had been replaced by deuterium.

1-Methyl-2-phenyl-4-chloro-pyrazolium tosylate 1f (X = Cl) (572 mg) was heated to reflux with 1 N sodium hydroxide (5.01 ml) and the mixture was worked up as described above for the bromo-compound *1f*. After chromatographic purification 7.6 mg (3 %) of 1-phenyl-2-methyl-pyrazol-4-in-3-one *5f*, identified through its spectra, was obtained.

1-Methyl-2-phenyl-4-iodo-pyrazolium tosylate 1f (X = I). Similarly, *1f* (X = I) (997 mg), after treatment with 1 N sodium hydroxide (4.37 ml) and working up as described above for the bromo-compound *1f* afforded 54 mg (14 %) of 1-phenyl-2-methyl-pyrazol-4-in-3-one *5f*, m.p. 108 – 111°C. Filtration through activated carbon and recrystallization from ethyl acetate-hexane raised the melting point to 123 – 124°C. IR- and NMR-spectra proved the identity with the material described above. As shown by an NMR-spectrum the residue from the ethyl acetate extraction contained, among other compounds, the 1-methyl-2-phenyl-pyrazolium salt *1e*. The latter was identified by addition of the pure substance to the solution.

1,3-Dimethyl-2-phenyl-4-bromo-pyrazolium tosylate 11f A. 11f (679 mg) and 1 N sodium hydroxide (3.2 ml) were heated to reflux for 3 h. The solvent was then removed *in vacuo* and the residue was extracted with boiling chloroform (50 + 4 × 10 ml). The chloroform was removed leaving 87 mg (29 %) of 1-phenyl-2,5-dimethyl-pyrazol-4-in-3-one *14f* ("isoantipyrin") as colourless crystals, m.p. 96 – 100°C. Recrystallization from ethyl acetate-hexane raised the melting point to 117°C (reported [11] m.p. 113°C). IR- and NMR-spectra were identical with those of an authentic sample.[24]

B. 11f (1.22 g) was treated with 1 N sodium hydroxide (5.8 ml) and the mixture worked up as described above for 1-methyl-2-phenyl-4-bromo-pyrazolium tosylate *1f*. The first fraction to leave the column (20 g of silica gel, elution with ethyl acetate) contained 128 mg of a brown oil. (NMR-data: δ 2.05, doublet, (3H) ($J = 1.2$ Hz); δ 2.80, singlet, (3H); δ 4.33, quartet, (1H) ($J = 1.2$ Hz); δ 7.2 – 7.5, multiplet, (*ca.* 7H)). The compound was unstable, even at room temperature, and attempts to purify it were unsuccessful.

Therefore, the material was not identified further. The column was then eluted with ethyl acetate-methanol (1:1). This gave 73 mg (13 %) of 1-phenyl-2,5-dimethyl-pyrazol-4-in-3-one *15f*, m.p. 104 – 106°C. Recrystallization from ethyl acetate-hexane raised the melting point to 117°C.

1-Phenyl-2,3-dimethyl-4-bromo-pyrazolium tosylate 13f (955 mg) was treated with 1 N sodium hydroxide (4.5 ml) as described above for 1-methyl-2-phenyl-4-bromo-pyrazolium tosylate *1f*. The water was then removed *in vacuo* and the residue was extracted with boiling chloroform ($50 + 4 \times 10$ ml). Removal of the chloroform and extraction with boiling ethyl acetate ($50 + 3 \times 20$ ml) gave a residue which was dissolved in water and passed through Amberlite IRA 400 (40 ml) in the *p*-toluenesulfonate form. Removal of the water gave 378 mg (40 %) of unchanged starting material as a brown oil. The ethyl acetate extract was filtered through activated carbon and the solvent was removed leaving 14 mg of a yellow oil. An NMR-spectrum indicated that no 1-methyl-2,5-dimethyl-pyrazol-4-in-3-one *15f* was present.

1-Methyl-2-benzyl-4-bromo-pyrazolium tosylate 1d (1.33 g) and 1 N sodium hydroxide (12.4 ml) were heated to reflux for 3 h. The solvent was evaporated and the residue was extracted with chloroform and with ethyl acetate as described above. The ethyl acetate extract contained 298 mg (51 %) of a mixture of 1-methyl-2-benzyl-pyrazol-4-in-3-one *9d* and 1-benzyl-2-methyl-pyrazol-4-in-3-one *5d* in the ratio 1.62 as shown by the NMR-spectrum in deuteriochloroform solution. The pyrazolones *9d* and *5d* were purified by preparative TLC using methylethyl ketone saturated with water as the eluent. The first fraction contained *9d* contaminated with *5d*. Rechromatography afforded the pure compounds. The second fraction contained pure *5d*. The total yield of *9d* was 93 mg (16 %) as a yellow oil which was dissolved in ethyl acetate and filtered through activated carbon. Removal of the solvent and two reprecipitations from ethyl acetate-hexane raised the melting point to 74 – 80°C. IR- and NMR-spectra proved the identity with the material described below. The total yield of *5d* was 178 mg (30 %) as yellow crystals, m.p. 53 – 55°C. Purification as described for the isomeric compound raised the melting point to 67 – 69°C. The compound was identical with the material described below.

1-Methyl-2-benzyl-4-chloro-pyrazolium tosylate 1d (X = Cl) (1.26 g) and 1 N sodium hydroxide (10.6 ml) similarly gave an ethyl acetate extract which was purified by preparative TLC (methylethyl ketone, one elution). The adjoining zones containing the pyrazolones *9d* and *5d* ($R_F = 0.29$) were combined. Yield 24 mg (3.8 %). An NMR-spectrum indicated that the ratio between *5d* and *9d* was 1.99.

1-Methyl-2-benzyl-4-iodo-pyrazolium tosylate 1d (X = I) (434 mg) and 1 N sodium hydroxide (3.0 ml) similarly gave an ethyl acetate extract which contained 34 mg (20 %) of a mixture of *5d* and *9d* in the ratio 1.66 as indicated by the NMR-spectrum. The residue from the extraction with ethyl acetate consisted of 58 mg (21 %) of 1-methyl-2-benzyl-pyrazolium iodide *1c* (A = I). The latter compound was identified by NMR with addition of the pure compound to the solution.

Reaction of 3-halogeno-substituted pyrazolium tosylates with sodium hydroxide

The pyrazolium salt (*ca.* 1 g) and 1 N aqueous sodium hydroxide (3.2 equiv.) were heated to reflux for 3 h. The solvent was then removed *in vacuo* and the residue was extracted with boiling methylene chloride (5×10 ml). The methylene chloride was removed and the residue was extracted with boiling ethyl acetate (4×10 ml). The solution was filtered through activated carbon. Removal of the ethyl acetate gave the crude pyrazolone which was crystallized from ethyl acetate-hexane. Yields, melting points, and analytical data are given in Table 4. IR- and NMR-data of the pyrazolones are presented in Table 5.

Reactions with sodium methoxide

1-Methyl-2-phenyl-5-bromo-pyrazolium tosylate 1f (250 mg) and 1 N sodium methoxide (2.0 ml) were heated to reflux for 10 min. The mixture was worked up as described for the reaction of *1f* with sodium hydroxide. The yield of 1-phenyl-2-methyl-pyrazol-4-in-3-one *5f* was 5.3 mg (5.0 %).

Kinetic experiments. The pyrazolium tosylate was dissolved in 1 N aqueous potassium hydroxide (0.88 ml per mmol of pyrazolium salt). The solution was placed in a bath the temperature of which was kept at 59.6°C. At intervals samples of 0.45 ml were taken; they were quenched immediately with three drops of conc. hydrochloric acid. The solvent was removed, the residue was dissolved in deuterium oxide and NMR-spectra were measured. The conversion of starting material to pyrazol-4-in-3-one was evaluated from mean-values of several integrations of the *N*-methyl signals. The results are given in Table 6. The total amount of byproducts was estimated by comparing the sum of the integrals of the *N*-methyl group signals of the starting material and of the pyrazol-4-in-3-one with the integral of the *C*-methyl group signal of the tosylate ion.

REFERENCES

1. Begtrup, M. *Acta Chem. Scand.* **24** (1970) 1819.
2. Kauffmann, T. *Angew. Chem.* **77** (1965) 557.
3. Kauffmann, T. and Wirthwein, R. *Angew. Chem.* **83** (1971) 21.
4. Bunnett, J. F. and Scorrano, G. *J. Am. Chem. Soc.* **93** (1971) 1190.
5. Reinecke, M. G. and Adickes, H. W. *J. Am. Chem. Soc.* **90** (1968) 511.
6. Begtrup, M. *To be published.*
7. Harries, C. and Loth, G. *Ber.* **29** (1896) 513.
8. O'Brien, D. F. and Gates, J. W. *J. Org. Chem.* **31** (1966) 1538.
9. Hoffmann, R. W. *Dehydrobenzene and Cycloalkynes*, Verlag Chemie, Weinheim 1967.
10. Begtrup, M. and Venø Poulsen, K. *Acta Chem. Scand.* **25** (1971) 2087.
11. Knorr, L. and Köhler, A. *Ber.* **39** (1906) 3257.
12. Knorr, L. and Weidel, A. *Ber.* **42** (1909) 3523.
13. Maas, W., Jansson, M. J., Stamhuis, E. J. and Wynberg, H. *J. Org. Chem.* **32** (1967) 1111.
14. Aubagnac, J.-L., Elguero, J., and Jaquier, R. *Bull. Soc. Chim. France* **1969** 3306.
15. Elguero, J., Jaquier, R., and Tizané, D. *Bull. Soc. Chim. France* **1969** 1687.
16. Lingens, F. and Schneider-Bernlöhr, H. *Ann.* **686** (1965) 134.
17. Dorn, H. and Arndt, D. *J. prakt. Chem.* **313** (1971) 115.
18. Grandberg, I. I., Gorbachova, L. I., and Kost, A. N. *J. Gen. Chem.* **33** (1963) 503.
19. Michaelis, A. *Ann.* **385** (1911) 1.
20. Jones, R. G. *J. Am. Chem. Soc.* **71** (1949) 3994.
21. Severini, O. and Balbiano, L. *Atti Reale Accad. Lincei* [5] **1 II** (1892) 391.
22. Claisen, L. and Roosen, P. *Ann.* **278** (1894) 261.
23. v. Auwers, K. and Hollmann, H. *Ber.* **59** (1926) 1282.
24. Michaelis, A. *Ann.* **338** (1904) 267.
25. Finar, I. L. and Godfrey, K. E. *J. Chem. Soc.* **1954** 2293.
26. v. Auwers, K. and Kohlhaas, W. *Ann.* **437** (1924) 36.
27. Balbiano, L. *Gazz. Chim. Ital.* **19** (1889) 128.
28. Begtrup, M. *Acta Chem. Scand.* **25** (1971) 249.
29. *Ber.* **28** (1895), Ref. 78.
30. Bodendorf, K. and Popelak, A. *Ann.* **566** (1950) 84.
31. Fensmeyer, L. G. and Ainsworth, C. *J. Org. Chem.* **31** (1966) 1878.
32. Miller, J. *Aromatic Nucleophilic Substitution*, Elsevier, London 1968.

Received January 26, 1973.

ACTA CHEMICA SCANDINAVICA 27 (1973) 2075–2082

A Comparative Study on the Ionization of Catechol Amines in Aqueous Solutions

P. J. ANTIKAINEN and ULLA WITIKAINEN

Department of Basic Instruction in Chemistry, Medical Faculty, University of Helsinki, 00170 Helsinki 17, Finland

The acid ionization constants of four protonated catechol amines (dopa, dopamine, α-methyldopa and isoprenaline) in aqueous 0.1 M potassium chloride solutions at 25°C were determined by a potentiometric method. The results are compared with earlier results concerning the ionization of other catechol amines. The first and second protolytic constants of catechol were determined.

A simple correlation is noted between the protolytic constants of *o*-diphenols (and of the corresponding catechol amines) and the formation constants of their boric acid chelates. From this the phenolic group of the catechol amines is proved to be a stronger acid than the protonated amino group. The effect of the structure of the catechol amines on their protolysis is examined.

Although the pharmacological properties of common catechol amines are well known, their ionization and chelate formation reactions seem to have been little investigated.[1–8] In studies of chelate formation reactions of inorganic acids with di- and polyphenols [9–11] it has been found that these phenols, and the similar catechol amines, form chelates with boric acid. Boric acid has been found to stabilize aqueous solutions of the diphenolic drug, adrenaline.[4] This has been explained as due to the chelate formation between boric acid and adrenaline. In order to clarify the possible chelation reactions of the other catechol amines with boric acid it is necessary to determine the protolytic constants of these catechol amines. The evaluation of these constants is also important for an understanding of the biological activity and stability of catechol amines.

The common catechol amines may be considered as substituted diphenols, and their ionization and chelation can be compared to the corresponding properties of the diphenols studied previously.[9–11]

According to Riegelman [4] it can be assumed that the protonated form (H_2L^+) occupies a central position in the chemistry of catechol amines in aqueous solutions. Here the first phenolic group is assumed to be more acidic than the protonated amino group. According to Rajan *et al.*[6] and Karpel *et al.*,[8] however, the protonated amino groups are more acidic.

EXPERIMENTAL

The measurements were carried out at 25°C on aqueous solutions containing various concentrations of protonated (hydrochlorides) catechol amines, in which the ionic strength was stabilized by making the solutions 0.1 M in potassium chloride. Dopa, dopamine, and isoprenaline sulphate were products of Fluka AG and α-methyldopa a product from Merck Sharp & Dohme.

All solutions were prepared in distilled water free from dissolved oxygen. The vessels used for storage of the solutions were flushed with purified nitrogen to remove the air. The catechol amines studied were titrated with 0.01 – 0.1 N sodium hydroxide in solutions containing the corresponding protonated (hydrochlorides) catechol amines. The temperature was maintained at 25°C by a water bath. The pH was measured during the titrations with a Radiometer Type PHM 4c pH meter using a Beckman Type E2 No 41263 glass electrode. A Beckman Type K 100 calomel electrode was used as a reference electrode. A 0.05 M potassium hydrogen phthalate solution (pH = 4.008) was used as reference solution. The value of the apparent activity coefficient $pf_{H^+} = 0.081$ (0.1 M KCl) [12] was used when calculating the hydrogen ion concentrations from the measured pH values.

The protolytic constants were calculated by a computer program written in ALGOL.

RESULTS

The acid ionization constants (first phenolic and protonated amino groups) for the protonated catechol amines studied here were determined potentiometrically as described earlier.[9] Some of the typical titration data are presented in Tables 1 – 4, where C_A is the stoichiometric concentration of the protonated catechol amine and C_B that of the added base (0.1 N NaOH). The protolytic

Table 1. Determination of the values for the protolytic constants K_1 and K_2 of protonated dopa (DH_2^+) in aqueous 0.1 M potassium chloride solutions at 25°C.

C_B/C_A	0.008 M DH_2^+ pH	0.008 M DH_2^+ pK_1	0.005 M DH_2^+ pH	0.005 M DH_2^+ pK_1	0.003 M DH_2^+ pH	0.003 M DH_2^+ pK_1	0.0015 M DH_2^+ pH	0.0015 M DH_2^+ pK_1
0.35	8.443	8.754	8.435	8.748	8.411	8.732	8.414	8.724
0.40	8.525	8.754	8.513	8.744	8.493	8.734	8.501	8.729
0.45	8.603	8.756	8.593	8.748	8.573	8.741	8.657	8.820
0.50	8.676	8.758	8.668	8.752	8.645	8.745	8.582	8.650
0.55	8.742	8.755	8.736	8.752	8.711	8.745	8.804	8.831
0.60	8.809	8.756	8.801	8.752	8.777	8.749	8.792	8.735
0.65	8.873	8.756	8.867	8.753	8.838	8.750	8.855	8.733
		pK_2		pK_2		pK_2		pK_2
0.85	9.118	9.847	9.110	9.840	9.066	9.743	9.097	9.850
0.90	9.177	9.845	9.167	9.834	9.119	9.737	9.155	9.849
0.95	9.236	9.844	9.227	9.837	9.173	9.735	9.214	9.853
1.00	9.295	9.844	9.281	9.827	9.227	9.734	9.270	9.850
1.05	9.352	9.841	9.340	9.829	9.277	9.726	9.325	9.846
1.10	9.411	9.841	9.397	9.827	9.372	9.719	9.382	9.848
1.15	9.473	9.846	9.455	9.827	9.376	9.711	9.635	10.209
Average	$pK_1 = 8.756$		8.750		8.742		8.742	
	$pK_2 = 9.844$		9.832		9.729		9.886	

Table 2. Determination of the values for the protolytic constants K_1 and K_2 of protonated dopamine (DAH_2^+) in aqueous 0.1 M potassium chloride solutions at 25°C.

C_B/C_A	0.01 M DAH_2^+ pH	0.01 M DAH_2^+ pK_1	0.005 M DAH_2^+ pH	0.005 M DAH_2^+ pK_1	0.0015 M DAH_2^+ pH	0.0015 M DAH_2^+ pK_1	0.001 M DAH_2^+ pH	0.001 M DAH_2^+ pK_1
0.10	7.881	8.839	7.890	8.849	7.895	8.858	7.923	8.888
0.15	8.076	8.835	8.087	8.848	8.088	8.854	8.112	8.879
0.20	8.230	8.840	8.242	8.854	8.229	8.848	8.256	8.875
0.25	8.350	8.838	8.358	8.848	8.347	8.846	8.374	8.873
0.30	8.455	8.837	8.465	8.850	8.453	8.846	8.477	8.872
0.35	8.551	8.838	8.558	8.849	8.543	8.846	8.570	8.872
0.40	8.640	8.840	8.645	8.849	8.624	8.842	8.655	8.872
		pK_2		pK_2		pK_2		pK_2
0.60	8.956	10.366	8.954	10.283	8.920	10.106	8.952	10.226
0.65	9.030	10.350	9.030	10.294	8.990	10.122	9.022	10.238
0.70	9.105	10.344	9.105	10.304	9.056	10.120	9.094	10.259
0.75	9.184	10.356	9.178	10.299	9.125	10.136	9.165	10.278
0.80	9.261	10.352	9.255	10.310	9.195	10.149	9.233	10.282
0.85	9.342	10.358	9.332	10.315	9.263	10.158	9.300	10.283
0.90	9.422	10.356	9.408	10.314	9.335	10.178	9.368	10.289
Average	pK_1 =	8.838		8.850		8.849		8.876
	pK_2 =	10.355		10.302		10.138		10.246

Table 3. Determination of the values for the protolytic constants K_1 and K_2 of protonated α-methyldopa (MDH_2^+) in aqueous 0.1 M potassium chloride solutions at 25°C.

C_B/C_A	0.008 M MDH_2^+ pH	0.008 M MDH_2^+ pK_1	0.005 M MDH_2^+ pH	0.005 M MDH_2^+ pK_1	0.003 M MDH_2^+ pH	0.003 M MDH_2^+ pK_1	0.001 M MDH_2^+ pH	0.001 M MDH_2^+ pK_1
0.10	7.913	8.874	7.916	8.880	7.902	8.866	7.970	8.941
0.15	8.120	8.884	8.122	8.890	8.101	8.869	8.150	8.926
0.20	8.263	8.880	8.448	9.081	8.253	8.874	8.289	8.920
0.25	8.391	8.889	8.892	8.897	8.377	8.880	8.404	8.918
0.30	8.489	8.883	8.495	8.900	8.479	8.881	8.496	8.910
0.35	8.584	8.887	8.585	8.900	8.566	8.877	8.590	8.916
0.40	8.666	8.885	8.667	8.901	8.651	8.880	8.665	8.911
		pK_2		pK_2		pK_2		pK_2
0.60	8.960	10.110	8.954	9.942	9.013	8.932	8.939	9.927
0.65	9.025	10.095	9.020	9.955	9.077	8.996	8.999	9.929
0.70	9.090	10.089	9.081	9.957	9.139	9.058	9.062	9.946
0.75	9.157	10.095	9.143	9.966	9.199	9.118	9.121	9.955
0.80	9.211	10.091	9.205	9.976	9.260	9.179	9.178	9.960
0.85	9.285	10.089	9.265	9.980	9.320	9.239	9.234	9.964
0.90	9.348	10.086	9.324	9.983	9.378	9.297	9.291	9.973
Average	pK_1 =	8.883		8.917		8.875		8.920
	pK_2 =	10.093		9.965		9.999		9.950

Table 4. Determination of the values for the protolytic constants K_1 and K_2 of protonated isoprenaline (IPH_2^+) in aqueous 0.1 M potassium chloride solutions at 25°C.

	0.008 M IPH_2^+		0.005 M IPH_2^+		0.003 M IPH_2^+		0.001 M IPH_2^+	
C_B/C_A	pH	pK_1	pH	pK_1	pH	pK_1	pH	pK_1
0.35	8.366	8.674	8.348	8.650	8.347	8.647	8.338	8.639
0.40	8.450	8.672	8.430	8.647	8.432	8.648	8.415	8.631
0.45	8.528	8.671	8.509	8.647	8.510	8.647	8.503	8.642
0.50	8.602	8.671	8.583	8.646	8.586	8.648	8.567	8.630
0.55	8.669	8.667	8.656	8.648	8.658	8.648	8.646	8.638
0.60	8.737	8.666	8.724	8.646	8.727	8.646	8.714	8.636
0.65	8.806	8.668	8.795	8.648	8.793	8.643	8.780	8.634
		pK_2		pK_2		pK_2		pK_2
0.85	9.068	9.926	9.059	9.880	9.063	9.905	9.048	9.865
0.90	9.131	9.926	9.127	9.886	9.131	9.910	9.116	9.870
0.95	9.195	9.930	9.192	9.884	9.198	9.911	9.182	9.870
1.00	9.254	9.922	9.258	9.885	9.264	9.911	9.246	9.866
1.05	9.314	9.920	9.323	9.884	9.324	9.900	9.305	9.854
1.10	9.375	9.922	9.387	9.882	9.389	9.900	9.368	9.851
1.15	9.432	9.918	9.452	9.883	9.455	9.903	9.430	9.847
Average	$pK_1 = 8.670$		8.647		8.647		8.636	
	$pK_2 = 9.924$		9.883		9.905		9.860	

constants of the four catechol amines studied here are collected in Table 5. In Table 6 the protolytic constants of some common catechol amines are compared to the protolytic constants of catechol and pyrogallol.[13] The protolytic constant of catechol has been previously determined by several investigators, but their results are divergent.[14–24] Hence the protolytic constants of catechol were redetermined using the potentiometric method described earlier.[9] The results are shown in Table 7.

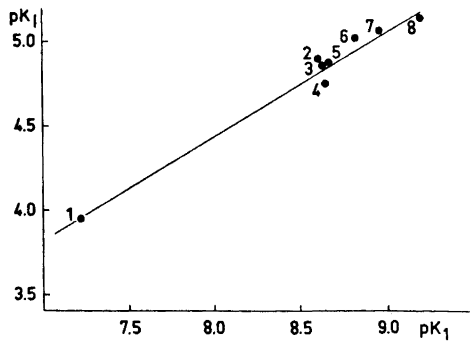

Fig. 1. The dependence of *o*-diphenol-boric acid chelate formation on the protolysis of the first phenolic group in *o*-diphenols. 1 Protocatechualdehyde. 2 DL-Noradrenaline. 3 L-Noradrenaline. 4 Adrenaline. 5 Gallic acid. 6 Protocatechuic acid. 7 Pyrogallol. 8 Catechol.

In Fig. 1 is shown the relationship between the first protolytic constants of some *o*-diphenols and the formation constants of the boric acid chelates of the corresponding phenols [9] (points 1, 5 – 8). According to this the formation of the boric acid chelates of the phenols is promoted by the acid strength of the ligand. Because the catechol amines considered in this paper also form such boric acid chelates,[9] the same correlation should be expected to hold for them too. In Fig. 1, the points 2 – 4 depict the catechol amines studied earlier with the first protolytic constant of the catechol amine taken as the protolytic constant. If, on the other hand, the corresponding second protolytic constants were used, the expected correlation would not be realized (*cf.* Table 6). It is obvious from this that the first protolytic constant of the catechol amines is due to the phenolic group and the second one to the protonated amino group. Riegelman [5] has earlier come to the same conclusion, whereas Rajan [6] and Karpel [8] have taken the opposite view.

An examination of the results in Table 6 reveals that the catechol amines are stronger acids than the simple *o*-diphenols. An amine chain attached to the diphenol ring thus clearly strengthens the acidic character of the phenolic group. Changes in the amine chain, however, seem to have a clear effect only on the second protolytic constant of the catechol amines (protonated amino

Table 5. Values of the protolytic constants (protonated amino and phenolic groups) of four protonated catechol amines in aqueous solutions at various concentrations (0.1 M KCl, 25°C).

	Dopamine			α-Methyldopa	
$[DAH_2^+]$	pK_1	pK_2	$[MDH_2^+]$	pK_1	pK_2
0.001	8.876	10.264	0.001	8.926	9.950
	8.858	10.072		8.845	9.965
0.005	8.850	10.302		8.890	10.038
0.015	8.849	10.138	0.003	8.875	9.999
0.010	8.838	10.355	0.005	8.917	9.965
	8.865	10.357	0.008	8.868	10.035
	8.865	10.375		8.883	10.093
	8.851	10.477	Average	8.886	9.996
	8.850	10.336			
	8.836	10.378			
	8.838	10.282			
	8.890	10.402			
Average	8.855	10.312			
	Dopa			Isoprenaline	
$[DH_2^+]$	pK_1	pK_2	$[IPH_2^+]$	pK_1	pK_2
0.0015	8.742	9.886	0.001	8.670	9.924
0.003	8.742	9.729	0.003	8.647	9.906
0.005	8.750	9.832		8.647	9.905
	8.766	9.830	0.005	8.647	9.883
Average	8.750	9.819		8.657	9.915
			0.008	8.636	9.860
			Average	8.651	9.899

Table 6. The protolytic constants (phenolic and protonated amino groups) of catechol, pyrogallol, and some common protonated catechol amines.

	pK_1	pK_2	Medium (I and °C)	References
Catechol	9.43	13	0.1 – 0.15, 20	20
	9.15	11.23	0.06, 25	14
	9.17	13.4	0.1, 18 – 22	21
	9.37	12.8	0.1, 25	17
	9.33	12.62	0.1, 25	20, 23
	9.25	–	0.09, 25	15
	9.85	–	?, 26	16
	9.20	11.93	0.1, 25	18
	9.39	13.1	0.1, 25	19
	9.21	11.70	0.1, 25	This work
Pyrogallol	8.82	11.09	?, ?	22
	9.01	11.64	?, ?	23
	9.05	11.19	0.1, 20	24
	8.98	–	0.1, 25	13
Adrenaline	8.71	9.90	0.1, 25	25
	8.66	9.95	0.1, 25	17
	8.78	10.02	0.06, 25	26
	8.73	10.17	1.0, 25	6
	8.62	10.05	0.1, 25	9
L-Noradrenaline	8.82	9.98	0.06, 25	26
	8.57	9.93	1.0, 25	6
	8.64	9.70	0.1, 25	17
	8.62	9.64	0.1, 25	9
DL-Noradrenaline	8.57	9.73	1.0, 25	6
	8.60	9.62	0.1, 25	9
Dopamine	8.96	10.50	1.0, 25	6
	8.86	10.31	0.1, 25	This work
Isoprenaline	8.65	9.90	0.1, 25	This work
Dopa	9.19	10.24	?, ?	3
	8.71	9.74	1.0, 25	7
	8.67	9.88	0.0, 25	2
	8.75	9.82	0.1, 25	This work
α-Methyldopa	9.12	10.61	?, ?	3
	8.87	10.00	0.1, 25	This work

group). It can be noted, *e.g.*, that methylation of the amino group clearly weakens the acidic character of the protonated amino group (*cf.* adrenaline/noradrenaline), but seems to have no effect on the protolysis of the phenolic group. This effect on the protonated amino group is readily understood by analogy with the basic protolytic constants of alkyl amines. The attachment

Table 7. Determination of the values for the protolytic constants K_1 and K_2 of catechol in aqueous 0.1 M potassium chloride solutions at 25°C.

C_B/C_A	0.008 M Catechol pH	0.008 M Catechol pK_1	0.005 M Catechol pH	0.005 M Catechol pK_1	0.003 M Catechol pH	0.003 M Catechol pK_1
0.35	8.934	9.210	8.950	9.226	8.735	9.220
0.40	9.022	9.208	9.034	9.218	8.908	9.220
0.45	9.109	9.208	9.124	9.221	9.061	9.221
0.50	9.193	9.208	9.210	9.222	9.199	9.217
0.55	9.273	9.205	9.295	9.223	9.336	9.216
0.60	9.354	9.202	9.378	9.221	9.475	9.214
0.65	9.435	9.198	9.465	9.219	9.622	9.211
		pK_2		pK_2		pK_2
0.85	9.798	11.161	9.864	11.821	9.622	11.604
0.90	9.909	11.199	9.991	11.910	9.783	11.626
0.95	10.035	11.261	10.121	11.897	9.965	11.716
1.00	10.168	11.315	10.269	12.009	10.156	11.774
1.05	10.312	11.386	10.404	12.027	10.342	11.852
1.10	10.468	11.488	10.530	12.069	10.499	11.895
1.15	10.614	11.584	10.638	12.093	10.629	11.942
Average		$pK_1 = 9.206$ $pK_2 = 11.342$		$pK_1 = 9.221$ $pK_2 = 11.975$		$pK_1 = 9.217$ $pK_2 = 11.773$

of an alkyl group to the amine markedly strengthens the basic character of the latter, or correspondingly weakens the acidic character of the protonated amino group. It is just this weakening of protolysis that is observed in passing from noradrenaline to adrenaline. Moreover, by comparing isoprenaline and adrenaline, it can be observed that the radical attached to nitrogen has no significant effect on the protolytic constants. Neither here nor in the case of alkyl amines has the size of the alkyl group any substantial effect on the protolytic constants.

It may be noted as a general feature of this argument that the structure of the amine chain on the whole has but little effect on the protolysis of the catechol amines. A remarkable exception, however, is a methyl group in the α-position (*cf.* dopa and dopamine), which quite clearly exerts an influence on both the phenolic and the protonated amino group by decreasing their corresponding protolytic constants. On the other hand, changes in the structure of the amine chain affect primarily the protolysis of the protonated amino group.

One of the authors (P. J. A.) shortly intends to continue investigating the formation of boric acid chelates of the catechol amines.

REFERENCES

1. Axelrod, J. *Science* **173** (1971) 598.
2. Miyamoto, S. and Schidt C. L. A. *J. Biol. Chem.* **90** (1930) 165.
3. Stein, G. A., Bronner, H. A. and Pfister, K. *J. Am. Chem. Soc.* **77** (1955) 165.
4. Riegelman, S. and Fischer, E. Z. *J. Pharm. Sci.* **51** (1962) 206, 210.

5. Riegelman, S., Strait, L. A. and Fischer, E. Z. *J. Pharm. Sci.* **51** (1962) 129.
6. Rajan, K. S., Davis, J. M., Colburn, R. W. and Jatkar, F. H. *J. Neurochem.* **18** (1971) 345; **19** (1972) 1099.
7. Gorton, J. E., Jameson, R. F. *J. Chem. Soc.* **A 1968** 2615.
8. Karpel, R. L., Kustin, K., Kowalak, A. and Pasternack, R. F. *J. Am. Chem. Soc.* **93** (1971) 1085.
9. Antikainen, P. J., Kauppila, A., Lundgren, G., Mälkönen, P. J., Rossi, V. M. K., Tevanen, K., Viro, M., Witikainen, U., Katila, R. and Viitala, A. *Suomen Kemistilehti* **B 32** (1959) 141, 175, 185, 211; **B 37** (1964) 213; **B 39** (1966) 2, 285; **B 41** (1968) 206; **B 42** (1969) 178; **B 44** (1971) 173, 256, 259.
10. Antikainen, P. J. and Oksanen, H. *Acta Chem. Scand.* **22** (1968) 2867.
11. Näsänen, R., Tilus, P. and Helander, P. *Suomen Kemistilehti* **B 33** (1960) 1; **B 43** (1970) 331.
12. Näsänen, R., Lumme, P. and Mukula, A.-L. *Acta Chem. Scand.* **5** (1951) 1199.
13. Antikainen, P. J. and Katila, R. *Suomen Kemistilehti* **B 44** (1971) 256.
14. Timberlake, C. F. *J. Chem. Soc.* **1957** 4987.
15. Näsänen, R. and Markkanen, R. *Suomen Kemistilehti* **B 29** (1956) 119.
16. Haight, G. P. and Pargamian, V. *Anal. Chem.* **32** (1960) 642.
17. Jameson, R. F. and Neillie, W. F. S. *J. Inorg. Nucl. Chem.* **27** (1965) 2623; **28** (1966) 2667.
18. L'Heuveux, G. A. and Martell, A. E. *J. Inorg. Nucl. Chem.* **28** (1966) 481.
19. Pichet, P. and Benoit, R. L. *Inorg. Chem.* **6** (1967) 1505.
20. Perrin, D. D. *Nature* **182** (1958) 741.
21. Sommer, L. *Coll. Czech. Chem. Commun.* **28** (1963) 2102.
22. Sheppard, S. E. *Trans. Am. Electrochem. Soc.* **39** (1921); *Chem. Abstr.* **15** (1921) 2329.
23. Abichandani, C. T. and Jatkar, S. K. K. *J. Indian Inst. Sci.* **A 21** (1938) 417.
24. Bartusek, M. *Coll. Czech. Chem. Commun.* **30** (1965) 2746.
25. Lewis, G. B. *Brit. J. Pharmacol.* **9** (1954) 488.
26. Andrews, A. C., Lyons, T. D. and O'Brien, T. D. *J. Chem. Soc.* **1962** 1176.

Received January 15, 1973.

ACTA CHEMICA SCANDINAVICA 27 (1973) 2083–2094

The Reactions of Lignin during Sulphate Pulping

Part XIII.* Reactions of Episulphide Structures with Alkali and with White Liquor** under Pulping Conditions

JOSEF GIERER, INGEGERD PETTERSSON, LEIF-ÅKE SMEDMAN*** and INGER WENNBERG†

Swedish Forest Products Research Laboratory, Chemistry Department, Box 5604, S-114 86 Stockholm, Sweden

Episulphide I, an intermediate in the cleavage of phenolic β-aryl ether structures by white liquor, was subjected to the conditions of alkali and sulphate pulping. Plausible formation pathways have been outlined for the low-molecular reaction products which were separated and identified (see Schemes 1 and 2). Experimental support for the validity of the schemes was provided by treating several of the proposed intermediates in a similar way and isolating identical reaction products. The reactions of compound I are illustrative of the final degradation steps of β-aryl ether structures leading to monomeric and polymeric phenolic products with concomitant partial elimination of sulphur.

On treatment with white liquor, milled wood lignin afforded the same monomeric phenolic degradation products as did episulphide I. This result lends further support for the presence of β-aryl ether structures in lignin and their mode of reaction during sulphate pulping as suggested in previous communications of this series.

In previous communications of this series [1,2] the mechanism of cleavage of β-aryl ether linkages in phenolic phenylpropane units of lignin during sulphate pulping has been described. It has been shown by model experiments that the reaction proceeds *via* methylene quinone, benzylthiol, and episulphide structures and yields mixtures of phenolic degradation products which have not yet been characterised. The sulphur incorporated during the initial step

* Part XII, see Gierer, J., Pettersson, I. and Smedman, L.-Å. *Acta Chem. Scand.* **26** (1972) 3366.

** The term "white liquor" refers to a solution of NaOH (3.5 g) and $Na_2S.9H_2O$ (3.1 g) in water (100 ml).

*** Present address: MoDoCell AB, Forskningslaboratoriet, Örnsköldsvik, Sweden.

† Present address: Stockholms Universitet, Wallenbergslaboratoriet, Strålningsbiologiska avdelningen, Stockholm, Sweden.

of the reaction sequence (formation of benzylthiol structures) is to a large extent eliminated subsequent to episulphide formation.[1–3]

When model compounds representing episulphide structures (*e.g.* I, see Scheme 1), or their precursors, benzylthiol structures, are treated with 2 N alkali at temperatures between 20 and 100°, *p*-dithianes (*e.g.* III) are formed as final products.[1,2] It is probable that the episulphide ring is opened between the α-carbon atom and the sulphur atom, giving rise to β-mercaptomethylene quinone structures (*e.g.* II) which spontaneously dimerise.[1,2] *p*-Dithianes are also obtained in good yields, when model compounds of the α-hydroxy-β-thiol type (*e.g.* XIX, see Scheme 2) are treated in the same manner.[1] However, if the treatment with alkali or white liquor is carried out at higher temperatures (about 140° or above), the episulphide, as well as the hydroxythiol and dithiane structures, are converted into mixtures of phenolic products with loss of most of the sulphur.[1–3]

During sulphate pulping "uncondensed" [4] phenolic units of the β-aryl ether type [5,6] should form episulphide I as an intermediate.[1,3] Therefore, this compound (in the form of its diacetate) was chosen as starting material in the present study for an investigation of the reactions involving the elimination of sulphur and the subsequent fragmentation to lower molecular weight products. Treatment of this compound with 2 N sodium hydroxide or white liquor at 180° for 2 h gave mixtures of phenolic products which were acetylated or methylated and separated by thin-layer, column and/or gas chromatographic methods. The main components of the monomeric fraction were identified by comparison with authentic samples (chromatographic behaviour, and mass spectral fragmentation patterns). The degradation products from both milled wood lignin and from some of the proposed intermediates (designated by asterisks in Schemes 1 and 2) were separated and identified in essentially the same manner.

RESULTS AND DISCUSSION

In Schemes 1 and 2 the low-molecular weight products formed from compound I are summarised and plausible routes of their formation are tentatively outlined. As is the case for the dimerisation [2] of episulphide I, the processes of sulphur elimination and fragmentation should be preceded by an alkali-promoted opening of the thiirane ring giving rise to the reactive intermediate II, a β-mercaptomethylene quinone.[3] At pulping temperature (180°), the latter may undergo two types of elimination as depicted in Schemes 1 and 2, both yielding conjugated intermediates (styrene derivatives).

In the *first type* of these eliminations (see Scheme 1) elemental sulphur is split off [3] from episulphide (I) giving rise to coniferyl alcohol (IV). The predominant formation of coniferyl alcohol has been demonstrated (TLC) by mild alkaline treatment of the episulphide at 90°. Extensive desulphurisation of episulphide I in the form of the diacetate was also achieved in the absence of alkali or any other solvent by simply heating a sample to 90° for 4 h. In this instance the diacetate of coniferyl alcohol formed was isolated in a high yield and identified. The fact that aromatic derivatives of thiiranes readily

part with their sulphur to yield the corresponding substituted styrenes is well documented both in early and recent literature.[7,8] The loss of sulphur was also observed during the preparation and purification of epithio compounds described in Part X of this series.[2]

The facile elimination of sulphur from the episulphide or from the β-mercaptomethylene quinone II may be regarded as a disproportionation, where the organic part is reduced to the olefin, and the inorganic part, sulphur, is oxidised from the −II to the 0-oxidation state. An attempt was therefore made to establish the elimination of elemental sulphur by heating appropriate model compounds with alkali or white liquor in the presence of metallic copper with exclusion of air. Activated copper and other activated metals (iron, zinc, nickel) are known to trap elemental sulphur.[9,10] and, thus, the sulphur is prevented from reacting according to the scheme

$$n\mathrm{S}(0) + \mathrm{HS}^- + \mathrm{OH}^- \rightarrow \mathrm{S}_n\mathrm{S}^{2-} + \mathrm{H}_2\mathrm{O}$$
$$\mathrm{S}_n\mathrm{S}^{2-} + (n-1)\mathrm{OH}^- + (1-n/4)\mathrm{H}_2\mathrm{O} \rightarrow (1+n/2)\mathrm{HS}^- + n/4\mathrm{S}_2\mathrm{O}_3^{2-}$$

with the formation of sulphide and thiosulphate ions.[11] The cupric sulphide formed was decomposed with hydrochloric acid and the liberated hydrogen sulphide estimated titrimetrically.[12] In separate runs it was established by GLC and TLC analyses of the resulting reaction mixtures that the presence of copper in the samples did not influence the process of sulphur elimination and the subsequent fragmentations (see below) to any noticeable degree.

Table 1.

Compound	Yield S^0 (%)
α-Thioglycerol	13
α,β-Dithioglycerol	1[a]
α,γ-Dithioglycerol	17
Tetraacetate of dithiane (III)	80
Diacetate of dithiane (III, CH_3 replacing CH_2OH)	88
Triacetate of hydroxythiol XIX	87
Diacetate of episulphide I	99[a]

[a] Determined with the improved method (see experimental section).

In Table 1 the yields of elemental sulphur eliminated from several appropriate model and reference compounds are given. The figures are mean values from at least two different runs with either 2 N sodium hydroxide or white liquor. Corresponding blanks were run with the respective cooking liquor omitting the model compound. Due to incomplete exclusion of oxygen which causes the formation of copper sulphide from S(−II), the reproducibility of the results was poor. However, much better values were obtained when the reaction was performed at lower temperature and in the presence of pyrogallol to absorb the small amount of oxygen present. From the values in Table 1 it may be concluded that the majority of the sulphur present in intermediate I, as well as in the dimerisation products (dithianes), is eliminated in elemental form, whereas the reference compounds only loose quantities hardly exceeding the limits of error of the determination methods.

Recently, evidence for the elimination of elemental sulphur from intermediates of the β-thiol [13,14] and benzyl thiol [15] types during treatment with alkali has been provided. The desulphurisation was followed indirectly by measuring the changes in thiol and sulphide concentrations by potentiometric titration.[14] The reaction has been interpreted [13–15] in terms of an intramolecular redox reaction of the previously [1,2] suggested methylene quinone intermediates. In the present work another type of model compound (episulphide) and a direct method of determination of eliminated elemental sulphur was used. In spite of these differences, the results obtained in this study concerning sulphur elimination are in good agreement with those recently published.

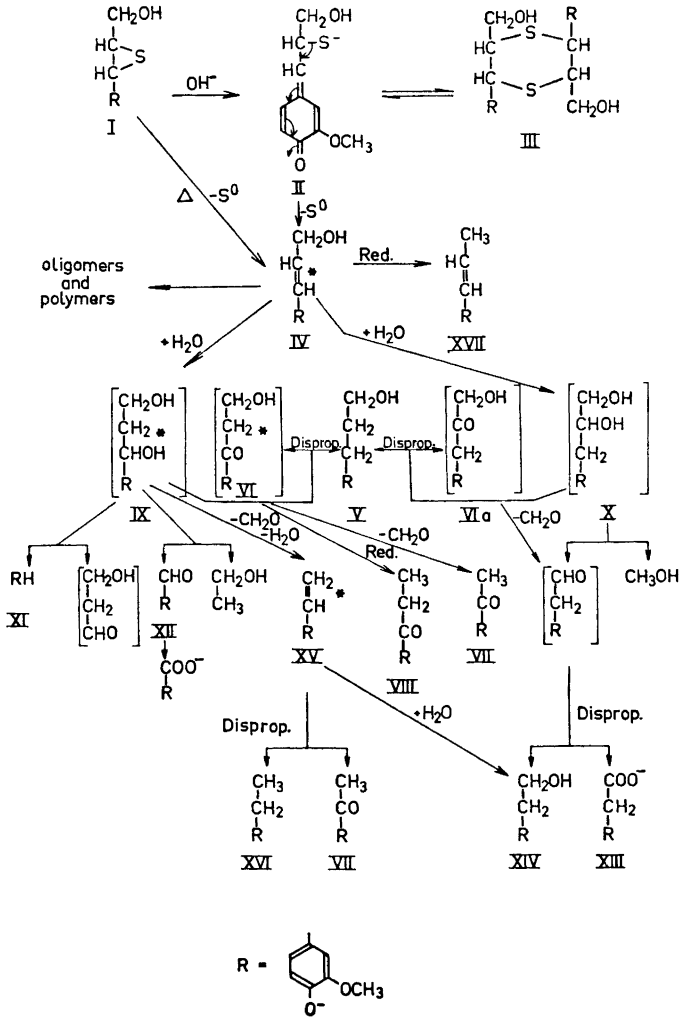

Scheme 1.

After the removal of sulphur from episulphide I, the resulting coniferyl alcohol exhibits various reactions under the strongly alkaline conditions of alkali and sulphate pulping which are tentatively interpreted as follows (see Scheme 1): About two thirds of this intermediate polymerise and the remaining third adds the elements of water giving rise to the α,γ- and β,γ-diols IX and X, respectively. Parts of these diols undergo disproportionation, diol IX yielding dihydroconiferylalcohol (V) and hydroxyconiferylalcohol (β-ketol) VI and diol X affording V and the α-ketol VIa. Other parts of the diols IX and X undergo alkaline cleavage of carbon-carbon bonds [16,17] yielding phenolic fragments of the C_6, C_6-C_1 and C_6-C_2 types. These include guaiacol (XI), vanillin (XII) and vanillic acid, vinylguaiacol (XV) and its disproportionation products 4-ethylguaiacol (XVI) and acetoguaiacone (VII), and the disproportionation products of homovanillin, homovanillic acid (XIII) and 2-(4-hydroxy-3-methoxyphenyl)-ethanol (XIV). Acetoguaiacone (VII) and homovanillin may also arise by elimination of formaldehyde from the ketols VI and VIa, respectively. In the presence of sulphide ions small amounts of ketol VI and of coniferylalcohol (IV) are reduced to propioguaiacone (VIII) and isoeugenol (XVII), respectively.

In addition to the previously mentioned phenolic reaction products the aliphatic fragments methanol and ethanol were obtained after treatment of episulphide I with alkali or white liquor at 180°.

Compounds V, VII, VIII and XI–XVII, as well as methanol and ethanol, were also obtained after appropriate treatment of coniferyl alcohol (IV). This result, together with the formation of IV after mild alkali or heat treatment of episulphide I, strongly strengthens the view that structures of the coniferyl alcohol type constitute important intermediates in the conversion of episulphide structures into low- and high-molecular sulphur-free products during sulphate pulping (see Scheme 1) (*cf.* also Ref. 15).

Further experimental support for the validity of Scheme 1 was provided by subjecting authentic samples of other proposed intermediates (VI, IX, and XV) to the conditions of alkali and sulphate pulping and by demonstrating the formation of the expected reaction products (compounds VII and VIII from VI, compounds V, VII, XI, XII, XIV–XVI, and ethanol from IX and compounds VII, XIV, and XVI from XV) (see Table 2).

Treatment of the α,γ-diol IX with alkali gave, in addition to high molecular weight fractions and the compounds mentioned above, 1,1-bis-(4-hydroxy-3-methoxyphenyl)ethane, most likely arising by addition of guaiacol (XI) to vinylguaiacol (XV). This reaction between a conjugated compound and a reactive site in a phenol indicates a possible mode of repolymerisation of lignin degradation products formed during alkali and sulphate pulping.

The remaining compounds in Scheme 1 (depicted within parentheses) (VI, VIa, IX, X, β-hydroxypropionaldehyde and homovanillin) are likely to be intermediates but have not been identified. Compounds VII and VIII have been previously obtained from sulphate spent liquors and have been suggested to originate from β-aryl ether structures in lignin.[18]

The fragmentation reactions of coniferyl alcohol outlined in Scheme 1 are in many respects analogous to those reported previously for other conjugated intermediates, *e.g.* a stilbene [19,20] and a 1,4-diarylbutadiene.[21]

Of the aliphatic fragmentation products, methanol may be liberated by alkaline cleavage of methyl aryl ether bonds and by cleavage of C_β-C_γ-bonds. However, ethanol which is formed in appreciable amounts from episulphide I and from the intermediates IV and IX can only arise by cleavage of $C_\alpha - C_\beta$-bonds in a reaction which also affords vanillin (XII) (see Scheme 1). The presence of ethanol in sulphate spent liquors has been considered to be due to microbial degradation of carbohydrate constituents *prior* to the pulping process.[22] The present study provides a plausible explanation for its formation also *during* the process by alkaline fragmentation of coniferyl alcohol type intermediates formed in lignins. The fact that ethanol, present in kraft spent liquors, originates from lignin was confirmed by treating milled wood lignin with white liquor under pulping conditions and demonstrating the formation of considerable amounts of ethanol. After a similar treatment, holocellulose gave only traces of ethanol and cotton gave no ethanol at all.

A third aliphatic cleavage product, formaldehyde, should originate from terminal hydroxymethyl groups in intermediary methylene quinone structures. This elimination reaction, resulting in the cleavage of $C_\beta - C_\gamma$-bonds is common to methylene quinone intermediates and is particularly pronounced with those

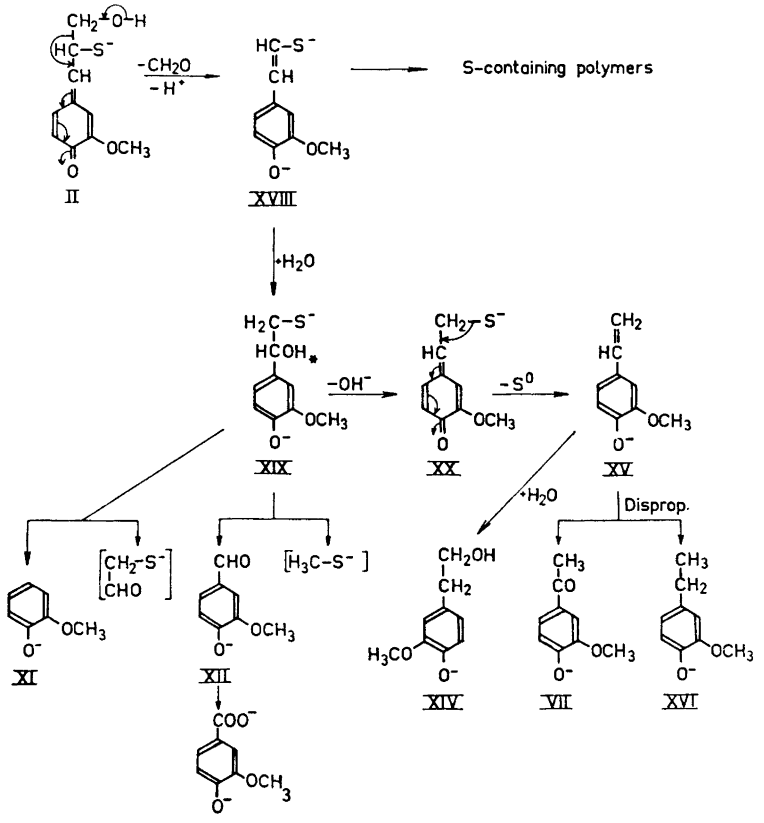

Scheme 2.

carrying an electron-attracting substituent, such as an aroxyl [23], an aryl [24,25] or a thiol group (see Scheme 2) in the β-position. However, in spite of the general character of this elimination reaction, only traces of formaldehyde were occasionally detected in the sulphate spent liquors from model compounds. This is probably due to the immediate consumption of formaldehyde in various condensation reactions, particularly with phenolic nuclei [3] ("Lederer-Manasse reactions"), self-condensation [26] and disproportionation (Cannizzaro) reactions.[26]

The *second type* of elimination reaction exhibited by intermediate II also leads to the liberation of formaldehyde (see Scheme 2). The resulting styrene-β-thiol (XVIII) may in part polymerise yielding a sulphur-containing high molecular weight polymer. The other part may add the elements of water to give the α-hydroxy-β-thiol XIX. The latter intermediate can be expected to undergo analogous types of fragmentation as intermediate IX yielding guaiacol, vanillin and the appropriate aliphatic fragments (thiols). Another possible reaction path leads *via* methylene quinone XX to 4-vinylguaiacol (XV), in analogy to the desulphurisation of II (see Scheme 1). 4-Vinylguaiacol may add the elements of water to give XIV or disproportionate to yield VII and XVI in analogy to the corresponding reactions of coniferyl alcohol (IV). Thus, compounds VII, XI, XII, XIV – XVI and vanillic acid may have been formed *via* routes outlined in both Schemes 1 and 2.

Further support for the validity of Scheme 2 was obtained by treating an authentic sample of the proposed intermediate XIX with 2 N sodium hydroxide at 180° for 2 h and identifying the expected compounds (VII, XI, XII, XIV – XVI and vanillic acid) (see Table 2).

The reliability of the above results was verified by treating milled wood lignin with white liquor or 2 N sodium hydroxide under pulping conditions. The resulting mixtures of degradation products contained essentially the same monomeric and aliphatic compounds as were obtained from episulphide I and from coniferyl alcohol (IV) (see Table 2).[27] This result further confirms the validity of Schemes 1 and 2 and previous suppositions in this series on the mechanism of lignin degradation during sulphate pulping. The fact that the same phenolic and aliphatic products are formed on treatment of milled wood lignin with white liquor and with sodium hydroxide indicates that the degradation with the latter cooking liquor may also proceed to a certain extent *via* intermediates of the coniferyl alcohol type.

The secondary condensation and polymerisation reactions of the intermediary conjugated structures of the types IV and XV during alkali and sulphate pulping are currently being studied.

EXPERIMENTAL

Melting points are corrected. Evaporations were carried out under reduced pressure.

Thin-layer (TLC) and column chromatography. For thin-layer chromatography silica gel HF_{254} (E. Merck A.G., Darmstadt) was used as adsorbant and mixtures of petroleum ether-ethyl acetate in suitable ratios as solvent systems. The spots were developed by spraying with a 1 % solution of vanillin in conc. sulphuric acid and heating at 120° for about 10 min. The preparative separations were carried out by column chromatography using silicic acid (SilicAR CG-7 100 – 200 mesh, Mallinckrodt) as adsorbant and mixtures

Table 2. Products separated by column and/or gas chromatography and identified by mass spectrometry.

Starting compound (cooking liquor)	Guaiacol (XI)	Vanillin (XII)	Aceto-guaiacone (VII)	Propio-guaiacone (VIII)	Dihydro-coniferyl alcohol (V)	4-Ethyl guaiacol (XVI)	4-Vinyl guaiacol (XV)	4-(2-Hydroxy-ethyl)-guaiacol (XIV)	Iso-eugenol (XVII)	Methanol	Ethanol
Episulphide I (NaOH)	+	+	+	+	+	+	+	+		+	+
Coniferylalcohol (NaOH)	+	+	+		+	+	+	+		+	+
Coniferylalcohol (white liquor)	+	+	+	+	+	+	+	+	+	+	+
β-Hydroxy-propio-guaiacone (VI) (NaOH)			+	+							
4-(1,3-Dihydroxy-propyl)-guaiacol (IX) (NaOH)	+	+	+		+	+	+	+		+	+
4-Vinyl-guaiacol (XV) (NaOH)			+			+		+			
4-(1-Hydroxy-2-mercapto-ethyl)-guaiacol (XIX) (NaOH)	+	+	+			+	+	+		+	+
Milled wood lignin (NaOH)	+	+	+	+	+	+	+	+		+	+
Milled wood lignin (white liquor)	+	+	+	+	+	+	+	+	+	+	+

of ethyl acetate-petroleum ether in appropriate ratios as solvents. The elutions were followed by TLC.

Gas chromatography and mass spectrometry. The gas chromatographic separations were carried out with a Perkin-Elmer model 270 instrument (combination with a mass spectrometer). Column dimensions: 150 × 0.1 cm i.d. Column: 3 % silicon OV-1 Gaschrom. Q. washed with conc. hydrochloric acid and treated with dimethyldichlorosilane. Injection temperature: 180°. Detector: flame ionisation, 280°. Carrier gas: N_2 20 ml/min. The mass spectra were recorded at 70 eV.

Model and reference compounds. The compounds used in this study were prepared as previously described (I,[2] III,[2] IV,[28] V,[29] VI,[30] VIII,[31] IX,[32] XIII,[33] XIV,[34] XV,[29,35] XVI [34]). Compound XIX was synthesised as follows:

α-Thioacetoxy-4-acetoxy-3-methoxy-acetophenone. 4-Acetoxy-3-methoxy-α-bromo-acetophenone [36] (9.34 g) was treated with potassium thioacetate (7.43 g) in dimethylformamide (100 ml) at room temperature for 5 h. The reaction mixture was poured into water and extracted with chloroform. The chloroform extract was washed with water (10 times) and dried with sodium sulphate. Evaporation of the solvent gave a slightly yellowish oil (8.75 g, 95.7 %) which crystallised in the refrigerator after some days. Recrystallisation from chloroform-hexane or from isopropyl ether (twice) yielded colourless crystals (4.0 g, 43.5 %), m.p. 70.5 – 71.5°. (Found: C 55.83; H 5.28; O 28.07; S 12.07. $C_{13}H_{14}O_5S$ requires: C 55.30; H 5.00; O 28.34; S 11.36).

1-Hydroxy-1-(4-hydroxy-3-methoxy-phenyl)-ethane-2-thiol (XIX). α-Thioacetoxy-4-acetoxy-3-methoxy-acetophenone (3.50 g) was dissolved in dry ethyl ether (150 ml). The solution was added dropwise to a solution of lithium aluminium hydride (0.80 g) in the same solvent (100 ml). The reaction mixture was kept in an ice-bath until all starting material had been added and then at room temperature for another 2 h. The usual working-up procedure gave a yellowish oil (2.65 g, 98.4 %) which was purified by preparative thin-layer chromatography on silica gel HF_{254} using chloroform as solvent. The pure compound XIX, a colourless oil, turned yellowish on standing at room temperature. (Found: S 15.05. $C_9H_{12}O_3S$ requires: S 16.01.) It was identified by NMR and IR spectra and by conversion into its triacetate.

1-Acetoxy-1-(4-acetoxy-3-methoxy-phenyl)-2-thioacetyl-ethane (triacetate of XIX) was obtained by acetylation of XIX with acetic anhydride-pyridine. The compound was identified by NMR and mass spectra.

The remaining reference compounds were commercially available.

Cooking liquors. Sodium hydroxide (2 N) and "white liquor" were used as cooking liquors.

Treatment of model compounds with cooking liquors and working-up procedure

The treatment of the model compounds (0.1 – 1.0 g) with the cooking liquors was carried out at 180° for 2 h in an atmosphere of nitrogen. The resulting reaction mixtures were worked up in the following way:

After neutralisation with dry ice the mixture was extracted with ethyl acetate. The ethyl acetate layer was washed with water, dried (Na_2SO_4) and evaporated, and the residue was acetylated with acetic anhydride-pyridine.

The acetates were separated into several fractions by column and/or preparative thin-layer chromatography and the fractions were analysed by gas liquid chromatography combined with mass spectroscopy. The identifications were based on the retention times and on the mass spectral fragmentation patterns (comparison with the corresponding data of authentic samples). Fractions containing unsatisfactorily separated mixtures of acetylated degradation products were subjected to further separation(s) by column or thin-layer chromatography until the main components of the fractions obtained could be unambiguously identified using the above mentioned method.

Thus, many of the degradation products given in the general part (see Schemes 1 and 2) were found in several fractions. In this work no attempt was made to determine the proportions of the various monomeric reaction products. Their total amount varied between about 33 and 38 % calculated on the amount of starting material.

The formation of methanol and ethanol was demonstrated in separate runs. The sample (250 or 500 mg) was treated with cooking liquor (10 or 20 ml) in the usual way. Before opening, the autoclave was cooled first in a freeze box and then in powdered dry ice. The uppermost layer of the resulting solid mass was transferred into a 2 ml volumetric flask which was closed with a membrane. After heating the flask at 70° for about 30 min a sample of the gaseous content was withdrawn with a syringe and injected into the gas chromatograph. The chromatographic separation was performed using a Porapak Q column at 130°. The alcohols were identified by comparison of their retention times with those of authentic samples and of mixtures with authentic samples.

The formation of vanillic acid and homovanillic acid was demonstrated separately using an ion pair methylation method.[37] An aliquot of the reaction mixture was withdrawn and concentrated until a humid solid mass was obtained. Methylene chloride (2 ml) and tetrabutylammonium hydrogen sulphate (> 1.1 equiv.) were added and the mixture was triturated with ether (3 times) with ultrasonic agitation. After 20 min methyl iodide (1 ml > 4 equiv.) was added, the shaking was continued for another 10 min and then the mixture was refluxed for 1 h on a steam bath. Careful evaporation of the bulk of methylene chloride gave a residue which was exhaustively extracted with ether. Filtration through a small column (4 × 10 mm) of alumina yielded a solution of the mixture of methylated compounds which was investigated by GLC using an OV-1 column. In addition to the methyl esters of vanillic acid and homovanillic acid the presence of several other methylation products was indicated [27] but these products have not been included in the schemes.

Treatment of milled wood lignin with cooking liquors and working-up procedure

Milled wood lignin [38] (500 mg) was similarly treated with white liquor and sodium hydroxide. The resulting mixtures were worked up in the same way and the mixtures of acetates and methylation products obtained were analysed as mentioned above. The results are given in Table 2.

Demonstration of the formation of coniferyl alcohol (IV)

(a) *By mild alkaline treatment of episulphide I.* A mixture of dioxan (3 ml) and 0.01 N sodium hydroxide (3 ml) was saturated with nitrogen at 90°. Episulphide I in the form of its diacetate (60 mg) was added at the same temperature and allowed to react for 4 h. The resulting mixture was acetylated and investigated by TLC [benzene (75 %)-ethyl-acetate (15 %), run three times]. The diacetate of IV was shown to be the main component in the mixture which also contained some diacetate of the starting material (I).

(b) *By simple heat treatment of the diacetate of episulphide I.* The elimination of sulphur from the diacetate of episulphide I was brought about by heating a sample (60 mg) without any solvent to 90° for 4 h. The diacetate of IV was isolated by column chromatography as a colourless oil (yield 70 %) and identified by TLC and NMR (comparison with authentic diacetate of IV).

Determination of S^0

Granulated copper was treated with boiling conc. hydrochloric acid, carefully washed with water, activated with conc. nitric acid (vigorous stirring) and again washed with water. The activated copper was immediately transferred to a glove-box filled with argon (careful exclusion of air). Glass ampoules were charged with the compound (50 – 100 mg), copper (25 g), and cooking liquor (5 ml) and temporarily closed by stoppers. During the sealing argon was passed into the ampoules. The latter were then treated as described in Refs. 11 and 12. After cooling, the ampoules were opened and their content was added to water. The CuS-containing copper was treated with conc. hydrochloric acid (200 ml) at 90° until all hydrogen sulphide had been released. The latter was passed into a receiver

and reacted with a solution (30 ml) of $CdSO_4$ (89.25 g $CdSO_4.8H_2O$) in conc. ammonia (650 ml, diluted with water 1:1). When the evolution of hydrogen sulphide had ceased, nitrogen was passed through the apparatus to assure complete removal of hydrogen sulphide from the reaction vessel and absorption in the receiver. Conc. hydrochloric acid (45 ml) and 0.1 N iodine solution (25 ml) were added to the suspension in the receiver to dissolve the precipitate. The resulting solution was titrated with 0.1 N sodium thiosulphate.

The determination of elemental sulphur eliminated from episulphide I under milder conditions was carried out using an improved method: The diacetate of compound I (170 mg), together with pyrogallol (200 mg) and purified copper (50 g), was treated with 1 N sodium hydroxide (20 ml) at 100° for 1 h in a nitrogen atmosphere using a three-necked, round-bottomed flask, equipped with a reflux condenser and nitrogen inlet and outlet tubes. The liberation of hydrogen sulphide from the CuS-containing copper and the iodometric titration were carried out as described above (Found: elemental sulphur eliminated 18.30 mg (99.5 % of the theoretical yield.) A sample of 2,3-dimercaptopropanol (200 mg), when treated in a similar way gave off only 1.0 mg elemental sulphur (1.0 % of the theoretical yield).

Acknowledgement. The authors are indebted to "*1959 års fond*" for financial support.

REFERENCES

1. Gierer, J. and Smedman, L.-Å. *Acta Chem. Scand.* **19** (1965) 1103.
2. Gierer, J. and Smedman, L.-Å. *Acta Chem. Scand.* **20** (1966) 1769.
3. Gierer, J. *Svensk Papperstidn.* **71** (1970) 571.
4. Leopold, B. *Acta Chem. Scand.* **6** (1952) 38; *Svensk Kem. Tidskr.* **64** (1952) 18.
5. Freudenberg, K. In Freudenberg, K. and Neish, A. C. *Constitution and Biosynthesis of Lignin*, Springer Verlag, Berlin-Heidelberg-New York 1968, p. 45.
6. Adler, E. *Svensk Kem. Tidskr.* **80** (1968) 279.
7. Staudinger, H. and Siegwart, J. *Helv. chim. Acta* **3** (1920) 840.
8a. Reid, E. E. *Organic Chemistry of Bivalent Sulfur*, Chemical Publishing Co, New York 1960, Vol. 3, p. 19, 167.
b. Schönberg, A. and v. Vargha, L. *Ber.* **64** (1931) 1390.
c. Campaigne, E. In Patai, S. *The Chemistry of the Carbonyl Group*, Interscience, London-New York-Sydney 1966, p. 938.
9. Ref. 8a., p. 116.
10. Schönberg, A. and Nickel, S. *Ber.* **64** (1931) 2323.
11. Teder, A. *Svensk Papperstidn.* **70** (1969) 294.
12. Ahlgren, P. and Hartler, N. *Svensk Kem. Tidskr.* **78** (1966) 404.
13. Brunow, G. and Miksche, G. E. *Acta Chem. Scand.* **23** (1969) 1444.
14. Brunow, G., Ilus, T. and Miksche, G. E. *Acta Chem. Scand.* **26** (1972) 1117.
15. Brunow, G. and Miksche, G. E. *Acta Chem. Scand.* **26** (1972) 1123.
16. Shemyakin, M. M. and Shchukina, L. A. *Quart. Rev. Chem. Soc.* **10** (1956) 261.
17. Salomaa, P. In Patai, S. *The Chemistry of the Carbonyl Group*, Interscience, London – New York – Sydney 1966, p. 197.
18. Enkvist, T., Åshorn, T. and Hästbacka, K. *Paper and Timber* (Finland) **44** (1962) 395.
19. Turunen, J. *Comment. Phys. Math.* **28** (1963) No. 9; Enkvist, T. and Turunen, J. *Chim. Biochem. Lignin, Cellulose, Hemicellulose*, Grenoble 1964, p. 177.
20. Gierer, J. Pettersson, I. and Smedman, L.-Å. *Acta Chem. Scand.* **26** (1972). 3366.
21. Gierer, J. and Opara, A. E. *Unpublished work.*
22. Wilson, D. F. and Hrutfiord, B. F. *Tappi* **54** (1971) 1094.
23. Gierer, J. and Norén, I. *Acta Chem. Scand.* **16** (1962) 1713.
24. Adler, E., Marton, J. and Falkehag, S. I. *Acta Chem. Scand.* **18** (1964) 1311.
25. Nimz, H. *Chem. Ber.* **98** (1965) 3160.
26. Marton, J., Marton, T., Falkehag, S. I., and Adler, E. *Advan. Chem. Ser.* **59** (1966) 125.
27. Gierer, J. and Pettersson, I. *Unpublished work.*
28. Freudenberg, K. and Hübner, H. H. *Chem. Ber.* **85** (1952) 1181.

29. Coscia, C. J., Schubert, W. J. and Nord, F. F. *J. Org. Chem.* **26** (1961) 5085.
30. Fisher, H. E. and Hibbert, H. *J. Am. Chem. Soc.* **69** (1947) 1208.
31. Belg. Pat. 614,525 Aug. 28, 1962, U.S. Appl., March 1, 1961, Mead Johnson and Co., *Chem. Abstr.* **59** (1963) 512d.
32. Kratzl, K. and Miksche, G. E. *Monatsh.* **94** (1963) 530.
33. Muszynski, E. *Acta Pol. Pharm.* **18** (1961) 471; *Chem. Abstr.* **58** (1963) 3334h.
34. Arlt, H. G., Gross, S. K. and Schuerch, C. *Tappi* **41** (1958) 64.
35. Hachihama, Y. and Shono, T. *Chem. Abstr.* **56** (1962) 10380 f.
36. Erdtman, H. and Leopold, B. *Acta Chem. Scand.* **3** (1949) 1358.
37. Strömberg, S. *Personal communication.*
38. Björkman, A. *Svensk Papperstidn.* **59** (1956) 477.

Received January 31, 1973.

ACTA CHEMICA SCANDINAVICA 27 (1973) 2095–2106

Bromination and Thiocyanation of 4-Cyano-2-methyl-1,3,6-triazacycl[3.3.3]azine under Photochemical Conditions

OLOF CEDER and MARIE LOUISE SAMUELSSON

Department of Organic Chemistry, University of Göteborg and Chalmers Institute of Technology, Fack, S-402 20 Göteborg 5, Sweden

The bromination and thiocyanation of 4-cyano-2-methyl-1,3,6-triazacycl[3.3.3]azine, *1a*, with free bromine and with thiocyanogen in the presence of light, results in ring as well as in side-chain substitution. The structures of eight brominated compounds, *5–12*, and of three thiocyanocyclazines, *16–18*, are reported. In chlorinated solvents the bromination yields mixtures of chlorinated and brominated compounds. The photochemical displacement of chlorine for bromine is briefly discussed.

We have recently described the electrophilic bromination of 4-cyano-2-methyl-1,3,6-triazacycl[3.3.3]azine, *1a*, with *N*-bromosuccinimide in chloroform and with bromine in glacial acetic acid, in both cases in the absence of light and peroxides.[1]

In agreement with results from HMO calculations [2] (performed on *1b*) the electrophilic substitution in *1a* occurred exclusively in positions 7 and 9. Free-valence values estimated by the same method [2] suggested that free-radical attack would be preferred in the same positions and also at C-5 (*cf.* Fig. 1).

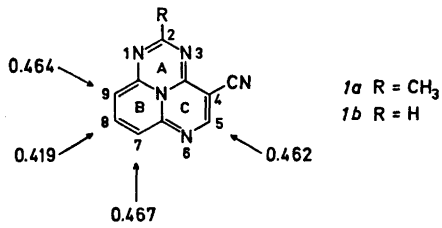

Fig. 1. Free-valence values at positions 5, 7, 8, and 9 in *1b*.

The first part of the present communication describes the isolation and structural assignment of eight bromine-containing compounds formed when a solution of the easily prepared cyclazine *1a* [2] was treated with free bromine

under the influence of light from a medium pressure mercury arc (Hanau Q-81). The rate of the dark reaction under the conditions used in this investigation is considerable and all compounds described are probably not formed exclusively by a free-radical path. This point will be elaborated later in the present paper.

The following compounds substituted in the ring (*2–4*), in the side-chain (*5–6*), or in both (*7–11*) were isolated.

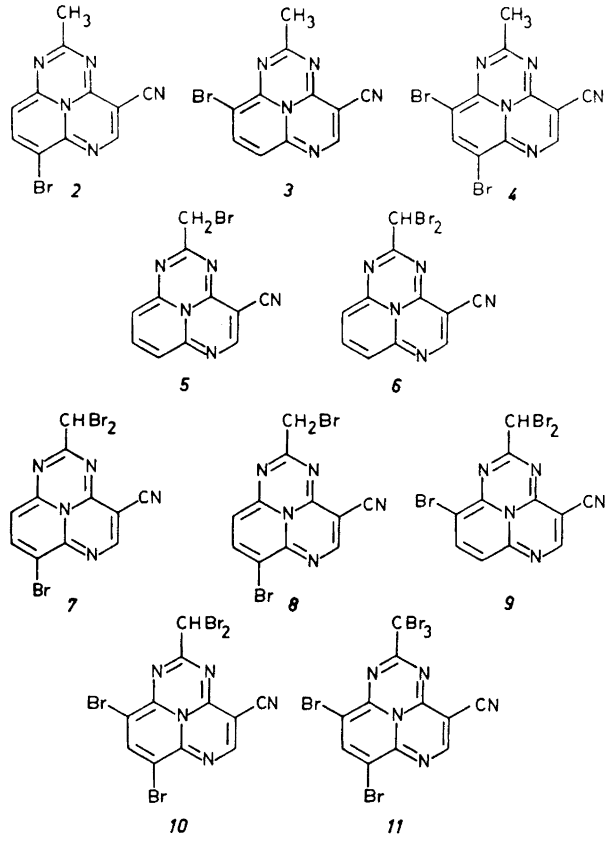

The structures of the new compounds (*5–11*) were supported by mass-spectral, infrared, ultraviolet, and, where sufficient amounts were available, by NMR data. The details are to be found in the Experimental section. In some cases, where the substitution pattern could not be unambiguously determined from the spectra of the compounds, the structures were derived by synthesis from a derivative with an already secured structure. These correlations are outlined in Chart 1.

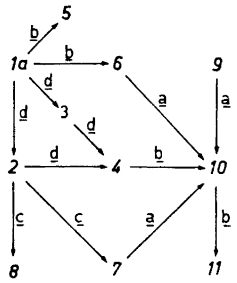

Chart 1. Reagents: *a* Br_2 in $CHCl_3$ or CCl_4; *b* Br_2 in $CHCl_3$ or CCl_4, *hν*; *c* NBS in "non-purified" $CHCl_3$; (*cf.* the Experimental section); *d* NBS in $CHCl_3$.[1]

The number of bromine atoms in a molecule was immediately determined from the element profile in the molecular-ion region, showing doublets (intensities 1:1), triplets (1:2:1), quartets (1:3:3), quintets (1:4:6:4:1), and sextets (1:5:10:10:5:1) for mono-, di-, tri-, tetra-, and pentasubstituted derivatives, respectively.[3]

All the brominated compounds have, like *1a*, high melting points (*2 – 11* melt above 350°). Their solubilities and chromatographic mobilities are rather similar to those of *1a*.

The electronic spectra of the brominated compounds show the pattern typical of a 1,3,6-triazacycl[3.3.3]azine with about seven high-intensity absorption maxima between 220 and 400 nm and low-intensity bands at 450 – 700 nm (*cf.* the Experimental section). Compounds with bromine in the side-chain are blue to violet in the solid state and in solution; compounds with bromine in the aromatic positions are green in the solid state but blue in solution; finally, compounds brominated both in the methyl group and in the ring are green both in the solid state and in solution.

The IR spectra of compounds *2 – 11* all show the strong absorption band characteristic of the cyano group (2210 – 2230 cm^{-1}).

The mass spectra of *5 – 11* are characterized by successive losses of bromine atoms (*cf.* Ref. 1, p. 631), eventually leading to bromine-free fragments, whose fragmentation patterns are very similar to those obtained from *1a – 4*.[1,4] The spectrum of *5* with assignments of fragment structures and proposed modes of fragmentation, supported by metastable ion peaks, is illustrated in Fig. 2.

In the mass spectra of *2* and *3*,[1] one atom of bromine is lost from the molecular ion and the resulting fragment then loses CH_3CN, which is supported by a metastable ion at $m/e = 135.2$. This type of fragmentation is observed for *N*-heteroaromatic systems with a methyl group on the adjacent ring-carbon atom.* In the mass spectrum of *5*, however, this metastable ion is found at $m/e = 135.6$, corresponding to a loss of CH_2CN, which indicates that the bromine atom in *5* was originally located in the side chain.

The NMR-spectra of *6 – 11* are easily interpreted, and the chemical shift values and coupling constants are summarized in Table 1.

* see Ref. 4, p. 614 and further references therein.

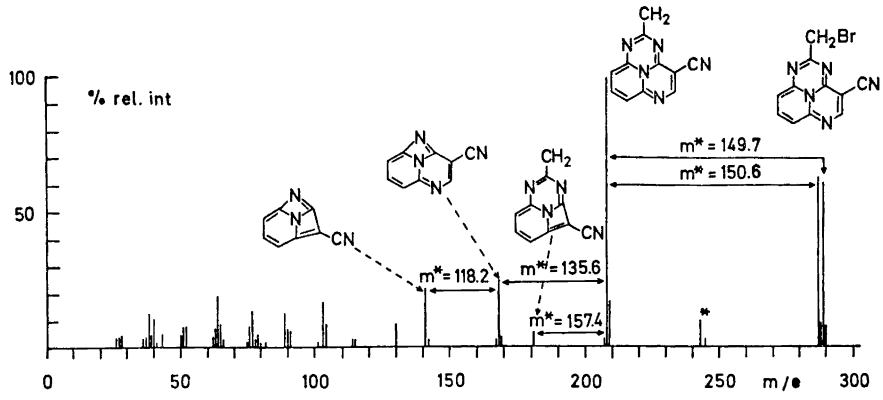

Fig. 2. Mass spectrum of *5*. The sample contained *ca.* 10 % of $C_{11}H_6N_3Cl$.

Table 1. NMR spectral data (δ-values and coupling constants) for compounds *6*–*11* (solvent: trifluoroacetic acid).

Compound	Side-chain protons	H-5	H-7	H-8	H-9	J_{7-8} (Hz)	J_{8-9} (Hz)	J_{7-9} (Hz)
6	6.12	7.83	7.12 or 7.04	8.08	7.04 or 7.12	7.5 or 8.8	8.8 or 7.5	0.9
7	6.07	7.84	–	8.20	7.04	–	9.0	–
8	4.07	7.93	–	8.17	6.95	–	9.0	–
9	6.09	7.77	6.88	8.19	–	9.0	–	–
10	6.13	7.85	–	8.45	–	–	–	–
11	–	7.86	–	8.52	–	–	–	–

Solutions of *1a* in carbon tetrachloride, chloroform, and methylene chloride were used for the photochemical brominations. The following solvents were also tried but found unsuitable: hydrocarbons like hexane (low solubility of *1a* and generation of HBr leading to the formation of insoluble cyclazine hydrobromides), methanol (formation of methoxy derivatives), and ethyl acetate (destruction of the cyclazine system). In all these three solvents, however, low yields of compounds *2*–*11* were obtained.

The composition of the reaction mixtures varied depending on the solvent, as well as on the irradiation time. In chloroform, aromatic substitution dominated in the beginning of the irradiation period with initial formation of *2*, *3*, and *4*. In carbon tetrachloride, *5* and *6* were formed after a short induction period (*ca.* 15 min) together with small amounts of *2* and *3*. After longer irradiation times (in chloroform, carbon tetrachloride and mixtures thereof) *7*, *9*, *10*, and *11* were formed, *10* being the major product.

Bromination of *1a* with NBS or bromine in the absence of radical promoters gave exclusively substitution in the aromatic ring.[1] Under the conditions used in the present investigation it was found, however, that after a longer period

(several months), *10* and *11* could sometimes be obtained from the dark reaction in fairly good yields.

The marked acceleration of the side-chain substitution under the influence of light and the induction period observed for the formation of *5* and *6*, clearly demonstrate that a free-radical mechanism is operating. The description of the reaction path for the aromatic substitution is not equally simple. Attempts were made to find conditions under which no "dark bromination" would occur (in methylene chloride at $-80°$ and in carbon tetrachloride at $-15°$), but *2*, *3*, and *4* were always detected. Irradiation of *1a* in carbon tetrachloride at $-15°$ gave the same products and, in addition, *5*, which is monobrominated in the side chain. A small increase in the yield of products substituted in the ring was observed when the reaction mixture was irradiated. Under the conditions used in this investigation, however, it has not been possible to separate homolytic and heterolytic aromatic substitution.

A compound formed in low yield in the photochemical bromination reaction of *1a* was shown by spectrometric methods (IR, MS, *cf.* the Experimental section) to be the amide *12*. The same compound was also obtained from

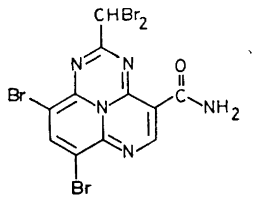

12

irradiation of *10*; therefore the positions of the bromine atoms in the proposed structure seem to be correct. It is possible that this represents a photochemical conversion of a nitrile to an amide, but we are not aware of any other cases of the same type. Attempts to achieve the same reaction by irradiation of *10* in a chloroform solution containing dilute hydrochloric acid were, however, unsuccessful.

When the monobromo compound *3* was irradiated in a bromine-containing chloroform solution, *3* was completely converted to two chlorinated compounds.* For these we propose structures *13* and *14*, since their mass spectro-

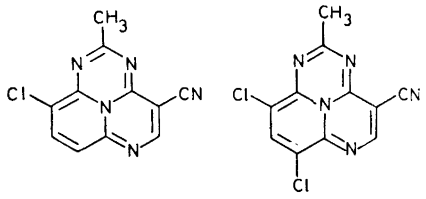

13 *14*

* A compound containing one chlorine and one bromine atom was also formed, though in very low yield (less than 1 % of the yield of *14*, as estimated from the mass spectrum).

metrical fragmentation patterns are analogous with those of the corresponding bromine derivatives *3* and *4*.[1] When the 7-bromo isomer *2* was irradiated under the above-mentioned conditions, *14* was formed, plus a compound very similar to *13* (TLC), which we believe is the 7-chloro isomer *15*. In addition, partly chlorinated compounds were observed as impurities (MS) in the brominated analogues, when these were formed in chlorinated solvents.

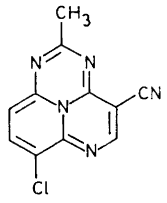

15

Similar observations for the system bromobenzene-chlorine were originally reported by Eibner [5] and the same reaction was later studied by Miller and Walling [6] and by Milligan *et al.*[7] In their studies free chlorine (dissolved in carbon tetrachloride) was present, and in the mechanism proposed the chlorine atom is attached to the aromatic ring *via* a π-complex type of bond. To our knowledge no reports on similar photochemical aromatic halogen exchange in chloroform or carbon tetrachloride solutions in the absence of added chlorine have appeared. It is not unlikely, however, that sufficient amounts of free chlorine (or bromine chloride) are formed during the irradiation to cause a halogen exchange in compounds substituted with bromine in the aromatic nucleus.

Arylalkyl hydrocarbons have been successfully thiocyanated with thiocyanogen in light-induced reactions [8] giving products substituted exclusively in the side-chain. The mechanism has been depicted [8] as a photo-initiated, radical chain reaction:

$$(SCN)_2 \rightarrow 2\,SCN$$

$$\cdot SCN + ArCHRR \rightarrow HSCN + Ar-\overset{\displaystyle R}{\underset{\displaystyle R}{\overset{|}{\underset{|}{C}}}}\cdot$$

$$Ar-\overset{\displaystyle R}{\underset{\displaystyle R}{\overset{|}{\underset{|}{C}}}}\cdot + (SCN)_2 \rightarrow Ar-\overset{\displaystyle R}{\underset{\displaystyle R}{\overset{|}{\underset{|}{C}}}}-SCN + \cdot SCN$$

With *1a* as substrate a similar reaction with thiocyanogen occurred in the presence of light, and a low yield of *16* was isolated. Compound *16* was the only product obtained in detectable amounts from photolysis in benzene, but in chlorinated solvents (methylene chloride, chloroform, and carbon tetrachloride) products substituted in the aromatic nucleus were also formed. Two of these, *17* and *18*, were isolated, but at least five other products, probably thiocyanated or isothiocyanated in the ring and/or in the side chain, were

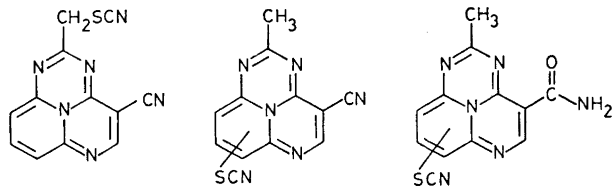

16 *17* *18*

detected. Compounds *16*–*18* were characterized by spectrometrical methods and by comparison with spectra for the corresponding bromo compound.

The side-chain substituted compound *16* was easily identified from its mass spectrum by a reasoning analogous with that used for compound *5* above. For *17* and *18*, the exact positions of the thiocyanate groups could not be determined, but *17* and *18* must be substituted in the *B*-ring, since the substituents can be placed neither at the methyl carbon (loss of CH_3CN in the mass spectra) nor at position 5 (loss of HCN from the *C*-ring). The mass spectrum of *18* differs from the spectra of *16* and *17*, since loss of CO as well as of S is observed here.

The UV spectra of compounds *16*, *17*, and *18* show the typical pattern with six to seven high-intensity bands at 500–220 nm and low-intensity peaks at 700–500 nm (*cf.* Table 2). Characteristic peaks in the infrared region are presented in the Experimental section.

Table 2. Electronic spectral data for *5*–*7*, *9*–*12*, and *16*–*18*.

	nm ($\varepsilon \times 10^{-4}$)						
5	388 (0.82)	371 (0.92)	354s(0.74)	335 (1.09)	271 (1.35)	237 (1.39)	216s(1.13)
6	389 (1.55)	380 (1.48)	372 (1.71)	355 (1.41)	338 (1.94)	272 (2.62)	236 (2.38)
7	397 (1.03)	388s(1.10)	378 (1.27)	346 (2.01)	282 (2.13)	241 (1.82)	222 (1.99)
9	398 (1.14)	381 (1.28)	363 (1.05)	345 (1.48)	285 (1.54)	234 (2.03)	224 (2.03)
10	404 (1.18)	398s(1.22)	387 (1.44)	353 (2.24)	292 (2.10)	243s(1.92)	231 (2.20)
11	398s(1.35)	385s(1.60)	370s(1.82)	354 (2.21)	293 (2.36)	242s(2.41)	227 (2.93)
12	400 (1.56)	382 (1.86)	360s(1.97)	346 (2.41)	285 (2.30)	241 (2.91)	224 (2.78)
16	390 (0.75)	372 (0.80)	356 (0.67)	333 (0.94)	269 (1.05)	234 (1.62)	
17	402s(0.75)	387 (0.80)	363s(1.17)	346 (1.68)	293 (0.69)	287 (0.67)	239 (1.90)
18	383 (0.40)	342 (0.44)	327 (0.58)	383 (0.52)	277s(0.50)	228 (1.40)	
	nm (ε).						
5	662s(111)	610 (260)	575 (277)	535s(190)			
6	670s(145)	621 (367)	578 (412)	544s(296)	455 (87)		
7	696s(205)	641 (413)	595 (401)	558s(257)	474 (45)		
9	698s(140)	645 (342)	596 (342)	554s(205)			
10	720 (155)	662 (406)	611 (302)	568s(157)			
11	719 (272)	660 (491)	614 (695)	575s(462)	512 (226)	479 (83)	
12	690s(268)	636 (532)	600 (501)	497 (338)	467 (359)		
16	642 (1400)	602 (2384)	572 (2400)	526s(895)			
17	665 (864)	614 (1183)	580s(895)				
18	550 (1323)	519 (1195)	483s(770)				

EXPERIMENTAL

General. The NMR spectra have been measured in trifluoroacetic acid with tetramethyl silane as internal reference using a Varian Model A-60 spectrometer. Mass spectra were recorded with a GEC–AEI 902 mass spectrometer at the Department of Medical Biochemistry, University of Göteborg. The IR spectra were determined in KBr with a Beckman IR 9 spectrophotometer or with a Perkin-Elmer 337 infrared spectrophotometer, and the UV and visible spectra in absolute ethanol with a Cary Model 15 spectrophotometer. For column chromatography, silica gel (0.02 – 0.5 mm) was used, and for TLC, Silica Gel GF_{254} (Merck) according to Stahl. The irradiations were carried out with a medium-pressure mercury arc (Hanau Q-81) placed in a quartz container cooled with water. The solution in the reaction vessel was magnetically stirred, and a stream of nitrogen was bubbled through the solution.

Methylene chloride, chloroform, and carbon tetrachloride used in the photochemical reactions were distilled and passed over aluminium oxide, if not otherwise stated. 4-Cyano-2-methyl-1,3,6-triazacycl[3.3.3]azine was prepared as described in Ref.2.

General bromination procedure

The conditions chosen for the photochemical bromination reactions varied slightly, but in general the following procedure was used. A solution (1 – 5 mM) of *1a* in carbon tetrachloride and/or chloroform was irradiated with ultraviolet light. The irradiation time varied from one to several hours, and the composition of the reaction mixture was followed by TLC. Before this analysis could be performed, the reaction solution, in which the products were present as cyclazine hydrobromides, was evaporated to dryness. An ethanol solution of the residue was stirred with the weakly basic ion-exchange resin Amberlite IR-4B (OH form). The mixture of the free bases of the bromocyclazines was then separated by chromatography (column or TLC).

Bromination of *1a*

Under "dark" conditions; (a) with excess of bromine. The dark-blue solution of 150 mg (0.72 mmol) of *1a* in 50 ml of chloroform was mixed with a solution of 300 mg (1.87 mmol) of bromine in 50 ml of chloroform. A red precipitate was immediately formed, and after a few minutes the solution became colourless. Three products, *2*, *3*, and *4*, had been formed; they were identified by comparison with authentic samples (TLC).

(b) At low temperatures with bromine. (i) In methylene chloride at −80°. A solution of 6 mg of *1a* in 50 ml of methylene chloride was cooled to −80° and 5 ml of methylene chloride, containing 1 drop of bromine, was slowly added. After 10 min, *2* and *3* had formed and after 1 h, *4* was also detected (TLC). (ii) In carbon tetrachloride at −15°. A solution containing 7 mg of *1a* and 1 drop of bromine in 100 ml of carbon tetrachloride was left at −15° for 1 h. Small amounts of *2* – *4* could be detected by TLC.

Under photochemical conditions; (a) with excess of bromine. A solution of 140 mg (0.67 mmol) of *1a* and 400 mg (2.5 mmol) of bromine in 100 ml of carbon tetrachloride reacted as described under (a) above. This heterogeneous mixture was irradiated for 17 h. The red precipitate of hydrobromides, treated as described above, and the green-violet solution were investigated by TLC. About half a dozen compounds were detected, among them *7* and *10*, identified by TLC.

(b) With continuously added bromine. To avoid extensive electrophilic bromination by having excess of halogen present, the bromine was introduced continuously over the entire period in the following way. A thin stream of nitrogen was passed through a gas-washing bottle containing bromine, and the mixture of nitrogen and bromine was bubbled *via* a gas-inlet tube through the solution of *1a*. This procedure resulted in lower initial yields of *2*, *3*, and *4* (substituted in the *B*-ring). (i) In carbon tetrachloride. A solution of 200 mg of *1a* in 500 ml of carbon tetrachloride was brominated with *ca.* 0.5 ml of bromine as just described. After 5 h, when the starting material was almost consumed (TLC), the irradiation was interrupted. The reaction mixture, containing a red-green precipitate, was evaporated to dryness under reduced pressure. The residue was then

dissolved in 50 ml of absolute ethanol, and treated over-night with 5 g of IR-4B resin (OH form). After filtration the solvent was evaporated *in vacuo* and the residue chromatographed on 20 g of silica gel, using chloroform-ethyl acetate 10:1 as the eluent. Further purification was performed with TLC. The following compounds were isolated: *5* (10 mg; 3.6 %), *6* (40 mg; 11 %), *7* (main product; *ca.* 30 %), *8* and *9* (30 mg together; 7 %), *10* (20 mg; 4 %), and *12* (5 mg; 1 %).

The above procedure was repeated until enough material was obtained for identification of the compounds by spectroscopic methods. Infrared data for the cyano groups, chromatographic mobilities, and molecular weights (MS) for compounds *5*–*10* are summarized in Table 3.

Compound *12* had infrared absorption at 3340, 3150, and 1650 ($CONH_2$) cm^{-1}. TLC: $R_F = 0.38$ ($CHCl_3$–EtOAc, 6:1). MS: $M^+ = 542.713 \pm 0.011$. Calc. for $C_{11}H_5N_5O^{79}Br_2{}^{81}Br_2$: 542.719.

The NMR data of *6*–*10* are summarized in Table 1 and the electronic spectra of *5*–*12* in Table 2.

Table 3. Infrared, chromatographic, and mass spectral properties of *5*–*10*.

	5	*6*	*7*	*8*	*9*	*10*
–CN (IR)	2220	2220	2210	2220	2220	2215
R_F (TLC)	0.30[a]	0.47[a]	0.37[b]	0.21[b]	0.21[b]	0.57[b]
M^+ (MS)	287–289	365–369	443–449	365–369	443–449	521–529

[a] Eluent EtOAc. [b] Eluent $CHCl_3$–EtOAc, 6:1.

(ii) In chloroform. To a solution of 100 mg of *1a* in 100 ml of chloroform, 2 ml of bromine was added continuously, as described above, during irradiation for 4 h. After evaporation and ion exchange as described under (i), 214 mg of a bromocyclazine mixture was obtained. Preparative TLC ($CHCl_3$–EtOAc, 6:1) of 5.2 mg of the crude product gave six bands, which were extracted with chloroform. Compounds *4*–*12* were obtained in the following yields, determined from UV-measurements: *4*, 62 %; *4*+*12*, 20 % (mainly *4*); *7*, 6 %; *10*, 8 %. Only very minute amounts of *8* and *9* were formed. No compounds with less than two bromine atoms could be detected (TLC).

In this experiment, the concentration of bromine was considerable, which probably accounts for the high percentage of *4* formed. However, in other experiments in chloroform, the initial yield of *4* was also substantial, but after prolonged irradiation time the amount of *4* decreased and mainly *10* was obtained.

(iii) In mixtures of chloroform and carbon tetrachloride. Over a period of 3.5 h, 1 ml of bromine was bubbled with a stream of nitrogen into a solution of 209 mg of *1a* in 500 ml of a 1:1 mixture of chloroform and carbon tetrachloride. After 1 h, *5* and *6* were detected (TLC) but after 3.5 h, only traces of these compounds could be observed and mainly *7* and *10* were present. After purification by column chromatography 265 mg (54 %) of *10* was isolated.

In a second experiment a solution of 200 mg of *1a* in a mixture of 350 ml of chloroform and 150 ml of carbon tetrachloride was irradiated for 50 min, while 0.5 ml of bromine was continuously added as described above. Only the mono- and dibromosubstituted compounds *2*–*6* were obtained (TLC).

(c) At low temperature with bromine. In an open vessel 7 mg of *1a* in 50 ml of carbon tetrachloride at −15° was irradiated and 3 drops of bromine in 50 ml of carbon tetrachloride was slowly added during the irradiation. After 1 h, the reaction mixture was analyzed by TLC. Three monobromides, *2*, *3*, and *5*, and one dibromide, *4*, were detected (TLC).

Bromination of derivatives of *1a*

Under "dark" conditions; (a) of *6* to *7* and *10* with bromine. A mixture of 5 mg of *6* and 1 drop of bromine in 10 ml of chloroform was stirred for 1 h. Isolation by preparative TLC yielded mainly *10* plus minor amounts of *7* (TLC).

(b) of *7* to *10* with bromine. A solution of 5 mg of *7* and 1 drop of bromine in 25 ml of carbon tetrachloride was stirred in the dark. After 4 h no new products could be detected and all starting material remained unreacted (TLC). After 1 week compound *10* had been formed in about 50 % yield (TLC).

(c) of *9* to *10* with bromine. Compound *9* brominated as described under (b) gave after 3 h *10* in about 50 % yield.

(d) of *2* to *7*, *8*, and *10* with NBS in "non-purified" chloroform.* Refluxing of 9.3 mg of NBS and 10 mg of *2* in 2 ml of chloroform for 30 min gave *7*, *8*, and *10* (TLC).

(e) of *3* to *4* with NBS in "non-purified" chloroform. Compound *3* was treated as described under (d). Only the ring-substituted compound *4* was formed.

Under photochemical conditions; (a) of *10* to *11* and *12* with bromine. To 25 mg of *10* in 50 ml of chloroform, 200 mg of bromine dissolved in 50 ml of chloroform was added and the mixture irradiated for 3.5 h. After evaporation and ion-exchange as described above, *11* and *12* (MS, TLC) were isolated. Separation of unreacted *10* and *11* was performed on a silica gel plate (CH_2Cl_2), developed twice.

Compound *11* was identified as a pentabromide from its mass spectrum. MS: $M^+ = 599-609$ (sextet: relative intensities 1:5:10:10:5:1). IR: 2230 (CN) cm^{-1}. TLC: $R_F = 0.57$ ($CHCl_3$ – EtOAc, 6:1). For NMR and electronic spectra, see Tables 1 and 2, respectively.

A colour change from green to red, observed when the TLC-plates were left in the air for some minutes, was earlier in this investigation attributed to *10*, but was here discovered to come from *11*. Apparently, *11* had been formed in many photochemical experiments described above, but it had been destroyed upon standing on a column of silica gel, or on the TLC-plate. The red conversion product of *11* could not be eluted with chloroform, ethyl acetate, or methanol and its nature has not been investigated.

(b) of *3* to *13* and *14* with bromine. Irradiation for 30 min of 12 mg of *3* and 1 drop of bromine dissolved in 100 ml of chloroform gave two products, which were separated by preparative TLC and identified as *13* and *14* by mass spectrometry. No brominated compounds and no starting material could be detected by TLC.

(c) of *2* to *14* and *15* with bromine. The same procedure was followed as described under (b). All starting material was consumed and *14* (TLC) plus a compound having almost the same R_F-value as *13* (0.24 compared to 0.26 for *13*; EtOAc) were formed. The new compound is supposed to have the structure *15*.

(d) of *4* to *10* with bromine. A solution of 10 mg of *4* and 1 drop of bromine in 100 ml of chloroform was irradiated for 45 min. The following compounds, separated by preparative TLC, were isolated and identified: *10* (MS, TLC), *12* (TLC), one compound with $R_F = 0.50$ ($CHCl_3$-EtOAc, 6:1) and with the molecular formula $C_{11}H_3N_5Br_2Cl_2$ and one with $R_F = 0.54$ and the molecular formula $C_{11}H_3N_5Br_3Cl$ (MS). Minor amounts of a not identified compound ($R_F = 0.40$; $CHCl_3$-EtOAc, 6:1) were also isolated.

Irradiation of *10* in the presence of H_2O/HCl.

In 100 ml of chloroform, containing 0.1 ml 2 M HCl, 39 mg of *10* was dissolved and irradiated for 50 min. No amide, *12*, was formed (TLC). Two products were observed and separated by TLC, but both showed strong infrared absorption at 2220 (CN) cm^{-1}.

General thiocyanation procedure

Thiocyanogen was prepared from bromine and lead thiocyanate as described by Söderbäck.[9] Addition of thiocyanogen in equimolar amounts to a solution of *1a* immediately resulted in the formation of a red precipitate and gradual decolourization of the

* Analytical grade, not passed over Al_2O_3.

blue solution. The solid was shown (by IR, NMR, and elemental analysis) to be the thiocyanate *19*, $C_{11}H_7N_5.(HSCN)_n$; $n \approx 2$.

The formation of *19* probably depends on the formation of HSCN from thiocyanogen and small amounts of water present in the solvents.[10] When these were carefully dried and the thiocyanogen solution, protected from moisture, was added slowly to the reaction mixture in portions, no formation of *19* was observed.

Salt formation between *1a* and HSCN

Addition of 5 mmol of thiocyanogen in 50 ml of carbon tetrachloride to 500 mg (2.4 mmol) of *1a* in 50 ml of carbon tetrachloride immediately led to the precipitation of a red solid. The solution, which initially was strongly coloured, gradually became pale, and after 15 min it was almost colourless. The reaction mixture was filtered, the solid washed repeatedly with chloroform, and the remaining material dried in the air. The red solid was identified as *19*. IR: 2060 (SCN), 2230 (CN), 2300–2800 (broad absorption peak, $-\overset{|}{\underset{|}{N^+}}-H$) cm^{-1}. M.p.: sublimation, accompanied by loss of HSCN, gives a blue material, which melts at 265°(=m.p. of *1a*). NMR ($AsCl_3$): singlet at 2.30 (3 H), multiplet at 7.02 (2 H), triplet at 7.80 (1 H), singlet at 7.98 (1 H), and $-\overset{|}{\underset{|}{N^+}}-H$ at 8.17 (2–3 H). The coupling pattern of *19* is analogous with that observed for *1a*. (Found: S 20.3. Calc. for $C_{13}H_9N_7S_2$: S 19.6).*

Thiocyanation of *1a*

Under photochemical conditions; (a) in carbon tetrachloride. A solution of 0.24 mmol (50 mg) of *1a* in 350 ml of carbon tetrachloride and 0.50 mmol of thiocyanogen in 50 ml of the same solvent (the thiocyanogen solution added dropwise over a period of 1 h) was irradiated for 3 h, after which no starting material remained (TLC). The larger portion of the solvent was evaporated *in vacuo* and the residue was dissolved in methylene chloride and allowed to stand for 2 days (to complete the polymerization of unreacted thiocyanogen).[10] Chromatography on 20 g of silica gel with methylene chloride removed a large amount of yellow impurities, and ethyl acetate eluted a blue-green band, which was further purified by preparative TLC (CH_2Cl_2-EtOAc, 6:1). Three products, *16–18*, were isolated, but at least five other coloured bands (blue, green, violet, and red) were observed on TLC.** The yield of *16* was 3 % (1.9 mg), and *17* and *18* were isolated in less than 1.5 % each. M.p.: for *16*, 206–208°; for *17*, 213–215°; for *18*, 235–237°.*** IR: for *16* and *17*, 2220 (CN) and 2160 (sharp peak, –SCN) cm^{-1}; for *18*, 2165 (–SCN), 3370, 3290, 3210, and 1655 ($CONH_2$) cm^{-1}. TLC: for *16*, $R_F = 0.36$; for *17*, $R_F = 0.62$; for *18*, $R_F = 0.55$ (EtOAc). The compounds are violet (*16*), blue (*17*), and red (*18*). Electronic spectral data are summarized in Table 2.

(b) In benzene. Over a period of 1 h 0.5 mmol of thiocyanogen in 10 ml of benzene was added to an irradiated solution of 50 mg (0.24 mmol) of *1a* in 100 ml of benzene. No coloured products were formed during this time (TLC). Another 0.25 mmol of thiocyanogen in 5 ml of benzene was added and the irradiation was continued for 5 h. The reaction mixture was worked up as described above, and *16* was the only product formed (< 2 %).

Several irradiation experiments in carbon tetrachloride and in methylene chloride with varying concentrations of the reactants were performed, giving the same products and the same low yields. Attempts to scale up the thiocyanation procedure were not successful. This resulted only in increasing amounts of the yellow by-products.

---

* The results obtained are in poor agreement with the calculated values, probably because of inhomogeneity of the material.

** Under "dark" conditions no coloured products were obtained.

*** Melting points are uncorrected.

Acknowledgments. Financial Support from the *Swedish Natural Science Research Council* and from the grant *Främjande av ograduerade forskares vetenskapliga verksamhet* to the University of Göteborg is gratefully acknowledged. We thank Mrs. Inger Nilsson for technical assistance.

REFERENCES

1. Ceder, O., Andersson, J. E. and Johansson, L.-E. *Acta Chem. Scand.* **26** (1972) 624.
2. Ceder, O. and Andersson, J. E. *Acta Chem. Scand.* **26** (1972) 596.
3. Beynon, J. H., Saunders, R. A. and Williams, A. E. *The Mass Spectra of Organic Molecules*, Elsevier, Amsterdam 1968, p. 375.
4. Ceder, O. and Andersson, J. E. *Acta Chem. Scand.* **26** (1972) 611.
5. Eibner, A. *Ber.* **36** (1903) 1229.
6. Miller, B. and Walling, C. *J. Am. Chem. Soc.* **79** (1957) 4187.
7. (a) Echols, J. T., Chuang, V. T.-C., Parrish, C. S., Rose, J. E. and Milligan, B. *J. Am. Chem. Soc.* **89** (1967) 4081; (b) Milligan, B., Bradow, R. L., Rose, J. E., Hubbert, H. E. and Roe, A. *J. Am. Chem. Soc.* **84** (1962) 158.
8. *E.g.* Bacon, R. G. R. and Irwin, R. S. *J. Chem. Soc.* **1961** 2447.
9. Söderbäck, E. *Ann. Chem.* **419** (1919) 217.
10. Wood, J. L. *Org. Reactions* **3** (1946) 252.

Received February 2, 1973.

ACTA CHEMICA SCANDINAVICA 27 (1973) 2107–2114

Tobacco Chemistry

18. Absolute Configuration of (9*R*)-9-Hydroxy-4,7*E*-megastigmadien-3-one (3-Oxo-α-ionol)

ARNE J. AASEN, BJARNE KIMLAND and CURT R. ENZELL

Research Department, Swedish Tobacco Co., S-104 62 Stockholm 17, Sweden

The absolute configuration of (9*R*)-9-hydroxy-4,7-*E*-megastigmadien-3-one has been shown to be R both in position 6 and 9. The MS fragmentation and possible biogenesis of this compound is discussed.

In a recent publication in this series dealing with the volatile constituents of Greek tobacco, *Nicotiana tabacum* L., the structure of one of the major neutral components (3-oxo-α-ionol), now named* (9*R*)-9-hydroxy-4,7*E*-megastigmadien-3-one (I),[1] was reported but without stereochemical assignments.[2] Subsequent studies have revealed the absolute configuration at the two asymmetric centres in this compound and the results are discussed below.

The structure (I) was deduced principally from MS ($C_{13}H_{20}O_2$, accurate mass measurement), UV (235 nm, disubst, conj. ketone), and IR data (3400 cm^{-1}, OH; 1657 cm^{-1}, conj. C=O; 1376 and 1369 cm^{-1}, *gem.* dimethyl; 976 cm^{-1}, *trans* disubst. C=C) and from NMR data of this compound, its acetate (II) and the corresponding diketone (III) as detailed in Table 1 (*cf.* Experimental). The spectral assignments were confirmed by comparison with synthetic (±)-9-hydroxy-4,7*E*-megastigmadien-3-one (I), the corresponding acetate (II) and diketone (III) which were prepared from (±)-*trans*-α-ionone (IV) as indicated in Scheme 1. The diketone (III) has previously been prepared from (±)-*trans*-α-ionone by Prelog and Osgan [3] and later by Roberts [4] who also obtained (±)-9-hydroxy-4,7*E*-megastigmadien-3-one (I), without characterization, as an intermediate in the synthesis of a tobacco additive.

Stereochemistry. (9*R*)-9-Hydroxy-4,7*E*-megastigmadien-3-one (I) isolated from tobacco displayed a fairly high optical rotation ($[\alpha]_D + 177°$) due to the two asymmetric centres, C(6) and C(9). Oxidation of this compound under mild conditions employing a two phase system [5] furnished the optically active diketone III, which exhibited a rotation ($[\alpha]_D + 293°$) very similar to that of the same diketone ($[\alpha]_D + 299°$) prepared from (+)-*trans*-α-ionone (IV). Since

* Nomenclature and stereochemistry as defined in Ref. 1.

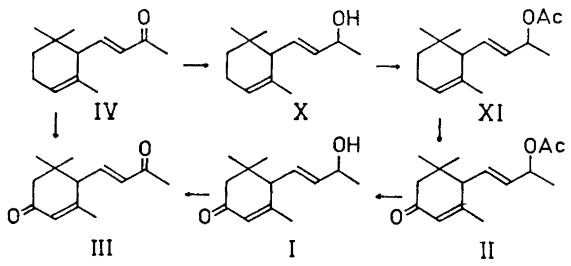

Scheme 1.

the absolute configuration of (+)-*trans*-α-ionone has recently been shown to be *R* by Eugster *et al.*[6] by correlating (−)-*trans*-α-ionone with (+)-manool, it follows that the configuration at C(6) is *R* in the tobacco isolate.

It may be noted that although the rotations of our 4,7*E*-megastigmadien-3,9-dione (III) preparations were higher than that reported by Buchecker *et al.*[7] for this compound ($[\alpha]_D + 235°$), the activity of an optically pure specimen might be still higher since the C(6) proton is labile as demonstrated by the fact that almost complete racemization was observed even under mild conditions such as oxidation of the alcohol function of the natural compound under Jones' conditions, which do not normally cause racemization.[8] The lability of this proton might account for the somewhat varying specific rotations reported for (+)-*trans*-α-ionone (IV, see Experimental).[9–11] It cannot be excluded that some racemization might have occurred at C(6) in (9*R*)-9-hydroxy-4,7*E*-megastigmadien-3-one (I) during its isolation from tobacco since alkali was used in the separation of the organic acids from the extracts.

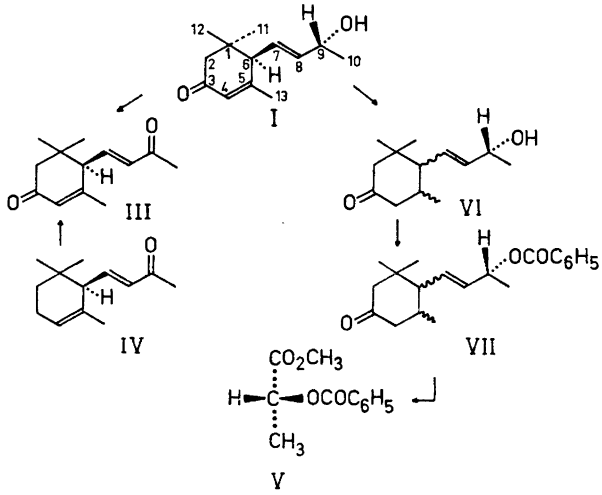

Scheme 2.

The absolute configuration at C(9) was shown to be *R* by comparison of methyl benzoyloxypropanoates (V) derived on the one hand from I, and on the other from (*S*)-lactic acid (L(+)-lactic acid). Selective catalytic hydrogenation of the 4,5-double bond of I under alkaline conditions [12] followed by conversion of the resulting dihydro compound (VI) to the corresponding benzoate (VII) was performed to simplify the isolation of the lactic acid derivative in the subsequent ozonolytic cleavage of the side chain double bond. The ozonolysis of the benzoate (VII) was carried out in methanol at $-70°$ and methyl benzoyloxypropanoate (V), exhibiting a negative rotation ($[\alpha]_D$ $-8.5°$), was obtained after successive treatment with performic acid and diazomethane. The optical activity of the product (V), when compared with that of methyl (2*S*)-2-benzoyloxypropanoate ($[\alpha]_D + 13.9°$) indicated a preponderance of the *R*-isomer to the *S*-isomer of 4:1.

This result is consistent with the fact that the NMR spectrum of the tobacco isolate after the addition of $Eu(DPM)_3$ revealed the presence of two diastereoisomers in the ratio 3:1. It may be concluded therefore that in addition to the main constituent, (9*R*)-9-hydroxy-4,7*E*-megastigmadien-3-one (I), there is some 20 % of the 9*S*-epimer present in this tobacco and eventually, but less likely, minor amounts of the 6*S*-isomer.

Mass spectra. The main feature of the mass spectra of (9*R*)-9-hydroxy-4,7*E*-megastigmadien-3-one (I) and 4,7*E*-megastigmadien-3,9-dione (III) is the dominance of the *m/e* 108 ion for which fragment the genesis shown in Scheme 3 may be invoked. The initial loss of 56 mass units, corresponding to C_4H_8, is readily explained by fissions of the 2,3-bond (α-cleavage) and the doubly allylic 1,6-bond. Subsequent cyclization of the resulting ions, *m/e* 152 and 150, accompanied by expulsion of acetaldehyde and ketene, respectively, yield the stable *m/e* 108 ion corresponding to *m*-cresol. Appropriate metastable peaks were observed for the latter transitions, and the elemental compositions of these ions were confirmed by high resolution mass spectrometry. Replacement of the hydroxyl proton in I by deuterium caused a shift of the base peak and the *m/e* 152 peak by one mass unit supporting the proposed mechanism.

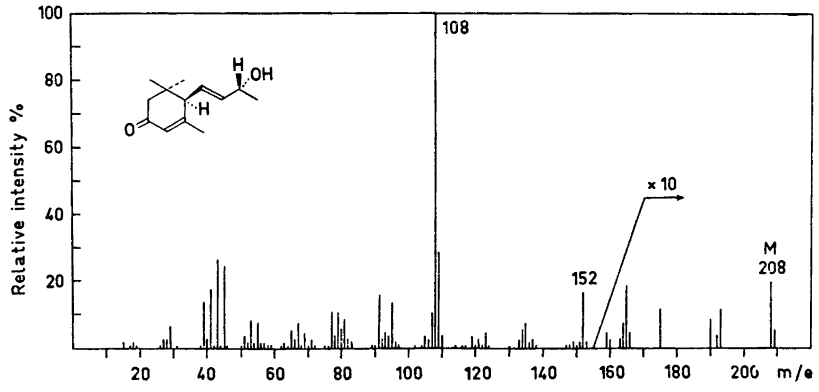

Fig. 1.

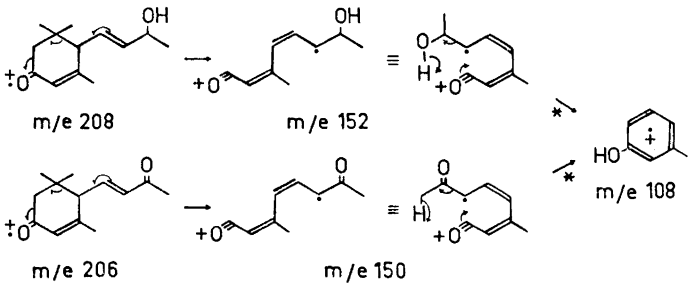

Scheme 3.

Biosynthetic considerations. It has previously been suggested that many isoprenoid cyclic and acyclic tobacco constituents might have higher terpenoids as precursors.[13,14] The constitution of the present compound (I) indicates that it is possibly derived from carotenoids. It is noteworthy that carotenoids like α-carotene [6] and lutein [7,15,16] (VIII) which are both known to be present in tobacco,[17] possess the same absolute configuration in position 6 as the new tobacco compound. (9*R*)-9-Hydroxy-4,7*E*-megastigmadien-3-one (I) might in turn be the precursor of the recently described megastigmatrienones which have been isolated from the same tobacco.[1]

Prelog *et al.*[18,19] studied the fate of α-ionone (IV) when fed to rabbits and they found that an oxygen atom was introduced into position 3. The structure of the product(s) was not determined. Since α-ionone (IV) is not known to be a tobacco constituent,[20] (9*R*)-9-hydroxy-4,7*E*-megastigmadien-3-one (I) might rather originate from hydroxylated carotenoids.

Very recently a structurally related compound, vomifoliol (IX), has been isolated from *Rauwolfia vomitoria*,[21] *Croton sparsiflorus*,[22] and *Podocarpus blumei*.[23] In the last case it was given the name 'blumenol A'.

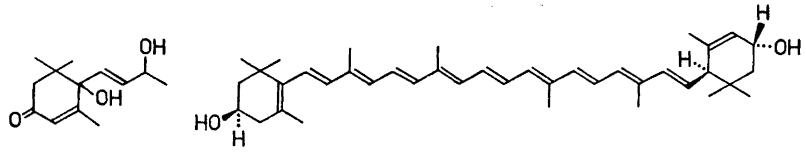

IX VIII

EXPERIMENTAL

NMR spectra were recorded on a Varian A60-A instrument using $CDCl_3$ as solvent, unless otherwise stated, and TMS as internal reference. Mass spectra were obtained on an LKB 9000 instrument operated at 70 eV. IR and UV spectra were recorded on a Perkin-Elmer 257 and a Beckman DK-2A instrument. Optical activities were measured on a Perkin-Elmer 141 polarimeter. Melting points were determined on a Leitz Wetzlar instrument and are uncorrected. Accurate mass determinations were carried out at the Laboratory for Mass Spectrometry, Karolinska Institutet, Stockholm.

Isolation. (9*R*)-9-Hydroxy-4,7*E*-megastigmadien-3-one (I) was isolated from an extract of 295 kg sun-cured Greek tobacco, grown in Serres 1968. The fractionation of this extract

Table 1. NMR data of megastigmane derivatives.

Compound	Chemical shifts[a] H-2	H-4	H-5	H-6	H-7	H-8	H-9	H-10	H-11	H-12	H-13
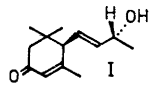 I	2.06 2.32 AB (16.5)	5.89 q (1.4)	–	2.51 m (7.8)	5.50 m (8[e],15)	5.70 m (5.5[e],15)	4.33 m (5.3)	1.31 d (6.3)	0.99 s	1.04 s	1.91 d (1.4)
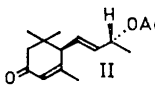 II [b]	2.17 2.25 AB (*ca.* 16)	5.95 q (1.5)	–	2.58 m	*ca.* 5.65 m	*ca.* 5.65 m	*ca.* 5.5 m	1.33 d (6.0)	0.97 s	1.05 s	1.90 d (1.5)
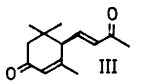 III	2.32 2.25 AB (16)	(6.04 q (1.5)	–	2.78 d (9.0)	6.72 q (9,15.5)	6.18 d (15.5)	–	2.32 s	1.05 s	1.11 s	1.94 d (1.5)
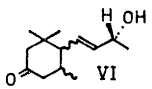 VI	2.1–2.5 m		1.2–2.0 m		*ca.* 5.7 m	*ca.* 5.7 m	4.4 m	1.27 d (6.5)	0.85–1.0 m		
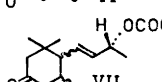 VII [c]	2.2–2.4 m		1.3–2.0 m		*ca.* 5.7 m	*ca.* 5.7 m	*ca.* 5.4 m	1.49 d (6.5)	0.8–1.0 m		

[a] Chemical shifts in ppm. Coupling constants (in Hz) in parenthesis. Multiplicity of signal: AB = AB-pattern, s = singlet, d = doublet, q = quartet, m = multiplet. [b] CH_3CO at δ 2.05 (s) [c] C_6H_5 at δ 7.5 (3H,m) and δ 8.05 (2H,m) [e] Measured after addition of $Eu(DPM)_3$.

into ten main subfractions, B1–B10, has been described in detail elsewhere.[24] 3 g of fraction B9 (6.9 g) was chromatographed on a column containing 210 g silica gel impregnated with silver nitrate[25] using ether-pentane mixtures as eluents. The main fraction (1.32 g), eluted with 60 % ether in pentane, was rechromatographed on 100 g silica gel. Fraction 4 (506 mg) appeared to be homogeneous by thin layer chromatography (TLC) but it could not be induced to crystallize; $[\alpha]_D^{20}$ +177° (*c* 1.5 in $CHCl_3$); λ_{max} (EtOH) 235 nm (ε 9000); ν_{max}(film) 3400 (broad), 2960 (s), 2865 (m), 1657 (s), 1630 (shoulder), 1376 (m), 1369 (m), 1253 (m), 1140 (m), 1065 (m), 976 (m) cm^{-1}; MS: 208 (M^+, 2), 108 (100), 109 (28), 43 (26), 45 (25), 41 (18), 152 (17), 91 (16), 95 (14), 39 (14), 107 (11), 77 (11), 79 (11), 81 (9), 53 (9); accurate mass determinations: *m/e* 208.1457, $C_{13}H_{20}O_2$ requires 208.1463; *m/e* 152.0823, $C_9H_{12}O$ requires 152.0837; *m/e* 108.0563, C_7H_8O requires 108.0575; NMR, see Table 1.

*(9*R)-9-*Acetoxy-4,7*E-*megastigmadien-3-one (II).* Acetic anhydride (1.5 ml) was added to a solution of the tobacco compound (I, 59 mg) in dry pyridine (3.5 ml) and kept at room temperature for 2 h. Excess anhydride was destroyed by addition of a few drops of methanol, followed by dilution with water and extraction with ether. The ether solution was washed with dilute acid (HCl), water, and evaporated. Chromatography on silica gel gave TLC pure acetate (II, 37 mg) as a colourless oil. ν_{max}(film) 2960 (s), 2940 (s), 2870 (m), 1735 (s), 1665 (s), 1630 (m), 1440 (m), 1370 (s), 1240 (s), 1145 (m), 1045 (s), 978 (m), 953 (m), 913 (m) cm^{-1}; MS: 250 (M^+, 2), 108 (100), 43 (100), 134 (85), 91 (45), 41 (32), 77 (20), 79 (20), 69 (18), 190 (18), 55 (17), 51 (15); NMR, see Table 1.

*4,7*E-*Megastigmadien-3,9-dione (III).* Treatment of natural (9*R*)-9-hydroxy-4,7*E*-megastigmadien-3-one (I) with Jones' reagent [8] furnished the corresponding, almost completely racemic diketone (III), while the optically active compound was obtained when employing the two-phase system recently communicated by Brown *et al.*[5] To the alcohol (I, 140 mg) in ether (30 ml) was added 0.8 ml of a solution containing sodium dichromate (1 g), water (5 ml) and sulphuric acid (1.36 g). After stirring for 1 h at room temperature water was added and the mixture extracted with ether. The ether solution was washed with water, dried and evaporated. The product (116 mg) was purified on a silica gel column to give TLC pure diketone (III, 73 mg). M.p. 74–75°; $[\alpha]_D^{20}$ +293° (*c* 1.0 in $CHCl_3$), lit.[7] $[\alpha]_D^{20}$ +235 (EtOH); λ_{max}(EtOH) 236 nm (ε 21 400), [lit.[3] *ca.* 236 nm (ε *ca.* 21 000)]; The infrared spectrum was closely similar to that (in nujol) published by Prelog and Osgan [3] and indistinguishable from that obtained for an authentic sample [3] recorded under indentical conditions (KBr); MS: 206 (M^+, 2), 108 (100), 43 (62), 150 (21), 109 (18), 77 (9), 107 (7), 39 (6), 41 (6), 79 (5); NMR, see Table 1. When acetone-d_6 was used as solvent, the four-proton signal at δ 2.32 in the $CDCl_3$-spectrum was resolved into a three-proton singlet at δ 2.28 and a one-proton doublet at δ 2.37 (AB-system).

*Preparation of (±)-9-acetoxy-4,7*E-*megastigmadien-3-one (II).* (±)-*trans*-α-Ionone (IV, 5 g) and sodium borohydride (290 mg) in ethanol (50 ml) were stirred for 3 h at room temperature. The mixture was diluted with water and extracted with ether which was dried and evaporated. The product was purified on a silica gel column to give the corresponding alcohol (X, 3.19 g). This (350 mg) was treated with acetic anhydride (1.5 ml) in pyridine (3 ml) at room temperature for 4 h and excess anhydride subsequently removed by the addition of a few drops of methanol. The acetate XI (366 mg) was isolated and purified as described above for II derived from the natural compound. Both the alcohol (X) and the acetate (XI) exhibited appropriate NMR spectra. Chromium trioxide (170 mg) was added to a solution of the acetate (XI, 200 mg) in acetic acid (5 ml). The mixture was stirred for 2 h at room temperature, diluted with water and extracted with ether. The residue obtained after removal of the solvent was chromatographed on a silica gel column to give homogeneous (±)-9-acetoxy-4,7*E*-megastigmadien-3-one (II, 36 mg). The physical properties of the product (NMR, IR, MS) were identical to those given above for II derived from natural (9*R*)-9-hydroxy-4,7*E*-megastigmadien-3-one (I).

*Preparation of (±)-9-hydroxy-4,7*E-*megastigmadien-3-one (I).* The ketoacetate II (25 mg) was saponified by treatment with 2 % KOH in methanol (5 ml) for 30 min. The mixture was diluted with water and extracted with ether. Removal of the solvent followed by purification on a silica gel column yielded the ketoalcohol I (12 mg). The spectral (NMR, IR, MS, UV) and chromatographic properties of the product were indistinguishable from those of the tobacco constituent except for being racemic.

*Preparation of 4,7*E-*megastigmadien-3,9-dione (III).* (±)-*trans*-α-Ionone (IV, 1 g) was added to a solution of chromium trioxide (1 g) in acetic acid (16 ml) and stirred

at ambient temperature for 6 h. Work up as outlined above for (±)-9-acetoxy-4,7*E*-megastigmadien-3-one (II) gave the desired dione III (80 mg). M.p. 73 – 73.5°, undepressed when admixed with authentic [3] material. NMR, IR, UV, and mass spectra were superimposable on those of the diketone derived from the natural ketoalcohol (I). Optically active 4,7*E*-megastigmadien-3,9-dione (III) was prepared from (*R*)-*trans*-α-ionone (IV, 300 mg) and chromium trioxide (400 mg) in acetic acid (10 ml). The product (III, 58 mg) was isolated and purified as detailed above. M.p. 73°; $[\alpha]_D^{20}$ +299° (*c* 0.7 in $CHCl_3$). The (*R*)-*trans*-α-ionone (IV) was obtained from its racemate using the method of Sobotka *et al.*[9] (±)-*trans*-α-Ionone (IV, 57.6 g) was reacted with (−)-menthydrazide[26] (64.2 g) to give the corresponding menthydrazones. (+)-*trans*-α-Ionone (−)-menthydrazone (3.7 g) having constant rotation and melting point was obtained after recrystallization nineteen times from ethanol. M.p. 182 – 183°, [lit. 176°,[9] 178.5°,[10] 183°[11]]; $[\alpha]_D^{20}$ +229° (*c* 1.5 in EtOH), [lit. +230° (EtOH),[9] +232° (C_6H_6),[10] +245° (EtOH)[11]]. In contrast to us Sobotka *et al.*[9] found (−)-*trans*-α-ionone (−)-menthydrazone to be the least soluble of these diastereoisomers. The hydrazone was hydrolyzed by subjecting it to steam distillation in the presence of phthalic anhydride. The distillate was extracted with ether which was dried and evaporated to give (+)-*trans*-α-ionone (IV, 1.6 g). $[\alpha]_D^{20}$ +369° (*c* 3.8 in EtOH), lit. +347° (EtOH),[9] +401° (C_6H_6),[10] +415° (EtOH).[11] The NMR spectrum was superimposable on that of racemic IV.

*(9*R*)-5ξ,6ξ-9-Hydroxy-7*E*-megastigmen-3-one (VI).* (9*R*)-9-Hydroxy-4,7*E*-megastigmadien-3-one (I, 300 mg) in 0.3 N NaOH/EtOH (5 ml) was hydrogenated at ambient temperature and atmospheric pressure in the presence of 10 % Pd/C (75 mg).[12] The theoretical amount of hydrogen was consumed in 2 h, after which the solution was extracted with ether. Removal of the solvent left a colourless oil (305 mg). $[\alpha]_D^{20}$ +4.3° (*c* 1.5 in $CHCl_3$); NMR, see Table 1.

*(9*R*)-5ξ,6ξ-9-Benzoyloxy-7*E*-megastigmen-3-one (VII).* (9*R*)-5ξ,6ξ-9-Hydroxy-7*E*-megastigmen-3-one (VI, 298 mg) and benzoyl chloride (300 mg) in dry pyridine (10 ml) were kept at room temperature overnight. The mixture was diluted with water and extracted with ether. The extract was washed with 5 % H_2SO_4, 5 % $NaHCO_3$, water, and dried over sodium sulphate. Removal of the solvent, followed by chromatography on silica gelfurnished the benzoate VII as a colourless oil (225 mg). $[\alpha]_D^{20}$ −10.4° (*c* 0.8 in $CHCl_3$); NMR, see Table 1.

*Ozonolysis of (9*R*)-5ξ,6ξ-9-benzoyloxy-7*E*-megastigmen-3-one (VII).* The benzoate VII (210 mg) dissolved in methanol (10 ml) was treated with excess ozone at −65° for 10 min. The reaction mixture was allowed to reach room temperature and the solvent distilled *in vacuo* to leave a colourless oil to which was added a mixture of formic acid (7 ml) and 30 % H_2O_2 (4 ml).[27] The mixture was refluxed for 30 min, cooled and extracted with ether. The extract was dried with sodium sulphate and concentrated *in vacuo*. Most of the formic acid which had been extracted, was distilled and the residue was treated with excess diazomethane in ether at room temperature for 10 min. Removal of solvent and excess reagent left a colourless oil which was chromatographed on a silica gel column. Elution with 7 % ether in pentane furnished pure methyl 2-benzoyloxypropanoate (V, 34 mg, 25 %). $[\alpha]_D^{20}$ −8.5° (*c* 1.0 in $CHCl_3$); δ 1.61 (3H, d, *J* 7.1 Hz), 3.76 (3H, s), 5.35 (1 H, quartet, *J* 7.1 Hz), 7.52 (3H, m), *ca.* 8.07 (2H, m); ν_{max}(film) 1759 (s), 1725 (s), 1604 (m), 1453 (s), 1360 (m), 1320 (m), 1273 (s), 1218 (s), 1179 (m), 1114 (s), 1072 (m), 1049 (m), 1028 (m), 971 (w), 859 (w), 838 (w), 717 (s), 691 (w) cm^{-1}.

*Methyl (2*S*)-2-benzoyloxypropanoate (V)* (a) Crystalline (*S*)-lactic acid (L(+)-lactic acid, 150 mg, Sigma No. L 1750) was methylated with excess diazomethane in ether solution. After standing for 10 min, the solvent was removed by distillation and the residue chromatographed on a silica gel column. Elution with 15 % ether in pentane gave pure methyl (2*S*)-2-hydroxypropanoate. $[\alpha]_D^{20}$ −13.3° (*c* 2.6 in ether), [lit.[28] −9.5° (neat)]; δ 1.4 (3 H, d, *J* 7 Hz), 3.5 (OH), 3.78 (3H, s), 4.31 (1 H, quartet, *J* 7 Hz). The methyl ester was dissolved in dry pyridine (5 ml) and benzoyl chloride (100 mg) and kept at room temperature overnight. The product was isolated as described above for VII and chromatographed on a silica gel column to give pure methyl (2*S*)-2-benzoyloxypropanoate (V, 135 mg). $[\alpha]_D^{20}$ +13.9° (*c* 4,5 in $CHCl_3$). NMR and IR spectra were identical to those of the corresponding compound derived from (9*R*)-5ξ,6ξ-9-benzoyloxy-7*E*-megastigmen-3-one (VII). (b) 90 % (*S*)-Lactic acid (2 g, Fluka No. 69773) was dissolved in methanol (100 ml) and refluxed for 24 h in the presence of H_2SO_4 (0.2 ml). The solvent was distilled off and the residue extracted with ether. The extract was washed with water, 5 % $NaHCO_3$, and subsequently

distilled. The methyl ester (300 mg, $[\alpha]_D^{20}$ −16.4° (*c* 2.8 in EtOH)) was dissolved in dry pyridine (5 ml) and treated with benzoyl chloride (300 mg) at room temperature overnight followed by isolation and chromatography as described above. $[\alpha]_D^{20}$ +11.2° (*c* 1.3 in $CHCl_3$). NMR and IR spectra were identical to those of the compound derived from VII.

Acknowledgements. The authors are indebted to Miss A.-M. Eklund for skilful technical assistance, to Professor K. Olsson, the Agricultural College of Sweden, Uppsala, for placing the NMR instrument at their disposal, to the Swedish Forest Products Research Laboratory, Stockholm, for lending them the ozone generator, and to Professor V. Prelog, Technischen Hochschule, Zürich, for a gift of 4,7*E*-megastigmadien-3,9-dione.

REFERENCES

1. Aasen, A. J., Kimland, B., Almqvist, S.-O. and Enzell, C. R. *Acta Chem. Scand.* **26** (1972) 2573.
2. Aasen, A. J., Kimland, B. and Enzell, C. R. *Acta Chem. Scand.* **25** (1971) 1481.
3. Prelog, V. and Osgan, M. *Helv. Chim. Acta* **35** (1952) 986.
4. Roberts, D. L. *U. S. Patent* 3,217,718, Nov. 16, 1965; *Chem. Abstr.* **64** (1966) 5466.
5. Brown, H. C., Garg, C. P. and Lin, K.-T. *J. Org. Chem.* **36** (1971) 387.
6. Eugster, C. H., Buchecker, R., Tscharner, Ch., Uhde, G. and Ohloff, G. *Helv. Chim. Acta* **52** (1969) 1729.
7. Buchecker, R., Hamm, P. and Eugster, C. H. *Chimia* **25** (1971) 192.
8. Bowden, K., Heilbron, I. M., Jones, E. R. H. and Weedon, B. C. L. *J. Chem. Soc.* **1946** 39; Jones, J. B. and Grayshan, R. *Chem. Commun.* **1970** 141.
9. Sobotka, H., Bloch, E., Cahnmann, H., Feldbau, E. and Rosen, E. *J. Am. Chem. Soc.* **65** (1943) 2061.
10. Naves, Y.-R. *Helv. Chim. Acta* **30** (1947) 769.
11. Tscharner, Ch., Eugster, C. H. and Karrer, P. *Helv. Chim. Acta* **41** (1958) 32.
12. Augustine, R. L. *Catalytic Hydrogenation*, Marcel Dekker, New York 1965.
13. Kimland, B., Appleton, R. A., Aasen, A. J., Roeraade, J. and Enzell, C. R. *Phytochemistry* **11** (1972) 309.
14. Demole, E. and Berthet, D. *Helv. Chim. Acta* **54** (1971) 681.
15. Goodfellow, D., Moss, G. P. and Weedon, B. C. L. *Chem. Commun.* **1970** 1578.
16. Buchecker, R., Hamm, P. and Eugster, C. H. *Chimia* **26** (1972) 134.
17. Wright, H. E., Burton, W. W. and Berry, R. C. *Arch. Biochem. Biophys.* **82** (1959) 107.
18. Prelog, V. and Meier, H. L. *Helv. Chim. Acta* **33** (1950) 1276.
19. Prelog, V. and Würsch, J. *Helv. Chim. Acta* **34** (1951) 859.
20. Stedman, R. L. *Chem. Revs.* **68** (1968) 153.
21. Pousset, J.-L. and Poisson, J. *Tetrahedron Letters* **1969** 1173.
22. Satish, S. and Bhakuni, D. S. *Phytochemistry* **11** (1972) 2888.
23. Galbraith, M. N. and Horn, D. H. S. *Chem. Commun.* **1972** 113.
24. Kimland, B., Aasen, A. J. and Enzell, C. R. *Acta Chem. Scand.* **26** (1972) 2177.
25. Norin, T. and Westfelt, L. *Acta Chem. Scand.* **17** (1963) 1828.
26. Woodward, R. B., Kohman, T. P. and Harris, G. C. *J. Am. Chem. Soc.* **63** (1941) 120.
27. Cornforth, J. W., Cornforth, R. H., Popjak, G. and Yengoyan, L. *J. Biol. Chem.* **241** (1966) 3790.
28. Timmermans, J., v. Lancker, T. and Jaffe, J. *Bull. Soc. Chim. Belg.* **48** (1939) 33.

Received February 17, 1973.

ACTA CHEMICA SCANDINAVICA 27 (1973) 2115–2120

A Qualitative Demonstration of the Degradation of Folic Acid by *Pseudomonas fluorescens* UK-1

JUHANI SOINI and KARIN MAJASAARI

Department of Biochemistry, University of Turku, SF-20500 Turku 50, Finland

The degradation of folic acid *in vitro* has been studied by using a cell free extract obtained from *Pseudomonas fluorescens* UK-1 after ultrasonic treatment and streptomycin sulphate precipitation. The degradation products have been separated chromatographically. With folic acid as the substrate *p*-aminobenzoylglutamic acid and a substituted pteridine were formed. The degradation increased as a function of time and protein concentration. A weak spontaneous degradation occurred without cell extract. The pteridine moiety formed in the reaction was eluted from paper after chromatographic run and examined both spectrophotometrically and fluorometrically. On the basis of these studies it is obvious that pterin-6-carboxylic acid is formed during incubation. When *p*-aminobenzoyl-L-glutamic acid was the substrate the appearance of *p*-aminobenzoic acid was noted. However, the degradation of *p*-aminobenzoyl-L-glutamic acid was slower than that of folic acid.

It has earlier been shown[1,2] that some pseudomonads isolated from soil are capable of degrading methotrexate and folate to 4-{*N*[(2,4-diamino-6-pteridyl)methyl]-*N*-methylamino} benzoic acid and pteroic acid, respectively. The enzyme carboxypeptidase G_1 which catalyzes the degradation has been isolated and purified 1050-fold.[2] We have found that still another splitting of the folic acid molecule occurs, resulting in a substituted pteridine, *p*-aminobenzoylglutamic acid, and *p*-aminobenzoic acid.* In our studies we have used *Pseudomonas fluorescens* strain UK-1, which was isolated from sea water in Hietalahti harbour, Helsinki.

EXPERIMENTAL

Reagents. Folic acid and PABA were purchased from British Drug Houses Ltd., and PABGA, pterin, and pterin-6-carboxylic acid from Sigma Chemical Co.

Culture conditions. Ps. fluorescens UK-1 was grown in a basal mineral medium containing (per litre) 20 mmol KH_2PO_4, 1 mmol $MgSO_4.7H_2O$ and 10 μmol $FeSO_4.7H_2O$.

* In this publication the following abbreviations are used: PABA=*p*-aminobenzoic acid; PABGA=*p*-aminobenzoyl-L-glutamic acid.

The medium contained 10 mmol of folic acid as a source of carbon and nitrogen and the pH was adjusted to 6.8. The precultivation of the organism was carried out in glutamate (20 mM) or pantothenate (5 mM) media. The culture was aerated during several days with an aquarium pump and incubated at 30°.

Preparation of cell extract and determination of degradation products. The cells were preserved on an agar slant whose salt composition was the same as above. It contained 5 mmol of pantothenate per litre and 1.5 % agar. The culture was kept at 2°C. From the agar slant the cells were transferred aseptically to 200 ml of sterile pantothenate medium in which they grew for 24 h under aeration at 30°C. The whole culture was poured into 500 ml of the same medium where it continued to grow for 12 h in similar conditions. The cells were separated by centrifugation (4000 *g*, 10 min), washed with cold saline, and transferred to 2000 – 5000 ml of medium which was 10 mM in folic acid. In this final medium the culture grew for 4 – 7 days at 30° under aeration. During this time the culture medium became yellow and turbid due to the precipitated pteroic acid.[1] The cells, together with the precipitate, were separated by centrifugation (4000 *g*, 15 min). A 2 % Na_2CO_3 solution was added in order to dissolve the yellow material, 100 ml per litre of medium being required. The remaining cells were washed with cold saline and ruptured for 15 min in 15 ml of 0.05 M TRIS–HCl buffer, pH 7.3, using the Raytheon Sonic Oscillator 10 kc, 250 W. The suspension was centrifuged at 17 300 *g* for 30 min, after which was added 0.5 ml of 5 % streptomycin sulphate solution per 3 ml of clear supernatant. After standing for 30 min, the precipitate was centrifuged at 17 300 *g* for 30 min and discarded. The protein content of the clear supernatant was estimated with sulphosalicylic acid,[3] employing crystalline bovine serum albumin as standard.

The reaction mixture contained 10 mg of folic acid or PABGA in 10 ml of 0.05 M TRIS–HCl buffer, pH 7.3. The reaction, which took place at 30°, was started by adding the enzyme preparation and stopped by putting the reaction tube into an ice bath. 200 µl of reaction mixture was pipetted onto a Whatman No. 3 paper. The spots were dried in an air stream and the chromatogram was run using the ascending technique. The solvent used was a 1:2 1 % NH_3 – 1-propanol mixture.[4]

After drying, the chromatograms were photographed in ultraviolet light employing a Desaga MinUVIS lamp at a wave lenght of 254 nm. Parallel chromatograms were diazo-stained.[5]

The spots that exhibited a blue fluorescence at 254 nm and whose R_F-value was 0.2 were cut off and eluted with 0.1 N NaOH or 0.1 M KH_2PO_4-KOH buffer, pH 8, for determination of their spectra spectrophotometrically or fluorometrically, respectively.

RESULTS AND DISCUSSION

Fig. 1 shows the degradation of folic acid as a function of time and enzyme preparation concentration. It can be seen that the amount of folic acid (dark spots) decreases when the enzyme concentration increases. The decrease has reached a constant level after 30 min when the protein concentration is 0.9 mg/10 ml. The decrease of folic acid is slower when lowest protein concentration (0.225 mg/10 ml) is used. In every reaction spot in Fig. 1, a white spot above the dark spot can be seen (in the original chromatogram the spot, in UV-light, is light blue). We believe that this spot is due to a substituted pteridine moiety (designated as Compound P) derived from the folic acid molecule. The spots cannot be seen in reaction mixtures that lack the protein (blank). PABGA is represented in the uppermost light spots, which in the original chromatogram in the UV-light appear as red-violet. Using pure PABGA and 1 % NH_3 – 1-propanol 1:2 as solvent, we obtained an R_F-value of 0.43 for PABGA. It is obvious that, during the reaction, the PABGA moiety is split off by the action of the enzyme preparation. As can be seen from the blank spots, a weak spontaneous splitting increasing as a function of time also occurs. Commercial folic acid always contains a little PABGA.

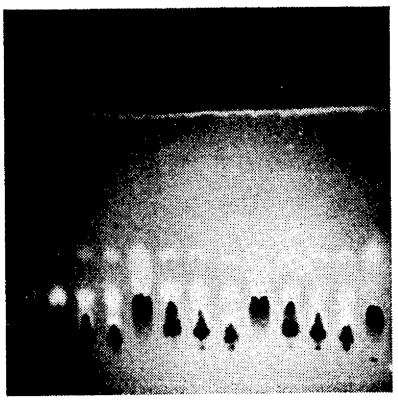

Fig. 1. Degradation of folic acid with time and protein concentration. Reaction times in spots 1–4, 5–8, and 9–12 were 30, 60, and 90 min, respectively. Protein concentration in spots 2, 6, and 10 was 0.09 mg/ml; in spots 3, 7, and 11, 0.045 mg/ml; and in 4, 8, and 12, 0.023 mg/ml. No protein was used in 1, 5, and 9. Each spot contained 200 µl of reaction mixture. As a reference, spot 13 is folic acid. The chromatogram was illuminated with UV-light.

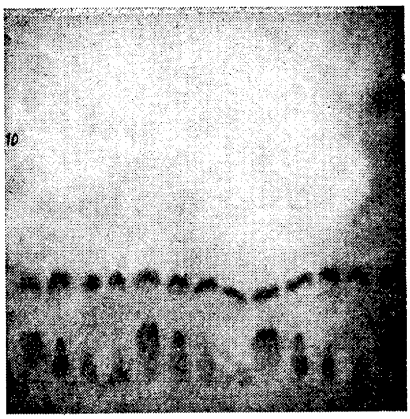

Fig. 2. Conditions are as in Fig. 1 except that the chromatogram has been diazo-stained.

The formation of PABGA during the course of the reaction is shown in Fig. 2, which represents a diazo-stained chromatogram. The strenght of the colour increases during 60 min as the protein concentration increases. The weakest spots belong to the blank mixtures and the pure standard.

The degradation of PABGA was also studied, with results shown in Figs. 3 and 4. The splitting of PABGA to PABA and glutamic acid increases as a function of time and a weak spontaneous splitting during the incubation occurs here, too. In the photographs, the lower dark spots represent PABGA and the spots above them PABA (in the original chromatogram the spots are dark red). For pure PABA we obtained an R_F-value of 0.56. The weak spots at the top of the chromatogram were originally greenish-brown and they probably represent non-diazotizable compounds.

In chromatographic runs we obtained an R_F-value of 0.2 both for Compound P and for a pure pterin-6-carboxylic acid standard. However, when the chromatograms, after drying, were run a second time for a better separation, the spot of Compound P moved faster than that of the pterin-6-carboxylic acid standard.

In preliminary spectrophotometric and fluorometric studies, Compound P behaved in a manner like pterin-6-carboxylic acid (Figs. 5–8). In Figs. 5 and 6 the absorption maxima for Compound P are 365 nm and 260 nm and those for pterin-6-carboxylic acid, 366 nm and 263 nm (lit.[6] 365 nm and 262

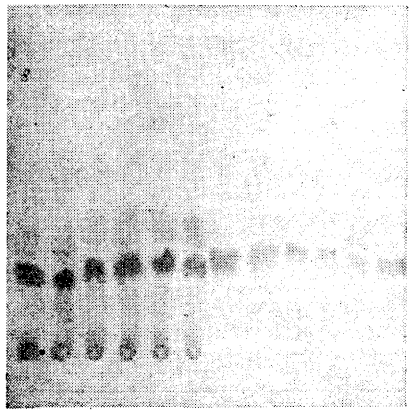

Fig. 3. Degradation of *p*-aminobenzoylglutamic acid with time by the action of cell protein. The reaction mixture contained 5 mg/10 ml of protein. 200 µl specimens were taken from the reaction mixture at intervals of 30 min and applied onto paper. Spot 1 represents the specimen taken at the beginning of reaction, whereas spots 7 – 12 represent those taken at intervals of 30 min from a reaction mixture that did not contain protein.

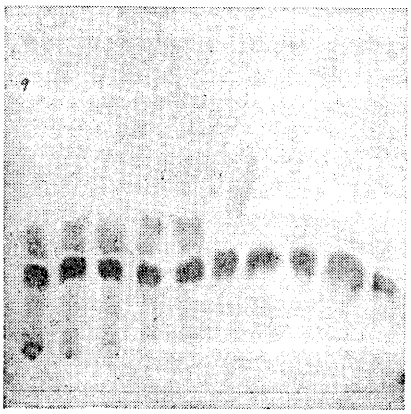

Fig. 4. Continuation of Fig. 3. Spots 1 – 5 represent specimens taken from the reaction mixture between 3 and 5 h after the reaction was initiated. Spots 6 – 10 are specimens taken from a reaction mixture not containing protein.

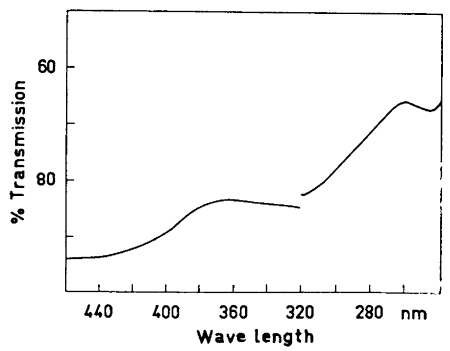

Fig. 5. Absorption spectrum of Compound P.

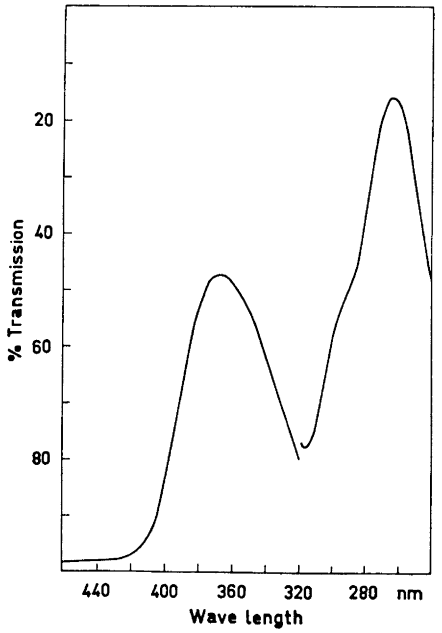

Fig. 6. Absorption spectrum of pterin-6-carboxylic acid.

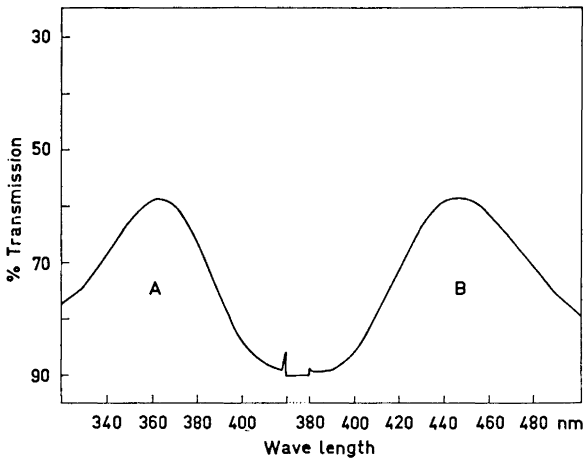

Fig. 7. Excitation spectrum A and fluorescence spectrum B of Compound P.

nm). For pure pterin we got values of 363 nm and 252 nm which agree with the literature values.[6] A third compound that could represent Compound P is 6-methylpterin. It was not available, but the literature values for it at pH 13 are 365 nm and 253 nm.[7]

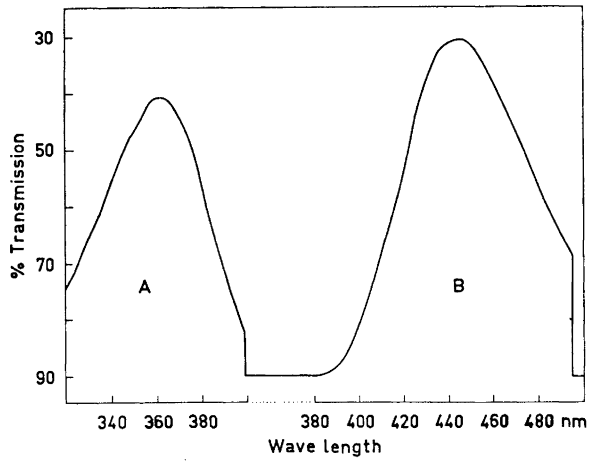

Fig. 8. Excitation spectrum A and fluorescence spectrum B of pterin-6-carboxylic acid.

Figs. 7 and 8 show the results of fluorometric measurements. Both Compound P and pterin-6-carboxylic acid exhibited the same excitation and fluorescence maxima, 363 nm and 447 nm. The literature values are 360 nm and 450 nm.[8]

The appearance of Compound P was noted only when *Ps. fluorescens* UK-1 had grown in the presence of folic acid. When glutamate or pantothenate were the only sources of carbon and nitrogen, Compound P did not form in the reaction mixture. We intend to investigate the nature of Compound P in future studies.

REFERENCES

1. Levy, C. C. and Goldman, P. *J. Biol. Chem.* **242** (1967) 2933.
2. McCullough, J. L., Chabner, B. A. and Bertino, J. R. *J. Biol. Chem.* **246** (1971) 7207.
3. Heepe, F., Karte, H. and Lambrecht, E. *Z. Kinderheilk.* **69** (1951) 331; ref. Layne, E. In Colowick, S. P. and Kaplan, N. O., Eds., *Methods in Enzymology*, Academic, New York 1957, Vol. 3 p. 447.
4. Goto, M., Forrest, H. S., Dickerman, L. H. and Urushibara, T. *Arch. Biochem. Biophys.* **111** (1965) 8.
5. *Data for Biochemical Research*, Eds. Lawson, R. M., Elliot, W. H., Elliot, D. C. and Jones, K. M., 2nd Ed. Clarendon Press, Oxford 1969, pp. 521–522.
6. Stokstad, E. L., Hutchings, B. L., Mowat, J. H., Boothe, J. H., Waller, C. W., Angier, R. B., Semb, J. and SubbaRow, Y. *J. Am. Chem. Soc.* **70** (1948) 5.
7. Mowat, J. H., Boothe, J. H., Hutchings, B. L., Stokstad, E. L., Waller, C. W., Angier, R. B., Semb, J., Cosulich, D. B. and SubbaRow, Y. *J. Am. Chem. Soc.* **70** (1948) 14.
8. Uyeda, K. and Rabinowitz, J. C. *Anal. Biochem.* **6** (1963) 100.

Received February 9, 1973.

ACTA CHEMICA SCANDINAVICA 27 (1973) 2121–2130

Reaction Rate Studies of the Acid Hydrolysis of Some Chromium(III) Complexes I. The Acid Hydrolysis of Monoamminepentaaquachromium(III) Ions and of *cis*- and of *trans*-Diamminetetraaquachromium(III) Ions in Aqueous Perchloric Acid

L. MØNSTED and O. MØNSTED

Chemistry Department I, Inorganic Chemistry, The H. C. Ørsted Institute, University of Copenhagen, DK-2100 Copenhagen, Denmark

The acid hydrolysis of monoamminepentaaquachromium(III) and of *cis*- and of *trans*-diamminetetraaquachromium(III) cations has been investigated in 0.5 to 1.0 M $HClO_4$ at an ionic strength of 1.0 in the temperature range 60 – 80°C.

In the reaction scheme:

$$\begin{array}{l} cis\text{-}[Cr(NH_3)_2(OH_2)_4]^{3+} \\ \quad k_{2tc} \Big\| \; k_{2ct} \quad [Cr(NH_3)(OH_2)_5]^{3+} \xrightarrow[\nearrow k_{2t}]{\searrow k_{2c}} [Cr(OH_2)_6]^{3+} \quad k_1 \\ trans\text{-}[Cr(NH_3)_2(OH_2)_4]^{3+} \end{array}$$

all reaction pathways were well defined, except the *cis*- to *trans*-diamminetetraaquachromium(III) isomerization reaction, and rate constants at 70°C and activation energies were found to be:

k_1:	$(1.110 \pm 0.012) \times 10^{-6}$ sec^{-1},	28.8 ± 0.3 kcal/mol
k_{2c}:	$(3.30 \pm 0.19) \times 10^{-6}$ sec^{-1},	27.8 ± 0.3 kcal/mol
k_{2t}:	$(17.6 \pm 0.3) \times 10^{-6}$ sec^{-1},	26.3 ± 0.4 kcal/mol
k_{2tc}:	$(5.2 \pm 0.2) \times 10^{-6}$ sec^{-1},	28.1 ± 1.1 kcal/mol

For the *cis* to *trans* isomerization reaction the rate constant was found to have an upper limit of 0.6×10^{-6} sec^{-1} at 70°C. Hence this path contributes less than 20 % to the disappearance of the *cis*-diamminetetraaquachromium(III) ion, and the equilibrium value for the concentration of *trans*-diamminetetraaquachromium(III) isomer is estimated to be less than 10 % of the total amount of diamminetetraaquachromium(III) ions present.

All rate constants were found to be independent of the hydrogen ion concentration in the acidity range studied.

As all the isomers in the ammineaquachromium(III) system are known, this system should prove ideal for a systematic investigation of some of the geometrical factors which influence the kinetic behaviour of octahedral substitution reactions. We report here, as the first part of an investigation of the acid hydrolysis of all the ammineaquachromium(III) ions, results for the acid hydrolysis of *cis*- and *trans*-diamminetetraaquachromium(III) and of monoamminepentaaquachromium(III) ions in 0.5 to 1.0 M perchloric acid at an ionic strength of 1.0, adjusted with sodium perchlorate.

This system has been studied previously by Jørgensen and Bjerrum [1] and also by Jørgensen [2] in nitrate containing media. However, later results of Espenson and Carlyle [3] for the monoamminepentaaquachromium(III) hydrolysis, show that nitrate ions have an accelerating effect on this reaction. The easy accessibility of the *cis*-diamminetetraaquachromium(III) [4] and the monoamminepentaaquachromium(III) ions,[5] compounds not readily available to Jørgensen and Bjerrum at the time of their investigations, together with the catalytic effect of nitrate ions, made a reinvestigation in perchlorate containing media seem worthwhile.

EXPERIMENTAL

Chemicals. Ion exchanged water, distilled from alkaline permanganate in an all quartz apparatus, was employed throughout. Sodium perchlorate (Fluka *puriss. p.a.*) and perchloric acid (Merck 70 % *p.a.*) were used without further purification for the kinetic experiments.

Chromium complexes were prepared by literature methods [1,4-6] with insignificant modifications, except that the previously unreported *trans*-$[Cr(NH_3)_2(OH_2)_2(OH)_2]ClO_4$ was prepared from *trans*-$[Cr(NH_3)_2(OH_2)_2(OH)_2]Br$ by dissolving this compound in dilute perchloric acid, and precipitating the perchlorate by addition of pyridine. After two reprecipitations with pyridine from dilute perchloric acid, no trace of bromide ions could be detected. Small amounts of polymeric chromium species were not readily removed by this method of purification, but were easily removed by the ion exchange chromatographic method described below, so that no further purification of the solid compound was attempted.

Preparation of solutions. $K_2Cr_2O_7$, $Cs[Cr(NH_3)(OH_2)_5](SO_4)_2.12H_2O$, *cis*-$[Cr(NH_3)_2(OH_2)_2Cl_2]Cl$ and *trans*-$[Cr(NH_3)_2(OH_2)_2(OH)_2]ClO_4$, were used as the initial materials for the preparation of $[Cr(OH_2)_6]^{3+}$, $[Cr(NH_3)(OH_2)_5]^{3+}$, *cis*-$[Cr(NH_3)_2(OH_2)_4]^{3+}$, and *trans*-$[Cr(NH_3)_2(OH_2)_4]^{3+}$ ions, respectively, in solution. Except for the dichloro complex, where the diamminetetraaqua complex was obtained after mercury(II) assisted chloride hydrolysis, and for potassium dichromate, where the hexaaquachromium(III) ion was obtained by reduction with hydrogen peroxide in dilute perchloric acid solution, the other ammineaqua complexes were formed directly by dissolving the substances in dilute perchloric acid.

Further purification of solutions obtained in this way was carried out as follows: an amount of solution containing about 1 mequiv. of chromium complex was charged onto a column (2 cm × 10 cm) packed with Dowex 50 W X8 200/400 mesh cation-exchanger prewashed with 2 M sulphuric acid and water. Excess hydrogen peroxide was now removed from the column with water, and excess mercury(II) with 0.5 M hydrochloric acid. The complexes were then displaced with 2 M sulphuric acid, as this solvent was able to separate the diammines from the monoammine and the monoammine from the hexaaquachromium(III) complex. The complexes were eluted in the following order: first hexaaqua-, then monoamminepentaaqua-, and last the diamminetetraaquachromium(III) ions. Although the separation of complexes with different numbers of coordinated ammonia molecules proceeded without difficulties, it proved rather difficult by this method to achieve separation between the isomeric diamminetetraaquachro-

mium(III) complexes. All separations were conducted at 15 – 20°C, as further cooling proved to be unnecessary (see Table 2). They were, however, made in the dark, as the *trans*-diammine when illuminated by daylight, but much less so in artificial light, isomerized to form the *cis*-isomer. After elution on the Dowex-column the main fraction was diluted approximately 100 times with water and adsorbed on about 5 ml of Sephadex SE-C-25. After washing with water, the chromium(III) complexes were displaced with 1 M sodium perchlorate solution. This last purification serves a multiple purpose. Firstly, it removes the sulphuric acid necessary for the separation of the tripositive ions, but unwanted in the kinetic investigations. Secondly, if small amounts of sulphato complexes were present, these complexes would by this treatment, because of their lower charge, be separated from the tripositive main species. However, spectral comparison between the sulphuric acid effluents and solutions of the purified compounds, gave no indication of sulphate complex formation during the time necessary for the elution to take place. Also the results of Table 2, which do not show any difference between elution experiments at 0°C and 20°C, indicate the absence of sulphato complexes. Thirdly, the small amount of UV-absorbing materials given off by the Dowex column are being disposed of. After dilution with an appropriate amount of 1 M perchloric acid, the solutions obtained were used either to measure the spectra of the purified ammineaqua complexes, see Table 1 and Fig. 1, or for the kinetic investigations.

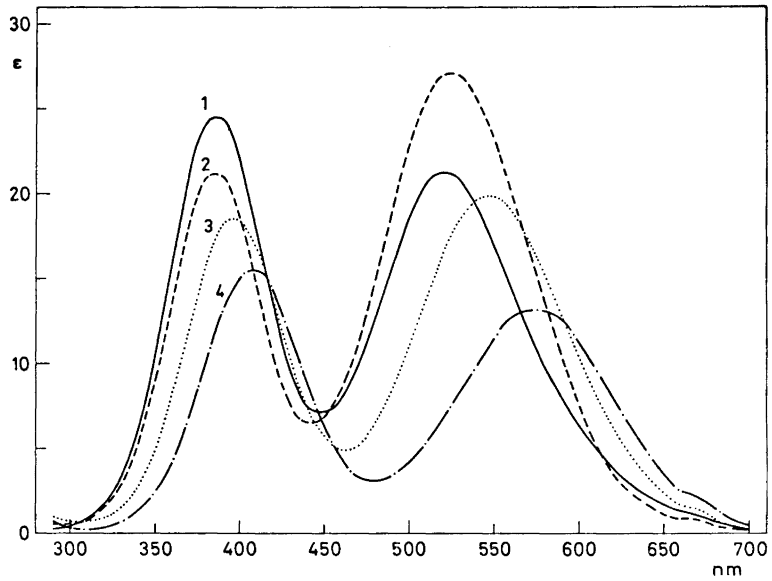

Fig. 1. Visible absorption spectra of compounds prepared and purified as described in the text. 1: *trans*-$[Cr(NH_3)_2(OH_2)_4]^{3+}$, 2: *cis*-$[Cr(NH_3)_2(OH_2)_4]^{3+}$, 3: $[Cr(NH_3)(OH_2)_5]^{3+}$ and 4: $[Cr(OH_2)_6]^{3+}$. The spectra measured are identical in 1.0 M $HClO_4$ and in 0.5 M $HClO_4$ + 0.5 M $NaClO_4$.

For different methods of purification the differences in reaction rates were insignificant. This is seen from experiments 1, 3, and 4 (Table 3) where the initial solutions of the *trans*-diamminetetraaquachromium(III) ion were obtained in three different ways: by direct dissolution of the *trans*-$[Cr(NH_3)_2(OH_2)_2(OH)_2]ClO_4$ in perchloric acid (expt. 1), by purification of the *trans* solution by passing it through a Sephadex column only (expt. 3), and by the method used for all remaining experiments and described above (expt. 4).

Table 1. Comparison of spectral characteristics of compounds, prepared and purified as described in the text, with literature values.

Complex	Medium	λ_1 max nm	ε_1 max l/(mol cm)	λ_2 max nm	ε_2 max l/(mol cm)	ε_1 max/ε_2 max	Ref.
trans-$[Cr(NH_3)_2(OH_2)_4]^{3+}$	0.5 M $HClO_4$ + 0.5 M $NaClO_4$	522	21.3	387	24.6	0.865	*a*
	0.5 M HNO_3	520	22	385	24.5	0.895	1[b]
	3 M $HClO_4$	530	21.0	390	18.9	1.11	8[c]
cis-$[Cr(NH_3)_2(OH_2)_4]^{3+}$	0.5 M $HClO_4$ + 0.5 M $NaClO_4$	526	27.0	386	21.3	1.27	*a*
	0.4 M $HClO_4$ + 0.4 M $Hg(ClO_4)_2$	525	26.8	386	21.5	1.25	4
$[Cr(NH_3)(OH_2)_5]^{3+}$	0.5 M $HClO_4$ + 0.5 M $NaClO_4$	547	19.9	396	18.6	1.07	*a*
	~0.5–2 M $HClO_4$	547	20.5	397	19.0	1.08	3
	1 M $HClO_4$	545	22.1	397	21.8	1.03	5
	0.5 M HNO_3	550	19	390	18	1.06	1[b]
$[Cr(OH_2)_6]^{3+}$	0.5 M $HClO_4$ + 0.5 M $NaClO_4$	574	13.2	407	15.5	0.852	*a*
	1 M $HClO_4$	574	13.4	408	15.8	0.848	5

[a] This work. [b] Estimated from the graph in this reference. [c] Reported as the *trans*-$[Cr(NH_3)_2(OH_2)_4]^{3+}$, but see text.

Table 2. Separation behaviour of *trans*- and a mixture of *cis*- and *trans*-diamminetetraaquachromium(III) ions. Absorbances of first and second spin-allowed band (A_1 and A_2) of the fractions, measured in 2.0 M H_2SO_4.

	Experiment at 20°C						Experiment at 0°C					
Fraction		*trans*			Mixture			*trans*			Mixture	
No.	A_2	A_1	Δ[a]	A_2	A_1	Δ[a]	A_2	A_1	Δ[a]	A_2	A_1	Δ[a]
0	0	0	−0.8	0	0	−1.5	0	0	0.5	0	0	−0.1
1	0.557	0.476	0.9	0.508	0.450	−2.2	0.042	0.036	0.6	0.010	0.009	0.0
2	0.880	0.749	−1.1	0.803	0.712	−1.9	0.180	0.153	−0.2	0.047	0.040	−1.8
3	0.708	0.604	0.4	0.568	0.509	3.6	0.306	0.261	0.2	0.230	0.202	−2.3
4	0.346	0.296	0.6	0.287	0.258	1.9	0.241	0.205	−0.3	0.281	0.250	0.4
5	—	—	—	—	—	—	0.151	0.129	0.6	0.227	0.202	0.3
6	—	—	—	—	—	—	0.065	0.054	−1.0	0.157	0.141	1.5
7	—	—	—	—	—	—	0.022	0.018	−0.3	0.100	0.091	2.1
8	—	—	—	—	—	—	—	—	—	0.053	0.047	−0.1
α		0.8515 ± 0.0015			0.887 ± 0.005			0.854 ± 0.002			0.888 ± 0.005	

[a] $\Delta = 1000(A_1 - \alpha A_2 - \beta)$; with α and β determined as slope and intercept of a straight line, determined by the method of least squares, through the points.

Table 3. Rate constants and initial complex concentrations calculated for individual kinetic experiments in a reaction scheme with *cis*- to *trans*-diamminetetraaquachromium(III) isomerization absent.

Run No.	$10^6 \times C_0$ (M)	$10^6 \times k_{2t}$ (sec^{-1})	$10^6 \times k_{2tc}$ (sec^{-1})	$10^6 \times k_{2c}$ (sec^{-1})	$10^6 \times k_1$ (sec^{-1})	Temp (°C)	t_{max}(h)
	trans-$[Cr(NH_3)_2(OH_2)_4]^{3+}$						
1	2260±16	55.4±1.4	16.8±1.4	10.0±1.4	3.7±0.3	80.20	29
2[a]	1959±11	50.2±2.3	14.5±2.5	8.8±1.0	— [b]	80.00	7
3	2431±19	53.3±1.3	17.4±1.5	11.2±1.6	3.5±0.3	80.20	29
4	1278±6	56.9±1.8	17.8±1.8	11.1±1.6	3.4±0.2	80.35	47
5	1285±4	17.4±0.3	4.5±0.3	2.9±0.3	0.91±0.09	69.70	98
6	1611±4	5.54±0.10	1.53±0.11	1.10±0.17	0.258±0.023	60.18	336
	cis-$[Cr(NH_3)_2(OH_2)_4]^{3+}$						
7	1021±4	—	—	11.51±0.18	3.50±0.10	80.20	264
8[a]	862±4	—	—	10.7±0.3	3.82±0.15	80.35	311
9	854±4	—	—	3.15±0.05	1.07±0.03	69.70	98
10	1586±6	—	—	1.026±0.013	0.315±0.009	60.18	819
	$[Cr(NH_3)(OH_2)_5]^{3+}$						
11	1654±4	—	—	—	3.83±0.06	80.20	167
12[a]	1808±4	—	—	—	3.86±0.04	80.20	168
13	3661±9	—	—	—	0.327±0.004	60.18	819

[a] Kinetic runs in 0.5 M $HClO_4$ + 0.5 M $NaClO_4$; all other in 1.0 M $HClO_4$.
[b] Experiment followed for too short a time for this constant to be well defined.

It is also noteworthy that the calculated total chromium concentrations are the same for experiments 4 and 5 and for experiments 8 and 9 (Table 3) and that both pairs were prepared from the same stock solutions.

Kinetic measurements. Aliquots of solutions prepared as described above in a suitable number of sealed glass ampoules were immersed into a thermostated water bath maintained at the desired temperature with an accuracy of ± 0.05°C. During the advancing hydrolysis the solutions were kept protected from light. At suitable time intervals ampoules were withdrawn from the thermostat, and the reactions quenched by cooling the reaction mixtures in an ice bath. Spectra of the reacted solutions were measured on a Cary 14 recording spectrophotometer equipped with a $0-0.2$ A slidewire. These measurements were performed at room temperature, that is 23 ± 2°C, as the temperature independence of the spectra in the range measured, $700-290$ nm, made a more careful thermostating unnecessary. Spectra of the pure substances were obtained analogously, except that these stronger solutions permitted the use of a $0-1$ A or $0-2$ A slidewire.

Methods of analysis. Chromium concentrations were determined by spectrophotometric measurements at the chromate(VI) absorption maximum at 373 nm after oxidation of the chromium(III) containing solutions with hot alkaline hydrogen peroxide solution. In good agreement with earlier results the molar extinction coefficient for our particular instrument was found to be 4826 ± 8 l/(mol cm).

Hydrogen ion concentrations and the sum of concentrations of hydrogen and sodium ions were determined by titrating with sodium hydroxide solution prior to and after exchange of sodium ions with hydrogen ions.

Method of calculation. The method of calculation was that of a nonlinear regression analysis. This will be described at length elsewhere.[7] Here we direct attention only to some points of particular interest for the present study.

The large number of individual measurements (approximately 5000) obtained over an extended period of time precluded the simultaneous reduction of all the primary data, and the datareduction, which ultimately yielded the contents of Tables 4 and 5 was

Table 4. Rate constants and activation energies for all kinetic experiments of Table 3.

	60°C	70°C	80°C	E_A(kcal/mol)
$10^6 \times k_{2t}$ (sec^{-1})	5.51 ± 0.15	17.6 ± 0.3	52.5 ± 1.0	26.4 ± 0.4
$10^6 \times k_{2tc}$ (sec^{-1})	1.52 ± 0.12	5.2 ± 0.2	16.8 ± 0.9	28.0 ± 1.2
$10^6 \times k_{2c}$ (sec^{-1})	0.986 ± 0.018	3.34 ± 0.04	10.6 ± 0.2	27.7 ± 0.4
$10^6 \times k_1$ (sec^{-1})	0.315 ± 0.006	1.115 ± 0.012	3.67 ± 0.05	28.7 ± 0.3

Table 5. Rate constants and activation energies calculated for all kinetic experiments in a reaction scheme with the *cis*- to *trans*-diamminetetraaquachromium(III) isomerization reaction included.

	60°C	70°C	80°C	E_A(kcal/mol)
$10^6 \times k_{2t}$ (sec^{-1})	5.51 ± 0.17	17.6 ± 0.3	52.4 ± 1.0	26.3 ± 0.4
$10^6 \times k_{2tc}$ (sec^{-1})	1.51 ± 0.11	5.2 ± 0.2	16.7 ± 0.8	28.1 ± 1.1
$10^6 \times k_{2c}$ (sec^{-1})	0.97 ± 0.06	3.30 ± 0.19	10.5 ± 0.6	27.8 ± 0.3
$10^6 \times k_{2ct}$ (sec^{-1})	0.00 ± 0.09	0.0 ± 0.3	0.0 ± 0.9	–
$10^6 \times k_1$ (sec^{-1})	0.313 ± 0.006	1.110 ± 0.012	3.66 ± 0.04	28.8 ± 0.3

therefore carried out in the following three steps. Firstly, the composition of quenched reaction mixtures was calculated from the spectra of these solutions and those of the four pure components. Absorption spectra from 290 nm to 700 nm measured at 10 nm intervals were employed in all the experiments. In this reduction of the primary data to yield concentrations of reaction products as function of time, the additional requirement, that in order to be chemically significant the concentrations had to be greater than or equal to zero, was applied.

Secondly, the concentrations as function of time permitted the calculation of the rate constants and of the initial complex concentrations for kinetic runs at various temperatures and hydrogen ion concentrations (Table 3).

Thirdly, rate constants (k_{T_0}) at a series of fixed temperatures (T_0), which were close to those at which the actual experiments were made, were calculated together with activation energies (E_A). These calculations were based upon the rate constants estimated for the individual kinetic runs (k_T), as a function of temperature(T), according to eqn. (1):

$$k_T = k_{T_0} \exp[-E_A(1/RT - 1/RT_0)] \quad (1)$$

Table 4 gives rate constants at 80, 70, and 60°C and activation energies calculated from the data of Table 3.*

RESULTS AND DISCUSSION

When a solution approximately 50 mM in *trans*-diamminetetraaquachromium(III) and 1 M in perchloric acid was kept in the dark at 80°C for 4 h, and the resulting mixture separated as described in the experimental section, three bands resulted. The two substances eluted first were identified as the hexaaquachromium(III) and the monoamminepentaaquachromium(III) ions, respectively. As the total amount of hexaaquachromium(III) in this particular experiment amounted to only a few percent of the total chromium ions present, this ion was only identified from its elution behaviour (known of course from columns with greater hexaaquachromium(III) ion content) whereas the monoamminepentaaquachromium(III) ion was identified through its visible absorption spectrum. The last eluate was identified from the visible absorption spectrum as containing a mixture of the *cis* and the *trans*-diamminetetraaquachromium(III) ions. The *cis*-diamminetetraaqua- and the monoamminepentaaquachromium(III) ions were studied in the same way except for reaction times of 24 and 48 h, respectively. With the former no *trans* was observed but *cis*-diamminetetraaqua-, monoamminepentaaqua-, and hexaaquachro-

* It should be noted that nondiagonal variance matrices were always employed in the latter two data reductions described above. Consequently, the data of Table 4 are not directly obtainable from those of Table 3 without knowledge of nondiagonal elements of the variance matrix for the data of Table 3.

The importance of these nondiagonal elements is particularly well illustrated by the data obtained when k_{2ct} is included in the calculations. As no significant amounts of *trans*-diamminetetraaquachromium(III) was ever obtained in experiments started with the *cis*-diamminetetraaquachromium(III) the normal equations became almost singular for these kinetic runs. Consequently rather large standard deviations were always obtained upon the highly correlated rate constants (k_{2t}, k_{2tc}, k_{2c}, and k_{2ct}) in these experiments. This can be illustrated by values of 12.7 ± 3.1, 6.1 ± 5.4, 3.3 ± 0.6, and 0.99 ± 0.15 sec^{-1} found for 10^6 k_{2c} in experiments 7 to 10. Had correlation terms been neglected in the following computation, the significantly better defined values for k_{2c} of Table 5 would never have been obtained. This of course is also the reason why the data reductions described by the above modified equation of Arrhenius (eqn. 1), resulting in Tables 4 and 5 in this investigation, have been chosen, as rate constants for individual kinetic runs seldom reflect the total content of information in a kinetic investigation when reaction schemes become sufficiently complicated.

mium(III) ions were all three identified from their visible absorption spectra. In the monoammine experiment only monoamminepentaaqua- and hexaaquachromium(III) ions could be detected.

The following reaction scheme:

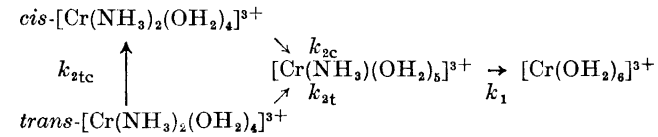

although it could have accommodated the experimental results was not immediately accepted because isomerization reactions of chromium(III) complexes, in which monodentate ligands only are present, are not commonly encountered. As the absence of the isomerization reaction would require contamination of the supposed *trans*-isomer with the *cis*-isomer, the isomeric purity of the *trans*-diamminechromium(III) compounds employed to generate the *trans*-diamminetetraaquachromium(III) ion in solution was investigated in more detail.

cis-Diamminechromium(III) compounds may in fact be obtained as products of the oxidation of Reinecke salt (ammonium *trans*-diamminetetrakis-(isothiocyanato)chromate(III) monohydrate). This is demonstrated by the results of House:[8] by oxidation of Reinecke salt with *aqua regia*, and treatment of the oxidation product with concentrated hydrobromic acid a dibromo compound precipitated, and after hydrolysis of the bromide ligands in this compound he obtained a diamminetetraaquachromium(III) solution, said to be that of the *trans*-isomer. The visible absorption spectrum of solutions thus generated did not agree with that of neither the *cis*- nor the *trans*-diamminetetraaquachromium(III) ions prepared by other methods (Table 1 and Fig. 1). Therefore solutions obtained by the method of House were investigated further. Ion exchange experiments revealed appreciable amounts of the monoamminepentaquachromium(III) ion, and from the visible absorption spectrum of the diammine fraction this was interpreted as a mixture of the isomeric diamminetetraaquachromium(III) ions with the *cis*-isomer as main constituent. This result indicates that *cis*-diamminechromium(III) compounds may well be present in the *trans*-diamminechromium(III) compounds prepared by the oxidation of Reinecke salt. In order to answer this question some separation experiments using the supposed *trans*-isomer product prepared according to Werner and Klien [6] and also this product mixed with a known amount of the *cis*-isomer prepared according to Andersen and Berg [4] were carried out.

It was found that diamminediaquadihydroxochromium(III) perchlorate prepared from a mixture of the dichloro compounds of the two diammines, containing the *cis*- and the supposed *trans*-diammine in the ratio 1:4, was indistinguishable from that prepared from the dichloro compound of the supposed *trans*-diammine alone. This was shown by comparing the visible absorption spectra of the diamminetetraaquachromium(III) ion generated by dissolving the dihydroxo compounds in dilute perchloric acid. As this spectrum did not change on further reprecipitation it must either be concluded that we have a pure isomer or a crystal reprecipitating with a constant ratio

between *cis*- and *trans*-isomer. From kinetic experiments the content of *cis*-isomer in *trans*-diamminetetraaquachromium(III) solutions prepared as described in the experimental part is found to be 25.0 ± 0.8 %, if the isomerization reaction is disregarded as a source of the *cis*-isomer. Thus a *cis*- to *trans* ratio of 1:3 in diamminediaquadihydroxochromium(III) perchlorate is predicted.

Ion exchange experiments with the *trans*-isomer and a mixture containing about 85 % of the *trans*- and about 15 % of the *cis*-isomer gave, when the diamminetetraaquachromium(III) effluent was fractionated, the results of Table 2. In this table results of a plot of the absorbance at the maximum of the second band against the absorbance at the maximum of the first band are shown for four fractionation experiments. The deviations from linearity are seen to be particularly systematic in the solutions known to be mixtures, whereas in the fractionation of the *trans*-solutions, no systematic trends are observed. The separation results are seen to be in agreement with the *cis trans* assignment of the isomeric diamminetetraaquachromium(III) ions based upon their mode of formation and visible absorption spectra, as *trans*-complexes are generally eluted more readily than the corresponding *cis*-isomers. From the 1:3 ratio of *cis* to *trans*, predicted from the kinetic experiments, *trans*-isomer contents in the two sets of solutions employed in the ion exchange experiments of 75 % and 64 % were calculated. These values are far too little different to account for the observed elution behaviour. It is therefore concluded that the *trans*-compounds prepared by bromine and chlorine oxidation of Reinecke salt are isomerically pure, and consequently that *trans* to *cis* isomerization does occur in the absence of light in diamminetetraaquachromium(III) solutions. Also the high reproducibility of the visible absorption spectrum of the *trans*-diamminetetraaquachromium(III) ion, whether this was prepared from dibromo-, dichloro-, or dihydroxo-diamminediaquachromium(III) compounds,[6] renders possible reprecipitation of the dihydroxo compound with a constant ratio of *cis*- to *trans*-isomer unlikely.

Table 3 shows rate constants and initial complex concentrations calculated for a series of kinetic experiments. The reaction rates are seen to be the same within the experimental error in 0.5 M and 1.0 M acid, when some small temperature differences are taken into consideration, so that at these high acidities reactions of deprotonated species need not be considered.

From Table 4 it is seen that k_{2t} is appreciably larger than k_{2c}. This means that a significant amount of *cis*-isomer may well hydrolyze *via* the *trans*-isomer, as the magnitude of k_{2t} prevents the build up of significant concentrations of the *trans*-isomer. In order to estimate to what extent this took place the *cis* to *trans* isomerization rate constant, k_{2ct}, was included in the calculations. Results of these calculations are shown in Table 5. As could be expected, no well defined value of k_{2ct} was obtained, as the kinetic experiments were already adequately described within the simpler reaction scheme with k_{2ct} absent. Some important conclusions may, however, be drawn by comparing Tables 4 and 5. The significant difference between the two tables lies in the standard deviation associated with k_{2c}, which is seen to be about three times larger in Table 5 than in Table 4. This is not unexpected since the high negative correlation between k_{2c} and k_{2ct} (as a result of the magnitude of k_{2t}) with a

correlation coefficient of about -0.98 should have this effect. Had k_{2t} been much greater almost complete correlation between k_{2c} and k_{2ct} would have existed. This would have rendered standard deviations upon k_{2c} and k_{2ct} as individual parameters so large as to invalidate the quantitative information in these separated parameters completely. In this case only the sum $k_{2c}+k_{2ct}$ could have been obtained with reasonable accuracy from the experiments. This is in agreement with the intuitive chemical considerations on the reaction scheme and also with the data of Table 4 as values of k_{2c} in this table are values of the sum $k_{2c}+k_{2ct}$ when the *cis* to *trans* isomerization reaction is included in the reaction scheme.

If two standard deviations are taken as an upper limit for k_{2ct} two interesting results emerge from Table 5. Firstly, less than about 20 % of the *cis*-diammine disappears *via* the *trans*-diammine, and secondly, in solutions at equilibrium with respect to the diamminetetraaquachromium(III) ions less than 10 % is present as the *trans*-isomer.

A more thorough discussion from a stereochemical and kinetic point of view, of the data presented here will be presented when our current studies of the acid hydrolysis of the other $[Cr(NH_3)_n(OH_2)_{6-n}]^{3+}$ ions ($n=3$, 4, 5, and 6) have been concluded.

REFERENCES

1. Bjerrum, J. and Jørgensen, E. *Acta Chem. Scand.* **12** (1958) 1047.
2. Jørgensen, E. *International Conference on Coordination Chemistry*, London 1959, p. 172.
3. Espenson, J. H. and Carlyle, D. W. *Inorg. Chem.* **5** (1966) 586.
4. Andersen, P. and Berg, T. *To be published.*
5. Ardon, M. and Mayer, B. E. *J. Chem. Soc.* **1962** 2816.
6. Werner, A. and Klien, J. *Ber.* **35** (1902) 277.
7. Mønsted, L. and Mønsted, O. *To be published.*
8. House, D. A. *Austral. J. Chem.* **22** (1969) 647.

Received February 13, 1973.

ACTA CHEMICA SCANDINAVICA 27 (1973) 2131–2134

Selfcondensation of Propionylpyruvic Ethyl Ester

ODD ANTONSEN and ENDRE BERNER

Kjemisk Institutt, Universitetet i Oslo, Blindern, Oslo 3, Norway

The condensation of propionylpyruvic ester proceeded analogous to that of acetopyruvic esters. The condensation product on degradation led to several acids amongst which a β-ketoacid $C_{12}H_{12}O_6$ on sublimation or by dissolving in conc. sulphuric acid split off one molecule of water. This reaction was found to be due to the occurrence of the lactol-form of the β-ketoacid.

The bimolecular condensation of acetopyruvic esters was first described by Claisen [1] but only quite recently a satisfactory scheme for the condensation process has been put forward by Berner and Kolsaker.[2] It has now been found that the ethyl ester of propionylpyruvic acid undergoes a similar condensation. The new condensation product (called PPE) is a crystalline substance with m.p. 67 – 70°C and the composition $C_{14}H_{18}O_7$. Contrary to the condensation products from acetopyruvic esters, it does not contain crystal water. Based upon the results obtained with the acetopyruvic esters, PPE is assigned the structural formula I.

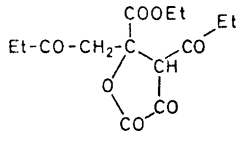

I

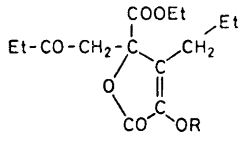

IIa: R = H
IIb: R = CH_3

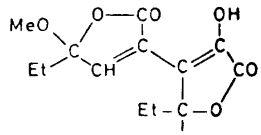

III

As in the case of the condensation products of acetopyruvic esters, PPE on catalytic hydrogenation took up 2 mol of hydrogen and split off 1 mol of water giving a crystalline product $C_{14}H_{20}O_6$ which is given formula IIa. It could be titrated as a monovalent acid and on treatment with diazomethane gave a methoxy derivative (IIb).

Similarly PPE on treatment with methanol containing hydrogen chloride gave a so-called isoester with the same composition as PPE and assigned formula III.

Formula I was verified by the results of a degradation which took place on heating PPE with barium hydroxide. Besides ethanol and water also oxalic and propionic acids were split off, and, although with considerable difficulty, the following three aromatic acids were isolated: *A*, $C_{12}H_{12}O_6$, containing all the carbon atoms from the original carbon-skeleton and obviously being 2-propionyl-4-methyl-5-hydroxyisophthalic acid (IVa). *B*, $C_{10}H_{12}O_3$, arising when oxalic acid is lost. It is accordingly homologous to the 3-methyl-5-hydroxybenzoic acid obtained from the condensation product of acetopyruvic ester and has the formula 3-ethyl-4-methyl-5-hydroxybenzoic acid. *C*, $C_9H_8O_5$, which as a propionyl group has been split off, must be 4-methyl-5-hydroxy-isophthalic acid.

The separation of these acids could not be effected by crystallization alone, but sublimation in a vacuum had alternately to be used. The least volatile of the acids (*A*) was isolated as a rest after a partial sublimation and after recrystallization had the composition $C_{12}H_{12}O_6$ (IVa). But even this acid could be sublimated by using sufficiently high temperature, resulting, however, in a crystalline substance with the formula $C_{12}H_{10}O_5$ (VIa). A similar dehydration took place when *A* was dissolved in conc. sulphuric acid. Recently it has been found in this institute [3] that even other β-ketoacids on dissolving in conc. sulphuric acid split off water. The explanation for this must be that β-ketoacids occur at least in part in the lactol-form (*e.g.* Va) in accordance with the fact that the esters of such acids are known both in open and cyclic forms. The dehydration in question proceeds as demonstrated in the formulæ IVa, Va, and VIa, which was verified by means of PMR. (Alternatively, the other carboxylic group could be engaged in the cyclization.)

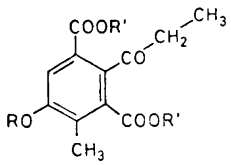

IVa: R = H, R' = H
IVb R = H, R' = CH_3
IVc R = CH_3, R' = CH_3

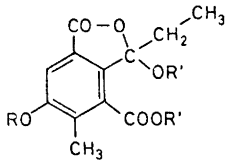

Va: R = H, R' = H
Vb: R = H, R' = CH_3
Vc: R = CH_3, R' = CH_3

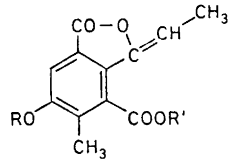

VIa: R = H, R' = H
VIb: R = CH_3, R' = CH_3

It should be added that also the iso-ester (III) was degraded similarly on heating with barium hydroxide, but in this case only the acid $C_9H_8O_5$ was isolated and identified with the acid obtained directly from PPE.

EXPERIMENTAL

Ethyl propionylpyruvate. The ester was first prepared according to Diels *et al.*[4] and later according to Mumm and Böhme.[5] The last mentioned method gave best results especially when working with small portions.

Condensation of ethyl propionylpyruvate. The condensation took place when the ester was shaken at room temperature with an aqueous solution of sodium acetate (equimolecular amounts of acetate and ester). In the course of a few days, the ester had dissolved

and an excess of hydrochloric acid was added. The condensation product separated as an oil which was dried in a vacuum above calcium chloride. All attempts to purify the product at first failed; it was only when the oil after several months spontaneously crystallized that the pure PPE could be isolated. The partly crystallized oil was pressed on a porous plate and the crystals recrystallized from ethyl acetate-ligroin. Yield about 15 %. M.p. 69–70°.* 53.8 mg req. 1.79 ml 0.1004 N NaOH. (Found: C 56.30; H 6.10; M 299. Calc. for $C_{14}H_{18}O_7$: C 56.37; H 6.08; M 298.3.)

Degradation of PPE. 20 g PPE, 40 g barium hydroxide (hydrate) and 400 ml water were heated in a water-bath under stirring for 30 min. The barium oxalate which had separated after reprecipitation weighed 3.2 g (oxalic acid, m.p. 101°, isolated and identified), showing that 22.5 % of PPE had split off oxalic acid. (In a separate experiment, the presence of propionic acid in the filtrate was proved using the method of McNair.[6]) The filtrate from the oxalate on adding 55 ml of 5 N HCl became strongly violet, and on standing until the next day, 8.8 g of a crystalline mixture of acids had separated which showed the equiv. weight 116.

The first acid to be isolated was *B*, *viz.* by sublimating the mixture of acids in a vacuum (12 mmHg) at about 170°. The sublimate after recrystallization from dilute ethanol had m.p. 192°. 51.1 mg req. 2.76 ml 0.101 N NaOH. (Found: C 66.69; H 6.75; M 183. Calc. for $C_{10}H_{12}O_3$: C 66.65; H 6.67; M 180.2.) The acid gave no derivative with dinitrophenylhydrazine and no colour with ferric chloride. The methyl ester, prepared by means of diazomethane, had m.p. 106°. (Found: C 68.00; H 7.33. Calc. for $C_{11}H_{14}O_3$: C 68.02; H 7.27.)

Rising the temperature during sublimation to about 250° a second fraction was obtained containing mainly the acid *C*. As it was futile to purify by crystallization, the acid was first esterified by boiling a 10 % solution in methanol containing 5 % sulphuric acid. The ester after recrystallization from dilute methanol had m.p. 168°. (Found: C 58.85; H 5.10. Calc. for $C_{11}H_{12}O_5$: C 58.92; H 5.40.) PMR showed the following singlets: π 7.47 (s,3H), 6.05 (s,6H), 1H at 4.08, 2.31 and 192.

By saponifying the ester, m.p. 168°, the pure acid *C* was obtained. Recrystallized from dilute ethanol, m.p. 310°. 75.6 mg req. 3.84 ml 0.2 N NaOH. (Found: C 55.00; H 4.16; E 98.5. Calc. for $C_9H_8O_5$: C 55.05; H 4.11; E 98.1.)

A solution of the ester, m.p. 168°, in ether containing a little methanol gave with diazomethane the fully methylated derivative of *C*, m.p. 82° after crystallization from dilute ethanol. (Found: C 60.19; H 5.85; CH_3O 39.78. Calc. for $C_{12}H_{14}O_5$: C 60.50; H 5.92; CH_3O 39.08.) PMR: π 7.53 (s,3H), 6.1 (s,9H), 2.41 (s,1H), and 192 (s,1H). By saponifying the ester, m.p. 82°, the 5-methoxy-4-methylisophthalic acid was isolated, m.p. 310°.

The rest after the sublimation of the mixture of the acids contained mostly both *A* and dehydrated *A*. In order to isolate *A* itself, the mixture was esterified by boiling a solution of it (5.7 g) in 80 ml methanol and 2 ml conc. sulphuric acid for 5 h. After removing the sulphuric acid with barium carbonate and evaporating the solvent, the solid residue was recrystallized many times, partly from ethyl acetate and partly from dilute ethanol. The pure cyclic ester (Vb) had m.p. 207°. (Found: C 60.30; H 5.88; CH_3O 22.41. Calc. for $C_{14}H_{16}O_6$: C 59.99; H 5.76; CH_3O 22.14.) PMR: π 9.24 (t,3H), 7.31 (s,3H), 6.90 (s,3H), 6.06 (s,3H), 3.80 (s,1H) 3.24 (s,1H) and a quartet at 7.65 (2H). Saponification: 0.85 g ester, a little methanol and 8 ml 2 N NaOH heated a short time to 50°. On adding 10 ml 2 N H_2SO_4, *A* separated immediately and was recrystallized from water, m.p. 325°. 63.0 mg req. 2.43 ml 0.2 N NaOH. (Found: C 57.36; H 4.92; E 130. Calc. for $C_{12}H_{12}O_6$: C 57.14; H 4.80; E 126.)

The dehydration af *A* was effected either by sublimation in a vacuum at 250–260° or by dissolving the acid in conc. sulphuric acid, and after 15 min pouring the solution in ice-water. In both cases, crystalline VIa was obtained which after recrystallization from dilute ethanol had m.p. 335°. (Found: C 61.73; H 4.47. Calc. for $C_{12}H_{10}O_5$: C 61.54; H 4.30.) PMR in DMSO: π 8.05 (d, 3H), 7.51 (s, 3H), a quartet at 3.33 (1H), 2.24 (1H) and besides 2 mobile H. When VIa was treated with diazomethane in the presence of methanol, a crystalline ester (m.p. 187°) was obtained which as expected from the formula contained two methoxyl groups. PMR: π 7.98 (d, 3H), 7.36 (s, 3H), 6.03 (s, 6H), 3.28 (q, 1H), and 2.28 (s, 1H).

* All melting points are in °C.

When *A* (IVa) was treated with diazomethane in the presence of methanol, the methoxy-derivative of the open ester (IVc) was obtained, m.p. 117°. (Found: C 60.92; H 5.98; CH_3O 31.75. Calc. for $C_{15}H_{18}O_6$: C 61.22; H 6.16; CH_3O 31.64.) PMR: π 8.82 (t, 3H), 7.74 (s, 3H), 6.08–6.14 (s, 9H), 7.26 (q, 2H), and 2.54 (s, 1H).

Transformation of open into cyclic ester. A solution of 0.5 g ester, m.p. 117°, in 5 ml methanol containing 0.2 ml conc. sulphuric acid was boiled for 5 h. On dilution with water the ester Vc separated and was recrystallized from dilute ethanol, m.p. 112°. (Found: C 61.08; H 6.15; CH_3O 32.05. Calc. for $C_{15}H_{18}O_6$: C 61.22; H 6.16; CH_3O 31.64.) PMR: π 9.25 (t, 3H), 7.36 (s, 3H), 6.92 (s, 3H), 6.03 (s, 6H), 7.62 (q, 2H), and 2.32 (s, 1H).

Hydrogenation of PPE. 10 g PPE and 0.5 g platinum oxide in 100 ml methanol during 22 h took up 1345 ml hydrogen (0°, 760 mm); calc. for 2 mol 1420 ml. The filtrate from platinum on evaporation gave 8.9 g crystalline product (IIa) which after successive crystallizations from benzene, water, and dilute methanol had m.p. 123°. 54.6 mg required 0.96 ml 0.2 N NaOH. (Found: C 59.47; H 6.83; CH_3O 16.21; E 285. Calc. for $C_{14}H_{20}O_6$: C 59.14; H 7.09; CH_3O 15.85; E 284.3.) A methoxy-derivative obtained by treatment with diazomethane had m.p. 55°. PMR is rather complex but obviously supporting formula IIb.

Preparation of the isoester. To a solution of 10 g PPE in 50 ml methanol, 2.5 ml conc. HCl were added. After 4 days crystallization started and after 9 days 3.4 g isoester (III) was filtered off. From the mother liquor a little more crystals separated; yield in all, 40 %. Recrystallized from ethyl acetate, m.p. 126°. 41.9 mg req. 1.41 ml 0.102 N NaOH. (Found: C 56.53; H 6.10; CH_3O 21.0; E 292. Calc. for $C_{14}H_{18}O_7$: C 56.37; H 6.08; CH_3O 20.80; E 298.3.) Degradation of III with barium hydroxide was carried out as described for PPE, but in this case only the most volatile of the acids was isolated. M.p. 192°, mixed m.p. 192°. (Found: C 66.36; H 6.72. Calc. for $C_{10}H_{12}O_3$: C 66.65; H 6.67.)

The authors want to thank universitetslektor Per Kolsaker for his keen interest and valuable suggestions, and Mrs. Grete Wøien Larsen for recording the PMR spectra.

REFERENCES

1. Claisen, L. *Ber.* **22** (1889) 3271.
2. Berner, E. and Kolsaker, P. *Acta Chem. Scand.* **23** (1969) 597.
3. Kolsaker, P. and Berner, E. *Tetrahedron* **29** (1973) 1095.
4. Diels, O., Sielisch, J. and Müller, E. *Ber.* **39** (1906) 1333.
5. Mumm, O. and Böhme, O. *Ber.* **54** (1921) 729.
6. McNair, J. B. *J. Am. Chem. Soc.* **54** (1932) 3249.

Received January 11, 1973.

ACTA CHEMICA SCANDINAVICA 27 (1973) 2135–2145

NMR Studies on Cyclic Arsenites

Spectral Analysis of the Geometrical Isomers of 2-Chloro- and 2-Phenyl-4-methyl-1,3,2-dioxarsolane and -1,3,2-dithiarsolane

DAGFINN W. AKSNES and OLAV VIKANE

Chemical Institute, University of Bergen, N-5000 Bergen, Norway

The proton NMR spectra of the four title compounds have been fully analyzed on the basis of an $ABCD_3$ spin system. The chemical shifts and coupling constants of the CH_3CHCH_2 moiety are reported and discussed. It is shown that these compounds are a mixture of *cis* and *trans* isomers with the latter predominating. Approximate values of the ring torsional angles have been obtained. The NMR data suggest that these five-membered rings can be adequately described in terms of flexible twist-envelope conformations. Only the *cis* isomers show signs of specific steric interactions in that a particular conformation appears to be favoured.

The application of NMR spectroscopy to the determination of the conformations and configurations of five-membered rings presents considerable difficulties owing to facile interconversions which occur between numerous equi-energy conformers.[1] It is generally believed that the five-membered rings exist in highly flexible puckered conformations. The process by which the puckering moves about the ring is termed pseudo-rotation.[1,2]

Although external substitution of the five-membered ring may prevent complete pseudo-rotation, conformational changes are still quite facile when one or even two small substituents are introduced into the ring. In more highly substituted systems, however, the steric requirements of the substituents may confine the ring to definite energy minima not necessarily associated with a specific conformation of the ring.[2,3]

In preceding papers the NMR spectra of several arsolanes have been studied.[4–6] The NMR data indicate that these five-membered rings exist in rapidly interconverting non-planar forms but that inversion at arsenic is slow.

This paper reports preparation and NMR investigations of the five-membered arsenites I–IV.

I; R = Cl, X = O
II; R = Cl, X = S
III; R = Ph, X = O
IV; R = Ph, X = S

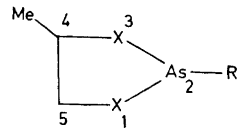

These compounds are presumably a mixture of two geometrical isomers, *cis* and *trans* forms, owing to the configurational stability about the arsenic atom. The spectral analysis of the NMR spectra is, therefore, expected to be tricky due to overlap of spectral lines from both geometrical isomers.

The existence of two geometrical isomers of 2-chloro-4-methyl-1,3,2-dioxaphospholane has been reported by Goldwhite.[7] At the inception of this investigation, however, detailed information regarding preferred conformations of similar di-substituted oxygen or sulphur containing heterocycles was limited largely to 2,4-dialkyl-1,3-dioxolanes.[3]

Our studies of the title compounds were undertaken in order to (1) verify the existence of geometrical isomers, (2) analyze these complex spin systems, (3) determine if any dominant conformations existed, and (4) examine whether rapid exchange of chlorine and pseudo-rotation were occurring on the NMR time scale.

EXPERIMENTAL

Phenyl dichloroarsine was prepared from diphenyl mercury and trichloroarsine according to a procedure of Blicke and Smith.[8] Compounds I, III, and IV were synthesized by the method of Kamai and Chadaeva [9] using trichloroarsine or phenyl dichloroarsine and 1,2-propanediol or 1,2-propanedithiol. Compound II was prepared from trichloroarsine and 1,2-propanedithiol, according to a method of Ruggeberg *et al.*[10] The boiling points of the prepared compounds are as follows: B.p.$_{12}$ 69.5 – 70.5°C, b.p.$_{0.8}$ 106 – 107°C, b.p.$_{10}$ 121 – 123°C, and b.p.$_{1.3}$ 149 – 150°C for compounds I, II, III, and IV, respectively.

The NMR spectra of these four compounds were examined either as neat liquids or else in benzene or deuteriochloroform solutions. The NMR samples were prepared as previously described. [4–6] TMS and deuteriochloroform served as internal locking substances for the 60 MHz and 90 MHz spectra, respectively.

The 60 MHz spectra were run on a JEOL-C-60H spectrometer. Line positions were obtained by averaging the results of four frequency-calibrated spectra of 54 Hz sweep width.

The 90 MHz spectra were recorded on a Bruker HX 90 E spectrometer using heteronuclear lock on deuterium. The spectra used in the calculations were recorded at the calibrated sweep range 1 Hz/cm.

Computations were performed on the IBM/50H computer at the University of Bergen. The graphical output was obtained on a Calcomp Plotter.

SPECTRAL ANALYSIS

The spectra of the four compounds were analyzed as $ABCD_3$ systems using the computer programs UEANMR II [11] and UEAITR.[12] The former program was only used in conjunction with the subroutine KOMBIP [13] to obtain "stick"- and line-shape plots. The "stick"- plots based on trial parameters facilitated the analyses, in particular the rather tricky analyses of compounds III and IV. The iterative fitting of experimental and calculated transitions was performed by means of the UEAITR program.

Several of the spectra can be approximately analyzed as $ABPX_3$ systems with $J_{BX} \approx J_{PX} \approx 0$. The methyl spectrum should then resemble the X_3 part of an ABX_3 system. This spin system is conveniently treated by the composite particle technique,[14] thus

$$ABX_3 = DDQ + 2DDD \quad (1)$$

The composite particles are referred to in the order A, B, and X_3. The transition frequencies of the DDD sub-system which is identical with the ABX system, have been listed previously.[15] The six X-transitions are given by

$$\nu_X \pm D(m_X) - \varepsilon D(m_X - 1) \quad (2)$$

$$\nu_X \pm N \quad (3)$$

where

$$D(m_X) = [(\tfrac{1}{2}\nu_{AB} + m_X N)^2 + \tfrac{1}{4}J_{AB}^2]^{\frac{1}{2}} \quad (4)$$

$$N = \tfrac{1}{2}(J_{AX} + J_{BX});\ \nu_{AB} = \nu_A - \nu_B \quad (5)$$

with $m_X = \frac{1}{2}$ and $\varepsilon = \pm 1$.

The DDQ sub-system gives the energy level groupings (1:1:1:1) and (2:2:2:2) in the X spectrum corresponding to the values ± 1 and 0, respectively, of the magnetic quantum number m_{AB}. For the extreme values $m_{AB} = \pm 1$ the DDQ sub-system thus contains two x_2 sub-spectra with effective Larmor frequencies given by eqns. (3) and (5). It is readily shown that the transition $(m_X - 1) \rightarrow m_X$ within the (2:2:2:2) sub-pattern, results in twelve lines given

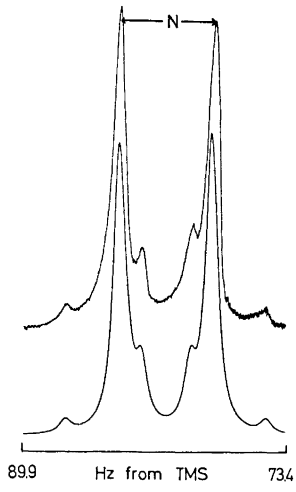

Fig. 1. Experimental (upper trace) and calculated (lower trace) 60 MHz spectrum of the methyl protons in compound I subjected to rapid exchange of chlorine. The "N-doublet" is shown.

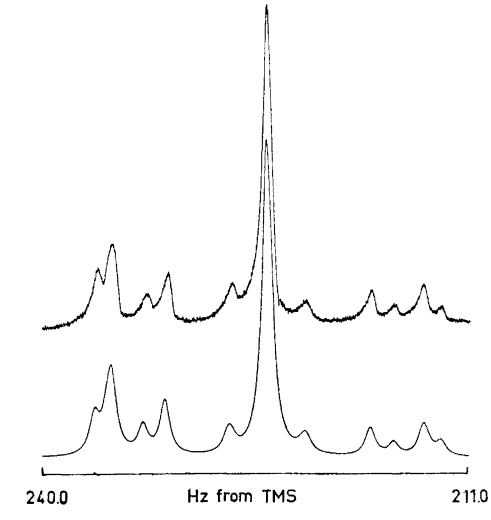

Fig. 2. Experimental (upper trace) and calculated (lower trace) 60 MHz spectrum of the H_C proton in compound I subjected to rapid exchange of chlorine.

by eqns. (2), (4), and (5) with $m_X = \frac{3}{2}$ and $\pm\frac{1}{2}$. The four lines arising from the $m_X = -\frac{1}{2} \rightarrow \frac{1}{2}$ transition thus occur in both sub-spectra. These four lines together with the "*N*-doublet" constituting all X-transitions of the ABX system,[15] should thus be easily discerned in the experimental methyl spectrum.

Only the average NMR spectra resulting from rapid exchange of chlorine were analyzed for compounds I and II. The trial parameters of these spin systems were easily obtained by using the $ABPX_3$ approximation. In Fig. 1 the methyl spectrum of I clearly shows the six X-transitions which are common for the ABX and ABX_3 systems. From this spectrum good trial values of ν_X, ν_{AB}, N, and J_{AB} were obtained.

The refined spectral parameters of I and II are listed in Table 1. Figs. 1 – 3 show excellent fit between the experimental and calculated spectra of I.

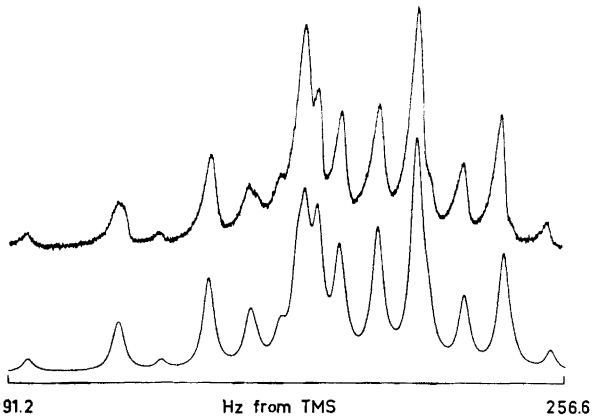

Fig. 3. Experimental (upper trace) and calculated (lower trace) 60 MHz spectrum of the H_A and H_B protons in compound I subjected to rapid exchange of chlorine.

The analyses of III and IV were more tricky owing to partial overlap of spectral lines from the *cis* and *trans* isomers. It will be shown later that the *trans* isomer predominates in the present compounds. Again some trial parameters of both isomers of III were found by analyzing directly the spectra as $ABPX_3$ systems. The high-field and low-field parts of the spectrum in Fig. 4 were assigned to the H_P proton (labelled H_C in Table 1) in the *trans* and *cis* isomers, respectively. This assignment gives ν_P and $|J_{AP} + J_{BP}|$. Approximate values of ν_X, ν_{AB}, N, and J_{AB} followed from the methyl signals. However, the uncertainties in ν_{AB} and J_{AB} are considerable due to severe overlap of the methyl signals of both isomers. Furthermore, since the AB regions of both isomers are superimposed (Fig. 5) it was also difficult to obtain ν_A, ν_B, and J_{AB} from this part of the spectrum. Only a tedious trial-and-error analysis yielded acceptable trial values. The final parameters obtained from the iterative analysis are listed in Table 1. The contributions from the individual isomers are shown in Figs. 4 and 5 together with the calculated and experimental total spectra.

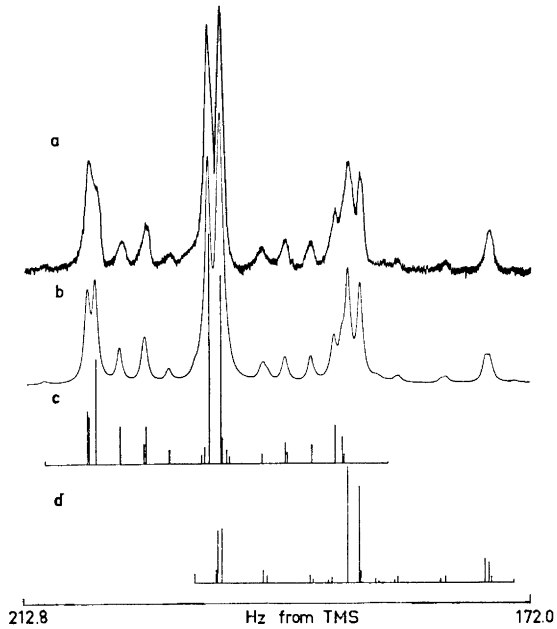

Fig. 4. The C region of the 60 MHz spectrum of compound III: a, experimental spectrum b, computed total line-shape spectrum for a *cis*:*trans* intensity distribution of 1:1.6; c, computed stick-plot of the H_C proton in the *trans* isomer; d, computed stick-plot of the H_C proton in the *cis* isomer.

From the experimental 90 MHz spectrum of IV in Fig. 6 it is seen that the spectrum of the *trans* and *cis* isomer can be approximately analyzed as $APQX_3$ and $ABPX_3$ systems, respectively. Trial values of ν_X and J_{AX} are directly obtainable from the methyl signals. The multiplet consisting of eight lines centered at *ca.* 272 Hz from TMS (Fig. 6) has been assigned to the two PQ protons (labelled BC in Table 1) of the *trans* isomer. Direct analysis of this spectrum region gives trial values for ν_P, ν_Q, J_{AP}, J_{AQ}, and J_{PQ}. A coupling scheme of the A region of the predominating isomer was then drawn on the basis of the known coupling constants. This procedure made it possible to pick out the extreme lines in the A spectrum and hence ν_A, in spite of severe overlap of spectral lines from the *cis* isomer.

The doublet of doublets centered at *ca.* 228 Hz from TMS (Fig. 6) was assigned to the H_P (labelled H_C in Table 1) proton of the *cis* isomer. This assignment yielded ν_P, J_{AP}, and J_{BP}. The doublet of doublets centered at *ca.* 306 Hz from TMS (Figs. 6 and 7) is due to the H_B proton and thus gives ν_B, J_{AB}, and J_{BP}. ν_A was obtained from the experimental spectrum after disregarding lines from the predominating isomer.

After having found all the necessary trial parameters iterative analyses were carried out on the experimental 90 MHz and 60 MHz spectra of both

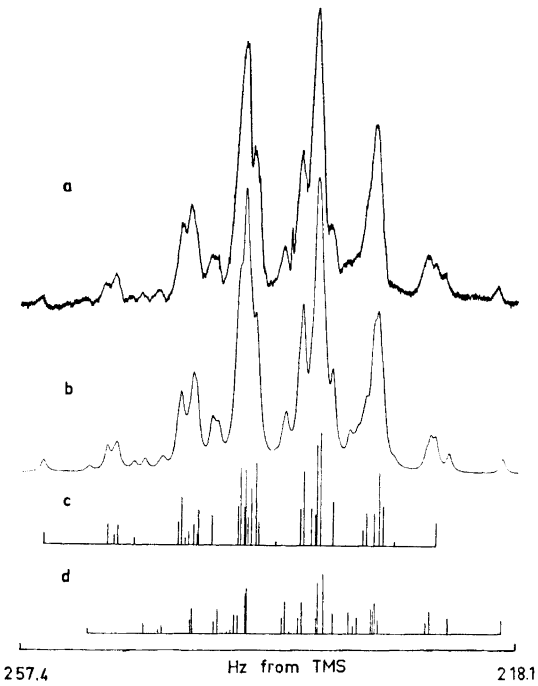

Fig. 5. The AB region of the 60 MHz spectrum of compound III: a, experimental spectrum; b, computed total line-shape spectrum for a *cis:trans* intensity distribution of 1:1.6; c, computed stick-plot, of the H_A and H_B protons in the *trans* isomer; d, computed stick-plot of the H_A and H_B protons in the *cis* isomer.

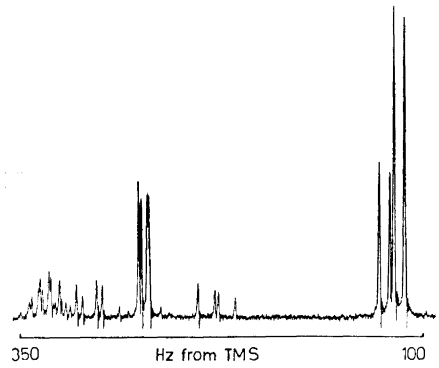

Fig. 6. Experimental 90 MHz spectrum of the CH_3CHCH_2 protons in compound IV.

isomers. The agreement between the 60 MHz and 90 MHz parameters of IV is satisfactory. Fig. 7 shows experimental and calculated 90 MHz spectra of IV for the only region where spectral lines from both isomers overlap.

RESULTS AND DISCUSSION

The methyl NMR spectrum of compounds II, III, and IV (Fig. 6) consists of two doublets that partly overlap in the 60 MHz spectrum. The two individual methyl signals show that these compounds are a mixture of two geometrical isomers, *cis* (A) and *trans* (B) forms, which are interconvertible by inversion at arsenic.

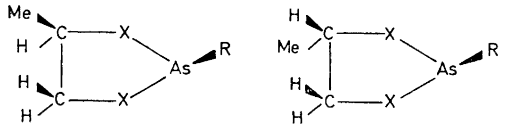

The predominant isomer displays an upfield chemical shift for the methyl signal in comparison with the other isomer. The actual intensity ratios of the low-field:high-field doublets are approximately 1:1.3, 1:1.6 and 1:2 for the examined samples of II, III, and IV, respectively. The high-field and low-field methyl signals have been assigned to the *trans* (B) and *cis* (A) forms, respectively, that is, the *trans* isomer is predominating. This assignment has been made on the basis of the reported paramagnetic shift effect of chlorine and phenyl substituents in arsolanes,[4–6] and phospholanes. [16,17] The remaining chemical shift values in Table 1 then followed from the spectral analysis.

Table 1. 60 MHz NMR parameters (in Hz) and ring torsional angles (ψ) of compounds I, II, III and IV.[a]

Compound	I	II	III		IV		IV[b]	
			cis	*trans*	*cis*	*trans*	*cis*	*trans*
Solvent[c]	Neat	C_6H_6	C_6H_6		neat		$CDCl_3$	
Temp.°C	60	30	30		75		30	
ν_A[d]	272.85	250.92	235.10	239.80	219.30	221.00	330.08	332.58
ν_B	267.20	216.69	236.75	236.25	201.41	178.88	305.46	268.82
ν_C	225.63	203.11	187.16	198.23	154.13	181.58	228.38	274.51
ν_{Me}	80.64	81.38	68.01	62.61	80.78	76.14	123.83	114.28
J_{BC}	−9.14	−12.04	−9.22	−8.77	−12.65	−11.97	−12.66	−11.91
J_{AB}	5.74	4.04	4.52	5.17	3.83	4.37	3.65	4.55
J_{AC}	8.88	7.18	10.02	7.61	10.22	6.10	10.35	5.98
J_{AMe}	6.04	6.63	5.98	5.93	6.57	6.66	6.43	6.59
J_{BMe}	−0.11	−0.02	−0.07	−0.04	−0.07	−0.02	−0.11	−0.01
J_{CMe}	−0.09	−0.04	−0.06	−0.07	−0.07	−0.01	−0.04	−0.02
Assigned transitions	93	102	85	89	104	78	96	91
RMS error	0.086	0.059	0.076	0.061	0.094	0.065	0.068	0.073
R	1.55	1.78	2.22	1.47	2.67	1.39	2.83	1.31
ψ (deg.)	53	55	58	52	61	51	62	50

[a] The methine and methylene protons are labelled A and BC, respectively. [b] Measured at 90 MHz. [c] 50 % v/v. [d] Chemical shifts downfield from TMS.

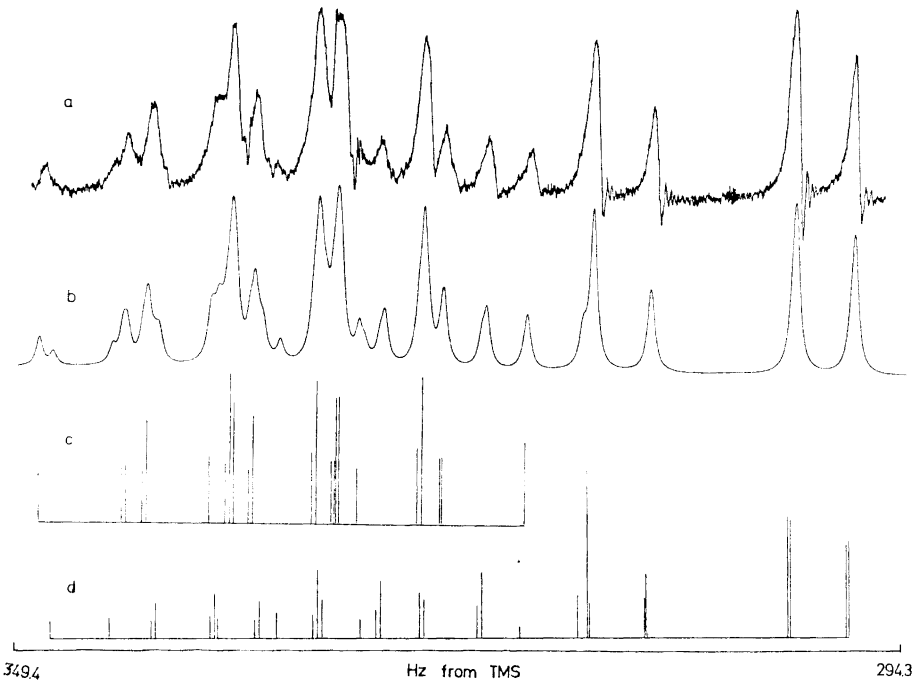

Fig. 7. The lower region (Fig. 6) of the 90 MHz spectrum of compound IV; a, experimental spectrum; b, computed total line-shape spectrum for a *cis*:*trans* intensity distribution of 1:2; c, computed stick-plot of the H_A proton in the *trans* isomer; d, computed stick-plot of the H_A and H_B protons in the *cis* isomer.

It is seen that the methine proton signals of the *trans* isomers (H_A *cis* to As–R) appear at lower field than the corresponding signals of the *cis* isomers (H_A *trans* to As–R) in agreement with the stereospecific anisotropy effect.[4–6]

However, only one methyl doublet was observed at room temperature for neat as well as diluted samples of I. The methyl signal of a neat sample of II showed, similarly, a single doublet at 135°C. Coalescence of the signal occurred at *ca.* 110°C whereas two distinct methyl doublets were observed at 70°C. However, when a small amount of tetraphenylarsonium chloride was added to a 50 % v/v solution of II in dry benzene, the methyl spectrum showed only one doublet. These observations indicate that exchange of chlorine proceeds with inversion at arsenic since retention of configuraton at arsenic would preserve the two kinds of methyl signals. Similar observations have been made for 2-chloro substituted 1,3,2-dioxarsolanes[4] and several 1,3,2-dioxaphospholanes.[16–19] The rate of chlorine exchange is considerably faster for the oxygen containing arsolanes than for their sulphur analogues. This observation should be conferred with the reported stability of the ring As–S bond as compared to the As–O bond in arsolanes. The observed dependence of chlorine exchange upon concentration of solute or tetraphenylarsonium chloride suggests that exchange occurs by a bimolecular process,[18] *viz.*

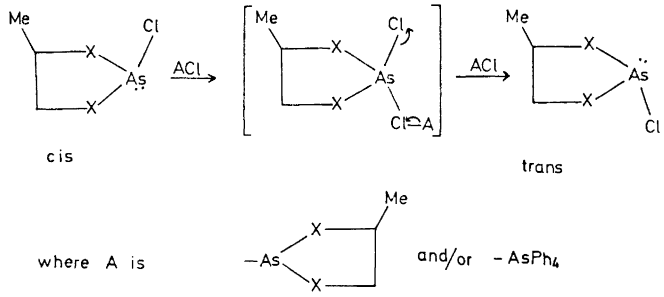

Previous studies of 1,3,2-dioxarsolanes [4,5] and 1,3,2-dithiarsolanes [6] have shown that these five-membered rings exist in rapidly interconverting non-planar forms with a stable configuration at arsenic. We believe that the predominating pseudo-rotamers of the four arsolanes examined in this work, can be adequately described by the twist-envelope conformations below:

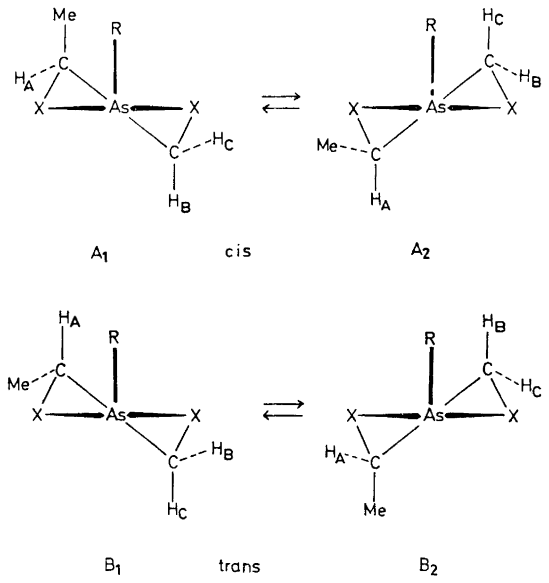

Evidence for this assumption is presented in the following discussion. At the outset, however, it should be pointed out that, since pseudo-libration is expected to occur in these systems,[2,3] each of the above pseudo-rotamers represents the average of a range of conformations of similar energies.

The X – C – C – X torsional angle, ψ, of these ring systems can be calculated from the J_{AB} and J_{AC} coupling constants of the CH_2CHCH_3 moiety using the R-value method due to Lambert.[20] The obtained R-values and corresponding torsional angles, however, represent the average of the conformational extremes

and thus characterize the mean geometry of the *cis* or *trans* isomers. The calculated R-values and the corresponding torsional angles are given in Table 1.

Since exchange of chlorine interconverts the *cis* and *trans* forms the spectral parameters of I and II listed in Table 1 are weighted average values of the two geometrical isomers. This makes it difficult to gain configurational information about the individual forms. The average torsional angle of II is, however, close to the values reported for 2-chloro- and 2-phenyl-1,3,2-dithiarsolane.[6]

The vicinal coupling constants of III and IV indicate that the preferred conformations of the ring are probably nearly the same for the two *cis* isomers, and for the two *trans* forms are likewise nearly the same. The X–C–C–X portion of the ring seems to assume a nearly staggered conformation in the *cis* forms whereas the *trans* forms are less puckered by 6–10°. The weighted average values of ψ in III and IV have been estimated to be 56° and 58°, respectively, that is, 3–4° more than in I and II.

The sulphur heterorings are more puckered than their oxygen counterparts except for *trans*-IV. This is consistent with the greater degree of flexibility conferred by the presence of sulphur rather than oxygen atoms in the ring. Similar observations have been reported previously for 1,3,2-dithiarsolanes,[6] 1,3,2-dithiaphospholanes,[21] and 1,3-dithiolanes[22] relative to their oxygen analogues.[6,16,22] The presence of methyl at carbon 4, however, seems to equalize, to some extent, the difference in ring puckering of the corresponding oxygen and sulphur containing rings.

The J_{AC} coupling constant is appreciably greater than J_{AB} in *cis*-III and *cis*-IV. Similar results have also been observed by Bergesen and Bjorøy in the *cis* forms of 2-chloro- and 2-phenyl-4-methyl-1,3,2-dithiaphospholane.[23] This is, however, not the case in the corresponding 2,4-dialkyl-1,3-dioxolanes.[3] It can be anticipated from the Dreiding model and the Karplus relationship [20] that the largest vicinal coupling constant (J_{AC}) involves the pseudo-axial protons. This indicates predominance of the A_2 pseudo-rotamers for *cis*-III and *cis*-IV. The equatorial preference of the 4 methyl groups is probably caused by *syn*-axial interactions of the 4-methyl and 2-R substituents which are greater in the A_1 conformer possessing a pseudo-axial methyl group.

Willy and co-workers [3] have found that the *cis* isomers of a series of 2,4-dialkyl-1,3-dioxolanes are thermodynamically favoured over the corresponding *trans* isomers. They have explained this on the basis of an unfavourable steric interaction of a pseudo-axial substituent at carbon 4 with a pseudo-axial hydrogen at carbon 2 (envelope conformation) in the *trans* isomer. This interaction is, however, absent in the arsolanes since carbon 2 has been replaced by trivalent arsenic. This may explain the observed predominance of the *trans* isomer in the present arsolanes in contrast to the situation in 2,4-dialkyl-1,3-dioxolane.[3]

The measured coupling constants in 2-chloro- and 2-phenyl-4-methyl-1,3,2-dithiaphospholane [23] also indicate, when related to the estimated S–C–C–S and P–S–C–H dihedral angles, predominance of A_2-like conformations for the *cis* isomers.

Owing to the anisotropy effect of the phenyl group the NMR signal of the H_C proton in *cis*-III and *cis*-IV was expected to appear at lower field

than the H_B signal since these protons are respectively *cis* and *trans* to the As-Ph bond. The reverse observation suggests that the anisotropy effect of the methyl group at carbon 4 predominates.

The similar values of J_{AB} and J_{AC} in *trans*-III and *trans*-IV indicate comparable contributions from the B_1 and B_2 pseudorotamers. An analogous situation seems to prevail in the *trans* forms of 2-chloro- and 2-phenyl-4-methyl-1,3,2-dithiaphospholane [23] judging from the coupling constants. This implies that the stability of the *trans* isomer is less affected (in comparison with the *cis* isomer) by non-bonded interactions involving the substituents on the ring.

The authors thank Mr. R. Bosvik at Bruker Spectrospin AB, Sweden, for obtaining the 90 MHz spectra of 2-phenyl-4-methyl-1,3,2-dithiarsolane.

REFERENCES

1. See, for example, Booth, H. *Progr. NMR Spectrosc.* **5** (1969) 149, and references therein.
2. Altona, C., Buys, H. R. and Havinga, E. *Rec. Trav. Chim. Pays-Bas* **85** (1966) 973.
3. Willy, W. E., Binsch, G. and Eliel, E. L. *J. Am. Chem. Soc.* **92** (1970) 5394.
4. Aksnes, D. W. and Vikane, O. *Acta Chem. Scand.* **26** (1972) 835.
5. Aksnes, D. W. and Vikane, O. *Acta Chem. Scand.* **26** (1972) 2532.
6. Aksnes, D. W. and Vikane, O. *Acta Chem. Scand.* **26** (1972) 4170.
7. Goldwhite, H. *Chem. Ind. (London)* **1964** 495.
8. Blicke, F. F. and Smith, F. D. *J. Am. Chem. Soc.* **51** (1929) 3479.
9. Kamai, G. and Chadaeva, N. A. *Chem. Abstr.* **47** (1953) 3792 c-f, 10470 c-h.
10. Ruggeberg, W. H. C., Grinsburg, A. and Cook, W. A. *J. Am. Chem. Soc.* **68** (1946) 1860.
11. Woodman, C. M. *Personal communication.*
12. Johannesen, R. B., Ferretti, J. A. and Harris, R. K. *J. Magn. Resonance* **3** (1970) 84.
13. Aksnes, W. A. KOMBIP, Quantum Chemistry Program Exchange, Indiana University, Chemistry Department, Indiana, U.S.A.
14. Diehl, P., Harris, R. K. and Jones, R. G. *Progr. NMR Spectrosc.* **3** (1967) 1.
15. Emsley, J. W., Feeny, J. and Sutcliffe, L. H. *High Resolution Nuclear Magnetic Resonance Spectroscopy*, Pergamon, New York 1966, Vol. 1, p. 360.
16. Haake, P., McNeal J. P. and Goldsmith, E. J. *J. Am. Chem. Soc.* **90** (1968) 715.
17. Bergesen, K. and Vikane, T. *Acta Chem. Scand.* **26** (1972) 2153.
18. Fontal, B. and Goldwhite, H. *Tetrahedron* **22** (1966) 3275.
19. Gagnaire, D., Robert, J.-B. and Verrier, J. *Bull. Soc. Chim. France* **1966** 3719.
20. Lambert, J. B. *Accounts Chem. Res.* **4** (1971) 87.
21. Peake, S. C., Fild, M., Schmutzler, R., Harris, R. K., Nichols, J. M. and Rees, R. G. *J. Chem. Soc. Perkin 2* **1972** 380.
22. Sternson, L. A., Coviello, D. A. and Egan, R. S. *J. Am. Chem. Soc.* **93** (1971) 6529.
23. Bergesen, K. and Bjorøy, M. *Personal communication.*

Received February 15, 1973.

ACTA CHEMICA SCANDINAVICA 27 (1973) 2146–2160

An X-Ray Investigation of the Coordination and the Hydrolysis of the Uranium(IV) Ion in Aqueous Perchlorate Solutions

STEVAN POCEV* and GEORG JOHANSSON

Department of Inorganic Chemistry, Royal Institute of Technology, S-100 44 Stockholm 70, Sweden

The coordination of the uranium(IV) ion in acid and hydrolyzed water solutions of uranium(IV) perchlorate has been investigated by means of X-ray scattering measurements. Analysis of the scattering data indicates a well-defined inner coordination sphere around the uranium(IV) ion with a coordination number which is not significantly different from eight. The perchlorate groups do not enter the inner coordination sphere but seem to form outer-sphere complexes. In hydrolyzed solutions polynuclear hydrolysis complexes are formed with a shortest U–U distance within the complexes of 4.0 Å. This is indicative of the formation of a double hydroxo bridge between the uranium atoms.

An X-ray investigation of the structures of the hydrolysis products of thorium(IV) in aqueous nitrate solutions has been reported in a previous paper.[1] The polynuclear hydrolysis complexes were found to be built up from thorium atoms joined by double hydroxo bridges and the nitrate groups were bonded to the thorium atoms as bidentate ligands in inner-sphere complexes. A similar investigation of uranium(IV) perchlorate solutions is reported in the present paper. Polynuclear hydrolysis complexes are formed in this case also, and the metal-metal distances within the complexes indicate the same type of bridging as for thorium. The perchlorate ions, however, do not seem to enter the first coordination sphere.

Because of its high charge the U^{4+} ion hydrolyzes easily. Several investigators have found evidence for the ion $U(OH)^{3+}$.[2] An early investigation by emf methods by Hietanen,[3] carried out in a 3 M perchlorate medium with U(IV) concentrations between 2 mM and 40 mM, showed that polynuclear complexes are also formed. The results were interpreted in terms of the "core +

* Permanent address: University of "Kiril and Methodi", Faculty of Technology and Metallurgy, Skoplje, Yugoslavia.

link" hypothesis, assuming the formation of an infinite series of complexes with the general formula $U[(OH)_3U]_n^{(n+4)+}$.

In the present work the X-ray scattering from three different uranium(IV) perchlorate solutions has been measured.The uranium concentration was kept constant at about 2 M in all of the solutions, but the acidity was varied. Because of precipitation the hydrolysis could not be carried as far as was possible for Th^{4+}. For the most hydrolyzed of the solutions investigated, however, it was found that polynuclear complexes are formed and the shortest metal-metal distances within the complexes could be determined.

EXPERIMENTAL

Preparation of solutions. Uranium(IV) perchlorate was prepared by cathodic reduction of uranyl(VI) perchlorate. The uranyl perchlorate was prepared from uranyl nitrate (Merck, *p.a.*) in the following way: Hydrogen peroxide was added to an aqueous solution of the uranyl nitrate. The precipitate of uranium peroxide was filtered off and was ignited at 850°C. The U_3O_8, which was thus formed, was dissolved in an excess of perchloric acid, H_2O_2 being added simultaneously. The resulting uranyl perchlorate solution was evaporated until crystallization occurred. The crystals were dissolved in doubly-distilled water, and the uranium concentration and the acidity were adjusted to give suitable starting solutions for the reduction to uranium(IV) perchlorate.

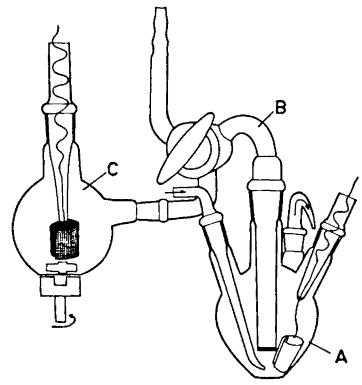

Fig. 1. The apparatus used for the reduction of the uranyl(VI) perchlorate solutions.

Cathodic reduction. The apparatus used for the reduction is illustrated in Fig. 1. The uranyl perchlorate solution was introduced into the vessel A. The anode compartment, C, was filled with a solution of ferrous perchlorate. The bridge, B, which contained 1 M perchloric acid, was separated from the anode compartment by a sintered glass disc (G-3). A gold cathode and a platinum net anode were used. A Regatron power supply (C633CMK) was used to obtain a 100 mA constant current, corresponding to a current density of about 7 mA/cm² and a voltage of about 30 V. A stream of oxygen-free nitrogen was bubbled through the cathode compartment before and during the reduction. Any residual traces of oxygen were removed from the nitrogen by passing the gas through a column of dispersed metallic copper at 200°C. The nitrogen gas was saturated with water vapor before being passed into the cathode compartment. The solution at the anode was stirred with a magnetic stirrer in order to decrease the concentration polarization.

The time needed for the reduction was estimated from the constant current used and from the amount of uranyl perchlorate. Hydrolyzed solutions were prepared by decreasing the concentration of $HClO_4$ in the starting solution. If this decrease was carried too far

a black precipitate, probably UO_2, appeared at the cathode. This limit, which determines the maximum degree of hydrolysis that can be obtained by this method, was found by trial and error.

Analysis of the solutions. The solutions were analyzed for U(IV), U(VI), and ClO_4^- both before and after the X-ray measurements. The hydrogen ion excess, H, was obtained from the material balance. No significant change in composition was caused by the X-ray irradiation.

Uranium(VI) was determined gravimetrically by precipitation as uranium peroxide, igniting at 850°C and weighing as U_3O_8. Uranium(IV) was determined, after acidifying the solution with 1 M H_2SO_4, by titration with $KMnO_4$ under nitrogen atmosphere. The $KMnO_4$ solution was standardized against sodium oxalate.

Perchlorate was determined with a cation exchange resin (Dowex 50W-X8). The uranium(IV) perchlorate was oxidized by a stream of oxygen and was then passed through a column of the H^+ saturated ion exchanger. The eluate was titrated with a sodium hydroxide solution.

The compositions of the solutions are given in Table 1. About 2 % of the uranium in the solutions investigated was present as uranium(VI), but this amount is too small to have any noticeable effect on the results.

Table 1. Composition of the solutions investigated.

Solution	A		B		C	
Concentration	g atom/l	atom/V	g atom/l	atom/V	g atom/l	atom/V
U(IV)	2.044	1	2.130	1	2.283	1
U(VI)	0.035	0.017	0.032	0.015	0.061	0.027
Cl	8.95	4.38	8.82	4.14	7.69	3.37
O	72.9	35.7	71.6	33.6	71.1	31.2
H	74.8	36.6	72.8	34.2	79.0	34.6
Hydrogen ion excess	0.71	0.35	0.23	0.11	−1.57	−0.69
Stoichiometric volume, V Å^3	812.4		779.6		727.4	

X-Ray measurements. The diffractometer used for the X-ray measurements has been described in previous papers.[5] During the irradiation the solutions were kept in a nitrogen atmosphere to prevent oxidation of the uranium(IV).

Because of the presence of strong fluorescence radiation when Mo$K\alpha$ radiation is used, the measurements were made with Ag$K\alpha$ radiation ($\lambda = 0.5608$ Å). Even then, some fluorescence radiation seemed to be present, as was also found in a previous investigation of uranium(VI).[6] Opening slits of 1°, 1/4°, and 1/12° were used. A recalculation of the measured data to a common slit width was made from measurements in overlapping regions. Measurements were made at intervals of 0.25° except in the low angle region ($\theta < \sim 4°$) where 0.1° intervals were used. About 40 000 counts were measured for each point, corresponding to a statistical accuracy of 0.5 %. Long-time variations in the X-ray source and the counting equipment were checked by measurements at larger intervals. No significant variations were observed.

DATA TREATMENT

The measured data were corrected in the usual way for polarization in the sample and in the monochromator. The incoherent part of the scattering was estimated from the spectrum of the X-ray tube. The final correction curve used was adjusted by a comparison with results obtained for a concentrated

mercury(II) iodide solution, which does not give fluorescence radiation and which was measured with both Ag$K\alpha$ and Mo$K\alpha$ radiation. The amount of fluorescence radiation was estimated in the way described in a previous paper.[6] It amounted to about 10 % of the intensity measured at the largest scattering angles, roughly corresponding to an intensity of 2 cps. No corrections were made for multiple scattering ($\mu \approx 60$ cm^{-1}), as it could be assumed to be negligible.

The scattering factors used were those given by Cromer and Waber [7] for U and Cl. For O and H the values were taken from the International Tables.[8] They were corrected for the real and the imaginary part of the anomalous dispersion according to Cromer.[9] The incoherent radiation was taken from Cromer [10] for U, O, and Cl and from Compton and Allison [11] for H and was corrected for the Breit-Dirac factor.

The scaling constant, K, was estimated from the high-angle portion ($\theta > 45°$) of the measured data according to the formula:

$$KI_{obs} = \sum_i n_i f_i^2 + \sum_i n_i I_{inc}$$

Here, I_{obs} are observed data corrected for fluorescence radiation and for polarization, f_i are the scattering factors corrected for the real and imaginary part of the anomalous dispersion,[12] I_{inc} the incoherent radiation reaching the counter, and n_i the number of atoms "i" in the stoichiometric volume chosen.

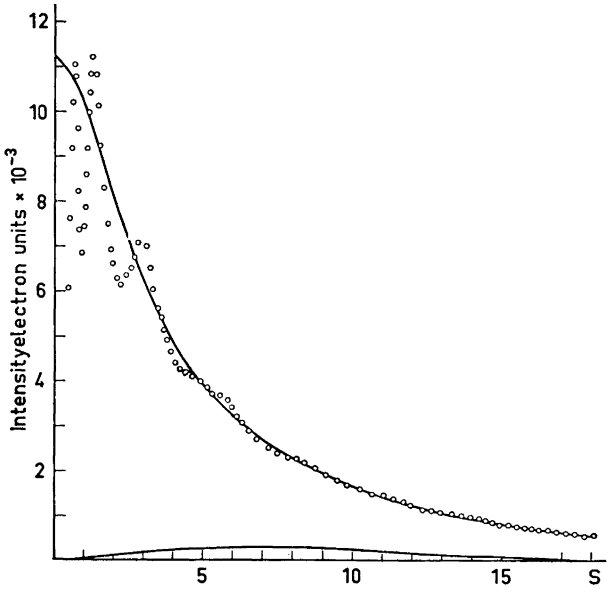

Fig. 2. Survey of the X-ray scattering measurements for solution A. Some of the observed normalized intensities, marked by dots, are compared with the corresponding calculated independent coherent scattering. The lower full-drawn curve gives the estimated amount of incoherent radiation reaching the counter.

Table 2. Observed intensity values, $I(s)$, after scaling and subtraction of incoherent radiation, and reduced intensity values, $i(s)$, given as functions of $s = 4\pi \sin \theta/\lambda$ for the three solutions investigated.

	A		B		C			A		B		C	
s	I	i	I	i	I	i	s	I	i	I	i	I	i
0.403	4304	-7292.0	-	-	9444	-1663.6	4.056	4572	-416.5	4529	-448.5	4401	-470.7
0.442	5095	-6459.1	5977	-5546.3	10165	-903.9	4.094	4502	-439.9	4459	-452.0	-	-
0.481	6639	-4870.4	-	-	11200	265.0	4.130	4472	-423.6	-	-	-	-
0.520	8183	-3277.9	-	-	12604	1624.9	4.133	-	-	4451	-435.4	4314	472.7
0.559	8245	-3163.1	8614	-2766.1	14232	3300.6	4.171	4450	-401.1	4408	-433.5	4308	-436.0
0.598	9748	-1607.3	9440	-1886.6	15908	5026.3	4.210	4408	-398.9	4391	-405.4	4276	-426.0
0.637	10750	-548.3	10399	- 870.6	15471	4645.2	4.248	4377	-385.8	4346	-406.5	4240	-418.7
0.676	11638	399.1	10829	- 380.7	12150	1367.7	4.287	4369	-350.3	4324	-387.1	4192	-426.6
0.715	11351	176.5	10068	-1076.0	10430	-269.9	4.325	4347	-330.3	4340	-329.8	4201	-377.7
0.755	10206	-901.9	8745	-2330.9	9537	-1099.2	4.363	4329	-305.1	4328	-299.6	4167	-370.9
0.794	8785	-2252.8	7981	-3024.9	8048	-2521.6	4.402	4308	-285.9	4263	-323.1	4176	-322.4
0.833	7890	-3076.4	7206	-3723.0	7688	-2815.9	4.440	4296	-257.0	4255	-281.3	4168	-295.9
0.872	7552	-3342.6	6976	-3886.7	7687	-2748.7	4.478	4277	-255.3	4243	-265.0	4125	-288.6
0.911	7408	-3413.4	7011	-3778.9	7907	-2460.7	4.517	4269	-203.3	4210	-257.0	4125	-258.7
0.950	7686	-3081.6	7216	-3499.0	8299	-1998.8	4.555	4250	-183.7	4220	-208.0	4107	-238.5
0.989	8004	-2667.9	7605	-3035.4	8644	-1582.5	4.593	4233	-161.9	4207	-182.4	4142	-167.2
1.028	8407	-2187.8	8193	-2371.3	9151	-1023.7	4.631	4227	-129.9	4202	-150.3	-	-
1.067	9124	-1393.0	8687	-1799.8	9713	- 369.2	4.670	4201	-115.3	4176	-138.0	4105	-130.9
1.106	9698	- 741.0	9100	-1308.6	10153	145.7	4.708	4186	-113.5	4185	- 92.6	-	-
1.145	10499	140.0	10138	- 192.3	10343	410.9	4.746	4184	- 58.7	4179	- 62.8	-	-
1.184	10959	681.1	10787	535.9	10422	567.2	4.784	4132	- 17.6	4135	- 71.1	-	-
1.223	11371	1174.4	11084	915.3	10360	582.9	4.823	4126	- 47.0	4134	- 36.9	-	-
1.262	11689	1575.6	10953	867.1	10425	725.4	4.861	4118	- 20.0	4109	- 26.7	4077	15.1
1.301	11647	1617.3	11147	1145.0	10190	569.8	4.899	4117	13.3	4081	- 40.7	-	-
1.340	11541	1695.1	11153	1235.3	9971	430.6	4.937	4074	4.9	4083	15.0	-	-
1.379	11320	1460.5	10934	1100.7	9863	401.9	4.956	-	-	-	-	4043	61.1
1.419	11030	1255.7	10719	971.9	9514	133.8	4.975	4073	37.6	4050	16.3	-	-
1.458	10577	889.1	10267	606.9	9268	- 31.3	5.013	4033	31.2	4032	0.9	-	-
1.497	10019	418.2	9978	403.9	9053	-165.4	5.051	4009	39.6	4019	50.6	4015	113.1
1.536	9681	156.4	9617	129.3	8951	-186.4	5.089	3978	41.4	3979	41.9	-	-
1.575	9431	3.4	9360	- 40.6	8720	-336.2	5.128	-	-	3951	86.5	-	-
1.614	9139	-202.3	9059	-255.1	8713	-263 0	5.147	3953	63.7	-	-	3964	138.8
1.653	8729	- 525.2	8652	-574.7	8476	-418.3	5.166	3923	50.1	3935	61.5	-	-
1.692	8559	-603.9	8417	-723.1	8342	-471.1	5.204	3895	52.8	3942	99.4	-	-
1.731	8242	-839.6	8113	-940.9	8216	-516.1	5.242	3861	50.1	-	-	3834	153.4
1.770	7923	-1071.5	7847	-1120.5	7989	-662.9	5.260	-	-	3891	98.6	-	-
1.809	7752	-1156.9	7631	-1230.3	7844	-726.9	5.318	-	-	3858	105.6	-	-
1.848	7560	-1262.9	7468	-1327.8	7742	-748.4	5.337	3821	85.3	-	-	3810	132.3
1.886	7335	-1402.5	7193	-1517.9	7620	-790.6	5.356	3805	84.0	3865	141.6	-	-
1.925	7180	-1472.7	7177	-1449 3	7465	-868.6	5.394	-	-	3812	117.5	-	-
1.964	6988	-1579.7	6988	-1553.5	-	-	5.432	3779	116.1	3818	152.2	3764	156.4
2.003	6860	-1624.1	6823	-1534.1	7129	-1044.1	5.470	-	-	3794	156.5	-	-
2.042	6768	-1632.3	6702	-1671.1	7009	-1085.1	5.507	-	-	3773	163.4	-	-
2.081	6677	-1640.0	6615	-1675.6	6780	-1235.3	5.526	3783	190.3	-	-	3681	141.2
2.120	6603	-1631.3	6551	-1657.4	6655	-1283.4	5.545	-	-	3782	199.5	-	-
2.159	6555	-1596.5	6447	-1679.0	6518	-1342.9	5.563	-	-	3750	194.5	-	-
2.198	6485	-1585.6	6416	-1628.1	6441	-1342.9	5.621	3725	201.0	3714	185.3	3643	168.1
2.237	6509	-1480.1	-	-	6394	-1313.9	5.659	3701	203.3	3678	175.7	-	-
2.276	6556	-1352.4	6465	-1418.6	6423	-1210.2	5.697	-	-	3694	218.4	-	-
2.315	6582	-1247.5	6527	-1278.1	6366	-1192.4	5.716	3704	245.9	-	-	3554	142.8
2.354	6570	-1180.3	6488	-1237.6	6335	-1148.3	5.735	-	-	3680	229.5	-	-
2.392	6628	-1043.1	6523	-1125.2	6349	-1061.0	5.772	-	-	3628	202.8	-	-
2.431	6684	- 910.2	6505	- 984.9	6354	- 982.9	5.810	3642	248.3	3601	201.0	3461	112.7
2.470	6710	-696.9	6917	-577.2	6404	-860.2	5.848	3610	241.1	3571	196.4	-	-
2.509	6726	-714.2	6767	-650.8	6383	-809.9	5.886	3555	211.5	3551	200.6	-	-
2.548	6736	-627.8	6817	-525.0	6379	-742.1	5.904	3552	220.4	-	-	3409	120.4
2.587	6854	-434.9	6872	-395.6	6459	-592.2	5.923	3546	226.3	3524	197.8	-	-
2.626	6922	-292.7	6937	-256.3	6502	-478.5	5.961	3511	215.4	3491	189.5	-	-
2.664	6965	-176.5	6991	-120.0	6629	-283.2	5.999	3466	194.9	3423	144.8	3308	77.8
2.703	7067	- 1.4	7057	9.6	6695	-147.9	6.036	-	-	3415	160.1	-	-
2.742	7202	205.8	7223	247.2	6759	- 16.0	6.039	3406	158.1	-	-	-	-
2.781	7252	326.8	7298	332.8	6921	212.9	6.074	-	-	3384	151.9	-	-
2.820	7353	499.1	7441	606.1	7009	367.2	6.093	3364	151.7	-	-	3274	99.7
2.858	7428	643.2	7483	717.6	7131	555.4	6.112	-	-	3339	130.7	-	-
2.897	7471	755.5	7551	853.7	7222	711.0	6.149	3299	120.5	3268	82.6	-	-
2.936	7480	833.3	7581	951.8	7257	810.5	6.187	3250	94.3	-	-	3208	89.1
2.975	7492	912.5	7551	989.8	7306	923.6	6.224	3252	118.7	-	-	-	-
3.014	7474	961.4	7474	979.1	7327	1007.5	6.262	3196	84.9	3212	92.7	-	-
3.052	7405	958.4	7380	951.3	7234	977.0	6.281	3159	58.1	-	-	3103	37.6
3.091	7239	858.4	7277	913.2	7194	999.0	6.300	-	-	3147	49.3	-	-
3.130	7111	795.6	7126	826.6	7100	966.0	6.337	3107	39.1	3107	30.7	-	-
3.168	6093	641.6	6986	750.7	7036	962.1	6.375	3057	10.0	3058	2.4	3064	50.2
3.207	6751	562.8	-	-	6835	819.4	6.412	3020	-6.0	3055	20.6	-	-
3.246	6591	465.0	6648	538.1	6678	723.5	6.468	2969	-26.2	-	-	2987	23.0
3.285	6376	312.0	6457	409.1	6531	634.3	6.487	-	-	2988	-5.6	-	-
3.323	6251	248.2	-	-	6397	557.7	6.521	2928	-36.3	2951	-22.5	-	-
3.362	6111	167.6	6166	238.3	6245	462.6	6.562	2900	-44.3	2922	-31.1	2906	-8.3
3.401	5929	45.5	6025	157.2	6097	371.7	6.599	-	-	2903	-30.1	-	-
3.439	5835	10.5	5917	107.0	597	307.2	6.655	2812	-83.7	-	-	2833	-34.3
3.478	5777	9.6	5808	49.8	5853	241.0	6.674	-	-	2832	-68.0	-	-
3.516	5691	-19.2	5675	-20.0	5743	182.1	6.711	-	-	2813	-57.7	-	-
3.555	5610	-44.4	5585	-54.5	5642	134.0	6.748	2756	-91.2	2781	-75.0	2782	-38.5
3.594	5527	-71.2	5471	-112.7	5518	63.5	6.786	-	-	2758	80.0	-	-
3.632	5409	-134.0	5424	-105.6	5408	5.3	6.823	-	-	2750	-69.4	-	-
3.671	5335	-154.4	5299	-176.9	5248	-103.0	6.842	2700	-100.8	-	-	2717	-57.6
3.709	5253	-183.5	5223	-200.3	5139	-162.1	6.860	-	-	2728	-72.6	-	-
3.748	5164	-220.1	5148	-222.3	5068	-182.6	6.897	-	-	2681	-101.0	-	-
3.787	5082	-249.9	5038	-280.8	4945	-257.1	6.935	2661	-94.4	2622	-142.5	-	-
3.825	4985	-295.7	4933	-334.6	4875	-278.4	6.990	-	-	2615	-122.5	-	-
3.864	4889	-341.5	4881	-337.1	4711	-394.4	7.027	2631	-79.8	-	-	2608	-79.5
3.902	4832	-348.0	4786	-382.6	4666	-391.4	7.083	-	-	2569	-125.1	-	-
3.941	4731	-400.5	4699	-421.2	4607	-403.6	7.120	2561	-106.9	-	-	2538	-107.8
3.979	4652	-430.4	4646	-426.2	-	-	7.213	2525	-100.0	2541	- 92.9	2499	-104.9
4.018	4643	-392.3	4581	-443.6	4452	-467.2	7.305	2498	- 86.0	2502	- 90.8	2451	-112.2

Table 2. Continued.

	A		B		C			A		B		C	
s	I	i	I	i	I	i	s	I	i	I	i	I	i
7.342	2483	- 84.2	-	-	-	-	13.956	961	6.1	951	6.0	945	6.1
7.379	2470	- 81.7	-	-	-	-	14.033	949	4.2	944	8.2	927	-2.9
7.398	2448	- 96.0	2476	-76.1	2434	-90.4	14.109	940	3.8	945	17.5	932	11.0
7.490	2416	-88.1	-	-	2405	-80.7	14.185	925	-2.2	922	3.8	909	-3.8
7.582	2412	-52.8	2405	-67.3	2371	-75.9	14.260	925	6.6	915	5.3	909	4.7
7.674	2353	-73.3	-	-	2343	-66.9	14.335	905	-5.3	-	-	898	1.9
7.766	2362	-26.8	2337	-58.9	2326	-46.6	14.410	899	-3.1	887	-6.1	882	-5.6
7.857	2319	-32.9	2327	-32.1	2320	-16.6	14.485	879	-4.2	874	-10.5	882	2.7
7.949	2318	2.0	2310	-12.4	2324	22.3	14.560	884	-1.5	872	- 4.7	869	-2.2
8.040	2301	20.0	2290	3.8	2284	17.0	14.634	870	-7.4	859	- 9.4	861	-2.6
8.131	2260	14.1	2267	15.4	2254	21.6	14.708	858	-11.8	849	-12.1	849	-7.4
8.222	2214	2.5	2260	42.7	2222	22.9	14.781	845	-16.5	837	-16.3	844	-4.0
8.313	2209	30.0	2200	17.0	2216	49.7	14.855	838	-16.2	842	- 4.1	830	-10.9
8.404	2192	46.2	2171	21.1	2178	44.5	14.928	836	-10.2	833	- 4.7	827	-6.3
8.494	2139	25.0	2144	25.3	2135	33.2	15.000	837	- 2.1	811	-19.7	826	-0.8
8.585	2100	17.2	2126	40.9	2099	27.9	15.073	825	- 7.2	812	-12.2	815	-4.1
8.675	2098	46.2	2099	45.4	2069	28.6	15.145	814	-10.7	799	-17.8	809	-3.9
8.765	2048	26.7	2044	20.9	2018	7.1	15.217	813	- 4.5	802	- 7.2	798	-7.4
8.855	2018	26.3	-	-	1991	9.4	15.289	810	- 0.9	794	- 8.4	-	-
8.945	1997	32.9	1981	16.6	1954	0.5	15.360	797	-6.7	783	-12.9	790	-2.3
9.034	1956	20.6	1956	20.5	1916	-9.4	15.431	795	-2.1	780	-9.3	780	-5.9
9.124	1910	1.6	1907	-0.9	1888	-10.3	15.502	788	-2.7	776	-7.0	777	-2.5
9.213	1884	-0.7	1876	-4.0	1850	-21.7	15.572	777	-7.1	778	1.9	767	-5.8
9.302	1842	-12.9	1847	-6.2	1824	-20.6	15.642	771	-6.4	765	-5.3	764	-3.0
9.391	1806	-23.8	1821	-6.4	1800	-18.6	15.712	762	-9.0	763	-0.4	756	-4.5
9.479	-	-	1797	-4.3	1775	-19.1	15.782	765	0.0	760	2.4	748	-6.7
9.568	-	-	1755	-20.7	1765	4.3	15.851	-	-	753	1.8	757	11.4
9.656	1735	-19.8	1737	-13.4	1731	-12.9	15.920	752	-0.3	741	-4.1	743	0.6
9.744	1714	-17.7	1700	-27.0	1706	-14.6	15.988	748	1.4	738	-1.4	735	-2.0
9.832	1692	-16.0	1691	-11.7	1685	-12.1	16.057	733	-7.1	733	-0.4	730	-1.4
9.920	1672	-13.5	1651	-28.6	1673	- 1.0	16.125	738	3.7	731	3.0	729	3.4
10.007	-	-	1646	-12.2	1648	- 3.8	16.192	728	-0.7	721	-0.8	722	2.4
10.095	1623	-17.8	1601	-32.9	1625	- 4.9	16.260	723	0.1	-	-	-	-
10.182	1613	- 6.5	1603	- 9.4	1598	-10.0	16.271	-	-	-	-	711	2.4
10.269	1595	- 3.3	1582	- 8.6	1597	10.8	16.327	726	8.6	716	5.5	714	4.9
10.356	1578	0.8	-	-	1570	4.0	16.394	714	1.8	710	4.4	711	7.2
10.425	-	-	1556	3.7	-	-	16.460	707	0.2	707	7.2	697	-0.8
10.442	1571	14.0	-	-	1548	3.5	16.526	710	8.6	693	-1.6	694	1.4
10.529	1546	9.1	1523	-5.5	1520	-3.7	16.592	701	5.0	697	6.9	692	4.2
10.615	1534	16.9	-	-	1510	5.5	16.658	700	9.6	680	-3.9	693	10.1
10.701	1505	7.4	1496	7.7	1478	-6.4	16.723	689	4.4	669	-9.9	672	-5.8
10.787	1486	7.3	1482	12.3	1484	18.4	16.788	686	6.3	678	3.3	675	3.1
10.872	1479	19.4	1468	17.4	1449	3.0	16.853	677	1.5	669	-0.4	671	3.2
10.958	1450	8.0	1452	19.9	1444	15.4	16.917	676	5.6	660	-4.7	668	4.9
11.043	1471	47.7	1422	8.0	1441	31.0	16.981	668	2.7	661	1.8	658	0.2
11.111	-	-	-	-	1412	16.9	17.044	661	1.1	652	-2.9	657	4.2
11.125	1432	25.7	1414	18.5	-	-	17.108	658	2.4	646	-3.9	-	-
11.213	1408	20.3	1395	16.5	1392	17.3	17.171	653	2.4	-	-	644	0.3
11.297	1377	5.1	1359	-2.2	1364	6.9	17.233	647	1.1	643	1.4	644	4.5
11.381	1355	-1.5	1337	-6.9	1344	4.1	17.296	639	-1.9	637	0.7	632	-2.8
11.465	1341	2.3	1322	-6.2	1326	2.2	17.357	637	0.6	631	-1.0	627	-2.9
11.549	1324	2.0	1307	-4.2	1302	-5.3	17.419	636	4.0	629	1.7	623	-2.8
11.633	1301	-5.3	1273	-22.7	1290	6.3	17.480	626	-2.3	622	-1.3	618	-3.2
11.716	1284	-6.9	1263	-16.8	1264	-12.0	17.541	624	0.5	618	-0.8	616	-0.8
11.800	1262	-13.9	1259	- 6.2	1242	-18.0	17.602	615	-3.5	614	-1.2	613	0.7
11.883	1252	- 8.6	1238	-12.5	-	-	17.662	609	-5.7	612	1.7	607	-1.5
11.916	-	-	-	-	1232	-7.6	17.722	608	-2.5	609	3.0	603	-1.0
11.965	1221	-25.4	1208	-27.0	1217	-13.3	17.782	599	-7.5	602	-0.2	602	1.6
12.048	1209	-22.6	1194	-26.6	1203	-12.7	17.841	598	-5.7	603	5.1	597	0.5
12.130	1189	-25.0	1180	-26.5	1173	-23.4	17.900	595	-3.0	596	1.7	590	-2.4
12.212	1175	-28.6	1164	-29.3	1175	-12.6	17.959	589	-4.6	587	-2.9	592	4.0
12.294	1170	-20.4	1153	-25.9	1156	-17.3	18.017	598	8.2	589	2.5	582	-2.3
12.376	1163	-13.0	-	-	1152	- 8.4	18.075	592	6.3	-	-	580	-0.3
12.457	1140	-23.0	1127	-25.4	1130	-17.1	18.133	587	5.0	-	-	575	-1.5
12.538	1136	-19.0	1133	-7.5	1123	-10.8	18.190	583	5.0	579	3.5	575	2.7
12.619	-	-	1106	-21.6	-	-	18.247	584	10.2	578	6.3	569	0.2
12.700	1104	-21.9	1101	-13.5	1105	-3.6	18.303	578	7.2	576	8.2	569	3.9
12.780	1103	-10.1	1096	- 6.9	1084	-12.6	18.360	565	-1.4	566	2.4	568	7.0
12.860	1094	- 7.0	1089	- 1.8	1087	2.0	18.415	568	4.5	569	9.3	559	1.3
12.940	1085	- 4.1	1083	3.2	1071	-2.1	18.471	554	-5.5	562	5.1	555	0.3
13.020	1070	- 7.6	-	-	1063	1.4	18.526	567	10.8	560	7.0	552	1.5
13.099	-	-	1054	-2.8	1041	+9.6	18.581	568	15.3	-	-	549	1.9
13.179	1064	8.7	1064	17.9	1044	5.5	18.635	559	9.6	551	5.1	547	3.0
13.258	1050	5.2	1047	12.0	1034	6.0	18.689	556	10.2	550	7.4	539	-0.3
13.336	1048	14.1	1043	18.8	1023	5.1	18.743	543	0.7	546	6.6	530	-6.9
13.415	1041	17.6	1023	9.0	1014	6.9	18.797	557	17.8	540	3.8	530	-3.7
13.493	1021	8.5	-	-	1014	17.0	18.850	542	6.3	542	8.5	529	-1.6
13.571	1008	5.1	1002	8.7	1000	13.1	18.902	538	5.3	539	9.2	529	2.0
13.648	1006	13.1	988	4.4	979	2.4	18.955	532	3.3	540	13.1	523	-1.5
13.726	1000	17.1	989	15.4	980	12.8	19.007	532	6.5	529	5.2	523	1.6
13.803	987	13.9	984	20.2	-	-	19.058	531	7.6	523	2.7	512	-5.8
13.880	974	10.6	959	4.2	945	-2 7							

The scaled intensity values were corrected for the incoherent part of the radiation and from the resulting intensity values, $I(s)$, the reduced intensities, $i(s)$, were calculated according to the expression [12]

$$i = I - \sum n_i f_i^2$$

All calculations were normalized to correspond to a stoichiometric volume of solution, V Å^3, containing one uranium(IV) atom. The I values are given in Table 2 as a function of $s = 4\pi \sin\theta/\lambda$. The reduced intensity values were corrected for spurious peaks below 1 Å in the radial distribution curves, as described in previous papers,[5,6] and the resulting $i(s)$ values are given in Table 2 as a function of s. Observed and reduced intensities are also shown in Figs. 2 and 3.

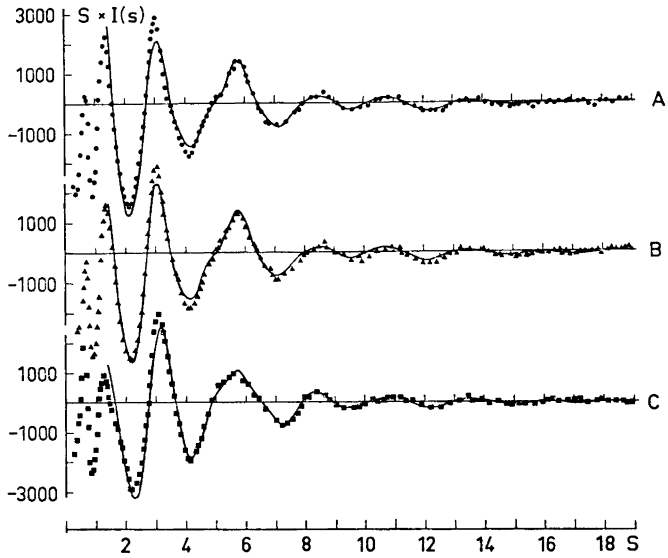

Fig. 3. Reduced intensity values, $i(s)$, multiplied by s, given as a function of $s = 4\pi \sin\theta/\lambda$. Between one half and one third of the observed intensities are given as dots. The full-drawn curves represent $si(s)$ values calculated with parameters from the least squares refinements.

Electronic radial distribution curves, $D(r)$, were calculated from the reduced intensities using the expression:[12]

$$D(r) = 4\pi r^2 \varrho_0 + \frac{2r}{\pi}\int_0^{s_{max}} si(s)\{f_U^2(0)/f_U^2(s)\exp(-ks^2)\}\sin(rs)\mathrm{d}s$$

In the sharpening factor, given within brackets, the first part compensates for the electron distribution within the atoms. The sharpening effect obtained in this way is reduced by the exponential part, in which the constant k for the following calculations has been chosen to be 0.01.

Theoretical intensity curves were calculated from [12]

$$i(s) = \sum_m \sum_n f_m f_n \frac{\sin(rs)}{rs} \exp(-b_{mn}s^2)$$

All calculations were carried out on an IBM 360/75 computer with the KURVLR program, which is an extended version,[12] written in Fortran, of the previously used Algol programs.[13]

ANALYSIS OF THE DATA

The radial distribution curves. Radial distribution curves, $D(r)$, for the solutions investigated are shown in Fig. 4. The variation of the $D(r)$ functions around the average, $4\pi r^2\varrho_0$, are given in Fig. 5.

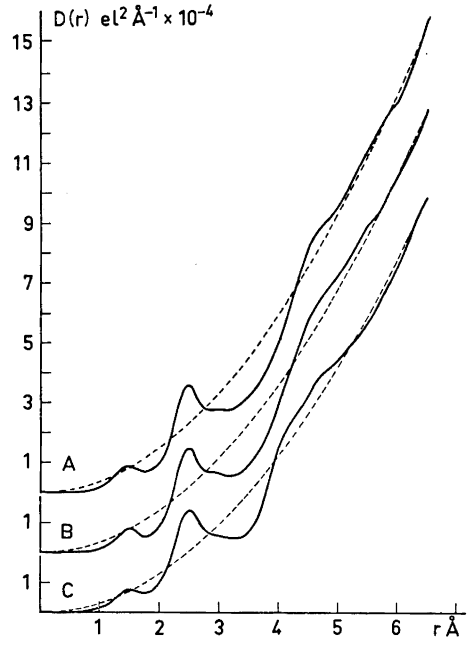

Fig. 4. Radial distribution curves, $D(r)$, for the solutions investigated. Broken lines are the corresponding $4\pi r^2\varrho_0$ functions.

The Cl – O peak at 1.4 Å in the perchlorate group is easily recognized. The first coordination sphere around the U^{4+} ion is represented by the peak at 2.5 Å. The broad peak at about 4.5 Å can probably be taken to indicate distances between the U^{4+} ion and atoms in a second coordination sphere. This peak is the only one that is noticeably different for the acid and the hydrolyzed solutions.

Polynuclear complexes. The changes in the distribution curves, when the hydrolysis is increased, are best brought out by taking the difference between the curves. The differences were calculated after subtracting the $4\pi r^2\varrho_0$ functions, including the light atoms only, from the $D(r)$ functions, and are given in Fig. 6. The significant differences are limited to the region around 4 Å and, possibly, around 5.5 Å. The changes in the region corresponding to the first coordination sphere of the uranium atom are too small to allow any quantitative analysis.

The peak at 4.0 Å in Fig. 6 is close to the corresponding position of the Th – Th peak in the polynyclear complexes found in the thorium nitrate solutions previously investigated which occurred at 3.95 Å. Thus it seems likely that the 4 Å peak indicates the formation of polynuclear complexes in solution

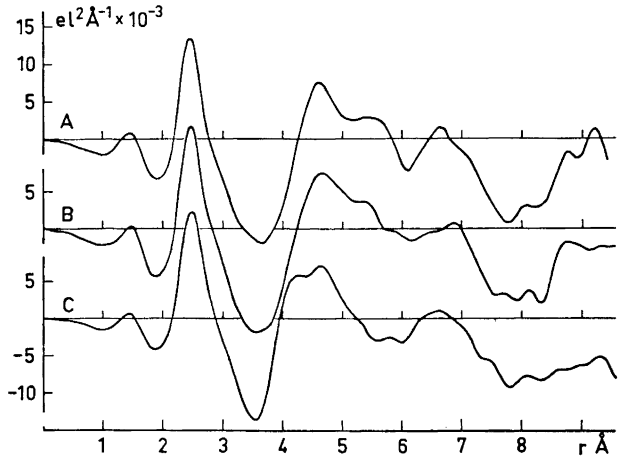

Fig. 5. $[D(r) - 4\pi r^2 \varrho_0]$ functions for the three solutions investigated.

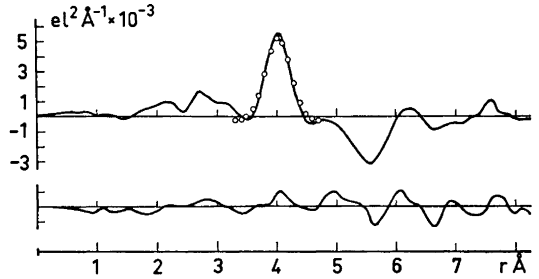

Fig. 6. Differences between distribution functions. The upper curve gives the difference between the solutions C and A and the lower curve that between the solutions B and A. Calculated values for an U – U interaction, assuming 0.34 U – U distances per U atom and a temperature factor of 0.013, are indicated on the upper curve.

C. By analogy with the Th^{4+} results this would indicate that the uranium atoms in the complexes are joined by double hydroxo bridges.

Comparison with calculated peak shapes for U – U interactions (Fig. 6) indicates that the average number of U atoms bound to each other U atom in solution C is about 0.7. In solution B no significant peak occurs at 4.0 Å (Fig. 6) indicating that no significant amount of polynuclear complexes has formed in this solution.

Coordination of the U^{4+} ion. The radial distribution curve for the acid solution, A, and to a somewhat lesser extent, the corresponding curves for solutions B and C, show irregularities in the region of the broad peak between about 4 and 6 Å, interpreted as indicating a concentration of distances corresponding to a second coordination sphere around the U^{4+} ion. This is particularly evident when these results are compared with the results from the thorium nitrate solutions previously investigated, for which no pronounced peaks were

found corresponding to those at 5.5 Å and 6.7 Å (Fig. 5) in the uranium(IV) solutions. On the other hand, the peak at 2.5 Å representing the first coordination sphere of the U^{4+} ion, is more regular than the corresponding peak for the acid thorium nitrate solution.

For the thorium nitrate solutions it was concluded that inner-sphere complexes are formed with the nitrate groups bound as bidentate ligands. The resulting Th – N distances were clearly indicated in the radial distribution curves. If the perchlorate groups form similar complexes with the U^{4+} ion, the corresponding U – Cl distances should be even more pronounced, because of the higher atomic number of the chlorine atom. The effects to be expected are illustrated in Fig. 7, where calculated peak shapes are given for an eight-

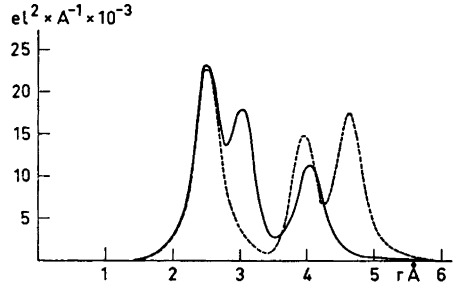

Fig. 7. Calculated peak shapes for uranium-light atom interactions within a $U-ClO_4$ complex. The U atom is assumed to be 8-coordinated (U – O distance 2.4 Å) with two perchlorate groups bound either as monodentate (broken curve) or as bidentate ligands (solid curve).

coordinated uranium atom with perchlorate groups bound either as bidentate or as monodentate ligands. A comparison with the observed distribution curves gives no support for a formation of any significant amount of these types of complexes.

If, on the other hand, formation of an outer-sphere complex is assumed, the peaks at 5.5 Å and 6.7 Å are easily explained. A perchlorate group orientated as a bidentate ligand would give U – O contributions to the peaks at 4.6 Å and 6.7 Å and U – Cl contributions to the peak at 5.5 Å. As the peaks at these comparatively large distances correspond only to small variations in the very large number of background interactions in this region (Fig. 5), this conclusion is not, of course, very firmly based. Some support for it, in addition to that obtained from the comparison with the results for the thorium nitrate solutions, is obtained from the observation that the supposed U – Cl peak at 5.5 Å, decreases when the perchlorate concentration is decreased (Fig. 6).

Least-squares refinement of the intensity curves. The dominant frequencies in the observed intensity curves (Fig. 3) were further analyzed by a least squares method with which a comparison was made with calculated intensity curves, obtained by including the Cl – O and O – O interactions of the perchlorate groups and interactions involving the uranium atoms. For each type of interaction the distance, d, a temperature factor, b, and a frequency factor, n, were introduced. A minimum was sought for the function $\sum[si(s)_{obs} - si(s)_{calc}]^2$, the summation being taken over the observed points. For the ClO_4 interactions the parameters obtained in a previous investigation of tin(II) perchlorate solutions [14] were used. The low-angle part of the intensity curves, where other

types of interactions are the main contributors, was not included in the refinement. In order to check the constancy of the frequencies the refinement was carried out using different values for the lower s limit.

Table 3. Results of the least squares refinement for solutions A and B, when two different U – O interactions are included. The longer U – O distance has significant contributions only for the two lower s limits.

s_{min}	sol.	$(U-O)_1$ d	b	n	$(U-O)_2$ d	b	n
1.9	A	2.519[6]	0.012[2]	9.5[3]	4.57[2]	0.018[7]	6.0[6]
	B	2.530[5]	0.016[2]	10.5[3]	4.55[2]	0.038[8]	7.7[7]
3.5	A	2.472[5]	0.003[1]	7.0[3]	4.43[1]	0.019[6]	7.0[9]
	B	2.480[5]	0.003[1]	6.9[3]	4.42[2]	0.046[12]	9.8[23]
6.6	A	2.432[6]	0.003[1]	7.2[7]			
	B	2.430[5]	0.001[1]	6.4[7]			
7.8	A	2.425[6]	0.004[1]	8.9[13]			
	B	2.427[5]	0.003[1]	7.7[10]			
8.8	A	2.419[6]	0.005[2]	10.1[24]			
	B	2.426[6]	0.002[1]	7.0[12]			
10.3	A	2.423[9]	0.002[2]	5.9[6]			
	B	2.426[6]	0.002[1]	7.0[12]			

Table 3 gives the results of the first part of this refinement. The number of U – O interactions corresponding to the 2.5 Å peak in the distribution curve does not differ significantly from eight. The introduction of a second U – O interaction at about 4.5 Å, as an approximation of a second coordination sphere, does not affect this result. Thus the coordination of the uranium atom does not differ significantly from that which has been found in crystal structures.[15]

Table 4. Results of the least squares refinements for solutions A and B, when U – ClO_4 interactions are included in addition to the two U – O and the intramolecular ClO_4 interactions.

s_{min}	sol.	$(U-O)_1$ d	b	n	$(U-O)_2$ d	b	n	U – ClO_4 d	b	n
1.9	A	2.495[4]	0.005[1]	7.9[2]	4.46[1]	0.021[5]	8.5[5]	5.74[3]	0.031[5]	3.3[4]
	B	2.510[4]	0.009[2]	9.2[3]	4.47[2]	0.038[7]	9.6[9]	5.77[5]	0.036[9]	2.5[6]
3.5	A	2.457[4]	0.004[1]	7.8[3]	4.40[1]	0.045[8]	16 [3]	5.69[2]	0.07[1]	8.2[12]
	B	2.472[4]	0.005[1]	8.0[4]	4.38	0.046[6]	13 [2]	5.67[4]	0.06[1]	4.3[7]

In the second part of the refinement an attempt was made to include interactions between a U atom and an outer-sphere perchlorate group. This refinement converged but significant parameter values were obtained only for the lower s limit where systematic errors can be expected to be large. The results are given in Table 4.

Introduction of O – O interactions within the first coordination sphere of the uranium atom, assuming an antiprismatic arrangement of the oxygen atoms, did not affect the results of the refinements, although it led to a small decrease in the least squares error sum. A parameter introduced to allow a change in the orientation of the ClO_4 group did not show any significant deviation of the ClO_4 group from the assumed bidentate orientation.

The final agreement between observed and calculated intensity curves is shown in Fig. 3. The contributions of the various interactions to the intensity curves and the distribution functions are shown in Figs. 8 and 9.

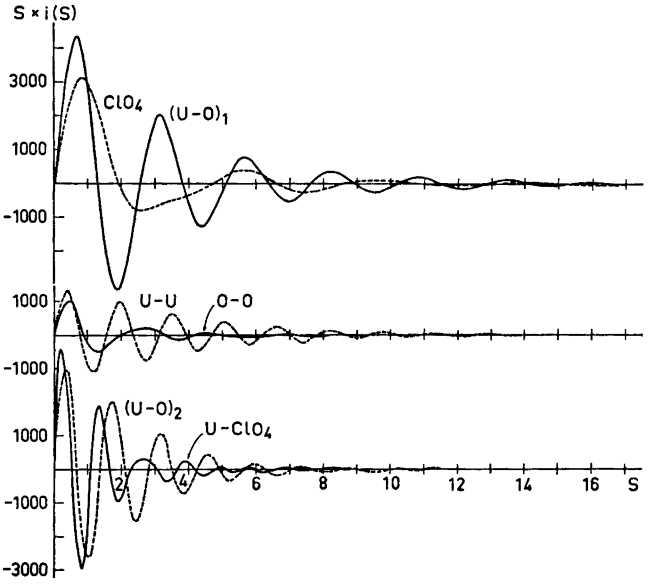

Fig. 8. The contributions from the separate interactions used to calculate $si(s)$ values for solution C. The following parameters were used:
ClO_4: $d = 2.43$ Å (Cl – O), $b = 0.003$ (Cl – O) (broken line); $(U-O)_1$: $d = 2.46$ Å, $b = 0.005$, n = 8.0 (solid line); U – U: $d = 4.00$ Å, $b = 0.013$, $n = 0.34$ (broken line); O – O: an Archimedean antiprism surrounding the U atom (solid line); $(U-O)_2$: $d = 4.46$ Å, $b = 0.03$, $n = 9.6$ (broken line); $U-ClO_4$; $d = 5.75$ Å (U – Cl), $b = 0.034$, $n = 2.5$ (solid line).

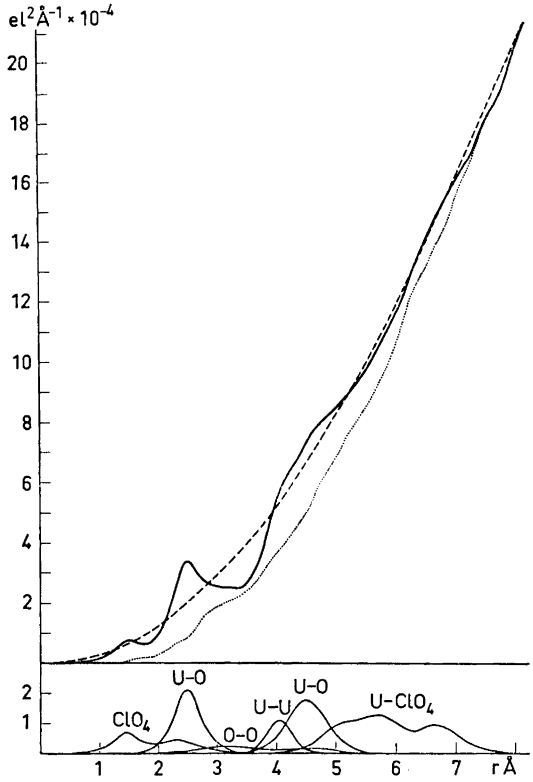

Fig. 9. A comparison between the $D(r)$ function for solution C and the peak shapes for the separate interactions calculated with the parameters given in Fig. 8. The dotted line shows the difference between observed and calculated curves. The broken line shows the $4\pi r^2\varrho_0$ function.

DISCUSSION OF THE RESULTS

The analysis of the scattering data shows the uranium(IV) ion to have a well-defined first coordination sphere with a coordination number which is not significantly different from eight. The least-squares analysis with the use of the high-angle parts of the intensity curves, which should be the least affected by systematic errors, gives a value of 2.43 Å for the corresponding U – O distance (Table 3). Similar distances have been reported for crystals of uranium(IV) compounds.[15] In UO_2, which has the fluorite structure, the U – O bonding distance has been found to be 2.37 Å.[16] In several other crystals, such as $U(OH)_2SO_4$,[17] $U_6O_4(OH)_4(SO_4)_6$,[18] and $U(SO_4)_2(H_2O)_4$,[19] the uranium(IV) ion has also been found to be eight-coordinated, but with the oxygen atoms arranged at the corners of an Archimedean antiprism. The U – O distances in these crystals are close to those found in the UO_2 structure, but the oxygen positions were derived from mainly geometrical reasoning.

It has not been possible to deduce from the solution scattering data the arrangement of oxygen atoms in the inner sphere, as the contributions from the corresponding O – O distances to the scattered intensities are too small (Figs. 8 and 9). No evidence is, however, found for inner-sphere complex formation with the perchlorate ions.

Well-defined distances, which can be related to a second coordination sphere, are found in the analysis of the scattering data. Water molecules at a distance of 4.4_6 Å from the uranium ion and ClO_4 groups with a U – Cl distance of 5.7_2 Å seem to form a relatively well-defined second coordination sphere around the uranium ion. If the water molecules in the inner coordination sphere are assumed to form a cube or a square antiprism around the uranium atom as has been found in crystals, the distances between the water molecules in the first and the second sphere can be estimated. If the water molecules in the second sphere are assumed to be situated outside an edge of the cube or the antiprism, the shortest distances to the two water molecules of the inner sphere, which define that edge, will be about 2.9 Å. Such a position seems likely as it would allow the formation of hydrogen bonds from the two water molecules in the inner sphere. For a perchlorate group in a similar position, that is with an edge of the ClO_4 tetrahedron parallel to an edge of the cube or the antiprism the O – O distances would be about the same, when the U – Cl distance is 5.7 Å. Thus, the distances derived from the X-ray scattering data and assigned to atoms in a second coordination sphere of the uranium atom lead to reasonable O – O contact distances, which supports our interpretation. Other positions for the oxygens than those now discussed lead either to too long or to too short O – O distances. We have found no crystal structure determinations of uranium(IV) perchlorates reported in the literature with which a comparison can be made. A crystal structure determination of the compound $U(OH)(ClO_4)_3(H_2O)_6$ has therefore been started.

Although only relatively weakly hydrolyzed solutions of the uranium(IV) perchlorate could be prepared, the formation of polynuclear hydrolysis complexes in the most hydrolyzed of the solutions investigated, is clearly indicated (Fig. 6). The shortest U – U distance within the complexes is 4.00 Å, which is close to the distance 3.95 Å found for the Th – Th distance in the polynuclear hydrolysis complexes of thorium,[1] where the thorium atoms are joined by two hydroxo bridges. A similar distance, 3.90 Å, has been found by Lundgren[17] in a crystal structure investigation of $U(OH)_2SO_4$ in which the uranium atoms are joined by double hydroxo bridges into infinite chains. In crystals of $U_6O_4(OH)_4(SO_4)_6$,[18] which contain discrete complexes in which the uranium atoms are octahedrally arranged with each uranium atom sharing two oxygens with a neighboring uranium atom, the U – U distances have been reported to be 3.85 Å. Thus it seems likely that the uranium atoms in the polynuclear complexes formed in hydrolyzed solutions are joined by double hydroxo bridges. A dinuclear complex should therefore have a structure analogous to the one previously found for thorium.[1] The formation of larger complexes cannot be excluded on the basis of the scattering data only, as longer interactions in such complexes would probably be too weak to be distinguished in the distribution curves.

Acknowledgements. The work has been supported by *Statens Naturvetenskapliga Forskningsråd (Swedish Natural Science Research Council)*. Computer time has been made available by the *Computer Division of the National Swedish Office for Administration, Rationalization and Economy*. A scholarship from *The Scientific and Research Council*, Skoplje, Yugoslavia, to one of us (S.P.) is gratefully acknowledged. We thank Dr. Derek Lewis for revising the English text.

REFERENCES

1. Johansson, G. *Acta Chem. Scand.* **22** (1968) 399.
2. Sillén, L. G. and Martell, A. E. *Stability Constants of Metal-Ion Complexes*, Special Publication No. 17, The Chemical Society, London 1964, and Supplement No. 1, London 1970.
3. Hietanen, S. *Acta Chem. Scand.* **10** (1956) 1531.
4. El-Shamy, H. K. and El-Dinzayan, S. *J. Chem. Soc.* **1953** 384.
5. Johansson, G. *Acta Chem. Scand.* **20** (1966) 553; **25** (1971) 2787.
6. Åberg, M. *Acta Chem. Scand.* **24** (1970) 2931.
7. Cromer, D. T. and Waber, J. T. *Acta Cryst.* **18** (1965) 104.
8. *International Tables for X-Ray Crystallography*, The Kynoch Press 1962, Vol. III.
9. Cromer, D. T. *Acta Cryst.* **18** (1965) 17.
10. Cromer, D. T. *J. Chem. Phys.* **50** (1969) 4857.
11. Compton, A. H. and Allison, S. K. *X-Rays in Theory and Experiment*, Van Nostrand, New York 1935.
12. Johansson, G. and Sandström, M. *Chemica Scripta. In press.*
13. Johansson, G. Programs with accession Nos. 6037 and 6038 in *IUCr World List of Crystallographic Computer Programs*, 2nd Ed. 1966.
14. Johansson, G. and Ohtaki, H. *Acta Chem. Scand.* **27** (1973) 643.
15. Chernyaev, I. I., Ed., *Complex Compounds of Uranium*. Israel Program for Scientific Translations, Jerusalem 1966.
16. Zachariasen, W. H. *Phys. Rev.* **78** (1948) 1104.
17. Lundgren, G. *Arkiv Kemi* **2** (1950) 535.
18. Lundgren, G. *Arkiv Kemi* **5** (1953) 349.
19. Kierkegaard, P. *Acta Chem. Scand.* **10** (1956) 599.

Received February 3, 1973.

ACTA CHEMICA SCANDINAVICA 27 (1973) 2161–2170

Reaktionen von Trichlormethansulfenylchlorid mit Stickstoffverbindungen. IV.* Substituenteneffekte in 5-Aryl-1,3,4-oxathiazol-2-onen

ALEXANDER SENNING und JAKOB SCHMIDT RASMUSSEN

Chemisches Institut der Universität Aarhus, DK-8000 Århus C, Dänemark

Durch Ringschluss der entsprechenden Amide wurden 27 neue 5-Aryl-1,3,4-oxathiazol-2-one *I* und aus diesen durch Substitution weitere 11 neue *I* erhalten. Durch Bestimmung der integralen IR-Carbonylabsorption von *I* ($R = C_6H_5$), der σ-Konstanten des 1,3,4-Oxathiazol-2-on-5-yl-Rings und durch halbquantitative Nitrierungsversuche mit repräsentativen *I* wurde der 1,3,4-Oxathiazol-2-on-5-yl-Ring als Substituent aromatischer Ringsysteme charakterisiert. In *I* selbst ist er überwiegend als –I,–M zu bezeichnen, während sein Einfluss auf die Stabilisierung des σ-Komplexes der Nitrierung von I der eines –I,+M-Substituenten entspricht.

Die 5-Alkyl- bzw. 5-Aryl-1,3,4-oxathiazol-2-one *I* wurden erstmals 1965 unabhängig voneinander von uns[1] und in den Laboratorien der Farbenfabriken Bayer[2] dargestellt. Die bisher erschienene Literatur über diese Verbindungsklasse ist noch wenig umfangreich.[1–10]

Die bequemste Synthese von *I* ist zweifellos die aus Carbonsäureamiden und Chlorcarbonylsulfenylchlorid[2,8–10] (1); andere Synthesewege, die vom Trichlormethansulfenylchlorid ausgehen,[1,3–5] können damit nur in Sonderfällen konkurrieren.

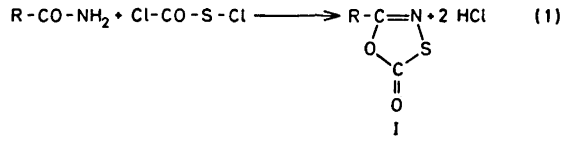

(1)

I

Besonderes Interesse knüpft sich an folgende Eigenschaften von *I*: die Säurestabilität und Basenlabilität von *I*[3] legt ihre Verwendung als Schutz-

* Vorläufige Mitteilung siehe Literaturzitat 6. Teil III siehe Literaturzitat 3.

gruppe für die Amidfunktion nahe, *I* sind eine bequeme Quelle für die 1,3-dipolaren Nitril-*N*-sulfide [7] und schliesslich ist die Charakterisierung des 1,3,4-Oxathiazol-2-on-5-yl-Restes als Elektronendonor bzw. -acceptor ein spektroskopisches bzw. chemisches Problem.[6]

Tabelle 1. Aus Carbonamiden erhaltene 5-substituierte 1,3,4-Oxathiazol-2-one *I*.

Verbindung Nr.	R	Summenformel	Methode	Ausbeute (%)*	F: (umkr.aus)	Analysenwerte
I-1	(1-Naphthoxy)-methyl	$C_{13}H_9NO_3S$	A	38	98-100° (Äthanol)	Gef. C 61,05; H 3,65; N 5,60 Ber. C 60,22; H 3,50; N 5,40
I-2	(2-Naphthoxy)-methyl	$C_{13}H_9NO_3S$	A	31	84-86° (Äthanol)	Gef. C 60,50; H 3,30; N 5,60 Ber. C 60,22; H 3,50; N 5,40
I-3	2-Hydroxyphenyl	$C_8H_5NO_3S$	D	51	80-81° (Äthanol)	Gef. C 49,31; H 2,65; N 7,11; S 16,56 Ber. C 49,24; H 2,58; N 7,18; S 16,40
I-4	2-Acetoxyphenyl	$C_{10}H_7NO_4S$	B	50	70-71° (Äthanol)	Gef. C 50,55; H 3,27; N 5,87 Ber. C 50,61; H 2,98; N 5,90
I-5	2-Methoxyphenyl	$C_9H_7NO_3S$	B	53	69-70° (Methanol)	Gef. C 51,60; H 3,28; N 6,54; S 15,27 Ber. C 51,68; H 3,37; N 6,70; S 15,30
I-6	3-Methoxyphenyl	$C_9H_7NO_3S$	B	67	93-94° (Methanol)	Gef. C 51,65; H 3,50; N 6,52; S 15,30 Ber. C 51,68; H 3,37; N 6,70; S 15,30
I-7	4-Methoxyphenyl	$C_9H_7NO_3S$	B	41	99-101° (Methanol)	Gef. C 51,44; H 3,49; N 6,58 Ber. C 51,68; H 3,37; N 6,70
I-8	2-Fluorphenyl	$C_8H_4FNO_2S$	B	40	47,5-50° (Äthanol)	Gef. C 48,39; H 2,20; S 16,58 Ber. C 48,77; H 2,05; S 16,26
I-9	3-Fluorphenyl	$C_8H_4FNO_2S$	B	72	57-58° (Methanol)	Gef. C 48,42; H 2,10; S 17,09 Ber. C 48,77; H 2,05; S 16,26
I-10	4-Fluorphenyl	$C_8H_4FNO_2S$	B	74	99-101° (Äthanol)	Gef. C 48,13; H 1,90; N 7,05 Ber. C 48,77; H 2,05; N 7,11
I-11	2-Brompheny1	$C_8H_4BrNO_2S$	B	48	54-55,5° (Äthanol)	Gef. C 37,91; H 1,52; N 5,32 Ber. C 37,24; H 1,56; N 5,45
I-12	2-Jodphenyl	$C_8H_4JNO_2S$	B	59	64-65,5° (Methanol)	Gef. C 31,25; H 1,22; N 4,46 Ber. C 31,49; H 1,32; N 4,59
I-13	3-Jodphenyl	$C_8H_4JNO_2S$	A	38	98-100° (Äthanol)	Gef. J 41,90; S 11,03 Ber. J 41,60; S 10,51
I-14	4-Jodphenyl	$C_8H_4JNO_2S$	B	48	145-146,5° (Äthanol)	Gef. C 31,62; H 1,39; N 4,55 Ber. C 31,49; H 1,32; N 4,59
I-15	2-Methylphenyl	$C_9H_7NO_2S$	C	71	ca. 15° (Methanol)	Gef. C 54,98; H 3,81; S 16,71 Ber. C 55,94; H 3,65; S 16,60
I-16	2-(Chlormethyl)-phenyl	$C_8H_6ClNO_2S$	B	15	69-71,5° (Äthanol)	Gef. C 47,38; H 2,88; N 6,10; Cl 15,23 Ber. C 47,47; H 2,66; N 6,15; Cl 15,57
I-17	3-(Chlormethyl)-phenyl	$C_8H_6ClNO_2S$	B	69	114-115° (Chloroform/Äthanol)	Gef. C 47,28; H 2,67; N 6,10; S 14,13 Ber. C 47,47; H 2,66; N 6,15; S 14,08
I-18	4-(Chlormethyl)-phenyl	$C_8H_6ClNO_2S$	B	57	118-120° (Äthanol)	Gef. C 47,46; H 2,72; N 5,99 Ber. C 47,47; H 2,66; N 6,15
I-19	2-(Dichlormethyl)-phenyl	$C_8H_5Cl_2NO_2S$	B	27	74,5-75,5° (Äthanol)	Gef. C 40,59; H 2,07; N 5,42; S 12,66 Ber. C 41,24; H 1,92; N 5,35; S 12,23
I-20	3-(Dichlormethyl)-phenyl	$C_8H_5Cl_2NO_2S$	B	31	80-84° (Äthanol)	Gef. C 40,85; H 1,99; N 5,31; S 12,30 Ber. C 41,24; H 1,92; N 5,35; S 12,23
I-21	3-(Trichlormethyl)-phenyl	$C_9H_4Cl_3NO_2S$	B	31	60-62° (Äthanol)	Gef. C 36,48; H 1,55; N 4,72; S 10,86 Ber. C 36,44; H 1,36; N 4,72; S 10,82
I-22	4-(Trichlormethyl)-phenyl	$C_9H_4Cl_3NO_2S$	B	42	122-124° (Äthanol)	Gef. C 36,51; H 1,52; N 4,70; S 10,98 Ber. C 36,44; H 1,36; N 4,72; S 10,82
I-23	2-Cyanphenyl	$C_9H_4N_2O_2S$	B	8	166-169°(Zers.) (Acetonitril)	Gef. C 52,80; H 2,15; N 13,47; S 15,77 Ber. C 52,95; H 1,98; N 13,72; S 15,68
I-24	3-Nitro-4-chlor-phenyl	$C_8H_3ClN_2O_4S$	B	63	112,5-114° (Äthanol)	Gef. C 36,95; H 1,26; N 10,54 Ber. C 37,15; H 1,17; N 10,83
I-25	2-Thienyl	$C_6H_3NO_2S_2$	A	44	82,5-84° (Äthanol)	Gef. C 38,47; H 1,20; N 7,47 Ber. C 38,93; H 1,63; N 7,57
I-26	2-Thiazolyl	$C_5H_2N_2O_2S_2$	A	41	93-96° (Äthylacetat/Acetonitril)	Gef. C 32,65; H 1,10; N 15,40 Ber. C 32,26; H 1,08; N 15,04
I-27	5-Methyl-2-thiazolyl	$C_6H_4N_2O_2S_2$	A	38	110,5-112,5° (Äthanol)	Gef. S 32,29 Ber. S 32,02

* Korrigiert für zurückgewonnenes Carbonsäureamid.
Methode A: nach Literaturzitat.[3]
Methode B: nach Literaturzitat.[2]
Methode C: wie B, aber bei Zimmertemperatur (Reaktionsdauer 144 Stunden).
Methode D: wie B, aber bei 40–45° (Reaktionsdauer 144 Stunden).

Tabelle 2. Durch Modifizierung der Seitenkette erhaltene 5-substituierte 1,3,4-Oxathiazol-2-one *I*.

Verbindung Nr.	R	Summenformel	Ausbeute (%)	F: (umkr. aus)	Analysenwerte
I – 29	3-(JCH_2)-C_6H_4-	$C_9H_6JNO_2S$	87	155,5 – 156,5° (Äthanol)	Gef. C 34,20; H 1,96; N 4,40 Ber. C 33,85; H 1,90; N 4,39
I – 30	4-(JCH_2)-C_6H_4-	$C_9H_6JNO_2S$	81	132,5 – 134° (Chloroform/ Methanol)	Gef. C 33,95; H 1,82; N 4,19 Ber. C 33,85; H 1,90; N 4,39
I – 31	4-HOOC-C_6H_4-	$C_9H_5NO_4S$	80	220 – 222° (Zers.)	Gef. C 48,36; H 2,60; N 6,40; S 15,03 Ber. C 48,44; H 2,26; N 6,28; S 14,36
I – 32	Cl^-4-[$^+$(H_5C_5N)-CH_2]-C_6H_4-	$C_{14}H_{11}ClN_2O_2S$. 0,5 C_2H_5OH	84	172 – 176° (Zers.)	Gef. C 53,82; H 4,15; Cl 11,11; Ber. C 54,43; H 4,00; Cl 11,00; Gef. N 8,53; S 9,87 Ber. N 8,70; S 9,95
I – 33	4-[C_2H_5O-CH(OH)]-C_6H_4-	$C_{11}H_{11}NO_4S$	38	120 – 122°	Gef. C 52,25; H 4,45; N 5,48; S 12,64 Ber. C 52,17; H 4,38; N 5,53; S 12,64

Tabelle 3. Durch Nitrierung erhaltene 5-substituierte 1,3,4-Oxathiazol-2-one *I*.

Verbindung Nr.	R	Summenformel	Ausbeute (%) [a]	F: (umkr. aus)	Analysenwerte
I – 34	2-CH_3-5-NO_2-C_6H_3	$C_9H_6N_2O_4S_2$	34 [b]	89 – 91,5° (Äthanol)	Gef. C 45,18; H 2,69; N 11,61; S 13,24 Ber. C 45,39; H 2,54; N 11,76; S 13,44
I – 35	3-CH_3-4-NO_2-C_6H_3	$C_9H_6N_2O_4S_2$	20 [c]	114,5 – 116° (Äthanol)	Gef. C 45,61; H 2,65; N 11,59; S 13,42 Ber. C 45,39; H 2,54; N 11,76; S 13,44
I – 36	4-CH_3-3-NO_2-C_6H_3	$C_9H_6N_2O_4S_2$	51 [b]	104 – 106° (Äthanol)	Gef. N 11,47; S 13,41 Ber. N 11,76; S 13,44
I – 37	2-F-5-NO_2-C_6H_3 [d]	$C_8H_3FN_2O_4S$	64 [b]	133 – 134° (Chloroform/ Äthanol)	Gef. C 39,58; H 1,32; N 11,40; S 13,52 Ber. C 39,67; H 1,25; N 11,57; S 13,24
I – 38	3-F-6-NO_2-C_6H_3 [d]	$C_8H_3FN_2O_4S$	78 [b]	78 – 80° (Chloroform/ Äther)	Gef. C 39,72; H 1,37; N 11,51; S 13,38 Ber. C 39,67; H 1,25; N 11,57; S 13,24
I – 39	2-(5-Nitrofuryl)- [d]	$C_6H_2N_2O_5S$	47 [b]	121,5 – 124° (Äthanol)	Gef. C 33,71; H 0,92; N 12,69 Ber. C 33,66; H 0,94; N 13,09

[a] Nicht für zurückgewonnenes Ausgangsmaterial korrigiert. [b] Mit Nitriersäure (0 – 15°). [c] Mit rauchender Salpetersäure (0°). [d] Siehe Schlussbemerkung.

Die vorliegende Arbeit beschäftigt sich vor allem, über die bereits mitgeteilten Befunde [6] hinausgehend, mit der systematischen Untersuchung der Nitrierung einer Reihe von 5-Aryl-1,3,4-oxathiazol-2-onen *I* (R = Ar). Ausserdem wurde eine Reihe von *I* (R = Ar) durch Modifizierung der Seitenkette am Arylrest in neue *I* überführt.

Darstellung der Ausgangsverbindungen. Wie aus Tabelle 1 hervorgeht, stellten wir 27 neue *I* dar, die zum Teil zur Abrundung unserer Kenntnisse dieser Verbindungsklasse dienen sollten und zum Teil für die weiter unten beschriebenen Untersuchungen benötigt wurden.

Die nach (1) erforderlichen Carbonsäureamide waren durchwegs bekannt. Interessant ist die Darstellung von *I-3* (R = 2-HOC_6H_4), die nach der Standardmethode nicht gelang, aber durch Einhaltung einer niedrigen Reaktionstemperatur und einer langen Reaktionszeit ohne Schutz der Hydroxylfunktion durchgeführt werden konnte. Besondere Probleme bot die Darstellung von *I-16* (R = 2-$CH_3C_6H_4$). Auch hier war es notwendig, die Umsetzung über lange Zeit bei niedriger Temperatur ablaufen zu lassen. Obwohl das Produkt bei Zimmertemperatur flüssig ist, liess es sich auch im Ölpumpenvakuum nicht unzersetzt destillieren und musste durch Umkristallisation gereinigt werden.

Modifizierung von Seitenketten in I. 5-(3-Methylphenyl)-1,3,4-oxathiazol-2-on lässt sich in Gegenwart von Peroxiden in der Seitenkette mit Sulfurylchlorid chlorieren und mit *N*-Bromsuccinimid bromieren, die Reaktionen sind jedoch langsam und die Trennung der Reaktionsprodukte ist schwierig.

Die 5-(Chlormethyl-phenyl)-1,3,4-oxathiazol-2-one lassen sich in der üblichen Weise mit Natriumjodid in Aceton in die entsprechenden 5-(Jodmethyl-phenyl)-1,3,4-oxathiazol-2-one überführen.

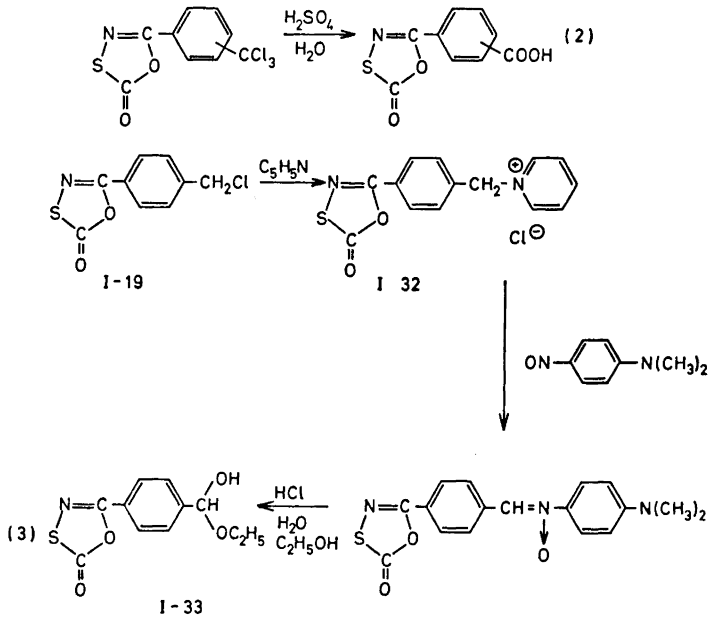

Die 5-(Trichlormethyl-phenyl)-1,3,4-oxathiazol-2-one lassen sich, ohne dass der heterocyclische Ring Schaden nimmt, in saurer Lösung zu den entsprechenden Carbonsäuren hydrolysieren (2).

5-[4-(Chlormethyl)-phenyl]-1,3,4-oxathiazol-2-on *I-19* bildet als typisches Benzylhalogenid mit Urotropin ein stabiles Salz und lässt sich in einer Kröhnke-Synthese[11] (3) über das entsprechende Pyridiniumsalz *I-32* und Nitron in den entsprechenden Aldehyd überführen, der allerdings nur als Halbacetal mit Äthanol *I-33* erhalten wurde.

Diese Reaktionen illustrieren deutlich die grosse Stabilität des 1,3,4-Oxathiazol-2-on-5-yl-Rings und zeigen den Weg zu zahlreichen neuen, durch Ringschluss von Carbonsäureamiden nicht unmittelbar zugänglichen, *I*.

Die spektralen Eigenschaften der Carbonylgruppe von I. In diesem Zusammenhang war auch ein Vergleich von *I* (R = C_6H_5) mit dem isomeren 4-Phenyl-1,3,2-oxathiazolium-5-olat *II* von Interesse, d.h. welches Gewicht eventuelle mesoionische Resonanzformeln von *I* (R = C_6H_5) haben (siehe Fig. 1). Nach Gotthardt[12] lässt sich die integrale IR-Absorption der Carbo-

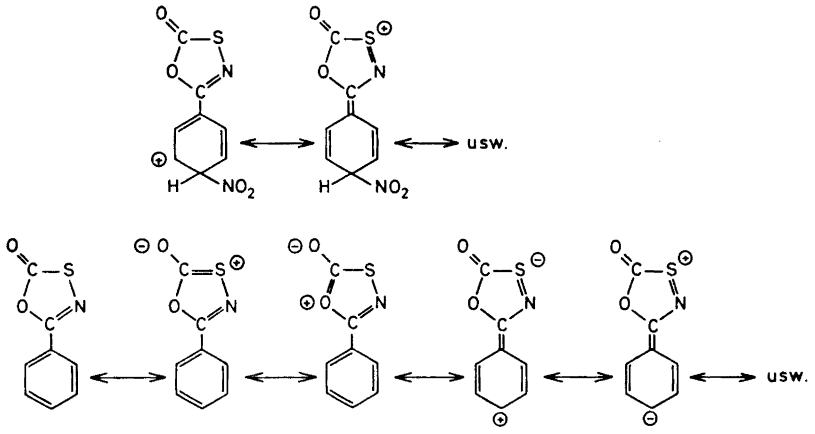

Fig. 1. Resonanzmöglichkeiten im σ-Komplex der Nitrierung von *I* (R = C_6H_5) bzw. in *I* (R = C_6H_5).

nylgruppe zur Beurteilung des mesoionischen Charakters von *II* heranziehen. Wir führten entsprechende Messungen mit *I* (R = C_6H_5) durch[13] und stellten dabei fest, dass dieses nach dem Kriterium der integralen Absorption in

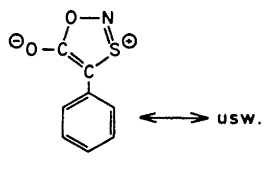

II

dieselbe Kategorie fällt wie das mesoionische *II*. Tabelle 4 enthält die entsprechenden Messdaten.

Tabelle 4. Integrale Absorption der infraroten Carbonylschwingungen von *I* (R = C_6H_5), *II* und Diisobutylketon.

Verbindung	Intensität A ($CHCl_3$, 1 $mmol^{-1}$ cm^{-2}) gemessen [13,a]	Literaturwert [12]
I (R = C_6H_5)	18,6; 19,9	–
II	18,8	51
Diisobutylketon	6,3	15 – 18

[a] Diese Messreihe entstand unter identischen Versuchsbedingungen. Der Ursache der Diskrepanz zwischen diesen Werten und den Literaturwerten wurde nicht näher nachgegangen.

Der 1,3,4-Oxathiazol-2-on-5-yl-Rest als Substituent. Wie wir bereits mitteilten,[6] lässt sich der 1,3,4-Oxathiazol-2-on-5-yl-Rest NMR-spektroskopisch eindeutig als Elektronenacceptor charakterisieren, was wohl überwiegend auf den –I-Effekt dieses Substituenten zurückzuführen ist. Tabelle 5 enthält u.a. die aus den NMR-Daten von *I* (R = C_6H_5) nach der Methode von Hayamizu und Yamamoto [14] bzw. aus den entsprechenden Daten von *I-9* nach Taft *et al.*[15] berechneten σ-Konstanten des 1,3,4-Oxathiazol-2-on-5-yl-Restes.

Betrachtet man die durch diesen Heterocyclus verursachte Desaktivierung des Benzolrings gegenüber der elektrophilen Substitution sowie die Isomerenverteilung bei der Nitrierung von *I*, gelangt man zu der Auffassung, dass der

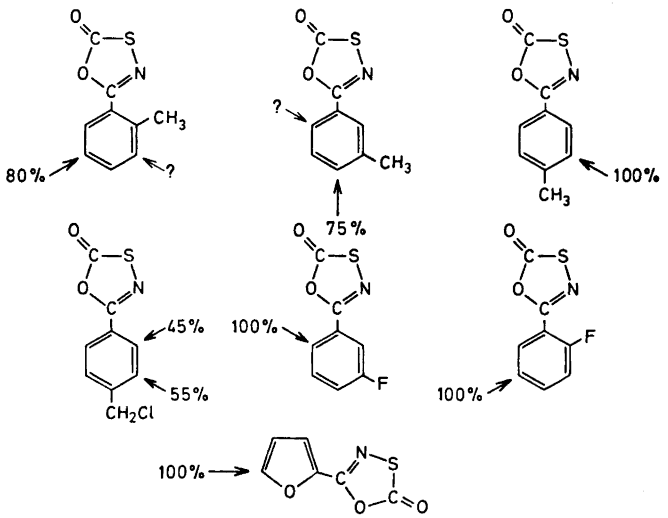

Fig. 2. Die Orientierung bei der Nitrierung von I (R = Ar) mit Nitriersäure bzw. rauchender Salpetersäure.

Fig. 3. Partielle Geschwindigkeitsfaktoren für die Nitrierung von Benzylchlorid [18] und *I* (R = C_6H_5) mit Acetylnitrat in Essigsäureanhydrid bei 25°. Da sich das Isomerenverhältnis bei der Nitrierung mit Acetylnitrat nicht genügend genau bestimmen liess (siehe Versuchsteil), wurde es dem bei der Nitrierung mit Nitriersäure bestimmten [6] gleichgesetzt.

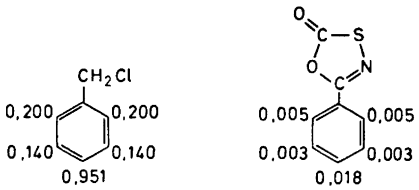

1,3,4-Oxathiazol-2-on-5-yl-Rest zur Kategorie der desaktivierenden, *o-p*-dirigierenden –I, + M-Substituenten gehört, zu der man sonst noch die Halogene und die Halogenmethylgruppen rechnet [16–19] (siehe Figur 2 und 3). Die Isomerenverteilung bei der Nitrierung von *I* (R = C_6H_5) [6] ähnelt weitgehend der Isomerenverteilung bei der Nitrierung des Benzylfluorids und des Benzylchlorids.[18] Die Geschwindigkeit der Nitrierung von *I* (R = C_6H_5) mit Acetylnitrat in Essigsäureanhydrid bei 25° beträgt 0,0056 (relativ zu Benzol), während der entsprechende Wert für Benzylchlorid 0,302 beträgt.[18] Halbquantitative Nitrierungsversuche mit *I* (R = $CH_3C_6H_4$) und *I* (R = FC_6H_4) zeigten, dass in beiden Fällen die *o-p*-dirigierende Wirkung der Methylgruppe bzw. die ganz überwiegend *p*-dirigierende Wirkung des Fluoratoms dominierte, d.h. also, dass, wie üblich, bei Anwesenheit einer aktivierenden und einer desaktivierenden Gruppe die aktivierende Gruppe die Orientierung bestimmt (Figur 2). Besonders aufschlussreich war die Nitrierung von *I-19* in rauchender Salpetersäure bei 10°. Die beiden möglichen Nitroderivate werden im Mengenverhältnis 45:55 gebildet, was wiederum die Ähnlichkeit des 1,3,4-Oxathiazol-2-on-5-yl-Restes mit der Chlormethylgruppe illustriert (siehe Figur 2 und 3).

Tabelle 5. Die σ-Konstanten des 1,3,4-Oxathiazol-2-on-5-yl-Restes.

σ_R^0	σ_I	σ_m	σ_p	σ_m^+	σ_p^+	Bestimmt nach Methode
0,14	0,44	0,49	0,64			A [14,19]
	0,39					B [15]
				0,42	0,29	C [17]

Wie aus Tabelle 5 hervorgeht, spielt der + M-Effekt des 1,3,4-Oxathiazol-2-on-5-yl-Restes für die Stabilisierung von *I* selbst keine Rolle, sondern man kann eher von einem –M-Effekt sprechen. Im σ-Komplex der Nitrierung von *I* tritt der + M-Effekt, zumindest relativ, stärker in den Vordergrund und führt zur beobachteten überwiegenden *o-p*-Orientierung (vgl. Figur 1). Beim Vergleich der σ- mit den σ^+-Werten der Tabelle 5 erhält man einen quantitativen Eindruck von diesen Zusammenhängen.

Die Bestimmung der Dissoziationskonstante von *I-31* scheiterte an der extremen Schwerlöslichkeit dieser Verbindung.

Es ist bemerkenswert, dass *I-3* und *I-39* trotz ihrer erheblichen strukturellen Ähnlichkeit mit *III* bzw. *IV* keine praktisch verwertbaren therapeutischen Eigenschaften aufweisen.

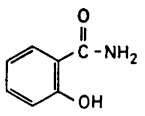

Salicylamid

III

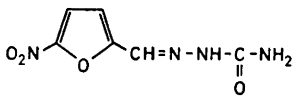

„Nitrofurazon"

IV

Der Bayer AG, Leverkusen (Deutschland) sind wir für Chemikalienspenden, biologische Prüfungen von *I* und die Aufnahme von NMR-Spektren zu Dank verpflichtet. Herr Dr. J. Eggers, Laboratorium für Chemische Physik der Universität Aarhus, stellte uns freundlicherweise die in Tabelle 4 wiedergegebenen Messergebnisse zur Verfügung.

Herrn Dr. Arne Holm, Chemisches Laboratorium II, H. C. Ørsted-Institut der Universität Kopenhagen, haben wir für die Überlassung einer Probe von *II* zu danken.

Durch eine Verkettung unglücklicher Umstände ging ein Teil unserer Originalunterlagen, darunter eine Reihe von NMR-Spektren, verloren. Die auf diesen Spektren fussenden Strukturbestimmungen der Verbindungen *I-37*, *I-38* und *I-39* spielen aber im vorliegenden Zusammenhang eine so untergeordnete Rolle, dass wir auf die Rekonstruktion dieses Versuchsmaterials verzichtet haben.

RESCHREIBUNG DER VERSUCHE

Die Schmelzpunkte sind unkorrigiert. Auf präparative chromatographische Trennungen von *I* musste verzichtet werden, da sie sowohl an Aluminiumoxid als auch an Kieselgel Schwefel abspalten.

Darstellung von I-1 bis I-28. Siehe Tabelle 1.

Darstellung von I-29 bis I-33 (siehe auch Tabelle 2).

5-[3-(Jodmethyl)-phenyl]-1,3,4-oxathiazol-2-on I-29: 2,28 g (0,01 Mol) *I-18* und 15 g Natriumjodid wurden 3 Std. in Aceton gerührt. Die Lösung wurde eingedampft und der Rückstand mit 100 ml Chloroform extrahiert. Die Chloroformlösung wurde mit 250 ml Wasser gewaschen, über Calciumsulfat getrocknet und eingedampft.

5-[4-(Jodmethyl)-phenyl]-1,3,4-oxathiazol-2-on I-30: Aus *I-19* wie oben.

4-(1,3,4-Oxathiazol-2-on-5-yl)-benzoesäure I-31: 4,0 g (0,013 Mol) *I-23*, 15 ml Wasser und 85 ml konz. Schwefelsäure wurden 3 Std. bei Zimmertemperatur gerührt. Das Reaktionsgemisch wurde auf 500 g Eis gegossen, die Fällung abfiltriert und mit Wasser und Aceton gewaschen.

Kröhnke-Salz I-32: 13,7 g (0,06 Mol) *I-19*, 12 ml Pyridin und 200 ml Äthanol wurden 3,5 Std. am Rückfluss gekocht. Danach wurden etwa 75 ml Äthanol abdestilliert und der Rest in 800 ml Äther gegossen (bei 0°). Die Fällung wurde abfiltriert und mit Äther gewaschen.

4-(1,3,4-Oxathiazol-2-on-5-yl)-benzaldehydäthylhalbacetal I-33: 14,05 g (0,046 Mol) *I-32* wurden in 600 ml Äthanol gelöst und mit 8,50 g (0,056 Mol) 4-Nitroso-*N*,*N*-dimethylanilin und 1,84 g (0,046 Mol) Natriumhydroxid versetzt. Nach 5 Std. Rührens bei Zimmertemperatur war die Farbe nach rotbraun umgeschlagen. Das Nitron (15,2 g) wurde durch Verdünnen mit Wasser ausgefällt und mit Wasser und Äther gewaschen. Es schmolz unter Zersetzung bei 162 – 164° und wurde ohne weitere Reinigung in 400 ml Benzol gelöst und bei Zimmertemperatur 4 Std. mit 200 ml 2 N Salzsäure gerührt. Danach wurde die benzolische Lösung mit Wasser neutral gewaschen, getrocknet und das Halbacetal mit Äther ausgefällt.

Nitrierungsversuche (siehe auch Tabelle 3)

Die Nitrierung von *I* ($R = C_6H_5$) mit Nitriersäure wurde bereits beschrieben.[6]

Nitrierung von I-16: 2,90 g (0,015 Mol) *I-16* wurden bei – 10° unter Rühren in 60 ml konz. Schwefelsäure gelöst. Die Temperatur wurde auf – 15° gesenkt und ein Gemisch von 7,5 ml konz. Salpetersäure und 15 ml konz. Schwefelsäure langsam zugesetzt. Nach

insgesamt 45 Min. Rührens bei −15° wurde auf 250 g Eis gegossen. Die klebrige Fällung wurde mit Äther und Chloroform aufgenommen, die vereinigten organischen Phasen mit Wasser säurefrei gewaschen, getrocknet und eingedampft. Das Rohprodukt (3,55 g, 99 %) bestand nach dem NMR-Spektrum aus 80 % A und 20 % B, während *I-16* nicht nachzuweisen war. Durch Umkristallisieren des Rohproduktes aus Chloroform wurden 1,23 g (38 %) A, F: 85,5–90,5° erhalten. Durch Hydrolyse mit wässrigem Natriumhydroxid liess sich A in das bekannte 2-Methyl-5-nitrobenzamid und die ebenfalls bekannte 2-Methyl-5-nitrobenzoesäure überführen [20] und damit als *I-34* identifizieren.

Nitrierung von I (R = 3-$CH_3C_6H_4$): 12,0 g (0,062 Mol) *I* (*R* = 3-$CH_3C_6H_4$) [3] wurden unter Rühren bei 0° langsam in 200 ml rauchende Salpetersäure eingetragen. Nach weiteren 30 Min. wurde die klare Lösung auf Eis gegossen. Die Fällung wurde abfiltriert und mit Wasser säurefrei gewaschen. Das so erhaltene Rohprodukt wog 10,0 g und hatte F: 82–101°. Das NMR-Spektrum des Rohprodukts in $CDCl_3$ enthielt folgende Methylsignale:

Produkt	δ (ppm)	Integral %	Bemerkungen
A	2,38	15	Ausgangsstoff
B	2,47	5	
C	2,53	8	
D	2,60	3	
E	2,65	64	
F	2,78	5	

Das analysenreine Produkt E wurde durch Umkristallisieren aus Äthanol erhalten und durch alkalische Hydrolyse zum bekannten 3-Methyl-4-nitrobenzamid und der ebenfalls bekannten 3-Methyl-4-nitrobenzoesäure [21] als *I-35* identifiziert.

Nitrierung von I (R = 4-$CH_3C_6H_4$): 6,0 g (0,031 Mol) *I* (R = 4-$CH_3C_6H_4$) [3] wurden bei 0° in 400 ml konz. Schwefelsäure gelöst. Bei dieser Temperatur wurde unter Rühren im Laufe von 15 Min. ein Gemisch von 50 ml konz. Salpetersäure und 100 ml konz. Schwefelsäure zugesetzt. Nach weiteren 15 Min. Rührens wurde auf Eis gegossen, die Fällung abfiltriert und mit Wasser säurefrei gewaschen. Es wurden so 4,2 g Rohprodukt, F: 99–105°, erhalten. Dem NMR-Spektrum nach enthielt es nur *I-36*.

Nitrierung von I-8: 2,96 g (0,015 Mol) *I-8* wurden in 60 ml konz. Schwefelsäure gelöst und bei −15° unter Rühren mit einem Gemisch von 7,5 ml konz. Salpetersäure und 15 ml konz. Schwefelsäure versetzt. Nach insgesamt 40 Min. Rührens bei −15° wurde auf 200 g Eis gegossen. Die Fällung wurde abfiltriert und mit Wasser säurefrei gewaschen. Rohausbeute 3,14 g (64 %). Dem ^{1}H- und ^{19}F-NMR-Spektrum nach handelt es sich um *I-37*.

Nitrierung von I-9: Wie oben, nur wurde die Fällung nicht abfiltriert, sondern mit Chloroform aufgenommen. Rohausbeute 78 %. Dem ^{1}H- und ^{19}F-NMR-Spektrum nach handelt es sich um *I-38*.

Nitrierung von I-19: 2,6 g (0,011 Mol) *I-19* wurden bei 10° unter Rühren in 50 ml rauchende Salpetersäure eingetragen. Nach insgesamt 30 Min. Rührens wurde auf Eis gegossen, die Fällung mit Chloroform aufgenommen, die organische Phase mit Wasser säurefrei gewaschen, getrocknet und eingedampft. Es hinterblieb ein Öl, das beim Anreiben mit Äthanol auskristallisierte, F: 80–90°, 0,85 g (28 %). Das NMR-Spektrum in $CDCl_3$ enthielt drei Methylensignale und zwar bei $\delta = 4{,}63$ ppm (*I-19*, Integral ≈ 0), $\delta = 4{,}72$ ppm (*I* (R = 2-NO_2-4-(CH_2Cl)-C_6H_3), Integral = 45) und $\delta = 5{,}03$ ppm (*I* (R = 3-NO_2-4-(CH_2Cl)-C_6H_3), Integral = 55). Auf eine präparative Trennung der Isomeren wurde wegen der zu erwartenden Schwierigkeiten verzichtet.

Nitrierung von I (R = 2-Furyl): 12,7 g (0,075 Mol) *I* (R = 2-Furyl) [2] wurden in 300 ml konz. Schwefelsäure gelöst und bei −13° unter Rühren mit einem Gemisch von 12,5 ml konz. Salpetersäure und 25 ml konz. Schwefelsäure versetzt. Nach weiteren 25 Min. Rührens wurde die kräftig gelbe Lösung auf Eis gegossen. Das Nitrierungsprodukt wurde mit Chloroform aufgenommen, die organische Phase mit Wasser säurefrei gewaschen, getrocknet und eingedampft. Nach zweimaligem Umkristallisieren aus Acetonitril/Wasser und einmal aus Äthanol betrug die Ausbeute 7,5 g (47 %). Dem NMR-Spektrum nach handelte es sich um *I-39*.

Bestimmung der Reaktionsgeschwindigkeit der Nitrierung von I ($R=C_6H_5$): Bei 0° wurden 50 ml (1,19 Mol) 100-proz. stickoxidfreie Salpetersäure *p.a.* in 300 ml frisch destilliertem Essigsäureanhydrid gelöst. Nach Thermostatieren auf 25° wurde rasch eine Lösung von 5,810 g (0,0324 Mol) *I* ($R=C_6H_5$) in 100 ml Essigsäureanhydrid zugesetzt und das Volumen der Lösung mit Essigsäureanhydrid auf 500 ml gebracht. (Molarität der Salpetersäure 2,48). Alle 6 Min. wurde eine 50-ml-Probe entnommen (insgesamt 8) und in 300 ml Wasser eingegossen. Nach 24-stündigem Stehen (zur Hydrolyse des Essigsäureanhydrids) wurde mit 100 ml Chloroform ausgeschüttelt und die organische Phase zweimal mit je 200 ml Wasser gewaschen. Nach Trocknen und Eindampfen wurde der Rückstand gewogen und in 250 ml absolutem Alkohol gelöst. In dieser Lösung wurde die Summe der Nitroverbindungen durch Titrieren mit Titan(III)chlorid-Lösung [23] quantitativ bestimmt. Blindversuche mit den drei Isomeren *I* ($R=NO_2C_6H_4$) [2,3] ergaben, dass diese Bestimmung durch die Anwesenheit des 1,3,4-Oxathiazol-2-on-5-yl-Restes nicht gestört wird.

Die Auswertung der Messwerte geschah nach Paul.[24]

Die Geschwindigkeitskonstante erster Ordnung für Benzol ergab sich zu $28{,}4\times10^{-2}$ sec^{-1} und die entsprechende Konstante für *I* ($R=C_6H_5$) zu $0{,}158\times10^{-4}$ sec^{-1}. Damit beträgt die relative Reaktionsgeschwindigkeit 0,056.

Bestimmung der σ-Konstanten aus den chemischen Verschiebungen der Ringprotonen von I ($R=C_6H_5$) bzw. des Fluoratoms von I-9 (vgl. Tabelle 5): Die Auswertung des auf unendliche Verdünnung extrapolierten NMR-Spektrums von *I* ($R=C_6H_5$) in CCl_4 nach Hayamizu und Yamamoto [14] führt zu folgenden Ergebnissen: $\delta_o=7{,}95$ ppm, $\delta_m=7{,}46$ ppm, $\delta_p=7{,}54$ ppm, $\delta_{C_6H_6}=7{,}26$ ppm. $\sigma_R^\circ=0{,}14$, $\sigma_I=0{,}44$.

Das ^{19}F-NMR-Spektrum von *I-9* wurde in C_6D_6 mit C_6F_6 als Hilfsstandard mit einem Varian 100-XL-15-Gerät aufgenommen.

δ_m ergab sich zu $-52{,}8$ ppm. Rechnet man diesen Wert auf C_6H_5F als Standard um, ergibt sich $\delta_m=-2{,}2$ ppm und damit $\sigma_I=0{,}39$.[15]

LITERATUR

1. Senning, A. *Chem. Commun.* **1965** 551.
2. Mühlbauer, E. und Weiss, W. (Farbenfabriken Bayer AG), Belg. Patent 680 644 (1966).
3. Senning, A. und Kelly, P. *Acta Chem. Scand.* **21** (1967) 1871.
4. Badische Anilin- und Soda-Fabrik AG, Belg. Patent 710 988 (1968).
5. Becke, F. und Gnad, J. *Ann.* **726** (1969) 110.
6. Senning, A., Rasmussen, J. S. und Jakobsen, H. J. *Tetrahedron Letters* **1969** 5131.
7. Franz, J. E. und Black, L. L. *Tetrahedron Letters* **1970** 1381.
8. Zumach, G. und Kühle, E. *Angew. Chem.* **82** (1970) 63.
9. Haase, H. J., DDR-Patent 77227 (1970); *Chem. Abstr.* **75** (1971) 88616.
10. Kühle, E. *Synthesis* **1971** 617.
11. Angyal, S. J. *Org. Reactions* **8** (1954) 197.
12. Gotthardt, H. *Chem. Ber.* **105** (1972) 105 und dort zitierte Literatur.
13. Dr. J. Eggers, Chemisches Institut der Universität Aarhus, private Mitteilung.
14. Hayamizu, K. und Yamamoto, O. *J. Mol. Spectrosc.* **29** (1969) 183.
15. Taft, Jr., R. W., Price, E., Lewis, J. C., Andersen, K. K. und Davis, G. T. *J. Am. Chem. Soc.* **85** (1963) 709.
16. Norman, R. O. C. und Taylor, R. *Electrophilic Substitution in Benzenoid Compounds*, Elsevier, Amsterdam 1965.
17. Stock, L. M. *Aromatic Substitution Reactions*, Prentice-Hall, Englewood Cliffs 1968.
18. Ingold, C. K., *Structure and Mechanism in Organic Chemistry*, Cornell University Press, Ithaca 1953.
19. Hammett, L. P. *Physical Organic Chemistry. Reaction Rates, Equilibria, and Mechanisms*, McGraw, New York 1970.
20. Beilstein *IX*, H 471, 472, E I 189, E III 2313.
21. Beilstein *IX*, H 481, E I 192, E II 326, E III 2331.
22. Beilstein *IX*, H 502, E I 196, E II 334, E III 2359, 2363.
23. Houben-Weyl, *Methoden der organischen Chemie II* (1953) 627.
24. Paul, M. A. *J. Am. Chem. Soc.* **80** (1958) 5329.

Eingegangen am 22. Januar 1973.

ACTA CHEMICA SCANDINAVICA 27 (1973) 2171–2178

Pseudomonas Cytochrome *c* Peroxidase

VII. Kinetics of the Peroxidatic Reaction Mechanism

NILS ELLFOLK, MARJAANA RÖNNBERG and RITVA SOININEN

Department of Biochemistry, University of Helsinki, SF-00170 Helsinki 17, Finland

Initial rate data are reported for the *Pseudomonas* cytochrome *c* peroxidase reaction with substrates *Pseudomonas* ferrocytochrome *c* and hydrogen peroxide at pH 5.0, 6.0, and 7.0. The results indicate a sequential reaction mechanism involving a kinetically significant ternary complex for this enzyme.

In 1931 Mann [1] postulated the existence of a ternary complex in the reaction mechanism of horse radish peroxidase (HRP) on the basis of hyperbolic relationships between the over-all rate of reaction and the donor concentration. Chance [2] has later pointed out, however, that such a "saturation effect" could be expected even with binary complexes alone. Only with the arrival of the kinetic method of Alberty [3] and Dalziel [4] was it possible to detect ternary complexes of even very short life-times. Using the kinetic method of Dalziel,[4] Yonetani and Ray [5] have recently confirmed the presence of a ternary complex in the reaction mechanism of yeast cytochrome *c* peroxidase (YCCP).

The properties of *Pseudomonas* cytochrome *c* peroxidase (PsCCP) differ clearly from those of YCCP, *e.g.* the enzyme molecule of PsCCP contains two heme moieties present in the low spin form.[6] In addition, PsCCP does not form those spectrally distinguishable complexes with hydrogen peroxide which are characteristic of other peroxidases,[7] *e.g.* YCCP. Consequently, a somewhat different kinetic behaviour may be expected for PsCCP as compared with that of YCCP.

In order to simplify the interpretation of the kinetic data, these studies concern only that part of the peroxidatic reaction in which the enzyme was initially incubated with reduced cytochrome *c* before addition of H_2O_2, *i.e.* the phase of initial delay was excluded.[8]

MATERIALS AND METHODS

Pseudomonas cytochrome c peroxidase (PsCCP) was prepared from acetone-dried cells of *P. aeruginosa* as previously described.[6] The ratio A_{407}/A_{280} of the preparation used

was 4.4. The concentration of the enzyme was determined spectrophotometrically using $A(1\ \%,\ 1\ cm)$ equal to 12.1 at 280 nm.[9] The molar concentrations of the enzyme were calculated on the basis of a molecular weight of 43 200.[9]

Yeast cytochrome c peroxidase (YCCP) was prepared as described previously.[10] The ratio A_{407}/A_{280} of the preparation was 1.30. The concentration of the enzyme was determined on the basis of the total hematin content, measured as pyridine ferrohemochrome according to Paul *et al.*[11]

Pseudomonas cytochrome c-551 (Ps-cyt-551) was prepared from acetone-dried cells of *P. aeruginosa* by the method of Ambler.[12] The purity of the cytochrome preparations $[A_{551}(\text{red.}) - A_{570}(\text{red.})/A_{280}]$ were 1.12 – 1.19, while those of Ambler were 1.13 – 1.17. The cytochrome preparations were found to be homogeneous on disc electrophoresis. The concentration of Ps-cyt-551 was determined spectrophotometrically applying the extinction coefficients $\varepsilon_{551}(\text{red.}) = 26.9\ \text{mM}^{-1}\ \text{cm}^{-1}$ and $\Delta\varepsilon_{551}(\text{red.-ox.}) = 19.0\ \text{mM}^{-1}\ \text{cm}^{-1}$.[8]

Horse heart cytochrome c was a commercial preparation from Sigma (Type III, 98 %), and was used without further purification. The extinction coefficients $\varepsilon_{550}(\text{red.}) = 27.6\ \text{mM}^{-1}\ \text{cm}^{-1}$ and $\Delta\varepsilon_{550}(\text{red.-ox.}) = 19.6\ \text{mM}^{-1}\ \text{cm}^{-1}$ were used for the spectrophotometric determination of the cytochrome concentration.[13]

Reduced Ps-cyt-551 and horse heart cytochrome c were prepared according to Yonetani and Ray [14] using anaerobic gel filtration on Sephadex G-25.

Hydrogen peroxide solutions were prepared from Merck Perhydrol (30 % H_2O_2). Peroxide concentration was determined enzymatically with YCCP using horse heart cytochrome *c* as substrate according to the method of Yonetani.[13]

Measurements of reaction rates. The activity of *Pseudomonas* cytochrome *c* peroxidase was assayed spectrophotometrically by measuring the rate of peroxidatic oxidation of fully reduced *Pseudomonas* cytochrome *c*-551 by the enzyme in acetate and phosphate buffers, pH 5.0, 6.0, and 7.0, all at $\mu = 0.01$. The reaction was initiated by mixing 10 μl of hydrogen peroxide solution with the reaction mixture (2.0 ml) containing 5 μl of suitably diluted enzyme and varying amounts of Ps-cyt-551. No appreciable oxidation of ferrocytochrome *c* was observed in the absence of the enzyme under the experimental conditions used. The reaction was followed by measuring the decrease in absorbance of Ps-cyt-551 at 551 nm with time. Initial rates (v_0/e) were calculated from the slope of the reaction curve at zero time and were expressed in terms of mol ferrocytochrome *c* oxidized per mol of enzyme per second.

Disc electrophoresis of Ps-cyt-551 was carried out in polyacrylamide gel according to the procedure of Ornstein and Davis [15] and Maurer.[16] The basic gel system No. 1a of Maurer (pH 8.9; 7 % gel) was used.

Instruments. Spectrophotometric measurements were performed with a Beckman DU spectrophotometer. Enzymatic activities were measured with a Beckman DK-1 A or a Cary 15 recording spectrophotometer equipped with cell compartment thermostated at 25°C. pH was measured with a Radiometer TTT 1 C meter fitted with a combination glass-calomel electrode; Beckman pH 7 buffer No. 3581 was used for standardization.

Reagents used were of analytical grade if not otherwise stated.

THEORETICAL BASIS OF KINETIC ANALYSIS

Alberty,[3] as well as Dalziel,[4] has suggested a number of mechanisms for two-substrate enzyme reactions. They have also given criteria for evaluating different mechanisms on the basis of kinetic data. For two-substrate reaction systems in which both substrates interact with the enzyme before dissociation of either product, the following rate equation, in Dalziel's notation, should be obeyed:

$$\frac{e}{v_0} = \phi_0 + \frac{\phi_1}{[S_1]} + \frac{\phi_2}{[S_2]} + \frac{\phi_{12}}{[S_1][S_2]} \qquad (1)$$

where e is the enzyme concentration, S_1 and S_2 are the two substrates and ϕ_0, ϕ_1, ϕ_2, and ϕ_{12} represent the kinetic coefficients. The kinetic coefficients,

which are functions of rate constants in the mechanism, can be evaluated from primary and secondary plots of initial-rate data according to Dalziel.[4]

The Mann [1] mechanism of the peroxidatic reaction of HRP is a general form of compulsory order mechanism for two-substrate reactions involving a rate-limiting ternary complex. When the ternary complex becomes non-rate-limiting, the Chance mechanism [2] is obtained, which is a special case of the general compulsory order mechanism (eqn. 2).

$$\frac{e}{v_0} = \frac{\phi_1'}{[S_1]} + \frac{\phi_2'}{[S_2]} + \frac{\phi_{12}'}{[S_1][S_2]} \qquad (2)$$

In the Mann mechanism, the secondary plot of intercepts has an intercept value of ϕ_0 and a slope of ϕ_2; while in that of Chance, the replot of intercepts gives an intercept value of zero and a slope value of ϕ_2'. The two mechanisms are, therefore, clearly distinguishable from each other by determining an intercept value for the secondary plot of primary intercepts.

RESULTS

Initial rate data measurements were made in phosphate buffer, pH 6.0 ($\mu = 0.01$), with concentrations of Ps-cyt-551 in the range 5 – 30 μM and of hydrogen peroxide in the range 10 – 200 μM. Lineweaver-Burk plots with each reactant as variable substrate (Fig. 1) are linear within the experimental error, and secondary plots of the slopes and intercepts (Figs. 2 and 3) are also linear. Since the ϕ_0 value was found to be positive it was concluded that the

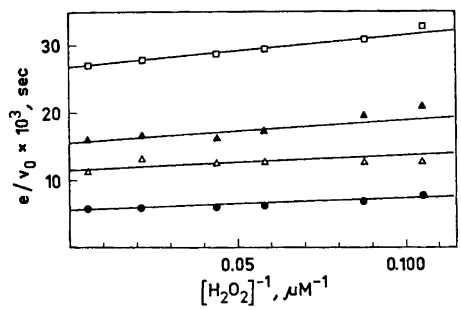

Fig. 1. Plot of reciprocal of specific initial rate at 25°C in sodium phosphate buffer, $\mu = 0.01$, pH 6.0 *versus* the reciprocal of H_2O_2 concentration at various concentrations of reduced Ps-cyt-551. [Ps-ferrocyt-551]: □, 5.2 μM; ▲, 10.2 μM; △, 15.0 μM; ●, 30.0 μM. The concentrations of other reagents used were: H_2O_2 10 – 200 μM and PsCCP 1.56 nM. Kinetic coefficients calculated from the plot are given in Table 1.

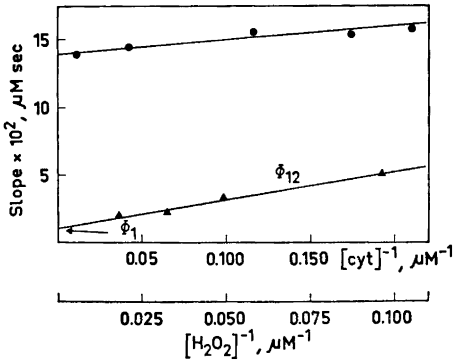

Fig. 2. Secondary plots of primary plot slopes *versus* the reciprocal of fixed substrate concentration in phosphate buffer, pH 6.0. Triangles and circles, respectively, represent data taken with Ps-cyt-551 and H_2O_2 as the fixed substrate.

Table 1. Kinetic coefficients for the peroxidatic oxidation reaction catalyzed by *Pseudomonas* cytochrome *c* peroxidase at 25°C in sodium acetate and sodium phosphate buffers. The kinetic coefficients are those in the initial-rate equation

$$\frac{e}{v_0} = \phi_0 + \frac{\phi_1}{[S_1]} + \frac{\phi_2}{[S_2]} + \frac{\phi_{12}}{[S_1][S_2]}.$$

Substrate	pH	Buffer	ϕ_0 sec	ϕ_1 M sec	ϕ_2 M sec	ϕ_{12} M^2 sec	ϕ_2/ϕ_0 M	ϕ_{12}/ϕ_2 M	$\phi_{12}/\phi_1\phi_2$ sec^{-1}
Ps-cyt-551	5.0	Acetate, $\mu = 0.01$	0.8×10^{-3}	6.0×10^{-8}	1.5×10^{-7}	0.4×10^{-12}	1.9×10^{-4}	2.7×10^{-6}	41
Ps-cyt-551	6.0	Phosphate, $\mu = 0.01$	1.6×10^{-3}	1.0×10^{-8}	1.4×10^{-7}	0.2×10^{-12}	8.8×10^{-5}	1.4×10^{-6}	365
Ps-cyt-551	7.0	Phosphate, $\mu = 0.01$	0.4×10^{-3}	3.8×10^{-8}	2.1×10^{-7}	0.3×10^{-12}	5.3×10^{-4}	1.4×10^{-6}	41

Pseudomonas cytochrome *c* peroxidase reaction follows the reaction scheme given in eqn. (1). The kinetic coefficients in eqn. (1), estimated from the slopes and intercepts of the secondary plots, are shown in Table 1.

Similar experiments were made in phosphate buffer, pH 7.0 ($\mu = 0.01$) and acetate buffer, pH 5.0 ($\mu = 0.01$). The Lineweaver-Burk plots for the first of these experiments, Fig. 4, are linear in the range of substrate concentrations

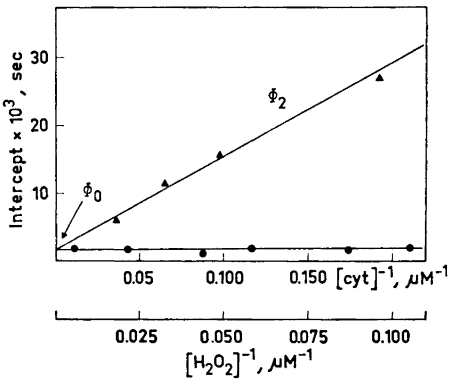

Fig. 3. Secondary plots of primary plot intercepts *versus* the reciprocal of fixed substrate concentration in phosphate buffer, pH 6.0. Triangles and circles, respectively, represent data taken with Ps-cyt-551 and H_2O_2 as the fixed substrate.

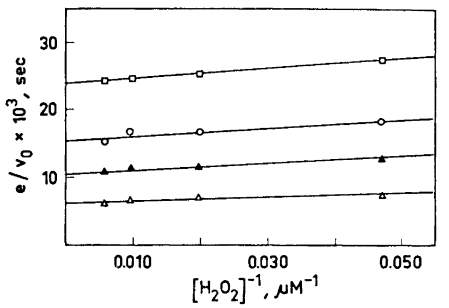

Fig. 4. Plot of the reciprocal of specific initial rate at 25°C in sodium phosphate buffer, $\mu = 0.01$, pH 7.0 *versus* the reciprocal of H_2O_2 concentration at various concentrations of reduced Ps-cyt-551. [Ps-ferrocyt-551]: □, 9.1 μM; ○, 13.8 μM; ▲, 18.4 μM; △, 34.4 μM. The concentrations of other reagents used were: H_2O_2 20 – 200 μM and PsCCP 1.56 nM. Kinetic coefficients calculated from the plot are given in Table 1.

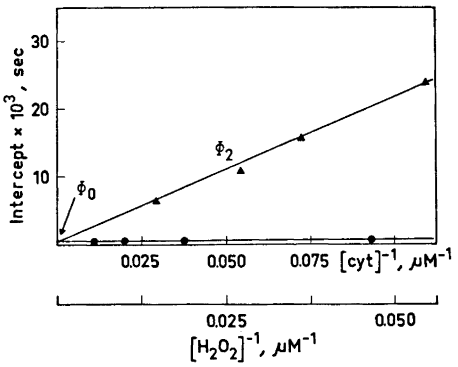

Fig. 5. Secondary plots of primary plot intercepts *versus* the reciprocal of fixed substrate concentration in phosphate buffer, pH 7.0. Triangles and circles, respectively, represent data taken with Ps-cyt-551 and H_2O_2 as the fixed substrate.

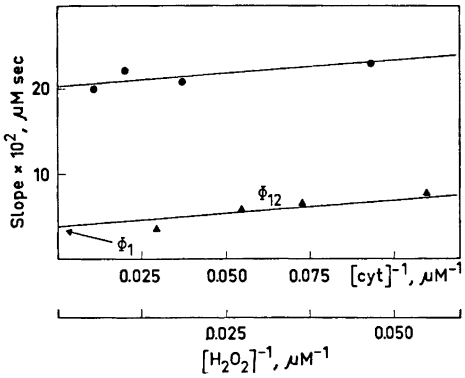

Fig. 6. Secondary plots of primary plot slopes *versus* the reciprocal of fixed substrate concentration in phosphate buffer, pH 7.0. Triangles and circles, respectively, represent data taken with Ps-cyt-551 and H_2O_2 as the fixed substrate.

used, and the slopes and intercepts (Figs. 5 and 6) allowed reliable estimates of the kinetic coefficients to be made from the secondary plots. This was also true of the experiments performed at pH 5 (Figs. 7, 8, and 9). The values obtained for the kinetic coefficients are given in Table 1.

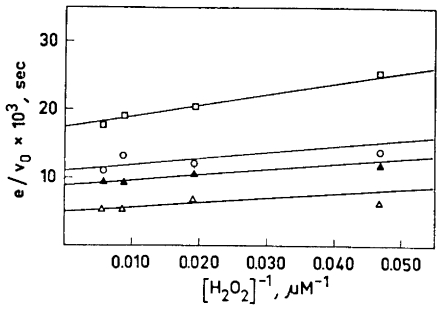

Fig. 7. Plot of the reciprocal of specific initial rate in sodium acetate buffer, $\mu = 0.01$, pH 5.0 *versus* the reciprocal of H_2O_2 concentration at various concentrations of reduced Ps-cyt-551. [Ps-ferrocyt-551]: □, 9.1 μM; ○, 14.4 μM; ▲, 16.9 μM; △, 34.1 μM. Other experimental conditions as given in the text of Fig. 4.

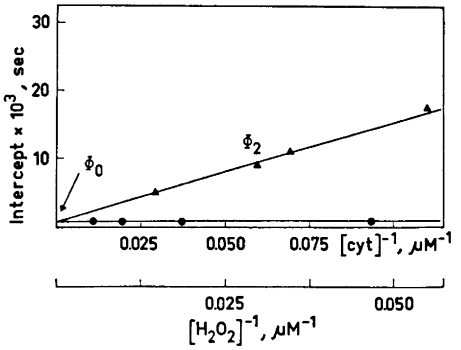

Fig. 8. Secondary plots of primary plot intercepts *versus* the reciprocal of fixed substrate concentration in acetate buffer, pH 5.0. Triangles and circles, respectively, represent data taken with Ps-cyt-551 and H_2O_2 as the fixed substrate.

The inhibition of the reaction by *Pseudomonas* ferricytochrome *c*, *i.e.* the product of one of the substrates, was studied by measuring initial rates of reaction in the presence of oxidized Ps-cyt-551 as well as in the absence of the inhibitor (Fig. 10). The primary Lineweaver-Burk plot indicates a competitive product inhibition.

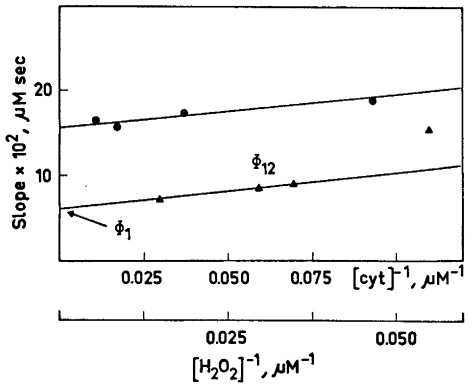

Fig. 9. Secondary plots of primary plot slopes *versus* the reciprocal of fixed substrate concentration in acetate buffer, pH 5.0. Triangles and circles, respectively, represent data taken with Ps-cyt-551 and H_2O_2 as the fixed substrate.

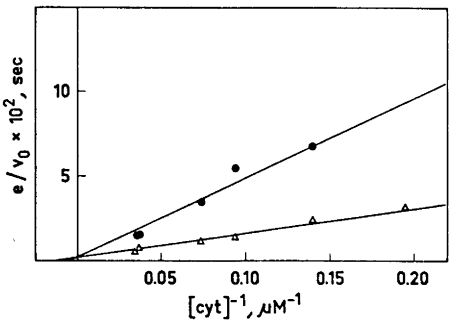

Fig. 10. Product inhibition of *Pseudomonas* cytochrome *c* peroxidase by oxidized Ps-cyt-551 with reduced Ps-cyt-551 as variable substrate. The concentration of H_2O_2 was kept constant, 143 μM. [Ps-ferricyt-551]: △, none; ●, 25.3 μM. The K_i value calculated is equal to 11.1 μM. Other experimental conditions as given in the text of Fig. 1.

DISCUSSION

The results of the kinetic studies indicate the reaction scheme given in eqn. (1) for the *Pseudomonas* cytochrome *c* peroxidase reaction, in agreement with the Mann [1] mechanism and excluding that of Chance.[2] The Mann mechanism involves the formation of a rate-limiting ternary complex according to the following equations:

$$E + S_1 \underset{k_{-1}}{\overset{k_1}{\rightleftarrows}} ES_1 \tag{3}$$

$$ES_1 + S_2 \underset{k_{-2}}{\overset{k_2}{\rightleftarrows}} ES_1S_2 \tag{4}$$

$$ES_1S_2 \xrightarrow{k_3} E + P \tag{5}$$

where E = PsCCP, S_1 and S_2 are the two substrates, P = product, k_1, k_{-1}, k_2, k_{-2}, and k_3 = rate constants of the indicated reactions.

On the basis of our data, it cannot be decided whether S_1 represents H_2O_2 or Ps-cyt-551. In the Mann mechanism the following relationships exist between the kinetic coefficients and the rate constants: $\phi_0 = 1/k_3$; $\phi_1 = 1/k_1$; $\phi_2 = 1/k_2$; $\phi_2/\phi_0 = K_m$; $\phi_{12}/\phi_2 = k_{-1}/k_1 = K_s$; $\phi_{12}/\phi_1\phi_2 = k_{-1}$. The association rate of cytochrome *c* peroxidase and H_2O_2 at pH 6.0 ($k_1 = 1.0 \times 10^8$ $M^{-1}sec^{-1}$) was determined to be about the same as that of YCCP ($k_1 = 1.4 \times 10^8$ $M^{-1}sec^{-1}$).[5]

Most hematin-containing peroxidases are known to form two types of enzymatically active ES-complexes with peroxides,[2] Complex I and Complex II. Yeast cytochrome *c* peroxidase appears to form only one type of ES-complex with peroxide (Complex II).[13,17] With PsCCP no such hydrogen peroxide complexes have been identified.[7] It has earlier been shown [8] that with the experimental conditions used, 2 mol of ferrocytochrome *c* appear to be necessary to convert 1 mol of PsCCP-H_2O_2-complex into 1 mol of free cytochrome *c* peroxidase. However, a simultaneous interaction between a PsCCP-H_2O_2 complex and 2 molecules of reduced cytochrome *c* to form a quaternary complex PsCCP-H_2O_2-(cytochrome)$_2$ is excluded since the primary plots of e/v_0 *versus* reciprocal of cytochrome *c* at fixed H_2O_2 were found to be linear. It therefore seems that the PsCCP-H_2O_2 complex formed under the present conditions interacts with 2 molecules of ferrocytochrome *c* in a consecutive two step sequence. The ternary complex E-H_2O_2-cytochrome *c* is assumed to be the rate-determining Michaelis-complex when the concentration of $H_2O_2 \geq K_m$.

Alberty [18] has introduced the product inhibition method as an additional tool in deciding between different mechanisms, and it has shown its value in kinetic studies of, *e.g.*, ribitol dehydrogenase,[19] malic dehydrogenase,[20] as well as yeast and liver alcohol dehydrogenases.[21] With yeast cytochrome *c* peroxidase a mixed competitive (noncompetitive-competitive) inhibition has been observed for ferricytochrome *c*, and the inhibition pattern obtained confirms the compulsory order mechanism of that enzyme.[5] The inhibition studies of PsCCP showed Ps-ferricyt-551, one of the products, as a competitive inhibitor for

Ps-ferrocyt-551 in the reaction and this agrees with a random ternary complex sequence. However, the case of PsCCP is complicated. The end product might influence the reaction velocity in two different ways; by affecting the retardation phase or then competing with the ferrocytochrome *c* for the enzyme in the peroxidatic reaction. This ambiguity makes the diagnostic method less valuable for this particular case.

Acknowledgement. This investigation was in part supported by grants from the *Finnish National Research Council for Sciences (N.E.).*

REFERENCES

1. Mann, P. J. G. *Biochem. J.* **24** (1931) 918.
2. Chance, B. *Advan. Enzymol.* **12** (1951) 153.
3. Alberty, R. A. *J. Am. Chem. Soc.* **75** (1953) 1928.
4. Dalziel, K. *Acta Chem. Scand.* **11** (1957) 1706.
5. Yonetani, T. and Ray, G. J. *J. Biol. Chem.* **241** (1966) 700.
6. Ellfolk, N. and Soininen, R. *Acta Chem. Scand.* **24** (1970) 2126.
7. Soininen, R. and Ellfolk, N. *Acta Chem. Scand.* **27** (1973) 35.
8. Soininen, R. and Ellfolk, N. *Acta Chem. Scand.* **26** (1972) 861.
9. Ellfolk, N. and Soininen, R. *Acta Chem. Scand.* **25** (1971) 1535.
10. Ellfolk, N. *Acta Chem. Scand.* **20** (1966) 1427; **21** (1967) 175.
11. Paul, K. G., Theorell, H. and Åkeson, Å. *Acta Chem. Scand.* **7** (1953) 1284.
12. Ambler, R. P. *Biochem. J.* **89** (1963) 341.
13. Yonetani, T. *J. Biol. Chem.* **240** (1965) 4509.
14. Yonetani, T. and Ray, G. S. J. *J. Biol. Chem.* **240** (1965) 3392.
15. Ornstein, L. and Davis, B. J. *Disc electrophoresis*, Distillation Product Industries, Eastman, Kodak Co., 1962.
16. Maurer, H. R. *Disk-Elektrophorese*, Walter de Gruyter & Co., Berlin 1968.
17. Yonetani, T. and Ray, G. S. J. *J. Biol. Chem.* **240** (1965) 4503.
18. Alberty, R. A. *J. Am. Chem. Soc.* **80** (1958) 1777.
19. Fromm, H. and Nelson, D. *J. Biol. Chem.* **237** (1962) 215.
20. Raval, D. N. and Wolfe, R. G. *Biochemistry* **1** (1962) 1112.
21. Wratten, C. and Cleland, W. *Biochemistry* **2** (1963) 935.

Received February 2, 1973.

ACTA CHEMICA SCANDINAVICA 27 (1973) 2179–2183

Synthesis of Brominated Imidazoles

KARL-ERLAND STENSIÖ, KERSTIN WAHLBERG and ROBERT WAHREN*

Research Institute of National Defence, Dept. 1, S-172 04 Sundbyberg, Sweden

Bromination of imidazole in acetic acid containing sodium acetate gives 2,4,5-tribromoimidazole in a good yield. 4(5)-(2-Chloroethyl)imidazole, imidazole-4(5)-carbaldehyde, and 4(5)-hydroxymethylimidazole have been brominated by the same method. Debromination of 2,4,5-tribromoimidazole with sodium sulphite or butyllithium gives 4(5)-bromoimidazole. A simple synthesis of 4(5)-(2-bromoethyl)-imidazole is described.

In connection with studies on compounds capable of reactivating phosphorylated acetylcholinesterase, some imidazole derivatives were prepared because of their known catalytic activity.[1] In the present communication the synthesis of some imidazole derivatives containing bromo substituents is reported.

Bromination of imidazole to 2,4,5-tribromoimidazole occurs readily.[2] Attempted monobromination,[3,4] however, gives mixtures containing mono-, di-, and tribromo derivatives, indicating that deactivation of the imidazole ring by a bromo substituent is insignificant. Neither did we, using several different bromination procedures, achieve monobromination (see Experimental).

The yield of 2,4,5-tribromoimidazole is reportedly about 30 %.[2] This low figure is probably explained by a formation of unreactive imidazole hydrobromide and, to some extent, degradation.[5] We therefore investigated bromination in the presence of a base, which should neutralise the hydrogen bromide formed, as has been done in the bromination of other heterocyclics.[6]

Bromination of imidazole in acetic acid containing sodium acetate gave a good yield of 2,4,5-tribromoimidazole (78 %). Bromination of 4(5)-(2-chloroethyl)imidazole using the same method was also efficient and yielded the dibromo compound (76 %). Imidazole 4(5)-carbaldehyde, however, gave only a moderate yield of a monobrominated product. This proved to be the 5(4)-bromoimidazole 4(5)-carbaldehyde, as indicated by its NMR spectrum (Table

* Present address: Dept. of Organic Chemistry, Royal Institute of Technology, S-100 44 Stockholm, Sweden.

1) and by its oxidation to the known 5(4)-bromoimidazole 4(5)-carboxylic acid. In the latter bromination, 2,4,5-tribromoimidazole was also formed. This was also the main product isolated on bromination of 4(5)-hydroxymethylimidazole.

Selective debromination of 2,4,5-tribromoimidazole with sodium sulphite has been described by Balaban and Pyman,[2] who obtained 4(5)-bromoimidazole (57 %) together with dibromo- and sulphonated derivatives. On debromination of the crude reaction product, containing the tribromo derivative obtained on bromination of imidazole, 4(5)-bromoimidazole was formed in a 62 % yield. The same compound was also prepared by treatment of 2,4,5-tribromoimidazole with butyllithium at 0°, followed by hydrolysis of the trilithiated imidazole with methanol at −70°. Small amounts of 4(5)-bromo-5(4)-butylimidazole and 4,5-dibromoimidazole were also obtained. Also 4(5)-Bromoimidazole reacted with butyllithium. In a separate experiment a 98 % yield of imidazole was isolated after debromination. When the hydrolysis was carried out with deuteriated methanol, 4(5)-deuterio-imidazole was isolated.

For the synthesis of various *N*-substituted aminoethyl imidazoles we needed 4(5)-(2-bromoethyl)imidazole. This substance, which is more reactive than the corresponding chloro derivative, has been prepared in low over-all yields by multistep synthesis.[7–10] We prepared it by deamination of histamine in the presence of bromide. Deamination of primary amines generally gives a mixture of products and is of limited value in synthesis. However, 4(5)-(2-bromoethyl)imidazole was isolated in a 47 % yield after treatment of histamine with nitrous acid and potassium bromide. The bromoethylimidazole was extracted with chloroform, leaving the main by-product 4(5)-(2-hydroxyethyl)-imidazole in the aqueous phase. A minor by-product also extracted with chloroform was 4(5)-bromo-5(4)-(2-bromoethyl)imidazole. 4(5)-(2-Bromoethyl)-

Table 1. δ-Values (ppm) for ring- and aldehyde protons in some substituted imidazoles.

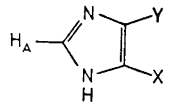

X	Y	H_A	H_Y	H_X	CHO	Solvent
COOH [11]	H	9.03	8.52	–	–	CF_3COOH
Br [11]	H	8.90	7.67	–	–	CF_3COOH
CHO	H	9.05	8.43	–	10.07	CF_3COOH
CHO	H	8.03	8.03	–	9.82	DMSO(d_6)
CHO	Br	8.15	–	–	9.75	DMSO(d_6)
CHO	Br	9.02	–	–	9.88	CF_3COOH
CH_2CH_2Br	H	8.68	7.43	–	–	CF_3COOH
CH_2CH_2Br	Br	8.68	–	–	–	CF_3COOH
H	H	8.78	7.56	7.56	–	D_2O [a]
D	H	8.87	7.62	–	–	D_2O [a]

[a] As the hydrochloride. Internal standard sodium trimethylsilylpropane-sulphonic acid.

imidazole is very reactive and should be stored as the hydrobromide salt. *N*-Alkylated derivatives may otherwise be formed from the free base by interalkylation.

Relevant NMR resonances from the imidazole derivatives prepared are given in Table 1.

EXPERIMENTAL

Melting points are corrected. NMR-spectra were recorded on a Varian A-60 instrument. Chemical shifts are given in ppm (δ) relative to TMS as an internal standard. Mass spectra were obtained on an LKB 9000 instrument at 70 eV (direct inlet). All compounds containing bromine and/or chlorine gave molecular ions with the expected isotope distribution. Reactions involving butyllithium were carried out anhydrously under purified argon. Tetrahydrofuran was distilled from lithium aluminium hydride immediately before use. Solutions of butyllithium (Merck, 20 % in hexane) were analysed by the double titration procedure of Gilman and Haubein.[12] The sodium acetate used contained about 1 % water. Concentrations were performed under reduced pressure.

Chromatography. TLC was performed on layers of silica gel (HF_{254} or DC-Fertigplatten F_{254}, Merck) and column chromatography on silica gel (0.05 – 0.2 mm, Merck). Imidazoles were detected by spraying with a 1 % solution of Echtblausaltz B (Merck) and then with M NaOH. Dragendorff's reagent and 2,4-dinitrophenylhydrazine (2,4-DNPH) were also used. TLC of imidazole, mono-, di-, and tribromoimidazole was obtained with ethyl acetate or ethyl acetate-water-methanol-acetone (95:5:5:25) as eluent.

2,4,5-Tribromoimidazole. Bromine (9.6 g) in anhydrous acetic acid (20 ml) was added during 30 min to a stirred solution of imidazole (1.36 g) and sodium acetate (20 g) in acetic acid (180 ml). When about one third of the bromine had been consumed, more sodium acetate (5 g) was added. Stirring was continued for 2.5 h. During this time tribromoimidazole began to separate. The acetic acid was evaporated and water (600 ml) was added. The white precipitate, consisting of tribromoimidazole, was collected, washed with water and dried. Yield: 4.30 g, 71 %, m.p. 221 – 222° (lit.[2] 220 – 222°). The mother liquor was concentrated and extracted with ether, yielding a mixture (0.75 g) containing imidazole, dibromoimidazole and tribromoimidazole. Fractional precipitation [2] permitted the isolation of dibromoimidazole (0.08 g, 2 %) and tribromoimidazole (0.40 g, 7 %).

Bromination of 4(5)-(2-chloroethyl)imidazole. The hydrochloride of the title compound (1.0 g) was brominated with bromine (2.2 g in 10 ml acetic acid) and sodium acetate (5.9 g) in acetic acid (125 ml) as described above for imidazole. The concentrated product was extracted with ether (3 × 150 ml). The presence of two Echtblau positive compounds in the ether extract was demonstrated with TLC (ethyl acetate). Chromatography on a silica gel column (80 g) with chloroform-ethyl acetate 1:1 yielded 2,4(5)-dibromo-5(4)-(2-chloroethyl)imidazole, 1.31 g, 76 %. Recrystallisation from benzene gave the pure compound, m.p. 102 – 105°. (Found: C 20.90; H 1.75; N 9.79. Calc. for $C_5H_5N_2ClBr_2$: C 20.83; H 1.75; N 9.72.) The other component is probably a monobromo derivative.

Bromination of imidazole 4(5)-carbaldehyde. The title compound (1.04 g) was brominated with bromine (3.95 g in 20 ml acetic acid) and sodium acetate (9.39 g) in acetic acid (100 ml) as above. The concentrated product was extracted with ether (3 × 150 ml) and then with acetone (3 × 150 ml). From the combined extracts a solid (2.0 g) containing three compounds (TLC, ethyl acetate) was obtained. These were separated on silica gel (80 g) using ethyl acetate, as eluent. One fraction (0.506 g) according to TLC (toluene-ethyl acetate, 1:1) and GLC-MS (5 % Lexan on Chromosorb W, 200°) contained a mixture of 2,4,5-tribromoimidazole (14 % total yield) and 2,5(4)-dibromoimidazole 4(5)-carbaldehyde (2 %). The main fraction (0.590 g) contained 5(4)-bromoimidazole 4(5)-carbaldehyde (32 %). An analytical sample, m.p. 216 – 217°, was prepared by crystallisation from butanone. (Found: C 27.67; H 1.62; N 16.42; Br 45.76. Calc. for $C_4H_3N_2OBr$: C 27.46; H 1.73; N 16.01; Br 45.67.) Part of the latter product was oxidised with permanganate to 5(4)-bromoimidazole 4(5)-carboxylic acid, m.p. 255 – 256° (lit.[13] 255°). The ethyl ester has m.p. 170 – 171° (lit.[14] 171°).

Bromination of 4(5)-hydroxymethylimidazole. The hydrochloride of the title compound (2.0 g) was brominated with bromine (4.79 g in 20 ml acetic acid) and sodium acetate (18.5 g) in acetic acid (125 ml) as above. The concentrated reaction mixture was extracted with ether (3 × 150 ml). The extract (1.84 g) contained at least six components according to TLC (ethyl acetate-water-methanol-acetone 95:5:5:25). One of these, 2,4,5-tribromoimidazole, was isolated in a yield of 23 % by chromatography on a silica gel column.

4(5)-Bromoimidazole (debromination with sulphite). Imidazole (1.36 g) was brominated as described above and the reaction mixture concentrated to dryness. The crude product and sodium sulphite (25 g) in water (125 ml) were refluxed for 3.5 h, cooled with ice water and extracted with ether (about 5 × 200 ml). The completeness of the extraction was checked by TLC. The ether solution was dried, concentrated and the crystalline product washed with light petroleum, yielding 4(5)-bromoimidazole, 1.82 g, 62 %, m.p. 130° (lit.[2] 130°).

4(5)-Bromoimidazole (debromination with butyllithium). Butyllithium (0.0144 mol in hexane, 8 ml) was transferred with a syringe to a solution of tribromoimidazole (1.10 g) in tetrahydrofuran (30 ml). The mixture was stirred for 1.25 h at 0° and then added with a syringe to methanol (50 ml) kept at −70°. The pale yellow solution was neutralised with hydrochloric acid, silica gel (0.5 g) was added and the solution was evaporated to dryness. Separation on a silica gel column using 40 g SiO_2/g substrate and chloroform-methanol (19:1) as eluent afforded 4(5)-bromoimidazole, m.p. 128 − 130° (lit.[2] 130°) 0.440 g, 83 %. A mixture (0.065 g) of 4(5)-bromo-5(4)-butylimidazole, 4(5)-bromoimidazole, and 4,5-dibromoimidazole in the approximate proportions 4:3:1 was eluted before the main fraction. The compounds were identified and their proportions determined by NMR and mass spectroscopy.

Attempted direct synthesis of 4(5)-bromoimidazole. The following methods have been tried without success. Bromination with dioxan.Br_2,[15] tetrahydrofuran.Br_2,[15] pyridine.Br_2,[15] iodine monobromine,[15] pyrrolidone-2-hydrotribromide,[15] copper(II) bromide,[15] bromination *via* thallium compounds,[16] and *via* *N*-lithioimidazole and *N*-acetyl imidazole. The method in alkaline medium described for nitroimidazoles by Kochergin *et al.*[17] was also tried.

Imidazole from 4(5)-bromoimidazole and butyllithium. A solution of 4(5)-bromoimidazole (0.522 g) in tetrahydrofuran (15 ml) was cooled to −70° and butyllithium (9.5 ml, 17.1 mmol) was added with a syringe. After 1 h at room temperature, the mixture was cooled to −70° and hydrolysed with 2 ml methanol. Concentrated hydrochloric acid (50 ml) was added and the solution evaporated to dryness, dissolved in 200 ml water and added to a Dowex 50W X-8 (200 − 400 mesh, H^+) column (21 × 3 cm). Elution with M HCl afforded first lithium salts and then imidazole hydrochloride, 0.365 g (98 %). 4(5)-Deuterio-imidazole was obtained in the same way using CH_3OD and careful neutralisation with 4 M HCl.

4(5)-(2-bromoethyl)imidazole. A saturated aqueous solution of sodium nitrite (2.42 g) was added during 2.5 h to a solution of histamine (3.0 g, free base) and potassium bromide (10.8 g) in 1.5 M sulphuric acid (40 ml) kept at −5°. After 3 h at room temperature, the pH was adjusted to 10 by adding 5 M sodium hydroxide, and the solution was extracted with chloroform (4 × 40 ml). Concentration of the chloroform extract yielded the title compound as a yellow oil (2.2 g, 47 %) which crystallised on cooling. This substance, which is not very stable due to intermolecular alkylation, was transferred to the hydrobromide. An analytical sample was prepared by silica gel chromatography (chloroform-methanol 9:1) of the free base. The eluted fractions were treated with hydrobromic acid before concentration. Recrystallisation from acetonitrile gave m.p. 149 − 150° (lit.[10] 156 − 158°). (Found: C 23.7; H 3.2; N 11.1. Calc. for $C_5H_7N_2Br_2$: C 23.5; H 3.2; N 10.9.) When an evaporated sample of the free base was left at room temperature overnight, intermolecular alkylation occurred. One component (10 %) was obtained from column chromatography and identified (NMR, MS) as a 4(5)-(2-bromoethyl)imidazole, *N*-alkylated by reaction with another monomer. The main by-product, 4(5)-(2-hydroxyethyl)imidazole, was obtained by extraction of the alkaline aqueous phase with butanol. When the nitrosation was carried out at 50°, another by-product, 4(5)-bromo-5(4)-(2-bromoethyl)imidazole, was obtained (15 %). The compound was identified by its NMR spectrum. Crystallisation from acetonitrile yielded the pure compound, m.p. 128 − 129°. (Found: C 23.7; H 2.4; N 11.2. Calc. for $C_5H_6N_2Br_2$: C 23.7; H 2.4; N 11.0.)

Acknowledgements. We thank Professor Bengt Lindberg and Dr. Magnus Sandström for their interest and valuable discussions. The English was checked by Patrick Hort.

REFERENCES

1. Bruice, T. C. and Benkovic, S. *Bioorganic Mechanisms*, Benjamin, New York 1966.
2. Balaban, E. and Pyman, F. L. *J. Chem. Soc.* **121** (1922) 947.
3. Hofmann, K. *Imidazole and its Derivatives*, Interscience, New York 1953.
4. Caló, V., Ciminale, F., Lopez, L., Naso, F. and Todesco, P. E. *J. Chem. Soc. Perkin Trans. 1* **1972** 2567.
5. Schmir, G. L. and Cohen, L. A. *Biochemistry* **4** (1965) 533.
6. Eisch, J. J. *Advan. Heterocycl. Chem.* **7** (1966) 1.
7. Turner, R. A. *J. Am. Chem. Soc.* **71** (1949) 3476.
8. Huebner, C. F. *J. Am. Chem. Soc.* **73** (1951) 4667.
9. Garforth, R. and Pyman, F. L. *J. Chem. Soc.* **1935** 489.
10. Bloemhoff, W. and Kerling, K. E. T. *Rec. Trav. Chim.* **89** (1970) 1181.
11. Barlin, G. B. and Batterham, T. J. *J. Chem. Soc.* **B 1967** 516.
12. Gilman, H. and Haubein, A. J. *J. Am. Chem. Soc.* **66** (1944) 1515.
13. Balaban, E. *J. Chem. Soc.* **1932** 2423.
14. King, H. and Murch, W. O. *J. Chem. Soc.* **1923** 621.
15. Fieser, M. and Fieser, L. F. *Reagents for Organic Synthesis*, Wiley-Interscience, Vol. I–III.
16. McKillop, A., Bromley, D. and Taylor, E. L. *Tetrahedron Letters* **1969** 1623.
17. Kochergin, P. M., Tsyganova, A. M. and Shlikhunova, V. S. *Khim. Farm. Zh.* **2** (1968) 22.

Received January 17, 1973.

ACTA CHEMICA SCANDINAVICA 27 (1973) 2184–2192

Pyrylium Salts

II. [1] Reactions of the 2,6-Dimethoxycarbonylpyrylium Cation with Carbon Nucleophiles

EILIF TERJE ØSTENSEN[a] and KJELL UNDHEIM[b]

[a]*Organic Chemistry Laboratories, Norwegian Institute of Technology, University of Trondheim, Trondheim, Norway and* [b] *Department of Chemistry, University of Oslo, Oslo 3, Norway*

The 2,6-dimethoxycarbonylpyrylium cation reacts with carbonyl activated methyl or methylene carbon in the cold to 4H-pyrans. A concurrent redox process may occur whereby the more stabilised pyrylium ion is formed. Of the 1,3-dicarbonyl-4H-pyrans prepared, only a cyclohexane-1,3-dione was largely enolised in chloroform. The NMR spectra in chloroform of the 4-acetonylidene- and the 4-phenacylidene-4H-pyrans are interpreted to mean preference for s-*cis*-conformation, this tendency decreasing with further substitution.

Recently we reported on the synthesis of the 2,6-dimethoxycarbonylpyrylium cation and some of its reactions with hydroxy and amino nucleophiles and bases.[1] The work reported in this paper deals with studies of its reactivity towards carbon nucleophiles. Dissolution of the perchlorate of the pyrylium cation I in acetone resulted in immediate formation of an acetone adduct. The NMR spectrum ($CDCl_3$) shows the β-pyranyl protons as a doublet at 4.0 τ ($J = 3.5$ cps) and the γ-proton at about 6.3 τ coupled (7.0 cps) to methylene protons at 7.3 τ. The methoxy protons and the additional methyl protons appear as singlets at 6.2 and 7.8 τ, respectively. These data are only consistent with the 4H-pyran IIa (Scheme 1). The acetophenone (IIb) and the acetylacetone (IIc) derivatives were also prepared using the ketone both as solvent and reagent. The dibenzoylmethane (IId) and the cyclic dimedone (IIe) derivatives were synthesised in liquid SO_2. Using equivalent amounts of reagents in liquid SO_2, the monoketones IIa and IIb reacted further, as discussed below, to the methylene analogues (IIIa and IIIb).

To relate the reactivity of the 2,6-dimethoxycarbonylpyrylium ion to that of other previously studied pyrylium ions, 2,6-diphenylpyrylium perchlorate was synthesised.[2] The latter was found not to react with acetone. With stronger nucleophiles such as carbanions and Grignard reagents, however, the 2,6-

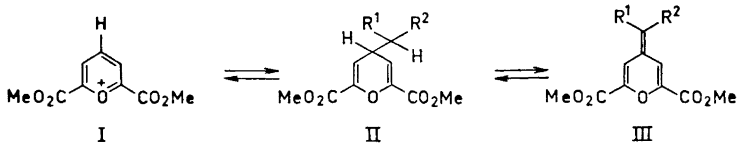

I II III

a $R^1 = H$, $R^2 = COCH_3$
b $R^1 = H$, $R^2 = COC_6H_5$
c $R^1 = R^2 = COCH_3$
d $R^1 = R^2 = COC_6H_5$
e $R^1, R^2 = COCH_2 \diagup\!\diagdown CH_3$ (spiro)

Scheme 1.

diphenylpyrylium cation undergoes addition to the 4-position.[3,4] A further comparison is available with the tropylium ion. The latter has been reported to react slowly with acetone on heating but is readily attacked by more activated compounds such as malonic acid and acetoacetic acid.[5] The lower reactivity of the tropylium ion is in good agreement with the relative redox potential as discussed below.

The reaction between I and acetone at room temperature is very fast. By lowering the temperature it was found that below about $-10°C$ no significant reaction rate was observed. At this temperature region, however, the reaction is rapid once initiated which suggests autocatalysis through the perchloric acid liberated in the reaction. Kinetic studies of the reaction between the tropylium ion and aldehydes have shown that the rate constant was independent of the tropylium ion concentration but proportional to the hydrogen ion concentration. From these observations it was concluded that the tropylium ion reacts with the enolised carbonyl compound and that enol formation is the rate determining step.[6] We have not carried out quantitative studies but have qualitatively demonstrated acid catalysis in agreement with enolisation of the carbonyl reagent as the rate determining step. Thus passage of dry HCl gas into an acetone solution of the dimethoxycarbonylpyrylium salt at $-40°C$ resulted in very rapid conversion to the 4H-pyran.

Reversibility in the formation of 4H-pyrans in acid solution, especially in the case of 2,6-diphenyl-4H-pyrans, has been reported.[2] This was also demonstrated for the acetonyl derivative IIa by heating in trifluoroacetic acid (TFA) with added perchloric acid at $60-70°C$, presumably because the liberated acetone is distilled off. In cold solution the equilibrium was too far in favour of the 4H-pyran for detection of the pyrylium ion I by NMR. For corresponding 2,6-diphenyl-4H-pyrans the equilibrium is in favour of the pyrylium salt. This difference in behaviour is caused by the different electronic effects of the 2,6-substituents on the stabilisation of the pyrylium cation. The breakage of the exocyclic carbon-carbon bond with regeneration of aromaticity bears some resemblance to acid catalysed enolisation where in this case the pyranyl oxygen acts as an intramolecular base (Scheme 2).

Treatment of the 4H-pyrans II with triphenylmethyl perchlorate in liquid SO_2, the reagent used for hydride abstraction in the preparation of I and the 4-methyl analogue VII (Scheme 5) from the respective 4H-pyrans, resulted in the isolation of the anhydro-bases III. The acid strength of IV is such that it

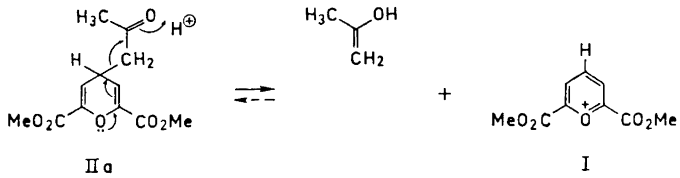

IIa I

Scheme 2.

is largely dissociated. In the 4-methyl analogue VII, however, the lack of carbonyl activation required treatment with a base such as an amine for anhydro-base formation (III, $R^1 = R^2 = H$).[1] The acetylacetonylidene IIIc is an exception to the above reaction in that it was best prepared from IIc through dehydrogenation by 2,3-dichloro-5,6-dicyano-1,4-benzoquinone in benzene solution.

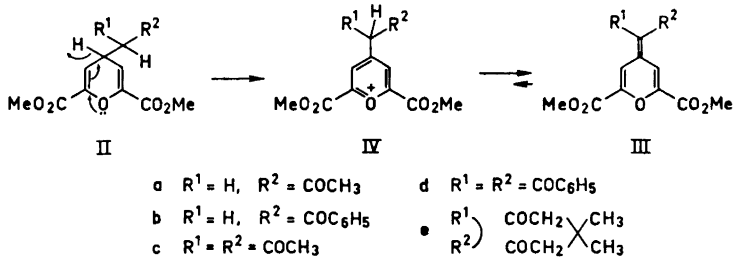

II IV III

a $R^1 = H$, $R^2 = COCH_3$ d $R^1 = R^2 = COC_6H_5$

b $R^1 = H$, $R^2 = COC_6H_5$ e R^1, R^2 = $COCH_2CH_3$, $COCH_2CH_3$

c $R^1 = R^2 = COCH_3$

Scheme 3.

The acetonylidene IIIa in TFA contains an exocyclic proton but no apparent methylene protons from protonation of the exocyclic α-carbon. The β-pyranyl protons are non-equivalent occurring at 1.2 and 2.5 τ in TFA and at 1.4 and 3.1 τ in $CDCl_3$, respectively. The 4-methylpyrylium analogue VII has its β-protons at 1.0 τ (TFA).[1] In TFA-*d*, however, the exocyclic vinyl proton was exchanged in the course of 1 – 2 min. The relative chemical shifts and nonequivalence of the pyranyl protons together with the rapid deuteriation must mean that IIIa is protonated only to a small extent in TFA. This low basicity is in accordance with low pyrylium resonance contribution to the ground state of IIIa as discussed below.

As mentioned above, in the reaction between equivalent amounts of the dimethoxycarbonylpyrylium ion and acetone or acetophenone in liquid SO_2, the anhydro-base III was obtained directly. The product composition in this reaction shows that the initial 4H-pyran II suffers hydride abstraction to the pyrylium salt IV, the hydride abstractor being the pyrylium ion I. The presence in the product of nearly equivalent amounts of the ketone reagent, 2,6-dimethoxycarbonyl-4H-pyran and the anhydro-base III shows that hydride abstraction from IIa and IIb is a much faster reaction than adduct formation. For the 1,3-dicarbonyl derivatives, however, the order is reversed presumably for sterical reasons.

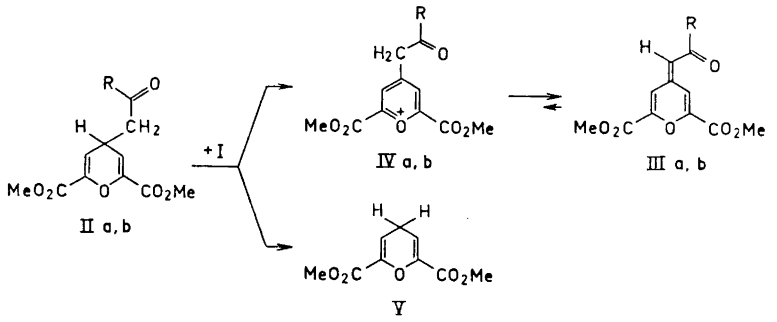

Scheme 4.

The driving force in the hydride exchange between the 4H-pyran II and I lies in the relative stabilities of the pyrylium ions I and IV. A 4-substituent will stabilise the pyrylium cation. This was readily seen in an NMR experiment with equivalent amounts of the cation I and the 4-methyl-4H-pyran VI in TFA. Thus after 2 days all the pyrylium cation I had been reduced to its 4H-pyran (V) with concurrent oxidation of VI to the 4-methylpyrylium ion VII. Similarly the greater stability of the tropylium ion was demonstrated by dissolving the cation I and cycloheptatriene in acetonitrile. The NMR spectrum, recorded after 20 min, contained only proton signals from the tropylium ion and the 4H-pyran.

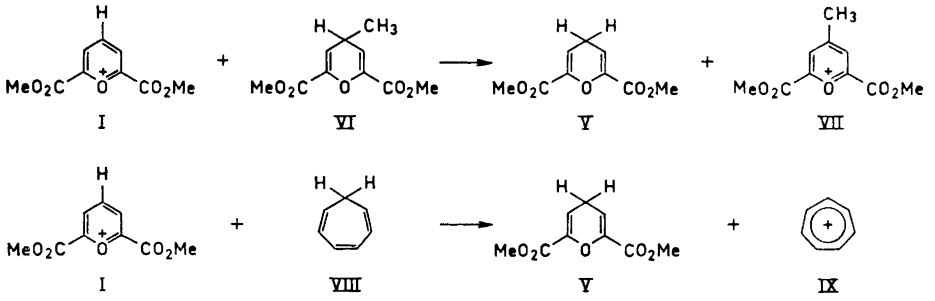

Scheme 5.

Integration of the NMR spectra (Table 1) of the pyranyl ketones (II) showed that both the mono-carbonyl and the acyclic 1,3-dicarbonyl derivatives exist almost entirely in the ketone form. The keto-enol equilibria of 1,3-dicarbonyl compounds are solvent sensitive, the enol tautomer being the more important in non-polar solvents.[7,8] In the present case the *cis*-enol, however, will be destabilised relative to the ketone because of steric repulsion between the pyranyl group and the substituents on the carbonyl groups (Scheme 6). In the *trans*-enol, the main interaction is between the R-groups. On the other hand the NMR spectrum of the cyclic 1,3-dicarbonyl derivative IIe shows this

to be about 80 % enolised. In this case the steric interaction between the dimedone and the pyran ring is little affected by the degree of enolisation, and IIe is therefore enolised very much as dimedone itself.[9,10]

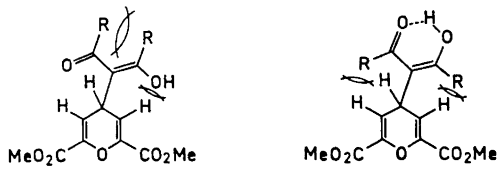

Scheme 6.

The chemical shifts for the β-pyranyl protons in the pyranyl ketones II have been shifted slightly upfield (up to 0.2 τ) relative to the corresponding shift in the 4-methyl derivative (VI). The shifts are probably caused by anisotropy effects from the carbonyl group, the shift being largest in the acyclic dicarbonyl compounds. In the anhydro-bases III, however, the chemical shifts for the β-pyranyl protons have been moved considerably downfield. These shifts are also at lower field than in the parent methylene derivative III ($R^1 = R^2 = H$).[1]

Table 2. NMR spectra of 4H-dehydropyrans recorded in $CDCl_3$.

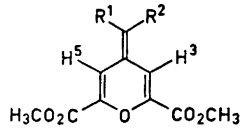

Comp.	Substituents R^1	R^2	Chemical shift in τ values H^3	H^5	R^1	R^2	OCH_3	Coupling in cps
IIIa	H	CH_3CO	1.40	3.07	4.10	7.75	6.08	$J_{3,5}=2.0$
b	H	C_6H_5CO	1.25	2.92	3.38	2.0–2.6	6.07	$J_{3,5}=2.0$
c	CH_3CO	CH_3CO	2.33	2.33	7.67	7.67	6.08	–
d	C_6H_5CO	C_6H_5CO	2.17	2.17	2.2–2.9		6.10	–
e	$(CH_3)_2C(CH_2CO)_2$		0.87	0.87	CH_3:8.92; CH_2:7.45		6.02	–

Table 2 shows that the β-protons appear at different fields in the monocarbonyl derivatives, the signal at about 3 τ being comparable with 3.2 τ in the methylene analogue (III, $R^1 = R^2 = H$). In the cyclic diketone IIIe both β-pyranyl protons resonate at 0.9 τ. The carbonyl groups in the cyclohexylidene system (IIIe) are prevented from moving far away from the coplanarity of the pyranyl ring. The β-pyranyl protons are therefore in the deshielding zone of the carbonyl group resulting in a downfield chemical shift. Application of this to the monoketone IIIa leads to the assignment of the lower chemical shift signal to the

Table 1. NMR spectra of 4H-pyrans recorded in $CDCl_3$.

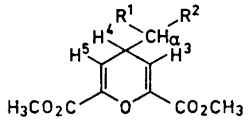

Comp.	Substituents R¹	Substituents R²	Chemical shifts in τ values H³	H⁵	H⁴	Hα	R¹	R²	OCH_3	Couplings in cps
IIa	H	CH_3CO	4.00[b]	4.00[b]	6.2–6.5[d]	7.28[b]	7.28[b]	7.83[a]	6.18[a]	$J_{3,4}=3.5$ $J_{4,\alpha}=7.0$
b	H	C_6H_5CO	3.88[b]	3.88[b]	5.6–6.3[d]	6.78[b]	6.78[b]	1.9–2.7[d]	6.18[a]	$J_{3,4}=3.5$ $J_{4,\alpha}=7.0$
c	CH_3CO	CH_3CO	4.05[b]	4.05[b]	6.0–6.2[d,e]		7.77[a]	7.77[a]	6.17[a]	$J_{3,4}=4.0$ $J_{4,\alpha}=7.0$
d	C_6H_5CO	C_6H_5CO	3.97[b]	3.97[b]	5.5–5.8[d]	4.43[b]	1.9–2.8[d]	1.9–2.8[d]	6.27[a]	$J_{3,4}=4.0$ $J_{4,\alpha}=8.0$
e	CH_3, CH_3, CH_2CO, CH_2CO		3.90[b]	3.90[b]	6.1–6.3[d,e]		CH_3:8.90;	CH_2:7.62[a]	6.18[a]	$J_{3,4}=3.5$
f	CH_3, CH_3, CH_2CO, $CH=C(OH)$		4.05[b]	4.05[b]	5.33[c]	2.5–2.9[f]	CH_3:8.90;	CH_2:7.62[a]	6.18[a]	$J_{3,4}=3.5$

[a] Singlet, [b] doublet, [c] triplet, [d] multiplet, [e] superimposed, [f] enolic OH.

β-pyranyl proton which is in front of the carbonyl group in the s-*cis* conformation (Scheme 7).

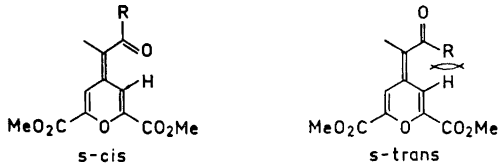

Scheme 7.

The s-*trans* conformation is thought destabilised by steric repulsion between the carbonyl methyl group and the β-pyranyl hydrogen atom. The preferential assignment of a s-*cis* conformation also agrees well with conclusions reached in conformational studies of related simple open-chain α,β-unsaturated ketones by means of infrared and Raman spectroscopy.[11] The higher field (0.5 τ) signal for the deshielded pyranyl proton in IIIa than in the cyclohexylidene derivative IIIe, however, suggests a greater deviation from coplanarity of the exocyclic α,β-unsaturated carbonyl system for the former.

Steric repulsion between the substituents on the carbonyl carbons in the acyclic 1,3-dicarbonyl compound IIIc will force the carbonyl groups considerably out of plane in both s-*cis* and s-*trans* conformations resulting in an upfield shift (0.5 τ) of the now equivalent β-pyranyl protons. The NMR data in Table 2 show that the aromatic analogues IIIb and IIId behave similarly to the discussed aliphatic derivatives IIIa and IIIc.

The chemical shifts for the pyranyl protons in IIIa were not affected by increase in temperature. The energy barrier for rotation around the exocyclic double bond in IIIa was not reached by heating in dimethyl sulphoxide-d_6 to 150°C. In the literature a somewhat related 2,6-dimethylpyran has been reported to behave similarly while the superior electron releasing properties of the nitrogen in the pyridine analogue results in low energy barrier for rotation.[12] This indicates a relatively low ground state contribution to resonance from the pyrylium form (Scheme 8) which is not unexpected because of the destabilising effect from the methoxycarbonyl groups on the pyrylium cation.

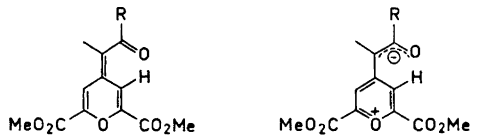

Scheme 8.

EXPERIMENTAL

The NMR spectra were recorded on a 60 Mc/s instrument.

4-Acetylmethyl-2,6-dimethoxycarbonyl-4H-pyran (IIa). 2,6-Dimethoxycarbonylpyrylium perchlorate (2.96 g, 0.01 mol) was added to acetone (50 ml) with stirring and the

solution was left in the cold overnight. The solvent was then evaporated and the residual oil dissolved by warming in ethanol; a colourless, crystalline material was separated on cooling. The yield was 75 % (1.92 g), m.p. 125°C. (Found: C 56.46; H 5.84. Calc. for $C_{12}H_{14}O_6$: C 56.69; H 5.55.) Molecular weight by MS: Found 254.0796. Calc. for $C_{12}H_{14}O_6$: 254.0790.

4-Benzoylmethyl-2,6-dimethoxycarbonyl-4H-pyran (IIb) was prepared as IIa using acetophenone. The yield was 75 %, m.p. 167–169°C (EtOH). Molecular weight by MS: Found 316.0948. Calc. for $C_{17}H_{16}O_6$: 316.0946.

4-Diacetylmethyl-2,6-dimethoxycarbonyl-4H-pyran (IIc) was prepared as IIa using acetylacetone. The yield was 91 %, m.p. 175°C (MeOH). Molecular weight by MS: Found 296.0897. Calc. for $C_{14}H_{16}O_7$ 296.0896.

4-Dibenzoylmethyl-2,6-dimethoxycarbonyl-4H-pyran (IId). 2,6-Dimethoxycarbonylpyrylium perchlorate (1.48 g, 0.005 mol) was dissolved in liquid sulphur dioxide (25 ml) at −30°C and dibenzoylmethane (1.12 g, 0.005 mol) added with stirring. The SO_2 was then allowed to evaporate off, and the residual material was dissolved by heating in ethanol. The title compound crystallised out on cooling. The yield was 57 % (1.20 g), m.p. 163–165°C (EtOH). (Found: C 68.74; H 5.07. Calc. for $C_{24}H_{20}O_7$: C 68.56; H 4.80.) Molecular weight by MS: Found 420.1201. Calc. for $C_{24}H_{20}O_7$: 420.1209.

4-(5,5-Dimethyl-1,3-dione-2-cyclohexyl)-2,6-dimethoxycarbonyl-4H-pyran (IIe) was prepared from dimedone in SO_2 as described for IId. The yield was 81 %, m.p. 220°C (dilute EtOH). Molecular weight by MS: Found 336.1213. Calc. for $C_{17}H_{20}O_7$ 336.1209.

4-Benzoylmethylene-2,6-dimethoxycarbonylpyran (IIIb). 2,6-Dimethoxypyrylium perchlorate (1.48 g, 0.005 mol) was dissolved in liquid SO_2 at −30°C and acetophenone (0.3 g, 0.0025 mol) added with stirring. The SO_2 was then allowed to evaporate in the cold and the residual material dissolved in ethanol by heating. The yellow crystalline title compound was precipitated on cooling; yield 62 % (0.48 g), m.p. 155°C (EtOH). (Found: C 64.88; H 4.79. Calc. for $C_{17}H_{14}O_6$: C 64.94; H 4.49.) Molecular weight by MS; Found 314.0793. Calc. for $C_{17}H_{14}O_6$ 314.0790.

4-Acetylmethylene-2,6-dimethoxycarbonylpyran (IIIa) was prepared from acetone in 82 % yield, m.p. 185–187°C (EtOH). Molecular weight by MS: Found 252.0628. Calc. for $C_{12}H_{12}O_6$ 252.0633.

4-Dibenzoylmethylene-2,6-dimethoxycarbonylpyran (IIId). A solution of 4-dibenzoylmethyl-2,6-dimethoxycarbonyl-4H-pyran (0.57 g, 0.0014 mol) and triphenylmethyl perchlorate (0.46 g, 0.0014 mol) in anhydrous acetonitrile (10 ml) was refluxed for 30 min before evaporation of the solvent. The residual material was redissolved by heating with ethanol. Yellow needles crystallised out from the ethanol solution on cooling; yield 0.59 g (49 %), m.p. 187–190°C. (Found: C 68.87; H 4.37. Calc. for $C_{24}H_{18}O_7$: C 68.89; H 4.34.) Molecular weight by MS: Found 418.1052. Calc. for $C_{24}H_{18}O_7$ 418.1053.

4-(5,5-Dimethyl-1,3-dione-2-cyclohexylidene)-2,6-dimethoxycarbonylpyran (IIIe) was prepared from IIe and triphenylmethyl perchlorate as described for IIId in 71 % yield, m.p. 210°C (EtOH). Molecular weight by MS: Found 334.1061. Calc. for $C_{17}H_{18}O_7$334.1052.

4-Diacetylmethylene-2,6-dimethoxycarbonylpyran (IIIc). A solution of 4-diacetylmethyl-2,6-dimethoxycarbonyl-4H-pyran (0.89 g, 0.003 mol) and 2,3-dichloro-5,6-dicyano-1,4-benzoquinone (0.68 g, 0.003 mol) in benzene (25 ml) was heated at 60°C for 20 min. The precipitated material was filtered off from the cold solution and the filtrate evaporated. The residue was redissolved by heating with ethanol. Yellow needles were precipitated from the cold ethanol solution; yield 0.70 g (70 %), m.p. 130°C (EtOH). Molecular weight by MS: Found 294.0731. Calc. for $C_{14}H_{14}O_7$ 294.0740.

REFERENCES

1. Part I. Undheim, K. and Østensen, E. T. *Acta Chem. Scand.* **27** (1973) 1385.
2. Dimroth, K. and Wolf, K. H. In Foerst, W. and Kirchner, F. K., Eds., *Newer Methods of Preparative Organic Chemistry*, Academic, New York 1964, Vol. III, p. 357.
3. Dimroth, K. and Neubauer, G. *Angew. Chem.* **69** (1957) 720.
4. Kröhnke, F. and Dickoré, K. *Chem. Ber.* **92** (1957) 46.
5. Vol'pin, M. E., Akhrem, I. S. and Kursanov, D. N. *Zh. Obshch. Khim.* **30** (1960) 1187.

6. Vol'pin, M. E., Akhrem, I. S., Teret'eva, E. A. and Kursanov, D. N. *Izvest. Akad. Nauk. SSSR. Otd. Khim. Nauk.* **5** (1963) 802.
7. Allen, G. and Dwek, R. A. *J. Chem. Soc.* **B 1966** 161.
8. Rogers, M. T. and Burdett, J. L. *Can. J. Chem.* **43** (1965) 1516.
9. Natsuko, C. and Reeves, L. W. *Can. J. Chem.* **43** (1965) 3057.
10. Yogev, A. and Mazyr, Y. *J. Org. Chem.* **32** (1967) 2162.
11. Noack, K. and Jones, R. N. *Can. J. Chem.* **39** (1961) 2225.
12. Seitz, G. *Angew. Chem.* **81** (1969) 518.

Received January 16, 1973.

ACTA CHEMICA SCANDINAVICA 27 (1973) 2193–2198

Pseudomonas Cytochrome *c* Peroxidase

VIII. The Amino Acid Composition of the Enzyme

RITVA SOININEN and NILS ELLFOLK

Department of Biochemistry, University of Helsinki, SF-00170 Helsinki 17, Finland

The amino acid composition of *Pseudomonas* cytochrome *c* peroxidase has been determined. The analyses indicate the presence of the following amino acid residues: Asp_{36}, Thr_{16}, Ser_{22}, Glu_{39}, Pro_{28}, Gly_{29}, Ala_{37}, Val_{24}, Met_4, $Ileu_9$, Leu_{31}, Tyr_8, Phe_{19}, Lys_{23}, His_9, Arg_{13}, Cys_3, Trp_4,$(\text{-CONH}_2)_{35}$. No neutral sugars, amino sugars or sialic acids were detected in the enzyme. The molecular weight of 44 047 computed from the amino acid composition corresponds to the values based on the iron and heme content. A value of 0.711 ml/g for the partial specific volume was calculated from the weight percentages of the amino acid residues and their respective specific volumes. The electrophoretic mobility of the enzyme can be satisfactorily explained by the amino acid composition.

Homogeneous cytochrome *c* peroxidase (cytochrome *c*:H_2O_2-oxidoreductase, EC 1.11.1.5) has recently been purified from *Pseudomonas aeruginosa*.[1,2] It differs from plant and animal peroxidases in containing heme *c* (two molecules per mol) as the prosthetic group.[1,3] In the present publication we report the results of the analyses of its amino acid composition and the possible presence of carbohydrates, common constituents of plant and animal peroxidases.

MATERIALS AND METHODS

Pseudomonas cytochrome *c* peroxidase (PsCCP) was prepared from the acetone-dried cells of *P. aeruginosa* as previously described.[1,2] The preparation was homogeneous when analyzed by disc electrophoresis [4] (7 % gel, pH 8.9, staining according to Weber and Osborne [5]) and its absorbance ratio A_{407}/A_{280} was 4.53.

Amino acid analyses. Samples of PsCCP were extensively dialyzed against twice-distilled water before analysis. The acid hydrolysis of the protein was performed in 6 N HCl at 110°C in evacuated sealed Pyrex tubes for periods of 20 and 70 h. To prevent the loss of tyrosine during hydrolysis, 10 µl of 0.1 M phenol was added to the samples.[6] After hydrolysis, HCl was removed in a rotary evaporator. Aliquots containing 0.4 – 0.6 mg hydrolysate were analyzed according to the procedure of Moore *et al.*[7] using a Beckman Spinco Model 120 B amino acid analyzer. A Beckman standard amino acid mixture was used to standardize the columns. The analysis of tryptophan was carried out on samples

of unhydrolyzed protein according to "procedure K" of Spies and Chambers.[8] Cyst(e)ine and methionine were determined in the amino acid analyzer as cysteic acid and methionine sulfone following performic acid oxidation according to Moore.[9] The number of residues was calculated by reference to the molar quantities of amino acids stable to oxidation.

Amide ammonia was determined after the hydrolysis of PsCCP samples in 1 N HCl for 4 h in a stoppered test tube at 100°C. The Conway microdiffusion technique was employed as previously described.[10,11] The ammonia liberated from amide groups and trapped in 0.01 N HCl in the inner chamber of the Conway vessel was determined in the amino acid analyzer.

Total nitrogen content of dried samples of PsCCP was determined using a Coleman 29 A C Nitrogen Analyzer II which is based on the Dumas method.

Carbohydrate analyses. Neutral sugars were analyzed in the unhydrolyzed protein by the Winzler orcinol-sulfuric acid procedure [12] and by the anthrone method.[13] Hexosamine analyses were performed on the neutralized hydrolysate (hydrolysis in 4 N HCl at 100°C for 4 h) by the Rondle and Morgan procedure. [14,15] Sialic acids were analyzed after the hydrolysis of samples in 0.05 M H_2SO_4 at 80°C for 1 h by the thiobarbituric acid method.[16] Optical absorption difference spectra (sample *minus* protein blank) of the reaction products were recorded on a Cary 15 recording spectrophotometer at the appropriate wavelengths. The spectra obtained from PsCCP were compared with those of standard monosaccharides and glycoproteins (lactoperoxidase, prepared from milk according to Carlström,[17] containing 4.1 – 5.4 % neutral sugars and 4.8 % amino sugars,[18] ovalbumin, Grade V, Sigma, containing 2 % neutral sugars and 1.2 % amino sugars,[19] and casein, Merck, containing 0.2 % neutral sugars, 0.2 % amino sugars, and 0.3 – 0.5 % sialic acids [20]).

Dry weights. Protein samples were extensively dialyzed against twice-distilled water and dried to constant weight at 105°C. Weighing was performed in a Cahn microbalance.

Chemicals were of analytical grade.

Table 1. Amino acid recoveries after acid hydrolysis of *Pseudomonas* cytochrome *c* peroxidase. The results are given as grams of amino acid residues per 100 g of protein. The values for 20 h represent the mean of three separate determinations and those of 70 h that of two.

Amino acid residue	Time of hydrolysis		Average or extrapolated values
	20 h	70 h	
Aspartic acid	9.56	9.62	9.59
Threonine	3.67	3.60	3.70[a]
Serine	4.04	3.38	4.34[a]
Glutamic acid	11.75	11.75	11.75
Proline	6.19	6.21	6.20
Glycine	3.82	3.86	3.84
Alanine	6.16	6.12	6.14
Valine	5.42	5.53	5.53[b]
Methionine	(1.04)[c]	(0.47)[c]	–
Isoleucine	2.25	2.25	2.25
Leucine	8.03	7.96	8.00
Tyrosine	2.62	2.02	2.91[a]
Phenylalanine	6.17	6.34	6.34[b]
Lysine	6.71	6.74	6.73
Histidine	2.74	2.72	2.73
Arginine	4.66	4.72	4.69
Cystine	0	0	–

[a] Obtained by extrapolation to zero hydrolysis time. [b] 70 h value. [c] Sum of methionine and methionine sulfoxides.

RESULTS

Table 1 presents the amino acid recoveries from the samples of PsCCP hydrolyzed for 20 and 70 h. Decomposition with increasing hydrolysis time occurred with serine, tyrosine and, to a slight extent, threonine. The concentration of these amino acids was obtained by extrapolation to zero hydrolysis time by assuming first-order kinetics of destruction.[21] The yield of valine and phenylalanine was found to increase with increasing hydrolysis time. The values of the 70 h hydrolysates were used in the final calculation of these two amino acids. A tryptophan content of 1.65 % per unit weight of protein was obtained by analyzing colorimetrically the unhydrolyzed samples of PsCCP.[8] During the acid hydrolysis of PsCCP, cyst(e)ine is completely oxidized or

Table 2. Composition and molecular weight of *Pseudomonas* cytochrome *c* peroxidase.

Amino acid residue	Grams of amino acid residues per 100 g of protein[a]	Minimum molecular weight[b]	Amino acid residues per 43 200 g[c] of protein	Nearest integral No. of amino acid residues per 43 200 g of protein	Nearest integral No. multipl. by min. mol. weight
Aspartic acid	9.59	1 200	36.00	36	43 200
Threonine	3.70	2 732	15.81	16	43 712
Serine	4.34	2 006	21.54	22	44 132
Glutamic acid	11.75	1 099	39.31	39	42 861
Proline	6.20	1 566	27.59	28	43 848
Glycine	3.84	1 486	29.07	29	43 094
Alanine	6.14	1 157	37.34	37	42 809
Valine	5.53	1 793	24.09	24	43 032
Isoleucine	2.25	5 029	8.59	9	45 261
Leucine	8.00	1 414	30.55	31	43 834
Tyrosine	2.91	5 607	7.70	8	44 856
Phenylalanine	6.34	2 321	18.61	19	44 099
Lysine	6.73	1 904	22.69	23	43 792
Histidine	2.73	5 023	8.60	9	45 207
Arginine	4.69	3 330	12.97	13	43 290
Tryptophan	1.65[d]	11 300	3.83	4	45 200
Half cystine	0.65[e]	15 868	2.72	3	47 604
Methionine	1.22[e]	10 753	4.02	4	43 012
Amide ammonia	1.30[f]		35.10	35[f]	
	88.26				
Heme	2.85[g]				
Total	91.11[h]		350.80	354	44 047[i]

[a] From the last column of Table 1. [b] (Molecular weight of amino acid residue × 100)/percent amino acid residue in protein. [c] Molecular weight of PsCCP based on iron content.[3] [d] Determined by the method of Spies and Chambers.[8] [e] Determined after the performic acid oxidation according to Moore.[9] [f] Omitted from the total. [g] Calculated on the basis of iron content of PsCCP.[1,3] [h] Recovery on the basis of dry weight. The recovery of nitrogen calculated from the amino acid residues plus heme is 15.28 % nitrogen per unit weight of protein, which represents 97.4 % of the independently determined nitrogen content, 15.7 %. [i] Average molecular weight for all residues.

decomposed and methionine partially oxidized to methionine sulfoxides. Consequently, the sum of cysteine and cystine was determined as cysteic acid and methionine as methionine sulfone after performic acid oxidation.[9] Because no significant amounts of methionine, methionine sulfoxides or cystine were observed, the oxidation was considered to be complete. A cyst(e)ine content of 0.65 % and a methionine content of 1.22 % per unit weight of protein was so obtained. The amide ammonia analyses indicate the presence of 1.30 % amide residues per unit weight of protein. This corresponds to 35 amide groups per mol of PsCCP.

The nitrogen content of PsCCP calculated from the amino acid recoveries and including the nitrogen of heme groups is 15.28 %. An independent value of 15.7 % was obtained experimentally by the Dumas method.

No neutral sugars, amino sugars, or sialic acids were detected in carbohydrate analyses of PsCCP.

The composition and molecular weight of PsCCP is shown in Table 2. The accuracy with which the number of amino acids can be estimated depends on the number of residues present in the protein. The permitted variation would be $n \pm 0.4$ with n amino acid residues, and the accuracy therefore $\pm 0.4/n$.[22] The precision of the amino acid analyses may be estimated as better than 3 %, so that amino acid residues up to 13 per mol of protein can be calculated with reliability to the nearest integer. The total of amino acid residues in one molecule of the protein was estimated to be 354 and the average molecular weight, calculated from all amino acid residues, was found to be 44 047 with the standard deviation of 1212.

A value of 0.711 ml/g was calculated for the partial specific volume of PsCCP from the composition of the molecule using the weight percentages of

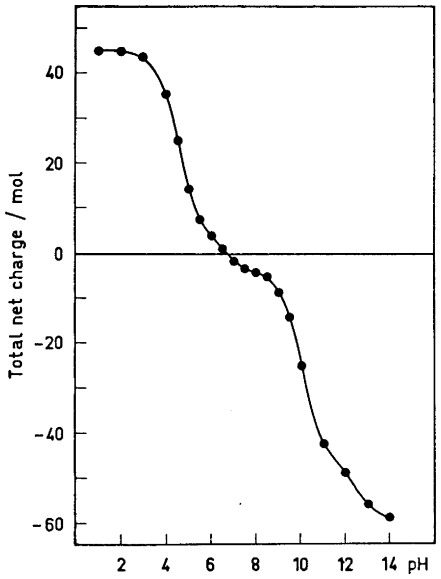

Fig. 1. A theoretical titration curve for *Pseudomonas* cytochrome *c* peroxidase. The calculation is based on the following pK values.[24,25]

Ionizable group	Total number in PsCCP	pK assumed
γ- and δ-Carboxyl	40	4.5
Imidazole	9	6.5
ε-Amino	23	10.0
Phenolic hydroxyl	19	10.0
Guanidine	13	12.5

The terminal amino and carboxyl groups and sulfhydryl groups assumed to be covalently bound to the heme groups were not considered. The titrateable carboxyl groups were obtained by subtracting the number of amide groups from the total of carboxyl groups.

the amino acid residues and their respective specific volumes [23] (heme groups omitted).

A theoretical titration curve for a total of 104 ionizable groups in the protein is shown in Fig. 1. For this hypothetical case an isoionic point of approximately 6.8 is obtained.

DISCUSSION

Acid hydrolysis of PsCCP was performed using the intact protein with the heme groups attached. The presence of iron in the hydrolysate may contribute to abnormal decomposition of amino acids during the hydrolysis. It is possible that the rate of decomposition of free amino acids may follow higher orders under these conditions.[26,27] Despite the addition of phenol to prevent the chlorination of tyrosine,[6] the loss of this amino acid during hydrolysis was considerable. No cystine and only traces of cysteic acid were detected in the chromatograms of the unoxidized hydrolysate; and methionine was partially oxidized to sulfoxides.

A considerable proportion of the acidic amino acid residues of PsCCP is in the amidated form (35 residues out of 75, the sum of aspartic acid and glutamic acid). Although the enzyme is soluble in aqueous solution at neutral pH, it contains an excess of hydrophobic amino acids (188 hydrophobic residues against 166 hydrophilic ones). The tyrosine and tryptophan as well as the cysteine and methionine content of PsCCP is quite low. Surprisingly, only three half cystines were recovered (if no unexpected losses of cysteine had occurred in the presence of iron) in a protein which, according to iron and heme analysis, contains two groups of heme *c* per molecule.[1,3] In C-type cytochromes there are generally two cysteine residues covalently linked with the vinyl groups of one protoheme; however, some exceptions are known. The hemopeptide of *Chromatium* cytochrome *cc'* contains two heme groups and three cysteine residues.[28] One heme is bound to two cysteine residues and the other, as deduced from the amino acid sequence of the hemopeptide, to one cysteine and presumably a threonine residue by an oxyether linkage.[28] This cytochrome yields a normal alkaline pyridine ferrohemochrome of heme *c* with an α-band at 551 nm.[29] Two other cytochromes containing one cysteine residue per heme are *Crithidia* cytochrome *c* [30] and *Euglena* cytochrome *c*.[31] These cytochromes, however, yield an alkaline pyridine ferrohemochrome with an α-band at 553 nm, thus differing from *Chromatium* cytochrome *cc'*. The linkages of the heme groups to the protein moiety in PsCCP require further study.

No neutral sugars, amino sugars, or sialic acids were detected in PsCCP. It thus differs in this respect too from plant peroxidases and lactoperoxidase which contain carbohydrates (neutral sugars and amino sugars) up to about 20 % of the dry weight.[18,32,33] PsCCP is similar to yeast cytochrome *c* peroxidase in containing no carbohydrates.[34]

The total recovery of amino acids on a dry weight basis was somewhat low. The recovery of nitrogen was, however, satisfactory. The low recovery on a dry weight basis may indicate the presence of some non-nitrogeneous component (not carbohydrate) in PsCCP, representing less than 6 % of dry weight.

The molecular weight, about 44 000, obtained from amino acid analyses, corresponds to the values based on the iron and heme analyses, 43 200 and 48 800, respectively.[3] The partial specific volume calculated from the chemical composition of PsCCP, 0.711 ml/g, is somewhat higher than the experimental value of 0.695 ml/g.[3]

The isoionic point, 6.8, obtained from the theoretical titration curve based on the amino acid composition of PsCCP, agrees well with the experimentally determined isoelectric point, 6.7.[1]

Acknowledgement. Automated nitrogen analyses were performed in the Biotechnical Laboratory of the Technical Research Centre of Finland, Helsinki, with the kind permission of Prof. T. M. Enari.

REFERENCES

1. Ellfolk, N. and Soininen, R. *Acta Chem. Scand.* **24** (1970) 2126.
2. Soininen, R. *Acta Chem. Scand.* **26** (1972) 2535.
3. Ellfolk, N. and Soininen, R. *Acta Chem. Scand.* **25** (1971) 1535.
4. Maurer, H. R. *Disk-Elektrophorese*, Walter de Gruyter, Berlin 1968.
5. Weber, K. and Osborne, M. *J. Biol. Chem.* **244** (1969) 4406.
6. Sanger, F. and Thompson, E. O. P. *Biochim. Biophys. Acta* **71** (1963) 468.
7. Moore, S., Spackman, D. H. and Stein, W. H. *Anal. Chem.* **30** (1958) 1190.
8. Spies, J. R. and Chambers, D. C. *Anal. Chem.* **21** (1949) 1249.
9. Moore, S. *J. Biol. Chem.* **238** (1963) 235.
10. Laki, K., Kominz, D. R., Symonds, P., Lorand, L. and Seegers, W. H. *Arch. Biochem. Biophys.* **49** (1954) 276.
11. Ellfolk, N. *Acta Chem. Scand.* **21** (1967) 2736.
12. Francois, C., Marshall, R. D. and Neuberger, A. *Biochem. J.* **83** (1962) 335.
13. Roe, J. E. *J. Biol. Chem.* **212** (1955) 335.
14. Rondle, C. J. M. and Morgan, W. T. J. *Biochem. J.* **61** (1955) 586.
15. Kraan, J. G. and Muir, H. *Biochem. J.* **66** (1957) 55P.
16. Aminoff, D. *Biochem. J.* **81** (1961) 384.
17. Carlström, A. *Acta Chem. Scand.* **19** (1965) 2387.
18. Carlström, A. *Acta Chem. Scand.* **23** (1969) 185.
19. Neuberger, A. and Marshall, R. D. In Gottschalk, A. *Glycoproteins*, Elsevier, Amsterdam 1966, p. 299.
20. Johansson, B. and Svennerholm, L. *Acta Physiol. Scand.* **37** (1956) 324.
21. Hirs, C. H. W., Stein, W. H. and Moore, S. *J. Biol. Chem.* **211** (1954) 941.
22. Tristram, G. R. *Biochem. J.* **40** (1946) 721.
23. Cohn, E. J. and Edsall, J. T. In Cohn, E. J and Edsall, J. T. *Proteins, Amino Acids and Peptides as Ions and Dipolar Ions*, Reinhold, New York 1943, p. 370.
24. Edsall, J. T. In Cohn, E. J. and Edsall, J. T. *Proteins, Amino Acids and Peptides as Ions and Dipolar Ions*, Reinhold, New York 1943, p. 444.
25. Edsall, J. T. and Wyman, J. *Biophysical Chemistry*, Academic, New York 1958, Vol. *1*, p. 406.
26. Kossel, B. and Laskowski, M. *J. Biol. Chem.* **236** (1961) 1996.
27. Bargetzi, J. P., Sampath Kamar, K. S. V., Cox, D. J., Walsh, K. A. and Neurath, N. *Biochemistry* **2** (1963) 1468.
28. Dus, K., Bartsch, R. and Kamen, M. *J. Biol. Chem.* **237** (1962) 3083.
29. Bartsch, R. G. and Kamen, M. D. *J. Biol. Chem.* **235** (1960) 825.
30. Pettigrew, G. *FEBS Letters* **22** (1972) 64.
31. Meyer, T. E. and Cusanovich, M. A. *Biochim. Biophys. Acta* **267** (1972) 383.
32. Shannon, L. M., Kay, E. and Lew, J. Y. *J. Biol. Chem.* **241** (1966) 2166.
33. Morita, Y. and Kameda, K. *Bull. Agr. Chem. Soc. Japan.* **23** (1959) 28.
34. Ellfolk, N. *Acta Chem. Scand.* **21** (1967) 175.

Received February 14, 1973.

ACTA CHEMICA SCANDINAVICA 27 (1973) 2199–2210

The Donnan Potential II

TORMOD FØRLAND[a] and TERJE ØSTVOLD[b]

[a] *The University of Trondheim, Norwegian Institute of Technology, Division of Physical Chemistry, Trondheim, Norway and* [b] *The University of Trondheim, College of Arts and Science, Chemistry Department, Trondheim, Norway*

The Donnan potential is calculated on the basis of classical irreversible thermodynamics for the following galvanic cell:

$$\mathrm{Ag}\,|\,\mathrm{AgCl}\,|\,\underset{C_{\mathrm{K(3\,M)}}}{\mathrm{KCl}}\,\|\,\underset{C_{\mathrm{KCl(1)}}}{\mathrm{KCl}}\ \underset{C_{\mathrm{K_2SO_4}}}{\mathrm{K_2SO_4}}\ \underset{C_{\mathrm{M}}}{\mathrm{MCl}}\,\|\,\underset{}{\text{Mem-brane}}\,\|\,\underset{C_{\mathrm{KCl(2)}}}{\mathrm{KCl}}$$

$$\underset{C_{\mathrm{S}}}{\text{Sugar}}\,\|\,\underset{C_{\mathrm{K(3\,M)}}}{\mathrm{KCl}}\,|\,\mathrm{AgCl}\,|\,\mathrm{Ag}$$

The membrane is permeable to water, K^+ and Cl^- ions, but impermeable to the M^+ and SO_4^{2-} ions. When chemical equilibrium is obtained across the membrane, the emf for the present cell can be approximated by the equation

$$E = \frac{RT}{F}\left\{\ln\frac{C_{\mathrm{Cl(2)}}}{C_{\mathrm{Cl(1)}}} + \frac{u_{\mathrm{K}} - \frac{1}{2}u_{\mathrm{SO_4}}}{u_{\mathrm{K}} - u_{\mathrm{SO_4}}}\ln\left(1 - \frac{u_{\mathrm{SO_4}} - u_{\mathrm{K}}}{u_{\mathrm{K}}}\frac{C_{\mathrm{SO_4}}}{C_{\mathrm{K(3\,M)}}}\right) - \ln\left(1 - \frac{C_{\mathrm{M}}(u_{\mathrm{K}} - u_{\mathrm{M}})}{2C_{\mathrm{K(3\,M)}}u_{\mathrm{K}} + 2C_{\mathrm{SO_4}}(u_{\mathrm{SO_4}} - u_{\mathrm{K}})}\right)\right\}$$

In the present cell the concentration of potassium sulfate in the left hand half cell is much smaller than the concentration of potassium chloride in the 3 molar (3 M) potassium chloride salt bridge. The second term on the right hand side of the above equation is therefore negligible. Since the metal chloride concentration in the left hand half cell also is negligible compared to 3 M the third term in the above equation is also negligible and the emf of the above cell can be further approximated by

$$E \simeq \frac{RT}{F}\ln\frac{C_{\mathrm{Cl(2)}}}{C_{\mathrm{Cl(1)}}}$$

which is the result obtained experimentally for cells of the above type.

In a recent paper Førland and Østvold[1] calculated the Donnan potential for the following galvanic cell

$$\mathrm{Ag}\,|\,\mathrm{AgCl}\,|\,\mathrm{KCl(3\,M)}\,\|\,\underset{C(1)\ C_{\mathrm{R}}}{\mathrm{KCl\ KR}}\,|\,\underset{}{\text{Mem-brane}}\,|\,\underset{C(2)}{\mathrm{KCl}}\,\|\,\mathrm{KCl(3\,M)}\,|\,\mathrm{AgCl}\,|\,\mathrm{Ag}$$

The membrane was considered permeable to water, K^+, and Cl^- ions, but impermeable to the large organic anion R^-. In the calculation of the Donnan potential for the present cell

$$\mathrm{Ag} \mid \mathrm{AgCl} \mid \underset{C_{\mathrm{K(3\,M)}}}{\mathrm{KCl}} \parallel \underset{C_{\mathrm{KCl(1)}}}{\mathrm{KCl}} \; \underset{C_{\mathrm{K_2SO_4}}}{\mathrm{K_2SO_4}} \; \underset{C_{\mathrm{MCl}}}{\mathrm{MCl}} \mid \mathrm{Membrane} \mid \underset{C_{\mathrm{KCl(2)}}}{\mathrm{KCl}} \; \underset{C_{\mathrm{S}}}{\mathrm{Sugar}} \parallel \underset{C_{\mathrm{K(3\,M)}}}{\mathrm{KCl}} \mid \mathrm{AgCl} \mid \mathrm{Ag}$$

the only assumptions introduced are the ideal solution approximation, the assumption of zero mobilities for SO_4^{2-} and M^+ ions in the membrane phase and the assumption of constant relative mobilities in electrolyte solutions. The Donnan potential is a concept very frequently used in the discussion of biological systems, and it is introduced in the calculations of transport processes in biological membranes. Fig. 1 shows a schematic diagram of a galvanic cell with a membrane separating the two half cells. The membrane is permeable to the K^+ and Cl^- ions, but impermeable to the SO_4^{2-} and M^+ ions.

The potential established over the membrane is called the Donnan potential. As K^+ and Cl^- are free to migrate between the two compartments of the cell separated by the membrane, the chemical potential of KCl, μ_{KCl}, must after some time be equal on both sides of the membrane. If the solutions are sufficiently dilute, they can be treated as ideal ionic solutions, and we may write

$$RT \ln C_{K(1)} C_{Cl(1)} = RT \ln C_{K(2)} C_{Cl(2)}$$

or

$$C_{K(1)} C_{Cl(1)} = C_{K(2)} C_{Cl(2)} \qquad (1)$$

which is the Donnan equilibrium. This equation was derived by Donnan and Guggenheim.[2]

When an equation for an electric potential difference, or the emf of a cell, is written, it should be said how it can be measured, and what the electrodes should be like. If the electrodes of the cell in Fig. 1 were reversible to Cl^- (*e.g.*

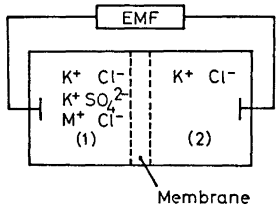

Fig. 1. A schematic diagram of a galvanic cell constructed to study the Donnan potential. The membrane is permeable to water molecules and K^+ and Cl^- ions, but not to the M^+ and SO_4^{2-} ions.

Ag/AgCl electrodes), the total cell reaction would be the transfer of KCl from the left hand side to the right hand side of the cell. (The quantity transferred per Faraday would be given by the transport number of K^+ in the membrane.) But since the chemical potential of KCl is equal on both sides of the membrane, the total cell reaction gives no change in Gibbs energy, and the emf must be zero. The same result would be obtained if the electrodes were reversible to the K^+ ion. This type of reasoning was also used by Babcock and Overstreet [3]

in their discussion of the use of calomel half cells to measure Donnan potentials in 1953, but seems to have been ignored by most scientists discussing Donnan potentials in later years.

Most of the measurements in biology of potentials over membranes are carried out with micro electrodes consisting of a pipette filled with a high concentration KCl-solution, into which an electrode reversible to Cl^- is introduced. In such cases it has been assumed that processes taking place in the liquid junction at the tip of the pipettes would not contribute to the measured emf by any significant amount. It will be shown that this assumption is far from beeing valid.

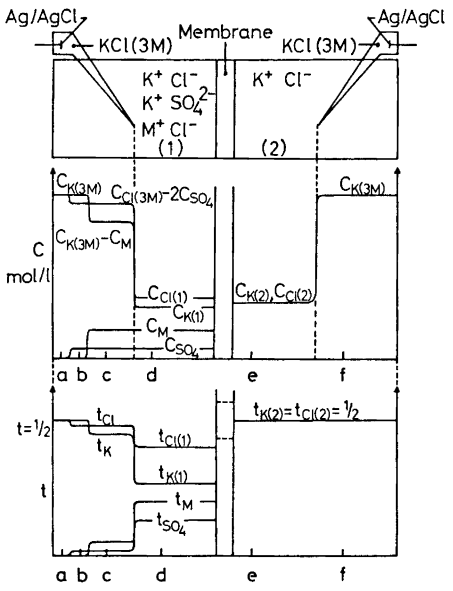

Fig. 2. A schematic diagram of a special galvanic cell constructed to study the Donnan potential together with diagrams of the variations of the concentration of the K^+, M^+, Cl^-, and SO_4^{2-} ions and the transport numbers of the K^+, M^+, Cl^-, and SO_4^{2-} ions through the cell.

To calculate the emf of the cell shown in Fig. 2, a small positive charge, ΔQ, is allowed to pass under reversible conditions from left to right in the cell during a short period of time, Δt. It has been shown in previous papers by Førland [4] and by Førland *et al.*,[5] that the outer electric work (in the potentiometer) ΔQE, where E is the emf of the cell, is connected to that part of the Gibbs energy change occurring in the cell which is dependent on ΔQ, but not on Δt. One may thus write

$$\Delta QE + \frac{\Delta Q}{F}\Delta G_Q = 0 \qquad (2)$$

where ΔG_Q is the change in Gibbs energy following the cell reaction per Faraday of charge transferred. ΔG_Q can be calculated when the cell reaction is known and when the transport number, t_i, and the chemical potentials, μ_i,

of the components of the cell have been measured. ΔG_Q is given by the following equations (see Førland *et al.* [5]):

$$\Delta G_Q = \Delta G_{el} - \int \sum_{\substack{i \\ \text{over} \\ \text{cell}}} \mu_i dt_i \tag{3}$$

where ΔG_{el} is the change in Gibbs energy close to the two electrodes. In the present cell the two electrodes and their close surroundings are identical and $\Delta G_{el} = 0$.

The integral $-\int \sum_i \mu_i dt_i$ gives the change in Gibbs energy due to change in composition by charge transfer in the different sections of the cell. In any region where all t_i are constant the change in Gibbs energy is zero. To describe the change in composition of the electrolyte in the different sections of the cell, the choice of frame of reference for all transports have no influence on the final result. For the region of concentration gradients in the electrolyte it is most practical to refer to water as frame of reference.

In the region of the membrane it may sometimes be more practical to refer all transport to the membrane as a frame of reference. Knowing the transport numbers of the components KCl and H_2O one will then be able to tell how much of each component was added to each side of the membrane by the charge transfer. In the present case, however, this is of no interest for the emf calculation since the chemical potential is constant both for KCl and for H_2O in the region from d to e. This may be obtained by adding a neutral molecule like sugar to the right hand side of the cell, or by keeping a pressure difference, which has to be corrected for in the emf. So in the region of the membrane we may just as well use water as frame of reference as was done in the other regions of the cell.

With water as the frame of reference eqn. (3) becomes

$$\Delta G_Q = -\int_a^f \mu_{KCl} dt_{KCl} - \int_a^f \mu_{MCl} dt_{MCl} - \int_a^f \mu_{K_2SO_4} dt_{K_2SO_4} \tag{4}$$

With electrodes reversible to the Cl^- anions, t_{MCl} obtained from the Hittorf experiment is the same as the transport numbers of M^+ ions, t_M. The transport coefficient for potassium sulfate, $t_{K_2SO_4}$, obtained from the Hittorf experiment, is the same as minus one half times the transport number of SO_4^{2-} ions, t_{SO_4}, because the negative divalent sulfate ion is migrating in the negative direction. The change in KCl content following the Hittorf experiment can be expressed by t_{KCl} and it is easily seen that t_{KCl} is related to the transport numbers of the K^+ and SO_4^{2-} ions through the following equation:

$$t_{KCl} = t_K + t_{SO_4}$$

When ionic transport numbers are introduced eqn. (4) attains the form

$$\Delta G_Q = -\int_a^f \mu_{KCl} d(t_K + t_{SO_4}) - \int_a^f \mu_{MCl} dt_M + \tfrac{1}{2}\int_a^f \mu_{K_2SO_4} dt_{SO_4} \tag{5}$$

With water as our frame of reference, the membrane (and the walls of the container) will move by the charge transfer. If t_{H_2O} with membrane as frame of reference is positive, then the membrane will move from right to left with water as frame of reference. Since the membrane is assumed to be impermeable to SO_4^{2-} and M^+, this means that MCl and K_2SO_4 must be transported in the same direction as the membrame in a region close to the membrane. As, however, this is transport of components over a region where their chemical potentials are constant, it gives no contribution to the emf.

Principally we should also have a term $-\int\mu_{\text{membrane}}\mathrm{d}t_{\text{membrane}}$ in ΔG_Q. However, the membrane is supposed to be in equilibrium with the KCl and water during the whole process of charge transfer. Thus any movement of these components between d and e with respect to the membrane does not contribute to $\Delta G_Q'$, or any movement, with respect to water, of membrane and KCl within the same region does not contribute to ΔGQ. Therefore the term $-\int\mu_{\text{membrane}}\mathrm{d}t_{\text{membrane}}$ is zero. Further it is sufficient to know the transport coefficient of KCl at the points d and e. The variation in transport coefficient between these points will have no influence on ΔG_Q.

It is thus shown that the change in Gibbs energy by charge transfer can be calculated by eqn. (5) and detailed knowledge about transports in the region from d to e is not needed for the emf calculation.

The transport number t_K is a function of composition and may change along the length of the galvanic cell in a way similar to what is shown in Fig. 2. This means that KCl will be added to the region where the left hand side electrolyte comes in contact with the KCl-solution of the KCl salt bridge. In this region one can observe from Fig. 2 that $\mathrm{d}t_K$ is negative. The major change will take place at concentrations close to $C_{KCl(1)}$ since the changes in transport number with distance along the length of the cell is greatest in this region. In this region KCl is transported from a high to a low concentration. This is a source of free energy which is transformed to electric energy in the outer circuit of the galvanic cell.

It should be mentioned that the left hand side KCl salt bridge has been given a MCl and K_2SO_4 content in that part of the bridge which is close to electrolyte(1) of the cell. This is to make the liquid junction reproducible and well defined, and it simplifies the calculation of the integral in eqn. (5), and diffusion data are not needed. It is reasonable to assume that this type of liquid junction will give the same potential as the one usually made. An experimental test of the above assumptions is now in progress. Similar assumptions were made in a previous paper by Førland and Østvold [6] where the emf of a concentration cell containing a KCl salt bridge was calculated.

The major drop in t_K back to the value $\frac{1}{2}$ takes place in the region of the membrane. The quantities of salt coming to either side of the membrane is determined by the transport number, t_K, in the membrane. Due to the Donnan equilibrium established across the membrane μ_{KCl} is constant from one side to the other, and we do not have to know the transport number in the membrane to calculate the chemical work, ΔG_Q, caused by the charge transfer.

As the major part of the transport takes place in concentration ranges around $C_{KCl(1)}$ and since the activity coefficients are usually not known for

such systems, we may operate with low values of C_{KCl} and assume that the solutions are close to ideal. We will then have from eqn. (5) remembering that

$$t_K + t_{SO_4} = 1 - t_{Cl}$$

$$\begin{aligned}\Delta G_Q = &\int_a^b(\mu^\circ_{KCl} + RT\ln C_K C_{Cl})dt_{Cl} + \tfrac{1}{2}\int_a^b(\mu^\circ_{K_2SO_4} + RT\ln C_K{}^2 C_{SO_4})dt_{SO_4} \\ &- \int_b^e(\mu^\circ_{KCl} + RT\ln C_K C_{Cl})d(t_K + t_{SO_4}) - \int_b^e(\mu^\circ_{MCl} + RT\ln C_M C_{Cl})dt_M \\ &+ \tfrac{1}{2}\int_b^e(\mu^\circ_{K_2SO_4} + RT\ln C_K{}^2 C_{SO_4})dt_{SO_4} \qquad (6)\end{aligned}$$

or

$$\begin{aligned}\Delta G_Q = RT\{&\int_a^b \ln C_K C_{Cl}dt_{Cl} + \tfrac{1}{2}\int_a^b \ln C_K{}^2 C_{SO_4}dt_{SO_4} - \int_b^e \ln C_K C_{Cl}dt_K \\ &- \int_b^e \ln C_M C_{Cl}dt_M + \int_b^e(\tfrac{1}{2}\ln C_K{}^2 C_{SO_4} - \ln C_K C_{Cl})dt_{SO_4}\} \qquad (7)\end{aligned}$$

If we assume that the mobility ratios u_i/u_j of the ions K^+, M^+, SO_4^{2-}, and Cl^- are independent of the concentrations, the transport number of these ions will be simple functions of the concentrations. We thus have

$$t_K = \frac{u_K C_K}{u_K C_K + u_{Cl}C_{Cl} + u_M C_M + 2u_{SO_4}C_{SO_4}} \qquad (8)$$

and similarly for the other transport numbers. These transport numbers will change in the following regions of the galvanic cell; (a – b), (b – c), (c – d) and (d – e) (see Fig. 2). In the region (a – b) we have

$$dt_{Cl} = -\frac{2u_{K_2SO_4}u_{Cl}C_{K(3\,M)}}{[C_{K(3\,M)}u_{KCl} + 2C(u_{SO_4} - u_{Cl})]^2}dC \qquad (9)$$

$$dt_{SO_4} = \frac{2u_{KCl}u_{SO_4}C_{K(3\,M)}}{[C_{K(3\,M)}u_{KCl} + 2C(u_{SO_4} - u_{Cl})]^2}dC \qquad (10)$$

In these equations $u_{KCl} = u_K + u_{Cl}$, $u_{K_2SO_4} = u_K + u_{SO_4}$ and C is the concentration of SO_4^{2-} in the electrolyte. In the region (b – c) we have

$$dt_K = -\frac{u_K(C_{K(3\,M)}u_{MCl} + 2C_{SO_4}(u_{SO_4} - u_{Cl}))}{[C_{K(3\,M)}u_{KCl} + C(u_M - u_K) + 2C_{SO_4}(u_{SO_4} - u_{Cl})]^2}dC \qquad (11)$$

$$dt_M = \frac{u_M[C_{K(3\,M)}u_{KCl} + 2C_{SO_4}(u_{SO_4} - u_{Cl})]}{[C_{K(3\,M)}u_{KCl} + C(u_M - u_K) + 2C_{SO_4}(u_{SO_4} - u_{Cl})]^2}dC \qquad (12)$$

$$dt_{SO_4} = -\frac{2u_{SO_4}(u_M - u_K)C_{SO_4}}{[C_{K(3\,M)}u_{KCl} + C(u_M - u_K) + 2C_{SO_4}(u_{SO_4} - u_{Cl})]^2}dC \qquad (13)$$

In eqn. (11) to eqn. (13) $u_{MCl} = u_M + u_{Cl}$ and C is the concentration of M^+ in the electrolyte.

In the region (c – d) the M^+ and SO_4^{2-} concentrations are constant and we can express the variation the ionic transport numbers as functions of the variations in the concentration of K^+ ions.

We thus have

$$dt_K = \frac{u_K(C_M u_{MCl} + 2C_{SO_4}(u_{SO_4} - u_{Cl})}{[Cu_{KCl} + C_M u_{MCl} + 2C_{SO_4}(u_{SO_4} - u_{Cl})]^2} dC \quad (14)$$

$$dt_M = -\frac{C_M u_M u_{KCl}}{[Cu_{KCl} + C_M u_{MCl} + 2C_{SO_4}(u_{SO_4} - u_{Cl})]^2} dC \quad (15)$$

$$dt_{SO_4} = -\frac{2C_{SO_4} u_{SO_4} u_{KCl}}{[Cu_{KCl} + C_M u_{MCl} + 2C_{SO_4}(u_{SO_4} - u_{Cl})]^2} dC \quad (16)$$

In these equations C is the concentration of K^+ ions in the electrolyte.

Since potassium chloride is the only component transported across the membrane during charge transfer the integral from d to e in eqn. (7) can be simplified. Since μ_{KCl} is constant from one side of the membrane to the other, that part of the integral which is due to potassium chloride transport can be simplified to $-RT(t_{KCl(2)} - t_{KCl(1)}) \ln C_{K(1)} C_{Cl(1)}$. The metal chloride, MCl, is transported to the membrane at the left hand side and since the transport numbers of the metal ion is zero in the membrane the chemical work occurring at the membrane interface due to MCl-transport is given approximately by $-RT(-t_{MCl(1)}) \ln C_M C_{Cl(1)}$. The contribution to the integral from d to e in eqn. (7) from potassium sulfate transport is analogously given by $-RT(-t_{K,SO_4(1)}) \ln C_{K(1)}^2 C_{SO_4}$.

In the half cell on the right hand side the concentrations of potassium and chloride are equal and as a consequence of this t_K is constant in this region. Introducing these results and eqns. (8 – 16) into eqn. (7) gives the following equation for the change in Gibbs energy per Faraday for the cell reaction (see Appendix for calculations):

$$\Delta G_Q = RT\left[\ln\frac{C_{Cl(1)}}{C_{Cl(2)}} - \frac{u_{Cl} - \frac{1}{2}u_{SO_4}}{u_{Cl} - u_{SO_4}} \ln\left(1 - \frac{u_{SO_4} - u_{Cl}}{u_{Cl}} \frac{C_{SO_4}}{C_{K(3\,M)}}\right) + \ln\left(1 - \frac{C_M(u_{Cl} - u_M)}{2C_{K(3\,M)}u_{Cl} + 2C_{SO_4}(u_{SO_4} - u_{Cl})}\right)\right] \quad (17)$$

and the emf of the cell is

$$E = \frac{RT}{F}\left[\ln\frac{C_{Cl(2)}}{C_{Cl(1)}} + \frac{u_{Cl} - \frac{1}{2}u_{SO_4}}{u_{Cl} - u_{SO_4}} \ln\left(1 - \frac{u_{SO_4} - u_{Cl}}{u_{Cl}} \frac{C_{SO_4}}{C_{K(3\,M)}}\right) - \ln\left(1 - \frac{1}{2}\frac{C_M(u_{Cl} - u_M)}{C_{K(3\,M)}u_{Cl} + C_{SO_4}(u_{SO_4} - u_{Cl})}\right)\right] \quad (18)$$

The last two terms in this equation are very small since $C_{SO_4}^{2-}$ and C_M^+ are very small compared to 3 M and they can therefore probably be neglected in view of the approximation introduced by assuming ideal solution behaviour of the electrolyte. We thus obtain an equation for the emf of the cell which

is identical to an equation usually presented as the Donnan potential equation. This equation is, however, constructed by operating with single ion activities which are not measurable quantities and by neglecting processes taking place at the liquid junction of the KCl bridge (see, *e.g.*, Aidly [7]), processes which in this case are the major sources of free energy change contributing to the emf.

In the paper mentioned above by Førland and Østvold [1] the Donnan potential was calculated for the cell containing KCl and KR only. Zero mobility for the R^- ion in the membrane was assumed. The following result was obtained

$$E = \frac{RT}{F}\left[\ln\frac{C_{\mathrm{Cl}(2)}}{C_{\mathrm{Cl}(1)}} + \ln\left(1 + \frac{u_{\mathrm{R}} - u_{\mathrm{Cl}}}{2u_{\mathrm{Cl}}}\frac{C_{\mathrm{R}}}{C_{\mathrm{K}(3\,\mathrm{M})}}\right)\right] \qquad (19)$$

showing that the emf of the cell can be approximated by the first term in this equation as long as $C_{\mathrm{R}} \ll 3\,\mathrm{M}$. If we had used saturated KCl salt bridges in these emf calculations, the equation for the emf would have been slightly different, but the difference can be neglected in view of the ideal solution approximation used in the calculations.

Yuasa *et al.*[8] measured the emf of the cell

$$\mathrm{Hg} \mid \mathrm{Hg_2Cl_2} \mid \begin{matrix}\mathrm{KCl}\\(\mathrm{satd.})\end{matrix} \Vert \begin{matrix}\mathrm{K^+PSS^-}(x)\\ \mathrm{K^+Cl^-}\end{matrix} \mid \text{Membrane} \mid \mathrm{KCl\ (C)} \Vert \begin{matrix}\mathrm{KCl}\\(\mathrm{satd.})\end{matrix} \mid \mathrm{Hg_2Cl_2} \mid \mathrm{Hg}$$

where the membrane is permeable to water K^+ and Cl^- but not to the polystyrene-sulfonate ion. The emf of the cell was measured as a function of C (concentration of KCl in the right hand half cell) and X (concentration of potassium polystyrenesulfonate in the left hand half cell). Their results agree with eqn. (19) within 0.2 mV. Instead of making the emphasis on undefined or irrelevant local electric potential differences in the galvanic cell by the calculation of an emf, as is very frequently done, it is demonstrated in this paper that the emphasis should be on the gradients of chemical potential of neutral components of the cell and how the concentration of these components is changed by charge transfer, that means on the coupling between transport of charge and transport of components.

The method outlined above will be applied to other potential calculations related to biological membranes.

APPENDIX

When eqns. (8 – 16) are introduced into eqn. (7) and the integral over the membrane from d to e is calculated as outlined in the text, the change in Gibbs energy per Faraday in the above galvanic cell following the transfer of positive charge from the left to the right hand electrode at equilibrium conditions is given by the following equation:

$$\frac{\Delta G_Q}{RT} = -\frac{2u_{K_2SO_4}u_{Cl}C_{K(3\,M)}}{4(u_{SO_4}-u_{Cl})^2}\int_0^{C_{SO_4}}\frac{\ln C_{K(3\,M)}+\ln(C_{K(3\,M)}-2C)}{\left(C+\frac{u_{KCl}}{2(u_{SO_4}-u_{Cl})}C_{K(3\,M)}\right)^2}\mathrm{d}C$$

$$+\frac{u_{SO_4}C_{K(3\,M)}}{4(u_{SO_4}-u_{Cl})^2}\int_0^{C_{SO_4}}\frac{2\ln C_{K(3\,M)}+\ln C}{\left(C+\frac{u_{KCl}}{2(u_{SO_4}-u_{Cl})}C_{K(3\,M)}\right)^2}\mathrm{d}C$$

$$+\frac{u_K(C_{K(3\,M)}u_{MCl}+2C_{SO_4}(u_{SO_4}-u_{Cl})}{(u_M-u_K)^2}\times$$

$$\int_0^{C_M}\frac{\ln(C_{K(3\,M)}-C)+\ln(C_{K(3\,M)}-2C_{SO_4})}{\left(C+\frac{2C_{SO_4}(u_{SO_4}-u_{Cl})+C_{K(3\,M)}u_{KCl}}{u_M-u_K}\right)^2}\mathrm{d}C$$

$$-\frac{u_M[C_{K(3\,M)}u_{KCl}+2C_{SO_4}(u_{SO_4}-u_{Cl})]}{(u_M-u_K)^2}\times$$

$$\int_0^{C_M}\frac{\ln C+\ln(C_{K(3\,M)}-2C_{SO_4})}{\left(C+\frac{2C_{SO_4}(u_{SO_4}-u_{Cl})+C_{K(3\,M)}u_{KCl}}{u_M-u_K}\right)^2}\mathrm{d}C$$

$$-\frac{u_{SO_4}C_{SO_4}}{u_M-u_K}\int_0^{C_M}\frac{2\ln(C_{K(3\,M)}-C)+\ln C_{SO_4}}{\left(C+\frac{2C_{SO_4}(u_{SO_4}-u_{Cl})+C_{K(3\,M)}u_{KCl}}{u_M-u_K}\right)^2}\mathrm{d}C$$

$$+\frac{2u_{SO_4}C_{SO_4}}{u_M-u_K}\int_0^{C_M}\frac{\ln(C_{K(3\,M)}-C)+\ln(C_{K(3\,M)}-2C_{SO_4})}{\left(C+\frac{2C_{SO_4}(u_{SO_4}-u_{Cl})+C_{K(3\,M)}u_{KCl}}{u_M-u_K}\right)^2}\mathrm{d}C$$

$$-\frac{u_K[C_Mu_{MCl}+2C_{SO_4}(u_{SO_4}-u_{Cl})]}{u_{KCl}^2}\times$$

$$\int_{C_{K(3\,M)}-C_M}^{C_{K(1)}}\frac{\ln C+\ln(C+C_M-2C_{SO_4})}{\left(C+\frac{C_Mu_{MCl}+2C_{SO_4}(u_{SO_4}-u_{Cl})}{u_{KCl}}\right)^2}\mathrm{d}C$$

$$+\frac{C_Mu_M}{u_{KCl}}\int_{C_{K(3\,M)}-C_M}^{C_{K(1)}}\frac{\ln C_M+\ln(C+C_M-2C_{SO_4})}{\left(C+\frac{C_Mu_{MCl}+2C_{SO_4}(u_{SO_4}-u_{Cl})}{u_{KCl}}\right)^2}\mathrm{d}C$$

$$-\frac{C_{SO_4}u_{SO_4}}{u_{KCl}}\int_{C_{K(3\,M)}-C_M}^{C_{K(1)}}\frac{2\ln C+\ln C_{SO_4}}{\left(C+\frac{C_Mu_{MCl}+2C_{SO_4}(u_{SO_4}-u_{Cl})}{u_{KCl}}\right)^2}\mathrm{d}C$$

$$+\frac{2C_{SO_4}u_{SO_4}}{u_{KCl}}\int_{C_{K(3\,M)}-C_M}^{C_{K(1)}}\frac{\ln C+\ln(C+C_M-2C_{SO_4})}{\left(C+\frac{C_Mu_{MCl}+2C_{SO_4}(u_{SO_4}-u_{Cl})}{u_{KCl}}\right)^2}\,dC$$

$$+\ln C_{K(1)}C_{Cl(1)}\left(\frac{C_{K(1)}u_K+2C_{SO_4}u_{SO_4}}{C_{K(1)}u_{KCl}+C_Mu_{MCl}+2C_{SO_4}(u_{SO_4}-u_{Cl})}-\tfrac{1}{2}\right)$$

$$+\ln C_MC_{Cl(1)}\frac{C_Mu_M}{C_{K(1)}u_{KCl}+C_Mu_{MCl}+2C_{SO_4}(u_{SO_4}-u_{Cl})}$$

$$-\tfrac{1}{2}\ln C_{K(1)}{}^2C_{SO_4}\frac{2C_{SO_4}u_{SO_4}}{C_{K(1)}u_{KCl}+C_Mu_{MCl}+2C_{SO_4}(u_{SO_4}-u_{Cl})} \qquad (A1)$$

When the above integrals are solved * the following result is obtained

$$\frac{\Delta G_Q}{RT}=\frac{2u_K(u_{SO_4}-u_{Cl})C_{SO_4}\ln C_{K(3\,M)}}{u_{KCl}[C_{K(3\,M)}u_{KCl}+2C_{SO_4}(u_{SO_4}-u_{Cl})]}-\frac{u_{Cl}}{u_{KCl}}\ln C_{K(3\,M)}$$

$$+\frac{u_{Cl}}{u_{SO_4}-u_{Cl}}\ln\left(1+\frac{2C_{SO_4}}{C_{K(3\,M)}}\,\frac{u_{SO_4}-u_{Cl}}{u_{KCl}}\right)$$

$$+u_{Cl}\frac{(C_{K(3\,M)}-2C_{SO_4})\ln(C_{K(3\,M)}-2C_{SO_4})}{C_{K(3\,M)}u_{KCl}+2C_{SO_4}(u_{SO_4}-u_{Cl})}$$

$$+u_{SO_4}\frac{C_{SO_4}\ln C_{SO_4}}{C_{K(3\,M)}u_{KCl}+2C_{SO_4}(u_{SO_4}-u_{Cl})}$$

$$-\tfrac{1}{2}\frac{u_{SO_4}}{u_{SO_4}-u_{Cl}}\ln\left(1+\frac{2C_{SO_4}}{C_{K(3\,M)}}\,\frac{u_{SO_4}-u_{Cl}}{u_{KCl}}\right)-\frac{u_Ma}{u_M-u_K}\left[\frac{C_M\ln C_M}{a(a+C_M)}\right.$$

$$\left.-\frac{1}{a}\ln\left(1+\frac{C_M}{a}\right)\right]-\frac{u_Kd}{(u_M-u_K)(C_{K(3\,M)}+a}\left[\frac{(C_{K(3\,M)}-C_M)\ln(C_{K(3\,M)}-C_M)}{C_M+a}\right.$$

$$\left.-\frac{C_{K(3\,M)}\ln C_{K(3\,M)}}{a}+\ln\left(1+\frac{C_M}{a}\right)\right]$$

$$+\frac{C_M}{a(u_K-u_M)}\left(u_{Cl}\frac{(C_{K(3\,M)}-2C_{SO_4})\ln(C_{K(3\,M)}-2C_{SO_4})}{C_M+a}+u_{SO_4}\frac{C_{SO_4}\ln C_{SO_4}}{C_M+a}\right)$$

$$-\frac{u_K}{u_{KCl}}\left(\frac{C_{K(1)}\ln C_{K(1)}}{C_{K(1)}+b}-\frac{(C_{K(3\,M)}-C_M)\ln(C_{K(3\,M)}-C_M)}{C_{K(3\,M)}-C_M+b}\right.$$

$$\left.+\ln\frac{C_{K(3\,M)}-C_M+b}{C_{K(1)}+b}\right)+\frac{u_{Cl}}{u_{KCl}}\left(\frac{C_{Cl(1)}\ln C_{Cl(1)}}{C_{K(1)}+b}\right.$$

$$\left.-\frac{(C_{K(3\,M)}-2C_{SO_4})\ln(C_{K(3\,M)}-2C_{SO_4})}{C_{K(3\,M)}-C_M+b}+\ln\frac{C_{K(3\,M)}-C_M+b}{C_{K(1)}+b}\right)$$

* To solve these integrals we used the equation

$$\int\frac{\ln x}{(a+x)^2}\,dx=\frac{x\ln x}{a(a+x)}-\frac{1}{a}\ln(a+x)$$

$$+\frac{u_{SO_4}C_{SO_4}\ln C_{SO_4}}{C_{K(1)}u_{KCl}+C_M u_{MCl}+2C_{SO_4}(u_{SO_4}-u_{Cl})}$$
$$-\frac{u_{SO_4}C_{SO_4}\ln C_{SO_4}}{C_{K(3\,M)}u_{KCl}+C_M(u_M-u_K)+2C_{SO_4}(u_{SO_4}-u_{Cl})}$$
$$+\frac{u_M C_M\ln C_M}{C_{K(3\,M)}u_{KCl}+C_M(u_M-u_K)+2C_{SO_4}(u_{SO_4}-u_{Cl})}$$
$$-\frac{u_M C_M\ln C_M}{C_{K(1)}u_{KCl}+C_M u_{MCl}+2C_{SO_4}(u_{SO_4}-u_{Cl})}$$
$$-\frac{u_{SO_4}C_{SO_4}\ln C_{SO_4}-u_M C_M\ln C_M}{C_{K(1)}u_{KCl}+C_M u_{MCl}+2C_{SO_4}(u_{SO_4}-u_{Cl})}$$
$$+\left(\frac{C_{K(1)}u_K}{C_{K(1)}u_{KCl}+C_M u_{MCl}+2C_{SO_4}(u_{SO_4}-u_{Cl})}-\tfrac{1}{2}\right)\ln C_{K(1)}$$
$$+\tfrac{1}{2}\frac{C_{K(1)}(u_K-u_{Cl})+C_M(u_M-u_{Cl})+2C_{SO_4}(u_{SO_4}-u_{Cl})}{C_{K(1)}u_{KCl}+C_M u_{MCl}+2C_{SO_4}(u_{SO_4}-u_{Cl})}\ln C_{Cl(1)} \qquad \text{(A2)}$$

In this equation

$$a=\frac{C_{K(3\,M)}u_{KCl}+2C_{SO_4}(u_{SO_4}-u_{Cl})}{u_M-u_K},\quad b=\frac{C_M u_{MCl}+2C_{SO_4}(u_{SO_4}-u_{Cl})}{u_{KCl}}$$

and $$d=\frac{C_{K(3\,M)}u_{MCl}+2C_{SO_4}(u_{SO_4}-u_{Cl})}{u_M-u_K}$$

In aqueous electrolytes $u_{Cl}\simeq u_K$. If this approximation is introduced in the above equation and terms with the same logaritmic functions are gathered, the following result is obtained

$$\frac{\Delta G_Q}{RT}=\tfrac{1}{2}\ln\frac{C_{Cl(1)}}{C_{K(1)}}-\frac{u_{Cl}-\frac{1}{2}u_{SO_4}}{u_{Cl}-u_{SO_4}}\ln\left(1-\frac{u_{SO_4}-u_{Cl}}{u_{Cl}}\frac{C_{SO_4}}{C_{K(3\,M)}}\right)$$
$$+\ln\left(1-\tfrac{1}{2}\frac{C_M(u_{Cl}-u_M)}{C_{K(3\,M)}u_{Cl}+C_{SO_4}(u_{SO_4}-u_{Cl})}\right) \qquad \text{(A3)}$$

The Donnan equilibrium is established across the membrane, and the chemical potential of potassium chloride is therefore the same on both sides of the membrane. Using eqn. (1) we get

$$\frac{C_{Cl(1)}}{C_{K(1)}}=\frac{C^2_{Cl(1)}}{C_{K(1)}C_{Cl(1)}}=\frac{C^2_{Cl(1)}}{C^2_{Cl(2)}} \qquad \text{(A4)}$$

Combining eqns. (A3 and A4) we have

$$E=-\frac{\Delta G_Q}{F}=\frac{RT}{F}\left[\ln\frac{C_{Cl(2)}}{C_{Cl(1)}}+\frac{u_{Cl}-\frac{1}{2}u_{SO_4}}{u_{Cl}-u_{SO_4}}\ln\left(1-\frac{u_{SO_4}-u_{Cl}}{u_{Cl}}\frac{C_{SO_4}}{C_{K(1\,M)}}\right)\right.$$
$$\left.-\ln\left(1-\tfrac{1}{2}\frac{C_M(u_{Cl}-u_M)}{C_{K(3\,M)}u_{Cl}+C_{SO_4}(u_{SO_4}-u_{Cl})}\right)\right] \qquad \text{(A5)}$$

Since the concentration of metal chloride and potassium sulfate is very small compared to 3 M, the electromotive force of the above cell can be expressed by the equation

$$E = \frac{RT}{F} \ln \frac{C_{Cl(2)}}{C_{Cl(1)}} \qquad (A6)$$

REFERENCES

1. Førland, T. and Østvold, T. *Electrochim. Acta. Submitted for publication.*
2. Donnan, F. G. and Guggenheim, E. A. *Z. Phys. Chem. Leipzig* **162** (1932) 346.
3. Babcock, K. L. and Overstreet, R. *Science* **117** (1953) 686.
4. Førland, T. *Acta Chem. Scand.* **14** (1960) 1381.
5. Førland, T., Thulin, L. U. and Østvold, T. *J. Chem. Educ.* **48** (1971) 741.
6. Førland, T. and Østvold, T. *Trans. Royal Inst. Technol.* Stockholm, Sweden; *Pure Appl. Chem.* **34** (1972) 585.
7. Aidley, D. J. *The Physiology of Excitable Cells*, Cambridge University Press 1971, pp. 13–36.
8. Yuasa, M., Kobatake, Y. and Fujita, H. *J. Phys. Chem.* **72** (1968) 2871.

Received January 29, 1973.

ACTA CHEMICA SCANDINAVICA 27 (1973) 2211–2216

The Contribution of Charge Fluctuation at the Second Virial Coefficients of Human Serum Albumin

JØRGEN F. HANSEN*

Department of Blood Fractionations, Statens Seruminstitut, DK-2300 Copenhagen S, Denmark

The second virial coefficients of human serum albumin at zero charge in 0.01 to 0.1 M sodium acetate have been obtained by osmotic pressure measurements, and found to be considerably smaller than expected from the contribution of the non-electrostatic excluded volume. The discrepancy can, however, be explained when the effect of charge fluctuation is taken into consideration.

The second virial coefficient of serum albumin in salt solution has been considered as the sum of the non-electrostatic excluded volume and the Donnan term.[1,2] However, it has not been possible to explain the low value of the second virial coefficient measured at zero charge.[2]

In this work measurements of the second virial coefficient at zero charge in 0.01 – 0.1 M sodium acetate has been compared with values obtained by theoretical expressions. In these expressions account has been taken of the non-electrostatic excluded volume, and of the effect of the charge fluctuation from the protein molecules. The charge fluctuation is due to local fluctuations in the binding of ions – especially hydrogen ions – to the protein molecules. It is known that in isoionic salt-free solutions the charge fluctuation gives a considerable contribution to the osmotic pressure.[2–5] However, in salt solutions the contribution has until now been considered negligible compared to the non-electrostatic excluded volume.

EXPERIMENTAL

Material. Human serum albumin from Statens Seruminstitut, Copenhagen, Denmark. Lot Asf 700527, fractionated according to Cohn's 6th method. The contents of dimer was 5 %, determined by polyacrylaminelectrophoresis.

Measurements of the osmotic pressure. The osmometer was the type described by Tybjærg-Hansen,[6] thermostated to 25.0 ± 0.1°C. Sartorius membrane type SM 11536 was used. The membrane was completely tight to serum albumin. pH was measured on

* Present address: Steno Hospital and Nordisk Insulinlaboratorium, Research Laboratory, Ved Stadion 2, DK-2820 Gentofte, Denmark.

a Radiometer Titrator TTT 1e, calibrated with a Radiometer standard buffer S 1201 (pH 6.5 at 20.0°C) and S 1221 (pH 4.65 at 20.0°C).

Conductivity was measured on a Philips Conductivity Meter Type PR 9501 with Celle PR 9513, calibrated with 0.100 M KCl (Merck *p.a.*).

Deionization was performed on a mixed bed ion-exchanger Amberlite IR 120 and IRA 400. Column: 3.5 × 10 cm. Flow rate 1 ml/min.

Serum albumin concentrations were determined spectrophotometrically, E_{280} (1 %, 1 cm): 5.5 ± 1 %. This value was determined by the Kjeldahl method. The content of nitrogen in human serum albumin is taken as 16 %.

RESULTS

Measurement of charge fluctuation of human serum albumin. The measurement of the osmotic pressure of human serum albumin in isoionic salt-free solutions is shown in Table 1.

Table 1. Osmotic pressure of human serum albumin in isoionic salt-free solution. 25.0°C.

c g/ml	$10^{-2}(\pi/c)$ measured values cm_{H_2O} ml/g	pH	Corrections excluded volume cm_{H_2O} ml/g × 10^{-2}	Corrections progressive ionisation cm_{H_2O} ml/g × 10^{-2}	$10^{-2}(\pi/c)$ corrected values cm_{H_2O} ml/g
0.0228	2.80	5.05	0.24	0.02	2.54
0.0149	3.02	5.08	0.16	0.03	2.83
0.0113	3.12	5.10	0.12	0.04	2.96
0.0074	3.31	5.12	0.08	0.05	3.18
0.0045	3.45	5.14	0.05	0.07	3.33
0.0030	3.51	5.15	0.03	0.10	3.38
0.0020	3.75	5.17	0.02	0.14	3.59

After correction of the measured osmotic pressure for the non-electrostatic excluded volume and the progressive ionisation, Timasheff *et al.*[5] have shown that in isoionic salt-free solution the osmotic pressure divided by the serum albumin concentration can be expressed by the following equation:

$$\frac{\pi}{c} = \frac{RT}{\langle M_n \rangle}\left(1 - \frac{\pi N \varepsilon^3 (\bar{Z}^2)^{3/2}}{3(DkT)^{3/2}\langle M_n \rangle^{1/2}} c^{1/2}\right) \quad (1)$$

π, the osmotic pressure;
c, protein concentration in g/ml;
R, the gas constant;
T, the absolute temperature;
$\langle M_n \rangle$, the number average molecular weight;
N, Avogadro's number;
ε, the charge of the hydrogen ion;
$(\bar{Z}^2)^{1/2}$, the charge fluctuation of the protein molecules;
D, the dielectric constant of water;
k, the constant of Boltzmann.

The corrections shown in Table 1 are calculated by the following equations:

The non-electrostatic volume:

$$\frac{RT}{\langle M_n \rangle} 4\bar{v}_{sp} c \tag{2}$$

Serum albumin is here supposed to be an impermeable sphere. $\bar{v}_{sp}$ is the partial specific volume of serum albumin, taken to be 0.735 ml/g.[7]

The progressive ionisation, including the Donnan term, is:

$$\frac{RT}{\langle M_n \rangle} 2\langle M_n \rangle S(\sqrt{1 + ([H^+/2S)^2} - 1)\frac{1}{c} \tag{3}$$

S, salt concentration in the non-protein solution of the osmometer.

Eqn. 3 is derived from the conditions of electroneutrality, and equal salt activity on both sides of the membrane.

$[H^+]$ is calculated from the pH values of Table 1.

S could not be measured directly. The value used has been calculated from the conductivity of water deionised on the same column as the serum albumin. The conductivity was 1.3×10^{-6} mho. Using the equivalent conductance of NaCl, S is 1×10^{-5} mol/l. This value is in agreement with the one used by Timasheff *et al.*[5]

$\langle M_n \rangle = 70\,000$ g/mol is taken from Table 2.

The corrected π values are obtained by subtracting the corrections from the measured values.

In Fig. 1 the corrected osmotic pressures are plotted as a function of the square root of the serum albumin concentration. The shown straight line is calculated according to the method of least squares.

$\langle M_n \rangle$ is found to 64 000 g/mol. A charge fluctuation of 4.07 is calculated from the slope and eqn. 1. The values determined by Timasheff *et al.*[5] are from 3.5 to 4.0, depending on the preparation of serum albumin.

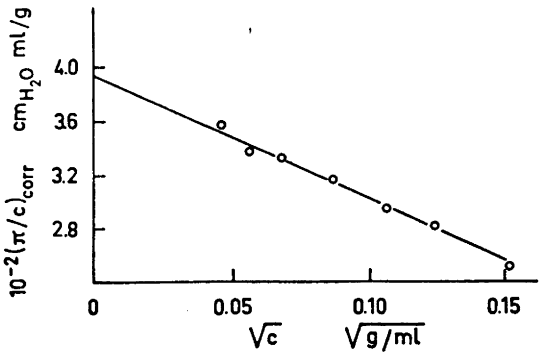

Fig. 1. The corrected osmotic pressures of human serum albumin in isoionic salt-free solutions, plotted as function of the square root of protein concentration. 25.0°C.

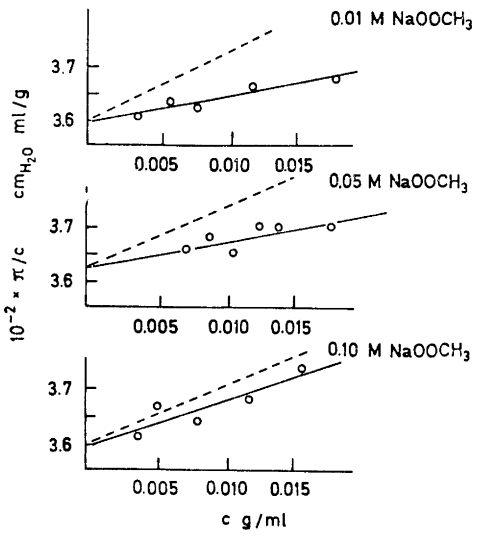

Fig. 2. Osmotic pressure of human serum albumin at zero charge in solutions of sodium acetate. 25.0°C. The dotted lines represent $\Gamma_2 = 3$ ml/g.

The second virial coefficient measured in sodium acetate solutions at zero charge. The concentration-dependence of the osmotic pressure in dilute solution of serum albumin can be expressed by the equation:

$$\frac{\pi}{c} = \frac{RT}{\langle M_n \rangle}(1 + \Gamma_2 c) \tag{4}$$

Γ_2, the second virial coefficient.

Fig. 2 shows measurements of osmotic pressure of human serum albumin in sodium acetate solutions at zero charge.

As π/c depends linearly on c, eqn. (4) can be used to calculate Γ_2.

The straight lines shown in Fig. 2 are calculated according to the least squares method.

Γ_2^{m} in Table 2 is calculated from the slope of the straight lines.

Table 2. Parameters derived from osmotic pressure measurements of human serum albumin in sodium acetate at zero charge.

	Measured values					Calculated values			
I	pH	$\bar{Z}$	$\langle M_n \rangle$ g/mol	Γ_2^{m} ml/g	Γ_2^{ms}[a] ml/g	Term of excluded volume ml/g	Donnan term ml/g	Term of charge fluctuation ml/g	Γ_2^{c} ml/g
0.10	4.75	0	70 100	2.4	2.0	3.0	0	−1.0	2.0
0.05	4.76	0	69 700	1.1	1.6	3.0	0	−2.1	0.9
0.01	4.96	0	70 300	1.3	0.9	3.0	0	−5.0	−2.0

[a] Γ_2^{ms}, values calculated with $\langle M_n \rangle = 70\,000$ g/ml.

The molecular weight is obtained from the intercept on the ordinate axis.

The isoelectric points shown in Table 2 are obtained from measurements on bovine serum albumin in sodium acetate.[6] These isoelectric pH values are supposed to be applicable for human serum albumin, as Tanford *et al.*[9] could find no differences in the number and distribution of the acid and the basic groups of the two serum albumins.

Γ_2^m is below 3 ml/g. Statistical analyses show that Γ_2 measured in 0.05 and 0.01 M sodium acetate are different from $\Gamma_2 = 3$ ml/g at 99 % level, and that Γ_2 measured in 0.1 M is different at 75 % level. 3 ml/g is the values expected at zero charge, when only the non-electrostatic excluded volume is considered.[2]

Γ_2^m is in accordance with the measurements of Scatchard *et al.*,[10] see also Tanford.[2] In addition they agree with the measurements of Timasheff *et al.*[5] as they also find decreasing values with decreasing ionic strength.

The equation for the osmotic pressure of serum albumin in salt solution at zero charge is, when the term of charge fluctuation is taken into account:[11,12]

$$\frac{\pi}{c} = \frac{RT}{\langle M_n \rangle}\left(1 + 4\bar{v}_{sp}c - \frac{\pi N \varepsilon^3 (\bar{Z}^2)^2 \sqrt{1000}}{4\sqrt{2}\,(DkT)^{3/2}\sqrt{I}\,\langle M_n \rangle\,(1 + a\varkappa)^2}c\right) \quad (5)$$

a is the Debye-Hückel parameter.

$$\varkappa^2 = \frac{4\pi N \varepsilon^2}{DkT}\left(\frac{2I}{1000} + \frac{\bar{Z}^2 c}{\langle M_n \rangle}\right) \quad (6)$$

I, the ionic strength of the salt.

The first term in eqn. (6) expresses the contribution of the salt ions to the screening of the electric potential between the protein molecules. The second term expresses the contribution of the protein molecules. The Γ_2^c shown in Table 2 is obtained from eqns. (5, 6) by use of the following values: $\bar{v}_{sp} = 0.735$ ml/g;[7] $a\varkappa$, the values calculated for pure salt solutions, are applied. This means that screening of protein molecules is neglected.

The values for $1/(1 + a\varkappa)$ are:

in 0.10 M salt 0.56
0.05 M salt 0.77
0.01 M salt 0.82

$\langle M_n \rangle = 70\,000$ g/mol.

$(\bar{Z}^2) = 16.5$. This value is the one obtained from measurements of osmotic pressure in isoionic salt-free solution. The use of this value is supposed to be a good approximation in sodium acetate solutions. The reason is that acetate ions are weakly bound to serum albumin.[13]

DISCUSSION

The non-electrostatic excluded volume in Table 2 is determined assuming that serum albumin is an impermeable sphere. However, serum albumin is shown to be an ellipsoid with axial ratio of about 4.[2] This means that the non-electrostatic excluded volume must exceed 3 ml/g. If this is the case the

discrepancy between the experimental Γ_2 and the values calculated from the non-electrostatic excluded volume may be even greater than previously assumed.

In the isoionic salt-free solution a molecular weight of 64 000 g/mol is obtained. This is less than the 70 000 g/mol measured in sodium acetate solutions. Furthermore from Table 2 it follows that at low ionic strength the Γ_2^c is smaller than the Γ_2^m. These two discrepancies are at least partly caused by the approximate value of S in the correction for progressive ionisation. If S is 0.2×10^{-5} mol/l a molecular weight of 69 000 g/mol and a charge fluctuation of 3.85 are obtained. If these values are used in the calculations of Table 2, the term for the charge fluctuation will increase with approximately 20 % and the differences between Γ_2^m and Γ_2^c become less pronounced.

To obtain a better accordance between the measured and calculated values of second virial coefficients, more accurate determinations of the ionic strength and the Debye-Hückel parameters will be necessary.

CONCLUSION

By including the term of charge fluctuations at least a qualitative agreement between the measured and calculated values of the second virial coefficients in salt solutions has been obtained. It is concluded that the charge fluctuation gives a non-vanishing contribution to the second virial coefficient in salt solutions.

REFERENCES

1. Scatchard, G. and Pigliacampi, J. *J. Am. Chem. Soc.* **84** (1961) 127.
2. Tanford, C. *Physical Chemistry of Macromolecules*, Wiley, New York 1961, Chapters 14, 23 d.
3. Timasheff, S. N., Dintzis, H. M., Kirkwood, J. G. and Coleman, B. D. *Proc. Nat. Acad. Sci. U.S.* **41** (1955) 710.
4. Kirkwood, J. G. and Timasheff, S. N. *Arch. Biochem. Biophys.* **65** (1956) 50.
5. Timasheff, S. N., Dintzis, H. M., Kirkwood, J. G. and Coleman, B. D. *J. Am. Chem. Soc.* **79** (1957) 782.
6. Tybjærg-Hansen, A. *Acta Physiol. Scand.* **53** (1961) 197.
7. Charlwood, P. A. *J. Am. Chem. Soc.* **79** (1957) 776.
8. Longsworth, L. G. and Jacobsen, C. F. *J. Phys. Colloid. Chem.* **53** (1949) 1261.
9. Tanford, C., Swanson, S. A. and Shore, W. S. *J. Am. Chem. Soc.* **77** (1955) 6414.
10. Scatchard, G., Batchelder, A. C. and Brown, A. *J. Am. Chem. Soc.* **68** (1946) 2320.
11. Kirkwood, J. G. and Shumaker, J. B. *Proc. Nat. Acad. Sci. U.S.* **38** (1952) 863.
12. Hill, T. *Introduction to Statical Thermodynamics*, Addison Wesley, London 1960, Chapters 18, 19.
13. Teresi, S. D. and Luck, J. M. *J. Biol. Chem.* **194** (1952) 823.

Received January 23, 1973.

ACTA CHEMICA SCANDINAVICA 27 (1973) 2217–2256

Short Communications

Oxidation of Carbohydrate Derivatives with Silver Carbonate on Celite. IX. Oxidation of 1,2-*O*-Isopropylidene-α-D-glucofuranose

SVEIN MORGENLIE

Agricultural University, Department of Chemistry, N-1432 Ås-NLH, Norway

In previous papers in this series, oxidation of ketoses,[1,2] aldoses,[3,4] and derivatives of aldoses [5–7] with silver carbonate on Celite has been described. At temperatures below 60°C, the oxidant seems to have negligible effect on nonreducing carbohydrate derivatives. In boiling methanol, however, some 1,2-*O*-isopropylidene derivatives of aldohexofuranoses have been found to undergo a slow oxidation, involving the exocyclic glycol group. The present paper reports the oxidation of 1,2-*O*-isopropylidene-α-D-glucofuranose (I) to methyl 1,2-*O*-isopropylidene-α-D-xylofuranuronate (II).

After 10 h in boiling methanol, 1,2-*O*-isopropylidene-α-D-glucofuranose (I) is completely oxidized by silver carbonate on Celite, and the xyluronic acid derivative

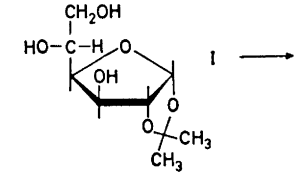

I →

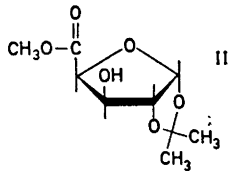

II

(II) is the only product, obtained in about 70 % yield. Small amounts of an other compound are chromatographically detectable during the course of the reaction. This compound undergoes, however, a relatively rapid further oxidation, and it is presumably an intermediate in the oxidation of 1,2-*O*-isopropylidene-α-D-glucofuranose (I) to the xyluronic acid derivative (II).

The physical data of the product are in good agreement with those previously reported for methyl 1,2-*O*-isopropylidene-α-D-xylofuranuronate.[8] The identity is further established by borohydride reduction and subsequent acid hydrolysis to xylose, and by spectroscopy. The proton magnetic resonance spectrum shows coupling constants $J_{1,2} = 3.5$ Hz, $J_{2,3} < 0.5$ Hz, and $J_{3,4} = 3.0$ Hz, in good agreement with those reported for other 1,2-*O*-isopropylidene-furanoses with *xylo*-configuration. The small coupling constant between the *trans* oriented protons at C-2 and C-3 is generally observed in spectra of this type of compounds.[9]

A more detailed investigation of this reaction and its applicability to analogous compounds is in progress.

Experimental. Paper chromatography was run on Whatman No. 1 paper in the solvent system (v/v) butanol-pyridine-water 5:3:2, thin layer chromatography on silica gel G plates in benzene-ethanol 4:1, and electrophoresis on Whatman No. 1 paper in borate buffer, pH 10. The proton magnetic resonance spectrum was recorded on a Varian HA-100 spectrometer.

Oxidation of 1,2-O-isopropylidene-α-D-glucofuranose (I). 1,2-*O*-Isopropylidene-α-D-glucofuranose (I) (500 mg) was stirred in boiling methanol (250 ml) with silver carbonate on Celite [10] (12 g) for 5 h. More oxidant (5–6 g) was then added, and the oxidation continued until thin layer chromatography showed complete oxidation of the starting material (3–4 h). A single spot was observed on the thin layer plate, detectable with diphenyl-

amine-aniline-phosphoric acid[11] as well as with hydroxylamine-ferric chloride.[12] The solution was filtered, the solvent evaporated and the residue extracted with chloroform. Evaporation of the chloroform gave crystalline methyl 1,2-*O*-isopropylidene-α-D-xylofuranuronate (II) (337 mg, 68 %). After sublimation *in vacuo*, it had m.p. 104–106°C (lit.[8] 103–104°C), and $[\alpha]_D$ −30° (*c* 2, methanol) (lit.[8] −32.8°). Strong infrared absorption was observed at 1745 cm^{-1} (KBr), NMR signals were located at δ 1.30, 1.46, 3.74 (3 protons, singlets), 2.42 (1 proton, broad), 4.39, 4.48, 4.68, 5.95 (1 proton, doublets).

The product (20 mg) in water (3 ml) was treated with sodium borohydride (100 mg) over night. The solution was then treated with Dowex 50 W ion exchanger (H^+), filtered and the solvent evaporated. Boric acid was removed by repeated distillations of methanol from the residue, which subsequently was hydrolyzed in 30 % acetic acid for 4 h at 100°C. Removal of the water and acetic acid under reduced pressure gave a syrup which appeared homogeneous by paper chromatography and electrophoresis, indistinguishable from authentic xylose.

Acknowledgments. The author is indebted to Miss Astrid Fosdahl for skilled technical assistance, and to Mrs. Grete Wöien Larsen for assistance with NMR spectroscopy.

1. Morgenlie, S. *Acta Chem. Scand.* **26** (1972) 2146.
2. Morgenlie, S. *Acta Chem. Scand.* **27** (1973) 1557.
3. Morgenlie, S. *Acta Chem. Scand.* **26** (1972) 1709.
4. Morgenlie, S. *Acta Chem. Scand. To be published.*
5. Morgenlie, S. *Acta Chem. Scand.* **25** (1971) 1154.
6. Morgenlie, S. *Acta Chem. Scand.* **25** (1971) 2773.
7. Morgenlie, S. *Acta Chem. Scand.* **26** (1972) 2518.
8. Reichstein, T., Pedolin, A. and Grüssner, A. *Helv. Chim. Acta* **18** (1935) 598.
9. Abraham, R. J., Hall, L. D., Hough, L. and McLauchlan, K. A. *J. Chem. Soc.* **1962** 3699.
10. Balogh, V., Fetizon, M. and Golfier, M. *Angew. Chem.* **81** (1969) 423.
11. Schwimmer, S. and Bevenue, A. *Science* **123** (1956) 543.
12. Abdel-Akher, M. and Smith, F. *J. Am. Chem. Soc.* **73** (1951) 5859.

Received June 22, 1973.

Formation and Crystal Structure of 3,3′-Spirobi(3-selenaphthalide)

BIRGITTA DAHLÉN[a] and BJÖRN LINDGREN[b]

[a] *Crystallography Group, Swedish Medical Research Council Unit for Molecular Structure Analysis, University of Göteborg, Fack, S-400 33 Göteborg 33, Sweden, and* [b] *Institute of Chemistry, University of Uppsala, Box 531, S-751 21 Uppsala 1, Sweden*

The 3,3′-spirobi(3-selenaphthalide) (II) was first synthesized by Lesser and Weiss[1] by warming 2,2′-dicarboxy-diphenyl selenide (I) with concentrated sulphuric acid. This synthesis has now been re-investigated. Compound II has also been obtained when oxidizing I with hydrogen peroxide in acetic acid (Scheme 1). Infrared spectra and elemental analysis data of II are in good agreement with the proposed spiro-dilactone structure.

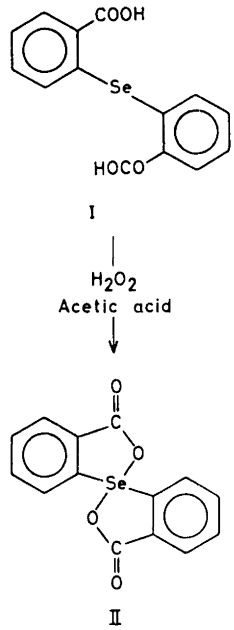

Scheme 1.

The analogous spiro-thia-dilactone has recently been synthesized and its crystal structure determined.[2,3]

amine-aniline-phosphoric acid[11] as well as with hydroxylamine-ferric chloride.[12] The solution was filtered, the solvent evaporated and the residue extracted with chloroform. Evaporation of the chloroform gave crystalline methyl 1,2-*O*-isopropylidene-α-D-xylofuranuronate (II) (337 mg, 68 %). After sublimation *in vacuo*, it had m.p. 104–106°C (lit.[8] 103–104°C), and $[\alpha]_D$ −30° (*c* 2, methanol) (lit.[8] −32.8°). Strong infrared absorption was observed at 1745 cm^{-1} (KBr), NMR signals were located at δ 1.30, 1.46, 3.74 (3 protons, singlets), 2.42 (1 proton, broad), 4.39, 4.48, 4.68, 5.95 (1 proton, doublets).

The product (20 mg) in water (3 ml) was treated with sodium borohydride (100 mg) over night. The solution was then treated with Dowex 50 W ion exchanger (H^+), filtered and the solvent evaporated. Boric acid was removed by repeated distillations of methanol from the residue, which subsequently was hydrolyzed in 30 % acetic acid for 4 h at 100°C. Removal of the water and acetic acid under reduced pressure gave a syrup which appeared homogeneous by paper chromatography and electrophoresis, indistinguishable from authentic xylose.

Acknowledgments. The author is indebted to Miss Astrid Fosdahl for skilled technical assistance, and to Mrs. Grete Wöien Larsen for assistance with NMR spectroscopy.

1. Morgenlie, S. *Acta Chem. Scand.* **26** (1972) 2146.
2. Morgenlie, S. *Acta Chem. Scand.* **27** (1973) 1557.
3. Morgenlie, S. *Acta Chem. Scand.* **26** (1972) 1709.
4. Morgenlie, S. *Acta Chem. Scand. To be published.*
5. Morgenlie, S. *Acta Chem. Scand.* **25** (1971) 1154.
6. Morgenlie, S. *Acta Chem. Scand.* **25** (1971) 2773.
7. Morgenlie, S. *Acta Chem. Scand.* **26** (1972) 2518.
8. Reichstein, T., Pedolin, A. and Grüssner, A. *Helv. Chim. Acta* **18** (1935) 598.
9. Abraham, R. J., Hall, L. D., Hough, L. and McLauchlan, K. A. *J. Chem. Soc.* **1962** 3699.
10. Balogh, V., Fetizon, M. and Golfier, M. *Angew. Chem.* **81** (1969) 423.
11. Schwimmer, S. and Bevenue, A. *Science* **123** (1956) 543.
12. Abdel-Akher, M. and Smith, F. *J. Am. Chem. Soc.* **73** (1951) 5859.

Received June 22, 1973.

Formation and Crystal Structure of 3,3′-Spirobi(3-selenaphthalide)

BIRGITTA DAHLÉN[a] and BJÖRN LINDGREN[b]

[a] *Crystallography Group, Swedish Medical Research Council Unit for Molecular Structure Analysis, University of Göteborg, Fack, S-400 33 Göteborg 33, Sweden, and* [b] *Institute of Chemistry, University of Uppsala, Box 531, S-751 21 Uppsala 1, Sweden*

The 3,3′-spirobi(3-selenaphthalide) (II) was first synthesized by Lesser and Weiss[1] by warming 2,2′-dicarboxy-diphenyl selenide (I) with concentrated sulphuric acid. This synthesis has now been re-investigated. Compound II has also been obtained when oxidizing I with hydrogen peroxide in acetic acid (Scheme 1). Infrared spectra and elemental analysis data of II are in good agreement with the proposed spiro-dilactone structure.

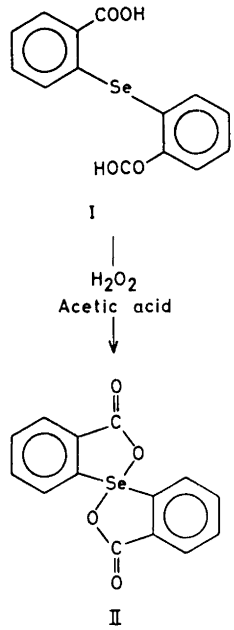

Scheme 1.

The analogous spiro-thia-dilactone has recently been synthesized and its crystal structure determined.[2,3]

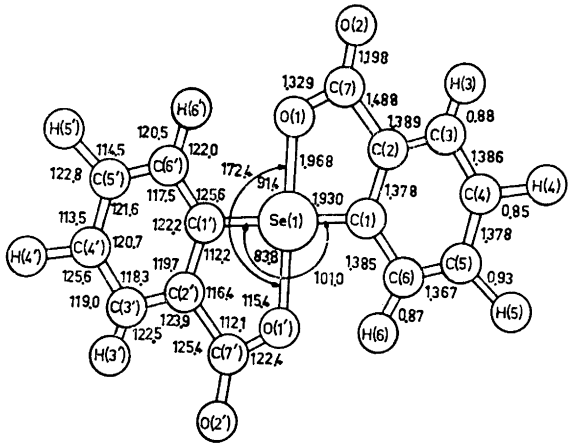

Fig. 1. Bond lengths and angles.

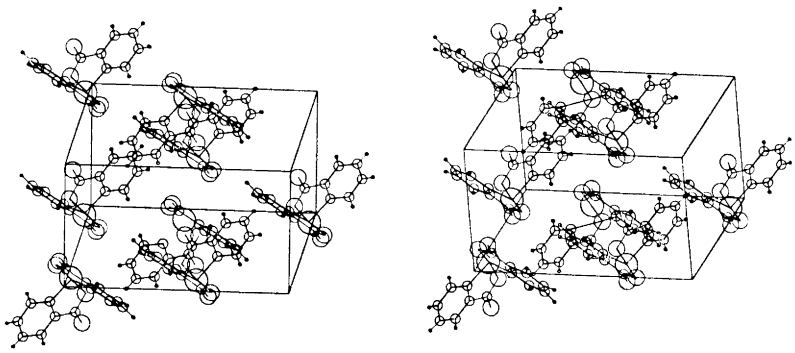

Fig. 2. Stereoscopic pair of 3,3′-spirobi(3-selenaphthalide) viewed along the *c* axis.

A number of papers dealing with similar problems have been published recently. An aliphatic spiro-selena-dilactone has been isolated by oxidizing 3,3′-selenodipropionic acid.[4] The 2-carboxyphenyl methyl sulphoxide and selenoxide systems have been studied by one of us with reference to different interactions between the carboxy group and the sulphinyl and seleninyl groups, respectively.[5] Interactions have also been found in 2-nitrobenzene-seleninyl compounds between the selenium atom and an oxygen atom of the nitro group.[6]

The interatomic distances and angles of II are given in Fig. 1. The molecular packing is shown by a stereoscopic drawing in Fig. 2. The standard deviations of the bond lengths and angles involving non-hydrogen atoms are approximately 0.01 Å and 0.06° respectively.

The two identical halves of the molecule are related by a twofold axis with the selenium atom located on the axis. The configuration around the selenium atom is a trigonal bipyramid very similar to that found in the sulphur analogue.[2] The dihedral angle between the best planes through the two benzene rings is 102.7°. The corresponding angle in the sulphur analogue is 106.7°.

The O – Se – O angle is 172.4° and the value obtained in the sulphur compound is 178.5°. These values are in good agreement with other values reported for O – Se – O,[5] O – S – O,[3,5,6] and S – Se – O [7]

angles which are all close to 180°. The configuration around the selenium atom is also similar to that found in 2-carboxyphenyl methyl selenoxide [5] where a ring closure has taken place by migration of the hydrogen atom from the carboxyl group to the selenoxide oxygen.

The Se–C distance is 1.930(7) Å which is normal for Se–C single bonds.[5,8] The Se–O bond is 1.968 Å which is considerably longer than the Se–O 'normal' single bond of 1.774 Å found in 2-carboxyphenyl methyl selenoxide but it is much shorter than the corresponding Se–O bond of 2.378 Å in the latter compound. The shorter Se–O bond in this structure has lead to a substantial decrease of the valence angles in the five-membered ring.

The Se–O bond can not extend due to the short intramolecular contact between O(1) and H(6′) of 2.46 Å. The O(1)···C(6′) distance is 2.914 Å which is much shorter than the sum of the van der Waals radii which is approximately 3.2 Å [9] and this close C–H···O interaction may indicate a hydrogen bond.

Experimental. The selenium analyses were performed by a microanalytical method developed by Bengtsson [10] and very similar to that of Gould.[11] The melting points are uncorrected.

2,2′-Dicarboxy-diphenyl selenide (I). Sodium formaldehydesulphoxylate 4.2 g (0.027 mol) was added to a solution of 9.6 g (0.024 mol) unpurified 2,2′-dicarboxy-diphenyl diselenide [12,13] in 60 ml 2 M ammonia. The solution was discoloured upon the addition. 2-Iodobenzoic acid 12 g (0.048 mol) was dissolved in 30 ml 2 M ammonia and added to the discoloured solution. The mixture was heated together with 0.5 g of copper powder in a glass vessel immersed in an autoclave for 5–6 h at 160–180°C, then filtered and acidified. Yield 10 g (65 %). M.p. 210–217°C (d). The product can be recrystallized from acetic acid.

3,3′-Spirobi(3-selenaphthalide) (II). Hydrogen peroxide (30 %), 0.6 g (0.0053 mol), was added dropwise with cooling and stirring to a suspension of 1.6 g (0.005 mol) unpurified 2,2′-dicarboxy-diphenyl selenide (I) in 20 ml of acetic acid. After the addition the temperature of the reaction mixture was allowed to rise to room temperature standing over night. The product was filtered and dried. Yield 1.4 g (88 %). M.p. 310–322°C. The product was purified by dissolving in warm diluted sodium hydroxide and slowly acidifying the warm solution with diluted sulphuric acid. (Found: Se 24.65. $C_{14}H_8O_4Se$ requires: Se 24.73).

Crystal data. The compound crystallizes in the monoclinic spacegroup $C2/c$ with 4 molecules in the unit cell. The cell dimensions are $a = 13.646(2)$, $b = 8.639(3)$, $c = 10.034(2)$ Å, and $\beta = 96.64(2)°$; $D_c = 1.804$ g cm^{-3} and $D_m = 1.803$ g cm^{-3}. Intensity data were collected on a Picker FACS I automatic diffractometer using the Vanderbilt disc oriented diffractometer system by Dr. P. G. Lenhert. The reflexions were measured by step scanning using 8 steps of 2 sec with a step size of 0.3°. 891 intensities recorded were more than 2σ above background and used in the calculations. The structure was solved by the heavy atom method and refined by full matrix least-squares treatment. The final R-value is 0.043. Full details of the X-ray investigation will be published elsewhere.

Acknowledgements. We thank Prof. S. Abrahamsson, Prof. A. Fredga and Dr. L.-B. Agenäs for valuable discussions and for their interest in this project. Grants in support of the Crystallography Group were obtained from the *Swedish Medical* and the *Swedish Natural Science Research Councils*, the *Swedish Board for Technical Development*, the *Tricentennial Fund of the Bank of Sweden*, and the *U. S. Public Health Service* (GM-11653.)

1. Lesser, R. and Weiss, R. *Ber.* **47** (1914) 2510.
2. Kapovits, I. and Kálmán, A. *Chem. Commun.* **1971** 649.
3. Kálmán, A., Sasvári, K. and Kapovits, I. *Acta Cryst.* **B 29** (1973) 355.
4. Agenäs, L. -B. and Lindgren, B. *Acta Chem. Scand.* **24** (1970) 3301.
5. Dahlén, B. *Acta Cryst.* **B 29** (1973) 595.
6. Dahlén, B. *To be published.*
7. Eriksen, R. and Hauge, S. *Acta Chem. Scand.* **26** (1972) 3153.
8. Aleby, S. *Acta Cryst.* **B 28** (1972) 1509.
9. Pauling, L. *The Nature of the Chemical Bond*, Cornell Univ. Press, Ithaca 1960, p. 260.
10. Bengtsson, A. *To be published.*
11. Gould, E. S. *Anal. Chem.* **23** (1951) 1502.
12. Lesser, R. and Weiss, R. *Ber.* **46** (1913) 2640.
13. Schoeller, A. *Ber.* **52** (1919) 1517.

Received June 16, 1973.

On the Structure of Ethyl 4-Imidazolidone-2-acetate

OLOF CEDER and URBAN STENHEDE

Department of Organic Chemistry, University of Göteborg and Chalmers Institute of Technology, Fack, S-402 20 Göteborg 5, Sweden

Investigations on the 2-substituted 4-thiazolidone system have shown [1-3] that the $\Delta^{2\alpha}$-isomer *1a*, having an exocyclic double bond, is the predominating tautomer.* No trace of the Δ^{2}-thiazolidinone *1b* could be detected. The isolation of two geometrical isomers of *1a* (R = COOR′) has also been described.[2]

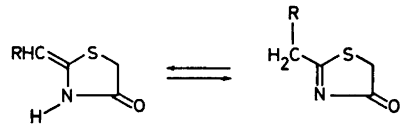

1a 1b

The present communication describes the synthesis of and similar investigations on the analogous 4-imidazolidone system *2*, for which four tautomeric structures, *2a*, *2b*, *2c*, and *2d* are possible.*

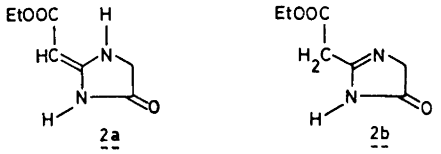

2a 2b

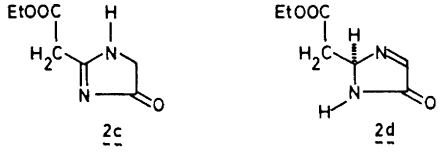

2c 2d

Condensation of ethyl carbethoxyacetimidate [4] and glycine ethyl ester gave the expected substance *2*. The IR spectrum contained two carbonyl bands (1730 and 1695 cm^{-1}; KBr) and NH absorption (3230 cm^{-1}, broad; 3510 and 3580 cm^{-1}, sharp; dioxane).

The NMR spectrum of *2* (in dimethyl sulfoxide-d_6) displayed two broad NH bands at 7.80 and 10.90 ppm, as well as unsplit olefinic and CH_2 (ring) absorption at 4.19 and 3.94 ppm, respectively. The last two bands overlap with the CH_2 quartet generated by the ethyl group. These data indicate that *2* exists as *2a* in dimethyl sulfoxide, and that only one geometrical isomer is present.

A solution of *2* in pyridine-d_5, however, gave rise to two identical, only slightly displaced, sets of signals in the ratio 1:6. Each set contained the same number and types of resonances as did the spectrum of *2* recorded in dimethyl sulfoxide. The chemical shifts (in pyridine-d_5) for the two olefinic proton signals are 4.79 and 4.82 ppm, respectively. These values are too close to be used for assignment of geometrical configurations. It is perhaps reasonable to predict, that the *Z* isomer *2a″*, containing a hydrogen bond involving the more acidic proton, would be the more stable isomer.

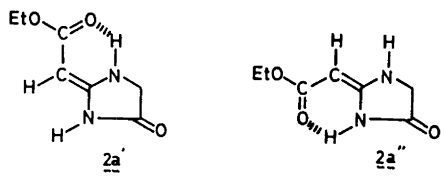

2a′ 2a″

The UV spectrum of *2* in ethanol (213 nm; $\varepsilon = 11\,900$ and 278 nm; $\varepsilon = 30\,000$) is very similar to that of *1a*.[2] The spectral changes observed for *2* on addition of base (228 nm; $\varepsilon = 16\,100$ and 295 nm; $\varepsilon = 45\,000$) and acid (282 nm; $\varepsilon = 8\,100$) are slightly different from those observed for *1a*.[2] We therefore propose the following equilibria to explain the acid-base behaviour of *2*.

Participation of the amide proton requires exchange of the olefinic proton in the presence of base. This has earlier been observed in *1a* [3] and is also found in *2* along with exchange of the ring-methylene protons when *2* is treated with D_2O and a base such as triethylamine or pyridine.

* Additional tautomeric structures can be written for *1* and *2*, but they do not contain a ring carbonyl group.

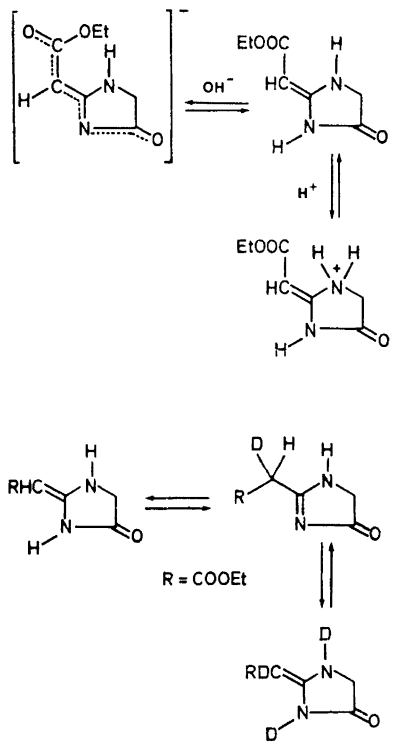

Our NMR investigations on the 4-imidazolidones were extended also to the 2-methyl and 2-benzylderivatives *3* and *4*, respectively. While our work was in progress, a detailed report [5] on the same subject appeared. We have arrived at essentially the same results as Jacquier *et al.*, namely that *3* and *4* have the double bond in the ring and not in the exocyclic position. Apparently, electron-withdrawing groups in the 2-position of the side chain stabilize the double bond in the exocyclic position. In *4*, the resonances for the benzylic and ring-methylene protons appear rather close to one another and Jacquier *et al.*[5] have assigned them δ-values of 4.05 and 3.77, resectively. Based on lanthanide-shift and spin-decoupling studies, we propose that these assignments should be reversed.

Addition of Eu(fod)$_3$-d_{27} [6] to a chloroform-*d* solution of *4* affected the two methylene resonances very differently. The induced shifts for the lower-field signal (4.05 ppm) is 14.0 ppm and for the higher-field signal (3.77 ppm) 6.3 ppm. The phenyl protons were divided into two groups with Δ_{Eu}-values of 2.3 and 1.0 ppm. Good, linear correlation between Δ_{Eu} and $(3\cos^2\theta_i - 1)/r_i^3$ (*cf.* Fig. 1) [7] is obtained for

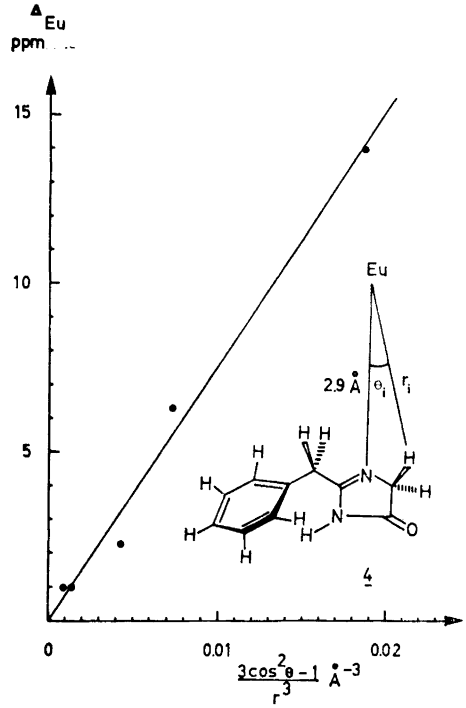

Fig. 1. Plots of the Δ_{Eu}-values for *4* *vs.* $(3\cos^2\theta - 1)/r^3$ and model showing the localization of the lanthanide ion in *4*.

all protons in *4* if the Eu-atom is placed at a distance of 2.9 Å from N-1 (*cf.* Fig. 1). The amide-proton signal is too broad to be followed. The diagram published by Wing *et al.*[8] was used, in combination with Dreiding models, to place the Eu-atom in a position which gave a good, over-all linear correlation. The angles θ_i and distances r_i were then refined by error computations. The results indicate that the methylene signal at 3.77 ppm should be assigned to the benzylic protons.

Further support for the above conclusion was rendered by double-resonance studies on *4*. Irradiation of the phenyl protons resulted in distortion of the higher-field

methylene triplet (3.77 ppm), while the lower-field one (4.05 ppm) remained unchanged. Finally, decoupling studies showed that the protons in the two methylene groups indeed coupled with each other.

Synthesis of ethyl 4-imidazolidone-$\Delta^{2,\alpha}$-acetate, 2. Ten g (0.097 mol) of glycine ethyl ester was slowly (*ca.* 20 min) added to 15.0 g (0.095 mol) of cold (0°C) carbethoxyacetimidic ethyl ester [4] in a 100 ml argon-flushed, three-necked, round-bottomed flask, equipped with a gas-inlet tube, a dropping funnel and a drying tube (magnesium sulfate). When the addition was complete, the gas stream was interrupted, the flask stoppered and kept at room temperature in the dark. After 24 h a brown, crystalline solid had precipitated. It was separated by filtration and triturated thoroughly, first with methylene chloride and then with diethyl ether. The brown solid was dried, then recrystallized four times from ethanol. Yield: 3.9 g (24 %) of brownish, flaky crystals. Sublimation of this material (140°C/1 torr) gave white crystals, which turned pink after a short exposure to air and/or light. Freshly sublimed samples were used for all measurements. M.p. 177–180°C, IR (KBr): 3380 (NH), 3300–3100 (NH), 1730 (ring C=O), 1695 (ester C=O), and 1595 cm^{-1} (C=C), UV (ethanol): λ_{max} at 278 (ε=30 000) and 213 nm (ε=11 900), NMR (dimethyl sulfoxide-d_6): triplet (J=7 Hz) at 1.17 (3H, CH_3), singlet at 3.94 (2H, SCH_2), quartet (J=7 Hz) at 4.00 (2H, OCH_2), singlet at 4.19 (1H, =CH), broad peak at 7.80 (1H, NH), and a broad peak at 10.90 ppm (1H, NH). (Found: C 49.03; H 5.81; N 16.12. Calc. for $C_7H_{10}N_2O_3$: C 49.41; H 5.92; N 16.46). MS: M^+=170.

1. Taylor, P. J. *Spectrochim. Acta* **A 26** (1970) 153.
2. Ceder, O., Stenhede, U., Dahlquist, K.-I., Waisvisz, J. M. and van der Hoeven, M. G. *Acta Chem. Scand.* **27** (1973) 1914.
3. Ceder, O. and Stenhede, U. *Acta Chem. Scand.* **27** (1973) 1923.
4. Lehr, H., Karlan, S. and Goldberg, M. W. *J. Am. Chem. Soc.* **75** (1953) 3640.
5. Jacquier, R., Lacombe, J.-M. and Maury, G. *Bull. Soc. Chim. France* **1971** 1040.
6. Rondeau, R. E. and Sievers, R. E. *J. Am. Chem. Soc.* **93** (1971) 1522.
7. Demarco, P. V., Elzey, T. K., Lewis, R. B. and Wenkert, E. *J. Am. Chem. Soc.* **92** (1970) 5734.
8. Wing, R. M., Early, T. A. and Uebel, J. J. *Tetrahedron Letters* **1972** 4153.

Received March 17, 1973.

A New Method for the Preparation of Dianionobis(diamine)cobalt (III) Complexes. Preparation of Carbonatobis(trimethylenediamine)cobalt(III) Salts

JOHAN SPRINGBORG [a] and CLAUS ERIK SCHÄFFER [b]

[a] *Department of General and Inorganic Chemistry, Royal Veterinary and Agricultural University, Thorvaldsensvej 40, 2, opg. 4, DK-1871 Copenhagen V, Denmark and* [b] *Chemistry Department I (Inorganic Chemistry), University of Copenhagen, H. C. Ørsted Institute, Universitetsparken 5, DK-2100 Copenhagen Ø, Denmark*

Various methods for the preparation of bis(diamine)cobalt(III) complexes are known. In the following, a new method of preparation for this type of complexes is given. We illustrate the method by giving the preparations of the chloride and nitrate salts of the carbonatobis(trimethylenediamine)cobalt(III) ion.

The traditional method of preparation of the carbonatobis(trimethylenediamine)-cobalt(III) ion is based upon the action of carbonate on an aqueous solution of *trans*-dichlorobis(trimethylenediamine)cobalt-(III) chloride, possibly combined with removal of chloride by treatment with silver carbonate.[1,2] *trans*-Dichlorobis(trimethylenediamine)cobalt(III) chloride is obtained by air-oxidation of an ethanolic solution of trimethylenediamine (tn) with an excess of anhydrous cobalt(II) chloride in a yield of 43 %.[3]

The following new method of preparation of carbonatobis(trimethylenediamine)cobalt(III) chloride utilizes hydrated cobalt(II) chloride directly as the starting material and provides a high yield (67 %) of an almost pure sample. An aqueous solution of cobalt(II) chloride (1 mol) is made to react with the carbamate of trimethylenediamine (2 mol) to give a green, not further identified cobalt(II) solution. This cobalt(II) solution is oxidized with hydrogen peroxide. The resulting mixture of bis(trimethylenediamine)cobalt(III) species is by addition of lithium hydroxide combined with a stream of carbon dioxide converted to the red carbonato complex.

methylene triplet (3.77 ppm), while the lower-field one (4.05 ppm) remained unchanged. Finally, decoupling studies showed that the protons in the two methylene groups indeed coupled with each other.

Synthesis of ethyl 4-imidazolidone-$\Delta^{2,\alpha}$-acetate, 2. Ten g (0.097 mol) of glycine ethyl ester was slowly (*ca.* 20 min) added to 15.0 g (0.095 mol) of cold (0°C) carbethoxyacetimidic ethyl ester [4] in a 100 ml argon-flushed, three-necked, round-bottomed flask, equipped with a gas-inlet tube, a dropping funnel and a drying tube (magnesium sulfate). When the addition was complete, the gas stream was interrupted, the flask stoppered and kept at room temperature in the dark. After 24 h a brown, crystalline solid had precipitated. It was separated by filtration and triturated thoroughly, first with methylene chloride and then with diethyl ether. The brown solid was dried, then recrystallized four times from ethanol. Yield: 3.9 g (24 %) of brownish, flaky crystals. Sublimation of this material (140°C/1 torr) gave white crystals, which turned pink after a short exposure to air and/or light. Freshly sublimed samples were used for all measurements. M.p. 177–180°C, IR (KBr): 3380 (NH), 3300–3100 (NH), 1730 (ring C=O), 1695 (ester C=O), and 1595 cm^{-1} (C=C), UV (ethanol): λ_{max} at 278 (ε=30 000) and 213 nm (ε=11 900), NMR (dimethyl sulfoxide-d_6): triplet (J=7 Hz) at 1.17 (3H, CH_3), singlet at 3.94 (2H, SCH_2), quartet (J=7 Hz) at 4.00 (2H, OCH_2), singlet at 4.19 (1H, =CH), broad peak at 7.80 (1H, NH), and a broad peak at 10.90 ppm (1H, NH). (Found: C 49.03; H 5.81; N 16.12. Calc. for $C_7H_{10}N_2O_3$: C 49.41; H 5.92; N 16.46). MS: M^+=170.

1. Taylor, P. J. *Spectrochim. Acta* **A 26** (1970) 153.
2. Ceder, O., Stenhede, U., Dahlquist, K.-I., Waisvisz, J. M. and van der Hoeven, M. G. *Acta Chem. Scand.* **27** (1973) 1914.
3. Ceder, O. and Stenhede, U. *Acta Chem. Scand.* **27** (1973) 1923.
4. Lehr, H., Karlan, S. and Goldberg, M. W. *J. Am. Chem. Soc.* **75** (1953) 3640.
5. Jacquier, R., Lacombe, J.-M. and Maury, G. *Bull. Soc. Chim. France* **1971** 1040.
6. Rondeau, R. E. and Sievers, R. E. *J. Am. Chem. Soc.* **93** (1971) 1522.
7. Demarco, P. V., Elzey, T. K., Lewis, R. B. and Wenkert, E. *J. Am. Chem. Soc.* **92** (1970) 5734.
8. Wing, R. M., Early, T. A. and Uebel, J. J. *Tetrahedron Letters* **1972** 4153.

Received March 17, 1973.

A New Method for the Preparation of Dianionobis(diamine)cobalt (III) Complexes. Preparation of Carbonatobis(trimethylenediamine)cobalt(III) Salts

JOHAN SPRINGBORG [a] and CLAUS ERIK SCHÄFFER [b]

[a] *Department of General and Inorganic Chemistry, Royal Veterinary and Agricultural University, Thorvaldsensvej 40, 2, opg. 4, DK-1871 Copenhagen V, Denmark and* [b] *Chemistry Department I (Inorganic Chemistry), University of Copenhagen, H. C. Ørsted Institute, Universitetsparken 5, DK-2100 Copenhagen Ø, Denmark*

Various methods for the preparation of bis(diamine)cobalt(III) complexes are known. In the following, a new method of preparation for this type of complexes is given. We illustrate the method by giving the preparations of the chloride and nitrate salts of the carbonatobis(trimethylenediamine)cobalt(III) ion.

The traditional method of preparation of the carbonatobis(trimethylenediamine)-cobalt(III) ion is based upon the action of carbonate on an aqueous solution of *trans*-dichlorobis(trimethylenediamine)cobalt-(III) chloride, possibly combined with removal of chloride by treatment with silver carbonate.[1,2] *trans*-Dichlorobis(trimethylenediamine)cobalt(III) chloride is obtained by air-oxidation of an ethanolic solution of trimethylenediamine (tn) with an excess of anhydrous cobalt(II) chloride in a yield of 43 %.[3]

The following new method of preparation of carbonatobis(trimethylenediamine)cobalt(III) chloride utilizes hydrated cobalt(II) chloride directly as the starting material and provides a high yield (67 %) of an almost pure sample. An aqueous solution of cobalt(II) chloride (1 mol) is made to react with the carbamate of trimethylenediamine (2 mol) to give a green, not further identified cobalt(II) solution. This cobalt(II) solution is oxidized with hydrogen peroxide. The resulting mixture of bis(trimethylenediamine)cobalt(III) species is by addition of lithium hydroxide combined with a stream of carbon dioxide converted to the red carbonato complex.

The use of the carbamate of the amine is essential. A single experiment utilizing the free amine was carried out. Besides a large amount of a water-soluble red by-product, which was not identified, only a yield of 25 % impure carbonato complex was obtained.

The nitrate salt is prepared analogously to the chloride (yield 72 %). The perchlorate salt is obtained in high yield (88 %) from the chloride.

These carbonato salts are all excellent starting materials for the preparation of other dianionobis(trimethylenediamine)cobalt(III) compounds; *e.g.* treatment of the chloride salt with concentrated hydrochloric acid yields *trans*-dichlorobis(trimethylenediamine)cobalt(III) chloride almost quantitatively.

With ethylenediamine the above method has been used with success resulting in new preparations of carbonato- and other dianionobis(ethylenediamine)cobalt(III) salts in high yields.[4]

This new method is probably also useful for preparations of dianionobis(diamine)-cobalt(III) complexes with other aliphatic diamines. A single experiment in which trimethylenediamine was replaced by propylenediamine showed that also carbonatobis(propylenediamine)cobalt(III) salts may be obtained in high yields by this method.

Experimental. Materials. Trimethylenediamine with the description *purissimum* was purchased from Fluka. All other chemicals were of reagent grade and were used without further purification.

Spectra. Absorption spectra in the 300–650 nm region, recorded using a Cary Model 14 spectrophotometer, were used as a check of purity and as characterization of the compounds. Data for maxima and minima have been given below as (ε,λ) the absorbancy ε in liter/mol cm and the wavelength λ in nm.

Preparations. 1. Carbonatobis(trimethylenediamine)cobalt(III) chloride. $[Cotn_2CO_3]Cl\cdot H_2O$. A mixture of trimethylenediamine (55.0 ml, 0.656 mol) and water (400 ml) was cooled in ice, and a stream of carbon dioxide was bubbled through the solution for 2–3 h. The stream of carbon dioxide was maintained during the entire preparation. A solution of cobalt(II) chloride 6-hydrate (78,0 g, 0.328 mol) in water (80 ml) at room temperature was then added to the solution with stirring. The addition of the cobalt(II) salt caused a violent evolution of carbon dioxide gas, and the solution became green and gel-like. With continued cooling and manual stirring, hydrogen peroxide (80 ml, 30 %) was then added dropwise during 15 min. During the addition the temperature increased to about 25° and the reaction mixture became a green homogeneous solution.

To complete the reaction the mixture was heated to 80–85°, and kept at that temperature for half an hour. During this time the colour changed from green to redviolet. The solution was cooled in ice to approximately 25°. At that temperature, finely powdered lithium hydroxide monohydrate (13.76 g, 0.328 mol) was added with thorough stirring and a vigorous stream of carbon dioxide. The solution became red. The cooling was continued for 3 h, when the stream of carbon dioxide was stopped and the solution left overnight at 0–5°. The filtered solution was then evaporated in a rotating vacuum evaporator at approximately 70° to a volume of 160 to 170 ml. It was found to be important to evaporate to this volume. Evaporation to a volume much larger than 170 ml decreased the yield substantially, and evaporation to a volume less than approximately 150 ml gave an oily product. This super saturated solution was then transferred (while hot) to a preheated beaker and heated to the boiling point with thorough stirring for a few minutes. This caused precipitation of red crystals of carbonatobis(trimethylenediamine)cobalt(III) chloride. The mixture was then cooled in ice for 2 h. The precipitate was filtered, washed with 96 % ethanol (three 100 ml portions) and allowed to dry in air. This yielded 70 g (67 %). This product was not pure, but still suitable for further synthetic work. The pure product was obtained by reprecipitation from water. The crude product (10 g) was dissolved in water (30 ml) at room temperature and filtered. A mixture of acetone (60 ml) and methanol (20 ml) was then added to the stirred solution within a period of 10 min., and red crystals of the chloride salt precipitated. The content of methanol was found to be essential in order to avoid the formation of an oil. The mixture was allowed to stand for another 10 min at room temperature, and was then filtered and washed with 96 % ethanol (three 5 ml portions). Drying in air yielded 7.6 g (76 %). (Found: Co 18.48; C 26.16; N 17.48; H 6.90; Cl 10.99. Calc. for $[Cotn_2CO_3]Cl.H_2O$: Co 18.38; C 26.21; N 17.47; H 6.92; Cl 11.06). $(\varepsilon,\lambda)_{max}$: (108.7,520); (126.7,360). $(\varepsilon,\lambda)_{min}$: (12.1,430); (51.2,327). Medium: water. Literature:[2] $(\varepsilon,\lambda)_{max}$: (108.5,520); (127.7,360).

2. Carbonatobis(trimethylenediamine)cobalt(III) nitrate, $[Cotn_2CO_3]NO_3$. Carbonatobis(trimethylenediamine)cobalt(III) nitrate was

prepared analogously to the chloride salt. With the quantities given in preparation No. 1, the cobalt(II) chloride solution was replaced by a solution of cobalt(II) nitrate 6-hydrate (95.5 g, 0.328 mol) in water (80 ml), and the procedure given in preparation No. 1 was followed exactly. The nitrate salt was isolated analogously by evaporation to a volume of 160 to 170 ml. The crude product was washed with 70 % v/v ethanol (three 80 ml portions) and allowed to dry in air. The yield was 82 g of red crystals of the nitrate salt (72 %). This product was not pure. The pure salt was obtained by reprecipitation from water. The crude product (20 g) was dissolved in water (40 ml) at 100° and filtered. Then 96 % ethanol (120 ml) was added quickly to the stirred solution (while hot), and the mixture was cooled for 2 h in ice. The precipitate was filtered and washed with 70 % v/v ethanol (two 20 ml portions). Drying in air yielded 16 g (80 %). (Found: Co 17.11; C 24.25; N 20.45; H 6.43. Calc. for $[Cotn_2CO_3]NO_3$: Co 16.98; C 24.21; N 20.18; H 6.39). $(\varepsilon,\lambda)_{max}$: (107.5,520); (124.9,360); $(\varepsilon,\lambda)_{min}$: (11.4,430); (50.2,327). Medium: water.

3. *Carbonatobis(trimethylenediamine)cobalt-(III) perchlorate*, $[Cotn_2CO_3]ClO_4$. Crude carbonatobis(trimethylenediamine)cobalt(III) chloride (20.0 g, 0.062 mol) was dissolved in water (50 ml) at room temperature and the solution was filtered. A saturated solution of sodium perchlorate in water (20 ml) was then added to the stirred solution with cooling in ice. The precipitation of red crystals of the perchlorate salt immediately commenced, and the cooling was continued for half an hour. The precipitate was filtered, washed with ice cold ethanol (50 % v/v, 20 ml) and 96 % ethanol (three 20 ml portions). Drying in air yielded 20.1 g (88 %). (Found: Co 16.06; C 22.74; N 15.46; H 5.52; Cl 9.65. Calc. for $[Cotn_2CO_3]ClO_4$: Co 16.07: C 22.93; N 15.28; H 5.50; Cl 9.67). $(\varepsilon,\lambda)_{max}$; (107.3,520); (124.7,360). $(\varepsilon,\lambda)_{min}$: (11.3,430); (49.2,327). Medium: water.

1. Werner, A. *Ann.* **386** (1912) 264.
2. Boyle, J. E. and Harris, C. M. *J. Am. Chem. Soc.* **80** (1958) 782.
3. Bailar, J. C. and Work, J. B. *J. Am. Chem. Soc.* **68** (1946) 232.
4. Springborg, J. and Schäffer, C. E. *Inorg. Syn.* **14** (1973) 63.

Received June 22, 1973.

Inhibition of Duodenal Pancreatic Enzymic Activities by Polyphloretin Phosphate with Special Reference to Phospholipase A_2

B. ARNESJÖ, I. IHSE and I. QVIST

Department of Surgery, University Hospital of Lund, S-221 85 Lund, Sweden

Polyphloretin phosphate (PPP) is a substance capable of inhibiting the effects of prostaglandins, trombin, and certain enzymes such as alkaline phosphatase and hyaluronidase. Hyaluronidase is completely inhibited in an environment containing 1 – 2 μg/ml PPP. The molecular weight of PPP is about 15 000 and it is only to a minor extent – if any – split or absorbed from the intestine.[1,2] It has been shown to be useful in cases with ulcerative colitis.[2] This beneficial effect in cases with ulcerative colitis has been ascribed its membrane tightening effect as in this disease the permeability of the colonic mucosa is increased with protein leakage as a consequence. This membrane tightening effect of PPP might be explained by its capability of inhibiting hyaluronidase. Lecithin is another compound that is one of the main components of cell membranes. In the present investigation, therefore, we have found it interesting to study the effect of PPP on the *in vitro* activity of pancreatic enzymes, especially on phospholipase A_2 which in the intestine splits lecithin to lysolecithin the latter of which might be highly toxic to cell membranes in patients with inflammatory intestinal diseases.

Materials and methods. Polyphloretin phosphate (PPP standard IV batch number Leo 101K) was a gift from AB Leo, Helsingborg, Sweden. It contained 93.5 % PPP. Contaminants were pyridine (2.7 %) sodium chloride (2.4 %), phosphoric acid (0.2 %) and water.

Phospholipase A_2 acitivity was estimated according to Ihse and Arnesjö,[3] lipase according to Erlansson and Borgström,[4] and trypsin by a modified version of the method of Hummel.[5] All enzyme assays were run using a pH-stat (Radiometer, Copenhagen) with a TTT2 titrator connected to an ABU11 Burette Unit with a 0.25 ml burette and a thermostatically controlled TTA31 titrator assembly.

Sodium taurodeoxycholate (NaTDC) was synthezised according to Norman [6] as modified

prepared analogously to the chloride salt. With the quantities given in preparation No. 1, the cobalt(II) chloride solution was replaced by a solution of cobalt(II) nitrate 6-hydrate (95.5 g, 0.328 mol) in water (80 ml), and the procedure given in preparation No. 1 was followed exactly. The nitrate salt was isolated analogously by evaporation to a volume of 160 to 170 ml. The crude product was washed with 70 % v/v ethanol (three 80 ml portions) and allowed to dry in air. The yield was 82 g of red crystals of the nitrate salt (72 %). This product was not pure. The pure salt was obtained by reprecipitation from water. The crude product (20 g) was dissolved in water (40 ml) at 100° and filtered. Then 96 % ethanol (120 ml) was added quickly to the stirred solution (while hot), and the mixture was cooled for 2 h in ice. The precipitate was filtered and washed with 70 % v/v ethanol (two 20 ml portions). Drying in air yielded 16 g (80 %). (Found: Co 17.11; C 24.25; N 20.45; H 6.43. Calc. for $[Cotn_2CO_3]NO_3$: Co 16.98; C 24.21; N 20.18; H 6.39). $(\varepsilon,\lambda)_{max}$: (107.5,520); (124.9,360); $(\varepsilon,\lambda)_{min}$: (11.4,430); (50.2,327). Medium: water.

3. *Carbonatobis(trimethylenediamine)cobalt-(III) perchlorate*, $[Cotn_2CO_3]ClO_4$. Crude carbonatobis(trimethylenediamine)cobalt(III) chloride (20.0 g, 0.062 mol) was dissolved in water (50 ml) at room temperature and the solution was filtered. A saturated solution of sodium perchlorate in water (20 ml) was then added to the stirred solution with cooling in ice. The precipitation of red crystals of the perchlorate salt immediately commenced, and the cooling was continued for half an hour. The precipitate was filtered, washed with ice cold ethanol (50 % v/v, 20 ml) and 96 % ethanol (three 20 ml portions). Drying in air yielded 20.1 g (88 %). (Found: Co 16.06; C 22.74; N 15.46; H 5.52; Cl 9.65. Calc. for $[Cotn_2CO_3]ClO_4$: Co 16.07: C 22.93; N 15.28; H 5.50; Cl 9.67). $(\varepsilon,\lambda)_{max}$; (107.3,520); (124.7,360). $(\varepsilon,\lambda)_{min}$: (11.3,430); (49.2,327). Medium: water.

1. Werner, A. *Ann.* **386** (1912) 264.
2. Boyle, J. E. and Harris, C. M. *J. Am. Chem. Soc.* **80** (1958) 782.
3. Bailar, J. C. and Work, J. B. *J. Am. Chem. Soc.* **68** (1946) 232.
4. Springborg, J. and Schäffer, C. E. *Inorg. Syn.* **14** (1973) 63.

Received June 22, 1973.

Inhibition of Duodenal Pancreatic Enzymic Activities by Polyphloretin Phosphate with Special Reference to Phospholipase A_2

B. ARNESJÖ, I. IHSE and I. QVIST

Department of Surgery, University Hospital of Lund, S-221 85 Lund, Sweden

Polyphloretin phosphate (PPP) is a substance capable of inhibiting the effects of prostaglandins, trombin, and certain enzymes such as alkaline phosphatase and hyaluronidase. Hyaluronidase is completely inhibited in an environment containing 1 – 2 μg/ml PPP. The molecular weight of PPP is about 15 000 and it is only to a minor extent – if any – split or absorbed from the intestine.[1,2] It has been shown to be useful in cases with ulcerative colitis.[2] This beneficial effect in cases with ulcerative colitis has been ascribed its membrane tightening effect as in this disease the permeability of the colonic mucosa is increased with protein leakage as a consequence. This membrane tightening effect of PPP might be explained by its capability of inhibiting hyaluronidase. Lecithin is another compound that is one of the main components of cell membranes. In the present investigation, therefore, we have found it interesting to study the effect of PPP on the *in vitro* activity of pancreatic enzymes, especially on phospholipase A_2 which in the intestine splits lecithin to lysolecithin the latter of which might be highly toxic to cell membranes in patients with inflammatory intestinal diseases.

Materials and methods. Polyphloretin phosphate (PPP standard IV batch number Leo 101K) was a gift from AB Leo, Helsingborg, Sweden. It contained 93.5 % PPP. Contaminants were pyridine (2.7 %) sodium chloride (2.4 %), phosphoric acid (0.2 %) and water.

Phospholipase A_2 acitivity was estimated according to Ihse and Arnesjö,[3] lipase according to Erlansson and Borgström,[4] and trypsin by a modified version of the method of Hummel.[5] All enzyme assays were run using a pH-stat (Radiometer, Copenhagen) with a TTT2 titrator connected to an ABU11 Burette Unit with a 0.25 ml burette and a thermostatically controlled TTA31 titrator assembly.

Sodium taurodeoxycholate (NaTDC) was synthezised according to Norman [6] as modified

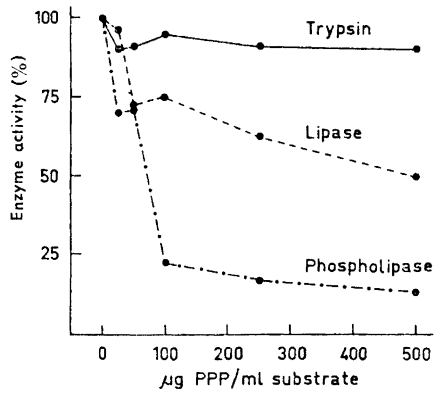

Fig. 1. Inhibition of trypsin, lipase, and phospholipase A by different concentrations of polyphloretin phosphate.

by Hofman.[7] Purity better than 98 % as judged by thin layer chromatography.

All experiments were run *in* vitro. The enzyme source was fresh human duodenal contents aspirated *via* a duodenal tube positioned in the ascendent part of the duodenum under fluoroscopic control and after testmeal stimulation of the pancreatic secretion. PPP in different concentrations was added to the substrate solution.

All numerical values given in results represent the average of three determinations.

Results. As is shown in Fig. 1 the phospholipase A activity was inhibited about 30 % with a PPP concentration of the substrate solution of 25 µg/ml, 85 % with a PPP concentration of 500 µg/ml and 100 % with 1 mg PPP/ml. Fig. 2 demonstrates the PPP inhibition with different concentrations of bile salt. The parallellity between the phospholipase activity measurements with or without PPP at different bile salt concentrations indicates that the inhibitory effect is independent of the bile salt concentrations. Duodenal phospholipase A activity is dependent on the presence of calcium.[3] As is shown in Fig. 2 the PPP inhibition of phospholipase A is the same irrespective of the calcium concentrations. The pH-optimum for the phospholipase A activity of duodenal contents is 7.5 pH.[3] This optimum was not shifted in the presence of

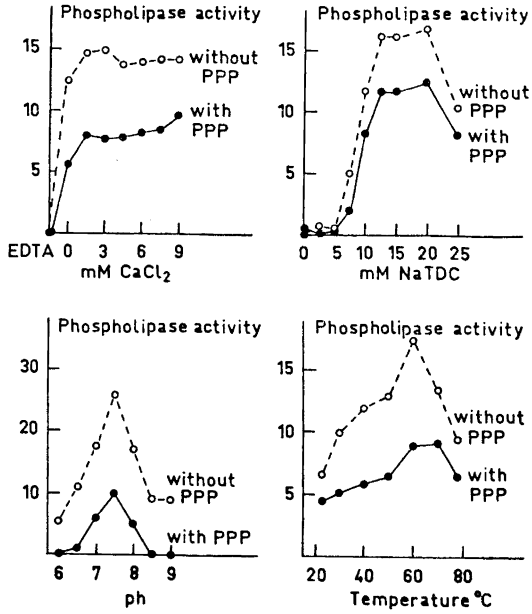

Fig. 2. The influence of calcium, bile salt, pH, and temperature on polyphloretin phosphate inhibition of duodenal phospholipase A.

PPP (Fig. 2). The temperature optimum was also unaltered in the presence of PPP (Fig.2).

Fig. 1 shows that the lipase activity of duodenal contents was found to be incompletely inhibited by relatively high concentrations of PPP. The inhibitory effect with a concentration of 100 μg PPP/ml substrate solution was 25 % while it was 50 % with 500 μg PPP/ml.

A maximal inhibition of the trypsin activity of duodenal contents of about 10 % was found even with high concentrations of PPP.

Discussion. The results of the present study indicate that PPP is a potent inhibitor of pancreatic phospholipase A in intestinal contents. This inhibitions seems to be independent of the bile salt concentrations, the calcium concentration, the pH, and the temperature of the incubation medium. Also duodenal pancreatic lipase was inhibited to a certain extent, whereas only slight inhibition, if any, of trypsin was found. PPP has been shown to exert a beneficial effect upon the protein losses *via* the colonic mucosa in patients with ulcerative colitis.[2] A subdivided dose of 2 g PPP/day was given. Under such circumstances a total inhibition of the intestinal phospholipase A_2 activity and, in addition, an moderate inhibition of the lipase activity should be expected. This latter possibility might explain that in cases with non-tropical sprue a beneficial effect on the protein leakage but no effect on the feacal fat excretion was obtained after peroral PPP administration.[2]

The membrane tightening effect of PPP has been ascribed its capability of inhibiting hyaluronidase.[1] Considering the fact that lecithin is a main component of cell membranes and that it is split by phospholipase A the beneficial effect of PPP in cases of ulcerative colitis may also be ascribed an inhibition of this latter enzyme by PPP.

1. Fredholm, B. AB Leo, Helsingborg, Sweden. *Personal communication.*
2. Krook, H. *Personal communication.*
3. Ihse, I. and Arnesjö ,B. *Acta Chem. Scand.* **27** (1973). *In press.*
4. Erlansson, C. and Borgström, B. *Scand. J. Gastroenterol.* **5** (1970) 293.
5. Hummel, B. C. W. *Can. J. Biochem. Physiol.* **37** (1959) 1393.
6. Norman, A. *Arkiv Kemi* **32** (1955) 331.
7. Hofman, A. F. Thesis, Lund 1964, p. 32.

Received June 29, 1973.

An Electron-Diffraction Investigation of the Molecular Structure of 1,2,4,5-Hexatetraene (Biallenyl) in the Vapour Phase

MARIT TRÆTTEBERG,[a] GUNNAR PAULEN [a] and HENNING HOPF[b]

[a]*Department of Chemistry, University of Trondheim, NLHT, N-7000 Trondheim, Norway and* [b]*Institute of Organic Chemistry, University of Karlsruhe, 7500 Karlsruhe 1, German Federal Republic*

The molecular structure of 1,2,4,5-hexatetraene (in the following called biallenyl) has been studied by the gas electron diffraction method. The compound used in the present study was synthesized from 3-bromo-1-propyne and magnesium metal with tetrahydrofuran as solvent.[1]

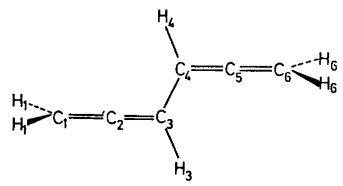

Fig. 1. Biallenyl. Molecular model which shows the numbering of the atoms.

A complete spectroscopic study of the compound was recently carried out by Powell *et al.*,[2] based on a sample originating from the same source. They concluded from examination of the infrared and Raman spectra that the molecule has a center of symmetry corresponding to C_{2h} symmetry in which the hydrogen atoms of the CH_2 groups are twisted out of the molecular plane by 90°.

The electron-diffraction intensity data were obtained with the Oslo diffraction camera.[3] Diffraction photographs were taken at two camera lengths (approximately 48 cm and 20 cm) at room temperature. For each camera length four plates were selected for the structure analyses. The data were treated in the usual way [4] and yielded an experimental molecular intensity ($sM(s)$) function in the region from $s = 1.25$ Å^{-1} to about 44 Å^{-1}.

PPP (Fig. 2). The temperature optimum was also unaltered in the presence of PPP (Fig.2).

Fig. 1 shows that the lipase activity of duodenal contents was found to be incompletely inhibited by relatively high concentrations of PPP. The inhibitory effect with a concentration of 100 μg PPP/ml substrate solution was 25 % while it was 50 % with 500 μg PPP/ml.

A maximal inhibition of the trypsin activity of duodenal contents of about 10 % was found even with high concentrations of PPP.

Discussion. The results of the present study indicate that PPP is a potent inhibitor of pancreatic phospholipase A in intestinal contents. This inhibitions seems to be independent of the bile salt concentrations, the calcium concentration, the pH, and the temperature of the incubation medium. Also duodenal pancreatic lipase was inhibited to a certain extent, whereas only slight inhibition, if any, of trypsin was found. PPP has been shown to exert a beneficial effect upon the protein losses *via* the colonic mucosa in patients with ulcerative colitis.[2] A subdivided dose of 2 g PPP/day was given. Under such circumstances a total inhibition of the intestinal phospholipase A_2 activity and, in addition, an moderate inhibition of the lipase activity should be expected. This latter possibility might explain that in cases with non-tropical sprue a beneficial effect on the protein leakage but no effect on the feacal fat excretion was obtained after peroral PPP administration.[2]

The membrane tightening effect of PPP has been ascribed its capability of inhibiting hyaluronidase.[1] Considering the fact that lecithin is a main component of cell membranes and that it is split by phospholipase A the beneficial effect of PPP in cases of ulcerative colitis may also be ascribed an inhibition of this latter enzyme by PPP.

1. Fredholm, B. AB Leo, Helsingborg, Sweden. *Personal communication.*
2. Krook, H. *Personal communication.*
3. Ihse, I. and Arnesjö ,B. *Acta Chem. Scand.* **27** (1973). *In press.*
4. Erlansson, C. and Borgström, B. *Scand. J. Gastroenterol.* **5** (1970) 293.
5. Hummel, B. C. W. *Can. J. Biochem. Physiol.* **37** (1959) 1393.
6. Norman, A. *Arkiv Kemi* **32** (1955) 331.
7. Hofman, A. F. Thesis, Lund 1964, p. 32.

Received June 29, 1973.

An Electron-Diffraction Investigation of the Molecular Structure of 1,2,4,5-Hexatetraene (Biallenyl) in the Vapour Phase

MARIT TRÆTTEBERG,[a] GUNNAR PAULEN [a] and HENNING HOPF[b]

[a]*Department of Chemistry, University of Trondheim, NLHT, N-7000 Trondheim, Norway and* [b]*Institute of Organic Chemistry, University of Karlsruhe, 7500 Karlsruhe 1, German Federal Republic*

The molecular structure of 1,2,4,5-hexatetraene (in the following called biallenyl) has been studied by the gas electron diffraction method. The compound used in the present study was synthesized from 3-bromo-1-propyne and magnesium metal with tetrahydrofuran as solvent.[1]

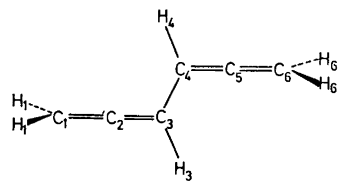

Fig. 1. Biallenyl. Molecular model which shows the numbering of the atoms.

A complete spectroscopic study of the compound was recently carried out by Powell *et al.*,[2] based on a sample originating from the same source. They concluded from examination of the infrared and Raman spectra that the molecule has a center of symmetry corresponding to C_{2h} symmetry in which the hydrogen atoms of the CH_2 groups are twisted out of the molecular plane by 90°.

The electron-diffraction intensity data were obtained with the Oslo diffraction camera.[3] Diffraction photographs were taken at two camera lengths (approximately 48 cm and 20 cm) at room temperature. For each camera length four plates were selected for the structure analyses. The data were treated in the usual way [4] and yielded an experimental molecular intensity ($sM(s)$) function in the region from $s = 1.25$ Å^{-1} to about 44 Å^{-1}.

Preliminary values for the bond distances and bond angles were obtained from the experimental radial distribution curve (Fig. 3). The peak at about 1.3 Å corresponds to the carbon carbon bond distances, while the shoulder at the short distance side of this peak contains contributions from the carbon-hydrogen bonds. Non-bonded C···H distances over one bond angle are found at 2.1 Å, while the composite peak at about 2.5 Å contains contributions from the C_1C_3 and C_2C_4 distances. The other nonbonded carbon carbon distances are found at 3.6 Å (C_1C_4 and C_2C_5), 4.9 Å (C_1C_5) and 6.1 Å (C_1C_6).

The molecular structure was determined by a least squares analysis of the diffraction data. During this procedure the r_a, r_g, and r_α structures were studied independently. This implies that for example in an r_a structure study the dependent distances and derivatives were calculated from r_a-parameters. As the $C_1=C_2$ and $C_2=C_3$ distances were assumed to be equal during the refinements, the r_a values for these bonds will be different in an r_α refinement and so on.

The following approximate relationships exist between the different r values:

$$r_a \approx r_e + \langle \Delta z \rangle + K - u^2/r_e \approx r_\alpha + K - u^2/r_e \simeq r_g - u^2/r_e$$

where $\Delta z (= r - r_e)$ is directed along the internuclear distance.[9] r_α gives the distance between average positions of two atoms. An r_α structure is therefore geometrical consistent. r_g represents an average internuclear distance. r_g and r_a structures are not geometrical consistent and shrinkage effects might be observed.

In order to determine an r_α structure it is necessary to know the perpendicular amplitude correction coefficients (K values) and the mean amplitudes of vibrations (u values). The u values for the most dominant internuclear distances are usually obtained quite accurately from electron diffraction data. It is, however, ordinarily not possible to determine all vibrational amplitudes by this method. Both u and K values may be calculated from spectroscopic data. In the present case these quantities have been calculated by Gwinn's method [6] which is based on an expansion of interatomic distances in terms of cartesian displacement coordinates. The computer program has been adjusted for use in an electron diffraction analysis by Stölevik *et al.*[6] The assumed force field was taken from data published by Allinger *et al.*[7] The results of the calculations are presented in Table 1, which also lists the experimentally determined mean vibrational amplitudes ($u_{ij}^{obs.}$).

Table 1. Biallenyl. Observed and calculated mean amplitudes of vibrations (u_{ij}) and calculated perpendicular amplitude correction coefficients (K_{ij}) for distances between carbon atoms. The numbers in parentheses are standard deviation values as obtained in the least squares analyses. All values are given in Å.

Distance	$u_{ij}^{obs.}$	$u_{ij}^{calc.}$	$K_{ij}^{calc.}$
$C_1=C_2$	0.0423(6)	0.0404	0.01113
$C_2=C_3$		0.0403	0.00807
C_3-C_4	0.0595(30)	0.0494	0.00253
C_1-H_1	0.0841(26)	0.0790	0.01382
C_3-H_3		0.0790	0.01210
C_2C_7	0.0784(36)	0.0929	0.00344
C_1C_3	0.0573(26)	0.0487	0.00678
C_1C_4	0.0976(66)	0.0961	0.00439
C_2C_5		0.0911	0.00257
C_1C_5	0.1019(91)	0.0910	0.00199
C_1C_6	0.1065(240)	0.0902	0.00039

The correspondence between observed and calculated mean vibrational amplitudes is reasonably good. The observed u values for bond distances are often found to be higher than those calculated by

Table 2. Structural parameters for biallenyl. The results in columns 2–4 represent values obtained from least squares intensity refinements based on an r_α-structure, while column 5 shows results based on an r_a-structure. The values in brackets are standard deviation values obtained when the geometrical and vibrational parameters were varied simultaneously.

	r_a, Å	r_g, Å	r_α, Å	r_a, Å
$C_1=C_2$	1.3144	1.3158	1.3046(5)	1.3123(5)
$C_2=C_3$	1.3113	1.3127	1.3046(5)	1.3123(5)
C–C	1.4682	1.4706	1.4681(35)	1.4656(40)
C–H	1.1058	1.1122	1.0992(32)	1.1043(36)
∠C=C–C			124.0° (0.31°)	123.5° (0.35°)
∠C=C=C			(180°)	(180°)
$\angle C_2=C_1-H_1$			(120°)	(120°)
$\angle C_2=C_3-H_3$			(118°)	(118°)

Gwinn's method, while the opposite is more often true for the non-bonded distances. The same trend is observed for the bond distance amplitudes of biallenyl, while the differences between observed and calculated u values for non-bonded distances are scattered in both directions.

Table 2 shows results based on refinements on r_α and r_a structures, respectively. The experimental data are consistent with a molecular structure with C_{2h} symmetry, a planar carbon skeleton with CH_2 groups that lie in planes at right angles to this plane. The carbon skeleton is well determined, but it was not possible to determine the C=C−H bond angles accurately. The length of the carbon-carbon double bond is found to be the same as in allene (r_a: 1.312 Å).[9]

The experimental and theoretical molecular intensity curves are shown in Fig. 2, while Fig. 3 shows the corresponding radial-distribution (RD) curves. It is seen that the deviation between the experimental and theoretical RD functions is quite large in some regions. This fairly large deviation is, however, mostly outside the regions where the CC distances contribute and are probably connected with the difficulties in obtaining reliable CCH bond angles.

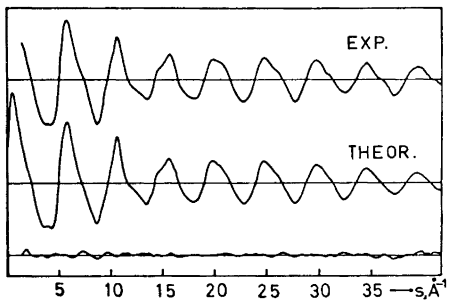

Fig. 2. Biallenyl. Experimental and theoretical molecular intensity functions and the differences between the two.

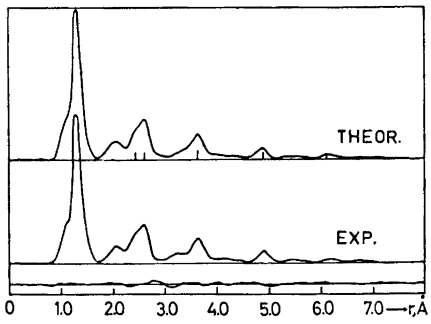

Fig. 3. Biallenyl. Experimental and theoretical radial distribution functions. Artificial damping constant $k = 0.0015$ Å^2.

Several factors may contribute to explain the fact that shrinkage effects within the allenyl groups could not be clearly demonstrated in the present case. The important C_1C_3 distance is not very different from another carbon carbon distance (C_2C_4), and the accuracy with which each of them is determined is therefore reduced. Further the assumed force field that was applied in calculating the perpendicular amplitude correction coefficients might not be accurate enough to give K values of the required precision. Finally experimental errors in the scattering data should be mentioned.

The investigation will be continued by carrying out a more elaborate calculation of K and u values from spectroscopic data for application in further refinements of the electron-diffraction data.

Acknowledgements. The authors are greatly indebted to cand.real. Arne Almenningen who made all the electron diffraction diagrams. Financial support from *Norges Almenvitenskapelige Forskningsråd* is gratefully acknowledged.

1. Hopf, H. *Angew. Chem.* **17** (1970) 703.
2. Powell, D. L., Klœboe, P., Christensen, D. H. and Hopf, H. *Spectrochim. Acta* **A 29** (1973) 7.
3. Almenningen, A., Bastiansen, O., Haaland, A. and Seip, H. M. *Angew. Chem.* **77** (1965) 877.
4. Andersen, B., Seip, H. M., Strand, T. G. and Stölevik, R. *Acta Chem. Scand.* **23** (1969) 3224.
5. Gwinn, W. D. *J. Chem. Phys.* **55** (1971) 477.
6. Stölevik, R., Seip, H. M. and Cyvin, S. J. *Chem. Phys. Letters* **15** (1972) 263.
7. Allinger, N. L. and Sprague, J. T. *J. Am. Chem. Soc.* **94** (1972) 5734.
8. Almenningen, A., Bastiansen, O. and Trætteberg, M. *Acta Chem. Scand.* **13** (1959) 1699.
9. Cyvin, S. J. *Molecular Vibrations and Mean Square Amplitudes*, Universitetsforlaget, Oslo and Elsevier, Amsterdam 1968.

Received July 14, 1973.

The Crystal Structure of $Tl(ZnSO_4Cl)$

BENGT BOSSON

Division of Inorganic Chemistry 2, The Lund Institute of Technology, Chemical Center, Box 740, S-220 07 Lund 7, Sweden

The crystal structure of $Tl(ZnSO_4Cl)$ has been determined from X-ray single crystal data. The crystals are monoclinic, space group $P2_1/c$ (No. 14) with four formula units in a unit cell with the dimensions $a = 7.278$, $b = 9.551$, $c = 8.092$ and $\beta = 93.97°$. X-Ray intensity data were collected with an integrating Weissenberg camera using Mo$K\alpha$ radiation. 656 independent reflections were observed in the layers $hk0 - hk7$.

The coordinates of the thallium atom were obtained from a three-dimensional Patterson function. The other atoms were located from three-dimensional electron density difference syntheses. A correction for the absorption was performed; the linear absorption coefficient was 340 cm^{-1}. A least-squares full matrix refinement was performed including anisotropic temperature factors for the thallium and zinc atoms, isotropic temperature factors for chlorine, sulphur, and oxygen atoms, and an overall scale factor. The discrepancy factor $R = \sum||F_o| - |F_c||/\sum|F_o| = 0.073$ (656 reflections). The final positional and thermal parameters are given in Table 1 and selected interatomic distances and

Table 1. Final positional and thermal parameters with standard deviations (within brackets). The temperature factor expression used for the thallium and zinc atoms is $\exp-(h^2\beta_{11}+k^2\beta_{22}+l^2\beta_{33}+2hk\beta_{12}+2hl\beta_{13}+2kl\beta_{23})$. The point position of all atoms is 4(*e*).

	x	y	z	B (Å^2)
Tl	0.3690(2)	0.0894(2)	0.2099(2)	–
Zn	0.9037(5)	0.2014(4)	0.4612(5)	–
Cl	0.6232(11)	0.1853(9)	0.5418(12)	1.85(13)
S	0.1109(8)	0.4369(6)	0.2687(9)	0.71(9)
O1	0.1071(31)	0.3552(26)	0.1099(31)	2.00(38)
O2	−0.0294(36)	0.3826(28)	0.3655(35)	2.51(44)
O3	0.2903(40)	0.4155(36)	0.3525(41)	3.25(51)
O4	0.0591(27)	0.5823(24)	0.2386(29)	1.54(32)

	β_{11}	β_{22}	β_{33}	β_{12}	β_{13}	β_{23}
Tl	0.0103(2)	0.0069(2)	0.0094(3)	−0.0013(2)	0.0007(2)	0.0023(2)
Zn	0.0060(5)	0.0021(3)	0.0023(6)	0.0005(3)	0.0014(4)	0.0012(3)

Table 2. Selected distances (Å) and bond angles (°) with standard deviations (within brackets) in the structure of $Tl(ZnSO_4Cl)$.

Tl–O3	2.91(3)	Zn–O1	1.92(2)
Tl–O3	3.06(3)	Zn–O2	1.97(3)
Tl–O4	3.17(2)	Zn–O4	2.01(2)
Tl–O2	3.19(3)	Zn–Cl	2.19(1)
Tl–Cl	3.20(1)		
Tl–O1	3.24(2)	S–O2	1.43(3)
Tl–Cl	3.28(1)	S–O3	1.44(3)
Tl–Cl	3.30(1)	S–O4	1.46(2)
Tl–O3	3.38(3)	S–O1	1.50(3)
∠O1–S–O2	108.0(1.5)	∠Cl–Zn–O1	119.2(0.8)
∠O1–S–O3	107.0(1.6)	∠Cl–Zn–O2	116.1(0.8)
∠O1–S–O4	111.3(1.4)	∠Cl–Zn–O4	112.3(0.6)
∠O2–S–O3	110.4(1.7)	∠O1–Zn–O2	107.0(1.0)
∠O2–S–O4	104.6(1.4)	∠O1–Zn–O4	101.8(1.0)
∠O3–S–O4	115.4(1.6)	∠O2–Zn–O4	97.5(1.1)

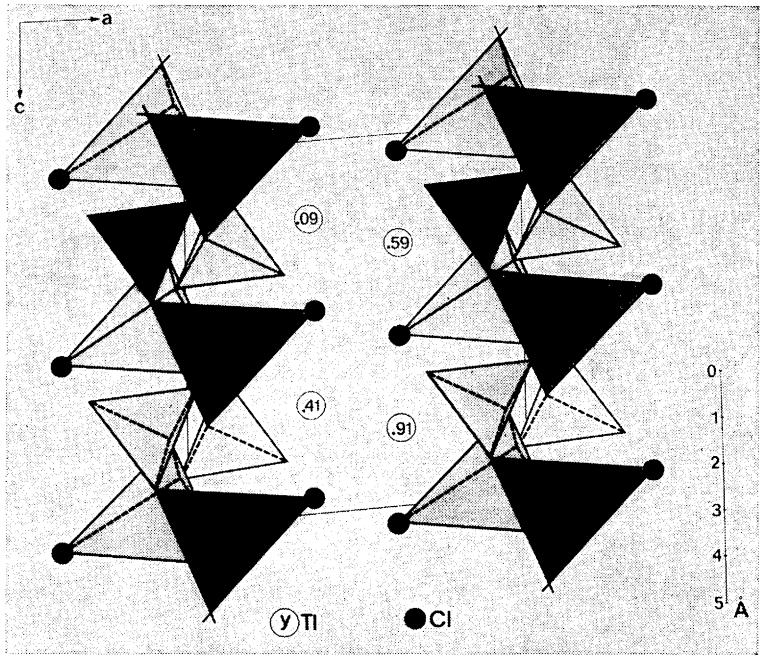

Fig. 1. Part of the infinite layers $(ZnSO_4Cl)_n^{n-}$ and the Tl^+ ions in the crystal structure of $Tl(ZnSO_4Cl)$, viewed along the *b*-axis. The small tetrahedra denote the sulphate groups and the larger ones the "ZnO_3Cl tetrahedra". The *y*-coordinates of the Tl^+ ions are given.

angles in Table 2.

The crystal structure of $Tl(ZnSO_4Cl)$ is built up of infinite layers of the composition $(ZnSO_4Cl)_n^{n-}$, held together by thallium ions, Tl^+. The thallium atoms are surrounded by three chlorine and six oxygen atoms in an irregular way. The Tl – Cl distances vary between 3.20(1) and 3.30(1) Å and five Tl – O distances range between 2.91(4) and 3.24(2) Å. The distances are normal as compared to the values 3.33 Å for Tl – Cl [1] and 2.57 to 3.19 Å for Tl – O.[2] The sixth Tl – O distance is 3.38(3) Å. A next nearest oxygen atom is then situated at the distance of 3.90(3) Å from the thallium atom. The architecture of the sheets can be described as follows. In a distorted tetrahedral arrangement the zinc atoms are each coordinated to one chlorine and to three oxygen atoms, the latter belonging to three different sulphate groups. In this way every "ZnO_3Cl tetrahedron" is linked by sharing three corners to sulphate tetrahedra and each of the sulphate tetrahedra is linked to three "ZnO_3Cl tetrahedra", forming the infinite layers of the composition $(ZnSO_4Cl)_n^{n-}$ (Fig. 1). The layers are parallel to the *bc* plane. The average bond distance S – O in the sulphate group is 1.46(2) Å and the mean distance O – O 2.38(2) Å. The Zn – O distances in the "ZnO_3Cl tetrahedra" are between 1.92(3) and 2.01(3) Å and the distance Zn – Cl is 2.19(1) Å. The distances are normal compared to those in Refs. 1 and 3.

In order to obtain more accurate values of the interatomic distances a diffractometer study has been started. A full report of this work will be published elsewhere.

The author is very grateful to Professor Bengt Aurivillius for his stimulating interest and for valuable discussions.

This investigation forms part of a research program on compounds of heavy metals, financially supported by the *Swedish Natural Science Research Council.*

1. *International Tables for X-Ray Crystallography*, Kynoch Press, Birmingham 1965, Vol. III.
2. Alcock, N. W. *Acta Cryst.* **B 29** (1973) 498.
3. Allmann, R. *Z. Kristallogr.* **126** (1968) 417.

Received June 18, 1973.

Tobacco Chemistry

21. Three New Volatile Tobacco Constituents of Probable Isoprenoid Origin

JOSEPH R. HLUBUCEK, ARNE J. AASEN, SVEN-OLOF ALMQVIST and CURT R. ENZELL

Research Department, Swedish Tobacco Co., Box 17 007, S-104 62 Stockholm 17, Sweden

We recently reported the isolation of the three new naturally occurring compounds *1*, *2*, and *3* from the volatile fraction of an extract from Greek tobacco, *Nicotiana tabacum L.*[1] Our continued interest in tobacco flavour constituents of terpenoid origin has led to the identification of three new compounds structurally related to *1* and *2*. The isolation, structural elucidation, and synthesis of these constitute the subject of the present communication.

The first two compounds were diastereomers isolated as a mixture which on high resolution gas chromatography in combination with mass spectrometry (GC–MS) was partially resolved into two compounds exhibiting almost identical mass spectra. The elemental composition of the heaviest fragment observed in the mass spectrum, *m/e* 171 (M – 15), indicated the formula $C_{11}H_{22}O_2$ for the two diastereomers. The presence of a tertiary hydroxyl group was apparent from IR absorption at 3450 cm^{-1}, two methyl singlets at δ 1.38 and δ 1.43, and the absence of signals in the δ 3.0 – 4.5 region in the NMR spectrum. On addition of $Eu(fod)_3$, these two magnetically non-equivalent methyl groups gave rise to four distinct, strongly downfield-shifted methyl signals providing further evidence for the diastereomeric nature of the mixture.

A *trans* oxirane ring accounted for the second oxygen atom as judged from resonances in the NMR spectrum appearing as two sets of signals due to the presence of two diastereomers: doublet of doublets at δ 2.87 and δ 2.88 (J 2.5 and 8.5 Hz), and doublets at δ 2.73 and δ 2.74 (J 2.5 Hz). The $J_{vic.}$ 2.5 Hz for the protons on both epoxides is consistent with *trans* disubstitution since spin-spin coupling constants across oxirane rings possessing no electronegative substituents have invariably been found in the range +1.9 to +2.5 Hz and +4.0 and +5.0 Hz for *trans* and *cis* configurations,[2,3] respectively. The presence of the electronegative hydroxyl function one carbon atom removed from the coupling path would be expected to cause an increase in $J_{vic.}$ for the oxirane protons,[4] further supporting the *trans*-disubstituted epoxide assignment on the basis of the observed $J_{vic.}$ The trisubstituted carbon atom α to the oxirane ring carried either a methyl and a *sec.*-butyl group, or an ethyl and an isopropyl group which were indicated in the NMR spectrum as two overlapping doublets at δ 0.97 and δ 0.99 (J 7 Hz), and an obscured triplet at δ 0.99 (J *ca.* 7 Hz). Since the induced shift ratios[5] observed on addition of the shift reagent were of the same magnitude for these signals the latter alternative, structure *4* was favoured for these new tobacco compounds. Strong *m/e* 59 and 85 ions in the mass spectrum arising from cleavages α to the epoxide group support the proposed structure. The dominant *m/e* 72 ion could be ascribed to transannular cleavage of the oxirane ring.[6]

Synthesis of the racemic epoxyalcohol *4* confirmed the proposed gross structure (*4*) and stereochemical assignments. Treatment of the (±)-ketone *1*[1] with methylmagnesium iodide in ether solution gave the alcohol *5*, which on overnight reaction with *m*-chloroperbenzoic acid in methylene chloride gave *4* as a mixture of diastereomers. The synthetic mixture appeared as two partially resolved peaks on high resolution gas chromatography and did not separate from the natural products on coinjection. The NMR, IR, and mass spectra of the synthetic and natural materials were indistinguishable.

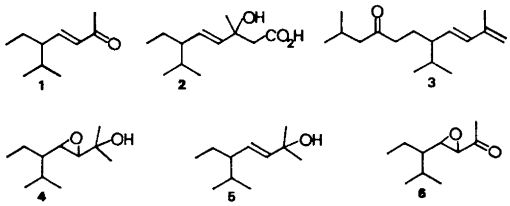

The occurrence of the epoxyalcohols *4* in the tobacco extract prompted us to investigate if the related compounds *5* and *6* were also present in Greek tobacco. A search of our mass spectral data located a

minor component in fraction B-3,[7,8] having a mass spectrum identical to that of authentic (±)-*6*, conveniently prepared by epoxidation of the ketone *1* with 30 % hydrogen peroxide in alkaline methanolic solution. The natural product was isolated by preparative gas chromatography and its structure confirmed by comparison of its NMR, IR, and mass spectra with those of the synthetic epoxyketone *6*, and co-injection on a capillary GC-column with authentic *6*. It was not clear from NMR or high resolution gas chromatography whether the natural epoxyketone *6* was a diastereomeric mixture. We have not as yet been able to conclusively identify the alcohol *5* as a component of Greek tobacco.

Experimental. Materials and methods. NMR, IR, and mass spectra were recorded on Varian HA 100D and A60-A, Digilab FTS-14, and LKB 9000 (70 eV) instruments, respectively. Columns used for combined capillary GC-MS, analytical and preparative GC, and purification of solvents, silica gel, and drying agents were as previously described.[1]

Isolation. The extraction and fractionation of the Greek tobacco (*N. tabacum* L.) has previously been described.[7] Compounds *4* and *6* were isolated by column chromatography on silica and silica impregnated with 20 % $AgNO_3$, followed by preparative GC, from fractions B-5,[7] and B-3,[7,8] respectively.

3,4E-Epoxy-5ξ-isopropyl-2-methylheptan-2-ol (*4*, 10 mg). MS: M^+ at *m/e* 186 not observed, 43 (100), 72 (66), 85 (49), 59 (43), 41 (42), 55 (40), 69 (36), 57 (35), 83 (15); accurate mass measurement: $C_{10}H_{19}O_2$ (M−15), found 171.1383, calc. 171.1385; δ ($CDCl_3$): 0.97 (3H, d, *J* 7 Hz), 0.99 (3H, d, *J* 7 Hz), 0.99 (3H, t, *J* 7 Hz), 1.38 (3H, s), 1.43 (3H, s), 1.1−2.0 (4H, m), 2.74 (1H, d, *J* 2.5 Hz), 2.88 (1H, dd, *J* 2.5 and 8.5 Hz); oxirane protons of second diastereomer: δ 2.73 (1H, d, *J* 2.5 Hz), 2.87 (1H, dd, *J* 2.5 and 8.5 Hz). Addition of $Eu(fod)_3$: *r* (relative induced shift ratio [5])= 1 and 1.13 (C(2) $(CH_3)_2$) for the first diastereomer, and *r*= 1.04 and 1.21 for the second isomer. *ν*(film): 3450 (broad), 1255 (m), 1150 (broad), 965 (m), 910 (s), 815 (m) cm^{-1}.

3,4E-Epoxy-5ξ-isopropylheptan-2-one (*6*, 1 mg). MS: 170 (M^+, 0.2), 85 (100), 43 (83), 41 (33), 55 (30), 57 (30), 69 (17); accurate mass measurement: $C_{10}H_{18}O_2$ (M−15), found 155.1065, calc. 155.1072; δ ($CDCl_3$) 0.97 (6H, 2d, *J* 6.5 Hz), 0.96 (3H, obscured), 1.1−2.0 (4H, m), 2.04 (3H, s), 2.9 (1H, dd, *J* 2.0 and 8.0 Hz), 3.16 (1H, d, *J* 2.0 Hz); *ν* (film): 1715 (s), 1360 (m), 1250 (m), 875 (m) cm^{-1}.

Synthetic products. (±)-5-Isopropyl-2-methylhept-3E-en-2-ol (5). (±)-5-Isopropylhept-3*E*-en-2-one [1] (*1*), 1.54 g) in dry ether (5 ml) was added to a suspension of methylmagnesium iodide (from 0.26 g Mg, 10 % excess) in ether (20 ml) and the reaction mixture refluxed for 30 min. Decomposition of the complexes with cold dilute H_2SO_4 and ether extraction gave essentially pure *5* (1.6 g). Material purified by column chromatography on silica gel gave MS: 170 (M^+, 0.1), 43 (100), 71 (45), 85 (19), 41 (18), 59 (14), 55 (13), 69 (11), 39 (7), 101 (7); *ν* (film): 3380 (broad), 1150 (m), 975 (s) cm^{-1}.

(±)-3,4E-Epoxy-5-isopropyl-2-methylheptan-2-ol (4). *m*-Chloroperbenzoic acid (330 mg) was added to a solution of the allylic alcohol (*5*, 300 mg) in methylene chloride (10 ml). After 3 h at room temperature TLC showed no unreacted starting material and the reaction mixture was worked up to yield, after column chromatography on silica, TLC-pure (±)-epoxy-alcohol (*4*, 210 mg). The synthetic mixture of diastereomers (ratio 2:3) was shown to be identical to the mixture of diastereomers of *4* isolated from the tobacco by their identical NMR, IR, and mass spectra and successful co-injection on a capillary GC column.

(±)-3,4E-Epoxy-5-isopropylheptan-2-one (6). Aqueous 1 M NaOH solution (2 ml) was added over 4 h to a stirred solution of (±)-5-isopropylhept-3*E*-en-2-one (*1*, 300 mg) and 30 % hydrogen peroxide (0.6 ml) in methanol (4 ml) at room temperature. After 5 h total reaction time TLC indicated no unreacted starting material and the reaction mixture was worked up to yield, after chromatography on silica, pure (±)-*6* (250 mg) as a colourless liquid. The NMR, IR, and mass spectra of synthetic (±)-*6* were indistinguishable from those of *6* isolated from the tobacco and the compounds did not separate when co-injected on a capillary GC-column.

(±)-3-Isopropylpent-1E-en-1-yl acetate (7). From the overnight reaction of (±)-5-isopropylhept-3*E*-en-2-one (*1*) with *m*-chloroperbenzoic acid in methylene chloride solution at room temperature in the absence of added alkali the vinyl acetate *7* was isolated in 30 % yield after column chromatography on silica. δ (neat): 0.80 (3H, d, *J* 6.5 Hz), 0.86 (3H, d, *J* 6.5 Hz), *ca.* 0.83 (3H, obscured) 1.0−1.9 (4H, m), 2.02 (3H, s), 5.06 (1H, dd, *J* 9 and 12.5 Hz), 6.99 (1H, d, *J* 12.5 Hz); *ν* (film): 1760 (s), 1674 (m), 1225 (s), 1090 (s), 940 (m) cm^{-1}.

Acknowledgements. The authors are indebted to Miss A.-M. Eklund for skilful technical assistance, and Professor O. Theander, Agri-

cultural College of Sweden, Uppsala, for placing the NMR instrument at their disposal.

1. Aasen, A. J., Hlubucek, J. R., Almqvist, S.-O., Kimland, B. and Enzell, C. R. *Acta Chem. Scand.* **27** (1973). *In press.*
2. Bovey, F. *Nuclear Magnetic Resonance Spectroscopy.* Academic, New York 1969, p. 361.
3. Lyle, G. G. and Keefer, L. K. *J. Org. Chem.* **31** (1966) 3921.
4. Sternhell, S. *Quart. Rev. Chem. Soc.* **23** (1969) 236.
5. Wineburg, J. P. and Swern, D. *J. Am. Oil. Chem. Soc.* **49** (1972) 267.
6. Budzikiewicz, H., Djerassi, C. and Williams, D. H. *Mass Spectrometry of Organic Compounds.* Holden-Day, San Fransisco 1967.
7. Kimland, B., Aasen, A. J. and Enzell, C. R. *Acta Chem. Scand.* **26** (1972) 2177.
8. Hlubucek, J. R., Aasen, A. J., Kimland, B. and Enzell, C. R. *Phytochemistry*, **12** (1973) 2555.

Received June 25, 1973.

On the Structures of Two Crystalline Forms of Oxydiacetic Acid

HARALD HERBERTSSON and CARL-ERIK BOMAN

Inorganic Chemistry 1, Chemical Center, University of Lund, P.O.B. 740, S-220 07 Lund, Sweden

The structure of the oxydiacetate group has been investigated in several compounds. It has been determined as hydrogen oxydiacetate ion in alkali salts,[1,2] and as oxydiacetate ion in cadmium [3] and lanthanoid [4] compounds. In these structures the ligand is planar, except in one of the three known cadmium oxydiacetate phases.[3] In the alkali compounds, hydrogen bond systems with very short hydrogen bonds were found.[1,2] We considered it therefore to be of interest to examine the free acid especially with regard to planarity and hydrogen bonds.

From aqueous solutions of oxydiacetic acid two different crystalline phases, one orthorhombic and one monoclinic, are formed side by side at room temperature. In order to determine space groups and preliminary cell dimensions, rotation and Weissenberg photographs were taken for both phases. Some important crystal data are summarized in Table 1. The orthorhombic crystals are effloresent at room temperature. From the observed density, 1.54 g cm^{-3}, and the cell volume given in Table 1, it is concluded that there is at least one water of crystallization in this compound.

Powder photographs for the monoclinic phase were obtained from a Guinier-Hägg camera with Cu$K\alpha_1$ radiation and aluminium (cubic $a = 4.04934$ Å) as internal standard. Least-squares refinement of the data gave the accurate cell constants shown in Table 1.

Table 1. Crystal data for the two phases of oxydiacetic acid.

Space group	Monoclinic $C2/c$	Orthorhombic $Pna2_1$ or $Pnam$
a	9.706(2) Å	7.52 Å
b	3.941(1)	8.24
c	15.027(2)	10.84
β	104.79(2)°	—
V	555.75 Å^3	671 Å^3
Z	4	4

Powder photographs of the orthorhombic phase, showed, among other lines, also those characteristic of the monoclinic phase. The orthorhombic crystals are thus rather quickly transformed into the monoclinic phase, when powdered. For this reason we have not been able to refine the orthorhombic cell constants.

So far we have determined the structure of the monoclinic phase only. Three-dimensional intensity data have been collected by the use of the Weissenberg multiple film technique with Cu$K\alpha$ radiation. The number of observed, independent reflexions was 396. The method of symbolic addition was used (GAASA) for the structure determination. The systematic extinctions were consistent with the space groups $C2/c$ (No. 15) and Cc (No. 9). The E statistics were decidedly in favour of the centrosymmetrical space group $C2/c$.

The positions of the oxygen and carbon atoms were obtained from the E map. It

cultural College of Sweden, Uppsala, for placing the NMR instrument at their disposal.

1. Aasen, A. J., Hlubucek, J. R., Almqvist, S.-O., Kimland, B. and Enzell, C. R. *Acta Chem. Scand.* **27** (1973). *In press.*
2. Bovey, F. *Nuclear Magnetic Resonance Spectroscopy.* Academic, New York 1969, p. 361.
3. Lyle, G. G. and Keefer, L. K. *J. Org. Chem.* **31** (1966) 3921.
4. Sternhell, S. *Quart. Rev. Chem. Soc.* **23** (1969) 236.
5. Wineburg, J. P. and Swern, D. *J. Am. Oil. Chem. Soc.* **49** (1972) 267.
6. Budzikiewicz, H., Djerassi, C. and Williams, D. H. *Mass Spectrometry of Organic Compounds.* Holden-Day, San Fransisco 1967.
7. Kimland, B., Aasen, A. J. and Enzell, C. R. *Acta Chem. Scand.* **26** (1972) 2177.
8. Hlubucek, J. R., Aasen, A. J., Kimland, B. and Enzell, C. R. *Phytochemistry*, **12** (1973) 2555.

Received June 25, 1973.

On the Structures of Two Crystalline Forms of Oxydiacetic Acid

HARALD HERBERTSSON and CARL-ERIK BOMAN

Inorganic Chemistry 1, Chemical Center, University of Lund, P.O.B. 740, S-220 07 Lund, Sweden

The structure of the oxydiacetate group has been investigated in several compounds. It has been determined as hydrogen oxydiacetate ion in alkali salts,[1,2] and as oxydiacetate ion in cadmium [3] and lanthanoid [4] compounds. In these structures the ligand is planar, except in one of the three known cadmium oxydiacetate phases.[3] In the alkali compounds, hydrogen bond systems with very short hydrogen bonds were found.[1,2] We considered it therefore to be of interest to examine the free acid especially with regard to planarity and hydrogen bonds.

From aqueous solutions of oxydiacetic acid two different crystalline phases, one orthorhombic and one monoclinic, are formed side by side at room temperature. In order to determine space groups and preliminary cell dimensions, rotation and Weissenberg photographs were taken for both phases. Some important crystal data are summarized in Table 1. The orthorhombic crystals are effloresent at room temperature. From the observed density, 1.54 g cm^{-3}, and the cell volume given in Table 1, it is concluded that there is at least one water of crystallization in this compound.

Powder photographs for the monoclinic phase were obtained from a Guinier-Hägg camera with Cu$K\alpha_1$ radiation and aluminium (cubic $a = 4.04934$ Å) as internal standard. Least-squares refinement of the data gave the accurate cell constants shown in Table 1.

Table 1. Crystal data for the two phases of oxydiacetic acid.

Space group	Monoclinic $C2/c$	Orthorhombic $Pna2_1$ or $Pnam$
a	9.706(2) Å	7.52 Å
b	3.941(1)	8.24
c	15.027(2)	10.84
β	104.79(2)°	—
V	555.75 Å^3	671 Å^3
Z	4	4

Powder photographs of the orthorhombic phase, showed, among other lines, also those characteristic of the monoclinic phase. The orthorhombic crystals are thus rather quickly transformed into the monoclinic phase, when powdered. For this reason we have not been able to refine the orthorhombic cell constants.

So far we have determined the structure of the monoclinic phase only. Three-dimensional intensity data have been collected by the use of the Weissenberg multiple film technique with Cu$K\alpha$ radiation. The number of observed, independent reflexions was 396. The method of symbolic addition was used (GAASA) for the structure determination. The systematic extinctions were consistent with the space groups $C2/c$ (No. 15) and Cc (No. 9). The E statistics were decidedly in favour of the centrosymmetrical space group $C2/c$.

The positions of the oxygen and carbon atoms were obtained from the E map. It

turned out that the ether oxygen occupied the special position 4(*e*), and thus only one-half of the other atoms in the molecule were independent and situated in 8(*f*). A least-squares refinement of the preliminary coordinates, followed by a difference Fourier synthesis with $\sin\theta/\lambda \leq 0.5$ (Å^{-1}), gave the positions of the hydrogen atoms in the methylene group. The hydrogen atom in the carboxyl group involved in the hydrogen bonding could not be located, however.

The structure was refined isotropically by least-squares methods, the temperature factors for the hydrogen atoms being fixed to 5.0 Å^2. A difference synthesis at this stage indicated anisotropic temperature vibrations for the non-hydrogen atoms. A final anisotropic least-squares refinement, with $B=5.0$ (Å^2) for the hydrogen atoms, resulted in a weighted R-value of 0.081. The weights used in these calculations were assigned according to Cruickshank. The atomic parameters are given in Tables 2 and 3.

Table 2. Atomic coordinates with standard deviations (× 10^4).

Atom	x	y	z
O(1)	0	4832(10)	2500
O(2)	−650(3)	2325(8)	4032(2)
O(3)	1416(3)	−401(8)	4468(2)
C(1)	1029(4)	2830(12)	3114(2)
C(2)	511(3)	1581(10)	3918(2)
H(1)	2057(92)	4104(250)	3451(70)
H(2)	1091(96)	432(250)	2838(75)

A schematic picture of the planar oxydiacetate ion is shown in Fig. 1, and a stereoscopic view of the structure of monoclinic oxydiacetic acid in Fig. 2.

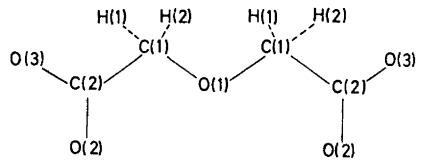

Fig. 1. A schematic picture of the oxydiacetate ion.

As seen from Fig. 2, the molecule is twisted about the ether oxygen O(1), so that the O(2) atoms are *trans* to each other. The non-hydrogen atoms in the independent half of the molecule are coplanar (Table 4), and the angle between the two ligand halves is 72°. The interatomic distances and angles given in Table 5 agree very well with those found in the alkali hydrogen oxydiacetates.[1,2]

Table 4. Least-squares plane for the oxydiacetic molecule and distances of atoms from this plane.

Atoms defining plane
O(1), O(2), O(3), C(1), C(2)

Equation
$-0.279x-0.806y-0.522z+3.182=0$

Displacement from the plane.	
O(1)	0.019 Å
O(2)	−0.005
O(3)	0.017
C(1)	−0.023
C(2)	−0.009

Table 3. Anisotropic thermal parameters with standard deviations (× 10^4). The form of the temperature factor is $\exp(-\beta_{11}h^2-\ldots-2\beta_{12}hk-\ldots)$; the root-mean square components R_i(× 10^3) in Å of thermal displacement along the ellipsoid axes are also listed.

Atom	β_{11}	β_{22}	β_{33}	β_{12}	β_{13}	β_{23}	R_1	R_2	R_3
O(1)	96(5)	230(33)	19(1)	0	2(2)	0	216	135	141
O(2)	82(4)	507(30)	28(1)	57(7)	13(2)	29(4)	224	156	179
O(3)	84(3)	456(29)	27(1)	46(7)	9(1)	27(5)	213	149	190
C(1)	67(4)	245(35)	21(1)	−16(9)	2(2)	0(5)	186	135	146
C(2)	60(3)	236(34)	15(1)	−14(7)	8(2)	−22(4)	166	106	152

Table 5. Interatomic distances and angles for monoclinic oxydiacetic acid.

Distances	Å	Angles	°
O(1)–C(1)	1.415(5)	C(1)–O(1)–C(1)	112.2(4)
C(1)–C(2)	1.505(5)	O(1)–C(1)–C(2)	112.3(3)
C(2)–O(2)	1.218(4)	C(1)–C(2)–O(2)	123.0(3)
C(2)–O(3)	1.302(4)	C(1)–C(2)–O(3)	113.4(3)
O(2)–O(3)	2.221(4)	O(2)–C(2)–O(3)	123.6(3)
C(1)–H(1)	1.12(9)	O(1)–C(1)–H(1)	116(5)
C(1)–H(2)	1.04(10)	O(1)–C(1)–H(2)	111(6)
		C(2)–C(1)–H(1)	103(5)
		C(2)–C(1)–H(2)	95(6)
		H(1)–C(1)–H(2)	117(7)

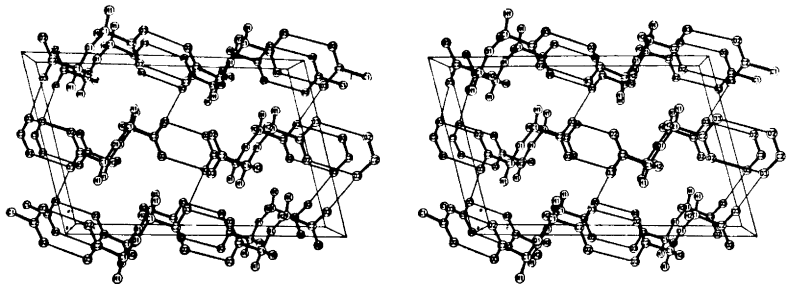

Fig. 2. A stereoscopic drawing of the structure of the monoclinic oxydiacetic acid.

As seen from Table 5, the distances C(2)–O(2) and C(2)–O(3) are 1.218(4) and 1.302(4) Å, respectively. The hydrogen atom in the carboxyl group should thus be closer to O(3) than to O(2). The structure may be described in two different ways, depending on the position of the carboxyl hydrogen atom. If it is situated on a line between the atoms O(2) and O(3), which are 2.65 Å apart, infinite chains are formed along the *c*-axis; the chains are held together by van der Waals forces. On the other hand, the distances O(3)–O(2) and O(3)–O(3), which are 2.65 and 2.83 Å, respectively, might indicate a bifurcated hydrogen bond, with the hydrogen atom situated within the triangle formed by the atoms O(3), O(3), and O(2). If this is the case, the structure is hydrogen-bonded in three dimensions.

We will later try to find the position of the hydrogen atom in the carboxyl group by the use of a more refined technique, and so be able to decide which one of the two models is the correct one.

For the orthorhombic phase, three-dimensional X-ray intensity data have been collected as for the monoclinic phase. Possible space groups are *Pnam* (No. 62) and $Pna2_1$ (No. 33), and the *E* statistics indicate $Pna2_1$ as the more probable one. Attempts to solve the structure of this compound are being continued.

1. Albertsson, J., Grenthe, I. and Herbertsson, H. The Crystal Structures of Sodium and Potassium Hydrogen Oxydiacetate. *Acta Cryst.* **B 29** (1973) 1855.
2. Albertsson, J., Grenthe, I. and Herbertsson, H. The Crystal and Molecular Structure of Rubidium Hydrogen Oxydiacetate. *To be published.*
3. Boman, C.-E. On the Structures of Three Different Forms of Solid Cadmium Oxydiacetate Hydrate. *To be published.*
4. Albertsson, J. *On the Stereochemistry of Nine-coordinate Lanthanoid Compounds.* Diss., Lund 1972, Sweden.

Received July 12, 1973.

Xanthone Studies

V.* Hydroxyl Proton Chemical Shifts of Hydroxyxanthones with Allylic Substituents

PER HELBOE and PETER ARENDS

Chemical Laboratory B, The Royal Danish School of Pharmacy, DK-2100 Copenhagen, Denmark

In a previous communication[1] the hydroxyl proton chemical shifts in DMSO-d_6 of hydroxy- and methoxy-substituted xanthones were reported and correlated with the oxygenation patterns. Several naturally occurring xanthones also have allylic side chains, which may be cyclized to pyrano or furano ring systems.[2] An investigation of the influence of these substituents upon the hydroxyl proton chemical shifts measured in DMSO-d_6 has therefore been undertaken. The results reported here (Table 1) are for thirteen xanthones with one or two hydroxyl groups and one or two allylic substituents in the same ring, and for jacareubin (I), isojacareubin (II), maculatoxanthone (III), mangostin (IV), and an oxidatively-cyclized derivative (V) of mangostin.

The resonance of the 1-hydroxyl ** proton is shifted 0.25 – 0.35 ppm to lower field when an allylic substituent is introduced into the *ortho* position, *e.g.* 1-hydroxy-2-allyl- and 1,3-dihydroxy-2-allylxanthone, while this is not the case for a 2- or 3-hydroxyl proton (see later); a *para*-substituent produces no shift, *e.g.* 1,3-dihydroxy-4-allylxanthone. This may be interpreted mainly as a steric effect. The *ortho* substituent forces the 1-hydroxyl group closer to the xanthone carbonyl, thereby augmenting the chelation of the hydroxyl proton. The same effect is operative with even greater magnitude when the steric crowding is increased, as for example in 1,3-dihydroxy-2,4-diallylxanthone (shifted by 0.45 ppm) and 1-hydroxy-2-(1,1-dimethyl-2-propenyl)-xanthone (shifted by 0.85 ppm). The presence of the dimethyl-chromen moiety with the pyrano ring linearly fused to the xanthone nucleus, as in

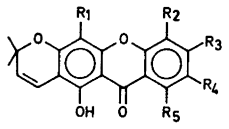

I $R_1=R_4=R_5=H$, $R_2=R_3=OH$

III $R_4=R_5=H$, $R_2=R_3=OH$
R_1=Lavandulyl

V $R_1=R_2=H$ $R_3=OH$, $R_4=OCH_3$
$R_5=CH_2-CH=C(CH_3)_2$

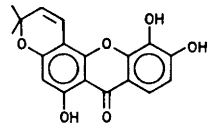

II

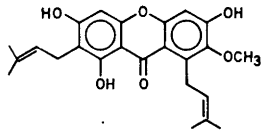

IV

jacareubin (I) and maculatoxanthone (III), also causes a large shift (0.6 – 0.7 ppm). This can be interpreted as arising from a combination of a steric and a resonance effect since, for isomers in which the pyrano ring is angularly fused, *e.g.* isojacareubin (II), the resonance of the 1-hydroxyl proton is shifted to lower field to a lesser extent (0.4 ppm), steric effects being absent.

The steric diminution of the hydrogen bonding distance between the chelating groups may also be effected by an allylic substituent in the 8-position; this again leads to a downfield shift of the 1-hydroxyl proton, for example 0.35 ppm for 1,5-dihydroxy-8-(3-methyl-2-butenyl)-xanthone. When resonance effect or/and steric compression operates from both the 2- and the 8-position as in mangostin(IV) and its oxidatively cyclized derivative(V), the chemical shifts of the 1-hydroxyl proton are the lowest measured.

The chemical shifts of the 2- or 3-hydroxyl protons are not influenced by the presence of a single *ortho*-situated allyl group, *e.g.* 2-hydroxy-1-allyl-, 3-hydroxy-4-allyl-, and 1,3-dihydroxy-2-allyl-xanthone. However, when surrounded by two allyl-substituents as in 2-hydroxy-

* Part IV see Ref. 1.

** The numbering system is based on 9-xanthenone as the parent compound.

Table 1. Chemical shifts of xanthone hydroxyl protons in DMSO-d_6.

	δ for OH at position (the value for the corresponding hydroxy xanthone [1] is given in parenthesis)			
	1(8)	2(7)	3(6)	4(5)
1-Hydroxy-2-allyl [4]	12.90(12.55)			
1-Hydroxy-2-(1,1-dimethyl-2-propenyl) [5]	13.40(12.55)			
2-Hydroxy-1-allyl [5]		9.80(9.85)		
2-Hydroxy-1,3-diallyl [5]		8.75(9.85)		
3-Hydroxy-4-allyl [5]			10.95(10.90)	
3-Hydroxy-2,4-diallyl [5]			9.90(10.90)	
4-Hydroxy-3-allyl [6]				10.00(10.35)
1,3-Dihydroxy-2-allyl [7]	13.00(12.70)		11.00(10.95)	
1,3-Dihydroxy-4-allyl [7]	12.75(12.70)		11.00(10.95)	
1,3-Dihydroxy-2,4-diallyl [7]	13.15(12.70)		10.00(10.95)	
1,3-Dihydroxy-2-(3-methyl-2-butenyl) [5]	13.00(12.70)		11.00(10.95)	
1,3-Dihydroxy-2,4-bis(3-methyl-2-butenyl) [5]	13.05(12.70)		9.95(10.95)	
1,5-Dihydroxy-8-(3-methyl-2-butenyl) [8]	12.95(12.60)			10.20(10.40)
Jacareubin (I) [5]	13.65(12.95)			
Isojacareubin (II) [5]	13.35(12.95)			
Maculatoxanthone (III) [9]	13.55(12.95)			
Mangostin (IV) [10]	13.90(13.05)			
V [11]	13.95(13.05)			

1,3-diallyl- and 3-hydroxy-2,4-diallyl-xanthone these hydroxyl protons show *upfield* shifts (1.1 and 1.0 ppm, respectively), which may be attributed to the partial inhibition of intermolecular hydrogen bonding between the phenolic proton and a solvent molecule. An alternative explanation, which has been presented for the observation of an upfield shift (1.2 ppm) of the hydroxyl proton in 2,6-dimethylphenol,[3] is that resonance has been inhibited by the hydrogen bonded hydroxyl group not being coplanar with the ring. This explanation does not seem valid for the xanthones, however, since the 2- and the 3-hydroxyl protons experience nearly the same shifts in the *o,o'*-disubstituted compounds. If the 3-hydroxyl group, situated *para* to the carbonyl group, is sterically hindered from being coplanar with the aromatic nucleus its proton would be expected to show an upfield shift. For the 2-hydroxyl group, being *para* to the ether bridge, the same situation should, if anything, lead to a shift in the opposite direction.

The 4-hydroxyl group can only have a single *ortho*-situated allylic substituent, yet its presence also causes an upfield shift in, for example, 4-hydroxy-3-allyl-xanthone (shifted by 0.35 ppm). In this case the other *ortho*-position is occupied by an ether bridge instead of an allylic substituent so that the steric crowding might be expected to be less.

Experimental. ^{1}H-NMR-spectra were recorded as previously described.[1] All compounds were synthesized or isolated in this laboratory (references in Table 1).

1. Arends, P. and Helboe, P. *Acta Chem. Scand.* **26** (1972) 4180.
2. Carpenter, I., Locksley, H. D. and Scheinmann, F. *Phytochemistry* **8** (1969) 2013.
3. Tribble, M. T. and Traynham, J. G. *J. Am. Chem. Soc.* **91** (1969) 379.
4. Scheinmann, F. and Suschitzky, H. *Tetrahedron* **7** (1959) 31.
5. Helboe, P. and Arends, P. *Arch. Pharm. Chem. Sci. Ed.* **1** (1973) 69.
6. Mustafa, A., Sidky, M. M., Zayed, S. and Soliman, F. M. *Tetrahedron* **19** (1963) 1335.
7. Jain, A. C., Khanna, V. K. and Seshadri, T. R. *Indian J. Chem.* **7** (1969) 1182.
8. Quillinan, A. J. and Scheinmann, F. *J. Chem. Soc. Perkin Trans.* **1 1972** 1382.
9. Arends, P. *Tetrahedron Lett.* **1969** 4893.
10. Yates, P. and Stout, G. H. *J. Am. Chem. Soc.* **80** (1958) 1691.
11. Locksley, H. D., Quillinan, A. J. and Scheinmann, F. *J. Chem. Soc.* **C 1971** 3804.

Received May 11, 1973.

The Inhibition of the Electrochemical Oxidation of Glucose at Platinum at pH = 7.4 by Chloride Ions

E. M. SKOU

Fysisk-Kemisk Institut, The Technical University of Denmark, DK-2800 Lyngby, Denmark

In their attempt to develop an implantable fuel cell as power source for an artificial heart or a cardiac pacemaker, several workers [1-3] have studied the electrochemical oxidation of glucose on platinum in neutral media. Their experiments were carried out either in physiological solutions [2,3] or in phosphate or carbonate buffers,[1] where high ionic strengths were obtained by addition of KCl. Glucose showed very little activity in all cases. It will be shown in this communication that chloride ions have a strong inhibitory effect on the electrochemical oxidation of glucose, so the low activity found in the experiments reported was probably caused by the chloride ions in the buffers used.

Experimental. The experiments were carried out at pH = 7.4 in a 0.2 M phosphate buffer. The ionic strength was set to 1.0 M by addition of Na_2SO_4. All chemicals were analytical grade from Riedel de Haën, and the water was redistilled from an alkaline $KMnO_4$ solution. The buffer solution is equivalent to the one used by Rao and Drake [1] in their investigation of the electrooxidation of glucose, except that the KCl is replaced by Na_2SO_4. The temperature was maintained at 25°C by means of a thermostat, and the solution was degassed by bubling with oxygenfree nitrogen. The electrodes used were either a platinum disk electrode or a platinum wire in the form of a flat spiral of diameter 0.6 cm. The disk electrode was made of a 0.5 cm long platinum cylindrical stud with a diameter of 0.5 cm soldered to a stainless steel rod. The electrode was then covered with a PTFE tube of 1.2 cm external diameter, which was heated to 160°C before it was press fitted over the cold electrode. The end of the electrode was ground with water proof silicon carbide paper and polished with diamond paste. The platinum spiral electrode was made of a piece of 0.7 mm diameter wire. The wire except the spiral was covered with a piece of shrinkable PTFE tube. The counter electrode was a platinum spiral placed in a pyrex gas dispenser (Sovirel 4.853 – 2). The sintered glass disk in the dispenser was placed opposite the exposed area of the electrodes. When the disk electrode was used, the reference electrode was a dynamic Pt-black hydrogen electrode loaded with 100 $\mu A/cm^2$ (geometrical area) and placed in a Lugin capillary, while a standard mercurous sulfate electrode (Radiometer type K 601) was placed at the edge of the platinum spiral electrode. The ohmic drop was determined by measuring the impedance at 1 kHz and 3 kHz. It was *ca.* 4 ohm with the disk electrode and *ca.* 15 ohm with the spiral electrode. The potentiostat was made at the Fysisk-Kemisk Institut by use of an operational amplifier (Motorola MC 1433) with an input bias current of 0.2 μA. The signal generator was an Exact Waveform Generator type 505B. The current was measured as the potential drop across a resistance in the counter electrode circuit, and the current potential curve was recorded at an X–Y recorder (Omnigraphic 2000 from Houston Instruments). The electrodes were pretreated with a periodic triangular sweep between 0.05 and 1.5 V *vs.* a standard hydrogen electrode in the same solution (NHE) with a sweep rate of 0.3 V/sec until reproducibility was obtained. The electrode area was determined coulombmetrically from the hydrogen coverage using a sweep rate of 0.3 V/sec. The current potential curve was recorded at 0.3 V/sec and 0.03 V/sec between 0.05 V and 1.5 V *vs.* NHE in a 0.25 M glucose solution with chloride concentrations between 0 and 5×10^{-2} M. Both electrode types gave similar results, and the curves were reproducible after a few sweeps.

Results. Current potential curves for buffer solutions, which were 0.25 M in glucose and from 5×10^{-4} M to 5×10^{-2} M in chloride, are shown in Figs. 1 to 3. The curves were corrected for double layer charging as well as formation and removal of the Pt-H layer by subtracting the values obtained during the sweep made in the pure buffer solution. This procedure introduces a small error, because the correction is dependent on glucose and chloride concentrations. The effect of glucose is not known, but sweeps made on glucose in 1 M H_2SO_4 (where glucose is not oxidized between 0 V and 0.5 V *vs.* NHE) showed that the effect is small in that medium. The effect of the chloride ions has been checked by making sweeps in a buffer solution which was 0.5 M in KCl. The chloride ions lowered the hydrogen peaks

between 0.25 V and 0.4 V *vs.* NHE, but the error should not be greater than approx. 20 % with the highest chloride concentration. It is seen from the curves in the Figs. 1 to 3 that glucose (or intermediary products) is oxidized by two mechanisms, the associated current peaks of which are separated in the anodic scan ($dV/dt > 0$) in Fig. 1 but overlap in the cathodic scans

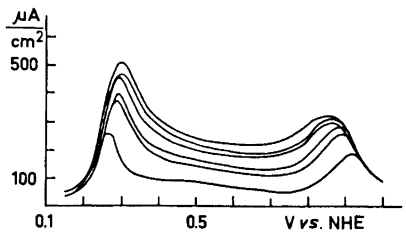

Fig. 1. The oxidation of glucose on platinum in phosphate buffer at pH = 7.4 and different chloride concentrations: 0 (largest current), 5×10^{-4}, 10^{-3}, 5×10^{-3}, 10^{-2}, and 5×10^{-2} M (smallest current). Anodic scan. Sweep rate: 0.3 V/sec.

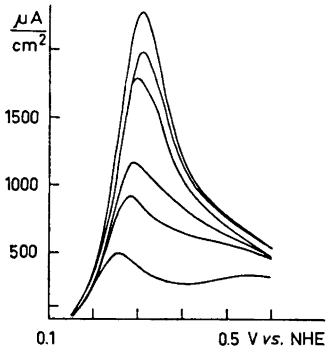

Fig. 2. As Fig. 1. Cathodic scan. Sweep rate: 0.3 V/sec.

($dV/dt < 0$) in Figs. 2 and 3. It can also be seen that the peaks associated with the two mechanisms have differing sweep rate dependencies. There is a third current peak (not shown in Fig. 1) in the anodic scan between 1.1 V and 1.5 V *vs.* NHE, but this is almost unaffected by the chloride ions. The nature of the current peaks will be discussed in a later communication. The effect of the chloride ions is seen to dis-

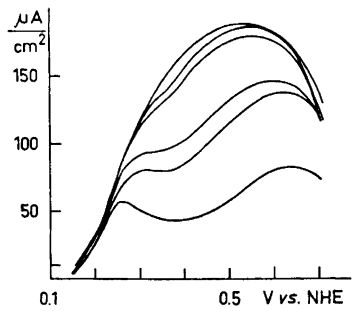

Fig. 3. As Fig. 1. Cathodic scan. Sweep rate: 0.03 V/sec.

appear at 0.95 to 1.0 V *vs.* NHE in the anodic scan, where they probably are removed during the formation of the Pt-O layer. The Pt-O layer is reduced in the cathodic scan from 0.9 V to 0.4 *vs.* NHE.

The dependence of the current on the chloride concentration can be used to find the chloride adsorption isotherms, if it is assumed that the current at a given potential is proportional to the electrode area not covered with chloride ions:

$$i = i_0(1 - \theta)$$

where θ is the surface coverage of chloride ions, and i_0 is the current obtained for the chloride concentration $c_{Cl^-} = 0$.

Rearrangement gives:

$$\theta = 1 - i/i_0$$

The adsorption isotherm $\theta = f(c_{Cl^-})$ can be found by plotting $1 - i/i_0$ against different functions of c_{Cl^-} at constant potential.

A plot of $1/\theta$ against $1/c_{Cl^-}$ corresponding to Langmuir adsorption did not give a straight line, whereas a plot of θ against log c_{Cl^-} did give reasonable straight lines, indicating that chloride adsorbs through a logarithmic isotherm: $Kc_{Cl^-} = e^{(b\theta)}$ or

$$\theta = \frac{2.303}{b} \log K + \frac{2.303}{b} \log c_{Cl^-}$$

where K is the absorption konstant and b an interaction parameter. The slope of such lines gives b and the extrapolation to $\theta = 0$ gives $K = 1/c_{Cl^-}(\theta = 0)$. Plots of θ (calculated from the curves in Figs. 1, 2, and 3) *vs.* log c_{Cl^-} at 0.275, 0.375, and 0.500 V *vs.* NHE are shown in Fig. 4 (a–c), and the corresponding b values and K values are shown in Table 1. The results show,

Table 1. Adsorption constant K and interaction parameter b corresponding to a logarithmic isotherm for the adsorption of chloride on platinum in phosphate buffer at pH = 7.4. Subscripts c and a refer to cathodic and anodic scans.

$\pi - \pi_{NHE}$ V	dV/dt V/sec	b_c	b_a	K_c l/mol	K_a l/mol
0.275	0.3	6.2	11	2.2×10^3	2.0×10^3
	0.03	9.6		1.4×10^3	
0.375	0.3	6.1	7.9	2.9×10^3	3.3×10^3
	0.03	6.6		2.3×10^3	
0.500	0.3	13	9.2	3.3×10^3	4.3×10^3
	0.03	6.8		1.5×10^3	

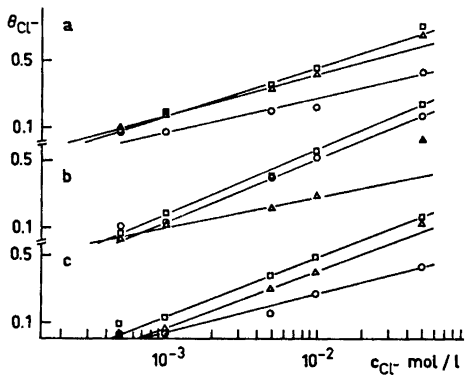

Fig. 4. a. The surface coverage of chloride as function of log c_{Cl^-} at different potentials. ○ ~0.275 V, □ ~0.375 V and △ ~0.500 V *vs.* NHE. Anodic scan. Sweep rate: 0.3 V/sec. b. As Fig. 4a. Cathodic scan. Sweep rate: 0.3 V/sec. c. As Fig. 4a. Cathodic scan. Sweep rate: 0.03 V/sec.

that the chloride ion adsorption is higher at 0.375 V than at 0.275 V *vs.* NHE in all cases. These findings are in agreement with the results obtained by Horanyi, Solt and Nagy [4] for the chloride adsorption on platinum in 1 N $HClO_4$ measured with a tracer technique.

Although their results indicate adsorption through a logarithmic isotherm, an increase in adsorption with potential and b values close to the values found in this work, the K values were of the order of 10^5 to 10^6 l/mol. Also, they reported the hysteresis between the anodic and cathodic scans, which can be seen from Figs. 4a and b. The rise in chloride adsorption at 0.500 V *vs.* NHE when the sweep rate is changed from 0.3 V/sec to 0.03 V/sec (Figs. 4b and c), can be caused by the time dependence of the reduction of the Pt-O layer, which has been investigated by Vetter and Schultze.[5]

1. Rao, M. L. B. and Drake, R. F. *J. Electrochem. Soc.* **116** (1969) 334.
2. Yao, S. J., Appleby, A. J., Geisel, A., Cash, H. R. and Wolfson, S. K. *Nature* **224** (1969) 921.
3. Appleby, A. J. and VanDrunen, C. *J. Electrochem. Soc.* **118** (1971) 95.
4. Horanyi, G., Solt, J. and Nagy, F. *J. Electroanal. Chem.* **31** (1971) 95.
5. Vetter, K. J. and Schultze, J. N. *J. Electroanal. Chem.* **34** (1972) 131; 141.

Received June 27, 1973.

Ring-opening Reactions of Heterocyclic Metal-organics. IV. The Synthesis of Acetylenic Mixed Ketenethioacetals and Thio-seleno-acetals

SALO GRONOWITZ and TORBJÖRN FREJD

Chemical Center, Division of Organic Chemistry 1, University of Lund, Box 740, S-220 07 Lund 7, Sweden

It has previously been demonstrated that certain 3-lithiothiophenes, and especially 3-lithioselenophenes, ring-open to give *Z*-1-butene-3-yne-1-thiolates and *Z*-1-butene-3-yne-1-selenolates.[1-4] These products are alkylated by the alkyl halides formed in the preparation of the lithio derivatives by halogen-metal exchange, or by alkyl halides intentionally added to the reaction mixture.

We have now found that this ring-opening reaction proceeds smoothly with 2-methylthio-4-thienyllithium, and especially with 2-methylthio-4-selenienyllithium derivatives, to give a type of organic compounds which as far as we could find have not been described before, namely acetylenic ketenethioacetals or mixed acetylenic ketenethio-seleno-acetals (*cf.* Formula scheme).

Thus the reaction of 3-bromo-2-methyl-5-methylthiothiophene (Ia) with ethereal ethyllithium at room temperature, followed by the addition of ethyl bromide, gave a mixture consisting of three components (VPC) in about 80 % yield. The main component (70 %), which was obtained pure by TLC, was shown by NMR, IR, and mass spectral data and by elemental analyses to be *Z*-1-ethylthio-1-methylthio-1-penten-3-yne. The two by-products, which were formed in 25 % and 5 % yields, both had molecular weight of 200, and judging from their fragmentation pattern, these compounds are most probably 1-methylthio-1-ethylthio-1-heptene-3-yne, formed by alkylation at the acetylenic methyl group, and 3-ethyl-2-methyl-5-methylthiothiophene, formed by Wurtz reaction between the initially formed 2-methyl-5-methylthio-3-thienyllithium and ethyl bromide. It should perhaps be stressed that if halogen-metal exchange between 2-methylthio-4-bromothiophenes is carried out at −70°, the 2-methylthio-4-thienyl-lithium derivatives are stable enough to allow the preparation of many different 4-substituted-2-methylthiothiophenes.[5,6]

3-Bromo-2-methyl-5-methylthioselenophene reacted more smoothly and gave an 85 % yield of 95 % pure *Z*-1-ethylseleno-1-methylthio-1-pentene-3-yne (IIb). (The structure proof is given in the experimental part.) It has been demonstrated that the ring-opening is stereospecific [2-4] (the acetylenic bond and the thiolate group being *cis*-situated), so the *Z*-structure is assigned to IIa and IIb. It was, however, observed that isomerization to a 50:50 mixture of *cis-trans* isomer occurred during attempts to prepare pure Ia by preparative VPC at 190°C. (For an investigation of barriers to rotation around the carbon-carbon double bond in 1,1-bisalkylthio-ethylenes, *cf.* Refs. 7 – 8.) Compound Ia was prepared from 2-methylthiophene by dibromination to give 3,5-dibromo-2-methylthiophene,[9] followed by halogen-metal exchange and reaction with dimethyldisulphide. 3,5-Dibromo-2-methylselenophene could not be prepared in a completely analogous way, as decomposition occurred upon attempted bromination of 2-methylselenophene under conditions used successfully in the thiophene series. However, by using *N*-bromosuccinimide, 2-methylselenophene [10] could be dibrominated in the 5- and 3-positions. Halogen-metal exchange and reaction with dimethyldisulphide, as in the thiophene series, gave compound Ib.

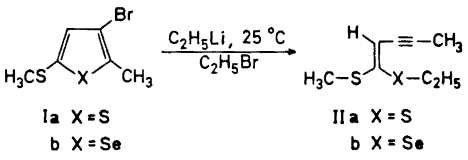

Ia X = S
b X = Se

IIa X = S
b X = Se

As mentioned above, compounds such as IIa and IIb have as far as we could find not been described in the literature. Addition of alkylthiolates or alkylselenolates to methyl-methylthiodiacetylenes occurs at the acetylenic carbon to which the methyl group is bonded, giving 2-methylthio-5-alkylthio-2-pentene-4-yne or the corresponding alkylseleno derivative, respectively.[11] It would perhaps be possible to apply the method used for the synthesis

of 1,1-dialkylthioethylenes,[12-14] consisting in the condensation of carbanions from active methylene derivatives with carbon disulphide, followed by alkylation. This method, has, as far as we are aware, not been applied to dialkylacetylenes, but even if it would be successful, it would certainly not be useful for the stereospecific synthesis of mixed ketenethioacetals or ketene thio-seleno acetals such as IIa and IIb.

The scope of this ring-opening route to acetylenic ketene mercaptals appears to be broad. It should be possible to use different alkylthio or arylthio groups in the thiophenes and selenophenes. It is also feasible to alkylate the thiolate or selenolate functionality formed in the ring-opening with a variety of reagents, if the halogen-metal exchange is carried out with phenyllithium followed by any alkylating agent.[15] We are currently persuing these aspects of the ring-opening reaction.

Experimental. 3,5-Dibromo-2-methylselenophene. To a stirred solution of 9.6 g (0.066 mol) of 2-methylselenophene in 70 ml of acetic acid, 25.8 g (0.145 mol) of *N*-bromosuccinimide was added in portions at room temperature. When the addition was complete, the mixture was stirred for 30 min and poured into water. The mixture was extracted several times with ether and the combined ether phases washed with sodium hydrogen carbonate solution and water to neutral reaction. The ether phase was dried and fractionated to yield 11.0 g (55 %) of 2,4-dibromo-5-methylselenophene, b.p. 81–82°/1 mmHg. NMR (CCl_4): $\delta_{CH_3}=2.35$ ppm; $\delta_4=6.96$ ppm. [Found: C 19.86; H 1.28; Br 52.87; Se 26.07. Calc. for $C_5H_4Br_2Se$ (302.84): C 19.83; H 1.33; Br 52.77; Se 26.07].

3-Bromo-2-methyl-5-methylthioselenophene. To a stirred solution of 7.74 g (0.0256 mol) of 3,5-dibromo-2-methylselenophene at −70°, 16.0 ml of 1.6 N butyllithium in hexane was added at −70°. After 10 min the reaction mixture was pressed into 2.45 g (0.0260 mol) of dimethyldisulphide in 25 ml of anhydrous ether and the mixture stirred for 3 h and then hydrolyzed with water. The ether phase was washed with dilute sodium hydroxide solution and water, dried and fractionated to yield 4.42 g (64 %) of the title compound, b.p. 89–93°/0.8 mmHg. NMR (CCl_4): $\delta_{SCH_3}=2.86$ ppm, $\delta_{CH_3}=2.82$ ppm, $\delta_4=7.55$ ppm. [Found: C 26.60; H 2.55; Br 29.56; S 11.78; Se 29.40. Calc. for C_6H_7BrSSe (270.05): C 26.69; H 2.61; Br 29.59; S 11.87; Se 29.24].

3-Bromo-2-methyl-5-methylthiothiophene. From 36.0 g (0.141 mol) of 3,5-dibromo-2-methylthiophene [9] in 100 ml of anhydrous ether, 81.5 ml of 1.6 N butyllithium in hexane and 14.1 g (0.150 mol) of dimethyldisulphide, 22.2 g (70 %) of the title compound, b.p. 79–81°/1.4 mmHg was obtained, following the procedure described above. NMR (CCl_4) δ_{SCH_3}, $\delta_{CH_3}=2.29$ and 2.36 ppm, $\delta_4=6.78$ ppm. [Found: C 32.22; H 3.19; Br 35.80; S 28.80; Calc. for $C_6H_7BrS_2$ (223.15): C 32.29; H 3.16. Br 35.81; S 28.71].

Z-1-Ethylseleno-1-methylthio-1-pentene-3-yne. To a stirred solution of 2.70 g (0.0100 mol) of 3-bromo-2-methyl-5-methylthioselenophene in 50 ml of anhydrous ether, 15.8 ml of 0.7 N ethereal ethyllithium was added, and the mixture stirred for 15 min. Then 7.6 g (0.070 mol) of ethyl bromide was added and the mixture stirred for 4 h. Water was added, the ether phase separated, washed with water and dried. The ether was evaporated, and VPC (OV 17 (5 %), 2 m × 3 mm, 170°) showed that the crude product (1.85 g; 84 %) consisted to 95 % (area %) of the title compound. Distillation yielded 1.2 g (55 %) of pure *Z*-1-ethylseleno-1-methylthio-1-pentene-3-yne, b.p. 66–67°/5×10^{-3} mmHg. IR: 2205 cm^{-1} (C≡C), 1530 cm^{-1} (C=C). NMR (CCl_4): $\delta_{CCH_3}=1.95$ ppm; $\delta_2=5.68$ ppm; $\delta_{SCH_3}=2.16$ ppm; $\delta_{Se-CH_2}=2.84$ ppm; $\delta_{CH_2-CH_3}=1.37$ ppm; $J_{CCH_3-H}=2.40$ Hz; $J_{CH_2-CH_3}=7.0$ Hz. Mass spectrum: M^+; $m/e=220$. Calc. for $C_8H_{12}S^{80}Se$ $m/e=220$. [Found: C 43.78; H 5.52; S 14.58; Se 36.21. Calc. for $C_8H_{12}SSe$ (219.21): C 43.83; H 5.52; S 14.63; Se 36.02].

Z-1-Ethylthio-1-methylthio-1-pentene-3-yne. When 10.0 g (0.0448 mol) of 3-bromo-2-methyl-5-methylthiothiophene in 150 ml of ether was treated with 75 ml of 0.6 N ethyllithium and then with 23.4 g (0.150 mol) of ethyl iodide and worked up as above, 7.5 g of product was obtained which according to VPC (BDS (10 %); 2 m × 3 mm; 130–190°, 16°/min) and combined VPC-mass spectrometry showed three components (in order of increasing retention time) with the area percentage 5 (m/e 200), 70 ($m/e=172$, the title compound), and 25 ($m/e=200$). The crude product was distilled at 91–94°/1.2 mmHg and pure *Z*-1-ethylthio-1-methylthio-1-pentene-3-yne was obtained through preparative thin layer chromatography (1 mm silica gel; hexane:ether 10:1). IR: 2205 cm^{-1} (C≡C); 1540 cm^{-1} (C=C). NMR (CCl_4): $\delta_{CCH_3}=2.00$ ppm; $\delta_2=5.58$ ppm; $\delta_{SCH_3}=2.28$ ppm; $\delta_{SCH_3}=2.86$ ppm; $\delta_{CH_2-CH_3}=1.28$ ppm; $J_{CCH_3-H}=2.40$ Hz; $J_{CH_2-CH_3}=7.0$ Hz. [Found: C 55.7; H 7.04; S 36.4. Calc. for

$C_8H_{12}S_2$ (172.32): C 55.76; H 7.02; S 37.22]. VPC analyses were performed on a Perkin Elmer 900 Gas Chromatograph. IR spectra were recorded on a Perkin Elmer 257 Grating Infrared Spectrophotometer, NMR spectra on a Varian A-60 spectrometer and mass spectra on an LKB 9000 mass spectrometer.

Acknowledgements. Grants from the *Swedish Natural Science Research Council* to S.G. and from the *Royal Physiographic Society* to T.F. are gratefully acknowledged.

1. Gronowitz, S. and Frejd, T. *Acta Chem. Scand.* **23** (1969) 2540.
2. Gronowitz, S. and Frejd, T. *Acta Chem. Scand.* **24** (1970) 2656.
3. Jacobsen, H. J. *Acta Chem. Scand.* **24** (1970) 2663.
4. Gronowitz, S. and Frejd, T. *Int. J. Sulfur Chem. Part A* **2** (1972) 165.
5. Gronowitz, S., Moses, P. and Håkansson, R. *Arkiv Kemi* **16** (1960) 267.
6. Gronowitz, S., Moses, P. and Hörnfeldt, A.-B. *Arkiv Kemi* **17** (1961) 237.
7. Isaksson, G., Sandström, J. and Wennerbeck, I. *Tetrahedron Letters* **1967** 2233.
8. Sandström, J. and Wennerbeck, I. *Acta Chem. Scand.* **24** (1970) 1191.
9. Gronowitz, S., Moses, P., Hörnfeldt, A.-B. and Håkansson, R. *Arkiv Kemi* **17** (1961) 165.
10. Yur'ev, Yu.K., Mezentzova, N. N. and Vaskovskii, V. E. *J. Gen. Chem. USSR* **27** (1957) 3193.
11. Brandsma, L. *Preparative Acetylenic Chemistry*, Elsevier, New York 1971, p. 92.
12. Gompper, R. and Töpfl, W. *Chem. Ber.* **95** (1962) 2861.
13. Gompper, R. and Töpfl, W. *Chem. Ber.* **95** (1962) 2871.
14. Jensen, K. A. and Henriksen, L. *Acta Chem. Scand.* **22** (1968) 1107.
15. Gronowitz, S. and Frejd, T. *To be published.*

Received August 23, 1973.

Reactivation of Phosphorylated Cholinesterase by Some Imidazole-substituted Oximes

TOM KARLSSON, KARL-ERLAND STENSIÖ and KERSTIN WAHLBERG

Research Institute of National Defence, Department 1, S-172 04 Sundbyberg 4, Sweden

Nucleophilic agents such as oximes have been employed in restoring the activity of cholinesterase (ChE) which has been inactivated by organophosphorus compounds. Methyl-quaternized pyridinium aldoximes have been found particularly effective.[1] By a suitable modification of the substituent on the nitrogen, an increase in the reactivation rate was obtained.[2] Our intention has been to study the effect of an imidazole substituent in the pyridine aldoxime.

There is strong evidence that imidazole is part of the active site of ChE.[3] Furthermore, imidazole has a well documented catalytic capacity, *e.g.* for ester hydrolysis, both as a nucleophile itself and as a catalyst in a general acid-base catalyzed reaction.[3] Thus it would be of interest to study the effect on the reactivation process of a properly spaced imidazole group.

Moreover, imidazole-substituted oximes may participate in the degradation of organophosphorus compounds before they reach the active site of the enzyme.

The syntheses were performed by reacting 4(5)-chloromethylimidazole hydrochloride or 4(5)-(2-bromoethyl)imidazole hydrobromide with the appropriate pyridine aldoxime in dimethylformamide. However, it was not possible to obtain the 2-aldoxime of *N*-(imidazolylethyl)pyridinium bromide by this procedure. The difficulties with quaternization of 2-pyridine aldoximes have been pointed out previously by Poziomek *et al.*[4]

The reactivator potency against BuChE inhibited by methylisopropoxyphosphoryl fluoride (Sarin) is illustrated in Table 1. It is evident that I and II are slightly more active than 2-(hydroxyimino)-methylpyridinium methanesulphonate (P2S), a compound used as an antidote in nerve gas poisoning and as a standard in reactivation experiments. None of the compounds I – V is able to reactivate the enzyme after inhibition with dimethylamidoethoxy-

$C_8H_{12}S_2$ (172.32): C 55.76; H 7.02; S 37.22]. VPC analyses were performed on a Perkin Elmer 900 Gas Chromatograph. IR spectra were recorded on a Perkin Elmer 257 Grating Infrared Spectrophotometer, NMR spectra on a Varian A-60 spectrometer and mass spectra on an LKB 9000 mass spectrometer.

Acknowledgements. Grants from the *Swedish Natural Science Research Council* to S.G. and from the *Royal Physiographic Society* to T.F. are gratefully acknowledged.

1. Gronowitz, S. and Frejd, T. *Acta Chem. Scand.* **23** (1969) 2540.
2. Gronowitz, S. and Frejd, T. *Acta Chem. Scand.* **24** (1970) 2656.
3. Jacobsen, H. J. *Acta Chem. Scand.* **24** (1970) 2663.
4. Gronowitz, S. and Frejd, T. *Int. J. Sulfur Chem. Part A* **2** (1972) 165.
5. Gronowitz, S., Moses, P. and Håkansson, R. *Arkiv Kemi* **16** (1960) 267.
6. Gronowitz, S., Moses, P. and Hörnfeldt, A.-B. *Arkiv Kemi* **17** (1961) 237.
7. Isaksson, G., Sandström, J. and Wennerbeck, I. *Tetrahedron Letters* **1967** 2233.
8. Sandström, J. and Wennerbeck, I. *Acta Chem. Scand.* **24** (1970) 1191.
9. Gronowitz, S., Moses, P., Hörnfeldt, A.-B. and Håkansson, R. *Arkiv Kemi* **17** (1961) 165.
10. Yur'ev, Yu.K., Mezentzova, N. N. and Vaskovskii, V. E. *J. Gen. Chem. USSR* **27** (1957) 3193.
11. Brandsma, L. *Preparative Acetylenic Chemistry*, Elsevier, New York 1971, p. 92.
12. Gompper, R. and Töpfl, W. *Chem. Ber.* **95** (1962) 2861.
13. Gompper, R. and Töpfl, W. *Chem. Ber.* **95** (1962) 2871.
14. Jensen, K. A. and Henriksen, L. *Acta Chem. Scand.* **22** (1968) 1107.
15. Gronowitz, S. and Frejd, T. *To be published.*

Received August 23, 1973.

Reactivation of Phosphorylated Cholinesterase by Some Imidazole-substituted Oximes

TOM KARLSSON, KARL-ERLAND STENSIÖ and KERSTIN WAHLBERG

Research Institute of National Defence, Department 1, S-172 04 Sundbyberg 4, Sweden

Nucleophilic agents such as oximes have been employed in restoring the activity of cholinesterase (ChE) which has been inactivated by organophosphorus compounds. Methyl-quaternized pyridinium aldoximes have been found particularly effective.[1] By a suitable modification of the substituent on the nitrogen, an increase in the reactivation rate was obtained.[2] Our intention has been to study the effect of an imidazole substituent in the pyridine aldoxime.

There is strong evidence that imidazole is part of the active site of ChE.[3] Furthermore, imidazole has a well documented catalytic capacity, *e.g.* for ester hydrolysis, both as a nucleophile itself and as a catalyst in a general acid-base catalyzed reaction.[3] Thus it would be of interest to study the effect on the reactivation process of a properly spaced imidazole group.

Moreover, imidazole-substituted oximes may participate in the degradation of organophosphorus compounds before they reach the active site of the enzyme.

The syntheses were performed by reacting 4(5)-chloromethylimidazole hydrochloride or 4(5)-(2-bromoethyl)imidazole hydrobromide with the appropriate pyridine aldoxime in dimethylformamide. However, it was not possible to obtain the 2-aldoxime of *N*-(imidazolylethyl)pyridinium bromide by this procedure. The difficulties with quaternization of 2-pyridine aldoximes have been pointed out previously by Poziomek *et al.*[4]

The reactivator potency against BuChE inhibited by methylisopropoxyphosphoryl fluoride (Sarin) is illustrated in Table 1. It is evident that I and II are slightly more active than 2-(hydroxyimino)-methylpyridinium methanesulphonate (P2S), a compound used as an antidote in nerve gas poisoning and as a standard in reactivation experiments. None of the compounds I – V is able to reactivate the enzyme after inhibition with dimethylamidoethoxy-

Substance	m.p.	Crude yield %	Recrystallization	Elemental analysis
I	215–217	78	EtOH-H_2O (9:1) plus acetone until turbid	Found: C 43.7; H 4.41; N 20.5. Calc. for $C_{10}H_{12}N_4OCl_2$; C 43.71; H 4.40; N 20.4.
II	212–213	85	MeOH	Found: C 43.7; H 4.44; N 20.5.
III	242–243	88	EtOH-H_2O (9:1) plus acetone until turbid	Found: C 43.4; H 4.42; N 20.4.
IV	231–232	73	95 % EtOH	Found: C 35.0; H 3.81; N 15.0. Calc. for $C_{11}H_{14}N_4OBr_2$; C 35.0; H 3.73; N 14.82.
V	232–234	68	95 % EtOH	Found: C 35.0; H 3.81; N 15.0.

Table 1. Structural formulae of some imidazole substituted pyridine oximes and their reactivating effect on Sarin inhibited BuChE. The inhibiting effect of the oximes alone on BuChE are expressed in molar I_{50} values.

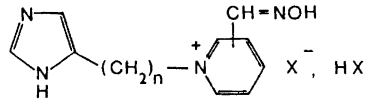

Substance	n	Substitution in the pyridine ring	Reactivation: Conc. of reactivator M	Reactivation: Restored enzyme activity %	I_{50} BuChE M
I	1	2	1.25×10^{-4}	57	6.2×10^{-4}
II	1	3	1.25×10^{-4}	54	6.0×10^{-4}
III	1	4	2.5×10^{-4}	40	1.9×10^{-3}
IV	2	3	2.5×10^{-4}	25	7.7×10^{-4}
V	2	4	2.5×10^{-4}	37	3.7×10^{-3}
P2S	–	–	3.67×10^{-4}	55	8.1×10^{-4}

phosphoryl cyanide (Tabun) or methylpinacoloxyphosphoryl fluoride (Soman).

An interesting feature is that compound II with the oxime group in the 3-position is equally effective as a reactivator as the isomers (I, III) substituted in the 2- and 4 positions. This is in contrast to the behaviour of (hydroxyimino)methylpyridinium isomers, where the 3-isomer has a very small reactivation capacity.[5] The relatively good effect of II and also of IV can be attributed to the catalytic assistance of the imidazole group in the reactivation procedure and to a modification of the acid strength of the oxime group. Most of the compounds which are effective reactivators are also ChE inhibitors. This reflects the fact that a certain fit to the active site is required in order to get a reactivation. Table 1 gives the I_{50} values for the inhibition of BuChE by compounds I–V. The 4-substituted compounds III and V have only about 15–30 % of the inhibiting activity given by the other substances but show a reasonable reactivation capacity. A preliminary pharmacological investigation shows that II is not very toxic having an LD_{50} (mice, i.p.) of 184 mg/kg compared to 216 mg/kg for P2S.[6]

Experimental. Lyophilized horse serum pseudocholinesterase (BuChE) with the activity 5232 Warburg units per mg was purchased from Diosynth International NV, the Netherlands. The phosphorus compounds were synthesized in this laboratory.

Reactivation experiments. The ChE activity was measured by an electrometric method[7]

with acetylcholine (14×10^{-3} M) as substrate. ChE was completely phosphorylated by incubation with 10^{-5} M Sarin, Soman, or Tabun and excess inhibitor removed by dialysis. After dialysis a check was made that no phosphorus compound was left.[8] The reactivation experiments were performed at 25° for 90 min in a Michels buffer[7] at pH 8.14. Reactivation is given as a percentage of the ChE activity in an enzyme control containing the reactivator but no phosphorus compound.

Synthesis. 4(5)-Chloromethylimidazole hydrochloride was prepared according to Turner *et al.*[9] 4(5)-Bromoethylimidazole hydrobromide was prepared from histamine.[10] The pyridinealdoximes used have the following m.p.: 2-aldoxime 109–111° (lit.[11] 114°), 3-aldoxime 148–150° (lit.[11] 150–151°), 4-aldoxime 130–132° (lit.[11] 132°). The quaternizations were performed in dimethylformamide at 50° for about 12 h using two equivalents of aldoxime. After cooling and chloroform addition, the precipitate was filtered, washed with chloroform and recrystallized.

The reactions could be followed by TLC on silica gel with pentanol-acetic acid-acetone-water (56:6:24:14) as eluent. Compounds containing the imidazole ring were detected by spraying with a diazonium salt (Echtblausalz B). For the other compounds, Dragendorffs reagent was used.

1. O'Brien, R. D. *Toxic Phosphorus Esters*, Academic, New York 1960.
2. Ashani, Y. and Cohen, S. *Israel J. Chem.* **5** (1967) 59.
3. Bruice, T. C. and Benkovic, S. J. *Bioorganic Mechanisms*, Benjamin, New York 1966, Vol. 1.
4. Poziomek, E. J., Hackley, Jr., B. E. and Steinberg, G. M. *J. Org. Chem.* **23** (1958) 714.
5. Hobbiger, F., O'Sullivan, D. G. and Sadler, P. W. *Nature* **182** (1958) 1498.
6. Davies, D. R. and Willey, G. L. *Brit. J. Pharmacol.* **13** (1958) 202.
7. Tammelin, L.-E. and Strindberg, B. *Acta Chem. Scand.* **6** (1952) 1041.
8. Heilbronn, E. *Biochem. Pharmacol.* **12** (1963) 25.
9. Turner, R. A., Huebner, C. F. and Scholz, C. R. *J. Am. Chem. Soc.* **71** (1949) 2801.
10. Stensiö, K.-E., Wahlberg, K. and Wahren, R. *Acta Chem. Scand.* **27** (1973). *In press.*
11. Ginsburg, S. and Wilson, I. B. *J. Am. Chem. Soc.* **79** (1957) 481.

Received August 7, 1973.

X-Ray Investigation of *N,N*-Dimethyl-*p*-nitrosoaniline, a Disordered Structure

CHR. RØMMING and H. J. TALBERG

Department of Chemistry, University of Oslo Oslo 3, Norway

Recent investigations have shown the dimers of organic nitroso compounds to be azodioxy-derivatives:[1-3]

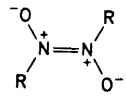

The correlation between the electron donor ability of R and the stability of these compounds has been demonstrated by Lüttke.[4-6] In *para*-substituted nitrosobenzenes a shift to the right in the equilibrium

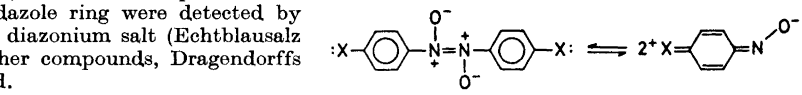

was found when X is a strong electron donor.

In view of the powerful electron donating property of the dimethylamino group, *N,N*-dimethyl-*p*-nitrosoaniline was selected as the subject of the present investigation. A comparison of the bonds in this molecule and in those with X = H, Br, I [2,3,7] and X = OH (now being investigated in this laboratory) should be of importance for the understanding of the dimerisation process.

Owing to the disorder observed in crystals of the title compound two structure refinements were carried out with crystals grown in different ways; both gave the same results with exception of small differences in the thermal parameters. The crystals were formed (I) by slow evaporation of a diethyl ether solution and (II) by cooling a similar solution in liquid nitrogen. A third attempt was carried out by a zone melting technique; X-ray photographs proved also these crystals to be disordered. The crystal data are as follows: *N,N*-Dimethyl-*p*-nitrosoaniline, triclinic, space group $P\bar{1}$. Cell dimensions (II): $a =$

with acetylcholine (14×10^{-3} M) as substrate. ChE was completely phosphorylated by incubation with 10^{-5} M Sarin, Soman, or Tabun and excess inhibitor removed by dialysis. After dialysis a check was made that no phosphorus compound was left.[8] The reactivation experiments were performed at 25° for 90 min in a Michels buffer[7] at pH 8.14. Reactivation is given as a percentage of the ChE activity in an enzyme control containing the reactivator but no phosphorus compound.

Synthesis. 4(5)-Chloromethylimidazole hydrochloride was prepared according to Turner *et al.*[9] 4(5)-Bromoethylimidazole hydrobromide was prepared from histamine.[10] The pyridinealdoximes used have the following m.p.: 2-aldoxime 109–111° (lit.[11] 114°), 3-aldoxime 148–150° (lit.[11] 150–151°), 4-aldoxime 130–132° (lit.[11] 132°). The quaternizations were performed in dimethylformamide at 50° for about 12 h using two equivalents of aldoxime. After cooling and chloroform addition, the precipitate was filtered, washed with chloroform and recrystallized.

The reactions could be followed by TLC on silica gel with pentanol-acetic acid-acetone-water (56:6:24:14) as eluent. Compounds containing the imidazole ring were detected by spraying with a diazonium salt (Echtblausalz B). For the other compounds, Dragendorffs reagent was used.

1. O'Brien, R. D. *Toxic Phosphorus Esters*, Academic, New York 1960.
2. Ashani, Y. and Cohen, S. *Israel J. Chem.* **5** (1967) 59.
3. Bruice, T. C. and Benkovic, S. J. *Bioorganic Mechanisms*, Benjamin, New York 1966, Vol. 1.
4. Poziomek, E. J., Hackley, Jr., B. E. and Steinberg, G. M. *J. Org. Chem.* **23** (1958) 714.
5. Hobbiger, F., O'Sullivan, D. G. and Sadler, P. W. *Nature* **182** (1958) 1498.
6. Davies, D. R. and Willey, G. L. *Brit. J. Pharmacol.* **13** (1958) 202.
7. Tammelin, L.-E. and Strindberg, B. *Acta Chem. Scand.* **6** (1952) 1041.
8. Heilbronn, E. *Biochem. Pharmacol.* **12** (1963) 25.
9. Turner, R. A., Huebner, C. F. and Scholz, C. R. *J. Am. Chem. Soc.* **71** (1949) 2801.
10. Stensiö, K.-E., Wahlberg, K. and Wahren, R. *Acta Chem. Scand.* **27** (1973). *In press.*
11. Ginsburg, S. and Wilson, I. B. *J. Am. Chem. Soc.* **79** (1957) 481.

Received August 7, 1973.

X-Ray Investigation of *N,N*-Dimethyl-*p*-nitrosoaniline, a Disordered Structure

CHR. RØMMING and H. J. TALBERG

Department of Chemistry, University of Oslo Oslo 3, Norway

Recent investigations have shown the dimers of organic nitroso compounds to be azodioxy-derivatives:[1-3]

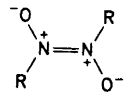

The correlation between the electron donor ability of R and the stability of these compounds has been demonstrated by Lüttke.[4-6] In *para*-substituted nitrosobenzenes a shift to the right in the equilibrium

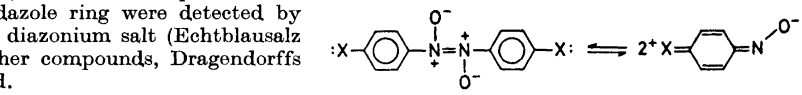

was found when X is a strong electron donor.

In view of the powerful electron donating property of the dimethylamino group, *N,N*-dimethyl-*p*-nitrosoaniline was selected as the subject of the present investigation. A comparison of the bonds in this molecule and in those with X = H, Br, I [2,3,7] and X = OH (now being investigated in this laboratory) should be of importance for the understanding of the dimerisation process.

Owing to the disorder observed in crystals of the title compound two structure refinements were carried out with crystals grown in different ways; both gave the same results with exception of small differences in the thermal parameters. The crystals were formed (I) by slow evaporation of a diethyl ether solution and (II) by cooling a similar solution in liquid nitrogen. A third attempt was carried out by a zone melting technique; X-ray photographs proved also these crystals to be disordered. The crystal data are as follows: *N,N*-Dimethyl-*p*-nitrosoaniline, triclinic, space group $P\bar{1}$. Cell dimensions (II): $a =$

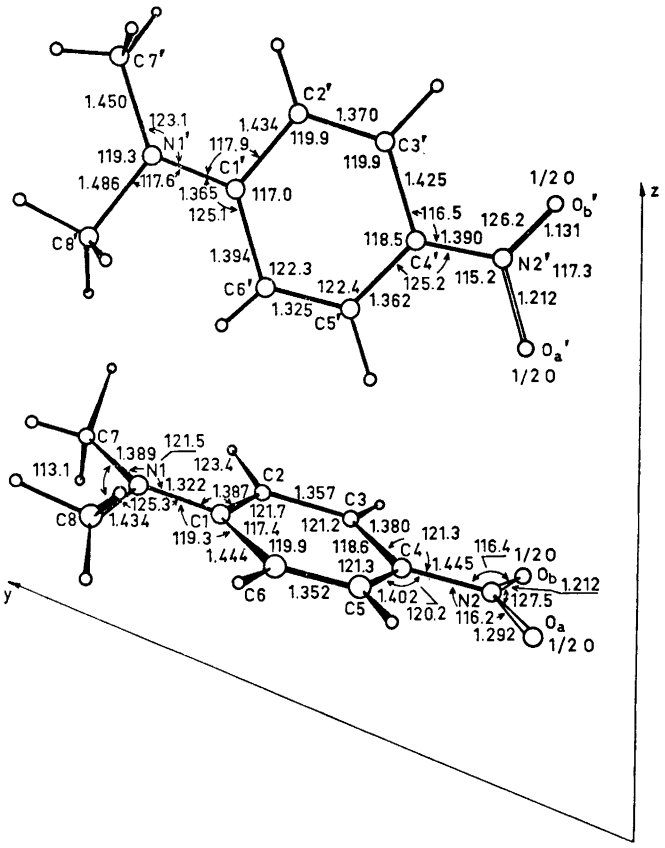

Fig. 1. *N,N*-Dimethyl-*p*-nitrosoaniline. Bond lengths (Å) and angles (°), $R = 8.8$ %.

9.617(2) Å, $b = 10.137(2)$ Å, $c = 9.817(2)$ Å, $\alpha = 68.21(1)°$, $\beta = 68.51(1)°$, $\gamma = 76.61(1)°$. $D_{obs} = 1.19$ g cm^{-1}, $Z = 4$, $D_{calc} = 1.21$ g cm^{-1}.

The intensity data were collected using an automatic Picker diffractometer with graphite crystal monochromated Mo$K\alpha$-radiation. Reflections with sin θ/λ up to 0.6 Å^{-1} were measured; data set I comprised 1036 observed reflections ($I > 1.5\ \sigma(I)$) and data set II 1702 observed reflections ($I > 2\sigma(I)$).

Cell dimensions in crystal I did not deviate significantly from those of crystal II. A conventional agreement factor between the two data sets of 5 % was determined after scaling the data set I with a factor $C \exp(\Delta B \sin^2\theta/\lambda^2)$. ΔB was found to be 0.58 Å^2 by a least-squares procedure.

The transformation $\mathbf{a}' = \mathbf{b}$, $\mathbf{b}' = \mathbf{a} - \mathbf{c}$, $\mathbf{c}' = \mathbf{a} + \mathbf{c}$ gives a cell with dimensions $a' = 10.1$ Å, $b' = 5.5$ Å, $c' = 8.2$ Å, $\alpha' = 91°$, $\beta' = 68°$, $\gamma = 84°$. This is a pseudo monoclinic cell with an intensity distribution resembling that of the space group $P2_1/c$.

With data set I a three-dimensional Patterson function and subsequent Fourier refinements revealed the positions of the two independent molecules. Both showed the same kind of disorder resulting in a pseudo two-fold axis of symmetry passing through the nitrogen atoms of each molecule. The disorder was maintained when refining the model against the second data set. Least-squares refinements were terminated (parameter shifts less than 10 % of the e.s.d.) with $R = 14.6$ % using data set I and $R = 8.8$ % with data set II.

All hydrogen atoms were located. The results of the structure analysis for data set II are given in Fig. 1. The estimated standard deviations are 0.008 – 0.015 Å in bond lengths and 0.5 – 1.0° in angles. Apparently significant differences in the bond lengths and large thermal parameters of the oxygen atoms are probably due to the disorder in the structure.

Both of the independent molecules appear to be almost planar with respect to the heavy atoms; this is even the case for the "half" oxygen atoms. At the present stage of the refinement there are indications of a weak quinonoid character in the molecule.

1. Darwin, C. and Hodgkin, D. C. *Nature* **166** (1950) 825.
2. Hiramatsu, M., Furusaki, A., Noela, T., Naya, K., Tomie, Y. and Nitta, I. *Bull. Chem. Soc. Japan* **43** (1970) 1966.
3. Dieterich, D. A., Paul, I. C. and Curtin, D. Y. *Chem. Commun.* **1970** 1710.
4. Lüttke, W. *Z. Elektrochem.* **61** (1957) 302.
5. Lüttke, W. *Z. Elektrochem.* **61** (1957) 976.
6. Kaissler, V. v. and Lüttke, W. *Z. Elektrochem.* **63** (1959) 614.
7. Webster, M. S. *J. Chem. Soc.* **1956** 2841.

Received July 3, 1973.

Antigenic Relationship between Lysozymes and its Use in Isolation and Purification of this Type of Enzyme

ARNE GROV

The University of Bergen, School of Medicine, The Gade Institute, Department of Microbiology, Bergen, Norway

Lysozymes or endo-β-*N*-acetylmuramidases (E.C. 3.2.1) have been isolated from a variety of sources including mammalian tissues, birds, insects, plants, and microorganisms.[1-3] These enzymes hydrolyze the glycan of the bacterial cell walls to oligosaccharides of the *N*-acetylglucosaminyl-*N*-acetylmuramic acid structure.

Immunological cross-reaction is a widespread phenomenon, and several cases of serological cross-reactions between related enzymes have been reported in recent years, *e.g.* between trypsin and chymotrypsin [4,5] and between papain and chymopapain.[6]

The many immunological studies carried out on hen egg-white lysozyme (E.C. 3.2.1.17), of which the primary as well as tertiary structures have been fully characterized, have given us a considerable knowledge of the antigenic determinants of this enzyme.[7-14] Comparative immunological studies of lysozyme from different sources have, in spite of the striking similarity in amino acid sequences and three-dimensional structures, detected few or no cross-reactions.[15-19] This is the case also for human lysozyme and hen egg-white lysozyme, which have also been found to differ in amino acid sequences at a considerable number of points near the catalytic site.[20,21] However, cross-reactions between human and chicken lysozymes have been detected by methods necessitating only one antigenic determinant in common.[17,19] Immunoadsorbents, therefore, are expected to be a useful tool in isolation and purification of related enzymes. In the present study rabbit anti-hen egg-white lysozyme has been used to isolate lysozymes from human milk and saliva.

Materials and methods. Antiserum to hen egg-white lysozyme (EL) (Sigma; Grade I, 3 × crystalline) was raised in rabbits given injections of a saline solution of the enzyme emulsified in an equal volume of Freund's complete adjuvant (Difco). Three injections (5 mg of antigen/dose) were given 3 weeks apart, the first one in a foot pad (0.5 ml), the two other intramuscularly (1 ml into 2 sites). IgG was precipitated from rabbit anti-EL sera at 1.33 M $(NH_4)_2SO_4$ concentration, chromatographed on a column of DEAE-cellulose (Eastman),[22] and coupled to Sepharose 4B (Pharmacia) and Sephadex G-15 (Sigma) activated with cyanogen bromide following the procedure described by Porath *et al.*[23] Casein-free milk whey was prepared by acidifying (to pH 4.6 with 1 N HCl) skimmed human milk (kindly provided by Dr. B. Haneberg, The University Hospital) which was subsequently centrifuged to sediment the precipitated casein. The whey

All hydrogen atoms were located. The results of the structure analysis for data set II are given in Fig. 1. The estimated standard deviations are 0.008 – 0.015 Å in bond lengths and 0.5 – 1.0° in angles. Apparently significant differences in the bond lengths and large thermal parameters of the oxygen atoms are probably due to the disorder in the structure.

Both of the independent molecules appear to be almost planar with respect to the heavy atoms; this is even the case for the "half" oxygen atoms. At the present stage of the refinement there are indications of a weak quinonoid character in the molecule.

1. Darwin, C. and Hodgkin, D. C. *Nature* **166** (1950) 825.
2. Hiramatsu, M., Furusaki, A., Noela, T., Naya, K., Tomie, Y. and Nitta, I. *Bull. Chem. Soc. Japan* **43** (1970) 1966.
3. Dieterich, D. A., Paul, I. C. and Curtin, D. Y. *Chem. Commun.* **1970** 1710.
4. Lüttke, W. *Z. Elektrochem.* **61** (1957) 302.
5. Lüttke, W. *Z. Elektrochem.* **61** (1957) 976.
6. Kaissler, V. v. and Lüttke, W. *Z. Elektrochem.* **63** (1959) 614.
7. Webster, M. S. *J. Chem. Soc.* **1956** 2841.

Received July 3, 1973.

Antigenic Relationship between Lysozymes and its Use in Isolation and Purification of this Type of Enzyme

ARNE GROV

The University of Bergen, School of Medicine, The Gade Institute, Department of Microbiology, Bergen, Norway

Lysozymes or endo-β-*N*-acetylmuramidases (E.C. 3.2.1) have been isolated from a variety of sources including mammalian tissues, birds, insects, plants, and microorganisms.[1-3] These enzymes hydrolyze the glycan of the bacterial cell walls to oligosaccharides of the *N*-acetylglucosaminyl-*N*-acetylmuramic acid structure.

Immunological cross-reaction is a widespread phenomenon, and several cases of serological cross-reactions between related enzymes have been reported in recent years, *e.g.* between trypsin and chymotrypsin [4,5] and between papain and chymopapain.[6]

The many immunological studies carried out on hen egg-white lysozyme (E.C. 3.2.1.17), of which the primary as well as tertiary structures have been fully characterized, have given us a considerable knowledge of the antigenic determinants of this enzyme.[7-14] Comparative immunological studies of lysozyme from different sources have, in spite of the striking similarity in amino acid sequences and three-dimensional structures, detected few or no cross-reactions.[15-19] This is the case also for human lysozyme and hen egg-white lysozyme, which have also been found to differ in amino acid sequences at a considerable number of points near the catalytic site.[20,21] However, cross-reactions between human and chicken lysozymes have been detected by methods necessitating only one antigenic determinant in common.[17,19] Immunoadsorbents, therefore, are expected to be a useful tool in isolation and purification of related enzymes. In the present study rabbit anti-hen egg-white lysozyme has been used to isolate lysozymes from human milk and saliva.

Materials and methods. Antiserum to hen egg-white lysozyme (EL) (Sigma; Grade I, 3 × crystalline) was raised in rabbits given injections of a saline solution of the enzyme emulsified in an equal volume of Freund's complete adjuvant (Difco). Three injections (5 mg of antigen/dose) were given 3 weeks apart, the first one in a foot pad (0.5 ml), the two other intramuscularly (1 ml into 2 sites). IgG was precipitated from rabbit anti-EL sera at 1.33 M $(NH_4)_2SO_4$ concentration, chromatographed on a column of DEAE-cellulose (Eastman),[22] and coupled to Sepharose 4B (Pharmacia) and Sephadex G-15 (Sigma) activated with cyanogen bromide following the procedure described by Porath *et al.*[23] Casein-free milk whey was prepared by acidifying (to pH 4.6 with 1 N HCl) skimmed human milk (kindly provided by Dr. B. Haneberg, The University Hospital) which was subsequently centrifuged to sediment the precipitated casein. The whey

samples were then neutralized using 1 N NaOH. Portions of whey (5 ml) and human mixed saliva (5 ml) were applied to immunoadsorbent columns of anti-EL IgG (1.5 cm × 20 cm). The columns were washed thoroughly with 0.2 M borate-buffer, pH 8.0, and then eluted with 3 M NaSCN.[24] Fractions (2 ml) were collected on a Minirac connected with a Uvicord (LKB Produkter) reading at 280 nm. Enzymatic activity was measured either as reduction in turbidity at 600 nm of a suspension of *Micrococcus lysodeikticus* whole cells in 0.1 M phosphate buffer, pH 6.2, or as lysis of *M. lysodeikticus* mucopeptide, prepared according to the method described in Ref. 25, in agar plates (0.5 mg/ml of 1 % agar). Enzymatically active fractions were bulked, concentrated by evaporation *in vacuo*, desalted on a column of Sephadex G-15 and freeze-dried. Enzyme specificity was tested by digestion of mucopeptide followed by reduction with sodium borohydride (Merck),[26,27] hydrolysis in 3 N HCl (4 h at 95°C), and chromatography on thin layer (cellulose plates) in solvent systems BuOH:HOAc:H_2O (4:1:1) and pyridine:H_2O (4:1). Hydrolysate of non-reduced digests, standard glucosamine and muramic acid (Koch-Light) and their $NaBH_4$-reduced forms (glucosaminitol and muraminitol) were included as references. Ninhydrin was used as colour reagent. Electrophoresis in dodecyl sulphate-polyacrylamide gels was carried out according to the method of Weber and Osborn.[28] The serological tests; double diffusion in agar, ring test examinations, inhibition of precipitation, and indirect haemagglutination using tanned sheep erythrocytes (TSE), were carried out as described previously.[29]

Results and discussion. The anti-EL serum gave one single line in double diffusion in agar against homologous antigen. The line could be detected at a serum dilution of 1/4. The haemagglutination titre was 1/320 and the ring test titre (dilution of antigen) was 1/160.

Neither whey nor saliva gave precipitation with anti-EL serum. However, when whey and saliva were applied to immunoadsorbent columns, materials having the capability to lyse *M. lysodeikticus* were eluted with NaSCN. In contrast to Sephadex G-15, Sepharose 4B, without coupled antibodies, apparently bound small amounts of lysozyme which could be released by 3 M NaSCN.

Portions of *M. lysodeikticus* mucopeptide were digested with (1) EL, (2) the lytic material isolated from whey (ML), and (3) the lytic material isolated from saliva (SL). Reduction of digested materials by $NaBH_4$, followed by acid hydrolysis and chromatography, showed that in all the three portions muraminitol, the reduced form of muramic acid, had been formed. On dodecyl sulphate-polyacrylamide gel electrophoresis both ML and SL showed a single band with an electrophoretic mobility corresponding to that of EL. These results strongly indicate that isolated ML and SL are pure muramidases. Although untreated Sepharose fixed some EL, no difference could be observed in the corresponding preparations isolated on columns of Sephadex- and Sepharose-coupled antibodies.

Precipitation reaction could not be detected between anti-EL and ML or SL, but both enzyme preparations inhibited anti-EL to precipitate with EL. Thus, when equal volumes of anti-EL and ML or SL (approximately 2.5 mg/ml) had been incubated for 2 h at 37°C and overnight at 4°C, this mixture, in contrast to anti-EL (1/2 in saline), showed no line in agar diffusion against EL.

Rabbits were also immunized with ML and SL (a total of approx. 1.5 mg of enzyme preparation) according to the schedule described for EL. The antisera obtained were very weak. No precipitation was detected either with homologous or heterologous antigen. However, both antisera agglutinated TSE sensitized with homologous as well as heterologous antigen (Table 1). The cross-reactions between ML and SL were relatively strong, whereas that between EL and the two human lysozymes seemed to be rather weak. However, in spite of an apparently slight immunological resemblance it seemed possible to isolate pure lysozymes from human milk and saliva on a column of antibodies to egg-white lysozyme.

Table 1. Indirect haemagglutination titres (reciprocal values) of lysozyme antisera using tanned sheep erythrocytes (TSE) sensitized with the lysozymes.

TSE sensitized with	Antisera to EL	ML	SL
EL (from egg-white)	320	10	10
ML (from milk)	10	80	80
SL (from saliva)	20	160	160

1. Jollès, P. *Angew. Chem.* **76** (1964) 20.
2. Jollès, P. *Proc. Roy. Soc. London. Ser. B* **167** (1967) 350.
3. Chipman, D. M. and Sharon, N. *Science* **165** (1969) 454.
4. Arnon, R. and Schechter, B. *Immunochemistry* **3** (1966) 451.
5. Sanders, M. M., Walsh, K. A. and Arnon, R. *Biochemistry* **9** (1970) 2356.
6. Arnon, R. and Shapira, E. *Biochemistry* **7** (1968) 4196.
7. Fujio, H., Imanishi, M., Nishioka, K. and Amano, T. *Biken J.* **11** (1968) 207.
8. Arnon, R. and Sela, M. *Proc. Natl. Acad. Sci. (U.S.)* **62** (1969) 163.
9. Imanishi, M., Miyagawa, N., Fujio, H. and Amano, T. *Biken. J.* **12** (1969) 85.
10. Bonavida, B. *Federation Proc.* **28** (1969) 326.
11. Atassi, M. Z. and Habeeb, A. F. S. A. *Biochemistry* **8** (1969) 1385.
12. Habeeb, A. F. S. A. and Atassi, M. Z. *Immunochemistry* **6** (1969) 555.
13. Young, J. D. and Leung, C. Y. *Biochemistry* **9** (1970) 2755.
14. Strosberg, A. D. and Kanarek, L. *Eur. J. Biochem.* **14** (1970) 161.
15. Faure, A. and Jollés, P. *FEBS Lett.* **10** (1970) 237.
16. Maron, E., Arnon, R., Sela, M., Perin, J. P. and Jollés, P. *Biochim. Biophys. Acta* **214** (1970) 222.
17. Prager, E. M. and Wilson, A. C. *J. Biol. Chem.* **246** (1971) 5978.
18. Prager, E. M. and Wilson, A. C. *J. Biol. Chem.* **246** (1971) 7010.
19. Arnheim, N., Sobel, J. and Canfield, R. *J. Mol. Biol.* **61** (1971) 237.
20. Canfield, R. E., Kammerman, S., Sobel, J. H. and Morgan, F. J. *Nature New Biol.* **232** (1971) 16.
21. Maron, E., Eshdat, Y. and Sharon, N. *Biochim. Biophys. Acta* **278** (1972) 243.
22. Levy, H. B. and Sober, H. A. *Proc. Soc. Exp. Biol. Med.* **103** (1960) 250.
23. Porath, J., Axén, R. and Ernback, S. *Nature* **215** (1967) 1491.
24. de Saussure, V. A. and Dandliker, W. B. *Immunochemistry* **6** (1969) 77.
25. Helgeland, S. M. and Grov, A. *Acta Pathol. Microbiol. Scand.* **B 79** (1971) 819.
26. Ghuysen, J.-M., Tipper, D. J. and Strominger, J. L. *Methods Enzymol.* **8** (1966) 685.
27. Tipper, D. J. and Strominger, J. L. *Biochem. Biophys. Res. Commun.* **22** (1966) 48.
28. Weber, K. and Osborn, M. *J. Biol. Chem.* **244** (1969) 4406.
29. Grov, A., Oeding, P., Myklestad, B. and Aasen, J. *Acta Pathol. Microbiol. Scand.* **B 78** (1970) 106.

Received August 7, 1973.

On the Structure of β-$Dy(NH_4)_3(SO_3)_3.H_2O$

LAURI NIINISTÖ* and
LARS OLOF LARSSON

Department of Structural Chemistry, Arrhenius Laboratory, University of Stockholm, Fack, S-104 05 Stockholm, Sweden

Several ammonium lanthanoid sulphites can be prepared in the system $NH_4^+ - Ln^{3+} - SO_2 - H_2O$ where Ln = Sm, Gd, or Dy.[1] Because of the low solubility of these phases the crystals are usually very small and cannot be studied by single crystal X-ray methods. After many unsuccessful attempts, however, crystals with suitable dimensions (approximately $0.02 \times 0.02 \times 0.15$ mm^3) were obtained of the high temperature polymorph of $Dy(NH_4)_3(SO_3)_3.H_2O$ by precipitating the compound at 75°C and then gradually warming to 90 – 95°C. The crystals were kept in a tightly sealed vessel for a week in this temperature range.

Weissenberg and rotation photographs indicated that the needle-shaped crystals have monoclinic symmetry, with the following unit cell dimensions: $a = 8.88$ Å, $b = 3.98$ Å, $c = 9.48$ Å and $\beta = 117.4°$. The powder pattern was satisfactorily indexed with these unit cell parameters. The measured density, 2.60 g cm^{-3}, corresponds to one formula unit in the cell (calculated density 2.65 g cm^{-3}). Single crystal intensity data were collected on a Philips PW 1100 computer-controlled four-circle diffractometer, using graphite monochromatized CuK radiation. 439 independent reflections were obtained, representing all observed ($\sigma(I_{net})/I_{net} < 0.25$) reflections with $\theta < 55°$. There were no systematically absent reflections. The net intensities were corrected for Lorentz and polarization effects as well as for absorption ($\mu = 338$ cm^{-1}).

The structure determination was started by assuming the centrosymmetric space group $P2/m$ (No. 10). A three-dimensional Patterson synthesis revealed presence of the dysprosium atom at the special position 1(g) ($\frac{1}{2}$,0,$\frac{1}{2}$), and the subsequent Fourier synthesis gave the positions of the

* Present address: Department of Chemistry, Helsinki University of Technology, SF-02150 Otaniemi, Finland.

1. Jollès, P. *Angew. Chem.* **76** (1964) 20.
2. Jollès, P. *Proc. Roy. Soc. London. Ser. B* **167** (1967) 350.
3. Chipman, D. M. and Sharon, N. *Science* **165** (1969) 454.
4. Arnon, R. and Schechter, B. *Immunochemistry* **3** (1966) 451.
5. Sanders, M. M., Walsh, K. A. and Arnon, R. *Biochemistry* **9** (1970) 2356.
6. Arnon, R. and Shapira, E. *Biochemistry* **7** (1968) 4196.
7. Fujio, H., Imanishi, M., Nishioka, K. and Amano, T. *Biken J.* **11** (1968) 207.
8. Arnon, R. and Sela, M. *Proc. Natl. Acad. Sci. (U.S.)* **62** (1969) 163.
9. Imanishi, M., Miyagawa, N., Fujio, H. and Amano, T. *Biken. J.* **12** (1969) 85.
10. Bonavida, B. *Federation Proc.* **28** (1969) 326.
11. Atassi, M. Z. and Habeeb, A. F. S. A. *Biochemistry* **8** (1969) 1385.
12. Habeeb, A. F. S. A. and Atassi, M. Z. *Immunochemistry* **6** (1969) 555.
13. Young, J. D. and Leung, C. Y. *Biochemistry* **9** (1970) 2755.
14. Strosberg, A. D. and Kanarek, L. *Eur. J. Biochem.* **14** (1970) 161.
15. Faure, A. and Jollés, P. *FEBS Lett.* **10** (1970) 237.
16. Maron, E., Arnon, R., Sela, M., Perin, J. P. and Jollés, P. *Biochim. Biophys. Acta* **214** (1970) 222.
17. Prager, E. M. and Wilson, A. C. *J. Biol. Chem.* **246** (1971) 5978.
18. Prager, E. M. and Wilson, A. C. *J. Biol. Chem.* **246** (1971) 7010.
19. Arnheim, N., Sobel, J. and Canfield, R. *J. Mol. Biol.* **61** (1971) 237.
20. Canfield, R. E., Kammerman, S., Sobel, J. H. and Morgan, F. J. *Nature New Biol.* **232** (1971) 16.
21. Maron, E., Eshdat, Y. and Sharon, N. *Biochim. Biophys. Acta* **278** (1972) 243.
22. Levy, H. B. and Sober, H. A. *Proc. Soc. Exp. Biol. Med.* **103** (1960) 250.
23. Porath, J., Axén, R. and Ernback, S. *Nature* **215** (1967) 1491.
24. de Saussure, V. A. and Dandliker, W. B. *Immunochemistry* **6** (1969) 77.
25. Helgeland, S. M. and Grov, A. *Acta Pathol. Microbiol. Scand.* **B 79** (1971) 819.
26. Ghuysen, J.-M., Tipper, D. J. and Strominger, J. L. *Methods Enzymol.* **8** (1966) 685.
27. Tipper, D. J. and Strominger, J. L. *Biochem. Biophys. Res. Commun.* **22** (1966) 48.
28. Weber, K. and Osborn, M. *J. Biol. Chem.* **244** (1969) 4406.
29. Grov, A., Oeding, P., Myklestad, B. and Aasen, J. *Acta Pathol. Microbiol. Scand.* **B 78** (1970) 106.

Received August 7, 1973.

On the Structure of β-$Dy(NH_4)_3(SO_3)_3.H_2O$

LAURI NIINISTÖ* and
LARS OLOF LARSSON

Department of Structural Chemistry, Arrhenius Laboratory, University of Stockholm, Fack, S-104 05 Stockholm, Sweden

Several ammonium lanthanoid sulphites can be prepared in the system $NH_4^+ - Ln^{3+} - SO_2 - H_2O$ where Ln = Sm, Gd, or Dy.[1] Because of the low solubility of these phases the crystals are usually very small and cannot be studied by single crystal X-ray methods. After many unsuccessful attempts, however, crystals with suitable dimensions (approximately $0.02 \times 0.02 \times 0.15$ mm^3) were obtained of the high temperature polymorph of $Dy(NH_4)_3(SO_3)_3.H_2O$ by precipitating the compound at 75°C and then gradually warming to 90 – 95°C. The crystals were kept in a tightly sealed vessel for a week in this temperature range.

Weissenberg and rotation photographs indicated that the needle-shaped crystals have monoclinic symmetry, with the following unit cell dimensions: $a = 8.88$ Å, $b = 3.98$ Å, $c = 9.48$ Å and $\beta = 117.4°$. The powder pattern was satisfactorily indexed with these unit cell parameters. The measured density, 2.60 g cm^{-3}, corresponds to one formula unit in the cell (calculated density 2.65 g cm^{-3}). Single crystal intensity data were collected on a Philips PW 1100 computer-controlled four-circle diffractometer, using graphite monochromatized CuK radiation. 439 independent reflections were obtained, representing all observed ($\sigma(I_{net})/I_{net} < 0.25$) reflections with $\theta < 55°$. There were no systematically absent reflections. The net intensities were corrected for Lorentz and polarization effects as well as for absorption ($\mu = 338$ cm^{-1}).

The structure determination was started by assuming the centrosymmetric space group $P2/m$ (No. 10). A three-dimensional Patterson synthesis revealed presence of the dysprosium atom at the special position 1(g) ($\frac{1}{2}$,0,$\frac{1}{2}$), and the subsequent Fourier synthesis gave the positions of the

* Present address: Department of Chemistry, Helsinki University of Technology, SF-02150 Otaniemi, Finland.

Table 1. Fractional atomic coordinates and temperature factors. Estimated standard deviations are given within parentheses.

Atom	Position	x	y	z	B
Dy	1(*g*)	0.5	0.0	0.5	2.2(1)
S(1)	2(*n*)[a]	0.1702(25)	0.5	0.2657(24)	4.0(4)
S(2)	2(*n*)[a]	0.4037(25)	0.5	0.7334(24)	4.1(4)
N(1)	2(*m*)	0.7623(61)	0.0	0.0245(58)	4.7(1.0)
N(2)	1(*c*)	0.0	0.0	0.5	4.2(1.3)

[a] Occupation number is 0.75.

sulphur and nitrogen atoms. The sulphur atoms were placed at a 2(*n*) position: $\pm(x,\frac{1}{2},z)$ with an occupancy of 0.75, and the nitrogen atoms N(1) and N(2) at position 2(*m*): $\pm(x,0,z)$ and 1(*c*): $(0,0,\frac{1}{2})$, respectively. A least-squares refinement with isotropic temperature factors resulted in an R-value of 12.7 %. The atomic parameters are presented in Table 1.

It was not possible, however, to locate the oxygen atoms from the difference Fourier maps, which did not show distinct maxima at expected distances from the sulphur atoms. A careful examination of long exposure Weissenberg and rotation films of several crystals revealed weak superstructure reflections indicating a fourfold b-axis. A least-squares refinement of powder data obtained at 25°C with Cu$K\alpha_1$ radiation ($\lambda = 1.54050$ Å) in a Guinier-Hägg camera, using KCl as an internal standard, gave the following unit cell dimensions for the superstructure (*cf.* Table 2): $a = 8.863(6)$, $b = 15.919(5)$, $c = 9.467(5)$ Å and $\beta = 117.38(5)°$. The powder pattern was measured and interpreted up to $\sin^2\theta = 0.44$.

The complete structure determination of β-$Dy(NH_4)_3(SO_3)_3.H_2O$ will have to be postponed until intensity data on the superstructure reflections have been measured. However, on the basis of the substructure it can be stated that the atoms are situated in layers $b/4$ apart and that the sulphite groups are coordinated to dysprosium through oxygen. The Dy – S distances of 3.40 Å and 3.41 Å exclude other possibilities. The IR absorption spectrum gives further support for the bonding through oxygen. In the region 2000 – 400 cm^{-1} there are, besides maxima due to water (1665w) and ammonium (1395s), four bands (1020m, 960s, 890vs, 820s) in the S – O stretching region

Table 2. X-Ray powder data of β-$Dy(NH_4)_3(SO_3)_3.H_2O$. Cu$K\alpha_1$ radiation ($\lambda = 1.54050$ Å).

h	k	l	$10^5 \sin^2\theta_{obs}$	$10^5 \sin^2\theta_{obs}$	I_{obs}
0	0	1	837	839	s
1	0	0	963	958	s
1	2	0	1890	1894	vw
1	0	1	2624	2622	m
2	0	0	3837	3831	w
0	4	1	4576	4585	w
1	4	0	4702	4704	m
1	4	1	6364	6368	s
−2	4	1	6736	6767	m
0	4	2	7074	7104	m
0	0	3	7561	7555	w
2	4	0		7577	
3	0	0	8599	8620	w
−3	2	3	9698	9690	w
1	4	2		9711	
2	4	1	10070	10066	w
2	0	2	10501	10488	w
−2	0	4	10670	10665	w
1	0	3	10964	10987	vw
1	6	1	11045	11051	vvw
1	1	3	11253	11222	vw
−2	6	2	12338	12319	w
−4	1	2		12319	
3	4	0		12366	
2	4	2	14240	14234	w
1	4	3	14709	14733	w
−4	3	1	14966	14973	m
3	4	1	15683	15680	w
−4	1	4	15792	15795	w
2	5	2	16341	16241	vw
−2	5	4	16531	16518	w
−1	5	4	16949	16944	vvw
1	8	1	17599	17606	w
−1	2	5	18781	18758	w
2	8	0		18815	
0	7	3	19010	19027	w
3	3	2		19034	

(ν_1 and ν_3 vibrations). The maximum at 630 cm^{-1} can be attributed to the ν_2 vibration, and the last two modes (525m, 460m) are probably due to the ν_4 vibration. The nondegeneracy of the ν_3 and ν_4 vibrations as well as the existence of a high intensity maximum at 960 cm^{-1} are in agreement with oxygen coordination,[2,3] although the occurrence of a band at 1020 cm^{-1} (if not an overtone or a combination band) complicates the interpretation.

The ammonium ions are situated at the edges of the unit cell and are possibly connecting the structure in the directions of the *a* and *c* axes *via* hydrogen bonding.

As the superstructure reflections are very weak they may be due to the oxygen atoms only. On the other hand, the temperature factors for the sulphur and nitrogen atoms are high, although not unreasonable (*cf.* Table 1).

Acknowledgements. We are indebted to Professor Peder Kierkegaard and Professor Arne Magnéli for their encouraging interest and many valuable discussions. We also wish to thank Dr. Sven Westman for his correction of the English of this paper. This investigation has been performed with financial support from the *Tri-Centennial Fund of the Bank of Sweden* and from the *Swedish Natural Science Research Council*. Financial aid from the *Neste Oy Foundation* for one of us (L.N.) is gratefully acknowledged.

1. Erämetsä, O., Niinistö, L. and Korvela, T. *Suomen Kemistilehti* **B 45** (1972) 394.
2. Newman, G. and Powell, D. B. *Spectrochim. Acta* **19** (1963) 213.
3. Nyberg, B. and Larsson, L. *Acta Chem. Scand.* **27** (1973) 63.

Received August 9, 1973.

The Acid-catalyzed Reactions of Triphenylallene. A Reexamination

TYGE GREIBROKK*

Department of Chemistry, University of Oslo, Oslo 3, Norway

Acid-catalyzed rearrangement of triphenylallene (I) has been reported to give a dimeric product, $C_{42}H_{32}$.[1] To this product, which also was formed by acid-catalyzed dehydration of 1,3,3-triphenylprop-2-en-1-ol and 1,1,3-triphenylprop-2-en-1-ol,[2,3] Jones [4] and Rewicki [5] independently assigned structure II. In analogy with the formation of 1,3,3-triphenylindene from tetraphenylallene,[6] 1,3-diphenylindene (III) was the expected product; this was isolated in 40 % yield from the reaction of the above mentioned allylic alcohols with phosphorus pentoxide.[2] We want to report that compound III is also formed by treatment of triphenylallene with acid.

The reaction of I with HCl/acetic acid gave besides the dimer a small amount of another component which was isolated. The NMR spectrum showed a vinyl proton at δ 6.6 coupled to a methine proton at δ 4.6 ($J = 2$ Hz) and aromatic protons at δ 7.0 – 7.7. The mass spectrum (*m/e* 268) corresponded to the indene III. The isomeric 3,3-diphenylindene was not present.

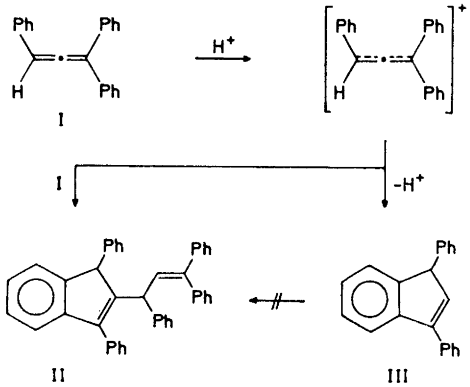

The formation of the dimer has been suggested to proceed through the addition of an allylic carbonium ion to another

* Present address: Institute for Biomedical Research, University of Texas, Austin, Texas 78712, U.S.A.

(ν_1 and ν_3 vibrations). The maximum at 630 cm^{-1} can be attributed to the ν_2 vibration, and the last two modes (525m, 460m) are probably due to the ν_4 vibration. The nondegeneracy of the ν_3 and ν_4 vibrations as well as the existence of a high intensity maximum at 960 cm^{-1} are in agreement with oxygen coordination,[2,3] although the occurrence of a band at 1020 cm^{-1} (if not an overtone or a combination band) complicates the interpretation.

The ammonium ions are situated at the edges of the unit cell and are possibly connecting the structure in the directions of the *a* and *c* axes *via* hydrogen bonding.

As the superstructure reflections are very weak they may be due to the oxygen atoms only. On the other hand, the temperature factors for the sulphur and nitrogen atoms are high, although not unreasonable (*cf.* Table 1).

Acknowledgements. We are indebted to Professor Peder Kierkegaard and Professor Arne Magnéli for their encouraging interest and many valuable discussions. We also wish to thank Dr. Sven Westman for his correction of the English of this paper. This investigation has been performed with financial support from the *Tri-Centennial Fund of the Bank of Sweden* and from the *Swedish Natural Science Research Council*. Financial aid from the *Neste Oy Foundation* for one of us (L.N.) is gratefully acknowledged.

1. Erämetsä, O., Niinistö, L. and Korvela, T. *Suomen Kemistilehti* **B 45** (1972) 394.
2. Newman, G. and Powell, D. B. *Spectrochim. Acta* **19** (1963) 213.
3. Nyberg, B. and Larsson, L. *Acta Chem. Scand.* **27** (1973) 63.

Received August 9, 1973.

The Acid-catalyzed Reactions of Triphenylallene. A Reexamination

TYGE GREIBROKK*

Department of Chemistry, University of Oslo, Oslo 3, Norway

Acid-catalyzed rearrangement of triphenylallene (I) has been reported to give a dimeric product, $C_{42}H_{32}$.[1] To this product, which also was formed by acid-catalyzed dehydration of 1,3,3-triphenylprop-2-en-1-ol and 1,1,3-triphenylprop-2-en-1-ol,[2,3] Jones [4] and Rewicki [5] independently assigned structure II. In analogy with the formation of 1,3,3-triphenylindene from tetraphenylallene,[6] 1,3-diphenylindene (III) was the expected product; this was isolated in 40 % yield from the reaction of the above mentioned allylic alcohols with phosphorus pentoxide.[2] We want to report that compound III is also formed by treatment of triphenylallene with acid.

The reaction of I with HCl/acetic acid gave besides the dimer a small amount of another component which was isolated. The NMR spectrum showed a vinyl proton at δ 6.6 coupled to a methine proton at δ 4.6 ($J = 2$ Hz) and aromatic protons at δ 7.0 – 7.7. The mass spectrum (*m/e* 268) corresponded to the indene III. The isomeric 3,3-diphenylindene was not present.

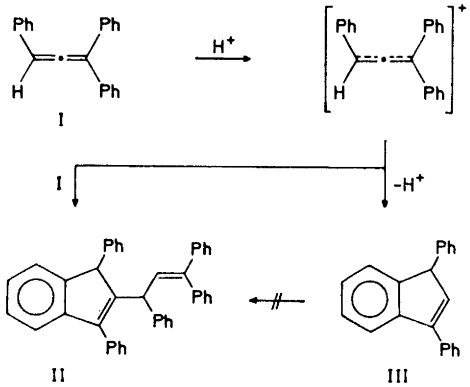

The formation of the dimer has been suggested to proceed through the addition of an allylic carbonium ion to another

* Present address: Institute for Biomedical Research, University of Texas, Austin, Texas 78712, U.S.A.

molecule of triphenylallene;[5] however, an electrophilic attack at the 2-position of the indene (III) cannot be excluded. In order to examine this possibility III was reacted with I in HCl/acetic acid. After 4 h at 100°C unreacted 1,3-diphenylindene was recovered quantitatively. Hence, the reaction takes place as previously suggested, which is not unexpected in view of the high reactivity of allenes towards electrophilic reagents.[7,8]

In an attempt to raise the yield of III compared to the dimer, some experiments were performed. When a 0.1 M solution of triphenylallene in benzene was refluxed with *p*-toluenesulfonic acid, II and III were formed in a ratio of about 2:1. Since III is formed by a monomolecular mechanism, a dilute solution would be expected to prefer this reaction. This indeed was found to be true. With an actual concentration of triphenylallene in benzene less than 0.02 M, the indene (III) was isolated in 73 % yield and the dimer in 11 % yield.

Experimental. Triphenylallene (2.68 g, 0.01 mol) in benzene (500 ml) was added dropwise to a refluxing solution of *p*-toluenesulfonic acid (0.5 g) in benzene (300 ml) over a period of 1.5 h. After heating for another 0.5 hour, the solution was cooled, washed with aqueous Na_2CO_3, dried and evaporated. The residue was treated with hexane whereby most of the dimer precipitated, 0.30 g (11 %), m.p. 213–215°C (lit.[5] m.p. 214–216°C). The filtered solution was chromatographed on neutral alumina (activity III) and the pure indene was eluted with hexane, 1.95 g (73 %), m.p. 68–69°C (lit.[2] m.p. 71–72°C).

1. Jacobs, T. L., Dankner, D. and Singer, S. *Tetrahedron* **20** (1964) 2177.
2. Ziegler, K., Grabbe, H. and Ulrich, F. *Ber.* **57** (1924) 1983.
3. Dufraisse, C., Etienne, A. and Goffinet, B. *Compt. Rend.* **238** (1954) 861.
4. Jones, D. W. *J. Chem. Soc.* **C 1966** 1026.
5. Rewicki, D. *Chem. Ber.* **99** (1966) 392.
6. Vorländer, D. and Siebert, S. *Ber.* **39** (1906) 1024.
7. Taylor, D. R. *Chem. Rev.* **67** (1967) 317.
8. Grimaldi, J. and Bertrand, M. *Bull. Soc. Chim. France* **1971** 957.

Received February 27, 1973.

Complex Dibenzofurans

XV.* Mass Spectra of the Isomeric Benzobisbenzofurans

BRIAN G. PRING

Research and Development Laboratories, Astra Läkemedel AB, S-151 85 Södertälje, Sweden

The mass spectra of the five isomeric benzobisbenzofurans have been recorded and are now reported. The relative intensities of the most important peaks in the spectra are given in Table 1.

Table 1. Relative intensities of the main peaks in the mass spectra of the five isomeric benzobisbenzofurans.

	Relative intensity (%)				
m/e	I	II	III	IV	V
260	3.1	3.0	2.8	2.8	2.9
259	20.9	21.3	20.9	20.8	21.0
258	100.0	100.0	100.0	100.0	100.0
230	1.7	2.0	1.9	2.1	1.8
229	7.2	7.5	8.6	8.9	7.4
202	7.2	5.3	4.5	4.7	4.7
201	6.0	4.3	3.6	3.8	4.3
200	9.6	7.7	7.1	7.6	7.4
176	4.6	2.3	1.8	1.9	1.9
175	2.3	2.2	1.4	1.6	1.6
174	2.4	2.3	1.5	1.7	1.7
129.5	3.1	4.1	3.6	3.8	4.2
129	12.9	17.6	16.7	17.6	17.5
114.5	2.3	2.7	2.9	3.2	2.5
101.5	2.2	1.6	1.4	1.4	1.1
101	7.9	4.9	3.9	4.2	3.7
100.5	3.1	2.7	1.9	1.9	2.2
100	8.2	5.8	5.5	6.0	5.5
88.5	1.7	1.5	1.1	1.2	1.1
88	6.5	5.8	5.5	5.8	5.7
87.5	1.7	1.5	1.1	1.1	1.6
87	3.4	2.7	2.2	2.4	2.6
86.33	0.15	0.16	0.15	0.13	0.16
86	1.7	1.6	1.4	1.4	1.7
75	3.1	2.9	2.9	3.0	2.8
74	2.3	2.0	1.6	2.1	1.8
63	1.7	1.9	1.6	1.6	1.8
51	1.4	1.4	1.4	1.6	1.0
39	1.8	1.6	1.4	1.1	1.5

I, Benzobis[1,2-b:4,3-b′]benzofuran; II, benzobis[1,2-b:3,4-b′]benzofuran; III, benzobis[1,2-b:5,4-b′]benzofuran; IV, benzobis[1,2-b:4,5-b′]benzofuran; V, benzobis[1,2-b:6,5-b′]benzofuran.

* Part XIV. *Acta Chem. Scand.* **27** (1973). *In press.*

molecule of triphenylallene;[5] however, an electrophilic attack at the 2-position of the indene (III) cannot be excluded. In order to examine this possibility III was reacted with I in HCl/acetic acid. After 4 h at 100°C unreacted 1,3-diphenylindene was recovered quantitatively. Hence, the reaction takes place as previously suggested, which is not unexpected in view of the high reactivity of allenes towards electrophilic reagents.[7,8]

In an attempt to raise the yield of III compared to the dimer, some experiments were performed. When a 0.1 M solution of triphenylallene in benzene was refluxed with *p*-toluenesulfonic acid, II and III were formed in a ratio of about 2:1. Since III is formed by a monomolecular mechanism, a dilute solution would be expected to prefer this reaction. This indeed was found to be true. With an actual concentration of triphenylallene in benzene less than 0.02 M, the indene (III) was isolated in 73 % yield and the dimer in 11 % yield.

Experimental. Triphenylallene (2.68 g, 0.01 mol) in benzene (500 ml) was added dropwise to a refluxing solution of *p*-toluenesulfonic acid (0.5 g) in benzene (300 ml) over a period of 1.5 h. After heating for another 0.5 hour, the solution was cooled, washed with aqueous Na_2CO_3, dried and evaporated. The residue was treated with hexane whereby most of the dimer precipitated, 0.30 g (11 %), m.p. 213–215°C (lit.[5] m.p. 214–216°C). The filtered solution was chromatographed on neutral alumina (activity III) and the pure indene was eluted with hexane, 1.95 g (73 %), m.p. 68–69°C (lit.[2] m.p. 71–72°C).

1. Jacobs, T. L., Dankner, D. and Singer, S. *Tetrahedron* **20** (1964) 2177.
2. Ziegler, K., Grabbe, H. and Ulrich, F. *Ber.* **57** (1924) 1983.
3. Dufraisse, C., Etienne, A. and Goffinet, B. *Compt. Rend.* **238** (1954) 861.
4. Jones, D. W. *J. Chem. Soc.* **C 1966** 1026.
5. Rewicki, D. *Chem. Ber.* **99** (1966) 392.
6. Vorländer, D. and Siebert, S. *Ber.* **39** (1906) 1024.
7. Taylor, D. R. *Chem. Rev.* **67** (1967) 317.
8. Grimaldi, J. and Bertrand, M. *Bull. Soc. Chim. France* **1971** 957.

Received February 27, 1973.

Complex Dibenzofurans

XV.* Mass Spectra of the Isomeric Benzobisbenzofurans

BRIAN G. PRING

Research and Development Laboratories, Astra Läkemedel AB, S-151 85 Södertälje, Sweden

The mass spectra of the five isomeric benzobisbenzofurans have been recorded and are now reported. The relative intensities of the most important peaks in the spectra are given in Table 1.

Table 1. Relative intensities of the main peaks in the mass spectra of the five isomeric benzobisbenzofurans.

	Relative intensity (%)				
m/e	I	II	III	IV	V
260	3.1	3.0	2.8	2.8	2.9
259	20.9	21.3	20.9	20.8	21.0
258	100.0	100.0	100.0	100.0	100.0
230	1.7	2.0	1.9	2.1	1.8
229	7.2	7.5	8.6	8.9	7.4
202	7.2	5.3	4.5	4.7	4.7
201	6.0	4.3	3.6	3.8	4.3
200	9.6	7.7	7.1	7.6	7.4
176	4.6	2.3	1.8	1.9	1.9
175	2.3	2.2	1.4	1.6	1.6
174	2.4	2.3	1.5	1.7	1.7
129.5	3.1	4.1	3.6	3.8	4.2
129	12.9	17.6	16.7	17.6	17.5
114.5	2.3	2.7	2.9	3.2	2.5
101.5	2.2	1.6	1.4	1.4	1.1
101	7.9	4.9	3.9	4.2	3.7
100.5	3.1	2.7	1.9	1.9	2.2
100	8.2	5.8	5.5	6.0	5.5
88.5	1.7	1.5	1.1	1.2	1.1
88	6.5	5.8	5.5	5.8	5.7
87.5	1.7	1.5	1.1	1.1	1.6
87	3.4	2.7	2.2	2.4	2.6
86.33	0.15	0.16	0.15	0.13	0.16
86	1.7	1.6	1.4	1.4	1.7
75	3.1	2.9	2.9	3.0	2.8
74	2.3	2.0	1.6	2.1	1.8
63	1.7	1.9	1.6	1.6	1.8
51	1.4	1.4	1.4	1.6	1.0
39	1.8	1.6	1.4	1.1	1.5

I, Benzobis[1,2-b:4,3-b′]benzofuran; II, benzobis[1,2-b:3,4-b′]benzofuran; III, benzobis[1,2-b:5,4-b′]benzofuran; IV, benzobis[1,2-b:4,5-b′]benzofuran; V, benzobis[1,2-b:6,5-b′]benzofuran.

* Part XIV. *Acta Chem. Scand.* **27** (1973). *In press.*

As can be seen from the data in the table, there is very little difference in the mass spectra. The molecular ions at *m/e* 258 are very stable and form the base peaks. In fact, the tendency of the molecules to fragment is so little that the next most intense peaks in the spectra are the doubly-charged molecular ions at *m/e* 129 (12.9 – 17.6 %), as indicated by the accompanying ^{13}C-, ^{17}O-, and ^{2}H-containing peaks at *m/e* 129.5. This may be compared to the situation in dibenzofuran [1] where a doubly-charged molecular ion is also prominent. Triply-charged molecular ions at *m/e* 86 (1.4 – 1.7 %) are also present together with the corresponding isotope peak at *m/e* 86.33. The presence of triply-charged and even quadruply-charged ions in the mass spectra of molecules with extended aromatic systems is known.[2]

Fragmentation of the benzobisbenzofuran molecular ions takes place by loss of carbon monoxide and a hydrogen atom (*cf.* dibenzofuran [1]) to give *m/e* 229 (7.2 – 8.9 %) followed by a second loss of carbon monoxide and a hydrogen atom to give *m/e* 200 (7.9 – 9.6 %). The corresponding doubly-charged ions at *m/e* 114.5 (2.3 – 3.2 %) and *m/e* 100 (5.5 – 8.2 %) are also present in the spectra.

Thus, it can be concluded that the isomeric benzobisbenzofurans give very similar mass spectra, in which the dominating feature is the stability of the molecular ion towards fragmentation.

Experimental. The mass spectra were recorded on an LKB 9000 mass spectrometer, the electron energy being 70 eV. The benzobisbenzofurans were prepared according to literature methods [3–5] and purified by sublimation *in vacuo*.

Acknowledgements. The author thanks Docent Nils E. Stjernström for his kind interest in this work and Ing. Hans Thorin, Astra Nutrition, Mölndal, for recording the mass spectra.

1. Pring, B. G. and Stjernström, N. E. *Acta Chem. Scand.* **22** (1968) 549.
2. Bursey, M. M., Rogerson, P. F. and Bursey, J. M. *Org. Mass Spectrom.* **4** (1970) 615.
3. Stjernström, N. E. *Acta Chem. Scand.* **14** (1960) 2191.
4. Stjernström, N. E. *Acta Chem. Scand.* **16** (1962) 553.
5. Pring, B. G. *Acta Chem. Scand.* **27** (1973). *In press.*

Received July 4, 1973.

Note on Anion and Cation Disorder in $NaNO_3$

J. H. FERMOR and A. KJEKSHUS

Kjemisk Institutt, Universitetet i Oslo, Blindern Oslo 3, Norway

The solid state transition in $NaNO_3$, which occurs continuously over the temperature range ~420 to ~550 K, is known to be associated with the onset of dynamic disorder of the nitrate groups between two non-equivalent orientations, and a random movement of the Na^+ ions between equivalent lattice positions. Some of the evidences which establish this description of the thermally disordered lattice are calorimetric investigations,[1–3] X-ray determinations,[4–8] infrared and Raman spectroscopic data,[9–11] NMR (^{23}Na) measurements,[12,13] low frequency dielectric dispersion experiments,[14] and entropy considerations.[8,15–19]

Above ~550 K the cation sublattice is disordered in the sense that Na^+ ions have statistical lattice positional lifetimes of $\sim 5 \times 10^{-4}$ s, after which interval the ion jumps to a new site.[12,13] This repetitive jumping of the ions produces a fluidity which appears to be restricted to the cation sublattice, and which has implications for the electrical conductivity.[20] In a perfect lattice in which all ions are at normal sites, cations are able to jump from one site to another only if the movements are coordinated to occur over closed loops involving two or more cation sites.

(Ion movements of this kind are electrically neutral, since they involve neither a translation of charge nor a reorientation (of formation) of electric dipoles.) Positional jumping is greatly facilitated by the presence of cation vacancies, which largely removes the requirement of correlated cation movements.[21] Cation vacancies may be created thermally by the activation of cations to interstitial positions to form Frenkel defects in the lattice, and electrical conductivity results from the migration of the interstitial ions or the vacancies. It seems likely that interstitial positions of the cations will be involved in inter-site jumping because of the greatly increased number of ways in which the jumps may then occur, bearing in mind that in order to pass from one lattice site

As can be seen from the data in the table, there is very little difference in the mass spectra. The molecular ions at *m/e* 258 are very stable and form the base peaks. In fact, the tendency of the molecules to fragment is so little that the next most intense peaks in the spectra are the doubly-charged molecular ions at *m/e* 129 (12.9 – 17.6 %), as indicated by the accompanying ^{13}C-, ^{17}O-, and ^{2}H-containing peaks at *m/e* 129.5. This may be compared to the situation in dibenzofuran [1] where a doubly-charged molecular ion is also prominent. Triply-charged molecular ions at *m/e* 86 (1.4 – 1.7 %) are also present together with the corresponding isotope peak at *m/e* 86.33. The presence of triply-charged and even quadruply-charged ions in the mass spectra of molecules with extended aromatic systems is known.[2]

Fragmentation of the benzobisbenzofuran molecular ions takes place by loss of carbon monoxide and a hydrogen atom (*cf.* dibenzofuran [1]) to give *m/e* 229 (7.2 – 8.9 %) followed by a second loss of carbon monoxide and a hydrogen atom to give *m/e* 200 (7.9 – 9.6 %). The corresponding doubly-charged ions at *m/e* 114.5 (2.3 – 3.2 %) and *m/e* 100 (5.5 – 8.2 %) are also present in the spectra.

Thus, it can be concluded that the isomeric benzobisbenzofurans give very similar mass spectra, in which the dominating feature is the stability of the molecular ion towards fragmentation.

Experimental. The mass spectra were recorded on an LKB 9000 mass spectrometer, the electron energy being 70 eV. The benzobisbenzofurans were prepared according to literature methods [3–5] and purified by sublimation *in vacuo*.

Acknowledgements. The author thanks Docent Nils E. Stjernström for his kind interest in this work and Ing. Hans Thorin, Astra Nutrition, Mölndal, for recording the mass spectra.

1. Pring, B. G. and Stjernström, N. E. *Acta Chem. Scand.* **22** (1968) 549.
2. Bursey, M. M., Rogerson, P. F. and Bursey, J. M. *Org. Mass Spectrom.* **4** (1970) 615.
3. Stjernström, N. E. *Acta Chem. Scand.* **14** (1960) 2191.
4. Stjernström, N. E. *Acta Chem. Scand.* **16** (1962) 553.
5. Pring, B. G. *Acta Chem. Scand.* **27** (1973). *In press.*

Received July 4, 1973.

Note on Anion and Cation Disorder in $NaNO_3$

J. H. FERMOR and A. KJEKSHUS

Kjemisk Institutt, Universitetet i Oslo, Blindern Oslo 3, Norway

The solid state transition in $NaNO_3$, which occurs continuously over the temperature range ~420 to ~550 K, is known to be associated with the onset of dynamic disorder of the nitrate groups between two non-equivalent orientations, and a random movement of the Na^+ ions between equivalent lattice positions. Some of the evidences which establish this description of the thermally disordered lattice are calorimetric investigations,[1–3] X-ray determinations,[4–8] infrared and Raman spectroscopic data,[9–11] NMR (^{23}Na) measurements,[12,13] low frequency dielectric dispersion experiments,[14] and entropy considerations.[8,15–19]

Above ~550 K the cation sublattice is disordered in the sense that Na^+ ions have statistical lattice positional lifetimes of $\sim 5 \times 10^{-4}$ s, after which interval the ion jumps to a new site.[12,13] This repetitive jumping of the ions produces a fluidity which appears to be restricted to the cation sublattice, and which has implications for the electrical conductivity.[20] In a perfect lattice in which all ions are at normal sites, cations are able to jump from one site to another only if the movements are coordinated to occur over closed loops involving two or more cation sites.

(Ion movements of this kind are electrically neutral, since they involve neither a translation of charge nor a reorientation (of formation) of electric dipoles.) Positional jumping is greatly facilitated by the presence of cation vacancies, which largely removes the requirement of correlated cation movements.[21] Cation vacancies may be created thermally by the activation of cations to interstitial positions to form Frenkel defects in the lattice, and electrical conductivity results from the migration of the interstitial ions or the vacancies. It seems likely that interstitial positions of the cations will be involved in inter-site jumping because of the greatly increased number of ways in which the jumps may then occur, bearing in mind that in order to pass from one lattice site

to another the ion necessarily passes through such interstitial positions, and they must therefore be accessible at the energies encountered. In the absence of an electric field, the majority of cation movements are likely to consist of translation to an interstitial position, followed by a return to the original lattice site. It seems clear that this type of positional disorder of the cations, *viz.* jumping between normal and interstitial sites, must be closely connected with orientational disorder of the anions in *inter alia* $NaNO_3$. It may be incorrect to say that the cation disorder results from anion disorder, but the existence of the latter does imply fluctuations in lattice potential which would favour the former. At all events, the anion and cation movements are both manifestations of thermal disorder in the lattice which have a fundamental effect on the physical properties of the crystal.

The anion disorder is detectable calorimetrically, since the disordered orientations are non-equivalent, and therefore give rise to an entropy contribution. This disorder is not in itself directly detectable by electrical means, since the anion group is assumed not to migrate, and to have no electrical dipole moment. The cation disorder, on the other hand, does influence the conductivity, because interstitial sites are involved, as described above. There is no (first order) calorimetric effect however, because of the equivalence of the initial and final sites which the cations occupy for most of the time.

The increased probability that a cation will be found at an interstitial site in the disordered $NaNO_3$ lattice is clearly reflected in the high electrical conductivity and low frequency dielectric constant found $> \sim 550$ K. The effect is consistent with conduction either by interstitial ions or vacancies. If the lattice potential is assumed to remain constant over the order-disorder transformation, the increase in conductivity provides a direct measure of the increase in the number of interstitial ions, since $\sigma = nq\mu$ with q and μ constant. In this case, the effect of the transformation is to increase the number of carriers by approximately two orders of magnitude, since this is the increase in conductivity over the region, beyond that which would normally be accounted for by the increase in temperature alone. A correction of this value, which will not be attempted here, is possible by taking into account the changes in force constants which result from the transformation, subject to a reasonable assumption regarding the relationship between the force constants (*cf.*, *e.g.*, Ref. 22) and the activation and translation barrier energies.

The adoption of interstitial positions by cations in disordered $NaNO_3$, which may be expected on general grounds, is supported by the increased d.c. conductivity of the crystal which has been found experimentally.[20] Low frequency dispersion experiments [14] also support this conclusion and show that the jump rate between normal and interstitial sites has an upper frequency limit of $\sim 10^4$ Hz.

In conclusion, the above considerations, which attribute the temperature variation of the NMR parameters [12,13] at the phase I to II transition in $NaNO_3$ to a jumping between lattice and interstitial sites, remove the apparent inconsistency with the d.c. conductivity [20] data. Moreover, this provides an interesting example of the way in which d.c. and a.c. measurements can be used as sources of information on the statistical and dynamic aspects of the behaviour of the crystal lattice associated with the onset of thermal disorder.

Acknowledgement. This work was made possible by the financial support of *Nansenfondet.*

1. Mustajoki, A. *Ann. Acad. Sci. Fennicæ Ser. A VI* **1957** No. 5.
2. Sokolov, V. A. and Schmidt, N. E. *Izv. Sektora Fiz.-Khim. Analiza, Inst. Obshch. Neorgan. Khim., Akad. Nauk SSSR* **26** (1955) 123.
3. Reinsborough, V. C. and Wetmore, F. E. V. *Aust. J. Chem.* **20** (1967) 1.
4. Tahvonen, P. E. *Ann. Acad. Sci. Fennicæ A I* **1947** No 42.
5. Siegel, L. A. *J. Chem. Phys.* **17** (1949) 1146.
6. Sass, R. L., Vidale, R. and Donohue, J. *Acta Cryst.* **10** (1957) 567.
7. Shinnaka, Y. *J. Phys. Soc. Japan* **19** (1964) 1281.
8. Strømme, K. O. *Acta Chem. Scand.* **23** (1969) 1616.
9. Pattabhiramayya, P. *Proc. Indian Acad. Sci.* **A 7** (1938) 229.
10. Nedungadi, T. M. K. *Proc. Indian Acad. Sci.* **A 8** (1938) 397; **A 10** (1939) 197.
11. Hexter, R. M. *Spectrochim. Acta* **10** (1958) 291.

12. Eades, R. G., Hughes, D. G. and Andrew, E. R. *Proc. Phys. Soc.* **71** (1958) 1019.
13. Andrew, E. R., Eades, R. G., Hennel, J. W. and Hughes, D. G. *Proc. Phys. Soc.* **79** (1962) 954.
14. Fermor, J. H. and Kjekshus, A. *Acta Chem. Scand.* **26** (1972) 3235.
15. Janz, G. J., Kelly, F. J. and Perano, J. L. *J. Chem. Eng. Data* **9** (1964) 133.
16. Newns, D. M. and Stavely, L. A. K. *Chem. Rev.* **66** (1966) 267.
17. Fermor, J. H. and Kjekshus, A. *Acta Chem. Scand.* **24** (1970) 1015.
18. Strømme, K. O. *Acta Chem. Scand.* **26** (1972) 477.
19. Fermor, J. H. and Kjekshus, A. *Acta Chem. Scand.* **26** (1972) 2039.
20. Fermor, J. H. and Kjekshus, A. *Acta Chem. Scand.* **22** (1968) 1628.
21. Manning, J. R. *Diffusion Kinetics for Atoms in Crystals*, Van Nostrand, Princeton, Toronto, London, Melbourne 1968.
22. Kornfel'd, M. I. and Chubinov, A. A. *Soviet Phys. JETP (English Transl.)* **6** (1958) 26.

Received June 28, 1973.

ACTA CHEMICA SCANDINAVICA 27 (1973) 2257–2270

Heterocyclic Fused Tropylium Ions

IV. Stabilities and Electrophilic Deuteriation of Some Dithieno- and Furothienoannelated Tropylium Ions*

SALO GRONOWITZ, BARUCH YOM-TOV and URI MICHAEL**

Division of Organic Chemistry, University of Lund, Chemical Center, P.O. Box 740, S-220 07 Lund 7, Sweden

Unusually stable tropylium ions with pK_{R^+} values of 6.65, 5.40, 6.9 and 6.8 have been found in dithieno[2,1-b;4,5-b']tropylium perchlorate (V), dithieno[2,1-b;5,4-b']tropylium perchlorate (VI), furo-[3,2-a]thieno[2',3'-d]tropylium perchlorate (VII) and furo[2,3-a]-thieno[3',2'-d]tropylium perchlorate (VIII), respectively. Thus thieno- and furoannelation stabilize the tropylium ion, while the result of the corresponding benzoannelations is strong destabilization. Attempts are made to explain these differences.

It was found that V, VI, and VII smoothly underwent deuterium exchange with concentrated deuteriosulphuric acid in the heterocyclic β-positions. This was proven in the case of V and VI by the synthesis of authentic 3-deuterio derivatives.

A few years ago Pettit *et al.*[1] made the interesting observation that the fusion of a thiophene ring with its b-side onto the tropylium ion increased the stability (pK_{R^+} of $I = +6.0$), while it was known that benzoannelation decreased the stability[2] ($pK_{R^+} = +1.7$), compared to that of the tropylium ion[3] ($pK_{R^+} = 4.7$). Further annelation of benzene rings decreased the stability of the carbonium ion even more ($pK_{R^+} = -1.9$ for the dibenzotropylium ion IV).[4] The reason for the destabilizing effect of benzoannelation is not well understood.[4,5] It has been suggested that fusion of benzene rings, which in principle should cause an extension of the conjugated system, stabilizes the conjugate base or bases to a greater extent than the ion itself. One contribution to the relative destabilization has in some cases been ascribed to *peri* hydrogen interference, which could cause deviation from coplanarity.[6–8] Angular strain has also been mentioned as a factor contributing to the lower stability of benzoannelated systems.[8]

* Taken in part from the Ph.D. theses of U. Michael, University of Lund 1971 and B. Yom-Tov, University of Lund 1972.

** Present address: N. Clauson-Kaas, Chemical Research Laboratory, Rugmarken 28, 3520 Farum, Denmark.

SYNTHESES AND QUALITATIVE OBSERVATIONS

In order to obtain a better understanding of the annelation effects in tropylium ion chemistry, we have prepared some dithieno- and furothieno-annelated tropylium ions and studied their stabilities, their spectroscopical properties and electrophilic deuteriation. We were also interested in such compounds in connection with investigations on isoelectronic borepins.[9] The syntheses of dithieno[2,1-b;4,5-b′]tropylium perchlorate (V) and dithieno[1,2-

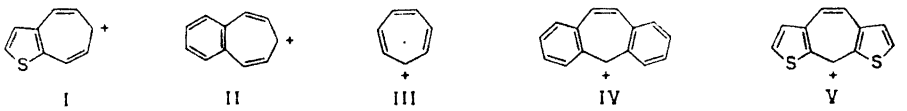

I II III IV V

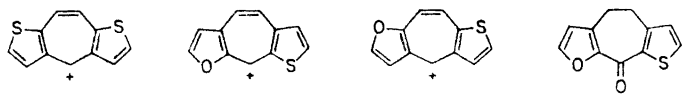

VI VII VIII IX

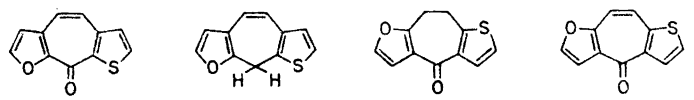

X XI XII XIII

b;5,4-b′]tropylium perchlorate (VI) have been described previously,[10,11] and preliminary reports of some physical and chemical properties have been given.[10] Furo[2,1-b]thieno[4,5-b]tropylium perchlorate (VII) and furo[1,2-b]-thieno[5,4-b]tropylium perchlorate (VIII) were prepared [12] in a similar way as that described for the dithieno analogues.[11] Thus 4,5-dihydro-9H-thieno-[4,5-b′]cyclohepta[2,1-b]furan-9-one (IX)[12] was transformed to 9H-thieno-[4,5-b′]cyclohepta[2,1-b]furan-9-one (X) by side-chain bromination-dehydrobromination. Reduction of X with lithium aluminium hydride gave 9H-thieno-[4,5-b′]cyclohepta[2,1-b]furan (XI), which was difficult to obtain pure and therefore was directly transformed to the tropylium perchlorate VII, by reaction with triphenylmethyl perchlorate. Following the same reaction sequence, VIII was prepared *via* 8,9-dihydro-4H-thieno[5,4-b′]cyclohepta[1,2-b]furan-4-one (XII),[12] 4H-thieno[5,4-b′]cyclohepta[1,2-b]furan-4-one (XIII) and 4H-thieno[5,4-b′]cyclohepta[1,2-b]furan (XIV). The structures of the compounds were evident from the mode of synthesis, and from IR, NMR, and mass spectral data.

Qualitatively, the high stability of the tropylium ions V to VIII is demonstrated by several observations. The first indication stems from the ease with which IX, XII, 4,5-dihydro-9H-cyclohepta[2,1-b;4,5-b′]dithiophene-9-one (XV) [13] and 8,9-dihydro-4H-cyclohepta[1,2-b;5,4-b′]dithiophene-4-one (XVI),[13] in contrast to 8,9-dihydro-4H-cyclohepta[2,1-c;4,5-c′]dithiophene-4-one

(XVII),[13] underwent bromination-dehydrobromination to the cycloheptatrienone derivatives. The driving force for the spontaneous dehydrobromination is probably the fact that the newly introduced unsaturation is part of an aromatic system. (The unsaturated ketones have tropylium ion structures in one of their dipolar forms.)

The lithium aluminium hydride reduction of X, XIII, 9H-cyclohepta[2,1-b;4,5-b']dithiophene-9-one (XVIII)[10] and 4H-cyclohepta[1,2-b;5,4-b']dithiophene-9-one (XIX)[10] yields the methylene derivatives and not the carbinols, corresponding to the ketones. A mixture of lithium aluminium hydride and aluminium chloride reduces some ketones to the methylene stage.[14] In this reducing mixture the aluminium chloride enhances the electrophilicity of the carbonyl carbon and eases the C–O bond cleavage. In the cases of ketones X, XIII, XVIII, and XIX, the carbon is electrophilic enough so that the Lewis acid is not necessary. The tropylium ions might be intermediates in these cases. The saturated ketone XII yielded only the corresponding carbinol upon reaction with lithium aluminium hydride. Furthermore the dibenzocycloheptatrienone (XX) also yielded the corresponding carbinol. This is understandable if it is considered that the corresponding dibenzotropylium ion IV is $10^8 - 10^9$ times less stable than the corresponding dithieno- or furothienoannelated tropylium ions (*cf.* below). The difficulty experienced in the reduction of 4H-cyclohepta[2,1-c;4,5-c']dithiophene-4-one (XXI)[13] might also be associated with the expected lower stability of the corresponding tropylium ion.

Additional evidence for the stability of the tropylium ions and the delocalization of the positive charge in the tricyclic system is obtained from a study of the C=O stretching region in the IR spectra of the ketones. Due to the high contribution of dipolar resonance forms having C–O single bonds, low frequencies for the C=O stretching are expected. However, the situation is somewhat complicated as several bands are observed in the pertinent region

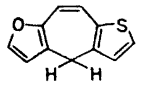
XIV

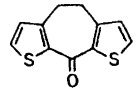
XV

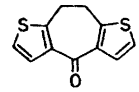
XVI

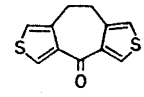
XVII

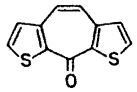
XVIII

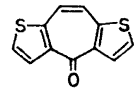
XIX

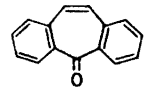
XX

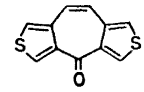
XXI

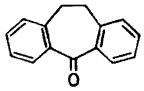
XXII

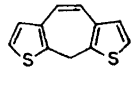
XXIII

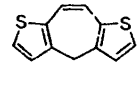
XXIV

for the unsaturated ketone. This was already found by Doering and Detert [15] in their classical work on tropone, for which they observed two bands at 1638 cm^{-1} and 1582 cm^{-1}. By extrapolation from benzoannelated derivatives, Heilbronner *et al.* assigned the lower frequency band to carbonyl stretching.[5] For the unsaturated ketones X, XIII, XVIII, and XIX, we have assigned the broad high-intensity bands to the carbonyl stretching frequency (Table 1). The sharper peaks of lower intensity (given in parentheses) are most probably due to C=C stretching, or perhaps are ring stretching bands. For XXI only one band was observed in this region.

The IR spectra were measured both in the solid state and in $CHCl_3$ solution. It is obvious that on going from the saturated to the unsaturated b-annelated dithieno or furothieno systems a shift of about 50 cm^{-1} towards lower frequency is observed. This effect is absent in the c-annelated dithieno derivatives XXI and XVII, and in the dibenzo systems XX and 10,11-dihydro-5H-dibenzo[a,d]cyclohepta-5-one (XXII).

Table 1. Frequencies in the C=O stretching region of some dithieno- and furothieno-annelated cycloheptanones.

Unsaturated ketone No.	Frequency cm^{-1} in KBr	Frequency cm^{-1} in $CDCl_3$ (≈5 %)	Saturated ketone No.	Frequency cm^{-1} in KBr	Frequency cm^{-1} in $CDCl_3$ (≈5 %)
X	1565 (1622)	1573 (1613)	IX	1612	1618 (1575)
XIII	1582 (1612)	1575 (1604)	XII	1630	1625
XVIII	1545 (1602)	1550 (1575) (1600) (1612)	XV	1595	1598
XIX	1568 (1598)	1568 (1598) (1612) (1585)	XVI	1621	1618 (1595)
XXI	1617	1616	XVII	1621	1625
XX	1650 (1600)		XXII	1648 (1595)	

It has recently been shown by X-ray analysis that compound XX is not planar.[16] The more extensive conjugation of a carbonyl group attached to the 2-position of thiophene or furan, compared to one attached through the 3-position, first pointed out for 2- and 3-thiophene aldehyde,[17] is also evident from the data given in Table 1.

pK_{R^+} Values

The pK_{R^+} values of V, VI, and VIII could easily be determined by titrating dilute ($< 2 \times 10^{-4}$ molar) aqueous carbon dioxide-free solutions of the perchlorate with dilute sodium hydroxide solution. Under these conditions reproducible ∫-shaped curves were obtained. The pH at half neutralization was taken as pK_{R^+}. Solutions with higher concentration of tropylium ion became turbid on standing, and the titration curves obtained from such solutions deviated more from the classical ∫ shape the more concentrated the

solution was. The pK_{R^+} value of tropylium ion VII could not be determined by this technique, since this ion did not show a normal response towards added base. However, the pK_{R^+} value for VII was determined by measuring initial pH values of the aqueous solutions of the perchlorate, a method used by Pettit and coworkers.[1] The stability constant can be estimated, if it is assumed that $(H_3O^+) \approx (ROH)$ and that the concentration of the carbonium ion is given by the difference between the concentration of added R^+ and the concentration of hydronium ion. This method is not very suitable for the determination of the pK_{R^+} of this particular tropylium ion, since over a wide range of concentrations the initial pH values were between 5.0 – 5.3, a region where small amounts of dissolved carbon dioxide can introduce a significant error. When the water was carefully treated to remove dissolved carbon dioxide and the measurements were carried out under an argon atmosphere, a reproducible value of $pK_{R^+} = 6.9 \pm 0.3$ was obtained. Application of the same method to the isomeric tropylium ion VIII and to tropylium ion (III)[18] gave pK_{R^+} values in excellent agreement with those obtained from potentiometric titrations.

The difficulties in determining the pK_{R^+} values of the tropylium salts at higher concentration is most probably due to some irreversible reactions of the tropylium ion-carbinol system. One possibility consists in a bimolecular hydride transfer between the carbinol and the tropylium ion, giving the methylene derivative and the ketone (after proton loss). These difficulties could perhaps be circumvented by using alkoxide in the corresponding alcohol as solvent (provided the carbonium ion is in rapid equilibrium with the corresponding ether).

The pK_{R^+} values measured in this investigation, together with some pertinent values of other tropylium ions, are given in Table 2. The dithieno- or furothienoannelated tropylium ions are thus 10^7 to 10^9 times more stable (less acidic) than the corresponding dibenzotropylium ion, and are among the most stable carbonium ions known.

The higher stability of VIII than V could also be demonstrated by hydride ion transfer experiments.[18] The NMR spectrum of an equimolar mixture of VIII and 9H-cyclohepta[2,1-b;4,5-b']dithiophene (XXIII), which was allowed to equilibrate (30 min at room temperature in anhydrous acetonitrile) revealed that the ratio of V to VIII was 2.0 – 2.2. The same ratio was obtained when XIV and V were allowed to equilibrate.

Several factors may contribute to the *increased* stabilization upon thieno- or furoannelation as compared to benzoannelation. Firstly it is well known that the π-excessive five-membered heterocyclic rings stabilize a positive charge of benzylic type much more efficiently than the benzene ring[19] and this has also been confirmed quantitatively by comparing pK_{R^+} values for dithienyl and trithienyl carbonium ions with those for analogous benzene derivatives.[1] MO calculations carried out by Pettit *et al.* also are in agreement with this observation.[1] In general, greater resonance stabilization can always be expected upon annelation of strongly π-excessive aromatic rings onto strongly π-deficient rings. It is possible that the same factors also are involved in tropylium ions. Secondly, as indicated by others,[8] ring-strain effects could operate upon the

annelation of benzene rings onto tropylium ions. The ideal angle of the six-membered ring is 120°, and that of the regular seven-membered ring is 129°. In thiophene the $H_2-C_2-C_3$ angle is 128.68° and the $C_2-C_3-H_3$ angle is 123.28°.[20] On this basis one might expect less angular strain upon annelation of thiophene rings onto tropylium ions. The same geometrical considerations are also true for furan rings.[21] Thirdly, due to the hetero atoms *peri* interactions between hydrogens are diminished or completely excluded. X-Ray analysis shows that V is planar.[22] No point of the cation's surface deviates more than 0.05 Å from the best plane.

Heilbronner and coworkers [5] and Pettit and coworkers [1] have found linear correlations between the "excessive" π-energy ΔE_π of the cation and the pK_{R^+} values for tropylium ions and for other types of carbonium ions with varying pK_{R^+} values. An estimation of ΔE_π may be obtained from the difference between the calculated π-energies of the cation and a model of its conjugate base. As a model for the conjugate bases of the dithienotropylium and furothienotropylium ions we chose the corresponding dithienyl- and furylthienylethylenes. Calculations were carried out by the HMO method and by the ω-technique.[23] The following set of parameters for oxygen and sulphur were used:[23] $h_O = 2.0$; $k_{CO} = 0.6$; $h_S = 1.0$; $k_{CS} = 0.4$. The ΔE_π values obtained are given in Table 2. The calculated ΔE_π values do not show a linear correlation with the pK_{R^+} values, which might be due to the few values and small interval of the latter. Calculations, however, predict which of the two dithieno- and furothienotropylium ions are the more stable. This can also be inferred from simple considerations of "good resonance structure".[19]

Table 2. pK_{R^+} values of some tropylium ions and calculated ΔE_π values for the furothieno- and dithienotropylium ions.

Tropylium ion, No.	pK_{R^+}	Ref.	ΔE_π (in β-units) HMO	ω-techn.
III	4.7	3		
II	1.7 ±0.1	5		
I	6.0	1		
IV	−1.9 ±0.1	4		
V	6.65±0.05		1.50	2.64
VI	5.40±0.05		1.37	2.58
VII	6.9 ±0.3		1.50	2.63
VIII	6.8 ±0.1		1.37	2.57

A comparison of the NMR spectra of the four tropylium ions V – VIII and their methylene precursors XXIII, 9H-cyclohepta[1,2-b;5,4-b']dithiophene (XXIV), XI and XIV also indicates an extensive delocalization of the charge in the tropylium ions. The heterocyclic ring hydrogens are shifted 1.25 to 2.8 ppm towards lower field, and the formal ethylenic hydrogens 2.50 – 3.13 ppm, on going from the methylene derivatives to the tropylium ions. Attempts to correlate these chemical shift differences with the corresponding π-electron

density differences [24] led to poor correlations. However, a rough correlation was obtained between the chemical shifts of the hydrogens of the tropylium ions in deuteriosulphuric acid and the π-electron densities on the carbons bearing these hydrogens (calculated by the ω-technique). Least square calculations gave a regression line with a proportionality constant of 7.1 ppm/electron and with a correlation coefficient of 0.84. In recent work, a proportionality constant of 13.56 ppm/electron was obtained for trithienylmethylcarbonium ions.[25] The electron densities and superdelocalizabilities for electro-

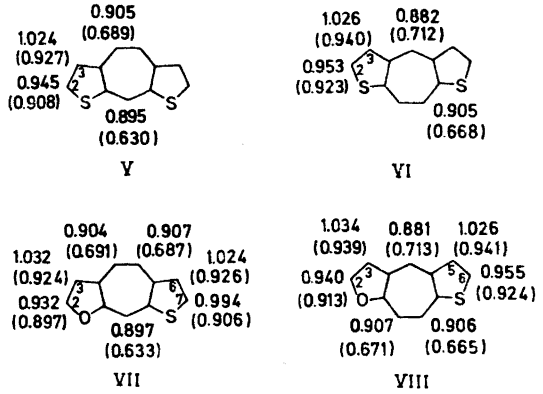

Fig. 1.

philic substitution (S_r^+, in parentheses) of the tropylium ions are given in the diagrams in Fig. 1.

The UV spectra of the tropylium ions and their precursors will be discussed in a separate paper.

ELECTROPHILIC DEUTERIATIONS

The NMR spectra of the tropylium ions V and VI run in D_2SO_4 at 68° showed that the high-field thiophenic doublets at δ 8.74 in V and 8.67 in VI, gradually disappeared, while a singlet simultaneously grew up in the middle of the lower field doublets, finally replacing these. Similarly with VII, the doublets at δ 8.21 (furanic) and δ 8.73 (thiophenic) gradually disappeared, while singlets grew up in the middle of the corresponding doublets at δ 9.17 and δ 9.35. From these results, it is quite obvious that deuterium exchange is occurring. Tropylium ion VIII, on the other hand, decomposed in concentrated D_2SO_4 before any exchange reaction could be observed. When mixtures of trifluoroacetic anhydride and D_2O or D_2SO_4 were used, no reaction could be detected. In order to prove the position of deuterium exchange, authentic 3-deuterio derivatives of V and VI were prepared.

Starting from 3-bromo-4-deuteriothiophene,[26] 4-deuterio-3-thiophene aldehyde (XXV) was prepared, which was transformed to 1-(2-bromo-3-thienyl)-

2-(4′-deuterio-3′-thienyl)ethene (XXVI) through the phosphonate carbanion [27,28] reaction with diethyl-2-bromo-3-thenylphosphonate. Catalytic hydrogenation using tris triphenylphosphine chlororhodium(I) gave 1-(2-bromo-3-thienyl)-2-(4′-deuterio-3′-thienyl)ethane (XXVII), which by halogen-metal exchange followed by carbonation yielded 1-(2-carboxy-3-thienyl)-2-(4′-deuterio-3′-thienyl)ethane (XXVIII). The acid XXVIII was ring-closed to 4,5-dihydro-3-deuterio-9H-cyclohepta[2,1-b;4,5-b′]dithiophene-9-one (XXIX) upon reaction with phosphorus pentachloride and tin tetrachloride. Ketone XXIX was brominated-dehydrobrominated with *N*-bromosuccinimide to give 3-deuterio-9H-cyclohepta[2,1-b;4,5-b′]dithiophene-9-one (XXX). Reduction of XXX with lithium aluminium hydride gave 3-deuterio-9H-cyclohepta[2,1-

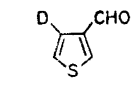
XXV

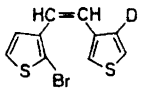
XXVI

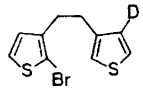
XXVII

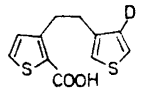
XXVIII

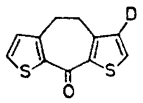
XXIX

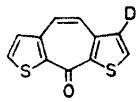
XXX

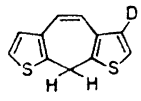
XXXI

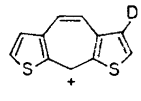
XXXII

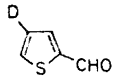
XXXIII

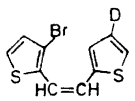
XXXIV

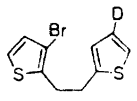
XXXV

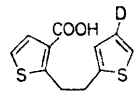
XXXVI

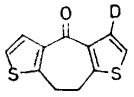
XXXVII

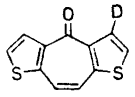
XXXVIII

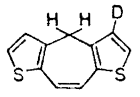
XXXIX

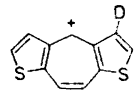
XL

b;4,5-b′]dithiophene (XXXI), which finally through hydride transfer with trityl perchlorate was transformed to 3-deuterio-9H-dithieno[2,1-b;4,5-b′]-tropylium perchlorate (XXXII). 3-Deuterio-4H-dithieno[1,2-b;5,4-b′]tropylium perchlorate (XL) was prepared by an approach quite similar to that described for XXXII. The necessary 4-deuterio-2-thiophene aldehyde (XXXIII) was prepared in a one-pot procedure [29] from 2,4-dibromothiophene by halogen-metal exchange with butyllithium followed by reaction with *N*,*N*-dimethylformamide, renewed halogen-metal exchange and methanolysis with CH_3OD. Reaction of XXXIII with diethyl-3-bromo-2-thenylphosphonate gave

1-(3-bromo-2-thienyl)-2-(4′-deuterio-2′-thienyl)ethene (XXXIV), which *via* 1-(3-bromo-2-thienyl)-2-(4′-deuterio-2′-thienyl)ethane (XXXV), 1-(3-carboxy-2-thienyl)-2-(4′-deuterio-2′-thienyl)ethane (XXXVI), 8,9-dihydro-3-deuterio-4H-cyclohepta[1,2-b;5,4-b′]dithiophene-4-one (XXXVII), 3-deuterio-4H-cyclohepta[1,2-b;5,4-b′]dithiophene-4-one (XXXVIII) and 3-deuterio-4H-cyclohepta[1,2-b;5,4-b′]dithiophene (XXXIX), was transformed to XL. The full details of the synthetic approach have previously been discussed for the unlabelled compounds.[11,13]

From the NMR spectra of XXXII and XL it follows that hydrogen exchange has occurred in the β-positions of the two dithienotropylium ions (3- and 6-positions of V and 3- and 5-positions of VI). The assignments of the ring protons in the NMR spectrum of VII were not proven as rigorously. It is, however, evident that by analogy with V, the high-field thiophenic doublet of VII should be assigned to hydrogen 6. With the known larger shift difference between the high-field β-hydrogens and the low-field α-hydrogens in furans than in thiophenes,[31,32] it seems reasonable to also assume that the high-field furanic band of VII is that of the 3-hydrogen. In addition, a long-range coupling of 0.8 Hz to hydrogen 9 was observed in this band. Such long-range couplings across five bonds following the straightest zig-zag path from a β-hydrogen have for instance been observed in benzothiophenes,[32] benzofurans,[32,33] thienopyridines,[34] 4,5-borazarothieno[2,3-c]pyridines,[35] 4,5-borazarofuro[2,3-c]-pyridines,[36] thienobenzofurans,[37,38] and in benzodithiophenes [38] support the assignment of the δ 8.21 band to the 3-hydrogen. Similar long-range couplings ($J_{39}=1.0$ Hz and $J_{58}=0.6$ Hz), following the same pattern, are also observed in the NMR spectrum of VIII. It is thus clear that also in VII, it is the β-hydrogens (3- and 6-hydrogens), that are exchanged.

We have not yet undertaken a detailed kinetic investigation of the deuteriation. However, at 68°C half-lives in 97 % D_2SO_4 are around 5 h and exchange as far as can be seen by the NMR technique is complete in 24 h, except for the 3-hydrogen of VII, which is exchanged somewhat more slowly. The β-exchanged ions V and VI behaved differently on further heating with D_2SO_4. While no additional changes were observed in the NMR spectrum of V after heating for 100 h, two or more new peaks near each of the three original peaks of the fully β-deuteriated molecule appeared in the NMR spectrum of VI. These new peaks, which amounted to roughly 10 – 15 % of the original sample, could perhaps be attributed to mono- and disulphonated products.

Nothing is known about electrophilic substitution in the benzene derivatives isoelectronic with the tropylium ions, *viz.* benzodithiophenes and thienobenzofurans.[37–39] The closest related systems which have been studied in detail are benzo[b]thiophene and benzo[b]furan.[40] However, recent work by Marino and coworkers [40] on the influence of benzoannelation onto thiophene and furan upon electrophilic substitution, has shown that although the orientation in the two bicyclic systems is different, *i.e.* predominant substitution in the 3-position of benzo[b]thiophene and in the 2-position of benzo[b]furan, the effect caused by annelation on the reactivity of the α- and β-positions is substantially the same in the two rings. The reactivity of the α-position is always decreased by a similar factor and the reactivity of the β-position is in-

creased in both systems. The different orientation observed in benzo[b]-thiophene and benzo[b]furan is therefore not a consequence of a different effect of benzo-fusion, but must be attributed to the different α:β-ratios in the two monocyclic systems. A consequence of this annelation effect is that in many electrophilic substitutions the β-position of benzo[b]thiophene is more reactive than the β-position of benzo[b]furan. Annelation of a tropylium ring onto furan as in VII apparently deactivates the α-position to a greater extent than the β-position, so that orientation is reversed.

MO calculations of electron-densities and superdelocalizabilities [41] for V – VIII by the ω-technique, given in the diagrams in Fig. 1, predict that electrophilic reagents should enter the β-positions, which is in agreement with the hydrogen-deuterium exchange experiments carried out with V – VII.

As far as we know, this is the first case in which electrophilic substitution has been carried out with tropylium ions, and we hope to be able to study hydrogen exchange in more detail and also to extend our investigations to other substitution reactions.

EXPERIMENTAL

4H-Thieno[5,4-b']cyclohepta[1,2-b]furan-4-one (XIII). A mixture of 8.0 g (39 mmol) of 8,9-dihydro-4H-thieno[5,4-b']cyclohepta[1,2-b]furan-4-one (XII) [12] and 100 mg of azobisisobutyronitrile (ABN) dissolved in 120 ml of anhydrous carbon tetrachloride was refluxed. A mixture of 7.0 g (39 mmol) of *N*-bromosuccinimide (NBS) and 150 mg of ABN was added in portions within 30 min. A red precipitate began to form 10 min after the addition was started. A few minutes later the evolution of hydrogen bromide could be detected. The mixture was refluxed for 6 h and was then cooled. The solid was filtered off (12.5 g), treated with water (3 × 50 ml at 45°) and dried, yielding 6.0 g of slightly greenish XIII. The carbon tetrachloride filtrate was treated with charcoal and evaporated, yielding 2.0 g of XII brominated in the side-chain. This product was dissolved in methanol containing 1.0 g of sodium methoxide and refluxed for 90 min. The methanol was evaporated, water was added and the solution was neutralized and extracted with ether. After drying over magnesium sulphate and evaporation, an additional 0.70 g of XIII was obtained, making a total yield of 84 %, m.p. 117 – 119° after recrystallization from hexane. NMR ($CDCl_3$): $\delta = 7.25$ ppm, centre of complex multiplet due to hydrogens 3, 8, and 9, $\delta_2 = 7.62$ ppm, $\delta_5 = 7.53$ ppm, $\delta_6 = 8.08$ ppm. $J_{23} = 2.0$ Hz, $J_{56} = 5.5$ Hz. [Found M. wt. 202: C 64.8; H 2.99; S 15.5. Calc. for $C_{11}H_6O_2S$ (202.2): C 65.33; H 2.99; S 15.86].

9H-Thieno[4,5-b']cyclohepta[2,1-b]furan-9-one (X). A mixture of 4.0 g (20 mmol) of 4,5-dihydro-9H-thieno[4,5-b']cyclohepta[2,1-b]furan-9-one (IX) and 80 ml of anhydrous carbon tetrachloride was refluxed. 70 mg of ABN was added, and then 3.5 g (20 mmol) of NBS was added in two portions. 2 min later, a vigorous reaction started and solid material precipitated from the solution. A few minutes later the evolution of hydrogen bromide could be observed. After 30 min the carbon tetrachloride was evaporated and methanol was added. The mixture was then refluxed for 2 h, the methanol evaporated and 50 ml of water was added. The slightly yellow solid was filtered off, washed with water (3 × 50 ml at 45°) and dried thoroughly, yielding 3.9 g (98 %) of the title compound X, m.p. 170 – 172° after recrystallization from isopropanol. NMR (CD_3SOCD_3): $\delta_3 = 7.27$ ppm, δ_4 or $\delta_5 = 7.57$ ppm, δ_5 or $\delta_4 = 7.86$ ppm, $\delta_6 = 7.77$ ppm, $\delta_7 = 8.28$ ppm, $\delta_2 = 8.43$ ppm. $J_{23} = 1.9$ Hz, $J_{45} = 11.5$ Hz, $J_{67} = 5.3$ Hz. [Found M. wt. 202: C 65.6; H 3.09; S 16.1. Calc. for $C_{11}H_6O_2S$ (202.2): C 65.33; H 2.99; S 15.86].

4H-Thieno[5,4-b']cyclohepta[1,2-b]furan (XIV). 3.0 g (15 mmol) of 4H-thieno[5,4-b']-cyclohepta[1,2-b]furan-4-one (XIII) in 75 ml of anhydrous ether was refluxed with 1.5 g of lithium aluminium hydride for 6 h. The excess of lithium aluminium hydride was decomposed with methanol, and cold dilute hydrochloric acid was added until the layers were clearly separated. The aqueous phase was extracted a few times with ether and the combined organic phases were dried over magnesium sulphate and evaporated, yielding

2.7 g (96 %) of the title compound XIV, m.p. 65 – 68° after recrystallization from hexane. The compound should be stored in a cold dark place due to its instability to heat and light. NMR ($CDCl_3$): $\delta_{CH_2}=3.87$ ppm, $\delta_2=7.35$ ppm, $\delta_3=6.18$ ppm, $\delta_5=6.71$ ppm, $\delta_6=7.20$ ppm, δ_8 and $\delta_9=6.47$ ppm. $J_{23}=1.9$ Hz, $J_{56}=5.0$ Hz. [Found M. wt. 188: C 70.1; H 4.34; S 16.9. Calc. for $C_{11}H_8OS$ (188.3): C 70.18; H 4.28; S 17.03].

Furo[1,2-b]thieno[3,4-b]tropylium perchlorate (VIII). 2.0 g (11 mmol) of 4H-thieno-[5,4-b']cyclohepta[1,2-b]furan (XIV) was dissolved in 200 ml of anhydrous ethyl acetate and a hot solution of 3.6 g (10.5 mmol) of triphenylmethyl perchlorate [42] dissolved in the minimum amount of anhydrous acetonitrile was added dropwise within 5 min. An immediate precipitation occurred. The mixture was stirred for another 5 min, filtered and dried, yielding 3.0 g (98 %) of the title compound, m.p. 271 – 275° after recrystallization from an ethyl acetate-acetonitrile mixture. NMR (CF_3COOH): $\delta_2=8.60$ ppm, $\delta_3=7.83$ ppm, $\delta_4=10.00$ ppm, $\delta_5=8.46$ ppm, $\delta_6=8.81$ ppm, $\delta_8=9.60$ ppm, $\delta_9=9.00$ ppm. $J_{23}=2.2$ Hz, $J_{39}=1.0$ Hz, $J_{56}=5.4$ Hz, $J_{58}=0.6$ Hz, $J_{89}=10.8$ Hz. [Found: C 46.4; H 2.61; Cl 12.3; S 11.1. Calc. for $C_{11}H_7ClO_5S$ (286.7): C 46.08; H 2.46; Cl 12.37; S 11.18].

Furo[2,1-b]thieno[4,5-b]tropylium perchlorate (VII). 1.5 g (7.0 mmol) of 9H-thieno-[4,5-b']cyclohepta[2,1-b]furan-9-one (X) in 100 ml of anhydrous ether was refluxed for 6 h with 350 mg of lithium aluminium hydride and worked up as described for hydrocarbon XIV. 1.3 g of crude labile 9H-thieno[4,5-b']cyclohepta[2,1-b]furan (XI) was obtained, which without purification was used in the next step. NMR ($CDCl_3$): $\delta_9=4.23$ ppm, $\delta_3=6.33$ ppm, δ_4 or $\delta_5=6.33$ ppm, δ_5 or $\delta_4=6.62$ ppm, $\delta_6=6.86$ ppm, $\delta_7=7.05$ ppm, $\delta_2=7.25$ ppm. $J_{23}=2.0$ Hz, $J_{39}\approx0.4$ Hz, $J_{29}\approx0.3$ Hz, $J_{67}=5.0$ Hz, $J_{45}=11.5$ Hz. 850 mg of crude XI was converted into the title compound in the same way as described above for the isomeric tropylium ion VIII. 820 mg (58 % based on the unsaturated ketone X) of furo[2,1-b]thieno[4,5-b]tropylium perchlorate, m.p. 236 – 239° after recrystallization from a mixture of ethyl acetate-acetonitrile, was obtained. NMR (CF_3COOH): $\delta_3=7.84$ ppm, $\delta_6=8.41$ ppm, $\delta_2=8.80$ ppm, $\delta_7=9.00$ ppm, δ_4 or $\delta_5=9.06$ ppm, δ_5 or $\delta_4=9.36$ ppm, $\delta_9=9.95$ ppm. $J_{23}=2.0$ Hz, $J_{39}\approx0.8$ Hz, $J_{45}=10.5$ Hz, $J_{67}=5.5$ Hz, $J_{69}\approx0.4$ Hz. NMR (D_2SO_4): $\delta_3=8.21$ ppm, $\delta_6=8.73$ ppm, $\delta_2=9.17$ ppm, $\delta_7=9.35$ ppm, δ_4 or $\delta_5=9.40$ ppm, δ_5 or $\delta_4=9.68$ ppm, $\delta_9=10.23$ ppm. [Found: C 46.5; H 2.41; Cl 12.4; S 11.4. Calc. for $C_{11}H_7ClO_5S$ (286.7): C 46.08; H 2.46; Cl 12.37; S 11.18].

4-Deuterio-3-thiophene aldehyde (XXV). To 475 ml of 0.7 N ethereal butyllithium cooled to −70°, 49.2 g (0.30 mol) of 3-bromo-4-deuteriothiophene [26] in 200 ml of anhydrous ether was added in a slow stream. After stirring for 5 min, 36.0 g of anhydrous *N,N*-dimethylformamide in 100 ml of anhydrous ether was added during 5 min with efficient stirring. The cooling bath was removed after 30 min, stirring was continued until the reaction mixture reached room temperature, and it was then decomposed by pouring it into a 20 % ice-water solution of ammonium chloride. After the usual work-up, the ether phase was fractionated, yielding 24 g (70 %) of 4-deuterio-3-thiophene aldehyde, b.p. 40 – 45°/1 mmHg. NMR ($CDCl_3$): $\delta_5=7.30$ ppm, $\delta_2=8.07$ ppm, $\delta_{CHO}=9.83$ ppm. $J_{25}=2.9$ Hz, $J_{CHO-5}=0.8$ Hz.

4-Deuterio-2-thiophene aldehyde (XXXII). To a solution of 42.2 g (0.17 mol) of 2,4-dibromothiophene [43] in 100 ml of anhydrous ether cooled to −70°, 110 ml of 1.6 N commercial butyllithium in hexane was added during 20 min under nitrogen. The mixture was stirred at −70° for an additional 5 min, and 13 g of anhydrous *N,N*-dimethylformamide in 100 ml of ether was added quickly. The cooling bath was removed, the mixture stirred for 30 min, and cooled again to −70°. 172 ml of 1.6 N butyllithium in hexane was added dropwise during 15 min. Stirring was continued for 75 min and 8.0 g of deuteriomethanol in 50 ml of anhydrous ether was added. The cooling bath was removed and the mixture poured into 20 % ice-cold ammonium chloride solution and worked up as usual. Distillation gave 10 g of 4-deuterio-2-thiophene aldehyde, b.p. 90 – 110°/15 mmHg, which VPC analysis showed to contain 20 % 2,4-dibromothiophene. Fractionation gave 8.0 g (41 %) of 4-deuterio-2-thiophene aldehyde, which was pure enough (> 95 %) for further use. NMR ($CDCl_3$): δ_3 and $\delta_5=7.78$ ppm, $\delta_{CHO}=9.92$ ppm. $J_{CHO-5}=1.0$ Hz.

1-(2-Bromo-3-thienyl)-2-(4'-deuterio-3'-thienyl)ethene (XXVI). This compound (25.6 g, 94 %) was prepared according to the general description given in Ref. 11 from 11.4 g (0.10 mol) of 4-deuterio-3-thiophene aldehyde and 31.3 g (0.10 mol) of diethyl-2-bromo-3-thenylphosphonate.

1-(2-Bromo-3-thienyl)-2-(4'-deuterio-3'-thienyl)ethane (XXVII). 20.0 g (73.5 mmol) of recrystallized 1-(2-bromo-3-thienyl)-2-(4'-deuterio-3-thienyl)ethene in 250 ml of 96 %

ethanol was hydrogenated using 0.6 g of tris triphenylphosphine chlororhodium(I) as catalyst, following the general procedure given in Ref. 11. 19.0 g (95 %) of the title compound, b.p. $100-115°/5\times10^{-3}$ mmHg, was obtained. NMR ($CDCl_3$): $\delta_{CH_2-CH_2}=2.84$ ppm, $\delta_4=6.65$ ppm, $\delta_{2'}=6.84$ ppm, $\delta_5=7.05$ ppm, $\delta_{5'}=7.15$ ppm. $J_{45}=5.7$ Hz, $J_{2',5'}=3.0$ Hz.

1-(2-Carboxy-3-thienyl)-2-(4'-deuterio-3'-thienyl)ethane (XVIII). From 6.8 g (2.5 mmol) of 1-(2-bromo-3-thienyl)-2-(4'-deuterio-3'-thienyl)ethane and 42 ml of 0.8 N ethereal ethyllithium and carbon dioxide, following the general procedure given in Ref. 11, 5.0 g (93 %) of the title compound, m.p. 176° after recrystallization from chloroform, was obtained. NMR (DMSO): $\delta_{CH_2-CH_2}=2.8-3.2$ ppm (broad multiplet), $\delta_4=7.04$ ppm, $\delta_{2'}=7.14$ ppm, $\delta_{5'}=7.41$ ppm, $\delta_5=7.67$ ppm. $J_{2',5'}=2.7$ Hz, $J_{45}=5.0$ Hz.

4,5-Dihydro-3-deuterio-9H-cyclohepta[2,1-b;4,5-b']dithiophene-9-one (XXIX). From 4.25 g (17.8 mmol) of 1-(2-carboxy-3-thienyl)-2-(4'-deuterio-3'-thienyl)ethane in 100 ml of anhydrous benzene, 4.4 g of phosphorus pentachloride and 4 ml of tin tetrachloride, 3.7 g (94 %) of the title compound, m.p. 105 – 106° after recrystallization from methanol, was obtained following the procedure given for the unlabelled compound in Ref. 11. NMR ($CDCl_3$): $\delta_{CH_2-CH_2}=3.08$ ppm, $\delta_2=7.40$ ppm (singlet), $\delta_7=7.50$ ppm (doublet), $\delta_6=6.90$ ppm. $J_{67}=5.0$ Hz.

3-Deuterio-9H-cyclohepta[2,1-b;4,5-b']dithiophene-9-one (XXX). Following the procedure for the unlabelled compound in Ref. 13, 3.0 g (13.6 mmol) of 4,5-dihydro-3-deuterio-9H-cyclohepta[2,1-b;4,5-b']dithiophene-9-one in 75 ml of carbon tetrachloride was heated with 2.43 g of *N*-bromosuccinimide and 0.4 g azobisisobutyronitrile, followed by treatment with 3 g of sodium methoxide, yielding 2.7 g (90 %) of the title compound, m.p. 151 – 152° after recrystallization from acetonitrile. NMR ($CDCl_3$): $\delta_2=7.70$ ppm (singlet), $\delta_4=7.36$ ppm, $\delta_6=7.35$ ppm, $\delta_7=7.70$ ppm (doublet). $J_{67}=5.2$ Hz.

3-Deuterio-9H-cyclohepta[2,1-b;4,5-b']dithiophene (XXXI). This compound was prepared in quantitative yield by reaction of 1.5 g of 3-deuterio-9H-cyclohepta[2,1-b;4,5-b']dithiophene-9-one in 200 ml of anhydrous ether with 0.5 g of lithium aluminium hydride, according to the procedure in Ref. 13, m.p. 98 – 99° after recrystallization from hexane. NMR ($CDCl_3$): $\delta_2=7.00$ ppm (singlet), $\delta_4=\delta_5=6.73$ ppm, $\delta_6=6.87$ ppm, $\delta_7=7.00$ ppm (doublet), $\delta_9=4.05$ ppm. $J_{67}=5.3$ Hz.

3-Deuterio-9H-dithieno[2,1-b;4,5-b']tropylium perchlorate (XXXII). From 0.5 g of 3-deuterio-9H-cyclohepta[2,1-b;4,5-b']dithiophene in 75 ml of anhydrous ethyl acetate and 2 g of triphenylmethyl perchlorate in the minimum amount of acetonitrile, 0.7 g of the title compound was obtained, m.p. 288° after recrystallization from acetonitrile. NMR (H_2SO_4): $\delta_2=9.38$ ppm (singlet), $\delta_4=\delta_5=9.43$ ppm, $\delta_6=8.67$ ppm, $\delta_7=9.38$ ppm (doublet), $\delta_9=10.34$ ppm. $J_{67}=5.5$ Hz.

1-(3-Bromo-2-thienyl)-2-(4'-deuterio-2'-thienyl)ethene (XXXIV). From 11.4 g (0.10 mol) of 4-deuterio-2-thiophene aldehyde, 31.3 g diethyl-3-bromo-2-thenyl phosphonate and 8.1 g of sodium methoxide, 24.8 g (91 %) of the title compound was obtained, following the general procedure given in Ref. 11.

1-(3-Bromo-2-thienyl)-2-(4'-deuterio-2'-thienyl)ethane (XXXV). 15.0 g (55.1 mmol) of recrystallized 1-(3-bromo-2-thienyl)-2-(4'-deuterio-2'-thienyl)ethene in 200 ml of 96 % ethanol was hydrogenated, using 0.5 g of tris triphenylphosphine chlororhodium(I) as catalyst and following the general procedure given in Ref. 11. 14.0 g (93 %) of the title compound, b.p. $105-110°/5\times10^{-3}$ mmHg, was obtained. NMR ($CDCl_3$): $\delta_{CH_2-CH_2}=3.13$ ppm, $\delta_4=6.83$ ppm, $\delta_5=7.03$ ppm, $\delta_{3'}=6.90$ ppm, $\delta_{5'}=7.07$ ppm. $J_{45}=5.2$ Hz, $J_{3',5'}=1.4$ Hz.

1-(3-Carboxy-2-thienyl)-2-(4'-deuterio-2'-thienyl)ethane (XXXVI). From 11.5 g (42.3 mmol) of 1-(3-bromo-2-thienyl)-2-(4'-deuterio-2'-thienyl)ethane and 70 ml of 0.8 N ethereal ethyllithium and carbon dioxide, following the general procedure given in Ref. 11, 9.5 g (90 %) of the title compound was obtained, m.p. 135° after recrystallization from aqueous acetone. NMR (CD_3COCD_3): $\delta_{CH_2-CH_2}=3.0-3.8$ ppm (broad multiplet), $\delta_{5'}=7.18$ ppm, $\delta_{3'}=6.90$ ppm, δ_4 or $\delta_5=7.21$ ppm, δ_5 or $\delta_4=7.43$ ppm. $J_{3',5'}=1.5$ Hz, $J_{45}=5.4$ Hz.

8,9-Dihydro-3-deuterio-4H-cyclohepta[1,2-b;5,4-b']dithiophene-4-one (XXXVII). From 4.25 g (17.8 mmol) of 1-(3-carboxy-2-thienyl)-2-(4'-deuterio-2'-thienyl)ethane in 100 ml of anhydrous benzene, 4.4 g of phosphorus pentachloride and 4 ml of tin tetrachloride, 3.6 g (92 %) of the title compound was obtained, m.p. 95° after recrystallization from methanol, following the procedure given for the unlabelled compound in Ref. 11. NMR

($CDCl_3$): $\delta_{CH_2-CH_2} = 3.27$ ppm, $\delta_2 = 7.00$ ppm (singlet), $\delta_5 = 7.70$ ppm (doublet). $J_{56} = 5.5$ Hz.

3-Deuterio-4H-cyclohepta[1,2-b;5,4-b']dithiophene-4-one (XXXVIII). Following the procedure for the unlabelled compound in Ref. 13, 3.0 g (13.6 mmol) of 8,9-dihydro-3-deuterio-4H-cyclohepta[1,2-b;5,4-b']dithiophene-4-one in 75 ml of carbon tetrachloride was reacted with 2.43 g of NBS and 0.4 g ABN, followed by treatment with 3 g of sodium methoxide, yielding 2.55 g (85 %) of the title compound, m.p. 172 – 173° after recrystallization from acetonitrile. NMR ($CDCl_3$): $\delta_2 = 7.50$ ppm (singlet), $\delta_5 = 8.09$ ppm, $\delta_6 = 7.50$ ppm (doublet), $\delta_8 = \delta_9 = 7.24$ ppm. $J_{56} = 5.5$ Hz.

3-Deuterio-4H-cyclohepta[1,2-b;5,4-b']dithiophene (XXXIX). 1.4 g (100 %) of the title compound, m.p. 132 – 133° after recrystallization from hexane, was obtained from 1.5 g (6.9 mmol) of 3-deuterio-4H-cyclohepta[1,2-b;5,4-b']dithiophene-4-one in 200 ml of anhydrous ether and 0.5 g of lithium aluminium hydride, according to the procedure in Ref. 13. NMR ($CDCl_3$): $\delta_2 = 7.24$ ppm (singlet), $\delta_4 = 3.85$ ppm, $\delta_5 = 6.78$ ppm, $\delta_6 = 7.24$ ppm (doublet), $\delta_8 = \delta_9 = 6.72$ ppm. $J_{56} = 5.2$ Hz.

3-Deuterio-4H-dithieno[1,2-b;5,4-b']tropylium perchlorate (XL). From 0.5 g of 3-deuterio-4H-cyclohepta[1,2-b;5,4-b']dithiophene in 75 ml of anhydrous ethyl acetate and 2 g of triphenylmethyl perchlorate in the minimum amount of acetonitrile, 0.7 g of the title compound was obtained, m.p. 310° after recrystallization from acetonitrile. NMR (H_2SO_4): $\delta_2 = 9.04$ ppm (singlet), $\delta_4 = 10.31$ ppm, $\delta_5 = 8.74$ ppm, $\delta_6 = 9.04$ ppm (doublet), $\delta_8 = \delta_9 = 9.59$ ppm. $J_{56} = 5.5$ Hz.

Hydrogen-deuterium exchange experiments with the tropylium ions V, VI, and VII. 40 mg of the tropylium ion was dissolved in 0.5 ml of conc. D_2SO_4 (97 %) and the solution kept at 68°. The progress of the reaction was followed by NMR. The average value of four integrations of each absorption was taken. During the night the sample was stored at −25°. No exchange reaction could be detected at this temperature.

In the pK_{R^+} determinations, sample titrations were made in a titration assembly consisting of a Radiometer Autoburette, ABU 11, in conjunction with a Radiometer pH-meter 26. Radiometer electrodes G202C and K410 were used. NMR spectra were recorded on a Varian A-60 NMR spectrometer, mass spectra on an LKB 9000 mass spectrometer and IR spectra on Perkin-Elmer 257 and Perkin-Elmer 221 spectrophotometers.

The elementary analyses were carried out by Miss Ilse Beetz, Mikroanalytisches Laboratorium, Kronach.

Acknowledgements. Grants from the *Swedish Natural Science Research Council* (to S.G.) and from the *Faculty of Science, University of Lund,* (to U.M. and B.Y.-T.) are gratefully acknowledged.

REFERENCES

1. Turnbo, R. G., Sullivan, D. L. and Pettit, R. *J. Am. Chem. Soc.* **86** (1964) 5630.
2. Renhard, H. H., Heilbronner, E. and Eschenmoser, A. *Chem. Ind. (London)* **1955** 415.
3. Doering, W. V. E. and Knox, L. H. *J. Am. Chem. Soc.* **76** (1954) 3203.
4. Berti, G. *J. Org. Chem.* **22** (1957) 330.
5. Naville, G., Strauss, H. and Heilbronner, E. *Helv. Chim. Acta* **43** (1960) 1221.
6. Meuche, D., Simon, W. and Heilbronner, E. *Helv. Chim. Acta* **41** (1958) 57.
7. Meuche, D., Simon, W. and Heilbronner, E. *Helv. Chim. Acta* **41** (1958) 414.
8. Stiles, M. and Libbey, A. J. *J. Org. Chem.* **22** (1957) 1243.
9. Gronowitz, S., Gassne, P. and Yom-Tov, B. *Acta Chem. Scand.* **23** (1969) 2927.
10. Gronowitz, S. and Yom-Tov, B. *Z. Chem.* **10** (1970) 390.
11. Yom-Tov, B. and Gronowitz, S. *Chemica Scripta* **3** (1973) 165.
12. Michael, U. and Gronowitz, S. *Chemica Scripta* **4** (1973) 126.
13. Yom-Tov, B. and Gronowitz, S. *Chemica Scripta* **3** (1973) 37.
14. Brown, B. R. and White, A. M. S. *J. Chem. Soc.* **1957** 3755.
15. Doering, W. v. E. and Detert, F. L. *J. Am. Chem. Soc.* **73** (1951) 876.
16. Shimanouchi, H., Hata, T. and Sasada, Y. *Tetrahedron Letters* **1968** 3573.
17. Gronowitz, S. and Rosenberg, A. *Arkiv Kemi* **8** (1955) 23.

18. For a review *cf.* Nenitzescu, C. D. *Intermolecular Hydride Transfer Reactions.* In Olah, G. A. and Schleyer, P. von R. *Carbonium Ions*, Wiley-Interscience, New York 1970, Vol. II, Chapter 13, p. 463.
19. Gronowitz, S. *Arkiv Kemi* **13** (1958) 295.
20. Bak, B., Christensen, D., Hansen-Nygaard, L. and Rastrup-Andersen, J. *J. Mol. Spectry.* **7** (1961) 58.
21. Bak, B., Christensen, D., Dixon, W. B., Hansen-Nygaard, L., Rastrup-Andersen, J. and Schottländer, M. *J. Mol. Spectry.* **9** (1962) 124.
22. Aurivillius, B. *Private communication.*
23. Streitwieser, Jr., A. *Molecular Orbital Theory for Organic Chemists.* Wiley, New York 1961.
24. Fraenkel, G. and Farnum, D. G. *Nuclear Magnetic Resonance Spectra.* In Olah, G. A and Schleyer, P. von R., Eds., *Carbonium Ions*, Wiley-Interscience, New York 1968, Vol. I, Chapter 7.
25. Taddei, F., Spagnolo, P. and Tiecco, M. *Org. Magn. Resonance* **2** (1970) 159.
26. Gronowitz, S., Moses, P. and Håkansson, R. *Arkiv Kemi* **16** (1960) 267.
27. Wadsworth, D. H., Schupp, O. E., Sens, E. J. and Ford, J. A. *J. Org. Chem.* **30** (1965) 680.
28. Horner, L., Hoffman, H., Wipple, H. and Klahre, G. *Chem. Ber.* **92** (1958) 2499.
29. Michael, U. and Gronowitz, S. *Acta Chem. Scand.* **22** (1968) 1353.
30. Hoffman, R. A. and Gronowitz, S. *Arkiv Kemi* **15** (1959) 45.
31. Gronowitz, S., Sörlin, G., Gestblom, B. and Hoffman, R. A. *Arkiv Kemi* **19** (1962) 483.
32. Elvidge, J. A. and Foster, R. G. *J. Chem. Soc.* **1964** 981.
33. Elvidge, J. A. and Foster, R. G. *J. Chem. Soc.* **1963** 590.
34. Gronowitz, S. and Sandberg, E. *Arkiv Kemi* **32** (1970) 269.
35. Gronowitz, S. and Namtvedt, J. *Acta Chem. Scand.* **20** (1966) 1448.
36. Gronowitz, S. and Michael, U. *Arkiv Kemi* **32** (1970) 283.
37. Kellogg, R. M., Groen, M. B. and Wynberg, H. *J. Org. Chem.* **32** (1967) 3093.
38. Blackburn, F. V., Cholerton, T. J. and Timmons, C. J. *J. Chem. Soc. Perkin Trans 2* **1972** 101.
39. Timmons, C. J. and Lodder, C. E. *J. Chem. Soc.* **C 1967** 1677.
40. Clementi, S., Linda, P. and Marino, G. *J. Chem. Soc.* **B 1971** 79.
41. Ref. 23, pp. 330–331.
42. Dauben, Jr., H. J., Gadecki, F. A., Harmon, K. M. and Pearson, D. L. *J. Am. Chem. Soc.* **79** (1957) 4557.
43. Lawesson, S.-O. *Arkiv Kemi* **11** (1957) 317.

Received March 7, 1973.

ACTA CHEMICA SCANDINAVICA 27 (1973) 2271–2278

Preparation and Characterization of 1-Alkyl-5-hydroxy-Δ^2-1,2,3-triazolines

CARL ERIK OLSEN and CHRISTIAN PEDERSEN

Department of Organic Chemistry, Technical University of Denmark, DK-2800 Lyngby, Denmark

A number of 1-methyl- and 1-benzyl-5-hydroxy-Δ^2-1,2,3-triazolines have been prepared by reaction of ketones with methyl or benzyl azide in the presence of potassium *tert*-butoxide. Some of the triazolines exist in solution as an equilibrium mixture of diastereomers, most likely interconvertible *via* triazenes. The structures of the triazolines, including the diastereomeric pairs, have been determined by NMR spectroscopy in chloroform and pyridine.

The reaction of alkyl or aryl azides with ketones in the presence of potassium *tert*-butoxide leads to the formation of 5-hydroxy-Δ^2-1,2,3-triazolines (I), as described in a preliminary communication.[1] The reaction has now been further studied, and the products obtained by treating a number of ketones with methyl and benzyl azide are described in the present paper. The analogous reaction with aryl azides forms the subject of a forthcoming paper.

Methyl or benzyl azide react smoothly with ketones and potassium *tert*-butoxide at room temperature to give 1-methyl- or 1-benzyl-5-hydroxy-Δ^2-1,2,3-triazolines (I) in mostly good yields (Table 1). Sterically unhindered ketones react with azides in the course of a few hours whereas hindered ketones, such as diisopropyl ketone, require longer reaction times. For certain ketones the reaction takes a different course.[2,3]

The highly hindred triazoline (Ig) was prepared by treatment of the α-azido ketone (III) with methyl magnesium iodide, a reaction probably proceeding with the triazene (IIg) as an intermediate,[4] which subsequently undergoes ring-closure to (Ig). The α-azido alcohol (IV) was obtained as a by-product from this reaction.

Triazolines in which R_a[4] and R_b[4] are different may obviously exist in two diastereomeric forms (I′) and (I″), and NMR spectra in fact showed that many of the compounds in Table 1 gave a mixture of two products when dissolved in chloroform or pyridine. When an NMR spectrum of 1-benzyl-4,5-dimethyl-5-hydroxy-Δ^2-1,2,3-triazoline (Ik) was determined immediately after it was dissolved in deuteriochloroform almost only one isomer (I′k) was present.

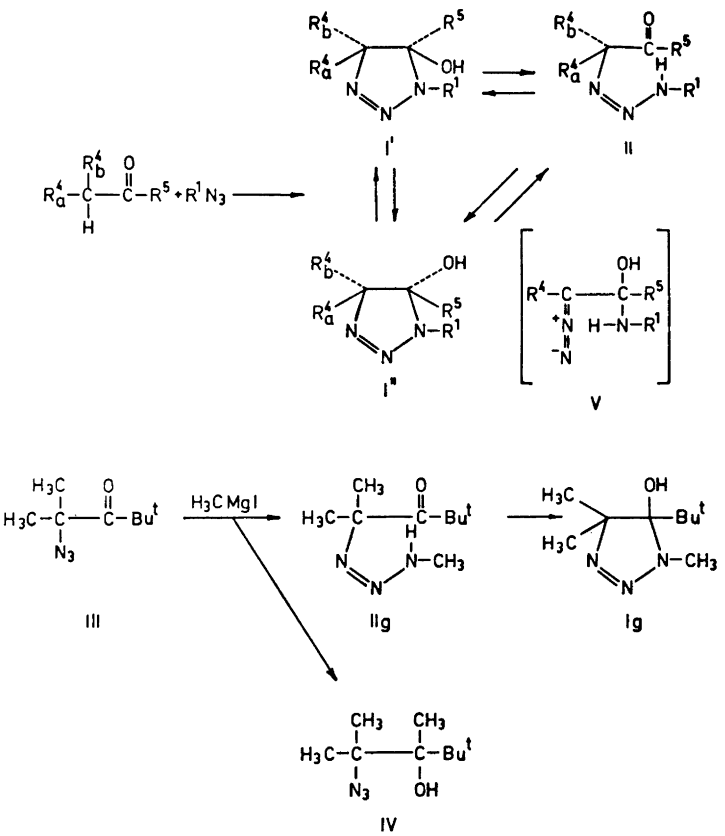

After a few minutes, however, an equilibrium mixture of (I'k) and (I''k) had been formed. This indicates that in the crystalline phase only (I'k) is present, whereas in solution it isomerizes to a mixture of (I'k) and (I''k). Presumably all the triazolines listed in Table 1 crystallize as the I'-isomers (the assignment of structures to the (I') and (I'') isomers is described below).

The equilibrium mixtures of (I') and (I'') were determined in deuteriochloroform solution by NMR spectroscopy (Table 2). The position of the equilibrium is determined by the interaction of R^5 with R_a^4 and R_b^4. When the two substituents at C-4 are different R_b^4 is chosen to be the smaller of the two groups (Table 1).

The reversible isomerization of (I') and (I'') in solution probably proceeds *via* the triazenes (II). When R^1 is an aryl group, the latter can be detected through IR and NMR spectra.[1] The hydroxy-triazolines described in the present paper (R^1 = methyl or benzyl), however, did not contain the triazene (II) in amounts sufficiently large to be detected. This even applies to the highly hindered compound (Ig). Since the 1-phenyl-triazoline corresponding to (Ig) is almost entirely on the triazene form[2] it may be concluded that the

Table 1. 1-Alkyl-5-hydroxy-Δ^2-1,2,3-triazolines (I).

I	R^1	R_b^4	R_a^4	R^5	Reaction time, h	Isolation procedure	% Yield	m.p. °C.	Formula	C % Calc.	C % Found	H % Calc.	H % Found	N % Calc.	N % Found
a	Me	H	Me	Me	3	D	33	106–7	$C_5H_{11}N_3O$	46.48	46.56	8.59	8.48	32.53	32.37
b	Me	H	Me	Et	7	D	58	94–95	$C_6H_{13}N_3O$	50.32	50.35	9.15	9.07	29.35	29.25
c	Me	H	Me	i-Pr	24	C	74	109–10	$C_7H_{15}N_3O$	53.48	53.62	9.62	9.44	26.74	26.80
d	Me	H	Me	*t*-Bu	150	C	77	134–35	$C_8H_{17}N_3O$	56.12	56.25	10.01	9.80	24.55	24.78
e	Me	H	$-(CH_2)_4-$		18	D	78	120–22[a]	$C_7H_{13}N_3O$	54.17	54.27	8.44	8.21	27.08	27.28
f	Me	Me	Me	i-Pr	900	C	75	100–01	$C_8H_{17}N_3O$	56.12	56.21	10.01	10.16	24.55	24.47
g[b]	Me	Me	Me	*t*-Bu			32	118–20	$C_9H_{19}N_3O$	58.33	58.40	10.33	10.10	22.68	22.85
h	Me	H	Me	Ph	3	C	84	138–39[a]	$C_{10}H_{13}N_3O$	62.81	62.72	6.85	6.84	21.98	22.04
i	Me	H	Et	Ph	26	C	78	112–13[a]	$C_{11}H_{15}N_3O$	64.35	64.38	7.37	7.43	20.47	20.38
j	Me	Me	Me	Ph	220	C	63	190–91[a]	$C_{11}H_{15}N_3O$	64.35	64.54	7.37	7.30	20.47	20.69
k	$PhCH_2$	H	Me	Me	7	B	57	108–9[a]	$C_{11}H_{15}N_3O$	64.35	64.21	7.37	7.38	20.47	20.63
l	$PhCH_2$	H	Me	Et	3	A	65	104–5	$C_{12}H_{17}N_3O$	65.72	65.71	7.81	7.62	19.16	19.33
m	$PhCH_2$	H	Me	i-Pr	28	A	72	110–11[a]	$C_{13}H_{19}N_3O$	66.92	67.07	8.21	8.06	18.02	18.17
n	$PhCH_2$	H	Me	*t*-Bu	100	A	73	130–31[a]	$C_{14}H_{23}N_3O_2$[d]	63.38	63.30	8.74	8.64	15.84	16.00
o	$PhCH_2$	H	$-(CH_2)-$		8	A	81	121–22[a]	$C_{13}H_{17}N_3O$	67.50	67.33	7.41	7.28	18.17	18.11
p	$PhCH_2$	Me	Me	i-Pr	600	B[c]	91	99–102[a]	$C_{14}H_{21}N_3O$	68.00	68.15	8.56	8.47	16.99	17.19
q	$PhCH_2$	H	Me	Ph	7	A	92	153[a]	$C_{16}H_{17}N_3O$	71.89	71.76	6.41	6.22	15.72	15.84
r	$PhCH_2$	Me	Me	Ph	220	A	74	134–35[a]	$C_{17}H_{19}N_3O$	72.58	72.58	6.81	6.77	14.94	14.89

[a] Melts with evolution of nitrogen. [b] Prepared from the α-azido ketone (III) and Grignard reagent. [c] Recrystallized from cyclohexane. [d] Contains one mol water of crystallization.

equilibrium between triazolines (I) and triazenes (II) is determined largely by electronic factors.

Since some Δ^2-1,2,3-triazolines can undergo ring opening to diazo compounds (V),[5] such intermediates might conceivably also account for the interconversion of (I′) and (I″). However, when (Ia) was dissolved in deuterium oxide it gave a mixture of (I′a) and (I″a) without exchange of H-4 with deuterium. In the presence of a trace of potassium hydroxide the isomerization took place at such a rate that an averaged NMR spectrum of the two diastereomers was obtained; yet, no deuterium was incorporated at C-4. This necessarily excludes (V) as an intermediate in the interconversion.

In Tables 3 and 4 are presented NMR data of all the 5-hydroxy-Δ^2-1,2,3-triazolines (I) described in the present paper. In the cases where two diastereomers are present in solution (Table 2), NMR data of both isomers

Table 2. Content (%) of I′ in the equilibrium mixtures of I′ and I″ in deuteriochloroform (4 % w/v-concentration) as determined from NMR spectra.

	1-Methyl-Δ^2-1,2,3-triazoline					1-Benzyl-Δ^2-1,2,3-triazoline				
Solvent	a	b	c	d	h	k	l	m	n	q
Deuterio-chloroform	68	85	100	100	78	70	90	100	100	80

(I′ and I″) are given. The δ-values of the methyl groups at C-4 fall into two groups, namely at 1.41 – 1.57 or at 1.05 – 1.21. They can be oriented either *cis* or *trans* relative to the hydroxy group at C-5. The compounds with bulky substituents at C-5 (Ic, d, m, and n) exist in only one form in chloroform solution (Table 2), and this is undoubtedly the I′-isomer in which the bulky group at C-5 is *trans* to the methyl group at C-4. The signals of the C-4-methyl groups in compounds (I″h) and (I″q) and of one of the two methyl groups in (Ij) and (Ir) are found at unusually high field. Since these compounds have a phenyl group at C-5 the upfield shift must be due to shielding by ring currents in the phenyl group. Consequently, the phenyl and the methyl groups are *cis* oriented in (I″h) and (I″q).

From the spectra of the above mentioned compounds it may be concluded that the methyl groups with δ-values of about 1.48, are positioned *cis* to the hydroxy group at C-5, whereas *trans* methyl groups give rise to signals at *ca.* 1.13. Similar conclusions have been arrived at by Huisgen and Szeimies [6] in the case of 5-alkoxy-Δ^2-1,2,3-triazolines. Furthermore, in agreement with the finding of Demarco *et al.*[7] it is observed that the chloroform-pyridine solvent shifts are larger (*ca.* −0.22) for the *cis* than for the *trans* methyl groups (only −0.06 to −0.15) (Tables 3 and 4). By using these δ-values and solvent shifts, structures were assigned to the remaining pairs of diastereomers (Ia, b, k, and l) as shown in Tables 3 and 4. The assignments are confirmed by the

Table 3. NMR spectra of 1-methyl-5-hydroxy-Δ^2-1,2,3-triazolines. The spectra have been recorded in deuteriochloroform and pyridine as 4 % w/v solutions. The general effect of dilution is a small downfield shift; thus the signals of Ia are shifted 0.01 – 0.05 ppm downfield on dilution four times (to 1 %). In Table 3 and 4 are given δ-values in deuteriochloroform as well as solvent shifts, $\Delta = \delta_{CDCl_3} - \delta_{pyridine}$. In a few cases solvent shifts in benzene are also given; these are shown in parentheses (Δ) = $\delta_{CDCl_3} - \delta_{benzene}$.

	R_b^4	R_a^4	R^5	Me[1]		Me-groups in 4-position *cis*		Me-groups in 4-position *trans*		H in 4-position *cis*		H in 4-position *trans*		Other signals
				δ	Δ	δ	Δ	δ	Δ	δ	Δ	δ	Δ	
I'a				3.27s	−0.10	1.44d	−0.20					3.63q	−0.20	1.47(s,−0,11,3H)
	H	Me	Me											
I''a				3.27s				1.05d	−0.06	4.22q	−0.39			1.38(s,−0,12,3H)
I'b				3.24s	−0.09	1.44d	−0.22					3.78q	−0.20	ca. 0.9("t",3H) *ca.* 1.83("q",2H)
	H	Me	Et											
I''b				3.24s				1.05d		4.24q				
I'c	H	Me	i-Pr	3.24s	−0.07	1.44d	−0.22					3.84q	−0.23	1.03(d,−0,11,3H)0.83(d,−0,04,3H) 2.19(sept.,−0,14,1H)
I'd	H	Me	*t*-Bu	3.37s	−0.06	1.41d	−0.22					4.10q	−0.23	1.02(s,−0,10,9H)
I''e	H	$-(CH_2)_4-$		3.28s	−0.10					4.11dd	−0.38			0−2.5(m,8H)
If	Me	Me	i-Pr	3.26s	−0.09	1.52s	−0.21	1.13s	−0.10					1.07(d,3H)1.18(d,3H)2.18(sept,1H)
Ig	Me	Me	*t*-Bu	3.34s	−0.08	1.57s	−0.20	1.20s	−0.10					1.17(s,9H)
I'h				3.22s	−0.10	1.48d	−0.18					3.92q	−0.21	}
	H	Me	Ph											7.2−7.7(m)
I''h				3.30s				0.67d	−0.11	4.48q	−0.39			}
I'i				3.19s	−0.05							3.76q	−0.23	0.8−1.3(m,3H) 1.6−2.2(m,2H)
	H	Et	Ph											}
I''i				3.29s										7.2−7.7(m,5H)
Ij	Me	Me	Ph	3.26s	−0.06	1.54s	−0.25	0.63s	−0.14					7.42("s",5H)

$J_{H^4Me^4} = 7.0 - 7.4$ cps. *cis* and *trans* refer to position relative to the hydroxy group at C-5. (Δ) values for H^4, Me^4, and Me^5 in I'a are +0.30, +0.11, and +0.40. In I''a they are +0.08, +0.26, and +0.31. Ia is, however, very sparingly soluble in benzene.

Table 4. NMR data of 1-benzyl-5-hydroxy-Δ^2-1,2,3-triazolines (4 % w/v, magnet temperature).

	R_b^4	R_a^4	R^5	Benzylic protons A δ	Δ	B δ	Δ	Me-groups in 4-position *cis* δ	Δ	*trans* δ	Δ	H in 4-position *cis* δ	Δ	*trans* δ	Δ	Other signals
I'k				4.62	−0.26	4.99	−0.17	1.48d	−0.19					3.73q	−0.21	1.34(s,−0,19,3H)
	H	Me	Me													
I''k				4.71	−0.22	4.98	−0.18			1.08d	−0.08	4.28q	−0.39			1.28(s,−0.20,3H)
I'l				4.60	−0.22	4.92	−0.16	1.48d	−0.21					3.86q	−0.22	0.6−1.2(m)1,5−2.0(m)
	H	Me	Et													
I''l				4.68		4.98				1.10d	−0.07	4.31q				
I'm	H	Me	i-Pr	4.60	−0.17	4.82	−0.15	1.47d	−0.23					3.93q	−0.21	0.69 0.99(d,3H)2.14(sept,1H)
I'n	H	Me	*t*-Bu	4.64	−0.25	4.90	−0.02	1.42d	−0.25					4.21q	−0.25	0.96(s,9H)
I''o	H	$-(CH_2)_4-$		4.68	−0.23	5.00	−0.18					4.15dd	−0.40			0−2.7(m,8H)
Ip	Me	Me	i-Pr	4.63	−0.27	4.83	−0.16	1.55s	−0.23	1.21	−0.09					0.99 1.09(d,3H)2.18(sept,1H)
I'q				4.69	−0.25	4.54	−0.08	1.47d	−0.17					4.02q	−0.22	
	H	Me	Ph													
I''q										0.72d	−0.11	4.22q				
Ir	Me	Me	Ph	4.70	−0.28	4.55	−0.11	1.55s	−0.28	0.68s	−0.15					
Is[2]	H	H	Me	4.70	−0.23	4.98	−0.20					4.26	−0.42	3.78	−0.29	1.43(s,−0.15,3H)
It[2]	H	H	Ph	4.63	−0.30	4.63	−0.07					4.49	−0.41	4.08	−0.27	

$J_{H^4Me^4} = 7.2-7.5$ cps. $|J_{AB}| = 15-16$ cps. δ_A and δ_B have been calculated from the equation $\delta_A - \delta_B = \sqrt{(\nu_4-\nu_1)(\nu_3-\nu_2)}$.
The aromatic protons lie within the range 7.2−7.6 ppm usually as multiplets.
cis and *trans* refer to position relative to the hydroxy group at C-5. (Δ) values for H^4, Me^4, and Me^5 are the following: I'k: +0.31, +0.09, +0.26; I''k: +0.02, +0.02, +0.26, +0.20, and −0.01 and +0.16 for the *cis* and *trans* methyl groups of Ip, respectively.

δ-values of H-4. These fall into two ranges, namely 3.6 – 4.0 (except for the two *tert*-butyl derivatives (I'd) and (I'n)) when H-4 is *trans* to the hydroxy group (I'-isomers) and 4.1 – 4.5 when H-4 is *cis* oriented (I''-isomers). The two cyclohexane derivatives, (Ie) and (Io), must necessarily possess the I''-form; in agreement herewith their H-4-protons give signals at δ 4.11 and 4.15, respectively.

Because of restricted solubility it has not been possible to utilize benzene induced solvent shifts in general for the assignment of structures. Spectra of (Ia), (Ik), and (Ip) in benzene solution, however, show that hydrogen atoms or methyl groups, which are *trans* to the hydroxy group, are shielded much more than the corresponding *cis* oriented groups. This is consistent with the association of a molecule of benzene to the triazoline opposite to the hydroxy group.[8–10]

The diastereotopic benzylic protons in compounds (Ik to p) give signals which fall into two ranges, the A-protons at 4.6 – 4.7 δ and the B-protons at 4.8 – 5.0 (Table 4). The pyridine induced solvent shifts (Δ-values) are quite constant for the A-protons, but vary considerably for the B-protons. In compounds (Iq and r) the B-protons give signals at rather high field, probably due to shielding by the phenyl groups at C-5.

EXPERIMENTAL

Melting points are uncorrected. NMR spectra were recorded on Varian A-60 or HA-100 spectrometers. Unless otherwise stated deuteriochloroform was used as solvent. Chemical shifts are given in ppm (δ-values) relative to tetramethylsilane.

tert-Butyl alcohol. A FLUKA *purissimum* grade was used without further purification.

Methyl azide, prepared according to the literature,[11] was used as an approximately 20 % w/v solution in *tert*-butyl alcohol. The solution was dried with molecular sieve 4A.

Benzyl azide was prepared according to Curtius and Ehrhardt.[12]

The ketones were commercially available with the exception of 2,2,4-trimethyl-3-pentanone, which was prepared in analogy with the method of Cook and Percival.[13]

General procedure for the preparation of 1-benzyl- and 1-methyl-5-hydroxy-Δ^2-1,2,3-triazolines. Benzyl azide (0.02 mol) was added to a solution of potassium (1.0 g) in *tert*-butyl alcohol (20 ml). With methyl azide the following procedure was used: a 20 % solution of methyl azide (0.024 mol) in *tert*-butyl alcohol was added to potassium *tert*-butoxide, prepared from 1.0 g of potassium. To the solution of the azide the appropriate ketone (0.02 mol) was added, and the mixture was shaken until a homogeneous solution was obtained. The mixture turned yellow or orange after a short time. The reaction was followed by NMR spectroscopy, and when it was complete the product was isolated by one of the following procedures:

A. If the product crystallized on pouring the reaction mixture into 200 ml of ice-water, it was filtered off, washed with water and pentane, and recrystallized from ethyl acetate-pentane.

B. If the product did not crystallize when the reaction mixture was poured into 200 ml of ice-water it was extracted with methylene chloride. The extract was dried with sodium sulfate (magnesium sulfate should not be used because of its acidic nature) and the solvent was removed *in vacuo* at room temperature. The product usually crystallized on cooling, if not it was dissolved in ether, cooled to – 75°C, and induced to crystallize by scratching. Recrystallization from ethyl acetate-pentane afforded the pure products.

C. Ice (*ca.* 10 g) was added to the reaction mixture; *tert*-butyl alcohol was removed *in vacuo*, and the aqueous phase was extracted with methylene chloride.

D. In some cases extraction of the triazoline from its aqueous solution was very difficult. Procedure C was then used, but the extraction was performed continuously for 20 h. The methylene chloride was renewed after 1 and 7 h.

2-Bromo-2,4,4-trimethyl-3-pentanone. 2,2,4-Trimethyl-3-pentanone (12.8 g) was heated to 40 – 50°C and bromine (5.1 ml) was added dropwise. When the evolution of hydrogen bromide had ceased the reaction mixture was distilled yielding 19.0 g (92 %) of a product with b.p. 70°C (12 – 15 mmHg) (reported [14] 65 – 66°C (13 – 14 mmHg). NMR-spectrum: 1.41 δ (s, 9H) and 1.96 δ (s, 6H).

2-Azido-2,4,4-trimethyl-3-pentanone (III). To a stirred solution of sodium azide (3.9 g) in 30 ml of dimethyl sulfoxide was added 2-bromo-2,4,4-trimethyl-3-pentanone (8.28 g). The temperature rose to *ca*. 40°C and the mixture solidified after 2 min due to separation of sodium bromide. The stirring was continued for 3 h. Ice was then added and the mixture was extracted with ether (50 ml). The ether phase was washed with water and dried with magnesium sulfate. Removal of the ether and distillation of the residue (caution) gave 6.43 g (95 %) of a colourless liquid with b.p. 33°C (2 mmHg). (Found: C 56.89; H 8.94; N 24.95. Calc. for $C_8H_{15}N_3O$: C 56.78; H 8.94; N 24.84.) NMR spectrum: 1.26 δ (s, 9H) and 1.48 δ (s, 6H).

Reaction of 2-azido-2,4,4-trimethyl-3-pentanone (III) with methylmagnesium iodide. Methylmagnesium iodide (3.5 mmol) in ether (6 ml) was added to a solution of (III) (0.508 g, 3 mmol) in 25 ml of ether with stirring. The mixture was stirred at reflux temperature for 1.5 h. A solution of ammonium chloride (0.7 g) and conc. ammonia (0.3 ml) in 2 ml of water was added, and stirring was continued until the precipitated magnesium salt had dissolved. The ether phase was separated, washed with water, and dried over sodium sulfate. Removal of the ether in vacuum left 0.63 g of a mixture of crystals and liquid which was placed in a water bath at 70°C; the liquid was distilled off at 0.01 mmHg. Yield of the azido alcohol (IV); 0.33 g (60 %). (Found: C 57.76; H 10.24; N 22.14. Calc. for $C_9H_{19}N_3O$: C 58.33; H 10.33; N 22.68.) The IR spectrum revealed the azido group at 2110 cm^{-1}. The NMR spectrum showed signals at 1.08 δ (s, 9H), 1.19 (s, 3H), 1.43 (q, 3H), and 1.47 (q, 3H). The two methyl groups geminal to the azido group couple with a coupling constant of 0.4 Hz. IR and NMR spectra revealed that (IV) was slightly contaminated with the starting material (III).

The residue from the distillation consisted of the triazoline (Ig), 0.176 g (32 %), m.p. 117 – 119°C. Recrystallization from ethyl acetate-pentane gave the pure product (Table 1).

Microanalyses were performed by Dr. A. Bernhardt.

REFERENCES

1. Olsen, C. E. and Pedersen, C. *Tetrahedron Letters* **1968** 3805.
2. *To be published*.
3. Dimroth, O., Frisoni, E. and Marshall, J. *Ber*. **39** (1906) 3920.
4. Dimroth, O. *Ber*. **38** (1905) 670.
5. Huisgen, R., Szeimies, G. and Möbius, L. *Chem. Ber*. **99** (1966) 475.
6. Huisgen, R. and Szeimies, G. *Chem. Ber*. **98** (1965) 1153.
7. Demarco, P. V., Farkas, E., Doddrell, D., Mylari, B. L. and Wenkert, E. *J. Am. Chem. Soc*. **90** (1968) 5480.
8. Ronayne, J. and Williams, D. H. *J. Chem. Soc*. **B 1967** 540.
9. Ledaal, T. *Tetrahedron Letters* **1968** 1683.
10. Wilczynski, J. J., Daves, G. D. and Folkers, K. *J. Am. Chem. Soc*. **90** (1968) 5593.
11. Houben-Weyl: *Methoden der organischen Chemie*, Vol. **10** part 3, p. 802.
12. Curtius, T. and Ehrhardt, G. *Ber*. **55** (1922) 1559.
13. Cook, N. C. and Percival, W. C. *J. Am. Chem. Soc*. **71** (1949) 4141.
14. Sacks, A. A. and Aston, J. G. *J. Am. Chem. Soc*. **73** (1951) 3902.

Received January 11, 1973.

ACTA CHEMICA SCANDINAVICA 27 (1973) 2279–2286

Preparation of 1-Aryl-5-hydroxy-Δ^2-1,2,3-triazolines

CARL ERIK OLSEN and CHRISTIAN PEDERSEN

Department of Organic Chemistry, Technical University of Denmark, DK-2800 Lyngby, Denmark

A number of 1-aryl-5-hydroxy-Δ^2-1,2,3-triazolines have been prepared by reaction of ketones with aryl azides in the presence of potassium *tert*-butoxide. Some of the triazolines with two different substituents at C-4 exist in solution as a mixture of the two diastereomeric forms. In other cases, especially when two methyl groups are present at C-4, the triazoline ring is partly opened in solution to give a triazene. The structures of the triazolines and of the triazenes were determined by IR- and NMR-spectroscopy.

In the preceding paper a number of 1-methyl- and 1-benzyl-5-hydroxy-Δ^2-1,2,3-triazolines were described.[1] In the present paper the corresponding 1-aryl-compounds (I) are described and some of their properties are discussed.

It was found that phenyl azide reacted smoothly with ketones in the presence of potassium *tert*-butoxide to give high yields of 1-phenyl-5-hydroxy-Δ^2-1,2,3-triazolines (I) (Table 1). Phenyl azide reacts considerably faster than methyl or benzyl azide,[1] and the reaction times shown in Table 1 should be observed since lower yields and impure products may otherwise result. Similarly, *p*-nitrophenyl, *p*-bromophenyl, and *p*-methoxyphenyl azide yielded triazolines by reaction with ketones (Table 1). The triazolines (Iq,r,s, and t), which contain a *p*-aminophenyl group, were prepared by catalytic hydrogenation of the corresponding nitro-compounds.

The triazolines thus prepared are undoubtedly homogeneous compounds in the solid state as seen from the sharp melting points (Table 1). However, NMR spectra of these compounds in chloroform or in pyridine solution show, in many cases, that two isomeric compounds are present. When R_a^4 is different from R_b^4, the triazolines may exist in two diastereomeric forms, I′ and I″. These two are readily interconvertible, presumably *via* a ketotriazene (II) as discussed in the preceding paper. This type of isomerism was observed in many cases and structures were assigned to the two isomers on the basis of their NMR spectra (Tables 2 and 3) following the principles used previously.[1]

Triazolines in which R_a^4 and R_b^4 are identical cannot exhibit diastereoisomerism. Nevertheless, a number of compounds of this type were found to consist of a mixture of two products in chloroform or in pyridine solution, as

Table 1. 1-Aryl-5-hydroxy-Δ^2-1,2,3-triazolines (I).

I	R^1	R_b[4]	R_a[4]	R^5	Reaction time, min	Isolation method	Yield %	M.p. °C.	Formula	% C Calc.	% C Found	% H Calc.	% H Found	% N Calc.	% N Found
a	Ph	H	Me	Me	2	B	72	84–85	$C_{10}H_{13}N_3O$	62.81	62.99	6.85	6.82	21.98	22.43
b	Ph	H	Me	Et	3	B	85	119–20	$C_{11}H_{15}N_3O$	64.35	64.37	7.37	7.17	20.47	20.36
c	Ph	H	Me	i-Pr	7	A	50	147–48	$C_{12}H_{17}N_3O$	65.72	65.66	7.81	7.86	19.16	19.33
d	Ph	H	Me	*t*-Bu	15	A	35	124–25	$C_{13}H_{19}N_3O$	66.92	66.82	8.21	8.35	18.02	18.05
e	Ph	H	$-(CH_2)_4-$		8	B	87	106–8	$C_{12}H_{15}N_3O$	66.32	66.15	6.96	7.00	19.34	19.29
f	Ph	H	$PhCH_2$	Me	7	B	61	121–22	$C_{16}H_{17}N_3O$	71.89	71.88	6.41	6.41	15.72	15.82
g	Ph	Me	Me	i-Pr	180	C[a]	71	65–66	$C_{13}H_{19}N_3O$	66.92	66.92	8.21	8.00	18.02	18.17
h	Ph	Me	Me	*t*-Bu	50 days	C	58	57–59	$C_{14}H_{21}N_3O$	68.00	67.61	8.56	8.59	16.99	16.84
i	Ph	H	Me	Ph	5	A	87	149–50	$C_{15}H_{15}N_3O$	71.13	70.99	5.97	6.12	16.59	16.42
j	Ph	H	Et	Ph	15	A	86	153–54	$C_{16}H_{17}N_3O$	71.89	71.81	6.41	6.30	15.72	15.79
k	Ph	Me	Me	Ph	180	A	89	147–48	$C_{16}H_{17}N_3O$	71.89	71.78	6.41	6.40	15.72	15.91
l	*p*NO_2Ph	H	Me	Me			69	111–12	$C_{10}H_{12}N_4O_3$	50.86	50.85	5.12	4.98	23.72	23.86
m	*p*NO_2Ph	H	Me	i-Pr	4	A	79	125–26	$C_{12}H_{16}N_4O_3$	54.53	54.27	6.10	6.18	21.20	21.35
n	*p*NO_2Ph	H	Me	*t*-Bu	10	A	90	127–28	$C_{13}H_{18}N_4O_3$	56.10	55.92	6.52	6.68	20.14	19.92
o	*p*NO_2Ph	Me	Me	i-Pr	8	A	84	98–99	$C_{13}H_{18}N_4O_3$	56.10	56.01	6.52	6.51	20.14	20.22
p	*p*NO_2Ph	Me	Me	Ph	5	A	92	111–12	$C_{16}H_{16}N_4O_3$	61.53	61.41	5.16	5.41	17.94	17.67
q	*p*NH_2Ph	H	Me	Me				110–13	$C_{10}H_{14}N_4O$	58.24	57.97	6.84	7.02	27.17	26.38
r	*p*NH_2Ph	H	Me	i-Pr			100	142–43	$C_{12}H_{18}N_4O$	61.51	61.41	7.74	7.59	23.92	23.77
s	*p*NH_2Ph	H	Me	*t*-Bu			97	129–30	$C_{13}H_{20}N_4O$	62.88	62.73	8.12	7.91	22.56	22.75
t	*p*NH_2Ph	Me	Me	i-Pr			100	101–2	$C_{13}H_{20}N_4O$	62.88	62.73	8.12	8.14	22.56	22.45
u	*p*BrPh	Me	Me	i-Pr	240	A	93	104–5	$C_{13}H_{18}N_3OBr$	50.01	49.86	5.82	5.74	13.46	13.38
v	*p*MeOPh	Me	Me	i-Pr	2 days	C	60	69–71	$C_{14}H_{21}N_3O_2$	63.86	63.79	8.04	8.18	15.96	15.87

The 1-phenyl triazolines (a–k) are colourless compounds. All triazolines in this table melt with evolution of nitrogen. [a] Recrystallized from pentane.

Table 2. NMR data of 1-phenyl-5-hydroxy-Δ^2-1,2,3-triazolines (4 % w/v, $CDCl_3$, magnet temp.)

	R_b[4]	R_a[4]	R^5	Me-groups in 4-position *cis* δ	*cis* Δ	*trans* δ	*trans* Δ	H in 4-position *cis* δ	*cis* Δ	*trans* δ	*trans* Δ	Other signals
I'a				1.45d	−0.26							
	H	Me	Me							3.91q	−0.25	1.68(s,−0.15,3H)
I''a						1.12d	−0.16	4.33q				
I'b				1.44d	−0.28							1.51(s,−0.17,3H)
	H	Me	Et							4.10q	−0.24	
I''b						1.18d	−0.13					0.87("t",3H), 2.05("q",2H)
I'c	H	Me	i-Pr	1.42d	−0.30							
I'd	H	Me	*t*-Bu	1.44d	−0.23					4.18q	−0.27	1.03(d,3H),0.69(d,3H),2.63(sept,1H)
I''e	H	$-(CH_2)_4-$								4.42q	−0.26	0.91(s,9H)
I'f								4.31dd	−0.39			0.6−2.7(m,8H)
	H	$PhCH_2$	Me							4.10dd	−0.30	1.48(s,3H) 3.25(m,2H)
I''f								4.59dd				1.53(s,3H)
Ig	Me	Me	i-Pr	1.58s	−0.23	1.33s	−0.06					
Ih	Me	Me	*t*-Bu	1.67s	−0.17	1.42s	−0.07					1.06(d,3H),1.06(d,3H),2.41(sept,1H)
I'i				1.47d	−0.21							1.06(s,9H)
	H	Me	Ph							4.18q	−0.26	
I''i						0.68d	−0.22	4.62q	−0.46			
I'j	H	Et	Ph									
Ik	Me	Me	Ph	1.54s	−0.29	0.70s	−0.14			4.02"t"	−0.26	1.6−2.2(m,3H),1.87("q",2H)

$J_{H_4Me_4}$ = 7.2−7.5 cps. *cis* and *trans* refer to position relative to the hydroxy group at C-5.
The aromatic protons occur within the range 6.8−7.8. $\Delta = \delta_{CDCl_3} - \delta_{pyridine}$.

Table 3. NMR data of 1-aryl-5-hydroxy-Δ^2-1,2,3-triazolines (2 % in $CDCl_3$,[a] 4 % in pyridine, magnet temp.)

	p-substit. of 1-aryl group	R_b^4	R_a^4	R^5	Aromatic protons[b] *ortho*	*para*	Me-groups in 4-position *cis* δ	Δ	*trans* δ	Δ	H in 4-position *cis* δ	Δ	*trans* δ	Δ	Other signals
I'l	NO_2	H	Me	Me	7.65	8.24	1.53d	−0.18					4.14q	−0.17	1.80(s, −0.10,3H)
I''l	NO_2	H	Me	i-Pr	7.67	8.21	1.47d	−0.23	1.30d	−0.04	4.48q	−0.44			1.63(s, −0.11,3H)
I'm	NO_2	H	Me	*t*-Bu	7.79	8.20	1.44d	−0.18					4.35q	−0.23	0.63(d,3H),1.08(d,3H)2.77(sept,1H)
I'n	NO_2	H	Me	i-Pr	7.72		1.56s		1.44s				4.63q	−0.20	0.95(s,9H)
Io	NO_2	Me	Me	i-Pr	7.39	8.10	1.60s		0.77s						7.39("s",5H)
Ip	NO_2	Me	Me	Ph											
I'q	NH_2	H	Me	Me	6.69	7.19	1.53d	−0.20	1.21d	−0.05	4.41q		3.90q	−0.16	1.61(s, −0.15,3H)
I''q	NH_2	H	Me	i-Pr	6.67	7.22	1.49d	−0.26					4.15q	−0.22	1.45(s, −0.20,3H)
I'r	NH_2	H	Me	*t*-Bu	6.66	7.25	1.49d	−0.21					4.35q	−0.23	0.85(d,3H),1.04(d,3H)
I's	NH_2	H	Me	i-Pr	6.66	7.20	1.60s	−0.23	1.29s	−0.09					0.94(s,9H)
It	NH_2	Me	Me	i-Pr											
Iu	Br	Me	Me	i-Pr			1.58s	−0.21	1.33s	−0.05					0.99(d,3H),1.11(d,3H)2.26(sept,1H)
Iv	MeO	Me	Me	i-Pr	6.90	7.35	1.60s	−0.23	1.30s	−0.10					

$J_{H,Me_2} = 7.0 - 7.5$ cps.
cis and *trans* refer to position relative to the hydroxy group at C-5.
[a] Except Iu and Iv which were measured as 4 % solutions.
[b] The centres of the doublets are given. These do not, of course, represent the true δ-values.
$\Delta = \delta_{CDCl_3} - \delta_{pyridine}$.

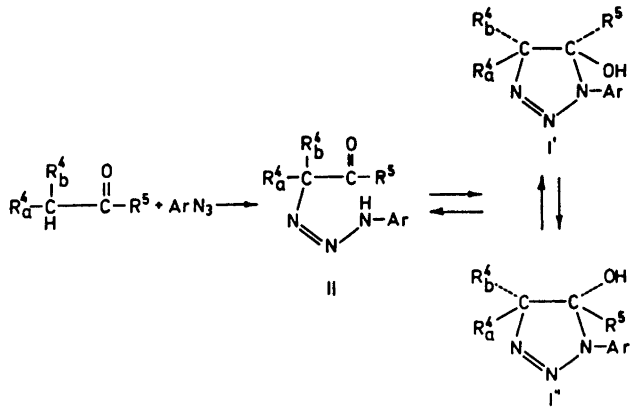

seen from their NMR spectra. IR spectra of the chloroform solutions of these compounds were found to exhibit carbonyl group absorption at 1710 cm^{-1} and an NH band at 3330 cm^{-1}. This seems to indicate that the ketotriazene (II) is present in equilibrium with the hydroxytriazoline (I). The equilibration of (I′) and (I″) is assumed to take place *via* (II), but with 1-methyl- or 1-benzyl-substituted triazolines the ketotriazene (II) could not be detected.[1] With an aromatic substituent at N-1, on the other hand, appreciable amounts of (II) may apparently be present in solution in some cases. In the solid state only one of the compounds listed in Table 1 (namely I h) showed carbonyl absorption (in potassium bromide), indicating that the triazene (II) is usually only present in solution. Apart from (Ih), the solid products listed in Table 1 presumably all have the I′-form. When these products are dissolved in chloroform or in pyridine they may isomerize to give a mixture of the diastereomeric forms (I′) and (I″) or they may give a mixture of (I′) and the ketotriazene (II). In no cases were (I″) and (II) observed simultaneously.

In (Ia), which has one methyl group at C-4 and C-5, 70 % of the (I′) isomer is present (Table 4), showing that the two methyl groups tend to be as far apart

Table 4. Equilibrium content of I′ in $CDCl_3$ solution as determined from the NMR spectra. (Ia-j 4 %, Il-s 2 %, magnet temp.)

1-Ph							1-*p*NO_2-Ph			1-*p*NH_2-Ph		
a	b	c	d	f	i	j	l	m	n	q	r	s
70	~90	100	100	~80	82	?	70	100	100	70	100	100

as possible. The steric interactions become more pronounced in the 5-ethyl and the 5-isopropyl compounds (Ib) and (Ic), which contain 90 and 100 % of the (I′) isomer, respectively. None of these compounds gave detectable amounts of the triazenes (II). The *tert*-butyl derivative (Id) would not be ex-

Table 5. NMR data of β-keto-triazenes (II) in $CDCl_3$-solution. (Measuring conditions as in Tables 2 and 3).

	R^1	R_a^4	R_b^4	R^5
n	(7.3) – 8.20	1.45(d,3H)	5.30(1H)	1.25(s,9H)
d	7.1 – 7.8	1.40(d,3H)	5.27(q,1H)	1.24(s,9H)
s				1.26(s)
o	7.29 – 8.25	1.51(s,6H)		1.07(d,6H)3.07(sept,1H)
u	7.0 – 7.7	1.51(s,6H)		1.06(d,6H)3.10(sept,1H)
g	7.0 – 7.6	1.49(s,6H)		1.07(d,6H)
v	6.90 – 7.35	1.52(s,6H)		1.07(d,6H)
	3.83(s,3H)			
t	6.66 – 7.20	1.50(s,6H)		
h	6.8 – 7.6	1.49(s,6H)		1.21(s,9H)

Table 6. Equilibrium content of II in $CDCl_3$ and in pyridine solution as determined from the NMR spectra. (Measuring conditions as in Table 2).

R_b^4	H			Me					
R^5		*t*-Bu				i-Pr			*t*-Bu
	n	d	s	o	u	g	v	t	h
$CDCl_3$	42	24	11	70	56	53	37	34	91
Pyridine		< 5	< 2		11	8	5	5	71

pected to give any of the (I″) isomer when dissolved in chloroform, and this was indeed found to be the case. However, NMR spectra (Tables 5 and 6) showed that a solution of (Id) contained 24 % of the ketotriazene (IId). Apparently the steric hindrance in this case causes ring opening to some extent.

In the *p*-nitrophenyl derivatives (Il) and (Im) the same ratio between the diastereomeric forms (I′) and (I″) was found as between (Ia) and (Ic) (Table 4). However, the 5-*tert*-butyl derivative (In) gave 42 % of the triazene (IIn) when dissolved in deuteriochloroform. Since a *p*-nitro-group would not be expected to have any steric effects, the increased amounts of the triazene (IIn) over that of (IId) indicates that electronic factors are involved in the equilibrium between the hydroxy-triazolines (I) and the triazenes (II). This is further seen from the fact that the *p*-aminophenyl derivative (Is) gave only 11 % of the triazene (IIs) in chloroform solution.

In the 4,4-dimethyl derivatives only one isomer of the hydroxy-triazoline is possible. The 4,4-dimethyl-5-isopropyl derivative (Ig) was found to give 53 % of the triazene (IIg) in solution. Comparison of this with the corresponding 4-monomethyl derivative (Ic), which did not give any triazene, show again that steric factors play a part in the equilibrium between hydroxytriazolines and triazenes. This is further confirmed by the *tert*-butyl compound (Ih),

which gave 91 % of the triazene IIh at equilibrium in solution. It may be noted, that (Ih) is the only compound which contains the triazene isomer in the solid state as seen from the IR spectrum, which showed absorption at 1680 cm^{-1} (carbonyl) and at 3270 cm^{-1} (NH). The sharp melting point (Table 1) could indicate that it is completely in the (IIh) form.

The 4,4-dimethyl-5-isopropyl derivatives (It, v, g, u, and o), which have increasing electronegative substitution of the phenyl-group, contain increasing amounts of the triazenes (II) at equilibrium in solution (Table 6). This shows again that, besides steric factors, electronic factors have an effect on the equilibrium between hydroxy-triazolines and triazenes. It is therefore understandable why the 1-alkyl substituted triazolines, described in the preceding paper, do not yield detectable amounts of triazenes.

It may be noted that when a phenyl group is present at C-5 a triazene is not formed in solution (compounds Ii,j, and k), not even in case of the 1-(*p*-nitrophenyl) derivative (Ip). This may be explained by an enhanced electrophilicity of the carbonyl group in the triazene (II) due to the electronegativity of the phenyl group.

When pyridine or dimethyl sulfoxide was used as the solvent, smaller amounts of the triazenes (II) were formed. Nitrobenzene, on the other hand, did not affect the triazene formation. The increased formation of hydroxy-triazolines in pyridine or in dimethyl sulfoxide may therefore be due to a stabilization by hydrogen bonding of the solvent to the hydroxy group (*cf.* Ref. 2).

The ring-opening reaction (I→II) is rather rapid. Thus repeated integration of the range 1.20 – 1.70 ppm in the NMR spectrum of (Ig) immediately after it was dissolved showed that equilibrium was attained within a few seconds. The reaction is accelerated by base. A solution of (Ig) in dimethyl sulfoxide showed two separate signals for the methyl groups at C-4. On addition of a trace of potassium hydroxide these signals collapsed to a singlet. This indicates that (Ig⇌IIg) takes place at such a rate that the two methyl groups become magnetically equivalent.

Some methyl ketones react in a more complicated manner with azides, and this will be the subject of a forthcoming paper.

EXPERIMENTAL

Melting points are uncorrected. NMR spectra were recorded on Varian A-60 or HA-100 spectrometers. Unless otherwise stated deuteriochloroform was used as solvent. Chemical shifts are given in ppm (δ-values) relative to tetramethylsilane.

All ketones were commercially available with the exception of 2,2,4-trimethyl-3-pentanone.[1]

The organic azides were prepared by methods described in the literature: Phenyl azide,[3] *p*-nitrophenyl azide and *p*-bromophenyl azide,[4] and *p*-methoxyphenyl azide.[5]

General procedure for the preparation of 1-aryl-5hydroxy-Δ^2-1,2,3-triazolines

The appropriate azide (0.02 mol) (or when *p*-nitrophenyl azide is used, a suspension in 20 ml of *tert*-butyl alcohol) is added with stirring to a solution of potassium (1.0 g) in *tert*-butyl alcohol (20 ml). The mixture is cooled in ice-water until crystallization begins

and the ketone (0.02 mol) is then added. The reaction mixture usually turns dark, and a slight evolution of nitrogen is often observed. The temperature should not exceed 30°C, and permanent cooling in ice-water is frequently necessary for the first couple of minutes. After this first period only occasional cooling is employed. The reaction mixture is stirred magnetically or shaken vigorously by hand.

After the appropriate reaction time (Table 1) the product is isolated by one of the following procedures:

Procedure A. The reaction mixture is poured into ice-water (200 ml), and the crystalline product is filtered off and washed with water and pentane. Recrystallization from ethyl acetate-pentane gives the pure product.

Procedure B. If the product fails to crystallize when poured into ice-water, it is extracted with methylene chloride. Drying over sodium sulfate and removal of the solvent gives a syrup which crystallizes when treated with pentane. The product is recrystallized from ethyl acetate-pentane.

Procedure C. In some cases a potassium salt precipitates during the reaction, and a very pure product is obtained by the following procedure. The reaction mixture is diluted with ether (20 ml) and cooled to 0°C. The potassium salt is filtered off, washed rapidly with dry ether (moisture hydrolyses the salt), and transferred to a mixture of ice-water (20 ml) and ether (20 ml). After stirring for some time the hydrolysis of the potassium salt is complete, and the product is present in the ether phase. The aqueous phase is further extracted two or three times with ether, and the combined extracts are dried over sodium sulfate. Removal of the solvent leaves a syrup, which can be crystallized in ether-pentane at −70°C. Recrystallization from ethyl acetate-pentane gives the pure product.

*1-(*p*-Nitrophenyl)-4,5-dimethyl-5-hydroxy-Δ²-1,2,3-triazoline* (II). *p*-Nitrophenyl azide (0.82 g) in ether (25 ml) was added to a solution of potassium (0.5 g) in *tert*-butyl alcohol (10 ml). Butanone-2 (1.34 ml), previously dried over Drierite and diluted with ether (15 ml), was added and the mixture was shaken vigorously. The reaction mixture turned black at once, and fine, dark crystals separated. After 1 min the mixture was poured in a mixture of ice-water (100 ml) and ether (100 ml). The two phases were separated and the aqueous phase was extracted twice with ether. The combined ether-extracts were dried and evaporated. The residue was a mixture of 1-(*p*-nitrophenyl)-4,5-dimethyl-1,2,3-triazole and the triazoline (I l). Crystallization from ether (5 ml) at 0°C gave 151 mg (14 %) of the triazole, m.p. 202 – 203°C (reported [6] m.p. 206°C). Crystallization of the material in the mother liquor from ether-pentane at −76°C gave 815 mg (69 %) of (I l) as light brown crystals, m.p. 85 – 97°C (dec.). Recrystallization from ethyl acetate-pentane gave the pure product (Table 1).

*1-(*p*-Aminophenyl)-5-hydroxy-Δ²-1,2,3-triazolines.* These products were prepared from the corresponding 1-*p*-nitrophenyl compounds in the following way:

The 1-(*p*-nitrophenyl)-triazoline (*ca.* 300 mg) and platinum oxide (3 mg) was suspended in methanol (3 ml) and hydrogenated for 30 min at a hydrogen pressure of 2.5 atm. During this time the nitro compound dissolved. The catalyst was then filtered off and the solvent was evaporated giving the crystalline 1-(*p*-aminophenyl)-triazoline. Recrystallization from ethyl acetate-pentane gave the pure products (Table 1).

Microanalyses were performed by Dr. A. Bernhardt.

REFERENCES

1. Olsen, C. E. and Pedersen, C. *Acta Chem. Scand.* **27** (1973) 2271.
2. Paukstelis, J. V. and Hammaker, R. M. *Tetrahedron Letters* **1968** 3557.
3. *Org. Syn.* Coll. Vol. III (1965) 710.
4. *Ibid.* Coll. Vol. IV, p. 75.
5. Walker, P. and Waters, W. A. *J. Chem. Soc.* **1962** 1632.
6. Bianchetti, G., Ferruti, P. and Pocar, D. *Gazz. Chim. Ital.* **97** (1967) 579.

Received January 11, 1973.

ACTA CHEMICA SCANDINAVICA 27 (1973) 2287–2303

Phthalic Acid as a Reagent in Inorganic Qualitative Analysis of Metal Ions. Part. II. Thermogravimetric, Differential Thermal and Infrared-spectral Studies of Iron(III), Chromium(III), and Aluminium(III) Compounds Precipitated with Hydroxyl and Phthalate Ions and of Potassium Biphthalate

PAAVO LUMME and JOUNI TUMMAVUORI

Department of Chemistry, University of Jyväskylä, Jyväskylä, Finland

Precipitates were formed when 2 M sodium hydroxide and 0.5 M potassium biphthalate solutions were added to 100 ml of 0.01 M iron (III) chloride, chromium(III) chloride, or aluminium(III) chloride solutions. These, after drying in air and in a desiccator, had the compositions $Fe_3O_5(OH)_5(O_2C)_2C_6H_4$, $Cr_3(OH)_{12}(O_2C)_2C_6H_4$, and $Al_2O_3.5H_2O$, respectively. If 0.5 M potassium biphthalate only was added to the iron(III) chloride solution, the precipitate formed had the composition $Fe_2(OH)_2[(O_2C)C_6H_4(CO_2H)]_2$. With 2 M sodium hydroxide solution, the hydroxides $Fe(OH)_3$, $Cr(OH)_3.1.75H_2O$ and the oxyhydrate $Al_2O_3.6H_2O$ were formed. The TG and DTA curves and IR spectra of the compounds and potassium biphthalate were recorded and the results are discussed.

In the qualitative analysis system which was described in the first part of this series [1] and is being used in our inorganic chemistry teaching laboratory, the division of the metal ions into analytical groups is to a certain degree based on the adjustment of the pH of the solutions studied. In the analytical scheme, the cation group II is precipitated with sodium hydroxide from the solution buffered with potassium biphthalate. The pH of the solution is in this way held between 4 and 5. The cation group II consists of the following ions: tin(II), tin(IV), antimony(III), bismuth(III), iron(II), iron(III), chromium(III), and aluminium(III).

According to the values of the solubility products taken from the literature,[2] the hydroxides of these metals begin to precipitate from 0.01 M solutions of the metal salts at roughly the following pH's at room temperature (25°C):

tin(II) hydroxide ($pK_{S,0} = 25.0 - 25.7$) at pH 2.3 and tin(IV) hydroxide ($pK_{S,0} = 56$) at pH 0.5. The tin(II) ion is usually oxidized in the solution to the tin(IV) ion, and precipitated as this. The antimony(III) hydroxide ($pK_{S,0} = 41.4$) precipitates at pH 1, but is immediately converted to the basic salt SbOX, where X may be Cl^-, NO_3^-, *etc.*, depending on the solution. Bismuth-(III) hydroxide ($pK_{S,0} = 30.4$) precipitates at pH 4.6, but changes immediately to the BiOX salt. The compounds mentioned have such low solubility products that they are almost completely precipitated from the solutions at pH 5.

The iron(II), iron(III), chromium(III), and aluminium(III) ions form an interesting quartet because they are strongly complex-forming ions and additionally their hydroxides are precipitated near the pH range which divides the metal ions into different analytical groups. Iron(II) hydroxide ($pK_{S,0} = 14.0 - 15.1$) precipitates at about pH 7.7, but iron(II) ions are easily oxidized by air in the solutions and therefore precipitate as iron(III) hydroxide. Iron(III) hydroxide ($pK_{S,0} = 36.4 - 39.4$), chromium(III) hydroxide ($pK_{S,0} = 29.8 - 30.8$), and aluminium(III) hydroxide ($pK_{S,0} = 31.7 - 33.5$) are precipitated in the conditions described above at about the pH values 2.1, 4.6, and 3.8, respectively.[2]

In the light of this examination, the metal ions of the cation group II with the precipitation conditions used in the qualitative analysis scheme [1] would precipitate as hydroxides, hydroxy hydrates or basic phthalates. The basic phthalate, however, was formed only with iron(III) and chromium(III) ions and, with the latter ions only when sodium hydroxide was also added to the solution. This may be seen from the following comparison of precipitation conditions and the composition of the precipitates.

EXPERIMENTAL

Preparation of the compounds. The compounds studied were precipitated in three ways, by adding to 100 ml of 0.01 M iron(III), chromium(III), or aluminium(III) chloride solutions: (1) according to the analytical scheme,[1] 0.5 M potassium biphthalate and 2 M sodium hydroxide solutions, or (2) a 0.5 M potassium biphthalate solution, or (3) a 2 M sodium hydroxide solution. The precipitation method is indicated by the symbols (I), (II), or (III) after the chemical formulas of the compounds.

The precipitations were performed at room temperature, after which the samples were warmed for 10 min in a water bath at 90 – 95°C. They were then cooled to room temperature, filtered and washed with water. The precipitates were allowed to dry in the air for a day, and for two weeks in a silica gel desiccator at room temperature. The results of the experiments are shown in Table 1.

The micro combustion analyses of the phthalate complexes gave the following results:

Complex	Precipitation method	Found C	Found H	Analysis formula	Calcd C	Calcd H
Iron	I	19.59	1.77	$C_8H_9O_{14}Fe_3$	19.35	1.83
Iron	II	40.52	2.45	$C_8H_6O_5Fe$	40.38	2.54
Chromium	I	18.19	2.91	$C_8H_{16}O_{16}Cr_3$	18.33	3.08

Apparatus and measurements. The TG analyses were performed with a Fisher TGA System Series 100. The recorder was a two pen type Hewlett Packard model Moseley 7100 BM. About 7 – 9 mg samples were used with a platinum pan and static air conditions. The rate of heating was 10°C/min.

Table 1. The results of the precipitation experiments.

Precipitation method	Precipitate colour	Precipitate colour	Precipitate colour
I	Brown	Dark green	White
II	Light brown	No	No
III	Dark brown	Green	White
Metal ion	Fe^{3+}	Cr^{3+}	Al^{3+}

The DTA analyses were made with a Fisher DTA System Series 200 A, the recorder being the one mentioned above. The differential thermocouple was the "Platinel I" of the equipment. As reference compound, aluminium oxide, "Alumina", from the Fisher Scientific Co. was used. The reference was dried at 600°C and then kept in a silica gel desiccator. The samples were from 30 to 40 mg and the heating rate was 10°C/min.

The IR spectra were run on a Perkin Elmer Model 457 spectrophotometer. Potassium bromide disks were used, consisting of 1 mg of the sample per 300 mg of potassium bromide. Potassium bromide was a guaranted reagent "Uvasol" from E. Merck AG. Before use, the reagent was first seived (mesh diameter 0.044 mm) and then dried at 120°C.

Reagents. The guaranteed reagents of E. Merck AG were used.

RESULTS AND DISCUSSION

The thermograms of the compounds studied are shown in Fig. 1, and the detailed analysis of the curves in Table 2. The DTA curves are seen in Fig. 2 with the peak temperatures and their assignments in Table 3. The IR spectra are represented in Fig. 3 and the absorption bands with their assignments in Tables 4 – 6.

Potassium biphthalate. The thermal decomposition of potassium biphthalate is thought to occur in two main stages which are independent of the decomposition atmosphere. Firstly, dipotassium phthalate is formed by volatilization of phthalic anhydride and water, and secondly, dipotassium phthalate is decomposed to give potassium carbonate and volatile products.[3–7] The initial decomposition temperature for potassium biphthalate found by different workers varies from 145°C[7] to 240°C,[6] depending on the decomposition conditions and the heating rate. The decomposition and sublimation temperature in static air, 228°C, observed in this study (Fig. 1, curve 1 and Table 2) is well within this range. Further observations of the decomposition processes from the thermogravimetric curve were impossible because of the strong sublimation effects.

The DTA curve (Fig. 2, curve 1) and peak temperatures (Table 3) reported here may be compared with those of Belcher *et al.*[4] and with their derivatographic TG curves. Thus, the endothermic peaks at 90°, 125°, and 185°C may be assigned to changes in structure and the melting of potassium biphthalate. The peak at 305°C corresponds to the decomposition of potassium biphthalate, sublimation of phthalic anhydride and removal of water. The endothermic peak at 437°C marks the melting of dipotassium phthalate. The exothermic peaks at 460°, 517° and 540°C are due to the decomposition of dipotassium phthalate and formation of potassium carbonate, and the peaks at 580° and

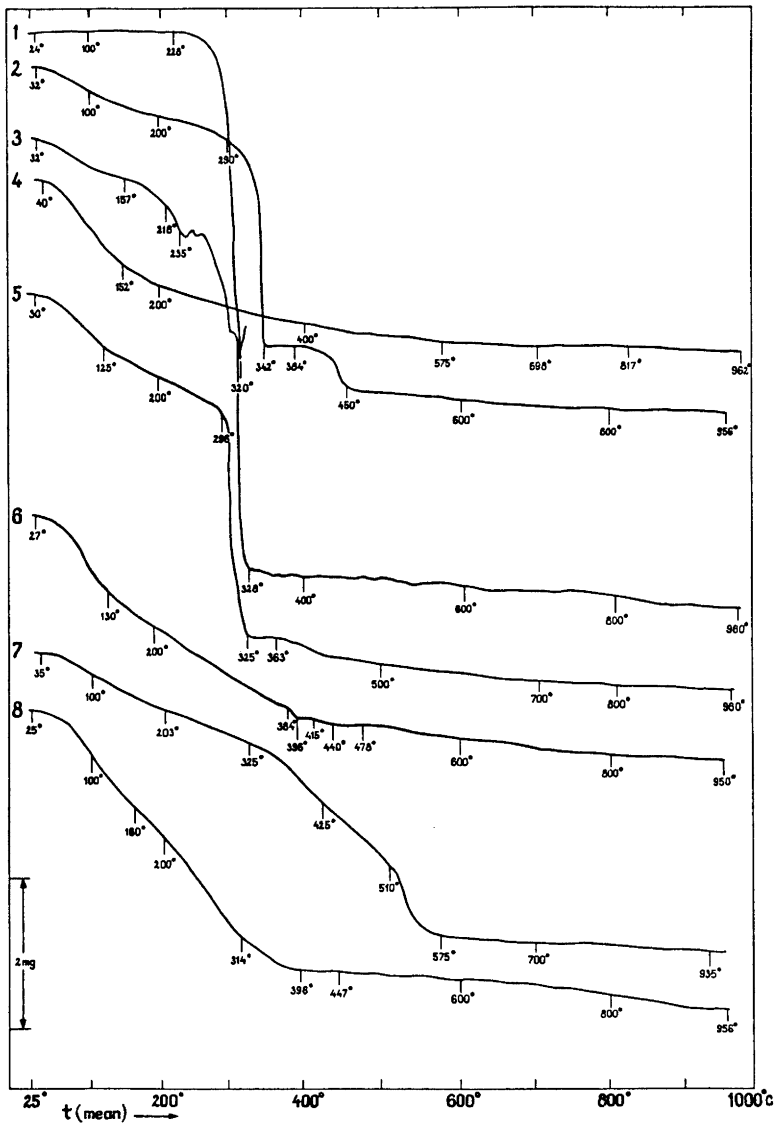

Fig. 1. The thermograms of potassium biphthalate and of the precipitated iron(III), chromium(III), and aluminium(III) salts.
Curve: 1, $KH(O_2C)_2C_6H_4$; 2, $Fe_3O_5(OH)_5(O_2C)_2C_6H_4$, (I);
3, $Fe_2(OH)_2[(O_2C)C_6H_4(CO_2H)]_2$, (II); 4, $Fe(OH)_3$, (III);
5, $Cr_3(OH)_{12}(O_2C)_2C_6H_4$, (I); 6, $Cr(OH)_3.1.75H_2O$, (III);
7, $Al_2O_3.5H_2O$, (I); 8, $Al_2O_3.6H_2O$, (III).

Table 2. The detailed analyses, weight losses and temperature ranges of the thermal processes of the metal salts studied.

Salt	Reaction	Weight loss, % Calc.	Found	Temperature range, °C
$KH(O_2C)_2C_6H_4$				
	Decomposition and sublimation	–	–	228–
$Fe_3O_5(OH)_5(O_2C)_2C_6H_4$, (I)				
	$Fe_3O_5(OH)_5(O_2C)_2C_6H_4 \rightarrow$			
	$Fe_3O_{7.5}(O_2C)_2C_6H_4 + 2.5H_2O$	9.1	10.6	32 – 290
	$Fe_3O_{7.5}(O_2C)_2C_6H_4 \rightarrow Fe_2O_2CO_3$	32.3	34.2	290 – 342
	$Fe_2O_2CO_3 \rightarrow Fe_2O_3$	21.6	17.3	384 – 956
	Yield (%) of Fe_2O_3: 48.7 (found); 48.2 (calc.)			
$Fe_2(OH)_2[(O_2C)C_6H_4(CO_2H)]_2$, (II)				
	$Fe_2(OH)_2[(O_2C)C_6H_4(CO_2H)]_2 \rightarrow Fe_2[(O_2C)_2C_6H_4]_2$	7.6	6.1	32 – 157
	$Fe_2((O_2C)_2C_6H_4)_2 \rightarrow Fe_2O_3$	63.7	71.1	157 – 960
	Yield (%) of Fe_2O_3: 27.1 (found); 33.6 (calc.).			
$Fe(OH)_3$, (III)				
	$2Fe(OH)_3 \rightarrow Fe_2O_{1.5}(OH)_3 + 1.5H_2O$	12.6	12.5	40 – 152
	$Fe_2O_{1.5}(OH)_3 \rightarrow Fe_2O_3 + 1.5H_2O$	14.5	13.9	152 – 962
	Yield (%) of Fe_2O_3: 75.3 (found); 74.7 (calc.).			
$Cr_3(OH)_{12}(O_2C)_2C_6H_4$, (I)				
	$Cr_3(OH)_{12}(O_2C)_2C_6H_4 \rightarrow$			
	$Cr_2O_3.CrO_3(O_2C)_2C_6H_4 + 6H_2O$	20.6	18.4	30 – 296
	$Cr_2O_3.CrO_3(O_2C)_2C_6H_4 \rightarrow Cr_2O_3.CrO_3$	39.4	40.7	296 – 325
	$2Cr_2O_3.CrO_3 \rightarrow 3Cr_2O_3 + 1.5O_2$	9.5	16.7	363 – 960
	Yield (%) of Cr_2O_3: 40.4 (found); 43.5 (calc.).			
$Cr(OH)_3.1.75H_2O$, (III)				
	$2Cr(OH)_3.1.75H_2O \rightarrow 2Cr(OH)_3.0.75H_2O + 2H_2O$	13.4	13.4	27 – 130
	$2Cr(OH)_3.0.75H_2O \rightarrow Cr_2O_3 + 4.5H_2O$	34.8	34.9	130 – 950
	Yield (%) of Cr_2O_3: 56.4 (found); 56.5 (calc.).			
$Al_2O_3.5H_2O$, (I)				
	$Al_2O_3.5H_2O \rightarrow Al_2O_3.4H_2O + H_2O$	9.4	9.3	35 – 203
	$Al_2O_3.4H_2O \rightarrow Al_2O_3.3.5H_2O + 0.5H_2O$	5.2	5.0	203 – 325
	$Al_2O_3.3.5H_2O \rightarrow Al_2O_3.2.5H_2O + H_2O$	10.9	10.8	325 – 425
	$Al_2O_3.2.5H_2O \rightarrow Al_2O_3.1.5H_2O + H_2O$	12.3	12.3	425 – 510
	$Al_2O_3.1.5H_2O \rightarrow Al_2O_3 + 1.5H_2O$	21.0	19.5	510 – 935
	Yield (%) of Al_2O_3: 54.2 (found); 53.1 (calc.)			
$Al_2O_3.6H_2O$, (III)				
	$Al_2O_3.6H_2O \rightarrow Al_2O_3.4H_2O + 2H_2O$	17.2	17.1	25 – 160
	$Al_2O_3.4H_2O \rightarrow Al_2O_3.1.5H_2O + 2.5H_2O$	25.9	25.9	160 – 314
	$Al_2O_3.1.5H_2O \rightarrow Al_2O_3.H_2O + 0.5H_2O$	7.0	9.3	314 – 396
	$Al_2O_3.H_2O \rightarrow Al_2O_3 + H_2O$	15.0	12.1	447 – 956
	Yield (%) of Al_2O_3: 49.0 (found); 48.5 (calc.)			

636°C correspond to the decomposition of potassium carbonate and formation of potassium oxide.

The infrared spectrum of potassium biphthalate in the region 4000 – 2000 cm^{-1} shows two very weak bands at 2910 and 2460 cm^{-1} (Fig. 3, curve 1 and Table 4), which may be assigned to the OH stretching bands of the unionized carboxylic group. This suggests dimerization or polymerization of the salt through the carboxylic groups.[8–15]

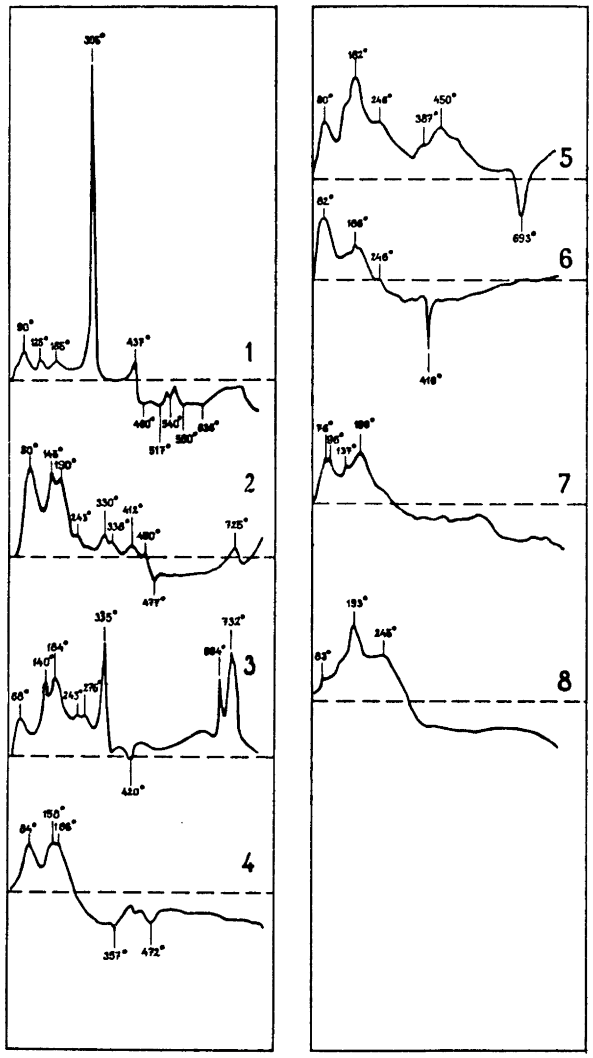

Fig. 2. The differential thermal analysis curves of potassium biphthalate and of the precipitated iron(III), chromium(III), and aluminium(III) salts.
Curve: 1, $KH(O_2C)_2C_6H_4$; 2, $Fe_3O_5(OH)_5(O_2C)_2C_6H_4$, (I);
3, $Fe_2(OH)_2[(O_2C)C_6H_4(CO_2H)]_2$, (II); 4, $Fe(OH)_3$, (III);
5, $Cr_3(OH)_{12}(O_2C)_2C_6H_4$, (I); 6, $Cr(OH)_3.1.75H_2O$, (III);
7, $Al_2O_3.5H_2O$, (I); 8, $Al_2O_3.6H_2O$, (III).

There are several strong bands in the region 2000 – 1300 cm^{-1}. The medium and broad band at 1945 cm^{-1} is obviously due to the CH out-of-plane bending vibrations of the benzene ring, typical of *o*-disubstituted benzenes.[16–18] The

Table 3. The DTA peak temperatures and their comparison with the TG temperature ranges of the thermal decomposition processes of the metal salts studied.

Salt	Process	DTA peak temperature, °C	TG temperature range, °C
$KH(O_2C)_2C_6H_4$			
	Changes in structure, melting, endoth.	90, 125, 185	24 – 228
	Decomposition, sublimation, »	305	228 –
	Melting of $(KO_2C)_2C_6H_4$, »	437	
	Decomposition, formation of K_2CO_3, exoth.	460, 517 540	
	Decomposition, formation of K_2O, »	580, 636	
$Fe_3O_5(OH)_5(O_2C)_2C_6H_4$, (I)			
	Changes in structure, melting, loss of water, endoth.	90, 145, 190, 243	32 – 290
	Decomposition, endoth.	330, 338	290 – 342
	Decomposition, »	412, 450	384 – 450
	Decomposition, formation of Fe_2O_3, exoth.	477	450 – 956
	Decomposition, endoth.	725	450 – 956
$Fe_2(OH)_2[(O_2C)C_6H_4(CO_2H)]_2$, (II)			
	Changes in structure, melting, loss of water, endoth.	68, 140	32 – 157
	Decomposition, sublimation, endoth.	184, 243, 276	157 – 328
	Decomposition, endoth.	335	328 – 960
	Decomposition, formation of Fe_2O_3, exoth.	420	»
	Decomposition, endoth.	694, 732	»
$Fe(OH)_3$, (III)			
	Changes in structure, loss of water, endoth.	84, 158, 186	40 – 200
	Decomposition, loss of water, formation of Fe_2O_3, exoth.	357, 472	200 – 962
$Cr_3(OH)_{12}(O_2C)_2C_6H_4$, (I)			
	Changes in structure, melting, loss of water, endoth	80, 182, 246	30 – 296
	Decomposition, endoth.	387, 450	296 – 960
	Decomposition, formation of Cr_2O_3, exoth.	693	»
$Cr(OH)_3.1.75H_2O$, (III)			
	Changes in structure, loss of water, endoth.	82	27 – 130
	Decomposition, loss of water, »	186, 246	130 – 384
	Decomposition, formation of Cr_2O_3, exoth.	410	384 – 950
$Al_2O_3.5H_2O$, (I)			
	Changes in structure, loss of water, endoth.	76, 96, 137,190	35 – 203
$Al_2O_3.6H_2O$, (III)			
	Changes in structure, loss of water, endoth.	83	25 – 160
	Decomposition, loss of water, endoth.	193, 245	160 – 314

band at 1668 cm^{-1} is due to the asymmetric CO stretching modes of the unionized carboxylic group, which shows further that the salt is dimerized or polymerized through the carboxylic groups.[8–15,19–28] The intensity of the CO stretching band dominates that of all other double bond bands so that the overtone and combination bands of the substituted benzene ring is masked.[8,16] The low wavenumber of the band also points to internal hydrogen bonding and so to the dimerization or polymerization of the salt.[8–12,19–26]

The strong band at 1555 cm^{-1} arises from the antisymmetric COO^- stretching modes, [23,24,29–33] the medium band at 1480 cm^{-1} from the CC stretching

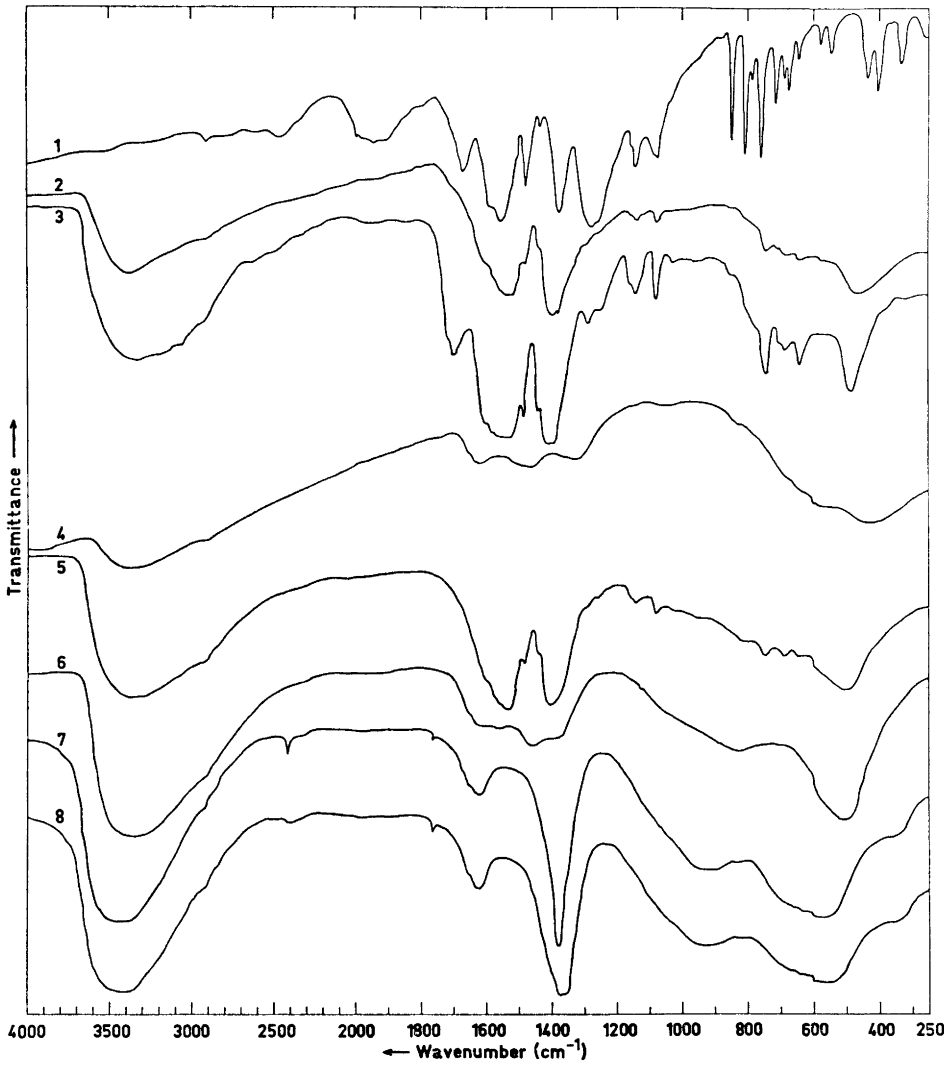

Fig. 3. The infrared absorption spectra of potassium biphthalate and of the precipitated iron(III), chromium(III), and aluminium(III) salts in the range 4000 – 250 cm^{-1} recorded in potassium bromide discs (1 mg of the compound per 300 mg of KBr) at room temperature (about 22°C).

Spectrum: 1, $KH(O_2C)_2C_6H_4$; 2, $Fe_2O_5(OH)_5(O_2C)_2C_6H_4$, (I);
3, $Fe_2(OH)_2((O_2C)C_6H_4(CO_2H))_2$, (II); 4, $Fe(OH)_3$, (III);
5, $Cr_3(OH)_{12}(O_2C)_2C_6H_4$, (I); 6, $Cr(OH)_3.1.75H_2O$, (III);
7, $Al_2O_3.5H_2O$, (I); 8, $Al_2O_3.6H_2O$, (III).

Table 4. The wave numbers and assignments of the infrared absorption bands of the precipitated iron(III) salts and of potassium biphthalate.

$Fe_3O_5(OH)_5 \cdot (O_2C)_2C_6H_4$, (I)		$Fe_2(OH)_2 \cdot [(O_2C)C_6H_4(CO_2H)]_2$, (II)		$Fe(OH)_3$, (III)		$KH(O_2C)_2C_6H_4$		Assignment[b]	Ref.
cm^{-1}	Comments[a]	cm^{-1}	Comments	cm^{-1}	Comments	cm^{-1}	Comments		
3380	s,bd	3350	vs,bd	3360	m,bd			ν(FeOH)+ ν(HOH)	19, 35 45-61, 63, 67, 69
		3050	sh					ν(OH)	10, 61
		2920	sh			2910	vw	ν(OH), (COOH)	8-15
2900	sh			2900	sh			ν(OH)	8-15
						2460	vw	ν(OH), (COOH)	8-15
						1945	m,bd	π(CH)	8, 16-18
		1700	m			1668	m	ν_a(OCO), (COOH)	8-15, 19-28
				1620	w,bd			δ(HOH)	46, 53, 54-58, 62, 63, 67
1600	sh	1600	sh			1595	sh	ν(CO) or ν(CC)	14, 17, 20, 23, 24, 26, 31, 32, 34
1530	s	1540	vs			1555	s	$\nu_a(CO_2^-)$	8, 11, 14, 23, 24, 34, 29, 32, 35
1480	sh	1487	w			1480	m	ν(CC)	8, 14, 16, 17, 34
				1465	w,bd			δ(FeOH)	51, 63-71
1438	sh	1440	sh			1437	vw	ν_s(CO)+ ν(CC)	9-11, 14, 17, 23, 25-27, 29, 32
1400	s	1400	vs					$\nu_s(CO_2^-)$+	8, 11, 14, 17, 19, 20, 23-27
1380	sh					1377	s	ν(CC)	32, 33, 35
				1330	w,bd			δ(FeOH)	51, 63-71
1290	sh	1290	w			1278	s	ν_s(CO)+ δ(OCO)	9, 10, 20, 23, 25-27, 35
1260	sh	1250	sh			1257	sh	»	25, 33
1140	vw	1145	m			1144	w	δ(OH)	13, 35
1080	vw	1082	m			1076	w	»	13, 35
		1030	vw					δ(OH)	8-13
		850	sh			848	vs	ν(CO)+ν(CC), (COOH)	14, 17, 23, 26
						806	vs	δ(OCO)+ ν(CC)	33, 35
						785	vw	»	19, 25, 26
745	vw	745	m			758	vs	δ(OCO)+ δ(CH)	17, 20, 33, 35
		706	sh			716	m	»	»
685	vw	688	vw			688	vw	(OCO)+ ring def.	14, 20, 25-27, 32, 33, 35-39
						673	m	»	»
644	vw	644	w			644	w	»	14, 20, 29
						578	w	»	14, 20, 32
						546	w	»	14

Table 4. Continued.

468	m,bd	485	s					
						434	s	$\varrho_r(CO_2^-)$+ ring def.
				425	m,bd			
						403	s	ϱ_r(OCO)+ ring. def.
						333	m	ϱ_r(OCO)

		ν(FeO)	51, 63-72	
		$\varrho_r(CO_2^-)$+ ring def.	21, 25-27	
		ν(FeO)	25, 51, 63-72	
		ϱ_r(OCO)+ ring. def.	21, 25-27	
		ϱ_r(OCO)	20, 23, 25, 26, 33	

[a] The intensity abbreviations are: vs = very strong, s = strong, m = medium, w = weak, vw = very weak, bd = broad, sh = shoulder.

[b] The following abbreviations are used for the different vibrations: ν(stretching), ν_a(antisymmetric stretching), ν_s(symmetric stretching), δ(bending), ϱ_r(rocking), π(out-of-plane bending), ring def. (ring deformation), (Ref. 27, p. 218).

Table 5. The wave numbers and assignments of the infrared absorption bands of the precipitated chromium(III) salts.

$Cr_3(OH)_{12}(O_2C)_2C_6H_4$, (I)		$Cr(OH)_3.1.75H_2O$, (III)		Assignment	Reference
cm^{-1}	Comments	cm^{-1}	Comments		
3350	vs, bd	3350	vs, bd	ν(CrOH)+ν(HOH)	45, 53, 70
2915	sh	2920	sh	ν(OH)	45, 53, 70
		1620	sh	δ(HOH)	53, 77
1600	sh			ν(CO) or ν(CC)	17, 31,32
1535	vs			$\nu_a(CO_2^-)$	23, 24, 29-32
1482	vw			ν(CC)	8, 16, 17, 34
		1458	m, bd	δ(CrOH)	51, 63-71
1440	sh			ν_s(CO)+ν(CC)	17, 25-27
1400	vs			$\nu_s(CO_2^-)$+ν(CC)	17, 25-27, 33
		1380	sh	δ(CrOH)	51, 63-71
1290	sh			ν_s(CO)+δ(OCO)	25, 27, 33
1260	sh			»	»
1142	vw			δ(OH)	13
1090	vw			δ(OH)	13
		825	w, bd	ν(CrO)	51, 63-71
747	w			δ(OCO)+δ(CH)	17, 33
690	vw			δ(OCO)+ ring def.	20, 25-27, 33, 36-39
650	vw			»	»
500	m, bd	507	s, bd	ν(CrO)	51, 63-71, 78

modes of the benzene ring,[8,16,17,34] and the strong band at 1377 cm^{-1} from the symmetric CO stretching and CC stretching vibrations.[25-27] The band at 1278 cm^{-1} is due to CO stretching and OCO deformation vibrations.[25-27] The very strong bands at 848 cm^{-1} and 806 cm^{-1} are not generally found in the spectra of the precipitated iron(III) and chromium(III) phthalates, but could obviously derive from the OCO stretching or deformation modes of the COOH group and the CC stretching vibrations of the benzene ring.[17,33,35]

Table 6. The wave numbers and assignments of the infrared absorption bands of the precipitated aluminium(III) salts.

$Al_2O_3.5H_2O$, (I)		$Al_2O_3.6H_2O$, (III)		Assignment	Reference
cm^{-1}	Comments	cm^{-1}	Comments		
3420	vs, bd	3420	vs, bd	ν(AlOH) + ν(HOH)	45, 53,59-62, 81
2920	sh	2920	sh	ν(OH)	46-61
2415	w	2400	vw	ν(OH)	46-61
1762	vw	1762	w	ν(OH)	46-61
1620	m	1622	m	δ(HOH)	53, 55-58, 62,81
1377	vs	1377	vs	δ(AlOH)	51, 63-71
915	w, bd	930	w, bd	δ(AlOH)	51, 59-71, 81
830	vw	830	vw	ν(AlO)	51, 62-71
570	s, bd	560	s, bd	ν(AlO)	25, 68, 72, 82
350	sh	350	sh	Vibration modes of lattice H_2O or ν(AlOH)	59, 66-68, 82

In the spectral region 800 – 250 cm^{-1}, the bands at 758 cm^{-1} and 716 cm^{-1}, which are observed as medium, weak, or absent in the spectra of the basic iron(III) and chromium(III) phthalates, are obviously also due to the OCO deformation vibrations of the unionized carboxylic group and the CH deformation vibrations of the benzene ring.[17,33] The medium or strong bands at 673, 434, 403, and 333 cm^{-1}, which are not observed in the spectra of the other phthalates investigated are possibly due to the OCO and ring deformation vibrations.[25–27,36–39]

The iron(III) compounds. It is to be noted that an iron precipitate was obtained with all three precipitation methods. With the first, a brown precipitate was formed, which was easily separable from the mother liquor (Table 1). After standing for a few days, the precipitate dissolved completely in the mother liquor, which became dark red-brown. When the second method was used, precipitation with 0.5 M potassium biphthalate solution, an easily separable, pale-brown precipitate was obtained (Table 1). This did not dissolve upon standing in the mother liquor, which remained colourless for a longer time. The precipitation with sodium hydroxide (method III) gave a heavy, dark-brown product (Table 1).

It seems to be typical of the precipitations that in the first case (method I), a complicated basic iron oxide hydroxide phthalate and in the second case (method II), a basic iron hydroxy biphthalate are formed. These may be polymerized and have very complicated structures. In the third case (method III), the formation of ferric hydroxide is most probable.

Although performed in ethanolic (50 or 90 %) water solutions, the heterometric studies by Bobtelsky and Bar-Gadda [40] of iron, chromium, and aluminium phthalate complexes and their mixtures indicate that individual metal phthalate complexes are also precipitated from the mixed solutions of the metals, either successively or simultaneously. This observation supports the accepted research method of analytical precipitation, although it does not exclude the possible formation of mixed basic metal phthalate complexes during the analytic procedure.[1]

It is interesting to note that Galwey,[41] following the observations of Bobtelsky and Bar-Gadda,[40] precipitated a pale brown product of the composition $C_8H_5FeO_5 \cdot 0.5H_2O$ by adding ferric chloride (dissolved in 50 % ethanol-water) to a phthalic acid-ammonium hydroxide solution (50 % ethanol-water). This formula is very close to the composition of the precipitate obtained by method II in the present study (Table 2).

According to the literature quoted in Gmelin,[42] alkaline hydroxides precipitate from ferric salt solutions as hydrated ferric oxide gel having a varying water content. The thermogravimetric results (Fig. 1, Table 2) suggest that the precipitated ferric hydroxide with the procedure used in the present study, reaches the composition $Fe_2O_3.3H_2O$, which corresponds to the hydroxide $Fe(OH)_3$. The later studies of Dey and Ghosh [43] on precipitations with sodium hydroxide from ferric chloride solutions support the present conclusions concerning the hydroxide precipitation.

The probable compositions and possible decomposition reactions derived from the thermogravimetric curves (Fig. 1, curves 2 – 4) and from the combustion analyses of the iron precipitates prepared by the three different precipitation methods (I, II, and III) are presented in Table 2. The temperature ranges of the reactions are compared with those of the DTA peaks (Fig. 2, curves 2 – 4) in Table 3.

In the thermal decomposition of the basic iron phthalate (Fig. 1, curve 2 and Table 2), an interesting plateau between 342° and 384°C can be seen. The suggested intermediate corresponding to this feature may be formulated [44] as $Fe_2O_3.CO_2$.

The DTA curves show an exothermic peak in the temperature range 400 – 500°C (Table 3) from the decompositions of all iron compounds. This is obviously connected with the formation of a stable product (Fe_2O_3) from more reactive intermediates.

The IR spectra of the iron(III) compounds precipitated by the three different methods show a strong, broad band at 3700 – 3000 cm^{-1} (Fig. 3, curves 2 – 4 and Table 4), which is strongest for the iron hydroxide biphthalate complex and weakest for iron(III) hydroxide. These bands are due to the OH stretching vibrations of the metal hydroxide groups.[45–61] From the intensity of the band, these stretching vibrations are especially unrestrained in the iron hydroxide biphthalate complex. To some extent, the bands may also be due to the OH stretching vibrations of lattice water.[46–52] Potassium biphthalate shows no band in this region.

The shoulders in the spectra at about 2900 cm^{-1} are obviously also due to the OH stretching vibrations of metal hydroxide groupings or lattice water, depending on the composition of the compound. The medium band at 1700 cm^{-1} in the spectrum of the iron(III) hydroxide biphthalate complex, confirms the presence of the unionized carboxylic group.[8–15,19–28]

The appearance or absence of a band at about 1620 cm^{-1} in the spectra of metal hydroxides (due to the HOH bending modes of water) has been used to prove, respectively, the existence of water of the hydroxide form.[53] Using this criterion, the weakness of the band in the spectrum of the ferric compound precipitated with sodium hydroxide only (method III) shows that the

compound is better represented by the $Fe(OH)_3$ form than the $Fe_2O_3.3H_2O$, at least after treatment of the precipitate.[55–58,62]

The strong bands at 1530, 1400, 1380 cm^{-1} and 1540, 1400 cm^{-1}, respectively, in the spectra of the basic iron(III) phthalate and biphthalate, have the same designations as in potassium biphthalate. The medium bands at 1145 and 1082 cm^{-1} in the spectrum of iron(III) biphthalate indicate an increase in the OH deformation vibrations compared to the other phthalates studied.

The medium band at 468 cm^{-1} and the strong band at 485 cm^{-1} in the spectra of the basic iron(III) phthalate and biphthalate, respectively, and which are not found for potassium biphthalate, should have their origin in the FeO stretching vibrations.[63–71]

The weak or medium broad bands at 1465, 1330 and 425 cm^{-1} in the spectrum of iron(III) hydroxide are apparently also due to the FeOH bending and FeO stretching vibrations,[63–71] respectively.

The absence of bands [46–51,62,72] typical of α-Fe_2O_3, γ-Fe_2O_3 and Fe_3O_4 in the spectral range $800-250$ cm^{-1} in the spectrum of the precipitated iron(III) hydroxide confirms that it is not a question of a hydrated iron(III) oxide, but mainly of the iron(III) hydroxide. On the contrary the iron(III) phthalates show a medium or strong band at $460-490$ cm^{-1}, which appears as a strong band in the spectrum of α-Fe_2O_3 and as a weak band or shoulder for the other iron oxides. These observations indicate the iron oxide contents of the basic iron phthalates.

The chromium(III) compounds. By precipitation of chromium(III) ions according to the analytical scheme [1] (method I), a dark-green, easily separable precipitate was formed (Table 1). When allowed to stay several days in the mother liquor, it dissolved completely and the colourless solution became dark-green. No precipitate was formed when potassium biphthalate alone was used as the precipitating agent (method II), but the solution was coloured dark green (Table 1). With sodium hydroxide (method III), a green precipitate was formed (Table 1).

The precipitate formed by the method I has a very complicated composition and is obviously a polymer. It decomposes on heating in three stages, the probable processes for which are interpreted from the thermogram (Fig. 1, curve 5) and presented in Table 2. The results point to a partial sublimation of the product during the decomposition. The thermogravimetric temperature ranges are compared with the DTA peaks (Fig. 2, curve 5) in Table 3. The exothermic peak found (693°C) obviously corresponds to the formation of Cr_2O_3.

The thermogravimetric results (Fig. 1, curve 6 and Table 2) clearly show that the precipitate obtained with sodium hydroxide has, after the treatment described, a composition corresponding to a hydrated chromium(III) hydroxide. Its DTA curve (Fig. 2, curve 6) also shows an exothermic peak (Table 3) at 410°C (*cf.* the iron compound above), which again clearly corresponds to the formation of chromium(III) oxide.

The studies of Higashi *et al.*[73] on chromium(III) complexes with phthalic acid show the difficulties of precipitating a basic chromium(III) phthalate complex containing potassium. This is obviously still more difficult when sodium hydroxide is used to adjust the pH of the solution, as in the analytical

scheme [1] (method I). From the consistancy of the present combustion analysis with respect to carbon and hydrogen and the thermogravimetric chromium residue, it follows that the alkali metal content of this precipitate is probably negligible or zero, as has been accepted.

In their heterometric experiments, Bobtelsky and Bar-Gadda [40] found that excess phthalate or chromium(III) ions dissolved the precipitate of chromium phthalate formed. It is therefore easily understood that no precipitate was obtained by using potassium biphthalate alone as the precipitating agent (method II).

On the basis of polarographic rate studies, Hamm *et al.*[74] have concluded that the rate determining step in the reaction process of carboxylic acids (among others the phthalate anion) with chromium(III) ions is the escape of a water molecule from the hexahydrated chromium(III) ion. Conversely, the slow uptake of water molecules by the chromium(III) ions in the basic chromium phthalate precipitate may explain its slow back-solubility into the mother liquor.

According to Franco and Sing,[75] no pronounced exothermic peak associated with a glow phenomenon has been observed in the DTA curve of the transformation of CrO_2 to α-Cr_2O_3. However, since both DTA curves of the present chromium precipitates show an exothermic peak, it is evident that although the precipitates could to some extent contain CrO_2 as an intermediate during the decomposition processes, they should nevertheless leave chromium(III) oxide as the decomposition end-product,[76] as is accepted in Table 2.

Both the precipitated chromium(III) compounds show a very strong and broad band at 3350 cm^{-1} and weak shoulders at about $2915-2920$ cm^{-1} (Fig. 3, curves 5 and 6, and Table 5). These are due to the OH stretching vibrations of the CrOH groupings [45,53,70] and lattice water.

The almost complete absence of the band at 1620 cm^{-1} due to the HOH bending vibrations in the spectrum of the chromium hydroxide precipitate confirms the product to be almost wholly in the $Cr(OH)_3$ form.[53,77]

The strong bands at 1535 and 1400 cm^{-1} in the spectrum of the basic chromium(III) phthalate complex should have the same origin as those of potassium biphthalate in the same region. The medium, broad band at 500 cm^{-1} supposedly arises from the CrO stretching modes.[51,63–71]

The medium and strong bands at 1458 and 507 cm^{-1} in the spectrum of $Cr(OH)_3$ are due to the CrOH bending and CrO stretching vibrations,[51,63–71] respectively. The complete lack of the bands in the region $800-250$ cm^{-1}, typical of chromium(III) oxide,[51,78] shows the precipitate to consist rather of the hydroxide form than of a hydrated oxide.

The aluminium(III) compounds. Aluminium(III) ion was precipitated as white amorphous products both according to the analytical scheme [1] (method I) and with sodium hydroxide solution (method III), but not when precipitating with potassium biphthalate alone when no changes were observed in the clear solution (Table 1).

The thermogravimetric analyses showed that the products precipitated both by method I (Fig. 1, curve 7 and Table 2) and by method III (Fig. 1, curve 8 and Table 2) were aluminium oxide hydrates, the former containing five and the latter six water molecules. The proposed dehydration processes

for both hydrates are presented in Table 2. These and their temperature limits are compared with the DTA peaks (Fig. 2, curves 7 and 8) of the products in Table 3. In contrast to the iron and chromium compounds discussed above, the DTA curves do not show any exothermic processes. This confirms the opinion that the precipitates are already in the hydrated aluminium oxide forms at the beginning of the thermal processes.

For general views on the dehydration processes of precipitated aluminium hydroxides or oxide hydrates the reader is reffered to Gmelin.[79]

The potentiometric studies on the complexing of aluminium ions with phthalate ions performed by Napoli and Liberti [80] support the nonprecipitation of aluminium phthalate complexes observed here. They found two successive soluble aluminium phthalate complexes, the stability constants of which were determined.

The precipitated aluminium compounds also exhibit both a strong, broad band at 3420 cm^{-1} and a weak shoulder at 2920 cm^{-1} (Fig. 3, curves 7 and 8, and Table 6), which are due to the OH stretching vibrations of the aluminium hydroxyl groupings [46,53] and the lattice water. Two weak bands are seen in both spectra at 2400 – 2415 cm^{-1} and 1762 cm^{-1}, obviously corresponding to the OH stretching vibrations of the AlOH groupings and the lattice water.[46,61]

It can be seen from the spectra in Fig. 3 and Tables 4 – 6 that the frequency of the OH stretching mode of the MOH grouping in the region 3700 – 3000 cm^{-1} increases in the series Cr(III) < Fe(III) < Al(III). The OH bond is obviously shortened, the bond strength increased and the hydrogen bond O – H···O formation decreased in this series.[27,53]

The medium HOH bending bands at 1620 cm^{-1} in the spectra of both aluminium precipitates show the compositions to be closer to the oxide hydrates than to the hydroxides.[53,55–58,62,81]

Both aluminium compounds show strong bands at 1377 cm^{-1} and 570 – 560 cm^{-1}, contributed by the AlOH bending [51,63–71] and AlO vibrations,[72,82] respectively. This latter band is also found in the spectrum of α-Al_2O_3 [51,66–68,82] which further indicates that we are dealing more with hydrated aluminium oxides than with hydroxides.

SUMMARY

The main conclusions of the present study may be summarized as follows:

1. For simplicity, the iron, chromium, and aluminium precipitates obtained by the analytical procedure (method I) were presented in the analytical scheme [1] in the forms $[Fe(OH)Ph]_n$, $[Cr(OH)Ph]_n$, and $Al(OH)_3$. These ought now be considered in the light of this study.

2. The iron(III) and chromium(III) ions are most probably precipitated in the analytical scheme [1] as polymerized hydroxy phthalates, whereas the aluminium(III) ions are precipitated as hydrated aluminium(III) oxides.

3. The micro combustion analyses and thermogravimetric results of the basic iron(III) and chromium(III) phthalates studied are parallel, and confirm the conclusions about the compositions.

4. The DTA curves show considerably more structural and composition changes than would generally be concluded from the TG curves. The DTA

curves of iron(III) and chromium(III) compounds show an exothermic peak in the temperature range 400° – 700°C, which indicates the formation of the oxides Fe_2O_3 and Cr_2O_3.

5. The infrared spectra confirm the conclusions drawn concerning the compositions of the compounds studied.

REFERENCES

1. Lumme, P. and Tummavuori, J. *Acta Chem. Scand.* **27** (1973) 851.
2. *Stability Constants of Metal-ion Complexes*, Spec. Publ. No. 17, The Chem. Coc., London 1964; *Stability Constants of Metal-ion Complexes*, Suppl. No. 1, Spec. Publ. No. 25, The Chem. Soc., London, 1971.
3. Newkirk, A. E. and Laware, R. *Talanta* **9** (1962) 169.
4. Belcher, R., Erdey, L., Paulik, F. and Liptay, G. *Talanta* **5** (1960) 53.
5. Duval, C. and Wadier, C. *Anal. Chim. Acta* **23** (1960) 541.
6. Duval, C. *Anal. Chim. Acta* **13** (1955) 32.
7. Caley, E. R. and Brundin, R. H. *Anal. Chem.* **25** (1953) 142.
8. Flett, M. St. C. *Characteristic Frequencies of Chemical Groups in the Infra-red*, Elsevier, London 1963, pp. 34 – 35.
9. Hadzi, D. and Sheppard, N. *Proc. Roy. Soc. London* **A 216** (1953) 247.
10. Flett, M. St. C. *J. Chem. Soc.* **1951** 962.
11. Flett, M. St. C. *Spectrochim. Acta* **18** (1962) 1537.
12. Lusi, H. *Anal. Chem.* **31** (1959) 910.
13. Colthup, N. B., Daly, L. H. and Wiberley, S. E. *Introduction to Infrared and Raman Spectroscopy*, Academic, London 1964, pp. 257 – 262.
14. Bentley, F. F., Ryan, M. T. and Katon, J. E. *Spectrochim. Acta* **20** (1964) 685.
15. Bentley, F. F., Smithson, L. D. and Rozek, A. L. *Infrared Spectra and Characteristic Frequencies* ~ 700 – 300 cm^{-1}, Interscience, London 1968, pp. 136, 137, 150 and 151.
16. Bellamy, L. J. *The Infra-red Spectra of Complex Molecules*, Methuen, London 1958, p. 90.
17. Ref. 13, pp. 220 – 230.
18. Whiffen, D. H. *Spectrochim. Acta* **7** (1955) 253.
19. Schmelz, M. J., Nakagawa, I., Mizushima, S. and Quagliano, J. V. *J. Am. Chem. Soc.* **81** (1959) 287.
20. Itoh, K. and Bernstein, H. J. *Can. J. Chem.* **34** (1956) 170.
21. Green, J. H. S., Kynaston, W. and Lindsey, A. S. *Spectrochim. Acta* **17** (1961) 486.
22. Vrätny, F., Rao, C. N. R. and Dilling, M. *Anal. Chem.* **33** (1961) 1455.
23. Hester, R. E. and Plane, R. A. *Inorg. Chem.* **3** (1964) 513.
24. Nakamoto, K., Morimoto, Y. and Martell, A. E. *J. Am. Chem. Soc.* **83** (1961) 4528.
25. Fujita, J., Martell, A. E. and Nakamoto, K. *J. Chem. Phys.* **36** (1962) 324, 331.
26. Schmelz, M. J., Miyazawa, T., Mizushima, S., Lane, T. J. and Quagliano, J. V. *Spectrochim. Acta* **9** (1957) 51.
27. Nakamoto, K. and McCarthy, P. J. *Spectroscopy and Structure of Metal Chelate Compounds*, Wiley, London 1968, pp. 270 – 273.
28. Nakamoto, K. *Infrared Spectra of Inorganic and Coordination Compounds*, 2nd Ed., Wiley-Interscience, London 1970, pp. 244 – 246.
29. Wilmhurst, J. K. *J. Chem. Phys.* **23** (1955) 2463.
30. Ref. 27, p. 269.
31. Condrate, R. A. and Nakamoto, K. *J. Chem. Phys.* 42 (1965) 2590.
32. Tsuboi, M., Onishi, T., Nakagawa, I., Shimanouchi, T. and Mizushima, S. *Spectrochim. Acta* **12** (1958) 253.
33. Ref. 28, pp. 222 – 223, 232 – 243.
34. Wexler, A. S. *Spectrochim. Acta* **A 23** (1967) 1319.
35. Lumme, P. *Suomen Kemistilehti* **B 31** (1958) 294; **B 30** (1957) 204.
36. Bentley, F. F. and Wolfarth, E. F. *Spectrochim. Acta* **15** (1959) 165.
37. Ref. 13, p. 342.
38. Jones, L. A. and McLaren, E. *J. Chem. Phys.* **22** (1954) 1796.

39. Ref. 15, pp. 45, 69.
40. Bobtelsky, M. and Bar-Gadda, I. *Anal. Chim. Acta* **9** (1953) 446.
41. Galwey, A. K. *J. Chem. Soc.* **1965** 4235.
42. *Gmelins Handbuch der anorg. Chemie*, 8 Aufl., Eisen, Syst. Nr. 59, Teil B, Liefer. 1, Verlag Chemie, Weinheim 1930, pp. 26, 34, 36, 63, 122–131, 134.
43. Dey, A. K. and Ghosh, S. *J. Ind. Chem. Soc.* **27** (1950) 65.
44. Ref. 42, Liefer. 2, pp. 508, 509, 512.
45. Busing, W. R. and Morgan, H. W. *J. Chem. Phys.* **28** (1958) 998.
46. Lucchesi, P. J. and Glasson, W. A. *J. Am. Chem. Soc.* **78** (1956) 1347.
47. Brink, G. *Spectrochim. Acta* **A 28** (1972) 1151.
48. Miller, F. A. and Wilkins, C. H. *Anal. Chem.* **24** (1952) 1253.
49. Hunt, J. M., Wisherd, M. P. and Bonham, L. C. *Anal. Chem.* **22** (1950) 1478.
50. Brame, E. G., Jr., Margrave, J. L. and Meloche, V. W. *J. Inorg. Nucl. Chem.* **5** (1957) 48.
51. McDevitt, N. T. and Baun, W. L. *Spectrochim. Acta* **20** (1964) 799.
52. Ref. 28, pp. 166, 167.
53. Siebert, H. *Anwendungen der Schwingungsspektroskopie in der anorganischen Chemie*, Springer-Verlag, Berlin 1966, pp. 90–92 and 145.
54. Glemser, O. *Angew. Chem.* **73** (1961) 785.
55. Glemser, O. and Rieck, G. *Z. anorg. allgem. Chem.* **297** (1958) 175.
56. Cannon, C. G. *Spectrochim. Acta* **10** (1958) 341.
57. Maurin, M. *Bull. Soc. Chim. France* **1962** 1497.
58. Schwarzmann, E. *Z. anorg. allgem. Chem.* **317** (1962) 176.
59. Frederickson, L. D., Jr. *Anal. Chem.* **26** (1954) 1883.
60. Glemser, O. and Hartert, E. *Z. anorg. allgem. Chem.* **283** (1956) 111.
61. Braunholtz, J. T., Hall, G. E., Mann, F. G. and Sheppard, N. *J. Chem. Soc.* **1959** 868.
62. Hartert, E. and Glemser, O. *Z. Elektrochem.* **60** (1956) 746.
63. Glemser, O. *Nature* **183** (1959) 1476.
64. Glemser, O. and Hartert, E. *Naturwiss.* **40** (1953) 552.
65. Dupuis, T. *Rec. Trav. Chim.* **79** (1960) 518.
66. Van der Elsken, J. and Robinson, D. W. *Spectrochim. Acta* **17** (1961) 1249.
67. Gamo, I. *Bull. Chem. Soc. Japan* **34** (1961) 760, 765, 1430, 1433.
68. Nakagawa, I. and Shimanouchi, T. *Spectrochim. Acta* **20** (1964) 429.
69. Scargill, D. *J. Chem. Soc.* **1961** 4444.
70. Ferraro, J. R., Driver, R., Walker, W. R. and Wozniak, W. *Inorg. Chem.* **6** (1967) 1586.
71. Hewkin, D. J. and Griffith, W. P. *J. Chem. Soc.* **A 1966** 472.
72. Ref. 15, the spectra N os. 1528–1530.
73. Higashi, K., Hori, K. and Tsuchiya, R. *Bull. Chem. Soc. Japan* **40** (1967) 2569.
74. Hamm, R. E., Johnson, R. L., Perkins, R. H. and Davis, R. E. *J. Am. Chem. Soc.* **80** (1958) 4469.
75. Franco, M. A. A. and Sing, K. S. W. *J. Thermal Anal.* **4** (1972) 47.
76. *Gmelins Handbuch der anorg. Chemie*, 8 Aufl., Chrom, Syst. Nr. 52, Teil B, Verlag Chemie, Weinheim 1962, pp. 8, 9, 11, 13–15, 26–29, 42, 59–60, 64–66, 71–74, 80–81, 90, 95, 99, 100, 103, 105, 107, 113.
77. Benoit, A. *Spectrochim. Acta* **19** (1963) 2011.
78. Ref. 15, the spectrum No. 1515.
79. *Gmelins Handbuch der anorg. Chemie*, 8 Aufl., Aluminium, Syst. Nr. 35, Teil B, Liefer. 1, Verlag Chemie, Weinheim 1933, pp. 102, 107, 114.
80. Napoli, A. and Liberti, A. *Gazz. Chim. Ital.* **100** (1970) 906.
81. Ginsberg, H., Hüttig, W. and Stiehl, H. *Z. anorg. allgem. Chem.* **309** (1961) 233; **318** (1962) 238.
82. Ref. 15, the spectrum No. 1507.

Received January 10, 1973.

ACTA CHEMICA SCANDINAVICA 27 (1973) 2304–2308

Mean Amplitudes of Vibration and Related Quantities for Halo Propiolaldehydes and Propiolic Acid Chloride

ASTRI ROGSTAD[a] and S. J. CYVIN[b]

[a]*Kjemisk institutt, Universitetet i Oslo, Oslo 3, Norway and*
[b]*Institutt for teoretisk kjemi, Norges tekniske høgskole, N-7034 Trondheim, Norway*

The following molecular constants were calculated from spectroscopic data for the halopropiolaldehydes CHOCCCl, CHOCCBr and CHOCCI, and for propiolic acid chloride (CClOCCH): (i) mean amplitudes of vibration, (ii) perpendicular amplitude correction coefficients, and (iii) Bastiansen-Morino linear shrinkage effects. The mean amplitudes were compared with the corresponding values for propiolaldehyde, and characteristic values for some distance types are listed.

Three halopropiolaldehydes have recently been studied spectroscopically.[1] The harmonic force fields previously developed were used to calculate the mean amplitudes of vibration [2] and related quantities, which are reported here. These data are of great interest in gas electron diffraction studies of molecular structures. Similar calculations were also performed for the propiolic acid chloride molecule. They are based on a vibrational assignment of experimental frequencies for this molecule from an original investigation.

HALOPROPIOLALDEHYDES

The halopropiolaldehydes (halopropynals) CHOCCCl, CHOCCBr and CHOCCI have been investigated recently by infrared and Raman spectroscopy.[1] That work includes normal coordinate analyses for the molecules in question, and the main stretching and bending force constants from the developed harmonic force fields are reported. The corresponding vibrational frequencies are shown in Table 1. The force fields were used to calculate the mean amplitudes of vibration (u) and perpendicular amplitude correction coefficients (K),[2] which are given in Tables 2, 3, and 4 for the chloro-, bromo-, and iodo compound, respectively. The interatomic separations (R) are included in these tables. They give implicit information on the structural parameters applied in the analysis. The Bastiansen-Morino shrinkage effects (δ) for the linear chains in the three halopropiolaldehydes may be obtained very simply from the K values.[2] Their magnitudes are listed in Table 5.

Table 1. Vibrational frequencies (cm^{-1}) for chloro-, bromo-, and iodopropiolaldehyde and for propiolic acid chloride.

Species	CHOCCCl	CHOCCBr	CHOCCI	CClOCCH
a′	2860	2858	2850	3326
	2220	2196	2159	2132
	1694	1692	1676	1767
	1387	1386	1385	1003
	1077	1030	1005	696
	738	691	670	655
	473	395	360	482
	312	290	276	414
	114	105	107	157
a″	945	950	960	703
	352	340	330	665
	152	143	131	224

PROPIOLIC ACID CHLORIDE (PROPIOLYL CHLORIDE)

A normal coordinate analysis was performed for the CClOCCH molecule on the basis of the vibrational assignment of experimental frequencies shown in Table 1. These values are gas infrared frequencies, which have not been published previously. A detailed report on the experimental work is to be communicated later. The developed harmonic force field was used to calculate the u and K values with the results given in Table 6. The linear shrinkage effects are shown in Table 7.

Table 2. Mean amplitudes of vibration (u) and perpendicular amplitude correction coefficients (K) for chloropropiolaldehyde, CHOCCCl.

Distance	(R, Å)	u, Å		K, Å	
		$T=0$	298 K	$T=0$	298 K
C_1-H	(1.080)	0.080	0.081	0.019	0.027
$C_1=O$	(1.210)	0.041	0.042	0.003	0.007
C_1-C_2	(1.460)	0.049	0.051	0.005	0.011
$C_2\equiv C_3$	(1.204)	0.036	0.037	0.006	0.009
C_3-Cl	(1.628)	0.038	0.039	0.006	0.018
$C_1\cdots C_3$	(2.664)	0.052	0.055	0.004	0.010
$C_2\cdots Cl$	(2.832)	0.043	0.044	0.002	0.006
$C_1\cdots Cl$	(4.292)	0.054	0.058	0.000_3	0.000_5
$O\cdots H$	(1.984)	0.098	0.100	0.010	0.020
$C_2\cdots H$	(2.208)	0.098	0.100	0.014	0.029
$C_3\cdots H$	(3.338)	0.108	0.111	0.009	0.022
$Cl\cdots H$	(4.922)	0.114	0.130	0.003	0.005
$C_2\cdots O$	(2.316)	0.059	0.066	0.003	0.009
$C_3\cdots O$	(3.433)	0.066	0.082	0.003	0.008
$Cl\cdots O$	(5.008)	0.071	0.108	0.000_1	0.000_2

Table 3. Mean amplitudes of vibration (u) and perpendicular amplitude correction coefficients (K) for bromopropiolaldehyde, CHOCCBr.

Distance	(R, Å)	u, Å		K, Å	
		$T=0$	298 K	$T=0$	298 K
C_1-H	(1.080)	0.080	0.081	0.020	0.031
$C_1=O$	(1.210)	0.040	0.041	0.003	0.008
C_1-C_2	(1.460)	0.049	0.050	0.005	0.013
$C_2\equiv C_3$	(1.204)	0.036	0.037	0.006	0.010
C_3-Br	(1.793)	0.039	0.042	0.005	0.015
$C_1\cdots C_3$	(2.664)	0.052	0.054	0.004	0.013
$C_2\cdots Br$	(2.997)	0.043	0.046	0.002	0.005
$C_1\cdots Br$	(4.457)	0.052	0.060	0.000_2	0.000_4
$O\cdots H$	(1.984)	0.098	0.099	0.011	0.024
$C_2\cdots H$	(2.208)	0.098	0.099	0.016	0.035
$C_3\cdots H$	(3.338)	0.108	0.112	0.011	0.027
$Br\cdots H$	(5.084)	0.115	0.134	0.004	0.007
$C_2\cdots O$	(2.316)	0.058	0.065	0.004	0.011
$C_3\cdots O$	(3.433)	0.066	0.081	0.003	0.011
$Br\cdots O$	(5.169)	0.069	0.110	0.000_1	0.000_3

Table 4. Mean amplitudes of vibration (u) and perpendicular amplitude correction coefficients (K) for iodopropiolaldehyde, CHOCCI.

Distance	(R, Å)	u, Å		K, Å	
		$T=0$	298 K	$T=0$	298 K
C_1-H	(1.080)	0.080	0.080	0.020	0.034
$C_1=O$	(1.210)	0.040	0.041	0.003	0.008
C_1-C_2	(1.460)	0.048	0.050	0.005	0.014
$C_2\equiv C_3$	(1.204)	0.037	0.037	0.006	0.010
C_3-I	(1.991)	0.042	0.047	0.004	0.013
$C_1\cdots C_3$	(2.664)	0.051	0.054	0.005	0.014
$C_2\cdots I$	(3.195)	0.045	0.051	0.002	0.004
$C_1\cdots I$	(4.655)	0.053	0.063	0.000_3	0.000_6
$O\cdots H$	(1.984)	0.098	0.099	0.012	0.027
$C_2\cdots H$	(2.208)	0.098	0.099	0.017	0.040
$C_3\cdots H$	(3.338)	0.108	0.111	0.012	0.031
$I\cdots H$	(5.279)	0.115	0.134	0.004	0.008
$C_2\cdots O$	(2.316)	0.057	0.063	0.004	0.011
$C_3\cdots O$	(3.433)	0.066	0.081	0.003	0.011
$I\cdots O$	(5.363)	0.068	0.109	0.000_1	0.000_4

DISCUSSION OF THE MEAN AMPLITUDES

All of the four molecules studied display very similar magnitudes of mean amplitudes for corresponding distance types. This feature might be expected *a priori* and supports the reliability of the analysis. The present results are

Table 5. Linear shrinkage effects (δ) for the halopropiolaldehydes CHOCCCl, CHOCCBr, and CHOCCI.

Molecule	Distance	δ, Å	
		$T=0$	298 K
CHOCCCl	$C_1\cdots C_3$	0.007	0.010
	$C_2\cdots Cl$	0.010	0.021
	$C_1\cdots Cl$	0.017	0.038
CHOCCBr	$C_1\cdots C_3$	0.007	0.011
	$C_2\cdots Br$	0.009	0.021
	$C_1\cdots Br$	0.016	0.038
CHOCCI	$C_1\cdots C_3$	0.007	0.011
	$C_2\cdots I$	0.009	0.019
	$C_1\cdots I$	0.016	0.038

Table 6. Mean amplitudes of vibration (u) and perpendicular amplitude correction coefficients (K) for propiolic acid chloride, CClOCCH.

Distance	(R, Å)	u, Å		K, Å	
		$T=0$	298 K	$T=0$	298 K
C_1-Cl	(1.789)	0.045	0.047	0.002	0.003
$C_1=O$	(1.192)	0.039	0.039	0.003	0.004
C_1-C_2	(1.426)	0.049	0.051	0.003	0.003
$C_2\equiv C_3$	(1.205)	0.036	0.036	0.007	0.014
C_3-H	(1.060)	0.074	0.074	0.033	0.046
$C_1\cdots C_3$	(2.631)	0.053	0.055	0.002	0.004
$C_2\cdots H$	(2.265)	0.079	0.079	0.022	0.040
$C_1\cdots H$	(3.691)	0.088	0.089	0.011	0.021
$O\cdots Cl$	(2.602)	0.055	0.063	0.000_7	0.002
$C_2\cdots Cl$	(2.683)	0.057	0.070	0.001	0.003
$C_3\cdots Cl$	(3.708)	0.076	0.116	0.000_4	0.000_7
$H\cdots Cl$	(4.681)	0.126	0.177	0.007	0.011
$C_2\cdots O$	(2.346)	0.054	0.056	0.002	0.004
$C_3\cdots O$	(3.482)	0.060	0.069	0.001	0.002
$H\cdots O$	(4.511)	0.102	0.115	0.008	0.014

Table 7. Linear shrinkage effects (δ) for propiolic acid chloride, CClOCCH.

Distance	δ, Å	
	$T=0$	298 K
$C_1\cdots C_3$	0.007	0.013
$C_2\cdots H$	0.018	0.020
$C_1\cdots H$	0.031	0.043

Table 8. Characteristic values of mean amplitudes at 298 K from the present calculations.

Distance type	u, Å
C – H(aldehyde)	0.080 – 0.081
C – H(ethynyl)	0.074
C≡C	0.036 – 0.037
C – C	0.050 – 0.051
C = O	0.039 – 0.042
$C_1 \cdots C_3$	0.053 – 0.055
$C_2 \cdots O$	0.06 – 0.07
$C_3 \cdots O$	0.07 – 0.08

very well consistent with the calculated mean amplitudes for propiolaldehyde (propynal) reported recently.[3]

Some of the characteristic values of mean amplitudes are listed in Table 8. Sugié *et al.*[3] have reported the calculated C – H(aldehyde) and C – H(ethynyl) mean amplitudes in CHOCCH at 20°C equal to 0.0797 Å and 0.0742 Å, respectively. These values are seen to be consistent with those listed in Table 8. This is also the case for [3] u(C≡C) = 0.0363 Å, and approximately for [3] u(C – C) = 0.0476 Å, u(C = O) = 0.0385 Å and $u(C_1 \cdots C_3) = 0.0513$ Å. For $u(C_2 \cdots O)$ in CHOCCH Sugié *et al.*[3] have calculated the value of 0.0572 Å (20°C) being similar to the present value of 0.056 Å (25°C) in CClOCCH. In the halopropiolaldehydes the corresponding values are slightly higher, *viz.* 0.063 – 0.066 Å. For $u(C_3 \cdots O)$ on the other hand Sugié *et al.*[3] give the relatively high value of 0.0858 Å (20°C), which is slightly above the characteristic value for the halopropiolaldehydes, *viz.* 0.081 – 0.082 Å at 25°C. In CClOCCH the corresponding value is somewhat lower, *viz.* 0.069 Å.

Sugié *et al.*[3] have deduced mean amplitudes of vibration for CHOCCH from electron diffraction data and found good agreement with the spectroscopic values. No electron diffraction mean amplitudes are available so far for the molecules of the present study.

REFERENCES

1. Lagset, E., Klaboe, P., Kloster-Jensen, E., Cyvin, S. J. and Nicolaisen, F. M. *Spectrochim. Acta* **A 29** (1973) 17.
2. Cyvin, S. J. *Molecular Vibrations and Mean Square Amplitudes*, Universitetsforlaget, Oslo, and Elsevier, Amsterdam 1968.
3. Sugié, T., Fukuyama, T. and Kuchitsu, K. *J. Mol. Structure* **14** (1972) 333.

Received February 26, 1973.

ACTA CHEMICA SCANDINAVICA 27 (1973) 2309–2320

On the Crystal Structure of $[Pb_4(OH)_4]_3(CO_3)(ClO_4)_{10}.6H_2O$

SAM-HYO HONG and ÅKE OLIN

Institute of Chemistry, University of Uppsala, S-751 21 Uppsala, Sweden

The crystal structure of $[Pb_4(OH)_4]_3(CO_3)(ClO_4)_{10}.6H_2O$ has been determined from three-dimensional X-ray data. The crystals are hexagonal and the space group is $P6_3/m$. The unit cell contains two formula units (24 lead atoms) and has the dimensions: $a=b=14.121\pm0.003$ Å and $c=16.316\pm0.006$ Å.

The crystals contain discrete $[Pb_4(OH)_4^{4+}]$-units. The four lead atoms occupy the corners of a slightly distorted tetrahedron and the hydroxide groups are located outside the faces of this tetrahedron. The unit is probably closely related to one of the main species formed in hydrolyzed lead(II)perchlorate solutions.

Complex formation between Pb^{2+} and OH^- in the acid and neutral pH-range yields two main species. The composition and structure of one of these species, $[Pb_6O(OH)_6]^{4+}$, is well established by the combined results from the crystal structure determinations [1,2] of the two known polymorphs of $[Pb_6O(OH)_6](ClO_4)_4.H_2O$ and an X-ray scattering study [3] on hydrolyzed lead(II)perchlorate solutions. The six lead atoms in the complex occupy the corners of three distorted tetrahedra connected by common faces. There is an oxygen atom at the center of the central tetrahedron and an hydroxide oxygen outside each of the six unshared faces of the outer tetrahedra.

The other complex formed has been shown from emf measurements [4] to contain four lead atoms and its composition is usually written $Pb_4(OH)_4^{4+}$. X-Ray scattering measurements [3,5] on solutions containing this complex indicate that the lead atoms are at the corners of a tetrahedron. The hydroxide groups have been assumed to be situated outside the faces of the Pb_4-tetrahedron. Since emf measurements at constant water activity cannot differentiate between two OH^- and one O^{2-} some uncertainty exists as to the exact formula and structure of the complex.

There have been no crystal structure determinations made on solids formed from solutions containing $Pb_4(OH)_4^{4+}$. Several such solids have been described [6,7] but the compound $[Pb_4(OH)_4]_3(CO_3)(ClO_4)_{10}.6H_2O$ whose crystal structure is reported in this paper has apparently not been prepared before.

EXPERIMENTAL

Preparation, description and analysis of the crystals

Crystals of the compound $[Pb_4(OH)_4]_3(CO_3)(ClO_4)_{10}.6H_2O$, henceforth for convenience called *A*, were incidently obtained in experiments which aimed at the preparation of $PbOHClO_4$ from hydrolyzed lead(II) perchlorate solutions. In some of these solutions, which were not sufficiently concentrated for $PbOHClO_4$ to crystallize, *A* was formed in small amounts on long standing. No method of preparation, which gave good yields, was found even when it later became obvious that the crystals contained carbonate. The following recipe may, however, be given. 0.2 mol of PbO is dissolved in 0.28 mol of $HClO_4$ and the resulting solution diluted to 50 cm^3 and filtered. No precaution should be taken to exclude the carbon dioxide of the air during these operations. On standing in a closed vessel, crystals of *A* are formed after a couple of weeks. They consist of transparent, hexagonal prisms terminated by pyramidal faces, $\{10\bar{1}1\}$, and are not changed in contact with the atmosphere.

The lead content of the compound was determined by evaporation with H_2SO_4 and weighing the residue as $PbSO_4$. The number of basic groups was found by a potentiometric titration with standard $HClO_4$ in the following way. A known amount of the solid was added to a known volume of water. The acid was then gradually added, allowing sufficient time for it to react with the solid. The emf's beyond the equivalence point, where all the solid had disappeared, were used to determine this point by a Gran extrapolation. The analytical results obtained were: Pb 64.58 %; mol H^+ consumed/mol Pb 1.17. Calculated values for $[Pb_4(OH)_4]_3(CO_3)(ClO_4)_{10}.6H_2O$:Pb 64.54 %; mol H^+ consumed/mol Pb 1.17.

When *A* was dissolved in acid, whilst observing the process under the microscope, gas bubbles (CO_2) were seen. It was left as a matter for the structure analysis to determine how many of the basic groups that were carbonate groups.

X-Ray diffraction measurements

The space group was determined from oscillation and equi-inclination Weissenberg photographs. The unit cell dimensions were calculated from 59 indexed lines on a powder photograph talen with a Guinier-Hägg focussing camera using Cr$K\alpha_1$ ($\lambda = 2.28962$ Å)[8] with silicon ($a = 5.4305$ Å)[9] as internal standard.

The intensity data were collected with a Stoe Weissenberg diffractometer using Ni-filtered Cu$K\alpha$ radiation and equi-inclination geometry. The crystals were rotated about the *c*-axis. The diffractometer, which is paper-tape controlled, was programmed to collect the data as if the crystal was monoclinic ($\beta = 120°$). Thus each independent reflection was recorded three times. The scan rate varied from 0.25°/min for the weakest to 4°/min for the strongest reflections. The angle scanned was 1° for the lowest values of *l* and then gradually increased to 1.4°. The background was measured for 30 sec at the beginning and at the end of the scan interval. The data were corrected for background and converted to the standard scan rate 1°/min. In the calculations of the corrected intensities, *I*, and their standard deviations, $\sigma(I)$, the expressions presented in Ref. 2 were used. 1414 independent reflections were measured from 14 layers. A new crystal was used for each layer in order to avoid the introduction of a correction for the decomposition of the crystals in the X-ray beam. Inter-layer scale factors, which should take account of the different crystal sizes, were obtained from measurements of three "standard reflections" chosen from the zero-layer. These measurements were done twice, once before and once after the data had been collected for a layer. When these experimental scale factors were refined at the end of the least squares treatment of the data, it was found that they changed by less than 5 %.

An *I*-value is generally based on the mean of the three measurements of a reflection as described above. $|F|$- and $\sigma(F)$-values were calculated from *I*- and $\sigma(I)$-values by applying absorption, Lorentz and polarization corrections. The linear absorption coefficient is estimated to be 738 cm^{-1}. It was therefore necessary to use small crystals. Very small crystals, besides being difficult to handle, had less welldeveloped faces and were

unsuitable for that reason. The crystals used were ca 0.1 mm long and had a very regular hexagonal cross-section. The distance between the $\{10\bar{1}0\}$ faces was 0.04 mm.

Computation

The main programs used in this work were CELSIUS, DRF, LALS (UPALS), DISTAN, and ORTEP: The calculations have been performed on the CDC 3600, IBM 370/155 and 1800 computers in Uppsala. The atomic scattering factors were taken from Hanson *et al.*[10] and the real part of the dispersion correction [11] was introduced.

CRYSTAL DATA

Formula unit:	$[Pb_4(OH)_4]_3(CO_3)(ClO_4)_{10}.6H_2O$
Diffraction symmetry:	$6/m$
Crystal system:	hexagonal
Lattice parameters (σ):*	$a=b=14.121(1)$ Å
	$c=16.316(2)$ Å
	$V=2818$ Å^3
Density (measured):	4.54(2) g cm^{-3}
Number of formula units per unit cell:	2
Density (calculated):	4.541 g cm^{-3}
Linear absorption coefficient:	738 cm^{-1}
Systematic absences:	$00l$ for $l=2n+1$
Space group:	$P6_3/m$ or $P6_3$
Coordinates of equivalent positions:	$P6_3$: x,y,z; $-y$, $x-y$, z; $y-x$, $-x,z$; $-x$, $-y$, $1/2+z$; y, $y-x$, $1/2+z$; $x-y$, x, $1/2+z$
	$P6_3/m$: Above plus centrosymmetric positions

DETERMINATION OF THE STRUCTURE

A rather detailed description of the structure determination will be given since some uncertainty as to the correct space group arose during this part of the work. Furthermore the exact composition of the compound had to be established from the structure determination as this was not possible from the chemical analysis alone.

From a three-dimensional Patterson synthesis one set of lead atoms was found to occupy a general twelve-fold position and two other sets to occupy two special six-fold positions in the mirror plane of the assumed space group, $P6_3/m$. After refinement of these positions the chlorine atoms were next located from a ΔF synthesis. The positions found have the following notations in $P6_3/m$: 12(i) x,y,z; 4(f) 1/3, 2/3, z; 2(d) 1/3, 2/3, 3/4, and 2(b) 0, 0, 0. Thus all of the twenty chlorine atoms have been located. The last two positions are, however, not consistent with the geometry of the perchlorate group. For

* Estimated standard deviations here and elsewhere in the paper refer to the least significant digits.

instance the latter position is at a center of symmetry. This symmetry element is not present in the perchlorate ion.

The symmetry was therefore lowered and the space group was assumed to be $P6_3$, *i.e.* the center of symmetry was removed. After the lead atom positions had been refined in this space group, they were used to calculate difference syntheses from which all the lighter atoms were located. These atoms were found to take up nearly centrosymmetric positions. The light atom parameters did, however, not refine properly. The B-values of several pairs of nearly centrosymmetric atoms moved in different directions ending in one low and one high value. A few B-values even became negative. This behaviour is probably not caused by poor data, since each $|F|$-value is based on the mean of three I-values, which very seldom differed by more than $3\sigma(I)$ or $0.05I$ from the mean. The space group $P6_3$ was abandoned and an approximate structure solution with two disordered perchlorate groups was sought in the higher space group.

From the difference syntheses calculated in $P6_3/m$ the following assignments beside the perchlorate oxygens were made. Four well-defined maxima were assigned to oxygens bound to lead. A peak in the special position 0, 0, $-1/4$ was assigned to the carbon atom and an adjacent peak also on the mirror plane to an oxygen atom in a carbonate group. The two other oxygen atoms in the carbonate group are generated from this atom by the symmetry operations. There would then be two carbonate groups in the unit cell. Since the chemical analysis had shown that the number of equivalents of acid consumed per mol of Pb was $1.17 = 7/6$, the number of base equivalents per unit cell is 28. The CO_3^{2-}-groups take care of 4 of these leaving 24, which fit in if the 24 oxygens bound to lead are hydroxide oxygens.

Only one peak now remained to be assigned. It was assumed to be due to a water molecule. No chemical analysis for water has been made, but the assumption is supported by the lead analysis. The calculated lead content of the material is 66.39 % without any water included. With the amount of water of crystallization indicated by the structure analysis it is 64.58 %. The experimental value is 64.54 %, which thus is in very close agreement with the expected value for the hypothesis advanced.

The later ΔF syntheses also showed that the chlorine atom, which had originally been placed at 1/3, 2/3, 3/4, was better approximated by two half chlorine atoms slightly off the mirror plane. The structure would then be disordered with respect to this chlorine atom and to the oxygen atoms of the perchlorate group at the origin.

In the final refinements data with $|F| < 3\sigma(F)$ were excluded and the weight, w, was calculated as $w^{-1} = \sigma^2(F) + (kF)^2$ and $w(|F_o| - |F_c|)^2$ minimized. k was varied until $w(|F_o| - |F_c|)^2$ did not show a systematic trend with $|F_o|$. The value of k used in the final cycles was 0.05 and the estimated standard deviation of an observation of unit weight was 1.10. No correction for extinction was introduced. The refinement was continued until the shifts, with few exceptions, were less than 0.2σ. The R-value ($R = \sum||F_o| - |F_c||/\sum|F_o|$) became 0.060 for the 1095 reflections with $|F_o| > 3\sigma(F)$. The final parameters are listed in Table 1 with the following exceptions. O(42) was found to oscillate and its z-coordinate was therefore so fixed that the Cl(4) – O(42) distance became

Table 1. Final positional and thermal parameters with standard deviations (σ) within parenthesis.

Atom	x	y	z	B (Å^2)
Pb(1)	0.22033(14)	0.22285(14)	−0.13474(10)	
Pb(2)	0.44783(12)	0.21413(13)	−1/4	See below
Pb(3)	0.42327(13)	0.47349(13)	−1/4	
O(1)	0.2611(18)	0.1460(19)	−1/4	2.8(4)
O(2)	0.2427(17)	0.3329(17)	−1/4	2.0(4)
O(3)	0.4191(14)	0.3282(14)	−0.1668(11)	3.3(3)
O(4)	0.1309(22)	0.6696(22)	−0.0978(16)	7.0(6)
C(1)	0	0	−1/4	2.1(9)
O(5)	0.0422(25)	0.1099(24)	−1/4	4.5(6)
Cl(1)	0.3335(5)	0.3272(5)	0.0928(5)	2.8(1)
O(11)	0.3233(40)	0.2559(40)	0.1530(28)	13.8(13)
O(12)	0.2358(25)	0.3288(25)	0.0803(18)	8.3(7)
O(13)	0.4098(50)	0.4277(47)	0.1168(34)	16.3(17)
O(14)	0.3713(38)	0.3093(38)	0.0195(27)	13.3(13)
Cl(2)	1/3	2/3	0.0632(7)	2.7(2)
O(21)	0.4242(19)	0.6631(20)	0.0346(13)	5.9(5)
O(22)	1/3	2/3	0.1519(22)	5.2(8)
Cl(3)	0	0	0	3.7(3)
O(31)	0.0946(42)	0.0017(41)	−0.0376(29)	6.6(11)
O(32)	0	0	0.090(−)	10.5(32)
Cl(4)	1/3	2/3	−0.2296(12)	2.9(4)
O(41)	0.4462(25)	0.7119(24)	−1/4	4.7(6)
O(42)	1/3	2/3	−0.141(−)	8.9(23)

Coefficients ($\times 10^4$) in the expression exp $-(B_{11}hh+...+2B_{12}hk+...)$ for the anisotropic temperature factors for lead.

Atom	B_{11}	B_{22}	B_{33}	B_{12}	B_{13}	B_{23}
Pb(1)	118(1)	123(2)	43(3)	92(1)	45(1)	42(1)
Pb(2)	44(1)	52(1)	44(3)	31(1)	0	0
Pb(3)	48(1)	34(1)	61(3)	13(1)	0	0

1.45 Å. One of the perchlorate oxygens, O(32), with a bond length differing by more than 0.1 Å from the expected value was moved to the positions indicated by the ΔF map. The C−O bond length in the carbonate group was 1.36 Å ($3\sigma = 0.08$ Å) with the oxygen position obtained from the least squares treatment. With the oxygen atom coordinates from the ΔF synthesis it was 1.31 Å. Since this value is closer to the value (1.294 Å) [13] expected for a free carbonate ion, the latter set of coordinates was accepted. The R-value was unaffected by these changes. The observed and with the parameters in Table 1 calculated structure factors are given in Table 2. The final ΔF synthesis showed 25 peaks with heights greater than 1 $e^-/Å^3$. The largest values, slightly less than 2 $e^-/Å^3$, were found close to the lead and one of the oxygen atoms. The last atom, O(13), was originally located from a rather broad peak with a peak height of *ca.* 4 $e^-/Å^3$.

Table 2. Observed and calculated structure factors. Columns are in order h, k, $10F_o$, $10F_c$. Reflexions with $|F_o| < 3\sigma(F)$ are not included. Reflexions with $0.5 < F_o/F_c > 1.5$ are marked with an asterisk.

H,K,0

1	0	1842	1734
1	1	2404	2402
1	2	2902	2761
1	3	404	575
1	4	2757	2491
1	5	1824	1846
1	6	1595	1543
1	7	549	408
1	8	1624	1647
1	9	1295	1275
1	10	1053	925
1	11	701	799
1	12	869	845
2	0	763	851
2	1	499	374
2	2	925	837
2	3	1230	1365
2	4	3525	3449
2	5	1016	972
2	6	1455	1499
2	7	1865	1858
2	8	2396	2383
2	9	1609	1679
2	11	975	1041
2	12	1707	1710
3	0	2285	2282
3	1	2046	2052
3	2	2776	2911
3	3	456	879
3	4	2999	2957
3	5	853	967
3	6	437	175*
3	10	1114	1077
3	11	723	794
4	0	7460	8417
4	1	5554	5711
4	2	821	785
4	3	493	579
4	4	2003	1945
4	5	6036	6117
4	6	506	499
4	7	1283	1290
4	8	664	604
4	9	1978	1928
5	0	5680	5717
5	1	2679	2694
5	2	2575	2728
5	3	1748	1751
5	4	3777	3734
5	5	1691	1512
5	7	2176	2219
5	8	2325	2325
5	9	1072	1185
5	10	571	467
6	0	684	462
6	1	2993	3215
6	2	1893	1853
6	3	1836	1811
6	4	1249	1283
6	5	1150	1137
6	6	1448	1336
6	7	1420	1468
7	0	1836	1700
7	1	762	505
7	2	2924	3071
7	3	985	1008
7	4	1431	1481
7	5	694	704
7	6	698	618
7	7	1230	1170
7	8	434	155*
8	1	2000	1962
8	3	1168	1213
8	5	1442	1392
8	6	417	283
8	7	442	498
9	0	6173	6194
9	1	591	399
9	2	2108	2241
9	4	1733	1705
9	5	639	682
10	1	962	942
10	2	445	310
10	3	398	328
10	4	2000	1932
10	5	356	3*
11	0	1020	1024
11	1	1480	1394
11	2	1932	1854
11	3	924	851
11	4	1138	1095
12	0	875	747
12	1	772	691
13	0	1255	1335
13	1	614	655

H,K,1

1	0	1368	1333
1	1	3786	3953
1	2	1804	1774
1	3	1315	1383
1	4	3738	3667
1	5	2514	2468
1	7	1876	1808
1	8	1018	1002
1	9	731	791
1	11	1459	1482
1	13	880	842
2	0	1622	1574
2	1	3668	3624
2	2	3843	3747
2	3	3313	3340
2	4	1800	1794
2	5	2054	2088
2	6	4246	4179
2	7	2045	2106
2	8	1494	1531
2	10	1511	1491
2	12	1013	1027
2	13	738	597
3	0	4792	5056
3	1	5691	6099
3	2	2254	2162
3	3	3435	3290
3	4	5624	5871
3	6	882	915
3	7	2188	2246
3	8	1819	1779
3	9	2361	2414
3	10	792	887
3	12	486	524
4	0	997	1059
4	1	1422	1335
4	2	2694	2773
4	4	726	733
4	7	648	598
5	0	1759	1676
5	1	444	359
5	2	2394	2432
5	3	1698	1832
5	5	714	816
5	7	709	706
5	8	483	541
5	9	767	758
5	10	588	595
5	11	495	549
6	0	614	664
6	1	2203	2174
6	2	1108	1030
6	3	2199	2189
6	4	1526	1581
6	5	1384	1293
6	6	2061	2007
6	9	1819	1672
7	0	1273	1202
7	1	2763	2740
7	2	1345	1348
7	3	2539	2443
7	4	539	418
7	5	1489	1494
7	6	1630	1736
7	7	2265	2274
7	9	1091	1023
8	0	3363	3436
8	1	2003	1968
8	2	1566	1453
8	3	1321	1322
8	4	2192	2161
8	5	1128	1225
8	6	643	611
8	7	379	184*
8	8	980	898
9	0	1306	1207
9	1	995	1016
9	2	1675	1687
9	4	833	824
9	5	780	842
10	2	711	757
10	3	1048	994
10	6	393	384
11	0	1331	1375
11	1	893	894
11	2	1213	1282
11	3	764	868
11	4	1141	1068
11	5	316	220
12	0	1648	1651
12	1	760	818
12	3	874	941
13	0	791	741
13	2	457	372

H,K,2

0	1	1428	1430
0	2	1114	1132
0	3	3777	3982
0	4	3437	3546
0	5	1877	1972
0	6	2501	2687
0	7	1018	1055
0	8	1397	1386
0	9	1269	1376
0	10	939	921
0	11	972	848
0	12	913	916
1	1	1341	1297
1	2	474	489
1	3	1692	1612
1	4	529	477
1	5	520	154*
1	8	457	444
1	9	478	466
1	10	976	835
1	12	654	591
2	1	2073	2093
2	2	1285	1314
2	3	435	331
2	4	1181	1306
2	5	1778	1902
2	6	577	454
2	7	559	548
2	8	1795	1880
2	9	918	779
2	10	1002	869
2	12	987	975
2	13	615	583
3	1	2974	3178
3	2	1474	1546
3	3	1951	1699
3	4	2820	2841
3	5	1288	1192
3	6	1517	1477
3	7	993	980
3	8	1278	1274
3	9	1609	1558
3	10	1010	958
3	12	1501	1516
4	1	1936	1835
4	2	1212	1151
4	3	1772	1789
4	4	501	525
4	5	2818	2719
4	6	1052	1082
4	7	1413	1470
4	8	1197	1371
4	9	598	492
4	10	705	777
5	1	2209	2154
5	2	1301	1130
5	3	2332	2411
5	4	1884	1776
5	5	512	364
5	7	1791	1791
5	8	1493	1481
5	9	654	542
5	11	386	398
6	1	4515	4490
6	3	674	757
6	4	1180	1278
6	5	1562	1505
6	6	1183	1246
6	7	537	505
	9	811	837
6	10	870	884
7	1	568	578
7	2	2188	2116
7	4	1202	1228
7	5	691	704
7	6	507	450
7	7	652	442
7	9	460	489
8	1	745	792
8	3	1936	1818
8	4	538	615
8	6	549	420
8	7	896	874
8	8	337	231
9	1	521	489
9	2	1397	1423
9	3	1395	1315
9	4	691	707
9	6	840	886
9	7	496	630
10	1	654	672
10	4	1343	1278
10	6	1273	1277
11	1	1664	1685
11	2	1314	1293
11	4	984	974
11	5	423	390
12	1	953	910
12	2	502	598
12	3	342	234

H,K,3

1	0	417	286
1	1	1150	1110
1	2	3645	3740
1	3	1547	1467
1	4	1817	1745
1	5	479	460
1	6	4460	4486
1	7	471	445
1	8	769	750
1	10	1122	1158
1	12	442	582
1	13	649	776
2	0	2729	2591
2	1	3878	4024
2	2	3731	3662
2	3	746	818
2	4	4509	4560
2	5	2195	2232
2	6	1482	1581
2	7	1846	1758
2	8	2339	2288
2	9	539	555
2	11	1194	1306
2	12	512	453
3	0	4444	4663
3	1	4530	4593
3	3	4963	4768
3	4	2243	2248
3	5	1702	1721
3	6	1513	1478
3	7	688	624
3	9	1731	1635
3	10	1038	1034
4	0	1261	1157
4	3	2237	2259
4	4	843	935
4	5	706	680
4	6	840	756
4	7	1433	1374
4	8	1326	1321
4	10	773	772
4	11	720	717
5	0	1372	1322
5	1	1645	1854
5	2	2407	2406
5	3	1473	1522
5	5	2730	2777
5	6	1440	1440
5	7	723	487
5	9	913	912
5	10	1346	1290
6	0	931	843
6	1	1851	1808
6	2	3119	3024
6	3	1469	1496
6	4	2541	2479
6	5	597	507
6	6	673	474
6	9	1238	1290
7	0	915	874
7	2	1562	1540
7	3	487	294
7	4	2212	2147
7	5	1674	1796
7	6	937	813
7	7	818	847
7	8	1087	1203
8	0	2236	2187
8	1	894	852
8	2	1054	1082
8	3	1399	1339
8	4	1395	1319
8	5	679	535
8	6	763	882
8	7	799	842
9	0	1260	1200
9	1	1598	1598
9	2	554	702
9	3	489	641
9	4	1239	1171
9	5	1274	1360
9	6	937	831
10	1	779	846
10	2	507	554
10	3	1076	1089
10	4	662	751
11	0	1995	1975
11	1	856	858
11	4	1454	1568
12	0	1432	1417
13	0	642	681

H,K,4

1	0	4242	4485
1	1	2316	2334
1	2	3414	3531
1	3	1995	2020
1	4	4150	3825
1	6	1768	1684
1	7	1523	1434
1	10	1654	1502
1	12	426	587
2	0	3686	3454
2	1	5228	5410
2	2	4847	4639
2	3	2697	2646
2	5	3661	3629
2	6	2548	2571
2	7	987	946
2	10	1725	1799
2	11	793	793
3	0	3084	3099
3	1	3006	3019
3	3	4737	4566
3	4	939	998
3	5	1711	1743
3	6	1265	1248
3	7	2530	2509
3	8	2330	2224
3	9	1540	1435
3	10	844	858
3	12	1738	1835
4	0	1960	2011
4	1	2463	2196
4	2	969	912
4	3	2591	2478
4	4	3009	2982
4	5	449	179*
4	6	1770	1773
4	7	2328	2231
4	8	1551	1621
4	9	782	811
4	10	1261	1389
5	0	2995	2929
5	1	3076	3000
5	2	1042	860
5	3	1945	1886
5	4	1150	1031
5	5	2344	2327
5	7	990	929
5	8	833	840
5	9	474	560
6	0	2861	3024
6	1	5870	5885
6	2	1851	1840
6	3	1277	1275
6	4	1319	1405
6	5	1652	1709
6	6	2088	2180
6	7	516	477
6	9	832	798
6	10	825	1074
7	1	597	567
7	3	1537	1506
7	7	747	698
7	8	682	666
8	0	2558	2570
8	1	566	616
8	2	1504	1429
8	3	2807	2898
8	4	597	684
8	5	580	672
8	7	1431	1441
9	0	1587	1516
9	1	1749	1789
9	2	432	338
9	3	872	824
9	5	1299	1323
9	6	972	961
9	7	482	347
10	0	2119	2233
10	1	1251	1177
10	2	1332	1280
10	4	856	755
10	5	854	884
10	6	1150	1437
11	0	761	720
11	1	2076	2029
11	3	544	511
11	4	764	823
12	0	1191	1146
12	1	921	991
12	2	1022	1019
12	3	680	789
13	0	505	508
14	0	407	517

H,K,5

1	0	1362	1476
1	1	2708	2514
1	2	6359	6660
1	3	2000	1693
1	4	2009	2126
1	6	4509	4399
1	7	2011	1986
1	8	1526	1586
1	9	563	512
1	10	1415	1852
1	11	816	742
1	12	544	650
2	0	1236	1396
2	1	3820	3786
2	2	2658	2665
2	4	4995	5088
2	5	1387	1183
2	6	695	783
2	7	2177	2216
2	8	3003	3064
2	9	791	578
2	11	1007	1123
2	12	811	754
3	0	3728	3841
3	1	2331	2382
3	2	579	386
3	3	5203	5434
3	4	1065	1116
3	5	1466	1479
3	6	1011	1083
3	7	573	503
3	8	1339	1293
3	9	1058	1093
3	10	752	693
4	0	1625	1560
4	3	2809	2810
4	4	1002	833
4	6	994	969
4	7	958	1007
4	8	1402	1387
4	10	510	401
5	0	730	729
5	1	1304	1191
5	2	1641	1619
5	5	1894	1894
5	6	1794	1785
5	7	522	548
5	8	444	173*
5	9	790	877
5	10	1182	1078
6	0	1201	1172
6	1	2783	2877
6	2	3373	3525
6	3	1650	1609
6	4	2203	2163
6	6	868	1026
6	7	1054	1079
6	9	1244	1223
7	0	741	788
7	1	1048	970
7	3	817	720
7	4	1966	1907
7	5	1707	1738
7	6	525	456
7	7	1263	1259
8	0	2282	2304
8	1	862	808
8	3	1450	1513
8	4	490	496
8	5	926	885
8	6	575	475
8	7	1023	1047
9	0	1104	1154
9	1	1672	1608
9	2	1481	1405
9	3	876	797
9	4	1326	1245
9	5	883	833
9	6	878	863
10	0	457	161*
10	1	1593	1543
10	2	968	1169
10	3	890	983
10	5	662	450
11	0	1420	1448
11	1	866	933
11	3	429	333
12	0	1170	1165
13	0	657	731

H,K,6

0	1	2630	2813
0	2	1304	1296
0	3	1022	600
0	4	1558	1258
0	5	1346	1184
0	6	1524	1613
0	8	772	860
0	9	1428	1103
0	10	1991	2051
0	11	1142	1028
1	1	901	833
1	2	473	50*
1	3	1235	1342
1	4	2165	2246
1	5	1134	1102
1	6	534	534
1	7	503	485
1	8	594	564
1	10	453	429
1	12	788	808
2	1	3941	4066
2	2	2098	2000
2	3	978	1001
2	4	1090	1060
2	5	1934	1993
2	6	650	648
2	8	1016	1084
2	9	811	768
2	10	799	869
2	12	645	656
3	1	1858	1847
3	2	1188	1181
3	3	3627	3868
3	4	796	758
3	5	859	905
3	7	1240	1327
3	8	1426	1501
3	10	766	692
3	11	645	537
4	1	1020	822
4	2	662	726
4	3	1984	2110
4	4	1338	1325
4	5	1220	980
4	6	1646	1672
4	7	1317	1320
4	8	429	500
4	9	394	231
4	10	1174	1256
5	1	3161	3385
5	2	377	528
5	3	1433	1429
5	4	433	26*
5	5	1907	1851
5	6	811	804
5	7	1204	1236
5	8	1094	1008
5	9	406	419
6	1	3391	3349
6	2	848	886
6	3	1921	1877
6	4	1834	1826
6	5	672	703
6	6	1912	1973
7	2	901	925
7	3	461	419
7	4	836	743
8	3	2158	2226
8	7	725	870
9	1	1749	1776
9	2	1031	1020
9	4	405	333
9	5	839	945
9	6	559	565
10	2	532	564
10	4	650	624
11	1	1533	1504
11	2	780	766
12	1	660	708
12	2	643	618

H,K,7

0	2	1681	1745
0	3	3355	3333
0	4	1307	1439
0	5	682	417
0	6	700	715
0	7	985	990
0	8	1768	1761
0	9	880	867
0	10	533	386
0	11	1196	1223
0	12	1028	1106
1	1	1697	1558
1	2	291	322
1	3	454	442
1	4	2542	2603
1	5	1935	2074
1	8	1026	970
1	11	727	774
1	12	479	323
2	1	1263	1268
2	2	788	744
2	3	2219	2313
2	4	2521	2646
2	5	1496	1440
2	6	2140	2059
2	7	2553	2550
2	8	1431	1457
2	9	1057	1010
2	10	989	885
2	11	506	510
3	1	3495	3556
3	2	1663	1632
3	3	491	598
3	4	2497	2462
3	6	474	435
3	7	1586	1559
3	8	832	760
3	9	1086	1246
3	10	677	732
3	11	403	327
4	1	1209	1247
4	2	1099	1080
4	3	1444	1294
4	4	372	376
4	5	656	762
4	6	700	656
5	1	478	510
5	2	1412	1362
5	3	1628	1594
5	4	538	389
5	8	395	457
6	1	1060	1083
6	3	1937	2055
6	4	1304	1337
6	5	1209	1149
6	6	1002	892
6	7	668	575
7	1	770	736
7	3	1882	1844
7	5	801	884
7	7	1999	1974
8	1	554	626
8	2	866	857
8	4	1315	1314
8	5	997	1151
9	1	631	436
9	2	1706	1581
9	3	717	590
9	4	921	1018
9	5	598	474
10	2	518	455
10	3	1023	1073
11	2	538	507
11	3	963	961
12	1	510	534

H,K,8

1	0	1072	1236
1	1	1679	1638
1	2	1702	1592
1	4	1358	1201
1	5	460	303
1	6	971	918
1	8	1508	1475

Table 2. Continued.

1	9	819	917	11	0	704	662	8	1	1296	1100	5	2	762	655	7	3	576	425	9	2	441	2*
1	12	706	658	11	1	1077	1087	8	2	1681	1724	5	3	1455	1408	7	5	1227	1148	9	3	416	225
2	0	275	221	11	2	1253	1288	8	3	970	1127	5	4	1707	1740	7	6	1004	1088	10	1	733	602
2	1	411	395					8	4	1703	1700	5	5	1055	1152	8	0	1509	1576	10	2	652	788
2	2	752	653			H,K,9		8	5	421	410	5	7	1284	1292	8	1	1384	1201	11	0	399	56*
2	3	383	263					8	6	534	533	5	8	872	1010	8	4	1033	936				
2	4	1794	1731	1	0	709	836	9	0	761	680	6	1	2083	1981	8	5	443	377			H,K,13	
2	7	1094	1103	1	1	3575	3814	9	1	656	806	6	2	1032	982	9	0	544	507				
2	8	1722	1643	1	2	2613	2582	9	2	793	799	6	3	453	9*	9	1	1049	1103	1	0	339	370
2	9	1004	985	1	3	722	678	9	4	401	401	6	5	957	877	10	1	649	596	1	1	1389	1499
2	10	395	265	1	4	1300	1300	9	5	622	580	6	6	561	386	10	2	405	266	1	2	2528	2525
2	11	636	549	1	5	1750	1625	10	1	681	729	6	7	793	712	11	0	597	607	1	3	975	995
3	0	1476	1297	1	6	972	855	10	2	721	952	7	2	1548	1556					1	4	1021	875
3	1	831	786	1	7	2246	2152	10	3	568	439	7	4	610	749			H,K,12		1	6	2607	2445
3	2	1698	1625	1	9	596	486	11	0	840	829	7	5	623	726					1	7	1177	1204
3	4	1520	1632	1	10	779	690	11	1	796	840	7	6	628	498	1	0	1005	1470	1	10	1138	1129
3	6	979	961	1	11	1390	1448	12	0	573	650	8	1	448	523	1	2	1328	1381	2	0	604	769
3	8	734	636	2	0	607	660	12	0	1094	1057	8	2	575	495	1	3	975	971	2	1	2203	2293
3	9	613	649	2	1	3088	3057					8	4	580	674	1	4	1331	1354	2	2	583	716
3	10	730	867	2	2	1285	1285			H,K,10		9	1	465	386	1	5	586	456	2	3	597	562
4	0	5591	5995	2	3	2498	2411					9	2	812	891	1	6	1169	1152	2	4	2028	2014
4	1	2910	2764	2	5	596	618	0	1	209	286	9	3	1009	1059	1	10	623	609	2	6	591	653
4	2	921	914	2	6	3299	3346	0	2	407	356	10	1	1021	957	2	0	1097	1189	2	7	963	881
4	3	926	971	2	7	1149	1031	0	3	2017	2059	10	3	525	311	2	1	2124	2171	2	8	1707	1766
4	4	1413	1348	2	10	1222	1311	0	4	2736	2643	11	1	660	682	2	2	1152	1129	2	9	496	406
4	5	4007	4045	3	0	2804	2791	0	5	2709	2643					2	3	596	655	3	0	1434	1437
4	6	557	543	3	1	4093	3940	0	6	1121	1046			H,K,11		2	5	1458	1396	3	1	857	847
4	7	617	542	3	2	1875	1772	0	7	1216	1320					2	6	1077	1018	3	2	867	764
4	9	1485	1603	3	3	2131	2038	0	8	899	834	1	0	706	887	2	10	982	888	3	3	2304	2265
5	0	3947	4058	3	4	3870	3793	0	9	1633	1756	1	1	273	290	3	0	528	592	3	5	577	771
5	1	1177	1205	3	5	564	488	0	12	697	698	1	2	1185	1185	3	1	1552	1469	3	6	827	451
5	2	1938	1973	3	6	884	952	1	1	292	167	1	3	563	602	3	3	2775	2522	3	7	1119	976
5	3	891	783	3	7	1850	1837	1	2	1096	973	1	4	840	908	3	4	887	809	3	8	832	841
5	4	3079	3125	3	8	1922	1950	1	3	1079	1223	1	6	1355	1287	3	5	1094	1017	3	9	476	574
5	5	507	438	3	9	1657	1560	1	4	1018	1015	1	7	608	517	3	7	1290	1226	4	0	525	450
5	6	488	504	3	10	645	660	1	5	759	751	1	10	877	752	3	8	720	746	4	1	536	434
5	7	1186	1225	4	0	634	703	1	6	500	640	2	0	612	741	3	9	502	512	4	2	610	454
5	8	1567	1583	4	2	1677	1984	1	8	409	240	2	1	378	397	4	0	1078	982	4	3	1320	1261
5	9	853	1020	4	3	747	725	1	9	522	633	2	2	371	274	4	1	800	769	4	7	440	364
6	0	1688	1774	4	5	435	339	1	10	918	895	2	4	1692	1618	4	2	630	563	4	8	521	524
6	1	1863	1785	5	0	797	862	1	11	451	540	2	5	774	783	4	3	853	799	5	1	1196	1098
6	2	1022	995	5	1	469	166*	2	1	383	109*	2	6	986	1007	4	4	1811	1686	5	2	589	449
6	4	697	719	5	2	1007	951	2	2	416	342	2	8	1118	1092	4	5	476	218*	5	3	1099	18*
6	5	625	677	5	3	1655	1601	2	3	557	410	3	0	2058	2114	4	7	869	922	5	5	513	403
6	6	452	253	5	5	1022	1065	2	4	1193	1159	3	1	2061	2072	4	8	1144	976	5	6	1016	923
6	7	618	691	5	6	547	413	2	5	958	877	3	2	1007	941	5	0	863	884	6	0	719	582
6	8	840	900	5	7	892	832	2	7	986	962	3	3	741	699	5	1	942	839	6	1	1364	1340
7	2	1581	1626	5	9	362	386	2	8	783	851	3	4	2402	2370	5	3	1300	1176	6	2	1760	1908
7	3	690	651	6	0	515	471	2	9	662	680	3	6	1288	1200	5	5	595	584	6	3	853	758
7	4	1172	1175	6	1	2179	2004	2	10	446	330	3	9	1327	1304	5	6	646	676	6	4	1412	1430
7	6	1148	1154	6	2	1139	1175	3	1	1508	1474	4	2	891	1018	5	7	694	542	6	5	463	331
7	7	938	763	6	3	1115	994	3	2	1327	1253	4	3	649	612	6	1	2839	2765	6	6	736	816
8	0	1057	943	6	4	612	638	3	4	2074	2174	4	6	572	442	6	2	962	948	7	1	718	860
8	1	1755	1758	6	5	717	777	3	5	945	938	5	0	744	618	6	3	945	831	7	3	793	689
8	3	1043	986	6	6	1498	1616	3	6	876	799	5	1	777	744	6	4	472	452	7	4	710	714
8	4	572	467	6	7	418	400	3	9	1005	1042	5	2	652	615	6	5	1106	1013	7	5	793	893
8	5	892	910	6	8	390	257	3	10	566	515	5	3	512	469	6	6	1456	1558	8	0	1031	958
8	6	369	329	7	0	729	730	4	1	2350	2220	5	5	1118	1173	7	2	486	278	8	1	468	324
9	0	2921	2949	7	1	2695	2630	4	2	602	587	5	6	1110	1015	7	3	1036	997	8	3	905	987
9	1	458	185*	7	2	995	984	4	3	393	317	6	0	632	492	8	0	1788	1631	9	1	647	427
9	2	1209	1317	7	3	1889	1905	4	5	2190	2360	6	1	757	772	8	1	788	697	10	1	971	920
9	3	614	529	7	5	514	479	4	6	829	763	6	4	1008	947	8	2	885	880				
9	4	1656	1660	7	6	1250	1324	4	8	1243	1209	6	7	375	228	8	3	1281	1176				
9	5	474	613	7	7	1071	1076	4	9	411	517	7	1	839	816	8	4	973	842				
10	4	1055	1181	8	0	1510	1571	5	1	523	496	7	2	1335	1289	9	1	595	572				

DESCRIPTION AND DISCUSSION OF THE STRUCTURE

The lead atoms, Pb(1) – Pb(3), occur in groups of four, which form the corners of a nearly regular tetrahedron. By virtue of the assumed space group this arrangement has a plane of symmetry. Five of the six lead-lead distances are almost equal (*ca.* 3.76 Å) as can be seen from Table 3, whereas the sixth

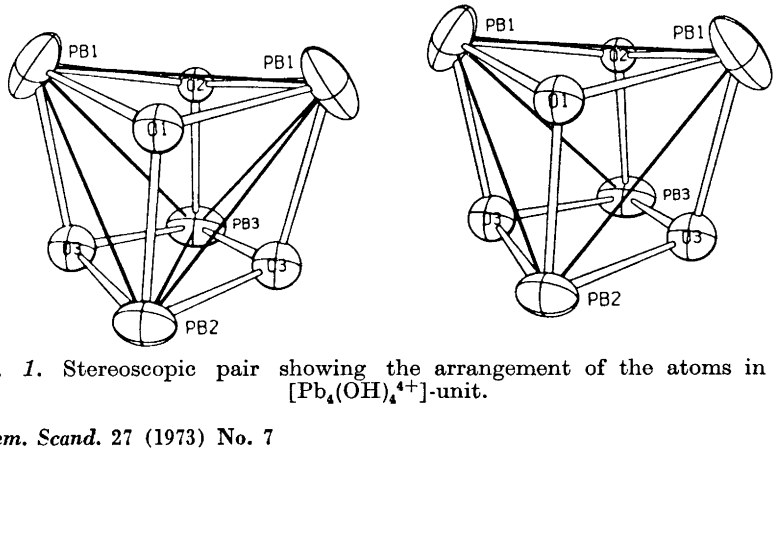

Fig. 1. Stereoscopic pair showing the arrangement of the atoms in the $[Pb_4(OH)_4^{4+}]$-unit.

Table 3. Some distances and angles in the $[Pb_4(OH)_4^{+4}]$-unit.[a]

A. Distances (Å). Standard deviations (σ) within parenthesis.

Atoms	Distance	Atoms	Distance
Pb(1)–Pb(1)′	3.761(3)	Pb(2)–Pb(3)	3.848(2)
–Pb(2)	3.777(2)	–O(1)	2.311(22)
–Pb(3)	3.759(2)	–O(3)	2.293(17)
–O(1)	2.381(14)	Pb(3)–O(2)	2.319(20)
–O(2)	2.358(16)	–O(3)	2.436(17)
–O(3)	2.488(16)		

B. Angles (°). The estimated standard deviation of a Pb–Pb–Pb angle is ± 0.1° and ± 2° of a Pb–O–Pb or O–Pb–O angle.

Atoms	Angle	Atoms	Angle
Pb(1)′–Pb(1)–Pb(2)	60.1	Pb(1)–O(1)–Pb(1)′	104
Pb(1)′– –Pb(3)	60.0	Pb(1)– –Pb(2)	107
Pb(2) – –Pb(3)	61.4		
O(1) – –O(2)	72		
O(1) – –O(3)	69		
O(2) – –O(3)	73		
Pb(1) –Pb(2)–Pb(1)′	59.7	Pb(1)–O(2)–Pb(1)′	106
Pb(1) – –Pb(3)	59.1	Pb(1)– –Pb(3)	107
O(1) – –O(3)	74		
O(3) – –O(3)′	73		
Pb(1) –Pb(3)–Pb(1)′	60.0	Pb(1)–O(3)–Pb(2)	104
Pb(1) – –Pb(2)	59.5	Pb(1)– –Pb(3)	100
O(2) – –O(3)	74	Pb(2)– –Pb(3)	109
O(3) – –O(3)′	68		

[a] Atoms with primed and unprimed symbols are related by the mirror plane at $z = -1/4$.

distance is *ca.* 0.1 Å longer. These values fall within the rather broad range of Pb–Pb distances found in the lead(II) oxides[14,15] and in α- and β-$[Pb_6O(OH)_6](ClO_4)_4.H_2O$.[1,2] There are four hydroxide oxygens, O(1)–O(3), associated with the Pb_4-unit. They are situated outside the four faces of the lead tetrahedron and the whole unit can be written $[Pb_4(OH)_4]^{4+}$, Fig. 1. The lead-oxygen distances are less regular than the Pb–Pb distances and vary between 2.29 and 2.49 Å; see Table 3. Each oxygen atom coordinates three lead atoms and neighbouring lead atoms in the Pb_4-cluster can be considered held together by two hydroxide bridges. It should, however, be noted that each hydroxide group is involved in three bridges. The cluster may be further stabilised by metal-metal bonds as discussed by Maroni and Spiro.[16] The hydroxide oxygens form a somewhat distorted tetrahedron. The six oxygen-oxygen distances lie between 2.72 and 2.87 Å (mean 2.80 Å) indicating van der Waals contacts between these atoms.

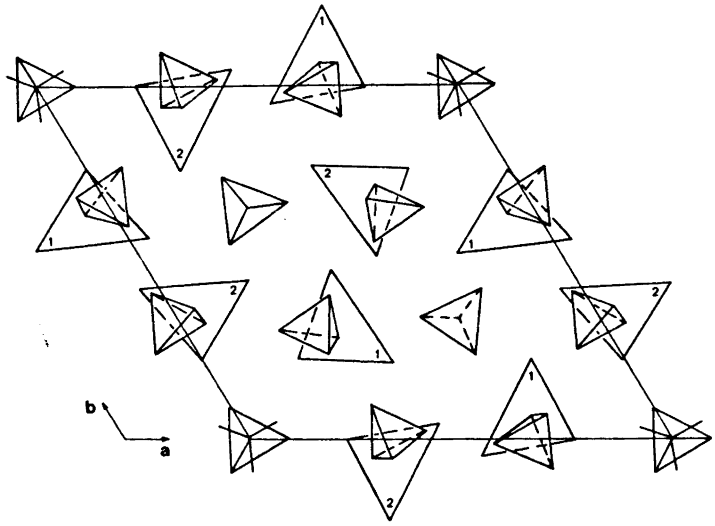

Fig. 2. Projection of the structure of $[Pb_4(OH)_4]_3(CO_3)(ClO_4)_{10}.6H_2O$ along the *c*-axis. For clarity some of the CO_3^{2-} and ClO_4^--groups along the symmetry axes as well as the OH^--groups in the $[Pb_4(OH)_4^{4+}]$-units have been excluded. The Pb_4-units appear as triangles and the units on and around the mirror planes at $z = -1/4$ and $1/4$ are marked with 1 and 2, respectively.

The $[Pb_4(OH)_4^{4+}]$-units are arranged in a pattern resembling hexagonal close-packing, Fig. 2. The shortest Pb–Pb and Pb–OH distances between atoms belonging to different units but in the same layer are 4.40 and 4.51 Å, respectively. The corresponding distances between atoms belonging to different layers exceed 5 Å. Thus, since there is no extended Pb–OH–Pb network in the structure the group $[Pb_4(OH)_4^{4+}]$ definitely occurs as a discrete unit.

The arrangement of the above units leads to "channels" in the structure centered around the axes of symmetry. The unit cell contains two carbonate and twenty perchlorate groups. Of these anions, eight of the perchlorates, $ClO_4(2)$–$ClO_4(4)$, and the two carbonates are found in these channels with the chlorine and carbon atoms situated on the axes. The arrangement of the various groups is indicated in Fig. 2 which is supplemented by Fig. 3, which gives the heights of the atoms along the *c*-axis.

The Cl–O bond lengths in the perchlorate groups are within $2\sigma(\sigma_{max} = 0.05$ Å) equal to the expected value 1.45 Å.[17] The closest distance between a lead atom and a perchlorate oxygen is 2.96 Å. If oxygens closer than 3.25 Å are considered coordinated, the coordination numbers towards the perchlorate oxygens are five, four, and four for Pb(1), Pb(2), and Pb(3), respectively. The perchlorate group in general position, $ClO_4(1)$, is situated in a "tetrahedral hole" in the arrangement of the Pb_4-groups and is coordinated to the four surrounding Pb_4-groups. $ClO_4(3)$, which is in an "octahedral hole", is coordinated to six such groups. $ClO_4(2)$ and (4) are coordinated to only three

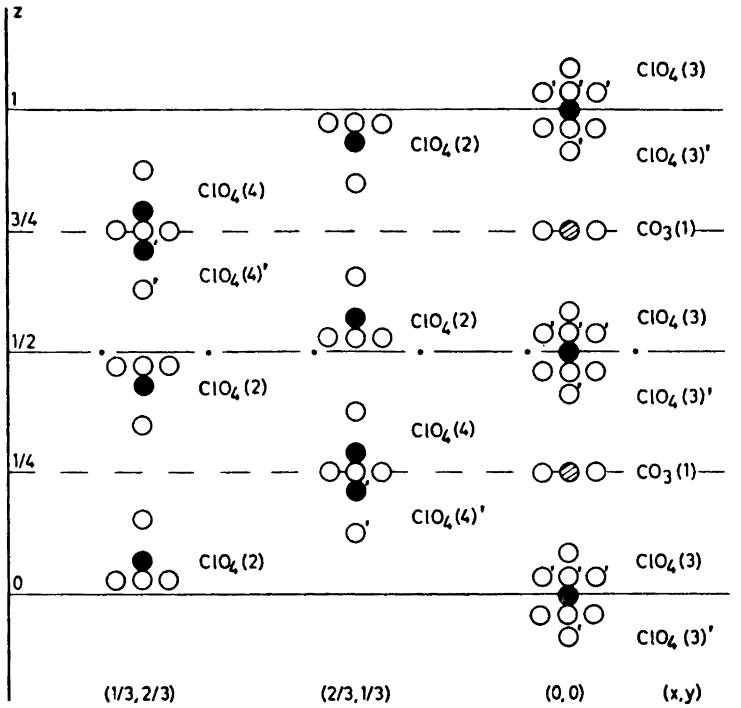

Fig. 3. Arrangement of the anions along the symmetry axes. Alternative positions are primed. O oxygen, ● chlorine, ● carbon.

groups and here O(21) and O(42) are uncoordinated. The closest distances between the hydroxide and perchlorate oxygens range between 2.88 and 3.14 Å. Although the shortest distance may indicate some hydrogen bonding from one of the hydroxide oxygens no definite conclusion can be drawn, partly because of the uncertainties in the bond lengths (σ *ca.* 0.05 Å). The observed atomic distances between the perchlorate groups and the $[Pb_4(OH)_4^{4+}]$-groups fall in the same ranges as was found for α- and β-$[Pb_6O(OH)_6](ClO_4)_4.H_2O$. These distances indicate that the interactions between these groups are weak.

In the carbonate group both the bond lengths (1.31 Å) and the bond angles (120°) are equal by symmetry. The carbonate oxygen, O(5), coordinates two Pb(1) atoms at 2.91 Å. This distance is appreciably longer than the values found in $2PbCO_3.Pb(OH)_2$ (2.75 Å) [18] and in $PbCO_3.PbO.2H_2O$ (2.65 Å) [19] from electron diffraction studies. Probably, the interaction is weak between the $[Pb_4(OH)_4^{4+}]$-unit and the carbonate ion.

The water molecule, O(4), may be considered attached to the Pb_4-cluster through interactions with Pb(3) and Pb(1), which are 2.78 and 2.98 Å distant, respectively. Its nearest oxygen neighbours are O(2), O(3), and O(42), which all are at a distance of *ca.* 2.96 Å from O(4).

The positional disorder of $ClO_4(3)$ and $ClO_4(4)$ may be explained by the fact that the interatomic distances are the same for the two alternative ways to place each of them; see Fig. 3. The suggested arrangement of anions along the symmetry axes results in a rather loose packing. The largest distance between two levels of oxygen atoms is *ca.* 3.6 Å along the screw axis and *ca.* 4.6 Å along the three-fold axes. If the disorder is static rather than dynamic, the holes on the latter axes are just big enough to have room for a water molecule. The presence of this water molecule cannot be decided upon from the *F* map, since its location can be expected to be close to an O(42) position in the centrosymmetric approach. Its presence should add extra electron density to this position and be reflected in the *B*-value of O(42). The temperature factor of O(42) is, however, not low compared to those of O(22) and O(32). When the electron densities are compared one finds for the not disordered O(22) 4.0 $e^-/Å^3$ and for O(32) 1.9 $e^-/Å^3$ and for O(42) 2.1 $e^-/Å^3$. There is thus no extra electron density at the O(42) position. The lead analysis, which should be quite accurate, does not either suggest that two additional water molecules should be included in the unit cell.

The general features of the arrangement of the atoms in the $[Pb_4(OH)_4^{4+}]$-unit are the same as those suggested for this unit in aqueous solution. The Pb–Pb distances are, however, significantly different in the two cases. In solution, where the diffraction data have been interpreted on the assumption of a regular Pb_4-tetrahedron, the Pb–Pb distance is 3.85 Å. This is 0.07 Å longer than the mean distance found in the solid. The Pb–O distance can be determined with much less accuracy and in Ref. 3 only a mean value of *ca.* 2.6 Å was reported for this distance in solution. The radial distribution curve, in fact, shows two peaks at 2.4 and 2.9 Å, respectively. These peaks can now be interpreted as arising from Pb–O interactions within the tetramer and between the tetramer and water and perchlorate oxygens. The mean Pb–O distance in the solid for the $[Pb_4(OH)_4^{4+}]$-unit is 2.38 Å. The $[Pb_6O(OH)_6^{4+}]$-unit in the structure of α- and β-$[Pb_6O(OH)_6](ClO_4)_4.H_2O$ may be considered as built from two $[Pb_4(OH)_4^{4+}]$-units with two lead and one oxygen atom in common. In it the Pb–Pb and Pb–O distances are quite varied and somewhat different in the two structures. The observed differences in bond lengths for $[Pb_4(OH)_4^{4+}]$ in the solid and in solution may thus be due to the difference in environment and the less regular Pb_4-unit in the solid caused by the unequal sets of nearest neighbours of the lead atoms.

Acknowledgements. We thank Professor Ivar Olovsson and his group for their generous help. We also wish to thank Drs. Rolf Hesse and Georg Johansson for helpful discussions and Dr. Marcus Richardson for correcting the English of this paper.

This work has been financially supported by grants from the *Swedish Natural Science Research Council.*

REFERENCES

1. Spiro, T. G., Templeton, D. H. and Zalkin, A. *Inorg. Chem.* **8** (1969) 856.
2. Olin, Å. and Söderquist, R. *Acta Chem. Scand.* **26** (1972) 3505.
3. Johansson, G. and Olin, Å. *Acta Chem. Scand.* **22** (1968) 3197.
4. Olin, Å. *Acta Chem. Scand.* **14** (1960) 126.

5. Esval, O. E. *Thesis*, University of North Carolina 1962.
6. Groth, P. *Chemische Krystallographie 2. Teil*, Engelmann, Leipzig 1908, p. 186.
7. Weinland, R. and Stroh, R. *Ber.* **55** (1922) 2706.
8. Lonsdale, K. *Acta Cryst.* **3** (1950) 400.
9. Parrish, W. *Acta Cryst.* **13** (1960) 838.
10. Hanson, H. P., Herman, F., Lea, J. D. and Skillman, S. *Acta Cryst.* **17** (1964) 1040.
11. Saravia, L. R. and Caticha-Ellis, S. *Acta Cryst.* **20** (1966) 927.
12. Wilson, A. J. C. *Nature* **150** (1942) 151.
13. Sass, R. L., Vidale, R. and Donohue, J. *Acta Cryst.* **10** (1957) 567.
14. Moore, W. J. and Pauling, L. *J. Am. Chem. Soc.* **63** (1941) 1392.
15. Kay, M. I. *Acta Cryst.* **14** (1961) 80.
16. Maroni, V. A. and Spiro, T. G. *Inorg. Chem.* **7** (1968) 188.
17. Olovsson, I. *J. Chem. Phys.* **49** (1968) 1063.
18. Cowley, J. M. *Acta Cryst.* **9** (1956) 391.
19. Voronova, A. A. and Vainshtein, B. K. *Kristallografiya* **9** (1964) 197.

Received February 28, 1973.

ACTA CHEMICA SCANDINAVICA 27 (1973) 2321–2334

Bacterial Carotenoids

XLI.* C_{50}-Carotenoids. 11.** C_{45}- and C_{50}-Carotenoids from *Sarcina lutea* — Sarcinaxanthin

N. ARPIN,*** S. NORGÅRD, G. W. FRANCIS† and S. LIAAEN-JENSEN

Organic Chemistry Laboratories, Norwegian Institute of Technology, University of Trondheim, 7034-Trondheim, Norway

Previous work on the carotenoids of the common air contaminant *Sarcina lutea* is reviewed.

The carotenoids of *S. lutea* have been re-examined by modern chemical and spectroscopic methods including PMR and mass spectroscopy.

Major carotenoids were a mono-D-glucoside (*2*) of a C_{50}-diol, probably sarcinaxanthin, and the C_{50}-diol sarcinaxanthin (*3*). Decaprenoxanthin (*1*) and sarcinaxanthin (*3*) are structural isomers ($C_{50}H_{72}O_2$), probably differing only in the location of one of two primary, allylic hydroxy groups.

In one of two pilot-plant batches a carotenoid considered to be a 7,8- or 7′,8′-dihydrosarcinaxanthin (*5*) was one of three major carotenoids.

Minor carotenoids were the C_{40}-carotene lycopene (*4*) and three C_{45}-mono-ols (tentative assignments *6*,*7* and *8*).

The biosynthesis of the isolated carotenoids is considered.

The carotenoids of the common air contaminant, the yellow gram-positive bacterium *Sarcina lutea*, have been studied by several investigators. Chargaff and Dieryck [1] and Chargaff [2] described the presence of the epiphasic sarcinene, presumably a hydrocarbon, as well as a xanthophyll with the same absorption spectrum in visible light (corresponding to an aliphatic nonaene chromophore). Later Nakamura [3] isolated a yellow pigment with absorption maxima at slightly shorter wavelengths than sarcinene. Nakamura considered his pigment to be a xanthophyll ester. Still later Takeda and Ohta [4] isolated

* No. XL. *Acta Chem. Scand.* **26** (1972) 2526.

** No. 10. *Acta Chem. Scand.* **26** (1972) 2528.

*** On leave of absence from Departement de Biologie Végétale, Service de Phytochemie et Phytophysiologie, Université de Lyon, 69 Villeurbanne, France.

† Present address: Chemistry Department, University of Bergen, 5000 Bergen, Norway.

in the crystalline state a xanthophyll, sarcinaxanthin, m.p. 149 – 150°C, presumably identical with the xanthophyll described by Chargaff.[1,2,5] The only carotene isolated was lycopene.[4] Sobin and Stahly [6] found no ester or carotenoic acid, but two yellow xanthophylls. Mathews and Sistrom [7] reported the presence of sarcinene and sarcinaxanthin. In recent years Thirkell and Strang [8] have claimed the presence in both *S. lutea* and *S. flava* of a carotene, a mono-ol, a diol, and a polyol, all with nonaene-type absorption spectra in visible light. In an independant investigation [9] sarcinaxanthin from *S. flava* and sarcinaxanthin from *S. lutea* which were considered identical [8] were compared with *dehydrogenans*-P439, to which structure, *1*, $C_{50}H_{72}O_2$, had been assigned.[10,11]

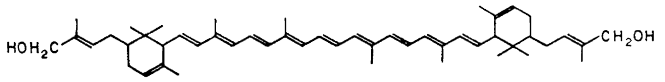

①

The comparative study, performed by means of micro methods involving electronic and mass spectrometry and co-chromatography of the parent compounds and various derivatives, was taken to support identity of sarcinaxanthin and *dehydrogenans*-P439 (*1*).[9] From further mass-spectrometric studies Thirkell, Strang and Chapman [12] later suggested that their sarcinaxanthin might be a mixture of the three compounds $C_{50}H_{72}O_2$, $C_{50}H_{70}O_2$, and $C_{50}H_{68}O_2$. Although M – 2 and M – 2 – 2 peaks, as well as combination peaks therewith, have been observed for carotenoids on electron impact,[13,14] it was felt that a further examination of the structure of crystalline sarcinaxanthin ought to be carried out.

The present paper describes further studies on the carotenoids of *S. lutea*. Some preliminary data [15,16] and parts of this project [17,18] have been reported elsewhere.

RESULTS AND DISCUSSION

Whereas all previous studies were made on cells cultivated on agar plates, large scale submerged culture grown with high aeration was employed in the present work. Cell yields from 1.4 – 3.0 g dry cells per liter culture were obtained. In previous work, *e.g.* Ref. 8, extraction difficulties had been considerable. This was overcome by lysing the cells by means of lysozyme prior to solvent extraction, thereby allowing facile and complete pigment extraction. Even so the pigment content was low, constituting 0.008 – 0.011 % of the dry weight. In total 24 mg (spectrophotometrically determined) carotenoids were obtained from a 150 l culture (Batch 1, 215 g dried cells) and 41 mg from a 170 l culture (Batch 2, 519 g dried cells). For comparison Takeda and Ohta [4] obtained 3.4 mg crystalline sarcinaxanthin from 385 g dried cells.

Batch 1 provided pure crystalline sarcinaxanthin, m.p. 160 – 161°C, for structural studies. The characterization of the polar carotenoid and the minor carotenoids was mainly effected with pigments from Batch 2.

Experimental details on the polar carotenoid are included in the Experimental Part. Results and arguments leading to the mono-D-glucoside structure *2a* (or *2b*) have been presented separately [17] and are not repeated here. In the absence of PMR data it is emphasized that since no *retro*-Diels Alder fragmentations were observed on electron impact the attachment of the two extra C_5-units of the C_{50}-aglucone to 2,2′-position is not proved. However, the location of the two oxygen atoms of the aglucone at two different ends of the main chromophore is considered demonstrated by the observed in-chain cleavages on electron impact (indicated on structures *2a* and *2b*) of the penta-acetate and the corresponding penta(trideutero)acetate. That the C_{50}-diol aglucone is indeed identical with sarcinaxanthin, the main xanthophyll of *S. lutea* remains an assumption.

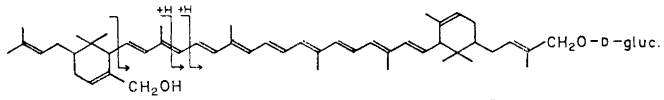

(2a)

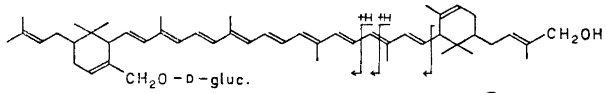

(2b)

Crystalline sarcinaxanthin (2 mg) was obtained from the present isolation. *Dehydrogenans*-P439, later renamed decaprenoxanthin,[19] was available for further direct comparison.

Judged from the crystalline shapes of sarcinaxanthin (small hexagonal plates) and of decaprenoxanthin (large needles) when obtained from the same solvent system, melting points and mixed melting point determination, and finally co-chromatography tests of the pure *trans* isomers, of their mono- and diacetates as well as their dialdehydes here prepared (Table 1), the two compounds are not identical, contrary to our previous assumption.[9] This conclusion is substantiated by further spectral data given below. However, the physical and chemical data obtained do indicate a close structural relationship.

Both compounds possess the same aliphatic nonaene chromophore *3* as evidenced by their electronic spectra (see Ref. 10) and PMR spectra (Fig. 1). Also sarcinaxanthin (*3*) contains four in-chain methyl groups (τ 8.03, *ca.* 12 H) and exhibits no end-of-chain methyl signals at τ 8.19. Instrumental factors may explain the fact that the two methyl groups closest to the end of the polyene chain in sarcinaxanthin (*3*) do not produce separate signals at τ 8.08 as for decaprenoxanthin (*1*). Furthermore the τ 3 – 4 complex defining the olefinic protons of the C-8, C-8′ polyene system appears identical in the two compounds (Fig. 1). The intensity ratio (1.64) of the M – 92 and M – 106 peaks in the mass spectrum of sarcinaxanthin (*3*) is also as expected for an aliphatic nonaene chromophore.[20]

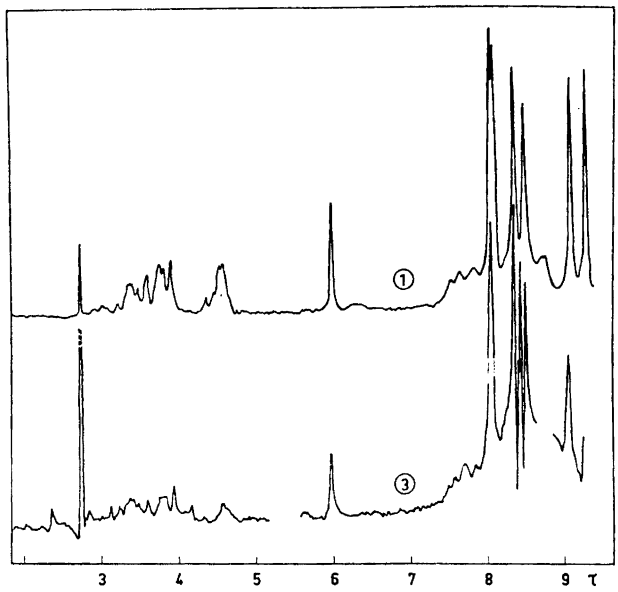

Fig. 1. Proton magnetic resonance spectrum ($CDCl_3$) of sarcinaxanthin (*3*) and decaprenoxanthin (*1*).

Mass spectrometry confirmed that sarcinaxanthin (*3*) has the same molecular weight (M = 704) as decaprenoxanthin (*1*). As reported by Thirkell *et al.*[12] dehydrogenation losses (M − 2, M − 2 − 2 and combination peaks therewith) are observed. The presence of two hydroxy groups was indicated by two consecutive losses of water from the molecular ion, and the formulation of the peracetate as a diacetate by following the course of acetylation was confirmed by the mass spectrum of the diacetate (M = 788, M − 42, M − 60). That the two hydroxy groups of sarcinaxanthin (*3*) are primary, allylic ones follows from the OH deformation/C − O stretching absorption at 1005 cm^{-1} in the IR spectrum (Fig. 2) and the 5.96 τ singlet in the PMR spectrum (Fig. 1) of sarcinaxanthin. The hydroxy groups, in common with those in decaprenoxanthin (*1*), are not allylic to the polyene chain, since selective oxidation of the allylic hydroxy groups with nickel peroxide, *cf.* Ref. 10, yields products with unchanged visible light absorption spectra. Judged from the similarity in polarity of *3* with decaprenoxanthin (*1*) and a negative silylation test for its diacetate further hydroxy groups are disregarded. No other functional groups are disclosed by the IR spectra of sarcinaxanthin (*3*) and its diacetate. In the absence of high-precision measurements the molecular formula of sarcinaxanthin (*3*) is therefore formulated as $C_{50}H_{72}O_2$, *cf.* Ref. 12, as for decaprenoxanthin (*1*).[10]

Further information about the structure of sarcinaxanthin (*3*) is obtained from the PMR spectrum (Fig. 1). Methyl signals not yet discussed are observed at τ 8.32 (*ca.* 6H), 8.41 (*ca.* 3H), 8.49 (*ca.* 3H), 9.05 (*ca.* 6H), and *ca.*

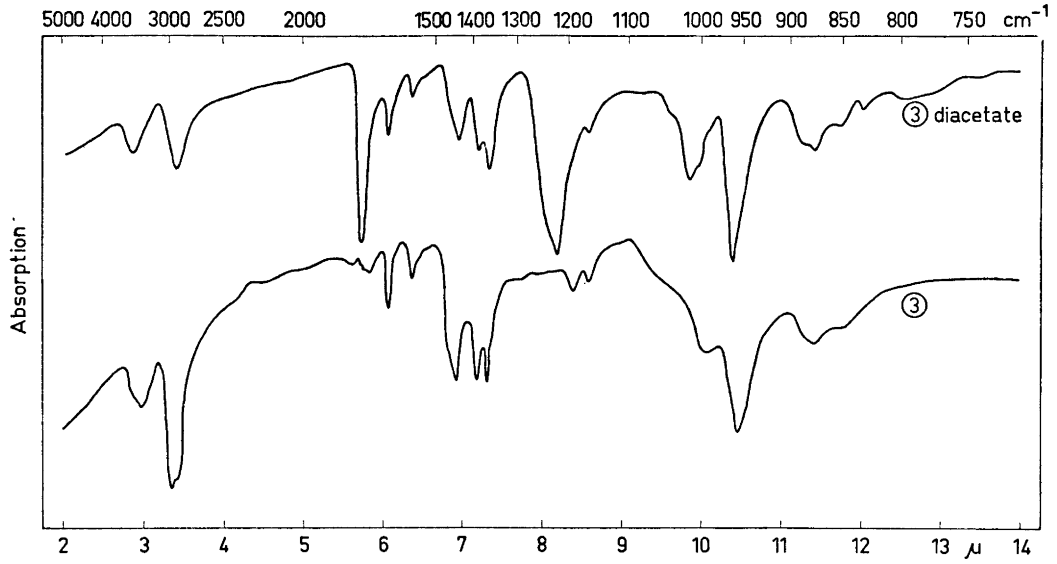

Fig. 2. Infrared spectrum (KBr) of sarcinaxanthin (*3*) and sarcinaxanthin diacetate.

9.25 (*ca.* 6H). The latter signal, not included in the spectrum presented in Fig. 1, was present also on a time-averaged 60 Mc/sec spectrum and must originate from the end-groups. The two signals at high field (τ 9.05 and 9.25)

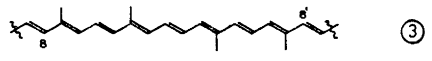

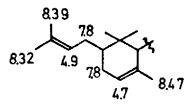

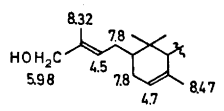

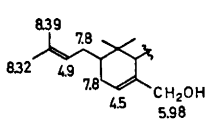

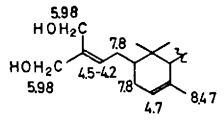

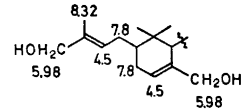

coincide with those of decaprenoxanthin (*1*) and are assigned to the *gem.* dimethyl groups of two ε-rings.

The remaining four methyl groups must be attached to isolated double bonds, and the intensity ratio of their PMR signals (2:1:1) reflects an unsymmetrical molecule.

Various combinations of the end-groups $a-e$ to be considered (predicted signals are indicated in the formula) are all compatible with the allylic CH_2-region in the PMR spectrum of sarcinaxanthin (analogous to that of decaprenoxanthin *1* = *3bb*). The methyl signals observed can best be accomodated with *3ea* or *3bc*, whereas the symmetrical combinations *3cc* and *3bb* (= decaprenoxanthin *1*) can be ruled out. For *3da* the expected intensity ratio is different from that observed. Moreover, failure to form an acetonide, and more particularly resistance towards formation of a condensation product with benzaldehyde [21] do not sustain a grouping of type *d*. Compound *3da* may also exhibit decreased polarity relative to, *e.g.*, *3bb*. Structures *3ea* or *3bc* consequently remain as likely possibilities.

The main peaks in the upper region of the mass spectra of sarcinaxanthin (*3*) and sarcinaxanthin diacetate are compiled in the Experimental Part together with some possible assignments. Exact mass measurements were unfortunately not available. Sarcinaxanthin (*3*) shows the already mentioned dehydrogenation losses and losses due to the two primary allylic hydroxy functions (M − 16, M − 18, M − 18 − 18) in addition to the characteristic losses of toluene, xylene, and dimethylcyclodecapentaene. Other losses compatible with in-chain cleavages will be discussed below.

A major difference in the mass spectra of sarcinaxanthin (*3*) and decaprenoxanthin (*1*) (*cf.* Ref. 10) is that the characteristic loss of 140 mass units from the molecular ion of decaprenoxanthin (*1*), resulting from a RDA-rearrangement [10,11] is not observed for sarcinaxanthin (*3*). Nor does a corresponding loss of 182 mass units occur from sarcinaxanthin diacetate, *cf.* Ref. 10. This was for some time considered evidence against the presence of end-group *b* in sarcinaxanthin and hence the structure *3 ea* was preferred for sarcinaxanthin.[15,16] It seemed reasonable that the hydroxymethyl group at C-18 of end group *a* could prevent the common RDA-rearrangement provided this hydroxy group on electron impact showed a strong tendency to (i) expulsion of oxygen or (ii) elimination of water:

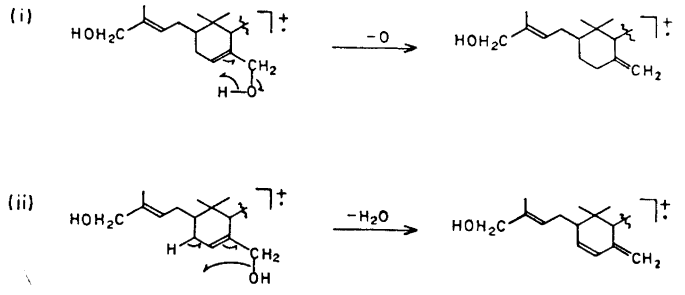

Moreover, previous evidence for RDA-fragmentation for hydrocarbon end-groups of type *a* is not conclusive.[22]

However, in light of the results obtained for the C_{50}-D-glucoside (*2a* or *2b*) discussed above, structure *3bc* must be reconsidered. Fragment ions at M − 207 (a), M − 261 (b), and M − 274 (c) of *3* compatible with the corresponding in-chain cleavages of the *2* pentaacetate are observed. Corresponding cleavages, resulting in ions of type a′,b′,c′ appear to occur in the *3* diacetate.

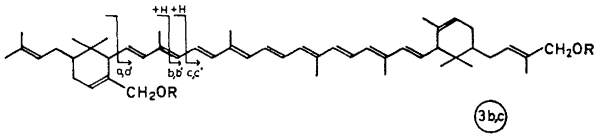

R=H: a,b,c
R=Ac: a',b',c'

Although the losses observed for *3* and *3* diacetate could alternatively be explained by combined losses of atomic oxygen and a hydrocarbon fragment (required by *3ea*), the analogy with the proved in-chain fragmentations of *2* pentaacetate may be taken to support structure *3bc* for sarcinaxanthin. The lacking preference for RDA-rearrangement for the molecular ions of sarcinaxanthin and its acetate may only reflect an unsymmetrical molecule with other preferred fragmentations.

The differentiation between *3ae* and *3bc* could easily be made by the PMR Europium shift technique[23,24] provided large enough samples could be obtained.

The data presented contain no support other than the appearance of the allylic methylene region in the PMR spectrum (Fig. 1) for the attachment of the C_5-units of *3* to the 2- rather than 3-position. 2-Substitution is preferred by analogy with decaprenoxanthin (*1*).[10,11]

The close similarity between decaprenoxanthin (*1*) and sarcinaxanthin (*3*) in chromatographic properties, necessitating the preparation of acetylated (or aldehydic) products for a clear distinction to be made on the micro scale, calls for caution in the identification of these pigments from bacteria, *cf.* Refs. 9, 25.

Sarcinene[1,2,7,8] was not encountered. The only carotene isolated was lycopene (*4*), identified from its electronic spectrum, mass spectrum (M = 536, M − 69, M − 92, M − 106, *m/e* 69) and by co-chromatography, with authentic lycopene.

The most abundant minor carotenoid is considered to be a 7,8- or 7′,8′-dihydro-sarcinaxanthin (*5*), which exhibited aliphatic octaene chromophore, judged by its electronic spectrum. The mass spectrum exhibited the molecular ion at *m/e* 706 (compatible with $C_{50}H_{74}O_2$), M − 2, M − 18, and M − 92 ions. The PMR spectrum of a lipid-contaminated sample (for assignments see Experimental Part) supported structure *5* and ruled out the possibility of a substituted β-end group. The presence of primary allylic hydroxy group(s) was further

supported by IR absorption at 1005 cm^{-1}. *5* gave a diacetate on acetylation (*m/e* 790 = M, M − 2, M − 42, M − 60, and M − 92). The diacetate could not be silylated.

The mono-ol fraction comprised three minor carotenoids *6*, *7*, and *8*. Carotenoid *6* again had an aliphatic octaene chromophore and was a new C_{45}-carotenoid (*m/e* 622 = M, corresponding to $C_{45}H_{66}O$, M − 2, M − 18, M − 92, and base peak *m/e* 69). Acetylation provided a monoacetate (*m/e* 664 = M, corresponding to $C_{45}H_{65}OCOCH_3$, M − 92 and base peak *m/e* 43). With this limited information structure *6* seems plausible for this C_{45}-mono-ol.

Another minor carotenoid *7* may represent a 7′,8′-dihydro derivative of *6* or an entirely aliphatic carotenoid. *7* exhibited aliphatic heptaene chromophore with molecular ion at *m/e* 624 corresponding to $C_{45}H_{68}O$ and base peak at *m/e* 69.

The final minor carotenoid *8* exhibited an electronic spectrum characteristic of β-carotene, and gave on acetylation a monoacetate (*m/e* 662 = M, corresponding to $C_{45}H_{63}OCOCH_3$, M − 92 and M − 106, base peak *m/e* 43). The tentative structure *8* may be considered.

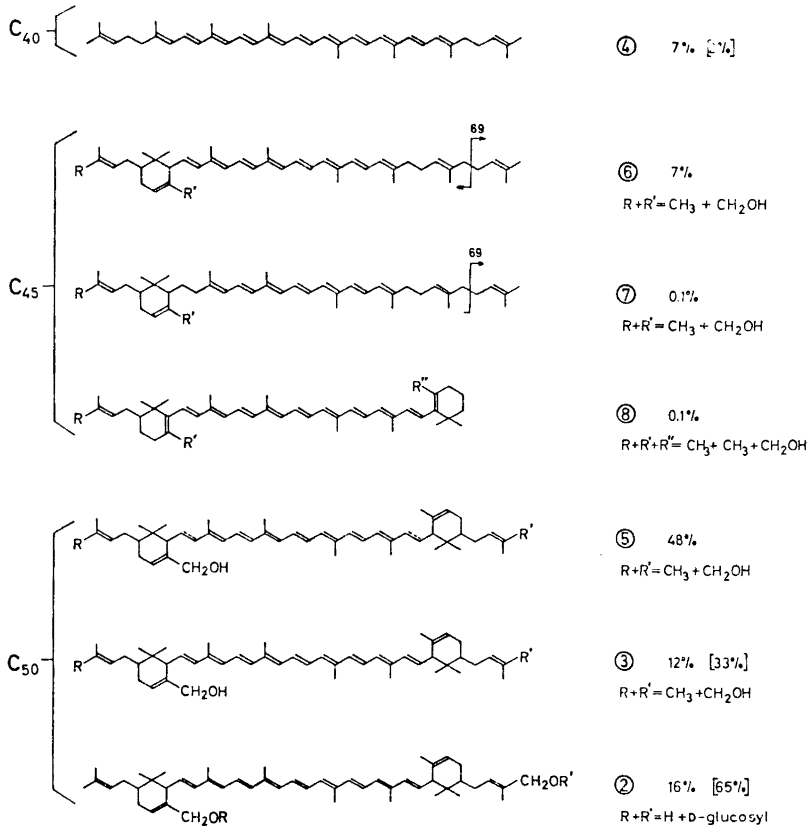

Scheme 1.

BIOSYNTHETIC CONSIDERATIONS

For convenience the carotenoids here isolated from *S. lutea* are compiled in Scheme 1. The close biosynthetic relationship between these structures is apparent.

The occurrence of both C_{40}- (*4*), C_{45}- (*6,7,8*), and C_{50}-carotenoids (*5,3,2*) in the same organism may be taken to support the postulated biosynthetic pathway of C_{45}- and C_{50}-carotenoids *via* C_{40}-carotenoids.[10,16] The tentative structure *7* would imply cyclization at the dehydrogenation level of ζ-carotene and may be biosynthetically unsound.

The percentage figures on Scheme 1 refer to the carotenoid composition of Batch 2; those in brackets to Batch 1. Since the carotenoids of highest dehydrogenation level normally represent the ultimate products of carotenoid biosynthesis, it is reasonable to assume that sarcinaxanthin (*3*) and the D-glucoside (*2*) represent the biosynthetic end-products (*cf.* Batch 1). The growth conditions of Batch 2 therefore appear to have depressed complete dehydrogenation to the nonaene system characteristic of *3* and glucoside formation, even though the same medium and growth period were employed for each pilot-plant batch. However, the degree of aeration was probably higher for Batch 1. Considerably higher cell density was obtained in Batch 2.

The location of the carotenoids in the cell membrane of *S. lutea* and their protective effect against photodynamic destruction of the cell have been demonstrated by Mathews and Sistrom.[28,29] No specific function of glycosidic carotenoids is yet known.

EXPERIMENTAL

Materials and general methods. Solvents and instruments used were as specified elsewhere [30] except that some of the mass spectra were obtained with an LKB-9000 instrument (70 eV, direct inlet system, ion source temperature 290°C) and IR-spectra of *3* and *3*-acetate were recorded on a Perkin Elmer Model 21 Instrument.

Column chromatography was carried out on Woelm neutral alumina, May and Baker magnesium oxide or Schleicher and Schüll cellulose powder No. 124. For TLC Merck Kieselgel G and for paper chromatography Schleicher and Schüll No. 287 (Kieselguhr paper), No. 288 (alumina paper) or No. 996 ($CaCO_3$ paper) were used. Chromatographic properties of the individual compounds are compiled in Table 1.

Acetylations, silylations, and saponifications were carried out by standard procedures [31] commonly used in this laboratory.

Cultivation. Sarcina lutea, isolated by Reistad [32] and obtained from the Department of Biochemistry, this University, was used. The medium consisted of 2 % casamino acids, 1 % glycerol, 0.5 % yeast extract, 0.5 % NaCl and tap water; pH 7.0 – 7.2. Batch 1 (150 l) was cultivated at the Karolinska Institute, Stockholm, and Batch 2 (170 l) at the Department of Biochemistry, this University. Both cultures were grown at 30°C with aeration using *ca.* 5 % inoculum. Batch 1 was harvested by centrifugation after 24 h of growth; cell yield after lyophilization 215 g. Batch 2 reached the stationary phase after 16 h of growth and was harvested by centrifugation after 26 h and frozen; yield 516 g cell residue after acetone extraction.

Pigment extraction. Wet cells (3.1 kg; Batch 2) suspended in phosphate buffer (1800 ml) pH 7.2 (560 ml 0.4 M $NaH_2PO_4.H_2O$ and 1440 ml 0.4 M $Na_2HPO_4.12H_2O$) were treated with lysozyme (1 g) in phosphate buffer (200 ml) for 46 h at 30°C. The lysed cells were repeatedly and completely extracted with acetone at room temperature and the pigments transferred to benzene-ether in a separatory funnel.

The pigments of the lysed cells of Batch 1 were less favourably extracted with methanol, necessitating subsequent precipitation of extracted proteins with acetone.

Table 1. Chromatographic properties of the carotenoids of *Sarcina lutea* and their derivatives and of decaprenoxanthin (*1*) and derivatives thereof.

Carotenoid	Required eluent from cellulose column	Required eluent from alumina grade 3 column	R_F-values TLC kieselgel 20 % [c]	TLC kieselgel 40 % [c]	TLC kieselgel 1 % [a]	Kieselguhr paper 2 % [a]	Kieselguhr paper 5 % [a]	Kieselguhr paper 10 % [a]	Kieselguhr paper 50 % [b]	Al_2O_3 paper 30 % [a]	$CaCO_3$ paper 10 % [a]
C_{50}-Mono-D-glucoside (*2*)	30—100 % [a]	pet.ether							0.45		
2 pentaacetate				[e]							
Sarcinaxanthin (*3*)	10—20 % [a]	75 % [d]		[e]				0.64		0.57	0.75
3 monoacetate							0.58	0.83			
3 diacetate						0.60	0.85	0.98			
3 monoaldehyde								0.78			
3 dialdehyde							0.76				
3 di TMS ether					0.77						
Lycopene (*4*)	pet.ether	pet.ether				0.62					
Dihydrosarcinaxanthin (*5*)		50 % [d]						0.65			
5 monoacetate							[e]				
5 diacetate							0.95				
Carotenoid *6*		40 % [d]					0.68				
6 monoacetate						0.84					
Carotenoid *7*		40 % [d]	[e]								
Carotenoid *8*		40 % [d]	[e]								
8 monoacetate				[e]							
Decaprenoxanthin (*1*)								0.66		0.57	0.75
1 monoacetate							0.64				
1 diacetate							0.67				
1 dialdehyde							0.84				

[a] acetone-petroleum ether, [b] acetone-benzene, [c] Suitable system, [d] ether-pet.ether [e] Appropriate system; R_F-value not measured.

Even so transfer of the pigments to chloroform in a separatory funnel was hampered by continuous precipitation of proteins.

Spectrophotometrically determined total yield of carotenoids was: Batch 1, 24 mg (0.011 % of dried cells), and Batch 2, 41.6 mg (0.008 % of acetone-extracted cell residue).

Separation of individual carotenoids. The pigment extract of Batch 1 was chromatographed on alumina activity grade 2. Carotenes were eluted with 10 – 12 % ether in petroleum ether and sarcinaxanthin (*3*) with 0.5 – 2 % methanol in benzene. The polar carotenoid (*2*) could not be eluted with methanol or pyridine.

The pigments of Batch 2 were chromatographed on two cellulose columns (recovery 89 %), effecting separation of the strongly polar xanthophyll (*2*, 18 %) from the less polar carotenoids (82 %, eluted jointly with 0 – 20 % acetone in petroleum ether). The less polar carotenoids of Batch 2 (30.3 mg) were saponified with 5 % KOH in methanol-ether for 1 h in the usual manner; pigment recovery 68 %. The saponified pigment mixture was chromatographed on alumina, activity grade 3, see Scheme 1 for quantitative carotenoid composition of each batch.

C_{50}-Mono-D-glucoside (*2*). The purest fractions from the cellulose columns above (5.7 mg) were used. The paper-chromatographically homogeneous carotenoid exhibited λ_{max} (acetone) 417, 439, and 468 nm, % III/II [33] = 85.

2 (1.1 mg) was acetylated in standard manner for 24 h; pigment recovery 12 %. The pentaacetate, purified by TLC, exhibited the same electronic spectrum as *2*; *m/e* 1072(M), M – 2, M – 42, M – 44, M – 60, M – 79, M – 92, M – 106, M – 60 – 92, M – 60 – 106, M – 92 – 106, M – 60 – 60 – 92, M – 249, 827.4704 (calc. 827.4734 for $C_{50}H_{67}O_{10}$) = M – 275, M – 289, M – 302, M – 303, M – 316, M – 330, M – 334, M – 346, M – 347, M – 348, 331 (18 %), 169 (31 %), 109 (27 %), 43 (100 %).

2 (1.0 mg) in pentadeuteriopyridine (2.0 ml) was acetylated with hexadeuterioacetic anhydride (0.3 ml) for 24 h; pigment recovery 17 %. The fully acetylated product exhibited the same electronic spectrum and R_F-value on TLC and kieselguhr paper as the undeuterated pentaacetate; *m/e* 1091(M), M – 45, M – 47, M – 61, M – 63, M – 79, M – 92, M – 106, M – 61 – 92, M – 63 – 92, M – 158, M – 92 – 106, 839.5548 (calc. 839.5487 for $C_{50}H_{55}D_{12}O_{10}$) = M – 252, M – 272, M – 286, M – 288, M – 305, M – 306, M – 319, M – 343, M – 358, M – 359, M – 360, 343 (18 %), 251, 172 (43 %), 119, 109 (43 %), 43 (100 %).

2 (2.0 mg) was hydrolyzed [34,35] in 0.15 N HCl/methanol (5 ml) for 21 h. Methanol (5 × 10 ml) was added and evaporated. The residue was refluxed with 0.04 N polystyrenesulphonic acid (0.4 ml) for 2 h. The residue was filtered and extracted with warm methanol. The hexose liberated on hydrolysis was identified as glucose or galactose by co-chromatography with galactose, glucose, and mannose in systems 1 and 4 [35] (development with aniline-phthalic acid reagent). The hexose was further purified by chromatography in System 1 with glucose as reference. The reference was localized by spraying with the aniline-phthalic acid reagent and the unknown hexose extracted with hot water. To the hexose (*ca.* 5 μg) in water (0.02 ml) was added tris buffer (1.0 ml) and D-glucose reagent [35] (1.0 ml). After 30 min at room temperature, H_2SO_4 (1.0 ml of a 50 % aqueous solution) was added and the light absorption measured at 546 nm against a blank reference containing no hexose. The same test was carried out with a D-glucose standard solution (0.02 ml of a 0.025 % aqueous solution). Both the test and standard developed the bluish colour specific for D-glucose.[24]

Sarcinaxanthin (3). trans-Sarcinaxanthin from Batch 1 crystallized as small, regular hexagonal plates from acetone-petroleum ether, m.p. 160 – 161°C, yield *ca.* 1 mg. The absorption spectrum in visible light was identical with that of decaprenoxanthin (*1*).[10] The IR-spectrum (Fig. 1) had ν_{max} (KBr) 3330 (OH), 3000 (CH), 1640, 1580 (double bonds), 1440 (CH_2), 1385 and 1370 (*gem.* CH_3CH_3), 1000, 955 (*trans* disubst. C=C), 870 and 830 (trisubst. C=C) cm^{-1} very similar to that of decaprenoxanthin (*1*).[10] The PMR-spectrum (Fig. 2) had τ ($CDCl_3$) 9.25, 9.05 (*ca.* $2CH_3$), 8.72 (lipid impurity), 8.49 (*ca.* $1CH_3$), 8.41 (*ca.* $1CH_3$), 8.32 (*ca.* $2CH_3$), 8.04 (*ca.* $4CH_3$ in-chain), 5.98 (*ca.* 4H, CH_2OH) and 4.8 – 3 (olefinic H). The mass spectrum (Fig. 3) exhibited *m/e* 704(M), 702(M – 2), 700(M – 2 – 2), 688(M – 16), 686(M – 18 and M – 2 – 16), 684(M – 2 – 18), 672(M – 18 – 18), 670(M – 2 – 18 – 18), 625(M – 79 [26]), 612(M – 92 [13]), 610(M – 2 – 92), 598(M – 106 [13]), 596(M – 2 – 106), 594(M – 2 – 2 – 106), 582 (M – 16 – 106), 580(M – 18 – 106), 546(M – 158 [14]), 544(M – 2 – 158), 506(M – 106 – 92), 498(M – 206,?), 497(M – 207) = a, 481(M – 16 – a), 479(M – 18 – a), 443(M – 261) = b, 430(M – 274) = c, 351(b – 92). The mass spectrum is described in Fig. 3 and Table 3.

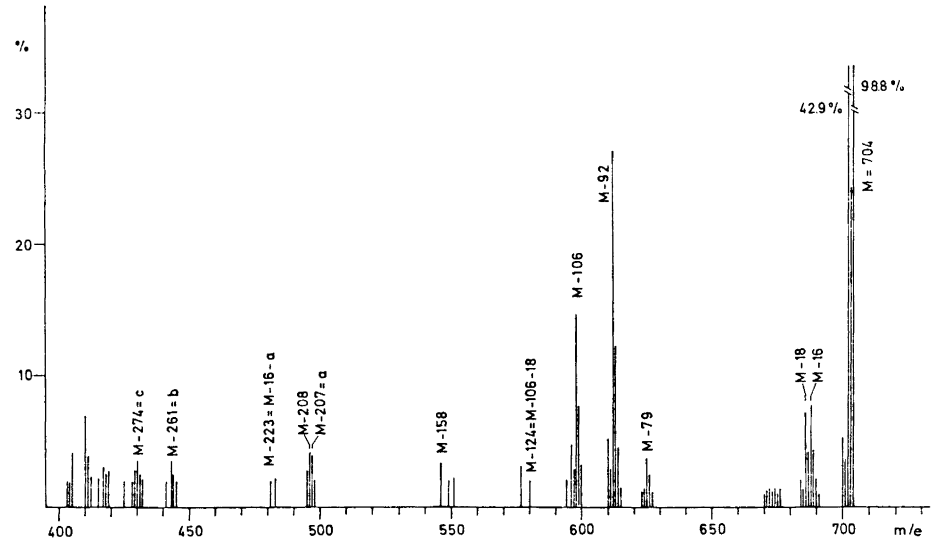

Fig. 3. Mass spectrum of sarcinaxanthin (*3*).

Acetylation of *3* in pyridine was effected in several experiments in the standard manner with acetic anhydride; pigment recoveries *ca.* 95 %. The formation of an intermediary monoacetate was observed when the acetylation reaction was monitored by paper chromatography (Table 1). The monoacetate and the diacetate exhibited unchanged electronic spectra. The IR-spectrum of the diacetate (Fig. 2) had ν_{max} (KBr) 3000, 1740 (acetate), 1640, 1570 (double bonds), 1440 (CH_2), 1385, 1365 (*gem.* CH_3, CH_3), 1220 and 1030 (acetate), 960 (*trans* disubst. C=C), 870 and 830 (trisubst. C=C) cm^{-1}, differing only in minor bands from that of decaprenoxanthin diacetate.[10]

The diacetate had *m/e* 788(M), 786(M−2), 746(M−42), 744(M−44), 730(M−58), 728(M−60), 709(M−79), 696(M−2−92, $m^*=616$), 682(M−106), 669(M−121,?), 661(M−129,?), 630(M−158), 622(M−106−60, $m^*=568$), 590(M−106−92), 576(M−106−106), 538(M−92−158), 512(M−60−60−158), 485(M−2−303=b′−2), 479(a′−2−60), 472(c′−2). The diacetate could not be silylated.

3 (0.53 mg) was silylated in the usual manner; pigment recovery 94 %. The di(trimethylsilyl) ether, purified by TLC had the same electronic spectrum as *3*, *m/e* 848 (M), M−72, M−92, M−106, M−144, M−164, M−178, 73 (100 %).

Allylic oxidation of *3* (1 mg) by the procedure used for *1* for 2 h gave 70 % pigment recovery. Paper chromatography revealed the formation of a monoaldehyde (45 %) and a dialdehyde (5 %) beside unreacted *3*. The new products exhibited the same electronic spectra as *3*.

Acetonide formation [21] was attempted with *3* (0.5 mg) in dry acetone (1.8 ml) and anhydrous $CuSO_4$ (10 mg) for 44 h at room temperature. No less polar products were formed.

Condensation of *3* (1.5 mg) with benzaldehyde [38] (1 ml) at 45°C for 40 h also failed.

Direct comparison of sarcinaxanthin (3) *and decaprenoxanthin* (1)

Decaprenoxanthin (*1*) for comparison was obtained from *Flavobacterium dehydrogenans*.[10] On slow crystallization from acetone-petroleum ether *1* afforded long needles forming branches, m.p. 153−154°C. Mixed m.p. with sarcinaxanthin (*3*, m.p. 160−161°C) gave depression (144°C).

Separate iodine catalyzed stereomutation of *3* and *1* in benzene caused the same spectral shift and reduction in spectral finestructure, *cf.* Ref. 10. Both *trans* isomers gave rise to a neo U isomer (kieselguhr paper), *cf.* Ref. 9. Separation of *trans 3* and *trans 1* was not possible on $CaCO_3$-containing, Al_2O_3-containing, or kieselguhr paper.

The result of co-chromatography tests of the mono- and diacetates of *1* and *3* is given in Table 1, also including R_F-values for co-chromatography tests with the dialdehyde of *1* left from a previous study.[10] The PMR-spectrum of *1* is included in Fig. 1.

Lycopene (*4*), purified by TLC or paper chromatography had λ_{max} 347, 363, 447, 472, and 503 nm, *m/e* 536(M), M − 69, M − 92, M − 106, 69 (100 %). Co-chromatography (kieselguhr paper) of the stereomutation mixture containing *trans*, neo A, and neo B isomers with the stereomutation mixture of synthetic lycopene gave no separation of the corresponding isomers.

Dihydrosarcinaxanthin (*5*). *5* (3.5 mg) was rechromatographed on magnesium oxide and crystallized from acetone-petroleum ether; yield 0.6 mg. The visible light absorption spectrum (acetone) had λ_{max} 398, 421, and 446 nm, % III/II $^{33} = 65$, ν_{max} (KBr) 3500 (OH), 2900 (CH), 1640 (double bonds), 1440 (CH_2) 1385, 1370 (methyl, *gem.* dimethyl) 1005, 960 (*trans* disubst. C=C) and 890 cm^{-1}, τ($CDCl_3$) 9.27 (*ca.* $2CH_3$), 9.03 (*ca.* $2CH_3$), 8.73 (lipid impurity), 8.40 (*ca.* $2CH_3$), 8.34 (*ca.* 2 CH_3), 8.17 (*ca.* 1 CH_3, end-of-chain), 8.03 (*ca.* 3 CH_3, in-chain), 5.98 (*ca.* 4H, CH_2OH) and 3 − 5 (olefinic protons); *m/e* 704(M), M − 2, M − 18, M − 92, 43 (100 %).

Acetylation of *5* (0.41 mg), monitored by paper chromatography revealed one intermediary acetate. Pigment recovery was 90 %. The final product, purified by TLC, exhibited the same electronic spectrum as *5* and *m/e* 790 (M), M − 2, M − 42, M − 60, M − 92, 43 (100 %). The diacetate could not be silylated. Saponification of the diacetate gave *5* (90 % recovery).

Minor carotenoid 6. *6* (1.6 mg), purified by TLC, had λ_{max} (acetone) (357), 376, 397, 421 and 447 nm; *m/e* 622(M), M − 2, M − 18, M − 92, and 69 (100 %). Acetylation of *6* (0.21 mg) gave a monoacetate (no intermediary products); recovery 95 %, *6* monoacetate had the same electronic spectrum as *6*, *m/e* 664 (M), M − 92, 43 (100 %).

Minor carotenoid 7. *7* (0.02 mg), less polar than *6* on TLC, had λ_{max} (acetone) 354, 373, 396 and 419 nm; *m/e* 624 (M), 69 (100 %).

Minor carotenoid 8. *8* was isolated after acetylation of a mixture with *6*, as a monoacetate (0.02 mg) more polar than *6* monoacetate. *8* monoacetate had λ_{max} (acetone) 346, (426), 450, and (480) nm; *m/e* 662 (M), M − 92, 43 (100 %).

Acknowledgements. The cultivations were carried out by the Bacteriological Department, Karolinska Institutet, Stockholm, by the courtesy of Dr. C.-G. Hedén, and by the Department of Biochemistry, this University, under the supervision of Docent K. E. Eimhjellen. Docent Eimhjellen suggested the lysozyme treatment used. Some of the mass spectra were obtained from the Research Department, Swedish Tobacco Co., Stockholm, by the courtesy of Docent C. R. Enzell and the time-averaged PMR-spectrum of sarcinaxanthin was recorded by Varian Ass., London, through Dr. J. Feeney. N. A. was supported by a research grant from Hoffmann-La Roche, Basle, to S. L. J., S. N. and G. W. F. received maintenance grants from the Norwegian Institute of Technology.

REFERENCES

1. Chargaff, E. and Dieryck, J. *Naturwiss.* **20** (1932) 872.
2. Chargaff, E. *Compt. Rend.* **197** (1933) 946.
3. Nakamura, Y. and Ohta, T. *Hoppe-Seyler's Z. Physiol. Chem.* **268** (1941) 1.
4. Takeda, Y. and Ohta, T. *Hoppe-Seyler's Z. Physiol. Chem.* **268** (1941) 1.
5. Karrer, P. and Jucker, E. *Carotinoide*, Birkhäuser, Basel p. 329.
6. Sobin, B. and Stahly, G. L. *J. Bacteriol.* **44** (1942) 265.
7. Mathews, M. and Sistrom, W. R. *J. Bacteriol.* **78** (1959) 778.
8. Thirkell, D. and Strang, R. H. C. *J. Gen. Microbiol.* **49** (1967) 53.
9. Liaaen-Jensen, S., Weeks, O. B., Strang, R. H. C. and Thirkell, D. *Nature* **214** (1967) 379.
10. Liaaen-Jensen, S., Hertzberg, S., Weeks, O. B. and Schwieter, U. *Acta Chem. Scand.* **22** (1968) 344.
11. Schwieter, U. and Liaaen-Jensen, S. *Acta Chem. Scand.* **23** (1969) 1057.
12. Thirkell, D., Strang, R. H. C. and Chapman, J. R. *J. Gen. Microbiol.* **49** (1967) 157.

13. Schwieter, U., Bolliger, H. R., Chopard-dit-Jean, L. H., Englert, G., Kofler, M., König, A., v. Planta, C., Rüegg, R., Vetter, W. and Isler, O. *Chimia* **19** (1965) 294.
14. Enzell, C. R., Francis, G. W. and Liaaen-Jensen, S. *Acta Chem. Scand.* **23** (1969) 727.
15. Francis, G. W., *Thesis*, Norw. Inst. Technology, Trondheim 1969.
16. Liaaen-Jensen, S. *Pure Appl. Chem.* **20** (1969) 421.
17. Norgård, S., Francis, G. W., Jensen, A. and Liaaen-Jensen, S. *Acta Chem. Scand.* **24** (1970) 1460.
18. Norgård, S. *Thesis*, Norw. Inst. Technology, Trondheim 1972.
19. Weeks, O. B., Andrewes, A. G., Brown, B. O. and Weedon, B. C. L. *Nature* **224** (1969) 879.
20. Enzell, C. R., Francis, G. W. and Liaaen-Jensen, S. *Acta Chem. Scand.* **22** (1968) 1054.
21. Gerhardt, W. *Chem. Zentr.* **1912** 1953.
22. Liaaen-Jensen, S. In Goodwin, T. W. *Biochemistry of Terpenoids*, Academic, New York 1970, p. 223.
23. Hinckley, C. C. *J. Am. Chem. Soc.* **91** (1969) 5160.
24. Kjøsen, H. and Liaaen-Jensen, S. *Acta Chem. Scand.* **26** (1972) 2185.
25. Weeks, O. B. and Garner, R. J. *Arch. Biochem. Biophys.* **121** (1967) 35.
26. Kjøsen, H. *Thesis*, Norw. Inst. Technology, Univ. Trondheim 1973.
27. Straub, O. In Isler, O. *Carotenoids*. Birkhäuser, Basle 1972, Chpt. XII.
28. Mathews, M. M. and Sistrom, W. R. *Nature* **184** (1959) 1892.
29. Mathews, M. M. and Sistrom, W. R. *Arch. Mikrobiol.* **35** (1960) 139.
30. Kjøsen, H., Arpin, N. and Liaaen-Jensen, S. *Acta Chem. Scand.* **26** (1972) 3053.
31. Liaaen-Jensen, S. and Jensen, A. *Methods Enzymol.* **23** (1971) 586.
32. Reistad, R. *Arch. Mikrobiol.* **71** (1970) 353.
33. Ke, B., Imsgard, F., Kjøsen, M. and Liaaen-Jensen, S. *Biochim. Biophys. Acta* **210** (1970) 139.
34. Painter, T. J. *Chem. Ind. London* **1960** 1214.
35. Hertzberg, S. and Liaaen-Jensen, S. *Phytochemistry* **8** (1969) 1259.
36. Richterich, R. *Klinische Chemie, Theorie und Praxis*, Karger, Basle 1965.
37. Tallent, W. H. *J. Org. Chem.* **29** (1964) 2756.

Received February 21, 1973.

ACTA CHEMICA SCANDINAVICA 27 (1973) 2335–2343

Outer-sphere Complex Formation between the Hexaamminecobalt(III) Ion and Bromide Ion in Aqueous Solution

LARS JOHANSSON

Division of Inorganic Chemistry 1, Chemical Center, University of Lund, P.O.B. 740, S-220 07 Lund 7, Sweden

The complex formation between $Co(NH_3)_6^{3+}$ and Br^- has been studied at 25°C, at the constant ionic strengths ($NaClO_4$) $I = 1$ M and 4 M, and in NaBr of varying ionic strength. The solubility measurement data give evidence for the formation of outer-sphere complexes with one, two, and three bromide ions. At the constant ionic strengths, the following constants fit the data (errors within parentheses): $I =$ 1 M: $\beta_1 = 0.40(2)$ M^{-1}, $\beta_2 = 0.04(2)$ M^{-2} $I = 4$ M: $\beta_1 = 0.43(5)$ M^{-1}, $\beta_2 = 0.045(10)$ M^{-2}, $\beta_3 = 0.006(4)$ M^{-3}. Possible systematic errors are discussed. The results are compared with earlier studies on the same and similar systems.

This study is part of a series of investigations on outer-sphere complexes formed by inert complex cations. Previously, iodide complexes of $Coen_3^{3+}$ and $Co(NH_3)_6^{3+}$ have been studied.[1,2] These systems differ in the respect that $Coen_3^{3+}$ prefers one or three iodide ions while $Co(NH_3)_6^{3+}$ forms iodide complexes in a more regular manner. The differences are thought to be due to the different shapes of the inert cations. If this is true, the hexaamminecobalt bromide system should be similar to the hexaamminecobalt iodide system.

The present system has been subject to several earlier studies.[3–11] The majority of these have dealt with the formation of the first complex only. However, Larsson [9] challenged the commonly adopted view that predominantly electrostatic forces are responsible for outer-sphere complex formation. For $Co(NH_3)_6^{3+}$ and a number of ligands, including Br^-, he attempted to show that a series of consecutive complexes is formed, and not only those explicable by electrostatic attraction. Thus, for Br^- it was inferred from anion exchange measurements that the complexes ML^{2+}, ML_2^+, ML_3 and ML_4^- were formed. Since the ionic strength could not be kept constant, no evaluation of stability constants was attempted.[9]

In the present investigation, the hexaamminecobalt bromide system has been studied by solubility measurements in mixtures of NaBr and $NaClO_4$ of constant ionic strengths (1 M and 4 M). A quantitative interpretation should

then be possible. On the other hand, ClO_4^- probably forms, as discussed below, complexes with $Co(NH_3)_6^{3+}$, a fact which affects the results of the measurements. To see if the picture is substantially different when ClO_4^- is omitted, at the cost of the constant ionic strength, the solubility has also been measured in pure NaBr. A closer comparison with Larsson's results [9] is then also possible.

It would have been desirable to study this weak complex formation with different methods, but no suitable complement to the solubility measurements has been found. Spectrophotometric [1,12] measurements, for instance, are rendered impracticable by the low solubility of $Co(NH_3)_6(ClO_4)_3$.

EXPERIMENTAL

Chemicals. Analytical grade chemicals were used when available. $Co(NH_3)_6Cl_3$ and $Co(NH_3)_6(ClO_4)_3$ were prepared and analyzed as described earlier.[2] $Co(NH_3)_6Br_3$ was precipitated from the chloride by HBr and recrystallized several times. Its bromide content was found to be 59.6(3) % (calculated 59.80 %).

Solubility measurements. Solutions were equilibrated in a saturator and analyzed spectrophotometrically as described earlier.[2] The same precautions as before were taken to assure good reproducibility. The wavelengths 470 and 340 nm were chosen when $I = 1$ M, and 270 nm in the remainder of the measurements. The solubilities were reproducible within 1 % when $I = 1$ M otherwise within 1 – 2 %. Below $C_L = 1.0$ M ($I =$ 4 M) no reproducible solubilities could be obtained.

Samples of the solid phase were frequently withdrawn and analyzed for bromide in the same manner as described for iodide [2] (Table 1).

Table 1. Bromide content in the solid phase equilibrated with solutions of various compositions.

Phase	I M	C_L M	% Br
ML_3		*Theoretical*	*59.80*
	1	0.90	60.0
	4	4.00	59.3
ML_2A		*Theoretical*	*38.01*
	1	0.90	38.3
	1	0.50	38.4
	1	0.47	38.1
	4	2.8	37.6
	4	1.5	37.7
MA_3	1	0.44	0
	4	1.5	0

RESULTS, CALCULATIONS

The same notation is used as in Refs. 1 and 2. For the two constant ionic strengths 1 M and 4 M, the observed solubilities are given in Tables 2 and 3, respectively. A striking difference between the present system and the iodide system [2] is the appearance of a well-defined intermediate phase, $MBr_2(ClO_4)$(s), between MBr_3(s) at high $[Br^-]$ and $M(ClO_4)_3$(s) at low $[Br^-]$. As is obvious from Table 1, no solid solution formation [1] was observed. All three phases had,

Table 2. $I = 1$ M. Solubilities: experimentally observed (S_o), and calculated from the constants of Table 4 (S_c), *vs.* bromide ([L]) and perchlorate ([A]) concentration. Deviation $= 100(S_o - S_c)/S_c$. Ligand number: by eqn. (4) or eqn (5) ($\bar{n}_o$) and calculated from the constants ($\bar{n}_c$). Metastable points are marked (*).

Phase	C_L M	[L] M	[A] M	$S_o \times 10^3$ M	$S_c \times 10^3$ M	Dev. %	$\bar{n}_o$	$\bar{n}_c$
ML_3	1.000	1.005	0.000	1.918	1.906	+0.6	0.3	0.33
	0.960	0.965	0.040	2.111	2.125	−0.7		
	0.920	0.926	0.080	2.355	2.373	−0.8		
	0.900*	0.906	0.100	2.536	2.517	+0.8	0.3	0.31
ML_2A	0.900	0.903	0.1022	2.225	2.227	−0.1		
	0.850	0.853	0.1516	1.649	1.654	−0.3		
	0.800	0.802	0.2014	1.393	1.385	+0.6		
	0.700	0.702	0.3012	1.169	1.167	+0.2		
	0.600	0.602	0.401	1.153	1.150	+0.2	0.2	0.20
	0.500	0.502	0.501	1.277	1.277	0.0		
	0.470	0.472	0.531	1.340	1.345	−0.4	0.2	0.17
MA_3	0.450	0.450	0.554	1.339	1.343	−0.3	0.1	0.16
	0.440	0.440	0.564	1.271	1.268	+0.2		
	0.3000	0.2999	0.702	0.621	0.625	−0.6		
	0.1000	0.1000	0.901	0.275	0.2739	+0.4	0.04	0.04
	0	0	1.001	0.192	0.1922	−0.1		

Table 3. $I = 4$ M. *Cf.* Table 2. Here, $[L] = C_L$ and $[A] = 4.000 - C_L$.

Phase	C_L M	$S_o \times 10^4$ M	$S_c \times 10^4$ M	Dev. %	$\bar{n}_o$	$\bar{n}_c$
ML_3	4.000	1.96	1.956	+0.2	1.1	1.13
	3.900	2.05	2.052	−0.1		
	3.800	2.17	2.156	+0.6		
	3.700	2.27	2.270	0.0		
	3.600	2.40	2.395	+0.2		
	3.500*	2.51	2.532	−0.9	1.1	1.02
ML_2A	3.500	2.360	2.379	−0.8		
	3.400	2.065	2.041	+1.1		
	3.300	1.780	1.803	−1.3		
	3.200	1.618	1.629	−0.7		
	3.000	1.392	1.397	−0.4	0.8	0.91
	2.800	1.276	1.258	+1.4		
	2.600	1.172	1.176	−0.4		
	2.200	1.138	1.127	+1.0		
	2.000	1.155	1.150	+0.4	0.6	0.65
	1.600	1.306	1.311	−0.4		
	1.500	1.384	1.384	0.0		
MA_3	1.500*	1.495	1.513	−1.2		
	1.200	0.970	0.958	+1.3	0.5	0.38
	1.000	0.724	0.725	−0.2		

however, a tendency to be metastable just outside their stability ranges. Once a transition had started, though, it proceeded rapidly and completely, in the saturator. The phase transition points generally were approached both from

high and from low [Br^-]. It was always possible to return over a phase transition point and, once the earlier phase was reestablished, obtain the same solubilities as before.

When $I = 1$ M, some indications of the formation of the phase $MBr(ClO_4)_2(s)$ around $C_L = 0.45$ M were observed. Later attempts to confirm these findings failed, however. This could possibly be due to a persistent metastability of the adjacent phases, and we shall not exclude the possibility that $MBr(ClO_4)_2(s)$ has a narrow range of existence between $MBr_2(ClO_4)(s)$ and $M(ClO_4)_3(s)$.

If Br^- is denoted by L and ClO_4^- by A, the solubility of the solid phase ML_jA_{3-j} $(0 \leq j \leq 3)$ is given by

$$S = K_s(j)\, X[L]^{-j}[A]^{j-3} \tag{1}$$

where $X = \sum_{n=0}^{N} \beta_n[L]^n$

represents the complex formation in the solution, and $K_s(j)$ is the solubility product. Complexes involving ClO_4^- are assumed to be absent.

At equilibrium, [L] and [A] may differ slightly from the initial values, C_L and $I - C_L$:

$$[L] = C_L + (j - \bar{n})S \tag{2}$$

$$[A] = I - C_L + (3 - j)S \tag{3}$$

(See Tables 2 and 3.)
The minor changes in ionic strength have been neglected.

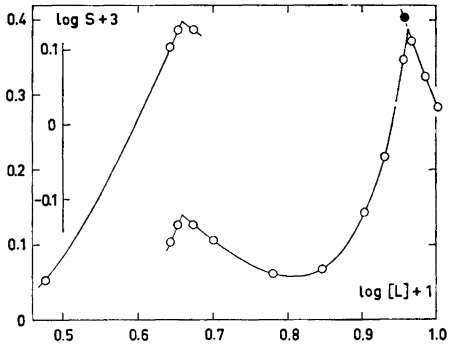

Fig. 1. 1 M ionic strength: log S *vs.* log [L]. The points are the observed values; the curves are calculated from the constants given in Table 4. The left part is raised and conforms to the inner ordinate scale. Metastability is indicated by dashed curve and filled symbols.

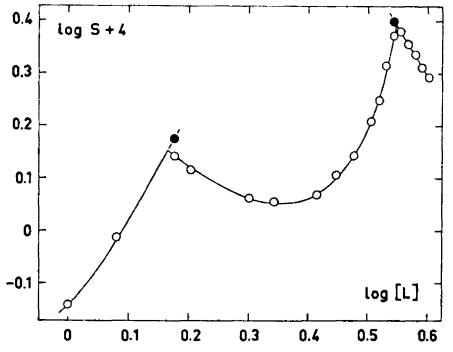

Fig. 2. 4 M ionic strength: log S *vs.* log [L]. See Fig. 1.

The slope of a plot of log S *vs.* log [L] (Figs. 1 and 2) yields important information [13] on the complex formation as well as on changes in the solid phase. The following derivative is obtained from eqn. (1) (provided $I = [L] + [A]$)

$$D = \frac{\mathrm{d}\log S}{\mathrm{d}\log[\mathrm{L}]} = \bar{n} - j + (3-j)\frac{[\mathrm{L}]}{I-[\mathrm{L}]} \tag{4}$$

Thus, as soon as the composition (*i.e.* j) of the solid phase is known, $\bar{n}$ can be estimated from the slope of the solubility curve. A few $\bar{n}$ values estimated in this way are given in Tables 2 and 3.

For MA_3(s) it may be an advantage to plot log S *vs.* log [A]. From eqn. (1) ($j=0$) then

$$\frac{\mathrm{d}\log S}{\mathrm{d}\log[\mathrm{A}]} = -\left(\frac{\bar{n}}{[\mathrm{L}]}[\mathrm{A}] + 3\right) \tag{5}$$

The limiting value of this derivative as [L] approaches zero is $-(\beta_1 I + 3)$. When $I = 1$ M, the $\bar{n}$ values for MA_3(s) given in Table 2 were obtained from a plot of log S *vs.* log [A]. The limiting value of the slope was -3.4, indicating a value of $\beta_1 \approx 0.4$.

As eqn. (4) shows, an intermediate phase like ML_2A(s) may exhibit a minimum solubility, even if no complex formation takes place ($\bar{n}=0$) or, as in the present case, $\bar{n}$ is small and varies only slightly. If no complexes were formed, the minimum would occur at $[\mathrm{L}] = 2/3\ I$; it is found here at somewhat lower values, $[\mathrm{L}] \approx 0.65$ M and $[\mathrm{L}] \approx 2.26$ M, when $I = 1$ and 4 M, the displacements being caused by the complex formation.

Close to a phase transition point, the slopes for both phases (characterized by j_1 and j_2, respectively) can be estimated at the same [L]. Eqn. (4) then gives

$$D_1 - D_2 = (j_2 - j_1)\ I/(I - [\mathrm{L}]) \tag{6}$$

Thus, when $I = 1$ M, we find at $[\mathrm{L}] = 0.89$ M $D_1 = 6.2(3)$ and $D_2 = -2.7(1)$ (estimated errors in the last digit given within parentheses). Hence, $j_2 - j_1 = 0.98(4)$. For $[\mathrm{L}] = 0.45$ the slopes are 2.7(1) and $-0.92(3)$, respectively, giving a change in j of 1.99(6). The corresponding changes in j when $I = 4$ M are 0.96(4) and 2.0(2), respectively. The changes found by analysis of the solid phase (Table 1) are thus amply confirmed by the solubility data.

The stability constants were computed in the following way. According to eqn. (1)

$$S[\mathrm{L}]^j[\mathrm{A}]^{3-j} = K_s(j)X \tag{7}$$

S, [L], and [A] being known, $K_s(j)X$ can thus always be computed. When $I = 1$ M, $K_s(j)X$ was plotted *vs.* [L] separately for the phases MA_3(s) and ML_2A(s). Good straight lines resulted, thus implying that only the first complex, ML, is formed. However, the values of β_1 obtained were slightly different: 0.42(1) and 0.48(2). This fact, in conjunction with the findings when $I = 4$ M (below), leads one to conclude that also ML_2 is formed to a slight degree. It was found that an assumed value of $\beta_2 = 0.10\ \beta_1$ (*cf.* 4 M ionic strength, Table 4) gave the same value of $\beta_1 = 0.40(2)$ for both phases, MA_3(s) and ML_2A(s). The phase ML_3(s) has too narrow a range of existence to allow an independent evaluation of β_1 (and β_2). However, the $K_s(3)X$ values for this phase were divided by X, as calculated from the β_1 and β_2 values just obtained. The re-

sulting $K_s(3)$ showed no systematic variation. Thus, the $ML_3(s)$ data also fit to these stability constant values (Table 2).

When $I = 4$ M, only $ML_2A(s)$ could be studied in a broad range of [L] (Fig. 2). For this phase, $K_s(2)X$ was plotted vs. [L]. Then, $K_s(j)X$ for $MA_3(s)$ and $ML_3(s)$ were multiplied by suitable factors, a and b respectively, so that they fell on the same curve as $K_s(2)X$. From the resulting data set the constants $K_s(2)$, β_1, β_2, and β_3 were extracted (graphically). The other solubility products were obtained as

$$K_s(0) = K_s(2)/a \text{ and } K_s(3) = K_s(2)/b$$

As is obvious from Table 3, the data for all three phases fit to the common set of stability constants.

Table 4. Solubility products of $Co(NH_3)_6Br_3(s)$, $Co(NH_3)_6Br_2(ClO_4)(s)$, and $Co(NH_3)_6(ClO_4)_3(s)$. Stability constants of the $Co(NH_3)_6^{3+} - Br^-$ system. The estimated error of the last digit is given within parentheses.

I M	$K_s(3) \times 10^3$ M	$K_s(2) \times 10^3$ M	$K_s(0) \times 10^3$ M	β_1 M^{-1}	β_2 M^{-2}	β_3 M^{-3}
1	1.34(2)	0.133(2)	0.193(1)	0.40(2)	0.04(2)	–
4	3.3(2)	0.44(3)	1.32(10)	0.43(5)	0.045(10)	0.006(4)

From the solubility products now being known, [L] of the phase transition points can be determined. In a transition point, eqn. (1) is valid for both phases, with S, [A], and [L] and hence also X equal. This gives the following expression

$$K_s(j_1)/K_s(j_2) = ([L]/[A])^{j_1 - j_2} \quad (8)$$

By eqn. (8) it was found that $MA_3(s)$ changes to $ML_2A(s)$ for $[L] = 0.455$ M and $ML_2A(s)$ changes to $ML_3(s)$ for $[L] = 0.915$ M, when $I = 1$ M. The corresponding points at 4 M ionic strength are 1.46 M and 3.53 M.

Table 4 summarizes the various constants obtained.

Table 5. Floating ionic strength. Solubility of $Co(NH_3)_6Br_3(s)$ *vs.* bromide concentration: C_L, $S \times 10^4$; 4.0, 1.96; 3.5, 2.54; 3.0, 3.45; 2.5, 4.50; 2.0, 6.39; 1.5, 10.47; 1.0, 19.18.

The solubility of $ML_3(s)$ in NaBr (floating ionic strength) is given in Table 5. In the plot of log S *vs.* log [L] (Fig. 3), the slope tends to *decrease* with increasing [L]. This unexpected behaviour can be explained only by medium effects. Probably, it mainly reflects a maximum in the solubility product of $ML_3(s)$ caused by the minimum in activity factors usually encountered around $I = 2$ M.[16] It may be noted that the same trend was found in the $Co(NH_3)_6^{3+} - [I^-]$ system (Table 2 of Ref. 2: $[I^-] = 1$, 2, and 4 M).

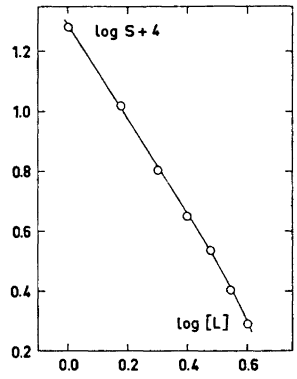

Fig. 3. Floating ionic strength: log S *vs.* log [L]. Best curve drawn.

DISCUSSION

Table 6 shows the result of earlier determinations of β_1 in the hexaammine-cobalt bromide system. In addition, some more qualitative studies have been reported.[9–11]

Table 6. Earlier studies on the $Co(NH_3)_6^{3+} - Br^-$ system at 25°C.

Reference	Method	I M	β_1 M^{-1}
Bjerrum [14,6]	Theory	0	66
Nancollas *et al.*[3,15]	Spectr.	0.054	46
»	»	→0	240
King *et al.* (35°C) [4]		0.9	< 0.2
»	»	→0	< 5
Tanaka *et al.*[5]	»	0.07	2.2
»	»	→0	9
Katayama *et al.*[6]	Cond.	0	45
Miranov *et al.*[7]	Soly.	~0.2	0.8
»	»	→0	95
Heck [8]	Spectr.	0.0120	35.7
»	»	0.0048	37.7
»	»	0.0024	40.5
»	»	→0	60

In all studies summarized in Table 6, attempts have been made to assign a value to β_1 at zero ionic strength. When these values are compared, it is obvious that the spectrophotometric L-method gives, as explained earlier,[12] completely irrelevant values of β_1. Disregarding these values,[4,5] the remainder fall in the range 45 to 240 M^{-1}. Bearing in mind that none of the latter studies are completely unambiguous, and that the extrapolations to zero ionic strength are always more or less uncertain, the agreement is satisfactory. There is little doubt that the correct value is positioned somewhere within this range.

With reference also to the present work, the spectacular decrease of β_1, when the ionic strength is increased from zero to ≈ 1 M, is noted. At least three factors can be mentioned as possible causes of this decrease: the decrease of activity factors with increasing ionic strength, medium effects at constant ionic strength, and perchlorate association. The first is the most significant factor and is the one that should be eliminated on extrapolation to zero ionic strength. The other two may be termed systematic errors and have been discussed in detail earlier.[2] In the present study, activity factors may change, at constant ionic strength, due to the exchange of $NaClO_4$ for NaBr. The effect is probably not negligible, as it was in the iodide case, but the crude estimates outlined [2] indicate it to be of a modest magnitude (~ 10 % in β_1). Moreover, the medium effects in this case tend to increase the stability constants, the observed values being higher than the "true" ones.

Perchlorate association, on the other hand, necessarily decreases the observed stability constants.[1,2] The effect is believed to be of some significance as far as β_1 is concerned.[2,8] From a comparison with the measurements in perchlorate-free solutions (Table 5), no safe conclusions can be drawn about the perchlorate effect, as strong medium effects are evidently on hand here.

Regarding the higher complexes, ML_2 and, especially, ML_3, the effects of medium changes as well as of perchlorate association should reasonably be smaller. Therefore, there cannot be any doubt about the existence of these species. On the other hand, there is no indication of the formation of ML_4, either at constant (Fig. 2) or floating (Fig. 3) ionic strength. Actually, the curves are far from any minimum ($\bar{n} = 3$) in both cases. It might be argued that the appearance of ML_4 is masked by perchlorate association and medium changes. However, it is difficult to imagine these effects to be of the required magnitude. It seems safe to conclude that ML_4 is formed only in negligible amounts for $[L] \leq 4$ M. This naturally does not mean to say that ML_4 *cannot* be formed. That question has to be left unanswered by the present measurements. The views held by Larsson [9] are thus partially confirmed: species higher than ML do exist. It is probable, however, that the degree of complex formation at high ligand concentration, as inferred from the anion exchange measurements,[9] is strongly overestimated.

The smooth decrease of β_n as n increases confirms the earlier findings [2,1] that $Co(NH_3)_6^{3+}$ forms halide complexes in a more regular way than does $Coen_3^{3+}$.

In conclusion, the present study gives reliable evidence for the existence of ML_2 and ML_3. Together with a suitably weighted average value of β_1 at zero ionic strength (Table 6), this is believed to give a fairly true description of the hexaamminecobalt bromide system. From various lines of evidence it is inferred that ClO_4^- associates to $Co(NH_3)_6^{3+}$ (and similar ions). A more quantitative knowledge of the degree of this association at different ionic strengths is lacking but would be very valuable.

This work was supported by a grant from the *Swedish Natural Science Research Council*. The author is indebted to Dr. Ragnar Larsson for stimulating discussions. The skilful technical assistance of Mrs. Agneta Nilsson is gratefully acknowledged.

REFERENCES

1. Johansson, L. *Acta Chem. Scand.* **25** (1971) 3752.
2. Johansson, L. *Acta Chem. Scand.* **27** (1973) 1637.
3. Evans, M. G. and Nancollas, G. H. *Trans. Faraday Soc.* **49** (1953) 363.
4. King, E. L., Espenson, J. H. and Visco, R. E. *J. Phys. Chem.* **63** (1959) 755.
5. Tanaka, N., Kobayashi, Y. and Kamada, M. *Bull. Chem. Soc. Japan* **40** (1967) 2839.
6. Katayama, S. and Tamamushi, R. *Bull. Chem. Soc. Japan* **41** (1968) 606.
7. Mironov, V. E., Lyubomirova, K. N. and Ragulin, G. K. *Zh. Fiz. Khim.* **44** (1970) 416.
8. Heck, L. *Habilitationsschrift*, Saarbrücken 1972.
9. Larsson, R. and Tobiasson, I. *Acta Chem. Scand.* **16** (1962) 1919.
10. Mazzei, M. and Lederer, M. *J. Chromatog.* **31** (1967) 196.
11. Yoneda, H., Muto, M., Baba, T. and Miura, T. *Bull. Chem. Soc. Japan* **44** (1971) 689.
12. Johansson, L. *Acta Chem. Scand.* **25** (1971) 3569.
13. Johansson, L. *Coord. Chem. Rev.* **3** (1968) 293.
14. Bjerrum, N. *Kgl. Danske Videnskab. Selskab, Mat.-Fys. Medd.* **7** (1926) No. 9.
15. Nancollas, G. H. *J. Chem. Soc.* **1955** 1458.
16. Harned, H. S. and Owen, B. B. *Physical Chemistry of Electrolytic Solutions*, 3rd Ed., Reinhold, N.Y. 1967.

Received March 14, 1973.

ACTA CHEMICA SCANDINAVICA 27 (1973) 2344–2350

Thermodynamic Properties of Rare Earth Complexes

XV. Enthalpy and Heat Capacity Changes for the Formation of Rare Earth EDTA Complexes from $MgEDTA^{2-}$ at 10, 20, 30 and 40°C

HEIKKI OTS

Division of Physical Chemistry 1, Chemical Center, University of Lund, P.O.B. 740, S-220 07 Lund 7, Sweden

The changes in enthalpy and heat capacity for the formation of La(III), Pr(III), Nd(III), Sm(III), Eu(III), Gd(III), Tb(III), Ho(III), and Yb(III) EDTA complexes according to the reaction

$$MgEDTA^{2-} + Ln^{3+} \rightarrow LnEDTA^{-} + Mg^{2+}$$

have been determined at 10.00, 20.00, 30.00, and 40.00°C. In addition, for La(III), Eu(III), and Tb(III), determinations have also been made at 15.00, 25.00, and 35.00°C. All data refer to an aqueous sodium perchlorate solvent with the sodium ion concentration equal to 1.00 M. The enthalpy changes at the various temperatures were obtained from direct calorimetric determinations and these data have been fitted to polynomials of the type

$$\Delta H^\circ = A + BT + CT^2 + DT^3$$

From these functions, the corresponding heat capacity changes have been obtained. The heat capacity data for the rare earth EDTA complexes indicate the presence of a hydration equilibrium of the same type as previously found for the second rare earth diglycolate complexes.

In previous communications,[1,2] we have discussed the relative merits of spectroscopic and thermodynamic methods to establish the occurrence of hydration equilibria among rare earth complexes. The spectroscopic method has been used very successfully in the study of hydration equilibria among the rare earth EDTA complexes.[3,4] However, it is quite clear that this method is useful only in systems where the absorption bands of the metal ion are changed substantially by changes in the coordination shell. Changes in the surroundings normally show only a small influence on the $f-f$ transitions, a fact which severely restricts the use of the spectroscopic method in lanthanoid systems.[2] Geier's study [3,4] of europium EDTA complexes is one case where the method has been applied with good results. It seemed worthwhile to

investigate this system also with the thermodynamic method, that is, a determination of ΔC_P° as outlined in Refs. 1 and 2, in order to compare the results of the two methods.

In the present investigation the enthalpy changes for the reaction

$$MgEDTA^{2-} + Ln^{3+} \rightarrow LnEDTA^- + Mg^{2+} \quad (1)$$

have been determined by a direct calorimetric method at 10, 20, 30, and 40°C. This method gives the same information on the occurrence of hydration equilibria among the $LnEDTA^-$-complexes as the direct determination

$$Ln^{3+} + EDTA^{4-} \rightarrow LnEDTA^- \quad (2)$$

but is experimentally much easier to use.

The investigation has included nine lanthanoids, *i.e.* La(III), Pr(III), Nd(III), Sm(III), Eu(III), Gd(III), Tb(III), Ho(III), and Yb(III). In order to investigate the accuracy of the $\Delta H^\circ - T$ functions normally obtained from four experimental temperatures only, determinations of the enthalpy changes have been made for La(III), Eu(III), and Tb(III) also at 15, 25, and 35°C.

The stability constants for reaction (1) are large [6] and a quantitative amount of $LnEDTA^-$ is thus formed when Ln^{3+} is added to a solution of $MgEDTA^{2-}$. All measurements refer to an aqueous perchlorate medium with 1.00 M total sodium ion concentration. All concentrations, volumes and additions in this study refer to 25°C as discussed in a preceding publication.[1]

EXPERIMENTAL

Chemicals. Rare earth oxides were obtained from the American Potash & Chemical Corp. Stock solutions of the rare earth perchlorates were prepared and standardized as described by Grenthe *et al.*[7] The $Na_2MgEDTA$ used was obtained from the Siegfried Company. Standardization of the stock solutions of the salt was done by addition of known amounts of Zn^{2+}-ions in excess to the solutions, this excess being then back-titrated with a standard EDTA-solution using xylenol orange as an indicator. Sodium perchlorate was obtained from Baker ($NaClO_4.H_2O$, *p.a.*).

Calorimetric titrations. The calorimeter used has been recently described.[5] The experimental procedure was the same as before.[5,8] The calorimeter was filled with 100.054 cm^3 (V_0) of a solution S. From calibrated piston burettes, known volumes (v) of a solution T were added. The solutions S and T had the following compositions:

$$S \left\{ \begin{array}{l} C_M\ Ln(ClO_4)_3 \\ pH = 7.0 \\ 1.00\ M\ NaClO_4 \end{array} \right. \qquad T \left\{ \begin{array}{l} C_A\ Na_2MgEDTA \\ pH = 7.0 \\ (1.00\ M - 2\ C_A)\ NaClO_4 \end{array} \right.$$

All the concentrations, C_M, were about 10 mM. The concentration, C_A, of $MgEDTA^{2-}$ in solution T was 0.08317 M. The sodium ion concentration was 1.00 M in all the measurements.

The solution T was added in portions of 2.000 cm^3 at all temperatures. The enthalpy change (not corrected for the dilution) for reaction (1) can be calculated directly for each addition. At least four additions were made for each system at each temperature. From the concentrations given above it follows that the titrations are performed at excess of metal ion.

The solutions S were prepared just before use by a potentiometric neutralisation of the slightly acid ($\approx 10^{-3}$ M $HClO_4$) stock solutions by titration with NaOH. When the calorimetric titrations are performed at a low and constant hydrogen ion concentration, enthalpy changes associated with the protonation reactions of the EDTA-ions can be neglected. The same principle has been used previously by Spedding *et al.*[9]

However, the method used in this study has one disadvantage. The formation of hydrolytic products in the rare earth perchlorate solutions cannot be avoided. The investigations by Biedermann *et al.*[10,11] on Ce^{3+} and Y^{3+} indicate, on the other hand, that the hydrolysis at pH = 7.0 and [M] = 10 mM is negligible in the first half of the rare earth series. In the second half of the series the hydrolysis is gradually increasing so that at the end at most 1.5 % of the metal ions are present as hydroxo complexes. The predominating hydrolysis products are MOH^{2+} and $M_2(OH)_2^{4+}$ which occur in approximately equal amounts in the solutions used. The concentration of the hydroxo complexes varies with the change of concentration of the free lanthanoid ions, *i.e.* with the amount of $MgEDTA^{2-}$ complex added in the titrations. The enthalpy change associated with the dissociation of the hydroxo complexes is estimated [12–14] to 10 – 12 kJ mol^{-1} for a reaction of the type

$$MOH \rightarrow M + OH \qquad (3)$$

The influence of the hydroxo complexes on the measured enthalpy changes for reaction (1) can be estimated from Biedermann's stability constants and the above value of the enthalpy change for reaction (3). The correction is at most 200 J mol^{-1} for the elements with an ionic radius close to that of yttrium (*i.e.* the elements around erbium). This is approximately 1 % of the total heat evolved at complex formation with EDTA and cannot affect the general picture.

The heats of dilution of the T-solution have been determined and were found to be small in the whole temperature range used. The heats of dilution of the rare earth perchlorate solutions have been neglected.

The thermodynamic standard state in this study is chosen as before.[2]

RESULTS

The experimental Q-values obtained from the calorimetric titrations ranged from 2.5 to 4 J. The correction for the dilution of the $Na_2MgEDTA$-solution was largest at 10°C and at most 3 % of the total heat evolved. At higher temperatures, the correction never exceeded 1 %. The enthalpy changes calculated from the corrected Q-values for the various systems are given in Table 1. The error is given as one standard deviation and is based on five determinations, except at 40°C where only four determinations have been made. The uncertainties in the experimental $\Delta H°$-values are approximately the same for all the systems at all temperatures.

The temperature dependence of the enthalpy changes for the formation of the rare earth EDTA complexes was described by the same type of functions as for the rare earth diglycolate complexes,[2] *i.e.* polynomials of the type:

$$\Delta H° = A + BT + CT^2 + DT^3 \qquad (4)$$

The constants in the equation have been based on four experimental temperatures for all systems except for La(III), Eu(III), and Tb(III). In order to check the accuracy of such a fit, a comparison has been made for these elements between the constants obtained from experimental values at four and at seven temperatures. This comparison showed that the agreement between the two sets of constants was satisfactory and hence no significant error is introduced if the temperature dependence of the enthalpy changes are based on only four experimental values. In fact, an inspection of the results obtained for, *e.g.*, Eu, will show that the temperature variation of $\Delta C_P°$ will differ *at most* by 2 J/K mol depending on which of the two sets of constants that is used.

Table 1. The enthalpy changes $\Delta H°$ with their corresponding standard deviations for the various rare earth EDTA complexes at 10, 15, 20, 25, 30, 35, and 40°C.

Metal ion	$-\Delta H_{283}°$ / kJ mol^{-1}	$-\Delta H_{288}°$ / kJ mol^{-1}	$-\Delta H_{293}°$ / kJ mol^{-1}	$-\Delta H_{298}°$ / kJ mol^{-1}	$-\Delta H_{303}°$ / kJ mol^{-1}	$-\Delta H_{308}°$ / kJ mol^{-1}	$-\Delta H_{313}°$ / kJ mol^{-1}
La	22.113±0.045	21.512±0.061	21.004±0.023	20.579±0.059	20.111±0.050	19.614±0.034	18.989±0.060
Pr	22.825±0.026		21.886±0.065		21.182±0.052		20.351±0.052
Nd	24.391±0.050		23.304±0.095		22.560±0.037		21.672±0.097
Sm	25.334±0.070		23.946±0.041		22.716±0.061		21.354±0.020
Eu	23.270±0.040	22.540±0.103	21.881±0.039	21.242±0.050	20.651±0.012	20.014±0.039	19.369±0.021
Gd	20.323±0.025		19.133±0.010		18.181±0.029		17.067±0.029
Tb	16.658±0.052	16.489±0.079	16.385±0.034	16.275±0.027	16.177±0.017	15.933±0.032	15.649±0.019
Ho	16.834±0.045		16.928±0.017		17.052±0.009		16.798±0.017
Yb	19.976±0.092		20.003±0.031		20.206±0.016		20.140±0.044

Table 2. The enthalpy changes and heat capacity changes at 25°C calculated from the eqns. (4) for the various rare earths.

Metal ion	$-\Delta H_{298}^{\circ}$ / kJ mol^{-1}	ΔC_{p298}° / J K^{-1} mol^{-1}
La	20.567	87.5
Pr	21.528	68.9
Nd	22.920	72.4
Sm	23.330	121.8
Eu	21.251	122.8
Gd	18.651	93.5
Tb	16.284	21.5
Ho	17.012	−14.1
Yb	20.110	−22.2

The enthalpy and heat capacity changes at 25.0°C obtained from the functions of type (4) for the various rare earths are given in Table 2. The ΔH°-values at 25°C in this study are not in agreement with those reported by Spedding *et al.*[9] for the corresponding reaction (1). However, this is not unexpected because of differences in both ionic strength and ionic medium.

The variation through the rare earth series of the heat capacity change ΔC_p° at 25.0°C for reaction (1) is shown in Fig. 1. The ΔC_p°-values pass through

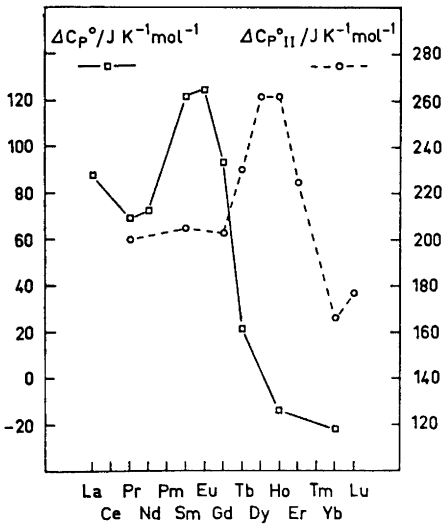

Fig. 1. The heat capacity changes at 25° for the reactions $Ln(ClO_4)_3 + Na_2MgEDTA \rightarrow NaLnEDTA + NaClO_4 + Mg(ClO_4)_2$ (□) and $Ln(ClO_4)_3 + 2Na_2(diglyc) \rightarrow NaLn(diglyc)_2 + 3NaClO_4$ (○).

a maximum at europium. The appearance of a maximum is a strong indication for the presence of a hydration equilibrium for the LnEDTA complexes. The conclusion from this investigation is in agreement with that drawn by Geier [3] on the basis of his spectroscopic investigation of the europium-EDTA system.

Thus, both the thermodynamic and spectroscopic methods give in this case compatible results.

For comparison, also the variation of the over-all heat capacity change $\Delta C_P^\circ{}_{II}$ for the diglycolate system is shown in Fig. 1. This heat capacity change corresponds to the reaction

$$Ln^{3+} + 2A^{2-} \rightarrow LnA_2^+ \quad (5)$$

The reason for the comparison between $\Delta C_P^\circ{}_{II}$ for the diglycolate system and ΔC_P° for the EDTA system is, that the geometries of the coordination shells of both complexes are expected to be similar. Both ligands in the second diglycolate complex are expected to occupy positions in the same half of the coordination sphere which results in a geometry similar to that found by Hoard *et al.*[16] in the rare earth EDTA complexes.

DISCUSSION

In a recent study, we have determined the partial molal heat capacities for various rare earth perchlorates.[15] The $\bar{C}_P^\circ$-values are very near constant through the rare earth series, from which we conclude that there are no hydration equilibria for the hydrated rare earth ions. This conclusion is in agreement with the results of previous investigations.[3,17,18] The most important result of this is that the variations of ΔC_P° with Z for complex formation reactions between the rare earth ions and ligands always will reflect the changes of the partial molal heat capacity of the complex formed.

An exception from the near constancy in $\bar{C}_P^\circ$ was found for $La(ClO_4)_3$ for which the $\bar{C}_P^\circ$-value was lower than for the other rare earths. The difference is 29 ± 6 J K^{-1} mol^{-1} which is in good agreement with the difference between the ΔC_P°-values for Pr and La found in this study. The high value of ΔC_P° for the formation of the LaEDTA complex has thus nothing to do with the hydration equilibrium discussed here, but is a reflection of the different properties of lanthanum as compared with the other rare earths. For this reason, lanthanum will be excluded from further discussion here.

The variations of $\Delta C_P^\circ{}_{II}$ and $\Delta C_P^\circ{}_{EDTA}$ with Z in Fig. 1 are very similar; *e.g.* the height of the maximum is about the same in both cases. The most obvious difference between the two systems is that the maxima occur in different parts of the rare earth series, for the EDTA complexes at Eu and for the second diglycolate complexes at Dy-Ho. (It must be pointed out once more that for the formation of the first diglycolate complexes, no hydration equilibria seem to be involved.[2]) The element for which the two differently hydrated complexes have the same free energy obviously varies with the geometry of the ligand, *e.g.* from Pr – Nd in the 1,3-diaminopropane-*N*,*N*,*N*′,*N*′-tetraacetate complexes [18] ("TMTA") *via* Eu in the EDTA complexes to Dy – Ho in the second oxydiacetate complexes.

In a recent spectroscopic investigation on lanthanoid EDTA-complexes Ternovaya and Kostromina [19] found two "isomeric forms" of europium-EDTA complexes in solution. According to their interpretation of the ex-

perimental data these two forms are: $EuEDTA(H_2O)_x$ (five-coordinated EDTA) and $EuEDTA(H_2O)_{x-1}$ (six-coordinated EDTA). Furthermore, the five-coordinated and six-coordinated forms should be the dominating species at the beginning and at the end of the rare earth series, respectively, with a region of equilibrium in between.

The Russian authors have based their interpretation on a comparison of spectra of solid lanthanoid EDTA-complexes with the corresponding spectra in solution. A necessary assumption is that there is a change in the number of bonded carboxylate groups in the solid NaLnEDTA-complexes between La and Lu. No X-ray data are supplied to corroborate this assumption. On the other hand, Hoard *et al.*[16] have made structure determinations of $KLaEDTA.8H_2O$ and $KTbEDTA.8H_2O$ and found no evidence of a change in the number of coordinated carboxylate groups.

The Russian interpretation is certainly in agreement with our thermodynamic data but, in view of the available X-ray data, we prefer our own. A change in the number of coordinated carboxylate groups might be acceptable in the EDTA-system in which the ligand has many binding sites. However, for the diglycolate complexes, for which we have found the same thermodynamic behaviour as for the EDTA-complexes, it is hard to understand how such a change of the coordination number vis-à-vis the ligand could be explained.

This project has been sponsored by a grant from the *Swedish Natural Science Research Council*.

REFERENCES

1. Grenthe, I. and Ots, H. *Acta Chem. Scand.* **26** (1972) 1217.
2. Grenthe, I. and Ots, H. *Acta Chem. Scand.* **26** (1972) 1229.
3. Geier, G., Karlén, U. and v. Zelewsky, A. *Helv. Chim. Acta* **52** (1969) 1967.
4. Geier, G., and Jörgensen, C. K. *Chem. Phys. Letters* **9** (1971) 263.
5. Ots, H. *Acta Chem. Scand.* **26** (1972) 3810.
6. Betts, R. H. and Dahlinger, O. F. *Can. J. Chem.* **37** (1959) 91.
7. Grenthe, I. and Hansson, E. *Acta Chem. Scand.* **23** (1969) 611.
8. Grenthe, I., Ots, H. and Ginstrup, O. *Acta Chem. Scand.* **24** (1970) 1067.
9. Mackey, J. L., Powell, J. E. and Spedding, F. H. *J. Am. Chem. Soc.* **84** (1962) 2047.
10. Biedermann, G. and Newman, L. *Arkiv Kemi* **22** (1964) 303.
11. Biedermann, G. and Ciavatta, L. *Arkiv Kemi* **22** (1964) 253.
12. Arnek, R. and Schlyter, K. *Acta Chem. Scand.* **22** (1968) 1327.
13. Arnek, R. and Kakolowicz, W. *Acta Chem. Scand.* **21** (1967) 1449.
14. Hardwick, T. J. and Robertsson, E. *Can. J. Chem.* **29** (1951) 818.
15. Grenthe, I., Hessler, G. and Ots, H. *Acta Chem. Scand.* **27** (1973) 2543.
16. Hoard, J. L., Byunkook, L. and Lind, M. D. *J. Am. Chem. Soc.* **87** (1965) 1612.
17. Reuben, J. and Fiat, D. *J. Chem. Phys.* **51** (1969) 4909.
18. Anderegg, G. and Wenk, F. *Helv. Chim. Acta* **54** (1971) 216.
19. Ternovaya, T. V. and Kostromina, N. A. *Russ. J. Inorg. Chem.* **18** (1973) 190.

Received February 23, 1973.

ACTA CHEMICA SCANDINAVICA 27 (1973) 2351–2360

Thermodynamic Properties of Rare Earth Complexes

XVI. Thermodynamic Model for the Description of Hydration Equilibria among Rare Earth EDTA and Oxydiacetate Complexes

HEIKKI OTS

Division of Physical Chemistry, Chemical Center, University of Lund, P.O.B. 740, S-220 07 Lund 7, Sweden

A model is used to describe the variation of ΔC_P° with both Z an T in rare earth complexation reactions where hydration equilibria are involved. The results from both the EDTA and oxydiacetate investigations are discussed according to this model.

In a previous communication,[1] we have given a qualitative description of the effect of an equilibrium between two different states of hydration in a certain complex and the changes in some thermodynamic functions for the over-all reaction. In the following we will elaborate this description and eventually make a quantitative comparison between model and experiment.

The enthalpy change ΔH° for the over-all reaction

$$M(aq) + jA(aq) \rightarrow (1 - n)MA_j(H_2O)_x + nMA_j(H_2O)_y \quad (1)$$

is obtained experimentally. $(1-n)$ and n denote the number of mol (properly the fraction of mol) of the two different states of hydration, "x" and "y", of the complex MA_j.

If the enthalpy change for the reaction

$$MA_j(H_2O)_x \rightarrow MA_j(H_2O)_y + (x - y)H_2O \quad (2)$$

is denoted ΔH_H°, one obtains

$$\Delta H^\circ = \Delta H^{\circ(x)} + n\Delta H_H^\circ \quad (3)$$

where $\Delta H^{\circ(x)}$ is the change in enthalpy for the formation of one mol of the complex MA_j in the "x"-form and n is the number of mol of the complex in the "y"-form.

Derivation of expression (3) gives

$$\frac{d\Delta H^\circ}{dT} = \frac{d\Delta H^{\circ(x)}}{dT} + n\frac{d\Delta H_H^\circ}{dT} + \Delta H_H^\circ \frac{dn}{dT}$$

or

$$\Delta C_P^\circ = \Delta C_P^{\circ(x)} + n\Delta C_{PH}^\circ + \Delta H_H^\circ \frac{dn}{dT} \quad (4)$$

ΔC_P° is a quantity which is obtained experimentally from the temperature variation of ΔH°. $\Delta C_P^{\circ(x)}$ is the heat capacity change in a reaction where only the species $MA_j(H_2O)_x$ is formed and ΔC_{PH}° is the heat capacity change for reaction (2). dn/dT is the temperature derivate of n for the element "M".

The equilibrium constant for a possible hydration equilibrium of type (2) will be a function of both the ionic radius (or the atomic number Z) and the temperature. As will be discussed below, the second term in the right hand of eqn. (4) will be mainly dependent on Z while the third term will be strongly dependent on T.

It is obvious that the observed non-monotonic variation of ΔH° through the rare earth series for a number of rare earth complexation reactions might be a result of a hydration equilibrium with a positive value of ΔH_H°, if n is gradually increasing with Z (see eqn. (3)). Regarding the terms in eqn. (4), we then know that the third term is positive as both ΔH_H° and consequently also dn/dT are positive. The second term must be negative as all molecular theories will give ΔC_{PH}° a negative value for $x > y$. The opposite signs of the last two terms in eqn. (4) result in the appearance of a maximum in ΔC_P° plotted as a function of Z *if a hydration equilibrium is present.* The maximum is situated at the element for which dn/dT is largest.

A derivation of eqn. (4) gives the following result after rearranging:

$$\frac{d\Delta C_P^\circ}{dT} - \frac{d\Delta C_P^{\circ(x)}}{dT} = 2\Delta C_{PH}^\circ \frac{dn}{dT} + n\frac{d\Delta C_{PH}^\circ}{dT} + \Delta H_H^\circ \frac{d^2n}{dT^2} \quad (5)$$

This expression is a measure of the contribution to the temperature variation of ΔC_P° caused by the presence of hydration equilibria. Thus, the difference on the left hand side in eqn. (5) represents the difference in curvature between the $\Delta C_P^\circ(T)$- and $\Delta C_P^{\circ(x)}(T)$-functions, since $\Delta C_P^{\circ(x)}$ is the heat capacity change for a reaction where only the species $MA_j(H_2O)_x$ is formed (see p. 2358).

Test of the model. Let us now investigate how well the experimental ΔC_P°-(T,Z)-data can be described with this model. Unfortunately, there is no possibility of making any *a priori* statements about the various quantities in eqns. (4) and (5). They have instead to be determined from the experimental data. The procedure we will follow is to determine the quantities in the equations from the ΔH°-data obtained at only *one* temperature, supplemented with the temperature variation of ΔH° for two elements in the series chosen so that the form $MA_j(H_2O)_x$ dominates for one element and $MA_j(H_2O)_y$ for the other at *all* the investigated temperatures.

The EDTA-system. In Fig. 1 we have plotted the enthalpy changes for the formation of the various rare earth EDTA complexes against Z.[2] The plots have been made for all four temperatures investigated. The basis for our test

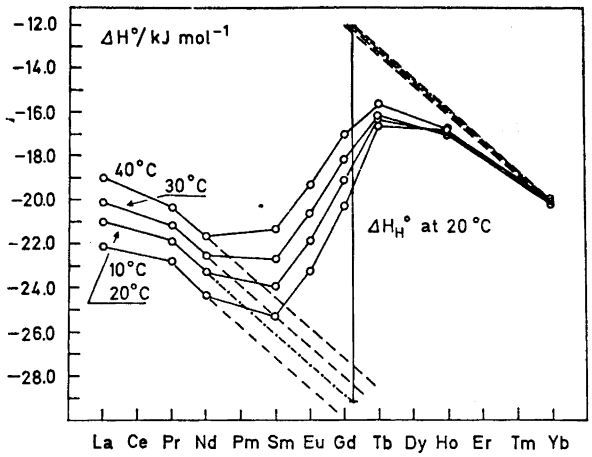

Fig. 1. The enthalpy changes $\Delta H°$ *versus* Z for the formation of rare earth EDTA complexes at 10, 20, 30, and 40°C. The figure demonstrates the determination of $\Delta H_H°$. The full-drawn curves at 10, 30, and 4°0C are calculated according to the model.

is the $\Delta H° - Z$ curve at 20°C. The enthalpy change, $\Delta H_H°$, for reaction (2) is determined on the following assumptions:

1. There is a linear dependence of both $\Delta H^{\circ(x)}$ and $\Delta H^{\circ(y)}$ on Z. $\Delta H^{\circ(y)}$ is the enthalpy change for the formation of one mol of the complex MA_j in the "y" form (*i.e.* $n = 1$ in eqn. (3)).
2. The two lines are parallel, *i.e.* the $\Delta H_H°$-value is the same for all elements in the series.
3. The slopes of the lines $\Delta H^{\circ(x)} - Z$ and $\Delta H^{\circ(y)} - Z$ are constant in the temperature range studied.

These assumptions are supported by empirical findings, *e.g.* a large number of investigations on the complex formation between rare earth ions and various ligands.

Under these conditions, the $\Delta H_H°$-value at 20°C is determined as shown in Fig. 1. As indicated by the $\Delta H° - Z$ curve at 20°C in this figure, the dominating species for Pr is the "x"-form and for Yb the "y"-form. From the temperature variation of $\Delta H°$ for these two elements, the $\Delta H_H°$-values at 10, 30, and 40°C are obtained on the same assumptions as above, *i.e.* parallel lines are drawn to the lines at 20°C. The $\Delta H_H°$-values are given in Table 1. Normally, these values should have been fitted to the same type of function as in the preceding publication[2] (*i.e.* a polynomial of the third degree; Ref. 2, p. 2346), but for simplicity the temperature variation of $\Delta H_H°$ is described by a polynomial of only the second degree. This can be done without any significant loss in accuracy. From this function the value at 25°C given in Table 1 is obtained. The $\Delta C_{PH}°$- and $d\Delta C_{PH}°/dT$-values in the same table are obtained from the $\Delta H_H°$-function by derivation.

Table 1. ΔH_H°, ΔC_{PH}° and $\frac{d(\Delta C_{PH}^\circ)}{dT}$ for reaction (2) at 5, 10, 20, 25, 30, 35, 40, and 50°C for the EDTA and diglycolate complexes obtained from the functions of the type

EDTA: $\Delta H_H^\circ = A + BT + CT^2$
Diglyc.: $\Delta H_H^\circ = A + BT + CT^2 + DT^3$

	EDTA			Diglyc.	
T / K	ΔH_H° / J mol^{-1}	ΔC_{PH}° / J K^{-1} mol^{-1}	$\frac{d(\Delta C_{PH}^\circ)}{dT}$ / J K^{-2} mol^{-1}	ΔH_H° / J mol^{-1}	ΔC_{PH}° / J K^{-1} mol^{-1}
278.15				15900	−67
283.15	18200	−115	1.3		
293.15	17175	−102	1.3	15350	−15
298.15	16650	−95	1.3	15300	−9
303.15	16150	−89	1.3		
308.15				15200	−13
313.15	15375	−76	1.3		
323.15				14700	−62

If the equilibrium constant for reaction (2) is K, we can apply the relation

$$\frac{d \ln K}{dT} = \frac{d}{dT} \ln \frac{n}{1-n} = \frac{\Delta H_H^\circ}{RT^2} \tag{6}$$

and calculate the n-values for each element in the series at any temperature in the range 10 – 40°C, provided that the n-values at *one* temperature are known. The necessary information can be obtained from the $\Delta H^\circ - Z$ curve at 20°C in Fig. 1. This is done by calculation of that fraction of the total enthalpy change, ΔH_H°, which each of the experimental ΔH°-values constitutes. The n-values obtained from eqn. (6) are used for the determinations of the derivatives dn/dT and d^2n/dT^2 which are necessary for the calculations according to eqns. (4) and (5).

Relation (6) can be transformed to

$$\frac{dn}{dT} = \frac{\Delta H_H^\circ n (1-n)}{RT^2} \tag{7}$$

which describes the variation of dn/dT with temperature. The values of n and dn/dT at 10, 20, 25, 30, and 40°C are given in Table 2. From these data the second and third terms on the right in eqn. (4) can be calculated at the above temperatures. The consequence of the three assumptions (p. 2353), under which the temperature dependence of ΔH_H° was determined, is that the $\Delta C_P^{\circ(x)}$-values vary with temperature but are at each temperature equal for all elements within the rare earth series. As the temperature variation of ΔH° for Pr is known (Ref. 2, p. 2347), the $\Delta C_P^{\circ(x)}$-values in (4) can be calculated from the experiment. The values used are 118, 76, 69, 71, and 102 J/K^{-1} mol^{-1} at 10, 20, 25, 30, and 40°C, respectively.

Table 2. The values of n and dn/dT for the various rare earth EDTA complexes at 10, 20, 25, 30, and 40°C.

Metal ion	283 K n / mol	283 K $\frac{dn}{dT} \times 10^3$ / mol K^{-1}	293 K n / mol	293 K $\frac{dn}{dT} \times 10^3$ / mol K^{-1}	298 K n / mol	298 K $\frac{dn}{dT} \times 10^3$ / mol K^{-1}	303 K n / mol	303 K $\frac{dn}{dT} \times 10^3$ / mol K^{-1}	313 K n / mol	313 K $\frac{dn}{dT} \times 10^3$ / mol K^{-1}
La	–	–	–	–	–	–	–	–	–	–
Pr	0	0	0	0	0	0	0	0	0	0
Nd	0	0	0	0	0	0	0	0	0	0
Sm	0.100	2.46	0.125	2.63	0.138	2.68	0.152	2.73	0.180	2.79
Eu	0.273	5.42	0.326	5.28	0.352	5.14	0.377	4.97	0.426	4.61
Gd	0.502	6.83	0.566	5.91	0.594	5.44	0.620	4.98	0.666	4.20
Tb	0.764	4.93	0.807	3.75	0.825	3.25	0.840	2.84	0.865	2.20
Ho	0.920	2.01	0.937	1.42	0.944	1.19	0.949	1.02	0.958	0.76
Yb	1.000	0	1.000	0	1.000	0	1.000	0	1.000	0

The values of ΔC_P° calculated from eqn. (4) using the data above show a satisfactory agreement with the experimental data at all temperatures (some values at 10°C are exceptions). In Fig. 2 the calculated $\Delta C_P^\circ - Z$ curve at

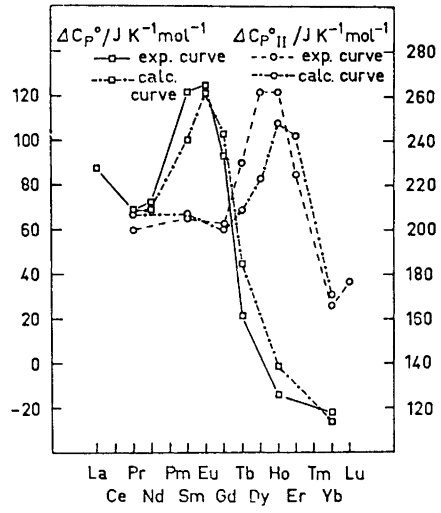

Fig. 2. The heat capacity changes at 25°C for the reactions $Ln(ClO_4)_3 + Na_2MgEDTA \rightarrow NaLnEDTA + NaClO_4 + Mg(ClO_4)_2$ (–□–) and $Ln(ClO_4)_2 + 2Na_2(diglyc) \rightarrow NaLn(diglyc)_2 + 3NaClO_4$ (--O--). The calculated curves for EDTA (·····□·····) and diglycolate (-·-·-O-·-·-) are also included.

25°C is plotted together with the experimental data for the EDTA-system. It must be kept in mind that the deviations shown in Fig. 2 are a result both of errors in the model and in the experimental data. The satisfactory agreement between experimental and calculated data is a good indication for the validity of the assumptions made and consequently the model and the parameters used can be considered to be essentially correct. The same conclusion is obtained

by comparing the ΔH°-values calculated from eqn. (3), using the data in Tables 1 and 2, with the corresponding experimental quantities. (The $\Delta H^{\circ(x)}$-values are taken from Fig. 1). The deviation between the two quantities is in general less than 1 % (1σ) at all temperatures.

The oxydiacetate system. A. From our previous investigations,[1] we know that hydration equilibria are present for the second rare earth diglycolate complexes. On the basis of the experimental determinations of the stepwise enthalpy changes, ΔH_2°, versus Z at 20°C, we tested the model presented above on the same assumptions as for the EDTA system (p. 2353). From the temperature variation of ΔH_2° for Pr and Yb (representing the "x"-form and "y"-form, respectively) it is obvious that the temperature variation of ΔH_H° is smaller here than in the EDTA system. Nevertheless, the temperature variation of ΔH_H° had to be described with a polynomial of the third degree (Ref. 2, p. 2346) in order to fit the data with sufficient accuracy. The values of ΔH_H° and ΔC_{PH}° are given in Table 1. The ΔC_{PH}°-values for the diglycolate complexes are approximately ten times lower than the corresponding values obtained for the EDTA complexes, while the ΔH_H°-values are almost the same.

Using the set of parameters given in Table 1, the ΔC_{P2}°-values were calculated from eqn. (4) as described earlier. The $\Delta C_{P2}^{\circ(x)}$-values used were the ΔC_{P2}°-values for Pr at the various temperatures.

These calculations show that the differences between the experimental and calculated ΔC_{P2}°-values are larger for the diglycolate complexes than for the EDTA complexes. We believe that this is a result of larger experimental uncertainties in the diglycolate measurements caused by the presence of three consecutive equilibria.

B. As pointed out earlier,[1] the variation of ΔH_1°, the enthalpy change for the formation of the first diglycolate complex, through the rare earth series is about as large as the variation of ΔH_2°. However, no hydration equilibrium of the type discussed above seems to be present in the formation of the first complexes as no maximum for the variation of ΔC_{P1}° with Z is obtained. This would imply that the term dn/dT in relations (4) and (7) is zero.

One possible way to explain this behaviour is to assume a gradual change of geometry in the hydration shells of the complexes. This change must result in *one* definite geometry for each lanthanoid. If the total geometrical change results in an enthalpy change ΔH_α° (see below), then the enthalpy change for each element can be described as a certain fraction of this quantity.

The variation of ΔH_1° with Z can, in a purely formal way, be described by eqn. (3) whether a hydration equilibrium is present or not. However, the temperature dependence of the ΔH° *vs.* Z curves can be used to distinguish between the two possibilities. If no temperature variation in n is observed there can be no equilibrium with a non-zero enthalpy change present in the system.

The quantities n in eqn. (3) have been determined from the experimental $\Delta H_1^\circ(Z)$ curves at the various temperatures investigated, in the same way as described earlier for the EDTA system at 20°C (p. 2354). From these calculations one can conclude, that the quantities n, for the various rare earths, are constant with temperature; *i.e.* no solvation equilibrium is present in this step. In systems where no change in hydration occurs when the temperature is changed, we will in the following use the symbol α instead of n. The constant

Table 3. The quantity α for the various rare earths.

	Pr	Sm	Gd	Tb	Dy	Ho	Er	Yb	Ln
α	0	0	0.282	0.605	0.789	0.920	0.979	1.000	–

α-values obtained from the above calculations for each element are given in Table 3.

Eqn. (3) can now be written as

$$\Delta H_1^\circ = \Delta H_1^{\circ(\circ)} + \alpha \Delta H_\alpha^\circ \quad (8)$$

where $\Delta H_1^{\circ(\circ)}$ is the enthalpy change for a complex formation reaction with no additional changes involved whatsoever. Derivation of eqn. (8) will give

$$\Delta C_{P1}^\circ = \Delta C_{P1}^{\circ(\circ)} + \alpha \Delta C_{P\alpha}^\circ \quad (9)$$

where $\Delta C_{P\alpha}^\circ$ is obtained from the temperature variation of the corresponding enthalpy change ΔH_α°. The ΔH_α°-values have been determined from the experimental data as described before (p. 2353), *i.e.* the $\Delta H_1^\circ - Z$ curve at 20°C and the temperature variation of ΔH_1° for the elements Sm and Yb. The temperature variation of ΔH_α° have been described by a polynomial of the third degree (see above) and the results are given in Table 4. On the same assumptions as before (pp. 2353 and 2354), the $\Delta C_{P1}^{\circ(\circ)}$-values in relation (9) are equal for all elements in the rare earth series.

Table 4. ΔH_α° and $\Delta C_{P\alpha}^\circ$ according to eqns. (8) and (9) for the formation of the first rare earth diglycolate complexes at 5, 20, 25, 35, and 50°C.

T / K	ΔH_α° / J mol^{-1}	$\Delta C_{P\alpha}^\circ$ / J K^{-1} mol^{-1}
278	14770	21
293	14690	−26
298	14542	−33
308	14180	−37
323	13770	−12

The heat capacity changes calculated using eqn. (9) (and with $\Delta C_P^{\circ(\circ)}$ equal to ΔC_{P1}° for Sm) show satisfactory agreement with the experimental quantities. The values at 25°C are given in Table 5. By addition of the calculated heat capacity changes for the first two consecutive steps, the over-all heat capacity changes, $\Delta C_{P\,II}^\circ$, are obtained which also are given in Table 5 at 25°C. The variation of $\Delta C_{P\,II\,calc}^\circ$ with Z at 25°C has been plotted in Fig. 2 in comparison with the experimental curve. In our opinion, the agreement is satisfactory except for Dy for which we believe the experimental values are in error.

Table 5. The experimental and calculated heat capacity changes at 25°C for the reactions:

1. $Ln^{3+} + A^{2-} \rightarrow LnA^{+}$
2. $Ln^{3+} + 2A^{2-} \rightarrow LnA_2^{-}$

Metal ion	ΔC_{P1}°exp / J K^{-1} mol^{-1}	ΔC_{P1}°calc / J K^{-1} mol^{-1}	ΔC_{PII}°exp / J K^{-1} mol^{-1}	ΔC_{PII}°calc / J K^{-1} mol^{-1}
Pr	132	138	201	207
Sm	138	138	205	207
Gd	140	131	203	200
Tb	121	118	230	209
Dy	127	112	262	223
Ho	113	108	262	248
Er	113	106	225	242
Yb	117	105	166	171
Ln	117	–	177	–

We have now seen that the model can be applied to two different types of systems. In both cases the results are in fair agreement with the experimental data. In order to decide whether hydration equilibria or some other effects (*e.g.* geometrical changes) cause the typical variation of ΔH° with Z, the following quantities have to be determined.

1. The variation of ΔH° with Z at *one* temperature.
2. The temperature variation of ΔH° for one element at the beginning and one at the end of the rare earth series. (Representing $n = 0$ and $n = 1$ or $\alpha = 0$ and $\alpha = 1$, respectively.)
3. ΔH° at two temperatures for an element in that part of the rare earth series where the change in ΔH° with Z is largest. From the last determination, information is obtained as to whether n (or α) is constant with temperature or not.

The temperature variation of ΔC_P° for the rare earth EDTA complexes. In the previous investigation of the rare earth diglycolate system,[1] we found that the ΔC_{P2}°-values for the various lanthanoid complexes varied with temperature and had in all cases minima around 30°C. From the model then presented, one would expect a positive contribution to ΔC_P° for a hydration equilibrium. Such a contribution should be detectable experimentally in the temperature variation of ΔC_P° if the experimental data are accurate enough. One of the aims of EDTA investigation[2] was to establish whether such an effect is detectable or not.

The experimental $\Delta C_P^{\circ}(T)$ curves from the EDTA measurements[2] indicate contribution to the temperature variation of ΔC_P° from the presence of hydration equilibria. The curve for the elements Sm and Eu, for which we have the largest contribution according to eqn. (4), seem to be less curved than those for the other elements (see Fig. 3).

Using the praseodymium system as a reference as before, we can now compare the quantities $d\Delta C_P^{\circ}/dT - d\Delta C_P^{\circ(x)}/dT$ determined from the experiments, with the corresponding quantities calculated from the model.

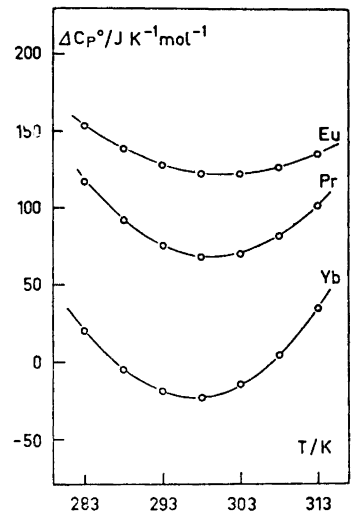

Fig. 3. The temperature variation of ΔC_P° for the formation of some rare earth EDTA complexes.

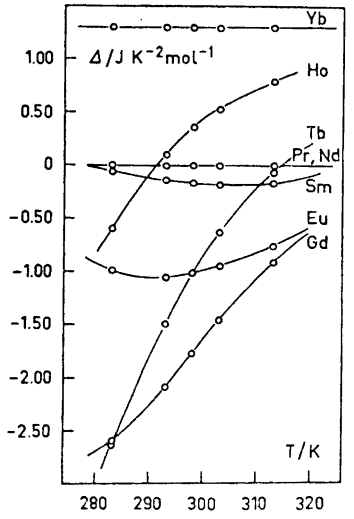

Fig. 4. The variation of Δ with temperature for the formation of the rare earth EDTA complexes in the range 10 – 40°C.

The difference $d\Delta C_P^\circ/dT - d\Delta C_P^{\circ(x)}/dT$, is denoted Δ. From (7) we obtain by derivation

$$\frac{d^2n}{dT^2} = \frac{\Delta C_{PH}^\circ\, n(1-n)T + \Delta H_H^\circ\, dn/dT(1-2n)T - 2\Delta H_H^\circ\, n(1-n)}{RT^3} \qquad (10)$$

which together with the data in Tables 1 and 2 makes the determination of the right hand side in (5) possible. The calculations are made on the same assumptions as before (p. 2353). In Fig. 4 the variation of Δ with temperature is shown for the various elements.

The slopes obtained from Fig. 4 for the various rare earths can be compared with the experimental results. With praseodymium as a reference (with only the "x"-form present) we obtain from relation (4) in Ref. 2 by derivation

$$\frac{d(\Delta_{exp})}{dT^2} = 6D_{Ln} - 6D_{Pr} = 6(D_{Ln} - D_{Pr}) \qquad (11)$$

Such calculations confirm the *qualitative* description given by the model above. The only exception is Yb. The constant value of Δ with temperature in Fig. 4 for this element is due to the use of a second degree polynomial for the description of the temperature variation of ΔH_H°. If instead a third de gree polynomial is used to describe ΔH_H° *vs.* T, the slope of Δ *vs.* T for Yb will be positive (as given by (11)), while the qualitative picture for the rest of the elements will be unchanged.

Whichever of the polynomials above is used for the description of the temperature variation of ΔH_H°, the quantitative agreement between the slopes of Δ in Fig. 4 and those obtained from (11) is not particularly good. This is

of course not unexpected as the quantities discussed are very sensitive towards experimental errors.

Conclusions. 1. The observed non-monotonic variation of $\Delta H°$ with Z can be due to either solvation equilibria or discrete changes in geometry. One can distinguish between these two possibilities by the determination of the variation of $\Delta C_P°$ with Z.

2. Both the above situations can be described by the use of the model presented.

3. The success or failure in the agreement between the model and the experimental data is very much dependent on the accuracy with which the temperature derivatives of $\Delta H°$ and $\Delta H_H°$ (or $\Delta H_\alpha°$) can be determined.

4. As $\Delta G_H°$ varies through the rare earth series, one or both of the quantities $\Delta H_H°$ and $\Delta S_H°$ must also be varying. In the model presented above $\Delta H_H°$ has been assumed to be constant, *i.e.* the variation in $\Delta G_H°$ is entirely due to a variation in $\Delta S_H°$. Alternatively $\Delta S_H°$ can be assumed to be a constant (see Ref. 3) with a variation in $\Delta H_H°$ through the rare earth series as a result. We prefer the first description as it makes a *direct* comparison possible between the predictions of the model and the *experimental* data.

5. As seen above the assumption of a constant $\Delta H_H°$-value throughout the rare earth series at each temperature need not necessarily be quite correct. However, the fair agreement between the model and the experimental data indicates that a possible variation of $\Delta H_H°$ with Z must be small.

Acknowledgements. I am indebted to Dr. Ingmar Grenthe for many useful discussions and helpful advice. I also thank Professor Ido Leden for his valuable suggestions and kind interest in this work. This project has been sponsored by a grant from the *Swedish Natural Science Research Council.*

REFERENCES

1. Grenthe, I. and Ots, H. *Acta Chem. Scand.* **26** (1972) 1229.
2. Ots, H. *Acta Chem. Scand.* **27** (1973) 2344.
3. Geier, G., Karlén, U. and v. Zelewsky, A. *Helv. Chim. Acta* **52** (1969) 1967.

Received February 23, 1973.

ACTA CHEMICA SCANDINAVICA 27 (1973) 2361–2366

Metabolic Changes Induced by Ethanol in Muscle and Liver Tissue of the Rat *in vivo*

ERIK FELLENIUS, ULLA BJÖRKROTH and KARL-HEINZ KIESSLING

Institute of Zoophysiology, University of Uppsala, Uppsala, Sweden

The metabolic changes in the rat liver and skeletal muscle after infusion of ethanol into the rat *in vivo* were studied. Samples of the liver and muscle tissue were taken simultaneously by the freeze-clamp technique and analyzed for content of lactate, pyruvate, α-glycerophosphate, dihydroxyacetonephosphate, malate, adenine nucleotides, inorganic phosphate, creatinephosphate and creatine. The changes in the redox-state in the cytoplasm and mitochondria of the liver were measured as the [lactate]/[pyruvate]-ratio, and the [β-hydroxybutyrate]/[acetoacetate]-ratio, respectively. The ratios in the liver varied with the total amount of ethanol infused. The [lactate]/[pyruvate]-ratio of the muscle was not affected by the oxidation of ethanol. Thus the reduced state of the liver caused by the oxidation of ethanol and which partly can be exported to extrahepatic tissues will be readjusted in the resting muscle cell. The [β-hydroxybutyrate]/[acetoacetate]-ratio of the liver was, however, not restored to its normal value in the muscle. This was probably due to a low activity of the β-hydroxybutyrate dehydrogenase in the muscle.

The changes of the adenine nucleotides were mainly in the level of AMP. These changes occurred both in the liver and in the muscle tissue and were related to the metabolism of acetate, the main product during oxidation of ethanol in the liver.

Most work has been done on the effect of ethanol on liver and brain.[1] Little is known about the effect on skeletal muscle although it has been demonstrated that long-term ethanol intake leads to serious damage in skeletal muscle.[2,3] The aim of the present study was therefore to investigate the simultaneous metabolic changes in the liver and skeletal muscle of the rat during short-term exposure to ethanol.

METHODS

Animal treatment and sampling procedure. Female Wistar rats (150 – 250 g) from the laboratory's stock were used. The animals were starved for 48 h and anaesthetized by intraperitoneal injection of Evipan-Sodium®, 50 mg/200 g rat weight, dissolved in 0.9 %

Table 1. Changes of the concentrations of redox substrates and energy-rich compounds in liver and skeletal muscle tissue after infusion of ethanol and sodium acetate. Two different solutions of ethanol (0.95 M and 2.84 M) were infused into the saphenous vein at a rate of 2.2 ml/h per 200 g rat weight during 30 min to 48 h starved animals. Sodium

Substrate infused	Tissue	Malate	α-GP	Lactate	Pyruvate	DAP	β-OH
None	L	0.277 ± 0.025	0.211 ± 0.019	0.374 ± 0.075	0.045 ± 0.005	0.038 ± 0.003	0.907 ± 0.171
	M	0.188 ± 0.011	0.046 ± 0.011	1.20 ± 0.14	0.078 ± 0.007	0.035 ± 0.007	0.485 ± 0.086
Ethanol (0.95 M)	L	0.996 ± 0.086[a]	0.743 ± 0.083[a]	0.671 ± 0.081	0.063 ± 0.009	0.041 ± 0.003	0.504 ± 0.095
	M	0.155 ± 0.005[a]	0.076 ± 0.008	1.50 ± 0.15	0.105 ± 0.012	0.017 ± 0.003	0.361 ± 0.075
Ethanol (2.84 M)	L	1.20 ± 0.13[a]	0.827 ± 0.051[a]	0.985 ± 0.106[a]	0.052 ± 0.004	0.035 ± 0.004	1.05 ± 0.11
	M	0.146 ± 0.020	0.063 ± 0.010	1.04 ± 0.08	0.075 ± 0.010	0.019 ± 0.003	0.475 ± 0.102
Sodium-acetate (2.84 M)	L	0.221 ± 0.009	0.185 ± 0.011	0.291 ± 0.040	0.065 ± 0.007	0.064 ± 0.004[a]	0.831 ± 0.047
	M	0.076 ± 0.006[a]	0.062 ± 0.005	0.798 ± 0.074	0.048 ± 0.006[a]	0.028 ± 0.002	0.435 ± 0.051

[a] = Significance of difference ($p < 0.01$) compared with control

sodium chloride. After continuous infusion of the different agents for 30 min, the liver and skeletal muscle were at the same time rapidly frozen between small aluminium clamps cooled in liquid nitrogen.[4] The rate of infusion was 2.2 ml/h. Prior to the sampling of the muscle tissue, which was mainly the posterior-inferior thigh muscles, visible fat pads were removed.

The further treatment of the tissues for the determination of different metabolites has been described by others.[5]

Determination of metabolites. The concentrations of the following compounds were estimated in the neutralized perchloric acid extract: lactate, malate, α-glycerophosphate (α-GP), dihydroxyacetonephosphate (DAP) and pyruvate,[6] acetoacetate (AcAc) and β-hydroxybutyrate (β-OH),[7] adenosinetriphosphate (ATP),[8] adenosinediphosphate (ADP) and adenosinemonophosphate (AMP),[9] inorganic phosphate (P),[10] creatinephosphate (CP),[11] creatine,[12] and ethanol.[13]

Definitions. The term redox-state is used as a description of the ratio free [NADH]/free [NAD^+] in a cell compartment. According to this concept [14] the ratio can be assumed to be in equilibrium with these metabolite pairs which are interconverted by means of sufficiently active NAD-coupled dehydrogenases located in the corresponding compartment. In this paper evidence is presented of the existence of two functional compartments regarding the redox-state within the cytoplasm, one represented by the [lactate]/[pyruvate]-ratio and one by the [α-GP]/[DAP]-ratio. The [β-OH]/[AcAc]-ratio represents that of the mitochondrial compartment.

Statistical analyses. Student's *t*-test was used for statistical analyses, $p < 0.01$ being considered significant.

RESULTS

Ethanol, acetate and "redox substrates". The changes of the concentration of lactate, malate, α-GP, pyruvate, and DAP in the liver and skeletal muscle after a 30 min infusion of various amounts of ethanol are shown in Table 1. At the lower dose of ethanol, giving a final ethanol concentration in the liver of 4.08 ± 0.40 μmol/g wet wt (mean ± S. E. of 5 observations) the amount of

acetate (2.84 M) was infused at the same rate. All the substances were dissolved in 0.9 % sodium chloride. 0.9 % sodium chloride was infused in the control animals. The concentrations are expressed as μmol/g wet weight of the liver (L) or skeletal muscle (M) tissue and are given as mean ± S. E. of 5 observations.

AcAc	ATP	ADP	AMP	P_i	CP	Creatine
.956± 0.050	3.35± 0.09	1.02 ± 0.06	0.149± 0.017	2.81± 0.24		
.119± 0.018	6.70± 0.11	0.860± 0.008	0.029± 0.003	11.8 ± 0.4	21.1± 0.7	8.89± 0.31
.516± 0.093[a]	3.38± 0.17	0.967± 0.022	0.230± 0.013[a]	2.68± 0.26		
.106± 0.025	6.44± 0.09	0.824± 0.015	0.049± 0.004[a]	11.7 ± 1.0	18.1± 0.8[a]	6.91± 0.82
.264± 0.027[a]	3.56± 0.12	0.870± 0.051	0.228± 0.015[a]	2.11± 0.23		
.058± 0.010[a]	7.01± 0.15	0.790± 0.051	0.048± 0.004[a]	11.3 ± 1.0	21.3± 0.8	4.39± 0.41[a]
.03 ± 0.04	2.88± 0.05[a]	1.22 ± 0.035	0.787± 0.027[a]	3.27± 0.99		
.183± 0.034	7.57± 0.12[a]	0.936± 0.026	0.076± 0.008[a]	9.78± 1.1	24.5± 0.7[a]	4.55± 0.18[a]

malate and α-GP increased significantly in the liver, while lactate and β-OH were less affected. This is also seen in the changes of the [α-GP]/[DAP]-[lactate]/[pyruvate]-, and [β-OH]/[AcAc]-ratios (Table 2). Thus, the [α-GP]/[DAP]-ratio increased significantly while the [lactate]/[pyruvate]- and the [β-OH]/[AcAc]-ratios were only slightly affected. At the higher concentration of ethanol, giving a final concentration in the liver tissue of 14.7 ± 0.9

'able 2. Changes of the redox-state and the "energy charge" in liver and skeletal muscle after infusion of ethanol nd sodium acetate. From the concentrations presented in Table 1 different ratios have been calculated. The ratios are given as mean ± S. E. of 5 observations. L = liver, M = skeletal muscle.

ubstrate infused	Tissue	$\frac{[Lactate]}{[Pyruvate]}$	$\frac{[\alpha\text{-GP}]}{[DAP]}$	$\frac{[\beta\text{-OH}]}{[AcAc]}$	$\frac{[ATP]}{[ADP][P_i]}$	$\frac{[ADP]^2}{[ATP][AMP]}$	$\frac{[ATP][Creatine]}{[ADP][CP]}$
one	L	8.5± 1.7	5.4± 0.5	1.2± 0.2	1.2± 0.1	3.0± 0.5	
	M	13.7± 1.8	3.5± 0.6	4.2± 0.6	0.8± 0.1	4.0± 0.4	3.3± 0.2
thanol	L	12.3± 1.2	21.5± 1.6[a]	1.4± 0.3	1.2± 0.2	1.3± 0.6[a]	
).95 M)	M	13.4± 0.8	4.5± 0.6	3.6± 0.4	0.7± 0.1	2.3± 0.2[a]	3.0± 0.4
thanol	L	20.3± 1.5[a]	29.8± 2.0[a]	4.0± 0.3[a]	1.8± 0.2[a]	1.2± 0.2[a]	
?.84 M)	M	14.8± 2.2	2.9± 0.4	8.1± 0.7[a]	1.0± 0.2	2.2± 0.1[a]	1.9± 0.3[a]
odium cetate	L	4.8± 1.0	2.8± 0.2[a]	0.8± 0.6	0.8± 0.1	0.7± 0.03[a]	
?.84 M)	M	17.5± 2.5	2.1± 0.3	3.2± 0.4	0.9± 0.1	1.6± 0.1[a]	1.5± 0.1[a]

[a] = Significance of difference ($p < 0.01$) compared to control

μmol/g wet wt. (mean $\pm$ S. E. of 5 observations) a significant increase of all the redox-ratios was obtained. This shows that the changes of the [lactate]/[pyruvate]-ratio and the [β-OH]/[AcAc]-ratio, representing the redox-state in the cytosol and the mitochondria, respectively, are dependent upon the amount of ethanol infused.

With the exception of the [β-OH]/[AcAc]-ratio the redox-ratios in the skeletal muscle were not much influenced by infusion of the two doses of ethanol. The increased ratio was mainly due to a decrease in the level of AcAc.

Infusion of acetate did not change the content of the various redox substrates in the liver significantly except for DAP (Table 1). This caused the [α-GP]/[DAP]-ratio to decrease.

In the skeletal muscle a significant decrease of malate and pyruvate was found. The changes did not, however, affect the [lactate]/[pyruvate]-ratio.

Ethanol, acetate and the "energy charge". The content of ATP and ADP was practically unchanged in the liver and skeletal muscle 30 min after the infusion of ethanol (Table 1). The concentration of AMP was increased in both tissues by ethanol infusion, while the amount of CP was practically unchanged.

The ratio $[ADP]^2/[ATP]\,[AMP]$ (Table 2), which represent the mass action ratio of the adenylate kinase reaction, was slightly decreased. The ratio should be compared with the ratio 1.5 – 3.5 obtained *in vitro*.[15]

In spite of the fact that the amount of ATP, ADP, and P_i was not significantly changed after ethanol infusion, the changes were large enough to give an elevated "phosphate potential" ($[ATP]/[ADP]\,[P_i]$)[16] at the higher concentration of ethanol.

Acetate influenced the amount of ATP and AMP significantly (Table 1) both in liver and muscle tissue, causing the equilibrium ratio of the adenylate kinase reaction to decrease (Table 2). The "phosphate potential" was not much changed.

DISCUSSION

It is clearly shown in the present investigation that the influence of ethanol on the different redox ratios in the liver depends on the amount of ethanol infused. This is evidently not due to the alcohol dehydrogenase system not being saturated with ethanol. The amount of ethanol found in the liver at the lower dose of ethanol was about twice as high as the reported K_m-value for alcohol dehydrogenase with ethanol as substrate.[17] Moreover, with the two doses of ethanol infused there was a steady increase with time of this compound in the blood. Thus, at the lower dose the following concentrations of ethanol were found in the blood after 10, 30, 60, 120, and 180 min infusion: 5.0, 11.0, 17.7, 20.6, and 20.3 mM, respectively.

A possible explanation for the difference in effect of the different doses of ethanol would be that no immediate equilibrium is established between the α-glycerophosphate and the lactate dehydrogenase systems. This is a consequence of a functional compartmentation. Such disequilibria between the two enzymes has been reported to occur during ethanol oxidation.[18]

The preliminary regulator of the redox state in the cytoplasm is suggested to be the state of phosphorylation,[19] which in turn depends on the concentration of the components of the glyceraldehyde-3-phosphate dehydrogenase and the 3-phosphoglycerokinase reactions. The ratio [ATP]/[ADP] [P_i], the "phosphate potential", is one part of the cited reactions and can be expected to move parallel with any change in the redox state. Our results indicate that the redox state shown in the changes in the [lactate]/[pyruvate]-ratio is regulated by the phosphorylation state, while the redox state of the α-glycerophosphate dehydrogenase system is not primarily regulated by this factor.

This conclusion presupposes that the ratio [3-phosphoglycerate]/[glyceraldehyde-3-phosphate], which can also influence the redox state,[19] is constant.

The compounds malate, lactate, pyruvate, β-OH, and AcAc penetrate the membranes of the mitochondria and the liver cell more or less freely. In this way the reduced state, governed by the oxidation of ethanol, can be exported to extrahepatic tissues. As no changes in the [lactate]/[pyruvate]-ratio occur in the skeletal muscle after infusion of ethanol it follows that the muscle tissue has a great capacity even during rest to readjust the reduced state carried in the circulation from the sites of ethanol metabolism. The situation is somewhat different for the [β-OH]/[AcAc]-ratio. A significant increase in the ratio was found in the muscle tissue after infusion of the higher dose of ethanol. This should not be interpreted as a limited capacity of the muscle to adjust the redox state, since the [β-OH]/[AcAc]-ratio of the muscle sample is not necessary a good indicator of the redox state of this tissue. The activity of the β-hydroxybutyrate dehydrogenase in skeletal muscle is quite low [20] compared to that of the liver. This might be the rate-limiting factor in the readjustment of the [β-OH]/[AcAc]-ratio.

To summarize: There appears to be no dramatic change in the metabolic pattern of compounds related to the redox state in the skeletal muscle during oxidation of ethanol in the liver.

The changes of the level of AMP in the muscle tissue should be considered as one effect that might have consequences for the muscle metabolism in the chronic state. This compound is a powerful modifier of the flow through important metabolic steps.[21] The changes of the AMP level is due to the activation of acetate in the muscle tissue. This acetate is formed in the liver during oxidation of ethanol and carried in the circulation to the muscle. This was clearly demonstrated when only acetate was infused. Similar changes of the level of AMP occur when ethanol alone in infused. The changes in the liver tissue seem to be dependent upon the amount of ethanol adminstrated.[22–25] In the present investigation the doses of alcohol were low enough to prevent any toxic effect of ethanol.

In conclusion it may be said that any alterations in the metabolic pattern of skeletal muscle after administration of ethanol result from an indirect effect *via* the metabolites carried in the circulation from the sites of ethanol metabolism. At this point it is impossible to decide the chronic effects of the metabolism of acetate. However, in evaluating the reason for the muscle derangements occurring in alcoholism, it may be fruitful to consider the consequences of unilateral combustion of acetate.

Acknowledgements. This work was supported by *Helge Ax:son Johnson's Foundation*, the *Faculty of Mathematics and Science of the University of Uppsala* and the *Swedish Medical Research Council*, Sweden, grant No. B 73-03X-575-09B.

REFERENCES

1. Wallgren, H. and Barry, H. III, *Actions of Alcohol*, Elsevier, Amsterdam 1970.
2. Hed, R., Lundmark, C., Fahlgren, H. and Orell, S. *Acta Med. Scand.* **171** (1962) 585.
3. Kiessling, K.-H. and Pilström, L. *Clin. Science. In press.*
4. Wollenberger, A., Ristau, O. and Schoffa, G. *Pflügers Arch. ges. Physiol.* **270** (1960) 399.
5. Lowry, O. H., Passonneau, J. V., Hasselberger, F. X. and Schulz, D. W. *J. Biol. Chem.* **239** (1964) 18.
6. Hohorst, H. J., Kreutz, F. H. and Bücher, Th. *Biochem. Z.* **332** (1959) 18.
7. Williamson, D. H., Mellanby, J. and Krebs, H. A. *Biochem. J.* **82** (1962) 90.
8. Lamprecht, W. and Trautschold, I. In Bergmeyer, H.-U., Ed., *Methoden der Enzymatischen Analyse*, Verlag Chemie, Weinheim 1962, p. 543.
9. Adam, H. *Ibid.* p. 573.
10. Harper, A. E. *Ibid.* p. 788.
11. Lamprecht, W. and Stein, P. *Ibid.* p. 610.
12. Bernt, E., Bergmeyer, H.-U. and Möllering, H. *Ibid.* p. 407.
13. Dickinson, F. M. and Dalziel, K. *Biochem. J.* **104** (1967) 165.
14. Krebs, H. A. *Advan. Enzyme Regul.* **5** (1967) 409.
15. Egglestone, L. V. and Hems, R. *Biochem. J.* **52** (1952) 156.
16. Atkinson, D. E. In Goodwin, T. W., Ed., *Metabolic Roles of Citrate*, Academic, London 1969, p. 23.
17. Marshall, E. K. and Fritz, W. F. *J. Pharmacol. Exptl. Therap.* **109** (1953) 431.
18. Schimassek, H., Walli, A. K. and Höfer, G. In Martini, G. A. and Bode, Ch., Eds., *Metabolic Changes Induced by Alcohol*, Springer, Berlin-Heidelberg-New York 1971, p. 157.
19. Stubbs, M., Veech, R. L. and Krebs, H. A. *Biochem. J.* **126** (1972) 59.
20. Lehninger, A. L., Sudduth, H. C. and Wise, J. B. *J. Biol. Chem.* **235** (1960) 2450.
21. Newsholme, E. A. In Bartley, W., Kornberg, H. L. and Quayle, J. R., Eds., *Essays in Cell Metabolism*, Wiley-Interscience, London 1970, p. 189.
22. Oura, E., Räihä, N. C. R. and Suomalainen, H. *Ann. Med. Exp. Fenn.* **45** (1967) 57.
23. Lindros, K. and Aro, H. *Abstr. 5th Meeting Fed. Europ. Biochem. Soc.*, Prague 1968, p. 461.
24. Scholz, R. In Staib, W. and Scholz, R., Eds., *Stoffwechsel der isolierten perfundierten Leber*, Springer, Berlin-Heidelberg-New York 1968, p. 225.
25. Thieden, H. I. D. *FEBS Lett.* **2** (1968) 121.

Received March 14, 1973.

ACTA CHEMICA SCANDINAVICA 27 (1973) 2367–2374

The Crystal Structure of $HfTe_5$

SIGRID FURUSETH, LEIF BRATTÅS and ARNE KJEKSHUS

Kjemisk Institutt, Universitetet i Oslo, Blindern, Oslo 3, Norway

The crystal structure of $HfTe_5$ has been determined from three dimensional X-ray data. The structure is orthorhombic, space group *Cmcm*. The pycnometric density at 25.00°C is 6.806 gcm^{-3}, the unit cell contains four formula units, and has the dimensions: $a = 3.9743(5)$ Å, $b = 14.492(2)$ Å, $c = 13.730(2)$ Å. The following values were found for the positional parameters: $y = 0.3143(1)$ for Hf in 4(*c*); $y = 0.6635(2)$ for Te_I in 4(c); $y = 0.9299(2)$, $z = 0.1494(2)$ for Te_{II} in 8(*f*); $y = 0.2099(2)$, $z = 0.4353(2)$ for Te_{III} in 8(*f*).

$ZrTe_5$ is shown to be isostructural with $HfTe_5$ ($d_{pycn.} = 6.079$ gcm^{-3}; $a = 3.9876(11)$ Å, $b = 14.502(4)$ Å, $c = 13.727(3)$ Å); both compounds are diamagnetic.

The $HfTe_5$ type structure comprises distinct layers arranged approximately parallel to (010). Within the layers distorted bi-capped trigonal prisms are linked together by zig-zag chains of Te atoms. The structure and bonding in $HfTe_5$ are discussed in relation to the $ZrSe_3$ type structure.

Some few years ago the development of inorganic chemistry had approached a stage when it was considered profitable to discuss the non-existence of particular compounds. However, the probable discovery of further compounds as a result of the *systematic* application of conventional and modern techniques of synthesis renders such an approach ill advised at the present time. Among the new compounds which continue to be discovered, some unexpected and strange compositions emerge at intervals. The recent preparation[1] of $HfTe_5$ has provided an interesting addition to the latter category. At first sight, the tellurium content of this compound seemed revolutionary high, but after a little while one gets accustomed to its existence and one aspires to place $HfTe_5$ in an ulterior chemical connection. The present report on the determination of its crystal structure represents a first step in this direction.

EXPERIMENTAL

Samples were prepared from 99.9 % Zr and Hf (turnings from crystal bars; the analytical figure for Hf excludes a content of ~3 % Zr) and 99.999 % Te from Koch-Light Laboratories, Ltd. Polycrystalline samples of $ZrTe_5$ and $HfTe_5$ were obtained by heating weighed quantities of the components in sealed, evacuated silica tubes at 450°C for 7 d

and cooling to room temperature over a period of 3 d. In preliminary [1] experiments, the use of too high temperature, $\geqq 500$°C, prevented the preparation of $HfTe_5$ by direct reaction.

Single crystals of both compounds were obtained by means of chemical transport reactions, using iodine as the transport agent in a concentration of 5 mg/ml capsule volume. The most suitable transport conditions were obtained by applying temperature gradients of ~ 1 ($\sim \frac{1}{3}$) °C/mm along ~ 150 mm long evacuated and sealed silica capsules, with the hot ends containing mixtures of Zr and Te (Hf and Te) at ~ 580 (~ 500) °C. These conditions produced a considerable number of needle shaped crystals at the cold ends of the capsules after 7 days.

In analogy with $ZrTe_5$ and $HfTe_5$ attempts have also been made to prepare $TiTe_5$. A variety of different thermal and transport conditions were tried during these syntheses, but this endeavour has hitherto failed.

X-Ray powder photographs of all samples were taken in a Guinier type camera of 80 mm diameter with monochromatized Cu$K\alpha_1$-radiation using KCl as internal standard.

Three dimensional single crystal data for $HfTe_5$ were collected (from the layers $0kl$ to $5kl$) in an integrating Weissenberg camera of 57.3 mm with Zr-filtered Mo$K\alpha$-radiation, using the multiple-film technique. The intensities were measured microphotometrically except for the weakest reflections, which were estimated visually. The intensities were corrected for the combined Lorentz and polarization factors, and for absorption according to the actual shape of the crystal. (No corrections for dispersion and secondary extinctions were carried out.)

The computational work, including least squares refinements of the unit cell dimensions, corrections, data reductions, scalings, Patterson- and Fourier-syntheses, full matrix least squares refinements of the structure factors, and calculations of interatomic distances and angles, was carried out on a CDC 3300 computer using, in most cases, the programmes of Dahl *et al.*[2]

Atomic scattering factors were taken from Hanson *et al.*[3] Anisotropic thermal motion of the atoms were allowed for according to the expression $\exp[-(\beta_{11}h^2+\beta_{22}k^2+\beta_{33}l^2+\beta_{12}hk+\beta_{13}hl+\beta_{23}kl)]$. The extent of the agreement between the observed and calculated structure factor data is judged from the average and weighted reliability factors $R=\sum||F_o|-|F_c||/\sum|F_o|$ and $R^*=[\sum w(|F_o|-|F_c|)^2/\sum w|F_o|^2]^{\frac{1}{2}}$ where w denotes the weight factor. The unobserved reflections were not included in the calculations of R and R^*, and were omitted from the least squares refinements. (The observed and calculated structure factor data are available from the authors upon request.)

Density measurements were carried out pycnometrically at 25.00°C with kerosene as displacement liquid. To remove gases adsorbed by the samples (weighing ~ 2 g), the pycnometer was filled with kerosene under vacuum.

Magnetic susceptibilities were measured between 80 and 725 K by the Faraday method (maximum field ~ 8 kØ) using $50-100$ mg samples.

Diffuse reflectance measurements were made in the range 2200 to 22 000 Å using a Cary 14 dual-beam spectrophotometer fitted with a diffuse reflectance accessory. $MgCO_3$ was used as a standard, and the integrating sphere was coated with MgO.

CRYSTAL DATA

$ZrTe_5$, $M=729.22$; $HfTe_5$, $M=816.49$.

Needle shaped single crystals with approximately rectangular cross section, a-axis along the needle axis.

Orthorhombic.

$ZrTe_5$: $a=3.9876(11)$ Å, $b=14.502(4)$ Å, $c=13.727(3)$ Å, $V=793.8(6)$ Å^3

$HfTe_5$: $a=3.9743(5)$ Å, $b=14.492(2)$ Å, $c=13.730(2)$ Å, $V=790.8(3)$ Å^3

Observed densities at 25.00°C.
$ZrTe_5$: 6.079 gcm^{-3}
$HfTe_5$: 6.806 gcm^{-3}
Unit cell content: 4 TX_5 groups.
Systematic extinctions:
hkl absent when $h+k=2n+1$
$h0l$ absent when $l=2n+1$ (and/or $h=2n+1$)
Space group: $Cmcm$ (the possible space groups $C2cm$ and $Cmc2_1$ were excluded as a result of the structure determination).

STRUCTURE DETERMINATION OF $HfTe_5$

With great zest the structure determination of $HfTe_5$ was started before no more than the intensity data from the layer $0kl$ had been evaluated. The (100) Patterson projection contains a large number of poorly resolved peaks. However, the composition $HfTe_5$ in relation to the space group symmetry and the short a-axis greatly aids the interpretation of the Patterson map. Furthermore, on taking advantage of postulated similarities with key fragments of the crystal structures of $ZrSe_3$ [4,5] and elemental Te [6,7] and the expected values for the Hf–Te and Te–Te bond lengths it was in fact a relatively simple task to devise a useful trial structure. The tentative atomic positions were improved by application of the minimum residual method, by Fourier syntheses, and finally by least squares refinements until termination at $R=0.083$.

The three dimensional atomic arrangement of $HfTe_5$ is approximately fixed on the basis of the coordinates in the (100) projection. There is, in fact, only a slight degree of freedom for the variations of the x parameters from the fixed values of 0 and $\frac{1}{2}$ prescribed by space group $Cmcm$. (Space group $Cmc2_1$ was eliminated from the (100) projection and at this stage there was accordingly a choice between $Cmcm$ and $C2cm$.)

Refinements of the three dimensional structure factor data, according to the method of least squares, were carried out assuming a description of the

Table 1. Final positional and thermal parameters for the crystal structure of $HfTe_5$.
(Hf and Te_I in position 4(*c*) and Te_{II} and Te_{III} in position 8(*f*) of space group $Cmcm$. The symmetry of $Cmcm$ imposes the restraint $\beta_{12}=\beta_{13}=0$ on all atoms and in addition $\beta_{23}=0$ on Hf and Te_I. According to the calculations β_{23} is zero for Te_{II} and Te_{III}, thus confining the principal axes of the vibrational ellipsoids to coincide with the crystallographic axes for all atoms.)

	Hf	Te_I	Te_{II}	Te_{III}
y	0.3143(1)	0.6635(2)	0.9299(2)	0.2099(2)
z	$\frac{1}{4}$	$\frac{1}{4}$	0.1494(2)	0.4353(2)
β_{11}	0.0121(12)	0.0064(17)	0.0109(13)	0.0134(13)
β_{22}	0.0010(1)	0.0010(1)	0.0017(1)	0.0013(1)
β_{33}	0.0010(1)	0.0011(1)	0.0017(1)	0.0012(1)

structure in terms of space group $C2cm$. The least squares iterations were continued until no shifts were obtained in any of the variables for each computational model. Using the Hamilton [8] test it was found that the model specified by the positional and thermal parameters listed in Table 1 ($R = 0.053$ and $R^* = 0.034$ for 484 independent reflections), is superior to all models based on variable x parameters at a significance level < 0.005. The conclusion reached by application of the Hamilton test concurs with that derived from the values of the parameters for the various models and their associated standard deviations, *viz.* that space group *Cmcm* gives the most correct description of the crystal structure of $HfTe_5$. The correctness of the structure was finally also ascertained by a difference Fourier synthesis.

Obvious relationships in dimensions, content, and symmetry of the unit cells (*vide supra*) and nearly matching intensities on Guinier and Weissenberg photographs unambiguously demonstrate that $ZrTe_5$ is isostructural with $HfTe_5$. The positional parameters for $ZrTe_5$ must clearly be very similar to those for $HfTe_5$, but no attempt has been made to determine their actual values.

DESCRIPTION AND DISCUSSION OF THE $HfTe_5$ STRUCTURE

Important interatomic distances and angles calculated from the unit cell dimensions and the positional parameters in Table 1 are given in Table 2. Fig. 1 shows the structural arrangement projected along [100]. A left hand coordinate system is adopted in order to facilitate comparison with the $ZrSe_3$ type structure (Fig. 2). Apart from the more customary structural merits of such a comparison, this particular one is of considerable interest because $ZrTe_3$ and $HfTe_3$ crystallize with the $ZrSe_3$ type structure.[9]

Table 2. Interatomic distances (< 3.5 Å) and angles in the crystal structure of $HfTe_5$. (The standard deviations correspond to those in the positional parameters.)

Interatomic distances (Å)

$Hf-Te_I$	2.954(3)	$Te_{II}-Te_{II}$	2.763(4)
$-Te_{II}$	2.944(2)		
$-Te_{III}$	2.960(2)	$Te_{III}-Te_{III}$	2.908(3)

Interatomic angles (°)

$Te_I-Hf-Te_I$	84.57(9)	$Hf-Te_I-Hf$	84.57(9)
$-Te_{II}$	88.12(5)		
$-Te_{II}$	151.09(5)		
$-Te_{III}$	67.79(4)		
$Te_{II}-Hf-Te_{II}$	55.97(8)	$Hf-Te_{II}-Te_{II}$	62.01(4)
$-Te_{II}$	84.90(7)		
$-Te_{II}$	110.58(10)		
$-Te_{III}$	83.55(5)		
$-Te_{III}$	133.96(4)		
$Te_{III}-Hf-Te_{III}$	118.53(10)	$Hf-Te_{III}-Te_{III}$	108.72(9)
		$Te_{III}-Te_{III}-Te_{III}$	86.20(11)

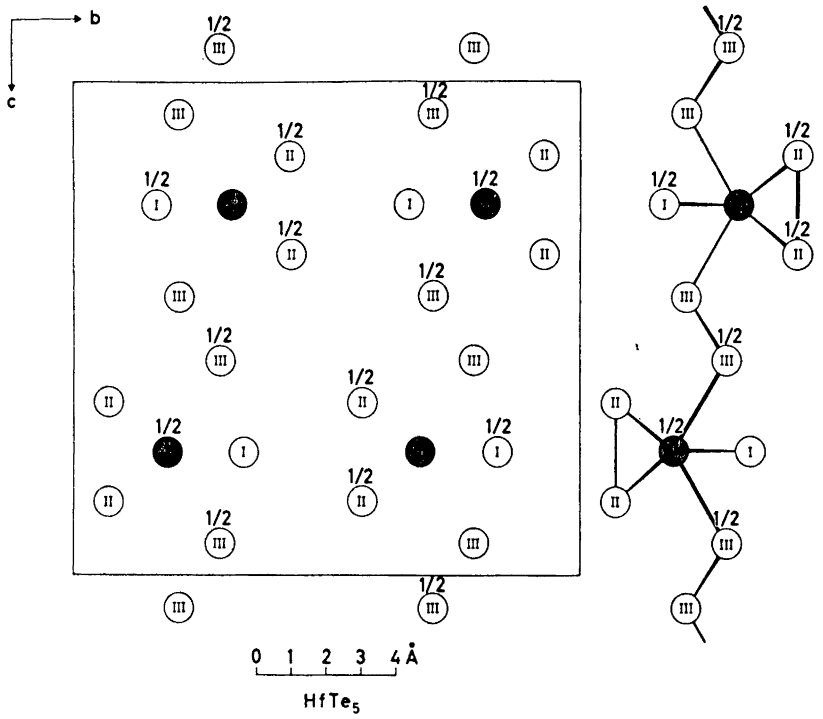

Fig. 1. The crystal structure of $HfTe_5$ projected along [100]. In this and the following diagram filled and open circles represent the metal (T) and non-metal (X) atoms, respectively. The numbers indicate fractions of the projection axis.

Each T atom in the $HfTe_5$ and $ZrSe_3$ type structures have nearly identical coordinations of eight close X neighbours. Six X atoms are at the corners of a triangular prism and two lie outside rectangular faces of the prism. These coordination polyhedra (which are distorted variants of the type named bi-capped trigonal prism) are linked together by $X-X$ zig-zag chains (running parallel to [100]) in the case of $HfTe_5$ and by X atoms which belong to neighbouring prisms in $ZrSe_3$. The latter distinction accounts for the difference in composition between the two compounds. Moreover, as clearly apparent from Figs. 1 and 2, both structure types consist of distinct layers arranged approximately parallel to (010) and (100) in $HfTe_5$ and $ZrSe_3$, respectively. Each such slab comprises a single sheet of T atoms in the case of $HfTe_5$ as opposed to the twinned T sheets in the $ZrSe_3$ type structure. However, despite this dissimilarity in internal architecture, the $HfTe_5$ and $ZrSe_3$ slabs are both virtually two dimensional, *i.e.* of infinitesimal thickness in proportion to area. The mutual interactions between adjacent slabs in both structure types are weak as clearly demonstrated by the long interlayer $X-X$ contacts ($\geqq$4.161(3) Å in $HfTe_5$ and $\geqq$3.87 Å in $ZrSe_3$, which are only slightly shorter than the corresponding van der Waals distances of 4.4 Å for Te–Te and 4.0 Å for Se–Se).

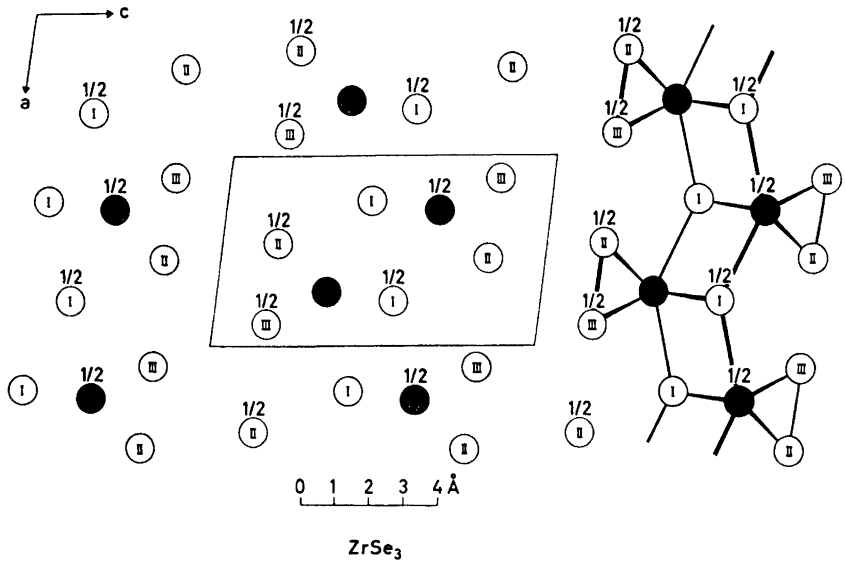

Fig. 2. The crystal structure of $ZrSe_3$ projected along [010]. Data from Krönert and Plieth,[5] the origin being shifted to 0,¼,0.

Since the X atoms unquestionably play the leading part in compounds of this type their situation must also be discussed in some detail. The three crystallographically non-equivalent X atoms of the $HfTe_5$ type structure exhibit different immediate surroundings. Each X_I in the $HfTe_5$ type structure is coordinated to only two T, each X_{II} to two T and another X_{II}, and each X_{III} to one T and two other X_{III}. In the $ZrSe_3$ type structure each X_I is coordinated to four T and each X_{II} and X_{III} have nearly identical configurations of two T and, respectively, one X_{III} and one X_{II} as near neighbours. Hence, the coordination numbers for the X atoms in these structure types range between two and four, and according to the $T-X-T$ and $X-X-T$ bond angles (in Table 2 for $HfTe_5$) the corresponding coordination polyhedra may be regarded as distorted tetrahedra with zero, one, or two of the corners vacant. Consequently, each X atom in the two structure types may obtain a complete octet in its valence shell, implying that, apart from X_I of the $ZrSe_3$ type structure, all X atoms must carry one or two lone electron pairs. The latter deduction is clearly open to future experimental and/or theoretical verification.

In order to form an idea about the valence situation in these compounds it is convenient to test them in terms of the generalized (8−N) rule (*cf.*, *e.g.*, Ref. 10). The correct mathematical formulation of the rule is in this case (*viz.* assuming complete octets on all X atoms) $n+P-Q=8a$, where, per formula unit, n is the total number of electrons involved in bonding, P and Q are the number of electrons in $X-X$ and $T-T$ bonds, respectively, and a is the number of X atoms. Most of the compounds with the $ZrSe_3$ type structure

are diamagnetic semiconductors and all of them satisfy the generalized (8 – N) rule with $a = 22$, $P = 2$, $Q = 0$, and $a = 3$ (*cf.*, *e.g.*, Ref. 9). $ZrTe_5$ and $HfTe_5$ are diamagnetic with temperature dependent susceptibilities as shown in Fig. 3. Hence, and in accordance with previous experience, each T atom is assumed

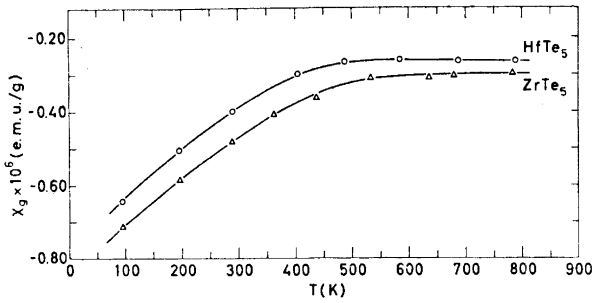

Fig. 3. Magnetic susceptibility *versus* temperature for $ZrTe_5$ and $HfTe_5$. The observations are not corrected for induced diamagnetism.

to contribute 4 electrons and each X atom 6 electrons to $n(=34)$ for $ZrTe_5$ and $HfTe_5$. Neglecting the distinction between the $X_{II}-X_{II}$ and $X_{III}-X_{III}$ bond lengths in the $HfTe_5$ type structure (Table 2 and *vide infra*) and assigning a single electron pair to each such bond, the structural data give $P = 2 + 2 \times 2 = 6$ and $Q = 0$. The composition TX_5 (crystallographic formula $TX_I(X_{II}X_{III})_2$) yields $a = 5$. The values $n = 34$, $P = 6$, $Q = 0$, and $a = 5$ show that the generalized (8 – N) rule is fulfilled for $ZrTe_5$ and $HfTe_5$. The rule is often used as a necessary, but insufficient criterion for the prediction of semiconduction. Thus, $ZrTe_5$ and $HfTe_5$ are potential semiconductors, although this was not brought out in their diffuse reflectance spectra, which show a uniform decrease with increasing wave length apart from a slight irregularity at the long wave length limit. Electrical conductivity measurements on $ZrTe_5$ and $HfTe_5$ single crystals will be carried out in order to shed further light on this problem.

The mutual differences between the $Hf-Te_I$, $Hf-Te_{II}$, and $Hf-Te_{III}$ bond distances in Table 2 is not significant according to the significance test of Cruickshank.[11,12] The same applies to the Zr – Se bond distances in $ZrSe_3$.[5] This together with the values of the corresponding bond angles lead one to propose d^5sp^2 as the idealized hybridization scheme for the T atoms in these compounds. (The valence bond language is used for convenience, but a similar statement can also be given in terms of the molecular orbital formalism.) No useful explanation can be given, however, as to why these compounds favour this somewhat complex hybridization for the T atoms. The information conveyed by the average Hf – Te and Zr – Se bond distances of 2.950 and 2.73_8 Å, respectively, cannot be appraised owing to the lack of suitable data for comparison.

The difference between the $Te_{II}-Te_{II}$ and $Te_{III}-Te_{III}$ bond distances (Table 2) is to be classified as highly significant. The cause of this distinction

is rather obscure. The $Te_{II}-Te_{II}$ and $Se_{II}-Se_{III}$ bond lengths of 2.763(4) and 2.34 Å, respectively, which are analogously situated in the atomic arrangements of $HfTe_5$ and $ZrSe_3$ (*cf.* Figs. 1 and 2), match almost perfectly the single bond (tetrahedral) Te – Te and Se – Se distances (2.74 and 2.34 Å, respectively) listed by Pauling.[13] The $Te_{III}-Te_{III}$ bond length of 2.908(3) Å, on the other hand, conforms with the Te – Te distances found in a number of other transition metal polytellurides (*e.g.* 2.923 Å in $TaTe_4$ [14] and 2.926(1) Å in $FeTe_2$ [15]). The bond distance of 2.835(2) Å in elemental Te falls half way between the values for the $Te_{II}-Te_{II}$ and $Te_{III}-Te_{III}$ distances. Further progress in the clarification of this problem is clearly intimately associated with the assessment of the normal, single bond Te – Te distance appropriate to $HfTe_5$. This evidently requires data which are not available at present.

REFERENCES

1. Brattås, L. and Kjekshus, A. *Acta Chem. Scand.* **25** (1971) 2783.
2. Dahl, T., Gram, F., Groth, P., Klewe, B. and Rømming, C. *Acta Chem. Scand.* **24** (1970) 2232.
3. Hanson, H. P., Herman, F., Lea, J. D. and Skillman, S. *Acta Cryst.* **17** (1964) 1040.
4. Krönert, W. and Plieth, K. *Naturwiss.* **45** (1958) 416.
5. Krönert, W. and Plieth, K. *Z. anorg. allgem. Chem.* **336** (1965) 207.
6. Bradley, A. J. *Phil. Mag.* **48** (1924) 477.
7. Cherin, P. and Unger, P. *Acta Cryst.* **23** (1967) 670.
8. Hamilton, W. C. *Acta Cryst.* **18** (1965) 502.
9. Brattås, L. and Kjekshus, A. *Acta Chem. Scand.* **26** (1972) 3441.
10. Kjekshus, A. *Acta Chem. Scand.* **18** (1964) 2379.
11. Cruickshank, D. W. J. *Acta Cryst.* **2** (1949) 65.
12. Cruickshank, D. W. J. and Robertson, A. P. *Acta Cryst.* **6** (1953) 698.
13. Pauling, L. *The Nature of the Chemical Bond*, Cornell University Press, Ithaca 1960.
14. Bjerkelund, E. and Kjekshus, A. *J. Less-Common Metals* **7** (1964) 231.
15. Brostigen, G. and Kjekshus, A. *Acta Chem. Scand.* **24** (1970) 1925.

Received February 22, 1973.

ACTA CHEMICA SCANDINAVICA 27 (1973) 2375–2382

Electrochemistry in Media of Intermediate Acidity

Part VI.[1] Coupling Reactions of Simple Aryl Ethers

ALVIN RONLÁN,[a] KLAUS BECHGAARD[b] and VERNON D. PARKER[b]

[a]*Department of Organic Chemistry, Lund Institute of Technology, Chemical Center, Box 740, S-220 07 Lund S, Sweden and* [b]*Department of General and Organic Chemistry, The H. C. Ørsted Institute, University of Copenhagen, Universitetsparken 5, DK-2100 Copenhagen, Denmark*

The anodic oxidation of anisole and several substituted anisoles as well as diphenyl ether in media containing trifluoroacetic acid is accompanied by the formation of the corresponding biphenyl and the cation radical of the biphenyl. Conditions for optimum yield of coupled products were examined. The solvent system of choice consists of dichloromethane-trifluoroacetic acid (2:1). The limiting factor for the yield of coupled products is the concentration of product in the anolyte. Up to concentrations of about 1 mM, both yield and current efficiency is very high. The reactions were found to be highly specific with only *para* coupling observed.

The low yields observed during oxidative coupling of simple aryl ethers [2] is readily understood when one considers the relative ease of oxidation of the substrate and the dimeric product. The increased conjugation in the biaryl in addition to the strong electron releasing tendency of the ether group renders the biaryl product much more easily oxidized than the simple aryl ether. The initial oxidation product of an aryl ether by electron transfer is the corresponding cation radical. In addition to dimerisation, the cation radical is highly susceptible to electrophilic reactions with even trace quantities of nucleophiles present in the medium, thus further lowering the yields of desired products. Furthermore, the *ortho-para* directing ether linkage contributes to the complexity of the reaction by favoring the production of isomeric mixtures.

The most successful coupling reactions of the simplest aryl ether, anisole, which have previously been reported involve the action of benzoyl peroxide and aluminium chloride on anisole in nitrobenzene [3] giving 4,4′-dimethoxybiphenyl in 23 % yield and the lead(IV) tetraacetate-boron trifluoride etherate oxidation of anisole in dichloromethane [4] which resulted in the formation of all three possible biphenyls with 4,4′-dimethoxybiphenyl predominating (30 % yield).

It is apparent from the discussion above that what is necessary for a successful biaryl synthesis from simple aromatic ethers is that (a) a medium be employed in which the isomer distribution favors the desired product and (b) in which the initial intermediate is restricted to dimerisation and (c) in which the coupled product is stabilised toward further oxidation and other reactions. Here, we report the results of a study of the coupling of simple aryl ethers in media containing trifluoroacetic acid (TFA). The study was restricted to anisole, diphenyl ether, and simple substituted anisoles since more complex ethers such as the trimethoxybenzenes [2,5,6] or alkoxynaphthalenes [2,7,8] are readily coupled in high yield using conventional techniques.

RESULTS

Voltammetry of anisoles in CH_2Cl_2-TFA (2:1). In general, anisole and substituted anisoles are considerably more difficult to oxidize than the corresponding biphenyls. The latter fact gives rise to a characteristic voltammetric behaviour for this series of compounds which is illustrated by the voltammograms in Fig. 1. For example, anisole is oxidized in CH_2Cl_2-TFA (2:1) with an oxidation peak potential (O_1) equal to +1.55 V (Fig. 1a). On the cathodic

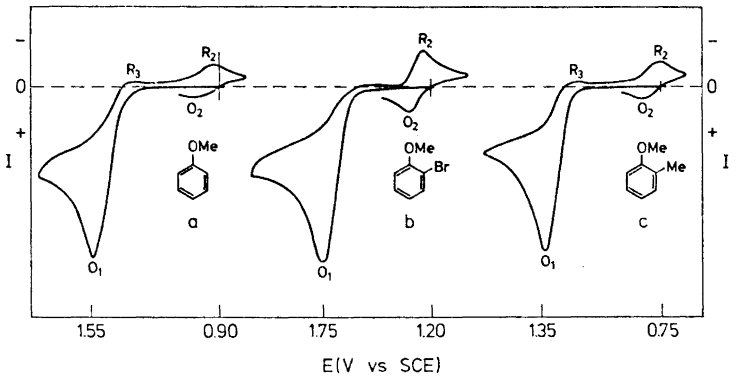

Fig. 1. Cyclic voltammetry for the anodic coupling of anisoles in CH_2Cl_2 – TFA (2:1) containing n-Bu_4NBF_4 (0.2 M). (a) Anisole, (b) 2-bromoanisole, (c) 2-methylanisole. Voltage sweep rate = 156 mV/sec.

going sweep, a very small reduction peak (R_3) is first seen and then more cathodic a larger reduction peak (R_2) appears with a corresponding oxidation peak (O_2) being observed on the second anodic sweep. The redox couple, $R_2 - O_2$, was found to be due to the oxidation-reduction of 4,4′-dimethoxybiphenyl and the corresponding cation radical by comparison with the authentic compound. Furthermore, the small reduction peak, R_3, was found to appear at the same potential as the reduction peak for the dication of 4,4′-dimethoxybiphenyl. This behaviour appears to be general for compounds having a free position *para* to a methoxy group. Two other typical examples are illustrated

by the voltammograms for 2-bromoanisole (Fig. 1b) which exhibits an initial oxidation peak (O_1) at +1.76 V. In the case of 2-methylanisole in the same solvent system, the oxidation of the substrate occurs with a peak potential of +1.33 V (Fig. 1c). Both the latter voltammograms have the characteristic reversible couple, $R_2 - O_2$, as seen in the case of anisole. In addition to the above examples, a similar behaviour was observed for the following compounds: 2,6-dimethylanisole, 2,3,5,6-tetramethylanisole, diphenylether, and 4-methoxybiphenyl. Compounds substituted in the position *para* to methoxy such as 4-methylanisole failed to give voltammograms showing the reversible couple, $R_2 - O_2$, due to the corresponding dimeric product.

Exhaustive electrolysis of 1.0 mM solutions of all the compounds listed above in CH_2Cl_2-TFA (2:1) using constant current coulometric techniques,[9] resulted in coulometric n values ranging from 1.5 to 1.7. The theoretical n value for oxidation of an anisole to the cation radical of the corresponding biaryl is equal to 1.5. Yields of the dimers could be determined readily by a comparison of the voltammetry of the resulting coulometric solution with that of solutions of known concentrations of the dimers. Yields of 90 – 100 % were observed.

The effect of solvent composition on the yield of coupling products. Anisole was selected as the model compound for the study of the conditions to give optimum yields of coupling products. Previous results had shown that significant yields of coupling products from simple aryl ethers could not be attained by anodic oxidation in acetonitrile.[10] However, it had not been established whether or not dichloromethane, which has been found to be a suitable medium for the coupling of aromatic hydrocarbons,[11] could also be of utility in the coupling of aryl ethers. Thus, the anodic oxidation of anisole (1.0 mM) in dichloromethane containing n-Bu_4NBF_4 (0.2 M) was carried out until 1.5 F/mol had been passed. Only traces of the desired product, 4,4′-dimethoxybiphenyl, could be detected. Thus, TFA is a necessary and essential part of the CH_2Cl_2-TFA solvent mixtures if coupling of aryl ethers is to be observed. The data in Table 1 indicate how the yield of 4,4′-dimethoxybiphenyl from the anodic oxidation of anisole varies with solvent composition during preparative scale (2 mmol) electrolysis. Table 2 gives data for the yield of product and current efficiency during electrolysis under coulometric conditions as a func-

Table 1. Effect of solvent composition on the yield of 4,4′-dimethoxybiphenyl. 3.0 F/mol passed at 20°. Supporting electrolyte = n-Bu_4NBF_4 (0.1 M).

TFA (ml)	Dichloromethane (ml)	% Yield
0	100	4
10	90	22
17	83	30
25	75	58
33	67	63
50	50	61
100	0	57

tion of the current passed. The data in Table 1 indicate that the preferred medium for the preparation of 4,4′-dimethoxybiphenyl by anodic oxidation of anisole contains about 66 % by volume of dichloromethane. Going to solutions containing higher percentage of TFA resulted in a slight lowering of the yield. Increasing the proportion of dichloromethane to 75 % resulted in a lowering of the yield and still higher proportions caused the yield of product to decrease drastically. The data in Table 2 show the same trend regarding the

Table 2. Yield and current efficiency for formation of 4,4′-dimethoxybiphenyl during oxidation of anisole.[a]

Faraday ($\times 10^4$)[b]	TFA		CH_2Cl_2–TFA (2:1)		CH_2Cl_2–TFA (5:1)	
	Yield[c] %	Current[d] Efficiency	Yield[c] %	Current[d] Efficiency	Yield[c] %	Current[d] Efficiency
1	90	103	100	100	96	58
2	81	94	99	91	59	60
3	77	78	85	89	48	61
4	69	80	80	79	41	57
5	62	78	74	76	40	50
6	57	76	65	73	36	53
7	53	74	60	70	33	52
8	47	72	54	68	29	49

[a] Substrate (0.4 mmol) dissolved in solvent containing n-Bu_4NBF^4 (0.2 mM). [b] Constant current electrolysis at 25 mA for 6.44 min = 10^{-4} Faraday. [c] Based on anisole consumed. [d] Expressed in % based on 1.5 F/mol anisole = 100 %.

solvent composition. Best results were obtained with a CH_2Cl_2-TFA ratio of 2:1. The *data* clearly show that both yield and current efficiency is high at low conversion but falls off drastically with increasing degree of conversion. The latter effect is even more clear from the graphs of Fig. 2. When the solvent

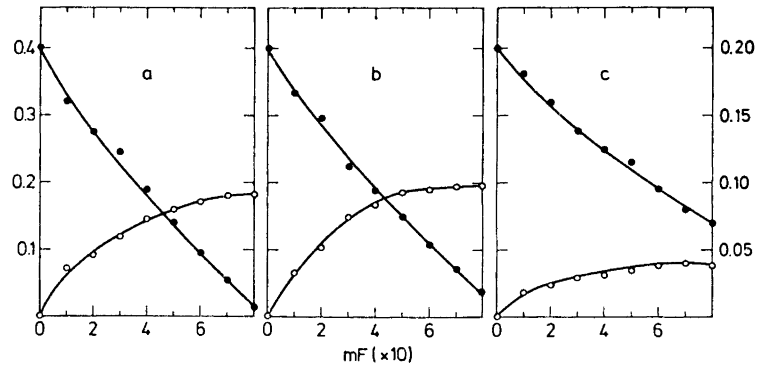

Fig. 2. Consumption of anisole and formation or 4,4′-dimethoxybiphenyl as a function of number of Faraday passed. ● Anisole, ○ 4,4′-dimethoxybiphenyl. Solvent: (a) TFA, (b) CH_2Cl_2–TFA (2:1), (c) CH_2Cl_2–TFA (5:1). Left hand scale refers to mmol anisole and right hands scale refers to mmol 4,4′-dimethoxybiphenyl.

was TFA the amount of product rose rather sharply and then leveled off at about 0.09 mmol (maximum possible = 0.2 mmol). The same general trend is seen with CH_2Cl_2-TFA (2:1) as solvent (Fig. 2b) with the maximum being approached after the consumption of 0.5 mF and then remaining level at about 0.1 although the anisole continued to be consumed. A much lower level of product (0.04 mmol) was attained in CH_2Cl_2-TFA (5:1). It is also seen that the comsumption of anisole was less efficient in the latter case (Fig. 2c). In order to determine whether the level to which the amount of product reached was determined by an optimum concentration of product or by the amount of substrate oxidized, an experiment identical to that giving the data for Fig. 2b was carried out with one major change, *i.e.* the amount of anisole used was increased by a factor of 10 (4.0 mmol). The results were nearly the same as those in Fig. 2b with amount of product formed leveling off at about 0.11 mmol.

Several experiments were carried out at different temperatures ranging from $-20°$ to $+30°$. No significant change in the yield of product was observed upon changing the temperature.

DISCUSSION

Clearly, an important factor contributing to the complexity of aryl ether and phenol oxidation is that the coupled products are invariably more easily oxidized than the substrates. This fact is demonstrated by the cyclic voltammograms (Fig. 1) for anisoles in CH_2Cl_2-TFA (2:1). The three examples shown: anisole, 2-bromoanisole, and 2-methylanisole, are all oxidized about 600 mV more anodic than their corresponding dimers. Thus, at the potential necessary for anisole oxidation to occur, all the reactions in Scheme 1 take

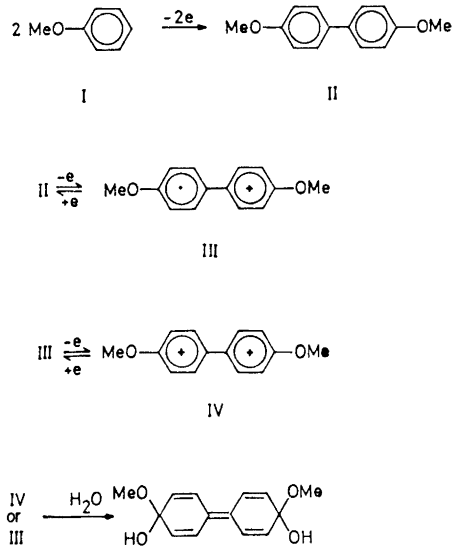

Scheme 1.

place. The cation radical (III) and the dication (IV) are both reactive species and react with any nucleophiles present. An expected reaction, when water is present, is the formation of cyclohexadienones [12] of type V which would undergo loss of methanol to give the quinone. Reactions of this type have been observed previously during oxidation of methoxybenzenes in both aqueous [13] and non-aqueous [14] systems. Water is nearly always present in solvents used for electrolytic reactions and has been implicated in reactions of a variety of aromatic cation radicals in "dry" acetonitrile.[15–20] Other possible reactions such as polymerisation are also likely when cation radical concentrations become high.

The success of coupling reactions of simple aryl ethers in media containing trifluoroacetic acid must be attributed to the stabilizing influence of TFA on the cation radicals and dications of the dimers. The stabilishing influence of TFA on aromatic cation radicals as well as the deactivation of water as a nucleophile toward aromatic cation radicals has recently been described.[21] While the potential for oxidation of the anisole is sufficient to oxidize the biaryl to the dication, it is not necessary for the dication to be stable for long times in the medium since it behaves as a potent oxidant, most likely oxidizing both the substrate and the biaryl in homogeneous electron transfer reactions. The dications of several biaryls are sufficiently stable in media containing TFA to show reversible behavior for the cation radical-dication couple.[22]

As indicated by the data in both Tables 1 and 2, best results were obtained using a mixed solvent and the optimum ratio of CH_2Cl_2-TFA appears to be about 2:1. The latter is of practical importance since our reason for going to the mixed solvent system was to use the inexpensive dichloromethane as a diluent for the more expensive TFA.

The data in Table 2 and Fig. 2 indicate that the formation of biaryls is a very efficient, high yield process until a certain concentration of the product is achieved after which the concentration of product remains nearly the same while the substrate is continuing to be consumed. This is also seen from the coulometric experiments where nearly quantitative yields of the dimers were obtained during oxidation of 1.0 mM solutions of the substrates. When the solvent was CH_2Cl_2-TFA (2:1), the yield was essentially quantitative up until about 0.2 mF had been consumed. The concentration of dimer at that point (Fig. 2) was equal to about 1.0 mM. Thus if one were to oxidize an aryl ether which was sufficiently valuable to warrant use of dilute solutions to achieve the maximum yield, our data suggest that a 2 mM solution of the ether should be exhaustively oxidized, following the reaction by voltammetry to determine the stopping point. In this manner it should be possible to obtain nearly 400 mg of product (for a substrate of molecular weight 200) per liter of solution oxidized.

EXPERIMENTAL

TFA was reagent grade and used without further purification. Dichloromethane was passed through a column of neutral alumina before use. The aryl ethers were either reagent grade or prepared from the corresponding phenols by standard procedures. The apparatus used for voltammetry and coulometry has been described.[23]

General procedure for yield and current efficiency experiments (Table 2). Anisole (0.4 mmol) was dissolved in the solvent (50 ml) containing n-Bu_4NBF_4 (0.2 M) and placed

in the cell which consisted of a 100 ml beaker equipped with magnetic stirring and a platinum gauze electrode which fit snugly into the beaker. Solvent containing electrolyte was placed in a tube, the bottom of which was a sintered glass disk (G–4). The tube was supported in the electrolytic solution with the liquid levels adjusted to be the same in both solutions. The tube served as the cathode compartment and was equipped with a platinum gauze electrode. The peak voltammogram of the anolyte was recorded at a Beckman platinum button electrode. The reference electrode was an aqueous saturated calomel electrode and was placed in the cathodic compartment while the large platinum gauze served as the counter electrode. Constant current electrolysis was carried out for 6.45 min at 25.0 mA which corresponds to 0.1 mF. The peak voltammogram, showing a peak for anisole as well as for 4,4'-dimethoxybiphenyl was recorded. The concentration of 4,4'-dimethoxybiphenyl was determined by comparison of the peak current with that obtained from a voltammogram of a solution of known concentration of the compound in the solvent system. The above procedure was repeated at 0.1 mF intervals until a total of 0.8 mF had been consumed.

General procedure for preparative scale oxidations (Table 1). Anisole (2.0 mmol) was dissolved in the solvent (100 ml) containing n-Bu_4NBF_4 (0.1 M) and placed in a two compartment water jacketed cell. The compartments were separated by a sintered glass disk (G–4). The anode was a platinum sheet (area = 75 cm^2) and the cathode was a coiled platinum wire. Electrolysis was conducted at constant current (200 mA) under an atmosphere of nitrogen * until 3 F/mol had been passed. The anolyte was stirred magnetically and kept at 8° by external cooling. After treatment of the anolyte with zinc dust to reduce any of the product present as an oxidized form, the solution was filtered and evaporated to dryness *in vacuo* at 40°. The residue was treated with dry ether to precipitate the supporting electrolyte. After evaporation of the ether, the yield was determined from the NMR spectrum and the peak voltammogram of the crude product. Further purification was carried out either by vacuum sublimation or preparative thin layer chromatography.

2,2',3,3',5,5',6,6'-Octamethyl-4,4'-dimethoxybiphenyl was prepared as described above. Yield 53 %, m.p. 131 – 131.5°, NMR ($CDCl_3$); 1.73 (s, 12 H), 2.22 (s, 12 H) and 3.77 (s, 6 H). (Found C 81.3; H 9.0. Calc. for $C_{22}H_{30}O_2$: C 81.0; H 9.2).

4,4'''-Dimethoxyquaterphenyl was obtained in 48 % yield as described above. M.p. 336 – 339° (lit.[24] 336 – 339°).

3,3'-Dibromo-4,4'-dimethoxybiphenyl was obtained in 43 % yield in the manner described above. M.p. 167 – 168° (lit.[25] 167°).

4,4'-Diphenoxybiphenyl was prepared in 56 % yield as described above. M.p. 155 – 157° (lit.[26] 150 – 151°).

3,3'-Dimethyl-4,4'-dimethoxybiphenyl was obtained in 42 % yield by the standard procedure. M.p. 155 – 156° (lit.[27] 154.5°).

3,4,3',4'-Tetramethoxy-2,2'-dimethylbiphenyl was obtained in 86 % yield as described above. M.p. 115 – 116° (lit.[28] 115 – 116°).

REFERENCES

1. Part V: Hammerich, O. and Parker, V. D. *J. Electroanal. Chem.* **38** (1972) App. 9; For preliminary account of this work see: Bechgaard, K., Hammerich, O., Moe, N. S., Ronlán, A., Svanholm, U. and Parker, V. D. *Tetrahedron Letters* **1972** 2271.
2. Musgrave, O. C. *Chem. Rev.* **69** (1969) 499.
3. Edward, J. T., Chang, H. S. and Samad, S. A. *Can. J. Chem.* **40** (1962) 804.
4. Aylward, J. B. *J. Chem. Soc.* **B 1967** 1268.
5. Erdtman, H. *Proc. Roy. Soc.* **A 143** (1933) 191.
6. Davidson, I. M., Musgrave, O. C and Manson, D. L. *J. Chem. Soc.* **1965** 3040.
7. Scholl, R. and Seer, C. *Ber.* **55** (1922) 330.
8. Marschalk, C. *Bull. Soc. Chim. France* **3** (1936) 121.
9. Parker, V. D. *Acta Chem. Scand.* **24** (1970) 2768.
10. Parker, V. D. and Adams, R. N. *Unpublished results.*

* Similar results were obtained in runs conducted under air.

11. Nyberg, K. *Acta Chem. Scand.* **24** (1970) 1609; **25** (1971) 2499.
12. Ronlán, A. and Parker, V. D. *J. Chem. Soc.* **C 1971** 3214.
13. Papachoudo, L., Bacon, J. and Adams, R. N. *J. Electroanal. Chem.* **24** (1970) App. 1.
14. Parker, V. D. *Chem. Commun.* **1969** 610.
15. Sioda, R. E. *J. Phys. Chem.* **72** (1968) 2322.
16. Majeski, E. J., Stewart, J. D. and Ohnesorge, W. E. *J. Am. Chem. Soc.* **90** (1968) 633.
17. Parker, V. D. *Acta Chem. Scand.* **24** (1970) 2757.
18. Parker, V. D. *Acta Chem. Scand.* **24** (1970) 3171.
19. Shine, H. J. and Murata, Y. *J. Am. Chem. Soc.* **91** (1969) 1872.
20. Parker, V. D. and Eberson, L. *J. Am. Chem. Soc.* **92** (1970) 7488.
21. Hammerich, O., Moe, N. S. and Parker, V. D. *Chem. Commun.* **1972** 156.
22. Ronlán, A., Coleman, J., Hammerich, O. and Parker, V. D. *Submitted for publication.*
23. Hammerich, O. and Parker, V. D. *J. Chem. Soc. Perkin Trans.* **1 1972** 1718.
24. Harly-Mason, J. and Mann, F. G. *J. Chem. Soc.* **1940** 1379.
25. Van Alphen, J. *Rec. Trav. Chim.* **49** (1940) 769.
26. Kotlyarrskii, K. L., Shcartsberg, M. S., Andrievskol, V. N. and Kruglor, B. G. *Izv. Akad. Nauk SSSR, Ser. Khim.* **11** (1963) 2032.
27. Winston, J. H. C. *Am. Chem. J.* **31** (1909) 119.
28. Cromartie, R. I. T., Harley-Mason, J. and Wanningama, D. C. P. *J. Chem. Soc.* **1958** 1982.

Received March 10, 1973.

ACTA CHEMICA SCANDINAVICA 27 (1973) 2383–2395

Xanthomonas Pigments

2.* The *Xanthomonas* "Carotenoids" — Non-carotenoid Brominated Aryl-polyene Esters

A. G. ANDREWES,[a] S. HERTZBERG,[a] S. LIAAEN-JENSEN[a] and M. P. STARR[b]

[a]*Organic Chemistry Laboratories, Norwegian Institute of Technology, University of Trondheim, Trondheim, Norway and* [b]*Department of Bacteriology, University of California, Davis, California 95616, USA*

The pigments of *Xanthomonas juglandis* strain XJ103, previously reported to be carotenoids, have been further investigated.

Two pigment complexes (I and II), each of estimated molecular weight *ca.* 2200, provided on saponification brominated aryl octaene methyl esters. Partial structures for the four components of the saponified pigment mixture are presented (*1a*, *1b*, *2a*, *2b*). The monobromides (*1a*, *2a*) could not be separated from the corresponding dibromides (*1b*, *2b*). The proposed structures are based on chemical data and physical properties including electronic, infrared and mass spectra, and comparison with dimethylcortisalin (*3b*) and model compounds (*4* – *7*) synthesized for this purpose.

Structures such as those proposed are unique and support the premise that the pigments may serve as a significant taxonomic marker for the genus *Xanthomonas*.

The genus *Xanthomonas* is a group of Gram-negative bacteria which cause diseases in plants.[1–4]

Although a few non-pigmented bacteria have been occasionally assigned to the genus *Xanthomonas*, and colourless mutants of *Xanthomonas* spp. are known, the yellow colour of their colonies has been of diagnostic importance for distinguishing *Xanthomonas* spp. from other bacteria occurring in the same habitats.

From previous studies, it appears that the same pigments occur in many nomenspecies of *Xanthomonas*,[5,6] that they are membrane-bound,[7] that they are different from other previously reported bacterial pigments,[5,6] and that they have some properties which led to their classification as carotenoids.[5,8]

* No. 1. *J. Bacteriol.* **87** (1964) 293.

We now report partial structures for the pigments isolated from *Xanthomonas juglandis* strain XJ103 which, in fact, are not carotenoids but are unique aryl octaene methyl esters distinguished by carrying one or two bromine atoms.

The present work is restricted to *X. juglandis* strain XJ103. However, on the basis of previous work,[5,6] it seems likely that the results may be extended to other *Xanthomonas* nomenspecies.

RESULTS AND DISCUSSION

Members of the genus *Xanthomonas* form from glucose a complex polysaccharide [9–11] which interferes with pigment analysis. *X. juglandis* XJ103 was therefore cultivated in a sugar-free medium.

Pigments were extracted from lyophilized cells and isolated according to the scheme shown in Fig. 1. Pigments *1* and *2* obtained after mild saponification of the extracts correspond to the material isolated from the same strain of *X. juglandis* in previous investigations.[5–7]

Complexes I and II were obtained when the saponification procedure was omitted. Treatment of the complexes I and II with mild base afforded pigments *1* and *2*, respectively. Pigments *1* and *2* and the corresponding complexes exhibited virtually identical electronic spectra (*cf.* Fig. 2), but differed

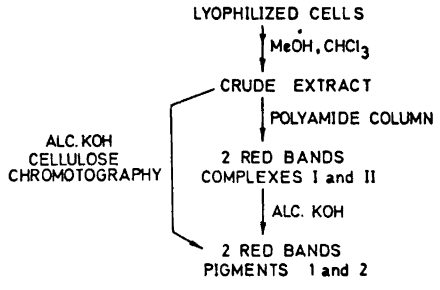

Fig. 1. Scheme for isolation of pigments from *X. juglandis* XJ103.

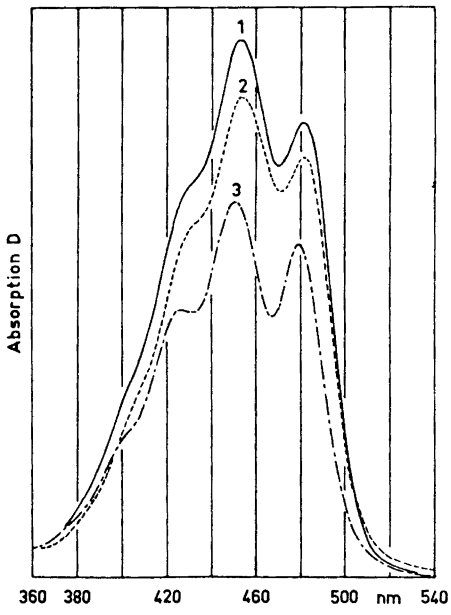

Fig. 2. Absorption spectra in visible light of *X. juglandis* XJ103 pigment *1* (curve 1), XJ103 pigment *2* (curve 2), and synthetic *4* (curve 3).

Table 1. Chromatographic properties of the *X. juglandis* XJ103 pigment complexes I and II, of the *trans* pigments *1* and *2* and of the acetate of *2*.

Chromatographic system	Required eluent or R_F-value				
	I	II	*1*	*2*	*2*-acetate
Polyamide 6-AC column	4 % MeOH-benzene	6–10 % MeOH-benzene			
Merck kieselgel column			benzene	$CHCl_3$ ether [a]	
$CaCO_3$ column	[b]			[b]	
Alumina activity grade 2 column					
Cellulose (Schleicher & Schüll No. 124) column			5 % acetone-pet.ether	20–100 % acetone-pet.ether	2–5 % acetone-pet.ether
Schleicher & Schüll No. 287 (kieselguhr) paper					
benzene	0.40	0.25	0.78	0.47	
20 % acetone in petroleum ether			0.80	0.50	0.80
Silicagel G plates: benzene			0.80	0.45	
2 % methanol in benzene	0.60	0.40			
chloroform			0.92	0.60	

[a] For development, zones extruded. [b] Not eluted with methanol.

in other physical properties. The complexes were readily soluble in most common organic solvents. Their mass and IR spectra were inconclusive, and the PMR spectra showed only a strong band characteristic of methylene groups in saturated environments. Pigments *1* and *2*, however, had minimum solubility in all common solvents to such an extent that the PMR spectra could not be obtained. A single attempt to obtain a time-averaged spectrum was unsuccessful because of degradation during the time required.

Considering now only the products obtained after mild saponification, Pigments *1* and *2* constituted 0.04 % of the lyophilized cells in the approximate ratio of 2:1. Pigment *1* crystallized as needles of m.p. 220°C, whereas *2* was obtained as an amorphous powder. The chromatographic behaviour is summarized in Table 1. The difference in polarity of *1* and *2* indicates that *2* has at least one polar group not present in *1*. Representative electronic absorption spectra of *1* and *2* are shown in Fig. 2. Absorption maxima for both compounds in various solvents are listed in Table 2. The general shape of

Table 2. Spectral properties of the *X. juglandis* XJ103 pigment complexes I and II and the *trans* pigment *1* and *2* in visible light.

Solvent	Absorption maxima in nm											
	I			II			*1*			*2*		
Methanol	420	442.5	469	420	442	469	(418)	442	470			
Acetone	(421)	444	472	(421)	443	471	(423)	445	473	420	444	472
Chloroform							(428)	453	482	(428)	453	480
Benzene	433	456	483	430	455	483						
Pyridine							(435)	460	489			
Dimethyl sulfoxide							(435)	462	490			

the absorption curves are typical for conjugated polyenes and resemble the spectra of aromatic polyene aldehydes characterized by Zechmeister's group.[12]

Mass spectrometric analysis of *1* showed the molecular ion as a triple peak at *m/e* 530, 532, and 534 with relative intensities 1 : 2 : 1, indicative of a dibromo-compound. Accurate mass measurement established the molecular formula $C_{25}H_{24}Br_2O_3$. Fragment ions centered at *m/e* 501 and *m/e* 473 were compatible with loss of methoxy and carbomethoxy radicals, respectively. Also noted were ions attributed to the loss of HBr and probably benzene. Pigment *2* gave a molecular ion centered at *m/e* 518 with isotopic distribution precisely that of a dibromo-compound. The molecular formula $C_{24}H_{22}Br_2O_3$ determined by high precision measurements indicated that *2* differs from *1* by an extra methyl or methylene group.

Bands in the IR spectrum of *1* (Fig. 3) at 1710 cm^{-1} and 1135 cm^{-1} are attributed to an α,β-unsaturated ester.[13] Absorption at 1010 cm^{-1} was assigned to out-of-plane C–H vibrations on *trans*-double bonds, the position of which is shifted to somewhat higher frequencies than that noted for carotenoids,[14] but consistent with the same assignment made here for cortisalin (*3a*)[15] which has no methyl substituents on the polyene chain. The IR spectra of dimethyl-

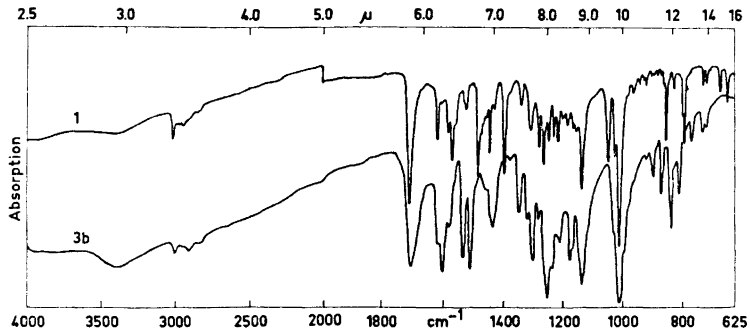

Fig. 3. Infrared spectra (KBr) of *Xanthomonas juglandis* XJ103 pigment *1* and dimethylcortisalin (*3b*).

cortisalin (*3b*) and *1* have many features in common (Fig. 3). Thus absorption at 1250 cm^{-1} in *3b* and *1* may be associated with an aromatic methoxy group.[13] The band at 855 cm^{-1} of *1* was originally attributed to the vibration of isolated C–H in an aromatic ring. We have been unable to assign the prevalent bands at 1396 cm^{-1} and 1050 cm^{-1}. The IR spectrum of *2* was less distinct. Strong absorption at 3410 cm^{-1} indicated a hydroxy group [13] and additional bands were present which suggested a conjugated ester and conjugated *trans*-disubstituted double bonds at the same frequencies noted in the spectrum of *1*.

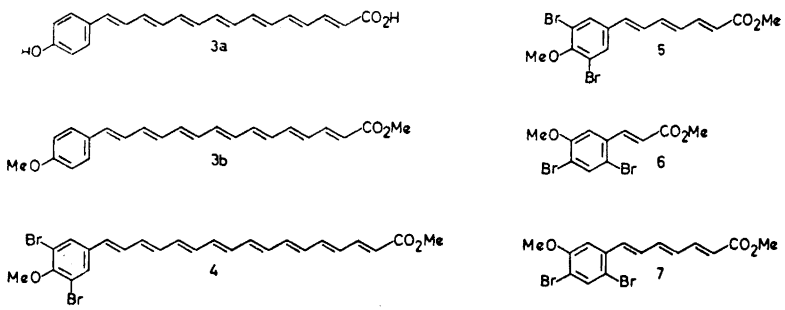

The molecular formulas for *1* and *2* (13 double bond equivalents) in conjunction with the observed electronic spectrum dictate that in all probability the pigments contain one aromatic ring. The loss of methoxy and carbomethoxy fragments in the mass spectra [16] and the aforementioned IR data suggest that the chromophore terminates in a conjugated methyl ester function. Comparison of the electronic spectra with that of dimethylcortisalin (*3b*, λ_{max} 444 nm *vs.* 461 nm for *1* in pyridine) indicated that *1* and *2* have a polyene system longer than 7 conjugated double bonds. The difference in the absorption maxima of dimethylcortisalin (*3b*) and *1* or *2* suggested that the polyene system of *1* and *2* consists of 8 double bonds. Moreover, considering

the molecular formula and chromophore, *1* could contain at most one methyl group. Oxidation studies to be discussed below showed that this methyl group is connected with the aryl ring and not with the polyene chain. Thus the initial supposition was that *1* and *2* were aryl octaenes terminated by a conjugated methyl ester and further distinguished by having two bromine atoms incorporated in the structure, presumably on the phenyl ring. The presence of a phenolic hydroxy group in *2*, methylated in *1*, was consistent with the spectral data.

A model compound *4* was synthesized [17] and the properties compared with that of *1*. Compound *4* had solubility properties similar to and chromatographic properties identical with those of *1* in the systems tested. The electronic absorption spectrum of *4* closely resembled, but was not identical to, that of *1* (Fig. 2); the maximum of *4* was hypsochromically displaced by 3 nm in chloroform and the spectrum of *4* showed slightly more fine-structure. Comparison of the IR spectra (*cf.* Ref. 17) showed similarities in the bands assigned to the ester and methoxy groups and the *trans*-disubstituted double bonds. Differences were observed in the region 800 – 900 cm^{-1} and the bands at 1395 cm^{-1} and 1050 cm^{-1}, noted for, but not assigned for *1* were absent. With respect to the mass spectrum of *4* the expected molecular ion and isotopic peaks were present. Losses of methoxy and carbomethoxy fragments were noted along with a prominent loss of C_6H_6 (benzene from the polyene chain [17]), but no loss of HBr was detectable. Thus, *1* and *4* were not identical, but the similarities in the general characteristics of the synthetic pigment (*4*) and *1* are supporting evidence for the basic proposed structures of *1* and *2*.

Turning now to the chemical properties of *1* and *2:* Saponification of a mixture of *1* and *2* in methanol-chloroform (1:1) containing 10 % KOH gave a mixture of the corresponding carboxylic acids, confirmed by mass spectrometry and by the change in partition properties. Neither pigment *1* nor *2* reacted with diazomethane. This result does not disprove the presence of a phenolic hydroxy group in *2* since neither *3a* nor phenolic carotenoids [18] provide a methyl ether under the same conditions. Pigment *1* could not be acetylated or silylated. Pigment *2* gave a monoacetate, judged by chromatographic properties and mass spectrometry (M = *m/e* 558, 560, 562).

Reduction with complex metal hydrides were complicated by the low solubility of the pigments and low recoveries. As expected the ester group was not reduced with $NaBH_4$. A product obtained with $NaBH_4$ exhibited the same electronic spectrum as the starting material (*1*), but was chromatographically more strongly adsorbed. Its formation may involve displacement of bromine by hydride,[19] although mass spectrometric results were inconclusive.

When *1* was reduced with $LiAlH_4$, at least two products were obtained. One product could not be distinguished from the $NaBH_4$-product mentioned above. Reduction of the ester function can account for the second major acetylable product with λ_{max} 405, 422, and 448 nm in acetone. Other products, less consistently obtained, had shorter chromophores.

Oxidation of *1* with $KMnO_4 - CaCO_3$,[20] slow under reflux condition, gave an acid with molecular formula $C_8H_7BrO_3$ (high precision mass spectrometry), explicable by a benzoic acid substituted by a methoxy group and one bromine

atom. $KMnO_4-H_2SO_4$ oxidation was rapid and gave the same $C_8H_7BrO_3$ moiety. Ozonolysis of a mixture of *1* and *2* gave products with molecular ions corresponding to $C_8H_7BrO_3$ and $C_7H_5BrO_3$. The oxidation data thus support the idea that *2* is a phenol and *1* its methyl ether derivative.

The absence of any dibromo acid in the oxidation mixture was unexpected, and may be explained in a number of ways:

First of all, the second bromine may be located on the polyene chain and not on the ring. However, vinylic bromides of the required type might be expected to suffer elimination under the alkaline conditions used for preparation of the free carboxylic acids of *1* and *2*.[21]

A second possibility would be that *1* and *2* each were mixtures of mono- and dibromo compounds and that (i) the dibromo compounds did not survive the oxidation conditions or (ii) that the dibromo compounds only represented a minor portion of the total pigment mixture. Alternative (i) is disregarded for *1* since $KMnO_4$ oxidation of the two model dibromomethoxy aryl compounds *5* and *6* gave the expected dibromo acids.

Careful re-examination of the mass spectra of *2* under different conditions and from different batches of cells indeed confirmed that *2* is, in fact, a mixture of the mono- and dibromo compounds: *2a*, $C_{24}H_{23}BrO_3$ *m/e* 438, 440, and *2b*, $C_{24}H_{22}Br_2O_3$ *m/e* 516, 518, 520. This conclusion was not reached earlier because the fragment ions at *m/e* 436, 438, caused by loss of HBr from the molecular ion of *2b*, give peaks in the same region. The relative quantities of *2a* and *2b* cannot be judged from the mass spectra and are not known, since we have been unable to separate the mixture although a number of chromatographic systems have been examined.

Consequently, it appears that *X. juglandis* strain XJ103 contains four pigments (*1a*, *1b*, *2a*, *2b*), two of which are monobromides (*1a*, *2a*) and two dibromides (*1b*, *2b*). In the case of the monobromides, the bromine atom must be located on the aromatic ring. With respect to the dibromides, one of the bromine atoms is on a phenyl ring while the position of the second bromine is not established.

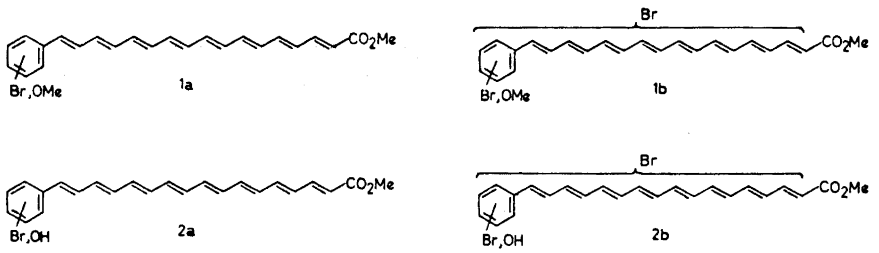

The observed loss of HBr from *1b* and *2b* on electron impact may support the presence of bromine in *ortho* position to the polyene chain. The required hydrogen transfer for HBr elimination from an aryl bromide is best accommodated with *ortho* substitution, for example by the following mechanism:

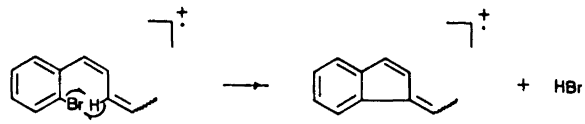

Loss of a bromine radical from the model compounds *6* and *7* indicates that bromine substituted *ortho* to the polyene chain is labile on electron impact. Further support for an *ortho* bromine substituent in *1* and *2* follows from a comparison of the electronic spectra of *5* and *7*. Compounds *5* and *7* exhibit absorption at about the same wavelength. However, *7* displays less spectral fine-structure than *5*. The same situation is observed with respect to *1* and *2* *versus* the synthetic model *4*. Finally the IR-band at 1050 cm^{-1}, observed for *1* and *2* was also noted for synthetic *7*, and not for *4* and *5*.

The *Xanthomonas* complexes consist of the pigments *1a*, *1b*, *2a*, *2b*, or precursors thereof, bound in as yet an unknown fashion to a lipid-like moiety. Considering the extinction coefficient of the complexes, I and II and the corresponding pigments *1* and *2*, a rough calculation of the unit weight of the attached moiety can be made and gives a value of 1700 for complex I as well as II. It then appears that the same moiety is attached to each pigment. The PMR spectrum of the complexes indicates that the attached group is largely lipid in nature, and the fact that base is required to break the complex suggests that the bond between the chromophore moiety and the attached group is chemical in nature. Phospholipid/fatty alcohol esters of a coloured carboxylic acid, suffering re-esterification on alkali treatment in methanol to give the methyl esters *1* and *2*, have been considered. However, alkali treatment of the complexes I and II in ethanol did not result in the corresponding ethyl esters, thus disproving the above hypothesis.

One remaining possibility is that complexes I and II contain a hydroaromatic ring which gives rise to the aromatic structure on alkali treatment.

CHEMOTAXONOMICAL CONSIDERATIONS

Naturally occurring bromine compounds in living organisms are comparatively rare although several have been reported from marine sources, *e.g.* Refs. 22 – 33. Some of these marine compounds have bromine substituents on an aromatic ring,[22,23,29–33] but none have extended polyene chains. The instances of bromine compounds isolated from non-marine sources [34–37] are scarce and in each of the cases referred to the incorporation of bromine was accomplished by the addition of potassium bromide to a synthetic medium as a replacement for chloride ion.

In the present cultivation of *X. juglandis* no bromide was deliberately added to the complex culture medium, and the precise source of the bromine incorporated into the *Xanthomonas* pigments is so far not known. It is probably safe to assume that the concentration of chloride ion was higher than that of bromide in the beef extract-peptone nutrient broth used. If this is indeed the case, then these *Xanthomonas* bacteria must have a capacity for specific

enrichment of bromide over chloride. This in itself would constitute a novel feature of a non-marine organism.

With respect to the general features of the *Xanthomonas* pigments other than the presence of bromine in the molecule, we have found relatively few instances of naturally occurring compounds with related structures. Cortisalin (*3a*) isolated from the fungus *Corticium salicinum* [15] is a phenol *para* substituted by a conjugated polyene carboxylic acid, which has features common to the *Xanthomonas* pigments. An unbranched polyene dicarboxylic acid, corticrocin,[38] has been isolated from the related species *Corticium croceum*, but this lacks an aromatic ring. From *Aspergillus niger* two aromatic polyenes [39–41] have been reported, but both these pigments have substituents on the polyene chain and lack substituents on the aryl ring.

Thus, the *Xanthomonas* pigments, not yet encountered outside the bacterial genus *Xanthomonas*, represent unique structures of significant chemotaxonomic value and considerable chemo-ecological interest.

EXPERIMENTAL

Xanthomonas pigments

Biological material. Xanthomonas juglandis strain XJ103 [6,7] was obtained from the International Collection of Phytopathogenic Bacteria maintained at the Department of Bacteriology, University of California at Davis.

Cultivation. The cultures were grown in several 200 l batches of double-strength Difco nutrient broth (16 g/l) with aeration (7 l/min) and agitation. Initial pH of the broth was 6.9. During growth the pH was maintained at 7.2. The cells of one typical batch were harvested after 29 h of growth and the total yield was 1280 g wet weight; after lyophilization 150 g.

Materials and methods. Instrumentation and solvents were as generally used in the Norwegian laboratory.[17] Chromatographic properties are compiled in Table 1.

Pigment extraction. Lyophilized cells were exhaustively extracted with MeOH, then MeOH – $CHCl_3$ (1:1) and the extracts pooled and concentrated under vacuum. The resultant viscous oil was dispersed in benzene and filtered through Celite to eliminate insoluble material.

Chromatography of non-saponified extracts. Benzene solutions of the extracts were chromatographed on columns of polyamide 6-AC resin (Machery, Nagel & Co., Germany). The individual complexes of I and II were further purified by preparative thick layer chromatography on silica gel G plates developed with benzene.

Characterization of complexes I and II. I and II were isolated as deep red, amorphous powders from chilled MeOH solutions. Both were soluble in petroleum ether, ether, benzene, acetone, MeOH, $CHCl_3$, and CH_2Cl_2. The absorption maxima for I and II in visible light are listed in Table 2. In MeOH solution complexes I and II had E (1 %, 1 cm) = 515 and 505, respectively, at 443 nm. Assuming E (1 %, 1 cm) = 2200 and M = 530 and 516 for *1* and *2*, respectively, this corresponds to molecular weights of 2236 and 2212 for complexes I and II, respectively, provided only one chromophore unit is present in each complex.

The PMR spectra for both I and II ($CDCl_3$) showed only a single signal at τ 8.72; the mass spectra gave no identifiable molecular ion. The IR spectra (KBr) of I and II showed bands at 3320 (broad, s, OH), 2910 – 2840 (s, CH), 1715 (broad, vs., C=O), 1615 (m, C=C), 1580 (m), 1455 (m), 1130 (broad, s), 1010 (*trans*-disubstituted double bonds), 955 (s), 890 (m) and 850 (m) cm^{-1}.

Hydrolysis of complex I with ethanolic KOH. Complex I (0.2 mg) in ethanol (5 ml) containing 5 % KOH was stirred for 1 h at room temperature, whereupon the pigment precipitated. The pigment was extracted with $CHCl_3$ and, after drying and concentrating

the extract, was purified on silica gel plates. The mass spectrum of the product showed the molecular ion at *m/e* 534, 532, 530 (1:2:1, $C_{25}H_{24}Br_2O_3$).

Saponification of extracts. Extracts containing I and II were saponified in MeOH solution containing 5 % KOH at room temperature for 1 h. Under these conditions most of the pigments precipitated. Water was added and the pigments extracted with $CHCl_3$. Occasionally a small amount of NH_4Cl was necessary to transfer all pigments to the organic phase. The organic extracts were combined, dried over NaCl and concentrated under vacuum.

Chromatography of saponified extracts. Benzene solutions of pigments *1* and *2* were chromatographed on cellulose columns developed with benzene. The individual fractions were further purified by preparative thick layer chromatography on silica gel G plates developed with benzene. The handling and chromatography of *1* and *2* was continually hampered by the low solubility of these pigments. The approximate ratio of *1* and *2* was 2:1.

Characterization of 2. *2* was precipitated as an amorphous red powder from MeOH solution; total amount available from several isolations *ca.* 6 mg. *2* was chromatographically homogeneous in all systems tested. Upon chromatography on Al_2O_3 columns activity grade 3, *2* could not be eluted with pure MeOH.

Absorption characteristics in visible light are given in Fig. 2 and Table 2.

The IR-spectrum (KBr) exhibited ν_{max} 3410 (OH), 3020 – 2820 (C–H), 1710 (conj. C=O), 1010 (*trans*-disubstituted double bonds), 858 (aromatic C–H) and 800 cm^{-1}.

The mass spectrum showed molecular ions at *m/e* 516, 518, 520 (1:2:1, $M_{2a} = C_{24}H_{22}Br_2O_3$) and 438, 440 (1:1, $M_{2b} = C_{24}H_{23}BrO_3$).

Acetylation of 2. *2* (0.32 mg) was submitted to standard acetylation in acetic anhydride/pyridine; pigment recovery 82 %. The reaction mixture contained a single product less polar than *2* and slightly more polar than *1*. *2*-acetate was purified on cellulose columns and TLC; λ_{max} ($CHCl_3$) 430, 451, 479 nm; *m/e* 558 (M, 3 % of base), 530 (M – 28), 516 (M – 42), 470 (M′, 17 % of base) and 438 (M′ – 42).

Other attempted reactions of 2. *2* (0.26 mg) in 2.5 % methanolic KOH was resistant to ester hydrolysis overnight.

Careful $LiAlH_4$ reduction in ether of **2** (0.1 mg) for 2 min gave 43 % recovery. No new coloured products were formed.

2 (0.1 mg) in $CHCl_3$ was treated with diazomethane (10 ml, 1.5 % solution in ether) at room temperature for 2 h. Starting material (84 %) was recovered, and TLC analysis showed no methylation to have occurred. The methylation reaction was repeated and the reaction heated at 35°C for 4 h. Again the reaction was negative.

Characterization of 1. *1* crystallized from acetone-MeOH or $CHCl_3$-petroleum ether as red needles with metallic sheen, m.p. sharp 218°C. The needles were imperfect and not suitable for X-ray analysis. The total amount of crystalline *1* available from several isolations was *ca.* 15 mg.

Crystalline *1* was insoluble in petroleum ether, ether and MeOH; slightly soluble in DMSO, pyridine, $CHCl_3$, CH_2Cl_2, benzene, and acetone.

The visible light absorption spectrum of *1* is given in Fig. 2 and absorption maxima in various solvents in Table 2. In a mixed solvent system ($CHCl_3$-pyridine-DMSO, 4:4:92), *1* had *E* (1 %, 1 cm) = 2200 at the main maximum (462 nm). In the same solvent system crystalline β-carotene exhibited *E* (1 %, 1 cm) = 2190 at λ_{max}.

The IR-spectrum (KBr) of *1* (Fig. 3) had ν_{max} 3020 – 2820 (C – H), 1712 (conj. C=O), 1620 (C=C), 1395, 1260 (OCH_3), 1135 (C – O), 1050, 1010 (*trans*-disubstituted double bonds), 855 (aromatic C – H), and 792 cm^{-1}.

An attempt to record a time-averaged PMR spectrum failed due to decomposition of the sample over 24 h.

The mass spectrum of *1* showed peaks at *m/e* 530, 532, 534 (1:2:1, $M = C_{25}H_{24}{}^{79}Br^{81}BrO_3$: obs. 532.0086 calc. 532.0088). Fragment ions were observed at M – 31 (OCH_3), M – 59 ($COOCH_3$), M – 78 (C_6H_6), M – 80 (HBr), M – 111 (OCH_3 + HBr or $HOCH_3$ + Br), M – 139 (CH_3COO + HBr or CH_3COOH + Br).

1 (0.1 mg.) was stereoisomerized by stirring in benzene solution for 20 h in daylight with a catalytic amount of I_2. Paper chromatography on S&S 287 (benzene) showed the formation of a *neo* A isomer (15 %); λ_{max} (acetone) 420, 442 and 468 nm; $R_F = 0.89$.

Attempted acetylation of 1. *1* (0.2 mg) in dry pyridine was treated with acetic anhydride (0.2 ml) at room temperature; pigment recovery was 90 %. No new products were formed.

Lithium aluminium hydride reduction of 1. *1* (0.2 mg) partially dissolved in ether (3 ml) was reduced with $LiAlH_4$ for 5 min; pigment recovery 80 %. Traces of a new product were observed.

1 dissolved in tetrahydrofuran (THF) was in two experiments reacted with $LiAlH_4$ at room temperature with pigment recoveries 25 – 42 %.

1 (0.28 mg) in THF (10 ml) was reacted with $LiAlH_4$ for 2 h at −40°C; pigment recovery was 62 %. The reaction mixture contained unreacted *1*, a product inseparable from the $NaBH_4$-reduction product described below and a product which after purification on TLC had λ_{max} ($CHCl_3$) 415, 436, and 450 nm. The latter product was acetylated with acetic anhydride in pyridine to a less polar product with R_F-value near that of *1*.

Sodium borohydride reduction of 1. *1* (0.87 mg) in benzene (3 ml) and ethanol (3 ml) was treated with $NaBH_4$ for 12 h at 20°C; pigment recovery 40 %. After work-up in the usual manner, chromatography on a cellulose column gave *1* (30 %) and a product (70 %) more strongly adsorbed. The product was separated into two zones on kieselguhr paper (benzene); $R_F = 0.32$ (minor), λ_{max} (415), 437, and (465) nm in acetone and $R_F = 0.45$ (major), λ_{max} (420), 443, and (469) nm in acetone and (428), 453, and 480 nm in $CHCl_3$. The main product, further purified by TLC, appeared on mass spectrometry to have molecular ions at *m/e* 466, 468 (1:1).

Permanganate oxidation of 1. *1* (8 mg) in a benzene (5 ml) and water (5 ml) mixture containing $KMnO_4$ (90 mg) and $CaCO_3$ (140 mg) was refluxed for 10 h and the reaction mixture worked up according to the procedure described by Karrer *et al.*[20] About 60 % of starting material was recovered. The acid fraction was purified by GLC and the mass spectrum obtained; *m/e* 232, 230 (1:1, $M = C_8H_7BrO_3$, obs. 231.9557, calc. 231.9555 for ^{81}Br ion, 217, 215 (M − 15), 215, 213 (M − 17), 187, 185 (M − 45) and 161, 159 (M − 71).

1 (5 mg) was oxidized as described above in acid solution (0.1 N H_2SO_4). After 1 h of refluxing, the benzene layer was totally decolorized and the solution worked up. The organic acid was isolated, purified and analyzed by mass spectrometry. The spectrum was identical to that obtained for the product from the above oxidation.

Ozonization of 1 *and* 2. A mixture of *1* and *2* (10 mg) in acetic acid (2.5 ml) and $CHCl_3$ (2.5 ml) at 0°C was subjected to a 3 % stream of ozone for 4 min. The ozonides were oxidatively decomposed with H_2O_2 (30 %), water added and the organic acids extracted into ether. The ether solution was extracted with an aqueous sodium carbonate solution from which the organic acids were again extracted with ether after acidification with H_3PO_4. Mass spectrometry revealed ions at *m/e* 232, 230 (1:1, $M = C_8H_7BrO_3$), 217, 215 (M − 15), 215, 213 (M − 17), 187, 185 (1:1, M − 45); 218, 216 (1:1, $M' = C_7H_5BrO_3$) and 173, 171 (1:1, M′ − 45).

Hydrolysis of 1 *and* 2 *to the corresponding carboxylic acids.* A mixture of *1* and *2* (0.8 mg) in MeOH–$CHCl_3$ (1:1, 5 ml) containing 10 % KOH was stirred at room temperature for 5 h. After the addition of water and $CHCl_3$ the pigments were entirely in the aqueous phase. Dilute acetic acid was added until the aqueous layer was adjusted to pH 7.3 and the pigments extracted into $CHCl_3$. The organic extracts were dried with Na_2SO_4 and the solvent evaporated under vacuum. Mass spectrometry showed ions corresponding to $C_{24}H_{22}Br_2O_3$ and $C_{23}H_{20}Br_2O_3$, compatible with the expected carboxylic acids. The mixed carboxylic acids had λ_{max} (MeOH) 419, 443, and 472 nm.

In several other experiments where $CHCl_3$ was omitted, no hydrolysis of *1* or *2* was achieved.

Model compounds

Methyl 7-(3,5-dibromo-4-methoxyphenyl)-heptatrienoate (5). 3,5-Dibromo-4-methoxybenzaldehyde was prepared and characterized according to the procedure described by Andrewes.[17] Reaction with the phosphoran derived from methyl sorbate [17] gave *5*; m.p. 142 – 144°C; λ_{max} (MeOH) 325 shoulder, 337, 350 nm, (ether) 322, 338, 352 nm; ν_{max} (KBr) 3020 – 2840 (CH), 1708 (C=O), 1604 (C=C), 1270 (OCH_3), 1140 (C – O), 1000 (*trans*-disubstituted double bonds), 875 (aromatic C – H); τ ($CDCl_3$) 6.22 (3 H, OCH_3 on ring), 6.09 (3 H, OCH_3 in ester), 4.2 – 2.8 (6 H, olefinic protons), 2.43 (2 H, aromatic protons); *m/e* triple peaks centered at 402 (M), 387 (M − 15), 371 (M − 31), 343 (M − 59), no ions at M − 79, M − 80, M − 81 or M − 82.

Permanganate oxidation of 5. *5* (50 mg) in benzene (25 ml) and water (25 ml containing $KMnO_4$ (250 mg) and H_2SO_4 (0.1 N) was refluxed for 1 h. The cooled mixture was extracted with ether and the organic acid transferred into an aqueous solution of 5 % K_2CO_3. The aqueous solution was acidified with H_3PO_4 (0.5 N) and the organic acid transferred to ether. After drying the organic extracts with Na_2SO_4 and concentrating under vacuum, mass spectrometry of the residue showed a molecular ion as a triple peak at *m/e* 310, 312, 314 (M, $C_8H_6Br_2O_3$) and no ion corresponding to $C_8H_7BrO_3$.

Methyl 3-(2,4-dibromo-5-methoxyphenyl)-acrylate (6). 3-Hydroxybenzaldehyde was brominated according to the procedure described by Brink [42] and methylated using the procedure described by Lindemann.[43] The resulting 3,5-dibromo-4-methoxybenzaldehyde was added to a stirred methanolic solution of ethyl diethylphosphonoacetate [44] and NaOMe. After 20 h at 40°C, water was added and the mixture extracted with ether. The ether extracts were concentrated under vacuum and chromatographed on a deactivated Al_2O_3 column to give *6*; m.p. 162–164°C; λ_{max} (MeOH) 283, 327 nm; ν_{max} (KBr) 3095–2840 (C–H), 1710 (C=O), 1240 (OCH_3), 1170 (C–O), 870 (aromatic C–H); τ($CDCl_3$) 6.17 (3 H, OCH_3 on ring), 6.08 (3 H, OCH_3 in ester), 3.62 d (1 H, J = 16 Hz, H-1), 2.93 (1 H, aromatic, H-6), 2.23 (1 H, aromatic, H-3), 2.05 d (1 H, J = 16 Hz, H-3); *m/e* 348, 350, 352 (1:2:1, M), 319 (M–31) and 269, 271 (M–Br).

Permanganate oxidation of 6. *6* (50 mg) was oxidized with $KMnO_4$ as described above. Mass spectrometry of the product showed a molecular ion as a triple peak corresponding to $C_8H_6Br_2O_3$.

Methyl-7-(2,4-dibromo-5-methoxyphenyl)-heptatrienoate (7). 3,5-Dibromo-4-methoxybenzaldehyde was reacted with the phosphoran derived from methyl sorbate.[17] After work-up and purification by column chromatography on deactivated Al_2O_3, *6* crystallized from MeOH-$CHCl_3$ solution melted at 154–156°C; λ_{max} (MeOH) 352 nm, (broad band with inflection at 352 nm), (ether) 352 nm, (broad band with inflections at 322 and 337 nm); ν_{max} (KBr) 3075–2840 (C–H), 1710 (C=O), 1625 (C=C), 1135 (C–O), 1010, 1050 (*trans*-disubstituted double bonds), 880, 858, 820 (aromatic C–H) cm^{-1}; τ($CDCl_3$) 6.23 (3 H, OCH_3 on ring), 6.08 (3 H, OCH_3 in ester), 4.05 d (1 H, J = 15 Hz, H–2), 3.5–3.0 (5 H, olefinic protons), 2.95 (1 H, aromatic H-6), 2.17 (1 H, aromatic H-3); *m/e* triple peak centered at 402 (M), 385 (M–15), 371 (M–31), 329, 331 (1:1, M–79), 289, 291 (1:1, M–31–80 or M–32–79), 281 (M–123) and 265 (M–138).

Cortisalin (3a). Methylation of *3a* with diazomethane under the conditions used for *2* gave no product.

Dimethylcortisalin (3b). *3b* had λ_{max} (pyridine) at 418, 443, and 466 nm; ν_{max} see Fig. 3. Attempted hydrolysis of *3b* (0.3 mg) in 10 % methanolic KOH overnight at room temperature or at reflux temperature for 2 h failed.

Methyl 17-(3,5-dibromo-4-methoxyphenyl)-heptadeca-2,4,6,8,10,12,14,16-heptaenoate.[17] On co-chromatography with *1* on kieselguhr paper or silicagel plates (*cf.* Table 1), no separation was achieved.

Acknowledgements. Gifts of cortisalin and dimethylcortisalin were obtained from Professor J. Gripenberg, Chemistry Department, Tekniska Högskolan, Otnäs, Finland.

A.G.A. was supported by a postdoctoral fellowship from the *Royal Norwegian Council for Scientific and Industrial Research*. S. H. was maintained by a research grant from Hoffmann-La Roche, Basel, to S.L.J.

The project was supported in part by research grant AI-08426 from the *U.S. Public Health Service* to M.P.S. who acknowledges technical assistance by Gladys Cosens, Carolyn Whitenack and C. S. Campbell.

REFERENCES

1. Starr, M. P. *Ann. Rev. Microbiol.* **13** (1959) 211.
2. Stolp, H., Starr, M. P. and Baigent, N. L. *Ann. Rev. Phytopathol.* 3 (1965) 231.
3. Lelliott, R. A. In Maas Geesteranus, H. P. *Proc. Third Int. Conf. Plant Pathogenic Bacteria, Wageningen*, 1971, p. 269, Centre for Agricultural Publishing and Documentation, Wageningen 1972.
4. Murata, N. and Starr, M. P. *Phytopathol. Z.* **77** (1973) 285.
5. Starr, M. P. *Cornell Univ. Abstr. Theses* **1943** (1944) 349.

6. Starr, M. P. and Stephens, W. L. *J. Bacteriol.* **87** (1964) 293.
7. Stephens, W. L. and Starr, M. P. *J. Bacteriol.* **86** (1963) 1070.
8. Straub, O. In Isler, O. *Carotenoids*, Birkhaüser, Basel 1972, p. 832.
9. Rogovin, S. P., Anderson, R. F. and Cadmus, M. C. *J. Biochem. Microbiol. Technol. Eng.* **3** (1961) 51.
10. Sloneker, J. H. and Jeanes, A. *Can. J. Chem.* **40** (1962) 2066.
11. Orentas, D. G., Sloneker, J. H. and Jeanes, A. *Can. J. Microbiol.* **9** (1963) 427.
12. Gansser, C. and Zechmeister, L. *J. Am. Chem. Soc.* **79** (1957) 3854.
13. Bellamy, L. J. *The Infra-red Spectra of Complex Molecules*, 2nd Ed., Methuen, London 1964.
14. Lunde, K. and Zechmeister, L. *J. Am. Chem. Soc.* **77** (1955) 1647.
15. Gripenberg, J. *Acta Chem. Scand.* **6** (1952) 580.
16. Budzikiewicz, H., Djerassi, C. and Williams, D. H. *Mass Spectrometry of Organic Compounds*, Holden-Day, San Francisco 1967.
17. Andrewes, A. G. *Acta Chem. Scand.* **27** (1973) 2574.
18. Nybraaten, G. and Liaaen-Jensen, S. *Acta Chem. Scand.* **25** (1971) 370.
19. Bell, H. M., Vanderslice, W. and Spehar, A. *J. Org. Chem.* **34** (1969) 3923.
20. Karrer, P., Helfenstein, A., Wehrli, H. and Wettstein, A. *Helv. Chim. Acta* **13** (1930) 1084.
21. Hendrickson, J. B., Cram, D. J. and Hammond, G. S. *Organic Chemistry*, 3rd Ed., McGraw, London 1970.
22. Friedländer, P. *Ber.* **42** (1909) 765.
23. Morner, C. T. *Z. physiol. Chem.* **88** (1913) 138.
24. Sharma, G. M. and Burkholder, P. R. *Tetrahedron Letters* **1967** 4142.
25. Irie, T., Suzuki, M., Kurosawa, E. and Masamune, T. *Tetrahedron* **6** (1970) 3271.
26. Suzuki, M., Kurosawa, E. and Irie, T. *Tetrahedron Letters* **1970** 4995.
27. Sharma, G. M. and Burkholder, P. R. *Chem. Commun.* **1970** 151.
28. a. Sharma, G. M., Vig, B. and Burkholder, P. R. *J. Org. Chem.* **35** (1970) 2823; b. Fattorusso, E., Minale, L. and Soldano, G. *Chem. Commun.* **1970** 751; c. Moody, K., Thompson, R. H., Fattorusso, E., Minale, L. and Soldano, G. *J. Chem. Soc.* **I 1972** 18.
29. Mastagli, P. and Augier, J. *Compt. Rend.* **209** (1939) 775.
30. Saito, T. and Ande, Y. *Nippon Kagaku Zasshi* **76** (1955) 478; *Chem. Abstr.* **51** (1957) 17810i.
31. Tanaka, T. and Toyama, Y. *Mem. Fac. Eng. Nagoya Univ.* **11** (1959) 187; *Chem. Abstr.* **55** (1961) 19036i.
32. Hodgkin, J. H., Craigie, J. S. and McInnes, A. G. *Can. J. Chem.* **44** (1966) 74.
33. Ashworth, R. B. and Cormier, M. J. *Science* **155** (1967) 1558.
34. MacMillan, J. *J. Chem. Soc.* **1959** 2586.
35. Patterson, E. L., Andres, W. W. and Mitscher, L. A. *Appl. Microbiol.* **15** (1967) 528.
36. Smith, G. G. *J. Bacteriol.* **75** (1958) 577.
37. Doerschuk, A. P., McCormick, J. R. D., Goodman, J. J., Szumski, S. A., Growich, J. A., Miller, P. A., Bitler, B. A., Jensen, E. R., Matrishin, M., Petty, M. A. and Phelps, A. S. *J. Am. Chem. Soc.* **81** (1959) 3069.
38. Erdtman, H. *Acta Chem. Scand.* **2** (1948) 209.
39. Jefferson, W. E. *Biochemistry* **6** (1967) 3479.
40. Patterson, G. *Tetrahedron Letters* **1969** 4049.
41. Rabache, M., Laborey, F., Neumann, J. and Lavollay, J. *Compt. Rend.* **271** (1970) 795.
42. Brink, M. *Acta Univ. Lund.* **2** (1965) 3.
43. Lindemann, H. *Ann.* **431** (1923) 270.
44. Wadsworth, W. S. and Emmons, W. D. *J. Am. Chem. Soc.* **83** (1961) 1733.

Received February 26, 1973.

ACTA CHEMICA SCANDINAVICA 27 (1973) 2396–2398

Fungal Extractives

V.* The Stereostructure of two Sesquiterpene Lactones from *Lactarius*

GÖRAN MAGNUSSON and SVANTE THORÉN

Organic Chemistry 2, Chemical Center, The Lund Institute of Technology, Box 740, S-220 07 Lund 7, Sweden

The stereostructures of two sesquiterpene lactones from *Lactarius vellereus* and *L. pergamenus* have been determined by interrelation with the dialdehyde "velleral" of known relative configuration.

In a previous publication [2] we have reported the structure of two sesquiterpene lactones from the basidiomycetes *Lactarius vellereus* and *L. pergamenus* (Russulaceae). Spectroscopic evidence and chemical synthesis of a degradation product showed that these two compounds had the basic structures *1* and *2*, respectively, but did not permit assignment of the stereochemical configuration. The relative stereostructure of "velleral" [1] was determined by applying extensive NMR techniques and is shown in formula *3*. By chemical interrelation of lactone *1* and "velleral" we have now been able to deduce the stereoarrangement of the two lactones.

It was realised that a comparison of compounds *1* and *3* could be based on their reduction products, preferably the diols. The reduction agent of choice seemed to be AlH_3 known to give pure 1,2-addition to α,β-unsaturated carbonyl systems without secondary rearrangements.[3] AlH_3 reduction of "velleral" (*3*) gave as anticipated the diol *4* in moderate yield. A similar reduction of lactone *1* also yielded a diol with the same R_F-value on TLC as *4* and with IR and NMR spectra superimposable on those of *4*. Furthermore, these diols had practically the same optical rotation: $[\alpha]_D^{25} + 201°$ for the diol from *1* and $[\alpha]_D^{25} + 203°$ for *4*. The identity was thus firmly established.

It has previously been shown that lactone *1* can be converted to lactone *2* by heat-induced isomerisation.[2] The relative stereostructures of the two lactones are therefore as shown in formulate *1* and *2*, respectively.

* Part IV, see Ref. 1.

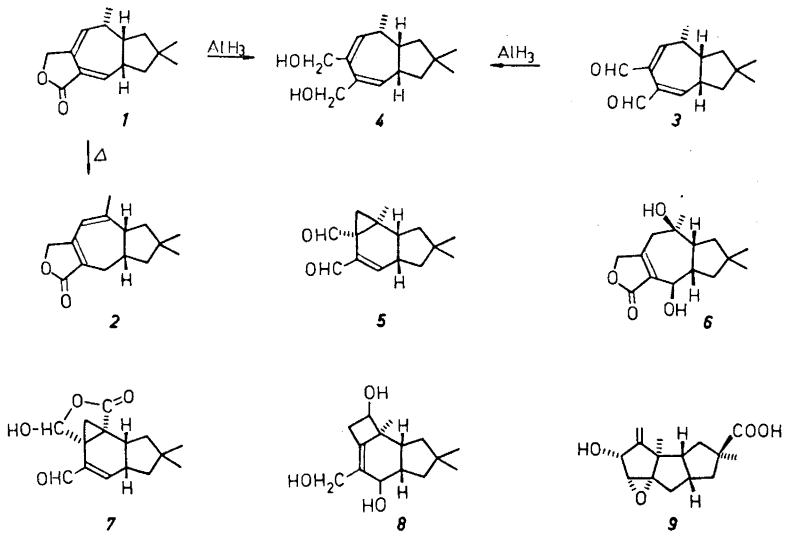

Many of the known sesquiterpenoids of basidiomycetes origin have a fused cyclopentane ring with geminal substituents. Some of these compounds which have been fully elucidated have hydrogens in the ring junction and a methyl group or its equivalent on a carbon atom adjacent to one of the bridgeheads. It is perhaps not surprising that the *Lactarius* compounds "isovelleral" (5),[4] the lactones *1* and *2*, and "velleral" from *L. vellereus* and *L. pergamenus* and lactarorufin A (*6*) [5] from *L. rufus* have the same relative configuration. However it might be noted that a number of compounds, for instance marasmic acid (*7*),[6,9] illudol (*8*),[7,9] and hirsutic acid (*9*),[8] of diverse structures and origins, have the same steric arrangement at the three carbons concerned even though not always with the same absolute configuration.

EXPERIMENTAL

The NMR spectra were recorded on a Varian T-60 spectrometer. The high resolution mass spectrum was measured on a MS 902/DS 30 instrument by the kind cooperation of Dr. G. Hvistendahl, Kjemisk Institutt, The University of Oslo, Norway.

AlH_3 reduction of "velleral" (3).[3] "Velleral" (239 mg; 0.001 mol) dissolved in dry ether (5 ml) was added dropwise to a magnetically stirred, ice-cold solution of AlH_3 (0.001 mol) in dry ether (10 ml). After the addition was complete, the reaction mixture was stirred at room temperature for 24 h. Thereafter $Na_2SO_4.10H_2O$ (2 g) was added followed by water (1 ml) and 2 M NaOH (2–3 drops). The mixture was filtered and the organic phase was dried (Na_2SO_4) and evaporated. The residue was chromatographed on a silica gel column with toluene-ethyl acetate (1:1) as eluent to yield *diol 4* (80 mg). The *diol* had b.p.$_{0.001}$ 115°; $[\alpha]_D^{25}$ + 203° (*c.* 1.6; $CHCl_3$); IR: ν_{max} (neat) 3600–3100 (broad, –OH), 3040, 1390, 1380, 1372, 1020, 845, 730, 695 cm^{-1}; NMR: δ_{TMS} ($CDCl_3$) 5.92 (2 H, m; vinyl protons), 4.26 4.08 (4 H, two coincident AB doublets with J = |12.5| Hz; $-CH_2OH$, $-CH_2OH$), 1.08 (3 H, s; $-CH_3$), 0.98 (3 H, d J = 6.0 Hz; $CH-CH_3$), 0.93 (3 H, s; $-CH_3$); MS (70 eV): *m/e* 236 (M^+, 11 %; $C_{15}H_{24}O_2$), 218 ($M^+ - H_2O$; 58 %), 203 (44 %), 189 (56 %), 119 (77 %), 105 (100 %), 91 (83 %). (Found: M.wt. 236.1779. Calc.

for $C_{15}H_{24}O_2$: M.wt. 236.1775). The *diol 4* gave an oily *diacetate* and an oily *bis-p-nitrobenzoate* which were not further characterized.

AlH_3 reduction of lactone 1. The lactone was reduced according to the same procedure as above and gave after work-up a *diol* which had identical IR and NMR spectra as *diol 4* and had the optical rotation $[\alpha]_D^{25} + 201°$ (*c.* 1.2; $CHCl_3$).

Acknowledgement. We thank Professor Börje Wickberg for stimulating discussions and Dr. Brian Thomas for helpful linguistic criticism. This work was in part supported by a grant from *Längmanska Kulturfonden* (to S. T.) and by the *Swedish Natural Science Research Council.*

REFERENCES

1. Drakenberg, T., Magnusson, G. and Thorén, S. *Tetrahedron* **29** (1973) 1621.
2. Magnusson, G. and Thorén, S. *Acta Chem. Scand.* **27** (1973) 1573.
3. Jorgensen, M. J. *Tetrahedron Lett.* **1962** 559.
4. Magnusson, G., Thorén, S. and Wickberg, B. *Tetrahedron Letters* **1972** 1105.
5. Daniewski, W. M., Ejchart, A., Jurczak J., Kozerski, L. and Pyrek, J. S. *Bull. Acad. Pol. Sci. Ser. Chim.* **20** (1972) 131.
6. Dugan, J. J., deMayo, P., Nisbeth, M., Robinson, J. R. and Anchel, M. *J. Am. Chem. Soc.* **88** (1966) 2838.
7. McMorris, T. C., Nair, M. S. R., Singh, P. and Anchel, M. *Phytochemistry* **10** (1971) 3341.
8. Comer, F. W., McCapra, F., Qureshi, I. H., Trotter, J. and Scott, A. I. *Chem. Commun.* **1965** 310.
9. Cradwick, P. D. and Sim, G. A. *Chem. Commun.* **1971** 431.

Received March 22, 1973.

ACTA CHEMICA SCANDINAVICA 27 (1973) 2399–2404

Putrescine Metabolizing Enzyme Activities in Some Rat Tissues during Postnatal Development

JUHANI JÄNNE and ERKKI HÖLTTÄ

Department of Medical Chemistry, University of Helsinki, SF-00170 Helsinki 17, Finland

Four enzyme activities, ornithine decarboxylase (EC 4.1.1.17), *S*-adenosylmethionine decarboxylase, spermidine synthase and diamine oxidase (EC 1.4.3.6), involved in the metabolism of putrescine and spermidine have been followed in some rat tissues during the postnatal development and subsequent ageing of the animal. In thymus and small intestine, known to contain high diamine oxidase activity, ornithine decarboxylase and diamine oxidase activities showed roughly an opposite mode of behavior during the postnatal development of the rat. The activity of diamine oxidase increased markedly at the time ornithine decarboxylase activity decreased. Both S-adenosylmethionine decarboxylase and spermidine synthase activities decreased with age even though the changes were not very marked.

The biosynthesis and accumulation of putrescine and spermidine undergo dramatic changes after application of various growth stimuli, *e.g.* in rat liver after partial hepatectomy,[1–5] and in several target tissues after appropriate hormone administration.[6–10] In general, young and growing tissues are rich in spermidine and putrescine [3,11,12] whereas during ageing of the animal the tissue spermidine concentration markedly decreases.[11] The main role attributed to putrescine in mammalian tissues is to serve as the natural precursor in the synthesis of spermidine. Little is known of the metabolic fate of putrescine aside from its function in spermidine biosynthesis. Radioactive putrescine, when injected into the intact animal, was rapidly oxidized to expired carbon dioxide,[3] however, the mechanisms involved in this oxidation are not known. Recent observations indicate that the enzyme histaminase (also known as diamine oxidase, EC 1.4.3.6) may play a role in the metabolism of putrescine in some mammalian tissues. During pregnancy in the rat there is a marked rise in ornithine decarboxylase activity (EC 4.1.1.17), the enzyme responsible for the synthesis of putrescine in animal tissues, in the fetal placenta with a concomitant increase in diamine oxidase activity in the maternal placenta.[13] This may suggest that the natural substrate for the high levels of diamine oxidase activity found during pregnancy was putrescine rather than hista-

mine.[13] Furthermore, it has also been suggested that putrescine serves as the major substrate for the high diamine oxidase activity found in rat thymus.[14,15]

In the present communication we have followed the changes of enzyme activities directly or indirectly involved in the metabolism of putrescine in specific rat tissues during postnatal development and ageing of the animal. In agreement with earlier observations [14] we found high diamine oxidase activity in rat thymus and in addition found unusually high activity in the small intestine. An opposite pattern of enzyme activity changes was apparent for ornithine decarboxylase and diamine oxidase during the postnatal development. *S*-Adenosylmethionine decarboxylase and spermidine synthase, the enzymes involved in the synthesis of spermidine from putrescine and adenosylmethionine, showed much smaller changes.

MATERIALS AND METHODS

Labelled and unlabelled adenosylmethionine were synthesized and purified according to Pegg and Williams-Ashman.[16] Decarboxylated adenosylmethionine was prepared with the aid of *Escherichia coli* adenosylmethionine decarboxylase and purified on ion exchange columns and by preparative paper electrophoresis as described earlier.[17,18] DL-Ornithine-^{14}C (specific radioactivity 37 mCi/mmol) was purchased from the Radiochemical Centre, Amersham. Putrescine-1,4-^{14}C (specific radioactivity 17.5 mCi/mmol) was purchased from the New England Nuclear Corporation and purified before use on a Dowex 50-H^+ column.[19]

Female rats of the Wistar strain were used in all experiments. The rats were killed by decapitation and the tissues were immediately removed and homogenized with ice-cold 0.25 M sucrose – 0.3 mM EDTA – 1 mM 2-mercaptoethanol. Before homogenization the small intestine was opened and thoroughly rinsed with cold water. The homogenates were centrifuged for 60 min at 100 000 g_{max} and the supernatant fractions were used for enzyme assays.

Diamine oxidase was assayed in the presence of 0.4 mM putrescine-1,4-^{14}C by the method of Okuyama and Kobayashi [20] as modified by Tryding and Willert.[21] The incubation time was 60 min at 37°.

The activity of ornithine decarboxylase was assayed in the presence of 2 mM L-ornithine-^{14}C [22,23] and that of adenosylmethionine decarboxylase in the presence of 0.2 mM adenosylmethionine and 2.5 mM putrescine.[18,24] Spermidine synthase activity was assayed in the presence of 0.5 mM putrescine-1,4-^{14}C and 0.1 mM decarboxylated adenosylmethionine.[18,25]

RESULTS AND DISCUSSION

The different enzyme activities involved in the biosynthesis of putrescine and spermidine together with the activity of diamine oxidase in rat thymus during the postnatal development and subsequent ageing of the animal are shown in Fig. 1. Ornithine decarboxylase activity was found to be remarkably high in young rats; in fact, the maximum activity was found at the age of one month, with a rapid decrease thereafter. The activity of diamine oxidase followed an opposite pattern, *i.e.* a marked increase at the time ornithine decarboxylase activity decreased. Using crude thymic extracts as the source of enzyme the diamine oxidase was roughly characterized. The production of toluene-extractable radioactive material was linear for at least 60 min. The enzyme showed a broad pH optimum between 7.0 and 7.6 in potassium phosphate buffer. An apparent K_m value for putrescine was approximately

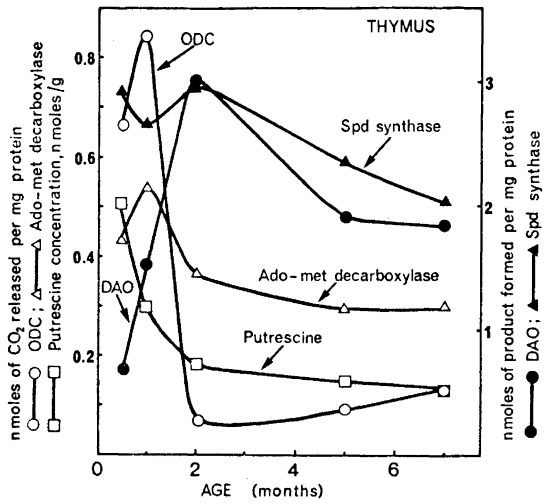

Fig. 1. Diamine oxidase (DAO), ornithine decarboxylase (ODC), *S*-adenosylmethionine (Ado-met) decarboxylase, spermidine (Spd) synthase activities and putrescine concentration in rat thymus during postnatal development. The enzyme activities were assayed under standard incubation conditions as described in Materials and methods. Each value represents a pooled sample obtained from at least six rats.

0.1 mM. Spermidine and spermine were apparently not oxidized by the enzyme since the inclusion of 1 mM spermidine or spermine (unlabelled) to the incubation mixture did not decrease the formation of radioactive product from putrescine-1,4-^{14}C.

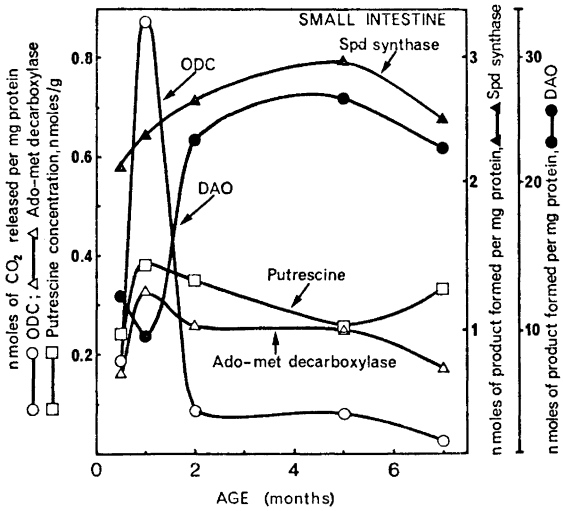

Fig. 2. Putrescine metabolizing enzyme activities and the concentration of putrescine in rat small intestine during postnatal development. For details, see legend of Fig. 1.

Adenosylmethionine decarboxylase, most probably the rate limiting enzyme in the synthesis of spermidine in animal tissues,[26,27] behaved much like ornithine decarboxylase even though the changes in enzyme activity during development were not marked. Spermidine synthase activity seemed to decrease with increasing age. The concentration of putrescine in the thymus continuously decreased with age.

The corresponding enzyme activities in the small intestine are shown in Fig. 2. The pattern of the enzyme activities in this tissue differed only slightly from that found in the thymus; an opposite pattern of ornithine decarboxylase and diamine oxidase activities could be seen again.

It is of interest to note that two tissues, namely thymus and small intestine tissue, which had high ornithine decarboxylase activity also contained high diamine oxidase activity. At the time when ornithine decarboxylase activity dropped most markedly, *i.e.* between the first and the second month of the life, the activity of diamine oxidase increased sharply (Figs. 1 and 2). The role of diamine oxidase activity in the metabolism of putrescine is not known as yet. The changes in ornithine decarboxylase and diamine oxidase activities as well as putrescine concentration in thymus during the postnatal development are interesting (Fig. 1) as the thymus of the young rat appears to contain exceptionally high concentration of putrescine and also high ornithine decarboxylase activity. Between the first and second months of the life the ornithine decarboxylase activity decreased to a fraction of the activity found in young animals and, in addition, the concentration of putrescine was decreased to less than half the concentration found in very young rats. During the same period the activity of diamine oxidase more than tripled. It is possible that the putrescine content of thymus is regulated by the activities of both ornithine decarboxylase and diamine oxidase. The patterns of ornithine decarboxylase and diamine oxidase activities were similar in small intestine

Table 1. Putrescine and spermidine synthesizing enzyme activities and diamine oxidase activity in liver and spleen during the postnatal development of the rat. The enzyme activities are expressed as pmoles of product formed per mg protein per 30 min (ornithine decarboxylase, Ado-met decarboxylase and spermidine synthase) or 60 min (diamine oxidase). Ado-met = *S*-adenosylmethionine. For details, see legend of Fig. 1.

	Age of the animal (months)	Diamine oxidase	Ornithine decarboxylase	Ado-met decarboxylase	Spermidine synthase
Liver	0.5	< 1	111	128	1612
	1	9	87	362	1509
	2	< 1	36	284	1237
	5	5	10	309	1117
	7	< 1	16	234	1229
Spleen	0.5	21	274	365	2232
	1	51	49	325	1932
	2	14	38	192	1344
	5	10	10	174	1518
	7	20	26	139	1315

and thymus; however, it seems more likely that the high diamine oxidase activity in small intestine functions to metabolize exogenous rather than endogenous putrescine.

Liver and spleen contained very low diamine oxidase activities at any time during development (in kidney and brain the activity was not measurable) as compared with the high activity found in thymus and small intestine (Table 1). Also in these tissues (liver and spleen) ornithine decarboxylase and adenosylmethionine decarboxylase activities decreased after the first month of life. The activity of spermidine synthase also tended to decrease with age, however, the changes were not very marked.

In all tissues studied spermidine synthase activity assayed under optimal conditions was much greater than adenosylmethionine decarboxylase activity further suggesting that adenosylmethionine decarboxylase activity together with the concentration of putrescine is the rate limiting step in the enzymatic synthesis of spermidine in mammalian tissues.[27]

The stimulation of putrescine and spermidine synthesis seems to be, almost without exception, associated with a rapid growth of animal tissues. The significance of these phenomena for the general metabolism of an animal cell is not known. However, a better understanding of the metabolism of these compounds may also provide further insight to the physiological function of the polyamines.

Acknowledgements. This study has been supported by a grant from the *National Research Council for Medical Sciences*, Finland. The excellent technical assistance of Mrs. Riitta Sinervirta and Mrs. Sirkka Kanerva is gratefully acknowledged.

REFERENCES

1. Raina, A., Jänne, J. and Siimes, M. *Biochim. Biophys. Acta* **123** (1966) 197.
2. Dykstra, W. G., Jr. and Herbst, E. J. *Science* **149** (1965) 428.
3. Jänne, J. *Acta Physiol. Scand. Suppl.* **300** (1967) 1.
4. Jänne, J. and Raina, A. *Acta Chem. Scand.* **22** (1968) 1349.
5. Russell, D. and Snyder, S. H. *Proc. Natl. Acad. Sci. U.S.* **60** (1968) 1420.
6. Jänne, J., Raina, A. and Siimes, M. *Biochim. Biophys. Acta* **166** (1968) 419.
7. Jänne, J. and Raina, A. *Biochim. Biophys. Acta* **174** (1969) 769.
8. Pegg, A. E., Lockwood, D. H. and Williams-Ashman, H. G. *Biochem. J.* **117** (1970) 17.
9. Kobayashi, Y., Kupelian, J. and Maudsley, D. V. *Science* **172** (1971) 379.
10. Cohen, S., O'Malley, B. W. and Stastny, M. *Science* **170** (1970) 336.
11. Jänne, J., Raina, A. and Siimes, M. *Acta Physiol. Scand.* **62** (1964) 352.
12. Raina, A. and Jänne, J. *Federation Proc.* **29** (1970) 1568.
13. Maudsley, D. V. and Kobayashi, Y. *Federation Proc.* **30** (1971) 204.
14. Beaven, M. A. and Jacobsen, S. *J. Pharmacol. Exp. Ther.* **176** (1971) 52.
15. Beaven, M. A. and de Jong, W. *Federation Proc.* **31** (1972) 532.
16. Pegg, A. E. and Williams-Ashman, H. G. *J. Biol. Chem.* **244** (1969) 682.
17. Jänne, J., Williams-Ashman, H. G. and Schenone, A. *Biochem. Biophys. Res. Commun.* **43** (1971) 1362.
18. Raina, A. and Hannonen, P. *FEBS Letters* **16** (1971) 1.
19. Raina, A., Jänne, J., Hannonen, P. and Hölttä, E. *Ann. N. Y. Acad. Sci.* **171** (1971) 697.
20. Okuyama, T. and Kobayashi, Y. *Arch. Biochem. Biophys.* **95** (1961) 242.
21. Tryding, N. and Willert, B. *Scand. J. Clin. Lab. Invest.* **22** (1968) 29.

22. Raina, A. and Jänne, J. *Acta Chem. Scand.* **22** (1968) 2375.
23. Jänne, J. and Williams-Ashman, H. G. *J. Biol. Chem.* **246** (1971) 1725.
24. Jänne, J. and Williams-Ashman, H. G. *Biochem. Biophys. Res. Commun.* **42** (1971) 222.
25. Jänne, J., Schenone, A. and Williams-Ashman, H. G. *Biochem. Biophys. Res. Commun.* **42** (1971) 758.
26. Hannonen, P., Raina, A. and Jänne, J. *Biochim. Biophys. Acta* **273** (1972) 84.
27. Hölttä, E. and Jänne, J. *FEBS Letters* **23** (1972) 117.

Received February 19, 1973.

ACTA CHEMICA SCANDINAVICA 27 (1973) 2405–2410

Tobacco Chemistry

20. Structures and Syntheses of Three New Tobacco Constituents of Probable Isoprenoid Origin

ARNE J. AASEN, JOSEPH R. HLUBUCEK, SVEN-OLOF ALMQVIST, BJARNE KIMLAND and CURT R. ENZELL

Research Department, Swedish Tobacco Co., Box 17007, S-104 62 Stockholm 17, Sweden

The structures of three new tobacco isolates, 5ξ-isopropyl-3*E*-hepten-2-one (1), 3ξ-hydroxy-3ξ-methyl-6ξ-isopropyl-4*E*-octenoic acid (2), and 2,10-dimethyl-7ξ-isopropyl-8*E*,10-undecadien-4-one (3) have been elucidated on the basis of their spectral data and subsequently confirmed by total syntheses. The possible isoprenoid origin of these compounds is discussed.

Earlier work in this laboratory on the volatiles of Greek tobacco, *Nicotiana tabacum* L., has led to the isolation of three new minor constituents.[1–3] In the present communication we wish to report their structures, which on account of the small amounts available were deduced solely from their spectral data, and syntheses.

*5ξ-Isopropyl-3*E*-hepten-2-one (1).* The presence of a 2-oxo-3*E*-pentenylidene moiety, $CH_3CO–CH=CH–CH$, in this tobacco isolate having the elemental composition $C_{10}H_{18}O$ (accurate mass determination), was apparent from its IR (1677 cm^{-1}, conj. CO; 987 cm^{-1}, *trans* disubst. C=C), UV (223 nm, monosubst. conj. CO), and NMR spectra [δ 2.24, CH_3CO; δ 6.04 (d, J 16 Hz) and δ 6.6 (q, J 8.5 and 16 Hz), $CO–CH=CH–CH$]. The remaining two saturated alkyl residues accounting for C_5H_{12}, attached to the vinylic carbon atom, had to be either an ethyl group and an isopropyl group, or a methyl group and a *sec*-butyl group since the NMR spectrum exhibited one triplet (δ 0.83, J 7 Hz) and two doublets (δ 0.86, J 6.5 Hz and δ 0.91, J 6.5 Hz) in the methyl region. The ethyl-isopropyl alternative was favoured on account of bands at 1361 cm^{-1} and 1369 cm^{-1} indicative of a *gem.* dimethyl grouping and since an allylic methyl group would resonate further downfield, *i.e.* at *ca.* 1 ppm.[4] Synthesis of the racemate of this compound performed by an aldol condensation of 2-isopropylbutyraldehyde (*4*) with acetone followed by *in situ* de-

hydration furnished a product with IR, NMR, and mass spectra identical to those of the tobacco isolate thereby confirming the assigned structure.

*3ξ-Hydroxy-3ξ-methyl-6ξ-isopropyl-4*E*-octenoic acid (2).* The methyl ester (*9*) of this acid, for which the spectral data were obtained, displayed hydroxyl absorption in the infrared (3500 cm^{-1}) clearly suggesting that it had

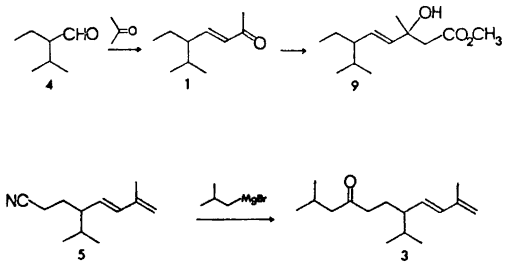

the composition $C_{13}H_{24}O_3$ rather than $C_{13}H_{22}O_2$ (M − 18) determined by accurate mass measurement for the heaviest mass, *m/e* 210, observed in the mass spectrum. A three-proton singlet at δ 1.31 was ascribed to a methyl group attached to a tertiary carbinol group which, from the NMR spectrum after addition of $Eu(DPM)_3$, had as further substituents a $-CH_2COOR$ (δ 2.56, s) and a $-CH=CH-CHR_1R_2$ grouping (δ 5.45, m and 1.58, m). The addition of the shift reagent separated the methylene protons of the $-CH_2COOR$ group into an AB system ($r = 1.28$ and 1.21, J 16 Hz) and resolved the olefinic proton multiplet into a doublet ($r = 0.87$, J 16 Hz) and a quartet ($r = 0.68$, J 9 and 16 Hz), thereby revealing the *trans* configuration of the double bond. The partial structure $R_1R_2CH-CH=CH-C(OH,CH_3)-CH_2-COOCH_3$ follows from these data and also that R_1 and R_2 must be two saturated alkyl substituents to account for the remainder of the molecule, C_5H_{12}. Three three-proton signals constituting one triplet and two doublets (δ 0.78, 0.79, 0.84; all J's 7 Hz), left the same two possible sets of alkyl residues as for 5ξ-isopropyl-3*E*-hepten-3-one (1). The ethyl-isopropyl alternative was favoured over that comprising a methyl and *sec*-butyl group for the following reasons: the infrared spectrum suggested the presence of a *gem.* dimethyl grouping (1384 and 1369 cm^{-1}), irradiation of the olefinic proton at $r = 0.68$ simplified the multiplet of the methine proton ($r = 0.26$) to a doublet of triplets demonstrating further spin-spin coupling to three rather than four protons, and none of the methyl signals occurred at sufficiently low field to correspond to an allylic methyl group.[4] It follows therefore that the tobacco constituent is 3ξ-hydroxy-3ξ-methyl-6ξ-isopropyl-4*E*-octenoic acid (*2*), which judging from the NMR spectrum after addition of shift reagent is partly racemic (ratio 1:4). This structural assignment was confirmed by comparison of the methyl ester of the tobacco acid with a synthetic specimen prepared by a Reformatsky reaction of (±)-5-isopropyl-3*E*-hepten-3-one (*1*) with methyl bromoacetate.

*2,10-Dimethyl-7ξ-isopropyl-8*E*,10-undecadien-4-one (3).* A small quantity of this compound was isolated about two years ago but no structure could then be deduced. In the light of subsequent work and deepening interest in the

biogenesis of tobacco nor-isoprenoids, we recently reconsidered its NMR and mass spectra. Due mainly to the presence of signals in the NMR spectrum corresponding to a 2-methyl-1,3E-pentadienylidene moiety (three-proton triplet at δ 1.82, J 1.1 Hz; two-proton narrow multiplet at δ 4.86; one-proton quartet at δ 5.33, J 8 and 16 Hz; one proton doublet at δ 6.06, J 16 Hz), and the striking resemblance of its mass spectrum to that of solanone (*6*, R = CH_3), we were able to postulate two possible structures for this compound, namely 2,10-dimethyl-7ξ-isopropyl-8*E*,10-undecadien-4-one (*3*) or 8ξ-isopropyl-11-methyl-9*E*,11-dodecadien-5-one (*7*).

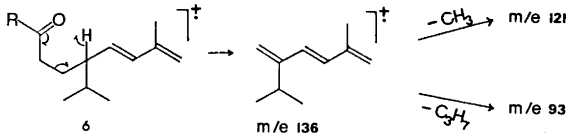

Scheme 1.

The mass spectral fragmentation of solanone (*6*, R = CH_3) is depicted in Scheme 1 accounting for the formation of the three characteristic ions at *m/e* 93, 121, and 136 which presumably are present irrespective of which saturated alkyl residue (R) is attached to the carbonyl group. The molecular weight of the tobacco compound, 236, corresponds to R = C_4H_9, *i.e.* butyl, isobutyl, *sec*-butyl, or *t*-butyl. The last two possibilities were excluded since the NMR spectrum disclosed the presence of four protons adjacent to the carbonyl group (δ 2.1 – 2.45). Considerable overlap in the methyl region of the NMR spectrum did not enable us to clearly distinguish between the butyl and isobutyl alternatives. Although consideration of the integrated methyl region favoured the latter, the previously advanced hypothesis that the structurally related solanone (*6*, R = CH_3) and other tobacco constituents are degradation products of diterpenoids possessing the thunbergane skeleton * (*10*),[5–7] made the butyl possibility also appear likely. Subsequent synthesis of 8ξ-isopropyl-11-methyl-9*E*,11-dodecadien-5-one (*7*) performed by reacting 2-methyl-5-isopropyl-7-cyano-1,3*E*-heptadiene (*5*) [8] with butylmagnesium bromide in analogy with the last step in Johnson and Nicholson's [8] elegant synthesis of solanone (*6*, R = CH_3), furnished a product which exhibited a mass spectrum nearly identical to that of the tobacco constituent. However, the two specimens separated when co-injected on a capillary GC column and their NMR spectra displayed differences. The isobutyl-isomer was therefore prepared next by the same procedure using isobutylmagnesium bromide. The product displayed NMR and mass spectra which were indistinguishable from those recorded for the tobacco constituent and no separation could be observed when co-injected on a capillary GC column. It follows therefore that the tobacco constituent is 2,10-dimethyl-7ξ-isopropyl-8*E*,10-undecadien-4-one (*3*).

The compound with the *sec*-butyl end group – 3,10-dimethyl-7-isopropyl-8*E*,10-undecadien-4-one (*8*) – was also prepared and its mass spectrum

* Nomenclature according to J. W. Rowe, Oct. 1968; personal communication.

exhibited, in addition to the expected set of ions at *m/e* 93, 121 and 136, an intense *m/e* 57 ion due to cleavage of the C(3) – C(4) bond which is α both to the carbonyl and a disubstituted carbon atom.

Biogenetic considerations

Several tobacco constituents possessing an isopropyl group protruding from a methyl substituted chain, *e.g.* solanone (*6*, R = CH_3), have been postulated to be degradation products of tobacco diterpenoids belonging to the thunbergane (cembrane, *10*) class.[5–7] The skeletons of the present three compounds may formally be derived from that of thunbergane, requiring for the enone (*1*) and the acid (*2*), if not more directly interrelated, cleavages of the 4,5- and 12,13-bonds and of the 6,7- and 12,13-bonds, respectively. The dienone (*3*), which has many structural features in common with solanone (*6*, R = CH_3), would require more elaborate changes such as formation of a bond between C(6) and C(13) and cleavages of the 5,6- and 12,13-bonds, plus cleavage of the 9,10-bond. In view of the multiplicity of functional groups encountered in these macrocyclic diterpenoids and the number of reactions

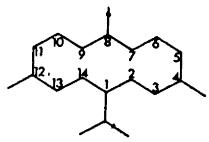

10

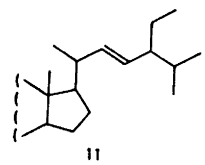

11

that can be envisaged, a variety of routes to *1*, *2*, and *3* may be postulated. However, further examples and preferably a knowledge of the steric relationships, not presently at hand, seem desirable before considering these in detail.

Presently, alternative pathways might also be considered, notably those involving alkylation such as encountered in certain isoprenoids, *e.g.* irones,[9] juvenile hormones,[10] steroids,[11] and C_{50}-carotenoids.[12] Of particular interest in this context is the structural similarity between the side chain of stigmasterol (*11*), a steroid known to occur in tobacco,[13] and the enone (*1*) and the acid (*2*).

EXPERIMENTAL

NMR, IR, UV, and mass spectra were recorded on Varian HA 100D and A60-A, Digilab FTS-14, Perkin-Elmer 257, Beckmann DK-2A and LKB 9000 (70 eV) instruments, respectively. The mass spectra were obtained by gas chromatography in combination with the mass spectrometer (GLC–MS) using steel capillary columns (0.5 mm × 50 m, Handy and Harman grade 316-S) coated with emulphor using the dynamic packing method.[14] Preparative GLC was performed with a Varian 1700 instrument using a 3.2 mm × 3 m glass column packed with 5 % Carbowax 20 M on Chromosorb G. Fractions were collected at −70° in U-shaped teflon tubes (i.d. 5 mm) equipped with an electrostatic precipitator.[15] Accurate mass determinations were carried out at the Laboratory for Mass Spectrometry, Karolinska Institutet, Stockholm. The solvents, silica gel, and drying agents were purified as previously described.[16]

Isolation

5ξ-Isopropyl-3E-hepten-2-one (*1*, 3 mg) was isolated from fraction "B 3" [1] by preparative gas chromatography.[3] MS: 154 (M^+, 3.5) 43 (100), 97 (45), 55 (34), 111 (34), 112 (34), 69 (30), 41 (23), 39 (11), 125 (11), 84 (7); accurate mass determination: $C_{10}H_{18}O$, found 154.1361, calc. 154.1358; λ_{max} (EtOH) 223 nm (ε 14 600); $[\alpha]_D^{20}+4.7°$ (*c* 0.4 in ether); ν(film): 2961 (s), 2931 (m), 2872 (m), 1696 (m), 1677 (s), 1625 (m), 1460 (m), 1387 (w), 1369 (m), 1361 (m), 1255 (s), 1180 (w), 987 (m); $\delta(CDCl_3)$: 0.83 (3 H, t, *J* 7 Hz), 0.86 (3 H, d, *J* 6.5 Hz), 0.91 (3 H, d, *J* 6.5 Hz), 1.1–2.0 (4 H, m), 2.24 (3. H, s), 6.04 (1 H, d, *J* 16 Hz), 6.6 (1 H, quartet, *J* 8.5 and 16 Hz).

3ξ-Hydroxy-3ξ-methyl-6ξ-isopropyl-4E-octenoic acid (*2*, 17 mg) was isolated as the corresponding methyl ester (*9*) from 'Acids' [1] by preparative gas chromatography.[2] MS: M^+ at *m/e* 228 was not seen, 43 (100), 97 (39), 111 (28), 55 (27), 112 (24), 69 (23), 41 (23), 71 (14); accurate mass determination: $C_{13}H_{22}O_2$ (M−18), found 210.1620, calc. 210.1620; ν(film): 3500 (broad), 2959 (s), 2931 (m), 2875 (m), 1730–1720 (s), 1440 (m), 1384 (m), 1369 (m), 1338 (m), 1209 (s), 1175 (m), 1128 (w), 1012 (w), 978 (m), 939 (w) cm^{-1}; $\delta(CDCl_3)$: 0.78 (3 H, t, *J* 7 Hz), 0.79 (3 H, d, *J* 7 Hz), 0.84 (3 H, d, *J* 7 Hz), 1.2–1.8 (4 H, m), 1.31 (3 H, s), 2.56 (2 H, s), 3.66 (3 H, s), 3.82 (OH, broad singlet), 5.42 (2 H, m). Addition of $Eu(DPM)_3$: *r* (relative induced shift ratio) [17] = 1.28 (1 H, d, *J* 16 Hz), r = 1.21 (1 H, d, *J* 16 Hz), *r* = 1 (3 H, s), r = 0.87 (1 H, d, J 16 Hz), *r* = 0.68 (1 H, quartet, *J* 9 and 16 Hz), *r* = 0.26 (1 H, m), *r* = 0.13 (3 H, t, *J* 7 Hz), *r* = 0.11 (6 H, d, *J* 7 Hz), *r* = 0.31 (3 H, s). Extrapolation to zero addition of $Eu(DPM)_3$ indicated the chemical shift of C(6)H having *r* = 0.26 to be δ 1.58. The coupling (*J* 9 Hz) between this proton and C(5)H with *r* = 0.68 was demonstrated in spin decoupling experiments. Irradiation of C(5)H in the LIS-doped sample simplified the multiplet having r = 0.26 to a doublet of triplets. $[\alpha]_D^{25}-0.8°$ (*c* 0.5 in chloroform). The NMR spectra obtained after addition of $Eu(DPM)_3$ indicated a diastereomeric mixture 1:4.

2,10-Dimethyl-7ξ-isopropyl-8E,10-undecadien-4-one (*3*, 3.4 mg) was isolated about two years ago from fraction "C 9" [1] by preparative gas chromatography. MS: *m/e* 236 (M^+, 8), 93 (100), 121 (53), 57 (53), 136 (48), 85 (42), 41 (35), 43 (28), 79 (20), 81 (17); NMR was found identical to that of synthetic *3*.

Synthesis

(±)-5-Isopropyl-3E-hepten-2-one(1). A mixture of (±)-2-isopropylbutyraldehyde (*4*), (3.4 g), acetone (25 ml) and 10 % aqueous KOH solution (3 ml) was refluxed on a steam-bath for 16 h. The cooled reaction mixture was concentrated *in vacuo*, extracted with pentane, and the combined pentane extracts washed with water and dried over sodium sulphate. The solvent was removed under reduced pressure to leave *1* as a straw-coloured liquid (3.9 g, purity: > 95 %, yield 85 %). The physical properties of the product were indistinguishable from those of the natural compound (*vide supra*).

(±)-3-Hydroxy-3-methyl-6-isopropyl-4E-octenoic acid (2). A mixture of (±)-5-isopropyl-3*E*-hepten-2-one (*1*, 1.54 g), methyl bromoacetate (1.68 g) and activated [18] zinc powder (0.7 g) in dry benzene (40 ml) was refluxed with stirring under nitrogen. A vigorous reaction started shortly after refluxing began and the reaction mixture turned a dark green colour. The refluxing and stirring was continued for 1 h after which the reaction mixture was cooled, treated with ice-cold 10 % aqueous acetic acid and extracted with ether. The ether-benzene solution was washed with 10 % aqueous acetic acid, 5 % $NaHCO_3$ solution, water and finally dried over anhydrous sodium sulphate. The solvents were removed *in vacuo* to leave *9* as a pale yellow liquid (2.1 g). The NMR, IR, and mass spectra of a sample purified by chromatography on silica gel were identical to those of the methyl ester isolated from tobacco (*vide supra*).

(±)-2,10-Dimethyl-7-isopropyl-8E,10-undecadien-4-one (3). (±)-2-Methyl-5-isopropyl-7-cyano-1,3*E*-heptadiene [8] (*5*, 405 mg) in dry ether (10 ml) was slowly added to a stirred solution of isobutylmagnesium bromide prepared from isobutyl bromide (2 g) and magnesium (340 mg) in 30 ml dry ether. After the addition, dry benzene (25 ml) was added and the ether removed by distillation. The mixture was refluxed for 24 h after which the solution was cooled and poured over crushed ice to hydrolyze the intermediate ketimine.

After stirring for 4 h at room temperature the benzene layer was removed and the aqueous phase extracted with ether. The solvent was removed by distillation and the residue chromatographed on a silica gel column. Elution with 1 % ether in pentane furnished 85 mg (16 %) of *3*, which was found indistinguishable from the tobacco compound when co-injected on a capillary column. Furthermore, the NMR and mass spectra (*vide supra*) were superimposable. At this stage the tobacco compound was only available in a reference sample of the fraction from which it had been isolated, and an IR spectrum of the natural compound could not be obtained for comparison. λ_{max} (EtOH): 230 nm (ε 23 600); ν(film): 2960 (s), 2875 (s), 1712 (s), 1609 (w), 1469 (m), 1410 (w), 1386 (m), 1369 (s), 1170 (w), 1142 (w), 1068 (w), 1037 (w), 972 (s), 884 (m) cm^{-1}; $\delta(CDCl_3)$: 0.85 (3 H, d), 0.89 (6 H, d), 0.90 (3 H, d), 1.3 – 1.8 (5 H, m), 1.82 (3 H, t, *J* 1.1 Hz), 2.1 – 2.45 (4 H, m), 4.86 (2 H, m), 5.33 (1 H, quartet, *J* 8 and 16 Hz), 6.06 (1 H, d, *J* 16 Hz).

(±)-*8-Isopropyl-11-methyl-9*E,*11-dodecadien-5-one* (*7*). *7* was prepared as described for *3* except that butylmagnesium bromide was used in the Grignard reaction. *7* disclosed a longer retention time than the tobacco compound (*3*) when co-chromatographed on a capillary column. MS: *m/e* 236 (M^+, 17), 93 (100), 136 (66), 121 (65), 85 (37), 57 (34), 41 (26), 79 (15), 43 (14), 81 (13). $\delta(CDCl_3)$: 0.86 (3 H, d), 0.90 (3 H, t), 0.91 (3 H, d), 1.2 – 1.8 (8 H, m), 1.82 (3 H, t, *J* 1.1 Hz), 2.34 (6 H, two triplets, *J* 7 Hz), 4.85 (2 H, m), 5.32 (1 H, quartet, *J* 8 and 16 Hz), 6.07 (1 H, d, *J* 16 Hz).

(±)-*3,10-Dimethyl-7-isopropyl-8*E,*10-undecadien-4-one* (*8*). *8* was synthesized as outlined for *3* except for using *sec*-butylmagnesium bromide in the Grignard coupling. MS: *m/e* 236 (M^+, 9.5), 93 (100), 57 (98), 121 (54), 136 (46), 41 (38), 85 (37), 43 (31), 79 (24), 81 (22). $\delta(CDCl_3)$: 0.7 – 1.1 (12 H, m), 1.2 – 2.0 (6 H, m), 1.82 (3 H, t, *J* 1.1 Hz) 2.36 (2 H, t, *J* 6.5 Hz), 4.85 (2 H, m), 5.32 (1 H, quartet, *J* 8 and 16 Hz), 6.05 (1 H, d, *J* 16 Hz).

Acknowledgements. The authors are indebted to Miss A.-M. Eklund for skilful technical assistance, Prof. K. Olsson, Agricultural College of Sweden, Uppsala, for placing the NMR instrument at their disposal, and Dr. R. R. Johnson, Brown and Williamson Tobacco Corporation, Louisville, Kentucky, for a generous gift of (±)-2-methyl-5-isopropyl-7-cyano-1,3*E*-heptadiene.

REFERENCES

1. Kimland, B., Aasen, A. J. and Enzell, C. R. *Acta Chem. Scand.* **26** (1972) 2177.
2. Kimland, B., Aasen, A. J., Almqvist, S.-O., Arpino, P. and Enzell, C. R. *Phytochemistry* **12** (1973) 835.
3. Hlubucek, J. R., Aasen, A. J., Kimland, B. and Enzell, C. R. *Phytochemistry* **12** (1973) 2555.
4. Slomp, G. and MacKellar, F. *J. Am. Chem. Soc.* **84** (1962) 204.
5. Kinzer, G. W., Page, T. F., Jr. and Johnson, R. R. *J. Org. Chem.* **31** (1966) 1797.
6. Kimland, B., Appleton, R. A., Aasen, A. J., Roeraade, J. and Enzell, C. R. *Phytochemistry* **11** (1972) 309.
7. Roberts, D. L. and Rohde, W. A. *Tobacco Science* **16** (1972) 107.
8. Johnson, R. R. and Nicholson, J. A. *J. Org. Chem.* **30** (1965) 2918.
9. Whiting, D. A. and Harper, S. H. In Coffey, S., Ed., *Rodd's Chemistry of Carbon Compounds*, Elsevier, Amsterdam 1968, Vol. II, part B, p. 153.
10. Karlson, P. In Goodwin, T. W., Ed., *Natural Substances Formed Biologically From Mevalonic Acid*, Academic, London 1970, p. 145.
11. Goad, L. J. *Ibid.* p. 45.
12. Straub, O. In Isler, O., Ed., *Carotenoids*, Birkhäuser, Basel 1971.
13. Carruthers, W. and Plimmer, J. R. *Chem. Ind. (London)* **1959** 48.
14. Dijkstra and de Goey, J. In Desty, D. H., Ed., *Gas Chromatography* 1958, Butterworths, London 1958, p. 56.
15. Kratz, P., Jacobs, M. and Mitzner, B. M. *Analyst* **84** (1959) 671.
16. Appleton, R. A., Enzell, C. R. and Kimland, B. *Beitr. Tabakforsch.* **5** (1970) 266.
17. Wineburg, J. P. and Swern, D. *J. Am. Oil. Chemists' Soc.* **49** (1972) 267.
18. Hauser, C. R. and Breslow, D. S. *Org. Syn. Coll. Vol.* **3** (1955) 408.

Received March 17, 1973.

ACTA CHEMICA SCANDINAVICA 27 (1973) 2411–2414

Synthesis of Some Aryl α-Diketones and Aryl Glyoxylic Acid Derivatives by Acylation of Electron-rich Aromatics

DAN BEHR, SVANTE BRANDÄNGE and BJÖRN LINDSTRÖM

Department of Organic Chemistry, The Arrhenius Laboratory, P.O.B., S-104 05 Stockholm 50, Sweden

N-Acylpyridinium salts, prepared from pyridine and oxalyl chloride or ethoxalyl chloride, have been used for acylation of electron-rich aromatics of the pyrrole, indole, and furan groups.

Acylation of electron-rich heteroaromatics is sometimes complicated by the acid-sensitivity of the starting aromatic. Some reactions, without a catalyst, between oxalyl chloride and aromatics such as indole,[1,2] pyrrole,[3–5] *N*-methylpyrrole,[3] and 2,4-dimethylpyrrole [6] have been performed with varying degrees of success.

Treibs and Kreuzer [3] used the *N*-acylammonium salt obtained on reaction between oxalyl chloride and triethylamine (1:1) for acylation of *N*-methylpyrrole. After quenching with methanol, methyl *N*-methyl-2-pyrrolylgly-

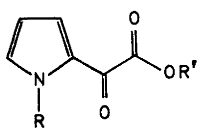

I R = CH_3, R' = CH_3
III R = H, R' = C_2H_5

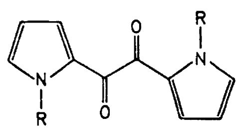

II R = CH_3
IV R = H

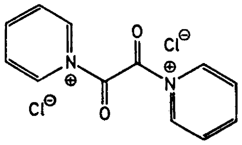

V

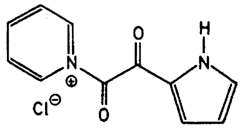

VI

oxylate (I) and bis(*N*-methyl-2-pyrrolyl)-ethanedione (II) were obtained in moderate yields (30 and 37 %, respectively). We have reported a similar acylation reaction.[7] Ethyl 2-pyrrolylglyoxylate (III) was obtained in 64 % isolated yield from the reaction between pyrrole, pyridine, and ethoxalyl chloride at $-80°$ for 3 h. We now report further studies on this and related acylations.

When the above reaction was carried out at $-70°$ for 17 h, the yield of III, determined by GLC, was 96 %. Lower yields (75 and 70 %, respectively) were obtained when the temperature was allowed to rise from $-70°$ to room temperature or when the reagents were kept at room temperature throughout. Ethyl 3-indolylglyoxylate was prepared (92 % yield) in an analogous reaction.

When equimolar amounts of pyridine, oxalyl chloride, and pyrrole were used, and the reaction was quenched with ethanol, III was also obtained. Ethyl 3,5-dimethyl-4-ethoxycarbonyl-2-pyrrolylglyoxylate was prepared in an analogous reaction. When, however, pyridine, oxalyl chloride, and pyrrole were used in the molar proportions 2:1:1, different results were obtained depending upon the dilution of the reaction mixture. At high concentrations, when the mixture was heterogeneous, bis(2-pyrrolyl)-ethanedione (IV) was the main product (53 % yield), and the ketoester III was formed in low yield (< 4 %). In dilute homogeneous solution, III was obtained in 60 % yield. The yield of III raised to 92 % when the bis-pyridinium salt was used in excess. A reasonable explanation of this difference in result is that at higher concentrations the major part of the bis-pyridinium salt V is precipitated and the mono-pyridinium salt VI becomes the main acylating agent. In dilute solutions, however, all V is in solution and this compound then becomes the main acylating agent. The presence of a bis-pyridinium salt was demonstrated by mixing oxalyl chloride (0.010 mol) with pyridine (0.022 mol) in methylene chloride at $-70°$, followed by filtration and determination of the amount of pyridine in the mother liquor.

The less reactive 2-methylfuran, on reaction with equimolar amounts of pyridine and oxalyl chloride and quenching with methanol, gave the corresponding methyl glyoxylate in good yield (77 %). Poor yields were, however, obtained with the even less reactive furan and 2-methylthiophene.

α-Diketones were also prepared from *N*-methylindole and 2-methylfuran by reacting the aromatic, oxalyl chloride, and pyridine in the molar proportions 2:1:2.

EXPERIMENTAL

Analytical GLC was performed using a 3 % JXR on Gas-Chrom Q column (0.2 × 180 cm) mounted in a Perkin-Elmer 900 chromatograph. Melting points are corrected. IR spectra were recorded with a Perkin-Elmer 257 instrument. Methylene chloride was distilled over P_2O_5, and pyridine was distilled over KOH and stored over molecular sieves (3 Å).

Ethyl 2-pyrrolylglyoxylate[7] *(III).* A solution of pyridine (0.95 g, 12 mmol) in methylene chloride (25 ml) and thereafter a solution of pyrrole (0.67 g, 10 mmol) in methylene chloride (25 ml) were slowly added (15 min for each) to a stirred and cooled ($-70°$ to $-80°$) solution of ethoxalyl chloride (1.50 g, 11 mmol) in methylene chloride (25 ml). The reaction mixture was stirred for 17 h ($-70°$) and washed with dilute hydrochloric acid, and the organic layer was then dried (Na_2SO_4). Quantitative GLC analysis (internal standard) revealed that III was formed in 96 % yield.

Ethyl 3-indolylglyoxylate (VII). A solution of pyridine (2.85 g, 0.036 mol) in methylene chloride (50 ml) and thereafter a solution of indole (3.51 g, 0.030 mol) in methylene chloride (100 ml) were added to a stirred and cooled (−80°) solution of ethoxalyl chloride (4.50 g, 0.033 mol) in methylene chloride (100 ml). The cooling bath was then removed and the mixture was stirred for 20 h. Crystals of VII were filtered off (3.71 g, m.p. 185−186.5°, lit.[8] m.p. 187°), and a second crop (2.28 g, m.p. 185−186.5°) was obtained from the mother liquor. The total yield was 5.99 g (92 %).

Ethyl 2-pyrrolylglyoxylate (III). A solution of pyridine (2.61 g, 33 mol) in methylene chloride (50 ml) and thereafter a solution of pyrrole (2.01 g, 30 mmol) in methylene chloride (50 ml) were added to a stirred and cooled (−80°) solution of oxalyl chloride (4.19 g, 33 mmol). The reaction mixture was stored at −20° for 18 h and ethanol (4.6 g) was then added. After 3 h at room temperature the mixture was washed with dilute hydrochloric acid, and the organic layer was dried (Na_2SO_4) and concentrated. Chromatography on silica gel (methylene chloride) yielded pure III (4.17 g, 83 % yield), indistinguishable (IR, NMR, GLC) from an otherwise prepared [7] sample.

Ethyl 3,5-dimethyl-4-ethoxycarbonyl-2-pyrrolylglyoxylate (VIII). The reaction between 2,4-dimethyl-3-ethoxycarbonylpyrrole [9] (167 mg, 1.0 mmol), oxalyl chloride (141 mg, 1.1 mmol), and pyridine (95 mg, 1.2 mmol) in methylene chloride (10 ml) was started at −80° and was then allowed to reach room temperature. Ethanol was added after 1 h, and the reaction mixture was worked up as above. Purification on silica gel (chloroform) gave 245 mg of VIII (92 % yield, m.p. 74−76°, lit.[3] m.p. 80°).

Bis(2-pyrrolyl)-ethanedione (IV). A solution of pyridine (10.0 g, 0.12 mol) in methylene chloride (25 ml) and thereafter a solution of pyrrole (3.3 g, 0.050 mol) in methylene chloride (25 ml), were added with stirring to a cooled (−80°) solution of oxalyl chloride (6.4 g, 0.050 mol) in methylene chloride (25 ml). After 15 min the mixture was washed with dilute hydrochloric acid, and the organic layer was dried (Na_2SO_4) and concentrated. Purification on a silica gel column (acetone) gave IV as yellow crystals (2.5 g, 53 %, m.p. 203−205°, lit.[10] m.p. 199−200°).

Ethyl 2-pyrrolylglyoxylate (III). Oxalyl chloride (0.64 g, 5.0 mmol), pyridine (1.0 g, 12 mmol) and methylene chloride (450 ml) were mixed at −80°, and when warmed to −10° the mixture became homogeneous. A solution of pyrrole (0.165 g, 2.5 mmol) in methylene chloride was then added dropwise, and after 10 min ethanol (10 ml) was added. Part of the solvent was evaporated and the resulting solution was washed with dilute hydrochloric acid. After drying (Na_2SO_4) and concentration of the organic layer a blue crystalline mass was obtained. NMR showed that this consisted of reasonably pure III (92 % yield).

Methyl 5-methylfurylglyoxylate (IX). A solution of pyridine (4.35 g, 55 mmol) in methylene chloride (50 ml) and thereafter a solution of 2-methylfuran (4.11 g, 50 mmol) were added dropwise with stirring and cooling (−80°) to a solution of oxalyl chloride (7.61 g, 60 mmol). The cooling bath was removed and the mixture was stirred at room temperature for 18 h. After reaction with methanol and the usual work-up a brown oil (8.8 g) was obtained. Purification on silica gel (methylene chloride) gave IX as yellow needles (6.50 g, 77 % yield), m.p. 56−57°. An analytical sample, m.p. 56−57°, was obtained on recrystallisation from light petroleum. (Found: C 57.4; H 4.94. Calc. for $C_8H_8O_4$: C 57.1; H 4.80.) IR ($CHCl_3$): 1740 and 1662 cm^{-1}.

Bis(5-methyl-2-furyl)-ethanedione (X). A solution of pyridine (6.96 g, 88 mmol) in methylene chloride (50 ml) and thereafter a solution of 2-methylfuran (6.57 g, 80 mmol) in methylene chloride (50 ml) were added dropwise with stirring to a solution of oxalyl chloride (5.08 g, 40 mmol) in methylene chloride (50 ml) at −70°. The cooling bath was removed and the reaction mixture was stirred at room temperature for 16 h. A dark brown residue was obtained after extraction with hydrochloric acid, drying (Na_2SO_4) and concentration of the organic layer. Purification on a silica gel column (methylene chloride) gave X as yellow crystals (4.41 g, 51 % yield, m.p. 166.5−167°). An analytical sample, m.p. 166.5−167°, was obtained from ethanol. (Found: C 65.9; H 4.81. Calc. for $C_{12}H_{10}O_4$: C 66.1; H 4.62.) IR ($CHCl_3$): 1642 cm^{-1}.

Bis(N-methyl-3-indolyl)-ethanedione (XI). Methylene chloride solutions (50 ml) of oxalyl chloride (0.65 g, 5.1 mmol), pyridine (0.95 g, 12 mmol) and *N*-methylindole (1.31 g, 10 mmol) were mixed at −70°, and the mixture was stirred at room temperature (18 h) producing an orange colour. After washing with dilute hydrochloric acid, drying and

concentration, the residue was crystallised from benzene giving pale yellow crystals, m.p. 272–273.5° (0.70 g, 45 %, lit.[8] m.p. 268–269°).

Acknowledgement. This work has been supported by the *Hierta-Retzius' forskningsfond.*

REFERENCES

1. Giua, M. *Gazz. Chim. Ital.* **54** (1924) 593.
2. Shaw, K., McMillan, A., Gudmundson, A. and Armstrong, M. *J. Org. Chem.* **23** (1958) 1171.
3. Treibs, A. and Kreuzer, F.-H. *Ann.* **721** (1969) 105.
4. Archibald, J. L. and Freed, M. E. *J. Heterocycl. Chem.* **4** (1967) 335.
5. Birchall, G. R. and Rees, A. H. *Can. J. Chem.* **49** (1971) 919.
6. Nenitzescu, C. D., Necsoin, I. and Zalman, M. *Comun. Acad. Rep. Populare Romine* **8** (1958) 659; *Chem. Abstr.* **53** (1959) 17092.
7. Brandänge, S. and Lundin, C. *Acta Chem. Scand.* **25** (1971) 2447.
8. Millich, F. and Becker, E. I. *J. Org. Chem.* **23** (1958) 1096.
9. Knorr, L. *Ann.* **236** (1886) 325.
10. Oddo, B. *Gazz. Chim. Ital.* **41** (1911) 248.

Received March 3, 1973.

ACTA CHEMICA SCANDINAVICA 27 (1973) 2415–2420

Isoelectric Focusing of Acidic Proteins

Studies on Pepsin

O. VESTERBERG

Chemical Division, Occupational Health Department, The National Board of Occupational Safety and Health, S-100 26 Stockholm 34, Sweden

The development of acidic carrier ampholytes (Ampholine) for the pH range 2.5 – 4 will allow studies on isoelectric focusing of most acidic proteins. These carrier ampholytes are of the aliphatic polyamino-polycarboxylic acid type. Isoelectric focusing in density gradient and polyacrylamide gel have been used for studies on multiple molecular forms of pepsin of hog and human origin. Detection of the enzymatic activity after focusing in gel using a modified zymogram procedure is described. Samples of human gastric juices show different patterns at a high degree of resolution, that might be promising for further studies on possible relationships between specific patterns and ulcers and cancer.

Isoelectric focusing has been used for separation and characterising many different proteins (for review articles see Refs. 1 – 4). Most of the proteins studied up to now have been isoelectric in the pH range 3.5 – 10. The principal reason why very few studies have been made outside this pH range is that buffer substances, carrier ampholytes, have not been commercially available to cover very acidic and basic pH regions. Recently, it was possible to extend the useful pH range on the alkaline side up to about pH 11.[5] During the last years the problem with the acidic pH region has been tackled. This has resulted in the development of a suitable system of aliphatic polyaminopolycarboxylic acids for the acidic pH, analogous to the carrier ampholytes for other pH ranges.[6,7] (Vesterberg, to be published in more detail elsewhere.)

There are many interesting acidic proteins with isoelectric point (pI) < 4, *e.g.* glycoproteins in serum, from micro organisms, and cell membranes. One of the best known acidic proteins is pepsin. A correlation between increased concentration of pepsin and the incidence of duodenal ulcers [8] and cancer in the stomach [9] has been found. This protein has been shown to occur in multiple molecular forms,[10,11] one of which has been shown to be more prominent in some patients with peptic ulcers.[12] Because isoelectric focusing has been shown to give a resolution comparable to or surpassing carefully conducted electrophoresis in gels, it was of interest to apply the method on pepsin.

MATERIALS, METHODS, AND RESULTS

Pepsin was purchased from Merck, Germany, types Crude DABG, and pepsin krist. lyophilisiert 100 mU/mg, and from Sigma Chem. Co., Mo., USA, type 2 × Crystallized and Lyophilized, 2700 U/mg. The samples of gastric juice were obtained by aspiration from different patients with complaints indicating gastritis and in some cases ulcers, courtesy of Professor H. Lagerlöf at Karolinska sjukhuset, Stockholm. Some samples were obtained after stimulation with gastrin. All samples had been stored at $-20°$ for about one month. Isoelectric focusing in density gradient was performed essentially as described earlier.[4] A gradient mixer was used. A column of 110 ml capacity (Type 8101 LKB-Produkter AB, S-161 25 Bromma, Sweden) was used with circulating cooling water at +4°C. The dense solution contained 24 g of sucrose, 2 ml of carrier ampholytes 20 % (w/v) pH 2.4 – 4 and distilled water to make a final volume of 49 ml; the less dense solution contained 0.5 ml of carrier ampholytes 20 % (w/v) pH 2.5 – 4 in a final volume of 49 ml. 15 mg of pepsin was dissolved in this solution. The anode solution for the central tube and the bottom of the column comprised 20 ml of a sucrose solution 55 % (w/v) to which 1.0 ml 1 M H_3PO_4 was added. After filling the column 10 ml of water containing 0.25 ml of Ampholine 20 % (w/v) pH 2.5 – 4 was added to provide the cathode solution. A potential of 500 V was applied for 2 h and was then increased to 700 V for 46 h. Fractions of 2.0 ml were collected. The pH of the fractions was measured at +4°. Pepsin was assayed on hemoglobin as substrate essentially as described earlier.[10]

The result of focusing a purified preparation of pepsin in a density gradient column is shown in Fig. 1. The total yield of pepsin after focusing was often close to 90 %. Two

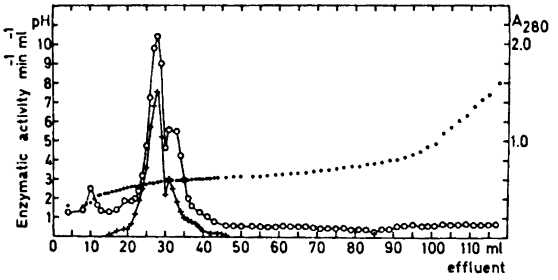

Fig. 1. The result of isoelectric focusing at +4° of 15 ml of pepsin (Sigma). Symbols: pH at +4° ··· ; absorbance, A_{280} O; enzymatic activity measured as increase in A_{280} min^{-1} ml^{-1}, +.

components with enzymatic activity were resolved, characterised by isoelectric points (pI's) at 2.86 and 2.94, respectively. The protein concentration as estimated by A_{280} correlated well with the enzymatic activity in the fractions showing significant activity. The elevated A_{280} values in the very acidic fractions were probably caused by impurities in the sucrose, or products formed at the anode. Thus the results indicated that the pepsin preparation used was probably not contaminated by protein impurities to any high extent.

Isoelectric focusing in thin layer polyacrylamide gels (IFPAG) was done in principle as described elsewhere.[13] The gels contained 1 % (w/v) of Ampholine (LKB) pH 2.5 – 4 and were polymerized with riboflavin as catalyst. The anode was soaked in 1 M H_3PO_4 and the cathode was soaked in 0.1 % of Ampholine pH 2.5 – 4. The distance between the electrodes was 10.5 cm. Protein samples were usually applied after beeing soaked into small rectangular pieces of filter paper, *e.g.* Whatman 3 MM, and usually placed close to the cathode. A potential of 800 V was used for 4 h.* In some cases protein was applied close to both electrodes in the same strip of the gel. After focusing for 2, 3, and 3.5 h,

* *Note added in proof.* For further details and recommendations see Vesterberg, O. *Science Tools* **20** (1973) probably in No. 2.

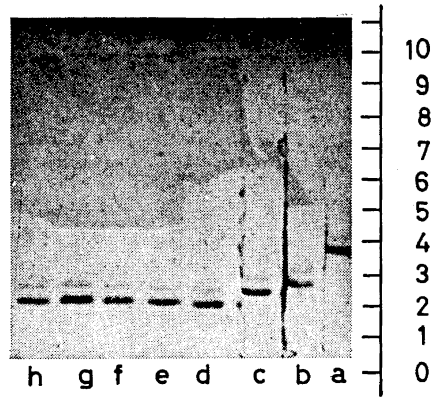

Fig. 2. The result obtained after staining of the protein zones of pepsin preparations after isoelectric focusing in polyacrylamide gel. The distance from the anode is shown to the right (cm scale).
a – d, Sample application: 25 μl containing 50 μg of pepsin (Sigma) was soaked into each of two pieces of filter paper measuring 5 × 0.5 cm, which were placed close to each electrode. Focusing time in hours: (a) 2,(b) 3,(c) 3.5, and (d) 4. e – h, Sample application: Protein solutions were soaked into rectangular pieces of filter paper measuring 1.0 × 1.0 cm, and placed close to the cathode. e, 25 μl containing 50 μg of pepsin (Sigma). f, Same as e. g, 100 μl containing 50 μg of pepsin (Merck "krist"). h, 50 μl of the same solution as in g.

narrow strips were cut out. During this operation the current was switched off. The strips were strained for protein as described earlier.[13] By this procedure it was possible to see when protein zones migrating from either electrode had coalesced and focused sharply (Fig. 2). With the voltage used, this occurred within 2 h although the proteins continued to migrate slowly towards the anode. Nevertheless a high degree of resolution could be obtained (Fig. 2). A main component was always obtained. When sufficient protein was applied a faint band was also seen on the cathodic side of the main component. This component was more pronounced in impure preparations. By using a zymogram procedure (*vide infra*) it was possible to show that both zones contained enzymatic activity.

After switching off the current, pH was measured on the surface with a surface pH electrode [13] (Fig. 3). Fastening the electrode with a clamp fixed to a stand, which can be moved a little for each pH measurement, aids the process. When these pH values were compared to the corresponding positions of the stained protein zones, the main component possessed a pI of 2.8 and the minor one a pI of 2.9.

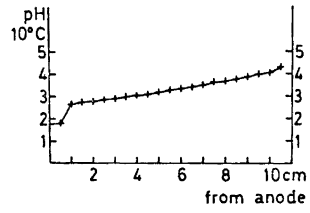

Fig. 3. Record of pH measurements at +10° from anode to cathode of the experiment shown in Fig. 2(e – h).

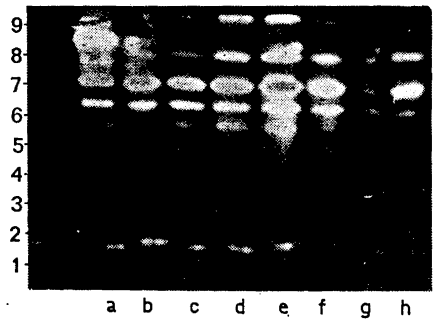

Fig. 4. Zymogram detection of proteolysis after isoelectric focusing. The samples of gastric juice (10 μl) were applied to pieces of filter paper measuring 1.0 × 0.3 cm and placed close to the cathode.
The zones with enzymatic activity can be seen as white unstained zones against the stained background, which represents undigested albumin. Distance from the cathode (in cm) is shown to the left.

As was mentioned earlier, proteins were usually detected by staining. However, in some experiments protein samples were applied to the gel to permit slicing into two identical halves. One of the pieces was then used for detection of enzymatic activity by a modified zymogram procedure.[14] It was only necessary to incubate the gel in albumin solution for 30 min. This is a shorter time than recommended earlier.[14] Sharper zones are obtained with the new procedure because diffusion is reduced. Staining and fixing were done as described earlier.[13] The patterns obtained with samples of gastric juice from different persons often showed differences in the number of zones detected, and also in the relative activities of particular zones. Up to 6 zones of activity were seen (Fig. 4).

DISCUSSION

As can be seen from Fig. 1 the useful pH range with these new carrier ampholytes extends down to about pH 2.2, which should be low enough to allow studies of most acidic proteins. A very important property of the carrier ampholytes is a sufficient buffering capacity.[6,15] Measurements have shown that the carrier ampholytes forming the acidic pH region show more than twice the buffering capacity of those used earlier for the neutral pH range when compared on a weight for weight basis. This is due to the abundance of carboxylic groups dissociating in the acidic region, and is the principal reason why half the usual concentration of carrier ampholytes can be used for focusing in the acidic pH region. Another reason is that it is important to try to avoid too high a current at the voltage necessary for focusing. A lower concentration of Ampholine results in a smaller current, and thus a reduced total electrical load, minimising the risk of excessive heating that could otherwise destroy the density gradient.

The degree of focusing, *i.e.* the width of a protein zone, is determined among other factors by the local field strength.[15] Quite good distribution of the field strength can be obtained with these new acidic carrier ampholytes judging from the width of the zones obtained after focusing in the column as well as in the gel. However, very critical inspection might perhaps indicate that the width of the main zones obtained after focusing both in the column and in the gel are somewhat larger than could be expected for homogeneous proteins. Some of the results obtained indicate that minor components are present close to the major ones and make them look somewhat broader than they actually should be. As was mentioned earlier pepsin has been proven by independent methods, such as ion change chromatography and electrophoresis in agarose gels, to occur in many multiple molecular forms, formed by cleavage of the peptide chain at different points during activation, and perhaps also differing in the number of amide groups. (For a summary of the most usual explanations for multiple molecular forms of proteins see Ref. 16).

During the IFPAG of pepsin it has been found that this protein migrates slowly in the direction of the anode. This is probably caused by electroendosmosis. Therefore, no stable final focusing position in the acidic pH region of the gel should be awaited before stopping any particular experiment. A method of determining the duration of an experiment has already been indicated. Proteins substantially larger than pepsin may require a somewhat longer time for optimal resolution than pepsin due to a lower electrophoretic mobility in the gel.

The pH measurement with the surface electrode has certain limitations. However, it can be seen by comparison of Figs. 1 and 3, that fairly good agreement between the values obtained in column and gel was obtained.

The fact that pepsin occurs in different molecular forms makes it difficult to make an exact comparison of the pI obtained by isoelectric focusing with that from electrophoresis. However, a value of 2.7 with the latter method has been reported,[17] which is in good agreement with the pI for the main component obtained here. Earlier electrophoretic data which estimate the pI in the vicinity of 1 are most probably false, and probably resulted from binding of anions to the protein. Moreover, such a low value is not in accord with the amino acid composition of the protein. Another interesting fact is that an isoionic point close to pH 3 has been reported for pepsin.[18] This is also close to the pI obtained here for the main component and may be considered additional evidence for the earlier proposed statement that the pI obtained by isoelectric focusing is also close to the isoionic point of a protein.[7,15]

The patterns obtained with the different samples of gastric juice (Fig. 4) show many different zones of activity in accord with earlier observations.[11,12] The resolution obtained by isoelectric focusing is very high and seems very promising for continued studies, *e.g.* on the significance of different patterns and their possible correlation with ulcers and cancer.

When this manuscript was completed a paper appeared on isoelectric spectra of pepsin.[19] In this investigation pH gradients below pH 3 were created by using mixtures of acids. Three components of pepsin were detected. It is not possible to make a strict comparison of the pI values of that study with those reported in this investigation, because different brands of pepsin have been used. However, M. Jonsson indicated that the pI of the most acidic component was too low, which could have been caused by binding of some of the anions used to obtain the pH gradient. He was also of the opinion that a pI obtained in the presence of carrier ampholytes was closer to the isoionic point than the pI obtained in the presence of acids. The use of ordinary acids to create a pH gradient has many drawbacks, some of which may be mentioned here:

(1) the pI obtained is influenced by the type of acids and concentrations thereof used;
(2) a very long time (about 150 h) may be required for separation of proteins;
(3) the distribution of the field strength is unfavourable;
(4) it is difficult to obtain a good shallow pH course which means among other things that the useful part of the column is very short;
(5) no stable final pH gradient is obtained; instead there is a slow drift against the anode;
(6) the resolution of proteins with a considerable difference in pI is not good.

The new carrier ampholytes for the acidic pH range circumvent all the mentioned drawbacks.

Acknowledgements. Thanks are due to Miss Vesna Gasparich for preparation of the carrier ampholytes, and also to Mrs. Gun Nise and Miss Birgitta Karlsson for skilful technical assistance in the experiments with pepsin and gastric juice. Dr. Cyril Smyth is acknowledged for valuable criticism and revision of the English text.

REFERENCES

1. Haglund, H. *Methods Biochem. Anal.* **19** (1971) 1.
2. Catsimpoolas, N. *Separ. Sci.* **5** (1970) 523.
3. Wrigley, C. W. In Niederwieser, A. and Pataki, G. *New Techniques in Amino Acid Peptide, and Protein Analysis*, Ann Arbor Science Publ. Inc. 1971, pp. 291 – 339.
4. Vesterberg, O. *Methods Enzymol.* **22** (1971) 389, 412.
5. Lundblad, G., Vesterberg, O., Zimmerman, R. and Lind, J. *Acta Chem. Scand.* **26** (1972) 1711.
6. Vesterberg, O. *Acta Chem. Scand.* **23** (1969) 2653.
7. Vesterberg, O. In Catsimpoolas, O. *Conference on Isoelectric Focusing and Isotachophoresis, Ann. N.Y. Acad. Sci.* **209** (1973) 23.
8. Cheret, A.-M. and Bonfils, S. *Pathol. Biol.* **18** (1970) 317.
9. Pastore, J. O., Kato, H. and Belsky, J. I. *N. Engl. J. Med.* **286** (1972) 279.
10. Rajagopalan, T. G., Moore, S. and Stein, W. H. *J. Biol. Chem.* **241** (1966) 4940.
11. Etherington, D. J. and Taylor, W. H. *Biochem. J.* **113** (1969) 663.
12. Taylor, W. H. *Nature* **227** (1970) 76.
13. Vesterberg, O. *Biochim. Biophys. Acta* **257** (1972) 11.
14. Hirsch-Marie, H., Burtin, P. and Conte, M. *Acta Gastro-Enterol. Belg.* **28** (1965) 373.
15. Vesterberg, O. and Svensson, H. *Acta Chem. Scand.* **20** (1966) 820.
16. Vesterberg, O. In Renoz, M. *Proc. VII Symp. Chromatogr. and Electrophoresis*, Presses Académiques Européennes, Brussels 1973.
17. Polonovski, M., Boulanger, P., Macheboef, M. and Roche, J. *Biochemie médicale*, 5° éd., Masson, Paris 1952, Vol. 1, p. 299.
18. Bovey, F. A., Yanarig, S. S. In *The Enzymes*, Academic 1960, Vol. 4, p. 63.
19. Jonsson, M. *Acta Chem. Scand.* **26** (1972) 3435.

Received February 28, 1973.

ACTA CHEMICA SCANDINAVICA 27 (1973) 2421–2425

Synthesis and Electrophilic Bromination of 2-Methyl-9-carbethoxy-1,3,4,7-tetraazacycl[3.3.3]azine

OLOF CEDER and KENNETH ROSÉN

Department of Organic Chemistry, University of Göteborg and Chalmers Institute of Technology, Fack, S-402 20 Göteborg, Sweden

The synthesis of the 1,3,4,7-tetraazacycl[3.3.3]azine, *7*, is described. Electrophilic bromination of this compound occurs in position 6.

The condensation between equimolar amounts of 2,4-diaminopyrimidine, *1*, and ethyl 2-cyano-3-ethoxyacrylate, *2*,[1] can occur either at the 2- or 4-amino group. In the first case the recently reported[2] 1,3,6,7-tetraazacycl-azine *8* (*cf.* Chart 1) is eventually formed and in the second the isomeric system *7* should finally result. The present communication describes the synthesis, proof of structure, and electrophilic bromination of 2-methyl-9-carbethoxy-1,3,4,7-tetraazacycl[3.3.3]azine, *7*, along with spectral studies on *7* and its 6-bromoderivative *9*. The sequence utilized to prepare *7* is the same as the one earlier[2] used to obtain *8*.

Condensation of 2,4-diaminopyrimidine, *1*, with one mol of ethyl 2-cyano-3-ethoxyacrylate, *2*, in refluxing benzene led to a *ca.* 1:3 mixture of *3* and *4*, from which *3* was isolated by fractional crystallization from methanol. The two isomers could not be separated by thin-layer chromatography. The structural proof of *3* is based on the following data. The mass spectrum shows a molecular ion peak at $m/e = 233$ and in the IR spectrum, bands at 2180 (CN), 3200 – 3400 (NH_2), and 1680 cm^{-1} (ester carbonyl) are present. The NMR spectrum displays the expected types of protons (*cf.* Experimental) and it is very similar to the spectrum of *4*.[5] In the spectrum of *3* no evidence for a mixture of geometrical isomers, which is present in the spectrum of *4*, can be discovered.

On acetylation of an aromatic, primary amine, the proton adjacent to the amino group suffers a considerable chemical-shift change.[2,3] This method, earlier used[2] to determine the structure of *4*, was now applied to *3*. In an aminopyrimidine system the above-mentioned change is 97 – 117 Hz (at 60 MHz).[4] The present results are summarized in Chart 1. The shift-changes,

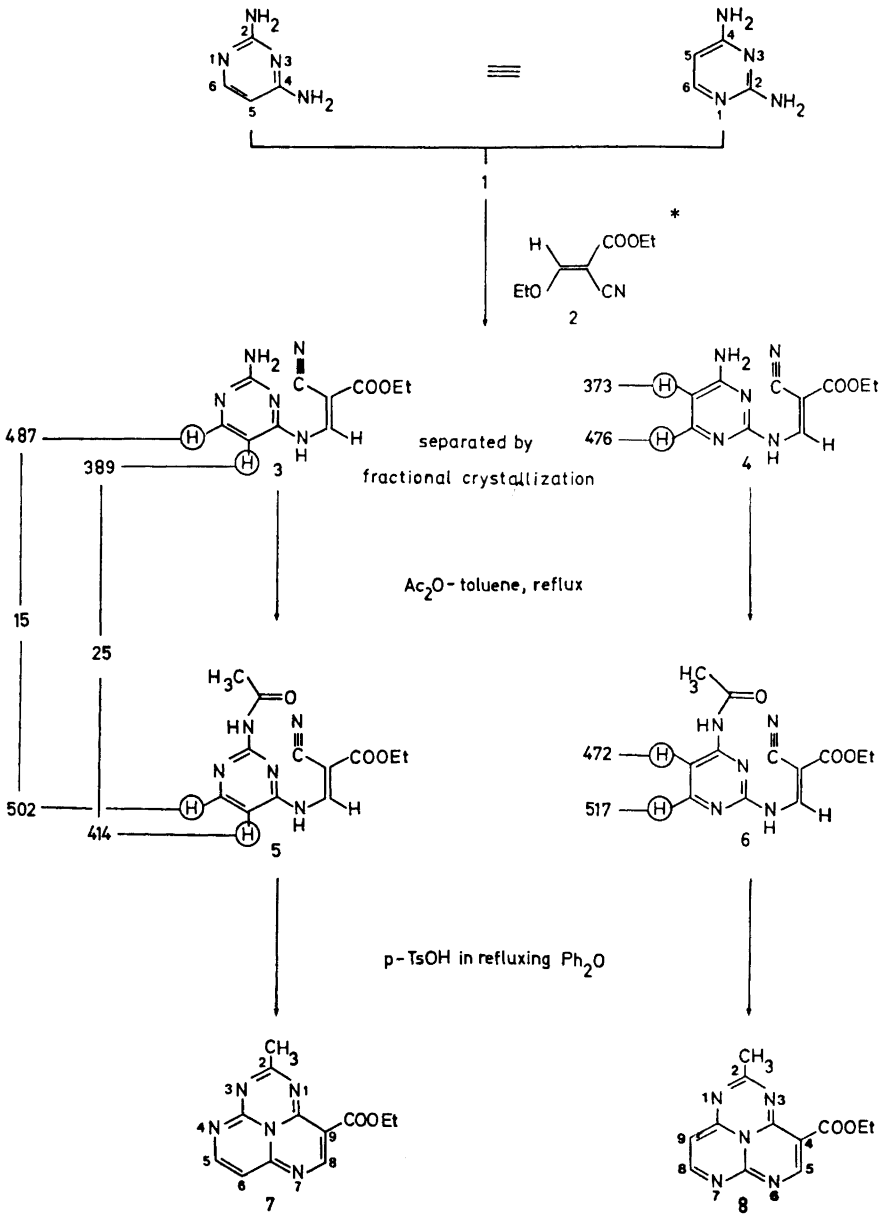

Chart 1. Reaction scheme for the formation of *7* and chemical-shift changes of H-5 and H-6 in *3* and *4* on acetylation. * For configurational assignment of *2*, *cf.* Ref. 2.

25 and 15 Hz for H-5 and H-6, respectively, are in complete accord with structures *3* and *5*.

The final ring closure of *5* to *7* was achieved, as before,[2] in diphenyl ether at 250° in the presence of a catalytic amount of *p*-toluenesulfonic acid. The yield in the last step was 45 %. The deep-red cyclazine *7* has a molecular weight of 257 (MS) and the elemental analyses are in agreement with the molecular formula $C_{12}H_{11}N_5O_2$. The IR spectrum, which lacks amino and cyano absorption, has a carbonyl band at 1638 cm^{-1}. The UV spectrum (*cf.* Experimental) is very similar to the spectrum of *8*.[6] The chemical shifts for the "corresponding" protons in *7* and in *8* are, as would be expected, very similar (*cf.* Table 1). The mass spectra of *7* and *8*[2] show identical fragmentation patterns, including an abundance of doubly-charged ions.

Table 1. Chemical-shift values for the protons in *7* and *8* ($CDCl_3$).

Cpd.	"Corresponding" aromatic protons						CH_3	CH_3-CH_2-O	
7	8.10	(H-8)	7.67	(H-5)	6.12	(H-6)	2.20	1.33,	4.29
8	8.22	(H-5)	7.74	(H-8)	5.75	(H-9)	2.09	1.29,	4.20

Attempts to decarboxylate *7* by the method used to prepare 1,3,6-triazacycl[3.3.3]azine and its 2-methyl homolog [7] from their 4-carbethoxy derivatives (diphenyl ether, traces of *p*-toluenesulfonic acid, 100 – 258°, 1 – 3 h) were not successful, since *7* is unstable under these conditions.

From an argument using resonance structures, one can predict that an electrophile (E) should attack at C-6. For the intermediates resulting from substitution in this position one can draw, in addition to the six resonance forms with the positive charge on carbon atoms as represented by *7a*, three structures with the charge on the central nitrogen atom. These, represented by *7b*, are the only ones where all atoms have full octets. For substitution in position 5, there are four resonance forms with the positive charge on peripheral nitrogen atoms and two with the charge on carbon atoms. In all these forms, represented by *7c*, the atom carrying the charge contains a sextet and no resonance structure with the charge on the central nitrogen atom can be drawn.

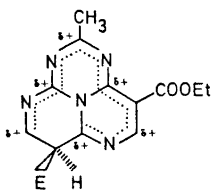

7a

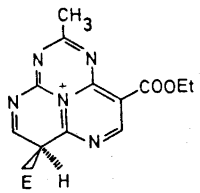

7b

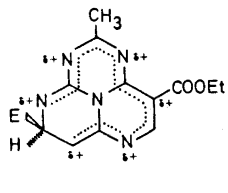

7c

In order to verify the above prediction, *7* was treated with *N*-bromosuccinimide in chloroform at room temperature. A 86 % yield of 6-bromo-9-carbethoxy-2-methyl-1,3,4,7-tetraazacycl[3.3.3]azine, *9*, was obtained. Its mass spectrum shows molecular ion peaks at $m/e = 335$ and 337 (intensity 1:1), which is in agreement with the formula $C_{12}H_{10}N_5O_2Br$. In the NMR spectrum of *7* the H-5 and H-6 signals appear as two doublets centered at 7.67 and 6.12 ppm, respectively. In the spectrum of *9*, the signal at higher field has vanished and the lower-field signal remains as a singlet at 7.96 ppm. Therefore, substitution has occurred at C-6. The H-8 singlet is found at 8.25 ppm.

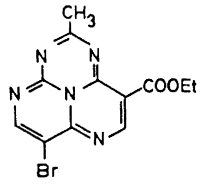

9

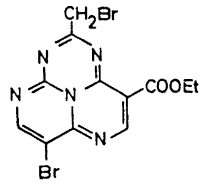

10

There seems to be no significant difference between the strength of the conditions necessary to monobrominate *7* and *8*. The monobromo compound *9* seems to be much more stable than the 9-bromoderivative of its isomer *8*, and it can be handled and stored without any particular precautions. The higher stability of system *7* is also demonstrated by bromination with bromine in glacial acetic acid. In that medium at room temperature, *8* was completely destroyed and no identifiable products could be isolated. The same treatment of *7* at 20° or 50° yielded a blue dibromo compound (molecular ion peaks at 413, 415, and 417, intensities 1:2:1), stable under normal conditions (*cf.* Experimental). This compound also resulted when *9* was treated with bromine in glacial acetic acid as described above. We believe that it has structure *10* since electrophilic bromination is not likely to occur on carbon atoms adjacent to a nitrogen atom (*cf. 7a* and *7c*) and since the corresponding methyl group in the 1,3,6-triazacycl[3.3.3]azine system reacts easily under these conditions.[8]

EXPERIMENTAL

General. Nuclear magnetic resonance (NMR) spectra were recorded with a Varian Model A-60 spectrometer, using tetramethylsilane as internal reference. Ultraviolet and visible spectra were measured in ethanol with a Cary Model 15 spectrophotometer. Mass spectra were determined with a GEC-AEI MS 902 instrument at the Department of Medical Biochemistry, University of Göteborg. Thin-layer chromatography (TLC) was performed on Silica Gel GF_{254} (Merck) according to Stahl and the spots were visualized by means of short-wave ultraviolet light. For column chromatography, silica gel (0.05 – 0.2 mm; Merck), and neutral aluminium oxide (Fluka) were used.

Condensation of 2,4-diaminopyrimidine with ethyl 2-cyano-3-ethoxyacrylate. To a suspension of 8.8 g (0.08 mol) of 2,4-diaminopyrimidine, *1*, in 1 l of benzene was added 13.5 g (0.08 mol) of ethyl 2-cyano-3-ethoxyacrylate, *2*. The reaction mixture was heated under reflux for 72 h. After cooling to room temperature, the reaction mixture was filtered to remove a small amount of brown, solid material and the benzene was evaporated under reduced pressure. The solid residue was dissolved in boiling methanol, cooled in an ice bath and the precipitate (of *4*) then formed was removed by filtration.

The mother liquor was evaporated under reduced pressure and the remaining solid was washed with cold methanol to remove traces of starting material. This evaporation-washing procedure was repeated three times. After drying at 70°/2 torr, 1.7 g (9 %) of yellow, solid *3*, m.p. 184 – 186°, showing one spot on TLC (EtOAc; $R_F = 0.63$) was obtained. IR (KBr): 3200 – 3400 (NH), 2180 (CN), 1680 (C=O) cm^{-1}; NMR (dimethyl sulfoxide-d_6): doublet ($J = 5$ Hz) at 8.08 (1 H, H-6), doublet ($J = 5$ Hz) at 6.45 (1 H, H-5), vinyl singlet at 9.02 and NH absorption at 6.58 ppm; MS: *m/e* 233 (M^+). No NMR signals arising from compound *4* were detectable.

Acetylation of 3 to 5. A suspension of 1.0 g (0.004 mol) of *3* in 70 ml of *p*-xylene and 3 ml of acetic anhydride was heated under reflux for 24 h. The resulting solution was allowed to cool to room temperature and the white, crystalline solid, which had precipitated, was separated by filtration. Yield: 0.6 g of pure *5* (51 %). NMR (dimethyl sulfoxide-d_6): broad NH at 10.10 (2 H), vinyl singlet at 9.01 (1 H), doublet ($J = 5$ Hz) at 8.33 (1 H, H-6), doublet ($J = 5$ Hz) at 6.88 (1 H, H-5), quartet at 4.20 (2 H, CH_2), singlet at 2.22 (3 H, CH_3), and triplet at 1.26 (3 H, CH_3) ppm. MS: *m/e* 275 (M^+).

Cyclization of 5 to 7. To a solution of 210 mg of *5* in 30 ml of refluxing diphenyl ether was added 5 mg of *p*-toluenesulfonic acid. The solution immediately became deeply red-brown. Refluxing was continued for 15 min. The now turbid reaction mixture was allowed to cool to room temperature, and was then poured on to a column of 8 g of aluminium oxide, packed in petroleum ether. A red band was eluted with 250 ml of chloroform. The eluate containing this material was collected and evaporated under reduced pressure to yield 90 mg (45 %) of a deep-red solid, m.p. 157 – 159°. The NMR spectrum ($CDCl_3$), IR, and mass spectral data are reported above. UV: λ_{max} at 221 ($\varepsilon = 13\,900$), 236 ($\varepsilon = 10\,150$), 315 ($\varepsilon = 12\,050$), 337 ($\varepsilon = 15\,720$), 348 ($\varepsilon = 13\,200$), 492 ($\varepsilon = 490$), 521 ($\varepsilon = 744$), and 556 ($\varepsilon = 639$). (Found: C 55.96; H 4.58; N 27.03. Calc. for $C_{12}H_{11}N_5O_2$: C 56.03; H 4.31; N 27.22).

Bromination of 7 with NBS. A solution of 40 mg of *7* and 90 mg of *N*-bromosuccinimide in 8 ml of chloroform was stirred at *ca.* 25°. The formation of *9* was followed by TLC (EtOAc; $R_F = 0.27$). After 30 h, all starting material had been converted to *9*. The volume of the reaction solution was reduced to *ca.* 5 ml under reduced pressure and succinimide and unreacted NBS were then removed by filtration. The filtrate was poured on to a column of silica gel (2.5 × 25 cm) and the product was eluted with 150 ml of chloroform-ethyl acetate (1:3). Yield: 45 mg (86 %). Mass and NMR spectral data are reported above.

Bromination of 7 with bromine in glacial acetic acid. To a solution of 5 mg of *7* in 0.5 ml of glacial acetic acid was added a solution of 7 mg of bromine in 0.2 ml of glacial acetic acid. The mixture was allowed to stand at room temperature and the reaction was followed by analytical TLC (EtOAc). A blue-violet band appeared and after 4 h the acetic acid was removed *in vacuo* and the brown residue was applied on to a preparative silica-gel plate, which was developed in ethyl acetate. The blue-violet band was scraped off and extracted with chloroform. MS: *m/e* 413, 415, and 417 (M^+, intensity 1:2:1), in agreement with the composition $C_{12}H_9N_5O_2Br_2$.

Acknowledgements. Financial support from the *Swedish Natural Science Research Council* and a fellowship (to K. R.) from *Stiftelsen Bengt Lundqvists Minne* are gratefully acknowledged. We thank Prof. C. L. Perrin for constructive discussions and Miss Gun Myrne for technical assistance.

REFERENCES

1. Ceder, O. and Stenhede, U. *Tetrahedron* **29** (1973) 1585.
2. Ceder, O. and Witte, J. F. *Acta Chem. Scand.* **26** (1972) 635.
3. Ceder, O., Andersson, J. E. and Johansson, L. E. *Acta Chem. Scand.* **26** (1972) 624.
4. For model studies, *cf.* pp. 638 – 639 in Ref. 2.
5. *Cf.* p. 636 in Ref. 2.
6. *Cf.* p. 640 in Ref. 2.
7. Ceder, O. and Andersson, J. E. *Acta Chem. Scand.* **26** (1972) 596.
8. Ceder, O. and Samuelsson, M. L. *Acta Chem. Scand.* **B 28** (1974). *In press.*

Received March 22, 1973.

ACTA CHEMICA SCANDINAVICA 27 (1973) 2426–2430

Analytical Isotachophoresis in Capillary Tubes Used for the Separation of Ions Involved in the Enzymatic Transformation of Glucose to 6-Phosphogluconate

ANN KOPWILLEM

LKB-Produkter AB, Fack, S-161 25 Bromma 1, Sweden

The ions involved in the enzymatic transformation of glucose to 6-phosphogluconate have been separated by means of analytical isotachophoresis. The reactants and the reaction products simultaneously analysed were ATP, ADP, $NADP^+$, NADPH, glucose-6-phosphate, and 6-phosphogluconate. Nanomol quantities of these ions were separated within 30 min. Detection of the sample ions was done with a thermal and a UV-detector.

A two-step enzymatic reaction, the transformation of glucose to 6-phosphogluconate, has been chosen as a model system to demonstrate the separability of some biochemically important ions by isotachophoresis in capillary tubes. The method gives qualitative as well as quantitative information about the ion species involved. A great number of reactants and reaction products can be followed simultaneously, *e. g.* ATP, ADP, $NADP^+$, NADPH, glucose-6-phosphate, and 6-phospho-gluconate. Nanomol quantities of these ions were analysed in 30 min. In addition to the compounds mentioned a number of impurities were also found. No pre-treatment, *i.e.* deproteinization or concentration of the sample, was necessary. Previously, isotachophoresis has also been used for the separation of nucleotides in capillary tubes [1] and for the separation of glucose metabolites on thin layer.[2–3]

In isotachophoresis, as in all electrophoretic separation methods, the ion species migrate in an electric field. In contrast to ordinary electrophoresis, the sample ions, when the steady state is reached, migrate with the same velocity and form zones according to their electrophoretic mobilities. In isotachophoresis, the electrolyte system consists of a leading electrolyte, containing a leading ion with a mobility higher than that of the sample ions and a terminating electrolyte, containing a terminating ion with a lower mobility than that of the sample ions. The leading electrolyte also contains a counter-ion, generally buffering, which migrates into the terminating electrolyte, and thus is common to both electrolytes. A constant current is applied to the system

creating a discontinuous electric field and the sample ions separate and form zones of constant concentrations. In the steady state, the electric field rises step-wise at each zone boundary. A high electric field in a sample zone is associated with a low mobility of the sample ion and *vice versa*. In isotachophoresis, the boundaries between the sample zones remain sharp due to the high and discontinuous electric field.

The concentration and pH in the sample zones are regulated by the concentration and mobility of the leading ion and the pH in the leading electrolyte. The separability of the sample ions is based on the differences in their net mobilities. The net mobility is defined as: ionic mobility × degree of dissociation. It is therefore pH-dependent. Consequently, the net mobility of the sample ion is dependent on the pH in the leading electrolyte.

A more detailed theoretical treatment of isotachophoresis is given by Haglund [4] in a review, which also contains different applications.

EXPERIMENTAL

The capillary apparatus used in this investigation was the LKB 2127 Tachophor (LKB-Produkter AB, Bromma 1, Sweden). The separations took place in a 62 cm long, teflon capillary with 0.5 mm I. D., which was kept at a constant temperature of 19°C. The apparatus [5] was equipped with a thermal detector, which was also used in a differential manner, and with a UV-detector set at 254 nm.

The ATP and glucose were obtained from British Drug Houses Ltd., Poole, Dorset, U.K. $NADP^+$ was purchased from Boehringer und Söhne, Mannheim, Germany, as well as the enzyme preparation containing both hexokinase and glucose-6-phosphate dehydrogenase activity. In all incubation mixtures the enzyme was present in a final dilution of 1:30.

Two series of experiments were carried out. First, a 1.2 mM glucose solution was transformed to glucose-6-phosphate in the presence of ATP (3 mM). In the second series, glucose (2 mM) was transformed to 6-phosphogluconate in the presence of ATP (3 mM) and $NADP^+$ (1 or 3 mM). All experiments were performed in triethanolammonium chloride buffer (24 – 36 mM) at pH 7.5. The incubation mixtures were kept at 25°C for at least 10 min to complete the reactions. The reaction products were then stoichiometrically formed. 5 µl samples were used for analytical isotachophoresis in all experiments. The quantities of the ion species are given in the figure texts.

The leading electrolyte consisted of 0.01 M chloride with different amounts of β-alanine as a counter-ion, giving varying pH-values in the leading electrolyte. The terminating electrolyte was 0.01 M caproic acid. The experiments were run at a constant current of 100 µA for about 30 min. The voltage increased from 4 kV at the beginning to 23 kV at the end of the experiment.

RESULTS AND DISCUSSION

Fig. 1 shows the thermal step-heights of the ions to be separated at different pH-values of the leading electrolyte. The thermal step-height is a measure of the net mobility [6–8] and thus also separability.

In the separation of the ions involved in the transformation of glucose to glucose-6-phosphate the pH in the leading electrolyte was 3.8, whereas in the separation of the ions present in the two-step enzymatic reaction, the leading electrolyte pH was 4.2 in order to ensure full separation.

Results of separations of different mixtures of ions are shown in Figs. 2 and 4. The curves with sharp peaks in Fig. 2 (bottom) are the differential

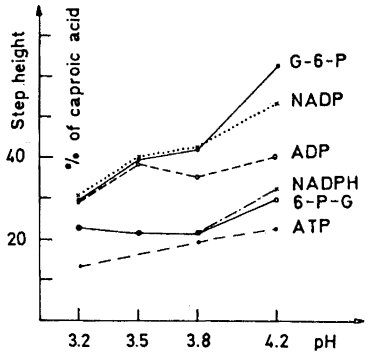

Fig. 1. Thermal step-heights of the ions involved in the enzymatic transformation of glucose to 6-phosphogluconate related to the step-height of the terminator, caproic acid, as a funtion of pH in the leading electrolyte.

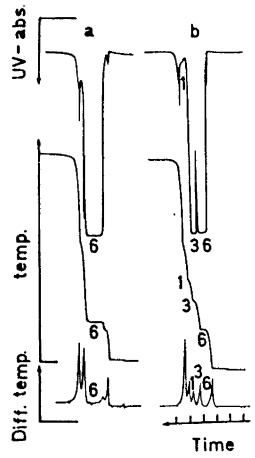

Fig. 2. Separation of ATP (zone 6), ADP (zone 3) and glucose-6-phosphate (zone 1). Leading electrolyte was 0.01 M HCl and 0.027 M β-alanine. (pH = 3.8). Terminator was 0.01 M caproic acid. UV-absorption (254 nm), thermal and differentiated thermal detectors were used.
Sample ions were: (a) ATP 15 nmol; (b) ATP 9 nmol, ADP 6 nmol, G-6-P 6 nmol.

temperature recordings. The distance between two peaks is easily measured from this type of curves. This distance is proportional to the zone length in the capillary tube. Since the concentration of an ion is uniform throughout its zone, quantitative determination of an ionic species can be made by simply measuring the length of the zones. The curves with steps in Fig. 2 (intermediate position) are the temperature recordings. The step-height is a function of the net mobility of the isotachophoretically moving ion in the corresponding zone. The UV-recordings in Fig. 2 (top) show, in addition to the nucleotide peaks of more or less rectangular shape a number of small peaks of different shapes. These small peaks represent UV-absorbing impurities either in the leading or terminating electrolyte or in the sample. For reference a sample containing no glucose is separated (Fig. 2a), where in addition to the ATP (6) zone of 15 nmol, the first low thermal step that occurs is derived from the sulphate ions in the enzyme solution. Another reproducible non-UV-absorbing zone comes from the impurities in the counter-ion, β-alanine. This zone can be seen following the ATP zone on all detector signals. The UV detector also resolves another three UV-absorbing impurities, which are separated by less UV-absorbing components.

The enzymatic consumption of ATP and glucose is seen in Fig. 2b by the occurrence of the glucose-6-phosphate (1) and ADP (3) zones and also from the decreased ATP (6) zone length. The zone lengths are directly related to the quantities of the ions involved in separation (Fig. 3). The UV detector signals

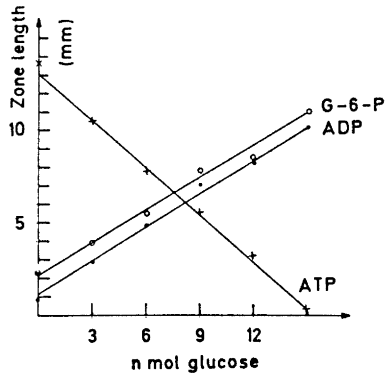

Fig. 3. The zone length (mm) of ATP, ADP, and glucose-6-phosphate as a function of initial glucose quantity in the reaction mixtures. Initial quantity of ATP was 15 nmol. Chart speed 10 mm/min.

were used to measure the zone lengths. Since the glucose-6-phosphate zone was measured together with the impurities in β-alanine up to the well-defined UV-peak (Fig. 2), the zone length function did not pass the origin. Similarly, the ADP zone length is enlarged due to the UV-absorbing zone following the ATP zone (Fig. 2a).

In the separation including $NADP^+$ used in the transformation of glucose-6-phosphate to 6-phosphogluconate, a large UV-absorbing impurity is present in front of $NADP^+$ (Fig. 4a). This impurity can be followed as the UV-absorbing peak following the 6-phosphogluconate (5) zone (Figs. 4b and 4c).

Figs. 4b and 4c show the separation of ions involved in the two-step enzymatic reaction, where glucose (10 nmol), ATP (15 nmol) and $NADP^+$ (5, 15 nmol) react with the enzymes. The reaction products, glucose-6-phos-

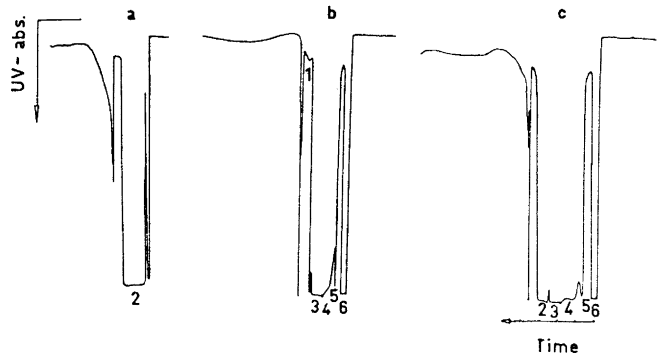

Fig. 4. Separation of glucose-6-phosphate (zone 1), $NADP^+$ (zone 2), ADP (zone 3), NADPH (zone 4), 6-phosphogluconate (zone 5), and ATP (zone 6). Leading electrolyte was 0.01 M HCl and 0.055 M β-alanine (pH = 4.2). Terminator was 0.01 M caproic acid. UV-absorption (254 nm) was measured.
Sample ions were: (a) $NADP^+$ 15 nmol; (b) G-6-P 5 nmol, ADP 10 nmol, NADPH 5 nmol, 6-P-G 5 nmol, ATP 5 nmol; (c) $NADP^+$ 5 nmol, ADP 10 nmol, NADPH 10 nmol, 6-P-G 10 nmol, ATP 5 nmol.

phate (1), ADP (3), NADPH (4), and 6-phosphogluconate (5), and the reactants ATP (6) and $NADP^+$ (2), are separable and recognizable as distinct zones. In addition to the compounds mentioned, a number of impurities are found, which act as markers of the zone boundaries. In fact, each predicted sample zone is surrounded by impurities. This can be most useful when two adjoining zones have the same UV-adsorption (*e.g.* zones 2 and 3 in Fig. 4c).

Acknowledgements. I am greatly indebted to Tekn. Lic. L. Arlinger and to Fil. lic. A. Vestermark for stimulating discussions. Dr. A. Vestermark is also acknowledged for initiating this investigation. Many thanks are due to Mr. H. Lundin for skilfull technical assistance.

REFERENCES

1. Beckers, J. L. and Everaerts, F. M. *J. Chromatogr.* **71** (1972) 380.
2. Vestermark, A. and Sjödin, B. *J. Chromatogr.* **71** (1972) 588.
3. Vestermark, A. and Sjödin, B. *J. Chromatogr.* **73** (1972) 211.
4. Haglund, H. *Sci. Tools* **17**, No. 1 (1970) 2.
5. Arlinger, L. In Peeters H., Ed., *Protides of Biological Fluids* **19** (1971) 513.
6. Kaimakov, E. A. and Sharkov, V. I. *Russian J. Phys. Chem.* **38** (1964) 893.
7. Martin, A. J. P. and Everaerts, F. M. *Anal. Chim. Acta* **38** (1967) 233.
8. Konstantinov, B. P. and Oshurkova, O. V. *Sov. Phys. Techn. Phys.* **12** (1968) 1280.

Received March 9, 1973.

ACTA CHEMICA SCANDINAVICA 27 (1973) 2431–2440

Thermodynamic Properties of Rare Earth Complexes

XVIII. Free Energy, Enthalpy, and Entropy Changes for the Formation of Some Lanthanoid Thiodiacetate and Hydrogen Thiodiacetate Complexes

INGEMAR DELLIEN, INGMAR GRENTHE and GUNNEL HESSLER

Division of Physical Chemistry 1, Chemical Center, University of Lund, P.O.B. 740, S-220 07 Lund 7, Sweden

The changes in free energy, enthalpy and entropy for the formation of Ce, Pr, Sm, Tb, Er, and Yb thiodiacetate and hydrogen thiodiacetate complexes with the compositions MA, MA_2, MHA and MHA_2 have been determined. The changes in free energy were calculated from stability constants, obtained from a potentiometric determination of the concentration of free hydrogen ion, using a glass electrode. The enthalpy values were measured calorimetrically. The measurements were performed at 25.0°C in an aqueous sodium perchlorate medium with the total sodium ion concentration equal to 1.00 M.

The possible formation of a complex MA_3 has been investigated in the praseodymium and ytterbium systems, using 4.00 M $Na(ClO_4)$ as ionic medium.

The changes in thermodynamic functions such as ΔG_j°, ΔH_j°, and ΔS_j° for the formation of lanthanoid(III)-complexes usually do not follow the monotonic dependence on the size of the metal ion as is suggested by simple electrostatic models of bonding. This non-monotonic size dependence is not a consequence of differences in electron configuration, as all the tervalent rare earth ions have a "noble gas" like configuration of the outer electron shells. Hence, one should try to base models which describe the observed size specificity in the complexation reactions on factors such as the size of the central ion, the geometrical requirements of the ligand, and the coordination of solvent molecules to the species participating in the complex formation reactions.

The coordinated donor atoms in the ligands may be described as forming a cavity, the size of which depends on the size of the central ion and the way in which the donor atoms are interconnected in the ligand. In general, one must expect that a coordinated ligand can not be arranged as freely as the solvent molecules in the coordination shell. Hence, the cavities formed by the coor-

dinated donor atoms in multidentate ligands cannot contract to the same extent as the cavities formed by the coordinated solvent molecules as the size of the metal ion decreases. The resulting differences in the geometry of the coordination spheres will give rise to a size specificity in the complexation reactions.

In previous parts of this series we have reported thermodynamic data for complexation reactions in aqueous solution between rare earths and the terdentate ligands 2,6-pyridinedicarboxylate (=dipicolinate[1]), iminodiacetate,[2] and oxydiacetate.[3] They all form stable chelates with a maximum of three ligands coordinated in each case, presumably giving rise to ninecoordinated complexes in solution. The variations through the rare earth series of the thermodynamic quantities are also very similar, *e.g.* the pronounced difficulty for the third complex to be formed for the central ions with the smallest ionic radius. The observed similarities are probably due to a similar coordination geometry for the three ligands, as judged from the structures of solids containing the complexes.[4,5]

We have extended the previous investigations to include the terdentate ligand thiodiacetate, which contains a sulphur atom as the third donor atom. As the rare earths are typical *a*-acceptors and thus have a much smaller affinity to sulphur than to nitrogen and oxygen, a substantial decrease in stability is expected for the thiodiacetate complexes as compared to those with nitrogen and oxygen donors.

The radius of the sulphur atom is about 30 % larger than the radii of nitrogen and oxygen. Sulphur atoms in the equatorial plane of a tricapped trigonal prism, which is the most common coordination polyhedron in solid rare earth complexes are, because of their size, expected to be closer to one another than the equatorial atoms in the dipicolinate, iminodiacetate and oxydiacetate complexes. Thus, purely geometrical constraints might give an additional decrease in stability for the higher thiodiacetate complexes.

In systems containing polyprotic acids and their conjugate bases, the possibility of complex formation with all these various ligands must be kept in mind. This will lead to an increased difficulty in the interpretation of the experimental data, especially when the concentration of free ligand can not be measured directly. Acid complexes have been found only for the iminodiacetate systems,[2] a fact that undoubtedly is due to the high basicity of iminodiacetate as compared to the other ligands. Thiodiacetate has very nearly the same base strength as oxydiacetate. On the other hand, the expected decrease in stability of the thiodiacetate complexes ought to increase the possibility for acid complexes to appear in noticeable amounts.

Because of the similarity in geometry of oxydiacetate, iminodiacetate, dipicolinate, and thiodiacetate, it is expected that they will interact in a similar way with a given lanthanoid ion. The pronounced similarities in the variations of the ΔH_j° and ΔS_j° values through the lanthanoid series for the oxydiacetate, iminodiacetate, and dipicolinate complexes can thus be expected to include also the thiodiacetate complexes.

This study of lanthanoid thiodiacetates has been undertaken mainly in order to obtain quantitative information about the coordinating ability of various donors in rare earth complexes of similar geometry. Measurements have

been performed in solutions with a high concentration of hydrogen thiodiacetate ion in order to get information concerning the formation of acid complexes. The changes in ΔG_j°, ΔH_j° and ΔS_j° have been determined for six lanthanoid ions, *viz.* Ce^{3+}, Pr^{3+}, Sm^{3+}, Tb^{3+}, Er^{3+}, and Yb^{3+}, which should give sufficient information on the variation pattern of these properties across the lanthanoid series. The stability constants have been calculated from potentiometric determinations of the concentration of free hydrogen ion by means of a glass electrode. The various enthalpies of complexation have been determined calorimetrically. Most data refer to a temperature of 25.0°C and an aqueous sodium perchlorate medium with the sodium ion concentration equal to 1.00 M. However, in order to obtain information on the possible formation of a third complex, accurate experimental data at high ligand concentrations are needed. This is not easy, as changes in the composition of the medium will cause changes in the activity coefficients of the reacting species and/or the appearance of diffusion potentials in the emf measurements. In order to minimize these effects and get as accurate emf-data as possible, even at high concentrations of the ligand, stability constants for the praseodymium and ytterbium systems have also been measured in 4.00 M $NaClO_4$.

NOTATIONS AND CALCULATIONS

The notations have been defined previously.[2,8]

The stability constants and enthalpy values have been calculated from the experimentally determined values of (v/ml, E/mV) and (v/ml, Q_{corr}/J), respectively, by the least-squares procedures "Etiter" and "Kalle" in the "Letagrop" series.[6,7] The proton thiodiacetate system has also been treated with standard graphical procedures.

EXPERIMENTAL

Chemicals used. A stock solution of cerium perchlorate was prepared by dissolving cerium(III) nitrate (BDH, 99 %) in perchloric acid, precipitating the cerium as carbonate and redissolving the precipitate in perchloric acid. The other metal perchlorate solutions were prepared and analyzed as described before.[8] Thiodiacetic acid (Schuchard, 98 %) was purified with active charcoal and recrystallized twice from water. The purity was checked by alkalimetric titration and the formula weight was found to be 150.4 (calc. 150.1).

The various buffers were obtained by mixing the appropriate amounts of solutions of thiodiacetic acid and sodium hydroxide. The sodium ion concentration was adjusted to 1.00 M (or 4.00 M, respectively) by addition of sodium perchlorate solution.

Potentiometric measurements. The equipment and experimental procedure in the potentiometric measurements were the same as described earlier.[8]

The protonation constants of the thiodiacetate ion were determined in solutions with $C_M = 0$ and with different, constant values of C_A. In 1 M $Na(ClO_4)$, these values of C_A were equal to 20 mM, 40 mM, and 100 mM, respectively. For the corresponding measurements in 4 M $Na(ClO_4)$, the C_A-values were 50 mM, 100 mM, and 200 mM, respectively.

About six titration series have been made on each of the lanthanoid thiodiacetate systems, using solutions with different compositions. A wide concentration range with respect to thiodiacetate and hydrogen thiodiacetate ion must be covered in order to get solutions containing measurable amounts of the various complexes. The ratio C_H/C_A in the different solutions varied from 2 to 1/10, and the total metal ion concentration varied from 8 mM to 35 mM. Table 1 shows the compositions of the solutions used for the measurements on the terbium system.

Table 1. Experimental results of the potentiometric measurements on the terbium system. The results are given as v/ml, E/mV, $\bar{n}_H$, $(\bar{n}_{H,calc} - \bar{n}_{H,exp}) \times 10^3$. The sodium ion concentration is 1.00 M in all solutions. Approximately one half of the experimental data are given.

Series 1. S: $C_H = 0.00068$ M, $C_M = 0.03184$ M, $C_A = 0$; T: $C_H = 0.06098$ M, $C_M = 0$, $C_A = 0.1906$ M; $V_0 = 20.00$ ml, $E_0 = 361.1$ mV.

0.900, 147.9, *0.369*, 1.21; 1.400, 145.3, *0.353*, 2.53; 2.500, 141.1, *0.340*, 5.42; 3.900, 136.4, *0.333*, 6.80; 5.300, 132.1, *0.330*, 6.80; 6.800, 127.9, *0.328*, 4.65; 8.500, 123.9, *0.327*, 1.97; 10.60, 120.1, *0.325*, −0.18; 13.60, 116.0, 0.324, −4.47; 17.00, 112.9, *0.323*, −7.46; 22.00, 109.8, *0.323*, −11.88; 28.00, 107.6, *0.322*, −14.32; 35.00, 105.9, *0.322*, −16.89;

Series 2. S: $C_H = 0.05061$ M, $C_M = 0.01990$ M, $C_A = 0.02509$ M; T: $C_H = 0.00064$ M, $C_M = 0.01990$ M, $C_A = 0.05018$ M; $V_0 = 20.00$ ml, $E_0 = 361.5$ mV.

0.0, 226.1, *1.812*, −1.18; 0.400, 221.2, *1.774*, −1.19; 0.800, 216.6, *1.732*, −1.77; 1.300, 211.5, *1.677*, −1.22; 1.800, 206.9, *1.622*, −2.70; 2.500, 201.5, *1.545*, −2.63; 3.200, 196.9, *1.473*, −3.28; 4.100, 191.9, *1.388*, −4.16; 5.200, 186.8, *1.295*, −5.02; 6.500, 181.8, *1.198*, −5.09; 8.000, 117.0, *1.103*, −3.90; 10.00, 171.6, *0.997*, −3.12; 12.10, 166.8, *0.905*, −2.64; 14.60, 161.9, *0.816*, −2.43; 17.70, 156.8, *0.727*, −0.83; 21.20, 151.8, *0.648*, −1.03; 25.40, 146.8, *0.573*, 0.48; 30.20, 141.9, *0.507*, 1.14; 36.00, 136.9, *0.445*, 1.88;

Series 3. S: $C_H = 0.1405$ M, $C_M = 0.01990$ M, $C_A = 0.07005$ M; T: $C_H = 0.00064$ M, $C_M = 0.01990$ M, $C_A = 0.05018$ M; $V_0 = 20.00$ ml, $E_0 = 361.5$ mV.

0.0, 234.7, 1.865, 0.02; 0.600, 229.3, 1.834, 0.46; 1.150, 224.7, 1.803, 0.77; 1.800, 219.8, 1.764, 1.30; 2.550, 214.8, 1.717, 1.44; 3.400, 209.9, 1.664, 1.27; 4.400, 205.0, 1.603, 1.09; 5.600, 200.0, 0.07; 7.100, 194.9, 1.455, 0.82; 8.800, 189.9, 1.373, −1.58; 10.90, 184.9, 1.284, −0.95; 13.40, 179.9, 1.191, −0.49; 16.40, 174.8, 1.095, −1.11; 20.00, 169.6, 0.999, −2.60; 24.00, 164.9, 0.910, −0.27; 29.00, 159.8, 0.819, −0.02; 35.20, 154.5, 0.729, 0.52;

Table 2. Experimental results of the calorimetric measurements on the terbium system. Corresponding values of v/ml, $Q_{corr,exp}$/J and $(Q_{corr,calc} - Q_{corr,exp}) \times 10^3$/J are given. The sodium ion concentration is 1.00 M in all solutions.

Series 1. S: $C_H = 0.000417$ M, $C_M = 0.02023$ M, $C_A = 0$; T: $C_H = 0.05870$ M, $C_M = 0$, $C_A = 0.2660$ M; $V_0 = 79.98$ ml.

1.000, 3.008, 50; 3.000, 5.886, 16; 5.000, 5.112, 12; 7.000, 4.326, −46; 9.000, 3.518, −42; 11.00, 2.824, −46; 13.00, 2.255, −42; 15.00, 1.585, 181; 17.00, 1.426, −8; 19.00, 1.100, 55;

Series 2. S: $C_H = 0.000417$ M, $C_M = 0.02023$ M, $C_A = 0$; T: $C_H = 0.05870$ M, $C_M = 0$, $C_A = 0.2660$ M; $V_0 = 79.98$ ml.

2.000, 6.054, 46; 4.000, 5.497, 29; 6.000, 4.723, −12; 8.000, 3.945, −76; 10.00, 5.150, −34; 12.00, 2.531, −55; 14.00, 1.995, −20; 16.00, 1.548, 29; 18.00, 1.246, 29; 20.00, 1.033, 12;

Series 3. S: $C_H = 0.2441$ M, $C_M = 0$, $C_A = 0.2374$ M; T: $C_H = 0.000417$ M, $C_M = 0.02023$ M, $C_A = 0$, $V_0 = 79.98$ ml.

1.000, 0.397, 16; 3.000, 0.790, 29; 5.000, 0.811, 4; 7.000, 0.803, 8; 9.000, 0.820, −16; 11.00, 0.774, 20; 13.00, 0.782, 4; 15.00, 0.799, −16; 17.00, 0.765, 8; 19.00, 0.761, 8;

Series 4. S: $C_H = 0.2441$ M, $C_M = 0$, $C_A = 0.2374$ M; T: $C_H = 0.000417$ M, $C_M = 0.02023$ M, $C_A = 0$; $V_0 = 79.98$ ml.

2.000, 0.832, −8; 4.000, 0.811, 8; 6.000, 0.824, −12; 8.000, 0.815, −8; 10.00, 0.757, 41; 12.00, 0.807, −12; 14.00, 0.794, −8; 16.00, 0.753, 25; 18.00, 0.728, 41; 20.00, 0.728, 37;

Series 5. S: $C_H = 0.000417$ M, $C_M = 0.02023$ M, $C_A = 0$; T: $C_H = 0.2441$ M, $C_M = 0$, $C_A = 0.2374$ M; $V_0 = 79.98$ ml.

3.000, 3.631, −25; 5.000, 2.096, 0; 7.000, 2.058, −134; 9.000, 1.962, −205; 11.00, 1.594, 4; 13.00, 1.489, −29; 15.00, 1.347, −20; 17.00, 1.171, 29; 19.00, 1.117, −25;

Series 6. S: $C_H = 0.000417$ M, $C_M = 0.02023$ M, $C_A = 0$; T: $C_H = 0.2441$ M, $C_M = 0$, $C_A = 0.2374$ M; $V_0 = 79.98$ ml.

2.000, 2.464, 71; 4.000, 2.196, −4; 6.000, 1.987, 25; 8.000, 1.849, −12; 10.00, 1.707, −33; 12.00, 1.460, 64; 14.00, 1.384, 4; 16.00, 1.280, −16; 18.00, 1.167, −20;

For the measurements in 4 M $Na(ClO_4)$, only one buffer solution with the ratio C_H/C_A equal to 1/5 was used, and three titration series were made for each system. A precipitate with the composition $M_2A_3.nH_2O$ is formed during the titration, but it was dissolved if T solution was added in excess at once.

Calorimetric measurements. The measurements were performed as titrations in the same way as described earlier.[9]

The heats of protonation of thiodiacetate ion were determined by titrating a disodium thiodiacetate solution with perchloric acid.

In order to determine the enthalpies of formation of the various lanthanoid-thiodiacetate complexes, titration series have been made with solutions of the following types:

Metal perchlorate solutions were titrated with thiodiacetate buffers with the ratio C_H/C_A equal to 1 or 1/4. In the third type of titration, a hydrogen thiodiacetate solution was titrated with a metal perchlorate solution.

The different solutions used for the measurements on the terbium system are given in Table 2. Most of the titrations were repeated once. The heats of dilution of the various T solutions were determined in separate experiments and were found to be negligible.

RESULTS

Determination of the stability constants

Measurements in 1 M $Na(ClO_4)$. A least-squares treatment of $(\bar{n}_H, h)$--data gave the following values of the two protonation constants of the thiodiacetate ion.

$$\beta_{0,1,1} = (9.84 \pm 0.10) \times 10^3 \text{ M}^{-1}$$
$$\beta_{0,2,1} = (1.34 \pm 0.01) \times 10^7 \text{ M}^{-2}$$

(The errors given above and in the following are equal to three standard deviations). The standard deviation in $\bar{n}_H$ was equal to 2.7×10^{-3}, and 102 experimental points were used in the calculation.

The constants vary somewhat with C_A; $\beta_{0,1,1}$ thus increased with approx. 1 % as C_A is increased from 20 mM to 40 mM. This variation might be caused by an uncompensated liquid junction potential.

Some experimental values of $\bar{n}^*$ *vs.* $-\log(a^*/\text{M})$ for the praseodymium thiodiacetate system are shown in Fig. 1 (a). The fact that different curves are obtained in titrations with different values of the ratio C_H/C_A, clearly indicates that complexes of the composition $M_pH_qA_r$ with $q > 0$ are formed.

The curves obtained at C_M equal to 19 mM and 35 mM are very nearly the same, indicating that polynuclear species are not formed in appreciable amounts. Since the highest value of $\bar{n}^*$ is 1.5, complexes with at least two ligands per metal ion must be formed, but no conclusions can be drawn about the existence of a third complex.

It is not possible in these systems to determine directly from experimental data the stoichiometry of the complexes formed; neither can standard graphical procedures be used. Instead, the results of using different "probable" models have been calculated.

In the first model, which was based on the results presented in Fig. 1 (a) the following assumptions were made:

i. Two binary complexes with the compositions MA and MA_2 are formed.
ii. One acid complex, *viz.* MHA, is formed.
iii. Polynuclear species are not formed.

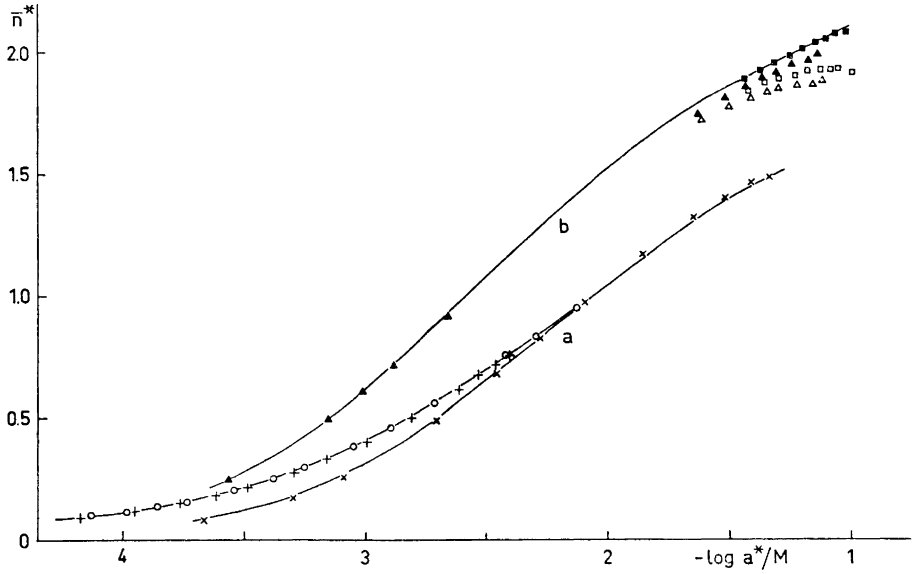

Fig. 1. Experimental $\bar{n}^*$ *vs.* $-\log (a^*/\mathrm{M})$ values for the praseodymium thiodiacetate system. *a.* Results from the measurements in 1 M $Na(ClO_4)$. The curves have been calculated with the constants given in Table 3. *b.* Results from the measurements in 4 M $Na(ClO_4)$. The curve is calculated with the constants given in Table 5. Values of $\bar{n}^*$ and $-\log (a^*/\mathrm{M})$ have been calculated for two titration series with different values of the protonation constant $\beta_{0,1,1}$; *viz.*

Series 1 ($V_0 = 10$ ml) $\beta_{0,1,1} = 3.93 \times 10^4$/M (■), $\beta_{0,1,1} = 3.74 \times 10^4$/M (□)
Series 2 ($V_0 = 20$ ml) $\beta_{0,1,1} = 3.84 \times 10^4$/M (▲), $\beta_{0,1,1} = 3.66 \times 10^4$/M (△)

		Solution S			Solution T		
		C_H/mM	C_M/mM	C_A/mM	C_H/mM	C_M/mM	C_A/mM
	○	122	19	60	1	19	60
a.	+	122	35	60	2	35	60
	×	0.7	15	0	42	15	181
b.	△ □	2	42	0	57	21	277

The calculated stability constants were positive and the standard deviation in C_H/C_A was equal to 7.75×10^{-3}. (The figures refer to the terbium system).

There is no reason to include the complex MA_3 in the calculations, but the possible presence of other acid complexes, *viz.* MHA_2 or MH_2A_2, has been investigated. The results are:

$\beta_{1,1,2} = (1.98 \pm 0.36) \times 10^7$ M^{-3}; *sig* $C_H/C_A = 4.48 \times 10^{-3}$
$\beta_{1,2,2} = (2.3 \pm 0.8) \times 10^9$ M^{-4}; *sig* $C_H/C_A = 6.90 \times 10^{-3}$

From these values of the stability constants, it is found that $\alpha_{1,1,2}$ amounts to 0.05 – 0.10 in some solutions, while $\alpha_{1,2,2}$ is always less than 0.01 in the solutions studied.

The possible presence of binuclear complexes M_2A and M_2HA has also been tested. These species did not improve the over-all description of the experimental data, *i.e.* the standard deviation in C_H/C_A was not lowered and the corresponding stability constants were zero or negative.

Thus, it can be concluded that the species MH_2A_2, M_2A, and M_2HA are not present in any significant amounts, if at all, in the solutions studied.

From the experimental data, stability constants for the formation of the complexes MA, MA_2, MHA, and MHA_2 have been calculated. The stability constants with their estimated errors are given in Table 3. Some of the experimental data for the terbium system are given in Table 1.

Table 3. Stability constants for the lanthanoid thiodiacetate systems studied. The errors are equal to three standard deviations.

Metal ion	Number of points	*sig* C_H/C_A	$\beta_{1,0,1} \times 10^{-2}$ M	$\beta_{1,0,2} \times 10^{-4}$ M^2	$\beta_{1,1,1} \times 10^{-5}$ M^2	$\beta_{1,1,2} \times 10^{-7}$ M^3
Ce	92	6.08×10^{-3}	4.53 ± 0.11	3.07 ± 0.22	2.30 ± 0.24	4.6 ± 1.2
Pr	140	5.08×10^{-3}	5.55 ± 0.17	2.43 ± 0.17	2.81 ± 0.21	4.4 ± 0.9
Sm	169	4.56×10^{-3}	8.01 ± 0.31	4.80 ± 0.24	3.91 ± 0.23	6.6 ± 1.3
Tb	110	4.48×10^{-3}	3.30 ± 0.06	1.33 ± 0.06	1.61 ± 0.11	1.98 ± 0.36
Er	120	4.07×10^{-3}	2.30 ± 0.030	0.704 ± 0.030	1.38 ± 0.07	1.61 ± 0.22
Yb	120	5.56×10^{-3}	2.30 ± 0.037	0.576 ± 0.038	1.25 ± 0.10	1.87 ± 0.30

It is assumed that the values of the protonation constants remain the same when $C_M \neq 0$ as when $C_M = 0$. This assumption was tested for the terbium system. When the protonation constants were varied with the other constants, the standard deviation in C_H/C_A was lowered from 4.48×10^{-3} to 4.01×10^{-3}, but the constants calculated in this way agreed, within the limits of error, with those given in Table 3. It can be concluded that any systematic variation of the protonation constants with C_M and C_A is less than the error limits given.

Measurements in 4 M Na(ClO_4). The protonation constants of the ligand must be accurately known if reliable values of $\bar{n}$ and a are to be obtained.

Table 4. The protonation constants of thiodiacetate ion in 4.00 M $Na(ClO_4)$, calculated for each experimental C_A-value separately.

C_A / mM	Number of points	$\beta_{0,1,1} \times 10^{-4}$ M	$\beta_{0,2,1} \times 10^{-8}$ M^2	*sig* (C_H/C_A)
50	69	3.66 ± 0.014	1.664 ± 0.010	1.37×10^{-3}
100	76	3.74 ± 0.012	1.668 ± 0.006	0.99×10^{-3}
200	77	3.95 ± 0.011	1.784 ± 0.006	1.02×10^{-3}

Table 4 shows the protonation constants, calculated for each experimental C_A-value separately. The increase in $\beta_{0,1,1}$ with C_A must be taken into account in the calculation of the stability constants.

For each of the praseodymium and ytterbium systems, about 30 experimental points were determined. If the presence of acid complexes is neglected in the calculations, the calculated values of the concentration of free ligand, a, and the ligand number, $\bar{n}$, are incorrect and will be denoted a^* and $\bar{n}^*$, respectively (*cf.* Ref. 8). From these ($\bar{n}^*$, a^*)-values "stability constants", β_j^*, are obtained, which are smaller than the true constants. However, the ratio $\beta_j^{*2}/(\beta_{j+1}^*\beta_{j-1}^*)$ should give a good estimate of the ratio of the stepwise stability constants, K_j/K_{j+1}. Hence, we have estimated the magnitude of the ratio K_2/K_3 from the experimental ($\bar{n}^*$, a^*)-values. For each titration series, two sets of ($\bar{n}^*$, a^*)-values have been calculated, using two different values of $\beta_{0,1,1}$. These values correspond to the smallest and largest value of C_A, respectively, which were used during the titration in the region where $\bar{n}^*$ is greater than 1.6. From the "upper limit" of ($\bar{n}^*$, a^*)-values thus obtained, the lower limit of the ratio K_2/K_3 is estimated. For the praseodymium system, experimental values of ($\bar{n}^*$, $-\log a^*/\mathrm{M}$) are shown in Fig. 1 (b), together with the $\bar{n}^*$ *vs.* $-\log (a^*/\mathrm{M})$ curve from which the lower limit of K_2/K_3 has been estimated. The ytterbium system was treated in a similar way. Table 5 gives the results and a comparison with the values obtained in 1 M $Na(ClO_4)$.

Table 5. Stability constants for the formation of the non-acid complexes MA_j and the ratios of the stepwise stability constants, determined in 1 M ($Na(ClO_4)$) and 4 M $Na(ClO_4)$, respectively.

Metal ion	Medium: 1.00 M $Na(ClO_4)$			Medium: 4.00 M $Na(ClO_4)$				
	$\beta_{1,0,1}$ M	$\beta_{1,0,2}$ M^2	K_1/K_2	$\beta^*_{1,0,1}$ M	$\beta^*_{1,0,2}$ M^2	$\beta^*_{1,0,3}$ M^3	K_1^*/K_2^*	K_2^*/K_3^*
Pr	5.55×10^2	2.43×10^4	12.7	1.10×10^3	1.4×10^5	3×10^5	8.7	60
Yb	2.296×10^2	5.76×10^3	9.2	7.0×10^3	5.4×10^4	8×10^4	9.1	51

A "Letagrop" calculation with the acid complexes included gave the same value of K_2/K_3 as the procedure described above.

Determination of the enthalpy values

The following values for the heats of protonation of the thiodiacetate ion were obtained:

$$\Delta H^\circ_{0,1,1} = (1.82 \pm 0.11) \text{ kJ mol}^{-1}$$
$$\Delta H^\circ_{0,2,1} = (1.36 \pm 0.15) \text{ kJ mol}^{-1}$$

The standard deviation in Q_{corr} was 0.10 J and 19 experimental points were measured.

The changes in free energy and entropy for the formation of the proton-thiodiacetate complexes at 25.0°C are:

$\Delta G^\circ_{0,1,1} = (-22.79 \pm 0.02)$kJ mol^{-1}
$\Delta G^\circ_{0,2,1} = (-40.68 \pm 0.02)$kJ mol^{-1}
$\Delta S^\circ_{0,1,1} = (82.5 \pm 0.4)$ J K^{-1} mol^{-1}
$\Delta S^\circ_{0,2,1} = (140.9 \pm 0.6)$ J K^{-1} mol^{-1}

The heats of formation of the various rare earth thiodiacetate complexes, calculated with the least-squares procedure, are given in Table 6. The standard deviations in the individual measurements, *sig* Q_{corr}, are of the magnitude expected from the precision of the calorimetric equipment.

Table 6. The overall values of ΔH°, ΔG°, and ΔS° for the lanhtanoid thiodiacetate systems studied. The enthalpy values are tabulated with their estimated maximum errors, equal to three standard deviations. The standard deviation *sig* Q_{corr} in the measured Q_{corr} values and the number of experimental points in the calorimetric titrations are also given. The ΔH° and ΔG°-values have been divided with kJ mol^{-1}, the ΔS°-values with J K^{-1} mol^{-1}.

	Ce	Pr	Sm	Tb	Er	Yb
$\Delta H^\circ_{1,0,1}$	12.80 ± 0.29	12.16 ± 0.45	11.38 ± 0.12	17.20 ± 0.39	20.96 ± 0.33	22.38 ± 0.18
$\Delta G^\circ_{1,0,1}$	−15.15	−15.65	−16.57	−14.39	−13.47	−13.47
$\Delta S^\circ_{1,0,1}$	93.7	93.3	93.7	105.9	115.5	120.1
$\Delta H^\circ_{1,0,2}$	20.29 ± 0.45	19.7 ± 1.1	20.63 ± 0.24	26.3 ± 0.8	33.1 ± 0.8	36.1 ± 0.5
$\Delta G^\circ_{1,0,2}$	−25.61	−25.03	−26.69	−23.56	−21.97	−21.46
$\Delta S^\circ_{1,0,2}$	154	150	159	167	185	193
$\Delta H^\circ_{1,1,1}$	8.5 ± 1.3	6.4 ± 2.6	5.4 ± 0.6	12.9 ± 2.6	15.3 ± 2.3	14.7 ± 1.1
$\Delta G^\circ_{1,1,1}$	−30.59	−31.09	−31.92	−29.71	−29.33	−29.08
$\Delta S^\circ_{1,1,1}$	131	126	125	143	150	147
$\Delta H^\circ_{1,1,2}$	15.7 ± 2.5	16 ± 5	14.5 ± 1.5	20 ± 6	25.2 ± 3.8	26.6 ± 1.6
$\Delta G^\circ_{1,1,2}$	−43.7	−43.6	−44.6	−41.6	−41.1	−41.5
$\Delta S^\circ_{1,1,2}$	200	200	198	207	222	228
sig Q_{corr}/J	0.045	0.082	0.023	0.066	0.053	0.027
Number of points	58	57	48	58	57	59

DISCUSSION

The stability constants for the lanthanoid thiodiacetate complexes are considerably smaller than those for the corresponding oxydiacetate,[3] dipicolinate,[1] or iminodiacetate [2] complexes. In the oxydiacetate complexes, two five-membered chelate rings are formed, which makes these complexes stronger than the corresponding oxalate complexes. The thiodiacetate complexes are even weaker than those formed with the bidentate malonate ion.[8] One can thus safely conclude that sulphur is a much poorer donor than oxygen in this case.

For the oxydiacetates and dipicolinates there is an increased difficulty for the third complex to be formed as the ionic radius of the lanthanoid decreases, as judged from the variation of the ratio K_2/K_3 of the stepwise stability constants. This ratio increases from 30 for the light lanthanoids to more than 100 for ytterbium and lutetium. Scandium does not form any third complex at all with these ligands. A comparison with the thiodiacetates is made difficult by the experimental problems in determining the stability constant of a third complex. However, the values given above show that the ratio K_2/K_3 is larger

than 60 for the thiodiacetates, *i.e.* it is indeed difficult for the third complex to be formed. The values of the ratio K_1/K_2 are about 10, which shows that there is no problem in forming the second complex. This ratio has also very nearly the same value as for the corresponding oxydiacetates. These findings indicate that the larger radius of the sulphur atom makes the formation of a third thiodiacetate complex difficult even for the lanthanoid ions with the largest ionic radii. The magnitude of the stepwise stability constant K_3 is small. This indicates that the ligand in the third complex, if this complex is formed at all, is bound only to one carboxylate group.

The stability constants for the complexation with the protonated ligand, *i.e.* $M+HA \rightleftharpoons MHA$, are in the range $12-40$ M^{-1} for the thiodiacetates, which is of the same order of magnitude as for the malonates.[8] For the hydrogen malonates, the strength of the acid MHA increases when the metal ion becomes smaller. This was described as due to an increased electrostatic repulsion between the central ion and the bonded proton when the size of the metal ion decreased. A similar result is not found for the hydrogen thiodiacetates, for which pK_a for MHA is roughly constant through the rare earth series. The larger distance between the carboxylate groups in the thiodiacetate ion as compared with the malonate ion might be an explanation for this finding.

The low stability of the thiodiacetates is mainly an enthalpy effect, whereas the entropy term is of the same order of magnitude as for the oxydiacetates. The variation pattern of the function ΔH_1° *vs.* Z and ΔS_1° *vs.* Z are very similar for the thiodiacetates, oxydiacetates,[10] dipicolinates,[10] and iminodiacetates.[2] It is reasonable to assume that these geometrically similar dicarboxylate ligands cause approximately the same changes in the hydration shell of a given metal ion, at least on the formation of the first complex. This will roughly account for the similarities in the entropy changes.

Acknowledgement. This work has been sponsored by grants from the *Swedish Natural Research Council* and *Kungl. Fysiografiska Sällskapet* in Lund.

REFERENCES

1. Grenthe, I. *J. Am. Chem. Soc.* **83** (1961) 360.
2. Grenthe, I. and Gårdhammar, G. *Acta Chem. Scand.* **26** (1972) 3207.
3. Grenthe, I. and Tobiasson, I. *Acta Chem. Scand.* **17** (1963) 2101.
4. Albertsson, J. *On the stereochemistry of nine-coordinate lanthanoid compounds*, Diss., Lund 1972.
5. Malmborg, T. and Oskarsson, Å. *To be published.*
6. Arnek, R., Sillén, L. G. and Wahlberg, O. *Arkiv Kemi* **31** (1969) 353.
7. Arnek, R. *Arkiv Kemi* **32** (1970) 81.
8. Dellien, I. and Grenthe, I. *Acta Chem. Scand.* **25** (1971) 1387.
9. Dellien, I. *Acta Chem. Scand.* **27** (1973) 733.
10. Grenthe, I. *Acta Chem. Scand.* **17** (1963) 2487.

Received March 7, 1973.

ACTA CHEMICA SCANDINAVICA 27 (1973) 2441–2454

Structural Studies on the Rare Earth Carboxylates

17. The Crystal and Molecular Structure of Hexa-aquo Tris-malonato Di-neodymium(III) Dihydrate

EVA HANSSON

Physical Chemistry 1, Chemical Center, University of Lund, P.O. Box 740, S-220 07 Lund 7, Sweden

The crystal and molecular structure of $Nd_2(C_3H_2O_4)_3.8H_2O$ has been determined from three-dimensional, photographic, X-ray intensity data. The crystals are orthorhombic with $a = 11.258(3)$ Å, $b = 12.602(3)$ Å, and $c = 14.689(3)$ Å. $Z = 4$. The space group is *Pbcn*. The structure is a three-dimensional neodymium-malonate network. Each neodymium ion is coordinated by six carboxylate and three water oxygens which form a monocapped square antiprism. The Nd – O bonds are in the range 2.41 – 2.72 Å. There are two independent malonate ions in the structure. They are both nonplanar. One of them has strict twofold symmetry and is bonded to four neodymium ions by six Nd – O bonds, *i.e.* two of its oxygens form two Nd – O bonds each. The other malonate ion forms a six-membered chelate ring with neodymium and one bridge of the type Nd – OCO – Nd. The chelate ring has boat conformation. The water molecules are hydrogen bonded with O – O distances in the range 2.63 – 2.85 Å.

Thermodynamic studies of the lanthanoid oxalate and malonate complexes formed in solution [1,2] show that the five-membered chelate ring of the oxalate complexes is more stable than the six-membered ring of the malonate complexes. Further a maximum of four oxalate groups are coordinated to the lanthanoids while the corresponding number of malonate groups is three. Knowledge of the structures of some related solid compounds would facilitate the understanding of these differences.

The structures of some lanthanoid oxalates, $M_2ox_3.nH_2O$ (M = lanthanoid, $ox = C_2O_4^{2-}$) have been reported previously.[3,4,5] The oxalate ions form planar five-membered chelate rings with the lanthanoids with a ligand bite, *i.e.* intra-ring distance between the two donor atoms, of about 2.65 Å.

The ligand bite of the malonate ion depends on its conformation and with normal bond distances and angles it may range from about 2.5 Å for a completely planar ion to about 3.5 Å when the carboxylate groups are twisted 90° out of the plane of the three carbon atoms. The only X-ray study of coor-

dinated malonate ions previously reported deals with malonate complexes of Co(III) and Cr(III).[6] The malonate ions in these complexes form six-membered chelate rings and are nonplanar with bites larger than 2.65 Å.

The compounds $M_2mal_3.nH_2O$ ($mal = CH_2(COO)_2^{2-}$) were chosen for a X-ray structure analysis in order to determine the conformation of the malonate ion when coordinated to the lanthanoids and to study the resulting coordination geometry around the lanthanoid ion. Azikov *et al.*[7] have studied the IR-spectra of these solids. Their interpretation of the spectra indicates the presence of six-membered chelate rings in the complexes.

The lanthanoid malonates, $M_2mal_3.nH_2O$, can be divided into three different isostructural groups; one with $n = 8$ and M = Ce – Gd (referred to as octahydrate type I below), another with $n = 6$ and M = Ce – Eu, and a third type with $n = 8$ and M = Eu – Lu (octahydrate type II). This paper deals with the structure of $Nd_2(CH_2(COO)_2)_3.8H_2O$ (NDO). The two other structure types will be reported in following communications.

EXPERIMENTAL

Preparation. The lanthanoid malonates, $M_2mal_3.nH_2O$, were precipitated from solutions of the various lanthanoid chlorides (10 mM) and malonic acid (15 mM) with the pH adjusted to about 5 by the addition of 0.1 M sodium hydroxide. Slow evaporation at room temperature resulted in the octahydrate type I for the elements Ce – Gd and the octahydrate type II for the elements Tb – Lu. The octahydrate type II with M = Eu and Gd were obtained by evaporation under a heating lamp. The hexahydrates with M = Ce – Eu form at low temperature (5°C) but also by chance at higher temperatures, *e.g.* $Nd_2mal_3.6H_2O$ has been obtained at 70°C.

The compounds $Nd_2mal_3.8H_2O$ (type I), $Nd_2mal_3.6H_2O$, and $Eu_2mal_3.8H_2O$ (type II) were analysed for M, C, and H with the following results (%):

		M	C	H
$Nd_2mal_3.8H_2O$	Found	39.1	14.6	3.2
	Calc.	39.0	14.6	3.0
$Nd_2mal_3.6H_2O$	Found	41.1	15.1	2.6
	Calc.	40.9	15.3	2.6
$Eu_2mal_3.8H_2O$	Found	40.5	14.9	3.2
	Calc.	40.2	14.3	2.9

The different phases of the other lanthanoid malonates were then identified by their X-ray powder patterns. When precipitated from the solutions described the crystals of the various phases are also easily recognized by their habits. The crystals of the octahydrates are orthorhombic; thick tabular (001) bounded by the faces {001}, {010}, and {110} for type I and acicular elongated *b* for type II, while the hexahydrate crystals are monoclinic and thick tabular (001) bounded by the faces {001}, {010}, and {100}.

All the hexahydrates and the octahydrates type II with M = Eu and Gd are transformed to octahydrate type I when stored in the mother liquor at room temperature for a long time (sometimes more than two years). Thus the octahydrate type I is the stable phase for M = Ce – Gd under these conditions.

X-Ray diffraction work. A crystal of the dimensions $0.22 \times 0.13 \times 0.13$ mm³ mounted along the 0.22 mm edge was used in recording the layers $0kl - 14kl$, with the integrated, Weissenberg, multi-film technique. Zr-filtered Mo-radiation was used. The intensities of 1876 independent reflexions were measured visually by comparison with a calibrated scale. 1390 of these reflexions were within the copper sphere representing 53 % of the possible number.

The intensities were corrected for the Lorentz, polarisation and absorption effects. The linear absorption coefficient, μ, is 50 cm^{-1} and the transmission factors, evaluated by numerical integration, were in the interval 0.54 – 0.61.

The powder photographs were taken at room temperature in a Guinier-Hägg focusing camera with Cu$K\alpha$-radiation ($\lambda = 1.54178$ Å). Lead nitrate (cubic $a = 7.857$ Å) was used as internal standard.

UNIT CELL AND SPACE GROUP

The crystals of NDO are orthorhombic with $a = 11.258(3)$ Å, $b = 12.602(3)$ Å, and $c = 14.689(3)$ Å and $Z = 4$. The accurate values of the cell parameters were determined from powder data by least squares refinement, as described in Ref. 5. The observed values of $\sin^2 \theta$ are compared with those calculated in the last cycle of refinement in Table 1.

Table 1. Powder data for $Nd_2(C_3H_2O_4)_3.8H_2O$. Observed and calculated values of $10^5 \sin^2 \theta$ are given together with the observed powder intensities.

h k l	obs	calc	I_{obs}	*h k l*	obs	calc	I_{obs}
1 1 0	847	843	s	1 4 2	7576	7558	w
0 0 2	1101	1102	vs	2 4 0	7861	7863	w
1 1 1		1119		4 1 1	8161	8152	m
0 2 0	1499	1497	w	3 2 3		8196	
2 0 0	1880	1876	w	4 0 2	8609	8604	w
1 1 2	1948	1945	m	3 3 2	8687	8690	vw
1 2 1	2237	2241	vs	1 2 5	8885	8853	m
2 1 1	2523	2525	s	2 4 2	8990	8965	m
2 0 2	2972	2978	w	4 2 0		8999	
1 2 2	3063	3068	vvw	2 1 5	9118	9137	vvw
2 2 0	3370	3372	w	0 0 6	9923	9918	vw
2 2 1	3645	3648	w	4 1 3		10356	
0 0 4	4446	4408	s	1 0 6	10384	10387	m
1 2 3		4445		0 4 4		10395	
2 2 2	4595	4594	w	1 1 6	10770	10761	w
2 1 3	4732	4729	m	4 0 4	11888	11910	vw
1 0 4	4868	4877	w	3 3 4	11992	11996	vw
1 3 2	4930	4939	w	2 3 5	12121	12131	s
1 1 4	5246	5251	s	3 2 5	12607	12604	vw
2 3 1	5514	5519	s	0 6 0		13471	
3 1 2	5699	5696	s	4 4 0	13487	13490	s
2 2 3	5846	5852	vw	5 2 1		13495	
0 4 0	5994	5987	m	3 5 0	13572	13575	w
3 2 1		5992		2 5 3	13719	13710	vw
1 4 1	6731	6732	vw	1 3 6		13755	
3 2 2	6816	6819	vw	1 6 1	14210	14216	m
0 4 2	7082	7089	s	1 5 4		14232	
4 0 0	7510	7502	w				

Weissenberg photographs show the systematic absences $0kl$: $k \neq 2n$, $h0l$: $l \neq 2n$ and $hk0$: $h + k \neq 2n$ and thus the only possible space group is $Pbcn$ (No. 60).[8]

DETERMINATION AND REFINEMENT OF THE STRUCTURE

The structure was determined by the heavy atom method. The position of neodymium was obtained from a three-dimensional Patterson synthesis and a subsequent difference electron density calculation revealed the positions of the remaining 15 non-hydrogen atoms.

The preliminary atomic coordinates and isotropic temperature factors together with the inter layer scale factors were improved by full-matrix least squares refinement. The quantity minimized was $\sum w(|F_o| - |F_c|)^2$ with

Table 2. Analysis of the weighting scheme $w = 1/(40 + |F_o| + 0.005|F_o|^2 + 0.0001\ |F_o|^3)$. The averages $\overline{w\Delta^2}$, where $\Delta = |F_o| - |F_c|$, are normalized.

Interval $\|F_o\|$	Number of reflexions	$\overline{w\Delta^2}$	Interval sin θ	Number of reflexions	$\overline{w\Delta^2}$
0 – 40	155	0.84	0.00 – 0.28	322	0.94
40 – 46	174	0.96	0.28 – 0.35	289	0.98
46 – 49	171	0.97	0.35 – 0.40	242	0.90
49 – 54	176	0.96	0.40 – 0.44	201	0.94
54 – 61	177	1.08	0.44 – 0.48	188	0.97
61 – 71	179	0.95	0.48 – 0.51	166	0.98
71 – 85	184	0.99	0.51 – 0.53	108	0.95
85 – 103	181	0.97	0.53 – 0.56	74	0.77
103 – 140	182	1.09	0.56 – 0.58	59	1.41
140 – 423	171	1.19	0.58 – 0.60	40	1.17

Table 3. Atomic parameters with estimated standard deviations for the compound $Nd_2(H_2C_3O_4)_3.8H_2O$.

Atom	Group	$x \times 10^4$	$y \times 10^4$	$z \times 10^4$	B/Å^2
Nd		1491.7(6)	1134.3(5)	74.1(3)	(1.37)[a]
O(1)	COO^-	1038(12)	850(10)	1750(8)	2.8(2)
O(2)	COO^-	−167(9)	−88(8)	911(7)	2.1(2)
O(3)	COO^-	2199(10)	−697(9)	307(7)	2.4(2)
O(4)	COO^-	3147(12)	−2155(11)	752(8)	3.1(2)
O(5)	COO^-	3545(11)	1162(9)	604(7)	2.7(2)
O(6)	COO^-	5343(15)	711(13)	952(10)	4.1(3)
O(7)	H_2O	−515(10)	2028(9)	188(6)	2.4(2)
O(8)	H_2O	1368(16)	2403(11)	−1195(9)	3.7(2)
O(9)	H_2O	2780(12)	662(10)	−1242(8)	2.9(2)
O(10)	H_2O	3551(17)	2565(10)	−1958(10)	4.3(3)
C(1)		0	−527(18)	1/4	2.2(3)
C(2)		325(13)	131(11)	1675(9)	2.0(2)
C(3)		3032(12)	−1160(12)	764(8)	1.8(2)
C(4)		3855(18)	−494(16)	1362(13)	3.3(3)
C(5)		4295(17)	546(15)	966(11)	2.8(3)

[a] The anisotropic thermal parameters for neodymium, calculated from the expression: $\exp -(h^2\beta_{11} + 2hk\beta_{12} + ...)$ are $\beta_{11} = 0.00269(6)$, $\beta_{22} = 0.00186(5)$, $\beta_{33} = 0.00185(3)$, $\beta_{12} = 0.00007(4)$, $\beta_{13} = 0.00005(2)$, and $\beta_{23} = -0.00000(2)$, resulting in root mean square displacements along the principal axis of the thermal ellipsoid $R_1 = 0.142$ (Å), $R_2 = 0.122$ (Å), and $R_3 = 0.132$ (Å).

Table 4. Observed and calculated structure factors in $Nd_2(C_3H_2O_4)_3.8H_2O$. In each group the running index l, $|F_o|$, and $|F_c|$ are given. The 126 reflexions not obeying the condition $0.80 \leq |F_o|/|F_c| \leq 1.25$ are denoted by asterisks.

H=-14 K= 0
2 63 1164
4 81 109*
6 81 84
8 90 93
10 78 75
12 56 53
14 47 49

H=-14 K= 1
1 21 41*
3 33 48*
5 44 51
7 39 44
9 40 35

H=-14 K= 2
2 21 27*
9 35 29
11 34 33
15 45 39

H=-14 K= 3
1 30 47*
3 37 48*
5 46 50
7 41 44
9 38 40
11 39 37

H=-14 K= 4
0 89 104
2 87 105
4 82 95
6 87 88
8 69 73
10 59 61
12 64 60
14 53 50
16 48 36*

H=-14 K= 5
1 30 28

H=-14 K= 6
0 58 53
2 47 43
4 42 40
6 45 38
8 40 36
9 42 34

H=-14 K= 7
1 42 47
3 48 51
5 50 54
7 53 52
9 48 41

H=-14 K= 8
0 76 74
2 71 75
4 70 68
6 54 63
8 48 54
10 55 53
12 45 42

H=-14 K= 10
0 47 44
2 56 56
4 49 52
6 50 46
8 48 42
10 46 36*

H=-14 K= 11
1 50 50
3 46 46
5 47 46
7 53 46

H=-14 K= 12
0 48 47
2 48 41
4 49 42

H=-14 K= 14
0 57 55
2 57 51
4 52 49
6 53 45

H=-13 K= 1
0 48 103*
2 63 107*
4 71 102*
6 61 77*
8 80 84
10 64 68
11 39 38
12 48 58
14 57 51
16 48 36*

H=-13 K= 2
1 29 50*
3 35 49*
5 29 37*
7 40 41
9 42 42
11 33 29

H=-13 K= 3
0 51 74*
2 47 67*
4 52 59
6 54 62
8 44 48
9 46 38
10 45 50
11 52 46
12 49 46
13 40 37
14 38 33
15 51 39*

H=-13 K= 5
0 118 117
2 111 115
4 103 111
6 92 104
8 85 90
10 79 77
12 61 69
14 56 51
16 50 37*

H=-13 K= 6
1 54 48
3 53 50
5 48 50
7 36 39

H=-13 K= 7
2 31 32
9 41 42
11 48 44
13 51 45
15 46 39

H=-13 K= 9
0 98 103
2 99 106
4 93 91
6 92 81
8 68 78
10 79 78
12 57 61
14 55 53
16 49 38*

H=-13 K= 11
13 47 35*

H=-13 K= 13
0 72 81
2 51 74*
4 79 71
6 69 70
8 71 63
10 56 54
12 53 49

H=-13 K= 17
0 54 55
2 59 52
4 50 51
6 55 46
8 51 42

H=-12 K= 1
1 39 76*
2 18 15
3 62 99*
4 29 35
5 79 92
7 100 97
8 32 30
9 77 82
10 51 51
11 64 58
12 40 41
13 42 49
14 43 41
15 45 40
16 56 48
18 46 35*

H=-12 K= 3
1 76 105*
3 91 137*

H=-12 K= 4
2 27 32
4 36 34
6 47 46

H=-12 K= 5
1 71 75
3 41 48
5 48 55
6 32 33
7 57 52
8 50 52
9 48 46
10 55 58
11 41 41
12 46 50
14 50 47
16 54 47
18 52 44

H=-12 K= 7
1 112 131
3 133 124
5 107 113
7 114 120
9 104 105
11 86 80
13 71 64
15 49 49
17 52 40*

H=-12 K= 8
0 38 30*
2 35 37

H=-12 K= 9
12 47 44
14 60 50
16 53 45

H=-12 K= 11
1 104 100
3 101 99
5 113 103
7 98 96
9 89 84
11 75 64
13 47 49
15 49 43

H=-12 K= 15
1 81 75
3 65 70
5 72 71
7 68 66
9 53 56
11 50 52

H=-12 K= 19
5 52 45

H=-11 K= 0
4 59 49
10 48 50
12 53 53

H=-11 K= 1
0 37 80*
2 61 98*
4 79 97
6 84 90
8 66 93
9 38 33
10 52 58
12 53 49

H=-11 K= 2
1 83 157*
3 124 144
5 97 109
7 92 101
9 92 99
11 86 83
13 73 74
15 61 58

H=-11 K= 3
0 61 76
2 60 68
4 50 56
6 36 42
8 53 54
10 45 48

H=-11 K= 4
1 48 52
3 45 47
8 54 53
9 40 35
10 51 49

H=-11 K= 5
0 67 72
2 89 94
4 91 96
6 80 78
8 87 78
10 68 67
12 52 52
14 52 45

H=-11 K= 6
1 124 120
3 117 116
5 105 106
7 87 87
9 73 76
11 67 73
13 66 62

H=-11 K= 8
6 126 126
7 32 27
8 103 103
9 34 27
10 90 79
11 36 33
12 65 68
14 52 57
15 45 37
16 55 56
18 45 41

H=-10 K= 10
0 101 95
2 99 98
4 110 102
6 97 91
7 38 38
8 85 84
10 58 55
12 51 51
13 41 39
14 46 43
15 47 39
16 44 36
17 45 38

H=-10 K= 12
0 93 82
2 93 86
4 83 81
6 75 77
8 60 62
10 57 55
11 41 31*
12 46 45

H=-10 K= 14
0 97 93
2 82 88
4 95 83
6 72 78
8 65 68
10 56 61
12 53 50
14 50 42

H=-10 K= 18
0 45 67*
2 64 68
4 60 66
6 72 65
8 51 54
10 52 48

H=-10 K= 22
0 53 50
2 53 47
4 49 47
6 49 44

H=-9 K= 0
6 56 56
8 97 96
10 62 68
12 44 44
14 53 51
16 53 46
18 57 53
20 47 55
22 46 43

H=-9 K= 1
2 52 84*
4 64 73
5 33 40
6 94 97
7 26 35*
8 94 91
9 35 35
10 57 56
11 36 37
12 34 35
14 45 54
15 36 35
16 41 40

H=-9 K= 2
1 156 204*
3 188 194
5 149 159
7 100 133*
9 106 115
11 93 105
13 109 100
15 94 82
17 61 57
19 42 38
21 41 25*

H=-9 K= 3
0 70 79
2 70 80
4 67 78
5 33 46*
6 53 52
7 38 34
8 40 55*
9 43 43
10 54 53
11 37 33
12 46 42
13 37 38
15 37 34

H=-9 K= 4
1 33 41
2 33 37
3 59 61
4 47 49
5 65 66
6 41 44
7 51 48
8 38 35
9 26 31
10 71 63
12 66 60
13 32 25*
14 51 47
16 55 55
18 54 46
20 44 42
22 47 42

H=-9 K= 5
0 84 84
2 86 94
4 72 75
6 61 62
8 80 82
10 67 71
12 52 54
14 52 53
16 43 37

H=-9 K= 6
1 175 163
3 151 153
4 28 26
5 141 130
7 122 112
9 102 106
11 86 90
13 79 76
15 69 64
17 49 45

H=-9 K= 7
0 31 33
4 35 37
9 41 33*
11 41 40

H=-9 K= 8
1 93 90
3 90 89
5 65 62
7 62 59
8 54 49
9 66 60
11 42 45
12 40 42
13 49 44
14 47 44
15 44 41

H=-9 K= 9
0 111 90
2 107 92
4 112 106
6 98 83
8 67 71
10 65 61
12 53 55

H=-9 K= 10
1 122 123
3 91 88
5 69 72
7 71 68
9 72 63
11 67 69
13 62 58
15 42 40

H=-9 K= 12
1 100 98
3 85 79
5 73 74
7 58 65
9 60 60
11 63 62
13 55 50

H=-9 K= 13
0 84 79
2 74 74
4 69 67
6 60 64
8 62 52
10 41 48
12 43 41

H=-9 K= 14
1 46 47
3 60 53
5 47 47
7 45 35*

H=-9 K= 16
3 81 76
5 56 65
7 48 59
9 49 55

H=-9 K= 20
1 48 58
3 52 50

H=-8 K= 0
2 23 46*
4 48 62*
6 90 87
8 81 79
10 39 46
12 37 31
14 37 27*
16 44 39

H=-8 K= 1
1 78 154*
3 108 150*
5 90 108
6 25 27
7 151 137
8 35 41
9 116 123
10 47 44
11 66 83
12 52 52
13 70 67
14 62 65
15 55 51
16 48 54
17 46 42
18 48 45
20 47 46

H=-8 K= 2
0 30 44*
2 32 35
3 35 35
7 33 35

H=-8 K= 3
1 214 218
3 185 196
4 23 34*
5 172 176
7 180 162
9 150 157
10 44 44
11 112 113
12 45 44
13 72 79
14 41 40
15 72 62
16 41 42
17 46 44
19 42 39

H=-8 K= 4
0 58 65
2 77 88
4 100 93
6 83 79
8 55 51
10 38 40
12 42 43

H=-8 K= 5
1 36 47*
3 80 76
4 50 57
5 109 110
6 39 37
7 80 71
8 30 28
9 49 54
10 65 67
11 49 54
12 72 72
13 45 45
14 72 72
16 84 73
18 54 51
20 48 44

H=-8 K= 6
0 46 45
4 38 35
6 53 50

H=-8 K= 7
1 167 168
3 204 191
5 172 165
7 176 168
8 51 47
9 155 146
11 107 101
13 85 88
15 74 73
17 59 53
19 48 41

H=-8 K= 8
0 84 74
2 68 70
4 56 48
6 32 44*
8 37 42
10 52 52

H=-8 K= 9
6 44 43
8 60 66
10 59 62
12 48 59
14 51 58
16 55 53
18 58 54

H=-8 K= 10
4 38 32

H=-8 K= 11
1 129 126
3 120 127
5 147 145
7 111 122
9 91 100
11 109 100
13 88 80
15 61 57
17 54 48

H=-8 K= 12
4 42 34

H=-8 K= 13
10 48 46
12 50 49
14 53 45
16 50 44

H=-8 K= 14
2 45 39
4 42 37

H=-8 K= 15
1 94 92
3 87 98
5 96 95
7 99 89
9 72 78
11 75 63
13 50 50

H=-8 K= 19
1 60 64
3 55 54
5 60 56
7 56 53

H=-7 K= 1
0 118 229*
2 135 177*
4 119 140
5 28 27
6 140 133
7 59 66
8 170 168
9 50 42
10 120 149
11 61 63
12 124 121
13 70 59
14 84 82
15 57 54
16 64 64
17 40 40
18 45 45

H=-7 K= 2
1 34 36
2 37 41
3 80 82
4 24 29
6 69 74
7 74 72
8 31 33
9 55 52

H=-7 K= 3
0 104 104
2 124 123
3 49 48
4 130 133
5 54 47
6 143 131
7 65 60
8 96 98
9 94 90
10 77 81
11 89 92
12 63 64
13 75 85
14 66 62
15 82 75
16 46 46
17 53 53
18 39 32
19 47 52

Table 4. Continued.

H= -7 K= 4
1 39 37
3 48 47
4 42 38
5 30 25

H= -7 K= 5
0 206 194
2 229 208
4 206 210
6 206 200
8 190 183
9 48 46
10 144 143
12 185 175
14 101 96
16 80 75
17 45 31*
18 40 52*

H= -7 K= 6
1 81 73
3 77 78
4 26 35*
5 58 54
7 44 42
9 44 49

H= -7 K= 7
0 62 61
2 75 81
4 87 78
5 40 40
6 63 65
7 60 62
8 34 37
9 73 69
10 36 40
11 86 77
13 82 77
15 62 67
17 67 63
19 55 50
21 57 49

H= -7 K= 8
3 58 45*
5 33 31

H= -7 K= 9
0 201 191
2 127 190*
4 218 174*
6 135 165
8 124 136
10 113 130
12 109 106
14 82 86
16 67 57
18 46 44

H= -7 K= 10
1 32 41*

H= -7 K= 11
9 59 62
11 62 57
13 42 51
15 44 45
17 51 49
19 49 48

H= -7 K= 13
0 125 128
2 137 134
4 149 137
6 124 120
8 111 104
10 100 90
12 81 81
14 65 62
16 52 47

H= -7 K= 15
11 50 45
13 52 43

H= -7 K= 17
0 102 95
2 86 84
4 83 76
6 71 71
8 67 71
10 53 64
12 54 54

H= -6 K= 0
4 176 216
6 130 135
8 151 142
10 144 149
12 144 138
14 98 108
16 76 80
18 49 52
20 48 43

H= -6 K= 1
5 119 127
6 45 46

7 155 163
9 106 109
11 53 54
12 49 49
13 40 37
14 64 55
16 45 46

H= -6 K= 2
3 38 45
4 40 55*
5 53 55
7 73 67
9 85 87
11 86 82
12 38 34
13 52 55
15 73 65
17 67 62
19 66 58
21 55 50

H= -6 K= 3
1 151 151
2 32 34
3 113 113
5 169 172
7 123 135
8 48 54
9 81 94
10 35 35
11 84 75
13 48 54
15 57 53

H= -6 K= 4
0 196 175
2 238 235
3 38 42
4 239 220
6 182 177
7 26 24
8 179 159
9 34 36
10 122 116
12 101 101
14 102 96
16 66 71
18 50 53

H= -6 K= 5
3 59 66
4 36 39
5 75 78
6 24 24
8 44 48
9 32 39
11 54 61
12 40 40
14 48 44

H= -6 K= 6
0 68 67
2 76 79
3 49 47
4 100 96
5 74 69
6 64 64
7 37 41
8 64 62
9 37 48*
10 49 50
11 47 52
13 66 67
14 45 44
15 66 58
17 50 54
19 49 46

H= -6 K= 7
1 119 120
3 115 121
5 135 127
7 125 130
9 109 102
10 47 35*
11 97 88
13 65 63

H= -6 K= 8
0 237 214
2 171 167
4 115 118
6 120 125
8 114 105
10 97 107
12 73 79
14 56 63
16 46 47

H= -6 K= 9
4 48 47
10 51 49
12 45 46
14 53 49
16 56 53

H= -6 K= 10
0 128 116
2 130 119

8 81 77
6 74 70
7 45 45
8 65 72
9 36 37
10 68 71
12 51 60
13 44 39
14 50 50

H= -6 K= 11
1 87 84
3 107 118
5 120 119
7 102 97
9 90 91
11 79 71
13 50 54
15 48 44

H= -6 K= 12
0 84 88
2 84 85
4 94 86
6 89 72
8 55 57
12 51 50

H= -6 K= 13
10 46 38

H= -6 K= 14
0 106 99
2 101 93
4 87 92
6 89 87
8 84 73
10 62 60
12 45 48

H= -6 K= 15
1 81 74
3 64 63
5 50 61
7 67 68
9 53 59
11 50 47

H= -6 K= 18
0 88 78
2 66 72
4 72 69
6 67 60
8 53 53
10 54 47

H= -6 K= 19
3 52 43
5 49 41

H= -6 K= 22
0 52 48
2 52 47

H= -5 K= 0
4 151 157
6 82 79
8 83 83
10 94 94
12 86 86
14 103 103
16 112 105
18 87 91
20 66 72
22 59 65
24 53 54

H= -5 K= 2
4 21 15*
5 310 302
6 33 32
7 257 236
9 193 199
11 180 173
13 92 159*
15 111 107
17 84 84
19 59 62
21 49 42

H= -5 K= 3
2 26 25
4 23 21
6 24 27

H= -5 K= 4
1 82 75
2 76 83
3 92 96
4 32 29
5 74 76
6 78 77
7 29 31
8 74 83
9 30 37
10 82 79
11 47 51
12 98 86
14 76 71
16 83 72

18 75 78
20 67 72
22 51 55

H= -5 K= 5
0 65 50*
4 32 34

H= -5 K= 6
1 282 263
3 244 209
5 201 192
7 199 171
8 44 40
9 152 151
11 139 139
13 120 120
15 112 97
17 93 75
19 52 55

H= -5 K= 7
0 48 45
4 53 45

H= -5 K= 8
1 198 186
3 139 132
4 67 70
5 121 118
6 70 68
7 131 116
8 48 53
9 98 94
10 47 51
11 71 80
12 55 56
13 71 62
14 59 68
15 47 42
16 63 60
17 42 38
18 48 49

H= -5 K= 9
0 34 28

H= -5 K= 10
1 130 152
2 34 33
3 161 154
4 49 45
5 156 132
6 46 49
7 133 131
8 37 34
9 117 114
10 51 49
11 68 81
12 54 58
13 75 73
14 48 50
15 64 70
16 47 49
17 44 53

H= -5 K= 12
1 114 137
3 138 134
5 142 121
6 43 42
7 123 107
8 53 48
9 99 99
10 47 42
11 62 78*
12 45 38
13 65 67
14 47 37*
15 57 62

H= -5 K= 14
1 86 85
3 83 81
5 85 81
6 43 38
7 62 62
8 53 47
9 42 48
9 45 48
11 61 51
13 49 43
14 50 43

H= -5 K= 16
1 98 100
3 99 100
5 101 95
7 73 89
9 69 75
11 60 69
13 57 60
15 54 48

H= -5 K= 20
1 80 77
3 85 81
5 63 75
7 53 65
9 54 58

H= -5 K= 24
1 56 53
3 47 48

H= -4 K= 0
4 297 254
6 282 287
8 215 168*
10 172 161
12 124 116
14 125 124
16 106 109
18 71 74
20 57 46

H= -4 K= 1
4 54 50
5 110 92
7 98 95
8 50 49
9 102 95
10 112 100
11 91 83
12 68 65
13 85 76
14 45 43
15 55 48
16 49 45

H= -4 K= 2
3 70 64
4 80 85
5 88 89
6 80 73
7 103 107
9 83 83
11 85 74
13 93 84
15 61 67
16 49 46*
17 72 75
19 65 68
21 54 54

H= -4 K= 3
2 41 41
3 189 147*
4 38 36
5 185 154
6 32 34
7 97 104
8 73 70
9 106 109
10 56 50
11 87 95
12 32 44*
13 70 77
15 56 59

H= -4 K= 4
0 305 279
1 42 41
2 311 285
3 24 28
4 286 247
5 35 36
6 225 199
7 39 37
8 138 152
9 43 42
10 141 140
12 170 156
14 93 96
16 60 70
18 59 64
20 49 43
22 44 31*

H= -4 K= 5
1 94 99
3 58 48
5 88 83
6 27 25
7 69 68
8 49 50
9 51 47
10 43 53
12 43 41
14 40 39
18 50 37*

H= -4 K= 6
0 159 165
2 60 70
3 58 59
4 65 62
5 56 42*
6 98 99
7 72 69
8 49 47
9 55 62
10 89 77
11 51 57
12 71 66
13 55 56
15 68 67
17 54 61
19 68 60

H= -4 K= 7
1 159 147
3 137 136
5 107 111
7 117 120
9 109 101
11 88 83
13 70 77
15 47 57

H= -4 K= 8
0 260 219
2 242 188*
4 193 177
6 131 141
7 67 62
8 138 141
10 107 107
12 67 68
13 38 33
14 60 68
16 65 69
18 49 42

H= -4 K= 9
8 31 43*
10 54 57
12 49 54
14 44 46
16 43 39

H= -4 K= 10
0 96 101
2 119 117
4 130 132
5 51 49
6 106 101
8 87 87
10 52 64
12 60 65
13 37 39
14 41 48
15 42 49
16 48 47

H= -4 K= 11
1 172 145
3 128 124
5 113 106
7 89 92
9 89 87
11 55 70*
13 49 57
15 44 49

H= -4 K= 12
0 99 104
2 111 113
4 86 81
6 81 72
8 74 74
10 56 61
12 59 53
14 44 47
15 41 42

H= -4 K= 13
12 40 40

H= -4 K= 14
0 141 135
2 123 115
4 86 93
6 105 90
8 88 86
10 73 75
12 49 56

H= -4 K= 15
1 81 82
3 63 66
5 50 65*
7 55 62
9 48 54
11 50 55

H= -4 K= 16
2 46 39

H= -4 K= 18
0 84 77
2 84 85
4 71 77
6 67 72
8 48 64*
10 45 54

H= -4 K= 22
0 56 51
2 51 52
4 52 51
6 48 44

H= -3 K= 0
4 85 83
6 37 39
8 47 47

H= -3 K= 1
5 53 49

6 328 267
7 58 50
8 227 196
10 181 172
11 55 48
12 107 107
13 72 69
14 111 84*
15 75 70
16 69 66
17 63 65
18 55 58
19 44 44

H= -3 K= 2
3 139 125
4 42 40
5 136 128
6 25 23
7 47 50
9 31 32
11 75 78
13 58 54

H= -3 K= 3
1 43 53
2 133 116
3 92 83
4 133 127
6 190 166
8 167 153
9 105 106
10 118 115
11 97 100
12 104 92
13 102 101
14 52 53
15 70 78
16 47 45
17 83 78
18 47 40
19 58 64
21 48 52
23 47 45

H= -3 K= 4
1 83 73
2 51 46
3 110 86*
5 103 109
6 30 35
8 30 25
11 36 41
12 37 40

H= -3 K= 5
1 58 55
2 365 307
4 274 254
6 274 241
7 51 48
8 215 201
9 51 64
10 189 191
11 43 48
12 181 165
13 33 40
14 118 95
16 58 63
18 57 58
20 47 43

H= -3 K= 6
1 118 119
3 93 89
5 83 87
7 85 87
9 58 64
11 41 40
13 37 43
15 41 47

H= -3 K= 7
0 27 29
2 62 68
4 94 95
5 44 48
6 54 70*
7 94 104
8 75 76
9 63 61
10 34 31
11 92 84
13 91 92
14 43 43
15 73 88
17 69 74
19 67 67
21 50 52

H= -3 K= 8
1 55 54
2 25 29
3 27 31
4 33 32
5 43 43
6 44 60*
7 35 34
8 39 49

H= -3 K= 9
0 190 179
2 176 178
4 246 223
6 265 228
8 225 210
10 135 141
12 102 98
14 80 90
16 75 86
18 52 58

H= -3 K= 10
1 66 65
3 53 61
5 36 36
7 41 42
9 55 55
11 63 65
13 61 67
15 65 73
17 69 62
19 47 50

H= -3 K= 11
5 47 51
7 41 42
9 55 55
11 63 65
13 61 67
15 65 73
17 69 62
19 47 50

H= -3 K= 12
1 44 49
7 43 39

H= -3 K= 13
0 129 141
2 155 151
4 172 147
6 149 143
8 129 130
10 123 113
12 83 93
14 57 71*
16 46 53
18 48 46

H= -3 K= 15
0 46 52
6 37 36
7 45 40
8 42 35
9 42 48
13 45 49
15 47 46

H= -3 K= 16
1 40 42
3 49 46

H= -3 K= 17
0 85 92
2 93 99
4 107 98
6 95 94
8 82 83
10 71 72
12 52 53
14 49 45

H= -3 K= 19
2 42 47
4 50 48
6 51 47

H= -3 K= 21
0 48 49
2 49 50
4 53 52
6 49 48

H= -3 K= 23
2 46 43

H= -2 K= 0
4 144 127
6 108 99
8 65 66
10 31 30
14 58 55
16 49 54

H= -2 K= 1
5 121 122
6 79 73
7 222 201
8 130 108
9 164 159
10 93 81
11 138 131
12 105 105
13 121 111
14 90 84
15 79 76
16 49 56
17 56 64
18 54 65
20 49 57

H= -2 K= 2
3 128 108
4 105 106

Table 4. Continued.

6 104 96	9 253 201*	13 53 68*	14 48 46	17 49 46	6 103 93	3 36 41	17 44 50
8 61 55	10 36 33	15 46 58*	15 39 38	21 47 34*	8 85 94	4 423 386	18 45 43
12 38 41	11 188 165		16 44 37		10 68 71	6 306 285	19 51 50
	13 124 122	H= -2 K= 17	17 50 45	H= -1 K= 8	12 46 55	8 223 216	
H= -2 K= 3	15 74 66	1 45 52	19 54 51	1 104 106	14 48 48	9 71 72	H= 0 K= 12
1 188 200*	17 86 73	3 45 51		3 101 92		10 171 165	0 134 125
2 27 23	19 55 50	5 46 47	H= -1 K= 4	4 56 58	H= -1 K= 14	12 189 163	2 144 152
3 293 226*			1 136 119	5 147 114*	1 66 64	13 36 43	4 127 137
7 274 245	H= -2 K= 8	H= -2 K= 19	2 116 105	6 29 34	3 73 71	14 137 142	6 94 92
8 44 42	0 79 66	1 75 76	3 26 30	7 111 120	5 65 61	16 115 110	7 56 60
9 185 177	2 68 65	3 75 74	4 70 58	8 47 44	7 48 53	18 78 79	8 105 100
10 76 66	4 85 81	5 59 69	5 44 49	9 82 84	9 45 52	20 52 50	9 90 80
11 199 188	6 33 40	7 54 61	6 101 100	10 46 46	11 47 40		10 60 73
12 71 59	8 46 46	9 56 57	7 49 52	11 52 60	13 41 33*	H= 0 K= 6	11 51 53
13 117 130	10 53 49	11 57 52	8 67 75	12 35 42		0 330 311	12 92 73*
14 50 53			9 52 54	13 47 48	H= -1 K= 16	1 48 51	13 42 47
15 101 94	H= -2 K= 9	H= -2 K= 21	10 88 78	14 49 56	1 106 103	2 134 141	14 72 74
16 46 47	3 47 52	1 51 47	11 55 62	16 53 58	3 122 107	3 84 82	15 48 41
17 68 68	6 42 36	3 56 47	12 98 89	17 46 43	5 92 91	4 90 89	16 45 51
19 47 48	7 51 51		13 36 42	18 47 58	7 83 82	5 78 73	17 46 51
	8 74 79	H= -1 K= 0	14 64 70	20 46 49	9 75 74	6 122 116	19 45 50
H= -2 K= 4	9 35 41	4 222 189	16 75 76		11 55 59	7 59 61	
0 217 191	10 74 84	6 211 179	18 62 73	H= -1 K= 9	13 48 48	8 93 101	H= 0 K= 14
1 49 47	12 87 83	8 159 121*	20 52 60	0 226 200		9 97 106	0 125 149
2 187 142*	14 81 81	12 72 65	22 46 48	2 158 154	H= -1 K= 17	10 83 90	2 122 126
3 58 59	16 67 66	14 111 112	24 45 39	4 100 101	0 60 57	11 76 74	4 128 135
4 83 83	18 55 58	16 86 88		6 141 136	2 51 57	12 33 42*	6 135 120
5 35 42	20 49 55	18 79 75	H= -1 K= 5	8 108 127	4 52 60	13 53 59	8 106 103
6 78 70	22 47 51	20 66 60	0 64 73	10 118 122	6 48 52	14 47 42	10 74 88
8 64 68			2 88 121*	12 76 85	8 54 53	15 75 67	11 47 42
10 60 62	H= -2 K= 10	H= -1 K= 1	3 61 60	14 50 55	10 47 44	16 60 56	12 57 74*
12 76 70	2 32 35	4 318 234*	4 231 196		12 44 37	17 81 84	13 53 51*
	4 43 44	5 33 33	5 47 48	H= -1 K= 10		19 67 67	14 77 72
H= -2 K= 5		6 253 221	6 188 185	1 153 142	H= -1 K= 20	21 60 58	16 47 59
1 101 102	H= -2 K= 11	7 123 115	7 39 47	2 33 40	1 68 66	23 53 49	17 48 25*
2 79 73	1 225 201	8 125 110	8 136 124	3 176 164	3 57 65	25 51 41	18 49 41
3 165 153	2 40 36	9 36 42	10 91 90	5 166 140	5 63 64		
4 33 32	3 143 190*	10 100 98	11 37 36	6 32 33	7 54 60	H= 0 K= 8	H= 0 K= 16
5 186 162	5 147 156	11 44 51	12 88 76	7 113 122	9 50 53	0 250 222	0 89 78
6 72 67	7 158 154	12 121 111	13 34 46*	9 107 98		2 235 211	2 63 60
7 89 83	9 147 144	13 49 54	14 71 71	11 62 72	H= 0 K= 0	4 212 204	4 42 43
8 102 88	11 138 129	14 40 43	16 59 66	13 60 59	4 239 222	6 194 175	6 43 38
9 98 97	13 109 103	15 58 54	18 41 42	14 40 33	6 271 274	7 60 58	8 44 46
10 84 99	15 78 78	17 45 49		15 41 45	8 316 258	8 115 121	10 45 39
11 71 83	17 43 54*	18 39 38	H= -1 K= 6	17 44 39	10 267 269	9 56 53	11 42 48
12 116 117	19 46 42		1 366 286*	18 45 42	12 239 212	10 151 149	13 44 39
13 42 51		H= -1 K= 2	3 265 270		14 124 129	11 57 56	
14 96 96	H= -2 K= 12	3 196 247*	4 68 60	H= -1 K= 11	16 124 111	12 136 133	H= 0 K= 18
15 42 40	0 42 47	4 55 49	5 305 235*	7 32 33	18 124 111	13 61 57	0 131 116
16 73 82	2 39 37	5 336 271	6 82 75	9 51 50	18 66 67	14 107 112	2 116 109
18 72 75	3 36 35	6 46 47	7 180 168	11 45 48	20 51 43	15 36 44	4 83 93
20 55 59		7 278 254	8 56 57	13 57 58		16 68 80	6 60 76*
22 49 51	H= -2 K= 13	8 53 49	9 117 133	15 39 48	H= 0 K= 2	17 46 45	8 79 81
24 51 46	1 41 37	9 207 195	11 123 122	17 41 39	3 58 48	18 56 65	10 57 71
	3 41 42	10 36 37	13 116 106		4 63 46*	20 42 42	12 59 65
H= -2 K= 6	10 65 62	11 164 156	14 47 51	H= -1 K= 12	5 89 84		14 55 54
0 100 126*	12 57 61	13 124 117	15 82 84	1 124 128	7 140 147	H= 0 K= 10	
1 29 30	14 46 55	15 118 103	17 52 59	2 37 34	8 56 55	0 156 168	H= 0 K= 22
2 73 74	16 53 54	17 83 95	19 47 45	3 126 130	9 74 68	2 205 189	0 89 76
3 75 69	18 51 46	19 58 65		4 38 36	11 116 104	4 159 166	2 88 74
4 30 25			H= -1 K= 7	5 134 126	12 51 54	5 59 42*	4 66 67
5 28 26	H= -2 K= 14	H= -1 K= 3	0 83 76	7 103 93	13 139 132	6 144 138	6 51 60
6 35 42	0 51 47	2 172 147	2 55 55	9 70 74	15 99 98	7 66 80	8 47 54
7 40 42	2 39 40	4 152 146	4 37 28*	11 70 72	17 95 79	8 80 86	10 48 48
9 31 40*		5 90 74	5 41 44	13 59 60	19 90 89	9 90 93	12 48 41
11 40 47	H= -2 K= 15	6 167 147	7 34 36	15 44 44	21 63 81*	10 92 101	
	1 121 126	7 66 64	8 35 31	16 45 40	23 61 71	11 67 70	H= 0 K= 26
H= -2 K= 7	3 151 134	8 130 129	10 49 50		25 46 53	12 107 112	0 48 41
1 316 284	5 120 118	9 75 81	11 46 50	H= -1 K= 13		13 50 48	2 48 41
3 297 265	7 142 120	10 76 90	12 37 40	0 89 86	H= 0 K= 4	14 73 74	
5 263 221	9 98 106	11 46 46	13 65 68	2 121 107	0 293 268	15 41 47	
7 246 231	11 60 75	13 46 37*	15 54 52	4 134 114	2 367 406	16 43 46	

weights chosen according to Cruickshank.[9] In addition, the reflexions not obeying the condition $0.80 \leq |F_o|/|F_c| \leq 1.25$ were given zero weight. The atomic scattering factors for the neutral atoms were taken from International Tables [10] for oxygen and carbon and from Cromer *et al.*[11] for neodymium.

The discrepancy indexes $R = \sum||F_o| - |F_c||/\sum|F_o|$ and $wR = [\sum w(|F_o| - |F_c|)^2/\sum w|F_o|^2]^{\frac{1}{2}}$ converged to 0.098 and 0.097, respectively. All observed reflexions were included in the calculation of R. Further refinement using anisotropic thermal parameters for neodymium and an over-all scale factor resulted in $R = 0.092$ and $wR = 0.091$. The shifts of all parameters were less than 5 % of their estimated standard deviations in the last cycle of refinement.

The weighting scheme used was satisfactory as indicated by the approximate constancy of the averages of $w(|F_o| - |F_c|)^2$ between different $|F_o|$ and $\sin\theta$ intervals (Table 2).

The final atomic parameters with their estimated standard deviations are given in Table 3. The electron density maps of a difference synthesis based upon these parameters showed a peak of about 4.5 e/Å^3 at the position of neodymium, and only spurious peaks less than 2 e/Å^3 in the other regions. The observed and calculated structure factors are compared in Table 4.

All computations were performed on the UNIVAC 1108 computer at Lund, Sweden, using the programs DRF, LALS, DISTAN, PLANE, CELSIUS, and ORTEP.[12]

DESCRIPTION OF THE STRUCTURE

The general features of the structure of NDO are shown in Figs. 1 and 2. Interatomic distances and angles are given in Table 5; some of them are also indicated in Figs. 4 and 5. The numbering of the atoms constituting the two

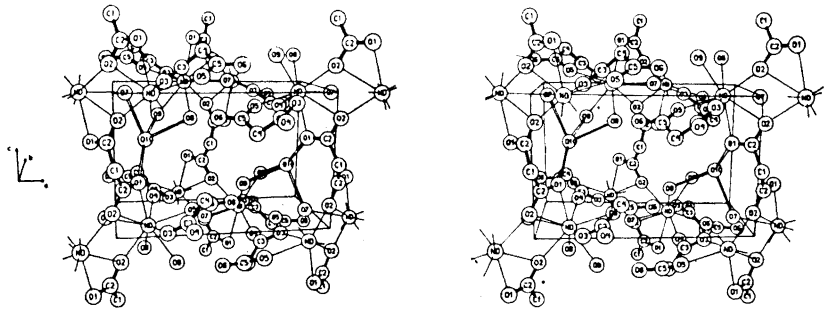

Fig. 1. A stereoscopic pair of drawings showing part of two adjacent neodymium-malonate networks and the bonding between them. Bonds within the malonate ions are filled, hydrogen bonds are open, and Nd – O bonds are single lines. The intra-network hydrogen bonds are omitted for clarity. The box outlined is $0 \leq x \leq 1$, $0 \leq y \leq 1/2$, $0 \leq z \leq 1/2$.

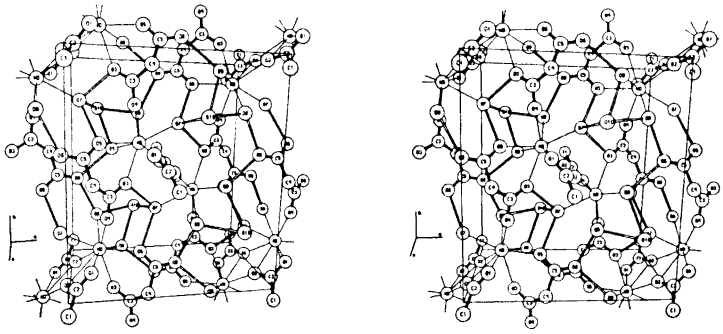

Fig. 2. A stereoscopic pair of drawings illustrating the neodymium-malonate network around $z = 0$. The bonds are indicated in the same way as in Fig. 1. The box outlined is $0 \leq x \leq 1$, $0 \leq y \leq 1$, $-1/4 \leq z \leq 1/4$.

Table 5. Selected distances (Å) and angles (°) with their estimated standard deviations.

A. The coordination polyhedron

Nd – O(1)	2.54(1)	$O(2^{i}) - O(7)$	3.03(2)
$Nd - O(2^{i})$	2.46(1)	$O(2^{i}) - O(8)$	3.24(2)
Nd – O(3)	2.47(1)	$O(2^{i}) - O(9)$	3.07(2)
$Nd - O(4^{vi})$	2.41(1)	$O(2^{i}) - O(2)$	2.71(2)
Nd – O(5)	2.43(1)	O(3) – O(5)	2.83(2)
Nd – O(7)	2.53(1)	O(3) – O(9)	2.92(2)
Nd – O(8)	2.46(1)	O(3) – O(2)	2.91(2)
Nd – O(9)	2.49(1)	$O(4^{vi}) - O(5)$	2.86(2)
Nd – O(2)	2.72(1)	$O(4^{vi}) - O(7)$	2.97(2)
O(1) – O(3)	3.16(2)	$O(4^{vi}) - O(8)$	2.97(2)
$O(1) - O(4^{vi})$	3.05(2)	O(5) – O(8)	3.93(2)
O(1) – O(5)	3.31(2)	O(5) – O(9)	2.92(2)
O(1) – O(7)	3.24(2)	O(7) – O(8)	2.97(2)
O(1) – O(2)	2.18(2)	O(7) – O(2)	2.90(2)
$O(2^{i}) - O(3)$	3.07(2)	O(8) – O(9)	2.71(2)

B. Ligand 1

C(1) – C(2)	1.51(2)	$\angle C(2) - C(1) - C(2^{ii})$	113(2)
C(2) – O(1)	1.22(2)	$\angle O(1) - C(2) - O(2)$	122(1)
C(2) – O(2)	1.28(2)	$\angle C(1) - C(2) - O(1)$	120(1)
		$\angle C(1) - C(2) - O(2)$	119(1)

C. Ligand 2

C(4) – C(3)	1.53(2)	$\angle C(3) - C(4) - C(5)$	117(1)
C(4) – C(5)	1.52(3)	$\angle O(3) - C(3) - O(4)$	121(1)
C(3) – O(3)	1.29(2)	$\angle C(4) - C(3) - O(3)$	119(1)
C(3) – O(4)	1.26(2)	$\angle C(4) - C(3) - O(4)$	120(1)
C(5) – O(5)	1.26(2)	$\angle O(5) - C(5) - O(6)$	123(2)
C(5) – O(6)	1.20(3)	$\angle C(4) - C(5) - O(5)$	118(2)
		$\angle C(4) - C(5) - O(6)$	119(2)

D. Possible hydrogen bonds

$O(7) - O(3^{i})$	2.63(2)	O(8) – O(10)	2.71(2)
$O(7) - O(5^{v})$	2.77(2)	$O(9) - O(6^{iii})$	2.76(2)
$O(7) - O(10^{v})$	2.85(2)	O(9) – O(10)	2.76(2)
$O(8) - O(6^{v})$	2.67(2)	$O(10) - O(1^{viii})$	2.79(2)

structurally independent malonate ions, referred to as ligand 1 and ligand 2, is shown in Fig. 4. The superscripts $(i) - (x)$ refer to the following equivalent sites in the structure:

	x,y,z	(iv)	$1/2+x,1/2-y,\bar{z}$	$(viii)$	$1/2-x,1/2-y,z-1/2$
(i)	$\bar{x},\bar{y},\bar{z}$	(v)	$x-1/2,1/2-y,\bar{z}$	(ix)	$x,\bar{y},1/2+z$
(ii)	$\bar{x},y,1/2-z$	(vi)	$1/2-x,1/2+y,z$	(x)	$1/2-x,y-1/2,z$
(iii)	$1-x,\bar{y},\bar{z}$	(vii)	$1/2-x,1/2-y,1/2+z$		

where x,y,z are the atomic coordinates given in Table 3.

The neodymium ions are situated at $z \approx 0$ and $z \approx 1/2$. Those at the same z-level are coupled in pairs by oxygen bridges Nd – O(2) – Nd, where O(2) is a carboxylate oxygen of ligand 1, as shown in Fig. 1. The methylene carbon of this ligand is situated on the twofold axis $x = 0$, $z = 1/4$, and hence ligand 1 connects the neodymium pairs in the z-direction. Ligand 2 links the neodymium pairs in layers parallel to (001) by bridges of the type Nd – OCO – Nd. As illustrated in Fig. 2, each neodymium pair is bonded in this way to four adjacent pairs.

There is a system of hydrogen bonds within the layer, formed by the coordinated water molecules O(7), O(8), and O(9) with the carboxylate oxygens of ligand 2 as acceptors. The uncoordinated water molecule O(10) is situated between the layers at $z \approx 1/4$ (see Fig. 1). It is hydrogen bonded to the coordinated water molecules in one layer and to the carboxylate oxygen O(1) in an adjacent layer. The layers are thus held together by ligand 1 as described above and by hydrogen bonds *via* O(10).

The coordination polyhedron. The coordination around the pair of neodymium ions is shown in Fig. 3, and the dimensions of the coordination polyhedron are given in Table 5 A. Each neodymium ion is coordinated by six carboxylate oxygens, from four malonate ions, and by three water oxygens. These nine oxygens form a distorted monocapped square antiprism.

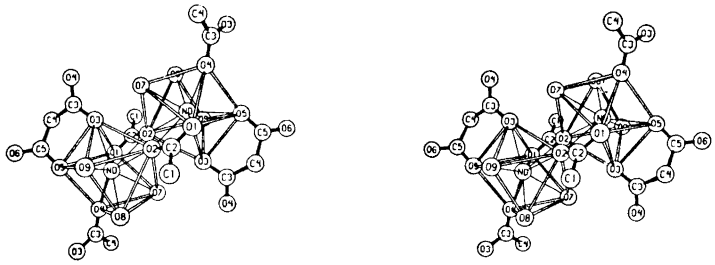

Fig. 3. A stereoscopic pair of drawings showing the coordination polyhedra around the neodymium ions Nd and Nd^{i}. Nd – O bonds are single lines, the bonds within the malonate ions are filled and the edges of the square antiprism are open.

The carboxylate oxygens O(2) and O(2^{i}) form asymmetric oxygen bridges between the two neodymium ions; the distances Nd – O(2) and Nd – O(2^{i}) are 2.72 Å and 2.46 Å, respectively. The other Nd – O bond distances are in the range 2.41 – 2.54 Å and the average of the nine Nd – O distances, 2.50 Å, is compatible with those found in other structures containing neodymium coordinated by nine oxygens.[13]

The "square" faces of the coordination polyhedron are O(8) – O(4^{vi}) – O(5) – O(9) and O(7) – O(1) – O(3) – O(2^{i}). The distant oxygen O(2) caps the latter square, which is larger than the first one, the edge lengths being in the intervals 2.71 – 2.97 Å and 3.02 – 3.24 Å, respectively. The "square" faces are approximately planar (see Table 6) and the least-squares planes through the atoms forming the "squares" are parallel. The neodymium ion is 0.2 Å closer to the capped square than to the uncapped one. The mean "contact"

Table 6. Deviations in Å from least squares planes within the malonate ions and the coordination polyhedron. The atoms defining the plane are in each case given above the asterisk.

A. The malonate ions

Atom	Distance	Atom	Distance	Atom	Distance	Atom	Distance
C(1)	−0.00	C(4)	−0.00	C(4)	0.01	C(3)	−0.03
C(2)	0.00	C(3)	0.01	C(5)	−0.03	C(5)	0.03
O(1)	−0.00	O(3)	−0.01	O(5)	0.01	O(3)	0.03
O(2)	−0.00	O(4)	−0.01	O(6)	0.01	O(5)	−0.03
*		*		*		*	
Nd	0.67	Nd	−0.03	Nd	0.49	Nd	−0.42
Nd	0.03	Nd^{x}	0.82			C(4)	−0.50

B. The coordination polyhedron

Atom	Distance	Atom	Distance
O(3)	0.22	O(8)	0.08
O(1)	−0.20	$O(4^{vi})$	−0.08
O(7)	0.21	O(5)	0.08
$O(2^{i})$	−0.23	O(9)	−0.08
*		*	
Nd	1.19	Nd	−1.38

distance between oxygens not belonging to the same malonate ion is 3.00 Å as compared to 2.98 Å in $Nd_2(C_2O_4)_3.10.5H_2O$.[2] Only two of the O − O distances are shorter than 2.8 Å, *viz.* O(2) − $O(2^{i})$ and O(8) − O(9), both being 2.71 Å.

Ligand 2 forms a six-membered chelate ring with neodymium. Its bite is 2.83 Å. The ring has a boat conformation with the four atoms O(3), C(3), C(5), and O(5) coplanar within ± 0.03 Å and the atoms Nd and C(4) situated 0.42 and 0.50 Å at the same side of this plane (Table 6). A similar conformation is found for the two structurally independent malonate rings of the complex $Comal_2en^{-}$ (en = $H_2NCH_2CH_2NH_2$), while the three equivalent rings of $Crmal_3^{3-}$ have the methylene carbon 0.69 Å out of the plane formed by the other five atoms.[5]

The polyhedra around Nd and Nd^{i} share the edge O(2)···$O(2^{i})$ and the distance Nd···Nd^{i} is relatively short, 4.42 Å. The carboxylate group C(2)O(1)O(2) may be described as bridging-chelating, *i.e.* both oxygens are bonded to the same metal ion in a four-membered ring and one of them, O(2), forms an additional bond to the second metal ion. This type of bridge is not uncommon in lanthanoid carboxylate structures. It is found, *e.g.*, in $Nd(OCOCH_2NHCH_2OCO)Cl.3H_2O$,[14] $K_2Ce(CH_3COO)_5.H_2O$,[15] and $Ce(CH_3COO)_3.0.7H_2O$.[16] The next shortest Nd···Nd distance, 6.70 Å, is between the neodymium ions Nd and Nd^{vi} which are connected by the bridging carboxylate group O(3)C(3)O(4) (see Fig. 2).

The malonate ions. The dimensions of the malonate ions are given in Table 5 B,C and in Fig. 4. The corresponding bond distances and angles in the two ions are equal within the limits of errors. There are no previous reports giving the

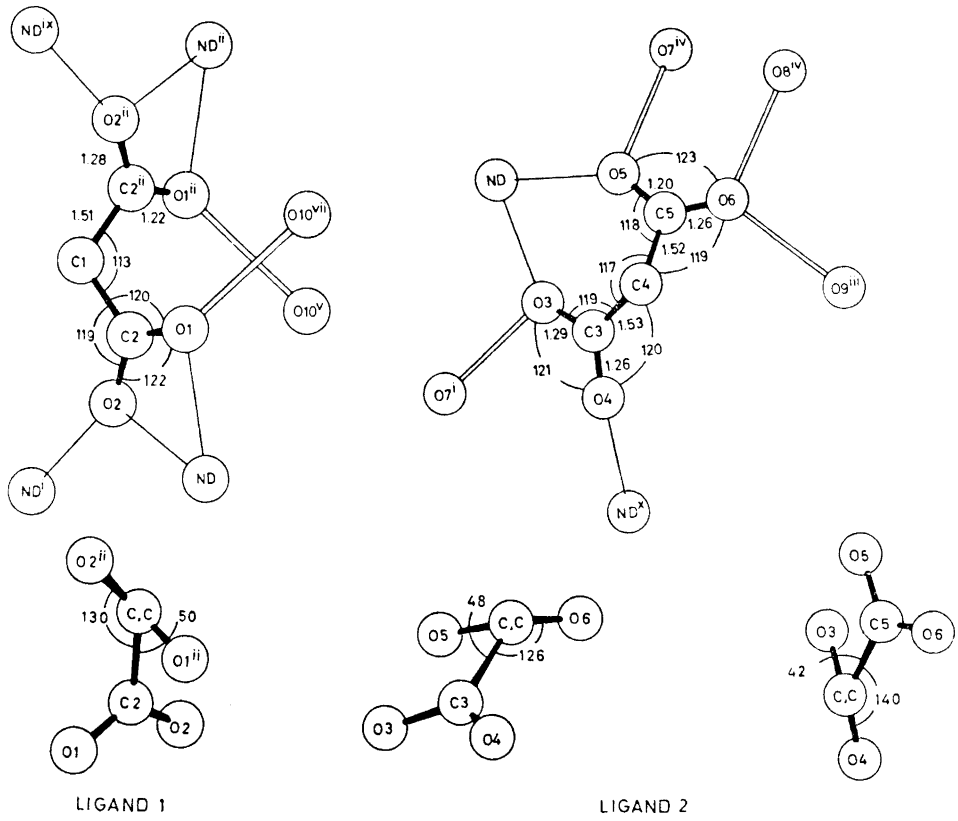

Fig. 4. The two malonate ions and their immediate surroundings, together with projections of each malonate ion along its C–C bonds. The angles indicated in the projections are the dihedral angles C–C–C–O.

dimensions of malonate ions. (The report of $Comal_2en^-$ and $Crmal_3^{3-}$ referred to above is only preliminary and contains no distances or atomic coordinates.) A comparison with the malonate residue in the compound $KOOCCH_2COOH$ [17] shows significant differences in the C – C – O bond angles attributable to the non-equivalence of the two C – O bonds in the hydrogen malonate ion, but otherwise the dimensions of the ions are compatible.

The three independent C–COO groups are planar within the limits of errors (Table 6) while the malonate ions are both nonplanar. In ligand 1 the dihedral angle $C(2^{ii}) - C(1) - C(2) - O(2)$ is 130°. Since the methylene carbon is situated on a two-fold axis, this means that the two COO-groups are twisted 50° in opposite directions out of the plane of the three central carbon atoms. Thus the two C–COO-planes are almost perpendicular to each other and the oxygens of the two COO-groups are well separated; the shortest distances are $O(1)\cdots O(1^{ii})$: 3.24 Å and $O(1)\cdots O(2^{ii})$: 3.78 Å.

In ligand 2, which forms the six-membered chelate ring, the dihedral angles O(3)–C(3)–C(4)–C(5) and C(3)–C(4)–C(5)–O(5) are 42° and 48°, respectively, *i.e.* the two COO-groups are twisted in the same direction out of the plane of the carbon atoms by about 45°. This twist results in one short O–O distance, *viz.* the ligand bite O(3)···O(5) which is 2.83 Å.

The conformations of the malonate ions may be compared with those found for the malonate residues in malonic acid [18] and potassium hydrogen malonate.[17] In malonic acid one COO-group but not the other is twisted about 90° out of the plane of the carbon atoms while the atoms of the malonate group in potassium hydrogen malonate are almost coplanar. In the latter compound, the shortest intramolecular separation of oxygens belonging to different COO-groups is 2.80 Å.

The hydrogen bonds. The possible hydrogen bond distances, *i.e.* the $(H_2)O-O$ distances shorter than 3.20 Å, between oxygens not belonging to the same coordination polyhedron [19] are given in Table 5 D. There is just one suitable distance for each of the active hydrogen atoms, and the longest of these distances is 2.85 Å. Thus the choice of a probable hydrogen bond system seems to be unequivocal even though the positions of the hydrogen atoms have not been located. The hydrogen bond system is illustrated in Fig. 5.

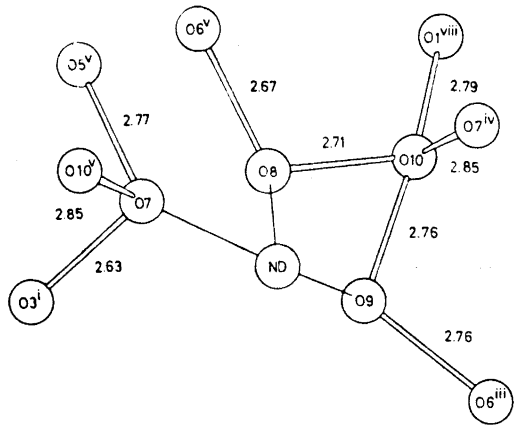

Fig. 5. The immediate surroundings of the four water molecules. Hydrogen bonds are open and Nd–O bonds are single lines.

The water molecule O(7) forms two hydrogen bonds to carboxylic oxygens within the neodymium malonate layer, *viz.* O(7)···O(3^i) and O(7)···O(5^v), and accepts one hydrogen bond from the uncoordinated water molecule O(10). The donor angle O(5^v)–O(7)–O(3^i) is 98°. The three hydrogen bonds and the bond Nd–O(7) are approximately tetrahedrally arranged around O(7) and the "tetrahedral" angles are in the range 95–133°. The oxygens O(7) and O(3^i) belong to different coordination polyhedra of an edge-sharing pair and thus the bond O(7)···O(3^i) constitutes an additional link between these polyhedra.

The water molecules O(8) and O(9) each form one intra-layer hydrogen bond to a carboxylic oxygen, *viz.* O(8)···O(6^{ii}) and O(9)···O(6^{iii}), and one to the water molecule O(10). The donor angles O(6^{ii}) – O(8) – O(10) and O(6^{iii}) – O(9) – O(10) are 111° and 112° respectively and the sum of the three bond angles is 341° around O(8) and 335° around O(9).

The uncoordinated water molecule O(10) is situated between the neodymium malonate layers and forms the only inter layer hydrogen bonds. It is bonded to the water oxygens O(8), O(9) and O(7^{iv}) of one layer and to the carboxylic oxygen O(1^{vii}) of an adjacent layer (see Fig. 1). These four oxygens form a distorted tetrahedron around O(10) with the "tetrahedral" angles in the range 59 – 159°. The donor angle O(1^{vii}) – O(10) – O(7^{iv}) is 116°.

Acknowledgements. I am indebted to Professor Ido Leden and Drs. Jörgen Albertsson and Ingmar Grenthe for many valuable discussions. This work is part of a research project supported by the *Swedish Natural Science Research Council.*

REFERENCES

1. Grenthe, I., Gårdhammar, G. and Rundcrantz, E. *Acta Chem. Scand.* **23** (1969) 93.
2. Dellien, I. and Grenthe, I. *Acta Chem. Scand.* **25** (1971) 1387.
3. Hansson, E. *Acta Chem. Scand.* **24** (1970) 2969.
4. Hansson, E. *Acta Chem. Scand.* **26** (1972) 1337.
5. Hansson, E. *Acta Chem. Scand.* **27** (1973) 823 .
6. Butler, K. R. and Snow, M. R. *J. Chem. Soc.* **D1971** 550.
7. Azikov, B. S., Kharzeeva, S. E., Grankina, Z. A. and Serebrennikov, V. V. *Russ. J. Inorg. Chem.* **13** (1968) 954.
8. *International Tables for X-Ray Crystallography*, Kynoch Press, Birmingham 1969, Vol. I.
9. Cruickshank, D. W. J. In Rollet, J. S. *Computing Methods in Crystallography*, Pergamon, Glasgow 1965, pp. 99 – 116.
10. *International Tables for X-Ray Crystallography*, Kynoch Press, Birmingham 1968, Vol. III.
11. Cromer, D. T., Larsson, A. C. and Waber, J. T. *Acta Cryst.* **17** (1964) 1044.
12. Liminga, R. *Acta Chem. Scand.* **21** (1967) 1206.
13. Albertsson, J. *On the Stereochemistry of Ninecoordinate Lanthanoid Compounds*, Thesis, Lund 1972, p. 37.
14. Oskarsson, Å. *Acta Chem. Scand.* **25** (1971) 1206.
15. Sadikov, G. G., Kukina, G. A., Porai-Koshits, M. A. and Pospelova, L. A. *J. Struct. Chem.* **9** (1967) 128.
16. Sadikov, G. G., Kukina, G. A. and Porai-Koshits, M. A. *J. Struct. Chem.* **8** (1967) 492.
17. Sime, J. G., Speakman, J. C. and Parthaserathy, R. *J. Chem. Soc.* **A 1970** 1919.
18. Goedkoop, J. A. and MacGillavry, C. H. *Acta Cryst.* **10** (1957) 125.
19. Baur, W. H. *Acta Cryst.* **B 28** (1972) 1456.

Received March 15, 1973.

ACTA CHEMICA SCANDINAVICA 27 (1973) 2455–2462

The Crystal Structure of $Hf(OH)_2SO_4$

MARGARETA HANSSON

Department of Inorganic Chemistry, Chalmers University of Technology and University of Göteborg, P.O. Box, S-402 20 Göteborg 5, Sweden

Single crystals of an orthorhombic modification of $Hf(OH)_2SO_4$ have been prepared in an autoclave at 325°C and the crystal structure has been determined from three-dimensional X-ray data. The unit cell has the dimensions $a = 11.085$ Å, $b = 5.517$ Å, and $c = 6.647$ Å, the space group being *Pnma*. The atomic positions were obtained from Patterson and Fourier syntheses and the structure was refined to an R value of 0.055, using 405 independent reflexions. $Hf(OH)_2SO_4$ contains infinite chains of composition $[Hf(OH)_2]_n^{2n+}$ which are joined by sulfate groups, each of which connects three chains. The Hf–Hf distance within the chain is 3.562 Å. Hafnium exhibits eightfold oxygen coordination, the coordination polyhedron being a somewhat distorted Archimedean square antiprism. The Hf–O bond distances range between 2.10_6 and 2.25_7 Å with an average distance of 2.17_5 Å.

During an investigation of the $HfO_2-SO_3-H_2O$ system, three basic salts have been prepared by hydrothermal hydrolysis. A note on $Hf(OH)_2SO_4\cdot(H_2O)_2$ [1] and the crystal structure of $Hf(OH)_2SO_4\ H_2O$ [2] have been published earlier, while the structure of $Hf(OH)_2SO_4$ is presented in this paper. For the $ZrO_2-SO_3-H_2O$ system, McWhan and Lundgren reported the structure of $Zr_2(OH)_2(SO_4)_3(H_2O)_4$.[3] Two modifications of $Zr(OH)_2SO_4$,[3] one orthorhombic (I) and one monoclinic (II), were also found and the refined structure of the orthorhombic phase will be published shortly.[4] Since the corresponding hafnium compound could now be prepared it was of interest to determine its structure in order to obtain more information concerning differences or resemblances between zirconium and hafnium.

PREPARATION AND ANALYSIS

The different basic hafnium sulfates have been prepared by means of hydrothermal hydrolysis. After dissolving HfO_2 in boiling concentrated sulfuric acid, the solutions were evaporated to dryness and the residues dissolved in water or dilute sulfuric acid. By varying the acidity and the temperature, hafnium sulfates with different water contents were obtained.

The crystals investigated were formed in 2 M sulfuric acid kept at 325°C for three weeks in an autoclave lined with metallic gold. At 300°C a sample containing crystals of $Hf(OH)_2SO_4$, together with crystals of the monoclinic form of $Hf(OH)_2SO_4H_2O$, was obtained.

The compound was analysed thermogravimetrically, the following results for the *hafnium* content (as HfO_2), the *sulfur* content (as SO_3) and the *water* content thus being obtained:

	%HfO_2	%SO_3	%H_2O	Density (g cm^{-3})
Found:	67.4	26.7	5.9	–
Calc. for $Hf(OH)_2SO_4$:	68.2	26.0	5.8	5.04

UNIT CELL AND SPACE GROUP

From Weissenberg films it was seen that $Hf(OH)_2SO_4$ crystallizes in the orthorhombic system, the following reflexions being systematically absent, $0kl$: $k+l=2n+1$; $hk0$: $h=2n+1$.
These extinctions indicate the space group to be either $Pna2_1$ or $Pnma$.[5]

The cell dimensions were obtained from Guinier powder photographs taken with Cu$K\alpha_1$ radiation and internally calibrated with $Pb(NO_3)_2$ ($a_{Pb(NO_3)_2}$ = 7.8566 Å at 21°C).[6] For the powder investigation crystals were picked out manually, because all the crystals in the sample were not quite transparent and well-developed. 37 reflexions were indexed and a least squares refinement with the programme POWDER [7] gave the following cell dimensions: a = 11.0850 ± 0.0012 Å; b = 5.5170 ± 0.0004 Å; c = 6.6474 ± 0.0007 Å and V = 406.5 Å^3. A list of observed and calculated $\sin^2\theta$ values is given in Table 1.

Assuming [4] that $Z=4$, the analysis and the volume of the cell give a calculated density of 5.04 g cm^{-3}.

INTENSITY DATA

$Hf(OH)_2SO_4$ crystallizes as rather large multi-faced crystals. The crystal chosen for the structure determination was cut off from an aggregate and had the maximum dimensions (in mm): 0.21 × 0.14 × 0.05. Three-dimensional X-ray data were collected with a Philips automatic four-circle diffractometer, PW 1100. Reflexions were registered with monochromated Cu$K\alpha$ radiation in the θ-interval 0 – 70°. The net intensities, I_{net}, and their estimated standard deviations, $\sigma(I_{net})$, based on counter statistics, were calculated. Only the 420 most significant reflexions with $\sigma(I_{net})/I \leq 0.25$ were used in the subsequent calculations. Corrections for Lorentz and polarization effects were performed with the program DATAP1.[8]

The absorption coefficient, $\mu_{CuK\alpha}$ = 530.1 cm^{-1}, was calculated from the values for the different elements given in the International Tables (1962), and a correction for absorption effects was performed with the program DATAPH.[8] Since the crystal had 18 faces a paper model was constructed to obtain an adequate picture of the crystal, and thus enable a correct calculation of the absorption factors. Because of requirements of the program used, the boundary planes were approximated to be 15. For the same reason fifteen reflexions measured at $\psi = 90°$, were not included in this correction. The remaining 405 reflexions were used in the final refinement of the structure.

Table 1. Guinier powder photograph of $Hf(OH)_2SO_4$.

$h\ k\ l$	$10^5 \sin^2\theta$ obs	$10^5 \sin^2\theta$ calc	F calc	I obs
1 0 1	1825	1825	112	s
2 0 0	1931	1931	184	s
0 1 1	3299	3292	174	vvs
1 1 1	3782	3775	126	vs
2 1 0	3881	3881	86	w
2 1 1	5221	5223	127	s
3 0 1	5696	5688	105	m
3 1 1	7640	7637	144	s
0 2 0 1 1 2	7807	7797 7803	225 212	vvs
4 0 1	9065	9068	109	m
2 1 2	9250	9251	55	w
4 1 0	9678	9674	222	s
2 2 0	9730	9728	135	m
2 2 1	11079	11071	108	m
3 1 2	11675	11665	50	vw
1 0 3	12570	12566	180	m
1 2 2	13651	13650	109	m
0 1 3	14036	14033	112	w
1 1 3	14509	14516	53	vw
2 1 3	15971	15964	77	w
3 0 3	16437	16429	95	w
4 2 1	16870	16865	171	s
3 2 2	17522	17513	184	s
3 1 3	18377	18378	133	w
0 3 1	18894	18886	157	m
1 3 1 5 1 2	19377	19368 19390	79 79	m
1 2 3	20356	20363	169	m
6 1 1	20669	20674	98	w
2 2 3	21821	21812	123	m
3 3 1	23243	23231	109	m
1 3 2	23402	23396	158	s
4 3 0	25261	25268	162	s
4 2 3	27606	27606	96	vvw
0 2 4	29283	29279	138	vw
7 1 2	30989	30978	111	m
2 4 0	33116	33119	111	w
4 4 1	40257	40255	86	vw

SOLUTION AND REFINEMENT OF THE STRUCTURE

From a three-dimensional Patterson synthesis, calculated with data yet uncorrected for absorption, the Hf and S parameters were obtained. A subsequent electron density calculation revealed the oxygen atoms and all parameters were seen to be consistent with the corresponding parameters in the structure of $Zr(OH)_2SO_4$.[4] A preliminary refinement of the atomic positions and isotropic temperature factors gave an R value of 0.143 ($R = \sum|F_o -$

$|F_c||/\sum F_o$). The Fourier summations were performed with the program *DRF*.[9]

After correction for absorption effects the isotropic refinement was repeated, including separate scale factors for three different θ-intervals in which the data were registered. The R value then dropped to 0.098.

From the intensities at low sin θ-values and the irregular shape of the crystal the diffraction from the crystal of $Hf(OH)_2SO_4$ could be suspected to be associated with extinction effects. A refinement of an isotropic secondary extinction factor, the scale factors and the atomic parameters, including isotropic thermal vibrations, was performed with the program LINUS.[9] An R value of 0.070 was obtained when the atomic scattering factors [10] for Hf and S were corrected for anomalous dispersion.[11] The final value of the isotropic extinction parameter was $g = (0.68 \pm 0.03) \times 10^4$.

Finally, the refinement was extended to include anisotropic thermal parameters, the scale factors being kept constant. The R value converged to 0.055, and the final parameters are given in Tables 2a,b. A weighting scheme according to Cruickshank was used in the refinements ($w = [60.0 + F_o + 0.018\ F_o^2 + 10^{-4}F_o^3]^{-1}$). The observed and calculated structure factors are compared in Table 3.

The accuracy of the structure was tested by means of a difference electron density calculation with the program FFT [9] which handles correction for

Table 2a. Atomic coordinates, expressed as fractions of the cell edges, and their standard deviations.

Atom and position	x	y	z
Hf in 4(*c*)	0.06016(8)	1/4	0.1366(1)
S in 4(*c*)	0.3635(4)	1/4	0.9435(7)
O_1 in 8(*d*)	0.4179(11)	−0.0004(33)	0.3938(16)
O_2 in 4(*c*)	0.4794(13)	1/4	0.0525(22)
O_3 in 4(*c*)	0.2615(14)	1/4	0.0855(21)
O_4 in 8(*d*)	0.3515(9)	0.0357(22)	0.8152(15)

Table 2b. Anisotropic thermal parameters and their standard deviations. The temperature coefficient is expressed as $\exp[-(h^2\beta_{11} + k^2\beta_{22} + l^2\beta_{33} + 2hk\beta_{12} + 2hl\beta_{13} + 2kl\beta_{23})]$.

Atom	β_{11}	β_{22}	β_{33}	β_{12}	β_{13}	β_{23}
Hf	0.0025(1)	0.0085(6)	0.0015(4)	0	−0.0001(1)	0
S	0.0021(4)	0.0106(16)	0.0012(11)	0	0.0003(5)	0
O_1	0.0034(8)	0.0166(48)	0.0068(24)	−0.0002(19)	−0.0006(11)	0.0009(30)
O_2	0.0030(12)	0.0121(47)	0.0069(40)	0	0.0001(19)	0
O_3	0.0048(13)	0.0094(52)	0.0006(27)	0	0.0018(18)	0
O_4	0.0023(8)	0.0179(42)	0.0081(20)	0.0004(16)	−0.0017(12)	−0.0048(31)

Table 3. Observed and calculated structure factors for $Hf(OH)_2SO_4$. (The columns are h, F_o and F_c, respectively.)

H 0 0	4 15 16	3 94 90
2 235 184	5 91 91	4 6 7
4 57 51	6 70 67	5 140 144
6 110 111	7 32 33	6 11 12
8 108 113	8 88 90	7 60 58
10 120 127	9 10 10	8 30 30
12 13 14	10 64 65	9 25 26
	11 48 48	
H 1 0		H 5 2
2 119 86	H 4 1	1 116 120
4 271 222	1 74 74	2 26 23
6 155 157	2 84 85	3 26 26
8 11 8	3 60 60	4 18 17
10 98 102	4 79 87	5 42 44
12 81 77	5 37 37	6 4 6
	6 54 55	7 63 66
H 2 0	7 96 100	
0 294 225	8 25 26	H 6 2
2 186 135	9 67 67	0 6 7
4 54 49	10 35 31	1 36 40
6 84 87		2 12 13
8 94 97	H 5 1	3 80 85
10 97 100	0 81 81	4 9 8
12 39 40	1 54 59	
	2 68 70	H 0 3
H 3 0	3 76 79	1 173 180
2 121 100	4 23 27	2 58 63
4 181 163	5 55 55	3 92 95
6 110 117	6 58 61	4 67 68
8 10 7	7 26 26	5 53 57
10 83 85	8 74 74	6 32 34
		7 107 119
H 4 0	H 6 1	8 31 28
0 281 242	1 34 38	9 94 90
2 127 112	2 55 62	10 23 21
4 19 17	3 33 38	11 44 43
6 70 78	4 71 77	12 61 58
8 80 84	5 10 10	
10 91 92		H 1 3
	H 0 2	0 117 112
H 5 0	0 15 16	1 55 53
2 45 47	1 28 30	2 75 77
4 118 126	2 11 8	3 130 134
6 90 98	3 104 110	4 58 58
8 6 11	4 8 8	5 138 141

H 6 3	2 62 63	
1 72 79	3 45 43	
2 53 52	4 150 146	
	5 9 6	
H 0 4	6 121 119	
0 209 209	7 42 43	
1 15 15	9 40 39	
2 121 128		
3 73 75	H 3 5	
4 7 8	0 151 142	
5 27 26	1 42 41	
6 106 115	2 84 81	
7 7 4	3 49 46	
8 131 130	4 29 29	
9 15 13	5 42 41	
10 80 78	6 58 57	
11 20 19	7 15 16	
	8 83 76	
H 1 4		
1 43 44	H 4 5	
2 120 122	1 58 55	
3 53 54	2 58 55	
4 160 160	3 20 20	
5 12 10	4 114 105	
6 98 100	5 23 26	
7 51 54	6 97 91	
8 21 20		
9 31 31	H 5 5	
10 60 56	0 99 100	
11 6 4	1 17 18	
	2 59 58	
H 2 4		
0 145 138	H 0 6	
1 42 41	0 33 34	
2 97 96	1 68 70	
3 59 61	2 40 45	
4 27 26	3 113 117	
5 21 21	4 4 3	
6 80 78	5 69 72	
7 18 18	6 15 18	
8 116 105	7 41 43	
9 20 20	8 58 58	
10 82 81		
	H 1 6	
H 3 4	1 109 110	

H 6 0	5 199 225	6 66 68
0 115 121	6 8 7	7 54 59
2 59 65	7 86 82	8 86 79
4 8 4	8 40 39	9 38 39
	9 35 35	10 38 37
H 0 1	10 13 13	11 78 76
1 106 112	11 75 72	12 6 7
2 140 158	12 7 5	
3 94 105		H 2 3
4 66 109	H 1 2	1 174 169
5 69 69	1 203 212	2 122 123
6 71 66	2 55 55	3 35 34
7 157 156	3 51 50	4 98 96
8 47 50	4 30 28	5 38 36
9 89 92	5 76 79	6 22 23
10 43 42	6 10 9	7 68 63
11 1 3	7 119 111	8 10 10
12 88 87	8 17 16	9 100 96
13 10 9	9 131 127	10 37 35
	10 13 11	11 60 63
H 1 1	11 65 66	
0 180 174	12 21 21	H 3 3
1 119 126		0 80 77
2 122 127	H 2 2	1 31 28
3 138 144	0 43 40	2 67 65
4 43 46	1 113 109	3 106 103
5 109 106	2 30 30	4 53 51
6 110 98	3 186 184	5 136 131
7 43 43	4 22 22	6 59 61
8 114 114	5 188 189	7 47 48
9 15 18	6 40 42	8 75 71
10 62 64	7 69 65	9 42 41
11 57 58	8 48 50	10 31 29
12 7 7	9 43 43	
	10 10 9	H 4 3
H 2 1	11 96 92	1 124 122
1 58 60	12 8 7	2 57 55
2 111 108		3 52 51
3 64 60	H 3 2	4 52 50
4 167 171	1 167 158	5 40 39
5 19 19	2 58 56	6 21 23
6 98 93	3 60 57	7 85 78
7 91 92	4 16 14	8 23 22
8 6 7	5 61 62	9 72 68
9 83 90	6 8 2	

1 26 25	2 56 56	
2 103 99	3 80 82	
3 59 58	4 51 52	
4 142 133	5 21 23	
5 10 8	6 30 34	
6 86 86	7 114 110	
7 60 58	8 9 11	
8 17 17		
9 23 23	H 2 6	
	0 32 30	
H 4 4	1 62 62	
0 144 138	2 57 58	
1 23 21	3 129 123	
2 89 88	4 13 10	
3 55 53	5 96 92	
4 17 6	6 47 47	
5 12 12	7 31 32	
6 81 79		
7 6 5	H 3 6	
8 100 91	1 107 100	
	2 55 54	
H 5 4	3 66 63	
1 27 27	4 42 42	
2 77 74	5 21 21	
3 26 27	6 26 24	
4 102 102		
5 5 6	H 4 6	
	0 25 24	
H 0 5	1 51 51	
1 84 87	2 34 35	
2 78 79	3 90 83	
3 19 18		
4 137 141	H 0 7	
5 35 37	1 145 138	
6 112 122	2 15 14	
7 42 47	3 31 34	
8 13 13	4 34 38	
9 53 52	5 33 40	
10 62 62	6 39 41	
H 1 5	H 1 7	
0 167 163	0 53 54	
1 36 37	1 22 21	
2 93 97	2 13 13	
3 49 49	3 102 101	

10 55 57	7 110 102	H 5 3
11 22 22	8 21 22	0 59 60
12 67 65	9 106 104	1 35 35
	10 10 10	2 45 44
H 3 1	11 56 54	3 82 81
0 170 157		4 26 28
1 80 79	H 4 2	5 79 82
2 94 92	0 14 11	6 42 42
3 114 109	1 33 33	7 38 36
	2 13 12	

4 32 32	4 14 16	
5 60 61	5 115 119	
6 67 69		
7 14 16	H 2 7	
8 97 90	1 141 129	
9 4 5	2 28 27	
10 86 79	3 34 36	
	4 42 43	
H 2 5		
1 28 27	H 3 7	
	0 38 39	
	1 23 19	

Table 4. Interatomic distances (Å) and angles (°) with their standard deviations in parentheses.

Within the antiprism:

$Hf-2O_1$	2.136(14)	O_1-Hf-O_1 (2x)	65.8(5)
$Hf-2O_1$	2.106(15)	O_1-Hf-O_1	82.0(8)
$Hf-O_2$	2.251(15)	O_1-Hf-O_1	80.3(8)
$Hf-O_3$	2.257(16)	$O_2-Hf-2O_1$	77.9(4)
$Hf-2O_4$	2.203(11)	$O_3-Hf-2O_1$	76.9(4)
Mean	2.175	$O_2-Hf-2O_4$	71.5(5)
		$O_3-Hf-2O_4$	69.0(4)
O_1-O_1 (2x)	2.763(37)	O_2-Hf-O_3	122.1(5)
O_1-O_1 (2x)	2.303(24)	O_4-Hf-O_4	91.4(6)
O_2-2O_4	2.601(16)		
O_3-2O_4	2.527(16)		
O_2-2O_1	2.742(19)		
O_3-2O_1	2.733(19)		
O_1-O_4 (2x)	2.903(15)		
O_1-O_4 (2x)	2.916(16)		

Within the sulfate group:

$S-O_2$	1.476(16)	O_2-S-O_3	110.8(9)
$S-O_3$	1.473(16)		
$S-2O_4$	1.464(12)	O_4-S-O_4	107.7(9)
O_2-O_3	2.428(22)		
O_4-O_4	2.364(25)	O_2-S-O_4 (2x)	111.4(5)
O_2-2O_4	2.429(17)		
O_3-2O_4	2.371(17)	O_3-S-O_4 (2x)	107.7(9)

Other distances:			
(within the chain)		(different chains):	
Hf–Hf	3.562(1)	O_1-O_4	3.038(16)
O_4-O_4	3.153(25)	O_1-O_3	3.020(19)

extinction effects. No unexpected maxima or minima were obtained, and the maximum electron density found was 4 e/Å^3.

Interatomic distances and angles were calculated with the program DISTAN [9] and the results are given in Table 4.

DISCUSSION

The structure may be considered to be composed of layers of zig-zag chains of somewhat distorted square antiprisms, the layers being connected by sulfate groups. Two chains of antiprisms from different layers are shown in Fig. 1 together with some of the connecting sulfate tetrahedra. This arrangement is also found in the isomorphous salts $Zr(OH)_2SO_4$(I),[4] $Th(OH)_2SO_4$,[12] and $U(OH)_2SO_4$,[13] and all of the structures have the characteristic $[Me(OH)_2]_n^{2n+}$ chains running along the *b* axis.

The distortion of the antiprismatic configuration about Hf is mainly due to the double oxygen bridges between the hafnium atoms. The short distances between the oxygen atoms in the bridges (cf. Table 4) cause a compression of the oxygen square on one side of the metal atom. In $Hf(OH)_2SO_4$ the O_1-O_1

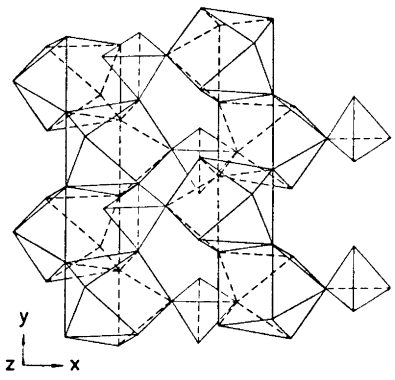

Fig. 1. Parts of two infinite chains of distorted square antiprisms connected by sulfate groups.

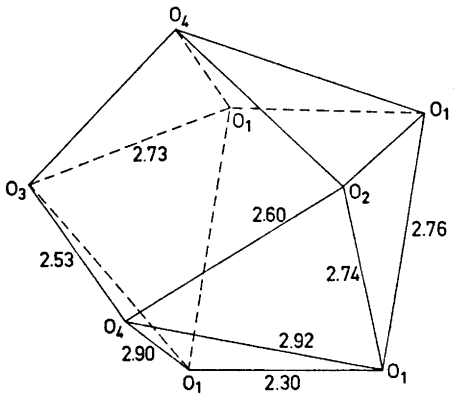

Fig. 2. Antiprismatic configuration of oxygen atoms about hafnium in $Hf(OH)_2SO_4$. (Distances in Å).

bridge distance is noticeably short, *i.e.* 2.30 ± 0.02 Å. This can be compared with the distances in $Zr(OH)_2SO_4$[4] (2.40 Å), $Zr_2(OH)_2(SO_4)_3(H_2O)_4$[3] (2.34 Å), $Hf(OH)_2SO_4H_2O$[2] (2.33 Å), $Zr(OH)_2CrO_4$[14] (2.35 Å) and $Zr_4(OH)_6(CrO_4)_5H_2O$[15] (2.37 – 2.40 Å). The shortest distances mentioned above (2.33 – 2.35 Å) are, however, found in structures with planar $[Me(OH)_2]_n^{2n+}$ chains.

On the other side of the hafnium atom an approximate square rotated through 45° is built up from oxygen atoms (O_2, O_3, $2O_4$), belonging to four different sulfate ions (*cf.* Fig. 2). Since this square was not quite planar, the plane of best fit was calculated by the program PLANEFIT,[9] the following equation being obtained (in Å and fractional coordinates): $6.720x + 5.286z = 2.441$. The distances of the sulfate oxygen atoms and of the hafnium atom from the plane are: O_2 0.21 Å; O_3 0.23 Å; $2 \times O_4$ −0.22 Å; and Hf 1.31 Å. The distance of Hf from the plane through the O_1 atoms was found to be 1.13 Å and the angle between the two planes 0.5°. These values are in agreement with those found for $Zr(OH)_2SO_4$(I),[4] the angles between the two planes differing, however, slightly in the two compounds. The angle is a little larger (1.2°) in the zirconium salt, but the difference is not quite significant.

The sulfate tetrahedra in the two isomorphous hafnium and zirconium salts are somewhat distorted but not in the same manner. The sulfate groups are bonded through all four vertices to four different metal atoms belonging to three different chains (*cf.* Fig. 1). In $Zr(OH)_2SO_4$ the tetrahedra are elongated along the chains, the distance between the two O_4 atoms belonging to the same chain being 2.48 Å. The distance between the layer-connecting oxygens, O_2 and O_3, is 2.37 Å. Corresponding distances in $Hf(OH)_2SO_4$ are 2.36 and 2.43 Å, respectively.

Despite the short distance between the bridging oxygen atoms, the distance between the bridged Hf-atoms, 3.562 Å, is shorter than the corresponding distance in $Zr(OH)_2SO_4$, *i.e.* 3.576 Å. Moreover, the planar chains in $Hf(OH)_2SO_4H_2O$ exhibit the shortest Me – Me distance (3.553 Å) found in basic compounds containing $[Me(OH)_2]_n^{2n+}$ chains (Me = Hf,Zr).

Acknowledgements. The author wishes to thank Professor Georg Lundgren for his support and great interest in this work. Thanks are also due to Professor Peder Kierkegaard and Fil. kand. Bengt Karlsson, Stockholm, for making it possible to collect the intensity data with the Philips automatic four-circle diffractometer, PW 1100, and for helpful assistance. The author is also indebted to Dr. Susan Jagner for revising the English text.

This work has been supported by the *Swedish Natural Science Research Council* (NFR, Contract No. 2318).

REFERENCES

1. Hansson, M. and Lundgren, G. *Acta Chem. Scand.* **22** (1968) 1683.
2. Hansson, M. *Acta Chem. Scand.* **23** (1969) 3541.
3. McWhan, D. B. and Lundgren, G. *Inorg. Chem.* **5** (1966) 284.
4. Hansson, M., Lundgren, G. and McWhan, D. B. *To be published.*
5. *International Tables for X-Ray Crystallography*, 2nd Ed., Kynoch Press, Birmingham 1965, Vol. I.
6. *International Tables for X-Ray Crystallography*, Kynoch Press, Birmingham 1962, Vol. III, p. 122.
7. Lindqvist, O. and Wengelin, F. *Arkiv Kemi* **28** (1967) 179.
8. Modified in Stockholm. Originally written by Coppens, P., Leiserowitz, L. and Rabinowich, D.
9. The program library of the Dept. of Inorg. Chem. Göteborg. *DRF* and *DISTAN* were originally written by Zalkin, A., *FFT* by Ten Eyck, L. and *PLANEFIT* by Wengelin, F. *LINUS* is the Busing, Martin & Levy (1962) LS program modified for refinement of extinction parameters by Coppens & Hamilton, 1970.
10. Cromer, D. T. and Waber, J. T. *Acta Cryst.* **18** (1965) 104.
11. Cromer, D. T. *Acta Cryst.* **18** (1965) 17.
12. Lundgren, G. *Arkiv Kemi* **2** (1950) 535.
13. Lundgren, G. *Arkiv Kemi* **4** (1952) 421.
14. Mark, W. *Acta Chem. Scand.* **26** (1972) 3744.
15. Mark, W. *Acta Chem. Scand.* **27** (1973) 177.

Received February 22, 1973.

ACTA CHEMICA SCANDINAVICA 27 (1973) 2463–2484

Influence of Cosolutes upon the Conformation of Carbohydrates in Aqueous Solutions. I. Dependence upon the Anion of the Relative Rates of Hydrolysis of the Anomeric Methyl Glucopyranosides in Aqueous Mineral Acids

TERENCE PAINTER

Institute of Marine Biochemistry, N-7034 Trondheim-NTH, Norway

The ratio (K_β/K_α) of the rates of hydrolysis of β- and α-methyl D-glucopyranoside in aqueous sulphuric, phosphoric, hydrochloric, and hydrobromic acids increased markedly with increasing concentration of acid, and, for a given value of the Hammett acidity function (H_0), the magnitude of the effect decreased in the order in which the acids are named.

For values of $-H_0$ between 1.0 and 3.0, separate plots of log (K_β) and log (K_α) against $-H_0$ were virtually rectilinear in each acid, but they had different slopes. A more detailed study of hydrolysis in sulphuric acid showed that, outside this range, the plots were parallel. In the region in which the slopes deviated, the respective activation energies, E_β and E_α, both decreased with increasing acidity, but E_β decreased more than E_α. Simultaneously, the entropies of activation decreased, but to the same extent.

The increase in K_β/K_α was attributed to the anomeric effect, which, as the activity of water decreases, would be expected to stabilise the α-anomer and de-stabilise the β-anomer relative to the transition state.

The overall decrease in E_β and E_α was attributed to the stripping of water of solvation from the hydroxyl groups, leading to a decrease in their effective conformational size. The concomitant decrease in the entropy of activation supports this, and implies that water of solvation is released in passing through the transition state.

In an attempt to learn more about the biological role of carbohydrates in marine organisms, a study was undertaken of the effect of inorganic ions and other relevant cosolutes upon the conformation of polysaccharides and simple, model glycosides in aqueous solutions. In the first instance, attention was focussed upon the effect of inorganic ions upon reactions of simple glycosides, whose mechanisms are well understood, and which are known to entail conformational changes in the transition state. The work now described is

concerned with the influence of anions, and consists simply in a study of the relative rates of hydrolysis of α- and β-methyl D-glucopyranoside in different mineral acids.

EXPERIMENTAL

Materials. The two glycosides were commercial products, and were recrystallised to constant melting point from absolute ethanol. The acids were of Merck analytical grade. The normalities of the acids were determined by titration at 20° with standard sodium hydroxide, prepared from Merck ampoules. The indicator was methyl red.

Method. Hydrolysis was carried out in a 2 dm, centre-filling polarimeter tube, fitted with a heavy copper heating jacket, which was insulated with cotton wool. Water from a thermostatically controlled water-bath was pumped through the jacket at a rate of 1.5 l/min. The temperature was measured with a thermometer fitted into the polarimeter tube, and could be held constant to within ±0.02°. A conventional Zeiss polarimeter was used, which permitted measurement of the angle of rotation to within 0.01°.

To start an experiment, the polarimeter tube was first brought to the desired temperature. Identical volumes (measured at 20°) of a 2 % w/v aqueous solution of the glycoside and of the acid were then separately heated in the water-bath to the same temperature. The two solutions were then rapidly mixed, and transferred to the polarimeter tube. Complete thermal equilibrium was normally established inside the tube within 2 min, after which the first readings were taken. In experiments with very concentrated acids, there was some heat of dilution liberated upon mixing the two reactants. In these cases, prior to mixing, the reactants were warmed to a lower temperature than that desired, the exact temperature being determined by trial and error.

To avoid errors due to the acid-catalysed reversion and dehydration of the liberated glucose, only the first 50 – 70 % of the hydrolysis was followed, and normally, 30 to 50 readings were taken in the time (30 to 240 min) required for this. An "infinite time" reading was obtained with a freshly prepared solution of D-glucose in the acid under the same conditions. These experiments additionally confirmed that the mutarotation of D-glucose was virtually instantaneous in all the acids studied, and that the rate of destruction of the glucose was not of significant importance compared to its rate of liberation from the parent glycosides under the same conditions.

In the more concentrated acids, the "initial" optical rotation differed significantly from that in water at the same temperature, and was estimated by extrapolation of the hydrolysis-curve to zero time.

Thin-layer chromatography of the glycosides and of p-*nitroaniline in strong mineral acids.* This was carried out at room temperature on glass plates (20 × 5 cm) coated with a 0.75 mm thick layer of silica gel (Merck Kieselgel nach Stahl). Portions (200 μg) of material were applied to the origin as 1 % w/v solutions in methanol. After the acid had ascended 15 – 18 cm, the plates were placed horizontally on asbestos mats, and heated about 30 min in an oven at 110°. The glycosides were then revealed as dark spots, due to charring.

In low concentrations of acid, the *p*-nitroaniline migrated as a visible, yellow spot, and its position was marked on the developed plate before heating. In high concentrations of acid, it was colorless, but could be localised after heating by examination under UV light, when it appeared as a black spot. In low concentrations of acid, the glycosides did not char sufficiently upon heating to be clearly visible, but in these cases they were plainly visible, after heating, as fluorescent spots under UV light.

When chromatography was carried out in pure water as the solvent, the developed plates were first dried completely in the oven, then sprayed with 10 N sulphuric acid, and then heated again. When the acids themselves were chromatographed in water, they were localised by spraying the dried plates with aqueous sucrose (20 % w/v), followed by further heating.

THEORY

Mechanism of hydrolysis. The extensive literature on the mechanism of hydrolysis of glycosides has been comprehensively reviewed by BeMiller.[1]

It is generally accepted that, for pyranosides, hydrolysis takes place by the "cyclic", A-1 mechanism (Fig. 1), in which a rapid, equilibrium-controlled protonation of the glycosidic oxygen atom to give the conjugate acid (I) is followed by a unimolecular, rate-controlling heterolysis of the bond between this oxygen atom and C(1) of the pyranose ring. This liberates the aglycone, and generates a carbonium ion at C(1) of the glycose moiety, forcing it into the highly strained, half-chair form (II). This then reacts rapidly with water to give free glucose and a proton.

The Edward hypothesis. It is also widely accepted [1] that the well-known difference in the rates of hydrolysis of anomeric pairs of glycopyranosides is due to the effect first suggested by Edward,[2] and now generally known as *the anomeric effect*.[3,4]

The anomeric effect can be most simply regarded as a special case of the general proposition that a polar molecule in a non-polar solvent will tend to adopt a conformation in which the net dipole moment is as small as possible. This tendency will normally be opposed by other non-bonded interactions, and will weaken as the polarity of the solvent increases, and polar solvent-solute interactions become dominant.

Edward [2] pointed out that a glycopyranoside in which the glycosidic oxygen atom is axial should have a lower net dipole moment than one in which it is equatorial. This should stabilise the *C-1* conformation in methyl α-D-glucopyranoside relative to the *C-1* conformation in methyl β-D-glucopyranoside. Edward further assumed that the transition state in the heterolysis step would be the same for both anomers, and would correspond to the carbonium ion (II) in Fig. 1. The β-anomer would then be expected to hydrolyse faster than the α-anomer, as is the case.

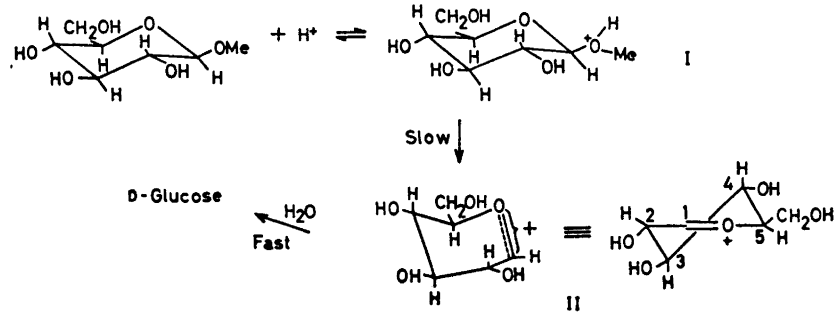

Fig. 1. Accepted mechanism for the acid hydrolysis of the methyl glucopyranosides.

In connection with a discussion of the preferred position of protonation in glycosidic hydrolysis, Lemieux and Morgan [5] subsequently pointed out that the stability of the conjugate acid would be governed by the reverse of the anomeric effect, essentially because, after protonation, the dipole along the C(1)–O(1) bond is in the opposite direction. This implies that the β-anomer, after protonation at the glycosidic oxygen atom, would be more stable than

the α-anomer, protonated in the same position. Expressed in other terms, the β-anomer is the stronger base, and the concentration of its conjugate acid at equilibrium is therefore higher.

There is no evidence that Lemieux and Morgan [5] regarded these statements as amounting to a negation of Edward's hypothesis in its original form, but their acceptance by others has led to the assumption that the β-anomer is hydrolysed faster, simply because it is the stronger base.[6] This is wrong, because the rate of the reaction is determined not only by the concentration of the conjugate acid at equilibrium, but also by the free energy of activation of the heterolysis step.

The theory of the transition state provides that the rate of reaction is proportional to the concentration of molecules in that state. This can be expressed in terms of the concentration of the conjugate acid at equilibrium, together with the free energy of activation of the heterolysis, but it can also be expressed in terms of the activities of the reactants, the activity coefficient of the conjugate acid, and the total change in free energy incurred in passing from the unprotonated glycoside to the transition state. This last quantity is the sum of the change in free energy upon protonation and the free energy of activation of the heterolysis.

Thus, we have: $G + H^+ \rightleftharpoons GH^+$; $GH^+ \rightarrow$ Products.

Whence:

$$K = \frac{\{GH^+\}}{\{G\}\{H^+\}} \times \frac{f_{GH^+}}{f_G f_{H^+}} \tag{1}$$

and

$$\text{Rate} = kC^{\ddagger} = k'\{GH^+\} \tag{2}$$

Hence:

$$\text{Rate} = k'K\{G\}\{H^+\}(f_G f_{H^+}/f_{GH^+}) \tag{3}$$

But $k' = (\varkappa kT/h)e^{-\Delta F^{\ddagger}/RT}$ and $K = K_0 e^{-\Delta F/RT}$, from which it is seen that the product, $k'K$ in eqn. (3) contains the relevant energetic term, $\exp[-(\Delta F^{\ddagger} + \Delta F)/RT]$.

The ratio of the rates of hydrolysis of the two anomers is then given by:

$$\frac{K_\beta}{K_\alpha} = \frac{(f_G)_\beta (f_{GH^+})_\alpha}{(f_G)_\alpha (f_{GH^+})_\beta} \times \exp[(\Delta F_\alpha^{\ddagger} - \Delta F_\beta^{\ddagger} + \Delta F_\alpha - \Delta F_\beta)/RT] \tag{4}$$

It is, therefore, a valid hypothesis to suggest that the β-anomer is hydrolysed faster because, in its unprotonated state, it is less stable than the unprotonated α-anomer. It rests, of course, upon the stated assumption that the transition state is identical for both anomers, and it also implies the assumption that the term containing the activity coefficients in eqn. (4) is unity. For hydrolysis in dilute mineral acids, this last assumption is plausible, but it is not known to be true, and it is certainly not known to be true in strong mineral acids. An attempt was therefore made in the present work to show whether or not it is true.

It is not a valid alternative to the hypothesis of Edward to suggest that the β-anomer is the stronger base without making any statement about the

free energy of activation. This applies, regardless of whether the reason for the greater basicity is that advanced by Lemieux and Morgan,[5] or whether, as others[1] have suggested, the glycosidic oxygen atom of the β-anomer is more easily protonated because it is "more accessible".

Alternatives to Edward's hypothesis. It must be explained at this point that it is not our purpose to question, or seek further evidence for, the existence of the anomeric effect.[3,4] We shall investigate the effect of various anions upon the relative rates of hydrolysis of the two glucosides, and in order to understand these effects, it will be necessary to know, in every instance, whether the observed difference in rates is due solely to the anomeric effect, or to what extent it is due also to other effects.

It must be recognised that Edward's hypothesis requires not merely that the β-anomer be less stable than expected on the basis of van der Waals forces alone, or the α-anomer more stable than otherwise expected, but that the β-anomer be less stable than the α-anomer in the absolute sense, even in dilute, aqueous mineral acid. Water is known to have a strong capacity to quench the anomeric effect, apparently because it is able to form hydrogen bonds with the ring and glycosidic oxygen atoms.[7,8]

We may begin by questioning Edward's first assumption, namely, that the transition state is identical for both anomers. Assuming that the mechanism is A-1 in both instances, it is difficult to see how it could not be. There can be no doubt that the half-chair form of the carbonium ion represents an energy maximum in passing from conjugate acid to products. It is significant, however, that the most definitive mechanistic studies favouring the A-1 mechanism have been carried out on α-anomers.[9,10,11] If the possibility that the β-anomer is hydrolysed, even partly, by a bimolecular mechanism is admitted, the situation changes. Moreover, there is a serious reason for believing that it may do so.

This is because of the Hassel-Ottar effect, a hypothesis originally advanced to explain why, in the hydrohalogenolysis of penta-*O*-acetyl-hexopyranosides, the α-glycopyranosyl halide is formed to the almost complete exclusion of the corresponding β-anomer.[12] This reaction is thought to proceed by an S_N2 mechanism, entailing Walden inversion at the anomeric centre. Both anomeric forms of the penta-*O*-acetate react, but since the only product is the α-halide, the α-acetate must first anomerise to the β-acetate before reaction can occur. Expressed in other terms, the β-anomer is again the more reactive, but in this case overwhelmingly so.

Hassel and Ottar pointed out that, for the α-acetate to react, the attacking halide ion would have to approach the ring on the side which would bring it into a *cis*-configuration with respect to C(6), and that there would be a particularly strong steric interaction with this atom in the transition state, because of the relative shortness of the bonds adjoining C(5), O(5) and C(1). In fact, they went further, and suggested that, in order to make room for the acetoxyl ion to leave, the ring would temporarily have to convert into the alternative chair-conformation, thus making the interaction a *syn*-diaxial one. On the other hand, there would be no such interaction in the conversion of the β-acetate into the α-halide.

The corollary of ring-conversion would appear to be a necessary one, because, in the case of glucose, for example, conversion of the β-acetate into the α-halide would, in the transition state, entail a strong interaction between the entering halide ion and O(2). This can be seen in Fig. 1.

The existence of the Hassel-Ottar effect, which is now generally regarded as referring to the especially strong syn-diaxial interaction between substituents at C(1) and C(5), is, of course, just as indisputable as the existence of the anomeric effect. It is interesting, however, that this particular reaction, which Hassel and Ottar sought to explain in terms of such an interaction, has a rival explanation. Thus, the proposed mechanism implies kinetic control, but if it is assumed that anomerisation of acetylglycopyranosyl halides can occur rapidly under the conditions of the reaction, the reaction will be equilibrium-controlled, and the high yield of the α-halide would then be a direct result of the anomeric effect.

Returning to the question of glycosidic hydrolysis, it is evident that the molecularity of the hydrolysis of the β-anomer must be examined very carefully. The attacking species could be either the anion of the mineral acid used for hydrolysis, or it could be a water molecule, in which case the mechanism would be an A-2 one.

Turning to the second assumption implied by Edward's hypothesis, namely, that the term containing the activity coefficients in eqn. 4 is unity, we come to a consideration of primary salt effects. Even if there were no difference between the free energies of the two glycosides in the unprotonated state, the β-anomer would still be hydrolysed faster than the α-anomer if its activity coefficient were higher than that of the α-anomer, or if the activity coefficient of its conjugate acid were lower than that of the conjugate acid of the α-anomer. It is already known [1] that the activation energy for hydrolysis of the β-anomer is lower than that of the α-anomer, so it is certain that the facts cannot be explained solely in terms of salt effects. It will still be necessary, however, to ascertain to what extent any new results are due to salt effects.

Finally, brief comment must be made regarding the possibility that the effects to be described are spurious, that is, an artefact of the polarimetric method of analysis. This could come about if anomerisation occurred as a reaction competitive with hydrolysis. Such anomerisation could occur either through ring-scission between O(5) and C(1), or as a result of a cave effect, that is, recombination of the carbonium ion (II in Fig. 1) with the molecule of methanol before it has escaped from the site of reaction. Against this may be cited the following facts:

(*a*) The position of the equilibrium between the α- and β-glycosides would certainly be different from that between the α- and β-anomers of free glucose.[3,4] Therefore, the kinetics indicated by the polarimetric method would not be of the first order.

(*b*) The kinetics of the acid-hydrolysis of simple glycosides and disaccharides, measured both polarimetrically and by chemical methods, have invariably been found to be of the first order, with good agreement between the two methods. This holds true, even for hydrolysis in concentrated mineral acids (see, for example, results given for cellobiose and maltose in 18 N sulphuric acid by Freudenberg *et al.*[13]). Clearly, if anomerisation occurred, neither method

would indicate first-order kinetics, and nor would they agree.

As a corollary to these well-known facts, it may be pointed out that they also exclude the "acyclic" mechanism of hydrolysis that has been discussed [1] as an alternative to the "cyclic" one. If the "acyclic" mechanism operated, anomerisation would be expected to take place as a reaction competitive with hydrolysis, and it could be expected to be at least as fast, if not more so.*

Criteria of molecularity. To determine whether or not the observed results can be attributed in any degree at all to the Hassel-Ottar effect, it is necessary to have a sensitive criterion of molecularity. If the assumptions of the Zucker-Hammett hypothesis [15] held true, a plot of the logarithm of the first-order rate-coefficient against $-H_0$ would give a straight line of unit slope for an A-1 mechanism. For an A-2 mechanism, a curve would be obtained whose slope decreased as the numerical value of $-H_0$ increased. This would happen, of course, because the activity of the water molecules decreases with increasing values of $-H_0$ (increasing concentration of acid). If, on the other hand, bimolecularity resulted because of nucleophilic attack by the anion of the acid, a curve would be expected whose slope increased with increasing values of $-H_0$.

In practice, it has been found that, for glycosides and other acetals in strong mineral acids, the plots are usually linear, but not of unit slope. [15] This has led some authors [16] to describe the criterion as "useless". There are, however, a number of additional points to be considered before reaching such a conclusion.

The first of these was raised by McIntyre and Long,[17] who pointed out that deviation from unit slope would be expected if either the activity coefficient of the unprotonated substrate relative to that of the unprotonated base changed with increasing acid-concentration, or if the activity coefficients of the protonated substrate and Hammett base changed relative to one another with increasing acid-concentration.

Thus, starting with the Brønsted equation for the dependence of the first-order rate-coefficient upon changes in the medium:

$$k_h = k_{h0}' C_{H^+}(f_{H^+} f_S / f_{S^+}) \tag{5}$$

in which f_S and f_{S^+} are the activity coefficients of the unprotonated and protonated substrate respectively, McIntyre and Long [17] deduced an expanded expression of the Zucker-Hammett relationship:

$$\log k_h = -H_0 + \log \frac{f_S f_{BH^+}}{f_{S^+} f_B} + \text{const.} \tag{6}$$

in which f_{BH^+} and f_B are the activity coefficients of the protonated and free Hammett base, respectively.

* Reference is made to Lindberg's work [14] on the acetolysis of the anomeric ethyl glucopyranosides. This reaction is definitely known to proceed partly by the "acyclic" mechanism, because a small amount of hepta-*O*-acetyl-glucose is formed. The catalytic species in this reaction is the acetonium ion instead of a proton, and steric hindrance may account for the different mechanism. The rate of anomerisation was extremely high compared to the rate of acetolysis.

These authors then studied the effect of neutral salts upon the activity coefficient of methylal, by measuring its distribution ratio between benzene and the aqueous phase, and also upon the activity coefficient of *p*-nitroaniline, by measurements of solubility.[18] They then studied the hydrolysis of methylal in dilute hydrochloric acid containing various proportions of salt, and found that the correlation between rate and H_0 could be satisfactorily expressed by eqn. (6), on the assumption that f_{BH^+}/f_{S^+} was consistently unity.[18] No attempt was made to measure these last quantities, but the work nevertheless shows that the Hammett criterion of molecularity can still be used if measurements of activity coefficients are also carried out.

Apart from primary salt effects, it is also necessary, in any complete analysis of molecularity, to consider the possibility that changes in the medium may bring about changes in the total free energy of activation ($\Delta F^{\neq} + \Delta F$). This could come about, without implying any change of mechanism, if the possibility is admitted that the substrate may exist in solution as one or more hydrated species as well as an unhydrated molecule. As the concentration of acid increases, and the activity of the water molecules decreases, the relative proportions of these species would be expected to change. Moreover, it is readily seen why both the enthalpy and entropy of activation might be different for these different species, because the conformational change (from chair to half-chair) that takes place on passing through the transition state might well entail decomposition of the hydrate.

For simplicity, we may consider a two-component system of unhydrated glycoside, G, and a hydrate, $G(H_2O)_n$, which will be referred to as GS for purposes of notation. Then, $G + nH_2O \rightleftharpoons G(H_2O)_n$ whence $K_{solv} = a_{GS}/a_G(a_{H_2O})^n = [(1-\alpha)/\alpha(a_{H_2O})^n]f_{GS}/f_G$ where α represents the degree of dissociation of the hydrate.

It follows that $\alpha = [1 + K_{solv}(a_{H_2O})^n f_G/f_{GS}]^{-1}$, and hence:

$$\text{Rate} = k_1\alpha C_{H^+}(f_G f_{H^+}/f_{GH^+}) + k_2(1-\alpha)C_{H^+}(f_{GS}f_{H^+}/f_{GSH^+}) \quad (7)$$

Applying the unmodified assumptions of the Zucker-Hammett hypothesis, we now get:

$$\log\ (\text{Rate}) = -H_0 + \log[k_1\alpha + k_2(1-\alpha)] = \\ = -H_0 + \log\left[\frac{k_1 + k_2 K_{solv}(a_{H_2O})^n f_G/f_{GS}}{1 + K_{solv}(a_{H_2O})^n f_G/f_{GS}}\right] \quad (8)$$

On the assumption that f_G/f_{GS} is independent of the medium, examination of eqn. (8) shows that there are two special cases in which a plot of log (Rate) against $-H_0$ would give a straight line of unit slope. Thus, when $k_1 = 0$ and K_{solv} is large, eqn. (8) simplifies to:

$$\log\ (\text{Rate}) = -H_0 + \log\ k_2 \quad (9)$$

and when $k_2 = 0$ and K_{solv} is small:

$$\log\ (\text{Rate}) = -H_0 + \log\ k_1 \quad (10)$$

Two other special cases of interest arise when $k_1 = 0$ and K_{solv} is small:

$$\log (\text{Rate}) = -H_0 + n \log (a_{H_2O}) + \log k_2 + \text{const.} \quad (11)$$

and when $k_2 = 0$ and K_{solv} is large:

$$\log (\text{Rate}) = -H_0 - n \log (a_{H_2O}) + \log k_1 + \text{const.} \quad (12)$$

Eqns. (11) and (12) are identical with those arrived at empirically by Bunnett,[19–22] n being, in these particular cases, identical with his parameter, w. Bunnett tried to interpret all examples of acid-hydrolysis in terms of these two special cases, and hence in terms of a single parameter, w.

In the general case, all curves described by eqn. (8) are sigmoid in shape, and have unit slopes at both low concentrations of acid ($-H_0$ less than zero) and very high concentrations of acid ($-H_0$ greater than about 3.5 – 5.0, depending on the value of n). In the intermediate range of acid-concentration, which is normally chosen in mechanistic studies, the slopes of the curves are greater than unity when $k_1 > k_2$, and less than unity when $k_1 < k_2$. Two examples are shown in Fig. 2. Bearing in mind that in this figure, rather extreme

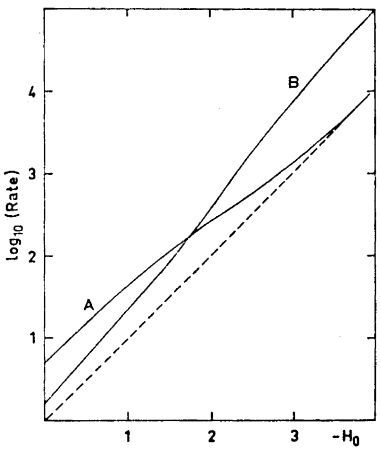

Fig. 2. Theoretical plots of the logarithm of *pseudo*-first-order rate-coefficients against $-H_0$, according to eqn. (8). In curve A, $k_1 = 1$, $k_2 = 10$, and $K_{solv} = 1$, while in curve B, $k_1 = 10$, $k_2 = 1$, and $K_{solv} = 10$. In both curves, $n = 4$, and values for the activity of water are taken from the table compiled by Bunnett.[29]

examples have been chosen for purposes of illustration, and the existence of experimental error, it is readily understood why straight-line plots are usually reported: *it is because they are drawn through points of inflexion in what are really sigmoid curves.*

Given that a study of the type described by McIntyre and Long [17,18] allows possible salt effects to be either discounted or corrected for, it is now necessary to decide how a plot of log (Rate) against $-H_0$ will be helpful in determining the reason for the higher rate of hydrolysis of the β-glucoside. With regard to the possibility of direct participation by the anion of the acid, the criterion is fortunately simple: without participation, the slope will eventually, with increasing values of $-H_0$, return to unity, while with participation, it will increase indefinitely.

As regards our ability to detect the operation of an A-2 mechanism, the situation is impossible. This is because eqns. (7) and (8) refer not only to the hydrolysis, by an A-1 mechanism, of mixtures of free and solvated molecules, but also to the hydrolysis of a single species that reacts partly by an A-1 mechanism, and partly by an A-2 mechanism (or a multimolecular mechanism when $n > 1$). The only difference is that, in the latter case, K_{solv} would refer to the transition state. This proves that it is impossible, from kinetic data alone, to distinquish between a reaction in which water acts as a nucleophile and one in which closely-associated water undergoes some other change of state as the molecule passes through the transition state. Bunnett clearly saw this, in his third paper.[21]

If it is objected that at least the high entropy of activation characteristic of the hydrolysis of glycopyranosides [1] is evidence for an A-1 mechanism, as has been suggested,[23] we must point out that this idea also ignores entropic changes in the water of hydration. Results to be described in this paper will show that the argument is invalid.* Bunnett [21] has previously noted an inverse correlation between $\Delta S^{\ddagger}$ and his parameter, w.

The only operational criterion of an A-2 mechanism is the ability to demonstrate a Walden inversion at the carbon atom attacked, and, since anomerisation is extremely fast in strong acids, there is no possibility of doing this. (The possibility of nucleophilic attack by water on the aglycone is, of course, ruled out by the ^{18}O tracer studies of Bunton *et al.*,[24] and the fact that isomerisation of sugar residues does not occur during the acid-hydrolysis of polysaccharides).

This situation fortunately does not prevent a reasonably definitive answer to our question. If the higher rate of hydrolysis of the β-glucoside is due to a Hassel-Ottar effect associated with an A-2 mechanism, then, even though K_{solv} may be very large, it is at least certain that the *ratio* of the rates of hydrolysis of the β- and α-anomers (K_β/K_α) will not increase as $-H_0$ increases. If it can be additionally shown that K_{solv} is not large, and that K_β/K_α does not *decrease* with increasing acid-concentration, this will confirm that the higher rate of hydrolysis of the β-anomer is not due to an A-2 mechanism, or to the presence of closely-associated water of any kind.

RESULTS

The principal result that prompted this paper is shown in Fig. 3, where K_β/K_α is plotted against molarity for hydrolysis in sulphuric, phosphoric, hydrochloric, and hydrobromic acids. In Fig. 4, the same data are plotted against $-H_0$. The remainder of the work consisted in an attempt to understand (*a*) why K_β/K_α increases with increasing acid-concentration, (*b*) why, for a given value of $-H_0$, the magnitude of the effect is different for the four different acids, and (*c*) why, for a particular glucoside at a given value of $-H_0$, the absolute rate of hydrolysis is different in the four different acids. (This last effect had previously been noted by Timell for the α-glucoside.[25])

* Even a negative entropy of activation, such as is found in the acid-hydrolysis of glycofuranosides,[1] cannot prove an A-2 mechanism, because it is possible for water of hydration to become more highly ordered in the transition state.

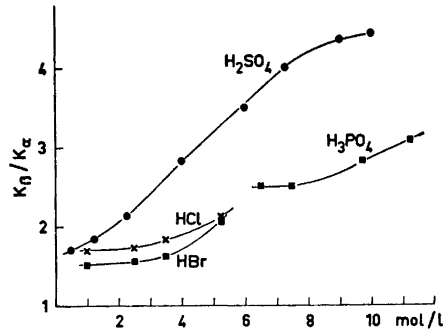

Fig. 3. Dependence upon acid-concentration of the ratio (K_β/K_α) of the rates of hydrolysis of the anomeric methyl glucopyranosides at 68.5°.

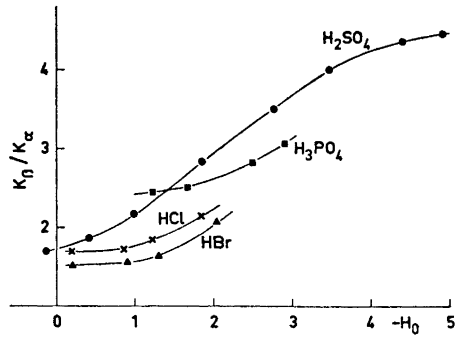

Fig. 4. The data of Fig. 3, re-plotted with $-H_0$ as the measure of acid-concentration.

The following, preliminary conclusions could be drawn: (*i*) Since the activity of water at a given value of $-H_0$ is known to be independent of the nature of the anion,[26,27] the phenomenon is not a simple function in the activity of water alone.

(*ii*) The magnitude of the effect increases in proportion to the affinity of the anion for water, as judged by its position in the Hofmeister lyotropic series, and the heat of dilution of the acid.

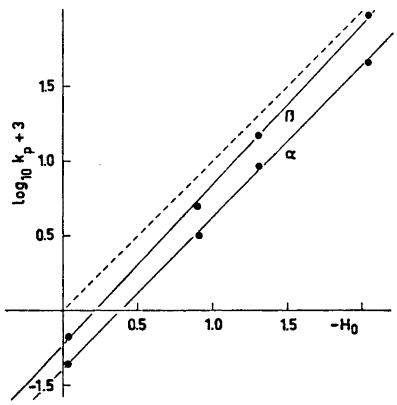

Fig. 5. Hydrolysis of the anomeric methyl glucopyranosides in hydrobromic acid at 68.5°. The *pseudo*-first-order rate-coefficients (k_p) were obtained by use of logarithms to the base 10, and were expressed in min^{-1}. The values of $-H_0$ were taken from published tables [28] and are valid at 25°. The broken line indicates unit slope.

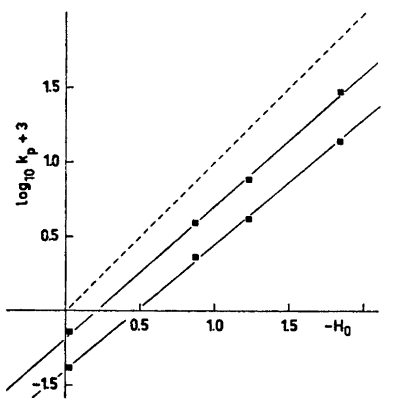

Fig. 6. Hydrolysis of the anomeric methyl glucopyranosides in hydrochloric acid at 68.4°. The values of $-H_0$ were taken from published tables [18] and were corrected, to be valid at 68.4°, from published values of the temperature coefficient of H_0 in this acid.[18]

(*iii*) The bromide ion, which is the strongest nucleophile, has the weakest effect.

Investigation of the possibility that the phenomenon is due to a Hassel-Ottar effect. In Figs. 5 – 8, the logarithms of the *pseudo*-first order rate-coefficients

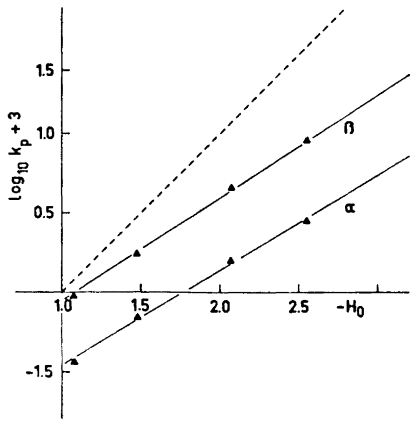

Fig. 7. Hydrolysis of the anomeric methyl glucopyranosides in phosphoric acid at 68.5°. The values of $-H_0$ were corrected [28] to be valid at that temperature.

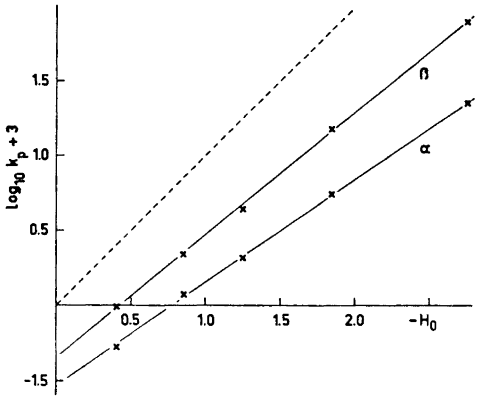

Fig. 8. Hydrolysis of the two anomers in moderately concentrated sulphuric acid at 68.5°. The values of $-H_0$ were corrected for temperature.[28]

are plotted against $-H_0$ for hydrolysis in the four acids at 70°. Straight lines are drawn through the points, because this is uncontroversial, and because an insufficient number of points was obtained to justify any other action. The reader will decide for himself whether or not to believe our claim that the curves are really sigmoid. The following comments must, however, be made:

(A) The sizes of the experimental points give a realistic estimate of the accuracy of the ordinates at about the 2σ level.

(B) The values of H_0 are corrected for temperature from published values [28] for the temperature coefficient of H_0, except in the case of hydrobromic acid, for which the temperature coefficient could not be found. In that case, the plotted values are valid at 25°.

(C) Although they were unbiassed by theoretical considerations, De Bruyne and Wouters-Leysen [16] concluded, from a very detailed study of the hydrolysis of α-methyl-D-glucopyranoside and β-phenyl-D-glucopyranoside in hydrochloric and sulphuric acids that the plots showed slight curvature, the slope decreasing with increasing acid-concentration. They did not investigate acidities higher than about $-H_0 = 2$.

(D) A careful examination of the data of Timell [25] will perhaps suggest that the experimental points could be more easily accommodated in a sigmoid curve than a straight one. In every case, and again in Figs. 6 – 8,* the slope

* But not Fig. 5, which seems to do the opposite. This may be due to uncertainties about the correct values of H_0 at 70°, but our experience suggests that hydrobromic acid is very different also in other ways, and should be studied separately.

initially decreases with increasing acidity, and then increases again. The magnitude of the effect is greatest for sulphuric and phosphoric acids.

Because of the importance of attaching the correct significance to the slopes of these curves, a special study was carried out of hydrolysis in sulphuric acid at very low and also at very high acid-concentrations. This could not be done at the same temperature of 70°, however, because the rate of hydrolysis was then too low to be measured conveniently in weak acid, and too high to be measured accurately in strong acid.

Hydrolysis in weak sulphuric acid was therefore carried out at 80°, 90°, and 100°, and, from the activation energy obtained, the expected rate at 70° was calculated. The results (Fig. 9) show that the slopes are almost parallel,

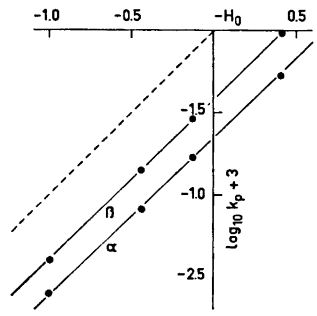

Fig. 9. Hydrolysis of the two anomers in dilute sulphuric acid at 68.5°. The values of k_p for $-H_0 = 0.41$ were measured directly at 68.5°. The others were calculated to be valid for 68.5°, from measurements made at 77.9°, 86.6°, and 95.4°.

and very close to unity. The value of K_β/K_α at infinite dilution is apparently 1.6 as judged by this experiment. (In hydrobromic acid, the ratio initially *decreases* to about 1.5, and then slowly increases again with increasing acid-concentration. A special study of this will be reported elsewhere. In any acid the actual value of K_β/K_α is, of course, temperature-dependent, because the energies of activation are different for the two anomers.[25] The results just reported refer to a temperature of 70°.)

Hydrolysis in very concentrated sulphuric acid (normality greater than 12) was carried out at 30°, 40°, and 50°, and in one case at 40°, 50°, and 60°. At concentrations higher than 15 N, plots of log $a/(a-x)$ against time deviated from strict linearity after degrees of hydrolysis (x/a) of about 50 – 70 %. This is illustrated in Fig. 10, which compares the results obtained at 50° in 15 N and 18 N sulphuric acid. Such effects were accompanied by darkening of the reaction mixture. There is little doubt that they were due to further modification of the liberated glucose, rather than of the glycoside, because the β-anomer was always less affected; this would be expected, since it hydrolyses faster. The initial slope was therefore taken as a correct measure of the rate-coefficient.

The expected rates at 70° were calculated from the activation energies, and the results are shown in Fig. 11. Again, straight lines have been drawn through the points, to avoid theoretical bias. Their slopes are about 0.85 in both cases. It is at least clear that the slope for the α-anomer is now higher,

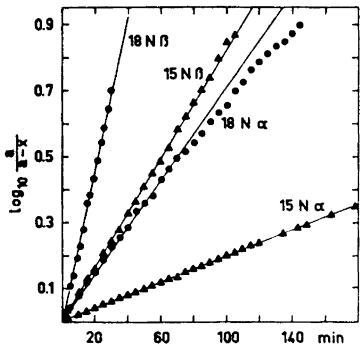

Fig. 10. Illustration of the onset of serious departure from first-order kinetics in very concentrated sulphuric acid. The temperature in all four experiments was 49.3°.

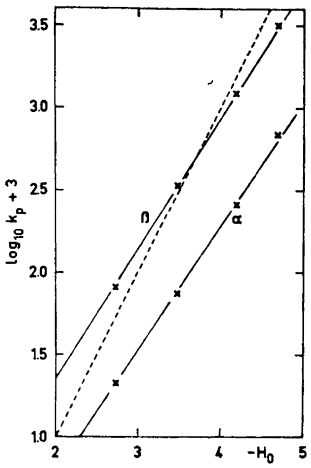

Fig. 11. Hydrolysis of the two anomers in very concentrated sulphuric acid at 68.5°. The values of $-H_0$ were corrected for temperature.[28] The values of k_p for $-H_0 = 2.67$ were measured at the stated temperature. The others were calculated to apply at that temperature from measurements made at 39.6°, 49.3°, and 58.6°.

and that the plots have become almost parallel again. The final value of K_β/K_α at 70° is about 4.6. It is clearly impossible to say whether or not the slopes would eventually increase to unity. With the onset of serious deviation from first-order kinetics, it was not worthwhile to investigate still-higher concentrations of acid.

The entire behaviour in sulphuric acid can be summarised as follows. Even in 0.1 N acid, the β-anomer is hydrolysed faster than the α-anomer. For values of $-H_0$ between -1 (pH = $+1$) and $+0.4$ (corresponding to about 2.5 N acid), plots of log (Rate) against $-H_0$ are linear and of unit slope. In this region, the activity of water suffers only a 10 % decrease.[29]

For values of $-H_0$ between 1 and 3, the plots are approximately linear. The average slope for the β-anomer is 0.82, and that for the α-anomer is 0.68. The activity of water in the same region decreases from about 0.85 to about 0.35. As $-H_0$ increases further up to 5, the slope of the plot for the α-anomer increases markedly, until the two plots become virtually parallel again. The activity of water at $-H_0 = 5$ is about 0.1. The "final" rate of hydrolysis of the β-anomer is about 30 %, and that of the α-anomer is about 10 %, of the rate at which they would have been hydrolysed, had unit slope been maintained throughout.

It will be noted that, throughout the entire range studied, the concentration of the anion has increased by a factor of 200, while the activity of water has decreased to 10 %.

Investigation of primary salt effects. This was undertaken, firstly to determine whether the increase in K_β/K_α with increasing acidity could be due to any change in the term containing the activity coefficients in eqn. (4), and secondly to determine to what extent the deviations from unit slope in Figs. 5 – 8 should be attributed to the effects described by McIntyre and Long.[17,18]

McIntyre and Long found that methylal was, relatively to the Hammett base studied, salted-out by strong acids [17] and neutral salts,[18] and therefore the plot of log (Rate) against $-H_0$ had a slope greater than unity. The methyl glucopyranosides are, compared to methylal, very polar compounds, and it is therefore possible that they may be salted-in relatively to the Hammett base, thus giving slopes less than unity.

The method of investigation was chromatographic. Preliminary experiments showed that thin-layer chromatography on silica gel could be carried out successfully with aqueous mineral acids or even water as the mobile phase. The quality of the separations was generally comparable with that obtainable in conventional solvent-systems. The selection of R_F values shown in Table 1 makes it clear that separation takes place on a basis of the polarity of the compounds, with the silica gel acting as the less-polar phase.

Table 1. Chromatographic mobilities of various carbohydrates in 10 N sulphuric acid. The stationary phase was silica gel, and the mobilities are calculated relative to the solvent front.

Compound	R_F value
Glycolaldehyde	0.81
D-Glucose	0.88
2-Deoxy-D-glucose	0.89
3-*O*-Methyl-D-glucose	0.89
2-Deoxy-D-ribose	0.82
6-*O*-Methyl-D-galactose	0.70
Methyl β-L-arabinopyranoside	0.69
2,3,4,6-Tetra-*O*-methyl-D-glucose	0.34
Methyl 2,3,4,6-Tetra-*O*-methyl-D-glucopyranoside	0.14
Maltose	0.95
Cellobiose	0.96

In agreement with this, it was next found that, when sulphuric, phosphoric, hydrochloric, or hydrobromic acid was chromatographed with water as the mobile phase, the acid was completely excluded from the silica gel, migrating at the solvent front. This implied that, when chromatography of organic compounds is carried out with these acids as the mobile phase, the silica gel would act like an immiscible organic solvent. Partition would then occur between this and a mobile phase whose composition could be varied at will. Any tendency for the acids to salt-in or salt-out one compound relatively to another should then be reflected in a change in the relative chromatographic mobilities of the two compounds.

The results obtained with the two methyl glucopyranosides and a Hammett base (*p*-nitroaniline) are shown in Table 2. Although the absolute mobilities vary a little, as could be expected, the relative mobilities are remarkably insensitive to both the nature of the anion and its concentration.

Table 2. Chromatographic mobilities of α- and β-methyl D-glucopyranoside (α/β-Me-G), *N*-acetyl-D-glucosamine (GNAc), and *p*-nitroaniline (p-NA) in various acids. The stationary phase was silica gel.

Acid	α-Me-G	β-Me-G	GNAc	p-NA
2 N H_2SO_4	0.87	0.88	0.86	0.87
4 N H_2SO_4	0.81	0.82	0.89	0.83
6 N H_2SO_4	0.78	0.80	0.89	0.79
8 N H_2SO_4	0.74	0.78	0.91	0.76
10 N H_2SO_4	0.75	0.79	0.91	0.80
12 N H_2SO_4	0.80	0.82	0.91	0.80
14 N H_2SO_4	0.75	0.77	0.91	0.79
16 N H_2SO_4	0.77	0.78	0.94	0.78
4 M H_3PO_4	0.78	0.81	0.93	0.74
6 M H_3PO_4	0.76	0.78		0.72
8 M H_3PO_4	0.75	0.76	0.90	0.71
11 M H_3PO_4	0.80	0.81		0.76
1 N HBr	0.82	0.82		0.76
3.6 N HBr	0.81	0.82		0.84
5 N HBr	0.83	0.83	0.90	0.81
2.5 N HCl	0.85	0.86		0.84
3.5 N HCl	0.82	0.85		0.84
5 N HCl	0.74	0.75	0.89	0.76
Water	0.83	0.83		0.75

The purpose of the experiment was to find out not only whether the unprotonated glycosides and Hammett base were salted-in or salted-out relatively to one another, but also whether this occurred with their conjugate acids. This was the purpose in varying the concentration of mineral acid in the mobile phase over a wide range. This was undoubtedly successful with regard to the Hammett base, whose yellow colour faded as the concentration of acid in the mobile phase increased.

The glycosides are, however, much weaker bases than *p*-nitroaniline, and it is doubtful whether they would have been sufficiently highly protonated even in the most concentrated acid for their mobilities to be significantly affected by any change in the activity coefficients of their conjugate acids. This is why data for 2-acetamido-2-deoxy-D-glucose are also included in Table 2. The reasoning was as follows.

The behaviour of *p*-nitroaniline was in good agreement with the general experience [30] that protonation of a relatively large organic, basic molecule has little effect upon its activity coefficient. To ascertain whether or not this was also likely to be true for a glycoside, it was necessary to find a molecule that was structurally very similar to a glycoside, but a stronger base. Amides are

well known to be highly protonated in moderately concentrated mineral acids.[31] The chromatographic behaviour of 2-acetamido-2-deoxy-D-glucose (Table 2) therefore indicates that any change in the activity coefficients of the protonated glycosides, relatively to one another and to *p*-nitroaniline, with increasing acid-concentration, is very unlikely.

Dependence of activation parameters upon acid-concentration. Table 3 gives the energies and entropies of activation for hydrolysis of both anomers in sulphuric acid of different concentrations. The results given for hydrolysis in 2.5 N and 12.0 N acid are based upon measurements of the rate of hydrolysis at five different temperatures, while the others are based upon measurements at three different temperatures. The limits of error were estimated by drawing the two "worst possible" straight lines through the plots of log (Rate) against $1/T$, and measuring the deviation of their slopes from that of the best straight line.

Table 3. Activation parameters for hydrolysis of α- and β-methyl D-glucopyranoside in sulphuric acid at 70°. The possible error in the activation energies (E_α and E_β) is consistently about ± 0.5 kcal mol^{-1}, while that in the entropies of activation ($\Delta S_\alpha^{\ddagger}$ and $\Delta S_\beta^{\ddagger}$) is about ± 1 e.u. The "theoretical" values of $E_\alpha - E_\beta$ are calculated from the ratio (K_β/K_α) of the rates of hydrolysis of the two glucosides on the assumption that the difference in the rates of hydrolysis is due solely to differences in the energy (and hence enthalpy) of activation.

Normality	K_β/K_α	E_α	E_β	$\Delta S_\alpha^{\ddagger}$	$\Delta S_\beta^{\ddagger}$	$E_\alpha - E_\beta$ Found	$E_\alpha - E_\beta$ Calc.
0.100	1.60	35.6	35.3	19.9	20.0	0.3	0.32
0.500	1.65	35.8	35.4	20.3	20.3	0.4	0.34
1.00	1.70	34.8	34.5	17.4	17.6	0.3	0.36
2.50	1.84	34.6	34.2	16.7	16.7	0.4	0.41
12.00	3.50	32.5	31.7	7.7	7.8	0.8	0.85
15.00	4.00	32.3	31.4	5.9	6.3	0.9	0.94
18.00	4.35	32.0	31.0	4.2	4.4	1.0	1.00
20.00	4.42	31.8	30.7	3.3	3.1	1.1	1.01

It is at least clear that, as the concentration of acid increases, the entropy of activation goes down for both anomers, the energy of activation goes down for both anomers, and the energy of activation of the β-anomer goes down significantly more than that of the α-anomer.

If the assumption is now permitted, that the estimated limits of error correspond to about 3σ, and that the probable error is about two-ninths of this, a further conclusion is strongly indicated. This is that, *at any acid-concentration, the higher rate of hydrolysis of the β-anomer is due entirely to its lower activation energy*. In other words, the phenomenon is entirely enthalpic.*

* It may be noted that, for small substituents attached to a fairly rigid pyranoid ring, the difference in free energy between two configurational isomers would be expected to be almost entirely enthalpic in nature.

Accepting this, and that salt effects are unimportant, eqn. (4) can be re-written:

$$K_\beta/K_\alpha = \exp[(E_\alpha - E_\beta)/RT] \quad (13)$$

From the experimental values for K_β/K_α at 70° (Figs. 3 and 4), expected values of $E_\alpha - E_\beta$ were calculated from this equation, and are included in Table 3 for comparison with the experimental values.

DISCUSSION

The possibility that the higher rate of hydrolysis of the β-anomer is due to direct nucleophilic attack by the anion of the acid on the anomeric centre, and to a consequent Hassel-Ottar effect, is discounted for the following reasons:

(*a*) Even in 0.1 N acid, the β-anomer is hydrolysed faster, and the value of K_β/K_α does not change significantly as the normality of the acid increases by a factor of 10 to 1 N (Fig. 9).

(*b*) The value of K_β/K_α tends to become constant again as the normality of the sulphuric acid increases from 15 to 20 (Figs. 3 and 11). In this region, the slope of the plot of log (Rate) against $-H_0$ increases more for the α-anomer than for the β-anomer (Figs. 8 and 11).

(*c*) The bromide ion, which is the strongest nucleophile, has the weakest effect. Both sulphuric and phosphoric acid are relatively weak nucleophiles.

(*d*) If the sulphate or bisulphate ion selectively attacked the β-anomer as a nucleophile, it is not very likely that the entropies of activation for the two anomers would be consistently the same at all concentrations of acid (Table 3).

The possibility that the higher rate of hydrolysis of the β-anomer is due to a primary salt effect is discounted for the following reasons:

(*a*) A close examination of the R_F values in Table 2 suggests that there is a slight, but probably significant, tendency for the α-anomer to be salted out, relatively to the β-anomer and the Hammett base, by sulphuric and phosphoric acid. On this basis, one would expect the α-anomer to be hydrolysed slightly faster than the β-anomer.

(*b*) On the basis of a fairly reasonable assumption about experimental accuracy, the data in Table 3 indicate that the higher rate of hydrolysis of the β-anomer is due largely, if not completely, to its lower energy of activation.

The increase in K_β/K_α with increasing acidity cannot be attributed to a Hassel-Ottar effect arising from an A-2 mechanism, because on this basis, K_β/K_α would have to be at a maximum when the activity of water is maximal, that is, in dilute acid. In the case of hydrobromic acid, the plot of log (Rate) against $-H_0$ is very close to unity, showing that K_{solv} in eqn. (8) is very large for this acid. In this particular acid, therefore, it would be possible for an A-2 mechanism to operate throughout the range of acidity studied. In the other acids, however, the plots are sigmoid, and for these it is certain that any contribution that an A-2 mechanism may make to the total rate of hydrolysis would have to diminish with increasing acidity. Any associated Hassel-Ottar effect would therefore also decrease with increasing acidity, and in sulphuric

acid, it would be expected to disappear entirely as $-H_0$ increases above 3 (Fig. 11).

The possibility that the higher rate of hydrolysis of the β-anomer in *dilute* acid may be due *partly* to a Hassel-Ottar effect, associated with an A-2 mechanism, cannot be completely excluded, but two facts oppose it:

(i) If, in dilute acid, the β-anomer were *selectively* hydrolysed by an A-2 mechanism, because of the Hassel-Ottar effect, it would be surprising to find that the entropies of activation were the same for the two anomers, as is the case. If there is any evidence against the A-2 mechanism, it is perhaps this lack of *selectivity* in the entropies of activation, rather than their absolute magnitudes.

(ii) As has been briefly mentioned, and will be reported in detail elsewhere, the value of K_β/K_α in hydrobromic acid initially goes *down* with increasing acid-concentration. In terms of the anomeric effect, this can be explained by assuming that low concentrations of bromide ion increase the activity of water, but it is impossible to explain on the assumption that a Hassel-Ottar effect is operating.

Finally, before attributing the entire phenomenon to the anomeric effect alone, it is necessary to consider whether accepted values for the magnitude of the anomeric effect are able to account for it. Angyal [4] has estimated that, on the basis of van der Waals interactions alone, the β-anomer should be *more* stable than the α-anomer by about 0.9 kcal mol^{-1}. In order to explain the present results, for hydrolysis in sulphuric acid at 70°, entirely in terms of the anomeric effect, it would therefore be necessary to assume that it has a magnitude of about 1.2 kcal mol^{-1} in dilute acid, and about 1.9 kcal mol^{-1} in 20 N acid.

It is, of course, known [32] that, for pyranosyl halides in inert solvents, the anomeric effect can have a magnitude of 3.2 kcal mol^{-1} or more, but this is not very helpful. A more realistic picture is given by the following facts:[3,4]

(a) The optical rotation, at equilibrium, of glucose in water indicates that the anomeric affect has a value of 0.55 kcal mol^{-1} while in anhydrous methanol it has a value of 0.9 kcal mol^{-1}.

(b) It is well known that the magnitude of the anomeric effect is higher for glycosides than for reducing sugars.

(c) An indication of how much higher it may be is given by the fact [3] that a solution of methyl 2,3,4,6-tetra-*O*-methyl-α-D-glucopyranose in methanolic hydrogen chloride anomerises, and gives, at equilibrium, the α- and β-anomers in a ratio of about 3:1. Depending slightly on the temperature, this indicates a value for the anomeric affect of about 1.6 kcal mol^{-1}.

If, therefore, the anomeric effect in methanol is 0.7 kcal mol^{-1} higher for the glycoside than for the reducing sugar, it is a reasonable speculation that a similar increment will apply in water. Accepting this, the expected value for the glycoside in water would be $0.55+0.7=1.25$ kcal mol^{-1}, as was found.

It is now possible to suggest answers to the three questions asked at the beginning of the section on results:

(a) The value of K_β/K_α increases with increasing acidity because the magnitude of the anomeric effect increases as the activity of water in the system decreases, leading to desolvation of the glycosides.

(b) For a given value of H_0, that is to say, for a given activity of water, the magnitude of the effect is different for different anions because the anions differ in their capacity to desolvate the glycosides. This must be explained further. The quantity, K_{solv}, in eqn. (8) will be a constant, independent of the medium, only if the activity coefficients, f_G and f_{GS} of the free and solvated glycoside are measured, with a dilute solution in pure water as the reference state. It is, however, impossible to do this, and therefore it is operationally meaningless to keep f_G/f_{GS} as a term, separate from K_{solv}. It is therefore better to set f_G/f_{GS} equal to a constant, or to unity, and to regard K_{solv} as an operational parameter, dependent upon the medium. It is not yet known whether K_{solv} is dependent upon the concentration of the anion as well as its identity, but the ability of eqn. (8) to explain the experimental results suggests that it may be nearly independent of concentration.

(c) For a given glycoside, at a given value of H_0, the absolute rate of hydrolysis is different in the presence of different anions because the glycoside exists in solution as a mixture of solvated and desolvated species, which are hydrolysed at different rates. The relative amounts of the solvated and desolvated species are different in the presence of different anions, for the reason just discussed. In the case of the α-anomer, the solvated species is hydrolysed about 10 times faster than the desolvated species, while in the case of the β-anomer, it is hydrolysed 3 times faster. The solvated species is hydrolysed faster than the desolvated species because its higher enthalpy of activation is more than offset by the very favourable entropic change associated with the release of solvent in the transition state.

It is not known, of course, that desolvation of the glycosides is complete in 20 N sulphuric acid, when K_β/K_α has again become constant, but it would certainly appear that those water molecules that diminish the magnitude of the anomeric effect, by forming hydrogen bonds with the ring and glycosidic oxygen atoms, have been removed in acid of that strength. It is possible that other water molecules, more firmly bound than these, are still present, and that an expanded form of eqn. (8), including more than one solvation constant, would give a better fit with the experimental data. In particular, this would explain why the slopes of the plots of log (Rate) againts $-H_0$ in Fig. 11 have not returned to unity, even though they are almost parallel. To judge from the value of n that would make the term $(a_{H_2O})^n$ in eqn. (8) vanishingly small for values of $-H_0$ between 4 and 5, it would appear that four, or possibly three, molecules of water are removed from the glycosides relatively easily, while a smaller number, if present, may be removed with greater difficulty.

It must be recognised that, in dilute, aqueous solutions, all these water molecules of solvation are in a very different state from those of the ambient solvent. Their entropy is much lower, which points to the existence of a fairly well-defined, ordered structure. This structure stabilises the chair form of the pyranoid ring, relative to the half-chair form of the transition state, to the extent of about 3 kcal per mol of glycoside. Exactly how it does this, is not known, but effectively, water can be regarded as increasing the conformational size of the oxygen atoms attached to the pyranoid ring.

Concentrated solutions of mineral acids do not exist in Nature, but sulphated polysaccharides are ubiquitous in marine plants and animals, while

phosphorylated sugars are important in intermediary metabolism, teichoic acids and nucleic acids. In the immediate vicinity of a sulphate half-ester group, or a phosphate mono- or di-ester group, the activity of water must be very low. The analogy with moderately concentrated solutions of sulphuric and phosphoric acids is perhaps quite good, because the principal anions in these solutions are the bisulphate and the dihydrogen phosphate ions, respectively.

The analogy breaks down, of course, insofar as the only cations in the present systems were hydrogen ions. A logical extension of the work would therefore be to introduce metallic and organic cations. Previous work in this laboratory by Haug and Smidsrød [33,34] on the salting-out and salting-in of anionic and neutral polysaccharides has demonstrated a remarkable sensitivity to both the nature of the anionic group and the identity of the cation. These solubility phenomena may or may not, in some cases, be associated with changes in the conformation of the pyranoid ring, but it is certain, in every case, that they represent profound changes in the state of the solvent molecules in the vicinity of the chains, and the purpose of future papers in this series will be to explore all the consequences of this.

Almost all the experimental work in this paper was carried out by Kjersti Andresen, to whom I am most deeply indebted. I am also deeply grateful to Prof. A. Haug and Prof. N.A. Sørensen for their interest, patience and understanding. It is especially appropriate that I should dedicate this manuscript to Prof. Sørensen, who retires this year as chairman of our Institute. Prof. Sørensen was one of the earliest pioneers of the mechanism of glycosidic hydrolysis.[35] Through his inspiring chairmanship, he helped to create the atmosphere in which it was possible to undertake this work.

REFERENCES

1. BeMiller, J. N. *Advan. Carbohyd. Chem.* **22** (1967) 25.
2. Edward, J. T. *Chem. Ind. (London)* **1955** 1102.
3. Lemieux, R. U. In De Mayo, P., Ed., *Molecular Rearrangements*, Interscience, New York, London and Sydney 1964, Vol 2, p. 733.
4. Angyal, S. J. In Eliel, E. L., Allinger, N. L., Angyal, S. J. and Morrison, G. A., Eds., *Conformational Analysis*, Interscience, New York, London and Sydney 1965, p. 375.
5. Lemieux, R. U. and Morgan, A. R. *Can. J. Chem.* **43** (1965) 2205.
6. BeMiller, J. N. and Doyle, E. R. *Carbohyd. Res.* **20** (1971) 23.
7. Lemieux, R. U., Pavia, A. A., Martin, J. C. and Watanabe, K. A. *Can. J. Chem.* **47** (1969) 4427.
8. Lemieux, R. U. and Pavia, A. A. *Can. J. Chem.* **47** (1969) 4441.
9. Hammett, L. P. and Paul, M. A. *J. Am. Chem. Soc.* **56** (1934) 830.
10. Armour, C., Bunton, C. A., Patai, S., Selman, L. H. and Vernon, C. A. *J. Chem. Soc.* **1961** 412.
11. Withey, R. J. and Whalley, E. *Can. J. Chem.* **41** (1963) 1849.
12. Hassel, O. and Ottar, B. *Acta Chem. Scand.* **1** (1947) 929.
13. Freudenberg, K., Kuhn, W., Dürr, W., Bolz, F. and Steinbrunn, G. *Ber.* **63** (1930) 1510.
14. Lindberg, B. *Acta Chem. Scand.* **3** (1949) 1153.
15. Zucker, L. and Hammett, L. P. *J. Am. Chem. Soc.* **61** (1939) 2791.
16. De Bruyne, C. K. and Wouters-Leysen, J. *Carbohyd. Res.* **17** (1971) 45.
17. McIntyre, D. and Long, F. A. *J. Am. Chem. Soc.* **76** (1954) 3240.
18. Long, F. A. and McIntyre, D. *J. Am. Chem. Soc.* **76** (1954) 3243.
19. Bunnett, J. F. *J. Am. Chem. Soc.* **83** (1961) 4956.
20. Bunnett, J. F. *J. Am. Chem. Soc.* **83** (1961) 4968.

21. Bunnett, J. F. *J. Am. Chem. Soc.* **83** (1961) 4973.
22. Bunnett, J. F. *J. Am. Chem. Soc.* **83** (1961) 4978.
23. Overend, W. G., Rees. C. W. and Sequeira, J. S. *J. Chem. Soc.* **1962** 3429.
24. Bunton, C. A., Lewis, T. A., Llewellyn, D. R. and Vernon, C. A. *J. Chem. Soc.* **1955** 4419.
25. Timell, T. E. *Can. J. Chem.* **42** (1964) 1456.
26. Wyatt, P. A. H. *Discuss. Faraday Soc.* **24** (1957) 162.
27. Yates, K. and Wai, H. *J. Am. Chem. Soc.* **86** (1964) 5408.
28. Rochester, C. H. *Acidity Functions*, Academic, London and New York 1970.
29. Bunnett, J. F. *J. Am. Chem. Soc.* **82** (1960) 499; **83** (1961) 4967.
30. Hammett, L. P. and Paul, M. A. *J. Am. Chem. Soc.* **56** (1934) 827.
31. Rosenthal, D. and Taylor, I. T. *J. Am. Chem. Soc.* **79** (1957) 2684.
32. Anderson, C. B. and Sepp, D. T. *J. Org. Chem.* **32** (1967) 607.
33. Smidsrød, O. and Haug, A. *J. Polymer Sci.* **C 16** (1967) 1587.
34. Haug, A. and Smidsrød, O. In *Solution Properties of Natural Polymers*, Special Publication No 23, Chemical Society, London 1968, p. 273.
35. Riiber, C. N. and Sørensen, N. A. *Kgl. Norske Videnskab. Selskabs Skrifter* **1938**.

Received March 5, 1973.

ACTA CHEMICA SCANDINAVICA 27 (1973) 2485–2494

Heterocyclic Fused Tropylium Ions

V. UV Spectra of Some Dithieno- and Furothienoannelated Tropones and Tropylium Ions

TOMMY LILJEFORS, URI MICHAEL, BARUCH YOM-TOV and SALO GRONOWITZ

Division of Organic Chemistry, University of Lund, Chemical Center, P.O. Box 740, S-220 07 Lund 7, Sweden

The ultraviolet spectra of a number of furan- and thiophene-annelated tropylium cations and tropones have been measured and compared to theoretical spectra calculated within the Pariser-Parr-Pople approximation. The calculated spectra are in good agreement with the experimental ones. The ultraviolet spectrum of an unknown thiophene-annelated tropylium cation (X) is predicted.

A number of furan- and thiopheneannelated tropylium cations and tropones have recently been prepared by Gronowitz and coworkers. The infrared and proton magnetic resonance spectra of these compounds have been reported.[1] In this paper we wish to report a study of the ultraviolet spectra of the annelated tropylium cations I–IV and the related annelated tropones V–VIII.

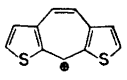

I

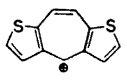

II

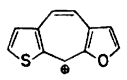

III

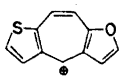

IV

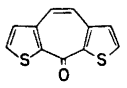

V

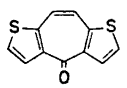

VI

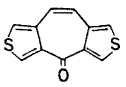

VII

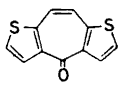

VIII

It is of interest to compare the spectral properties of the cations I–IV with those of the ketones V–VIII, since IR data indicate a pronounced tropylium cation character of the central ring in most of the latter compounds.[1]

The general complexity of the experimental spectra makes it interesting to test the ability of molecular orbital calculations to reproduce them. Calculations may also cast some light on questions concerning the number and positions of transitions making up a band in spectrum. Most successful calculations of ultraviolet spectra of conjugated organic compounds have been made by use of the π-electron approximation of Pariser, Parr and Pople (PPP),[2,3] and this method has been used to calculate the electronic transitions of the molecules considered in this work. Fabian *et al.*,[4,5] by extensive comparisons of ultraviolet spectra of heterocyclic sulphur compounds and the corresponding iso-π-electronic hydrocarbons, have shown the remarkable similarities in the spectra properties of these two classes of compounds. This approach will be used in the present paper to compare the ultraviolet spectra of compounds I – IV with that of 1,2:4,5-dibenzotropylium cation IX.

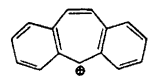

IX

METHODS OF CALCULATION

As mentioned above, the molecular orbital calculations were made using the PPP π-electron scheme, employing two different sets of parameters A and B. Set A was proposed by Fabian *et al.*[4,5] and is based on a systematic adjustment of the parameters $U_{\mu\mu}$, $\beta_{\mu\nu}$ and $\gamma_{\mu\mu}$ (for notation see Ref. 4) until a good fit between the calculated and experimental ultraviolet spectra of some reference compounds, including cations, was obtained. The parameter values used in the present calculations are given in Table 1. It should be noted that

Table 1. Parameters of set A (eV).

μ	$-U_{\mu\mu}$	$\gamma_{\mu\mu}$	$\mu\nu$	$-\beta_{\mu\nu}$
C	11.42	10.84	CC	2.318
O	27.17	14.58	CO	2.550
S	20.00	10.84	CS	1.623

in set A the resonance integral, $\beta_{\mu\nu}$, is kept constant for a given type of bond, thus neglecting the influence of variations of bond length on this integral. This may be a drastic simplification, but it is at least partly justified by the successful simulation of the ultraviolet spectra of a large number of heterocyclic compounds, by calculations using set A.[4,5] The two-centre repulsion integrals, $\gamma_{\mu\nu}$, were calculated by the Nishimoto-Mataga approximation.[6]

Parameter set B is based on a theoretical investigation of the Zero Differential Overlap approximation made by Fischer-Hjalmars.[7] The parameters

in this set were obtained through a least-squares fit to experimental ionization potentials and singlet π-π^* transitions of chosen reference compounds.[8–11] The main feature of the method proposed by Fischer-Hjalmars is the dependence of the diagonal elements, $H_{\mu\mu}^{\text{core}}$, on the neighbouring atoms through formulas (1) [12] and (2)

$$H_{\mu\mu}^{\text{core}} = W_\mu - (n_\mu - 1)\gamma_{\mu\mu} - \sum_\nu n_\nu \gamma_{\mu\nu} \quad (1)$$

$$W_\mu = W_\mu^\circ + \sum_\nu \{\Delta W_\mu^\circ(\nu) + \delta_{\mu\nu}{}^W (R_{\mu\nu} - R_{\mu\nu}^\circ)\} \quad (2)$$

where n_μ is the number of electrons contributed by atom μ and the sum in (2) is a correction due to neighbouring atoms ν and bond distances $R_{\mu\nu}$. The resonance integrals, $\beta_{\mu\nu}$, and the electron repulsion integrals, $\gamma_{\mu\nu}$, for nearest neighbours depend linearly on bond distances according to formulas (3) and (4).

$$\beta_{\mu\nu} = \beta_{\mu\nu}{}^\circ + \delta_{\mu\nu}{}^\beta (R_{\mu\nu} - R_{\mu\nu}^\circ) \quad (3)$$

$$\gamma_{\mu\nu} = \gamma_{\mu\nu}{}^\circ + \delta_{\mu\nu}{}^\gamma (R_{\mu\nu} - R_{\mu\nu}^\circ) \quad (4)$$

The values for W_μ°, $\Delta W_\mu^\circ(\nu)$, $\gamma_{\mu\mu}$, $\gamma_{\mu\nu}{}^\circ$, $\delta_{\mu\nu}{}^W$, $\delta_{\mu\nu}{}^\gamma$, $\beta_{\mu\nu}{}^\circ$, and $\delta_{\mu\nu}{}^\beta$ were obtained as described above. For non-neighbours $\gamma_{\mu\nu}$ is calculated using the ball approximation.[13] The parameters making up set B are summarized in Table 2.

Table 2. Parameters of set B (eV).

Atom	$-W_\mu{}^\circ$	$\gamma_{\mu\mu}$	Bond μ–x	$-\beta_{\mu\nu}{}^\circ$	$\gamma_{\mu\nu}{}^\circ$	$\delta_{\mu\nu}{}^W$	$\delta_{\mu\nu}{}^\beta$	$-\delta_{\mu\nu}{}^\gamma$	$\Delta W_{\mu(\nu)}{}^\circ$	$\Delta W_{\nu(\mu)}{}^\circ$	R_0(Å)
C	9.84	11.97	C–C	2.42	6.91	9.22	3.05	3.99	0.07	0.07	1.397
Ȯ	19.60	18.89	C–Ȯ	2.46	9.33	0	0	0	−0.71	0	1.22
Ö	11.18	18.89	C–Ö	1.80	6.20	0	0	0	−0.09	1.51	1.35
S	10.62	9.58	C–S	1.37	7.28	9.22	3.05	3.99	−0.70	0	1.714

The excited states were obtained by a limited configuration interaction, including a maximum of 20 configurations in calculations with set A, and all singly excited configurations in calculations using set B.

GEOMETRIES USED IN THE CALCULATIONS

All compounds were assumed to be planar. Preliminary X-ray investigations have shown that compounds I and II are planar in the crystalline state.[14] The geometries used in the calculations on these compounds were based on the X-ray analysis. Bond lengths and bond distances of the other compounds were estimated from the geometries of the tropylium cation,[15] tropone,[16] furan,[17] and thiophene.[18] Table 3 summarizes the values for bond lengths and bond angles used in the calculations. The numbering of the atoms is shown below.

Table 3. Bond distances (a) and bond angles (b) for compounds I – IV and X. The ring structures in compounds V – VIII were assumed to be the same as in the corresponding tropylium cations I, II, and IV. The carbonyl oxygen was placed 1.26 Å from atom 8 on a line bisecting the angle 7–8–9.

(a) Bond distances (Å)

Compound	1–2	2–3 1–13	3–4 12–13	4–5 11–12	5–6 10–11	6–7 9–10	7–8 8–9	3–7 9–13
I	1.37	1.41	1.44	1.33	1.72	1.735	1.415	1.39
II	1.40	1.42	1.71	1.715	1.365	1.47	1.395	1.46
X	1.41	1.41	1.37	1.714	1.714	1.37	1.409	1.423
			3–4	4–5	5–6	6–7		
III[a]			1.431	1.361	1.362	1.337		
IV[a]			1.362	1.362	1.361	1.420		

(b) Bond angles (°)

Compound	1–2–3 2–1–13	2–3–7 1–13–9	3–7–8 13–9–8	7–8–9	4–3–7 12–13–9	3–7–6 13–9–10	3–4–5 11–12–13	4–5–6 10–11–12	5–6–7 9–10–11
I	129	127	132.5	123	111.5	111.5	112	115	90.5
II	128	131	126	131	110	111.5	93	114.5	110.5
X	128.6	128.6	128.6	128.6	112.4	112.4	111.5	92.2	111.5
					4–3–7	3–7–6	3–4–5	4–5–6	5–6–7
III[a]					106	108.6	106	110.7	108.7
IV[a]					110.7	102	106.6	110.7	110

[a] The geometries of the thiophene and seven-membered rings in these compounds were assumed to be the same as in compounds I and II, respectively.

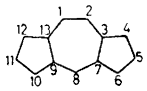

EXPERIMENTAL

The ultraviolet spectra were recorded on a Unicam SP 800 B UV spectrophotometer. Compounds I – III (as perchlorate) were dissolved in conc. suphuric acid, compound IV (perchlorate) in 0.2 N HCl and compounds V – VIII in abs. ethanol. The calculations were performed on a Univac 1108 computer using programs written by Professor Rolf Manne, University of Bergen, Norway (set A) and Dr. Marianne Sundbom, Institute of Theoretical Physics, University of Stockholm (set B).

Table 4. Experimental ultaviolet spectra of compounds I–VIII.

I		II		III		IV		V		VI		VII		VIII	
λ_{max} (nm)	$\varepsilon \times 10^{-3}$	λ_{max} (nm)	$\varepsilon \times 10^{-3}$	λ_{max} (nm)	$\varepsilon \times 10^{-3}$	λ_{max} (nm)	$\varepsilon \times 10^{-3}$	λ_{max} (nm)	$\varepsilon \times 10^{-3}$	λ_{max} (nm)	$\varepsilon \times 10^{-3}$	λ_{max} (nm)	$\varepsilon \times 10^{-3}$	λ_{max} (nm)	$\varepsilon \times 10^{-3}$
471	4.68	470(sh)	1.11	414(sh)	4.13	404(sh)	3.66	370	6.50	373	12.5	380	0.448	376	10.9
460.5	5.0	440(sh)	2.88	368	17.3	378	8.0	362	6.50	352	16.0	311	2.83	355	15.3
447	4.65	411	7.70	306	42.5	296	52.0	350	6.88	337	15.4	295(sh)	3.58	337	12.0
395	15.7	374	6.0	275	16.5	263(sh)	12.8	330	7.26	254	30.9	269.5	14.2	322(sh)	8.62
375	7.25	312	80.9	220	12.8	210	10.5	289	25.8	205	8.19	264	13.0	285(sh)	5.75
330.5	46.2	230(sh)	15.5					250	25.2			250	10.0	273	7.77
301.5	37.5	223	17.7					204	7.28			205	2.31	250(sh)	18.3
265.5	8.42	205	17.7											243	20.9
235	14.6														
208	17.4														

RESULT AND DISCUSSION

Preliminary calculations showed that only calculations using set A could account for the experimental spectra of compounds I – IV. Calculations using set B gave transition energies which were far too high. The failure of set B to reproduce the spectra of these cations is not unexpected since the parameters making up this set are primarily adjusted to give a good fit between calculated and experimental spectra of *neutral* compounds in the vapour phase, and should thus not be suited for calculations on ions in a solvent such as conc. sulphuric acid. The spectra of the *neutral* compounds V – VIII are, as will be seen later, well accounted for, using parameter set B.

1. Annelated tropylium cations (I – IV). Figs. 1 a-d show the experimental spectra of compounds I – IV superimposed on the calculated transitions (set A). (Calculated transitions with intensities corresponding to $\log f < -1.6$ are indicated with dots.) The experimental absorption maxima (λ_{max}) and intensities (ε) are tabulated in Table 4.

As can be seen in Figs. 1 a-d, the calculated transitions account very well for the experimental spectra. The positions and relative intensities of the two

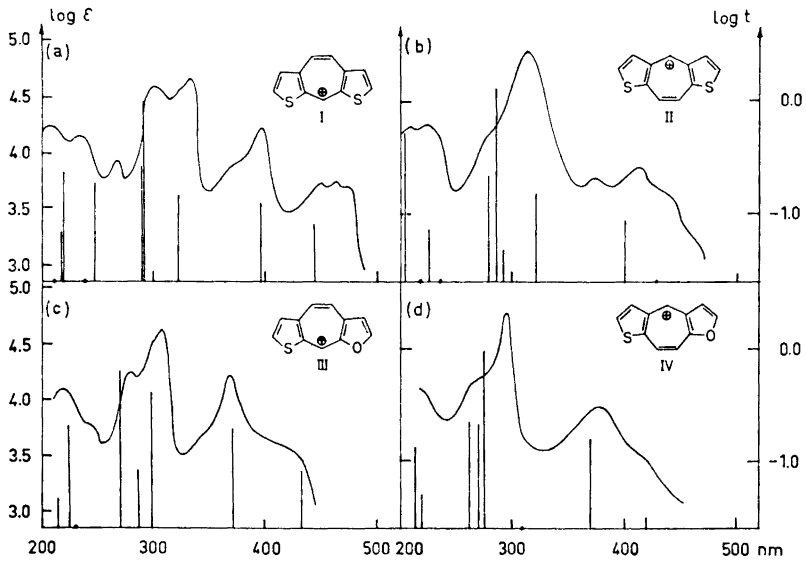

Fig. 1. Experimental and calculated UV spectra of

(a) dithieno[2,1-b:4,5-b']tropylium perchlorate,
(b) dithieno[2,1-b:5,4-b']tropylium perchlorate,
(c) furo[3,2-a]thieno[2',3'-d]tropylium perchlorate, and
(d) furo[2,3-a]thieno[2',3'-d]tropylium perchlorate.

bands at longest wavelength are especially well reproduced. The spectrum of compound I shows two well-resolved bands centred at 395 and 460 nm, respectively. The calculation indicates that these bands are due to two transi-

tions with partly resolved vibrational fine structure. This pattern is repeated in the spectra of compounds II – IV with variations in the separation between the two transitions. The small calculated separation between these transitions in the spectrum of compound II, as well as the low frequency of the first transition, accounts very well for the failure to observe two separate bands in this spectrum. Changing one of the sulphur atoms in compounds I and II to an oxygen atom, to give compounds III and IV, has no drastic influence on the ultraviolet spectra. Figs. 1 c and 1 d show that except for a loss of fine structure, the exchange results in small hypsochromic shifts of most of the transitions. This is a common observation in comparisons between the ultraviolet spectra of sulphur heterocycles and those of the corresponding oxygen heterocycles. Benzothiophene, for instance, absorbs at longer wavelengths than benzofuran.[4] This shift has been attributed to the smaller overlap between the p_z orbitals of sulphur and the neighbouring carbon atoms than between the corresponding orbitals of oxygen and carbon. Another factor of importance is the difference in the valence electron ionization potentials of sulphur and oxygen.[4] Both factors show up in the parameter set A, that is $U_O > U_S$, $|\beta_{CO}| > |\beta_{CS}|$ (Table 1).

The experimental spectra show only small differences due to the annelation pattern. The calculations indicate a small bathochromic shift of the first transition in I and III compared to the corresponding transition in II and IV, and also a greater separation between the first two transitions of the former compounds. The calculated closely lying transitions in the region of 280 – 300 nm in the spectrum of compound II, and at 260 – 280 nm in that of compound IV account well for the lower resolution of the corresponding experimental bands in these spectra compared to the equivalent bands in the spectra of compounds I and III.

The ultraviolet spectra of compounds I – IV show a general similarity to spectrum of 1,2:4,5-dibenzotropylium cation (IX), which is shown in Fig. 2 a (solvent: conc. sulphuric acid).[19] Each of the first two bands in this spectrum consists of one transition, according to calculations made by Heilbronner.[20] The position of the second band, centred at about 388 nm, is close to that of the corresponding band in the spectra of I – IV, and this is also true for the band with absorption maximum at 306 nm. The first transition, however, occurs at significantly longer wavelengths in the spectrum of IX than in the spectra of compounds I – IV. In this context it is interesting to study the calculated transitions (set A) of the unknown compound X, the synthesis of which is in progress in our laboratories.

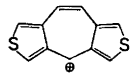

X

The predicted spectrum is given in Fig. 2 b. The annelation pattern in compound X gives, according to the calculations, some significant changes in the ultraviolet spectrum compared to the spectra of compounds I – IV. The first transition of X, for instance, is predicted to occur at 639 nm, which should

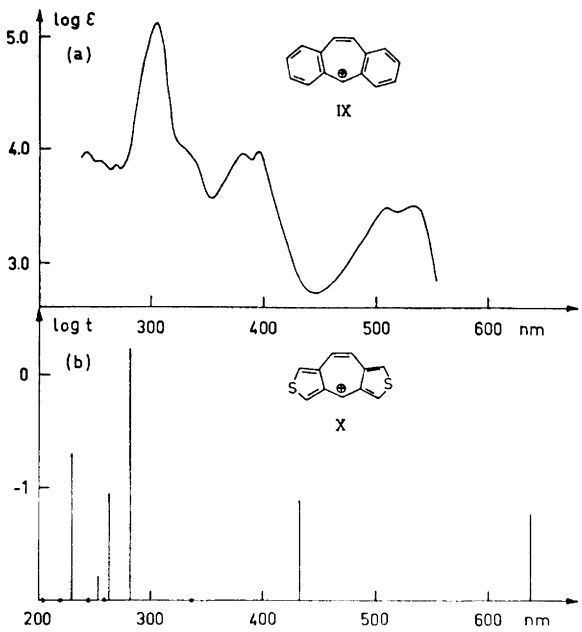

Fig. 2. (a). Experimental UV spectrum of 1,2:4,5-dibenzotropylium perchlorate. (b). Calculated UV spectrum of dithieno[2,1-c:4,5-c']tropylium perchlorate.

be compared to the first transitions in the spectra of I – IV, all of which come below 450 nm. The annelation pattern of compound X is thus predicted to have a similar effect on the ultraviolet spectrum as the exchange of the heterocyclic rings in I – IV for benzene rings. The prediction that compound X absorbs at longer wavelengths than compounds I – IV is not wholly unexpected. Resonance theory indicates restricted conjugation in compound X since more resonance structures with high probability can be written for compounds I – IV than for compound X. This should lead to a higher ground state energy of X than of any of the compounds I – IV, and consequently to lower transition energies of X than of I – IV, assuming that the energies of the excited states are not affected to the same extent.

2. Annelated tropones (V – VIII). The tropone molecule has been shown to be planar, [16] while dibenzotropone is nonplanar, at least in the crystalline state.[21] A thiophene ring is for geometrical reasons more suited than a benzene ring to be annelated to the tropone ring system without destroying the planarity of this ring, and it makes possible a coplanar arrangement of the rings. The experimental and calculated spectra of compounds V – VIII are given in Figs. 3 a – d; the experimental values are given in Table 4. The calculations were made using parameter set B. (No calculations with set A were made since this set does not include parameters for the carbonyl oxygen.) As can be seen in Fig. 3, the ultraviolet spectra of compounds V, VI, and VIII can satisfactorily be reproduced assuming planar systems.

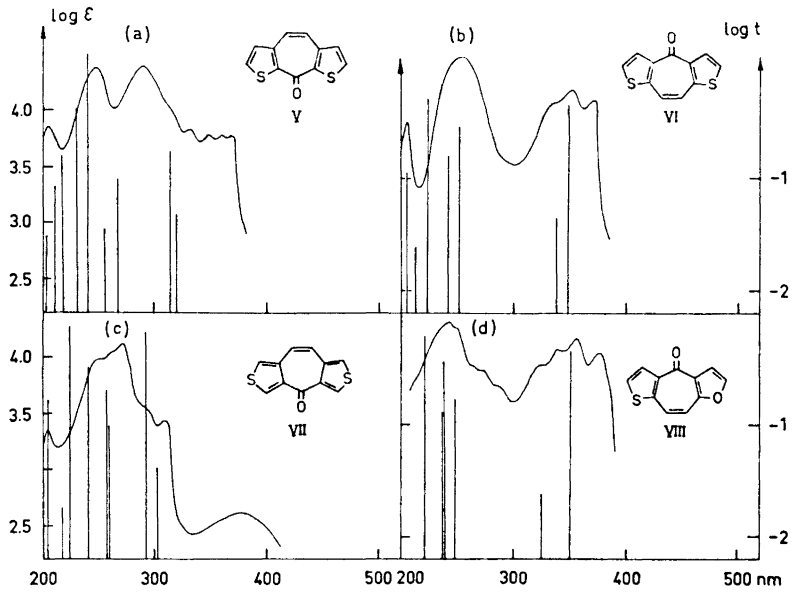

Fig. 3. Experimental and calculated UV spectra of
(a) 9H-cyclohepta[2,1-b:4,5-b′]dithiophene-9-one,
(b) 4H-cyclohepta[1,2-b:5,4-b′]dithiophene-4-one,
(c) 4H-cyclohepta[2,1-c:4,5-c′]dithiophene-4-one, and
(d) 4H-thieno[5,4-b′]cyclohepta[1,2-b]furan-4-one.

The overall similarities between the pattern of the ultraviolet transitions of compounds I – IV (Figs. 1 a – d) and that for compounds V, VI, and VIII, taking into consideration the fact that different solvents were used for the two groups of compounds, suggest a significant tropylium cation character of the central ring in V, VII, and VIII, in accordance with the previously reported IR data.[1] Further support for the proposed tropylium cation character of these compounds comes from the calculated carbon-oxygen bond orders, which are 0.6896, 0.6681, and 0.6824 for compounds V, VI, and VIII, respectively. These values are very low compared to the values for other carbonyl compounds calculated in the same way,[10] indicating an unusually strong polarity of the carbon-oxygen bond in V, VI, and VIII.

The low intensity band at 380 nm ($\varepsilon = 448$) in the spectrum of compound VII can not be reproduced by the calculations. An analogous band in the spectrum of benzophenone, which is displaced towards shorter wavelengths with increasing polarity of the solvent,[22] makes it probable that the low intensity band in the spectrum of VII is due to an $n - \pi^*$ transition. The calculated carbon-oxygen bond order of compound VII is 0.7577, which is significantly higher than the corresponding bond orders in the other ketones. This is in good agreement with the conclusion made from IR data that the tropylium cation character of the central ring is lower in compound VII than

in either of the compounds V and VI,[1] due to the restricted conjugation in the former compound. The ultraviolet spectrum of compound VII is also quite different from the spectra of the other annelated tropones (Fig. 3). Furthermore, the spectrum of VII shows no similarities to the predicted spectrum of the corresponding tropylium cation derivative X.

REFERENCES

1. a. Yom-Tov, B. and Gronowitz, S. *Chemica Scripta.* **3** (1973) 165; b. Michael, U. and Gronowitz, S. *Chemica Scripta.* **4** (1973) 126. c. Gronowitz, S., Yom-Tov, B. and Michael, U. *Acta Chem. Scand.* **27** (1973) 2257.
2. Pariser, R. and Parr, R. G. *J. Chem. Phys.* **21** (1953) 466, 767.
3. Pople, J. A. *Trans. Faraday Soc.* **49** (1953) 1375.
4. Fabian, J., Mehlhorn, A. and Zahradnik, R. *J. Phys. Chem.* **72** (1968) 3975.
5. Fabian, J., Mehlhorn, A. and Zahradnik, R. *Theoret. Chim. Acta* **12** (1968) 247.
6. Nishimoto, K. and Mataga, N. *Z. Phys. Chem. Frankfurt am Main* **13** (1957) 140.
7. Fischer-Hjalmars, I. *J. Chem. Phys.* **42** (1965) 1962.
8. Roos, B. *Acta Chem. Scand.* **21** (1967) 2318.
9. Skancke, A. and Skancke, P. N. *Acta Chem. Scand.* **24** (1970) 23.
10. Jensen, H. and Skancke, P. N. *Acta Chem. Scand.* **22** (1968) 2899.
11. Höjer, G. *Acta Chem. Scand.* **23** (1969) 2589.
12. Goeppert-Mayer, M. and Sklar, A. L. *J. Chem. Phys.* **6** (1938) 645.
13. Parr, R. G. *J. Chem. Phys.* **20** (1952) 1499.
14. Aurivillius, B., Div. of Inorganic Chemistry II, University of Lund. *Personal communication.*
15. Fateley, W. G. *Diss. Abstr.* **16** (1956) 464.
16. Kimura, K., Suzuki, S., Kimura, M. and Kubo, M. *J. Chem. Phys.* **27** (1957) 320.
17. Bak, B., Christensen, D., Dixon, W. B., Hansen-Nygaard, L., Rastrup-Andersen, J. and Schottländer, M. *J. Mol. Spectry.* **9** (1962) 124.
18. Bak, B., Christensen, D., Hansen-Nygaard, L. and Rastrup-Andersen, J. *J. Mol. Spectry.* **7** (1961) 58.
19. Navill, G., Strauss, H. and Heilbronner, E. *Helv. Chim. Acta* **43** (1960) 1221.
20. Heilbronner, E. and Murrell, J. N. *Mol. Phys.* **6** (1963) 1.
21. Shimanouchi, H., Hata, T. and Saseda, Y. *Tetrahedron Letters* **1968** 3573.
22. Ley, H. and Wingcken, H. *Ber.* **67** (1934) 501.

Received March 14, 1973.

ACTA CHEMICA SCANDINAVICA 27 (1973) 2495–2502

Fungal Carotenoids

9.* Total Synthesis of Aleuriaxanthin

HELGE KJØSEN and SYNNØVE LIAAEN-JENSEN

Organic Chemistry Laboratories, The Norwegian Institute of Technology, University of Trondheim, Trondheim, Norway

The total synthesis of aleuriaxanthin acetate (*8*, 13 % over-all yield) and aleuriaxanthin (*9*, 1′,2′-dihydro-1′,16′-didehydro-β,ψ-carotene-2′-ol) starting with linalool (*1*) is reported. Photosensitised autoxidation of linalool (*1*) constituted the key step.

Comparison of the synthetic pigments with those of natural origin proved their identity.

We have recently reported on the structure elucidation of aleuriaxanthin (*9*, 1′,2′-dihydro-1′,16′-didehydro-β,ψ-carotene-2′-ol)[1] which is the major xanthophyll of the ascomycete *Aleuria (Peziza) aurantia* of the family Pezizaceae.[2]

Aleuriaxanthin (*9*) contains an end group with a terminal methylene and an allylic hydroxyl, which has so far not been encountered in carotenoids, although other natural products with this type of end group have been isolated.[3,4] Among the carotenoids terminal methylene groups have so far been encountered in bicyclic carotenes isolated from the fungus *Caloscypha fulgens*[5] and the aphid *Macrosiphium liriodendri*.[6] The structures of these carotenes have been confirmed by total synthesis.[7]

We now report a total synthesis of aleuriaxanthin (*9*) hereby confirming the structure assigned to this new fungal carotenoid.

RESULTS AND DISCUSSION

For the synthetic formation of the desired end group photosensitised autoxidation of an isopropylidene structural element seemed to offer advantages over more conventional approaches.[4] Due to the relative reaction rates of tetra-, tri-, di-, and mono-substituted olefins with singlet oxygen [8]

* No. 8. *Phytochemistry. In press.*

specific reaction of the tri-substituted double bond of linalool (*1*) was considered feasible.

The synthesis of aleuriaxanthin (*9*) *via* the acetate (*8*) is depicted in Scheme 1, including yields.

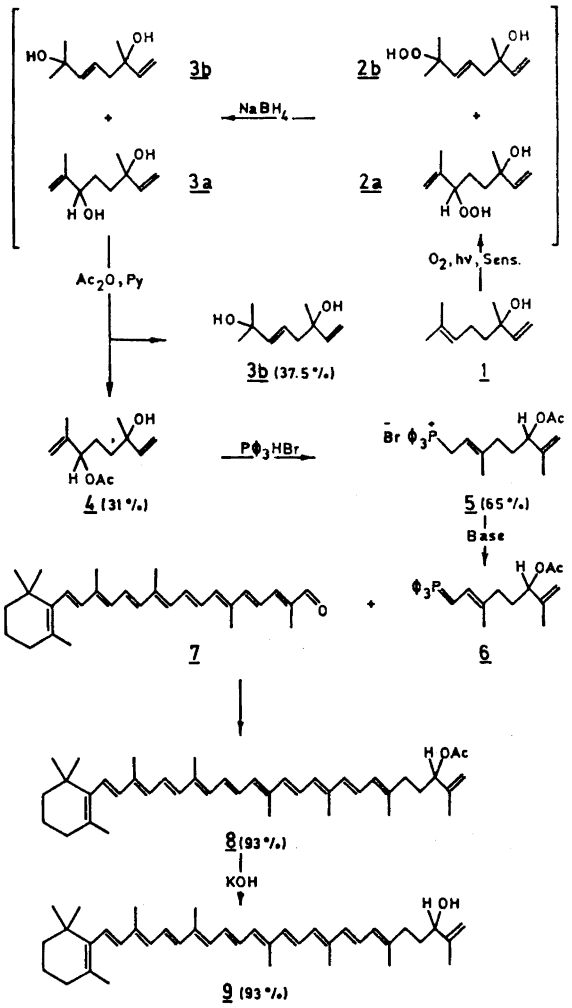

Scheme 1.

Linalool (*1*) was autoxidised with methylene blue as sensitiser to afford a *ca.* 1:1 mixture of the hydroperoxides *2a* and *2b*. This mixture was reduced with sodium borohydride to give a mixture of the diols *3a* and *3b* which on acetylation provided the acetate *4* and unreacted *3b*. The diol *3b* and

the acetate *4* were separated by column chromatography on silica. The acetate *4* was reacted with triphenylphosphonium bromide to give the phosphonium salt *5*. Condensation of the ylid *6*, generated *in situ* from *5* through the action of an appropriate base, with 8'-apo-β-caroten-8'-al (*7*) afforded a mixture of aleuriaxanthin acetate (*8*) and free aleuriaxanthin (*9*). Judged by the PMR spectrum the phosphonium salt *5* appeared to be homogeneous and it was therefore assumed that the acetoxy function had suffered nucleophilic attack by the base. In order to check this assumption bases of different nucleophilicity were employed. When butyl lithium was used *8* and *9* were obtained in a 20:80 ratio; with trityl lithium the ratio was 63:37 and with sodium hydride in a heterogeneous system the acetate *8* only was obtained. These results confirmed that the presence of free aleuriaxanthin (*9*) in the reaction mixture could be ascribed to nucleophilic attack by the base and was not due to an inhomogeneous phosphonium salt.

Aleuriaxanthin acetate (*8*), obtained as thin plates of m.p. 133–134°C from acetone-methanol, had identical physical properties, including mixed melting point and adsorptive properties, with aleuriaxanthin acetate derived from the natural carotenoid. The visible light absorption spectrum is reproduced in Fig. 1. Apart from the common carotenoid CH absorptions the

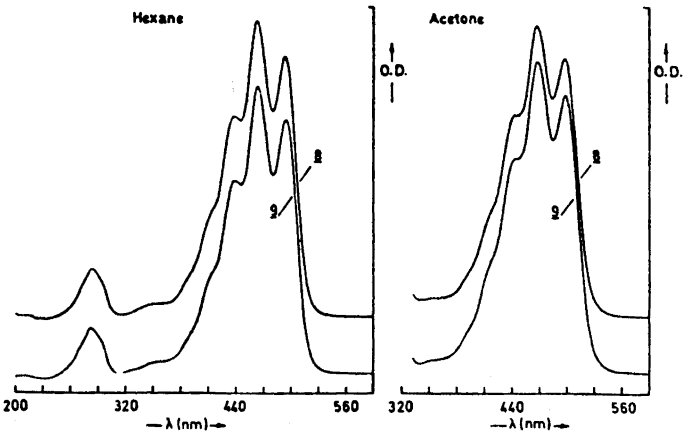

Fig. 1. Absorption spectrum in visible light of synthetic aleuriaxanthin acetate (*8*) and synthetic aleuriaxanthin (*9*) in hexane and acetone solutions.

IR spectrum exhibited acetate carbonyl frequency at 1735 cm^{-1} and an absorption at 900 cm^{-1} caused by the terminal methylene group and was indistinguishable from that of the acetate derived from natural aleuriaxanthin. The PMR spectrum (Fig. 2) exhibited the spectral characteristics which were expected.[1] The methine and terminal methylene signals at τ 4.86 and 5.04, respectively, correspond well with the values obtained for other compounds with this type of end group.[3] Addition of $Eu(dpm)_3$[9] to the PMR sample caused all the signals assigned to the oxygenated end group to move down-

field, thereby confirming the assignments, whereas the signals from the polyene chain and the cyclic end group remained virtually unshifted. The induced shifts relative (in per cent) to the induced shift of the 17′-methyl group were as follows (*cf.* Ref. 10): 16′-H_2 (135 and 61.2), 17′-H_3 (100), 2′-H (491), 18′-H_3 (25.5), 19′-H_3 (0.0), 20′-H_3 (0.0), 20-H_3 (0.0), 19-H_3 (0.0), 18-H_3 (0.0), 16,17-H_6 (0.0), acetate-CH_3 (307).

The mass spectrum (Fig. 3) had the molecular ion at *m/e* 594.4432 (calc. for $C_{42}H_{58}O_2$ 594.4436) and fragments at *m/e* 502, 488, and 436 corresponding to the common losses of toluene, xylene, and dimethylcyclodecapentaene,

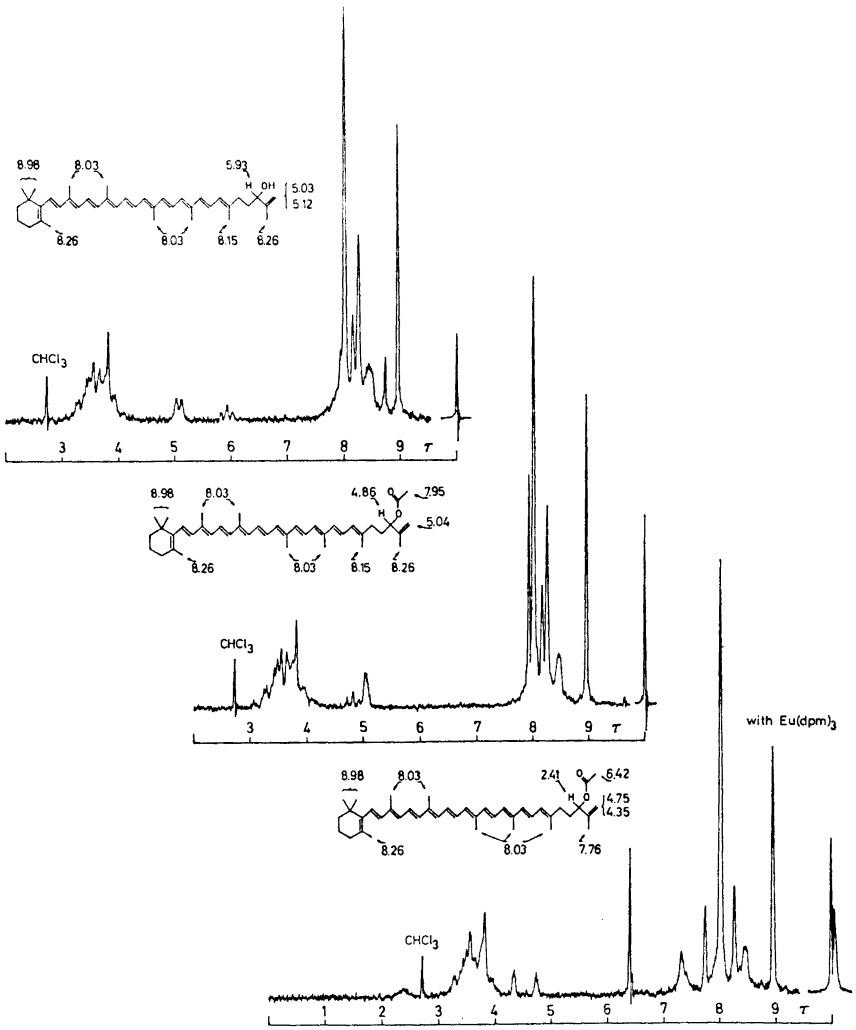

Fig. 2. PMR-spectra ($CDCl_3$) of synthetic aleuriaxanthin (*9*) and synthetic aleuriaxanthin acetate (*8*) alone and in the presence of 0.5 equiv. $Eu(dpm)_3$.

respectively.[11] Other losses of 42, 43, and 60 mass units correspond to the losses of ketene, acetyl, and acetic acid consistent with an acetate.[9]

Hydrolysis of the acetate *8* afforded aleuriaxanthin (*9*) which was obtained as clusters of prisms of m.p. 125–126°C from ether-petroleum ether. Synthetic aleuriaxanthin (*9*) was indistinguishable from the natural pigment in all its physical properties, except rotation. The visible light absorption spectrum (Fig. 1) exhibited the same maxima and spectral fine structure as the acetate *8*. The IR spectrum was identical with that of natural aleuriaxanthin and showed bonded OH and terminal methylene absorptions at 3300 and 900 cm^{-1}, respectively. The PMR spectrum (Fig. 2, including assignments) had skeletal methyl signals in the same positions as the acetate (and was identical with that of the natural pigment, *cf.* Ref. 1). The terminal

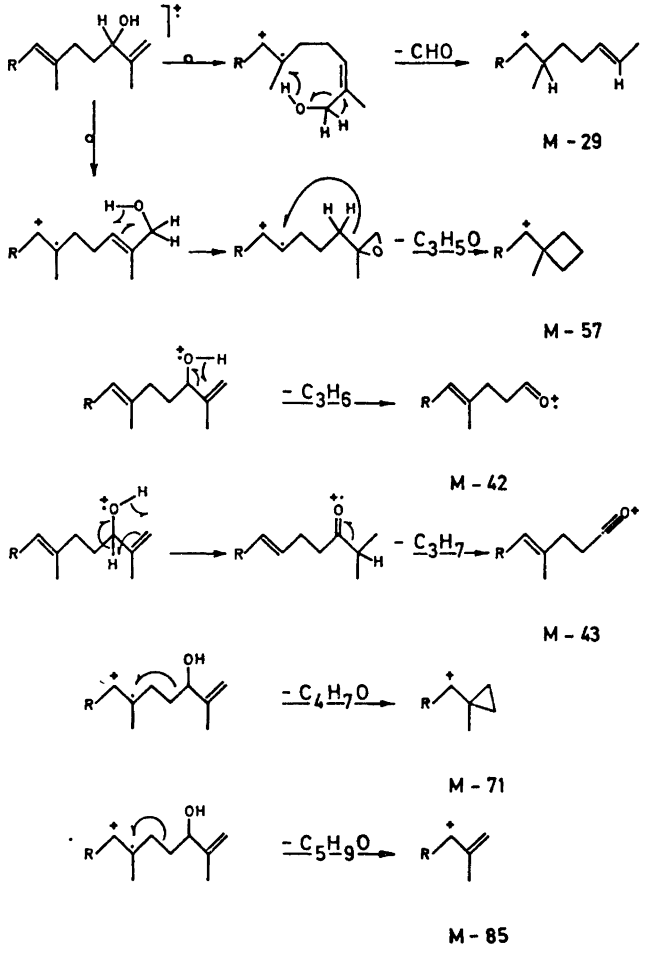

Scheme 2.

methylene protons gave rise to two signals at τ 5.03 and 5.12 due to the magnetic non-equivalence of these protons. Compatible with a secondary, allylic alcohol the methine proton resonated at τ 5.93 (triplet, J = 6 Hz). The anisotropic influence of the acetate function on the terminal methylene protons (two signals in *9* and only one in *8*) noted previously [1] was also observed for the synthetic pigments. On electron impact the molecular ion occurred at *m/e* 552.4334 (calc. 552.4331 for $C_{40}H_{56}O$). The fragmentation pattern of synthetic aleuriaxanthin (Fig. 3) was identical with that of the natural pigment.[1] Losses of 29 (CHO), 57 (C_3H_5O), 42 (C_3H_6), 43 (C_3H_7), 71 (C_4H_7O), and 85 (C_5H_9O) mass units are rationalised in Scheme 2. The losses of CHO and C_3H_5O may be derived by initial allylic rearrangement of the hydroxy group, whereas the losses of C_3H_6, C_4H_7O, and C_5H_9O involve simple cleavages. The loss of C_3H_7 requires double hydrogen transfer. Of special importance is the loss of C_4H_7O since it reflects the location of the hydroxy group (*cf.* Ref. 1).

EXPERIMENTAL

Materials and methods, summarised elsewhere,[12] were as generally used in our laboratory.

Photosensitised autoxidation of linalool (*1*). Linalool (*1*, 15.4 g) and methylene blue (30 mg) in methanol (300 ml) were irradiated externally with a tungsten lamp (Philips Argaphoto BM, 500 W) and oxygen was circulated through the solution. The oxygen uptake was monitored with a gas buret. The reaction was stopped after 2.31 l of oxygen had been absorbed (*ca.* 4 h). The crude reaction products, obtained by extraction with chloroform and evaporation, were reduced with sodium borohydride (4 g) in ethanol (150 ml) for 17 h. The reaction products were extracted with chloroform, the solvent evaporated and the crude mixture acetylated with acetic anhydride (7.5 g) in dry pyridine (25 ml) for 40 h at room temperature. Extraction with chloroform and evaporation of the solvent gave 17.4 g crude products which were separated by chromatography on silica (150 g).

6-Acetoxy-3,7-dimethylocta-1,7-diene-3-ol (*4*) was eluted from the column with benzene. Evaporation of the solvent gave 6.31 g (31 %) crude *4*. A small sample for analysis was distilled, b.p. 55–60°C/0.001 torr; n_D^{19} = 1.4627; ν_{max}(liq) 3460 (bonded OH), 3100–2820 (CH), 1740 (C=O), 1650 (C=C), 1450 (CH_2, CH_3), 1372 (CH_3), 1240 (C–O–), 1021 (OH), and 920 (=CH_2) cm^{-1}; τ ($CDCl_3$) 4.07 dd (1 H, $J_{1,2}$ = 17.5 Hz, $J_{1',2}$ = 10.5 Hz, H-2), 4.81 dd (1 H, $J_{1,2}$ = 17.5 Hz, $J_{1',2}$ = 2 Hz, H-1 *trans*), 4.83 t (1 H, J = 6 Hz, H-6), 4.95 dd (1 H, $J_{1',2}$ = 10.5 Hz, $J_{1,1'}$ = 2 Hz, H-1′ *cis*), 5.09 m (2 H, J = 1.5 Hz, H-8), 7.57 s (1 H, OH), 7.97 s (3 H, acetate), 8.29 d (3 H, J = 1.5 Hz, CH_3 at C-7), 8.42 m (4 H, H-4, H-5), 8.73 s (3 H, CH_3 at C-3); *m/e* 212.1408 (M, calc. for $C_{12}H_{20}O_3$ 212.1413).

3,7-Dimethylocta-1,5-diene-3,7-diol (*3b*) was eluted with chloroform. Evaporation of the solvent gave 6.36 g (37.5 %) crude *3b*. Distillation of a small sample for analysis gave b.p. 58–60°C/0.001 torr; n_D^{21} = 1.4758; ν_{max}(liq) 3380 (bonded OH), 3100–2820 (CH), 1460 (CH_2, CH_3), 1410, 1370 (CH_3), 1230, 1155 (OH), 975 (*trans* –CH=CH–), and 920 (=CH_2) cm^{-1}; τ ($CDCl_3$) 4.03 dd (1 H, $J_{1,2}$ = 17.5 Hz, $J_{1',2}$ = 10.5 Hz, H-2), 4.32 m (2 H, H-5, H-6), 4.81 dd (1 H, $J_{1,2}$ = 17.5 Hz, $J_{1,1'}$ = 2 Hz, H-1 *trans*), 4.95 dd (1 H, $J_{1',2}$ = 10.5 Hz, $J_{1,1'}$ = 2 Hz, H-1′ *cis*), 7.04 (broad 2 H, OH), 7.75 m (2 H, H-4), 8.70 s (6 H, H-8 and CH_3 at C-7), 8.73 s (3 H, CH_3 at C-3); *m/e* 170.1303 (M, calc. for $C_{10}H_{18}O_2$ 170.1307).

(6-Acetoxy-3,7-dimethylocta-2,7-dien-1-yl)triphenylphosphonium bromide (*5*). A solution of *4* (1.96 g) and triphenylphosphonium bromide (3.43 g) in chloroform (10 ml) was stirred at room temperature for 24 h. Addition of water, extraction with chloroform and evaporation of the solvent gave a sirup which was triturated with ether. Crys-

tallisation from chloroform-petroleum ether gave 3.23 g (65 %) *5* of m.p. 169 – 170°C; ν_{max} (KBr) 3050 – 2800 (CH), 1740 (C=O), 1650, 1587 (C=C), 1483, 1438 (CH_2, CH_3), 1370 (CH_3), 1240 (C – O –), 1220, 1112 (C – P –), 1015, 995, 935, 895 (=CH_2), 850, 750, 725 and 692 (arom. CH) cm^{-1}; τ ($CDCl_3$) *ca.* 2.20 (15 H, aromatic), 4.87 t (1 H, J = 6 Hz, H-6), 4.97 t (1 H, J = 7 Hz, H-2), 5.17 (2 H, H-8), 5.40 dd (2 H, J_{H-H} = 8 Hz, J_{H-P} = 16 Hz, H-1), 7.97 s (3 H, acetate), *ca.* 8.1 m (2 H, H-5), 8.43 s (6 H, CH_3 at C-3 and C-7), *ca.* 8.60 (2 H, H-4).

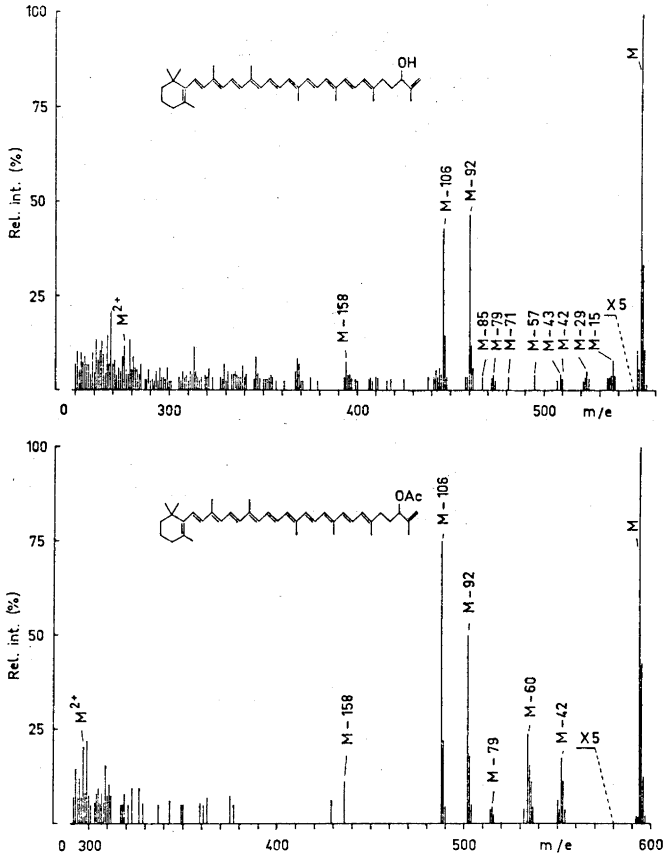

Fig. 3. Mass spectra of synthetic aleuriaxanthin acetate (*8*) and synthetic aleuriaxanthin (*9*).

Aleuriaxanthin acetate (*8*). 8′-Apo-β-caroten-8′-al (*7*, 93.2 mg), *5* (250 mg), and sodium hydride (250 mg) in dry methylene chloride (5 ml) was stirred at room temperature under nitrogen for 9.5 h. Excess sodium hydride was decomposed with acetic acid and the products extracted into ether. Chromatography on TLC (silica) afforded 83.5 mg (93 %) aleuriaxanthin acetate (*8*). Crystallisation from acetone-methanol and recrystallisation from acetone gave 16.2 mg *8* of m.p. 133 – 134°C, undepressed on admixture with aleuriaxanthin acetate (m.p. 134.5 – 135.5°C) of natural origin;[1] λ_{max} (acetone) (440), 464 [E(1 %, 1 cm) = 2570], and 495 nm; % III/II [13] = 58; (hexane) 282, 350, 436.5, 461, 492; % III/II = 60.5 (Fig. 1); ν_{max}(KBr) 3040 – 2800 (CH), 1740 (C=O),

1650, 1625, 1550 (C=C), 1440 (CH_2, CH_3), 1370 (CH_3), 1230 (C–O–), 1020, 963 and 953 (–CH=CH–), 900 (=CH_2), and 825 (>C=CH–) cm^{-1}; τ ($CDCl_3$) 3.0–4.2 (15 H, olefinic), 4.86 t (1 H, J=6 Hz, H-2′), 5.04 m (2 H, W_H=6 Hz, H-16′), 7.59 s (3 H, acetate CH_3), 8.03 s (4×3 H, in-chain CH_3), 8.15 s (3 H, CH_3 at C-5′), 8.26 s (2×3 H, CH_3 at C-5 and C-1′), 8.47 (2×2 H, non-allylic CH_2), and 8.98 s (2×3 H, *gem.* CH_3 at C-1), for the Eu(dpm)$_3$ experiment the procedure previously [10] used was followed with additions of 0.5 equiv. (Fig. 3) and 1 equiv. Eu(dpm)$_3$; *m/e* 594.4432 (M, calc. for $C_{42}H_{58}O_2$ 594.4436), 552 (M–42), 551 (M–43), 550 (M–44), 534 (M–60), 502 (M–92), 488 (M–106), and 436 (M–158).

Aleuriaxanthin (*9*). Crystalline aleuriaxanthin acetate (*8*, 30 mg) was saponified with 5 % KOH in methanol-ether (1:1, 100 ml) at room temperature for 5 h. The products were extracted with ether, the extract washed with water until neutral, dried and evaporated. Recovered 28 mg (93 %). Purification by TLC (silica) and crystallisation from chloroform-methanol gave 10 mg aleuriaxanthin (*9*) of m.p. 125–126°C, undepressed on admixture with natural aleuriaxanthin of m.p. 122–122.5°C;[1] λ_{max} (acetone) (440), 465 [E(1 %, 1 cm)=2630] and 496 nm; % III/II [13]=58; (hexane) 282, (350), 435.5, 460, 490.5; % III/II=64 (Fig. 1); ν_{max}(KBr) 3300 (bonded OH), 3040–2800 (CH), 1650, 1625, 1550 (C=C), 1440 (CH_2, CH_3), 1370 (CH_3), 1010, 960 (–CH=CH–), 900 (=CH_2), and 825 (>C=CH–) cm^{-1}; τ ($CDCl_3$) 3.0–4.2 (15 H, olefinic), 5.03 and 5.12 (1+1 H, W_H=4 Hz, H-16′), 5.93 t (1 H, J=6 Hz, H-2′), 8.03 s (4×3 H, in-chain CH_3), 8.15 s (3 H, CH_3 at C-5′), 8.26 s (2×3 H, CH_3 at C-5 and C-1′), 8.47 (2×2 H, non-allylic CH_2), 8.73 imp. and 8.98 s (2×3 H, *gem.* CH_3 at C-1); *m/e* 552.4334 (M, calc. for $C_{40}H_{56}O$ 552.4331), 537 (M–15), 534 (M–18), 523 (M–29), 510 (M–42), 495 (M–57), 481 (M–71), 467 (M–85), 460 (M–92), 446 (M–106) and 394 (M–158).

Acknowledgements. Professor N. A. Sørensen drew our attention to the previous use of photosensitised autoxidation for this type of end groups. The 8′-apo-β-carotene-8′-al used in this synthesis was a generous gift from Dr. O. Isler, F. Hoffmann-LaRoche, Basle. The support of H. K. by a grant from *The Norwegian Research Council for Science and Humanities* to S. L. J. is gratefully acknowledged.

REFERENCES

1. Arpin, N., Kjøsen, H., Francis, G. W. and Liaaen-Jensen, S. *Phytochemistry. In press.*
2. Ursing, B. *Svenska Växter i Text och Bild. Kryptogamer.* Nordisk Rotogravyr, Stockholm 1949.
3. Basa, S. L., Chatterjee, J. and Chatterjee, A. *Tetrahedron Letters* **1971** 1977.
4. Fourrey, J. L., Rondest, J. R. and Polonsky, J. *Tetrahedron* **26** (1970) 3839.
5. Arpin, N., Fiasson, J-L., Bouchez-Dangye-Caye, M. P., Francis, G. W. and Liaaen-Jensen, S. *Phytochemistry* **10** (1971) 1595.
6. Andrewes, A. G., Kjøsen, H. and Liaaen-Jensen, S. *Acta Chem. Scand.* **25** (1971) 3878.
7. Andrewes, A. G. and Liaaen-Jensen, S. *Acta Chem. Scand.* **25** (1971) 1922.
8. Foote, C. S. *Accounts Chem. Res.* 1 (1968) 104.
9. Sanders, J. K. M. and Williams, D. H. *Chem. Commun.* **1970** 422.
10. Kjøsen, H. and Liaaen-Jensen, S. *Acta Chem. Scand.* **26** (1972) 2185.
11. Enzell, C. R., Francis, G. W. and Liaaen-Jensen, S. *Acta Chem. Scand.* **23** (1969) 727.
12. Kjøsen, H. and Liaaen-Jensen, S. *Acta Chem. Scand.* **26** (1972) 4121.
13. Ke, B., Imsgard, F., Kjøsen, H. and Liaaen-Jensen, S. *Biochim. Biophys. Acta* **210** (1970) 139.

Received February 21, 1973.

ACTA CHEMICA SCANDINAVICA 27 (1973) 2503–2510

Phosphinodithioformates

V. *P,P*-Disubstituted Thiophosphinoylthioformhydrazides

OTTO DAHL, JAN ANDERSEN and OLE LARSEN

Department of General and Organic Chemistry, The H. C. Ørsted Institute, University of Copenhagen, DK-2100 Copenhagen, Denmark

The title compounds II have been prepared from $R_2P(S)CSSMe$ ((I), R = Et, Ph) and hydrazine, various methyl-substituted hydrazines, and phenylhydrazine. The structures of these compounds have been studied by IR and ^1H NMR spectroscopy. The reaction of (I) with methylhydrazine gives rise to a mixture of $R_2P(S)CSN(Me)NH_2$ and (mostly) $R_2P(S)CSNHNHMe$. In addition these and other compounds II exhibit *E–Z* isomerism about the C(S)–N bond. Tautomerism between apolar and dipolar isomers has been demonstrated for the compounds II derived from 1,1-dimethylhydrazine. Shielding effects from phenyl groups and the magnitude of coupling constants have been used in the assignment of ^1H NMR signals to *E–Z* isomers. The pK_A values of several of the compounds and the barrier to rotation about the C(S)–N bond of one of the compounds II have been estimated.

As part of a study of the chemistry of derivatives of phosphinodithioformic acid [1] we have investigated the preparation and properties of *P,P*-disubstituted thiophosphinoylthioformhydrazides (II). This type of compound,

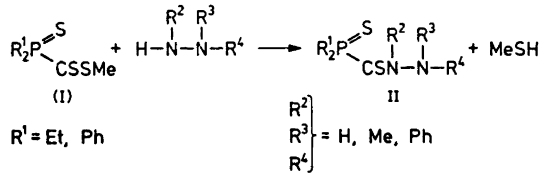

which to our knowledge has not been described previously, was obtained from methyl *P,P*-disubstituted thiophosphinoyldithioformates (I)[2] and hydrazines. The reaction of (I) with hydrazine and methylhydrazine is fast at room temperature, whereas 1,1- and 1,2-dimethylhydrazine and phenylhydrazine react more slowly. Trimethylhydrazine, 1-methyl-2-phenylhydrazine and 1,1-diphenylhydrazine do not give detectable amounts of II. The reaction probably

Table 1. Yields, melting points and elemental analyses for thiophosphinoylthioformhydrazides.

No.	Compound	Method	Yield, %	M.p., °C	Formula	Analyses (C, H, N, S)				
IIa	$Et_2P(S)CSNHNH_2$	A	70[a]	66.5– 67.5	$C_5H_{13}N_2PS_2$	Found:	30.67;	6.67;	14.26;	32.88
						Calc.:	30.59;	6.67;	14.28;	32.67
IIb	$Et_2P(S)CSNHNHMe$	B	50[b]	49.5– 50.5	$C_6H_{15}N_2PS_2$	Found:	34.38;	7.19;	13.36;	30.40
						Calc.:	34.26;	7.19;	13.32;	30.49
IIc	$Et_2P(S)CSN(Me)NH_2$	B+C	20[b]	76 – 77	»	Found:	33.98;	7.21;	13.22;	30.35
IId	$Et_2P(S)CSN(Me)NHMe$	C	35[c]	48 – 49	$C_7H_{17}N_2PS_2$	Found:	37.38;	7.65;	12.48;	28.31
						Calc.:	37.47;	7.64;	12.49;	28.59
IIe	$Et_2P(S)CSNHN(Me)_2$	B′	45[c]	*ca.* 55[g]	»	Found:	37.46;	7.70;	12.42;	28.33
IIf	$Et_2P(S)CS^-NN^+H(Me)_2$	B′	40[a]	62 – 63	»	Found:	37.43;	7.57;	12.38;	28.68
IIg	$Et_2P(S)CSNHNHPh$	A′	75[d]	107 – 108	$C_{11}H_{17}N_2PS_2$	Found:	48.30;	6.37;	10.13;	23.40
						Calc.:	48.50;	6.29;	10.29;	23.54
IIh	$Ph_2P(S)CSNHNH_2$	A	80[e]	153.5– 154.5	$C_{13}H_{13}N_2PS_2$	Found:	53.42;	4.57;	9.60;	21.73
						Calc.:	53.39;	4.48;	9.58;	21.93
IIi	$Ph_2P(S)CSNHNHMe$	B	50[e]	159 – 160	$C_{14}H_{15}N_2PS_2$	Found:	54.80;	5.04;	9.05;	20.70
						Calc.:	54.88;	4.94;	9.14;	20.93
IIj	$Ph_2P(S)CSN(Me)NH_2$	B+C	10[e]	154 – 155	»	Found:	54.95;	5.05;	9.07;	20.71
IIk	$Ph_2P(S)CSN(Me)NHMe$	C	35[e]	145 – 146	$C_{15}H_{17}N_2PS_2$	Found:	56.45;	5.44;	8.87;	19.86
						Calc.:	56.22;	5.35;	8.74;	20.01
IIl	$Ph_2P(S)CS^-NN^+H(Me)_2$	B′	30[f]	150.5– 151.5	»	Found:	56.35;	5.41;	8.76;	19.92
IIm	$Ph_2P(S)CSNHNHPh$	D	60[e]	133.5– 134	$C_{19}H_{17}N_2PS_2$	Found:	62.05;	4.71;	7.67;	17.34
						Calc.:	61.93;	4.65;	7.61;	17.40

Recrystallized from [a] 2-propanol, [b] 80 % methanol, [c] hexane, [d] methanol, [e] ethanol, [f] 1-propanol. [g] When quickly heated. Tautomerize to IIf upon melting.

fails with the higher substituted hydrazines due to steric hindrance from the $R_2P(S)$ group. Steric hindrance likewise explains the product distribution of the reaction of (I), R^1 = Et and Ph with methylhydrazine. The main product is the 3-methylhydrazide instead of the 2-methylhydrazide * expected [3] from considerations of the relative nucleophilic reactivity of the two nitrogen atoms of methylhydrazine. This steric control prevails even in the case of (I), R^1 = Me.[4] The hydrazides were isolated in variable yields (Table 1) due to side reactions, *e.g.* between (I) and the reaction product methanethiol. These side reactions are under further investigation. The hydrazides II were characterized by elemental analyses (Table 1), and by IR and ^{1}H NMR spectroscopy (Table 2).

Table 2. ^{1}H NMR chemical shifts [a] (τ) and coupling constants (J, Hz) of thiophosphinoylthioformhydrazides (*ca.* 5 % solutions in $CDCl_3$ at *ca.* 40°C).

Compound		$N(2)CH_3$	J_{PCNCH}	$N(3)CH_3$	J_{PCNNCH}	J_{HNCH}	NH[b]	%[c]
IIa							2.7	
IIb	*Z*			7.14 (d)[d]	*ca.* 0.7[d]	not obs.	−0.5	
							3.5	
IIc	*Z*	5.88 (d[e])	0.9				3.7	65
	E	6.35 (d)	1.3				4.2	35
IId[f]	*Z*	5.97 (d)	0.5	7.31 (dd)	1.1	6.1	2.3 (q)	40
	E	6.44 (d)	1.3	7.21 (d)	< 0.3	5.9	4.0 (q)	60
IIe	*Z*			7.22 (s)			−0.1	
IIg							−1.4	
							1.7	
IIh							3.3	
IIi	*Z*			7.10 (d)[d]	*ca.* 0.8[d]	not obs.	−1.1	
							3.3	
IIj	*Z*	6.40 (d)	0.9				3.9	75
	E	6.37 (d)	1.3				4.9	25
IIk[f]	*Z*	6.49 (d)	*ca.* 0.7	7.33 (dd)	1.2	6.1	not obs.[g]	60
	E	6.51 (d)	*ca.* 1.2	7.79 (d)	< 0.3	5.8	5.5 (q)	40
II*l*[h]	*Z*			7.18 (s)			not obs.	
IIm							−1.9	
							1.7[g]	

[a] The values given are the centres of the multiplets. [b] In order to obtain separate NH signals from *E* and *Z* isomers or from $N(2)$-H and $N(3)$-H's the solution was shaken with solid Na_2CO_3 in the NMR tube. [c] Estimated from the integral values. [d] Doublet only when $N(3)-H$ exchange rapidly (a little water added). [e] Multiplicity of signals, s = singlet, d = doublet, q = quartet. [f] Obtained at 90 MHz because of overlapping signals at 60 MHz. [g] Covered or partly covered by the phenyl signals. [h] Apolar isomer.

STRUCTURE OF II

Three types of isomerism are possible for compounds with a thiohydrazide structure,[5] namely structural isomerism when the reacting hydrazine is unsymmetrical, *E–Z* isomerism due to hindered rotation about the C(S)–N

* The IUPAC numbering $\overset{1}{C}(S)-\overset{2}{N}-\overset{3}{N}$ has been used throughout this work.

bond, and tautomerism (between apolar and dipolar isomers) due to the simultaneous presence of an acidic proton (II, $R^2 = H$) and a basic nitrogen atom:

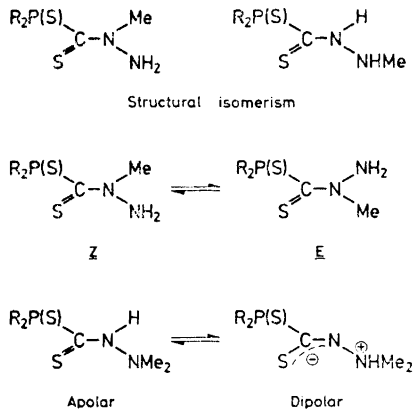

The occurrence of isomerism of these types is demonstrated in this series by IR and ^1H NMR spectroscopy.

The *N*-unsubstituted hydrazides IIa and IIh are at least 90 % apolar in the solid state and in $CHCl_3$ solution, as shown by the absence of NH^+ bands (2500 – 2800 cm^{-1}) in the IR spectra.[5] The ^1H NMR spectra ($CDCl_3$) showed only one, broad signal from the NH protons, leaving the question of *E*–*Z* isomerism open for these compounds.

The products from methylhydrazine and (I) are mixtures of 2- and 3-methylhydrazides. These isomers were separated by utilization of the fact that only the last type has acidic properties and dissolves in aqueous NaOH. This extraction procedure established IIb and IIi as the 3- and IIc and IIj as the 2-methylhydrazides.

The 3-methylhydrazides IIb and IIi were shown by IR spectroscopy to be apolar in the solid state and in $CHCl_3$ solution. The ^1H NMR spectra ($CDCl_3$) show two NH signals and one broadened *N*-CH_3 signal. On addition of a little water the NH signals collapse to one signal, and the *N*-CH_3 signal becomes narrower and shows a splitting. The splitting of the *N*-CH_3 signal is due to a coupling to phosphorus ($J = 0.7 - 0.8$ Hz), because it collapses to a singlet on strong irradiation at the ^{31}P frequency. Long-range couplings from phosphorus spanning 4 or 5 bonds are known in similar systems.[2,6] The fact that different *N*-CH_3 signals from *E* and *Z* isomers are not observed may be due to (i) accidental coincidence of signals, (ii) a low barrier for rotation about the C(S) – N bond, or (iii) the presence of only one of the *E*–*Z* isomers. The first possibility is considered unlikely since only one set of signals was observed when the spectra of IIb and IIi were recorded in C_6D_6. The second possibility is also unlikely since the barrier for rotation probably is comparable to that for IIc (21.1 kcal/mol, see below). Although IIb and IIi, contrary to IIc, are capable of dissociate the *N*(2)-H, the anions formed are expected to have higher bar-

riers for rotation than IIc. A dissociation would therefore, if anything, rise the barrier. It is therefore likely that one isomer prevails in the equilibrium mixture. Consequently the two NH signals observed must arise from the $N(2)$-H and the $N(3)$-H in the same isomer. The low field signal is assigned the more acidic $N(2)$-H.

The ^1H NMR spectra ($CDCl_3$) of the 2-methylhydrazides IIc and IIj show two NH signals and two N-CH_3 doublets. Since dipolar forms are impossible for these hydrazides the two set of signals must arise from the presence of E–Z isomers. When comparing the N-CH_3 signals from IIc with those from IIj (Fig. 1) it is seen that one of the doublets has approximately the same

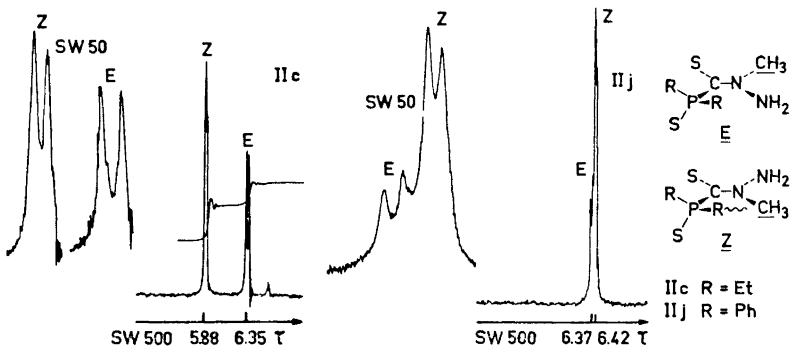

Fig. 1. Part of the ^1H NMR spectra (60 MHz) of the thiophosphinoylthioformhydrazides IIc and IIj showing the N-CH_3 signals. At the left: Signals expanded ten times.

chemical shift for both compounds, whereas the other is shifted upfield for IIj. Inspection of models of E and Z isomers suggests that this upfield shift may be explained by phenyl group shielding of the N-CH_3 protons of the Z isomer, whereas the N-CH_3 group of the E isomer is well away from the shielding area above the planes of the phenyl groups. Furthermore the coupling constants J_{PCNCH} are very similar for the doublets so correlated, and largest when phosphorus is *trans* to the N-CH_3 group (E isomers). The assignments of signals from IIc and IIj to E and Z isomers given in Table 2 are based on these arguments.

The 2,3-dimethylhydrazides IId and IIk also exist as equilibrium mixtures of E and Z isomers in $CDCl_3$. The ^1H NMR spectra show signals due to the $N(2)$-CH_3 groups which correspond well with the analogous signals from the 2-methylhydrazides IIc and IIj, and the shielding effect and the magnitude of the coupling constants J_{PCNCH} allow likewise the assignment to E and Z isomers (Table 2). The $N(3)$-CH_3 signals are doublets due to coupling to $N(3)$-H, one of the doublets being further splitted due to long-range coupling to phosphorus. The assignment to E and Z isomers follows from the integral values. A shielding is found for the $N(3)$-CH_3 group of the E isomer of IIk relative to IId, in accordance with models which show that this methyl group is close to a phenyl group in the most probable conformations. The finding of a shielding effect for $N(3)$-CH_3 groups indicate that the 3-methylhydrazides, the

structures of which was discussed above, are *Z* isomers, because the methyl group of IIi is not shielded relative to that of IIb.

The 3,3-dimethylhydrazides IIf and III are dipolar in the solid state as shown by the broad IR NH^+ bands in the 2550 – 2750 cm^{-1} region and the absence of bands above 3050 cm^{-1}. In $CHCl_3$ the apolar isomers prevail (NH bands in the 3070 – 3150 cm^{-1} region ($CDCl_3$) and absence of bands in the 2500 – 2780 cm^{-1} region). By recrystallizing IIf from hexane the apolar isomer IIe could be isolated (NH band at 3130 cm^{-1} (KBr)), whereas 2-propanol gave the dipolar IIf. Isomerization of IIe to IIf in the solid state took place within a few hours at room temperature, but IIe was rather stable at −25°C. All attempts to isolate the apolar isomer of III were fruitless. The ^1H NMR spectra ($CDCl_3$) of IIe and IIf are identical in accord with rapid isomerization of IIf to IIe in this solvent. The spectra of IIe and III show one broadened *N*-CH_3 signal and a very broad NH signal. The lack of shielding of the *N*-CH_3 group of III indicate that IIe and apolar III are *Z* isomers.

The phenylhydrazides IIg and IIm are apolar in the solid state and in $CHCl_3$ solution (IR). The compounds are soluble in 2 N NaOH and are therefore 3-phenylhydrazides, as found for other thiohydrazides prepared from phenylhydrazine.[3] The two NH signals observed in the ^1H NMR spectra most likely arise from *N*(2)-H and *N*(3)-H of one isomer, as found for IIb and IIi, although the presence of *E*–*Z* isomerism cannot be excluded.

The assignment of ^1H NMR signals to *E* and *Z* isomers, which is based primarily on the observed shielding of *N* – CH_3 groups by *P*-phenyl groups, is supported by several other observations: (1) The 3-methyl- and 3,3-dimethylhydrazides exist mainly as the sterically least hindered *Z* isomers. (2) The J_{PCNCH} coupling constant is largest when the *N*(2)-CH_3 group is *trans* to phosphorus about the C(S) – N bond (*E* isomers). This is in accord with the findings for the analogous J_{HCNCH} coupling constants in *N*-methyl thioformamides.[7,8] (3) The ^1H NMR spectra of the closely related thioamides III

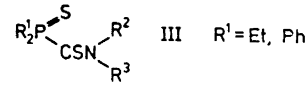

III R¹ = Et, Ph

described earlier [6] may be assigned similarly. Thus (III, $R^2 = R^3 = Me$) shows a large upfield shift of one of the *N*-CH_3 signals and virtually no shift of the other *N*-CH_3 signal when R^1 is changed from Et to Ph.[6] The *N*-CH_3 group, the signal of which is shifted, is assigned *cis* to the $R_2P(S)$ group and shows accordingly the smallest J_{PCNCH} value (1.0 Hz; the other is 1.6 Hz). No shielding is observed for (III, $R^2 = H$, $R^3 = Me$, Et) when R^1 is changed from Et to Ph and J_{PCNCH} is rather large (1.7 – 1.9 Hz). These findings are in agreement with the alkyl group being *trans* to the $R_2P(S)$ group, which is also the sterically least hindered position.

PROPERTIES OF II

The thiohydrazides II are colourless or yellow solids, *e.g.* the dipolar IIf is colourless and the apolar isomer IIe is sulfur yellow. The compounds are nearly insoluble in water except IIa and the dipolar IIf. All the thiohydrazides

Table 3. Dissociation constants for thiophosphinoylthioformhydrazides, determined by potentiometric titration of the hydrazides (*ca.* 5×10^{-4} mol in 50 ml, 20°C) with 0.1 M aqueous NaOH.

Compound	pK_A, H_2O	pK_A, 1:1 (vol.) EtOH-H_2O
$Et_2P(S)CSNHNH_2$	5.6[a]	6.6[a]
$Et_2P(S)CSNHNHMe$		6.4[a]
$Et_2P(S)CS^-NN^+H(Me)_2$	9.5[a]	10.0[a]
$Et_2P(S)CSNHNHPh$		4.9[b]
$Ph_2P(S)CSNHNH_2$		7.1[a]

[a] pH at half-neutralisation. [b] Calc. from $pK_A = 2pH - 14 - \log C_B$ at the equivalence point, since the hydrazide was poorly soluble.

with an *N*(2)H are freely soluble in 2 N NaOH showing the acidic character general for such thiohydrazides.[3] Apart from the dipolar IIf, however, their pK_A-values are 4 – 5 p*K*-units lower than those for simple thiohydrazides[3] (Table 3). This remarkable acid strength reflects the electron-attracting power of the $R_2P(S)$ group. It is obscure to us that such strong acids are not isomerized to their dipolar isomers irrespectively of the degree of substitution at N(3). The compounds are somewhat weaker bases than simple thiohydrazides and could not be titrated as bases in 1:1 ethanol-water, although salts are formed with HCl in ether.

The barrier for rotation about the C(S) – N bond in dimethyl sulfoxide has been estimated for the thiohydrazide IIc. From the coalescence temperature for the *N*-CH_3 signals (140 ± 2°C) and the chemical shift difference at slow exchange (26.5 Hz at 40°C) an approximate $\Delta G^{\ddagger}$ value of 21.1 kcal/mol is calculated. This value is close to the two $\Delta G^{\ddagger}$ values published for the isomerization of *E* to *Z* (21.0) and *Z* to *E* isomers (22.4 kcal/mol) of 3-methyl-3-phenylthioformhydrazide.[9] The $R_2P(S)$ group thus seems to have no significant effect on the barrier for rotation about the C(S) – N bond in the thiohydrazides II.

EXPERIMENTAL

Analyses were carried out by the Microanalysis Department of this laboratory. Infrared spectra were recorded on a Perkin Elmer 337 Grating Infrared Spectrophotometer, and the proton magnetic resonance spectra on a Varian A-60 A or (in case of IId and IIk) a Bruker HX-90 E instrument. The $\Delta G^{\ddagger}$ was calculated by the method given by Kessler.[10]

S-*Methyl* P,P-*diethylthiophosphinoyldithioformate* (Ia) was prepared as previously described.[2] S-*Methyl* P,P-*diphenylthiophosphinoyldithioformate* (Ib) was prepared from reaction of potassium diphenylthiophosphinoyldithioformate[2] suspended in ether with methyl iodide. Filtration and evaporation of the solvent gave (Ib) (*ca.* 70 %) which was sufficiently pure for preparation of the hydrazides.

Thiophosphinoylthioformhydrazides IIa-m. The following methods A–D have been used for the preparations. The choice of method and of solvent for recrystallization is shown in Table 1.

A. The ester (10^{-2} mol) in acetonitrile (50 ml) was mixed with an equimolar amount of the hydrazine at room temperature. After one minute the red colour of the reaction mixture had disappeared, and the mixture was evaporated to dryness at reduced pressure to give the crude product.

A'. The procedure is identical to A except that the reaction mixture was allowed to stand for 24 h before evaporation.

B. The ester (10^{-2} mol) in methylene chloride (50 ml) and the hydrazine (2×10^{-2} mol) were mixed at room temperature. The red colour disappeared immediately. The solution was extracted with 2 M aqueous NaOH (3×25 ml), the aqueous phase acidified (conc. HCl), extracted with methylene chloride (3×50 ml), and dried ($MgSO_4$). Evaporation of the solvent gave the crude product.

B'. The procedure is identical to B except that the reaction mixture was allowed to stand for 24 h before extraction.

C. The ester (10^{-2} mol) in dry ether (150 ml) was mixed with the hydrazine (2×10^{-2} mol) at room temperature. After 30 min the reaction mixture was evaporated to dryness in order to remove methanethiol. The residue was redissolved in dry ether (75 ml), and a solution of HCl in dry ether (*ca.* 4 M, 10 ml) was added with stirring. The precipitated hydrochloride was isolated by filtration, washed with HCl-ether, and dried. Treatment at 0°C with 2 M NaOH liberated the hydrazide, which was extracted with methylene chloride and isolated by evaporation of the solvent.

B+C. The reaction was performed as described in B, but the compound was isolated from the reaction mixture after the extraction with NaOH. The reaction mixture was evaporated to dryness, the residue dissolved in ether, and the hydrazide precipitated with HCl as described in *C*.

D. The ester (10^{-2} mol) in acetonitrile (70 ml) was mixed with phenylhydrazine (5×10^{-2} mol) at room temperature. After 10 min 4 M aqueous HCl (20 ml) was added with stirring, and the resulting precipitate was isolated by filtration, washed several times with 4 M HCl and then water to give the crude product.

REFERENCES

1. Part IV: Dahl, O. *Acta Chem. Scand.* **25** (1971) 3163.
2. Dahl, O. and Larsen, O. *Acta Chem. Scand.* **23** (1969) 3613.
3. Jensen, K. A., Baccaro, H. R., Buchardt, O., Olsen, G. E., Pedersen, C. and Toft, J. *Acta Chem. Scand.* **15** (1961) 1109.
4. Larsen, O. *Unpublished result.*
5. Walter, W. and Reubke, K. J. In Zabicky, J., Ed., *The Chemistry of Amides*, Interscience, London 1970, Chapter 9.
6. Dahl, O. and Larsen, O. *Acta Chem. Scand.* **24** (1970) 1094.
7. Neuman, Jr., R. C. and Young, L. B. *J. Phys. Chem.* **69** (1965) 1777.
8. Walter, W., Maerten, G. and Rose, H. *Ann.* **691** (1966) 25.
9. Walter, W. and Weiss, H. *Angew. Chem.* **81** (1969) 1050.
10. Kessler, H. *Angew. Chem.* **82** (1970) 237.

Received March 1, 1973.

ACTA CHEMICA SCANDINAVICA 27 (1973) 2511–2516

Conformational Analysis

VI. 6,6-Dialkyl- and 2,6,6-Trialkyl-4-oxo-1,3-dioxans

PERTTI ÄYRÄS and KALEVI PIHLAJA

Department of Chemistry, University of Turku, SF-20500 Turku 50, Finland

Several 6,6-dialkyl- and 2,6,6-trialkyl-substituted 4-oxo-1,3-dioxans were prepared and their PMR spectra recorded. The PMR data together with the results given by chemical equilibration reveal that the ring conformation depends greatly on the substitution pattern. For instance, *trans*-2,6-dimethyl-6-*tert*-butyl-4-oxo-1,3-dioxan exists mainly in a 2,5-boat form whereas the *cis* epimer adopts a distorted half-chair conformation. Obviously, the 6,6-dialkyl derivatives are conformational mixtures of half-chair and 2,5-boat forms.

The effect of the lactone grouping on the ring conformation of some five- and six-membered rings has been the subject of several recent investigations.[1–4] It has also been reported that certain 6-alkyl substituted 4-oxo-1,3-dioxans exist predominantly in half-chair or (twist) boat conformations.[4] To further clarify the energetics and structural properties of these interesting oxalactones, a number of 6,6-dialkyl and 2,6,6-trialkyl derivatives were prepared from suitable 3-hydroxy acids [5] and aldehydes (Table 1) by the method described previously.[6]

Table 1. Physical properties of the 4-oxo-1,3-dioxans synthesised.

R(2)	^{1}R(6)	^{2}R(6)	B.p. °C/torr	n_D^{25} or m.p.°C	d_4^{20}	Yield from hydroxy acid, %	Notes
H	Me	Me	102–4/12	1.4397	1.1063	54	[a]
H	Me	i-Pr	109–114/9	1.4508		65	[a]
H	Me	*t*-Bu	88–90/3	53–55		42	[a]
Me	Me	Me	102–4/12	1.4348	1.0519	33	[a]
Me	Me	i-Pr	107–9/8	1.4450		60	[a,b]
Me	Me	*t*-Bu	107–9/8	1.4493		65	[a,c]
i-Pr	Me	*t*-Bu	127–8/8	1.4507		60	[a,d]

[a] Catalyst *p*-TOS. [b,c,d] Two isomers; isomer ratio 47:53, 38:62 and 36:64, respectively.

Chemical equilibrations of epimeric *cis* and *trans* 2,6-dimethyl-6-isopropyl-, 2,6-dimethyl-6-*tert*-butyl- and 2-isopropyl-6-methyl-6-*tert*-butyl-4-oxo-1,3-dioxans were carried out using the normal procedure.[4] The results are shown in Table 2. The diastereoisomeric 2,6-dimethyl-6-isopropyl-4-oxo-1,3-dioxans

Table 2. Equilibration of the 2,6,6-substituted 4-oxo-1,3-dioxans. Catalyst *p*-TOS. (For experimental details, see Ref. 4.)

R(2)	^{1}R(6)	^{2}R(6)	°C	K[a]	$-\Delta G°$ kJ mol^{-1}	$-\Delta H°$ kJ mol^{-1}	$\Delta S°$ J mol^{-1}K^{-1}
Me	Me	i-Pr	33.5	1.2[b]	0.4		
Me	Me	*t*-Bu	23	1.611	1.18		
			−1.5	1.709	1.21		
			−11	1.744	1.21	1.55 ± 0.08[c]	−1.21 ± 0.29[c]
i-Pr	Me	*t*-Bu	51	1.908	1.74		
			23	1.965	1.665		
			12	1.980	1.62	0.71 ± 0.04[c]	3.26 ± 0.17[c]
			−10	2.025	1.54		

[a] *cis*-R(2), ^{2}R(6)/*trans*-R(2), ^{2}R(6). [b] from NMR-spectrum. [c] Standard deviation.

could not be separated by preparative gas chromatography. The equilibrium ratio had to be determined from the NMR spectrum of the isomer mixture by integrating the signals of the 2 protons which have slightly different chemical shifts in CCl_4.

On the basis of IR spectra Saint-Martino [7] suggested that 6,6-disubstituted 4-oxo-1,3-dioxans exist in a 2,5-boat structure with a planar lactone group, one of the 6-substituents occupying a pseudo-equatorial orientation and the other a pseudo-axial orientation. From our compounds, the *cis*-2,6-dimethyl-6-*tert*-butyl derivative might adopt a 2,5-boat form, whereas the *trans* epimer could hardly exist in a 2,5-boat conformation where either both methyl groups or a *tert*-butyl group would have to be in pseudo-axial positions.

Table 3. The chemical shifts (Hz from internal TMS) of the 6,6- and 2,6,6-substituted 4-oxo-1,3-dioxans.

R(2)	^{1}R(6)	^{2}R(6)	δ_{2a}	δ_{2e}	δ_{5a}	δ_{5e}	$\delta_{6\text{-CH}_3}$	$\delta_{2\text{-CH}_3}$	$\delta_{6\text{-}t\text{-Bu}}$
H	Me	Me[a]	318.0		155.0		80.5		
H	Me	i-Pr	313.5	313.5	157.0	145.0	73.6		
H	Me	*t*-Bu	315.5	313.0	168.5	139.0	75.8		58.0
Me	Me	Me	332.0		156.0	147.5	77.0 80.5	84.3	
Me	Me	*t*-Bu[b]	326.5		158.5	134.0	75.9	87.0	57.2
Me	Me	*t*-Bu[c]	324.0		174.0	135.5	71.6	83.9	59.2
i-Pr	Me	*t*-Bu[b]	299.5		160.5	132.0	75.3		57.0
i-Pr	Me	*t*-Bu[c]	317.5		173.0	137.0	71.3		59.1

[a] An average spectrum. [b] *cis*-R(2), ^{2}R(6). [c] *trans*-R(2), ^{2}R(6).

Table 4. The coupling constants (Hz) of the 6,6- and 2,6,6-substituted 4-oxo-1,3-dioxans. The notations "a" and "e" mean (pseudo)-axial and (pseudo)-equatorial, respectively.

R(2)	^{1}R(6)	^{2}R(6)	$^2J_{2a2e}$	$^2J_{5a5e}$	$^3J_{2aCH_3}$	$^3J_{2aCH(CH_3)_2}$	$^4J_{5aCH_3}$	$^3J_{CH(CH_3)_2}$
H	Me	i-Pr	c	−16.08			>0	6.5
H	Me	*t*-Bu	−6.26	−16.23			>0	
Me	Me	Me		−16.10	5.20		>0	
Me	Me	*t*-Bu[a]		−16.64	4.95		~0	
Me	Me	*t*-Bu[b]		−15.15	4.98		1.0	
i-Pr	Me	*t*-Bu[a]		−16.60		4.1	~0	6.4
i-Pr	Me	*t*-Bu[b]		−15.00		4.7	1.0	6.2

[a] *cis*-R(2), ^{2}R(6). [b] *trans*-R(2), ^{2}R(6). [c] $\Delta\nu = 0$ in both CCl_4 and C_6H_6.

The ^{1}H NMR spectra were recorded in 10 % CCl_4 solutions (40 mg solute in 400 μl solvent). Chemical shifts and coupling constants are shown in Tables 3 and 4. In the *cis*-2,6-dimethyl-6-*tert*-butyl and the corresponding 2-isopropyl derivatives, the 5a proton signal is a poorly resolved quartet while the signal of the 6 methyl protons is a clearly resolved doublet. This indicates a long range coupling $^4J_{5aCH_3}$ of 1.0 Hz between these protons. A ^4J of this type was not found in the corresponding *trans* epimers. 1,3-Dioxans exhibit the same type of ^4J between a 5 axial methyl group and the 6 axial proton.[8] The protons are necessarily in a W-arrangement for a long range coupling of this order of magnitude.[9,10]

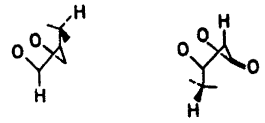

(1)

The NMR spectra of the previously [4] described *cis* and *trans* forms of 2-methyl-6-*tert*-butyl-4-oxo-1,3-dioxan will be compared with those of the corresponding isomers of 2,6-dimethyl-6-*tert*-butyl-4-oxo-1,3-dioxan (Table 5).

Table 5. The solvent induced shifts ($\delta_{CCl_4} - \delta_{C_6H_6}$, Hz) and coupling constants for the "*cis*" and "*trans*" epimers of 2-methyl-6-*tert*-butyl and 2,6-dimethyl-6-*tert*-butyl-4-oxo-1,3-dioxan.

	^{1}R (6)		$\Delta\delta_{2a}$	$\Delta\delta_{2-CH_3}$	$\Delta\delta_{5a}$	$\Delta\delta_{5e}$	$\Delta\delta_{6-t-Bu}$	$\Delta\delta_{6-CH_3}$	$^2J_{5a5e}$	$^3J_{2aCH_3}$
I	H	*cis*[a]	27.0	14.7	9.0	13.5	14.6	—	−17.9	4.98
II	Me	*cis*[a]	29.5	14.2	5.5	23.5	9.2	25.6	−16.6	4.95
III	H	*trans*[b]	27.5	12.9	26.0	11.0	18.0	—	−15.5	5.00
IV	Me	*trans*[b]	30.0	12.2	30.0	10.0	19.2	10.6	−15.2	4.98

[a] *cis*-2-methyl-6-*tert*-butyl. [b] *trans*-2-methyl-6-*tert*-butyl.

The benzene-induced solvent shifts were measured to get further information.[11] The values for the "*trans*" compounds (III and IV) show that the ring conformations are similar. All the respective parameters are nearly equal. A slightly twisted boat form (2,5-boat) has been suggested [4] for III. If the 6 proton is replaced by a methyl group, the orientation of the methyl protons with respect to the 5a proton allows the fragment $H_a-C_5-C_6-C_{Me}-H$ to attain an exactly planar W-arrangement. This structure (IV) is further sup-

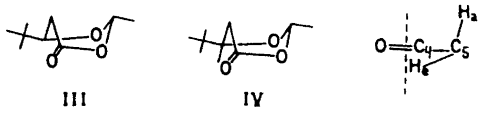

(2)

ported by the value of J_{gem} of the 5 protons since the angle $H_e-C=O$ should be about 15° and the angle $H_a-C=O$ close to 105.°[4,12] The solvent shifts also confirm this: the 5e proton lies near the reference plane [13] used to predict the magnitude of ASIS for carbonyl compounds, and the 5a proton lies well above this plane in accordance with its *ca.* three times greater solvent shift.

Comparison of the NMR spectra of the "*cis*" compounds (I and II) shows that their ring conformations are different. We found a half-chair structure for *cis*-2-methyl-6-*tert*-butyl-4-oxo-1,3-dioxan (I).[4] In II, the axial methyl substituent obviously distorts the ring conformation towards a twist-boat (2,5-twist [14]).

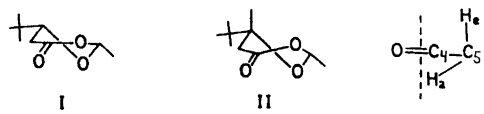

(3)

The slightly increased value of J_{gem} and the special solvent shifts for the 5 protons can also be explained by this kind of distortion. It can be seen from Tables 3–4 that an isopropyl substituent in position 2 does not alter the NMR parameters appreciably and so has little or no effect on the epimer conformations suggested above for the 2 methyl derivatives.

The other compounds studied are very likely equilibrium mixtures of different ring conformations in agreement with the above structural considerations and demonstrated by the value of J_{gem} for the 5 protons: the values around −16.2 Hz are intermediates between the limiting values of −15.3 and −17.9 Hz.[4] The J_{gem} value, −6.26 Hz, of the 2 protons in 6-methyl-6-*tert*-butyl-4-oxo-1,3-dioxan is very similar to those of the 1,3-dioxans (chair conformation) [15] and about 0.5–1.0 Hz lower than those of 6-alkyl substituted 4-oxo-1,3-dioxans having a half-chair conformation.[16] In a chair (as in 1,3-dioxan) or a boat (2,5-boat), the C(2)–H bonds are staggered against the lone-pair orbitals of the ring oxygen atoms, but in a half-chair conformation the C(2)–H bonds are eclipsed with one of the two pairs of lone-pair orbitals in accordance with the more positive value of J_{gem} for the latter.[17]

Consequently, the energy parameters shown in Table 2 seem to reflect mainly enthalpy and entropy differences between different ring conformations.

An isopropyl substituent in position 2 does not appreciably alter the enthalpy value, but the entropy difference is considerably greater than the value for the corresponding 2 methyl epimers (Table 2) and, moreover, is of different sign. This is certainly due to a slightly hindered rotation of the isopropyl group in the *trans* form (boat conformation),[18] and is also demonstrated by the coupling constants $^3J_{2H,CH(CH_3)_2}$ being slightly increased in the *trans* epimer (4.7 *vs.* 4.1 Hz).[19]

Johnson and Riggs have prepared several *gem*-dimethylphenylvalerolactones which are structurally related to the 4-oxo-1,3-dioxans.[3] They observed that the compounds could be divided into two classes on the basis of the J_{gem} values of the protons in an α position to the carbonyl group (the 5 protons in 4-oxo-1,3-dioxans). Some examples are given below:

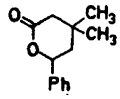
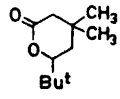
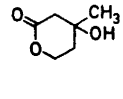
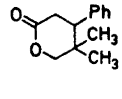
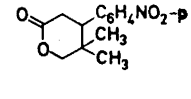

	I	II	III	IV	V
J_{gem} at C(2)	−16.1	−16.0	−17.0	−18.1	−17.9

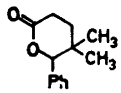
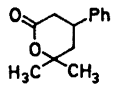

	VI	VII
J_{gem} at C(2)	−18.3	−17.9

(4

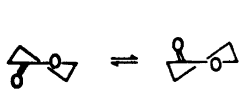

III-VI

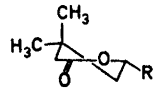

I, II

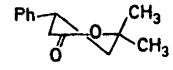

VII

(5)

The first three compounds have a J_{gem} which is clearly larger than the others and carry a geminal substitution in a β-position to the carbonyl group. Compounds IV–VI form a freely inter-converting system of two half-chair structures, compound VII exists predominantly in a half-chair conformation with a pseudoequatorial phenyl group, whereas compound III is an equilibrium mixture of two half-chair conformations ($\Delta G = 2.9$ kJ/mol = free energy difference between a pseudo-axial methyl and a hydroxyl group).[3] Johnson and Riggs suggested half-chair conformations with a pseudo-equatorial phenyl or *tert*-butyl group for compounds I and II. However, in the light of our investigations, it seems more probable that compounds I–III as well exist to a considerable extent in boat forms.

We conclude once again that the ring conformation of 4-oxo-1,3-dioxan depends very greatly on the ring substitution. In general the ring adopts a conformation in which the steric interactions are minimized – usually a half-chair, a slightly twisted boat (2,5-boat), a twist-boat (2,5-twist[14]), or a dynamic equilibrium state between all of these.

Acknowledgements. One of the authors (P.Ä.) thanks the *Foundation of Neste Co.* and the *Foundation of Emil Aaltonen* for financial support. K. P. thanks the *Finnish National Science Foundation* for a *Senior Research Grant.*

REFERENCES

1. Sheppard, R. C. and Turner, S. *Chem. Commun.* **1968** 77.
2. Carroll, F. I. and Blackwell, J. T. *Tetrahedron Letters* **1970** 4173; Carroll, F. I., Sibti, A. and Meck, R. *Ibid.* **1971** 405.
3. Johnson, R. N. and Riggs, N. V. *Tetrahedron Letters* **1967** 5119; *Aust. J. Chem.* **24** (1971) 1643, 1959.
4. Äyräs, P. and Pihlaja, K. *Tetrahedron* **29** (1973) 1311.
5. Pihlaja, K. and Ketola, M. *Suomen Kemistilehti B* **41** (1968) 299.
6. Äyräs, P. and Pihlaja, K. *Tetrahedron Letters* **1970** 4095.
7. Saint-Martino, M.-A. *Thesis*, Centre Universitaire de Perpignan, 1971.
8. Anderson, J. E. *J. Chem. Soc. B* **1967** 712.
9. Meinwald, J. and Lewis, A. *J. Am. Chem. Soc.* **83** (1961) 2769.
10. Barfield, M. *J. Chem. Phys.* **41** (1964) 3825.
11. Engler, E. M. and Laszlo, P. *J. Am. Chem. Soc.* **93** (1971) 1317.
12. Barfield, M. and Grant, D. M. *J. Am. Chem. Soc.* **85** (1963) 1899; Cookson, K. C., Crabb, T. A., Frankel, J. J. and Hudec, J. *Tetrahedron, Suppl.* **7** (1966) 355; Anteunis, M., Swaelens, G. and Gelan, J. *Tetrahedron* **27** (1971) 1917.
13. Connolly, J. D. and McGrindle, R. *Chem. Ind. (London)* **1965** 379.
14. Pihlaja, K., Kellie, G. M. and Riddell, F. G. *J. Chem. Soc. Perkin Trans. 2* **1972** 252.
15. Pihlaja, K. and Äyräs, P. *Acta Chem. Scand.* **24** (1970) 204, 531.
16. Äyräs, P. *Unpublished results.*
17. Cookson, R. C. and Crabb, T. A. *Tetrahedron* **24** (1968) 2385; Anteunis, M., Swaelens, G., Anteunis-De Ketelaere, F. and Dirinck, P. *Bull. Soc. Chim. Belges* **80** (1971) 409.
18. Pihlaja, K. and Äyräs, P. *Suomen Kemistilehti B* **43** (1970) 171.
19. Tavernier, D. and Anteunis, M. *Bull. Soc. Chim. Belges* **80** (1971) 219.

Received March 2, 1973.

ACTA CHEMICA SCANDINAVICA 27 (1973) 2517–2523

Structures of Linear Multisulphur Systems

IV. The Crystal and Molecular Structure of 2,6-Bis(5-*t*-butyl-1,2-dithiole-3-ylidene)cyclohexanethione

REIDAR KRISTENSEN and JORUNN SLETTEN

Chemical Institute, University of Bergen, N-5000 Bergen, Norway

Crystals of 2,6-bis(5-*t*-butyl-1,2-dithiole-3-ylidene)cyclohexanethione, $C_{20}H_{26}S_5$, are monoclinic, space group $C2/c$ with $Z=8$ in a unit cell of dimensions $a=35.00(1)$ Å, $b=6.34(1)$ Å, $c=20.87(1)$ Å, $\beta=110.65(1)°$. The structure was solved by three-dimensional Patterson synthesis and refined by full-matrix least-squares to $R=0.106$. The refinement comprises 1989 unique $h0l-h3l$ and $hk0$ reflections including 847 unobserved.

The five sulphur atoms are lying almost on a linear row with S–S bond distances in the region between a single bond and van der Waals distance, S(1)–S(2) = 2.183 Å, S(2)–S(3) = 2.580 Å, S(3)–S(4) = 2.583 Å, S(4)–S(5) = 2.172 Å. The molecule possesses a pseudo mirror plane perpendicular to the least-squares plane of the five membered rings and passing through S(3) and C(6).

The present investigation was undertaken as part of a program of X-ray crystallographic studies of linear multisulphur compounds. So far five four-sulphur compounds and two five-sulphur compounds have been investigated.[1–6] In these compounds sulphur-sulphur distances in the region between single bond and van der Waals distance have been found. The first structure determination of a linear five-sulphur compound (I) clearly indicates that partial covalent bonding exists between all five sulphur atoms.[5] In the present investigation the structure of a symmetrically substituted five-sulphur compound (II) is determined. A preliminary note on this work has been published.[6]

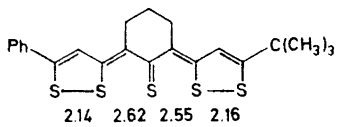

(I)

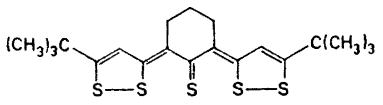

(II)

CRYSTAL DATA

$C_{20}H_{26}S_5$, M. W. = 414.75
Crystal system: monoclinic
Systematic absences: hkl: $h+k=2n+1$
$h0l$: $l=2n+1$
Space group: $C2/c$ (or Cc)
a = 35.00(1), b = 6.34(1), c = 20.87(1) Å
β = 110.65(1)°
V = 4330 Å^3
D_x = 1.309 g cm^{-3}, $Z=8$
F_{000} = 1760
$\mu_{(CuK\alpha)}$ = 47.2 cm^{-1}

EXPERIMENTAL

The compound was synthesized by Stavaux and Lozac'h.[7] Needle shaped tiny crystals grew from a solution of cyclohexane by slow evaporation at room temperature. The crystals were of poor quality and gave reflections which were partly split. A crystal with dimensions 0.022 × 0.670 × 0.044 mm^3 was used to collect integrated equi-inclination Weissenberg photographs of the $h0l-h3l$ levels employing the multiple film method. Correlation data were obtained from $hk0$ Weissenberg photographs using a crystal of dimensions 0.015 × 0.340 × 0.030 mm^3. A total of 1989 independent reflection were measured visually by comparison with a calibration strip. Space group and cell dimensions were deduced from oscillation and Weissenberg $h0l$ and $hk0$ photographs. Nickel filtered CuK radiation was used throughout the data collection.

The data were corrected for Lorentz, polarization and absorption effects. The absorption correction was made by the procedure described by Coppens *et al.*[8] the absorption integral being evaluated by the numerical method of Gauss.[9]

The density was not experimentally determined due to lack of material.

STRUCTURE DETERMINATION AND REFINEMENT

The statistical distribution of the intensity data indicated a centrosymmetric space group. Therefore, as a working hypothesis it was assumed that the space group is $C2/c$. The orientation of the approximately linear row of sulphur atoms was easily found from a three-dimensional Patterson synthesis. However, in order to locate the actual position of the row in the unit cell it was necessary to consider several possibilities. This problem arose mainly because the relative heights of the peaks due to vectors between centrosymmetrically related sulphur rows, did not correspond to the theoretically expected peak heights. All together four possible solutions were tested, three of which are closely related; from one of the possibilities the two others may be derived by translating the sulphur row by half a S – S distance in one direction or the other. In each case phases determined by the sulphur atoms were used to calculate a three-dimensional Fourier map, and all four maps showed electron density peaks in positions for atoms C(2) through C(10) (Fig. 1). Each possibility was then tested by including these carbon atoms, refining atomic positions by least squares and calculating new electron density maps. Three of the possibilities were discarded as the Fourier maps did not reveal the remaining atoms. For

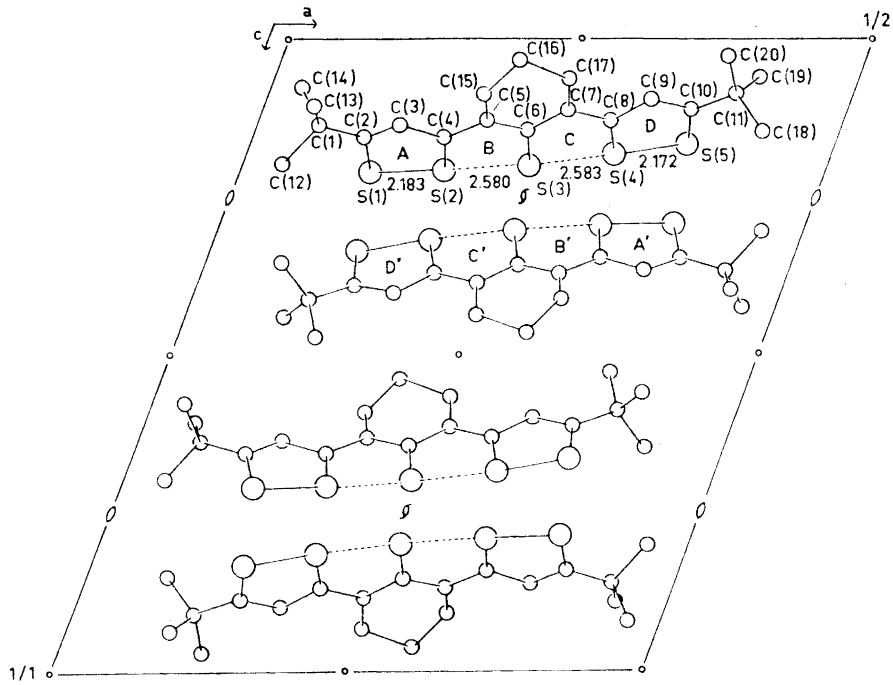

Fig. 1. Packing of molecules. The content in half a unit cell is shown.

the fourth possible solution all non-hydrogen atoms were found in successive Fourier maps, and this structure was successfully refined by a full-matrix least-squares procedure, minimizing the function $\sum w(|F_o|-|(1/k)F_c|)^2$ and giving all observed reflections, and unobserved reflections with $|F_c|>|F_o|$, unit weight. Interlayer scale factors were introduced as variables in the refinement. In the final stages of refinement the sulphur atoms were given anisotropic thermal parameters. Hydrogen atoms were not located. The refinement converged at an R of 0.107 ($R=\sum(||F_o|-|F_c||)/\sum|F_o|$). The atomic scattering factors used are for sulphur those of Dawson [10] and for carbon those of Berghuis *et al.*[11]

The calculations were carried out on an IBM 360/50 computer using programs made available by the Chemistry Department, Weizmann Institute of Science, Rehovoth, Israel and modified by D. Rabinovich and K. Åse. Programs for calculating interatomic distances and least-squares planes have been written by K. Maartmann-Moe.

RESULTS AND DISCUSSION

Atomic coordinates and thermal parameters are listed in Tables 1a and b. Bond lengths and angles are given in Tables 2 and 3. The sulphur atoms are lying approximately on a linear row, the angles S(1)–S(2)–S(3),

Table 1a. Fractional atomic coordinates and isotropic thermal parameters with standard deviations in parentheses. Thermal parameters are multiplied by 10^3. Isotropic temperature factor $T = \exp(-8\pi^2 U \sin^2\theta/\lambda^2)$

Atom	X/a	Y/b	Z/c	U
S(1)	0.1130(1)	0.0559(10)	0.2090(3)	
S(2)	0.1753(1)	0.0739(9)	0.2092(2)	
S(3)	0.2474(1)	0.0941(9)	0.2023(3)	
S(4)	0.3163(1)	0.0578(9)	0.1838(3)	
S(5)	0.3737(1)	0.0424(11)	0.1658(3)	
C(1)	0.0500(5)	0.3348(33)	0.1378(8)	46(5)
C(2)	0.0959(4)	0.2740(32)	0.1595(8)	42(5)
C(3)	0.1232(4)	0.3848(32)	0.1393(8)	44(4)
C(4)	0.1653(4)	0.3029(30)	0.1566(8)	37(4)
C(5)	0.1945(4)	0.3860(32)	0.1328(8)	40(4)
C(6)	0.2335(4)	0.2988(30)	0.1471(8)	38(4)
C(7)	0.2610(4)	0.3689(32)	0.1165(8)	43(5)
C(8)	0.2996(4)	0.2850(31)	0.1302(8)	39(4)
C(9)	0.3294(5)	0.3683(32)	0.1009(8)	44(5)
C(10)	0.3685(4)	0.2555(33)	0.1146(8)	43(5)
C(11)	0.4003(5)	0.3271(35)	0.0885(9)	58(5)
C(12)	0.0346(5)	0.3055(35)	0.1988(9)	61(6)
C(13)	0.0432(6)	0.5650(41)	0.1077(10)	84(7)
C(14)	0.0257(6)	0.1801(37)	0.0779(10)	71(6)
C(15)	0.1840(5)	0.6001(35)	0.0915(9)	54(5)
C(16)	0.2043(6)	0.5974(38)	0.0378(10)	73(6)
C(17)	0.2506(5)	0.5588(36)	0.0679(9)	68(6)
C(18)	0.4337(7)	0.4369(43)	0.1493(11)	98(8)
C(19)	0.4164(5)	0.1373(37)	0.0626(9)	66(6)
C(20)	0.3841(6)	0.4956(39)	0.0285(10)	77(6)

Table 1b. Anisotropic thermal parameters for the sulphur atoms with standard deviations in parentheses. The numbers are multiplied by 10^3.

$T_i = \exp[-2\pi^2(U_{11}h^2a^{*2} + U_{22}k^2b^{*2} + U_{33}l^2c^{*2} + 2U_{12}hka^*b^* + 2U_{13}hla^*c^* + 2U_{23}klb^*c^*)]$

Atom	U_{11}	U_{22}	U_{33}	U_{12}	U_{23}	U_{13}
S(1)	53(3)	52(6)	99(4)	6(3)	34(4)	43(3)
S(2)	51(2)	40(5)	66(3)	5(3)	18(3)	33(2)
S(3)	44(2)	50(5)	71(3)	12(3)	34(4)	24(2)
S(4)	42(2)	38(5)	81(4)	17(3)	25(4)	25(2)
S(5)	45(2)	71(6)	107(4)	26(3)	37(4)	34(3)

S(2) – S(3) – S(4) and S(3) – S(4) – S(5) being 176.9°, 170.6° and 177.5°, respectively. Each of the five-membered rings A, B, C, and D (see Fig. 1) is almost planar. However, there is a significant bending of the molecule around S(3) – C(6), the angle between the least-squares planes through rings A + B and C + D being 7.8°. A similar geometry was found in molecule I.[5] Molecule II possesses a pseudo mirror plane perpendicular to the least-squares plane of rings A, B, C, D and passing through S(3) – C(6). The corresponding

Table 2. Bond distances (Å) with standard deviations referring to the last decimal places listed in parentheses.

S(1) – S(2)	2.183(7)	C(1) – C(12)	1.56(3)	C(7) – C(17)	1.53(3)
S(1) – C(2)	1.70(2)	C(1) – C(13)	1.57(3)	C(8) – C(9)	1.48(3)
S(2) – S(3)	2.580(7)	C(1) – C(14)	1.58(3)	C(9) – C(10)	1.40(2)
S(2) – C(4)	1.78(2)	C(2) – C(3)	1.37(3)	C(10) – C(11)	1.56(3)
S(3) – S(4)	2.583(7)	C(3) – C(4)	1.48(2)	C(11) – C(18)	1.55(3)
S(3) – C(6)	1.69(2)	C(4) – C(5)	1.39(3)	C(11) – C(19)	1.51(3)
S(4) – S(5)	2.172(7)	C(5) – C(6)	1.40(2)	C(11) – C(20)	1.59(3)
S(4) – C(8)	1.79(2)	C(5) – C(15)	1.58(3)	C(15) – C(16)	1.52(3)
S(5) – C(10)	1.70(2)	C(6) – C(7)	1.40(3)	C(16) – C(17)	1.54(3)
C(1) – C(2)	1.55(2)	C(7) – C(8)	1.38(2)		

Table 3. Bond angles (°) with the corresponding standard deviations in parentheses.

S(2) – S(1) – C(2)	95.6(6)	C(4) – C(5) – C(15)	118(1)
S(1) – S(2) – S(3)	176.9(2)	C(6) – C(5) – C(15)	118(1)
S(1) – S(2) – C(4)	93.5(6)	S(3) – C(6) – C(5)	118(1)
S(3) – S(2) – C(4)	84.8(6)	S(3) – C(6) – C(7)	118(1)
S(2) – S(3) – S(4)	170.6(2)	C(5) – C(6) – C(7)	124(1)
S(2) – S(3) – C(6)	91.3(6)	C(6) – C(7) – C(8)	124(1)
S(4) – S(3) – C(6)	91.5(6)	C(6) – C(7) – C(17)	121(1)
S(3) – S(4) – S(5)	177.5(3)	C(8) – C(7) – C(17)	115(2)
S(3) – S(4) – C(8)	84.6(6)	S(4) – C(8) – C(7)	121(1)
S(5) – S(4) – C(8)	93.0(6)	S(4) – C(8) – C(9)	115(1)
S(4) – S(5) – C(10)	96.5(6)	C(7) – C(8) – C(9)	124(1)
C(2) – C(1) – C(12)	111(1)	C(8) – C(9) – C(10)	117(1)
C(2) – C(1) – C(13)	110(1)	S(5) – C(10) – C(9)	118(1)
C(2) – C(1) – C(14)	107(1)	S(5) – C(10) – C(11)	119(1)
C(12) – C(1) – C(13)	113(2)	C(9) – C(10) – C(11)	123(2)
C(12) – C(1) – C(14)	109(1)	C(10) – C(11) – C(18)	107(2)
C(13) – C(1) – C(14)	107(1)	C(10) – C(11) – C(19)	109(2)
S(1) – C(2) – C(1)	119(1)	C(10) – C(11) – C(20)	112(1)
S(1) – C(2) – C(3)	118(1)	C(18) – C(11) – C(19)	112(2)
C(1) – C(2) – C(3)	123(1)	C(18) – C(11) – C(20)	107(2)
C(2) – C(3) – C(4)	119(1)	C(19) – C(11) – C(20)	109(2)
S(2) – C(4) – C(3)	114(1)	C(5) – C(15) – C(16)	108(2)
S(2) – C(4) – C(5)	121(1)	C(15) – C(16) – C(17)	113(2)
C(3) – C(4) – C(5)	125(1)	C(7) – C(17) – C(16)	111(2)
C(4) – C(5) – C(6)	124(1)		

bond lengths and angles in the two halves of the molecule are equal within the experimental error; however, the *t*-butyl groups are twisted in opposite directions relative to the molecular plane.

The S – S, S – C, and C – C bond lengths in the molecule resemble those found in some of the unsymmetrically substituted thiathiophthenes.[12,13] It is therefore natural to assume that the bonding schemes in thiathiophthenes and the five-sulphur compounds are quite similar. One of the concepts used to describe the S – S σ-bonding in the thiathiophthenes is "the 4-electron 3-center bond".[14] Similarly one may combine one orbital from each of the five sulphur atoms in, *e.g.*, molecule II obtaining five molecular orbitals which are occupied by

six electrons. Thus the sulphur-sulphur σ-bonding in this type of molecules might be described in terms of "6-electron 5-center bonds." The sum of the four S–S bond lengths in molecule I is 9.47 Å and in molecule II 9.52 Å which is slightly longer than twice the S–S–S distances found in thiathiophthenes. This may indicate that on the average the S–S bonds in five-sulphur compounds are somewhat weaker than in thiathiophthenes.

While in thiathiophthenes and five-sulphur compounds both the results of structure determinations and theoretical models clearly suggest delocalized σ-bonding across the sulphur atoms, this is not the case for the four-sulphur compounds studied so far. X-Ray results for, *e.g.*, compounds III[3] and IV[1] indicate that the four-sulphur sequence may adequately be described in terms

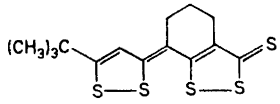

(III)

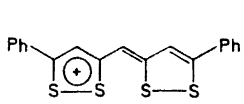

(IV)

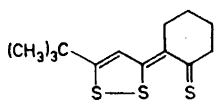

(V)

of two separate disulphide systems. Simple Hückel MO theory also predicts two localized S–S σ-bonds to be energetically more favourable than a delocalized 4-center bond.

In addition to the σ-system, a delocalized system of 10 π-electrons may be envisaged in thiathiophthenes. Results from MO calculations suggest that π-bonding exists between the three sulphur atoms.[15] With this model the visible band in the spectra of thiathiophthenes may be attributed to a $\pi \rightarrow \pi^*$ transition. NMR data are also consistent with π-conjugation in the system. The ring protons are deshielded to the same extent as in benzene, indicating ring current and aromaticity.[16] The signal from the dithiol hydrogen in, *e.g.*, compound V has a chemical shift of $\delta = 7.58$ ppm [17] compared to the δ value of 7.27 ppm for hydrogen in benzene.

In the five-sulphur compounds a delocalized π-system with 18 electrons may exist. The features of the ultraviolet and visible spectra of five-sulphur compounds [18,19] are similar to those of thiathiophthenes, the absorption bands being shifted to longer wavelength. It is possible that the bands in the visible region also in this case may be due to $\pi \rightarrow \pi^*$ transitions. The dithiol hydrogen in II has a chemical shift of $\delta = 7.04$ ppm,[18] which is somewhat lower than the benzene value, but this may still be compatible with π-bonding throughout the rings.

In the crystal there are no intermolecular contacts shorter than van der Waals distance. The shortest intermolecular sulphur-sulphur distance occurs between molecules related by a screw axis, S(3)···S(3)′ being 3.71 Å (the primed atom refers to the molecule in position $\frac{1}{2}-x$, $\frac{1}{2}+y$, $\frac{1}{2}-z$).

The least-squares plane through rings A′, B′, C′, D′ of the primed molecule makes an angle of approximately 70° with the corresponding plane of the reference molecule. S(1)′ through S(5)′ are situated above the plane through A, B, C, D at distances in the range 3.5 – 3.7 Å. Similar packing arrangements are often found in thiathiophthenes and related compounds. The reason for the difference in the twist of the *t*-butyl groups is probably packing forces.

If the butyl group at C(2) were twisted the same way as the C(10) group, C(14) would come too close to its inversion through (0,0,0). Similarly, if the group attached to C(10) were twisted as the C(2)-group, C(20) and C(16)'' (double prime refers to inversion through ($\frac{1}{4}$, $\frac{3}{4}$, 0)) would come too close.

Lists of structure factors may be obtained from the authors.

Acknowledgement. The authors wish to thank Drs. M. Stavaux and N. Lozac'h for supplying a sample of the compound.

REFERENCES

1. Hordvik, A. *Acta Chem. Scand.* **19** (1965) 1253; Hordvik, A., Sletten, E. and Sletten, J. Paper given at *The 6th Nordic Structure Chemistry Meeting* in Århus, Denmark, Jan. 1967.
2. Sletten, J. *Chem. Commun.* **1969** 688; *Acta Chem. Scand.* **25** (1971) 3577.
3. Sletten, J. *Acta Chem. Scand.* **26** (1972) 873.
4. Sletten, J. *Acta Chem. Scand.* **27** (1973) 229, and unpublished results.
5. Sletten, J. *Acta Chem. Scand.* **24** (1970) 1464.
6. Kristensen, R. and Sletten, J. *Acta Chem. Scand.* **25** (1971) 2366.
7. Stavaux, M. and Lozac'h, N. *Bull Soc. Chim. France* **1968** 4273.
8. Coppens, P., Leiserowitz, L. and Rabinovich, D. *Acta Cryst.* **18** (1965) 1035.
9. Busing, W. R. and Levy, H. A. *Acta Cryst.* **10** (1957) 180.
10. Dawson, B. *Acta Cryst.* **13** (1960) 403.
11. Berghuis, J., Haanappel, I. M., Potters, M., Loopstra, B. O., MacGillavry, C. H. and Veenendaal, A. L. *Acta Cryst.* **8** (1955) 478.
12. Hordvik, A., Sletten, E. and Sletten, J. *Acta Chem. Scand.* **23** (1969) 1852.
13. Johnson, S. M., Newton, M. G. and Paul, I. C. *J. Chem. Soc.* **B 1969** 986.
14. Gleiter, R. and Hoffmann, R. *Tetrahedron* **24** (1968) 5899.
15. Johnstone, R. A. W. and Ward, S. D. *Theoret. Chim. Acta* **14** (1969) 420.
16. Dingwall, J. G., McKenzie, S. and Reid, D. H. *J. Chem. Soc.* **C 1968** 2543.
17. Stavaux, M. and Lozac'h, N. *Bull. Soc. Chim. France* **1971** 4419.
18. Stavaux, M. *Bull. Soc. Chim. France* **1971** 4429.
19. Klingsberg, E. *Chem. Ind. (London)* **1968** 1813.

Received March 12, 1973.

ACTA CHEMICA SCANDINAVICA 27 (1973) 2524–2530

The Crystal and Molecular Structure of 1-Methyl-3-methoxy-6-pyridazone

T. OTTERSEN[a] and K. SEFF[b]

[a]*Department of Chemistry, University of Oslo, Oslo 3, Norway and* [b]*Department of Chemistry, University of Hawaii, Honolulu, Hawaii 96822, U.S.A.*

The crystal and molecular structure of 1-methyl-3-methoxy-6-pyridazone (monolactim dimethyl maleic hydrazide) has been determined by X-ray methods using 1125 reflections above background level collected by counter methods. The crystals are monoclinic, space group $P2_1/c$, with cell dimensions $a = 4.07_4$ Å; $b = 11.54_1$ Å; $c = 14.97_1$ Å; $\beta = 97.3_3°$. The carbon-oxygen and the nitrogen-nitrogen bond lengths are found to be shorter when all reflections with $\sin\theta/\lambda < 0.40$ are excluded from the refinement. Estimated standard deviations in bond lengths are about 0.006 – 0.007 Å, and in angles 0.4 – 0.5°. The heterocycle is planar, and the bond lengths indicate some resonance stabilization. The pyridazinedione moiety is significantly different from that in 4,5-dichloro-3,6-pyridazinedione.

The structure determination of 1-methyl-3-methoxy-6-pyridazone (monolactim dimethyl maleic hydrazide) (MDMH) was carried out as part of a series of structure investigations of 3,6-pyridazinediones.

In the X-ray structure determination of 4,5-dichloro-3,6-pyridazinedione [1] (DCMH) the molecule is found to be in the monolactim form (I). It is planar

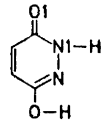

I

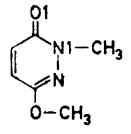

II

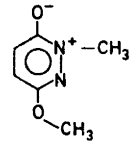

III

and the bond lengths indicate considerable resonance stabilization of the heterocycle. A similar resonance stabilization may occur in MDMH (II, III).

In the crystal structure of DCMH, N1 and both oxygen atoms were engaged in hydrogen bonds. The present structural work was carried out to determine the effect of the replacement of the two hydrogens by methyl groups. An electron diffraction study indicated a shortening of the C – O1 bond length.[2]

EXPERIMENTAL

MDMH was synthesized from 3,6-pyridazinedione by the method of Eichenberger *et al.*[3] The product was recrystallized by sublimation. Rectangular, colorless plate-shaped crystals were formed. The crystals are extremely fragile and have a high vapour pressure.

Oscillation, Weissenberg and precession photographs indicated monoclinic symmetry; all reflections ($h0l$) for l odd, and ($0k0$) for k odd, were systematically absent. This uniquely defines the space group as $P2_1/c$.

Unit cell parameters were determined on a Syntex-P$\bar{1}$ automatic diffractometer using Mo$K\alpha$ ($\lambda = 0.71069$ Å) radiation. Fifteen reflections were measured. The computer program used in the refinement of cell parameters is part of the diffractometer program library.

Three-dimensional intensity data were recorded using an automatic Syntex-P$\bar{1}$ four-circle diffractometer with graphite monochromated Mo$K\alpha$ radiation. The take-off angle was 4°, and the temperature was kept constant within 1° at 19°C.

A crystal of dimensions $0.9 \times 0.2 \times 0.1$ mm mounted in a lithium glass capillary tube, was used for the data collection. The $\omega - 2\theta$ scanning mode was utilized with scan speed variable from $1 - 12°$ min^{-1} depending on the peak intensity of the reflection. Background counting time was equal to the scan time. Reflections for which the counts exceeded 10^5 cps were remeasured with reduced primary beam intensity. The intensities of three standard reflections were measured after every 50 reflections, and the data were adjusted according to the variations in the test reflection intensity. The estimated standard deviations were taken as the square root of the total count with a 2 % addition for experimental uncertainty.

Of the 4519 unique reflections measured ($2\theta_{max} = 80°$), 1125 had intensities larger than twice their standard deviations. These were regarded as "observed" reflections, and the remaining reflections were excluded from further calculations. The intensities were corrected for Lorentz and polarization effects.

The atomic scattering factors used were those of Doyle and Turner [4] for carbon, nitrogen, and oxygen.

CRYSTAL DATA

1-Methyl-3-methoxy-6-pyridazone, $C_6H_8N_2O_2$, melting point: 68°C; monoclinic. $a = 4.074$ (0.002) Å; $b = 11.541$ (0.006) Å; $c = 14.971$ (0.007) Å; $\beta = 94.33°$ (0.04°). Figures in parentheses are estimated standard deviations. $V = 698.1$ Å^3; $M = 140.1$; $Z = 4$; $D_{calc} = 1.333$ g/cm^3; $F(000) = 296$. Absent reflections: ($h0l$) for l odd; ($0k0$) for k odd; space group $P2_1/c$.

STRUCTURE DETERMINATION

The phase problem was solved by a computer procedure [5] based on direct methods, utilizing Sayre's equation.[6]

The structure model was refined [7] to an R of 0.165, using all 849 observed structure factors with $\sin\theta/\lambda < 0.70$. Introduction of anisotropic thermal parameters for all non-hydrogen atoms and full-matrix least-squares [8] refinement yielded a conventional R of 0.079, and a weighted R_w of 0.085.

Attempts to locate the hydrogen atoms were not successful. A difference Fourier map [7] indicated that the methyl hydrogen atoms were disordered.

Some of the results from this refinement (A) are given in Fig. 1 and Table 3. The overdetermination ratio was 9.4.

The total discrepancy between the atomic vibration tensor components and those calculated from the rigid-body parameters found by analysis of the librational, translational, and screw motion [9] of the molecule, is 0.0024 Å^2,

Table 1. Observed and calculated structure factors. The columns are l, $10|F_o|$, $10\ F_c$.

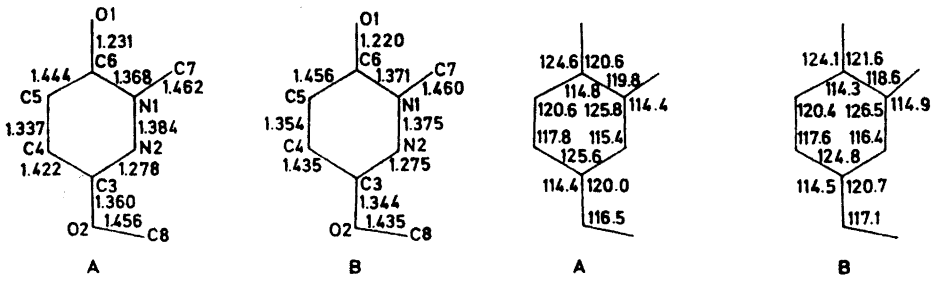

Fig. 1. Bond lengths (Å) (corrected for thermal vibration effects), and bond angles (°). A: Results from low-angle data. B: Results from high-angle data.

This indicates that the molecule may be regarded as a rigid body. The atomic positions were accordingly corrected for the librational motion. The r.m.s. librational amplitudes are 5.8°, 2.9°, and 2.7°.

In both DCMH and 1,2-dimethyl-3,6-pyridazinedione [10] it was found that the nitrogen and oxygen atomic positions were influenced by the valence electrons. In order to reduce this influence it was decided to exclude all structure factors with $\sin\theta/\lambda < 0.40$, and to include observed structure factors with $\sin\theta/\lambda > 0.70$ (to give 802 F_o's). Least-squares refinement (B) of all positional and anisotropic thermal parameters resulted in a conventional R of 0.090,

Table 2. Fractional atomic coordinates and thermal parameters with estimated standard deviations ($\times 10^5$) for nonhydrogen atoms (high angle data refinement). The temperature factor is given by exp $-(B_{11}h^2+B_{22}k^2+B_{33}l^2+B_{12}hk+B_{13}hl+B_{23}kl)$,

Atom	x	y	z	B_{11}	B_{22}	B_{33}	B_{12}	B_{13}	B_{23}
O1	3387	17369	49069	9690	866	431	−1072	2514	−57
	144	43	29	382	34	17	173	138	39
O2	61467	11386	19606	9770	703	441	367	2497	81
	138	39	29	384	32	18	151	139	35
N1	25798	24505	37160	6021	514	371	−60	1415	−37
	121	34	29	296	27	17	143	112	34
N2	40703	23505	29474	5299	628	299	110	1153	145
	110	38	25	293	28	15	131	106	32
C3	47362	13253	27106	6059	570	340	−101	1386	60
	145	44	33	339	30	18	170	130	39
C4	40536	2936	31874	7125	464	425	−67	1343	70
	155	42	35	427	29	21	161	153	41
C5	25671	4155	39391	6580	571	380	−455	1298	126
	156	45	34	392	33	20	168	147	41
C6	17383	15609	42475	5693	683	298	−687	1032	40
	150	45	32	342	36	17	171	125	39
C7	18197	36347	39618	9097	603	595	80	2360	−36
	193	53	47	519	35	31	222	213	53
C8	67879	21320	14387	8416	812	434	110	2247	230
	185	53	39	448	40	22	215	176	50

and a weighted R_w of 0.090. This structure model (B) yielded a conventional R of 0.116 for the total data set. The final parameters are listed in Table 2. The overdetermination ratio is 8.9. A comparison between observed and calculated structure factors is given in Table 1.

The total discrepancy between the atomic vibrational tensor components and those calculated from the rigid-body parameters found by analysis of the librational, translational, and screw motion [9] of the molecule, is 0.0022 Å^2. This indicates again that the molecule may be regarded as a rigid body, and the atomic positions were accordingly corrected for the librational motion. The eigenvalues of **T** are 0.22, 0.19, and 0.16 Å^2. The r.m.s. librational amplitudes are 5.4°, 2.8, and 1.7°. The major axis of libration is nearly parallel to the N2 – C5 line.

Standard deviations were calculated from the correlation matrix ignoring standard deviations in cell parameters.

Differences between the results from the two refinements are significant. The thermal parameters are generally smaller in refinement B, in agreement with previous results.[11] The three carbon-oxygen bonds are found to be shorter in refinement B (Fig. 1, Table 3), as is expected.[12] However, this shortening

Table 3. Bond lengths (Å) and bond angles (°). Estimated standard deviations are in parentheses. Results from the low angle data are given on the second line for each bond or angle.

	Bond length	e.s.d. ($\times 10^4$)	Corrected bond length		Bond angle	e.s.d.
O1 – C6	1.218	(70)	1.220	O1 – C6 – C5	124.1	(.59)
	1.229	(55)	1.231		124.6	(.40)
O2 – C3	1.343	(70)	1.344	O1 – C6 – N1	121.6	(.48)
	1.357	(54)	1.360		120.6	(.40)
N1 – N2	1.373	(60)	1.375	O2 – C3 – N2	120.7	(.49)
	1.382	(49)	1.384		120.0	(.41)
N2 – C3	1.274	(67)	1.275	O2 – C3 – C4	114.5	(.47)
	1.276	(58)	1.278		114.4	(.38)
C3 – C4	1.434	(72)	1.435	N1 – N2 – C3	116.4	(.45)
	1.419	(64)	1.422		115.4	(.37)
C4 – C5	1.352	(77)	1.354	N2 – C3 – C4	124.8	(.46)
	1.335	(64)	1.337		125.6	(.40)
C5 – C6	1.454	(74)	1.456	C3 – C4 – C5	117.7	(.47)
	1.442	(64)	1.444		117.8	(.45)
N1 – C6	1.369	(66)	1.371	C4 – C5 – C6	120.4	(.56)
	1.366	(55)	1.368		120.6	(.46)
N1 – C7	1.459	(74)	1.460	C5 – C6 – N1	114.3	(.52)
	1.460	(63)	1.462		114.8	(.36)
O2 – C8	1.430	(75)	1.435	C6 – N1 – N2	126.5	(.41)
	1.454	(62)	1.456		125.8	(.36)
				C6 – N1 – C7	118.6	(.50)
					119.8	(.40)
				N2 – N1 – C7	114.9	(.45)
					114.4	(.36)
				C3 – O2 – C8	117.1	(.52)
					116.5	(.37)

of the carbon-oxygen bonds was not found in DCMH,[1] where the oxygen atoms participated in hydrogen bonds. The shortening of nitrogen-nitrogen bonds which is observed here has been noted previously in similar structures.[1,10]

In the discussion, only results from the refinement based on high-angle data are considered.

DISCUSSION

Bond lengths and bond angles are listed in Table 3 and also in Fig. 1, where the numbering of the atoms is indicated.

Table 4. Deviations from a least-squares plane through the six ring atoms.

Atom	Deviations (Å)	Atom	Deviations (Å)
N1	0.002	C6	−0.001
N2	−0.001	O1	−0.034
C3	−0.002	O2	−0.025
C4	0.004	C7	−0.012
C5	−0.002	C8	−0.077

The heterocycle is planar, the atoms being displaced from a least-squares plane through the six ring-atoms by less than 0.004 Å (see Table 4). The oxygen atoms deviate significantly from the plane; the same displacement was found in DCMH.[1]

The N1–C6 bond length of 1.371 Å is shorter than the nitrogen-carbon bonds reported for phenylhydrazine [13] and phenylhydrazine hydrochloride.[14] Also C7 is close to the plane of the heterocycle, and the nitrogen-nitrogen bond length of 1.375 Å is significantly shorter than the corresponding bond length of 1.406 Å found in 1,2-dimethyl-3,6-pyridazinedione.[10] On this basis it may be concluded that N1 is sp^2-hybridized.

The bond lengths, the planarity of the molecule and the sp^2-hybridized N1-atom indicate that the heterocycle is resonance stabilized. However, the short C6–O1 bond length of 1.220 Å and the long C6–N1 bond length of 1.371 Å (which is significantly longer than the carbon-nitrogen bond length of 1.325 Å found in diformylhydrazine [15]) indicate only a small contribution from resonance structure III.

The differences between MDMH and DCMH are significant. The double bonds are more localized in MDMH. The N1–C6 single bond (1.371 Å) is longer in MDMH than it is in DCMH (1.345 Å), and the N2–C3 double bond is shorter (1.275 Å in MDMH, 1.305 Å in DCMH). Also the nitrogen-nitrogen bond (1.375 Å) is longer (1.353 Å in DCMH), while the C4–C5 bond (1.354 Å) is shorter (1.362 Å in DCMH). The differences may indicate that the hydrogen bonds in DCMH, which involve N1 and both oxygen atoms, establish an electronic structure between the monolactim and the dilactim. This would

give a large contribution from a resonance structure similar to III in the solid state.

The O2 – C8 bond length of 1.435 Å is as expected for bonds between oxygen and an sp^3-hybridized carbon atom. The deviation of C8 from the molecular plane is probably caused by packing effects.

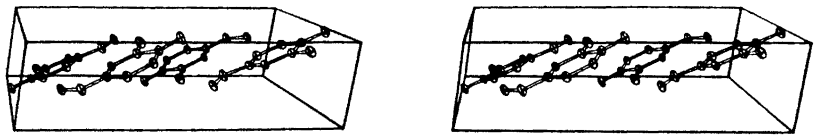

Fig. 2. Stereoview of the packing of 1-methyl-3-methoxy-6-pyridazone molecules in the unit cell, showing ellipsoids of 20 % probability. C. K. Johnson, ORTEP, Report ORNL-3794, Oak Ridge National Laboratory, Oak Ridge, Tennessee, 1965.

The molecular arrangement in the crystal is visualized in Fig. 2, and may be described as layers perpendicular to (102). Many short intermolecular van der Waals contacts (3.15 – 3.55 Å) are observed, the interplanar spacing is approximately 3.25 Å.

REFERENCES

1. Ottersen, T. *Acta Chem. Scand.* **27** (1973) 797.
2. Ottersen, T. and Strand, T. *To be published.*
3. Eichenberger, K., Staehelin, A. and Druey, J. *Helv. Chim. Acta* **37** (1954) 837.
4. Doyle, P. A. and Turner, P. S. *Acta Cryst.* **A 24** (1968) 390.
5. Long, R. E. Ph.D. Thesis, University of California at Los Angeles 1965, Part III, pp. 87 – 126.
6. Karle, J. *Advan. Struct. Res. Diffr. Methods* **1** (1964) 55.
7. Hubbard, C. R., Quicksall, C. O. and Jacobson, R. A. ALFF, Ames Laboratory, USAEC, Iowa State Univ. 1971.
8. Gantzel, P. K., Sparks, R. A. and Trueblood, K. N. UCLALS4, American Crystallographic Association Program Library (old) No. 317, modified.
9. Schomaker, V. and Trueblood, K. N. *Acta Cryst.* **B 24** (1968) 63.
10. Ottersen, T. *Acta Chem. Scand.* **27** (1973) 835.
11. Coppens, P. *Acta Cryst.* **B 24** (1968) 1272.
12. Coppens, P. and Coulson, C. A. *Acta Cryst.* **23** (1967) 718.
13. Srinivasan, S. and Swaminathan, S. *Z. Krist.* **127** (1968) 442.
14. Koo, C. H. *Bull. Chem. Soc. Japan* **38** (1965) 286.
15. Tomiie, Y., Koo, C. H. and Nitta, I. *Acta Cryst.* **11** (1958) 774.

Received March 21, 1973.

ACTA CHEMICA SCANDINAVICA 27 (1973) 2531–2535

Infrared and Raman Spectra of Phenylisocyanide $C_6H_5N \equiv C$

BØRGE BAK and CECILIA KIERKEGAARD

Chemical Laboratory V, H. C. Ørsted Institut, Universitetsparken 5, DK-2100 Copenhagen, Denmark

Infrared and Raman spectra of phenylisocyanide have been recorded and a vibrational analysis attempted in three stages. First, the experimental results alone were used for assignment of all A_1-class and 5 B_1-class fundamentals. Secondly, 9 B_2-class and 1 A_2-class fundamentals were assigned using their spectral positions close to phenyl*cyanide* fundamentals as a criterium. Finally, the 2 unassigned B_1-fundamentals, the 2 unassigned B_2-fundamentals, and 1 of the 2 unassigned A_2-vibrations were inferred from a study of the remaining experimental material. The assigned 32 fundamentals are summarized in Tables 2 and 3. Their positions are very close to normal vibration frequencies of phenylcyanide (mostly within 1 %).

In literature only one experimental infrared (IR) spectrum (4000 – 667 cm^{-1}) of unstable, liquid phenylisocyanide $C_6H_5N \equiv C$ (I) has appeared.[1] No Raman (Ra) spectrum has been reported and no identification of normal vibrations has been published. In this paper we intend to verify the expected very close agreement between the normal vibration frequencies of I and of related phenylcyanide (II). We want to use the result as one argument in a discussion on the structure of I in a following paper.

INSTRUMENTATION AND PREPARATION

IR spectra of gaseous I were recorded at room temperature at $p \sim 1$ mmHg in a 1 m cell on a Perkin-Elmer 125 grating spectrophotometer from 4000 to 400 cm^{-1}, and on a Fourier spectrometer (FS-500) from 450 to 20 cm^{-1} in a 6 m gas cell.[2] The IR spectrum of the pure liquid at 20° in a KBr cell with 0.012 mm spacing was recorded on the Perkin-Elmer 125 instrument from 4000 to 400 cm^{-1}. For the region 400 to 30 cm^{-1} a Perkin-Elmer FIS-3 instrument was used, the sample now being a 20 % sufficiently stable solution of I in hexane. A polyethylene cell with 1 mm spacing was applied. Pure I undergoes chemical change in the He-Ne laser light of the Coderg PH-1 Ra instrument used for the Ra measurements. However, the above-mentioned 20 % solution proved to be stable for hours. The sample volume applied was 300 μl. Measurements were performed perpendicular to the laser beam, depolarization measurements being carried out by rotation of the polarization analyzer by 90°. In a majority of cases (Table 1) the polarization results were unambiguous.

Table 1. Observed vibrational spectra of phenylisocyanide, C_6H_5NC.

Band No.	Infrared spectra at 20°: Gas at 1 mmHg Position cm^{-1}	P,R sep. and type	Intensity[a]	Liquid Position cm^{-1}	Intensity[a]	Assignment[c]	Raman spectrum at 20°: 20 % sol. in hexane Position cm^{-1}	Polar.	Intensity[a]
1	3040 – 3110[d]		m	3060	m	A_1,ν_2,ν_3,ν_4	3078	pol.	s
2	»		m	3040	w	$B_2,\alpha_{25},\alpha_{26}$	3047	depol.	w
3				2280	w				
4	2130		s	2120	s	A_1,ν_5	2126	pol.	vs
5				1950	w				
6				1880	w				
7				1795	w				
8				1745	w				
9				1670	w				
10	1600		m	1595	m	A_1,ν_6	1600	pol.	s
11				1585	m	B_2,α_{27}			
12				1500	w				
13	1489	*ca.*12.A	m	1485	s	A_1,ν_7	1487	pol?	w
14				1455	m	B_2,α_{28}			
15	1394		vw	1390	vw				
16				1325	vw	B_2,α_{29}			
17				1285	vw	B_2,α_{30}			
18				1240	vw		1244	pol?	vw
19	1193	*ca.*12,A	w	1185	m	A_1,ν_8	1190	pol.	vs
20	1170	*ca.*13,A	w	1165	m	A_1,ν_9	1168	pol.	vs
21				1155	vw	B_2,α_{31}			
22				1095	w				
23	1071	*ca.*9,B?	w	1070	m	B_2,α_{32}			
24	1029	*ca.*10,A?	w	1025	m	A_1,ν_{10}	1029	pol.	s
25				1010	w				
26				1000	vw	A_1,ν_{11}	1003	pol.	vs
27	913	?,C	s	910	m	B_1,ν_{18}			
28				880	vw				
29				840	vw	A_2,α_{15}			
30	770		vw	765	m	A_1,ν_{12}	770	pol.	s
31	756	*ca.*14,C	s	755	s	B_1,ν_{19}	757	depol?	vw
32	685	?,C	m	680	s	B_1,ν_{20}			
33				660	w				
34				620	vvw	B_2,α_{34}	621	depol.	w
35	510	?,C	m	510	m	B_1,ν_{22}	512	depol.	w
36				475	w	A_1,ν_{13}	473	pol.	m
37				470	vw				
38				327[b]	w		329	depol.	m
39				312[b]	w				
40	149	?,C	m	161[b]	s	B_1,ν_{24}	164	depol.	s

[a]Estimated. w = weak, m = medium, s = strong, v = very. [b]20 % solution in hexane. [c]ν_i: pure experimental assignment. Species and ν_i notation in agreement with Ref. 6. α_i: assignment by comparison with spectrum of C_6H_5CN.[5] Subindex i in agreement with Ref. 6. [d]Several, unidentified maxima.

Our sample of I was prepared according to Ref. 3. Its IR spectrum was consistent with the one earlier published.[1]

ANALYSIS OF SPECTRA

I has C_{2v} symmetry with a normal vibration distribution of A_1 (12, IR+Ra, A-type), A_2 (3, Ra), B_1 (7, IR+Ra, C-type), and B_2 (11, IR+Ra, B-type), the parentheses giving the number, spectral activity, and IR band fine-structure type of the fundamentals. From a microwave investigation [4] rotational constants were taken as A=5660, B=1640, and C=1271 Mc/s. P, R separations of IR gas phase bands of 11, 9, and 16 cm^{-1} were calculated for A, B, and C type contours. Observed and assigned vibrational frequencies are given in Table 1. Bands Nos. 1, 4, 10, 13, 19, 20, 24, 30 were assigned as A_1-fundamentals because they correspond to Ra lines which are polarized and of medium or strong intensity (except band No. 13) and to IR (liq.) lines of medium or strong intensity. They all appeared in the IR gas spectrum, but their identification as A type bands was not always possible (Table 1). Bands Nos. 26 and 36 were adopted as A_1 fundamentals solely on the Ra criterium. Thus, the assignment of all 12 A_1 fundamentals has been reached ($\nu_2-\nu_{13}$).

Bands Nos. 27, 31, 32, 35, and 40 were adopted as B_1-fundamentals mainly due to their appearance as C-type bands in the IR gas spectrum, and as medium or strong lines in the IR (liq.) spectrum. Bands Nos. 31, 35, and 40 also occurred as depolarized Ra-lines. Of the remaining depolarized Ra-lines (bands Nos. 2, 34, 38) band No. 2 must correspond to the 2 expected B_2-hydrogen stretching frequencies. It is an open question, whether bands Nos. 34 and 38 are B_1 and/or B_2-vibrations. They are less likely to be A_2-vibrations since they both appear in IR liq. Thus, 5 out of 7 expected B_1-fundamentals have been assigned.

Table 2 shows the close agreement between normal vibration frequencies, so far assigned, for I, and for II.[5] This agreement suggests that the mere appearance of a band in our experimental spectra of I unassigned above, but close to an assigned band in the spectrum of II, may be taken as a tentative assignment criterium. Bands assigned as fundamentals in this way which, of course, is second to our first assignment criterium, are in Table 1 denoted by their species and by α_i instead of ν_i for the sake of clarity. In this way, 9 out of 11 expected B_2-fundamentals were assigned [$\alpha_{25}-\alpha_{32}$, (α_{33} appears only in $C_6H_5C{\equiv}CH$), and α_{34}]. The assignment of band No. 29 as α_{15} assumes a sometimes occurring break-down of selection rules for liquids. Table 3 shows the satisfactory agreement obtained.

The 6 missing fundamental vibration frequencies are now γ_{17} and γ_{23} (B_1), γ_{35} and γ_{36} (B_2), and γ_{14} and γ_{16} (A_2). They must be looked for by analyzing the so far unassigned experimental bands Nos. 3, 5, 6, 7, 8, 9, 12, 15, 18, 22, 25, 28, 33, 37, 38, and 39 (Table 1). Bands Nos. 5–9 can be interpreted in close analogy with Ref. 6. 1950 (exp.)$=\gamma_{14}+\gamma_{17}$, 1880 (exp.)$=\gamma_{14}+\gamma_{18}$, and 1795 (exp.)$=\gamma_{14}+\alpha_{15}$ yields $\gamma_{14}=967$ or 955 in agreement with ν_{14} of II (Table 3), ignoring anharmonicity effects. Correspondingly, $\gamma_{17}=983$ or 995. 1745 (exp.)$=\alpha_{15}+\nu_{18}=840+913=1753$. 1670 (exp.)$=\nu_{18}+\nu_{19}=913+755=1668$. 1500 (exp.)$=\nu_{10}+\nu_{13}=1029+475=1504$. 1390 (exp.)$=\nu_{18}+\nu_{13}=913+475=1388$. 1240 (exp.)$=\nu_{12}+\nu_{13}=770+473=1243$.

Table 2. Comparison of experimentally assigned fundamental frequencies in cm^{-1} of phenylisocyanide and of phenylcyanide.[5] ν_i notation as in Ref. 6.

	i	Phenylisocyanide	Phenylcyanide	Per cent deviation
A_1	2		3080	
In plane	3	3040 – 3110	3062	
	4		3042	
	5	2130	2232	5
	6	1600	1599	0.07
	7	1489	1492	0.2
	8[c]	1193	1192	0.2
	9	1170	1178	0.6
	10	1029	1027	0.2
	11	1003	1001	0.2
	12[c]	770	769	1.5
	13[c]	473	461	2.5
B_1	17	γ_{17}[b]	(989)	(2.0)
Out of	18	913	925	1.4
plane	19	756	758	0.4
	20	685	686	0.2
	(21)		Only in $C_6H_5C{\equiv}CH$	
	22[c]	510	548	7.5
	23[c]	γ_{23}[b]	172	(7)
	24	149[a]	162	9.1(0.07)

[a]IR gas. For a solution in hexane: 161 cm^{-1}. [b]γ_i's are normal vibration frequencies unassigned by the methods producing Tables 2 and 3. A tentative assignment of combination bands (see text) results in $\gamma_{17} = 1010$ and $\gamma_{23} = ca.$ 160 or 329. [c]Sensitive to substitution such as $C_6H_5CN \rightarrow C_6H_5F$.[5]

Table 3. Phenylcyanide fundamental frequencies[5] in cm^{-1} (ν_i) and fundamental frequencies (α_i) of phenylisocyanide as suggested by simple comparison. ν_i notation as in Ref 6.

	i	ν_i	α_i	Per cent deviation
B_2	25	3072	3040 – 3110	
In plane	26	3027		
	27	1584	1585	0.07
	28	1448	1455	0.5
	29	1337	1325	1.0
	30	1289	1285	0.3
	31	1163	1155	0.7
	32	1071	1070	0.1
	(33)		Only in $C_6H_5C{\equiv}CH$	
	34	629	620	1.5
	35	551	γ_{35}[a]	(0)
	36[b]	381	γ_{36}[a]	(15)
A_2	14	978	γ_{14}[a]	(1.0)
Out of	15	848	840	1.0
plane	16	401	γ_{16}[a]	

[a]Unassigned fundamental frequency γ_i. A tentative assignment of combination bands (see text) results in $\gamma_{35} = 551$, $\gamma_{36} = 329$, and $\gamma_{14} = 955$. [b]Sensitive to substitution.[5]

Since band No. 34 was assigned as a B_2-vibration α_{34}, it is tempting to assign band No. 38 at 329 to another B_2-vibration, γ_{35} or γ_{36}, and preferably the latter which is close to ν_{36} (at 381) in the spectrum of II. 1095 (exp.) can now be taken as $\nu_{12}+\gamma_{36}=770+329=1099$. Band No. 25 at 1010 may be γ_{17} so that $\gamma_{17}=995$ and $\gamma_{14}=955$ (above) are the better choices. Setting band No. 28 at $880=\gamma_{35}+\gamma_{36}$ means $\gamma_{35}=551$, identical with γ_{35} in the spectrum of II. Band No. 33 at $660=2\gamma_{36}=658$. Unassigned experimental bands Nos. 3, 37, 39 remain. The frequency ratio of the 2 latter is 3:2 suggesting their interpretation as first and second overtones of a fundamental at *ca.* 160, perhaps ν_{24} already assigned, or the so far unassigned γ_{23}. In Ref. 6, $\nu_{23}=\nu_{36}$ is assumed for the spectrum of $C_6H_5C{\equiv}CH$.

Following the same procedure, $\gamma_{23}=329$. Finally, band No. 3 (2280 exp.) must be taken as $\nu_5+\nu_{24}=2280$ (exp.).

We have no suggestion whatsoever how to assign the last fundamental γ_{16}. Ref. 5 reports that this vibration is insensitive to substitution such as $C_6H_5CN \rightarrow C_6H_5F$. There is no observed band in our spectra closer to 400 than bands Nos. 37 and 38 at 470 and 329.

In summary, the vibrational spectra of phenylisocyanide may be assigned in very close agreement with the spectra of phenylcyanide.

DISCUSSION

The 3N-6 dimensional potential energy surfaces of phenylisocyanide and of phenylcyanide are, of course, not congruent. However, their *curvatures* in almost all 3N-6 separate points of normal coordinate null-values must be very much alike, the normal vibration frequencies being so close. Since major structural differences must mean less similarity of energy surface curvature we shall use the results of Tables 2 and 3 as one argument in favour of great structural resemblence of I and II assuming, in a forthcoming paper on the structure of I, equal phenyl ring structure in both molecules, presenting additional evidence for this.

Acknowledgements. We are highly indebted to Daniel H. Christensen, Flemming Nicolaisen, and Ole Faurskov Nielsen of this department for their active interest in this work and for help in the experiments.

REFERENCES

1. Ugi, I. and Meyer, R. *Chem. Ber.* **93** (1960) 239.
2. Stroyer-Hansen, T. *Infrared Phys.* **10** (1970) 159.
3. Appel, R., Kleinstück, R. and Ziehn, K. D. *Angew. Chem.* **83** (1971) 143.
4. Bak, B., Kierkegaard, C. and van Eijck, B. P. *Private communication.*
5. Jacobsen, R. J. *Spectrochim. Acta* **21** (1965) 127.
6. King, G. W. and So, S. P. *J. Mol. Spectry*, **36** (1970) 468.

Received February 22, 1973.

ACTA CHEMICA SCANDINAVICA 27 (1973) 2536–2542

Crystal Structure of Bis-pyrimidyl-2,2′-disulfide Dihydrate

S. FURBERG and J. SOLBAKK

Department of Chemistry, University of Oslo, Oslo 3, Norway

The crystal structure of bis-pyrimidyl-2,2′-disulfide dihydrate has been derived from 1690 observed reflections measured by counter methods. The final value of R is 0.030 and the estimated standard deviations in distance between non-hydrogen atoms are 0.001 – 0.003 Å. The C–S–S–C dihedral angle is 82.5°, and both sulfur atoms lie approximately in the plane of both pyrimidine rings. The S–S bond length is 2.016 Å. The bonds C2–N1 and C2–N3 appear to be significantly different.

Continuing our investigations of the structure of pyrimidine derivatives [1] we have carried out an X-ray analysis of bis-pyrimidyl-2,2′-disulfide. The structure of this compound is of interest because it is a derivative of the 2-*thiol* rather than the usual 2-*thio* tautomer of pyrimidine. It would also appear to be of interest to compare the structure of this simple disulfide with those of other aromatic disulfides, such as diphenyl disulfide.[2]

EXPERIMENTAL. STRUCTURE ANALYSIS

The compound was prepared by solving 2-thiopyrimidine in hot ammoniacal water. Oxidation takes place and after some time a crystalline precipitate was formed, which was shown by the structure analysis to be the dihydrate of the disulfide. The crystals disintegrate in air and were sealed off in glass capillaries containing some water during the X-ray exposures.

Unit cell dimensions are $a = 11.835(4)$ Å, $b = 6.944(1)$ Å, $c = 18.655(3)$ Å, and $\beta = 128.94(1)°$. The space group is $P2_1/c$, with four disulfide and eight water molecules in the unit cell. The density was measured by flotation in KI-solutions and found to be 1.44 g/cm.[3] The calculated value is also 1.44 g/cm.[3]

The intensity measurements were carried out on a crystal of dimensions $0.24 \times 0.36 \times 0.40$ mm using a Syntex automatic diffractometer and Mo$K\alpha$ radiation ($\lambda = 0.71069$ Å, graphite monochromator). The $\omega/2\theta$ scan technique (rates 1 – 12°/min) was used and 1690 reflections with 2θ less than 55° were recorded with measurable intensities, using a cut-off limit of 2σ. No breakdown of the crystal could be observed. Corrections for absorption or secondary extinction were not made.

The structure was solved by Patterson methods and refined by block diagonal least squares calculations to $R = 0.030$ ($R_w = 0.032$). The weighting scheme was based on standard deviations from counter statistics and an assumed 2 % fluctuation in diffractometer stability. Anisotropic temperature factors were applied to the non-hydrogen atoms,

common isotropic ones to the hydrogen atoms. Observed and calculated structure factors are given in Table 1, positional and thermal parameters in Table 2 and corresponding bond lengths and angles in Table 3 and Fig. 1.

Table 1. Observed and calculated structure factors.

Table 1. Continued.

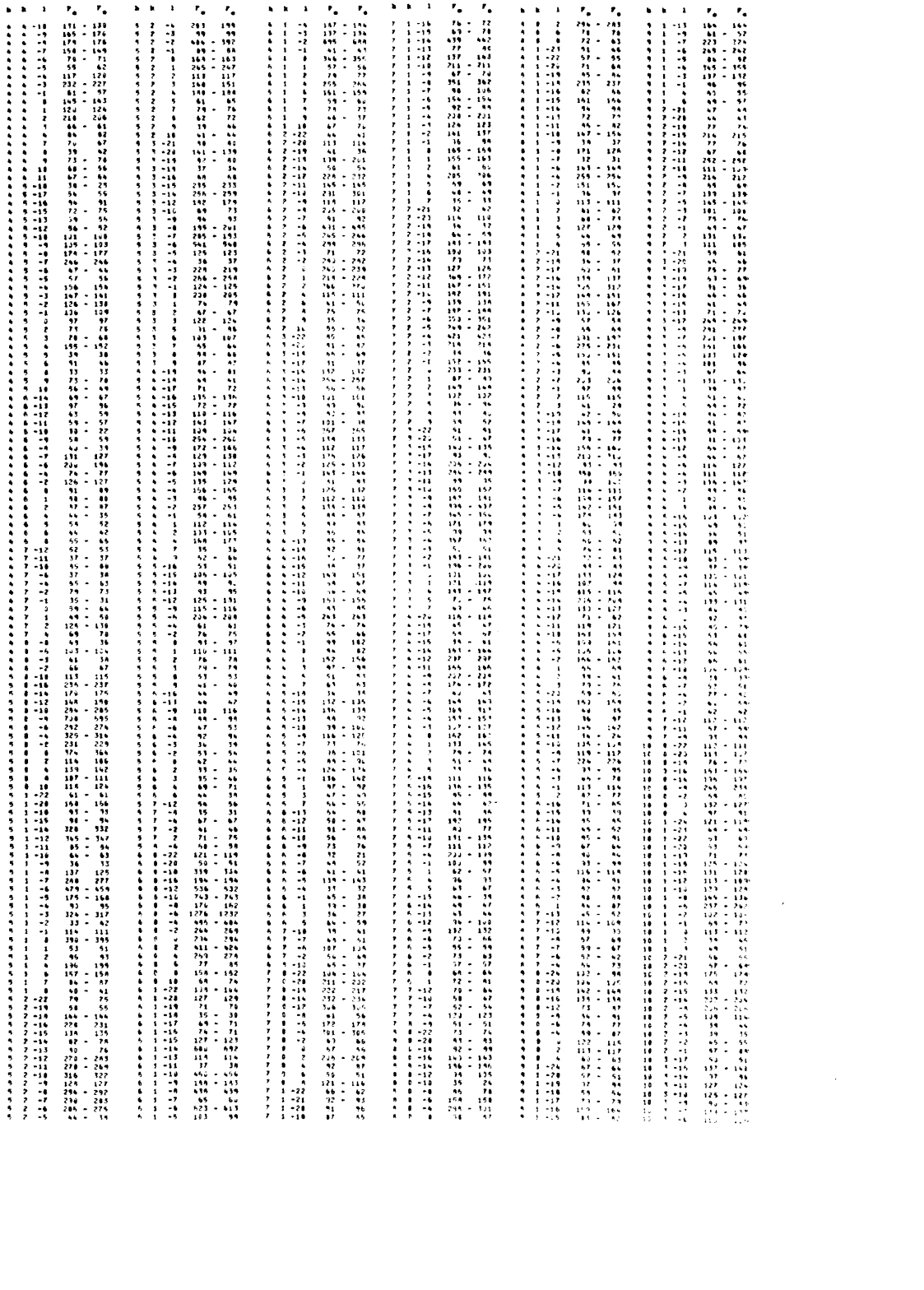

Table 1. Continued.

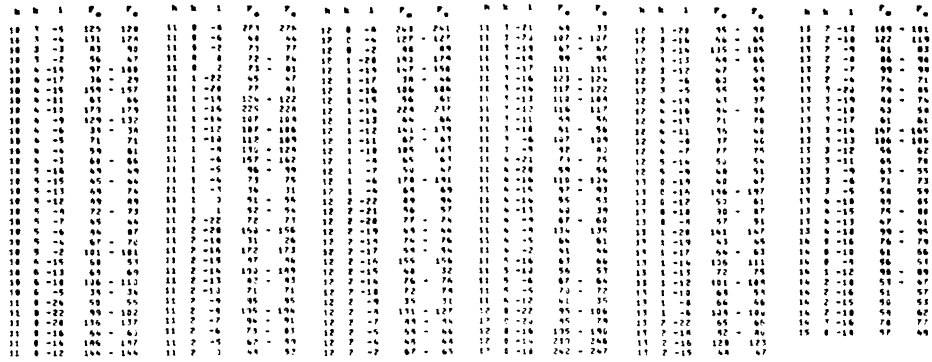

Table 2. Positional ($\times 10^5$ for non-hydrogens, $\times 10^4$ for hydrogens) and thermal ($\times 10^5$ for non-hydrogens) parameters with estimated standard deviations. The anisotropic temperature factor is $\exp[-(B_{11}h^2+B_{22}k^2+B_{33}l^2+B_{12}hk+B_{23}hl+B_{23}kl)]$.

Atom	x	y	z	B_{11}(B)	B_{22}	B_{33}	B_{12}	B_{13}	B_{23}
Ring A									
S	−2459	69050	32958	1022	3059	400	864	751	−2
	5	8	3	6	15	2	16	6	10
N1	−4284	71924	45977	1105	1811	600	311	1199	155
	15	20	10	19	37	9	43	23	29
C2	5323	74542	44556	981	1475	439	617	868	222
	17	23	11	21	37	9	48	24	33
N3	18956	80218	50536	1004	2450	490	−96	913	−110
	15	23	10	19	42	8	45	22	30
C4	23345	83735	59019	1208	2529	507	−25	851	−213
	20	30	13	25	53	11	63	29	40
C5	14526	81567	61339	1696	2413	499	634	1284	114
	22	30	13	31	51	11	68	32	40
C6	630	75539	54557	1663	1911	668	729	1705	444
	21	27	13	29	45	12	61	34	39
H4	3325	8725	6333	5.3					
	19	26	12	0.2					
H5	1827	8386	6732	5.3					
	18	28	12	0.2					
H6	−608	7355	5551	5.3					
	20	26	13	0.2					
Ring B									
S	13482	74597	32197	1836	2232	615	1390	1700	790
	6	7	3	8	12	3	17	9	11
N1	34725	54857	35648	1310	2411	543	152	1291	65
	15	23	10	21	42	9	49	25	31
C2	24534	53549	36630	982	1914	346	71	777	−86
	17	25	10	21	42	9	50	24	31
N3	22281	39382	40284	1128	1999	451	139	948	210
	14	21	9	19	37	8	44	22	28

Table 2. Continued.

C4	31308	24325	43125	1545	2126	553	368	1176	336
	22	28	13	29	49	11	63	32	40
C5	42027	23844	42280	1578	2700	655	1587	1318	423
	23	31	14	31	58	13	71	35	44
C6	43474	39617	38571	1300	3282	654	657	1365	86
	21	33	14	27	63	13	68	33	47
H4	3005	1378	4581	5.3					
	19	28	12	0.2					
H5	4806	1332	4409	5.3					
	18	28	12	0.2					
H6	5081	4116	3808	5.3					
	18	28	12	0.2					
Water molecules									
W1	46851	87353	32207	1524	2638	893	−107	1651	14
	14	21	10	20	40	10	47	26	33
W2	35345	14793	18496	1186	5313	1168	124	1266	2195
	15	29	13	20	65	14	60	29	49
H1W1	4255	7982	3278	6.9					
	23	33	15	0.3					
H2W1	5180	8077	3185	6.9					
	22	33	14	0.3					
H1W2	2695	1469	1418	6.9					
	22	32	14	0.3					
H2W2	3720	758	2186	6.9					
	21	32	14	0.3					

Table 3. Bond lengths (Å) and angles (°). Estimated standard deviations in parentheses. Corrected bond lengths in brackets {}.

	Ring A		Ring B			Ring A	Ring B
S–S	2.016(1)						
C2–S	1.781(2)	{1.788}	1.781(2)	{1.789}	C2–S–S	104.6(1)	104.9(1)
N1–C2	1.332(2)	{1.342}	1.332(2)	{1.342}	N1–C2–S	111.0(1)	110.1(1)
C2–N3	1.319(2)	{1.329}	1.316(2)	{1.325}	N3–C2–S	121.0(1)	121.7(1)
N3–C4	1.342(2)	{1.347}	1.343(2)	{1.350}	N1–C2–N3	128.0(2)	128.2(2)
C4–C5	1.366(3)	{1.374}	1.373(3)	{1.381}	C2–N3–C4	114.4(1)	114.6(1)
C5–C6	1.366(3)	{1.374}	1.363(3)	{1.370}	N3–C4–C5	123.1(2)	122.5(2)
C6–N1	1.339(2)	{1.345}	1.334(3)	{1.341}	C4–C5–C6	117.1(2)	117.3(2)
C4–H	0.95(2)		0.95(2)		C5–C6–N1	122.0(2)	122.2(2)
C5–H	0.92(2)		0.92(2)		C6–N1–C2	115.4(2)	115.3(2)
C6–H	0.93(2)		0.93(2)		N3–C4–H4	114(1)	117(1)
					C5–C4–H4	123(1)	120(1)
					C4–C5–H5	119(1)	122(1)
W1–H1	0.78(2)		$N1_A$···W2	2.928(2)	C6–C5–H5	124(1)	120(1)
W1–H2	0.78(2)		$N1_B$···W1	2.953(2)	C5–C6–H6	123(1)	124(1)
W2–H1	0.79(2)		W1···W2	2.766(2)	N1–C6–H6	115(1)	114(1)
W2–H2	0.72(2)		W1···W2′	2.694(2)			

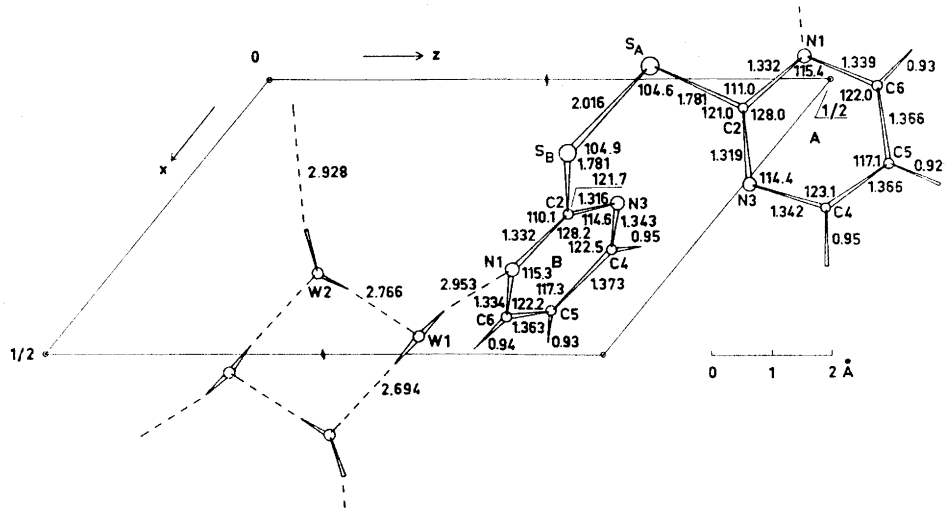

Fig. 1. The *b* projection of one molecule.

The effect of libration was examined by assuming each pyrimidine ring and its sulfur atom to be a rigid body. The root mean square differences between atomic vibration tensor components calculated from Table 1 and those derived from the rigid body model were 0.0019 Å² and 0.0015 Å², respectively. Corrected bond lengths are included in Table 2.

The atomic scattering factors were those of Hanson *et al.*[3] for non-hydrogen atoms and of Stewart *et al.*[4] for hydrogen atoms. All programs used are described in Ref. 5.

DISCUSSION

Because of the inherent uncertainties in the correction procedure, the discussion is based on uncorrected values of bond lengths and angles.

In Table 4 deviations from least square planes are given for the two pyrimidine residues A and B. It is seen that one ring (A) is almost exactly planar, whereas some of the atoms of the other are significantly displaced from planarity. The angle between the two planes is 80.7°. The hydrogen atoms lie in the ring planes to within 0.06 Å. Those at C4 and C6 appear to be bent away from that at C5.

Table 4. Deviation of atoms from least squares planes defined by the ring atoms and one sulfur atom.

	Ring A	Ring B	Ring A	Ring B
N1	0.004 Å	0.017 Å	C5 − 0.003 Å	− 0.024 Å
C2	0.005	0.009	C6 − 0.003	0.001
N3	0.001	0.016	S_A − 0.002	− 0.220
C4	0.000	− 0.002	S_B 0.052	− 0.009

The dihedral angle C–S–S–C is 82.5°, which is within the range of $90 \pm 10°$ usually found for organic disulfides. It has been pointed out,[6] that the values of the angle between the ring plane and the C–S–S plane fall into two general classes, being either *ca.* 0° or *ca.* 90°. The present compound clearly belongs to the former class, as the angles are 1.7° and 6.1° for rings A and B, respectively. This means that both sulfur atoms lie approximately in the plane of both pyrimidine rings. There would seem to be considerable strain in the molecule caused by steric repulsion between N3 and the sulfur atom of the other ring. This is shown by the great distortion of the external angles at C2, which differ by about 10°. The distances $N3_A \cdots S_B$ and $N3_B \cdots S_A$ are 3.08 Å and 3.11 Å, respectively, still somewhat shorter than the sum of van der Waals radii (about 3.3 Å). The length of the S–S bond is 2.016 Å, of the C–S bonds 1.781 Å. The S–S–C angles are 104.6° and 104.9°, respectively. These structural parameters are very similar to those found in other aromatic disulfides of this class, such as diphenyl disulfide[2] (2.03 Å, 1.80 Å, 106°), and 4,4′-di(thiouridine)[7] (2.022 Å, 1.79 Å, 104°) but different from those of the other class (2.074 Å, 1.75 Å, 101°).[6] The corresponding parameters in $(CH_3)_2S_2$ are 2.022 Å, 1.806 Å, and 104.4°, with a dihedral angle of 84° about S–S.[9]

Corresponding bond lengths and bond angles in the two pyrimidine rings agree very well. The angle N1–C2–N3 is large (128.2° and 128.0°), as is found in pyrimidine itself (128.2°),[8] but widely different from that in 2-*one* and 2-*thio* derivatives (near 120°). Each pyrimidine ring should be expected to have a plane of symmetry through C2···C5. Within the limits of error this is also found except that C2 – N3 is shorter than C2 – N1 by 0.013 Å in ring A and by 0.016 Å in ring B. A full matrix least squares refinement of the parameters of C2, N1, N3, and S did not give significant changes and the relevant correlation coefficients were small. The observed differences are therefore probably significant. They may be related either to the angular deformation at C2 or to a N3···S interaction. The effect has apparently not been observed in other structures of this class,[2,7] which, however, all are less accurately determined than the present one.

The water molecules are linked together in infinite spirals around the two-fold screw axes by nearly linear O–H···O hydrogen bonds of lengths 2.694 Å and 2.766 Å (Fig. 1). Each water molecule is also linked to N1 by an O–H···N bond of length 2.953 Å or 2.928 Å. The angles at the hydrogen atoms involved in hydrogen bonding are 167°, 178°, 164°, and 168° for H1W1, H2W1, H1W2, and H2W2, respectively.

REFERENCES

1. Furberg, S. and Petersen, C. S. *Acta Chem. Scand.* **26** (1972) 760.
2. Lee, J. D. and Bryant, M. W. R. *Acta Cryst.* **25** (1969) 2094.
3. Hanson, H. R., Hermann, F., Lea, J. D. and Skillman, S. *Acta Cryst.* **17** (1964) 1040.
4. Stewart, R. F., Davidson, E. R. and Simpson, W. T. *J. Chem. Phys.* **42** (1965) 3175.
5. Dahl, T., Gram, F., Groth, P., Klewe, B. and Rømming, C. *Acta Chem. Scand.* **24** (1970) 2232.
6. Shefter, E. *J. Chem. Soc.* **B 1970** 903.
7. Shefter, E. and Kalman, T. I. *Biochem. Biophys. Res. Commun.* **32** (1968) 878.
8. Wheatley, P. J. *Acta Cryst.* **13** (1960) 80.
9. Beagley, B. and McAloon, K. T. *Trans. Faraday Soc.* **67** (1971) 3216.

Received March 7, 1973.

ACTA CHEMICA SCANDINAVICA 27 (1973) 2543–2553

Thermodynamic Properties of Rare Earth Complexes

XVII. The Partial Molar Heat Capacities of Rare Earth Perchlorates and Oxydiacetate Complexes

INGMAR GRENTHE, GUNNEL HESSLER and HEIKKI OTS

Division of Physical Chemistry, Chemical Center, University of Lund, P.O.B. 740, S-220 07 Lund 7, Sweden

The partial molar heat capacities of some rare earth perchlorates and rare earth oxydiacetate complexes have been determined by direct calorimetry at 25°C using aqueous 1.000 mol/kg $NaClO_4$ as the solvent. From the near constancy of the $\bar{C}_P°$-values obtained for the various rare earth perchlorates it may be concluded that no ionic radius dependent hydration equilibria of the type

$$M(H_2O)_x^{3+} \rightleftharpoons M(H_2O)_y^{3+}$$

are present for the hydrated rare earth ions. This finding is in agreement with NMR data obtained by other authors. The previous interpretations of maxima in $\Delta C_P°$ *vs.* $\bar{Z}$ data for the formation of rare earth EDTA and oxydiacetate complexes as beeing due to hydration equilibria for the species $M(EDTA)^-$ and $M(oxydiacetate)_2^-$, have been confirmed.

The consistency of the partial molar heat capacity data has been checked by a comparison of the experimental $\Delta C_P°$-values for the formation of the complexes $Na_3M(oxydiacetate)_3$, M = Pr and Gd, with the same quantity calculated from the partial molar heat capacities of reactants and products. The agreement was satisfactory.

The observed variations of thermodynamic quantities such as $\Delta H_j°$ and $\Delta S_j°$ for various rare earth complexation reactions have frequently been interpreted in terms of changes of hydration of the species participating in the reactions.[1,2] The fact that the variations throughout the rare earth series are very similar for a number of different ligands has been taken as evidence that the variation is due to some property of the central ion, *viz.* its state of hydration. Spedding and his coworkers [3] have studied various properties such as molar volumes, activity coefficients, transference numbers, partial molar heat capacities, *etc.* for a number of simple rare earth salts, and claim that their results indicate a change of hydration of the hydrated rare earth ions within the lanthanoid series. On the other hand, the observation of Reuben

and Fiat [4] of a linear proportionality between the oxygen-17 chemical shifts and the molal concentration of lanthanoid perchlorate solutions, indicates that only a single hydrated species exists over a wide range of concentrations, *i.e.* no hydration equilibrium of the type

$$M(H_2O)_x^{3+} \rightleftharpoons M(H_2O)_y^{3+} \quad (1)$$

is present.

Most molecular interpretations (at least by solution chemists) of rare earth complexation reactions are based on thermodynamic data. There are two main obstacles to the interpretation of such thermodynamic data. Firstly, it is difficult to decide whether an observed variation in a "Δ" quantity is due to one or several of the species participating in the reaction studied. Secondly, at investigations of complex formation equilibria in solution one cannot, in general, obtain information about the complexes formed between the reaction species and the ions and molecules of the medium and the solvent. One possible way to circumvent these difficulties is to obtain further information on the systems by non-thermodynamic methods, *e.g.* by spectroscopic [4,5] or kinetic studies. The spectroscopic method has been used successfully by Geier *et al.*[5] in a study of hydration equilibria among rare earth EDTA complexes. Spectroscopic [6] and kinetic [7] methods have also been used to determine the relative amounts of inner and outer sphere complexes among the lanthanoids.

The molecular interpretation of the properties of a system obtained, *e.g.*, from spectroscopic studies must not contradict the thermodynamic properties of the macroscopic system, so thermodynamics can be used as a guide in the development of molecular theories. In the previous parts of this series [8–10] we have discussed the use of ΔC_p data to obtain information on the presence of equilibria of the type discussed above. Our experimental results from the rare earth oxydiacetate and EDTA systems gave strong evidence for the occurrence of hydration equilibria in these complexes. These measurements have now been extended by a study of partial molar heat capacities of a number of rare earth perchlorates and some rare earth oxydiacetate complexes. We have two aims with this study. The first is to establish, by the methods outlined in Ref. 11, whether hydration equilibria of the type (1) are present for the hydrated rare earth ions or not. The second is to decide whether the previously observed variations in ΔC_p° throughout the rare earth series are due to a variation in the partial molar heat capacity of the central ion and/or the various complexes.

Some experimental determinations of partial molar heat capacities for a number of simple rare earth salts in water solution have previously been reported by Spedding *et al.*[3,12] In order to obtain heat capacities which were compatible with our other thermodynamic data, we have chosen to use an aqueous 1.000 mol/kg $NaClO_4$ solution as the solvent. An advantage with this solvent as compared to pure water is the decreased concentration dependence of the apparent and partial molal heat capacities of the solute.

The most accurate heat capacity data for solutions are probably obtained by using a twin calorimeter as described, *e.g.*, by Gucker *et al.*[13] However, our previous experience with isothermal jacket calorimeters indicated that de-

terminations of partial molar heat capacities in 0.1 mol/kg solutions were possible with an accuracy of 10 – 15 J/K mol. This was considered to be sufficient in order to establish whether a maximum in the partial molar heat capacity, $\overline{C}_P$, occurred within the lanthanoid series or not; *cf.* Ref. 8, p. 1218. The height of the maximum is expected to be approx. 80 J/K mol.

EXPERIMENTAL

Description of the calorimeter. The calorimeter used is of the isothermal jacket type and is a development of the previously described reaction calorimeter.[14] The main changes are the removal of the addition unit (capillaries and heat exchange system) and the use of a larger calibration resistance. The inner vessel has a total volume of 115 cm³. It is made of 18 carat gold in order to ensure a rapid temperature equilibration. The calorimeter is heated electrically by using a manganin resistance enclosed in a gold spiral. The temperature is measured by a thermistor enclosed in a gold thimble. The two bladed stirrer is operated at 750 rpm. The calorimeter is thermostated at 25.00°C by using a thermostat bath similar to the LKB 7603 A. The stability is within 2.5×10^{-4} K/h. The calorimeter system and part of the electronic equipment was placed in an air thermostat at 25.00 ± 0.05°C.

The calorimeter heater has a resistance of 250 Ω. Electrical energy is supplied from a constant current source (Guildline 9770 B). A four-lead system is used by which a simultaneous measurement of voltage and current can be made. The voltage was measured with an accuracy better than 30 ppm by a digital voltmeter (S.E. Laboratories, SM 213 Mk 2).

The current was determined by measuring the voltage drop over a thermostated standard resistance (Tinsley 3504 B). This voltage was measured with an accuracy of 25 ppm by a differential voltmeter (Fluke, model 885 AB) which had been calibrated against a voltage standard.

The current through the heater is switched on and off *via* a timer (Elesta Digital Counter) and a relay. The timer has a quartz crystal as frequency standard, the accuracy of which is better than 10 ppm. All electrical calibrations are made over 240 s and the total error in this quantity, including the errors in closing and releasing the relay (at most 650 μs), is less than 12 ppm. From the above quantities, we estimate the maximum error in the added energy quantity to be less than 50 ppm.

The bridge circuit. The bridge described in Ref. 14 has been modified as described by Ginstrup.[15] After several tests we found that an increased precision could be obtained by feeding the bridge with a square-wave voltage instead of the original DC voltage. This method has been used previously by Faulkner *et al.*[16] A frequency of 120 Hz was chosen for the square wave source and the unbalance voltage was detected by a phase sensitive detector (Brookdeal Electronics Ltd, Type 411). In this way we were able to decrease noise and drift by a factor of ten as compared with the DC bridge. The unbalance voltage from the phase sensitive detector is recorded on a Mosley 680 recorder to give a resistance *vs.* time curve. The bridge, except the thermistor and the 100 – 0.01 Ω decades, is made as a micro circuit placed on a card and immersed in a thermostated oil bath. By thermostating the large resistance (6 000 Ω in our case) in the decade one can get a substantial reduction of the resistance errors due to fluctuations in the ambient temperature.

Calculation of the partial molar heat capacities. The apparent molar heat capacity ϕ_{C_P} is obtained from the experimental heat capacity of the solution by using the expression

$$\phi_{C_P} = [c_P(1\,000 + mM) - 1\,000 c_P^\circ]/m \qquad (2)$$

where c_P and c_P° are the specific heat capacities of solution and solvent, respectively, m is the molality of the solute with the formula weight M.

Two methods can be used to determine the specific heat capacity. In one the thermistor is calibrated against a platinum resistance thermometer so that its resistance directly can be converted to temperature. In the other, which is the method we have used, solutions of known specific heat capacities are used to calibrate the system in the following way:

A quantity of energy Q which corresponds to a certain change of state (27.000 Ω as measured by the change in resistance, ΔR, of the thermistor) is added to the system. The heat capacity of the system is

$$Q/\Delta T = C_{PC} + gc_P \quad (3)$$

where ΔT is the change in temperature of the system, C_{PC} and c_P are the heat capacity of the calorimeter and the specific heat capacity of the solution, respectively, while g is the mass of the solution. In systems where the change of state, as measured by ΔR, always is the same, $\Delta T = k\Delta R$. Eqn. (3) can then be written as

$$Q/\Delta R = kC_{PC} + kgc_P \quad (4)$$

From experimental values of Q, ΔR, and g in solutions with known values of c_P, the constants k and kC_{PC} can be determined. These constants can then be used to calculate unknown specific heat capacities. We have used Randall and Rossinis' [17] specific heat capacity data on NaCl and KCl solutions to calculate the constants. A comparison of our specific heat capacity data using experimental calorimeter constants with those obtained by Randall and Rossini is given in Table 1. The agreement is in general within 0.008 J/K g which is satisfactory. An equally satisfactory agreement is obtained for the specific heat capacity of water where our experimental value was 4.1769 ± 0.0002 J/K g as compared to 4.1769 J/K g given by Osborne, Stimson and Ginnings.[18]

Experimental procedure. All solutions were weighed into the calorimeter which then was allowed to stand over night in the thermostat bath. Five to ten electrical calibrations were made with a rate of 1 calibration/1.5 h. In each calibration the calorimeter was brought to a predetermined temperature and an initial period of about 10 min duration was then recorded. At a given temperature energy was added to the system from the constant current source for a period of 240.00 s. The current was adjusted to give a change in the thermistor resistance of 27.000 Ω. This figure corresponds to a temperature change of approx. 0.1 K. The after period was recorded over a period of 30 min. From this record of resistance *vs.* time the value of ΔR was obtained.

Analysis and preparation of solutions. Stock solutions of the various rare earth perchlorates were prepared by dissolving the corresponding oxides (American Potash and Chemical Co, purity better than 99.9 %) in warm concentrated perchloric acid. The excess of acid was removed by evaporation with a heat lamp. The rare earth and hydrogen ion concentrations were determined as described before.[19] The sodium perchlorate molality in the stock solutions was 1.000 mol/kg and the rare earth and hydrogen ion molalities had values in the ranges $0.8 - 1.0$ mol/kg and $5 \times 10^{-3} - 10 \times 10^{-3}$ mol/kg, respectively. The solutions in the calorimeter were prepared from these stock solutions and a 1.000 mol/kg sodium perchlorate stock solution by weighing. A stock solution of oxydiacetate was prepared by partial neutralization of oxydiacetic acid with sodium hydroxide.

Table 1. A comparison of specific heat capacities at 25°C of aqueous sodium chloride and potassium chloride solutions obtained in this study with the corresponding values obtained by Randall and Rossini (R & R).

Molality of NaCl	c_P/J K^{-1} g^{-1} R & R	c_P/J K^{-1} g^{-1} this work	Molality of KCl	c_P/J K^{-1} g^{-1} R & R	c_P/J K^{-1} g^{-1} this work
0.0500	4 1585	4 1601	0.1604	4 1141	4.1133
0.1010	4.1430	4.1442	0.1609	4.1137	4.1141
0.1498	4.1284	4.1288	0.1628	4.1129	4.1125
0.4995	4.0296	4.0313	0.5029	3.9853	3.9878
0.7495	3.9656	3.9664	0.5032	3.9848	3.9849
1.0028	3.9066	3.9083	1.0047	3.8187	3.8177
1.5095	3.8003	3.7991	1.0050	3.8187	3.8166
			1.5065	3.6694	3.6702
			1.5068	3.6694	3.6710

Oxydiacetic acid was purified by recrystallization from ethyl acetate and had an equivalent weight of 67.10, calcd. 67.03. The solution had the following composition $C_{NaClO_4} = 1.0000$ mol/kg, $C_{Na_2A} = 2.3093$ mol/kg and $C_{NaHA} = 0.0480$ mol/kg. The solutions containing the complexes Na_3MA_3 were prepared from the metal and ligand stock solutions with addition of water to make the sodium perchlorate molality equal to 1.000 mol/kg. These solutions had an excess of ligand sufficiently large to make the concentrations of the first and second complexes negligible.

RESULTS AND DISCUSSION

The accuracy of the specific heat capacity values is in general within 0.02 % as indicated by the data given in Table 1. The errors in the specific heat capacity values are in our case not influenced significantly by analytical errors. They are instead dominated by the errors in Q and ΔR. However, the error in Q is not large enough to explain the observed spread in the c_p values. The two main sources of error in ΔR are due to temperature dependent variations in the decade resistance, an error we have tried to decrease by keeping the large resistances well thermostated, and errors due to a slow (and not sufficiently reproducible) attainment of thermal equilibrium within the calorimeter. From the graphs of the after period we have reason to believe that the second factor is the most important source of error.

The rare earth perchlorate solutions. The specific heat capacities of the various solutions with their estimated errors, equal to 3σ, are given in Table 2.

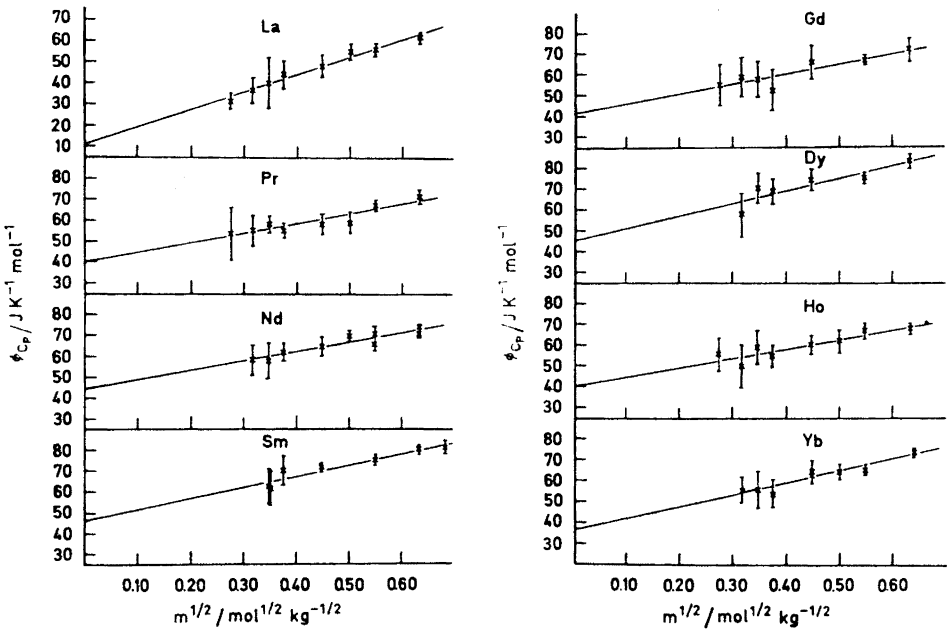

Fig. 1. ϕ_{C_p} *versus* the square root of the molality for the various rare earth perchlorates.

Table 2. c_P and ϕ_{CP} for $M(ClO_4)_3$, Na_2A, $NaClO_4$ and Na_3MA_3. The difference in the specific heat capacity of the solvent (1.000 m $NaClO_4$) between the various systems is due to the use of different stock solutions.

La, $c_{P\,solv.}$ = 3.7887±0.0008 $J\cdot K^{-1}\cdot g^{-1}$

m / $mol\cdot kg^{-1}$	c_P / $J\cdot K^{-1}\cdot g^{-1}$	ϕ_{cp} / $J\cdot K^{-1}\cdot mol^{-1}$
[illegible]	[illegible]±0.0010	62.3±[illegible]
[illegible]	[illegible]±0.0008	[illegible]
[illegible]	[illegible]±0.0013	[illegible]
[illegible]	[illegible]	48.4±[illegible]
[illegible]	[illegible]	44.2±6.9
[illegible]	[illegible]	40.4±1[illegible]
.1000	[illegible]±0.0006	36.9±6.3
[illegible]	3.6704±0.00[illegible]	31.7±1.1

Pr, $c_{P\,solv.}$ = 3.7887±0.0008 $J\cdot K^{-1}\cdot g^{-1}$

m / $mol\cdot kg^{-1}$	c_P / $J\cdot K^{-1}\cdot g^{-1}$	ϕ_{cp} / $J\cdot K^{-1}\cdot mol^{-1}$
0.4002	3.2446±0.0010	71.5±3.[illegible]
0.3001	3.3653±0.0007	67.4±2.[illegible]
0.2400	3.4273±0.0010	53.2±5.3
0.1999	3.4976±0.0003	59.4±4.[illegible]
0.1402	3.5762±0.0001	55.3±3.8
0.1200	3.6054±0.0005	58.4±4.4
0.0909	3.6247±0.0007	55.2±7.[illegible]
0.07[illegible]	3.6718±0.0009	[illegible].9±10.[illegible]

Nd, $c_{P\,solv.}$ = 3.7887±0.0008 $J\cdot K^{-1}\cdot g^{-1}$

m / $mol\cdot kg^{-1}$	c_P / $J\cdot K^{-1}\cdot g^{-1}$	ϕ_{cp} / $J\cdot K^{-1}\cdot mol^{-1}$
0.4017	3.2413±0.000[illegible]	74.[illegible]
0.4003	3.2424±0.000[illegible]	70.9±[illegible]
0.3000	3.3623±0.001[illegible]	70.[illegible]
0.2993	3.3630±0.000[illegible]	66.3±[illegible].4
0.2[illegible]	3.4258±0.000[illegible]	69.9±[illegible]
0.20[illegible]	3.4917±0.000[illegible]	64.9±[illegible]
0.1400	3.5755±0.00[illegible]	60.1±1.[illegible]
0.1202	3.6059±0.001	57.0±[illegible]
0.1000	3.6337±0.000[illegible]	58.[illegible]

Sm, $c_{P\,solv.}$ = 3.7887±0.0008 $J\cdot K^{-1}\cdot g^{-1}$

m / $mol\cdot kg^{-1}$	c_P / $J\cdot K^{-1}\cdot g^{-1}$	ϕ_{cp} / $J\cdot K^{-1}\cdot mol^{-1}$
[illegible]	[illegible]	[illegible]
[illegible]	[illegible]	[illegible]
[illegible]	[illegible]	[illegible].8±[illegible]
[illegible]	[illegible]±0.000[illegible]	[illegible]
[illegible]	[illegible]	[illegible]
[illegible]	[illegible].6089±0.0009	[illegible].7±8.[illegible]
[illegible]	[illegible]	[illegible].6±8.[illegible]

Gd, $c_{P\,solv.}$ = 3.7887±0.0008 $J\cdot K^{-1}\cdot g^{-1}$

m / $mol\cdot kg^{-1}$	c_P / $J\cdot K^{-1}\cdot g^{-1}$	ϕ_{cp} / $J\cdot K^{-1}\cdot mol^{-1}$
0.3984	3.2307±0.0019	71.3±5.7
0.2995	3.3512±0.0006	66.6±2.2
0.2002	3.4840±0.0015	65.4±8.[illegible]
0.1400	3.568[illegible]±0.0015	52.3±10.[illegible]
[illegible]	3.5988±0.0010	[illegible].3±8.[illegible]
[illegible]	3.6293±0.001[illegible]	[illegible].7±9.4
[illegible]	3.6670±0.00[illegible]	[illegible]

Dy, $c_{P\,solv.}$ = 3.7887±0.0008 $J\cdot K^{-1}\cdot g^{-1}$

m / $mol\cdot kg^{-1}$	c_P / $J\cdot K^{-1}\cdot g^{-1}$	ϕ_{cp} / $J\cdot K^{-1}\cdot mol^{-1}$
0.4005	3.2266±0.0012	82.9±3.6
0.3006	3.3475±0.0007	75.0±2.8
0.2007	3.4815±0.0011	74.0±5.4
0.14[illegible]	3.5676±0.0008	68.7±6.2
0.1200	3.5978±0.0008	70.7±7.2
[illegible]	3.6269±0.0010	[illegible]

Ho, $c_{P\,solv.}$ = 3.7878±0.0008 $J\cdot K^{-1}\cdot g^{-1}$

m / $mol\cdot kg^{-1}$	c_P / $J\cdot K^{-1}\cdot g^{-1}$	ϕ_{cp} / $J\cdot K^{-1}\cdot mol^{-1}$
0.4004	3.2181±0.0009	67.9±[illegible]
0.3003	3.2428±0.0010	66.9±[illegible]
0.2505	3.4079±0.001[illegible]	62.[illegible]
0.1998	3.4779±0.00[illegible]	60.[illegible]
0.1599	3.5645±0.000[illegible]	54.[illegible]
0.1199	3.5952±0.0009	58.3±[illegible]
0.1001	3.6247±0.001[illegible]	49.9±1[illegible]
0.0753	3.6646±0.0006	55.5±8.1

Yb, $c_{P\,solv.}$ = 3.7887±0.0008 $J\cdot K^{-1}\cdot g^{-1}$

m / $mol\cdot kg^{-1}$	c_P / $J\cdot K^{-1}\cdot g^{-1}$	ϕ_{cp} / $J\cdot K^{-1}\cdot mol^{-1}$
0.4099	3.2017±0.0008	[illegible].7±[illegible]
0.3005	3.3362±0.0005	65.6±2.[illegible]
0.2502	3.4035±0.0008	64.5±[illegible]
0.2000	3.4736±0.001	64.[illegible]±5.[illegible]
0.2000	3.47[illegible]±0.0006	62.8±[illegible]
0.1400	3.5610±0.0009	54.2±[illegible]
0.1201	3.5921±0.001[illegible]	56.2±8.[illegible]
0.1000	3.6232±0.0006	56.1±6.[illegible]

Na_2A, $c_{P\,solv.}$ = 3.7900±0.0008 $J\cdot K^{-1}\cdot g^{-1}$

m / $mol\cdot kg^{-1}$	c_P / $J\cdot K^{-1}\cdot g^{-1}$	ϕ_{cp} / $J\cdot K^{-1}\cdot mol^{-1}$
[illegible]	3.3987±0.0006	265.2±1.[illegible]
[illegible]	3.5060±0.0004	245.[illegible]±1.[illegible]
[illegible]	3.5867±0.0008	232.1±1.[illegible]
[illegible]	3.6795±0.0011	215.7±4.[illegible]
[illegible]	3.7[illegible]54±0.000[illegible]	194.3±9.[illegible]

$NaClO_4$, $c_{P\,solv.}$ = 3.7877±0.0008 $J\cdot K^{-1}\cdot g^{-1}$

m / $mol\cdot kg^{-1}$	c_P / $J\cdot K^{-1}\cdot g^{-1}$	ϕ_{cp} / $J\cdot K^{-1}\cdot mol^{-1}$
1.[illegible]	3.3540±0.0006	136.1±0.6
0.9[illegible]	3.4964±0.0009	135.6±0.9
[illegible].6999	3.5734±0.0010	131.4±1.9
0.4699	3.6386±0.0008	128.3±1.8
0.2500	3.7050±0.0012	125.0±5.1
[illegible].1000	3.7528±0.0007	111.0±7.3

$NaClO_4$(rel. H_2O), c_{P,H_2O} = 4.1769 $J\cdot K^{-1}\cdot g^{-1}$

m / $mol\cdot kg^{-1}$	c_P / $J\cdot K^{-1}\cdot g^{-1}$	ϕ_{cp} / $J\cdot K^{-1}\cdot mol^{-1}$
2.4524	3.3540±0.0006	1[illegible].8±0.3
2.1288	3.4964±0.000[illegible]	104.9±0.[illegible]
1.7875	3.5734±0.001[illegible]	10[illegible].[illegible]±0.5
1.5392	3.6386±0.000[illegible]	9[illegible].[illegible]±0.7
1.2811	3.7050±0.00[illegible]	8[illegible].2±1.0
1.1130	3.7528±0.000[illegible]	78.2±2.0
1.0000	3.7687±0.0008	7[illegible].6±1.4

Na_3PrA_3, $c_{P\,solv.}$ = 3.7900 $J\cdot K^{-1}\cdot g^{-1}$

$m_{complex}$ / $mol\cdot kg^{-1}$	m_{Na_2A} / $mol\cdot kg^{-1}$	c_P / $J\cdot K^{-1}\cdot g^{-1}$	ϕ_{cp} / $J\cdot K^{-1}\cdot mol^{-1}$
0.1494	0.2893	3.4527±0.0006	541.0±6.[illegible]
[illegible]	0.2893	3.4902±0.0008	538.5±7.8
[illegible]	0.2893	[illegible].5213±0.0010	[illegible].5±11.[illegible]
[illegible]	0.2893	[illegible]±0.0006	528.[illegible]±6.6
[illegible]	0.2894	[illegible]±0.0006	[illegible].8±6.[illegible]

Na_3GdA_3, $c_{P\,solv.}$ = 3.7900±0.0008 $J\cdot K^{-1}\cdot g^{-1}$

$m_{complex}$ / $mol\cdot kg^{-1}$	m_{Na_2A} / $mol\cdot kg^{-1}$	c_P / $J\cdot K^{-1}\cdot g^{-1}$	ϕ_{cp} / $J\cdot K^{-1}\cdot mol^{-1}$
0.1516	0.2872	3.4410±0.0006	557.7±4.2
0.1230	0.2844	3.4810±0.0002	549.8±2.[illegible]
0.1022	0.2844	3.5127±0.0005	534.7±5.4
0.08091	0.2843	3.5441±0.0009	528.9±11.[illegible]
0.06079	0.2843	3.5741±0.0009	512.5±8.4

The relation between the apparent molal heat capacity (also given in Table 2) and the square root of the molality is assumed to be linear. It is a well established experimental fact that $\bar{C}_P$ and many other partial molar properties of strong electrolytes vary linearly with $m^{\frac{1}{2}}$ over a concentration range far beyond that at which the limiting laws might be expected to hold.[20] Thus, the experimental ϕ_{C_P} data in Table 2 were fitted to functions of the type

$$\phi_{CP} = a + bm^{\frac{1}{2}} \tag{5}$$

by a least-squares method.

The constants a and b with their corresponding standard deviations are given in Table 3. The ϕ_{C_P} data are very sensitive towards systematic errors, particularly in the most dilute solutions.[21] The fact that the slope b turns out to have about the same values for all the investigated rare earth perchlorate solutions is a good indication that the experimental procedure is not seriously affected by such errors.

Table 3. Least-squares refined parameters from eqn. (5). a is the partial molal heat capacity of the solute at infinite dilution.

Metal ion	a / J K^{-1} mol^{-1}	b / J K^{-1} mol^{-1} $m^{-\frac{1}{2}}$
La	10.7 ± 2.4	84.2 ± 5.3
Pr	39.9 ± 3.6	46.6 ± 8.0
Nd	43.9 ± 3.1	45.9 ± 6.3
Sm	46.2 ± 3.8	52.8 ± 7.6
Gd	41.2 ± 4.8	47.3 ± 10.9
Dy	44.9 ± 7.2	59.7 ± 15.6
Ho	40.4 ± 3.9	44.6 ± 8.8
Yb	36.5 ± 3.5	56.7 ± 7.5
Na_2A	170.5 ± 1.0	87.5 ± 1.3
$NaClO_4$	75.6 ± 1.4	–
Na_3PrA_3	477.9 ± 7.5	170.9 ± 22.6
Na_3GdA_3	438.3 ± 8.1	308.6 ± 25.1

Since the parameters in eqn. (5) are not evaluated from data at high dilution, the intercept and slope may differ numerically from the correct values at infinite dilution in the solvent 1.000 mol/kg $NaClO_4$. For the intercept this difference is usually small,[20] while it can be fairly large for the slope. Small errors in the $\bar{C}_P^\circ$ values at infinite dilution due to errors in the extrapolation procedure should be nearly equal for all the rare earth perchlorates. Hence, the variation of the extrapolated ϕ_{C_P}-values ought to be very nearly the same as the variation of the "true" $\bar{C}_P^\circ$-values at infinite dilution.

An experimental finding worth mentioning is that the slope b is smaller in 1.000 mol/kg $NaClO_4$ than in pure water (see Ref. 12), thus making the solution appear more "ideal" in the former case. This is a well known fact, at least to solution chemists who often use an ionic medium to keep activity

coefficients approximately constant for moderate variations in the composition of a solution.

As seen in Fig. 3 the values of $\bar{C}_P^\circ$ for the perchlorates are very nearly constant from praseodymium to ytterbium. Spedding *et al.*[12] found this behaviour for rare earth nitrates while the corresponding chlorides and perchlorates seemed to form two groups with a region of transition in between. The authors interpreted the latter finding in terms of an equilibrium between rare earth ions with different hydration numbers. However, it follows from our arguments in the preceding publications that an equilibrium of the type (1), where the equilibrium constant varies through the rare earth series, must give rise to a maximum in $\bar{C}_P^\circ$. Such a maximum is found neither in our data nor in Spedding's.

Hence, one may conclude that these thermodynamic data give no indications for the presence of a Z-dependent hydration equilibrium for the hydrated rare earth ions. This conclusion is supported by the previously mentioned NMR study of Reuben and Fiat.[4] The differences between our data for the rare earth perchlorates and those of Spedding *et al.*[12] might be due to the difference in solvents, *viz.* 1.000 mol/kg $NaClO_4$ *vs.* pure water.

The tris-(oxydiacetato)lanthanoidate(III) complexes. The reaction in which the third rare earth oxydiacetate complex is formed can be written as

$$M(ClO_4)_3(aq) + 3\ Na_2A(aq) \rightarrow Na_3MA_3(aq) + 3\ NaClO_4(aq)$$

The change in heat capacity $\Delta C_P^\circ{}_{III}$, for this reaction is

$$\Delta C_P^\circ{}_{III} = \bar{C}_P^\circ{}_{Na_3MA_3} + 3\ \bar{C}_P^\circ{}_{NaClO_4} - 3\ \bar{C}_P^\circ{}_{Na_2A} - \bar{C}_P^\circ{}_{M(ClO_4)_3} \qquad (6)$$

The value of $\Delta C_P^\circ{}_{III}$ is known from previous calorimetric determinations. The partial molar heat capacities of the various reactants and products can, as we have described above, be determined experimentally. In this section we will report values of $\bar{C}_P^\circ{}_{NaClO_4}$, $\bar{C}_P^\circ{}_{Na_2A}$ and $\bar{C}_P^\circ{}_{Na_3MA_3}$. A comparison between the experimental values of $\Delta C_P^\circ{}_{III}$ and the corresponding quantity calculated from eqn. (6) will give a check of the consistency of our partial molal heat capacity data.

The values of $C_P^\circ{}_{Na_3MA_3}$, with M = Pr and Gd, were determined in solutions containing an excess of ligand sufficiently large to make the concentrations of lower oxydiacetate complexes negligible. From eqn. (2) one obtains

$$\phi_{C_P} = \frac{c_P(1\,000 + m_{Na_2A}M_{Na_2A} + m_{Na_3MA_3}M_{Na_3MA_3}) - m_{Na_2A}\bar{C}_{PNa_2A} - 1\,000c_P^\circ}{m_{Na_3MA_3}} \qquad (7)$$

where the meaning of the various symbols is evident from the context.

The apparent molar heat capacity values for Na_2A are given in Table 2 and in Fig. 2. The $\bar{C}_P$-values at the various molalities, m_{Na_2A}, were calculated from the eqn.

$$\bar{C}_{PNa_2A} = \phi_{C_{PNa_2A}} + 1/2\sqrt{m_{Na_2A}}\,\frac{d\phi_{C_{PNa_2A}}}{d\sqrt{m_{Na_2A}}} \qquad (8)$$

The variation of $\bar{C}_{PNa_2A}$ with $\sqrt{m_{Na_2A}}$ is shown in Fig. 2.

The experimental results for the praseodymium and gadolinium complexes are shown in Table 2, while the corresponding partial molar heat capacities at infinite dilution are given in Table 3.

In order to calculate a value of $\Delta C_P^\circ{}_{III}$ from eqn. (6) we must also determine the partial molar heat capacity of sodium perchlorate *referred to* 1.000 mol/kg $NaClO_4$ *as the solvent*. The experimental data for sodium perchlorate in Table 2 have been given relative to both 1.000 mol/kg $NaClO_4$ (ϕ'_{C_P}) and pure water (ϕ''_{C_P}) as the solvent. These data are also shown in Fig. 2. The value of $\bar{C}_P^\circ{}_{NaClO_4}$ in 1.000 mol/kg $NaClO_4$ is given in Table 3.

The changes in heat capacity calculated from eqn. (6) are 153 J/K mol and 113 J/K mol for the praseodymium and gadolinium complexes, respectively. The same quantities obtained from the temperature variation of the corresponding enthalpy changes [9] are 167 J/K mol and 139 J/K mol, respectively. The fair agreement between the two sets of data is a good criterion of the reliability of the various $\bar{C}_P^\circ$-values obtained in this study. However, it must be pointed out that the agreement for the gadolinium system is less satisfactory at finite concentrations of solute. This is probably due to a small error in the slope b for this system. Small errors in this quantity do not affect the $\bar{C}_P^\circ$-values very much, but will lead to fairly large errors in the $\bar{C}_P$-data at finite concentrations (see p. 2549 and Ref. 20).

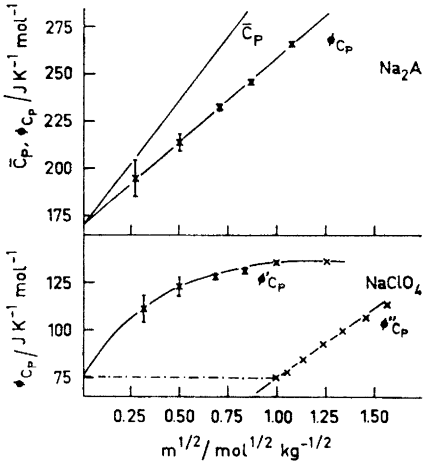

Fig. 2. ϕ_{C_P} and $\bar{C}_P$ *versus* the square root of the molality for Na_2A. For $NaClO_4$ two different curves are shown. ϕ'_{C_P} refers to a 1.000 mol/kg $NaClO_4$ solution as the solvent, whereas for ϕ''_{C_P} pure water is used as the solvent (see above).

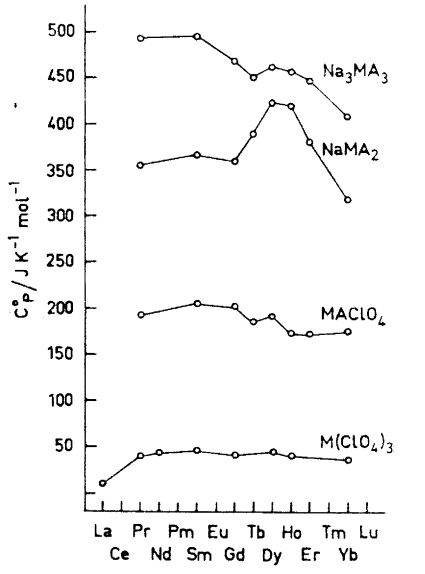

Fig. 3. The partial molar heat capacities at infinite dilution for the various rare earth perchlorates and the corresponding oxydiacetate complexes.

A better agreement with the previously found ΔC_P-values [9] would be obtained for Gd by using a smaller slope for the complex. This would also make the magnitudes of the *b*-values for the praseodymium and gadolinium complexes more equal (see Table 3).

By use of the $\overline{C}_P$-values for the rare earth perchlorates, Na_2A and $NaClO_4$, together with the $\Delta\overline{C}_P°$-data for the complexation reactions from the preceding investigation, one can calculate the $\overline{C}_P°$-values for all the various rare earth oxydiacetate complexes. These values given in Table 4 and in Fig. 3. The $\overline{C}_P°$-

Table 4. The partial molar heat capacities at infinite dilution for the various rare earth perchlorates and the corresponding oxydiacetate complexes.

Metal ion	$C_P°_{M(ClO_4)_3}$ J K^{-1} mol^{-1}	$C_P°_{MAClO_4}$ J K^{-1} mol^{-1}	$C_P°_{NaMA_2}$ J K^{-1} mol^{-1}	$C_P°_{Na_3MA_3}$ J K^{-1} mol^{-1}
Pr	40	191	354	492
Sm	46	204	365	494
Gd	41	201	358	466
Tb	43	184	387	449
Dy	45	191	421	460
Ho	40	172	417	455
Er	39	171	378	445
Yb	37	173	316	406

values for the terbium and erbium perchlorates were obtained by interpolation between the corresponding values for the adjacent elements in the rare earth series. The $\overline{C}_P°$-data show conclusively that the maximum found in $\Delta C_P°_2$ for the formation of the second rare earth oxydiacetate complex is due to the second complex alone, thus confirming the conclusion drawn previously.[9]

Acknowledgements. This work has been supported by a grant from the *Swedish Natural Science Research Council.* We also wish to thank Mrs. Gunilla Johnmark for all her help with the very time-consuming experimental part of this study.

REFERENCES

1. Grenthe, I. *Acta Chem. Scand.* **18** (1964) 293.
2. Choppin, G. and Graffeo, *Inorg. Chem.* **4** (1965) 1254.
3. Spedding, F. H. In Hamer W. J., Ed., *The Structure of Electrolytic Solutions*, McGraw, New York 1953, Chapter 22.
4. Reuben, J. and Fiat, D. *J. Chem. Phys.* **51** (1969) 4918.
5. Geier, G., Karlén, U. and v. Zelewsky, A. *Helv. Chim. Acta* **52** (1969) 1967.
6. Larsson, R. *Acta Chem. Scand.* **19** (1965) 783.
7. Silber, H. B., Scheinin, N., Atkinson, G. and Grecsek, J. R. H. *Faraday Trans. I* **1972** 1200.
8. Grenthe, I. and Ots, H. *Acta Chem. Scand.* **26** (1972) 1217.
9. Grenthe, I. and Ots, H. *Acta Chem. Scand.* **26** (1972) 1229.
10. Ots, H. *Acta Chem. Scand.* **27** (1973) 2344.
11. Ots, H. *Acta Chem. Scand.* **27** (1973) 2351.

12. Walters, J. P. and Spedding, F. H. *United States Atomic Energy Commission Research and Development Reports* IS-1988, 1968.
13. Gucker, F. T., Jr., Ayres, F. D. and Rubin, T. R. *J. Am. Chem. Soc.* **58** (1936) 2118.
14. Ots, H. *Acta Chem. Scand.* **26** (1972) 3810.
15. Ginstrup, O. *Chemica Scripta* **3** (1973) 97.
16. Faulkner, E. A., McGlashan, M. L. and Stubley, D. *J. Chem. Soc.* **1965** 510, 2837.
17. Randall, M. and Rossini, F. D. *J. Am. Chem. Soc.* **51** (1929) 323.
18. Osborne, N. S., Stimson, H. F. and Ginnings, D. C. *B. of S. Jour.* **23** (1939) 238.
19. Grenthe, I. and Hansson, E. *Acta Chem. Scand.* **23** (1969) 611.
20. Harned, H. S. and Owen, B. B. *The Physical Chemistry of Electrolytic Solutions*, 3rd Ed., Reinhold, New York 1958, p. 353.
21. Gucker, F. T., Jr. and Schminke, K. H. *J. Am. Chem. Soc.* **54** (1932) 1358.

Received March 3, 1973.

ACTA CHEMICA SCANDINAVICA 27 (1973) 2554–2558

A Spectrophotometric Study of the Complex Formation between Vanadium(V) and Hydroxylamine in Strongly Acidic Perchlorate Solutions

GÖSTA BENGTSSON

Division of Inorganic Chemistry 1, Chemical Center, University of Lund, S-220 07 Lund 7, Sweden

The complex formation between vanadium(V) and hydroxylamine has been studied within the hydrogen ion concentration range $[H^+] = 0.010 - 0.900$ M by two spectrophotometric methods, the so-called M-method and the L-method. The former method gives $\beta_1 = 19 \pm 11$ M^{-1} and the latter $\beta_1 = 12.5 \pm 0.4$ M^{-1}. The results agree within the experimental errors and it seems probable that only one complex is present in appreciable concentrations. The value of $\beta_1 = [ML]/[M][L]$ is independent of $[H^+]$ within the hydrogen ion concentration range studied. Thus the complex formed seems to be $VO_2NH_3OH^{2+}$.

In a previous paper [1] the kinetics of the reaction between vanadium(V) and hydroxylamine within the hydrogen ion concentration range $[H^+] = 0.2 - 1.0$ M was studied. The reaction was found to follow a two term rate law,

$$-\frac{d[V(V)]}{dt} = k[V(V)][NH_2OH] + k'[V(V)]^2[NH_2OH] \quad (1)$$

where $[V(V)]$ and $[NH_2OH]$ represent the over-all concentrations of vanadium(V) ($=[VO_2^+]$) and hydroxylamine ($=[NH_3OH^+]$), respectively. At sufficiently low $[V(V)]$ ($[V(V)] \leq 5 \times 10^{-4}$ M) the third order term becomes negligible. The first step in the reaction seems to be the rapid formation of a complex between the two reactants. This complex formation manifests itself in an immediate increase of the absorbance as compared with a vanadium(V) solution of the same concentration at wave lengths below about 250 nm when the reactant solutions are mixed. The present paper describes a spectrophotometric study of the complex formation equilibria within the hydrogen ion concentration range 0.010 – 0.900 M. However, optical methods are not the most general for the determination of stability constants of complex ions in solution. But in the present case there was not, however, any more reliable method available.

SYMBOLS AND NOTATIONS

C_M over-all concentration of the central ion M ($=VO_2^+$) (mol/l).
C_L over-all concentration of the ligand L ($=NH_3OH^+$) (mol/l).
ε_X molar absorption coefficient of the species X (M^{-1} cm^{-1}).
A absorbance ($A=\sum\varepsilon_X c_X l$; c_X = concentration; l = path length).
a absorption coefficient ($a=A/l$) (cm^{-1}).
ε formal molar absorption coefficient ($\varepsilon=a/C_M$) (M^{-1} cm^{-1}).
λ wave length (nm).

EXPERIMENTAL

The chemicals used were of the same kind as those described in Ref. 1, and so were the procedures used for the preparation of the solutions and determination of their concentrations. The temperature was 25.00 ± 0.05°C, the ionic strength 1.00 M. Sodium perchlorate and perchloric acid were used to keep the ionic strength constant.

The measurements were carried out spectrophotometrically within the ultraviolet region of the spectrum ($\lambda=225-235$ nm). The narrow wave length range used was due to two factors: (1) The absorption of the ligand should be as small as possible. (2) The effect of the complex formation on ε should not be too small. At each series of measurements performed the slit width was kept constant and the wave length knob was not touched until the whole series was completed. Thereby the effects of small differences in the wave length (which can give large errors, if the wave length is on the slope of an absorption curve) were eliminated as far as possible.

THEORY

The most reliable spectrophotometric method for the study of complex formation is the method of corresponding solutions.[3,4] This method requires, however, optimal conditions which were not met with in the present study. Thus two less reliable methods, the M-method and the L-method (*cf.* Ref. 5) had to be applied. In both these methods it is assumed that only one mononuclear complex is formed.

In the M-method [6] $C_M \gg C_L$. C_L is kept constant while the difference $(\varepsilon-\varepsilon_M)$ is determined as a function of C_M. ε is the formal molar absorption coefficient of a solution containing both M and L. If the absorbance of the ligand can be neglected, the following relations can be derived:

$$\frac{1}{\varepsilon-\varepsilon_M}=\frac{1+\beta_1 C_L}{(\varepsilon_{ML}-\varepsilon_M)\beta_1 C_L}+\frac{[M]}{(\varepsilon_{ML}-\varepsilon_M)C_L} \quad (2)$$

$$[M]\approx\frac{C_M}{1+\beta_1 C_L} \quad (3)$$

As a first approximation we put $[M]\approx C_M$ and β_1 is evaluated from the straight line representing $1/(\varepsilon-\varepsilon_M)$ *versus* C_M. If necessary, the calculations can be repeated using the approximate value of β_1 for the calculation of [M]. If polynuclear complexes can be neclected, the assumption of only one complex formed seems justified. A disadvantage of this method is, however, that $(\varepsilon-\varepsilon_M)$ often represents a small difference between two large numbers. It is therefore very sensitive even to small experimental errors.

In the L-method $C_L \gg C_M$ and $(\varepsilon - \varepsilon_M)$ is determined as a function of C_L, while C_M is kept constant. If the concentrations of higher complexes than ML can be neglected, the following relation can be derived:

$$\frac{C_L}{\varepsilon - \varepsilon_M} = \frac{1 + \beta_1[M]}{(\varepsilon_{ML} - \varepsilon_M)\beta_1} + \frac{C_L}{(\varepsilon_{ML} - \varepsilon_M)} \quad (4)$$

Since $\beta_1[M] \ll 1$ the stability constant is obtained from $C_L/(\varepsilon - \varepsilon_M)$ *versus* C_L. The validity of the assumption that the higher complexes can be neglected is often less certain in this method. It yields often too low values of β_1 due to this neglect (*cf.* Refs. 3 and 5). Since it has been misused on several occasions it has obtained a bad reputation and should be used with great care. It yields, however, sometimes a better precision to the obtained stability constants, and if the result agrees with the result obtained by the M-method, it seems reasonable to accept the former value. Furthermore, the formation of polynuclear complexes may be eliminated, since it is possible to perform the measurements at very low central ion concentrations.

MEASUREMENTS AND RESULTS

The complex formation between vanadium(V) and hydroxylamine is rapid ("momentaneous") and is succeeded by a slow oxidation of hydroxylamine.[1] The absorbances considered in this paper are therefore absorbances extrapolated to the time $t = 0$ after mixing the reactant solutions. Since the redox reaction is slow at $[H^+] > 0.050$ M this does not affect the precision noticeably, except at low hydrogen ion concentrations ($[H^+] < 0.050$ M) where the kinetics of the succeeding reactions becomes more complicated with a rather rapid change of the absorbance with time.[7]

The M-method was applied at $[H^+] = 0.200$ M and $\lambda = 228$ nm. The results are shown in Fig. 1. During these measurements special care was taken to ascertain that the corresponding values of ε and ε_M were measured at equal conditions. The path lengths were chosen such that the absorbances would not change too much when C_M was changed. The validity of Lambert-Beer's

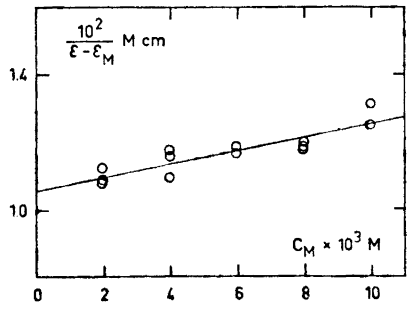

Fig. 1. $1/(\varepsilon - \varepsilon_M)$ *versus* C_M. $\lambda = 228$ nm; $C_L = 2.00$ mM; $C_{HClO_4} = 0.200$ M.

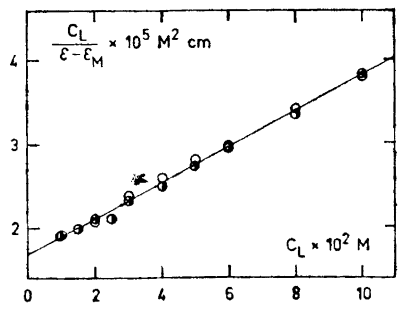

Fig. 2. $C_L/(\varepsilon - \varepsilon_M)$ *versus* C_L. $\lambda = 225$ nm; ○ $C_M = 1.00$ mM, $C_{HClO_4} = 0.200$ M; ◑ $C_M = 0.050$ mM, $C_{HClO_4} = 0.900$ M.

law was established as concerns the central ion. The slope and the intercept of the straight line $1/(\varepsilon - \varepsilon_M)$ *versus* C_M was calculated by a least squares program on a desk-top computer. $\beta_1 = 19 \pm 11$ M^{-1} and $(\varepsilon_{ML} - \varepsilon_M) = (2.5 \pm 1.3) \times 10^3$ M^{-1} cm^{-1}. The error limits throughout this paper represent three standard deviations.

The results of the L-method, applied at two hydrogen ion concentrations (0.200 and 0.900 M) and two wave lengths (225 and 235 nm) are shown in Table 1 and Fig. 2. The values of β_1 and $(\varepsilon_{ML} - \varepsilon_M)$ were calculated from

Table 1. The L-method. Experimental conditions and stability constants obtained.

$C_M \times 10^3$ M	λ nm	C_{HClO_4} M	β_1 M^{-1}	$(\varepsilon_{ML} - \varepsilon_M) \times 10^{-3}$ M^{-1} cm^{-1}
1.00	225	0.200	12.7 ± 1.6	4.68 ± 0.31
0.150	225	0.200	12.2 ± 1.4	4.66 ± 0.33
0.150	235	0.200	12.4 ± 3.1	1.66 ± 0.25
0.150	225	0.900	12.9 ± 2.5	4.72 ± 0.55
0.050	225	0.900	12.4 ± 1.6	4.78 ± 0.37
		Mean value	12.5 ± 0.4	

$C_L/(\varepsilon - \varepsilon_M)$ *versus* C_L by the least squares program. The differences between the formal molar absorption coefficients $(\varepsilon - \varepsilon_M)$ from some of the series of measurements, including those at $[H^+] = 0.010$ and 0.020 M, are shown in Fig. 3. The full drawn line has been calculated using the mean values of β_1 and $(\varepsilon_{ML} - \varepsilon_M)$ from Table 1.

DISCUSSION

The values of the stability constant β_1 obtained by the two methods used agree within the experimental error. The fact that the value obtained by the M-method is larger than that obtained by the L-method might indicate an influence on the absorbances from higher complexes (*cf.* Refs. 3 and 5). Both the reactants are, however, positively charged (VO_2^+ and NH_3OH^+, *cf.* below) and it seems reasonable to believe that the higher complexes are very weak. Since the L-method yields the most precise values, the mean value $\beta_1 = 12.5 \pm 0.4$ M^{-1} is accepted.

As can be seen from Table 1, β_1 is independent of $[H^+]$ within the hydrogen ion concentration range 0.2 – 0.9 M, and Fig. 3 shows that $(\varepsilon - \varepsilon_M)$ as a function of C_L at $[H^+] = 0.010$ M and 0.020 M can be accomodated to the same line as the values for higher $[H^+]$ (within the large experimental errors at these $[H^+]$). At 25°C and the ionic strength 1 M the hydroxylammonium ion NH_3OH^+ has a pK_a-value of about 6,[8] so at the hydrogen ion concentrations used in this study hydroxylamine is present almost entirely as NH_3OH^+. The complex formation therefore occurs without any loss of the proton from NH_3OH^+. It does not seem very likely that VO_2^+ should be able to accept a proton

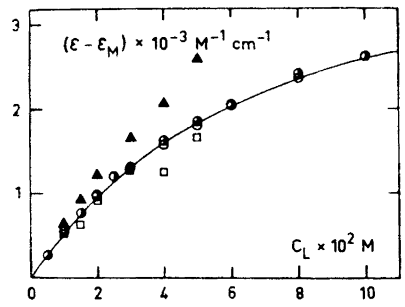

Fig. 3. $(\varepsilon - \varepsilon_M)$ *versus* C_L. $\lambda = 225$ nm;
○ $C_M = 1.00$ mM, $C_{HClO_4} = 0.200$;
◑ $C_M = 0.050$ mM, $C_{HClO_4} = 0.900$;
□ $C_M = 0.100$ mM, $C_{HClO_4} = 0.020$ M;
▲ $C_M = 0.100$ mM, $C_{HClO_4} = 0.010$ M.

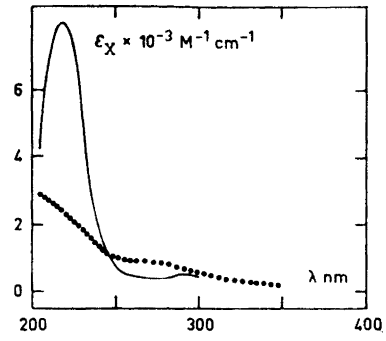

Fig. 4. Absorption curves of VO_2^+ ··· and $VO_2NH_3OH^{2+}$ ——.

within this hydrogen ion concentration range. It might therefore be concluded that the oxygen atom of the hydroxylammonium ion is the ligand atom (as might be guessed from other considerations).

Fig. 4 shows the absorption curves of VO_2^+ and $VO_2NH_3OH^{2+}$ within the wave length range 200 – 350 nm. The curve of the complex has been calculated using extrapolated absorbance values for a solution with $C_M = 1.00 \times 10^{-4}$ M, $C_L = 0.020$ M in 1.000 M $HClO_4$, known values of ε_M, and the β_1-value given above. The curve has been interrupted at 300 nm since at larger wave lengths the experimental errors have too strong an influence for the results to be meaningful.

The author is indebted to Professor Sture Fronæus for valuable comments, to Mrs. Christina Oskarsson for technical assistance in some of the measurements, and to Dr. Peter Sellers for linguistic revision of the manuscript.

REFERENCES

1. Bengtsson, G. *Acta Chem. Scand.* **26** (1972) 2494.
2. Rossotti, F. J. C. and Rossotti, H. *The Determination of Stability Constants*, McGraw, New York 1961.
3. Olerup, H. *Järnkloridernas komplexitet*, Diss., Lund 1944.
4. Fronæus, S. In Jonassen, H. B. and Weissberger, A., Eds., *Technique of Inorg. Chem.* **1** (1963) 1, and references therein.
5. Johansson, L. *Acta Chem. Scand.* **25** (1971) 3569.
6. Evans, M. G. and Nancollas, G. H. *Trans. Faraday Soc.* **49** (1953) 363.
7. Bengtsson, G. *Acta Chem. Scand. To be published.*
8. Lumme, P., Lahermo, P. and Tummavuori, J. *Acta Chem. Scand.* **19** (1965) 2175.

Received March 24, 1973.

ACTA CHEMICA SCANDINAVICA 27 (1973) 2559–2566

Cyclo-oligomerization of Quinones

V.* The Acid Catalyzed Reactions of α-Naphthoquinone with Phenols

HANS-ERIK HÖGBERG

Department of Organic Chemistry, Royal Institute of Technology, S-100 44 Stockholm 70, Sweden

In the presence of catalytic amounts of strong acid α-naphthoquinone reacts with several polyhydric phenols to yield at room temperature 2-(polyhydroxyphenyl)-1,4-naphthoquinones. At higher temperatures good yields of polyhydroxybenzo[b]naphtho[2,1-d]furans are formed.

Many quinones readily undergo acid catalyzed condensations with phenols to give biphenyl derivatives or analogous compounds. The reaction products are often highly coloured hydroxyphenylquinones formed by oxidation of the primary phenolic condensation products by unchanged starting quinone. The reaction mixtures therefore also contain the hydroquinone corresponding to the original quinone.

Similar treatment of pure quinones frequently yields phenolic oligomers containing one or more dibenzofuran elements.[1–6] In these cases small amounts of the hydroquinone are obviously formed by some side reaction. This serves to start the condensation reactions which proceed to completion because the relevant hydroquinones are produced during the process. Therefore the condensation reactions are inhibited if oxidizing agents of sufficiently high oxidation potential are added to the reaction mixtures.[5] *p*-Benzoquinone gives, for example, small amounts of the tri- and tetramerization products *1* and *2* but 2,3-dialkylquinones and α-naphthoquinone give larger yields of analogous products.[4–6] It should be noted that during these reactions the condensation products are formed already at low temperatures and in the presence of small to moderate amounts of, *e.g.*, sulphuric acid. Under such conditions no dehydration of *o,o'*-dihydroxybiphenyls to dibenzofurans occurs. Much more drastic conditions, *e.g.*, prolonged boiling with strong hydrobromic acid, are normally required to bring about such ring closures. The relations between structure and ease of dibenzofuran formation have recently been studied in

* Part IV: Ref. 6.

this laboratory by Stjernström.[7,8] Clearly the furan rings in the above quinone condensation products must have been formed in a quite different way.

In this paper we describe reactions during which either quinones or phenols containing dibenzofuran elements are formed depending upon the reaction conditions used.

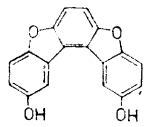

1

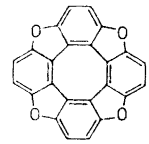

2

Long ago Blumenfeld and Friedländer[9] noted that on addition of sulphuric acid to an acetic acid solution of α-naphthoquinone and resorcinol at room temperature a sparingly soluble, black product is formed. On heating, however, a colourless solution is obtained. The black product was easily obtained in an 80 % yield. The mass spectrum was in agreement with that expected for the quinone *4* contaminated with somewhat of the hydroquinone *3*. Recrystallization from ethanol in the presence of *p*-benzoquinone furnished the brown-red quinone *4*. The black product could be reduced to a tetraphenol (m.p. 169–171°) which gave a tetramethyl ether and a tetraacetate whose spectral properties (UV, NMR) clearly showed that *3* is the correct structure of the phenol. The quinone *4* dissolves in alkali giving a deep blue colour, typical for *o*- or *p*-hydroxyphenyl-1,4-naphthoquinones.[11] The UV and visible spectra of the quinone *4* in neutral or alkaline solution is shown in Fig. 1. The phenol,

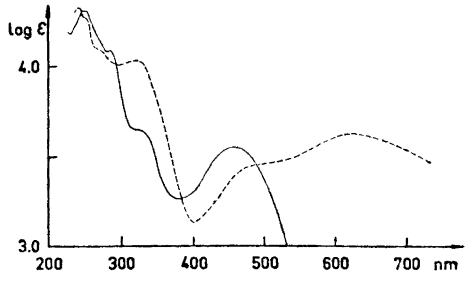

Fig. 1. UV and visible absorption curve of the quinone *4* in ethanol —— (λ_{max}/log ε = 460/3.55) and in 1 % sodium carbonate solution in water – – – (λ_{max}/log ε = 623/3.63).

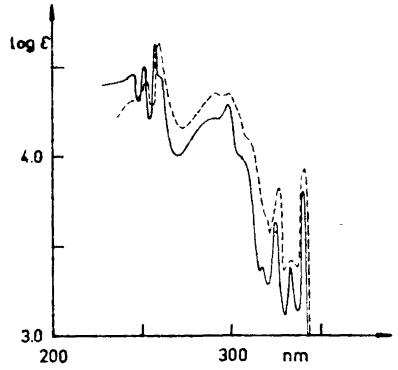

Fig. 2. UV absorption curve of α-brazan (*5*)[12] —— and of diacetoxybenzonaphthofuran (*6*, OAc instead of OH) – – – in ethanol. The latter is displaced 0.1 log ε unit upwards.

m.p. 169–171°, is obviously identical with a product, m.p. 167°, obtained by Pummerer and Huppmann and assigned structure *3*.[9] So far we have not been able to repeat their experiment.

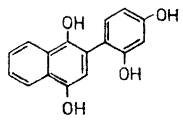

3

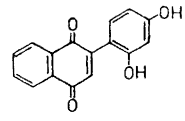

4

When naphtoquinone and an excess of resorcinol (1.5 mol) were similarly treated at reflux temperatures a colourless phenolic product (m.p. 210–211°) could be isolated in 70 % yield *via* its acetate. The UV-spectrum of the acetate was very similar to that of α-brazan (*5*) (Fig. 2).[12] The phenol, therefore, must be 5,9-dihydroxybenzo[b]naphtho[2,1-d]furan (*6*) and this conclusion is corroborated by the NMR investigation of its dimethyl ether.

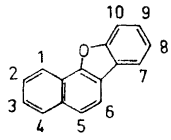

5

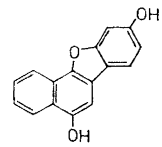

6

Two additional phenolic products A (about 2 %) and B (about 20 %) were isolated from the reaction mixture. Compound A was probably a condensation product of 2 mol of naphthoquinone and 1 mol of resorcinol minus 2 mol of water as evidenced by the MS ($m/e = 390$; $M^{+\cdot}$). One of the possible structures is *7*.

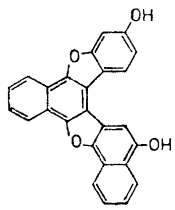

7

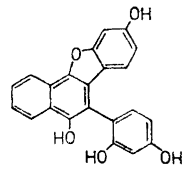

8

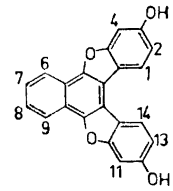

9

Compound B was obtained in almost quantitative yield by condensing the quinone *4* with resorcinol. Its structure, *8*, follows from its spectral properties and from the fact that it is dehydrated to a dihydric phenol when refluxed with hydrobromic acid. The NMR spectrum of this compound clearly shows that it must have the structure *9*.

Pyrogallol and methoxyhydroquinone both react with naphthoquinone in the same way as resorcinol. At room temperature the quinones *10* and *11* were obtained but at reflux temperature compounds *12* and *13* were formed.

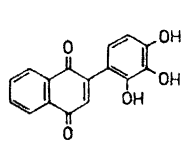

10

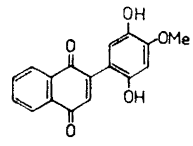

11

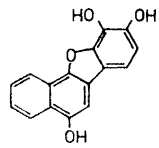

12

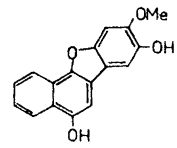

13

When introduced into a benzenesulphonic acid melt compound *11* underwent cyclodimerization to give a dimethoxydibenzotetraphenylenotetrafuran in 40 % yield ($m/e = 520$; $M^{+\cdot}$).

One of the two possible structures for this compound is *14*. The properties of the substance were very similar to those of similar quinone tetramers.[3,5,6] This cyclodimerization parallels the formation of the naphthoquinone tetramer from 2-(1,4-dihydroxy-2-naphthyl)-1,4-naphthoquinone.[5]

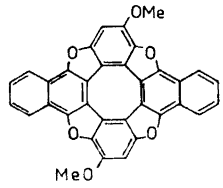

14

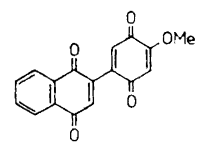

15

Sufficiently reactive phenol ethers also give condensation products with naphthoquinone. With resorcinol dimethyl ether it gave the red 2-(2,4-dimethoxyphenyl)-1,4-naphthoquinone (*4*, OMe instead of OH), identical with the product formed by chromic acid oxidation of the tetramethyl ether of the phenol *3*. Hydroxyhydroquinone trimethyl ether gave the deep blue 2-(2,4,5-trimethoxyphenyl)-1,4-naphthoquinone (*11*, OMe instead of OH) which on oxidation with nitric acid gave the diquinone *15* which is also formed upon similar oxidation of the quinone *11*.

In these condensation reactions the quinones, *e.g.* *4*, are formed as intermediates at higher temperatures. Samples withdrawn at early stages of the reaction displayed the intense absorption at 460 nm typical of compound *4*. At a lower temperature (50°) the quinone *4* first precipitated but slowly dissolved again to give a colourless solution from which a 20 % yield of furan *6*

could be isolated. There is certainly no mechanistic difference between the high and low temperature reactions. The reason why hydroxyphenylquinones can be isolated is obviously that, at low temperatures, they are insoluble in the reaction medium.

EXPERIMENTAL

Melting points are uncorrected. Instruments: UV, Beckmann DK2; MS, LKB 9000 (ion source temp. 290°, 70 eV); NMR, Varian A-60A (TMS internal standard).

2-(2,4-Dihydroxyphenyl)-1,4-naphthoquinone (4). Naphthoquinone (15.8 g, 0.1 mol) was dissolved in acetic acid (400 ml) and a solution of resorcinol (6.1 g, 0.055 mol) in acetic acid (300 ml) was added. The light red solution was cooled to 20° and 2 M sulphuric acid (1 ml) was added. The reaction mixture immediately turned dark brown. It was cooled to 20° and the walls of the reaction flask were scratched with a glass rod to induce rapid crystallization. If cooling and scratching were omitted the yield was lowered. In some experiments the reaction was complicated by the coprecipitation of naphthoquinhydrone. After 2 h the mixture was filtered and the brownish-black product was washed with acetic acid and dried. Yield: 10.8 g, 80 %. The MS showed the product to be a 2:1 mixture of compounds *4* and *3*. The product was therefore recrystallized from ethanol containing enough benzoquinone to ensure complete oxidation to compound *4*. The brown-red product melted with decomposition at 202 – 204° (evacuated capillary). (Found: C 72.0; H 3.8. Calc. for $C_{16}H_{10}O_4$: C 72.2; H 3.8. Mw = 266). MS, $m/e = 266$ ($M^{+\cdot}$, base peak); 249 ($M^{+\cdot} - OH^{\cdot}$); 238 ($M^{+\cdot} - CO$); 104 ($C_6H_4CO^{+\cdot}$); 76 ($C_6H_5^+$). UV, see Fig. 1. With conc. sulphuric acid the compound gave an intense blue colour which slowly turned to green. The alkaline solution was deep blue (see Fig. 1 for absorption curve).

2-(2,4-Dihydroxyphenyl)-4,4-naphthoquinone (3). The quinone *4* (2 g) was boiled with a 20 % sodium dithionite solution (25 ml), charcoal was added and the solution filtered. On cooling colourless needles (1 g) separated. The compound was very sensitive to oxidation. Sublimed (150°/0.1 mm) material melted at 171 – 173° (Dec., evacuated capillary). (Found: C 71.0; H 4.5. Calc. for $C_{16}H_{12}O_4$ = C 71.6; H 4.5. Mw = 268). MS, $m/e = 268$ ($M^{+\cdot}$, base peak). Colour reaction with sulphuric acid, blue violet.

2-(2,4-Diacetoxyphenyl)-1,4-diacetoxynaphthalene (3, OAc instead of OH). On reductive acetylation (Ac_2O, Zn, traces of pyridine) the above crude condensation product gave the acetate of *3* in a quantitative yield. M.p. 155 – 156° (EtOH). (Found: C 65.9; H 4.8. Calc. for $C_{24}H_{20}O_8$: C 66.1; H 4.6. Mw = 436). MS, $m/e = 436$ ($M^{+\cdot}$). UV (ethanol) λ_{max} (nm)/log ε = 242/4.60; 283/3.92. The UV spectrum was very similar to that of 2-phenylnaphthalene.[13]

2-(2,4-Dimethoxyphenyl)-1,4-dimethoxynaphthalene (3, OMe instead of OH). The phenol *3* was methylated with excess dimethyl sulphate and alkali. Needles m.p. 120 – 121° (EtOH). (Found: C 73.9; H 6.2. Calc. for $C_{20}H_{20}O_4$: C 74.1; H 6.2. Mw = 324). MS, m/e = 324 ($M^{+\cdot}$, base peak). NMR ($CDCl_3$), δ (ppm) = 3.52, 3.68, 3.75, and 3.86 (12 H, four $-OCH_3$); 6.42 – 7.86 (3 H, complex multiplets, ArH *ortho* to $-OCH_3$); 7.20 – 7.60 (3 H, complex multiplets, ArH); 8.05 – 8.35 (complex multiplets, 2 H, ArH).

5,9-Diacetoxybenzo[b]naphtho[2.1-d]furan (6, OAc instead of OH). A solution of naphthoquinone (3.2 g) and resorcinol (3.3 g) in acetic acid (10 ml) was heated to boiling. Addition of sulphuric acid (2 M, 1 ml) started a strongly exothermal reaction. A deep brown colour developed which faded within a couple of minutes. A sample withdrawn immediately after addition of acid was diluted with ethanol and the resulting solution displayed the typical absorption maximum of the quinone *4* at 460 nm. After refluxing for 1 h the mixture was poured into water (0.5 l). The precipitate was collected and washed with water (1 l). The product (4.4 g) was acetylated (Ac_2O, pyridine). From the hot reaction mixture 0.1 g of crystals separated (filtrate = A). The MS of the collected acetate indicated that it had the structure *7* (OAc instead of OH) or isomer ($m/e = 474$ ($M^{+\cdot}$); 432; 390 (base peak). (Calc. for $C_{30}H_{18}O_5$: **Mw = 474**)). After cooling the filtrate A deposited the diacetate of compound *6*. Colourless needles (3.5 g, 60 %). M.p. 202 – 204° (HOAc). (Found: C 71.7; H 4.2. Calc. for $C_{20}H_{14}O_5$: C 71.8; H 4.2.) MS: $m/e = 334$ ($M^{+\cdot}$); 292; 250 (base peak). UV, see Fig. 2. The mother liquors were poured into water and the solid collected was dissolved in the smallest possible amount of ethanol. After some

days the product that had separated (0.35 g) was recrystallized from acetic acid. This product was identical (MS, m.p.) with the acetate of compound *8* (see below).

In a similar experiment the reaction mixture was directly acetylated and filtered while hot to give the acetate of compound *7* or isomer (2 %). The filtrate was poured into water. The solid was collected and chromatographed on silica gel. Methylene chloride eluted the acetate of compound *6* (66 %) and chloroform/methylene chloride (1/3) eluted the acetate of compound *8* (17 %).

5,9-Dihydroxybenzonaphthofuran (6). The diacetate was refluxed with acidified (H_2SO_4) aqueous methanol. M.p. 210 – 211° (dilute ethanol). (Found: C 76.8; H 4.0. Calc. for $C_{16}H_{10}O_3$: C 76.8; H 4.0. Mw = 250). MS, *m/e* = 250 ($M^{+\cdot}$, base peak); 222 ($M^{+\cdot} - CO$, metastable peak at *m/e* = 197.3, calc. for 250 – 222: *m/e* = 197.1); 221; 164; 125 (M^{2+}). Colour reaction with sulphuric acid, intense red-violet.

5,9-Dimethoxybenzonaphthofuran (*6*, OMe instead of OH). The phenol *6* was methylated (Me_2SO_4, NaOH). M.p. 111 – 111.5° (ethanol). (Found: C 77.8; H 5.1. Calc. for $C_{18}H_{14}O_3$: C 77.6; H 5.1. Mw = 278). MS, *m/e* = 278 ($M^{+\cdot}$, base peak). NMR ($CDCl_3$), δ (ppm) = 3.80 and 4.94 (6 H, two $-OCH_3$); 6.87 (H_8, quartet, $J_{7-8} = 8.5$ cps, $J_{8-10} = 2.5$ cps); 7.01 (H_6, singlet); 7.09 (H_{10}, doublet, $J_{8-10} = 2.5$ cps); 7.64 (H_7, doublet, $J_{7-8} = 8.5$ cps); 7.4 – 7.8 (H_2 and H_3, complex multiplets); 8.15 – 8.40 (H_1 and H_4, complex multiplets).

6-(2,4-Dihydroxyphenyl)-5,9-dihydroxybenzonaphthofuran (8). To a boiling solution of resorcinol (5.0 g) in acetic acid (50 ml) containing sulphuric acid (2 M, 2 ml) the quinone *4* (2.7 g) was added in portions. After each addition a deep brown-red colour developed which soon faded. After boiling for 10 min the solution was poured into water and the precipitate was collected. Yield: 3.2 g, 90 %. M.p. after sublimation 275 – 278° (Dec., evacuated capillary). (Found: C 74.3; H 3.8. Calc. for $C_{22}H_{14}O_5$: C 73.7; H 3.9. Mw = 358). MS, *m/e* = 358 ($M^{+\cdot}$, base peak); 249.

6-(2,3-Diacetoxyphenyl)-5,9-diacetoxybenzonaphthofuran (*8*, OAc instead of OH) was obtained from the preceding phenol. Prisms m.p. 201 – 202° (HOAc). (Found: C 68.4; H 4.2. Calc. for $C_{30}H_{22}O_9$: C 68.4; H 4.2. Mw = 526). MS, *m/e* 526 ($M^{+\cdot}$). UV (ethanol): λ_{max} (nm)/log ε = 263/4.81; 290/4.33; 300/4.28; 329/3.62; 344/3.66.

6-(2,4-Dimethoxyphenyl)-5,9-dimethoxybenzonaphthofuran (*8* OMe instead of OH) was obtained by methylation of the phenol *7*, in the usual way. Prisms m.p. 170 – 171° (HOAc). (Found: C 75.2; H 5.4. Calc. for $C_{26}H_{22}O_5$. C 75.3; H 5.4. Mw = 414). MS, *m/e* = 414 ($M^{+\cdot}$, base peak). NMR ($CDCl_3$): δ (ppm) = 3.56, 3.61, 3.73, and 3.82 (12 H, four $-OCH_3$ groups); 6.50 – 7.71 (8 H, complex multiplets, aromatic H); 8.02 – 8.38 (2 H, complex multiplets, aromatic H). The singlet at δ = 7.02 ppm observed in the spectra of the 5-methoxybenzonaphthofurans described here and arising from H_6 was not present in this spectrum.

3,12-Dihydroxynaphtho[1,2-b:4,3-b']bisbenzofuran (9). The phenol (*7*) (3 g) was refluxed with constant boiling hydrobromic acid (50 ml) and acetic acid (20 ml) for 60 h under nitrogen. The product (2.7 g) was sublimed (270°/0.1 mm) and did not melt below 360°. (Found: C 77.9; H 3.5. Calc. for $C_{22}H_{12}O_4$: C 77.6; H 3.6. Mw = 340). MS, *m/e* = 340 ($M^{+\cdot}$, base peak). NMR (DMSO d_6), δ (ppm) = 7.19 (H_2 and H_{13}, quartet, $J_{2-1} = 8.5$ cps, $J_{2-4} = 2.0$ cps); 7.31 (H_4 and H_{11}, doublet, $J_{2-1} = 2.0$ cps); 7.51 – 7.74 (H_7 and H_8, quartet); 8.28 (H_1 and H_4, doublet, $J_{1-2} = 8.5$ cps); 8.21 – 8.45 (H_6 and H_9, quartet); 10.10 (two phenolic H; singlet).

3,12-Diacetoxynaphthobisbenzofuran (*9*, OAc instead of OH) was obtained from the phenol *8*. M.p. 261 – 262° (pyridine). (Found: C 73.9; H 3.6. Calc. for $C_{16}H_{16}O_6$ = C 73.6; H 3.8. Mw = 424). MS, *m/e* = 424 ($M^{+\cdot}$). UV (ethanol), λ_{max} (nm)/log ε = 281/4.84; 347/3.82; 365/3.90. Absolute intensities slightly uncertain due to low solubility.

3,12-Dimethoxynaphthobisbenzofuran (*9* OMe instead of OH). The methylated phenol *9* melted at 236 – 237° (pyridine). (Found: C 78.3; H 4.3. Calc. fo $C_{24}H_{16}O_4$: C 78.3; H 4.4. Mw = 368). MS, *m/e* = 368 ($M^{+\cdot}$, base peak).

2-(2,3,4-Trihydroxyphenyl)-1,4-naphthoquinone (10). Naphthoquinone and pyrogallol were treated at 20° as above. A brown-black material separated in 80 % yield which was shown by MS to consist of a 4/1 mixture of quinone *10* and the corresponding hydroquinone. Recrystallization from acetic acid containing benzoquinone gave the deep brown-red quinone *10*, which undergoes a phase transition at 129 – 130° and finally melts at 172 – 173° (Dec., evacuated capillary). (Found: C 67.8; H 3.6. Calc. for $C_{16}H_{10}O_5$: C 68.1; H 3.7. Mw = 282). MS, *m/e* = 282 ($M^{+\cdot}$, base peak), 266, 265, 244, 237, 226, 197,

104, 76. UV (ethanol), λ_{max} (nm)/log ε = 248/4.26; 327/3.74; 454/3.42. Colour reaction with sulphuric acid, olive green.

2-(2,3,4-Triacetoxyphenyl)-1,4-diacetoxynaphthalene was obtained from the quinone *10* (Ac_2O, Zn dust, trace of pyridine). M.p. 143 – 145° (HOAc). (Found: C 63.3; H 4.6. Calc. for $C_{26}H_{22}O_{16}$: C 63.1; H 4.5. Mw = 494). MS, *m/e* = 494 (M+·).

2-(2,3,4-Trimethoxyphenyl)-1,4-dimethoxynaphthalene. The preceding acetate was saponified (MeOH, trace H_2SO_4 under N_2, reflux 2 h) and after neutralization of the solution (NaOAc) it was methylated (Me_2SO_4, NaOH) as above. The product was distilled at reduced pressure and recrystallized from acetic acid. M.p. 117 – 118°. (Found: C 70.8; H 6.2. Calc. for $C_{21}H_{22}O_5$: C 71.2; H 6.2. Mw = 354). MS, *m/e* = 354 (M+·, base peak). NMR ($CDCl_3$), δ (ppm) = 3.56; 3.71; 3.81; 3.88, and 3.91 (15 H of 5 $-OCH_3$ groups); 6.66 (1 H, doublet, position 3 of phenyl group, J_{2-3} = 8.8 cps); 6.76 (1 H, position 3 of the naphthyl group); 7.11 (1 H, doublet, position 2 of the phenyl group, J_{2-3} = 8.8 cps); 7.32 – 7.58 (2 H, positions 6 and 7 of the naphthyl group); 8.03 – 8.37 (2 H, positions 5 and 8 of the naphthyl group).

5,9,10-Triacetoxybenzo[b]naphtho[2,1-d]furan (*12*, OAc instead of OH). Naphthoquinone (6.3 g) and pyrogallol (7.6 g) were refluxed with a mixture of acetic acid and sulphuric acid. The phenolic product obtained on acetylation as described above gave three acetates: (a) A sparingly soluble triacetate (0.26 g) [probably the triacetate of the pyrogallol analogue of compound *7* as judged by its MS, *m/e* = 532 (M+·) (calc. for $C_{32}H_{20}O_8$: Mw = 532)]. (b) The triacetate of compound *12* (5.3 g, 34 %). M.p. 174 – 175°, resolidifying and finally melting at 191 – 193° (HOAc). (Found: C 67.4; H 4.1. Calc. for $C_{22}H_{10}O_6$: C 67.3; H 4.1. Mw = 392). MS, *m/e* = 392 (M+·); 350; 308; 266. UV (ethanol). λ_{max} (nm)/log ε = 245/4.55, 254/4.66; 262/4.90; 295/4.26; 326/3.76; 334/4.48; 3.41/3.87. This spectrum is very similar to that of α-brazan [12] and to that of the diacetate of compound *6*. (c) The hexaacetate of the pyrogallol analogue of compound *8* ((*m/e* = 644 (M+·) and peaks corresponding to successive losses of 6 CH_2CO groups (calc. for $C_{32}H_{26}O_{13}$: Mw = 644)].

5,9,10-Trihydroxybenzonaphthofuran (12) was obtained from the acetate ($MeOH/H_2O$, trace H_2SO_4, reflux 2 h). M.p. 267 – 269° after sublimation (evacuated capillary). (Found: C 72.3; H 3.7. Calc. for $C_{16}H_{10}O_4$: C 72.2; H 3.8. Mw = 266). MS, *m/e* = 266 (M+·). Colour reaction sulphuric acid, red-violet.

5,9,10-Trimethoxybenzonaphthofuran (*12*, OMe instead of OH). M.p. 119.5 – 120° (EtOH). (Found: C 74.0; H 5.2. Calc. for $C_{19}H_{16}O_4$: C 74.0; H 5.2. Mw = 308). MS, *m/e* = 308 (M+·). NMR ($CDCl_3$), δ (ppm) = 3.89, 3.96, and 4.25 (9 H, three $-OCH_3$ groups); 6.85 (H_8, doublet, J_{7-8} = 8.5 cps); 7.00 (H_6 singlet); 7.34 (H_7, doublet, J_{7-8} = 8.5 cps); 7.40 – 7.70 (H_3 and H_7); 8.28 – 8.42 (H_1 and H_4).

2-(2,5-Dihydroxy-4-methoxyphenyl)-1,4-naphthoquinone (11). 1,4-Naphthoquinone (3.2 g) and methoxyhydroquinone (1.7 g) were treated as above at 20°. After recrystallization from ethanol reddish brown prisms (2.0 g) were obtained. M.p. 230 – 233° (Dec., evacuated capillary). (Found: C 68.9; H 4.0. Calc. for $C_{17}H_{12}O_5$: C 68.9; H 4.1. Mw = 296). MS, *m/e* = 296 (M+·, base peak); 281, 279; 268; 253; 225; 211; 104; 76; 69. UV (ethanol), λ_{max} (nm)/log ε = 246/4.30; 302/4.11/ 503/3.32. Colour reaction with sulphuric acid, green.

2-(2,5-Diacetoxy-4-methoxyphenyl)-1,4-diacetoxynaphthalene. Needles from acetic acid. M.p. 160 – 161° (HOAc). (Found: C 64.5; H 4.7. Calc. for $C_{25}H_{22}O_9$: C 64.4; H 4.8).

2-(2,4,5-Trimethoxyphenyl)-1,4-dimethoxynaphthalene was obtained from the quinone *11* by reduction with sodium dithionite in methanol. After filtering, the phenol solution was treated directly with dimethyl sulphate and alkali. M.p. 99 – 101° (ethanol). (Found: C 70.6; H 6.2. Calc. for $C_{21}H_{22}O_5$: C 71.3; H 6.3).

5,8-Diacetoxy-9-methoxybenzo[b]naphtho[2,1-d]furan (*13*, OAc instead of OH). Naphthoquinone (7.9 g) and methoxyhydroquinone (10.5 g) were refluxed in acetic acid/sulphuric acid, worked up and acetylated as described above. Three products were obtained: (a) A diacetate in low yield [*m/e* = 504 (M+·). Calc. for $C_{34}H_{26}O_{13}$: Mw = 504] probably corresponding to the acetate of compound *7*. (b) A tetraacetate in low yield [*m/e* = 586 (M+·). Calc. for $C_{32}H_{26}O_{11}$: Mw = 586) corresponding to the methoxyhydroquinone analogue of compound *8*. (c) The diacetate of compound *13* (5.0 g, 28 %). Needles m.p. 178 – 179° (HOAc). (Found: C 69.1; H 4.4. Calc. for $C_{21}H_{16}O_6$: C 69.2; H 4.4. Mw = 364). MS, *m/e* = 364 (M+·); 322; 280 (base peak); 265.

5,8-Dihydroxy-9-methoxybenzonaphthofuran (*13*) was obtained from the acetate. M.p. 226–227°. (Found: C 72.8; H 4.3. Calc. for $C_{17}H_{12}O_4$: C 72.8; H 4.3. Mw = 280). MS, *m/e* = 280 (M+·, base peak); 265.

5,8,9-Trimethoxybenzonaphthofuran (*13*, OMe instead of OH) was obtained from the phenol *13*. M.p. 142–143° (EtOH). (Found: C 74.2; H 5.3. Calc. for $C_{21}H_{16}O_6$: C 74.0; H 5.2). NMR ($CDCl_3$), δ (ppm) = 3.81, 3.84, and 3.86 (9 H, 3 $-OCH_3$ groups); 6.82 (H_7 or H_{10}, singlet); 6.93 (H_{10} or H_7, singlet); 7.02 (H_6, singlet); 7.30–7.60 (H_2 and H_3); 8.05–8.30 (H_1 and H_4).

Dimethoxydibenzotetraphenylenotetrafuran (*14* or isomer). The quinone *11* (1.0 g) was dissolved in a benzenesulphonic acid melt at 60°. From the intensely green solution a product soon precipitated. After 10 min ethanol was added and the solid collected by centrifugation. After washing with ethanol and pyridine the product (0.4 g, 40 %) was sublimed (400°/0.01 mm) to give a slightly yellow product, no m.p. below 360°. (Found: C 78.6; H 3.2. Calc. for $C_{34}H_{16}O_6$: C 78.5; H 3.1. Mw = 520). MS, *m/e* = 520 (M+·, base peak); 505; 490; 260.0 (M^{2+}); 252.5; 245. This compound exhibits a greenish yellow fluorescence in UV light.

2-(4-Methoxybenzoquinonyl)-1,4-naphthoquinone (*15*). 2-(2,5-Dihydroxy-4-methoxyphenyl)-1,4-naphthoquinone and 2-(2,4,5-trimethoxyphenyl)-1,4-naphthoquinone were treated with conc. nitric acid. As soon as the reaction mixtures turned yellow, water was added. The products were recrystallized from Ac_2O. Yellow needles charring at 326–330°. The IR and MS of the two products were identical. The substance could be sublimed under reduced pressure. (Found: C 69.2; H 3.4. Calc. for $C_{17}H_{10}O_5$: C 69.4; H 3.4. Mw = 294). MS, *m/e* = 294 (M+·, base peak).

2-(2,4,5-Trimethoxyphenyl)-1,4-naphthoquinone (*11*, OMe instead of OH). Naphthoquinone (3.2 g) in acetic acid (15 ml) was mixed with a solution of hydroxyhydroquinone trimethyl ether (1.7 g) in acetic acid (5 ml) and sulphuric acid (2 M in H_2O, 10 ml) was added. After 8 h the product was collected. Yield: 90 %. Blue dimorphous needles from ethanol. M.p. 168–169° and 183–184°. (Found: C 70.0; H 4.9. Calc. for $C_{19}H_{14}O_4$: C 70.3; H 5.0.) UV (ethanol), λ_{max} (nm)/log ε = 246/4.49; 294/4.24; 468/3.18. Colour reaction with sulphuric acid, green.

2-(2,4-Dimethoxyphenyl)-1,4-naphthoquinone (*4*, OMe instead of OH). Naphthoquinone (3.2 g) and resorcinol dimethyl ether (4 ml) in acetic acid (30 ml) were treated with sulphuric acid (2 M, 1.0 ml) in water (15 ml). After 8 h the red product (1.0 g, 36 %) was collected. Recrystallization and sublimation gave bright red needles. M.p. 160–160.5°. (Found: C 73.6; H 4.8. Calc. for $C_{18}H_{14}O_4$: C 73.5; H 4.8). UV (ethanol), λ_{max} (nm)/log ε = 246/4.37; 252/4.37; 329/3.65; 425/3.45. Colour reaction with sulphuric acid, green.

Acknowledgements. I thank Professor Holger Erdtman for many interesting discussions. Some of the compounds described here were prepared by him during the early phases of this research. I am grateful to Miss Gurli Hammarberg for running the NMR spectra.

REFERENCES

1. Erdtman, H. *Proc. Roy. Soc.* **A 143** (1933) 228.
2. Erdtman, H. and Stjernström, N.-E. *Acta Chem. Scand.* **13** (1959) 653.
3. Erdtman, H. and Högberg, H. E. *Tetrahedron Letters* **1968** 3389.
4. Stjernström, N.-E. *Arkiv Kemi* **21** (1967) 73.
5. Högberg, H. E. *Acta Chem. Scand.* **26** (1972) 309.
6. Högberg, H. E. *Acta Chem. Scand.* **26** (1972) 2752.
7. Pettersson, E. and Stjernström, N.-E. *Arkiv Kemi* **21** (1963) 49.
8. Stjernström, N.-E. and Pring, B. G. *Acta Chem. Scand.* **22** (1968) 538.
9. Pummerer, R. and Huppmann, G. *Ber.* **60** (1927) 1442.
10. Blumenfeld, S. and Friedländer, P. *Ber.* **30** (1897) 2563.
11. Thomson, R. H. and Shand, A. J. *Tetrahedron* **19** (1963) 1919.
12. Badger, G. M. and Christie, B. J. *J. Chem. Soc.* **1956** 3438.
13. Clar, E. *Tetrahedron* **16** (1961) 113.

Received February 23, 1973.

ACTA CHEMICA SCANDINAVICA 27 (1973) 2567–2573

Hindered Internal Rotations in *N*-Arylthioncarbamates and *N*-Aryldithiocarbamates

A. LIDÉN and J. SANDSTRÖM

Division of Organic Chemistry, Chemical Center, University of Lund, P.O.Box 740, S-220 07 Lund 7, Sweden

The thioamide type rotation in some *p*-substituted *N*-arylthion- and *N*-aryldithiocarbamates has been studied by monitoring the temperature-dependent ^{1}H-NMR spectra of the aryl and alkoxy (alkylthio) protons. The evaluation of the rate constants was carried out by approximate methods, the validity of which for the aromatic protons was checked by calculations with the density matrix program DNMR 3. The *N*-aryl groups are barrier-lowering compared to methyl groups. The identification of the spectra of *Z* and *E* isomers was made on the basis of the expected effects of the anisotropy of the thiocarbonyl group.

The comparatively high barriers to rotation of the amino group in amides and thioamides, which have been extensively studied by NMR lineshape methods,[1] are ascribed to an electronic interaction between the nitrogen lone pair and the carbonyl (thiocarbonyl) group, which stabilizes the initial state but is absent in the transition state of the rotation. Substituents that interfere with this interaction also affect the barrier. Thus, substituents with double bonds [2] or hetero atoms with lone pairs [3,4] attached to the (thio)amide carbon atom lower the barrier, because they conjugate with the (thio)carbonyl group. As discussed in Ref. 3, the main reason for the lowering of the barrier is that the substituents interact more strongly with the (thio)carbonyl group in the transition state than in the initial state, where a competing cross-conjugation with the amino group is operative.

A similar effect should be expected when a substituent with double bonds or an aromatic ring is attached to the nitrogen atom. Gehring *et al.*[5] reported a considerable lowering in barrier on going from *N*,*N*-dialkylamides to *N*-alkyl-*N*-vinylamides. However, the great differences in E_a (6.2 – 14.3 kcal/mol for formamides, 6.2 – 8.7 kcal/mol for acetamides) are probably mostly due to the method of evaluation. The line-separation method [6] was used, and the log *A* values vary from 11.4 to 17.4. However, when the $\Delta G^{\ddagger}$ values at coalescence are calculated from the given coalescence temperatures and non-exchanging

chemical shifts ($\Delta\nu_0$), smaller but probably more significant differences in the expected direction are obtained (*ca.* 1.5 kcal/mol for both formamides and acetamides).

A study of the effect of an *N*-aryl group is rendered difficult by steric factors. In *N*-alkylanilides [7] and in *ortho*-substituted anilides [8] the aromatic ring is perpendicular to the amide plane, and in *N*-unsubstituted anilides without *ortho* substituents the *E*/*Z* ratio is often unfavourable for NMR lineshape studies.[9] Carter [10] has measured the amide type rotational barriers by NMR technique in a series of para-substituted formanilides with an *E*/*Z* ratio close to unity, and he has found $\Delta G^{\ddagger}$ values at the coalescence temperature in the range 17.7 – 18.3 kcal/mol. These barriers are not much different from that reported for formamide, 17.8 kcal/mol.[11]

However, it should be noted that the effect of the vinyl group in the *N*-vinylamides [5] is compared to that of a methyl group, whereas the effect of an aryl group is compared to that of a hydrogen atom. Since *N*-methyl groups in amides are barrier-increasing relative to hydrogen, the aryl group, like the vinyl group, is barrier-decreasing relative to a methyl group. The choice of reference barriers will be further discussed in connection with the results of the present investigation.

The small effect of *N*-aryl substitution in formamide cannot be due to a nearly perpendicular arrangement of the aromatic ring and the amide group, since the angle between these two planes in crystalline acetanilide is 17.6°[12,13] and there is no reason to expect a larger angle in formanilide.

The present work was undertaken because some *para*-substituted thioanilides with favourable *E*/*Z* ratios became available (Ia – e), and the temperature-dependence of the aromatic proton NMR signals provided an extra opportunity to measure the barriers. It was anticipated that the results would give information on the effect of *N*-aryl substitution in thioamides.

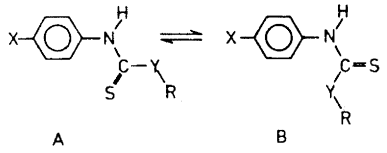

A B

I

a. X = $(CH_3)_2N$, Y = S, R = CH_3.
b. X = $(CH_3)_2N$, Y = O, R = CH_3.
c. X = $(CH_3)_2N$, Y = O, R = C_2H_5.
d. X = $(CH_3)_2N$, Y = O, R = i-C_3H_7.
e. X = CH_3O, Y = S, R = CH_3.

EXPERIMENTAL

Preparative part. The preparation of Ia has been described previously,[14] and Ie was prepared as described in Ref. 15.

Methyl p-*dimethylaminophenylthioncarbamate (Ib).* Methyl chlorothionformate [16] (0.04 mol) was added dropwise with stirring and external cooling to a solution of *N*,*N*-dimethyl-*p*-phenylenediamine (0.04 mol) in dry acetone (50 ml). The solution was left overnight at +5°, and the resulting pale yellow crystals (hydrochloride of Ib) were filtered off and treated with sodium bicarbonate solution to give colourless crystals (2.61

g, 31 % yield), m.p. 137 – 138° after recrystallization from chloroform-ligroin (b.p. 80 – 100°). (Found: C 57.1; H 6.92; N 13.2; S 15.3. $C_{10}H_{14}N_2OS$ (210.30) requires C 57.1; H 6.71; N 13.3; S 15.3).

Ethyl p-*dimethylaminophenylthioncarbamate (Ic)* was prepared in an analogous fashion. However, ethyl chlorothionformate could not be prepared as described in Ref. 16. Instead, the preparation of Ic was performed as follows. Sodium ethoxide (0.05 mol) in absolute ethanol was added dropwise with stirring to a solution of thiophosgene (0.05 mol) in absolute ethanol (3 ml) under nitrogen with external cooling to −20°. The mixture was allowed to warm to room temperature, and the precipitated sodium chloride was removed by filtration. *N,N*-Dimethyl-*p*-phenylenediamine (0.05 mol) in absolute ethanol (50 ml) was added dropwise with stirring under nitrogen.

On the following day the ethanol was removed by evaporation, and the residue was brought to crystallization by trituration with acetone. The product (hydrochloride of Ic) was dissolved in water, and addition of sodium acetate precipitated colourless prisms (4.5 g, 40 % yield), m.p. 100 – 101° after recrystallization from toluene-ligroin (b.p. 80 – 100°). (Found: C 59.3; H 7.36; N 12.5; S 14.4. $C_{11}H_{16}N_2O_5$ (224.33) requires C 58.9; H 7.19; N 12.5; S 14.3).

2-Propyl p-*dimethylaminophenylthioncarbamate (Id)*. *p*-Dimethylaminophenyl isothiocyanate [17] (0.02 mol) in hexamethylphosphoric triamide (HMPT, 100 ml) was added dropwise with stirring and cooling to −10° to a solution of sodium 2-propoxide (0.02 mol) in 2-propanol (200 ml). The mixture was left overnight at −20° and then poured onto ice. After extraction with chloroform and washing of the chloroform solution with dilute hydrochloric acid, bicarbonate solution, and water, some HMPT still remained. This was removed by evaporation, dissolution of the residue in benzene, and repeated extractions with water. Evaporation of the benzene solution gave a pale brown crystalline residue (0.29 g, 6 % yield), which crystallized from toluene-ligroin (b.p. 80 – 100°) as colourless prisms, m.p. 105 – 106°. (Found: C 60.1; H 7.69; N 11.7; S 13.5. $C_{12}H_{18}N_2OS$ (238.35) requires C 60.5; H 7.61; N 11.8; S 13.5).

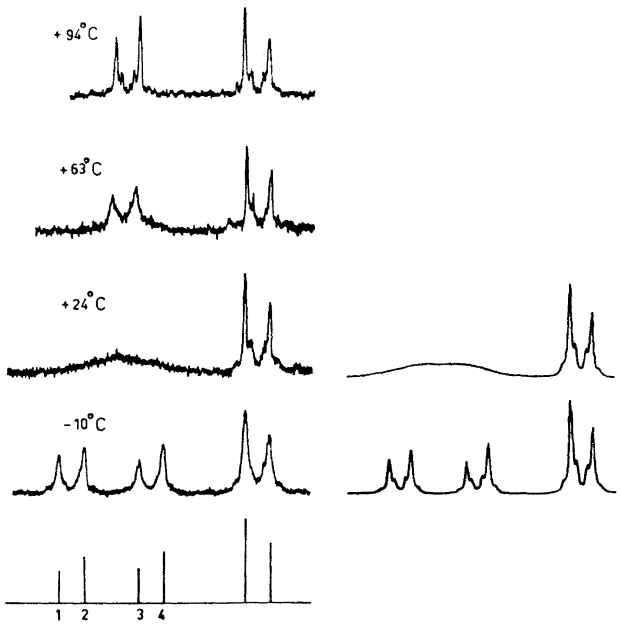

Fig. 1. Experimental and calculated spectra of the aromatic protons of Ia (in pyridine-d_5).

NMR spectra and evaluation of rate constants. The spectra were recorded on Varian Models A-60 and XL-100 NMR spectrometers equipped with variable temperature probes and V-6040 temperature controllers. The temperatures were measured from the internal chemical shifts of capillaries filled with methanol (low temperature) or ethylene glycol (high temperature) and placed concentrically in the sample tubes. The capillaries were calibrated with a copper-constantan thermocouple as previously described.[18] The samples were measured in 0.5 M solutions.

The evaluation of the rate constants from the lineshape of the *S*- and *O*-methyl proton signals was carried out by the approximate method developed by Shanan-Atidi and Bar-Eli [19] for uncoupled two-site cases with unequal populations. In Ic the ethyl methylene proton signals were observed with simultaneous decoupling of the methyl protons.

In the evaluation of the rate constants from the aromatic proton signals, the latter were treated as two AB spectra with different populations in the slow exchange limit, which change to one AB spectrum in the fast exchange limit. The chemical shift differences between the protons *meta* to the thiocarbamoyl group in the *E* and *Z* forms is quite small, and therefore the exchange has been treated as one between site 1 and site 3 and between site 2 and site 4 (Fig. 1). To check the validity of this approximation, the lineshape of the AA'BB' $\rightleftharpoons$ CC'DD' exchange system in Ia was calculated by the density matrix method (program DNMR 3).[20] The rate constant used was that found by the approximate method at coalescence; the chemical shifts (ν_A to ν_D) and the population ratio were obtained from the low temperature spectrum, and the appropriate coupling constants ($J_{ortho} = 8.0$ Hz, $J_{meta} = 2.5$ Hz, $J_{para} = 0.5$ Hz,) were taken from the literature.[21] As can be seen in Fig. 1, the agreement between the calculated and the experimental lineshapes is quite satisfactory, and the approximate method can be regarded as reliable. The rate constants and $\Delta G^{\ddagger}$ and $\Delta\nu_0$ values are summarized in Table 1.

Table 1.

Compound	Solvent	p_A[a]	$\Delta\nu_0$ Hz	T_c K	$\Delta G^{\ddagger}_{B\rightarrow A}$ kcal/mol	Frequency MHz	^{1}H signals observed
Ia	Pyridine-d_5	0.48	29.5	297	15.0	60	Aromatic
Ia	$CDCl_3$	0.14	11.4	267	14.8	100	*S*-Methyl
Ib	Pyridine-d_5	0.44	24.9	314	16.1	60	Aromatic
Ib	$CDCl_3$	0.25	3.5	288	16.3	60	*O*-Methyl
Ic	Pyridine-d_5	0.46	23.1	316	16.2	60	Aromatic
Ic	Pyridine-d_5	0.46	7.5	307	16.3	100	*O*-Methylene
Id	Pyridine-d_5	0.41	23.5	319	16.5	60	Aromatic
Ie	Pyridine-d_5	0.67	26.5	288	14.9	60	Aromatic
Ie	$CDCl_3$	0.10	10.8	256	14.4	100	*S*-Methyl

[a] Mol fraction of form A.

RESULTS AND DISCUSSION

A possible set of reference compounds for I is the corresponding *N*-methylthion- and dithiocarbamates (II), in which case the effect of the aryl group is compared with that of a methyl group. Whereas the barriers for II are still unknown, those for the corresponding *N*,*N*-dimethylthioamides (III) are 17.7 and 15.6 kcal/mol, respectively [3] (in *ortho*-dichlorobenzene). The difference between IIa and IIIa, and between IIb and IIIb, may be estimated by a comparison with the pair *N*-methylthioacetamide and *N*,*N*-dimethylthioacetamide. The first of these compounds has been extensively studied by Walter and Schaumann.[22] These authors could separate the *E* and *Z* forms

II III

IIa, IIIa. Y = O.
IIb, IIIb. Y = S.

by TLC and follow their isomerization by IR and UV spectroscopy. In chloroform solution a UV-kinetic investigation gave $\Delta G^{\ddagger}_{E\rightarrow Z} = 21.2$ kcal/mol, $\Delta G^{\ddagger}_{Z\rightarrow E} = 23.4$ kcal/mol. A complicating factor in this comparison is the relatively larger stabilization of the *Z* forms. This is found also in amides [23] and esters,[24] and a recent *ab initio* calculation on methyl formate indicates that it is due to electrostatic attraction between the oxygen and the methyl hydrogen atoms.[25] On the other hand, the *E* form of *N*-methylthioacetamide is destabilized by about 1 kcal/mol by a repulsive interaction between the methyl groups.[26] A similar repulsion must be expected in the *Z* form of IIb, since the van der Waals radii of methyl and sulphur are rather similar, and a somewhat smaller repulsion is expected in the *E* form of IIa.* For *N*,*N*-dimethylthioacetamide $\Delta G^{\ddagger}$ values of 21.6 [3] and 21.8 kcal/mol [28] have been reported, both in *ortho*-dichlorobenzene. Roughly, the difference between the $\Delta G^{\ddagger}$ values for *N*,*N*-dimethylthioacetamide and the *E* form of *N*-mehylthioacetamide, 0.4 – 0.6 kcal/mol, can be used as a correction from compounds III to the corresponding compounds II, *i.e.* $\Delta G^{\ddagger}_{E\rightarrow Z}$ should be 17.2 ± 0.1 and 15.1 ± 0.1 kcal/mol for IIa and IIb, respectively. The real deviations may of course be somewhat larger than ± 0.1 kcal/mol.

An inspection of the $\Delta G^{\ddagger}$ values in Table 1 reveals in most cases slightly higher values in pyridine-d_5 than in deuteriochloroform solution. This is at variance with the behavior of the *N*,*N*-dimethyl-*N'*-arylthioureas, where the barriers to rotation of the dimethylamino group were found to be *ca.* 1 kcal/mol lower in pyridine than in deuteriochloroform.[18] The solvent effect in the latter example was explained by hydrogen bonding between NH protons and pyridine nitrogen atoms, which should lead to a strengthening of the (Ar)N – C = S interaction in competition with the $(CH_3)_2$N – C = S interaction. The same mechanism can evidently account for the solvent effect in the present work, since the rotation observed is around the (Ar)N – C = S bond.

Comparison of the $\Delta G^{\ddagger}$ values in deuteriochloroform in Table 1 with the assumed values for IIa and IIb shows a small barrier-lowering effect (*ca.* 0.3 kcal/mol) of the *p*-dimethylaminophenyl group in the dithiocarbamates, and a somewhat larger effect of the *p*-methoxyphenyl group, as expected from the electron-donating effects of the dimethylamino and methoxy groups. The barrier-lowering effect of the *p*-dimethylamino group is larger (*ca.* 0.9 kcal/mol) in the thioncarbamate series.

* The *E*–*Z* nomenclature [27] is slightly confusing in systems I and II, since the *Z* form when Y = O is the *E* form when Y = S. Therefore, the symbols A and B are used for I in the present work.

Surprisingly, the effect of increasing the size of the group R (Ib – Id) is an increased stabilization of form B. (For assignments of forms A and B, *vide infra.)* No explanation for this effect can be offered at present.

It has been found in several anilides and thioanilides that the aromatic protons *ortho* to the anilide nitrogen atom are considerably more deshielded in the *Z* (A) form than in the *E* (B) form, due to the anisotropy of the carbonyl or thiocarbonyl group.[29] In the present case, therefore, the group of aromatic proton signals found at lowest field is assigned to the *ortho* protons in form A. With the approximation that the aromatic proton spin systems in the slow exchange limit can be treated as two AB spectra, the effect of the anisotropy of the thiocarbonyl group can be measured by the difference, Δ, between the internal chemical shifts $|\nu_A - \nu_B|$ for the A and B forms. The pertinent data are recorded in Table 2. It is apparent that the Δ values are much smaller for

Table 2. Internal chemical shifts and shift differences (at 60 MHz) for I, forms A and B.

Compound	Solvent	$\lvert\nu_A - \nu_B\rvert$ Hz[a] A	B	Δ^b Hz
Ia	Pyridine-d_5	69.2	39.0	30.2
Ia	$CDCl_3$	38.8	29.0	9.8
Ib	Pyridine-d_5	63.4	38.4	25.0
Ib	$CDCl_3$	38.4	27.8	10.6
Ic	Pyridine-d_5	64.2	42.6	21.6
Id	Pyridine-d_5	63.8	41.8	22.0
Ie	Pyridine-d_5	52.2	24.4	27.8
Ie	$CDCl_3$	29.8	19.7	10.1

[a] Note that A and B here are the common NMR symbols. [b] $\Delta = |\nu_A - \nu_B|_A - |\nu_A - \nu_B|_B$ ($c = 0.5$).

deuteriochloroform than for pyridine-d_5 solution. This may be due to the orientation of solvating pyridine molecules by the molecular electric dipole moment (ASIS effect [30]). In A, the negative end of the dipole is close to the *ortho* hydrogen atoms, and consequently a solvating pyridine molecule should preferentially shield the *meta* protons. In form B the negative end of the dipole is directed away from the aromatic ring, and shielding of the *ortho* protons becomes possible. The effect of hydrogen bonded pyridine molecules should to a first approximation be the same in forms A and B.

The Δ values observed in deuteriochloroform solution are less than half of the values observed for *N*,*N*-dimethyl-*N'*-arylthioureas,[18] and also for formanilides.[10] For *p*-nitrothioformanilide in acetone solution Rae [31] has observed a Δ value of 39 Hz. The lower values in the compounds studied here must reflect a difference in the anisotropy of the thiocarbonyl group.

Since it was found that the aryl groups in I are barrier-lowering compared to a methyl group, it was of interest to perform a similar comparison for the formanilides discussed in Ref. 10. For these, the reference is the $E \rightarrow Z$ barrier in *N*-methylformamide, 18.0 kcal/mol in 1,2-dichloroethane.[32] Evidently, the aryl groups are not significantly barrier-lowering compared to a methyl group

in the formanilides. The *p*-methoxyphenyl and *p*-dimethylaminophenyl groups are even slightly barrier-raising. A possible explanation for the difference between the formanilides and compounds I may be that the thiocarbonyl group is more polarizable in both directions by substituents on the nitrogen atom than the carbonyl group.

Acknowledgement. We are grateful to *the Swedish Natural Science Research Council* for financial support.

REFERENCES

1. Stewart, W. E. and Siddall III, T. H. *Chem. Rev.* **70** (1970) 517.
2. Rogers, M. T. and Woodbrey, J. C. *J. Phys. Chem.* **66** (1962) 540.
3. Sandström, J. *J. Phys. Chem.* **71** (1967) 2318.
4. Brown, B. T. and Katekar, G. F. *Tetrahedron Letters* **1969** 2343.
5. Gehring, D. G., Mosher, W. A. and Reddy, G. S. *J. Org. Chem.* **31** (1966) 3436.
6. Gutowsky, H. S. and Holm, C. H. *J. Chem. Phys.* **25** (1956) 1228.
7. Pedersen, B. F. *Acta Chem. Scand.* **21** (1967) 1415.
8. Siddall III, T. H. *J. Phys. Chem.* **70** (1966) 2249.
9. Kessler, H. and Rieker, A. *Ann.* **708** (1967) 57.
10. Carter, R. E. *Acta Chem. Scand.* **22** (1968) 2643.
11. Drakenberg, T. and Forsén, S. *J. Phys. Chem.* **74** (1970) 1.
12. Brown, C. J. and Corbridge, D. E. C. *Acta Cryst.* **7** (1954) 711.
13. Brown, C. J. *Acta Cryst.* **21** (1966) 442.
14. Lidén, A. and Sandström, J. *Tetrahedron* **27** (1971) 2893.
15. Burrows, A. A. and Hunter, L. *J. Chem. Soc.* **1952** 4118.
16. Delépine, M. M. *Bull. Soc. Chim. France* [4] **9** (1911) 901.
17. Dyson, G. M., George, H. J. and Hunter, R. F. *J. Chem. Soc.* **1927** 436.
18. Isaksson, G. and Sandström, J. *Acta Chem. Scand.* **24** (1970) 2565.
19. Shanan-Atidi, H. and Bar-Eli, K. H. *J. Phys. Chem.* **74** (1970) 961.
20. Kleier, D. A. and Binsch, G. J. *J. Magn. Resonance* **3** (1970) 146.
21. Martin, J. and Dailey, B. P. *J. Chem. Phys.* **37** (1962) 2594.
22. Walter, W. and Schaumann, E. *Chem. Ber.* **104** (1971) 3361.
23. La Planche, L. A. and Rogers, M. T. *J. Am. Chem. Soc.* **86** (1964) 337.
24. Miyazawa, T. *Bull. Chem. Soc. Japan* **34** (1961) 691.
25. Wennerström, H., Forsén, S. and Roos, B. *J. Phys. Chem.* **76** (1972) 2430.
26. Sandström, J. and Uppström, B. *Acta Chem. Scand.* **21** (1967) 2254.
27. Blackwood, J. E., Gladys, C. L., Loening, K. L., Petrarca, A. E. and Rush, J. E. *J. Am. Chem. Soc.* **90** (1968) 509.
28. Siddall III, T. H., Stewart, W. E. and Knight, F. D. *J. Phys. Chem.* **74** (1970) 3580.
29. Brown, R. F. C., Radom, L., Sternhell, S. and Rae, I. D. *Can. J. Chem.* **46** (1968) 2577; See also Ref. 1, p. 518 ff.
30. Laszlo, P. *Progr. Nucl. Magn. Resonance Spectrosc.* **3** (1967) 231.
31. Rae, I. D. *Personal communication.*
32. Drakenberg, T. and Forsén, S. *Chem. Commun.* **1971** 1404.

Received April 11, 1973.

ACTA CHEMICA SCANDINAVICA 27 (1973) 2574–2580

Synthesis of Methyl 17-(3,5-Dibromo-4-methoxyphenyl)-heptadeca-2,4,6,8,10,12,14,16-octaenoate

A. G. ANDREWES

Organic Chemistry Laboratories, Norwegian Institute of Technology, University of Trondheim, Trondheim, Norway

The synthesis of methyl 17-(3,5-dibromo-4-methoxyphenyl)-heptadeca-2,4,6,8,10,12,14,16-octaenoate (*10*) is reported. The pertinent physical data associated with this type of structure is given and includes electronic absorption, infrared and mass spectra.

The intermediates, some of which are new compounds, have been fully characterized.

In the course of the investigations on the pigments of the phytopathogenic bacterium *Xanthomonas juglandis*,[1] one of the structures considered for the main pigment was a conjugated aryl octaene methyl ester in which the aromatic ring was substituted by two bromine atoms and one methoxy group. The substitution pattern on the phenyl ring was not known with certainty but IR data suggested the presence of isolated hydrogens on the ring. From biosynthetic considerations a 3,5-dibromo-4-methoxy substitution pattern was considered plausible. The various physical properties associated with this type of structure could not, on the basis of the available literature, be precisely predicted and necessitated total synthesis in order to compare physical and chemical properties. The synthesis was so designed that alternative substitution patterns on the ring could be achieved with only slight changes in the general scheme. Of particular importance is the intermediate phosphonium salt *8* from which a number of aromatic polyenes can be constructed *via* a one step reaction.

RESULTS AND DISCUSSION

Pent-2-en-4-yn-1-ol (*1*) was coupled in a Glaser [2] reaction to give the acetylenic C_{10}-diol *2*, Scheme 1. Attempts to hydrogenate *2* to the corresponding tetraene with Lindlar [3] catalyst met with difficulty, but after MnO_2 oxidation to the dial *3* selective hydrogenation to the dial *4* proceeded smoothly. The conjugated system of *4* was extended by a Wittig reaction with the triphenylphosphonium salt of methyl sorbate (*5*) to give the heptaene *6*. Selective

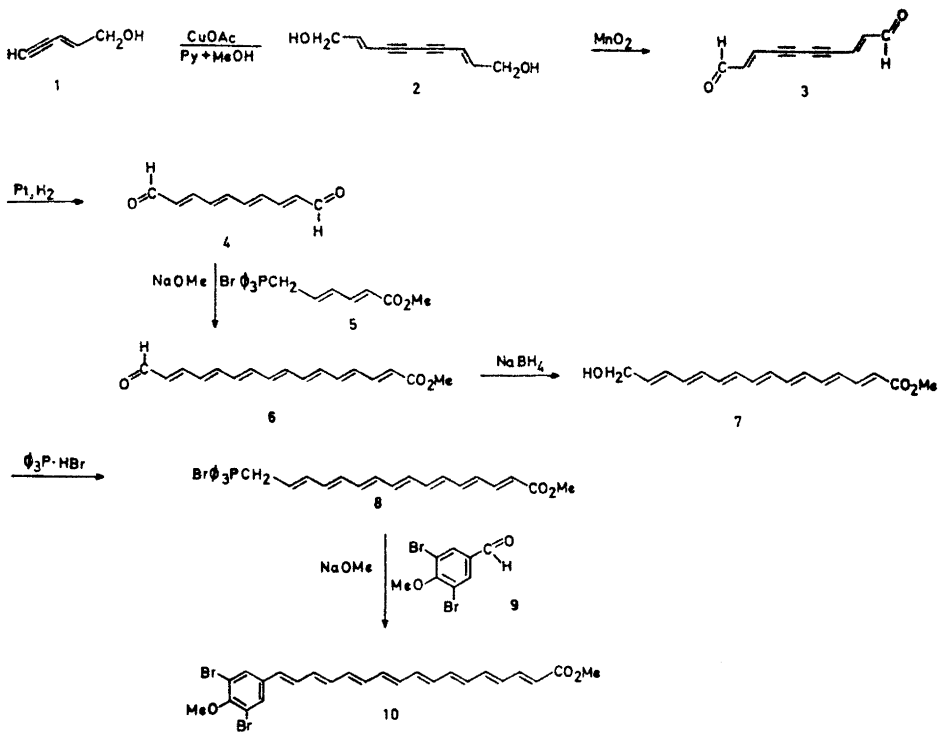

Scheme 1.

reduction of the aldehyde function with sodium borohydride gave *7* which was converted to the phosphonium salt *8*. Finally, condensation of the phosphoran of *8* with the aromatic aldehyde *9* gave the desired product *10*.

10 melted at 245 – 247°. The *trans*-isomer was extremely insoluble in all common organic solvents and as a result no PMR spectrum was obtained. The same solubility property was noted for dimethylcortisalin (*11*) and *Xanthomonas* pigment *1* (*12*).[1,4]

Synthetic *10* could not be separated from *Xanthomonas 1* (*12*) when chromatographed on silica gel G plates or kieselguhr paper.

The visible absorption spectrum of *10* had λ_{max} 429, 450, and 478 nm in chloroform and 430, 455, and 483.5 nm in pyridine (Fig. 2). Compared to the pigments isolated from *Xanthomonas juglandis*,[1] which have similar proposed structures, the visible spectrum of *10* was hypsochromically displaced by 3 nm in chloroform and showed slightly more fine-structure. These small differences may reflect a difference in the substitution pattern on the phenyl rings. Compared to dimethylcortisalin (*11*),[1,4] which has a chromophore one double bond shorter (Fig. 1), the visible spectrum of *10* displayed much more fine-structure. Some of the increase in fine-structure can be accounted for by the extended chromophore of *10 vs. 11*.[5] However, it is also possible that

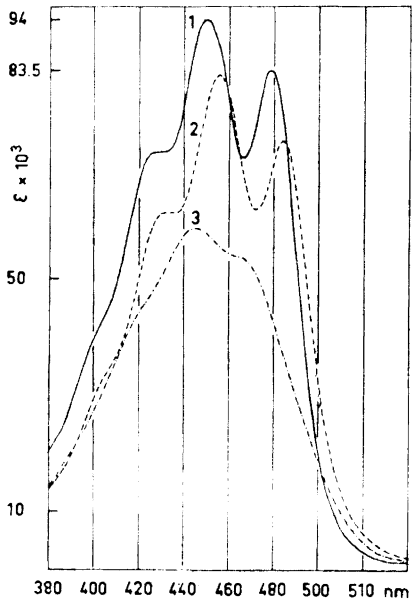

Fig. 1. Absorption spectra in visible light of *10* in $CHCl_3$ (curve 1), *10* in pyridine (curve 2) and *12* in pyridine (curve 3). Extinction values valid only for *10* in $CHCl_3$.

the bromine substituents on the phenyl ring of *10* may influence the fine-structure.

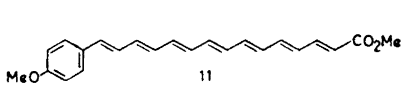

11

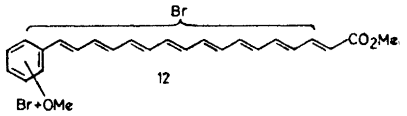

12

The IR-spectrum of *10* is given in Fig. 2. Bands at 1710 and 1010 cm^{-1} assigned to α,β-unsaturated ester [6] and C–H out of plane vibrations of *trans*-disubstituted double bounds are consistent with the same assignments made

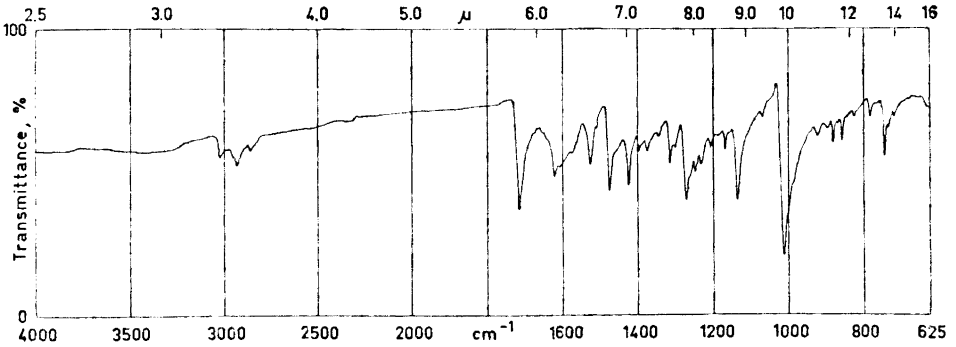

Fig. 2. Infrared spectrum (KBr) of *10*.

for dimethylcortisalin (*11*) and the pigments isolated from *Xanthomonas juglandis*.[1] The latter band, as previously noted,[1] is shifted to higher frequencies than those associated with conjugated polyenes of the carotenoid type. A band at 1265 cm^{-1} is attributed to a phenolic methoxy group [6] and absorption at 1138 cm^{-1} assigned to the C–O ester stretch.[6] Corresponding assignments have been made for bands noted in the spectra of *11* and Xanthomonas pigment *1*.[1] Absorption arising from C–H out of plane deformations on an aromatic ring occurred at 880 and 855 cm^{-1} in the spectrum of *10*. No bands occurred at 1395 or 1450 cm^{-1} at which positions strong absorption was found in the spectrum of *Xanthomonas* pigment *1* (*12*).[1]

Of particular interest was the mass spectrometric fragmentation pattern for *10* (Fig. 3). Loss of C_6H_6 from the molecular ion probably reflects the thermal

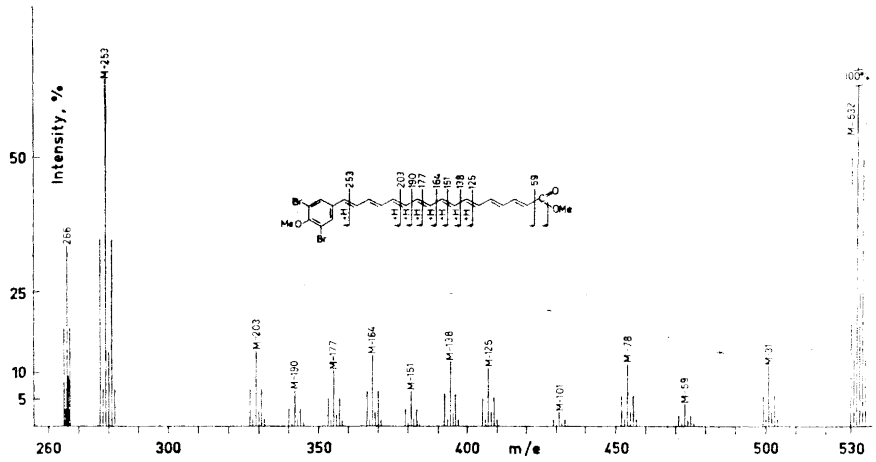

Fig. 3. Mass spectrum of *10*.

expulsion (no metastable ion) of benzene easily envisioned after *trans-cis*-isomerization of the polyene chain, *cf.* Ref. 7. There was no observable loss of HBr or bromine radical from the molecular ion or any fragment ion in the upper region of the spectrum. All prominent ions in the upper mass region were associated with fragmentation of the polyene chain or from the ester function. The fragmentation of *10* is then different from that observed for the Xanthomonas pigment *1* (*12*),[1] which shows a strong ion attributed to loss of HBr from the molecular ion.

In conclusion, comparison of the physical properties of synthetic *10* with pigment *1* isolated from *Xanthomonas juglandis* clearly showed that they are not identical. The difference in structures of *10* and *Xanthomonas* pigment *1* (*12*) probably lies in the substitution pattern on the aromatic ring.

EXPERIMENTAL

General. Solvents were either of analytical grade or distilled before use. All of the reactions involving polyenes were carried out under a blanket of nitrogen and in dim light.

Comparative chromatography was carried out on silica gel HF_{254} plates developed with mixtures of petroleum ether and acetone or Schleicher & Schüll paper No. 287 (kieselguhr paper) developed with benzene.

Melting points were determined on an Electrothermal Melting Point Apparatus in sealed evacuated tubes and are uncorrected.

Electronic absorption spectra were recorded on a Coleman Hitachi 124 Spectrometer. IR spectra were obtained from KBr disks or liquid films on a Perkin Elmer 257 instrument and PMR spectra were generally recorded in $CDCl_3$ solutions in a Variant A-60 A instrument. Mass spectra were registered with an AEI MS902 instrument at 70 eV.

Deca-2,8-diene-4,6-diyne-1,10-diol (*2*). Pent-2-en-4-yn-1-ol (15 g) was slowly added over a period of 30 min to a stirred solution of copper(I) acetate (30 g) in pyridine-MeOH (300 ml, 1:1).[8] The mixture was stirred for an additional 2 h after which water was added and the solution extracted with ether. After drying over Na_2SO_4 the organic solvents were removed under vacuum leaving a solid which was recrystallized from methanol and yielded a total of 9.75 g (65 %) of *2*. The diol *2* was kept in the dark under nitrogen since when exposed to light and air *2* rapidly turned dark brown. *2*[8,9] had an m.p. of 160 – 161°, λ_{max} (methanol) 312, 292, 275, and 260 nm; ν_{max} (KBr) 3300 broad (OH), 2120 (C≡C), 1630 (C=C), 1090 (C–O), 950 (CH=CH) and 900 cm^{-1}; τ (deuterated acetone) 7.02 (2 H, O*H*), 5.80 dd (4 H, $J_{1,2}$ = 4 Hz, $J_{1,3}$ = 1.5 Hz, CH_2OH), 4.15 dt (2 H, unresolvable, H-3), 6.5 dt (2 H, $J_{2,3}$ = 16 Hz, $J_{1,2}$ = 4Hz, H-2); *m/e* 162 (M), 144(M – 18), 133(M – 29), 121(M – 41) and 115(M – 18 – 29).

Deca-2,8-diene-4,6-diyne-1,10-dial (3). *2* (9 g) in acetone (50 ml) was cooled to 5° and treated with MnO_2 (4 g) at that temperature with stirring for 1 h. The reaction was monitored by TLC and additional MnO_2 was added as required allowing 1 h between the additions of MnO_2. When the chromatogram showed no starting material, the mixture was filtered and the solvent removed under vacuum. The resulting solid was recrystallized from CH_2Cl_2-acetone solution to give 6.3 g (70 %) of dial *3*; m.p. 144°;[10] λ_{max} (ether) 346, 323, 302, and 277 nm; ν_{max} (KBr) 3000 (=CH), 2118 (C≡C), 1675 (conj. C=O), 1115 (C–O), 2850 (C–H) and 970 (HC=CH) cm^{-1}; τ($CDCl_3$) 3.40 – 3.32 (4 H, olefinic), 0.35 d, 0.43 d (J_{H-H} = 5 Hz, equal quantities of *cis-* and *trans*-isomers, aldehydic H); *m/e* 158 (M), 129(M – 29) and 102(M – 56).

Deca-2,4,6,8-tetraene-1,10-dial (4). *3* (5 g) in 50 ml of acetone-ethyl acetate (1:1) and Lindlar catalyst (0.5 g) was hydrogenated at room temperature in the dark. After the calculated uptake of hydrogen the solution was filtered and the solvent evaporated. The brownish semisolid was dissolved in $CHCl_3$, a trace of I_2 added and the solution refluxed for 2 h to effect isomerization to the *trans*-isomer.[11] After evaporating the solution to dryness the product was crystallized from acetone-CH_2Cl_2 solution to give 2.25 g (45 %) of *4*; m.p. 134°; λ_{max} (methanol) 339, 352, (ethyl ether) 320, 335, 352 nm; ν_{max} (KBr) 3040 (=CH), 2820, 2740 (C–H), 1670 (C=O), 1620 (C=C), 1135 (C–O) and 975 (*trans* CH=CH) cm^{-1}; τ($CDCl_3$) 2.1 – 4.0 (8 H, olefinic, non-resolvable), 0.32 d (J = 8 Hz, aldehydic); *m/e* 162 (M), 129(M – 29) and 121(M – 49).

5-Carbomethoxy-2,4-pentadienyl-triphenylphosphonium bromide (*5*). Methyl sorbate (50 g), *N*-bromosuccinimide (70 g) and benzoyl peroxide (0.2 g) were mixed with CCl_4 (25 ml) in a 3-necked round bottom flask fitted with a condenser. The mixture was heated while stirring and the CCl_4 allowed to distill off until the temperature of the reaction mixture rose to 111°. Stirring was stopped and the reaction mixture held at 111 – 115° while the mixture turned orange in color. After 15 min a small aliquot (0.05 ml) was withdrawn which showed no activity when tested against KI in dilute H_2SO_4. The reaction mixture was cooled and worked-up in the normal manner. Double distillation gave methyl ε-bromosorbate (19 g, 15 %); b.p. 81 – 84°/0.75 Torr.[12,13]

Methyl ε-bromosorbate (10 g) and triphenylphosphine (20 g) were refluxed in benzene (50 ml) for 20 h. The salt *5* crystallized from solution as it was formed but later could not be recrystallized after a number of attempts and was used without further purification; yield 15 g (64 %); τ($CDCl_3$) 6.32 (3 H, OCH_3, 4.98 dd (2 H, J_{H-P} = 17 Hz, J_{H-H} = 8 Hz, CH_2 – 1), 4.4 – 3.6 (4 H, olefinic) and 2.4 – 2.1 (15 H, aromatic).

Methyl 16-oxo-hexadeca-2,4,6,8,10,12,14-heptaenoate (6). Sodium methoxide was slowly added to a stirred methanolic solution of *5* (3 g) under a blanket of nitrogen until the phosphonium salt was totally converted to the corresponding phosphoran. Two-fold excess of *4* (2 g) in methanol was rapidly added and the solution allowed to stir at room temperature for 1 h and then for an additional 1 h at 50 °. Water was added and the mixture extracted with $CHCl_3$, the organic phase dried over NaCl and evaporated under vacuum. The solid residue was chromatographed on an Al_2O_3 (1 % H_2O) column developed with benzene from which *6* (1 g, 58 %) was isolated; crystallized from ether *6* melted at 154°; λ_{max} ($CHCl_3$) 405, 423, 450, (ethyl ether) 392, 409, 433 and (acetone) 395, 414, 439 nm; ν_{max} (KBr) 2930 – 3020 (CH), 1720 (conj. ester), 1665 (conj. aldehyde), 1620, 1590 (C=C), 1140 (C – O) and 1010 (CH=CH) cm^{-1}; τ ($CHCl_3$) 6.23 (3 H, OCH_3), 2.9 – 4.1 (14 H, olefinic), 0.35 d (1 H, $J = 7$ Hz, aldehydic H); *m/e* 270(M), 255(M – 15), 239(M – 31) and 211(M – 59).

Methyl 16-hydroxy-hexadeca-2,4,6,8,10,12,14-heptaenoate (7). A methanolic solution of *6* (1 g) cooled to 0° was treated with $NaBH_4$ until TLC analysis showed complete conversion to the mono-ol *7*. The solution was worked up in the normal manner and *7* (0.9 g, 89 %) isolated and purified on a deactivated Al_2O_3 (2 % H_2O) column developed with benzene-5 % ether; λ_{max} (ether) 375, 389, 407, ($CHCl_3$) 380, 397, 416 nm; ν_{max} (KBr) 3260 (OH), 2960 – 3030 (CH), 1715 (conj. ester), 1620 (C=C),1335 (C – O), 1140 (C – O) and 1010 (CH=CH) cm^{-1}; τ ($CDCl_3$) 6.25 (3 H, OCH_3), 5.75 d (2 H, $J = 6$ Hz, $CH_2 - 1$), 3.0 – 4.3 (14 H, olefinic); *m/e* 272(M), 257(M – 15), 241(M – 31), 213(M – 59), and 196 (M – 78).

15-Carbomethoxypentadeca-2,4,6,8,10,12,14-heptenyl-triphenylphosphonium bromide (8). *7* (0.9 g) in $CHCl_3$ (5 ml), was stirred with triphenylphosphine hydrobromide (2.5 g) at 20° in the dark for 15 h. The solvent was evaporated and the residue triturated with ethyl ether from which the Wittig salt *8* (0.75 g, 38 %) was collected as a finely divided solid. No attempt was made to further purify the product.

3,5-Dibromo-4-methoxybenzaldehyde (9). *p*-Hydroxybenzaldehyde (15 g) was brominated according to the procedure described by Brink [14] to obtain 3,5-dibromo-4-hydroxybenzaldehyde, m.p. 182 – 183° from MeOH – H_2O; λ_{max} (MeOH) 273 nm; ν_{max} (KBr) 3140, 1665, 1595, 1570, 1550, 1300, 1230, 1040, 900 and 830 cm^{-1}; τ($CDCl_3$) 4.67 (1 H, O*H*), 1.92 (2 H, aromatic), 0.13 (1 H, aldehydic); *m/e* 278, 280, 282 (1:2:1, M). 3,5-Dibromo-4-hydroxybenzaldehyde was converted into the sodium salt and thence to the methoxy derivative *9* using the procedure described by Lindemann;[15] m.p. 85 – 87° from petroleum ether, λ_{max} (MeOH) 271 nm; ν_{max} (KBr) 1680, 1550, 1470, 1260, 1205, 1185, 980, and 875 cm^{-1}; τ ($CDCl_3$) 6.04 (3 H, OCH_3), 1.97 (2 H, aromatic), 0.15 (1 H, aldehydic); *m/e* 292, 294, 296 (1:2:1, M).

Methyl 17-(3,5-dibromo-4-methoxyphenyl)-heptadeca-2,4,6,8,10,12,14,16-octaen-1-oate (10). Sodium methoxide was slowly added to a stirred solution of *8* (200 mg) and *9* (200 mg) and the mixture allowed to stir for 1 h at 20° and then 2 h at 50°. Water was added and the solution was filtered to remove *10* some of which had precipitated. The solution was extracted with $CHCl_3$ and the extract combined with the solid product isolated from the filtration. The product was chromatographed on silica gel G from which all *trans-10* was isolated and crystallized; m.p. 245 – 247° from MeOH-$CHCl_3$. The crystalline product was slightly soluble in $CHCl_3$, CH_2Cl_2, pyridine, DMSO, and acetone; insoluble in petroleum ether, MeOH, ethyl ether, CCl_4, and dioxane. The visible absorption spectrum had λ_{max} ($CHCl_3$) 429, 450 ($\varepsilon = 94\,000$), and 478 nm ($\varepsilon = 83\,500$), (pyridine) 430, 455, and 483.5 nm; ν_{max} (KBr) 3050 – 2900 (CH), 1710 (conj. ester), 1620 (C=C), 1265 (OMe), 1038 (C – O), 1010 (HC=CH), 880 (isolated aromatic CH), 855 and 745 cm^{-1} (aromatic, CH); *m/e* 530, 532, 534 (1:2:1, M, for fragmentation pattern see structure *10*), 499, 501, 503 (M – 31), 471, 473, 475 (M – 59), 452, 454, 456 (M – 78), 405, 407, 409 (M – 125), 392, 394, 396 (M – 138), 379, 381, 383 (M – 151), 366, 368, 370 (M – 164), 353, 355, 357 (M – 177), 340, 342, 344 (M – 190), 327, 329, 331 (M – 203), 277, 279, 281 (M – 253), 265, 266, 267 (doubly charged ion).

Synthetic *10* could not be separated from *Xanthomonas 1* (*12*) when co-chromatographed on S & S kieselguhr paper developed with benzene ($R_F = 0.78$) or on silica gel G plates developed with petroleum ether-acetone, 80:20 ($R_F = 0.80$).

Acknowledgements. Dimethylcortisalin was kindly provided by Dr. J. Gripenberg, Chemistry Dept., Tekniska Högskolan, Otnäs, Finland. A post-doctoral fellowship from *The Royal Norwegian Council for Scientific and Industrial Research* is gratefully acknowledged.

REFERENCES

1. Andrewes, A. G., Hertzberg, S., Liaaen-Jensen, S. and Starr, M. *Acta Chem. Scand.* **27** (1973) 2383.
2. Eglenton, G. and McCrae, W. *Advan. Org. Chem.* **4** (1963) 225.
3. Lindlar, H. *Helv. Chim. Acta* **35** (1952) 446.
4. Gripenberg, J. *Acta Chem. Scand.* **6** (1952) 580.
5. Aasen, A. J. and Liaaen-Jensen, S. *Acta Chem. Scand.* **21** (1967) 970.
6. Bellamy, L. J. *The Infra-red Spectra of Complex Molecules*, 2nd Ed., Methuen, London 1964.
7. Vetter, W., Englert, G., Ragissi, N. and Schwieter, U. In Isler, O. *Carotenoids*, Birkhaüser, Basel 1971.
8. Weedon, B. C. L. *J. Chem. Soc.* **1954** 4168.
9. Heilbron, I., Jones, E. R. H. and Sondheimer, F. J. *J. Chem. Soc.* **1947** 1586.
10. Nakano, H. *J. Antibiot.* **14** (1961) 68.
11. Mayer, H., Montavon, M., Rüegg, R. and Isler, O. *Helv. Chim. Acta* **50** (1967) 1606.
12. Karrer, P. and Schwyzer, R. *Helv. Chim. Acta* **25** (1964) 1191.
13. Heilbron, I., Jones, E. R. H. and O'Sullivan, D. G. *J. Chem. Soc.* **1946** 866.
14. Brink, M. *Acta Univ. Lund* **2** (1965) 3.
15. Lindemann, H. *Ann.* **431** (1923) 284.

Received February 26, 1973.

ACTA CHEMICA SCANDINAVICA 27 (1973) 2581–2585

Dihydrocornin, a Novel Natural Iridoid Glucoside

S. ROSENDAL JENSEN, A. KJÆR and B. JUHL NIELSEN

Department of Organic Chemistry, Technical University of Denmark, DK-2800 Lyngby, Denmark

Leaves and twigs of *Cornus Nuttallii* and *C. florida* contain, besides the long-known glucoside cornin *1a*, a minor constituent, dihydrocornin *3*, characterized as the pentaacetate *7*. Reduction of cornin tetraacetate *1b* with $LiAlH(t\text{-}BuO)_3$ yields a 2:1 mixture of two tetraacetates, assigned the structure *4* and *5*, respectively, on the assumption of a more facile approach of the reagent from the convex face of the substrate. The pentaacetate derived from *5* is indistinguishable from that of natural derivation, a conclusion necessitating revision of assignments in the literature. NMR-data for a series of natural and synthetic iridoid glucosides are presented.

In the course of phytochemical studies within the genus *Cornus* (Cornaceae), the species *C. Nuttallii* Aud. and *C. florida* L. have been found to contain a novel, natural iridoid glucoside, additional to cornin *1a*,[1]* a long known constituent of the latter species.[2] The new glucoside, dihydrocornin, $C_{17}H_{26}O_{10}$, was obtained in crystalline form by repeated chromatography of a purified

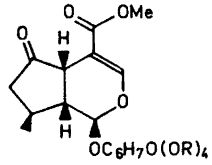

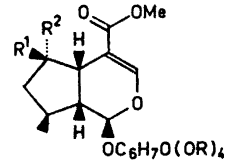

1a; R = H

1b; R = Ac

2; R = R¹ = H, R² = OH

3; R = R² = H, R¹ = OH

4; R = Ac, R¹ = H, R² = OH

5; R = Ac, R¹ = OH, R² = H

6; R = Ac, R¹ = H, R² = AcO

7; R = Ac, R² = H, R¹ = AcO

* The name cornin applies to a β-glucoside, isolated in 1902 in pure form from *C. florida* L. and characterized by elemental composition, $C_{17}H_{24}O_{10}$, m.p., optical rotation, and a number of chemical reactions (*cf.* Ref. 3). Its identity with 'verbenalin', described as a constituent of *Verbena officinalis* L. in 1908,[4] has been established.[5] In agreement with other authors,[2,5] we propose to delete the name 'verbenalin' as redundant.

iridoid glucoside fraction, isolated from leaves and twigs of the above *Cornus* species. Its structure elucidation rests heavily on ^{1}H NMR data, displaying a considerable overall similarity to those of cornin *1a*, yet with a higher multiplicity of the methine proton at C-5 as a distinctly deviating feature. Successive decouplings from the vinylic proton (at C-3) and the hidden methine proton at C-9, recognized by its coupling to the easily distinguishable acetalic proton at C-1, revealed the existence of residual coupling (J 3 Hz) to a proton at δ 4.17 ppm, obviously residing in a hydroxy-substituted methine group at C-6. In keeping with this conclusion, acetylation of the glucoside afforded a pentaacetate, m.p. 166 – 168°.

Partial synthesis of the 6-epimeric carbinols, (*2*) and (*3*), was accomplished by reduction of cornin (*1a*) with $NaBH_4$ in methanol. The epimer, moving at the slowest rate on chromatography and constituting about 50 % of the mixture, was indistinguishable from dihydrocornin from natural sources. The second epimer did not crystallize, but was characterized as a pentaacetate, m.p. 141 – 142°. Similarly, $NaBH_4$ reduction of cornin tetraacetate (*1b*) yielded a *ca.* 1:1 mixture of the epimeric carbinol tetraacetates *4* and *5*, one crystalline (m.p. 150°), the other amorphous. Reduction with $LiAlH(t\text{-}BuO)_3$, a reputed stereoselective reagent,[6] afforded the same products, yet in the ratio 2:1 in favour of the amorphous product. On the assumption that preferential approach of the bulky reducing agent occurs from the least hindered, *i.e.* the convex face, the crystalline tetraacetate possesses the structure *5*. On acetylation, *5* affords a pentaacetate, *7*, m.p. 166 – 168°, indistinguishable from that of natural derivation, whereas *4* yields the epimeric acetate *6*, m.p. 141 – 142°. Hence, dihydrocornin possesses the structure *3*.

This assignment is at variance with statements in the literature. Thus, Büchi and Manning[1] formulated a pentaacetate, m.p. 172 – 174°, obtained in 39 % yield by $NaBH_4$ reduction of cornin (*1a*), followed by acetylation, as *6*. Similarly, reduction of cornin tetraacetate (*1b*), with subsequent epimerization and acetylation, gave a pentaacetate, m.p. 134 – 138°, formulated as *7*.[1] The present evidence suggests that these assignments should be interchanged.

Table 1. Optical rotations, UV-maxima, and analytical data.

Compound	$[\alpha]_D^{20}$ (c in EtOH)	UV-data (EtOH) λ_{max} in nm (ε)	Formula	Analyses Calculated C	Calculated H	Found C	Found H
1b	−135[a] (0.4)	237[b] (9 300)					
3	−126 (0.5)	238 (11 200)	$C_{17}H_{26}O_{10}$	52.30	6.71	52.14	6.68
4	−67 (1.4)	238 (11 200)	$C_{25}H_{34}O_{14}$	53.75	6.15	53.77	6.21
5	−113 (0.4)	236 (10 700)	$C_{25}H_{34}O_{14}$	53.75	6.15	54.05	6.20
6	−86 (0.5)	234[d] (11 700)	$C_{27}H_{36}O_{15}$	54.00	6.04	54.21	6.09
7	−115 (0.5)	233[c] (10 400)					

[a] Reported:[9] −134° (*c* 1.2, EtOH). [b] Reported:[1] 235 nm (9370). [c] Reported:[1] 232 nm (11 200). [d] Reported:[1] 234 nm (11 500).

Table 2. ^{1}H NMR-data (*cf.* Experimental).

Compound (solvent)		δ-Values[a] H-1	H-3	H-5	H-6	OCH_3	10-CH_3	Coupling constants[b] $J_{1,9}$	$J_{3,5}$	$J_{5,6}$	$J_{5,9}$
1a	(D_2O)[c]	5.38	7.58	~3.5	–	3.78	1.22	5.5	1.2	–	–
1b	($CDCl_3$)	~5.2	7.40	3.50	–	3.77	1.22	–	1.5	–	8
2	(D_2O)[c]	5.21	7.70	2.99	4.52	3.81	1.16	8.5	1.3	4	9.5
3	(D_2O)[c]	5.52	7.48	2.88	4.17	3.81	1.15	2.5	1.0	3	8
4	($CDCl_3$)	~5.1	7.60	2.88	4.48	3.75	1.12	–	1.2	4	9
5	($CDCl_3$)	5.22	7.36	2.49	4.01	3.78	1.12	3.0	1.0	4	9
6	($CDCl_3$)	5.06	7.51	3.08	5.52	3.75	1.13	8	1.2	4	9
7	($CDCl_3$)	5.37	7.38	3.00	5.25	3.73	1.13	2.0	1.0	2	9

[a] In ppm ±0.02 ppm. [b] $J_{3,5}$ ±0.1 Hz; others ±0.5 Hz. [c] DDS = 0 ppm.

Analytical data and physical constants are presented in Tables 1 and 2. Certain consistencies in the ^{1}H NMR data are apparent: (*i*) in members of the 6α-series, the methine proton at C-6 is more deshielded than in the 6β-series; (*ii*) the proton at C-1 appears at lower field in the 6β- than in the 6α-series (*cf.* Table 3); (*iii*) the vinylic proton at C-3 is most deshielded in the 6α-

Table 3. Differences in δ-values of epimeric 6-OH-iridoids.

Compound	δH-1 (α) − δH-1 (β)	δH-3 (α) − δH-3 (β)
2 and *3*	−0.31	0.22
4 and *5*	–	0.24
6 and *7*	−0.31	0.13
9 and *8*	−0.36	0.20
11 and *10*	−0.10	0.06

series (*cf.* Table 3). Two related pairs of epimers: scandoside methyl ester-daphylloside (*8,9*),[7,8] and anthirrinoside-procumbide (*10,11*),[9,10] conform to these regularities (*cf.* Table 3).

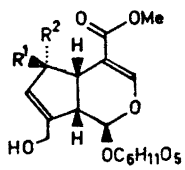

8 ; R^1=OH, R^2=H

9 ; R^1=H, R^2=OH

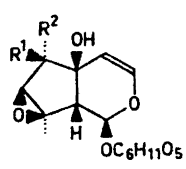

10; R^1=OH, R^2=H

11 ; R^1=H, R^2=OH

EXPERIMENTAL

When not otherwise indicated, melting points are uncorrected and determined in capillary tubes in a heated bath. NMR-Spectra are recorded on a Varian HA-100 instrument, with TMS as an internal or external standard in $CDCl_3$ or D_2O, respectively. Preparative thin layer chromatography (TLC) was performed on 20×40 cm plates covered with a 1 mm thick layer of silica gel PF_{254} (Merck); detection: UV-light. Analyses were performed at Dr. A. Bernhardt, Mikroanal. Labor., Germany.

Isolation of glucosides. Frozen foliage (50 g) of *C. Nuttallii* or *C. florida*, collected in the summer of 1972 and stored at $-28°$ in polyethylene bags, was homogenized in EtOH (150 ml). After filtration, extraction was repeated with another 150 ml-portion of EtOH. The combined filtrates were concentrated *in vacuo*, and the residue was partitioned between water (50 ml) and ether (150 ml). The aqueous phase was extracted with an additional amount of ether (150 ml) and the organic phases were discarded. The aqueous solution was filtered through a column of neutral alumina (50 g); the column was eluted with water (500 ml). After evaporation to dryness, the residue was dissolved in the minimum amount of MeOH:H_2O and applied to a column of silica gel. Acetone (400 ml) eluted a glycoside fraction which was further subjected to separation into two UV-absorbing zones on preparative TLC in $CHCl_3$:MeOH (4:1). A faster, major zone afforded pure cornin *1a* after recrystallization from EtOH, m.p. 178°, $[\alpha]_D^{20}$ $-170°$ (*c* 0.4, EtOH) [reported: m.p. $182-183°$ (corr.);[1,11] $[\alpha]_D^{24}$ $(-165°)-(-166°)$ (EtOH),[11] $(-171°)-(-173°)$ (H_2O);[1,11] others quote numerically higher rotation values, *viz.* $[\alpha]_D^{25}$ $-198°$ (*c* 1.41, H_2O) [12] and $(-184°)-(-185°)$ (H_2O) [13]]. A slightly slower-moving, minor zone contained dihydrocornin. Rechromatography, under the same conditions, of the combined material from several isolations, afforded a yellowish, sirupy fraction which was adsorbed on charcoal. After rinsing with water, the glucoside was eluted with MeOH; it separated from water-saturated EtOAc as colourless crystals, m.p. $90-100°$, containing *ca.* 0.75 mol of H_2O. A specimen dried at room temperature over P_2O_5 at 2 mm for 24 h was employed for analysis (Table 1). Rotation and UV-absorption are likewise reported in Table 1.

Leaves and twigs of *C. Nuttallii* contained $0.2-0.3$ % and 0.5 % of cornin, respectively. The corresponding contents of dihydrocornin were 0.03 and 0.04 %, respectively. In *C. florida*, leaves were found to contain $0.12-0.13$ % of cornin and 0.03 % of dihydrocornin, twigs 0.14 % and 0.08 %, respectively.

Dihydrocornin pentaacetate 7. A solution of dihydrocornin (35 mg) in pyridine (0.5 ml), containing Ac_2O (0.3 ml), afforded, after work up, a crude pentaacetate (55 mg) which was recrystallized twice from EtOH to give colourless crystals of *7*, m.p. $166-168°$ (on Kofler Micro Hot Stage, $172-173°$) [reported [1] m.p. $172-174°$ (Kofler)]. For other data, *cf.* Tables $1-3$.

Reduction of cornin 1a. Cornin (300 mg) was dissolved in MeOH (10 ml) and $NaBH_4$ (100 mg) was added. After stirring for 10 min, 2 drops of AcOH were added. The reaction mixture was concentrated *in vacuo* and the residue subjected to two developments on TLC plates in Bz:EtOH:EtOAc, 1:1:4, resulting in the separation of two zones. The fastest moving of these, containing *2* (143 mg), was separated from the slower moving fraction, chiefly *3*, contaminated with traces of *2*. Both fractions were freed of AcONa by adsorption on charcoal, washing with H_2O, and elution with MeOH. The α-epimer, *2*, could not be induced to crystallize from a number of solvents tried, and apart from recording of its NMR-spectrum (Table 2), further characterization was abandoned. Recrystallization of the β-epimer, *3*, from wet EtOAc, gave colourless needles, indistinguishable from dihydrocornin (m.p., m.m.p., NMR-spectrum).

epi-*Dihydrocornin pentaacetate* 6. On acetylation with Ac_2O in pyridine solution, the amorphous α-epimer from the above reduction yielded a crystalline pentaacetate, m.p. (from MeOH) $141-142°$, (Kofler, m.p. $141.5-142.5°$), assigned the structure *6* (reported:[1] $134-138°$, Kofler). For further data, *cf.* Tables $1-3$.

Reduction of cornin tetraacetate 1b *with* $NaBH_4$. Cornin tetraacetate *1b* (190 mg), obtained by acetylation of cornin,[1] was dissolved in MeOH (10 ml), and a mixture of $NaBH_4$ (35 mg) and H_3BO_3 (50 mg) was added with stirring. After 5 min at ambient temperature, AcOH (6 drops) and H_2O (40 ml) were added. The solution was concentrated to 20 ml and extracted with two 40-ml portions of ether. The ether-soluble residue (178 mg), containing the two epimeric dihydro-derivatives *4* and *5* and some unreduced *1b*,

in the ratio 2:2:1 according to NMR-analysis (in CCl_4; low-field region), was subjected to TLC-separation (3 plates) with Bz:Et_2O (1:2) as the eluant (two developments). The fastest migrating zone contained unchanged *1b* (35 mg). The next zone afforded the pure *β*-carbinol *5* (44 mg), recrystallized from Et_2O to give an analytical specimen, m.p. 150° (*cf.* Tables 1 – 3). The slowest moving band, not completely separated, gave the *α*-carbinol *4*, contaminated with the epimer *5*. All attempts to induce rechromatographed *4* to crystallize proved abortive. An analytical specimen was produced by filtering a CH_2Cl_2-solution through charcoal, followed by high-vacuum drying of the residue. For further data, *cf.* Tables 1 – 3.

On acetylation with Ac_2O in pyridine solution, *5* yielded a pentaacetate, m.p. 166 – 168°, indistinguishable from *7*, deriving from dihydrocornin. Under the same conditions, *4* afforded a crystalline pentaacetate, m.p. 141 – 142°, identical with *6* described above.

Reduction of cornin tetraacetate 1b *with LiAlH*(t-*BuO*)$_3$. A solution of $LiAlH_4$ (150 mg) in anhydrous ether (25 ml) was refluxed under N_2 for 1 h and then siphoned, through a plug of glass wool, into another flask, containing *t*-BuOH (900 mg) in ether (25 ml). After 1 h, the solution was decanted from the precipitate, which was dissolved in freshly distilled THF (25 ml). Under stirring, the tetraacetate (70 mg) was added to the clear solution, and after 30 min the reaction was stopped by adding AcOH (10 drops) and water (40 ml). In this case the reduction was complete, the epimeric carbinols *4* and *5* being present, according to NMR-analysis, in the ratio 2:1.

Acknowledgement. The authors are grateful to Dr. E. Hartmann of the Arboretum, Hørsholm, Denmark, for supplying the plant material used in the present study. Herbarium specimens of the species studied will be deposited at the Botanical Museum of the University of Copenhagen.

REFERENCES

1. Büchi, G. and Manning, R. E. *Tetrahedron* **18** (1962) 1049.
2. Hegnauer, R. In *Beiträge zur Biochemie und Physiologie von Naturstoffen*, Festschrift für K. Mothes, G. Fischer, Jena 1965, p. 235.
3. Miller, E. R. *J. Am. Pharm. Assoc.* **17** (1928) 744.
4. Bourdier, L. *Arch. Pharm.* **246** (1908) 272.
5. Reichert, B. *Arch. Pharm.* **273** (1935) 357.
6. Brown, H. C. and McFarlin, R. F. *J. Am. Chem. Soc.* **78** (1956) 252.
7. Inouye, H., Inouye, S., Shimokawa, N. and Okigawa, M. *Chem. Pharm. Bull.* **17** (1969) 1942.
8. Inouye, H., Okigawa, M. and Shimokawa, N. *Chem. Pharm. Bull.* **17** (1969) 1949.
9. Cheymoll, J. *Bull. Soc. Chim. France* **1938** 642.
10. Bianco, A., Esposito, P., Guiso, M. and Scarpati, M. L. *Gazz. Chim. Ital.* **101** (1971) 764.
11. Chatterjee, A. and Parks, L. M. *J. Am. Chem. Soc.* **71** (1949) 2249.
12. Battersby, A. R., Hall, E. S. and Southgate, R. *J. Chem. Soc.* **C 1969** 721.
13. Karrer, P. and Salomon, H. *Helv. Chim. Acta* **29** (1946) 1544.

Received March 26, 1973.

ACTA CHEMICA SCANDINAVICA 27 (1973) 2586–2590

Permanganate Oxidation of the Ethanol Extract of Raw Humus

GUNNAR OGNER

The Forest Soil Fertilization Research Group, The Norwegian Forest Research Institute, N-1432 Ås-NLH, Norway

Methylated and unmethylated ethanol extracts of raw humus were oxidized by potassium permanganate at pH 9–10. The methylated extract gave four benzenecarboxylic acid methyl esters (3 % yield), seven methoxy-benzenecarboxylic acid methyl esters (9 % yield), 3,4-dimethoxy-benzoic acid methyl ester (22 % yield) and five dicarboxylic acid dimethyl esters (57 % yield). The unmethylated extract gave four benzenecarboxylic acid methyl esters (5 % yield), 2-methoxy-1,4-benzenedicarboxylic acid dimethyl ester (1 % yield) and eight dicarboxylic acid dimethyl esters (94 % yield). The compounds identified have also been found after oxidation of other humic fractions. Compared to these fractions, methylated and unmethylated ethanol extracts yielded a higher amount of aliphatic structures and the number of aromatic methoxy compounds obtained from methylated extract was considerable reduced. It is concluded that carboxyl and/or alkyl polysubstituted humic phenols or condensed structures evidently contribute less to the structure of the ethanol extract of raw humus than to other humic fractions of the same soil material.

The chemistry of the ethanol extractable soil organic matter is not well known. The material is believed to consist of resins, fats and waxes.[1] The purpose of the present work was to investigate the ethanol extractable material from raw humus by potassium permanganate oxidation of methylated and unmethylated samples. This method has proved useful for other humic fractions like raw humus, humin, humic acids and fulvic acids [2–4] and acid boiled raw humus.[5]

Gel filtration of the ethanol extract confirmed that it, like all other humic fractions, is a mixture of components of different chemical and physical properties with relatively high molecular weights.

The oxidation products identified are represented in Table 1. The same compounds have previously been found among the oxidation products of a number of humic fractions together with other aromatic and aliphatic

Table 1. Yields of compounds isolated from methylated and non-methylated ethanol extractable humic material after oxidation. Yields refer to 100 g extract.

Component No.	Compound	Methylated extract mg	Unmethylated extract mg
1	1,2-Benzenedicarboxylic acid dimethyl ester	11	
2	1,2,4-Benzenetricarboxylic acid trimethyl ester	24	11
3	1,2,3,4-Benzenetetracarboxylic acid tetramethyl ester	14	40
4	1,2,4,5-Benzenetetracarboxylic acid tetramethyl ester		26
5	Benzenepentacarboxylic acid pentamethyl ester	9	20
6	4-Methoxy-benzoic acid methyl ester	73	
7	3-Methoxy-1,2-benzenedicarboxylic acid dimethyl ester	37	
8	4-Methoxy-1,3-benzenedicarboxylic acid dimethyl ester	67	
9	2-Methoxy-1,4-benzenedicarboxylic acid dimethyl ester		17
10	4-Methoxy-1,2,3-benzenetricarboxylic acid trimethyl ester	14	
11	6-Methoxy-1,2,4-benzenetricarboxylic acid trimethyl ester	12	
12	2-Methoxy-1,3,5-benzenetricarboxylic acid trimethyl ester	3	
13	5-Methoxy-1,2,3,4-benzenetetracarboxylic acid tetramethyl ester	7	
14	3,4-Dimethoxy-benzoic acid methyl ester	500	
15	Adipic acid dimethyl ester	37	34
16	Pimelic acid dimethyl ester	200	270
17	Suberic acid dimethyl ester	480	480
18	Azelaic acid dimethyl ester	520	660
19	Sebacic acid dimethyl ester	100	250
20	Hendecanedioic acid dimethyl ester		180
21	Dodecanedioic acid dimethyl ester		57
22	Tridecanedioic acid dimethyl ester		10
23	Dimethoxy-carbomethoxy-diazine I	180	
24	Dimethoxy-carbomethoxy-diazine II	27	
25	Benzoyl-benzenetricarboxylic acid trimethyl ester		32
	Not identified	650	430

carboxylic acids.[2-5] A number of not identified compounds constitute a significant part of the oxidation products.

In general, the differences between the yields of oxidation products from methylated and unmethylated ethanol extract correspond to the differences found for methylated and unmethylated raw humus, humin, humic acid and fulvic acid [4] and acid boiled raw humus [5] although the number of compounds identified from the ethanol extractable material is smaller, and their yields differ from that of the above mentioned humic fractions. The discussion will therefore be limited to a comparison of the main differences found between the ethanol extractable material and other humic fractions of the same soil material.[4,5]

The chromatographic behavior (GLC and TLC) of the extracted material and the similarity to other humic fractions regarding the composition of oxidation products, indicate that the ethanol extractable matter is related to humic materials. No significant amounts of waxes or fats have been found.

Permanganate oxidation of methylated samples, recently demonstrated that the total amount of dicarboxylic acid dimethyl esters increased (from

17 to 44 %) and the amount of dimethoxy-benzenecarboxylic acid methyl esters decreased (from 54 to 30 %) in the order humin, humic acid, "high molecular weight" fulvic acid and "low molecular weight" fulvic acid.[5] Thus, the more soluble humic fractions had a higher contribution of aliphatic structures. As seen from Table 2, summarizing the compounds isolated, this trend is even more pronounced for the ethanol extractable material.

Table 2. Groups of compounds isolated from methylated and non-methylated ethanol extractable humic material after oxidation. Yields refer to 100 g samples. The contribution of each group relative to the total amount of identified compounds is given in per cent.

	Methylated extract		Unmethylated extract	
	g	% [a]	g	% [a]
Benzenepolycarboxylic acid polymethyl esters	0.06	3	0.10	5
Methoxy-benzenepolycarboxylic acid polymethyl esters	0.21	9	0.02	1
Dimethoxy-benzenecarboxylic acid methyl ester	0.50	22		
Dicarboxylic acid dimethyl esters	1.33	57	1.93	94
Dimethoxy-carbomethoxy-diazines	0.21	9		
Total	2.31	100	2.05	100

[a] Represented as % of total yield.

Between methylated and unmethylated ethanol extractable material, the difference in yield of benzenecarboxylic acids found by oxidation is small (Table 2). This is in contrast to results found from other humic materials, and might indicate a smaller contribution of the condensed structures expected to be present in soil organic matter.[3–6]

The decrease in amount of condensed structures might be connected to the smaller number of methoxy-benzenecarboxylic acid methyl esters detected. The usually relatively important 3-methoxy-1,2,4-benzenetricarboxylic acid trimethyl ester and 4-methoxy-1,2,3,5-benzenetetracarboxylic acid tetramethyl ester are not at all found among the products of the methylated ethanol extractable material.

The most striking difference between the ethanol extractable material and other humic fractions of the same raw humus material was found for the dimethoxy derivatives isolated. The methylated ethanol extract yields exclusively 3,4-dimethoxy-benzoic acid methyl ester (compound 14) by oxidation and methylation, whereas also six other dimethoxy-benzenepolycarboxylic acid polymethyl esters are usually found from other humic fractions.[4,5] The yields and number of aromatic methoxy and dimethoxy compounds clearly indicate that alkyl and/or carboxyl polysubstituted phenols contribute relatively little, and carboxyl substituted or alkyl polysubstituted *o*-diphenols nothing, to the composition of the ethanol extractable material. This will also apply to the condensed structures.

The relative contribution of the different dicarboxylic acid dimethyl esters identified, compound 15–22, Table 1, corresponds well with results found earlier [4,5] and will not be discussed here.

The significance of the dimethoxy-carbomethoxy-diazines (compounds 23 and 24) has been described elsewhere.[5] The fact that they are isolated in relatively high yield from the methylated sample, shows that the structures yielding these compounds are of significant importance also for the ethanol extractable material.

Compound 25 is most probably a benzoyl-benzenetricarboxylic acid trimethyl ester. The mass spectrum shows peaks at *m/e* 105, 77, and 51 due to the benzoyl cation and its decomposition products. The base peak is at *m/e* 279 representing a tricarbomethoxyl-benzoyl cation. Peaks at *m/e* 356 and 325 represent the molecular ion and M – 31, respectively. The infra-red spectrum gives a strong ester carbonyl absorption (1725 cm^{-1}) and a weaker carbonyl absorption (1675 cm^{-1}).

Further investigations showed that compound 25 is an oxidation product of a number of unmethylated humic fractions, the same as earlier investigated.[4,5] Compound 25 was not detected in humic materials methylated prior to oxidation. Thus, the original humic structure, probably phenolic, yielding compound 25 by oxidation, is apparently stabilized toward permanganate oxidation by methylation to give other oxidation products. It might therefore well constitute a part of the condensed phenolic structures of humic materials previously reported.[5]

The results obtained here indicate that the ethanol extractable material is similar to other humic fractions in composition, although more aliphatic. Its occurrence in soil, therefore, probably originates from biochemical reactions in humus formation and/or degradation.

EXPERIMENTAL

Material. Details of the raw humus and the extraction are given elsewhere.[6] The dry raw humus was extracted with ether and thereafter ethanol. The ethanol extract is a dark waxy substance extracted in 1.8 % yield. (C 63.6; H 8.98; OCH_3 6.2). After methylation with diazomethane in methanol the methoxyl content increased to 14.0 %.

Oxidation. The sample (5 g extract or methylated extract) was oxidized by potassium permanganate at pH 9–10 according to the method outlined elsewhere.[5] Yields: 5 g ethanol extract gave 0.70 g acids, after methylation the yield was 0.50 g of esters; 5 g methylated extract gave 0.84 g acids which were methylated to give 0.68 g esters. The loss of matter by methylation is due to volatile esters; these have not been analyzed.

The ester mixture obtained by methylation of the extracted oxidation products was analyzed by preparative thin-layer and gas chromatography, followed by micro infra-red and mass spectroscopy. Details of the procedure are given elsewhere.[5]

Acknowledgements. This work was supported by the *Agricultural Research Council of Norway*. Thanks are due to ing. W. Sørensen and Mr. W. George for technical assistance.

REFERENCES

1. Waksman, S. A. In *Humus, origin, chemical composition, and importance in nature*, William and Wilkins Company, Baltimore 1936, p. 156.
2. Kahn, S. U. and Schnitzer, M. *Can. J. Soil Sci.* **52** (1972) 43.
3. Matsuda, K. and Schnitzer, M. *Soil Sci.* **114** (1972) 185.
4. Ogner, G. *Acta Chem. Scand.* **27** (1973) 1601.
5. Ogner, G. *Soil Sci.* **116** (1973) 93.
6. Ogner, G. *Soil Sci.* **109** (1970) 86.

Received April 13, 1973.

ACTA CHEMICA SCANDINAVICA 27 (1973) 2591–2596

Cyclo-oligomerization of Quinones

VI.* The Synthesis and Cyclization of a Furohelicene

HANS-ERIK HÖGBERG

Department of Organic Chemistry, Royal Institute of Technology, S-100 44 Stockholm 70, Sweden

The synthesis of furo[3.2-a:4.5-a′]bisdibenzofuran (*3*) and its cyclization to tetraphenyleno[1.16-bcd:4.5-b′c′d′:8.9-b″c″d″]trifuran (*4*) is described. The spectral properties of these compounds are discussed.

The properties of several complex dibenzofurans, obtained by the action of strong acids on *p*-benzoquinones, have recently been studied in this laboratory. Examples are the compounds *2a* [1] and *5*.[2,3] Compound *3* was

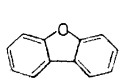

1

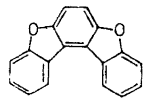

2

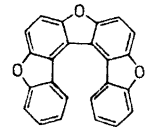

3

2a: OH instead of H in the positions para to the oxygen atoms

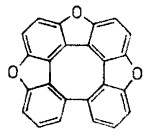

4

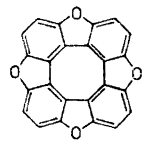

5

expected to provide valuable information about the steric requirements for the formation of macrocyclic tetramers of the type *5* and has now been synthesized.

* Part V: Ref. 14.

2-Hydroxydibenzofuran (*6*, R = R′ = H) is known to undergo preferential substitution in position 1 [4,5] and reacted with iodine chloride to give a monoiodo derivative whose structure, 2-hydroxy-1-iododibenzofuran (*6*, R = H, R′ = I), was corroborated by its NMR spectrum. The corresponding methyl ether was heated with copper bronze to give compound *7* (R = CH_3). When this dimethyl ether was boiled with hydriodic acid demethylation to phenol *7* (R = H) occurred. Ring closure to compound *3* was eventually effected by prolonged

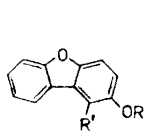

6

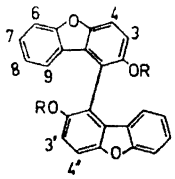

7

heating of the phenol with hydrobromic acid at 280°. When this furanobisdibenzofuran was fused with sodium chloroaluminate, cyclization to the tetraphenylenotrifuran *4* occurred. Like the tetraphenylenotetrafurans (*e.g.* compound *5*) the cyclized compound was light yellow and exhibited a greenish yellow fluorescence in UV light.

The UV spectra (Fig. 1) of compounds *1*, *2*, and *3* were very similar to those of various sulphur heterohelicenes which have been discussed by Groen and Wynberg.[6] The α-, *p*-, and β-bands (*cf.* Clar [7]) were therefore easily identified.

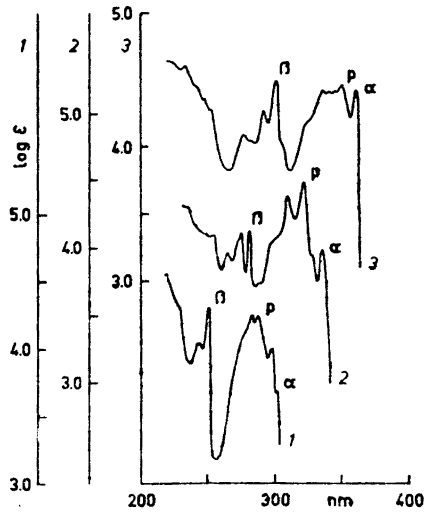

Fig. 1. UV absorption curve of dibenzofuran (*1*) (bottom), benzobisbenzofuran (*2*) (middle) and furobisdibenzofuran (*3*) (top) (all in EtOH).

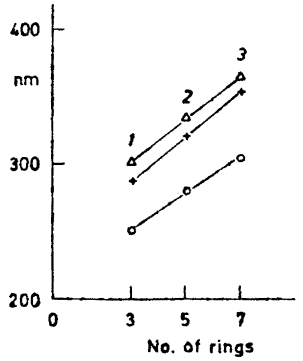

Fig. 2. λ_{max} of the α-, *p*-, and β-band sof compounds *1*, *2*, and *3* *versus* number of rings (△ = α-, + = *p*-, and ○ = β-bands).

As seen from Fig. 2 increasing annelation causes systematic red shifts of the absorption bands. The presence of the furan rings in compounds *1*, *2*, and *3* is reflected in their UV spectra, the α- and β-bands being less split ($\lambda_\alpha/\lambda_\beta = 1.21$, 1.20, and 1.20, respectively) than in the sulphur heterohelicenes ($\lambda_\alpha/\lambda_\beta = 1.25$)[6] and in the series phenanthrene-hexahelicene ($\lambda_\alpha/\lambda_\beta = 1.3$).[7] (For a discussion of this heteroatom effect see Ref. 6).

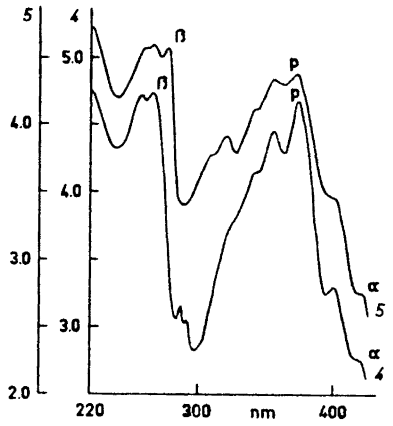

Fig. 3. UV absorption curve of tetraphenylenotrifuran (*4*) (in cyclohexane) (top) and of tetraphenylenotetrafuran (*5*) (in dioxan) (bottom).

A comparison of the very similar UV spectra of the macrocyclic compounds *4* and *5* (Fig. 3) with that of the "open" compound *3* shows that the *p*-bands are shifted to longer wavelengths and that the α- and β-bands have become separated ($\lambda_\alpha/\lambda_\beta = 1.6$). The latter effect is probably due to the higher symmetry of the macrocyclic compounds (*cf.* hexahelicene: $\lambda_\alpha/\lambda_\beta = 1.3$ and coronene: $\lambda_\alpha/\lambda_\beta = 1.4$).[7]

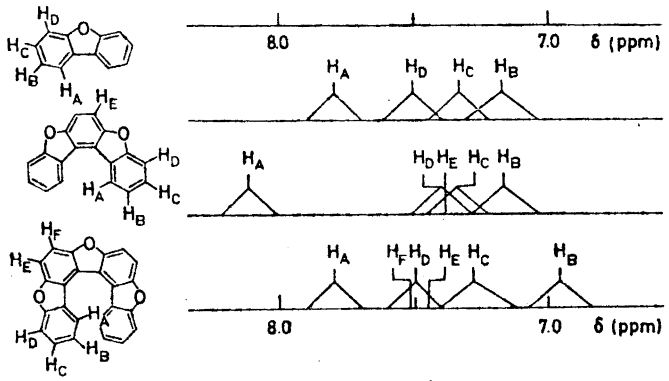

Fig. 4. Schematic NMR spectra of dibenzofuran (*1*), (top), benzobisbenzofuran (*2*) and of furobisdibenzofuran (*3*) (bottom) (all in $CDCl_3$, 60 Mhz).

A diagrammatic representation of the NMR spectra of the compounds *1*, *2*, and *3* is shown in Fig. 4. The chemical shifts assigned to the resonances of the dibenzofuran protons are based upon the detailed discussion in Ref. 8. Those of the protons of compound *2* are assigned on the basis of the close similarity of its NMR spectrum to those of compounds *1* and *3* (Fig. 5). As

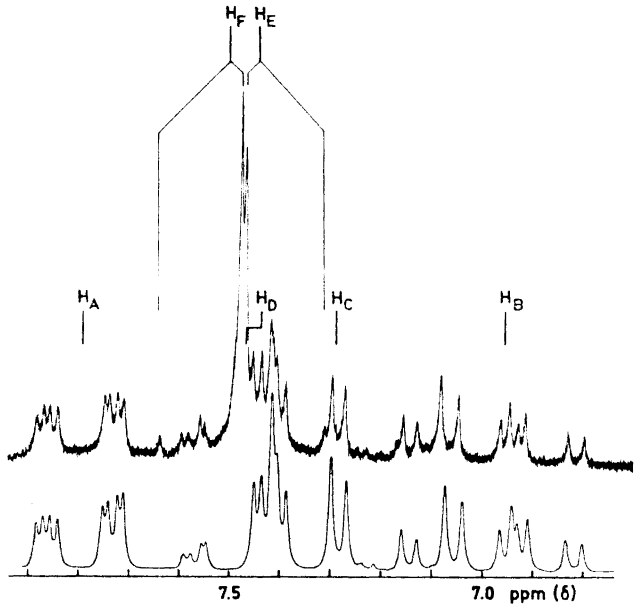

Fig. 5. Experimental (top) and calculated (H_E and H_F not included) (bottom) NMR spectrum of compound *3*. δ (ppm) = 7.79 (H_A); 6.96 (H_B); 7.29 (H_C); 7.47 (H_D); 7.44 (H_E); 7.50 (H_F); $J_{A-B} = 8.2$ cps; $J_{A-C} = 1.6$ cps; $J_{A-D} = 0.6$ cps; $J_{B-C} = 7.2$ cps; $J_{B-D} = 1.2$ cps; $J_{C-D} = 8.6$ cps; $J_{E-F} = 9.6$ cps.

expected the resonance frequency of the proton H_A is shifted to a lower field in the spectrum of compound *2* as compared with that of dibenzofuran (*1*). However, in the spectrum of compound *3* the resonance frequency of the corresponding proton is shifted to a higher field instead of a lower as would be anticipated had compound *3* had a planar structure. Therefore it should have a non-planar helical structure, the proton H_A being located more or less within the shielding zone of the neighbouring terminal benzene ring. This effect is typical for the helicenes and heterohelicenes.[9,10]

Further support for a non-planar structure for the open compound *3* is provided by the fact that anomalous peaks (M − 1, M − 2, and M − 15) occur in its mass spectrum but not in those of compounds *8*,[11] *2*, and *4* (see experimental). The successive loss of 2 H atoms from the molecular ion of *3* gives a fragment ion M − 2, the molecular ion of compound *4*.

The M – 15 peak is probably due to the loss of a methyl radical with formation of the ion *9* as judged by the presence of a metastable peak at $m/e = 318.4$. (Calc. for the transition $m/e = 348 - 333$, $m/e = 318.64$). Similar complex fragmentations and rearrangements have been observed in the helicene and heterohelicene series.[10,12]

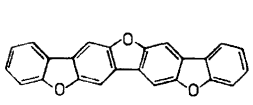

8

9

The cyclic compound *2* does not undergo such abnormal fragmentations.

The facile cyclization of compound *3* to give compound *4* and the spectroscopic results discussed above indicate a close proximity of the carbon atoms of compound *3* involved in the formation of the biphenyl linkage in compound *4*. Macrocyclic compounds such as *4* and *5* therefore seem to differ little in strain from dibenzofuran or compound *8*. The ease with which tetramers of type *5* are formed from suitably substituted *p*-benzoquinones is perhaps not surprising as the reaction leads to highly conjugated products of low energy.

EXPERIMENTAL

Melting points were measured on a micro hot stage. The mass spectra were run at 70 eV, ion source temperature 290° (LKB 9000). The NMR spectra were run at 60 MHz and chemical shifts are given relative to TMS (Varian A60).

1-Iodo-2-hydroxydibenzofuran (*6*, R = H; R′ = I). A solution of 2-hydroxydibenzofuran [4] (18.4 g) in acetic acid (100 ml) was treated with a mixture of conc. hydrochloric acid (25 ml) and iodine chloride (19 g) in acetic acid (50 ml). The iodo compound slowly precipitated in the form of long colourless needles. After 24 h the crystals were collected and washed with a little acetic acid, then with water containing sodium bisulphite and finally with water. The product (25 g) melted at 150 – 155°. Recrystallization from acetic acid gave long colourless needles (19 g, 59 %). M.p. 161 – 162°. (Found: C 46.4; H 2.2. Calc. for $C_{12}H_7IO_2$: C 46.5; H 2.3. Mw = 310). MS, $m/e = 310$ ($M^{+\cdot}$, base peak); 281 ($M^{+\cdot} - CO - H\cdot$); 183 ($M^{+\cdot} - I\cdot$); 155 ($M^{+\cdot} - CO - I\cdot$); 127; 126. NMR (acetone d_6): δ (ppm) = 7.19 (H_3, doublet); 7.48 (H_4, doublet); $J_{3-4} = 8.6$ cps; 7.35 – 8.65 (H_6, H_7, and H_8, complex multiplets); 8.65 – 9.00 (H_9 plus phenolic H, complex multiplet).

1-Iodo-2-methoxydibenzofuran (*6*, R = CH_3; R′ = I) was obtained in almost quantitative yield by methylation of the phenol *5* (R = H; R′ = I) with dimethyl sulphate and alkali. Distillation (160 – 167°, 2 mm) and recrystallization from acetic acid gave colourless prisms melting at 124.5 – 125°. (Found: C 48.2; H 2.8; I 39.0. Calc. for $C_{13}H_9IO_2$: C 48.2; H 2.8; I 39.2. Mw = 324). MS, $m/e = 324$ ($M^{+\cdot}$, base peak); 309 ($M^{+\cdot} - CH_3\cdot$); 281 ($M^{+\cdot} - CH_3\cdot - CO$); 182 ($M^{+\cdot} - CH_3\cdot - I\cdot$); 139; 126.

2,2′-Dimethoxybidibenzofuranyl-1,1′ (*7*, R = CH_3). 1-Iodo-2-methoxydibenzofuran (4.0 g) was mixed with copper bronze (30 g) and slowly heated to 220° when an exothermic reaction started. The mixture was then heated to 250° for 0.5 h. The ether extract (4 l) from 10 batches gave a sticky product (18.2 g) which was triturated with cold ethanol to give a solid (A, 12.7 g) and a solution which contained 2-methoxydibenzofuran (5.5 g). Recrystallization of product A from acetic acid gave crystals (9.8 g, yield 50 %) melting at 207 – 208°. (Found: C 79.1; H 4.6. Calc. for $C_{26}H_{18}O_4$: C 79.2; H 4.6. Mw = 394). MS, $m/e = 394$ ($M^{+\cdot}$, base peak); 379 ($M^{+\cdot} - CH_3\cdot$); 364 ($M^{+\cdot} - 2CH_3\cdot$); 348 ($M^{+\cdot} - CH_3OCH_3$, the largest fragment peak, corresponding to the formation of compound *3*). NMR,

δ(ppm) = 3.70 (6 H, two OCH_3 groups); 7.22 (doublet, H_3 and $H_{3'}$); 7.73 (doublet, H_4 and $H_{4'}$); J_{3-4} = 9.0 cps; the two doublets were clearly distinguished from the peaks in the region 6.60 – 7.50 (complex multiplets, H_6 and $H_{6'}$, H_7 and $H_{7'}$, H_8 and $H_{8'}$, and H_9 and $H_{9'}$).

2,2'-Dihydroxybidibenzofuranyl-1,1' (*7*, R = H) 2,2'-Dimethoxybidibenzofuranyl-1,1' (9.0 g) in a solution of conc. hydriodic acid in acetic acid (1:1, 200 ml) was refluxed for 24 h. After cooling, water was added. The yield of the precipitated diphenol was almost quantitative. Recrystallization from acetic acid/water gave colourless needles. M.p. 238 – 240°. (Found: C 78.7; H 3.8. Calc. for $C_{24}H_{14}O_4$: C 78.5; H 3.8. Mw = 366). MS, m/e = 366 ($M^{+\cdot}$, base peak); 348 ($M^{+\cdot} - H_2O$, corresponds to compound *3*); 337 ($M^{+\cdot} - CO - H^{\cdot}$); 311; 309; 291; 289; 183 (M^{2+}).

Furo[3.2-a:4.5-a']bisdibenzofuran (3). A mixture of 2,2'-dihydroxybidibenzofuranyl-1,1' (440 mg), conc. hydrobromic acid (4 ml) and red phosphorus (100 mg) was heated with shaking at 285° for 60 h in a sealed glass tube under nitrogen. After cooling the reaction product was finely ground and washed with 2 M sodium hydroxide to remove any phenolic products. The alkali-insoluble product was sublimed (190°/0.1 mm) and the sublimate (224 mg, 54 %) was recrystallized from acetic acid giving long colourless needles melting at 189 – 190°. (Found: C 82.9; H 3.5. Calc. for $C_{24}H_{12}O_3$: C 82.8; H 3.5. Mw = 348). MS, *m/e* (rel. intensity) = 348(100) ($M^{+\cdot}$); 347(23); 346(19); 333(4); 320(4); 319(11); 317(3); 290(4); 263(2); 261(4); 174.0)12) (M^{3+}). Efforts to resolve this compound into optical enantiomers have so far been unsuccessful.

Furo[2.3-b:5.4-b']bisdibenzofuran (8) [11] gave the following MS, *m/e* (rel. intensity) = 348(100) ($M^{+\cdot}$); 319(3); 292(4); 263(3); 261(2); 174.0(10) (M^{2+}).

Tetraphenyleno[1.16-bcd:4.5-b'c'd':8.9-b''c''d'']trifuran (4). Furanobisdibenzofuran (*3*) (100 mg) was added to a sodium aluminium chloride melt [13] kept at 140°. After 5 min the reaction mixture was cautiously poured into 2 M hydrochloric acid and the precipitate was collected. Sublimation (250°/0.1 mm) gave a small amount of starting material and a less volatile yellow material (30 mg, 30 %). Recrystallization from pyridine afforded yellow needles, exhibiting a greenish yellow fluorescence in ultraviolet light. M.p. 317 – 320°. (Found: C 83.2; H 3.0. Calc. for $C_{24}H_{10}O_3$: C 83.3; H 2.9. Mw = 346). MS; *m/e* (rel. intensity) = 346(100) ($M^{+\cdot}$); 317(9) ($M^{+\cdot} - CO - H^{\cdot}$); 290(2); 288(3); 261(4); 259(3); 173.0(20) (M^{2+}); 158.5(3); 145.0(4); 230.5(7).

Benzo[2.1-b:3.4-b']bisbenzofuran (2). This compound was prepared as described by Erdtman and Stjernström.[1] MS; m/e (rel. intensity) = 258(100) ($M^{+\cdot}$); 229(8) ($M^{+\cdot} - CO - H^{\cdot}$); 202(9) ($M^{+\cdot} - 2CO$); 200(12) ($M^{+\cdot} - 2CO - 2H^{\cdot}$); 176(5); 150(2); 129(8) (M^{2+}).

Acknowledgements. I thank Professor H. Erdtman for stimulating discussions, Miss G. Hammarberg for running the NMR spectra, Prof. Dr. W. Kern, Department of Chemistry, University of Mainz, for a generous gift of compound *8*, and Dr. P. Forslind for help with the calculation of the NMR spectrum of compound *3*.

REFERENCES

1. Erdtman, H. and Stjernström, N.-E. *Acta Chem. Scand.* **13** (1959) 653.
2. Erdtman, H. and Högberg, H. E. *Tetrahedron Letters* **1970** 3389.
3. Högberg, H. E. *Acta Chem. Scand.* **26** (1972) 2752.
4. Gilman, H. and van Ess, P. R. *J. Am. Chem. Soc.* **61** (1939) 1365.
5. Schimmelschmidt, K. *Ann.* **566** (1950) 184.
6. Groen, M. B. and Wynberg, H. *J. Am. Chem. Soc.* **93** (1971) 2968.
7. Clar, E. *Polycyclic Hydrocarbons*, Academic, London 1964.
8. Black, P. J. and Heffermann, M. L. *Austr. J. Chem.* **18** (1965) 353.
9. Martin, R. H., Defay, N., Figeys, H. P., Flammang-Barbieux, M., Coryn, J. P., Gelbcke, M. and Schurter, J. J. *Tetrahedron* **25** (1969) 4985.
10. Groen, M. B., Schadenberg, H. and Wynberg, H. *J. Org. Chem.* **19** (1971) 2797.
11. Wirth, H. O., Waese, G. and Kern, W. *Makromol. Chem.* **36** (1965) 139.
12. Dougherty, R. C. *J. Am. Chem. Soc.* **90** (1969) 5788.
13. Dopper, J. H. and Wynberg, H. *Tetrahedron Letters* **1972** 763.
14. Högberg, H. E. *Acta Chem. Scand.* **27** (1973) 2559.

Received February 23, 1973.

ACTA CHEMICA SCANDINAVICA 27 (1973) 2597–2606

Acid Degradation of Lignin

Part VIII.* Low Molecular Weight Phenols from Acidolysis of Birch Lignin

KNUT LUNDQUIST

Department of Organic Chemistry, Chalmers University of Technology and University of Göteborg, Fack, S-402 20 Göteborg 5, Sweden

Refluxing of Björkman lignin from birch (*Betula verrucosa*) with 0.2 M hydrogen chloride in dioxan-water (9:1) for 4 h gives considerable amounts of phenols with one and two aromatic rings (about 30 % of the original lignin). A number of phenols has been identified. Most of them can be related to structural elements of the arylglycerol-β-aryl ether, 1,2-diaryl-1,3-propanediol, and syringaresinol types.

Acidolysis [refluxing with 0.2 M hydrogen chloride in dioxan-water (9:1)**] for 4 h of Björkman lignin gives considerable amounts of low molecular weight phenols.[1] The degradation proceeds mainly by cleavage of ether linkages, particularly those in arylglycerol-β-aryl ether structures.[2]

Phenols, carbonyl compounds, and, at least at an early stage of the acidolysis, benzyl alcohols are present in the lignin acidolysis mixture. It is very likely that condensation reactions occur in such a mixture. Experiments have been carried out which indicate that the formaldehyde liberated is partly consumed due to condensation.[3] Studies with model compounds of the arylglycerol-β-aryl ether type indicate that the benzyl alcohol groups present in such structures condense only to a limited extent during acidolysis.[1,2] As judged from studies of carboxylic acids formed on permanganate oxidation of acidolysed lignin condensation with aromatic rings occur to a minor extent only.[4] Coniferyl alcohol polymerizes under acidic conditions.[5] Since lignin contains minor amounts of cinnamyl alcohol end groups, this reaction should be of some importance in the acidolysis of lignin. The latter reaction and condensation reactions decrease the yield of low molecular weight phenols on acidolysis.

* Part VII, Ref. 2.

** Throughout this paper the term acidolysis is used specifically for this treatment.

Upon acidolysis of aspen wood Pepper and co-workers [6] obtained evidence for the occurrence of condensation reactions by studying the yields of vanillin and syringaldehyde formed on alkaline nitrobenzene oxidation of the lignin samples isolated. In connection with the present studies it has been found that carbohydrates give 2-furaldehyde and 5-hydroxymethyl-2-furaldehyde on acidolysis.[7,8] Due to the difference in carbohydrate content, considerably larger amounts of such aldehydes should be formed from wood than from Björkman lignin (concerning content of carbohydrates, see Refs. 8 and 9) on acidolysis. It seems possible that furaldehydes react with lignin in condensation reactions during acidolysis conditions. The difference in formation of such compounds may therefore explain why the results obtained on acidolysis of wood [6] (difficulties with the dissolution of the lignin, alkaline nitrobenzene oxidation studies) seem to indicate the importance of condensation reactions more than the results with Björkman lignin [1,2,4] do (gel filtration experiments, permanganate oxidation studies).

The major part of the work in this series deals with lignin from spruce (*Picea abies*), but results obtained with lignin from birch (*Betula verrucosa*) have been discussed to some extent. The present paper describes the identification of low molecular weight phenols from acidolysis of birch lignin. The relation of the compounds to structural elements in lignin is discussed. A study of the acidolysis products from bamboo and beech lignins has recently been published.[10] These lignins show structural resemblance to birch lignin and it is therefore of interest to compare these results with those obtained from the acidolysis of birch lignin.

As in the acidolysis experiments with spruce lignin,[1] the separation methods used included removal of the major part of the polymeric material on a silica gel column (the eluted material was 42 % of the original lignin) and division of the eluted material by gel filtration into fractions of monomers, dimers, and high molecular weight material (Fig. 1). The monomer fraction (20 % of

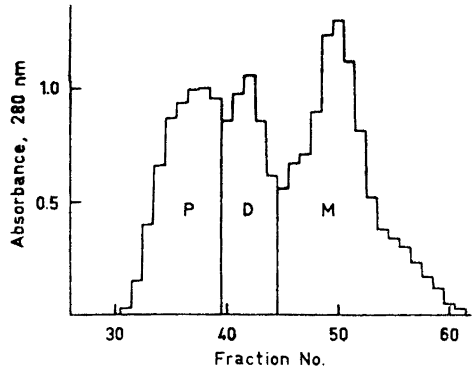

Fig. 1. Gel filtration of an essentially low molecular weight fraction separated by column chromatography from the reaction mixture obtained on 4 h acidolysis of Björkman lignin from birch [Sephadex G-25, eluent: dioxan-water (1:1)].

the original lignin) and the dimer fraction (10 % of the original lignin) were investigated to identify individual components. (The terms monomer and dimer in this paper refer to the number of aromatic rings present in the compounds.)

Composition of the monomer fraction. Compounds detected in the monomer fraction are shown in Fig. 2. Compounds *1*, *2*, *6*, *8*, *9*, and *11* were obtained in a crystalline state and identified with authentic samples by IR and mixed

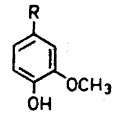
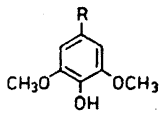

1 R = CH_2COCH_2OH
2 R = $COCH(OH)CH_3$
3 R = $CH(OH)COCH_3$
4 R = $COCOCH_3$
5 R = CHO
6 R = COOH
7 R = CH=CHCHO

8 R = CH_2COCH_2OH
9 R = $COCH(OH)CH_3$
10 R = $COCOCH_3$
11 R = CHO
12 R = CH=CHCHO

Fig. 2. Compounds detected in the monomer fraction.

m.p. For the identification of compounds *3–5*, *7*, *10*, and *12* paper chromatography was used. Ketols *1* and *8* were the most abundant constituents; their yields were 5 % and 2.6 % of the original lignin, respectively.

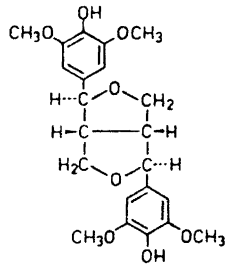
13

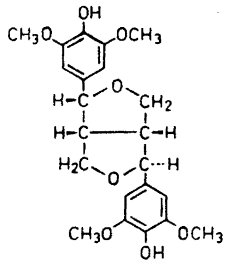
14

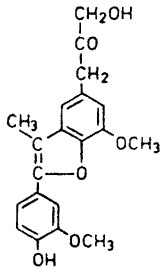
15

Composition of the dimer fraction. From two of the sub-fractions obtained by column chromatography crystalline compounds were obtained. These were (±)-syringaresinol (*13*) and a product, m.p. 185°, denoted compound Y in the following paragraph, which for reasons given below is proposed to be (±)-episyringaresinol (*14*). Each of the fractions was 0.9 % of the original lignin.

The IR spectrum of compound Y was identical with the IR spectrum reported for certain stereoisomers of syringaresinol (lirioresinol A and B [11]). Acidolysis (4 h) of (±)-syringaresinol gave a reaction product consisting of about equal amounts of compound *13* and compound Y. The fact that similar acidolysis of (+)-pinoresinol results in a mixture of (+)-pinoresinol and (+)-epipinoresinol [1] makes it likely that compound Y is identical with compound *14*. This is further supported by the fact that the dimethyl ether of (±)-syringaresinol on acid treatment gives a mixture of the dimethyl ethers of (±)-syringaresinol and (±)-episyringaresinol.[12] Additional work [13] on the structure of syringaresinol and its stereoisomers (including "lirioresinols" discussed in Ref. 11) can also be interpreted to indicate that compound Y is identical with compound *14*.

The remaining sub-fractions (constituting a total of 3.5 % of the original lignin) were reduced with sodium borohydride and acetylated; by this procedure carbonyl groups were replaced by $>CHOCOCH_3$ groups and hydroxy groups by acetoxy groups. The products were examined by GLC, GLC–MS, and thin layer chromatography. Proof for the presence of a number of derivatives of

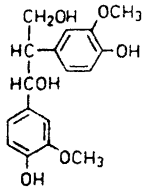

16

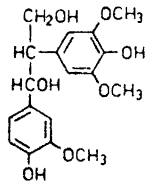

17

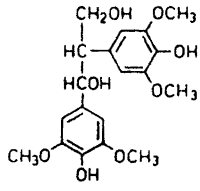

18

acidolysis products of 1,2-diaryl-1,3-propanediols *16*, *17*, and *18* was obtained by GLC and GLC-MS. Evidence for the presence of the derivative of phenylcoumarone *15* was obtained by gas chromatography and thin layer chromatography.

Compounds found in the dimer fraction which have been found to be acidolysis products of compounds *16*, *17*, and *18* are shown in Fig. 3. The structures of several of the compounds are not fully proved. Acidolysis products from *16*, (*19*–*21*, and *22*) have previously been detected in acidolysis mixtures from spruce lignin,[14,1] and the identification of *19*, *21*, and *22*, *via*

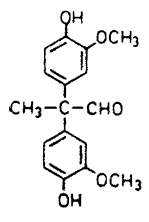

19

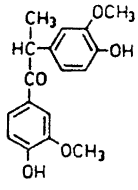

20

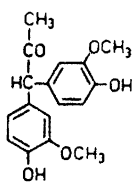

21

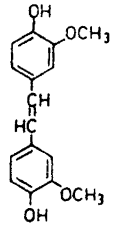

22

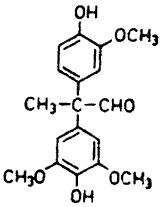

23

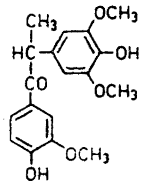

24

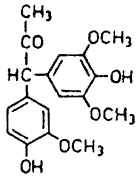

25

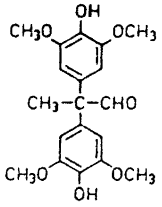

26

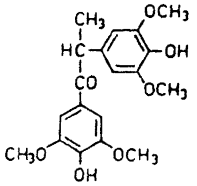

27

Fig. 3. Compounds in the dimer fraction which are formed on acidolysis of the 1,2-diaryl-1,3-propanediols *16-18*.

derivatives obtained on reduction-acetylation, by gas chromatography-mass spectrometry has been described in this connection.[1] (The structure of *19* is tentative, see Ref. 1.) In the present work gas chromatography-mass spectrometry was also used for the detection of compound *20 via* its derivative obtained on reduction-acetylation (*28*). The MS of the derivative was in accord with structure *28*, *e.g.* the molecular ion was *m/e* 430.

Structural evidence for compounds *23 – 25* comes from a striking analogy of the mass spectra of the derivatives with those of the corresponding derivatives of *19 – 21*. Similarly, evidence for the structure of compounds *26* and *27* was obtained from mass spectral data. The derivative of compound *27* was obtained in a crystalline state, m.p. 220°. This made it possible to obtain

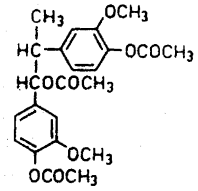

28

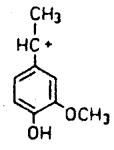

(m/e 151)

29

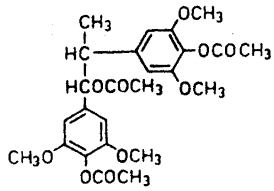

30

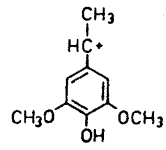

(m/e 181)

31

more conclusive structural evidence. Precise mass measurements of the molecular ion (*m/e* 490) gave the elemental composition $C_{25}H_{30}O_{10}$, which is in accord with structure *30*. The base peak was *m/e* 181 (fragment *31*); other peaks were less than 50 % of the base peak. Analogously, the base peak in the mass spectrum of derivative *28* was *m/e* 151 (fragment *29*), which strongly dominated the spectrum.

Acidolysis of the 1,2-diaryl-1,3-propanediols *16 – 18* followed by reduction-acetylation and subsequent examination of the mixtures by GLC supported the view that the lignin acidolysis products shown in Fig. 3 arise on acidolysis of compounds *16 – 18*.

DISCUSSION

The monomer fraction and the dimer fraction correspond to 30 % of the original lignin. The corresponding fractions obtained from spruce lignin constituted 17 % of the original lignin.[1] Thus considerably more low molecular weight material is formed from birch lignin than from spruce lignin on acidolysis. This difference should be essentially due to the fact that many of the units in birch lignin are of the syringyl type (*34*); in this type of units the 3- and the 5-positions are occupied by methoxyl groups and the aromatic rings are therefore linked to adjacent units by acid-stable biphenyl and diaryl ether linkages only to a small extent. Such a difference in formation of low molecular weight material has been encountered in several comparative degradations of softwood and hardwood lignins. Of particular interest in connection with this work is the observation that larger amounts of "Hibbert ketones" are formed from hardwoods.[15]

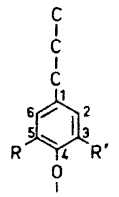

32 R = R' = H
33 R = H, R' = OCH_3
34 R = R' = OCH_3

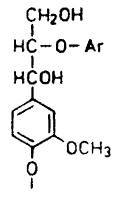

35

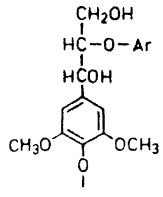

36

Ar = aromatic ring in adjacent unit

A comparison of the low molecular weight phenols from spruce lignin with those from birch lignin can roughly be interpreted to indicate that both lignins have similar structures with the exception of a different ratio of units *32 – 34* and differences due to the lack of condensation possibilities in syringyl units discussed above. However, other structural differences between birch and spruce lignin of interest for the formation of low molecular weight material on hydrolysis have been observed. Thus the frequency of hydrolysable ether bonds has been found to be higher in birch lignin.[4b] Similar results have been obtained in studies of beech lignin [16] which in all likelihood is closely related to birch lignin. NMR studies indicated that the guaiacyl units in birch lignin are condensed to a great extent.[17] This is not supported by the present study, since guaiacyl monomers constitute a rather large portion of the monomer fraction. Similarly, estimations made on the basis of the formation of aromatic acids on oxidative degradation suggest the presence of a considerable portion of noncondensed guaiacyl units in birch lignin.[4b]

The formation of ketols *1 – 3*, *8*, and *9* can be explained by the occurrence of structural elements of types *35* and *36* in the lignin.[2] Since the yield of ketols is rather high, birch lignin should contain a considerable number of units of these types. According to model experiments, compounds *4* and *5* originate – at least in part – from units of type *35*.[2] Analogously units of type *36* can be expected to give rise to compounds *10* and *11*.

Concerning the relation of acidolysis products *5 – 7* and the syringyl analogues of *5* and *7*, namely *11* and *12*, to lignin structures, *cf.* the discussion [1] of the origin of compounds *5 – 7* on acidolysis of spruce lignin.

The formation of (±)-syringaresinol (*13*) and its acidolysis product, (±)-episyringaresinol (*14*), shows that birch lignin contains structural elements of the syringaresinol type. Evidence for this type of structural elements has been obtained by the fact that (±)-syringaresinol is formed on hydrolysis of pre-extracted wood from beech [18] (*Fagus silvatica*) and *Fraxinus mandshurica*.[19] However, compound *13* has also been found in an ethanol extract from wood of *Fraxinus mandshurica*.[20] Therefore, the formation of compounds *13* and *14* on acidolysis of isolated birch lignin complements the earlier evidence for the occurrence of structural elements of the syringaresinol type in lignin.

The yields of *13* and *14* were rather small, suggesting that birch lignin contains only a small percentage of syringaresinol structures. The total number of units involved in "resinol" structures (including syringaresinol, pinoresinol,

and analogous structures consisting of one unit of type *33* and one unit of type *34*) may be of the order of 10 % (yield of "dilactone" on oxidation [21]).

Sinapyl alcohol yields almost exclusively (±)-syringaresinol on oxidation.[22] The low yields of compounds *13* and *14*, as well as the formation of considerable amounts of other syringyl compounds on acidolysis, suggest that oxidative dimerization of sinapyl alcohol is very much suppressed in the formation of birch lignin. This can be explained by co-polymerization with coniferyl alcohol or reaction of sinapyl alcohol radicals with radicals of units containing a saturated side chain. The latter reaction is presumably the most important one. For a discussion of aspects of the biosynthesis of lignin of interest in this connection, see Ref. 23. Interestingly, it has been demonstrated that the oxidative dimerization of *p*-hydroxycinnamyl alcohols is suppressed when the oxidation is performed under suitable conditions in media containing a great excess of a phenol with a saturated side chain.[24]

Acidolysis products originating from 1,2-diaryl-1,3-propanediols *16 – 18* incorporated in the lignin constitute a rather large portion of the dimer fraction. The amount seems to agree fairly well with the amount of degradation products related to 1,2-diaryl-1,3-propanediols obtained on degradation of beech wood.[25]

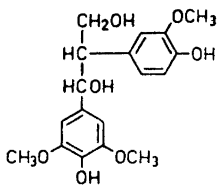

37

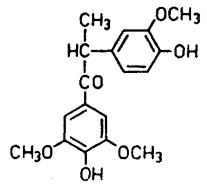

38

In addition to compounds *16 – 18*, a fourth 1,2-diaryl-1,3-propanediol conceivably may be incorporated into the lignin, namely compound *37*. Compounds *23* and *25* can be expected to be formed from *17* as well as *37* on acidolysis. Compound *37* should, however, give rise to *38* rather than *24* on acidolysis. Mass spectral evidence (*e.g.* a large peak at *m/e* 181, fragment *31*) suggests that the compound detected in the birch acidolysis mixture is *24*. Thus evidence for the occurrence of structures related to compound *37* has not been obtained. Interestingly, only *16 – 18* have been obtained on hydrolysis of beech wood.[26]

The occurrence of phenylcoumarone *15* in the dimer fraction suggests the presence of phenylcoumaran structures in birch lignin of the same type as previously found in spruce lignin.[27] A degradation product which can be derived from phenylcoumaran structures containing a syringyl unit has recently been obtained in studies with beech wood.[25] Such structures are probably also present in birch lignin, but corresponding acidolysis products have not been detected. The failure to detect these and possibly other products may be due to decomposition of the derivatives during gas chromatography. Therefore the dimer fraction from birch lignin deserves further investigation.

EXPERIMENTAL

GLC was accomplished with a Varian Aerograph 1200 instrument. Column dimensions: 100 × 0.3 cm o.d. stainless steel tubing. Solid support: Chromosorb G, acid-washed and treated with dimethyldichlorosilane, 80 – 100 mesh. Stationary phase OV-1 (2 %). Temperatures: Injector 290°, detector 250°, and column 240° (in a few experiments 250°). Carrier gas: N_2, 25 ml/min. Detector: FID. Internal standard: Retention times are given relative that of dotriacontane. For *GLC–MS* an LKB 9000 instrument was used.

For *paper chromatography* (PC) the solvent system employed by Kratzl and Schweers [28] was used. For the detection of *3 – 5*, and *7* with this system, see Refs. 29 and 1. Compounds *10* (R_F 0.55), *11* (R_F 0.30), and *12* (R_F 0.20) were also detected by PC. Compound *10* is yellow and the spot could therefore be seen on the paper. On spraying with diazotised sulphanilic acid in 2 % aqueous Na_2CO_3, *10* and *11* gave pink spots. Compound *12* appeared as a purple spot on spraying with phloroglucinol in hydrochloric acid/ethanol.

Thin layer chromatography (TLC) was performed on plates covered with a 0.3 mm thick layer of silica gel (Merck HF_{254}). Eluent, benzene-ethyl acetate (1:1). Spots were made visible by exposing them to iodine vapour and by spraying with formalin-H_2SO_4 (1:9).

Preparative TLC was performed on plates similar to those used in analytical experiments. Eluent, ethyl acetate. The zones of silica gel containing the materials of interest, detected by UV light, were scratched off and eluted with acetone.

Standard procedure for column chromatography on silica gel using gradient elution. The procedure described in Ref. 1 was followed, but with ethyl acetate instead of benzene-ethyl acetate (2:3) in the reservoir.

Acidolysis of syringaresinol (13). (±)-Syringaresinol (*13*) [prepared by oxidation of sinapyl alcohol with peroxidase, m.p. 170° (lit.[22] 169.5°)] was refluxed for 4 h with 0.2 M hydrochloric acid in dioxan-water (9:1). The reaction product, extracted with chloroform was chromatographed according to the standard procedure. Two fractions of about equal weight were obtained. These were starting material and a compound, m.p. 183°, proposed to be (±)-episyringaresinol (*14*), *cf.* p. 2599.

Acidolysis of birch lignin

Björkman lignin (4.1 g, OCH_3 = 21.1 %) from birch (*Betula verrucosa*) was acidolysed according to the procedures described for the examination of acidolysis mixtures from spruce lignin.[1] Work-up procedures were also essentially the same. Polymeric material was removed by chromatography on silica gel (40 g SiO_2) with benzene-dioxane (3:1) as eluent. Elution was continued until the absence of material with $R_F < 0.05$ was shown by TLC. Gel filtration on a Sephadex G-25 (fine) column (180 g) with dioxan-water (1:1) as solvent (see Fig. 1) gave a monomer fraction (0.82 g) and a dimer fraction (0.38 g).

Examination of the monomer fraction

The monomer fraction was chromatographed on silica gel according to the standard procedure, but initially (315 ml eluate) with benzene-ethyl acetate (2:3) in the reservoir. Crystalline compounds were identified by IR and mixed m.p. *Tubes 19 – 23* gave 10 mg of an oil. PC revealed the presence of *1-(4-hydroxy-3-methoxyphenyl)-1,2-propanedione (4)*. *Tubes 24 – 32* gave 66 mg of an oil. PC indicated the presence of *vanillin (5)*, *coniferaldehyde (7)*, and *1-(4-hydroxy-3,5-dimethoxyphenyl)-1,2-propanedione (10)*. *Tubes 33 – 41* gave 12 mg of an oil. From dichloromethane a small amount of crystals were obtained with m.p. about 200°, identified as *vanillic acid (6)* (m.p. 210° [30]). *Tubes 36 – 41* gave 47 mg of a partially crystalline product. PC indicated the presence of syringaldehyde. Preparative TLC gave a fraction from which impure crystals were obtained from benzene. After washing with ether, a product of m.p. 108° was obtained. This was identified as *syringaldehyde (11)* (m.p. 113° [31]). *Tubes 42 – 47* gave 69 mg of an oil. The presence of *sinapaldehyde (12)* was demonstrated by PC. From benzene crystals were obtained with m.p. 106°, identified as *2-hydroxy-1-(4-hydroxy-3-methoxyphenyl)-1-propanone (2)* (m.p. 109 – 110° [32]). *Tubes 48 – 54* gave *32* mg of an oil. The presence of *1-hydroxy-1-(4-*

hydroxy-3-methoxyphenyl)-2-propanone (*3*) was indicated by PC. *Tubes 55 – 65* gave 182 mg of an oil. Preliminary examinations indicated the presence of compound *1*. Extraction with 15 % hydrogen sulphite solution from a solution of the fraction in ether-dichloromethane (2:1) and recovery of the extracted material (acidification, extraction by chloroform) gave 105 mg crystals with m.p. 71 – 75°, identified as *1-hydroxy-3-(4-hydroxy-3-methoxyphenyl)-2-propanone* (*1*) (m.p. 81 – 82° [33]). The residue obtained from the organic layer gave crystals from benzene melting at 118 – 120°, identified as *2-hydroxy-1-(4-hydroxy-3,5-dimethoxyphenyl)-1-propanone* (*9*) (m.p. 126 – 127° [34]). *Tubes 66 – 75* gave 48 mg of an oil containing unidentified products. *Tubes 76 – 86* gave 202 mg crystals of m.p. 102 – 103°. From chloroform-benzene, 146 mg of product melting at about 105° was obtained. Repeated recrystallisation raised the m.p. to 106 – 107°. The product was identified as *1-hydroxy-3-(4-hydroxy-3,5-dimethoxyphenyl)-2-propanone* (*8*) (m.p. 106.5 – 107.5° [35]). *Tubes 87 – 94* gave 31 mg of an oil. TLC indicated that compound *8* may be present in the fraction.

Examination of the dimer fraction

The dimer fraction was chromatographed on silica gel according to the standard procedure.

Sub-fractions obtained from tubes 19 – 23 (10 mg), tubes 24 – 31 (30 mg), 32 – 39 (43 mg), 40 – 44 (31 mg), and 45 – 50 (30 mg) were reduced and acetylated as described for fractions of dimers from spruce lignin [1] and, subsequently, examined by GLC and GLC–MS. No prominent peaks other than those discussed below appeared. Concerning the identification of compounds *19 – 27*, see p. 2600.

Tubes *19 – 23* showed peaks with rel. ret. times 0.43 (the derivative of *stilbene 22*) and 0.38 (the derivative of *aldehyde 19*). *Tubes 24 – 31* showed peaks with rel. ret. times 0.27 (the derivatives of *ketones 20* and *21*) and 0.40 (the derivative of *aldehyde 23*). *Tubes 32 – 39* showed a peak with rel. ret. time 0.36 (the derivatives of *ketones 24* and *25*) and a stronger peak with rel. ret. time 0.50 (the derivative of *aldehyde 26*). An additional peak (rel. ret. time 2.11, in this run the temperature of the column was 250° instead of 240°) corresponded to the derivative of *phenylcoumarone 15*. Confirmation by GLC–MS failed due to decomposition in the molecule separator. However, according to TLC the derivative of *15* was present in the fraction. *Tubes 40 – 44* showed a peak with rel. ret. time 0.47 (the derivative of *ketone 27*). From acetone, crystals (m.p. 220°) were obtained; this product was identical with the major component of the fraction. The elemental composition was determined as $C_{25}H_{30}O_{10}$ by mass measurements of the molecular ion (measured: 490.1865, calculated: 490.1839); an AEI model MS 902 was used. This is in accord with structure *30*. *Tubes 45 – 50* showed a peak with rel. ret. time 0.47 (the derivative of *27*?).

Further sub-fractions were obtained from tubes 51 – 56 (36 mg) and tubes 58 – 63 (36 mg). The material in *tubes 51 – 56* gave crystals from methanol, m.p. 185°. The product is proposed to be (±)-*episyringaresinol* (*14*), see p. 2599.

Crystalline (±)-*syringaresinol* (*13*) (m.p. 166 – 170°, lit.[22] 169.5°) was obtained from the material in *tubes 58 – 63*. The product was identified with an authentic sample by IR and mixed m.p.

Acknowledgements. The author thanks Prof. E. Adler and Prof. M. Nilsson for their interest and for valuable criticism. Dr. H. Nimz, Karlsruhe, is thanked for gifts of compounds *17* and *18*.

REFERENCES

1. Lundquist, K. *Acta Chem. Scand.* **24** (1970) 889.
2. Lundquist, K. and Lundgren, R. *Acta Chem. Scand.* **26** (1972) 2005.
3. Lundquist, K. and Ericsson, L. *Acta Chem. Scand.* **24** (1970) 3681.
4. a. Larsson, S. and Miksche, G. E. *Acta Chem. Scand.* **21** (1967) 1970; b. Larsson, S. and Miksche, G. E. *Acta Chem. Scand.* **25** (1971) 647.
5. Freudenberg, K., Maercker, G. and Nimz, H. *Chem. Ber.* **97** (1964) 903.

6. Pepper, J. M., Baylis, P. E. T. and Adler, E. *Can. J. Chem.* **37** (1959) 1241; Pepper, J. M. and Siddiqueullah, M. *Can. J. Chem.* **39** (1961) 1454.
7. Hemrå, L. and Lundquist, K. *Unpublished results.*
8. Björkman, A. *Svensk Papperstid.* **59** (1956) 477.
9. Björkman, A. and Person, B. *Svensk Papperstid.* **60** (1957) 158.
10. Higuchi, T., Tanahashi, M. and Sato, A. *Nippon Mokuzai Gakkaishi* **18** (1972) 183.
11. Dickey, E. E. *J. Org. Chem.* **23** (1958) 179.
12. Weinges, K. *Chem. Ber.* **94** (1961) 2522.
13. Briggs, L. H., Cambie, R. C. and Couch, R. A. F. *J. Chem. Soc.* **C 1968** 3042.
14. Lundquist, K. and Miksche, G. E. *Tetrahedron Letters* **1965** 2131.
15. West, E., MacInnes, A. S. and Hibbert, H. *J. Am. Chem. Soc.* **65** (1943) 1187; Kulka, M., Fisher, H. E., Baker, S. B. and Hibbert, H. *J. Am. Chem. Soc.* **66** (1944) 39. See also Brauns, F. E. *The Chemistry of Lignin*, Academic, New York 1952, p. 465.
16. Nimz, H., Das, K. and Minemura, N. *Chem. Ber.* **104** (1971) 1871.
17. Klemola, A. *Suomen Kemistilehti* **B 41** (1968) 99.
18. Nimz, H. and Gaber, H. *Chem. Ber.* **98** (1965) 538.
19. Omoro, S. and Sakakibara, A. *Nippon Mokuzai Gakkaishi* **17** (1971) 464.
20. Terazawa, M. and Sasaya, T. *Nippon Mokuzai Gakkaishi* **17** (1971) 167.
21. Ogiyama, K. and Kondo, T. *Nippon Mokuzai Gakkaishi* **14** (1968) 416.
22. Freudenberg, K., Harkin, J. M., Reichert, M. and Fukuzumi, T. *Chem. Ber.* **91** (1958) 581.
23. Sarkanen, K. V. In Sarkanen, K. V. and Ludwig, C. H., Eds., *Lignins*, Wiley, New York 1971, p. 95.
24. Erickson, M. and Miksche, G. E. *Acta Chem. Scand.* **26** (1972) 3085.
25. Nimz, H. and Das, K. *Chem. Ber.* **104** (1971) 2359.
26. Nimz, H. *Chem. Ber.* **99** (1966) 469.
27. Lundquist, K. and Hedlund, K. *Acta Chem. Scand.* **25** (1971) 2199.
28. Kratzl, K. and Schweers, W. *Monatsh.* **85** (1954) 1046.
29. Lundquist, K. and Hedlund, K. *Acta Chem. Scand.* **21** (1967) 1750.
30. Vogel, A. I. *Practical Organic Chemistry*, 3rd Ed., Wiley, New York 1966.
31. *Handbook of Chemistry and Physics*, The Chemical Rubber Co., 1971.
32. Cramer, A. B. and Hibbert, H. *J. Am. Chem. Soc.* **61** (1939) 2204.
33. Fisher, H. E. and Hibbert, H. *J. Am. Chem. Soc.* **69** (1947) 1208.
34. Hunter, M. J. and Hibbert, H. *J. Am. Chem. Soc.* **61** (1939) 2190.
35. Gorecki, E. W. and Pepper, J. M. *Can. J. Chem.* **37** (1959) 2089.

Received February 28, 1973.

ACTA CHEMICA SCANDINAVICA 27 (1973) 2607–2613

Oxidation of Carbohydrate Derivatives with Silver Carbonate on Celite. VII. Aldopentoses

SVEIN MORGENLIE

Department of Chemistry, Agricultural University, N-1432 Ås-NLH, Norway

Aldopentoses are oxidized by silver carbonate on Celite in methanol to give formic esters of tetroses as major products. Pentonolactones are also formed primarily. Prolonged reaction time and higher temperatures cause extensive degradation beyond the tetrose stage, and tetronolactones as well as methyl esters of carboxylic acids with two and three carbon atoms are formed. The aldonolactones show greater resistance to the oxidant in methanol. Possible pathways for formation of most of the different products are suggested.

In a previous communication in this series the formation of tetroses as major products on oxidation of D-xylose and L-arabinose with silver carbonate on Celite in methanol and subsequent mild alkaline hydrolysis was described.[1] The yields of the tetroses were about 40 %, and spectroscopy and chromatography showed the presence also of other compounds. A more detailed investigation of the oxidation of aldopentoses with the oxidant has therefore been undertaken and is reported in the present paper.

RESULTS AND DISCUSSIONS

As in the case of D-xylose and L-arabinose,[1] tetroses were formed initially from D-ribose and D-lyxose on oxidation in methanol and subsequent mild alkaline hydrolysis. Infrared spectra of the product mixtures after oxidation of the pentoses before hydrolysis showed a great band at 1725 cm^{-1}. This absorption is due to formic ester groups resulting from glycol cleavage of the aldopentoses in cyclic form between C-1 and C-2. In addition, substantial absorption was observed at 1770 – 1780 cm^{-1}, indicating the presence of γ-lactones. In order to isolate these compounds, the aldopentoses were subjected to prolonged oxidation which led to further degradation of the initially formed *O*-formyl tetroses; the lactones showed greater resistance to the oxidant. This facilitated their isolation by paper chromatography. From L-arabinose (I) were obtained in 20 % yield L-arabino-1,4-lactone (II) and small amounts of erythrono-1,4-lactone (III).

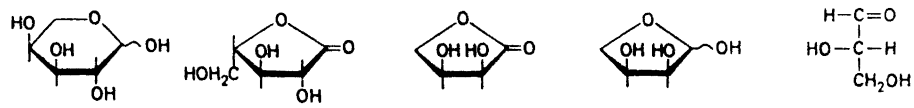

I II III IV V

After prolonged oxidation of L-arabinose (I) at 40°C, hydrolysis and removal of acidic products, column chromatography on silica gel gave four fractions. One contained L-erythrose (IV), an other contained L-glyceraldehyde (V), both in low yields. The fastest moving fractions contained small amounts of products with chromatographic and electrophoretic behaviour corresponding to those of glycolaldehyde (VI) and glyoxal (VII), both were contaminated with at least one additional unidentified compound.

D-Ribose, D-xylose, and D-lyxose give analogous reaction mixtures on oxidation. Some of the products have been detected by chromatography and electrophoresis only (Table 1).

The observation that aldonolactones were formed and that lower carbon sugars gradually disappeared, made an examination of the nature of the final degradation products interesting. After oxidation for 1 h at 40 – 45°C of D-xylose (VIII) with an excess of oxidant, chromatography showed the presence of several compounds detectable with hydroxylamine-ferric chloride, in addition to xylono-1,4-lactone (IX) and threono-1,4-lactone (X). Methyl glycerate (XI), methyl glyoxylate (XII), and dimethyl oxalate (XIII) have been characterized as components of the reaction mixture, and a compound with chromatographic mobility as methyl glycolate (XIV), giving an acid indistinguishable from glycolic acid on hydrolysis, was also detected.

The presence of glyceraldehyde and products assumed to be glycolaldehyde and glyoxal in the reaction mixture after oxidation of the pentoses, suggested a possible relationship between these compounds and the methyl esters of the two- and three-carbon acids which have been found to be final products in these oxidations. An investigation of the possibility of such a relationship has been performed in this laboratory, and is to be published separately.[2] This investigation has shown that α-hydroxy aldehydes are rapidly oxidized to the methyl esters of the corresponding carboxylic acids, and that glyoxal gives methyl glyoxylate with the oxidant in methanol. Methyl glycerate has been found to give a mixture of methyl glyoxylate and dimethyl oxalate at 45 – 50°C. In accordance with these results, possible routes to most of the different oxidation products from D-xylose (VIII) are shown in Scheme 1. It is, however, necessary to take into consideration the fact that several of the intermediate products exist in *O*-formylated form during parts of the reaction time, and this may alter the ease with which the reactions occur, and even the type of reaction undergone.

The rates with which the pentoses are oxidized have been compared, it has been found that L-arabinose and D-ribose are oxidized more slowly than D-xylose and D-lyxose (Fig. 1). The yields of pentonolactones from the two first mentioned pentoses are about 20 %, whereas the yield from D-xylose is only about 10 %. This fact suggests that the differences in oxidation rate are due mainly to differences in the ease with which the pentoses are degraded.

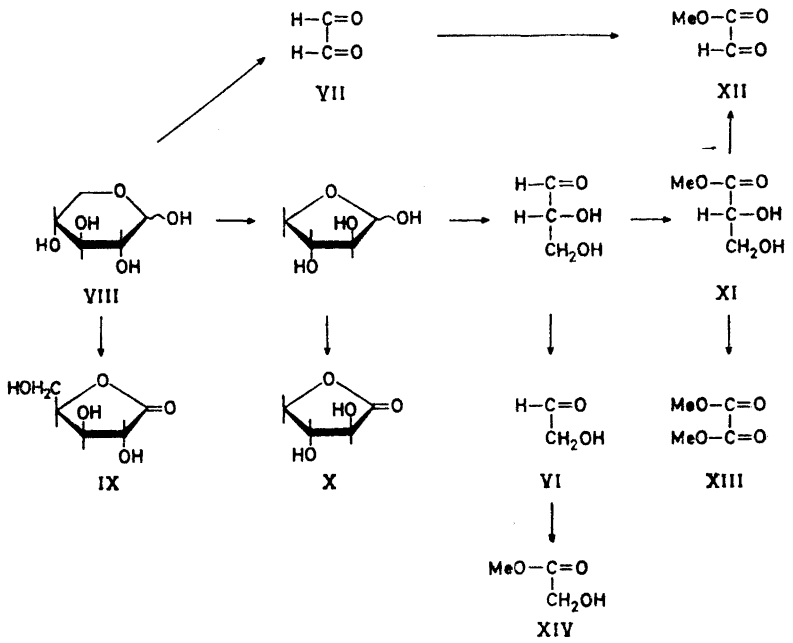

Scheme 1.

The instability of the formic ester group under the reaction conditions and particularly under the conditions necessary for work up makes an isolation of the primary degradation products difficult, and it has been impossible to

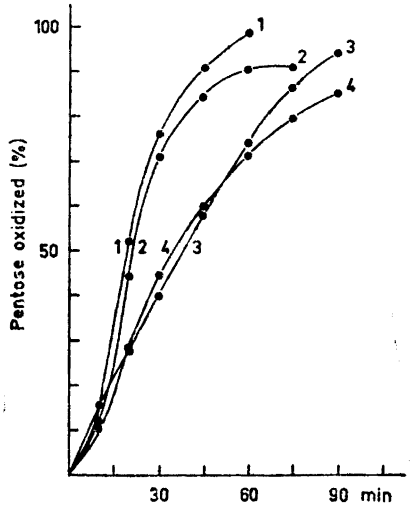

Fig. 1. Oxidation of aldopentoses at 30°C. Rates of disappearance of the pentoses: 1, D-xylose; 2, D-lyxose; 3, D-ribose; 4, L-arabinose.

establish in what form or forms the pentoses are degraded. Suggestions about the configurational factors to which the differences in degradation rate are to be ascribed are thus prevented.

It has previously been found that 2-*O*-methyl pentoses are stable to the oxidant in methanol at a temperature as high as 60°C.[3] The present work has shown that an unsubstituted hydroxyl group at C-2 of the aldopentoses greatly enhances the tendency to oxidation to aldonolactone; degradation is nevertheless the dominating reaction when the aldopentoses are treated with silver carbonate on Celite in methanol. It is in this connection of interest that galactono-1,4-lactone was the main product on oxidation of galactose in ethanol at 80°C, as reported recently by Fetizon and Moreau.[4]

EXPERIMENTAL

Paper chromatography was performed on Whatman No. 1 and 3 MM papers in the following solvent systems (v/v): (A) Butanol – ethanol – water 40:11:19, (B) butanol – pyridine – water 5:3:2, and (C) butanone – acetone – formic acid – water 40:2:1:6. Thin layer chromatography (TLC) was run on Silica gel G in (D) benzene – ethanol 3:1, (E) benzene – ethanol 5:1, (F) benzene – ethanol 10:1, and (G) chloroform – methanol 50:1. Electrophoresis was performed on Whatman No. 1 paper in borate buffer, pH 10, M_G-values refer to the mobilities relative to glucose. As spray reagents were used diphenylamine – aniline – phosphoric acid,[5] aniline oxalate and aniline hydrogen phthalate for the sugars, hydroxyl amine – ferric chloride[6] for the esters and lactones, and sulphanilamide – β-naphthol – sodium nitrite [7] for the acids.

Oxidation of aldopentoses. A. Identification of lower carbon sugars. Pentose (500 mg) in methanol (100 ml) was stirred with silver carbonate on Celite [8] (12 g) at 40°C for 10 – 25 min. The solution was filtered, and sodium bicarbonate (0.5 g) in water (50 ml) was added. After 1 h, the solution was treated with Dowex 50W (H^+) and subsequently with Dowex 1 (HCO_3^-) ion exchangers, and the solvents were removed. The composition of the residue was examined by paper chromatography (solvent B), TLC (solvent D), and electrophoresis. Treatment of the residue with acetone sulphuric acid and isolation of the resulting *O*-isopropylidene tetrose was performed as described previously;[1] the results are shown in Table 1.

B. Identification of aldonolactones. Pentose (500 mg) in methanol (100 ml) was treated with silver carbonate on Celite (12 g) for 40 min at 40°C. After filtration of the solution and evaporation of the solvent, the residue was subjected to preparative paper chromatography (solvent A). Two main fractions were obtained, the fraction with the lowest mobility, which contained pentonolactone, was eluted with water. Aldonic acid phenylhydrazides were prepared from the lactones with phenylhydrazine (100 mg to 100 mg of the lactones) in ethanol (1 ml) at 80°C for 3 h. The products were recrystallized from ethanol – ethylacetate. The results are shown in Table 2.

The fastest moving fraction obtained after the preparative paper chromatography contained as one component products with chromatographic mobilities (paper chromatography solvents A and B, TLC solvent D) corresponding to those of the tetronolactones (Table 2).

Identification of erythrono-1,4-lactone after oxidation of L-*arabinose.* The tetronolactone-containing fraction obtained from L-arabinose was treated with acetone-sulphuric acid. Neutralization of most of the sulphuric acid with solid sodium bicarbonate, filtration and evaporation yielded after purification by preparative TLC (solvent F) and crystallization from petroleum ether (b.p. 40 – 65°C), 2 mg of a product with chromatographic mobility (TLC, solvents F and G) corresponding to that of 2,3-*O*-isopropylidene-L-erythrono-1,4-lactone, m.p. 66 – 68°C, (lit.[1] 66.5 – 68°C).

Prolonged oxidation of L-*arabinose.* L-Arabinose (500 mg) in methanol (500 ml) was stirred with silver carbonate on Celite (15 g) for 40 min at 40°C. The solution was filtered and the solvent evaporated. The residue was hydrolyzed in 0.1 M sulphuric acid for 48 h at room temperature, the solution was neutralized and the acidic products were

Table 1. Oxidation of aldopentoses at 40°C for 10–25 min; lower-carbon sugars obtained.

Pentose	Tetrose	Isopropylidene derivatives			Glyceraldehyde
		Yield (%)	$[\alpha]_D$	M.p.	
L-Arabinose	L-Erythrose	41	+75° (*c* 1, MeOH), lit.[11] +72°	–	[b]
D-Ribose	D-Erythrose	19	−60° (*c* 1, water), lit.[12] −66°	–	[b]
D-Xylose	D-Threose	38 [a]	−13° (*c* 2, acetone), lit.[13] −15°	81–83°C, lit.[13] 84°C	[b]
D-Lyxose	Threose [b]	–	–	–	[b]

[a] Oxidation at room temperature. [b] Detected by TLC and electrophoresis.

Table 2. Aldolactones formed on oxidation of aldopentoses at 40°C for 40 min.

Pentose	Pentonolactones			Tetronolactones
	Yield (%)	$[\alpha]_D$ (equil.)	M.p. of phenylhydrazides	
L-Arabinose	20	−33° (*c* 1, water), lit.[14] −36.1°	212–214°C, lit.[15] 215°	Erythrono-
D-Ribose	21	+7° (*c* 2, water), lit.[16] +8.4°	159–161°C, lit.[16] 162°	Erythrono-[a]
D-Xylose	<12	not pure	–	Threono-[a]
D-Lyxose	[a]	–	–	Threono-[a]

[a] Detected chromatographically.

removed with Dowex 1 (HCO_3^-) ion exchanger. The residue after removal of the water under reduced pressure was chromatographed on a Silica gel column with benzene–ethanol 3:1 (v/v), benzene–ethanol 5:2, and finally benzene–ethanol 2:1. Four fractions were obtained.

Fraction 1 (15 mg) contained a compound indistinguishable by chromatography (TLC, solvent E) and electrophoresis (M_G 1.17) from glyoxal; the colours obtained with the spray reagents were identical with those obtained from glyoxal. This fraction in addition contained an other, unidentified component.

Fraction 2 (11 mg) contained a compound indistinguishable by TLC (solvent E) and electrophoresis (M_G 0.65) from glycolaldehyde. This fraction also contained an unidentified component, presumably the same as the unidentified compound in fraction 1.

Fraction 3 contained L-glyceraldehyde (12 mg), $[\alpha]_D$ −8° (*c* 1, water) [lit.[9] −8.7°], mobilities by TLC (solvent D) and electrophoresis (M_G 0.78) and colours obtained with the spray reagents corresponded to those of authentic D-glyceraldehyde.

Fraction 4 contained erythrose (41 mg), indistinguishable by chromatography (paper, solvent B; TLC, solvent D) and electrophoresis from authentic erythrose.

Oxidation of D-*xylose; identification of the methyl esters of oxalic and glyoxylic acid.* D-Xylose (250 mg) in methanol (50 ml) was stirred at 45°C with silver carbonate on Celite (15 mg) for 1 h. The solution was then filtered, the solvent evaporated and the residue dissolved in chloroform (30 ml). The chloroform solution was extracted with water (6 × 5 ml), the water extracts 3 to 6 were combined and the solvent was removed. The resulting oily residue (14 mg) was chromatographically homogeneous and indistinguishable (TLC, solvent E) from authentic methyl glyoxylate, and the infrared spectrum ($CHCl_3$, strong absorption at 1740 cm^{-1}) was identical with that of the authentic sample. The methyl ester was hydrolyzed in 0.5 M trifluoroacetic acid at 60°C overnight, and water and trifluoroacetic acid were removed under reduced pressure. The product was indistinguishable from authentic glyoxylic acid by paper chromatography (solvent C), both samples gave somewhat elongated spots.

The chloroform solution was dried with anhydrous sodium sulphate, the solution was filtered and the solvent evaporated. The residual syrup (19 mg) was chromatographically (TLC, solvent F) homogeneous and indistinguishable from authentic dimethyl oxalate. The infrared spectrum ($CHCl_3$, strong absorptions at 1740 and 1765 cm^{-1}) was identical with that of the authentic dimethyl oxalate. Hydrolysis in 0.5 M trifluoroacetic acid as described for methyl glyoxylate, gave a compound indistinguishable from oxalic acid by paper chromatography (solvent C).

Oxidation of D-*xylose. B. Identification of methyl glycerate.* D-Xylose (500 mg) in methanol (100 ml) was oxidized with silver carbonate on Celite (12 g) at 40°C for 40 min, the solution was filtered and the solvent evaporated. The residue was shown by TLC (solvent E) to contain at least five components detectable with hydroxylamine–ferric chloride. Two of the products had mobilities corresponding to those of glyceric acid methyl ester and glycolic acid methyl ester (traces). The product mixture was hydrolyzed in 0.5 M trifluoroacetic acid overnight at 60°C. After removal of the solvent and trifluoroacetic acid under reduced pressure, the residue was subjected to preparative paper chromatography (solvent B). Two zones with high mobility and two with very low mobility were obtained. The zones with low mobility were eluted with water and rechromatographed on paper (solvent C). Three fractions were obtained, the one with highest mobility contained a compound with chromatographic mobility as glycolic acid (4 mg), the next fraction (5 mg) contained a product with mobility corresponding to that of authentic D-glyceric acid, the third fraction was a mixture of the acid from the second fraction and an acid with mobility as glyoxylic acid. The acid from fraction 2 was stirred with Dowex 50W (H^+) ion exchanger in methanol for 24 h. Filtration of the solution and evaporation of the solvent yielded a syrup, chromatographically (TLC, solvent E) indistinguishable from methyl D-glycerate. The infrared spectrum ($CHCl_3$, strong absorption at 1735 cm^{-1}) was identical with that of the authentic sample.

Measurements of the rate of oxidation. The pentoses (50 mg) in methanol (10 ml) were stirred with silver carbonate on Celite (1.2 g) at 30°C. Aliquots (25 µl) were withdrawn at intervals, and the amount of unoxidized pentose determined by the paper chromatographic–colorimetric method described by Wilson.[10] The results are shown in Fig. 1.

Acknowledgement. The author wishes to thank Miss Astrid Fosdahl for valuable technical assistance.

REFERENCES

1. Morgenlie, S. *Acta Chem. Scand.* **26** (1972) 1709.
2. Morgenlie, S. *Acta Chem. Scand. To be published.*
3. Morgenlie, S. *Acta Chem. Scand.* **25** (1971) 2773.
4. Fetizon, M. and Moreau, N. *C. R. Acad. Sci. Ser. C* **275** (1972) 621.
5. Schwimmer, S. and Bevenue, A. *Science* **123** (1956) 543.
6. Abdel-Akher, M. and Smith, F. *J. Am. Chem. Soc.* **73** (1951) 5859.
7. Schmidt, G. C., Fischer, C. and McOwen, J. M. *J. Pharm. Sci.* **52** (1963) 468.
8. Balogh, V., Fetizon, M. and Golfier, M. *Angew. Chem.* **81** (1969) 423.
9. Perlin, A. S. *Methods Carbohyd. Chem.* **1** (1962) 62.
10. Wilson, C. M. *Anal. Chem.* **31** (1959) 1199.
11. Baxter, J. N. and Perlin, A. S. *Can. J. Chem.* **38** (1960) 2217.
12. Schaffer, R. *J. Res. Natl. Bur. Std.* **A 65** (1961) 507.
13. Steiger, M. and Reichstein, T. *Helv. Chim. Acta* **19** (1936) 1016.
14. Hauers, R. and Tollens, B. *Ber.* **36** (1903) 3306.
15. Fischer, E. *Ber.* **23** (1890) 2625.
16. Levene, P. A. and LaForge, F. B. *Ber.* **45** (1912) 608.

Received March 14, 1973.

ACTA CHEMICA SCANDINAVICA 27 (1973) 2614–2622

The Crystal Structure of $Zr(OH)_2SO_4H_2O$

MARGARETA HANSSON

Department of Inorganic Chemistry, Chalmers University of Technology and University of Göteborg, P.O. Box, S-402 20 Göteborg 5, Sweden

The crystal structure of $Zr(OH)_2SO_4H_2O$ has been determined from three-dimensional X-ray data. The symmetry is monoclinic, space group $C2/c$, with $a = 6.497$ Å, $b = 12.460$ Å, $c = 6.826$ Å, $\beta = 96.31°$ and $Z = 4$. Intensity data were collected with an automatic single crystal diffractometer, and, using a total of 986 independent reflexions, least squares full matrix refinements yielded a final R value of 0.060.

The structure consists of almost planar, infinite $[Zr(OH)_2]_n^{2n+}$ chains, which are joined in one direction by sulfate groups, thus constituting layers held together merely by hydrogen bonds and van der Waals contacts. Zr exhibits sevenfold oxygen coordination, the coordination polyhedron being a somewhat distorted pentagonal bipyramid. The Zr–O bond distances range between 2.10_7 and 2.19_0 Å with an average distance of 2.13_8 Å.

The crystal structure of $Hf(OH)_2SO_4H_2O$ has recently been determined.[1] The close resemblance between Hf and Zr suggested that the isomorphous compound $Zr(OH)_2SO_4H_2O$ ought to exist. During an investigation of the $ZrO_2-SO_3-H_2O$ system, McWhan and Lundgren found other zirconium hydroxide salts,[2] but not $Zr(OH)_2SO_4H_2O$. The experiments were, however, carried out using more basic solutions than those used for the preparation of $Hf(OH)_2SO_4H_2O$. Attempts were therefore made to prepare the zirconium salt under conditions more alike those under which the hafnium compound is obtained.

PREPARATION AND ANALYSIS

Solutions of 0.8 g $ZrOCl_2.8H_2O$ in concentrated sulfuric acid were evaporated to dryness and the residues dissolved in 2 M sulfuric acid. After heating in sealed Pyrex glass tubes for a month, no crystals were obtained. Experiments with solutions containing both hafnium and zirconium indicates, however, that the distribution factor for the crystals obtained, was in favour of Hf under these conditions. Guinier powder photographs showed the phase to be identical with $Hf(OH)_2SO_4H_2O$, and electron probe microanalysis indicated that with a Zr:Hf mol ratio of 3:1 in the original solution, the elements were distributed statistically in approximately equal amounts in the crystals.

Some experiments were then carried out in which only the volume of dilute sulfuric acid was varied, between 3 and 12 ml. In the more dilute zirconium solutions, crystals of $Zr_2(OH)_2(SO_4)_3(H_2O)_4$ were obtained,[2] while in the more concentrated ones $Zr(OH)_2SO_4H_2O$ crystallized as elongated prisms.

The compound was analysed with a Mettler Recording Thermoanalyzer, the following results for the *zirconium* content (as ZrO_2), the *sulfur* content (as SO_3) and the amount of *water* thus being obtained:

	% ZrO_2	% SO_3	% H_2O	Density (g cm^{-3})
Found:	52.0	33.3	14.8	2.88
Calc. for $Zr(OH)_2SO_4H_2O$:	51.5	33.5	15.0	2.89

The density was determined by the flotation method.

UNIT CELL AND SPACE GROUP

From rotation and Weissenberg photographs it was seen that $Zr(OH)_2SO_4H_2O$ crystallizes in the monoclinic system, the following reflexions being systematically absent: hkl, $h+k=2n+1$; $h0l$, $l=2n+1$. These extinctions are characteristic for space groups Nos. 9, Cc, and 15, $C2/c$.[3]

Accurate cell dimensions were obtained from Guinier powder photographs taken with $CuK\alpha_1$ radiation and internally calibrated with $Pb(NO_3)_2$ ($a=7.8566$ Å at 21°C).[4] 52 reflexions were indexed and least squares refinement with the program POWDER [5] gave the following cell dimensions:

$a = 6.4969 \pm 0.0004$ Å $\beta = 96.311° \pm 0.004°$
$b = 12.4598 \pm 0.0010$ Å $V = 549.2$ Å^3
$c = 6.8262 \pm 0.0004$ Å

A list of observed and calculated $\sin^2\theta$ values is given in Table 1. Assuming that $Z=4$, the calculated density of $Zr(OH)_2SO_4H_2O$ is 2.89 g cm^{-3} which is in good agreement with the experimental value (*cf.* above).

INTENSITY DATA

Three-dimensional X-ray data were collected with a Philips PAILRED single crystal diffractometer. A single crystal of the dimensions (in mm): $0.087 \times 0.062 \times 0.062$ was mounted along the a-axis in a sealed glass capillary, and reflexions from the layer lines $0kl - 9kl$ were recorded with $MoK\alpha$ radiation. The intensities were processed using the program DATAP1.[6] Standard deviations, $\sigma(I)$, based on counter statistics, were evaluated, and the reflexions with $\sigma(I)/I \leq 0.5$ were regarded as observed, thus yielding a data set of 1050 reflexions to be used in the subsequent calculations. Corrections for Lorentz', polarization and absorption effects were calculated with the programs DATAP1 and DATAP2,[6] the linear absorption coefficient being 23.0 cm^{-1}.

SOLUTION AND REFINEMENT OF THE STRUCTURE

A three-dimensional Patterson function and a subsequent electron density calculation (program DRF [6]) yielded parameters for all atoms in accordance with the corresponding parameters in the structure of $Hf(OH)_2SO_4H_2O$. The

Table 1. Guinier powder photograph of $Zr(OH)_2SO_4H_2O$.

$h\ k\ l$	$10^5 \sin^2\theta$ obs	$10^5 \sin^2\theta$ calc	d (calc) Å	I obs
0 2 0	1531	1529	6.230	s
1 1 0	1804	1805	5.733	vs
0 2 1	2821	2817	4.589	vvs
1 3 0	4865	4862	3.493	s
0 0 2	5163	5155	3.392	s
2 0 0	5684	5691	3.229	vvs
1 1 2	6360	6365	3.053	m
0 2 2	6675	6684	2.979	s
2 2 0	7219	7219	2.867	m
0 4 $\bar{1}$	7408	7403	2.831	s
2 2 $\bar{1}$	7918	7913	2.738	s
2 2 1	9109	9104	2.553	m
1 3 $\bar{2}$	9421	9422	2.509	m
2 0 $\bar{2}$	9660	9655	2.479	m
0 4 2	11272	11270	2.294	vw
1 5 $\bar{1}$	11966	11968	2.227	s
2 0 2	12039	12037	2.220	vvw
1 1 $\bar{3}$	12511	12511	2.178	w
1 5 1	12557	12563	2.173	m
0 2 3	13135	13128	2.126	m
3 1 0	13190	13187	2.121	s
2 2 2	13561	13565	2.091	w
2 4 1	13694	13690	2.082	w
1 1 3	14302	14297	2.037	vw
0 6 1	15055	15046	1.986	s
1 5 $\bar{2}$	15546	15536	1.954	m
3 3 0	16251	16244	1.911	s
3 1 $\bar{2}$	16553	16556	1.893	m
1 5 2	16725	16727	1.883	m
2 2 $\bar{3}$	17039	17032	1.866	w
0 4 3	17718	17714	1.830	s
3 3 $\bar{2}$	19615	19613	1.739	m
3 1 2	20129	20128	1.717	m
2 2 3	20608	20605	1.697	s
1 7 $\bar{1}$	21142	21139	1.675	w
1 1 $\bar{4}$	21239	21235	1.672	vw
2 4 $\bar{3}$	21625	21618	1.657	w
1 5 $\bar{3}$	21676	21683	1.654	w
1 7 1	21733	21735	1.652	w
0 2 4	22142	22149	1.637	m
3 5 $\bar{1}$ / 4 0 0	22754	22754 / 22764	1.615 / 1.614	vvs
3 3 2	23191	23185	1.600	vw
1 5 3	23466	23469	1.590	m
2 0 $\bar{4}$	23934	23930	1.575	vw
1 3 $\bar{4}$ / 4 2 0	24293	24292 / 24293	1.563 / 1.563	m
3 5 1	24541	24540	1.555	m
2 4 3	25190	25191	1.535	m
4 0 $\bar{2}$	25544	25538	1.524	w
3 5 $\bar{2}$ / 0 8 1	25735	25728 / 25747	1.518 / 1.518	m
2 0 4	28699	28693	1.438	m
2 2 4	30222	30222	1.401	w
4 2 $\bar{3}$	32311	32319	1.355	w

Table 2. Observed and calculated structure factors for $Zr(OH)_2SO_4H_2O$. (The columns are l, F_o, F_c and the phase angles, respectively.)

	0 0 L			1 3 L			-4	32	24	-3.10	-2	47	45	0.05	0	47	52	0.06
2	159	176	-3.12	10	39	39	-3.08	-3	41	50	-3.09	-3	68	64	0.03	2	67	64	-3.13
4	159	160	0.02	8	39	40	0.06	-1	51	56	0.05	-4	41	41	-3.08	5	79	84	0.06
6	131	134	-3.12	6	59	63	-3.10	0	45	44	-3.12	-5	62	62	-3.11	4	51	46	-3.12
8	62	62	0.05	4	65	61	0.04	1	56	52	-3.09	-6	30	27	0.09	3	98	102	-3.11
10	65	68	-3.09	2	51	45	-3.08	3	47	45	0.06	-11	34	30	0.05	2	44	45	0.02
12	44	42	0.07	0	134	131	0.02	5	41	44	-3.08	-12	33	28	-3.06	1	136	135	0.03
	0 2 L			-2	88	91	-3.11	6	34	27	0.04		2 12 L			0	73	77	-3.13
0	126	129	0.02	-3	61	59	0.03	7	41	40	0.06	-10	39	41	0.07	-1	110	112	-3.11
1	169	166	0.01	-4	65	69	0.04		1 10 L			-9	68	67	-3.10	-2	45	44	0.02
2	116	120	-3.12	-6	77	84	-3.11	7	43	40	0.07	-6	55	57	0.06	-3	106	103	0.03
3	117	120	-3.12	-7	43	47	0.04	3	49	53	0.05	-4	73	76	-3.10	-4	53	47	-3.12
4	99	93	0.03	-8	45	54	0.04	-3	52	55	-3.09	-2	96	92	0.06	-5	105	102	-3.11
5	68	68	0.03	-10	46	40	-3.09	-7	35	42	-3.08	0	69	71	-3.09	-6	37	41	0.03
6	52	54	-3.09		1 5 L				1 11 L			2	95	102	0.03	-7	50	56	0.06
7	69	67	-3.11	-11	48	50	0.06	0	33	36	0.06	4	72	75	-3.10	-9	53	57	-3.09
8	43	45	0.06	-9	62	65	-3.10	6	26	24	-3.06	6	69	69	0.05	-11	41	45	0.06
9	36	36	0.05	-8	50	46	0.02		2 0 L			8	57	65	-3.09		3 0 L		
10	44	40	-3.08	-7	91	90	0.03	-10	66	69	-3.09		2 14 L			-8	44	45	-3.09
12	34	26	0.09	-5	109	107	-3.11	-8	64	66	0.05	6	47	44	0.06	-6	45	46	0.05
	0 4 L			-4	72	68	0.02	-6	104	118	-3.11	5	58	52	-3.11	-5	47	41	-3.11
1	121	99	0.03	-3	124	123	0.03	-4	84	93	0.04	4	52	52	-3.09	-4	76	77	-3.11
2	69	63	-3.13	-2	106	106	-3.13	-2	111	118	-3.11	3	46	31	0.06	-2	89	81	0.03
3	147	146	-3.12	-1	143	138	-3.12	2	92	91	-3.10	2	51	45	0.06	-1	73	68	-3.11
4	27	22	0.04	1	116	110	0.03	4	156	159	0.02	1	47	44	-3.10	0	74	74	-3.11
5	39	42	0.06	2	126	122	-3.13	6	120	122	-3.11	0	64	57	-3.10	1	42	37	0.05
7	57	58	-3.10	3	89	89	-3.10	8	74	70	0.05	-1	57	50	0.04	2	91	91	0.03
9	48	46	0.06	4	53	47	0.03	10	39	35	-3.10	-2	53	49	0.05	3	26	25	-3.07
	0 6 L			5	81	78	0.04		2 2 L			-4	39	43	-3.08	4	57	58	-3.12
0	34	33	-3.14	6	33	27	-3.10	11	36	31	-3.09	-5	41	41	0.04	5	54	52	0.01
1	132	127	0.02	7	62	67	-3.09	10	41	44	-3.09	-6	42	45	0.06	6	69	69	0.05
3	72	69	-3.11	8	45	45	0.02	9	42	40	0.05	-7	30	27	-3.08	8	37	43	-3.09
5	74	73	0.03	9	47	55	0.05	8	50	54	0.05	-8	37	35	-3.07		3 11 L		
7	45	46	-3.09	11	49	45	-3.08	7	65	64	-3.11	-9	27	24	0.07	6	43	45	0.05
9	34	34	0.07		1 7 L			6	56	62	-3.10		2 16 L			4	51	57	-3.12
11	35	31	-3.06	11	37	43	-3.07	5	66	69	0.03	-7	41	36	-3.07	2	69	70	0.06
	0 8 L			9	59	60	0.05	4	78	73	0.04	-5	46	46	0.05	0	60	61	-3.12
0	60	66	-3.13	7	52	60	-3.09	3	101	99	-3.12	-4	50	52	0.05	-2	81	83	0.03
1	82	81	0.03	6	30	29	0.03	2	87	84	-3.11	-3	43	43	-3.09	-4	43	50	-3.09
3	43	39	-3.08	5	79	77	0.04	1	87	86	0.03	-2	48	45	0.06	-6	45	45	0.06
5	62	69	0.04	4	39	40	-3.11	0	60	60	0.05	-1	52	51	-3.08	-8	49	48	-3.09
7	36	34	0.07	3	95	92	-3.10	-2	34	32	-3.06	0	35	36	0.07		3 13 L		
11	35	32	-3.07	2	38	30	0.04	-3	88	85	0.03	1	35	33	-3.07	-4	33	43	-3.03
	0 10 L			1	107	105	0.03	-4	67	62	0.04		3 1 L			-3	36	38	0.04
0	47	45	-3.09	0	74	69	-3.13	-5	47	43	-3.09	-10	39	40	-3.08	-1	31	31	0.03
1	74	74	0.03	-1	98	102	-3.11	-6	41	44	-3.08	-8	58	58	-3.10	0	34	39	-3.07
2	82	84	0.03	-2	40	40	0.03	-7	63	66	0.03	-6	86	81	0.01	2	51	49	0.06
3	76	69	-3.11	-3	113	116	0.03	-8	34	39	0.07	-3	49	50	0.01	3	32	33	-3.07
4	54	55	-3.10	-4	60	56	-3.12	-9	38	39	-3.09	-2	85	77	-3.11		3 15 L		
5	61	59	0.03	-5	105	106	-3.11	-10	42	45	-3.09	2	88	86	-3.11	10	32	25	0.08
6	36	35	0.07	-6	45	45	0.02	-11	34	29	0.06	3	40	35	-3.13	6	35	36	0.06
7	43	42	-3.10	-7	68	70	0.05		2 4 L			4	77	75	0.03	1	34	27	-3.09
8	39	42	-3.09	-9	62	69	-3.10	-9	42	49	-3.09	6	55	54	-3.10	0	46	49	-3.10
9	36	38	0.05	-11	47	49	0.06	-7	43	44	0.06	8	33	36	0.07	-2	35	40	0.05
	0 12 L				1 9 L			-5	35	32	-3.06	10	36	37	-3.07	-6	41	35	0.04
0	93	88	-3.10	-12	38	30	-3.07	-3	95	94	0.03		3 3 L			-10	34	27	0.07
2	114	116	0.03	-9	31	24	-3.06	-2	35	31	-3.11	8	44	40	0.06		3 17 L		
4	82	85	-3.10	-8	61	57	-3.10	1	79	76	0.04	6	53	59	-3.10	-6	35	39	0.03
6	61	66	0.05	-7	34	31	0.06	2	48	44	-3.12	4	88	86	0.01	-5	50	49	0.06
8	63	67	-3.10	-6	59	56	0.04	3	110	110	-3.12	3	55	58	-3.11	-3	48	51	-3.09
	0 14 L			-5	60	54	-3.11	5	44	42	0.06	2	79	74	-3.11	-1	56	58	0.05
0	74	66	-3.10	-4	80	72	-3.11	7	75	73	-3.11	1	49	47	0.04	0	33	36	-3.11
1	63	61	-3.11	-2	87	82	0.03	9	45	49	0.05	0	119	118	0.02	1	58	52	-3.09
2	53	51	0.05	-1	67	62	-3.11	11	35	32	-3.07	-1	51	44	-3.10	3	44	49	0.05
3	33	34	0.05	0	53	46	-3.08		2 6 L			-2	120	116	-3.12	4	35	28	-3.12
4	51	51	-3.09	1	47	44	0.04	9	41	43	0.06	-3	67	66	0.03	5	42	46	-3.08
5	50	52	-3.11	2	77	73	0.04	7	48	49	-3.09	-4	60	59	0.04	7	41	37	0.07
6	41	47	0.05	4	54	47	-3.09	5	66	74	0.03	-6	68	67	-3.11		3 19 L		
7	30	28	0.06	5	51	52	0.04	3	57	55	-3.10	-8	47	49	0.05	5	32	34	-3.06
	0 16 L			6	41	43	0.06	1	68	61	0.04	-10	33	31	-3.07	3	48	51	0.05
1	62	61	-3.10	8	53	47	-3.09	0	25	22	-3.14	-12	37	31	0.07	1	47	48	-3.08
3	47	48	0.05		1 11 L			-1	78	74	-3.11		3 5 L			-1	47	45	0.06
5	49	53	-3.09	8	43	42	-3.08	-3	36	30	0.08	-13	36	35	-3.06	-3	49	53	-3.09
7	40	36	0.07	6	36	44	0.06	-5	43	44	-3.09	-11	39	40	0.07		3 21 L		
	0 18 L			4	41	43	-3.08	-7	39	43	0.06	-9	51	53	-3.08	0	43	39	0.05
1	39	34	-3.07	2	63	57	0.05	-9	30	36	-3.07	-8	39	40	0.03	2	35	30	-3.07
3	48	44	0.05	0	53	54	-3.09	-11	34	34	0.07	-7	80	76	0.04		4 0 L		
	0 20 L			-2	73	74	0.04		2 8 L			-5	95	87	-3.10	-12	51	48	0.06
3	33	28	0.07	-4	52	54	-3.09	-5	50	56	-3.10	-4	71	69	0.02	-11	67	69	-3.11
1	24	23	-3.06	-6	52	58	0.04	-1	61	59	-3.10	-3	131	123	0.03	-8	82	81	0.04
	0 22 L			-8	52	54	-3.09	1	52	51	0.05	-2	71	66	-3.12	-6	122	126	-3.11
4	23	24	0.08		1 13 L			3	30	37	-3.08	-1	153	152	-3.12	-4	113	111	0.01
	1 1 L			-2	41	43	0.05	5	63	66	0.04	0	33	28	0.06	-2	146	149	-3.12
10	44	52	-3.09	2	42	44	0.05	6	29	24	0.04	1	132	133	0.02	2	73	66	-3.09
-8	52	47	0.05	8	38	35	-3.08	9	45	40	0.06	2	98	107	-3.13	4	114	112	0.03
-6	69	73	-3.11		1 15 L			11	38	32	-3.07	3	120	120	-3.11	6	75	74	-3.13
-4	95	95	0.03	6	42	37	0.05		2 10 L			4	33	29	0.04	8	56	53	0.06
-3	75	75	0.01	4	34	41	-3.09	6	40	41	0.06	5	91	89	0.04	10	62	60	-3.09
-2	64	61	-3.10	2	39	38	0.06	5	55	53	0.04	6	27	32	-3.11	12	36	35	0.08
2	27	30	-3.06	0	50	52	-3.10	4	39	45	-3.09	7	68	66	-3.10		4 2 L		
3	58	52	-3.13	-2	48	40	0.05	3	64	60	-3.11	8	40	33	0.01	12	29	27	0.08
4	48	49	0.05	-4	39	41	-3.09	2	69	69	0.03	9	49	51	0.06	10	33	34	-3.07
6	40	43	-3.08		1 17 L			1	74	75	0.03	11	38	38	-3.07	9	38	32	0.06
8	38	34	0.07	-7	42	47	-3.09	0	30	22	-3.11		3 7 L			7	48	44	-3.10
10	36	43	-3.08	-5	52	48	0.06	-1	67	64	-3.11	11	40	37	-3.07	6	37	44	-3.08

Table 2. Continued.

5	44	44	0.05			4 20	L		-5	37	44	0.08	-6	38	40	-3.08	0	31	34	-3.08
4	47	40	0.06	3	24	25	0.10	-3	37	43	-3.08	-2	45	48	0.05	4	24	30	-3.08
3	76	72	-3.11		5 1	L		-2	39	36	0.04	-1	46	47	0.04		7 17	L					
2	59	54	-3.09	-6	47	46	-3.09	-1	41	44	0.06	0	37	43	-3.08	-1	61	58	0.07
1	61	57	0.04	-4	33	37	0.07	0	44	42	-3.11	1	34	37	-3.09	-3	33	42	-3.09
-1	85	86	-3.12	-2	24	22	-3.03	1	36	40	-3.08	2	39	43	0.06	-5	31	34	0.07
-2	52	52	-3.09	0	60	62	0.06	2	43	43	0.06	3	36	34	0.05		8 0	L					
-3	105	101	0.02	1	24	24	0.02	3	33	25	-3.10	4	49	43	-3.08	-12	32	38	0.08
-4	84	81	0.03	2	42	40	-3.08	4	35	39	-3.08	5	35	36	-3.10	-10	56	61	-3.08
-5	57	52	-3.10	4	54	56	0.06	5	36	33	0.08	8	35	29	-3.06	-8	53	53	0.06
-6	67	67	-3.10	6	53	52	-3.09		8 2	L				6 16	L		-6	65	63	-3.09
-7	70	71	0.03	8	42	39	0.06	10	49	48	-3.08	7	32	27	0.08	-4	63	63	0.06
-8	37	45	0.06	10	40	39	-3.08	8	50	52	0.06	5	44	37	-3.08	-2	69	72	-3.10
-9	43	46	-3.10		5 3	L		6	65	67	-3.09	3	41	41	0.06	0	66	68	0.05
-10	46	47	-3.09	9	24	22	0.08	4	110	109	0.03	1	38	43	-3.08	2	65	66	-3.09
-11	32	30	-3.09	8	44	42	0.05	2	101	96	-3.11	-1	46	49	0.05	4	78	74	0.04
	4 4	L		6	47	49	-3.09	-2	123	127	-3.11	-3	33	30	-3.08	6	53	54	-3.08
-9	52	53	-3.09	4	68	69	0.03	-4	90	91	0.04	-7	35	34	-3.07	8	50	49	0.06
-7	56	55	0.05	3	42	36	-3.09	-6	84	87	-3.10		7 1	L		10	44	41	-3.07
-5	69	68	-3.10	2	60	56	-3.10	-8	59	61	0.05	6	37	34	0.07		8 2	L	
-3	99	96	0.03	0	55	53	0.05	-10	59	53	-3.08	5	51	54	0.04	9	26	26	0.07
-2	22	27	-3.11	-2	74	74	-3.11		6 2	L		-2	41	42	-3.08	8	34	32	0.07
-1	37	34	-3.06	-3	27	29	0.06	-10	39	33	-3.07	-4	47	48	0.05	7	38	35	-3.09
1	79	76	0.04	-4	45	42	0.06	-9	38	38	-3.09	-6	52	57	-3.10	6	43	41	-3.08
2	27	26	-3.11	-6	50	47	-3.09	-7	51	50	0.04	-8	32	33	0.07	5	31	31	0.06
3	59	56	-3.09	-8	48	49	0.05	-6	50	52	-3.09	-10	36	38	-3.08	4	45	42	0.06
7	48	54	-3.09	-10	33	32	-3.07	-5	44	40	-3.09		7 3	L		3	49	49	-3.10
9	30	33	0.08	-12	32	30	0.07	-4	55	58	0.04	-9	30	27	-3.08	2	38	36	-3.07
	4 6	L			5 5	L		-3	86	85	0.02	-8	46	49	0.05	1	47	43	0.04
9	41	34	0.07	-13	40	37	-3.07	-2	59	56	-3.09	-7	28	27	0.06	0	49	47	0.05
5	48	44	0.06	-11	37	41	0.07	-1	87	88	-3.11	-6	48	47	-3.09	-1	35	36	-3.08
3	37	38	-3.08	-9	53	54	-3.09	0	84	84	0.03	-4	57	56	0.04	-2	33	32	-3.06
1	66	59	0.06	-7	63	64	0.05	1	67	64	0.03	-3	41	41	0.04	-3	56	55	0.04
0	25	25	-3.14	-6	26	29	-3.10	2	66	64	-3.10	-2	65	67	-3.11	-4	32	33	0.08
-1	70	72	-3.11	-5	57	59	-3.09	3	73	73	-3.11	-1	15	13	-3.02	-5	31	31	-3.08
-3	61	59	0.04	-4	51	54	0.02	4	58	54	0.05	0	45	44	0.05	-6	47	41	-3.08
-5	58	57	-3.10	-3	81	77	0.04	5	43	42	0.04	1	20	19	0.09	-7	33	35	0.05
-7	53	54	0.04	-2	40	41	-3.11	6	53	49	-3.09	2	48	50	-3.09	-8	32	28	0.08
-9	42	43	-3.09	-1	79	79	-3.10	7	46	41	-3.10	3	26	22	-3.06	-9	35	36	-3.09
-11	32	33	0.07	0	34	37	0.03	8	29	35	0.07	4	42	46	0.05	-11	25	22	0.08
	4 8	L		1	77	75	0.04	9	32	27	0.06		7 5	L		-12	33	27	0.08
-11	34	35	0.07	2	71	66	-3.12		8 4	L		9	40	36	0.08		8 4	L	
-9	62	60	-3.10	3	69	67	-3.11	7	47	50	-3.09	7	38	43	-3.08	-7	35	35	0.07
-7	29	32	0.08	5	73	72	0.04	5	49	45	0.06	5	41	45	0.06	-5	36	34	-3.07
-5	59	62	-3.10	6	37	33	-3.11	3	59	66	-3.10	3	55	61	-3.09	-3	34	35	0.07
-3	42	40	0.06	7	61	63	-3.09	2	25	26	-3.10	2	42	41	-3.11	-1	36	35	-3.07
-1	30	31	-3.06	9	45	51	0.06	1	87	87	0.03	1	61	62	0.05	1	48	47	0.06
1	50	47	0.05	11	32	38	-3.07	-1	58	58	-3.10	0	36	35	0.03	3	43	38	-3.08
3	30	24	-3.05		5 7	L		-2	21	19	-3.09	-1	70	71	-3.10	5	47	40	0.06
	4 10	L		11	31	37	-3.07	-3	67	68	0.04	-2	34	32	-3.11	7	45	42	-3.08
7	43	36	-3.09	9	45	49	0.06	-5	55	54	-3.09	-3	84	83	0.04		9 6	L	
5	43	47	0.04	7	56	60	-3.09	-7	37	39	0.07	-4	34	39	0.03	5	29	34	0.07
3	49	47	-3.10	6	30	27	0.04	-9	40	35	-3.07	-5	65	68	-3.10	3	35	36	-3.08
2	46	52	0.04	5	73	75	0.04		6 6	L		-6	33	29	-3.10	1	27	28	0.08
1	62	67	0.03	4	36	34	-3.11	-9	34	30	-3.06	-7	63	66	0.05	0	18	14	-3.13
0	27	32	-3.07	3	73	69	-3.09	-6	34	40	-3.08	-8	33	28	0.04	-1	25	27	-3.04
-1	54	58	-3.11	1	92	92	0.04	-4	56	54	0.04	-11	44	37	0.07	-3	28	29	0.08
-2	51	49	0.05	0	42	44	-3.12	-1	61	63	-3.10		7 7	L		-5	26	26	-3.05
-3	54	52	0.04	-1	81	75	-3.10	0	28	27	-3.14	-11	46	44	0.06		8 8	L	
-4	59	54	-3.10	-2	26	22	0.05	1	49	52	0.05	-9	45	46	-3.08	-9	29	22	-3.04
-5	63	62	-3.11	-3	60	60	0.05	3	53	55	-3.10	-7	56	58	0.05	-7	30	28	0.04
-6	32	41	0.06	-4	28	26	-3.10	5	47	46	0.05	-6	37	36	0.03	-5	30	31	-3.07
-7	39	37	0.05	-5	83	83	-3.10	7	30	31	-3.06	-5	62	61	-3.10	-3	25	23	0.10
-8	49	43	-3.09	-6	39	34	0.03		6 8	L		-4	35	27	-3.10	-1	37	37	-3.08
-11	31	31	0.05	-7	49	51	0.06	9	33	30	0.07	-3	65	61	0.05	1	26	29	0.08
-12	34	27	-3.06	-9	50	51	-3.08	7	29	26	-3.06	-2	22	28	0.04	3	31	32	-3.07
	4 12	L		-11	48	48	0.06	5	46	46	0.05	-1	77	77	-3.10	5	36	36	0.06
-10	39	43	0.07		5 9	L		3	44	42	-3.09	0	36	35	-3.11	9	29	27	0.08
-8	73	68	-3.10	-8	32	40	-3.08	1	47	46	0.05	1	69	70	0.04		8 10	L	
-6	53	62	0.05	-6	33	39	0.06	-1	55	59	-3.10	3	49	49	-3.08	8	27	27	-3.06
-4	87	84	-3.10	-4	54	51	-3.09	-2	29	25	0.06	5	52	56	0.05	6	35	32	0.07
-2	84	87	0.04	-3	29	18	0.10	-3	26	33	0.07	7	42	41	-3.07	5	31	34	0.06
0	66	68	-3.09	-2	40	46	0.05	-5	43	45	-3.09	9	39	36	0.08	3	32	30	-3.08
2	83	84	0.04	-1	48	44	-3.10	-9	30	23	-3.04		7 9	L		2	35	34	0.06
4	50	58	-3.09	0	55	50	-3.09		6 10	L		8	31	27	-3.06	1	37	38	0.05
6	55	56	0.06	2	62	62	0.04	-5	57	54	-3.11	6	34	33	-3.07	0	27	27	-3.06
8	46	51	-3.08	4	43	47	-3.09	-4	37	43	-3.09	2	43	45	0.05	-1	46	45	-3.10
10	32	32	0.09	5	42	41	0.04	-3	47	40	0.05	0	52	49	-3.09	-2	37	36	0.08
	4 14	L		6	57	51	0.05	-2	49	46	0.05	-1	34	34	-3.08	-3	28	30	0.06
10	31	28	0.08	8	42	41	-3.09	-1	57	53	-3.11	-2	56	60	0.05	-4	28	26	-3.06
8	35	31	-3.07		5 11	L		0	47	46	-3.09	-3	28	25	0.07	-5	41	41	-3.10
6	38	35	0.07	8	41	40	-3.08	1	55	54	0.03	-4	50	55	-3.10	-6	27	29	-3.07
5	37	39	-3.10	6	39	40	0.06	2	60	56	0.04	-5	29	29	-3.08	-11	28	25	0.06
4	38	47	-3.09	4	49	47	-3.09	3	31	38	-3.09	-6	43	48	0.05		8 12	L	
2	36	41	0.06	2	47	53	0.05	5	42	42	0.04	-7	30	24	0.07	-10	36	35	0.09
1	38	34	-3.09	-2	53	55	0.05	6	39	36	0.06	-8	45	41	-3.09	-8	43	44	-3.08
0	52	49	-3.09	-6	33	31	0.08	7	29	29	-3.09		7 11	L		-6	46	41	0.07
-1	54	50	0.04	-8	46	47	-3.09	8	34	31	-3.07	-8	44	46	-3.09	-4	52	53	-3.08
-2	46	52	0.05		5 13	L			6 12	L		-6	29	33	0.07	-2	49	50	0.06
-3	39	33	-3.09	-8	31	25	-3.05	8	35	43	-3.07	-4	49	47	-3.09	0	47	49	-3.08
-4	44	43	-3.08	2	34	38	0.06	6	48	53	0.06	-2	47	51	0.05	2	52	56	0.06
-5	51	45	0.04	6	34	31	0.07	4	61	57	-3.09	0	32	29	-3.06	4	43	44	-3.07
-6	40	44	0.06		5 15	L		2	75	79	0.04	2	45	44	0.06	6	38	43	0.07
-7	37	33	-3.09	6	34	29	0.07	0	65	66	-3.10	6	28	27	0.09	8	35	36	-3.07
-11	31	24	-3.08	4	39	36	-3.09	-2	74	75	0.04		7 13	L			8 14	L	
	4 16	L		2	29	31	0.06	-4	72	72	-3.10	2	30	28	0.08	6	29	27	0.09
-5	53	48	0.05	0	40	41	-3.09	-6	45	50	0.06	0	35	28	-3.06	4	35	33	-3.07
-3	40	42	-3.08	-2	41	35	0.06	-8	53	53	-3.08	-4	28	31	-3.07	3	27	26	0.08
-1	47	52	0.05	-4	33	36	-3.09		8 14	L		-6	27	27	0.08	2	35	35	0.07
3	37	38	0.07	-8	32	25	-3.06	-8	31	33	-3.07	-8	28	26	-3.06	1	24	23	-3.07
	4 18	L			5 17	L		-7	30	24	-3.07		7 15	L		0	28	32	-3.07
-1	33	26	0.09	-7	40	38	-3.07	-5	33	36	0.05	-2	31	30	0.07	-2	36	36	0.07

Table 2. Continued.

-5	29	27	0.06	-4	47	46	0.05	-3	44	44	0.05	5	49	52	3.05	0	37	31	-3.07
-10	28	24	0.09	-3	31	31	0.05	-4	31	27	0.04	7	32	35	-3.06	2	46	45	3.05
	8 16	L		-2	52	50	-3.10	-5	44	49	-3.08	9	33	30	0.09	6	26	28	0.08
-5	29	28	0.08	-1	16	18	-3.05	-6	21	22	-3.09		9 8	L			9 13	L	
-3	30	29	-3.06	0	42	43	0.05	-7	40	42	0.07	8	23	23	-3.06	8	22	18	-3.03
1	28	30	-3.06	1	29	30	0.05	-8	22	23	0.04	6	36	32	0.06	6	23	23	0.09
3	35	31	0.07	2	51	51	-3.10	-9	34	37	-3.07	4	34	37	-3.08	-2	24	25	3.09
	9 1	L		3	28	28	-3.08		9 7	L		3	25	25	-3.08		9 15	L	
8	23	24	0.10	4	40	40	0.05	-11	31	33	0.08	2	40	44	3.05	-6	29	25	0.07
4	41	42	0.06	6	32	31	-3.07	-9	28	31	-3.05	1	22	22	0.09	-4	25	25	-3.07
2	33	36	-3.08	8	27	28	0.07	-7	40	44	0.07	0	47	47	-3.09	0	30	28	-3.08
0	48	51	0.05		9 5	L		-6	26	23	0.04	-1	29	27	-3.08		9 17	L	
-2	38	40	-3.08	9	34	29	0.09	-5	52	56	-3.09	-2	45	44	0.05	1	31	32	-3.07
-4	32	31	0.07	7	30	39	-3.07	-4	24	18	-3.09	-3	24	21	0.09	-1	30	31	0.08
-6	36	36	-3.08	5	40	45	0.06	-3	52	49	0.06	-4	36	40	-3.08	-3	35	34	-3.07
-12	24	19	0.12	3	57	59	-3.09	-1	72	69	-3.10	-6	29	34	0.07	-5	25	29	3.09
	9 3	L		2	28	27	-3.10	0	26	30	-3.11	-8	23	27	-3.06				
-10	26	24	-3.06	1	63	64	0.05	1	61	60	0.05		9 11	L					
-8	32	33	0.07	0	30	28	0.04	2	21	19	0.05	-8	26	30	-3.07				
-7	17	12	0.13	-1	60	60	-3.09	3	49	51	-3.08	-6	37	39	-3.09				
-6	31	32	-3.07	-2	30	27	-3.10	4	28	23	-3.10	-2	38	39	0.06				

space group was therefore assumed to be $C2/c$. Preliminary refinement of the scale factors between the layers and the atomic parameters gave an R value of 0.069. After correction for absorption effects there were still some discrepancies between observed and calculated structure factors with high values, and a secondary extinction factor was therefore included in the refinement. The following parameters were thus refined with the program LINUS:[6] scale factors, atomic positions including isotropic thermal vibrations and an isotropic secondary extinction factor. An R value of 0.065 was obtained when the scattering factors [7] for Zr and S were corrected for anomalous dispersion.[8]

Since the crystal was very symmetric in shape, the values of the average path lengths in the crystal, used to calculate the extinction corrections, are approximately the same for the reflexions $0kl$ and $0k\bar{l}$. Hence, mean values of F_{0kl} and $F_{0k\bar{l}}$ could be calculated, giving a final data set of 986 independent reflexions. The final refinement was then extended to include anisotropic thermal parameters while the scale factors were held constant. When the shifts of the parameters were less than 2 % of the standard deviations the refinement was terminated, the R value having converged to 0.060. A weighting scheme according to Cruickshank was used in the refinement, which yielded a weighted R value of 0.074. The final value of the isotropic extinction parameter was $g = (1.12 \pm 0.10) \times 10^4$. Observed and calculated structure factors are listed in Table 2. Because of the small size of the crystal used in the collection of the intensity data, there were more reflexions with $\sigma(I)/I > 0.5$ than for the hafnium salt. Calculated structure factors for the unobserved reflexions

Table 3a. Atomic coordinates, expressed as fractions of the cell edges, and their standard deviations.

Atom and position	x	y	z
Zr in 4(*e*)	0.0	0.95831(7)	1/4
S in 4(*e*)	0.0	0.3800(2)	1/4
O_1 in 8(*f*)	0.0142(8)	0.0894(4)	0.4460(7)
O_2 in 8(*f*)	0.0606(11)	0.3160(6)	0.4237(11)
O_3 in 8(*f*)	0.1733(8)	0.4510(6)	0.2105(9)
O_4 in 4(*e*)	1/2	0.2826(8)	1/4

Table 3b. Anisotropic thermal parameters and their standard deviations. The temperature coefficient is expressed as exp $[-(h^2\beta_{11}+k^2\beta_{22}+l^2\beta_{33}+2hk\beta_{12}+2hl\beta_{13}+2kl\beta_{23})]$.

Atom	β_{11}	β_{22}	β_{33}	β_{12}	β_{13}	β_{23}
Zr	0.0014(1)	0.00051(3)	0.0007(1)	0	0.00011(6)	0
S	0.0035(4)	0.0013(1)	0.0057(4)	0	0.0014(3)	0
O_1	0.0089(10)	0.0010(3)	0.0041(8)	−0.0004(4)	0.0013(6)	0.0008(3)
O_2	0.0097(13)	0.0033(5)	0.0111(12)	−0.0006(5)	0.0014(9)	0.0025(6)
O_3	0.0038(9)	0.0036(4)	0.0085(9)	0.0002(5)	0.0014(7)	0.0001(5)
O_4	0.0146(21)	0.0019(5)	0.0082(16)	0	0.0042(14)	0

have not therefore been included in the table. The final atomic parameters, together with their standard deviations, are given in Table 3a, b.

Finally, a three-dimensional electron difference density calculation was performed with the program FFT.[6] Only negligible rest peaks around the zirconium atoms were obtained.

Interatomic distances and angles were calculated with the program DISTAN [6] and the results are given in Table 4.

Table 4. Interatomic distances and angles with their standard deviations in parentheses.

Zr – Zr	3.568(1) (Å)		
Within the bipyramid:			
Zr – 2O$_1$	2.107(5) (Å)	O$_1$ – Zr – O$_1$	78.4(3)°
Zr – 2O$_1$	2.170(5)	O$_1$ – Zr – O$_1$ (2×)	66.9(2)
Zr – 2O$_3$	2.112(5)	O$_1$ – Zr – O$_3$ (2×)	88.8(2)
Zr – O$_4$	2.190(10)	O$_1$ – Zr – O$_3$ (2×)	90.8(2)
Mean	2.138	O$_1$ – Zr – O$_3$ (2×)	95.0(2)
O$_1$ – O$_1$	2.662(10)	O$_1$ – Zr – O$_3$ (2×)	87.9(2)
O$_1$ – O$_1$ (2×)	2.359(11)	O$_4$ – Zr – 2O$_1$	74.1(1)
O$_1$ – O$_3$ (2×)	3.049(8)	O$_4$ – Zr – 2O$_3$	87.5(2)
O$_1$ – O$_3$ (2×)	2.971(8)	O$_3$ – Zr – O$_3$	175.1(4)
O$_1$ – O$_3$ (2×)	2.952(8)		
O$_1$ – O$_3$ (2×)	3.111(8)		
O$_4$ – 2O$_1$	2.627(8)		
O$_4$ – 2O$_3$	2.977(10)		
Within the sulfate group:			
S – 2O$_2$	1.448(8)	O$_2$ – S – O$_2$	113.1(6)°
S – 2O$_3$	1.480(6)	O$_3$ – S – O$_3$	106.6(6)
O$_2$ – O$_2$	2.415(15)	O$_2$ – S – O$_3$ (2×)	108.9(4)
O$_2$ – O$_3$ (2×)	2.382(10)	O$_2$ – S – O$_3$ (2×)	109.6(4)
O$_2$ – O$_3$ (2×)	2.392(10)		
O$_3$ – O$_3$	2.372(11)		
Other distances and angles (different layers):			
O$_4$ – 2O$_2$	2.611(9)	O$_2$ – O$_4$ – O$_2$	123.9(5)°
O$_1$ – O$_2$	2.846(9)	Zr – O$_1$ – O$_2$	109.8(2)

DESCRIPTION AND DISCUSSION OF THE STRUCTURE

The zirconium atoms constitute, together with the oxygen atoms, O_1, infinite, almost planar zigzag chains lying in the *yz* plane and running parallel to the *z* direction. The metal atoms are joined by double hydroxide bridges and the Zr – Zr distance within the chains are 3.568 Å (*cf.* Table 4). This is significantly longer than the corresponding distance (3.553 Å) in $Hf(OH)_2SO_4H_2O$.[1]

The $[Zr(OH)_2]_n^{2n+}$ chains are connected in the *x* direction by sulfate groups, each of which is in contact with zirconium atoms in two different chains. A water oxygen atom, O_4, completes the pentagonal bipyramidal arrangement about zirconium. This oxygen atom is at coordination distance from Zr and lies in the same plane as the metal atom and the hydroxide oxygen atoms, O_1. The structure can thus be visualised as being composed of chains of condensed pentagonal bipyramids linked in one direction by sulfate tetrahedra. These layers, which are parallel to the *xz* plane, are held together only by means of hydrogen bonds (2.61 Å and 2.85 Å) and van der Waals contacts. The structure is described in more detail in the paper on $Hf(OH)_2SO_4H_2O$.[1]

The deviation of the Zr coordination polyhedron from the ideal D_{5h} symmetry is illustrated in Figs. 1 and 2. A comparison with Fig. 3 and Table 5

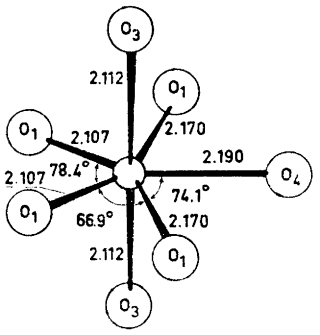

Fig. 1. The coordination polyhedron of $Zr(OH)_2SO_4H_2O$. The Zr – O distances (in Å) and some O – Zr – O bond angles are indicated.

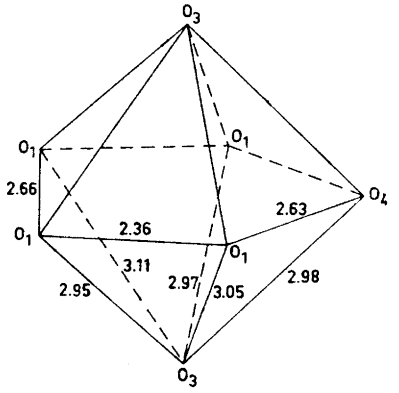

Fig. 2. Pentagonal bipyramidal configuration of oxygen atoms about zirconium in $Zr(OH)_2SO_4H_2O$. (Distances in Å.)

in the paper on $Hf(OH)_2SO_4H_2O$ shows the distortion of the bipyramids to be about the same in the two compounds. There are, however, some differences. The Me – O distances are, for example, on the whole slightly longer in the zirconium compound, and the difference is significant for the axially coordinated O_3 atoms, the distances being 2.11_2 and 2.07_6 Å in the zirconium and hafnium compounds, respectively. This is reflected in the somewhat smaller $O_3 - Me - O_3$ angle in the zirconium compound, 175.1°, compared with 177.0° in the hafnium salt, as well as in the discrepancies in the $O_1 - O_3$ bond distances, as can be seen from the tables.

The plane of best fit through the four O_1 oxygen atoms around Zr was calculated with the program PLANEFIT,[6] the following equation being obtained (Cartesian coordinates, Å):

$$0.9926X + 0.1216Z = 3.2443$$

Transformation to fractional coordinates is performed by $X = 6.4969x$, $Z = -0.7504x + 6.7848z$.

Two O_1 atoms are situated 0.10_7 Å and 0.06_7 Å above the plane while the other two are at the same distances under the plane. This is in good agreement with corresponding values in the structure of the hafnium compound. The metal atoms and the water oxygen atoms are situated on a twofold axis and thus lie in the plane.

The sulfate tetrahedra in the two isomorphous zirconium and hafnium compounds are somewhat deformed due to their chain-connecting function. The type of distortion appears to be slightly different in the two compounds, but the differences in the geometry are not quite significant.

Acknowledgements. The author would like to thank Professor Georg Lundgren for his kind interest in this work. Thanks are also due to Dr. Susan Jagner for revising the English text.

This work has been supported by the *Swedish Natural Science Research Council* (NFR, Contract No. 2318).

REFERENCES

1. Hansson, M. *Acta Chem. Scand.* **23** (1969) 3541.
2. McWhan, D. B. and Lundgren, G. *Inorg. Chem.* **5** (1966) 284.
3. *International Tables for X-Ray Crystallography*, 2nd Ed., Kynoch Press, Birmingham 1965, Vol. I.
4. *International Tables for X-Ray Crystallography*, Kynoch Press, Birmingham 1962, Vol. III, p. 122.
5. Lindqvist, O. and Wengelin, F. *Arkiv Kemi* **28** (1967) 179.
6. The program library of the Dept. of Inorg. Chem. Göteborg. DATAP1 has been written locally by O. Lindgren, DATAP2 was originally written by Coppens, Leiserowitz and Rabinowich (1965), DRF and DISTAN by A. Zalkin, Berkeley, California, FFT by Ten Eyck, L. and PLANEFIT by Wengelin, F. LINUS is the Busing, Martin and Levy (1962) LS program modified for refinement of extinction parameters by Coppens and Hamilton, 1970.
7. Cromer, D. T. and Waber, J. T. *Acta Cryst.* **18** (1965) 104.
8. Cromer, D. T. *Acta Cryst.* **18** (1965) 17.

Received March 23, 1973.

ACTA CHEMICA SCANDINAVICA 27 (1973) 2623–2633

ESCA Studies of Ag, Ag_2O and AgO

GUNNAR SCHÖN

Division of Chemical Technology, The Lund Institute of Technology, Chemical Center, P.O. Box 740, S-220 07 Lund, Sweden

Ag, Ag_2O, and AgO have been studied with X-ray photoelectron spectroscopy (ESCA). Attention has been paid to both photoelectrons and Auger electrons. Ag 3*d* binding energies decrease in the order Ag, Ag_2O, and AgO. The chemical shift is thus in an opposite direction here compared to all other metal-metal oxide systems reported in the literature. The chemical shift between Ag and Ag_2O is 0.4 eV and between Ag and AgO 0.7 eV. An Ag $3d4d4d$ Auger electron energy shift of 0.7 eV exists between silver in the metallic and the oxide state. In metallic Ag the $3d_{5/2}4d4d$ Auger signal is split into at least three components. The oxygen signal is the most characteristic feature of a particular compound; Ag has one O 1*s* peak at 532.2 eV, Ag_2O two peaks at 529.0 and 530.4 eV and AgO two peaks at 528.4 eV and 530.3 eV. The thermal decomposition of Ag_2O and AgO was also studied.

In X-ray photoelectron spectroscopy (XPS) or electron spectroscopy for chemical analysis (ESCA), information is gained not only from directly excited photoelectrons but also from Auger electrons. This implies that XPS is not a very informative designation of the method, since Auger electrons are excluded. For this reason the expression ESCA is used here.

In this work metallic Ag, Ag_2O, and AgO have been studied over the temperature range 25 – 400°C. Attention has been paid to both photoelectrons and Auger electrons. The investigation has been carried out in order to get basic information that can be utilized when analyzing silver catalysts with electron spectroscopy.

EXPERIMENTAL

The experiments were performed with an AEI ES 100 electron spectrometer and the results presented here were obtained with $AlK\alpha_{1,2}$ radiation (1486.6 eV). The instrumental calibration has previously been described in detail,[1] according to which the binding energy of Au $4f_{7/2}$ electrons is 84.0 eV. A quadrupole mass spectrometer, AEI QMS 40, was attached to the source chamber.

Electron binding energies and Auger electron energies are given in relation to the Fermi level throughout this work.

Metallic silver studied as foil (BDH, 0.13 mm thick) whereas Ag_2O (Schuchardt, Laboratory Reagent) and AgO (BDH, Laboratory Reagent) were studied as powders fastened to a copper gauze. All three substances were studied in a temperature range from 25°C to 400°C. Information about the decomposition of the oxides was gained not only from the ESCA spectra but also from the residual gas analysis carried out by the mass spectrometer.

RESULTS AND DISCUSSION

Ag core electron spectra. The electron binding energies in metallic silver measured in this work are summarized in Table 1 together with some previously published results. Comparison with X-ray data from Bearden [5] shows a very good consistency; the energy of Ag $M_{II}M_{IV}$ X-rays is 229.5 eV [5] and Table 1 gives an energy separation of 229.6 eV. Ag $M_{III}M_{V}$ X-rays have an energy of 204.8 eV [5] and exactly the same energy separation is obtained from Table 1.

Table 1. Silver electron binding energies.

Electron level	Binding energy (eV) This work	FWHM (eV) This work	Siegbahn *et al.*[2]	Johansson *et al.*[3]	Baer *et al.*[4]
Ag 3*s*	718.4 ± 0.5	8.5	717		
Ag $3p_{1/2}$	603.8 ± 0.1	3.3	602		
Ag $3p_{3/2}$	572.9 ± 0.1	3.2	571	573.0	
Ag $3d_{3/2}$	374.2 ± 0.1	1.15	373		
Ag $3d_{5/2}$	368.1 ± 0.1	1.15	367	368.2	
Ag 4*s*	96.9 ± 0.2	4.9	95		
Ag $4p_{1/2}$	62.7 ± 0.5	12.9	62		
Ag $4p_{3/2}$	57.6 ± 0.5		56		
Ag 4*d* (max.)	4.8 ± 0.1	3.4	3		4.7
Ag Fermi level	0.0				

Table 2. $3d_{5/2}$ electron binding energies in Ag, Ag_2O, and AgO.

Compound	Binding energy (eV)	FWHM (eV)
Ag	368.1 ± 0.1	1.15
Ag_2O	367.7 ± 0.2	1.4
AgO	367.4 ± 0.2	1.8

Ag $3d_{5/2}$ electron binding energies and FWHM (full width half maximum) for Ag, Ag_2O, and AgO are given in Table 2. Normally the electron binding energy increases when a metal is oxidized, but here it is found that the Ag 3*d* electron binding energy decreases in the order $Ag - Ag_2O - AgO$. This has not been reported for any metal earlier. For copper [6] no Cu $2p_{3/2}$ chemical shift was found between Cu and Cu_2O whereas in CuO a small shift to a higher binding energy was observed. FWHM for Cu $2p_{3/2}$ signals increased from 1.4

eV in Cu to 3.7 eV in CuO. A change in signal width is also found here in the silver-silver oxide system (Table 2).

AgO is considered to contain two kinds of silver atoms, and the formula $Ag^{I}Ag^{III}O_2$ is often used.[7] Ag^{I} is coordinated with two oxygen atoms and Ag^{III} with four oxygen atoms. The presence of chemically inequivalent silver atoms can be an explanation as to why the Ag 3*d* signals from AgO are broader than those from Ag and Ag_2O. However, chemically inequivalent atoms are not the only possible explanation for a broadened signal. Vacancy lifetimes also affect the line widths [8] and multiplet splittings [9] can give rise to broad signals. Nevertheless, the binding energy shifts are in an unexpected direction, but it should also be mentioned that the chemical shift is not a direct measure of the oxidation state, but is primarily determined by the Hartree potential.[10]

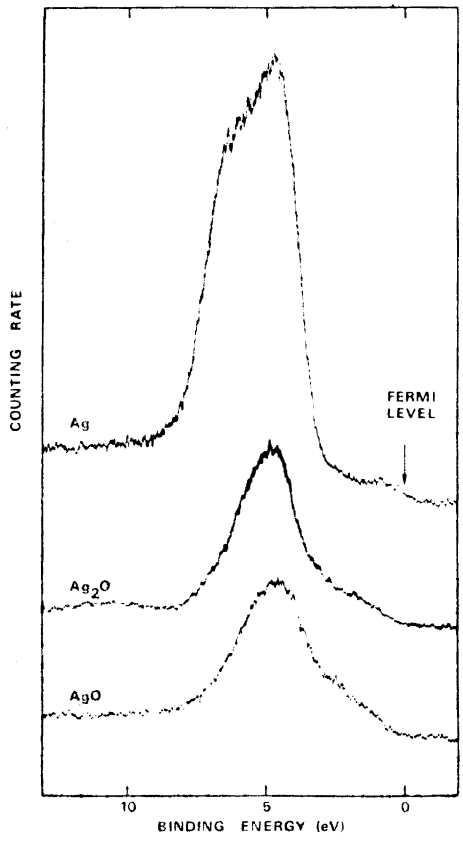

Fig. 1. Band spectra from metallic Ag, Ag_2O, AgO. Spectrum from metallic Ag recorded at 400°C. Spectra from silver oxides recorded at room temperature.

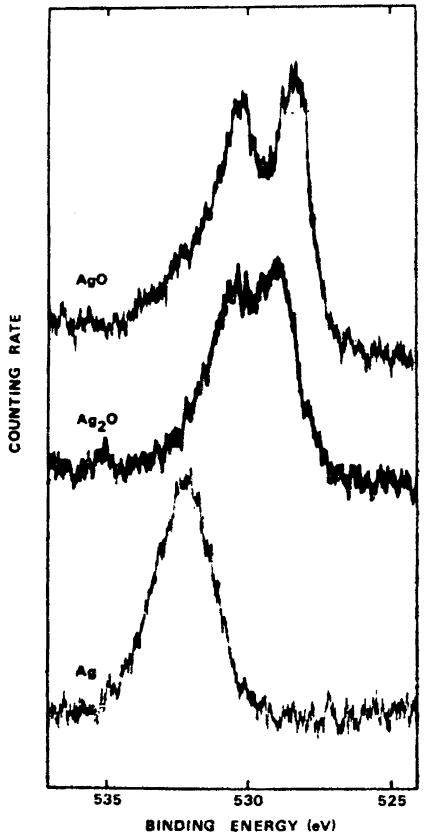

Fig. 2. Oxygen 1*s* spectra from metallic Ag, Ag_2O, and AgO. Spectra recorded at room temperature.

The three compounds were studied several times. Mostly no charging of the sample was found. This conclusion was drawn since the contamination carbon peak appeared at the same kinetic energy within 0.2 eV for all three compounds. The C 1*s* electron binding energy thus found was 284.6 ± 0.1 eV. A few times, however, the oxide samples indicated a charging of at most 0.6 eV. Both Ag 3*d* and C 1*s* electron signals were then shifted. With reference to this discussion it is concluded that the anomalous chemical shifts cannot be an effect of sample charging.

Band spectra. Distinct differences are found in the band spectra from Ag, Ag_2O, and AgO (Fig. 1). Ag_2O and AgO have a valence band structure of the same character with a maximum at 4.7 eV. The half-width in Ag_2O (2.5 eV) is smaller than in AgO (3.0 eV) and the low binding energy hump is more intense in AgO than in Ag_2O. The maximum in Ag is found at a binding energy of 4.8 eV in accordance with Baer *et al.*[4] The Fermi level of Ag can be seen in the band spectrum at a binding energy of 0.0 eV. In Ag_2O and AgO the valence band boundary is observable at a binding energy of about 0.6 eV. Since the band gap in Ag_2O is 1.2 eV at room temperature [11] the Fermi level is positioned in the middle of the band gap. No band structure calculations for Ag_2O or AgO have been found in the literature with which to compare these experimental valence band structures.

Oxygen 1s electron spectra. Very characteristic differences between the three compounds are found in the oxygen 1*s* signals (Fig. 2). The oxygen binding energies are summarized in Table 3. In metallic silver the oxygen

Table 3. Oxygen 1*s* electron binding energies.

Compound	Binding energy (eV)	
Ag (25°C)	532.2 ± 0.2	
Ag (400°C)	531.4 ± 0.2	
Ag_2O (25°C)	530.4 ± 0.2	529.0 ± 0.2
AgO (25°C)	530.3 ± 0.2	528.4 ± 0.2

signal is due to adsorbed (or absorbed) oxygen. It is, however, possible that some other oxygen-containing molecules also contribute to the O 1*s* signal. When the temperature is raised to 400°C the oxygen signal decreases and changes its position from a binding energy of 532.2 eV to one of 531.4 eV. This indicates different modes of adsorbed oxygen on silver, in agreement with the general view of oxygen adsorption on silver.[12]

Oxygen found in metallic silver is quite different from oxygen present in the oxides. In both Ag_2O and AgO two distinct peaks are present. The separation in Ag_2O is 1.4 eV compared to 1.9 eV in AgO. The interpretation of these oxygen signals will be discussed in the next two sections.

Ag_2O decomposition. Ag_2O was studied at room temperature, 100, 200, 300, and 400°C. The oxygen spectra were not recorded until the sample had been kept at a particular temperature for at least 3 h. At 100°C the low-binding energy part of the oxygen signal had decreased a little, but no further

changes occurred at either 200 or 300°C. Not until 400°C was reached was an oxygen signal characteristic of metallic Ag obtained. FWHM of the Ag $3d_{5/2}$ signal decreased from 1.4 eV to 1.2 eV when 400°C was reached, which also indicates metallic Ag instead of Ag_2O at this temperature (Table 2).

The equilibrium oxygen partial pressure over Ag_2O is 1 atm at 190°C,[13] but the decomposition rate is very slow at this temperature as shown by Allen,[14] according to whom 5 % of the total oxygen in Ag_2O is evolved between 100 and 200°C and a further 1 – 2 % between 200 and 300°C. Metallic silver crystallized first above 300°C. This decomposition scheme of Ag_2O is supported by the oxygen electron spectra recorded in this work.

Since a distinct change occurred in the temperature interval 300 – 400°C, the decomposition was closely examined in this region. The result is shown in Fig. 3. At 300°C, as mentioned above, the O 1*s* spectrum is very similar to that

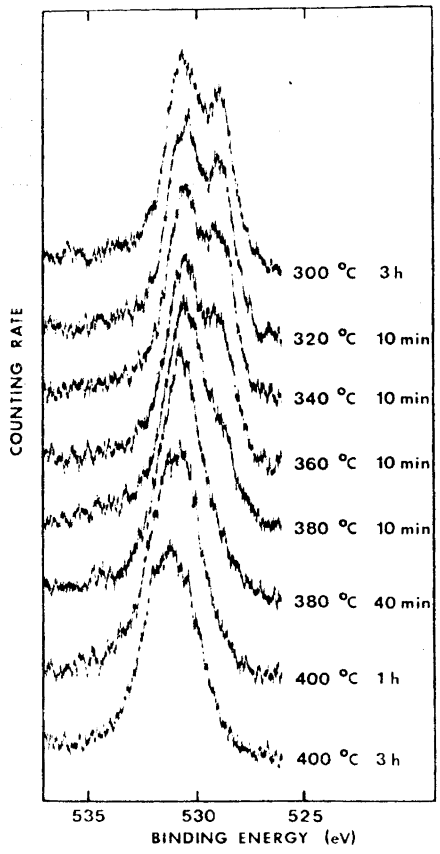

Fig. 3. Oxygen 1*s* spectra from Ag_2O during thermal decomposition. The figure indicates how long time the sample was kept at a particular temperature before the spectrum was recorded.

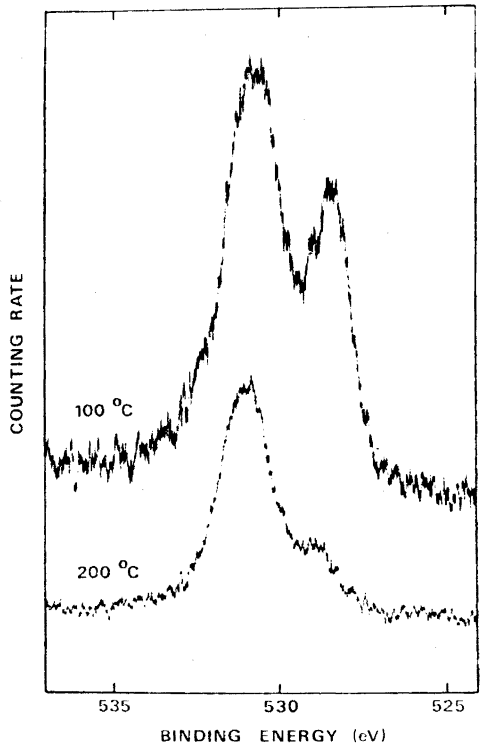

Fig. 4. Oxygen 1*s* spectra from AgO during thermal decomposition.

at 25°C shown in Fig. 2. The only difference is that the low-binding energy part of the signal has become somewhat smaller. Upon raising the temperature the low-binding energy peak continually decreases, and above 360°C a more rapid change is observed. After 40 min at 380°C only one oxygen peak is present. This single signal is narrow, but as the temperature is raised to 400°C a broader signal appears, simultaneously with a slight shift of the signal to a higher binding energy. The last spectrum gives an O 1*s* binding energy of 531.3 eV, which agrees with the O 1*s* binding energy observed on metallic silver foil at 400°C (Table 3).

These results indicate that the low-binding energy O 1*s* peak is due to lattice oxygen, since this peak decreases simultaneously with the oxide decomposition. The high-binding energy oxygen is interpreted as due to adsorded oxygen. The binding energy of this oxygen peak changes continuously from oxygen adsorbed on Ag_2O to oxygen adsorbed on metallic Ag. The same interpretation of O 1*s* doublets from metal-oxygen systems have been given for, *e.g.*, Ni,[15,16] Cu,[6,15,17] and Zn.[18]

The decomposition rate was also followed by the mass spectrometer. By comparing the oxygen partial pressures at 300°C and at 380°C and relating these partial pressures with decomposition rates, an activation energy of 55 kcal/mol was calculated, in good agreement with the value given by Allen.[14]

AgO decomposition. AgO is much less stable than Ag_2O. It readily decomposes according to the reaction,

$$4\ AgO(s) \rightleftharpoons 2\ Ag_2O(s) + O_2(g) \qquad (1)$$

Allen [19] studied this reaction over the temperature region 83 – 134°C and found an activation energy of 30 kcal/mol.

In Fig. 2 the O 1*s* electron spectrum from AgO at room temperature is shown. Fig. 4 shows O 1*s* spectra at 100 and 200°C. Already at 100°C the low-binding energy peak, which again is interpreted as due to lattice oxygen, has decreased but is still characteristic of AgO. At 200°C the lattice oxygen signal is very small and has changed its position to that of Ag_2O.

According to reaction (1), Ag_2O is present after the decomposition, which means that the position of the lattice oxygen peak at 200°C is correct. However, when comparing this spectrum with that from Ag_2O at 300°C in Fig. 3, the lattice oxygen signal is obviously much smaller in decomposed AgO than in heated Ag_2O. The spectrum of Ag_2O at 200°C was almost identical to that at 300°C. The surface composition of decomposed AgO is thus not identical to that of Ag_2O. The oxygen evolved upon AgO decomposition might give a very oxygen-rich surface layer, and this oxygen is not lattice oxygen but adsorbed or absorbed oxygen.

Both position and half-width of the Ag $3d_{5/2}$ signal at 200°C indicated Ag_2O and not metallic Ag. The narrow signal (1.2 eV) of metallic Ag was not found until 400°C. This excludes the possiblility of metallic Ag in the surface region at 200°C, which also could have been an explanation for the low lattice oxygen signal.

Ag Auger electron spectra. In electron spectroscopy, Auger electrons are analyzed as well as directly excited photoelectrons. Fig. 5 shows Auger signals from metallic silver at 400°C. The intense doublet is due to 3*d*4*d*4*d* ($M_{IV,V}N_{IV,V}$

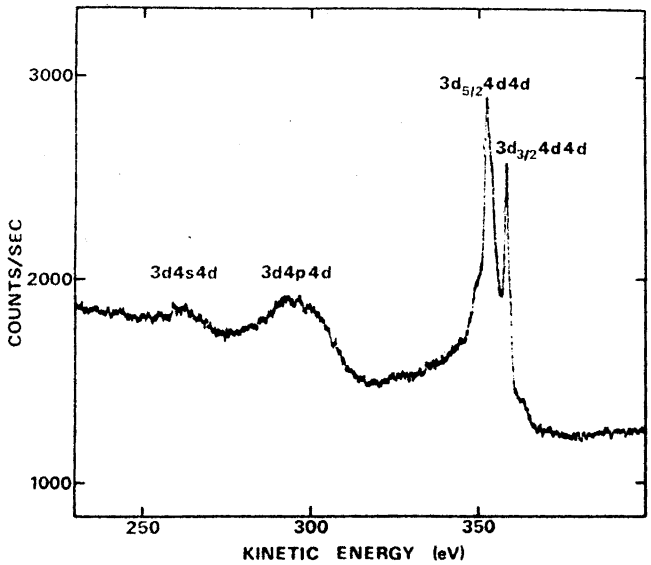

Fig. 5. Auger electron spectrum from metallic Ag. Spectrum recorded at 400°C.

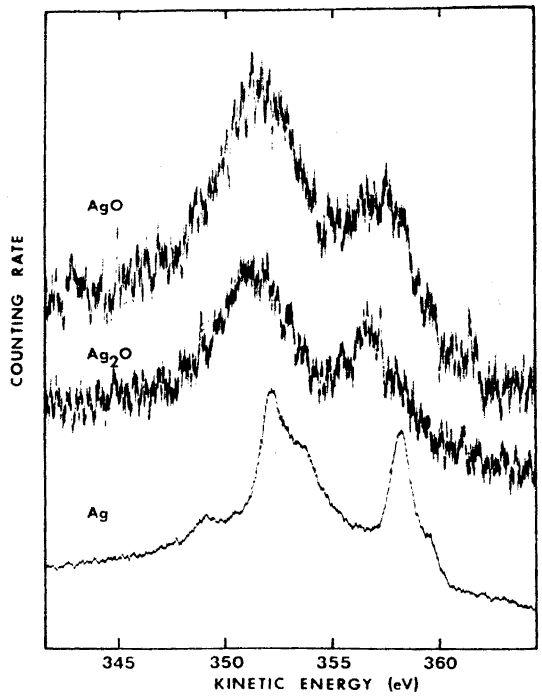

Fig. 6. Ag 3*d*4*d*4*d* electron spectra from metallic Ag, Ag_2O, and AgO. Spectrum from metallic Ag recorded at 400°C. Spectra from silver oxides recorded at 25°C.

$N_{1V,V}$) Auger electrons and is shown in greater detail in Fig. 6. This designation means that a 3*d* vacancy is filled by a 4*d* electron with simultaneous ejection of another 4*d* electron. The two main peaks are separated by 6.1 eV, which is exactly the same difference as between Ag $3d_{5/2}$ and Ag $3d_{3/2}$ electron binding energies (Table 1). The $3d_{5/2}4d4d$ Auger signal is split into at least three components, and a similar splitting is indicated for the $3d_{3/2}4d4d$ signal.

The splittings are due to spin-orbit couplings which give rise to different final states in the Auger process.[20,21] High resolution MNN spectra from gases have been studied extensively by, *e.g.*, Werme *et al.*[22] High resolution Auger spectra from solids are not very often presented. The fine structure of the Ag 3*d*4*d*4*d* Auger electron signal was, however, partially resolved by Aksela [23] and Pattinson and Harris.[24] Their results are included in Table 4. According to the interpretation by Siegbahn *et al.*[20] the main peaks are due to $^1D_2$ terms.

No change in the silver Auger spectra during the temperature rise, when the adsorbed mode of oxygen changes, was observed. This supports the study by Bradshow *et al.*[27] on silver, where attempts to observe chemical shifts of the silver Auger peaks were unsuccessful.

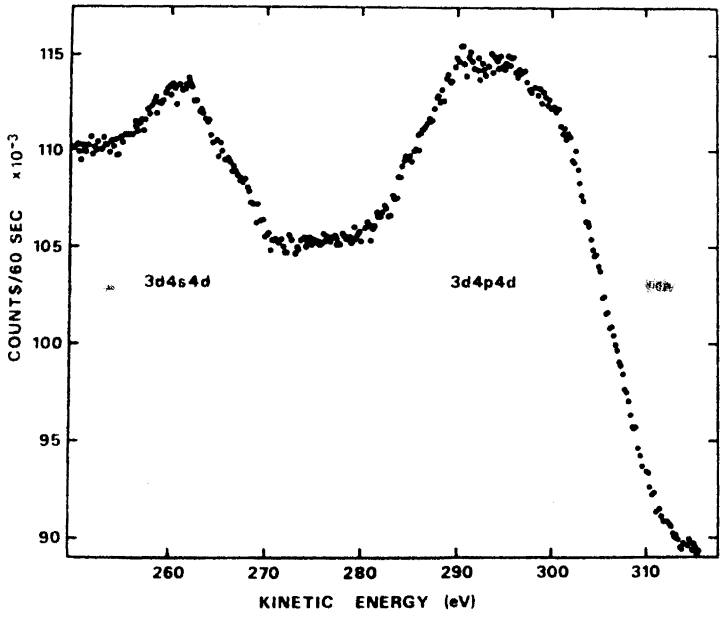

Fig. 7. 3*d*4*s*4*d* and 3*d*4*p*4*d* Auger electron signals from metallic Ag. Spectrum recorded at 400°C.

In Fig. 7 Ag 3*d*4*s*4*d* and Ag 3*d*4*p*4*d* Auger signals are shown in greater detail. The spectrum was not continuously recorded as in the previous spectra. Each point represents the number of counts during 60 sec. In the 3*d*4*s*4*d* signal a doublet is indicated by the hump about 6 eV from the main peak, which is in

accordance with a splitting due to the difference in binding energy between Ag $3d_{3/2}$ and $3d_{5/2}$ electrons. The $3d4p4d$ signal is very broad, which agrees with the broad $4p$ photoelectron signal (Table 1). No definite fine structure is resolved in this signal.

The $3d4d4d$ Auger signals from metallic Ag are very narrow, as seen in Fig. 6. The width of the $4d$ band is 3.4 eV which means that the Auger signals are narrower than a level doubly involved in the transition giving rise to the Auger electrons. This is a behaviour previously observed and discussed for Cu,[1] Zn,[18] and Ga.[18]

In Table 4 calculated Auger electron energies are also included. The energies were calculated by the equation:

$$E_{vxy(z)} = E_{v(z)} - E_{x(z)} - E_{y(z+1)}$$

where $E_{vxy(z)}$ is the Auger electron energy in element z when a v vacancy is filled by an x electron under ejection of an y electron, $E_{v(z)}$ and $E_{x(z)}$ are binding energies of electrons v and x in element z and $E_{y(z+1)}$ is the binding energy of electron y in element $z+1$. Compared to Ag the element $z+1$ is Cd. The Cd $4d$ electron binding energy in metallic Cd is measured to 11.1 eV in this work. The Ag electron binding energies in Table 1 are used for the calculation, with an Ag $4p$ binding energy of 59.6 eV. The agreement between calculated and experimental Auger energies is very good as is shown in Table 4. The consistency between different investigations is also good.

Table 4. Silver Auger electron energies (eV).

Assignment	This work		Palmberg and Rhodin[25]	Aksela[23]	Pattinson and Harris[24]	Wagner[26] (Ag_2O)
	Measured	Calculated				
$3d_{5/2}4s4d$	261.0 ± 0.5	260.1	268			
$3d_{3/2}4s4d$	267.0 ± 0.5	266.2				
$3d_{5/2}4p4d$	296 ± 1	297	308			
$3d_{3/2}4p4d$		303				
$3d_{5/2}4d4d$	349.1 ± 0.2 352.2 ± 0.2 353.7 ± 0.2	352.2	362	353.4 354.6	352.5 354	351
$3d_{3/2}4d4d$	358.2 ± 0.2 359.5 ± 0.2	358.3		359.3	358.5	356

In Fig. 6 Ag $3d4d4d$ Auger spectra from Ag_2O and AgO are also shown. These signals are broader than from metallic Ag and no fine structure is resolved. An Auger electron energy shift between metallic Ag and the silver oxides is also found, as can be deduced from Table 5. The shift of 0.7 eV is smaller than the Auger shift found between Cu and Cu_2O (1.3 eV),[6] Zn and ZnO (4.3 eV),[18] and Ga and Ga_2O_3 (5.7 eV),[18] but this shift of 0.7 eV is in an opposite direction compared to the binding energy shifts discussed earlier in this paper.

Table 5. Ag $3d4d4d$ Auger electron energies in Ag, Ag_2O, and AgO.

Assignment	Auger electron energy (eV) Ag	Ag_2O	AgO
$3d_{5/2}4d4d$	352.2 ± 0.2	351.4 ± 0.3	351.7 ± 0.3
$3d_{3/2}4d4d$	358.2 ± 0.2	356.8 ± 0.3	357.4 ± 0.3

CONCLUSIONS

The $3d$ electron binding energy decreases in the order Ag, Ag_2O, and AgO although the formal oxidation number increases. This has not been observed for any metal – oxygen system earlier. The Ag $3d4d4d$ Auger electron energies are 0.7 eV lower in the oxide state than in the metal state. Thus electron binding energies and Auger electron energies are shifted in opposite directions, which shows that the relation between Auger shifts and binding energy shifts is complex.

Different binding energies for adsorbed oxygen on silver are found, but ultrahigh vacuum conditions are necessary to make definite adsorption studies with ESCA. Oxygen signals from Ag_2O and AgO are interpreted as due to lattice oxygen and adsorbed oxygen. When the temperature is increased the lattice oxygen disappears due to decomposition, but the adsorbed mode changes its position only slightly.

Acknowledgement. The author is grateful to Professor Sten T. Lundin for his generous support during the course of this work. Collaboration with Docent R. Larsson and Dr. B. Folkesson is also appreciated. The work is supported by the *Swedish Board for Technical Development* and the *Bank of Sweden Tercentenary Fund.*

REFERENCES

1. Schön, G. *J. Electron Spectrosc.* **1** (1972/73) 377.
2. Siegbahn, K., Nordling, C., Fahlman, A., Nordberg, R., Hamrin, K., Hedman, J., Johansson, G., Bergmark, T., Karlsson, S.-E., Lindgren, I. and Lindberg, B. *ESCA – Atomic, Molecular and Solid State Structure Studied by Means of Electron Spectroscopy*, Almqvist & Wiksells Boktryckeri AB, Uppsala 1967.
3. Johansson, G., Hedman, J., Berndtsson, A., Klasson, M. and Nilsson, R. *UUIP*-769 (1972).
4. Baer, Y., Hedén, P. F., Hedman, J., Klasson, M., Nordling, C. and Siegbahn, K. *Phys Scr.* **1** (1970) 55.
5. Bearden, J. A. *Rev. Mod. Phys.* **39** (1967) 78.
6. Schön, G. *Surface Sci.* **35** (1973) 96.
7. McMillan, J. A. *Chem. Rev.* **62** (1962) 65.
8. Friedman, R. M., Hudis, J. and Perlman, M. L. *Phys. Rev. Lett.* **29** (1972) 692.
9. Fadley, C. S. In Shirley, D. A., Ed., *Electron Spectrosc., Proc. Int. Conf. 1971*, North-Holland Publ. Co., Amsterdam 1972, p. 781.
10. Jørgensen, C. K. *J. Phys. (Paris), Colloq.* **C 4** (1971) 274.
11. Fortin, E. and Weichman, F. L. *Phys. Status Solidi* **A 5** (1964) 515.
12. Sachtler, W. M. H. *Catal. Rev.* **4** (1970) 27.
13. Benton, A. F. and Drake, L. C. *J. Am. Chem. Soc.* **54** (1932) 2186.
14. Allen, J. A. *Aust. J. Chem.* **13** (1960) 431.
15. Robert, T., Bartel, M. and Offergeld, G. *Surface Sci.* **33** (1972) 123.
16. Schön, G. and Lundin, S. T. *J. Electron Spectrosc.* **1** (1972) 105.

17. Novakov, T. and Prins, R. *Solid State Commun.* **9** (1971) 1975.
18. Schön, G. *J. Electron Spectrosc.* **2** (1973) 75.
19. Allen, J. A. *Aust. J. Chem.* **14** (1961) 20.
20. Siegbahn, K., Nordling, C., Johansson, G., Hedman, J., Hedén, P. F., Hamrin, K., Gelius, U., Bergmark, T., Werme, L. O., Manne, R. and Baer, Y. *ESCA Applied to Free Molecules*, North-Holland Publ. Co., Amsterdam 1969.
21. Yin, L., Tsang, T., Adler, I. and Yellin, E. *J. Appl. Phys.* **43** (1972) 3464.
22. Werme, L. O., Bergmark, T. and Siegbahn, K. *Phys. Scr.* **6** (1972) 141.
23. Aksela, S. *Z. Physik* **244** (1971) 268.
24. Pattinson, E. B. and Harris, P. R. *J. Phys.* **D 5** (1972) 59.
25. Palmberg, P. W. and Rhodin, T. N. *J. Appl. Phys.* **39** (1968) 2425.
26. Wagner, C. D. *Anal. Chem.* **44** (1972) 967.
27. Bradshaw, A. M., Engelhardt, A. and Menzel, D. *Ber. Bunsenges. Phys. Chem.* **76** (1972) 500.

Received March 24, 1973.

ACTA CHEMICA SCANDINAVICA 27 (1973) 2634–2638

The Utilization of Immobilised Substrate/Product in Affinity Chromatography. A Model Study using α-Chymotrypsin

PETER BRODELIUS and KLAUS MOSBACH

Biochemical Division, Chemical Centre, University of Lund, P.O. Box 740, S-220 07 Lund 7, Sweden

The use of an immobilised substrate, L-tryptophan methyl ester, bound to Sepharose extended with ε-aminocaproic acid in affinity chromatography of α-chymotrypsin (EC 3.4.4.5) has been studied. The enzyme was significantly retarded on this column material, permitting complete separation from serum albumin and DFP-chymotrypsin. A purification of the crystalline chymotrypsin preparation of about 20 per cent was also achieved.

Separation of chymotrypsin from trypsin (EC 3.4.4.4) was possible using a corresponding column material prepared by coupling α-*N*-(ε-aminocaproyl)-L-tryptophan methyl ester to Sepharose.

Affinity chromatography or biospecific adsorption has received increasing attention during the last few years,[1,2] but two factors hinder the wider use of this technique. One of these factors is the elaborate chemistry often required to immobilise the ligand while the second is that knowledge of specific competitive inhibitors is often lacking. Use of a more general ligand such as the cofactor NAD^+ or an AMP analogue, *e.g.* N^6-(6-aminohexyl)-adenosine 5′-monophosphate, which has affinity for a great number of enzymes, at least partially overcomes the first difficulty.[3,4] Here the specificity associated with affinity chromatography can be preserved by elution of one enzyme at a time.[4,5]

Since substrate and product are generally established a solution to the second difficulty, which applies particularly to the application of affinity chromatography in the purification of an un-characterised enzyme, may be the coupling of one or the other to a matrix, provided that the binding strength between enzyme and affinity adsorbent is strong enough to bind or at least retard the enzyme of interest. In fact, since binding can be expected to be weak in many instances, this could have the additional advantage that drastic elution methods might not be necessary. With these considerations in mind we started the present investigation by covalently attaching the α-chymotrypsin substrate, L-tryptophan methyl ester, to Sepharose extended by a "spacer", ε-aminocaproic acid. The choice of this compound was in part influenced by previous work [6] on affinity chromatography of this enzyme using the corresponding D-enantiomer, a competitive inhibitor of α-chymotrypsin.

MATERIALS AND METHODS

Sepharose 4B was obtained from Pharmacia, Uppsala, Sweden, and DFP-chymotrypsin from Worthington Biochemical Corporation, Freehold, New Jersey, USA. Trypsin (bovine pancreas, type III, 11.000 benzoyl-L-arginine ethyl ester units/mg), α-chymotrypsin (bovine pancreas, type II, 46 benzoyl-L-tyrosine ethyl ester units/mg), bovine serum albumin, *N*-benzoyl-L-tyrosine ethyl ester, α-*N*-benzoyl-L-arginine ethyl ester HCl, L-tryptophan methyl ester HCl, ε-aminocaproic acid, and carbobenzoxychloride were purchased from Sigma Chemical Company, St. Louis, Mo., USA. 1-Cyclohexyl-3-(2-morpholinoethyl)-carbodiimide metho-*p*-toluene-sulphonate was obtained from Aldrich Chemical Company Inc., Milwaukee, Wis., USA. *N*,*N*′-Dicyclohexylcarbodiimide, benzoyl chloride, and triethylamine were supplied by British Drug House Chemicals Ltd., Poole, England. Palladium on charcoal (9.7 %) was purchased from Degussa, Hanau, West Germany. Chymotrypsin activity was measured according to the method described by Hummel [7] using *N*-benzoyl-L-tyrosine ethyl ester as substrate. Trypsin was assayed with α-*N*-benzoyl-L-arginine ethyl ester as substrate according to the method described by Schwert and Takenaka.[8] The amount of chymotrypsin was determined spectrophotometrically at 280 nm by using $E_{280}(1\ \%) = 20.0$ to relate molar absorptivity to protein concentration.[9] The affinity material was prepared by two methods. In the first method (A) ε-aminocaproic acid (1.0 g) was coupled to Sepharose suspension (10 ml) using the cyanogen bromide method,[10] and then L-tryptophan methyl ester (250 mg) was attached to the terminal carboxyl group of the spacer using 1-cyclohexyl-3-(2-morpholinoethyl)-carbodiimide metho-*p*-toluene sulphonate (1.0 g). In the second method (B) α-*N*-(ε-aminocaproyl)-L-tryptophan methyl ester was synthesized through condensation of *N*-carbobenzoxy-ε-aminocaproic acid with L-tryptophan methyl ester.[11]

It was prepared by the procedure of Winitz *et al.*[12] for formation of peptide bonds by using *N*,*N*′-dicyclohexylcarbodiimide or by the mixed anhydride method described by Vaughan and Osato.[13] In either case the carbobenzoxy group was removed by hydrogenolysis with palladium charcoal as catalyst. The synthetic substrate analogue (200 mg) was then coupled to Sepharose suspension (20 ml) by the cyanogen bromide method. Since the ester is insoluble in water, coupling was carried out in a 1:1 mixture of dimethylformamide and 0.1 M $NaHCO_3$.

In preparation (A) the amount of ligand bound was determined either chemically or enzymically. In the chemical procedure the quantity of bound ligand was determined spectrophotometrically by measuring the tryptophan ($\varepsilon_{280} = 5.56 \times 10^3$, pH 7.0)[14] liberated when the gel was hydrolysed in 5 M NaOH for 24 h at room temperature. This procedure indicated that each ml of packed gel contained 3 μmol of tryptophan methyl ester. In the enzymic method the gel was incubated with an excess of α-chymotrypsin and the hydrolysis of tryptophan ester was followed using the pH-stat method with an automatic titrator at pH 7.8. It was found that 1 μmol of ester was hydrolysed per ml of packed gel. In preparation (B), the bound substrate (20 μmol/ml of packed gel) was calculated from the difference of tryptophan ester in solution before and after coupling, as determined spectrophotometrically (280 nm).

RESULTS AND DISCUSSION

The chromatographic patterns depicted in Fig. 1 (a – c) were obtained by subjecting various mixtures containing α-chymotrypsin to chromatography on the affinity adsorbent (A). The enzyme separated well from a mixture with bovine serum albumin, being significantly retarded, while the albumin (not defatted sample) appeared in the void volume (Fig. 1 (a)). Using such columns, purification of crystalline chymotrypsin preparations was achieved with an approximate increase in specific activity of 20 % (Fig. 1 (b)). Separation of active chymotrypsin from diisopropylfluorophosphate-treated enzyme (DFP-chymotrypsin) could also be effected (Fig. 1 (c)). Here a slight retardation of the inactivated enzyme was observed. Control experiments run with either un-

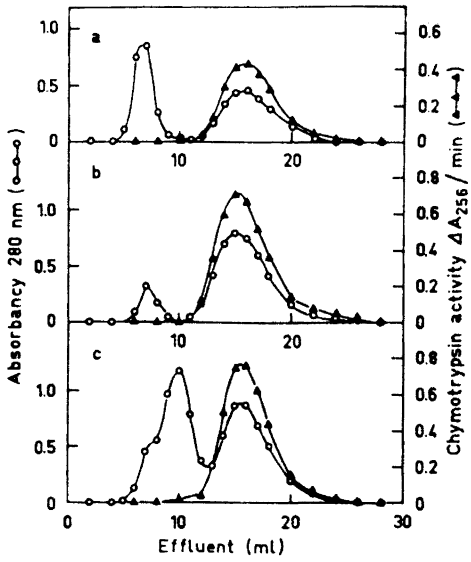

Fig. 1. Chromatography of protein mixtures containing α-chymotrypsin on adsorbent (A) packed in a column (0.9 × 15 cm, containing 4.5 ml of packed gel) equilibrated and eluted with 0.05 M Tris-HCl buffer, pH 7.8, at room temperature. 1.0 ml fractions were collected at a rate of 6 ml/h. The following mixtures were applied in 0.2 ml of this buffer: (a) bovine serum albumin (3.1 mg) and α-chymotrypsin (2.0 mg), (b) α-chymotrypsin (3.1 mg) and (c) DFP-chymotrypsin (2.6mg) and α-chymotrypsin (3.2 mg).

substituted Sepharose or "Sepharose-spacer" lacking the L-tryptophan methyl ester gave no retardation of the enzyme in any of the three cases discussed. Thus, immobilisation of the enzyme substrate yields an adsorbent which is sufficiently effective for affinity chromatography, but which, because of the relatively weak binding of the enzyme, requires no special elution procedure. The result of an attempted separation of chymotrypsin from trypsin on a column of adsorbent (B) is shown in Fig. 2. This synthetic material was chosen

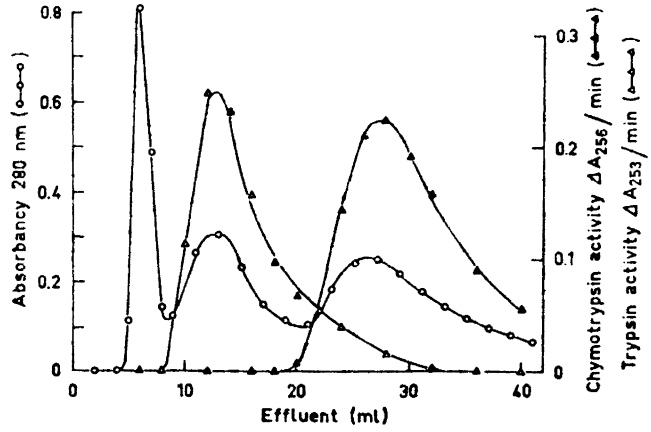

Fig. 2. Chromatography of a mixture of α-chymotrypsin (2.8 mg) and trypsin (3.0 mg) on a column of adsorbent (B). The column (0.9 × 15 cm, containing 1.5 ml of packed gel) was equilibrated and eluted with 0.05 M Tris-HCl buffer, pH 7.8, at room temperature. 1.0 ml fractions were collected at a rate of 6 ml/h.

to eliminate any possible contribution to the chromatographic pattern by ionic interaction between free carboxyl groups of unsubstituted ε-aminocaproic acid and the positively charged trypsin (isoelectric point 10.1).[15] Efficient separation of the two enzymic activities was obtained. The same synthetic preparation (B) was also used in the separation of chymotrypsin from DFP-chymotrypsin giving an elution pattern similar to that obtained in Fig. 1 (c).

In an interpretation of the observed affinity chromatographic separations the question of whether these are due to immobilised substrate or product is relevant. This investigation began as a pilot study for possible substrate affinity chromatography. It was found that on carrying out the chromatographic procedure a second time with the same sample of adsorbent the elution profiles changed, showing decreased retardation of the enzyme. Subsequent repetition, however, produced no further changes in the retardation. The elution profiles shown in Fig. 1 (a – c) were obtained by chromatography on previously used gels. We have shown that under these conditions all the enzymically available bound tryptophan methyl ester was hydrolysed during the first chromatographic use of the gel. This is not surprising in view of the relatively small amount (1 μmol/ml of packed gel) of ligand bound. In this context it is interesting to note that the chemically determined bound ligand was about three times as high as the enzymically determined ligand content. This difference is likely to be due to the fact that not all bound tryptophan methyl ester is sterically available for the enzyme. The fact that on repeated runs significant retardation is observed (Fig. 1. (a – c) we ascribe to the interaction of enzyme with the product *N*-ε-aminocaproyl-L-tryptophan. The literature K_i value for a related compound, *N*-acetyl-L-tryptophan, is 1.75×10^{-2} M;[16] the *N*-ε-aminocaproyl-L-tryptophan derivative is likely to have a similar or even lower K_i as indicated by a K_i of 0.88×10^{-2} M found for *N*-nicotinyl-L-tryptophan.[16] Apparently the low affinity of the enzyme for the ligand obtained is sufficient to give the separation observed.

In summary we suggest that in many cases a simple preliminary approach to affinity chromatographic purification, especially of new enzymes, should involve immobilisation of either enzyme substrate or product. Since turnover of substrate may often be complete after one cycle, direct coupling of the product may be the most rational choice, thus utilising the effect of product inhibition in affinity chromatography.

Acknowledgement. The authors wish to acknowledge the skilful help given by Mrs. Margaretha Scott and Dr. Hugh Guilford.

REFERENCES

1. Cuatrecasas, P. and Anfinsen, C. B. *Ann. Rev. Biochem.* **40** (1971) 259.
2. Porath, J. and Sundberg, L. *The Chemistry of Biosurfaces*, Marcel Dekker, New York 1972, Vol. 2, p. 633.
3. Mosbach, K., Guilford, H., Larsson, P.-O., Ohlsson, R. and Scott, M. *Biochem. J.* **125** (1971) 20 p.
4. Mosbach, K., Guilford, H., Ohlsson, R. and Scott, M. *Biochem. J.* **127** (1972) 625.
5. Ohlsson, R., Brodelius, P. and Mosbach, K. *FEBS Lett.* **25** (1972) 234.
6. Cuatrecasas, P., Wilchek, M. and Anfinsen, C. B. *Proc. Natl. Acad. Sci. U.S.* **61** (1968) 636.

7. Hummel, B. C. W. *Can. J. Biochem. Physiol.* **37** (1959) 1393.
8. Schwert, G. W. and Takenaka, Y. *Biochem. Biophys. Acta* **16** (1955) 570.
9. Dixon, G. H. and Neurath, H. *J. Biol. Chem.* **225** (1957) 1049.
10. Axén, R., Porath, J. and Ernback, S. *Nature* **214** (1967) 1302.
11. Bergmann, M. and Zervas, L. *Ber.* **65** (1932) 1192.
12. Winitz, M., Bloch-Frankenthal, L., Izumiya, N., Birnbaum, S. M., Baker, C. G. and Greenstein, J. P. *J. Am. Chem. Soc.* **78** (1956) 2423.
13. Vaughan, J. R. and Osato, R. L. *J. Am. Chem. Soc.* **73** (1951) 5553.
14. Sober, H. A., Ed. *Handbook of Biochemistry*, 2nd Ed., Chemical Rubber Company, Cleveland 1970, p. B-75.
15. Green, N. M. and Neurath, H. *The Proteins*, Academic, New York 1954, Vol. IIB, p. 1057.
16. Huang, H. T. and Niemann, C. *J. Am. Chem. Soc.* **73** (1951) 1541.

Received March 6, 1973.

ACTA CHEMICA SCANDINAVICA 27 (1973) 2639–2644

Benzylated Orthoesters in Glycoside Synthesis

The Synthesis of α-D-Glucopyranosides and β-D-Mannopyranosides

HANS B. BORÉN, GÖRAN EKBORG, KARIN EKLIND, PER J. GAREGG, ÅKE PILOTTI and CARL-GUNNAR SWAHN

Department of Organic Chemistry, The Arrhenius Laboratory, P.O.B., S-104 05 Stockholm 50, Sweden

3,4,6-Tri-*O*-benzyl-1,2-*O*-(methoxyethylidene)-α-D-glucopyranose and the corresponding β-D-mannopyranose are easily prepared from the corresponding 3,4,6-tri-*O*-acetyl-1,2-*O*-(methoxyethylidene) compounds by deacetylation followed by benzylation with benzyl bromide and silver oxide in dimethyl formamide. Glycoside syntheses using the Kochetkov orthoester method and the 3,4,6-tri-*O*-benzyl orthoesters, is followed by removal of the acetyl group in the 2-position. Oxidation and reduction produces inversion at C-2 and thereby new methods for the syntheses of α-D-glucopyranosides and β-D-mannopyranosides.

One of the classical topics of carbohydrate chemistry is the search for stereospecific, high-yield syntheses of glycosides and oligosaccharides. Access to such syntheses would be of considerable interest in both synthetic natural products chemistry and in biological chemistry. The topic can be divided into two separate problems, the synthesis of glycosides with 1,2-*trans*-configuration and those with 1,2-*cis*-configuration. The former of these is by far the easiest one, and therefore the one for which relatively satisfactory solutions have been found. The traditional way of preparing 1,2-*trans*-glycosides is the Koenigs-Knorr synthesis in which an acetoxy group in the 2-position exerts steric control in the reaction.[1] An important improvement has been described by Kochetkov and co-workers who developed the orthoester glycoside synthesis in which a 3,4,6-tri-*O*-acyl-1,2-(alkoxyethylidene)-hexose (or the corresponding pentose) is allowed to react with an alcohol or a suitably protected sugar in the presence of an acidic catalyst such as *p*-toluenesulphonic acid or mercuric bromide.[2] The steric outcome of the reaction normally is a 1,2-*trans*-glycoside, although exceptions have been noted.[3,4] Of the various attempts made in order to obtain 1,2-*cis*-glycosides [5–7] two recent approaches are particularly noteworthy. In the first of these, due to Lemieux and co-workers, nitrosyl chloride adducts of protected glycals are used in glycoside syntheses.[8] The reaction product of an alcohol (or a suitably protected monosaccharide)

with the nitrosyl chloride adduct of a 3,4,6-tri-*O*-acetyl-glycal normally is an α-D-glycoside with an oximino function in the 2-position. This is converted into a keto function by treatment with levulinic acid. Borohydride reduction affords the 1,2-*cis*-glycoside. The method works well in the *gluco*, *galacto*, and *talo* series and produces 1,2-*cis*-configuration,[9] although one exeption has been noted.[10] Another promising approach is that due to Ferrier and co-workers in which an acylated 2-hydroxyglycal is allowed to react with an alcohol or a suitably protected monosaccharide under catalysis with boron trifluoride.[11] The products are 3-deoxy-hex-2-enopyranosyl glycosides, with the α-anomers predominating. Here, the problem lies in the subsequent stereospecific conversion of the 3-deoxy-2-hexenopyranose unit (or a 2,3,-dideoxy-2-hexenopyranose unit, produced as above, but from acylated glycals instead of 2-hydroxyglycals) into a saturated pyranoside. The subject of *O*-glycoside synthesis has recently been reviewed by Ferrier.[12]

Of these various glycoside syntheses, the one with the generally highest yield and stereoselectivity is the orthoester synthesis, which leads to 1,2-*trans*-glycosides. One possible approach to the synthesis of 1,2-*cis*-glycosides would seem to be the use of this reaction, followed by the stereospecific inversion at the 2-position. This approach will be discussed in the present paper, as applied to the synthesis of α-D-glucopyranosides and of β-D-mannopyranosides. The work follows from the application of the principle of stereoselective 1,2-*trans*-glycoside synthesis followed by C-2 inversion in the synthesis of β-D-mannopyranosides previously communicated from this Department.[13] In that work, the key step consisted in the Koenigs-Knorr synthesis applied to 2-*O*-benzoyl-3,4,6-tri-*O*-benzyl-α-D-glucopyranosyl bromide, the product of which was converted into the corresponding β-D-mannoside by debenzoylation, oxidation and reduction.

3,4,6-Tri-*O*-acetyl-1,2-*O*-(methoxyethylidene)-α-D-glucopyranose [2] and the corresponding β-D-mannopyranose [14] are easily made from the appropriate 2,3,4,6-tetra-*O*-acetyl-α-D-hexosyl bromides. The orthoesters were deacetylated in the 3,4,6-positions by treatment with methanolic ammonia. The products were benzylated in the same positions by treatment with benzyl bromide and silver oxide in dimethyl formamide.[15] The yields from the orthoester starting materials were about 50 %. Each of the two tri-*O*-benzyl orthoesters underwent normal orthoester glycoside syntheses and produced the expected 1,2-*trans*-glycosides. Since the protecting group in the 2-position now was an acetyl group and those in the 3,4,6-positions were benzyl groups, the 2-hydroxyl group could be specifically generated with protecting groups in all other positions, offering an opportunity for inversion at the 2-position by oxidation followed by reduction. The result of this sequence of reactions therefore was an α-D-glucopyranoside (from the tribenzylmannose orthoester) or a β-D-mannopyranoside (from the tribenzylglucose orthoester).

The 1,2-*cis*-glycoside synthesis is illustrated by the syntheses of 6-*O*-α-D-glucopyranosyl-D-galactose and 6-*O*-β-D-mannopyranosyl-D-galactose.

2,3,4-Tri-*O*-benzyl-1,2,-*O*-(methyoxyethylidene)-β-D-mannopyranose (I) [16] was allowed to react with 1,2:3,4-di-*O*-isopropylidene-α-D-galactopyranose (II) [17] in nitromethane containing mercuric bromide under the general glycosylation conditions described by Kochetkov and co-workers.[2] The product III

was deacetylated in methanolic ammonia and the product, with a free hydroxyl group in the 2-position of the mannose residue was oxidized to the corresponding 2-hexosulose residue with dimethyl sulphoxide-acetic anhydride [18] yielding IV. The 2-hexosulose-containing disaccharide IV was reduced with diborane in tetrahydrofuran [19] to yield the glucosylgalactose derivative V. In the reduction of the 2-hexosulose moiety of IV to the glucose residue of V the ratio of glucose-mannose residue formed was 88:12. Reduction with sodium borohydride gave a ratio of 60:40 for the same sugars. The yield of the glucosylgalactose derivative V from I was 25 %. Removal of blocking groups from V afforded 6-*O*-α-D-glucopyranosyl-D-galactose with $[\alpha]_D + 126°$ (lit.[20,21] $[\alpha]_D + 125°$).

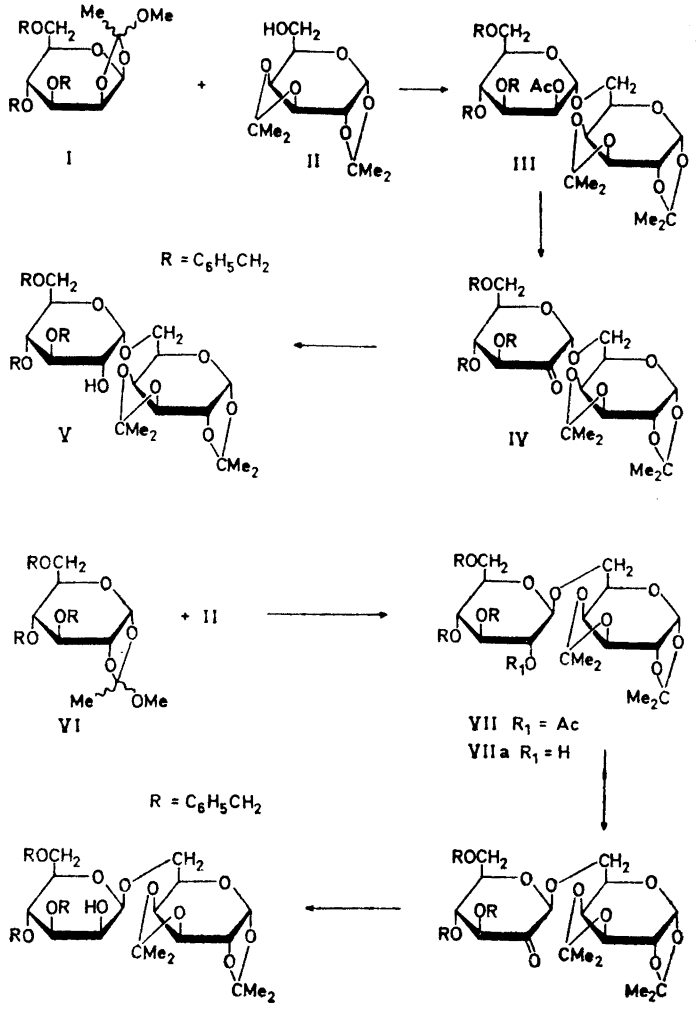

2,3,4-Tri-*O*-benzyl-1,2-*O*-(methoxyethylidene)-α-D-glucopyranose (VI) was condensed with 1,2:3,4-di-*O*-isopropylidene-α-D-galactopyranose (II) as described above for the corresponding mannose orthoester, to produce the glucosylgalactose derivative VII in 77 % yield. The deacetylated product (VIIa) was found to be identical to that previously synthesized in this Department by an alternative route.[13] Since the deacetylation of VII, the oxidation of the product VII and the highly stereoselective reduction with H_2/Pt has previously been demonstrated,[13] the synthesis of VII constitutes a synthesis of a β-D-mannopyranosyl disaccharide.

The stereoselectivity of the above sequence of reactions depends on two key steps, the orthoester glycoside synthesis [2] and on the reduction of the intermediate 2-hexosulose derivatives (IV and VIII). Despite occasional exceptions [3,4] the glycoside synthesis generally proceeds with a high degree of stereoselectivity. The problems associated with the stereochemical outcome of the reduction step are also encountered in the α-D-glycoside synthesis described by Lemieux and co-workers.[8,9] In instance where sodium borohydride offers poor selectivity, improved results may be obtained with diborane as described above. Even higher degrees of selectivity may be attainable with more sterically hindered boranes.

Some extensions from the above synthetic scheme are obvious. Since glycosides and disaccharides containing a 2-hexosulose residue are produced as intermediates, the conversion of these into the corresponding oximes and the reduction of the latter should lead to useful syntheses of 2-amino-2-deoxy-α-D-glucopyranosides and 2-amino-2-deoxy-β-D-mannopyranosides. Work on this particular aspect of the use of benzylated orthoesters in glycoside synthesis is in progress in this Department. A less general extension would be the synthesis, from the intermediates with a single hydroxyl group free in the hexose unit, of (1 → 2) linked oligosaccharides.

EXPERIMENTAL

General methods. Melting points are corrected. Concentrations were performed at reduced pressure. Optical rotations were recorded at room temperature (20 – 22°) at *c* 0.05 – 1.0 using a Perkin-Elmer 141 instrument. NMR spectra (in deuteriochloroform unless otherwise stated) were recorded with a Varian A60-A instrument, using tetramethylsilane as internal reference. The NMR spectra, determined for all new compounds were invariably in agreement with the postulated structures. TLC was performed on silica gel F_{254} (Merck) plates. When necessary, sulphuric acid was used as spray reagent. Silica gel column chromatography was performed using Mallinckrodt 100 mesh silicic acid. GLC was performed on a Perkin-Elmer F 11 instrument using XE-60 (3 % on Gas Chrom Q, 100 – 120 mesh) for disaccharide derivatives or ECNSS-M (3 % on Gas Chrom Q, 100 – 120 mesh), for monosaccharide analysis.

3,4,6-Tri-O-benzyl-1,2-O-(methoxyethylidene)-β-D-mannopyranose (I).[16] 3,4,6-Tri-*O*-acetyl-1,2-*O*-(methoxyethylidene)-β-D-mannopyranose was obtained in a 63 % yield from 2,3,4,6-tetra-*O*-acetyl-α-D-mannopyranosyl bromide by treatment with methanol and lutidine according to the general method described by Kochetkov and coworkers.[2] The material had m.p. 111 – 113° which corresponds to the major stereoisomer of this compound, obtained by another route.[14] NMR ($CDCl_3$) confirmed the presence of one stereoisomer only. The triacetyl orthoester (3.0 g) was deacetylated in methanol (25 ml) by the addition of ammonia-saturated methanol (5 ml) at room temperature overnight. The solution was concentrated to a chromatographically pure suryp (2.21 g). The product (1.15 g) was

dissolved in dimethyl formamide (8.6 ml) and benzylated with benzyl bromide (4.6 ml) and silver oxide (5 g) with stirring at room temperature in the dark for 20 h. Methanol (3.5 ml) was added and the mixture stirred for another 2 h. The mixture was filtered through kiselguhr. The filtrate was concentrated and the product purified by chromatography on silica gel (ethyl ether-hexane 2:1) to yield pure I (1.19 g) which crystallized from ethyl ether-light petroleum (40 – 60°) m.p. 75 – 77°, $[\alpha]_D$ +29° (chloroform) (Found: C 71.1; H 6.90. Calc. for $C_{30}H_{34}O_7$: C 71.1; H 6.77).

6-O-(2-O-Acetyl-3,4,6-tri-O-benzyl-α-D-mannopyranosyl)-1,2:3,4-di-O-isopropylidene-α-D-galactopyranose (III). The above orthoester I (1.45 g) and 1,2:3,4-di-*O*-isopropylidene-α-D-galactopyranose (II) (800 mg) were dissolved in nitromethane (20 ml). Solvent (*ca.* 200 ml) was removed by distillation with the continuous addition of nitromethane at constant volume. The trans-esterification was completed after 5.5 h (TLC, ethyl ether-hexane 2:1). Mercuric bromide (70 mg) was added and the mixture was refluxed overnight. The solution was concentrated and the product purified by TLC (ethyl ether-hexane 2:1) to yield pure III (800 mg), $[\alpha]_D$ −6° (chloroform). (Found: C 67.1; H 6.85. Calc. for $C_{41}H_{50}O_{12}$: C 67.0; H 6.85).

6-O-(3,4,6-Tri-O-benzyl-α-D-arabino-2-hexulopyranosyl)-1,2:3,4-di-O-isopropylidene-α-D-galactopyranose (IV). The above disaccharide derivative III (760 mg) in methanol (25 ml) was deacetylated by the addition of ammonia-saturated methanol (25 ml) for 24 h at room temperature. The solution was concentrated to a syrup (680 mg) $[\alpha]_D$ +9° (chloroform). The product (680 mg) was oxidized in dimethyl sulphoxide (68 ml) and acetic anhydride (3.4 ml) at room temperature for 96 h. The solution was lyophilized to yield a residue which was purified by TLC (ethyl ether-hexane 2:1) to give IV (555 mg), $[\alpha]_D$ +1° (chloroform), which was used directly in the next step.

6-O-(3,4,6-Tri-O-benzyl-α-D-glucopyranosyl)-1,2:3,4-di-O-isopropylidene-α-D-galactopyranose (V). The above disaccharide derivate IV (330 mg) in tetrahydrofuran (30 ml) in a serum bottle under nitrogen was reduced by the injection of a solution of diborane in tetrahydrofuran (0.75 M, 30 ml). The solution was kept at room temperature for 2.5 h, water was then added and the product concentrated. Boric acid was removed by repeated co-distillations with methanol. TLC (ethyl ether-hexane 3:1) showed the presence of a major component and a minor one, with lower R_F value (see below). The main component V was obtained by TLC in the same solvent as a chromatographically pure syrup (276 mg), $[\alpha]_D$ +31° (chloroform) (Found: C 67.4; H 6.86; O 25.6. Calc. for $C_{39}H_{48}O_{11}$: C 67.6; H 6.98; O 25.4).

6-O-α-D-Glucopyranosyl-D-galactose. The above disaccharide derivative V (35 mg) was hydrolyzed in 90 % aqueous trifluoroacetic acid (10 ml) at room temperature for 10 min and concentrated. The product (30 mg), $[\alpha]_D$ +64° (ethanol) was pure on TLC (ethyl acetate-methanol-water 85:10:5). The material (30 mg) was hydrogenated with 10 % palladium on carbon in ethanol to give a quantitative yield of 6-*O*-α-D-glucopyranosyl-D-galactose as a syrup $[\alpha]_D$ +126° (water). Goldstein and Whelan [20] have reported this disaccharide as a syrup, $[\alpha]_D$ +125° (water). Flowers [21] reports a syrup, $[\alpha]_D$ +123° (water).

The disaccharide on acid hydrolysis (0.25 M aqueous sulphuric acid at 100° overnight), conversion into an alditol acetate mixture (sodium borohydride reduction followed by acetylation with acetic anhydride in pyridine) and examination by GLC (on the ECNSS-M column) gave galactitol and glucitol hexa-acetates in a ratio of 1:1.

The above minor components (38 mg) obtained in the diborane reduction of IV to yield V was obtained pure by TLC as described above for V. An aliquot was subjected to treatment with, in sequence, palladium on carbon, aqueous sulphuric acid, sodium borohydride and finally, acetic anhydride in pyridine. Examination of the product by GLC (ECNSS-M) gave galactitol and mannitol in a ratio of 1:1. Another aliquot of the minor component on acetylation yielded III.

3,4,6-Tri-O-benzyl-1,2-O-(methoxyethylidene)-α-D-glucopyranose (VI). 3,4,6-Tri-*O*-acetyl-1,2-*O*-(methoxyethylidene)-α-D-glucopyranose [2] (6 g) was deacetylated in methanol (50 ml) by the addition of ammonia-saturated methanol (10 ml). After 20 h at room temperature, the solution was concentrated to a syrup (3.6 g). The product (2.0 g) was dissolved in dimethyl formamide (15 ml) and benzylated with benzyl bromide (8 ml) and silver oxide (8 g) with stirring at room temperature in the dark for 20 h. Methanol (6 ml) was added in portions and the stirring continued for another 2 h. The mixture was filtered through kiselguhr. The filtrate was concentrated and the product purified by

chromatography on silica gel (toluene-ethyl acetate 4:1) to yield pure IV (2.25 g) $[\alpha]_D$ +36° (chloroform) (Found: C 71.0; H 6.65. Calc. for $C_{30}H_{34}O_7$: C 71.1; H 6.77).

6-O-(2-O-Acetyl-3,4,6-tri-O-benzyl-β-D-glucopyranosyl)-1,2:3,4-di-O-isopropylidene-α-D-galactopyranose (VII). The above orthoester VI (1.1 g) and II (0.565 g) were dissolved in nitromethane (13 ml). Solvent was removed by distillation with the continuous addition of nitromethane at constant volume until no more methanol was found in the distillate (GLC). The trans-esterification was complete after 1.5 h (TLC, toluene-ethyl acetate 4:1). Mercuric bromide (42 mg) was added and the mixture was refluxed overnight. After the addition of a few drops of pyridine, the solution was concentrated and the product purified by TLC (toluene-ethyl acetate 4:1) to give pure VII (1.2 g), $[\alpha]_D$ −31° (chloroform) (Found: C 66.8; H 6.71. Calc. for $C_{41}H_{50}O_{12}$: C 67.0; H 6.86).

The disaccharide derivative VII (0.6 g) was deacetylated in methanol (10 ml) by the addition of ammonia-saturated methanol (2 ml) at room temperature overnight to give VIIa in a quantitative yield, $[\alpha]_D$ −42° (chloroform) (Found: C 67.9; H 7.13. Calc. for $C_{39}H_{48}O_{11}$: C 67.6; H 6.98). These values are in agreement with those previously found for this substance, from which 6-*O*-β-D-mannopyranosyl-D-galactose was made.[13]

Acknowledgements. The authors are indebted to Professor Bengt Lindberg for his interest, to *Hierta-Retzius stipendiefond* and to *Statens Naturvetenskapliga Forskningråd* for financial support, and to Mr. Lennart Holmqvist for skilful assistance.

REFERENCES

1. Koenigs, W. and Knorr, E. *Ber.* (1901) 957.
2. Kochetkov, N. K., Khorlin, A. J. and Bochkov, A. F. *Tetrahedron* **23** (1967) 693.
3. Alfredsson, G., Borén, H. B. and Garegg, P. J. *Acta Chem. Scand.* **26** (1972) 2531.
4. Garegg, P. J., Lindberg, B., Nilsson, K. and Swahn, C.-G. *Acta Chem. Scand.* **27** (1973) 1595.
5. Austin, P. W., Hardy, F. E., Buchanan, J. G. and Baddiley, J. *J. Chem. Soc.* **1964** 2128.
6. Fréchet, J. M. and Schuerch, C. *J. Am. Chem. Soc.* **94** (1972) 604.
7. Fréchet, J. M. and Schuerch, C. *Carbohyd. Res.* **22** (1972) 399.
8. Lemieux, R. U., Suemitsu, R. and Gunner, S. W. *Can. J. Chem.* **46** (1968) 1040.
9. Lemieux, R. U., Abstracts Papers IUPAC *VI Symp Carbohyd. Chem. Madison* **1972.**
10. Miyini, K. and Jeanloz, R. W. *Carbohyd. Res.* **21** (1972) 45.
11. Ferrier, R. J., Prasad, N. and Sankey, G. H. *J. Chem. Soc.* **1969** 587.
12. Ferrier, R. J. *Fortschr. chem. Forsch.* **14** (1970) 389.
13. Ekborg, G., Lindberg, B. and Lönngren, J. *Acta Chem. Scand.* **26** (1972) 3287.
14. Perlin, A. S. *Can. J. Chem.* **41** (1963) 399.
15. Kuhn, R., Löv, I. and Trischmann, H. *Chem. Ber.* **90** (1957) 203.
16. Franks, N. E. and Montgomery, R. *Carbohyd. Res.* **6** (1968) 286.
17. Tipson, S. *Methods Carbohyd. Chem.* **II** (1963) 246.
18. Lindberg, B. *Methods Carbohyd. Chem.* **VI** (1972) 323.
19. Brown, H. C., Heim, P. and Nung Min Yoon *J. Am. Chem. Soc.* **92** (1970) 1637.
20. Goldstein, I. J. and Whelan, W. J. *J. Chem. Soc.* **1963** 4264.
21. Flowers, H. M. *Carbohyd. Res.* **18** (1971) 211.

Received March 5, 1973.

ACTA CHEMICA SCANDINAVICA 27 (1973) 2645–2649

Structural Studies on the *Klebsiella* O Group 3 Lipopolysaccharide

MARGARETA CURVALL,[a] BENGT LINDBERG,[a] JÖRGEN LÖNNGREN[a] and WOLFGANG NIMMICH[b]

[a] *Department of Organic Chemistry, The Arrhenius, Laboratory, P.O.B., S-104 05 Stockholm 50, Sweden and* [b] *Institut für Medizinische Mikrobiologie und Epidemiologie der Universität Rostock, DDR-25 Rostock, German Democratic Republic*

The structure of the O-specific side chains in a *Klebsiella* O group 3 lipopolysaccharide has been investigated, using methylation analysis and Smith degradation as the principal methods. The results are consistent with the assumption that the side chains are composed of repeating units containing five α-D-mannopyranose residues, two which are (1→3)-linked and adjacent and the other three (1→2)-linked.

The O-specific side chains in the lipopolysaccharide (LPS) from two of the twelve serologically defined O groups of *Klebsiella*, O group 3 and O group 5, are composed of D-mannose residues.[1] Those from O group 5 contain in addition a low percentage of 3-*O*-methyl-D-mannose. The O-antigen from *E. coli* O8 also contains D-mannose and its 3-*O*-methyl ether,[2] and is serologically identical with the *Klebsiella* O5 antigen.[3] According to our recent studies,[4] the O-specific side chains in the *Klebsiella* O5 LPS should be composed of pentasaccharide repeating units of structure I, and be terminated by 3-*O*-methyl-D-mannose residues.

→2)-α-D-Man*p*-(1→2)-α-D-Man*p*-(1→3)-α-D-Man*p*-(1→2)-α-D-Man*p*-(1→3)-α-D-Man*p*-(1→

I

In a recent investigation of the *E. coli* O8 LPS a trisaccharide repeating unit (II) was proposed.[5]

→2)-α-D-Man*p*-(1→3)-α-D-Man*p*-(1→2)-α-D-Man*p*-(1→

II

We now report structural studies on the *Klebsiella* O3 LPS.

RESULTS AND DISCUSSION

The LPS was isolated from *Klebsiella* O3:K58 as previously described.[1] A hydrolysate of the LPS contained mannose and trace amounts of galactose, glucose, and a heptose. The three latter sugars, which are found in all *Klebsiella* LPS,[1] are probably components of the core region, whereas the mannose represents the sole component of the O-specific side chains. D-Arabinose was used as internal standard in the analysis and the percentage of mannose was found to be 43 %. Mannose was isolated from a hydrolysate and the D-configuration was assigned from its optical rotation. No significant absorption around 1735 cm^{-1} in the IR was observed, demonstrating the absence of *O*-acyl groups. This was confirmed by methylation analysis of the acetalated polysaccharide, according to the method devised by de Belder and Norrman.[6] The optical rotation of the LPS, $[\alpha]_{589}$ +38°, indicates that the D-mannose residues are α-linked, assuming that the rotation is essentially due to these residues. Sugar analysis of acetylated LPS that had been treated with chromium trioxide in acetic acid, using *myo*-inositol hexaacetate as internal standard, also showed that no D-mannose residues had been oxidized. These results indicate that the D-mannose residues are α-linked.[7]

Fully methylated polysaccharide, prepared by the Hakomori procedure,[8] was hydrolysed and the sugars in the hydrolysate analysed, as alditol acetates, by GLC-MS.[9] The results (Table 1) suggest that the O-specific side chains are composed of linear pentasaccharide residues, with two 3-*O*-substituted and

Table 1. Methyl ethers obtained in the methylation analysis of the *Klebsiella* O group 3 LPS.

Sugars[a]	T^b	Mol %[c]
2,3,4,6-G 2,3,4,6-Man	1.00	2
3,4,6-Man	1.95	56
2,4,6-Man	2.09	38
Others[d]	–	4

[a] 2,3,4,6-G = 2,3,4,6-tetra-*O*-methyl-D-glucose, *etc.* [b] Retention times of the corresponding alditol acetates on an ECNSS–M column at 170° relative to that of 1,5-di-*O*-acetyl-2,3,4,6-tetra-*O*-methyl-D-glucitol. [c] Average values from three determinations. [d] Some of these are probably non-sugar components.

three 2-*O*-substituted α-D-mannopyranose residues, as was also observed for the *Klebsiella* 05 LPS. The terminal D-mannose residue will give 2,3,4,6-tetra-*O*-methyl-D-mannose, and from the percentage of this sugar, which is not well separated from the corresponding D-glucose derivative, the average number of pentasaccharide repeating units in the O-specific side chains should be 9 or higher.

In this repeating unit the two 3-*O*-substituted α-D-mannopyranose residues could either be adjacent or separated. In order to distinguish between these alternatives, the LPS was subjected to a Smith degradation.[4,10] The products after periodate oxidation, reduction with sodium borohydride and hydrolysis under mild conditions were reduced with sodium borodeuteride. Sugar analysis, using D-arabinose as internal standard, of the material obtained after periodate oxidation and borohydride reduction revealed a mannose content similar to the original, (1→3)-linked D-mannose residues. In a methylation analysis of this product the only methyl ether obtained was 2,4,6-tri-*O*-methyl-D-mannose. These results demonstrate that the oxidation had gone to completion and that no significant amounts of material had been lost. Part of the product obtained after hydrolysis and borodeuteride reduction was subjected to methylation analysis. The only sugars obtained in significant quantities were 2,3,4,6-tetra-*O*-methyl-D-mannose and 2,4,6-tri-*O*-methyl-D-mannose, in the proportion 0.7:1.0. Another part of the product was trimethylsilylated and analysed by GLC-MS.[4,11] No trimethylsilyl (TMS) derivatives of mannitol, glycerol mannoside, or mannitol mannoside were observed. The main component, $T_{\text{melibiitol}} = 1.04$ (retention time relative to the TMS derivative of melibiitol) was identified as the TMS derivative of mannobiosyl glycerol (III), as it gave the same MS, except for the shifts caused by the deuterium labelling, as that of the mannosylgalactosyl glycerol (IV) ($T_{\text{melibiitol}} = 1.4$) isolated from a red alga.[12] The yield of III in the Smith degradation was estimated to ~35 % of the theoretical value, assuming that the response factor on GLC of its TMS derivative is the same as that of the melibiitol derivative. The estimate of the yield is also corrected for the finding that only about 85 % of the oxidized-reduced residues had been hydrolysed, as demonstrated by the methylation analysis of the degraded material.

α-D-Man*p*-(1→3)-α-D-Man*p*-O-CH(CHDOH)(CH$_2$OH)

III

α-D-Man*p*-(1→3)-α-D-Gal*p*-O-CH(CH$_2$OH)(CH$_2$OH)

IV

From the evidence presented above it is proposed that the O-specific side chains of the *Klebsiella* O3:K58 LPS are composed of pentasaccharide repeating units with the structure V. This is similar to the repeating unit of the *Klebsiella* O group 5 LPS (I) but the 3-*O*-substituted D-mannose residues are adjacent in the former and separated in the latter. This difference, and the absence of 3-*O*-methyl-D-mannose in the *Klebsiella* O group 3 LPS, could account for observed serological differences between the two species.

→2)-α-D-Man*p*-(1→3)-α-D-Man*p*-(1→3)-α-D-Man*p*-(1→2)-α-D-Man*p*-(1→2)-α-D-Man*p*-(1→

V

EXPERIMENTAL

General methods were the same as in the investigation of *Klebsiella* O group 5 LPS [4] except for the GLC analyses of TMS derivatives which were performed on a glass column (180 × 0.15 cm) containing 3 % XE-60 on Gas Chrom Q (100/120 mesh). Separations were performed at 175° or 120° to 180° (3°/min) for quantitative estimations.

The LPS was isolated from strain *Klebsiella* O3:K58 (636/52) as previously described.[1] The LPS showed $[\alpha]_{589}^{20}$ +38° (*c* 0.1, water). In the IR spectrum (KBr) no absorption around 1735 cm^{-1} was observed. The content of phosphorus in the material was < 0.1 %.

Sugar and methylation analyses were performed as previously described.[4,8,9,13,14] Mannose was isolated from a hydrolysate of LPS by preparative paper chromatography. The sample showed $[\alpha]_{578}^{20}$ +16° (*c* 0.1, water).

Methylation analysis of acetalated LPS. Preparation of the acetalated LPS by reaction with methyl vinyl ether and methylation analysis of the product was performed as previously described.[6,15] Only mannitol hexaacetate was obtained in the analysis.

Oxidation with chromium trioxide. LPS (20 mg) was dissolved in formamide (20 ml), acetic anhydride (5 ml) and pyridine (5 ml) were added and the solution was kept at room temperature overnight. The reaction mixture was added to the top of a Sephadex LH-20 column (25 × 3 cm) which was irrigated with chloroform:acetone (2:1). The eluate was monitored polarimetrically and the acetylated polysaccharide (28 mg) was eluted as a single peak with the void volume. The acetylated polysaccharide showed no absorption in the hydroxyl region in the IR. *myo*-Inositol hexaacetate (7 mg) was added to the polysaccharide material and this was divided into two equal portions. One portion was dissolved in acetic acid (0.4 ml), chromium trioxide (40 mg) was added and the mixture was treated in an ultrasonic bath at 50° for 1 h. The other portion was treated likewise but the chromium trioxide was omitted. The samples were recovered by partition between chloroform and water and subjected to sugar analysis as described earlier.[4,13,14] The proportion between mannitol hexaacetate and *myo*-inositol hexaacetate was the same in the two samples.

Smith degradation of the LPS. A mixture of LPS (30 mg) in 0.1 M acetate buffer of pH 3.9 (20 ml) and 0.2 M sodium metaperiodate (5 ml) was kept in the dark at 4° for 120 h. Excess periodate was destroyed with ethylene glycol (1 ml), the solution was dialysed overnight and concentrated to 50 ml, sodium borohydride (300 mg) was added and the solution was kept at room temperature for 9 h. Excess borohydride was decomposed with 50 % acetic acid and the solution dialysed overnight. Part of the recovered material (1/15) was used for sugar analysis with D-arabinose as internal standard. Another part (1/3) was lyophilized and subjected to methylation analysis. After addition of 0.5 mg of D-arabinose (internal standard) the main part was treated with 0.25 M sulphuric acid at room temperature for 60 h, neutralized with Dowex 3 (free base) and reduced with sodium borodeuteride (50 mg) during 3 h at room temperature. The solution was treated with acetic acid and boric acid was removed by repeated distillations with methanol. The material was divided into two equal parts which were lyophilized and dried in a vacuum over phosphorus pentoxide. One part was subjected to methylation analysis. The other part was dissolved in dry pyridine (2 ml) and treated with a mixture of trimethylchlorosilane (0.2 ml) and hexamethyldisilazane (0.4 ml). After 20 min at 40° the mixture was concentrated to dryness, dissolved in carbon tetrachloride, filtered and used for GLC-MS. The ratio of the responses for the TMS-derivatives of D-arabinitol and melibiitol, determined in a separate experiment, was 3.4:1. Using the same factor the main peak ($T_{\text{melibiitol}} = 1.04$) accounted for 0.4 mg. The mass spectrum of this component showed, *inter alia*, the following signals (relative intensities in brakets): 73(100), 103(37), 104(20), 129(23), 147(23), 204(30), 217(29), 361(33), 451(5) and 467(3).

Acknowledgements. The skilled technical assistance of Mrs. Jana Cederstrand (Stockholm) and Miss Karin Legand (Rostock) is acknowledged. This work was supported by *Statens Naturvetenskapliga Forskningsråd*, *Statens Medicinska Forskningsråd* (B72-40X-2522-04), *Harald Jeanssons Stiftelse* and *Stiftelsen Sigurd och Elsa Goljes Minne*.

REFERENCES

1. Nimmich, W. and Korten, G. *Pathol. Microbiol.* **36** (1970) 179.
2. Nimmich, W. *Biochim. Biophys. Acta* **215** (1970) 189.
3. Ørskov, I. *Acta Pathol. Microbiol. Scand.* **34** (1954) 145.
4. Lindberg, B., Lönngren, J. and Nimmich, W. *Acta Chem. Scand.* **26** (1972) 2231.
5. Reske, K. and Jann, K. *Eur. J. Biochem.* **31** (1972) 320.
6. de Belder, A. N. and Norrman, B. *Carbohyd. Res.* **8** (1968) 1.
7. Hoffman, J., Lindberg, B. and Svensson, S. *Acta Chem. Scand.* **26** (1972) 661.
8. Hakomori, S. *J. Biochem. (Tokyo)* **55** (1964) 205.
9. Björndal, H., Hellerqvist, C. G., Lindberg, B. and Svensson, S. *Angew. Chem.* **82** (1970) 643.
10. Goldstein, I. J., Hay, G. W., Lewis, B. A. and Smith, F. *Methods Carbohyd. Chem.* **5** (1965) 361.
11. Kärkkäinen, J. *Carbohyd. Res.* **11** (1969) 247.
12. Lindberg, B. *Acta Chem. Scand.* **9** (1955) 1093.
13. Sawardeker, J. S., Sloneker, J. H. and Jeanes, A. R. *Anal. Chem.* **37** (1965) 1602.
14. Chizhov, O. S., Golovkina, L. S. and Wulfson, N. S. *Izv. Akad. Nauk SSSR Ser. Khim.* **1966** 1915.
15. Lindberg, B., Lönngren, J. and Nimmich, W. *Carbohyd. Res.* **23** (1972) 47.

Received March 30, 1973.

ACTA CHEMICA SCANDINAVICA 27 (1973) 2650–2654

Nucleophilic Reactivity of Amines toward Ethylene Oxide

P. O. I. VIRTANEN and R. KORHONEN

Department of Chemistry, University of Oulu, 90100 Oulu 10, Finland

The rates of reaction of ethylene oxide with a series of primary, secondary, and tertiary amines with a wide pK_a range have been studied in aqueous solution. A logarithmic plot of the rate constants against the pK_a values of the amines is a curve with individual deviations, but against the nucleophilicity parameter N_+ a straight line of slope 0.60 is obtained. These correlations are discussed with reference to the reaction mechanism.

During kinetic studies on cation-anion combination reactions, the remarkably simple relationship

$$\log k_N^R = \log k_{H_2O}^R + N_+ \quad (1)$$

was shown to correlate the rates of reaction of different cations from triarylmethyl, benzenediazonium, and phenyltropylium systems with different anions over a reactivity range of six powers of ten.[1] $k_{H_2O}^R$ is the first-order rate constant of the reaction of a particular cation R with water in water as solvent and k_N^R is its second-order rate constant with the nucleophile N in a particular solvent. N_+ is the corresponding nucleophilicity parameter defined by the equation

$$N_+ = \log k_N^{PNMG} - \log k_{H_2O}^{PNMG} \quad (2)$$

where the rate constants refer to the reactions of *para*-nitro Malachite Green, *i.e.* the bis(*para*-dimethylaminophenyl)-*para*-nitrophenylmethyl cation.

Some support for the value of eqn. (1) in correlating the reactions between cations and neutral molecules and between neutral molecules has also been gathered.[2] These observations suggested that further study would yield more information about the detailed reaction process. We report here our kinetic results for the reaction of various amines and some anions with ethylene oxide, one of the cyclic ethers which has been studied for several years in these laboratories.

EXPERIMENTAL

Chemicals. Ethylene oxide, a product of *purum* grade from Fluka AG, Buchs, Switzerland, was used directly from its steel cylinder. Glycine, glycylglycine, phenylhydrazine hydrochloride, and potassium cyanide were guaranteed reagents from Fluka AG or

Merck AG, Darmstadt, BRD, and used without further purification. The hydrochlorides of ethylamine, ethylenediamine, hydrazine, semicarbazine, piperidine, and diethylamine were commercial chemicals or prepared by standard methods from the corresponding amines. They were recrystallized from appropriate solvents before use. Pyridine and triethylamine were products of *purum* grade from Fluka AG and were fractionally distilled. Water was purified by distillation and ion-exchange. Methanol, a guaranteed *purissimum p.a.* product from Fluka AG was used as received.

A stock solution of sodium hydroxide free from carbon dioxide was prepared by mixing equal weights of sodium hydroxide and water and allowing the solution to stand until a clear supernatant was obtained. A stock solution of sodium methoxide was prepared by adding freshly cut sodium to methanol.

Kinetic experiments. Ethylene oxide was passed through a capillary tube into water. This solution was mixed with the buffer solution prepared by partly neutralizing the amine hydrochloride solution with a solution of sodium hydroxide. In the case of pyridine and triethylamine the buffer solutions were prepared from amine and perchloric acid solutions. The addition reactions of cyanide anion in water and methoxide ion in methanol were studied in unbuffered solutions.

The reactions were followed by analyzing the concentration of ethylene oxide using either gas chromatography or the thiosulphate method of Roos.[3,4] The gas chromatograms were run on a Perkin-Elmer model F11 gas chromatograph equipped with a flame ionization detector and using a 2-meter column containing 10 % Silicone Gum Rubber SE-30 on Chromosorb W at 40°C with helium as carrier gas. This method was employed when the reactions of ethylamine, phenylhydrazine, semicarbazine, triethylamine, pyridine, and cyanide were studied. In the reactions of ethylamine, glycine, piperidine, diethylamine, and methoxide anion, the titrations were carried out visually to the cresol red end-point near pH 8. Potentiometric titrations were suitable for analyzing the reactions of ethylenediamine, 2-ammonioethylamine, glycylglycine, and hydrazine. Within the limits of experimental error the same value of the rate constant was obtained when both methods were employed for the analysis of ethylene oxide from the reaction of ethylamine.

Calculations. Pseudo-first-order overall rate constants were evaluated from the variation of the ethylene oxide concentration with time. Second-order rate constants were calculated by subtracting the first-order rate constants of possible side reactions from the overall rate constant and dividing the difference by the average concentration of free amine during the reaction. The aminium ions were not found to add ethylene oxide.

The rate constant for the reaction of ethylenediamine was corrected for the reaction of 2-ammonioethylamine. The uncatalyzed hydrolysis of ethylene oxide was taken into account in calculating the rate constants of reactions of phenylhydrazine, semicarbazine, and pyridine, as was the uncatalyzed reaction of chloride ion with ethylene oxide in the reactions of 2-ammonioethylamine, phenylhydrazine and semicarbazine.[4,5] In the semicarbazine buffers, the pH was so low that the contributions of acid-catalyzed hydrolysis and the reaction of chloride ion with ethylene oxide were significant.[4] The total contribution of these side-reactions was low. It amounted to less than 8 % of the overall reaction except in the case of semicarbazine for which it was about 40 %.

In the reactions of cyanide ion with ethylene oxide, the hydrolysis of cyanide ion was taken into account using a pK_a value of 9.14 for hydrocyanic acid.[6] The rate was corrected for small contributions from the uncatalyzed hydrolysis of ethylene oxide and its reaction with hydroxide ion.[4]

RESULTS

The work of Eastham *et al.* has shown that ethylene oxide reacts with amines in aqueous solutions of pH range from 4 to 14 without any significant basic catalysis or catalysis by hydrogen or ammonium-type ions. In agreement with this, the rates of the reactions studied in the present work were found to be strictly first-order in ethylene oxide and amine. The pH of the aqueous amine buffer solutions was adjusted to or near the pK_a value of the

Table 1. Rate constants for the reaction of ethylene oxide with amines in water at 25°C.

Amine	Initial conen of amine, M	pH	pK_a[a]	k_{amine} M^{-1} s^{-1}	N_+[d]
1. Ethylamine	0.313	11.00	10.97	1.08×10^{-3}	4.88
2. Ethylenediamine	0.463	10.71	10.18	1.30×10^{-3}	5.04
3. Glycine	0.300	9.76	9.76	1.12×10^{-3}	4.95
4. Glycylglycine	0.313	8.29	8.25	5.07×10^{-4}	4.25
5. Hydrazine	0.313	8.23	8.20	1.81×10^{-3}	5.60
6. 2-Ammonioethylamine	0.313	7.45	7.42	4.35×10^{-4}	3.39
7. Phenylhydrazine	0.156	5.30	5.27[b]	7.41×10^{-4}	4.36
8. Semicarbazine	0.313	3.89	3.89	3.57×10^{-5}	3.32
9. Piperidine	0.313	11.45	11.42	5.60×10^{-3}	6.25
10. Diethylamine	0.313	10.70	10.67	1.35×10^{-3}	5.87
11. Triethylamine	0.302	10.77	10.75[c]	5.46×10^{-4}	
12. Pyridine	0.310	5.54	5.52	1.90×10^{-4}	

[a] Ref. 8. [b] Ref. 9. [c] Ref. 6. [d] Ref. 2.

aminium ions, *i.e.* within the range 3.9 to 11.4. The results are collected in Table 1. Close agreement is found between our reaction rate constants for diethylamine, triethylamine, and pyridine and those measured dilatometrically by Eastham *et al.*, 1.1×10^{-3}, 5.2×10^{-4}, and 2.0×10^{-4} M^{-1} s^{-1}, respectively.[7]

Data for the reaction of ethylene oxide with some other nucleophiles than amines are collected in Table 2. Gee *et al.* have measured the rate of the reaction of methoxide ion in methanol at 29.8°C in 0.263 M sodium methoxide solution.[10] Because direct comparison with our other results was ambiguous, we repeated the experiments at 25°C using a lower concentration of the salt. Our result agrees with their value of 2.14×10^{-4} M^{-1} s^{-1} when the different experimental conditions are taken into account.

Table 2. Rate constants for the reactions of ethylene oxide with nucleophiles at 25°C.

Nucleophile	Solvent	Initial conc. of nucleophile, M	k_1 s^{-1}	k_2 M^{-1} s^{-1}	pK_a	N_+[g]
13. Hydroxide ion	water	2.04×10^{-2}		1.22×10^{-4} [a,b]	15.75[e]	4.5
14. Phenoxide ion	water	3.05×10^{-2}		9.50×10^{-5} [a]	10.00[f]	
15. Cyanide ion	water	4.66×10^{-2}		3.38×10^{-4}	9.14[d]	3.8
16. Azide ion	water			9.00×10^{-5} [c]	4.59[d]	
17. Water	water		6.18×10^{-7} [a]		−1.74	0.0
18. Methoxide ion	methanol	3.73×10^{-3}		2.11×10^{-4}	15.5[e]	7.5
19. Methanol	methanol		4.99×10^{-8} [a]		−1.39	0.5

[a] Ref. 4. [b] Ref. 5. [c] Ref. 11. [d] Ref. 6. [e] Ref. 8. [f] Ref. 12. [g] Ref. 1.

DISCUSSION

The logarithm of the rate constant for the reactions of ethylene oxide with the nucleophiles is plotted as a function of the basicity of the nucleophile in Fig. 1. When the reactions in water (circles) only are considered, the data show (despite some individual variations) a decreasing dependence of the rate on

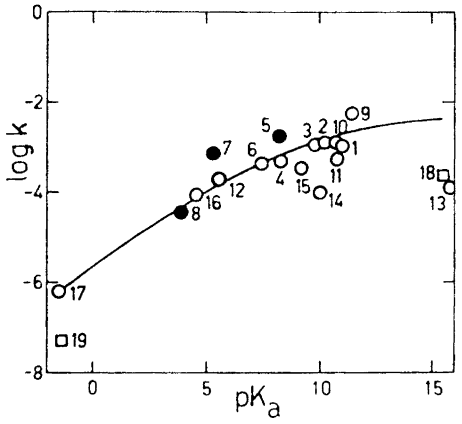

Fig. 1. Dependence of the rate constant for the reaction of ethylene oxide with nucleophiles on the basicity of the nucleophile. Notation as in Tables 1 and 2.

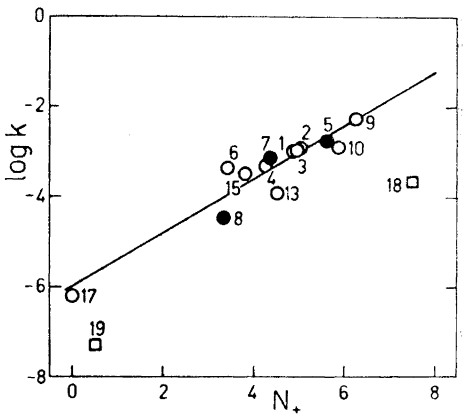

Fig. 2. Logarithm of the rate constant for the reaction of ethylene oxide with nucleophiles as a function of the parameter N_+. Numbers refer to the same nucleophiles as in Fig. 1.

the basicity of the nucleophile with increasing basicity. A similar levelling out of the reaction rate has been observed in the reactions of acetate esters [8] and substituted *N*-acetylpyridinium ions.[13] The phenomenon has been cited as evidence that the transition state occurs early along the reaction coordinate so that no significant change in the charge of the nucleophile occurs. The explanation warrants consideration, but it is well to remember that our knowledge of the relationship between carbon and hydrogen basicities is very limited. The reactions of oxirans are promoted by acid catalysis, and the catalyzed reactions are believed to proceed *via* transition states in which both partial bonds are long. The spontaneous reactions of oxirans are evidently facilitated by hydrogen or other bonds to the oxygen atom. The speculation is consistent with the interpretation that when the enhanced rate of oxiran reactions is caused by increased catalytic activity or by increased nucleophilicity of the nucleophile, the transition state has a looser structure. The above-mentioned catalytic effect in the stretching of the carbon-oxygen bond of the oxiran thus gives the reaction mechanism a more S_N1-like character.

There are several deviations from the rate-basicity curve. Hydroxide anion shows its characteristic negative deviation as does phenoxide ion.[13] Clearly the anions of strong acids like chloride, $k = 8.0 \times 10^{-6}$ M^{-1} s^{-1} at 30°C,[4] and bromide, $k = 7.0 \times 10^{-5}$ M^{-1} s^{-1} at 35°C,[11] also deviate from the plot.

When studying the reaction of Malachite Green with nucleophiles, Dixon and Bruice found that the Brønsted plots for α-effect nucleophiles (black points in Fig. 1) and for primary amines of similar pK_a fall on different lines,[14] and that the magnitude of the α-effect decreases with decreasing pK_a.[15] If the ratio k(hydrazine)/k(glycylglycine) is taken as a measure of the α-effect,[16] a value of 3.6 is obtained for the reactions of ethylene oxide. This low value is consistent with the gentle Brønsted slope of about 0.2 for the reaction rates of primary amines 1 – 4.

The logarithm of the rate constant for each reaction is plotted in Fig. 2 as a function of the nucleophilicity parameter N_+ where this is known. Comparison with Fig. 1 indicates that the rates in aqueous solution show no curvature and that the hydroxyl anion lies close to the line. The low reaction rate of methanol and methoxide anion in methanol (squares) is easily understood from the first paragraph of this discussion. These deviations arise from the low hydrogen bond donor ability of methanol compared with that of water.

Regression analysis of the data obtained in aqueous solution yields the equation

$$\log k_N = 0.60\, N_+ - 6.01 \qquad (3)$$

with a regression coefficient of 0.944. It has been noted that N_+ values are inherent properties of nucleophiles alone [17] and independent of the electrophilic component of the reaction system. Moreover, it has been suggested that the N_+ values are related to the desolvatation energy of the nucleophiles: the higher the N_+ value, the less is the amount of energy required for the reaction.[1] Thus eqn. (1) with unit slope correlates reactions which are controlled by the desolvation of the nucleophiles, *i.e.* typical S_N2 reactions. Consequently, a slope of less than unity directs attention to the changes occurring in ethylene oxide itself during the formation of the transition state. Points for clean S_N1 reactions would surely fall on a line with zero slope. When more data have been collected we hope to discuss the question of whether this kind of analysis of reaction rates can be used as a measure of reaction mechanism.

REFERENCES

1. Ritchie, C. D. and Virtanen, P. O. I. *J. Am. Chem. Soc.* **94** (1972) 4966.
2. Ritchie, C. D. and Virtanen, P. O. I. *J. Am. Chem. Soc.* **95** (1973) 1882.
3. Ross, W. C. J. *J. Chem. Soc.* **1950** 2257.
4. Virtanen, P. O. I. *Ann. Acad. Sci. Fennicae A II* **124** (1963).
5. Porret, D. *Helv. Chim. Acta* **24** (1941) 80E.
6. *Handbook of Chemistry*, Lange, N. A., Ed., 9th Ed., McGraw, New York 1956.
7. Eastham, A. M., Darwent, B., deB. and Beaubien, P. E. *Can. J. Chem.* **29** (1951) 575.
8. Jencks, W. P. and Gilchrist, M. *J. Am. Chem. Soc.* **90** (1968) 2622.
9. Stroh, H. and Westphal, G. *Chem. Ber.* **96** (1963) 184.
10. Gee, G., Higginson, W. C. E., Levesley, P. and Taylor, K. J. *J. Chem. Soc.* **1959** 1338.
11. Hardy, F. E. *J. Chem. Soc. B* **1971** 1899.
12. Biggs, A. I. *Trans. Faraday Soc.* **52** (1956) 35.
13. Fersht, A. R. and Jencks, W. P. *J. Am. Chem. Soc.* **92** (1970) 5442.
14. Dixon, J. E. and Bruice, T. C. *J. Am. Chem. Soc.* **93** (1971) 3248.
15. Dixon, J. E. and Bruice, T. C. *J. Am. Chem. Soc.* **93** (1971) 6592.
16. Dixon, J. E. and Bruice, T. C. *J. Am. Chem. Soc.* **94** (1972) 2052.
17. Ritchie, C. D. and Virtanen, P. O. I. *J. Am. Chem. Soc.* **94** (1972) 1589.

Received March 9, 1973.

ACTA CHEMICA SCANDINAVICA 27 (1973) 2655–2660

Synthesis of 3-Amino- and 3-Substituted Amino-2H-1,2,4-benzothiadiazine 1,1-Dioxides

HANS JØRGEN PETERSEN

Leo Pharmaceutical Products, DK-2750 Ballerup, Denmark

Various cyclization reactions were successfully adapted to the conversion of substituted 2-aminobenzenesulfonamides into some new 3-amino-2H-1,2,4-benzothiadiazine 1,1-dioxides.

The smooth exchange reaction of the 3-unsubstituted 6-trifluoromethyl member of the title group with amines afforded the corresponding 3-substituted amino derivatives, in the case of butyl- and cyclohexylamine constituting an independent synthesis of the compounds obtained by the fusion of 2-amino-4-trifluoromethylbenzenesulfonamide with butylcyanamide and with *N,N'*-dicyclohexylcarbodiimide, respectively.

A report by Raffa *et al.*[1] on hypotensive activity displayed by 3-amino-substituted members of the title ring system has stimulated the interest in preparing further substituted analogues, predominantly carrying 6- or 7-substituents, the main incentive being the enhancement and the singling out of this pharmacological property from the additional diuretic activity of 7-sulfamoyl derivatives.[2]

3-Unsubstituted amino derivatives were chiefly obtained by the fusion of 2-aminobenzenesulfonamides with guanidine carbonate.[3a,b] More specific synthetic procedures have involved alkaline hydrolysis of a 3-pyridinium salt[4] and ammonium carbonate fusion of a 3-methylmercapto derivative of the ring system.[5] A number of 3-substituted amino-2H-1,2,4-benzothiadiazine 1,1-dioxides bearing no substituents on the aromatic nucleus was synthesized by Raffa[4] from the 3-methylmercapto compound by heating with the requisite amines in a sealed tube at 130 – 180°C. Some 6-chloro-3-substituted amino derivatives resulted from condensing 2-amino-4-chlorobenzenesulfonamide with isothiocyanates.[3a] 6,7-Dimethoxy-3-di-substituted amino representatives were prepared by reacting the 3-chloro compounds with secondary amines.[6] The present paper reports some alternative synthetic pathways, essentially based on a study of reactions of 2-amino-4-trifluoromethylbenzenesulfonamide (Ia), as outlined in Scheme 1.

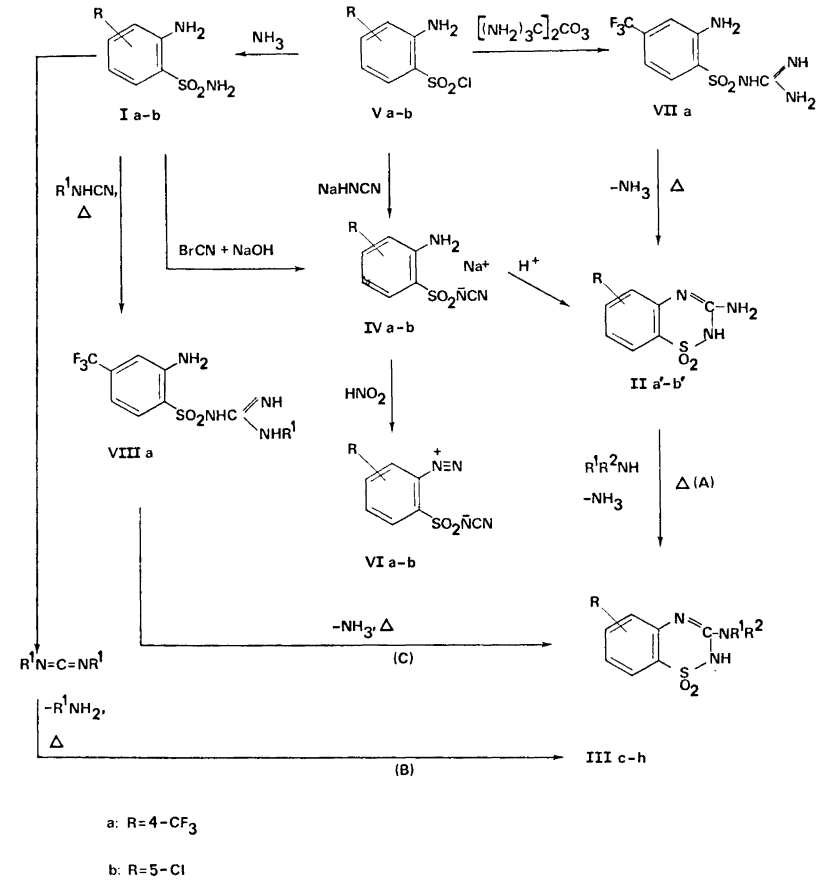

Scheme 1.

The structural formulae II and III are in accordance with the one established for analogous compounds in an extensive study of tautomerism.[7]

Action of cyanogen bromide on Ia in 2 N sodium hydroxide at 0°C furnished an aqueous solution of the sodium salt IVa. On evaporation it proved to have an IR spectrum identical with that of a sample, prepared by reacting 2-amino-4-trifluoromethylbenzenesulfonyl chloride (Va) with aqueous sodium cyanamide. Further verification of the structure of IVa – and consequently of the specific attack of cyanogen bromide at the sulfonamide nitrogen – was lent by acidifying an aqueous solution of IVa and sodium nitrite, causing quantitative precipitation of an inner diazonium salt (VIa). With some precaution VIa was isolable in the analytically pure state, displaying characteristic IR absorptions (KBr) at 2180 cm^{-1} ($-CN$) and at 2280 cm^{-1} ($-N^+\equiv N$). The 5-chloro-analogue (VIb) was obtained accordingly (Table 1).

Table 1.

	R	R^1	R^2	M.p. °C	IR (KBr) cm^{-1}	Yield % (Route)	Formula
IIa′	6-CF_3-			332-338[a]	3420-3190, 1670-1650	85	$C_8H_6F_3N_3O_2S$
IIb′	7-Cl-			390 (dec)[b]	3340, 3190, 1660-1650, 1615	79	$C_7H_6ClN_3O_2S$
IIIc	6-CF_3-	n-C_4H_9-	H	270-273	3310, 3180, 3120, 1645-1630	50(A); 42(C)	$C_{12}H_{14}F_3N_3O_2S$
IIId	6-CF_3-	C_6H_{11}-	H	334-338 (dec)	3400, 3300, 3200, 1645-1635	34(A); 43(B)	$C_{14}H_{16}F_3N_3O_2S$
IIIe	6-CF_3-	-$(CH_2)_2$-N$(C_2H_5)_2$	H	180.5-182.5	[c]	57(A)	$C_{14}H_{19}F_3N_4O_2S$
IIIe, HCl	6-CF_3-	-$(CH_2)_2$-N$(C_2H_5)_2$	H	180.5-182	3300, 1620-1615, 1605-1595		
IIIf	6-CF_3-	-$(CH_2)_2O(CH_2)_2$-		350-356 (dec)	3360, 1640-1635	34(A)	$C_{12}H_{12}F_3N_3O_3S$
IIIg	7-Cl-	C_6H_{11}-	H	290-293 (dec)	3310, 3180, 3100, 1640-1625	53(B)	$C_{13}H_{16}ClN_3O_2S$
IIIh	7-Cl-	$C_6H_5CH_2$-	H	249-251.5	3320, 3160, 3080, 1635-1620	56(B)	$C_{14}H_{12}ClN_3O_2S$
IVa	4-CF_3-			240 (dec)	3420, 3340, 2180	31	$C_8H_5F_3N_3NaO_2S$
IVb	5-Cl-			236 (dec)	3440, 3340, 2190	90[d]	$C_7H_5ClN_3NaO_2S$
VIa	4-CF_3-			dec → 300[e]	2280, 2180	98	$C_8H_3F_3N_4O_2S$
VIb	5-Cl-			[e]	2280, 2190	83	$C_7H_3ClN_4O_2S$
VIIa	4-CF_3-			191-192	3440, 3380, 3200, 1660-1610	42	$C_8H_9F_3N_4O_2S$
VIIIa	4-CF_3-			185.5-187	3460, 3400, 3180, 1665-1660, 1640-1635	48	$C_{12}H_{17}F_3N_4O_2S$

[a] Lit.[3a] 342-344°C. [b] Lit.[4] >360°C. [c] Broad absorptions, probably inner salt. [d] Prepared from Vb and Na HN-CN. [e] Violent decomposition on quick heating.

Acidification of an aqueous solution of IVa to pH ~ 1 afforded an 85 % yield of 3-amino-6-trifluoromethyl-2H-1,2,4-benzothiadiazine 1,1-dioxide (IIa').[3a] Analogously the 7-chlorosubstituted compound (IIb') was isolated. IIa' was also obtained by heating 2-amino-4-trifluoromethylbenzenesulfoguanidide (VIIa) to 220°C.

IIa' dissolved in 10 equiv. of the appropriate amine at reflux temperature, was converted into III by direct substitution and elimination of ammonia (Route A, Scheme 1). The successful reaction with n-butylamine implies that the displacement may be effectuated at a temperature as low as 80°C.

IIId (R = 6-CF_3; R^1 = cyclohexyl; R^2 = H) also resulted from gradual heating of a mixture of Ia and *N,N'*-dicyclohexylcarbodiimide to 200°C, eliminating cyclohexylamine (Route B, Scheme 1). The same approach was adopted with Ib and *N,N'*-dicyclohexyl- as well as *N,N'*-dibenzylcarbodiimide (Table 1).

Ia, heated with butylcyanamide to 120°C, gave rise to VIIIa (R^1 = n-C_4H_9),* while increasing the temperature to 190°C caused elimination of ammonia and left IIIc (R = 6-CF_3; R^1 = n-C_4H_9; R^2 = H) in a fair overall yield (Route C, Scheme 1), identical with the product of route A. In this context fusion of orthanilamide with cyanamide has been reported to proceed with a low yield of the unsubstituted title compound.[3a] Yields and some physical data of compounds prepared are compiled in Tables 1 and 2.

Table 2. Representative NMR data of III [$(CD_3)_2SO$].[a]

IIIc	3-NH-$(CH_2)_3$-CH_3: 0.93, t; 3-NH-$CH_2(CH_2)_2$-CH_3: 1.40, m; 3-NH-CH_2-: 3.25, m; 3-NH-: 7.40, t; 5-H + 7-H: 7.52, m; 8-H-: 7.97, d, J = 8.5; 2-NH-: 10.70, s
IIId	3-NH-$CH(CH_2)_5$: 0.90 – 2.20, m; 3-NH-$CH<$: 3.67, m; 3-NH-: 7.33, d, J = 8; 5-H + 7-H: 7.55, m; 8-H: 7.91, dd, J = 8.5, J = 1; 2-NH-: 10.49, s.
IIIe	$CH_3-CH_2>N$-: 1.02, t; -CH_2-N$<^{CH_2}_{CH_2}$: 2.60, m; 3-NH-CH_2-: 3.36, t, J = 5.5; 3-NH + 2-NH-: 6.88, broad s; 5-H: 7.47, m; 7-H: 7.55, m; 8-H: 7.92, m.
IIIf	-N = $(CH_2CH_2)_2$ = O: 3.72, s; 5-H: 7.87, m; 7-H: 7.67, m; 8-H: 7.98, m; 2-NH-: 10.80, s.

[a] Chemical shifts in the ppm δ scale; coupling constants in Hz; TMS as internal standard.

With the concession made that the applicability of the present methods and the substitution pattern of the aromatic ring may be closely interrelated, they still appear to present favourable options to previous procedures.

Pharmacology. In the screening for hypotensive activity in rats and cats compounds IIIc-d and IIIf-h were devoid of any reasonable activity. IIa'

* The proposed structure VIIIa is based on elemental analysis and an instantaneous diazotization and positive coupling reaction.

proved to have the same activity as "diazoxide", 3-methyl-7-chloro-2H-1,2,4-benzothiadiazine 1,1-dioxide,[8] an antihypertensive, nondiuretic agent. Compounds IIb′ and IIIe were somewhat weaker. The water and sodium retaining effect of "diazoxide" was shared by IIa′.

EXPERIMENTAL

Melting points are uncorrected. IR spectra were recorded with a Perkin-Elmer PE 21 spectrophotometer, NMR spectra with a Varian A60A spectrometer. For all compounds reported the C,H,N elemental analyses deviated by less than 0.25 % from theory.

2-Amino-4-trifluoromethylbenzenesulfonyl cyanamide, sodium salt (IVa). 8.0 g (0.033 mol) of Ia [9] was suspended in 50 ml of water, containing 5.3 g (0.133 mol) of sodium hydroxide. 7.1 g (0.066 mol) of cyanogen bromide in 75 ml of water was added at 0°C over 30 min. The mixture was stirred for 2.5 h at 0°C, pH was lowered to 7 with 12 N hydrochloric acid and unreacted sulfonamide was filtered off. The aqueous filtrate was extracted with ether, concentrated *in vacuo* and extracted with 30 ml of anhydrous ethanol. The sodium salt (IVa) was precipitated by adding 60 ml of ether to the extract. Recrystallization from ethanol-chloroform furnished an analytically pure sample.

2-Amino-4-trifluoromethylbenzenesulfoguanidide (VIIa). 2.60 g (0.01 mol) of 2-amino-4-trifluoromethylbenzenesulfonyl chloride (Va) (m.p. 70 – 73°C) was gradually added to a stirred mixture of 1.80 g (0.01 mol) of guanidine carbonate, 10 ml of 2 N sodium hydroxide and 50 ml of ether. After maintaining stirring at 25°C for 5½ h 25 ml of ether was added and the layers were separated.

The aqueous phase was extracted with 25 ml of ether, and the combined ethereal solution was dried over magnesium sulfate and evaporated to dryness. The residue was extracted with 10 ml of a 1:1 mixture of ether and petroleum ether to leave 1.9 g of material, which upon recrystallization from aqueous methanol gave 1.20 g (42 %) of VIIa.

Inner salt of 2-diazonium-4-trifluoromethylbenzenesulfonyl cyanamide (VIa). 1.45 g (0.005 mol) of IVa and 0.55 g (0.008 mol) of sodium nitrite were dissolved in 25 ml of water at 0°C. Dropwise addition of 4 N hydrochloric acid (a total of 3.2 ml) brought about rapid precipitation. After 15 min the crystalline product was collected on a filter and repeatedly washed with water and ether. Drying in a desiccator left 1.35 g (98 %) of VIa, which was recrystallized from methanol-ether. (*Warning!* Smaller quantities should be handled at a time, since on one occasion spontaneous decomposition was triggered by scratching of a specimen on a filter.)

3-Amino-6-trifluoromethyl-2H-1,2,4-benzothiadiazine 1,1-dioxide (IIa′). From IVa. To 1.15 g (0.004 mol) of IVa in 20 ml of water was added 12 N hydrochloric acid to pH ~ 1 while stirring at ambient temperature. After 1 h the precipitate was filtered and washed with water to yield 0.9 g (85 %) of IIa′. An analytical sample was obtained by recrystallizing from aqueous ethanol.

From VIIa. 0.56 g (0.002 mol) of VIIa was heated to 220 – 230°C for 5 h. The residue was washed with ether and recrystallized from ethanol to give 0.15 g (32 %) of IIa′.

3-Substituted amino-2H-1,2,4-benzothiadiazine 1,1-dioxides (III). Route A. General procedure. 1.33 g (0.005 mol) of IIa′ was heated to reflux in 0.05 mol of the appropriate amine for 24 h. After removal of excess amine *in vacuo* the residue was treated with 20 ml of 0.5 N hydrochloric acid (this treatment was omitted with IIIe), filtered and washed with ether. The crude product was recrystallized from ethanol.

Route B. General procedure. Ia-b (0.02 mol) was thoroughly mixed with carbodiimide (0.021 mol) and heated to 200°C for 3 h. The volatile fraction was gradually removed under reduced pressure, and the residue was triturated with 2 N acetic acid, filtered and washed with ether. Subsequent recrystallization from ethanol yielded pure III.

Route C. 3-Butylamino-6-trifluoromethyl-2H-1,2,4-benzothiadiazine 1,1-dioxide (IIIc). 48 g (0.2 mol) of Ia was added to 24.5 g (0.25 mol) of butylcyanamide [10] in 100 ml of ether, containing a trace of *p*-toluenesulfonic acid. After evaporation of the solvent the temperature was gradually elevated. After 1 h at 110 – 115°C solidification occurred

(intermediate formation of VIIIa). On further heating gas evolution from the liquefied mixture subsided after 9 h at 190°C. The residue was worked up as described for route A and recrystallized from glacial acetic acid to yield 27.0 g (42 %) of IIIc.

Acknowledgements. The author is indebted to Mr. F. Lund for valuable discussions, to Professor Dr. H.-H. Frey for providing the pharmacological data, and to Mr. N. Rastrup Andersen for interpretation of the NMR spectra.

REFERENCES

1. Grana, E., Lilla, L. and Raffa, L. *Farmaco. Ed. Sci.* **17** (1962) 974.
2. Lund, F. J. and Kobinger, W. *Acta Pharmacol. Toxicol.* **16** (1960) 297.
3. (a) Topliss, J. G. and Konzelman, L. M. *J. Org. Chem.* **28** (1963) 2313; (b) Raffa, L., Di Bella, M. and Monzani, A. *Farmaco. Ed. Sci.* **19** (1964) 47.
4. Raffa, L., Di Bella, M., Melegari, M. and Vampa, G. *Farmaco. Ed. Sci.* **17** (1962) 331.
5. Raffa, L., Melegari, M. and Vampa, G. *Farmaco. Ed. Sci.* **21** (1966) 839.
6. Cronin, T. and Hess, H.-J. *J. Med. Chem.* **11** (1968) 136.
7. Albazini, A. and Melegari, M. *Farmaco. Ed. Sci.* **23** (1968) 546.
8. Rubin, A. A., Roth, F. E. and Winbury, M. M. *Nature* **192** (1961) 176.
9. Holdrege, C. T., Babel, R. B. and Cheney, L. C. *J. Am. Chem. Soc.* **81** (1959) 4807.
10. Schmidt, H. *Ber.* **54** (1921) 2068.

Received February 7, 1973.

ACTA CHEMICA SCANDINAVICA 27 (1973) 2661–2685

Short Communications

Cyanogenic Glucosides in *Sambucus nigra* L.

S. ROSENDAL JENSEN and B. JUHL NIELSEN

Department of Organic Chemistry, Technical University of Denmark, DK-2800 Lyngby, Denmark

The cyanogenic glucoside sambunigrin (*1*) has been repeatedly identified as a constituent of common elder (*Sambucus nigra* L., Caprifoliaceae).[1] We report the additional occurrence in certain elder collections of prunasin (*2*) and the *m*-hydroxysubstituted glucosides zierin [2] and holocalin [3] (*3* and *4*).

Frozen leaf material was extracted with ethanol and worked up to give a mixture of cyanogenic glucosides which could be separated by chromatography into pairs of epimers (see Experimental). The mixture of sambunigrin *1* and prunasin *2*, was readily identified by PMR-analysis, the epimers differing conspicuously in the chemical shifts of the benzylic protons: δ 6.07 and 5.88 ppm, respectively. Acetylation, followed by chromatographic separation, gave the corresponding acetates *5* and *6*, possessing properties identical with those previously reported (see Table 1) including the characteristic differences in the PMR-spectra (*cf.* Ref. 4).

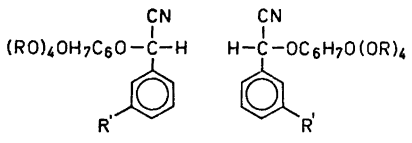

1 : R = R' = H 2 : R = R' = H
3 : R = H, R' = OH 4 : R = H, R' = OH
5 : R = Ac, R' = H 6 : R = Ac, R' = H
7 : R = Ac, R' = OAc 8 : R = Ac, R' = OAc

Analogously, PMR analysis revealed the identity of the second fraction as a mixture of *3* and *4*, again exhibiting benzylic proton signals at 6.07 and 5.88 ppm, respectively. Acetylation, followed by chromatographic separation of the mixture, afforded the pentaacetates *7* and *8*. Their PMR-spectra exhibited differences similar to those observed above for the pair *5* and *6*, and for the acetates *9* and *10*, derived from the epimeric pair of *p*-hydroxy-substituted isomers (dhurrin-taxiphyllin) [4] (see Table 1). Additional to the characteristic differences in the chemical shift of the benzylic protons, the acetoxy patterns of the epimers display differences which are diagnostically useful.

On this basis, *7* is considered a derivative of a member of the (*S*)-cyanohydrin series, thus far represented by sambunigrin and dhurrin. Consequently, *8* derives from an (*R*)-cyanohydrin, configurationally related to prunasin and taxiphyllin. The pairwise differences in melting points and specific rotations of the acetates are consistent with this assignment (*cf.* Table 1). Acetylation of holocalin, kindly provided by Dr. R. Gmelin, afforded a pentaacetate, indistinguishable (m.p., m.m.p., PMR-spectrum) from *8*. Hence, holocalin *4* belongs to the (*R*)-series, a conclusion opposite to that arrived at by Gmelin *et al.*[3] (Parallel to our work, Nahrstedt [5] has reached the same conclusion, based on the GLC-behaviour of TMS-ethers of the epimers.)

A number of collections of very young shoots from different localities have been examined. Out of six samples, collected on widely separated localities on the island of Sjælland, four contained *1* as the sole detectable cyanogenic glucoside, demonstrating that no isomerization had taken place during the standard work-up. Only two collections contained the *m*-hydroxy-substituted glucoside(s) as apparent from PMR-data. Further work to clarify the distributional pattern is in progress.

Table 1.

	m.p. °C	$[\alpha]_D^{21}$ (°; in $CHCl_3$)	PMR-data H_α	H_1'	H_6'	H_6'	H_5'	OAc-pattern	Glucoside content (% of fresh weight)
5	125–126[a]	−55[a]	5.71	5.00	4.32	4.25	3.83	1:1:1:1	0.044
6	137–138[b]	−17[b]	5.54	4.57	4.27	4.17	3.69	1:3	0.018
7	117.5–118.5[d]	−50[c]	5.73	4.98	4.30	4.23	3.81	1:1:1:1:1	0.016
8	129–130	−12	5.56	4.59	4.28	4.15	3.69	1:1:3	0.022
9[e]	132–133	−50[f]	5.69	5.02	4.28		3.84	1:1:1:1:1	
10[e]	144–145	−22[f]	5.54	4.62	4.20		6.68	1:1:3	

[a] Reported:[6] m.p. 125–126°; $[\alpha]_D^{21}$ −54° (EtOAc). [b] Reported:[6] m.p. 139–140°; $[\alpha]_D^{21}$ −24° (EtOAc). [c] In EtOH: −46°. [d] Reported:[2] m.p. 115–118°; no rotation data listed. [e] Quoted from Ref. 4. [f] Measured in EtOH.

Experimental. Melting points are corrected and determined in capillary tubes in a heated bath. PMR-spectra are recorded on a Varian HA-100 instrument, with TMS as an internal standard. Preparative TLC was performed on 20 × 40 cm plates coated with 1 mm layers of silica gel PF_{254} (Merck); detection by UV-light. Analyses were performed by Dr. A. Bernhardt.

Isolation of glucosides. Frozen plant material (210 g, collected in June 1972 and stored for 9 months in polyethylene bags at −25°) was homogenised with ethanol and worked up as previously described.[7] The mixture of cyanogenic glucosides (245 mg) was separated from the other glycosides (0.74 g) by preparative TLC, with EtOAc–Bz–EtOH (4:1:1) as an eluent. A second fractionation, this time with $CHCl_3$–MeOH (4:1) as the eluent, separated the mixture into two fractions, a faster moving, *A*, (*1* and *2*, 134 mg), and a slower moving, *B* (*3* and *4*, 83 mg). Fraction *A* was acetylated (Ac_2O/Py), and the resulting mixture of acetates was subjected to preparative TLC (ether–pentane; 9:1) to give, as the faster moving fraction, *sambunigrin tetraacetate* (*5*, 99 mg) and as the slower moving fraction, *prunasin tetraacetate* (*6*, 42 mg). Data are presented in Table 1. Fraction *B* was treated similarly to give *zierin tetraacetate* (*7*, 47 mg) (Found: C 55.35; H 5.34; N 2.80. Calc. for $C_{24}H_{27}NO_{12}$: C 55.28; H 5.22; N 2.69) and *holocalin tetraacetate* (*8*, 64 mg) (Found: C 55.14; H 5.28; N 2.80). Further data are presented in Table 1.

Vouchers (IOK 30/72: IOK 3/73; IOK 5/73; IOK 8/73 – IOK 12/73) have been deposited at the Botanical Museum of the University of Copenhagen, Denmark.

Added in proof. Collections made in September all contain holocalin, exclusively, or in admixture with zierin. The contents ofsambunigrin were low.

Acknowledgement. The authors are grateful to Dr. K. Rahn, the Botanical Museum, Copenhagen, for botanical identification of the plant material, and to Professor A. Kjær of this Institute for valuable discussions.

1. Bourquelot, E. and Danjou, E. *J. Pharm. Chim.* **22** [6] (1905) 154, 210, 219, 385; Finnemore, H. and Cox, C. B. *J. Proc. Roy. Soc. N. S. Wales* **62** (1928) 369.
2. Finnemore, H. and Cooper, J. M. *J. Proc. Roy. Soc. N. S. Wales* **70** (1936) 175.
3. Gmelin, R., Schüler, M. and Bordas, E. *Phytochemistry* **12** (1973) 457.
4. Towers, G. H. N., McInnes, A. G. and Neish, A. C. *Tetrahedron* **20** (1964) 71.
5. Nahrstedt, A. *Phytochemistry* **12** (1973) 2799.
6. Fischer, E. and Bergmann, M. *Ber.* **50** (1917) 1047.
7. Jensen, S. R., Kjær, A. and Nielsen, B. J. *Acta Chem. Scand.* **27** (1973) 2581.

Received August 31, 1973.

Carbon-13 Nuclear Magnetic Resonance of Tris(diamine)-cobalt(III) Complexes

SVEN BAGGER, OLE BANG and FLEMMING WOLDBYE

Chemistry Department A, The Technical University of Denmark, Building 207, DK-2800 Lyngby, Denmark

In our study of conformations in five- and sixmembered metal-diamine rings we have applied the technique of Fourier transform ^{13}C-NMR to a series of tris-(diamine)cobalt(III) complexes.

In the only previous ^{13}C-NMR study [1] of diamagnetic diamine complexes known to us it was reported that at 15.1 MHz the ^{13}C chemical shifts between some free 1,2-diamines and the same diamines coordinated to cobalt(III) were negligible within the experimental uncertainty of 5 ppm. This finding might suggest that constancy of chemical shifts would limit the structural information that could be obtained by the technique.

Furthermore, it is known that the ^{1}H-NMR spectra of tris(diamine)cobalt(III) consistently exhibit broad, rather unresolved bands (Fig. 1) due to spin-spin coupling over three bonds of the protons with ^{59}Co ($I = 7/2$, 100 % natural abundance); ^{59}Co decoupling is necessary to get sufficient resolution for accurate analysis.[2] A similar complication might arise in the ^{13}C-NMR spectra, especially because only two bonds separate the cobalt nucleus from its nearest carbon atoms.

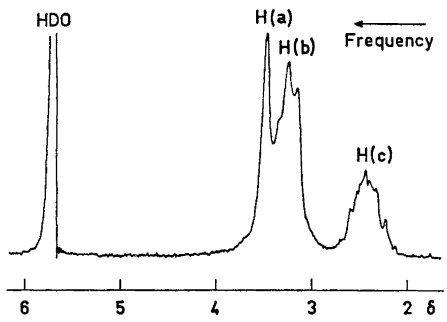

Fig. 1. 60 MHz ^{1}H NMR spectrum of [Co(en)(tn)$_2$]Cl$_3$.

The proton-decoupled 22.63 MHz ^{13}C-NMR spectra reported here were obtained by means of a Bruker WH 90 spectrometer using the Fourier transform technique, which allows measurement of samples with ^{13}C in natural abundance (1.1 %); the solvent was D_2O, and the spectra were run at ambient temperature. δ-Values are given relative to TMS; dioxane ($\delta = 67.40$) served as an internal standard.

$[Co(en)_2(i\text{-}bn)]^{3+}$ was prepared by reacting *trans*-$[Co(en)_2Cl_2]^{+}$ with i-bn. All other complexes were obtained by the general procedure described earlier [3] for preparation and chromatographic separation of "mixed" tris-complexes.

The carbon skeletons of the ligands involved and the letter indices used are shown in Fig. 2.

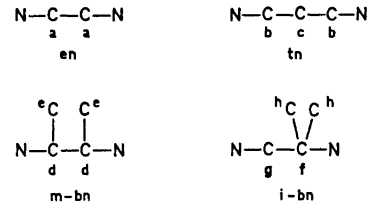

Fig. 2.

Fig. 3 illustrates the quality of the spectra obtained. The experimental uncertainty of peak positions is *ca.* 0.1 ppm.

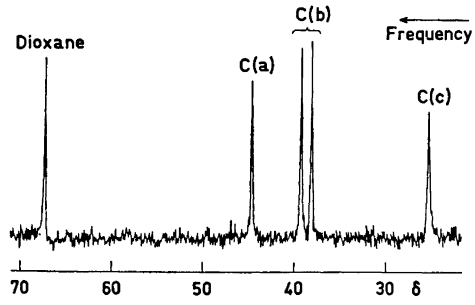

Fig. 3. Illustrative example of the 22.63 MHz ^{13}C NMR spectra. 0.246 g [Co(en)(tn)$_2$]Cl$_3$ and 20 μl dioxane in 1.3 ml D_2O. (4000 pulses, 4K input data points, 1 s sampling time.)

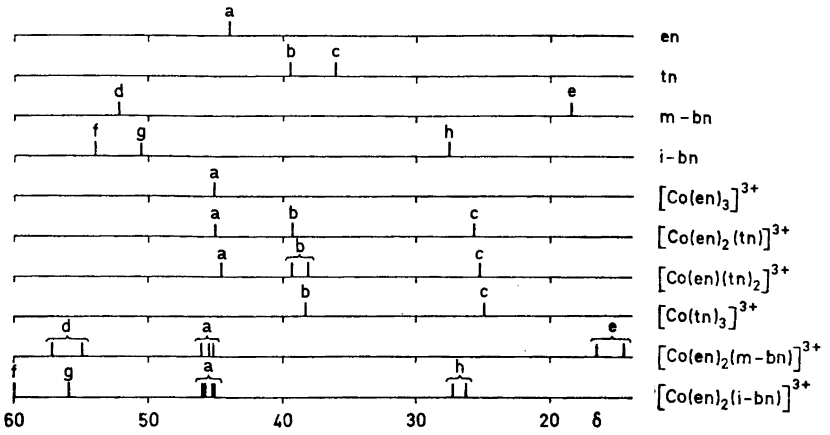

Fig. 4. Diagrammatic representation of the ^{13}C NMR spectra, showing the positions of resonance lines on a δ-scale.

In contrast to the ^{1}H spectrum (Fig. 1) the ^{13}C spectrum exhibits well-resolved and sharp lines, and thus ^{13}C-^{59}Co spin-spin coupling does not significantly influence the resolution.

Assignments and chemical shift data are outlined in Fig. 4.

It appears that chelation of the diamines causes distinct chemical shifts, and characteristic patterns for the different complexes result.

The ^{13}C-resonances of both the CH_3 (e) and CH (d) moieties in $[Co(en)_2(m\text{-}bn)]^{3+}$ are split into two lines, and this is consistent with the presence of both an equatorial and an axial methyl group on the puckered fivemembered Co-m-bn ring.[4] Similarly $[Co(en)_2(i\text{-}bn)]^{3+}$ contains an equatorial and an axial methyl group, but in this case they are bound to the same carbon atom, and this causes a smaller chemical shift difference between the two CH_3 lines (h).

The methylene groups bound to nitrogen in the sixmembered Co-tn rings in $[Co(en)(tn)_2]^{3+}$ give rise to two peaks (b). This is tentatively explained by assuming that different conformations, *e.g.* chair and skew-boat forms,[5,6] of the Co-tn rings are present.

Clearly, ^{13}C-NMR spectroscopy offers new possibilities for conformational studies of chelate diamine rings in diamagnetic complexes.

The NMR spectrometer was made available by *Statens Naturvidenskabelige Forskningsråd*; we thank Dr. Klaus Bock for advice in the use of the instrument.

1. Strouse, C. E. and Matwiyoff, N. A. *Chem. Commun.* **1970** 439.
2. Sudmeier, J. L. and Blackmer, G. L. *J. Am. Chem. Soc.* **92** (1970) 5238.
3. Bang, O., Engberg, A., Rasmussen, K. and Woldbye, F. *Proc. 3rd Symp. Coord. Chem.*, Akadémiai Kiadó, Budapest 1970, p. 63.
4. Hawkins, C. J. *Absolute Configuration of Metal Complexes*, Wiley-Interscience, New York 1971, p. 285.
5. Jurnak, F. A. and Raymond, K. N. *Inorg. Chem.* **11** (1972) 3149.
6. Niketić, S. R. and Woldbye, F. *Acta Chem. Scand.* **27** (1973) 621.

Received June 1, 1973.

On the Magnetic Properties of $Pr_2(DPM)_6$ and $Eu_2(DPM)_6$

A. KJEKSHUS and T. LEDAAL

Kjemisk Institutt, Universitetet i Oslo, Blindern Oslo 3, Norway

Among the various, currently used NMR shift reagents (*cf.*, *e.g.*, Ref. 1), the lanthanide chelate type reagents introduced by Hinckley [2] play an important role. Typical representatives for this class of complexes are tris-dipivalomethanato-praseodymium ($Pr(DPM)_3$) and -europium ($Eu(DPM)_3$). As a link in a protracted research programme [3,4] on the effects of these reagents, a thorough examination of the physical properties of the reagents themselves and a few suitable model adducts is being carried out in order to obtain further insight in the NMR shift mechanism. The present communication gives an account of the magnetic properties of the dimers $Pr_2(DPM)_6$ and $Eu_2(DPM)_6$, which prevail in the solid state, advertisement for such data being submitted by, *e.g.*, Weissman.[5]

Experimental. Samples of $Pr_2(DPM)_6$ and $Eu_2(DPM)_6$ were prepared and purified according to the procedure of Eisentraut and Sievers,[6] analysed, and identified as the dimeric [7] compounds on the basis of X-ray diffraction (Guinier) data.

Magnetic susceptibilities were measured between 80 and 500 K by the Faraday method (maximum field ~ 8 kØ) using 20–30 mg samples. In the low temperature range (15–293 K), additional measurements on 50–80 mg samples were performed at field strengths up to 16 kØ in a Princeton Applied Research Model FM-1 vibrating sample magnetometer.

Results. The reciprocal magnetic susceptibility *versus* temperature curves for $Pr_2(DPM)_6$ and $Eu_2(DPM)_6$ are shown in Fig. 1. Field strength dependent susceptibilities were not observed and the experimental points represent mean values at different field strengths without correcting for induced diamagnetism. The points refer to four samples and two different measuring techniques for each compound, thus demonstrating an excellent reproducibility of the characteristics.

The thermomagnetic curves of $Pr_2(DPM)_6$ and $Eu_2(DPM)_6$ obey the Curie-Weiss Law $\chi^{-1} = C^{-1}(T-\theta)$ over the approximate ranges 100 to 500 K and 50 to 500 K, respectively. (The upper temperature limits are imposed by the melting/decomposition points of the compounds in the sealed, evacuated measuring capsules.) Least squares fits of the experimental data over the linear sections of the curves give $\theta = 30 \pm 20$ K and $\mu_P = \sqrt{8C_{mol}} = 3.4 \pm 0.1\ \mu_B$ for $Pr_2(DPM)_6$ and $\theta = -140 \pm 20$ K and $\mu_P = 3.8 \pm 0.1\ \mu_B$ for $Eu_2(DPM)_6$. The μ_P values are accordingly in line with those commonly found in the literature (3.4 to 3.6 μ_B; *cf.*, *e.g.*, Ref. 8) for compounds of Eu^{3+} and Pr^{3+}. The minimum in $\chi^{-1}(T)$ at $T_{crit.} = 50 \pm 10$ and 100 ± 10 K

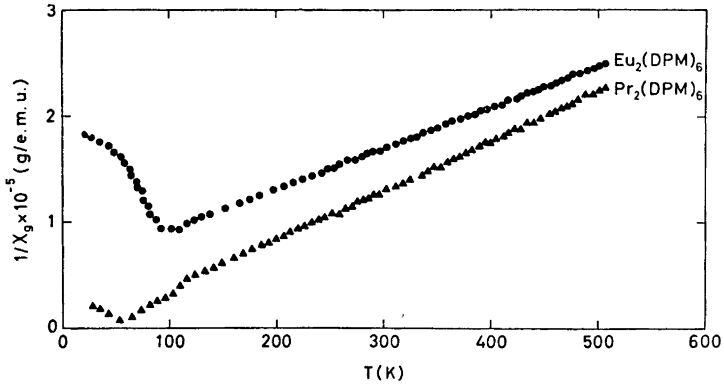

Fig. 1. Inverse magnetic susceptibility as a function of temperature for $Pr_2(DPM)_6$ and $Eu_2(DPM)_6$.

for $Pr_2(DPM)_6$ and $Eu_2(DPM)_6$, respectively, very strongly suggests that there is magnetic coupling between the lanthanide ions of the binuclear clusters. The fact that $T_{crit.} \approx |\theta|$ shows that essentially one exchange interaction is operative in both cases.

The above results are fully consistent with the recent theory of Bleaney [9] for NMR shifts in solutions containing lanthanide chelate reagents. It should be emphasized, however, that this theory is based on the anisotropy in the susceptibility of the *mononuclear*, paramagnetic complex which prevails in solution. Hence, the present study (which was started before Bleaney's paper came to hand) does not provide a critical test of the theory. Experimental confirmation of some of the more fundamental predictions of Bleaney's theory has, very recently, been published by Grotens *et al.*[10]

1. von Ammon, R. and Fischer, R. D. *Angew. Chem.* **84** (1971) 737.
2. Hinckley, C. C. *J. Am. Chem. Soc.* **91** (1969) 5160.
3. Kristiansen, P. and Ledaal, T. *Tetrahedron Letters* **1971** 2817.
4. Kristiansen, P. and Ledaal, T. *Tetrahedron Letters* **1971** 4457.
5. Weissman, S. I. *J. Am. Chem. Soc.* **93** (1971) 4928.
6. Eisentraut, K. J. and Sievers, R. E. *J. Am. Chem. Soc.* **87** (1965) 5254.
7. Erasmus, C. S. and Boeyens, J. C. A. *Acta Cryst.* **B 26** (1970) 1843.
8. Earnshaw, A. *Introduction to Magnetochemistry*, Academic, London, New York 1968.
9. Bleaney, B. *J. Magn. Resonance* **8** (1972) 91.
10. Grotens, A. M., Backus, J. J. M. and de Boer, E. *Tetrahedron Letters* **1973** 1465.

Received June 28, 1973.

The Structure of 2,3,4,5-Tetraphenyl-6a-thiathiophthene

ODDLEIV HJELLUM and ASBJØRN HORDVIK

Chemical Institute, University of Bergen, N-5000 Bergen, Norway

So far structure studies on 2-phenyl-, 2,4- and 3,4-diphenyl-, and 2,3,4-triphenyl-6a-thiathiophthene have been reported.[1-4]

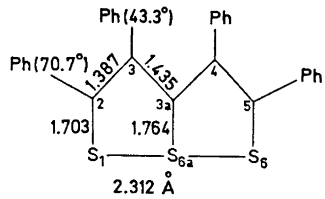

(I)

The present structure study of 2,3,4,5-tetraphenyl-6a-thiathiophthene (I) has been carried out in order to obtain further information about the degree to which phenyl substituents affect the S–S bonding in 6a-thiathiopthenes; the preliminary results are presented here.

The S(6a)–C(3a) bond in I lies along a crystallographic two-fold axis, and the two halves of the molecule are therefore exactly equal. The bond lengths in the 6a-thiathiophthene system of I are, S(1)–S(6a) = 2.312(2) Å, S(1)–C(2) = 1.703(7) Å, S(6a)–C(3a) = 1.764(10) Å, C(2)–C(3) = 1.387(10) Å, and C(3)–C(3a) = 1.435(8) Å. The phenyl groups in 2 and 3 positions are twisted 70.7° and 43.3° about the respective connecting bonds.

A sample of I was generously supplied by M. Stavaux.[5] The crystals are dark purple and belong to the monoclinic space group $Ic/2$. The cell dimensions are, $a = 20.6370(20)$ Å, $b = 9.7541(8)$ Å, $c = 11.3520(22)$ Å, and $\beta = 92.90(2)°$. There are four molecules per unit cell; density, calculated 1.352 g/cm³, found 1.36 g/cm³.

The structure analysis is based on X-ray data collected on a paper-tape controlled Siemens AED diffractometer using Mo$K\alpha$ radiation. 1952 reflections were observed within $\theta = 28°$.

for $Pr_2(DPM)_6$ and $Eu_2(DPM)_6$, respectively, very strongly suggests that there is magnetic coupling between the lanthanide ions of the binuclear clusters. The fact that $T_{crit.} \approx |\theta|$ shows that essentially one exchange interaction is operative in both cases.

The above results are fully consistent with the recent theory of Bleaney [9] for NMR shifts in solutions containing lanthanide chelate reagents. It should be emphasized, however, that this theory is based on the anisotropy in the susceptibility of the *mononuclear*, paramagnetic complex which prevails in solution. Hence, the present study (which was started before Bleaney's paper came to hand) does not provide a critical test of the theory. Experimental confirmation of some of the more fundamental predictions of Bleaney's theory has, very recently, been published by Grotens *et al.*[10]

1. von Ammon, R. and Fischer, R. D. *Angew. Chem.* **84** (1971) 737.
2. Hinckley, C. C. *J. Am. Chem. Soc.* **91** (1969) 5160.
3. Kristiansen, P. and Ledaal, T. *Tetrahedron Letters* **1971** 2817.
4. Kristiansen, P. and Ledaal, T. *Tetrahedron Letters* **1971** 4457.
5. Weissman, S. I. *J. Am. Chem. Soc.* **93** (1971) 4928.
6. Eisentraut, K. J. and Sievers, R. E. *J. Am. Chem. Soc.* **87** (1965) 5254.
7. Erasmus, C. S. and Boeyens, J. C. A. *Acta Cryst.* **B 26** (1970) 1843.
8. Earnshaw, A. *Introduction to Magnetochemistry*, Academic, London, New York 1968.
9. Bleaney, B. *J. Magn. Resonance* **8** (1972) 91.
10. Grotens, A. M., Backus, J. J. M. and de Boer, E. *Tetrahedron Letters* **1973** 1465.

Received June 28, 1973.

The Structure of 2,3,4,5-Tetraphenyl-6a-thiathiophthene

ODDLEIV HJELLUM and ASBJØRN HORDVIK

Chemical Institute, University of Bergen, N-5000 Bergen, Norway

So far structure studies on 2-phenyl-, 2,4- and 3,4-diphenyl-, and 2,3,4-triphenyl-6a-thiathiophthene have been reported.[1-4]

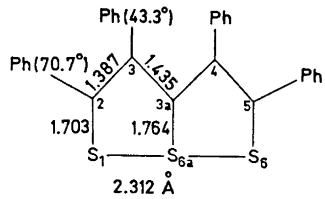

(I)

The present structure study of 2,3,4,5-tetraphenyl-6a-thiathiophthene (I) has been carried out in order to obtain further information about the degree to which phenyl substituents affect the S–S bonding in 6a-thiathiopthenes; the preliminary results are presented here.

The S(6a)–C(3a) bond in I lies along a crystallographic two-fold axis, and the two halves of the molecule are therefore exactly equal. The bond lengths in the 6a-thiathiophthene system of I are, S(1)–S(6a) = 2.312(2) Å, S(1)–C(2) = 1.703(7) Å, S(6a)–C(3a) = 1.764(10) Å, C(2)–C(3) = 1.387(10) Å, and C(3)–C(3a) = 1.435(8) Å. The phenyl groups in 2 and 3 positions are twisted 70.7° and 43.3° about the respective connecting bonds.

A sample of I was generously supplied by M. Stavaux.[5] The crystals are dark purple and belong to the monoclinic space group $Ic/2$. The cell dimensions are, $a = 20.6370(20)$ Å, $b = 9.7541(8)$ Å, $c = 11.3520(22)$ Å, and $\beta = 92.90(2)°$. There are four molecules per unit cell; density, calculated 1.352 g/cm³, found 1.36 g/cm³.

The structure analysis is based on X-ray data collected on a paper-tape controlled Siemens AED diffractometer using Mo$K\alpha$ radiation. 1952 reflections were observed within $\theta = 28°$.

The structure was solved by the heavy atom (S) method and refined by full matrix least squares. The R factor is 0.04.

The authors are indebted to Dr. M. Stavaux, Faculté des Sciences de Caen, France, for providing a sample of 2,3,4,5-tetraphenyl-6a-thiathiophthene.

1. Bezzi, S. *Gazz. Chim. Ital.* **92** (1962) 859.
2. Hordvik, A., Sletten, E. and Sletten, J. *Acta Chem. Scand.* **20** (1966) 2001; **23** (1969) 1852.
3. Johnson, P. L. and Paul, I. C. *Chem. Commun.* **1969** 1014.
4. Hordvik, A. *Acta Chem. Scand.* **25** (1971) 1822.
5. Stavaux, M. and Lozac'h, N. *Bull. Soc. Chim. France* **1967** 2082.

Received July 11, 1973.

Addition of Hydrogen Chloride and Deuterium Chloride to 2-*exo*-Methoxy-5-norbornene

ERKKI KANTOLAHTI

Department of Chemistry, University of Jyväskylä, Jyväskylä, Finland

Additions of hydrogen chloride and deuterium chloride to bicyclic bridge compounds have been very extensively studied.[1–4] In this work the reaction of 2-*exo*-methoxy-5-norbornene (I) with hydrogen chloride in methylene chloride at room temperature has been investigated and found to give two main products, 2-*endo*-methoxy-5-*exo*-chloronorbornane (IIIA) and 2-*exo*-methoxy- 5-*exo*-chloronorbornane (IVA). Addition of deuterium chloride to I under similar reaction conditions also gave two main products, 2-*endo*-methoxy-5-*exo*-chloro-7-*anti*-deuterionorbornane (IIIB) and 2-*exo*-methoxy-5-*exo*-chloro-6-*exo*-deuterionorbornane (IVB). The results were verified by NMR and mass spectroscopy.

Dehydronorbornyl methyl ether (I) was prepared by acid-catalyzed addition of methanol to norbornadiene.[5] The reaction yielded a mixture of I and *exo*-3-methoxy-nortricyclene (V) in the ratio 1:2. The methyl ethers (I) and (V) were separated by preparative gas chromatography.

exo-Dehydronorbornyl methyl ether (I) was treated with dry, gaseous hydrogen chloride in methylene chloride at room temperature for 24 h. Gas chromatographic analysis showed that the reaction had proceeded almost to completion. The reaction gave a mixture of IIIA and IVA in the ratio 52:48, as measured by the retention times and peak heights. Separation of IIIA and IVA was carried out by preparative gas chromatography.

The reaction of I with deuterium chloride was performed as above, using the labelled, dry gas prepared by the method of Dewar and Fahey.[6] In this case the reaction time was 48 h. The reaction gave a mixture of IIIB and IVB in the ratio 47:53. The stereochemical structure of IIIA, IIIB, IVA, and IVB could be deduced from the NMR spectra of the products of the reactions of I with hydrogen chloride and deuterium chloride. The correspondence of the product ratios reflects the mechanism for the stereochemical course of the additions of hydrogen chloride and deuterium chloride to I. It seems plausible that reaction proceeds *via* the "asymmetrically bridged" cation route:[7–9]

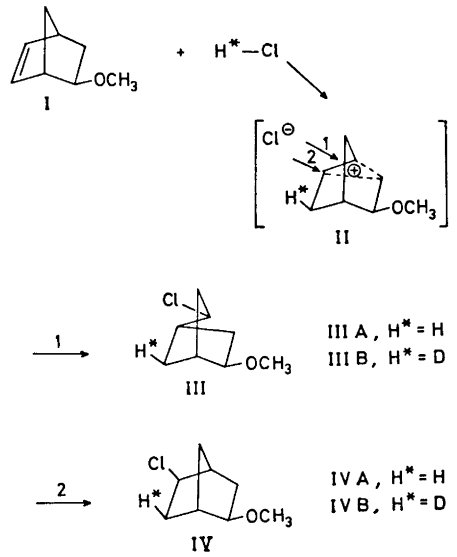

The proton resonance spectrum of 2-*endo*- methoxy-5-*exo*- chloronorbornane

The structure was solved by the heavy atom (S) method and refined by full matrix least squares. The R factor is 0.04.

The authors are indebted to Dr. M. Stavaux, Faculté des Sciences de Caen, France, for providing a sample of 2,3,4,5-tetraphenyl-6a-thiathiophthene.

1. Bezzi, S. *Gazz. Chim. Ital.* **92** (1962) 859.
2. Hordvik, A., Sletten, E. and Sletten, J. *Acta Chem. Scand.* **20** (1966) 2001; **23** (1969) 1852.
3. Johnson, P. L. and Paul, I. C. *Chem. Commun.* **1969** 1014.
4. Hordvik, A. *Acta Chem. Scand.* **25** (1971) 1822.
5. Stavaux, M. and Lozac'h, N. *Bull. Soc. Chim. France* **1967** 2082.

Received July 11, 1973.

Addition of Hydrogen Chloride and Deuterium Chloride to 2-*exo*-Methoxy-5-norbornene

ERKKI KANTOLAHTI

Department of Chemistry, University of Jyväskylä, Jyväskylä, Finland

Additions of hydrogen chloride and deuterium chloride to bicyclic bridge compounds have been very extensively studied.[1–4] In this work the reaction of 2-*exo*-methoxy-5-norbornene (I) with hydrogen chloride in methylene chloride at room temperature has been investigated and found to give two main products, 2-*endo*-methoxy-5-*exo*-chloronorbornane (IIIA) and 2-*exo*-methoxy- 5-*exo*-chloronorbornane (IVA). Addition of deuterium chloride to I under similar reaction conditions also gave two main products, 2-*endo*-methoxy-5-*exo*-chloro-7-*anti*-deuterionorbornane (IIIB) and 2-*exo*-methoxy-5-*exo*-chloro-6-*exo*-deuterionorbornane (IVB). The results were verified by NMR and mass spectroscopy.

Dehydronorbornyl methyl ether (I) was prepared by acid-catalyzed addition of methanol to norbornadiene.[5] The reaction yielded a mixture of I and *exo*-3-methoxy-nortricyclene (V) in the ratio 1:2. The methyl ethers (I) and (V) were separated by preparative gas chromatography.

exo-Dehydronorbornyl methyl ether (I) was treated with dry, gaseous hydrogen chloride in methylene chloride at room temperature for 24 h. Gas chromatographic analysis showed that the reaction had proceeded almost to completion. The reaction gave a mixture of IIIA and IVA in the ratio 52:48, as measured by the retention times and peak heights. Separation of IIIA and IVA was carried out by preparative gas chromatography.

The reaction of I with deuterium chloride was performed as above, using the labelled, dry gas prepared by the method of Dewar and Fahey.[6] In this case the reaction time was 48 h. The reaction gave a mixture of IIIB and IVB in the ratio 47:53. The stereochemical structure of IIIA, IIIB, IVA, and IVB could be deduced from the NMR spectra of the products of the reactions of I with hydrogen chloride and deuterium chloride. The correspondence of the product ratios reflects the mechanism for the stereochemical course of the additions of hydrogen chloride and deuterium chloride to I. It seems plausible that reaction proceeds *via* the "asymmetrically bridged" cation route:[7–9]

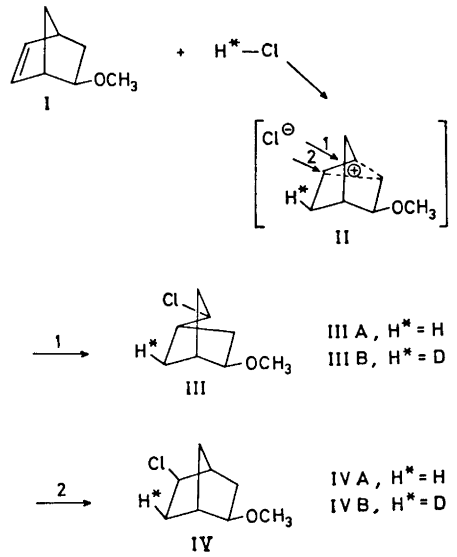

The proton resonance spectrum of 2-*endo*- methoxy-5-*exo*- chloronorbornane

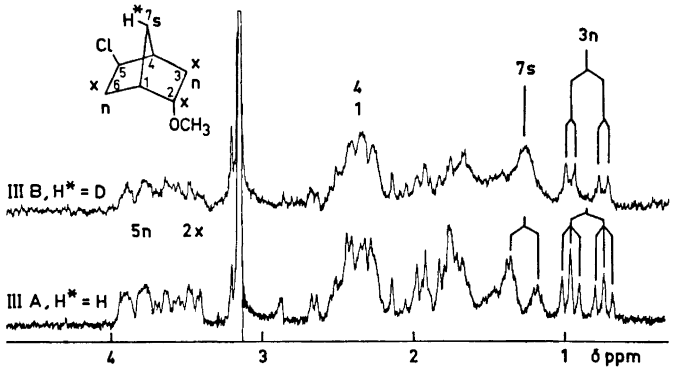

Fig. 1. Proton resonance spectrum of 2-*endo*-methoxy-5-*exo*-chloronorbornane (IIIA) and 2-*endo*-methoxy-5-*exo*-chloro-7-*anti*-deuterionorbornane (IIIB) in carbon tetrachloride measured with 60 Mc Perkin-Elmer R 12 B spectrometer. The following coupling constants (cps) were measured and confirmed by double resonance experimentents: $J_{3n3x}=13.5$, $J_{3n2x}=3.7$, $J_{3x2x}=10.0$, $J_{5n6n}=7.9$, $J_{6x6n}=13.5$, $J_{7a7s}=10.5$.

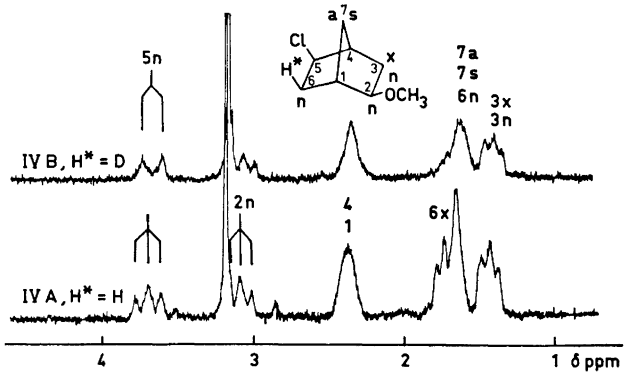

Fig. 2. Proton resonance spectrum of 2-*exo*-methoxy-5-*exo*-chloronorbornane (IVA) and 2-*exo*-methoxy-5-*exo*-chloro-6-*exo*-deuterionorbornane (IVB) in carbon tetrachloride recorded with a Perkin-Elmer Model R 12 B 60 Mc spectrometer. The signals of 5*n* and 2*n* in the spectrum of IVA appear as triplets, indicating a virtual coupling.[13] The signal of 5n in the spectrum of IVB is a doublet with $J=8.0$ cps. It arises from the *endo*-5-H and *endo*-6-H coupling.[3]

(IIIA) in CCl_4 (Fig. 1) shows the signals of the norbornane skeleton protons. The CH-signals at the lowest field arise from the α-protons (closest to chlorine and the methoxy group). In all the compounds studied the signal of the α-proton closest to chlorine appears at a lower field than that of the α-proton closest to the methoxy group. Accordingly, the 5*n* signal in the spectrum of IIIA in CCl_4 is at a lower field than the 2*x* signal. This was confirmed by using trifluoroacetic acid as solvent. All signals in the spectrum of IIIA in CF_3COOH move to a lower field compared to solution in CCl_4, and the signal of 2*x* moves much more (0.34 ppm) than the signal of 5*n* (0.17 ppm). Because the 2*x* proton is nearest the oxygen of the methoxy group, this solvent effect of CF_3COOH causes more deshielding of the

$2x$ signal than of the $5n$. Interpretation of other signals and couplings was verified by double resonance experiments, and comparing them with the NMR data of norbornadiols [10,13] and norbornatriols.[11,12] The results are presented in Figs. 1 and 2.

The mass spectra of IIIA and IVA ($C_8H_{13}ClO$) were quite similar; M^+ peaks at m/e 160 and 162 were detected. The base peak at m/e 66 can be attributed to the cyclopentadienyl cation ($C_5H_6^+$), as in the case of starting compound (I). The other characteristic peaks in the mass spectrum of IIIA and IVA were at m/e 124, 93, 92, 91, 79, 58, 45, and 36. M^+ peaks were at m/e 161 and 163 in the mass spectra of IIIB and IVB. In each case the base peak was at m/e 67 and was due to the cation ($C_5H_5D^+$). The other characteristic peaks in mass spectra of IIIB and IVB were at m/e 125, 94, 93, 92, 80, 67, 58, 45, and 36 (run with a Perkin-Elmer gas chromatograph mass spectrometer Model 270).

Acknowledgement. The author is grateful to Professor Jaakko Paasivirta for his interest and advice with this investigation.

1. Kwart, H. and Nyce, J. L. *J. Am. Chem. Soc.* **86** (1964) 2601.
2. Cristol, S. J. and Caple, R. *J. Org. Chem.* **31** (1966) 2741.
3. Brown, H. C. and Liu, K. T. *J. Am. Chem. Soc.* **89** (1967) 3898; **89** (1967) 3900.
4. Morrill, T. C. and Greenwald, B. E. *J. Org. Chem.* **36** (1971) 2769.
5. Cristol, S. J., Seifert, W. K., Johnson, D. W. and Jurale, J. B. *J. Am. Chem. Soc.* **84** (1962) 3918.
6. Dewar, M. J. S. and Fahey, R. C. *J. Am. Chem. Soc.* **85** (1963) 2245.
7. Paasivirta, J. *Acta Chem. Scand.* **22** (1968) 2200.
8. Winstein, S. and Trifan, D. S. J. *J. Am. Chem. Soc.* **71** (1949) 2953; **74** (1952) 79.
9. Olah, G. A. J. *J. Am. Chem. Soc.* **94** (1972) 808.
10. Paasivirta, J. and Äyräs, P. *Suomen Kemistilehti* **B 41** (1968) 51.
11. Paasivirta, J. and Äyräs, P. *Suomen Kemistilehti* **B 42** (1969) 379.
12. Paasivirta, J. and Äyräs, P. *Suomen Kemistilehti* **B 43** (1970) 82.
13. Äyräs, P. and Paasivirta, J. *Suomen Kemistilehti* **B 42** (1969) 61.

Received July 11, 1973.

A Comparison of *ab initio* and Semi-empirical Calculations on $Li^+(NH_3)$

ÅSE STØGÅRD

Department of Chemistry, University of Bergen, N-5014 Bergen, Norway

The comparison between the *ab initio* and CNDO/2 method on the hydration of Li^+ is reported in a separate paper.[1] The ammonia molecule is now substituted for the water molecule to investigate whether the *ab initio* calculations on $Li^+(NH_3)$ compared to the CNDO/2 method gives results similar to those found for the $Li^+(H_2O)$ and $Li^+(H_2O)_2$ systems.

During the calculations the geometry of the ammonia molecule was kept constant at the experimental values: $R_{N-H} = 1.01$ Å and $\angle HNH = 107°$. The three hydrogens lie in the xy-plane and N – Li lies on a line perpendicular to the xy-plane.

For the *ab initio* calculations the program IBMOL [2,3] was used. This program uses gaussian type functions

$$g = Nx^l y^m z^n e^{-\alpha r^2} \quad (1)$$

where α is the orbital exponent and N is a normalisation constant. The calculations were performed with the following basis set:

(H|4) contracted to ⟨H|2⟩
(N|7,3) contracted to ⟨N|4,2⟩
(Li|7,2) contracted to ⟨Li|4,2⟩

Orbital exponents and contraction coefficients are tabulated in Table 1. R_{Li-N} was varied to find the distance corresponding to minimum energy.

The semi-empirical calculations are based on the CNDO theory as developed by Pople and co-workers.[4-6] The computations were performed with the QCPE program.[7] All parameters were taken from the original papers without any modification.

The results are given in Table 2. The calculated ammoniation energies (ΔE) for the reaction

$$Li^+ + NH_3 = Li^+(NH_3) \quad (2)$$

are also listed here.

The ΔE for the CNDO/2 calculation is much greater than for the *ab initio*. The ΔE for *ab initio* calculation is sensitive to the basis set.[1] No experimental ΔE value is available for the $Li^+(NH_3)$ system.

$2x$ signal than of the $5n$. Interpretation of other signals and couplings was verified by double resonance experiments, and comparing them with the NMR data of norbornadiols [10,13] and norbornatriols.[11,12] The results are presented in Figs. 1 and 2.

The mass spectra of IIIA and IVA ($C_8H_{13}ClO$) were quite similar; M^+ peaks at m/e 160 and 162 were detected. The base peak at m/e 66 can be attributed to the cyclopentadienyl cation ($C_5H_6^+$), as in the case of starting compound (I). The other characteristic peaks in the mass spectrum of IIIA and IVA were at m/e 124, 93, 92, 91, 79, 58, 45, and 36. M^+ peaks were at m/e 161 and 163 in the mass spectra of IIIB and IVB. In each case the base peak was at m/e 67 and was due to the cation ($C_5H_5D^+$). The other characteristic peaks in mass spectra of IIIB and IVB were at m/e 125, 94, 93, 92, 80, 67, 58, 45, and 36 (run with a Perkin-Elmer gas chromatograph mass spectrometer Model 270).

Acknowledgement. The author is grateful to Professor Jaakko Paasivirta for his interest and advice with this investigation.

1. Kwart, H. and Nyce, J. L. *J. Am. Chem. Soc.* **86** (1964) 2601.
2. Cristol, S. J. and Caple, R. *J. Org. Chem.* **31** (1966) 2741.
3. Brown, H. C. and Liu, K. T. *J. Am. Chem. Soc.* **89** (1967) 3898; **89** (1967) 3900.
4. Morrill, T. C. and Greenwald, B. E. *J. Org. Chem.* **36** (1971) 2769.
5. Cristol, S. J., Seifert, W. K., Johnson, D. W. and Jurale, J. B. *J. Am. Chem. Soc.* **84** (1962) 3918.
6. Dewar, M. J. S. and Fahey, R. C. *J. Am. Chem. Soc.* **85** (1963) 2245.
7. Paasivirta, J. *Acta Chem. Scand.* **22** (1968) 2200.
8. Winstein, S. and Trifan, D. S. J. *J. Am. Chem. Soc.* **71** (1949) 2953; **74** (1952) 79.
9. Olah, G. A. J. *J. Am. Chem. Soc.* **94** (1972) 808.
10. Paasivirta, J. and Äyräs, P. *Suomen Kemistilehti* **B 41** (1968) 51.
11. Paasivirta, J. and Äyräs, P. *Suomen Kemistilehti* **B 42** (1969) 379.
12. Paasivirta, J. and Äyräs, P. *Suomen Kemistilehti* **B 43** (1970) 82.
13. Äyräs, P. and Paasivirta, J. *Suomen Kemistilehti* **B 42** (1969) 61.

Received July 11, 1973.

A Comparison of *ab initio* and Semi-empirical Calculations on $Li^+(NH_3)$

ÅSE STØGÅRD

Department of Chemistry, University of Bergen, N-5014 Bergen, Norway

The comparison between the *ab initio* and CNDO/2 method on the hydration of Li^+ is reported in a separate paper.[1] The ammonia molecule is now substituted for the water molecule to investigate whether the *ab initio* calculations on $Li^+(NH_3)$ compared to the CNDO/2 method gives results similar to those found for the $Li^+(H_2O)$ and $Li^+(H_2O)_2$ systems.

During the calculations the geometry of the ammonia molecule was kept constant at the experimental values: $R_{N-H} = 1.01$ Å and $\angle HNH = 107°$. The three hydrogens lie in the xy-plane and N – Li lies on a line perpendicular to the xy-plane.

For the *ab initio* calculations the program IBMOL [2,3] was used. This program uses gaussian type functions

$$g = Nx^l y^m z^n e^{-\alpha r^2} \quad (1)$$

where α is the orbital exponent and N is a normalisation constant. The calculations were performed with the following basis set:

(H|4) contracted to ⟨H|2⟩
(N|7,3) contracted to ⟨N|4,2⟩
(Li|7,2) contracted to ⟨Li|4,2⟩

Orbital exponents and contraction coefficients are tabulated in Table 1. R_{Li-N} was varied to find the distance corresponding to minimum energy.

The semi-empirical calculations are based on the CNDO theory as developed by Pople and co-workers.[4-6] The computations were performed with the QCPE program.[7] All parameters were taken from the original papers without any modification.

The results are given in Table 2. The calculated ammoniation energies (ΔE) for the reaction

$$Li^+ + NH_3 = Li^+(NH_3) \quad (2)$$

are also listed here.

The ΔE for the CNDO/2 calculation is much greater than for the *ab initio*. The ΔE for *ab initio* calculation is sensitive to the basis set.[1] No experimental ΔE value is available for the $Li^+(NH_3)$ system.

Table 1. Contracted Gaussian basis set for $Li^+(NH_3)$.

Atom	Type	Function No.	Coefficients C	Exponents α
H	*s*	1	0.01906	16.7019
			0.13424	2.51663
			0.47449	0.567196
		2	1.0	0.154146
N	*s*	1	0.004479	2038.41
			0.034581	301.689
			0.164263	66.4630
			0.453898	17.8081
		2	1.0	5.30452
		3	1.0	0.764993
		4	1.0	0.234424
	p	1	0.119664	5.9546
			0.474629	1.23293
		2	1.0	0.286752
Li	*s*	1	0.005889	284.399
			0.044471	42.3482
			0.194745	9.37924
			0.474138	2.50578
		2	1.0	0.733345
		3	1.0	0.073733
		4	1.0	0.039787
	p	1	1.0	0.154
		2	1.0	0.057

Table 2. Equilibrium distances and ΔE's for $Li^+(NH_3)$.

	NH_3 $-E$ (a.u.)	Li^+ $-E$(a.u.)	Li^+NH_3 $-E$(a.u.)	$-\Delta E$ (kcal/mol)	R_{Li-N} (Å)
ab initio	56.098647	7.233138	63.417165	53.6	1.98
CNDO/2	13.87307		14.01947	91.9	2.19

Experimental Li – N distances in four-coordinated lithium compounds are reported for $Li(NH_3)_4$ [8] where $R_{Li-N}=1.94$ Å, and for LiCN [9] with $R_{Li-N}=2.06$ Å. The *ab initio* result is closer to the experimental data than the CNDO/2 calculation. The same was found for the $Li^+(H_2O)$ and $Li^+(H_2O)_2$ systems,[1] but for these the differences between the equilibrium distances of the *ab initio* and the CNDO/2 method were greater.

1. Bauge, K. and Støgård, Å. *Acta Chem. Scand* **27** (1973) 2683.
2. Davies, D. R. and Clementi, E. QCPE 92, IBMOL.
3. Veillard, A. IBMOL: Computation of wavefunction for molecules of general geometry. Version 4, Special IBM Report 1968. Due to the small memory of our computer (an IBM 360/50 with 300 k bits available to the users) we had to modify these programs accordingly.
4. Pople, J. A., Santry, D. P. and Segal, G. A. *J. Chem. Phys.* **43** (1965) S129.
5. Pople, J. A. and Segal, G. A. *J. Chem. Phys.* **43** (1965) S136.
6. Pople, J. A. and Segal, G. A. *J. Chem. Phys.* **44** (1966) 3289.
7. Quantum Chemistry Program Exchange (QCPE) No. 141, CNINDO, Chemistry Department, Indiana University, Bloomington, Indiana 47401, U.S.A.
8. Mammano, N. and Sienko, M. J. *J. Am. Chem. Soc.* **90** (1968) 6322.
9. Lely, J. A. and Bijvoet, J. M. *Rec. Trav. Chim.* **61** (1942) 244.

Received June 20, 1973.

NMR-Studies of the Interaction of Metal Ions with Poly(1,4-hexuronates). II. The Binding of Europium Ions to Sodium Methyl α-D-Galactopyranosiduronate

THORLEIF ANTHONSEN,[a] BJØRN LARSEN[b] and OLAV SMIDSRØD[b]

[a]*Organic Chemistry Laboratories, Norwegian Institute of Technology, University of Trondheim, N-7034 Trondheim-NTH, Norway and* [b]*Institute of Marine Biochemistry, University of Trondheim, 7034 Trondheim-NTH, Norway*

Metal ions play an essential part in determining the physical and biological properties of many polyuronides, and we have recently [1] started an NMR-study in which lanthanide ions are used as probes for determining possible binding sites. The effect of Eu^{3+} on sodium D-galacturonate was shown to be markedly greater than on sodium D-glucuronate. This difference between the two C_4-epimeric sugars and other evidence, suggested that the binding site in D-galacturonic acid consisted of the carboxy group, together with O_4 and O_5. In an attempt to locate the Eu^{3+} ion more exactly we have now determined the induced shifts in sodium methyl α-D-galacturonate. The 60 MHz PMR-spectrum is given in Fig. 1a.

After the addition of europium nitrate to an equivalent ratio of 3.6, the resonances are shifted as shown in Fig. 1b. The assignments were confirmed by double resonance experiments and all coupling constants are in satisfactory agreement with earlier observations.[2] They indicate that no change in conformation ($^4C_1$) occurs during the addition of europium nitrate. The shift curves (Fig. 2) show that the resonance peaks are shifted both upfield and downfield. Even at high europium-to-sugar ratios, the magnitude of the shift still depends on the europium ion concentration.

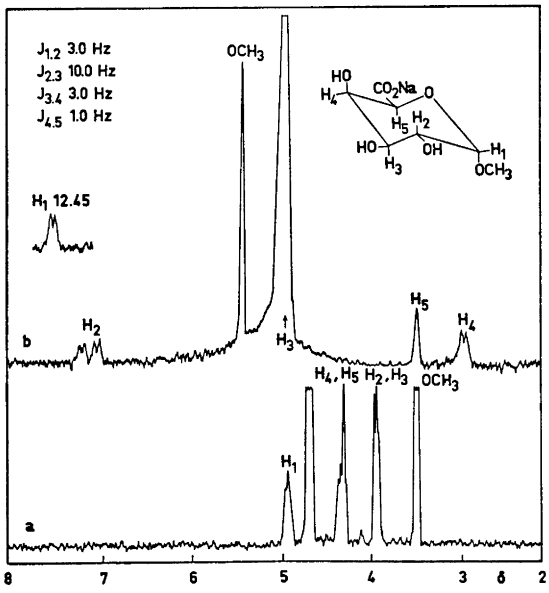

Fig. 1. The 60 MHz PMR-spectrum of sodium methyl α-D-galacturonate in D_2O before (a) and after (b) the addition of europium nitrate (equivalent ratio [Eu]/[S] = 3.6). The shifts are measured relative to sodium 3-(trimethylsilyl)propanesulfonate.

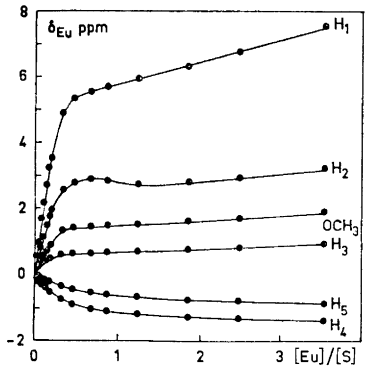

Fig. 2. The Eu^{3+} induced shift (δ_{Eu}) for the various protons in sodium methyl α-D-galacturonate as a function of the equivalent ratio [Eu]/[S]. ([S] = 0.335 M.)

Assuming axial symmetry of the Eu^{3+}-uronic-acid complex, we have calculated the relative shifts of protons $H_1 - H_5$ (space coordinates for the various atoms were taken from an X-ray study of methyl α-D-galacturonic acid methyl ester [3]) according to the equation [4]

$$\Delta\nu/\nu_0 = K(3\ \cos^2\phi - 1)/r^3 \qquad (I)$$

The experimental shifts were calculated from the initial slopes of the shift curves (Fig. 2) assuming 3:1 (sugar:Eu^{3+}) stoichiometry. The calculated shifts were scaled to the experimental ones by varying the value of K in eqn. I to obtain the minimum mean square deviation (R-factor) The best fit (Table 1) was obtained when the distances from the Eu^{3+} ion to O_4, O_5, and C_6 were set at 2.9, 2.0, and 2.2 Å, respectively, with the magnetic axis

Table 1. Observed and calculated europium induced shifts assuming 3:1 complex.

	Obs.	Calc.
H_1	5.50	5.50
H_2	3.00	3.01
H_3	0.80	0.74
H_4	−0.93	−0.96
H_5	−0.43	−0.41
OMe	1.42	—

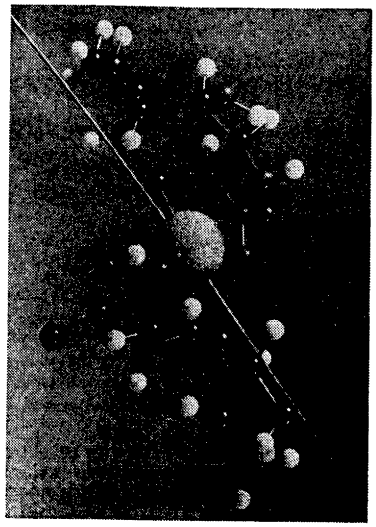

Fig. 3. Ball-stick-model where 2 of the three sugar molecules are arranged around the magnetic axis of Eu^{3+} according to the data. The third sugar ligand is omitted both for the sake of clarity in the figure and because of practical difficulties in building the 3:1 complex. The carboxy groups are rotated so as to give the smallest possible distance between one of the two oxygen atoms and the europium ion. The assumed position of the magnetic axis is indicated by the string through the center of the europium ion.

pointing towards H_1 (see Fig. 3). The calculated R-factor was 0.001.

Angyal [5] has recently remarked that the direction and magnitude of the induced shifts in methyl β-D-hamamelopyranoside did not seem to be related to eqn. I. However, the agreement between calculated and observed shifts in Table 1 is remarkably good. This suggests that the method will prove to be of great value for evaluating binding sites in metal-sugar complexes.

Bleaney *et al.*[6] have discussed the use of lanthanide-induced shifts (LIS) in aqueous solutions. They proposed that experimental tests for axial symmetry should be carried out and also that the LIS should be corrected for electrostatic shielding effects of the lanthanide ions. Such experiments are currently being carried out and will possibly lead to some small corrections in the positioning of the Eu^{3+} ion. However, the position of the europium ion that is indicated at present is reasonable from a

chemical viewpoint. The proximity of the europium ion to the carboxy group, the ring oxygen, and the axial O_4 is in agreement with our earlier proposal.[1] The essential part played by the carboxy group is clearly visible from the pH-dependence of the LIS of H_1 and H_2 in the α-anomer of D-galacturonic acid (Fig. 4). It is therefore

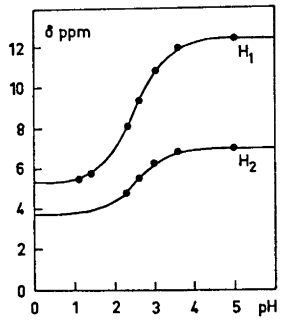

Fig. 4. The pH dependence of the Eu^{3+} induced shift (δ_{Eu}) of H_1 and H_2 in the α-anomer of sodium D-galacturonate (40.0 mg uronate and 21.7 mg europium nitrate in 0.3 ml D_2O).

very important to control the pH of the solution, and in the present experiments it was kept well above the critical value.

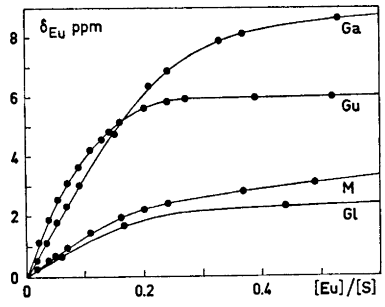

Fig. 5. The Eu^{3+} induced shift (δ_{Eu}) of H_1 in the α-anomers of sodium D-galacturonate (Ga), sodium L-guluronate (Gu), sodium D-mannuronate (M), and sodium D-glucuronate (GL) as a function of the equivalent ratio [Eu]/[S]. ([S] ≈ 0.4 M.)

We have also studied the effect of Eu^{3+} ions on the NMR spectra of the sodium salts of D-galacturonic acid, D-glucuronic acid, D-mannuronic acid, and L-guluronic acid. The spectra of the anomeric mixtures are too complex for complete analysis at present. However, it is obvious that the H_1 proton of the α-anomer in all four cases is subject to the most dramatic downfield shift (Fig. 5). It is also clear that this proton is most strongly influenced in the spectra of D-galacturonic acid and L-guluronic acid. We conclude that the reason for this is the presence of the proposed binding site in these two acids. Moreover, α-L-guluronic acid also possesses the ax-eq-ax sequence of three hydroxy groups which offers [7] an additional binding site.

A full analysis of the LIS curves (Fig. 2) in terms of the stoichiometry of the different possible complexes and the corresponding total shifts and equilibrium constants has not yet been carried out. This analysis and further studies in the field are in progress.

Acknowledgements. We are grateful to lic. techn. Johan Hjortås for X-ray diffraction data for methyl α-D-galacturonic acid methyl ester, to siv.ing. Hans Grasdalen for valuable discussions and for a grant from *Norges Tekniske Høgskoles fond* to T.A.

1. Anthonsen, T., Larsen, B. and Smidsrød, O. *Acta Chem. Scand.* **26** (1972) 2988.
2. Rees, D. A. and Wight, A. W. *J. Chem. Soc.* **1971** 1366.
3. Thanomkul, S. and Hjortås, J. *Private communication.*
4. Bleaney, B. *J. Magn. Resonance* **8** (1972) 91.
5. Angyal, S. J. *Carbohyd. Res.* **26** (1973) 271.
6. Bleaney, B., Dobson, C. M., Levine, B. A., Martin, R. B., Williams, R. J. P. and Xavier, A. V. *Chem. Commun.* **1972** 791.
7. Angyal, S. J. *Aust. J. Chem.* **25** (1972) 1957.

Received July 14, 1973.

Walden Inversion

III. The Crystal Structure and Absolute Configuration of Zn(II) (+)-Aspartate Trihydrate

LARS KRYGER and
SVEND ERIK RASMUSSEN

Department of Inorganic Chemistry, University of Aarhus, DK-8000 Aarhus C, Denmark

L-(+)-Aspartic acid can be converted into, *e.g.*, (−)-malic acid and (−)-chlorosuccinic acid according to the choice of reagents. These facts were used by Walden [1] for his discovery of the sequence of reactions called the Walden cycle. The structures and absolute configurations of (−)-chlorosuccinic acid and of (−)-malic acid have been determined recently [2,3] and we considered it desirable also to determine the absolute configuration of aspartic acid. Doyne, Pepinsky and Watanabe [4] reported cell dimensions of salts of L-aspartic acid with divalent zinc, cobalt, and nickel. They report that the salts crystallize as trihydrates and that they are isomorphous. They determined the structure and absolute configuration of the cobaltous salt and used the coordinates from this to refine the structural parameters of the zinc salt.

The report by Doyne *et al.*[4] is without details; no coordinates are listed. We aimed at a repetition of their work in order to check our results against theirs.

Experimental. We were unable to obtain crystals of cobalt (II) and nickel (II)-aspartate. We made several attempts using the prescriptions of Lifschitz and Schouteden [5] and several variants of their methods. Zinc(II)-aspartate, however, yielded crystals readily. The aspartic acid was a Fluka *puriss.* product of specific optical rotation $[\alpha]_D^{23.5} = +3.2°$/cm (1 % solution in 6 M HCl). Three-dimensional intensity data were collected using a linear diffractometer of Arndt-Phillips design. All reflections within a hemisphere of reciprocal space were recorded out to a Bragg angle of 27°. Mo$K\alpha$-radiation was selected by a graphite monochromator. The reflections which were recorded near the spindle axis of the linear diffractometer were remeasured using a four-circle Picker diffractometer. A set of non pinacoid Friedel related intensities $|F(hkl)|^2$ and $|F(\bar{h}\bar{k}\bar{l})|^2$ were measured using the Picker diffractometer and W$L\beta_1$-radiation.

Crystal data are as follows: $ZnC_4H_5O_4N.3H_2O$, $a = 9.443(5)$, $b = 7.862(4)$, $c = 11.696(6)$

Table 1. Fraction 1 coordinates x 10^4 and thermal parameters, $U_{ij}(A^2) \times 10^4$, as they appear in the temperature factor empression: $\exp(-2\pi^2 a_i^* a_j^* h_i h_j U_{ij})$. Estimated standard deviations in the last significant figures are in parentheses.

	x/a	y/b	z/c	U_{11}	U_{22}	U_{33}	U_{12}	U_{13}	U_{23}
Zn	452 (3)	1359 (3)	923 (2)	1453 (12)	1585 (12)	2161 (11)	91 (12)	-115 (12)	110 (12
O(1)	1510 (24)	2532 (27)	2416 (16)	2565 (104)	2120 (96)	3440 (91)	648 (87)	-692 (86)	-582 (82
O(2)	3477 (25)	2075 (30)	3451 (18)	3113 (116)	3420 (120)	3881 (98)	357 (105)	-1473 (101)	-932 (96
O(3)	2448 (21)	1800 (27)	33 (16)	1590 (90)	2588 (108)	2872 (82)	148 (79)	205 (73)	850 (78
O(4)	4705 (20)	1278 (26)	-458 (17)	2026 (94)	1947 (94)	3900 (90)	308 (93)	1044 (80)	601 (83
N	1348 (27)	-736 (32)	1729 (19)	2079 (107)	1679 (109)	2694 (95)	-227 (97)	117 (93)	213 (90
C(1)	2560 (30)	1635 (36)	2728 (21)	2197 (125)	2067 (138)	2088 (93)	57 (107)	-54 (98)	-106 (99
C(2)	2734 (29)	-154 (36)	2179 (20)	2028 (128)	1635 (120)	2128 (98)	144 (104)	-331 (97)	367 (104
C(3)	3868 (31)	-107 (40)	1227 (21)	2042 (138)	2200 (140)	2769 (116)	467 (117)	186 (100)	378 (104
C(4)	3623 (28)	1088 (33)	206 (20)	1754 (114)	1337 (126)	2542 (100)	-83 (101)	212 (95)	-59 (95
O(W1)	-310 (25)	263 (31)	-601 (18)	2027 (110)	3899 (123)	3281 (94)	44 (102)	97 (82)	-1085 (89
O(W2)	-1572 (26)	946 (35)	1763 (20)	2626 (115)	2510 (130)	3145 (101)	-299 (97)	217 (90)	-41 (92
O(W3)	1992 (26)	6041 (32)	385 (20)	2746 (115)	2656 (126)	3711 (110)	-261 (98)	-20 (92)	247 (99

	x/a	y/b	z/c	U		x/a	y/b	z/c	U
CH(2)	3084 (431)	-1144 (542)	2703 (329)	54 (12)	H2(W2)	-2198 (565)	1209 (710)	1240 (476)	71 (16
CH(31)	4745 (348)	239 (435)	1555 (258)	23 (8)	H1(W3)	1393 (529)	5329 (681)	523 (379)	45 (14
CH(32)	4144 (472)	-1268 (563)	868 (322)	50 (13)	H2(W3)	1976 (517)	6490 (617)	-137 (409)	52 (14
H1(W1)	285 (517)	-506 (668)	-935 (356)	56 (13)	NH(1)	771 (328)	-1031 (433)	2329 (257)	25 (8
H2(W1)	-1146 (416)	-147 (491)	-632 (282)	39 (9)	NH(2)	1451 (521)	-1721 (614)	1285 (379)	45 (13
H1(W2)	-1758 (616)	240 (770)	1946 (431)	65 (20)					

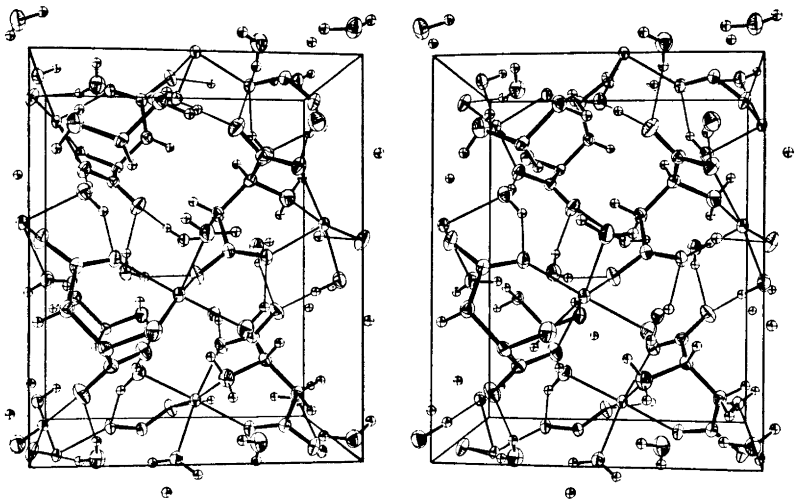

Fig. 1. Perspective drawing of the content of a unit cell of zinc(II) aspartate trihydrate

Å. $Vc = 686.3$ Å^3, density (calc) 1.92, exp.[4] 1.97 gcm^{-3}, $Z = 4$, space group $P2_12_12_1$ (No. 19 Int. Tables). Systematic absences $h00$ for $h =$ odd, $0k0$ for $k =$ odd, and $00l$ for $l =$ odd.

The structure was redetermined without using the preliminary data of Doyne *et al.* by direct methods employing the program system SYMBAD.[6] The first electron density map revealed the positions of all non-hydrogen atoms. By successive applications of least squares refinement and difference electron density maps the positions of the hydrogen atoms were determined also. The parameters from the least squares computations are given in Table 1. The structure was refined to a conventional R-value of 2.5 % using 1279 reflections considered to be of observable magnitude.* The crystal was regularly and almost centro symmetrically shaped with a radius less than 0.1 mm. No absorption correction was introduced, as $\exp(-\mu t)$ varies 2 % in the angular range of measurements. The linear absorption coefficient for Mo$K\alpha$ is 29.4 cm^{-1}. An isotropic extinction factor g was refined to a value of 213(14) (dimensionless), thus yielding extinction corrections to F_c^2 ranging from 0.65 to 1.00. This extinction factor corresponds to a mean domain size of 151 Å or a mosaic spread of 273 sec. A projection of the structure is shown in Fig. 1. Bond lengths are shown in Table 2.

Table 2. Interatomic distances in Å units. Estimated standard deviations in the last significant figures are in parentheses.

Bond lengths Å				Bond lengths Å			
O(1)	- C(1)	1.270	(4)	Zn	- N	2.077	(2)
O(2)	- C(1)	1.259	(3)	Zn	- O(W1)	2.106	(2)
C(1)	- C(2)	1.554	(4)	Zn	- O(W2)	2.173	(3)
C(2)	- N	1.482	(4)	O(W1)	- H1(W1)	0.913	(51)
C(2)	- CH(2)	1.044	(41)	O(W1)	- H2(W1)	0.853	(39)
C(2)	- C(3)	1.545	(4)	O(W2)	- H1(W2)	0.623	(58)
C(3)	- CH(31)	0.952	(33)	O(W2)	- H2(W2)	0.875	(58)
C(3)	- CH(32)	1.038	(44)	O(W3)	- H1(W3)	0.812	(53)
C(3)	- C(4)	1.536	(4)	O(W3)	- H2(W3)	0.706	(50)
C(4)	- O(3)	1.258	(3)	O(W3)	- O(2)	2.739	(3)
C(4)	- O(4)	1.292	(3)	O(W1)	- O(2)	2.756	(3)
N	- NH(1)	0.917	(32)	O(W1)	- O(W3)	2.757	(3)
N	- NH(2)	0.938	(47)	O(W3)	- O(4)	2.827	(3)
Zn	- O(1)	2.212	(2)	O(W2)	- O(1)	2.850	(4)
Zn	- O(3)	2.180	(2)	O(W2)	- O(3)	2.899	(3)
Zn	- O(4)	2.060	(2)	O(W2)	- O(4)	2.923	(3)
				O(W1)	- O(4)	2.988	(3)

The absolute configuration was found by computing the ratio $q_c = F_c^2\ (hkl)/F_c^2\ (\bar{h}\bar{k}\bar{l})$ using the W$L\beta_1$ wave length 1.2818 Å ($\Delta f' = -6{,}82$, $\Delta f'' = 4.21$ for the zinc atom) and comparing it with the ratio between observed data $q_o = F^2_{obs}(hkl)/F^2_{obs}(\bar{h}\bar{k}\bar{l})$.

The arbitrarily selected enantiomorph proved to be the correct one. A selection of observed and calculated q-ratios are shown in Table 3.

The computer programs employed in addition to SYMBAD were data reduction, G4,[7] Fourier Synthesis, FORDAP,[8] least squares refinement, LINUS,[9] plot program, ORTEP,[10] distance and angle calculations, ORFFE.[11]

* A structure factor table can be obtained from the authors at request.

Table 3.

Comparison of intensities used in the determination of absolute configuration.
The ratio q = I(hkl)/I($\bar{h}\bar{k}\bar{l}$) is given as observed with standard deviations x 100 in parentheses and as calculated. All together 49 q-ratios were measured. None of those left out was in contradiction to the results listed.

hkl	q(obs)	q(calc)	hkl	q(obs)	q(calc)
111	0.77 (1)	0.72	231	1.11 (3)	1.26
113	0.69 (2)	0.69	23$\bar{1}$	1.14 (2)	1.26
1$\bar{1}$3	0.88 (3)	0.69	234	1.40 (4)	1.66
1$\bar{1}$5	1.47 (6)	1.34	23$\bar{4}$	1.23 (3)	1.66
123	0.82 (2)	0.91	332	0.90 (3)	0.91
12$\bar{3}$	0.91 (2)	0.91	33$\bar{2}$	0.84 (3)	0.91
131	0.61 (1)	0.50	343	0.64 (12)	0.62
13$\bar{1}$	0.59 (1)	0.50	34$\bar{3}$	0.71 (14)	0.62
141	1.16 (5)	1.10	361	1.38 (6)	1.42
14$\bar{1}$	1.15 (5)	1.10	36$\bar{1}$	1.26 (6)	1.42
21$\bar{1}$	0.81 (1)	0.72	415	0.58 (2)	0.69
223	0.57 (1)	0.48	324	0.76 (2)	0.72
22$\bar{3}$	0.65 (1)	0.48	32$\bar{4}$	0.87 (3)	0.72

L-(+)-Aspartic acid has the *S*-configuration according to the Cahn-Ingold notation. As (−)-chlorosuccinic acid [2] and (−)-malic acid [3] also have the *S*-configuration, no inversion takes place in the reactions leading from aspartic acid to these two compounds. The structural results are in accordance with those of Doyne *et al.*[4] When our structural work was completed, we became aware of a subsequent refinement of the data reported in Ref. 4. Doyne reports refined parameters for Zn(II)-aspartate trihydrate in *Advan. Protein Chem.*[12] These data are probably less accurate than those reported here, but on the average there is a good agreement between the two sets of results.

Acknowledgement. *Carlsberg Fondet* is thanked for the linear diffractometer and Mrs. R. Grønbæk Hazell and Dr. J. Danielsen are thanked for advice on computing. Dr. A. C. Hazell is thanked for computing the anomalous dispersion of the zinc atom for W$L\beta_1$-radiation.

1. Walden, P. *Ber.* **29** (1896) 1692.
2. Kryger, L., Rasmussen, S. E. and Danielsen, J. *Acta Chem. Scand.* **26** (1972) 2339.
3. Kryger, L. and Rasmussen, S. E. *Acta Chem. Scand.* **26** (1972) 2349.
4. Doyne, T., Pepinsky, R. and Watanabe, T. *Acta Cryst.* **10** (1957) 438.
5. Lifschitz, I. and Schouteden, F. L. M. *Rec. Trav. Chim.* **58** (1939) 411.
6. Danielsen, J. *Studier over nogle af røntgenkrystallografiens direkte metoder*, Aarhus 1969.
7. Grønbæk Hazell, R. *Program G 404*, Department of Inorganic Chemistry, University of Aarhus, DK-8000 Aarhus, Denmark.
8. Zalkin, A. *FORDAP* unpublished, modified by Lundgren and Liminga.
9. Hamilton, W. C., Ibers, J. A. and Edmonds, J. *LINUS* Modified ORFLS program Busing, W. R., Martin, K. O. and Levy, H. A. ORNL-TM-305, Oak-Ridge National Laboratory, Oak Ridge Tennessee.
10. Johnson, C. K. *ORTEP*, ORNL-3794. Oak-Ridge National Laboratory, Oak Ridge, Tennessee 1965.
11. Busing, W. R., Martin, K. O. and Levy, H. A. *ORFFE*, ORNL-TM-306, Oak Ridge National Laboratory, Oak Ridge, Tennessee 1964.
12. Anfinsen, C. B., Anson, M. L., Edsall, J. T. and Richards, F. M. *Advan. Protein Chem.* **22** (1967) 410.

Received August 3, 1973.

The Effect of Oxygen Lone Pairs on $^1J(^{13}CH)$ Values in 1,3-Dioxanes

K. BOCK and L. WIEBE

Department of Organic Chemistry, Technical University of Denmark, DK-2800 Lyngby, Denmark

Recently we have shown that $^1J(^{13}CH)$ values can be used to determine the anomeric configuration in carbohydrate derivatives since the carbon-hydrogen coupling constant is *ca.* 10 Hz larger when the proton is equatorially oriented than when it is axial.[1,2]

We have now studied a number of 1,3-dioxane derivatives and have found that the $^1J(^{13}CH)$ values are dependent on the orientation of the protons relative to the ring oxygens.

The assignments of the ^{13}C-chemical shifts are based mainly on published values as shown in Table 1. Undecoupled spectra were obtained using gated decoupling technique.[3]

The $^1J(^{13}C-H2)$ value of *trans*-2-methyl-5-*t*-butyl-1,3-dioxane (*2*), or of the corresponding 2-phenyl derivative (*3*), was 158

Table 3.

Comparison of intensities used in the determination of absolute configuration.
The ratio q = I(hkl)/I($\bar{h}\bar{k}\bar{l}$) is given as observed with standard deviations x 100 in parentheses and as calculated. All together 49 q-ratios were measured. None of those left out was in contradiction to the results listed.

hkl	q(obs)	q(calc)	hkl	q(obs)	q(calc)
111	0.77 (1)	0.72	231	1.11 (3)	1.26
113	0.69 (2)	0.69	23$\bar{1}$	1.14 (2)	1.26
1$\bar{1}$3	0.88 (3)	0.69	234	1.40 (4)	1.66
1$\bar{1}$5	1.47 (6)	1.34	23$\bar{4}$	1.23 (3)	1.66
123	0.82 (2)	0.91	332	0.90 (3)	0.91
12$\bar{3}$	0.91 (2)	0.91	33$\bar{2}$	0.84 (3)	0.91
131	0.61 (1)	0.50	343	0.64 (12)	0.62
13$\bar{1}$	0.59 (1)	0.50	34$\bar{3}$	0.71 (14)	0.62
141	1.16 (5)	1.10	361	1.38 (6)	1.42
14$\bar{1}$	1.15 (5)	1.10	36$\bar{1}$	1.26 (6)	1.42
21$\bar{1}$	0.81 (1)	0.72	415	0.58 (2)	0.69
223	0.57 (1)	0.48	324	0.76 (2)	0.72
22$\bar{3}$	0.65 (1)	0.48	32$\bar{4}$	0.87 (3)	0.72

L-(+)-Aspartic acid has the *S*-configuration according to the Cahn-Ingold notation. As (−)-chlorosuccinic acid [2] and (−)-malic acid [3] also have the *S*-configuration, no inversion takes place in the reactions leading from aspartic acid to these two compounds. The structural results are in accordance with those of Doyne *et al.*[4] When our structural work was completed, we became aware of a subsequent refinement of the data reported in Ref. 4. Doyne reports refined parameters for Zn(II)-aspartate trihydrate in *Advan. Protein Chem.*[12] These data are probably less accurate than those reported here, but on the average there is a good agreement between the two sets of results.

Acknowledgement. *Carlsberg Fondet* is thanked for the linear diffractometer and Mrs. R. Grønbæk Hazell and Dr. J. Danielsen are thanked for advice on computing. Dr. A. C. Hazell is thanked for computing the anomalous dispersion of the zinc atom for W$L\beta_1$-radiation.

1. Walden, P. *Ber.* **29** (1896) 1692.
2. Kryger, L., Rasmussen, S. E. and Danielsen, J. *Acta Chem. Scand.* **26** (1972) 2339.
3. Kryger, L. and Rasmussen, S. E. *Acta Chem. Scand.* **26** (1972) 2349.
4. Doyne, T., Pepinsky, R. and Watanabe, T. *Acta Cryst.* **10** (1957) 438.
5. Lifschitz, I. and Schouteden, F. L. M. *Rec. Trav. Chim.* **58** (1939) 411.
6. Danielsen, J. *Studier over nogle af røntgenkrystallografiens direkte metoder*, Aarhus 1969.
7. Grønbæk Hazell, R. *Program G 404*, Department of Inorganic Chemistry, University of Aarhus, DK-8000 Aarhus, Denmark.
8. Zalkin, A. *FORDAP* unpublished, modified by Lundgren and Liminga.
9. Hamilton, W. C., Ibers, J. A. and Edmonds, J. *LINUS* Modified ORFLS program Busing, W. R., Martin, K. O. and Levy, H. A. ORNL-TM-305, Oak-Ridge National Laboratory, Oak Ridge Tennessee.
10. Johnson, C. K. *ORTEP*, ORNL-3794. Oak-Ridge National Laboratory, Oak Ridge, Tennessee 1965.
11. Busing, W. R., Martin, K. O. and Levy, H. A. *ORFFE*, ORNL-TM-306, Oak Ridge National Laboratory, Oak Ridge, Tennessee 1964.
12. Anfinsen, C. B., Anson, M. L., Edsall, J. T. and Richards, F. M. *Advan. Protein Chem.* **22** (1967) 410.

Received August 3, 1973.

The Effect of Oxygen Lone Pairs on $^1J(^{13}CH)$ Values in 1,3-Dioxanes

K. BOCK and L. WIEBE

Department of Organic Chemistry, Technical University of Denmark, DK-2800 Lyngby, Denmark

Recently we have shown that $^1J(^{13}CH)$ values can be used to determine the anomeric configuration in carbohydrate derivatives since the carbon-hydrogen coupling constant is *ca.* 10 Hz larger when the proton is equatorially oriented than when it is axial.[1,2]

We have now studied a number of 1,3-dioxane derivatives and have found that the $^1J(^{13}CH)$ values are dependent on the orientation of the protons relative to the ring oxygens.

The assignments of the ^{13}C-chemical shifts are based mainly on published values as shown in Table 1. Undecoupled spectra were obtained using gated decoupling technique.[3]

The $^1J(^{13}C-H2)$ value of *trans*-2-methyl-5-*t*-butyl-1,3-dioxane (*2*), or of the corresponding 2-phenyl derivative (*3*), was 158

Table 1. ^{13}C-Chemical shifts (ppm)[a] and observed 1 st. order one-bond coupling constants (Hz)[b].

1,3-Dioxane	C-2	C-4	C-5	C-6	5-Cα	5-Cβ	2-Cα	4-Cα	6-Cα	Reference
	93.15	68.22	43.76	68.22	30.36	27.19				
1. 5-*t*-Bu	158									4,9
	166	142.5	127.5	142.5		125				
2. *trans*-2-Me-	98.19	68.09	42.91	68.09	30.03	27.12	20.71			
5-*t*-Bu	158	141.3	127.5	141.3		125	125			4,9
3. *trans*-2-Ph-	100.85	68.87	43.30	68.87	30.23	27.32				
5-*t*-Bu	158	142.5	127.5	142.5		125				4,9
4. *cis*-Paraldehyde	97.78						20.11			4
	159						126.6			
5. *cis*-4,6-di-Me	93.02	72.30	40.98	72.30				21.56	21.56	
	157.5									4,10
	166.5	137	127.5	137				125	125	
6. *trans*-4,6-di-	86.38	67.19	37.38	67.19				19.13	19.13	
Me	161	142.5	127.5	142.5				125	125	4,10
7. 2-*cis*-4-*cis*-6-	97.81	71.79	40.00	71.79			20.97	21.36	21.36	
-tri-Me			123.5							4
	158	138	127.5	138			126.5	125.9	125.9	
8. 2-*trans*-4-*trans*-	93.11	63.76	40.13	63.76			16.70	21.62	21.62	
6-tri-Me	165	140	126	140			126	125.3	125.3	4
9. 2-*cis*-4-*trans*-6-	90.36	66.54	36.18	67.13			20.97	21.43	16.77	
tri-Me	158.5	137	126.5	150			125.8	126.5	125	4,10
10. *trans*-2-*O*-Me-	111.14	65.64	42.62	65.64	30.36	27.45	51.62			
5-*t*-Bu	186	142.5	127.5	142.5		125	144.2			11
11. *cis*-2-*O*-Me-5-	107.78	60.04	42.85	60.04	30.52	27.28	52.14			
t-Bu	193	142.5	127.5	142.5		125	142.5			11

[a] Measured at 22.63 MHz on a Bruker WH-90 instrument, *ca.* 25 % solutions in $CDCl_3$, used as internal reference = 76.90 ppm. [b] ± 0.7 Hz using pulsed decoupling technique.

Hz, whereas C-2 in the unsubstituted derivative (*1*) showed up as a double doublet with coupling constants of 158 and 166 Hz. It is known from previously published work [4] that the methyl or phenyl group is equatorially oriented and we therefore conclude that $^1J(^{13}C\text{-}H2_{ax})$ is 158 Hz and $^1J(^{13}C\text{-}H2_{eq})$ is 166 Hz. This is in accordance with the results found in the carbohydrate derivatives mentioned above.

Paraldehyde (*4*) gives a $^1J(^{13}CH)$ value of 159 Hz, consistent with an equatorial methyl group and an axial proton.[4]

cis-4,6-Dimethyl-1,3-dioxane (*5*) exhibits the same $^1J(^{13}C\text{-}H2)$ value as (*1*) (see Table 1). The *trans* isomer (*6*), on the other hand, gives a value of 161 Hz, but it is known from proton NMR spectroscopy that this compound is conformationally unstable [4] and a coupling constant of 158 – 166 Hz would therefore be expected. Substitution of one of the protons at C-2 in (*5*) with a methyl group as in 2-*cis*-4-*cis*-6-trimethyl-1,3-dioxane (*7*) or in 2-*trans*-4-*trans*-6-trimethyl-1,3-dioxane (*8*), confirms the assignments of the $^1J(^{13}C\text{-}H2)$ values in (*5*) (see Table 1).

Several authors have discussed the effect of electron lone pairs on ^{13}CH coupling constants, and the available evidence indicates that directly bonded ^{13}CH coupling constants are increased when neighbouring lone pairs are present at a position close to the proton.[5–8] This effect may explain the difference in $^1J(^{13}C\text{-}H2)$ values in 1,3-dioxanes since equatorial protons, which are close to the lone pairs of the ring oxygens have larger coupling constants than axial protons.

Both oxygen atoms do not necessarily have to be within the ring with fixed orientation of the lone pairs. This is seen in the carbohydrate derivatives mentioned above, where only one oxygen atom is in the pyranose ring. But also 1,3-dioxane derivatives with an OR-substituent at C-2 exhibit different coupling constants to an axial and to an equatotial proton. Thus 2-*O*-methyl-5-*t*-butyl-1,3-dioxane gives a $^1J(^{13}C\text{-}H2)$ value of 186 Hz for the *trans* isomer (*10*) with an axial proton at C-2

whereas the *cis* isomer (*11*) gives a coupling constants of 193 Hz.

2-*cis*-4-*trans*-6-Trimethyl-1,3-dioxane (*9*) exists mainly in the conformation with the methyl substituent at C-2 equatorial, as shown by Eliel and Knoeber from proton NMR spectra,[4] and we have in accordance herewith found that $^1J(^{13}C\text{-}H2)$ is 159 Hz. In this compound the coupling constants to H-4 and H-6 are 138 Hz and 150 Hz, respectively. The assignment of these coupling constants is based on the value of $^1J(^{13}C\text{-}H4) = 138$ Hz in (*5*) and (*7*), where H-4 must be axially oriented. We here see that the lone pairs from only one oxygen atom can have a large influence on ^{13}CH coupling constants. This effect has also been found in methyl-pentopyranosides.[2]

We conclude from these results that the difference in directly bonded ^{13}CH coupling constants to axial and equatorial protons is due to the effect of lone pairs on neighbouring oxygen atoms.

Acknowledgement. The Pulsed Fourier Transform spectrometer was provided by *The* Danish National Science Research Council.

1. Bock, K., Lundt, I. and Pedersen, C. *Tetrahedron Letters* **1973** 1037.
2. Bock, K. and Pedersen, C. *To be published.*
3. Freeman, R. and Hill, H. D. W. *J. Magn. Res.* **5** (1971) 278.
4. Eliel, E. L. and Knoeber, S. M. C. *J. Am. Chem. Soc.* **90** (1968) 3444.
5. Jennings, W. B., Boyd, D. R., Watson, C. G., Becker, E. D., Bradley, R. B. and Jerina, D. M. *J. Am. Chem. Soc.* **94** (1972) 8501.
6. Gil, V. M. S. and Teixeira-Dias, J. J. C. *Mol. Phys.* **15** (1968) 47.
7. Yonezawa, T., Morishima, I., Fukuta, K. and Ohmori, Y. *J. Mol. Spectry.* **31** (1969) 341.
8. Albrand, J. P., Cogne, A., Gagnaire, D. and Robert, J. B. *Tetrahedron* **27** (1971) 2453.
9. Jones, A. J., Eliel, E. L., Grant, D. M., Knoeber, M. C. and Bailey, W. F. *J. Am. Chem. Soc.* **93** (1971) 4772.
10. Kellie, G. M. and Riddell, F. G. *J. Chem. Soc. Perkin Trans. 2* **1971** 1030.
11. Nader, F. W. and Eliel, E. L. *J. Am. Chem. Soc.* **92** (1970) 3050.

Received September 14, 1973.

Structure of Bis-(1-ethynylcyclohexanol)-bis-(triphenylphosphine)platinum

R. A. MARIEZCURRENA* and S. E. RASMUSSEN

Department of Inorganic Chemistry, Aarhus University, DK-8000 Aarhus C, Denmark

Crystals of $Pt(P(C_6H_5)_3)_2(C_8H_{12}O)_2$ were kindly supplied by Dr. H. B. Jonassen of Tulane University, New Orleans. The complex has been subject to IR and NMR spectroscopic investigations by Roundhill and Jonassen.[1] Two kinds of crystals were found in the sample: a triclinic modification not yet extensively investigated and the monoclinic form reported here. The monoclinic crystals appear to be the more numerous.

Experimental. A plate-shaped crystal $0.3 \times \times 0.22 \times 0.51$ mm was mounted along *c*. Cell dimensions and systematic absences were obtained from Weissenberg and precession photographs and were confirmed by diffractometer measurements. The conditions limiting possible reflections were: $0k0$: $k=2n$, $h0l$: $h+l=2n$. hkl: no conditions. The crystals are monoclinic, space group $P2_1/n$, $Z=2$, F.W.= 966.0, $a=8.992$, $b=23.012$, $c=11.585$ Å, $\beta=105.35°$, $V=2311$ Å^3, $D_m=1.43$, $D_c=1.39$ g cm^{-3}, $\lambda(MoK\alpha)=0.7107$ Å, $\mu(MoK\alpha)=33.0$ cm^{-1}.

The density was measured by flotation in a mixture of heptane and carbon tetrachloride. Intensities were measured on an Arndt-Phillips linear diffractometer. Mo$K\alpha$ radiation was selected by a graphite monochromator. The counting chain included a scintillation counter and a pulse height analyzer. 6288 reflections with $l=0$ to 14 were measured to a $\sin\theta/\lambda$ limit of 0.64 Å^{-1}. Symmetry related reflections were averaged. 2898 independent reflections had intensities above two standard deviations as derived by counting statistics and were employed in subsequent computations. Lorentz and polarization factors were applied, assuming the graphite monochromator to behave as an ideal mosaic crystal. An absorption correction was applied, the correction factors ranging from 1.60 to 2.70.

* Now returned to Facultad de Quimica, Montevideo, Uruguay.

whereas the *cis* isomer (*11*) gives a coupling constants of 193 Hz.

2-*cis*-4-*trans*-6-Trimethyl-1,3-dioxane (*9*) exists mainly in the conformation with the methyl substituent at C-2 equatorial, as shown by Eliel and Knoeber from proton NMR spectra,[4] and we have in accordance herewith found that $^1J(^{13}C\text{-}H2)$ is 159 Hz. In this compound the coupling constants to H-4 and H-6 are 138 Hz and 150 Hz, respectively. The assignment of these coupling constants is based on the value of $^1J(^{13}C\text{-}H4) = 138$ Hz in (*5*) and (*7*), where H-4 must be axially oriented. We here see that the lone pairs from only one oxygen atom can have a large influence on ^{13}CH coupling constants. This effect has also been found in methyl-pentopyranosides.[2]

We conclude from these results that the difference in directly bonded ^{13}CH coupling constants to axial and equatorial protons is due to the effect of lone pairs on neighbouring oxygen atoms.

Acknowledgement. The Pulsed Fourier Transform spectrometer was provided by *The* Danish National Science Research Council.

1. Bock, K., Lundt, I. and Pedersen, C. *Tetrahedron Letters* **1973** 1037.
2. Bock, K. and Pedersen, C. *To be published.*
3. Freeman, R. and Hill, H. D. W. *J. Magn. Res.* **5** (1971) 278.
4. Eliel, E. L. and Knoeber, S. M. C. *J. Am. Chem. Soc.* **90** (1968) 3444.
5. Jennings, W. B., Boyd, D. R., Watson, C. G., Becker, E. D., Bradley, R. B. and Jerina, D. M. *J. Am. Chem. Soc.* **94** (1972) 8501.
6. Gil, V. M. S. and Teixeira-Dias, J. J. C. *Mol. Phys.* **15** (1968) 47.
7. Yonezawa, T., Morishima, I., Fukuta, K. and Ohmori, Y. *J. Mol. Spectry.* **31** (1969) 341.
8. Albrand, J. P., Cogne, A., Gagnaire, D. and Robert, J. B. *Tetrahedron* **27** (1971) 2453.
9. Jones, A. J., Eliel, E. L., Grant, D. M., Knoeber, M. C. and Bailey, W. F. *J. Am. Chem. Soc.* **93** (1971) 4772.
10. Kellie, G. M. and Riddell, F. G. *J. Chem. Soc. Perkin Trans. 2* **1971** 1030.
11. Nader, F. W. and Eliel, E. L. *J. Am. Chem. Soc.* **92** (1970) 3050.

Received September 14, 1973.

Structure of Bis-(1-ethynylcyclohexanol)-bis-(triphenylphosphine)platinum

R. A. MARIEZCURRENA* and S. E. RASMUSSEN

Department of Inorganic Chemistry, Aarhus University, DK-8000 Aarhus C, Denmark

Crystals of $Pt(P(C_6H_5)_3)_2(C_8H_{12}O)_2$ were kindly supplied by Dr. H. B. Jonassen of Tulane University, New Orleans. The complex has been subject to IR and NMR spectroscopic investigations by Roundhill and Jonassen.[1] Two kinds of crystals were found in the sample: a triclinic modification not yet extensively investigated and the monoclinic form reported here. The monoclinic crystals appear to be the more numerous.

Experimental. A plate-shaped crystal $0.3 \times \times 0.22 \times 0.51$ mm was mounted along *c*. Cell dimensions and systematic absences were obtained from Weissenberg and precession photographs and were confirmed by diffractometer measurements. The conditions limiting possible reflections were: $0k0$: $k=2n$, $h0l$: $h+l=2n$. hkl: no conditions. The crystals are monoclinic, space group $P2_1/n$, $Z=2$, F.W.= 966.0, $a=8.992$, $b=23.012$, $c=11.585$ Å, $\beta=105.35°$, $V=2311$ Å^3, $D_m=1.43$, $D_c=1.39$ g cm^{-3}, $\lambda(MoK\alpha)=0.7107$ Å, $\mu(MoK\alpha)=33.0$ cm^{-1}.

The density was measured by flotation in a mixture of heptane and carbon tetrachloride. Intensities were measured on an Arndt-Phillips linear diffractometer. Mo$K\alpha$ radiation was selected by a graphite monochromator. The counting chain included a scintillation counter and a pulse height analyzer. 6288 reflections with $l=0$ to 14 were measured to a $\sin\theta/\lambda$ limit of 0.64 Å^{-1}. Symmetry related reflections were averaged. 2898 independent reflections had intensities above two standard deviations as derived by counting statistics and were employed in subsequent computations. Lorentz and polarization factors were applied, assuming the graphite monochromator to behave as an ideal mosaic crystal. An absorption correction was applied, the correction factors ranging from 1.60 to 2.70.

* Now returned to Facultad de Quimica, Montevideo, Uruguay.

Table 1. Parameters from least squares analysis. Atomic coordinates are in fractions of cell edges. Where only one thermal parameter is given as $B11$, it is the conventional B-value: $B = 8\pi^2u^2$ where u^2 is the mean square vibration amplitude in Å². Where six parameters are given, the temperature factor is calculated as exp $-2\pi^2[a^{*2}h^2B11 + b^{*2}k^2B22 + c^{*2}l^2B33 + 2a^*b^*hkB12 + 2a^*c^*hlB13 + 2b^*c^*klB23]$ where the B_{ij} values are in Å².

Atom	x	y	z	$B11$	$B22$	$B33$	$B12$	$B13$	$B23$
C 1	.136016	.051529	.289122	2.68					
C 2	.209959	.040924	.412879	4.12					
C 3	.304188	.084035	.480158	4.40					
C 4	.323127	.137135	.422720	4.83					
C 5	.250531	.148355	.299925	5.06					
C 6	.156302	.105244	.232645	3.94					
C 7	−.180392	.010465	.222885	2.75					
C 8	−.308706	−.017504	.141909	3.99					
C 9	−.456262	−.010958	.158887	4.47					
C 10	−.473395	.023463	.256600	4.61					
C 11	−.347188	.051525	.337819	4.40					
C 12	−.199633	.044979	.320840	4.00					
C 13	.071904	−.068618	.283905	2.68					
C 14	.223037	−.090325	.289709	4.20					
C 15	.276804	−.139614	.359054	5.14					
C 16	.178670	−.166492	.421605	5.07					
C 17	.028305	−.145490	.416792	6.11					
C 18	−.025462	−.096201	.347447	4.26					
C 19	−.225490	.184791	−.015024	6.81					
O	−.162564	.216910	−.092584	7.42					
C 20	−.153873	.215639	.110858	8.98					
C 21	−.458344	.158097	.055605	10.93					
C 22	−.220675	.189462	.210805	12.55					
C 23	−.405000	.187983	−.044000	13.22					
C 24	−.394305	.188636	.167141	14.39					
C 25	−.165129	.121518	−.009427	.008540	.000998	.004181	−.000274	.002625	−.000256
C 26	−.110476	.076124	−.007809	.009251	.000941	.004976	−.000323	.003072	.000467
P	.007912	−.003362	.200547	.022177	.001163	.010503	.000058	.004901	.001942
Pt	.000000	.000000	.000000	.014859	.000981	.006730	.000175	.003322	.001023

Structure determination. The platinum atom is located at the origin. The position of the phosphorus atom was found from a Patterson function. As y_p is close to zero (0.003), the phosphorus atom, like the platinum atom, does not contribute to reflections with $h+k+l = 2n+1$. An electron density map phased on the platinum and the phosphorus positions therefore shows a false mirror plane perpendicular to y. The light atoms were poorly defined in this first map but approximate positions of the three phenyl rings were derived. As their geometry is known to an accuracy better than we could expect from our diffraction data, refinement by least squares was carried out with each phenyl group constrained to be planar with $2m$ symmetry. The Euler angles and the centers of gravity of the phenyl rings were refined. Convergence was obtained at $R = 12$ % when isotropic thermal movement was assumed for all atoms. When temperature factor parameters describing anisotropic vibration were assigned to the platinum and phosphorus atoms, R dropped to 9 %. A difference map still showed the effect of the pseudo mirror plane. It was, however, possible to find a group of atoms which corresponded to a 1-ethynylcyclohexanol molecule. Anisotropic thermal movement was assumed for the acetylene group and isotropic for the cyclohexanol group. The B-values of the atoms in the cyclohexanol group were large (9 − 14 Å²) indicating a certain degree of disorder. The final R is 5.2 %.

The final parameters are given in Table 1. A table of calculated and observed structure factors can be obtained from

S.E. Rasmussen at request.

Atomic scattering factors were taken from Ref. 2, $\Delta f'$ for Pt = −1.9.

The following computer programs were used: Data reduction: G4.[3] Absorption correction: Wells.[4] Fourier synthesis: Fordap (A. Zalkin, modified by Lundgren and Liminga), unpublished. Least squares constrained refinement: Pawley.[5] Plot program and distance calculations: ORTEP, Johnson.[6]

Discussion. This study was undertaken as a preliminary to a neutron diffraction investigation of the positions of the hydrogen atoms. According to Roundhill and Jonassen[1] an octahedral configuration round the platinum is expected with hydrogen atoms completing the octahedron. This investigation has so far confirmed that the triphenylphosphine and the hydroxyacetylene molecules are coordinated to platinum, but our data are not accurate enough to yield positions of the hydrogen atoms. In the sample crystals of the size of several mm³ occurred. These were intended for neutron investigation but proved to belong to the triclinic modification which is now being investigated by X-ray diffraction.

The molecule is depicted in Fig. 1. Interatomic distances are given in Table 2. The distances between the light atoms agree well with standard values in similar compounds. The distances found in the cyclohexanol group reflect the low accuracy of the determination of that part of the structure. The Pt−P distance of 2.307 Å compares well with an average of 2.293 Å in ten structures of platinum phosphine complexes (2.240 to 2.345 Å). The Pt-C distance is normal. It is not possible to draw conclusions about the valence state of the platinum atom.

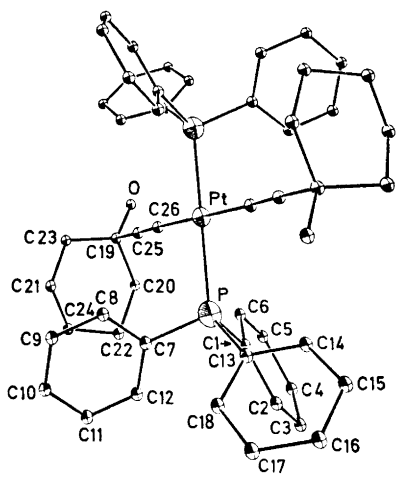

Fig. 1. Projection of a molecule of bis(1-ethynylcyclohexanol) bis (triphenylphosphine) platinum.

Table 2. Bond lengths (Å).

Triphenylphosphine group		
C	−C(as inserted)	(1.41)
P	−C(1)	1.808
P	−C(7)	1.796
P	−C(13)	1.830
Ethynylcyclohexanol group		
C(25)−C(26)		1.15
C(25)−C(19)		1.55
C(19)−C(23)		1.57
C(23)−C(21)		1.81
C(21)−C(24)		1.44
C(24)−C(22)		1.51
C(22)−C(20)		1.56
C(20)−C(19)		1.60
C(19)−O		1.39
Pt	−P	2.307
Pt	−C(26)	2.004

Acknowledgements. We thank the *Danish International Development Agency* for financial aid; the *Facultad de Quimica de Montevideo* for leave of absence to Raul A. Mariezcurrena; Dr. G. S. Pawley for use of his program for constrained refinement; Mrs. R. Grønbæk Hazell for helpful advice on computing; Dr. A. C. Hazell for discussions on structures of platinum complexes; and Dr. H. B. Jonassen of Tulane University for the crystals.

1. Roundhill, D. H. and Jonassen, H. B. *Chem. Commun.* **1968** 1233.
2. *International Tables for X-Ray Crystallography*, Kynoch Press, Birmingham 1962, Vol. III.
3. Grønbæk Hazell, R. ALGOL program, Department of Inorganic Chemistry, Aarhus University, Aarhus 1964.
4. Wells, M. *Acta Cryst.* **13** (1960) 722.
5. Pawley, G. S. Least Squares Constrained Program, Department of Physics, Edinburg University, Edinburg 1971.
6. Johnson, C. K. ORTEP, ORNL-3794. Oak Ridge National Laboratory, Oak Ridge, Tennessee.

Received August 20, 1973.

Spectrophotometric Studies on the Acid Dissociation of Anthocyanins in Aqueous Solutions

HEIKKI PYYSALO and OSMO MÄKITIE

Department of Chemistry, University of Helsinki, SF-00170 Helsinki 17, Finland and Technical Research Centre of Finland, Food Research Laboratory, SF-02150 Otaniemi, Finland

The acid dissociation reaction of an anthocyanin is reflected in absorption spectra of the compound in solutions where the pH is varied.[1-4] Although absorption spectra for solutions of different anthocyanins have been reported in several earlier studies, no precise measurements of the corresponding reaction equilibria seem to be available.

The absorption spectra of cyanidin-3-galactoside, delphinidin, pelargonidin, malvidin-3,5-diglucoside, and peonidin-3,5-diglucoside in aqueous solutions of various hydrogen ion concentration were recorded, and dissociation constants were evaluated by the common absorptiometric method.

The acid dissociation of anthocyanins can be represented as:

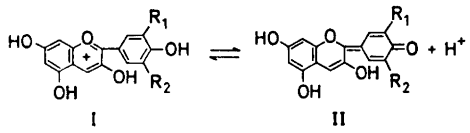

I II

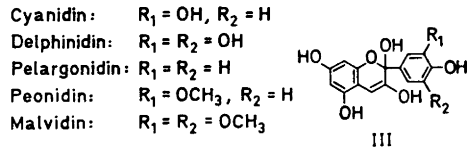

III

Table 1 lists the absorptivities of the spectra of cyanidin-3-galactoside and shows the precision with which the equilibrium constant is determined. Table 2 presents the results obtained for the other anthocyanins. It was not possible to determine any precise K_a value for pelargonidin; but it could be roughly estimated as $K_a \simeq 1.1 \times 10^{-2}$. The absorption spectra are presented in Figs. 1 and 2.

The spectrophotometric determinations of 1×10^{-4} M solutions of cyanidin-3-galactoside were also carried out in solu-

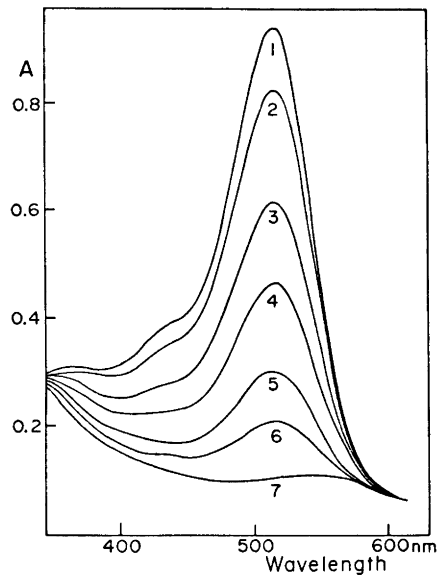

Fig. 1. Absorption spectra of cyanidin-3-galactoside in solutions of various hydrogen ion concentration ($c = 7 \times 10^{-5}$ M, 25°C). Curves: (1) $-\log [H^+]$ 1.0, (2) 2.2, (3) 2.8, (4) 3.1, (5) 3.4, (6) 3.7, and (7) 5.0.

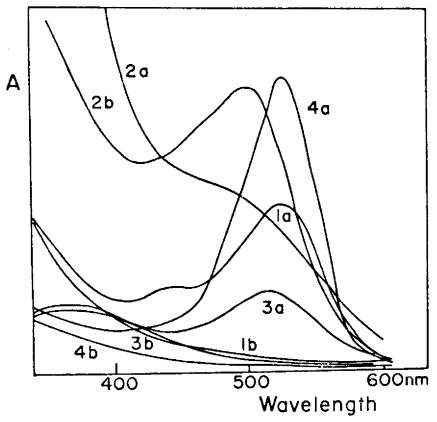

Fig. 2. Absorption spectra of aqueous solutions of anthocyanins at 25°C. Curves: (1) Delphinidin $c = 5 \times 10^{-4}$, $-\log [H^+] = 0$ (a) and 3.1 (b); (2) Pelargonidin $c = 3 \times 10^{-4}$, $-\log [H^+] = 0.3$ (a) and 3.9 (b); (3) Peonidin-3,5-diglucoside $c = 3 \times 10^{-4}$, $-\log [H^+] = 0$ (a) and 3.3 (b); (4) Malvidin-3,5-diglucoside $c = 2 \times 10^{-5}$ $-\log [H^+] = 0$ (a) and 3.5 (b).

Table 1. Determinations of pK_a values of cyanidin-3-galactoside in aqueous solution at 25°C. $c = 7 \times 10^{-5}$ M, $I = 0.005$.

$-\log [H^+]$	496 nm	506 nm	516 nm	526 nm	536 nm	Mean value
1.89	2.984	2.963	2.977	2.949	2.958	2.966
2.20	2.905	2.999	3.002	2.984	2.983	2.975
2.50	2.953	2.939	3.000	3.009	3.018	2.984
2.81	2.970	2.958	3.013	2.999	3.007	2.989
3.20	2.960	2.980	2.973	2.963	2.987	2.973
pK_a= (mean value)	2.954	2.967	2.993	2.981	2.991	2.977

Table 2. pK_a values obtained for different anthocyanins in aqueous solution at 25°C. $I = 0.005$.

	n	c, M	λ_{max}	pK_a
Cyanidin-3-galactoside	3	7×10^{-5}	516	2.98 ± 0.05
Delphinidin	4	$3-10 \times 10^{-4}$	524	1.56 ± 0.20
Peonidin-3,5-diglucoside	2	5×10^{-4}	512	2.09 ± 0.10
Malvidin-3,5-diglucoside	2	2×10^{-5}	524	1.75 ± 0.10
Pelargonidin	3	3×10^{-4}	500	–

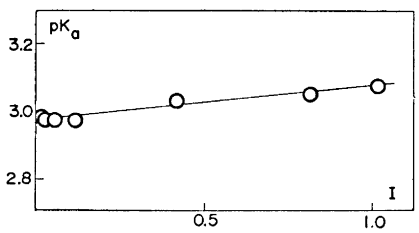

Fig. 3. Dependence of pK_a of cyanidin-3-galactoside on ionic strength of aqueous solutions at 25°C. $c = 1 \times 10^{-4}$ M, KCl as inert salt; pK_a° (extrapolated) $= 2.98 \pm 0.02$.

tions of various ionic strengths (potassium chloride was added as inert salt). The results are shown in Fig. 3. The dependence of the pK_a values on the ionic strength of the solutions is linear: $pK_a = [H^+][L]/[HL^+]$.

Anthocyanins are relatively unstable in aqueous solutions, and may form colourless pseudo-bases.[5] It appears that neither the acid dissociation reactions nor the disappearance of the red colour of anthocyanins proceed directly from forms I to II. Instead a colourless pseudo-base is formed as intermediate, the proposed structure of which is shown as form III.[6] In these experiments only pelargonidin proved unstable.

Experimental. Cyanidin-3-galactoside was isolated from the berries of mountain ash. The other anthocyanins were in the form of hydrochlorides obtained by the purification (paper chromatography) of commercial reagents from Fluka AG.

The absorption spectra were measured and recorded at 25°C with a Perkin-Elmer Model EPS-3T spectrophotometer.

The K_a values were obtained by the common absorptiometric method in which the absorptivities of solutions of various hydrogen ion concentration were measured at different wave lengths near the isoelectric point in the buffer range.

1. Willstätter, R. and Bolton, E. *Ann.* **408** (1915) 412.
2. Kuhn, H. and Sperling, W. *Experientia* **16** (1960) 237.
3. Bayer, E. *Chem. Ber.* **91** (1958) 1115.
4. Bayer, E. *Chem. Ber.* **92** (1959) 1062.
5. Willstätter, R. *Ann.* **412** (1917) 234.
6. Bayer, E. and Voelter, W. In Schormüller, L., Ed., *Handbuch der Lebensmittelchemie*, Part I, Springer, Berlin-Heidelberg 1965, p. 697.

Received July 5, 1973.

Calculations on the Hydration of Ions

KJELL BAUGE and ÅSE STØGÅRD

Department of Chemistry, University of Bergen, N-5014 Bergen, Norway

Several calculations, by both *ab initio* and semiempirical methods, on hydration of ions have been reported.[1-9]

We have performed calculations on Li^+H_2O and $Li^+(H_2O)_2$ both by *ab initio* and semiempirical methods using an IBMOL-program [10,11] and a CNDO/2 program.[12] The purpose has been to calculate the hydration energies and by comparison, investigate the possible utility of the CNDO/2 program for larger hydration aggregates.

In addition to these calculations we have also carried out CNDO/2 calculations on Li^+ with 4 and 6 water molecules, and on F^-, Cl^-, and Na^+ with 1,2, 4, and 6 water molecules attached to the ions.

The hydration energy was calculated from:

$$\Delta E = E_{A\pm(H_2O)n} - (E_{A\pm} + nE_{H_2O})$$

where $E_{A\pm(H_2O)n}$ is the calculated energy value for the hydrated ion, $E_{A\pm}$ is that of the isolated ion, E_{H_2O} that of the water molecule, and n is the hydration number.

The geometry of the water molecule wat kept constant with the H – O distance 1.0 Å and the H – O – H angle 104.5°. The ion-oxygen distance was varied so that minimum energy was detected. In the cases of more than one oxygen the ion-oxygen distances were varied in a symmetrical fashion so that for 2, 4, and 6 water molecules we had linear, tetrahedral, and octahedral symmetries.

The orbital exponents and expansion coefficients were taken in part from

Table 1. Orbital exponents (α) and expansion coefficients (c).

Type	H		O		Li	
	α	c	α	c	α	c
s	4.50038	0.07048	2714.89	0.004324	284.399	0.005889
	0.681277	0.40789	415.725	0.032265	42.3482	0.044471
	0.151374	1.0	91.9805	0.156410	9.37924	0.194745
			24.4515	1.447813	2.50578	0.474138
			7.22296	1.0	0.733345	1.0
			1.06314	1.0	0.073733	1.0
			0.322679	1.0	0.029787	1.0
p	0.33	1.0	7.75579	0.129373	0.154	1.0
			1.62336	0.481296	0.057	1.0
			0.36503	1.0		
d			0.72	1.0		
			0.1	1.0		

Table 2. Equilibrium values of *ab initio* calculation.

	H_2O $-E$ a.u.	Li^+ $-E$ a.u.	$Li^+(H_2O)_n$ $-E$ a.u.	$-\Delta E$ kcal/mol	$d(Li^+-O)$ Å
Li^+H_2O					
Basis set I	75.885733	7.233138	83.192775	45.5	1.78
Basis set II	75.885733	7.238503	83.197751	32.7	1.81
Basis set III	75.910831	7.238503	83.211633	38.9	1.84
$Li^+(H_2O)_2$	75.878167	7.233138	159.12827	88.5	1.79

Veillard [11] and from Siegbahn and Roos [18] and are given in Table 1.

In the case of Li^+H_2O three kinds of basis sets were used:

I (H|3)(O|7,3)(Li^+|7)
II (H|3)(O|7,3)(Li^+|7,2)
III (H|3,1)(O|7,3,2)(Li^+|7,2) contracted to (H|2,1)(O|4,2)(Li^+|4,2)

For the $Li^+(H_2O)_2$ case only one basis set was used:

(H|3)(O|7,3)(Li^+|7) contracted to (H|2)(O|4,2)(Li^+|4)

In actual cases d_{Z^2} orbital was added to the oxygen atom. Also in all cases calculations were performed on the Li^+ ion and on the H_2O molecule with the above mentioned geometry.

The results of the *ab initio* calculations are presented in Fig. 1 and Table 2 and of CNDO/2 in Fig. 2, and Table 3. The figures give the total energies as function of ion-oxygen distances. Only the case of Li^+ is presented for CNDO/2 but similar curves were obtained for the other calculations. In the figures the energy is given per water molecule according to:

$$E_{norm} = \frac{E_{A\pm(H_2O)n} - E_{A\pm}}{n} + E_{A\pm}$$

Table 3. Equilibrium values of CNDO/2 calculations.

	$-E_{tot}$ a.u.	$-\Delta E$ kcal/mol	$d(A_\pm - O)$ Å
Li^+H_2O	19.959	45.0	2.38
$Li^+(H_2O)_2$	39.914	86.9	2.59
$Li^+(H_2O)_4$	78.810	162.8	2.43
$Li^+(H_2O)_6$	119.667	216.6	2.49
Na^+H_2O	19.939	32.4	2.94
$Na^+(H_2O)_2$	39.877	63.8	2.95
$Na^+(H_2O)_4$	79.748	124.1	2.95
$Na^+(H_2O)_6$	119.611	178.9	2.98
$F^-(H_2O)$	47.40590	21.4	2.14
$F^-(H_2O)_2$	67.32238	39.4	2.16
$F^-(H_2O)_4$	107.14553	69.5	2.24
$F^-(H_2O)_6$	146.96814	99.1	2.28
$Cl^-(H_2O)$	36.02058	18.8	2.38
$Cl^-(H_2O)_2$	55.93481	34.6	2.41
$Cl^-(H_2O)_4$	95.76685	70.2	2.37
$Cl^-(H_2O)_6$	135.58944	99.8	2.42

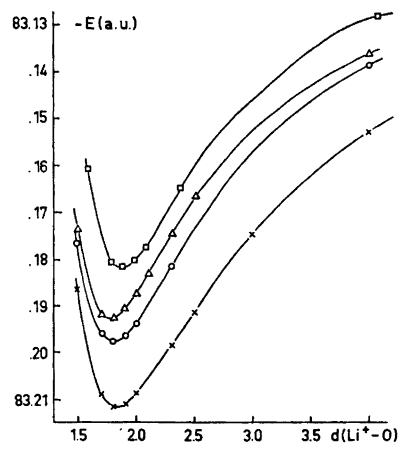

Fig. 1. Energy curves for the $d(Li^+ - O)$ variation of $Li^+(H_2O)$ and $Li^+(H_2O)_2$. ×: $Li^+(H_2O)$ basis set I, ○: $Li^+(H_2O)$ basis set II, △: $Li^+(H_2O)$ basis set III, □: $Li^+(H_2O)_2$.

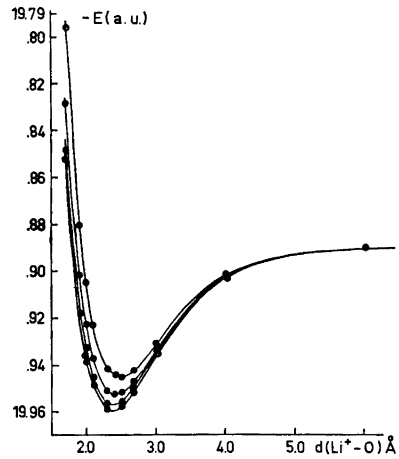

Fig. 2. Energy curves for the $d(Li^+ - O)$ variation of the systems $Li^+(H_2O)_n$. n= 1, 2, 4, 6.

so that the curves were adjusted to the same scale.

In Table 2 the first two columns are the calculated values for the energy of the water molecule and the Li^+ ion. In Table 2 the three last columns and the three columns of Table 3 are, respectively,

the total energies of the hydrated ion, the hydration energy, and the distance between the ion and the water-oxygen atom.

In the CNDO/2 calculations the total energies of H_2O, F^-, and Cl^- was found to be -19.88771, -27.48407, and -16.10429 a.u., respectively, and the total energies of Li^+ and Na^+ were taken to be zero.

Discussion. The basis set III in *ab initio* calculations is most closely related to the basis-set in CNDO/2 calculations. The ΔE's for $Li^+(H_2O)$ calculated by the CNDO/2 method and by basis set I agree very well, while ΔE for basis-set III is closer to the experimental value, which for Li^+H_2O is -34 kcal/mol.[14] ΔE seems to be very sensitive to the basis set.

For $Li^+(H_2O)_2$, the ΔE's from the *ab initio* and the CNDO/2 calculations are similar while the experimental value is -59.8 kcal/mol. [14]

The greatest difference in the CNDO/2 and *ab initio* results is in the equilibrium distances. For Li^+H_2O and $Li^+(H_2O)_2$ the difference in R_{Li-O} is about 30 %. Compared to the crystal structure determination ($R_{Li-O}=1.939$ Å) for 4-coordination on Li,[15] the *ab initio* calculations are closer to the experimental values than those obtained by the CNDO/2 method. Equilibrium distances do not seem to be greatly affected by the basis set as can be seen from Fig. 1.

1. Burton, R. E. and Daly, J. *Trans. Faraday Soc.* **66** (1970) 1281.
2. Burton, R. E. and Daly, J. *Trans Faraday Soc.* **66** (1970) 2408.
3. Burton, R. E. and Daly, J. *Trans. Faraday Soc.* **67** (1971) 1219.
4. Lischka, H., Plesser, T. and Schuster, P. *Chem. Phys. Letters* **6** (1970) 263.
5. Diercksen, G. H. F. and Kraemer, W. P. *Chem. Phys. Letters* **5** (1970) 570.
6. Schuster, P. and Preuss, H. W. *Chem. Phys. Letters* **11** (1971) 35.
7. Diercksen, G. H. F. and Kraemer, W. P. *Theor. Chim. Acta* **23** (1972) 387.
8. Diercksen, G. H. F. and Kraemer, W. P. *Theor. Chim. Acta* **23** (1972) 393.
9. Clementi, E. *J. Chem. Phys.* **57** (1972) 1077.
10. Davies, D. R. and Clementi, E. QCPE 92, IBMOL.
11. Veillard, A, IBMOL: Computation of wavefunction for molecules of general geometry. Version 4, Special IBM Report 1968. Due to the small memory of our computer (an IBM 360/50 with 300 k bits available to the users) we had to modify these programs accordingly.
12. Quantum Chemistry Program Exchange (QCPE) No. 141, CNINDO, Chemistry Department, Indiana University, Bloomington, Indiana 47401, U.S.A.
13. Roos, B. and Siegbahn, P. *Theor. Chim. Acta* **17** (1970) 209.
14. Dridic, I. and Kebarle, P. *J. Phys. Chem.* **74** (1970) 1466.
15. Durant, P. F., Piret, P. and van Meerssche, M. *Acta Cryst.* **22** (1967) 52.

Received June 20, 1973.

ACTA CHEMICA SCANDINAVICA 27 (1973) 2687–2693

Apparent Molal Volume of Aqueous Solutions of Propanoic Acid, Butanoic Acid, Isobutanoic Acid, and their Sodium Salts at Pressures up to 2000 bar at 25°C

HARALD HØILAND

Department of Chemistry, University of Bergen, N-5014 Bg-U, Norway

The compressions of aqueous solutions of propanoic acid, butanoic acid, and isobutanoic acid and their sodium salts were measured at pressures up to 2000 bar at 25°C. The apparent molal volume of the aqueous solutions of the carboxylic acids and their sodium salts was calculated from existing density values.

The apparent molal volume has been separated into three contributions: the intrinsic volume of the molecule, the volume due to hydrophilic hydration, and the volume due to hydrophobic hydration. When the hydrocarbon chain contains more than two carbon atoms, the volume due to hydrophilic hydration seems to become constant, independent of the length of the hydrocarbon chain. The volume increment from the addition of a CH_2-group is mainly due to the volume of the CH_2-group itself. The volume due to hydrophobic hydration is independent of pressure.

The partial molal volume of ionization is probably dependent on the conditions around the carboxylic group, and seems to approach a constant value as the hydrocarbon chain increases.

The apparent molal volume of solutions of electrolytes at infinite dilution has been investigated by a number of workers studying solute-solvent and solvent-solvent interactions.[1]

It seems likely that the apparent molal volume of solutions at finite concentration might provide valuable information as well. In this work the apparent molal volume and its dependence on pressure at a concentration of approximately 0.5 molal, have been used in studying structural relations in aqueous solution.

EXPERIMENTAL

The compression cell was made from an ordinary Pyrex glass cell with two fixed electrodes. A tube of approximately 4 mm diameter and length 12 cm was connected to this cell, Fig. 1. A spiral of 0.2 mm platinum wire was soldered on a small stainless steel cylinder forming a floating electrode on top of the mercury meniscus in the tube, the

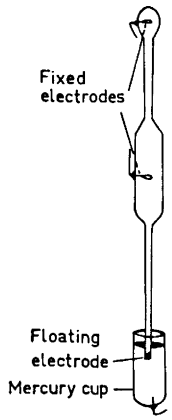

Fig. 1. Compression and conductivity cell.

mercury acting both as pressure transmitting fluid and as electrical lead for the floating electrode.

From the measured conductivity the cell constant between each of the fixed electrodes and the floating electrode was calculated at each pressure. The compression k was then calculated from an empirical equation

$$k = \alpha(K_p - K_0)/V_0 \quad (1)$$

Here K_p and K_0 represent the cell constants between one of the fixed electrodes and the floating electrode at pressure p and atmospheric pressure, respectively. V_0 is the starting volume of the cell and α a constant determined from measurements on the compression of dilute electrolyte solution using the values of Gibson and Loeffler [2] on the compression of water as calibrating standard. Parallel measurements indicated an error of ± 0.0002 in the compression values. Good results were obtained both with rising and falling pressures except at the lower pressures where hysteresis appeared.

Materials. The water used had conductivity less than 4×10^{-6} ohm^{-1} cm^{-1}. The propanoic acid was made by E. Merck A.G., the butanoic acid by The British Drug Houses Ltd., and the isobutanoic acid by Fluka AG, quality *puriss*. The acids were used without further purification. Sodium salts were prepared by titration by weight with sodium hydroxide solution. The conductivity of the butanoic acid solution was compared with values given by Grindley and Bury,[3] the difference being approximately 0.3 %.

Density. The density values were taken from King [4] and International Critical Tables.[5] The compression values of acetic acid were taken from Korpela [6] by interpolation.

The error in the apparent molal volumes due to errors in density and compression values is estimated to ± 0.1 cm^3/mol.

RESULTS

From Figs. 2 and 3 it is seen that the apparent molal volume of the aqueous solutions of acetic acid, propanoic acid, butanoic acid, and isobutanoic acid decreases with increasing pressure while the apparent molal volume of the salts increases. This seems to be a general result and is explained by the electrostriction due to ion-water interactions.[7,8]

The apparent molal volume of one acid solution is now subtracted from the apparent molal volume of the acid having one carbon atom more in the

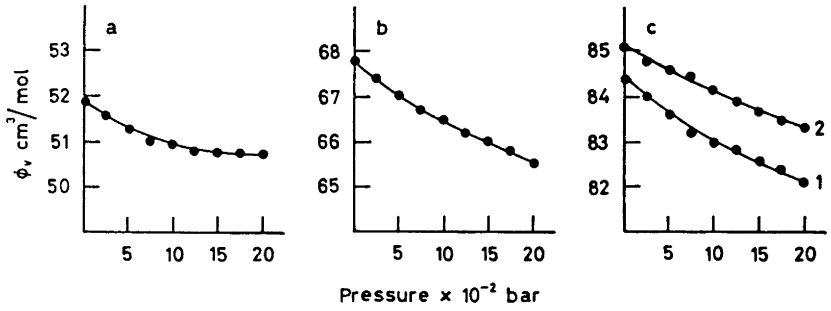

Fig. 2. a. Apparent molal volume of 0.5773 m acetic acid. b. Apparent molal volume of 0.6881 m propanoic acid. c. Apparent molal volumes. 1, 0.5606 m butanoic acid. 2, 0.5583 m isobutanoic Acid.

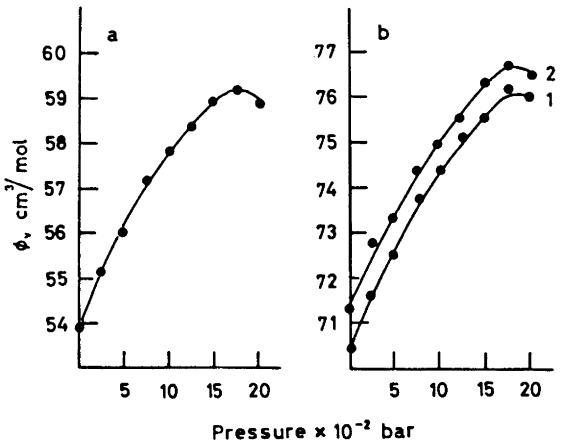

Fig. 3. a. Apparent molal volume of 0.5069 m sodium propanoate. b. Apparent molal volumes. 1, 04395 m sodium butanoate. 2, 0.4324 m sodium isobutanoate.

hydrocarbon chain. The overall volume increment due to the addition of a CH_2-group is then found:

$$\Delta\phi_v(m,m-1) = \phi_v(m) - \phi_v(m-1) \quad (2)$$

Here m and $m-1$ are the number of carbon atoms in the hydrocarbon chain of the two carboxylic acids.

The same was done with the apparent molal volumes of the sodium salt solutions. The contribution of the sodium ions cancels, and one is left with the overall volume increment of adding a CH_2-group to the carboxylic anion. The results are given in Tables 1 and 2.

Table 1. Differences in the apparent molal volumes between solutions of carboxylic acids, $\Delta\phi_v(m,m-1)$. The numbers in the brackets of $\Delta\phi_v(m,n)$ refer to the number of carbon atoms in the hydrocarbon chain of the two acids in question. The asterisk refers to isobutanoic acid.

Pressure bar	$\Delta\phi_v(2,1)$ cm³/mol	$\Delta\phi_v(3,2)$ cm³/mol	$\Delta\phi_v(4,3)$ cm³/mol	$\Delta\phi_v(4^*,3)$ cm³/mol
1	17.3	15.9	16.6	17.3
500		15.7	16.5	17.6
1000		15.6	16.5	17.6
1500		15.2	16.6	17.6
2000		14.9	16.5	17.7

Table 2. Differences in the apparent molal volumes between solutions of the sodium salts of carboxylic acids, $\Delta\phi_v(m,m-1)$. The numbers in the brackets of $\Delta\phi_v(m,n)$ refer to the number of carbon atoms in the hydrocarbon chain of the two acid anions in question. The asterisk refers to isobutanoate.

Pressure bar	$\Delta\phi_v(2,1)$ cm³/mol	$\Delta\phi_v(3,2)$ cm³/mol	$\Delta\phi_v(4,3)$ cm³/mol	$\Delta\phi_v(4^*,3)$ cm³/mol
1	14.3	13.4	16.5	17.4
500			16.5	17.4
1000			16.5	17.3
1500			16.6	17.4
2000			16.2	17.6

When m in eqn. 2 takes the values 4, $\Delta\phi_v(m,m-1)$ is equal for the acid and salt solutions within the limits of error and is independent of pressure.

The values of $\Delta\phi_v(m,m-1)$ are in good agreement with Traube's rule,[9] predicting an increment of 16.0 cm³ per CH_2-group. A somewhat larger increment is observed with the isobutanoic acid. This may be explained by a larger "empty volume"[10] due to the two CH_3-groups at the hydrocarbon end.

The volume increments per CH_2-group of pure liquid carboxylic acids and hydrocarbons are also of the same magnitude (Table 3).

Table 3. Differences in partial molal volumes of pure liquids $\overline{V} = M/d_4^{20}$. Density values d_4^{20} from Handbook of Chemistry and Physics, 51st. Ed., The Chemical Rubber Co, Cleveland, Ohio 1970–1971.

$\overline{V}(2,1)$	$\overline{V}$(Acetic acid) – $\overline{V}$(Formic acid)	19.54 cm³/mol
$\overline{V}(3,2)$	$\overline{V}$(Propanoic acid) – $\overline{V}$(Acetic acid)	17.36 cm³/mol
$\overline{V}(4,3)$	$\overline{V}$(Butanoic acid) – $\overline{V}$(Propanoic acid)	17.40 cm³/mol
$\overline{V}(4^*,3)$	$\overline{V}$(Isobutanoic acid) – $\overline{V}$(Propanoic acid)	16.41 cm³/mol
$\overline{V}(7,6)$	$\overline{V}$(Heptane) – $\overline{V}$(Hexane)	15.3 cm³/mol
$\overline{V}(8,7)$	$\overline{V}$(Octane) – $\overline{V}$(Heptane)	16.1 cm³/mol

The standard partial molal volume of ionization

$$\Delta\bar{V}^\circ = -RT\left(\frac{\partial \ln K}{\partial P}\right)_T \qquad (3)$$

was calculated by the method used by Lown, Thirsk and Lord Wynne-Jones.[11] The pressure dependence of the activity coefficients was neglected, however. Comparing the results with literature values,[4,16] it seems that this may be done without appreciable error in the $\Delta\bar{V}^\circ$ values.

The equivalent conductivities are shown as functions of pressure in Fig. 4. Limiting conductivities were taken from Ellis,[12] Belcher,[13] and Dippy.[14]

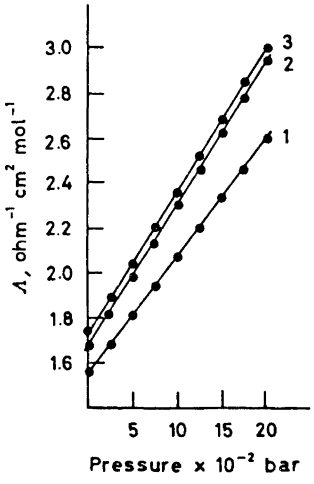

Fig. 4. Equivalent conductivities. 1, 0.6881 m propanoic acid. 2, 0.5583 isobutanoic acid. 3, 0.5606 m butanoic acid.

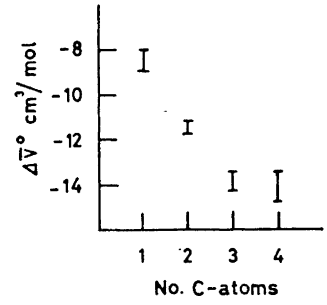

Fig. 2. Standard partial molal volumes of ionization.

Table 4. Standard partial molal volumes of ionization.

Formic acid cm³/mol	Acetic acid cm³/mol	Propanoic acid cm³/mol	Butanoic acid cm³/mol	Isobutanoic acid cm³/mol	Ref.
−8.43	−11.50		−14.22		4
−8.0	−12.5	−13.7	−13.7		16
−9.2	−11.6				17
	−11.46				18
	−11.47				19
	−11.2				11
		−14.1	−14.6	−14.8	This work

Values of $\Delta\overline{V}^{\circ}$ are given in Table 4. In Fig. 5 the values of the partial molal volume of ionization are plotted *versus* the number of carbon atoms in the hydrocarbon chain. It seems to approach a constant value with increasing length of the hydrocarbon chain.

DISCUSSION

The apparent molal volume may be written as the sum of two terms, first the volume due to the space occupied by the molecule or ion itself $\phi_v(\text{Mol})$ and the overall volume effect due to hydration $\phi_v(\text{H})$.

$$\phi_v = \phi_v(\text{Mol}) + \phi_v(\text{H}) \tag{5}$$

Two main types of hydration are described by Desnoyers and Jolicoeur.[15] Hydrophilic hydration is caused by the strong affinity existing between polar groups or ions and the solvent. Hydrophobic hydration results from strengthening the solvent-solvent interactions brought about by hydrophobic groups in the molecule. By this model hydrophilic hydration is expected at the carboxylic end and hydrophobic hydration at the hydrocarbon end of the carboxylic acids in aqueous solution.

Eqn. (5) may then be written as

$$\phi_v = \phi_v(\text{Mol}) + \phi_v(1) + \phi_v(2) \tag{6}$$

where $\phi_v(1)$ and $\phi_v(2)$ refer to the volume contributions of hydrophilic and hydrophobic hydration. Any volume effect due to electrostriction will have to be included in the hydrophilic term, $\phi_v(1)$.

Eqn. (2) may now be written

$$\Delta\phi_v(m,m-1) = \Delta\phi_v(\text{Mol}) + \Delta\phi_v(1) + \Delta\phi_v(2) \tag{7}$$

where $\Delta\phi_v(\text{Mol})$ is the volume of the added CH_2-group.

$$\Delta\phi_v(m,m-1) = \phi_v(CH_2) + \Delta\phi_v(1) + \Delta\phi_v(2) \tag{8}$$

By this hydration model, the addition of a CH_2-group has no effect on the volume due to hydrophilic hydration. This may be a realistic model provided that the carbon chain is not too short. This makes $\Delta\phi_v(1) = 0$.

$$\Delta\phi_v(m,m-1) = \phi_v(CH_2) + \Delta\phi_v(2) \tag{9}$$

The effect of pressure on the apparent molal volume difference is

$$\left[\frac{\partial\Delta\phi_v(m,m-1)}{\partial p}\right]_T = \left[\frac{\partial\phi_v(CH_2)}{\partial p}\right]_T + \left[\frac{\partial\Delta\phi_v(2)}{\partial p}\right]_T \tag{10}$$

Regarding the molecule as incompressible, the first term on the right of eqn. (10) is zero, and from Tables 1 and 2 it is seen that the second term must also be zero. Thus, the volume effects of hydrophobic hydration are independent of pressure at least over moderate pressures.

Acknowledgements. This work was supported by a grant from the *Norwegian Research Council for Science and the Humanities.* I also wish to thank Professor Dr. Thorvald Brun for his valuable advice and his interest in this work.

REFERENCES

1. Millero, F. J. *Chem. Rev.* **71** (1971) 147.
2. Gibson, R. E. and Loeffler, O. H. *J. Am. Chem. Soc.* **63** (1941) 898.
3. Grindley, J. and Bury, C. R. *J. Chem. Soc.* **1930** 1665.
4. King, E. J. *J. Phys. Chem.* **73** (1969) 1220.
5. International Critical Tables, Vol. III McGraw, N. Y. 1933.
6. Korpela, J. *Acta Chem. Scand.* **25** (1971) 2852.
7. Hamann, S. D. *Physico-Chemical Effects of Pressure*, Butterworths, London 1957.
8. Yayanos, A. A. *J. Phys. Chem.* **76** (1972) 1783.
9. Traube, J. *Samml. Chem. Vortr.* **4** (1899) 255.
10. Edward, J. T. *J. Chem. Educ.* **47** (1970) 261.
11. Lown, D. A., Thirsk, H. R. and Lord Wynne-Jones *Trans. Faraday Soc.* **66** (1970) 51.
12. Ellis, A. J. *J. Chem. Soc.* **1959** 3689.
13. Belcher, D. *J. Am. Chem. Soc.* **60** (1938) 2744.
14. Dippy, J. F. S. *J. Chem. Soc.* **1938** 1222.
15. Desnoyers, J. E. and Jolicoeur, C. In Bockris, J. O'M. and Conway, B. E., Eds., *Modern Aspects of Electrochemistry*, Butterworths, London 1968, No. 5.
16. Hamann, S. D. and Lim, S. C. *Aust. J. Chem.* **7** (1954) 329.
17. Disteche, L. and Disteche, P. *J. Electrochem. Soc.* **112** (1965) 350.
18. Wirth, H. *J. Am. Chem. Soc.* **70** (1948) 462.
19. Redlich, O. and Nielsen, L. E. *J. Am. Chem. Soc.* **54** (1942) 761.

Received March 12, 1973.

ACTA CHEMICA SCANDINAVICA 27 (1973) 2694–2700

An Electron Diffraction Investigation of the Molecular Structure of *anti-trans,trans*-2,2′-Dibromobicylopropyl in the Vapour Phase

R. STØLEVIK[a] and G. SCHRUMPF[b]

[a] *Department of Chemistry, University of Oslo, Blindern, Oslo 3, Norway and* [b] *Organisch-Chemisches Institut der Universität Göttingen, B. R. Deutschland*

The experimental intensities obtained for the title compound are best reproduced by assuming an equilibrium between an *s-trans* conformer (33 % at 80°C) and a *gauche* conformer with a multiplicity of two.

The following values were found for bond lenghts: r(C–Br) = = 1.926(.005) Å, r(C–C, ring) = 1.527(.004) Å, r(C–C, central) = = 1.490(.013) Å, and r(C–H) = 1.143(.009). Values in parentheses are estimated standard deviations, and bond lenghts are r_a-values.

Bond angles, torsional angles, and mean amplitudes of vibration are found in Table 1.

In a previous paper [1] we reported the structure of *anti-cis,cis*-2,2′-dibromobicyclopropyl investigated by electron diffraction. The subject of the present communication is the study of the geometry and the rotational equilibrium of the isomer *anti-trans,trans*-2,2′-dibromobicyclopropyl.

Table 1. Structural parameters of *anti-trans,trans*-2,2′-dibromobicyclopropyl. The values in parentheses are estimated standard deviations. The bond lengths (r) are r_a-values, and u is the root mean square amplitude of vibration.

	r (Å)	u (Å)
C–Br	1.926 (.005)	0.031 (.008)
C_1-C_2	1.527 (.004)	0.038 (.004)
C_1-C_1'	1.490 (.013)	0.043 (.005)
C–H	1.143 (.009)	0.048 (.010)
$Br_1\cdots C_1$	2.975 (.004)	0.068 (.006)
$Br_1\cdots C_1'$	4.262 (.005)	0.102 (.010)
$C_2\cdots C_1'$	2.611 (.007)	0.078 (.009)

Table 1. Continued.

θ	55.1 (1.0)°	($C_1'C_1C_2$ = 119.7°)
α	56.5 (0.5)°	($C_1C_2Br_1$ = 118.6°)
s-trans conformer:		
ϕ_t	160.0 (6.0)°	
$Br_1 \cdots Br_2$	7.158 (.005)	0.118 (.020)
Mol fraction	0.33 (0.03)	
gauche conformer:		
ϕ_g	58.8 (5.0)°	
$Br_1 \cdots Br_2$	6.462 (.011)	0.261 (.040)

EXPERIMENTAL AND CALCULATION PROCEDURE

The compound was synthesized and purified as described before.[2] The purity as determined by VLP chromatography was about 96 %. The main impurity probably is the isomer *anti-cis,trans*-2,2'-dibromobicyclopropyl, which has a gas chromatographic retention time very similar to the *anti-trans,trans* isomer. Diffraction photographs were obtained in the usual way with the Oslo apparatus.[3] The nozzle temperature was ap-

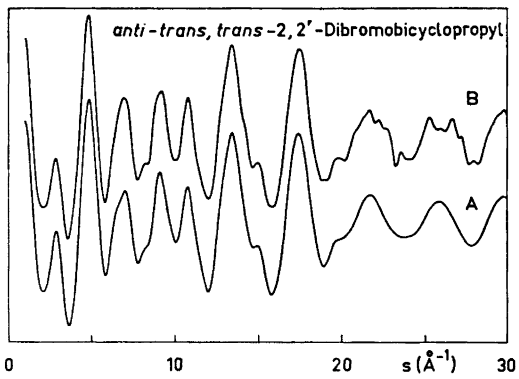

Fig. 1. Reduced molecular intensity curves of *anti-trans,trans*-2,2'-dibromobicyclopropyl. A: Theoretical curve calculated from the parameters in Table 1. B: Experimental curve.

proximately 80°C. Plates from three nozzle-to-plate distances of about 130, 48, and 19 cm were obtained. Four plates from each camera distance were photometered, and the intensity data treated in the usual way.[4] The 130 cm data cover the range 0.625 to 7.25 $Å^{-1}$ with $\Delta s = 0.125$ $Å^{-1}$, the 48 cm data extend from $s = 1.25$ to 18.0 $Å^{-1}$, and the 19 cm data from $s = 8.75$ to 45.5 $Å^{-1}$, both in intervals of $\Delta s = 0.25$ $Å^{-1}$. The modification function was normalized to the C – Br distances.[4] The curves from three different nozzle to plate distances were combined to give the experimental reduced molecular intensity curve (Fig. 1B). The intensity points in the s range between 0 and 0.625 $Å^{-1}$ were calculated. A Fourier transformation of this curve using a damping constant of $k = 0.0020$ yields the experimental radial distribution curve (RD curve) shown in Fig. 2B. The numbering of the atoms is given in Fig. 3.

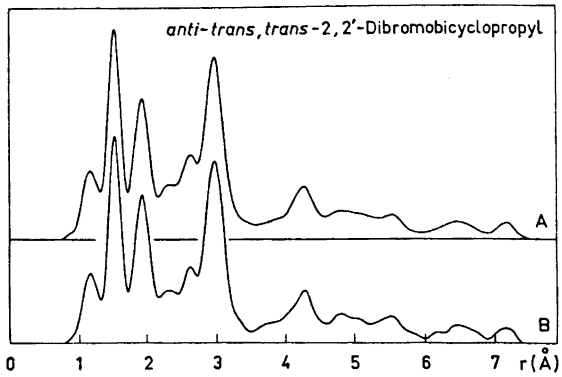

Fig. 2. Radial distribution curves of *anti-trans,trans*-2,2′-dibromobicyclopropyl. A: Theoretical curve. B: Experimental curve. The damping constant for both curves is 0.0015 Å².

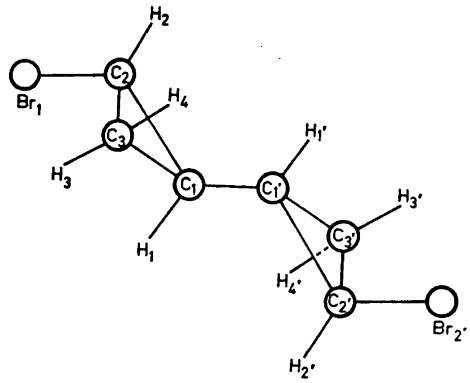

Fig. 3. Numbering of atoms in *anti-trans,trans*-2,2′-dibromobicyclopropyl.

The part from 0 to 3.0 Å is very similar to that of the *cis,cis* isomer,[1] showing the bond distances CH, CC, and CBr at 1.1, 1.5, and 1.9 Å, respectively. In addition, there are the peaks corresponding to distances across one angle, *i.e.* C···H at 2.2 Å, C···C at 2.6 Å, and C···Br at 3.0 Å. The *trans* position of bromine with respect to the neighbouring cyclopropane ring is verified by the shift of the C···Br distance over two angles from 3.3 Å in the *cis,cis* isomer to 4.2 in the *trans,trans* compound. The maxima at 6.5 and 7.2 Å originate from two different Br···Br distances indicating the presence of two rotational isomers, a *s-trans* and a *gauche* conformer. The maximum at 4.2 Å overlaps the various conformation dependent C···C distances. The broad peaks between 4.5 and 5.8 Å correspond to the different C···Br distances. There is extensive overlapping in the RD curve between 3.0 and 5.8 Å making a determination of the geometry from the RD curve difficult. The structure was calculated by the least squares procedure [4] using the molecular intensity. The data are weighted by a function being unity between 5.5 and 25.0 Å^{-1} and falling off exponentially beyond these limits ($w_1 = w_2 = 0.05$).[4] Reasonable changes in these limits do not influence the geometry significantly, but have an effect on the u values.

BASIC ASSUMPTIONS OF THE STRUCTURAL MODEL

The structure was determined by refining the bond distances and bond angles using a model with the following basic assumptions.

(1) As in the *anti-cis,cis* isomer, the cyclopropane ring was assumed to be an equilateral triangle.

(2) The substituents attached to the three-membered ring are oriented in a plane perpendicular to the ring and containing the bisector of the inner angles of the ring.

(3) The positions of the hydrogen atoms are those determined for the cyclopropane molecule.[5]

(4) The molecule exists in an *s-trans* conformation, which is in equilibrium with two *gauche* forms of equal structure, the torsional angle of which was to be determined. The concentration ratio of the two rotational isomers was also to be determined.

Some of these assumptions had to be dropped at a later stage of the least squares analysis in order to improve the fit between the experimental and the theoretical curve.

STRUCTURAL ANALYSIS

Because of the large number of independent parameters to be adjusted, the analysis of the electron diffraction data of this molecule is more complex than that of the *cis,cis* isomer described in the previous communication. Besides the torsional angle of the second rotational isomer and the concentration ratio of the conformers, there are two sets of torsion dependent distances and principally different u values. The u values of most distances depending on torsion had to be guessed and kept constant during the least squares adjustments. Some of them, in particular those involving only carbon atoms, could be taken from our previous investigation of the *cis,cis* isomer. Mean amplitudes of those distances involving bromine atoms have been estimated with the aid of a very approximate formula.[6] The intensity due to the H···H distances was calculated and subsequently treated as a constant contribution to the total intensity.

Initially, the length of the central CC bond was kept constant and put equal to the length of the bonds within the cyclopropane ring. The angle of the *s-trans* conformation was held constant at 180°. With these restrictions, the bond distances and bond angles refined to reasonable values. The torsional angle of the *gauche* conformer could be refined simultaneously. The RD curve of the model thus obtained deviated from the experimental one in several regions. One important conclusion was drawn from one of these deviations. The theoretical Br···C distance over two angles was found to be too long, when calculated with those bond distances and angles fitting the distances $C_2 \cdots C_1$, and $Br_1 \cdots C_1$ over one angle and equal CC bond lengths. This could not be improved by twisting the two BrCH groups out of the bisector planes. However, there was improved agreement when the length of the central CC bond between the two cyclopropane rings was shortened. A second observation on the RD curve was that the *trans* Br···Br distance computed from the initial

model was always too long compared to the experimental distance by about 0.03 Å. Introducing the torsional angle ϕ_t of the *s-trans* conformation as an additional independent parameter, ϕ_t refines to values less than the exact *s-trans* angle of 180° by 15° to 24° depending on the least squares scheme used. Probably, this result is due to the shrinkage effect originating for the most part from large amplitudes of torsional oscillation of the *s-trans* conformer.

In this investigation, we simulated the shrinkage effect by considering a non-*s-strans* equilibrium structure with an angle of rotation of ϕ_t. Basically, there is a difference between these two models.

An equilibrium angle less than 180° destroys the C_i symmetry of the molecule and splits up distances which are degenerate in the *s-trans* conformation (*cf.* the conformational structure of the *cis,cis* isomer [1]). However, a symmetrical torsion about the *s-trans* form with large amplitudes resembles the rigid *s-trans* form on the time average, but introduces a large asymmetric component to the total u value of conformation dependent distances. We did not differentiate between these two alternatives in the least squares treatment, because the number of parameters becomes too large compared to the usability of the data. We favour the model with a *s-trans* conformation and large amplitudes of torsion.

The u values of the distances between the heavy atoms, which do not depend on the angle of torsion, could be refined independently. However, this was not possible for all of the u values of the torsion dependent C···C and C···Br distances of both conformers. There is a strong coupling between the torsional angle of the *gauche* conformation, the relative concentration ratio of the conformers, and the u values of the heavy atom distances depending on the torsional angle. In later stages of the refinement these u values had to be varied in groups, *i.e.*, several of them are given the same shift in the least squares iterations. However, only the u values of the Br···C distances refined to reasonable numbers. The u values of the Br···H and C···H non bonded distances are difficult to refine. This was possible for the C···H distances over one angle only. All other u values were guessed or taken from the results of the hydrocarbon bicyclopropyl, which was recently reinvestigated by electron diffraction.[7] In that work, the u values of the non bonded distances had been calculated from spectroscopic data. We assumed that substitution of hydrogen in *trans* position to the central CC bond in bicyclopropyl by two bromine atoms does not change the overall geometry or the internal rotation very much. Therefore, we used the same u values for the C···C and C···H non bonded distances as in bicyclopropyl.

The mean amplitudes of vibration of the Br···H distances were approximated by setting them equal to the u value of the corresponding C···H distance involving the carbon atom bonded to the bromine atom under consideration.

The least squares refinement yielded an R-factor of 11.6 % The final theoretical molecular intensity curve is shown in Fig. 1A, its Fourier transform in Fig. 2A. The structural parameters are listed in Table 1 together with estimates of their standard deviations. An uncertainty in the wavelength (0.14 %) has been included in the standard deviations for distances. Corrections for the effect of correlation [11] in the experimental intensities are included, too.

DISCUSSION

The main interest in structural studies within the series of bicyclopropyls originates from the question of how the bonds between two cyclopropane carbon atoms, being largely unaffected by conjugative interaction, determine the properties of these molecules. We concentrated upon two aspects of this problem.

1. *Bond lengths.* One consequence of the constituent sp^2 orbitals which form the central CC bond in bicyclopropyls is a shortening of that bond compared to the CC bond of aliphatic hydrocarbons. This is confirmed by our results yielding 1.49 Å compared to 1.53 Å in aliphatic hydrocarbons.[8] It also holds for the CBr bond which is slightly shortened compared to that in alkyl bromides.[8] The CC and CBr bond lengths of both isomers are the same within the error bounds. The central bond length for both compounds observed in these investigations also compares favourably with the value of 1.487 Å obtained by an X-ray study of solid bicyclopropyl [9] and 1.499 Å for gaseous bicyclopropyl investigated by electron diffraction.[7]

The angles α and θ are a few degrees larger than those of the *cis,cis* isomer *i.e.*, the bond angles $C_2C_1C_1$ and $C_1C_2Br_1$ are correspondingly smaller. This opening of the bond angle in the *cis,cis* isomer probably reflects the steric repulsion between the substituents on the ring in *cis* position. The CH bond length appears to be somewhat too long. The u values are generally smaller than one would expect from general experience and also smaller than those of the *cis,cis* compound.

2. *Rotational isomerism.* The second aspect of the sp^2-sp^2 nature of the central bond in bicyclopropyl is its effect on the internal rotation mode. There are two main questions to be answered by the structural investigations regarding (1) the torsional angle ϕ_g of the *gauche* conformer and (2) the relative amount of both rotational isomers.

In a previous ED study of bicyclopropyl [10] the equilibrium angle of the *gauche* conformation was found to be 35° to 40°. New ED measurements [7] changed this value to $\phi_g = 48.7°$. The equilibrium angle of the *gauche* form obtained in the present study is 58.8°. Considering the large standard deviations in this angle of 7° and 5°, respectively, the results of the two measurements are not significantly different. It must be stated, however, that we feel our value to be more reliable than that of the hydrocarbon, if it were not for a real difference between the two molecules brought about by the bromine substitution. In the *trans,trans* derivative, the two rotational isomers exhibit two distinct maxima in the RD curve which are not obscured by overlapping peaks stemming from other distances in the molecule. Their position can be precisely located. Their u values determined from the least squares treatment of the intensity data do not depend significantly on assumptions as to u values of other distances or the hydrogen geometry. On the other hand, the region of the RD curve of bicyclopropyl which is significant for determining the *gauche* angle is a broad and quite unstructured area of heavily overlapping peaks.

The concentration of the *s-trans* conformer was obtained by integrating the areas below the two Br···Br peaks. By this method, we obtained 33 % *s-trans* form at 80°C.

If the entropy difference between the two conformers ($\Delta S = S_g - S_t$) is equal to R ln 2 (originating from the multiplicity of the *gauche* form) then the energy difference is approximately zero. However, we do not know the difference in entropy that might exist between the conformers due to differences in vibrational frequencies. Thus in order to get information about the energy difference between the conformers, a vibrational analysis of the molecule is desirable.

Acknowledgements. The authors thank Professor O. Bastiansen for the idea of studying this molecule. We also thank Cand. Real. A. Almenningen for having taken the diffraction photographs. We acknowledge Professor W. Lüttke for his continuing support in connection with this work.

Financial support from *Deutsche Forschungsgemeinschaft* and *Norges almenvitenskapelige forskningsråd* is gratefully acknowledged. The calculations were done at the *Gesellschaft für wissenschaftliche Datenverarbeitung*, Göttingen.

REFERENCES

1. Schrumpf, G. and Stølevik, R. *Acta Chem. Scand.* **27** (1973) 1950.
2. Schrumpf, G. and Lüttke, W. *Liebigs Ann. Chem.* **730** (1969) 100.
3. Almenningen, A., Bastiansen, O., Haaland, A. and Seip, H. M. *Angew. Chem.* **77** (1965) 877.
4. Andersen, B., Seip, H. M., Strand, T. G. and Stølevik, R. *Acta Chem. Scand.* **23** (1969) 3224.
5. Bastiansen, O., Fritsch, F. N. and Hedberg, K. *Acta Cryst.* **17** (1964) 538.
6. Stølevik, R. *Unpublished results.*
7. Hagen, K., Hagen, G. and Trætteberg, M. *Acta Chem. Scand.* **26** (1972) 3649.
8. Sutton, W. *Tables of Interatomic Distances and Configuration in Molecules and Ions*, The Chemical Society, London 1958, Supplement 1965.
9. Eraker, F. and Rømming, C. *Acta Chem. Scand.* **21** (1967) 2721.
10. Bastiansen, O. and de Meijere, A. *Acta Chem. Scand.* **20** (1966) 516.
11. Seip, H. M. and Stølevik, R. In Cyvin, S. J., Ed., *Molecular Structure and Vibrations*, Elsevier, Amsterdam 1972.

Received April 2, 1973.

ACTA CHEMICA SCANDINAVICA 27 (1973) 2701–2709

Reaction of Sugar Esters with Hydrogen Fluoride

XI. Preparation of 1,6-Anhydro-β-D-altropyranose from Methyl Tetra-*O*-benzoyl-α-D-glucopyranoside

KLAUS BOCK and CHRISTIAN PEDERSEN

Department of Organic Chemistry, Technical University of Denmark, DK-2800 Lyngby, Denmark

Treatment of the pentaacetates of D-glucopyranose, D-mannopyranose, and D-altropyranose with anhydrous hydrogen fluoride gave complicated mixtures of products. Among these were found derivatives of 1,6-anhydro-β-D-altropyranose and 1,6-anhydro-β-D-mannopyranose. When the tetraacetates of methyl α-D-glucopyranoside, methyl α-D-mannopyranoside, and methyl α-D-altropyranoside were reacted with hydrogen fluoride larger amounts of 1,6-anhydrides were formed. The mechanisms of these reactions are discussed. Treatment of methyl tetra-*O*-benzoyl-α-D-glucopyranoside with hydrogen fluoride gave a 45 % yield of 1,6-anhydro-β-D-altropyranose and 8 % of 1,6-anhydro-β-D-mannopyranose, the latter isolated as its triacetate.

In a previous paper it was shown that treatment of penta-*O*-acetyl-β-D-glucopyranose with anhydrous hydrogen fluoride gave derivatives of D-mannose and D-altrose.[1] The products were isolated as methyl α-D-mannopyranoside and 1,6-anhydro-β-D-altropyranose after treatment of the crude product with methanolic sodium methoxide. The same products were obtained when penta-*O*-acetyl-D-mannopyranose was treated with hydrogen fluoride.[2] These reactions and the reaction of other derivatives of glucose, mannose, and altrose with hydrogen fluoride have now been investigated more closely using NMR technique.

When penta-*O*-acetyl-β-D-glucopyranose (*1a*) was dissolved in anhydrous hydrogen fluoride at 0°C the α-fluoride (α-*2a*) was formed immediately as seen from an NMR spectrum of the solution. The spectrum showed signals at 2.30 and 2.40 ppm corresponding to 12 acetoxy-protons and a signal at 2.57, corresponding to one equivalent of acetic acid. The remaining part of the spectrum was very similar to that of (α-*2a*) in deuteriochloroform.[3] In agreement herewith (α-*2a*) may be isolated at this stage.[1] When the hydrogen fluoride solution was kept at room temperature further changes took place and after 24 h

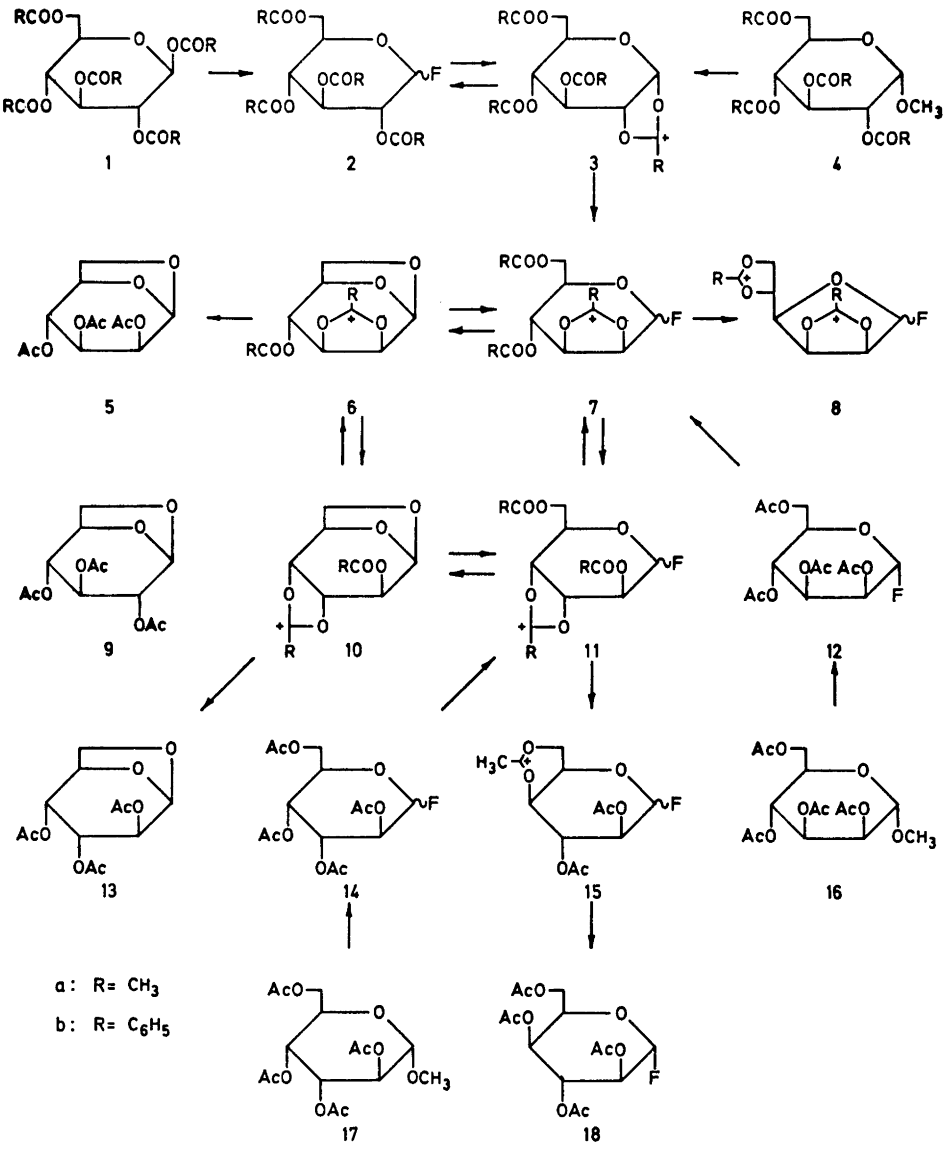

the reaction was completed. An NMR spectrum obtained at this stage was complex and showed that several compounds were present. Thus the signals of the acetoxonium ion (*10a*), derived from 1,6-anhydro-β-D-altropyranose, were seen (see below). Small amounts of the diacetoxonium ion (*8a*) were also present as seen from signals at 6.15, 6.34, 2.90, and 2.81 ppm. The NMR spectrum of the latter ion in hydrogen fluoride was known from previous

work.[4] Work up of this hydrogen fluoride solution and acetylation gave a crude product, which was a complicated mixture of compounds. Chromatography and NMR spectroscopy showed that the mixture contained the tetraacetates of α- and β-D-glucopyranosyl fluoride (α- and *β-2*), α-D-mannopyranosyl fluoride (*12*), α- and β-D-altropyranosyl fluoride (α- and *β-14*), and α-D-idopyranosyl fluoride (*18*). Besides, the triacetates of 1,6-anhydro-β-D-altro-

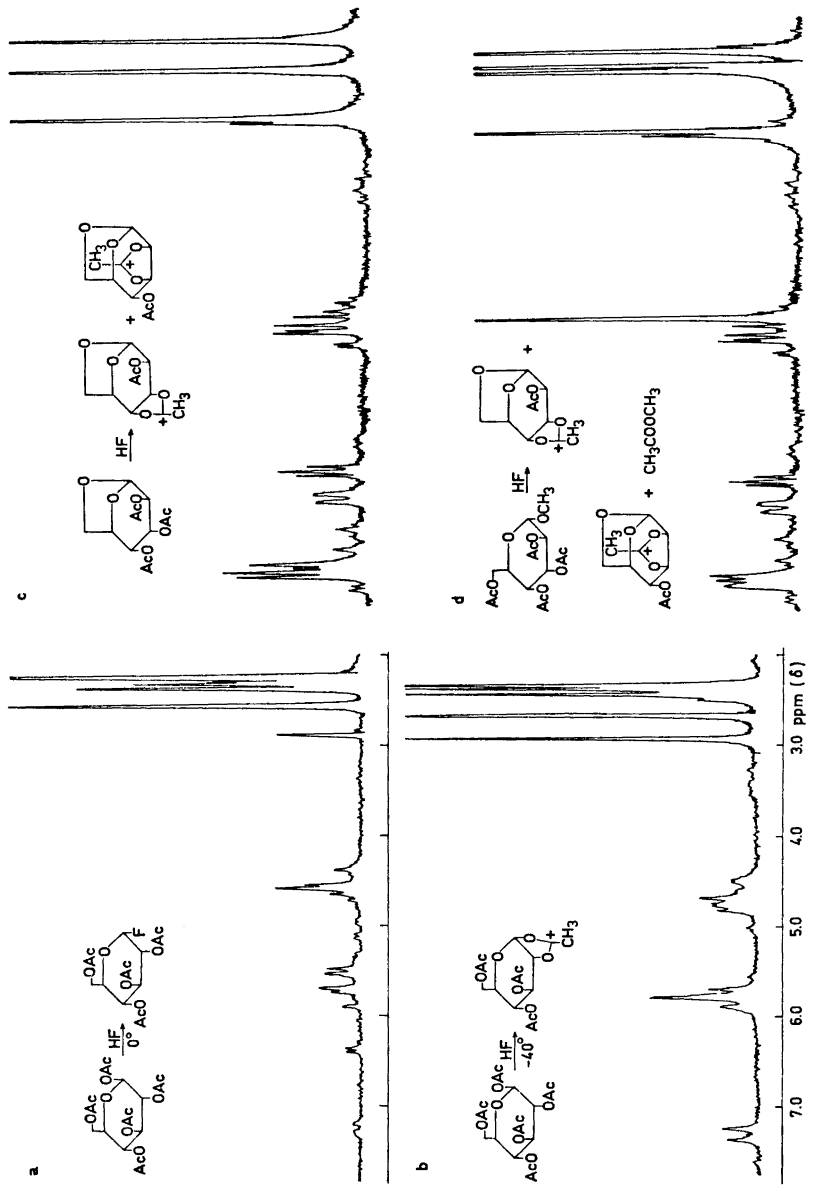

Fig. 1. a. 60 MHz. *b.* 60 MHz. *c.* 100 MHz, 0°C. *d.* 100 MHz, 0°C.

pyranose (*13*) and 1,6-anhydro-β-D-mannopyranose (*5*) were isolated from the mixture. These results thus show that 1,6-anhydrides are formed directly in the hydrogen fluoride solution and not, as assumed previously,[2] in a secondary reaction by treatment of the crude fluoride with sodium methoxide.

The pentaacetate (*1a*) gave the fluoride (α-*2a*) when dissolved in hydrogen fluoride at 0°C (Fig. 1a). When this hydrogen fluoride solution was prepared at −40°C the NMR spectrum changed completely, and it showed that at this temperature the acetoxonium ion (*3a*) (Fig. 1b) was formed. When the temperature was raised to 0°C the fluoride (α-*2a*) was reformed. In other cases dioxolanylium ions are observed when acylated carbohydrates are dissolved in hydrogen fluoride at 0°C. Thus penta-*O*-benzoyl-β-D-glucopyranose (*1b*) gives the benzoxonium ion (*3b*) as the only detectable product in hydrogen fluoride and the fluoride (*2b*) is not formed until the solution is hydrolyzed (see below). In general, it may be assumed that when an acylated carbohydrate is dissolved in hydrogen fluoride the acyloxy-group at C-1 is cleaved off at once, and an equilibrium is established between the fluoride and the 1,2-dioxolanylium ion, *e.g.* between (*2*) and (*3*). With acetylated pyranoses the equilibrium is generally shifted towards the fluoride at 0°C. This was found when the tetraacetates of arabinopyranose or ribopyranose were treated with hydrogen fluoride. With benzoylated pyranoses, and with both acetylated and benzoylated furanoses, the equilibrium is shifted towards the 1,2-dioxolanylium ion, and the fluorides can usually not be observed in the NMR spectra of the hydrogen fluoride solutions.[4–6]

The acetoxonium ion (*3a*) can, by further reaction with hydrogen fluoride, rearrange to the mannose-ion (*7a*) with loss of acetic acid and introduction of fluorine at C-1. The latter ion is in equilibrium with the altrose-ion (*11a*) and both these ions are in equilibrium with the corresponding 1,6-anhydrides (*6a*) and (*10a*), respectively. The spectrum shown in Fig. 1c is essentially an equilibrium mixture of the latter two ions with the altrose-ion (*10a*) predominating. As mentioned above, a small amount of the furanose derivative (*8a*) is also present. This is probably formed from the mannose-ion (*7a*) by ring contraction and loss of acetic acid in analogy to the pyranose-furanose rearrangements observed in other cases.[5,7]

When penta-*O*-acetyl-α-D-mannopyranose was dissolved in hydrogen fluoride the α-fluoride (*12*) was formed at once. The NMR spectrum showed signals of 4-acetoxy groups at 2.25, 2.33, 2.40, and 2.45 ppm and a signal at 2.59 ppm corresponding to one equivalent of acetic acid. The remaining part of the spectrum was identical with that of tetra-*O*-acetyl-α-D-mannopyranosyl fluoride (*12*) in deuteriochloroform.[3] After 24 h at room temperature the spectrum was identical with that obtained from glucose pentaacetate, in agreement with previous results.[2] The fluoride (*12*) contains a pair of *cis*-oriented acetoxy groups and it probably forms the acetoxonium ion (*7a*) by the mechanism by which *cis*-1,2-diacetoxycyclohexane reacts with hydrogen fluoride.[8]

Penta-*O*-acetyl-α-D-altropyranose gave the fluorides (*14*) at once when dissolved in hydrogen fluoride at 0°C, as seen from an NMR spectrum. Treatment of the pentaacetate with hydrogen fluoride at −70°C gave a mixture of the anomeric fluorides (*14*);[3] the pure fluoride (α-*14*) was obtained by chro-

matography. When penta-*O*-acetyl-α-D-altropyranose was kept in hydrogen fluoride for 24 h at room temperature an NMR spectrum showed that the ion (*10a*) was formed together with (*6a*) and other products. The furanose derivative (*8a*) could not be detected in the spectrum. Work up of the solution at this stage and acetylation of the crude product gave a complicated mixture of glycosyl fluorides. Besides, the acetates of 1,6-anhydro-β-D-altropyranose (*13*) and 1,6-anhydro-β-D-mannose (*5*) were isolated.

The initially formed tetra-*O*-acetyl-D-altropyranosyl fluorides (*14*) have the acetoxy-groups at C-3 and C-4 *cis*-oriented and they can therefore form the acetoxonium ions (*10a*) or (*11a*) by further reaction with hydrogen fluoride. Whether the 1,6-anhydride formation takes place prior to the acetoxonium ion formation or not could not be decided.

In analogy with the rearrangement of arabinose tetraacetate to ribose-derivatives [5] it might be expected that the altrosyl fluorides (*14*) should rearrange to D-allose derivatives by reaction with hydrogen fluoride. This was not observed; but it has been found that penta-*O*-benzoyl-D-altropyranose yields allose derivatives by treatment with hydrogen fluoride. These results will be described in a forthcoming paper.

Since 1,6-anhydrides were formed in hydrogen fluoride it was decided to study the reaction of tri-*O*-acetyl-1,6-anhydro-β-D-glucopyranose (*9*) and of the corresponding altrose derivative (*13*) with hydrogen fluoride.

The triacetate (*9*) reacted immediately with hydrogen fluoride to give a complicated mixture of products. In the course of *ca.* 48 h at room temperature the reaction was finished and rather large amounts of the acetoxonium ion (*10a*), derived from 1,6-anhydro-β-D-altropyranose, was formed together with the corresponding mannose derivative (*6a*). Appreciable amounts of the diacetoxonium ion (*8a*) and small amounts of other compounds were also present. Apparently (*9*) gives the same products as those obtained from glucose- and mannose-pentaacetate, but in a different ratio, larger amounts of the 1,6-anhydro-derivatives (*6a*) and (*10a*) being formed.

If an equilibrium exists between the fluorides (*7a*) and (*11a*) and the 1,6-anhydrides (*6a*) and (*10a*), respectively, then this equilibrium should be affected by the amount of acetic acid present in the hydrogen fluoride solution. It is therefore reasonable that the triacetate (*9*) should give more of the anhydro-ions (*6a*) and (*10a*) than glucose- or mannose-pentaacetate since the latter two compounds will liberate more acetic in hydrogen fluoride solution.

Tri-*O*-acetyl-1,6-anhydro-β-D-altropyranose (*13*), when kept in hydrogen fluoride solution at room temperature, was almost completely transformed into a mixture of the ions (*6a*) and (*10a*) in the course of 24 h. No other products could be seen in the NMR spectrum (Fig. 1c). Work up and acetylation gave the acetylated anhydrides (*5*) and (*13*) and small amounts of the fluorides (*12*) and (α- and β-*14*).

It was found previously that methanol and acetic acid react rapidly in hydrogen fluoride to give methyl acetate.[8] It might therefore be expected that tetraacetylated methyl glycosides should give the same products as those obtained from the triacetylated anhydrides since the methanol, which is initially liberated, should capture one equivalent of acetic acid.

This was actually found to be the case. When methyl tetra-*O*-acetyl-α-D-glucopyranoside (*4a*) was kept in hydrogen fluoride for *ca.* 48 h one equivalent of methyl acetate was formed as seen from the signals at 4.2 and 2.5 ppm. The remaining part of the spectrum was identical with that obtained from tri-*O*-acetyl-1,6-anhydro-β-D-glucopyranose and showed that the ions (*6a*) and (*10a*) were the main products together with (*8a*). The same result was obtained when methyl tetra-*O*-acetyl-α-D-mannopyranoside (*16*) was treated with hydrogen fluoride. Methyl tetra-*O*-acetyl-α-D-altropyranoside (*17*) gave the acetoxonium ions (*6a*) and (*10a*) and one equivalent of methyl acetate as the only products, that could be detected in the hydrogen fluoride solution (Fig. 1d).

Paulsen *et al.*[9,10] found that treatment of acetylated hexoses with antimony pentachloride gave acetoxonium ions, which rearranged in a manner similar to the one described above. However, whereas Paulsen [9] found that considerable amounts of a D-idose derivative was formed when tetra-*O*-acetyl-β-D-glucopyranosyl chloride was treated with antimony pentachloride the reaction with hydrogen fluoride gives only traces of idose derivatives. An idose derivative (*15*) would be formed by further rearrangement of the altrosyl fluoride (*11a*), but since it has now been found that this fluoride is largely converted to the 1,6-anhydride (*10a*) in hydrogen fluoride it is understandable that idose derivatives are only formed to a small extent. With antimony pentachloride 1,6-anhydrides are not formed.

The reactions described above with acetylated sugars are of little preparative value since low yields are obtained. This is probably due to the fact that partially acetylated products, which are formed by hydrolysis of the acetoxonium ions, are somewhat soluble in water, and therefore may be lost when the reaction mixtures are washed during the isolation. The reaction of some benzoylated compounds with hydrogen fluoride was therefore investigated.

The NMR spectrum, which was obtained from a solution of penta-*O*-benzoyl-β-D-glucopyranose (*1b*) in hydrogen fluoride, was not well resolved and the signal of the anomeric proton was hidden by the benzoyl group signals. It was, however, obvious that a fluoride was not present in the initial stage of the reaction. The spectrum probably represents the 1,2-benzoxonium ion (*3b*). When this solution was poured on ice tetra-*O*-benzoyl-β-D-glucopyranosyl fluoride (*β-2b*) was formed as the main product. Treatment of a dioxolanylium ion with water would be expected to give a hydroxy-compound. It has, however, been observed in several cases, that when hydrogen fluoride solutions of 1,2-benzoxonium ions, or 1,2-acetoxonium ions, are hydrolyzed then glycosyl fluorides are formed as the main products, usually with *trans*-opening of the dioxolanylium ring.[5,6]

Prolonged reaction of (*1b*) wih hydrogen fluoride gave a complicated mixture of products which was not investigated further. When methyl tetra-*O*-benzoyl-α-D-glucopyranoside (*4b*) was kept in hydrogen fluoride for *ca.* 72 h the ion (*10b*) was formed as the main product, as seen from NMR spectra. Besides, smaller amounts of (*6b*) and other products were present. The dibenzoxonium ion (*8b*) was not formed at all, in contrast to the result obtained with the corresponding acetate. Presumably, the ring-contraction of (*7*) to (*8*) is rather slow in the benzoate series.[5] When the hydrogen fluoride solution

was hydrolyzed and worked up a product was obtained which contained large amounts (50 – 60 %) of dibenzoylated 1,6-anhydro-β-D-altropyranose, smaller amounts of dibenzoylated 1,6-anhydro-β-D-mannopyranose, and a number of partially benzoylated glycosyl fluorides. These products were formed by hydrolysis of the benzoxonium ions, which were present in the hydrogen fluoride solution. Treatment of the crude reaction product with aqueous sodium hydroxide removed the benzoyl groups and destroyed the glycosyl fluorides and, after deionization, 1,6-anhydro-β-D-altropyranose could be isolated in 45 % yield. Besides, 8 % of 1,6-anhydro-β-D-mannopyranose was obtained, isolated as the triacetate (*5*). Thus the reaction of methyl tetra-*O*-benzoyl-α-D-glucopyranoside with hydrogen fluoride provides a convenient method for the preparation of 1,6-anhydro-β-D-altropyranose.

EXPERIMENTAL

Melting points are uncorrected. NMR spectra were obtained on Varian A-60 and HA-100 instruments. NMR spectra in anhydrous hydrogen fluoride were measured in Teflon sample tubes. Positions of signals in hydrogen fluoride are given in ppm relative to $(CH_3)_3SiCH_2CH_2CH_2SO_3Na$. ^{19}F spectra were measured at 94.1 MHz. Positions of signals (ΦF) are given in ppm relative to internal methyl trifluoroacetate. Thin layer chromatography (TLC) was performed on silica gel PF_{254} (Merck); for preparative work 1 mm layers were used on 20 × 40 cm plates. Zones were visualized under UV light or by charring with a hot wire.

Penta-O-acetyl-β-D-glucopyranose (1.06 g) was dissolved in anhydrous hydrogen fluoride (3 ml) and the solution was kept for 24 h at room temperature. It was then diluted with chloroform and poured on ice. The organic phase was washed with aqueous sodium hydrogencarbonate and dried with magnesium sulfate. The solvent was evaporated and the residue was acetylated by treatment with acetic anhydride (3 ml) in pyridine (10 ml) at room temperature over night. Work up in the usual way gave 594 mg of crude product. This was separated into four fractions by preparative TLC using ether-pentane (3:1) as eluent.

The fastest moving fraction (274 mg, 29 %) was a mixture of tetra-*O*-acetyl-α- and β-D-glucopyranosyl fluoride (α- and *β-2a*), tetra-*O*-acetyl-α- and β-D-altropyranosyl fluoride (α- and *β-14*), and tetra-*O*-acetyl-α-D-mannopyranosyl fluoride (*12*) in a ratio of 30:12:58. The next fraction (85 mg, 9 %) was a mixture of (*12*) and tetra-*O*-acetyl-α-D-idopyranosyl fluoride (*18*) in a 1:1 ratio. The fluorides were identified by comparing the proton and ^{19}F NMR spectra with those of authentic samples of the pure fluorides. Spectra of all these fluorides have been published [3] except that of tetra-*O*-acetyl-α-D-idopyranosyl fluoride, which is described below.

The third fraction gave 103 mg (13 %) of tri-*O*-acetyl-1,6-anhydro-β-D-altropyranose (*13*), m.p. 98 – 100°C, $[\alpha]_D^{20}$ −163° (*c* 1.8, $CHCl_3$) (reported [11] m.p. 100 – 101°C, $[\alpha]_D$ −172°). An NMR spectrum was identical with that of an authentic sample.[12] The last fraction gave 30 mg (4 %) of tri-*O*-acetyl-1,6-anhydro-β-D-mannopyranose (*5*), which was not quite pure, m.p. 75 – 80°C (reported [13] m.p. 90 – 91°). An NMR spectrum was identical with that of an authentic sample.[12]

Penta-O-acetyl-α-D-idopyranose [9] (550 mg) was kept in anhydrous hydrogen fluoride (1 ml) for 15 min at 0°C. Work up as described above gave 454 mg of crude product which was separated into two fractions by preparative TLC (ether-pentane 3:1). The fast moving fraction gave 210 mg (43 %) of tetra-*O*-acetyl-α-D-idopyranosyl fluoride (*18*) which was not quite pure. The product was further purified by preparative TLC, first with benzene-ether (1:1) as eluent and then with ether-pentane (3:1). This gave 80 mg of pure (*18*) as a syrup, $[\alpha]_D^{24}$ +15.8° (*c* 1.5, $CHCl_3$). (Found: C 48.24; H 5.44. Calc. for $C_{14}H_{19}FO_9$: C 48.00; H 5.47).

An NMR spectrum in deuteriochloroform gave the following δ-values: H-1 5.88; H-2 5.9 – 6.0; H-3 5.06; H-4 5.9 – 6.0; H-5 4.59; H-6 4.1 – 4.2. A ^{19}F-spectrum using

methyl trifluoroacetate as internal reference gave the fluorine signal at −58.2 ppm in good agreement with the value predicted by Hall *et al.*,[3] $J_{1F} = 48.0$ Hz, $J_{2F} = 4.9$ Hz.

Penta-O-*acetyl*-α-D-altropyranose (562 mg) was kept in hydrogen fluoride (1.5 ml) for 1 h at −70°C. Work up as described above gave 570 mg of a product which was purified by preparative TLC using ether-pentane (2:1) as eluent. This gave 456 mg (80 %) of a mixture of tetra-*O*-acetyl-α- and β-D-altropyranosyl fluoride (α- and *β-14*) in a 10:1 ratio as seen from an NMR spectrum.[3] Repeated chromatography gave pure (*α-14*) as a syrup, $[\alpha]_D^{20}$ +35.9° (*c* 4.3, $CHCl_3$). (Found: C 47.97; H 5.42. Calc. for $C_{14}H_{19}FO_9$: C 48.00; H 5.47). NMR data in deuteriochloroform: H-1 5.50 δ; H-2 5.05; H-3 5.35; H-4 5.20; H-5 4.48; H-6 4.1−4.4. J_{1F} 49.0; J_{12} 1.0; J_{13} 0.7; J_{2F} 2.7; H_{23} 3.0; J_{34} 3.2; J_{45} 10.0. Fluorine chemical shifts are in agreement with those described.[3]

Penta-O-*acetyl*-α-D-*altropyranose* (1.02 g) was kept in hydrogen fluoride (2 ml) for 24 h at room temperature. The solution was then worked up and the product was acetylated as described above. The product thus obtained (530 mg) was separated into 3 fractions by preparative TLC with ether-pentane (3:1) as eluent. The fastest moving fraction gave 280 mg of a mixture of the tetraacetates of α-D-altropyranosyl fluoride (*α-14*), β-D-altropyranosyl fluoride (*β-14*), α-D-mannopyranosyl fluoride (*12*), and α-D-idopyranosyl fluoride (*18*) in a ratio of 2:1:4:1 as seen from proton and ^{19}F spectra. The next fraction gave 160 mg (22 %) of tri-*O*-acetyl-1,6-anhydro-β-D-altropyranose (*13*), m.p. 97−99°C, $[\alpha]_D^{20}$ −164° (*c* 1.6, $CHCl_3$). An NMR spectrum was identical with that of an authentic sample. The last fraction gave 35 mg (5 %) of tri-*O*-acetyl-1,6-anhydro-β-D-mannopyranose (*5*), m.p. 76−79°C. The product was characterized through its NMR spectrum.[12]

Tri-O-*acetyl*-*1,6-anhydro*-β-D-*altropyranose* (*13*) (538 mg) was dissolved in hydrogen fluoride (1.5 ml) and the solution was kept at room temperature for 24 h. Work up and acetylation as described above gave 370 mg of a product which was separated into 3 fractions by preparative TLC with ether-pentane (3:1). The fast moving fraction gave 76 mg (10 %) of a mixture of the fluorides (*12*) and (α- and *β-14*) in a ratio of 4:2:1 as seen from NMR spectra. The next fraction gave 188 mg (36 %) of (*13*), m.p. 98−100°C, $[\alpha]_D^{24}$ −165° (*c* 0.9, $CHCl_3$). The last fraction gave 46 mg (8 %) of (*5*), m.p. 83−86°C. The latter two products were further identified through their NMR spectra.

Methyl tetra-O-*acetyl*-α-D-*altropyranoside* (*17*) (1.03 g) was kept in hydrogen fluoride (2.5 ml) for 24 h at room temperature. Work up and acetylation gave a product (700 mg) which was separated into 3 fractions by preparative TLC with ether-pentane (3:1). The fast moving fraction gave 62 mg (6 %) of a mixture of (α- and *β-14*) and (*12*) in a ratio of 2:1:4, identified through proton and ^{19}F spectra. The next fraction gave 420 mg (50 %) of (*13*), m.p. 98−100°C, $[\alpha]_D^{24}$ −163° (*c* 2.3, $CHCl_3$). The last fraction gave 55 mg (7 %) of (*5*), m.p. 85−86°C, $[\alpha]_D^{24}$ −121° (*c* 0.9, $CHCl_3$).

Penta-O-*benzoyl*-β-D-*glucopyranose* (*1b*) (2.0 g) was dissolved in anhydrous hydrogen fluoride (4 ml) and the solution was kept at −10°C for 30 min. It was then diluted with dichloromethane and poured on ice. The dichloromethane solution was washed with aqueous sodium hydrogen carbonate and water, dried and evaporated. The residue (1.70 g) was crystallized from ether-pentane to give 950 mg (55 %) of tetra-*O*-benzoyl-β-D-glucopyranosyl fluoride (*β-2b*), m.p. 147−149°C. An additional recrystallization from ethanol gave the pure product, m.p. 147−149°C, $[\alpha]_D^{21}$ +54° (*c* 1.2, $CHCl_3$), in agreement with the reported values.[14] An NMR spectrum of the material in the mother liquors indicated that it was a mixture of (*β-2b*) and the corresponding α-fluoride.

Methyl tetra-O-*benzoyl*-α-D-*glucopyranoside* (*4b*) (50 g) was dissolved in anhydrous hydrogen fluoride (100 ml) with cooling in dry ice-acetone and the solution was kept at room temperature for 72 h. It was then cooled in dry ice-acetone, diluted with dichloromethane, and poured on ice. The organic phase was washed with aqueous sodium hydrogen carbonate, dried and evaporated. The residue (38.0 g) was boiled with water (200 ml) and sodium hydroxide (20 g) for 3 h. The solution was then acidified with hydrochloric acid and the benzoic acid was extracted with ether. The aqueous phase was deionized by passage through columns of Amberlite IR-120 and IR-4B. The solution was then evaporated and the residue was dissolved in ethanol and filtered through activated carbon. Evaporation gave 9.0 g of a syrup which was crystallized from ethanol (20 ml) to give 6.0 g (45 %) of 1,6-anhydro-β-D-altropyranose, m.p. 130−135°C, $[\alpha]_D^{22}$ −200° (*c* 2.3, H_2O). An additional recrystallization from ethanol gave 5.4 g, m.p. 133−134°C, $[\alpha]_D^{22}$ −208° (*c* 2.3, H_2O). (Reported [15] m.p. 134−135°C, $[\alpha]_D$ −211°).

The material in the mother liquors was separated into two fractions by chromatography on a column of silica gel (150 g) using butanone-2 saturated with water as eluent. The fast moving fraction (1.96 g) was acetylated with acetic anhydride in pyridine, and the product (2.56 g) was crystallized from ether-pentane to give 1.9 g (8 %) of tri-*O*-acetyl-1,6-anhydro-β-D-mannopyranose (*5*), m.p. 82 – 84°C. An additional recrystallization gave a product with m.p. 84 – 86°C, $[\alpha]_D^{22}$ −119° (*c* 2, $CHCl_3$). (Reported [13] m.p. 90 – 91°C, $[\alpha]_D$ −123°).

The second fraction (502 mg) was crystallized from ethanol to give 300 mg of 1,6-anhydro-β-D-altropyranose, m.p. 120 – 130°C.

Microanalyses were performed by Dr. A. Bernhardt.

REFERENCES

1. Pedersen, C. *Acta Chem. Scand.* **16** (1962) 1831.
2. Pedersen, C. *Acta Chem. Scand.* **17** (1963) 673.
3. Hall, L. D., Manville, J. F. and Bhacca, N. S. *Can. J. Chem.* **47** (1969) 1.
4. Bock, K. and Pedersen, C. *Acta Chem. Scand.* **26** (1972) 2360.
5. Pedersen, C. *Acta Chem. Scand.* **22** (1968) 1888.
6. Gregersen, N. and Pedersen, C. *Acta Chem. Scand.* **22** (1968) 1307.
7. Jacobsen, S., Jensen, S. R. and Pedersen, C. *Acta Chem. Scand.* **26** (1972) 1561.
8. Lundt, I. and Pedersen, C. *Acta Chem. Scand.* **26** (1972) 1938.
9. Paulsen, H., Trautwein, W.-P., Espinosa, F. G. and Heyns, K. *Chem. Ber.* **100** (1967) 2822.
10. Paulsen, H. *Advan. Carbohyd. Chem.* **26** (1971) 127.
11. Richtmyer, N. K. and Hudson, C. S. *J. Am. Chem. Soc.* **63** (1941) 1727.
12. Hall, L. D. and Hough, L. *Proc. Chem. Soc.* **1962** 382. Hall, L. D., Manville, J. F. and Tracey, A. *Carbohyd. Res.* **4** (1967) 514.
13. Knauef, A. E., Hann, R. M. and Hudson, C. S. *J. Am. Chem. Soc.* **63** (1941) 1447.
14. Lundt, I. and Pedersen, C. *Mikrochim. Acta* **1966** 126.
15. Johansson, J. and Richtmyer, N. K. *Carbohyd. Res.* **10** (1969) 322.

Received March 23, 1973.

ACTA CHEMICA SCANDINAVICA 27 (1973) 2710–2716

The Biosynthesis of Nidulin and Trisdechloronornidulin

JULIAN SIERANKIEWICZ and STEN GATENBECK

Department of Pure and Applied Biochemistry, Royal Institute of Technology, S-100 44 Stockholm 70, Sweden

In contrast to earlier suggested theories experimental evidence has been obtained for the formation of nidulin and trisdechloronornidulin from acetate-malonate and one carbon units. The incorporations of L-isoleucine-4,5-^{3}H, L-methionine-$^{13}CH_3$, and L-methionine-$^{14}CH_3$ have been studied. Degradation of radioactive trisdechloronornidulin to 4,6-dinitroevernic acid and analysis of ^{13}C-NMR spectra conclusively localize the positions of the one carbon units in the structure.

The experiments supporting the earlier suggested theories are discussed and a hypothetical formation sequence of trisdechloronornidulin is presented.

A new fungal depsidone has recently been isolated by us from *Aspergillus nidulans*.[1] The structure of this depsidone was shown to correspond to that of trisdechloronornidulin (Fig. 1). The same compound has been isolated from *Aspergillus unguis* by two other groups of investigators [2,3] independent of each other. They call the depsidone yasimin and unguinol, respectively. *A. unguis* is an organism closely related to *A. nidulans*, both being members of the *Aspergillus nidulans* group.[4]

The structure of nidulin (Fig. 1) has been known since 1960,[5] and in 1963 Beach and Richards [6] made the first experiments in establishing its biosynthesis. The results of feeding experiments with acetate-1-^{14}C and uniformly labeled L-isoleucine-^{14}C made them suggest that ring A of nidulin, *i.e.* orsellinic acid, is derived from acetate and malonate and, more interesting, that ring B and its side chains are derived from a five-carbon fragment of isoleucine, tentatively tiglyl-coenzyme A, three acetate (or malonate) units, and an additional one carbon unit combined as shown in Fig. 2.

In contrast to the suggestion of Beach and Richards, in a recent publication Kamal *et al.*[7] propose that the eleven carbon atoms of B ring and its side-chains originate from two isoprene units and an additional one carbon unit. They find support for their proposal from feeding experiments with DL-mevalonic-2-^{14}C acid and L-methionine-CH_3-^{3}H. It is not evident how these three units are joined together to form the B ring system.

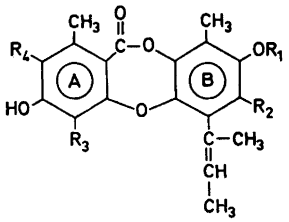

Fig. 1. $R_1 = CH_3$; $R_2 = R_3 = R_4 = Cl$, nidulin. $R_1 = R_2 = R_3 = R_4 = H$, trisdechloronornidulin.

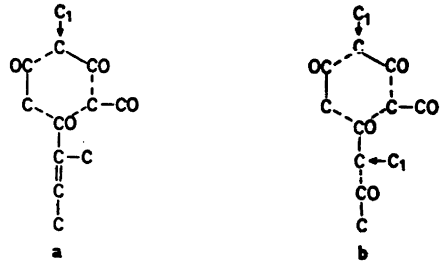

Fig. 2. Formation of the B ring system according to (a) Beach and Richards,[6] (b) "the acetate pathway".

The chemical structure represented by ring B and its side chains is rare among natural products. The skeletal feature of the 2-butenyl side chain is present in, *e.g.*, citrinin. In this case the side chain is derived from acetate-malonate and a one carbon unit.[8,9] The presented experimental results have not convinced us about the reliability of either of the suggested pathways of the biosynthesis of the B ring system so we have therefore tested the possibility of the formation of the system according to an "acetate pathway", *i.e.* from acetate-malonate and one carbon units as shown in Fig. 2. In our experiments we have studied the incorporation of L-isoleucine-4,5-^{3}H, L-methionine-$^{14}CH_3$, and L-methionine-$^{13}CH_3$ into trisdechloronornidulin and nidulin.

EXPERIMENTAL

Culture conditions. Aspergillus nidulans CMI 85, 473 (NRRL 2006) was grown at 28°C for 23 – 30 days as surface cultures in 1 l Fernbach's flasks each containing 350 ml of substrate medium ($NaNO_3$ 2.0 g, KH_2PO_4 1.0 g, $MgSO_4.7H_2O$ 0.5 g, $FeSO_4.7H_2O$ 0.01 g, yeast extract 1.0 g, glucose 40 g, and distilled water to 1 l).

Trisdechloronornidulin (I) from 4,5-^{3}H-L-isoleucine. After 22 days of growth 150 μCi (0.02 μmol) of 4,5-^{3}H-L-isoleucine were equally distributed between two flasks. The mycelia were filtered off and dried at 70°C over P_2O_5 after 16 h exposure to the radioactive precursor. Extraction with diethyl ether in a Soxhlet apparatus and repeated recrystallizations from hexane/diethyl ether of the solid residue obtained on evaporation of the diethyl ether solution yielded 200 mg (8.15×10^5 dpm/mmol) of labeled trisdechloronornidulin. The yield of incorporation of added radioactivity was 0.2 %.

O-*Methyl-trisdechloronidulin-^{3}H* (II). Tritium labeled I (200 mg) was methylated with an excess of diazomethane in methanol at room temperature for 3 h. The methanol was driven off *in vacuo* and the residue redissolved in ether. After washing with 2 M NaOH and water, the product crystallized on addition of hexane. Yield 150 mg, m.p. 136 – 139°C, specific radioactivity 7.5×10^5 dpm/mmol. Before degradation, II was diluted with 100 mg of cold *O*-methyl-trisdechloronidulin to a specific radioactivity of 4.2×10^5 dpm/mmol.

Methyl O-*methyl-trisdechloronidulinate-^{3}H* (III). 200 mg of II was dissolved in 20 ml of absolute methanol containing 20 mg of Na and heated for 15 min at 60 – 65°C under nitrogen. After cooling to 0°C the pH of the solution was adjusted to 2.5 with 1 M HCl. The precipitate was filtered off, washed with water and dried *in vacuo*. Yield 203 mg, m.p. 136 – 137°C, *m/e* 386. (Found: C 68.1; H 7.01. $C_{22}H_{26}O_6$ requires: C 68.4; H 6.79).

ν_{max} (KBr) 3400, 1708, 1605, and 1585 cm^{-1}; NMR (acetone-d_6) at δ 6.50, 6.40, 6.15 (aromatic protons), 5.76 (vinyl proton), 3.95, 3.86, 3.67 (*O*-methyls), 2.37, 2.07 (aromatic methyls), 1.93, 1.67 (vinyl methyls). UV: λ_{max} 280 nm (ε 4180), $\lambda_{infl.}$ 245 nm (ε 16700) Specific radioactivity 4.4×10^5 dpm/mmol.

Degradation of III to methyl 4,6-dinitroeverinate-^3H (IV). 100 mg of III were dissolved in 1 ml of glacial acetic acid at 60 – 65° and 125 µl of HNO_3 (*d*, 1.40) was added. After 2 min the reaction mixture was diluted with 50 ml of water followed by extraction with ether. The ether solution was washed several times with water and IV was then extracted with several small portions of aqueous $NaHCO_3$. The aqueous solution was extracted with ether after acidification with conc. HCl. The ether phase was washed with water, dried over anhydrous Na_2SO_4 and then evaporated to dryness. The residue was recrystallized from hexane/chloroform and finally from diethylether. Yield 30 mg, m.p. 155°C, *m/e* 286. (Found: C 41.86; H 3.42; N 9.94. $C_{10}H_{10}N_2O_8$ requires: C 41.94; H 3.52; N 9.79). ν_{max} (KBr) 1670, 1605, 1570, 1535, 1368, 1330, 1240 cm^{-1}; NMR (acetone-d_6) at δ 4.03 (ester methyl), 3.97 (ether methyl), 2.45 (aromatic methyl), no aromatic protons. UV: λ_{max} 306 nm (ε 2800), $\lambda_{infl.}$ 238 nm (28 000). Specific radioactivity 1.5×10^5 dpm/mmol.

O-Methyl-trisdechloronidulin from L-metionine-$^{14}CH_3$. Trace amounts of methionine-$^{14}CH_3$ (25 µCi) were added to two 25 days old cultures. After another 5 days the cultures were harvested and the dried mycelia were extracted with ether. The crude extract was recrystallized once from petroleum ether and then methylated with methyl iodide in acetone as described earlier.[1] The yield of crude labeled *O*-methyl-trisdechloronidulin was 115 mg. 34 mg of this labeled compound was recrystallized from methanol-water to constant specific radioactivity with 100 mg cold carrier substance. Yield 107 mg, specific radioactivity 2.5×10^6 dpm/mmol. Incorporation of ^{14}C-labeling 5.8 %. Degradation of *O*-methyl-trisdechloronidulin-^{14}C was performed as described above. The obtained methyl 4,6-dinitroeverinate contained practically no radioactivity.

Trisdechloronornidulin from L-methionine-$^{13}CH_3$. L-Methionine-$^{13}CH_3$ was prepared from $^{13}CH_3I$ (purchased from Wilmad Glass Company, N.J., USA) and L-homocystine as described by Jackman *et al.*[10] To each of two 25 days old cultures 10 mg/day of L-methionine-$^{13}CH_3$ was added for 5 days. The trisdechloronornidulin was isolated as described above. Yield 160 mg.

Nidulin from L-methionine-$^{14}CH_3$. Nidulin-^{14}C was prepared as described for *O*-methyl-trisdechloronidulin from L-methionine-$^{14}CH_3$ using two cultures with the substrate supplemented with KCl. The radioactive nidulin (specific radioactivity 4.5×10^6 dpm/mmol) was demethylated according to Zeisel.[11] The formed methyl iodide was trapped in trimethylamine and isolated as tetramethylammonium iodide (specific radioactivity 1.4×10^6 dpm/mmol.

Radioactive measurements. All radioactive determinations were performed in a Packard Scintillation Spectrometer (model 3375) using appr. 1 mg of substance dissolved in 0.1 ml of methanol and 20 ml of toluene containing standard amounts of PPO and POPOP.

RESULTS AND DISCUSSION

In one of their feeding experiments Beach and Richards used uniformly ^{14}C-labeled L-isoleucine.[6] They found that 13 % of the radioactivity incorporated into nidulin were localized to the orsellinic acid part of the molecule, which means that 87 % of the radioactivity was concentrated to the B ring system. Without further experimental evidence Beach and Richards suggest that most of this radioactivity is situated in the 2-butenyl side chain. If "the acetate pathway" is true one would expect an almost equal labeling of the orsellinic acid part and the B ring system from uniformly labeled isoleucine. This is on the assumption that the metabolic degradation of isoleucine follows the known route to acetyl-coenzyme A and propionyl-coenzyme A. On the other hand, if uniformly labeled isoleucine besides labeled acetyl CoA could deliver labeled one carbon units the experimental results of Beach and Richards could still support the formation of the B ring according to "the acetate

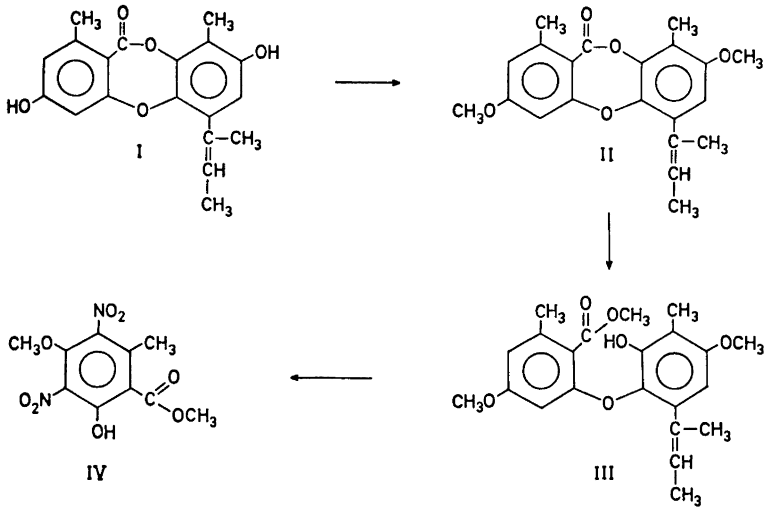

Fig. 3. Degradation scheme of trisdechloronornidulin.

pathway" as the one carbon units are entirely localized to the B ring system. In order to avoid possible formation of labeled one carbon units an incorporation experiment was performed with L-isoleucine-4,5-^{3}H, which should only give rise to acetyl-coenzyme A as a labeled catabolic product. Isolation of radioactive trisdechloronornidulin (specific radioactivity 4.4×10^5 dpm/mmol) and its subsequent degradation to 4,6-dinitroeverinate (specific radioactivity 1.5×10^5 dpm/mmol) indicated that the labeling from L-isoleucine was not specifically incorporated into the B ring system. The distribution of the radioactivity between the orsellinic acid part and the B ring system was in accordance with a degradation of isoleucine to labeled acetyl-coenzyme A and a formation of the ring B system as proposed in "the acetate pathway". The degradation reactions of isoleucine in the organism have apparently, as judged from the experiment of Beach and Richards, involved one carbon units that have effectively been transferred to methyl groups.

As seen from Fig. 2, two methyl groups are introduced into the B ring system during the biosynthesis of the depsidone according to "the acetate pathway". One of the methyl groups is attached to the aromatic nucleus and the other one is found in the 2-butenyl side chain on the carbon atom nearest the aromatic ring.

In their biosynthetic experiments Kamal *et al.*[7] have used L-methionine-CH_3-^{3}H as labeled precursor. They found that the orsellinic acid part did not contain any labeling from the one carbon metabolism and they claimed that only one of the three methyl groups of the B ring system is derived from methionine and they suggest the methyl group on the aromatic ring to be the labeled one. This is not in accordance with "the acetate pathway". On the other hand, we found that when methionine-$^{13}CH_3$ (60 % excess) is fed to *A. nidulans* the isolated trisdechloronornidulin contains an excess (3 %) of ^{13}C.

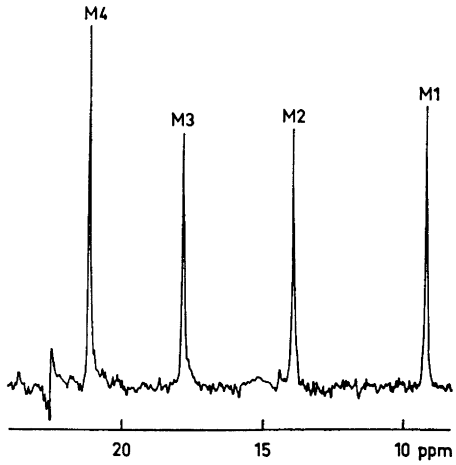

Fig. 4. ^{13}C-NMR spectra of trisdechloronornidulin (natural abundance). Varian X L-100 ^{13}C (25.2 MHz); sample 200 mg/3.0 ml CD_3OD; s.w. 1000 Hz; p.w. 60 μsec (30°); repetition 2 sec × 6800; lock = CD_3OD internal.

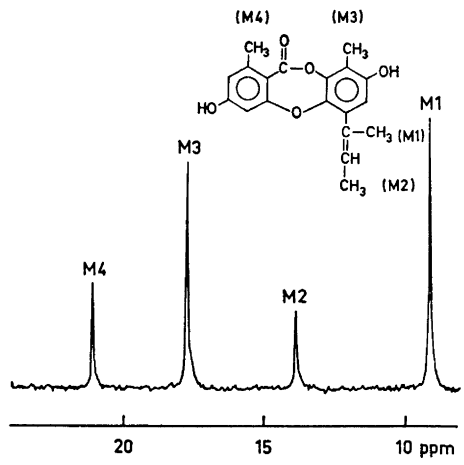

Fig. 5. ^{13}C-NMR Spectra of trisdechloronornidulin (^{13}C-enriched from methionine-$^{13}CH_3$). Varian X L-100 ^{13}C (25.2 MHz); sample 100 mg/3.0 ml CD_3OD; s.w. 1000 Hz, p.w. 60 μsec (30°); repetition 2 sec × 8300; lock = CD_3OD internal.

The localization in the structure of this excess of ^{13}C is seen from the ^{13}C-NMR spectrum in Fig. 4 which also shows the ^{13}C-NMR spectrum of the non-enriched compound. In these spectra the signals of the four methyl groups are found at δ 9.2 ppm, 14.0 ppm, 18.0 ppm, and 21.4 ppm from TMS. The two high-field signals are easily assigned to the methyl groups M1* (9.2 ppm) and M2 (14.0 ppm), respectively. The other two signals arise from the two aromatic methyl groups (M3, M4) and the assignments of their individual chemical shifts are not quite evident to us. Apparently two of the four methyl groups contain ^{13}C in excess of the natural abundance and are consequently derived from methionine. One of the ^{13}C-enriched methyl groups is attached to an aromatic nucleus. The other one is the methyl group designated Ml in Fig. 5 which is in full accordance with "the acetate pathway".

In order to be able to definitively establish which one of the aromatic methyl groups that is derived from a one carbon unit the incorporation of methionine-$^{14}CH_3$ was studied. After degradation of the radioactive trisdechloronornidulin to 4,6-dinitroeverinate the latter was shown to contain no radioactivity. From this follows that the methyl group M4 is not derived from the one carbon metabolism.

The described results all support the hypothesis that trisdechloronornidulin is synthesized from two polyketide units, (a) the orsellinic acid derived from one acetate unit and three malonate units, (b) the B ring system formed from one acetate unit and four malonate units and in addition two one carbon units.

* For designation of the methyl groups (M1, M2, M3, M4), see Fig. 4.

Even if there should be no doubt that nidulin is biosynthesized in a similar way, we have studied the incorporation of methionine-$^{14}CH_3$ into nidulin. The radioactive nidulin (specific radioactivity 4.5×10^6 dpm/mmol) was demethylated in a Zeisel reaction and the formed methyl iodide trapped as tetramethylammonium iodide (specific radioactivity 1.4×10^6 dpm/mmol).

From the specific activities can be calculated that the radioactive nidulin contained 3.2 labeled methyl groups, which indicates that "the acetate pathway" is valid also for the nidulin biosynthesis.

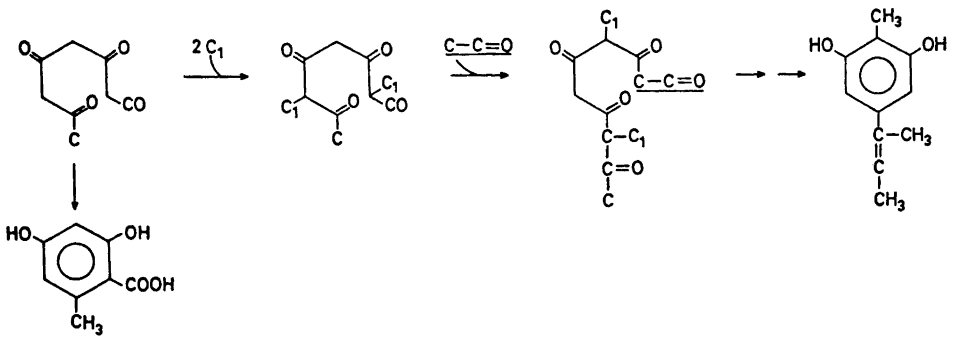

Fig. 6. Hypothetical formation sequence of the B ring system.

From the obtained results it is possible to speculate that in the formation of orsellinic acid and the B ring system a common intermediate is involved. This intermediate (a C-8 polyketomethylene chain) is in some cases methylated at positions that hinder the formation of a benzene derivative of orsellinic acid type or phloroglucinol type. If we assume that the products can only be released from the enzyme protein after aromatization, the methylated C-8 polyketomethylene chain has to be extended with one malonate unit to be able to form a benzoid compound. As seen from Fig. 6 this compound is easily transformed to the B ring system of trisdechloronornidulin.

Acknowledgements. This investigation was supported by a grant from the *Swedish Natural Science Research Council.* The authors are also grateful to Dr. T. Drakenberg, Chemical Centre, Lund, for running the ^{13}C-NMR spectra.

REFERENCES

1. Sierankiewicz, J. and Gatenbeck, S. *Acta Chem. Scand.* **26** (1972) 455.
2. Kamal, A., Haider, Y., Khan, Y. A., Qureshi, I. H. and Qureshi, A. A. *Pakistan J. Sci. Ind. Res.* **13** (1970) 244.
3. Stodola, F. H., Vesonder, R. F., Fenell, D. I. and Weisleder, D. *Phytochemistry* **11** (1972) 2107.
4. Thom, C. and Raper, K. B. *A Manual of the Aspergilli*, The Williams and Wilkens Company, 1945, p. 155.
5. Dean, F. M., Deorha, D. S., Erni, A. D. T., Hughes, D. W. and Roberts, J. C. *J. Chem. Soc.* **1960** 4829.
6. Beach, W. F. and Richards, J. H. *J. Org. Chem.* **28** (1963) 2746.

7. Kamal, A., Haider, Y., Akhtar, R. and Qureshi, A. A. *Pakistan J. Sci. Ind. Res.* **14** (1971) 79.
8. Birch, A. J., Fitton, P., Pride, E., Ryan, A. J., Smith, H. and Whalleg, W. B. *J. Chem. Soc.* **1958** 4576.
9. Schwenk, E., Alexander, G. J., Gold, A. M. and Stevens, D. F. *J. Biol. Chem.* **233** (1958) 1211.
10. Jackman, L. M., O'Brien, I. G., Cox, G. B. and Gibson, F. *Biochim. Biophys. Acta* **141** (1967) 1.
11. Kuster, W. and Maag, W. *Helv. Chim. Acta* **125** (1930) 190.

Received April, 26 1973.

ACTA CHEMICA SCANDINAVICA 27 (1973) 2717–2721

Copper-promoted Arylation of Pentafluorobenzene

HELENA LJUSBERG and ROBERT WAHREN

Department of Organic Chemistry, Royal Institute of Technology, S-100 44 Stockholm 70, Sweden

Pentafluorobiphenyls are formed in 40–70 % yields from pentafluorobenzene and iodobenzene, 2-nitro-, 4-nitro-, 2,6-dimethoxy- or 4-methoxy-iodobenzene, and copper(I) oxide in refluxing pyridine. At 80° 2-iodonitrobenzene gives pentafluoroiodobenzene in addition to the biaryl.

Copper-promoted arylations of electron-rich aromatic systems like 2-arylthiophenes and 2-arylfurans, leading to 2,5-diarylthiophenes and -furans, have been reported.[1,2] Benzthiazole gives 2-arylbenzthiazoles with iodobenzenes and copper(I) oxide.[3] Aromatic compounds with strongly electron-attracting substituents are likewise susceptible to copper-promoted reactions. 1,3,5-Trinitrobenzene and 1,3-dinitrobenzene form nitrobiaryls with iodoarenes and copper(I) oxide in quinoline.[4–8] The copper-promoted arylation of electron-deficient aromatic systems has now been extended to pentafluorobenzene.

Pentafluorobiphenyls are obtained in 40–70 % yields from pentafluorobenzene, an iodobenzene and copper(I) oxide or silver oxide in refluxing pyridine (reaction 1).

(1)

The experimental results of the coupling reactions are summarised in Table 1. Substituents in the iodobenzene significantly affect reaction rates. The reactivity of various substituted iodobenzenes towards pentafluorobenzene and copper(I) oxide in pyridine decreases in the following approximate order: 2-nitro > 4-nitro > none ≃ 2,6-dimethoxy > 4-methoxy. Similar orders have been observed for the reactions between iodobenzenes and phenylcopper,[9] 2-thienylcopper,[10] and phenylethynylcopper.[11] However, the corresponding order for iodoarenes towards 1,3-dinitrobenzene in the presence of copper(I) oxide in quinoline is: 2,6-dimethoxy > 4-methoxy > none > 4-nitro. In the latter case 2-iodonitrobenzene gave nitrobenzene and no biphenyl at all.[5]

Table 1. Yields of biphenyls from equimolar amounts of pentafluorobenzene, copper(I) oxide, and halogenoarenes in refluxing pyridine.

Halogenoarene	Product	Yield %	Reaction time h
2-Iodonitrobenzene	2,3,4,5,6-Pentafluoro-2′-nitrobiphenyl	69	4
2-Bromonitrobenzene	2,3,4,5,6-Pentafluoro-2′-nitrobiphenyl	10	24
4-Iodonitrobenzene	2,3,4,5,6-Pentafluoro-4′-nitrobiphenyl	37	50
Iodobenzene	2,3,4,5,6-Pentafluorobiphenyl	57	67
2,6-Dimethoxybenzene	2,3,4,5,6-Pentafluoro-2′,6′-dimethoxybiphenyl	52	72
4-Methoxyiodobenzene	2,3,4,5,6-Pentafluoro-4′-methoxybiphenyl	41	168

A nitro substituent in the iodobenzene, especially in the *ortho* position, increases the rate in reaction 1. Similar *ortho* effects are well known from the Ullmann reaction[12] and from copper-catalysed halogen exchange in haloarenes.[13]

Pentafluoroiodobenzene (32 %) is formed slowly, together with the unsymmetrical coupling product (24 %), when 2-iodonitrobenzene, pentafluorobenzene, and copper(I) oxide are reacted at 80°. To see whether pentafluoroiodobenzene was an intermediate in the unsymmetrical coupling between pentafluorobenzene and 2-iodonitrobenzene in refluxing pyridine, we followed the reaction by gas chromatography – mass spectrometry. Small samples were withdrawn at intervals, hydrolysed and analysed. As no pentafluoroiodobenzene was detected, it seems that this compound is formed in a reaction proceeding simultaneously with the coupling reaction at 80°. When pentafluorobenzene was treated with iodine in refluxing pyridine, pentafluoroiodobenzene was formed even in the absence of copper(I) oxide, but in a lower yield (25 %).

Dehalogenation of the iodoarene is a side reaction (1,3-dimethoxybenzene 3 %, nitrobenzene 2 % from 2-iodonitrobenzene, 13 % from 4-iodonitrobenzene). The reactions with 2-iodo- and 2-bromonitrobenzene also give 2-nitrophenol (15 and 35 %, respectively). When the reaction time is prolonged in these cases, fluorine substitution occurs. Thus, a small amount of 4-(2-nitrophenoxy)-2,3,5,6-tetrafluoro-2′-nitrobiphenyl (*1*) is formed, probably *via* copper assisted attack of a 2-nitrophenolate anion on pentafluoro-2-nitrobiphenyl. The position of fluorine substitution was determined by fluorine magnetic resonance. The copper-assisted nucleophilic displacement of fluorine has been studied recently.[14]

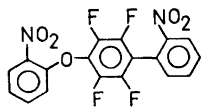

1

Silver oxide was found to be about as efficient as copper(I) oxide in promoting the reaction between pentafluorobenzene and 4-methoxyiodobenzene. Without copper- or silver oxide, no coupling reactions were observed. Nor did we find coupling products from reactions between pentachlorobenzene and 2-iodonitrobenzene or 4-methoxyiodobenzene in the presence of copper(I) oxide in pyridine or quinoline. Pentafluorobenzene reacts with 2-iodonitrobenzene more than twenty times faster in pyridine than in quinoline at 116°.

Pentafluorophenylcopper is a plausible intermediate in the coupling reactions. Both pentafluorophenylcopper and -silver react with iodoarenes [15–17] in dimethylformamide and tetrahydrofuran. If the formation of pentafluorophenylcopper were rate-determining, the couplings with different iodoarenes should all proceed at the same rate. The different reaction rates for the various halogenoarenes thus suggest that the iodoarene is also involved in the rate-determining step. The order of reactivity observed for iodobenzenes with pentafluorobenzene and copper(I) oxide in pyridine agrees with those found for iodobenzenes and organocopper compounds.[9–11]

An alternative reaction path might be the formation of an arylcopper-compound and copper(I) iodide from the iodoarene and copper(I) oxide. The arylcopper so formed would then react with pentafluorobenzene. However, we have not detected any reaction between 2,6-dimetoxyphenylcopper and pentafluorobenzene, even in refluxing pyridine. 2,6-Dimetoxyphenylcopper forms a σ-complex, with 1,3,5-trinitrobenzene which can be oxidised to the corresponding biaryl.[7]

Preliminary experiments show that thiophene may react similarly to pentafluorobenzene. Thiophene, copper(I) oxide, and 2-iodonitrobenzene give in refluxing pyridine 2(2-nitrophenyl)thiophene and 2-iodothiophene (about 10 % of each; GLC-MS evidence).

EXPERIMENTAL

Melting points were determined on a micro hot stage. NMR-spectra were recorded on a Varian A 60 A spectrometer and mass spectra on an LKB 9000 instrument. Pentafluorobenzene (Fluka) was used without purification. Pyridine (A.R.) was dried over sodium hydroxide and distilled from phosphorus pentoxide. 2,6-Dimethoxyphenylcopper was prepared according to Ref. 7. Previously known compounds were identified by spectral methods.

General procedure for the coupling reactions. Pentafluorobenzene (0.01 mol), halogenoarene (0.01 mol), copper(I) oxide (0.01 mol), and pyridine (about 50 ml) were mixed in a reaction vessel and refluxed (116°) under a nitrogen atmosphere. Ether (about 600 ml) was added to the cooled reaction mixture and the copper iodide pyridine complex was filtered off together with unreacted copper(I) oxide. The filtrate was extracted with 2 M hydrochloric acid to remove remaining pyridine, washed with water and dried ($MgSO_4$). The solution was then concentrated in vacuum and the components were separated by column chromatography or by vacuum distillation.

Coupling with 2-iodonitrobenzene. The reaction was terminated after 4 h, by which time no iodonitrobenzene remained. The products were separated by vacuum distillation. Nitrobenzene (0.02 g, 2 %) and 2-nitrophenol (0.21 g, 15 %) distilled together and were separated by extraction with 2 M sodium hydroxide. The yield of 2,3,4,5,6-pentafluoro-2′-nitrobiphenyl, pale yellow crystals, b. p. 100° 0.5 mmHg, m.p. 81 – 83° (lit. [18] 84 – 84.5°), was 2.00 g, 69 %. (Found: C 49.7; H 1.5; F 33.0; N 5.0. Calc. for $C_{12}H_4F_5NO_2$: C 49.9; H 1.4; F 32.9; N 4.8). IR, NMR, and mass spectra were in accordance with the suggested structure.

In another experiment the temperature was kept at 80° for 120 h. The reaction mixture was worked up in the usual way. Pentafluoroiodobenzene (0.94 g, 32 %) was distilled at about 50 mmHg. The distillation was continued in vacuum and gave a mixture of 2-iodonitrobenzene (0.90 g, 36 %) and pentafluoro-2-nitrobiphenyl (0.70 g, 24 %). The amount of each substance was determined by GLC.

When the reaction time in refluxing pyridine was prolonged to 14 h, the yield of pentafluoro-2-nitrobiphenyl decreased to 23 %. On vacuum distillation a higher boiling fraction was collected, from which 4-(2-nitrophenoxy)-2,3,5,6-tetrafluoro-2′-nitrobiphenyl (*I*) 0.11 g, 5 % (based on 2-iodonitrobenzene) was isolated by fractional sublimation, m.p. 198–199°. (Found: C 53.1; H 2.0; F 18.8; N 6.7. Calc. for $C_{18}H_8F_4N_2O_5$: C 53.0; H 2.0; F 18.6; N 6.7). Mass spectrum (20 eV): *m/e* 408 (48 %; molecular ion), 286 (95 %) and 122 (100 %). IR: 1530, 1350, 1230, 990 cm^{-1}. The fluorine magnetic resonance spectrum (94 MHz) showed an AA′BB′ pattern. One half of the spectrum showed an additional coupling (1.0 Hz) to a proton in the adjacent ring. The spectrum was recorded by Dr Torbjörn Drakenberg, Lund.

Coupling with 2-bromonitrobenzene. After 24 h no bromonitrobenzene remained. The products were separated by distillation and extraction as described for 2-iodonitrobenzene. 2,3,4,5,6-pentafluoro-2′-nitrobiphenyl (0.285 g, 10 %), 2-nitrophenol (0,486 g, 35 %) and nitrobenzene (0.174 g 14 %) were isolated.

Coupling with 4-iodonitrobenzene. After 50 h no iodonitrobenzene remained. The products were separated by vacuum distillation and fractional sublimation. The yield of 2,3,4,5,6-pentafluoro-4′-nitrobiphenyl was 1.07 g, 37 %, m.p. 90–92° (lit.[18] 92°). (Found: C 50.0; H 1.4; N 5.0. Calc. for $C_{12}H_4F_5NO_2$: C 49.9; H 1.4; N 4.8). Nitrobenzene (0.162 g, 13 %) was also isolated.

Coupling with iodobenzene. After 67 h no appreciable change occurred in the ratio of biphenyl to iodobenzene. GLC-MS indicated iodobenzene and pentafluorobiphenyl. Separation (vacuum distillation) gave 2,3,4,5,6-pentafluorobiphenyl, 1.39 g, 57 %, m.p. 110–111° (lit. [19] 111–112).

Coupling with 2,6-dimethoxyiodobenzene. The reaction was terminated after 72 h, by which time no pentafluorobenzene remained. Separation (silica gel, light petroleum b.p. 40°, toluene) yielded 2,3,4,5,6-pentafluoro-2′,6′-dimethoxybiphenyl, m.p. 84° 1.56 g, 52 %. (Found: C 55.3; H 3.1; F 31.4. Calc. for $C_{14}H_9F_5O_2$: C 55.3; H 3.0; F 31.2). IR, NMR, and MS were in accordance with the proposed structure. 1,3-Dimethoxybenzene (0.04 g, 3 %) was also obtained and 2,6-dimethoxyiodobenzene (0.71 g, 27 %) was recovered.

Coupling with 4-methoxyiodobenzene. The reaction was terminated after 168 h, when no appreciable increase was noted in the ratio coupling product to iodoarene. A light petroleum (b.p. 40°) solution of the crude reaction mixture was filtered through a short silica gel column and then distilled in vacuum. Separation is also readily achieved by fractional sublimation. The yield of 2,3,4,5,6-pentafluoro-4′-methoxybiphenyl m.p. 123–124°, was 1.15 g, 41 %. IR, NMR, and MS were in accordance with the proposed structure. (Found: C 56.9; H 2.7; F 34.4. Calc. for $C_{13}H_7F_5O$: C 57.0; H 2.6; F 34.6). 4-Methoxyiodobenzene (40 %) was recovered.

In another experiment, silver oxide replaced copper(I) oxide. Naphthalene was used as internal standard. The yield of pentafluoro-4-methoxybiphenyl (about 55 %) was determined by GLC after 170 h. Metallic silver deposited on the walls of the reaction vessel in addition to the silver iodide pyridine complex.

Pentafluoroiodobenzene. Pentafluorobenzene (2 mmol) and iodine (2 mmol) were refluxed in pyridine for 100 h. Naphthalene was used as internal standard. The yield of pentafluoroiodobenzene (25 %) was determined by GLC and was the same whether copper(I) oxide was present or not.

Acknowledgements. We thank Professor Martin Nilsson, Dr. Christer Björklund and Dr. Olof Wennerström for interesting discussions. This work has been supported by the *Swedish Board for Technical Development.* The English was checked by Patrick Hort.

REFERENCES

1. Nilsson, M. *Tetrahedron Letters* **1966** 679.
2. Nilsson, M. and Ullenius, C. *Acta Chem. Scand* **22** (1968) 1998.
3. Chodowska-Palicka, J. and Nilsson, M. *To be published.*
4. Björklund, C. and Nilsson, M. *Tetrahedron Letters* **1966** 675.
5. Björklund, C. and Nilsson, M. *Acta Chem. Scand.* **22** (1968) 2338.
6. Björklund, C. and Nilsson, M. *Acta Chem. Scand.* **22** (1968) 2581.
7. Björklund, C., Nilsson, M. and Wennerström, O. *Acta Chem. Scand.* **24** (1970) 3599.
8. Björklund, C. *Copper-promoted arylation of nitroarenes.* Diss. Stockholm 1972.
9. Nilsson, M. and Wennerström, O. *Acta Chem. Scand.* **24** (1970) 482.
10. Nilsson, M. and Ullenius, C. *Acta Chem. Scand.* **24** (1970) 2379.
11. Stephens, R. D. and Castro, C. E. *J. Org. Chem.* **28** (1963) 3313.
12. Fanta, P. E. *Chem. Rev.* **64** (1964) 613.
13. Bacon, R. G. R. and Hill, H. A. O. *Quart. Rev.* **19** (1965) 95.
14. Burdon, J., Coe, P. L., Marsh, C. R. and Tatlow, J. C. *J. Chem. Soc. Perkin 1* **1972** 763.
15. Cairncross, A. and Sheppard, W. A. *J. Am. Chem. Soc.* **90** (1968) 2186.
16. Sun, K. K. and Miller, W. T. *J. Am. Chem. Soc.* **92** (1970) 6985.
17. DePasqale, R. J. and Tamborski, C. *J. Org. Chem.* **34** (1969) 1736.
18. Brown, P. J. N., Chaudhry, M. T. and Stephens, R. *J. Chem. Soc.* **C 1969** 2747.
19. Birchall, J. M., Haszeldine, R. N. and Parkinson, A. R. *J. Chem. Soc.* **1962** 4966.

Received April 17, 1973.

ACTA CHEMICA SCANDINAVICA 27 (1973) 2722–2732

Electrolyte — Solvent Interaction

Conductance of Lithium Bromide in Acetone-Methanol Mixtures

ANN-MARGRET NILSSON

Division of Physical Chemistry, University of Umeå, S-901 87 Umeå, Sweden

The variation of conductance with concentration for lithium bromide in solvent mixtures of acetone and methanol containing between 0.1 and 100 % methanol has been studied at 25°C and the data obtained have been analyzed by means of the 1957 Fuoss-Onsager equation. In the acetone rich region the ion-pair association constant, K_A, and the limiting molar conductance, Λ_∞, decrease rapidly with increasing methanol concentration. These changes are correlated with the tendency to solvation of the bromide ion through hydrogen-bond formation. The ion-size parameter, $\mathring{a}$, increases with decreasing permittivity of the solvent. Comparison with corresponding parameters for lithium bromide in acetone-water solvent mixtures is made.

The theory of electrolyte conductance ascribes the decrease of molar conductance with increasing electrolyte concentration to the effects of decreasing mobility of the free ions and to the relative concentration of free ions. The ions are represented by charged spheres and the solvent is regarded as a structureless continuum. This model gives a theory for the variation in conductance with the electrolyte concentration and makes it possible to calculate an association constant for the formation of ion pairs from experimental data.

A very large number of investigators have tested the conductance theory using different electrolytes and both aqueous and nonaqueous solvents. Especially electrolytes forming large ions, *e.g.* quaternary ammonium salts, have been extensively investigated, and the theory has been quite successful in accounting for the observed behaviour of this systems.[1–4]

Alkali halides, with their small ions, comparable in size with the solvent molecules, in polar solvents systems show complex behaviour due to strong ion-solvent interactions. This interaction may be studied by conductance measurements in mixed solvents.

Extensive conductometric studies of alkali halides in dioxane-water mixtures,[5–11] in aqueous alcohol,[12] and in mixtures of primary alcohols,[13] have been undertaken during the last decade.

The purpose of the present paper, which is the second part in a series [14] dealing with ion-solvent interactions in binary protic-aprotic solvent mixtures, is to report the result of a conductometric investigation of the behaviour of lithium bromide in acetone-methanol mixtures at 25°C and to make a comparison with the behaviour of the salt in acetone-water mixtures at this temperature.

EXPERIMENTAL

Materials. Lithium bromide (Merck, *suprapur*) was dried at 200°C for 2 h immediately before use.

Commercial acetone (*p.a.*) was allowed to pass through a column packed with Linde Molecular Sieve 4A and then fractionally distilled.[15] By repeated measurements acetone purified in this manner was found to have the following properties: $\varkappa < 2 \times 10^{-8}$ Ω^{-1} cm^{-1}; $d_4^{25} = 0.78429$ g cm^{-3}, $\eta = 0.00304$ P; $\varepsilon = 20.7$. Methanol (*p.a.*) was purified in the same manner as acetone and had the following properties: $\varkappa < 11 \times 10^{-8}$ Ω^{-1} cm^{-1}; $d_4^{25} = 0.78674$ g cm^{-3}; $\eta = 0.00543$ P; $\varepsilon = 32.7$. All the solvent properties were determined as described below.

Table 1. Properties of acetone-methanol mixtures at 25°C.

Wt. % methanol	d g cm^{-3}	η cP	ε
0.100	0.78435	0.300	20.6
0.300	0.78447	0.300	20.6
1.00	0.78468	0.301	20.7
2.00	0.78491	0.301	20.8
5.00	0.78563	0.301	21.1
10.0	0.78662	0.304	21.6
20.0	0.78828	0.314	22.7
50.0	0.79060	0.370	26.3
100.0	0.78674	0.543	32.7

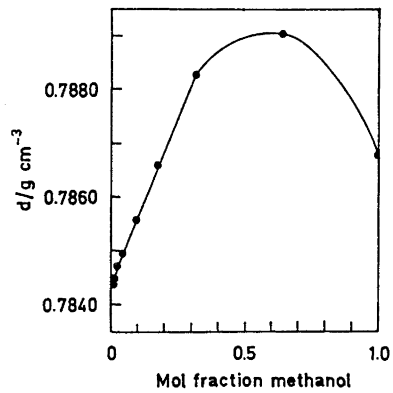

Fig. 1. Density of acetone-methanol mixtures at 25°C as a function of the mol fraction methanol.

Acetone-methanol mixtures were prepared by weight. In all weighings bouyancy corrections were applied. The density of acetone-methanol was measured with a Lipkin pycnometer. Viscosities were determined by means of a calibrated Ubbelohde viscosimeter and permittivities by a Ferrisol M 803 A Q-meter. The properties of the various acetone-methanol mixtures thus established are listed in Table 1. The density of acetone-methanol mixtures shows a positive deviation from linearity (Fig. 1) with a maximum between 50 and 60 mol % methanol. The system acetone-ethanol [16] shows the same deviation while for the acetone-propanol [17] system density is a linear function of the mol fraction as in the case of acetone-water mixtures.[14]

In Figs. 2 and 3 permittivities and viscosities, respectively, are plotted as a function of the mol fraction of methanol together with the acetone-water system.

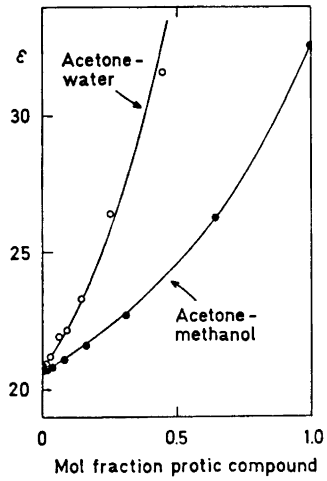

Fig. 2. Permittivity of the solvent mixtures at 25°C as a function of the composition (acetone-water mixtures according to Ref. 14).

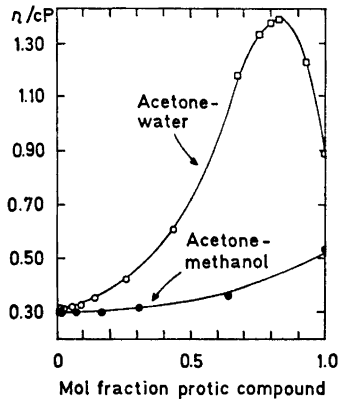

Fig. 3. Viscosity of the solvent mixtures at 25°C plotted against the mol fraction (open circles acetone-water (Ref. 14) and open squares acetone-water (Ref. 31)).

To enable exact calculations of lithium bromide concentrations, the density of solution was measured as a function of the salt concentration. For each solvent mixture investigated the density of the solution was found to vary lineary with the concentration of lithium bromide.

Conductivity measurements. The resistances of the solution were measured by means of a Leeds and Northrup 4666 conductivity bridge. A Dagget-Bair-Kraus conductivity cell fitted with two pairs of bright platinum electrodes [14] and a salt cup dispensing device was used.

The general technique for the conductance measurements was the same as previously described.[14] The temperature was determined by means of a Mueller temperature bridge 8069-B in connection with a high precision platinum resistance thermometer. The temperature was 25.000 ± 0.005°C.

RESULTS AND DISCUSSION

Conductance data for different molar concentrations, c, of lithium bromide are shown in Table 2, for the different acetone-methanol mixtures studied. The molar conductivities, Λ, have been corrected for the conductivity of the

Table 2. Molar conductivities of lithium bromide in acetone-methanol mixtures at 25°C.

Run A		Run B	
$c \times 10^4$ M	Λ cm² Ω^{-1} mol^{-1}	$c \times 10^4$ M	Λ cm² Ω^{-1} mol^{-1}
	0.100 wt. % methanol		
1.5441	139.51	2.0492	130.90
7.0899	93.225	6.4199	96.291
15.874	71.079	15.395	71.881
26.445	59.011	28.569	57.309
40.037	50.434	41.549	49.689
58.177	43.635		
	0.300 wt. % methanol		
0.8161	158.97	1.2973	149.06
2.7103	128.63	3.3883	122.19
6.7040	101.78	16.118	76.839
15.253	78.434	28.649	62.781
28.310	63.089	40.784	55.126
45.724	52.819		
62.656	46.856		
	1.00 wt. % methanol		
1.7786	148.48	1.1602	157.19
3.9249	128.90	3.3465	132.96
8.4896	107.07	7.5158	110.48
17.776	86.301	16.478	88.290
31.534	71.495	29.289	73.252
44.494	63.439	41.897	64.761
62.124	56.288	59.074	57.288
	2.00 wt. % methanol		
0.7696	164.11	1.0303	160.88
15.551	97.576	2.8180	142.39
28.700	81.448	6.6089	121.32
41.791	72.188	11.154	106.99
58.809	64.368	23.376	86.850
		35.473	76.184
		50.728	67.710
	5.00 wt. % methanol		
1.1958	157.55	1.1837	157.93
3.5135	141.57	3.6675	140.89
7.9386	124.33	8.3005	123.31
16.934	105.54	17.063	105.39
30.236	90.769	30.307	90.734
43.501	81.767	43.202	81.965
60.856	73.832	61.752	73.516

Table 2. Continued.

		10.0 wt. % methanol	
1.4282	153.07	2.1340	149.06
3.7624	141.94	6.1149	134.01
12.985	119.46	15.090	116.26
25.625	104.24	28.320	101.98
38.832	94.569	41.165	93.232
55.634	86.236	55.187	86.419
		20.0 wt. % methanol	
1.3539	145.41	0.9804	146.82
3.5373	138.79	2.9113	140.53
7.7014	130.59	15.884	120.08
16.790	119.33	28.544	110.01
30.003	109.19	41.804	102.70
41.294	103.10	58.582	96.196
59.165	96.011		
		50.0 wt. % methanol	
1.7538	122.96	1.4307	123.58
4.2070	119.52	21.470	108.37
8.2535	115.88	35.299	103.59
13.806	112.30	53.663	98.949
28.855	105.82		
40.784	102.18		
55.946	98.553		
		100.0 wt. % methanol	
1.6179	92.755	1.3243	93.024
3.8046	91.256	3.7439	91.298
8.3122	89.077	8.3533	89.022
17.604	86.255	17.787	86.174
31.455	83.437	31.433	83.408
45.083	81.377	45.520	81.290
63.398	79.238	64.263	79.090

solvent. The data in Table 2 were analyzed using a computer program previously described.[18] This program is based on the Fuoss-Onsager equation [19] of 1957:

$$\Lambda = \Lambda_\infty - S(c\alpha)^{1/2} + Ec\alpha^{10}\log c\alpha + Jc\alpha - K_A c\alpha\gamma^2\Lambda \qquad (1)$$

where Λ_∞, α, and K_A have their usual meanings. The parameters S, E, and J are definied in Ref. 20. The mean molar activity coefficient, γ, is approximated by the mean rational activity coefficient. The latter was evaluated from the Debye-Hückel equation in its more complete form.[21]

Table 3. Conductance parameters for lithium bromide in acetone-methanol mixtures at 25°C.

Wt. % methanol	Λ_∞ cm² Ω^{-1} mol^{-1}	K_A M^{-1}	$\mathring{a} \times 10^8$ cm	$\sigma\Lambda$ %
0.0 [14]	195.01 ± 0.02	4202 ± 0.6	9.3	0.04
0.100	193.59 ± 0.06	3457 ± 3	7.8	0.14
0.300	190.61 ± 0.08	2613 ± 4	6.3	0.16
1.00	185.37 ± 0.05	1542 ± 1	5.0	0.11
2.00	181.41 ± 0.07	1069 ± 4	4.7	0.14
5.00	173.91 ± 0.06	598.8 ± 1.7	4.4	0.15
10.0	166.16 ± 0.07	317.5 ± 1.3	4.3	0.16
20.0	153.91 ± 0.04	105.6 ± 0.7	3.9	0.11
50.0	128.68 ± 0.04	6.20 ± 0.75	3.7	0.11
100.0	95.80 ± 0.01		3.1	0.05

Eqn. (1) was fitted to the conductance data by an iterative method [18] similar to one outlined by Kay.[22] The results of these calculations are shown in Table 3, in which values of Λ_∞ and K_A, together with their standard deviations, and the parameter $\mathring{a}$ are quoted. The standard deviation in single value of Λ, σ_Λ, also is included.

According to Fuoss and Onsager,[19] eqn. (1) should not be used for 1:1 electrolytes for concentrations corresponding to $\varkappa\mathring{a} > 0.2$, where $\varkappa^2/c = \pi N e^2/\varepsilon kT$. Evans *et al.*[17] report for several electrolytes in acetone and acetone-propanol mixtures, if $\varkappa\mathring{a} > 0.1$ the conductance parameters depend upon the concentration range analyzed.

To investigate any dependence of Λ_∞, K_A, and $\mathring{a}$ on the concentration range of lithium bromide some of our conductance data where treated by means

Table 4. The dependence in the conductance parameters upon the concentration region analyzed.

Conc. interval $c \times 10^4$/M	Λ_∞ cm² Ω^{-1} mol^{-1}	KA M^{-1}	$\mathring{a} \times 10^8$ cm	$\sigma\Lambda$ %
	LiBr in acetone containing 0.100 wt % methanol			
1 – 15	194.30 ± 0.10	3544 ± 6	10.9	0.16
1 – 30	193.91 ± 0.08	3494 ± 5	8.9	0.14
1 – 41	193.70 ± 0.07	3469 ± 4	8.2	0.13
1 – 60	193.59 ± 0.06	3457 ± 3	7.8	0.14
	LiBr in acetone containing 50.0 wt. % methanol			
1 – 15	128.89 ± 0.01	34.7 ± 0.4	6.9	0.04
1 – 30	128.81 ± 0.03	19.4 ± 0.5	4.8	0.09
1 – 35	128.75 ± 0.04	13.6 ± 0.6	4.3	0.10
1 – 41	128.75 ± 0.03	13.5 ± 0.6	4.2	0.09
1 – 55	128.68 ± 0.04	6.2 ± 0.8	3.7	0.11

of eqn. (1) for successively broadening of the interval of concentration. This analysis was undertaken for two solvent compositions, *viz.* acetone containing 0.1 and 50 wt %, respectively of methanol. In the latter solvent the electrolyte is only slightly associated to ion pairs. The concentration intervals analyzed and the conductance parameters obtained are given in Table 4. In that table it can be seen that the parameters discussed are dependent upon the concentration interval analyzed even at low concentrations.

For acetone containing 0.1 wt % methanol the value of $\Lambda_\infty = 193.6$ cm^2 Ω^{-1} mol^{-1} calculated for the whole concentration interval ($1 \times 10^{-4} - 6 \times 10^{-3}$ M) may be compared with the corresponding $\Lambda_\infty = 194.3$ cm^2 Ω^{-1} mol^{-1} obtained on basis of the experimental points within the low concentration range ($1 \times 10^{-4} - 1.5 \times 10^{-3}$ M). The corresponding values for K_A are 3457 and 3544 M^{-1}, respectively, and for $\mathring{a}$ 7.8 and 10.9 Å.

A corresponding analysis for acetone containing 50 wt % methanol yields $\Lambda_\infty = 128.7$ cm^2 Ω^{-1} mol^{-1} ($1 \times 10^{-4} - 5.5 \times 10^{-3}$ M) and $\Lambda_\infty = 128.9$ cm^2 Ω^{-1} mol^{-1} ($1 \times 10^{-4} - 1.5 \times 10^{-3}$ M); $K_A = 6.2$ and 34.7 M^{-1}, respectively; $\mathring{a} = 3.7$ and 6.9 Å, respectively. Further systematic studies must be undertaken to determine if the observed effect is a consequence of the experimental precision or is a general inability in eqn. (1) to represent adequately the conductance data.

As can be seen in Table 3, K_A decreases rapidly with increasing methanol concentration. Fig. 4 shows that for a given mol fraction of protic compound

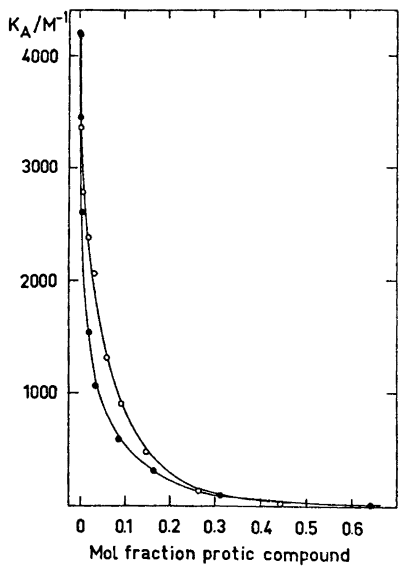

Fig. 4. Association constants at 25°C for lithium bromide in acetone-methanol and acetone-water mixtures plotted against the solvent composition (full circles acetone-methanol mixtures and open circles acetone-water mixtures (Ref. 14)).

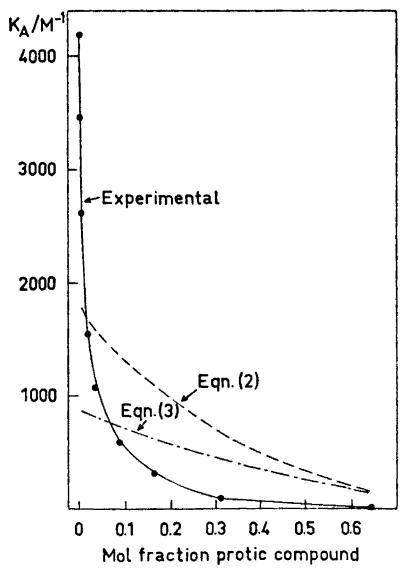

Fig. 5. Association constants for lithium bromide in acetone-methanol at 25°C.

in the acetone rich region, the association constant for the acetone methanol system is smaller than for the acetone-water mixture, although the permittivity of the former system is lower, see Fig. 2. The two isodielectric mixtures 5.00 wt. % methanol-acetone and 1.00 wt. % water-acetone [14] have association constants of 599 M^{-1} and 2073 M^{-1}, respectively. This may be an effect of different anion solvation from the protic compound in the solvent mixtures.

According to Fuoss [23] two ions may be regarded as an ion pair if they are in contact. Fuoss has derived the association constants of such ion pairs in a dielectric continuum to

$$K_A = \frac{4\pi N å^3}{3000} \exp\left(\frac{e^2}{å \varepsilon k T}\right) \tag{2}$$

where N is the Avogadro number and $å$ means the distance of closest approach between the centres of the two ions.

Alternatively, two ions may be regarded as paired if the distance between their centres is less than the Bjerrum critical distance, q, where q, for a given charge type of electrolyte, is a parameter dependent only on the solvent.

Regarding the solvent as a continuum with permittivity, ε, Bjerrum [24] derived for an 1:1 electrolyte:

$$K_A = \frac{4\pi N}{1000} \int_{å}^{q} r^2 \exp\left(\frac{e^2}{\varepsilon k T r}\right) \mathrm{d}r$$

or

$$K_A = \frac{4\pi N}{1000} \left(\frac{e^2}{\varepsilon k T}\right)^3 Q(b) \tag{3}$$

where $Q(b)$ stands for $\int_{2}^{b} x^{-4} e^x \mathrm{d}x$; $x = e^2/\varepsilon k T r$

r is the distance from the center of a reference ion. This integral has been tabulated in Ref. 25, as a function of $b = e^2/å k \varepsilon T$.

Values of K_A according to eqns. (2) and (3) has been calculated using $å = 2.55$ Å, the crystal radii sum of lithium bromide. Using the $å$-values in Table 3 obtained from eqn. (1) association constants of the magnitude 50 M^{-1} were obtained for both eqns. (2) and (3). The $å$-values obtained from eqn. (1) are not used in the following as a value for the distance of closest approach. The discrepancies between calculated and observed association constants are large as can be seen from Fig. 5. Both equations underestimate K_A in the acetone rich region, where the ion pair has greater stability than the theories above predict. Compare the opposite behaviour in the methanol rich region in which both equations overestimate K_A. This is not surprising as neither of eqns. (2) and (3) allow factors for solvent-solute interaction to appear in K_A. In addition there is the uncertainty about the values of the permittivity employed to account for the reduction of field strength in the immediate vicinity of an ion. The macroscopic permittivity is used.

Gilkerson [26,27] has elaborated eqn. (2) further in an attempt to include factors in K_A accounting for the solvent-solute interaction and for the free volume of the solute. He obtained the expression:

$$K_A = \frac{4\pi N \mathring{a}^3}{3000} \exp\left(\frac{\Delta G_s}{RT}\right) \exp\left(\frac{e^2}{\mathring{a}\varepsilon kT}\right) \quad (4)$$

where ΔG_s is the difference in molar free energy of solvation of the free ions and the ion-pair, and $\mathring{a}$ is the distance of closest approach. Variations in the solvent composition not only change the dielectric constant but also ΔG_s and $\mathring{a}$.

The distance of closest approach of two ions should not vary with the solvent if the ions are not separated by solvent molecules in the ion pair or if the solvent molecules separating the ions do not change. The addition of a small amount of a protic compound to acetone decreases the association constants very rapidly and this indicates a change to selective solvation of the ions by the protic compound. One may assume ΔG_s and $\mathring{a}$ to be constant over a wide concentration interval of the protic compound. Assuming ΔG_s and $\mathring{a}$ are constant a plot of log K_A against $1/\varepsilon$ should yield a straight line. As the plots in Fig. 6 is linear in the protic region down to a concentration of about 6 mol % protic compound one may conclude that the solvation shells of the protic solvent around the ions is fully developed when the content of the protic component exceeds about 6 mol %.

From the slope and intercept according to eqn. (4) the estimated value of $\mathring{a}$ and ΔG_s are, for lithium bromide in acetone-water mixtures, 2.3 Å and -2.5 kJ mol^{-1}, respectively and, for lithium bromide in acetone-methanol mixtures, 1.2 Å and -26 kJ mol^{-1}, respectively.

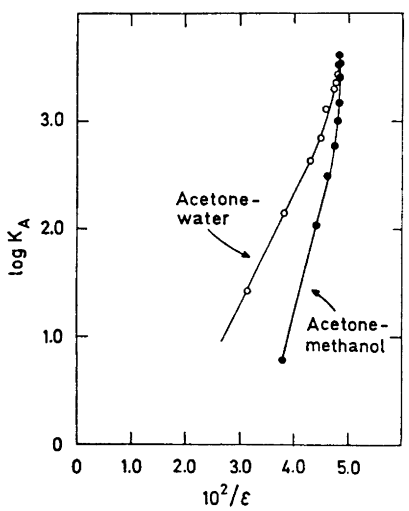

Fig. 6. The logarithms of the ion-pair association constants of lithium bromide *vs.* the reciprocal of the permittivity.

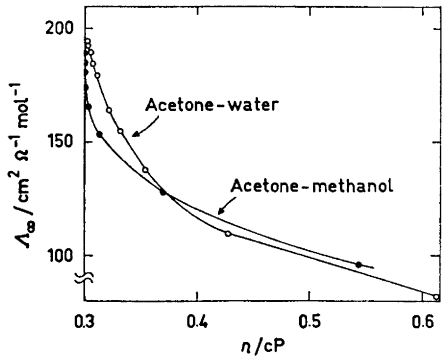

Fig. 7. Limiting molar conductivity at 25°C as a function of the viscosity of the solvent mixtures.

The distances of closest approach are unrealistically small, both less than the crystal radii sum for lithium bromide. The values of ΔG_s are negative indicating that the ions are more strongly solvated than the ion-pairs. The ΔG_s value for lithium bromide in acetone-methanol mixtures is ten times that in acetone-water, which may be correlated with a stronger hydrogen bonds formed by methanol.[28] The uncertainty in the quantitative results above is large because the linear part of the plots in Fig. 6 covers a rather small interval of the macroscopic permittivity of the solvent.

From values of Λ_∞ in Table 3 it can be seen that the limiting molar conductivity decreases with increasing methanol concentration. These values of Λ_∞ are reproduced in Fig. 7 as a function of the viscosity. From this figure it can be seen that for $\eta < 0.38$ cP the absolute value of Λ_∞ is significantly lower for the acetone-methanol system than for the acetone-water system. As transport numbers for the ions here concerned are not available in the literature no conclusions concerning differences in anion and cation solvation can be drawn.

As in most other solvents $\mathring{a}$ estimated from eqn. (1) seems more characteristic of the solvent than of the salt and can hardly be seen as the distance of closest approach between the centres of the ions in the ion pair. Recent spectroscopic studies [29] show that in anhydrous acetone the bromide ions compete with acetone molecules for a position in the solvent shell of the lithium ion, with the formation of a contact ion-pair. Eqn. (1) yields 9.3 Å as the distance of closest approach in anhydrous acetone while the crystal radii sum is 2.55 Å.

Justice [30] has recently suggested that Bjerrum's critical distance, q, should be used in the Fuoss-Onsager equation in place of the ion-size parameter $\mathring{a}$, and this has been experimentally verified by other authors.[13]

Bjerrum's critical distance, q, for the solvent mixtures investigated has been calculated from:

$$q = e^2/2\varepsilon kT \tag{5}$$

and is compared in Table 5 with the parameter, $\mathring{a}$, derived by means of eqn. (1) from experimental data. From this table it can be seen that though not un-

Table 5. Comparison between the parameters $\mathring{a}$ and Bjerrum critical distances, q, for the acetone-methanol mixtures at 25°C.

Wt. % methanol	$\mathring{a} \times 10^8$ cm	$q \times 10^8$ cm
0.100	7.8	13.6
0.300	6.3	13.6
1.00	5.0	13.5
2.00	4.7	13.5
5.00	4.4	13.3
10.0	4.3	13.0
20.0	3.9	12.3
50.0	3.7	10.7
100.0	3.1	8.6

expectedly different in magnitude, $\mathring{a}$, and q show the same tendency with changing solvent composition. A conclusion of this investigation is that none of the available theories for association gives an adequate representation of the association of lithium bromide in aprotic-protic solvent mixtures. The $\mathring{a}$-values obtained from eqn. (1) agree with Justice's interpretation and this suggests that a further development of the Bjerrum theory taking the ion-solvent interaction into account would be of interest.

Acknowledgements. The author thanks Dr. Per Beronius and Prof. Per-Olof Kinell for suggesting improvements of the manuscript and Miss Eva Borg for technical assistance. This work was supported by grants from the *Swedish Natural Science Research Council.*

REFERENCES

1. Sadek, H. and Fuoss, R. M. *J. Am. Chem. Soc.* **81** (1959) 4507.
2. Hirsch, E. and Fuoss, R. M. *J. Am. Chem. Soc.* **82** (1960) 1018.
3. Berns, D. S. and Fuoss, R. M. *J. Am. Chem. Soc.* **82** (1960) 5585.
4. Lind, Jr., J. E. and Fuoss, R. M. *J. Am. Chem. Soc.* **83** (1961) 1828.
5. Kay, R. L. and Broadwater, T. L. *Electrochim. Acta* **16** (1971) 667.
6. Pistoia, G., Polcaro, A. M. and Schiavo, S. *Ric. Sci.* **37** (1967) 228.
7. Fabry, T. L. and Fuoss, R. M. *J. Phys. Chem.* **68** (1964) 971.
8. Lind, Jr., J. E. and Fuoss, R. M. *J. Phys. Chem.* **65** (1961) 999.
9. Kunze, R. W. and Fuoss, R. M. *J. Phys. Chem.* **67** (1963) 911.
10. Kunze, R. W. and Fuoss, R. M. *J. Phys. Chem.* **67** (1963) 914.
11. Justice, J.-C. and Fuoss, R. M. *J. Phys. Chem.* **67** (1963) 1707.
12. Hawes, J. L. and Kay, R. L. *J. Phys. Chem.* **69** (1965) 2420.
13. DeRossi, C., Sesta, B., Battistini, M. and Petrucci, S. *J. Am. Chem. Soc.* **94** (1972) 2961.
14. Nilsson, A.-M. and Beronius, P. *Z. physik. Chem. Frankfurt am Main* **79** (1972) 83.
15. Smith, S. G., Fainberg, A. H. and Winstein, S. *J. Am. Chem. Soc.* **83** (1961) 618.
16. Pistoia, G. and Pecci, G. *J. Phys. Chem.* **74** (1970) 1450.
17. Evans, D. F., Thomas, J., Nadas, J. A. and Matesich, M. A. *J. Phys. Chem.* **75** (1971) 1714.
18. Beronius, P., Wikander, G. and Nilsson, A.-M. *Z. physik. Chem. Frankfurt am Main* **70** (1970) 52.
19. Fuoss, R. M. and Onsager, L. *J. Phys. Chem.* **61** (1957) 668.
20. Beronius, P., Nilsson, A.-M. and Wikander, G. *Acta Chem. Scand.* **24** (1970) 2826.
21. Robinson, R. A. and Stokes, R. *Electrolyte Solutions*, Butterworths, London 1959, p. 229.
22. Kay, R. L. *J. Am. Chem. Soc.* **82** (1960) 2099.
23. Fuoss, R. M. *J. Am. Chem. Soc.* **80** (1958) 5059.
24. Bjerrum, N. *Danske Vidensk. Selsk.* **7** (1926) No. 9.
25. Robinson, R. A. and Stokes, R. *Electrolyte Solutions*, Butterworths, London 1959, p. 549.
26. Gilkerson, W. R. *J. Chem. Phys.* **25** (1956) 1199.
27. Gilkerson, W. R. *J. Phys. Chem.* **74** (1970) 746.
28. Pauling, L. *The nature of the Chemical Bond*, 3rd Ed., Cornell University Press, pp. 468 and 474.
29. Ming Keong Wong, Mc Kenney, W. J. and Popov, A. I. *J. Phys. Chem.* **75** (1971) 56.
30. Justice, J.-C. *Electrochim. Acta* **16** (1971) 701.
31. Brentel, I. *Unpublished.*

Received April 17, 1973.

ACTA CHEMICA SCANDINAVICA 27 (1973) 2733–2739

The Vapour Pressure of Solid and Liquid $NbCl_5$

LARS-INGVAR STAFFANSSON[a] and PER ENGHAG[b]*

[a]*Dept. of Metallurgy, Royal Institute of Technology, P.O.B., S-100 44 Stockholm 70, Sweden and* [b]*Axel Johnson Institute for Industrial Research, S-149 01 Nynäshamn, Sweden*

The vapour pressure of solid and liquid $NbCl_5$ has been measured in the temperature range 462 to 494 K by a transpiration method. From the obtained data heats and entropies of fusion, vaporization, and sublimation have been calculated.

This work comprises measurement of the vapour pressure of solid and liquid $NbCl_5$ and is part in an attempt to provide accurate data for some of the most important refractory metal chlorides. Using the same method the vapour pressure of $WOCl_4$ [1] and $TaCl_5$ [2] have earlier been investigated.

EXPERIMENTAL

The $NbCl_5$ used came from Schuchard, München, and was delivered in sealed glass ampoules. It contained > 99.9 % $NbCl_5$ and < 0.03 % $TaCl_5$, other metallic impurities where < 0.02 %. The argon used as carrier gas in the experiments was delivered by AGA, Stockholm, and had a purity better than 99.99 %. The procedure for the purification of the argon as well as the transpiration method and the apparatus and experimental technique were the same as in the work on $TaCl_5$ and has been described elsewhere.[1,2]

RESULTS AND DISCUSSION

The results from the vapour pressure determinations on solid and liquid $NbCl_5$ are given in Table 1 where values from weighing as well as from chemical analysis are given. All values are corrected for blanks, *i.e.* the amount of $NbCl_5$ vaporized during the heating up period. The data from weighings are plotted in Fig. 1 as log P *versus* $1/T$. As the results from the weighings are more accurate they have been used for the calculation of the vapour pressure equations while the values from the chemical analysis are only given as a check. The vapour pressure equations corresponding to the two lines in Fig. 1 are

* Present address: AB Garphytte Bruk, S-710 16 Garphyttan, Sweden.

Table 1. Results from weighing and analysis.

Temperature K	$10^3/T$	From weighing: $NbCl_5$ mmol	Ar mmol	Mol fraction	Pressure torr	P_{NbCl_5} torr	log P_{NbCl_5}	From analysis: Mol fraction	P_{NbCl_5} torr	log P_{NbCl_5}	Notes
469.4	2.130	2.039	7.594	0.2117	752.0	159	2.201	0.2062	155	2.190	
469.4	2.130	1.880	6.796	0.2167	752.9	163	2.212	0.2153	162	2.210	
478.6	2.090	1.547	3.782	0.2903	760.0	221	2.344	0.2803	213	2.328	[a]
478.7	2.089	1.266	2.897	0.3041	760.8	231	2.364	0.2934	223	2.348	
462.7	2.161	1.625	9.076	0.1519	776.6	118	2.072	0.1545	120	2.079	
462.9	2.160	1.751	9.483	0.1559	776.1	121	2.083	0.1511	117	2.068	
477.5	2.094	2.931	7.284	0.2869	776.7	223	2.348	0.2903	225	2.352	
477.5	2.094	1.492	3.755	0.2844	776.8	221	2.344	0.2667	207	2.316	
487.2	2.052	1.221	2.612	0.3185	778.3	248	2.395	—	—	—	[a]
487.5	2.051	1.806	2.908	0.3831	777.6	298	2.474	—	—	—	
487.4	2.051	2.051	3.229	0.3884	761.9	296	2.471	0.3712	283	2.452	
494.1	2.024	2.065	2.216	0.4824	762.7	368	2.566	0.4682	357	2.553	
494.2	2.023	2.262	2.381	0.4872	762.7	372	2.571	0.4609	352	2.547	
483.7	2.067	1.880	3.535	0.3586	764.8	274	2.438	0.3349	256	2.408	
484.1	2.066	1.877	3.361	0.3583	766.0	274	2.438	0.3397	260	2.415	

[a] New charge.

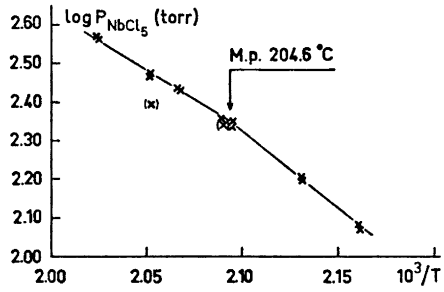

Fig. 1. Vapour pressures of $NbCl_5$ calculated from weighing results.

$$\log P_{NbCl_5(s)}(\text{torr}) = -4.033 \times 10^3/T + 10.794 \qquad (462\ \text{K} - 478\ \text{K}) \qquad (1)$$

$$\log P_{NbCl_5(l)}(\text{torr}) = -3.080 \times 10^3/T + 8.799 \qquad (478\ \text{K} - 494\ \text{K}) \qquad (2)$$

The intersection of the two lines corresponds to a melting point of 477.8 K. An extrapolation of eqn. (2) gives a boiling point of 520 K. From eqn. (1) the entropy of sublimation $\Delta S°_{subl.}$ is calculated to 36.20 cal deg.$^{-1}$ mol^{-1} and from the same equation the heat of sublimation in the temperature range investigated is obtained giving the value $\Delta H°_{subl.} = 18.45$ kcal/mol. For calculation of the $\Delta S°_{subl.(298)}$ and the $\Delta H°_{subl.(298)}$ the Δc_p value estimated by Schäfer and Kahlenberg [3] was used. According to their estimation

$$\Delta c_p = -6.4 - 0.7 \times 10^5/T^2 \text{ cal deg.}^{-1} \text{ mol}^{-1}$$

With this value $\Delta S°_{subl.(298)} = 39.4$ cal deg.$^{-1}$ mol^{-1} and $\Delta H°_{subl.(298)} = 19.64$ kcal mol^{-1} were calculated.

In the gas phase $NbCl_5$ has a similar structure as $TaCl_5$, consisting of monomeric trigonal bipyramidal $NbCl_5$ according to electron defraction measurements by Skinner and Sutton.[4] This structure has also been confirmed by Gaunt and Ainscough [5] from IR and Raman spectroscopy. The Nb – Cl distance in the trigonal bipyramid has been determined to 2.28 ± 0.02 Å by Spiridonov and Romanov.[6] In the solid state, however, Zalkin and Sands [7] have shown that crystallized niobium pentachloride forms dimeric molecules Nb_2Cl_{10}. Several investigations of the vapour pressure of $NbCl_5$ have been reported in the literature.[8–15]

Schäfer and Pölert [8] obtained with a transpiration method the relation

$$\log P_{NbCl_5(s)}(\text{atm}) = -5352.57/T + 19.3779 - 3.2204 \log T - 7648.9 \times T^{-2}$$

valid between 350 – 385 K. From results of Meyer, Oosterom and van Oeveren [9] on the system $NbCl_5 - Nb_2O_5$ Schäfer and Pölert [8] derived the equation

$$\log P_{NbCl_5(s)}\ (\text{torr}) = -4805/T + 12.446$$

Using a boiling point method Ainscough, Holt and Trowse [10] obtained results at vapour pressures between 680 – 900 torr which they related to the boiling points with the equation

$$\log P_{NbCl_5(s)}\ (\text{torr}) = -2770/T + 8.201$$

't Hart and Meyer [11] studied the vapour pressure of $NbCl_5$ with a static method in the range 540 – 695 K and gave the equation

$$\log P_{NbCl_5(l)}(\text{torr}) = 313.0179 - 15664.84/T - 112.9694 \log T + 0.0460236T$$

Johnson, Silva and Cubicciotti [12] used a boiling point method in the temperature range 504 – 800 K and obtained the relation

$$\log P_{NbCl_5(l)}(\text{atm}) = 6.11621 - 5.42391 \times 10^3/T + 2.10052 \times 10^6/T^2 - 0.48558 \times 10^9/T^3$$

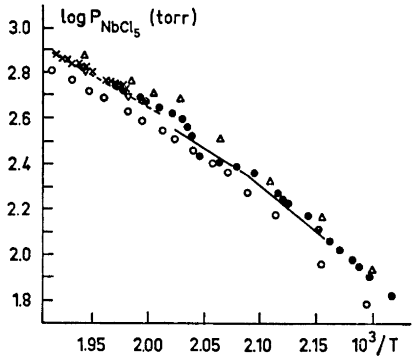

Fig. 2. Vapour pressures of $NbCl_5$ (comparison with earlier works).
△ Opichtina, Fleischer;[13]
● Tarasenkov, Komandin,[14] static method;
× Tarasenkov, Komandin,[14] boiling point method;
○ Alexander, Fairbrother;[15]
▽ Johnson, Silva, Cubicciotti;[12]
– – – Ainscough, Holt, Trowse;[10]
——— This work.

In Fig. 2 the present work – given as two lines corresponding to eqns. (1) and (2) – is compared with published results that fall within the same temperature range. In Table 2 the constants in the vapour pressure equation

$$\log P_{NbCl_5(l)}(\text{torr}) = -a \times 10^3/T + b$$

Table 2. Reported results for $NbCl_5(l)$

Temp. range K	Boiling point °C	a	b	$\Delta H°_{vap}$ kcal mol^{-1}	$\Delta S°_{vap}$ cal deg.$^{-1}$ mol^{-1}	Ref.
483 – 514	–	2.84	8.43	13.0	25.4	13
480 – 506	–	3.27	9.22	15.0	29.0	14 Static method
504 – 520	–	2.45	7.60	11.2	21.6	14 Boiling p. method
478 – 528	–	2.89	8.36	13.2	25.1	15
–	247	2.770	8.201	12.7	–	10
–	248	–	–	–	–	17
478 – 494	247	3.080	8.799	14.09	27.10	This work

and the thermodynamic quantities calculated from the constants are compared. Boiling points obtained at different investigations are also given. The values given from the work of Opichtina and Fleischer,[13] Tarasenkov and Komandin,[14] and Alexander and Fairbrother [15] have been obtained from a statistical treatment by Schäfer, Bayer and Lehman [16] and from these values Schäfer and Kahlenberg [3] have given the equation

$$\log P_{NbCl_5(l)}(\text{torr}) = -2.87 \times 10^3/T + 8.37$$

said to be valid for temperatures close to the melting point.

From Fig. 2 it can be seen that the present work shows a good agreement with the result from Ainscough, Holt and Trowse,[10] Tarasenkov and Komandin,[14] and Johnson *et al.*[12] for liquid $NbCl_5$.

The heat of vaporization, 14.09 kcal/mol, derived from the present work is in fair agreement with the value 13.8 kcal/mol which can be evaluated from the curve of ΔH°_{vap} *versus* temperature, given by Johnson, Silva and Cubicciotti,[12] and which they have derived with the aid of the Clapeyron equation from vapour pressures combined with the vapour and liquid densities. For solid $NbCl_5$ the corresponding constants in the vapour pressure equation

Table 3. Reported results for $NbCl_5$(s).

Mean temp. K	$10^3/T$	a	b	Ref.
434.4	2.30	4.38	11.57	13
462.7	2.16	4.01	10.77	14
449.0	2.23	4.36	11.38	15
457.4	2.19	4.805	12.446	9
469.9	2.13	4.033	10.794	This work

are given in Table 3. The a- and b-values from earlier results are taken from the article by Schäfer and Pölert.[8] As can be seen from this table the best agreement with the present work is obtained in the work by Tarasenkov and Komandin.[14] Over a large temperature range there is, however, likely to be a significant deviation from linearity in the log P *versus* $1/T$ relation. This was also found in the investigation of the vapour pressure of $WOCl_4$ [1], and has been discussed in connection with the work on $TaCl_5$.[2] It is therefore not surprising that at lower temperatures, not covered by the present work, Schäfer and Pölert from their own investigations in the range 350 to 384 K give an a-value of 4.875 at a $10^3/T$-mean value of 2.693 which indicates that the curvature of the log P *versus* $1/T$ curve is even greater for $NbCl_5$ than for $TaCl_5$.

To study the influence of temperature on the slope the log P results from different investigations near the melting point were plotted *versus* $1/T$ and compared to the results of Schäfer and Pölert at low temperatures. The slopes from these curves were evaluated graphically and are given in Table 4 together with the corresponding heats of sublimation.

Table 4. Slopes from published results and corresponding heats of sublimation.

Temp. range $10^3/T$	a graphically evaluated	$\Delta H°_{subl.}$ kcal mol^{-1}	Ref.
2.6 – 2.85	4.85	22.2	8
2.1 – 2.2	4.5	20.6	15
2.1 – 2.2	4.2	19.2	13
2.1 – 2.25	4.05	18.5	14
2.1 – 2.2	4.05	18.5	This work

If we assume that the low temperature values of Schäfer and Pölert are correct it is now possible to obtain an equation that takes into account the difference in slope of the log P curve at high and low temperature. With an a-value of 4.85 and 4.10 at $10^3/T = 2.7$ and 2.1, respectively, the following relations is obtained valid from 350 K to the melting point.

$$\log P_{NbCl_5(s)}(\text{torr}) = -7500/T - 16.45 \log T + 1.32 \times 10^3 T + 61.496 \quad (3)$$

This equation shows a good agreement with the present work as well as with the low temperature work of Schäfer and Pölert. The $\Delta H°_{subl.(298)} = 19.6$ kcal mol^{-1} and $\Delta S°_{subl.(298)} = 39.4$ cal K^{-1} mol^{-1} calculated from this work are smaller than the corresponding values from the work of Schäfer and Pölert which are 22.8 and 46.2, respectively. The reason for this descrepancy is probably the uncertainty in the Δc_p-value used for the integration. As the experimental values in this work are obtained at temperatures higher than those of Schäfer and Pölert the influence of the error in the Δc_p is also much greater why it is plausible to assume that the latter values are closer to the true values. The melting point 204.6°C obtained in the present work is in fair agreement with the results from previous investigations as can be seen in Table 5. The heat of fusion has been determined calorimetrically by Keneshea *et al.*[19] to 8.09 kcal/mol, cryoscopicly by Nisel'son and Perekhrest[21] to 9.95 kcal/mol, and from the difference in $\Delta H°_{subl.}$ and $\Delta H°_{vap.}$ by Alexander and Fairbrother[15] to 7.7 kcal/mol and by Meyer *et al.*[9] to 8.3 kcal/mol. The value in this work 4.36 kcal/mol shows a pronounced lower value than those mentioned. One should, however, not attach to much importance to this value as a calculation of the heat of fusion as a difference between $\Delta H°_{subl.}$ and $\Delta H°_{vap.}$ is not a very accurate method. The low heat of fusion obtained in this work corresponds to an entropy of fusion of 9.1 cal deg.$^{-1}$ mol^{-1} or about 1.8 cal K^{-1} g atom^{-1} which is low even for a molecular substance.

Table 5. Melting point for $NbCl_5$.

°C (Ref.): 204.7 (18); 204.4 (17); 206.8 (9); 205.7 (19); 205.3 (20); 204.6 (this work).

Acknowledgement. The authors wish to express their gratitude to professor Gotthard Björling for his interest in this work. They also wish to thank Mr. Arne Sundling at the Axel Johnson Institute who carried out the chemical analysis. This research was sponsored by the *Swedish Board for Technical Development.*

REFERENCES

1. Enghag, P. and Staffansson, L.-I. *Acta Chem. Scand.* **26** (1972) 1067.
2. Staffansson, L.-I. and Enghag, P. *Scand. J. Met. In press.*
3. Schäfer, H. and Kahlenberg, F. *Z. Anorg. Allgem. Chem.* **305** (1960) 178.
4. Skinner, H. and Sutton, L. E. *Trans. Faraday Soc.* **36** (1940) 668.
5. Gaunt, I. and Ainscough, J. B. *Spectrochim. Acta* **10** (1957) 52.
6. Spiridonov, V. P. and Romanov, G. V. *Vestn. Mosk. Univ. Khim.* **23** (1968) 10 [*Chem. Abstr.* **69** (1968) 100786].
7. Zalkin, A. and Sands, D. E. *Acta Cryst.* **11** (1958) 615.
8. Schäfer, H. and Pölert, W. *Z. Anorg. Allgem. Chem.* **353** (1967) 78.
9. Meyer, G., Oosterom, J. F. and van Oeveren, W. J. *Rec. Trav. Chim.* **80** (1961) 502.
10. Ainscough, J. B., Holt, R. J. W. and Trowse, F. W. *J. Chem. Soc.* **1957** 1034.
11. 't Hart, W. and Meyer, G. *Rec. Trav. Chim.* **83** (1964) 1233.
12. Johnson, J. W., Silva, W. J. and Cubicciotti, D. *High Temp. Sci.* **2** (1970) 20.
13. Opichtina, M. and Fleischer, N. A. *Zh. Obshch. Khim.* **7** (1937) 2016.
14. Tarasenkov, D. N. and Komandin, A. W. *Zh. Obshch. Khim.* **10** (1940) 1319.
15. Alexander, K. M. and Fairbrother, F. *J. Chem. Soc.* **1949** 223.
16. Schäfer, H., Bayer, L. and Lehman, H. *Z. Anorg. Allgem. Chem.* **268** (1952) 268.
17. Nisel'son, L. A. *Russ. J. Inorg. Chem.* **3** (1958) 14.
18. Schäfer, H. and Pietruck, Ch. *Z. Anorg. Allgem. Chem.* **267** (1951) 174.
19. Keneshea, F. J., Cubicciotti, D., Withers, G. and Ediny, H. *J. Phys. Chem.* **72** (1968) 1272.
20. Johnson, J. W. and Cubicciotti, D. *High. Temp. Sci.* **2** (1970) 9.
21. Nisel'son, L. A. and Perekhrest, G. L. *Zh. Neorg. Khim.* **3** (1958) 2150.

Received April 12, 1973.

ACTA CHEMICA SCANDINAVICA 27 (1973) 2740–2748

Circular Dichroism of Acetylated Methyl Glycosides. Part II*

HANS B. BORÉN, PER J. GAREGG, LENNART KENNE, ÅKE PILOTTI, SIGFRID SVENSSON and CARL-GUNNAR SWAHN

Avd. för organisk kemi, Arrheniuslaboratoriet, Fack, S-104 05 Stockholm 50, Sweden

The CD spectra, in ethanol, of twentytwo methyl-D-hexopyranoside acetates with the *O*-acetyl groups in the 4-, 6-, 2,3-, 2,6-, 3,4-, 3,6-, and 4,6-positions have been recorded. Possible relationships between the observed Cotton effects and the molecular geometry of the acetoxy groups and neighbouring oxygen atoms are discussed.

In a previous paper the circular dichroism of the 2-*O*-acetyl and 3-*O*-acetyl derivatives of the methyl D-hexopyranosides of D-galactose, D-glucose and D-mannose were recorded.[1] The signs of the observed Cotton effects were empirically correlated with the dihedral angle between the acetoxy group and a vicinal oxygen atom. Thus (1) was considered to give rise to a positive Cotton effect and (2) correspondingly a negative one.

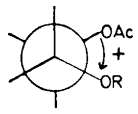

(1)

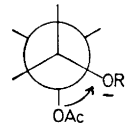

(2)

Arrangements with the acetoxy group and the vicinal oxygen in a *trans* relationship were considered to give no Cotton effect. Furthermore, it was found necessary to postulate that the contribution to the circular dichroism for R = H in (1) and (2) exceeded that for R = CH_3. Contributions from vicinal carbon (and hydrogen) atoms were neglected. Also, the orientation of the chromophore may be different in the substances studied. It is possibly for these reasons that correlations of molecular geometry with the signs, but not with the magnitudes of the observed CD could be obtained. In the present paper these studies have been extended to methyl D-hexopyranosides with the *O*-acetyl groups in the 4 and 6-positions, and to some di-*O*-acetyl derivatives.

* Part I, Ref. 1.

The various acetates were synthesized by conventional routes. The 4-acetates of methyl α-D-glucopyranoside, methyl β-D-glucopyranoside, methyl α-D-galactopyranoside, methyl β-D-galactopyranoside, and methyl α-D-mannopyranoside were prepared, starting from the appropriate methyl 4,6-*O*-benzylidene hexopyranosides. These were benzylated in the 2,3-positions. The benzylidene groups were removed by mild acid hydrolysis. The primary hydroxyls in the 6-positions were tritylated (glucosides and mannosides) or benzylated (galactosides) and the remaining hydroxyl groups in the 4-positions acetylated. Catalytic hydrogenation removed trityl and benzyl groups and afforded the 4-acetates. The 6-*O*-acetyl derivatives of the same methyl hexopyranosides were obtained from the above methyl 2,3-di-*O*-benzylhexopyranosides by partial acetylation and obtained in pure form by silica gel chromatography.

Table 1. Positions and amplitudes of CD maxima of some hexoside acetates.

Substance	Ref. [a]	CD maximum (nm)	θ (°)	Predicted sign for θ
Methyl 3-*O*-acetyl-2-*O*-methyl-α-D-glucopyranoside		nil		+
Methyl-4-*O*-acetyl-α-D-glucopyranoside		213	−725	−
Methyl-4-*O*-acetyl-β-D-glucopyranoside		212	−489	−
Methyl-4-*O*-acetyl-β-D-galactopyranoside		218	+174	+
Methyl-4-*O*-acetyl-α-D-mannopyranoside		214	−1650	−
Methyl-6-*O*-acetyl-α-D-glucopyranoside	8	234	+218	+
		217	−348	−
Methyl-6-*O*-acetyl-β-D-glucopyranoside	9	214	−286	−
Methyl-6-*O*-acetyl-α-D-galactopyranoside		217	−212	−
Methyl-6-*O*-acetyl-β-D-galactopyranoside	2	217	−180	−
Methyl 6-*O*-acetyl-α-D-mannopyranoside		242	+226	+
		217	−552	−
Methyl 2,3-di-*O*-acetyl-α-D-glucopyranoside	10	218	−835	−
Methyl 2,3-di-*O*-acetyl-β-D-glucopyranoside	11	217	+558	+
Methyl 2,3-di-*O*-acetyl-α-D-galactopyranoside	12	217	−3180	−
Methyl 2,3-di-*O*-acetyl-β-D-galactopyranoside	12	217	−2410	−
Methyl 2,3-di-*O*-acetyl-β-D-mannopyranoside	13	214	+1055	+
Methyl 2,6-di-*O*-acetyl-β-D-galactopyranoside		218	+101	−
		228	−81	−
Methyl 3,4-di-*O*-acetyl-β-D-galactopyranoside		215	−745	−
Methyl 3,6-di-*O*-acetyl-α-D-galactopyranoside		216	−1620	−
Methyl 4,6-di-*O*-acetyl-α-D-glucopyranoside		239	+600	+
		217	−1050	−
Methyl 4,6-di-*O*-acetyl-α-D-galactopyranoside		213	+864	+
Methyl 4,6-di-*O*-acetyl-β-D-galactopyranoside		213	+1120	+
Methyl 4,6-di-*O*-acetyl-α-D-mannopyranoside		211	−2210	−
		237	−2320	

[a] For new compounds see Table 2.

Table 2. New compounds.

Compound	Synthetic precursor	Method of synthesis	Yield from precursor (%)
Methyl 4-*O*-acetyl-2,3-di-*O*-benzyl-6-*O*-triphenylmethyl-α-D-glucopyranoside (I)	Methyl 2,3-di-*O*-benzyl-6-*O*-triphenylmethyl-α-D-glucopyranoside (II)[14]	*a*	90
Methyl 4-*O*-acetyl-α-D-glucopyranoside	I	*b*	100
Methyl 4-*O*-acetyl-2,3-di-*O*-benzyl-6-*O*-triphenylmethyl-β-D-glucopyranoside (III)	Methyl 2,3-di-*O*-benzyl-6-*O*-triphenylmethyl-β-D-glucopyranoside (IV)[15]	*a*	90
Methyl 4-*O*-acetyl-β-D-glucopyranoside	III	*b*	100
Methyl 2,3,6-tri-*O*-benzyl-β-D-galactopyranoside (IV)	Methyl 2,3-di-*O*-benzyl-β-D-galactopyranoside (V)[16]	*c*	35
Methyl 4-*O*-acetyl-2,3,6-tri-*O*-benzyl-β-D-galactopyranoside (VI)	IV	*a*	76
Methyl 4-*O*-acetyl-β-D-galactopyranoside	VI	*b*	100
Methyl 2,3-di-*O*-benzyl-4,6-*O*-benzylidene-α-D-mannopyranoside (VII)	Methyl 4,6-*O*-benzylidene-α-D-mannopyranoside (VIII)[17]	*d*	68
Methyl 2,3-di-*O*-benzyl-α-D-mannopyranoside (IX)	VIII	*e*	52
Methyl 2,3-di-*O*-benzyl-6-*O*-triphenylmethyl-α-D-mannopyranoside (X)	IX	*f*	66
Methyl 4-*O*-acetyl-2,3-di-*O*-benzyl-6-*O*-triphenylmethyl-α-D-mannopyranoside (XI)	X	*a*	88
Methyl 4-*O*-acetyl-α-D-mannopyranoside	XI	*b*	100
Methyl 6-*O*-acetyl-2,3-di-*O*-benzyl-α-D-glucopyranoside	Methyl 2,3-di-*O*-benzyl-α-D-glucopyranoside (XII)[18]	*g*	60
Methyl 6-*O*-acetyl-2,3-di-*O*-benzyl-β-D-glucopyranoside	Methyl 2,3-di-*O*-benzyl-β-D--glucopyranoside (XIII)[19]	*g*	58
Methyl 6-*O*-acetyl-2,3-di-*O*-benzyl-α-D-galactopyranoside	Methyl 2,3-di-*O*-benzyl-α-D-galactopyranoside (XIV)[20]	*g*	72
Methyl 6-*O*-acetyl-α-D-galactopyranoside	XIV	*b*	100
Methyl 6-*O*-acetyl-2,3-di-*O*-benzyl-α-D-mannopyranoside (XV)	IX	*g*	55
Methyl 6-*O*-acetyl-β-D-mannopyranoside	XV	*b*	100
Methyl 2,6-di-*O*-acetyl-β-D-galactopyranoside	Methyl 2,6-di-*O*-acetyl-3,4-*O* benzylidene-β-D-galactopyranoside [2]	*b*	86
Methyl 2,6-di-*O*-benzyl-β-D-galactopyranoside (XVI)	Methyl 3,4-*O*-benzylidene-β-D-galactopyranoside [2]	*h*	65
Methyl 3,4-di-*O*-acetyl-2,6-di-*O*-benzyl-β-D-galactopyranoside (XVII)	XVI	*a*	70
Methyl 3,4-di-*O*-acetyl-β-D-galactopyranoside	XVII	*b*	100
Methyl 4,6-di-*O*-acetyl-2,3-di-*O*-benzyl-α-D-glucopyranoside (XVIII)	XII	*a*	100
Methyl 4,6-di-*O*-acetyl-α-D-glucopyranoside	XVIII	*b*	100
Methyl 4,6-di-*O*-acetyl-2,3-di-*O*-benzyl-α-D-galactopyranoside (XIX)	XIV	*a*	100
Methyl 4,6-di-*O*-acetyl-α-D-galactopyranoside	XIX	*b*	100
Methyl 4,6-di-*O*-acetyl-2,3-di-*O*-benzyl-β-D-galactopyranoside (XX)	V	*a*	90
Methyl 4,6-di-*O*-acetyl-β-D-galactopyranoside	XX	*b*	100
Methyl 4,6-di-*O*-acetyl-2,3-di-*O*-benzyl-α-D-mannopyranoside (XXI)	IX	*a*	100
Methyl 4,6-di-*O*-acetyl-α-D-mannopyranoside	XXI	*b*	100
Methyl 3-*O*-acetyl-2-*O*-methyl-α-D-glucopyranoside	Methyl 3-*O*-acetyl-4,6-*O*-benzylidene-2-*O*-methyl-α-D-glucopyranoside [21]		100

Solvent for TLC Purification	Solvent for crystallization	$[\alpha]_D$ (°)	Solvent for rotation	m.p. (°)	Analysis C	Analysis H %	Required analysis C	Required analysis H %
$CHCl_3$ – Et_2O 9:1	MeOH – EtOAc	+23	$CHCl_3$	134 – 7	76.7	6.51	76.6	6.43
–	–	+119	H_2O	–				
$CHCl_3$ – Et_2O 9:1	MeOH – EtOAc	+5	$CHCl_3$	158 – 161	76.8	6.57	76.6	6.43
–	–	−20	H_2O	119 – 126	45.6	6.57	45.8	6.83
Light petr. [j] – EtOAc 2:1	–	+3	$CHCl_3$	–				
Light petr. [j] – EtOAc 3:1	–	+20	$CHCl_3$	–				
–		−4	EtOH					
Light petr. [j] – EtOAc 4:1	–	+25	$CHCl_3$	–	72.7	6.59	72.7	6.54
$PhCH_3$ – EtOAc 4:1	–	−2	$CHCl_3$	–	67.2	6.81	67.4	7.00
$PhCH_3$ – EtOAc 4:1	–	−9	$CHCl_3$	–	77.9	6.64	77.9	6.54
$CHCl_3$ – Et_2O 9:1	–	−5	$CHCl_3$	–	76.8	6.33	76.6	6.43
–	–	+55	H_2O	–				
$CHCl_3$ – Me_2CO 8:1	–	+18	$CHCl_3$	–	66.3	6.93	66.3	6.78
$CHCl_3$ – Me_2CO 5:1	–	−20	$CHCl_3$	–	66.5	6.80	66.3	6.78
Light petr. [j] – EtOAc 2:1	MeOH	+13	$CHCl_3$	139 – 141	66.9	7.09	66.3	6.78
–	Me_2CO	+160	EtOH	154 – 6	45.9	6.68	45.8	6.83
$CHCl_3$ – Me_2CO 85:15	–	−9	$CHCl_3$	–	66.2	6.75	66.3	6.78
–	–	+67	EtOH	–				
–	Et_2O	−12	$CHCl_3$	105 – 111	47.3	6.40	47.5	6.52
$CHCl_3$ – Et_2O 7:3	Et_2O light petr.	+10	$CHCl_3$	79 – 80	67.1	7.16	67.4	7.00
$CHCl_3$ – Et_2O 8:2	–	+14	$CHCl_3$	–	65.5	6.43	65.5	6.60
–	–	+32	$CHCl_3$	–	–	–		–
–	–	+13	$CHCl_3$	–	65.6	6.72	65.5	6.60
–	–	+96	$CHCl_3$	–	–	–	–	–
Light petr. [j] – EtOAc 2:1	–	+52	$CHCl_3$	–	–	–	–	–
–	–	+111	EtOH	–	–	–	–	–
Light petr. [j] – EtOAc 2:1	Pr^i_2O	+28	$CHCl_3$	108 – 9	65.7	6.97	65.5	6.60
–	Pr^i_2O	−1	EtOH	109 – 112	47.3	6.5	47.5	6.52
–	–	−5	$CHCl_3$	–	65.7	6.64	65.5	6.60
–	–	+38	$CHCl_3$	–	–	–	–	–
–	Pri_2O	+150	EtOH	84 – 6	47.9	7.30	48.0	7.25

[a] Ac_2O, C_5H_5N. [b] Pd/H_2. [c] 1 mol equiv. $PhCH_2Br$, Ag_2O, DMF. [d] $PhCH_2Br$, Ag_2O, DMF. [e] 90 % aq. CF_3COOH. [f] Ph_3CCl, C_5H_5N. [g] 1 mol equiv. Ac_2O, C_5H_5N. [h] $PhCH_2Br$, NaH, DMF. [j] 40 – 60° throughout.

The 2,3-di-*O*-acetyl derivatives of methyl α-D-glucopyranoside, methyl β-D-glucopyranoside, methyl α-D-galactopyranoside, methyl β-D-galactopyranoside, and methyl α-D-mannopyranoside were obtained by acetylation of the appropriate methyl 4,6-*O*-benzylidene hexopyranosides followed by catalytic hydrogenation.

Methyl 2,6-di-*O*-acetyl-β-D-galactopyranoside was obtained from methyl 2,6-di-*O*-acetyl-3,4-*O*-benzylidene-β-D-galactopyranoside [2] by catalytic hydrogenation. Methyl 3,4-di-*O*-acetyl-β-D-galactopyranoside was obtained from methyl 3,4-*O*-benzylidene-β-D-galactopyranoside [2] by benzylating the 2- and 6-positions, removing the benzylidene group with mild acid, acetylating the free hydroxyl groups in the 3- and 4-positions and finally removing benzyl groups from the 2- and 6-positions by catalytic hydrogenation.

The 4,6-di-*O*-acetyl derivatives of methyl α-D-glucopyranoside, methyl α-D-galactopyranoside, methyl β-D-galactopyranoside, and methyl α-D-mannopyranoside were prepared from the appropriate methyl 2,3-di-*O*-benzyl-hexopyranosides described above, by acetylation followed by catalytic hydrogenation.

Methyl 3,6-di-*O*-acetyl-α-D-galactopyranoside was produced from the 4,6-acetate by spontaneous acetyl migration by standing as a syrup. Its constitution follows from NMR evidence.

Methyl 3-*O*-acetyl-2-*O*-methyl-α-D-glucopyranoside was obtained by catalytic hydrogenation of the corresponding 4,6-*O*-benzylidene derivative.

Literature references for all known compounds are given in Table 1; the syntheses and pertinent data for all new compounds are summarized in Table 2.

Positions and amplitudes for the various CD maxima are given in Table 1. The results may be rationalized following the same argumentation as that previously presented. It is assumed that unit (3) gives a positive Cotton effect, while that of (4) gives a negative one.[1]

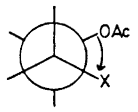

(3)

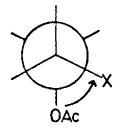

(4)

X = −O−, −OH, −OMe, −OAc, $-CH_2OH$, $-CH_2OAc$

The main contribution to the Cotton effect thus arises from the presence of a neighbouring oxygen or oxymethylene function. In order to explain the results in Table 1 it is furthermore necessary to propose that the magnitude of the effect of these groupings on the observed dichroism decreases in the order

$$CH_2OH \geq CH_2OAc \gg O\text{-}5 > OH > OCH_3 > OAc$$

The expected signs for the observed dichroism following from these empirical rules are given in the last column in Table 1.

The following two examples illustrate the reasoning used in the various correlations: For methyl 4-*O*-acetyl-α-D-glucopyranoside (as well as for the

β-anomer and for methyl 4-*O*-acetyl-α-D-mannopyranoside) the units (5) and (6) would be expected to determine the sign of the CD observed.

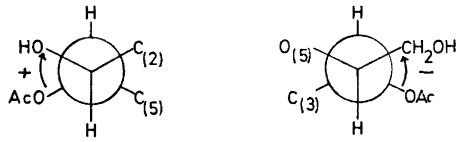

(5) (6)

Since the contribution from (6) is thought to dominate over that from (5) the sign of the CD is predicted to be negative, in agreement with the findings shown in Table 1. On the other hand, methyl 4-*O*-acetyl-β-D-galactopyranoside would, by the same reasoning, be expected to have positive CD, arising from contributions from the units (7) and (8) and this is in agreement with the CD observed.

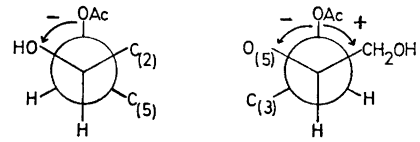

(7) (8)

In order to explain the observed CD for the 4-acetates it is therefore necessary to postulate the dominance of the influence from the primary oxymethylene group (acetoxy or hydroxy). By contrast, this dominating influence is not observed for ring oxymethylene functions. Thus, for example, the CD for an acetyl group in the 2-position of a mannopyranoside is assumed to be relatively unaffected by the CHOAc group attached to C – 3. The reason for this apparent anomaly is not clear, but could be associated with the rotational freedom of a primary acetoxy- or hydroxymethylene group which, by contrast to the corresponding group in the pyranose ring, can adopt conformations which affect the sign of the CD strongly.

Some of the 6-*O*-acetyl derivatives give rise to two CD bands. Whenever this occurs, a substantial separation of the wave-lenghts for the CD bands is observed. This separation effect has been described and accounted for previously.[3,ab] The occurrence of the double CD bands probably is best interpreted as being due to the presence, in solution, of two conformers. For the 6-*O*-acetyl derivatives, the above rationale requires that, in accordance with previous results, conformation (9) does not give rise to CD, while those of (10) and (11) give a positive and a negative CD band, respectively.

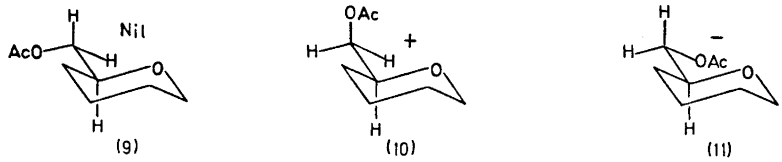

(9) (10) (11)

Hall and Manville, on the basis of NMR data, have concluded that (9) is the favoured conformation for acetylated D-*galacto*-hexopyranoses and that of (10) for the corresponding D-*gluco* isomers.[4] Lemieux and co-workers have, however, presented data from investigations of NMR and of optical rotation to support the view, that at least for D-*erythro*-hexopyranoses, conformation (11) is the favoured one.[5,6] The double CD band for methyl 6-*O*-acetyl-α-D-glucopyranoside is best explained by assuming the presence, in ethanol, of both conformations (10) and (11). For the corresponding β-anomer, however, the unfavourable dipolar interactions of conformation (10), shown in (12), should lead to the predominance, in ethanol solution, of conformation (11) and thereby a single, negative CD band, which is that observed.

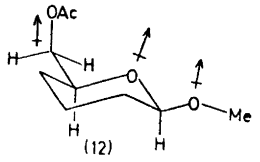

(12)

By analogy, methyl 6-*O*-acetyl-α-D-mannopyranoside gives two CD bands, presumably corresponding to conformations (10) and (11). For the anomeric methyl 6-*O*-acetyl-D-galactopyranosides, conformation (10) would necessitate an unfavourable 1,3-interaction, depicted in (13).

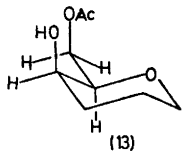

(13)

It is therefore possible that for these substances, conformation (11) predominates over (10) giving a negative, single CD band, which would fit the above generalization. In the crystalline state, methyl 6-*O*-acetyl-β-D-galactopyranoside, however, adopts conformation (9).[7] It should be noted that the presence, in the various conformational equilibria of the 6-acetates, of conformation (9) would remain undetected in the CD experiments, since (9) is expected to give a negligible contribution to the CD.*

The signs of the CD bands of the various diacetates listed in Table 1 are those expected from the above discussion, with two exceptions. The origin of the two negative CD bands for methyl 4,6-di-*O*-acetyl-β-D-mannopyranoside is not entirely clear. The sign of one CD band given by methyl 2,6-di-*O*-acetyl-β-D-galactopyranoside is opposite to that expected, since the above considerations would predict negative CD for this substance, as depicted in (14) – (17).

* The presence of several rotamers for the C(5)-CH_2OTMS groups in several monosaccharide pertrimethyl silyl derivatives has recently been demonstrated by 220 MHz ^1H NMR.[7b]

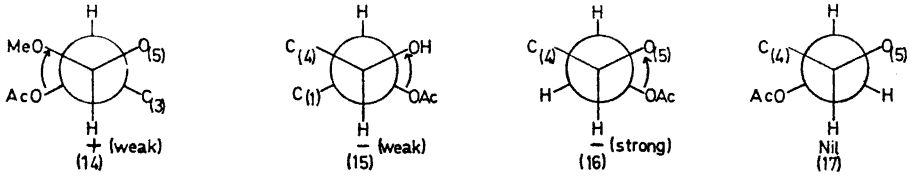

This indicates that other factors such as 1,3-diaxial type interactions may be of importance in determining the sign of the CD. In addition, methyl 3-*O*-acetyl-2-*O*-methyl-α-D-glucopyranoside does not show any detectable CD band, whereas the above rationale would predict it to be positive, (18) and (19):

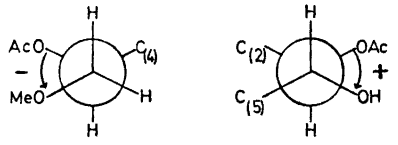

This emphasizes that these rules, being entirely empirical, should be used with caution.

EXPERIMENTAL

General methods. Concentrations were performed at reduced pressure. Melting points are corrected. Optical rotations were determined at room temperature (20 – 22°) with a Perkin-Elmer 141 polarimeter. NMR spectra were recorded with a Varian A-60 A spectrometer using tetramethylsilane as internal reference and deuteriochloroform or deuteriomethanol as solvents (the latter for glycoside mono- and diacetates). The NMR spectra were invariably in accordance with the presumed structures. TLC was performed on silica gel GF^{254} (Merck). Sulphuric acid was used as spray reagent. Mallinckrodt AR silicic acid (100 mesh) was used in preparative column separations. The CD spectra were determined on a Cary 60 apparatus equipped for CD. The solvent used was ethanol throughout.

Compounds. Pertinent data for the various new compounds synthesized in the course of the investigation are summarized in Table 2. References for the various known compounds, synthesized by previously described routes, are given in Table 1.

The purity of the various acetates was checked by examining the acetates by TLC immediately after running the CD spectra (TLC solvent: ethyl acetate). All substances were found to be sufficiently stable for the purposes of the investigation.

Acknowledgement. The authors are indebted to Professor Bengt Lindberg for his interest, to the Department of Organic Chemistry, University of Lund (Sweden) for placing the CD equipment at our disposal, to *Hierta-Retzius stipendiefond*, *Wallenberg-stiftelsens jubileumsanslag för befordrande av vetenskapligt arbete* and *Statens Naturvetenskapliga Forskningsråd* for financial support.

REFERENCES

1. Borén, H. B., Garegg, P. J., Kenne, L., Maron, L. and Svensson, S. *Acta Chem. Scand.* **26** (1972) 644.
2. Garegg, P. J. and Swahn, C.-G. *Acta Chem. Scand.* **26** (1972) 3895.

3. a. Wellman, K. M., Laur, P. A., Briggs, W. S., Moscowitz, A. and Djerassi, C. *J. Am. Chem. Soc.* **87** (1965) 66; b. Wellman, K. M., Briggs, W. S. and Djerassi, C. *J. Am. Chem. Soc.* **87** (1965) 87.
4. Hall, L. D. and Manville, J. F. *Can. J. Chem.* **47** (1969) 1.
5. Lemieux, R. U. and Stevens, J. D. *Can. J. Chem.* **43** (1965) 2059.
6. Lemieux, R. U. and Martin, J. C. *Carbohyd. Res.* **13** (1970) 139.
7. a. Lindberg, B., Garegg, P. J. and Swahn, C.-G. *Acta Chem. Scand.* **27** (1973) 380; b. Streefkerk, D. G., de Bie, M. J. A. and Vliegenhart, J. F. G. *Tetrahedron* **29** (1973) 833.
8. Hurst, D. T. and McInnes, A. G. *Can. J. Chem.* **43** (1965) 2004.
9. Bouveng, H. O. *Acta Chem. Scand.* **15** (1961) 87.
10. Whistler, R. L. and Kazeniac, S. J. *J. Am. Chem. Soc.* **76** (1954) 3044.
11. Oldham, J. W. H. and Rutherford, J. K. *J. Am. Chem. Soc.* **54** (1932) 366.
12. Müller, S., Moricz, M. and Verner, G. *Ber.* **72** (1939) 745.
13. Garegg, P. J. *Arkiv Kemi* **23** (1964) 255.
14. Kenner, J. and Richards, G. N. *J. Chem. Soc.* **1955** 1810.
15. McGilvray, D. I. *J. Chem. Soc.* **1952** 3648.
16. Bacon, J. S. D., Bell, D. J. and Lorber, J. *J. Chem. Soc.* **1940** 1147.
17. Buchanan, J. G. and Schwarz, J. C. P. *J. Chem. Soc.* **1962** 4770.
18. Freudenberg, K. and Plankenhorn, E. *Ber.* **73B** (1940) 621.
19. Dennison, J. C. and McGilvray, D. I. *J. Chem. Soc.* **1951** 1616.
20. Kiss, J. and Burkhardt, F. *Helv. Chim. Acta* **53** (1970) 1000.
21. Bourne, E. J., Stacey, M., Tatlow, C. E. M. and Tatlow, J. C. *J. Chem. Soc.* **1951** 826.

Received April 13, 1973.

ACTA CHEMICA SCANDINAVICA 27 (1973) 2749–2756

The Phospholipase A_2 Activity of Human Small Intestinal Contents

INGEMAR IHSE and BO ARNESJÖ

Department of Surgery, University Hospital of Lund, Lund, Sweden

Studies are presented dealing with the properties, substrate requirements, kinetics and the behaviour during gel chromatography of the phospholipase A_2 present in human intestinal contents.

Phospholipase A_2 present in duodenal contents is completely stable when stored at 25°C in spite of the presence of high proteolytic activity. As judged by gel chromatography experiments this protection seems to be independent of partition of these enzymes between the emulsion or micellar phases and the water phase.

Sodium dodecyl sulfate in combination with bile salts and calcium highly stimulated the enzymic hydrolysis of egg lecithin. This made it possible to design a sensitive, accurate, automatic, titrimetric method for the assay of the phospholipase A_2 activity of intestinal contents.

The phospholipase A activity of the small intestinal contents is derived from the pancreatic secretion.[1–13] In the pancreas and pancreatic juice, however, it is present mainly as an inactive precursor, prophospholipase.[1–6,10,11] When secreted into the duodenum this enzymic precursor is actived by trypsin.[2–8,10,11] The active form of phospholipase A hydrolyses exclusively the fatty acid ester linkage at the 2-position of lecithin.[2–5,10,11] No other physiologically important enzyme activities capable of hydrolyzing the fatty acid ester bonds of lecithin are present in the intestinal lumen.[5,14]

Several methods for the measurement of phospholipase A activity in intestinal contents have been suggested.[5,8,9,13,15] All these methods have involved disadvantages by reason of the necessity of adding too high concentrations of intestinal contents. This has lead to uncontrolled detergent and free or esterfied fatty acid concentrations in the incubation mixture resulting in varying and relatively high blank values.

In the present study the main purpose was to study the properties, substrate requirements, kinetics, and the behaviour during gel chromatography of small intestinal phospholipase A_2. This was performed in order to design a sensitive and rapid routine method for the assay of the enzyme.

MATERIALS AND METHODS

All solvents and chemicals were of reagent grade purity. Chloroform was stabilized with 2 % ethanol.

Sodium taurodeoxycholate (NaTDC), sodium taurocholate, and sodium deoxycholate were synthesized and crystallized according to Norman [16] as modified by Hofman.[17] Purity better than 97 % as judged by thin layer chromatography of the three bile salts.[18]

Egg lecithin was prepared from fresh egg yolks as described by Hanahan.[19] Purity better than 97 % as judged by thin layer chromatography.[20] The lecithin was stored either in powder form in a nitrogen atmosphere at -20°C in the dark, or in a chloroform solution at -20°C in the dark. Several control experiments were run after further purification of lecithin.[3] No differences were observed.

Sodium dodecyl sulfate (NaDS), purity better than 99.8 % ,was purchased from AB Kebo, Stockholm, Sweden, and used without further purification.

Small intestinal contents were obtained from healthy male persons by duodenal or jejunal aspiration after oral (testmeal) or intravenous (pancreozymin) stimulation of the pancreatic secretion.

Sephadex G 100 was a product of Pharmacia Fine Chemicals, Uppsala, Sweden. The columns were packed according to standard procedures and the size of the columns are given in the text to the figures. Blue dextran 200 was used for indication of the void volumes of the columns and measured at 600 mμ in a spectrophotometer.

Phospholipase A activity was estimated in the following optimal way. A mixture 4.5 mmol/l in $CaCl_2$, 12.5 mmol/l in sodium taurodeoxycholate, and 2.5 mmol/l in sodium dodecyl sulfate containing 12 mg lecithin/ml was prepared. After vigorous shaking or sonication to dissolve the lecithin the solution was temperature-equilibrated at 60°C for 30 min. This mixture was used within 12 h. Two ml were transferred to an incubation flask kept at 60°C. During stirring the pH of the mixture was automatically kept at pH 7.5 with 0.01 mol/l NaOH, using a pH-stat (Radiometer, Copenhagen) with a TTT2 titrator connected to an ABU II Burette Unit with a 0.25 ml burette and a thermostatically controlled TTA31 titration assembly. The titration curves were recorded by means of a SBR2 Titrigraph. After measurement of the spontaneous hydrolysis rate (max. 0.05 μmol fatty acid released per min) for at least $2-3$ min, the enzyme source diluted to 0.2 ml was added. The automatic titration was then run at pH 7.5 for at least $3-5$ min after pH correction for the added enzyme source. A hydrolysis rate higher than 2.0 and lower than 0.1 μmol fatty acid released per min was not used in order to record activities directly proportional to the added amount of intestinal contents. These hydrolysis rate limits corresponded to $1:10-1:1000$ dilution of normal human small intestinal contents aspirated during digestion of a standard testmeal as previously described. Small intestinal contents having low phospholipase A activities were precipitated in 90 % ethanol, centrifuged and redissolved in water prior to the phospholipase A assay. Repeated assays of different concentrations of intestinal aspirates gave a mean coefficient of variation of $\pm$ 2.5 %.

Lipase activity was measured by a scaled down version of the method described by Erlanson and Borgström.[21] Trypsin was assayed by automatic titration using TAME as the substrate.[22]

All values described in this paper represent the averages of three determinations.

RESULTS AND DISCUSSION

Properties, substrate requirements and kinetics of small intestinal content phospholipase A_2

Enzymic action of intestinal contents. The phospholipase A_2 activity of small intestinal aspirates stored for $3-4$ weeks at room temperature was found to be completely stable. This contrasts to the ready inactivation of purified active pancreatic juice phospholipase A_2 in the presence of trypsin at such concentrations as present in intestinal contents.[4] Thus the enzyme is

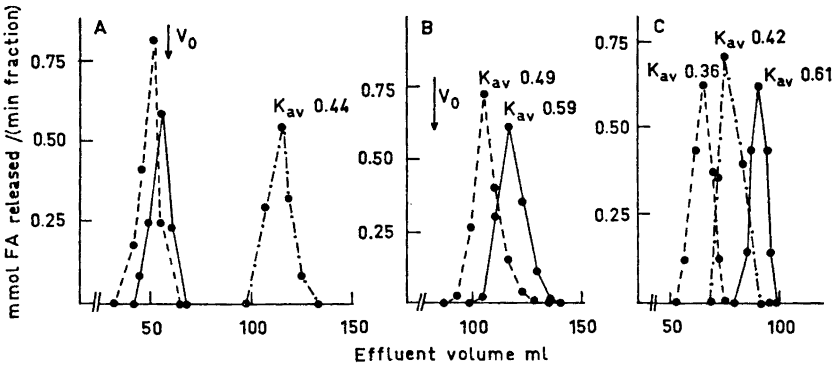

Fig. 1. One ml human intestinal contents was chromatographed on a Sephadex G 100 column (diameter 1.5 cm) equilibrated and eluted with 0.15 mol/l NaCl (A) and with 5.0 mmol/l sodium dodecylsulfate (B) or 6 mmol/l sodium taurodeoxycholate (C). Activity against micellar lecithin ——— , tributyrine – – – and TAME ·—·—·—· Flow rate approx, 6 ml/h.

protected against proteolytic inactivation in the intestinal lumen. This might depend either on the presence of bile salts [4] or on phase separation of the two enzymes or both. To test this, previously filtered intestinal contents were chromatographed on Sephadex G 100 equilibrated and eluted with 0.15 mol/l NaCl (Fig. 1A). Phospholipase A and lipase appeared in the void volume as previously observed for lipase by Erlanson and Borgström.[23] Trypsin was eluted at a K_{av} corresponding to its molecular weight. Accordingly both phospholipase A and lipase have a tendency to appear in fractions which under such circumstances contain the intestinal emulsion phase.[23] When chromatographed on Sephadex G 100 columns equilibrated and eluted with 5.0 mmol/l sodium dodecyl sulfate or 6 mmol/l NaTDC, however, phospholipase A, lipase, and trypsin were eluted at K_{av}'s corresponding to their molecular weights in previously tryptically digested human pancreatic juice [23] (Figs. 1B and 1C). In view of the results obtained in these latter experiments and in those by Erlanson and Borgström [23] phospholipase A and lipase in the presence of detergents were eluted in fractions which contained neither the emulsion nor the micellar phase of the intestinal contents. Therefore it seems that the protection of intestinal phospholipase A against tryptic inactivation is independent of phase separation.

Intestinal contents centrifuged at 55 000 g_{av} for 1 h exhibited exactly the same phospholipase A activity as before centrifugation. Ordinary filtration did not cause activity losses. It was completely precipitated in 90 % ethanol and quantitatively recovered after centrifugal sedimentation and consecutive solubilization of the sediment in water. In order to reduce the amount of base to be added for automatic pH correction when testing intestinal aspirates containing low phospholipase A activities but ordinary free or esterified fatty acid concentrations, a preceding alcohol precipitation is recommended.

The addition of different concentrations of human blood, serum, heparin, ε-amino caproic acid, tranexanic acid and of the reaction products in amounts corresponding to 50 % hydrolysis of the substrate did not alter the hydrolysis rate.

Influence of the volume of the incubation mixture. Routinely the assays of the phospholipase A_2 activity were run in 2.2 ml with vigorous stirring at constant temperature. After pH correction (50 – 100 μl 0.01 mol/l NaOH) the enzymic reaction was followed by the addition of 0.01 mol/l NaOH – with a maximal volume increase of 10 %. A dilution to 0.5 ml of an intestinal aspirate aliquot containing a suitable phospholipase A activity did, however, not change the constant hydrolysis rate. Therefore an increase of 22 % of the volume under the optimal conditions described above (see Materials and Methods) did not change the accuracy of the measurements.

Influence of incubation time on enzymic activity. Small intestinal aspirate aliquots exhibiting hydrolysis rates of 0.1 – 0.5 μmol fatty acid released per min gave a fatty acid release proportional to incubation time for at least 20 min, after pH correction of the whole incubation mixture. Routinely the enzymic activity was measured during 3 – 5 min and expressed as μmol fatty acid release per min. A hydrolysis of approximately 0.5 μmol fatty acid released corresponded to 5 – 10 % hydrolysis of the substrate. A spontaneous base catalyzed hydrolysis of the substrate mixture was observed especially above pH 8 and at high temperature (70 – 90°C). In all assays the proportion of the total hydrolysis rate dependent on this spontaneous hydrolysis was kept below one third of the enzymic hydrolysis and subtracted. When freshly prepared the pH of the substrate mixture was approximately 5. After storage a progressive decrease of the pH was found. Also, as the spontaneous hydrolysis rate increased with old mixtures only preparations made within 12 h were used.

Influence of pH on enzymic activity. The dependence of intestinal content phospholipase A on the pH of the incubation medium is shown in Fig. 2. A sharp optimum peak around pH 7.5 was found. Contrary to the findings by Borgström for lipase [24] and Vogel and Zieve for phospholipase A [13] no shift in the optimal pH was demonstrated when using different concentrations of bile salt. In previously tryptically digested human, pig, and rat pancreatic juice the phospholipase A has a rather broad pH optimum between pH 8 and 9 in the presence of bile salt.[4,10] This difference between pancreatic juice and intestinal content phospholipase A indicates an alteration of the physiochemical state of the enzyme when secreted into the duodenum. The details of this process cannot be judged at present.

Influence of calcium on enzymic activity. With the addition of an excess of EDTA no phospholipase A activity was found even with high concentrations of intestinal contents. An increase of the calcium concentration above the EDTA concentration increased the enzymic activity until an optimum level was reached at a final concentration above 3 mmol/l $CaCl_2$. At concentrations above 4.5 mmol/l $CaCl_2$ calcium was inhibitory (Fig. 3).

Influence of detergents on enzymic activity. In the absence of bile salt phospholipase A of small intestinal contents was inactive. This was demonstrated when testing phospholipase A containing fractions eluted with 0.15

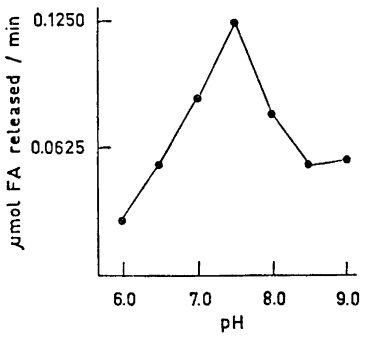

Fig. 2. Effect of pH on the rate of lecithin hydrolysis under optimal conditions (for details see text).

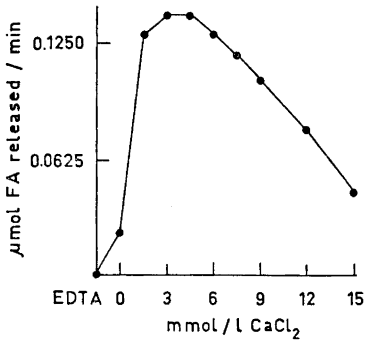

Fig. 3. Effect of calcium concentration on the rate of lecithin hydrolysis under optimal conditions (for details see text).

mol/l NaCl from a Sephadex G 100 column where during chromatography the enzyme is separated by size from bile salts in micellar as well as molecular solution (Fig. 1A). Both sodium taurocholate (NaTC) and sodium taurodeoxycholate (NaTDC) stimulated the reaction. Much higher concentration of NaTC was needed and therefore NaTDC was routinely used. Sodium deoxycholate (NaDC) was found not to stimulate the enzymic activity due to the fact that at both acid and alkaline pH it is precipitated in a calcium chloride solution. This latter observation might explain the varying previous results regarding the necessity of calcium as a co-factor for phospholipase A catalysis.[4,8,9,12,13,15] As partly demonstrated in Fig. 4, NaTDC at concentrations above 5.0 mmol/l initiate lecithin fatty acid hydrolysis with optimal

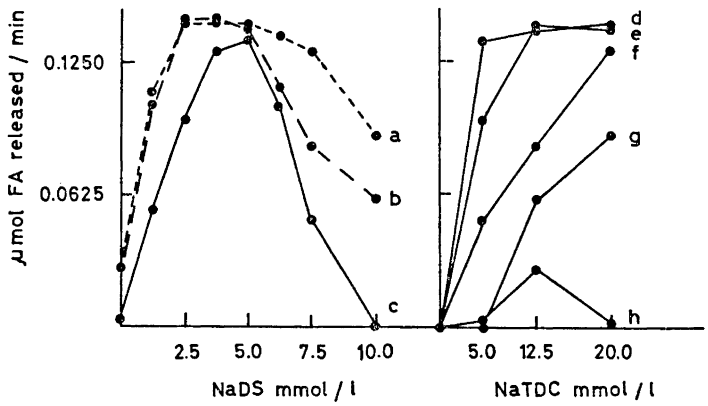

Fig. 4. Effect of varying relative concentrations of sodium taurodeoxycholate (NaTDC) and sodium dodecylsulfate (NaDS) on the rate of hydrolysis of lecithin (for details, see text). Concentrations of NaTDC (mmol/l): (a) 20.0; (b) 12.5; (c) 5.0. Concentrations of NaDS (mmol/l): (d) 5.0; (e) 2.5; (f) 7.5; (g) 100; (h) 0.0.

activity around 12.0 mmol/l NaTDC. At higher concentrations NaTDC is inhibitory. In contrast to tryptically activated phospholipase A from human and rat pancreatic juice the lowest concentration at which lecithin hydrolysis could be demonstrated did not correspond to the critical micellar concentration of the lecithin-bile salt mixture (turbidity measurements at 600 mμ).[4]

Although in concentrations high above the critical micellar concentration for its mixture with lecithin, sodium dodecyl sulfate (NaDS) *per se* had no stimulatory effect on the phospholipase A catalysis. In combination with NaTDC, however, the lecithin hydrolysis rate was stimulated between 5 and 50 times. This stimulation is demonstrated in Fig. 4. As can be seen there is maximal stimulation between 2.5 and 5.0 mmol/l NaDS in the incubation medium. This interaction between NaTDC and NaDS demonstrated in Fig. 4 might depend on several factors, such as that the combined detergents make the substrate more accessible for the enzyme or that NaDS alters the enzyme physicochemically, thus making it readily available for the lecithin substrate.

Influence of substrate concentration on the enzymic assays. In the presence of 4.5 mmol/l $CaCl_2$ and 12.5 mmol/l NaTDC and at 60°C optimal phospholipase A activity of small intestinal contents was obtained at 8 mg lecithin/ml (approx. 10 μmol/ml) (Fig. 5A). Higher concentrations of lecithin inhibited the reaction. At concentrations below the optimal an increase in the activity differences with increasing substrate concentration was observed. This resulted in a curvylinear Lineweaver-Burke representation at suboptimal substrate concentrations (Fig. 5B). The interpretation of such a substrate activation is difficult but might be explained either by a lecithin induced increase in enzymic solubilization or an increasing association of the enzyme with an increasing nonpolar phase of the mixed lecithin-bile salt micelles where the formation of enzyme-substrate complexes might take place.

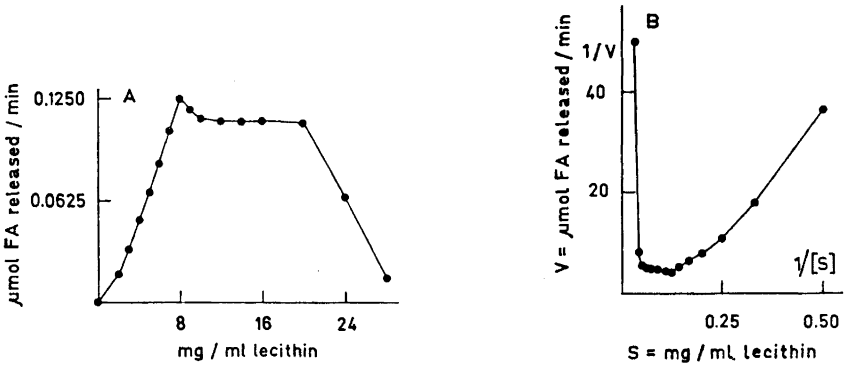

Fig. 5. Effect of lecithin concentration on the rate of lecithin hydrolysis at optimal concentration of sodium taurodeoxycholate. To the left: lecithin concentration *versus* hydrolysis rate. To the right: the corresponding Lineweaver-Burke representation (for details see text).

The addition of NaDS to the incubation mixture outlined in the preceding paragraph caused two modifications of the substrate concentration dependence.

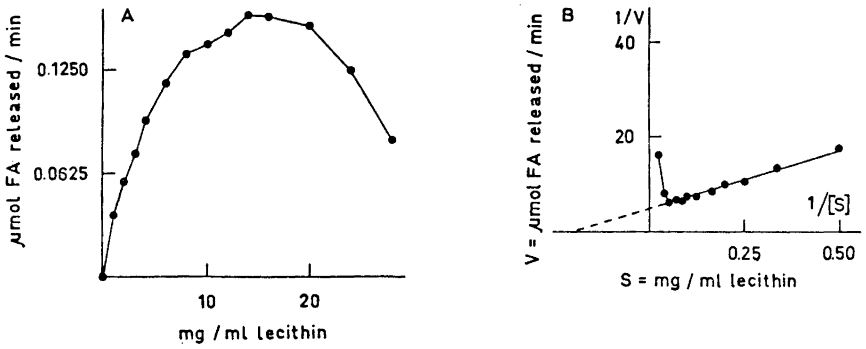

Fig. 6. Effect of lecithin concentration on the rate of lecithin hydrolysis at optimal concentration of sodium taurodeoxycholate and 5.0 mmol/l sodium dodecylsulfate. To the left: lecithin concentration *versus* hydrolysis rate. To the right: the corresponding Lineweaver-Burke representation(for details see text).

First, the optimal lecithin concentration was shifted towards higher values (Fig. 6A). Secondly, the activity difference at concentrations below the optimal decreased with increasing substrate concentrations and a straight line relationship in the Lineweaver-Burke diagram was obtained (Fig. 6B). These effects of NaDS might indicate that – in conformity with lecithin – it acts as a solubilizing agent for the phospholipase A in the water phase as well as in the micellar phase of the substrate mixture. Under these circumstances (12.5 mmol/l NaTDC, 4.5 mmol/l $CaCl_2$, 5.0 mmol/l NaDS and incubation at 60°C) the optimal lecithin concentration averaged 12 mg lecithin/ml and *Km* 5.8 mg/ml (approx. 7.25 µmol/l).

Influence of incubation temperature on enzymic reaction. Fig. 7 illustrates the effect of incubation temperature on the phospholipase A activity of small intestinal contents when tested under optimal conditions. The enzymic activity increased in an almost linear fashion with increasing temperature to 60°C above which a decreased activity was found. Routinely 60°C was used in the assays.

The fractions obtained in all the three types of gel chromatography described above (Figs. 1A, 1B, and 1C) were tested at 38°C and 60°C, respectively. At

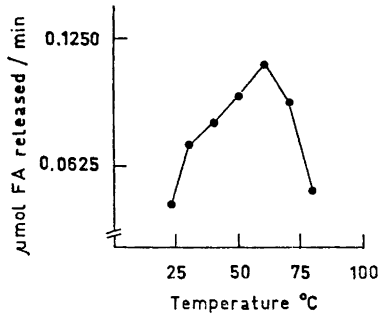

Fig. 7. Effect of incubation temperature on the rate of lecithin hydrolysis under optimal conditions (for details see text).

38°C no lecithin fatty acid release could be demonstrated in fractions other than those containing phospholipase A activity at 60°C. This result in combination with previous findings [5] indicates that the only lecithin fatty acid ester splitting enzyme activity in small intestinal contents is of the heat stable phospholipase A_2 type.

REFERENCES

1. Arnesjö, B. *Acta Physiol. Scand.* **81** (1971) 170.
2. Arnesjö, B., Barrowman, J. and Borgström, B. *Acta Chem. Scand.* **21** (1967) 2897.
3. Arnesjö, B. and Filipek-Wender, H. *Acta Physiol. Scand.* **74** (1968) 616.
4. Arnesjö, B. and Grubb, A. *Acta Chem. Scand.* **25** (1971) 577.
5. Arnesjö, B., Nilsson, Å., Barrowman, J. and Borgström, B. *Scand. J. Gastroenterol.* **4** (1969) 653.
6. Belleville, J. and Clément, J. *Compt. Rend.* **266** (1968) 959.
7. Van den Bosch, X. Thesis, Utrecht, The Netherlands, 1966.
8. Gjone, E and Björnstad, P. *Scand. J. Gastroenterol.* **1** (1966) 214.
9. Gjone, E., Björnstad, P., Marton, P. F. and Orning, O. M. *Scand. J. Gastroenterol.* **1** (1967) 228.
10. de Haas, G. H., Postema, N. M., Nieuwenhuizen, W. and van Deenen, L. L. M. *Biochim. Biophys. Acta* **159** (1968) 103.
11. de Haas, G. H., Postema, N. M., Nieuwenhuizen, W. and van Deenen, L. L. M. *Biochim Biophys. Acta* **159** (1968) 118.
12. Magee, W. L., Gallai-Hatchard, J., Saunders, H. and Thompson, R. H. S. *Biochem. J.* **83** (1962) 17.
13. Vogel, W. C. and Zieve, L. *J. Clin. Invest.* **39** (1960) 1295.
14. de Haas, G. H., Sarda, L. and Roger, J. *Biochim. Biophys. Acta* **106** (1965) 638.
15. Figarella, C. and Ribeiro, T. *Scand. J. Gastroenterol.* **6** (1971) 133.
16. Norman, A. *Arkiv Kemi* **32** (1955) 331.
17. Hofman, A. F. Thesis, Lund 1964, p. 32 ff.
18. Bruusgaard, A. *Clin. Chim. Acta* **28** (1970) 495.
19. Hanahan, D. J., Rodbell, M. and Turner, L. D. *J. Biol. Chem.* **206** (1954) 431.
20. Skipski, V. P., Peterson, R. E. and Barclay, M. *Biochem, J.* **90** (1964) 374.
21. Erlanson, C. and Borgström, B. *Scand. J. Gastroenterol.* **5** (1970) 293.
22. Hummel, B. C. W. *Can. J. Biochem. Physiol.* **37** (1959) 1393.
23. Erlanson, C. and Borgström, B. *Scand. J. Gastroenterol.* **5** (1970) 395.
24. Borgström, B. *Biochim. Biophys. Acta* **84** (1964) 228.

Received April 19, 1973.

ACTA CHEMICA SCANDINAVICA 27 (1973) 2757–2768

The Crystal and Electronic Structure of Isocoffeine, (1,3,9-Trimethyl-2,6-dioxypurine)

HARALD RASMUSSEN and EINAR SLETTEN

Department of Chemistry, University of Bergen, N-5014 Bergen, Norway

The crystal structure of 1,3,9-trimethyl-2,6-dioxypurine has been determined by X-ray diffraction methods. The structure was determined from three-dimensional diffractometer data and refined to $R = 0.039$ including 1720 reflections. Standard deviations in bond lengths involving only non-hydrogen atoms are approximately 0.002 Å and for those involving hydrogen atoms 0.02 Å. The corresponding standard deviations in angles are 0.1° and 1°, respectively. The methyl group in 9-position is nearly eclipsed relative to the methyl group on N(3) and to the hydrogen atom on C(8). The purine molecule is slightly, though significantly, bent around the C(4) – C(5) bond. The carbonyl group C(2) – O(2) is displaced out of the pyrimidine plane by about 0.04 Å for C(2) and 0.08 Å for O(2).

Bergmann and coworkers have carried out extensive conformational studies on substituted purines in solutions by spectroscopic and dielectric measurements.[1,2] Some of the problems encountered in these investigations could possibly be clarified by X-ray diffraction methods. The first compound in this series is the isocoffeine molecule (1,3,9-trimethyl-2,6-dioxypurine) where the steric interaction between the 3- and 9-methyl groups is of particular interest.

EXPERIMENTAL

A sample of 1,3,9-trimethyl-2,6-dioxypurine was kindly supplied by F. Bergmann. The compound was crystallized from chloroform by slow evaporation in a refrigerator. A fairly large crystal with dimensions $0.71 \times 0.34 \times 0.33$ mm^3 was mounted along the a^*-axis and used for intensity measurements. The space group is $P2_1/n$, $Z = 4$, with cell dimensions $a = 7.717(2)$ Å, $b = 7.915(5)$ Å, $c = 13.646(2)$ Å, $\beta = 92.86(1)°$, $\varrho_{obs} = 1.54(1)$ g cm^{-3}, $\varrho_{calc} = 1.549(3)$ g cm^{-3}.

Three-dimensional data were collected on a Siemens AED four-circle diffractometer using niobium-filtered Mo$K\alpha$ radiation. Within a sphere limited at $\sin\theta/\lambda < 0.64$, 1813 reflections were measured with $\theta - 2\theta$ scan employing the 5-value measurement procedure. All measurements start at the reflection peak to enable the instrument to test the maximum counting rate and automatically insert an appropriate attenuator in the

primary beam to avoid counting losses, or to select an appropriate measuring time per step to give a statistically suitable count. Except for the very weak reflections which are recorded with a constant maximum scan time, all the reflections are measured at approximately the same statistical accuracy. The X-ray tube was operated at 50 kV, 20 mA, except for the measurements of nine very strong low order reflections which had to be recorded with the minimum current setting of 8 mA. During the collection of data two standard reflections were re-measured after each set of 50 reflections. The fluctuations in net intensities were about ± 1 % with one single deflection for both standards of about 6 %. Lorentz and polarization corrections were applied to the intensity data. The linear absorption coefficient for the compound is 1.24 cm^{-1} and no absorption correction was deemed necessary.

STRUCTURE DETERMINATION AND REFINEMENT

The structure was solved by a symbolic addition procedure programmed by Long.[3] Three origin determining reflections and three reflections with variable signs were used in the initial phasing process. 102 normalized structure factors with $E > 2.0$ were used for sign determinations. In addition, signs were derived for reflections with E-values in the range $1.5 - 2.0$. The total number of reflections used in the process were 243.

An E map based on the set of phases with highest consistency revealed all non-hydrogen atoms unambigously. Structure factor calculations based on the coordinates of these atoms gave an R-factor of 0.32. Three cycles of least-squares refinement lowered R to 0.12. The hydrogen atoms were localized by three-dimensional difference synthesis. Two more refinement cycles using anisotropic temperature factors on non-hydrogen atoms and isotropic temperature factors on hydrogen atoms gave $R = 0.048$.

Correction for secondary extinction was carried out according to the formula given by Zachariasen.[4] Four very strong low order reflections which had been measured far outside the linear range of the counter had large ΔF's and were given zero weight in the two final refinement cycles. At this stage all shifts were less than 0.1 σ and the refinement was terminated at an R of 0.039.

The final atomic coordinates and thermal parameters along with the corresponding standard deviations are shown in Tables 1 and 2. Table 3 lists the observed and calculated structure factors. Atomic scattering factors for the heavier atoms were obtained from *International Tables for X-Ray Crystallography* (1962),[5] and those for the hydrogen atoms were from Stewart, Davidson and Simpson.[6]

A residual difference synthesis based on all atoms showed peaks of electron densities 0.1 to 0.25 $eÅ^{-3}$ approximately in the middle of the bonds. As in previous published purine structures the largest peak appears in the middle of the conjugated bond C(4) – C(5).

THERMAL ANALYSIS

The thermal parameters were used in a rigid body motion analysis [7] in which the xanthine part of the molecule was assumed to form the rigid body. The root-mean-square amplitudes about principal axes of librational motion are 23.1°, 8.5°, 6.5°, respectively. The root-mean-square deviation between

Table 1. Final positional parameters with the corresponding standard deviations in parentheses.

Atom	X/a	Y/b	Z/c
C(1)	0.06913(24)	0.77805(21)	0.12922(13)
C(2)	0.19287(19)	0.49956(19)	0.10826(10)
C(3)	0.30248(27)	0.21269(21)	0.09372(14)
C(4)	0.30084(18)	0.42132(18)	−0.04456(10)
C(5)	0.26343(19)	0.57569(18)	−0.08501(10)
C(6)	0.18436(20)	0.70455(18)	−0.03064(10)
C(8)	0.37536(23)	0.43245(21)	−0.19597(11)
C(9)	0.43771(25)	0.15407(22)	−0.11628(14)
N(1)	0.15080(16)	0.65437(15)	0.06555(8)
N(3)	0.26569(16)	0.37863(15)	0.04999(8)
N(7)	0.31193(18)	0.58181(18)	−0.18122(9)
N(9)	0.37463(17)	0.32783(16)	−0.11543(9)
O(2)	0.16437(16)	0.47178(15)	0.19360(8)
O(6)	0.14618(18)	0.84710(14)	−0.05904(8)
H(8)	0.4282(27)	0.3879(26)	−0.2580(15)
H(11)	0.0128(25)	0.8695(25)	0.0884(15)
H(12)	0.1530(27)	0.8355(26)	0.1797(15)
H(13)	−0.0150(28)	0.7236(26)	0.1723(17)
H(31)	0.2508(34)	0.2088(32)	0.1550(22)
H(32)	0.4349(34)	0.1945(30)	0.1117(18)
H(33)	0.2578(30)	0.1279(31)	0.0584(17)
H(91)	0.5233(28)	0.1378(25)	−0.0632(15)
H(92)	0.3552(28)	0.0728(27)	−0.1086(15)
H(93)	0.4720(28)	0.1285(28)	−0.1798(17)

Table 2. Thermal parameters with the corresponding standard deviations in parentheses. The anisotropic thermal parameters are defined by the expression $T_i = \exp[-2\pi^2(U_{11}h^2a^{*2} + U_{22}k^2b^{*2} + U_{33}l^2c^{*2} + 2U_{12}hka^*b^* + 2U_{13}hla^*c^* + 2U_{23}klb^*c^*)]$ and the isotropic parameters by $T_i = \exp[-8\pi^2U \sin^2\theta/\lambda^2]$. For non-hydrogen atoms the values are multiplied by a factor of 10^4, for hydrogen atoms by 10^3.

	U_{11}	U_{22}	U_{33}	U_{12}	U_{23}	U_{13}
C(1)	424(9)	317(8)	340(8)	49(7)	−77(7)	53(7)
C(2)	295(7)	297(8)	249(7)	−3(6)	9(6)	29(5)
C(3)	579(12)	253(8)	336(9)	50(8)	68(7)	43(8)
C(4)	260(7)	256(7)	234(7)	−15(6)	−19(5)	16(5)
C(5)	328(8)	275(7)	237(7)	−18(6)	24(6)	39(6)
C(6)	324(8)	251(7)	279(7)	−24(6)	18(6)	13(6)
C(8)	447(9)	395(9)	253(7)	−18(7)	−13(6)	85(6)
C(9)	417(10)	310(9)	393(9)	58(7)	−79(7)	55(8)
N(1)	321(7)	253(6)	257(6)	16(5)	−24(5)	35(5)
N(3)	356(7)	238(6)	236(6)	20(5)	29(5)	40(5)
N(7)	488(8)	374(7)	247(6)	−10(6)	32(5)	75(6)
N(9)	335(7)	296(7)	264(6)	−1(5)	−34(5)	53(5)
O(2)	579(8)	448(7)	247(6)	89(6)	53(5)	115(5)
O(6)	658(9)	256(6)	418(7)	77(6)	77(5)	73(6)
	U		U		U	
H(8)	53(6)	H(31)	83(8)	H(91)	52(6)	
H(11)	52(6)	H(32)	76(7)	H(92)	51(6)	
H(12)	55(6)	H(33)	68(7)	H(93)	61(6)	
H(13)	56(6)					

Table 3. Observed and calculated structure factors multiplied by 10. Unobserved reflections are marked with a minus sign in front of F_o.

H	K	L	F(O)	F(C)	H	K	L	F(O)	F(C)	H	K	L	F(O)	F(C)	H	K	L	F(O)	F(C)	H	K	L	F(O)	F(C)
0	0	2	690	669	0	6	7	76	74	1	2-14		22	-26	1	5-13		-10	0	1	8	7	48	-49
0	0	4	613	-661	0	6	8	77	81	1	2-13		24	-27	1	5-12		46	-44	1	8	8	35	-36
0	0	6	350	-342	0	6	9	31	35	1	2-12		276	-287	1	5-11		20	-25	1	8	9	25	24
0	0	8	469	-450	0	6	10	14	13	1	2-11		201	199	1	5-10		69	73	1	8	10	52	48
0	0	10	96	109	0	6	11	11	10	1	2-10		227	-224	1	5	-9	22	19	1	9	-7	34	-30
0	0	12	202	-209	0	6	12	52	-52	1	2	-9	189	185	1	5	-8	157	160	1	9	-6	21	17
0	0	14	155	-162	0	6	13	17	-15	1	2	-8	33	-37	1	5	-7	271	272	1	9	-5	61	-59
0	0	16	122	121	0	6	14	13	8	1	2	-7	-7	9	1	5	-6	78	-77	1	9	-4	15	8
0	1	1	859	-802	0	7	1	53	52	1	2	-6	100	94	1	5	-5	11	-15	1	9	-3	40	35
0	1	2	151	154	0	7	2	54	58	1	2	-5	115	-115	1	5	-4	79	82	1	9	-2	17	-17
0	1	3	370	354	0	7	3	47	45	1	2	-4	366	370	1	5	-3	193	-188	1	9	-1	18	13
0	1	4	266	-268	0	7	4	55	55	1	2	-3	160	-150	1	5	-2	46	-48	1	9	0	18	-19
0	1	5	304	-301	0	7	5	133	139	1	2	-2	185	176	1	5	-1	129	-124	1	9	1	20	-19
0	1	6	468	-453	0	7	6	56	-58	1	2	-1	123	-123	1	5	0	122	-118	1	9	2	-10	3
0	1	7	312	297	0	7	7	44	-44	1	2	0	134	133	1	5	1	-7	-10	1	9	3	37	36
0	1	8	94	-88	0	7	8	21	-20	1	2	1	74	-76	1	5	2	61	59	1	9	4	37	-36
0	1	9	103	89	0	7	9	84	-89	1	2	2	-6	10	1	5	3	103	104	1	9	5	20	-19
0	1	10	155	154	0	7	10	13	13	1	2	3	7	-4	1	5	4	212	-222	1	9	6	-10	7
0	1	11	115	-113	0	7	11	14	11	1	2	4	38	-37	1	5	5	159	-152	1	9	7	-10	-1
0	1	12	20	-24	0	7	12	-11	-9	1	2	5	71	-78	1	5	6	26	26	1	10	-1	19	19
0	1	13	181	184	0	8	0	57	-61	1	2	6	52	-54	1	5	7	19	22	1	10	0	23	23
0	1	14	138	-111	0	8	1	30	-31	1	2	7	9	-14	1	5	8	23	28	1	10	1	30	-29
0	1	15	22	-17	0	8	2	15	16	1	2	8	65	-68	1	5	9	162	167	2	0	-16	15	15
0	1	16	-10	-1	0	8	3	109	-107	1	2	9	40	43	1	5	10	112	-116	2	0	-14	94	-89
0	1	17	-11	-6	0	8	4	-10	0	1	2	10	37	-35	1	5	11	35	34	2	0	-12	169	170
0	2	0	47	-49	0	8	5	60	-60	1	2	11	58	-57	1	5	12	36	36	2	0	-10	19	12
0	2	1	89	85	0	8	6	18	-19	1	2	12	108	-109	1	5	13	-10	-4	2	0	-8	225	217
0	2	2	450	-454	0	8	7	33	-34	1	2	13	21	-20	1	5	14	-10	8	2	0	-6	56	46
0	2	3	167	-160	0	8	8	27	27	1	2	14	29	-30	1	6	13	45	44	2	0	-4	568	-572
0	2	4	209	200	0	8	9	25	-24	1	2	15	-10	10	1	6	12	35	-29	2	0	-2	375	380
0	2	5	274	-265	0	8	10	52	-46	1	2	16	62	59	1	6	11	37	33	2	0	0	952	-1025
0	2	6	148	150	0	9	1	-10	4	1	3	16	23	-22	1	6	10	41	43	2	0	2	1210	-1263
0	2	7	68	67	0	9	2	25	23	1	3	15	52	-54	1	6	-9	220	-229	2	0	4	315	323
0	2	8	262	-258	0	9	3	65	-65	1	3	14	29	-24	1	6	-8	27	29	2	0	6	252	250
0	2	9	9	9	0	9	4	15	16	1	3	13	90	90	1	6	-7	48	-49	2	0	8	509	502
0	2	10	161	162	0	9	5	25	-26	1	3	12	169	-173	1	6	-6	42	44	2	0	10	-8	-1
0	2	11	71	71	0	9	6	64	-59	1	3	11	244	248	1	6	-5	125	127	2	0	12	139	-137
0	2	12	24	16	0	9	7	-10	-5	1	3	10	153	-153	1	6	-4	75	-79	2	0	14	248	246
0	2	13	103	105	0	10	0	-11	-4	1	3	-9	48	43	1	6	-3	61	58	2	0	16	47	47
0	2	14	45	-46	0	10	1	41	42	1	3	-8	78	88	1	6	-2	346	-354	2	1	-17	25	-22
0	2	15	-10	2	0	10	2	-11	7	1	3	-7	41	-42	1	6	-1	196	194	2	1	-16	56	58
0	2	16	28	28	1	0	-17	24	-19	1	3	-6	245	228	1	6	0	91	-90	2	1	-15	79	78
0	2	17	-11	4	1	0	-15	66	62	1	3	-5	281	-268	1	6	1	66	-65	2	1	-14	-10	-5
0	3	1	193	-191	1	0	-13	12	10	1	3	-4	362	346	1	6	2	18	-16	2	1	-13	85	-89
0	3	2	175	-168	1	0	-11	104	-104	1	3	-3	137	-128	1	6	3	34	36	2	1	-12	174	-184
0	3	3	390	390	1	0	-9	214	-227	1	3	-2	86	-84	1	6	4	9	-8	2	1	-11	27	-31
0	3	4	145	148	1	0	-7	218	-239	1	3	-1	125	122	1	6	5	49	46	2	1	-10	67	-63
0	3	5	44	41	1	0	-5	-7	12	1	3	0	106	-109	1	6	6	89	95	2	1	-9	185	188
0	3	6	25	23	1	0	-3	207	225	1	3	1	313	-314	1	6	7	211	-219	2	1	-8	10	11
0	3	7	89	91	1	0	-1	-5	-15	1	3	2	191	196	1	6	8	-9	10	2	1	-7	384	-366
0	3	8	8	-7	1	0	1	145	141	1	3	3	206	-205	1	6	9	11	9	2	1	-6	293	-279
0	3	9	99	-102	1	0	3	224	225	1	3	4	213	-219	1	6	10	87	86	2	1	-5	134	-127
0	3	10	101	105	1	0	5	124	131	1	3	5	162	-158	1	6	11	28	32	2	1	-4	434	-435
0	3	11	116	-115	1	0	7	66	67	1	3	6	225	-222	1	6	12	20	24	2	1	-3	270	-278
0	3	12	27	29	1	0	9	55	-60	1	3	7	9	-12	1	6	13	26	-27	2	1	-2	111	-121
0	3	13	57	55	1	0	11	32	-34	1	3	8	114	-112	1	7	-12	13	-12	2	1	-1	73	14
0	3	14	28	26	1	0	13	121	126	1	3	9	60	60	1	7	-11	31	-32	2	1	0	969	1064
0	3	15	27	-26	1	0	15	45	46	1	3	10	109	108	1	7	-10	12	-2	2	1	1	1080	1262
0	3	16	-10	-1	1	0	17	-10	1	1	3	11	137	133	1	7	-9	81	-80	2	1	2	922	996
0	4	0	309	-290	1	1	-17	32	-30	1	3	12	236	240	1	7	-8	15	14	2	1	3	25	20
0	4	1	241	236	1	1	-16	37	34	1	3	13	175	174	1	7	-7	51	-53	2	1	4	78	-84
0	4	2	310	-295	1	1	-15	10	-9	1	3	14	63	60	1	7	-6	142	-144	2	1	5	68	64
0	4	3	240	227	1	1	-14	73	79	1	3	15	-10	-1	1	7	-5	51	-55	2	1	6	220	-226
0	4	4	80	-74	1	1	-13	90	95	1	3	16	32	-30	1	7	-4	107	-113	2	1	7	29	24
0	4	5	9	14	1	1	-12	40	46	1	4	-15	42	-40	1	7	-3	191	193	2	1	8	12	11
0	4	6	152	149	1	1	-11	88	88	1	4	-14	35	31	1	7	-2	259	-267	2	1	9	265	-262
0	4	7	84	-83	1	1	-10	75	-76	1	4	-13	35	-36	1	7	-1	131	131	2	1	10	32	-30
0	4	8	295	308	1	1	-9	123	-129	1	4	-12	48	-48	1	7	0	100	-98	2	1	11	72	68
0	4	9	257	-261	1	1	-8	-7	-7	1	4	-11	102	107	1	7	1	32	-36	2	1	12	63	-64
0	4	10	193	190	1	1	-7	53	-44	1	4	-10	45	48	1	7	2	351	360	2	1	13	117	-116
0	4	11	113	-113	1	1	-6	11	-4	1	4	-9	10	-3	1	7	3	110	103	2	1	14	18	-20
0	4	12	-10	11	1	1	-5	229	237	1	4	-8	79	-77	1	7	4	227	244	2	1	15	101	-103
0	4	13	56	54	1	1	-4	65	-60	1	4	-7	18	-9	1	7	5	35	25	2	1	16	30	28
0	4	14	28	-22	1	1	-3	232	243	1	4	-6	139	-138	1	7	6	120	124	2	2	-16	40	-43
0	4	15	-11	7	1	1	-2	27	-34	1	4	-5	167	-155	1	7	7	23	-27	2	2	-15	-10	-8
0	5	1	120	115	1	1	-1	119	113	1	4	-4	195	180	1	7	8	26	-28	2	2	-14	12	15
0	5	2	170	-163	1	1	0	52	49	1	4	-3	147	-138	1	7	9	85	-82	2	2	-13	66	72
0	5	3	25	-24	1	1	1	35	-40	1	4	-2	76	74	1	7	10	64	-68	2	2	-12	179	184
0	5	4	80	81	1	1	2	-6	-11	1	4	-1	381	372	1	7	11	121	-117	2	2	-11	49	53
0	5	5	33	-34	1	1	3	108	120	1	4	0	111	112	1	7	12	82	72	2	2	-10	157	-152
0	5	6	152	148	1	1	4	202	221	1	4	1	185	-186	1	8	-10	94	91	2	2	-9	73	-73
0	5	7	86	-86	1	1	5	41	40	1	4	2	86	83	1	8	-9	-10	5	2	2	-8	15	-20
0	5	8	150	153	1	1	6	59	59	1	4	3	261	-267	1	8	-8	22	-24	2	2	-7	161	155
0	5	9	125	-124	1	1	7	61	-59	1	4	4	179	180	1	8	-7	28	29	2	2	-6	317	307
0	5	10	42	42	1	1	8	83	-85	1	4	5	168	166	1	8	-6	-10	-2	2	2	-5	52	41
0	5	11	-10	6	1	1	9	170	-175	1	4	6	199	203	1	8	-5	45	48	2	2	-4	83	79
0	5	12	116	-112	1	1	10	25	-25	1	4	7	215	210	1	8	-4	70	78	2	2	-3	278	-288
0	5	13	46	42	1	1	11	91	-92	1	4	8	85	-87	1	8	-3	56	60	2	2	-2	350	353
0	5	14	51	-47	1	1	12	69	-71	1	4	9	193	193	1	8	-2	69	73	2	2	-1	27	22
0	5	15	28	26	1	1	13	72	74	1	4	10	93	-98	1	8	-1	148	153	2	2	0	339	-342
0	6	0	105	104	1	1	14	78	-81	1	4	11	102	-104	1	8	0	103	104	2	2	1	86	-83
0	6	1	29	29	1	1	15	82	79	1	4	12	120	-119	1	8	1	70	-69	2	2	2	102	-101
0	6	2	101	100	1	1	16	11	-14	1	4	13	141	-143	1	8	2	92	-91	2	2	3	60	-62
0	6	3	32	-33	1	1	17	18	17	1	4	14	67	-69	1	8	3	149	-156	2	2	4	256	261
0	6	4	104	-105	1	2	-17	-11	-2	1	4	15	23	27	1	8	4	122	-117	2	2	5	23	-24
0	6	5	-9	2	1	2	-16	34	31	1	5	-15	30	-27	1	8	5	60	-66	2	2	6	312	-315
0	6	6	128	-128	1	2	-15	79	-79	1	5	-14	59	58	1	8	6	-10	2	2	2	7	107	-115

Table 3. Continued.

H	K	L	F(O)	F(C)	H	K	L	F(O)	F(C)	H	K	L	F(O)	F(C)	H	K	L	F(O)	F(C)	H	K	L	F(O)	F(C)
2	2	8	41	43	2	6	-9	23	-16	3	1	-7	140	-144	3	4	3	25	23	3	8	8	-11	-2
2	2	9	39	37	2	6	-8	128	-132	3	1	-6	82	-76	3	4	4	11	-4	3	9	-6	21	-20
2	2	10	25	20	2	6	-7	-9	6	3	1	-5	64	-65	3	4	5	125	-128	3	9	-5	58	56
2	2	11	81	83	2	6	-6	158	-160	3	1	-4	144	-144	3	4	6	148	-143	3	9	-4	-11	-2
2	2	12	79	-82	2	6	-5	40	-44	3	1	-3	120	120	3	4	7	63	-63	3	9	-3	34	37
2	2	13	13	-14	2	6	-4	32	33	3	1	-2	123	-124	3	4	8	76	-79	3	9	-2	70	73
2	2	14	31	29	2	6	-3	130	-131	3	1	-1	83	84	3	4	9	138	-136	3	9	-1	14	13
2	2	15	14	-14	2	6	-2	72	74	3	1	0	98	-96	3	4	10	123	125	3	9	0	102	104
2	2	16	51	-48	2	6	-1	-9	1	3	1	1	128	134	3	4	11	48	-48	3	9	1	57	55
2	3	-16	-10	6	2	6	0	66	66	3	1	2	-7	3	3	4	12	148	148	3	9	2	43	-40
2	3	-15	-10	1	2	6	1	-8	2	3	1	3	178	186	3	4	13	156	155	3	9	3	31	-33
2	3	-14	42	36	2	6	2	16	-18	3	1	4	54	52	3	4	14	102	102	3	9	4	100	-101
2	3	-13	43	-43	2	6	3	31	-28	3	1	5	36	31	3	5	-14	78	-72	3	9	5	32	-33
2	3	-12	59	-64	2	6	4	41	-43	3	1	6	24	-27	3	5	-13	-10	6	4	0	-16	86	-85
2	3	-11	61	-54	2	6	5	23	-23	3	1	7	11	11	3	5	-12	10	-7	4	0	-14	25	25
2	3	-10	66	70	2	6	6	134	136	3	1	8	62	59	3	5	-11	65	-62	4	0	-12	21	20
2	3	-9	37	38	2	6	7	48	-47	3	1	9	-8	2	3	5	-10	66	62	4	0	-10	84	88
2	3	-8	-8	0	2	6	8	42	44	3	1	10	29	25	3	5	-9	129	139	4	0	-8	89	93
2	3	-7	121	-125	2	6	9	21	22	3	1	11	-9	1	3	5	-8	144	-154	4	0	-6	211	-220
2	3	-6	190	-180	2	6	10	58	-61	3	1	12	-9	9	3	5	-7	51	61	4	0	-4	275	273
2	3	-5	218	214	2	6	11	11	9	3	1	13	-10	5	3	5	-6	88	-91	4	0	-2	61	87
2	3	-4	162	161	2	6	12	13	-9	3	1	14	75	75	3	5	-5	115	-114	4	0	0	224	-216
2	3	-3	156	155	2	6	13	11	-7	3	1	15	-11	-1	3	5	-4	-8	0	4	0	2	179	171
2	3	-2	14	-15	2	7	-12	33	-37	3	1	16	-11	6	3	5	-3	33	-33	4	0	4	129	-138
2	3	-1	144	-153	2	7	-11	39	39	3	2	-16	-11	-6	3	5	-2	132	132	4	0	6	104	111
2	3	0	72	-74	2	7	-10	24	-30	3	2	-15	10	10	3	5	-1	87	-94	4	0	8	21	-17
2	3	1	22	-14	2	7	-9	-10	0	3	2	-14	-10	8	3	5	0	309	308	4	0	10	194	-195
2	3	2	177	172	2	7	-8	38	34	3	2	-13	75	82	3	5	1	26	26	4	0	12	96	93
2	3	3	405	-402	2	7	-7	15	8	3	2	-12	199	206	3	5	2	23	-28	4	0	14	44	-43
2	3	4	84	77	2	7	-6	39	-38	3	2	-11	123	-124	3	5	3	99	-99	4	1	-16	56	58
2	3	5	197	-192	2	7	-5	123	-124	3	2	-10	292	305	3	5	4	40	41	4	1	-15	32	-32
2	3	6	-7	5	2	7	-4	24	-24	3	2	-9	245	-247	3	5	5	55	-53	4	1	-14	28	-28
2	3	7	19	16	2	7	-3	132	-131	3	2	-8	-8	-16	3	5	6	113	118	4	1	-13	46	-42
2	3	8	114	-115	2	7	-2	78	78	3	2	-7	61	-56	3	5	7	203	209	4	1	-12	-10	11
2	3	9	75	74	2	7	-1	21	-17	3	2	-6	103	-102	3	5	8	50	-52	4	1	-11	130	130
2	3	10	190	-190	2	7	0	73	79	3	2	-5	198	188	3	5	9	88	86	4	1	-10	96	95
2	3	11	252	255	2	7	1	20	-18	3	2	-4	276	-264	3	5	10	13	11	4	1	-9	64	-63
2	3	12	31	-33	2	7	2	40	39	3	2	-3	363	349	3	5	11	20	-27	4	1	-8	78	78
2	3	13	62	65	2	7	3	63	67	3	2	-2	177	-171	3	5	12	63	-62	4	1	-7	65	63
2	3	14	30	27	2	7	4	79	-82	3	2	-1	58	57	3	5	13	72	-72	4	1	-6	59	61
2	3	15	21	-18	2	7	5	-10	-3	3	2	0	126	126	3	6	-13	39	43	4	1	-5	125	115
2	3	16	14	12	2	7	6	63	-63	3	2	1	49	48	3	6	-12	12	-11	4	1	-4	91	-98
2	4	-15	17	-20	2	7	7	16	-19	3	2	2	118	-121	3	6	-11	49	-48	4	1	-3	29	-25
2	4	-14	-10	-3	2	7	8	-10	4	3	2	3	151	157	3	6	-10	-10	-8	4	1	-2	88	-83
2	4	-13	10	14	2	7	9	109	110	3	2	4	56	61	3	6	-9	70	75	4	1	-1	255	269
2	4	-12	31	-35	2	7	10	20	22	3	2	5	70	67	3	6	-8	-10	0	4	1	0	105	-104
2	4	-11	36	33	2	7	11	-11	-4	3	2	6	88	89	3	6	-7	201	207	4	1	1	395	-407
2	4	-10	153	-152	2	8	-10	30	26	3	2	7	9	-13	3	6	-6	97	94	4	1	2	470	-480
2	4	-9	153	-154	2	8	-9	17	-19	3	2	8	19	19	3	6	-5	-9	4	4	1	3	349	-357
2	4	-8	126	-123	2	8	-8	15	-18	3	2	9	106	-103	3	6	-4	-9	10	4	1	4	244	-245
2	4	-7	78	-75	2	8	-7	42	-43	3	2	10	31	-31	3	6	-3	121	-124	4	1	5	130	132
2	4	-6	48	46	2	8	-6	32	-31	3	2	11	40	-40	3	6	-2	186	194	4	1	6	137	141
2	4	-5	41	-35	2	8	-5	58	53	3	2	12	44	-46	3	6	-1	332	-334	4	1	7	19	-10
2	4	-4	24	29	2	8	-4	21	27	3	2	13	14	-13	3	6	0	186	193	4	1	8	182	181
2	4	-3	85	78	2	8	-3	20	21	3	2	14	11	11	3	6	1	122	-129	4	1	9	159	162
2	4	-2	121	121	2	8	-2	29	-30	3	2	15	-10	-5	3	6	2	74	-78	4	1	10	62	62
2	4	-1	241	231	2	8	-1	11	-3	3	3	-16	66	65	3	6	3	183	186	4	1	11	-9	-5
2	4	0	73	65	2	8	0	22	18	3	3	-15	27	-23	3	6	4	117	-127	4	1	12	19	-13
2	4	1	192	-190	2	8	1	24	21	3	3	-14	29	-33	3	6	5	35	-28	4	1	13	57	-54
2	4	2	141	132	2	8	2	29	32	3	3	-13	19	20	3	6	6	151	-157	4	1	14	60	59
2	4	3	168	-158	2	8	3	78	74	3	3	-12	49	-54	3	6	7	46	51	4	1	15	114	111
2	4	4	132	124	2	8	4	26	-25	3	3	-11	168	-172	3	6	8	14	-18	4	2	-15	39	42
2	4	5	114	117	2	8	5	103	100	3	3	-10	46	50	3	6	9	85	87	4	2	-14	50	50
2	4	6	37	-34	2	8	6	40	37	3	3	-9	47	-54	3	6	10	18	22	4	2	-13	23	22
2	4	7	130	126	2	8	7	-10	-4	3	3	-8	22	-25	3	6	11	23	23	4	2	-12	120	-119
2	4	8	114	-122	2	8	8	-10	-5	3	3	-7	-8	3	3	6	12	67	-65	4	2	-11	106	-112
2	4	9	154	154	2	8	9	42	-41	3	3	-6	26	29	3	7	-11	-11	11	4	2	-10	118	-118
2	4	10	161	-161	2	9	-7	67	64	3	3	-5	8	1	3	7	-10	11	2	4	2	-9	93	92
2	4	11	69	68	2	9	-6	53	-48	3	3	-4	123	-111	3	7	-9	14	14	4	2	-8	88	83
2	4	12	-10	-4	2	9	-5	63	59	3	3	-3	289	278	3	7	-8	71	-74	4	2	-7	17	19
2	4	13	42	-40	2	9	-4	38	-31	3	3	-2	72	-61	3	7	-7	57	-59	4	2	-6	149	-147
2	4	14	78	72	2	9	-3	65	63	3	3	-1	45	-44	3	7	-6	66	69	4	2	-5	292	-288
2	4	15	34	-31	2	9	-2	24	24	3	3	0	221	219	3	7	-5	33	32	4	2	-4	109	-103
2	5	-14	50	-44	2	9	-1	69	68	3	3	1	-7	-16	3	7	-4	73	75	4	2	-3	161	-168
2	5	-13	48	-46	2	9	0	12	-7	3	3	2	138	-140	3	7	-3	10	12	4	2	-2	205	-206
2	5	-12	41	-37	2	9	1	25	-30	3	3	3	244	251	3	7	-2	43	-43	4	2	-1	75	-69
2	5	-11	48	-44	2	9	2	-10	5	3	3	4	162	-161	3	7	-1	130	-132	4	2	0	72	74
2	5	-10	77	75	2	9	3	34	-36	3	3	5	107	108	3	7	0	32	34	4	2	1	327	331
2	5	-9	188	186	2	9	4	17	-17	3	3	6	-11	-13	3	7	1	-9	4	4	2	2	535	536
2	5	-8	163	162	2	9	5	24	-22	3	3	7	14	-19	3	7	2	98	-96	4	2	3	425	424
2	5	-7	252	258	2	9	6	-11	-5	3	3	8	71	70	3	7	3	10	9	4	2	4	47	-45
2	5	-6	138	133	3	0	-15	40	37	3	3	9	139	-139	3	7	4	76	-83	4	2	5	100	97
2	5	-5	33	34	3	0	-13	-9	10	3	3	10	92	96	3	7	5	-10	7	4	2	6	100	-100
2	5	-4	187	186	3	0	-11	49	-49	3	3	11	91	-91	3	7	6	26	-33	4	2	7	50	52
2	5	-3	119	-113	3	0	-9	67	75	3	3	12	82	-83	3	7	7	-10	5	4	2	8	20	19
2	5	-2	119	-116	3	0	-7	214	216	3	3	13	58	-56	3	7	8	60	-60	4	2	9	59	-57
2	5	-1	103	-103	3	0	-5	54	-57	3	3	14	71	-71	3	7	9	39	-39	4	2	10	16	15
2	5	0	279	-285	3	0	-3	295	-309	3	3	15	37	-38	3	7	10	54	55	4	2	11	161	-161
2	5	1	63	-67	3	0	-1	299	-314	3	4	-15	-11	-16	3	7	11	89	83	4	2	12	115	113
2	5	2	63	-57	3	0	1	17	12	3	4	-14	69	-66	3	8	-9	34	-30	4	2	13	101	-100
2	5	3	43	38	3	0	3	31	-34	3	4	-13	36	33	3	8	-8	55	-51	4	2	14	27	-25
2	5	4	30	-28	3	0	5	-7	-9	3	4	-12	29	-27	3	8	-7	11	10	4	2	15	38	-40
2	5	5	-8	1	3	0	7	27	29	3	4	-11	14	-16	3	8	-6	67	-62	4	3	-15	-11	11
2	5	6	47	52	3	0	9	40	41	3	4	-10	17	13	3	8	-5	36	-42	4	3	-14	57	-58
2	5	7	40	-36	3	0	11	120	123	3	4	-9	32	33	3	8	-4	95	-93	4	3	-13	26	29
2	5	8	27	25	3	0	13	40	-39	3	4	-8	69	-70	3	8	-3	-10	-9	4	3	-12	87	91
2	5	9	30	28	3	0	15	122	-120	3	4	-7	18	-16	3	8	-2	-10	-12	4	3	-11	57	59
2	5	10	41	-43	3	1	-16	34	-33	3	4	-6	192	194	3	8	-1	73	-73	4	3	-10	97	98
2	5	11	18	-19	3	1	-15	62	59	3	4	-5	100	-101	3	8	0	73	-71	4	3	-9	103	-103
2	5	12	36	36	3	1	-14	40	-41	3	4	-4	41	40	3	8	1	39	-41	4	3	-8	90	-92
2	5	13	31	-28	3	1	-13	75	71	3	4	-3	181	189	3	8	2	27	28	4	3	-7	41	41
2	5	14	42	43	3	1	-12	34	32	3	4	-2	151	-144	3	8	3	120	118	4	3	-6	118	117
2	6	13	60	57	3	1	-11	200	-206	3	4	-1	64	63	3	8	4	207	208	4	3	-5	163	165
2	6	12	54	49	3	1	-10	179	183	3	4	0	27	-32	3	8	5	90	92	4	3	-4	47	46
2	6	11	62	62	3	1	-9	267	-272	3	4	1	69	-67	3	8	6	91	87	4	3	-3	85	-88
2	6	10	69	62	3	1	-8	86	88	3	4	2	81	-84	3	8	7	62	64	4	3	-2	33	-36

Table 3. Continued.

H	K	L	F(O)	F(C)	H	K	L	F(O)	F(C)	H	K	L	F(O)	F(C)	H	K	L	F(O)	F(C)	H	K	L	F(O)	F(C)
4	3	-1	-7	-8	4	7	0	-10	4	5	2	12	13	-15	5	7	-6	105	104	6	3	-2	17	-8
4	3	0	73	74	4	7	1	15	14	5	2	13	-11	10	5	7	-5	49	52	6	3	-1	94	-96
4	3	1	39	-39	4	7	2	12	-17	5	2	14	35	35	5	7	-4	14	8	6	3	0	80	-77
4	3	2	194	-154	4	7	3	25	-21	5	3	-14	12	-10	5	7	-3	48	-48	6	3	1	104	105
4	3	3	135	143	4	7	4	11	11	5	3	-13	-10	-4	5	7	-2	-10	0	6	3	2	116	120
4	3	4	63	-63	4	7	5	81	-80	5	3	-12	126	125	5	7	-1	-10	-5	6	3	3	186	193
4	3	5	141	140	4	7	6	59	60	5	3	-11	65	68	5	7	0	-10	-10	6	3	4	179	183
4	3	6	15	-14	4	7	7	21	20	5	3	-10	59	61	5	7	1	15	-6	6	3	5	-9	-5
4	3	7	125	-128	4	7	8	19	22	5	3	-9	63	65	5	7	2	17	16	6	3	6	-9	-3
4	3	8	-9	-1	4	7	9	-10	-1	5	3	-8	-9	7	5	7	3	-10	0	6	3	7	-9	2
4	3	9	85	-88	4	7	10	-11	-15	5	3	-7	97	-98	5	7	4	-10	8	6	3	8	17	15
4	3	10	164	164	4	8	-8	24	22	5	3	-6	77	-79	5	7	5	25	22	6	3	9	42	44
4	3	11	99	-96	4	8	-7	-10	-8	5	3	-5	109	107	5	7	6	86	-80	6	3	10	40	-44
4	3	12	83	81	4	8	-6	60	56	5	3	-4	87	-92	5	7	7	40	-41	6	3	11	20	20
4	3	13	55	-56	4	8	-5	96	-91	5	3	-3	-8	-1	5	7	8	-11	5	6	3	12	61	-61
4	3	14	38	-38	4	8	-4	-12	3	5	3	-2	119	119	5	8	-6	18	-17	6	4	-12	43	-38
4	4	-14	66	61	4	8	-3	122	-116	5	3	-1	116	-116	5	8	-5	-11	0	6	4	-11	53	55
4	4	-13	-10	7	4	8	-2	-10	-6	5	3	0	22	26	5	8	-4	101	97	6	4	-10	81	79
4	4	-12	18	-23	4	8	-1	33	-33	5	3	1	48	47	5	8	-3	13	11	6	4	-9	10	-9
4	4	-11	44	-42	4	8	0	47	46	5	3	2	-9	9	5	8	-2	-11	8	6	4	-8	-10	-10
4	4	-10	16	-9	4	8	1	-10	2	5	3	3	59	-56	5	8	-1	-11	8	6	4	-7	39	-37
4	4	-9	28	32	4	8	2	16	-12	5	3	4	86	84	5	8	0	73	-73	6	4	-6	43	-46
4	4	-8	92	91	4	8	3	28	29	5	3	5	-9	1	5	8	1	32	34	6	4	-5	170	173
4	4	-7	38	-40	4	8	4	-13	-3	5	3	6	58	54	5	8	2	11	9	6	4	-4	12	12
4	4	-6	33	-28	4	8	5	24	-23	5	3	7	-9	4	5	8	3	45	-43	6	4	-3	12	2
4	4	-5	23	-25	4	8	6	18	-18	5	3	8	30	31	5	8	4	31	-29	6	4	-2	29	30
4	4	-4	36	-35	4	8	7	21	-23	5	3	9	13	12	5	8	5	66	-67	6	4	-1	122	-121
4	4	-3	224	221	4	9	-3	20	21	5	3	10	106	-106	6	0	-14	30	-30	6	4	0	53	54
4	4	-2	22	-21	4	9	-2	-11	-6	5	3	11	86	83	6	0	-12	14	-13	6	4	1	14	10
4	4	-1	67	-66	4	9	-1	24	-23	5	3	12	85	-86	6	0	-10	30	27	6	4	2	26	-26
4	4	0	20	8	4	9	0	36	33	5	3	13	21	22	6	0	-8	113	-119	6	4	3	10	-9
4	4	1	107	-103	4	9	1	52	-45	5	4	-13	33	-31	6	0	-6	-13	4	6	4	4	-9	-11
4	4	2	34	35	4	9	2	60	55	5	4	-12	40	34	6	0	-4	85	82	6	4	5	53	54
4	4	3	29	29	4	9	3	25	26	5	4	-11	10	-11	6	0	-2	-8	8	6	4	6	24	24
4	4	4	63	-64	5	0	-15	58	-55	5	4	-10	99	-96	6	0	0	134	135	6	4	7	23	-27
4	4	5	80	-81	5	0	-13	130	-129	5	4	-9	20	-22	6	0	2	9	-12	6	4	8	26	27
4	4	6	49	-50	5	0	-11	50	52	5	4	-8	55	62	6	0	4	64	61	6	4	9	62	-60
4	4	7	33	-36	5	0	-9	297	306	5	4	-7	129	-135	6	0	6	76	75	6	4	10	27	29
4	4	8	34	-34	5	0	-7	156	153	5	4	-6	55	61	6	0	8	123	-122	6	4	11	38	37
4	4	9	65	-66	5	0	-5	37	37	5	4	-5	-9	3	6	0	10	13	18	6	5	-11	31	26
4	4	10	26	26	5	0	-3	16	-7	5	4	-4	80	-78	6	0	12	-10	6	6	5	-10	70	-69
4	4	11	24	-24	5	0	-1	24	-23	5	4	-3	35	33	6	1	-14	35	-32	6	5	-9	34	37
4	4	12	49	46	5	0	1	44	-43	5	4	-2	43	42	6	1	-13	19	18	6	5	-8	34	33
4	4	13	73	73	5	0	3	122	-128	5	4	-1	45	48	6	1	-12	31	30	6	5	-7	54	59
4	4	14	18	-18	5	0	5	29	-27	5	4	0	60	-60	6	1	-11	20	-19	6	5	-6	19	12
4	5	-13	48	-45	5	0	7	22	-22	5	4	1	101	97	6	1	-10	43	39	6	5	-5	36	37
4	5	-12	31	27	5	0	9	21	19	5	4	2	33	-32	6	1	-9	28	-25	6	5	-4	49	-46
4	5	-11	27	23	5	0	11	16	-16	5	4	3	15	11	6	1	-8	65	69	6	5	-3	20	18
4	5	-10	52	-50	5	0	13	17	-14	5	4	4	19	-17	6	1	-7	-9	7	6	5	-2	97	95
4	5	-9	52	-60	5	1	-15	25	23	5	4	5	97	96	6	1	-6	42	-43	6	5	-1	83	-82
4	5	-8	154	-144	5	1	-14	21	24	5	4	6	50	-50	6	1	-5	64	-66	6	5	0	47	45
4	5	-7	198	-201	5	1	-13	42	-41	5	4	7	38	36	6	1	-4	32	-36	6	5	1	108	-108
4	5	-6	24	25	5	1	-12	-10	2	5	4	8	93	91	6	1	-3	93	94	6	5	2	34	35
4	5	-5	137	-134	5	1	-11	53	56	5	4	9	59	-57	6	1	-2	102	95	6	5	3	31	-30
4	5	-4	16	-14	5	1	-10	199	-204	5	4	10	33	32	6	1	-1	21	-21	6	5	4	10	10
4	5	-3	77	78	5	1	-9	256	262	5	4	11	-10	3	6	1	0	-8	1	6	5	5	14	10
4	5	-2	56	-55	5	1	-8	149	-147	5	4	12	59	-60	6	1	1	49	-46	6	5	6	75	-75
4	5	-1	175	175	5	1	-7	188	189	5	5	-12	35	32	6	1	2	-9	11	6	5	7	28	-30
4	5	0	95	90	5	1	-6	66	65	5	5	-11	-10	6	6	1	3	114	115	6	5	8	-10	-17
4	5	1	54	52	5	1	-5	32	31	5	5	-10	39	-37	6	1	4	79	77	6	5	9	56	-55
4	5	2	11	9	5	1	-4	138	136	5	5	-9	15	11	6	1	5	61	-60	6	5	10	24	-26
4	5	3	23	-24	5	1	-3	209	-207	5	5	-8	31	34	6	1	6	59	59	6	6	-9	17	13
4	5	4	33	32	5	1	-2	144	137	5	5	-7	125	-128	6	1	7	29	-33	6	6	-8	67	-72
4	5	5	12	11	5	1	-1	240	-250	5	5	-6	89	94	6	1	8	14	16	6	6	-7	109	-103
4	5	6	9	7	5	1	0	29	-29	5	5	-5	-11	-9	6	1	9	26	-24	6	6	-6	79	-80
4	5	7	112	112	5	1	1	43	-41	5	5	-4	18	17	6	1	10	85	-87	6	6	-5	102	-100
4	5	8	61	-61	5	1	2	14	13	5	5	-3	52	54	6	1	11	20	-20	6	6	-4	53	-52
4	5	9	40	38	5	1	3	94	-86	5	5	-2	67	-63	6	1	12	76	-77	6	6	-3	54	-57
4	5	10	13	14	5	1	4	-8	-2	5	5	-1	187	193	6	1	13	98	95	6	6	-2	15	15
4	5	11	37	-36	5	1	5	60	-63	5	5	0	268	-272	6	2	-13	81	-80	6	6	-1	-10	-2
4	5	12	-11	10	5	1	6	16	-14	5	5	1	171	171	6	2	-12	-10	-3	6	6	0	71	69
4	5	13	-11	7	5	1	7	-9	5	5	5	2	125	-127	6	2	-11	46	48	6	6	1	54	51
4	6	-12	-11	1	5	1	8	16	-19	5	5	3	73	-76	6	2	-10	61	59	6	6	2	60	60
4	6	-11	113	-108	5	1	9	16	16	5	5	4	95	100	6	2	-9	100	100	6	6	3	-10	1
4	6	-10	14	14	5	1	10	30	-27	5	5	5	56	-59	6	2	-8	-9	-2	6	6	4	18	14
4	6	-9	-10	-2	5	1	11	40	41	5	5	6	12	-4	6	2	-7	29	-28	6	6	5	35	37
4	6	-8	90	94	5	1	12	36	38	5	5	7	97	-100	6	2	-6	43	50	6	6	6	36	-35
4	6	-7	147	138	5	1	13	15	17	5	5	8	10	-3	6	2	-5	55	54	6	6	7	51	52
4	6	-6	163	165	5	1	14	24	-21	5	5	9	116	-116	6	2	-4	45	45	6	6	8	-11	5
4	6	-5	101	103	5	2	-15	37	34	5	5	10	-10	-1	6	2	-3	29	27	6	7	-7	45	44
4	6	-4	69	69	5	2	-14	17	-13	5	5	11	29	-25	6	2	-2	-8	-8	6	7	-6	65	66
4	6	-3	125	126	5	2	-13	-10	-9	5	6	-11	20	-20	6	2	-1	62	67	6	7	-5	125	124
4	6	-2	96	-94	5	2	-12	33	32	5	6	-10	13	-9	6	2	0	51	50	6	7	-4	24	31
4	6	-1	39	37	5	2	-11	11	3	5	6	-9	21	21	6	2	1	16	-17	6	7	-3	111	108
4	6	0	152	-154	5	2	-10	161	-167	5	6	-8	54	55	6	2	2	190	-196	6	7	-2	13	-7
4	6	1	38	-37	5	2	-9	83	83	5	6	-7	38	-39	6	2	3	327	-341	6	7	-1	29	27
4	6	2	114	-115	5	2	-8	83	-84	5	6	-6	57	-56	6	2	4	156	-153	6	7	0	49	-48
4	6	3	13	-14	5	2	-7	11	-7	5	6	-5	24	-22	6	2	5	166	-169	6	7	1	11	-12
4	6	4	37	39	5	2	-6	-8	-3	5	6	-4	88	-89	6	2	6	56	60	6	7	2	49	-47
4	6	5	40	-40	5	2	-5	59	-55	5	6	-3	12	-12	6	2	7	32	34	6	7	3	43	-43
4	6	6	35	36	5	2	-4	-8	-5	5	6	-2	-10	-2	6	2	8	46	43	6	7	4	-10	2
4	6	7	10	7	5	2	-3	191	-188	5	6	-1	91	89	6	2	9	91	92	6	7	5	12	11
4	6	8	20	-19	5	2	-2	143	134	5	6	0	86	-87	6	2	10	22	19	6	7	6	-11	-6
4	6	9	20	-23	5	2	-1	105	-102	5	6	1	174	172	6	2	11	122	123	6	8	-1	16	18
4	6	10	38	38	5	2	0	79	-81	5	6	2	39	35	6	2	12	86	-81	6	8	0	12	-13
4	6	11	36	-37	5	2	1	79	82	5	6	3	65	-64	6	3	-13	64	60	7	0	-11	44	42
4	7	-10	49	51	5	2	2	-9	-2	5	6	4	43	42	6	3	-12	-11	-1	7	0	-9	254	-260
4	7	-9	32	30	5	2	3	41	-39	5	6	5	82	-81	6	3	-11	70	-74	7	0	-7	292	-295
4	7	-8	26	-23	5	2	4	191	198	5	6	6	71	75	6	3	-10	122	-119	7	0	-5	80	-79
4	7	-7	15	-17	5	2	5	79	-80	5	6	7	29	29	6	3	-9	24	-23	7	0	-3	100	104
4	7	-6	67	-67	5	2	6	49	45	5	6	8	91	95	6	3	-8	11	13	7	0	-1	204	196
4	7	-5	34	-36	5	2	7	42	-38	5	6	9	18	16	6	3	-7	100	98	7	0	1	61	63
4	7	-4	-10	-10	5	2	8	13	-12	5	6	10	-11	-7	6	3	-6	12	-15	7	0	3	54	53
4	7	-3	17	19	5	2	9	86	88	5	7	-9	-11	-4	6	3	-5	84	-84	7	0	5	54	56
4	7	-2	-9	-7	5	2	10	53	-54	5	7	-8	47	46	6	3	-4	103	-103	7	0	7	13	19
4	7	-1	-10	-2	5	2	11	89	87	5	7	-7	37	39	6	3	-3	154	-157	7	0	9	-11	-9

Table 3. Continued.

H	K	L	F(O)	F(C)	H	K	L	F(O)	F(C)	H	K	L	F(O)	F(C)	H	K	L	F(O)	F(C)	H	K	L	F(O)	F(C)
7	0	11	28	-27	7	3	-7	42	43	7	5	6	49	-49	8	2	-7	14	-12	8	5	-1	-10	10
7	1	-12	61	-61	7	3	-6	64	-65	7	5	7	58	55	8	2	-6	22	21	8	5	0	46	-43
7	1	-11	-10	-8	7	3	-5	40	42	7	5	8	14	-14	8	2	-5	28	-32	8	5	1	26	27
7	1	-10	57	61	7	3	-4	23	21	7	6	-7	-11	4	8	2	-4	41	-40	8	5	2	-11	-11
7	1	-9	40	-42	7	3	-3	99	-98	7	6	-6	44	-41	8	2	-3	12	9	8	5	3	21	21
7	1	-8	202	201	7	3	-2	22	-24	7	6	-5	-11	8	8	2	-2	-10	-3	8	5	4	29	-30
7	1	-7	19	-21	7	3	-1	-9	-8	7	6	-4	22	25	8	2	-1	68	66	9	0	-7	182	184
7	1	-6	55	57	7	3	0	30	-30	7	6	-3	15	12	8	2	0	10	4	9	0	-5	75	78
7	1	-5	-9	6	7	3	1	37	-38	7	6	-2	-10	10	8	2	1	54	-52	9	0	-3	21	-21
7	1	-4	27	-28	7	3	2	37	34	7	6	-1	26	23	8	2	2	25	27	9	0	-1	127	-126
7	1	-3	54	52	7	3	3	-10	-8	7	6	0	-10	-8	8	2	3	19	21	9	0	1	74	-74
7	1	-2	104	-102	7	3	4	33	30	7	6	1	33	-36	8	2	4	55	59	9	0	3	-10	7
7	1	-1	119	121	7	3	5	14	19	7	6	2	32	-33	8	2	5	98	99	9	0	5	57	-63
7	1	0	35	-34	7	3	6	47	46	7	6	3	27	-25	8	2	6	-11	1	9	1	-7	66	-64
7	1	1	14	7	7	3	7	47	-46	7	6	4	32	-32	8	2	7	22	21	9	1	-6	104	-103
7	1	2	34	32	7	3	8	16	-15	7	6	5	13	9	8	2	8	-11	-8	9	1	-5	65	-64
7	1	3	17	-16	7	3	9	35	35	7	6	6	21	17	8	3	-9	77	75	9	1	-4	37	-38
7	1	4	68	-68	7	3	10	23	-18	7	7	-2	37	-34	8	3	-8	28	27	9	1	-3	18	18
7	1	5	69	71	7	4	-10	65	64	7	7	-1	12	11	8	3	-7	-10	13	9	1	-2	20	25
7	1	6	56	-59	7	4	-9	13	17	7	7	0	49	50	8	3	-6	-10	-2	9	1	-1	17	13
7	1	7	34	34	7	4	-8	55	51	7	7	1	13	1	8	3	-5	47	-44	9	1	0	88	89
7	1	8	21	-18	7	4	-7	38	41	8	0	-10	42	-36	8	3	-4	92	94	9	1	1	-10	-7
7	1	9	15	-11	7	4	-6	117	-121	8	0	-8	64	-59	8	3	-3	-10	6	9	1	2	11	11
7	1	10	45	47	7	4	-5	62	60	8	0	-6	28	-6	8	3	-2	11	11	9	1	3	28	28
7	1	11	47	-46	7	4	-4	19	-23	8	0	-4	-10	2	8	3	-1	87	85	9	1	4	13	13
7	2	-12	39	-36	7	4	-3	12	14	8	0	-2	-10	-6	8	3	0	14	-9	9	1	5	-11	-6
7	2	-11	26	24	7	4	-2	36	38	8	0	0	70	-68	8	3	1	62	58	9	1	6	49	51
7	2	-10	34	-30	7	4	-1	63	-62	8	0	2	21	-20	8	3	2	17	-25	9	2	-7	41	39
7	2	-9	29	-30	7	4	0	100	101	8	0	4	34	31	8	3	3	126	-129	9	2	-6	54	52
7	2	-8	49	51	7	4	1	163	-162	8	0	6	65	-63	8	3	4	146	-148	9	2	-5	39	-35
7	2	-7	47	47	7	4	2	139	140	8	0	8	36	-35	8	3	5	131	-132	9	2	-4	-10	1
7	2	-6	32	30	7	4	3	50	-47	8	1	-10	-11	1	8	3	6	54	-53	9	2	-3	17	9
7	2	-5	40	37	7	4	4	17	-18	8	1	-9	-11	-9	8	3	7	-11	3	9	2	-2	51	-51
7	2	-4	107	107	7	4	5	46	46	8	1	-8	12	-13	8	3	8	-11	3	9	2	-1	14	8
7	2	-3	11	-11	7	4	6	13	-9	8	1	-7	29	-26	8	4	-8	14	-14	9	2	0	27	28
7	2	-2	23	-25	7	4	7	16	18	8	1	-6	48	-46	8	4	-7	25	23	9	2	1	-10	9
7	2	-1	48	49	7	4	8	11	-9	8	1	-5	22	23	8	4	-6	37	37	9	2	2	-11	6
7	2	0	92	-92	7	4	9	41	37	8	1	-4	30	27	8	4	-5	24	-28	9	2	3	16	21
7	2	1	27	-26	7	5	-9	35	-33	8	1	-3	21	20	8	4	-4	-12	0	9	2	4	16	-14
7	2	2	24	22	7	5	-8	14	-16	8	1	-2	18	17	8	4	-3	112	-110	9	2	5	-11	-1
7	2	3	16	-13	7	5	-7	-10	16	8	1	-1	19	-16	8	4	-2	44	-49	9	3	-5	35	-36
7	2	4	65	-67	7	5	-6	34	-34	8	1	0	15	13	8	4	-1	19	11	9	3	-4	77	74
7	2	5	19	16	7	5	-5	-10	6	8	1	1	17	18	8	4	0	89	-89	9	3	-3	-11	10
7	2	6	72	-73	7	5	-4	-10	5	8	1	2	19	20	8	4	1	53	52	9	3	-2	12	12
7	2	7	22	19	7	5	-3	21	-25	8	1	3	-10	4	8	4	2	25	-22	9	3	-1	30	31
7	2	8	25	-28	7	5	-2	15	16	8	1	4	13	-21	8	4	3	105	108	9	3	0	38	-37
7	2	9	-10	-3	7	5	-1	-10	-7	8	1	5	45	43	8	4	4	59	60	9	3	1	51	51
7	2	10	18	15	7	5	0	84	83	8	1	6	-10	-5	8	4	5	48	52	9	3	2	87	-84
7	2	11	67	-66	7	5	1	108	-106	8	1	7	46	43	8	4	6	30	33	9	3	3	70	68
7	3	-11	23	18	7	5	2	100	97	8	1	8	30	-25	8	5	-6	28	-26	9	3	4	38	-38
7	3	-10	35	-35	7	5	3	35	-29	8	1	9	24	-24	8	5	-5	20	16	9	4	-2	29	-32
7	3	-9	85	-84	7	5	4	31	-30	8	2	-10	-11	3	8	5	-4	27	29	9	4	-1	22	-22
7	3	-8	31	-34	7	5	5	74	72	8	2	-9	36	-31	8	5	-3	38	38	9	4	0	41	-43
										8	2	-8	27	26	8	5	-2	13	-11	9	4	1	50	49

observed and calculated U_{ij}'s are 0.0013 Å^2 and thus of the same order of magnitude as the e.s.d's of the thermal parameters obtained in the refinement. The libration tensor was used to calculate corrected bond lengths. The corrections are on the limit of significance being in most cases less than 3σ. A stereoscopic plot of the thermal ellipsoids at 50 % probability is shown in Fig. 1.

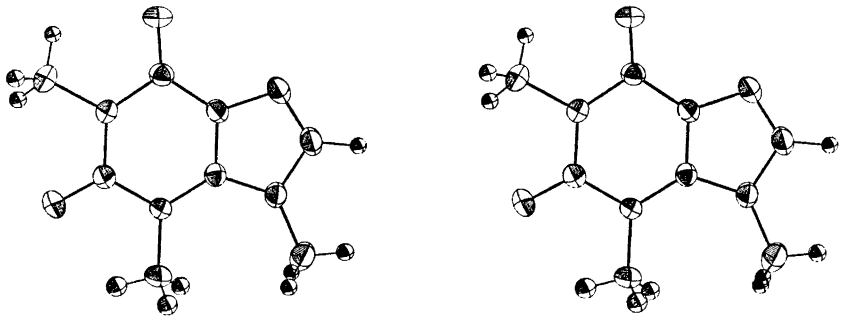

Fig. 1. The thermal ellipsoids plotted at the 50 % probability level. The isotropic thermal spheres of the hydrogen atoms are scaled down by a factor of four.

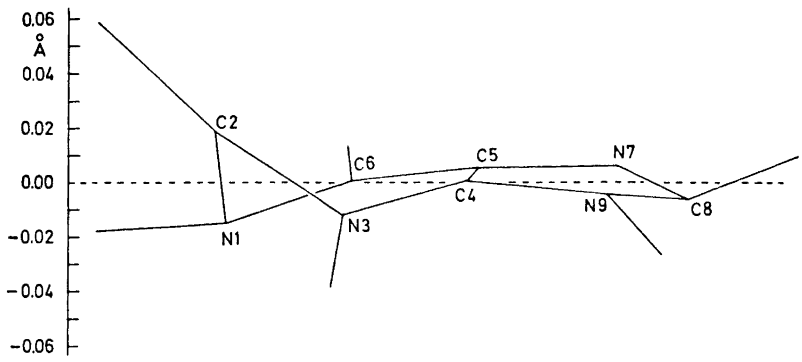

Fig. 2. The puckering of the molecule. The scale of the ordinate is greatly expanded relative to the abscissa.

MOLECULAR STRUCTURE

The molecule is not planar, as shown in Fig. 2. The methyl groups on N(3) and N(9) are displaced to the same side of the purine ring. The imidazole ring is planar within experimental error. Five of the atoms in the pyrimidine ring are lying in one plane, while the sixth atom, C(2), deviates significanly from this plane. There is a small though probably significant dihedral angle of 0.7° between the planes through the two rings. The same feature is observed in several other purine derivatives.[8]

The molecular dimensions are shown in Fig. 3. The bond lengths C(4) – C(5) and N(7) – C(8) have a large degree of double bond character which is consistent with the most probable canonical form (I).

The small variation in the extra-anular C – N-bonds is probably significant and related to the strength of the adjacent bonds and to the magnitude of the internal angle at the substituted nitrogen atom. The difference in bond lengths

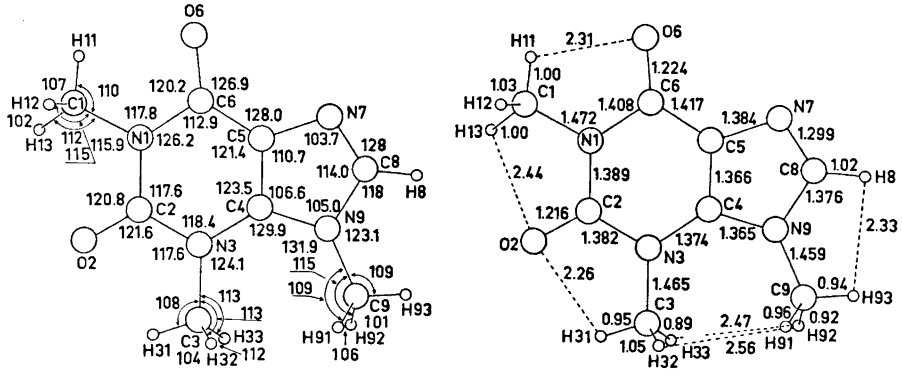

Fig. 3. Bond distances and angles. The estimated standard deviations are 0.002 Å and 0.1°, and 0.02 Å and 1° for non-hydrogen and hydrogen, respectively.

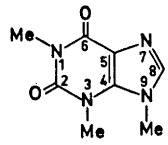

(I)

between the C=O bond in 6-position and the one in 2-position is also significant. The C(6)–O and C(2)–O distances found in three analogous purine structures are in average 1.234 and 1.216 Å, respectively.[9–11]

The substituent on C(6) in purines is always displaced so as to make the angle C(5)–C(6)–X greater than 120°. For carbonyl groups the average of the external angle C(5)–C(6)–O(6) is 127.8° (r.m.s. 0.3°) as calculated from 10 oxypurine structures.[8–15] In the present structure the angle is 126.9° and thus slightly reduced, probably because of the proximity of the methyl group on N(1). The steric interaction between the methyl group on N(3) and N(9) has caused an increase in the angle N(3)–C(4)–N(9) by approximately 2° compared to the average purine geometry.

MOLECULAR PACKING

A stereoscopic drawing of the crystal structure viewed along the *a* axis is shown in Fig. 4. There are no ordinary hydrogen bonds present in the structure, however, some of the C–H···O contacts between methyl and carbonyl groups may be classified as very week hydrogen bonds. In the stereodiagram three bonds of this type are indicated: C(9)–H(93)···O(2) = 3.35 Å, ∠CHO = 157°, C(9)–H(92)···O(6) = 3.43 Å, ∠CHO = 171°, and C(1)–H(12)··· O(2) = 3.45 Å, ∠CHO 176°.

The molecules related by unit translation along *a* are partially overlapping when viewed perpendicular to the purine plane (Fig. 5). The interplanar

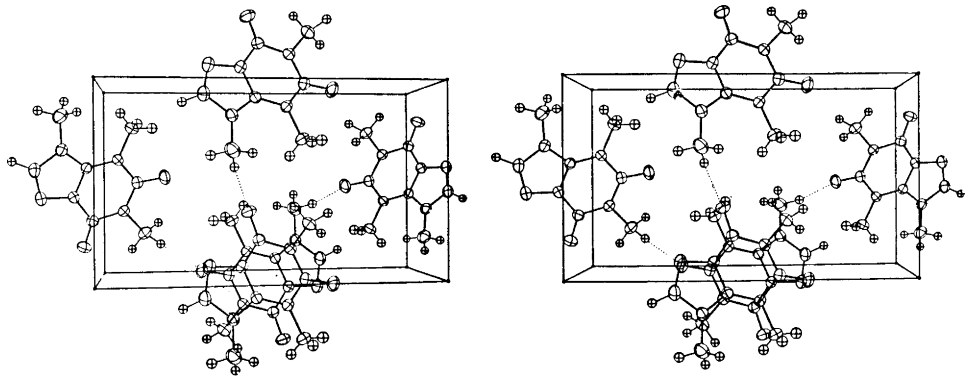

Fig. 4. Stereoscopic drawing of the packing of molecules in the unit cell. The *a* axis is nearly normal to the plane of the figure.

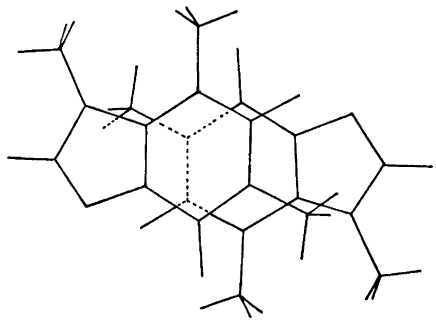

Fig. 5. Base stacking of TMX molecules viewed perpendicular to the least-squares plane of the purine ring. Interplanar spacing = 3.40 Å.

distance of 3.40 Å is slightly larger than what is normally found in stacks of simple purine-type molecules. The observed stacking pattern is not easily understood in terms of specific intermolecular forces. An excellent review on the subject of stacking interactions has recently been published.[8]

ELECTRONIC STRUCTURE

The usual CNDO/2 approximation and parameters were chosen to calculate charge distribution and dipole moment for the molecule. The theory of the CNDO/2 all valence electron calculation has been outlined by Pople *et al.*[16] The usefullness of this semiempirical method in predicting physical properties like dipole moment and rotation barriers seems to a certain degree to depend on the type of molecule and the atoms involved.

In Fig. 6 the calculated charge distribution and bond orders in TMX is given. The total dipole moment for the molecule is calculated to be 8.05 D. An experimental dipole moment is not yet determined due to solvation prob-

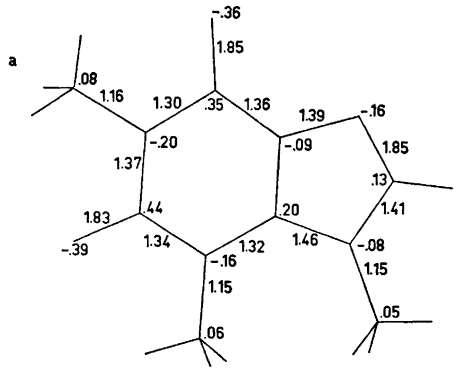

Fig. 6. Calculated charge distribution and bond orders obtained by the CNDO/2 method.

lems. However, in other xanthine molecules the dipole moments have been measured to be in the range 4.0 – 4.3 D for N(7) – H tautomers and 7.2 – 7.9 D for N(9) – H tautomers.[17] Introducing a methyl group instead of hydrogen on N(9) should not alter the dipole moment significantly, thus the calculated value of 8.05 D seems reasonable.

CONFORMATION OF THE METHYL GROUPS

The main interest in this investigation concerns the orientation of the methyl groups in 3 and 9 position. Due to packing effects conformational studies on molecules in the solid state must be regarded with caution. In cases where several closely related structures are compared the conclusion about conformational aspects may be valid. In the present case the 1,3,9-trimethyl compound (TMX) is compared to 1,3-bis(8-theophyline)propane (BTP)[9] and to the 9-methyl hypoxanthine ligand (MHX) in a copper(II) complex[18] (Fig. 7).

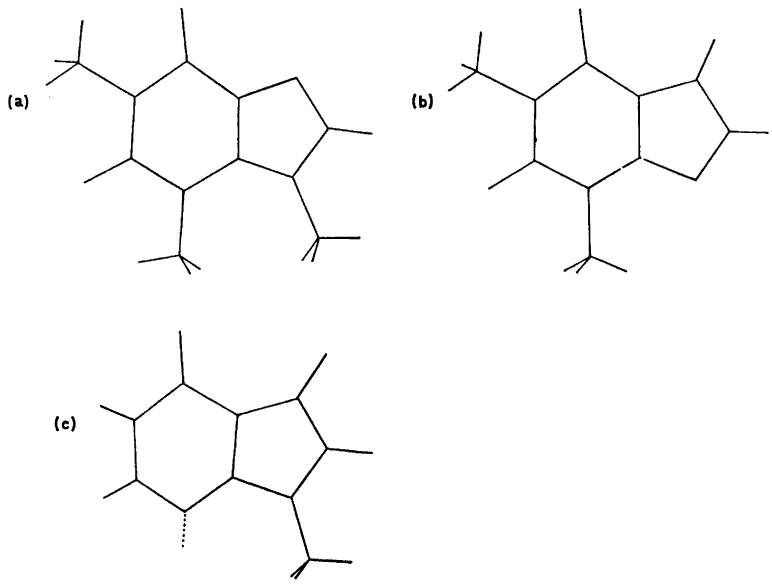

Fig. 7. Conformation of (a) 1,3,9-trimethyl-xanthine, (b) 1,3-bis(8-theophylline)propane, and (c) 9-methyl-hypoxanthine.

In the mono methyl substituted compound MHX the methyl group deviates 6° from an exactly eclipsed position relative to C(8) – H(8). The H(8)··· H(93) distance is only 2.3 Å. In TMX, Me(9) has exactly the same orientation within experimental error as in MHX despite the steric interference from Me(3). In BTP where the mutual methyl interaction is missing Me(3) is rotated 180° relative to the orientation in TMX. Thus the conformation with Me(3)

and Me(9) almost eclipsed seems to be more stable than the staggered conformation. In the observed eclipsed form the two shortest H···H distances between the methyl groups are 2.47 and 2.56 Å, respectively, and thus not significantly different from the van der Waals contact of 2.50 Å. The O(2)···H(31) distance on the other hand is only 2.26 Å compared to van der Waals distance O···H of 2.6 Å. In a staggered configuration the O(2)···Me(3) interaction is relieved somewhat, while the H(31)···Me(9) contact becomes critical.

The molecular packing of TMX shows no short intermolecular contacts that might be expected to significantly alter the conformation of the molecule. The environment of the methyl group on N(1) is quite different in TMX and BTP; however, the orientations of the methyl groups in the two compounds are identical within experimental error. The O(6)···H and O(2)···H distances are 2.34 and 2.44 in TMX and 2.31 and 2.44 in BTP.

The above results are in agreement with NMR-spectra obtained by Bergmann and coworkers.[2] They report down field shifts of the 3- and 9-methyl signals of 0.17 p.p.m. relative to the compounds with only 3- or 9-substitution. This is interpreted as due to steric interference. *A priori* one would not expect the shifts to be of the same magnitude since Me(3) has changed its orientation completely while Me(9) has almost the same orientation as in the monosubstituted compound.

REFERENCES

1. Lichtenberg, D., Bergmann, F. and Neiman, Z. *J. Chem. Soc.* **C 1971** 1676.
2. Lichtenberg, D., Bergmann, F. and Neiman, Z. *J. Chem. Soc.* **C 1971** 1940.
3. Long, R. E. *Ph. D. Dissertation*, University of California, Los Angeles, California 1965.
4. Zachariasen, W. *Acta Cryst.* **5** (1952) 68.
5. *International Tables for X-Ray Crystallography*, Kynoch Press, Birmingham 1962, Vol. III, p. 202.
6. Stewart, R. F., Davidson, E. R., and Simpson, W. T. *J. Chem. Phys.* **42** (1965) 3175.
7. Schomaker, V. and Trueblood, K. N. *Acta Cryst.* **B 24** (1968) 63.
8. Sletten, J. and Jensen, L. H. *Acta Cryst.* **B 25** (1969) 1608.
9. Rosen, L. S. and Hybl, A. *Acta Cryst.* **B 27** (1971) 952.
10. Ringertz, H. *Acta Cryst.* **20** (1966) 397.
11. Sutor, D. J. *Acta Cryst.* **16** (1963) 97.
12. Thewalt, U., Bugg, C. E. and Marsh, R. E. *Acta Cryst.* **B 27** (1971) 2358.
13. Sletten, J., Sletten, E. and Jensen, L. H. *Acta Cryst.* **B 24** (1968) 1692.
14. Munns, A. R. I. and Tollin, P. *Acta Cryst.* **B 26** (1970) 1101.
15. Thewalt, U., Bugg, C. E. and Marsh, R. E. *Acta Cryst.* **B 26** (1970) 1089.
16. Pople, J. A., Santry, D. P. and Segal, G. A. *J. Chem. Phys.* **43** (1965) 129.
17. Bergmann, E. D. and Weiler-Feilchenfeld, H. *The Purines – Theory and Experiment.* The Jerusalem Symposia on Quantum Chemistry and Biochemistry, The Israel Academy of Science and Humanities, Jerusalem, 1972, p. 21.
18. Sletten, E. *Chem. Commun.* **1971** 558.

Received April 5, 1973.

ACTA CHEMICA SCANDINAVICA 27 (1973) 2769–2780

The Use of Isocyanides for the Immobilization of Biological Molecules

PER VRETBLAD and ROLF AXÉN

Group of Applied Biochemistry (Swedish Board for Technical Development), Institute of Biochemistry, University of Uppsala, Box 531, S-751 21 Uppsala 1, Sweden

Isocyanides can be used for the preparation of immobilized enzymes and biospecific adsorbents. The technique is based on a four-component condensation involving an isocyanide, a primary amine, a carbonyl compound, and a carboxylate ion. The reaction proceeds in aqueous solution under physiological conditions.

The model substance human serum albumin has been immobilized on various carriers. The influence of reaction pH, temperature, and time on the immobilization has been studied. The immobilizations of several biological substances of various structure, *i.e.* nucleic acids, cofactors, peptides, steroids, and penicillins, are reported. The structures of the linkages between carrier and ligand are considered and also the possibilities to "direct" the reaction.

In recent years a number of methods for the preparation of immobilized biological activity have been developed and successfully applied to the preparation of immobilized enzymes and biospecific adsorbents. Several reviews have been written on the subject.[1–7]

As a part of our programme for development of methods for the covalent fixation of biologically active substances to polymers, we have investigated the four-component condensation of an isocyanide, a primary amine, a carbonyl compound, and an anion.[8] Many biological substances contain amino, carbonyl, or anionic groups or combinations of such groups and can thus be attached to a variety of polymeric carriers containing one or more of the other reaction components. In addition to ligand and carrier, the reaction mixture must contain the remaining components needed for the four-component condensation to take place. These are normally low-molecular weight substances.

The described procedure obviously implies a great flexibility in the choice of system for the immobilization of each individual compound. For example, the conditions of immobilization of biological molecules containing more than one class of the above mentioned reacting groups can be chosen so as to minimize modification of essential residues. Another feature giving the method a wide potential applicability is that the reaction proceeds readily, not only

in organic solvent systems, but also in aqueous solution at physiological pH values, thus decreasing the risk of denaturation or decomposition of pH-sensitive biological structures.

The mechanism of the condensation reaction has been thoroughly studied in homogeneous systems by Ugi and his associates.[9,10] A schematic representation is given in Fig. 1. The reaction is remarkable in the respect that a single end-product can be obtained from a reaction mixture containing all these reactive components.

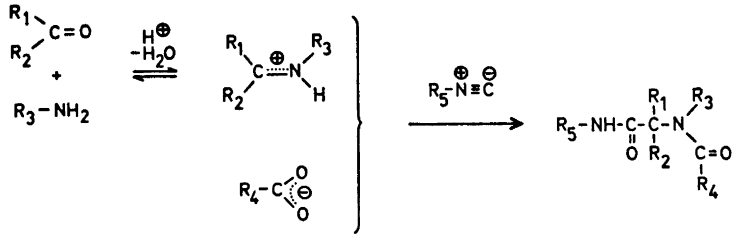

Fig. 1. Schematic representation of the four-component condensation exemplified by a primary amine and a carboxylate anion. The final product has a stable amide structure.

In this paper we present experiments performed in order to find conditions which allow high coupling efficiency. The protein human serum albumin (HSA)* has been used as a model substance. The properties of different carriers are discussed and comparison made between various low-molecular weight reagents which can be used as coupling mediators. The structures of the linkages between carrier and ligand are considered and also the possibilities to "direct" the reaction. The immobilizations of several biological substances of various structure, *i.e.* nucleic acids, cofactors, peptides, steroids, and penicillins, are reported.

In previous publications the preparations of immobilized enzymes of considerable catalytic efficiency and high stability have been described.[8,11,12]

EXPERIMENTAL

Preparation of carriers and immobilization of proteins. Sepharose® 6B (Pharmacia Fine Chemicals, Uppsala, Sweden) was cross-linked with epichlorohydrin and converted to an amino derivative by reaction with MDA (Aldrich Chem. Co., Milwaukee, Wisc.) as previously described [12] except that 50 % higher MDA concentration was used. 5 ml MDA-Sepharose (sedimented in 0.1 M NaCl) was diluted with 0.1 M NaCl to a total volume of 7 ml, and 50 mg HSA (Kabi, Stockholm, Sweden) was added, followed by 10 μl acetaldehyde and 25 μl cyclohexyl isocyanide (EGA-Chemie KB, Steinheim/Albuch, West Germany). Identical mixtures were incubated at different pH's and temperatures and for various periods of time (see Figs. 2 – 3). Excess reagents were removed on a glass filter and the gel packed in a column. It was washed at 23° at 10 ml/h with the following buffers: 0.1 M Na phosphate, pH 7.5 (24 h) and 0.1 M Na acetate, 0.2 M NaCl, pH 4.0

* Abbreviations: HSA, human serum albumin; MDA, *p,p'*-diaminodiphenylmethane (4,4'-methylene dianiline); CM, carboxymethyl; ECD, epichlorohydrin cross-linked and desulphated.

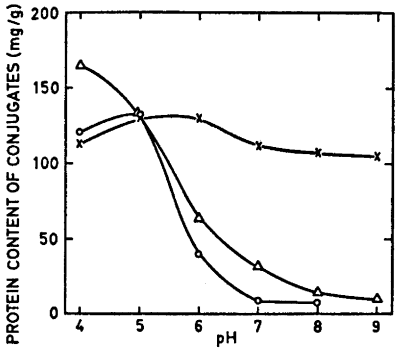

Fig. 2. The fixation of human serum albumin to various carriers as a function of reaction pH. ○, CM-Sephadex. ×, MDA-Sepharose. △, carbonyl-Sepharose. For composition of the reaction mixtures, see Experimental. Incubation for 6 h at 23°.

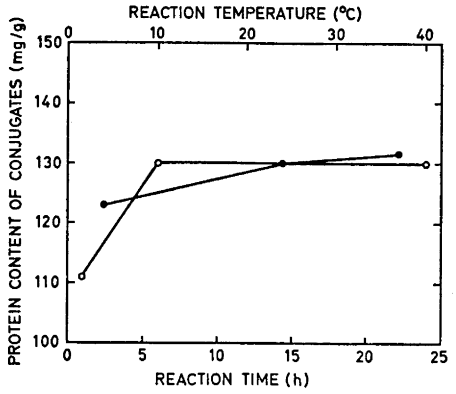

Fig. 3. The fixation of 50 mg human serum albumin to 5 ml MDA-Sepharose in a total volume of 7 ml 0.1 M NaCl at pH 6.0 as a function of reaction temperature (●) and reaction time (○). The immobilization was mediated by 25 μl cyclohexyl isocyanide and 10 μl acetaldehyde. The experiments performed at different temperatures were incubated for 6 h. The experiments performed for different periods of time were incubated at 23°.

(24 h). Samples of gel were treated with acetone, dried at 100° for 24 h, and subjected to amino acid analysis.[13] HSA was also coupled to 200 mg (dry weight) CM-Sephadex ® C-50 (Pharmacia) using the same amounts of reactants and the washing procedure as above; see Fig. 2.

A carbonyl polymer was prepared by dimethyl sulfoxide oxidation of ECD-Sepharose in the presence of P_2O_5 as previously described.[8] The product was washed in a column with 0.1 M NaCl at 10 ml/h for 24 h. To 1 ml sedimented gel in a total volume of 2 ml 0.1 M NaCl, were added 25 mg HSA, 25 μl cyclohexyl isocyanide, and 20 μl aniline. Incubation was carried out at various pH values at 23° for 6 h and the products washed as above; see Fig. 2.

A series of acetal- or aldehyde-substituted polyacrylamide carriers were used for the immobilization of α-chymotrypsin (3 × crystallized, Worthington Biochem. Corp., Freehold, N.J.). One acetal-polyacrylamide carrier, Enzacryl ® Polyacetal, is commercially available (Koch-Light, Colnbrook, Bucks., England). This polymer was hydrolyzed before application of the four-component reaction step. The hydrolysis was performed with 0.3 M HCl at 23° for 48 h. Chymotrypsin was attached to the hydrolyzed polymer as described in Table 2.

Enzacryl ® AA (Koch-Light) is a cross-linked polyacrylamide substituted by aromatic amino groups. Enzacryl AA was substituted with aldehyde or acetal groups using glutardialdehyde, *N*,*N*-bis(2,2-diethoxyethyl)amine, and 2,5-dihydro-2,5-dimethoxyfuran. The latter reagents were purchased from Aldrich Chem. Co. and Wolff and Kaaber, Farum, Denmark, respectively. The experiments were performed as follows: 50 mg polymer was suspended in 1.5 ml water and reacted with 50 mg Na acetate trihydrate, 50 μl cyclohexyl isocyanide, and 50 μl aldehyde or acetal reagent. The reaction mixture was stirred at 23° and pH 6.5 for 3 h. The product was washed free of soluble reagents with water on a glass filter and used for the attachment of chymotrypsin under the conditions given in Table 2. The conjugates were column washed as described earlier [14] and

Table 1. Immobilization of chymotrypsinogen A mediated by 10 μl acetaldehyde (omitted in the case of carbonyl polymer) and 25 μl cyclohexyl isocyanide. Incubation for 6 h at 23°.

Carrier	Amount of carrier dry weight (mg)	Amount of carrier sedimented gel (ml)	Amount of protein (mg)	Total volume of reaction mixture (ml 0.1 M NaCl)	Reaction pH	Protein content of conjugates (mg/g)
CM-Sephadex	200		50	7	5.0	184
CM-Sephadex	200		50	7	7.0	179
MDA-Sepharose		5	50	7	6.0	134
Carbonyl Sepharose		1	25	2	6.0	53

Table 2. Immobilization of α-chymotrypsin (20 mg) on acetal- or aldehyde-substituted polyacrylamide carriers (50 mg) mediated by cyclohexyl isocyanide (25 μl) at 23° and pH 6.5. Total reaction volume 2 ml. Reaction time 6 h. The specific activity of free chymotrypsin towards *N*-acetyl-L-tyrosine ethyl ester is 200 μmol min^{-1} mg^{-1}.

Carrier	Reagent for introduction of acetal or aldehyde groups	Esterolytic activity of chymotrypsin conjugates towards *N*-acetyl-L-tyrosine ethyl ester: Apparent pH-optimum	Specific activity (μmol min^{-1} mg $conjugate^{-1}$)
Enzacryl Polyacetal	–	9.6	6
Enzacryl AA	Glutardialdehyde	9.8	39
Enzacryl AA	*N*,*N*-Bis(2,2-diethoxyethyl)amine	9.8	42
Enzacryl AA	2,5-Dihydro-2,5-dimethoxyfuran	9.8	32

Table 3. Immobilization of nucleic acids and nucleotides on 3 ml sedimented MDA-Sepharose or 200 mg (dry weight) CM-Sephadex in a total volume of 7 ml H_2O, mediated by 100 μl cyclohexyl isocyanide and 50 μl acetaldehyde (50 μl and 25 μl, resp., in the case of poly-A). Incubation for 6 h at 23°.

Ligand	Amount of ligand (mg)	Carrier	Reaction pH	Ligand content of conjugates (mg/g)
RNA	50	CM-Sephadex	5.0	0.1
RNA	50	MDA-Sepharose	6.0	39
RNA	50	MDA-Sepharose	6.0	1[a]
poly-A	15	MDA-Sepharose	6.0	7
AMP	100	MDA-Sepharose	6.5	3
NAD	100	MDA-Sepharose	6.5	1
NAD	100	CM-Sephadex	6.5	0

[a] Isocyanide omitted.

characterized by their ability to catalyze the hydrolysis of *N*-acetyl L-tyrosine ethyl ester [14] at a substrate concentration of 15 mM.

Chymotrypsinogen A (Worthington) was immobilized and washed under the same conditions as given for HSA above. See Table 1.

Immobilization of nucleic acids and nucleotides. Yeast RNA (Worthington), polyadenylic acid (poly-A, Type I, Sigma Chem. Co., St. Louis, Mo.), 5'-AMP (Type III, Sigma), and NAD (Grade III, Sigma) were immobilized as described in Table 3. The conjugates were washed under the conditions given for HSA but with the phosphate buffer replaced by 0.1 M sodium borate buffer, pH 8.0. The ligand contents of the conjugates were estimated from their phosphorus content determined using ammonium molybdate.[15] Blank couplings without isocyanide were performed and the products always found to have a negligible phosphate content. The coenzymatic activity of free and immobilized NAD was determined using lactate dehydrogenase and lactate in the presence of semicarbazide.[16]

Immobilization of various low-molecular weight substances. Biotin (Merck AG, Darmstadt, West Germany), benzyl penicillin (sodium salt, Sigma), and 6-aminopenicillanic acid (Nutritional Biochem. Corp., Cleveland, Ohio) were fixed as described in Tables 4 and 6. The ligand contents of the conjugates were estimated from their content of sulphur determined as methylene blue.[17] All values are corrected for the sulphur content of the matrix; no additional sulphur was introduced in blank couplings performed in the absence of low-molecular weight coupling mediators.

Immobilization of peptides and amino acids is exemplified in Table 5. These conjugates were washed as described for HSA. Penicillanic acid conjugates were washed with 0.1 M Na phosphate, pH 6.2, and 0.1 M Na phosphate, pH 5.5.

Table 4. Immobilization of biological substances mediated by 25 μl cyclohexyl isocyanide (3-dimethylaminopropyl isocyanide in the case of biotin). Incubation for 6 h at 23°.

Ligand	Amount of ligand (mg)	Carrier	Total volume of reaction mixture (ml H_2O)	Amount of aldehyde (μl)	Additional reagent	Reaction pH	Ligand content of conjugates (μequiv./g)
Biotin	25	50 mg Enzacryl AA	2	25[a]	–	6.5	25
Benzylpenicillin	25	50 mg Enzacryl AA	2	25[a]	–	6.5	10
Benzylpenicillin	25	1 ml carbonyl Sepharose	2	–	20 μl butylamine	6.5	16
6-Aminopenicillanic acid	25	1 ml carbonyl Sepharose	3	–	30 mg Na acetate	6.0	34
6-Aminopenicillanic acid	50	5 ml MDA-Sepharose	7	25[b]	–	6.5	16
6-Aminopenicillanic acid	50	200 mg CM-Sephadex	7	25[b]	–	6.5	30

[a] Acetaldehyde. [b] Benzaldehyde.

Table 5. Immobilization of 35 mg amino acid ester or peptide on 50 mg (dry weight) CM-Sephadex mediated by 25 μl 3-dimethylaminopropyl isocyanide and 25 μl aldehyde in 2 ml H_2O at pH 7.0. Incubation for 6 h at 23°.

Ligand	Aldehyde	Amino acid content of acid hydrolysate of conjugate (μequiv./g conjugate)	
Phenylalanine ethyl ester	HCHO (35 %)	Phe: 84	Gly: 9
Phenylalanine ethyl ester	CH_3CHO	Phe: 57	Ala: 24
Glycyl leucine	CH_3CHO	Gly: 19 Leu: 275	Ala: 32

Table 6. The effect of the addition of a five-fold excess of aniline (100 μl) or Na acetate (150 mg) on the immobilization of benzyl penicillin (75 mg) and phenylalanine ethyl ester (40 mg). Incubation with 1 ml carbonyl-Sepharose and 25 μl cyclohexyl isocyanide in 3 ml water for 6 h at pH 6.0 and 23°.

Ligand	Ligand content of conjugates (μequiv./g)		
	standard experiment	amine added	acetate added
Benzyl-penicillin	12.2	15.0	0.5
Phenylalanine ethyl ester	5.3	0	3.7

Immobilization of cortisone (Sigma) was carried out as follows. 25 μl cyclohexyl isocyanide was added to 50 mg CM-Sephadex, 10 mg cortisone, and 25 μl aniline in 2 ml solvent mixture (50 % ethanol or dimethyl formamide in water). The pH was adjusted to 4.5 and the reaction allowed to proceed overnight at 23°. The product was washed on a glass filter and then in a column for 48 h at 10 ml/h with the same solvent mixture. IR spectra of dried samples in KBr were recorded and the steroid content of the conjugates estimated by comparisons with reference spectra recorded on mixtures of dry matrix and different amounts of steroid.

RESULTS AND DISCUSSION

The choice of carrier. Carriers containing amino, carbonyl, and carboxyl groups have been prepared and the isocyanide immobilization technique has been applied. A few commercially available derivatized polymers have also been used. The capacity of the polymers to take up ligands is important but the carrier must also satisfy requirements with regard to particle size and shape, mechanical rigidity, and permeability. As yet it has not been possible to prepare an isocyanide polymer with significant substitution.

The anionic polymers have exclusively been carboxyl-substituted. Carboxymethyl Sephadex has proved suitable in several cases (see tables, figures, and Ref. 8). Very high ligand uptakes can be obtained. We have earlier

used carboxymethyl agarose,[8] which has a lower capacity to take up protein. The relative activities of enzymes bound to these carriers, especially towards macromolecular substrates, are not very high which may be caused by intra- and intermolecular cross-linking effected by excess of low-molecular weight reagents (*cf.* below). Electrostatic repulsion between gel and substrate may also play a role in the case of casein hydrolysis.

The best amino polymers employed so far have been obtained by CNBr activation or bis-epoxide activation [18] of epichlorohydrin cross-linked Sepharose and subsequent coupling of aromatic diamines, *i.e.* MDA or occasionally *p*-phenylenediamine. The content of free amino groups in the MDA polymers is rather low,[12] but nevertheless good uptakes of proteins and other substances are obtained. Because of the low content of amino groups in the carrier, the proteins will be fixed by a small number of bonds which is advantageous since a large number of points of attachment may lead to destruction of the protein tertiary structure. Since aromatic amines are weak bases the charge density of the carrier is low at physiological pH values, which is important if the carrier is going to be used for the preparation of adsorbents for biospecific affinity chromatography. MDA-Sepharose has been used for the immobilization of pepsin,[11] β-amylase,[12] and several ligands discussed in this paper (see tables and figures).

The amino-substituted polymer Enzacryl AA has been used for the preparation of immobilized proteolytic enzymes with reasonable yields and with considerable activity in batch towards low-molecular weight substrates.[8] However, the proteolytic activity is low, probably because of steric hindrance. The powder-like conjugates are unsuitable for column use.

Structural proteins, *e.g.* keratin and wool, are examples of carriers containing both carboxyl and amino groups. They have been used for the preparation of catalytically active immobilized chymotrypsin.[8]

Carbonyl polymers can be prepared by dimethyl sulfoxide oxidation of alcoholic groups in polysaccharides in the presence of an activating electrophilic reagent such as acetic anhydride [19] or phosphorus pentoxide.[20] Using this reaction, carbonyl derivatives of ECD-Sepharose have been prepared which have been successfully used for the immobilization of biological molecules. The pH dependence of the fixation of HSA to such a polymer is shown in Fig. 2.

Aldehyde- and acetal-substituted polymers have been prepared by derivatizing Enzacryl AA with glutardialdehyde, *N*,*N*-bis(2,2-diethoxyethyl)amine, and 2,5-dihydro-2,5-dimethoxyfuran (see Experimental). These polymers, together with the commercial carrier Enzacryl Polyacetal, have been employed for the preparation of catalytically active immobilized chymotrypsin (Table 2).

Periodate-oxidized polysaccharide carriers have earlier been used for the immobilization of chymotrypsin.[8] In summary, proteolytic enzymes attached to carbonyl polymers exhibit high activities towards low-molecular weight substrates and, with the exception of Enzacryl derivatives, also have considerable proteolytic activities.

The choice of isocyanide. 3-Dimethylaminopropyl isocyanide, which is readily water-soluble but not commercially available, was used in early studies. Later cyclohexyl isocyanide has been used, which can be obtained commerci-

ally. This compound has a limited solubility in water, so that stirring or revolution of the reaction mixture must be efficient. Pepsin could be attached to Sepharose with equal yields using either of these isocyanides.[11] *t*-Butyl isocyanide and 1,1,3,3-tetramethyl butyl isocyanide (Kema Nord, Sweden) and also *N*-(3-isocyanidopropyl)-morpholine (prepared in our laboratory[21]) have also been used with no notable differences in the results.

The choice of carbonyl compound. The carbonyl function may be on the carrier (see above) or on the ligand, as exemplified by cortisone. Otherwise, a low-molecular weight aldehyde, such as acetaldehyde, is added to the reaction mixture. Several other aldehydes, *e.g.* formaldehyde, butyraldehyde, and benzaldehyde, have been used more occasionally. No significant differences in coupling yields have been found using these aldehydes. Ketones, however, give lower coupling yields.

The choice of amine. The amino component is usually present on the biological molecule to be immobilized or on the carrier. In other cases an amine is added as an additional component to make the system complete or to compete with an essential amino group. For such purposes we have used butylamine, ethanolamine, aniline, and *N*-(3-aminopropyl)-morpholine.

The choice of anion. Carboxylate anions have been regularly employed both on the carrier, on the ligand, and in the form of sodium acetate as an additional component. In a few cases anions of phosphate esters have been used (Table 3).

HSA is attached to MDA-agarose in exactly the same amount in 0.1 M Na phosphate buffer, pH 6.0 (131 mg/g) as in 0.1 M NaCl, adjusted to pH 6.0 (130 mg/g). This experiment indicates that phosphate ions do not participate in the immobilization reaction; no competition with carboxylate ions takes place.

The hydroxide ion is always present in the systems, although in low concentration at the pH at which the reaction is usually carried out. If this anion could compete efficiently with carboxylate anions it would not be possible to fix significant amounts of ligands to carboxylic carriers, or carboxylic ligands to amino carriers. However, at high pH the hydroxide ion may become important.

Optimal conditions for the immobilization of proteins. The attachment of HSA to MDA-Sepharose has been used as a model system for determing the optimal conditions for the immobilization of proteins. However, the results are probably representative for other classes of substances as well.

Identical reaction mixtures were incubated for 1, 6, and 24 h. The reaction was essentially complete in a few hours (Fig. 3). In earlier experiments with coupling of chymotrypsin to CM-Sephadex (unpublished) the protein uptake after 1 h was also 85 – 90 % of that after 6 h.

The temperature dependence of the immobilization reaction is not very marked. Only 8 % difference in protein content of the conjugates is observed if the coupling is performed at 4° or 37° (Fig. 3). This makes possible the immobilization of thermally unstable substances in good yields. Unless otherwise stated, a temperature of 23° has been used.

The pH-dependence of the extent of fixation of HSA to polymers substituted with amino, carbonyl, and carboxyl groups is illustrated in Fig. 2. The coupling of HSA to MDA-Sepharose proceeds with the same efficiency

over a wide range of pH. On the other hand, the fixation of HSA to CM-Sephadex and carbonyl-Sepharose is very dependent on pH. This is most likely due to electrostatic effects. MDA-Sepharose has a low charge density. CM-Sephadex carries many negative charges and repels the acidic protein HSA when the pH is significantly higher than the isoelectric point of the protein (pH 4.9). When the reaction pH is lowered, the protein loses its negative net charge and is attracted to the gel giving a high coupling yield. Contrary to HSA, the basic protein chymotrypsinogen A ($pI = 9.5$) is taken up in high yields by CM-Sephadex both at pH 5 and pH 7 (Table 1), which also may be explained by this charge effect. Chymotrypsin ($pI = 8.6$) has repeatedly been attached to CM-Sephadex at pH 6.5 in high yields.[8] When the carbonyl-Sepharose was synthesized, carboxyl groups were probably formed by oxidation of carbonyl functions. This gel thus repels HSA at neutral and alkaline pH analogous to CM-Sephadex. These results suggest that the four-component condensation is not very sensitive to pH but that electrostatic interactions between carrier and ligand can strongly affect the extent of coupling.

The reaction can be allowed to proceed in a pH-stat or in buffered solution. As stated above, some buffer anions (such as carboxylate) participate in the reaction, whereas others (such as phosphate) do not. This should be considered when an experiment is planned.

By varying the content of reactive groups in the carrier and the concentrations of soluble reactants, the uptake of ligand can be varied to a great extent.[8,11,12] However, high concentrations of reactants will not necessarily give the best products. A general observation is that there is an inverse relationship between the enzyme content of a conjugate and the relative activity of the fixed enzyme (compared to that of the free enzyme). For theoretical studies, the most desirable preparations may be those with high relative activity but, when practical applications are considered, the most important property of a conjugate is the percentage uptake of the total amount of catalytic activity added to the reaction mixture.[12]

Immobilization of substances other than proteins. The immobilization of nucleic acids and synthetic polynucleotides has received attention in the last few years. Such preparations, often with rather low ligand contents, have been employed as biospecific adsorbents.[6,22,23] The isocyanide method, used here for the immobilization of yeast RNA and polyadenylic acid (Table 3), should be a useful complement to the already existing methods.

The immobilization of various low-molecular weight substances (*i.e.* NAD, AMP, biotin, benzyl penicillin, 6-aminopenicillanic acid, glycyl leucine, and phenylalanine ethyl ester) is shown in Tables 3 – 6. The ligand uptakes of the carriers are low on a weight basis in comparison with the amounts of protein which can be taken up. However, an efficient biospecific adsorbent is not necessarily highly substituted. The immobilized NAD described in Table 3 was equally active as free NAD as coenzyme to lactate dehydrogenase.[16]

In addition to the substances mentioned above, matrix-bound cortisone has been prepared with a steroid content of approximately 20 mg/g conjugate. Because of the low water solubility of this substance the immobilization was carried out in mixtures of water and organic solvents. Immobilized hormones

and penicillins should be interesting objects for pharmacological investigations and studies on cellular metabolism. Immobilized peptide hormones have already been used for the latter purpose.[6]

The structure of the carrier-ligand linkage. The determinations of immobilized proteins, peptides and amino acids have been performed by amino acid analysis [13] of acid hydrolysates of the conjugates. It has been shown by hydrolyzing mixtures of carriers and amino acids that the presence of carrier does not normally influence the recovery of amino acids. However, the patterns of the chromatograms obtained from covalently linked ligands are often not identical with those of mere mixtures. The differences are understandable if it is assumed that attachment has taken place according to the four-component scheme and also that certain bonds are preferentially split upon hydrolysis.

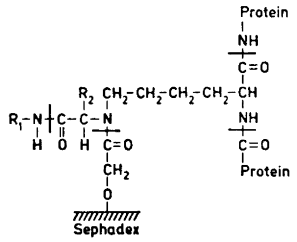

Fig. 4. Suggested structure and hydrolysis pattern of a CM-Sephadex-α-chymotrypsin conjugate. R_1: dimethylaminopropyl. R_2: H (formaldehyde). Hydrolytic cleavage indicated by heavy lines.

With the above assumptions, the study of amino acid chromatograms can give information about which functional groups participate in the condensation process. Fig. 4 gives an illustration. Chymotrypsin was attached to CM-Sephadex by means of formaldehyde and the conjugate analyzed. It was observed that the recovery of lysine was significantly reduced and that an extra peak had emerged. According to Fig. 4, the formation of carboxymethyl lysine could be expected and the extra peak was identified as this lysine derivative by comparison with a chromatogram of the products of hydrolysis of a bromoacetate-treated polylysine.

Analogous experiments have been performed with low-molecular weight substances (Table 5). When phenylalanine ethyl ester or glycyl leucine was immobilized on CM-Sephadex in the presence of acetaldehyde, alanine was formed in the hydrolysate; when phenylalanine ethyl ester was attached using formaldehyde, glycine was obtained. This is also in accordance with the model in Fig. 4, provided that all bonds of the tertiary amide nitrogen are susceptible to hydrolytic cleavage.

When proteins are attached to amino polymers, *e.g.* Enzacryl or MDA-agarose, and the linkage is mediated by acetaldehyde, the relative alanine content of the conjugates is significantly higher than in the native proteins. In experiments with carbonyl polymers no effects of this kind have been observed.

Blank couplings have been performed in the absence of isocyanide in order to estimate the amount of protein which becomes attached to different carriers by physical adsorption or electrostatic attraction. In all these experi-

ments, only very small amounts of protein have been found in the conjugates.

Inter- and intramolecular cross-linking. When isocyanides are used for the immobilization of biological molecules which contain more than one class of reactive group, and also all four reacting components are simultaneously present in the supernatant liquid, inter- and intramolecular cross-linking may occur. This can take place both in free solution and on the surface of the matrix. Such cross-linking will compete with the immobilization. Extensive cross-linking may affect the three-dimensional conformation of immobilized molecules, which can lead to destruction of the biological activity of these molecules.

Ways of directing the fixation. Biological molecules may contain more than one class of reactive group which can participate in the four-component condensation. For example, most proteins can react through either amino or carboxyl groups, one of which may be essential for the biological activity of the protein. However, the immobilization reaction can be directed so as to eliminate or diminish inactivation caused by modification of essential groups. This can be done in at least two ways: A protein which contains an essential carboxyl group can be attached to a carboxylic polymer, thereby utilizing the amino groups of the protein for fixation. Alternatively, it can be attached to a carbonyl polymer and an excess of carboxylate added to the reaction mixture to compete with the protein carboxyl groups.

A model experiment which illustrates the second of these methods of "direction" is shown in Table 6. Benzyl penicillin, which carries a free carboxyl group, and phenylalanine ethyl ester with a free amino group were incubated with carbonyl-Sepharose and cyclohexyl isocyanide. The uptakes of these ligands were estimated separately by sulphur and amino acid analysis of the conjugates, respectively. The uptake of benzyl penicillin could be almost completely inhibited by a five-fold excess of sodium acetate, and the uptake of phenylalanine ethyl ester was eliminated by a five-fold excess of aniline. A blank experiment performed in the absence of isocyanide showed no background adsorption of amino acid, but the carrier contained some sulphur for which correction was made.

Another series of experiments demonstrates the quantitative effect of the addition of "directing" reagents to a second model system, *viz.* the fixation of HSA to carbonyl-Sepharose at pH 6.0. When only cyclohexyl isocyanide was present in addition to these reagents, the protein uptake was 63 mg/g conjugate. When an excess of aniline was added, the uptake was identical. When the aniline was replaced by sodium acetate, the uptake was 38 mg/g.

Acknowledgements. We are indebted to Professor Jerker Porath for his continuous support. Our thanks are also due to Mrs. Marianne Lindström for technical assistance. The work has been supported by grants from *Sven and Lilly Lawski's Foundation for Scientific Research* and the *Swedish Board for Technical Development.*

REFERENCES

1. Katchalski, E., Silman, I. and Goldman, R. *Advan. Enzymol.* **34** (1971) 445.
2. Orth, H. D. and Brümmer, W. *Angew. Chem.* **84** (1972) 319.
3. Kay, G. *Process Biochem.* **3** (8) (1968) 36.

4. Lilly, M. D. and Dunnill, P. *Process Biochem.* **6** (8) (1971) 29.
5. Cuatrecasas, P. and Anfinsen, C. B. *Methods Enzymol.* **22** (1971) 345.
6. Cuatrecasas, P. *Advan. Enzymol.* **36** (1972) 29.
7. Porath, J. and Kristiansen, T. In Neurath, H., Ed., *The Proteins*, Academic, New York and London, 3rd Ed., Vol. 1. *In press.*
8. Axén, R., Vretblad, P. and Porath, J. *Acta Chem. Scand.* **25** (1971) 1129.
9. Ugi, I. *Angew. Chem.* **74** (1962) 9.
10. Ugi, I., Ed., *Isonitrile Chemistry*, Academic, N.Y. and London 1971.
11. Vretblad, P. and Axén, R. *FEBS Lett.* **18** (1971) 254.
12. Vretblad, P. and Axén, R. *Biotechnol. Bioeng.* **15** (1973) 783
13. Spackman, D. H., Stein, W. H. and Moore, S. *Anal. Chem.* **30** (1958) 1190.
14. Axén, R. and Ernback, S. *Eur. J. Biochem.* **18** (1971) 351.
15. Gustafsson, L. *Oikos. In press.*
16. Larsson, P.-O. and Mosbach, K. *Biotechnol. Bioeng.* **13** (1971) 393.
17. Gustafsson, L. *Talanta* **4** (1960) 227; 236.
18. Porath, J. and Sundberg, L. In Peeters, H., Ed., *Protides of the Biological Fluids*, Pergamon, Oxford 1971, Vol. 18, p. 401.
19. Albright, J. D. and Goldman, L. *J. Am. Chem. Soc.* **89** (1967) 2416.
20. Onodera, K., Hirano, S. and Kashimura, N. *Carbohyd. Res.* **6** (1968) 276.
21. Ugi, I., Betz, W., Fetzer, U. and Offermann, K. *Chem. Ber.* **94** (1961) 2814.
22. Wagner, A. F., Bugianesi, R. L. and Shen, T. Y. *Biochem. Biophys. Res. Commun.* **45** (1971) 184.
23. Rickwood, D. *Biochim. Biophys. Acta* **269** (1972) 47.

Received April 6, 1973.

ACTA CHEMICA SCANDINAVICA 27 (1973) 2781–2790

Effect of Ethanol on Fatty Acid Oxidation in the Perfused Livers of Starved, Fed, and Fat-fed Rats

ERIK FELLENIUS and KARL-HEINZ KIESSLING

Alcohol Research Group of the Swedish Medical Research Council, Institute of Zoophysiology, University of Uppsala, Uppsala, Sweden

On the basis of measurements of oxygen uptake, ethanol and oleate removal, and the production of ketone-bodies and acetate by the perfused liver, the effect of ethanol on the flow through the citric acid cycle and the β-oxidation pathways was calculated. Studies were carried out with livers from fed, 48 h starved, and fat-fed animals. Ethanol depressed flow through the citric acid cycle by 40 to 60 % depending on the nutritional state of the rat. The addition of pyruvate partly overcame this inhibition. The pathway of β-oxidation was also blocked by the addition of ethanol, although except for the fat-fed rats, ketone-body production was unaltered. The results suggest that, if inhibition of the citric acid cycle by ethanol favours an accelerated rate of ketogenesis, this effect may be concealed by a block in β-oxidation which limits the supply of acetyl-CoA for ketone-body formation.

Leloir and Muñoz [1] have calculated that in appropriate circumstances as much as three-quarters of the oxygen consumed by the liver may be used for the oxidation of ethanol. In more recent works [2–8] it has been proposed that the primary effect of ethanol oxidation in influencing lipid metabolism in the liver, results from its effect on the [free NAD^+]/[free NADH] ratio. However, the detailed nature of the interaction is still under debate.[9] Conflicting results have also appeared regarding the quantitative effects of ethanol oxidation on the β-oxidation pathway and on ketone-body metabolism. Thus Williamson *et al.*[7] indirectly showed that ethanol inhibited the β-oxidation of olelate while other authors [10] suggested unaltered flow through this step. Perfusion experiments [4] and investigations *in vivo* [9,11] indicate a tendency towards increased rate of ketone-body formation although an opposite effect has also been reported.[12]

Consequently, the present study of the perfused liver was undertaken to examine the interaction and its nature between ethanol oxidation and the metabolic steps related to fatty acid oxidation.

MATERIAL AND METHODS

Animal treatment. Female Wistar rats (180 – 230 g) from the laboratory's stock were used. The animals were divided into three groups and pretreated as follows: (1) starved for 48 h, (2) fed *ad libitum* the standard small-animal diet (Astra-Ewos, Södertälje, Sweden), (3) fed a high-fat diet [13] for 10 days. The high-fat diet consisted of 90 parts margarine and 10 parts casein, and was supplemented with salts and vitamins. During the first two days on this diet, the animals ate little and lost weight (10 – 30 g). After 2 or 3 days, the rats accepted the diet and their weights remained constant.

Chemicals. Oleic acid (*puriss.*) was obtained from Fluka AG Chemische Fabrik, Buchs, Switzerland. Oleic acid of very high purity, as shown by gas chromatography, was a generous gift from Prof. E. Stenhagen of the Institute of Medical Biochemistry, Gothenburg, Sweden. There were no notable differences in the results obtained with the two oleic acid compounds. Other substrates, co-enzymes, and crystalline enzymes were supplied by Biochimica Boehringer, Mannheim, West Germany, Sigma Chemical Co, St Louis, USA and E. Merck AG, Darmstadt, West Germany. Oleic acid was added to the perfusate as a neutral solution bound to albumin.[14] All other substrates were neutralized before addition.

Liver perfusions. The method of liver perfusion was that described by Hems *et al.*[15] The perfusion medium was composed of physiological saline,[16] to which had been added 2.6 % bovine serum albumin, fraction V (Armour Pharmaceutical Co. Ltd., Eastbourne, Sussex, U.K.), and aged washed human erythrocytes. The medium was gassed with CO_2:O_2 (6.5:93.5) during the perfusion. Unless otherwise stated, substrates were added to the medium 38 min after the start of the perfusion. At various time intervals, usually every 10 min, samples of perfusate were taken. These samples were used for the determination of different substances. Oxygenated samples (3 ml) were taken 5 min after the start of the perfusion. Venous samples (3 ml) were taken at 37, 53, and 68 min or more frequently. Oxygen was measured in the arterial and venous samples. In the presence of oleate (2 mM) the arterial oxygen content decreased 17.4 ± 2.5 S.E.M. %/h ($n = 7$), due to haemolysis. It was therefore necessary to estimate the arterial-oxygen content more frequently (at 15, 50, and 70 min) when a fatty acid had been added. The rates in the tables refer to maximum rates during 30 min after addition of substrate.

Analytical methods. The procedures for the determinations of β-hydroxybutyrate, acetoacetate, glucose, lactate, pyruvate, and ethanol were as previously described by Williamson *et al.*,[17] Ross *et al.*,[18,19] and Krebs *et al.*[20] Acetate was determined by a modifica-

Table 1. Rates of removal of ethanol and formation of acetate in perfused livers of starved, fed and fat-fed rats. After a preliminary perfusion period of 38 min, ethanol was added to a final concentration of 10 mM. Other substrates were also added at 38 min. The rats were starved for 48 h, fed a normal diet or fed a high-fat diet (see "Material and Methods"). In the experiment with starved rats, the ethanol which evaporated was caught in a trap containing cold destilled water (2°). The rate of evaporation was 11.5 ± 1.0 S.E.M. μmol/(h g wet wt), ($n = 7$). The rates, which have been corrected for evaporation, are given as means ± S.E.M. with the numbers of observations in parentheses.

	Metabolic changes (μmol/h per g wet wt)					
	Starved for 48 h		Normal diet		High-fat diet	
Substrate added	Ethanol	Acetate	Ethanol	Acetate	Ethanol	Acetate
None	118 ± 7.4 (7)	81 ± 4.5 (7)	137 ± 6.4 (6)	101 ± 6.3 (6)	89 ± 5.3 (4)	77 ± 4.3 (15)
Oleate (2 mM)	–	–	101 ± 6.3 (6)	95 ± 6.0 (6)	72 ± 3.0 (4)	62 ± 3.6 (4)
Pyruvate (10 mM)	169 ± 3.8 (7)	–	–	–	–	–

tion of the microdiffusion method fo Serlin and Cotzias [21] as described by Keane.[22] Fatty acids were estimated by the colorimetric method of Itaya and Ui.[23] Oxygen was measured manometrically according to Van Slyke and Neill.[24]

RESULTS

The effects of ethanol on approximate rates of β-oxidation of fatty acids and flow through the citric acid cycle are shown in Table 4. The data are based on measurements of ethanol uptake and acetate formation (Table 1), oxygen uptake and ketone-body metabolism (Table 2), and gluconeogenesis from pyruvate and lactate formation (Table 3). The flow through the different metabolic stages is expressed as flow of the two-carbon unit 'acetate'. For example the columns "changes of acetate calculated for total β-oxidation" and "changes of acetate calculated for citric acid cycle" equal the total production of acetyl-CoA in the β-oxidation step and the utilization of acetyl-CoA in the citric acid cycle, respectively. The calculations presuppose that oxygen-dependent reactions other than those listed in Table 4 do not occur. The assumption is also made that acetate derived from ethanol, which is not recovered in the medium (Table 1), is metabolized in the citric acid cycle. The figures in the column "β-oxidation resulting in acetate formation" (Table 4) have been calculated from the observed rates of acetate formation in the presence of oleate (2 mM). The rates are 27.5 ± 5.2 S.E.M. and 28.9 ± 2.7 S.E.M. μmol/(h g wet wt) ($n = 7$, resp. $n = 7$) for livers from rats on normal and high-fat diets, respectively. Endogenous rates of acetate production were very low (Fellenius and Kiessling, unpublished observations) and were therefore ignored.

The calculations used to obtain the data in Table 4 are illustrated by the following example in which ethanol (10 mM) and oleate (2 mM) were added to livers from normal-diet rats. In the first column "β-oxidation resulting in ketone-body formation" the rate of acetoacetate and β-hydroxybutyrate formation is expressed as rate of acetyl-CoA production according to the formula in Fig. 1 [$5.3 \times 9/4.5 + 32.7 \times 9/4.5 = 76$ μmol/(h g wet wt)]. The second column "β-oxidation not resulting in ketone-body formation" is obtained indirectly by substracting from the total oxygen uptake of 269 μmol/(h g wet wt) (Table 2) the sum of oxygen consumed in the following reactions: ethanol removal [Table 1, 101 μmol/(h g wet wt)], utilization of acetate in the citric acid cycle [the difference between ethanol removal and acetate formation shown in Table 1, 12 μmol oxygen/(h g wet wt)], and total ketone-body formation [Table 2, 48 μmol oxygen/(h g wet wt)]. The obtained rate of 108 ($269 - 161 = 108$) μmol oxygen/(h g wet wt) is equal to the rate of oxygen uptake due to complete oxidation of oleate. The proportions of this respiration associated with the β-oxidation is 32 [$(7.5/25.5) \times 108$] μmol oxygen/(h g wet wt) (Fig. 1). The remaining 76 μmol oxygen/(h g wet wt) is equivalent to the respiration in the citric acid cycle. If these two values are expressed as the production of acetyl-CoA by β-oxidation and the utilization of acetyl-CoA *via* the citric acid cycle (Fig. 1), the following rates are obtained: 38 ($32 \times 9/7.5$) and 38 ($76 \times 1/2$) μmol acetyl-CoA/(h g wet wt). The total rate of synthesis of acetyl-CoA (column 7, Table 4), is the sum of two-carbon units derived

Substrate	Overall reaction			
Oleate	$C_{18}H_{34}O_2 + 7.5\ O_2$	→	4.5	acetoacetate
	$C_{18}H_{34}O_2 + 5.25\ O_2$	→	4.5	β-hydroxybutyrate
	$C_{18}H_{34}O_2 + 7.5\ O_2$	→	9	acetate
	$C_{18}H_{54}O_2 + 25.5\ O_2$	→	18	cartbon dioxide
Ethanol	$C_2H_6O + O_2$	→		aceate
Acetate	$C_2H_4O_2 + 2\ O_2$	→	2	carbon dioxide
Pyruvate	$C_3H_4O_3 + 0.5\ O_2$	→		acetate + carbon dioxide
	$C_3H_4O_3 + 2.5\ O_2$	→	3	carbon dioxide

Fig. 1. Calculated quantitative relations between oxygen uptake and product formation from oleate, ethanol, acetate, and pyruvate.

from β-oxidation and ethanol oxidation, namely 120 (76 + 38 + 6) μmol acetyl-CoA/(h g wet wt). The total rate of utilization of acetyl-CoA by the citric acid cycle (column 8, Table 4) is 44 (38 + 6) μmol/(h g wet wt).

In the experiments with starved animals in the presence of ethanol the total sum of the oxygen-dependent reactions equals 237 (ethanol→acetate: 118, acetate→carbon dioxide: 74, oleate→ketone-body: 45) μmol oxygen/(h g wet wt), while the measured oxygen uptake is 200 μmol oxygen/(h g wet wt) (Table 2). To fulfil the condition that the measured oxygen uptake equals the calculated oxygen uptake it is, therefore, necessary to assume that only half of the acetate, *e.g.* 37 μmol/(h g wet wt), or 19 μmol 'acetate'/(h g wet wt) is completely oxidized in the citric acid cycle.

Ethanol, β-oxidation, and ketogenesis. In all experiments it was noted (Table 4) that ethanol depressed flow through the β-oxidation pathway. This is most directly shown in the experiments with livers from high-fat diet rats. Here the acetyl-CoA formed in the presence of oleate was exclusively used in the production of ketone-bodies. Thus, any effect of ethanol on β-oxidation will be reflected in ketone-body formation. As shown in Table 2 there was a significant ($p < 0.01$) decrease in ketone-body formation after the addition of ethanol to the perfusate. In livers from fed and starved animals ketogenesis was not depressed, but a lowered rate of β-oxidation could be demonstrated because of the decrease in "β-oxidation not resulting in ketone-body formation". As expected the [β-hydroxybutyrate]/[acetoacetate] ratio, an indicator of the redox state of the mitochondria, increased on the addition of ethanol or ethanol and oleate to the medium (Table 2).

Ethanol and the citric acid cycle. Inhibition of the citric acid cycle by ethanol varied with the nutritional state of the animals (Table 4). Inhibition was 64 % in livers from starved rats, but only 38 % when livers from normal fed rats were used. The decrease in flow through the citric acid cycle induced by ethanol in livers from fed rats was maintained in the presence of oleate. In livers from fat-fed rats, perfused with oleate, ethanol had no effect, since the citric acid cycle is already maximally inhibited by oleate oxidation.

It has been suggested [7] that the inhibition of the citric acid cycle by ethanol may be related to a decrease in oxaloacetate concentration. Pyruvate, one of the substrates for the synthesis of oxaloacetate in mitochondria *via*

Table 2. Effect of ethanol on oxygen uptake and ketone-body formation in the perfused livers of starved, fed and fat-fed rats. The experimental conditions were as described in Table 1. The initial concentration of ethanol was 10 mM. The term "total ketones" refers to the sum of β-hydroxybutyrate and acetoacetate. The rates are means ± S.E.M., with the numbers of observations in parentheses. The values for the [β-hydroxybutyrate]/[acetoacetate] ratio were determined from their concentrations in the medium 15 min after the addition of substrates. Metabolic changes are measured in μmol/(h g wet wt).

	Substrate added	Oxygen uptake		β-Hydroxybutyrate	
		Without ethanol	With ethanol	Without ethanol	With ethanol
Starved (48 h)	None	188 ±4.5 (5)	200 ±6.3 (4)	−1.1±0.9 (5)	11.5±1.8 (4)
	Pyruvate (10 mM)	271 ±6.8 (5)	287 ±6.1 (7)	−0.5±1.0 (5)	7.6±0.7 (7)
Normal diet	None	192 ±9.9 (5)	228 ±7.2 (6)	0.6±0.2 (7)	2.7±0.7 (6)
	Oleate (2 mM)	254 ±7.8 (7)	269 ±9.0 (6)	28.5±2.2 (7)	32.7±3.8 (6)
High-fat diet	None	203 ±8.5 (8)	196 ±8.2 (12)	−1.9±2.3 (8)	19.4±2.9 (15)
	Oleate (2 mM)	310 ±7.2 (7)	284 ±7.7 (8)	165 ±7.3 (7)	147 ±8.4 (8)

		Acetoacetate		Total ketones		[β-Hydroxybutyrate]/[Acetoacetate] ratio	
		Without ethanol	With ethanol	Without ethanol	With ethanol	Without ethanol	With ethanol
Starved (48 h)	None	24.5±2.4 (5)	18.3±2.1 (4)	23.4±1.6 (5)	29.8±2.5 (4)	0.15±0.01	0.48±0.07
	Pyruvate (10 mM)	2.8±2.0 (5)	−5.8±1.3 (7)	2.3±1.6 (5)	1.8±1.1 (7)	0.39±0.05	0.46±0.09
Normal diet	None	1.7±0.4 (7)	1.0±0.3 (6)	2.3±0.5 (7)	3.7±0.8 (6)	0.62±0.07	1.32±0.21
	Oleate (2 mM)	13.8±1.4 (7)	5.3±1.9 (6)	42.3±3.3 (7)	37.9±3.6 (6)	2.23±0.38	4.84±0.37
High-fat diet	None	52.7±2.1 (8)	24.5±2.7 (15)	50.8±2.4 (8)	43.9±2.7 (15)	0.27±0.04	0.57±0.13
	Oleate (2 mM)	17.9±2.4 (7)	−2.5±3.6 (8)	183 ±7.4 (7)	145 ±6.1 (8)	2.69±0.11	3.65±0.28

Table 3. Effect of ethanol on lactate formation and gluconeogenesis from pyruvate. The experimental conditions were as described in Table 1. The rats were starved for 48 h. The initial concentration of pyruvate and ethanol was 10 mM. The rates have been calculated from the linear part of the progress curve during 30 min. The results are given as means ± S.E.M., with the number of observations in parentheses.

Removal of pyruvate μmol/(h g wet wt)		Production of lactate μmol/(h g wet wt)		Rate of gluconeogenesis μmol/(h g wet wt)	
Without ethanol	With ethanol	Without ethanol	With ethanol	Without ethanol	With ethanol
320 ± 15 (5)	343 ± 8.4 (7)	115 ± 5.6 (5)	157 ± 8.1 (7)	50.1 ± 4.3 (5)	55.1 ± 5.6 (7)

Table 4. Effect of ethanol on the flow *via* the β-oxidation and the citric acid cycle in livers from rats fed various diets. The calculation of flow, which are expressed as changes of the two-carbon unit acetate, have been made from the results given in Tables 1, 2, and 3 and formulas in Fig. 1. The concentration of the added oleate was 2 mM and of pyruvate and ethanol 10 mM. The details of the calculations are given in the text. Figures are given in μmol/(h g wet wt).

	Substrate added	β-Oxidation resulting in ketone-body formation	β-Oxidation not resulting in ketone-body formation	β-Oxidation resulting in acetate formation	Total β-oxidation	Complete oxidation of acetate to CO_2 and H_2O	Oxidation of pyruvate to acetyl-CoA	Total synthesis of acetyl-CoA	Citric acid cycle
Starved (48 h)	None	47	52		99			99	52
	Ethanol	60	0		60	37		97	19
	Pyruvate	4	40		44		106	150	146
	Ethanol+ pyruvate	3	0		3	52	76	131	108
Normal diet	None	5	66		71			71	66
	Ethanol	7	5		12	36		48	41
	Oleate	84	89	28	174			174	61
	Ethanol+ oleate	76	38		114	6		120	44
High-fat diet	None	102	41		143			143	41
	Ethanol	88	7		95	12		107	19
	Oleate	366	50	30	416			416	20
	Ethanol+ oleate	290	7		297	10		307	17

Table 5. Quantitative relations between the removal and the oxidation of oleate in livers from fed and fat-fed rats. Ethanol (10 mM) and oleate (2 mM) were added 38 min after the start of the perfusions. The calculations of fatty acid oxidized have been made from the numbers shown in Table 4 ("total β-oxidation"), and the formulas in Fig. 1. The rates of oleate removed are means ± S.E.M., with the numbers of observations in parentheses. The calculations presuppose that the added oleate is oxidized in preference to endogenous fatty acids. A: Without ethanol. B: With ethanol.

	Oleate removed [μmol/(h g wet wt)]		Oleate oxidized [μmol/(h g wet wt)]		Oleate removed / Oleate oxidized	
	A	B	A	B	A	B
Normal diet	45.4 ± 1.8 (7)	44.5 ± 1.4 (6)	19	13	2.3	3.5
High-fat diet	55.8 ± 5.9 (5)	46.5 ± 3.8 (6)	46	33	1.2	1.4

pyruvate carboxylase [25] is known to decrease in the presence of ethanol [20] and can thereby decrease the rate of the pyruvate carboxylase reaction. The inhibition by ethanol of the flow in the citric acid cycle was therefore examined in the presence of pyruvate (Table 4). Pyruvate alone increases the cycle activity almost threefold. After the addition of ethanol, the inhibition is 26 %. The results also indicate that the pyruvate dehydrogenase step is inhibited by ethanol, since it was calculated that the oxidation of pyruvate to acetyl-CoA decreases about 25 %.

Ethanol and triglyceride synthesis. Knowing the amount of oleate oxidized (Table 4) and the observed rate of oleate removal (Table 5) it is possible to estimate approximately the amount of added oleate which is transferred to triglyceride. The results are shown in Table 5. Added oleate being oxidized is about 60 % less in livers from fed rats than in livers from fat-fed rats. Since the rates of oleate removal in the two types of livers are approximately the same it follows that oleate is incorporated into triglycerides. This reaction is accelerated by the addition of ethanol.

DISCUSSION

The interaction and its nature between ethanol and fatty acid oxidation was examined. With a knowledge of the over-all metabolic balance of the perfused liver it was possible to calculate approximate flow rates of the β-oxidation pathway, the citric acid cycle and triglyceride synthesis. The manner of expressing flow in the form of the two-carbon unit,[6] acetate' is to be preferred rather than rates of oxygen utilization,[7] because not all reactions giving rise to NADH are coupled to the electron transport chain and oxygen utilization. Thus, in the presence of pyruvate and ethanol it can be calculated from the rates in Tables 1 and 3 that about 80 % of the NADH formed when ethanol is oxidized to acetate is required for the synthesis of lactate and glucose. The

calculations presuppose that oxygen-dependent reactions other than those listed in Fig. 1 do not occur. Fritz [26] calculated that in livers from fed rats glucose and amino acid oxidation contributed to the fuel of respiration to about 20 %. It follows that the 80 % inhibition of the β-oxidation by ethanol in normal livers (Table 4) might be overestimated. However, the 40 % inhibition of the citric acid cycle in the same experiment is probably not overestimated, since the inflow of carbon-units derived from glucose [27] or amino acids [20,28] is strongly suppressed during ethanol oxidation.

In spite of a strong suppression of the activity of the citric acid cycle by ethanol (Table 4), which according to current views [29–32] should be related to an increased ketone-body formation, ethanol was shown to be antiketogenetic or without effect on ketogenesis (Table 2). The most likely explanation is that ethanol inhibits the β-oxidation pathway directly. This has been suggested by others [7,9] and is directly shown in the present investigation. Advantage was taken of the observation that livers from rats fed a high-fat diet almost quantitatively converted added oleate to ketone-bodies. Thus any effect of ethanol on the ketone-body formation of these livers will reflect the changes in the β-oxidation step. As shown in Table 2, the addition of ethanol significantly inhibits ketone-body formation in these livers. It is of interest that ethanol has been found to have a depressing effect on ketone-body production in diabetic patients.[33] In these patients, the turnover rate of fatty acid to ketone-body is very high and presumably the citric acid cycle is already inhibited.

The interpretation of the effect of ethanol on ketogenesis is thus complicated by an inhibition of both the β-oxidation and the citric acid cycle. Any inhibition of the citrate-synthetase reaction, leading to an accelerated ketogenesis, may be concealed by a block of the β-oxidation and, consequently, of the supply of acetyl-CoA for ketone-body formation. It is therefore not surprising that many authors have reported [11,34,35] almost unchanged ketone-body formation under the influence of ethanol.

The mechanism behind this effect of ethanol on the β-oxidation remains to be explored. Williamson *et al.*[7] suggest that, since the addition of ethanol in perfused liver supplemented with oleate causes a reduction of flavoproteins, the supply of reducing equivalents exceeds the rate at which they can be transferred from the flavin to the cytochrome system. This suggestion is probably also valid in the present investigation, when ethanol and oleate have been added, since the [β-hydroxybutyrate]/[acetoacetate] ratio increases above the normal range of 2 – 3. In addition, it is probable that ethanol oxidation competitively inhibits the β-oxidation of fatty acids by the formation of an excess of NADH. This is supported by the finding that ethanol oxidation is inhibited by oleate (Table 1), demonstrating the competitive nature of the interaction.

The redox state of the mitochondrial nicotinamide dinucleotides may be of importance in the regulation of ketone-body formation.[32] However, no correlation was found between the [β-hydroxybutyrate]/[acetoacetate] ratio and the ketone-body formation in liver supplemented with only oleate (Table 2). The ratio is about the same 15 min after the addition of oleate, despite a pronounced variation in ketone-body formation in all the livers tested. More-

over, in spite of an increase in the [β-hydroxybutyrate]/[acetoacetate] ratio, ethanol is antiketogenic when oleate is added to fat-fed rats.

The citrate-synthetase activity can be controlled by the mitochondrial concentration of oxaloacetate through its transformation to malate.[31,36,37] The production of oxaloacetate *via* the pyruvate-carboxylase reaction and the rate by which it is removed by gluconeogenesis are additional factors. Pyruvate concentration is one of the factors limiting the rate of the pyruvate-carboxylase reaction.[20] Addition of pyruvate (Table 4) partly overcomes the inhibition by ethanol of the flow through the citric acid cycle, probably by increasing the level of oxaloacetate. In addition to the concentration of oxaloacetate, the concentrations of adenine nucleotides may also play a key role in the regulation of the citrate-synthetase reaction.[38,39] Garland [40] pointed out that it is impossible to separate the significance of the intramitochondrial concentration of oxaloacetate from that of adenine nucleotides, since the K_m value of oxaloacetate in the citrate-synthetase reaction is dependent upon the concentrations of adenine nucleotides. The total inflow of two-carbon units to the citric acid cycle should be equivalent to the outflow of two-carbon units. This metabolic balance is not achieved in the experiment with the livers from starved animals, supplemented with ethanol (Table 4). The total synthesis of acetyl-CoA is 97 μmol/(h g wet wt) and the utilization of acetyl-CoA *via* the citric acid cycle and ketone-body formation is 79 μmol/(h g wet wt). This indicates that the flow through the cycle is decreased by inhibition of both citrate-synthetase and after the citrate-synthetase step, confirming the results of Williamson *et al.*[7] The latter proposed an inhibition at the isocitrate dehydrogenase step.

Ethanol is known to interfere with lipid metabolism in such a way that a single dose of ethanol causes a prompt increase in the triglyceride content of the liver.[41,42] The accumulation of α-glycerophosphate has been suggested to be one important mechanism responsible for the hyperlipemia.[43,44] It can be argued that the inhibition of the β-oxidation pathway might be an additional factor. However, as shown in Table 5 ethanol did not stimulate triglyceride synthesis in livers from animals on a high-fat diet, while the β-oxidation pathway was greatly inhibited (Table 4). As discussed elsewhere [45] the fraction of fatty acid undergoing esterification depends primarily on the level of α-glycerophosphate.

Acknowledgements. The authors are grateful to Prof. Sir H. A. Krebs for helpful discussions. Thanks are also due to Mr R. Hems for his advice on the perfusions and Mrs G.-B. Berglund for technical assistance. Mr Fellenius was in receipt of scholarships from the *C. F. Liljewalch, E. and K. G. Lennander, C. Groschinsky* and *Hierta-Retzius Foundations*. This work was supported by the *Swedish Medical Research Council*, (grant Nos. B69-13R-2782 and B70-13X-575-06B).

REFERENCES

1. Leloir, L. F. and Muñoz, J. M. *Biochem. J.* **32** (1938) 299.
2. Forsander, O., Räihä, N. and Suomalainen, H. *Hoppe-Seyler's Z. physiol. Chem.* **312** (1958) 243.
3. Lundquist, F., Tygstrup, N., Winkler, K., Mellemgaard, K. and Munck-Petersen, S. *J. Clin. Invest.* **41** (1962) 955.

4. Forsander, O., Räihä, N., Salaspuro, M. and Mäenpää, P. *Biochem. J.* **94** (1965) 259.
5. Lieber, C. S. *Federation Proc.* **26** (1967) 1443.
6. Lieber, C. S. In Maickel, R. P., Ed., *Biochemical Factors of Alcoholism*, Pergamon, Oxford 1967, p. 167.
7. Williamson, J. R., Scholz, R., Browning, E. T., Thurman, R. G. and Fukami, M. H. *J. Biol. Chem.* **244** (1969) 5044.
8. Lindros, K. O. and Aro, H. *Ann. Med. Exp. Fenn.* **47** (1969) 39.
9. Lindros, K. O. *Biochem. Biophys. Res. Commun.* **41** (1970) 635.
10. Zakim, D. and Green, J. *Proc. Soc. Exp. Biol. Med.* **127** (1968) 138.
11. Rawat, A. K. *Eur. J. Biochem.* **6** (1968) 585.
12. Kreisberg, R. A. *Diabetes* **16** (1967) 784.
13. Krebs, H. A. and Hems, R. *Biochem. J.* **119** (1970) 525.
14. Krebs, H. A., Wallace, P. G., Hems, R. and Freedland, R. A. *Biochem. J.* **112** (1969) 595.
15. Hems, R., Ross, B. D., Berry, M. N. and Krebs, H. A. *Biochem. J.* **101** (1966) 284.
16. Krebs, H. A. and Henseleit, K. *Hoppe-Seyler's Z. physiol. Chem.* **210** (1932) 33.
17. Williamson, D. H., Mellanby, J. and Krebs, H. A. *Biochem, J.* **82** (1962) 90.
18. Ross, B. D., Hems, R. and Krebs, H. A. *Biochem. J.* **102** (1967) 942.
19. Ross, B. D., Hems, R., Freedland, R. A. and Krebs, H. A. *Biochem. J.* **105** (1967) 869.
20. Krebs, H. A., Freedland, R. A., Hems, R. and Stubbs, M. *Biochem. J.* **112** (1969) 117.
21. Serlin, I. and Cotzias, G. C. *J. Biol. Chem.* **215** (1955) 263.
22. Keane, D. M. *Dissertation*, Oxford University, Oxford 1967.
23. Itaya, K. and Ui, M. *J. Lipid Res.* **6** (1965) 16.
24. Van Slyke, D. D. and Neill, J. M. *J. Biol. Chem.* **61** (1924) 523.
25. Keech, D. B. and Utter, M. F. *J. Biol. Chem.* **238** (1963) 2609.
26. Fritz, I. B. *Physiol. Rev.* **41** (1961) 52.
27. Forsander, O. and Himberg, J.-J. *Metabolism* **18** (1969) 776.
28. Fellenius, E., Carlgren, H. and Kiessling, K.-H. *Life Sci.* **13** (1973) 595.
29. Wieland, O., Weiss, L. and Eger-Neufeldt, I. *Advan. Enzyme Regul.* **2** (1964) 85.
30. Williamson, J. R., Browning, E. T. and Olson, M. S. *Advan. Enzyme Regul.* **6** (1968) 67.
31. Wotjtczak, A. B. *Biochem. Biophys. Res. Commun.* **31** (1968) 634.
32. Wieland, O. *Advan. Metab. Disord.* **10** (1968) 1.
33. Schlierf, G., Gunning, B., Uzawa, H. and Kinsell, L. W. *Am. J. Clin. Nutr.* **15** (1964) 85.
34. Warming-Larsen, A. *Acta Med. Scand.* **132** (1949) 458.
35. Arky, R. A. and Freinkel, N. *Arch. Intern. Med.* **114** (1964) 501.
36. Wieland, O. and Löffler, G. *Biochem. Z.* **339** (1963) 204.
37. Exton, J. H. *Biochem. J.* **92** (1964) 467.
38. Hathaway, J. A. and Atkinson, D. E. *Biochem. Biophys. Res. Commun.* **20** (1965) 661.
39. Shephard, D. and Garland, P. B. *Biochem. Biophys. Res. Commun.* **22** (1966) 89.
40. Garland, P. B. In Goodwin, T. W., Ed., *Metabolic Roles of Citrate*, Academic, London and New York 1968, p. 41.
41. Mallov, S. and Block, J. L. *Am. J. Physiol.* **184** (1956) 29.
42. Shapiro, R. H., Shimizu, Y., Drummery, G. D. and Isselbacher, K. J. *Clin. Res.* **10** (1962) 234.
43. Nikkilä, E. A. and Ojala, K. *Proc. Soc. Exp. Biol. Med.* **113** (1963) 814.
44. Ylikahri, R. H. *Metabolism.* **19** (1970) 1036.
45. Fellenius, E., Bengtsson, G. and Kiessling, K.-H. *Acta Chem. Scand.* **27** (1973) 2893.

Received April 5, 1973.

ACTA CHEMICA SCANDINAVICA 27 (1973) 2791–2796

Compounds with the Marcasite Type Crystal Structure

VIII.* Redetermination of the Prototype

G. BROSTIGEN, A. KJEKSHUS and CHR. RØMMING

Kjemisk Institutt, Universitetet i Oslo, Blindern, Oslo 3, Norway

The crystal structure of marcasite (FeS_2-*m*) has been redetermined, and contrary to an earlier suggestion the mirror plane perpendicular to [001] at $z = \frac{1}{2}$ (and $z = 0$) appears to be present. The different result is chiefly attributed to an improved absorption correction in the present case.

One problem connected with the detailed studies on compounds with the pyrite (FeS_2-*p*), marcasite (FeS_2-*m*), and arsenopyrite (FeAsS; binary prototype $CoSb_2$) type structures, which recently have been carried out at this Institute, concerns the proper crystallographic symmetry of the FeS_2-*m* type structure. Diffraction data for the compounds with this structure type show systematic extinctions consistent with the space groups *Pnnm* and *Pnn*2. The choice of space group has previously [1,2] been considered for $FeSb_2$, FeS_2, $FeTe_2$, and $CoTe_2$, with the conclusion that the mirror plane characteristic of the higher symmetric space group *Pnnm* is absent. Of the two ways in which the mirror plane may be absent (*viz.* in terms of positional or thermal parameters), it was reported that the absence is of the first kind for $FeSb_2$,[1] of the second for $CoTe_2$,[2] and of both kinds for $FeTe_2$ [2] and possibly FeS_2.[2]

The experimental and computational means employed in these investigations have been improved on in several respects. Firstly, counter techniques have been substituted for the photographic measurement of the intensities of the scattered X-rays. Secondly, the recent availability of more suitable computer programmes allows corrections for dispersion to be made. Also, the specimen used could be given a shape convenient for absorption correction. The prototype FeS_2-*m* was singled out for a careful reexamination in which these and other possible improvements could be taken into account. This choice was in part indicated by the anomalous thermal vibrational parameters previously found for the sulphur atoms in FeS_2-*m*.[2]

* Part VII. *Acta Chem. Scand.* **24** (1970) 3317.

EXPERIMENTAL

The single crystals were chosen from a natural *marcasite* sample (Joplin, U.S.A.) kindly donated by Mineralogisk-Geologisk Museum, Universitetet i Oslo. The analytical data for this specimen are given in the preceding paper.[2]

Three dimensional intensity data were collected with an automatic Picker diffractometer using monochromatized Mo$K\alpha$-radiation. The $\omega - 2\theta$ scan technique was utilized at a scan speed of 1° min^{-1}. The background was measured at each of the scan range limits. The intensities of three selected test reflections, measured for every 50th reflection during the data collection, demonstrated a systematic variation which was corrected for in the sets of observed intensities. A 1 % addition for the uncertainty in the rescaling as well as for reducing the effect of systematic errors in the strong reflections, was included in the estimated standard deviation of the intensities from counting statistics.

The first set of intensity data was collected for a carefully selected, but crude single crystal fragment as isolated from the natural specimen. The shape and orientation of the crystal in relation to the diffractometer ϕ axis were obtained with the aid of an optical goniometer in combination with a travelling microscope. A graphite crystal was used for monochromatization, the scan range was $2\theta(\alpha_1) - 0.9$ to $2\theta(\alpha_2) + 0.9°$, and the background was measured for 60 s on each side of the reflections. 791 independent reflections with sin θ/λ up to 1.35 were explored for this crystal, of which only four proved to have a net intensity smaller than twice the estimated standard deviation.

The second crystal was ground into a nearly perfect sphere of 0.44 mm diameter. In this case a quartz single crystal monochromator was used, the scan range was increased by 0.2° (*vide supra*), and the background was measured for 15 s at each of the scan range limits. Out of the 760 independent reflections with sin $\theta/\lambda < 1.28$, 726 were larger than twice their estimated standard deviations; these were regarded as "observed" reflections and used in the subsequent calculations.

The intensities were corrected for the combined Lorentz and polarization factors, and for absorption and secondary extinction according to the actual shape of the crystal.

Calculations were performed on a CD 3300 computer using a set of programmes by Dahl *et al.*[3] Atomic scattering factors were taken from Hanson *et al.*[4] and the values for the real and imaginary parts of the dispersion from Cromer.[5] Anisotropic thermal motion of the atoms were allowed for according to the expression $\exp[-(\beta_{11}h^2 + \beta_{22}k^2 + \beta_{33}l^2 + \beta_{12}hk + \beta_{13}hl + \beta_{23}kl)]$. The significance test of Hamilton [6] was used to assess the probable correctness of various computational models for the structure. (The observed and calculated structure factor data are available from the authors upon request.)

RESULTS AND DISCUSSION

Parallel with the presentation and discussion of the results it is convenient to comment on some more methodical and philosophical questions which arise in this connection.

The two marcasite crystals investigated here as well as that of the preceding study [2] were selected from adjacent spots on the same mineral specimen. Hence, it is probably reasonable to assume that these crystals are virtually identical with regard to chemical and physical perfection. The fact that one of the crystals had been subjected to light mechanical grinding does not apparently invalidate the assumption. On the other hand, this represents the first of a series of hypotheses or unevaluated approximations of the study.

One set of intensity data was collected for each of the crystals, *viz.* two sets of counter-diffractometer measurements and in addition the photographic recordings dealt with in Ref. 2. The question concerning whether one of the data sets *a priori* is more correct than the others immediately enforces a full discussion of systematic and random errors. These problems are considered in detail by, *e.g.*, Lonsdale *et al.*[7] and are not repeated here.

In relation to the absorption correction it is significant to dwell on the fact that two of the crystals had their natural shapes whereas the third had been ground to a nearly

perfect sphere. There is in the first place inevitable inaccuracies in the description of habits and the measurement of dimensions for the naturally shaped crystals. Secondly, limitations inherent in the available computer programme impose approximations in the mathematical definitions of the crystalline forms. The overall size of one of these crystals was, moreover, just amenable for treatment of the absorption correction by the computer programme. The absorption in the spherical crystal can, on the other hand, be corrected for completely, apart from more trivial errors caused by deviations from spherical symmetry, incorrect crystal diameter, and/or inaccurate linear absorption coefficients. Similar considerations apply to the correction for secondary extinction although the consequences of any inaccuracy are less important in the latter case.

Another source of uncertainty lies in the choice of atomic scattering factors. The complete electron distribution within the unit cell (*viz.* based on *ab initio* calculations or a hitherto unknown experimental technique) must be available in order to design entirely satisfactory scattering factors. However, even if the necessary information on the chemical bonding was at hand, the resulting "scattering factors" would become complicated and cumbrous multiparameter functions. Furthermore, the conventional crystallographic parameters are paradoxically explicitly contained in the more comprehensive conception of the complete electron distribution. The scattering factor problem can fortunately be considerably reduced by taking into account only those reflections with relatively large values for $\sin \theta/\lambda$ ($\geqq 0.6$ in the present case), where the contributions from the bonding electrons are small. The settling of the boundaries to the atomic cores is nevertheless a relevant source of ambiguity in the general case. However, the cores of sulphur and iron must, at any rate, contain a large proportion of the total number of electrons for the corresponding free atoms and according to calculations the actual selection of core boundaries appears to be rather unimportant. Thus, the customary scattering factors for neutral sulphur and iron could be employed, probably without any significant loss of accuracy.

The effects of dispersion may be taken into account by representing the atomic scattering factors of both kinds of atoms as complex variables of the diffraction angle. In the treatment of the photographic intensity data [2] it appeared to be a reasonable approximation to neglect these effects, whereas they ought not to be disregarded in connection with the improved accuracy of the two sets of counter data. In fact, a crucial part of the present problem centres around the dispersion effects (*vide infra*).

Anharmonic effects are clearly present in any real crystal, but in view of the time required to develop the theory for the general problem with anharmonicity in admixture with anisotropic thermal vibration and afterwards preparing a computer programme dealing with this considerably more complex case it was decided to utilize the facilities already at hand. The harmonic model appears to represent a useful approximation in the present case where the results show that the root mean square amplitudes in the direction of main axes of vibration are almost equal (0.063, 0.062, and 0.059 Å for Fe and 0.069, 0.069, and 0.064 Å for S are obtained for spherical crystal), implying that the thermal motions of both kinds of atoms are very nearly isotropic.

The weighting of the intensity data constitutes a side of the computational work which are open to some degree of freedom for subjective judgements. The weighting schemes in this work were based on counting statistics; careful analyses showed that this does not represent a relevant source of error.

The least squares refinement procedure was continued until no shifts were produced in any variable. Different sets of input parameters were tried in order to ascertain that none of the least squares refinements were terminated at secondary (false) minima.

Apart from making allowance for the effects of dispersion the computational models were essentially the same as those considered previously.[2] It should be emphasized, however, that the selection of certain useful models for testing does not in itself introduce any approximations into the treatment.

Typical results for some of the most relevant test models for the two sets of counter-diffractometer data are presented in Table 1. The table is arranged in order to facilitate direct comparison with the photographic data set considered in Ref. 2.

The final, but the most fundamental problem of the present study, is associated with the assessment of the relative correctness of the various models. As is commonly the case in crystallographic problems of this type it is difficult to design a suitable criterion for the comparison of the fitting of a large number of observed and calculated quantities.

Table 1. Positional parameters and temperature factors with standard deviations for different refinement models of FeS_2-*m*. Naturally shaped crystal: number of reflections 791. Spherically shaped crystal: number of reflections with $\sin\theta/\lambda \geqq 0.60$ is 610.

Crystal shape		Natural				Spherical	
Space group		*Pnnm*		*Pnn2*		*Pnnm*	*Pnn2*
Dispersion		Excl.	Incl.	Excl.	Incl.	Incl.	Incl.
Fe	β_{11}	0.00219(13)	0.00270(12)	0.00217(12)	0.00269(12)	0.00387(5)	0.00387(5)
	β_{22}	0.00166(7)	0.00199(7)	0.00167(7)	0.00200(7)	0.00238(3)	0.00238(3)
	β_{33}	0.00498(19)	0.00580(18)	0.00525(19)	0.00594(19)	0.00690(9)	0.00696(9)
	β_{12}	−0.00004(10)	−0.00001(10)	−0.00002(10)	−0.00002(10)	0.00007(6)	0.00007(6)
	x	0.20040(14)	0.20052(14)	0.20051(14)	0.20054(14)	0.20008(6)	0.20001(7)
	y	0.37826(9)	0.37827(9)	0.37831(9)	0.37833(9)	0.37820(5)	0.37824(5)
	z	0	0	0.00441(48)	0.00163(45)	0	−0.00128(33)
S	β_{11}	0.00365(16)	0.00366(16)	0.00367(16)	0.00369(16)	0.00456(7)	0.00456(7)
	β_{22}	0.00259(9)	0.00262(9)	0.00261(9)	0.00262(9)	0.00284(5)	0.00283(5)
	β_{33}	0.00733(25)	−0.00744(24)	−0.00711(27)	−0.00740(26)	−0.00805(12)	−0.00795(13)
	β_{12}	0.00098(18)	−0.00090(17)	−0.00087(17)	−0.00087(17)	−0.00051(9)	−0.00052(9)
	β_{13}	0	0	0.00425(87)	0.00369(85)	0	−0.00168(73)
	β_{23}	0	0	0.00283(63)	0.00246(65)	0	−0.00132(63)
	R	0.058_0	0.056_1	0.055_2	0.054_9	0.022_0	0.022_2
	R_w	0.079_7	0.076_3	0.076_5	0.074_8	0.025_2	0.024_8

An inherent, almost unsurmountable difficulty encountered in this connection is associated with the fact that crystallographic problems are generally non-linear and accordingly somewhat unsuitable for statistical treatments. The significance test of Hamilton [6] is the hitherto most widely accepted quantitative criterion for the kind of judgements which are to be performed. As is generally the case in statistics, the use of the Hamilton test is based on the supposition that there are no systematic errors in measurements, corrections, or computations (*vide supra*). Although there may be possible objections to the use of the Hamilton test, its unfailing correctness may be postulated for the present purpose. Hence, application of the test shows that the unrestrained model (Table 1) is superior to all the others at a significance level < 0.005 for each of the three data sets. Overlooking the distinction between statistical and physical significance, one may be led to the same inference on comparison of the values of the variable parameters with their associated standard deviations.

The superficial conclusion is accordingly that the mirror plane perpendicular to [001] at $z = \frac{1}{2}$ (and $z = 0$) is missing in FeS_2-*m*, implying that *Pnn*2 is the correct space group for this compound. It is gratifying to note that this conclusion is identical with that drawn in Ref. 2. However, there appears to be a fundamental drawback attached to the findings in that on applying more refined and copious data, corrections, and computations the key parameter z_S gradually approaches zero. This finding is rather suspect and suggests very strongly that the mirror plane in question may be present in the structure of FeS_2-*m* despite the verdict based on the Hamilton test. The space group ambiguity for FeS_2-*m* is therefore not removed although the problem can be said to be on a rather different level from what it was when this project was started. The possible deviation of z_S from zero is now so small that no practical significance is attached to it. The principal cause of the difference between the present and preceding [2] study appears to be associated with the absorption correction. Similar considerations may apply to the data [1,2] for the isostructural compounds $FeSb_2$, $FeTe_2$, and $CoTe_2$.

It may be of interest to those who are entertaining the possibility of similar studies to summarize our practical experiences. In rough terms the improvement in R_w (and R) resulting from the more correct account for the absorption in the spherical crystal amounts to 4 to 5 times that obtained by the substitution of counter for photographic technique of intensity measurements. (It should be emphasized that both natural crystal fragments were of a particular unfavourable wedgeform for absorption according to the present computer programme.) The shift from film to counter detection is of equal importance to the removal of the undesirable low angle data ($\sin \theta/\lambda < 0.6$) from the calculations. Each of these means of improvement is in turn 4 to 5 times more important than the effects of dispersion. Altogether, the absorption correction turned out to be far more important than anticipated in advance.

In connection with the present redetermination of FeS_2-*m* it is of interest to summarize the development in the bonding Fe–S and S–S distances over the years:

	Fe–S(Å)	S–S(Å)
Buerger [8] (1931)	2.21 and 2.24	2.25
Buerger [9] (1937)	2.23_1 and 2.25_0	2.21_0

Brostigen and Kjekshus [2] (1971)	2.230(6), 2.235(2) and 2.275(6)	2.223(3)
Present (1973)	2.2359(3) and 2.2540(2)	2.2151(4)

(The uncertainties in the unit cell dimensions are not taken into account in the present values for the bond distances.) The figures clearly demonstrate the remarkable correctness of the bond distances provided by Buerger [9] in 1937.

REFERENCES

1. Holseth, H. and Kjekshus, A. *Acta Chem. Scand.* **23** (1969) 3043.
2. Brostigen, G. and Kjekshus, A. *Acta Chem. Scand.* **24** (1970) 1925.
3. Dahl, T., Gram, F., Groth, P., Klewe, B. and Rømming, C. *Acta Chem. Scand.* **24** (1970) 2232.
4. Hanson, H. P., Herman, F., Lea, J. D. and Skillman, S. *Acta Cryst.* **17** (1964) 1040.
5. Cromer, D. T. *Acta Cryst.* **18** (1965) 17.
6. Hamilton, W. C. *Acta Cryst.* **18** (1965) 502.
7. Lonsdale, K., MacGillavry, C. H., Milledge, H. J., de Wolff, P. M. and Parrish, W. In *International Tables for X-Ray Crystallography*, Kynoch Press, Birmingham 1962, Vol. III, p. 133.
8. Buerger, M. J. *Am. Mineralogist* **16** (1931) 361.
9. Buerger, M. J. *Z. Krist.* **97** (1937) 504.

Received April 6, 1973.

ACTA CHEMICA SCANDINAVICA 27 (1973) 2797–2801

Alkaline Degradation of Methyl 2,4,6-Tri-*O*-methyl-α- and -β-D-*ribo*-hexosid-3-ulose. Part II. Isolation and Characterization of Degradation Products

LENNART KENNE, OLLE LARM and SIGFRID SVENSSON

Department of Organic Chemistry, The Arrhenius Laboratory, P.O.B., S-104 05 Stockholm 50, Sweden

Treatment of methyl 2,4,6-tri-*O*-methyl-α- or -β-D-*ribo*-hexosid-3-ulose with sodium ethoxide in ethanol-dichloromethane yielded a labile 4,6-di-*O*-methyl-1-deoxy-2-methoxy-D-hex-1-ene-3-ulose (A) and several isomeric ethyl 2,4,6-tri-*O*-methyl-hexosid-3-uloses (B – G).

The synthesis and alkaline degradation of methyl 2,4,6-tri-*O*-methyl-α-D-*ribo*-hexosid-3-ulose and the corresponding β-glycoside were reported in a previous communication.[1] Elimination of the aglycone was complete after 30 min at room temperature in 0.1 M ethanolic sodium ethoxide. The product was complex and isolation of the individual components was not attempted. We have now observed that a simpler reaction product is obtained when the reaction is performed with 0.1 M sodium ethoxide in ethanol-dichloromethane (1:1, v/v). GLC of the reaction product (Table 1) showed the presence of seven components (A – G). The proportions of these components were independent of whether the starting material had the α- or β-configuration.

Two of the main components (B and G) were obtained pure by Silica Gel chromatography. Two other components, D and F, were obtained pure by preparative GLC. Components C and E were enriched by this latter method but were still contaminated by B and D, respectively. Component A could not be isolated owing to its extreme lability. The response factors of B and G were determined, relative to an inert internal standard, and the yields of the various components were determined by GLC (Table 1).

The reaction products were further investigated by GLC-MS. The MS of A indicated that it was a 4,6-di-*O*-methyl-1-deoxy-2-methoxy-hex-1-ene-3-ulose. Possible routes for the formation of some fragments are given in Scheme 1.

Table 1. Composition and properties of the reaction products.

Compound	T^a	Yield[b]	$[\alpha]_D$ (c 0.3, $CHCl_3$)	τ, H-1	*J* 1.2	Derived alditols[c]	Configuration
A	0.34	5					
B	1.00	29	+113	4.89	1.8	D-altritol-D-mannitol (20:1)	α-D-*arabino*
C	1.19	4					
D	1.38	7	+ 33	4.72	4.0	D-galactitol-D-gulitol (1:11)	α-D-*xylo*
E	1.50	1					
F	2.00	6	− 19	5.60	8.0	D-allitol-D-glucitol (49:1)	β-D-*ribo*
G	3.59	42	+138	4.71	4.0	D-allitol	α-D-*ribo*

[a] Retention time, relative to ethyl 2,4,6-tri-*O*-methyl-α-D-*arabino*-hexosid-3-ulose.
[b] Response factors were determined for B and G relative to the internal standard (methyl 2,3,4-tri-*O*-methyl-β-D-xyloside). The response factors were the same for both B and G and they are therefore assumed to be valid for C–F.
[c] Obtained by reduction, hydrolysis, reduction and demethylation.

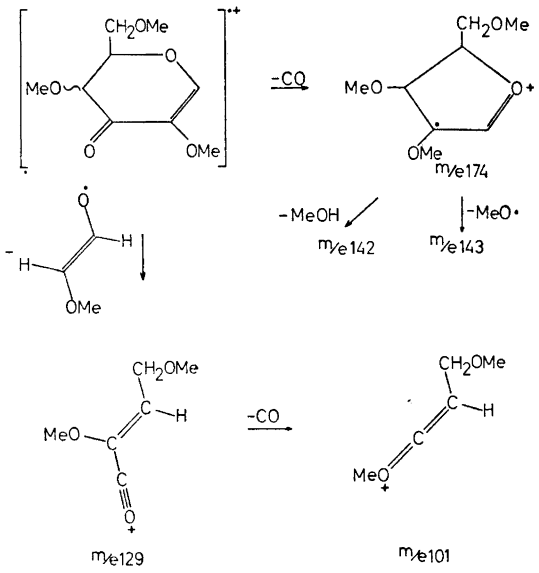

Components B – G all gave similar mass spectra, differing only in the intensities of some of the peaks. The composition of the molecular ion (for component F) as determined by high resolution MS was $C_{11}H_{20}O_6$. Authentic ethyl 2,4,6-tri-*O*-methyl-α/β-D-*ribo*-hexosid-3-ulose was prepared. This, on GLC gave two peaks with the same retention time as components F and G, and the corresponding MS were also indistinguishable. Components B – G are therefore isomeric ethyl 2,4,6-tri-*O*-methyl-hexosid-3-uloses.

The NMR data (relative proportions of methyl, ethyl, and other protons) were consistent with the proposed structures. Chemical shifts and coupling constants for the anomeric protons are given in Table 1.

Borodeuteride reduction of each isolated component and acid hydrolysis yielded mixtures of 2,4,6-tri-*O*-methyl-hexoses-3-*d*, which were analysed, as their alditol acetates, by GLC-MS.[2] The primary fragments formed on MS of these substances are indicated below.

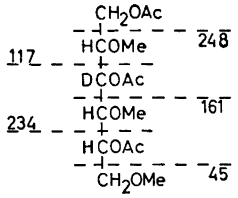

The alditol mixtures were also demethylated by treatment with boron tribromide [3] and analysed as acetates by GLC-MS [4,5] (Table 1). From these

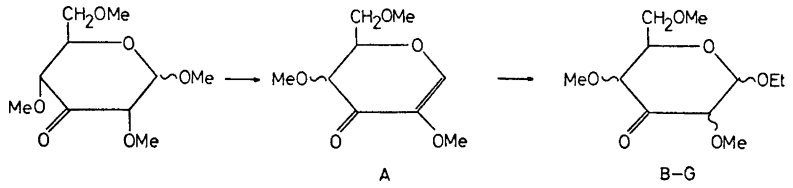

results, the NMR evidence and the optical rotations of the compounds, their configurations could be established (Table 1).

The formation of these compounds by β-elimination of methanol followed by addition of ethanol yielding B – G in a total yield of 90 %, is depicted below in Scheme 2. Reversible enolisation leading to epimerization at C-4 may also occur, at any stage of the transformation. Six of the eight possible ethyl 2,4,6-tri-*O*-methyl-hexosid-3-uloses were observed in the reaction product. The two missing isomers are probably formed in low percentages only and their GLC traces may be hidden in the peaks of other components. The predominating components were the α-glycosides with the D-*ribo*- and D-*arabino*-configurations. It seems reasonable that in an equilibrium mixture, the α-anomers should predominate because of the anomeric effect. Those with bulky equatorial substituents (D-*ribo*) at C-2, C-3, C-4, and C-5 should be favoured over those with one axial substituent only (D-*arabino* and D-*xylo*) as is actually observed.

EXPERIMENTAL

Concentrations were performed at reduced pressure at bath temperatures not exceeding 40°. Optical rotations were determined with a Perkin-Elmer 141 polarimeter. NMR spectra were recorded with a Varian A60 A and a Varian XL 100 spectrometer, using tetramethylsilane as internal reference. Chemical shifts (τ) are given as ppm downfield from tetramethylsilane. GLC separations were performed on a Perkin-Elmer model 990 instrument using a glass column packed with 3 % ECNSS-M on Gas-Chrom Q. Peak areas were measured with a Hewlett-Packard 3370 electronic integrator. The preparative GLC separations were performed on a Varian aerograph series 1400, column size: 0.3 × 250 cm. For GLC-MS the compounds were injected into a Perkin-Elmer 270 gas chromatograph-mass spectrometer fitted with the appropriate column. The mass spectra were recorded at a manifold temperature of 200°, ionisation potential of 70 eV, ionisation current of 80 μA and an ion source temperature of 120°. High resolution MS was performed by the peak matching technique on an Atlas SM 1 instrument.

Ethyl 2,4,6-tri-O-*methyl-α/β*-D-ribo-*hexosid-3-ulose* was prepared from 2,4,6-tri-*O* methyl-D-glucose, using the same procedure as previously described for the corresponding anomeric mixture of methyl glycosides.[1]

Alkaline degradation of methyl 2,4,6-tri-O-*methyl-α- and β*-D-ribo-*hexosid-3-ulose.* A. *Preparative experiments.* Ethanolic 0.1 M sodium ethoxide (12.5 ml) was added to a solution of methyl 2,4,6-tri-*O*-methyl-β-D-*ribo*-hexosid-3-ulose (500 mg) in dichloromethane (12.5 ml) and the solution was kept for 20 min at room temperature. The yellow solution was then neutralised by addition of Dowex 50 (H^+) and concentrated. The product, which gave seven peaks on GLC (Table 1) was fractionated on a silicic acid column (40 × 3 cm), irrigated with ethyl acetate-light petroleum (2:1). The separation was monitored by polarimetry and TLC. The first fraction eluted (36 mg) consisted of pure B. The second fraction (16 mg) contained B, D, and small amounts of C and E. Pure D was obtained from this fraction by preparative GLC. The third fraction (43 mg) contained F together with small amounts of D and E. Pure F, m.p. 83 – 84°, was ob-

tained by preparative GLC. It gave a molecular ion of *m/e* 248.1262, in agreement with the composition $C_{11}H_{20}O_6$ (248.1260). The last fraction (104 mg) consisted of pure G. All the isolated components showed a strong band at 1750 (C=O) in their IR spectra.

Each component (2 mg) was reduced with sodium borodeuteride (10 mg) in ethanol (5 ml) at room temperature overnight. The glycosides obtained after processing were hydrolysed in 0.25 M sulphuric acid at 100° for 18 h, and the product obtained after neutralization was reduced with sodium borohydride. One third of each alditol mixture was acetylated and analysed by GLC-MS,[2] using the ECNSS-M column at 170°. All components gave similar mass spectra, typical for the 2,4,6-tri-*O*-methyl-hexitol-3-*d* derivatives. The retention times, relative to 1,5-di-*O*-acetyl-2,3,4,6-tetra-*O*-methyl-D-glucitol, and percentages of the derivatives were: B, 2.00(95), 2.09(5); D, 2.00(91), 2.30(9); F, 1.45(98), 1.94(2); G, 1.45(100).

The remainder of the above products was demethylated with boron tribromide in dichloromethane,[3] acetylated and investigated by GLC-MS.[4,5] The products, which were all hexitol-3-*d* hexaacetates, had the following retention times (relative to peracetylated D-glucitol) on the ECNSS-M column at 200°: (B), D-altritol 0.785, D-mannitol 0.790 (separated at 170°); (D), D-galactitol 0.90, D-gulitol 1.00; (F), D-allitol 0.72, D-glucitol 1.00; (G), D-allitol 0.72.

B. *Quantitative experiments.* Ethanolic 0.1 M sodium ethoxide (0.5 ml) was added to a solution of methyl 2,4,6-tri-*O*-methyl-β-D-*ribo*-hexosid-3-ulose (19.6 mg) and methyl 2,3,4-tri-*O*-methyl-β-D-xyloside (1.8 mg) in dichloromethane (0.5 ml). Samples were withdrawn, neutralized (Dowex 50, H^+) and analysed by GLC. The composition of the product after 20 min, when no starting material remained, is given in Table 1. The response factors of B and G, relative to the xyloside, were determined in separate experiments. They were similar and it was assumed that the same response factors were valid for the other components. This is almost certainly incorrect for the extremely labile component A.

Almost identical results were obtained when the above experiment was repeated with methyl 2,4,6-tri-*O*-methyl-α-D-*ribo*-hexosid-3-ulose.

Acknowledgements. The authors are indebted to Miss Birthe Abrahamsson and Mrs Helena Liedgren for valuable technical assistance, to *Statens Naturvetenskapliga Forskningsråd* for financial support, to Pharmacia AB for a fellowship to one of us (L. K.) and to Professor Bengt Lindberg for his interest.

REFERENCES

1. Kenne, L., Larm, O. and Svensson, S. *Acta Chem. Skand.* **26** (1972) 2473.
2. Björndal, H., Hellerqvist, C. G., Lindberg, B. and Svensson, S. *Angew. Chem. Int. Ed.* **9** (1970) 610.
3. Bonner, T. G., Bourne, E. J. and McNally, S. *J. Chem. Soc.* **1960** 2929.
4. Sawardeker, J. S., Sloneker, J. H. and Jeanes, A. *Anal. Chem.* **12** (1965) 1602.
5. Chizhov, O. S., Golovkina, L. S. and Wulfson, N. S. *Izv. Akad. Nauk SSSR Ser. Khim.* **1966** 1915.

Received March 27, 1973.

ACTA CHEMICA SCANDINAVICA 27 (1972) 2802–2812

Organic Hydroxylamine Derivatives

VII.* Isoxazolin-5-ones. An Investigation of a Reaction Sequence Previously Stated to Give 3-Hydroxyisoxazoles

POVL KROGSGAARD-LARSEN, SØREN BRØGGER CHRISTENSEN and HANS HJEDS

The Royal Danish School of Pharmacy, Chemical Laboratory C, DK-2100 Copenhagen, Denmark

The acid catalyzed cyclization of the reaction products of hydroxylamine and β-ketoesters protected at the keto group with benzylamine has been reported [12] in some cases to give 3-hydroxyisoxazoles. A reinvestigation of these reaction sequences resulted in a revision of the structures of the compounds obtained in the different steps of the sequences, *e.g.* the final products claimed to be ethyl 3-hydroxy-5-methylisoxazolyl-4-acetate (IVb) and 3-hydroxy-4-(2-propynyl)-5-methylisoxazole (IVa) were shown to be ethyl 3-methylisoxazolin-5-on-4-yl-acetate (VIIIb) and 3-methyl-4-(2-propynyl)isoxazolin-5-one (VIIIa), respectively.

Analogous reaction sequences were investigated for the preparation of a number of known isoxazolin-5-ones, and one new, namely, 3-ethyl-4-methylisoxazolin-5-one (VIIIc). The extended investigation showed that the method is of general value for the preparation of isoxazolin-5-ones in a pure state.

The 3-hydroxyisoxazole derivatives muscimol (3-hydroxy-5-aminomethylisoxazole) and ibothenic acid [(±)-α-amino-3-hydroxyisoxazolyl-5-acetic acid], which are centrally acting constituents of *Amanita muscaria* [1] have been shown to be γ-aminobutyric acid and glutamic acid agonists, respectively, when applied to single neurones in the mammalian central nervous system.[2] These findings have stimulated the interest in the structural [3] as well as the synthetic aspects of the 3-hydroxyisoxazoles. During the last decade several synthetic routes leading to 3-hydroxyisoxazoles have been described,[4–7] but either the methods have been of limited scope or the yields have been very low.

Reactions between β-ketoesters and hydroxylamine under basic conditions followed by acidification normally afford mixtures of isoxazolin-5-ones and 3-hydroxyisoxazoles.[8] The reactions probably proceed by proton catalyzed

* Part VI. *Dansk Tidsskr. Farm.* **46** (1972) 97.

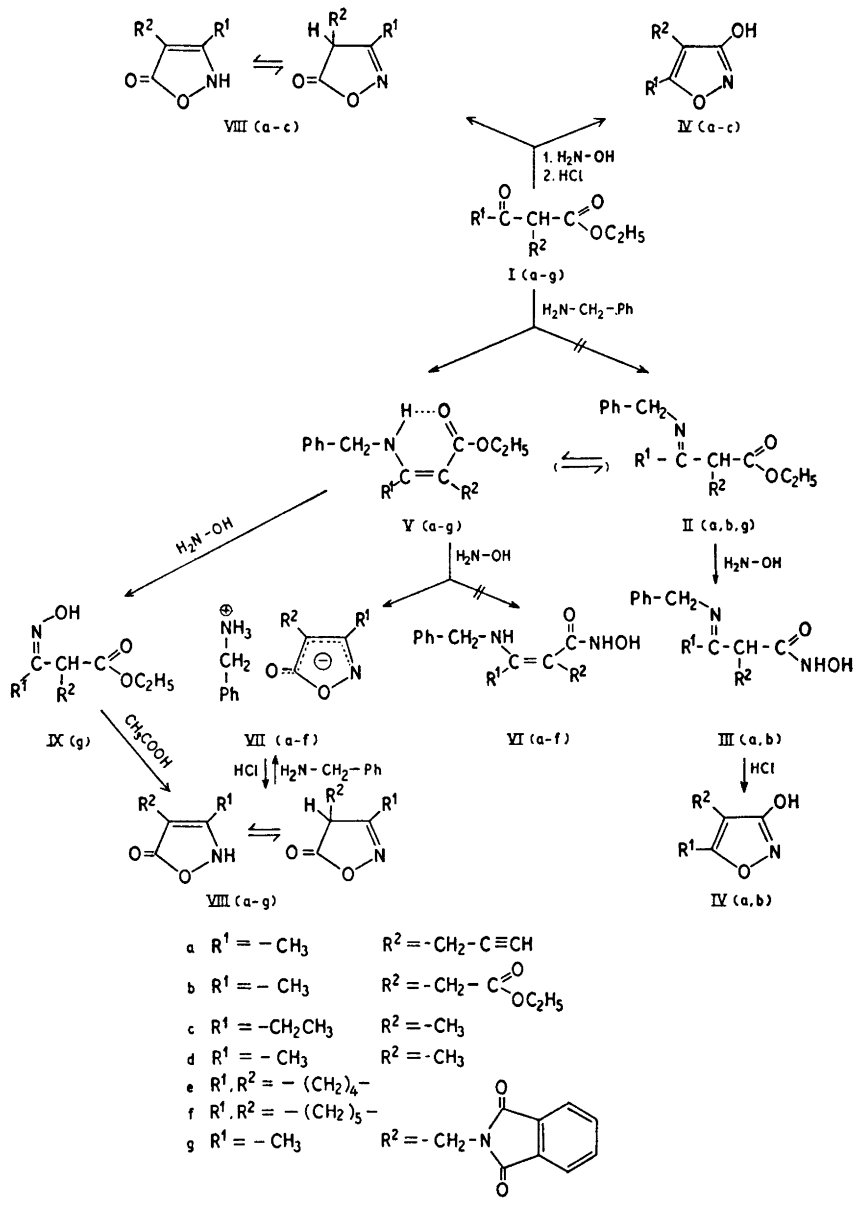

cyclization of the simultaneously formed oxime- and hydroxamic acid-intermediates, respectively.[8,9] The relative amounts of the two isomers strongly depend on the constitutions of the β-ketoesters.[8]

For that reason the preparation of 3-hydroxyisoxazoles, uncontaminated by the isoxazolin-5-one isomers, from β-ketoesters and hydroxylamine usually involves a previous conversion of the keto group into a base resistent derivative, which prior to the cyclization process can be easily cleaved by acid to give the β-ketohydroxamic acid-intermediates. As protection, *e.g.* ketalization of appropriate β-ketoesters with methanol, has been utilized in the syntheses of a few 3-hydroxyisoxazoles.[10,11] The use of this principle was extended by Jacquier *et al.*[4] who shielded the keto groups as ethylene ketals. The overall yields of the 3-hydroxyisoxazoles, especially of the 4,5-disubstituted ones, prepared in this way were rather poor.[4] On the other hand the reaction of ethyl enol ether of diethyl acetylmalonate with hydroxylamine followed by acid catalyzed cleavage and cyclization gave a mixture of 3-hydroxy-4-ethoxycarbonyl-5-methylisoxazole, and the unexpected isomer 3-methyl-4-ethoxycarbonylisoxazolin-5-one.[12]

The same authors [12] also described the syntheses of two compounds, which were assigned the structures 3-hydroxy-4-(2-propynyl)-5-methylisoxazole (IVa) and ethyl 3-hydroxy-5-methylisoxazolyl-4-acetate (IVb). The pertinent β-ketoesters (Ia) and (Ib) were treated with benzylamine to give compounds, which were assigned the structures (IIa) and (IIb). These were *via* the postulated hydroxamic acids (IIIa) and (IIIb) expected to be converted to the 3-hydroxyisoxazoles (IVa) and (IVb), respectively, as shown in the scheme. The structural assignments of (IVa) and (IVb) were supported by elemental analyses and were finally based on ^{1}H NMR spectroscopy and on IR and ^{1}H NMR spectroscopy, respectively. The constitution of compound (IVa) was claimed to be unambiguously established by the fact that it could be obtained by the above mentioned sequence *via* (IIa) and (IIIa). Furthermore (IVa) was stated to be obtained from the reaction of hydroxylamine with ethyl 2-(2-propynyl)acetoacetate (Ia). The structure of (IIb) was based on IR spectroscopy and on elemental analyses and those of (IIIa) and (IIIb) only on elemental analyses, exclusively.

In our hands, however, the reaction between ethyl 2-(2-propynyl)acetoacetate (Ia) and hydroxylamine only afforded small amounts of 3-hydroxy-4-(2-propynyl)-5-methylisoxazole (IVa) and almost exclusively 3-methyl-4-(2-propynyl)isoxazolin-5-one (VIIIa). The physical properties of the latter were consistent with those published by Bowden *et al.*[12] for the compound proposed as (IVa). These properties supported by our observations of a strong absorption band in the IR spectrum at 1800 cm^{-1} in chloroform solution and of a strong UV absorption at 259 nm provided conclusive evidence of the constitution of (VIIIa) in accordance with the general spectroscopic findings described by Jacquier *et al.*[13] for isoxazolin-5-ones. 3-Hydroxy-4-(2-propynyl)-5-methylisoxazole (IVa), as shown by elemental analysis, IR, UV, and ^{1}H NMR spectroscopy, was isolated from the reaction mixture by column chromatography.

These facts prompted us to reinvestigate the reaction sequences through the proposed intermediates (IIa)–(IIIa) and (IIb)–(IIIb), respectively, for the syntheses of the compounds, which by Bowden *et al.*[12] were assigned the structures 3-hydroxy-4-(2-propynyl)-5-methylisoxazole (IVa) and ethyl 3-hydroxy-5-methylisoxazolyl-4-acetate (IVb). Thus condensation of ethyl 2-

(2-propynyl)acetoacetate (Ia) and benzylamine turned out to give the enamine (Va) and not the proposed imine (IIa). A strong UV absorption at 295 nm, a carbonyl absorption band at 1640 cm^{-1} in the IR spectrum, and a ^1H NMR spin-spin splitting pattern for the N–H-proton (broadened triplet) and for the benzylic protons (doublet) as expected for compound (Va) provided evidence of the preferential existence of an intramolecular hydrogen bonded enamine form over the imine form. These structural features are in accordance with those generally accepted for related compounds.[14,15]

Reaction of the enamine (Va) with hydroxylamine gave as the only product a crystalline intermediate which upon treatment with hydrochloric acid afforded almost quantitatively a pure compound which was identical with 3-methyl-4-(2-propynylisoxazolin-5-one (VIIIa) as obtained from the above mentioned reaction of ethyl 2-(2-propynyl)acetoacetate (Ia) and hydroxylamine. This finding definitely ruled out a hydroxamic acid intermediate, and prompted us to examine the constitution of the above mentioned intermediate, which after the structure elucidation of compound (Va) was expected to exhibit the enamine hydroxamic acid structure (VIa) rather than the corresponding imine hydroxamic acid structure (IIIa) as proposed by Bowden *et al.*[12] The intermediate showed a transient purple colour with iron(III) chloride. In the IR spectrum, however, carbonyl group signals were absent, while broad absorption over the range 3200 – 2500 cm^{-1} and an absorption band at 2120 cm^{-1} suggested ammonium salt character of the compound. These findings together with the well known acidic properties of 3,4-disubstituted isoxazolin-5-ones [16] strongly pointed towards formula (VIIa) which is isomeric with the postulated products (VIa) and (IIIa). A UV maximum was observed at a wavelength of 255 nm, which is somewhat lower than that expected for the chromophoric system of formula (VIa), but in good agreement with that (255 nm) observed for the isoxazolin-5-one anion by Quin and Pinion.[17] Conclusive evidence could not be obtained from the ^1H NMR spectrum, but a final proof of the structural assignment was accomplished by synthesis of compound (VIIa) by mixing equivalent amounts of 3-methyl-4-(2-propynyl) isoxazolin-5-one (VIIIa) and benzylamine in tetrahydrofuran at room temperature. The precipitated salt was identical with the compound obtained from the enamine (Va) and hydroxylamine as shown by IR spectroscopy.

As mentioned before diethyl acetylsuccinate (Ib) was claimed to afford ethyl 3-hydroxy-5-methylisoxazolyl-4-acetate (IVb) *via* the proposed intermediates (IIb) and (IIIb).[12] A reinvestigation of this sequence disclosed a reaction pattern analogous with that described above for ethyl 2-(2-propynyl)-acetoacetate (Ia) leading to the formation of ethyl 3-methylisoxazolin-5-on-4-yl-acetate (VIIIb) through the intermediates (Vb) and (VIIb).

Ethyl 3-hydroxy-5-methylisoxazolyl-4-acetate (IVb) was detected by TLC as a minor compound together with the isoxazolin-5-one isomer (VIIIb) in the crude product from the reaction between diethyl acetylsuccinate (Ib) and hydroxylamine. It was isolated in a pure state by column chromatography and structure elucidated by spectroscopic methods. Similarly, the reaction between ethyl 2-methyl-3-oxovalerate (Ic) and hydroxylamine gave a mixture of 3-hydroxy-4-methyl-5-ethylisoxazole (IVc) and 3-ethyl-4-methylisoxazolin-5-one (VIIIc), both of which are new compounds.

Finally a series of 3,4-disubstituted isoxazolin-5-ones (VIIIc-f), were prepared in good yields through the not previously described intermediates (Vc-f) and (VIIc-f).

On the present basis this reaction sequence is considered to be of general value as a synthetic route to pure 3,4-disubstituted isoxazolin-5-ones.

The reaction between the enamines (Va-f) and hydroxylamine affording the corresponding isoxazolin-5-one benzylammonium salts (VIIa-f) is rather unusual. However, the reaction between the enamine 1,4,5,6-tetrahydronicotinamide and hydroxylamine leading to 4-(3-aminopropyl)-2-isoxazolin-5-one [17] is an analogous process. The mechanism of the process is unknown, but the first step is claimed to be an addition of the nucleophile to the enamine double bond,[17] and thus an oxime is a possible intermediate formed by an addition-elimination mechanism.

A compound assigned the oxime structure (IXg) has been isolated by Bowden *et al.*[12] from the reaction between hydroxylamine and the condensation product of ethyl 2-phthalimidomethylacetoacetate (Ig) and benzylamine. This compound was shown to cyclize to the corresponding isoxazolin-5-one in acidic media.[12]

The condensation product between ethyl 2-phthalimidomethylacetoacetate (Ig) and benzylamine turned out to be an enamine (Vg). A reinvestigation of the reaction between the enamine (Vg) and hydroxylamine confirmed the formation of the oxime intermediate (IXg). From a complex reaction mixture the compound (IXg) was isolated in a pure state by column chromatography and the structure proposed by Bowden *et al.*[12] was confirmed by spectroscopic methods.

EXPERIMENTAL

Melting points, determined in capillary tubes, are corrected. IR spectra were recorded on a Perkin-Elmer grating infrared spectrophotometer, Model 247. UV spectra were recorded in 99.9 % ethanol on a Perkin-Elmer grating ultraviolet-visible spectrophotometer, Model 402. ^{1}H NMR spectra were measured on a JEOL JMN-C-60HL instrument using TMS as an internal standard. The singlet, doublet, triplet, quartet, and multiplet patterns of the ^{1}H NMR spectra are designed s, d, t, q, and m, respectively. Microanalyses were made by Preben Hansen, Microanalytical Department of Chemical Laboratory II, University of Copenhagen.

Ethyl 2-(2-propynyl)acetoacetate (Ia). 20 g (0.10 mol) of ethyl β-morpholinocrotonate [18] were dissolved in excess of 2-propynyl bromide (40 ml). The solution was left at 65°C for 16 h, the excess of 2-propynyl bromide was removed *in vacuo*, and the residue was boiled with 40 ml of water for 15 min. The mixture was extracted with three 20 ml portions of ether. The combined, dried, and filtered ether phases were evaporated. The residue (17.3 g) was distilled to give 12.6 g (39 %) of a colourless oil, b.p. 102–110°C/13 mmHg (Ref. 18, b.p. 71°C/1 mmHg). The IR and ^{1}H NMR data were consistent with the structural assignments.

Ethyl 2-(2-propynyl)-3-benzylaminocrotonate (Va). A mixture of 5.0 g (30 mmol) of (Ia), 3.5 g (33 mmol) of benzylamine, and 15 g of molecular sieve, Union Carbide 3A, was refluxed in 60 ml of benzene for 4.5 h. The mixture was filtered and concentrated *in vacuo* to give 6.7 g (87 %) of a pale yellow oil. Distillation of an analytical sample at 0.05 mmHg afforded (Va) as a pale yellow oil. (Found: C 74.80; H 7.43; N 5.55. Calc. for $C_{16}H_{19}NO_2$: C 74.68; H 7.44; N 5.44). λ_{max} 298 nm ($\varepsilon = 1.72 \times 10^4$). IR data (neat) cm^{-1}: 3300, m (NH and HC≡C); 1640, s (C=O); 1600, s (C=C). ^{1}H NMR data (CCl_4) δ: 9.8 (broadened t ($J = 6$ cps), 1 H, CH_2-NH-C); 7.15 (slightly broadened s, 5 H, C_6H_5); 4.32 (d ($J = 6$ cps), 2 H, $C-CH_2-NH$); 4.02 (q ($J = 7$ cps), 2 H, $O-CH_2-CH_3$);

3.03 (d ($J=3$ cps), 2 H, C$-$CH_2-C); 1.90 (s, 3 H, CH_3-C=); 1.70 (t ($J=3$ cps), 1 H, $HC\equiv$C); 1.22 (t ($J=7$ cps), 3 H, CH_3-CH_2).

Benzylammonium salt of 4-(2-propynyl)-3-methylisoxazolin-5-one (VIIa). Method a. 115 mg (5 mmol) of sodium were reacted with methanol (12 ml) and to the solution were added 350 mg (5 mmol) of hydroxylammonium chloride. After stirring for 5 min 1.28 g (5 mmol) of (Va) were added and the mixture was refluxed for 4 h. After filtration and evaporation to dryness *in vacuo* a crystalline residue was obtained. Recrystallization from tetrahydrofuran (THF) afforded 500 mg (41 %) of (VIIa), m.p. 148$-$151°C (decomp.) (Ref. 12, m.p. 153$-$155°C for the proposed hydroxamic acid (IIIa)). λ_{max} 255 nm ($\varepsilon=0.89\times10^4$). IR data (KBr) cm^{-1}: 3200$-$2300 and 2160, m (NH_3^+); 1620, s and 1510$-$1470, several bands (isoxazole-ring). ^{1}H NMR data (DMSO-d_6) δ: 7.82 (perturbed s, 3 H, $CH_2-NH_3^+$); 7.32 (slightly broadened s, 5 H, C_6H_5); 3.92 (s, 2 H, C$-$C$H_2-NH_3^+$); 2.82 (d ($J=3$ cps), 2 H, C$-$CH_2-C); 2.40 (t ($J=3$ cps), 1 H, $HC\equiv$C); 1.89 (s, 3 H, C$-$CH_3).

Method b. To a solution of 137 mg (1 mmol) of the isoxazolin-5-one (VIIIa) in 1 ml of THF was added a solution of 107 mg (1 mmol) of benzylamine in 2.5 ml of THF. Upon standing at room temperature for 20 h 200 mg (82 %) of colourless crystals were isolated, m.p. 148$-$151°C (decomp.) (Found: C 68.95; H 6.69; N 11.52. Calc. for $C_{14}H_{16}N_2O_2$: C 68.83; H 6.60; N 11.47). The IR and UV spectra were identical with those of the product of method a.

3-Methyl-4-(2-propynyl) isoxazolin-5-one (VIIIa) and 3-hydroxy-4-(2-propynyl)-5-methylisoxazole (IVa). To 1.68 g (10 mmol) of ethyl 2-(2-propynyl)acetoacetate (Ia) was added a solution of 800 mg (20 mmol) of sodium hydroxide and 695 mg (10 mmol) of hydroxylammonium chloride in 5 ml of water at 0°C. The mixture was stirred until homogeneous and left at 4°C for 16 h. The mixture was acidified to pH ~2 with concentrated hydrochloric acid (*ca.* 1 ml) and left at 4°C for further 24 h. The crystalline precipitate (500 mg) was collected, dried, and recrystallized (ether) to give 400 mg (29 %) of compound (VIIIa) as colourless crystals, m.p. 90$-$93°C (Ref. 12, m.p. 91$-$93°C for the proposed 3-hydroxyisoxazole (IVa)). λ_{max} 259 nm ($\varepsilon=0.90\times10^4$). IR data ($CHCl_3$) cm^{-1}: 1800, s and 1740, s (ring C=O). The ^{1}H NMR data ($CDCl_3$-DMSO-d_6 (4:1)) supported the structural assignments of compound (VIIIa) and agreed with those published for the compound which was assigned the structure (IVa) [12] except for a broad peak which we observed at δ 11.5$-$10.5, 0.7 H (N*H*).

The aqueous mother liquor was evaporated and the residue was extracted with ether. Evaporation of the ether extract gave 700 mg of a residue, which by TLC (silica gel GF_{254} (Merck), benzene-ethyl acetate-formic acid (30:30:1)) was shown to be a mixture of two compounds, which were separated by column chromatography on silica gel (0.05$-$0.20 mm, Merck) (26 g). The eluent was benzene-ethyl acetate-formic acid (60:40:1) to which increasing amounts of ethyl acetate were added. 120 mg (9 %) of compound (IVa) and 300 mg (22 %) of compound (VIIIa) were isolated. (IVa) was recrystallized (cyclohexane) to give 100 mg of colourless needles, m.p. 102$-$104°C. (Found: C 61.15; H 5.20; N 10.42. Calc. for $C_7H_7NO_2$: C 61.31; H 5.15; N 10.21). λ_{max} 229 nm ($\varepsilon=3.5\times10^3$). IR data (KBr) cm^{-1}: 3200$-$2200, s (OH); 1660, s and 1550, s (isoxazole-ring). ^{1}H NMR data ($CDCl_3$) δ: 11.52 (s, 1 H, O*H*); 3.22 (d ($J=2$ cps), 2 H, C$-$CH_2-C); 2.32 (s, 3 H, C$-$CH_3; 2.02 (t ($J=2$ cps), 1 H, $HC\equiv$C).

3-Methyl-4-(2-propynyl)isoxazolin-5-one (VIIIa). 244 mg (1 mmol) of the benzylammonium salt (VIIa) were dissolved in 7.5 ml of water. Upon addition of 2.5 ml of concentrated hydrochloric acid the solution was continuously extracted with ether for 30 min. The extract was dried, filtered, and evaporated. Recrystallization of the residue afforded 100 mg (73 %) of (VIIIa) as pale yellow crystals, m.p. 90$-$93°C (ether), identical with (VIIIa) obtained from the above described reaction of ethyl 2-(2-propynyl)acetoacetate (Ia) and hydroxylamine as shown by IR spectroscopy.

Ethyl 3-ethoxycarbonyl-4-benzylamino-3-pentenoate (Vb). (Vb) was synthesized as described above for (Va) using 5.4 g (25 mmol) of diethyl acetylsuccinate (Ib) and 2.7 g (25 mmol) of benzylamine to give 7.8 g of crude product as a colourless oil. The oil was dissolved in 100 ml of petroleum ether and cooling overnight at $-$18°C gave colourless crystals, 3.9 g, m.p. 38$-$39°C (Ref. 12, described as an oil with the proposed structure (IIb)). λ_{max} 297 nm ($\varepsilon=1.93\times10^4$). IR data (KBr) cm^{-1}: 3280, m (NH); 1640, s (C=O); 1600 s (C=C). ^{1}H NMR data ($CDCl_3$) δ: 9.90 (broadened t, 1 H, C$-$N*H*$-$CH$_2$; 7.34 (s, 5 H, C_6H_5); 4.47 (d ($J=7$ cps), 2 H, NH$-$CH_2-C); 4.14 (q ($J=7$ cps), 4 H

($2\times O-CH_2-CH_3$); 3.30 (s, 2 H, $C-CH_2-C$); 1.95 (s, 3 H, $CH_3-C=$); 1.25 (t ($J=7$ cps), 6 H ($2\times CH_2-CH_3$)).

Benzylammonium salt of ethyl 3-methylisoxazolin-5-on-4-yl-acetate (VIIb). Method a. (VIIb) was synthesized as described above for (VIIa) using 3.0 g (10 mmol) of (Vb) and 0.76 g (11 mmol) of hydroxylammonium chloride to give 3.5 g of an oil which solidified upon standing. The crude product was recrystallized from ethyl acetate to give 1.7 g (58 %) of (VIIb), m.p. 122–124°C (decomp.). (Ref. 12, m.p. 120–122°C for the proposed hydroxamic acid (IIIb)). λ_{max} 255 nm ($\varepsilon=0.88\times10^4$). IR data (KBr) cm^{-1}: 3300–2300 and 2100, m (NH_3^+), 1720, s (C=O), 1625, s, and 1520–1480, several bands (isoxazole-ring). ^1H NMR data ($CDCl_3$-DMSO-d_6 (5:1)) δ: 7.93 (slightly broadened s, 3 H, $CH_2-NH_3^+$); 7.40–7.25 (m, 5 H, C_6H_5); 4.02 (q ($J=7$ cps), 2 H, $O-CH_2-CH_3$); 3.96 (s, 2 H, $NH_3^+-CH_2-C$); 3.00 (s, 2 H, $=C-CH_2-C$); 1.97 (s, 3 H, $CH_3-C=$); 1.20 (t ($J=7$ cps), 3 H, CH_2-CH_3).

Method b. To a solution of 74 mg (4 mmol) of the isoxazolin-5-one (VIIIb) in 0.2 ml of THF was added a solution of 43 mg (4 mmol) of benzylamine in 1 ml of THF. After standing overnight at room temperature 100 mg (85 %) of (VIIb) were isolated, m.p. 126.5–128.5°C (decomp.). The IR spectrum was identical with that of (VIIb) prepared according to method a.

Ethyl 3-methylisoxazolin-5-on-4-yl-acetate (VIIIb). 2.92 g (10 mmol) of (VIIb) were dissolved in a mixture of 6 ml of water and 1.5 ml of concentrated hydrochloric acid. The solution was continuously extracted with ether for 1 h and the extract was dried ($MgSO_4$), filtered, and evaporated to give 1.70 g of a pale yellow oil which crystallized upon standing. Recrystallization from ethyl acetate yielded 0.8 g (43 %) of colourless crystals, m.p. 75.5–76.5°C (Ref. 12, m.p. 78–79°C for a compound with the proposed structure (IVb)). λ_{max} 259 nm ($\varepsilon=1.02\times10^4$). IR data ($CHCl_3$) cm^{-1}: 1795, s (ring-C=O); 1740–1720, several strong bands (ring-C=O and ester-C=O). ^1H NMR data (DMSO-d_6) δ: 4.05 (q ($J=7$ cps), 2 H, $O-CH_2-CH_3$); 3.20 (s, 2 H, $=C-CH_2-C$); 2.09 (s, 3 H, $=C-CH_3$); 1.18 (t ($J=7$ cps), 3 H, CH_2-CH_3).

Ethyl 3-hydroxy-5-methylisoxazolyl-4-acetate (IVb). A mixture of 10 ml of 2 N NaOH, 0.70 g (10 mmol) of hydroxylammonium chloride, and 2.16 g (10 mmol) of diethyl acetylsuccinate (Ib) was stirred at 0°C for 1 h. The mixture was extracted with two 10 ml portions of ether and the pooled extracts were dried ($MgSO_4$) and evaporated *in vacuo* to give 0.3 g of an oil consisting mainly of diethyl acetylsuccinate (Ib). The aqueous phase was acidified to pH *ca.* 0 with concentrated hydrochloric acid and continuously extracted for 1 h with ether-methylene chloride (4:1). The extract was dried ($MgSO_4$) and evaporated to dryness *in vacuo* to give 1.5 g of an oil. TLC (silica gel GF_{254} (Merck), benzene-ethyl acetate-formic acid (50:50:1)) showed the oil to be a complex mixture containing a compound with the same R_F-value as (VIIIb) which like (VIIIb) gave a violet colour using $FeCl_3$ as a spraying reagent. The oil was submitted to column chromatography on 50 g of silica gel (0.05–0.20 mm, Merck) using benzene-ethyl acetate-formic acid (50:50:1) as an eluent. It was not possible to isolate any (VIIIb) as it is probably destroyed on the column during the elution. 379 mg of crude (IVb) were isolated. Recrystallization twice from cyclohexane-benzene (4:1) yielded colourless crystals, m.p. 100.5–102.5°C. (Found: C 51.50; H 5.80; N 7.57. Calc. for $C_8H_{11}NO_4$: C 51.88; H 5.99; N 7.56). λ_{max} 212 nm ($\varepsilon=5.04\times10^3$). IR data (KBr) cm^{-1}: 3300–2100, s (OH); 1715, s (C=O); 1663 and 1550, s (isoxazole-ring). ^1H NMR data ($CDCl_3$) δ: 10.20 (s, 1 H, $=C-OH$); 4.06 (q ($J=7$ cps), 2 H, $O-CH_2-CH_3$); 3.21 (s, 2 H, $=C-CH_2-C$); 2.20 (s, 3 H, $=C-CH_3$); 1.20 (t ($J=7$ cps), 3 H, CH_2-CH_3).

Ethyl 2-methyl-3-benzylamino-2-pentenoate (Vc). (Vc) was synthesized as described above for (Va) using 7.9 g (50 mmol) of ethyl 2-methyl-3-oxovalerate (Ic) [19] and 5.85 g (55 mmol) of benzylamine. Yield 4.2 g (30 %) of a colourless oil, b.p. 140–144°C/0.4 mmHg, m.p. *ca.* 8°C (Found: C 72.95; H 8.55; N 5.75. Calc. for $C_{15}H_{21}NO_2$: C 72.84; H 8.56; N 5.66). λ_{max} 303 nm ($\varepsilon=1.73\times10^4$). IR data (neat) cm^{-1}: 3250, m (NH); 1640, s (C=O); 1600, s (C=C). ^1H NMR data (CCl_4) δ: 9.6 (broadened t ($J=6$ cps), 1 H, $C-NH-CH_2$); 7.20 (slightly broadened s, 5 H, C_6H_5); 4.31 (d ($J=6$ cps), 2 H, $NH-CH_2-C$); 4.02 (q ($J=6$ cps), 2 H, CH_3-CH_2-O); 2.23 (q ($J=7$ cps), 2 H, $CH_3-CH_2-C=$); 1.75 (s, 3 H, CH_3-C); 1.22 (t ($J=6$ cps), 3 H, CH_3-CH_2-O); 1.00 (t ($J=7$ cps), 3 H, $CH_3-CH_2-C=$).

Benzylammonium salt of 3-ethyl-4-methylisoxazolin-5-one (VIIc). Method a. (VIIc) was synthesized as described above for (VIIa). As starting materials were used 12.4 g

(50 mmol) of (Vc) and 3.5 g (50 mmol) of hydroxylammonium chloride. After recrystallization (THF) 2.8 g (25 %) of colourless crystals of (VIIc) were obtained, m.p. 110–111°C (decomp.). (Found: C 66.40; H 7.81; N 11.90. Calc. for $C_{13}H_{18}N_2O_2$: C 66.64; H 7.74; N 11.96). λ_{max} 258 nm ($\varepsilon = 0.91 \times 10^4$). IR data (KBr) cm^{-1}: 3200–2300 and 2160, m (NH_3^+); 1630, s and 1500–1440, several bands (isoxazole-ring). ^1H NMR data (DMSO-d_6) δ: 7.88 (slightly broadened s, 3 H, $CH_2-NH_3^+$); 7.43 slightly broadened s, 5 H, C_6H_5); 3.98 (s, 2 H, $C-CH_2-NH_3^+$); 2.24 (q ($J = 6$ cps), 2 H, CH_3-CH_2-C); 1.54 (s, 3 H, CH_3-C); 1.04 (t ($J = 6$ cps), 3 H, CH_3-CH_2-C).

Method b. 25.4 mg (0.2 mmol) of the isoxazolin-5-one (VIIIc) were dissolved in a solution of 21.4 mg (0.2 mmol) of benzylamine in 100 µl of THF. After standing for 20 h at room temperature 28 mg (60 %) of (VIIc) were isolated, m.p. 110–111°C (decomp.). The IR spectrum was identical with that of (VIIc) as prepared by method a.

3-Ethyl-4-methylisoxazolin-5-one (VIIIc) and 3-hydroxy-4-methyl-5-ethylisoxazole (IVc). To a solution of 4.0 g (100 mmol) of sodium hydroxide and 3.45 g (50 mmol) of hydroxylammonium chloride in 25 ml of water were added 7.90 g (50 mmol) of ethyl 2-methyl-3-oxavalerate (Ic) at 0°C and the solution was stirred until homogeneous. After standing at 4°C for 16 h the mixture was acidified to pH ~2 with concentrated hydrochloric acid (7 ml) and the mixture was left at 4°C for further 24 h. The mixture was extracted with two 20 ml portions of ether. The combined, dried, and filtered extracts were evaporated to give 6.4 g of a mixture of two compounds as shown by TLC (silica gel GF_{254} (Merck), benzene-ethyl acetate-formic acid (30:30:1)). The mixture was submitted to column chromatography as described for the separation of (VIIIa) and (IVa) to give 2.6 g (41 %) of (VIIIc) and 3.3 g (52 %) of (IVc). Recrystallization of (IVc) (cyclohexane) afforded colourless crystals, m.p. 50–51°C. (Found: C 56.90; H 7.17; N 11.16. Calc. for $C_6H_9NO_2$: C 56.68; H 7.14; N 11.02). λ_{max} < 220 nm. IR data (KBr) cm^{-1}: 3200–2200, s (OH); 1660, s and 1530, s (isoxazole-ring). ^1H NMR data (CCl_4) δ: 11.22 (s, 1 H, O*H*); 2.52 (q ($J = 7$ cps), 2 H, CH_3-CH_2-C); 1.82 (s, 3 H, CH_3-C); 1.22 (t ($J = 7$ cps), 3 H, CH_3-CH_2-C). Compound (VIIIc) was distilled twice *in vacuo* to give a colourless oil, b.p. 98°C/0.5 mmHg. (Found: C 56.75; H 7.32; N 10.98. Calc. for $C_6H_9NO_2$: C 56.68; H 7.14; N 11.02). λ_{max} 264 nm ($\varepsilon = 8.2 \times 10^3$). IR data ($CHCl_3$) cm^{-1}: 1800, s and 1740, s (ring-C=O). ^1H NMR data (CCl_4) δ: 11.4–11.0 (broad signal, 0.7 H, N*H*); 2.51 (q ($J = 7$ cps), 2 H, CH_3-CH_2-C); 1.70 (s, 3 H, CH_3-C); 1.20 (t ($J = 7$ cps), CH_3-CH_2-C).

3-Ethyl-4-methylisoxazolin-5-one (VIIIc). (VIIIc) was obtained as described above for (VIIIa). 2.27 g (9.7 mmol) of the benzylammonium salt (VIIc) gave 700 mg of an oil, which was distilled to give 600 mg (49 %) of a colourless oil, b.p. 98°C/0.5 mmHg. The IR spectrum showed the product to be identical with (VIIIc) prepared as described above from ethyl 2-methyl-3-oxovalerate and hydroxylamine.

Ethyl 2-methyl-3-benzylaminocrotonate (Vd). (Vd) was synthesized as described above for (Va) using 7.2 g (50 mmol) of ethyl 2-methylacetoacetate (Id) and 5.9 g (55 mmol) of benzylamine as starting materials. Yield 10.2 g (88 %) of a pale yellow oil, b.p. 121–122°C/0.1 mmHg, m.p. *ca.* 8°C. (Found: C 72.65; H 8.13; N 6.50. Calc. for $C_{14}H_{19}NO_2$: C 72.07; H 8.21; N 6.00). λ_{max} 301 nm ($\varepsilon = 1.5 \times 10^4$). IR data (neat) cm^{-1}: 3250, m (NH); 1640, s (C=O); 1595, s (C=C). ^1H NMR data (CCl_4) δ: 9.6 (broadened t ($J = 6$ cps), 1 H, $C-NH-CH_2$); 7.15 (s, 5 H, C_6H_5); 4.26 (d ($J = 6$ cps), 2 H, $NH-CH_2-C$); 4.02 (q ($J = 6$ cps), 2 H, CH_3-CH_2-O); 1.78 (s, 3 H, $CH_3-C=$); 1.74 (s, 3 H, $CH_3-C=$); 1.00 (t ($J = 6$ cps), 3 H, CH_3-CH_2-O).

Benzylammonium salt of 3,4-dimethylisoxazolin-5-one (VIId). Method a. (VIId) was synthesized as described above for (VIIa) using 7.78 g (33 mmol) of (Vd) and 2.57 g (37 mmol) of hydroxylammonium chloride. Upon recrystallization (THF) 4.2 g (58 %) of (VIId) were obtained as colourless crystals, m.p. 101–103°C (decomp.). (Found: C 65.65; H 7.39; N 12.93. Calc. for $C_{12}H_{16}N_2O_2$: C 65.43; H 7.32; N 12.72). λ_{max} 258 nm ($\varepsilon = 0.86 \times 10^4$). IR data (KBr) cm^{-1}: 3300–2300 and 2200, m (NH_3^+); 1622, s and 1520–1420, several bands (isoxazole-ring). ^1H NMR data (DMSO-d_6) δ: 7.38 (slightly broadened s, 3 H, $CH_2-NH_3^+$); 7.31 (s, 5 H, C_6H_5); 3.92 (s, 2 H, $C-CH_2-NH_3^+$); 1.87 (s, 3 H, CH_3-C); 1.55 (s, 3 H, CH_3-C).

Method b. To 275 mg (2.4 mmol) of 3,4-dimethylisoxazolin-5-one (VIIId) dissolved in 0.5 ml of THF was added a solution of 260 mg (2.4 mmol) of benzylamine in 6 ml of THF. 11 ml of ether were added and upon standing at room temperature for 2 h 420 mg

(79 %) of colourless crystals, m.p. 105.5 – 106.5°C (decomp.), were isolated. The IR spectrum was identical with that of compound (VIId) as obtained by method a.

3,4-Dimethylisoxazolin-5-one (VIIId). To a solution of 3.6 g (16 mmol) of (VIId) in 20 ml of water were added 5 ml of concentrated hydrochloric acid and the solution was extracted continuously with ether-methylene chloride (4:1) for 1 h. The dried and filtered organic phase was evaporated. The crystalline residue (1.8 g) was sublimed twice *in vacuo* (70°C/0.2 mmHg) to give 1.2 g (65 %) of (VIIId) as colourless crystals, m.p. 47 – 50°C. λ_{max} 261 nm (log $\varepsilon = 4.0$). (Ref. 20, m.p. 49 – 51°C. λ_{max} 259 nm (log $\varepsilon = 3.9$) (CH_3OH)). The IR and ^1H NMR spectra were consistent with the structural assignments.

1-Benzylamino-2-ethoxycarbonylcyclohexene (Ve). (Ve) was synthesized as described above for (Va). As starting materials were used 45 g (0.27 mol) of 2-ethoxycarbonylcyclohexanone (Ie) [21] and 31 g (0.29 mol) of benzylamine. The yield of (Ve) was 57 g (83 %) obtained as a pale yellow oil, which crystallized by standing at – 18°C. An analytical sample was recrystallized (petroleum ether) to give (Ve) as colourless crystals, m.p. 20 – 22°C. (Found: C 74.15; H 8.33; N 5.51. Calc. for $C_{16}H_{21}NO_2$: C 74.10; H 8.16; N 5.40). λ_{max} 303 nm ($\varepsilon = 1.47 \times 10^4$). IR data (neat) cm^{-1}: 3260, m (NH); 1650, s (C=O); 1600, s (C=C). ^1H NMR data (CCl_4) δ: 9.3 (broadened t ($J = 6$ cps), 1 H, C – N*H* – CH_2); 7.14 (s, 5 H, C_6H_5); 4.28 (d ($J = 6$ cps), 2 H, NH – CH_2 – C); 3.98 (q ($J = 6$ cps), 2 H, CH_3 – CH_2 – O); 2.4 – 1.9 (m, 4 H, CH_2 – CH_2 – C=C – CH_2 – CH_2); 1.7 – 1.4 (m, 4 H, CH_2 – $(CH_2)_2$ – CH_2); 1.21 (t ($J = 6$ cps), 3 H, CH_3 – CH_2).

Benzylammonium salt of 3,4-tetramethyleneisoxazolin-5-one (VIIe). Method a. (VIIe) was synthesized as described above for (VIIa), using 10 g (39 mmol) of (Ve) and 2.8 g (39 mmol) of hydroxylammonium chloride to give 11.1 g of crystalline crude product. Recrystallization (THF) afforded 4.1 g (42 %) of (VIIe), m.p. 112 – 114°C (decomp.). (Found: C 68.10; H 7.54; N 11.25. Calc. for $C_{14}H_{18}N_2O_2$: C 68.27; H 7.37; N 11.37). λ_{max} 261 nm ($\varepsilon = 0.91 \times 10^4$). IR data (KBr) cm^{-1}: 3100 – 2250 and 2160, m (NH_3^+); 1610, s and 1500 – 1420, several bands (isoxazole-ring). ^1H NMR data (DMSO-d_6) δ: 7.76 (s, 3 H, CH_2 – NH_3^+); 7.4 (slightly broadened s, 5 H, C_6H_5); 3.94 (s, 2 H, C – CH_2 – NH_3^+); 2.6 – 1.8 (m, 4 H, CH_2 – CH_2 – C=C – CH_2 – CH_2); 1.8 – 1.3 (m, 4 H, CH_2 – $(CH_2)_2$ – CH_2).

Method b. (VIIe) was synthesized as described for (VIIa) from 13.9 mg (0.1 mmol) of the isoxazolin-5-one (VIIIe) and 10.7 mg (0.1 mmol) of benzylamine. Yield 8 mg (32 %) of (VIIe), m.p. 111 – 113°C (decomp.). The IR spectrum was identical with that of (VIIe) as prepared by method a.

3,4-Tetramethyleneisoxazolin-5-one (VIIIe). A solution of 1.0 g (40 mmol) of (VIIe) in 20 ml of an aqueous solution of sodium bicarbonate (5 %) was continuously extracted with ether for 3 h. Upon addition of 3 ml of 4 N hydrochloric acid the mixture was again continuously extracted with ether for 30 min. The extract of the acidified mixture was dried, filtered, and evaporated. After recrystallization of the residue (ether) were obtained 300 mg (54 %) of (VIIIe) as colourless crystals, m.p. 65 – 69°C. λ_{max} 262 nm ($\varepsilon = 0.97 \times 10^4$). (Ref. 22, m.p. 66 – 67°C. λ_{max} 258 nm ($\varepsilon = 0.906 \times 10^4$) (0.01 M sulphuric acid)). IR and ^1H NMR data were consistent with those reported in the literature.[22]

1-Benzylamino-2-ethoxycarbonylcycloheptene (Vf). (Vf) was synthesized as described above for (Va), using 7.6 g (41 mmol) of 2-ethoxycarbonylcycloheptanone (If) [23] and 4.8 g (45 mmol) of benzylamine as starting materials to give 11.9 g of crude product, which crystallized upon standing at – 18°C. Recrystallization (petroleum ether) afforded 6.8 g (61 %) of (Vf) as colourless crystals, m.p. 42 – 45°C. (Found: C 74.85; H 8.53; N 5.16. Calc. for $C_{17}H_{23}NO_2$: C 74.69; H 8.48; N 5.12). λ_{max} 309 nm ($\varepsilon = 1.52 \times 10^4$). IR data (neat) cm^{-1}: 3250, m (NH); 1640, s (C=O); 1600, s (C=C). ^1H NMR data (CCl_4) δ: 9.6 (broadened t ($J = 6$ cps), 1 H, C – N*H* – CH_2); 7.18 (s, 5 H, C_6H_5); 4.34 (d ($J = 6$ cps), 2 H, NH – CH_2 – C); 4.00 (q ($J = 7$ cps), 2 H, CH_3 – CH_2 – O); 2.6 – 2.1 (m, 4 H, CH_2 – CH_2 – C=C – CH_2 – CH_2); 1.8 – 1.1 (m, 6 H, CH_2 – $(CH_2)_3$ – CH_2); 1.22 (t ($J = 7$ cps), 3 H, CH_3 – CH_2).

Benzylammonium salt of 3,4-pentamethyleneisoxazolin-5-one (VIIf). Method a. (VIIf) was synthesized as described above for (VIIa), using 10.6 g (39 mmol) of (Vf) and 2.76 g (40 mmol) of hydroxylammonium chloride as starting materials to give 11.2 g of crystalline crude product. Recrystallization (THF) afforded 5.9 g (58 %) of (VIIf), m.p. 148 – 150°C (decomp.). (Found: C 68.95; H 7.79; N 10.83. Calc. for $C_{15}H_{20}N_2O_2$: C 69.20; H 7.74; N 10.76). λ_{max} 260 nm ($\varepsilon = 0.88 \times 10^4$). IR data (KBr) cm^{-1}: 3200 – 2200 and 2160, m (NH_3^+); 1630, s and 1500 – 1450, several bands (isoxazole-ring). ^1H NMR data (DMSO-d_6)

δ: 7.34 (perturbed s, 5 H, C_6H_5); 7.1 (s, 3 H, $CH_2-NH_3^+$); 3.88 (s, 2 H, $C-CH_2-NH_3^+$); 2.5 – 1.8 (m, 4 H, $CH_2-CH_2-C=C-CH_2$); 1.8 – 1.0 (m, 6 H, $CH_2-CH_2)_3-CH_2$).

Method b. (VIIf) was synthesized as described for (VIIa) from 15.3 mg (0.1 mmol) of the isoxazolin-5-one (VIIIf) and 10.7 mg (0.1 mmol) of benzylamine. Yield 15 mg (58 %) of (VIIf), m.p. 152 – 154°C (decomp.). The IR spectrum was identical with that of (VIIf) as prepared by method a.

3,4-Pentamethyleneisoxazolin-5-one (VIIIf). (VIIIf) was obtained as described above for (VIIIa). 700 mg (27 mmol) of the benzylammonium salt (VIIf) gave 300 mg of crude product. Recrystallization (ether) afforded 200 mg (49 %) of (VIIIf), m.p. 83 – 86°C (Ref. 8, m.p. 80°C). λ_{max} 264 nm (log $\varepsilon = 3.97$). (Ref. 13, λ_{max} 262 nm (log $\varepsilon = 3.90$)). IR and ^{1}H NMR data were consistent with those reported in the literature.[13]

Ethyl 2-phthalimidomethyl-3-benzylaminocrotonate (Vg). (Vg) was synthesized as described above for (Va) using 9.0 g (30 mmol) of ethyl 2-phthalimidomethylacetoacetate (Ig) [12] and 3.4 g (33 mmol) of benzylamine as starting materials to give a crystalline crude product. Recrystallization from ethanol gave 4.2 g (37 %) of pale yellow crystals, m.p. 157.5 – 158°C (Ref. 12, m.p. 160 – 162°C for the proposed compound (IIg)). λ_{max} 294 nm ($\varepsilon = 2.00 \times 10^4$). IR data (KBr) cm^{-1}: 3450, m (NH); 1770, m and 1710, s (phthalimido-C=O); 1645, s (ester-C=O); 1605, s (C=C). ^{1}H NMR data (CCl_4 – DMSO-d_6 (3:2)) δ: 9.95 (broadened t, 1 H, $=C-NH-CH_2$); 7.61 (s, 4 H, C_6H_4); 7.27 (s, 5 H, C_6H_5); 4.30 (perturbed d, 2 H, $NH-CH_2-C$); 3.94 (q ($J = 7$ cps), 2 H, $O-CH_2-CH_3$); 3.02 (s, 2 H, $N-CH_2-C$); 2.22 (s, 3 H, $CH_3-C=$); 1.12 (t ($J = 7$ cps), 3 H, CH_2-CH_3).

Ethyl 2-phthalimidomethyl-3-hydroxyiminobutyrate (IXg). A mixture of 2.26 g (6 mmol) of the enamine (Vg), 0.46 g (6.6 mmol) of hydroxylammonium chloride, 0.15 g (6.6 mmol) of sodium and 10 ml of methanol was refluxed for 2 h. After cooling the mixture was filtered and concentrated under reduced pressure to an oil which was column chromatographed (silica gel 0.05 – 0.20 mm, Merck, ethyl acetate-methanol (99:1)), to give 650 mg of crude product. Recrystallization from ether-petroleum ether yielded 240 mg of the oxime (IX), m.p. 149.5 – 151°C. (Ref. 12, m.p. 139 – 141.5°C). (Found: C 59.25; H 5.35; N 9.21. Calc. for $C_{15}H_{16}N_2O_5$: C 59.20; H 5.30; N 9.21). IR data (KBr) cm^{-1}: 3500, s (OH); 1790, m (phthalimido-C=O); 1720 – 1700, s, two bands (phthalimido-C=O and ester-C=O). ^{1}H NMR data ($CDCl_3$) δ: 8.28 (s, 1 H, $=N-OH$); 7.90 – 7.50 (m, 4 H, C_6H_4); 4.25 – 3.05 (complex pattern, 3 H, $N-CH_2-CH-C$); 4.13 (q ($J = 7$ cps), 2 H, $O-CH_2-CH_3$); 1.87 (s, 3 H, $CH_3-C=$); 1.20 (t ($J = 7$ cps), 3 H, CH_2-CH_3).

Treatment of (IXg) with acetic acid under reflux for 1 h yielded a compound of which the IR-spectrum (KBr) was identical with that of 3-methyl-4-phthalimidomethylisoxazolin-5-one (VIIIg) prepared as described by Bowden *et al.*[12]

Acknowledgement. The authors are grateful to the Head of this laboratory, professor B. Jerslev, and to professor A. Kjær, Department of Organic Chemistry, Technical University of Denmark, for their stimulating interest in this work and for valuable discussions. The authors wish to thank the *Danish Medical Research Council* for supporting this work.

REFERENCES

1. Eugster, C. H. *Fortschr. Chem. Org. Naturst.* **27** (1969) 261.
2. Johnston, G. A. R., Curtis, D. R., De Groat, W. C. and Duggan, A. W. *Biochem. Pharmacol.* **17** (1968) 2488.
3. Brehm, L., Hjeds, H. and Krogsgaard-Larsen, P. *Acta Chem. Scand.* **26** (1972) 1298.
4. Jacquier, R., Petrus, C., Petrus, F. and Verducci, J. *Bull. Soc. Chim. France* **1970** 1978.
5. Tomita, K., Nagano, M., Yanai, T., Oka, H., Murakami, T. and Sampei, N. *Ann. Sankyo Res. Lab.* **22** (1970) 215.
6. Ohata, K., Adachi, K., Hashimoto, M. and Kage, A. *Ger. Pat.* 2,032,809 (*Chem. Abstr.* **74** (1971) 76407 m).
7. Nakamura, N. *Chem. Pharm. Bull.* **19** (1971) 46.
8. Jacquier, R., Petrus, C., Petrus, F. and Verducci, J. *Bull. Soc. Chim. France* **1970** 2685.

9. Jacquier, R., Petrus, F., Verducci, J. and Vidal, Y. *Bull. Soc. Chim. France* **1971** 3664.
10. Gagneux, A. R., Häfliger, F., Eugster, C. H. and Good, R. *Tetrahedron Letters* **1965** 2077.
11. Göth, H., Gagneux, A. R., Eugster, C. H. and Schmid, H. *Helv. Chim. Acta* **50** (1967) 137.
12. Bowden, K., Crank, G. and Ross, W. J. *J. Chem. Soc.* **C 1968** 172.
13. Jacquier, R., Petrus, C., Petrus, F. and Verducci, J. *Bull. Soc. Chim. France* **1970** 2690.
14. Kuehne, M. E. In Cook, A. G., Ed., *Enamines: Synthesis, Structure, and Reactions*, Marcel Dekker, New York 1969, p. 343.
15. Saegusa, T., Murase, I. and Ito, Y. *Synth. Commun.* **1** (1971) 145.
16. DeSarlo, F. and Dini, G. *J. Heterocycl. Chem.* **4** (1967) 533.
17. Quin, L. D. and Pinion, D. O. *J. Org. Chem.* **35** (1970) 3130.
18. Tinker, J. F. and Whatmough, T. E. *J. Am. Chem. Soc.* **74** (1952) 5235.
19. Hanley, J. R., Kiliam, H. S., Lanyon, R. D. and McKenzie, S. *J. Org. Chem.* **23** (1958) 1461.
20. DeSarlo, F. *Tetrahedron* **23** (1967) 831.
21. Snyder, H. R., Brooks, L. A. and Shapiro, S. H. *Org. Syn. Coll. Vol.* **2** (1943) 531.
22. Katritzky, A. R., Øksne, S. and Boulton, A. J. *Tetrahedron* **18** (1962) 777.
23. Jacob, T. M., Vatakencherry, P. A. and Dev, S. *Tetrahedron* **20** (1964) 2815.

Received March 7, 1973.

ACTA CHEMICA SCANDINAVICA 27 (1973) 2813–2826

Structural Studies on the Rare Earth Carboxylates

18. The Crystal and Molecular Structure of Hexa-aquo Tris-malonato Di-neodymium(III)

EVA HANSSON

Physical Chemistry 1, Chemical Center, University of Lund, P.O. Box 740, S-220 07 Lund 7, Sweden

The crystal and molecular structure of $Nd_2(C_3H_2O_4)_3.6H_2O$ has been determined from three-dimensional, photographic, X-ray intensity data. Four formula units crystallize in a monoclinic unit cell with the dimensions $a = 11.210(2)$ Å, $b = 12.383(2)$ Å, $c = 13.696(3)$ Å, and $\beta = 93.01(2)°$. The space group is $I2/a$. The neodymium malonate hexahydrate is metastable and passes into the corresponding octahydrate when stored in the mother liquor. The structure is a three-dimensional neodymium-malonate network and is closely related to that of the octahydrate. The neodymium ion is coordinated by six carboxylate and three water oxygens forming a distorted monocapped square antiprism. The Nd–O bond distances are in the range 2.35–2.61 Å. One of the two independent malonate ions has strict twofold symmetry. The two oxygens of its carboxylate group are bonded to the same neodymium ion and one of them is also bonded to an adjacent neodymium ion. The other malonate ion forms a six-membered chelate ring with neodymium and also connects the neodymium ion with an adjacent one by a bridge of the type Nd–OCO–Nd. The chelate ring has a boat conformation and both malonate ions are nonplanar. The water molecules form hydrogen bonds with O–O distances in the range 2.74–2.85 Å.

This work is part of a systematic study of the structures of the lanthanoid malonate compounds $M_2mal_3 . nH_2O$ (M = lanthanoid, mal = $OOCCH_2COO^{2-}$, and $n = 6$ or 8) undertaken to get some information of the conformation of the malonate ions and the arrangement of the ligand atoms around the central ion in lanthanoid malonate complexes.

The structure of the compound $Nd_2mal_3.8H_2O$ (NDO) has been reported previously.[1] This paper deals with the structure of the compound $Nd_2mal_3.6H_2O$ (NDH) which is metastable relative to NDO at room temperature. The unit cell dimensions of NDH and NDO are closely related (see below) indicating that the two structures may be similar. With different numbers

of crystal water the hydrogen bond systems must, however, be different in the two compounds.

In NDO, one malonate ion forms a six-membered chelate ring with neodymium. Since very little is known about the preferred conformation of chelated malonate rings,[2] it was regarded with special interest. One of its non-chelating oxygens is bonded to an adjacent neodymium and the other oxygens are hydrogen bonded to water molecules. It must be assumed that this bonding plays an important part in determining the precise conformation of the ring, and it is then of interest to study the neodymium malonate chelate ring in a different hydrogen bond situation.

EXPERIMENTAL

The method of preparation and the habit of the crystals of NDH have been described in Ref. 1.

A crystal of the dimensions $0.10 \times 0.09 \times 0.20$ mm^3 mounted along the 0.20 mm edge was used in recording the layers $hk0-hk15$. 1869 measurable reflexions were recorded with the integrated multiple-film Weissenberg technique using Zr-filtered Mo$K\alpha$-radiation. 1520 of these reflexions were within the Cu-sphere representing 60 % of the possible number. The intensities were measured visually by comparison with a calibrated scale. The data were corrected for Lorentz, polarisation, and absorption effects. The linear absorption coefficient is 55 cm^{-1} and the transmission factors evaluated by numerical integration were in the range $0.58-0.62$.

UNIT CELL AND SPACE GROUP

The crystals of NDH are monoclinic. The unit cell is C-centered with $a=18.15$ Å, $b=12.38$ Å, $c=11.21$ Å, and $\beta=131.1°$. $Z=4$. The alternative choice of axis along [001], [010], and [$\bar{1}0\bar{1}$] results in a bodycentered cell with $a=11.210(2)$ Å, $b=12.383(2)$ Å, $c=13.696(3)$ Å, and $\beta=93.01(2)°$. This cell is similar to that of NDO which is orthorhombic with $a=11.26$ Å, $b=12.60$ Å, and $c=14.69$ Å, and was chosen for the description in order to facilitate the comparison between the two structures. The accurate values of the cell parameters were determined from powder data by least squares refinement as described before.[3] Table 1 gives the experimental values of $\sin^2\theta$ together with those calculated in the last cycle of refinement.

The systematically absent reflexions are hkl: $h+k+l\neq 2n$ and $h0l$: $h\neq 2n$. The possible space groups are then Ia and $I2/a$. The concentration of peaks in the Patterson section $P(x0z)$ indicated the space group $I2/a$. The structure was accordingly assumed to be centrosymmetric and the subsequent refinements gave no reason for changing this assumption. The general position of the space group $I2/a$ is eightfold: $(0,0,0;1/2,1/2,1/2)\pm(x,y,z;\ \bar{x},y,1/2-z)$. The conventional space group corresponding to $I2/a$ is $C2/c$. The transformation of indices from the bodycentered to the C-centered cell is given by $(h,k,l)=(-1,0,-1/0,1,0/1,0,0)(h',k',l')$ where h',k',l' refer to the body centered cell.

Table 1. Powder data for $Nd_2(C_3H_2O_4)_3.6H_2O$. Observed and calculated values of $10^5\sin^2\theta$ are given together with the observed powder intensities.

h k l	obs	calc	I_{obs}	*h k l*	obs	calc	I_{obs}
0 1 1	704	705	vvw	2 2 4	8869	8856	vw
1 1 0	860	862	s	−1 3 4		8882	
0 0 2	1267	1271	vs	−3 1 4	9250	9250	w
0 2 0	1547	1550	s	−1 4 3	9421	9412	vw
−1 1 2	2050	2051	s	2 4 2	9529	9531	vvw
−1 2 1	2380	2383	s	1 2 5	10166	10170	w
−2 1 1	2516	2521	s	3 1 4	10242	10227	vvw
2 1 1	2683	2684	s	−3 4 1	10675	10665	w
0 1 3	3242	3247	vvw	4 1 3	11338	11323	w
2 0 2	3331	3331	w	−1 5 2		11352	
3 1 0	4648	4656	m	0 3 5	11426	11430	vw
2 2 2	4886	4881	vw	−4 0 4	12011	12020	w
1 2 3	5003	5006	m	−1 1 6	12069	12054	w
−1 3 2	5152	5152	vw	1 1 6	12545	12542	w
2 1 3	5379	5388	m	−2 0 6	12861	12845	w
−2 3 1	5618	5621	m	−3 2 5	13163	13150	w
−3 2 1	6006	6014	w	2 4 4	13495	13506	m
3 1 2	6168	6171	m	−5 2 1		13521	
0 3 3	6340	6347	w	5 1 2		13922	
−1 4 1	6954	6952	w	5 2 1	13935	13928	s
2 0 4	7293	7305	vw	0 6 0		13952	
0 4 2	7483	7472	m	3 5 0		13957	
3 3 0	7767	7756	vvw	4 3 3	14429	14423	w
−2 3 3	7998	8000	w	−3 5 2	14974	14984	w
−3 2 3	8309	8311	m	−1 5 4	15074	15083	m
4 1 1	8464	8456	m	0 6 2	15224	15223	vw
−4 0 2	8528	8533	vvw	3 5 2	15476	15472	w
−3 3 2	8764	8783	vvw	−5 2 3	15668	15655	vw

DETERMINATION AND REFINEMENT OF THE STRUCTURE

The structure of NDH was determined by the heavy atom method. A three-dimensional Patterson synthesis revealed the position of neodymium and the positions of the remaining 14 non-hydrogen atoms were obtained from the subsequent difference electron density calculation.

The preliminary atomic coordinates, isotropic temperature factors, and inter layer scale factors were improved by least squares refinement. The function minimized was $\sum w(|F_o|-|F_c|)^2$. The weights, w, were chosen according to Cruickshank [4] and only the reflexions with $0.80 \leq |F_o|/|F_c| \leq 1.25$ were included in the refinement. The atomic scattering factors for the neutral atoms were for carbon and oxygen taken from International Tables [5] and for neodymium from Cromer *et al.*[6]

The discrepancy indexes $R = \sum||F_o|-|F_c||/\sum|F_o|$ and $wR = [\sum w(|F_o|-|F_c|)^2/\sum w|F|_o^2]^{\frac{1}{2}}$ converged to 0.094 and 0.098, respectively. All the observed reflexions were included in the calculation of R. Further refinement, now with anisotropic thermal parameters for neodymium and an over all scale-

factor, resulted in $R = 0.084$ and $wR = 0.088$. In the last cycle of refinement the shifts of all parameters were less than 1 % of their estimated standard deviations.

The approximate constancy of the averages of $w(|F_o| - |F_c|)^2$ between different $|F_o|$ and sin θ intervals indicated that the weighting scheme used was reasonable. (Table 2).

Table 2. Analysis of the weighting scheme $w = 1/(10 + |F_o| + 0.01|F_o|^2)$. The averages $\overline{w\Delta^2}$, where $\Delta = |F_o| - |F_c|$, are normalized.

Interval F_o	Number of reflexions	$\overline{w\Delta^2}$	Interval sin θ	Number of reflexions	$\overline{w\Delta^2}$
0 – 62	155	1.00	0.00 – 0.28	328	1.10
62 – 71	172	0.91	0.28 – 0.35	303	0.98
71 – 78	166	1.11	0.35 – 0.40	269	0.99
78 – 85	168	0.99	0.40 – 0.44	209	0.98
85 – 94	170	1.05	0.44 – 0.48	191	0.93
94 – 106	175	1.05	0.48 – 0.51	166	0.83
106 – 121	179	1.12	0.51 – 0.53	105	1.02
121 – 142	179	1.03	0.53 – 0.56	80	1.25
142 – 177	182	0.74	0.56 – 0.58	37	1.11
177 – 446	184	1.00	0.58 – 0.60	24	0.81

Table 3. Atomic parameters with estimated standard deviations for the compound $Nd_2(H_2C_3O_4)_3.6H_2O$.

Atom	Group	$x \times 10^4$	$y \times 10^4$	$z \times 10^4$	B/Å^2
Nd		1537.1(5)	1020.4(5)	335.1(5)	(1.14)[a]
O(1)	COO^-	1404(10)	78(10)	1990(9)	2.5(2)
O(2)	COO^-	−3(7)	−405(8)	898(7)	1.3(1)
O(3)	COO^-	2354(9)	−812(8)	254(8)	1.8(1)
O(4)	COO^-	3384(11)	−2322(11)	499(10)	2.8(2)
O(5)	COO^-	3610(10)	1033(10)	891(8)	2.3(2)
O(6)	COO^-	5502(13)	656(13)	1215(11)	3.5(2)
O(7)	H_2O	−460(11)	1854(11)	674(9)	3.0(2)
O(8)	H_2O	1724(15)	2473(12)	1653(12)	4.2(3)
O(9)	H_2O	2574(10)	687(10)	−1249(9)	2.5(2)
C(1)		0	−1238(21)	1/4	2.9(4)
C(2)		494(11)	−484(12)	1743(10)	1.6(2)
C(3)		3180(12)	−1335(12)	625(11)	1.9(2)
C(4)		4134(13)	−792(13)	1302(12)	2.1(2)
C(5)		4458(10)	383(11)	1086(9)	1.4(2)

[a] The anisotropic thermal parameters for neodymium, calculated from the expression: exp $[-(h^2\beta_{11} + 2hk\beta_{12} + ...)]$ are $\beta_{11} = 0.00234(4)$, $\beta_{22} = 0.00148(3)$, $\beta_{33} = 0.00190(3)$, $\beta_{12} = -0.00004(4)$, $\beta_{13} = -0.00023(2)$, and $\beta_{23} = 0.00009(4)$, resulting in root mean square displacements along the principal axis of the thermal ellipsoid $R_1 = 0.141$ (Å), $R_2 = 0.107$ (Å), and $R_3 = 0.116$ (Å).

Table 4. Observed and calculated structure factors in $Nd_2(C_2H_2O_4)_3.6H_2O$. The 139 reflexions not obeying the condition $0.80 \leq |F_o|/|F_c| \leq 1.25$ are denoted by asterisks. In each group the running index l, $|F_o|$, and $|F_c|$ are given.

H= 0 K=-17		
-11	79	76
-9	90	111
-7	105	105
-5	112	111
H= 0 K=-14		
-16	87	84
-14	99	93
-12	95	61*
-4	89	89
-2	156	147
H= 0 K=-13		
-11	75	74
-9	93	108
-7	153	149
-5	130	139
-3	100	109
H= 0 K=-11		
-11	99	92
-9	123	115
-7	124	133
-5	134	131
-3	114	113
H= 0 K=-10		
-18	100	82
-16	112	104
-14	96	110
-12	117	127
-10	92	80
-6	69	59
-4	186	186
-2	252	222
0	231	220
H= 0 K= -9		
-9	61	55
-7	96	98
-5	143	150
-3	116	101
H= 0 K= -8		
-12	60	46*
-10	60	51
-4	126	124
-2	90	71*
0	92	85
H= 0 K= -7		
-19	82	75
-13	79	93
-11	102	121
-9	180	171
-7	222	233
-5	173	186
-3	150	167
-1	68	75
H= 0 K= -6		
-18	78	67
-16	95	99
-14	132	131
-12	116	125
-10	95	100
-6	92	93
-4	93	98
-2	248	280
0	351	389
H= 0 K= -5		
-5	66	58
-3	94	80
H= 0 K= -4		
-18	91	80
-16	109	104
-14	121	124
-12	116	129
-10	119	113
-4	217	210
-2	351	351
0	285	277
H= 0 K= -3		
-19	85	79
-13	73	56*
-11	160	165
-9	230	198
-7	241	240
-5	330	327
-3	232	217
H= 0 K= -2		
-14	75	65
-12	74	63
-10	47	44
-8	54	56
H= 0 K= -1		
-13	71	57
-11	91	85
-9	133	109
-7	171	167
-5	121	126
H= 0 K= 0		
-18	89	95
-16	140	127
-14	173	186
-12	163	179
-10	113	115
-8	58	60
-6	59	38*
-4	82	85
H= 1 K=-18		
-11	87	71
-9	92	78
H= 1 K=-16		
-9	80	76
-3	74	52*
H= 1 K=-15		
-8	98	96
-6	123	124
-4	120	148
0	117	89*
10	121	122
12	89	97
H= 1 K=-13		
-4	77	71
-2	82	82
8	64	56
10	94	69*
H= 1 K=-12		
-15	80	80
-13	107	115
-11	170	131
-9	127	131
-7	110	106
-3	86	78
-1	165	152
5	160	165
7	92	103
13	76	67
15	80	88
17	85	82
19	89	62*
H= 1 K=-11		
-10	67	59
-8	82	89
-6	119	131
-4	149	151
-2	145	146
0	87	93
6	94	88
8	119	118
10	137	134
12	120	128
14	76	67
H= 1 K=-10		
7	65	45*
H= 1 K= -9		
-18	82	75
-14	78	59*
-10	68	68
-8	141	155
-6	203	212
-4	218	233
-2	211	210
0	107	116
4	81	64*
6	133	116
8	129	120
10	172	156
12	146	148
14	72	74
H= 1 K= -8		
-15	94	88
-13	137	133
-11	142	151
-9	152	151
-7	109	101
-1	130	140
3	254	261
5	172	179
7	123	121
9	58	51
13	67	52*
15	94	101
17	93	99
19	90	76
H= 1 K= -7		
-6	76	83
-4	112	108
-2	53	51
2	44	54
6	64	56
8	109	99
H= 1 K= -6		
-15	76	78
-13	120	121
-11	130	134
-9	122	115
-7	63	71
-3	42	46
-1	167	131*
1	241	237
3	285	262
5	114	134
7	96	82
15	83	88
17	89	88
H= 1 K= -5		
-20	82	83
-18	83	90
-16	84	93
-14	60	56
-10	70	71
-8	226	221
-6	288	317
-4	410	442
-2	320	290
0	88	100
2	41	47
4	98	89
6	159	161
8	217	214
10	274	234
12	173	181
14	153	149
16	71	59
H= 1 K= -4		
-15	87	59*
-13	80	75
-11	135	122
-9	156	143
-7	118	129
-5	47	43
-3	169	165
-1	257	266
1	128	121
3	35	42
5	67	80
7	109	96
9	71	78
13	73	71
15	67	54
H= 1 K= -3		
-8	127	115
-6	75	68
-4	216	179
-2	163	153
2	39	37
4	88	97
6	68	69
8	55	61
10	116	104
12	58	60
H= 1 K= -2		
-17	78	72
-15	122	122
-13	151	137
-11	188	176
-9	204	193
-7	200	193
-5	114	104
-3	59	66
1	154	270*
3	276	304
5	284	281
7	253	241
9	123	112
13	133	130
15	123	128
17	120	115
19	92	85
H= 1 K= -1		
-20	87	71
-18	96	100
-16	81	84
-14	62	44*
-12	56	56
-10	94	77
-8	128	105
-6	358	363
-4	446	425
6	251	241
8	292	277
10	162	180
12	143	142
14	127	110
16	74	58*
H= 2 K=-17		
-5	83	103
H= 2 K=-16		
-10	86	75
-8	90	83
-6	81	68
H= 2 K=-14		
-12	99	75*
-10	123	117
-8	144	135
-6	125	98*
8	151	130
10	104	62*
H= 2 K=-13		
-15	87	82
-13	90	84
-7	72	66
-5	138	130
-3	132	152
-1	162	160
9	98	85
11	102	104
13	108	94
15	87	79
H= 2 K=-11		
-5	135	134
-3	162	168
-1	152	145
9	90	89
11	95	104
11	113	104
H= 2 K=-10		
-14	85	65*
-12	103	112
-10	158	155
-8	163	177
-6	176	186
-4	120	112
0	106	106
4	217	200
6	213	224
8	157	171
10	134	138
H= 2 K= -9		
-13	87	72
-7	71	70
-5	80	74
-3	77	87
-1	69	70
3	65	78
11	81	73
H= 2 K= -8		
-10	82	74
-8	130	119
-6	107	97
0	105	92
2	95	91
6	108	86*
8	59	40*
10	69	49*
H= 2 K= -7		
-19	86	64*
-17	96	88
-15	124	131
-13	116	127
-11	82	83
-7	101	93
-5	174	195
-3	270	262
-1	312	332
3	157	150
5	66	62
9	173	170
11	177	174
13	148	148
15	117	112
17	81	61*
H= 2 K= -6		
-14	71	76
-12	109	110
-10	156	161
-8	177	206
-6	125	140
-4	85	88
-2	56	49
0	160	159
2	189	210
4	219	220
6	188	195
8	173	183
10	111	88*
16	86	66*
18	82	63*
20	88	59*
H= 2 K= -5		
-9	55	63
-3	48	49
3	38	28*
9	55	55
H= 2 K= -4		
-14	74	68
-12	117	124
-10	211	193
-8	267	236
-6	211	217
-4	187	205
-2	130	117
0	119	136
2	231	194
4	309	296
6	234	224
8	209	218
10	163	166
16	81	81
18	80	80
20	86	74
H= 2 K= -3		
-19	97	97
-17	107	113
-15	99	101
-13	100	119
-11	129	140
-7	144	141
-5	305	281
-3	285	299
1	303	277
3	244	228
7	60	51
9	81	75
11	162	165
13	170	180
15	109	112
17	83	74
H= 2 K= -2		
-12	78	64
-10	70	77
-8	67	69
-6	146	143
2	122	127
4	207	188
6	199	181
8	81	77
H= 2 K= -1		
-19	81	55*
-17	81	70
-15	81	75
-13	74	67
-11	87	88
-9	50	38*
-7	97	91
-5	146	131
3	206	206
5	141	122
9	123	117
11	116	136
13	123	141
15	90	87
H= 2 K= 0		
-20	77	54*
-14	78	88
-12	217	227
-10	287	276
-8	300	313
-6	206	182
-4	111	116
4	233	232
6	408	420
8	257	283
10	119	134
16	72	77
18	102	99
20	101	94
H= 3 K=-19		
-2	81	75
0	88	97
4	98	84
H= 3 K=-18		
-7	81	84
-5	87	73
-3	79	75
5	80	77
7	82	76
9	84	69
11	86	68*
H= 3 K=-16		
-9	78	80
-7	83	94
-5	74	76
5	96	88
7	76	84
9	79	74
11	82	69
H= 3 K=-15		
-14	99	88
-12	95	98
-10	92	83
-2	116	110
0	128	136
2	147	150
4	131	133
6	72	77
H= 3 K=-14		
-5	68	74
7	71	67
H= 3 K=-13		
-12	89	80
-10	78	57*
-2	74	70
2	81	87
4	83	76
6	67	51*
H= 3 K=-12		
-11	77	83
-9	136	141
-7	170	174
-5	157	153
-3	78	97
-1	84	87
3	66	66
5	122	130
7	138	148
9	144	143
11	132	128
13	75	81
H= 3 K=-11		
-14	81	76
-12	70	77
-10	93	81
-4	82	90
-2	125	132
0	189	185
4	114	124
6	66	63
12	77	71
14	82	84
H= 3 K=-10		
-1	53	61
3	77	68
5	94	88
H= 3 K= -9		
-16	98	93
-14	99	110
-12	110	114
-10	86	91
-8	62	66
-4	80	83
-2	132	150
0	200	212
2	181	190
4	216	185
6	144	133
12	86	85
14	100	99
16	76	89
H= 3 K= -8		
-11	79	96
-9	149	167
-7	219	217
-5	219	239
-3	132	182*
-1	95	84
5	133	138
7	208	220
9	238	226
11	132	125
H= 3 K= -7		
0	43	45
2	89	89
H= 3 K= -6		
-9	145	128
-7	167	176
-5	163	177
-3	91	79
-1	101	85
1	97	91
3	42	43
5	147	164
7	155	171
9	202	180
11	109	93
H= 3 K= -5		
-18	75	64
-16	107	115
-14	131	146
-12	149	153
-10	153	157
-8	62	66
-6	56	58
-4	141	129
-2	265	282
0	308	306
2	346	398
4	284	279
6	122	117
10	91	95
12	145	144
14	133	146
16	132	127
H= 3 K= -4		
-11	86	83
-9	100	75*
-7	82	67
-5	170	167
-3	323	281
-1	154	152
1	42	36
5	61	73
7	156	162
9	127	125
11	94	85
H= 3 K= -3		
-14	62	71
-10	60	60
-6	56	46
-2	174	155
2	76	59*
4	92	79
6	68	41
8	46	44
H= 3 K= -2		
-21	81	68
-19	82	74
-17	83	88
-15	64	72
-11	117	129
-9	227	211
-7	234	244
-5	325	345
3	45	49
5	197	185
7	252	284
9	212	254
11	148	158
13	92	95
H= 3 K= -1		
-18	72	53*
-16	94	81
-14	124	121
-12	209	199
-10	130	117
-6	164	144
-4	257	226
4	223	211
6	177	153
10	50	49
12	155	139
14	131	138
H= 4 K=-17		
1	110	104
3	101	122
5	113	115
7	106	92
H= 4 K=-16		
-4	90	87
-2	89	90
H= 4 K=-14		
-6	120	115
-4	152	150
-2	157	154
0	96	110
8	89	78
10	109	108
12	96	98
H= 4 K=-13		
-13	94	89
-11	106	113
-9	93	99
-7	98	90
-1	83	73
1	142	126
3	151	148
5	135	147
7	118	121
9	87	64*
H= 4 K=-11		
-13	88	84
-11	99	99
-9	94	72*
-7	69	71
-1	82	76
1	139	136
3	131	136
5	123	127
7	90	96
9	80	54*
H= 4 K=-10		
-16	94	88
-14	88	79
-8	113	108
-6	176	169
-4	185	188
-2	195	214
0	185	204
2	78	76
6	109	115
8	115	144*
10	102	124
12	141	127
14	90	97
H= 4 K= -9		
-11	77	86
-9	102	102
-7	96	89
3	145	147
5	127	126
7	82	82
9	67	64
H= 4 K= -8		
-6	63	59
-2	118	114
0	162	163
2	69	67
8	88	83
12	79	83
H= 4 K= -7		
-13	111	132
-11	174	182
-9	215	205
-7	130	140
-5	58	69
-1	117	116
1	229	201
3	269	264
5	262	265
7	197	189
9	96	96
17	93	96
H= 4 K= -6		
-16	87	76
-14	76	51*
-8	114	106
-6	119	120
-4	163	161
-2	222	213
0	153	150
2	131	120
6	106	93
8	179	165
10	139	166
12	116	112
14	98	97
H= 4 K= -5		
-5	51	51
-3	46	63*
-1	41	48
H= 4 K= -4		
-16	100	102
-14	77	76
-8	149	143
-6	159	166
-4	215	222
-2	192	257*
0	184	180
2	202	183
4	78	66
6	131	143
8	147	163
10	164	171
12	112	131
14	79	105*
16	86	71
H= 4 K= -3		
-15	79	100*
-13	147	160
-11	139	177*
-9	196	198
-7	190	191
-5	141	132
-3	50	37*
3	278	406*
5	386	359
7	160	183
9	117	108
17	88	94
H= 4 K= -2		
-6	94	98
-4	177	172
10	89	82
12	76	67
H= 4 K= -1		
-13	92	109
-11	118	134
-9	179	193
-7	152	140
5	177	182
7	95	84
H= 4 K= 0		
-20	96	66*
-18	115	103
-16	97	101
-14	88	77
-10	85	56*
-8	98	94
-6	240	262
-4	327	321
4	55	50
6	95	92
8	223	247
10	207	230
12	217	210
H= 5 K=-18		
-3	84	73
-1	84	92
1	84	91
3	85	76
H= 5 K=-16		
-3	92	72*
-1	100	94
1	92	88
3	72	66
H= 5 K=-15		
-8	112	127
-6	119	133
-4	116	102
2	74	67
4	107	110

Table 4. Continued.

Table 4. Continued.

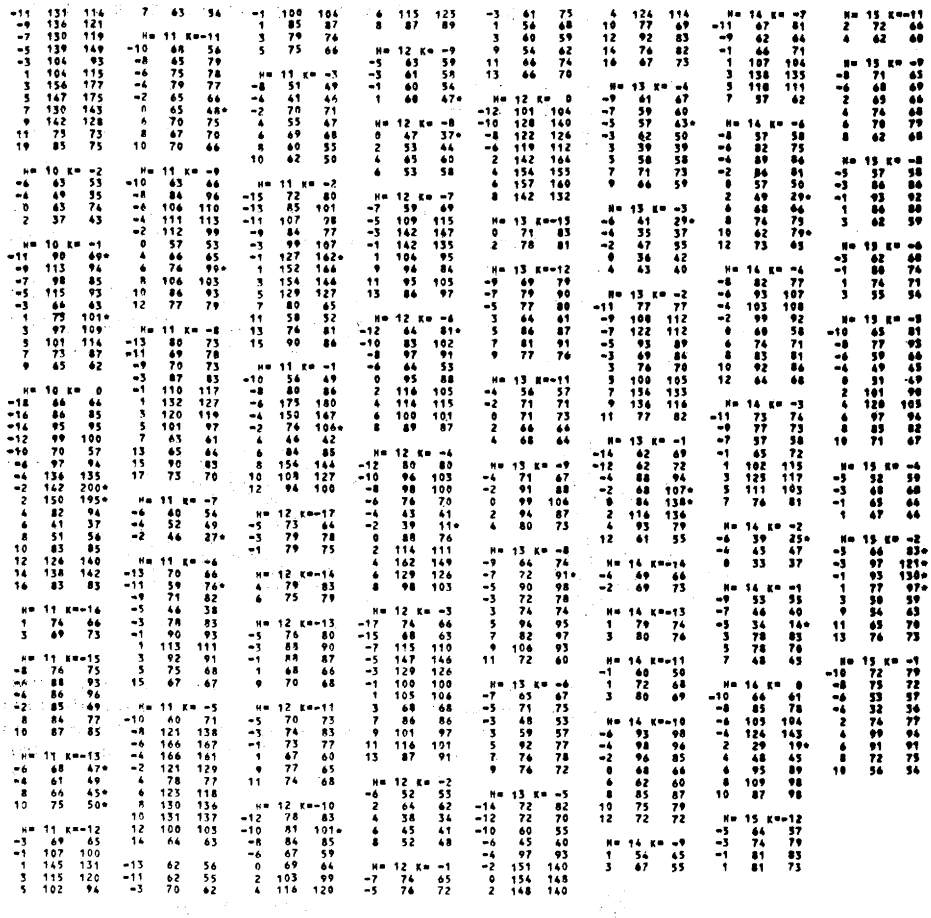

The final atomic parameters are given in Table 3 and the observed structure factors are compared with those calculated in the last cycle of refinement in Table 4. The electron density maps of a difference synthesis based on the parameters in Table 3 showed only spurious peaks, all less than 2 e/Å^3.

All computations were performed on the UNIVAC 1108 computer at Lund, Sweden, using the programmes DRF, LALS, DISTAN, PLANE, CELSIUS, and ORTEP.[7]

DESCRIPTION OF THE STRUCTURE

The structures of NDH and NDO are closely related. In the following description the structure of NDH is mainly compared to that of NDO which

was reported in Ref. 1. References to other related structures were given in that paper. The notation of the atoms is the same as that used in Ref. 1, and the superscripts $(i)-(x)$ indicate the following equivalent positions of the structure,

	x,y,z	(iv)	$1/2+x,1/2-y,z$	(viii)	$x,\bar{y},z-1/2$
(i)	$\bar{x},\bar{y},\bar{z}$	(v)	$x-1/2,1/2-y,z$	(ix)	$x,\bar{y},1/2+z$
(ii)	$\bar{x},y,1/2-z$	(vi)	$1/2-x,1/2+y,\bar{z}$	(x)	$1/2-x,y-1/2,\bar{z}$
(iii)	$1-x,\bar{y},\bar{z}$	(vii)	$1/2-x,1/2-y,1/2-z$		

where x,y,z are the atomic coordinates given in Table 3. The numbering of the atoms constituting the two independent malonate ions, referred to as ligand 1 and ligand 2, is given in Fig. 4.

The general features of the structure are shown in Figs. 1 and 2. The neodymium ions are held together in pairs by oxygen bridges formed by the carboxylate oxygen O(2) of ligand 1 (Fig. 1). These pairs are situated at

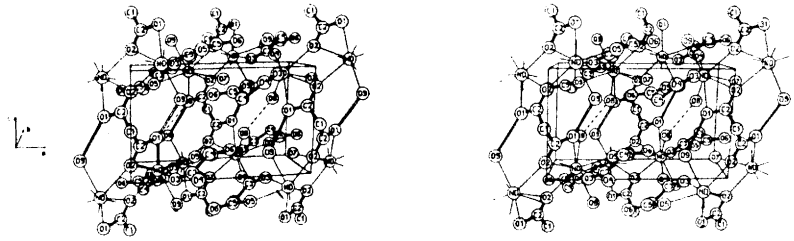

Fig. 1. A stereoscopic pair of drawings showing part of two adjacent neodymium malonate networks and the bonding between them. Bonds within the malonate ions are filled, hydrogen bonds are open and Nd–O bonds are single lines. The broken line indicates the possible hydrogen bond distance $O(8)-O(8^{vii})$. The intra-network hydrogen bonds are omitted for clarity. The box outlined is $0\leq x\leq 1$, $0\leq y\leq 1/2$, $0\leq z\leq 1/2$.

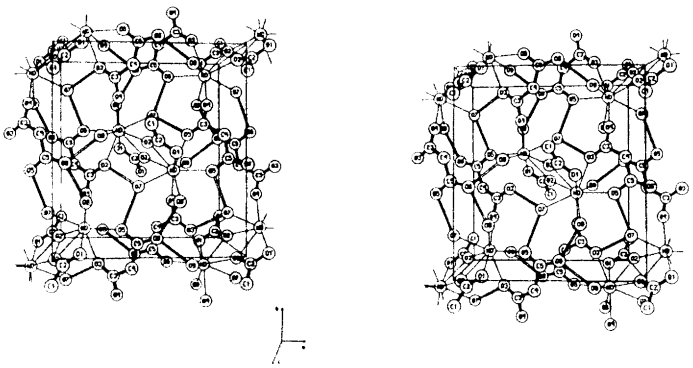

Fig. 2. A stereoscopic pair of drawings illustrating the neodymium malonate network around $z=0$. The bonds are indicated in the same way as in Fig. 1. The box outlined is $0\leq x\leq 1$, $0\leq y\leq 1$, $-1/4\leq z\leq 1/4$.

the levels $z=0$ and $z=1/2$. The methylene carbon of ligand 1, C(1), is situated on the twofold axis $x=0$, $z=1/4$ and ligand 1 thus connects the neodymium pairs in the z-direction.

Within the same z-level, each neodymium pair is bonded to four adjacent pairs by bridges of the type Nd – OCO – Nd, formed by ligand 2 (Fig. 2). In this way infinite neodymium-malonate networks parallel with (001) are formed.

The structure of NDO contains corresponding neodymium pairs bonded to each other in a similar manner, but while adjacent pairs at the same z-level are related by the a-glide in NDH, they are related by the b-glide in NDO.

The three water molecules are all coordinated to neodymium. They form hydrogen bonds to the oxygens of ligand 2 within the neodymium malonate network (Fig. 2) and one of them, O(9), is also hydrogen bonded to a carboxylate oxygen, O(1), of an adjacent network (Fig. 1). The intra-network hydrogen bonds are arranged in almost the same way as found in NDO, but corresponding distances between hydrogen bonded oxygens are about 0.1 Å longer in NDH than in NDO. The inter-network hydrogen bonds, which in NDH are formed directly between a water molecule of one network and a carboxylate oxygen of an adjacent one, are in NDO formed *via* a water molecule located between the networks. This is the essential difference between the two hydrogen bond systems, and results in a decrease in the distance between adjacent networks as indicated by the change in length of the c-axis from 14.69 Å in NDO to 13.69 Å in NDH.

The coordination polyhedron. Fig. 3 shows the coordination around the pair of neodymium ions. There are nine oxygens coordinated to each neo-

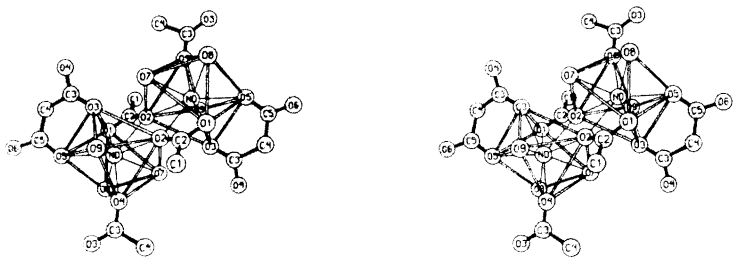

Fig. 3. A stereoscopic pair of drawings showing the coordination polyhedra around the neodymium ions Nd and Nd^{i}. Nd – O bonds are single lines, the bonds within the malonate ions are filled and the edges of the square antiprism are open.

dymium, six carboxylate oxygens from four malonate ions and three water oxygens. The coordination polyhedron is an intermediate between a monocapped square antiprism (CSAP) and a tricapped trigonal prism (TCTP). The "square" faces of the CSAP are O(1) – O(7) – O(2^{i}) – O(3) and O(4^{vi}) – O(9) – O(5) – O(8) and the TCTP has the triangular faces O(1) – O(3) – O(5) and O(2^{i}) – O(7) – O(4^{vi}). There is a close relationship between the idealized forms

of TCTP and CSAP [8] and with the rather irregular polyhedron dealt with here, the choice of description seems to be a matter of semantics. The CSAP model is chosen in order to facilitate a comparison with the distorted CSAP formed around neodymium in NDO. The dimensions of the coordination polyhedron are given in Table 5 A.

The average Nd – O bond distance is 2.50 Å; the same value as found in NDO. Two of the distances deviate considerably from this average, *viz.* Nd – O(4^{vi}): 2.35 Å, and Nd – O(2): 2.61 Å, while the others are in the range 2.41 – 2.56 Å. The bond Nd – O(2) is part of the oxygen bridge Nd···O(2)···Nd^{i}. The distance O(2) – Nd^{i} is 2.47 Å and Nd···Nd^{i} is 4.33 Å. This bridge is less asymmetric in NDH than in NDO where the corresponding distances are 2.72 Å, 2.46 Å, and 4.42 Å. The distance Nd···Nd^{i} is the shortest Nd···Nd distance of the structure. The next shortest one, 6.58 Å, is between the neodymium ions Nd and Nd^{vi} coupled by the bridging carboxylate group O(3)C(3)O(4).

The average "contact" distance between coordinated oxygens not belonging to the same malonate ion is 2.96 Å as compared to 3.00 Å in NDO. Two of these distances are shorter than 2.8 Å, *viz.* O(2)···O(2^{i}): 2.66 Å and O(3)···O(9): 2.79 Å.

The coordination around Nd is very similar in NDH and NDO (see Fig. 3 in Ref. 1 and Fig. 3). Apart from the fact that the oxygens O(8) and O(4^{vi}) change places between the two structures there are only minor rearrangements. The coordination polyhedron in NDO is best described as a distorted CSAP. The slight distortions that occur in going from NDO to NDH bring the polyhedron closer to the TCTP model. This change of the polyhedron may be described as follows: The quadrangle O(1) – O(7) – O(2^{i}) – O(3) is equilateral within 0.1 Å in NDO. In NDH it is approximately rectangular with the edges 3.48 Å, 2.87 Å, 3.36 Å, and 2.85 Å. In both structures the four atoms are coplanar within 0.2 Å. The other quadrangle, formed by the oxygens O(4^{vi}), O(9), O(5), and O(8) is equilateral within 0.1 Å in both structures. The four atoms are coplanar within 0.1 Å in NDO. In NDH they deviate ±0.3 Å from the least squares plane through them, in the directions expected in a TCTP. Further, the bond distance between neodymium and the capping oxygen O(2) is in NDO 2.72 Å, *i.e.* considerably longer than the other Nd – O bond distances. This feature is less pronounced in NDH where the distance Nd – O(2) is 2.61 Å.

Ligand 2 forms a six-membered chelate ring with neodymium. The ring has a boat conformation. The atoms O(3), C(3), C(5), and O(5) are coplanar within 0.06 Å and the atoms Nd and C(4) are situated 0.32 and 0.44 Å at the same side of the plane (Table 6). The corresponding values in NDO are 0.42 and 0.50 Å, and hence the changes in its crystallographic surroundings result in a flattening of the ring in going from NDO to NDH.

The malonate ions. The dimensions of the two independent malonate ions are given in Table 5 and are also indicated in Fig. 4. The bond distances and angles are in agreement with those found in NDO, with two exceptions, *viz.* the angle C(2) – C(1) – C(2^{ii}) which is 104° in NDH and 113° in NDO and the angle C(4) – C(3) – O(4) which is 112° in NDH and 120° in NDO.

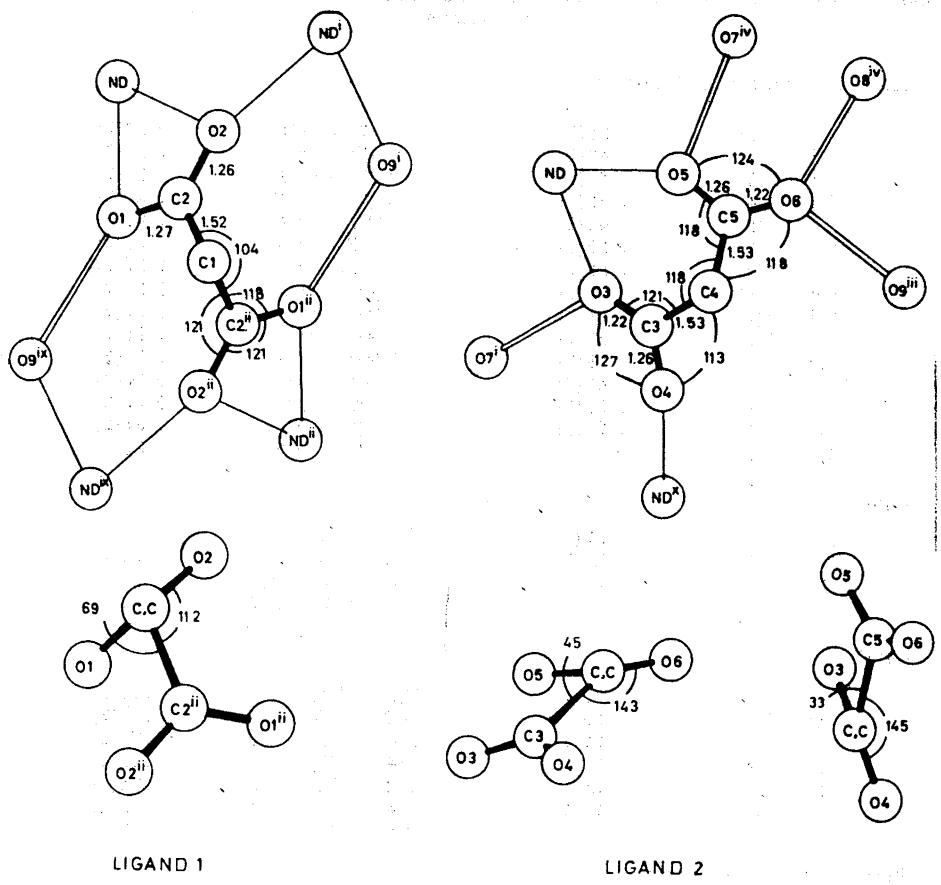

Fig. 4. The two malonate ions and their immediate surroundings, together with projections of each malonate ion along its C–C bonds. The angles indicated in these projections are the dihedral angles C–C–C–O.

The three independent C–COO groups are planar (Table 6). The methylene carbon C(1) of ligand 1 is situated on a twofold axis and the dihedral angle C(2^{ii})–C(1)–C(2)–O(1) is 69°, which means that the two COO-groups are twisted through this angle in opposite directions out of the carbon chain plane. The resulting intramolecular separations between oxygens of different COO-groups are O(1)···O(2^{i}): 3.42 Å and O(1)···O(1^{ii}): 3.51 Å. In NDO the corresponding twist is 50° and the O–O distances are O(1)–O(2): 3.78 Å and O(1)–O(1^{ii}): 3.24 Å.

In ligand 2, the dihedral angles O(3)–C(3)–C(4)–C(5) and O(5)–C(5)–C(4)–C(3) are 33° and 45°, respectively, and the carboxylate groups are twisted in the same direction out of the plane of the three carbon atoms. The shortest intramolecular separation between oxygens of different car-

Table 5. Selected interatomic distances (Å) and angles (°) with their estimated standard deviations.

A. The coordination polyhedron			
Nd – O(1)	2.56(1)	$O(2^{i}) - O(4^{vi})$	3.37(2)
$Nd - O(2^{i})$	2.47(1)	$O(2^{i}) - O(7)$	2.87(2)
Nd – O(3)	2.45(1)	$O(2^{i}) - O(9)$	2.97(2)
$Nd - O(4^{vi})$	2.35(1)	$O(2^{i}) - O(2)$	2.66(2)
Nd – O(5)	2.41(1)	O(3) – O(5)	2.80(2)
Nd – O(7)	2.53(1)	O(3) – O(9)	2.79(2)
Nd – O(8)	2.55(2)	O(3) – O(2)	2.87(2)
Nd – O(9)	2.55(1)	$O(4^{vi}) - O(5)$	3.51(2)
Nd – O(2)	2.61(1)	$O(4^{vi}) - O(7)$	3.07(2)
O(1) – O(3)	2.88(2)	$O(4^{vi}) - O(8)$	2.96(2)
O(1) – O(5)	3.19(2)	$O(4^{vi}) - O(9)$	2.90(2)
O(1) – O(7)	3.47(2)	O(5) – O(8)	3.00(2)
O(1) – O(8)	3.03(2)	O(5) – O(9)	3.12(2)
O(1) – O(2)	2.20(1)	O(7) – O(8)	2.84(2)
$O(2^{i}) - O(3)$	3.36(1)	O(7) – O(2)	2.86(2)
B. Ligand 1			
C(1) – C(2)	1.52(2)	$C(2) - C(1) - C(2^{ii})$	104(2)
C(2) – O(1)	1.27(2)	O(1) – C(2) – O(2)	121(1)
C(2) – O(2)	1.26(2)	C(1) – C(2) – O(1)	118(1)
		C(1) – C(2) – O(2)	121(1)
C. Ligand 2			
C(4) – C(3)	1.53(2)	C(3) – C(4) – C(5)	118(1)
C(4) – C(5)	1.53(2)	O(3) – C(3) – O(4)	127(2)
C(3) – O(3)	1.22(2)	C(4) – C(3) – O(3)	121(1)
C(3) – O(4)	1.26(2)	C(4) – C(3) – O(4)	113(1)
C(5) – O(5)	1.26(2)	O(5) – C(5) – O(6)	124(1)
C(5) – O(6)	1.22(2)	C(4) – C(5) – O(5)	118(1)
		C(4) – C(5) – O(6)	118(1)
D. Possible hydrogen bonds			
$O(7) - O(3^{i})$	2.74(2)	$O(8) - O(8^{vii})$	2.83(2)
$O(7) - O(5^{v})$	2.84(2)	$O(9) - O(6^{iii})$	2.72(2)
$O(8) - O(6^{v})$	2.74(2)	$O(9) - O(1^{viii})$	2.85(2)

boxylate groups, the ligand bite O(3) – O(5), is 2.80 Å. This conformation is slightly different from that found for ligand 2 in NDO where the twists are 42° and 48° and the bite 2.83 Å.

The hydrogen bonds. The distances suitable for hydrogen bond formation, *i.e.* the distances $(H_2)O - O$ between oxygens not belonging to the same coordination polyhedron [9] shorter than 3.20 Å, are collected in Table 5. They are also indicated in Fig. 5 which illustrates a probable hydrogen bond scheme.

The water molecule O(7) forms two hydrogen bonds, each to a carboxylate oxygen within the neodymium-malonate network, *viz.* $O(7) \cdots O(3^{i})$ and $O(7) \cdots O(5^{v})$. The water molecule O(9) also forms two hydrogen bonds, one

Table 6. Deviations in Å from least squares-planes within the malonate ions and the coordination polyhedron. The atoms defining the plane are in each case given above the asterisk.

A. The malonate ions

Atom	Distance	Atom	Distance	Atom	Distance	Atom	Distance
C(1)	0.00	C(4)	0.00	C(4)	−0.01	C(3)	−0.06
C(2)	−0.00	C(3)	−0.01	C(5)	0.04	C(5)	0.06
O(1)	0.00	O(3)	0.00	O(5)	−0.01	O(3)	0.06
O(2)	0.00	O(4)	0.00	O(6)	−0.02	O(5)	−0.05
*		*		*		*	
Nd	−0.07	Nd	−0.14	Nd	0.36	Nd	−0.32
Nd^{i}	0.10	Nd^{x}	0.55			C(4)	−0.44

B. The coordination polyhedron

Atom	Distance	Atom	Distance
O(3)	−0.23	O(8)	0.31
O(1)	0.22	$O(4^{vi})$	−0.33
O(7)	−0.22	O(5)	−0.28
$O(2^{i})$	0.23	O(9)	0.30
*		*	
Nd	−1.16	Nd	1.30

to the carboxylate oxygen $O(6^{iii})$ within the neodymium malonate network and the other to the carboxylate oxygen $O(1^{viii})$ of an adjacent network.

The hydrogen bond situation of the water molecule O(8) is less evident. One of its hydrogen atoms is engaged in an intra-network hydrogen bond to the carboxylate oxygen $O(6^{v})$. The position of the second hydrogen atom

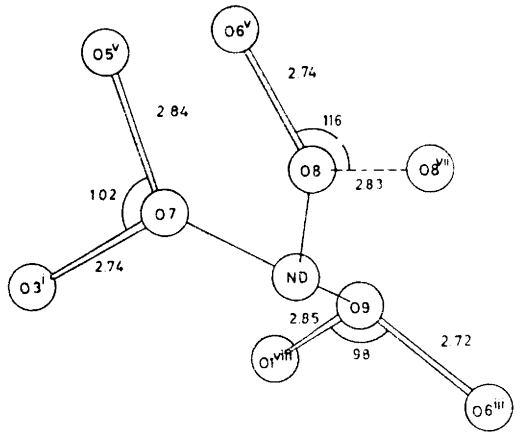

Fig. 5. The immediate surroundings of the three water molecules. Hydrogen bonds are open and Nd−O bonds are single lines. The possible bond $O(8)-O(8^{vii})$ is indicated by the broken line.

is more difficult to establish. The distance O(8)···O(8^{vii}) is 2.83 Å indicating a hydrogen bond. This interpretation implies a disordered structure in which the center of symmetry between O(8) and O(8^{vii}) is preserved by randomly assigning the shared hydrogen atom to one oxygen or the other. The next shortest O(8) – O distance outside the coordination polyhedron is O(8)···O(3^{vi}), 3.56 Å. If a hydrogen bond interaction O(8)···O(8^{vii}) exists, it constitutes an additional inter-network link.

Assuming a hydrogen bond O(8)···O(8^{vii}) each water oxygen is engaged in three bonds, one to neodymium and two hydrogen bonds. The sum of the three bond angles is 352° around O(7), 359° around O(8), and 341° around O(9). The O – O(W) – O donor angles are given in Fig. 5.

There are thus four intra-network hydrogen bonds in NDH, *viz.* O(7)··· O(3^{i}), O(7)···O(5^{v}), O(8)···O(6^{v}), and O(9)···O(6^{iii}). Corresponding hydrogen bonds are formed in NDO. In the latter structure they are about 0.1 Å shorter than in NDH except for the bond O(9)···O(6^{iii}) which is of equal length in the two structures. As mentioned earlier, the inter-network hydrogen bonds of NDO are formed *via* a water molecule situated between the networks. The insertion of this extra water molecule in the structure results in a hydrogen bond system where each of the water hydrogen atoms is engaged in a separate bond. These features probably contribute to making the lattice energy less for NDO than for NDH.

The hydrogen bond O(1^{ii})···O(9^{i}) is of some interest. It is seen in Fig. 4 that ligand 1 may be regarded as chelated to neodymium *via* this hydrogen bond to one of the coordinated water molecules. The existence of chelates of this type has been suggested for the lanthanoid glycolate complexes in solution. Both thermodynamic [10] and IR [11] data have been interpreted in this way. A thermodynamic study of the formation of lanthanoid malonate complexes in solution shows that the complexes formed are fairly weak for a chelate. Furthermore, the variation through the lanthanoid series in ΔH_j° and ΔS_j° deviates from that ordinarily found for lanthanoid chelates. This deviation might be explained if species with the malonate ion chelated *via* a water ligand of the metal ion are formed in increasing amounts through the series.[12] The existence of a corresponding chelate in the solid state supports this idea.

REFERENCES

1. Hansson, E. *Acta Chem. Scand.* **27** (1973) 2441.
2. Butler, K. R. and Snow, M. R. *J. Chem. Soc.* **D 1971** 550.
3. Hansson, E. *Acta Chem. Scand.* **27** (1973) 823.
4. Cruickshank, D. W. J. In Rollet, J. S. *Computing Methods in Crystallography*, Pergamon, Glasgow 1965, pp. 99 – 116.
5. *International Tables for X-Ray Crystallography*, Kynoch Press, Birmingham 1968, Vol. III.
6. Cromer, D. T., Larsson, A. C. and Waber, J. T. *Acta Cryst.* **17** (1964) 1044.
7. Liminga, R. *Acta Chem. Scand.* **21** (1967) 1206.
8. Muetterties, E. L. and Wright, C. M. *Quart. Revs.* **21** (1967) 109.
9. Baur, W. H. *Acta Cryst.* **B 28** (1972) 1456.
10. Grenthe, I. *Acta Chem. Scand.* **18** (1964) 283.
11. Larsson, R. *Acta Chem. Scand.* **19** (1965) 783.
12. Dellien, I. and Grenthe, I. *To be published.*

Received March 15, 1973.

ACTA CHEMICA SCANDINAVICA 27 (1973) 2827–2840

Structural Studies on the Rare Earth Carboxylates

19. The Crystal and Molecular Structure of Penta-aquo Tris-malonato Di-europium(III) Trihydrate

EVA HANSSON

Physical Chemistry 1, Chemical Center, University of Lund, P.O. Box 740, S-220 07 Lund 7, Sweden

The crystal structure of $Eu_2(C_3H_2O_4)_3.8H_2O$ has been determined from three-dimensional, photographic, X-ray intensity data. The crystals are orthorhombic, belong to the space group *Pnma*, and the cell parameters are $a = 12.220(5)$ Å, $b = 8.100(3)$ Å, and $c = 20.545(9)$ Å. $Z = 4$.

There are two non-equivalent europium ions and three non-equivalent malonate ions in the structure. They are linked to europium-malonate layers which are in turn held together by hydrogen bonds *via* water molecules between the layers.

One europium ion is coordinated by eight oxygens forming a distorted square antiprism and the other by nine oxygens forming a distorted tricapped trigonal prism. The average Eu – O bond distances are 2.42 Å and 2.51 Å, respectively.

The malonate ions possess mirror-symmetry, and the two carboxylate groups are in each ion twisted in the same direction out of the carbon chain plane. The twist angles are in the range 30 – 50°. The malonate ions form six-membered chelate rings with europium. Two of these rings have a boat conformation while the third ring adopts a chair conformation.

There are two different types of lanthanoid malonates of the composition $M_2mal_3.8H_2O$ (M = lanthanoid, mal = $OOC.CH_2COO^{2-}$); one with M = Ce – Gd and the other with M = Eu – Lu. The lighter lanthanoids also form a metastable hexahydrate, $M_2mal_3.6H_2O$.

The structure of the compounds $Nd_2mal_3.8H_2O$ and $Nd_2mal_3.6H_2O$ have been reported previously.[1,2] This paper deals with the structure of the heavier lanthanoid malonates represented by the europium compound $Eu_2mal_3.8H_2O$ (EUM).

The investigation of these structures was undertaken in order to study the coordination geometry around the lanthanoid ions and the conformation of the malonate ion in lanthanoid malonate complexes. The possible influence

of the lanthanoid contraction on the malonate ligands is also of interest. For the latter purpose it would have been more convenient to choose the isotypic compound formed by the smallest lanthanoid ion for the present study. However, the crystal quality which is poor for all the compounds becomes worse through the series and suitable single crystals could be prepared only of EUM.

The L_{II} absorption edge of europium lies just above $\lambda_{CuK\alpha}$ and hence the mass absorption coefficient of europium for Cu$K\alpha$-radiation is large and inaccurately known.[3] To avoid this disadvantage attempts were made to record the intensity material using Mo$K\alpha$-radiation. With the small crystals available the time of exposure needed was found to be at least 72 h per layer. During this long exposure the crystals disintegrated even when sealed in a glass capillary.

The possibility of using Cu$K\alpha$-radiation in spite of the large absorption was then considered. The influence of absorption errors in structure determinations has been studied by Werner [4] and by Srivastava *et al.*[5] Judging from their work the study of the small, needle shaped crystals of EUM using Cu$K\alpha$-radiation could be expected to give reliable information on the main features of the structure such as the coordination number of the europium ion, the type of coordination polyhedron formed around it, and the approximate conformation of the malonate ion. Since this information was considered valuable, it was decided to study the structure using Cu$K\alpha$-radiation.

EXPERIMENTAL

The method of preparation and the habit of the crystals of EUM were described in Ref. 1. They rapidly disintegrate when exposed to X-radiation and to prevent this they were sealed in Lindemann glass capillaries.

A crystal of the dimensions $0.16 \times 0.02 \times 0.04$ mm^3, mounted along the 0.16 mm edge, was used in recording the layers $h0l - h6l$ with the non-integrated Weissenberg, multi-film technique. Ni-filtered Cu-radiation was used.

The intensities of 692 independent reflexions were measured visually by comparison with a calibrated scale. Most of them, 650 reflexions, had $\sin\theta/\lambda \leq 0.5$. Thus 60 % of the possible reflexions within this limit were measured while only 20 % of the reflexions in the whole of the investigated region had measurable intensity. The data were corrected for Lorentz and polarisation effects.

An approximate value of the mass absorption coefficient of europium for Cu$K\alpha$-radiation is given in International Tables, Vol. III, 1st Ed. This value has been excluded in the 2nd Ed. since it was considered too unreliable. Nevertheless, it was used in an attempt to apply an approximate correction for absorption effects to the data (see below). The linear absorption coefficient of EUM used was 443 cm^{-1} and the transmission factors evaluated by numerical integration were then in the range $0.17 - 0.50$.

The powder photographs were taken at room temperature in a Guinier-Hägg focusing camera with Cu$K\alpha$-radiation ($\lambda = 1.54178$ Å). Lead nitrate (cubic $a = 7.857$ Å) was used as internal standard.

UNIT CELL AND SPACE GROUP

EUM crystallizes in the Laue class *mmm*. The systematically absent reflexions are $0kl$: $k+l \neq 2n$ and $hk0$: $h \neq 2n$. The possible space groups are then $Pna2_1$ and $Pnma$. The structure was assumed to be centrosymmetric

and the subsequent calculations did not contradict this assumption. Thus the space group is *Pnma* (No. 62).[6]

The unit cell dimensions were determined from powder data by least squares refinement as described before.[7] The observed powder pattern is given in Table 1 and the final cell parameters are $a = 12.220(5)$ Å, $b = 8.100(3)$ Å, and $c = 20.545(9)$ Å. $Z = 4$.

Table 1. Powder data for the compound $Eu_2(C_3H_2O_4)_3.8H_2O$. Observed and calculated values of $10^5\sin^2\theta$ are given together with the observed powder intensities.

h k l	obs	calc	I_{obs}	*h k l*	obs	calc	I_{obs}
1 0 1	537	539	s	2 1 5	6013	6018	vvw
0 0 2	560	563	s	4 0 0	6364	6368	vvw
1 0 2	960	961	vvw	4 0 1	6505	6509	w
1 1 1	1443	1445	vw	3 1 4	6751	6741	w
1 0 3	1665	1665	w	3 1 5	8017	8008	w
1 1 2	1866	1867	m	0 2 6	8697	8692	vvw
2 0 2	2148	2155	vvw	1 3 2	9115	9114	m
0 0 4	2240	2253	w	3 2 4	9465	9458	w
2 1 0	2498	2498	vvw	2 3 1	9899	9885	m
1 1 3	2567	2571	vvw	4 2 0	10018	9991	vw
2 1 1	2637	2639	s	2 2 6	10331	10284	vvw
2 1 2	3058	3061	vw	4 1 5	10817	10794	vvw
1 1 4	3547	3557	vvw	0 3 5	11691	11673	w
0 2 0	3640	3623	vvw	3 3 1	11847	11875	vvw
3 0 1	3713	3723	vvw	1 3 5	12046	12071	vvw
1 2 1	4177	4162	m	0 1 9	12282	12311	w
0 2 2		4187		0 2 8	12653	12635	vw
0 1 5	4431	4426	w	3 3 3	12995	13002	vw
1 2 2	4588	4585	m	1 2 8		13033	
3 0 3	4840	4849	m	2 3 5	13255	13265	vw
3 1 2	5054	5051	w	3 3 4	13954	13987	vvw
0 0 6		5069		0 4 0	14471	14494	w
1 2 3	5290	5289	m	5 2 3	14817	14841	vw
				4 2 6	15082	15060	vvw

DETERMINATION AND REFINEMENT OF THE STRUCTURE

The structure of EUM was determined by the heavy atom method. The three-dimensional Patterson synthesis showed the presence of two non-equivalent europium ions. They are situated in the mirror planes, *i.e.* in the positions 4*c*. From the first electron density difference synthesis it was possible to select the positions of the remaining non-hydrogen atoms except for half a water oxygen per asymmetric unit.

The deduced parameters were improved by full-matrix, least squares refinement. The discrepancy indexes $R = \sum||F_o| - |F_c||/\sum|F_o|$ and $wR = [\sum w(|F_o| - |F_c|)^2/\sum|F_o|^2]^{\frac{1}{2}}$ converged to 0.124 and 0.154, respectively. The electron density maps of the following difference synthesis showed a peak interpretable as a water oxygen at (0.02, 0.42, 0.50). Half an oxygen at this position was included in the following refinement of the atomic coordinates,

isotropic temperature factors and inter-layer scale factors, resulting in $R = 0.124$ and $wR = 0.152$.

At this stage the data were corrected for absorption using the approximate mass absorption coefficient of europium given in International Tables, Vol. III, 1st Ed. This treatment had the following effect: The values of R and wR decreased to 0.091 and 0.116, respectively, and the estimated standard deviations, σ, were reduced by about 25 %. The shifts in the positional parameters were less than σ except for $\Delta x_{O(5)}$ and $\Delta z_{O(6)}$ which were less than 2σ.

Table 2. Analysis of the weighting scheme $w = 1/(1.00 + |F_o| + 0.004|F_o|^2 + 0.00005|F_o|^3)$. The averages $\overline{w\Delta^2}$, where $\Delta = |F_o| - |F_c|$, are normalized.

Interval $\|F_o\|$	Number of reflexions	$\overline{w\Delta^2}$	Interval sin θ	Number of reflexions	$\overline{w\Delta^2}$
0 – 52	67	0.96	0.00 – 0.33	85	1.34
52 – 61	69	0.95	0.33 – 0.41	80	1.03
61 – 69	69	0.89	0.41 – 0.47	62	0.85
69 – 76	69	1.17	0.47 – 0.52	69	0.67
76 – 86	70	1.09	0.52 – 0.56	58	0.88
86 – 98	69	1.08	0.56 – 0.59	54	1.25
98 – 114	69	1.13	0.59 – 0.62	47	1.19
114 – 136	69	1.17	0.62 – 0.65	43	0.94
136 – 172	69	0.79	0.65 – 0.68	34	0.98
172 – 361	70	0.77	0.68 – 0.70	31	0.88

Table 3. Atomic parameters with estimated standard deviation for the compound $Eu_2(C_3H_2O_4)_3.8H_2O$.

Atom	Group	$x \times 10^4$	$y \times 10^4$	$z \times 10^4$	B/Å^2
Eu(1)		−5(2)	1/4	1598(1)	3.3(1)
Eu(2)		2218(2)	3/4	1970(1)	2.8(1)
O(1)	$-COO^-$	−1720(16)	5119(29)	3257(9)	2.5(4)
O(2)	$-COO^-$	−765(16)	4223(27)	2412(10)	3.3(4)
O(3)	$-COO^-$	−443(18)	4686(30)	838(10)	3.4(5)
O(4)	$-COO^-$	833(15)	5746(29)	1466(8)	1.8(4)
O(5)	$-COO^-$	1587(18)	5717(29)	2818(10)	3.7(5)
O(6)	$-COO^-$	1565(23)	4849(38)	3829(13)	5.7(6)
O(W1)	H_2O	1405(23)	1/4	2394(15)	3.3(6)
O(W2)	H_2O	1593(31)	1/4	843(17)	4.8(8)
O(W3)	H_2O	−1966(30)	1/4	1343(17)	4.5(8)
O(W4)	H_2O	2737(26)	3/4	841(15)	2.8(6)
O(W5)	H_2O	3656(28)	3/4	2821(15)	4.0(7)
O(W6)	H_2O	2742(24)	5080(39)	5004(15)	6.8(8)
O(W7)	H_2O	213(141)	4310(178)	4961(94)	19.1(4.6)
C(1)		−903(49)	1/4	3371(27)	4.9(1.3)
C(2)		−1115(23)	4108(43)	2989(15)	2.6(6)
C(3)		32(35)	3/4	663(20)	2.4(9)
C(4)		202(19)	5916(37)	998(12)	1.4(5)
C(5)		836(51)	3/4	3629(28)	5.3(1.4)
C(6)		1405(28)	5886(48)	3409(17)	3.7(7)

Table 4. Observed and calculated structure factors for the compound $Eu_2(C_2H_2O_4)_3.8H_2O$. In each group the running index h, $|F_o|$, and $|F_c|$ are given.

K= 0 L= 0
4 230 240
6 131 124
8 129 131
10 85 90
12 62 55
14 89 94

K= 0 L= 1
2 90 92
3 190 178
4 187 171
5 188 178
6 90 85
8 74 76
9 100 105
10 86 91
12 74 72
14 54 44

K= 0 L= 2
1 144 137
2 76 76
3 112 115
4 49 104
5 110 108
7 61 64
8 54 54
10 49 47
14 58 54

K= 0 L= 3
1 186 221
2 57 45
3 302 277
4 135 120
5 269 259
6 132 119
8 69 54
9 200 208
10 58 68
13 84 89

K= 0 L= 4
0 162 157
1 201 205
2 237 223
3 99 109
4 97 81
5 159 139
6 137 146
7 43 43
8 56 48
10 60 60
12 68 56

K= 0 L= 5
1 45 53
2 72 69
3 75 79
4 155 118
5 146 137
7 137 131
8 48 55
9 135 162
11 71 70
13 64 71

K= 0 L= 6
0 210 200
1 221 214
2 30 27
3 200 180
4 202 195
5 61 60
6 75 84
8 111 106
10 85 111
12 63 54
14 42 48

K= 0 L= 7
1 41 51
3 129 139
6 115 114
7 117 120
8 110 126
10 61 56
11 113 113
12 68 57

K= 0 L= 8
0 117 124
1 34 45
2 95 109
3 151 157
4 145 143
8 54 45

K= 0 L= 9
1 129 132
3 179 176
4 115 123
5 95 97
6 120 124
7 133 127
8 81 92
9 55 59
10 67 71
12 51 42
13 45 39

K= 0 L= 10
0 55 55
1 156 139
2 285 308
6 105 110
10 54 52
12 77 90

K= 0 L= 11
2 50 55
4 83 82
5 86 85
6 129 133
8 60 57
10 56 50
11 53 43

K= 0 L= 12
0 111 110
1 134 141
2 191 215
3 82 87
4 84 78
6 98 110
8 59 48
12 60 61

K= 0 L= 13
1 140 155
2 54 52
3 125 154
7 129 141
11 101 98

K= 0 L= 14
0 59 58
1 93 103
3 76 68
5 86 77

K= 0 L= 15
1 74 79
3 135 160
7 138 135
11 78 74

K= 0 L= 16
0 62 56
1 79 90
2 138 159
3 59 53
6 98 100
7 63 56
8 82 55

K= 0 L= 17
1 49 46
5 69 59
8 54 59

K= 0 L= 18
2 109 112
6 118 110

K= 0 L= 19
1 61 53
3 95 82
5 92 72
6 62 57
7 50 48
8 65 52
9 48 48

K= 0 L= 20
0 103 98
1 49 62
4 89 67

K= 0 L= 21
3 77 69
6 53 50
7 62 58

K= 0 L= 22
0 82 77
1 62 57
6 36 27
8 43 46

K= 0 L= 23
1 52 43
5 53 56

K= 0 L= 24
1 46 47
3 47 38

K= 0 L= 25
1 43 37

K= 1 L= 0
2 184 151
4 42 39
6 183 170
8 156 146
10 73 77
12 55 39

K= 1 L= 1
3 116 89
5 107 92
6 201 193
8 68 69
10 56 62
12 94 83

K= 1 L= 2
1 172 168
2 109 106
3 185 172
4 101 87
5 132 109
6 141 127
7 215 197
8 135 121
10 57 58
11 112 99
12 56 47
15 44 43

K= 1 L= 3
0 98 101
1 107 160
2 134 137
3 223 196
4 66 67
5 150 129

K= 1 L= 4
1 127 124
2 50 40
3 302 283
4 44 45
6 35 35
7 240 253
11 149 135

K= 1 L= 5
0 144 151
1 134 135
2 194 176
3 194 177
4 210 207
5 108 108
6 171 170
7 48 37
8 95 115
10 84 90

K= 1 L= 6
1 100 93
2 116 101
3 50 53
4 87 83
5 156 155
7 84 79
8 55 57
9 115 132

K= 1 L= 7
0 30 32
1 81 92
2 260 255
3 129 131
4 45 54
5 132 126
6 106 125
8 72 70
10 61 52
12 55 58

K= 1 L= 8
1 158 180
2 33 41
3 146 139
4 89 93
5 193 197
6 72 77
7 80 84
8 89 77
9 142 141
10 90 85
12 50 45

K= 1 L= 9
0 315 262
2 123 116
4 181 200
5 35 38
8 54 58

K= 1 L= 10
1 77 74
3 78 87
4 90 98
5 58 53
6 95 94
7 77 81
8 80 74
9 98 86

K= 1 L= 11
0 253 288
1 74 84
3 62 62
4 196 200
6 58 65
8 92 90
10 70 66

K= 1 L= 12
1 88 98
2 51 43
4 78 89
5 120 127
6 56 63
8 59 60
9 99 89

K= 1 L= 13
0 125 134
1 117 128
3 92 98
4 53 55

K= 1 L= 14
1 153 151
5 151 171
9 124 128

K= 1 L= 15
0 56 60
1 97 115
2 39 39
3 82 94
4 81 90
6 48 45

K= 1 L= 16
1 56 55
5 65 62
9 73 66

K= 1 L= 17
0 121 137
1 52 56
4 139 161
8 80 58
10 49 54

K= 1 L= 18
3 65 67
6 58 55
7 67 61
8 63 61

K= 1 L= 19
0 85 87
2 61 55
6 68 76

K= 1 L= 20
3 61 68
3 56 68
5 63 65

K= 1 L= 21
6 51 45

K= 2 L= 0
4 361 330
6 70 64
8 158 173
10 118 125

K= 2 L= 1
1 100 124
2 82 57
3 49 114
4 94 81
5 176 150
6 153 138
7 101 103
8 99 106
9 67 65
10 62 71

K= 2 L= 2
0 217 264
1 148 155
2 81 69
3 110 103
4 224 222
5 73 57
8 80 84
10 52 41

K= 2 L= 3
1 226 253
2 70 67
3 76 46
4 98 86
5 357 334
6 73 67
7 52 55
8 89 95
9 155 167
10 49 48

K= 2 L= 4
0 98 93
1 95 106
2 107 117
3 166 172
4 159 140
5 97 93
6 67 59
7 73 68
8 64 55
10 65 67

K= 2 L= 5
1 154 157
2 85 62
3 28 23
4 77 61
5 170 158
7 72 70
9 96 116

K= 2 L= 6
0 214 179
1 168 165
2 236 208
3 132 129
4 235 213
5 127 124
6 82 71
8 88 83
10 76 80

K= 2 L= 7
1 73 79
2 50 51
3 221 221
4 150 146
5 52 58
6 83 85
7 188 148
8 71 57
10 61 51
10 73 51
11 121 81

K= 2 L= 8
0 228 216
1 180 160
2 110 111
3 46 50
4 161 154
6 64 54

K= 2 L= 9
1 117 127
2 85 92
3 176 176
4 86 93
5 128 140
6 124 118
7 93 91
8 82 78
9 71 66
10 78 62
11 65 70

K= 2 L= 10
2 235 247
5 80 66
6 141 165
8 67 67

K= 2 L= 11
4 54 45
6 74 78
8 106 109

K= 2 L= 12
1 89 94
2 162 172
3 74 78
5 64 65
6 110 122
8 91 78

K= 2 L= 13
1 55 57
2 43 38
3 128 149
7 178 184

K= 2 L= 14
1 87 87
3 96 107

K= 2 L= 15
1 53 55
3 86 93
7 131 125

K= 2 L= 16
1 66 77
2 110 111
3 75 86
6 82 76

K= 2 L= 17
2 50 51

K= 2 L= 18
2 142 161

K= 2 L= 19
1 76 71
3 71 70
5 58 44

K= 2 L= 20
0 75 76
4 56 56

K= 2 L= 21
1 60 67
3 58 46

K= 2 L= 22
0 72 79
4 73 71

K= 2 L= 23
5 45 52

K= 2 L= 24
1 48 55

K= 3 L= 0
2 134 114
4 163 150
6 186 150
8 111 124
10 66 75

K= 3 L= 1
1 54 60
2 261 279
3 155 126
6 211 233
8 85 67
12 87 91

K= 3 L= 2
1 158 183
2 77 63
3 189 201
4 112 94
5 76 58
6 147 141
7 149 143
8 70 83
11 106 116

K= 3 L= 3
0 127 149
1 134 156
2 37 26
3 194 164
4 61 60
5 49 37
6 45 51

K= 3 L= 4
1 105 97
2 67 41
3 259 272
6 51 53
7 151 168
11 117 124

K= 3 L= 5
0 261 256
1 191 199
2 220 216
3 112 96
4 118 128
5 82 74
6 82 73
8 68 74
10 78 85

K= 3 L= 6
1 140 138
2 96 87
3 58 54
4 40 39
5 143 146
6 86 89
7 72 74
9 85 87

K= 3 L= 7
1 126 128
2 208 205
3 75 75
5 65 69
6 83 78
7 63 54

K= 3 L= 8
1 185 179
2 58 51
3 92 106
4 55 44
5 142 137
6 87 87
8 76 83
9 93 90

K= 3 L= 9
0 226 246
2 100 90
4 133 135

K= 3 L= 10
1 66 57
2 53 54
3 62 63
4 62 57
6 73 76
7 59 68
8 94 102

K= 3 L= 11
0 235 254
1 75 89
6 107 129
7 64 58
8 91 95

K= 3 L= 12
1 50 50
2 52 44
5 85 89
6 76 75

K= 3 L= 13
0 97 94
1 104 113
4 62 69
5 66 69

K= 3 L= 14
1 89 98
5 163 170

K= 3 L= 15
1 99 109
3 58 63

K= 3 L= 17
0 171 180
4 122 113

K= 3 L= 18
3 78 79

K= 3 L= 19
0 83 81
2 64 62

K= 3 L= 20
3 65 56

K= 4 L= 0
2 74 68
4 285 248
6 107 93
8 99 96
10 75 68

K= 4 L= 1
1 83 102
2 34 32
3 69 61
6 100 89
5 131 113
6 74 72
8 108 103
9 79 75
10 69 70

K= 4 L= 2
0 121 139
1 93 102
2 55 48
3 128 119
4 139 110
8 53 49

K= 4 L= 3
1 138 147
2 45 35
3 82 87
5 206 188
6 102 89
8 77 65
9 133 138

K= 4 L= 4
2 65 63
3 107 99
4 50 49
5 87 75

K= 4 L= 5
1 62 62
3 156 142
4 44 38
7 168 168

K= 4 L= 6
0 75 77
1 85 86
2 114 98
3 120 111
4 121 116
5 60 65
6 115 113
8 89 81

K= 4 L= 7
3 157 145
6 76 85
7 107 107
8 76 73

K= 4 L= 8
0 146 141
1 57 54
3 70 74
4 113 116

K= 4 L= 9
1 106 104
3 135 152
4 71 81
5 80 82
6 70 68
7 100 98

K= 4 L= 10
1 67 72
2 209 221
6 105 128

K= 4 L= 11
2 71 54
4 67 62
6 68 66

K= 4 L= 12
0 64 53
1 77 81
2 114 135
3 63 74
6 79 93

K= 4 L= 13
0 83 81
1 79 85
3 110 109
7 145 142

K= 4 L= 14
1 62 57
3 68 76

K= 4 L= 15
3 110 98

K= 4 L= 16
2 123 111

K= 4 L= 18
2 111 100

K= 5 L= 0
2 82 78
6 144 112
8 97 94

K= 5 L= 1
1 49 59
2 101 236
3 28 30
5 69 51
6 134 119
8 57 47

K= 5 L= 2
1 88 105
2 60 54
3 142 125
4 72 59
5 88 69
6 96 72
7 132 128
8 75 81

K= 5 L= 3
0 86 92
1 105 118
2 65 63
3 107 99
4 50 49
5 87 75

K= 5 L= 4
1 62 62
3 156 142
4 44 38
7 168 168

K= 5 L= 5
0 75 77
1 85 86
2 114 98
3 120 111
4 121 116
5 60 65
6 115 113
8 89 81

K= 5 L= 6
1 45 39
4 62 66
5 123 102
7 54 55

K= 5 L= 7
0 41 41

Table 4. Continued.

1	66	60	9	75	95	K= 5 L= 11		K= 5 L= 15		4	100	77	5	177	158	K= 6 L= 4		K= 6 L= 10	
2	139	146				0	152	180	1	69	73	5	96	79				0	92	96	2	132	143
3	84	81	K= 5 L= 9			4	114	130				6	94	71	K= 6 L= 6			1	70	73			
5	66	84	0	145	152				K= 5 L= 17						1	70	66	3	79	88	K= 6 L= 14		
6	86	78	2	90	85	K= 5 L= 13			4	84	95	K= 6 L= 2			2	82	87	4	102	92	2	108	115
			4	98	116	0	88	95				0	152	147	3	95	74						
K= 5 L= 8						1	89	83	K= 6 L= 0			1	82	72	4	80	71	K= 6 L= 7					
1	90	89	K= 5 L= 10			3	75	75	4	134	135	4	56	60	5	76	70	3	95	85			
3	72	76	1	61	55																		
4	67	60	3	62	57	K= 5 L= 14		K= 6 L= 1				K= 6 L= 3			K= 6 L= 5			K= 6 L= 8					
5	114	128	4	77	67	1	104	104	1	70	84	1	102	133	5	115	85	0	92	85			
6	61	58				5	105	118	2	55	54	4	91	84									

These results of absorption correction are consistent with those found by Werner and Srivastava *et al.* and the correction applied was considered to be better than no correction at all. Thus the atomic parameters obtained from the corrected material are used to describe the structure.

The function minimized in the refinements was $\sum w(|F_o|-|F_c|)^2$ with weights according to Cruickshank.[8] In addition the two reflexions not obeying the condition $0.33 \leq |F_o|/|F_c| \leq 3.00$ were given zero weight. All observed reflexions were included in the calculation of R. The atomic scattering factors for the neutral atoms were taken from International Tables [3] for oxygen and carbon and from Cromer *et al.*[9] for europium.

The weighting scheme used was satisfactory as indicated by the approximate constancy of the averages of $w(|F_o|-|F_c|)^2$ between different $|F_o|$ and sin θ intervals (Table 2). The shifts in all parameters were less than 5 % of their estimated standard deviations in the last cycle of refinement.

The final atomic parameters with their estimated standard deviations are given in Table 3. The isotropic temperature factor of O(W7) at (0.02, 0.42, 0.50) is very large, 19 Å^2, indicating a high degree of disorder for this water molecule. This interpretation seems reasonable when regarding the surroundings of O(W7) as discussed below.

The electron density maps of a difference synthesis based upon the parameters given in Table 3 showed only spurious peaks $1-2$ e/Å^3 above a slightly varying background. The observed and calculated structure factors are compared in Table 4.

All computations were performed on the UNIVAC 1108 computer at Lund, Sweden, using the programs PIRUM,[10] DRF, DATAP2, LALS, DISTAN, PLANE, CELSIUS, and ORTEP.[11]

DESCRIPTION OF THE STRUCTURE

The superscripts (i) – (viii) are used to indicate the following equivalent positions of the structure

	x,y,z	(iii)	$x-1/2,1/2-z$	(vi)	$1/2+x,3/2-y,1/2-z$
(i)	$x,1/2-y,z$	(iv)	$x-1/2,y-1,1/2-z$	(vii)	$1/2-x,1-y,1/2+z$
(ii)	$x,3/2-y,z$	(v)	$1/2+x,y,1/2-z$	(viii)	$-x,1-y,1-z$

where x,y,z are the atomic coordinates given in Table 3. The numbering of the atoms constituting the three independent malonate ions, referred to as ligand 1, ligand 2, and ligand 3, is given in Fig. 4.

The structure consists of europium-malonate layers parallel with (001) and located around $z=1/4$ and $z=3/4$. The layer around $z=1/4$ is illustrated in Fig. 1 and may be described in the following way. Ligand 2 connects the

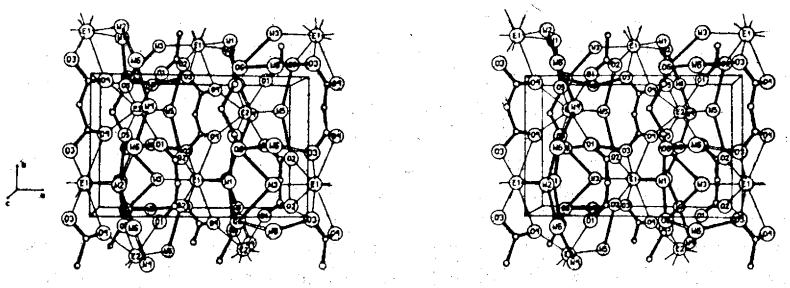

Fig. 1. A stereoscopic pair of drawings showing part of the europium malonate layer around $z=1/4$. The europium ions are denoted E1 and E2 and the water molecules W1, W2, *etc.* Bonds within the malonate ions are filled, hydrogen bonds are open, and Eu – O bonds are single lines. The box outlined is $-1/2\leq x\leq 1/2$, $0\leq y\leq 1$, $0\leq z\leq 1/2$.

europium ions by oxygen bridges Eu(1) – O(4) – Eu(2), in chains parallel with the b-axis. These chains are linked to layers by bridges of the type Eu(2) – O(1)C(2)O(2) – Eu(1) formed by ligand 1. Ligand 3 is not bridging. Each of the three malonate ions forms a six-membered chelate ring with europium.

There are seven non-equivalent water molecules in the structure. Five of them, O(W1) – O(W5), are coordinated to europium. O(W1), O(W3), and O(W5) are hydrogen bonded to carboxylate oxygens within the europium malonate layer, forming "water malonate" chains of the sequences – O(W1) – O(5) – CCC – O(5) – O(W1) –, – O(W3) – O(6) – CCC – O(6) – O(W3) –, and – O(W5) – O(2) – CCC – O(2) – O(W5) –, respectively. These chains run in the y-direction.

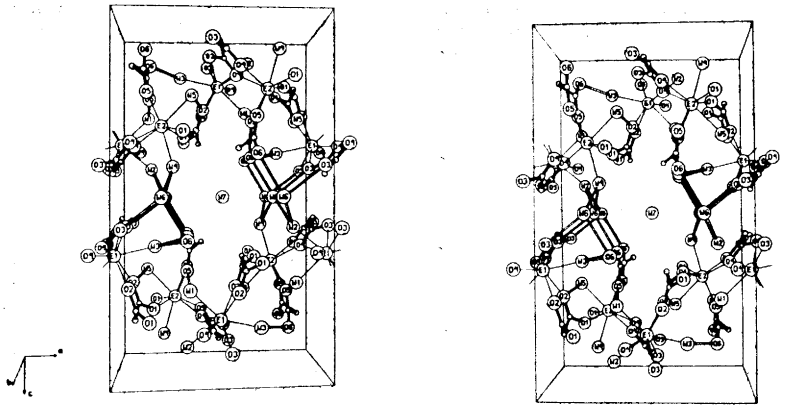

Fig. 2. A stereoscopic pair of drawings showing part of two adjacent europium malonate layers and the bonding between them. The atoms and bonds are indicated as in Fig. 1. The box outlined is $-1/2\leq x\leq 1/2$, $0\leq y\leq 1$, $0\leq z\leq 1$.

The water molecules O(W2) and O(W4) are bonded to the uncoordinated water molecule O(W6) forming a hydrogen bonded water chain of the sequence $-O(W2)-O(W6)-O(W4)-O(W6)-O(W2)-$. Also this chain runs in the y-direction.

The water molecule O(W6) is situated between the layers at $z \approx 0$ and $z \approx 1/2$, and adjacent layers are held together by hydrogen bonds *via* this water molecule, as illustrated in Fig. 2. The packing of the layers results in fairly wide oxygen bounded channels around $x = 0$, $z = 1/2$, and $x = 1/2$, $z = 0$. The disordered water molecule O(W7) is located in these channels.

The coordination polyhedra. The two crystallographically independent europium ions have different coordination numbers. Eu(1) is surrounded by nine oxygens forming a distorted tricapped trigonal prism (TCTP), while Eu(2) is surrounded by eight oxygens at the corners of a distorted square antiprism (SAP). The two polyhedra are illustrated in Fig. 3 and it is seen that they share the corner O(4). Their dimensions are given in Table 5 A and B.

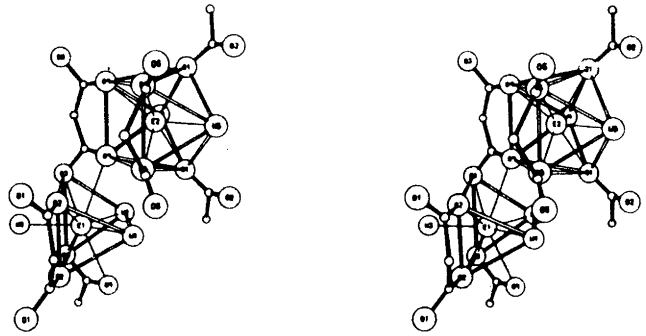

Fig. 3. A stereoscopic pair of drawings showing the coordination around the two europium ions. The notation of the atoms is as in Fig. 1. The edges of the square antiprism and the trigonal prism are open, bonds within the malonate ions are filled, and Eu – O bonds are single lines.

Table 5. Selected distances (Å) and angles (°) with their estimated standard deviations.

A. The coordination polyhedron around Eu(1)

Eu(1) – O(2)	2.37(2)	O(2) – O(W1)	3.00(3)
Eu(1) – O(3)	2.42(2)	O(2) – O(W3)	2.99(4)
Eu(1) – O(4)	2.84(2)	O(3) – O(3^{i})	3.54(5)
Eu(1) – O(W1)	2.38(3)	O(3) – O(4)	2.20(3)
Eu(1) – O(W2)	2.50(4)	O(3) – O(W2)	3.06(4)
Eu(1) – O(W3)	2.46(4)	O(3) – O(W3)	2.77(4)
O(2) – O(2^{i})	2.79(4)	O(4) – O(W1)	3.32(3)
O(2) – O(3)	3.28(3)	O(4) – O(W2)	3.07(3)
O(2) – O(4)	3.02(3)	O(W1) – O(W2)	3.19(5)

Table 5. Continued.

B. The coordination polyhedron around Eu(2)			
Eu(2) – O(1^{v})	2.37(2)	O(4) – O(4^{ii})	2.84(4)
Eu(2) – O(4)	2.44(2)	O(4) – O(5)	2.93(3)
Eu(2) – O(5)	2.39(2)	O(4) – O(W4)	3.02(3)
Eu(2) – O(W4)	2.41(3)	O(5) – O(5^{ii})	2.89(5)
Eu(2) – O(W5)	2.48(3)	O(5) – O(W5)	2.92(4)
O(1^{v}) – O(4)	3.09(3)	O(4) – Eu(2) – O(5^{ii})	116(1)
O(1^{v}) – O(5)	3.07(3)	O(W4) – Eu(2) – O(W5)	119(1)
O(1^{v}) – O(W4)	2.76(3)	O(1^{v}) – Eu(2) – O(1^{vi})	109(1)
C. Ligand 1			
C(1) – C(2)	1.54(5)	C(2) – C(1) – C(2^{i})	115(4)
C(2) – O(1)	1.23(4)	O(1) – C(2) – O(2)	125(3)
C(2) – O(2)	1.27(4)	O(1) – C(2) – C(1)	118(3)
O(2) – O(2^{i})	2.79(4)	O(2) – C(2) – C(1)	119(3)
Dihedral angles:	C(2^{i}) – C(1) – C(2) – O(1)		128
	C(2^{i}) – C(1) – C(2) – O(2)		45
D. Ligand 2			
C(3) – C(4)	1.47(4)	C(4) – C(3) – C(4^{ii})	122(3)
C(4) – O(3)	1.31(3)	O(3) – C(4) – O(4)	119(3)
C(4) – O(4)	1.24(3)	O(3) – C(4) – C(3)	117(2)
O(4) – O(4^{ii})	2.84(4)	O(4) – C(4) – C(3)	123(3)
	Dihedral angles	C(4^{ii}) – C(3) – C(4) – O(3)	146
		C(4^{ii}) – C(3) – C(4) – O(4)	28
E. Ligand 3			
C(5) – C(6)	1.55(5)	C(6) – C(5) – C(6^{ii})	115(5)
C(6) – O(5)	1.24(4)	O(5) – C(6) – O(6)	126(4)
C(6) – O(6)	1.22(5)	O(5) – C(6) – C(5)	117(4)
O(5) – (O(5^{ii})	2.89(5)	O(6) – C(6) – C(5)	117(3)
	Dihedral angles	C(6^{ii}) – C(5) – C(6) – O(5)	55
		C(6^{ii}) – C(5) – C(6) – O(6)	130
F. Possible hydrogen bonds			
O(W1) – O(5)	2.76(3)	O(W5) – O(2^{v})	2.79(2)
O(W2^{vii}) – O(W6)	2.74(4)	O(W6) – O(3^{v})	2.83(4)
O(W3) – O(6^{iii})	2.64(4)	O(W6) – O(6)	2.82(4)
O(W4^{vii}) – O(W6)	2.77(4)		
G. Distances shorter than 3.5 Å around O(W7)			
O(W7) – O(W6)	3.2(2)	O(W7) – O(W7^{i})	2.9(3)
O(W7) – O(6)	2.9(2)	O(W7) – O(W7^{viii})	1.2(3)
O(W7) – O(6^{viii})	3.4(2)	O(W7) – O(W4^{vii})	3.4(2)

The oxygens around Eu(1) are contributed by three malonate ions and three water molecules. The Eu(1)–O bond distances are in the range 2.37–2.84 Å. Their average value, 2.51 Å, is the same as found for ninecoordinated europium in europium trisglycolate.[12] The bond Eu(1)–O(4), 2.84 Å, is considerably longer than the average value. It is part of the oxygen bridge Eu(1)–O(4)–Eu(2) formed by the bridging-chelating carboxylate group –C(3)O(3)O(4). The distance Eu(2)–O(4) is not significantly different from the other Eu(2)–O bond distances. Similar asymmetric oxygen bridges are found in the malonates $Nd_2mal_3.nH_2O$, $n = 8$ and 6, and also in a number of other lanthanoid carboxylate structures.[1,2] The distance Eu(1)···Eu(2) is 4.20 Å and the next shortest Eu···Eu distance is Eu(2)···Eu(1^{v}), 6.05 Å.

The triangular faces of the TCTP – O(2)O(2^{i})O(W1) and O(3)O(3^{i})O(W2) – have the average edge length 3.08 Å. Two edges have lengths significantly different from this value *viz.* O(2)–O(2^{i}), 2.79 Å, and O(3)–O(3^{i}), 3.54 Å. O(2)–O(2^{i}) is the bite of ligand 1, and the oxygens O(3) and O(3^{i}) belong to bridging-chelating carboxylate groups of different malonate ions. The angle between the two triangular faces is 1° and the angles between each of these

Table 6. Deviations, in Å, from the least-squares planes within the coordination polyhedra and the malonate ions. The atoms defining the plane are in each case given above the asterisk.

A. The coordination polyhedra

Atom	Distance	Atom	Distance
O(1^{v})	0.08	O(2)	–0.10
O(1^{vi})	–0.02	O(W1)	0.10
O(W4)	–0.03	O(3)	0.10
O(W5)	–0.02	O(W2)	–0.10
*		*	

B. The carboxylate groups

Atom	Distance	Atom	Distance	Atom	Distance
C(1)	–0.01	C(3)	–0.01	C(5)	0.01
C(2)	0.04	C(4)	0.03	C(6)	–0.03
O(1)	–0.01	O(3)	–0.01	O(5)	0.01
O(2)	–0.01	O(4)	–0.01	O(6)	0.01
*		*		*	
Eu(1)	–0.47	Eu(1)	–0.15	Eu(2)	–1.01
Eu(2^{iii})	–0.43	Eu(2)	0.09		

C. The six-membered chelate rings

Atom	Distance	Atom	Distance	Atom	Distance
O(2)	0	O(4)	0	O(5)	0
C(2)	0	C(4)	0	C(6)	0
C(2^{i})	0	C(4^{ii})	0	C(6^{ii})	0
O(2^{i})	0	O(4^{ii})	0	O(5^{ii})	0
*		*		*	
C(1)	0.31	C(3)	0.67	C(5)	–0.45
Eu(1)	0.51	Eu(2)	0.29	Eu(2)	0.60

faces and the equatorial triangle, O(4)O(4^{i})O(W3), are 5° and 4°, respectively. The "rectangular" face O(2)O(2^{i})O(3)O(3^{i}) is planar for symmetry reasons and the other two "rectangular" faces are planar within 0.1 Å (Table 6A). Since O(3) and O(4) belong to the same carboxylate group the capping oxygen O(4) is restricted to a position far from equidistant from the four atoms of the capped face.

A regular TCTP is defined by the parameters ϱ and θ_{TP}.[13] ϱ is the ratio between the equatorial and prismatic metal-ligand bond lengths and θ_{TP} is the angle that the prismatic metal-ligand bonds make with the three fold axis. The average parameters of the present TCPT are $\varrho = 1.1$ and $\theta_{TP} = 48°$. The normal of the equatorial plane is taken as the three fold axis and the values of θ_{TP} range from 34° to 51°. The hard sphere value of θ_{TP} is 44° for $\varrho = 1.1$.

The oxygens coordinated to Eu(2) are contributed by four malonate ions and two water molecules. The Eu(2) – O bond distances are in the range 2.37 – 2.48 Å with the average 2.42 Å. This value is 0.05 Å less than that found in the eightcoordinated europium compound Eu(acetylacetonate)$_3$.3H$_2$O.[14] Variations of this magnitude in the average M – O bond distance are frequently found between different compounds of the same lanthanoid ion and coordination number (see Ref. 15, p. 37).

The two "square" faces of the SAP – O(4)O(4^{ii})O(5)O(5^{ii}) and O(1^{v})O(W4)O(1^{vi})O(W5) – are of about the same size. The average edge length is 2.87 Å with the maximum deviation 0.11 Å. The edges O(4)···O(4^{ii}) 2.84 Å, and O(5)···O(5^{ii}), 2.89 Å, are each spanned by a malonate ion forming a six-membered chelate ring with Eu(2). The corresponding square face is planar for symmetry reasons while the oxygens defining the other "square" face are coplanar within 0.1 Å (Table 6A). The angle between the two faces is 1°.

A regular SAP is defined by the angle, θ_{SAP}, that the metal-ligand bonds make with the eight fold inversion axis. The O-Eu(2) – O angles given in Table 5B represent $2\theta_{SAP}$. The average θ_{SAP} calculated from these angles is 57.5° as compared to the hard sphere value 59.3°.

Kepert[13] has shown that an increase in θ_{TP} and a decrease in θ_{SAP} both by 2 – 3° from the corresponding hard sphere value, minimize the ligand-ligand repulsive energy of a TCTP and a SAP, respectively. It is interesting to note that, even though the present polyhedra are irregular as a result of the geometrical constrains of the malonate ions and the interaction of the complexes with their crystallographic surroundings, the average values of θ_{TP} and θ_{SAP} are close to those predicted by Kepert's calculations.

There are three different six-membered europium-malonate chelate rings. In each ring the two C – O bonds are related by a mirror plane through the methylene carbon atom and the europium ion. Hence the four intra ring carboxylate atoms are coplanar. The rings formed by ligands No. 1 and 2 have a boat conformation with the europium ion and the methylene carbon atom at the same side of the OCCO-plane, while the ring formed by ligand 3 adopts a chair conformation with the europium ion and methylene carbon atom at opposite sides of the OCCO-plane (Table 6C). The boat conformation has invariably been found in previous X-ray structure analyses of malonate

complexes.[1,2,16] The chair conformation of the ring formed by ligand 3 is most probably determined by the possibilities of its uncoordinated oxygen, O(6), to be favourably hydrogen bonded.

The malonate ions. The dimensions of the malonate ions are given in Table 5C–E, and are also indicated in Fig. 4. They are in accordance with those found in other malonate structures.[1]

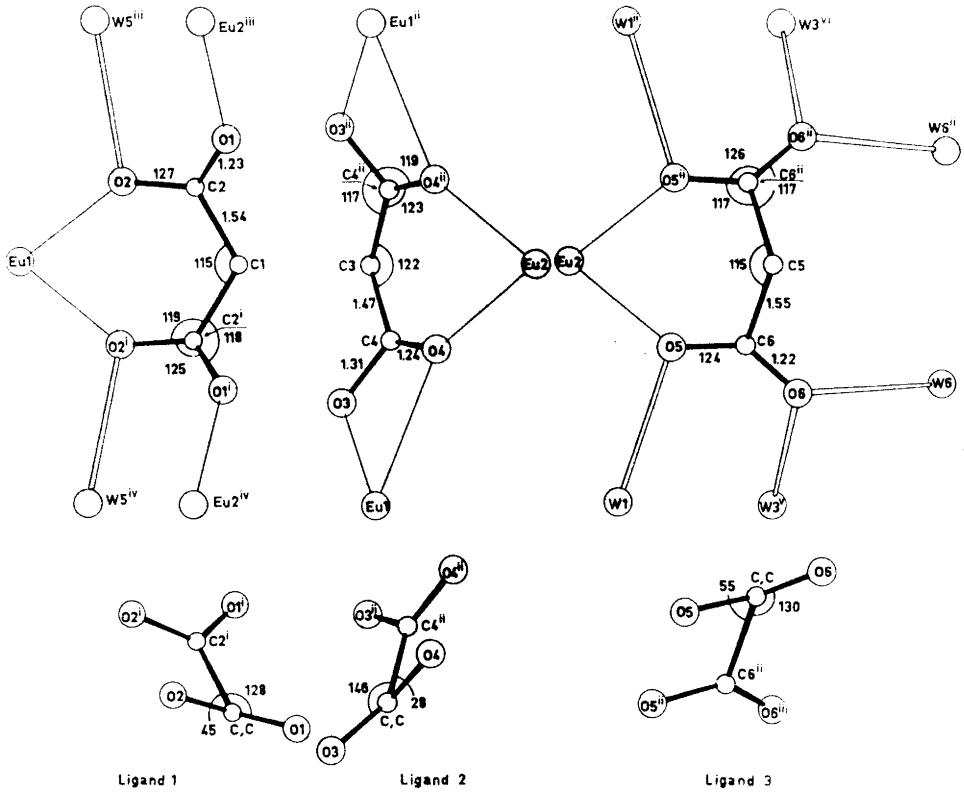

Fig. 4. The three malonate ions and their immediate surroundings, together with projections of each malonate ion along one of its C–C bonds. The angles indicated in these projections] are the dihedral angles C–C–C–O given in Table 5C, D, and E. The notation of the atoms and bonds is the same as in Fig. 1.

The three independent C–COO– groups are planar within the limits of errors (Table 6B). In each malonate ion the carboxylate groups are related by a mirror plane through the methylene carbon. The dihedral angles included in Table 5C–E and in Fig. 4 indicate that the two carboxylate groups are twisted in the same direction out of the carbon chain plane by about 30°, 50°, and 30° for ligands No. 1, 2, and 3, respectively. The corresponding ligand bites are 2.79 Å, 2.85 Å, and 2.89 Å.

The conformations of these malonate ions are similar to those found for the chelating malonate ions in $Nd_2mal_3.8H_2O$ [1] and $Nd_2mal_3.6H_2O$,[2] which have twist angles of about 40° and 45° and bites 2.80 Å and 2.83 Å.

The water molecules. The possible hydrogen bond distances around the water molecules O(W1) – O(W6) are given in Table 5F. They are selected by the criteria described before.[1]

The coordinated water molecules are situated in the mirror planes each forming two equivalent hydrogen bonds (see Fig. 1). Their donor angles, O···O(W)···O, are in the range 92 – 144° *i.e.* within the limits 60 – 150° found in other crystal hydrates.[17] The sum of the three bond angles around the water oxygen is 330° for O(W5), 344° for O(W4), and 350 – 360° for O(W1), O(W2), and O(W3).

The uncoordinated water molecule O(W6) is surrounded by four oxygens in an approximately tetrahedral arrangement *viz.* O(6) and O(3^{v}) which belong to one europium malonate layer and O($W4^{vii}$) and O($W2^{vii}$) which are coordinated to europium in an adjacent layer (see Fig. 2). Thus the hydrogen bonds of O(W6) link the layers together. The "tetrahedral" angles are in the range 83 – 138° and the donor angle O(6)···O(W6)···O(3^{v}) is 83°.

The water molecule O(W7) is situated in the channels running parallel with *b*. The channel centered at $x = 0$, $z = 1/2$ is illustrated in Fig. 2. It is bounded by oxygens at the levels $y = 0$ and $y = 1/2$ and by oxygen and methylene carbons at the levels $y = 1/4$ and $y = 3/4$, [*e.g.* O(1), O(6), O(W6), O(1^{viii}), O(6^{viii}) and O($W6^{viii}$) at $y = 1/2$ and O($W4^{vii}$), C(5^{viii}), and C(1) at $y = 1/4$]. Geometrically, any one of the bounding oxygens may act as an acceptor for a hydrogen bond from a water molecule in the channel. Regarding this fact, the fairly high temperature factor of O(W7) at (0.02, 0.43, 0.50) is interpreted as follows. The water molecules in the channel are distributed among a number of favourable positions around $x = 0$, $z = 1/2$, with a certain preference for the position (0.02, 0.43, 0.50). The latter position is surrounded by five oxygens at distances less than 3.4 Å (see Table 5G).

Acknowledgements. I am indebted to Professor Ido Leden and Drs. Jörgen Albertsson and Ingmar Grenthe for many valuable discussions. This work is part of a research project supported by the *Swedish Natural Science Research Council.*

REFERENCES

1. Hansson, E. *Acta Chem. Scand.* **27** (1973) 2441.
2. Hansson, E. *Acta Chem. Scand.* **27** (1973) 2813.
3. *International Tables for X-Ray Crystallography*, Kynoch Press, Birmingham 1968, Vol. III.
4. Werner, P. E. *Acta Chem. Scand.* **18** (1964) 1851.
5. Srivastava, R. C. and Lingafelter, E. C. *Acta Cryst.* **20** (1966) 918.
6. *International Tables for X-Ray Crystallography*, Kynoch Press, Birmingham 1969, Vol. I.
7. Hansson, E. *Acta Chem. Scand.* **27** (1973) 823.
8. Cruickshank, D. W. J. In Rollet, J. S., Ed., *Computing Methods in Crystallography*, Pergamon, Glasgow 1965, pp. 99 – 116.
9. Cromer, D. T., Larsson, A. C. and Waber, J. T. *Acta Cryst.* **17** (1964) 1044.
10. Werner, P. E. *Arkiv Kemi* **31** (1970) 513.
11. Liminga, R. *Acta Chem. Scand.* **21** (1967) 1206.

12. Grenthe, I. *Acta Chem. Scand.* **25** (1971) 3347.
13. Kepert, D. L. *J. Chem. Soc.* **1965** 4736.
14. Il'inskii, A. L., Aslanov, L. A., Ivanov, V. J., Khahilov, A. D. and Petrukhin, O. M. *J. Struct. Chem.* **10** (1969) 285.
15. Albertsson, J. *On the Stereochemistry of Ninecoordinate Lanthanoid Compounds*, Thesis, Lund 1972.
16. Butler, K. R. and Snow, M. R. *J. Chem. Soc.* **D 1971** 550.
17. Hamilton, W. C. and Ibers, J. A. *Hydrogen Bonding in Solids*, W. A. Benjamin, New-York-Amsterdam 1968, p. 213.

Received March 22, 1973.

ACTA CHEMICA SCANDINAVICA 27 (1973) 2841–2851

Structural Studies on the Rare Earth Carboxlates

20. The Crystal and Molecular Structure of Mono-Aquo Hydroxo Malonato Scandium(III) Monohydrate

EVA HANSSON

Physical Chemistry 1, Chemical Center, University of Lund, P.O. Box 740, S-220 07 Lund 7, Sweden

The crystal and molecular structure of $Sc(OH)C_3H_2O_4.2H_2O$ has been determined from three-dimensional, photographic, X-ray intensity data. The crystals are monoclinic with $a=6.276(1)$ Å, $b=15.353(4)$ Å, $c=7.776(2)$ Å, $\beta=99.90(3)°$. The space group is $P2_1/n$ and $Z=4$. The structure is composed of infinite scandium-hydroxo-malonate chains running in the x-direction and linked to each other by hydrogen bonds. Within each chain the scandium ions are bonded to pairs by double oxygen bridges formed by the hydroxy ions, and the scandium pairs are in turn linked by carboxylate bridges Sc–OCO–Sc. The malonate ion forms a six membered chelate ring with scandium and is nonplanar with the carboxylate groups twisted about 40° in the same direction out of the carbon chain plane. The chelate ring has a boat conformation. Each scandium ion is octahedrally surrounded by two hydroxy oxygens, three carboxylate oxygens and one water oxygen. The Sc–O bond distances are in the range 2.05–2.12 Å.

The conformation of the malonate ion in lanthanoid malonate complexes has been studied in a series of X-ray investigations, involving the noniso-structural compounds $Nd_2mal_3.8H_2O$ (NDO),[1] $Nd_2mal_3.6H_2O$ (NDH),[2] and $Eu_2mal_3.8H_2O$ (EUM),[3] ($mal=CH_2(COO)_2$). Poor crystal quality prevented the study of a malonate $M_2mal_3.nH_2O$ formed by the smaller lanthanoid ions, and for that reason it has not been possible to investigate changes in the geometry of the malonate ion, attributable to the lanthanoid contraction.

Scandium(III) has a similar outer electron shell to the trivalent lanthanoid ions and a smaller ionic radius. Thus a possible influence of a change in size of the central ion on the malonate ligand might be revealed in a crystal structure analysis of a solid scandium malonate complex.

The compound chosen for this investigation is $Sc(OH)mal.2H_2O$ (SCM). A number of basic scandium dicarboxylates $Sc(OH)R(COO)_2.nH_2O$ have been reported.[4] Their crystal structures seem to be unknown and the determina-

tion of the function of the hydroxy ion in a compound of this type confers additional interest to the present investigation.

EXPERIMENTAL

Preparation and analysis. Scandium hydroxide (4 mmol) and malonic acid (6 mmol) were dissolved in 100 ml water. The pH of the resulting solution was about 3 and crystals of SCM were precipitated after standing at room temperature for several weeks. (Found: Sc 22.0; C 18.4; H 3.8. Calc. for $Sc(OH)C_3H_2O_4.2H_2O$ (200.2): Sc 22.5; C 18.0; H 3.6).

X-Ray diffraction work. A crystal of the approximate dimensions $0.10 \times 0.02 \times 0.04$ mm^3 mounted along the 0.10 mm edge was used in recording the layers $0kl - 5kl$, with the integrated Weissenberg multi-film technique. Ni-filtered Cu-radiation was used. The intensities of 779 independent reflexions were measured visually by comparison with a calibrated scale. These reflexions represent about 55 % of the possible number in the investigated region.

The intensities were corrected for Lorentz and polarisation effects. The linear absorption coefficient is 87 cm^{-1} but no corrections for absorption were applied.

The powder photograph was taken at room temperature in a Guinier-Hägg focusing camera with Cu$K\alpha$-radiation ($\lambda = 1.54178$ Å). Lead nitrate (cubic $a = 7.8568$ Å) was used as an internal standard.

UNIT CELL AND SPACE GROUP

The crystals of SCM are monoclinic with $a = 6.276(1)$ Å, $b = 15.353(4)$ Å, $c = 7.776(2)$ Å, and $\beta = 99.90(3)°$. $Z = 4$. The accurate values of the lattice parameters were determined from powder data by least squares refinement, as described before.[5] The observed values of $\sin^2\theta$ are compared with those calculated after the last cycle of refinement in Table 1.

The reflexions $h0l$, $h+l \neq 2n$ and $0k0$, $k \neq 2n$ are systematically absent. Thus the only possible space group is $P2_1/n$, the general position of which is fourfold: $\pm(x,y,z;\ \frac{1}{2}+x,\frac{1}{2}-y,\frac{1}{2}+z)$.

DETERMINATION AND REFINEMENT OF THE STRUCTURE

The structure of SCM was determined by the heavy atom method. The position of the scandium ion was deduced from a three-dimensional Patterson synthesis and a following difference synthesis revealed the positions of the remaining ten non-hydrogen atoms.

The preliminary positional parameters, isotropic temperature factors and inter-layer scale factors were improved by full matrix least squares refinement. The discrepancy indices $R = \sum||F_o| - |F_c||/\sum|F_o|$ and $wR = [\sum w(|F_o| - |F_c|)^2/\sum w|F_o|^2]^{\frac{1}{2}}$ converged to 0.095 and 0.124, respectively. The inter-layer scale factors were now fixed and further refinement with anisotropic thermal parameters for all non-hydrogen atoms resulted in $R = 0.081$ and $wR = 0.104$. The structure is described with the anisotropic model even though the intensity material is not very accurate and hence the thermal parameters may have little physical significance.

The function minimized was $\sum w(|F_o| - |F_c|)^2$ with weights, w, chosen according to Cruickshank.[6] An analysis of the weighting scheme used in the

Table 1. Powder data for $Sc(OH)(C_3H_2O_4).2H_2O$. Observed and calculated values of $10^5 \sin^2 \theta$ are given together with the observed powder intensities.

h k l	obs	calc	I_{obs}	*h k l*	obs	calc	I_{obs}
0 2 0	1006	1008	m	2 0 2	11977	12008	vw
0 1 1	1266	1266	vs	0 7 1	13356	13357	vw
1 1 0	1806	1806	vs	−3 0 1	13694	13701	s
0 2 1	2021	2022	vs	1 7 0	13893	13897	vvw
1 0 1	2134	2134	m	3 1 0	14240	14241	w
−1 1 1	2386	2386	w	−1 7 1	14488	14477	vw
−1 2 1	3148	3142	vvw	−3 2 1	14700	14709	vw
1 1 1	3255	3254	m	3 2 0	14987	14996	s
0 4 0	4021	4030	m	−3 1 2	15691	15693	vw
0 4 1	5055	5044	m	−3 3 1	15953	15968	m
0 2 2		5063		0 0 4	16254	16222	vw
1 4 0	5590	5585	w	3 3 0		16256	
2 0 0	6218	6217	m	0 8 1	17113	17135	vvw
0 3 2	6329	6323	w	1 8 0	17687	17676	vvw
−2 1 1	6624	6615	vs	3 4 0	18031	18019	vvw
−1 3 2	7013	7009	vw	0 3 4	18505	18489	vvw
2 2 0	7229	7225	w	−2 7 1	18707	18707	vvw
1 5 0	7863	7852	vvw	−3 4 2	19471	19472	vw
0 4 2	8090	8086	vvw	3 5 0	20287	20286	w
−2 3 1	8637	8631	vw	3 1 2	20912	20899	w
−1 4 2	8772	8773	vw	−3 3 3	21487	21477	vvw
2 2 1	9099	9106	m	2 8 0	22345	22339	vvw
0 1 3	9370	9377	w	1 8 2	22599	22599	vvw
0 2 3	10112	10133	vvw	3 5 1		22601	
−1 6 1	11205	11203	vvw	−3 6 1	22770	22770	vvw
				−4 1 1	24396	24399	w
				−3 1 4	25253	25257	w

last cycle of refinement is given in Table 2. In this cycle the shifts in all parameters were less than 1 % of their estimated standard deviations. The atomic scattering factors for the neutral atoms were for O and C taken from International Tables [7] and for Sc from Cromer *et al.*[8]

Table 2. Analysis of the weighting scheme $w = 1/(5.0 + |F_o| + 0.02|F_o|^2 + 0.005|F_o|^3)$. The averages, $\overline{w\Delta^2}$, where $\Delta = |F_o| - |F_c|$, are normalized.

Interval $\|F_o\|$	Number of reflexions	$\overline{w\Delta^2}$	Interval $\sin \theta$	Number of reflexions	$\overline{w\Delta^2}$
0 – 7	77	0.79	0.00 – 0.37	71	2.38
7 – 9	78	0.86	0.37 – 0.47	68	1.12
9 – 10	78	0.96	0.47 – 0.54	72	0.92
10 – 12	78	1.38	0.54 – 0.59	61	1.03
12 – 14	78	1.10	0.59 – 0.64	62	0.62
14 – 16	78	1.05	0.64 – 0.68	51	0.74
16 – 19	78	0.81	0.68 – 0.71	47	1.00
19 – 24	78	0.92	0.71 – 0.74	46	0.75
24 – 35	78	0.65	0.74 – 0.77	39	0.51
35 – 130	78	1.49	0.77 – 0.80	40	0.93

Table 3. Atomic parameters with estimated standard deviations. The anisotropic thermal parameters, β_{ij}, have been obtained by using the expression $\exp[-(h^2\beta_{11}+2hk\beta_{12}+\ldots.)]$ and the root-mean-squares displacements along the principal axis of the thermal ellipsoids, R_i, have been calculated from the values of β_{ij}.

Atom	Group	$x\times10^4$	$y\times10^4$	$z\times10^4$	$\beta_{11}\times10^4$	$\beta_{22}\times10^4$	$\beta_{33}\times10^4$	$\beta_{12}\times10^4$	$\beta_{13}\times10^4$	$\beta_{23}\times10^4$	R_1/Å	R_2/Å	R_3/Å
Sc		391(2)	818(1)	6361(2)	154(6)	23(1)	115(3)	−3(1)	2(2)	−2(1)	0.185	0.164	0.174
O(1)	COO^-	3804(8)	741(3)	6701(7)	218(19)	32(2)	173(11)	−3(5)	1(11)	6(4)	0.236	0.194	0.202
O(2)	COO^-	7224(9)	1030(4)	6570(8)	194(22)	44(3)	202(13)	3(5)	4(12)	1(4)	0.245	0.193	0.229
O(3)	COO^-	2821(9)	3376(4)	5816(8)	316(18)	25(2)	191(13)	−16(5)	6(12)	7(4)	0.252	0.164	0.238
O(4)	COO^-	1052(9)	2131(4)	5978(9)	234(17)	29(2)	240(15)	−8(5)	6(12)	1(4)	0.267	0.182	0.213
O(5)	OH^-	265(8)	−533(3)	6264(7)	255(18)	29(2)	132(10)	−2(4)	3(10)	3(4)	0.223	0.180	0.200
O(6)	H_2O	832(9)	874(4)	9122(8)	264(19)	44(3)	135(10)	10(6)	3(10)	−12(5)	0.243	0.190	0.221
O(7)	H_2O	4169(11)	811(5)	11553(9)	341(24)	60(4)	211(15)	−18(7)	0(15)	24(6)	0.304	0.228	0.244
C(1)	COO^-	5255(12)	1222(5)	6247(10)	214(28)	34(3)	120(13)	1(7)	1(14)	−11(5)	0.221	0.173	0.201
C(2)	CH_2	4630(16)	2069(7)	5240(15)	349(33)	43(4)	266(26)	34(9)	11(23)	35(8)	0.316	0.196	0.234
C(3)	COO^-	2706(12)	2562(5)	5738(10)	279(26)	26(3)	131(13)	−9(6)	1(14)	12(5)	0.243	0.163	0.201

Table 4. Observed and calculated structure factors for the compound $Sc(OH)C_3H_2O_0.2H_2O$. In each group the running index l, $|F_o|$, and $|F_c|$ are given.

H= -5 K=-14	-2 9 8	0 10 9	3 18 19	H= -3 K= -3	-4 15 15	H= -1 K= 0	1 43 42
-2 6 7	-1 9 8	1 14 14	6 14 14	-5 10 11	-3 8 9	-7 26 29	2 11 12
0 10 10	0 11 11	2 11 10	5 6 7	-3 10 11	-2 38 37	-5 27 27	3 23 24
1 7 7	1 21 24	3 7 6		-2 15 16	-1 18 17	-3 88 104	4 7 8
2 13 13	2 9 8	4 19 17	H= -3 K=-12	-1 32 30	0 14 14	-1 12 11	5 26 26
4 10 13	4 11 10	5 9 10	-3 14 13	0 46 28	2 24 24	1 9 7	6 16 14
	5 20 20	6 11 9	-1 10 12	1 30 29	3 14 15	5 7 7	7 14 14
H= -5 K=-13	7 6 6	8 13 13	1 27 28	3 33 34	4 12 11	7 16 17	9 5 6
-2 10 12	8 8 7		3 14 14	4 23 20			
-1 6 6		H= -4 K= -5	5 19 19	5 25 25	H= -2 K= -8	H= -1 K= 1	H= -1 K= 9
0 9 9	H= -5 K= -1	-3 31 31		7 9 10	-6 8 8	-8 8 7	-5 18 17
2 7 8	-3 9 11	-2 8 7	H= -3 K=-11	9 11 10	-5 15 15	-7 11 11	-3 28 25
3 7 7	-2 20 18	0 5 5	-2 13 12		-4 21 20	-5 41 22	-1 38 33
4 13 11	0 9 10	1 47 45	0 18 17	H= -3 K= -2	-1 25 26	-4 19 22	0 16 13
	2 10 11	2 12 9	1 22 24	-4 44 42	0 40 41	-3 24 24	1 42 43
H= -5 K=-12	3 17 17	4 8 8	2 8 7	-3 34 32	1 8 7	-2 12 10	3 40 39
-3 13 14	4 11 12	5 28 27	3 22 21	-2 12 13	3 35 34	-1 53 62	4 20 20
-1 6 6	6 8 8		4 24 24	-1 4 4	4 16 15	0 27 28	5 26 26
1 15 17	8 7 8	H= -4 K= -4	5 9 9	0 95 87	5 8 8	1 12 10	7 21 17
3 6 6		-4 7 8	7 8 9	1 49 49	7 15 16	3 12 10	8 9 8
5 12 10	H= -5 K= 0	-2 6 6		2 17 17		6 10 12	
	-1 19 18	0 23 22	H= -3 K=-10	3 8 8	H= -2 K= -7	8 19 18	H= -1 K= 10
H= -5 K=-11	3 16 17	1 23 22	-4 20 20	4 17 16	-6 15 12		-8 7 7
-3 6 6	5 7 6	3 24 24	-3 18 19	5 14 13	-4 13 12	H= -1 K= 2	-4 10 11
-2 8 10		4 14 15	-2 16 17	6 12 13	-3 38 38	-8 7 6	-2 8 6
-1 11 12	H= -4 K=-16	6 15 16	-1 19 18	7 9 10	-2 23 23	-7 13 13	0 17 14
0 6 5	-1 10 11	7 15 16	0 26 28		0 28 23	-2 23 19	1 11 11
2 10 9	3 15 16	8 8 9	1 10 9	H= -3 K= -1	1 68 62	-1 44 43	2 25 25
3 8 9			2 28 28	-2 57 61	2 13 15	1 25 20	3 14 13
4 6 5	H= -4 K=-15	H= -4 K= -3	3 11 12	-1 17 16	5 15 14	2 13 9	6 21 21
6 5 6	0 12 14	-4 12 11	4 9 10	0 35 46	6 15 12	3 38 42	
	1 6 6	-2 18 18	6 19 17	1 10 11	6 12 12	5 15 14	H= -1 K= 11
H= -5 K=-10	3 4 7	0 16 17		2 44 41		6 15 15	-5 13 12
-4 13 13	4 13 11	1 12 11	H= -3 K= -9	3 21 18	H= -2 K= -6	7 16 17	-4 9 9
-2 12 13		2 15 13	-5 21 20	4 53 54	-6 13 13		-1 21 23
0 17 18	H= -4 K=-14	3 7 6	-3 38 41	5 14 15	-4 31 34	H= -1 K= 3	0 19 16
2 20 19	-2 6 6	4 19 15	0 12 12	7 12 11	0 60 59	-9 8 8	3 16 16
4 15 16	-1 7 9	6 14 15	2 6 5	8 18 20	1 5 6	-4 7 6	4 17 18
5 5 5	2 8 8	8 8 8	3 26 25		3 11 9	-3 27 25	8 9 8
6 9 8	3 7 8		4 8 7	H= -3 K= 0	4 34 35	-2 20 21	
	5 9 8	H= -4 K= -2	5 16 15	-3 55 55	5 14 14	-1 14 11	H= -1 K= 12
H= -5 K= -9		-3 15 15	7 10 12	-1 9 9	7 10 11	0 17 17	-7 17 15
-4 6 5	H= -4 K=-13	-2 6 6		3 23 21	8 13 15	1 69 69	-3 26 25
-3 7 8	-3 7 7	-1 13 13	H= -3 K= -8	5 39 37		2 29 29	1 20 21
-2 5 5	-2 15 15	0 6 6	-4 29 28	7 9 10	H= -2 K= -5	3 21 22	7 14 14
-1 11 12	-1 10 11	1 5 4	-3 28 31	9 7 7	-6 8 8	5 22 25	
0 16 17	0 8 9	3 20 19	-2 22 21		-3 26 29	7 9 9	H= -1 K= 13
2 9 9	1 10 10	4 22 22	0 47 49	H= -2 K=-18	-2 20 21	9 7 7	-5 11 11
3 12 11	2 12 11	5 12 12	1 35 33	0 12 11	-1 23 21		-3 13 12
4 12 12	4 6 7	6 13 14	2 33 31		1 12 13	H= -1 K= 4	-1 13 14
6 6 7	5 9 11	8 13 14	3 7 6	H= -2 K=-17	3 10 9	-8 7 6	0 25 23
7 13 13		9 7 7	4 17 17	1 12 13	5 20 21	-7 10 9	1 11 12
	H= -4 K=-12		5 14 14	-3 8 7	7 12 12	-4 16 18	2 9 9
H= -5 K= -8	-2 6 7	H= -4 K= -1	6 19 19	-2 13 13	9 9 9	-2 26 22	4 28 27
-4 13 13	0 8 7	-3 40 34		1 7 8		0 42 39	
-3 13 13	1 10 10	-2 19 16	H= -3 K= -7	2 10 12	H= -2 K= -4	1 23 22	H= -1 K= 14
0 18 18	2 14 12	-1 8 8	-6 16 17		-5 10 8	2 30 25	-6 10 9
1 19 18	4 7 8	0 18 21	-5 7 8	H= -2 K=-16	-4 9 10	4 8 8	-5 13 12
4 10 8	6 7 8	1 36 49	-4 10 11	-1 14 14	-3 6 6	5 12 12	-2 16 15
5 12 12		2 8 8	-2 43 44	1 10 9	-2 8 7	8 11 9	1 23 19
6 5 5	H= -4 K=-11	4 26 24	-1 16 17	3 11 12	-1 13 10		2 23 25
	-3 11 11	5 34 30	0 43 35	5 8 8	0 16 17	H= -1 K= 5	3 12 11
H= -5 K= -7	0 13 13	9 11 11	1 10 10		1 12 13	-3 8 9	5 16 15
-2 24 24	1 17 16		2 30 29	H= -2 K=-15	2 10 10	-2 16 16	6 20 17
0 5 6	4 13 13	H= -4 K= 0	3 22 20	-4 12 10	4 22 22	-1 20 22	
1 5 5	5 10 11	-2 22 21	4 48 42	-2 20 22	6 22 22	0 27 23	H= -1 K= 15
2 13 12		0 27 28	5 10 10	0 12 11	7 16 17	1 17 17	-5 17 16
4 9 9	H= -4 K=-10	2 34 34	6 7 8	2 15 16	8 10 10	2 14 13	-3 12 11
	-1 8 8	4 18 17	7 7 8		9 6 7	3 27 28	-2 13 14
H= -5 K= -6	2 9 9	6 17 16	8 15 17	H= -2 K=-14		4 18 18	-1 28 27
-3 18 16	5 7 6	R 11 12		-5 8 7	H= -2 K= -3	5 12 13	1 20 18
-1 5 5	6 5 5		H= -3 K= -6	-4 13 14	-4 14 14	8 13 12	3 25 25
1 25 21	7 14 14	H= -3 K=-18	-5 8 9	-3 8 8	-2 36 41		5 12 14
3 9 9		1 8 9	-3 45 46	0 24 22	-1 5 5	H= -1 K= 6	
4 6 7	H= -4 K= -9		-1 11 10	1 8 9	1 40 37	-7 19 21	H= -1 K= 16
5 19 16	-4 16 14	H= -3 K=-17	0 11 10	3 21 21	2 10 11	-5 10 9	-6 10 11
7 6 5	0 17 15	-2 8 8	1 73 59		3 28 26	-3 39 40	-3 10 10
	2 7 6	-1 8 9	2 16 16	H= -2 K=-13	6 12 11	-1 22 25	-2 14 16
H= -5 K= -5	4 14 14	0 7 7	3 6 6	-4 9 9		0 33 30	0 16 18
-3 6 6	5 7 9	1 7 8	5 26 21	-3 18 20	H= -2 K= -2	1 35 36	2 15 15
-2 12 13	6 7 8		7 9 9	1 19 19	-5 14 13	2 6 6	
-1 7 7		H= -3 K=-16	9 5 5	5 9 9	-4 28 30	3 28 31	H= -1 K= 17
0 8 7	H= -4 K= -8	-3 8 8		6 9 11	-3 15 15	4 11 12	-6 11 11
2 12 10	-5 12 14	-2 12 11	H= -3 K= -5		-2 10 10	5 12 13	-1 8 8
4 6 7	-3 8 9	0 12 14	-5 9 9	H= -2 K=-12	-1 36 42	7 20 20	0 10 12
6 7 7	-2 8 8	1 6 6	-4 8 7	-6 12 11	0 57 57		3 10 10
8 5 5	-1 24 22	2 15 15	-3 8 9	2 20 20	1 10 12	H= -1 K= 7	4 12 11
	2 13 12	4 7 6	-2 17 19	4 18 17	2 19 13	-8 9 10	
H= -5 K= -4	3 23 22		-1 15 18		3 65 68	-6 11 10	H= -1 K= 18
-4 15 15	6 7 7	H= -3 K=-15	0 53 47	H= -2 K=-11	4 35 35	-4 35 34	-3 10 9
-2 11 10	7 7 9	-1 22 22	2 18 18	-4 9 10	7 21 21	-3 23 25	1 9 8
0 18 17	9 7 8	3 15 16	3 12 10	-3 10 11	8 9 9	-2 26 28	3 10 8
1 6 5		5 7 8	4 58 53	-1 9 9		-1 9 11	
2 15 14	H= -4 K= -7		5 7 8	0 12 13	H= -2 K= -1	0 52 50	H= -1 K= 19
3 6 6	-4 9 8	H= -3 K=-14	8 17 18	1 9 8	-4 26 26	1 40 37	0 5 6
4 15 15	-3 20 20	-4 18 17		4 24 22	-3 56 57	2 35 38	1 5 6
5 8 7	-2 20 20	-3 15 16	H= -3 K= -4	6 8 9	-2 7 6	3 10 10	
7 6 5	-1 15 14	-2 14 15	-5 7 5		0 13 15	4 43 47	H= 0 K= 0
	0 13 13	-1 8 7	-4 22 24	H= -2 K=-10	1 86 84	5 11 11	2 19 17
H= -5 K= -3	1 34 34	0 21 23	-3 14 13	-5 12 11	2 6 3	6 13 12	4 101 114
-3 8 6	2 16 17	1 12 11	-2 12 13	-1 14 14	3 12 11	8 16 17	6 9 8
-2 9 9	3 16 15	2 17 16	0 54 33	0 18 17	5 32 34		8 16 14
0 8 8	4 13 9	4 12 11	2 62 57	1 17 16	9 9 10	H= -1 K= 8	
2 8 8	5 22 20	6 9 9	3 7 6	3 14 14		-7 12 12	H= 0 K= 1
3 12 10	6 8 8		4 20 19	5 12 10	H= -2 K= 0	-6 23 21	1 48 61
4 5 6		H= -3 K=-13	5 8 8	6 8 8	-4 37 39	-4 16 16	2 96 117
7 9 9	H= -4 K= -6	-2 18 21	6 21 22	7 8 9	-2 8 8	-3 35 32	3 62 74
	-3 8 10	0 14 15			4 50 46	-2 27 29	6 11 13
H= -5 K= -2	-2 11 11	1 18 18		H= -2 K= -9	8 23 25	-1 9 8	7 28 30
-3 10 9	-1 17 16	2 17 15		-6 16 16		0 35 35	

Table 4. Continued.

H= 0 K= 2			H= 0 K= 4			8 8 8			6 18 15			2 45 44			H= 0 K= 12			H= 0 K= 15			H= 0 K= 18		
0	44	39	0	75	72				7 18 16			4 28 28			8 38 38			1 15 14			0 11 11		
1	59	81	1	41	49	H= 0 K= 6			8 9 8			6 20 18			4 21 21			2 29 26					
2	42	50	2	23	24	0 130 134						8 17 14						4 9 7					
3	33	36	3	24	23	1 13 13			H= 0 K= 8						H= 0 K= 13			6 14 12					
4	33	39	4	35	37	2 17 21			0 58 54			H= 0 K= 10			2 14 13								
5	34	33	5	20	19	4 59 60			1 57 65			0 25 22			3 14 15			H= 0 K= 16					
6	22	20	6	13	11	5 13 13			3 63 50			1 14 16			7 11 10			0 11 10					
8	10	11	8	9	8	6 19 16			4 26 23			4 9 8						1 21 19					
9	10	10				8 9 10			5 20 19			5 17 14			H= 0 K= 14			3 19 16					
			H= 0 K= 5						6 10 10			6 10 9			0 21 21			5 10 8					
H= 0 K= 3			1 11 16			1 52 55			7 10 7						1 16 14								
2 53 61			2 18 18			2 46 45			8 8 7			H= 0 K= 11			4 15 12			H= 0 K= 17					
4 58 66			5 50 54			5 35 35						2 16 14			5 10 14			1 9 8					
6 26 25			4 15 17			6 19 20			H= 0 K= 9			5 16 14						2 12 10					
8 22 20			7 21 20			5 10 9			1 17 17			7 10 10						4 8 6					

The final atomic parameters are given in Table 3. The electron density maps of a different synthesis based on these parameters and calculated for F_o with $\sin\theta/\lambda \leq 0.5$ showed a broad maximum, 0.6 e/Å^3, in the region between the expected positions of the methylene hydrogens. Maxima of this height were also found in the region between the presumably hydrogen bonded oxygens O(5) and O(3), and O(6) and O(7). Attempts to refine the positions of these four hydrogen atoms failed however. All other peaks were less than 0.6 e/Å^3 and were judged as spurious.

The observed values of F_o are compared to those calculated in the last cycle of refinement in Table 4.

All computations were performed on the UNIVAC 1108 computer at Lund, Sweden, using the programmes DRF, LALS, DISTAN, PLANE, CELSIUS and ORTEP.[9]

DESCRIPTION OF THE STRUCTURE

The superscripts (i) – (x) are used to indicate the following equivalent positions in the structure

	x,y,z	(iv)	$x-1/2,1/2-y,1/2+z$	(viii)	$x-1/2,1/2-y,z-1/2$
(i)	$x-1,y,z$	(v)	$1-x,-y,2-z$	(ix)	$1/2+x,1/2-y,z-1/2$
(ii)	$-x,-y,1-z$	(vi)	$1/2+x,1/2-y,1/2+z$	(x)	$x-1,y,z$
(iii)	$1/2-x,y-1/2,3/2-z$	(vii)	$1/2-x,1/2+y,3/2-z$		

where x,y,z are the atomic coordinates given in Table 3.

The scandium ion is octahedrally surrounded by three carboxylate oxygens O(1), O(2), and O(3), contributed by two malonate ions, two hydroxy oxygens O(5), and one water oxygen O(6) as illustrated in Fig. 1. The octahedra are connected in pairs by the sharing of the edge O(5) – O(5). The resulting Sc···Sc distance is 3.27 Å. Carboxylate bridges like Sc – O(1)C(1)O(2) – Sc^x link the octahedra in infinite chains around the lines $y=0$, $z=1/2$ and $y=1/2$, $z=0$. The malonate ion forms a six-membered chelate ring with scandium and has one uncoordinated oxygen O(3) which points away from the chain in the y-direction.

The chains are hydrogen bonded to each other. This feature is shown in Fig. 2. The hydrogen bonds between chains at the same y-level are formed

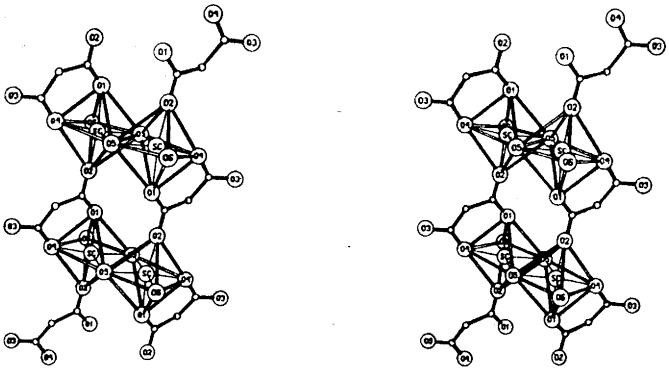

Fig. 1. A stereoscopic pair of drawings showing part of an infinite scandium-malonate chain. The Sc – O bonds are indicated by single lines, bonds within the malonate ions are filled and the edges of the octahedra are open.

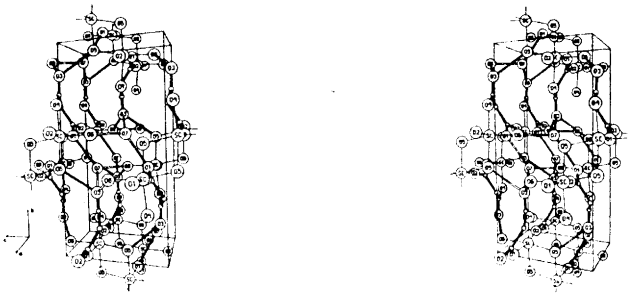

Fig. 2. A stereoscopic pair of drawings illustrating the hydrogen bond system and the packing of the scandium malonate chains. Hydrogen bonds are open and other bonds are indicated as in Fig. 1.

via the uncoordinated water molecule O(7) and those between chains at adjacent y-levels *via* the uncoordinated carboxylate oxygen O(3). Within the same y-level the chains are closely packed; the shortest inter-chain contact is $O(6^{ix})\cdots O(6^{vii})$, 3.27 Å. Furthermore the oxygens O(3) and O(7) are situated between these chains resulting in a crowding of oxygens around $y=0$, $z=0$ and $y=1/2$, $z=1/2$.

The coordination around scandium. The dimensions of the coordination polyhedron are given in Table 5 A. The Sc – O bond distances range from 2.05 to 2.12 Å with the average 2.08 Å. This value is within 0.02 Å equal to that reported for sixcoordinated scandium in $Sc(HCOO)_3$.[10] It may also be compared to the average Sc – O bond distance, 2.23 Å, found in $Sc_2(C_2O_4)_3.6H_2O$,[11] where the coordination number of scandium is eight. The difference in ionic radius of scandium(III) between eight and six coordination is 0.14 Å [12] and thus the agreement is good. These two structures seem to be the only scandium carboxylate structures previously reported.

The octahedron is somewhat distorted, with O – Sc – O bond angles in the range 76° – 98°. The distance between the bridging oxygens O(5)···O(5^{ii}) is 2.54 Å. All other O – O contact distances are within 0.21 Å from the average, 2.95 Å. Thus the malonate ion, with the bite O(1)···O(4), 2.74 Å, spans the next shortest edge of the distorted octahedron.

The chelate ring has a boat conformation; the carboxylate atoms C(1), O(1), C(3), and O(4) are coplanar within 0.04 Å and the scandium ion and the methylene carbon are situated at the same side of this plane (Table 6). This conformation is almost invariably found for six-membered malonate chelate rings.[3]

The malonate ion. The bond distances and angles within the malonate ion are given in Table 5B, and are also included in Fig. 3. They are in agreement with those found in other malonate structures.[1]

Table 5. Selected distances (Å) and angles (°) with estimated standard deviations.

A. The coordination polyhedron

Sc – O(1)	2.116(5)	O(1) – Sc – O(6)	85.6(2)
Sc – O(2^{i})	2.048(6)	O(2^{i}) – Sc – O(4)	94.4(2)
Sc – O(4)	2.090(6)	O(2^{i}) – Sc – O(5)	95.5(2)
Sc – O(5)	2.076(5)	O(2^{i}) – Sc – O(5^{ii})	94.6(2)
Sc – O(5^{ii})	2.059(5)	O(2^{i}) – Sc – O(6)	82.7(2)
Sc – O(6)	2.119(6)	O(4) – Sc – O(5^{ii})	94.3(2)
O(1) – Sc – O(4)	81.4(2)	O(4) – Sc – O(6)	96.3(2)
O(1) – Sc – O(5^{ii})	97.9(2)	O(5) – Sc – O(6)	94.3(2)

B. The malonate ion

C(1) – C(2)	1.533(13)	C(1) – C(2) – C(3)	115.7(8)
C(2) – C(3)	1.531(13)	O(1) – C(1) – O(2)	122.5(7)
C(1) – O(1)	1.270(9)	O(1) – C(1) – C(2)	120.2(7)
C(1) – O(2)	1.253(10)	O(2) – C(1) – C(2)	117.3(7)
C(3) – O(3)	1.253(10)	O(3) – C(3) – O(4)	123.6(7)
C(3) – O(4)	1.271(10)	O(3) – C(3) – C(2)	117.7(7)
O(1) – O(4)	2.743(8)	O(4) – C(3) – C(2)	118.6(7)
Dihedral angles:			
C(3) – C(2) – C(1) – O(1)	35.3	C(1) – C(2) – C(3) – O(3)	140.1
C(3) – C(2) – C(1) – O(2)	145.6	C(1) – C(2) – C(3) – O(4)	42.8

C. Possible hydrogen bonds

O(5) – O(3^{iii})	2.910(8)	O(1^{v}) – O(7) – O(3^{vi})	98.9(3)
O(6) – O(3^{iv})	2.736(8)	O(3^{iv}) – O(6) – O(7)	101.8(3)
O(6) – O(7)	2.570(9)	O(6) – O(7) – O(3^{vi})	115.6(3)
O(7) – O(1^{v})	2.922)9)	O(7) – O(3^{vi}) – O(6^{x})	125.3(3)
O(7) – O(3^{vi})	2.755(9)		
Sum of bond angles around:	O(5)	356.4	
	O(6)	357.2	
	O(7)	341.9	

Table 6. Deviations in Å, from the least-squares planes through the C–COO-groups and through the carboxylate atoms of the chelate ring. In each case the atoms defining the plane are given above the asterisk.

The C–COO-groups				The chelate ring	
Atom	Distance	Atom	Distance	Atom	Distance
C(2)	0.001	C(2)	0.004	C(1)	0.037
C(1)	−0.004	C(3)	−0.015	O(1)	−0.035
O(1)	0.002	O(3)	0.005	C(3)	−0.037
O(2)	0.002	O(4)	0.005	O(4)	0.035
*		*		*	
Sc	0.039	Sc	−0.321	Sc	0.324
Sc^{x}	0.426			C(2)	0.447

The two C–COO groups are planar within the limits of errors (Table 6). The dihedral angles included in Table 5B and in Fig. 3 indicate that the carboxylate groups are twisted in the same direction out of the carbon chain plane by about 40°. Similar twists have been found in all previously studied malonate chelates.

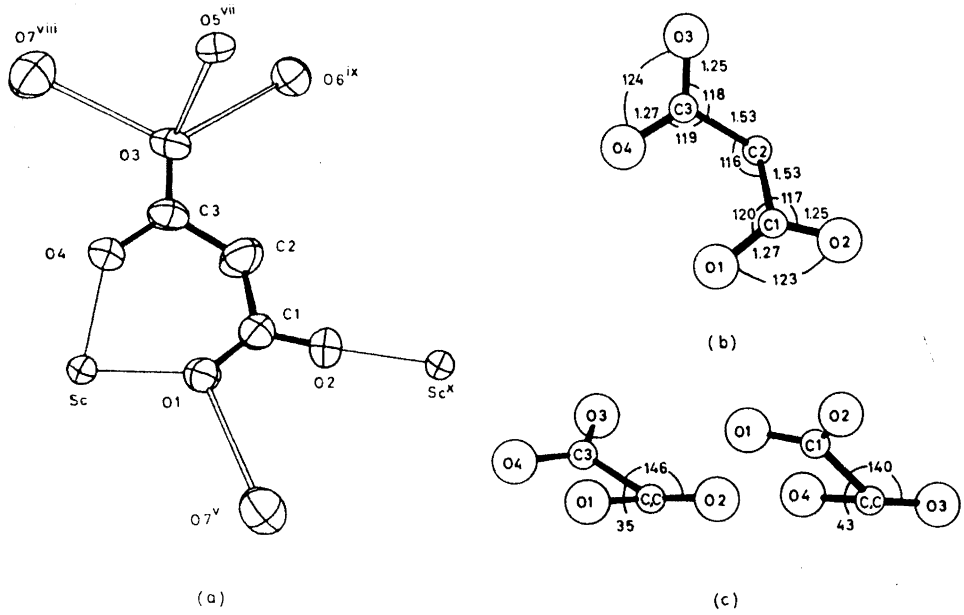

Fig. 3. (a) The malonate ion with its immediate surroundings. The "thermal ellipsoids" are scaled to include 50 % of the probability distribution. (b) Bond distances (Å) and angles (°) within the malonate ion. (c) Projections of the malonate ion along each of its C–C bonds. The angles included are the dihedral angles C–C–C–O.

The bonding situation of the malonate ion is approximately the same as found for the malonate ions forming six-membered chelate rings in NDO [1] and NDH,[2] *i.e.* one nonchelating oxygen is bonded to an adjacent metal ion and the other is hydrogen bonded in the structure. These three malonate ions are compared in Table 7. The ligand bite seems to be somewhat shorter in the sixcoordinated scandium complex than in the ninecoordinated neodymium complexes but it must be concluded that the influence of the change in size of the central ion is small.

Table 7. A comparison of the malonate ions forming six-membered chelate rings with neodymium(III) (NDO, NDH) and with scandium(III) (SCM). ϕ_1 is the angle between the plane of the bridging carboxylate group and the carbon chain plane, and ϕ_2 is the corresponding angle for the hydrogen bonded carboxylate group (see text).

	NDO	NDH	SCM
ϕ_1/°	41	34	35
ϕ_2/°	51	41	51
bite/Å	2.80(2)	2.83(2)	2.743(8)

The possible hydrogen bonds. The O – O distances suitable for hydrogen bond formation are given in Table 5C. They are selected by the same criteria as used before.[1]

Judging from these distances the scandium-malonate chains are held together by hydrogen bonds *via* the uncoordinated oxygens O(7) and O(3), as illustrated in Fig. 2. The water molecules O(6), coordinated to the scandium ions of one chain, form together with water molecules O(7) and carboxylate oxygens O(3), a hydrogen bonded chain with the sequence –O(6)–O(7)–O(3)–O(6)– and running in the x-direction. The O – O bond distances in this chain are 2.57 – 2.76 Å. Weaker hydrogen bonds, 2.9 Å, link O(3) and O(7) to the hydroxy oxygens O(5) and carboxylate oxygens O(1) of an adjacent scandium malonate chain.

The atoms O(5^{vi}), O(6^{ix}), O(7^{x}), and C(3) form a distorted tetrahedron around O(3) with "tetrahedral" angles in the range 80 – 129°. The sum of the three bond angles around the hydrogen bond donors O(5), O(6), and O(7) are given in Table 5C, which also includes the donor angles of O(6) and O(7) and the O – O – O angles within the hydrogen bonded chain.

Acknowledgements. I am indebted to Professor Ido Leden and Drs. Jörgen Albertsson and Ingmar Grenthe for many valuable discussions. This work is part of a research project supported by the *Swedish Natural Science Research Council.*

REFERENCES

1. Hansson, E. *Acta Chem. Scand.* **27** (1973) 2441.
2. Hansson, E. *Acta Chem. Scand.* **27** (1973) 2813.
3. Hansson, E. *Acta Chem. Scand.* **27** (1973) 2827.

4. Gmelin-Kraut, *Handbuch der anorganischen Chemie*, Heidelberg 1932, Band VI, Abteilung 2, p. 690.
5. Hansson, E. *Acta Chem. Scand.* **27** (1973) 823.
6. Cruickshank, D. W. J. In Rollet, J. S., Ed., *Computing Methods in Crystallography*, Pergamon, Glasgow 1965, pp. 99–116.
7. *International Tables for X-Ray Crystallography*, Kynoch Press, Birmingham 1962, Vol. III.
8. Cromer, D. T., Larsson, A. C. and Waber, J. T. *Acta Cryst.* **17** (1964) 1044.
9. Liminga, R. *Acta Chem. Scand.* **21** (1967) 1206.
10. Guseinova, A. S., Antsyshkina, M. A. and Porai-Koshits, M. A. *J. Struct. Chem.* **9** (1968) 926.
11. Hansson, E. *Acta Chem. Scand.* **26** (1972) 1337.
12. Shannon, R. D. and Prewitt, C. T. *Acta Cryst.* B **25** (1968) 925.

Received March 22, 1973.

ACTA CHEMICA SCANDINAVICA 27 (1973) 2852–2860

Structural Studies on the Rare Earth Carboxylates

21. On the Positions of the Water Molecules in Hexa-aquo Tris-oxalato Dineodymium(III) 4½-Hydrate at −50°C

EVA HANSSON

Physical Chemistry 1, Chemical Center, University of Lund, P.O. Box 740, S-220 07 Lund 7, Sweden

One third of the water molecules of $Nd_2(C_2O_4)_3.10\frac{1}{2}H_2O$ are disordered at room temperature. The structure has been redetermined at −50°C and several new water positions with occupancies in the range 0.3 – 0.5 have been found. They are located in cavities in the structure, and are within hydrogen bond distance (2.7 – 3.2 Å) from each other and from the oxygens surrounding the cavity.

According to chemical analysis the compound $Nd_2(C_2O_4)_3.nH_2O$ (NDOX) should contain 10.5 mol of water per formula unit. NDOX is commonly described as a decahydrate but values of n larger than 10 have been reported by Wylie [1] and by the present author.[2] An X-ray structure analysis [2] showed that six of the water molecules were coordinated to neodymium. Only one of the uncoordinated water molecules could be located and it became necessary to assume that the remaining water molecules (3.5 per formula unit) were disordered in the cavities formed by the packing of the neodymium oxalate complexes. This situation often arises when large "empty" spaces are left between layers, molecules or complex ions in compounds which crystallize from water solution.[3] The main function of such disordered water molecules seems to be that of filling space and they should be only weakly attached to the surrounding atoms and to each other.

In some structures of this type,[4–6] maxima in the electron density, interpretable as water molecules with temperature factors in the range 10 – 25 Å^2, are found in the appropriate regions. These high temperature factors cannot be attributed to the thermal movement of a single atom but may be simulated by a random distribution of the water molecules among a number of favourable positions around that obtained in the structure refinement. Even in cases where no significant electron density is found it must be assumed that the included water molecules are located to certain favourable regions of the actual space rather than being distributed completely at random.

This localized disorder may be statistical or dynamic. In the latter case it is possible that the water molecules may be fixed at the most favourable position of each region when their thermal mobility is reduced. Then it should be possible to detect these water positions in a low temperature study of the structure.

In an attempt to locate the missing water molecules the structure of NDOX has been reinvestigated at −50°C. Unfortunately the crystal structure may not be stable at low temperature as indicated by diffuse and sometimes split reflexions. Thus the accuracy in the determination is fairly low but since new water positions were actually found the result is given here.

EXPERIMENTAL

The preparation and analysis of the crystals have been described before.[2] A crystal of the dimensions $0.10 \times 0.10 \times 0.30$ mm^3 mounted in a glass capillary along the 0.30 mm edge was used in recording the layers $hk0-hk5$, with the Weissenberg, multi-film technique. Ni-filtered Cu-radiation was used and the temperature was −50°C. The low temperature equipment was of the type described by Olovsson.[7] The intensities of 756 independent reflexions were measured visually by comparison with a calibrated scale. Corrections for the Lorentz, polarisation and absorption effects were applied to the intensity data. The linear absorption coefficient was 371 cm^{-1} and the transmission factors were in the range 0.05 − 0.17.

The room-temperature unit cell parameters, $a = 11.68$ Å, $b = 9.65$ Å, $c = 10.28$ Å, and $\beta = 118.9°$ were used in the refinement. Judging from Weissenberg and oscillation photographs the changes in cell edges between room-temperature and −50°C were less than 0.05 Å and that in β less than 0.5°. The space group is $P2_1/c$ (No. 14)[8] and $Z = 4$.

All computation work was carried out on the UNIVAC 1108 computer at Lund, Sweden, using the programs DRF, DATAP2, LALS, DISTAN, and LINUS.[9]

DETERMINATION OF THE WATER POSITIONS

The electron density maps of a $F_o - F_c$ synthesis based on the room-temperature positions of the neodymium ion, the oxalate ions, and the coordinated water oxygens, revealed five peaks of height 1 − 2 e/Å^3, at positions suitable for water oxygens. These positions are denoted W1, W2, W3, W4, and W5 in Table 1. Several of them are too close together to be simultaneously occupied (see Table 4A).

The positional parameters of all atoms including W1 − W5, isotropic temperature factors, and inter layer scale factors together with the occupancies, G, of W1 − W5 were refined by full-matrix least squares calculations. After six cycles the shifts in all parameters were less than 10 % of their estimated standard deviations and the valus of the varied occupancies were $G_{w1} = 0.65(14)$, $G_{w2} = 0.52(13)$, $G_{w3} = 0.39(11)$, $G_{w4} = 0.32(11)$, and $G_{w5} = 0.30(13)$. It is obvious that the standard deviations are too large to permit any accurate determination of the water content.

Among the conditions on the occupancies derivable from the "too close" distances given in Table 4 A, are $G_{w1} + G_{w2} \leq 1$ and $G_{w3} + G_{w4} + G_{w5} \leq 1$. In view of the large estimated standard deviations both conditions appear to be met but in a following refinement the occupancies $G_{w1} - G_{w5}$ were fixed at the values 0.5, 0.5, 0.4, 0.3, and 0.3, respectively. The agreement factor

Table 1. Atomic parameters with estimated standard deviations for the compound $Nd_2(C_2O_4)_3.10\frac{1}{2}H_2O$ at −50°C. *B* denotes the isotropic temperature factor and *G* the occupancy of the position.

Atom	Group	*G*	$x \times 10^4$	$y \times 10^4$	$z \times 10^4$	B/Å^2
Nd			1887(2)	468(2)	3569(3)	2.4(1)
O(1)	COO^-		3934(23)	−704(20)	5548(34)	3.0(5)
O(2)	COO^-		3914(23)	1014(24)	3522(35)	3.5(5)
O(3)	COO^-		1265(24)	−989(23)	5065(36)	3.4(5)
O(4)	COO^-		89(22)	1454(23)	4000(33)	3.4(4)
O(5)	COO^-		−327(26)	−240(23)	1515(45)	3.5(5)
O(6)	COO^-		1653(29)	698(28)	929(44)	4.4(6)
O(7)	H_2O		2101(24)	−1866(22)	2812(36)	3.6(5)
O(8)	H_2O		2991(28)	1903(27)	5885(41)	4.5(6)
O(9)	H_2O		1630(25)	2938(26)	2791(40)	4.2(5)
C(1)			5010(36)	450(33)	4484(54)	3.5(6)
C(2)			324(29)	−680(26)	5329(47)	2.4(6)
C(3)			559(35)	178(33)	−305(72)	3.4(7)
W1	H_2O	0.5	4244(57)	−1898(58)	2273(83)	4.9(1.3)
W2	H_2O	0.5	4343(86)	−2904(86)	3009(117)	8.2(2.1)
W3	H_2O	0.4	3368(69)	−972(69)	6(100)	4.6(1.5)
W4	H_2O	0.3	3818(84)	552(81)	−1063(131)	3.6(1.6)
W5	H_2O	0.3	4155(87)	82(87)	176(133)	3.6(1.6)

$R = \sum||F_o| - |F_c||/\sum|F_o|$ converged to 0.122 and $wR = [\sum w(|F_o| - |F_c|)^2/\sum w|F_o|^2]^{1/2}$ to 0.155. The refinement procedure was the same as described in Ref. 2 and the weighting scheme used was $w = 1/(20 + |F_o| + 0.008|F_o|^2 + 0.0005|F_o|^3)$. The final atomic parameters are given in Table 1 and the observed structure factors are compared to those calculated in the last cycle in Table 2. The shifts in all parameters were less than 1 % of their estimated standard deviations in this cycle.

Judging from the conditions given above the sum of the occupancies used for W1 – W5 is the maximum possible. It corresponds to a total water content of 10 mol per formula unit *i.e.* lower than that indicated by chemical analysis. A difference synthesis based on the parameters given in Table 1 revealed, besides a peak of about 5 e/Å^3 at the position of neodymium, a number of peaks 1 – 2 e/Å^3. Three of them had positions suitable for additional water oxygens *viz.* (0.59, −0.06, 0.18), (0.37, −0.03, −0.11), and (0.48, −0.00,0.00), but it was not possible to refine oxygen at these positions. The structure may, however, contain disordered water even at low temperature and thus the hydration number 10.5 is not excluded by the present analysis.

The water position W1 was found already in the room-temperature study of NDOX.[2] The electron density maps of the final difference synthesis of that work showed a peak, 3e/Å^3, approximately at the position W4 and also wide regions of positive electron density, about 1 e/Å^3, around W2 and W3. The positions W2 – W5 were tentatively included in a new refinement of the room-temperature structure. This refinement was successful for W2 and W3 but not for W4 and W5. The positional parameters arrived at for W1, W2, and

Table 2. Observed and calculated structure factors in $Nd_2(C_2O_4)_3.10\frac{1}{2}H_2O$ at the temperature −50°C. In each group the running index h, $|F_o|$, and $|F_c|$ are given.

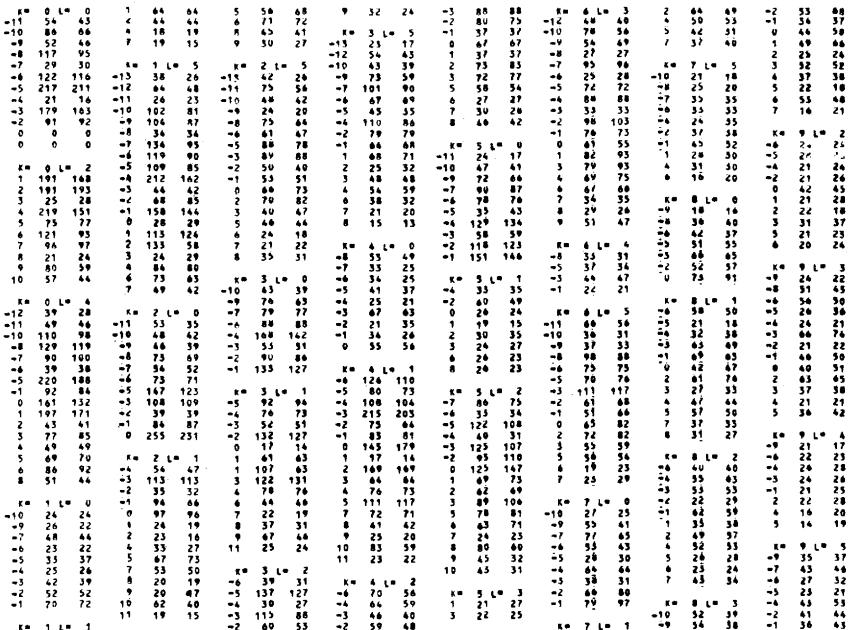

Table 3. Positional parameters of the disordered water molecules W1, W2, and W3 at room temperature. B denotes the isotropic temperature factor and G the occupancy of the position.

Atom	G	$x \times 10^4$	$y \times 10^4$	$z \times 10^4$	B/Å^2
W1	0.5	5685(52)	3098(60)	2812(60)	4.3(1.0)
W2	0.5	5719(95)	2431(112)	2190(112)	9.0(2.3)
W3	0.4	6797(197)	4166(209)	4995(209)	14.9(5.1)

W3 at room temperature are given in Table 3. The R-value was reduced by 0.002 by the introduction of W2 and W3.

The structure of NDOX has also been determined by Ollendorff and Weigel.[10] They found the water positions W1 ($G=0.5$, $B=8.0$) and W5 ($G=0.6$, $B=5.0$). Thus the low temperature study confirms the water positions discernible from the two room temperature investigations.

DESCRIPTION OF THE WATER ARRANGEMENT

The room temperature structure of NDOX has been described in detail in Ref. 2, and only a brief recapitulation of the general features will be given here. Superscripts of the following significance are used to indicate equivalent sites in the structure.

	x,y,z	(v)	$1-x,1/2+y,1/2-z$	(xi)	$1-x,\bar{y},1-z$
(i)	$1-x,\bar{y},\bar{z}$	(vi)	$1-x,\bar{y},1-z$	(xx)	$1+x,\bar{y},z$
(ii)	$x,1/2-y,z-1/2$	(ix)	$x,y,z-1$	(vv)	$\bar{x},\bar{y},\bar{z}$
(iii)	$x,-y-1/2,z-1/2$	(x)	$x,-y-1/2,z-1/2$		
(iv)	$1-x,y-1/2,1/2-z$				

The structure is composed from neodymium oxalate layers parallel with the *ac*-plane and located around $y=0$ and $y=1/2$. The layer around $y=0$ is shown in Fig. 1. The ligands Nos. 2 and 3 link the neodymium ions in zig zag chains running in the z-direction. These chains are in turn linked in layers by ligand 1. Three water molecules O(7), O(8), and O(9) are coordinated to neodymium and are situated above and below the layer at $y\approx 1/4$ and $y\approx -1/4$. Adjacent layers are related by the c-glide. They are held together by hydrogen bonds formed between the water molecules of one layer and the carboxylate oxygens in the zig zag chains of the next layer, *viz.* O(9^{ii}) – O(5^{vv}), O(8^{ii}) – O(6), and O(7^{iii}) – O(4^{vv}).

With this way of packing of the layers fairly large "empty" spaces are left around the symmetry centers (1/2,0,0) and (1/2,1/2,1/2). The uncoordinated water molecules are located in these cavities. Including W1 the cavity around (1/2,0,0) is surrounded by two water hexagons *viz.* W1^{i}, O(8^{ix}), O(9^{ii}), O(8^{ii}), W1^{v}, and O7^{v} at $y\approx 1/4$ and W1^{x}, O(7^{iii}), W1, O(8^{xi}), O(9^{iv}), O(8^{iv}) at $y\approx -1/4$ and by ligand 1^{ii} and ligand 1^{iv} at $y\approx 1/2$ and $y\approx -1/2$, respectively. The water hexagons around adjacent cavities share the edge O(8) – W1, *e.g.*

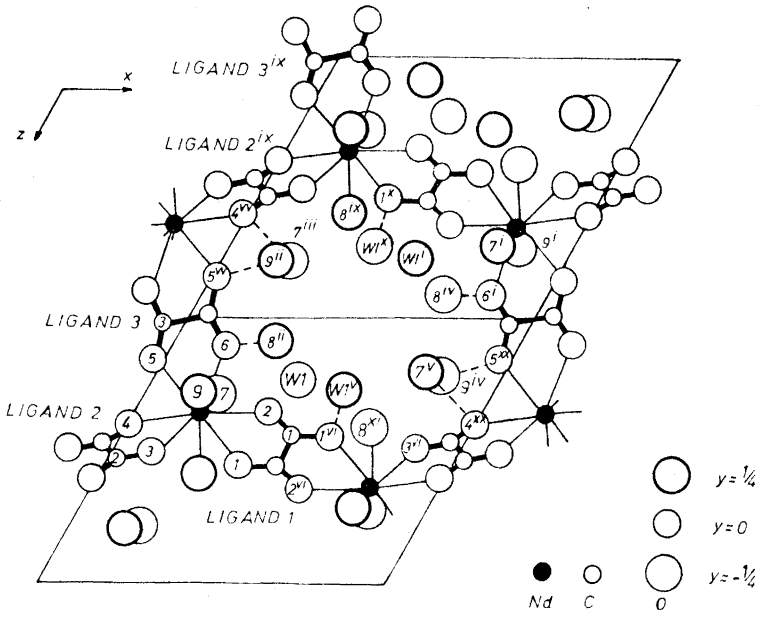

Fig. 1. The neodymium oxalate layer around $y=0$ projected onto (010), with $-0.32 \leq y \leq 0.32$, *i.e.* the water oxygens above and below the layer are included. Bonds within the oxalate ions are filled, metal-oxygen bonds are single lines, and possible hydrogen bonds are marked with dashes.

$O(8^{ix}) - W1^{i}$ of the upper hexagon around (1/2,0,0) belongs to the lower hexagon around (1/2,1/2,1/2).

This part of the structure is not drastically changed by the decrease in temperature. Because of the low accuracy obtained in both determinations it is not possible to make any detailed comparison of bond distances and angles between the two temperatures. This feature is illustrated in Table 4 B which gives the possible hydrogen bond distances of the coordinated water molecules at room temperature and at -50°C.

Table 4 C gives for each of the water molecules W1 – W5 the distances to all neighbours within the range 2.60 – 3.20 Å. These distances are regarded as representing possible hydrogen bonds.[11] W1 and W2 are hydrogen bonded to the coordinated water molecules O(7) and O(8) and to the carboxylate oxygen O(1); *cf.* $W1^{x}$ and $W2^{x}$ in Fig. 2 a and b, respectively. The distance W1 – W2 is 1.20 Å and thus either W1 or W2 is present. They may both be regarded as belonging to the hexagons surrounding the cavity. There are four pairs W1 – W2 around each cavity. Four water molecules may be distributed among these eight sites in ten non-equivalent ways. The possible arrangements around (1/2,0,0) are given in Table 5.

Within the cavity are six possible water sites, *viz.* W3, W4, W5, and their centrosymmetric equivalents $W3^{i}$, $W4^{i}$, and $W5^{i}$. These sites are close to

Table 4. Selected interatomic distances (Å) with estimated standard deviations in $Nd_2(C_2O_4)_3.10\frac{1}{2}H_2O$.

A. Distances shorter than 2.60 Å between possible water positions at −50°C.

W1 – W2	1.20(11)	W4 – W5	1.22(17)
W1 – W3	2.23(11)	W4 – $W5^{i}$	2.17(12)
W3 – W4	2.05(12)	W5 – $W5^{i}$	2.18(19)
W3 – W5	1.32(11)		

B. Possible hydrogen bond distances of the water molecules coordinated to Nd(III), at −50°C and at room temperature.

	−50°C	Room temperature		−50°C	Room temperature
$O(7^{v}) – O(4^{xx})$	2.83(3)	2.83(3)	$O(8^{ii}) – O(2)$	3.12(4)	3.12(3)
$O(7^{v}) – W1^{v}$	2.81(7)	2.96(6)	$O(8^{ii}) – O(6)$	2.81(4)	2.90(3)
$O(7^{v}) – W2^{v}$	2.72(9)	2.62(10)	$O(8^{ii}) – O(9)$	3.07(5)	3.03(3)
$O(7^{v}) – W3^{i}$	2.90(8)	2.89(20)	$O(8^{ii}) – W1^{v}$	2.85(7)	2.82(6)
$O(9^{ii}) – O(5^{vv})$	2.64(4)	2.69(3)	$O(8^{ii}) – W2^{v}$	2.92(9)	2.91(10)
$O(9^{ii}) – O(8^{ix})$	3.07(5)	3.00(3)	$O(8^{ix}) – W4$	3.09(12)	–
$O(9^{ii}) – W4$	2.67(9)	–			

C. Possible hydrogen bond distances at −50°C of the water molecules not coordinated to Nd(III).

$W1^{x} – O(1^{x})$	2.83(7)	$W3^{i} – W2^{v}$	2.99(13)
		$W3^{i} – W4$	2.95(11)
$W1^{x} – O(8^{iv})$	2.85(7)	$W3^{i} – W5$	3.11(12)
W1 – W5	2.84(13)		
		$W4 – O(8^{ix})$	3.09(12)
$W2^{x} – O(1^{x})$	2.70(11)	$W4 – O(9^{ii})$	2.67(9)
$W2^{x} – O(7^{iii})$	2.72(9)	$W4 – W2^{x}$	2.90(12)
$W2^{x} – O(8^{iv})$	2.92(9)	$W4 – W3^{i}$	2.95(11)
$W2^{x} – W3$	2.99(13)	$W4 – W4^{i}$	2.78(19)
$W2^{x} – W4$	2.90(12)	$W4 – W2^{v}$	3.19(15)
$W2 – W4^{i}$	3.19(15)		
$W2^{x} – W5$	3.15(14)	W5 – W1	2.84(13)
$W2^{v} – W5$	2.68(13)	$W5 – W2^{v}$	2.68(13)
		$W5 – W2^{x}$	3.15(14)
$W3^{i} – O(6^{i})$	3.06(8)	$W5 – W3^{i}$	3.11(12)
$W3^{i} – O(7^{v})$	2.90(8)		

each other and at most two of them may be simultaneously occupied. Four non-equivalent combinations are possible. They are denoted A, B, C, and D in Table 5. The distance W1 – W3 is 2.24 Å which means that those combinations of surrounding and included water molecules that contain the pair W1 – W3 or $W1^{i} – W3^{i}$ are not allowed. There remains 27 possible combinations and none of them seem to be more probable than the other.

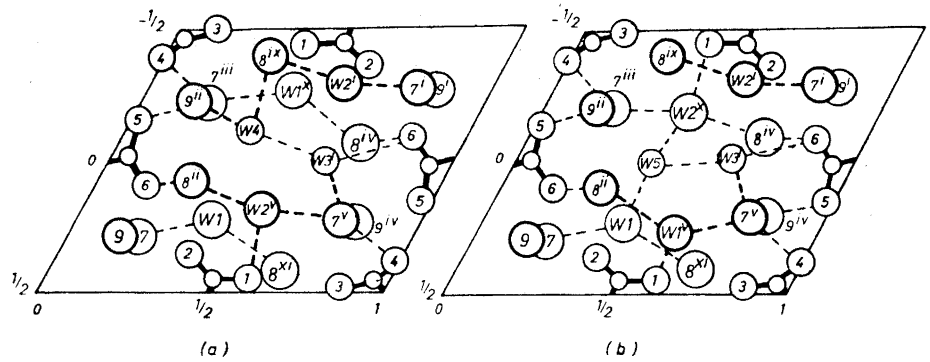

Fig. 2. Possible arrangements of water molecules around (1/2,0,0). The y-range projected and the notation of the atoms and bonds are the same as in Fig. 1.

Table 5. Possible arrangements of the disordered water molecules around (1/2,0,0). The signs + and − denote possible and impossible combinations, respectively.

Water molecules in the hexagons	Included water molecules A: W4 − W4^{i}	B: W3^{i} − W5	C: W3^{i} − W4	D: W3 − W3^{i}
I. W1,W2^{v},W2^{i},W1^{x}	+	+	+	−
II. W2,W1^{v},W2^{i},W1^{x}	+	+	+	+
III. W1,W1^{v},W2^{i},W2^{x}	+	+	+	−
IV. W1,W2^{v},W1^{i},W2^{x}	+	−	−	−
V. W2,W2^{v},W2^{i},W1^{x}	+	+	+	+
VI. W1,W2^{v},W2^{i},W2^{x}	+	+	+	−
VII. W1,W1^{v},W1^{i},W2^{x}	+	−	−	−
VIII. W1,W1^{v},W2^{i},W1^{x}	+	+	+	−
IX. W1,W1^{v},W1^{i},W1^{x}	+	−	−	−
X. W2,W2^{v},W2^{i},W2^{x}	+	+	+	+

The bonding situation of the water pairs A, B, and C may in all possible surroundings be described in the following way. The two water molecules are weakly attached to each other, with oxygen-oxygen distances of 2.7 − 3.1 Å. The distances to the surrounding oxygens are in the range 2.9 − 3.2 Å except for W4 − O(9^{ii}) and W5 − W2^{v} which are both 2.7 Å. The probable hydrogen bonds in the arrangements IIC and IIIB are shown as examples in Fig. 2 a and b, respectively. Some cavities may contain W3 and W3^{i}. In these cases the two included water molecules are not hydrogen bonded to each other since the distance W3 − W3^{i} is 4.25 Å.

The function of W1 and W2 seems to be different from that of W3, W4, and W5. W1 and W2 are engaged in hydrogen bonded water chains terminating at neodymium ions of adjacent neodymium oxalate chains, *e.g.* Nd^{ix} − O(8^{ix}) − W2^{i} − O(7^{i}) − Nd^{i} and Nd^{iii} − O(7^{iii}) − W1^{x} − O(8^{iv}) − Nd^{iv} (see Fig. 2 a). Thus the role played by W1 and W2 is that of linking adjacent neodymium

oxalate chains in the x-direction. W3 and W4 may also take part in chains of this type, *e.g.* $Nd^{ii}-O(9^{ii})-W4-W4^{i}-O(9^{iv})-Nd^{iv}$ and $Nd^{ii}-O(9^{ii})-W4-W3^{i}-O(7^{v})-Nd^{v}$ (see Fig. 2 a). Since these chains are not always present they are probably not essential as links in the structure and the main function of W3 and W4 seems to be that of filling space. W5 may link adjacent water chains in the y-direction, $W1-W5-W2^{v}$, or in the z-direction, $W1-W5-W2^{x}$ (see Fig. 2 b), but also W5 must be regarded as mainly filling out space.

Thus, even though the exact arrangement of the disordered water molecules has not been determined it is obvious that the preferred positions are those where they may be hydrogen bonded to each other and to the surrounding oxygens. In this way the included water molecules are involved in the linking of the structure at the same time as they fill out the space between the main structural elements.

Acknowledgements. I am indebted to Professor Ivar Olovsson, Uppsala, for the use of his low temperature equipment in the preliminary experiments and to Mr. Hilding Karlsson for helpful technical advice. I also wish to thank Professor Ido Leden and Drs. Jörgen Albertsson and Ingmar Grenthe for stimulating discussions. This work is part of a research project supported by the *Swedish Natural Science Research Council.*

REFERENCES

1. Wylie, A. W. *J. Chem. Soc.* **1947** 1687.
2. Hansson, E. *Acta Chem. Scand.* **24** (1970) 2969.
3. Albertsson, J. *On the Stereochemistry of Ninecoordinate Lanthanoid Compounds*, Thesis, Lund 1972.
4. Gerdil, R. *Acta Cryst.* **14** (1961) 333.
5. Mathern, G. and Weiss, R. *Acta Cryst.* **B 27** (1971) 1572.
6. Hansson, E. *Acta Chem. Scand.* **27** (1973) 2827.
7. Olovsson, I. *Arkiv Kemi* **16** (1960) 437.
8. *International Tables for X-Ray Crystallography*, Kynoch Press, Birmingham 1969, Vol. I.
9. Liminga, R. *Acta Chem. Scand.* **21** (1967) 1206.
10. Ollendorff, W. and Weigel, F. *Inorg. Nucl. Chem. Letters* **5** (1969) 263.
11. Ferraris, G. and Franchini-Angela, M. *Acta Cryst.* **B 28** (1972) 3572.

Received April 13, 1973.

ACTA CHEMICA SCANDINAVICA 27 (1973) 2861–2869

Mass Spectra of Some Aliphatic and Aromatic Selenides

ERIK REBANE

Chemical Institute, University of Uppsala, P.O.B. 531, S-751 21 Uppsala 1, Sweden

Mass spectra of a number of simple aliphatic and aromatic selenides are given. The spectrum of dimethyl selenide (I) exhibits, in addition to contributions from simple bond fissions, the two-carbon rearrangement-ions $[C_2H_5]^+$ and $[C_2H_3]^+$ and a one-step elimination of C_2H_4 from molecular ion with formation of $[SeH_2]^{+\cdot}$. In the spectra of dipropyl selenide (II) and dibutyl selenide (III) the most abundant selenious fragments are $[RSeH]^{+\cdot}$, but ions derived from C_1-C_2 and C_2-C_3 bond cleavages of one alkyl group also occur. In the spectrum of selenacyclohexane (IV) the dominating process is loss of a SeH radical from the molecular ion, but expulsion of hydrocarbon fragments containing one, two, or three carbon atoms is also observed. The fragmentation pattern of methyl phenyl selenide (V) is similar to that of the corresponding sulphide with elimination of $\cdot CH_3$, CH_2Se, and $\cdot SeH$ from the molecular ion as the main decomposition routes. In the spectra of the substituted aromatic selenides, $(XC_6H_4)_2Se$, X = *p*-CH_3, *p*-CH_3O, *p*-Cl, *p*-Br (VI–IX) the main degradation process implies elimination of the heteroatom. Alternatively, a stepwise elimination of the substituents followed by loss of the selenium atom is observed.

The selenides, R_2Se, are the largest and most extensively studied class of organic selenium compounds.[1] Their relative availability and stability also make them valuable precursors in the preparation of other types of selenium compounds, *e.g.* selenoxides, R_2SeO, and selenones, R_2SeO_2. Occasionally, selenides also occur as undesired by-products in syntheses or decompositions of other selenium compounds. For a mass spectrometric investigation on organic selenium-oxygen compounds,[2] a number of selenides were needed as starting materials in syntheses of selenoxides and selenones. However, with the exception of diethyl selenide,[3] dibenzyl selenide,[4] selenacyclopentane,[5] and diphenyl selenide,[6] the mass spectra of the prepared simple selenides seem not to have been reported in the literature but were of interest for comparative purposes during the interpretation of the spectra of their oxidation products. The purpose of the present paper is thus to discuss in some detail the spectra and fragmentation patterns of the selenides I–IX, the ions containing the main isotopes ^{80}Se, ^{35}Cl, and ^{79}Br being taken as representative of the fragment in question.

$(C_nH_{2n+1})_2Se$

Ia: n=1, Ib = D_6-Ia

II: n=3

III: n=4

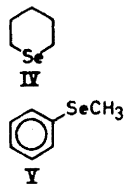

IV

V

$(XC_6H_4)_2Se$

VI : X = p-CH_3

VII : X = p-CH_3O

VIII : X = p-Cl

IX : X = p-Br

The mass spectrum of Ia, Fig. 1, is characterized by abundant selenious ions, the molecular ion at *m/e* 110 constituting the base peak. Investigation of the spectrum provides evidence for the fragmentation pattern proposed in Scheme 1.

Furthermore, evidence for some additional transitions is obtained from the spectrum of the deuterated analogue Ib (Fig. 2). Thus the fragments and the metastable transitions observed in these spectra indicate that, in addition to the main decompositions routes involving simple carbon-selenium and carbon-hydrogen bond fissions, skeletal rearrangements implying carbon-carbon bond formation occur. One such process, supported by the appearance of an appropriate metastable peak (*m/e* 61.2 in Ia, *m/e* 61.0 in Ib),

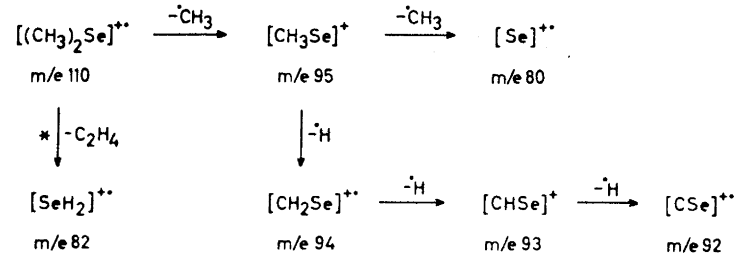

Scheme 1.

involves the elimination of the two-carbon fragment C_2H_4 from the molecular ion with formation of $[SeH_2]^{+\cdot}$ at *m/e* 82 and *m/e* 84 in Ib. This transition may proceed *via* an initial isomerization of the molecular ion and involve a hydrogen shift to selenium with a simultaneous methyl group migration forming the ion $[C_2H_5SeH]^{+\cdot}$. Loss of C_2H_4, in analogy with the *m/e* 110→*m/e* 82 process in the spectrum of diethyl selenide,[3] or simple carbon-selenium bond fission with formation of $[C_2H_5]^+$ at *m/e* 29 and *m/e* 34 in Ib, may then be obtained. However, elimination of C_2D_4 is also found, as indicated by metastable peaks at *m/e* 59.0 and *m/e* 57.2, from the $[M-D]^+$, *m/e* 114 and $[M-D_2]^{+\cdot}$, *m/e* 112, fragments of Ib (Fig. 2) with the formation of $[SeD]^+$ and $[Se]^{+\cdot}$, respectively. These processes might suggest the occurrence of a common selenacyclopropane intermediate in the eliminations of two-carbon fragments in the mass spectrum of dimethyl selenide. An alternative possibility for the generation of, for example, the $[SeH_2]^{+\cdot}$ fragment, implying the expulsion of two methylene units from the molecular ion, is very unlikely.[8] Similar skeletal

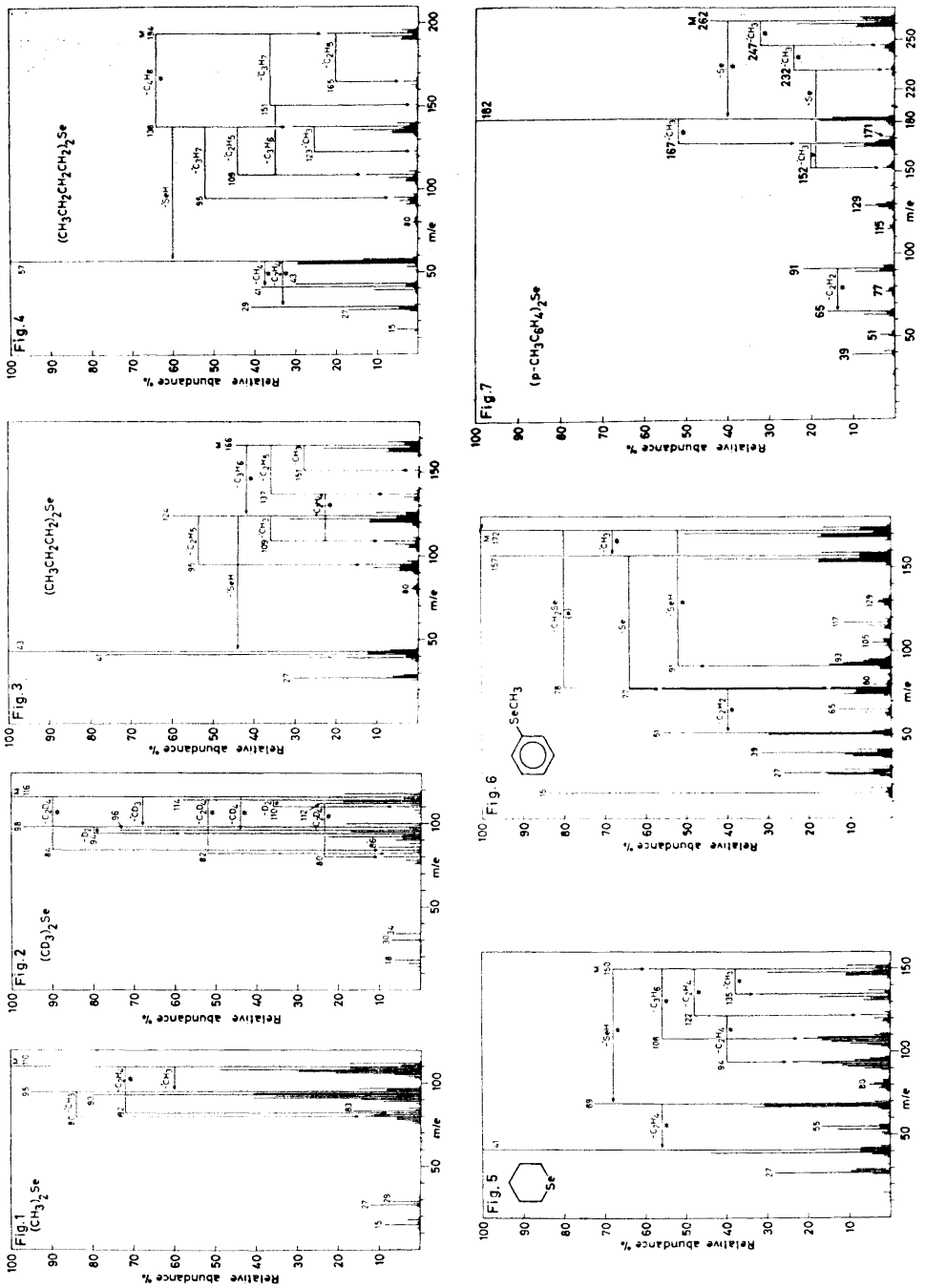
Fig.1
$(CH_3)_2Se$
Fig.2
$(CD_3)_2Se$
Fig.3
$(CH_3CH_2CH_2)_2Se$
Fig.4
$(CH_3CH_2CH_2CH_2)_2Se$
Fig.5
Fig.6
$SeCH_3$
Fig.7
$(p\text{-}CH_3C_6H_4)_2Se$
Relative abundance %
m/e

rearrangements with carbon-carbon bond formation are also observed in the mass spectra of dimethyl sulphide [9] and dimethyl phosphine.[10] Moreover, in the spectrum of Ib a somewhat unexpected elimination of CD_4 from the molecular ion

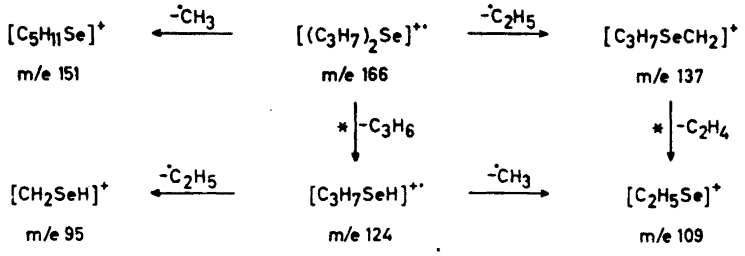

Scheme 2.

is observed, a transition which is supported by an appropriate metastable peak at *m/e* 79.5.

The mass spectra of II (Fig. 3) and III (Fig. 4) are characterized by abundant hydrocarbon ions, the selenious fragments giving peaks of lower intensity, particularly in the case of III. A detailed investigation of the spectra gives evidence for analogous fragmentation patterns as visualized for II in Scheme 2. The most abundant selenious fragments arise from cleavage of one carbon-selenium bond in the molecular ion with a simultaneous hydrogen migration to selenium from the expelled hydrocarbon fragment and the generation of the ions $[C_nH_{2n+1}SeH]^{+\cdot}$ at *m/e* 124, $n=3$ and *m/e* 138, $n=4$ in II and III, respectively. This process is analogous to that found for diethyl selenide [3] and the corresponding sulphides.[9]

Other selenious ions observed in the spectra of these selenides are derived from fragmentation processes in the alkyl groups. Thus, peaks due to C_1-C_2 and C_2-C_3 bond cleavages in one alkyl group of the molecular ion are found at *m/e* 137 and *m/e* 151 in II (Fig. 2) and at *m/e* 151 and *m/e* 165 in III (Fig. 3). Analogous degradation steps of the remaining alkyl group in the $[C_nH_{2n+1}SeH]^{+\cdot}$ ions are also observed, as indicated in Figs. 3–4. Part of the ions at *m/e* 109 $[C_2H_5Se]^+$ are also formed from the $[RSe=CH_2]^+$ fragments, a transition supported by an appropriate metastable peak in the case of II (*m/e* 86.7), probably by a McLafferty type of hydrogen migration with simultaneous cleavage of the C_1-C_2 bond and elimination of an alkene molecule. Thus the general mass spectrometric behaviour of these selenides resembles that of the corresponding sulphides and ethers.[9,11] However, pronounced differences also occur. The spectra of II and III do not exhibit to any considerable extent ions analogous to the $[RS]^+$ and $[RSH_2]^+$ fragments observed in the spectra of the corresponding sulphides, which are also much more strongly characterized by ions derived from C_1-C_2 bond cleavages.[9]

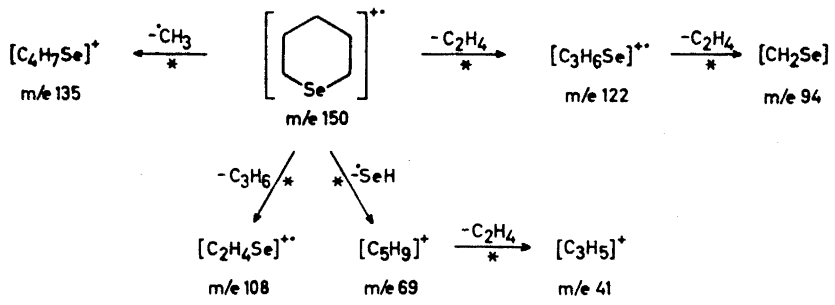

Scheme 3.

The spectrum of IV (Fig. 5) contains evidence for the fragmentation pattern given in Scheme 3. The dominating process is elimination of the heteroatom as a SeH radical, a process, which is also encountered in the spectrum of selenacyclopentane [5] but which seems to have no counterpart in the spectrum of the corresponding sulphide.[12] Other fragmentation modes of the molecular ion of IV, substantiated by appropriate metastable peaks, *m/e* 121.5, *m/e* 99.2, and *m/e* 77.8 involve elimination of hydrocarbon fragments containing one, two, and three carbon atoms and lead to the ions at *m/e* 135, 122 and *m/e* 108, respectively. The group of peaks around *m/e* 108 also contains selenious fragments at *m/e* 109 and 107, indicating the elimination of the fragments $\cdot C_3H_5$ and $\cdot C_3H_7$, respectively, from the molecular ion. Furthermore, at least part of the ions at *m/e* 94 $[CH_2Se]^{+\cdot}$ are generated by the two-step process $M-C_2H_4-C_2H_4$, although a concerted process with simultaneous loss of two molecules of ethylene may also be visualized. Remaining selenious ions in IV are observed at *m/e* 93 $[CHSe]^+$, *m/e* 81 $[SeH]^+$, and *m/e* 80 $[Se]^{+\cdot}$. These ions are often found in the spectra of aliphatic selenium compounds.[12]

The unsymmetrical selenide V, Fig. 6, exhibits an abundant molecular ion, the stability of which is reflected by the presence of doubly charged ions at *m/e* 86.[13] The dominating process is elimination of a methyl radical, Scheme 4, to form the ion at *m/e* 157, which in a second step gives rise to a phenyl ion at *m/e* 77 by loss of a selenium atom. No metastable peak has been detected to support the elimination of a CSe fragment from $[C_6H_5Se]^+$, although loss of CX is well-known from the corresponding sulphur and oxygen fragments.[14] A rearrangement of the molecular ion of V making the expulsion of a SeH radical possible, leads to the abundant ion at *m/e* 91, usually described as a tropylium ion. Another characteristic process in the spectrum of V involves a hydrogen migration to the aromatic ring with a simultaneous elimination of CH_2Se from the molecular ion and leads to the benzene ion at *m/e* 78. Both these rearrangements are also observed in the spectrum of the corresponding sulphide.[15] Finally, in the spectrum of V, there are the characteristic series of selenious fragments in low abundance at *m/e* 93 $[CHSe]^+$, *m/e* 105 $[C_2HSe]^+$, *m/e* 117 $[C_3HSe]^+$, and *m/e* 129 $[C_4HSe]^+$. These are frequently observed in the mass spectra of

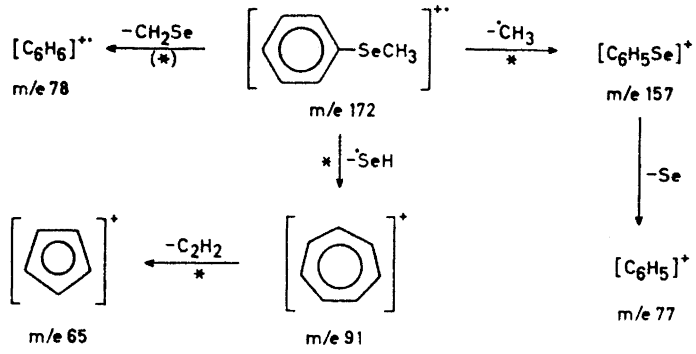

Scheme 4.

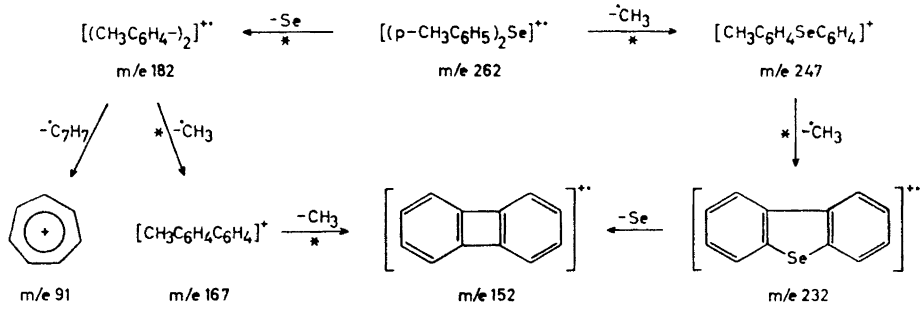

Scheme 5.

aromatic selenium compounds and apparently originate from fragmentation processes in the aromatic ring of the ion at *m/e* 157 $[C_6H_5-Se]^+$.[4]

Mass spectra of only a few aromatic selenides have been published.[7] The spectrum of diphenyl selenide has been recorded although the complete spectrum was not published.[6] The spectra of VI – IX, Figs. 7 – 10 are characterized by ions from fragmentations predominantly occurring around the selenium atom, but also by ions arising from loss of the substituents. The main fragmentation routes are formulated for VI in Scheme 5. In the spectrum of VI the dominating process is the $ABC^{+\cdot} \rightarrow AC^{+\cdot} + B$ type elimination of the selenium atom from the molecular ion leading to the ion at *m/e* 182, represented as a substituted biphenyl ion, Scheme 5.[4] This is also the principal process in the case of VII, Fig. 8, and VIII, Fig. 9, while in the spectrum of IX, Fig. 10, the alternative loss of a substituent gives rise to a peak of about equal intensity at *m/e* 311.[16] Cleavage of carbon-selenium bonds in the molecular ion occurs only to a minor extent to *m/e* 171 $[CH_3C_6H_4Se]^+$ in VI, with the analogous ions at *m/e* 187, *m/e* 191, and *m/e* 235 in the spectra of VII – IX, respectively.

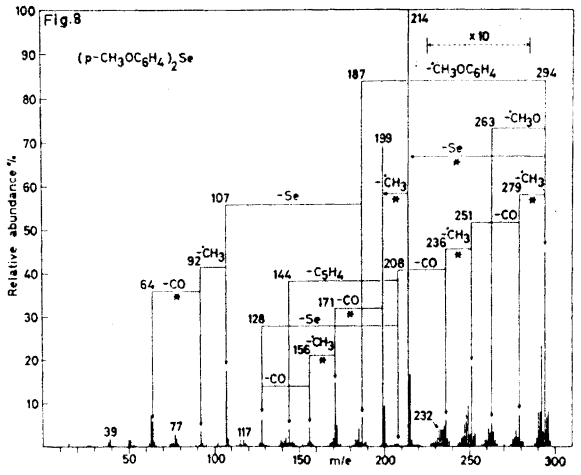

Fig. 8.

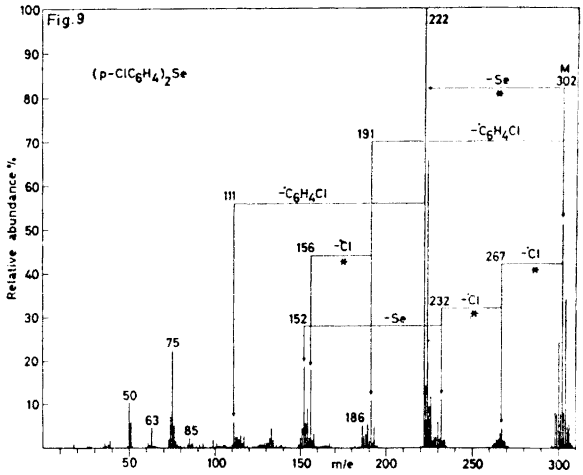

Fig. 9.

An alternative fragmentation route of the aromatic selenides VI–IX involves the stepwise elimination of the substituents from the molecular ion. This transition is shown for VI in Scheme 5 and leads to the ion at *m/e* 232. This fragment is rather abundant and associated with a doubly charged ion at *m/e* 116 in case of IX but is of very low abundance in the spectrum of VIII owing to alternative fragmentations as indicated in Fig. 8 around the ether function analogous to the degradation processes observed for anisole.[17] Finally,

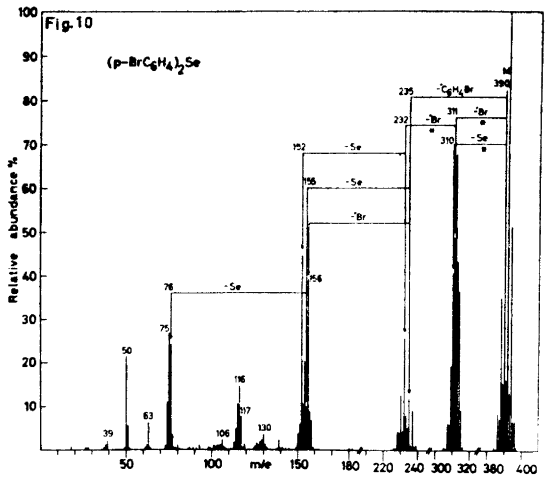

Fig. 10.

the fragment at *m/e* 232, described as a dibenzo[b,d]selenophene ion, Scheme 5, eliminates the selenium atom forming the biphenylene ion at *m/e* 152.[13] The remaining selenious fragments at lower masses in VI – IX are analogous to those usually found in the spectra of aromatic selenium compounds [4] and are not discussed further here. Finally, a number of low molecular hydrocarbon fragments are observed common to the mass spectra of aromatic compounds.[18]

EXPERIMENTAL

The mass spectra were recorded on an LKB model 9000 A gas chromatograph-mass spectrometer, operating at 70 eV. The spectra were recorded using the heated inlet system in case of I – IV, 50 – 100°, and the direct inlet system at 60 – 70°C for the selenides VI – IX. The purity of the selenides was checked by microanalysis for selenium and by TLC.

The aliphatic selenides I – IV were prepared from the corresponding alkyl halides and sodium selenide solution.[19] They were purified by redistillation and the fractions with boiling points in accordance with values in the literature were used. B.p. (°C) Ia: 53 – 54,[20] Ib: 52 – 54, II: 156 – 158,[21] III: 83.5 – 84/14, IV: 157 – 158.[22]

Methyl phenyl selenide, V, was prepared from selenophenol and dimethyl sulphate.[23] B.p. 89 – 91°/15.

The aromatic selenides VI – IX were obtained by treating the diazotized anilines with a potassium polyselenide solution as for the preparation of diphenyl selenide described in Organic Syntheses.[24] The selenides were purified by repeated recrystallizations from ethanol or methanol. VI and VII were distilled before recrystallization. M.p. (°C) VI: 68 – 69,[25] VII: 53 – 54,[25] VIII: 95.5 – 96.5,[26] IX: 114 – 115.[27]

Acknowledgements. I express my sincere gratitude to Professor Göran Bergson for the facilities put at my disposal and to Mr. O. Eriksson for skilled technical assistance with the figures. The mass spectra were recorded by Mr. P. Jahnke.

REFERENCES

1. Rheinboldt, H. In Houben-Weyl, *Methoden der Organischen Chemie*, G. Thieme, Stuttgart 1955, Vol. 9, p. 972.
2. Rebane, E. *Chemica Scripta. In press.*
3. Bogoljubov, G. H., Grishin, N. N. and Petrov, A. A. *Zh. Obshch. Khim.* **39** (1969) 2244.
4. Agenäs, L.-B. *Acta Chem. Scand.* **22** (1968) 1763.
5. Duffield, A. M., Budzikiewicz, H. and Djerassi, C. *J. Am. Chem. Soc.* **87** (1965) 2920.
6. Bergman, J. *Acta Chem. Scand.* **22** (1968) 1883.
7. Agenäs, L.-B. In Günther, W. H. H. and Klayman, D. L., Eds., *Organic Selenium Compounds: Their Chemistry and Biology*, Chapt. XV, Wiley, New York. *To be published.*
8. Budzikiewicz, H., Djerassi, C. and Williams, D. H. *Mass Spectrometry of Organic Compounds*, Holden-Day, San Francisco 1967, p. 23.
9. Levy, E. G. and Stahl, W. A. *Anal. Chem.* **33** (1961) 707.
10. Halmann, M. *J. Chem. Soc.* **1962** 3270.
11. McLafferty, F. W. *Anal. Chem.* **29** (1957) 1782.
12. Smakman, R. and deBoer, Th. J. *Advan. Mass Spectrom.* **4** (1968) 357.
13. Buu-Hoi, N. P., Mangane, M., Benson, M. and Christiaens, L. *J. Chem. Soc.* **B 1969** 751.
14. Bowie, J. H., Lawesson, S.-O., Madsen, J. Ø., Nolde, C. and Schroll, G. *Tetrahedron* **22** (1966) 3515.
15. Bowie, J. H., Lawesson, S.-O., Madsen, J. Ø., Schroll, G. and Williams, D. H. *J. Chem. Soc.* **B 1966** 951.
16. Reed, R. I. *Applications of Mass Spectrometry to Organic Chemistry*, Academic, London 1966, p. 87.
17. Barnes, C. S. and Occolowitz, J. H. *Austral. J. Chem.* **16** (1963) 219.
18. Ref. 8, p. 81.
19. Bird, M. L. and Challenger, F. *J. Chem. Soc.* **1942** 571.
20. Strecker, W. and Daniel, W. *Ann.* **462** (1928) 193.
21. Tschugaeff, L. *Ber.* **42** (1909) 49.
22. Morgan, G. T. and Burstall, F. H. *J. Chem. Soc.* **1929** 2201.
23. Gilman, H. and Webb, F. J. *J. Am. Chem. Soc.* **71** (1949) 4065.
24. Leicester, H. M. *Org. Syn.* **18** (1930) 27.
25. Leicester, H. M. and Bergstrom, F. W. *J. Am. Chem. Soc.* **53** (1931) 4433.
26. Lyons, R. E. and Bradt, W. E. *Ber.* **60** (1927) 60.
27. Bradt, W. E. and Green, J. E. *J. Org. Chem.* **1** (1937) 541.

Received April 18, 1973.

ACTA CHEMICA SCANDINAVICA 27 (1973) 2870–2876

The Mass Spectra of Some Aliphatic and Aromatic Selenium Dihalides

ERIK REBANE

Chemical Institute, University of Uppsala, P.O.B. 531, S-751 21 Uppsala 1, Sweden

The mass spectra of some representative organic selenium dibromides, R_2SeBr_2, and partial mass spectra of the corresponding selenium dichlorides, R_2SeCl_2, are given. Generally, peaks due to molecular ions are absent. The characteristic fragment is instead $[M-X]^+$. Two main fragmentation routes of the $[M-X]^+$ ions are observed. Elimination of the remaining halogen with formation of $[R_2Se]^+$ is an important process, being the only fragmentation mode of the $[M-X]^+$ ions in diarylselenium dihalides. In the spectra of dialkyl and alkyl aryl selenium dihalides, fission of one carbon-selenium bond with elimination of an alkyl group is observed, a process which may also be associated with hydrogen transfer to the charged selenious fragment. Further fragmentations of the resulting $[RSeX]^{+\cdot}$ ions involve selenium-halogen, selenium-carbon, and C_1-C_2 bond fissions.

Organic selenium dihalides, R_2SeX_2, particularly the dibromides, have long been utilized for the isolation and purification of selenides from other components in a reaction mixture.[1] Furthermore, they have been used as intermediates in syntheses of selenoxides, being of particular advantage for the preparation of pure aliphatic selenoxides.[2] During a mass spectrometric investigation of selenium-oxygen compounds, a number of selenium dibromides and selenium dichlorides were needed as precursors for selenoxides. Interest was also focused on the mass spectrometric behaviour of this type of compound during work on the preparation of aliphatic selenones by ozonization of the corresponding selenoxides in trichloromethane or tetrachloromethane solution. The products thus obtained were frequently contaminated by components, the mass spectra of which indicated the presence of both selenium and chlorine in the molecule. No descriptions, however, could be found in the literature on the fragmentation modes of organic selenium dihalides on electron impact. The mass spectra of some selenium dibromides, I – V, and partial spectra, Table 1, (including only ions containing Se – Cl bonds and some fragments obtained from their further degradation) of the corresponding selenium dichlorides, V – IX, of different types, Table 2, are given. In the following

discussion the ions containing selenium, bromine, or chlorine are represented by fragments containing the main natural isotopes ^{80}Se, ^{79}Br, and ^{35}Cl.

Compounds of the type, R_2SeX_2, X = Br, Cl, are slightly thermally unstable[3] and the question arises if the mass spectra of I – IX (Table 2) may be appreciably contaminated by fragments originating from thermal decomposition of the substances in the inlet system prior to ionization. Apparently there have been no exhaustive studies of the thermal properties of aliphatic selenium dihalides.[3] However, there are reports indicating that dialkylselenium dihalides may decompose into selenium and the corresponding alkylhalides upon heating.[3] Methyl phenylselenium dihalides are reported to give methyl halide and phenylselenium halide (C_6H_5SeX),[3] while in the case of diphenyl selenium dihalides the decomposition products are diphenyl selenide, diphenyl selenide, halogenated in one or both phenyl groups, and hydrogen halide.[3] Furthermore, in tetrachloromethane solution, the diphenylselenium dihalides have been shown to partly dissociate into the selenide and free halogen.[4]

The mass spectra of the freshly prepared pure selenium dihalides, I – IX, were recorded at rather low to moderate temperatures of the inlet system (25 – 65°). The mass spectra of the aliphatic compounds I – III and VI – VII do not exhibit fragments (Figs. 1 – 3) derivable from products which would be formed by the reported mode of their thermal decomposition.[3] The same is true for fragments which may originate from ring-halogenated diphenyl selenide in the case of V and IX. However, particularly in the spectra of IV and V, ions are found at *m/e* 158 $[Br_2]^{+\cdot}$ and abundant $[R_2Se]^{+\cdot}$ fragments at *m/e* 172 and *m/e* 234, respectively. Also, III exhibits a minor peak at *m/e* 158 due to $[Br_2]^{+\cdot}$. All the selenium dichlorides investigated, VI – IX, are also characterized by abundant $[R_2Se]^{+\cdot}$ fragments (Table 1). Small amounts of $[Cl_2]^{+\cdot}$ ions, however, are found only in the case of VIII (0.2 %) and IX (4.8 %). No metastable peaks for an electron-impact induced formation of

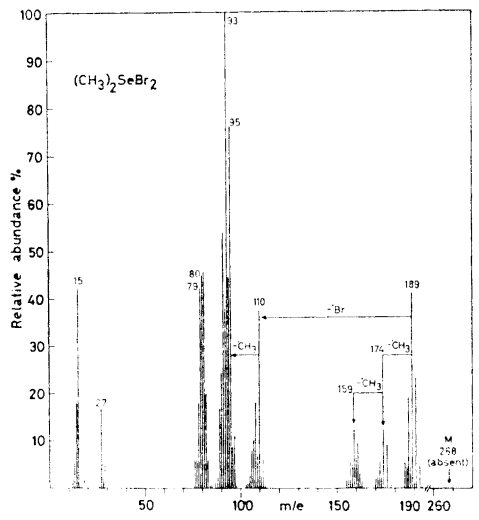

Fig. 1.

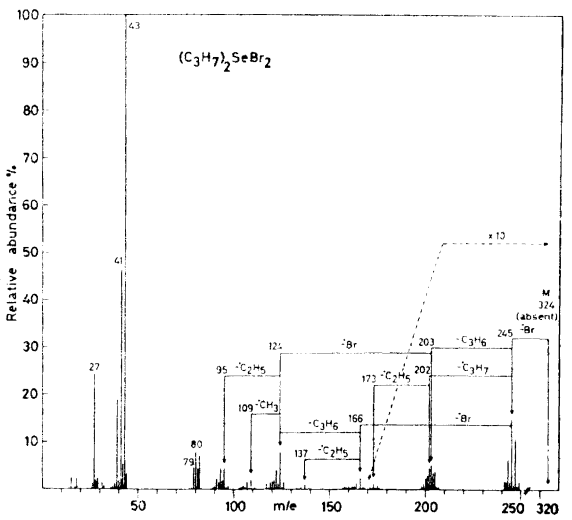

Fig. 2.

the $[M-X_2]^{+\cdot}$ ions are observed. Some dissociation of the selenium dihalides, particularly those containing aryl-selenium bonds, into the corresponding selenide and halogen before ionization thus cannot be excluded. However, the mode of the electron-impact induced degradations around the selenium dihalide function, as indicated by the recorded spectra, can in its essential parts be distinguished from the fragmentations of the decomposition products mentioned thus revealing a number of fragments which are characteristic for compounds of the type R_2SeX_2, X = Br, Cl.

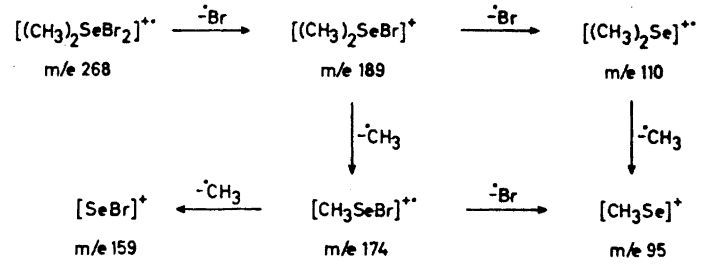

Scheme 1.

A general feature of the mass spectra of the selenium dihalides, I – IX, is absence of peaks due to molecular ions (Figs. 1 – 5). The only exception is VI, which exhibits a weak molecular ion, 0.1 %. Instead, these compounds are characterized by $[M-X]^+$ ions, X = Br, Cl. In the spectrum of I (Fig. 1) the abundant $[M-Br]^+$ fragment at *m/e* 189 is degraded by two alternative routes (Scheme 1). One fragmentation mode implies the preservation of the selenium-bromine bond and involves the elimination of methyl groups giving the ions $[CH_3SeBr]^{+\cdot}$ at *m/e* 174 and $[SeBr]^+$ at *m/e* 159. The alternative route implies cleavage of the selenium-bromine bond with charge retention on the selenide fragment at *m/e* 110. The subsequent degradation of this fragment is analogous to that already described for dimethyl selenide.[5] In addition, however, the group of peaks around *m/e* 80 contains the fragment $[Br]^+$ at *m/e* 79. In the spectrum of VI, fragments are observed in accordance with those mentioned for I which provides further support for the fragmentation pattern proposed in Scheme 1.

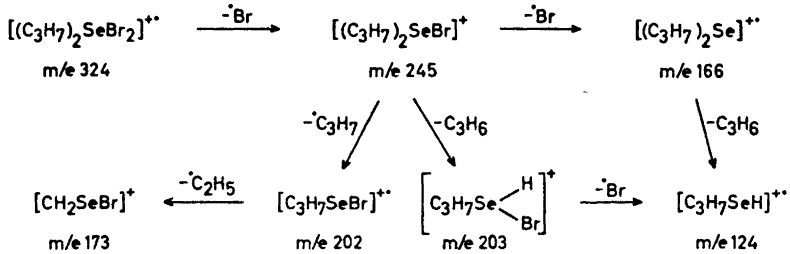

Scheme 2.

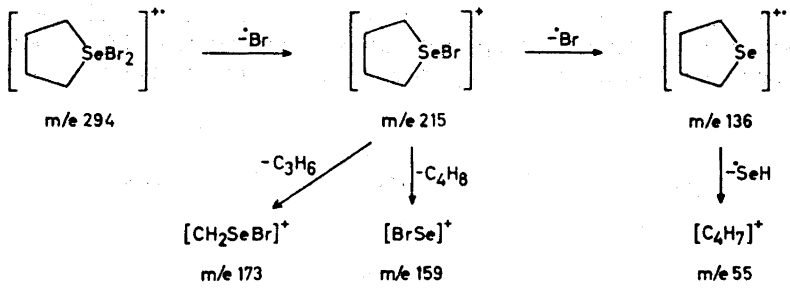

Scheme 3.

In the spectra of the other aliphatic selenium dihalides investigated, II (Fig. 2), III (Fig. 3), and VII (Table 1), fragments containing selenium-halogen bonds are of lower abundance. As in the case of I, simple Se – Br bond

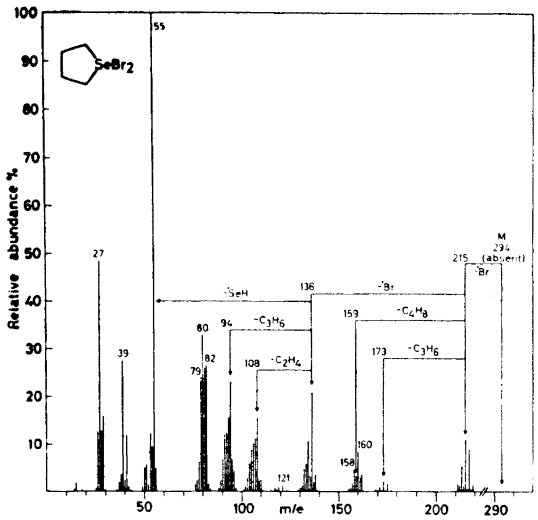

Fig. 3.

Table 1. Relative intensities (I) of ions containing Se – Cl bonds and their degradation fragments in the mass spectra of R_2SeCl_2.

VI		VII		VIII		IX	
m/e	% I	*m/e*	% I	*m/e*	% I	*m/e*	% I
180	0.1	206	–	242	–	304	–
145	14.0	171	2.5	207	1.8	269	0.2
130	3.4	136	42.5	192	0.5	234	53.8
115	0.9	129	1.1	172	100	192	0.1
110	100	115	0.4	157	84.4	157	6.8
95	91.1						

rupture in the $[M-Br]^+$ ions at *m/e* 245 and *m/e* 215 in II and III, respectively. is observed generating the fragments at *m/e* 166 and *m/e* 136 (Schemes 2 and 3). In addition, fragments arising from carbon-selenium bond cleavage of the

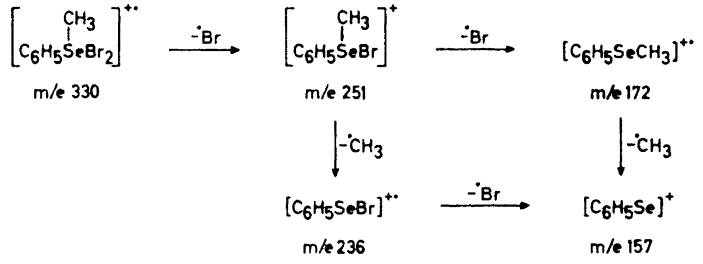

Scheme 4.

$[M-Br]^+$ ions are found. In the case of II (Fig. 2) elimination of a propyl radical leads to $[C_3H_7SeBr]^{+\cdot}$ at *m/e* 202 (Scheme 2). The transition is followed by a C_1-C_2 bond cleavage, forming $[CH_2SeBr]^+$ at *m/e* 173. Similar processes involving C_1-C_2 bond fissions are frequently observed in the spectra of, for example, selenides, sulphides, and ethers.[5-7] An analogous process is also proposed as the origin of the fragment at *m/e* 173 in the spectrum of III (Scheme 3). Furthermore, the carbon-selenium bond rupture in the $[M-Br]^+$ ion in II is also associated with hydrogen migration to the charged fragment forming $[C_3H_8SeBr]^+$ at *m/e* 203. This transition is similar to M→*m/e* 124 in the spectrum of dipropyl selenide.[5] In the spectrum of III, fission of both selenium-carbon bonds gives $[BrSe]^+$ at *m/e* 159 (Scheme 3), a fragment which is present to a minor extent in the case of II. The spectrum of VII (Table 2), reveals a fragmentation pattern in agreement with that given for III, although the relative abundance of ions containing Se–Cl bonds is, however, considerably lower. Finally, the spectra of II, III, and VII contain peaks at lower masses which, with the exception of peaks corresponding to $[X]^+$ and $[XH]^{+\cdot}$ ions, may also be recognized in the corresponding selenides.[5,8]

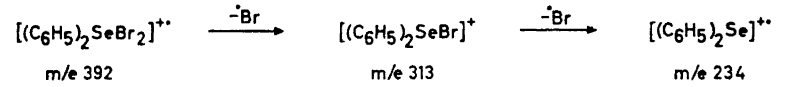

Scheme 5.

The spectra of IV (Fig. 4) and VIII (Table 1) are completely dominated by fragments which are also present in the spectrum of the corresponding selenide.[5] A detailed appraisal of these spectra gives evidence for fragmentation processes around the selenium dihalide function, as visualized for IV in Scheme 4, and which are very similar to the degradation pattern of I. Thus the $[M-X]^+$ ions at *m/e* 251 in IV and at *m/e* 207 in VIII are the origin of part of the abundant ions at *m/e* 172 $[C_6H_5SeCH_3]^{+\cdot}$, and by expulsion of a methyl radical

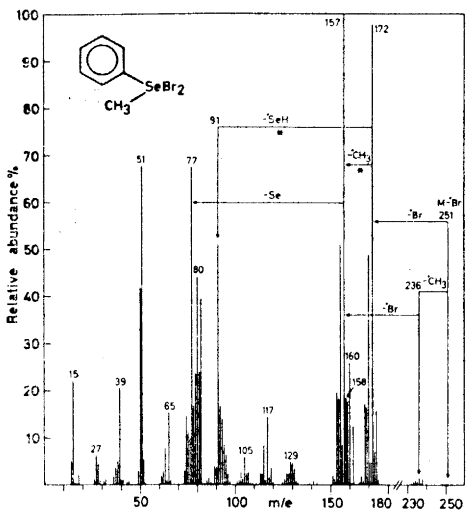

Fig. 4.

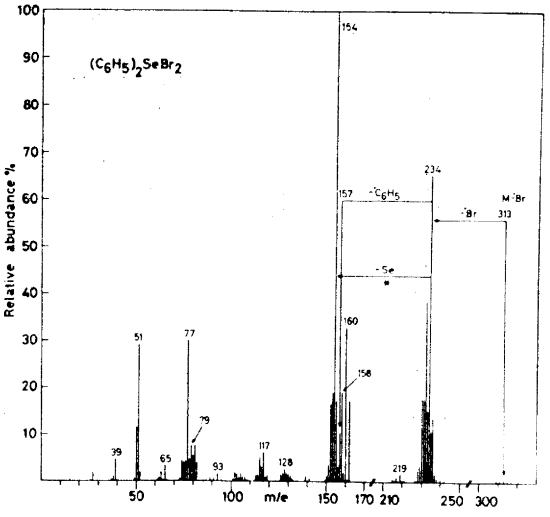

Fig. 5.

also of the $[C_6H_5SeX]^+$ fragments at *m/e* 236 and 192, respectively. Ions derived from the less favourable selenium-aryl bond cleavage in the $[M-X]^+$ fragment are not observed.

The mass spectra of the diarylselenium dihalides, V (Fig. 5) and IX (Table 1) are also dominated by fragments, which, with the exception of the $[X_2]^{+\cdot}$, $[X]^+$, and $[XH]^{+\cdot}$ ions are also present in the spectrum of the corresponding selenide.[9] The weak peaks present at *m/e* 313 (Fig. 5) and *m/e* 269 (Table 1), deriving from fragments containing both selenium and halogen, indicate that the electron-impact induced processes around the selenium dihalide function in these compounds mainly involve the stepwise elimination of the halogens (Scheme 5) from the molecular ion leading to *m/e* 234 $[(C_6H_5)_2Se]^{+\cdot}$. A weak peak at *m/e* 192 in the spectrum of IX is ascribed to $[C_6H_5SeCl]^{+\cdot}$.

EXPERIMENTAL

The mass spectra were recorded on an LKB 9000A gas chromatograph-mass spectrometer, operating at 70 eV. The spectra were recorded using the direct inlet technique. The purity of the selenium dihalides was checked by microanalysis for selenium. The melting points are uncorrected.

The selenium dibromides, I – V, were prepared by addition of bromine to the corresponding pure selenides [5] in tetrachloromethane solution.[1] The selenium dichlorides, VI – VIII, were prepared analogously by addition of chlorine to the selenides, while IX was obtained by oxidation of the selenide with nitric acid followed by addition of hydrochloric acid.[14] The selenium dihalides were purified by repeated recrystallizations from methanol or tetrachloromethane. The melting points are given in Table 2.

Table 2. Selenium dihalides, R_2SeX_2.

R		Selenium dibromides M.p. °C	Ref.		Selenium dichlorides M.p. °C	Ref.
CH_3	I	83.5–84 d	2	VI	60–61	15
C_3H_7	II	49–50	2	–	–	
$-(CH_2)_4-$	III	96–98	10	VII	91–92	10
C_6H_5	IV	115–116 d	11	VIII	133–134 d	13
CH_3 C_6H_5	V	150–151 d	12	IX	185–187	14

Acknowledgements. I express my sincere gratitude to Professor Göran Bergson for the facilities put at my disposal. Thanks are also due to Mr. O. Eriksson for skilled technical assistance with the figures. The mass spectra were recorded by Mr. K. Janné and Mr. L. Grehn.

REFERENCES

1. Rheinboldt, H. In Houben–Weyl, *Die Methoden der organischen Chemie*, G. Thieme, Stuttgart 1955, Vol. 9, p. 1005.
2. Paetzold, R. and Bochmann, G. *Z. anorg. allg. Chem.* **360** (1968) 293.
3. Rheinboldt, H. In Houben–Weyl, *Die Methoden der organischen Chemie*, G. Thieme, Stuttgart 1955, Vol. 9, p. 1015.
4. McCullough, J. D. *J. Am. Chem. Soc.* **64** (1942) 2672.
5. Rebane, E. *To be published.*
6. Levy, E. J. and Stahl, W. A. *Anal. Chem.* **33** (1961) 707.
7. McLafferty, F. W. *Anal. Chem.* **29** (1957) 1782.
8. Duffield, A. M., Budzikiewicz, H. and Djerassi, C. *J. Am. Chem. Soc.* **87** (1965) 2920.
9. Bergman, J. *Acta Chem. Scand.* **22** (1968) 1883.
10. Morgan, G. T. and Burstall, F. H. *J. Chem. Soc.* **1929** 1096.
11. Edwards, O. K., Gay-Thwaite, W. R., Kenyon, J. and Phillips, H. *J. Chem. Soc.* **1928** 2293.
12. Lyons, R. E. and Bush, G. C. *J. Am. Chem. Soc.* **30** (1930) 831.
13. Foster, D. G. and Brown, S. F. *J. Am. Chem. Soc.* **50** (1928) 1182.
14. Leicester, H. M. *Org. Syn. Coll. Vol.* **2** (1943) 240.
15. Jackson, C. L. *Ber.* **8** (1875) 109.

Received April 18, 1973.

ACTA CHEMICA SCANDINAVICA 27 (1973) 2877–2886

Thermodynamic Properties of Rare Earth Complexes

XIX. Free Energy, Enthalpy, and Entropy Changes for the Formation of Some Lanthanoid Maleate Complexes

INGEMAR DELLIEN and LARS-ÅKE MALMSTEN

Division of Physical Chemistry 1, Chemical Center, University of Lund, P.O.B. 740, S-220 07 Lund 7, Sweden

The changes in free energy, enthalpy, and entropy for the formation of Pr, Sm, Gd, Ho, and Yb maleate complexes with the composition MA and MA_2 have been determined. The changes in free energy were calculated from stability constants, determined by a standard potentiometric method, *viz.* the determination of the concentration of free hydrogen ion, using a glass electrode. The enthalpy changes were measured calorimetrically. All data refer to a temperature of 25.0°C and 1 M $Na(ClO_4)$ medium.

A fairly small number of investigations of the complex formation of tervalent lanthanoids with bidentate ligands containing oxygen donors have been published. In most of these investigations only the stability constants have been determined, but in some cases, *e.g.* for the glycolate,[1] malonate,[2,3] kojate,[4] tropolonate,[5] and acetylacetonate [6] systems, both free energy and enthalpy data for the complexation reactions have been obtained. The limited number of data is undoubtedly connected with the ease of formation of solid phases with this type of bidentate ligands.

Our series of investigations on lanthanoid dicarboxylate complexes has been extended to the maleate complexes in order to permit a further discussion of the following points:

a. We have been interested in the variation of thermodynamic quantities within the lanthanoid series. For the five ligands mentioned above, a regular and near linear variation of ΔG°_j, ΔH°_j and ΔS°_j with the ionic radius or the atomic number is found. This is at variance with the trends observed for a number of other ligands, *e.g.* oxydiacetate [7] and iminodiacetate,[8] where ΔH° (Z) and ΔS° (Z) increase rapidly in the region Sm – Tb. As the malonate ion is the only dicarboxylate in the group of bidentate ligands studied so far,[9] it seems motivated to investigate the complexation reactions of another bidentate ligand, *viz.* the maleate ion.

b. When the ligand is the anion of a polyprotic acid, there is a possibility for the formation of acid complexes of the type MH_qA_r, $q > 0$. Such acid complexes have been detected, *e.g.* in the malonate and thiodiacetate [10] systems. X-Ray studies of solid maleic acid have shown that there is a strong intramolecular hydrogen bond in the hydrogen maleate ion.[11] This bond must be broken when the hydrogen maleate ion forms a complex with a metal ion, thus rendering the formation of an acid complex energetically unfavoured. Hence, the corresponding stability constants ought to be small. It is of interest to investigate whether this is true or not.

c. A well-established structural effect in chelate complexes is the enhanced stability of five-membered rings as compared to six-membered ones. The lanthanoid complexes with oxalate ion,[12] which forms a five-membered ring, are much stronger than those formed with malonate ion [9] where a six-membered ring is formed. We have been interested to see, if a further decrease in stability is observed when a chelate containing a seven-membered ring is formed. When this comparison is made, one has to be aware of the difference in ligand geometry of the maleate ion as compared to oxalate and malonate, due to the presence of a double bond in the maleate ion.

There are some earlier investigations on rare earth maleate complexes. Roulet *et al.*[13] have determined stability constants for the 1:1 and 1:2 complexes at 25°C and ionic strength 0.1 M ($NaClO_4$).

Paramonova *et al.*[14] described the results of an ion-exchange study on the europium system by assuming that both maleate ion and hydrogen maleate ion formed 1:1 complexes with the metal ion.

Choppin *et al.*[22] have determined ΔH°_1 for the lanthanoid maleate complexes at ionic strength 0.1 M.

This paper describes the determination of the changes in free energy, enthalpy and entropy for the formation of the Pr^{3+}, Sm^{3+}, Gd^{3+}, Ho^{3+}, and Yb^{3+} maleates. The changes in free energy were calculated from the stability constants, which were determined from potentiometric measurements of the hydrogen ion concentration in solutions, containing metal perchlorate, maleic acid and disodium maleate. The enthalpy values were obtained in a direct calorimetric determination. The solvent was an aqueous sodium perchlorate medium with the total sodium ion concentration equal to 1.00 M. The temperature was 25.0 ± 0.1°C.

NOTATIONS AND CALCULATIONS

The notations have been defined earlier.[8,9]

The stability constants and enthalpy values have been calculated by least-squares programs in the "Letagrop" series.[15,16] Different error-carrying variables, *viz.* E/mV and $\bar{n}_H$, respectively, have been used in the calculation of the stability constants from (v/ml, E/mV)-data. A least-squares program, using weighted (a/M, $\bar{n}$)-data has also been used.[17] The weighting scheme assumes that the relative error in the determination of the concentration of free ligand is constant.

In addition, standard graphical procedures have been used for some systems.

EXPERIMENTAL

Chemicals used. The preparation and standardisation of the lanthanoid perchlorate and sodium perchlorate solutions have been described earlier.[9]

The formula weight of the maleic acid (Fluka, *p.a.*) was determined by alkalimetric titration as 116.3 (calc. 116.1). However, neither this method nor any electrometric titration with the equipment used here can be used to decide whether small amounts of fumaric acid are present or not. The presence of about 1 % fumaric acid in the Fluka sample was shown by thin layer chromatography.[18] Maleic acid can be separated from fumaric acid by using the fact that only maleic acid can form an anhydride, which can be distilled.[19] Thus, a 0.5 M stock solution of maleic acid was prepared after distilling the solid acid under reduced pressure, adding water to the anhydride obtained and standardising the solution with sodium hydroxide.

The potentiometric measurements on the proton and lanthanoid maleate systems were performed as titrations in the same way and with the same equipment as used before.[9] Contamination of the solutions with carbon dioxide was prevented by bubbling nitrogen through the solution in the titration vessel. The experimental emf-values were corrected for a hydrogen ion and a perchlorate ion dependent liquid junction potential in the same way as was described for the malonates.[9,p.1393] The perchlorate ion dependent liquid junction potential is a linear function of the perchlorate ion concentration with the slope 6.4 mV/M.

The stabilities of the proton maleate complexes were determined in solutions with $C_M = 0$ and with different constant values of the total maleate concentration, *viz.* $C_A =$ 25 mM, 50 mM, 100 mM, and 200 mM. With C_A-values greater than 125 mM, a precipitate with the composition $NaHA.\frac{1}{2}H_2O$ (after air-drying) is formed in solutions with $\bar{n}_H$ approximately equal to 1.

In order to get precise values of the stability constants of the various complexes, a wide concentration range must be covered in the titrations. The ratio C_H/C_A varies from 1 to about 1/5, and the total metal ion concentration is in the range 15 mM to 40 mM. In solutions with $C_M > 20$ mM, a precipitate is formed when the value of $\bar{n}$ in the solution is close to 1.5.

The calorimetric measurements were made with the calorimeter developed by Grenthe, Ots and Ginstrup,[20] using the same titrimetric technique as described for the malonates.[3]

The enthalpy values for the protonation of the maleate ion were determined by titrating disodium maleate solution with perchloric acid.

The heats of formation of the metal maleates were determined by titrating a metal solution with maleate buffers. The initial total metal ion concentration was about 20 mM, and two different buffer solutions with the ratio C_H/C_A equal to 2/5 and 1/3, respectively, were used. For each system, about 25 experimental points were measured.

RESULTS

Determination of the stability constants

The proton maleate system. The potentiometric measurements were described by assuming the existence of two proton maleate complexes, HA and H_2A, with the following stability constants:

$$\beta_{0,1,1} = (4.15 \pm 0.04) \times 10^5 \text{ M}^{-1}$$
$$\beta_{0,2,1} = (1.65 \pm 0.03) \times 10^7 \text{ M}^{-2}$$

These values were calculated in a "Letagrop" least-squares treatment of 182 experimental (v/ml, E/mV)-values. The standard deviation in C_H/C_A was equal to 6.3×10^{-3}. The experimental values are satisfactorily described by the calculated constants, except for some points with high $\bar{n}_H$-values ($\bar{n}_H >$ 1.35), where the values of $\bar{n}_{H,\,calc}$ exceed the $\bar{n}_{H,\,exp}$-values with at most

1.5 %. This deviation might in part be due to an error in the correction for the hydrogen ion dependent liquid junction potential in the very acid solutions used here.

The lanthanoid maleate systems. Fig. 1 shows calculated $\bar{n}$ *vs.* $-\log (a/\mathrm{M})$ curves for the samarium and ytterbium systems, together with some experi-

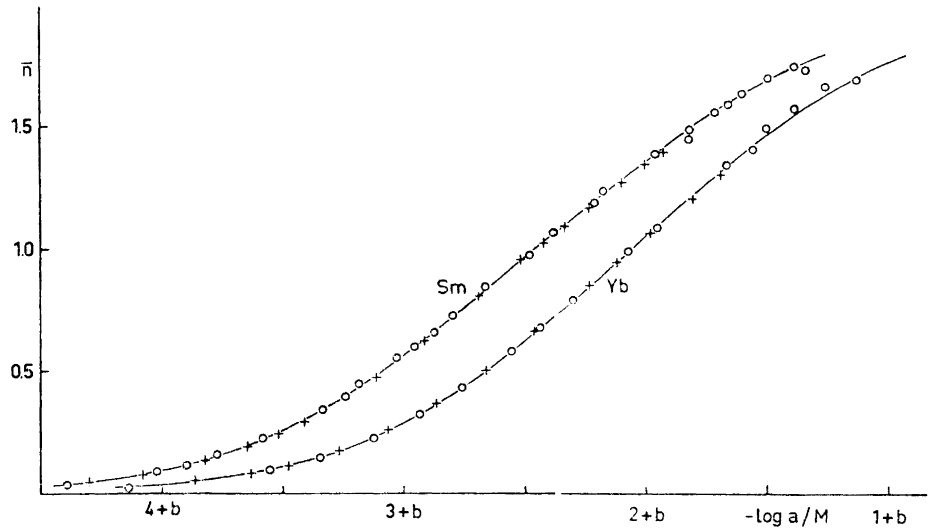

Fig. 1. Experimental $\bar{n}$ *vs.* $-\log (a/\mathrm{M})$ data for the samarium and ytterbium systems. The curves have been calculated with the constants in Table 2. The value of b is zero for the Sm system and 0.25 for the Yb system. Titrations with $C_M = 20$ mM and 40 mM are denoted with O and +, respectively.

mental points. Primary data for the praseodymium system are given in Table 1, and the calculated stability constants for the systems investigated are given in Table 2.

The stability constants have been calculated with the least-squares procedures using different error-carrying variables, *viz.* the measured emf E and C_H/C_A, respectively, in the "Letagrop" calculations. The same experimental points were used but the different choices of the error-carrying variable correspond to a different weighting of the data. The calculated values of the stability constants are the same in the two procedures, as they should be, but not the estimates of the corresponding standard deviations. Table 3 shows that the "Letagrop" procedure with the emf E as error-carrying variable gives the lowest values of the errors, especially for the stability constant $\beta_{1,1,1}$ of the acid complex MHA. The largest estimates are obtained by using weighted $(a/\mathrm{M}, \bar{n})$-data in the calculations. The limits of error for the constants, quoted in Table 2, have been calculated by multiplying these estimates of the standard deviations with three.

Table 1. Experimental results of the potentiometric measurements on the praseodymium maleate system. Values of v/ml and E/mV are given. The sodium ion concentration is 1.00 M in all solutions.

Series 1. S: $C_H = 0.00091$ M, $C_M = 0.01941$ M, $C_A = 0$;
T: $C_H = 0.06254$ M, $C_M = 0.01941$ M, $C_A = 0.1807$ M;
$V_0 = 19.96$ ml; $E_0 = 497.7$ mV.
0.250, 253.8; 0.500, 233.4; 0.750, 226.0; 1.000, 221.5; 1.500, 215.8; 2.000, 211.5; 3.000, 205.2; 4.000, 200.1; 5.000, 195.4; 7.000, 187.7; 9.000, 182.3; 12.00, 176.7.

Series 2. S: $C_H = 0.00148$ M, $C_M = 0.03115$ M, $C_A = 0$;
T: $C_H = 0.08322$ M, $C_M = 0.03115$ M, $C_A = 0.1908$ M;
$V_0 = 19.96$ ml; $E_0 = 497.3$ mV.
0.500, 265.0; 0.750, 254.0; 1.000, 248.6; 1.500, 242.1; 2.000, 238.3; 2.500, 235.2; 3.000, 233.3; 4.000, 229.7; 5.000, 226.9; 7.000, 221.5; 10.00, 214.6; 12.00, 210.7; 15.00, 205.7; 17.00, 203.0.

Series 3. S: $C_H = 0.05072$ M, $C_M = 0.02009$ M, $C_A = 0.02500$ M;
T: $C_H = 0.00081$ M, $C_M = 0.02009$ M, $C_A = 0.02500$ M;
$V_0 = 20.01$ ml; $E_0 = 389.5$ mV.
3.000, 275.2; 5.000, 269.3; 7.000, 263.3; 9.000, 257.1; 11.00, 250.5; 14.00, 239.5; 17.00, 226.1; 20.00, 208.8; 25.00, 178.8; 30.00, 159.9.

Series 4. S: $C_H = 0.02078$ M, $C_M = 0.02009$ M, $C_A = 0.02500$ M;
T: $C_H = 0.00081$ M, $C_M = 0.02009$ M, $C_A = 0.02500$ M;
$V_0 = 30.00$ ml; $E_0 = 389.3$ mV.
5.000, 140.8; 10.00, 129.1; 15.00, 120.4; 20.00, 113.9; 25.00, 108.5; 30.00, 103.7.

Series 5. S: $C_H = 0.0108$ M, $C_M = 0.02009$ M, $C_A = 0.02500$ M;
T: $C_H = 0.00081$ M, $C_M = 0.02009$ M, $C_A = 0.02500$ M;
$V_0 = 20.01$ ml; $E_0 = 389.3$ mV.
5.000, 93.1; 10.00, 85.7; 15.00, 79.8; 20.00, 75.2.

Series 6. S: $C_H = 0.00581$ M, $C_M = 0.02009$ M, $C_A = 0.02500$ M;
T: $C_H = 0.00081$ M, $C_M = 0.02009$ M, $C_A = 0.02500$ M;
$V_0 = 20.00$ ml; $E_0 = 389.2$ mV.
5.000, 68.1; 10.00, 63.0.

Series 7. S: $C_H = 0.1007$ M, $C_M = 0.02009$ M, $C_A = 0.05000$ M;
T: $C_H = 0.00090$ M, $C_M = 0.02009$ M, $C_A = 0.05000$ M;
$V_0 = 20.01$ ml; $E_0 = 389.4$ mV.
5.000, 279.3; 7.000, 272.4; 9.000, 265.4; 11.00, 258.2; 14.00, 245.8; 17.00, 230.4; 20.00, 209.7; 25.00, 174.2; 30.00, 153.2.

Series 8. S: $C_H = 0.04083$ M, $C_M = 0.02009$ M, $C_A = 0.05000$ M;
T: $C_H = 0.00090$ M, $C_M = 0.02009$ M, $C_A = 0.05000$ M;
$V_0 = 30.00$ ml; $E_0 = 389.0$ mV.
5.000, 131.7; 10.00, 117.8; 15.00, 107.5; 20.00, 99.4; 25.00, 92.8; 30.00, 87.3.

Series 9. S: $C_H = 0.02087$ M, $C_M = 0.02009$ M, $C_A = 0.05000$ M;
T: $C_H = 0.00090$ M, $C_M = 0.02009$ M, $C_A = 0.05000$ M;
$V_0 = 20.00$ ml; $E_0 = 388.9$ mV.
5.000, 75.0; 10.00, 66.4; 15.00, 59.9; 20.00, 54.7.

Table 2. The overall stability constants for the maleate complexes, calculated from ([A], $\bar{n}$)-data. The errors are equal to three standard deviations.

Metal ion	Number of experimental points	$\beta_{1,0,1} \times 10^{-2}$ M	$\beta_{1,0,2} \times 10^{-4}$ M^2
Pr	56	6.50 ± 0.22	4.96 ± 0.36
Sm	143	9.98 ± 0.09	8.00 ± 0.15
Gd	73	9.24 ± 0.10	6.10 ± 0.14
Ho	59	7.73 ± 0.34	4.73 ± 0.50
Yb	60	6.39 ± 0.13	4.44 ± 0.18

Table 3. "Letagrop" calculations of the stability constants for the Pr, Sm, and Gd maleate complexes with different error-carrying variable y, and with two different assumptions as to which complexes are formed. The number of experimental points is also given.

		$y = C_H/C_A$		$y = E$	
Metal ion	Assumed complexes	sig $y \times 10^3$	Calculated stability constants	sig y/mV	Calculated stability constants
Pr (67 p).	MA	3.81	$(6.22 \pm 0.10) \times 10^2$	0.44	$(6.27 \pm 0.10) \times 10^2$
	MA_2		$(5.05 \pm 0.21) \times 10^4$		$(5.01 \pm 0.17) \times 10^4$
	MA		$(6.42 \pm 0.16) \times 10^2$		$(6.36 \pm 0.10) \times 10^2$
	MA_2	3.33	5.1×10^4	0.45	5.1×10^4
	MHA		$(3.9 \pm 2.9) \times 10^4$		$(1.75 \pm 0.80) \times 10^5$
Sm (239 p).	MA	3.62	$(10.02 \pm 0.08) \times 10^2$	0.64	$(10.28 \pm 0.08) \times 10^2$
	MA_2		$(8.09 \pm 0.20) \times 10^5$		$(8.27 \pm 0.17) \times 10^4$
	MA		$(10.09 \pm 0.09) \times 10^2$		The calculations
	MA_2	4.33	8.1×10^4		did not converge.
	MHA		$(0 \pm 2.4) \times 10^5$		
Gd (132 p).	MA	2.67	$(9.14 \pm 0.09) \times 10^2$	0.41	$(9.02 \pm 0.04) \times 10^2$
	MA_2		$(5.97 \pm 0.13) \times 10^4$		$(6.00 \pm 0.01) \times 10^4$
	MA		$(9.31 \pm 0.12) \times 10^2$		$(9.17 \pm 0.09) \times 10^2$
	MA_2	2.43	6.0×10^4	0.37	6.0×10^4
	MHA		$(2.5 \pm 1.3) \times 10^5$		$(1.3 \pm 0.14) \times 10^5$

In the Pr, Sm, and Gd systems measurements were made with solutions containing a high concentration of hydrogen maleate ion, in order to obtain information on the possible formation and the stability of an acid complex MHA. (These points have not been used for the calculations presented in Table 2.) Table 3 shows that the calculated $\beta_{1,1,1}$-values are significantly positive for the praseodymium and gadolinium systems, though the estimated errors are fairly large. However, this fact is not sufficient to justify a claim as to the existence of this species; the effects of experimental errors must also be considered. For the acid solutions used, small concentration errors or small errors in the measured emf give large errors in the constant $\beta_{1,1,1}$. In fact,

the positive values found for the Pr and Gd systems disappear if the total concentrations and E_0-values are changed in a few titration series with at most 0.5 % or 0.2 mV. The equilibrium constant $K_{M,HA}$ for the reaction $M+HA \rightleftharpoons MHA$ is about 1 M^{-1}, according to the $\beta_{1,1,1}$-values found, and the experimental technique used here thus gives an upper limit for $K_{M,HA}$ of about 2 M^{-1}. This is the value found by Paramonova *et al.*[14] for the europium system in 0.5 M $NaNO_3$.

The accuracy of the calculated stability constants depends on the uncertainties in the protonation constants; an error of 1 % in $\beta_{0,1,1}$ thus corresponds to an error of 1 % in $\beta_{1,0,1}$ and 3 % in $\beta_{1,0,2}$.

Determination of the enthalpy values

The heats of protonation of the maleate ion were determined from 25 experimental points, and the following values were obtained:

$$\Delta H^\circ_{0,1,1} = (0.75 \pm 0.12) \text{ kJ mol}^{-1}$$
$$\Delta H^\circ_{0,2,1} = (1.38 \pm 0.25) \text{ kJ mol}^{-1}$$

Table 4. Experimental results of the calorimetric measurements on the praseodymium maleate system. Corresponding values of v/ml, $Q_{corr,exp}$/J and $(Q_{corr,calc} - Q_{corr,exp})$/J are given.

Series 1. S: $C_H = 0.00116$ M, $C_M = 0.02108$ M, $C_A = 0.001194$ M;
T: $C_H = 0.1042$ M, $C_M = 0$, $C_A = 0.3004$ M;
$V_0 = 100.60$ ml.
3.000, 5.700, 0.088; 6.000, 5.420, 0.074; 9.000, 5.093, −0.072; 12.00, 4.519, −0.105; 15.00, 3.760, −0.030; 18.00, 2.899, 0.150.

Series 2. S: $C_H = 0.00116$ M, $C_M = 0.02108$ M, $C_A = 0.001194$ M;
T: $C_H = 0.1042$ M, $C_M = 0$, $C_A = 0.3004$ M;
$V_0 = 100.60$ ml.
3.000, 5.688, 0.100; 6.000, 5.542, −0.048; 9.00, 5.172, −0.151; 12.00, 4.544, −0.130; 15.00, 3.710, 0.020; 18.00, 2.877, 0.172.

Series 3a. S: $C_H = 0.000436$ M, $C_M = 0.01837$ M, $C_A = 0$;
T: $C_H = 0.1032$ M, $C_M = 0$, $C_A = 0.3011$ M;
$V_0 = 79.93$ ml.
3.000, 5.188, 0.163; 6.000, 4.975, −0.033; 9.000, 4.092, −0.121; 12.00, 3.084, −0.134; 15.00, 2.067, 0.038; 18.00, 1.351, 0.125; 21.00, 0.937, 0.113.

Series 3b. S: $C_H = 0.02181$ M, $C_M = 0.01455$ M, $C_A = 0.06266$ M;
T: $C_H = 0.1032$ M, $C_M = 0$, $C_A = 0.3011$ M;
$V_0 = 81.93$ ml.
3.000, 0.686, 0.054; 6.000, 0.448, 0.075.

Series 4a. S: $C_H = 0.000436$ M, $C_M = 0.01837$ M, $C_A = 0$;
T: $C_H = 0.1032$ M, $C_M = 0$, $C_A = 0.3011$ M;
$V_0 = 79.93$ ml.
2.000, 3.410, 0.117; 5.000, 5.192, 0.021; 8.000, 4.481, −0.167; 11.00, 3.431, −0.151; 14.00, 2.393, −0.033; 17.00, 1.573, 0.088; 20.00, 1.063, 0.113.

Series 4b. S: $C_H = 0.02100$ M, $C_M = 0.01469$ M, $C_A = 0.06027$ M;
T: $C_H = 0.1032$ M, $C_M = 0$, $C_A = 0.3011$ M;
$V_0 = 84.93$ ml.
3.000, 0.628, 0.201; 6.000, 0.519, 0.063; 9.000, 0.347, 0.079.

Table 5. The changes in enthalpy, free energy and entropy for the formation of lanthanoid maleate complexes. The errors in the enthalpy values are equal to three standard deviations.

Metal ion	Standard deviation in Q_{corr}/J	$\Delta H^\circ_{1,0,1}$ kJ mol^{-1}	$\Delta G^\circ_{1,0,1}$ kJ mol^{-1}	$\Delta S^\circ_{1,0,1}$ J mol^{-1}K^{-1}	$\Delta H^\circ_{1,0,2}$ kJ mol^{-1}	$\Delta G^\circ_{1,0,2}$ kJ mol^{-1}	$\Delta S^\circ_{1,0,2}$ J mol^{-1}K^{-1}
Pr	0.116	10.80 ± 0.45	−16.06	90.1	20.0 ± 0.8	−26.80	157
Sm	0.044	10.67 ± 0.13	−17.12	93.2	17.74 ± 0.23	−28.00	153
Gd	0.043	12.51 ± 0.12	−16.94	98.8	19.83 ± 0.23	−27.32	158
Ho	0.076	15.44 ± 0.23	−16.47	107.0	24.1 ± 0.5	−26.60	170
Yb	0.055	16.32 ± 0.16	−16.01	108.4	27.03 ± 0.29	−26.53	179

The standard deviation in Q_{corr} was 0.20 J. The errors are fairly large, but as this does not affect the further calculations on the metal complexes very much, no further work has been done on this system.

The values of the changes in free energy and entropy for the formation of proton maleate complexes at 25°C are:

$$\Delta G^\circ_{0,1,1} = -32.14 \text{ kJ mol}^{-1}$$
$$\Delta G^\circ_{0,2,1} = -40.69 \text{ kJ mol}^{-1}$$
$$\Delta S^\circ_{0,1,1} = 110.3 \text{ J K}^{-1} \text{ mol}^{-1}$$
$$\Delta S^\circ_{0,2,1} = 141.1 \text{ J K}^{-1} \text{ mol}^{-1}$$

Experimental data for the determination of the heats of formation of the praseodymium maleate complexes are given in Table 4. The Q_{corr}-values include the small correction for the heats of dilution of the titrant. The overall enthalpy changes for the formation of the complexes are given in Table 5, together with the corresponding free energy and entropy changes. The standard deviation in the individual measurements, denoted *sig* Q_{corr}, is of the magnitude expected from the precision of the calorimetric equipment. The large error for the praseodymium system is an exception which cannot be explained, either as due to errors in the calorimetric procedure or to reasonable errors in the concentrations of the solutions.

DISCUSSION

The entropy of formation of lanthanoid maleate complexes is an approximately linear function of the atomic number, as is also the case for the malonates and other bidentate ligands with oxygen donors. The ΔH°_1-values are nearly the same for the malonates [3] and the maleates; the small differences are, however, larger than the experimental errors.

The non-monotonous, "normal" variation pattern of thermodynamic properties across the lanthanoid series as shown by, *e.g.*, the oxydiacetates,[7] has been interpreted as due to a release of different numbers of water molecules in the complex formation reactions. This in turn might be a result of different hydration numbers for the lanthanoid ions. According to Choppin *et al.*,[4] the

approximately linear behaviour of the $\Delta S°$ *vs.* Z function is a reflection of the fact that the mono-ligand complexes consist of species of different hydration in equilibrium. It is in principle possible to check this hypothesis, *e.g.* by measuring the temperature variation of $\Delta H°$. This will be difficult to do experimentally with this type of ligand, as solid phases are easily formed. Measurements of this type on some malonate systems are, however, in progress at this laboratory.

In some cases, when the ligand is the anion of a polyprotic acid, protonated forms of the ligand also form complexes with lanthanoid ions. Stability constants $K_{M,HA}$ for the formation of some such ternary complexes are given in Table 6. The correlation between $K_{M,HA}$ and the protonation constant

Table 6. The protonation constants ($K_{H,HA}$) and stability constants for europium (or samarium) complexes ($K_{M,HA}$) with some protonated ligands.

Ligand	log ($K_{H,HA}$ M)	log ($K_{M,HA}$ M)	Ref.
Hydrogen oxalate ion (M = Eu^{3+})	0.91	1.50	14
Hydrogen maleate ion (M = Eu^{3+})	1.53	0.3	14
Hydrogen maleate ion	1.60	< 0.3	This study
Iminodiacetic acid (M = Eu^{3+})	1.88	0.97	8
Hydrogen malonate ion (M = Eu^{3+})	2.55	1.42	9
Hydrogen iminodiacetate ion (M = Eu^{3+})	2.58	1.48	8
Hydrogen thiodiacetate ion (M = Sm^{3+})	3.13	1.60	10
Hydrogen succinate ion (M = Eu^{3+})	4.2	2.0	23

of the ligand HA is poor. According to experiments, the value of $K_{M,HA}$ is less than 2 M^{-1} for the maleates, *i.e.* hydrogen maleate ion forms the least stable complexes of the ligands quoted in Table 6. The formation of an acid maleate complex MHA with a chelated lanthanoid ion is energetically unfavoured, as a strong hydrogen bond in the hydrogen maleate ion has then to be broken. The large electrostatic repulsion from a chelated lanthanoid ion will also prevent a hydrogen ion from coordinating to any carboxylate oxygen.

The stability constants decrease in the order oxalates > malonates > maleates, *i.e.* the stability constants decrease when the size of the chelate ring increases. The enhanced stability of the malonates as compared to the maleates is almost entirely due to the more positive entropy change for the malonates. Nancollas *et al.*[21] have calculated thermodynamic functions for the formation of oxalate and malonate complexes of some transition metal ions. The lower stabilities of the malonates was nearly entirely an enthalpy effect. There are no determinations of enthalpy values for lanthanoid oxalate complexes, due to their low solubilities.

The effect on thermodynamic properties of changing the ionic medium can be assessed for the malonates and maleates, as complexes with both these ligands have been studied in different ionic media.[22] When the medium

is changed from 0.1 M $NaClO_4$ to 1.00 M $Na(ClO_4)$, there is a change in the ΔG°_1-values with about +5 kJ mol^{-1}, both for the malonates and maleates.[13] This is mainly due to a corresponding decrease in ΔS°_1, whereas the enthalpy changes, ΔH°_1, are less sensitive to changes in the ionic medium.

REFERENCES

1. Grenthe, I. *Acta Chem. Scand.* **18** (1964) 283.
2. Degischer, G. and Choppin, G. R. *J. Inorg. Nucl. Chem.* **34** (1972) 2823.
3. Dellien, I. *Acta Chem. Scand.* **27** (1973) 733.
4. Stampfli, R. and Choppin, G. R. *J. Coord. Chem.* **1** (1971) 173.
5. Campbell, D. L. and Moeller, T. *J. Inorg. Nucl. Chem.* **32** (1970) 945.
6. Dadgar, A. and Choppin, G. R. *J. Coord. Chem.* **1** (1971) 179.
7. Grenthe, I. *Acta Chem. Scand.* **17** (1963) 2487.
8. Grenthe, I. and Gårdhammar, G. *Acta Chem. Scand.* **26** (1972) 3207.
9. Dellien, I. and Grenthe, I. *Acta Chem. Scand.* **25** (1971) 1387.
10. Dellien, I., Grenthe, I. and Hessler, G. *Acta Chem. Scand.* **27** (1973) 2431.
11. Shahat, M. *Acta Cryst.* **5** (1952) 763.
12. Grenthe, I., Gårdhammar, G. and Runderantz, E. *Acta Chem. Scand.* **23** (1969) 93.
13. Roulet, R., Feuz, J. and Vu Duc, T. *Helv. Chim. Acta* **53** (1970) 1876.
14. Paramonova, V. I., Kereichuk, A. S. and Chizhov, A. V. *Radiokhimiya* **5** (1963) 63.
15. Arnek, R., Sillén, L. G. and Wahlberg, O. *Arkiv Kemi* **31** (1969) 353.
16. Arnek, R. *Arkiv Kemi* **32** (1970) 81.
17. Sandell, A. *Acta Chem. Scand.* **25** (1971) 2609.
18. Stahl, E. *Thin-Layer Chromatography*, Academic, New York and London 1965, p. 358.
19. Livingston, J. W. *U.S. Pat.* 1901914 (1931); (*Chem. Zentr.* **1933**-*I*, 3366).
20. Grenthe, I., Ots, H. and Ginstrup, O. *Acta Chem. Scand.* **24** (1970) 1067.
21. Nair, V. S. K. and Nancollas, G. H. *J. Chem. Soc.* **1961** 4367.
22. Choppin, G. R., Dadgar, A. and Stampfli, R. *J. Inorg. Nucl. Chem.* **35** (1973) 875.
23. Ke, C. H., Kong, P. C., Cheng, H. S. and Li, N. C. *J. Inorg. Nucl. Chem.* **30** (1968) 961.

Received March 23, 1973.

ACTA CHEMICA SCANDINAVICA 27 (1973) 2887–2892

Conformational Analysis

VIII. Separation and PMR Spectra of Some 4-Oxo-1,3-dioxans Derived from Diastereoisomeric 3-Hydroxy-2-methylbutyric Acids

PERTTI ÄYRÄS

Department of Chemistry, University of Turku, SF-205 00 Turku 50, Finland

Isomeric 5,6-dimethyl-, 2,5,6-trimethyl-, and 2,2,5,6-tetramethyl-4-oxo-1,3-dioxans have been prepared and separated. The ring conformations were determined by means of chemical equilibration and PMR spectroscopy. The data reveal that most of the compounds adopt a half-chair conformation. 2,2-*cis*-5,6-Tetramethyl-4-oxo-1,3-dioxan, however, seems to assume a twist-boat conformation and *r*-2-*cis*-5-*trans*-6-trimethyl-4-oxo-1,3-dioxan seems to be a mixture of half-chair and 2,5-boat conformations.

Alkyl-substituted 4-oxo-1,3-dioxans have two favoured ring conformations.[1–3] The half-chair form (1) with a planar lactone grouping is the most usual, but a proper substitution, *e.g.* an axial substituent in the 6 position, forces the ring (at least partly) into a 2,5-boat form (2) which still has an approximately planar lactone grouping.[1] Geminal substitution in the 6 position seems to have a similar effect as was noted earlier for 2,6,6-trialkyl and 2,5,6,6-tetra-alkyl derivatives.[2,3] An axial 2 or 6 substituent can, however, also change

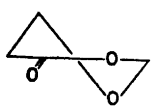

1

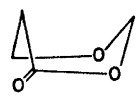

2

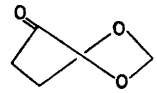

3

the ring conformation towards a 2,5-twist-boat form (3) in which the lactone atoms are not wholly coplanar.[2–4] In this paper derivatives with a methyl substituent in the 5 and 6 positions and with 0 to 2 methyl substituents in the 2 position will be considered. These derivatives were prepared from a mixture of *erythro*- and *threo*-3-hydroxy-2-methylbutyric acids and so exist in diastereomeric forms as well.

EXPERIMENTAL

The synthesis of all oxalactones except that of the 2,2,5,6-tetramethyl-4-oxo-1,3-dioxans has been described earlier (Table 1).[5] The exception was prepared conventionally [1] and had a boiling point of 82 – 94°C/12 Torr (partly decomposed during distillation).

Table 1. 4-Oxo-1,3-dioxans derived from *erythro*- and *threo*-3-hydroxy-3-methylbutyric acids.

I	*trans*-5,6-Dimethyl-4-oxo-1,3-dioxan[a]
II	*cis*-5,6-Dimethyl-4-oxo-1,3-dioxan[b]
III	*r*-2-*trans*-5-*cis*-6-Trimethyl-4-oxo-1,3-dioxan[a]
IV	*r*-2-*cis*-5-*trans*-6-trimethyl-4-oxo-1,3-dioxan[a]
V	*r*-2-*cis*-5-*cis*-6-Trimethyl-4-oxo-1,3-dioxan[b]
VI	*r*-2-*trans*-5-*trans*-6-Trimethyl-4-oxo-1,3-dioxan[b]
VII	2,2-*trans*-5,6-Tetramethyl-4-oxo1,3-dioxan[a]
VIII	2,2-*cis*-5,6-Tetramethyl-4-oxo1,3-dioxan[b]

[a] From *threo* acid. [b] From *erythro* acid.

The diastereoisomers were separated on a preparative gas chromatograph.[1] The epimer pairs of the isomeric 2,5,6-trimethyl-4-oxo-1,3-dioxans were obtained directly from *erythro*- and *threo*-3-hydroxy-2-methylbutyric acids *via* their 5,6-dimethyl derivatives in the way described earlier.[6] The chemical equilibrations were performed as before (catalyst *p*-TOS).[1] The PMR spectra were recorded with a 60 MHz Perkin-Elmer R 10 instrument and a variable temperature probe was used for recording the spectrum of *cis*-5,6-dimethyl-4-oxo-1,3-dioxan at different temperatures. The samples contained 40 mg solute in 400 µl solvent. TMS was used as internal standard. A first order analysis was used to evaluate the spectral parameters.

RESULTS AND DISCUSSION

2,5,6-Trimethyl-4-oxo-1,3-dioxans. Epimeric *r*-2-*trans*-5-*cis*-6- (III) and *r*-2-*cis*-5-*trans*-6-trimethyl-4-oxo-1,3-dioxans (IV) were obtained from *threo*-3-hydroxy-2-methylbutyric acid (*cf.* Table 1). Chemical equilibration (eqn. 1) revealed that the tri-equatorial epimer (III) is favoured by enthalpy whereas

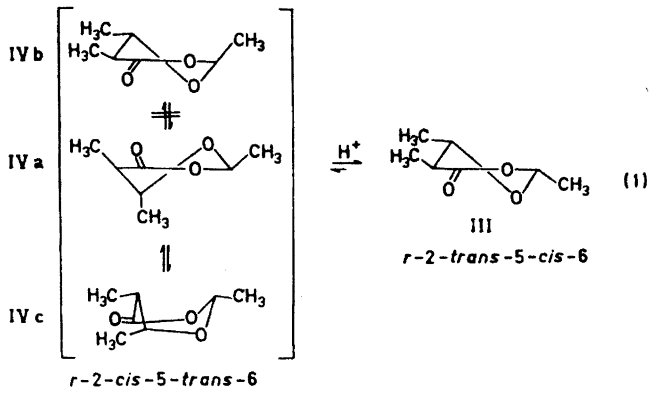

Table 2. The chemical equilibration of the epimer pairs of 2,5,6-trimethyl-4-oxo-1,3-dioxans.

°C	K III/IV[a]	$-\Delta G°$ kJ/mol	$-\Delta H°$ kJ/mol	$\Delta S°$ J mol^{-1} K^{-1}
65	3.28	3.34		
54	3.47	3.38		
45	4.10	3.75		
			4.98 ± 0.75[b]	-4.60 ± 2.38[b]
(25	5.02	4.00)		
11	4.61	3.61		
−9	5.51	3.75		
	V/VI[c]			
25	1.9	2.1		

[a] See eqn. 1. [b] Standard deviation. [c] See eqn. 2.

IV is favoured by entropy. The entropy difference (Table 2) is of opposite sign than for the 2,6-dialkyl-substituted derivatives.[1] In the latter the entropy was thought to arise from pseudo-libration of the half-chair conformation. In the present case the *gauche* interaction between the 5 and 6 substituents is thought to hinder pseudo-libration and hence the excess entropy of IV is mainly due to a conformational equilibrium between IVa and IVc (eqn. 1). We pointed out earlier[1] that an axial 6-substituent distorts the half-chair conformation towards a 2,5-boat form (IVc). In the half-chair form (IVa, IVb) the 5- and 6-substituents are (pseudo)-axial and the 2-methyl group pseudo-equatorial (IVa), or the 5- and 6-methyl groups are (pseudo)-equatorial and the 2-substituent pseudo-axial (IVb). The latter form makes a minor contribution as it includes a methyl-methyl *gauche* interaction and, moreover, the conformational free energy of an axial 2-methyl group is likely to be much greater than the sum of the conformational energies of the 5 and 6 axial methyl substituents (*cf.* 1,3-dioxans[7]).

Attempts were also made to equilibrate the other epimer pair (V and VI in Tables 1 – 2). Unfortunately, the compounds decomposed rapidly and only the free energy difference 2.1 kJ/mol at 25°C could be measured. This value is probably close to the energy difference between the conformations V and VI (eqn. 2). The other possible half-chair conformation on the right-hand side can be neglected, as in eqn. 1, because of a strong 1,3-interaction between the (pseudo)-axial 2 and 6 substituents. Similarly, 2,5-boat forms of V can be excluded on the basis of PMR data (see below) and those of VI because of

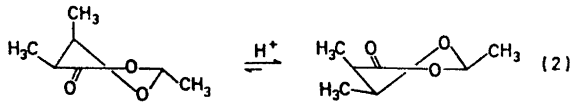

(2)

VI
r-2-*trans*-5-*trans*-6

V
r-2-*cis*-5-*cis*-6

Table 3. The chemical shifts (Hz from internal TMS in CCl_4) of 5,6-, 2,5,6-, and 2,2,5,6-substituted 4-oxo-1,3-dioxans.

	^{1}R(2)	^{2}R(2)	δ_{2H}	δ_{5H}	δ_{6H}	$\delta_{2\text{-}CH_3}$	$\delta_{5\text{-}CH_3}$	$\delta_{6\text{-}CH_3}$
I[a]	H	H	320.0 323.0	145.5	225.0		71.6	80.2
II[b]	H	H	325.0 319.0	169.5	257.0		70.7	72.1
III[a]	Me	H	328.0	136.5	222.5	86.2	70.6	78.4
IV[a]	Me	H	340.0	150.5	228.5	84.1	69.3	80.3
V[b]	Me	H	334.5	164.0	254.5	86.8	70.3	70.6
VI[b,c]	Me	H		144	223	87.0	71.5	77.9
VII[a]	Me	Me		131.5	238.5	91.9 91.9	69.5	76.5
VIII[b]	Me	Me		146.0	264.0	92.5 92.5	71.3	70.9

[a,b] See also eqns. 1 and 2. [a] From *threo* acid. [b] From *erythro* acid. [c] Impure.

Table 4. The coupling constants (Hz) of the compounds studied. Solvent CCl_4.

	^{1}R(2)	^{2}R(2)	$^2J_{2a2e}$	$^3J_{5,6}$	$^3J_{2H,CH_3}$	$^3J_{6H,CH_3}$	$^3J_{6H,CH_3}$
I[a]	H	H	−5.80	10.27		7.13	6.19
II[b]	H	H	−5.78	5.85		7.20	6.35
III[a]	Me	H		10.45	5.21	7.25	6.16
IV[a]	Me	H		9.51	5.18	6.81	6.21
V[b]	Me	H		5.50	5.06	7.30	6.66
VI[b,c]	Me	H			5.28	7.20	6.54
VII[a]	Me	Me		10.21		7.24	6.21
VIII[b]	Me	Me		3.10		7.55	6.43

[a,b,c] See Table 3.

Table 5. Solvent shifts ($\delta_{CCl_4} - \delta_{C_6H_6}$, Hz) of the 4-oxo-1,3-dioxans studied.

	^{1}R(2)	^{2}R(2)	$\Delta\delta_{2H}$	$\Delta\delta_{5H}$	$\Delta\delta_{6H}$	$\Delta\delta_{2\text{-}CH_3}$	$\Delta\delta_{5\text{-}CH_3}$	$\Delta\delta_{6\text{-}CH_3}$
I[a]	H	H	30.0 23.0	22.0	33.0		15.8	26.4
II[b]	H	H	25.5 25.5	28.0	40.0		14.6	24.2
III[a]	Me	H	27.0	17.5	33.5	12.7	13.4	24.5
IV[a]	Me	H	30.0	33.5	19.5	10.9	14.5	28.8
V[b]	Me	H	33.5	27.0	38.0	15.4	12.7	22.9
VI[b,c]	Me	H						
VII[a]	Me	Me		13.0	23.5	20.1 9.8	10.8	21.5
VIII[b]	Me	Me		13.0	31.5	20.2 12.1	8.7	22.6

[a,b,c] See Table 3.

Table 6. The temperature dependence of the coupling constants of *cis*-5,6-dimethyl-4-oxo-1,3-dioxan (II). Solvent CS_2.

T°C	$^3J_{5,6}$	$^3J_{5H,CH_3}$	$^3J_{6H,CH_3}$
−50	5.65	7.09	6.36
−35	5.43	7.40	6.42
−20	5.87	7.26	6.34
−10	5.84	7.12	6.40
10	5.84	7.12	6.37
25	5.27	7.08	6.40
50	5.77	7.12	6.38
75	5.85	7.08	6.30
100	5.46	7.14	6.43

trans-2,5-substitution. The alternative half-chair form of VI can also be neglected because of a pseudo-axial 2-methyl group, for reasons mentioned above.

The PMR parameters of the compounds studied. The PMR data (Tables 3 – 6) reveal that derivatives I, III, and VII (all from *threo* acid, see Table 1) have a similar conformation. The coupling constant $^3J_{5,6}$ is about the same as in *cis*-2,6-dialkyl-substituted derivatives [1] and evidently the 5 and 6 substituents are (pseudo)-equatorially orientated. J_{gem} of the 2 protons of I is −5.8 Hz, a typical value for a half-chair conformation.[3,4] Thus all these derivatives exist in a half-chair conformation like that of *r*-2-*trans*-5-*cis*-6-trimethyl-4-oxo-1,3-dioxan (III in eqn. 1). Compounds II and V (from *erythro* acid, Table 1) also have nearly equal parameters and most probably exist in a half-chair conformation with a pseudo-axial 5 substituent (V in eqn. 2). The solvent shifts of the 6 methyl protons of II and V (Table 5) are 24.2 and 22.9 Hz, respectively. This indicates a half-chair conformation since in a 2,5-boat the methyl group would occupy a pseudo-axial orientation and the solvent shift would be near to 10 Hz.[3,4] Moreover, the J_{gem} of 2 protons of the *cis*-5,6-dimethyl derivative (II) is −5.8 Hz, again a typical value for a half-chair conformation.[3,4] The spectrum of II was recorded at various temperatures (Table 6), but no significant changes were detected. Accordingly, the 5a6e conformation is clearly favoured in agreement with the close similarity of the PMR parameters of II and V.

The trimethyl derivative IV (see Table 1 and eqn. 1) seems to be a mixture of two conformations as mentioned above in discussing the equilibration results. $^3J_{5,6}$ 9.5 Hz, is close to the mean of the values for pure half-chair and 2,5-boat forms (IVa and IVc in eqn. 1),[1] an observation in accord with the entropy difference 4.6 kJ mol^{-1} K^{-1} between III and IV.

r-2-*trans*-5-*trans*-6-Trimethyl-4-oxo-1,3-dioxan (VI) contained too many impurities to allow a full analysis of its PMR spectra. $^3J_{5,6}$ for the tetramethyl derivative (VIII) is only 3.1 Hz, and the other PMR parameters clearly differ from the values for the other oxalactones derived from the *erythro* acid (II and V). Obviously, the *gem*-dimethyl grouping in the 2 position forces the ring

into a twist-boat conformation.[1,2] It is of interest that the other 2,2-disubstituted derivative (VII) has quite "normal" PMR parameters. This again demonstrates the fact that the conformation of the 4-oxo-1,3-dioxan ring is greatly dependent on substitution.

Acknowledgements. The author wishes to express his gratitude to the *Neste Oy* and *Emil Aaltonen Foundations* for financial aid.

REFERENCES

1. Äyräs, P. and Pihlaja, K. *Tetrahedron* **29** (1973) 1311.
2. Äyräs, P. *Advan. Mol. Relaxation Processes* **5** (1973) 219.
3. Äyräs, P. *Suomen Kemistilehti* **B 46** (1973) 151.
4. Äyräs, P. and Pihlaja, K. *Acta Chem. Scand.* **27** (1973) *In press.*
5. Äyräs, P. and Pihlaja, K. *Tetrahedron Letters* **1970** 4095.
6. Pihlaja, K., Launosalo T. and Äyräs, P. *Acta Chem. Scand.* **23** (1969) 2299.
7. Pihlaja, K. *Ann. Univ. Turkuensis Ser. A* **I** (1967) No. 114.
8. Pihlaja, K. and Luoma S. *Acta Chem. Scand.* **22** (1968) 2401.
9. Pihlaja, K. and Jalonen, J. *Org. Mass. Spectrom.* **5** (1971) 1363.

Received March 7, 1973.

ACTA CHEMICA SCANDINAVICA 27 (1973) 2893–2901

The Influence of Ethanol-induced Changes of the α-Glycerophosphate Level on Hepatic Triglyceride Synthesis

ERIK FELLENIUS, GUNNAR BENGTSSON and KARL-HEINZ KIESSLING

Alcohol Research Group of the Swedish Medical Research Council, Institute of Zoophysiology, University of Uppsala, Uppsala, Sweden

The correlation between the level of α-glycerophosphate and hepatic triglyceride synthesis was studied in rat liver. Livers were perfused *in situ* with and without oleate in the medium and the hepatic content of α-glycerophosphate was varied by using livers of rats in different nutritional states and by adding ethanol, pyruvate or glycerol to the perfusate.

It was observed that changes in triglycerides were not a function of the concentration of α-glycerophosphate in the absence of oleate. In the presence of oleate, alone or with other substrates, a correlation could be observed. Pyruvate tended to inhibit the ethanol-induced increase of α-glycerophosphate and malate. Oleate also decreased the ethanol-induced accumulation of α-glycerophosphate in the livers of starved rats but not in those of rats on normal diet.

The importance of the availability of proton acceptors for the regulation of the level of α-glycerophosphate is discussed. The capacity of the isolated liver mitochondria of rats fed a high-fat diet to oxidize α-glycerophosphate was twice as great as that of the liver mitochondria of rats on a normal diet. The result indicates a relationship between lipid metabolism and the activity of the mitochondrial α-glycerophosphate dehydrogenase.

Two major metabolic pathways are available to the free fatty acids entering the liver: catabolism *via* β-oxidation or esterification with α-glycerophosphate to form triglycerides. Obviously, the higher the proportion of free fatty acids which are converted into triglycerides, the less there is available for oxidation to acetyl-CoA. It has been suggested that the main factor controlling the intrahepatic fate of free fatty acids is the availability of α-glycerophosphate.[1–6] Indeed Howard and Lowenstein [7] presented evidence that the level of α-glycerophosphate might control the *de novo* synthesis of hepatic fatty acids. In certain nutritional states, fatty acid synthesized *de novo* may be a substrate of quantitative importance for triglyceride synthesis.[8]

Studies of the flux of carbon atoms from labelled glucose to glyceride-glycerol in hearts throw serious doubt on the assumption discussed above.[9,10]

A lack of correlation between the ability of various compounds to reverse starvation ketosis in the rat liver and their effects on the α-glycerophosphate concentration in the liver has also been reported.[11,12]

The purpose of the study reported here is to investigate quantitative relationship between the hepatic level of α-glycerophosphate and the triglyceride synthesis. For this purpose, livers were perfused *in situ* with or without equimolar quantities of oleate. The hepatic content of α-glycerophosphate was varied by the perfusion of the livers of rats in different nutritional states and by the addition of ethanol, pyruvate or glycerol. It is obvious from the results that net decrease of triglycerides in the liver is not a function of the level of α-glycerophosphate. However, during the net synthesis of neutral fat, a correlation was found between the changes in triglyceride content and the level of α-glycerophosphate at the end of the experiment. The factors affecting the level of α-glycerophosphate are discussed.

EXPERIMENTAL

Rats. Female Wistar rats (180 – 230 g) from the laboratory's stock were used. The animals were divided into fed, 48 h starved, and fat-fed groups as described in Ref. 13.

Reagents. Standard analytical-grade laboratory reagents were obtained from E. Merck AG, Darmstadt, West Germany. Oleic acid *(puriss.)* was obtained from Fluka AG, Chemische Fabrik, Buchs, Switzerland. All the enzymes and co-enzymes were obtained from Biochimica Boehringer, Mannheim, West Germany, or Sigma Chemical Co., St Louis, USA.

Liver perfusion and addition of agents. The method of liver perfusion was that described by Hems *et al.*,[14] except that fresh bovine erythrocytes, supplied by the slaughterhouse at Uppsala, Sweden, was used instead of aged human erythrocytes.

Substrates were added to the medium either as a single dose (ethanol, oleate) or by continuous infusion (glycerol, pyruvate) beginning 38 min after the start of the perfusion. Oleic acid was added as a neutral solution bound to albumin.[15] Before addition of substrates, one lobe of the liver was freeze-clamped. [16] The perfusion was continued for 45 min after the initial addition of substrate. At that time the rest of the liver was freeze-clamped. In the tables 0 min refer to the time of the first sampling of the liver, namely after 38 min of perfusion. Liver and perfusate were deproteinized with $HClO_4$ and were prepared for metabolite assays as described by Williamson *et al.*[17]

Warburg experiments. The rats on a normal diet and rats fed a high-fat diet were decapitated and the liver mitochondria were prepared for manometric studies according to the method of Ernster and Löw.[18] The mitochondria were suspended in sucrose (0.25 M), so that the 1 ml added to the Warburg vessel contained mitochondria from about 300 mg of liver.

The final concentration of substances in the incubation mixture was K-phosphate buffer, pH 7.4, 15.0 mM; ATP, 2.0 mM; $MgCl_2$, 5.0 mM; glucose, 25.0 mM; DL-α-glycerophosphate, 15.0 mM; hexokinase, 30 units.[19] The respiratory rate with DL-α-glycerophosphate (Sigma Chemical Co., St. Louis, USA) was determined manometrically. The rate of disappearance of α-glycerophosphate was also measured. Protein was estimated according to Lowry *et al.*[20]

Determination of metabolites. Lactate, malate, and α-glycerophosphate were determined by the method of Hohorst *et al.*[21] Triglycerides were estimated by a modification of the method described by Eggstein and Kreutz.[22]

The freeze-clamped liver tissue was ground in a cooled percussion mortar.[16] About 0.1 g of liver was transferred to a tube containing 2.0 ml of 0.50 M KOH dissolved in ethanol and previously weighed and chilled in liquid nitrogen. The tube was allowed to thaw and was weighed again. Hydrolysis of triglyceride was performed on a water bath (65 – 75°) for at least 1 h. Six millilitres of 0.10 M $MgSO_4$ were added and the solution was

chilled to 4°. After centrifugation for 15 min at 3000 g_{av}, the clear, neutralized supernatant was analyzed for its content of free glycerol (equivalent to the molar content of triglyceride) by the enzymatic method described by Eggstein and Kreutz.[22]

RESULTS

Changes of liver triglycerides. Hepatic triglyceride concentrations (Table 1) decreased significantly in starved, but not in fed animals during perfusion in the absence of oleate. While ethanol or pyruvate had no influence at all, a

Table 1. Changes of triglycerides in the perfused liver. Before the addition of substrates, one lobe of the liver was freeze-clamped. Thereafter, different substrates were added to the medium, either as a single dose (ethanol and oleate, final concentration 10 and 2 mM, respectively) or by continuous infusion of a 1.93 M pyruvate or 0.33 M glycerol solution at a rate of 1.83 ml/h. The livers were perfused for 45 min after the addition of substrates. The infusion of pyruvate was stopped after 40 min. At the end of the experiment, the rest of the liver was freeze-clamped. The rates are means ± S.E.M. for the number of observations stated in the parentheses.

Substrate added	Changes of liver triglycerides μmol/ (45 min g wet wt)		
	Normal diet	Starved for 48 h	High-fat diet
None	−0.14 ± 0.41(7)	−3.47 ± 0.53(7)	
Ethanol	+0.09 ± 0.43(9)	−2.43 ± 0.69(7)	
Oleate	+4.74 ± 0.29(9)	−0.37 ± 0.60(9)	
Ethanol + oleate	+7.50 ± 0.33(9)	+1.30 ± 0.48(7)	−1.62 ± 0.73(5)
Pyruvate		−3.99 ± 0.87(6)	
Pyruvate + ethanol		+0.16 ± 0.51(6)	
Pyruvate + oleate		−1.63 ± 0.73(7)	
Pyruvate + ethanol + oleate		+3.88 ± 0.74(8)	
Glycerol + oleate		+4.44 ± 0.67(9)	

net breakdown of triglyceride was eliminated in starved animals in the presence of oleate. A net increase of triglycerides could be demonstrated in the presence of oleate in the liver of normal diet rats. This increment was further augmented when ethanol was also present.

Correlation between changes of triglycerides and the level of α-glycerophosphate. When oleate was present, with or without other substrates, a correlation was found between the changes of triglycerides and the level of α-glycerophosphate (Fig. 1). The highest rate of triglyceride synthesis could be demonstrated in liver from normal-diet rats in the presence of ethanol and oleate. These tissues also had a very high level of α-glycerophosphate. The curve relating α-glycerophosphate concentration and net triglyceride synthesis tended to level off at high α-glycerophosphate concentrations possibly due to saturation of the enzyme system responsible for triglyceride synthesis. Whether the results from the experiments with glycerol and oleate represent such a saturation remains to be explored. It is noteworthy that the levels of α-glycerophosphate obtained in the present study were unphysiological and it is possible that

Table 2. The level of α-glycerophosphate, lactate and malate in the perfused liver. The experimental conditions were as described in Table 1. The values refer to the time of the addition of substrates (0 min) and after perfusion for 45 min. The values are means ± S.E.M. for the number of perfusions stated and are expressed as μmol/(g wet wt).

Animal treatment	Substrate added	Number of observations	α-Glycerophosphate 0 min	α-Glycerophosphate 45 min	Lactate 0 min	Lactate 45 min	Malate 0 min	Malate 45 min
Normal diet	None	7	0.230 ± 0.038	0.307 ± 0.021	1.69 ± 0.16	1.78 ± 0.18	0.435 ± 0.033	0.474 ± 0.091
	Ethanol	9	0.303 ± 0.050	0.652 ± 0.055	1.61 ± 0.11	1.94 ± 0.33	0.356 ± 0.039	0.517 ± 0.068
	Oleate	9	0.339 ± 0.043	0.385 ± 0.044	1.61 ± 0.27	0.58 ± 0.11	0.461 ± 0.051	0.890 ± 0.083
	Ethanol + oleate	9	0.333 ± 0.028	0.783 ± 0.079	1.72 ± 0.15	1.14 ± 0.13	0.384 ± 0.021	0.930 ± 0.114
Starved for 48 h	None	7	0.091 ± 0.021	0.092 ± 0.024	0.267 ± 0.031	0.211 ± 0.024	0.077 ± 0.016	0.069 ± 0.013
	Ethanol	7	0.080 ± 0.020	0.886 ± 0.068	0.217 ± 0.041	0.355 ± 0.059	0.053 ± 0.010	0.173 ± 0.016
	Oleate	9	0.049 ± 0.004	0.173 ± 0.021	0.199 ± 0.010	0.257 ± 0.037	0.064 ± 0.007	0.149 ± 0.013
	Ethanol + oleate	7	0.078 ± 0.009	0.124 ± 0.014	0.202 ± 0.028	0.429 ± 0.031	0.083 ± 0.011	0.156 ± 0.022
	Pyruvate	6	0.061 ± 0.010	0.053 ± 0.001	0.184 ± 0.018	2.67 ± 0.15	0.077 ± 0.020	0.657 ± 0.030
	Oleate + pyruvate	7	0.085 ± 0.009	0.120 ± 0.010	0.228 ± 0.004	3.85 ± 0.16	0.73 ± 0.006	1.64 ± 0.07
	Ethanol + pyruvate	6	0.069 ± 0.006	0.123 ± 0.014	0.268 ± 0.041	4.45 ± 0.31	0.060 ± 0.012	0.699 ± 0.039
	Ethanol + oleate + pyruvate	8	0.106 ± 0.017	0.319 ± 0.031	0.215 ± 0.047	3.49 ± 0.35	0.094 ± 0.035	2.00 ± 0.15
	Glycerol + oleate	9	0.086 ± 0.023	7.56 ± 0.51	0.200 ± 0.011	0.232 ± 0.024	0.078 ± 0.011	0.185 ± 0.012
High-fat diet	Ethanol + oleate	5	0.128 ± 0.027	0.155 ± 0.018	0.308 ± 0.054	0.940 ± 0.089	–	–

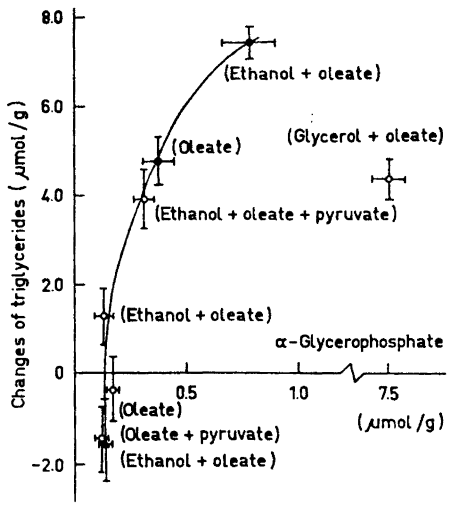

Fig. 1. Correlation between changes of hepatic triglycerides and the level of α-glycerophosphate. Livers from starved rats (○), rats on a normal diet (●) and rats on a high-fat diet (▲) were perfused as described in Table 1. The changes of hepatic triglycerides during 45 min in the presence of oleate have been plotted against the level of α-glycerophosphate after perfusion for 45 min. The values are means ± S.E.M. for 6 – 9 perfusions.

other factors were regulatory under these experimental conditions. Nevertheless, the results in those instances in which the amount of α-glycerophosphate varied within the physiological range, are consistent with the hypothesis that the concentration of this compound is a physiological regulator of the synthesis of neutral fat.

In livers perfused with a medium free of oleate, hepatic triglyceride stores either decreased or were unchanged (Table 1); no correlation was found between the magnitude of the change in triglyceride and the concentration of α-glycerophosphate.

Factors affecting the level of α-glycerophosphate. The level of α-glycerophosphate, malate, and lactate will depend to a large extent on the cytoplasmic [free NAD_+]/[free NADH] ratio.[21] One of the most characteristic events occurring in the liver during the oxidation of ethanol is a dramatic increase of this redox ratio.[23–26] Therefore, in order to investigate how the three compounds are interrelated during ethanol metabolism, an analysis was made of the content of α-glycerophosphate, malate, and lactate (Table 2).

In livers from starved and normal diet rats, the contents of α-glycerophosphate and malate increased in the presence of ethanol, while the level of lactate was less affected. Oleate decreased the lactate level, an effect which was slightly inhibited by ethanol. Oleate alone did not influence the concentration of α-glycerophosphate appreciably. During ethanol oxidation, however, oleate prevented the accumulation of α-glycerophosphate in the livers of starved rats but not in the livers of rats on a normal diet. Surprisingly, the oleate-induced accumulation of malate was not further increased by ethanol. When pyruvate was infused in the presence of ethanol, the amount of lactate increased while α-glycerophosphate and malate did not change appreaciably. Thus a considerable portion of the reducing equivalents derived from the oxidation of ethanol was transferred to pyruvate. Since pyruvate acts as gluconeogenetic precursor the NADH will also be consumed along this path-

way. In consequence, dihydroxyacetone phosphate and oxaloacetate will be ruled out as the proton acceptors.

Increased capacity of the mitochondria to oxidize α-glycerophosphate. The rate of disappearance of α-glycerophosphate and the uptake of oxygen by isolated mitochondria obtained from the livers of fat-fed and normal diet animals in Warburg experiments are presented in Table 3. The capacity to

Table 3. Induction of the liver mitochondria of rats fed a high-fat diet to oxidize α-glycerophosphate, as measured in Warburg experiments. Details of the experimental conditions have been given in the "Experimental" section. The values are means ± S.E.M. for the number of animals stated. The rates are expressed as μmol/(h 10 mg protein) and the concentrations of triglycerides as μmol/(g wet wt).

Animal treatment	Number of observations	Oxygen uptake	α-Glycero-phosphate consumption	Triglyceride content
Normal diet	6	7.2 ± 0.4	6.6 ± 0.4	11.7 ± 0.2
High-fat diet	6	19.5 ± 1.6	15.9 ± 1.0	52.2 ± 4.9

oxidize α-glycerophosphate was more than twice as great in the livers of rats on high-fat diets, compared with normal livers. The level of triglyceride was about five times higher in rats fed a high-fat diet compared with normal diet rats. The results suggest a relationship between the rate of triglyceride synthesis and the activity of the mitochondrial α-glycerophosphate dehydrogenase.

DISCUSSION

The results (Fig. 1) suggest that the concentration of α-glycerophosphate should be considered as one of the factors, but not the only one, influencing the hepatic triglyceride biosynthesis. In perfusions carried out in the absence of oleate, no correlation between the level of α-glycerophosphate and the rate of triglyceride synthesis was found. These were experiments in which the levels of triglycerides either decreased or were unchanged. In this instance the availability of fatty acid for triglyceride synthesis was probably rate limiting.

At very high, unphysiological levels of α-glycerophosphate, brought about by the infusion of glycerol, only a moderate increase in hepatic triglycerides was found in spite of the presence of oleate. Other factors were obviously rate limiting in this experiment.

Since it was found that the level of α-glycerophosphate may be a regulator of net triglyceride synthesis it is also of interest to know what factors influence the concentration of α-glycerophosphate. This may be the flux of α-glycerophosphate into mitochondria,[27] the supply from glycolysis, gluconeogenesis, lipid metabolism, the pentosphosphate pathway, the kinetic behaviour of α-glycerophosphate dehydrogenase[28,29] in the intact animal, the uptake of

glycerol from the blood and finally the redox state [21,30] or the availability of different proton acceptors.[31]

The NADH formed during ethanol oxidation may be utilized by the glyceraldehyde phosphate, lactate, malate, or α-glycerophosphate dehydrogenase systems, disregarding other biosynthetic or hydroxylation reactions which may directly utilize the NADH produced in the cell sap. Thus information on the interrelationship between α-glycerophosphate, malate, and lactate is of importance for a knowledge of the role of the availability of proton acceptors. It is clear from the results (Table 2) that the availability of pyruvate for different metabolic pathways is limited during ethanol oxidation. Lactate represents a metabolic end product and it would have increased more if the conversion of pyruvate to lactate was the main route of hydrogen transfer. Moreover, a net decrease of lactate was found with normal diet rats when oleate or oleate and ethanol had been added. Thus, hydrogen is mainly transferred to oxaloacetate and dihydroxyacetone phosphate during ethanol oxidation. As a consequence the corresponding reduced compounds, malate and α-glycerophosphate, increased. The powerful inhibition by α-glycerophosphate of α-glycerophosphate dehydrogenase [28,29] will prevent an indefinite accumulation of α-glycerophosphate. The suggested route for hydrogen transfer is further supported by the results when pyruvate was infused. Then, pyruvate availability is not the limiting factor and as a consequence the ethanol-induced rise in malate and α-glycerophosphate formation is prevented.

The importance of enzyme(s) located within the mitochondria on the level of α-glycerophosphate is not quite established. The activity of the flavin-dependent α-glycerophosphate dehydrogenase (EC 1.1.99.5) is considered to be too low to be of any significance.[32–34] In a recent report [35] it was shown that the rate of oxidation of α-glycerophosphate by the intact organ exceeded by far the calculated capabilities of isolated mitochondria. We found that liver mitochondria from fat-fed rats had an increased capacity to oxidize α-glycerophosphate (Table 3). The net sequence of this would be to limit the accumulation of α-glycerophosphate in the liver and in this way to inhibit the synthesis of triglycerides. A similar adaptation occurs after long-term feeding with ethanol.[36,37] Thus, there seems to exist a relationship between the relative disposition of fatty acid into the β-oxidative and triglyceride synthetic pathways and the activity of a mitochondrial enzyme, the flavin-dependent α-glycerophosphate dehydrogenase, which will influence the level of α-glycerophosphate.

Carnicero *et al.*[35] also presented evidence that the pathway by which extramitochondrial hydrogen in form of α-glycerophosphate is oxidized partly leads through a respiratory chain-linked NADH-dehydrogenase. Part of the disappearance of α-glycerophosphate may therefore be due to interaction between this dehydrogenase and other dehydrogenases as malate, β-hydroxybutyrate, or glutamate dehydrogenase within the mitochondria. Thus the small increase of α-glycerophosphate in starved and fat-fed rats supplemented with oleate and ethanol but not in fed rats (Table 2) can partly be explained by the higher rate of acetoacetate formation in the former group. The hydrogen formed during the oxidation of α-glycerophosphate will be reoxidized by the β-hydroxybutyrate dehydrogenase system in the livers of starved and fat-fed

rats but not in livers from normal diet rats, where the rate of ketone-body formation is fairly low. It should be noted that, when oleate was present, ethanol did not induce any accumulation of malate. Possibly the β-hydroxybutyrate dehydrogenase is more important than the malate dehydrogenase for the reoxidation of α-glycerophosphate under the present experimental conditions.

Acknowledgements. Thanks are due to Miss G.-B. Jönsson and Mrs Å. Paulin for excellent technical assistance and to Mrs B. Lundgren for typing the manuscript. Mr Erik Fellenius was in receipt of financial support from the *Helge Ax:son Johnson Foundation* and the *Faculty of Mathematics and Science of the University of Uppsala.* This work was also supported by the *Swedish Medical Research Council* (Grant No. B72-12Y-2364-05.)

REFERENCES

1. Fritz, I. B. *Physiol. Rev.* **41** (1961) 52.
2. Wieland, O. and Matschinsky, F. *Life Sci.* **1** (1962) 49.
3. Nikkilä, E. A. and Ojala, K. *Proc. Soc. Exp. Biol. Med.* **113** (1963) 814.
4. Nikkilä, E. A. and Ojala, K. *Life Sci.* **10** (1963) 717.
5. Tzur, R., Tal.E. and Shapiro, B. *Biochim. Biophys. Acta* **84** (1964) 18.
6. Ylikahri, R. H. *Metabolism* **19** (1970) 1036.
7. Howard, C. F., Jr. and Lowenstein, J. M. *J. Biol. Chem.* **240** (1965) 4170.
8. Windmueller, H. G. and Spaeth, A. E. *Arch. Biochem. Biophys.* **122** (1967) 362.
9. Denton, D. M. and Randle, P. J. *Biochem. J.* **104** (1967) 423.
10. Denton, D. M. and Halperin, M. L. *Biochem. J.* **110** (1968) 27.
11. Williamson, D. H., Veloso, D., Ellington, E. V. and Krebs, H. A. *Biochem. J.* **114** (1969) 575.
12. McGarry, J. D. and Foster, D. W. *J. Biol. Chem.* **246** (1971) 6247.
13. Fellenius, E. and Kiessling, K.-H. *Acta Chem. Scand.* **27** (1973) 2781.
14. Hems, R., Ross, B. D., Berry, M. N. and Krebs, H. A. *Biochem. J.* **101** (1966) 284.
15. Krebs, H. A., Wallace, P. G., Hems, R. and Freedland, R. A. *Biochem. J.* **112** (1969) 595.
16. Wollenberger, A., Ristau, O. and Schoffa, G. *Pflügers Arch. Gesamte Physiol. Menschen Tiere* **270** (1960) 399.
17. Williamson, D. H., Lund, P. and Krebs, H. A. *Biochem. J.* **103** (1967) 514.
18. Ernster, L. and Löw, H. *Exptl. Cell Res.*, Suppl. **3** (1955) 113.
19. Darrow, R. A. and Colowick, S. P. *Methods Enzymol.* Academic, New York and London (1962), p. 226.
20. Lowry, O. H., Rosebrough, N. H., Farr, A. L. and Randell, R. J. *J. Biol. Chem.* **193** (1951) 265.
21. Hohorst, H. J., Kreutz, F. H. and Bücher, Th. *Biochem. Z.* **332** (1959) 18.
22. Eggstein, M. and Kreutz, F. H. *Klin. Wschr.* **44** (1966) 262.
23. Forsander, O., Räihä, N. and Suomalainen, H. *Hoppe-Seyler's Z. physiol. Chem.* **312** (1958) 243.
24. Williamson, J. R., Scholz, R., Browning, E. T., Thurman, R. G. and Fukami, M. H. *J. Biol. Chem.* **244** (1969) 5044.
25. Lindros, K. O. and Aro, H. *Ann. Med. Exp. Fenn.* **47** (1969) 39.
26. Rawat, A. K. *Eur. J. Biochem.* **6** (1968) 585.
27. Lehninger, A. L. *The Mitochondrion*, Benjamin, New York 1964, p. 132.
28. Blanchaer, M. C. *Can. J. Biochem.* **43** (1965) 17.
29. Black, W. J. *Can. J. Biochem.* **44** (1966) 1301.
30. Veech, R. L., Guynn, R. and Veloso, D. *Biochem. J.* **127** (1972) 387.
31. Schimassek, H., Walli, A. K. and Höfer, G. In Martini, G. A. and Bode, Ch., Eds., *Metabolic Changes Induced by Alcohol*, Springer, Berlin, Heidelberg, New York 1971, p. 157.
32. Kleitke, B., Heier, G. and Wollenberger, A. *Biochim. Biophys. Acta* **130** (1966) 270.

33. Klingenberg, M. *Eur. J. Biochem.* **13** (1970) 247.
34. Hassinen, I., Ylikahri, R. and Kähönen, M. *Ann. Med. Exp. Fenn.* **48** (1970) 176.
35. Carnicero, H. H., Moore, C. L. and Hoberman, H. D. *J. Biol. Chem.* **247** (1972) 418.
36. Kiessling, K.-H. *Acta Pharmacol. Toxicol.* **26** (1968) 245.
37. Rawat, A. K. and Kyriyama, K. *Biochem. Biophys. Res. Commun.* **47** (1972) 517.

Received April 5, 1973.

ACTA CHEMICA SCANDINAVICA 27 (1973) 2902–2908

The Crystal and Molecular Structure of 9-Methyl-8-phenyl-6-thiopurine Hemihydrate

GUNNAR NYGJERD and EINAR SLETTEN

Chemical Institute, University of Bergen, N-5014 Bergen, Norway

The structure of 9-methyl-8-phenyl-6-thiopurine hemihydrate, $(C_{12}N_4SH_{10})\cdot\frac{1}{2}H_2O$, has been solved by X-ray crystallographic methods. The crystals are monoclinic, space group $C2/c$, with $a = 16.046$ Å, $b = 7.071$ Å, $c = 21.784$ Å and $\beta = 104.79°$. 2116 reflections were measured on a four-circle diffractometer using Mo$K\alpha$ radiation. The structure was refined to $R = 0.044$. Standard deviations in bond lengths and angles involving non-hydrogen atoms are in the range 0.003 – 0.006 Å and 0.2 – 0.3°, respectively. The phenyl group is twisted 28.5° relative to the purine ring. The molecules are piled on top of one another along the *b*-axis with alternate purine and phenyl rings in the stack. The interplanar spacing is 3.53 Å.

The present structure investigation was carried out to study the steric interactions in substituted purine bases. The structure of the unsubstituted 6-thiopurine molecule (I) has already been determined to high accuracy in two independent X-ray investigations.[1,2]

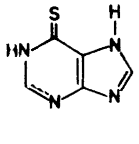

(I)

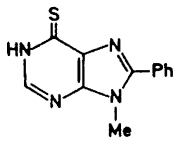

(II)

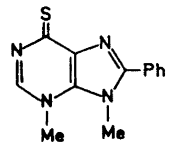

(III)

In the present paper the structure of II is reported. Further studies will include molecule III. F. Bergmann and co-workers have synthesized several compounds of this type and the results of UV, NMR and mass spectrometric measurements [3] will be discussed in relation to the structure obtained. Experimental dipole moments have also been obtained for some of the compounds [4] and will be correlated with theoretical calculations.[5]

EXPERIMENTAL

A sample of 9-methyl-8-phenyl-6-thiopurine (MPTP) was kindly supplied by F. Bergmann, the Hebrew University of Jerusalem. The crystals were grown from a 20 % solution of acetic acid in water by slow evaporation.

Weissenberg photographs showed the space group to be either $C2/c$ or Cc. The distribution of normalized structure factors indicated that $C2/c$ was the correct one. Cell parameters were determined by least-squares treatment of the 2θ settings for 12 reflections measured on the diffractometer. The density of the crystals was measured by flotation in a mixture of tetrachloromethane and benzene and the obtained value agreed satisfactorily with that calculated for the hemihydrate.

The crystal data are as follows:

$(C_{12}N_4SH_{10}).\frac{1}{2}H_2O$ M.W. = 251.31
Crystal system: monoclinic, space group $C2/c$.
$a = 16.046(5)$ Å, $b = 7.071(2)$ Å, $c = 21.784(4)$ Å, $\beta = 104.79(2)°$
$V = 2389(1)$ Å^3, $F_{000} = 524$, $Z = 8$
$D_m = 1.397$ g cm^{-3}, $D_x = 1.38$ g cm^{-3}
Linear absorption coefficient: $\mu = 2.57$ cm^{-1}.

Data were collected on a tape-operated four-circle diffractometer with niobium filtered Mo$K\alpha$ radiation. The crystal used had dimensions 0.65 mm × 0.10 mm × 0.07 mm, and was mounted along [010] which coincides with the needle axis. Integrated intensities were measured with the $\theta - 2\theta$ scan technique, the scan ranges being calculated as $\Delta\theta_1 = a_1 + b_1 \tan\theta$ and $\Delta\theta_2 = a_2 + b_2 \tan\theta$. Suitable scan ranges were obtained with $a_1 = 0.30°$, $b_1 = 0.20°$, $a_2 = 0.32°$ and $b_2 = 0.20°$. Both the peak and the background were measured twice and the net count was derived by subtracting the background counts from the peak counts. The error in the net intensity of each reflection was derived as

$$\sigma(I) = [\sigma_c^2 + (k\sigma_c^2)^2]^{\frac{1}{2}}$$

where σ_c is the error due to counting statistics. The factor k was set equal to 0.01 to include the error caused by electronic instability and misalignment of the crystal as reflected in the plot of standard reflections. Of the 2116 reflections measured in the interval $1° < \theta < 25°$, 678 were less than $2\sigma_c$. These reflections were set equal to the threshold value of $2\sigma_c$ and included in the refinement only if $F_{calc} > F_{threshold}$.

The structure was solved by a symbolic addition procedure and refined by full-matrix least-squares on an IBM 360/50 computer. The quantity minimized was $\sum w(|F_o| - |F_c|)^2$ with $w = 1/\sigma_F^2$. The atomic scattering factors for the heavier atoms were obtained from *International Tables for X-Ray Crystallography* (1962),[6] and those for the hydrogen atoms were from Stewart *et al.*[7] In the three initial cycles of refinement isotropic temperature parameters were used. Later the non-hydrogen atoms were included with anisotropic parameters. All the hydrogen parameters in the MPTP-molecule were well determined. However, some difficulties were encountered in refining the hydrogen atoms of the water molecule. The difference map indicated some kind of disorder in the orientation of the water hydrogens. Further refinement did not completely resolve this problem.

The refinement was terminated when all shifts were less than 0.1σ. The residual $R = (\sum||F_o| - |F_c||)/\sum|F_o|$ omitting unobserved reflections was 0.044. Final coordinates and temperature factors are listed in Tables 1 and 2, respectively. The thermal ellipsoids as shown in Fig. 3 seem to be physically meaningful. The phenyl group is seen to have an in-plane movement rather than an expected rotational movement around C(8)–C(10).

A rigid-body motion analysis [8] was carried out where the purine part of the molecule was treated separately. The r.m.s. deviation calculated between observed and calculated U_{ij}'s is 2.1×10^{-4} Å^2. The estimated standard deviation in U_{ij}'s from the full-matrix refinement is on the average 2.7×10^{-4} Å^2. The libration tensor were used to correct bond lengths between non-hydrogen atoms. The corrections are in the range 0.006 – 0.003 Å and are all less than 2σ.

Table 1. Final positional parameters with the corresponding standard deviations in parentheses.

Atom	*X/a*	*Y/b*	*Z/c*
S	0.51309(5)	0.02758(15)	0.39788(4)
O	0.50000(0)	0.27141(73)	0.25000(0)
N(1)	0.38878(16)	0.08445(37)	0.45727(11)
N(3)	0.24075(15)	0.14804(37)	0.41662(11)
N(7)	0.33271(15)	0.08282(34)	0.28474(10)
N(9)	0.20250(14)	0.14271(35)	0.30195(10)
C(2)	0.30879(20)	0.12170(48)	0.46341(14)
C(4)	0.25981(18)	0.12877(41)	0.36001(13)
C(5)	0.33917(17)	0.09161(42)	0.34883(12)
C(6)	0.41112(18)	0.06746(42)	0.40043(13)
C(8)	0.25023(18)	0.11371(40)	0.25790(13)
C(9)	0.11198(21)	0.19762(62)	0.29290(18)
C(10)	0.21485(19)	0.11256(42)	0.18819(13)
C(11)	0.13142(22)	0.05716(50)	0.15951(15)
C(12)	0.10301(25)	0.05725(55)	0.09358(17)
C(13)	0.15851(28)	0.10656(54)	0.05736(17)
C(14)	0.24190(27)	0.15824(53)	0.08600(16)
C(15)	0.27052(23)	0.16031(47)	0.15140(14)
H(0)	0.4805(30)	0.2008(61)	0.2708(21)
H(1)	0.4304(20)	0.0558(46)	0.4935(15)
H(2)	0.3071(17)	0.1406(42)	0.5076(13)
H(11)	0.0918(18)	0.0223(42)	0.1824(13)
H(12)	0.0440(19)	0.0120(44)	0.0754(13)
H(13)	0.1391(22)	0.1113(48)	0.0109(17)
H(14)	0.2818(20)	0.1976(46)	0.0611(14)
H(15)	0.3304(19)	0.1989(43)	0.1737(13)
H(91)	0.0796(21)	0.0667(52)	0.2890(14)
H(92)	0.1056(18)	0.2604(43)	0.3306(14)
H(93)	0.0946(18)	0.2803(44)	0.2547(15)

RESULTS AND DISCUSSION

Planarity of the molecule. The accumulation of accurate structural information on purines has revealed that the molecules are slightly bent around the conjugated bond C(4) – C(5).[9] In MPTP which has fairly large substituents, this feature is still present as shown in Fig. 1. The dihedral angle between the pyrimidine ring and the imidazole ring is 1.0°. In addition to the bending the purine part of the molecule is also slightly twisted around C(4) – C(5).

The phenyl group is rotated around C(8) – C(10) making a dihedral angle of 28.5° with the imidazole plane. In this conformation nearly symmetric short contacts appear between the *ortho*-hydrogen H(11) and the adjacent methyl hydrogen atoms. The lengths of the contacts H(11)···H(91) and H(11)···H(93) are 2.36(4) Å and 2.38(4) Å, respectively.

Methylation at N(7) or N(9) in 8-phenyl purines produces a large hypsochromic shift in contrast to the behaviour of the non-phenylated analogues, indicating a twist of the phenyl group.[3] The introduction of a second methyl

Table 2. Thermal parameters with the corresponding standard deviations in parentheses. The anisotropic thermal parameters are defined by the expression $T_i = \exp[-2\pi^2(U_{11}h^2a^{*2} + U_{22}k^2b^{*2} + U_{33}l^2c^{*2} + 2U_{12}hka^*b^* + 2U_{13}hla^*c^* + 2U_{23}klb^*c^*)]$ and the isotropic parameters by $T_i = \exp[-8\pi^2U \sin^2\theta/\lambda^2]$. For non-hydrogen atoms the values are multiplied by a factor of 10^4, for hydrogen atoms by 10^3.

	U_{11}	U_{22}	U_{33}	U_{12}	U_{23}	U_{13}
S	379(4)	955(8)	389(4)	149(5)	59(5)	141(3)
O	1018(34)	637(30)	890(31)	0	0	538(27)
N(1)	424(15)	533(18)	300(13)	95(13)	1(12)	104(12)
N(3)	437(15)	527(18)	353(13)	58(13)	14(12)	187(12)
N(7)	422(14)	444(17)	300(12)	55(12)	2(11)	132(10)
N(9)	326(12)	415(16)	361(13)	17(11)	−1(11)	107(10)
C(2)	524(20)	531(22)	313(17)	80(17)	−5(15)	170(15)
C(4)	382(16)	353(18)	325(15)	20(14)	1(13)	109(13)
C(5)	369(16)	372(18)	303(15)	24(14)	−1(13)	131(12)
C(6)	375(16)	428(20)	347(15)	48(14)	15(14)	132(12)
C(8)	374(15)	349(18)	356(16)	4(14)	−5(13)	134(13)
C(9)	369(18)	632(27)	480(21)	73(18)	6(20)	144(16)
C(10)	475(18)	347(18)	339(15)	46(15)	−9(14)	96(14)
C(11)	525(20)	479(23)	460(19)	−14(17)	−46(16)	93(16)
C(12)	595(24)	642(28)	506(21)	33(21)	−74(19)	−61(19)
C(13)	906(30)	601(26)	343(19)	96(23)	25(18)	74(21)
C(14)	791(28)	543(25)	393(19)	62(20)	7(17)	210(20)
C(15)	566(21)	432(21)	379(18)	38(17)	−9(15)	163(16)
	U		U		U	
H(1)	73(11)	H(13)	88(12)	H(92)	58(10)	
H(2)	58(9)	H(14)	65(10)	H(93)	55(10)	
H(11)	46(8)	H(15)	52(9)	H(0)	124(19)	
H(12)	63(10)	H(91)	73(12)			

group at N(3) is accompanied by a bathochromic shift of $\Delta\lambda_{max}$ +5 nm. N(3) methylation without the presence of Me N(9) gives a much larger shift, $\Delta\lambda_{max}$ +12. This is ascribed to an increased steric interference between 9-methyl and 8-phenyl substituents, when a methyl group is introduced at N(3). Further details of the stereochemistry have to await the structure determination of III.

Bond lengths and angles. The molecular dimensions are shown in Fig. 2. There is no known purine type tautomer directly comparable to the present

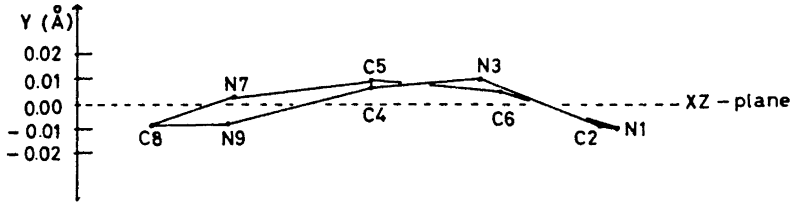

Fig. 1. The puckering of the purine ring. The scale of the ordinate is expanded relative to the abscissa.

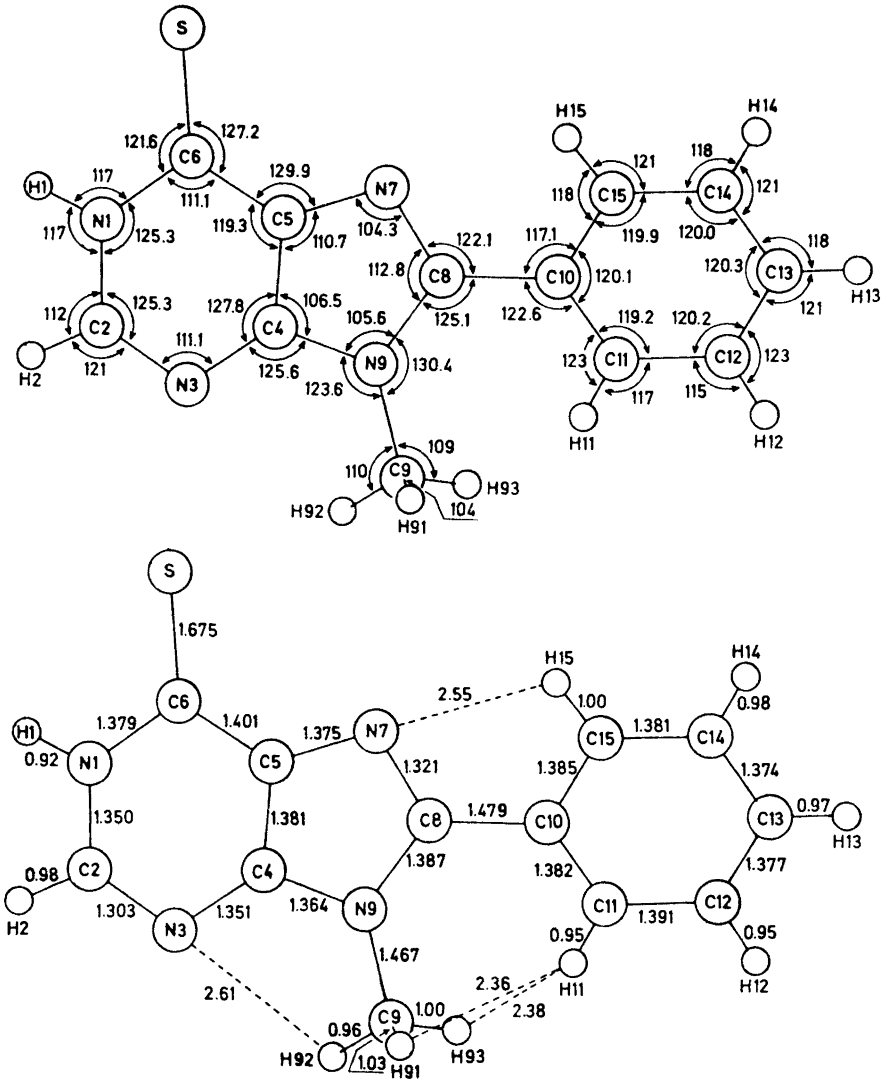

Fig. 2. Bond lengths and angles in 9-methyl-8-phenyl-6-thiopurine.

structure. The 6-thiopurine molecule [1,2] is a N(7) – H tautomer, thus only the pyrimidine parts in I and II are chemically equivalent. The structure of 1,3,9-trimethyl-xanthine (TMX) has recently been determined [10] and there the imidazole part may be compared to the present structure. In Table 3 pertinent bond lengths and angles in the three structures are listed. The dimensions of 6-thiopurine are most precise having been determined twice independently.[1,2] The pyrimidine parts in MPTP and 6-thiopurine, excluding

Table 3. Comparison of bond lengths (Å) and angles(°) in the purine part of 9-methyl-8-phenyl-6-thiopurine (MPTP), 6-thiopurine (TP)[1,2] and 1,3,9-trimethylxanthine (TMX).[19] The values of TP are the average of two independent determinations.

Bond	MPTP	TP	TMX
N(1) – C(2)	1.350	1.354	1.389
C(2) – N(3)	1.301	1.308	1.382
N(3) – C(4)	1.352	1.362	1.374
C(4) – C(5)	1.380	1.395	1.366
C(5) – C(6)	1.401	1.401	1.417
C(6) – N(1)	1.379	1.378	1.408
C(6) – S, (O)	1.676	1.677	1.216
C(5) – N(7)	1.375	1.371	1.384
N(7) – C(8)	1.321	1.349	1.299
C(8) – N(9)	1.387	1.329	1.376
N(9) – C(4)	1.365	1.365	1.365
Angles			
C(5) – C(6) – N(1)	111.1	110.8	112.9
C(5) – C(6) – S, (O)	127.2	126.8	126.9
N(1) – C(6) – S, (O)	121.6	122.4	120.2
C(6) – N(1) – C(2)	125.3	125.0	126.2
N(1) – C(2) – N(3)	125.3	125.0	117.6
C(2) – N(3) – C(4)	111.1	113.2	118.4
N(3) – C(4) – C(5)	127.8	124.1	123.5
C(4) – C(5) – C(6)	119.3	121.8	121.4
C(4) – C(5) – N(7)	110.7	105.9	110.7
C(6) – C(5) – N(7)	129.9	132.3	128.0
C(5) – N(7) – C(8)	104.3	106.1	103.7
N(7) – C(8) – N(9)	112.8	113.6	114.0
C(8) – N(9) – C(4)	105.6	104.3	105.0
N(9) – C(4) – C(5)	106.5	110.1	106.6

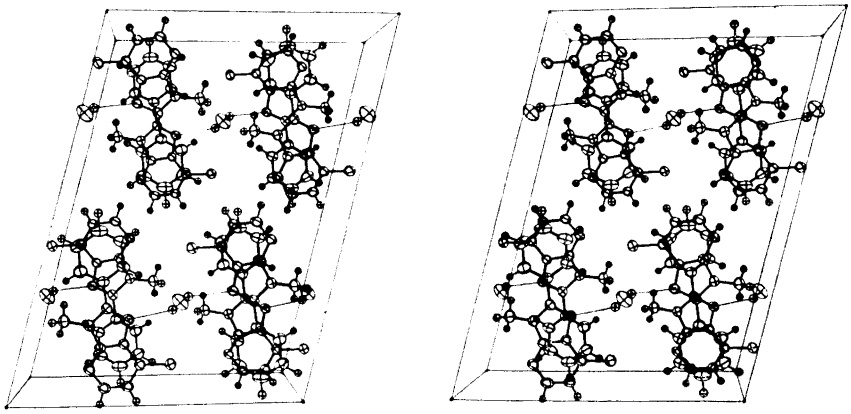

Fig. 3. Stereoscopic drawing of the contents of the unit cell viewed along the *b*-axis.

atoms C(4) and C(5) are identical within standard deviations. The effect of introducing a phenyl group in the imidazole ring is also apparently minor. The lengthenings of bonds N(7) – C(8) and C(8) – N(9) adjacent to the substitution site are probably significant. The steric interaction between methyl and phenyl has increased the external angles C(9) – N(9) – C(8) and N(9) – C(8) – C(10) though without significantly altering the internal angles at N(9) and C(8).

Molecular packing and hydrogen bonding. A stereoscopic drawing of the unit cell is shown in Fig. 3. The usual stacking pattern observed in purine structures is here replaced by alternate purine – phenyl stacking for molecules related by screw axis. The interplanar distance purine – phenyl is 3.53 Å and thus appreciably less than the van der Waals distance of 4.00 Å between aromatic rings. In the crystalline complex of 1,3,7,9-tetramethyluric acid and the carcinogene 3,4-benzpyrene the corresponding distance is 3.48 Å.[11] According to spectroscopic evidence the association between purines and aromatic hydrocarbons is not of the π-complex type but may be described as weak polarization-bonding interaction.[12]

The water molecule situated on the two-fold axis links the stacks together in the direction of the *a*-axis through weak hydrogen bonds to N(7), O – H··· N(7) = 3.255 Å. A normal oxygen-nitrogen hydrogen bond is in the range 2.7 – 2.9 Å. The loose hydrogen bonding found in the present structure may account for the apparent disorder of the water molecule.

Molecules related by a center of symmetry are connected by hydrogen bond N(1) – H···S = 3.24 Å, $\angle$N(1) – H – S = 143°. In thioguanine N – H···S distances are found slightly larger, 3.30 and 3.33, Å respectively.[13]

REFERENCES

1. Sletten, E., Sletten, J. and Jensen, L. H. *Acta Cryst.* **B 25** (1969) 1330.
2. Brown, G. M. *Acta Cryst.* **B 25** (1969) 1338.
3. Neiman, Z., Bergmann, F. and Lichtenberg, D. *J. Chem. Soc.* **C 1971** 1822.
4. Bergmann, E. D. and Weiler-Feilchenfeld, H. *The Purines – Theory and Experiment*, The Jerusalem Symposia on Quantum Chemistry and Biochemistry, The Israel Academy of Sciences and Humanities, Jerusalem 1972, p. 21.
5. Støgård, Å. *To be published.*
6. *International Tables for X-Ray Crystallography*, Kynoch Press, Birmingham 1962, Vol. III, p. 202.
7. Stewart, R. F., Davidson, E. R. and Simpson, W. T. *J. Chem. Phys.* **42** (1965) 3175.
8. Schomaker, V. and Trueblood, K. N. *Acta Cryst.* **B 24** (1968) 63.
9. Sletten, J. and Jensen, L. H. *Acta Cryst.* **B 25** (1969) 1608.
10. Rasmussen, H. and Sletten, E. *Acta Chem. Scand.* **27** (1973) 2757.
11. Damiani, A., Giglio, E., Liquori, A. M. and Ripamonti, A. *Acta Cryst.* **23** (1967) 675.
12. Wallwork, S. C. *J. Chem. Soc.* **1961** 494.
13. Bugg, C. H. and Thewalt, U. *J. Am. Chem. Soc.* **92** (1970) 7441.

Received May 7, 1973.

ACTA CHEMICA SCANDINAVICA 27 (1973) 2909–2922

Studies on the Enzymatic Degradation of Lignin

The Action of Peroxidase and Laccase on Monomeric and Dimeric Model Compounds*

JOSEF GIERER and AUGUSTINE E. OPARA

Swedish Forest Products Research Laboratory, Box 5604, S-114 86 Stockholm, Sweden

Monomeric and dimeric phenolic lignin model compounds were treated with one equivalent of hydrogen peroxide in the presence of *peroxidase*. During this treatment products of higher molecular weight were formed by oxidative carbon-to-carbon and carbon-to-oxygen coupling. The oligomeric components of the mixtures obtained were separated by chromatographic methods and characterised by NMR-spectra, mass spectra, and osmometric determination of the molecular weights. Non-phenolic model compounds remained unaffected by the enzyme system.

Oxidation of the phenolic models by *laccase* gave essentially the same pattern of reaction products as was obtained with peroxidase.

The results support the view that both enzymes are able to generate the mesomeric aryloxy radicals by hydrogen abstraction, the subsequent coupling reactions proceeding spontaneously. No indication was obtained that peroxidase or laccase are directly involved in the degradation of the aromatic moieties of lignin.

White rot fungi *(Basidiomycetes)* are well known for their ability to degrade wood lignins.[1–3] The fungi of this type produce varying amounts of extracellular phenol-oxidising enzymes,** of which peroxidase and laccase have been isolated. The good correlation between the production of these enzymes and the ability of the fungi to degrade lignin underlies the concept that these enzymes are directly involved in the degradation process.[4,5] This argument is strengthened by the fact that the taxonomically related species termed "brown-rot fungi" which do not exude any detectable amounts of phenol-oxidising enzymes, leave the lignin essentially undegraded. Other findings indicating a possible role of phenoloxidases in the fungal degradation of lignin

* The terms monomeric and dimeric refer to model compounds containing one and two aromatic nuclei, respectively.

** The terms phenol-oxidising enzymes and phenoloxidases are used interchangeably here and include peroxidase (EC. 1.11.1.7, Donor: H_2O_2 oxidoreductase) and laccase (EC. 1.10.3.1, *o*-Diphenol: oxygen oxidoreductase) which catalyse oxidation of phenols to polymeric dark products.

are the increased number of free radicals in wood after decay by white-rot fungi [6,7] and the oxidative cleavage of simple phenols with phenol-oxidising enzymes.[8]

Numerous studies on the effect of white-rot fungi or their enzymes on lignin and lignin model compounds have been carried out and have led to divergent theories on the microbial degradation of lignin. The main theories so far advanced have been reviewed recently [9–12] and may be summarised as follows:

(1) Side chains in lignin units are oxidised at the α- or β-carbon atoms with formation of structures containing keto groups and liberation of phenolic units. Methyl-aryl ether bonds are also cleaved in the process.

(2) β-Aryl ether linkages are cleaved hydrolytically giving rise to alcoholic and phenolic structures.

(3) The fragmentation of lignin is brought about by cleavage of alkyl aryl carbon-carbon bonds. In this type of reaction side-chains are removed from the aromatic nuclei by oxidative coupling between radical intermediates of the phenoxyl and cyclohexadienonyl types. Intermediary *p*-quinoid structures and aldehydic or acidic fragments are formed.

(4) The enzymes catalyse the cleavage of the aromatic nuclei. After introducing the required hydroxylation pattern (formation of *ortho*- or *para*-diphenol structures) by demethylation or hydroxylation, the phenolic rings are cleaved to give aliphatic degradation products (usually carboxylic acids).

Separately, or in coordination, reactions of these types should bring about extensive degradation of lignin. However, the pathway and mechanism of biodegradation of lignin is obscure and the results from many studies in this field are contradictory and confusing. No precise information is available as to the specific enzymes involved in the microbial degradation nor are the sequential changes occurring during the process known in detail. It is commonly held that the degradation of lignin is oxidative because the composition of degraded lignin resembles that of humic acid,[13,14] both products containing less methoxyl but more phenolic hydroxyl, carbonyl, and carboxyl groups. These changes apparently result from demethylations, hydroxylations, oxidative ring cleavages, and side chain oxidations. The extracellular enzymes, laccase and peroxidase, which are detected in culture media where lignin digestion has been demonstrated, are believed to play an important role in these transformations. Laccase is thought to be more involved in the degradation because of its wide distribution in fungi and other microorganisms effecting wood decay.[15,16] However, the significance of these enzymes in the process is uncertain.

This paper deals with model studies carried out with the aim of elucidating the role of peroxidase and laccase in the degradation of lignin. The low molecular weight components formed were separated by column chromatography after reductive acetylation of the crude mixtures. The structural assignments are based on molecular weight determinations and on NMR and mass spectra. In particular, the mode of coupling in the isolated compounds was deduced from the ratio of acetyl to methoxyl protons in the NMR-spectra. The identity of isolated compounds with previously known compounds was also corroborated by their melting points and mixed melting points.

RESULTS

Oxidation of monomeric models

Guaiacol. Peroxidase and laccase catalysed the conversion of guaiacol (I) into mixtures of products which precipitated from the buffered (pH 5) dark-brown solution. Thin-layer chromatography of the resulting mixtures showed the presence of residual guaiacol. Column chromatography after reductive acetylation gave a diaryl ether (II), two diaryl compounds (IV and V) and a trimeric compound (VII). The structures assigned to compounds II and VII are arbitrary, the choice between possible isomers (II – III) and (VII – X) being based solely on the preferential *p,p'*-coupling mode.* Compound VII should arise from the *p,p'*-coupled diaryl V by C – O coupling.

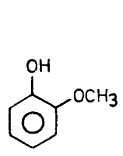

I

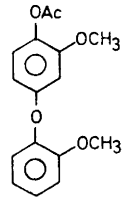

II

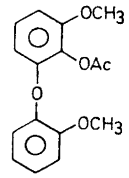

III

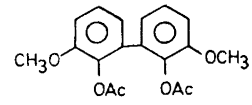

IV

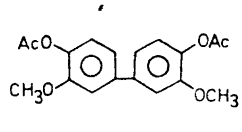

V

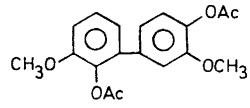

VI

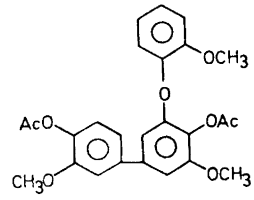

VII

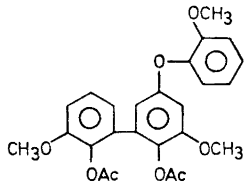

VIII

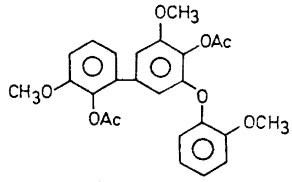

IX

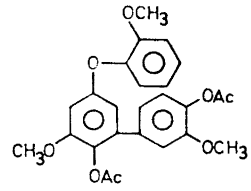

X

* The predominant yield of *p,p'*-coupled isomers is consistent with measurements of the electron density in various positions of phenoxy radicals (Scott, A. T. *Quart. Rev. Chem. Soc.* **19** (1965) 2–5). Compound VI resulting from *o-p'*-coupling was not isolated from the reaction mixture but cannot be ruled out.

The crude fraction from which the trimeric compound VII had been crystallised and the subsequent fractions could not be separated into their components. The first fraction containing residual compound VII showed at least two further spots on TLC and the mass spectrum contained peaks at m/e 410, 452, and 494. The two subsequent fractions also gave overlapping spots on TLC and the mass spectra contained peaks at *m/e* 532, 574, 616, 658 and 654 696, 738, respectively. The difference in 42 mass units may be due to the loss of ketene from acetylated compounds and/or to the presence in the reaction

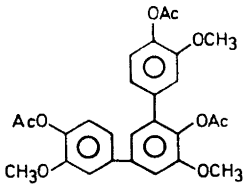

XI

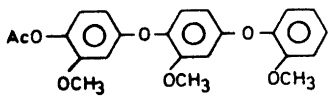

XII

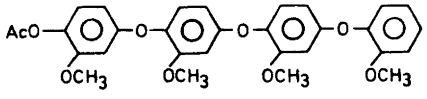

XIII

mixture of aryl-aryl and aryl-O-aryl linked oligomers differing by 42 units in molecular weight. For example, compounds VII and XII should give rise to molecular ion peaks at *m/e* 452 and 410, respectively. On the basis of the

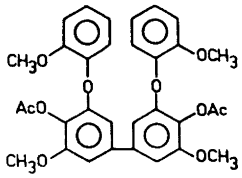

XIV

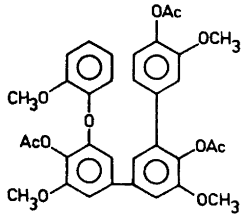

XV

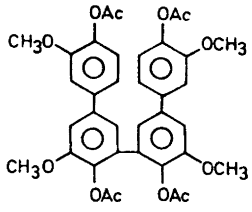

XVI

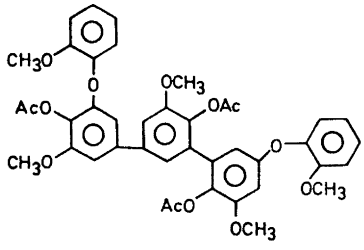

XVII

chromatographic behaviour (TLC) of the fractions eluted from the column it seems therefore most probable that some of these ions originate from non-separated oligomers with different modes of coupling between the aryl residues. Thus, the presence of different trimers (*e.g.* XI, M = 494, VII, M = 452, XII, M = 410), tetramers (*e.g.* XVI, M = 658, XV, M = 616, XIV, M = 574, XIII, M = 532) and of a pentamer (*e.g.* XVII, M = 738) is indicated.

The yields of the isolated components were considerably lower than the amounts actually formed, due to losses during the repeated chromatographic separation used in the purification procedure. Since the acetylated compounds were prepared from the reddish-brown reaction mixture under reducing conditions, it is likely that some of the parent phenolic components, particularly the biaryls and their carbon-to-carbon and carbon-to-oxygen coupled products, originated from the corresponding diphenoquinones.[17]

2,6-Dimethoxyphenol (XVIII). Oxidation of this compound by peroxidase-hydrogen peroxide afforded exclusively the *p,p'*-coupled quinoid product,

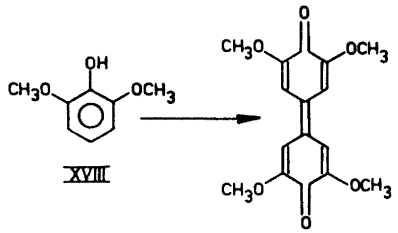

XVIII XIX

coerulignone (XIX), in almost quantitative yield. The same reaction catalysed by laccase had been reported previously.[18]

Glyceryl-aryl ethers. Treatment of the glyceryl-α- and β-guaiacyl ethers (XX and XXI, respectively) with peroxidase-hydrogen peroxide did not yield any

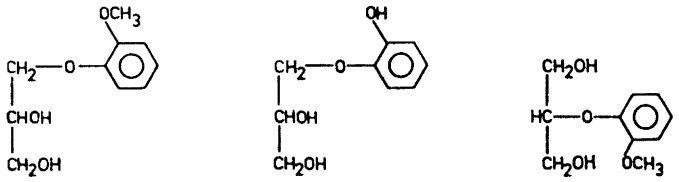

XX XXII XXI

detectable reaction product. The model compounds were recovered unchanged after the enzymatic treatment. The phenolic analogue to XX (XXII), however, gave a reddish-brown mixture of products similar to that observed in the enzymatically catalysed oxidation of guaiacol (see above). The mixture was shown to be free from both glycerol and catechol (TLC) showing that no oxidative or hydrolytic cleavage of the ether bond had taken place.

Oxidation of dimeric models

On treatment with peroxidase–hydrogen peroxide or with laccase the dimeric compounds XXV [1-(4-hydroxy-3-methoxyphenyl)-2-(2,6-dimethoxyphenoxy)-ethanol], XXIX (pinoresinol), and XXXII (dihydro-dehydrodiisoeugenol) underwent carbon-to-carbon and carbon-to-oxygen couplings

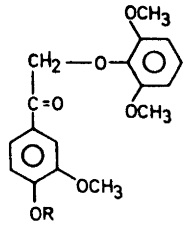

XXIII R = Ac
XXIV R = CH_2–C_6H_5

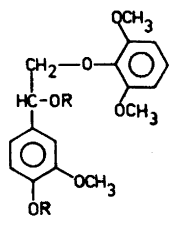

XXV R = H
XXVI R = Ac

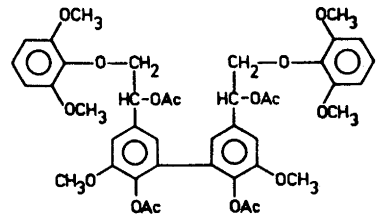

XXVII

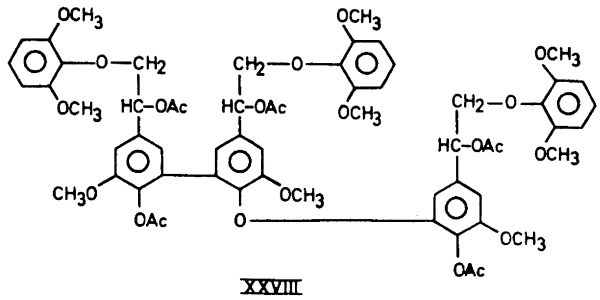

XXVIII

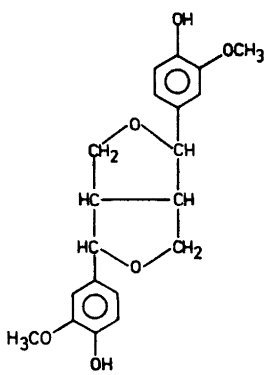

XXIX

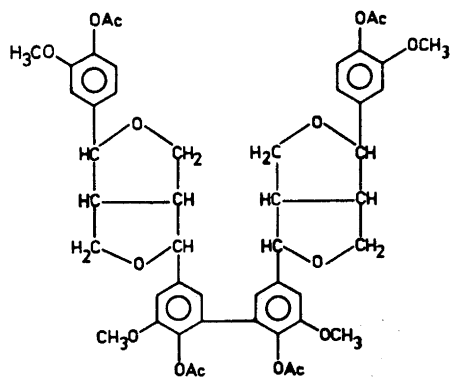

XXX

at the free positions *ortho* to the phenolic hydroxyl groups. The diaryl compounds XXVII, XXX, and XXXIV, respectively, constituted the main reaction products. In minor amounts, the oxygen-to-carbon coupling products between these diaryl compounds and the corresponding starting compounds were formed and isolated as their acetates (XXVIII, XXXI, and XXXVIII, respectively). From dihydro-dehydro-diisoeugenol (XXXII) an additional product of oxygen-to-carbon coupling was formed and characterised as the acetate XXXVI.

Most of these coupling products were unstable under electron impact and did not exhibit the expected molecular ions peaks. In these instances the molecular weights were determined using an osmometric method. Comparison of the thin-layer chromatograms of the acetylated mixtures of oxidation products with those of the reductively acetylated mixtures of the same oxidation products did not reveal any significant differences. This indicates that no oxidation of the *o,o'*-dihydroxy-diaryl compounds to the corresponding dipheno-quinones (*cf.* behaviour of I, see above) had taken place.

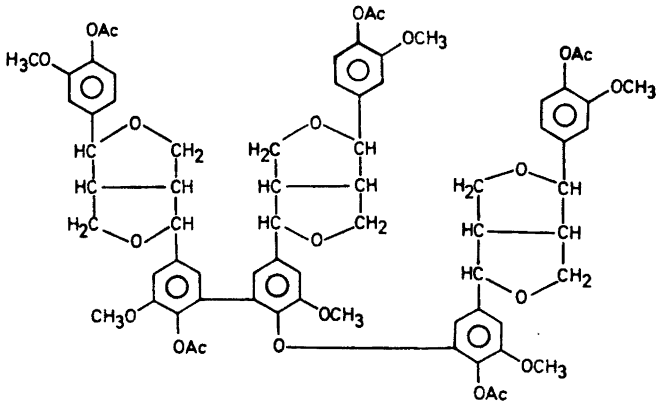

XXXI

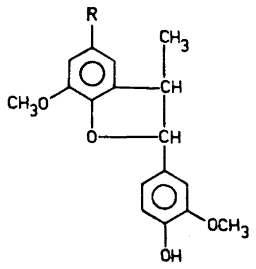

XXXII

R= propyl

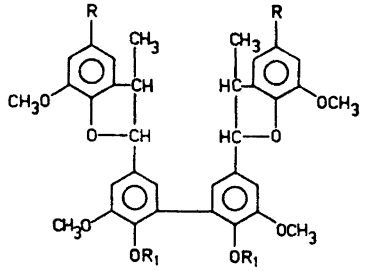

XXXIII R_1 = H

XXXIV R_1 = Ac

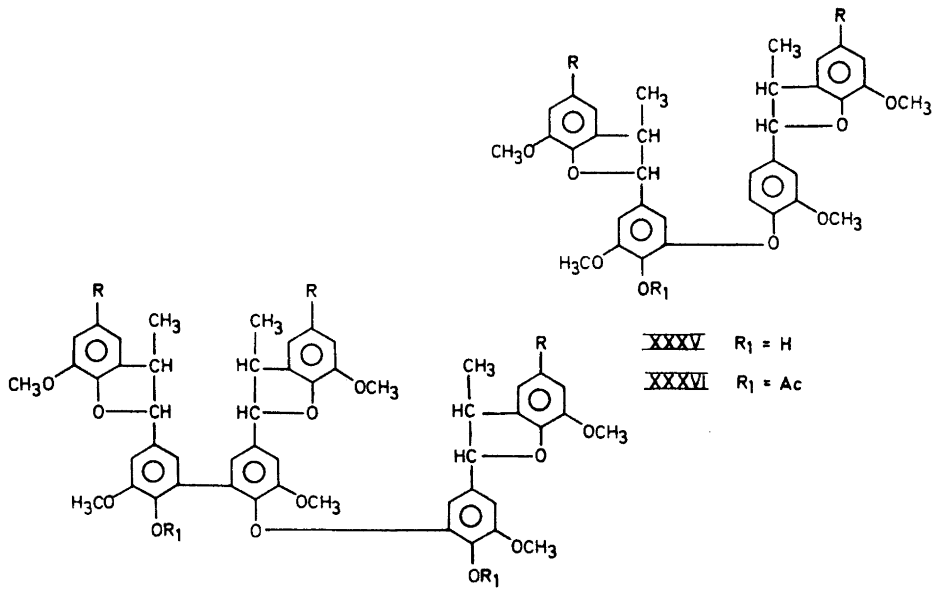

XXXV R_1 = H
XXXVI R_1 = Ac

XXXVII R_1 = H
XXXVIII R_1 = Ac

R = propyl

DISCUSSION AND CONCLUSION

Although guaiacol is commonly used as substrate in the assay of phenoloxidases,[19] no thorough investigation of its oxidation products has been undertaken so far. The bright red oxidation mixture was termed "tetraguaiacone" [20] and considered as a polymer constructed exclusively by carbon-to-carbon bonds.[17,21] The isolation of carbon-to-oxygen linked dimers and oligomers in the present investigation suggests that this type of interconnecting linkage is also an intrinsic structural feature of the high molecular weight tetraguaiacone.

The stability of the glycerylguaiacyl ethers XX and XXI and the sensibility of compound XXII towards peroxidase-hydrogen peroxide and laccase shows that the catalytic effect of these enzymes is oxidative rather than hydrolytic in nature. It appears to be restricted to phenolic structures.

The monomeric and dimeric phenolic models investigated here afforded only carbon-to-carbon and carbon-to-oxygen coupled products. Thus, it may be concluded that the two enzyme systems function primarily – if not exclusively – to catalyse oxidative coupling with the formation of aryl-aryl- and aryl-O-aryl linkages. No evidence for any extensive cleavage of ether linkages was obtained. The isolated coupling products contained all aryl alkyl ether bonds originally present. In particular, the methyl aryl ether and β-aryl ether bonds were shown to remain *essentially* unaffected.

Therefore, any degradative effect of these enzymes should be connected with the oxidative coupling reactions which they catalyse. Recently, de-

hydrogenative coupling reactions of this kind brought about by laccase (*p*-diphenol oxidase)[22] or peroxidase[23,24] have been observed using model compounds of the *p*-hydroxy-α-carbonyl[22,24] and *p*-hydroxy-α-carbinol[22,23] types. In these reactions the α-carbonyl- and α-carbinol side chains are displaced as carboxylic acids and aldehydes, respectively, by coupling of phenoxyl radicals to *p*-cyclohexadienonyl radicals. However, this elimination of side chains has been observed with phenolic units of the syringyl type only. Guaiacyl type units containing a free *ortho*- and an substituted *para*-position, undergo preferentially, if not exclusively, *o,o'*-coupling. The formation of such *o,o'*-dihydroxydiaryl structures has been described previously.[21,23–25,27] In the present work it is shown that, in addition to these carbon-to-carbon coupled compounds, carbon-to-oxygen coupled products are formed. (*cf.* the behaviour of compounds XXV, XXIX, and XXXII). The coupled products are remarkably stable towards further oxidation.

The identical pattern of coupling products obtained with peroxidase-hydrogen peroxide and with laccase, as well as the lack of substrate specificity of these two enzymes suggests that only the first step in the reactions, the abstraction of hydrogen from the phenolic hydroxyl group, is enzymatically catalysed. The subsequent couplings appear to proceed spontaneously. This behaviour of the two enzymes is well known from the extensive studies on the biosynthesis of lignin[26,27] in which coniferylalcohol and other *p*-hydroxycinnamyl alcohols have been used as substrates.

The features of the reactions described in this work are consistent with the view that the function of the extracellular enzymes peroxidase and laccase consists in detoxifying low molecular weight phenolic compounds which may be released from lignin during its fungal decomposition, and in maintaining the metabolic balance around the fungi.[28] No experimental evidence for a *direct* involvement of these enzymes in the microbial degradation of lignin was obtained (*cf.* also Ref. 28a). However, this result does not exclude the possibility that the above oxidative coupling reactions may constitute the first step of a reaction sequence, in which peroxidase and laccase in concert with other (unknown) enzymes participate in the microbial lignin breakdown.

EXPERIMENTAL

All melting points are corrected. Evaporations were carried out under reduced pressure.

Chromatography. Both analytical and preparative separations by thin-layer chromatography (TLC) were carried out using silica gel HF_{254} (E. Merck A G., Darmstadt) as adsorbant. The solvent systems used varied with the model compound under examination and are indicated below. Vanillin-sulphuric acid [vanillin (3.0 g), conc. sulphuric acid (0.5 ml)] in ethanol (100 ml) was used as spray reagent and gave characteristic color spots after 10 min heating (120°).

Silicic acid used for column chromatography was supplied by Mallinckrodt, USA (marketed as SilicAR CC-1 100 – 200 mesh).

Spectroscopy. The NMR spectra were run on a Perkin-Elmer R-12 spectrometer with deuteriochloroform ($CDCl_3$) as solvent and tetramethylsilane (TMS) as internal standard. The mass spectra were determined on a Perkin-Elmer 270 instrument at 20 – 35 eV using the direct inlet system with the temperature of the probe heater between 50 and 120°.

Acetylation. Acetylations and reductive acetylations were carried out according to standard procedures.[29]

Model compounds. 1-Guaiacoxy-2,3-dihydroxy-propane (XX) was commercially available. 2-Guaiacoxy-1,3-dihydroxy-propane (XXI),[30] 1-*o*-hydroxyphenoxy-2,3-dihydroxy-propane (XXII),[31] ω-bromo-4-acetoxy-3-methoxy-acetophenone,[32] ω-bromo-4-benzyloxy-3-methoxy-acetophenone,[32] pinoresinol (XXIX),[33] and dihydro-dehydro-diisoeugenol (XXXII)[34] have been prepared as previously described. Compound XXV was prepared as follows:

4-Acetoxy-3-methoxy-ω-(2,6-dimethoxyphenoxy)-acetophenone (XXIII). 2,6-Dimethoxyphenol (10.8 g, 0.7 mol) and ω-bromo-4-acetoxy-3-methoxyacetophenone (13.0 g, 0.045 mol) were reacted as described for the preparation of a related compound.[35] Recrystallisation of the crude product from ethanol gave compound XXIII as colourless prisms (7.4 g, 45 %), m.p. 95–96°. ν_{max} (KBr) 1760 cm^{-1} (ester C=O), 1700 cm^{-1} (ketone C=O). [Found: C 63.64; H 5.62; *m/e* 360. $C_{19}H_{20}O_7$ (M 360) requires C 63.70; H 5.55]. δ 7.85–7.60 (m, 3 H); 7.38–6.56 (m, 3 H); 5.20 (s, 2 H); 3.91 (s, 3 H); 3.82 (s, 6 H); 2.30 (s, 3 H).

1-(4-Hydroxy-3-methoxyphenyl)-2-(2,6-dimethoxyphenoxy)-ethanol (XXV). Compound XXIII (3 g) in THF (50 ml) was reduced with lithium aluminium hydride (1.2 g) in THF (80 ml) using a standard procedure.[36] The residue (2.7 g) obtained after working-up was recrystallised from benzene to give XXV as colourless prisms, m.p. 82–84°. ν_{max} (KBr) 3500–3200 cm^{-1} (OH). (Found: C 63.92; H 6.35. *m/e* 320. $C_{17}H_{20}O_6$ (M 320) requires: C 63.77; H 6.25). δ 7.30–6.80 (m, 3 H); 6.67–6.50 (m, 3 H); 5.85 (b, 2 H); 3.85 (s, 9 H).

The compound gave an intense blue colour with 2,6-dibromoquinone-4-chloroimide and alkali indicating the presence of a *p*-hydroxybenzyl alcohol grouping.[37]

The diacetate (XXVI) was obtained as needles, m.p. 122–125°. ν_{max} (KBr) 1750, 1725 cm^{-1} (ester C=O). δ 7.39–6.98 (m, 3 H); 6.75–6.50 (m, 3 H; 6.37 (t, 1 H; J=6 cps). 4.20 (d, 2 H; J=6 cps); 3.75 (s, 9 H); 2.25 (s, 3 H); 2.02 (s, 3 H.) *m/e* 404. Compound XXV was also prepared by hydrogenolysis (Pd/C) of the benzyl ether XXIV which was obtained by reacting ω-bromo-4-benzyloxy-3-methoxy-acetophenone[32] with 2,6-dimethoxyphenol as described above.

4-Benzyloxy-3-methoxy-ω-(2,6-dimethoxyphenoxy)-acetophenone (XXIV) was obtained as colourless crystals by reacting ω-bromo-4-benzyloxy-3-methoxy-acetophenone[32] with 2.6-dimethoxyphenol, m.p. 94–95°. δ 7.70–6.50 (m, 11 H); 5.19, 5.10 (s, 2 H, 2 H); 3.90, 3.89 (s, 3 H, 6 H). *m/e* 408.

Enzymes. The peroxidase (horseradish) type II used in this study was purchased from Sigma Chemical Co., St Louis, Mo. and contained approximately 135 purpurogallin units/mg. Laccase, isolated from *Neurospora crassa* was kindly supplied by Dr. K. E. Eriksson of this institute. The activity of this enzyme was measured using D,L-dopa as substrate,[38] 1 mg/ml, at pH 6 and 25°, gave 3500 KU (Klett units).

Solution. Acetate buffer solution (pH 5, 10 mM) was used. Acetone used to increase the solubility of some of the model compounds was purified by drying the technical grade solvent with P_2O_5 and distilling the decanted liquid over potassium permanganate.

Enzyme-catalysed reactions. The appropriate model compound (0.5–1.0 g) was dissolved in acetate buffer (pH 5.0), in some cases in a mixture of buffer and acetone, and a small amount (*ca.* 5 mg) of laccase or peroxidase and one equivalent of hydrogen peroxide was added. The solution was stirred (2 h) and then worked up by extraction with ethyl acetate. The major oligomeric products were characterised as the acetates. Evidence that the oxidation products described here resulted from enzymatic dehydrogenation rests upon controls carried out with a heat-denaturated solution of laccase and with a solution of active peroxidase omitting the addition of hydrogen peroxide.

Oxidation of guaiacol. (a) with peroxidase /H_2O_2. Hydrogen peroxide (30.0 ml, 1.0 %, 0.0088 mol) was added during 30 min to a stirred solution of guaiacol (2.1 g, 0.0169 mol) in acetate buffer (200 ml) containing peroxidase (4 mg). Stirring was continued for a further 30 min after which the brown mixture was extracted with ethyl acetate (3 × 100 ml). The combined ethyl acetate extracts were dried (Na_2SO_4) and evaporated to give a dark oily residue (1.7 g). Reductive acetylation of the residue gave a colourless solid (1.9 g) which showed several spots on TLC (benzene-ethyl acetate 15:1, developed four times with intermittent drying). The main oligomeric components were separated by chromatography on a silicic acid column (2 × 100 cm). Elution with benzene-ethyl acetate (15:1) gave in the following order:

(1) *4-Acetoxy-2',3-dimethoxydiphenyl ether* (II). The oil gave a yellow spot with vanillin-H_2SO_4. It was eluted simultaneously with guaiacol acetate (bright orange spot with vanillin-

H_2SO_4) and was separated from the latter by preparative thin-layer chromatography using benzene-chloroform (10:1) as eluent. The plate was developed three times with intermittent air drying. The oil gave only one spot (orange) on TLC (benzene-chloroform 10:1). Structure II was assigned to the compound which probably is indistinguishable from isomer III. ν_{max} 1765 cm^{-1} (ester C=O) [Found: C 64.61; H 5.55. *m/e* 288 $(M)^+$. $C_{16}H_{16}O_5$ (M 288) requires: C 64.43; H 5.38] δ 7.20 – 6.29 (m, 7 H); 3.80, 3.73 (s, 3 H, 3 H); 2.25 (s, 3 H). *m/e* 288 (40), 246/247 (100/70), 199 (20), 183 (12),171 (11), 149 (16), 136 (56), 92/91 (30/27), 79/77 (20/38), 51 (10), 43 (50).

(2) *2,2'-Diacetoxy-3,3'-dimethoxydiphenyl* (IV). Colourless prisms, m.p. 132 – 133° (lit: 133 – 134°),[17] gave a blue spot with vanillin-H_2SO_4. ν_{max} (KBr) 1760 cm^{-1} (ester C=O). δ 7.30 – 6.60 (m, 6 H); 3.84 (s, 6 H) 2.29 (s, 6 H). *m/e* 330 (2), 288 (65), 246/247), (100/56), 231 (15), 213/214 (22/15), 203 (20), 191 (8), 185/186 (8/5), 171 (4), 43 (7).

(3) *4,4'-Diacetoxy-3,3-dimethoxydiphenyl* (V). Colourless needles, m.p. 198 – 200° (lit: 195 – 198°),[17] gave a pale grey spot with vanillin-H_2SO_4. ν_{max} (KBr) 1765 cm^{-1} (ester C=O) δ 7.30 (s, 2 H); 7.19 (s, 4 H); 3.87 (s, 6 H); 2.20 (s, 6 H). *m/e* 330, 288 (15), 246 (100), 231 (10), 203 (9), 185 (3), 171 (2), 160 (2), 131 (4), 115 (4), 57 (3), 43 (20). The diaryls IV and V were eluted simultaneously and purified by fractional crystallisation from ethanol.

(4) *4,4'-Diacetoxy-3,3'-dimethoxy-5-guaiacoxydiphenyl* (VII) was obtained as fine needles, m.p. 172 – 173°, after several crystallisations of a fraction following the diaryls IV and V. It gave a pink spot with vanillin-H_2SO_4. ν_{max} (KBr) 1760, 1754 cm^{-1} (ester C=O). [Found: C 66.67; H 5.46. *m/e* 452 (M^+). $C_{25}H_{24}O_8$ (M 452) requires: C 66.40; H 5.31]. δ 7.05 – 6.95 (m, 9 H); 3.83, 3.80, 3.75 (s, 3 × 3 H); 2.25 (s, 3 H); 2.11 (s, 3 H). *m/e* 452 (78), 410 (83), 370 (83), 369/368 (55/95), 329/328 (40/85), 288 (26), 209 (60), 196 (44), 193 (60), 152/151 (82/100), 137/136 (82/83), 123 (57), 91 (25), 79/78 (32/32), 77 (48), 51 (40).

The crude fraction from which compound VII was separated showed mass ion peaks at *m/e* 410, 452, and 494. Indication that the fraction consisted of a mixture of different compounds was obtained from TLC, which showed overlapping coloured spots with the pink colour of compound VII, (*m/e* 452) predominating. Subsequent fractions showed ion peaks at higher mass numbers (*m/e* 532, 574, 616 and 658. Final elution with 25 – 50 % ethyl acetate produced fractions which exhibited mass ion peaks at *m/e* 654, 696, and 738. Each fraction showed at least two overlapping spots giving different colours with the spray reagent, indicating mixtures. Methoxyl analysis of the combined fractions gave a value of 17.05 %. (Calculated OCH_3 content for acetylated guaiacol 18.67 %) indicating that no extensive demethylation had taken place during the enzymatic treatment.

(*b*) *with laccase.* Laccase (2 mg) was added to a solution of guaiacol (0.6 g) in acetate buffer (100 ml) and the mixture was stirred for 30 min. Another batch containing laccase (3.2 mg) and guaiacol (2.8 g) in acetate buffer (250 ml) was stirred overnight. The preparations were worked up separately and the residues were reductively acetylated. The two resulting mixtures showed the same spots on TLC (*RF*-values and colours) as did a corresponding reaction mixture obtained by peroxidase/H_2O_2 oxidation.

Oxidation of 2,6-dimethoxyphenol (XVIII) with peroxidase/H_2O_2. 2,6-Dimethoxyphenol (1.0 g, 0.0065 mol) was dissolved in acetate buffer (200 ml) and peroxidase (5 mg) was added. To the stirred solution hydrogen peroxide (12 ml, 1 %, 0.0035 mol) was added during 30 min and the mixture was stirred for another 2 h. Purple crystals (0.6 g) precipitated [coerulignone (XIX, m.p. 293° (lit: 294°) [18] 0.6 g]. Reductive acetylation gave the diacetate, m.p. 231 – 233° (lit: 239°).[18] δ 6.73 (s, 4 H); 3.85 (s, 12 H); 2.83 (s, 6 H).

Oxidation of guaiacylglyceryl ethers with peroxidase/H_2O_2. 1-Guaiacoxy-2,3-dihydroxypropane (XX) and 2-guaiacoxy-1,3-dihydroxy-propane (XXI) (0.22 g of each) were separately dissolved in acetate buffer solution (100 ml) and peroxidase (5 mg) was added. To the stirred solutions a 1 % hydrogen peroxide solution (4 ml) was added during 30 min. The mixtures were stirred for 2 h and then worked up as described above. Compounds XX and XXI were recovered quantitatively. The identity of the unchanged compounds was proven by determination of melting points with admixture of authentic samples and also by TLC (chloroform-methanol-acetic acid 100:10:3).

A solution of 1-(*o*-hydroxyphenoxy)-2,3-dihydroxy-propane (XXII) (13 mg) in acetate buffer (20 ml), containing peroxidase (3 mg) was similarly treated with a solution of 1 % hydrogen peroxide (3 ml). The mixture turned reddish-brown. Extraction with ethyl acetate yielded a light oil. The TLC (chloroform, methanol, acetic acid (100:10:3) showed

residual starting material and coloured polymeric material but no glycerol or catechol.

Oxidation of 1-(4-hydroxy-3-methoxyphenyl)-2-(2,6-dimethoxyphenoxy)-ethanol (XXV). *(a) with peroxidase/H_2O_2.* Compound XXV (4.0 g, 0.0125 mol) was dissolved in acetone (120 ml) and acetate buffer solution (500 ml), followed by peroxidase (10 mg), was added. Hydrogen peroxide (36 ml, 1 %, 0.0105 mol) was then added dropwise during 30 min to the stirred solution. The stirring was continued for 2 h and the mixture was then extracted with ethyl acetate (3 × 100 ml). The oily residue (3.8 g) obtained after evaporation of the solvent, consisted of two major overlapping components (TLC, $CHCl_3$:EtOH, 100:1, developed three times). Better resolution of the mixture was obtained after acetylation, the TLC (benzene-ethyl acetate, 3:1, developed three times) showing three components. The acetylated mixture (1.8 g) was separated on a silicic acid column (2 × 75 cm) to yield in the order given:

(1) o,o-*Diaryl tetraacetate* XXVII (0.69 g) (37 %) solid resin, ν_{max} (KBr) 1760, 1740 cm^{-1} (ester C=O). [Found: C 62.51; H 5.91, *m/e* 806. $C_{42}H_{46}O_{16}$ (M 806) requires: C 62.53; H 5.73]. δ 7.35–6.43 (m, 10 H); 6.05 (t, 2 H, J = 6 cps); 4.25 (d, 4 H, J = 5 cps); 3.89, 3.76 (s, 6 H, 12 H); 2.05, 2.03 (s, 6 H, 6 H). Mol. wt. 881 (osmometry).

(2) *Compound XXVIII*, solid resin (0.15 g, 8.3 %). ν_{max} 1760, 1740 cm^{-1} (ester C=O). [Found: 62.66; H 5.87. $C_{61}H_{66}O_{23}$ (M 1166) requires: C 62.77; H 5.66]. δ 7.35–7.45 (m, 15 H); 6.20–5.90 (b, 3 H); 4.31–4.08 (b, 6 H); 3.85–3.70 (b, 27 H); 2.1, 2.0 (15 H). Mol. wt. 1095 (osmometry).

The third component was obtained in a small yield which did not allow identification.

(b) with laccase. Laccase (2.5 mg) was added to a solution of XXV (0.11 g) in acetone (10 ml) and acetate buffer (200 ml). The mixture was stirred for 2 h and worked up as described above. The mixture of acetylated products exhibited a TLC pattern identical to that of the mixture obtained by peroxidase/H_2O_2 oxidation.

Oxidation of pinoresinol (XXIX). (a) with peroxidase/H_2O_2. Pinoresinol (XXIX) (1.02 g, 0.0028 mol) was dissolved in acetone (50 ml) and acetate buffer solution (300 ml). To the stirred solution peroxidase (10 mg) and then during 20 min 1 % hydrogen peroxide solution (11 ml, 0.003 mol) was added. The mixture was stirred for 2 h and then worked up as described above. Acetylated and reductively acetylated samples of the resulting mixture showed an identical TLC pattern. The main components of the mixture were separated on a silicic acid column (2 × 70 cm) using benzene-ethyl acetate (3:2) as eluent to give:

(1) *Dehydro-dipinoresinol tetraacetate (XXX)*. Colourless needles (0.31 g), m.p. 202° (lit: 195°).[39] ν_{max} (KBr) 1760 cm^{-1} (ester C=O). (Found: C 64.93; H 5.57. Calc. for $C_{48}H_{52}O_{16}$ (M 884): C 65.01; H 5.84). δ 7.2–6.45 (m, 10 H); 4.70. [b, 4 H(α)]; 4.48–3.9 [m, 8 H(γ)]; 3.85 (s, 12 H); 3.08 [b, 4 H(β)]; 2.14, 2.02 (s, 6 H, 6 H).

(2) *Trimer (XXXI)* solid resin, 0.25 g. ν_{max} (KBr) 1760 cm^{-1} (ester C=O). (Found: C 66.6; H 6.30. $C_{70}H_{72}O_{23}$ (1280) requires: C 65.62; H 5.62). Mol. wt. 1303 (osmometry).

(b) with laccase. To a solution of compound XXIX (0.12 g) in acetone (20 ml) and acetate buffer solution (175 ml) laccase (1.5 mg) was added and the mixture stirred for 2 h. The mixture was worked up as described above. The acetylated mixture was indistinguishable from that obtained by peroxidase/H_2O_2 oxidation of XXIX (TLC).

Oxidation of dihydro-dehydro-diisoeugenol (XXXII). (a) with peroxidase/H_2O_2. Hydrogen peroxide (6 ml, 1 %, 0.0017 mol) was added during 15 min to a stirred solution of XXXII (1.02 g, 0.00305 mol) in acetone (100 ml) and acetate buffer (130 ml) containing peroxidase (10 mg). The mixture was kept with stirring for 2 h and then worked up in the usual way. TLC of the residue (chloroform, developed five times) showed four components which were separated both as phenols and as acetates by chromatography on a silicic acid column (2 × 50 cm). The following compounds were obtained in pure form:

(1) *Dihydro-dehydro-diisoeugenol (XXXII)*, m.p. 87–89°. The infrared spectrum was indistinguishable from that of the starting material. Mixed m.p. with authentic XXXII 87–89°.

(2) o,o-*Dihydroxy-diaryl XXXIII*.[40] Solid resin (0.3 g); ν_{max} 3550–3400 cm^{-1} (OH). (Found: C 73.52; H 6.97. *m/e* 654 (M^+). Calc. for $C_{40}H_{46}O_8$ (M 654): C 73.39; H 7.03). δ 7.0 (s, 4 H); 6.55 (s, 4 H); (b, 2 OH); 5.10 (d, 2 H, J = 7 cps), 3.82 (s, 12 H); 3.60–3.30 (m, 2 H); 2.50 (t, 4 H, J = 6 cps); 1.80–1.30 (m, 10 H); 0.95 (t, 6 H, J = 6 cps). *Diacetate XXXIV*, solid resin, ν_{max} (KBr) 1760 cm^{-1} (ester C=O) *m/e* 738(M^+).

(3) *o-Hydroxydiaryl ether XXXV*. Solid resin (0.1 g); ν_{max} (KBr) 3600–3300 cm^{-1} (OH). (Found: C 73.46; H 6.98. *m/e* 654 (M^+). $C_{40}H_{46}O_8$ (654) requires: C 73.39; H 7.03).

δ 7.35 – 6.55 (m, 10 H); 5.90 (s, 1 H); 5.05 (t, 2 H, $J = 6$ cps); 3.85 (s, 12 H); 3.10 – 3.30 (m, 2 H); 2.70 – 2.45 (t, 4 H, $J = 6$ cps); 1.90 – 1.30 (m, 10 H); 1.0 (t, 6 H, $J = 6$ cps). *Acetate XXXVI*, solid resin, ν_{max} 1760 cm^{-1} (ester C=O) *m/e* 696(M^+).

(4) *Compound XXXVII* was contaminated by the diaryl XXXIII. Purification was only accomplished by preparative TLC of the acetylated mixture using benzene-ethyl acetate (15:1). *Diacetate XXXVIII*, solid resin (0.1 g); ν_{max} (KBr) 1760 cm^{-1} (ester C=O). *m/e* 1064 (M^+). (Calc. for $C_{64}H_{72}O_{14}$: 1064).

(b) with laccase. Compound XXXII (84 mg) and laccase (3 mg) were dissolved in acetone (60 ml) and acetate buffer (150 ml). The mixture was stirred for 2 h and then worked up as described above. The mixture of acetylated products was indistinguishable from the corresponding mixture of acetylated products obtained by peroxidase/H_2O_2 oxidation (TLC).

REFERENCES

1. Davidson, R. W., Campbell, W. A. and Blaisdell, D. J. *J. Agr. Res.* **57** (1938) 683.
2. Lawsson, Jr., L. R. and Still, C. N. *Tappi* **40** (1957) 56A.
3. Cowling, E. B. *U. S. Dep. Agr. Tech. Bull.* **79** (1961) 1258.
4. Bavendamm, W. *Pflanzenkrankh., Pflanzenschutz* **38** (1928) 257.
5. Kirk, T. K. and Kelman, A. *Phytopathology* **55** (1965) 739.
6. Steelink, C. *Advan. Chem. Ser* **59** (1966) 51.
7. Caldwell, E. S. and Steelink, C. *Biochim. Biophys. Acta* **184** (1969) 420.
8. Farmer, V. C., Henderson, M. E. K. and Russel, J. D. *Biochim. Biophys. Acta* **52** (1961) 565.
9. Harkin. J. M. In Taylor, W. I. and Battersby, A. R., Eds., *Oxidative Coupling of Phenols*, Marcel Dekker, New York 1967, p. 300.
10. Christman, R. F. and Oglesby, R. T. In Sarkanen, K. V. and Ludwig, C. H., Eds., *Lignins*, Wiley-Interscience, New York 1971, p. 769.
11. Kirk, T. K. *Ann. Rev. Phytopathology* **9** (1971) 185.
12. Eriksson, K.-E. and Lindholm, U. *Svensk Papperstid.* **74** (1971) 701.
13. Steelink, C. and Green, G. *J. Org. Chem.* **27** (1962) 170.
14. Ref. 10, p. 782.
15. Fåhraeus, G. and Lundeberg, G. *Physiol. Plantarum* **6** (1953) 150.
16. *cf.* Harkin, J. M. in Ref. 9, p. 305.
17. Booth, H. and Saunders, B. C. *J. Chem. Soc.* **1956** 540.
18. Bocks, S. M., Brown, B. R. and Todd, A. H. *Proc. Chem. Soc. London* **1962** 117.
19. Maehly, A. G. *Methods Biochem. Anal.* **1** (1954) 357.
20. Bertrand. G. *Compt. Rend.* **137** (1903) 1270; *Bull. Soc. Chim. France* **31** (1904) 185.
21. Lindgren, B. O. *Acta Chem. Scand.* **14** (1960) 2089.
22. Kirk. T. K., Harkin, J. M. and Cowling, E. B. *Biochim. Biophys. Acta* **165** (1968) 145.
23. Pew, J. C. and Connors, W. J. *J. Org. Chem.* **34** (1969) 580.
24. Pew, J. C. and Connors, W. J. *J. Org. Chem.* **34** (1969) 585.
25. Kirk, T. K., Harkin, J. M. and Cowling, E. B. *Biochim. Biophys. Acta* **165** (1968) 134.
26. Freudenberg, K. and Neish, A. C. *Constitution and Biosynthesis of Lignin*, Springer, Berlin 1968, p. 83.
27. Freudenberg, K. *Science* **148** (1964) 595.
28. Lyr, H. *Nature* **195** (1962) 289.

28a. Konishi, K., Inoue, Y. and Higuchi, T. *J. Japan Wood Res. Soc.* **18** (1972) 571.

29. Vogel, A. I. *A. Textbook of Practical Organic Chemistry*, Longmans, London 1962, p. 749.
30. Gierer, J. and Kunze, I. *Acta Chem. Scand.* **22** (1968) 803.
31. Gellerstedt, G. and Gierer, J. *Acta Chem. Scand.* **22** (1968) 2510.
32. Leopold, B. *Acta Chem. Scand.* **4** (1950) 1523.
33. Erdtman, H. *Svensk Kem. Tidskr.* **46** (1934) 229.
34. Aulin-Erdtman, G. *Svensk Kem. Tidskr.* **54** (1942) 168.
35. Kratzl, K., Kisser, W., Gratzl, J. and Silbernagel, H. *Monatsh.* **90** (1959) 771.
36. Brown, W. G. *Org. Reactions*, **6** (1951) 469.

37. Gierer, J. *Acta Chem. Scand.* **8** (1954) 1319.
38. Fling, M., Horowitz, N. H. and Heineman, S. F. *J. Biol. Chem.* **238** (1963) 2045.
39. Freudenberg, K. and Sakakibara, A. *Ann. Chem.* **623** (1959) 129.
40. Pew, J. C., Connors, W. J. and Kunishi, A. *Chim. Biochim. Lignine, Cellulose, Hemicellulose*, Grenoble 1964, p. 224.

Received May 3, 1973.

ACTA CHEMICA SCANDINAVICA 27 (1973) 2923–2929

Structural Studies on the Rare Earth Carboxylates

22. The Crystal Structure of Tetra-aquo-thiodiacetatoneodymium(III) Chloride

THOM MALMBORG and ÅKE OSKARSSON

Inorganic Chemistry 1, Chemical Center, University of Lund, P.O.Box 740, S-220 07 LUND 7, Sweden

In order to determine the coordination geometry around the neodymium ion the crystal structure of $Nd(C_4H_4O_4S)(H_2O)_4Cl$ has been determined from three-dimensional X-ray intensity data. The compound crystallizes in the orthorhombic space group *Pnnm* with $Z = 4$. The unit cell dimensions are $a = 6.922$, $b = 17.69$, and $c = 10.226$ Å. The structure has been refined to $R = 0.127$. The neodymium ion is surrounded by four carboxylate oxygen atoms, four water molecules, and one sulfur atom, which form a distorted tricapped trigonal prism. The Nd – O distances are in the range 2.31 – 2.53 Å. The thiodiacetate ion forms two five membered rings with the metal ion, with the sulfur atom located in the equatorial plane of the prism. The Nd – S distance is 3.15 Å. The coordination polyhedra are connected by the carboxylate groups forming layers stacked in the *b*-direction. The chloride ion is situated between the layers and accepts two hydrogen bonds from each layer, thus holding the structure together in the *b*-direction.

The structures of a number of rare earth complexes in the solid state with ligands of the composition OCORCOO with $R = CH_2OCH_2$,[1] CH_2NHCH_2,[2] and C_5H_5N [3] have been described in previous communications in this series. These studies have now been extended to the ligand thiodiacetate ($R = CH_2SCH_2$). The formation constants in aqueous solution of the lanthanoid-thiodiacetate complexes have been reported by Dellien, Grenthe and Hessler.[4] The complexes found are comparatively weak, making it difficult to decide if a chelate is formed. Thus, it is of interest to study a complex in the solid state in order to obtain information of the coordination geometry around the lanthanoid ion.

The tri-aquo-iminodiacetate-lanthanoid(III) chlorides form an isostructural series of compounds for the elements Pr – Lu,[5] and a similar series can be prepared with the ligand thiodiacetate. In this paper the crystal structure

of tetra-aquo-thiodiacetato-neodymium(III) chloride is described, and it is referred to below as THIDAC.

EXPERIMENTAL

Preparation. Equimolar aqueous solutions of neodymium chloride and thiodiacetic acid were mixed and the pH of the resulting solution was adjusted to 2.5 with dilute sodium hydroxide. Slow evaporation at room temperature gave a crystalline compound. The composition $Nd(C_4H_4O_4S)(H_2O)_4Cl$ was determined by chemical analysis. If the pH was kept higher than 4 in the resulting solution, a microcrystalline compound of the composition $Nd_2(C_4H_4O_4S)_3(H_2O)_6$ was formed.

Single crystal work. The method of preparation resulted in crystals which were tabular (010). It was found that they slowly decomposed when exposed to X-rays. However, the rate of decomposition could be decreased by coating the crystals with Apiezon oil. A single crystal of the dimensions $0.22 \times 0.05 \times 0.16$ mm^3 was mounted along the b-axis. The intensities of 416 reflections of the layers $h0l - h10l$ were recorded using the integrated Weissenberg multifilm technique and Ni-filtered Cu-radiation ($\lambda = 1.5418$ Å). The intensities were estimated visually using a calibrated scale. The intensity data were corrected for Lorentz, polarization, and absorption effects. The linear absorption coefficient is 343 cm^{-1}. The transmission factor, evaluated by numerical integration, varied in the interval $0.010 - 0.188$.

UNIT CELL AND SPACE GROUP

The diffraction symmetry *mmm* and the systematic absences $0kl$: $k+l \neq 2n$ and $h0l$: $h+l \neq 2n$ indicate $Pnnm$ (No. 58) or $Pnn2$ (No. 34)[6] as possible space groups. Using Ni-filtered Cu-radiation the a and c parameters were determined from a zero layer Weissenberg photograph, and the b parameter was determined from an oscillation photograph. Both photographs were calibrated with a single crystal of quartz ($a = 4.9126$ and $c = 5.4043$ Å). The measured θ-values were used for a least squares refinement of the unit cell dimensions. The following crystal data were obtained.

$a = 6.922(3)$ Å*
$b = 17.69(3)$ Å
$c = 10.226(4)$ Å
$V = 1251(2)$ Å^3

$D_m = 2.2$ g/cm^3
$D_x = 2.12$ g/cm^3
$Z = 4$

The density D_m was determined by the displacement method using benzene.

STRUCTURE DETERMINATION AND REFINEMENT

The position of the neodymium ion was determined from a three-dimensional vector map. Assuming the centrosymmetric space group, the positional parameters and an isotropic temperature factor together with the interlayer scale factors, were improved by a full matrix least squares refinement. The quantity minimized was $\sum w(|F_o| - |F_c|)^2$, with weights w chosen according

* Numbers within parenthesis represent estimated standard deviations in the last significant digit.

to Cruickshank.[7] Due to the location of the neodymium ion close to $y = 1/4$, a three-dimensional difference electron density map showed two images of the structure related by a mirror plane at $y = 1/4$. Since the highest peak was at a possible coordination distance from the neodymium ion, the sulfur atom was placed at this position. The remaining ligand atoms were found from geometrical considerations. It was also possible to chose the position of the chloride ion belonging to the same image, since one of the two possible positions gave an improbable chloride carbon distance of 2.0 Å. A difference electron density map calculated after refining the parameters of the image chosen, revealed the positions of the four water molecules.

The preliminary positional coordinates, isotropic temperature factors and interlayer scale factors were improved by a series of least squares refinements. The convergency was followed by the agreement index R defined by $R = \sum||F_o| - |F_c||/\sum|F_o|$. All observed reflections were included in the calculations of R. The weights $w = 1/(40 + |F_o| + 0.0025|F_o|^2)$ in the last cycle of refinement gave a smooth weighting scheme. The shifts in the parameters were less than 1 % of the estimated standard deviations. The final agreement index obtained was $R = 0.127$. The interlayer scale factors increased from 0.5 for the zero layer to 3.2 for the tenth layer showing the decomposition of the crystal during the collection of the intensity data. The poor agreement between observed and calculated structure factors could mainly be ascribed to this circumstance. Since the main aim of this investigation was to determine the coordination geometry, no attempts were made to improve the results by collecting data from different crystals.

A final difference electron density map was featureless. The positional and thermal parameters are given in Table 1. Observed and calculated structure factors are compared in Table 2. The atomic scattering factors used in the calculations were taken from Ref. 8 (Cl, O, S, and C) and from Cromer *et al.*[9] (Nd).

An attempt to refine the structure in the non centrosymmetric space group $Pnn2$ was unsuccessful. All computations were made on the UNIVAC 1108 computor in Lund and the programs used are given in Ref. 10.

Table 1. Atomic parameters with estimated standard deviations. B denotes the isotropic temperature factor.

Atom	Group	$x \times 10^4$	$y \times 10^4$	$z \times 10^4$	B/Å^2
Nd		2123(5)	2467(5)	0	1.3(1)
Cl		0	5000	2725(27)	5.4(7)
O(1)	$-COO^-$	6447(64)	3268(32)	3015(40)	3.7(10)
O(2)	$-COO^-$	4806(61)	2731(30)	1471(41)	4.0(10)
O(3)	H_2O	4103(81)	1332(48)	0	3.4(14)
O(4)	H_2O	515(48)	3386(26)	1544(31)	1.9(7)
O(5)	H_2O	−1162(90)	2227(39)	0	3.3(13)
C(1)	$-COO^-$	5616(74)	3325(42)	2071(48)	1.9(10)
C(2)	$-CH_2-$	5554(104)	4069(61)	1440(75)	4.9(17)
S	$-C-S-C-$	3865(26)	4111(18)	0	1.9(4)

Table 2. Observed and calculated structure factors. The columns are k, $|F_o|$ and $|F_c|$.

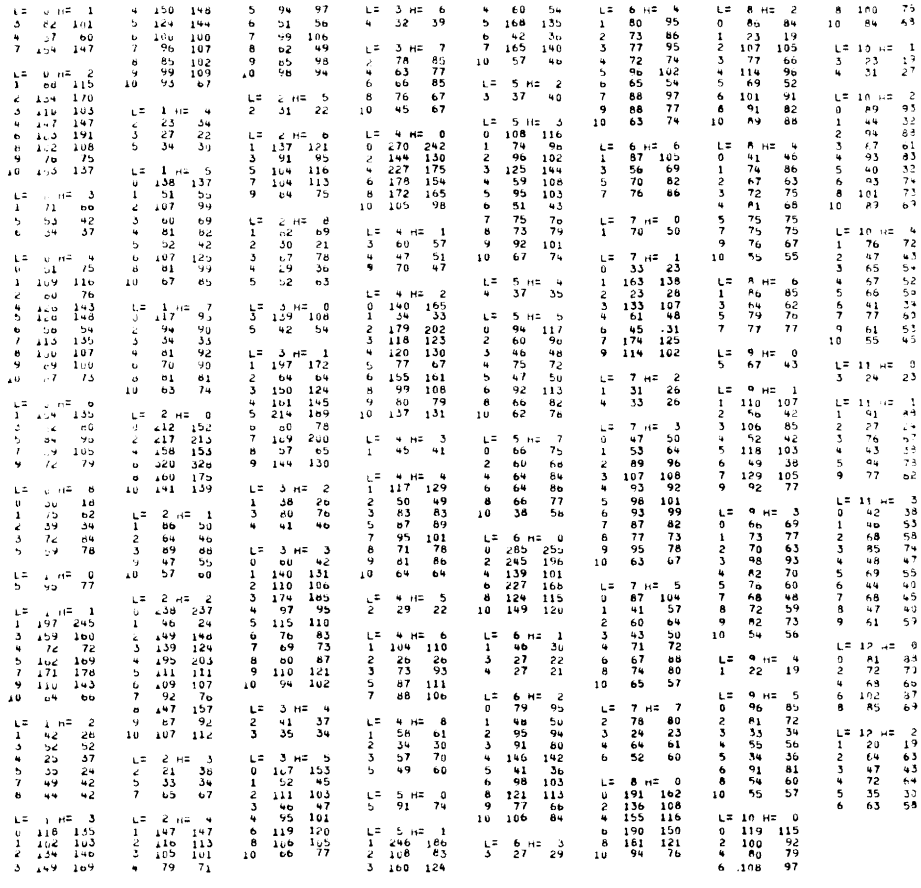

DESCRIPTION OF THE STRUCTURE

The structure is composed of layers of cross-linked neodymium ligand chains. These layers are stacked in the *b*-direction, and they are connected by hydrogen bonds *via* the chloride ion. A stereoscopic drawing of the contents of the unit cell is shown in Fig. 1. The superscripts $(i)-(x)$ are used to indicate the following equivalent sites in the structure:

(i)	$x,y,-z$	(ii)	$-1/2+x,1/2-y,1/2-z$
(iii)	$1/2+x,1/2-y,-1/2+z$	(iv)	$-1+x,y,z$
(v)	$-1+x,y,-z$	(vi)	$1/2-x,1/2+y,1/2+z$
(vii)	$-1/2+x,1/2-y,1/2-z$	$(viii)$	$-x,1-y,1-z$
(ix)	$-x,1-y,z$	(x)	$x,y,1-z$

where x,y,z are the atomic coordinates given in Table 1.

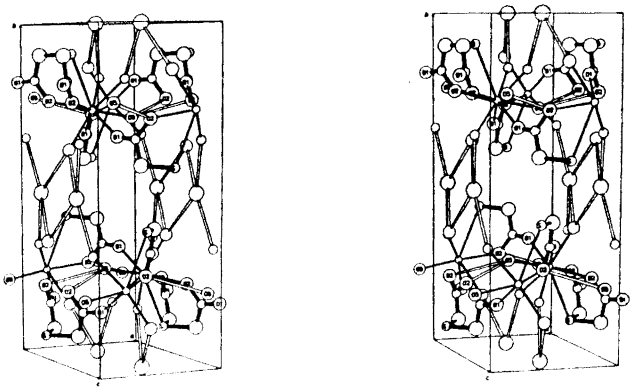

Fig. 1. A stereoscopic pair of drawings showing the contents of one unit cell. Figs. 1–3 were drawn by the program ORTEP.

The neodymium ion is coordinated by four water molecules, four carboxylate oxygen atoms, and one sulfur atom. The coordination polyhedron might be described as a distorted tricapped trigonal prism as is seen in Fig. 2. The thiodiacetate ligand is bent and has the oxygen atoms O(2) and O(2^{i}) on the same edge of the prism, and has the sulfur atom located outside the mid-

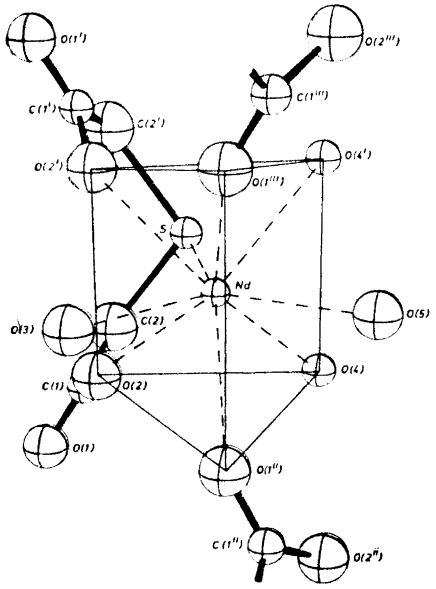

Fig. 2. The coordination polyhedron around the neodymium ion.

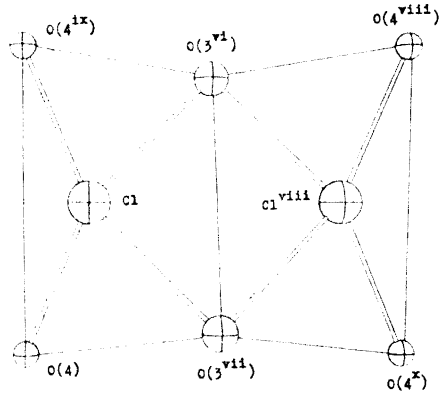

Fig. 3. The arrangement of the hydrogen bonded atoms around the chloride ions.

Table 3. Selected interatomic distances (Å) and angles (°) with estimated standard deviations.

A. The coordination polyhedron.

Distance		Distance	
Nd – O(1^{ii})	2.45(5)	O(3) – O(2)	2.94(9)
Nd – O(2)	2.44(4)	O(3) – O(1^{ii})	2.83(6)
Nd – O(3)	2.43(8)	O(5) – O(1^{ii})	2.85(6)
Nd – O(4)	2.53(4)	O(5) – O(4)	2.83(7)
Nd – O(5)	2.31(6)	O(1^{ii}) – O(2)	2.97(7)
Nd – S	3.15(3)	O(1^{ii}) – O(4)	3.19(6)
S – O(2)	2.94(6)	O(1^{ii}) – O(1^{iii})	4.06(10)
S – O(4)	3.09(4)	O(2) – O(2^{i})	3.01(9)
		O(4) – O(4^{i})	3.16(6)

B. The ligand.

Distance		Angle	
S – C(2)	1.88(8)	C(2) – S – C(2)	103(5)
C(2) – C(1)	1.46(12)	S – C(2) – C(1)	114(6)
C(1) – O(1)	1.13(7)	C(2) – C(1) – O(1)	118(7)
C(1) – O(2)	1.34(8)	C(2) – C(1) – O(2)	119(5)
		O(1) – C(1) – O(2)	122(7)

C. Possible hydrogen bonds.

Distance		Distance	
O(5) – O(2^{iv})	3.30(7)	Cl – O(3^{vi})	3.37(6)
O(4) – O(2^{ii})	2.87(6)	Cl – O(4)	3.12(5)

point of a "rectangular" face. A similar situation is found in $Nd(C_4H_5O_4N)(H_2O)_3Cl$.[2] Selected interatomic distances and angles within the coordination polyhedron are given in Table 3A. The large Nd – S distance, 3.15 Å, indicates only weak interaction between these two atoms. This supports the reported interpretation of the thermodynamic data for the rare earth thiodiacetate complexes, where a rather weak interaction has been assumed.[4] Of the 21 contact distances within the coordination polyhedron, four sulfur-oxygen and twelve oxygen-oxygen distances indicate van der Waals contacts.

The coordination polyhedra are connected by the carboxylate groups. This results in the formation of cross-linked chains aligned in the [101] and [10$\bar{1}$] directions, and the Nd – Nd distances within the chains are 6.175 Å.

In THIDAC the thiodiacetate ion exhibits the symmetry *m*, and the structure contains only one half independent ligand ion. The ligand forms two five-membered rings with the metal ion. The carboxylate oxygen atoms O(1) participate in the coordination of neighbouring metal ions. Bond distances

and angles within the thiodiacetate ion are given in Table 3B and they are not significantly different from those found in thiodiacetic acid.[11]

Judging from the oxygen-oxygen and oxygen-chloride distances, all water molecules are involved in hydrogen bonding (Table 3C). The water oxygen O(5) might be hydrogen bonded to $O(2^{iv})$ and $O(2^{v})$, thus connecting the coordination polyhedra in the *a*-direction. The chloride ion is situated between the metal-ligand layers and probably accepts hydrogen bonds from both layers, thus holding the structure together in the *b*-direction. The arrangement of the hydrogen bonded atoms around the chloride ion might be described as a distorted rectangle. Two rectangles are connected in pairs by sharing the edge $O(3^{vi})-O(3^{vii})$ as is seen in Fig. 3. The hydrogen atom at O(4) not involved in hydrogen bonding with the chloride ion is probably attracted by $O(2^{ii})$.

I am indebted to Professor Sture Fronæus and to Drs. Jörgen Albertsson and Ingmar Grenthe for useful discussions and many valuable suggestions. This work is part of a research project supported by the *Swedish Natural Science Research Council*.

REFERENCES

1. Albertsson, J. *Acta Chem. Scand.* **24** (1970) 3527.
2. Oskarsson, Å. *Acta Chem. Scand.* **25** (1971) 1206.
3. Albertsson, J. *Acta Chem. Scand.* **26** (1972) 1023.
4. Dellien, I., Grenthe, I. and Hessler, G. *Acta Chem. Scand.* **27** (1973) 2431.
5. Oskarsson, Å. *Acta Chem. Scand.* **26** (1972) 2126.
6. *International Tables for X-Ray Crystallography*, Kynoch Press, Birmingham 1952, Vol. I.
7. Cruickshank, D. W. J., In Pepinsky, R., Robertsson, J. M. and Speakman, J. C., Eds., *Computing Methods and the Phase Problem in X-Ray Crystal Analyses*, Pergamon, Glasgow 1961, p. 45.
8. *International Tables for X-Ray Crystallography*, Kynoch Press, Birmingham 1962, Vol. III.
9. Cromer, D. T., Larson, A. C. and Waber, J. T. *Acta Cryst.* **17** (1964) 1044.
10. Oskarsson, Å. *Acta Cryst.* **B 29** (1973) 1747.
11. Paul, S. *Acta Cryst.* **23** (1967) 491.

Received May 24, 1973.

ACTA CHEMICA SCANDINAVICA 27 (1973) 2930–2940

Reactions between Azolium Salts and Nucleophilic Reagents

X. The Reaction of 1,2-Disubstituted Pyrazolium Salts with *N*-Bromoacetamide and Sodium Hydroxide or Methoxide

MIKAEL BEGTRUP, NIELS CONRADSEN and JØRGEN HENRIK OLSEN

Department of Organic Chemistry, Technical University of Denmark, DK-2800 Lyngby, Denmark

1,2-Disubstituted pyrazolium salts *8* (X=H) with *N*-bromoacetamide and sodium methoxide, *via* bromination and substitution produce the four 1,2-disubstituted pyrazol-4-in-3-ones *3* and *16* (X=H or Br). The ratio between *3* and *16* (X=H), as expected, is reflected by the ratio between the base-catalyzed deuterium exchange rates of the heteroaromatic protons of the corresponding starting material *8*. The 4-halo-pyrazolium compounds *8* (X=Hal) with *N*-bromoacetamide and sodium methoxide, analogously, afford the halo-pyrazol-4-in-3-ones *3* and *16* (X=Hal), but in a ratio different from the relative D-exchange rate of the heteroaromatic protons of the starting material *8* (X=Hal). This difference is due to equilibration between the intermediate dihalo-compounds *1* and *14* (X=Hal). Thus, pure *1e* and sodium methoxide produces *3e* together with the *tele*-substitution product *16e*. The 4-halo-pyrazolium compounds *8* (X=Hal) with *N*-bromoacetamide and sodium hydroxide, *via* two successive brominations, giving rise to *9* (X=Hal), and subsequent substitution give the dihalo-pyrazol-4-in-3-ones *7* and *13* (X=Hal) in a ratio different from the relative substitution rates of the corresponding monohalo-compounds *1* and *14* (X=H), presumably for steric reasons.

When 1,3-disubstituted [1,2] or 1,2-disubstituted [3] 1,2,3-triazolium salts were treated with *N*-bromoacetamide in sodium hydroxide or methoxide a bromination of the heterocyclic ring, followed by substitution of the bromine atom with hydroxide or methoxide, took place. When the formation of isomeric products was possible the relative rates of the base-catalyzed deuterium exchange of the heteroaromatic protons of the starting material could usually be used to predict the product distribution. The reaction of some pyrazolium salts with *N*-bromoacetamide and sodium hydroxide or methoxide has now been investigated in order to examine if similar predictions about product distribution can be made in this series.

1-Methyl-2-benzyl-pyrazolium tosylate *8 a*, like the 1,2-dimethyl compound *8* ($R' = CH_3$)[4] did not react with *N*-bromoacetamide and aqueous sodium hydroxide. When the stronger base sodium methoxide in methanol was used a mixture of 1-methyl-2-benzyl-pyrazol-4-in-3-one *3a* and 1-benzyl-2-methyl-pyrazol-4-in-3-one *16a* was formed (total yield 21 %). Small amounts of the bromo-derivatives *3b* and *16b* were also isolated (total yield 4 %). Similarly, 1-methyl-2-phenyl-pyrazolium tosylate *8c*, *N*-bromoacetamide, and sodium methoxide produced 1-methyl-2-phenyl-pyrazol-4-in-3-one *3c* and 1-phenyl-2-methyl-pyrazol-4-in-3-one *16c* (total yield 6 %) together with the bromo-derivatives *3e* and *16e* (total yield 9 %).

When the reaction between *8* (X = H), *N*-bromoacetamide, and sodium methoxide was carried out in monodeuteriomethanol the 3- and 5-protons of *8* (X = H) were quantitatively, and almost instantaneously, exchanged with deuterium before any further reaction took place. This indicates that the solution contains a certain amount of the anions *4* and *10*.* These anions can react with either deuterons or with bromine cations delivered from the *N*-bromoacetamide.[1-4] The latter reaction, in analogy to previous considerations,[1-4] produces the bromo compounds *1* and *14*, respectively. Neither these, nor other intermediates, could, however, be observed in the reaction mixture by NMR-spectroscopy, most likely because they undergo a rapid substitution by a normal addition-elimination mechanism.[5] Subsequent *O*-demethylation then produces the pyrazol-4-in-3-ones *3* and *16*[2-4] (Scheme 1).

Since the anions *4* and *10* are very reactive the attack of bromine cations on a mixture of these anions is probably unselective. The ratio between the bromo compounds *1* and *14* will therefore be determined by the relative concentration of *4* and *10* and, hence, by their relative stability. This, in turn, is reflected by the relative deuterium exchange rate of the 3- and 5-protons of the starting material *8*.

Isomerizations between 3-halo-pyrazolium salts *1* (X = H) and *14* (X = H) have never been observed.[5] Thus, 1-methyl-2-phenyl-3-bromo-pyrazolium tosylate *1c* and base afforded the pyrazolone *3c* as the sole product. The isomeric pyrazolone *16c* was not formed. Similarly, the isomeric bromo compound *14c* produced the pyrazolone *16c*, exclusively.[5] Thus, in the present case, the ratio between the bromo compounds *1* and *14* will in its turn reflect the ratio between the final products *3* and *16*. Since the ratio of the exhange rates of the 3- and 5-protons of *8a* was found to be 1.13[5] the expected distribution between the pyrazol-4-in-3-ones *3a* and *16a* is 1.13. The distribution found was 1.04. According to the ratio of the exchange rates of the 3- and 5-protons of *8c*[5] the expected distribution between the pyrazol-4-in-3-ones *3c* and *16c* is 1.29. The distribution found was 1.53. The minor deviations between the predicted and obtained product ratio may be due to decomposition of the 3-bromo-pyrazolium salts *1* and *14*. Thus, considerable decomposition took place when the methylphenylbromopyrazolium tosylate *14c* was treated with potassium hydroxide.[5] The simultaneous formation of the bromo-pyrazol-4-in-3-ones may also influence the product distribution.

* The 3- and 5-protons of the starting material *8* (X = H) are replaced readily with deuterium in aqueous solution at pD = 12, whereas the 4-proton is not replaced at pD = 13 during three months.[5] This explains the lack of reactivity of the 4-position.

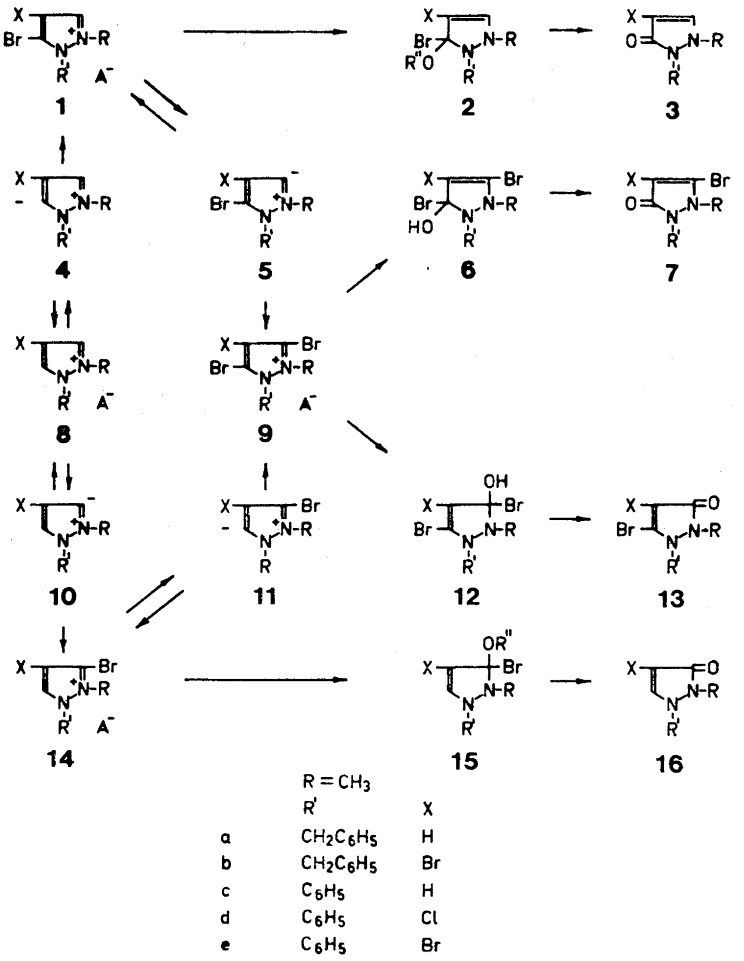

Scheme 1.

The 4-bromo-pyrazolones *3* (X = Br) and *16* (X = Br) do not arise *via* bromination of the initially formed pyrazolones *3* (X = H) and *16* (X = H) since separate experiments indicated that the latter compounds are not brominated by *N*-bromoacetamide under the conditions of the reaction. Since bromination at C-4 of the starting material *8* (X = H) is highly unlikely due to the slow deuterium exchange of H-4 of *8* (X = H) the bromopyrazolones probably arise *via* the initially formed 3-bromo-pyrazolium salts *1* (X = H) and *14* (X = H). In fact, pure 1-methyl-2-phenyl-3-bromo-pyrazolium tosylate *1c*, when treated with *N*-bromoacetamide and sodium methoxide, affords a mixture of 1-methyl-2-phenyl-pyrazol-4-in-3-one *3c* and the 4-bromo derivative *3e*. Similarly, 1-methyl-2-phenyl-5-bromo-pyrazolium tosylate *14c* gives rise to

the pyrazolones *16c* and *16e*. The mechanism of formation of the 4-bromo-pyrazolones *3e* and *16e* from the 3-bromo-pyrazolium compounds, *1c* and *14c*, is not evident. Apparently, *1c* and *14c*, *via* the 4-anions, are brominated at *C*-4 giving rise to *1e* and *14e* which in turn, by substitution, produce the bromopyrazolones *3e* and *16e*, respectively. According to the exchange rates of *1c* and *14c*, however, the 3-anions *5c* and *11c* are more stable than the 4-anions.[5] Consequently, the 3-bromo-pyrazolium compounds *1* (X = H) and *14* (X = H) should preferently, *via* *5* (X = H) and *11* (X = H) give rise to the 3,5-dibromo compound *9* (X = H). However, no pyrazolones *7* (X = H) or *13* (X = H) derived from *9* (X = H) could be detected. It is possible that *9* (X = H) decomposes or undergoes further bromination followed by debromination and subsequent substitution to give the isolated bromopyrazolones *3* (X = Br) and *16* (X = Br). This possibility is only speculative as yet. Since the mechanism of the formation of the bromo pyrazolones *3* (X = Br) and *16* (X = Br) from *8* (X = H) is unknown the ratio between *3* (X = Br) and *16* (X = Br) cannot be predicted.

The behaviour of 4-bromo-pyrazolium compounds *8* (X = Br) was now studied. When 1-methyl-2-benzyl-4-bromo-pyrazolium tosylate *8b* was treated with *N*-bromoacetamide and sodium methoxide 1-methyl-2-benzyl-4-bromo-pyrazol-4-in-3-one *3b* and 1-benzyl-2-methyl-4-bromo-pyrazol-4-in-3-one *16b* were produced (total yield 76 %). In analogy to the previous experiment, it is assumed that the dibromo compounds *1b* and *14b* arise initially *via* the anions *4b* and *10b* , respectively. Halogen in the 3-position of 1,2-disubstituted pyrazolium salts is replaced readily with nucleophilic reagents in contrast to halogen in the 4-position.[4,5] Therefore, the dibromo compounds *1b* and *14b* are expected to give *3b* and *16b*.

Provided that the conversion of the dibromo compounds to the bromo-pyrazol-4-in-3-ones *3b* and *16b* is kinetically controlled, the distribution between *3b* and *16b* should, as before, be reflected by the relative stability of the anions *4b* and *10b* and, hence, by the relative exchange rate of the 3- and 5-protons of the starting material *8b*. This exchange rate was determined to be 1.16. In contrast, the ratio between the methylbenzylbromopyrazolones *3b* and *16b* was found to be 0.74.

A similar difference between expected (1.35) and found (0.84) ratio was observed between the methylphenylbromopyrazolones *3e* and *16e*, produced by treatment of 1-methyl-2-phenyl-4-bromo-pyrazolium tosylate *8e* with *N*-bromoacetamide and sodium methoxide. The total yield of *3e* and *16e* was 59 %. Analogous results were obtained using 1-methyl-2-phenyl-4-chloro-pyrazolium tosylate *8d* as the starting material (see Experimental). These discrepancies may be explained by assuming that equilibration between the intermediate dihalo compounds *1* (X = Br) and *14* (X = Br) takes place. The ratio found being due to a net conversion of *1* (X = Br) to *14* (X = Br).

In order to investigate this possibility, pure 1-methyl-2-phenyl-3,4-dibromo-pyrazolium tosylate *1e*, prepared from 1-phenyl-4,5-dibromo-pyrazole and methyl tosylate, was treated with sodium methoxide. In fact, *1e* produced a mixture of the 4-bromo-pyrazol-4-in-3-one *3e* and the *tele*-substitution product *16e* in the ratio 8.2. A proposed mechanism for the *tele*-substitution of the dibromo compound *1e* is sketched in Scheme 2. Initially, *1e* loses a proton.

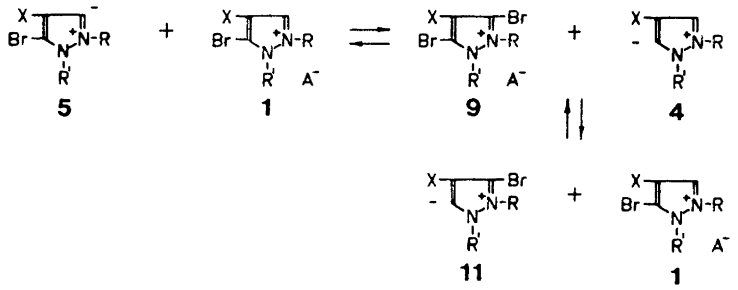

Scheme 2.

Since 3,4-di-bromo-pyrazolium salts may donate bromonium ions from the 3-position under basic conditions,[4] the anion *5e* may receive a bromonium ion from unchanged *1e*. The new anion *4e* thus produced may now receive a bromonium ion from the tribromo compound *9e*. If *9e* offers the bromine adjacent to the phenyl group the result is isomerization of the dibromo compound *1e* to *14e* as shown in Scheme 2. As a result a complex mixture arises. The highly different ratios between *3e* and *16e*, obtained from the monobromo compound *8e* or the dibromo compound *1e*, indicate that complete equilibration between the dibromo compounds is not reached. Therefore, predictions about the distribution between *3e* and *16e* in these cases are impossible. In the same way, the ratio between the methylphenylchloro-pyrazolones *3d* and *16d*, formed from *8c*, and analogously, the ratio between the methylbenzyl-bromo-pyrazolones *3d* and *16b*, formed from *8b*, cannot be predicted.

When 1-methyl-2-benzyl-4-bromo-pyrazolium tosylate *8b* was treated with *N*-bromoacetamide and sodium hydroxide 1-methyl-2-benzyl-4,5-dibromo-pyrazol-4-in-3-one *7b* and 1-benzyl-2-methyl-4,5-dibromo-pyrazol-4-in-3-one *13b* were obtained as the sole pyrazolones (total yield 28 %). Most likely, the dibromo compounds *1b* and *14b* are formed, as in the preceding experiment, *via* proton abstraction and bromination. The intermediates *1b* and *14b* then abstract a proton before substitution occurs producing the anions *5b* and *11b*, respectively. The latter species finally take up bromine cations to give the same tribromo-pyrazolium salt *9b*. This course is analogous to that found in the 1,2,3-triazolium salt series where substitution is slower than further bromination when the weaker nucleophile sodium hydroxide is used as the base.[1,3] The tribromopyrazolium salt *9b* in its turn, by substitution of the more reactive 3- and 5-halogen atoms, yields the dibromo-pyrazol-4-in-3-ones *7b* and *13b*, respectively. Since the latter process is product determining the distribution between *7b* and *13b* must depend on the relative reactivity of the 3- and the 5-halogens of the tribromo compound *9b* towards substitution. This ratio is expected to be reflected by the relative substitution rate of 1-methyl-2-benzyl-3-bromo-pyrazolium tosylate *1a* and 1-methyl-2-benzyl-5-bromo-pyrazolium tosylate *14a*, respectively, or by the rate of the chloro-analogs, as well. The latter substitution rate ratio was determined to be 0.30.[5] This ratio deviates somewhat from the ratio (0.21) between the dibromo-pyrazolones *7b* and *13b*, obtained by treatment of 1-methyl-2-benzyl-4-bromo-

pyrazolium tosylate *8b* with *N*-bromoacetamide and sodium hydroxide.

When 1-methyl-2-phenyl-4-bromo-pyrazolium tosylate *8e* was treated with *N*-bromoacetamide and sodium hydroxide 1-phenyl-2-methyl-4,5-dibromo-pyrazol-4-in-3-one *7e* and 1-methyl-2-phenyl-4,5-dibromo-pyrazol-4-in-3-one *13e* were obtained as the sole pyrazolones (total yield 62 %). The ratio between the rate of substitution of 1-methyl-2-phenyl-3-bromo-pyrazolium tosylate *1c* and 1-methyl-2-phenyl-5-bromo-pyrazolium tosylate *14c* was found to be 0.18.[5] Thus, this is the expected ratio between the dibromo-pyrazolones *7e* and *13e*, formed from *8e*. However, the ratio found was 0.35. A similar deviation between expected (0.18) and found (0.35) product distribution was found in the reaction of 1-methyl-2-phenyl-4-chloro-pyrazolium tosylate *8d* with *N*-bromoacetamide and sodium hydroxide (see Experimental).

These discrepancies may be due to decomposition of the tribromo compound similar to the decomposition of 1-methyl-2-phenyl-5-bromo-pyrazolium tosylate *14c*.[5] Steric effects may also alter the relative substitution rate of the 3- and 5-halogen in the trihalo compound *9* (X = Br) as compared to the relative substitution rate of the 3- and 5-halogen in the monohalo compounds *1* (X = H) and *14* (X = H).

The results described in the present paper indicate that 1,2-disubstituted pyrazolium salts, when treated with *N*-bromoacetamide and base yield the expected products. However, the product distribution cannot be predicted exactly on basis of the base catalyzed deuterium exchange of the hetero-aromatic protons of the starting material or the substitution rates of simple model compounds. In the reaction of 4-halo pyrazolium compounds *8* (X = Br) with *N*-bromoacetamide and sodium methoxide the process is not kinetically controlled. In the other cases discussed above competing decomposition and steric factors may influence the product distribution.

The pyrazol-4-in-3-ones described in the present paper were identified through their IR- and NMR-spectra (Table 1) which showed absorption characteristics of other 1,2-disubstituted pyrazol-4-in-3-ones.[4,5] As described previously, the NMR-signal of the phenyl group of 1-methyl-2-benzyl-pyrazol-4-in-3-one *3a*, the structure of which has been proven by chemical transformation, turned out to be a broad singlet.[5] In contrast, the phenyl group of the isomeric 1-benzyl-2-methyl-pyrazol-4-in-3-one *16a* appeared as a multiplet. This difference may be explained in terms of deshielding of the *ortho*-phenyl-protons by the pyrazole-ring.[6] The isomeric pairs of bromo- and dibromo-pyrazolones *3b* and *16b*, or *7b* and *13b* showed a similar difference on which the structure identification was based. These assignments were proved by chemical transformation. Thus 1-benzyl-2-methyl-4-bromo-pyrazol-4-in-3-one *16b*, and 1-benzyl-2-methyl-4,5-dibromo-pyrazol-4-in-3- one *13b*, when treated with sodium borohydride and palladium on charcoal, both produced 1-benzyl-2-methyl-pyrazol-4-in-3-one *16a* in high yield.

As described previously, the NMR-signal of the phenyl group of 1-methyl-2-phenyl-pyrazol-4-in-3-one *3c*, the structure of which has been proven by chemical transformations, turned out to be a broad singlet.[5] In contrast, the phenyl group signal of the isomeric 1-phenyl-2-methyl-pyrazol-4-in-3-one *16c* appeared as a broad multiplet. Again, the difference may be explained in terms of deshielding of the *o*-phenyl protons by the pyrazole-ring.[6] This

Table 1. NMR-spectra in deuteriochloroform with TMS as an internal standard (δ-values), and infrared absorptions of the carbonyl groups of 1,2-disubstituted pyrazol-4-in-3-ones.

Compound	IR[a] cm^{-1}	Phenyl group	H-4 ppm	H-5 ppm	N-CH_3 N-CH_2 ppm	$J_{^{13}C-H}$ Hz	$J_{H_4H_5}$ Hz
1-Methyl-2-benzyl-pyrazol-4-in-3-one *3a*[b]	1620	broad singlet	5.50	7.17	3.23 5.07	141	3.4
1-Benzyl-2-methyl-pyrazol-4-in-3-one *16a*[b]	1625	multiplet	5.46	7.39	3.30 4.83	141	3.4
1-Methyl-2-benzyl-4-bromo-pyrazol-4-in-3-one *3b*	1640	broad doublet		7.32	3.25 5.07	142	
1-Benzyl-2-methyl-4-bromo-pyrazol-4-in-3-one *16b*	1630	multiplet		7.43	3.37 4.82	141	
1-Methyl-2-benzyl-4,5-dibromo-pyrazol-4-in-3-one *7b*	1635	broad singlet			3.29 5.09		
1-Benzyl-2-methyl-4,5-dibromo-pyrazol-4-in-3-one *13b*	1655	multiplet			3.35 5.00		
1-Methyl-2-phenyl-pyrazol-4-in-3-one *3c*[b]	1645	broad singlet	5.56	7.45	3.14	142	3.6
1-Phenyl-2-methyl-pyrazol-4-in-3-one *16c*[b]	1630	broad multiplet	5.64	7.57	3.28	142	3.7
1-Methyl-2-phenyl-4-chloro-pyrazol-4-in-3-one *3d*	1670	broad singlet		7.59	3.11	142	
1-Phenyl-2-methyl-4-chloro--pyrazol-4-in-3-one *16d*	1635	broad multiplet	7.64	3.31		142	
1-Methyl-2-phenyl-4-bromo--pyrazol-4-in-3-one *3e*	1660	broad singlet	7.65	3.14		142	
1-Phenyl-2-methyl-4-bromo--pyrazol-4-in-3-one *16e*	1635	broad multiplet	7.65	3.32		142	
1-Methyl-2-phenyl-4-chloro-5-bromo-pyrazol-4-in-3-one *7d*	1680	singlet		3.19		142	
1-Phenyl-2-methyl-4-chloro-5-bromo-pyrazol-4-in-3-one *13d*	1660	multiplet		3.20		142	
1-Methyl-2-phenyl-4,5-dibromo-pyrazol-4-in-3-one *7e*	1675	singlet		3.22		142	
1-Phenyl-2-methyl-4,5-dibromo-pyrazol-4-in-3-one *13e*	1670	multiplet		3.22		142	

[a] IR-spectra were obtained in potassium bromide discs. [b] The data have been described previously [5] but are shown here for comparison.

difference could be used in the structure determination of the isomeric pairs of bromo-pyrazolones *3e* and *16e*, chloro-pyrazolones *3d* and *16d*, dibromo-pyrazolones *7e* and *13e*, and chlorobromo-pyrazolones *7d* and *13d*, respectively. In one case the identification was controlled by chemical conversion. Thus, the supposed 1-phenyl-2-methyl-4,5-dibromo-pyrazol-4-in-3-one *13e* when treated with sodium borohydride and palladium on charcoal afforded the parent 1-phenyl-2-methyl-pyrazol-4-in-3-one *16c* in 96 % yield.

EXPERIMENTAL

Column chromatography was carried out on silica gel (Merck, 0.05 – 0.2 mm). When non-aromatic eluents were used, 2 % of a fluorescent indicator (Riedl de Häen, Leucht-

pigment ZS Super) was added to the silica gel and tubes of clear quartz were used. The zones could then be visualized by illumination with a 254 mμ UV-lamp. Preparative thin layer chromatography (TLC) was carried out on 20 × 40 cm plates with a 1 mm layer of silica gel (Merck, PF_{254}). Melting points are uncorrected. NMR-spectra were obtained on a Varian A-60 or a HA-100 instrument. Position of signals are given in ppm (δ-values) relative to tetramethylsilane (TMS) when deuteriochloroform was used as the solvent. When deuterium oxide was used as the solvent 2,2-dimethyl-2-silapentane-5-sulfonate (DSS) was used as an internal standard. IR-spectra were measured in potassium bromide pellets. The purity of all non-ionic compounds were checked by TLC. All compounds were identified through their melting point, IR- and NMR-spectra.

1-Phenyl-4,5-dibromo-pyrazole. 1-Phenyl-5-bromo-pyrazole [5] (1.00 g) was dissolved in glacial acetic acid (1.00 ml) and a solution of bromine (0.28 ml) in glacial acetic acid (1.9 ml) was added with stirring during 15 min. Stirring was continued for 1 h, and water (40 ml) was then added. Filtration yielded 1.29 g (94 %) of 1-phenyl-4,5-dibromo-pyrazole. Recrystallization from ethanol-water (1:1) afforded 1.17 g (84 %) of colourless crystals, m.p. 106°C. The compound was identical with that described previously.[5]

1-Methyl-2-phenyl-3,4-dibromo-pyrazolium tosylate 1e. 1-Phenyl-4,5-dibromo-pyrazole (1.54 g), methyl tosylate (0.95 ml), and dry acetonitrile (1.00 ml) were heated to 100°C for 3 h. Ether (20 ml) was then added and the precipitate was washed 4 times with ether (20 ml). This afforded 646 mg (26 %) of 1-methyl-2-phenyl-3,4-dibromo-pyrazolium tosylate *1e* as colourless crystals, m.p. 167 – 170°C. Recrystallization from methanol-ether raised the melting point to 180 – 184°C. (Found: C 41.96; H 3.33; N 5.63; S 6.61; Br 32.57. Calc. for $C_{17}H_{16}N_2O_3SBr_2$: C 41.82; H 3.31; N 5.74; S 6.57; Br 32.76). NMR-data in D_2O: *H*-5 8.69, *N*-CH_3 3.94 ppm.

Reactions with sodium methoxide

1-Methyl-2-benzyl-pyrazolium tosylate 8a [5] (1.15 g), *N*-bromoacetamide (518 mg) and 1 N sodium methoxide (10.7 ml) were kept at room temperature for 14 days. Sodium thiosulfate (1.0 g) was then added. The solvent was removed, water (10 ml) was added, and the solution was extracted with methylene chloride (3 × 20 ml). The extract was dried (magnesium sulfate), the methylene chloride was removed and the residue was extracted with boiling ethyl acetate (50 + 20 + 2 × 10 ml). The ethyl acetate was removed and the residue was separated by preparative TLC using methylethyl ketone saturated with water as the eluent. This gave 20 mg (2.2 %) of 1-methyl-2-benzyl-4-bromo-pyrazol-4-in-3-one *3b* ($R_F = 0.66$) identical with the material described below. The next zone contained 13 mg (1.5 %) of 1-benzyl-2-methyl-4-bromo-pyrazol-4-in-3-one *16b* ($R_F = 0.53$) identical with the material described below. The last zone contained 134 mg (21 %) of a mixture of 1-methyl-2-benzyl-pyrazol-4-in-3-one *3a* and 1-benzyl-2-methyl-pyrazol-4-in-3-one *16a* in the ratio 1.04:1, as shown by an NMR-spectrum in deuteriochloroform solution. The pyrazolones were separated by preparative TLC as described previously [5] using methylethyl ketone as the eluent. The fast running fraction contained 35 mg (5.6 %) of 1-methyl-2-benzyl-pyrazol-4-in-3-one *3a*. The slow running fraction contained 44 mg (7.0 %) of 1-benzyl-2-methyl-pyrazol-4-in-3-one *16a*. The latter two compounds were identical with the materials described previously.[5]

1-Methyl-2-phenyl-pyrazolium tosylate 8c [5] *and N-bromoacetamide.* (1.03 g and 483 mg, respectively) were kept in 1 N sodium methoxide (9.7 ml) for 14 days. The mixture was then chromatographed on silica gel (50 g). Elution with ethyl acetate (200 ml) gave a mixture of 1-methyl-2-phenyl-4-bromo-pyrazol-4-in-3-one *3e* and 1-phenyl-2-methyl-4-bromo-pyrazol-4-in-3-one *16e* together with some impurities. The ratio between *3e* and *16e* was determined by NMR-spectroscopy in a 1:1 mixture of deuteriochloroform and benzene. The benzene causes upfield shifts of the *N*-methyl groups of 1,2-disubstituted pyrazol-4-in-3-ones. Methyl groups at *N*-1 are shifted much more than methyl groups at *N*-2.[6] The ratio between *3e* and *16e* determined in this way was 1:1.31. Preparative thin layer chromatography (ethyl acetate-ether 1:9) gave 25 mg (3.2 %) of *3e* ($R_F = 0.66$) as a yellow oil. Recrystallization from ethyl acetate-hexane afforded 21 mg of pure *3e*, m.p. 110 – 112°C. The compound was identical with the material described below. The next fraction ($R_F = 0.43$) from the thin layer chromatographically separation yielded 41 mg (5.3 %) of *16e*, m.p. 98 – 103°C. Recrystallization from ethyl acetate-hexane

raised the melting point to 117°C. The material was identical with that described below. The column was then eluted with ethyl acetate-methanol (1:1). This gave a mixture which was extracted with methylene chloride (5 × 8 ml). Removal of the solvent left 1-methyl-2-phenyl-pyrazol-4-in-3-one *3c* and 1-phenyl-2-methyl-pyrazol-4-in-3-one *16c* in the ratio 1.53:1 as shown by NMR-spectroscopy in a 1:1 micture of deuteriochloroform and benzene. The mixture was separated by preparative TLC using acetone as the eluent. The fast moving fraction contained 20 mg (3.6 %) of *3c*, m.p. 103 – 105°C. IR- and NMR-spectra were identical with those of the material described previously.[5] The slow moving fraction contained 11 mg (2.0 %) of *16c*, m.p. 104 – 105°C. IR- and NMR-spectra were identical with those of the material described previously.[5]

1-Methyl-2-benzyl-4-bromo-pyrazolium tosylate 8b [5] (743 mg), *N*-bromoacetamide (281 mg), and 1 N sodium methoxide (5.7 ml) were kept at room temperature for 14 days. Sodium thiosulfate (1.0 g) was then added. The methanol was removed, the residue was dissolved in water (5 ml), and the aqueous phase was extracted with methylene chloride (3 × 30 ml). The organic solution was dried (magnesium sulfate) and the methylene chlorid was removed. An NMR-spectrum of the residue dissolved in benzene-deuteriochloroform 1:1 indicated the presence of 1-methyl-2-benzyl-4-bromo-pyrazol-4-in-3-one *3b* and 1-benzyl-2-methyl-4-bromo-pyrazol-4-in-3-one *16b* in the ratio 1:1.36. The pyrazolones were separated on a column of silica gel (53 g) using ethyl acetate as the eluent. First, a minor amount of impurities left the column. Then, 112 mg (24 %) of 1-methyl-2-benzyl-4-bromo-pyrazol-4-in-3-one *3b* was collected. The compound was dissolved in ethyl acetate, filtered through activated carbon, and reprecipitated from ethyl acetate-hexane. This gave *3b* as a colourless oil. (Found: C 49.44; H 4.28; N 10.46; Br. 29.89. Calc. for $C_{11}H_{11}N_2OBr$: C 49.46; H 4.15; N 10.49; Br 29.92). The next fraction contained 242 mg (52 %) of 1-benzyl-2-methyl-4-bromo-pyrazol-4-in-3-one *16b* as colourless crystals, m.p. 98 – 103°C. Purification as described for the isomeric pyrazolone raised the melting point to 104 – 107°C. (Found: C 49.25; H 4.27; N 10.62; Br 29.79).

1-Methyl-2-phenyl-4-bromo-pyrazolium tosylate 8e [5] *and N-bromoacetamide* (1.05 g and 325 mg, respectively), were dissolved in 1 N methanolic sodium methoxide (8.2 ml). The solution was kept at room temperature for 14 days. It was then poured on a column of silica gel (50 g) packed with ethyl acetate. Elution with ethyl acetate gave 982 mg of brown crystals. An NMR-spectrum indicated the presence of 1-methyl-2-phenyl-4-bromo-pyrazol-4-in-3-one *3e* and 1-phenyl-2-methyl-4-bromo-pyrazol-4-in-3-one *16e* in the ratio 1:1.19. The two compounds were separated by preparative TLC eluting with ethyl acetate-ether (1:9). The fast moving fraction contained 218 mg (34 %) of 1-methyl-2-phenyl-4-bromo-pyrazol-4-in-3-one *3e*, m.p. 101 – 105°C. Filtration through activated carbon and recrystallization from ethyl acetate-hexane as above gave 160 mg (25 %), m.p. 119°C. (Found: C 47.62; H 3.60; N 11.17; Br 31.58. Calc. for $C_{10}H_9N_2OBr$: C 47.46; H 3.58; N 11.07; Br 31.57). The slow moving fraction contained 231 mg (36 %) of 1-phenyl-2-methyl-4-bromo-pyrazol-4-in-3-one *16e* as colourless crystals, m.p. 117C°. Filtration through activated carbon and recrystallization as above did not raise the melting point. (Found: C 47.59; H 3.67; N 11.14; Br 31.56).

1-Methyl-2-phenyl-4-chloro-pyrazolium tosylate 8d [5] *and N-bromoacetamide* (790 mg and 338 mg, respectively) were kept in 1 N sodium methoxide (7.0 ml) for 14 days at room temperature. Chromatography on silica gel (50 g) as described in the preceding experiment gave 479 mg of a mixture of the chloro-pyrazolones *3d* and *16d* in the ratio 1:1.37 as shown by NMR. Preparative TLC as described in the preceding experiment afforded a fast moving fraction containing 138 mg (31 %) of 1-methyl-2-phenyl-4-chloro-pyrazol-4-in-3-one *3d* as colourless crystals, m.p. 117 – 118°C. Filtration through activated carbon and recrystallization as above did not raise the melting point. (Found: C 57.60; H 4.20; N 13.26; Cl 16.85. Calc. for $C_{10}H_9N_2OCl$: C 57.54; H 4.35; N 13.42; Cl 16.99). The slow moving fraction contained 188 mg (42 %) of 1-phenyl-2-methyl-4-chloro-pyrazol-4-in-3-one *16d* as colourless crystals, m.p. 116 – 118°C. Filtration through activated carbon and recrystallization as before afforded 155 mg (34 %), m.p. 122°C. (Found: C 57.70; H 4.41; N 13.17; Cl 16.90).

1-Methyl-2-phenyl-3,4-dibromo pyrazolium tosylate 1e (322 mg) and 1 N sodium methoxide (2.10 ml) were kept at room temperature for 14 days. The mixture was then poured on a column of silica gel (30 g) packed with ethyl acetate. Elution with ethyl acetate gave a minor fraction which was not identified further. The second fraction contained 107 mg (41 %) of a mixture of 1-methyl-2-phenyl-4-bromo-pyrazol-4-in-3-one *3d* and

1-phenyl-2-methyl-4-bromo-pyrazol-4-in-3-one *16d* in the ratio 8.2:1 as shown by NMR in a mixture of deuteriochloroform and benzene (1:1). The compounds were identified by adding, one by the other, the pure substances to the solution. TLC (ethyl acetate-ether 9:1) confirmed the presence of *3d* and *16d*.

Reactions with sodium hydroxide

1-Methyl-2-benzyl-4-bromo-pyrazolium tosylate 8b (622 mg), *N*-bromoacetamide (1.11 g) and 1 N sodium hydroxide (8.8 ml) were kept at room temperature for 14 days. Sodium thiosulfate (1.0 g) was then added and the mixture was extracted with methylene chloride (3 × 30 ml). After drying (magnesium sulfate) the methylene chloride was removed. An NMR-spectrum of the residue dissolved in deuteriochloroform-benzene (1:1) indicated the presence of 1-methyl-2-benzyl-4,5-dibromo-pyrazol-4-in-3-one *7b* and 1-benzyl-2-methyl-4,5-dibromo-pyrazol-4-in-3-one *13b* in the ratio 1:4.70. The compounds were separated on a column of silica gel (45 g) using ether as the eluent. First, a minor amount of impurities left the column. Then, 35 mg (7 %) of 1-methyl-2-benzyl-4,5-dibromo-pyrazol-4-in-3-one *7b* was collected. The material was dissolved in ethyl acetate and filtered through activated carbon. Two reprecipitations from ethyl acetate-hexane yielded the pure compound as a colourless oil. (Found: C 38.31; H 3.01; N 8.18; Br 46.40. Calc. for $C_{11}H_{10}N_2OBr_2$: C 38.17; H 2.92; N 8.10; Br 46.18). The next fraction contained a mixture of 1-benzyl-2-methyl-4,5-dibromo-pyrazol-4-in-3-one *13b* and *N*-methyl-*N'*-acetyl-urea. The urea derivative was removed by refluxing the mixture for 3 h with 1 N aqueous sodium hydroxide and subsequent extraction with methylene chloride (3 × 20 ml). Removal of the methylene chloride afforded 108 mg (21 %) of the dibromo-pyrazolone *13b* which was purified as described for the isomeric compound. This gave 1-benzyl-2-methyl-4,5-dibromo-pyrazol-4-in-3-one *13b* as a colourless oil. (Found: C 38.25; H 2.97; N 8.28; Br 45.98).

1-Methyl-2-phenyl-4-bromo-pyrazolium tosylate 8e and N-bromoacetamide (1.72 g and 3.21 g, respectively) were dissolved in 1 N sodium hydroxide (25.0 ml) and the solution was kept at room temperature for 14 days. Sodium thiosulfate (1 g) was then added and the solution was extracted with methylene chloride (3 × 20 ml). Drying (magnesium sulfate), removal of the methylene chloride, dissolving in ethyl acetate, filtration through activated carbon, and removal of the solvent gave 1.00 g of yellow crystals. An NMR-spectrum, using chloroform-d_1-benzene-d_6 (1:1) as the solvent, indicated the presence of 1-methyl-2-phenyl-4,5-dibromo-pyrazol-4-in-3-one *7e* and 1-phenyl-2-methyl-4,5-dibromo-pyrazol-4-in-3-one *13e* in the ratio 1:2.82. The mixture was extracted with four 5 ml portions of boiling ethyl acetate. The extracts were poured into a column of silica gel (60 g) packed with ether. The column was then eluted with ether. The first fraction contained 307 mg (22 %) of 1-methyl-2-phenyl-4,5-dibromo-pyrazol-4-in-3-one *7e* as colourless crystals, m.p. 135 – 151°C. The compound was dissolved in ethyl acetate, filtered through activated carbon, and recrystallized from ethyl acetate-hexane giving 191 mg (14 %), m.p. 154 – 156°C. (Found: C 36.19; H 2.21; N 8.62; Br 48.03. Calc. for $C_{10}H_8N_2OBr_2$: C 36.18; H 2.43; N 8.44; Br 48.14). The next fraction contained 556 mg (40 %) of 1-phenyl-2-methyl-4,5-dibromo-pyrazol-4-in-3-one *13e* as colourless crystals, m.p. 150°C. Filtration through activated carbon and recrystallization from ethyl acetate-hexane did not raise the melting point. (Found: C 35.98; H 2.55; N 8.53; Br 48.05).

1-Methyl-2-phenyl-4-chloro-pyrazolium tosylate 8d and N-bromoacetamide (1.36 g and 2.84 g, respectively) dissolved in 1 N sodium hydroxide (23.0 ml) similarly gave 880 mg of a crude mixture of 1-methyl-2-phenyl-4-chloro-5-bromo-pyrazol-4-in-3-one *7d* and 1-phenyl-2-methyl-4-chloro-5-bromo-pyrazol-4-in-3-one *13d* in the ratio 1:2.85 as shown by NMR-spectroscopy. The product was dissolved in ethyl acetate and filtered through activated carbon. The ethyl acetate was removed and the mixture was chromatographed on silica gel (56 g) as described in the preceding experiment. This afforded 185 mg (17 %) of *7d*, m.p. 117 – 124°C, and 479 mg (45 %) of *13d*, m.p. 117 – 120°C. Filtration through activated carbon and recrystallization as described in the preceding experiment afforded 140 mg (13 %) of 1-methyl-2-phenyl-4-chloro-5-bromo-pyrazol-4-in-3-one *7d* as colourless crystals, m.p. 131°C. (Found: C 41.67; H 2.71; Br 27.95; Cl 12.28. Calc. for $C_{10}H_8N_2OBrCl$: C 41.75; H 2.81; N 9.74; Br 27.79; Cl 12.33). The yield of 1-phenyl-2-

methyl-4-chloro-5-bromo-pyrazol-4-in-3-one *13d* was 428 mg (40 %) after purification. Colourless crystals, m.p. 133 – 134°C. (Found: C 41.92; H 2.89; N 9.54; Br 27.85; Cl 11.25).

Dehalogenation of 1-benzyl-2-methyl-4-bromo-pyrazol-4-in-3-one. 16b (195 mg) was dehalogenated as described for [1-methyl-3-phenyl-5-bromo-4-(1,2,3-triazolio)]oxide [1] using 60 mg of palladium on charcoal and 119 mg of sodium borohydride. The acidification was omitted. The crude product was dissolved in ethyl acetate and filtered through activated carbon. Removal of the ethyl acetate afforded 123 mg (90 %) of 1-benzyl-2-methyl-pyrazol-4-in-3-one *16a*, m.p. 52 – 54°C. IR- and NMR-spectra proved the identity with the material described previously.[5]

Dehalogenation of 1-benzyl-2-methyl-4,5-dibromo-pyrazol-4-in-3-one. Similarly, *13b* (95 mg), palladium on charcoal (26 mg), and sodium borohydride (47 mg) produced 32 mg (62 %) 1-benzyl-2-methyl-pyrazol-4-in-3-one *16a*, identical with the material described previously.[5]

Dehalogenation of 1-phenyl-2-methyl-4,5-dibromo-pyrazol-4-in-3-one. Similarly, *13e* (287 mg), palladium on charcoal (71 mg), and sodium borohydride (137 mg) produced 145 mg (96 %) of 1-phenyl-2-methyl-pyrazol-4-in-3-one *16c*, m.p. 115 – 117°C, identical with the material described previously.[5]

REFERENCES

1. Begtrup, M. *Acta Chem. Scand.* **25** (1971) 249.
2. Begtrup, M. *Acta Chem. Scand.* **25** (1971) 795.
3. Begtrup, M. and Venø Poulsen, K. *Acta Chem. Scand.* **25** (1971) 2087.
4. Begtrup, M. *Acta Chem. Scand.* **24** (1970) 1819.
5. Begtrup, M. *Acta Chem. Scand.* **27** (1973) 2051.
6. Begtrup, M. *To be published.*

Received April 18, 1973.

ACTA CHEMICA SCANDINAVICA 27 (1973) 2941–2944

A Versatile Synthesis of α-Allenic Alcohols*

ALF CLAESSON, LARS-INGE OLSSON and CONNY BOGENTOFT

Department of Organic Chemistry, Faculty of Pharmacy, Box 6804 S-113 86 Stockholm, Sweden

The reaction of 4-alkoxy-2-butynols with $LiAlH_4$ afford α-allenic alcohols in good yields. Various types of alkoxy groups (*e.g.* methoxy, propoxy, *t*-butoxy, allyloxy, and diethylaminoethoxy) function well as leaving groups in this reaction. The number of easily obtainable α-allenic alcohols is extended by a procedure based upon this principle.

The reaction between $LiAlH_4$ and acetylenic derivatives of type I (*cf.* Scheme 1) affords α-allenic alcohols in good to excellent yields *via* an S_N2' reaction, X serving as a leaving group. To date, the following derivatives of type I have been explored: X = Cl[1,2], 2-tetrahydropyranyloxy (THP-oxy),[3] and R_3N^+.[4] The THP-derivatives have been most frequently used owing to the general applicability of their use and their convenient synthesis.[5,6]

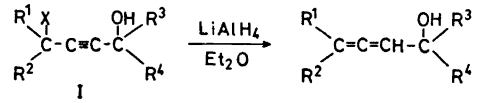

I

Scheme 1.

In this paper we report that equally good results are obtained with ordinary alkoxy groups as leaving groups. This makes the method more versatile and useful.

The acetylenic derivatives IIb – IId afforded the allenic alcohols IIIb and IIId upon treatment with $LiAlH_4$ in ether. The yields in these reactions (*cf.* Table 1) are comparable to that obtained by the original method[3] (IIa – IIIa). The acetylenic alcohols (IIb – IId) were obtained by reacting the Grignard derivatives of the corresponding acetylenic ethers (*e.g.* VII) with an appropriate ketone. The ethers required were prepared according to two principal routes, using acidic or basic conditions.

* Allenes and Acetylenes III. Part II: Olsson, L-I., Claesson, A. and Bogentoft, C. *Acta Chem. Scand.* **27** (1973) 1629.

Table 1.

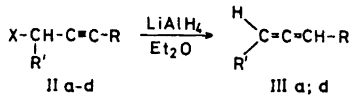

II a-d III a; d

Compound	X	R′	R	Yield %[a]
a	THP -oxy	H		72[7]
b	n-C_3H_7O	H		65
c	t-C_4H_9O	H		67
d	$(C_2H_5)_2N-(CH_2)_2O$	n-C_3H_7	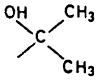	70

[a] After distillation.

Catalysis by strong acids is used in the synthesis of THP-derivatives applied in the method by Cowie *et al.*[3] On the other hand, no acidic conditions are necessary at any stage in the preparation of IIb and IId. The ethers used here (*e.g.* VII) were prepared according to the Williamson method.

Especially, *t*-butyl ethers offer some advantages over the corresponding THP-derivatives: (i) lower boiling points, (ii) *t*-butyl ethers can easily be obtained through the acid catalyzed addition of isobutene to primary and secondary propargylic alcohols,[8] (iii) the absence of an asymmetric center may be advantageous in special cases.

The method by Cowie *et al.*[3] requires a suitable acetylenic alcohol as starting material but the commercial availability of such compounds is limited. Thus it is usually necessary first to synthesize the desired acetylenic alcohol which makes the over-all route to the allenic alcohols tedious. In Scheme 2 we present a procedure which avoids this drawback of the THP-method and extends the number of easily obtainable α-allenic alcohols. A similar procedure, where a CH_3O functions as leaving group, was used for the synthesis of 6,6-dimethoxy-4-methyl-2,3-hexadienol (IX) from 4,6,6-trimethoxy-4-methyl-2-hexynol (VIII).

Reaction of magnesium halide alcoholates with halides in pure HMPA has been reported.[9] We used a mixture of THF and HMPA with good result in the present case (*cf.* Scheme 2).

EXPERIMENTAL. GENERAL

IR and NMR spectra were routinely recorded and in agreement with the expected structures. IR-spectra were run on a Perkin-Elmer 157 G spectrophotometer using liquid films on NaCl discs. NMR-spectra were obtained in $CDCl_3$ with a Varian A 60

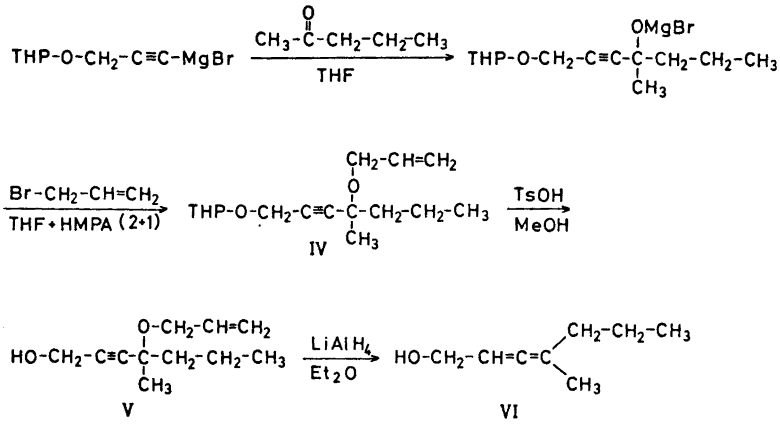

Scheme 2.

spectrometer and with tetramethylsilane as internal standard. Mass spectra were run on an AEI MS-30 mass spectrometer connected to a Pye 104 gas chromatograph. The ionizing energy was maintained at 70 eV, the accelerating energy at 4 kV, and the temperature of the ion source at 200°C.

Elemental analyses were performed in the laboratories of Dr. A. Bernhardt, Mülheim, West Germany. All reactions where Grignard reagents and $LiAlH_4$ were used, were performed under nitrogen.

1-(3-Propoxy-1-propynyl)cyclohexanol (IIb). To the Grignard reagent from magnesium (2.6 g, 0.107 mol) and ethyl bromide (11.7 g, 0.107 mol) in 100 ml of THF were added propyl propargyl ether (0.09 mol) with stirring during 15 min. After stirring for another 15 min, cyclohexanone (8.0 g, 0.082 mol) in 30 ml of THF was added during 20 min. Stirring was continued for 1 h and the reaction mixture poured on ice and the product taken up in light petroleum-ether (1:1), which was washed several times with saturated NH_4Cl, dried over Na_2SO_4-K_2CO_3 and distilled. B.p. 85°/0.15 mmHg. Yield: 68 %. (Found: C 73,2; H 9.9. Calc. for $C_{12}H_{20}O_2$: C 73.4; H 10.3).

1-(3-t-Butoxy-1-propynyl)cyclohexanol (IIc) was prepared similarly from *t*-butyl propargyl ether.[8] Yield: 69 %. B.p. 90°/0.15 mmHg. NMR ($CDCl_3$) δ (ppm) = 4.05 (s, 2 H), 2.70 (s, 1 H), 1.9 – 1.2 (m, 10 H), 1.18 (s, 9 H).

1-Propadienylcyclohexanol (IIIa).[7] IIc (3.3 g, 0.0157 mol) in 10 ml of ether was slowly added to an ice-cold, stirred mixture of $LiAlH_4$ (0.7 g, 0.0185 mol) in 40 ml of ether. The mixture was refluxed for 45 min and then cautiously poured on ice and taken up in ether, which was washed with saturated NH_4Cl and dried over Na_2SO_4-K_2CO_3. Distillation yielded 1.45 g (67 %) of IIIa. B.p. 93°/16 mmHg. IIIa was similarly prepared from IIb in 65 % yield.

3-(2-Diethylaminoethoxy)hexyne (VII). To a stirred suspension of 3.0 g (0.123 mol) of NaH in 100 ml of DMF was added dropwise 9.6 g (0.082 mol) of diethylaminoethanol at 0° during 15 min. The solution was stirred for another 2 h at 50° and then cooled to −40°. A solution of 15.6 g (0.082 mol) of tosyl chloride in 100 ml of benzene was added dropwise and stirring was continued for 2 h at −40°. An ice-cold solution of the sodium salt of 1-hexyn-3-ol, prepared from the alcohol (9.6 g, 0.098 mol) and NaH (2.6 g, 0.11 mol) in 100 ml of DMF, was then added and stirring continued overnight. The solution was then poured on ice and the product taken up in light petroleum, washed twice with 25 % Na_2SO_4, twice with water, dried over Na_2SO_4 and distilled. B. p. 105°/15 mmHg. Yield: 45 %. IR: 3310 cm^{-1} (≡C–H), 2100 cm^{-1} (–C≡C–). NMR: δ (ppm) 4.10 – 3.17 (m, 3 H), 2.77 – 2.28 (m, 7 H), 1.77 – 0.75 (m, 13 H).

5-(2-Diethylaminoethoxy)-2-methyl-3-octyn-2-ol (IId). To the Grignard reagent prepared in ether from magnesium (1.56 g, 0.064 mol) and ethyl bromide (6.5, 0.06 mol)

was added 75 ml of THF. A solution of VII (10 g, 0.051 mol) in 50 ml of THF was then added dropwise to the stirred solution at 15 – 20° during 0.5 h. The solution was stirred for another 15 min at room temperature and 2.7 g (0.0456 mol) of acetone in 25 ml of THF was added during 0.5 h. The mixture was kept at 50° for 5 h. After cooling, the reaction mixture was poured on ice. The alcohol was taken up in ether, washed twice with 25 % Na_2SO_4, twice with water, dried over Na_2SO_4 and distilled. B. p. 110°/1 mmHg. Yield: 50 %. IR: 2230 cm^{-1} (–C≡C–). NMR: δ (ppm) 4.40 (s, 1 H), 4.10 – 3.20 (m, 3 H), 2.76 – 2.30 (m, 6 H), 1.71 – 0.75 (m, 13 H), 1.46 (s, 6 H).

2-Methyl-3,4-octadien-2-ol (IIId). Prepared as described for 1-propadienylcyclohexanol (IIIa) from 6.0 g (0.024 mol) of IId. B.p. 82 – 86°/18 mmHg. Yield: 70 %. IR: 1960 cm^{-1} (C=C=C). (Found: C 76.9; H 11.4. Calc. for $C_9H_{16}O$: C 77.1; H 11.5).

4-Allyloxy-4-methyl-1-(tetrahydro-2-pyranyloxy)-2-heptyne (IV). To the Grignard reagent prepared in ether from magnesium (5.0 g, 0.206 mol) and ethyl bromide (22.4 g, 0.206 mol) was added 100 ml of THF. The solution was stirred at 15 – 20° and 3-(tetrahydro-2-pyranyloxy)propyne (22.6 g, 0.162 mol) in 100 ml of THF added during 20 min. The solution was stirred for another 15 min at room temperature and 12.6 g (0.147 mol) of 2-pentanone in 25 ml of THF was added during 1 h. Stirring was continued for 2 h at room temperature. To the solution was then added 21.4 g (0.177 mol) of allyl bromide in 25 ml of THF and 100 ml of HMPA. The mixture was refluxed (80°) for 5 h and poured on ice. The product was taken up in light petroleum, washed several times with 25 % $(NH_4)_2SO_4$, twice with water, dried over Na_2SO_4 and distilled. B.p. 126 – 132°/ 1 mmHg. Yield: 91 %. (Found: C 72.0; H 9.7. Calc. for $C_{16}H_{26}O_3$: C 72.1; H 9.8).

4-Allyloxy-4-methyl-2-heptynol (V). A solution of 3 g (0.0113 mol) of IV, 15 ml of methanol, and 50 mg of *p*-toluenesulfonic acid was stirred at room temperature for 10 h. The solution was diluted with light petroleum and ether (1:1), the organic phase was washed several times with water, dried over K_2CO_3 and distilled. B.p. 120°/4 mmHg. Yield: 90 %. (Found: C 72.2; H 9.9. Calc. for $C_{11}H_{18}O_2$: C 72.5; H 9.9).

4-Methyl-2,3-heptadienol (VI) was prepared as described for IIIa from 2.1 g (0.0115 mol) of V. B.p. 165 – 170°/760 mmHg. Yield: 60 %. (Found: C 75.9; H 11.0. Calc. for $C_8H_{14}O$: C 76.1; H 11.2).

4,6,6-Trimethoxy-4-methyl-2-hexynol (VIII) was prepared as described for V from 3-(tetrahydro-2-pyranyloxy)propyne (35.0 g, 0.25 mol) and acetoacetaldehyde dimethyl acetal (29.7 g, 0.225 mol) and dimethyl sulphate (46.2 g, 0.366 mol). Distillation (b.p. 116°/0.15 mmHg) yielded 74 % of the THP – protected intermediate, which was methanolyzed as above (*cf.* V). The over-all yield from the ketone was 69 %. B.p. 100°/0.4 mmHg. (Found: C 59.4; H 9.0. Calc. for $C_{10}H_{18}O_4$: C 59.4; H 9.0).

6,6-Dimethoxy-4-methyl-2,3-hexadienol (IX) was prepared from VIII (2.3 g, 0.013 mol) as described for IIIa. Yield: 70 % IR: 1960 cm^{-1} (C=C=C). NMR: δ (ppm) = 5.30 – 4.25 (m, 1 H), 4.40 (t, 1 H, J = 5.5 Hz), 3.94 (d, 2 H), 3.23 and 3.22 (two s, 6 H), 3.0 (s, 1 H), 2.20 (d, 2 H, J = 5.5 Hz, further split into doublets. J = 2.5 Hz), 1.70 (d, 3 H, J = 2.5 Hz). Mol.wt. 172 (MS).

Acknowledgement. We are indebted to Professor Bengt Danielsson for his kind interest in this work and for valuable discussions. This work has been supported financially by the *Swedish Natural Science Research Council.*

REFERENCES

1. Bailey, W. J. and Pfeifer, C. R. *J. Org. Chem.* **20** (1955) 1337.
2. Landor, P. D., Landor, S. R. and Pepper, E. S. *J. Chem. Soc.* **C 1967** 185.
3. Cowie, J. S., Landor, P. D. and Landor, S. R. *Chem. Commun.* **1969** 541.
4. Galantay, E. and Habeck, D. Belg. Pat. No. 742,137 (1969).
5. Biollaz, M., Landeros, R. M., Cuellar, L., Crabbé, P., Rocks, W., Edwards, J. A. and Fried, J. H. *J. Med. Chem.* **14** (1971) 1190.
6. Johnson, A. L. *J. Med. Chem.* **15** (1972) 854.
7. Claesson, A. and Bogentoft, C. *Acta Chem. Scand.* **26** (1972) 2540.
8. Mantione, R. *Bull. Soc. Chim. France* **1969** 4523.
9. Combret, J.-C. and Leroux, Y. *Compt. Rend.* **C 266** (1968) 1178.

Received April 28, 1973.

ACTA CHEMICA SCANDINAVICA 27 (1973) 2945–2954

The Crystal Structure of 1,4-Ethyleno-2,8-dihydroxy-2,4,6,8-tetramethyl-octahydronaphthal-5-en-3,7-dione

BENGT KARLSSON, ANNE-MARIE PILOTTI and ANNE-CHARLOTTE WIEHAGER

Institute of Inorganic and Physical Chemistry, University of Stockholm, S-104 05 Stockholm 50, Sweden

The crystal structure of 1,4-ethyleno-2,8-dihydroxy-2,4,6,8-tetramethyl-octahydronaphthal-5-en-3,7-dione, $C_{16}H_{20}O_4$, has been determined by three-dimensional single crystal X-ray diffraction methods. The monoclinic unit cell, $P2_1/c$, has lattice parameters $a = 8.470$, $b = 12.080$, $c = 14.995$ Å, $\beta = 108.69°$. The intensities of 2804 independent reflexions were measured by using the $\theta - 2\theta$ scan mode with a Siemens automatic diffractometer and monochromatized Cu$K\alpha$ radiation. The structure was solved by direct methods and refined to an R value of 0.066 for 2076 observed independent reflexions.

The compound is a Diels-Alder dimer of 2,6-dimethyl-*o*-quinol obtained by periodate oxidation of 2,6-dimethylphenol. The rather strained structure has C(sp^3)–C(sp^3) bond lengths of 1.589 and 1.554 Å, respectively, for the bonds C(4)–C(4a) and C(4a)–C(8a).

Oxidation of certain xylenols with sodium periodate results in the formation of *o*-quinols which undergo Diels-Alder dimerisation to yield substituted 1,4-ethylenonaphthalenes. Several isomeric dimers can arise but usually only one is observed. The steric orientation of these substituted 1,4-ethylenonaphthalenes have been discussed by Adler *et al.*[1,2] and structures have been proposed on the basis of chemical and spectral evidence as well as from considerations of steric requirements.

An X-ray analysis of the title compound has been undertaken as part of a program concerning crystal structure studies of Diels-Alder dimerisation of *o*-quinols.

EXPERIMENTAL

Crystal data from X-ray photographs and diffractometer measurements are summarized in Table 1. One molecule constitutes the asymmetric unit. Intensity data were collected on a Siemens four circle diffractometer with graphite-monochromatized Cu$K\alpha$ radiation by a $\theta - 2\theta$ scan technique in which the scan width was 150 steps of 0.01° in

θ and 0.02° in 2θ, at 0.6 sec per step. The reflexions were measured twice. Stationary background counts were taken for 90 sec at each end of the scan. By this method 2804 reflexions were measured out to $\theta = 70°$. The net intensities, I_{net}, and their estimated standard deviations, $\sigma(I_{net})$, based on counter statistics, were calculated. Only the 2076 most significant reflexions with $\sigma(I_{net})/I_{net} \leq 0.25$ were used in the subsequent calculations. The data were corrected for Lorentz and polarization factors but no correction for absorption was made. Two irregular crystals of approximate volumes 0.011 mm³ and 0.0053 mm³ were mounted with the b axis coincident with the ϕ axis of the diffractometer. The crystals deteriorated in the X-ray beam during the data collection. Three monitor reflexions measured at intervals of 40 reflexions showed a deviation of about 15 % in intensity on both crystals. Individual reflexions were corrected for this loss by fitting a linear function of time to the intensity of the monitor reflexions.

Table 1. Crystallographic data (estimated standard deviations in parentheses).

Space group $P2_1/c$
$a = 8.470(5)$ Å
$b = 12.080(7)$ Å
$c = 14.995(6)$ Å
$\beta = 108.69(7)°$
$Z = 4$

Graphite-monochromatized Cu$K\alpha$ radiation, 1.5418 Å.
Chemical formula $C_{16}H_{20}O_4$.
Calculated density 1.261 g cm^{-3}.

STRUCTURE DETERMINATION AND REFINEMENT

The absolute scale and the overall temperature factor for calculation of normalized structure factor magnitudes $|E|$ were estimated by Wilson's method.[3] The structure was solved by use of the MULTAN system.[4] Four combinations of signs of two reflexions as variables (in addition to three origin determining reflexions) were used to calculate probable phases for the 187 reflexions whose $|E|$ values were ≥ 1.90. The starting set of phases is given in Table 2. One combination of signs was better than the rest. This solution had a consistency index of 0.79. The E map of this best $|E|$ set yielded the coordinates of 17 out of the 20 non-hydrogen atoms in the asymmetric unit. The remaining three atoms were located from a difference Fourier synthesis. Introduction of anisotropic thermal parameters for all the non-hydrogen atoms

Table 2. Starting phase set.

h			$\|E_h\|$	Starting phase value	Correct phase value
2	3	−6	3.18	0	0
5	6	3	3.67	0	0
3	10	−6	3.12	0	0
9	5	−9	3.02	0,π	0
3	8	−7	3.27	0,π	0

Table 3. Observed and calculated structure amplitudes. The columns contain the index k, $10|F_o|$ and $10|F_c|$. The reflexions marked with an asterisk were not included in the refinement.

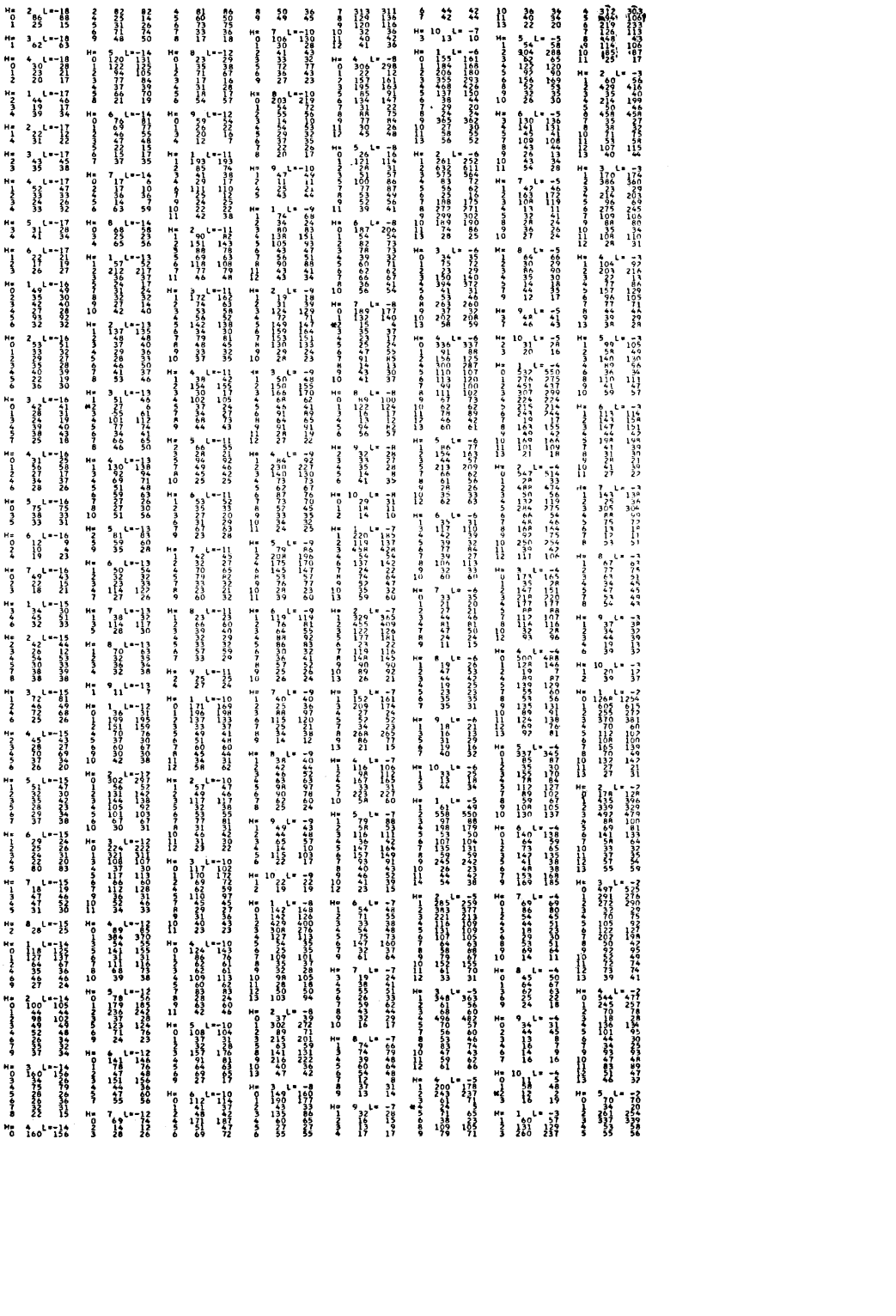

Table 3. Continued.

into the fullmatrix least-squares refinement reduced R to 0.117. The scattering factors of Freeman [5] were used for all atoms except hydrogens for which the scattering factors were those of Stewart, Davidson and Simpson.[6] All 20 hydrogen atoms showed well defined peaks in a difference Fourier synthesis. The hydrogens, given fixed isotropic thermal parameters equal to those of their parent atoms, were included in the refinement. 2076 reflexions were used in the refinement and Hughes' [7] weighting procedure with $F_{o,min} = 1.5$ was applied. The R value reduced to 0.066.

RESULTS

Observed and calculated structure factors are presented in Table 3, atomic coordinates and thermal parameters in Tables 4 and 5 and bond distances and angles involving the non-hydrogen atoms in Tables 6 and 7. Correction for thermal motion was not applied in the calculation of bond lengths and

Table 4. Positional and anisotropic thermal parameters of the non-hydrogen atoms. The β-values refer to the temperature factor expression exp $[-(h^2\beta_{11}+k^2\beta_{22}+l^2\beta_{33}+hk\beta_{12}+hl\beta_{13}+kl\beta_{23})]$. Estimated standard deviations are given in parentheses.

	$x\times10^4$	$y\times10^4$	$z\times10^4$	$\beta_{11}\times10^4$	$\beta_{22}\times10^4$	$\beta_{33}\times10^4$	$\beta_{12}\times10^4$	$\beta_{13}\times10^4$	$\beta_{23}\times10^4$
C(1)	8992(4)	1867(2)	4475(2)	167(5)	51(2)	35(2)	2(4)	58(4)	8(3)
C(2)	9724(4)	3040(3)	4711(2)	180(5)	59(2)	40(2)	−15(5)	71(4)	−11(3)
C(3)	9523(4)	3603(3)	3759(2)	183(5)	54(2)	48(2)	−21(5)	93(4)	−11(3)
C(4)	8930(4)	2846(2)	2908(2)	195(5)	56(2)	39(2)	−25(5)	88(4)	−3(3)
C(4a)	7108(4)	2473(3)	2867(2)	156(5)	59(2)	45(2)	42(5)	48(4)	20(3)
C(5)	6504(4)	1664(4)	2067(3)	197(6)	121(4)	40(2)	−63(7)	32(5)	6(4)
C(6)	6203(4)	599(3)	2132(3)	170(6)	102(3)	58(2)	−50(6)	46(5)	−39(4)
C(7)	6296(4)	153(3)	3059(3)	153(5)	66(3)	66(2)	−33(5)	26(5)	−11(3)
C(8)	6079(4)	973(3)	3777(2)	161(5)	86(3)	53(2)	−46(6)	67(5)	11(3)
C(8a)	7158(4)	2015(3)	3844(2)	146(5)	57(2)	46(2)	11(4)	81(4)	−4(3)
C(9)	9983(4)	1294(3)	3929(2)	144(5)	58(2)	55(2)	28(5)	44(4)	−6(3)
C(10)	9980(4)	1805(3)	3152(2)	149(5)	73(2)	54(2)	3(5)	86(4)	−34(3)
C(11)	11552(5)	3046(4)	5324(3)	211(7)	89(3)	58(2)	−50(7)	47(6)	−19(4)
O(12)	8737(3)	3615(2)	5168(2)	260(5)	74(2)	57(2)	−49(4)	137(4)	−46(2)
O(13)	9757(4)	4580(2)	3695(2)	406(7)	57(2)	64(2)	−88(5)	152(5)	−15(2)
C(14)	8996(6)	3429(4)	2018(3)	332(9)	78(3)	49(2)	−64(8)	142(7)	−1(4)
C(15)	5818(8)	−189(5)	1310(4)	321(11)	159(6)	78(3)	−159(12)	80(9)	−97(7)
O(16)	6394(4)	−833(2)	3234(3)	334(7)	76(2)	100(2)	−38(6)	10(6)	−9(3)
C(17)	4239(5)	1303(4)	3468(4)	175(7)	131(4)	113(4)	−57(8)	150(8)	−28(6)
O(18)	6508(4)	462(3)	4677(2)	317(6)	122(3)	67(2)	−158(7)	112(5)	34(3)

angles. Conformationally significant least-squares planes are given in Table 8, and intermolecular distances shorter than 3.8 Å in Table 9. Fig. 1 shows the numbering convention and all bond lengths of the non-hydrogen atoms. Fig. 2 is a perspective view [8] of the molecule. Fig. 3 is a projection of the crystal structure along the b axis.

Table 5. Positional and isotropic thermal parameters of the hydrogen atoms, with estimated standard deviations in parentheses.

	$x \times 10^3$	$y \times 10^3$	$z \times 10^3$	$B \times 10^2$ Å^2
H(C1)	903(3)	155(3)	500(2)	273
H(C4a)	657(4)	302(3)	273(2)	336
H(C5)	634(4)	194(3)	150(3)	441
H1(C8)	381(6)	165(4)	289(3)	647
H2(C8)	413(6)	170(4)	397(3)	647
H3(C8)	350(4)	61(3)	352(2)	647
H(C8a)	672(4)	256(3)	409(2)	287
H(C9)	1054(4)	62(3)	414(2)	331
H(C10)	1055(4)	154(3)	276(2)	345
H1(C11)	1194(5)	382(3)	545(3)	467
H2(C11)	1167(5)	267(3)	589(3)	467
H3(C11)	1220(5)	260(3)	505(3)	467
H(O12)	924(5)	405(3)	547(3)	391
H1(C14)	881(4)	299(3)	154(3)	431
H2(C14)	1016(4)	385(3)	213(3)	431
H3(C14)	804(5)	392(3)	181(3)	431
H1(C15)	589(6)	27(4)	68(3)	678
H2(C15)	465(6)	−34(4)	118(3)	678
H3(C15)	658(6)	−74(4)	143(4)	678
H(O18)	624(5)	−18(4)	458(3)	544

Table 6. Bond distances (Å) involving the non-hydrogen atoms, with estimated standard deviations in parentheses.

C(1)−C(2)	1.542(4)	C(4a)−C(5)	1.505(4)
C(1)−C(8a)	1.549(4)	C(4a)−(8a)	1.554(4)
C(1)−C(9)	1.515(4)	C(5)−C(6)	1.321(5)
C(2)−C(3)	1.539(4)	C(6)−C(7)	1.470(4)
C(2)−C(11)	1.528(4)	C(6)−C(15)	1.507(6)
C(2)−O(12)	1.420(3)	C(7)−C(8)	1.517(4)
C(3)−C(4)	1.519(4)	C(7)−O(16)	1.217(4)
C(3)−O(13)	1.205(3)	C(8)−C(8a)	1.540(4)
C(4)−C(4a)	1.589(4)	C(8)−C(17)	1.531(5)
C(4)−C(10)	1.517(4)	C(8)−O(18)	1.420(4)
C(4)−C(14)	1.526(4)	C(9)−C(10)	1.318(4)

DISCUSSION

The structural and conformational features of the dimer are illustrated in Fig. 2. The result is in agreement with the stereochemical considerations discussed by Adler *et al.*[1] A rewiew of the theory concerning Diels-Alder dimerisation, in conjunction with results from X-ray structure determinations, has been presented by Karlsson *et al.*[9] Most bond lengths in this structure are in agreement with usually observed values.[10] C(4)−C(4a) (1.589 Å) and C(4a)−C(8a) (1.554 Å) are, however, significantly longer ($\sim 5\sigma$ and $\sim 13\sigma$, respec-

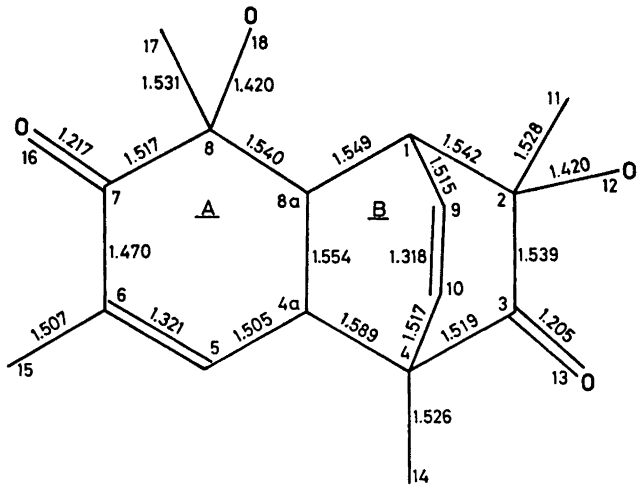

Fig. 1. Bond distances in the molecule

tively) than the average value, 1.536 Å, of the other C(sp^3)–C(sp^3) bonds in the structure. This is probably due to internal strain in the molecule. Effects of conjugation are apparent in the C(6)–C(7) bond adjacent to double bonds. The average value of the C(sp^2)–C(sp^3) bonds is 1.517 Å; $\sim 4\sigma$ longer than the accepted value of 1.50 Å.[11] This can probably be explained by the fact that

Table 7. Bond angles (°) involving non-hydrogen atoms, with estimated standard deviations in parentheses.

C(2)–C(1)–C(8a)	106.6 (2)	C(5)–C(4a)–C(8a)	114.9 (3)
C(2)–C(1)–C(9)	107.0 (3)	C(4a)–C(5)–C(6)	126.7 (3)
C(8a)–C(1)–C(9)	110.1 (2)	C(5)–C(6)–C(7)	118.3 (3)
C(1)–C(2)–C(3)	106.1 (2)	C(5)–C(6)–C(15)	123.4 (4)
C(1)–C(2)–C(11)	113.5 (3)	C(7)–C(6)–C(15)	118.3 (4)
C(1)–C(2)–O(12)	107.7 (3)	C(6)–C(7)–C(8)	116.8 (3)
C(3)–C(2)–C(11)	110.2 (3)	C(6)–C(7)–O(16)	122.8 (3)
C(3)–C(2)–O(12)	108.9 (3)	C(8)–C(7)–O(16)	120.1 (3)
C(11)–C(2)–O(12)	110.3 (3)	C(7)–C(8)–C(8a)	112.1 (3)
C(2)–C(3)–C(4)	114.9 (3)	C(7)–C(8)–C(17)	107.3 (3)
C(2)–C(3)–O(13)	122.3 (3)	C(7)–C(8)–O(18)	109.8 (3)
C(4)–C(3)–O(13)	122.7 (3)	C(8a)–C(8)–C(17)	109.4 (3)
C(3)–C(4)–C(4a)	105.0 (3)	C(8a)–C(8)–O(18)	109.1 (3)
C(3)–C(4)–C(10)	106.6 (3)	C(17)–C(8)–O(18)	109.1 (3)
C(3)–C(4)–C(14)	111.2 (3)	C(1)–C(8a)–C(4a)	109.7 (2)
C(4a)–C(4)–C(10)	105.2 (2)	C(1)–C(8a)–C(8)	113.8 (3)
C(4a)–C(4)–C(14)	113.8 (3)	C(4a)–C(8a)–C(8)	113.1 (3)
C(10)–C(4)–C(14)	114.2 (3)	C(1)–C(9)–C(10)	114.8 (3)
C(4)–C(4a)–C(5)	107.1 (3)	C(4)–C(10)–C(9)	115.9 (3)
C(4)–C(4a)–C(8a)	109.3 (2)		

Table 8. Least-squares planes and deviations. The planes are described in terms of axes (m, n, p) having $m \parallel a^*$, $n \parallel b$ and $p \parallel c$. The atoms indicated with asterisks were omitted from the calculations of the least-squares planes. Deviation in Å.

Plane A[a]		Plane B1[b]		Plane B2[c]		Plane B3[d]	
Atom	Deviation	Atom	Deviation	Atom	Deviation	Atom	Deviation
C(4a)	0.035	C(1)*	0.786	C(1)*	−0.736	C(1)*	0.627
C(5)	−0.035	C(2)	0.048	C(2)	0.034	C(4)*	0.752
C(6)	0.015	C(3)	−0.048	C(3)	−0.035	C(4a)	−0.040
C(7)	0.004	C(4)*	0.735	C(4)*	−0.628	C(8a)	0.040
C(8)*	−0.575	C(4a)	0.048	C(9)	−0.040	C(9)	−0.047
C(8a)	−0.018	C(8a)	−0.048	C(10)	0.040	C(10)	0.047

[a] Plane A : $0.9584m - 0.2400n - 0.1545p = 4.3480$.
[b] Plane B1: $0.9911m + 0.1331n - 0.0004p = 8.1852$.
[c] Plane B2: $0.3899m + 0.8450n + 0.3660p = 5.6554$.
[d] Plane B3: $0.5878m - 0.7254n - 0.3582p = 0.2892$.

Table 9. Intermolecular distances (Å) shorter than 3.8 Å, with estimated standard deviations in parentheses.

Code for symmetry related atoms.			
Superscript	Coordinates	Superscript	Coordinates
none	x,y,z	v	$2-x,1-y,1-z$
i	$1+x,y,z$	vi	$x,\frac{1}{2}-y,-\frac{1}{2}+z$
ii	$1-x,-y,-z$	vii	$1-x,\frac{1}{2}+y,\frac{1}{2}-z$
iii	$1-x,-y,1-z$	viii	$2-x,\frac{1}{2}+y,\frac{1}{2}-z$
iv	$2-x,-y,1-z$		

C(10) − C(17^{i})	3.537(5)	C(11) − O(13^{v})	3.559(4)
C(15) − C(15^{ii})	3.754(10)	O(12) − O(13^{v})	2.811(3)
C(17) − O(18^{iii})	3.716(6)	C(14) − O(12^{vi})	3.667(4)
O(18) − O(18^{iii})	3.209(6)	C(14) − O(18^{vi})	3.719(4)
C(9) − O(18^{iv})	3.706(4)	C(4a) − O(16^{vii})	3.547(4)
C(11) − O(16^{iv})	3.529(5)	O(13) − C(15^{viii})	3.761(7)
C(2) − O(13^{v})	3.675(3)		

many of the bonds involve a highly substituted carbon atom. The C − H bond distances range from 0.73 to 1.11 Å, mean value 0.92 Å, in good agreement with values found in some precisely determined X-ray structures.[6] The best plane for the ring A (Fig. 1) contains the atoms C(4a), C(5), C(6), C(7), and C(8a) which are coplanar within ± 0.035 Å. Atom C(8) deviates by 0.575 Å from the plane (Table 8). The rather strained ring system B consists of three boat-shaped rings, for which least-squares planes and deviations are given in Table 8. The A ring and the B ring system are connected in accordance with the *endo* rule.[12]

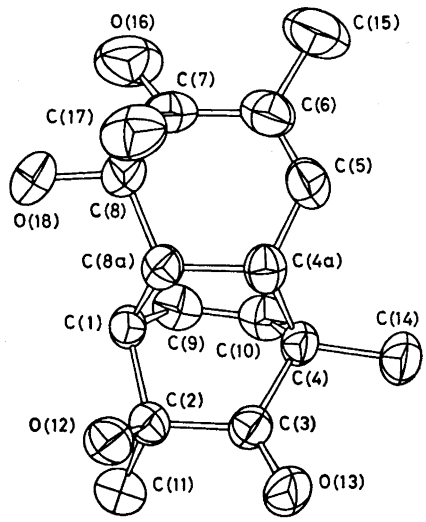

Fig. 2. A perspective view of the molecule.

An interaction, within the range of a possible intramolecular hydrogen bond, is observed between the hydroxyl group (18) and the ketone (16). The O(16)···H(O18) and O(16)···O(18) distances are 2.211 and 2.646 Å, respectively, and the O(16)···H(O18)−O(18) angle is 113.9°. The packing arrangement of the crystal viewed along the *b* axis is shown in Fig. 3. Those pairs of molecules related to each other by centers of symmetry at 0,0,0 and $0,\frac{1}{2},\frac{1}{2}$ form hydrogen bonded dimers. The O(13^{v})···H(O12) distance is 2.091 Å and the O(12)−H(O12)···O(13^{v}) angle is 169.4°. The intermolecular distances between the hydrogen bonded dimers are all longer than the sum of the van der Waals radii as shown in Table 9.

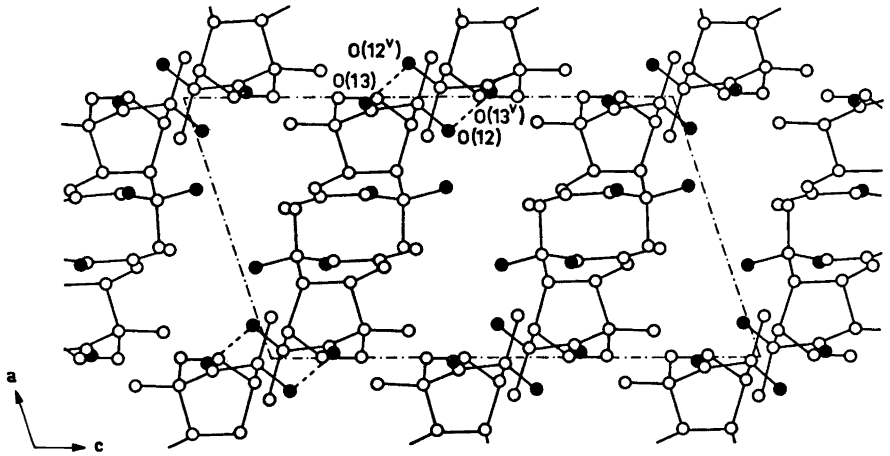

Fig. 3. Projection of the unit cell looking down the *b* axis. The dotted lines are hydrogen bonds. ○ carbon; ● oxygen.

This investigation has received financial support from the *Tri-Centennial Fund of the Bank of Sweden* and from the *Swedish Natural Science Research Council.*

The authors are indebted to Professor Peder Kierkegaard for his encouraging interest in this work and for the facilities placed at their disposal. Thanks are due to Dr. Bengt Lindgren for the supply of crystals used in the work and for valuable comments. Dr. Åke Pilotti is also thanked for valuable discussions and Dr. Don Koenig for his correction of the English of this paper.

REFERENCES

1. Adler, E., Brasen, S. and Miyake, H. *Acta Chem. Scand.* **25** (1971) 2055.
2. Adler, E. and Holmberg, K. *Acta Chem. Scand.* **25** (1971) 2775.
3. Wilson, A. J. C. *Nature*, **150** (1942) 151.
4. Germain, G., Main, P. and Woolfson, H. M. *Acta Cryst.* **B 26** (1970) 274.
5. Freeman, A. J. *Acta Cryst.* **12** (1959) 261.
6. Stewart, R. F., Davidson, E. R. and Simpson, W. T. *J. Chem. Phys.* **42** (1965) 3175.
7. Hughes, E. W. *J. Am. Chem. Soc.* **63** (1941) 1737.
8. Johnson, C. K. *ORTEP* Report *ORNL*-3794 (1965), Oak Ridge National Laboratory, Oak Ridge, Tennessee.
9. Karlsson, B., Kierkegaard, P., Pilotti, A.-M., Wiehager, A.-C. and Lindgren, B. *Acta Chem. Scand.* **27** (1973) 1428.
10. Sutton, L. E. *Tables of Interatomic Distances and Configuration in Molecules and Ions* (1965), Supplement 1956–1959. London: The Chemical Society.
11. Lide, D. R. *Tetrahedron* **17** (1962) 125.
12. Martin, J. G. and Hill, R. K. *Chem. Rev.* **61** (1961) 537.

Received April 18, 1973.

ACTA CHEMICA SCANDINAVICA 27 (1973) 2955–2964

The Crystal Structure of 1,4-Ethyleno-2,8-dihydroxy-2,4a,8,9-tetramethyl-octahydronaphthal-5-en-3,7-dione

BENGT KARLSSON, ANNE-MARIE PILOTTI and ANNE-CHARLOTTE WIEHAGER

Institute of Inorganic and Physical Chemistry, University of Stockholm, S-104 05 Stockholm 50, Sweden

The crystal structure of 1,4-ethyleno-2,8-dihydroxy-2,4a,8,9-tetramethyl-octahydronaphthal-5-en-3,7-dione, $C_{16}H_{20}O_4$, has been determined by single crystal X-ray diffraction analysis. The crystals are monoclinic, space group $P2_1/c$, with $a=12.421$, $b=7.142$, $c=16.412$ Å, $\beta=103.03°$, $Z=4$. The structure was solved by direct methods. The parameters were refined by a full-matrix least-squares method using 1540 observed intensities collected on the computer controlled Philips diffractometer PW 1100. The final R value is 0.044.

The compound is a Diels-Alder dimer of 2,4-dimethyl-*o*-quinol, obtained by periodate oxidation of 2,4-dimethylphenol. Two molecules of 2,4-dimethyl-*o*-quinol with the same absolute configuration about the tertiary carbon atom C(2) have dimerised. The structure is rather strained with $C(sp^3)-C(sp^3)$ bond lengths of 1.578 and 1.567 Å for the bonds C(4) – C(4a) and C(4a) – C(8a), respectively.

1,4-Ethyleno-2,8-dihydroxy-2,4a,8,9-tetramethyl-octahydronaphthal-5-en-3,7-dione is a dimer of 2,4-dimethyl-*o*-quinol, obtained by periodate oxidation of 2,4-dimethylphenol. Structures and steric orientations of Diels-Alder dimers of *o*-quinols have been discussed by Adler *et al.*[1,2] and X-ray structure determinations [3,4] have confirmed proposed structures based on chemical and spectral analysis.

The X-ray investigation of the title compound has been undertaken as part of a program concerning crystal structure studies of Diels-Alder dimerisation of *o*-quinols.

EXPERIMENTAL

Three-dimensional intensities were collected on the computer-controlled Philips diffractometer PW 1100, with monochromatized Cu$K\alpha$ radiation. A crystal of approximate volume 0.0047 mm³ was mounted arbitrarily on the diffractometer. Then 25 reflexions were found by the "Peak Hunting Program" and used by it to calculate the orientation matrix of the crystal relative to the coordinate system of the goniometer. The unit cell dimensions (Table 1) were derived from the matrix, the reflexions indexed, and the cell

dimensions then refined by the least-squares method. The moving crystal, moving counter method ($\omega/2\theta$) was used to measure the intensity data, 1.5° scans at 0.025°/sec, and background counts were recorded for 30 sec at the beginning and end of each scan. Three standard reflexions were monitored at intervals of approximately 1½ h. Of the 2673 reflexions with $2\theta < 130°$, 1540 had $\sigma(I)/I \leq 0.25$ and were used in the crystal structure refinements. The estimated standard deviation, $\sigma(I)$, of the net intensity, I, is based on counter statistics. Corrections were made for Lorentz and polarization factors, but not for absorption. An absolute scale factor and a mean isotropic temperature factor were estimated by Wilson's method [5] and normalized structure factor magnitudes $|E|$ were calculated.

Table 1. Crystal unit cell data. Figures in parentheses are calculated standard deviations.

Lattice constants	$a = 12.421(2)$ Å
	$b = 7.142(2)$ Å
	$c = 16.412(3)$ Å
	$\beta = 103.03(3)°$
Cell volume	$V = 1418.5$ Å^3
Calculated density	$d = 1.292$ g cm^{-3}
Molecules per unit cell	$Z = 4$
Space group	$P2_1/c$

STRUCTURE DETERMINATION AND REFINEMENTS

The structure was solved by using "variance-weighted" $\sum_2$-relationships, described by Norrestam.[6] Signs were determined for the 196 reflexions having $|E| \geq 1.75$. The starting set (Table 2) consisted of four variables and three origin-specifying reflexions. The E map corresponding to the solution with the highest "reliability index" displayed all the non-hydrogen atoms.

Table 2. Assignments of starting phases.

h			$\|E_h\|$	Starting phase value	Correct phase value
9	3	−2	4.97	0	0
3	3	−2	3.73	0,π	0
5	2	−13	3.40	0	0
10	3	0	3.37	0,π	0
6	3	−12	3.23	0	0
9	2	−6	3.10	0,π	0
0	6	1	3.03	0,π	π

Least-squares refinement was started with isotropic temperature factors, subsequent anisotropic cycles reduced R to 0.091. At this stage a difference Fourier synthesis revealed all the non-hydrogen atoms. After introduction of the hydrogen atoms with isotropic temperature factors, equal to those of the final isotropic values of their parent atoms, further refinement reduced the R value to 0.044.

The full-matrix least-squares refinements were performed by a modified version of program LALS.[7] Hughes' weighting scheme [8] was applied with $F_{o,min} = 3.3$. The atomic scattering factors for oxygen and carbon were taken from Freeman [9] and that for hydrogen from Stewart, Davidson and Simpson.[10]

Table 3. Observed and calculated structure amplitudes. The columns contain the index *l*, $10|F_o|$ and $10|F_c|$.

Table 3. Continued.

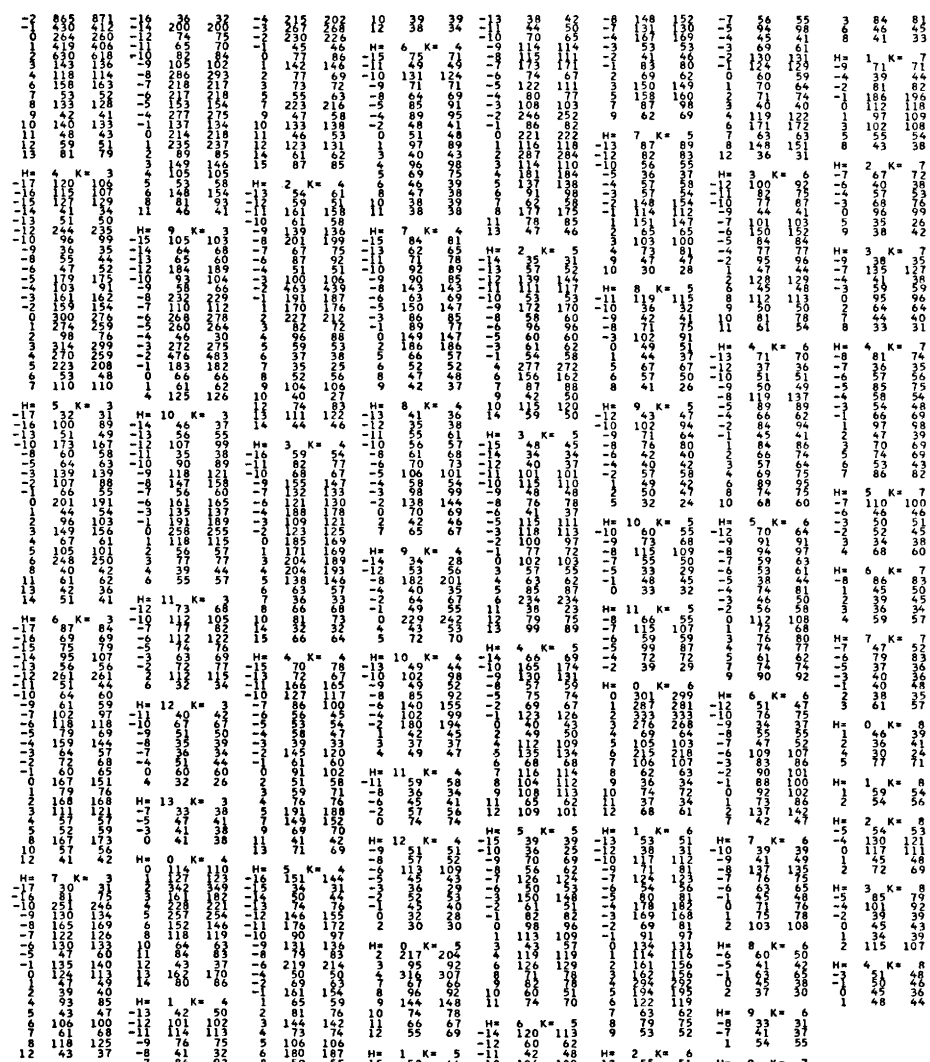

The observed and calculated structure factors are given in Table 3. The positional and thermal parameters of the non-hydrogen atoms with estimated standard deviations are listed in Tables 4 and 5, those for the hydrogen atoms in Table 6.

Table 4. Fractional atomic coordinates ($\times 10^4$) for non-hydrogen atoms with estimated standard deviations in parentheses.

	x	*y*	*z*
C(1)	2218(2)	5095(4)	3200(2)
C(2)	3164(2)	5571(4)	2768(2)
C(3)	3766(2)	3729(4)	2702(2)
C(4)	3260(2)	2065(4)	3044(2)
C(4a)	3323(2)	2411(4)	4003(2)
C(5)	2740(3)	744(4)	4272(2)
C(6)	1781(3)	790(4)	4487(2)
C(7)	1204(3)	2556(4)	4542(2)
C(8)	1932(3)	4293(4)	4664(2)
C(8a)	2743(2)	4330(4)	4082(2)
C(9)	1514(2)	3625(4)	2676(2)
C(10)	2071(2)	2075(4)	2593(2)
C(11)	2749(3)	6425(5)	1906(2)
O(12)	3905(2)	6811(3)	3291(2)
O(13)	4567(2)	3681(3)	2402(2)
C(14)	4545(3)	2423(6)	4465(3)
O(15)	234(2)	2647(4)	4554(2)
C(16)	2575(5)	4265(7)	5578(3)
O(17)	1294(3)	5939(3)	4503(2)
C(18)	329(3)	3979(6)	2273(3)

Table 5. Thermal parameters of the non-hydrogen atoms, with estimated standard deviations in parentheses. The β values refer to the temperature factor expression $\exp[-(h^2\beta_{11}+k^2\beta_{22}+l^2\beta_{33}+hk\beta_{12}+hl\beta_{13}+kl\beta_{23})]$. Values are $\times 10^4$.

	β_{11}	β_{22}	β_{33}	β_{12}	β_{13}	β_{23}
C(1)	49(2)	108(5)	32(1)	29(5)	35(2)	5(4)
C(2)	54(2)	118(5)	35(1)	0(5)	39(2)	1(4)
C(3)	52(2)	160(6)	38(1)	12(5)	43(3)	−8(4)
C(4)	58(2)	105(5)	41(2)	42(5)	36(3)	−8(4)
C(4a)	61(2)	126(5)	32(1)	1(5)	12(2)	18(4)
C(5)	87(3)	136(6)	35(1)	4(6)	17(3)	28(4)
C(6)	108(3)	132(6)	41(2)	−59(7)	56(3)	5(4)
C(7)	115(3)	188(6)	47(2)	−61(7)	106(4)	−27(5)
C(8)	135(3)	145(6)	40(2)	−55(7)	100(4)	−37(5)
C(8a)	70(2)	113(5)	26(1)	−44(5)	32(2)	−16(4)
C(9)	50(2)	153(6)	31(1)	−7(5)	19(2)	15(4)
C(10)	66(2)	142(5)	26(1)	−37(6)	28(2)	−23(4)
C(11)	96(3)	209(8)	46(2)	27(8)	58(4)	70(5)
O(12)	75(2)	176(4)	53(1)	−80(4)	71(2)	−25(3)
O(13)	95(2)	226(5)	91(2)	52(5)	135(3)	14(4)
C(14)	77(3)	241(8)	58(2)	8(8)	−18(4)	57(7)
O(15)	139(3)	254(6)	107(2)	−57(6)	180(4)	−59(5)
C(16)	246(8)	335(11)	39(2)	−261(15)	105(6)	−76(8)
O(17)	188(3)	173(5)	102(2)	10(6)	230(4)	−29(5)
C(18)	63(3)	231(8)	75(3)	−15(8)	−11(4)	37(7)

Table 6. Positional and isotropic thermal parameters of the hydrogen atoms, with estimated standard deviations in parentheses.

	$x \times 10^3$	$y \times 10^3$	$z \times 10^3$	$B \times 10^2$ Å^2
H(C1)	183(2)	618(4)	324(2)	240
H(C4)	363(2)	105(4)	297(2)	250
H(C5)	314(2)	−46(4)	422(2)	356
H(C6)	143(2)	−25(4)	457(2)	397
H(C8a)	331(2)	521(4)	431(2)	285
H(C10)	178(2)	108(4)	226(2)	276
H1(C11)	221(3)	572(4)	155(2)	419
H2(C11)	332(3)	666(4)	165(2)	419
H3(C11)	237(3)	762(5)	194(2)	419
H(012)	435(3)	719(4)	305(2)	322
H1(C14)	488(3)	129(5)	441(2)	521
H2(C14)	455(3)	258(5)	505(3)	521
H3(C14)	492(3)	349(5)	426(2)	521
H1(C16)	202(3)	435(6)	587(3)	728
H2(C16)	291(4)	316(6)	570(3)	728
H3(C16)	308(3)	472(6)	569(3)	728
H(O17)	92(3)	604(3)	480(2)	588
H1(C18)	30(3)	513(5)	190(2)	508
H2(C18)	0(3)	288(5)	194(2)	508
H3(C18)	−1(3)	420(5)	271(2)	508

RESULTS AND DISCUSSION

Fig. 1 is a perspective view of the molecule[11] with the atom numbering scheme. The Diels-Alder dimerisation of 2,4-dimethyl-*o*-quinol follows the *endo* addition rule.[12] The relative position of the two keto groups is such that

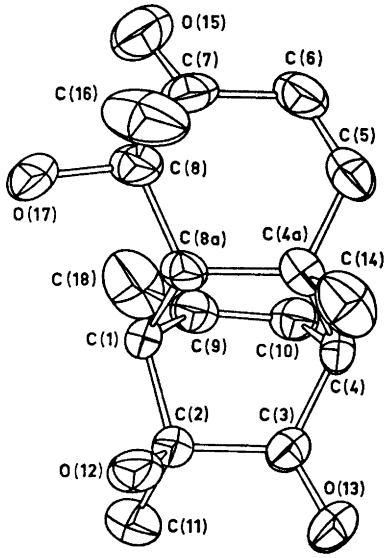

Fig. 1. A perspective view of the molecule.

the dipole moment of the transition state is lower than for any other structural isomers. This arrangement is favored according to Horner and Dürckheimer.[13] The configurations of the tertiary carbon atoms C(2) and C(8) reveal that the two molecules of 2,4-dimethyl-*o*-quinol which undergo dimerisation have the same configuration about the tertiary carbon atom C(2); this is probably a steric requirement.[14] The crystal structures of 1,4-ethyleno-2,8-dihydroxy-2,4,6,8-tetramethyl-octahydronaphthal-5-en-3,7-dione [15] and 1,4-ethyleno-2,8-dichloro-2,4,6,8-tetramethyl-octahydronaphthal-5-en-3,7-dione [16] have also been found upon X-ray investigation to follow the above mentioned rules.

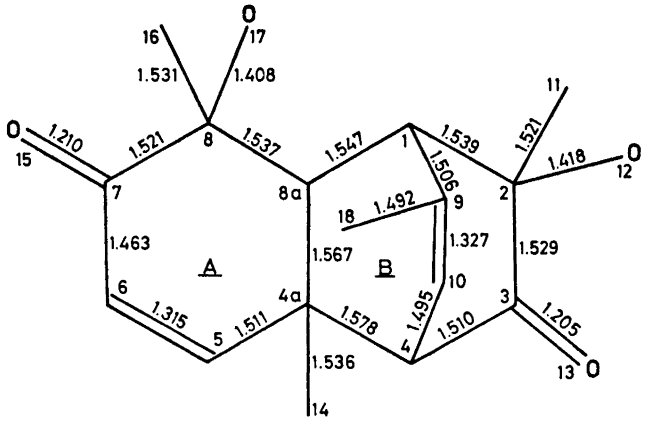

Fig. 2. Bond distances in the molecule.

Table 7. Bond distances (Å) involving the non-hydrogen atoms, with estimated standard deviations in parentheses.

C(1) – C(2)	1.539(3)	C(4a) – C(8a)	1.567(3)
C(1) – C(8a)	1.547(3)	C(4a) – C(14)	1.536(4)
C(1) – C(9)	1.506(3)	C(5) – C(6)	1.315(4)
C(2) – C(3)	1.529(3)	C(6) – C(7)	1.463(4)
C(2) – C(11)	1.521(4)	C(7) – C(8)	1.521(4)
C(2) – O(12)	1.418(3)	C(7) – O(15)	1.210(4)
C(3) – C(4)	1.510(3)	C(8) – C(8a)	1.537(4)
C(3) – O(13)	1.205(3)	C(8) – C(16)	1.531(5)
C(4) – C(4a)	1.578(4)	C(8) – O(17)	1.408(4)
C(4) – C(10)	1.495(3)	C(9) – C(10)	1.327(3)
C(4a) – C(5)	1.511(4)	C(9) – C(18)	1.492(4)

The bond distances for the molecule are displayed in Fig. 2. Corrections for thermal motion were not applied in the calculation of bond lengths or angles (Tables 7 and 8). The average estimated standard deviations in bond lengths and angles involving non-hydrogen atoms are 0.0036 Å and 0.3°. Most

Table 8. Bond angles (°) involving non-hydrogen atoms, with estimated standard deviations in parentheses.

C(2) – C(1) – C(8a)	107.7(2)	C(7) – C(8) – C(8a)	112.6(3)
C(2) – C(1) – C(9)	107.1(2)	C(7) – C(8) – C(16)	106.4(3)
C(8a) – C(1) – C(9)	110.8(2)	C(7) – C(8) – O(17)	111.3(3)
C(1) – C(2) – C(3)	106.2(2)	C(8a) – C(8) – C(16)	109.8(4)
C(1) – C(2) – C(11)	112.6(3)	C(8a) – C(8) – O(17)	106.8(3)
C(1) – C(2) – O(12)	108.5(2)	C(16) – C(8) – O(17)	110.0(3)
C(3) – C(2) – C(11)	110.3(3)	C(1) – C(8a) – C(4a)	109.7(2)
C(3) – C(2) – O(12)	108.6(2)	C(1) – C(8a) – C(8)	113.0(3)
C(11) – C(2) – O(12)	110.5(3)	C(4a) – C(8a) – C(8)	114.4(2)
C(2) – C(3) – C(4)	113.6(2)	C(1) – C(9) – C(10)	113.1(3)
C(2) – C(3) – O(13)	121.0(3)	C(1) – C(9) – C(18)	121.4(3)
C(4) – C(3) – O(13)	125.4(3)	C(10) – C(9) – C(18)	125.4(3)
C(3) – C(4) – C(4a)	108.5(2)	C(4) – C(10) – C(9)	115.6(3)
C(3) – C(4) – C(10)	105.0(2)		
C(4a) – C(4) – C(10)	108.3(2)		
C(4) – C(4a) – C(5)	104.5(2)		
C(4) – C(4a) – C(8a)	107.4(2)		
C(4) – C(4a) – C(14)	108.4(3)		
C(5) – C(4a) – C(8a)	114.0(2)		
C(5) – C(4a) – C(14)	110.2(3)		
C(8a) – C(4a) – C(14)	112.0(3)		
C(4a) – C(5) – C(6)	125.5(3)		
C(5) – C(6) – C(7)	121.5(3)		
C(6) – C(7) – C(8)	115.3(3)		
C(6) – C(7) – O(15)	123.3(3)		
C(8) – C(7) – O(15)	121.2(3)		

bond lengths are in good agreement with usually observed values.[17] The C–H bond distances range from 0.70 to 1.02 Å, mean value 0.91 Å, in good agreement with values found in some precisely determined X-ray structures.[10] C(sp^3) – C(sp^3) bond lengths, excluding C(4) – C(4a) and C(4a) – C8(a), have a mean value of 1.535 Å. The lengths of the two bonds C(4) – C(4a) and C(4a) – C(8a) are 1.578 Å and 1.567 Å, significantly longer ($> 10\sigma$) than this mean value. This lengthening, probably associated with internal strain in the molecule, has previously been observed in the crystal structure of 1,4-ethyleno-2,8-dihydroxy-2,4,6,8-tetramethyl-octahydronaphthal-5-en-3,7-dione, [15] a Diels-Alder dimer of 2,6-dimethyl-*o*-quinol, where the lengths of C(4) – C(4a) and C(4a) – C(8a) are 1.589 and 1.554 Å, respectively. The methyl group C(14), attached to the carbon atom C(4a) in the dimer of 2,4-dimethyl-*o*-quinol, has probably caused the lengthening of the C(4a) – C(8a) bond in the present structure relative to the structure of the dimer of 2,6-dimethyl-*o*-quinol.

A least-squares plane for ring A (Fig. 2) and the displacements of the atoms from this best plane are listed in Table 9. The conformation of the ring is puckered. Atom C(8) is significantly out of the plane of the other five atoms, as also was observed in the dimer of 2,6-dimethyl-*o*-quinol.[15] The three rings in the rigid B ring system (Fig. 2) are all boat-shaped and least-squares planes with deviations from them are also given in Table 9.

Fig. 3 is a view along the a^* axis of the arrangement of the molecules. The two hydrogen atoms bonded to oxygen participate in hydrogen bonds, forming

Table 9. Least-squares planes and deviations. The planes are described in terms of axes (m,n,p) having $m||a^*$, $n||b$ and $p||c$. The atoms indicated with asterisks were omitted from the calculations of the least-squares planes. Deviation in Å.

Plane A[a]		Plane B1[b]		Plane B2[c]		Plane B3[d]	
Atom	Deviation	Atom	Deviation	Atom	Deviation	Atom	Deviation
C(4a)*	−0.060	C(1)*	−0.779	C(1)*	0.728	C(1)*	0.646
C(5)	0.005	C(2)	−0.012	C(2)	−0.010	C(4)*	0.716
C(6)	−0.008	C(3)	0.012	C(3)	0.011	C(4a)	−0.026
C(7)	0.005	C(4)*	−0.716	C(4)*	0.688	C(8a)	0.025
C(8)*	0.554	C(4a)	−0.012	C(9)	0.012	C(9)	−0.030
C(8a)	−0.002	C(8a)	0.012	C(10)	−0.012	C(10)	0.030

[a] Plane A : $0.4808m+0.1028n+0.8708p=7.080$.
[b] Plane B1: $0.8557m+0.3806n+0.3505p=6.082$.
[c] Plane B2: $0.2119m-0.1041n+0.9717p=3.962$.
[d] Plane B3: $0.6448m+0.4914n-0.5855p=0.1596$.

the three-dimensional network shown in Fig. 3. Two molecules related to each other by a center of symmetry at $0,\frac{1}{2},\frac{1}{2}$ form a hydrogen-bonded dimer (Table 10). The O(15^{ii})···(O17) distance is 2.184 Å and the O(17)−H(O17)··· O(15^{ii}) angle is 158.7°. The hydrogen-bonded dimers are linked by hydrogen bonds along the *b* direction (Table 10). The O(13^{vi})···H(O12) distance is 1.986 Å and the O(12)−H(O12)···O(13^{vi}) angle is 166.1°.

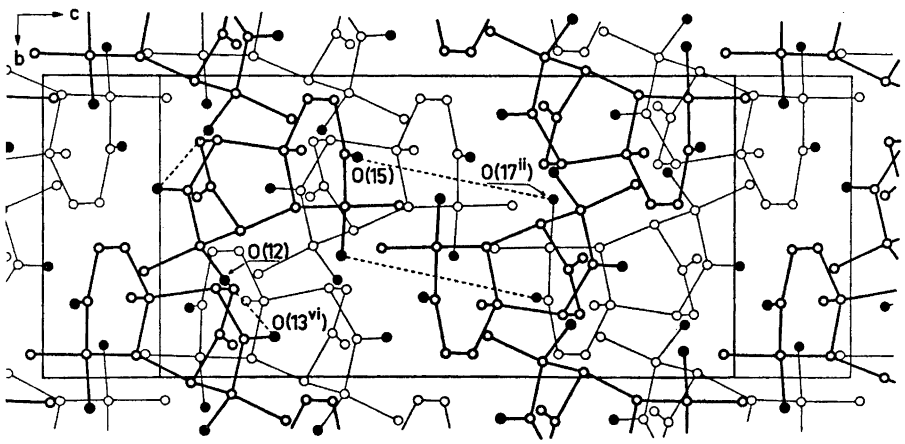

Fig. 3. Packing of molecules in the crystal as viewed along a^*. Molecules lying below the origin are marked with thin lines and hydrogen bonds with broken lines. ○ carbon; ● oxygen.

Table 10. Intermolecular distances (Å) shorter than 3.8 Å, with estimated standard deviations in parentheses.

Superscript	Code for symmetry related atoms. Coordinates	Superscript	Coordinates
none	x,y,z	iv	$x,1/2-y,-1/2+z$
i	$x,-1+y,z$	v	$-x,-1/2+y,1/2-z$
ii	$-x,1-y,1-z$	vi	$1-x,1/2+y,1/2-z$
iii	$1-x,1-y,1-z$	vii	$x,3/2-y,-1/2+z$

C(5) – O(12^{i})	3.691(3)	C(10) – C(18^{v})	3.756(4)
C(6) – O(17^{i})	3.518(4)	C(18) – C(18^{v})	3.775(2)
O(15) – O(15^{ii})	3.764(5)	C(2) – O(13^{iv})	3.647(3)
O(15) – O(17^{ii})	2.887(4)	C(11) – O(13^{vi})	3.644(4)
O(12) – C(14^{iii})	3.790(4)	O(12) – O(13^{vi})	2.765(3)
C(10) – C(16^{iv})	3.631(5)	O(13) – O(13^{vi})	3.722(1)
C(6) – C(18^{v})	3.669(5)	C(11) – C(16^{vii})	3.750(6)

This investigation has received financial support from the *Tri-Centennial Fund of the Bank of Sweden* and from the *Swedish Natural Science Research Council.*

The authors are indebted to Professor Peder Kierkegaard for his encouraging interest in this work and for the facilities placed at their disposal. Thanks are due to Dr. Bengt Lindgren for the supply of crystals used in the work and for valuable comments. Dr. Åke Pilotti is also thanked for valuable discussions and Dr. Don Koenig for his correction of the English of this paper.

REFERENCES

1. Adler, E., Brasen, S. and Miyake, H. *Acta Chem. Scand.* **25** (1971) 2055.
2. Adler, E. and Holmberg, K. *Acta Chem. Scand.* **25** (1971) 2775.
3. Vannerberg, N.-G. and Brasen, S. *Acta Chem. Scand.* **24** (1970) 1894.
4. Karlsson, B., Kierkegaard, P., Pilotti, A.-M., Wiehager, A.-C. and Lindgren, B. *Acta Chem. Scand.* **27** (1973) 1428.
5. Wilson, A. J. C. *Nature* **150** (1942) 151.
6. Norrestam, R. *Acta Cryst.* **A 28** (1972) 303.
7. Gantzel, P. K., Sparks, R. A. and Trueblood, K. N. *IUCr World List of Crystallographic Computer Programs*, 2nd Ed., Program 384 (1961).
8. Hughes, E. W. *J. Am. Chem. Soc.* **63** (1941) 1737.
9. Freeman, A. J. *Acta Cryst.* **12** (1959) 261.
10. Stewart, R. F., Davidson, E. R. and Simpson, W. T. *J. Chem. Phys.* **42** (1965) 3175.
11. Johnson, C. K. *ORTEP* Report *ORNL*-3794 (1965) Oak Ridge National Laboratory, Oak Ridge, Tennessee.
12. Alder, K. and Stein, G. *Angew. Chem.* **50** (1937) 514.
13. Horner, L. and Dürckheimer, W. *Chem. Ber.* **95** (1962) 1219.
14. Kende, A. S. and Mac Gregor, P. *J. Am. Chem. Soc.* **83** (1961) 4197.
15. Karlsson, B., Pilotti, A.-M. and Wiehager, A.-C. *Acta Chem. Scand.* **27** (1973) 2945.
16. Karlsson, B., Pilotti, A.-M. and Wiehager, A.-C. *To be published.*
17. Sutton, L. E. *Tables of Interatomic Distances and Configuration in Molecules and Ions*, The Chemical Society, London 1965, Supplement 1956 – 1959.

Received April 18, 1973.

ACTA CHEMICA SCANDINAVICA 27 (1973) 2965–2972

Molecular Structure of Gaseous Methylthio-dimethylborane

K. BRENDHAUGEN, E. WISLØFF NILSSEN and H. M. SEIP

Department of Chemistry, University of Oslo, Oslo 3, Norway

Methylthio-dimethylborane has been studied by gas electron diffraction. The skeleton is probably planar, though values for the torsional angle about the B–S bond up to about 25° cannot be ruled out. The results obtained for the most important parameters are (standard deviations in parentheses):
r_a(B–S) = 1.779(5) Å, r_a(C–S) = 1.825(4) Å, r_a(C–B) = 1.570(4) Å, ∠BSC = 107.2(10)°, ∠SBC4 = 124.0(8)°, ∠SBC5 = 115.3(6)°.
Mean amplitudes of vibration computed from spectroscopic data are also given.

Two compounds with B_2S_3 rings (dimethyl-1,2,4-trithia-3,5-diborolane [1] and dichloro-1,2,4-trithia-3,5-diborolane [2]) have recently been studied by electron diffraction in Oslo. Apart from methyl hydrogens, both molecules were found to be essentially planar. Considering the potential to internal rotation about S–S bonds,* one should expect a puckered B_2S_3 ring if the barrier to rotation about the B–S bonds is zero. Theoretical calculations using the CNDO/2 method indicated considerable π bond orders in the B–S bonds in the trithiadiborolane ring.[4] We have now studied this problem further by electron-diffraction investigations of methylthio-dimethylborane (Me_2BSMe), tris(methylthio)borane ($B(SMe)_3$),[5] and bis(dimethylboryl)-disulphane (Me_2BSSMe_2).[6]

EXPERIMENTAL

The sample of Me_2BSMe was kindly supplied by W. Siebert, University of Würzburg. The electron diagrams were recorded with the Balzer's Eldigraph KDG2 [7,8] in Oslo. The nozzle-temperature was about 20°C. Two sets of plates were used recorded with nozzle-to-plate distances of 50.0 cm and 25.0 cm and wavelengths of 0.05846 Å and 0.05833 Å (accelerating potential about 42kV) respectively. The data were treated in the usual way.[9] The levelled intensity curves obtained from each plate were plotted. We were not quite content with the quality of the data, but four curves from each set were considered fairly satisfactory, and composite intensity curves ranging from $s = 2.25$ Å^{-1} to $s = 29.0$ Å^{-1} were computed from these data. The s intervals were 0.125 Å^{-1} for $s < 7.25$ Å^{-1} and 0.25 Å^{-1} for $s < 7.25$ Å^{-1}.

* *ab initio* calulactions on H_2S_2 give a barrier of about 9.3 kcal/mol corresponding to the *syn* form.[3]

The elastic scattering amplitudes were calculated for an accelerating potential of 42 kV by the partial wave method.[9,10] The atomic potentials were taken from Ref. 11 except for hydrogen where the values in Ref. 12 were used. The modified molecular intensities were calculated using the modification function [9] $s/(|f'_B||f'_S|)$.

STRUCTURE REFINEMENT

The experimental radial distribution (RD) curve [9] in Fig. 1, obtained by Fourier transformation of the experimental intensity curve in Fig. 2, gives a rough idea of the main structural parameters. The structure was refined by

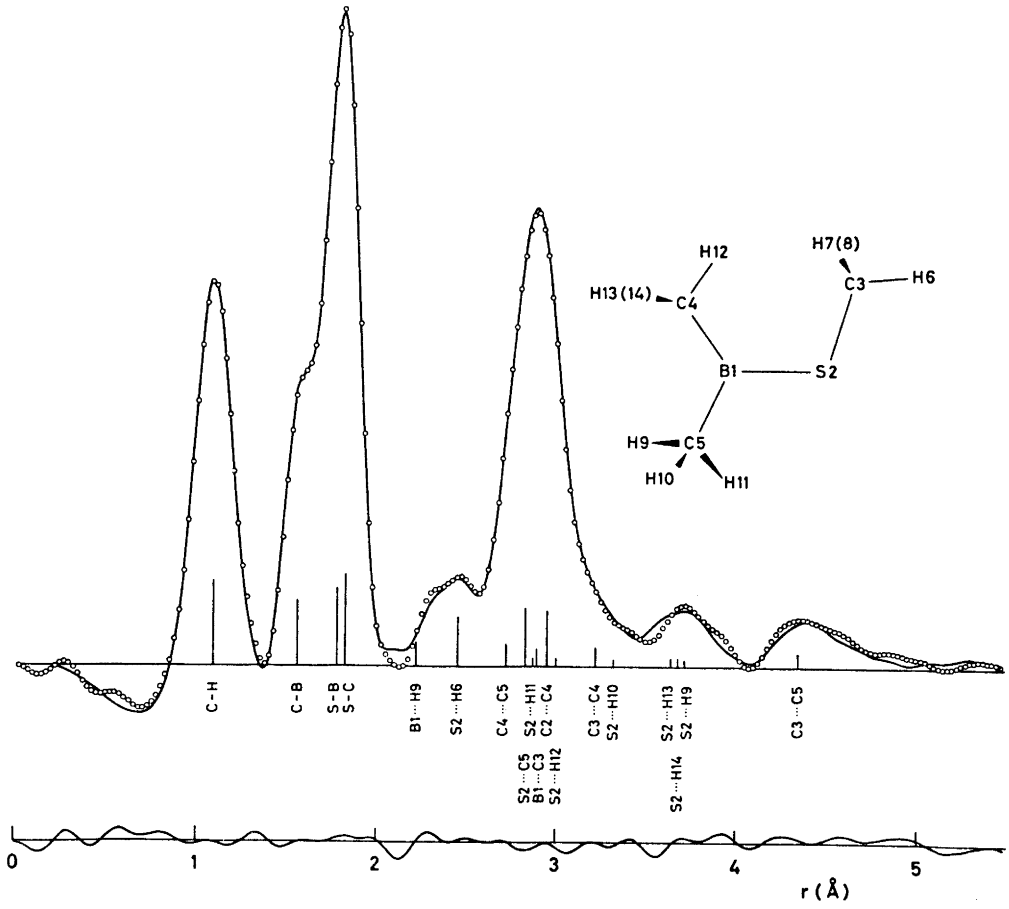

Fig. 1. Experimental (circles) and theoretical (full line) radial distribution functions for Me_2BSMe calculated by Fourier transformation of the curves in Fig. 2 with an artificial damping constant [9] $k = 0.002$ Å^2. The differences between experimental and theoretical values are also shown. The positions and approximate areas of the peaks corresponding to the most important distances are indicated.

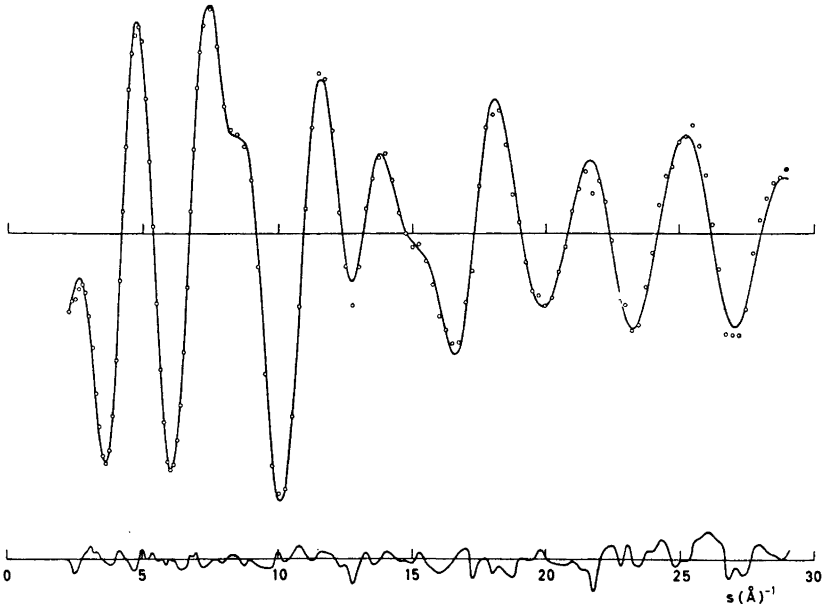

Fig. 2. Comparison of the experimental intensity values (circles) and the corresponding theoretical ones (full line) calculated with the parameters in Tables 1 and 2. The differences between experimental and theoretical values are also shown.

the least-squares method using a diagonal weight matrix. The molecule has little symmetry, at most a symmetry plane, and the number of parameters necessary to describe the geometry is large for a molecule of this size. Some assumptions were therefore necessary (*cf.* Tables 1 and 2). Thus the following parameters were assumed equal:

(1) B1 – C4 and B1 – C5
(2) All C – H bonds
(3) All BCH angles
(4) All SCH angles

The Bastiansen-Morino shrinkage effect [13–15] was neglected; this approximation is discussed in more detail later. Some assumptions about the mean amplitudes of vibration were also necessary (*cf.* the next section).

The possibility of tilt of the methyl groups was considered. However, this led to too many parameters, and it was necessary to assume threefold symmetry in the methyl groups with the axis coinciding with the B – C or S – C bonds. The thiomethyl group was assumed to be staggered with respect to the B – S bond. Free rotation was tried for the two other methyl groups, but with this assumption, we were unable to obtain satisfactory agreement in the outer part of the RD curve (Fig. 1). The experimental curve has a peak near 3.70 Å. To reproduce this peak theoretically several S···H distances must contribute in this region. If the torsional angle about B1 – C4 is such that one of the

hydrogens in this methyl group (say H12) lies *syn* to the sulphur atom (see Fig. 1), the distances S···H13 and S···H14 give contributions around 3.70 Å. The other methyl group is probably oscillating with a very large amplitude, avoiding positions where the torsional angle ϕ(SBC5H) for one of the hydrogens is close to zero. The distances given in Table 2 correspond to ϕ(SBC5H11) = $-30°$; S2···H9 is then about 3.75 Å. The agreement, as well as the other molecular parameters, was virtually independent of this angle within the interval $-20°$ to $-100°$.

VIBRATIONAL FREQUENCIES AND ROOT-MEAN-SQUARE AMPLITUDES OF VIBRATION

The IR and Raman spectra of Me_2BSMe have been given by Vahrenkamp.[16] A calculation of the fundamental frequencies was carried out using a computer program developed by Gwinn.[17] After some adjustments the force constants given in Table 4 were used. The force constants for torsional and out-of-plane motion, especially perhaps the force constant for methyl torsion about B–C bonds, are very uncertain. In Table 5 the computed frequencies are compared to the experimental values.

The value of the B–S stretching force constant is of some interest in the discussion of the π-bond order of the B–S bond. Unfortunately, values deviating considerably from 2.85 mdyn/Å may give reasonable fit for the frequencies if the B–C stretching constant and the BS/BC coupling constant are properly adjusted (*cf.* the discussion of the force field in $B(SMe)_3$ [5]).

The root-mean-square amplitudes of vibration were computed as described by Stølevik *et al.*[18] The results have been included in Tables 1 and 2. The u values which depend critically on one or more of the most uncertain

Table 1. Bond distances, angles, and mean amplitudes of vibration in methylthiodimethylborane. The standard deviations given in parentheses apply to the last decimal place. Mean amplitudes of vibration calculated from spectroscopic data are also given.

	r_a (Å)[19]	u (Å)	u_{calc} (Å)[b]		Angles (degrees)
$(C-H)_{av}$[a]	1.092(4)	0.074(3)	0.078	∠BSC	107.2(10)
C–B	1.570(4)	0.051	0.058	∠SBC4	124.0(8)
S–B	1.779(5)	0.047 (3)[b]	0.054	∠SBC5	115.3(6)
S–C	1.825(4)	0.047	0.053	∠BCH, ∠SCH	111.7[c]
				ϕ(C4BSC)	0[c]
				ϕ(SBC4H12)	−5[c]
				ϕ(SBC5H11)	−30[c]
				ϕ(BSC3H6)	180[c]

[a] An asymmetry constant, $\varkappa = 0.000020$ Å^3, was assumed for the C–H bond distances; for all other distances $\varkappa = 0$. [b] At 20°C. [c] The parameter was not refined at the same time as the other parameters. [d] The differences between the u-values were assumed.

Table 2. The most important non-bonded distances and mean amplitudes of vibration.

	r_a (Å)	u (Å)	u_{calc} (Å)[a]
B1···C3	2.901(18)	0.095[b]	0.095
S2···C4	2.959(8)	0.059 (10)[c]	0.073
S2···C5	2.831(6)	0.062	0.076
C3···C4	3.227(20)	0.125(19)	0.151
C3···C5	4.352(14)	0.120(20)	0.093
C4···C5	2.729(11)	0.077[b]	0.080
B1···H9	2.219(5)	0.150[b]	0.109
S2···H6	2.449(5)	0.098(9)	0.106
S2···H9	3.731	0.13[b]	0.12
S2···H10	3.330	0.20[b]	0.18
S2···H11	2.875	0.18[b]	0.17
S2···H12	3.006	0.16[b]	0.15
S2···H13	3.644	0.205 (60)[c]	0.16
S2···H14	3.706	0.205	0.14

[a] At 20°C. [b] The parameter was not refined at the same time as the other parameters. [c] The difference between the u values was assumed.

force constants (say u(S2···H10)) must be regarded as rough estimates only. The computer program gives also the terms necessary to obtain an r_α-structure,[19] and thus avoid the shrinkage problem. However, the mentioned uncertainties in some of the force constants lead to very unrealiable correction terms.

DISCUSSION

Our final results for the structure parameters are given in Tables 1 and 2. The standard deviations have been corrected for the effect of correlation between the intensity data,[20] and the uncertainty in the wavelength has been included. The atomic coordinates for the final model are given in Table 3.

Table 3. Atomic coordinates (Å) for Me_2BSMe.

	x	y	z
B1	0.0	0.0	0.0
S2	1.779	0.0	0.0
C3	2.319	1.743	0.0
C4	−0.878	1.302	0.0
C5	−0.671	−1.419	0.0
H6	3.407	1.829	0.0
H7	1.953	2.279	0.879
H8	1.953	2.279	−0.879
H9	−1.638	−1.409	−0.507
H10	−0.844	−1.784	1.015
H11	−0.049	−2.160	−0.507
H12	−0.266	2.202	−0.088
H13	−1.459	1.397	0.920
H14	−1.586	1.311	−0.831

Table 4. Force constants used in the calculation of frequencies and root-mean-square amplitudes of vibration.

Stretching force constants (mdyn/Å)			Bending force constants (mdyn Å/rad²)		Repulsion force constants (mdyn/Å)	
B–S	2.85		BSC	0.90	S···H	0.54
S–C	1.80		CBC	0.80	B···H	0.46
B–C	1.85		CBS	0.80	H···H	0.20
C–H	4.20	(B–CH_3 groups)	SCH, BCH	0.35		
C–H	4.30	(S–CH_3 group)	HCH	0.40		

Coupling constant (mdyn/Å)		Torsional force constants (mdyn Å/rad²)			Out-of-plane force constant (mdyn Å/rad²)
BS/BC	0.55	CBSC	0.10	(two contributions)	CB out of CBS plane: 0.18 (two contributions)
		BSCH	0.04	(three contributions)	BS out of CCB plane: 0.18
		SBCH	0.01	(three for each	
		CBCH	0.01	BC bond)	

Table 5. Observed [16] and calculated frequencies (cm^{-1}) for $(CH_3)_2BSCH_3$.

	IR	Raman	Calculated
τ(BS)			124
$\delta_s(BC_2)$		210	181
$\delta_{as}(BC_2)$		298	306
δ(BSC)		352	353
$\gamma(C_2BS)$	455	452	466
ν(BS)	575	574	573
ν(SC)	712	716	714
$\varrho(CH_3)$	824–961	825–964	769–1008
$\nu_s(BC_2)$[a]	1089/1119	1087	1097/1123
$\nu_{as}(BC_2)$[a]	1129/1161	1122	1121/1157
$\delta_s(CH_3)$	1301	1297	1364, 1367, 1389
$\delta_{as}(CH_3)$	1375, 1436	1432	1382–1402
ν(CH)	2890–3000	2890–2996	2911–2970

[a] Frequencies corresponding to ^{11}B and ^{10}B are given.

The agreement between experimental and theoretical intensity and RD curves is not entirely satisfactory (*cf.* Figs. 1 and 2). The discrepancies may be due to noise in the observed data or to unsatisfactory assumptions about the structure. By refining a very limited number of parameters simultaneously, it is possible to refine more parameters than are indicated in Tables 1 and 2, and thus obtain slightly better agreement. However, it is not obvious which new parameters to include, and we preferred to use u values in reasonable agreement with the computed ones, and the seemingly reasonable assumptions listed previously.

The value used for u(B···H) is somewhat larger than that calculated from spectroscopic data. If the latter value is used, the disagreement around 2.2 Å is more evident. The large u value may perhaps be regarded as an indication of tilt of these methyl groups.

The peak around 3.70 Å contains mainly S···H contributions. The peak was, as mentioned, rather difficult to reproduce theoretically. The peak seems to exclude free rotation about the B – C bonds though the actual equilibrium positions and the amplitudes of the oscillations of those methyl groups remain rather uncertain.

The C3···C5 distance gives the main contribution to the outer peak around 4.35 Å. The position of the peak shows that the heavy atom skeleton is essentially planar. However, the agreement is not much changed if ϕ(C4BSC3) is varied in the range 0 – 25°. An angle of 30° may be rejected a level well below 0.5 % according to Hamilton's R-factor test.[21] An equilibrium form with a planar skeleton is in agreement with theoretical calculations. A barrier to rotation about the B – S bond in H_2BSH of about 20 kcal/mol has been found both by *ab initio* and CNDO/2 calculations while the CNDO/2 method gives a slightly lower barrier in Me_2BSMe.[22]

The B – S bond seems to be slightly shorter than found in the trithiadiborolane system,[1,2] while the B – C bond is about twice the standard deviation smaller than found in $B(CH_3)_3$ (1.578(1) Å).[23] The C – S bond length and the bond angle BSC differ somewhat from the corresponding values in methyl vinyl sulphide (1.806(6) Å and 104.5(7)°),[24] but the standard deviations are rather large. The two CBS angles differ significantly, presumably for steric reasons.

REFERENCES

1. Seip, H. M., Seip, R. and Siebert, W. *Acta Chem. Scand.* **27** (1973) 15.
2. Almenningen, A., Seip, H. M. and Vassbotn, P. *Acta Chem. Scand.* **27** (1973) 21.
3. Veillard, A. and Demuynck, J. *Chem. Phys. Lett.* **4** (1970) 476.
4. Gropen, O. and Vassbotn, P. *Acta Chem. Scand.* **27** (1973) 3079.
5. Johansen, R., Wisløff Nilssen, E., Seip, H. M. and Siebert, W. *Acta Chem. Scand.* **27** (1973) 3015.
6. Siebert, W., Johansen, R. and Seip, H. M. *Acta Chem. Scand. To be published.*
7. Zeil, W., Haase, J. and Wegmann, L. *Z. Instrumentenk.* **74** (1966) 84.
8. Bastiansen, O., Graber, R. and Wegmann, L. *Balzers High Vacuum Report* **25** (1969) 1.
9. Andersen, B., Seip, H. M., Strand, T. G. and Stølevik, R. *Acta Chem. Scand.* **23** (1969) 3224.
10. Peacher, J. L. and Wills, J. G. *J. Chem. Phys.* **46** (1967) 4809.
11. Strand, T. G. and Bonham, R. A. *J. Chem. Phys.* **40** (1964) 1686.
12. Stewart, R. F., Davidson, E. R. and Simpson, W. T. *J. Chem. Phys.* **42** (1965) 3175.
13. Bastiansen, O. and Trætteberg, M. *Acta Cryst.* **13** (1960) 1108.
14. Morino, Y. *Acta Cryst.* **13** (1960) 1107.
15. Cyvin, S. J. *Molecular Vibrations and Mean-Square Amplitudes*, Universitetsforlaget, Oslo, and Elsevier, Amsterdam 1968.
16. Vahrenkamp, H. *J. Organomet. Chem.* **28** (1971) 181.
17. Gwinn, W. D. *J. Chem. Phys.* **55** (1971) 477.
18. Stølevik, R., Seip, H. M. and Cyvin, A. J. *Chem. Phys. Lett.* **15** (1972) 263.
19. Kuchitsu, K. and Cyvin, S. J. In Cyvin, S. J., Ed., *Molecular Structures and Vibrations*, Elsevier, Amsterdam 1972, Chapter 12.

20. Seip, H. M. and Stølevik, R. In Cyvin, S. J., Ed., *Molecular Structures and Vibrations*, Elsevier, Amsterdam 1972, Chapter 11.
21. Hamilton, W. C. *Acta Cryst.* **18** (1965) 502.
22. Gropen, O., Wisløff Nilssen, E. and Seip, H. M. *To be published.*
23. Bartell, L. S. and Carroll, B. L. *J. Chem. Phys.* **42** (1965) 3076.
24. Samdal, S. and Seip, H. M. *Acta Chem. Scand.* **25** (1971) 1903.

Received May 14, 1973.

ACTA CHEMICA SCANDINAVICA 27 (1973) 2973–2982

Hydrothermal Preparation of Rare Earth Hydroxycarbonates. The Crystal Structure of $NdOHCO_3$

A. NØRLUND CHRISTENSEN

Department of Inorganic Chemistry, University of Aarhus, DK-8000 Aarhus C, Denmark

The rare earth hydroxycarbonates, $MeOHCO_3$, of La, Nd, and Sm, were prepared by using hydrothermal technique. The crystal structure of neodymium hydroxycarbonate, $NdOHCO_3$, was solved using three dimensional Patterson and Fourier functions and was refined to a conventional R-value of 8.2 %. The space group is $P\bar{6}$ with $a = 12.32$ Å and $c = 9.88$ Å. The unit cell contains 18 formula units. The neodymium atom is nine fold coordinated with oxygen atoms, and the structure has layers of $(NdOH^{2+})_n$ ions held together by the carbonate ions. The average distance for the bonds metal to oxygen (carbonate) is 2.52(1) Å, and for metal to oxygen (hydroxyl) is the average distance 2.45(2) Å. The intensities were measured on a three circle diffractometer with Weissenberg geometry. The powder patterns of $LaOHCO_3$ ($a = 12.616$ Å, $c = 10.022$ Å) and of $SmOHCO_3$ ($a = 12.231$ Å, $c = 9.856$ Å) are similar to that of $NdOHCO_3$ and it is assumed that the two compounds have the $NdOHCO_3$ structure.

In a hydrothermal investigation of the system $Nd_2O_3 - H_2O - CO_2$ over the temperature range 360 – 675°C and at pressures up to 3000 atm, three crystalline neodymium compounds were prepared hydrothermally.[1] Neodymium trihydroxide was obtained over the entire temperature-pressure range. At temperatures greater than 550°C the hexagonal modification of $Nd_2O_2CO_3$ was found,[2] and at temperatures below 530°C a previously unidentified phase (called Nd(I) in Ref. 1) was obtained. The crystal structure determination of this phase is reported below. It shows that the compound is $NdOHCO_3$.

Hydrothermal preparation of the compound $PrOHCO_3 \cdot 0.1H_2O$ was reported by Caro *et al.*[3] The compound was obtained by using hydrolysis of praseodymium carbonate at 250°C and 400 bar. Haschke and Eyring [4] obtained the compound $PrOHCO_3$ hydrothermally at 500°C, and the compound was also obtained up to 800°C. Weissenberg data indicated that praseodymium hydroxycarbonate was hexagonal with a structure analogous to bastnaesite,[5] and it was further concluded by Haschke and Eyring that a previously reported high-pressure form of lanthanum trihydroxide [6] actually was the hexagonal form of lanthanum hydroxycarbonate. The unit cells of the mentioned rare earth hydroxycarbonates are listed in Table 1.

Table 1. Unit cell parameters of some rare earth hydroxycarbonates.

	a Å	*c* Å
$LaOHCO_3$, Ref. 6. (reported as high pressure $La(OH)_3$)	4.214	5.041
$CeFCO_3$, Bastnaesite, Ref. 5.	7.162	9.787
$PrOHCO_3.0.1\ H_2O$, Ref. 3.	7.152	9.862
$PrOHCO_3$, Ref. 4.	4.146	4.986

EXPERIMENTAL

Rare earth carbonates were precipitated with a 1 M $KHCO_3$ solution from dilute solutions of rare earth nitrates prepared by dissolving the oxides in nitric acid. The freshly precipitated carbonates were washed with water and treated with water saturated with carbon dioxide or with a 0.3 M $KHCO_3$ solution in pressure vessels lined with pure silver or pure gold at the experimental conditions listed in Table 2. The products were washed

Table 2. Experimental conditions for hydrothermal preparation of rare earth hydroxy carbonates.

Exp. No.	Initial conditions: Freshly precipitated	Liner of vessel	Temp °C	Pressure atm	Time h	Solvent	Product
1.	Lanthanum carbonate	Ag	300	75	48	0.3 M $KHCO_3$	$LaOHCO_3$ pure
2.	Neodymium hydroxide	Au	420	1800	44	H_2O+CO_2[a]	$NdOHCO_3+Nd(OH)_3$
3.	Samarium carbonate	Ag	300	75	48	0.3 M $KHCO_3$	$SmOHCO_3$ pure

[a] Water saturated with carbon dioxide.

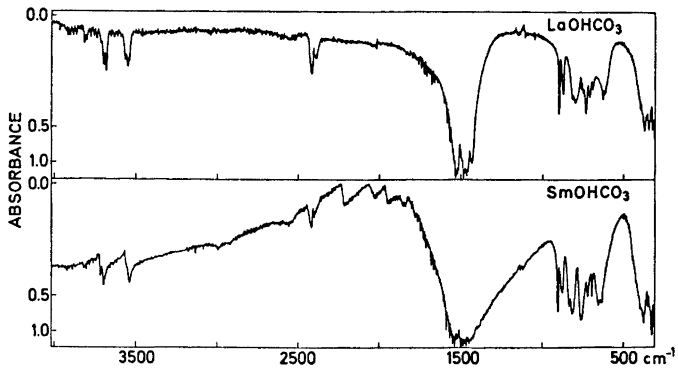

Fig. 1. Infra-red spectra of $LaOHCO_3$ and $SmOHCO_3$.

Table 3. X-Ray powder patterns of some rare earth hydroxycarbonates.

$LaOHCO_3$, a = 12.616(8) Å, c = 10.022(5) Å.

h	k	l	d_{obs}(Å)	d_{calc}(Å)	I
0	0	2	5.032	5.011	61
3	0	0	3.649	3.642	82
3	0	2	2.949	2.946	100
0	0	4	2.503	2.506	22
3	3	0	2.103	2.103	49
3	0	4	2.063	2.064	69
3	3	2	1.938	1.939	45
6	0	0	1.820	1.821	22
6	0	2	1.710	1.712	27
3	3	4	1.610	1.611	25
3	0	6	1.517	1.518	21
6	0	4	1.473	1.473	19
6	3	0	1.377	1.377	19
6	3	2	1.328	1.327	16
3	3	6	1.309	1.308	23

$NdOHCO_3$, a = 12.34(1) Å, c = 9.915(6) Å.

h	k	l	d_{obs}(Å)	d_{calc}(Å)	I
0	0	2	4.964	4.958	58
3	0	0	3.569	3.563	74
3	0	2	2.899	2.893	100
0	0	4	2.485	2.479	17
3	3	0	2.061	2.057	50
3	0	4	2.039	2.035	68
3	3	2	1.903	1.900	43
6	0	0	1.783	1.782	11
6	0	2	1.679	1.677	24
3	3	4	1.586	1.583	22
3	0	6	1.501	1.499	19
6	0	4	1.447	1.447	10
6	3	0	1.347	1.347	13
6	3	2	1.301	1.300	19
3	3	6	1.288	1.288	26

$SmOHCO_3$, a = 12.231(8) Å, c = 9.856(4) Å.

h	k	l	d_{obs}(Å)	d_{calc}(Å)	I
0	0	2	4.950	4.928	67
3	0	0	3.539	3.531	63
3	0	2	2.875	2.870	100
0	0	4	2.466	2.464	28
3	3	0	2.039	2.039	30
3	0	4	2.019	2.021	67
3	3	2	1.884	1.884	47
6	0	0	1.765	1.765	22
6	0	2	1.662	1.662	24
0	0	6	1.643	1.643	5
3	3	4	1.570	1.571	28
3	0	6	1.489	1.489	25
6	0	4	1.435	1.435	16
6	3	0	1.333	1.335	14
6	3	2	1.289	1.288	21
3	3	6	1.279	1.279	9

with water and dried in air at room temperature. Chemical analyses were made on samples that only contained one phase using EDTA titrations.[7] (Found: La 64.03. Calc. for $LaOHCO_3$: La 64.34. Found: Sm 66.14. Calc. for $SmOHCO_3$: Sm 66.13).

The IR spectra of the pure compounds were recorded over the frequency range 4000 to 400 cm^{-1} with a Perkin-Elmer 521 spectrophotometer using pellets of mixtures of 2 mg of sample and 200 mg of CsI. The spectra are recorded in Fig. 1.

X-Ray powder patterns were obtained with a Guinier camera using Cu$K\alpha_1$ radiation ($\lambda = 1.54051$ Å) with NaCl ($a = 5.6389$ Å) or Ge ($a = 5.6576$ Å) as internal standards. The intensities of the powder lines were measured using a Joyce double beam recording microdensitometer. The powder patterns are listed in Table 3.

A single crystal of $NdOHCO_3$ with the dimensions $0.1 \times 0.1 \times 0.35$ mm^3 was investigated using film technique. Weissenberg photographs were taken of *hk*0, *hk*1, and *hk*2, and precession photographs were taken of *h*0*l*, *h*1*l*, *h*2*l*, *h*3*l*, and 0*kl*. No systematic absences were found. A total of 1145 independent *hkl* reflections with $I > 3\ \sigma(I)$ were measured on a single crystal diffractometer with a scintillation counter using monochromatic Ag$K\alpha$-radiation ($\lambda = 0.5608$ Å) in conjunction with a pulse height analyzer. The diffractometer was a three circle diffractometer with Weissenberg geometry, using a ϕ-scan in the integration of the intensities. The monochromator was a graphite crystal. Lorentz-polarization corrections were applied and absorption corrections were made using Wells' method.[8]

STRUCTURE DETERMINATION

Several hexagonal space groups have no limiting conditions for the possible reflections. Attempts were made to refine the structure using all these possible hexagonal space groups. It was only possible to refine the structure using the space group $P\bar{6}$ (No. 174). A three-dimensional Patterson function showed strong maxima at the positions ($p/3$, $q/3$, $r/2$), where p and q have the values 0, 1, 2 and r the values 0 and 1. All these maxima had approximately the same heights and were interpreted as Nd-Nd-vectors. Of the observed *hkl* reflections strong intensities were only present when the conditions $h = 3n$, $k = 3n$, and $l = 2n$ was satisfied for the reflections. This indicates a layer structure with

neodymium atoms placed in layers parallel to the *ab*-plane, with Nd–Nd distances close to $a/3$ within the layers and with distances between the layers in the *c*-direction close to $c/2$. The weak *hkl* reflections may have scattering contributions from the metal atoms, if the metal-metal distances deviate from the distances $a/3$ and $c/2$, and will in all cases have scattering contributions from the light atoms in the structure.

From packing considerations where some of the oxygen atoms were placed in the special positions 2*i*, 2*h*, and 2*g* of the space group with *z* coordinates close to $\pm 1/4$, it was found that a model with neodymium atoms in the general position 6*l* at (0.22,0.12,0.25), (0.22,0.44,0.25), and (0.55,0.12,0.25) would give acceptable neodymium oxygen distances and would be in agreement with the calculated three-dimensional Patterson function. A combination of packing considerations and three-dimensional Fourier maps phased on this model gave after a series of refinement cycles and Fourier calculations the positions of all the oxygen and carbon atoms of the carbonate groups and the oxygen atoms of the hydroxyl groups. The refinements applied the methods of least squares and isotropic temperature factors. The program used was the Fortran crystallographic least squares program LINUS.[9] The refinement proceeded only to a conventional *R*-value of 17.5 %. The occupancy of two of the neodymium atoms was introduced as parameters and after a series of refinement cycles using isotropic temperature factors for all the atoms an *R*-value of 12.2 % was obtained. The oxygen and carbon atoms belonging to the carbonate ions had at this stage obtained positions corresponding to distorted and not planar carbonate ions. Further refinements proceeded with a least squares program (Pawley [10]) using constrained refinement of the atoms belonging to the carbonate ions and using anisotropic temperature factors for the metal atoms. The refinement proceeded to a conventional *R*-value of 8.2 %. No attempts were made to determine the position of the hydrogen atoms belonging to the hydroxyl ions. It was not possible to refine the structure in hexagonal space groups with higher symmetry than that of $P\bar{6}$.

CRYSTAL DATA

The unit cell of the compound $NdOHCO_3$ contains 18 formula units. The crystal system is hexagonal with the space group $P\bar{6}$ (No. 174). The axes determined from the diffractometer setting are $a = 12.32$ Å, $c = 9.88$ Å. The calculated density is 5.09 g/cm^3, and the absorption coefficient for Ag-radiation is 93 cm^{-1}. The structure factors for the atoms were calculated from the atomic scattering factors reported by Cromer and Mann.[11] Atomic coordinates and temperature factor parameters are listed in Table 4, interatomic distances and bond angles are in Table 5, and observed and calculated structure factors are listed in Table 6. Fig. 2 shows the positions of the atoms listed in Table 4 and the positions of the pertinent symmetry related atoms to form the metal oxygen coordination polyhedra of the three neodymium atoms.

Table 4. Atomic coordinates and temperature factors with standard deviations of $NdOHCO_3$. Diffractometer data, $R = 8.2$ %.

Atom	x	y	z	B (Å^2)
O_1	0.511(2)	0.755(2)	0.0	1.0(2)
C_1	0.510(3)	0.648(3)	0.0	1.7(4)
O_2	0.512(1)	0.596(1)	0.115(1)	1.0(3)
O_3	−0.101(3)	0.090(3)	0.0	3.0(5)
C_2	0.014(4)	0.185(4)	0.0	3.0(6)
O_4	0.073(1)	0.231(1)	0.115(1)	2.3(2)
O_5	0.529(4)	0.095(3)	0.0	3.0(6)
C_3	0.460(4)	0.149(4)	0.0	3.0(6)
O_6	0.428(1)	0.178(1)	0.115(1)	1.7(2)
O_7	0.501(1)	0.703(1)	0.5	0.2(2)
C_4	0.444(3)	0.580(3)	0.5	1.9(4)
O_8	0.419(1)	0.519(1)	0.615(1)	1.3(2)
O_9	0.572(3)	0.433(3)	0.5	3.0(5)
C_5	0.470(5)	0.322(5)	0.5	5.1(9)
O_{10}	0.422(1)	0.265(1)	0.615(1)	2.3(2)
O_{11}	0.183(2)	0.096(2)	0.5	2.3(4)
C_6	0.171(3)	0.196(3)	0.5	2.5(5)
O_{12}	0.169(2)	0.248(1)	0.615(1)	2.9(3)
O_{13}	0.0	0.0	0.272(2)	1.4(3)
O_{14}	1/3	2/3	0.230(2)	1.5(3)
O_{15}	2/3	1/3	0.230(3)	3.3(5)
O_{16}	0.339(1)	0.019(1)	0.321(1)	1.7(2)
O_{17}	0.654(2)	−0.012(2)	0.180(2)	3.0(3)
Nd_1	0.2284(1)	0.1226(1)	0.2375(1)	0.95(2)[a]
Nd_2	0.2092(2)	0.4363(1)	0.2638(2)	0.83(2)[a]
Nd_3	0.5515(3)	0.1060(1)	0.2537(3)	1.00[a]

Anisotropic temperature factor parameters of the neodymium atoms with standard deviations ($\times 10^5$).

	u_{11}	σu_{11}	u_{22}	σu_{22}	u_{33}	σu_{33}	u_{12}	σu_{12}	u_{13}	σu_{13}	u_{23}	σu_{23}
Nd_1	999	48	828	56	1400	46	770	41	259	39	−4	34
Nd_2	163	53	432	44	810	47	−104	35	760	31	348	38
Nd_3	2026	66	1137	53	2242	54	613	37	−353	52	456	51

[a] The values listed are the occupancy factor of the metal atoms.

DISCUSSION

The investigation shows that the hydroxycarbonates of lanthanum, neodymium, and samarium can be prepared by hydrothermal technique. The powder patterns of the three compounds are similar to each other, and it is assumed that the compounds all belong to the same hexagonal structure described above. In the powder patterns reflections are only observed with indices that satisfy the condition $h = 3n$, $k = 3n$, and $l = 2n$ (see Table 3). The

Table 5. Interatomic distances (Å) and bond angles (degrees). Standard deviations in parentheses.

Nd_1-O_3'	2.38	(1)	$O_{11}-Nd_1-O_{12}'$	52.5	(9)
Nd_1-O_4'	2.43	(2)	$O_{11}-Nd_1-O_{10}'$	66.3	(6)
Nd_1-O_6	2.51	(2)	$O_{11}-Nd_1-O_{16}$	75.0	(8)
Nd_1-O_{10}'	2.59	(1)	$O_{11}-Nd_1-O_{13}$	71.4	(7)
Nd_1-O_{11}	2.64	(1)	$O_3'-Nd_1-O_{17}'$	82.0	(8)
Nd_1-O_{12}'	2.49	(1)	$O_3'-Nd_1-O_6$	70.4	(9)
Nd_1-O_{13}	2.46	(1)	$O_3'-Nd_1-O_4'$	56.4	(9)
Nd_1-O_{16}	2.43	(2)	$O_{13}-Nd_1-O_{17}'$	121.5	(6)
Nd_1-O_{17}'	2.46	(2)	$O_{17}'-Nd_1-O_{16}$	123.2	(6)
			$O_{16}-Nd_1-O_{13}$	113.6	(3)
Nd_2-O_1'	2.67	(1)	$O_7'-Nd_2-O_{12}'$	79.0	(6)
Nd_2-O_2'	2.44	(1)	$O_7'-Nd_2-O_{16}'$	75.9	(4)
Nd_2-O_4	2.67	(1)	$O_7'-Nd_2-O_8'$	67.9	(5)
Nd_2-O_7'	2.47	(1)	$O_1'-Nd_2-O_4$	69.1	(5)
Nd_2-O_8'	2.55	(1)	$O_1'-Nd_2-O_2'$	52.7	(6)
Nd_2-O_{12}'	2.43	(2)	$O_1'-Nd_2-O_{14}$	69.9	(6)
Nd_2-O_{14}	2.48	(1)	$O_1'-Nd_2-O_{17}'$	73.6	(7)
Nd_2-O_{16}'	2.50	(1)	$O_{16}'-Nd_2-O_{14}$	123.9	(4)
Nd_2-O_{17}'	2.45	(3)	$O_{14}-Nd_2-O_{17}'$	107.7	(4)
			$O_{17}'-Nd_2-O_{16}'$	126.8	(5)
Nd_3-O_2''	2.53	(1)	$O_9'-Nd_3-O_{10}''$	55.8	(9)
Nd_3-O_5	2.52	(1)	$O_9'-Nd_3-O_8''$	67.9	(8)
Nd_3-O_6	2.52	(2)	$O_9'-Nd_3-O_{16}$	76.9	(8)
Nd_3-O_8''	2.58	(2)	$O_5-Nd_3-O_6$	53.7	(9)
Nd_3-O_9'	2.46	(1)	$O_5-Nd_3-O_{15}$	87.0	(9)
Nd_3-O_{10}''	2.40	(2)	$O_5-Nd_3-O_{17}$	75.4	(9)
Nd_3-O_{15}	2.44	(1)	$O_5-Nd_3-O_2''$	53.4	(7)
Nd_3-O_{16}	2.37	(2)	$O_{16}-Nd_3-O_{15}$	115.1	(5)
Nd_3-O_{17}	2.47	(3)	$O_{15}-Nd_3-O_{17}$	118.3	(5)
			$O_{17}-Nd_3-O_{16}$	126.1	(6)

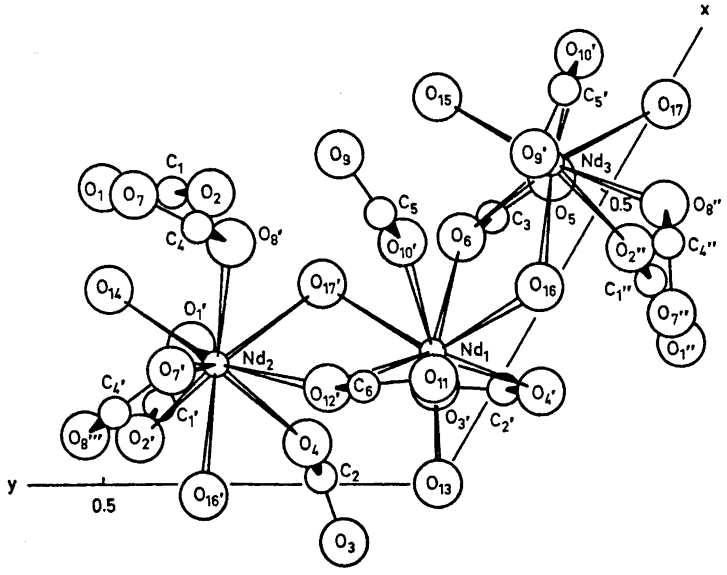

Fig. 2. Projection of the metal oxygen coordination polyhedra on (001).

Table 6. Observed and calculated structure factors of $NdOHCO_3$. Reading from the left to the right, the column contains the values h, k, l, F_{obs}, F_{calc}.

Table 6. Continued.

5	0	8	15	16	10	3	8	28	35	4	7	9	99	65	1	1	10	9	9	5	6	10	25	29	3	3	11	33	26	2	4	12	29	25
5	1	8	44	47	11	1	8	52	54	4	8	9	77	68	1	2	10	28	22	5	7	10	49	50	3	4	11	68	64	2	5	12	16	24
5	2	8	42	51	11	2	8	68	64	5	0	9	186	168	1	3	10	25	26	6	0	10	249	238	3	5	11	106	101	2	6	12	23	31
5	3	8	31	32	12	0	8	205	188	5	1	9	98	108	1	4	10	44	48	6	1	10	34	32	3	6	11	32	38	3	1	12	28	19
5	4	8	51	55	12	1	8	59	63	5	2	9	38	36	1	5	10	34	33	6	2	10	29	35	3	7	11	47	50	3	2	12	26	25
5	5	8	53	55	1	1	9	19	21	5	3	9	101	112	1	6	10	31	34	6	3	10	228	213	4	0	11	84	83	3	3	12	191	178
5	6	8	33	42	1	2	9	88	106	5	4	9	89	83	1	7	10	59	62	6	4	10	29	28	4	1	11	33	33	3	4	12	16	17
5	7	8	48	57	1	3	9	79	92	5	5	9	47	58	1	8	10	35	39	6	5	10	27	28	4	2	11	82	81	3	5	12	24	18
5	8	8	56	57	1	4	9	62	66	5	6	9	81	98	1	9	10	39	36	6	6	10	193	172	4	3	11	66	65	4	0	12	17	12
5	9	8	44	48	1	5	9	98	97	5	7	9	82	68	2	0	10	19	13	7	0	10	15	28	4	4	11	39	35	4	1	12	22	25
6	0	8	294	338	1	6	9	62	70	5	8	9	27	35	2	1	10	19	20	7	1	10	99	61	4	5	11	88	87	4	2	12	26	28
6	1	8	35	43	1	7	9	55	53	6	0	9	27	28	2	2	10	41	38	7	2	10	39	48	4	6	11	65	56	4	3	12	16	18
6	2	8	87	48	1	8	9	87	83	6	1	9	24	24	2	3	10	24	22	7	4	10	59	58	5	0	11	111	104	5	0	12	20	18
6	3	8	283	286	1	9	9	58	62	6	2	9	96	96	2	4	10	38	33	7	5	10	45	46	5	1	11	104	98	5	1	12	26	29
6	4	8	43	40	1	10	9	48	44	6	3	9	28	39	2	5	10	32	35	8	1	10	48	42	5	2	11	21	26	5	2	12	17	28
6	5	8	31	32	2	0	9	103	111	6	4	9	49	49	2	6	10	31	33	8	2	10	42	49	5	3	11	111	103	5	3	12	24	21
6	6	8	238	221	2	1	9	93	102	6	5	9	79	84	2	7	10	40	40	8	3	10	21	26	5	4	11	94	82	6	0	12	165	165
6	7	8	34	33	2	3	9	99	102	6	6	9	25	32	2	8	10	43	49	8	4	10	220	198	5	5	11	43	44	6	1	12	27	26
6	8	8	28	29	2	4	9	92	85	6	7	9	40	31	2	9	10	27	42	9	1	10	40	39	6	0	11	37	35	6	2	12	28	27
7	1	8	48	46	2	5	9	31	33	7	0	9	37	47	3	1	10	28	28	9	2	10	38	37	6	1	11	87	74	7	1	12	27	33
7	2	8	57	55	2	6	9	97	96	7	1	9	57	55	3	2	10	24	28	10	1	10	58	58	6	2	11	105	94	1	0	13	41	79
7	4	8	60	63	2	7	9	75	76	7	2	9	72	72	3	3	10	233	236	1	0	11	65	69	6	3	11	34	32	1	1	13	13	14
7	5	8	50	56	2	8	9	38	42	7	3	9	45	45	3	4	10	26	28	1	2	11	93	98	6	4	11	69	49	1	2	13	90	93
7	6	8	26	34	2	9	9	83	88	7	4	9	61	59	3	5	10	24	18	1	3	11	88	82	7	0	11	78	59	1	3	13	74	77
7	7	8	53	68	2	10	9	78	69	7	5	9	77	66	3	6	10	233	211	1	4	11	32	31	7	1	11	49	47	1	4	13	22	19
8	0	8	19	21	3	0	9	32	32	7	6	9	40	35	3	8	10	21	15	1	5	11	101	93	7	2	11	82	75	2	0	13	83	93
8	1	8	51	52	3	1	9	84	87	8	0	9	99	100	4	0	10	13	22	1	6	11	79	78	7	3	11	53	56	2	1	13	98	83
8	2	8	56	54	3	2	9	99	103	8	1	9	92	89	4	1	10	42	43	1	7	11	46	47	8	0	11	89	86	2	2	13	32	30
8	3	8	28	16	3	3	9	35	31	8	2	9	41	46	4	2	10	28	32	1	8	11	81	79	8	1	11	67	82	2	3	13	67	67
8	4	8	66	61	3	4	9	74	71	8	3	9	98	93	4	3	10	19	28	2	0	11	109	105	8	2	11	47	46	2	4	13	81	71
8	5	8	62	60	3	5	9	99	105	8	4	9	83	74	4	4	10	32	39	2	2	11	81	88	8	4	11	28	29	3	0	13	98	88
8	6	8	33	30	3	6	9	27	19	8	5	9	25	36	4	5	10	36	98	2	3	11	96	98	1	2	12	27	23	3	1	13	77	72
9	0	8	264	250	3	7	9	41	42	9	0	9	38	31	4	6	10	25	29	2	4	11	87	83	1	3	12	20	23	3	2	13	88	86
9	1	8	43	47	3	8	9	89	92	9	1	9	64	96	4	7	10	52	61	2	5	11	22	27	1	4	12	21	26	3	3	13	34	29
9	2	8	57	55	4	0	9	79	77	9	2	9	85	81	5	0	10	16	15	2	6	11	104	108	1	5	12	23	27	4	0	13	71	71
9	3	8	246	233	4	1	9	63	58	9	3	9	24	27	5	1	10	32	28	2	7	11	82	69	1	6	12	20	26	4	1	13	20	19
9	4	8	52	48	4	2	9	98	89	10	0	9	43	30	5	2	10	31	34	2	8	11	47	44	1	7	12	21	32	4	2	13	78	73
9	5	8	38	43	4	3	9	74	74	10	1	9	45	41	5	3	10	28	18	3	0	11	98	94	2	0	12	20	14					
10	1	8	56	59	4	5	9	83	80	10	2	9	63	65	5	4	10	49	47	3	1	11	82	86	2	1	12	26	18					
10	2	8	58	57	4	6	9	41	54	11	0	9	108	101	5	5	10	51	51	3	2	11	97	93	2	3	12	24	22					

powder patterns could thus be indexed on hexagonal cells with $a_H = a/3$, and $c_H = c/2$. Such cells would, however, only contain one formula unit of $MeOHCO_3$, which is in conflict with all the hexagonal space groups. From single crystal investigations of $NdOHCO_3$ the correct unit cell has been found, and it has been assumed that the correct unit cells of $LaOHCO_3$ and of $SmOHCO_3$ have the dimensions listed in Table 3. A plot of the unit cell parameters *vs.* the ionic radii [2] are shown in Fig. 3. which illustrates the lanthanide contraction.

Caused by the uneven scattering power of the heavy metal atom and the light oxygen and carbon atoms, it should not be expected that an X-ray investigation would give a structure with a high precision in the determination of the positions of the light atoms. Using the atomic numbers of the elements

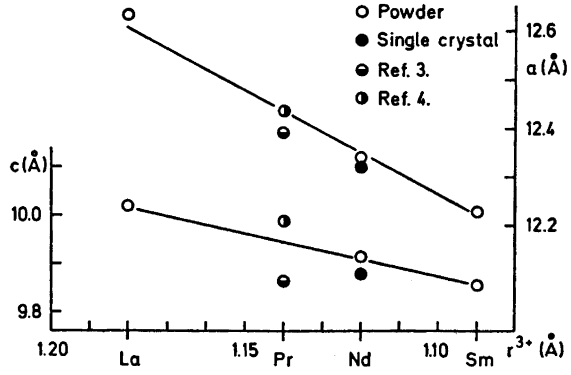

Fig. 3. Unit cell parameters (Å) of hexagonal rare earth hydroxycarbonates *vs.* ionic radii of Me^{3+} (Å). The unit cells from Refs. 3 and 4 are transformed to unit cells containing 18 formula units.

in $NdOHCO_3$ in a calculation of scattering contributions, it is found that the metal atom has an average scattering contribution of 92.5 % of the total intensity, and all the other atoms are only contributing with 7.5 % to the total intensity. In the last Fourier maps calculated, it was, however, possible to identify all the light atoms of the structure.

The occupancy factors of Nd_1 and Nd_2 have been used as parameters in the refinements and the occupancy factor of Nd_2 is significantly different from 1.0. Nd_2 is coordinated with the oxygen atoms of the carbonate ions in a way different from that of Nd_1 and Nd_3 (see Fig. 2). The carbonate ions $O_1'-C_1'-O_2'$ and $O_7'-C_4'-O_8'''$ are almost superimposed upon each other, and Nd_2 is bonded to the atoms O_1', O_2', and O_7'. The carbonate ions $O_3'-C_2'-O_4'$ and $O_{11}-C_6-O_{12}'$ are not superimposed upon each other, and Nd_1 is bonded to O_3', O_4', O_{11}, and O_{12}', and the carbonate ions $O_5-C_3-O_6$ and $O_9'-C_5'-O_{10}'$ are not superimposed upon each other, and Nd_3 is bonded to O_5, O_6, O_9', and O_{10}'. It is also observed (see below) that Nd_2 has the longest metal-oxygen distances. The coordination of Nd_2 is thus different from the coordination of Nd_1 and Nd_3. This can possibly explain that the number of vacancies at the position of Nd_2 is different from and greater than the number of vacancies at the positious of the atoms Nd_1 and Nd_3. No attempts have been made to introduce occupancy factors of the atoms to which Nd_2 is bonded as parameters in the refinements.

The three metal atoms are nine coordinated with oxygen atoms. Six oxygen atoms belong to carbonate ions and three oxygen atoms to hydroxyl ions. The average distances for the bonds metal to oxygen (carbonate) are Nd_1-O 2.51(1) Å, Nd_2-O 2.54(1) Å, and Nd_3-O 2.50(1) Å, and for metal to oxygen (hydroxyl) are the average distances Nd_1-O 2.45(2) Å, Nd_2-O 2.48(2) Å, and Nd_3-O 2.43(2) Å.

The neodymium-oxygen (carbonate) distances found in $NdOHCO_3$ are comparable with the corresponding distances of 2.47(3) Å and 2.64(2) Å found in $Nd_2O_2CO_3$.[2]

The crystal structure of $NdOHCO_3$ and that of $Nd_2O_2CO_3$ have common characteristics. Both structures are layer structures with the layers held together by the carbonate ions. Two of the three oxygen atoms of the carbonate ions are placed superimposed upon each other in the direction of the *c*-axis, and the third oxygen atom and the carbon atom are placed on mirror planes perpendicular to the *c*-axis. The carbonate ions are ordered in the $NdOHCO_3$ structure and are statistically arranged in the structure of $Nd_2O_2CO_3$. The carbon oxygen distances of 1.31(1) Å are in good agreement with distances of 1.28 Å found in the carbonate ions of $KHCO_3$ by neutron diffraction.[13]

REFERENCES

1. Christensen, A. N. In *Les Eléments des Terres Rares*, Colloques Internationaux du Centre National de la Recherche Scientifique No. 180. Edited by: Centre National de la Recherche Scientifique, Paris 1970, Vol. I, p. 279.
2. Christensen, A. N. *Acta Chem. Scand.* **24** (1970) 2440.
3. Caro, P. E., Lemaitre-Blaise, M., Dexpert, H. and Sawyer, J. *C. R. Acad. Sci., Ser. C* **272** (1971) 57.
4. Haschke, J. M. and Eyring, Le Roy. *Inorg. Chem.* **10** (1971) 2267.

5. Oftedal, I. *Z. Kristallogr.* **78** (1931) 462; **79** (1931) 437.
6. Shafer, M. W. and Roy, R. *J. Am. Ceram. Soc.* **42** (1959) 563.
7. Schwarzenbach, G. *Die komplexometrische Titration*, Stuttgart 1960, p. 69.
8. Wells, M. J. *Acta Cryst.* **13** (1960), 722.
9. Busing, W. R., Martin, K. O. and Levy, H. A. (1962) *ORFLS, A Fortran Crystallographic Least Squares Program*, Oak Ridge National Laboratory Report, ORNL-TM-305. *LINUS* is a 1971 version of *ORFLS*.
10. Pawley, G. S. *Constrained Refinements in Crystallography. Adv. Struct. Res. Diffr. Methods* **4** (1972) 1.
11. Cromer, D. T. and Mann, J. B. *Acta Cryst.* **A 24** (1968) 321.
12. Shannon, R. D. and Prewitt, C. T. *Acta Cryst.* **B 25** (1969) 925.
13. Herpin, P. and Meriel, P. *J. Phys. (Paris)* **25** (1964) 484.

Received May 8, 1973.

ACTA CHEMICA SCANDINAVICA 27 (1973) 2983–2988

Preparation of 1,2,3-Triazoles by Base-catalyzed Dehydration of 5-Hydroxy-Δ^2-1,2,3-triazolines

CARL ERIK OLSEN

*Department of Organic Chemistry, Technical University of Denmark, DK-2800 Lyngby, Denmark and Organic Chemical Laboratory, Royal Veterinary and Agricultural University, Thorvaldsensvej 40, DK-1871 Copenhagen, Denmark**

5-Hydroxy-Δ^2-1,2,3-triazolines are easily dehydrated to 1,2,3-triazoles on treatment with hot methanolic potassium hydroxide. The yield is very high when the substituent at the 1-position is an alkyl group, but rather low when it is a phenyl group. The potassium *tert*-butoxide catalyzed reactions of benzyl methyl ketone with organic azides give 1,2,3-triazoles directly. NMR spectra of the 1,2,3-triazoles are discussed.

The base-catalyzed reaction of organic azides with carbonyl compounds is a long known method for the preparation of 1,2,3-triazoles,[1–4] 5-hydroxy-Δ^2-1,2,3-triazolines being suspected intermediates (Scheme 1).[1,4,5] Using the particular base potassium *tert*-butoxide (PTB) we noted [6–8] that the reaction stopped at the stage of the triazoline. This could be due to either of two facts. First, the substituent R^4 is alkyl in our experiments, whereas it has been groups like RCO-, ROOC-, *etc.* in previous preparations. Assuming that the dehydration reaction (III→IV) is base-catalyzed, it is quite reasonably accelerated when R^4 is electronegative, since the adjacent proton, which is to be removed, is activated. Second, the lack of spontaneous dehydration could be due to the reaction conditions used. However, the PTB-catalyzed reactions of methyl benzyl ketone (R^4=Ph, R^5=Me) with methyl azide, benzyl azide, and phenyl azide, under conditions otherwise similar to those employed in the preparation of 5-hydroxy triazolines, resulted in the exclusive formation of 4-phenyl-5-methyl-1,2,3-triazoles, although R^4 in these cases is only moderately electronegative. The yields, which were very high in all three cases, appear from Table 2 in the experimental part.

Thus we conclude that in the presence of strong bases 5-hydroxy-Δ^2-1,2,3-triazolines may only be isolated if electronegative substituents are not present at the 4-position. Incidentally phenyl azide was also allowed to react

* Present address.

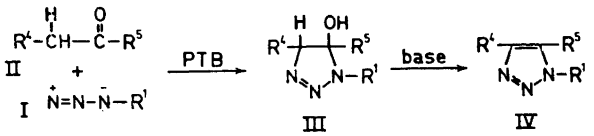

Scheme 1.

with benzyl phenyl ketone in the presence of sodium ethoxide. This resulted in a high yield of 1,4,5-triphenyl-1,2,3-triazole.

For R^4 being an alkyl group the proton at the 4-position of the hydroxy triazoline is not completely unactivated, however. There is still a proximate electron attracting azo group capable of activating it, and dehydration to 1,2,3-triazoles can be accomplished by treatment with hot methanolic potassium hydroxide (*cf.* Ref. 9). The results of a number of experiments are summarized in Table 3 in the experimental part. The yields of 1,2,3-triazoles are generally excellent for R^1 being alkyl but rather low for R^1 being phenyl. However, these yields are not necessarily the optimum obtainable, since a standard procedure, refluxing for 2 h, has been used all over, except in a few cases where an extension of the reaction time proved necessary to force the reaction to completion.

As to the mechanism of the dehydration reaction we can say safely only that the base-catalyzed removal of the proton at the 4-position is irreversible. When conducting the dehydration reaction in deuterated solvents (1,4,5-trimethyl-5-hydroxy-Δ^2-1,2,3-triazoline in deuterium oxide and 1-phenyl-4,5-dimethyl-5-hydroxy-Δ^2-1,2,3-triazoline in tetradeuteriomethanol) containing potassium hydroxide in such amounts as to make the reaction proceed with a rate convenient for an NMR study, the proton at the 4-position was not exchanged with deuterium (*cf.* Ref. 10 for experimental details). Consequently a 'preequilibrium' type E1cB mechanism[11] can be ruled out. It is more difficult to distinguish between an 'irreversible' type E1cB mechanism and an E2 mechanism. The preferred mode of elimination from the triazolines is apparently *trans*: dehydration of 1-benzyl-4,5-tetramethylene-5-hydroxy-Δ^2-1,2,3-triazoline, the only investigated hydroxy triazoline in which a *trans* orientation of the departing groups (H and OH) is impossible, required boiling for 30 h to go to completion, whereas 2 h was sufficient in almost all other cases (Table 3); but according to McLennan,[11] the stereochemistry of the elimination is a very unreliable criterion. The best means for deciding between the two possible mechanisms would probably be to determine the k_D/k_H isotope effect at the 4-position.[11,12].

Apparently a *tert*-butyl group at the 5-position retards the dehydration reaction (case c and l), possibly because a proper conformation of the triazoline ring is difficult to attain. A phenyl group seems to have the same effect.[8]

NMR spectra were recorded for all 1,2,3-triazoles prepared, and the data have been collected in Table 1. Some additional data for triazoles from the literature have also been included. The data in Table 1 (in conjunction with those for compounds IVd, XIIId, and XVIId of Ref. 8) confirm the observation

Table 1. Chemical shifts (δ-values) and coupling constants (cps) of some 1,2,3-triazoles (deuteriochloroform).

IV	R^1	R^4	R^5	R^1 [a]	R^4 [a]	R^5 [a]
a[13]	Me	H	H	4.10	7.74	7.59
b	Me	Me	Me	3.92s	2.22s 2.26s	
c	Me	Me	Bu^t	4.12s	2.44s	1.43s
d	Me	Me	Ph	3.97s	2.34s	7.2 – 7.7m
e	Me	Ph	Me	3.98s	7.2 – 7.9m	2.43s
f[14]	$PhCH_2$	H	H	7.33"s" 5.58s	7.50 7.70	(J = 1.0)
g[8]	$PhCH_2$	H	Me	7.0 – 7.5m 5.51s	7.48	2.19d (J = 0.8)
h[8]	$PhCH_2$	H	Bu^t	6.8 – 7.6m 5.71s	7.51s	1.28s
i[8]	$PhCH_2$	H	Ph	6.6 – 7.7m 5.52s	7.70	
j	$PhCH_2$	Me	Me	7.2 – 7.5m 5.45s	2.25s	2.08s
k	$PhCH_2$	Me	Et	7.0 – 7.5m 5.49s	2.29s	0.96t 2.55q
l	$PhCH_2$	Me	Bu^t	6.8 – 7.4m 5.70s	2.48s	1.29s
m	$PhCH_2$	Me	Ph	6.8 – 7.6m 5.46s	2.31s	
n	$PhCH_2$	$-(CH_2)_4-$		7.0 – 7.6m 5.44s	1.6 – 3.0m	
o	$PhCH_2$	Ph	Me	7.0 – 7.9m 5.55s		2.32s
p[15]	Ph	H	H	7.3 – 7.9m	7.86d 8.02d	(J = 1.0)
q[8]	Ph	H	Me	7.53"s"	7.60	2.38
r[9]	Ph	H	Ph	7.1 – 7.6m	7.86s	
s[15]	Ph	Me	H	7.3 – 7.9m	2.45d (J = 0.7)	7.74
t	Ph	Me	Me	7.50"s"	2.28 2.37	(J = 0.4)
u	Ph	Me	Et	7.53"s"	2.39s	1.08t 2.70q
ü	Ph	Me	Bu^t	7.2 – 7.7m	2.54s	1.23s
v	Ph	Me	Ph	7.0 – 7.6	2.46s	
w[15]	Ph	Et	H	7.2 – 7.9	1.36t 2.86q	7.74"s"
x[9]	Ph	Ph	H	7.2 – 8.1		8.19s
y	Ph	Ph	Me	7.55"s"	7.3 – 8.0m	2.49s
z	Ph	Ph	Ph	7.1 – 7.8		

[a] s, singlet; d, doublet; t, triplet; q, quartet; m, multiplet.

by Begtrup [16] that a phenyl group attached at the 1-position of a 1,2,3-triazole ring generally appears as a rather sharp singlet if a methyl group is present at the 5-position. An ethyl group, but not a *tert*-butyl group, seems to have the same effect.

The considerable downfield displacement of two of the protons of phenyl groups at the 4-position, observed with the triazoles IVe, o, x, y, z, possibly originates in a mesomeric effect from the triazole nucleus. These easily recognizable protons lie within the range 7.6 – 7.9 ppm.

An interesting feature of the NMR spectra is that an alkyl group at the 5-position is shielded by a benzyl group at the 1-position, as appears from a comparison of IVj with IVb, IVl with IVc, or IVo with IVe. This shielding effect must be due to the ring current of the phenyl group, and the conformation necessary for a proper action of this long-range shielding effect (Fig. 1) might be favored by *n*-π electron repulsion [17–19] between the lone-pair of the middle nitrogen atom and the electron cloud around the benzylic phenyl group. A *tert*-butyl group at the 5-position seems to be long-range shielded by a phenyl group at the 1-position, as may be seen on comparing IVü with IVc.

Fig. 1.

EXPERIMENTAL

Melting points are uncorrected. NMR spectra were recorded on a Varian A-60 instrument, using TMS as an internal standard. Chemical shifts are given as δ-values. All starting materials have been described in Ref. 7 or are commercially available.

Reaction of methyl azide with methyl benzyl ketone. Methyl azide (0.02 – 0.03 mol as an approx. 25 % solution in *tert*-butyl alcohol and methyl benzyl ketone (2.67 ml, 0.02 mol) were added to 20 ml of PTB stock solution.[8] The reaction mixture gradually turned red, and heat evolution was observed. After standing for 4 h, the mixture was poured into 150 ml of ice-water. The product was extracted with methylene chloride. Evaporation of the solvent and crystallization of the residue from ethyl acetate – pentane gave 3.18 g of a pure product (Table 2).

Table 2. 1-Substituted 4-phenyl-5-methyl-1,2,3-triazoles prepared from methyl benzyl ketone and organic azides.

IV	R^1	React. time h	Yield %	m.p. °C	Formula	Analyses % C Calc.	% C Found	% H Calc.	% H Found	% N Calc.	% N Found
e	Me	4	92	97 – 98	$C_{10}H_{11}N_3$	69.34	69.19	6.40	6.50	24.26	23.88
o	$PhCH_2$	2	85	93 – 94	$C_{16}H_{15}N_3$	77.08	77.03	6.06	6.15	16.86	16.78
y	Ph	0.5	79	155 – 156	$C_{15}H_{13}N_3$	76.56	76.40	5.57	5.78	17.86	17.96

Table 3. 1,4,5-Trisubstituted 1,2,3-triazoles (IV) prepared from 5-hydroxy-Δ^2-1,2,3-triazolines. When referring to picrates experimental data (yield, melting point, and solvent of recrystallization) are put in parenthesis. EtAc = ethyl acetate, P = pentane, cyHex = cylohexane.

IV	R^1	R^4	R^5	Reaction time h	Yield %	M.p. °C	Recryst. solvent	Formula	% C Calc.	% C Found	% H Calc.	% H Found	% N Calc.	% N Found
b	Me	Me	Me	2	90	50–51	EtAc–P	$C_5H_9N_3$	54.05	53.97	8.16	8.30	37.83	37.63
c	Me	Me	Bu^t	8	93	68–69	EtAc–P	$C_8H_{15}N_3$	62.72	63.11	9.87	10.18	27.43	26.87
d	Me	Me	Ph	2	95	103–104	EtAc–P	$C_{10}H_{11}N_3$	69.34	69.36	6.40	6.44	24.26	24.33
j	$PhCH_2$	Me	Me	2	93	108–109	EtAc–P	$C_{11}H_{13}N_3$	70.57	70.51	7.00	6.89	22.45	22.36
k	$PhCH_2$	Me	Et	2	(70)[a]	(95–96)	(Benzene)	$(C_{18}H_{18}N_6O_7)$	50.23	50.23	4.22	4.29	19.53	19.38
l	$PhCH_2$	Me	Bu^t	3	91[b]	(87–88)[c]	(EtAc–P)	$(C_{20}H_{22}N_6O_7)$	52.40	52.48	4.84	5.01	18.33	18.51
m	$PhCH_2$	Me	Ph	2	93[b]	65–66[d]	EtAc–P	$C_{16}H_{15}N_3$	77.08	76.98	6.06	6.27	16.86	16.83
n	$PhCH_2$	$-(CH_2)_4-$		30	9[d]	79[e]	cyHex	$C_{13}H_{15}N_3$	73.23	73.17	7.09	7.15	19.71	19.63
t	Ph	Me	Me	2	(21)[a]	(144–145)[f] 85–86[g]	(Benzene) P							
u	Ph	Me	Et	2	7[b,d]	(143–144)[h,c]	(Benzene)	$(C_{17}H_{16}N_6O_7)$	49.04	48.89	3.88	4.01	20.19	20.08
ü	Ph	Me	Bu^t	2	10	106–108	P	$C_{13}H_{17}N_3$	72.52	72.41	7.96	8.11	19.52	19.50
v	Ph	Me	Ph	2	33	120–121	EtAc–P	$C_{15}H_{13}N_3$	76.56	76.55	5.57	5.59	17.86	17.77

[a] Picrate obtained by successive treatment with acetic anhydride and picric acid. [b] Oil, purity tested by NMR. [c] Picrate obtained by treatment with picric acid. [d] After purification by TLC. [e] Reported [21] m.p. 77°C. [f] Reported [22] m.p. 131°C. [g] The free triazole was recovered by the method of Nicolaus and Testa.[23] [h] Reported [9] m.p. 144–145.5°C.

Reaction of benzyl azide with methyl benzyl ketone. Benzyl azide (2.48 ml, 0.02 mol) and methyl benzyl ketone (2.67 ml, 0.02 mol) were added to 20 ml of PTB stock solution. The reaction mixture turned red, and heat evolution was observed after a few minutes. After 2 h, the mixture was poured into 150 ml of ice-water. The crystalline product was washed with water and pentane, yielding 4.22 g (85 %) of a crude product with m.p. 92 – 93°C. Recrystallization from ethyl acetate – pentane gave the pure product (Table 2).

Reaction of phenyl azide with methyl benzyl ketone. Phenyl azide (2.2 ml, 0.02 mol) and methyl benzyl ketone (2.67 ml, 0.02 mol) were added to 20 ml of PTB stock solution, which had been previously cooled to beginning crystallization. Cooling was continued during the first minute of reaction. The product separated after half a minute, causing the mixture to solidify. After 15 min, 30 g of ice was added, and the crystalline product was filtered off, washed with water and pentane, yielding 3.74 g (79 %) of a product with m.p. 154 – 155°C. Recrystallization from ethyl acetate gave the pure product (Table 2).

Reaction of phenyl azide with benzyl phenyl ketone. Phenyl azide (2.2 ml, 0.02 mol) and benzyl phenyl ketone (3.9 g, 0.02 mol) were dissolved in a solution of 0.7 g of sodium in 15 ml of ethanol. Heat evolution occurred, and the mixture solidified after some minutes. After standing for 20 hours, the product was filtered off, washed with ethanol and water, leaving 5.0 g (84 %) of crude 1,4,5-triphenyl-1,2,3-triazole. After recrystallization from toluene the m.p. was 228 – 229°C (reported 230.5 – 231°C [20]).

General procedure for the conversion of 5-hydroxy-Δ^2-1,2,3-triazolines into 1,2,3-triazoles. The hydroxy triazoline [7] (*ca.* 2 mmol) and 1 g of potassium hydroxide are dissolved in 15 ml of methanol. The mixture is refluxed for a few hours (*cf.* Table 3). The solvent is removed, and 10 ml of water is added. Extraction with methylene chloride, drying over Na_2SO_4, and evaporation of the solvent gives the crude product, which can be purified by recrystallization, TLC, and/or by conversion into the picrate, eventually after treatment with acetic anhydride in order to avoid co-precipitation of amine picrate (*cf.* Table 3).

Acknowledgements. The author thanks Professor C. Pedersen for advice and inspiration and Dr. M. Begtrup for many fruitful discussions.

Microanalyses were performed by Dr. A. Bernhardt.

REFERENCES

1. Grundmann, C. In *Methoden der org. Chemie*, 4. Ed., Vol. 10/3, p. 813 (1965).
2. Benson, F. R. and Savell, W. L. *Chem. Rev.* **46** (1950) 1.
3. Boyer, J. H. In *Heterocyclic Compounds*, Wiley, New York 1961, Vol. 7, p. 384.
4. L'Abbe, G. *Ind. Chim. Belge* **36** (1971) 3.
5. Regitz, M. *Angew. Chem.* **79** (1967) 786.
6. Olsen, C. E. and Pedersen, C. *Tetrahedron Letters* **1968** 3805.
7. Olsen, C. E. and Pedersen, C. *Acta Chem. Scand.* **27** (1973) 2279.
8. Olsen, C. E. *Acta Chem. Scand.* **27** (1973) 1987.
9. Munk, M. E. and Kim, Y. K. *J. Am. Chem. Soc.* **86** (1964) 2213.
10. Olsen, C. E. *Acta Chem. Scand.* **27** (1973) 2989.
11. McLennan, D. J. *Quart. Rev.* **21** (1967) 490.
12. Crosby, J. and Stirling, C. J. M. *J. Am. Chem. Soc.* **90** (1968) 6869.
13. Elguero, J., Gonzalez, E. and Jacquier, R. *Bull. Soc. Chim. France* **1967** 2998.
14. Wiley, R. H., Hussung, K. F. and Moffat, J. *J. Org. Chem.* **21** (1956) 190.
15. Bertho, A. *Ber.* **58** (1925) 859.
16. Begtrup, M. *Unpublished results.*
17. Yonezawa, T., Morishima, I. and Fukuta, K. *Bull. Chem. Soc. Japan* **41** (1968) 2297.
18. Karabatsos, G. J. and Taller, R. A. *Tetrahedron* **24** (1968) 3923.
19. Bjørgo, J., Boyd, D. R., Watson, C. G. and Jennings, W. B. *Tetrahedron Letters* **1972** 1747.
20. Moulin, F. *Helv. Chim. Acta* **35** (1952) 177.
21. Bianchetti, G., Croce, P. D., Pocar D. and Vigevani, A. *Gazz. Chim. Ital.* **97** (1967) 301.
22. Rojahn, C. A. and Trieloff, H. *Ann.* **445** (1925) 302.
23. Nicolaus, B. J. R. and Testa, E. *Angew. Chem.* **73** (1961) 655.

Received May 2, 1973.

ACTA CHEMICA SCANDINAVICA 27 (1973) 2989–2996

Base Induced Conversions of 5-Hydroxy-Δ^2-1,2,3-triazolines, Intermediates in the Reaction of Organic Azides with Carbonyl Compounds

CARL ERIK OLSEN

*Department of Organic Chemistry, Technical University of Denmark, DK-2800 Lyngby, Denmark and Organic Chemical Laboratory, Royal Veterinary and Agricultural University, Thorvaldsensvej 40, DK-1871 Copenhagen, Denmark**

Treatment of 1-phenyl-4,5-dimethyl-5-hydroxy-Δ^2-1,2,3-triazoline with potassium hydroxide in methanol gives a mixture of 3-diazobutanone, aniline, and 1-phenyl-4,5-dimethyl-1,2,3-triazole. Anions of 5-hydroxy-Δ^2-1,2,3-triazolines are shown to be capable of existing in either a closed or an open form depending on substituents.

A unifying scheme for reactions of organic azides and carbonyl compounds is discussed with emphasis on the relation between reaction course, substituents, and medium.

In a previous paper[1] it was shown that 1-phenyl-5-hydroxy-Δ^2-1,2,3-triazolines gave much lower yields of 1,2,3-triazoles on treatment with potassium hydroxide in hot methanol than did the corresponding 1-alkyl triazolines. An explanation to this has now been found by using more gentle reaction conditions and by following the reaction by NMR spectroscopy. 1-Phenyl-4,5-dimethyl-5-hydroxy-Δ^2-1,2,3-triazoline[2] (IX, R^1=Ph, R_a^4=R^5=Me, R_b^4=H) (Scheme 1) was dissolved in tetradeuteriomethanol, a trace of potassium hydroxide was added, and NMR spectra were recorded at intervals. The results are shown in Fig. 1. The first spectrum (Fig. 1a) shows the two diastereomeric triazolines at equilibrium[2] prior to addition of KOH. Addition of a trace of KOH (Fig. 1b) accelerates the equilibration to such an extent that a time-averaged spectrum results (*cf.* Ref. 2). One day later (Fig. 1c) it is obvious that a conversion has begun to take place. This conversion is complete after three days (Fig. 1d). By adding a small amount of reference material, the signals at 2.26, 2.33, and 7.57 ppm were shown to be due to the expected[1] dehydration product, 1-phenyl-4,5-dimethyl-1,2,3-triazole (XVI). In a similar way the multiplet at 6.5–7.3 ppm was found to be due

* Present address.

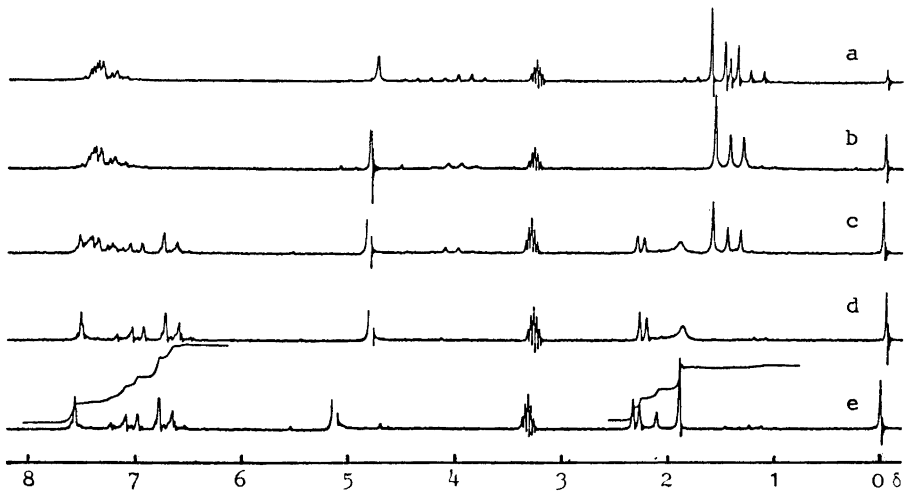

Fig. 1. NMR spectra showing conversions of 1-phenyl-4,5-dimethyl-5-hydroxy-Δ^2-1,2,3-triazoline (in CD_3OD). (a) prior to addition of KOH; (b) after addition of a trace of KOH; (c) one day later; (d) three days later; (e) after lowering the temperature to 0°C.

to aniline, a result that was confirmed by TLC. The molar ratio between these two compounds was measured to be 0.36.

Elimination of aniline from the triazoline or its ring-chain tautomer, the α-triazeno ketone IV, could result in 3-diazobutanone (V, $R_a^4 = R^5 = Me$), and the development of a yellow color supported this assumption. However, the broad signal at 1.92 ppm seemed unconsistent with this at first glance; but lowering the temperature to 0°C (Fig. 1e) caused the signal to split into two signals owing to the reduced rate of rotation about the partial double bond between the two carbon atoms in the grouping $N=N-C-C=O$.[3] The two signals stem from the methyl group adjacent to the diazo group in two conformers. The methyl group adjacent to the carbonyl group does not show up, because the hydrogen atoms have been exchanged with deuterium in the slightly alkaline deuteriomethanolic solution. It is to be noted that $R_b^4 = H$ is not exchanged with deuterium (Fig. 1b and c) in accordance with the statement made earlier[1] that there is no preequilibration between IV and its enol-anion. Undeuterated 3-diazobutanone resulted on carrying out a preparative scale experiment in regular methanol.

The overall conversion from butanone and phenyl azide[2] constitutes a diazo group transfer[4] from phenyl azide to a ketone, to our knowledge the first documented one. Tosyl azide is normally used as the donor of the diazo group in this kind of reaction.[4]

The experiment also illustrates that the use of phenyl azide from a synthetic point of view may be advantageous in cases where isomeric diazo compounds will result from the use of tosyl azide. In fact, the IR spectrum of the above diazobutanone showed one diazo band only, whereas that produced

using tosyl azide exhibits two.[5] The reason for this lies in the fact that the intermediate hydroxy triazoline in the phenyl case, in contrast to the tosyl case, is stable enough to be isolated; it may thus be purified before being converted into the diazo compound.

Using reaction conditions similar to those above, the corresponding reaction of 1-(*p*-nitrophenyl)-4,5-dimethyl-5-hydroxy-Δ^2-1,2,3-triazoline [2] was completed within an hour.

As described earlier,[2] 5-hydroxy-Δ^2-1,2,3-triazolines are in solution in equilibrium with α-triazeno ketones. But so far there has been no discussion of the structure of the anions of these compounds. A few potassium salts were mentioned in connection with the preparation of the triazolines, where they separated spontaneously.[2] A more general way of preparing them is to add the appropriate triazoline (or triazene) to a suspension of potassium *tert*-butoxide (PTB) in ether. The triazoline then dissolves, and after a few minutes the potassium salt precipitates. The salts are very sensitive to moisture, and many of them are relatively unstable, particularly those with $R_b^4 = H$.

The potassium salt of 1,5-diphenyl-4,4-dimethyl-5-hydroxy-Δ^2-1,2,3-triazoline [2] dissolved in dimethyl sulfoxide (DMSO) is clearly in the ring-closed form (alkoxide form, VIII), the NMR spectrum showing the two methyl groups at C-4 as two distinct, although a little broadened, signals at 1.2 and 0.48 ppm (the free triazoline in DMSO shows these signals at 1.47 and 0.58 ppm, respectively). The latter signal stems from that methyl group oriented *cis* to the phenyl group at C-5 (*cf.* Ref. 2). The enhanced shielding in the anion is probably due to the overall increased electron density in the molecule. In agreement with the above conclusion the IR spectrum does not show any C=O band (nujol).

In contrast, the potassium salt obtained by treatment of 1-phenyl-4,4-dimethyl-5-isopropyl-5-hydroxy-Δ^2-1,2,3-triazoline [2] with PTB in ether must be present in the ring-opened form (III), since the IR spectrum (nujol) shows a rather strong C=O band at 1695 cm^{-1}. The NMR spectrum taken in DMSO-d_6 (Fig. 2) is in agreement with this interpretation, the two methyl groups at C-4 now being equivalent (located at 1.23 ppm). The two isopropyl methyl

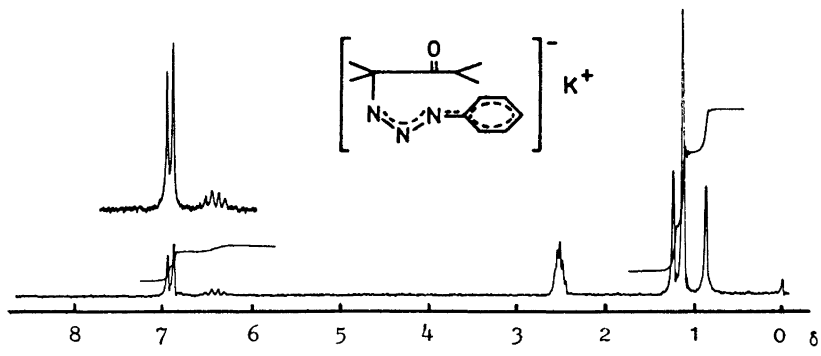

Fig. 2. NMR spectrum of the potassium salt obtained from 1-phenyl-4,4-dimethyl-5-isopropyl-5-hydroxy-Δ^2-1,2,3-triazoline (in DMSO-d_6).

groups are also equivalent as expected; but the signal from them is not split into a doublet, because the methine proton,which is adjacent to the carbonyl group, has been exchanged with deuterium from the solvent. Using undeuterated DMSO the signal appears as a doublet. The singlet at 1.13 ppm presumably comes from *tert*-butyl alcohol of crystallization; it persisted even after the K-salt had been thoroughly washed with ether. Perhaps the most interesting feature of the NMR spectrum (Fig. 2) is the appearance of the aromatic protons. Resonance considerations would predict high electron densities at both *ortho* and *para* positions, but seemingly only the *para* proton is being influenced, suffering an upfield shift of *ca.* 0.5 ppm relative to the other aromatic protons. This is presumably the effect of inter-electron repulsion,[6] which tends to disperse the charge to the extremities of the system, *i.e.* the *para* carbon atom and the Me_2C-N nitrogen atom. This effect was not observed with the corresponding 5-phenyl-triazoline anion in accordance with the assumed alkoxide structure (VIII) of this compound. The NMR spectrum of the analogous 5-*tert*-butyl triazoline potassium salt is almost identical to that shown in Fig. 2, the only major difference being that the signal at 0.86 ppm is replaced by a singlet at 1.08 ppm (*tert*-butyl).

Phenylallylpotassium, a salt containing a grouping isosteric with the phenyltriazene system, also shows the effect of inter-electron repulsion.[7] In passing, the amazing resemblance between the spectrum shown in Fig. 2 and that of diphenylmethyllithium (in tetrahydrofuran) [6] must be mentioned.

We conclude that anions of 5-hydroxy-Δ^2-1,2,3-triazolines, as well as the triazolines themselves, may exist in both an open and a closed form, III and VIII. In addition, since only a slight modification of R^5 (changing from Ph to iPr) is enough to change the state completely, it is reasonable to assume the existence of a very mobile equilibrium, A, between the two forms in solution, and that the position of this equilibrium is governed largely by the same effects that determine the triazoline/triazene equilibrium B.[2] However, there is no reason to expect the closed form, VIII, to be favored over III by solvents with high acceptor abilities in hydrogen bonding, as was the case with IX relative to IV.[2]

Regitz [8,9] also recognized the possibility of two structures, assigning closed and open structures to the potassium salts obtained from tosyl azide and desoxybenzoin ($R_a^4 = R^5 = Ph$) and trimethyldesoxybenzoin ($R_a^4 = Ph$, $R^5 = Me_3Ph$), respectively.

GENERAL CONSIDERATIONS ON BASE-CATALYZED REACTIONS OF ORGANIC AZIDES WITH CARBONYL COMPOUNDS (Scheme 1)

In the light of recent results with 5-hydroxy-Δ^2-1,2,3-triazolines [1,2,10,11] we believe there is a new basis for rationalizing the various known pathways that may be followed in base-catalyzed reactions of organic azides with carbonyl compounds as functions of substituents and medium used. The following is not claimed to be a comprehensive review for which the reader is referred to the existing ones;[4,12–15] rather only a few pertinent examples and references have been drawn out for purposes of illustration.

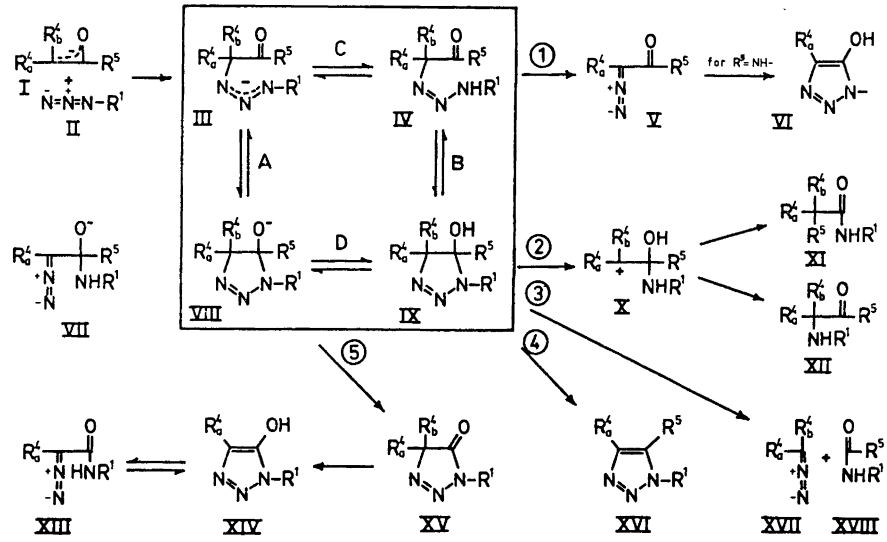

Scheme 1.

The principal feature of Scheme 1 is the four boxed equilibria A, B, C, and D, for which we have argued above and in previous papers. The existence of these equilibria implies that the species III, IV, VIII, and IX potentially are present in any reaction mixture. In addition the triazene IV is capable of existing in two tautomeric forms.[16] The relative concentrations of these species may vary with substituents and medium, and this in conjunction with differing reactivities gives variety to the product distribution.

The initial reaction (I + II→III) is presumably a one step nucleophilic attack on the terminal nitrogen atom of the azide by the appropriately generated carbanion.[15] Subsequent adjustment of the boxed equilibria is assumed to be fast relative to the reactions leading out from the box. The following examination of these irreversible reactions has been divided into sections according to substituents.

R^1 = alkyl or aryl; R_b^4 = H; R^5 = alkyl or aryl

Routes *1* and *4* are available, *4* being predominant for R^1 being alkyl.[1] Changing R^1 to aryl makes route *1* more favorable, at least as long as R_a^4 is an alkyl group. This is partly because ArNH is a better leaving group than RNH, and partly because equilibrium B is shifted upwards. A phenyl group at position 5 tends to neutralize this latter effect[2,10] and hence enhances *4* at the expense of *1*.[1,10]

The effect of R_a^4 being an electronegative group (aryl,[1] acyl, or alkoxycarbonyl[13]) is more straightforward. Now route *4* becomes the only passable,

irrespective of R^1 being aliphatic or aromatic. There are two reasons for this. First, an electronegative R_a^4 must be expected to exert a greater electron withdrawing effect on C-5 than on N-1, resulting in a downward shift of B.[2] Second, the kinetic acidity of $R_b^4 = H$ must increase much more in IX than in IV, because in IV the hydrogen atom is already activated by one carbonyl group (*cf.* Ref. 17). The reaction of acetoacetic ester with phenyl azide, known to produce XVI ($R^1 = Ph$, $R_a^4 = EtOOC$, $R^5 = Me$)[18] may serve as an example. This reaction also illustrates a situation where there are two possible directions of ring-closing III and IV, using either the keto C=O group or the ester C=O group. The former is the more electrophilic though, and the further reaction entirely follows route *4* rather than *5*, which would have become available if the ester C=O group were used (*vide infra*).

R^1 = aryl or alkyl; $R_b^4 = H$; $R^5 = OR$ or NHR (potential leaving groups)

Routes *1* and *5* may be used as exits from the box, the former only for R^1 being aryl, though. Reaction along route *4* has not been observed.

Working in strongly basic media it is conceivable that route *5*, if available, often gets preference over *1* and that XIV or its rearrangement product, XIII, then becomes the main product.[13] An example is the reaction of malonic ester with phenyl azide.[19] Base treatment of triazenes (IV), obtained by coupling esters of α-amino acids with benzene diazonium salts, also gives XIV as the major product.[20]

As pictured in Scheme 1 the formation of the postulated intermediate XV is analogous to a two step "olysis" of an ester group (Ref. 21, Ch. 12 and Ref. 22, Sect. 2.4), but a one step reaction (III→XV) cannot be excluded. On the other hand the route VIII→VII→XIII(⇌XIV) seems unlikely, since compounds of type XIV are formed irrespectively of the electronic character of R_a^4, which may be ROOC as well as Me or H.[19] Base-catalyzed ring-opening of triazolines to diazo compounds (VIII→VII) presumably requires that R_a^4 be electronegative.[23]

Reaction along route *1* may be increased at the expense of *5* by changing R^5 to a relatively poor leaving group, *e.g.* an amino group.[24,25] This may be because the conversion VIII→XV, in contrast to IV→V, will be slowed down, and possibly also because A and B are displaced upwards.[2]

We believe that the conversion IV→V is a one step reaction without intervention of an enol-anion;[24,26] the removal of $R_b^4 = H$ is involved in the rate limiting step. Therefore it is reasonable that the relative importance of *1* and *5* depends on the acidifying ability[17] of R_a^4. Thus the relatively poor acidifying phenyl group is observed to disfavor *1* relative to *5* when R^5 is NH_2.[24] For $R^5 = NHMe$ the effect is swamped by the much more important effect of a very poor leaving ability of NHMe and by a supposed upward shift of A; here route *1* becomes the only observed one.

For $R^5 = OR$ use of exit *1* has been inferred indirectly from observations on the reaction of malonic ester with phenyl azide;[27] but as mentioned above, *5* is most important.

R^1=aryl; R_a^4=alkyl or aryl; R_b^4=R'CO; R^5=OR or NHR

Assuming the triazene anion III to be the first intermediate, the formation of 1,2,3-triazoles requires an acyl cleavage to take place (R' may be an alkyl or alkoxy group). The predominant formation of products of type XIV in the reaction of phenyl azide with phenyl or methyl malonamides [24] (particularly for R^5=NHMe) suggests that the acyl cleavage mainly takes place under formation of some species that is not in equilibrium with the boxed ones in Scheme 1. If this were the case, we should get products of type VI (*cf.* the previous section, where R^5 being an amino group is mentioned to retard *5* in relation to *1*). Indeed an acyl cleavage is well possible in the assumed intermediate XV (XV(R_b^4=R'CO)→XV(R_b^4=H)), since three electronegative groups (two carbonyls and one azo group) are attached to the same carbon atom (*cf.* Refs. 28 and 21, Ch. 13). However, with the malonamides some acyl cleavage probably also takes place in IV [IV(R_b^4=R'CO)→IV(R_b^4=H)], since small amounts of VI are formed, particularly if R_a^4=Ph.[24]

For R^5=OR route *5* should be even more feasible, OR being a better leaving group than NHR. Subsequent acyl cleavage should lead to products of type XIV or XIII. This has been observed using diethyl α-methylmalonate and ethyl α-methylacetoacetate as starting materials.[19]

R^1=Tosyl (or other benzenesulfonyl derivatives)

In this case route *1* is highly favored for two reasons, namely the high leaving ability of NHTos [29] as compared with NHAr or NHR and an upward shift of B (and A). Actually, the reaction may often (when R_a^4 is R'CO) be carried out under conditions mild enough (aliphatic amines as catalysts [26,30]) to prevent the relatively sensitive diazo compounds V from undergoing subsequent reactions. Hence the reaction of tosyl azide with carbonyl compounds provides an excellent method for the preparation of α-diazocarbonyl compounds.[4]

Stronger bases (alkali metal bases) must be used as catalysts if R_a^4 differs from R'CO, and products of type V may then undergo further reactions. In some cases, however, such a change of base may have another effect, because it shifts C and D to the left and thus opens up for route *5* if R^5 is a potential leaving group, *e.g.*, OR. In fact, this reaction course then often becomes dominating,[8,9,30,31] unless R^5 is very bulky, *e.g.*, Bu^t–O.[30] NHR is too poor a leaving group, and with carboxamides one expectedly gets conversion *1*.[32]

In general 1-tosyl-Δ^2-1,2,3-triazolines are unstable compounds,[33,34] the conversions *2* and *3* taking place spontaneously. These reactions are expected to take place in weakly basic media,[26,35] in strongly protic media,[8,9] if B is shifted downward for one reason or another (R^5=H or Ph [5,26]), or simply if *1*, *4*, and *5* are precluded (R_b^4≠H).

EXPERIMENTAL

NMR spectra were recorded on a Varian A-60 instrument, using TMS as an internal standard. Chemical shifts are given as δ-values. IR spectra were recorded on a Perkin-Elmer model 421 instrument.

Treatment of 1-phenyl-4,5-dimethyl-5-hydroxy-Δ^2-1,2,3-triazoline with potassium hydroxide. To a solution of 0.34 g of the triazoline [2] in 5 ml of methanol was added 4 mg of KOH, and the mixture was let stand for two days at 35°C. It was then poured into 50 ml of water and extracted with methylene chloride. Drying (Na_2SO_4) and evaporation on a rotary evaporator (25°C, 60 mmHg) gave a mixture of 1-phenyl-4,5-dimethyl-1,2,3-triazole, aniline, and 3-diazobutanone. The latter compound was distilled at 1 mmHg (temp. of water bath: 25 – 35°C), giving 78 mg of a thin yellow liquid. NMR showed that it consisted of 3-diazobutanone and aniline in a molar ratio of 9:2. The NMR spectrum ($CDCl_3$) at 25°C showed broad singlets of equal integrals at 1.97 and 2.22 ppm. At – 20°C two conformers were observable. The preponderating form exhibited signals at 1.98 and 2.29 ppm, and the other form at 2.16 and 2.18 ppm. The IR spectrum showed the diazo band at 2075 cm^{-1}.

Acknowledgements. The author is grateful to Professor C. Pedersen and Professor P. Olesen Larsen for many valuable suggestions for the improvement of this manuscript.

REFERENCES

1. Olsen, C. E. *Acta Chem. Scand.* **27** (1973) 2983.
2. Olsen, C. E. and Pedersen, C. *Acta Chem. Scand.* **27** (1973) 2279.
3. Wentrup, C. and Dahn, H. *Helv. Chim. Acta* **53** (1970) 1637.
4. Regitz, M. *Angew. Chem.* **79** (1967) 786.
5. Regitz, M. and Menz, F. *Chem. Ber.* **101** (1968) 2622.
6. Sandel, V. R. and Freedman, H. H. *J. Am. Chem. Soc.* **85** (1963) 2328.
7. Sandel, V. R., McKinley, S. V. and Freedman, H. H. *J. Am. Chem. Soc.* **90** (1968) 495.
8. Regitz, M. *Chem. Ber.* **98** (1965) 1210.
9. Regitz, M. *Angew. Chem.* **78** (1966) 684.
10. Olsen, C. E. *Acta Chem. Scand.* **27** (1973) 1987.
11. Olsen, C. E. *Thesis*, Technical University of Denmark, DK-2800 Lyngby, Denmark, 1969 (in English).
12. Grundmann, C. In *Methoden der Org. Chemie*, Georg Thieme, Leipzig 1965, 4. Ed., vol. 10/3, p. 813.
13. Benson, F. R. and Savell, W. L. *Chem. Rev.* **46** (1950) 1.
14. Boyer, J. H. In *Heterocyclic Compounds*, Wiley, New York 1961, Vol. 7, p. 384.
15. L'Abbe, G. *Ind. Chim. Belge* **34** (1969) 519.
16. Hadzi, D. and Jan, J. *Spectrosc. Lett.* **1** (1968) 139.
17. Cram, D. J. *Fundamentals of Carbanion Chemistry*, Academic, 1965, pp. 8 – 20.
18. Dimroth, O. *Ber.* **35** (1902) 1029.
19. Dimroth, O. *Ber.* **35** (1902) 4041.
20. Olsen, C. E. *To be published.*
21. Hine, J. *Physical Organic Chemistry*, McGraw, New York 1962.
22. Gutsche, C. D. *The Chemistry of Carbonyl Compounds*, Prentice-Hall, 1967.
23. Huisgen, R., Szeimies, G. and Möbius, L. *Chem. Ber.* **99** (1966) 475.
24. Begtrup, M. and Pedersen, C. *Acta Chem. Scand.* **18** (1964) 1333.
25. Dimroth, O. *Ann.* **373** (1910) 336.
26. Hendrickson, J. B. and Wolf, W. A. *J. Org. Chem.* **33** (1968) 3610.
27. Begtrup, M., Larsen, P. S. and Pedersen, C. *Acta Chem. Scand.* **22** (1968) 2476.
28. Yao, H. C. and Resnick, P. *J. Am. Chem. Soc.* **84** (1962) 3514.
29. Fischer, W. and Anselme, J.-P. *J. Am. Chem. Soc.* **89** (1967) 5285.
30. Regitz, M. and Liedhegener, A. *Chem. Ber.* **99** (1966) 3128.
31. van Leusen, A. M., Smid, P. M. and Strating, J. *Tetrahedron Letters* **1965** 337.
32. Regitz, M. and Geelhaar, H. J. *Chem. Ber.* **102** (1969) 1743.
33. Fusco, R., Bianchetti, G., Pocar, D. and Ugo, R. *Chem. Ber.* **96** (1963) 802.
34. L'Abbe, G. *Ind. Chim. Belge* **32** (1967) 541.
35. Rosenberger, M., Yates, P., Hendrickson, J. B. and Wolf, W. *Tetrahedron Letters* **1964** 2285.

Received May 2, 1973.

ACTA CHEMICA SCANDINAVICA 27 (1973) 2997–3002

Intestinal Glycoproteins of Germfree Rats

II. Further Studies on the Chemical Composition of Water-soluble Extracts from Intestinal Mucus

JENS K. WOLD,[a] TORE MIDTVEDT[b] and RANDI WINSNES[a]

[a] *Institute of Pharmacy, Department of Pharmacognosy, University of Oslo, Oslo 3, Norway and* [b] *Kaptein W. Wilhelmsen og Frues Bakteriologiske Institutt, Rikshospitalet, Oslo 1, Norway*

Injection of glucose-^{14}C into germfree rats was followed, after 24 h, by removal of the entire gut and preparation of the aqueous non-dialysable extracts from contents of the small intestine, cecum, colon, and feces. The extracts were hydrolysed by acid for the release of sugars, which were then separated by paper chromatography and finally subjected to radioautography. In each of the extracts the following sugars were found to be radioactively labelled: galactose, mannose, fucose, *N*-acetylgalactosamine, *N*-acetylglucosamine, and sialic acid. Arabinose and xylose were not radioactive, and the presence of these sugars is ascribed to extraneous polymer carbohydrate in the intestinal contents. This material remained in the germfree rat intestinal tract even after a ten day dietary adjustment period during which the animals were fed a chemically defined diet, containing glucose as the only sugar.

The extracts of cecum and colon were similar in their contents of carbohydrate, protein, and sulphate. In comparison, the extract of the small intestine contained more protein, less carbohydrate, and no sulphate.

In an initial study [1] it was found that aqueous non-dialysable extracts of intestinal and fecal mucus from germfree rats, fed a chemically defined diet, consisted of carbohydrate and protein. The extracts contained the common glycoprotein sugars galactose, mannose, fucose, *N*-acetylgalactosamine, *N*-acetylglucosamine, and sialic acid.

The main amino acids present were serine and threonine, suggesting that a major part of the extracts might consist of mucin-type glycoproteins. This was consistent with the fact that mild alkali treatment of the material caused a marked decrease in the contents of serine and threonine.[2] In addition the extracts also contained significant quantities of the pentose sugars xylose and arabinose. There has been a number of reports on the occurrence of arabinose [3]

and xylose [4–6] in mammalian mucopolysaccharides and glycoproteins, but so far these pentoses have never been encountered as constituents of mucins. It has been clearly demonstrated that xylose is a structural component of mucopolysaccharides like heparin and chondroitin sulphate, were it serves as the point of linkage between carbohydrate and protein.[7,8]

However, in the case of other classes of glycoproteins the occurrence of pentose sugars as an integral part of the molecular structure has never been firmly established by chemical proof. At present it is thought that the occasional finding of pentoses in glycoproteins is due either to artefact formation, *e.g.* during acid hydrolysis, or more probably, to impure glycoprotein preparations. Our inability to completely remove the pentose-containing material from the glycoprotein fraction by ion exchange or gel chromatography necessitated an investigation into the origin of xylose and arabinose.

The monosaccharide components of mammalian glycoproteins, including the xylose residues of the mucopolysaccharides, are normally formed from D-glucose.[9] Thus by administering radioactively labelled glucose to the animals the label will appear in all the different sugars incorporated during glycoprotein biosynthesis. By using this method it was shown that the water-soluble, non-dialysable extracts from contents of different intestinal segments and of the feces from rats given glucose–^{14}C intraperitoneally were all radioactive. The relative levels of radioactivity in the four extracts were decreasing from the small intestinal to the fecal extract as measured on the lyophilized samples under identical conditions by the Geiger-Müller counter (Table 1).

Table 1. Relative amounts of radioactivity in non-dialysable extracts from the contents of the small intestine, cecum, colon, and from the feces. The measurements were done under identical conditions on lyophilized samples (10 mg) by a Geiger-Müller counter. Correction is made for background radiation, and the counts are adjusted to the nearest hundred.

Extract from	Counts per minute
Small intestine	2000
Cecum	1400
Colon	1300
Feces	600

The measurements can be regarded only as semiquantitative, but the trend is clear. The corresponding low-molecular weight fractions present in the respective dialysates, and also the lipid fractions (the combined acetone, chloroform-methanol, and ether extracts) all contained label but much less than the high-molecular weight material.

Thus it seems that the major part of the label is incorporated into macromolecular substances, and that the bulk of the radioactively labelled compounds secreted into the intestinal tract is not excreted from the animal during the 24 h after the injection of glucose-^{14}C.

Previous studies have demonstrated that epithelial cells of the rat small and large intestine incorporate labelled carbohydrate into glycoproteins [10–13] which are then gradually secreted into the intestinal lumen. Judging from the results obtained it seemed appropriate to collect the intestinal contents about 24 h after the injection of labelled sugar.

Each of the aqueous non-dialysable extracts was hydrolysed under the appropriate conditions for the release of neutral sugars, amino sugars, and sialic acid, respectively. Paper chromatography of the acid hydrolysates and subsequent radioautography, apparently, revealed label in all the sugars except arabinose, xylose, and the tiny amount of glucose present.

Larger quantities of the extracts were hydrolysed and the sugars fractionated by chromatography on thick filter paper. Each of the monosaccharides was isolated separately and then subjected to paper chromatography in at least three different solvent systems followed by radioautography. In every instance the dark spots visible on the X-ray film coincided both with the location and the shape of the spots revealed by the use of the appropriate spray reagents for sugars. The results clearly indicated that galactose, mannose, fucose, *N*-acetylglucosamine, *N*-acetylgalactosamine, *N*-acetylneuraminic acid, and *N*-glycolylneuraminic acid had become radioactively labelled after glucose-^{14}C injection. On the other hand paper chromatography of the isolated arabinose and xylose and subsequent radioautography revealed no trace of radioactivity, even when applying more than the normal amount of sugar to the chromatogram. Neither the trace amount of glucose isolated showed any sign of being radioactive.

No labelled carbohydrate could be detected in the intestinal and fecal extracts obtained from the animal that had received an injection of xylose-^{14}C. This finding is consistent with the general conception that xylose is not utilized as such by mammalian cells, but only after being formed by enzymic decarboxylation of uridine diphosphate glucuronic acid to uridine diphosphate xylose.[14,15]

The occurrence of non-labelled carbohydrate as part of the high-molecular weight intestinal contents from the animals that had received glucose-^{14}C suggests that this non-radioactive fraction is not produced by the animal. Thus the intestinal mucus of the rats that had been fed the synthetic diet for ten days probably contained exogenous polymer carbohydrate.

Extracts prepared separately of the intestinal contents from more than ten animals fed the chemically defined diet for ten days invariably proved to contain pentoses. The most likely source of a high-molecular weight carbohydrate contaminant would be the rat food used prior to the synthetic diet. The ordinary germfree rat diet was subjected to the general extraction procedure, and the non-dialysable extract obtained was analysed quantitatively for carbohydrate. Similarly, extracts of the contents of the small intestine, cecum and colon from the rats fed the synthetic diet for ten days were prepared and analysed under identical conditions. The extracts from the three segments of the gut all contained the same sugars although in somewhat different amounts and molar proportions (Table 2).

The rat food extract differed markedly from the intestinal extracts in its carbohydrate composition. It consisted mainly of glucose, xylose, and arabinose

Table 2. Composition of water-soluble, non-dialysable extracts from the contents of small intestine, cecum, and colon, and of the corresponding extract obtained from the ordinary germfree rat diet.

	Extract from							
	Small intestine		Cecum		Colon		Rat food	
	%[a]	Rel.am.[b]	%[a]	Rel.am.[b]	%[a]	Rel.am.[b]	%[a]	Rel.am.[b]
Arabinose	0.6	0.6	1.6	0.5	0.8	0.5	9.5	0.6
Xylose	1.0	1.0	3.0	1.0	1.5	1.0	15.3	1.0
Fucose	5.0	4.7	6.4	2.0	6.2	3.8	0.0	
Mannose	3.6	3.1	3.2	0.9	2.2	1.2	0.8	0.05
Galactose	11.0	9.4	15.1	4.2	14.7	8.2	1.7	0.1
N-Acetylgalactosamine	7.3	5.1	10.6	2.4	10.8	4.9	0.0	
N-Acetylglucosamine	11.5	8.4	12.3	2.8	12.2	5.5	0.0	
Sialic acid[c]	5.2	2.6	5.0	0.8	8.0	2.6	0.0	
Glucose	0.0		0.0		0.0		61.0	3.4
Total carbohydrate	45.2		57.2		56.4		88.3	
Protein	53.9		33.0		32.2		8.5	
Sulphate	0.0		0.4		0.3		0.0	
Total	99.1		90.6		88.9		96.8	

[a] Per cent of the lyophilized material, dried over phosphorus pentoxide *in vacuo*. [b] Molar proportions relative to xylose. [c] The content of sialic acid is calculated as *N*-acetylneuraminic acid.

and was devoid of fucose, hexosamine, and sialic acid. The molar ratio of xylose to arabinose is strikingly constant in all the four extracts. This makes it reasonable to conclude that the polymer material containing the two pentoses originates from the rat food and that this food component passes mainly unaltered through the gastrointestinal tract. On the other hand the greater proportion of the glucose-containing polymer in the rat food is obviously utilized by the animals.

No attempt was made to estimate the time required for the complete clearing of the pentose-containing diet from the intestinal tract. It seems likely that non-absorbable diet components are trapped, to some extent, in intestinal crypts, partly because of the reduced motility and propulsive activity of the germfree intestinal tract,[16] and partly because of the gel-like viscous mucoid material filling up the entire intestinal lumen.

Even if the analytical data presented in Table 2 are obtained on heterogeneous material consisting of a mixture of macromolecules, a comparison of the chemical composition of the three intestinal extracts still is informative. There is a significant difference between the extracts of the cecum and colon on one side and of the small intestine on the other side (Table 2). The small intestinal extract contains much more protein, no sulphate, and the sum of protein and carbohydrate makes up almost 100 % of the extract while these components account for only about 90 % of the extracts from the cecum and colon. This may be due to the presence in the cecum and colon mainly of mucin-type glycoproteins, giving an incomplete Lowry reaction because of the large number of carbohydrate side chains, thus resulting in a too low protein value.

Regarding the amount and composition of carbohydrate in the three extracts, again there is a rather close resemblance between the extracts of colon and cecum compared to that of the small intestine. The finding of sulphate ester groups in the two former extracts could be indicative of contamination with mucopolysaccharides, but all the intestinal extracts were devoid of uronic acid thus ruling out this possibility. On the other hand mucin glycoproteins frequently contain a small proportion of sulphate, and in the present case such substances would be the most probable source of the sulphate ester residues.

Fractionation experiments have revealed a considerable complexity in the composition of the extracts described in the present report. However, it appears that the intestinal mucin, which is regarded to be the predominant glycoprotein fraction of the germfree intestinal tract, can be obtained in a sufficient state of purity required for more detailed studies.

EXPERIMENTAL

Germfree rats of the CDF strain (The Charles River Breeding Laboratories, Wilmington, Mass., USA) were reared under the conditions described by Midtvedt and Trippestad.[17] Animals of both sexes, more than 40 days of age, were used in the experiments.

Two animals, fed the ordinary germfree rat diet, were given a single intraperitoneal injection of D-glucose-^{14}C, uniformly labelled, 0.5 mCi/animal. Similarly one animal, fed the same diet, was given a single intraperitoneal injection of D-xylose-^{14}C, uniformly labelled, 0.1 mCi. After 24 h the animals were anaesthesized by ether and sacrificed. The contents of the small intestine, cecum, colon, and the feces excreted during the 24 h were immediately collected separately under sterile conditions and stored at $-20°$.

In another experiment animals were fed the chemically defined diet under the same conditions as described previously.[1] After ten days the animals were sacrificed and the contents of the small intestine, cecum, and colon were collected and stored as above.

The conditions for the preparation of the intestinal extracts as well as for the acid hydrolysis and paper chromatography were as reported previously.[1] In addition neutral sugars were liberated from the polymer material by hydrolysis with 2 N sulphuric acid at 100° for 4 h. The deionized hydrolysates were subjected to preparative paper chromatography on Whatman No. 3 MM paper in either of the solvent systems, by volume: Ethyl acetate, acetic acid, formic acid, water, 18:3:1:4, or ethyl acetate, pyridine, acetic acid, water, 5:5:1:3. Three additional solvent systems were introduced for paper chromatography, by volume: Butanol, propanol, 0.1 N hydrochloric acid, 1:2:1; propanol, acetic acid, water, 7:1:2; ethyl acetate, pyridine, water, 8:2:1. Methanolysis was carried out by heating the lyophilized and dried sample, 1 mg, with 1 N hydrogen chloride in methanol at 85° for 20 h.

Gas-liquid chromatography of the derived trimethylsilylated methyl glycosides was performed on columns of 0.1 % OV-17 on glass beads using a Perkin-Elmer 900 gas chromatograph. The experimental details were as given by Reinhold.[18]

Radioactive compounds were located by a Geiger-Müller counter (Frieske & Hoepfner) or by radioautography.

When using radioautography the paper chromatograms were kept on X-ray film for three to four weeks.

Protein was estimated by the Lowry procedure,[19] bovine serum albumin being used as the standard. Sulphate was estimated by the barium chloroanilate method by Spencer.[20]

REFERENCES

1. Wold, J. K., Khan, R. and Midtvedt, T. *Acta Pathol. Microbiol. Scand.* **B 79** (1971) 525.
2. Anderson, B., Seno, N., Sampson, P., Riley, J. G., Hoffman, P. and Meyer, K. *J. Biol. Chem.* **239** (1964) 2716 PC.
3. Stary, Z., Wardi, A. H., Turner, D. L. and Allen, W. S. *Arch. Biochem. Biophys.* **110** (1965) 388.
4. Draper, P. and Kent, P. W. *Biochem. J.* **86** (1963) 248.
5. Weicker, H. and Grässlin, D. *Nature* **212** (1966) 715.
6. Weicker, H. and Jeanloz, R. W. *Federation Proc.* **26** (1967) 607.
7. Lindahl, U., Cifonelli, J. A., Lindahl, B. and Rodén, L. *J. Biol. Chem.* **240** (1965) 2817.
8. Lindahl, U. and Rodén, L. *J. Biol. Chem.* **240** (1965) 2821.
9. Hassid, W. Z. In Pigman, W. and Horton, D. *The Carbohydrates*, Academic, New York and London 1970, Vol. 2A, p. 301.
10. Peterson, M. and Leblond, C. P. *J. Cell Biol.* **21** (1964) 143.
11. Neutra, M. and Leblond, C. P. *J. Cell Biol.* **30** (1966) 119.
12. Neutra, M. and Leblond, C. P. *J. Cell Biol.* **30** (1966) 137.
13. Bennett, G. and Leblond, C. P. *J. Cell Biol.* **46** (1970) 409.
14. Bdolah, A. and Feingold, D. S. *Biochem. Biophys. Res. Commun.* **21** (1965) 543.
15. Grebner, E. E., Hall, C. W. and Neufeld, E. F. *Biochem. Biophys. Res. Commun.* **22** (1966) 672.
16. Abrams, G. D. and Bishop, J. E. *Proc. Soc. Exptl. Biol. Med.* **126** (1967) 301.
17. Midtvedt, T. and Trippestad, A. *Acta Pathol. Microbiol. Scand.* **B 78** (1970) 1.
18. Reinhold, V. N. *Methods in Enzymology* **25** (1972) 244.
19. Lowry, O. H., Rosebrough, N. J., Farr, A. L. and Randall, R. J. *J. Biol. Chem.* **193** (1951) 265.
20. Spencer, B. *Biochem. J.* **75** (1960) 435.

Received April 14, 1973.